सत्यमेव जयते

INDIAN AGRICULTURAL
RESEARCH INSTITUTE, NEW DELHI

30464

I.A.R.I.6.
GIP NLK—H-3 I.A.R.I.—10-5-55—15,000

TRANSACTIONS OF THE FARADAY SOCIETY

Founded in 1903 to promote the study of
Electrochemistry, Electrometallurgy, Chemical
Physics, Metallography, and Kindred Subjects

VOL. XLVI, 1950

30464
IARI

THE FARADAY SOCIETY

Agents for the Society's Publications
The Aberdeen University Press Ltd.
6 Upper Kirkgate
Aberdeen

PRINTED IN GREAT BRITAIN AT
THE UNIVERSITY PRESS
ABERDEEN

EXTRAPOLATION FORMULAE IN DIPOLE MOMENT MEASUREMENTS

By R. J. W. Le Fèvre

Received 25th May, 1949

The formula of Le Fèvre and Vine, and that afterwards proposed by Halverstadt and Kumler, are shown to be similar at all, and identical at zero, concentrations of solute. The discussion is illustrated by reference to data, mostly hitherto unpublished, for solutions of $PhNO_2$, PhCl, and $CHCl_3$, in C_6H_6. The variation of ϵ or d with weight fraction is found not to be rectilinear. The extrapolation procedures of Hedestrand or Cleverdon and Smith can, however, be applied successfully. Using the refractivity method, the following appparent dipole moments are recorded: $PhNO_2$, $\mu = 3{\cdot}9_5$ to $3{\cdot}9_7$, PhCl, $1{\cdot}5_9$, $CHCl_3$, $1{\cdot}2_1$ D.

During 1936-39, at University College, London, and to a less extent through the past two years in Sydney, we have accumulated concentration–dielectric constant–density measurements, in benzene at 25°, on 54 solutions of nitrobenzene, 22 of chlorobenzene, and 15 of chloroform. To date, only a few of these are available in other papers (e.g.[1, 2]). Cleverdon and Smith[3] have recently assembled and reviewed the data of other workers on the $PhNO_2 + C_6H_6$ system. We think it would be useful to add our unpublished material, since it confirms the conclusions of Cleverdon and Smith concerning nitrobenzene, and leads to analogous ones in the other two cases.

The original motive for the investigation came when Le Fèvre and Vine[4] rewrote the extrapolation formula of Hedestrand[5] for use with weight rather than molar fractions. Hedestrand had noticed that the dielectric constants ϵ or densities d of a series of solutions were often of a rectilinear form with f, e.g.

$$\epsilon_{12} = \epsilon_2(1 + \alpha f_1),$$

where f_1 is the molar fraction of the solute. From a number of constants, together with the practically accessible coefficients α and β (for ϵ_{12} and d_{12} respectively), the total molecular polarization at infinite dilution was theoretically calculable from determinations on *one* solution, in contrast to the older graphical method, which, to be dependable, required the examination of numerous mixtures ranging over the lower end of the concentration scale, i.e. the very region in which application of the simple additive rules magnifies experimental errors.

Hedestrand, however, was aware that the graphs of f_1 with ϵ_{12} or d_{12} were not always straight lines, and that expressions of the type

$$\epsilon_{12} = \epsilon_2 + \alpha f_1 + \alpha' f_1^2$$

were sometimes more satisfactory. For such instances he recommended that—since it is difficult to fit a tangent to a curve—the desired limiting slopes should be obtained by plotting the apparent coefficients against f_1, extrapolating to $f_1 = 0$, and using the values so obtained in the equation for $_\infty P_1$ (total polarization of solute at infinite dilution). Hedestrand thus forestalled both the subsequent criticisms of Svirbely, Ablard and Warner[6] and Otto's reply[7] to them.

---

[1] Le Fèvre and Russell, *J. Chem. Soc.*, 1936, 491.

[2] Le Fèvre and Le Fèvre, *ibid.*, 1936, 1136.

[3] Cleverdon and Smith, *Trans. Faraday Soc.*, 1949, **45**, 109.

[4] Le Fèvre and Vine, *J. Chem. Soc.*, 1937, 1805.

[5] Hedestrand, *Z. physik. Chem. B*, 1929, **2**, 428.

[6] Svirbely, Ablard and Warner, *J. Amer. Chem. Soc.*, 1935, **57**, 652.

[7] Otto, *ibid.*, 1935, **57**, 1147.

When, in 1937, we sought to add the arithmetical simplicity of weight fractions to the other advantages of Hedestrand's method we knew that, if d_{12} and ϵ_{12} were truly linear with f_1, then they could not also be so with w_1 (the weight fraction of the solute) unless $M_1 = M_2$ (M = molecular weight). In general, w_1 against f_1 is curved, towards or away from the f_1 axis as M_2/M_1 is less than or greater than unity. At the outset, therefore, we were prepared to find that the α and β coefficients of Le Fèvre and Vine [4] varied with concentration (w_1) and required extrapolation to $w_1 = 0$. The various sets of measurements then to hand, however, usually related to a few dilute solutions of each solute taken at concentrations insufficiently spaced from one another to enable definite drifts in α or β to be recognizable above the experimental errors.

For these reasons in 1938-39 we prepared the first series of

$$PhNO_2 + C_6H_6,\ PhCl + C_6H_6 \text{ and } CHCl_3 + C_6H_6$$

mixtures, where Ph denotes C_6H_5, falling within w_1 ranges 0·002 to 0·25, 0·003 to 0·15, and 0·004 to 0·19 respectively, and measured them at 25° by our (then) standard routine.[8] The expected effects were found, especially with weight fractions above about 2 %. Thus for the three substances we recorded for the multipliers of w_1, i.e. $\alpha\epsilon_2 = (\epsilon_{12} - \epsilon_2)/w_1$ and $\beta d_2 = (d_{12} - d_2)/w_1$, the following expressions :

(*a*) $PhNO_2$ (31 solutions)

$$\left.\begin{array}{l}(\epsilon_{12} - \epsilon_2)/w_1 = 14{\cdot}07 + 11{\cdot}60\, w_1\\ (d_{12} - d_2)/w_1 = 0{\cdot}2412 + 0{\cdot}075\, w_1\end{array}\right\} {}_\infty P_1 = 354{\cdot}8 \text{ cm.}^3$$

(*b*) PhCl (13 solutions)

$$\left.\begin{array}{l}(\epsilon_{12} - \epsilon_2)/w_1 = 2{\cdot}502 + 0{\cdot}6120\, w_1\\ (d_{12} - d_2)/w_1 = 0{\cdot}1844 + 0{\cdot}018\, w_1\end{array}\right\} {}_\infty P_1 = 83{\cdot}2 \text{ cm.}^3$$

(*c*) $CHCl_3$ (10 solutions)

$$\left.\begin{array}{l}(\epsilon_{12} - \epsilon_2)/w_1 = 1{\cdot}230 + 0{\cdot}5167\, w_1\\ (d_{12} - d_2)/w_1 = 0{\cdot}3554 + 0{\cdot}112\, w_1\end{array}\right\} {}_\infty P_1 = 51{\cdot}8 \text{ cm.}^3$$

From these, the polarizations when $w_1 = 0$, calculated as

$$M_1 p_2(1 - \beta) + M_1 C \alpha \epsilon_2,$$

where

$$\begin{aligned} p_2 &= (\epsilon_2 - 1)/(\epsilon_2 + 2)d_2,\\ C &= 3/d_2(\epsilon_2 + 2)^2,\\ d_2 &= 0{\cdot}87369 \text{ and } \epsilon_2 = 2{\cdot}2725,\end{aligned}$$

(cf. [4]) were as shown. Warned by this pre-war evidence, we have since adopted the practice of extrapolating $\alpha\epsilon_2$ and βd_2 to zero w_1 whenever these quantities seem to display a clear concentration dependence.[9]

During the past two years further measurements have been collected with apparatus [10] different from that formerly used,[8] both as regards the standard variable condensers and the designs of the replaceable capacities. The lower limits have been extended down to 0·1 %, and more examples of greater strengths added, so that there are now available for review the three groups of solutions, mentioned at the beginning of this paper, each comprising a roughly regularly graded series of w_1 figures from 0·1 % to 30 %, 18 %, and 21 %, for $PhNO_2$, PhCl, and $CHCl_3$, respectively. To provide a fixed basis for comparison, all results have been recalculated relatively to $\epsilon_2 = 2{\cdot}2725$ and $d_2 = 0{\cdot}87369$; it is satisfactory that, irrespective of sample, apparatus, time and place, they have proved to be, by this treatment, mutually harmonious.

---

[8] Le Fèvre, *Dipole Moments* (Methuen, 1938), Ch. II.

[9] Calderbank and Le Fèvre, *J. Chem. Soc.*, 1949, 199, 1462 ; Le Fèvre and Welsh, *ibid.*, 1909.

[10] Calderbank and Le Fèvre, *ibid.*, 1948, 1949.

It is unnecessary to record the numerous individual observations in the conventional tabular form; instead are quoted the equations for $\alpha\epsilon_2$ and βd_2, obtained by application of the method of least squares.[11] Taking the three solutes *seriatum*:

A. NITROBENZENE.

(i) 54 solutions ($w_1 = 0$ to $0{\cdot}3$)
$$\left.\begin{array}{l}\alpha\epsilon_2{}^* = 14{\cdot}07 + 11{\cdot}59\, w_1 \\ \beta d_2{}^* = 0{\cdot}2406 + 0{\cdot}0772\, w_1\end{array}\right\} \infty P_1 = 356{\cdot}1.$$

(ii) 26 solutions ($w_1 = 0{\cdot}01$ to $0{\cdot}30$)
$$\left.\begin{array}{l}\alpha\epsilon_2{}^* = 14{\cdot}19 + 10{\cdot}90\, w_1 \\ \beta d_2{}^* = 0{\cdot}2445 + 0{\cdot}0555\, w_1\end{array}\right\} \infty P_1 = 358{\cdot}6.$$

B. CHLOROBENZENE.

(i) 22 solutions ($w_1 = 0$ to $0{\cdot}18$)
$$\left.\begin{array}{l}\alpha\epsilon_2{}^* = 2{\cdot}5082 + 0{\cdot}613\, w_1 \\ \beta d_2{}^* = 0{\cdot}18429 + 0{\cdot}018\, w_1\end{array}\right\} \infty P_1 = 83{\cdot}34.$$

(ii) 10 solutions ($w_1 = 0{\cdot}02$ to $0{\cdot}18$)
$$\left.\begin{array}{l}\alpha\epsilon_2{}^* = 2{\cdot}5091 + 0{\cdot}598\, w_1 \\ \beta d_2{}^* = 0{\cdot}18432 + 0{\cdot}016\, w_1\end{array}\right\} \infty P_1 = 83{\cdot}35.$$

C. CHLOROFORM.

(i) 15 solutions ($w_1 = 0$ to $0{\cdot}21$)
$$\left.\begin{array}{l}\alpha\epsilon_2{}^* = 1{\cdot}2288 + 0{\cdot}517\, w_1 \\ \beta d_2{}^* = 0{\cdot}35528 + 0{\cdot}112\, w_1\end{array}\right\} \infty P_1 = 51{\cdot}74$$

(ii) 9 solutions ($w_1 = 0{\cdot}02$ to $0{\cdot}21$)
$$\left.\begin{array}{l}\alpha\epsilon_2{}^* = 1{\cdot}2290 + 0{\cdot}515\, w_1 \\ \beta d_2{}^* = 0{\cdot}35531 + 0{\cdot}110\, w_1\end{array}\right\} \infty P_1 = 51{\cdot}74.$$

With solutions weaker than *ca.* 1·5 % in each of the three cases, no trend of the coefficients could be discerned above the variations due to experimental errors. By ignoring curvature and taking mean values, in the manner we have often done since 1938 [12] the following are obtained:

(D) $PhNO_2$	(32 solutions)	$\alpha\epsilon_2 = 14{\cdot}09$	$\beta d_2 = 0{\cdot}2400$	$\infty P_1 = 356{\cdot}5$ cm.^{3}.
(E) $PhCl$	(9 „)	„ $= 2{\cdot}511$	„ $= 0{\cdot}1845$	„ $= 83{\cdot}4$ „
(F) $CHCl_3$	(5 „)	„ $= 1{\cdot}240$	„ $= 0{\cdot}3591$	„ $= 51{\cdot}8$ „

From these polarizations the apparent dipole moments of the solutes may be estimated by applying the refractivity method, taking $(R_L)_D$ as 32·74 cm.^{3} for nitrobenzene, 31·14 for chlorobenzene, 21·40 for chloroform, and $\mu = 0{\cdot}2198 \times (\infty P_1 - R_L)^{\frac{1}{2}}$ at 25°: †

Series	A(i)	A(ii)	B(i)	B(ii)	C(i)	C(ii)
μ in D . .	$3{\cdot}95_2$	$3{\cdot}96_7$	$1{\cdot}58_8$	$1{\cdot}58_8$	$1{\cdot}21_1$	$1{\cdot}21_1$

Series	*a*	*b*	*c*	D	E	F
μ in D . .	$3{\cdot}9_5$	$1{\cdot}5_9$	$1{\cdot}2_1$	$3{\cdot}9_5$	$1{\cdot}5_9$	$1{\cdot}2_1$

The above results illustrate the two routes to $(\alpha\epsilon_2)_{w_1=0}$ and $(\beta d_2)_{w_1=0}$, viz. the indirect and the direct. The former has the advantage of needing fewer solutions and allowing the use of concentrations at which the accuracies of most apparatus and techniques are adequate. It is seen that, with $CHCl_3$ or C_6H_5Cl, the results either way are identical. Even with the strongly polar $C_6H_5NO_2$, the difference (3·97 against 3·95 D) is of small consequence in the face of the unknown uncertainties introduced by taking $(R_L)_D$ as an approximation to the distortion polarization. This convention is common among dipole moment studies made with chemical or stereochemical objectives in mind. Nevertheless, it is now clear that arithmetic means of $\alpha\epsilon_2$ and βd_2 should only be taken when experimental indications cannot justify anything more than a rough constancy of these terms. In all other cases, the procedures exemplified in this paper should be applied. The advice given on pages 40 and 41 of ref. 8 needs amendment accordingly. As already stated we have made this our standard post-war practice since resuming work at Sydney.

---

[11] Mellor, *Higher Mathematics* (Longmans, 1931), 326.

[12] E.g., Hopf and Le Fèvre, *J. Chem. Soc.*, 1938, 1582.

* That is, the " constants " as determined, referred to above as the " multipliers of w_1".

† The latest values for Avogadro's number and Boltzmann's constant (Birge, *Reports Prog. Physics*, 1941, 8, 126) would require a slightly higher numerical factor, namely, 0·2212. The figure 0·2198 is retained here to assist comparison with the results of many previous workers, including Cleverdon and Smith. Multiplication by 1·006 will correct the moments shown.

Cleverdon and Smith [3] have further considered the proposals of Halverstadt and Kumler,[13] regarding (*a*) the derivation of the proper dielectric constant of the pure solvent, and (*b*) the evaluation of the specific polarizations p_1 of solutes at infinite dilution from ϵ_{12} and d_{12} measurements over a graded set of concentrations. With Cleverdon and Smith's remarks on (*a*) we agree, indeed, the possibility that the ϵ_{12} against w_1 graph is sometimes curved is basic to their paper and to this. As to point (*b*), it is interesting to note how the Halverstadt-Kumler and Le Fèvre-Vine, methods of calculation differ. The respective equations are :

$$\infty p_1 = (v_2 + \beta)(\epsilon_2 - 1)/(\epsilon_2 + 2) + 3\alpha v_2/(\epsilon_2 + 2)^2 \quad . \quad \text{H.-K.}$$

$$\infty p_1 = p_2(1 - \beta) + C\alpha\epsilon_2 \quad . \quad . \quad . \quad . \quad . \quad . \quad \text{L.-V.}$$

C (of L.-V.) has been expanded above. The *v*'s of H.-K. represent specific volumes; their α is $(\epsilon_{12} - \epsilon_2)/w_1$, i.e. the $\alpha\epsilon_2$ of Le Fèvre and Vine. The second terms of the expressions for ∞p_1 are therefore identical. H.-K. define β as $(v_{12} - v_2)/w_1$, whilst L.-V.'s β is $(d_{12} - d_2)/d_2 w_1$; hence $\beta_{\text{H.-K.}} = -\beta_{\text{L.-V.}}/d_{12}$. The H.-K. equation therefore becomes :

$$\infty p_1 = p_2(1 - \beta_{\text{L.-V.}} d_2/d_{12}) + \alpha C\epsilon_2.$$

In other words, in so far as d_2/d_{12} is close to unity (e.g. with dilute solutions) so should the same ∞p_1 be obtained by either process.

As an illustration the two groups listed under c(i) and c(ii) above have been recalculated by the H.-K. formula. Over both ranges, $\beta_{\text{H.-K.}}$. is notably more constant than is $\beta_{\text{L.-V.}}$ (this agrees with the remarks of Cleverdon and Smith, pp. 111 and 112 of ref. 3), but a slight numerical increase with dilution is obvious among the members of c(ii) (the sign of $\beta_{\text{H.-K.}}$ is negative). The $\beta_{\text{H.-K.}}$ against w_1 graph for c(ii) passes through the points for c(i) with a credible semblance to rectilinearity, although with small w_1 values there is scatter due to experimental errors, just as there is when $\beta_{\text{L.-V.}}$, is similarly plotted. By least squares, on c(i) $\beta_{\text{H.-K.}} = 0{\cdot}054\, w_1 - 0{\cdot}4656$, whence at infinite dilution, $\infty P_1 = 51{\cdot}7_2$ cm.^{3} (as a check on the calculations, we note that our βd_2 of 0·3553 divided by $-d_2^2$ gives $-$ 0·4655).

Between the two methods, therefore, there is little to choose. The use of specific volumes, rather than densities, because $\beta_{\text{H.-K.}}$ seems to be less concentration dependent than $\beta_{\text{L.-V.}}$, might sometimes be a disadvantage, by obscuring a trend which $\beta_{\text{L.-V.}}$ would reveal. On a given set of observed data, both treatments should yield the same ∞P_1.

Finally, both Hedestrand [5] and Cleverdon and Smith [3] mention that for very strong solutions powers of f_1 or w_1 higher than 2, or even other terms involving w_1, would be necessary. The concentrated mixtures, examined by Le Fèvre and Le Fèvre [14] provide some relevant information if they are recomputed with the benzene as solvent:

---

[13] Halverstadt and Kumler, *J. Amer. Chem. Soc.*, 1942, 64, 2988.

Solute	$PhNO_2$	$PhCl$	$CHCl_3$
Concentration range (100 w_1)	93-97	85-95	90-97
Apparent $\alpha\epsilon_2$ range	30-32	3·2-3·3	2·1-2·4
Apparent βd_2 range	0·31-0·32	0·21-0·22	0·56-0·58

Using the equations of this paper for $\alpha\epsilon_2$ and βd_2 for solutions of $w_1 = 0{\cdot}9$, these factors should have been $\alpha\epsilon_2 = 24{\cdot}5$, 3·0, 1·7 and $\beta d_2 = 0{\cdot}29$, 0·20 and 0·46, respectively; they are seen to be in all cases too small. Relations including w_1^3 might provide the necessary adjustment.

The author thanks the Chemical Society for various research grants made during the period 1936 to date.

School of Chemistry,
University of Sydney,
N.S.W., Australia.

---

[14] Le Fèvre and Le Fèvre, *J. Chem. Soc.*, 1936, 487.

KINETIC STUDIES IN HETEROGENEOUS BUFFER SYSTEMS

PART I.—THE SYSTEM ZINC HYDROXIDE AND ZINC SULPHATE

BY R. P. BELL AND J. E. PRUE

Received 10*th June*, 1949

Measurements have been made at 25°, 35° and 45° C of the hydroxyl ion concentrations in solutions of zinc sulphate partly precipitated by the addition of sodium hydroxide. The ionic strength was kept constant by the addition of sodium chloride or potassium iodide, and measurements were made with a cell without liquid junctions. The hydroxyl ion concentrations were stable and reproducible, but their dependence on the concentration of zinc ions could not be explained quantitatively in terms of a fixed stoichiometric composition for the solid phase. Measurements with a glass electrode showed that these systems have a rapid buffer action when acid is added.

The same buffer systems were used to study the initial rates of the reaction between acetone and iodine at 25°. The dependence of the rate on hydroxyl ion concentration gave a value for the catalytic constant of the hydroxyl ion in fair agreement with the most reliable previous value, but the system exerts other catalytic effects which are not completely understood.

In the usual type of homogeneous buffer system use is made of an equilibrium between dissolved species (including the solvent). In order that such a system should be little affected by small amounts of added substances it is necessary that the concentrations of all components except one should be relatively high. For example, in the buffer systems

$$CH_3COOH + H_2O \rightleftharpoons CH_3COO^- + H_3O^+$$

and

$$HPO_4^{=} + H_2O \rightleftharpoons H_2PO_4^- + OH^-$$

the concentrations of hydrogen and hydroxyl ions will only remain constant if the concentrations of CH_3COOH, CH_3COO^-, $HPO_4^=$ and $H_2PO_4^-$ are large compared with the amounts of acid or base added to the system. This condition is often disadvantageous, since it implies the presence in solution of considerable concentrations of acidic or basic species. In particular, if a reaction exhibiting general acid-base catalysis is studied kinetically in a buffer solution, the catalytic effect of the buffer constituents may far outweigh that of hydrogen or hydroxyl ions, and the latter can only be evaluated by measuring velocities at different concentrations of buffer and making an uncertain extrapolation to zero buffer concentration. In a few cases it is possible to measure catalysis by hydrogen or hydroxyl ions in dilute solutions of strong acids or bases, but the necessary concentrations are usually so low that they would be sensitive to minute traces of impurities, and the method is not suitable for reactions which produce or consume hydrogen ions.

There are two ways in which this difficulty may be avoided. In the first place it may be possible to use homogeneous equilibria which control the concentration of hydrogen and hydroxyl ions without involving appreciable concentrations of species which are individually acids or bases (in the sense of being proton donors or acceptors). For example, in the equilibrium

$$Br_2 + H_2O \rightleftharpoons Br^- + H^+ + HOBr$$

the hydrogen ion concentration is controlled by the concentrations of Br_2, Br^- and HOBr, though no basic species is present, and the weakly acidic function of HOBr plays no part in the equilibrium.[1] A less extreme example is afforded by the equilibrium

$$CO_2 + H_2O \rightleftharpoons H_2CO_3 \rightleftharpoons H^+ + HCO_3^-,$$

where the concentration of H_2CO_3 is very small, the buffer capacity of the system being provided by the non-acidic CO_2. Not only is the concentration of acid molecules very low, but because of the nature of the equilibrium involved the basic anion HCO_3^- has a much lower catalytic power [2] than would be expected from the apparent dissociation constant of H_2CO_3. Such buffer systems should therefore be particularly suitable for studying catalysis by hydrogen and hydroxyl ions, and the same may be true in general of buffers containing pseudo-acid-base systems, since it has been recently shown [3] that the catalytic power of pseudo-acids and bases may be several powers of ten lower than that of ordinary acids and bases of the same strength.

The other method of attacking the problem is to have the greater part of the acidic or basic component (or both) held in reserve in another phase, i.e. to use a buffer system which is heterogeneous. For example, if a sparingly soluble acid HX is in equilibrium with a solution containing the anion X^-, then the hydrogen ion concentration will be controlled by the value of $[X^-]$, although the amount of HX in solution may be very small indeed. Similarly, if a sparingly soluble hydroxide $X(OH)_n$ is in equilibrium with a solution containing the cation X^{n+}, then the value of $[OH^-]$ will be inversely proportional to $[X^{n+}]^{1/n}$. Similar relations will hold if the solid phase consists of an acidic or basic salt instead of a simple acid or hydroxide.

The existence of this buffering action is shown by the curves obtained by Britton [4] and others for the titration of heavy metal salts with alkali. However, although different workers are in general agreement as to the general form of these curves, there are discrepancies of up to ± 0·5 pH units in their absolute values. This suggests that there may be variations in the chemical or physical nature of the solid phase, or that equilibrium is reached only slowly. We have therefore made a rough survey of a number of metallic hydroxide systems, especially those with buffer ranges of pH 6-9, since this range would be useful for studying reactions sensitive to hydroxyl ions. Of the systems studied, only zinc hydroxide + zinc sulphate appeared to be sufficiently reproducible and adaptable, and the present paper describes a further investigation of this system. Firstly, the equilibrium hydroxyl ion concentrations have been measured as a function of the zinc ion concentration, using cells without liquid junctions. Secondly, the rate of adaptation of the system to the addition of acid was investigated and found to be satisfactory, and finally it was used for kinetic measurements in the reaction between acetone and iodine.

---

[1] Cf. Bell, Everett and Longuet-Higgins, *Proc. Roy. Soc. A.*, 1946, **186**, 443.

[2] Cf. Roughton and Booth, *Biochem. J.*, 1938, **32**, 2049. Olson and Youle, *J. Amer. Chem. Soc.*, 1940, **62**, 1027.

[3] Bell and Higginson, *Proc. Roy. Soc. A*, 1949, **197**, 141.

[4] Britton, *Hydrogen Ions*, 3rd ed., 1942, vol. 2, p. 35.

Experimental and Results

Measurements of Electromotive Force.—Earlier work[5] with the hydrogen, glass and quinhydrone electrodes showed that the buffer range of this system is in the neighbourhood of pH 7, though individual values vary within a whole pH unit. Several authors report difficulty in using a hydrogen or quinhydrone electrode in presence of zinc salts,[6] and the above measurements were carried out with cells involving liquid junctions and varying ionic strengths, thus making interpretation difficult.

The cells used in the present work were of the following types:

(*a*) $Pt(H_2) \mid CaSO_4, NaOH, NaCl \mid AgCl . Ag.$
(*b*) $Pt(H_2) \mid ZnSO_4, Na_2SO_4, Zn(OH)_2, NaCl \mid AgCl . Ag.$

The difference of the E.M.F.'s of these cells is given by

$$E_a - E_b = -\frac{RT}{F} \ln \frac{[H^+]_a[Cl^-]_a f^a_{H^+} f^b_{Cl^-}}{[H^+]_b[Cl^-]_b f^b_{H^+} f^b_{Cl^-}} \quad . \quad . \quad . \quad (1)$$

$$= -\frac{RT}{F} \ln \frac{[OH^-]_b[Cl^-]_a f^b_{OH^-} f^a_{Cl^-}}{[OH^-]_a[Cl^-]_b f^a_{OH^-} f^b_{Cl^-}} .$$

This expression can be much simplified if we can assume that the activity coefficients of OH^- and Cl^- are the same in the two cells: this was ensured as far as possible by making all solutions to a constant ionic strength of approximately 0·2, and by comparing solutions with the same concentration of $SO_4^=$, and in which $[Ca^{++}]_a = [Zn^{++}]_b$. Under these conditions eqn. (1) can be written

$$E_a - E_b = -\frac{RT}{F} \ln \frac{[OH^-]_b[Cl^-]_a}{[OH^-]_a[Cl^-]_b} \quad . \quad . \quad . \quad . \quad (2)$$

and $[OH^-]_b$ can be obtained in terms of known quantities. Similar experiments were carried out with Ag / AgI electrodes, and with potassium iodide replacing sodium chloride throughout, when an expression analogous to (2) will apply.

The value of $[OH^-]_a$ will not be exactly equal to the stoichiometric concentration of added NaOH, because of a partial formation of the species $CaOH^+$, $CaSO_4$, and $NaSO_4^-$ (or KSO_4^-). A correction was applied for this, using the dissociation constants given by Davies[7] for these species together with the appropriate expressions for their variation with ionic strength, and solving the three simultaneous quadratic equations by successive approximations. It will be seen from Table I that the correction is a small one (1—8 °/₀). It is also possible that the stoichiometric value of $[Cl^-]_b$ is decreased slightly by the formation of complexes with Zn^{++}, but the value of the dissociation constant of $ZnCl^+$ given by Sillén and Liljeqvist[8] (the lowest in the literature) indicates a correction of less than 1 °/$_0$. In iodide solutions the correction will be still smaller. It was also suspected that the concentration of halide ions might be affected by adsorption on the zinc precipitate, but this was shown to be inappreciable by electrometric titration of the solution after centrifuging off the precipitate.

---

[5] Kolthoff and Kameda, *J. Amer. Chem. Soc.*, 1931, **53**, 832; Britton and Robinson, *Trans. Faraday Soc.*, 1932, **28**, 531; Nikurashin, *J. Gen. Chem. Russ.*, 1938, **8**, 1454.

[6] E.g. Britton, *J. Sci. Instr.*, 1948, **23**, 89.

[7] Davies, *J. Chem. Soc.*, 1938, 276.

[8] Sillén and Liljeqvist, *Svensk Kem. Tidskr.*, 1944, **56**, 85.

TABLE I.—CALCIUM SOLUTIONS

Chloride electrodes

$$E' = E_a + \frac{RT}{F} \ln \frac{[\mathrm{Cl}^-]}{[\mathrm{OH}^-]_{\mathrm{corr.}}}.$$

$[\mathrm{Ca}^{++}]$	$[\mathrm{Cl}^-]$	[NaOH]	$[\mathrm{OH}^-]$(corr.)	E'		
				25°	35°	45°
0·01192	0·1738	0·01010	0·00920	1·0514	1·0529	1·0545
0·00497	0·2006	0·01000	0·00964	1·0507	1·0526	1·0544
0·00339	0·2055	0·01000	0·00970	1·0506	1·0522	1·0537
0·00202	0·2135	0·01000	0·00984	1·0506	1·0525	1·0544

Iodide electrodes

$$E' = E_a + \frac{RT}{F} \ln \frac{[\mathrm{I}^-]}{[\mathrm{OH}^-]_{\mathrm{corr.}}}.$$

$[\mathrm{Ca}^{++}]$	$[\mathrm{I}^-]$	[NaOH]	$[\mathrm{OH}^-]$(corr.)	E'		
				25°	35°	45°
0·00966	0·1517	0·00977	0·00897	0·6768	0·6817	0·6868
0·00682	0·1635	0·00978	0·00918	0·6764	0·6815	0·6864
0·00437	0·1730	0·00978	0·00948	0·6768	0·6816	0·6865
0·00329	0·1766	0·00977	0·00947	0·6764	0·6812	0·6864
0·00187	0·1820	0·00975	0·00965	0·6763	0·6812	0·6862

The measurements were carried out in a Harned type cell designed by Prof. D. H. Everett, containing duplicate electrodes for checking. It was filled by a vacuum technique to avoid the introduction of oxygen, and measurements were made at 25°, 35° and 45° ± 0·01° with a vernier potentiometer reading to 0·01 mV. Hydrogen electrodes were prepared as described by Popoff, Kunz and Snow [9] and the hydrogen used was passed over copper at 600° and presaturated with the vapour of the solution being measured. Silver/silver chloride electrodes were prepared as described by Smith and Taylor [10] and showed mutual agreement to within 0·04 mV. Silver/silver iodide electrodes prepared by an analogous procedure were less satisfactory, but were reproducible to ± 0·2 mV. Solutions were made up with conductivity water and A.R. materials, and the zinc solutions were prepared throughout by adding one equivalent of sodium hydroxide per mole of $\mathrm{ZnSO_4}$. The concentrations of zinc ion remaining in solution, given in Table II, are calculated on the assumption that the precipitate has the composition $3\mathrm{Zn(OH)_2} \,.\, \mathrm{ZnSO_4}$, for which there is good evidence [11] for concentrations of zinc ions greater than 0·00075 M.

The cells of type (*a*) came to equilibrium quickly, and potentials were reproducible to 0·1-0·2 mV. In cells of type (*b*) the presence of zinc ions had an adverse effect on the performance of the hydrogen electrode, which was very sluggish and frequently became poisoned. (After use in zinc solutions it was often necessary to clean the electrode with emery paper before a satisfactory deposit of platinum black could be obtained). However, by checking the

[9] Popoff, Kunz and Snow, *J. Physic. Chem.*, 1928, **32**, 1056.

[10] Smith and Taylor, *J. Res. Nat. Bur. Stand.*, 1938, **20**, 837.

[11] Feitknecht, *Helv. chim. Acta*, 1930, **13**, 22.

duplicate electrodes it was possible to obtain results reproducible to ± 0·5 mV, corresponding to about ± 2 °/₀ in the final hydroxyl ion concentrations. The results of all the electromotive force measurements are given in Tables I and II.

TABLE II.—ZINC SOLUTIONS

Chloride electrodes

$$E'' = E_b + \frac{RT}{F} \ln [\mathrm{Cl}^-].$$

$[\mathrm{Zn}^{++}]$	$[\mathrm{Cl}^-]$	E''			$-\log_{10}[\mathrm{OH}^-]$		
		25°	35°	45°	25°	35°	45°
0·01204	0·1168	0·6229	0·6182	0·6118	7·244	7·144	7·017
0·01052	0·1375	0·6249	0·6205	0·6166	7·207	7·074	6·940
0·00756	0·2125	0·6279	0·6249	0·6211	7·155	7·000	6·868
0·00499	0·1835	0·6350	0·6323	0·6279	7·031	6·877	6·759
0·00379	0·1975	0·6404	0·6374	0·6342	6·939	6·794	6·659
0·00304	0·2010	0·6450	0·6406	0·6379	6·865	6·723	6·601
0·00191	0·2101	0·6568	0·6499	—	6·661	6·588	—

Iodide electrodes

$$E'' = E_b + \frac{RT}{F} \ln [\mathrm{I}^-].$$

$[\mathrm{Zn}^{++}]$	$[\mathrm{I}^-]$	E''			$-\log_{10}[\mathrm{OH}^-]$		
		25°	35°	45°	25°	35°	45°
0·01050	0·0978	0·2507	0·2447	0·2414	7·207	7·153	7·060
*0·00906	0·1211	0·2523	0·2450	0·2421	7·180	7·147	7·047
0·00804	0·1507	0·2524	0·2493	0·2450	7·176	7·074	6·995
0·00586	0·1478	0·2563	—	—	7·108	—	—
0·00404	0·1670	0·2625	0·2603	0·2559	7·000	6·890	6·823
*0·00345	0·1657	0·2613	0·2587	0·2565	7·020	6·915	6·814
0·00253	0·1711	0·2707	0·2682	0·2647	6·860	6·759	6·682
*0·00246	0·1743	0·2664	0·2637	0·2595	6·933	6·831	6·764
0·00202	0·1798	0·2672	0·2721	0·2703	6·767	6·694	6·594

* indicates that an excess of precipitate has been added to the solution.

The E.M.F. of cell (*a*) is given by the expression

$$E_a = E_0 - \frac{RT}{F} \ln \frac{K_w[\mathrm{X}^-]f_{\mathrm{X}^-}}{[\mathrm{OH}^-]f_{\mathrm{OH}^-}}, \quad . \quad . \quad . \quad . \quad (3)$$

where X^- is the halide ion present, and the quantity E' in Table I is therefore

$$E' = E_a + \frac{RT}{F} \ln \frac{[\mathrm{X}^-]}{[\mathrm{OH}^-]} = E_0 - \frac{RT}{F} \ln \frac{K_w f_{\mathrm{X}^-}}{f_{\mathrm{OH}^-}}. \quad . \quad . \quad (4)$$

The right-hand side of this expression should be nearly constant at a given temperature and ionic strength, and the constancy of E' in Table I shows that the method of allowing for the incomplete dissociation of CaOH^+ and other species is justified.

There is a considerable difference, increasing with temperature, between the $[\mathrm{OH}^-]$ values for chloride and those for iodide. This is no doubt due to the different degree of complex formation by these two anions, and the sign of the difference corresponds to a smaller complex formation by iodide than by chloride, as has been suggested on other grounds. On the other hand, it is not easy to explain quantitatively the observed variation of $[\mathrm{OH}^-]$ with $[\mathrm{Zn}^{++}]$.

The systems were prepared by adding one equivalent of NaOH per mole of $ZnSO_4$, and if the solid phase precipitated is $3Zn(OH)_2 . ZnSO_4$, each solution should contain one-third of the original zinc ion concentration, and five-sixths of the sulphate ion concentration. The equilibrium governing the hydroxyl ion concentration is

$$3\,Zn(OH)_2 . ZnSO_4 \rightleftharpoons 6\,OH^- + 4\,Zn^{++} + SO_4^=,$$

and we should therefore have

$$\text{Const.} = [OH^-]^6[SO_4^=][Zn^{++}]^4 = 5/2[OH^-]^6[Zn^{++}]^5.$$

Actually, however, the slope of plots of $\log_{10}[OH^-]$ against $\log_{10}[Zn^{++}]$ is nearer to two-thirds than to five-sixths, with some tendency to curvature, especially at 25°. (The precipitation of a simple hydroxide $Zn(OH)_2$ would give a slope of one-half.) The discrepancy may be related to complex formation with the halide ions present, but this is not likely, since the slopes are the same for chloride as for iodide. It is more probable that the composition of the precipitate varies with that of the solution, and this explanation is supported by the fact that systems to which an excess of precipitate had been added gave pH values higher by 0·05-0·1 unit, corresponding to the removal of more zinc ions from solution. It should be noted that these uncertainties as to the exact nature of the solid phase do not affect the validity of the hydroxyl ion concentrations given in Table II. The system is stable and reproducible, and was always made up in the same way, while the values given for Zn^{++} were calculated throughout on the assumption that the precipitate is $3\,Zn(OH)_2 . ZnSO_4$.

Tests of Adaptability.—The reproducibility of the E.M.F. measurements shows that the buffer system responds rapidly to any chance acidic or basic impurities. A much more stringent test was carried out by running dilute acid into the well-stirred system at a constant rate, and observing the pH of the system. This was effected by means of a commercial pH meter using glass and calomel electrodes, which was found to respond immediately to pH changes in the region of pH 7 (phosphate buffer). The acid was added from a micro-burette through a long capillary, and the liquid stirred vigorously by a rotary glass stirrer. Experiments were carried out with varying rates of addition, and no appreciable displacement of pH was observed for rates up to about 5×10^{-5} mole l.$^{-1}$ min.$^{-1}$. The results of a typical experiment are shown in Fig. 1. In the kinetic experiments described below the rate of production of acid is 1 to 5×10^{-6} mole. l.$^{-1}$ min.$^{-1}$, so that the buffering power of the system is ample for this purpose.

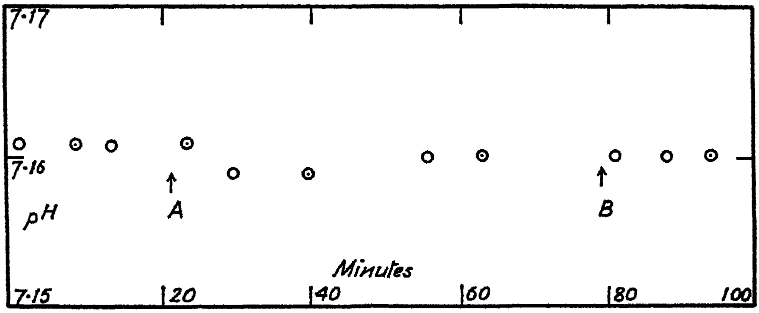

FIG. 1.

A. Addition of acid started ($3{\cdot}1 \times 10^{-5}$ mole l.$^{-1}$ min.$^{-1}$).
B. Addition of acid stopped.

Kinetic Measurements.—The reaction studied was that between acetone and iodine, which is well known to be catalyzed by both acids and bases and to be of zero order with respect to halogen. There is, however, considerable difficulty in obtaining a reliable catalytic coefficient for hydroxyl ions. Dawson and Key [12] gave $k_{OH^-} = 26$ at 25° (in mole halogen min.$^{-1}$, referred to a solution molar with respect to both acetone and hydroxyl ions). This value was obtained from measurements in phosphate buffers, and a re-calculation by Bell and Lidwell[13] gave $k_{OH^-} = 17$. Bell and Lidwell also derived a value of $k_{OH^-} = 15$ using the pH values of trichlorophenate buffers measured with a glass electrode. However, measurements with a hydrogen electrode[14] gave $3{\cdot}2 \times 10^{-6}$ as the dissociation constant of trichlorophenol, and if this value is used the same kinetic data lead to $k_{OH^-} = 34$. Probably the most reliable value to date is $k_{OH^-} = 31$, obtained by Bell and Longuet-Higgins[15] from experiments in very dilute solutions of sodium hydroxide.

---

[12] Dawson and Key, *J. Chem. Soc.*, 1928, 543.

The approximate magnitude of k_{OH^-} indicates that the reaction should proceed at a convenient speed in the zinc hydroxide + zinc sulphate buffers. Experiments were carried out in the systems already described (made up with iodide) with the addition of 0·07 M acetone, earlier measurements with 0·3 to 0·5 M acetone having shown that some displacement of pH is caused by these high concentrations. The system was stirred in the thermostat for 1 hr. at 25°, and enough N/10 iodine added to make the solution approximately 0·002 N in iodine. Stirring was continued, and 10 ml. samples withdrawn from time to time for titration with N/100 thiosulphate (using a micro-burette). Owing to the colloidal nature of the precipitate it was not found possible to filter samples of solution into the pipette, but the amount of precipitate removed with each sample is small and approximately constant. Precautions are necessary to obtain accurate titrations with these dilute solutions. It has been shown by Kolthoff[16] that there is a danger of oxidation of tetrathionate to sulphate

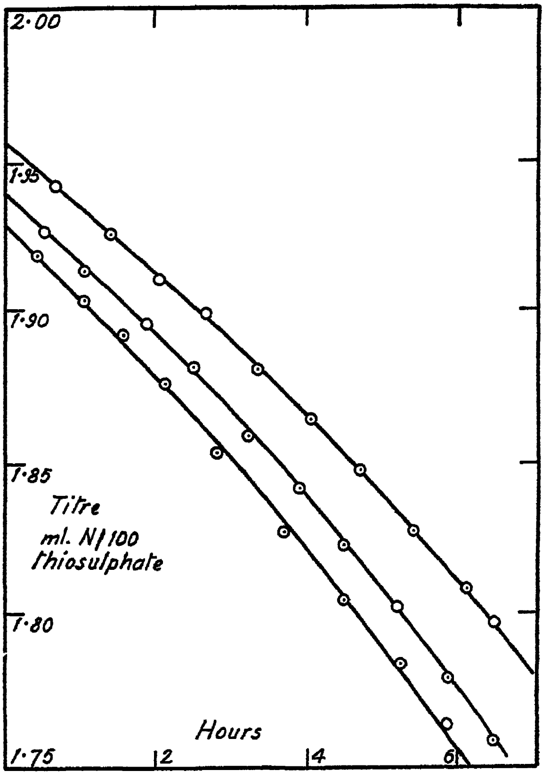

FIG. 2.

---

[13] Bell and Lidwell, *Proc. Roy. Soc. A*, 1940, **176**, 88.

[14] Ogston, *J. Chem. Soc.*, 1936, 1713.

[15] Bell and Longuet-Higgins, *ibid.*, 1946, 636.

[16] Kolthoff, *Z. anal. Chem.*, 1921, **60**, 341.

unless pH is kept sufficiently low, and this was effected by adding acetic acid until the solution was just clear. The end-point was determined by the " dead-stop " method,[17] in which a small current is passed between two platinum electrodes in the solution ; the removal of the last trace of iodine allows the cathode to polarize and the current then falls sharply to zero. By this procedure it was possible to obtain an accuracy of ± 0·003 ml. N/100 thiosulphate, as claimed by Evans.[17]

Fig. 2 shows typical results for the early part of the reaction ; it will be seen that the plots are curved, the rate increasing as the reaction proceeds. This is in the opposite direction to the effect which would be caused by a failure of the buffer to respond quickly enough, and a similar curvature was observed by Bergstein [18] in experiments with phosphate buffers in the region of pH 7. This behaviour differs from the linear plots normally obtained for this reaction, but can be accounted for in terms of the successive introduction of three iodine atoms into the acetone molecule. We shall consider first the simpler case in which only two atoms are introduced. The kinetic scheme can then be written as

$$\mathrm{RH_2}\ \text{-}$$

$$\mathrm{RHI} + \mathrm{I_2} \xrightarrow[k_2]{} \mathrm{RI_2}$$

where each stage is a zero-order reaction with respect to halogen, but first order with respect to ketone, the first-order constants k_1 and k_2 being proportional to the concentration of catalyst (here the hydroxyl ion). It is then easily shown that the amount of halogen h used up after time t is given by

$$h = \frac{a}{k_2 - k_1}\{2(k_2 - k_1) - (2k_2 - k_1)e^{-k_1 t} + k_1 e^{-k_2 t}\}, \quad . \quad . \quad (5)$$

where a is the initial concentration of ketone, and the rate of disappearance of halogen is

$$\frac{dh}{dt} = \frac{k_1 a}{k_2 - k_1}\{(2k_2 - k_1)e^{-k_1 t} - k_2 e^{-k_2 t}\}. \quad . \quad . \quad . \quad . \quad (6)$$

Eqn. (6) shows that the initial rate is given by

$$dh/dt = k_1 a.$$

If k_2 is considerably greater than k_1 the second exponential will eventually become negligibly small, and in a later phase of the reaction the rate will become

$$dh/dt = 2k_1 a\, e^{-k_1 t} \quad . \quad . \quad . \quad . \quad . \quad (7)$$

which is equivalent to

$$dh/dt = 2k_1 a$$

if the ketone is present in large excess. This second phase will be effectively reached when $e^{k_2 t} \gg 1$, i.e. when $t > 5/k_2$ for an accuracy of better than 1 %.

The halogenation of acetone can be treated similarly, except that there will now be three phases, and the velocity reached in the final phase will be $3k_1 a\, e^{-k_1 t}$. It has normally been assumed that in the base-catalyzed halogenation of acetone k_2 and k_3 are so large compared with k_1 that the final phase is reached almost immediately, and for catalysts like the acetate ion this is confirmed both by the linear nature of the halogenation plots and by direct measurements with halogen-substituted ketones. However, it is by no means certain that the same will be true for catalysis by hydroxyl ions, since there is evidence to show that the effect of halogen substitution on the reactivity of ketones is much smaller when either the ketone or the catalyst becomes highly reactive.[19] It is true that the experiments of Bell and Longuet-Higgins [15] in sodium hydroxide solutions followed a first-order course with an end-point corresponding to the introduction of three halogen atoms, indicating that the final phase had been effectively reached. However, this does not necessarily conflict with our results, since they used [OH$^-$] values of about 10^{-2} and times of 5 to 10 min., while we have used [OH$^-$] values of about 10^{-7} and times of 5 to 10 hr. : thus the fraction of the reaction observed in our experiments is less by a factor of about 1000 than that observed by Bell and Longuet-Higgins.

---

[17] Foulk and Bawden, *J. Amer. Chem. Soc.*, 1926, **48**, 2043. Evans, *Analyst*, 1947, **72**, 99.

[18] Bergstein, *J. Physic. Chem.*, 1927, **31**, 178.

[19] Bell and Lidwell, *loc. cit.* ; Bell, Gelles and Möller, *Proc. Roy. Soc. A*, 1949, **198**, 308.

We have therefore measured the initial reaction rates, corresponding to the introduction of one iodine atom, which can be done with some certainty thanks to the high accuracy of the titration method (cf. Fig. 2). The titres x were fitted to an equation of the type

$$x = x_0 + vt + at^2,$$

using the method of least squares, and the initial velocity is then given by the value of v. The results obtained are given in Table III, the values of [OH⁻] being obtained by interpolation from Table II.

TABLE III.—IODINATION OF ACETONE AT 25°

Initial velocities v in mole iodine/min., referred to 1 M acetone

10^3 [Zn⁺⁺]	10^8 [OH⁻]	$10^6\,v$
8·33	6·61	2·27
4·98	8·63	2·36
3·88	10·1	2·56
3·33	11·2	2·58
3·02	12·1	2·60
2·50	14·1	2·89
2·24	15·5	3·04
7·95	17·8	3·22

Fig. 3 shows a plot of v against [OH⁻]. It is linear within experimental error, its slope giving 9·3 as the catalytic coefficient of OH⁻ for the introduction of one iodine atom. This agrees reasonably well with the value 31 obtained by Bell and Longuet-Higgins[15] for the introduction of three iodine atoms, and serves to establish the value of this catalytic coefficient with some certainty.

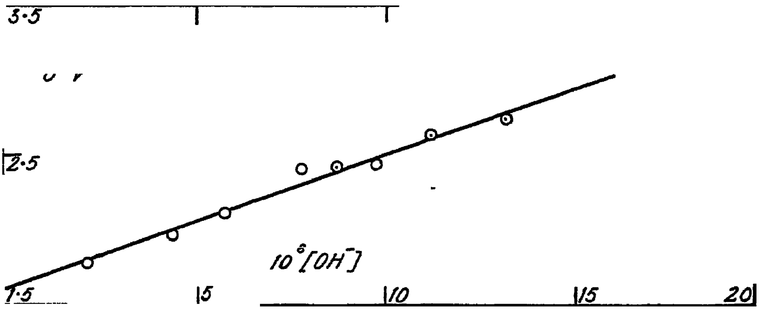

FIG. 3.

On the other hand, the large positive intercept in Fig. 3 is not easily explained, as it is about 100 times as great as the "spontaneous" or water-catalyzed reaction rate. It is not due to heterogeneous catalysis, since a change in the quantity of precipitate produces no measurable effect, nor do zinc ions alone produce any catalytic effect. It is probably due to catalysis by some dissolved species such as $Zn(OH)_2$ or ZnOH⁺, but it does not seem possible to settle this question in the absence of a complete understanding of the dependence of [OH⁻] upon [Zn⁺⁺].

Our thanks are due to Prof. D. H. Everett for advice and assistance in the measurements of electromotive force, and to the Department of Scientific and Industrial Research for a grant to one of us (J. E. P.).

Physical Chemistry Laboratory,
Oxford.

KINETIC STUDIES IN HETEROGENEOUS BUFFER SYSTEMS

PART II.—THE SYSTEM QUININE, QUININE SULPHATE AND POTASSIUM SULPHATE

BY R. P. BELL AND J. E. PRUE

Received 10*th June*, 1949

Buffer systems containing two solid phases are discussed, and a preliminary survey of a number of systems reported. The most satisfactory system was quinine + quinine sulphate + potassium sulphate, which exhibits buffer action in the region of pH 7-8, and responds rapidly to additions of acid or alkali. The dependence of the hydroxyl ion concentration on the concentration of sulphate ions was determined colorimetrically, using *m*-nitrophenol as indicator.

The buffer system was used for a kinetic study of the hydrolysis of methyl monochloroacetate and ethyl formate, and the mutarotation of glucose, all of which are very sensitive to hydroxyl ions. For the ester hydrolysis the observed velocity constants agree with those recalculated from earlier work. The catalytic constant obtained for the hydroxyl ion in the mutarotation of glucose is lower than the previous very divergent values, and is considered to be the most reliable value to date.

The first paper in this series[1] suggested the use of buffer systems containing one solid phase, and described measurements with one such buffer. This kind of system has the disadvantage that sparingly soluble acids and bases (including metallic hydroxides) are commonly weak electrolytes, so that the anion or cation added to control the pH of the system may itself have acidic or basic properties. The use of a buffer with one solid phase will thus usually cut down the concentration of either the acidic or the basic buffer component, while for some purposes it may be important to reduce the concentration of both components. This can be effected in principle by using a buffer system with two solid phases. For example, if a solution of sodium chloride is saturated simultaneously with a sparingly soluble acid HA and its sparingly soluble sodium salt NaA, then the pH will be controlled by the concentration of sodium ions, though there are no considerable concentrations of acidic or basic species in solution. The position is similar in a solution of sodium perchlorate saturated with a sparingly soluble base B and its perchlorate $BHClO_4$, the concentration of perchlorate ions being now the controlling factor. The stability and adaptability of such a system will vary greatly from one example to another, and the solubilities are in many cases not known. We have therefore made a rapid survey of a number of systems, mostly organic amines and their salts.

Experimental and Results

In this survey about 0·005 mole of each solid component was suspended with stirring in 50 ml. of a solution 0·1 M with respect to the controlling anion or cation, and pH observed with a glass electrode at room temperature. When this had become stready, small additions of acid and alkali were made alternately and the pH change observed after each addition. The results are summarized in Table I. A solubility was considered to be too high if it exceeded about 0·01 M.

---

[1] Bell and Prue, *Trans. Faraday Soc.* (preceding paper).

TABLE I.—BUFFER SYSTEMS WITH TWO SOLID PHASES

System	Approximate pH	Comments
Hexanitrodiphenylamine + potassium salt	6·0	Very slow adaptation
Tribenzylamine + hydrochloride	2·7	Rapid adaptation, but hydrochloride too soluble
α-Phenylcetylamine + hydrochloride	7	Slow adaptation
Brucine + perchlorate	8·8	Rapid adaptation, but perchlorate too soluble
Strychnine + perchlorate	8·2	Rapid adaptation, but not exactly reversible
Cinchonine + perchlorate	6·7	Moderate adaptation, but perchlorate too soluble
Acridine + picrate	8·7	Rapid adaptation, but pH rather erratic
5-Aminoacridine + hydrochloride	9·1	Fair adaptation, but rather erratic, and hydrochloride somewhat too soluble
Narcotine + picrate	5·8	No effective buffer action
Quinine + sulphate	8·3	Rapid adaptation and good stability

The most suitable of the systems in Table I appears to be quinine + quinine sulphate, and the solubilities are here reasonably low, being estimated at 1×10^{-3} M for quinine,[2] and $1{\cdot}6 \times 10^{-3}$ M for its sulphate.[2] (The solubility of the sulphate will, of course, be further depressed by the presence of an excess of sulphate ions.) Titration of the solution after centrifuging off the precipitate showed that these solubilities were not in fact exceeded. Typical results for the adaptability of this system are given in Table II.

TABLE II.—QUININE + QUININE SULPHATE IN 0·1 M K_2SO_4

Time (min.)	pH	Time (min.)	pH
0	8·27	111	†
80	8·32	111·5	8·35
86	*	112	8·32
86·5	8·24	117	8·31
87	8·28	120	8·30
90	8·30	140	8·30
109	8·30	—	—

* 1 ml. 0·2 N acid added at this point.
† 1 ml. 0·2 N alkali added at this point.

Measurement of Hydroxyl Ion Concentrations.—The glass electrode measurements are not suitable for obtaining absolute values of hydrogen or hydroxyl ion concentrations, and this was effected by colorimetric measurements with *m*-nitrophenol as an indicator. 0·1 g. quinine + 0·3 g. quinine sulphate was ground up with 50 ml. of a potassium sulphate solution of varying concentration (made up to an ionic strength of 0·2 with potassium chloride) and 4 ml. 0·02 M *m*-nitrophenol added. After standing and shaking at 25° the solution was filtered and its absorption for the 4360 Å mercury line measured with a Hilger photoelectric colorimeter, using a cell of 4 cm. depth. The absorption of the *m*-nitrophenate ion was also measured in solutions with an excess of alkali, and the indicator ratio can thus be calculated. No quinine *m*-nitrophenate was precipitated under these conditions, since if a solution of *m*-nitrophenol which had been treated with quinine buffer was made strongly alkaline, it gave the same absorption as a solution which had not been so treated. This also indicates that there is no appreciable adsorption of indicator by the precipitate, which is confirmed by the fact that the results obtained were independent of the amount of solid phase.

---

[2] Seidell, *Solubilities of Organic Compounds* (New York, 1941).

The results obtained are given in the first two columns of Table III. In the more dilute sulphate solutions two corrections are necessary to obtain the true sulphate concentration. In the first place the concentration of *m*-nitrophenate ion is an appreciable fraction of $[SO_4^{=}]$, and the latter is therefore reduced slightly on account of the reaction

$$\begin{gathered} 2\,C_6H_4(NO_2)OH + 2\,Q(s) + SO_4^{=} + 2\,H_2O \\ \rightarrow 2\,C_6H_4(NO_2)O^- + Q_2H_2SO_4(s) + 2\,OH^- \end{gathered}$$

where Q represents quinine. This correction does not exceed 4 %. In the second place the electroneutrality condition (omitting the potassium chloride) gives

$$2[K^+] + 2[QH^+] = [SO_4^{=}],$$

so that if $[QH^+]$ is an appreciable fraction of $[SO_4^{=}]$, the true sulphate ion concentration will be slightly greater than that of the original potassium sulphate solution, owing to dissolution of some quinine sulphate. Since the value of $[SO_4^{=}]$ is known to a first approximation, $[QH^+]$ can be obtained from the solubility product of quinine sulphate. The solubility of this salt in water (1·43 g./l.) gives

$$L = [QH^+]^2[SO_4^{=}] = 1{\cdot}77 \times 10^{-8}.$$

This figure refers to an ionic strength of $I = 0{\cdot}0054$, while all our measurements were carried out at $I = 0{\cdot}2$: hence if we use the standard expression

$$-\log_{10} f = \frac{0{\cdot}5\, z^2 \sqrt{I}}{1 + \sqrt{I}} \quad . \quad . \quad . \quad . \quad . \quad (1)$$

recommended by Guggenheim[3] for the activity coefficients of the QH^+ and $SO_4^{=}$ ions in the two solutions, the solubility product L' appropriate to our experiments is given by

$$\log_{10} \frac{L'}{L} = 3\left\{\frac{\sqrt{0{\cdot}2}}{1 + \sqrt{0{\cdot}2}} - \frac{\sqrt{0{\cdot}0054}}{1 + \sqrt{0{\cdot}0054}}\right\}, \quad . \quad . \quad . \quad (2)$$

whence $L' = 1{\cdot}06 \times 10^{-7}$. The value of $[SO_4^{=}]$ given in Table III and in all subsequent Tables have been corrected in this way for the solubility of the quinine sulphate. For values of $[SO_4^{=}] > 0{\cdot}01$ this correction is less than 7 %, but in the two most dilute solutions listed in Table III is 20 to 40 %. However, the value of the correction itself should be known to better than ± 10 %, and as the sulphate concentration enters into subsequent calculations as the square root no important error is introduced.

TABLE III.—INDICATOR RATIOS FOR *m*-NITROPHENOL IN QUININE + QUININE SULPHATE BUFFERS

$[SO_4^{=}]$ (corr.)	Ratio	Ratio/$[SO_4^{=}]^{\frac{1}{2}}$
0·0664	0·645	2·53
0·0496	0·546	2·45
0·0299	0·375	2·17
0·0163	0·294	2·29
0·0094	0·198	2·04
0·0052	0·185	2·56
		Mean = 2·34

---

[3] Guggenheim, *Phil. Mag.*, 1935, **19**, 588.

It is easily seen that the hydroxyl ion concentration in the quinine buffer is given by

$$[\mathrm{OH}^-] = \frac{K'_w Q'_s}{K'_Q \sqrt{L'}}[\mathrm{SO}_4^=]^{\frac{1}{2}} = K''[\mathrm{SO}_4^=]^{\frac{1}{2}}, \quad . \quad . \quad . \quad (3)$$

where K'_w = ionic product of water,
Q'_s = solubility of quinine,
K'_Q = concentration dissociation constant of QH^+,
L' = solubility product of quinine sulphate,
all at $I = 0{\cdot}2$.

Similarly for the *m*-nitrophenol equilibrium

$$[\mathrm{OH}^-] = \frac{K_w}{K_{NH}} \cdot \frac{f_{N^-}}{f_{OH^-}} \cdot \frac{[\mathrm{N}^-]}{[\mathrm{NH}]} \simeq \frac{K_w}{K_{NH}} \cdot \frac{[\mathrm{N}^-]}{[\mathrm{NH}]}, \quad . \quad . \quad . \quad (4)$$

where K_w and K_{NH} are thermodynamic constants, and $f_{OH^-} = f_{N^-}$ approximately. Comparison of eqn. (3) and (4) predicts that the indicator ratio should be proportional to $[\mathrm{SO}_4^=]^{\frac{1}{2}}$, and the last column of Table III shows that this is so with fair accuracy. Further, using the values,[4]

$$K_w = 1{\cdot}008 \times 10^{-14}, \; K_N = 5{\cdot}01 \times 10^{-9}$$

we find

$$[\mathrm{OH}^-] = 1{\cdot}008 \times 10^{-14} \times 2{\cdot}34[\mathrm{SO}_4^=]^{\frac{1}{2}}/5{\cdot}01 \times 10^{-9} \quad . \quad . \quad . \quad (5)$$
$$= 4{\cdot}70 \times 10^{-6}[\mathrm{SO}_4^=]^{\frac{1}{2}}.$$

This relation will be used in the remainder of this paper for calculating the hydroxyl ion concentrations in the quinine + quinine sulphate buffers.

Investigation of Adaptability.—Varying quantities of the two buffer components were stirred mechanically with 50 ml. 0·2 N potassium sulphate solution, and acid or alkali added at a slow constant rate through a long capillary so as to imitate the conditions in a system where acid is being produced or consumed by a reaction. The displacement of pH produced by different rates of addition was measured by means of a glass electrode, and the results are shown graphically in Fig. 1. It will be seen that the addition of alkali is dealt with more promptly than that of acid, so that the dissolution of quinine is probably the slowest process involved. This is confirmed by the fact that a reduction of the amount of quinine from 1 g. to 0·1 g. increased the pH displacement by about eight-fold.

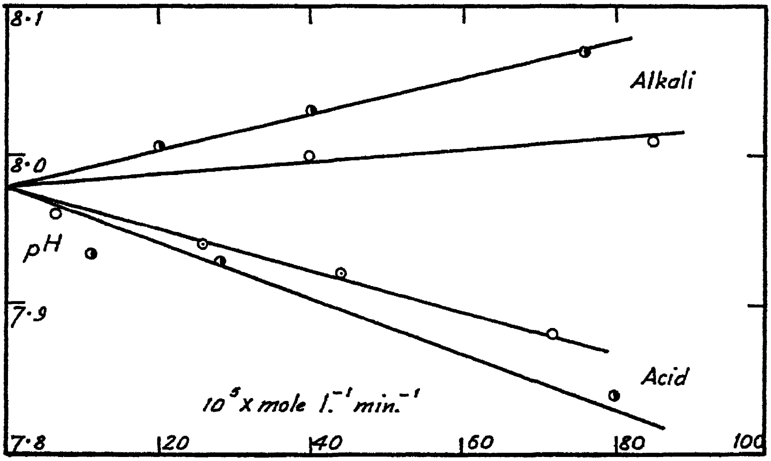

FIG. 1.

⊙ 1 g. quinine + 1 g. quinine sulphate.
◑ 1 g. quinine + 0·1 quinine sulphate.

---

[4] Kolthoff, *Acid-base Indicators* (New York, 1937).

Kinetic Measurements on Ester Hydrolysis.—Measurements of Skrabal and other workers[5] suggest that the alkaline hydrolysis of ethyl formate or methyl monochloroacetate should proceed at a convenient speed in these buffers, and this was found to be the case. The buffer system was stirred in a closed vessel at 25° for 1 hr., and the required amount of ester added from a small automatic pipette. At intervals samples were removed for the estimation of the remaining ester and filtered into a weighed excess of 0·05 N KOH. Hydrolysis is rapid, and the remaining alkali was titrated with 0·05 N HCl (indicator bromcresol green). Blank tests showed that the small amounts of quinine in solution did not interfere with this estimation.

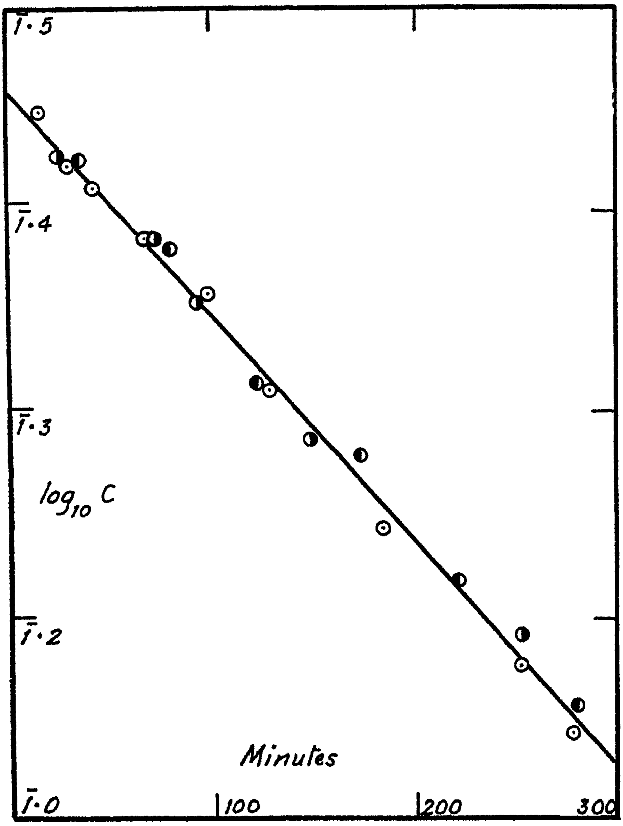

FIG. 2.

⊙ 2 g. quinine + 2 g. quinine sulphate.
◑ 6 g. quinine + 2 g. quinine sulphate.
◐ 2 g. quinine + 4 g. quinine sulphate.

Most of the experiments were done with the less volatile methyl monochloroacetate, and Fig. 2 shows the effect of varying the quantities of solid phase on the course of a reaction with 0·05 M K_2SO_4 and 0·025 M ester, c being the concentration of ester in arbitrary units. As would be expected from Fig. 1, the rate of production of acid (about 4×10^{-5} mole $l.^{-1}$ $min.^{-1}$) is not sufficient to disturb the buffering action. The rate is also independent of the amount of either solid phase, showing that there is no heterogeneous catalysis. In solutions containing less sulphate or more ester the plots of $\log_{10}c$ against t were considerably curved, because the acid liberated in the reaction causes appreciable changes in the value of $[SO_4^{=}]$ and hence in the equilibrium value of $[OH^-]$

---

[5] Skrabal *et al.*, *Monatsh.*, 1917, 38, 191; 1921, 42, 6; 1928, 50, 369; Leimu, Korte, Laaksonen and Lehmuskoski, *Kemistilehti*, *B*, 1946, 19, 93.

This can be taken into account as follows. If c is the concentration of ester after time t, then the kinetic expression is

$$-\,\mathrm{d}c/\mathrm{d}t = kc[\mathrm{OH}^-] = kK''c[\mathrm{SO}_4^=]^{\frac{1}{2}} \quad . \quad . \quad . \quad (6)$$

from (3). If S is the initial sulphate concentration, the concentration at a later stage of the reaction is

$$[\mathrm{SO}_4^=] = S - \tfrac{1}{2}(c_{0}{}_{4}^{=} - c),$$

where c_0 is the initial concentration of ester, and (6) thus becomes

$$-\,\mathrm{d}c/\mathrm{d}t = kK''c\{S - \tfrac{1}{2}(c_0 - c)\}^{\frac{1}{2}},$$

giving on integration

$$E^{\frac{1}{2}}kK''t = \ln\frac{(E + \frac{1}{2}c)^{\frac{1}{2}} + E^{\frac{1}{2}}}{(E + \frac{1}{2}c)^{\frac{1}{2}} - E^{\frac{1}{2}}} + \ln\frac{S^{\frac{1}{2}} - E^{\frac{1}{2}}}{S^{\frac{1}{2}} - E^{\frac{1}{2}}}, \quad . \quad . \quad (8)$$

where $E = S - \frac{1}{2}c_0$.

In order to test this equation a series of experiments was carried out with methyl monochloroacetate and a range of sulphate concentrations, the ionic strength being made up to 0·2 with potassium chloride. The initial sulphate concentrations (corrected as before for the solubility of quinine sulphate) are given in Table IV. In eqn. (8) the last term does not vary with time so that a plot of

$$\log_{10}\{(E + \tfrac{1}{2}c)^{\frac{1}{2}} + E^{\frac{1}{2}}\} - \log_{10}\{(E + \tfrac{1}{2}c)^{\frac{1}{2}} - E^{\frac{1}{2}}\}$$

against t should give a straight line of slope $0{\cdot}434\,kK''E^{\frac{1}{2}}$. Each experiment did in fact give an excellent straight line, the slopes of which are given in the third column of Table IV. From these slopes the value of k is obtained by using

$$K'' = 4{\cdot}70 \times 10^{-6} \text{ from } (5).$$

TABLE IV.—HYDROLYSIS OF METHYL MONOCHLOROACETATE IN QUININE + QUININE SULPHATE BUFFERS

Initial $[\mathrm{SO}_4^=]$ (corr.)	E	$0{\cdot}434\,kK''E^{\frac{1}{2}}$	k
0·0651	0·0551	0·00185	3910
0·0502	0·0396	0·00157	3890
0·0403	0·0298	0·00145	4130
0·0303	0·0196	0·00109	3810
0·0260	0·0123	0·00087	3830
0·0163	0·0057	0·00060	3900
			Mean = 3910

The constancy of k in Table IV is satisfactory. A smaller number of experiments was done with ethyl formate, but owing to the volatility of the ester only the early part of the reaction could be studied, and the accuracy is correspondingly lower. The mean value obtained for k was 2100.

These values cannot be compared directly with those given by Skrabal.[5] For methyl monochloroacetate he gives $k = 8170$, which is much greater than our value of 3910. His value is derived from two experiments in ammonia + ammonium chloride buffers in which the ionic strength varied from 0·1 to 0·2 and 0·2 to 0·3 respectively, but in calculating his hydroxyl ion concentrations he used the classical basic dissociation constant of ammonia, and did not take activity coefficients into account. An approximate correction can be applied by using activity coefficients calculated from eqn. (1), taking $I = 0{\cdot}15$ and $0{\cdot}25$ in the two experiments. The resulting values are then $k = 3850$, 4010, in excellent agreement with those in Table IV.

For ethyl formate Skrabal gives $k = 1080$ from experiments in a carbonate + bicarbonate buffer of average ionic strength $I = 0{\cdot}55$, using $K = 6 \times 10^{-11}$ for the second dissociation constant of carbonic acid and again neglecting activity coefficients. If we use the more accurate[6] value $K = 4{\cdot}7 \times 10^{-11}$ and estimate the value of the factor $\dfrac{f_{\mathrm{CO}_3^=}}{f_{\mathrm{HCO}_3^-}f_{\mathrm{OH}^-}}$ from eqn. (1), we obtain $k = 2200$. Skrabal gives a second value $k = 1400$ from experiments in a "kinetic buffer" of iodide and iodate at an ionic strength of $I = 0{\cdot}45$. Because of complicating reactions with iodine, only initial rates could be used. In this case the only weak electrolyte involved is water, and the value of $f_{H^+} f_{OH^-}$ in solutions of KBr or KCl of this ionic strength is about 0·54, leading to a corrected value of $k = 2600$. The Finnish workers [7] obtained $k = 1540$ from direct measurements in dilute alkali. This value is not subject to any activity corrections, but is probably not very accurate as the reactions studied had half-times of only a few seconds. The general agreement with our value of $k = 2100$ is as good as could be expected in view of the uncertainties involved.

---

[6] Harned and Scholes, *J. Amer. Chem. Soc.*, 1941, **63**, 1706.

Kinetic Measurements on the Mutarotation of Glucose.—This reaction is catalyzed by both acids and bases in general, but very divergent values have been given for the catalytic constant of the hydroxyl ion. It appears to be in the range 5,000 to 15,000, and the reaction should thus proceed at a convenient speed in quinine + quinine sulphate buffers. In order to follow the reaction polarimetrically it is necessary to remove the solid phase, and it was not found practicable to use a sampling technique. The following procedure was found to be satisfactory.

50 ml. of buffer system containing 0·5 g. quinine and 0·5 g. quinine sulphate was brought to equilibrium at 25° and 2·5 g. glucose added. After shaking for a few minutes to dissolve the glucose the solution was filtered rapidly into the water-jacketed polarimeter tube. By this means the hydroxyl ion concentration was adjusted in presence of the glucose and of any acidic or basic impurities which it may contain, and since no acid is produced or consumed during the reaction the small concentrations of dissolved buffer components should be sufficient to maintain constant conditions in the closed polarimeter tube. Velocity constants were evaluated by the method of Guggenheim [8] and all reactions were strictly of the first order. This circumstance, together with the good reproducibility of the velocity constants, demonstrates that the solution does not undergo any appreciable change after the removal of the solid phase.

The results obtained are given in Table V. The concentrations of sulphate ion have, as before, been corrected for the solubility of quinine sulphate, and a small correction (< 5 %) has been subtracted from the observed rates to allow for catalysis by sulphate ions and by glucosate ions.[9] The hydroxyl ion concentrations are again obtained from eqn. (5). The data in Table V are plotted in Fig. 3. It will be seen that the reaction velocity is a linear function of $[OH^-]$, and the slope of the line gives a value of $k_{OH^-} = 4300$ for the catalytic constant of the hydroxyl ion. This is lower than values previously given. Hudson [10] gives $k_{OH^-} = 9750$, calculated from experiments of Osaka [11] on ammonia + ammonium chloride buffers. This undoubtedly is too high, since Hudson neglected catalysis by ammonia molecules, and Brönsted and Guggenheim [9] derived the value $k_{OH^-} = 6200$ from the same data, putting $k_{NH_3} = 3{\cdot}2$. Osaka's results are equally well fitted by our value of $k_{OH^-} = 4300$ together with $k_{NH_3} = 4{\cdot}0$. Lowry and Wilson [12] made measurements in very dilute solutions of sodium hydroxide, and found $k_{OH^-} = 8000$ at 20°, corresponding

TABLE V.—MUTAROTATION OF GLUCOSE IN QUININE + QUININE SULPHATE BUFFERS

k = first-order velocity constant at 25° ($\log_{10}$, min.)

$[SO_4^=]$ (corr.)	10^7 $[OH^-]$	k (corr.)
0·0651	11·98	0·0161
0·0502	10·53	0·0156
0·0309	8·27	0·0151
0·0163	6·02	0·0136
0·00932	4·54	0·0132
0·00511	3·36	0·0124

---

[7] Leimu, Korte, Laaksonen and Lehmuskoski, *loc. cit.*

[8] Guggenheim, *Phil. Mag.*, 1926, **7**, 538.

[9] Cf. Brönsted and Guggenheim, *J. Amer. Chem. Soc.*, 1927, **49**, 2554; Smith, *J. Chem. Soc.*, 1936, 1824.

[10] Hudson, *J. Amer. Chem. Soc.*, 1910, **32**, 889.

[11] Osaka, *Z. physik. Chem.*, 1900, **35**, 661.

[12] Lowry and Wilson, *Trans. Faraday Soc.*, 1928, **23**, 683.

to about $k_{OH^-} = 14{,}000$ at 25°. This is likely to be too high, since Lowry did not attribute any catalytic effect to the glucosate ion, which has been shown by Smith[9] to contribute 20 to 40 $^{\circ}/_{\circ}$ of the observed catalysis: on the other hand Smith's own values (after allowing for glucosate catalysis) are close to those of Lowry. It is difficult to understand why the values of Smith and Lowry are so much higher than any of the others, but it may be because of an error in the acid dissociation constant of glucose, on which they depend directly. We regard our value $k_{OH^-} = 4300$ as more reliable than any of the earlier ones.

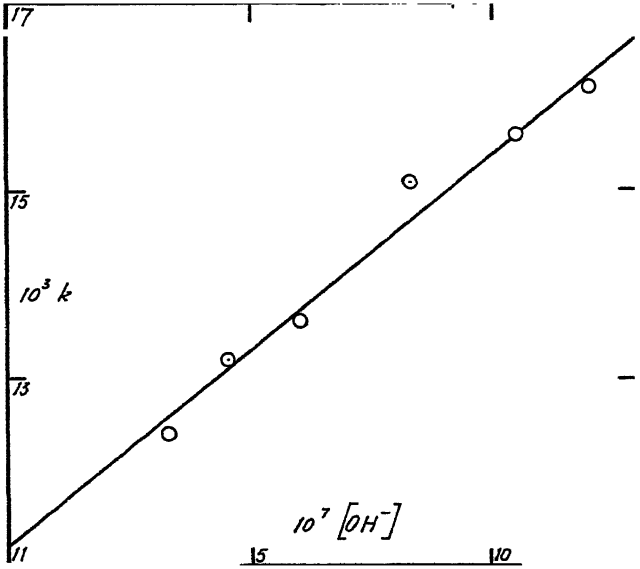

FIG. 3.

The intercept in Fig. 3 is 0·0112, which is slightly greater than the velocity of the water reaction at this temperature, 0·0096. The difference can be reasonably attributed to catalysis by the constant concentration of quinine molecules in the solution. Quinine has a pK of about 8, and a base of this strength would have a catalytic constant of about 1 to 2. Since its solubility is 1×10^{-3} M, it should contribute 1 to 2×10^{-3} to the observed velocity, in agreement with experiment. It is easily seen that the quininium ion is too weak an acid to exert any measurable catalytic effect at these concentrations.

Conclusions.—This paper and the preceding one show that it is possible to construct heterogeneous buffer systems which give accurately reproducible concentrations of hydrogen and hydroxyl ions, and which respond rapidly to additions of acid or alkali. It is, however, likely that satisfactory systems of this kind are not numerous, since it is necessary to compromise in the matter of solubilities: if these are too small the rate of adaptation of the system becomes too low, while if they are too great the whole purpose of using a heterogeneous system is defeated. Further, variations in the physical or chemical nature of the solid phase are likely to cause difficulty in many cases. In the four catalyzed reactions studied in these systems no indication was found of heterogeneous catalysis on the surface of the solid phase, and heterogeneous buffers may, therefore, be useful in the kinetic study of other reactions which are very sensitive to hydrogen or hydroxyl ions.

Our thanks are due to the Department of Scientific and Industrial Research for a grant to one of us (J. E. P.).

Physical Chemical Laboratory,
Oxford.

VIBRATION-ROTATION BANDS IN THE SPECTRUM OF METHYL THIOL

BY H. W. THOMPSON AND C. H. MILLER

Received 30*th June*, 1949

The vibrational spectrum of methyl thiol vapour has been re-measured using high dispersion. The rotational structure or contour of six bands has been analyzed. Two parallel bands at 2869 cm.$^{-1}$ and 2946 cm.$^{-1}$ have the contour expected for the molecular geometry which has been assumed on the basis of known dimensions, and have been assigned to a fundamental CH_3 group stretching vibration and the harmonic of a CH_3 group deformation. A perpendicular type band at 3010 cm.$^{-1}$ shows a well-marked series of *Q* branches with spacing close to the value expected, the Coriolis coupling being small. The essentially perpendicular-type band due to the S—H bond vibration at 2607 cm.$^{-1}$ has also been measured. The complex pair of overlapping perpendicular-type bands arising from the split degenerate skeleton vibration has been analyzed and discussed in relation to the molecular geometry. All these bands confirm the assignment of fundamentals made previously.

The infra-red spectrum of methyl thiol has been measured previously and correlated with data on the Raman spectrum to obtain an assignment of the molecular vibration frequencies.[1] The resolving power then used was insufficient to reveal the detailed rotational structure of vibration bands, and although the assignment of fundamentals from the bands observed seems satisfactory on other grounds, it seemed desirable to investigate this rotational structure with higher dispersion. The complex structure of the bands in the region of 10μ suggested, too, that interesting features might emerge. Also, the corresponding measurements on the structurally related molecule methyl alcohol and its deutero analogue CH_3OD have been made.[2]

Experimental

The spectrum was measured with a recording grating spectrometer which has been described in detail elsewhere.[3] For the region around 3·5μ and at 4μ, a 7200 line/inch grating was used, and between 8-11μ two gratings have respectively 2400 and 1200 line/inch. The effective slit widths are shown on the diagrams below. The absorption cell was either 10 cm. or 20 cm. in length, and pressures 100-700 mm. were used. The methyl thiol was a commercial sample which had been re-purified by repeated fractionation *in vacuo*.

Results and Discussion

Methyl thiol is almost a symmetrical rotator with least axis of inertia along the C—S bond. The moment of inertia of the methyl group about this axis can be assumed to be near $5{\cdot}5 \times 10^{-40}$ g. cm.^{2}, the value found spectroscopically for methyl halides, and assuming that the S—H bond length is 1·34 Å and the $C\widehat{S}H$ angle 100°, the moment of the rotating S—H bond will be $2{\cdot}9 \times 10^{-40}$, giving $I_A \sim 8{\cdot}4 \times 10^{-40}$. (The value quoted in the earlier paper was erroneous.) The other two, almost equal, moments of inertia I_B and I_C will be about 60×10^{-40} g. cm.^{2}.

---

[1] Thompson and Skerrett, *Trans. Faraday Soc.*, 1940, **36**, 812. Trotter and Thompson, *J. Chem. Soc.*, 1946, 481.

[2] Borden and Barker, *J. Chem. Physics*, 1938, **6**, 553. Barker and Bosschieter, *ibid.*, 1938, **6**, 563. Noether, *ibid.*, 1942, **10**, 693.

[3] Miller and Thompson, *Proc. Roy. Soc. A* (in press).

In reality, the slight degree of asymmetry will lead to a least axis slightly inclined to the C—S bond, but the three moments of inertia will not be much affected. The vibration bands will be essentially of two kinds, having a "parallel" or "perpendicular" rotational structure respectively. The former will have P, Q and R branches, the individual lines in the P and R branches being $h/8\pi^2 I_C$ apart. The latter will have an array of Q branches with "ideal" spacing $2(A—C)$, in which $A = h/8\pi^2 cI_A$ and $C = h/8\pi^2 cI_C$, unless these are special interactions. These arrangements of rotational lines may be somewhat affected by the asymmetry, and also some of the bands may show a hybrid structure consequent upon the change of electric moment having components along more than one axis.

Satisfactory values have been assigned to all the normal modes except that involving the mutual twisting of the end groups. No band in the spectrum appears suitable for this, and there still seems to be some doubt about its value in methyl alcohol, although it is very small.

In the region 3·2-3·6 μ, three bands have been measured, shown in Fig. 1. Two have the contour of parallel type bands and the third has a perpendicular structure. The parallel bands, centred at 2869 cm.$^{-1}$ and 2946 cm.$^{-1}$ have three clear sub-maxima, but the P and R contour has not been separated into individual lines. According to the above formulae, such lines should be 0·9 cm.$^{-1}$ apart, and using the lead telluride cell as detector, they should be resolvable. It is possible that at the pressures used the lines are broadened, but other factors may have prevented resolution. The $P—R$ spacings of the two bands are close to 32 cm.$^{-1}$ and 30 cm.$^{-1}$, which agrees excellently with the value calculated from the formula of Gerhard and Dennison.[4] The correlation of 2869 cm.$^{-1}$ with the Raman interval 2870, as the symmetrical C—H stretching mode, is thus confirmed. The band at 2946 cm.$^{-1}$ must be an overtone of a C—H deformational frequency. The two-fold degenerate CH_3 group deformation in methyl chloride may be expected to split as a result of the asymmetry in the case of methyl thiol, and in the earlier paper values of 1475 and 1430 were suggested for the two components. The band at 2946 cm.$^{-1}$ could therefore be explained immediately as the harmonic of 1475, which would have the parallel-type contour found. We might similarly expect the harmonic of 1430 to appear. It is worth

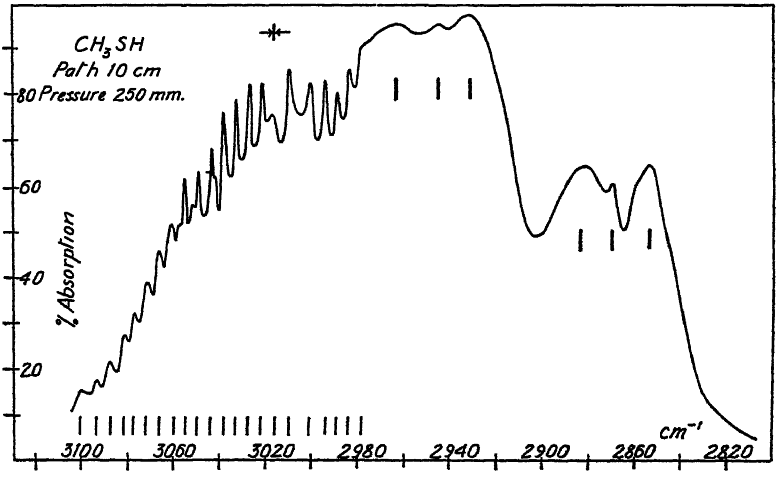

Fig. 1.

---

[4] Gerhard and Dennison, *Physic. Rev.*, 1933, 43, 197.

noting in this connection that the band of 2869 cm.$^{-1}$ has a perturbed contour, and there is a definite sub-maximum at 2860 cm.$^{-1}$, which might arise from the overlapping of two bands.

The perpendicular-type band between 2980-3100 cm.$^{-1}$ has well-marked *Q* branches, but the regular spacing is disturbed. Table I gives the positions of the peaks measured.

TABLE I.—POSITIONS OF MAIN *Q* BRANCHES, GIVEN IN CM.$^{-1}$. A FEW WEAK LINES HAVE BEEN OMITTED

ν	$\Delta\nu$	ν	$\Delta\nu$
3100·5	--	3038·4	5·0
3093·7	6·8	3032·9	5·5
3087·0	6·7	3027·0	5·9
3080·9	6·1	3021·9	5·1
3076·2	4·7	3017·0	4·9
3070·5	5·7	3010·2	6·8
3065·9	4·6	3000·2	10·0
3060·4	5·5	2994·4	5·8
3055·0	5·4	2989·1	5·3
3049·0	6·0	2983·9	5·2
3033·4	5·6	2978·8	5·1

The ideal spacing of *Q* branches given by $2(A—C)$ would be about 5·8 cm.$^{-1}$. The effect of Coriolis interaction will be to give a spacing $2\{(1 + \zeta)A—C\}$ in which the coupling coefficient ζ may be positive or negative. The observed spacings fluctuate noticeably, but a rough mean is about 5·5 cm.$^{-1}$, which would imply a very weak interaction with $\zeta = -0{\cdot}05$. It is certain, however, that the asymmetry leads to some of the irregularities near the centre of the band at about 3010 cm.$^{-1}$. This band, corresponding to the Raman interval 2999 cm.$^{-1}$, is correctly assigned to the asymmetrical stretching mode of the CH_3 group.

Between 3·7-4·0 μ the band due to the S—H stretching vibration occurs. Fig. 2 shows this to have an essentially perpendicular-type structure, which would be expected if the S—H bond is inclined at 100° to the C—S bond.

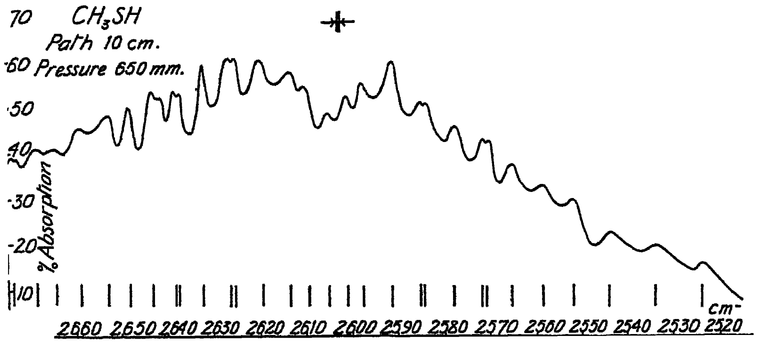

FIG. 2.

It is perhaps not surprising that the regular *Q* branch spacing here is more disturbed than in the previous case, since apart from the asymmetry, there will be partially hybrid character since the vibration will have a small component of electric moment change in the direction of the least axis of inertia. However, if the splitting of some of the Q branches is ignored, the band approximates very well to the perpendicular (B) type, and with loss of intensity near the band centre at 2607 cm.$^{-1}$. The spacings, given in Table II, are irregular, but there is a definite tendency to lower values at the higher frequency side, and a divergent trend towards the lower frequencies.

TABLE II.—Positions in cm.$^{-1}$

ν	$\Delta\nu$	ν	$\Delta\nu$
2673·5	—	2609·6	3·4
(2672·2)	—	2604·7	4·9
2668·5	5·0	2601·3	3·4
2663·9	4·6	2597·5	3·8
2658·7	5·2	2590·8	6·7
2652·4	6·3	2584·7	6·8
2647·9	4·5	2583·4	
2642·8	5·1	2577·3	6·2
(2640·6)	—	2571·1	6·6
2637·9	5·5	2570·2	
2636·6		2565·0	5·5
2632·0	5·9	2558·2	6·8
2626·5	6·2	2551·6	6·6
2625·0		2543·6	8·0
2619·6	6·2	2533·4	10·2
2613·0	6·6	2523·2	10·2

The mean spacing may be rather greater than 5·8 cm.$^{-1}$, implying a very small positive value for the coupling coefficient ζ. The contribution of parallel-type contour to this band at 2607 cm.$^{-1}$ must be small, so that the S—H bond must lie, as assumed, almost at right-angles to the C—S link. It is noteworthy that the corresponding Raman interval for the liquid lies at 2572 cm.$^{-1}$, much lower than the present value of 2607 cm.$^{-1}$, and this suggests a marked drop in frequency in the liquid state.

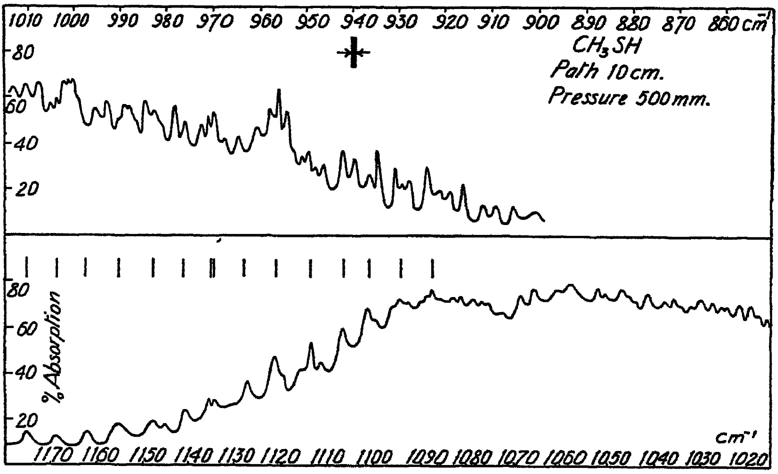

Fig. 3.

The region 8-11 μ is highly complex, as seen from Fig. 3. It certainly includes two overlapping perpendicular-type bands, which were previously estimated to lie near 950 cm.$^{-1}$ and 1060 cm.$^{-1}$. These are the components of the twofold degenerate skeleton mode of a methyl halide, split by the asymmetry. The positions of the lines are given in Table III. One band is centred near 1070 cm.$^{-1}$ and the other near 955 cm.$^{-1}$. At the higher frequency end there is a well-marked succession of *Q* branches between 1180-1080 cm.$^{-1}$. Although some perturbations and splittings occur, the intervals here are fairly regular and about 7 cm.$^{-1}$ in value. There is a loss of intensity near the centre of the band at 1070 cm.$^{-1}$, and to the lower frequency side of this a succession of *Q* branches which at first suggest a definite series, but from 1020 cm.$^{-1}$ to lower frequencies these lines become interlaced with those of the other perpendicular band at 955 cm.$^{-1}$. There seems to be a definite convergence of the main *Q* branches of the 1070 band as they progress towards the band at lower frequencies, reminiscent of the type of Coriolis interaction between two vibrations predicted by Nielsen and found in other cases, such as allene.[5]

TABLE III.—POSITIONS IN CM.$^{-1}$

ν	$\Delta\nu$	ν	$\Delta\nu$	ν
1182.3	—	1058.0	7.5	982.6
1175.3	7.0	1056.7	—	980.9
1168.5	6.8	1054.9	—	978.0
1162.0	6.5	1052.4	5.6	975.7
1154.7	7.3	1050.7	—	972.8
1147.3	7.4	1047.1	5.3	971.2
1144.7	—	1045.5	—	970.0
1141.2	6.1	1041.5	5.6	967.5
1135.6	—	1038.1	—	964.8
1134.1	7.1	1036.1	5.4	960.3
1131.2	—	1034.4	—	957.6
1127.2	6.9	1032.8	—	955.7
1121.2	6.0	1030.0	6.1	954.0
1120.0	—	1027.6	—	952.6
1115.8	—	1025.6	—	950.7
1114.0	7.2	1024.4	5.6	949.2
1111.5	—	1021.7	—	948.0
1106.7	7.3	1019.2	5.2	946.2
1101.5	5.2			941.9
1099.8	—	1017.8		939.5
1096.1	—	1016.1		936.5
1094.5	7.0	1013.8		934.5
1092.9	—	1013.0		930.4
1090.7	—	1010.6		929.1
1088.6	—	1007.7		927.5
1087.5	7.0	1005.3		923.7
1083.0	—	1003.8		922.8
1081.5	—	1002.2		920.8
1078.6	—	1001.1		918.7
1076.5	—	1000.2		916.0
1075.5	—	995.5		911.2
1072.5	—	992.9		909.4
1069.0	—	990.2		905.3
1065.5	—	989.0		900.1
1060.5	—	987.8		—
—	—	987.0		—
—	—	984.7		—

The band at 955 cm.$^{-1}$ appears to have increased intensity near its centre, which would agree with its being a perpendicular type having change of electric moment predominantly along the *C* (major) axis. There are, however, many more Q branches than can be explained, although even here on the lower frequency side a prominent set might be chosen with average spacing close to 7 cm.$^{-1}$. A possible reason for the extreme complexity might be that yet another band overlies that at 955 cm.$^{-1}$, this being the harmonic of the perpendicular twisting vibration. In methyl alcohol this lies at rather lower frequencies and extends over a wide range of frequencies. Further work at much longer wavelengths might help to settle this point.

---

[5] Thompson and Harris, *Trans. Faraday Soc.*, 1944, **40**, 295. Miller and Thompson, *Proc. Roy. Soc. A* (in press).

We are grateful to the Government Grant Committee of the Royal Society for a grant in aid of equipment, and to the Rhodes Trustees for a studentship to one of us (C. H. M.).

The Physical Chemistry Laboratory,
Oxford.

GENERAL VALENCE-FORCE DISPLACEMENT CO-ORDINATES

By P. Torkington

Received 4th July, 1949

General valence-force displacement co-ordinates for non-tetrahedral substituted methanes are obtained. From the equations given, symmetry co-ordinates for practically any system can be readily derived.

It has become customary to employ vector notation to describe the atomic displacements associated with the internal displacement co-ordinates used in molecular potential energy functions.[1] In the valence-force field, all the displacements can conveniently be described in terms of unit vectors directed along the chemical bonds. This system has the advantage of being independent of any internal co-ordinate system. But for some purposes it may still be more convenient to express the displacements in terms of the Cartesian components of the vectors. In this paper, formulae are given from which co-ordinates applicable to practically any system can be derived. The use of Cartesian co-ordinates has the advantage of being more explicit; it leads to longer formulae, but once these are obtained in general form, they may readily be reduced to satisfy any particular case and carried over to a given molecule with no further change other than in the subscripts. The formulae here may be used as such, or as checks on the vector method; it is in any case advisable to evaluate the elements of the kinetic energy matrix in two independent ways. The latter, and the secular equation for the molecular vibrations, is derived as follows.[1, 2] For an N-atomic molecule, with $n = 3N - 6$ internal degrees of freedom, the most general expression for the potential energy (if anharmonicity is neglected), is the following quadratic function of n internal displacement co-ordinates Δ_1 to Δ_n:

$$2V = \sum_{i=1}^{n}\sum_{j=1}^{n} d_{ij}\Delta_i\Delta_j \quad . \quad . \quad . \quad . \quad . \quad (1)$$

where the d_{ij} are the force constants. If the co-ordinates Δ_1 to Δ_n are expressed in terms of $3N$ subsidiary (e.g. Cartesian) displacement co-ordinates z_1 to z_{3N}, as

---

[1] Wilson, Jr., *J. Chem. Physics*, 1939, **7**, 1047; 1941, **9**, 76. Meister and Cleveland, *Amer. J. Physics*, 1946, **14**, 13.

[2] Torkington, *Nature*, 1948, **162**, 370, 607; *J. Chem. Physics* (in press).

$$\Delta_i = \sum_{j=1}^{3N} a_{ij} z_j, \quad . \quad . \quad . \quad . \quad . \quad (2)$$

the coefficients a_{ij} being determined by the geometry of the system as shown in this paper, then the secular equation for the molecular vibrations can be written

$$| dA - \lambda I | = 0, \quad . \quad . \quad . \quad . \quad (3)$$

where d is the force constant matrix, I is the unit matrix and the elements of A are defined as

$$A_{ij} = A_{ji} = \sum_{k=1}^{3N} a_{ik} a_{jk} (M/m_k), \quad . \quad . \quad . \quad (4)$$

where m_k is the mass of the atom whose subsidiary displacement co-ordinate is z_k and M is an arbitrary mass (usually chosen to be one of the m_k), introduced in order that the A_{ij} shall be dimensionless quantities of convenient magnitude. The n roots λ_1 to λ_n are related to the fundamental vibration frequencies ν_1 to ν_n as follows :

$$\lambda_i = 4\pi^2 \nu_i^2 c^2 M \quad . \quad . \quad . \quad . \quad (5)$$

where ν_i is in cm.$^{-1}$ and c is the velocity of light in cm. sec.$^{-1}$. The matrix A is simply related to the inverse kinetic energy matrix G of Wilson [1] as follows :

$$A = MG. \quad . \quad . \quad . \quad . \quad . \quad (6)$$

For molecules possessing elements of symmetry, the Δ_i of (2) will be such combinations of the valence-force displacement co-ordinates which satisfy the symmetry requirements of one species ; (3) will then be an nth order symmetry factor, the total secular equation being a product of such factors, one from each species, and each factor can be solved independently. The rules for forming symmetry co-ordinates are well-known ; the important step in setting up the secular equation is the writing down of the displacement co-ordinates.

Displacement Co-ordinates for Substituted Methanes with Non-Tetrahedral Angles.—These may all be derived from the system in Fig. 1. The various angles are related as follows :

$$\left.\begin{aligned} \cos \alpha_1 &= \cos \beta_1 \cos \beta_2 + \sin \beta_1 \sin \beta_2 \cos (\phi_1 + \phi_2) \\ \cos \alpha_2 &= \cos \beta_1 \cos \beta_3 - \sin \beta_1 \sin \beta_3 \cos \phi_1 \\ \cos \alpha_3 &= \cos \beta_2 \cos \beta_3 - \sin \beta_2 \sin \beta_3 \cos \phi_2 \end{aligned}\right\}, \quad . \quad (7)$$

where $\theta_{13} = \alpha_1$, $\theta_{14} = \alpha_2$, $\theta_{34} = \alpha_3$, $\theta_{15} = (\pi - \beta_1)$, $\theta_{35} = (\pi - \beta_2)$, $\theta_{45} = (\pi - \beta_3)$, and ϕ_1 and ϕ_2

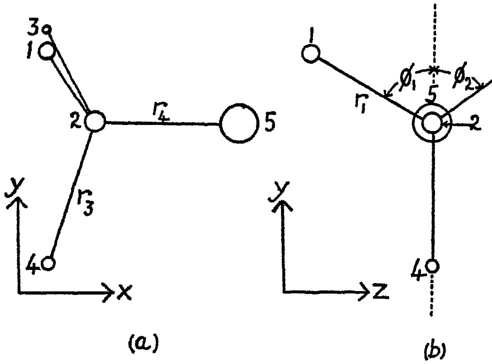

FIG. 1.—Displacement co-ordinates for substituted methanes with non-tetrahedral angles.

are the angles made by the planes through atoms 1, 2, 5 and 3, 2, 5 respectively with the xy plane. The bond r_{24} between atoms 2 and 4 lies parallel to the xy plane, and r_{25} is parallel to the x axis.

The co-ordinates for individual bond-stretchings are :

$$\left.\begin{aligned}
\Delta r_{12} &= (x_2 - x_1)\cos\beta_1 + (y_1 - y_2)\sin\beta_1\cos\phi_1 \\
&\qquad + (z_2 - z_1)\sin\beta_1\sin\phi_1 \\
\Delta r_{23} &= (x_2 - x_3)\cos\beta_2 + (y_3 - y_2)\sin\beta_2\cos\phi_2 \\
&\qquad + (z_3 - z_2)\sin\beta_2\sin\phi_2 \\
\Delta r_{24} &= (x_2 - x_4)\cos\beta_3 + (y_2 - y_4)\sin\beta_3 \\
\Delta r_{25} &= (x_5 - x_2)
\end{aligned}\right\}, \qquad (8)$$

where the x, y and z are the Cartesian displacement co-ordinates. The angular distortions of the system are governed by the following relations :

$$\begin{aligned}
&r_1\Delta\theta_{13} \\
&\quad = x_2\{(\cot\alpha_1 - b\operatorname{cosec}\alpha_1)\cos\beta_1 + (b\cot\alpha_1 - \operatorname{cosec}\alpha_1)\cos\beta_2\} \\
&\quad - x_1(\cot\alpha_1\cos\beta_1 - \operatorname{cosec}\alpha_1\cos\beta_2) - x_3 b(\cot\alpha_1\cos\beta_2 \\
&\quad - \operatorname{cosec}\alpha_1\cos\beta_1) + y_1(\cot\alpha_1\sin\beta_1\cos\phi_1 - \operatorname{cosec}\alpha_1\sin\beta_2\cos\phi_2) \\
&\quad + y_3 b(\cot\alpha_1\sin\beta_2\cos\phi_2 - \operatorname{cosec}\alpha_1\sin\beta_1\cos\phi_1) \\
&\quad - y_2\{(\cot\alpha_1 - b\operatorname{cosec}\alpha_1)\sin\beta_1\cos\phi_1 + (b\cot\alpha_1 - \operatorname{cosec}\alpha_1) \\
&\quad \times\sin\beta_2\cos\phi_2\} + z_2\{(\cot\alpha_1 - b\operatorname{cosec}\alpha_1)\sin\beta_1\sin\phi_1 \\
&\quad - (b\cot\alpha_1 - \operatorname{cosec}\alpha_1)\sin\beta_2\sin\phi_2\} - z_1(\cot\alpha_1\sin\beta_1\sin\phi_1 \\
&\quad - \operatorname{cosec}\alpha_1\sin\beta_2\sin\phi_2) + z_3 b(\cot\alpha_1\sin\beta_2\sin\phi_2 + \operatorname{cosec}\alpha_1\sin\beta_1\sin\phi_1) \qquad (9)
\end{aligned}$$

$$\begin{aligned}
&r_1\Delta\theta_{14} \\
&\quad = x_2\{(\cot\alpha_2 - c\operatorname{cosec}\alpha_2)\cos\beta_1 + (c\cot\alpha_3 - \operatorname{cosec}\alpha_2)\cos\beta_3\} \\
&\quad - x_1(\cot\alpha_2\cos\beta_1 - \operatorname{cosec}\alpha_2\cos\beta_3) - x_4 c(\cot\alpha_2\cos\beta_3 \\
&\quad - \operatorname{cosec}\alpha_2\cos\beta_1) + y_2\{(c\cot\alpha_2 - \operatorname{cosec}\alpha_2)\sin\beta_3 \\
&\quad - (\cot\alpha_2 - c\operatorname{cosec}\alpha_2)\sin\beta_1\cos\phi_1\} + y_1(\cot\alpha_2\sin\beta_1\cos\phi_1 \\
&\quad + \operatorname{cosec}\alpha_2\sin\beta_3) - y_4 c(\cot\alpha_2\sin\beta_3 + \operatorname{cosec}\alpha_2\sin\beta_1\cos\phi_1) \\
&\quad + z_2(\cot\alpha_2 - c\operatorname{cosec}\alpha_2)\sin\beta_1\sin\phi_1 - z_1\cot\alpha_2\sin\beta_1\sin\phi_1 \\
&\quad + z_4 c\operatorname{cosec}\alpha_1\sin\beta_1\sin\phi_1 \quad . \quad . \quad . \quad . \quad . \quad . \quad . \qquad (10)
\end{aligned}$$

$$\begin{aligned}
&r_2\Delta\theta_{34} \\
&\quad = x_2\{(\cot\alpha_3 - d\operatorname{cosec}\alpha_3)\cos\beta_2 + (d\cot\alpha_3 - \operatorname{cosec}\alpha_3)\cos\beta_3\} \\
&\quad - x_3(\cot\alpha_3\cos\beta_2 - \operatorname{cosec}\alpha_3\cos\beta_3) - x_4 d(\cot\alpha_3\cos\beta_3 \\
&\quad - \operatorname{cosec}\alpha_3\cos\beta_2) + y_2\{(d\cot\alpha_3 - \operatorname{cosec}\alpha_3)\sin\beta_3 \\
&\quad - (\cot\alpha_3 - d\operatorname{cosec}\alpha_3)\sin\beta_2\cos\phi_2\} + y_3(\cot\alpha_3\sin\beta_2\cos\phi_2 \\
&\quad - \operatorname{cosec}\alpha_3\sin\beta_3) - y_4 d(\cot\alpha_3\sin\beta_3 + \operatorname{cosec}\alpha_3\sin\beta_2\cos\phi_2) \\
&\quad - z_2(\cot\alpha_3 - d\operatorname{cosec}\alpha_3)\sin\beta_2\sin\phi_2 + z_3\cot\alpha_3\sin\beta_2\sin\phi_2 \\
&\quad - z_4 d\operatorname{cosec}\alpha_3\sin\beta_2\sin\phi_2 \quad . \quad . \quad . \quad . \quad . \quad . \quad . \qquad (11)
\end{aligned}$$

$$\begin{aligned}
&r_1\Delta\theta_{15} \\
&\quad = (x_2 - x_1)\sin\beta_1 + \{y_2(\cos\beta_1 + a_1) - y_1\cos\beta_1 - y_5 a_1\}\cos\phi_1 \\
&\quad + \{z_1\cos\beta_1 + z_5 a_1 - z_2(\cos\beta_1 + a_1)\}\sin\phi_1 \quad . \quad . \quad . \quad . \qquad (12)
\end{aligned}$$

$$\begin{aligned}
&r_2\Delta\theta_{35} \\
&\quad = (x_2 - x_3)\sin\beta_2 + \{y_2(\cos\beta_2 + a_2) - y_3\cos\beta_2 - y_5 a_2\}\cos\phi_2 \\
&\quad - \{z_3\cos\beta_2 + z_5 a_2 - z_2(\cos\beta_2 + a_2)\}\sin\phi_2 \quad . \quad . \quad . \quad . \quad . \qquad (13)
\end{aligned}$$

$$\begin{aligned}
&r_3\Delta\theta_{45} \\
&\quad = (x_2 - x_4)\sin\beta_3 + \{y_4\cos\beta_3 + y_5 a_3 - y_2(\cos\beta_3 + a_3)\}, \quad . \quad . \quad . \qquad (14)
\end{aligned}$$

where $a_1 = r_1/r_4$, $a_2 = r_2/r_4$, $a_3 = r_3/r_4$, $b = r_1/r_2$, $c = r_1/r_3$, $d = r_2/r_3$.

$$\left.\begin{aligned}
&\text{For tetrahedral angles,} \\
&\quad \cos\phi_1 = \cos\phi_2 = -\cos(\phi_1 + \phi_2) = \tfrac{1}{2}, \\
&\quad \sin\phi_1 = \sin\phi_2 = \sin(\phi_1 + \phi_2) = \tfrac{1}{2}\sqrt{3} \\
&\quad \cos\beta_1 = \cos\beta_2 = \cos\beta_3 = -\cos\alpha_1 = -\cos\alpha_2 = -\cos\alpha_3 = \tfrac{1}{3}, \\
&\quad \sin\beta_1 = \sin\beta_2 = \sin\beta_3 = \sin\alpha_1 = \sin\alpha_2 = \sin\alpha_3 = \tfrac{2}{3}\sqrt{2}.
\end{aligned}\right\} \qquad (15)$$

With these values, the displacement co-ordinates are :

$$\left.\begin{aligned} \Delta r_{12} &= \tfrac{1}{3}(x_2 - x_1) + \tfrac{1}{3}\sqrt{2}(y_1 - y_2) + \sqrt{\tfrac{2}{3}}(z_2 - z_1) \\ \Delta r_{24} &= \tfrac{1}{3}(x_2 - x_4) + \tfrac{2}{3}\sqrt{2}(y_2 - y_4) \\ \Delta r_{25} &= x_5 - x_2 \end{aligned}\right\} \quad . \quad (16)$$

$$\left.\begin{aligned} r_1\Delta\theta_{13} &= \tfrac{1}{3}\sqrt{2}\{x_1 + bx_3 - (1 + b)x_2\} + \tfrac{2}{3}\{(1 + b)y_2 - y_1 - by_3\} \\ &\qquad + \frac{1}{\sqrt{3}}\{(1 - b)z_2 - z_1 + bz_3\} \\ r_1\Delta\theta_{14} &= \tfrac{1}{3}\sqrt{2}\{x_1 + cx_4 - (1 + c)x_2\} + \tfrac{1}{6}\{5y_1 - (5 - c)y_2 - cy_4\} \\ &\qquad + \frac{1}{2\sqrt{3}}\{z_1 + 3cz_4 - (3c + 1)z_2\} \\ r_1\Delta\theta_{15} &= \tfrac{2}{3}\sqrt{2}(x_2 - x_1) + \tfrac{1}{6}\{(3a_1 + 1)y_2 - y_1 - 3a_1y_5\} \\ &\qquad + \frac{1}{2\sqrt{3}}\{z_1 + 3a_1z_5 - (3a_1 + 1)z_2\} \\ r_3\Delta\theta_{45} &= \tfrac{2}{3}\sqrt{2}(x_2 - x_4) + \tfrac{1}{3}\{y_4 + 3a_3y_5 - (3a_3 + 1)y_2\} \end{aligned}\right\} \quad (17)$$

Δr_{23} is obtained from Δr_{12} by replacing x_1 by x_3, y_1 by y_3 and $(z_2 - z_1)$ by $(z_3 - z_2)$. Similarly, $r_2\Delta\theta_{34}$ and $r_2\Delta\theta_{35}$ are derived from $r_1\Delta\theta_{14}$ and $r_1\Delta\theta_{15}$ respectively, the co-ordinates being as for Δr_{23}, and c and a_1 being replaced by d and a_2.

For small displacements from a tetrahedral configuration, the angle increments are related as follows :

$$\left.\begin{aligned} \Delta\alpha_1 &= \tfrac{1}{2}(\Delta\beta_1 + \Delta\beta_2) + \sqrt{\tfrac{2}{3}}(\Delta\phi_1 + \Delta\phi_2) \\ \Delta\alpha_2 &= \tfrac{1}{2}(\Delta\beta_1 + \Delta\beta_3) - \sqrt{\tfrac{2}{3}}\Delta\phi_1 \\ \Delta\alpha_3 &= \tfrac{1}{2}(\Delta\beta_2 + \Delta\beta_3) - \sqrt{\tfrac{2}{3}}\Delta\phi_2 \end{aligned}\right\} \quad . \quad . \quad (18)$$

Hence,

$$\Delta\alpha_1 + \Delta\alpha_2 + \Delta\alpha_3 = \Delta\beta_1 + \Delta\beta_2 + \Delta\beta_3 \,. \quad . \quad . \quad (19)$$

The displacement co-ordinates for the system X_3YZ, of symmetry C_{3v}, are readily derived from those obtained.[3] The conditions are :

$$\left.\begin{aligned} &\alpha_1 = \alpha_2 = \alpha_3, = \alpha\,;\ \beta_1 = \beta_2 = \beta_3, = \beta\,;\ \phi_1 = \phi_2 = (\pi/3) \\ &r_1 = r_2 = r_3\,;\ b = c = d = 1\,;\ a_1 = a_2 = a_3 = a. \end{aligned}\right\} \quad (20)$$

The geometry of the system then requires that

$$\left.\begin{aligned} 2 \sin\frac{\alpha}{2} &= \sqrt{3}\sin\beta \\ 4\cos^2\frac{\alpha}{2} &= 1 + 3\cos^2\beta \end{aligned}\right\} . \quad . \quad . \quad (21)$$

The co-ordinates are then :

$$\left.\begin{aligned} \Delta r_{25} &= x_5 - x_2 \\ \Delta r_{12} &= (x_2 - x_1)\cos\beta + \tfrac{1}{2}(y_1 - y_2)\sin\beta + \tfrac{1}{2}\sqrt{3}(z_2 - z_1)\sin\beta \\ \Delta r_{23} &= (x_2 - x_3)\cos\beta + \tfrac{1}{2}(y_3 - y_2)\sin\beta + \tfrac{1}{2}\sqrt{3}(z_3 - z_2)\sin\beta \\ \Delta r_{24} &= (x_2 - x_4)\cos\beta + (y_2 - y_4)\sin\beta \end{aligned}\right\} \quad (22)$$

$$\begin{aligned} r_1\Delta\theta_{13} &= (x_1 + x_3 - 2x_2)\tan\frac{\alpha}{2}\cos\beta + \tfrac{1}{2}(2y_2 - y_1 - y_3)\tan\frac{\alpha}{2}\sin\beta \\ &\qquad + \tfrac{1}{2}\sqrt{3}\,(z_3 - z_1)\cot\frac{\alpha}{2}\sin\beta \quad (23) \end{aligned}$$

$$r_1\Delta\theta_{14} = (x_1 + x_4 - 2x_2)\tan\frac{\alpha}{2}\cos\beta + [\tfrac{1}{4}\sqrt{3}\{(1 + \cos^2\beta)y_1 - 2y_4\cos^2\beta$$

$$- y_2 \sin^2 \beta\} + \tfrac{1}{4}\{(1 - 3\cos^2 \beta)z_1 + 2z_4 - 3z_2 \sin^2 \beta\}] \sec \frac{\alpha}{2} \quad (24)$$

$$r_1\Delta\theta_{34} = (x_3 + x_4 - 2x_2) \tan \frac{\alpha}{2} \cos \beta + [\tfrac{1}{4}\sqrt{3}\{(1 + \cos^2 \beta)y_3 - 2y_4 \cos^2 \beta$$
$$- y_2 \sin^2 \beta\} + \tfrac{1}{4}\{3z_2 \sin^2 \beta - (1 - 3\cos^2 \beta)z_3 - 2z_4\}] \sec \frac{\alpha}{2} \quad (25)$$

$$r_1\Delta\theta_{15} = (x_2 - x_1) \sin \beta + \tfrac{1}{2}\{(a + \cos \beta)y_2 - y_1 \cos \beta - ay_5\}$$
$$+ \tfrac{1}{2}\sqrt{3}\{z_1 \cos \beta + az_5 - (a + \cos \beta)z_2\} \quad (26)$$

$$r_1\Delta\theta_{35} = (x_2 - x_3) \sin \beta + \tfrac{1}{2}\{(a + \cos \beta)y_2 - y_3 \cos \beta - ay_5\}$$
$$+ \tfrac{1}{2}\sqrt{3}\{(a + \cos \beta)z_2 - z_3 \cos \beta - az_5\} \quad (27)$$

$$r_1\Delta\theta_{45} = (x_2 - x_4) \sin \beta + ay_5 + y_4 \cos \beta - (a + \cos \beta)y_2. \quad (28)$$

For tetrahedral angles,

$$(\alpha + \beta) = \pi, \quad \sin \frac{\alpha}{2} = \sqrt{\frac{2}{3}}, \quad \cos \frac{\alpha}{2} = \frac{1}{\sqrt{3}}, \quad \sin \beta = \frac{2\sqrt{2}}{3}, \quad \cos \beta = -\frac{1}{3}.$$

The co-ordinates for bond-stretching are then the same as for the totally unsymmetrical tetrahedral system; those for deformation of the angles become:

$$\left.\begin{aligned}
r_1\Delta\theta_{13} &= \tfrac{1}{3}\sqrt{2}(x_1 + x_3 - 2x_2) + \tfrac{2}{3}(2y_2 - y_1 - y_3) + \frac{1}{\sqrt{3}}(z_3 - z_1) \\
r_1\Delta\theta_{14} &= \tfrac{1}{3}\sqrt{2}(x_1 + x_4 - 2x_2) + \tfrac{1}{6}(5y_1 - y_4 - 4y_2) \\
&\qquad + \frac{1}{2\sqrt{3}}(z_1 + 3z_4 - 4z_2) \\
r_1\Delta\theta_{15} &= \frac{2\sqrt{2}}{3}(x_2 - x_1) + \tfrac{1}{6}\{(3a + 1)y_2 - y_1 - 3ay_5\} \\
&\qquad + \frac{1}{2\sqrt{3}}\{z_1 + 3az_5 - (3a + 1)z_2\} \\
r_1\Delta\theta_{45} &= \frac{2\sqrt{2}}{3}(x_2 - x_4) + \tfrac{1}{3}\{y_4 + 3ay_5 - (3a + 1)y_2\}
\end{aligned}\right\} \quad (29)$$

$r_1\Delta\theta_{34}$ and $r_1\Delta\theta_{35}$ are obtained from $r_1\Delta\theta_{14}$ and $r_1\Delta\theta_{15}$ respectively by replacing

x_1, y_1 by x_3, y_3 and z_1, z_2, z_4, z_5 by $-z_3, -z_2, -z_4$ and $-z_5$.

For deviations from the ideal tetrahedral configuration, $\Delta\alpha = \Delta\beta$.

Displacement Co-ordinates for Non-Tetrahedral Systems X_2YZ_2 of Symmetry C_{2v}.—These can be derived from the general system treated in the last section, but it is convenient to change the axes so that xx is parallel to the two-fold axis C_2, as in Fig. 2. The two planes of symmetry are parallel to the xy and xz planes. The various angles are related as follows:

$$\cos \beta = -\cos \alpha_1 \cos \alpha_2, \quad . \quad . \quad . \quad . \quad (30)$$

where $\theta_{14} = \theta_{34} = \theta_{15} = \theta_{35} = \beta$, and $\theta_{13} = 2\alpha_1$, $\theta_{45} = 2\alpha_2$.

The displacement co-ordinates are:

$$\left.\begin{aligned}
\Delta r_{12} &= (x_2 - x_1) \cos \alpha_1 + (y_1 - y_2) \sin \alpha_1 \\
\Delta r_{24} &= (x_4 - x_2) \cos \alpha_2 + (z_4 - z_2) \sin \alpha_2
\end{aligned}\right\} \quad . \quad (31)$$

$$\left.\begin{aligned}
r_1\Delta\theta_{13} &= (x_1 + x_3 - 2x_2) \sin \alpha_1 + (y_1 - y_3) \cos \alpha_1 \\
r_2\Delta\theta_{45} &= (2x_2 - x_4 - x_5) \sin \alpha_2 + (z_4 - z_5) \cos \alpha_2
\end{aligned}\right\} \quad . \quad (32)$$

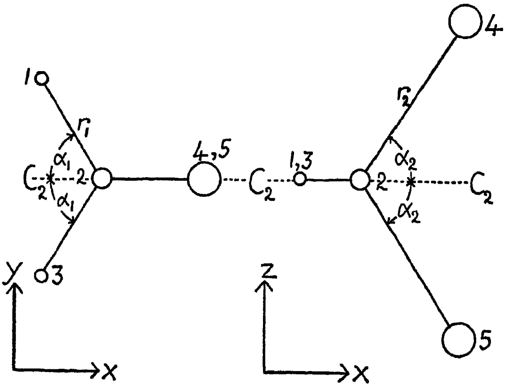

(a) (b)

FIG. 2.—Displacement co-ordinates for non-tetraheral systems X_2YZ_2, of symmetry C_{2v}.

$$\left.\begin{aligned} r_1\Delta\theta_{14} = {} & x_2\{(\cot\beta - a\operatorname{cosec}\beta)\cos\alpha_1 - (a\cot\beta - \operatorname{cosec}\beta)\cos\alpha_2\} \\ & - x_1(\cos\alpha_1\cot\beta + \cos\alpha_2\operatorname{cosec}\beta) \\ & + x_4a(\cos\alpha_1\operatorname{cosec}\beta + \cos\alpha_2\cot\beta) \\ & - y_2(\cot\beta - a\operatorname{cosec}\beta)\sin\alpha_1 + y_1\sin\alpha_1\cot\beta \\ & - y_4a\sin\alpha_1\operatorname{cosec}\beta - z_2(a\cot\beta - \operatorname{cosec}\beta)\sin\alpha_2 \\ & - z_1\sin\alpha_2\operatorname{cosec}\beta + z_4a\sin\alpha_2\cot\beta \end{aligned}\right\} \quad (33)$$

Δr_{23} and Δr_{25} are obtained from Δr_{12} and Δr_{24} respectively by replacing x_1, y_1 by x_3, $-y_3$; x_4, z_4 by x_5, $-z_5$; and y_2, z_2 by $-y_2$, $-z_2$. The remaining angles are obtained by the replacements indicated in Table I.

TABLE I

θ_{14}	$+x_2$	$-x_1$	$+x_4$	$-y_2$	$+y_1$	$-y_4$	$-z_2$	$-z_1$	$+z_4$
θ_{15}	$+x_2$	$-x_1$	$+x_5$	$-y_2$	$+y_1$	$-y_5$	$+z_2$	$+z_1$	$-z_5$
θ_{34}	$+x_2$	$-x_3$	$+x_4$	$+y_2$	$-y_3$	$+y_4$	$-z_2$	$-z_3$	$+z_4$
θ_{35}	$+x_2$	$-x_3$	$+x_5$	$+y_2$	$-y_3$	$+y_5$	$+z_2$	$+z_3$	$-z_5$

For tetrahedral angles,

$$\cos\alpha_1 = \cos\alpha_2 = \frac{1}{\sqrt{3}}, \quad \sin\alpha_1 = \sin\alpha_2 = \sqrt{\tfrac{2}{3}}.$$

The co-ordinates are then :

$$\left.\begin{aligned} \Delta r_{12} &= \frac{1}{\sqrt{3}}(x_2 - x_1) + \sqrt{\tfrac{2}{3}}(y_1 - y_2) \\ \Delta r_{24} &= \frac{1}{\sqrt{3}}(x_4 - x_2) + \sqrt{\tfrac{2}{3}}(z_4 - z_2) \end{aligned}\right\} \quad . \quad . \quad (34)$$

$$\left.\begin{aligned} r_1\Delta\theta_{13} &= \sqrt{\tfrac{2}{3}}(x_1 + x_3 - 2x_2) + \frac{1}{\sqrt{3}}(y_1 - y_3) \\ r_2\Delta\theta_{45} &= \sqrt{\tfrac{2}{3}}(2x_2 - x_4 - x_5) + \frac{1}{\sqrt{3}}(z_4 - z_5) \\ r_1\Delta\theta_{14} &= \frac{1}{\sqrt{6}}\{(1 - a)x_2 - x_1 + ax_4\} + \frac{1}{2\sqrt{3}}\{(3a + 1)y_2 - y_1 - 3ay_4\} \\ &\qquad + \frac{1}{2\sqrt{3}}\{(a + 3)z_2 - 3z_1 - az_4\} \end{aligned}\right\} \quad (35)$$

For deviations from the tetrahedral,

$$\Delta\alpha_1 + \Delta\alpha_2 + 2\Delta\beta = 0. \tag{36}$$

Applications of the Formulæ.—(*a*) THE SYMMETRIC TRIATOMIC MOLECULE.[4] The required co-ordinates are identical with those for either half of the non-tetrahedral system X_2YZ_2, of symmetry C_{2v}. Taking the left-hand side, they are:

$$\left.\begin{array}{ll} \text{For symmetrical stretching,} & \Delta_1 = \Delta r_{12} + \Delta r_{23} \\ \text{For angular deformation,} & \Delta_2 = r_1\Delta\theta_{13} \end{array}\right\} \text{Class } A_1$$

$$\text{For asymmetrical stretching, } \Delta_3 = \Delta r_{12} - \Delta r_{23} \;\} \text{ Class } B_1.$$

If it is required to normalize the co-ordinates, so that the force constants going with them are straight valence-force constants, Δ_1 and Δ_3 must be multiplied by a factor $(1/\sqrt{2})$. With the unnormalized co-ordinates, the kinetic energy matrix has the following form:

A, $(M = m_2)$, =

$$\begin{bmatrix} 2\{(m_2/m_1) + 2\cos^2\alpha)\} & -2\sin 2\alpha & 0 \\ -2\sin 2\alpha & 2\{(m_2/m_1 + 2\sin^2\alpha\} & 0 \\ 0 & 0 & 2\{(m_2/m_1 + 2\sin^2\alpha\} \end{bmatrix} \tag{37}$$

where $2\alpha = \theta$ is the angle of the triatomic molecule. The valence-force constants in the expanded potential energy function are related to the elements of the matrix $\boldsymbol{d}$ going with the above matrix $\boldsymbol{A}$ as follows:

Principal stretching constant .	$(d_{11} + d_{33})$
Principal bending constant .	d_{22}
Stretching-stretching interaction	$(d_{11} - d_{33})$
Stretching-bending interaction .	d_{12}

(*b*) SYSTEMS X_3YZ OF SYMMETRY C_{3v}.[3]—The required co-ordinates have already been obtained; the combinations satisfying the symmetry requirements of the two symmetry factors are:

$$\begin{array}{lll} & \textit{Class } A & \textit{Class } E \\ X-Y \text{ stretching} & \Delta_1 = \Delta r_{12} + \Delta r_{23} + \Delta r_{24} & \Delta_4 = \Delta r_{12}+\Delta r_{23}-2\Delta r_{24} \\ \text{Angular deformation} & \Delta_2 = r_1(\Delta\theta_{13}+\Delta\theta_{14}+\Delta\theta_{34} & \Delta_5 = r_1(\Delta\theta_{14}+\Delta\theta_{34}-2\Delta\theta_{13}) \\ & \quad -\Delta\theta_{15}-\Delta\theta_{35}-\Delta\theta_{45}) & \Delta_6 = r_1(\Delta\theta_{15}+\Delta\theta_{35}-2\Delta\theta_{45}) \\ Y-Z \text{ stretching} & \Delta_3 = \Delta r_{25}. & \end{array}$$

The factors of the matrix A are then:

$$\boldsymbol{A}_1 \begin{bmatrix} 3(\mu_1+3\cos^2\beta) & \begin{array}{r} -9[\sqrt{3}\sec(\alpha/2)\cos\beta+1] \\ \times\sin\beta\cos\beta \end{array} & -3\cos\beta \\ & \begin{array}{r} 3(\mu_1+3\sin^2\beta)\times \\ [\sqrt{3}\sec(\alpha/2)\cos\beta+1]^2 \end{array} & \begin{array}{l} 3[\sqrt{3}\sec(\alpha/2) \\ \cos\beta+1]\times\sin\beta \end{array} \\ & & (1+\mu_3) \end{bmatrix} \tag{38}$$

$$\mathrm{E} \begin{bmatrix} 3(2\mu_1+3\sin^2\beta) & \tfrac{9}{2}(\sqrt{3})\sin^3\beta\sec(\alpha/2) & -9(a+\cos\beta)\sin\beta \\ & \begin{array}{l} \dfrac{9}{4}\{2(1+\cos^2\beta)\mu_1 \\ \quad +3\sin^4\beta\}\sec^2(\alpha/2) \end{array} & \begin{array}{l} \dfrac{3\sqrt{3}}{2}\{2\mu_1\cos\beta-3\times \\ (a+\cos\beta)\sin^2\beta\}\sec(\alpha/2) \end{array} \\ & & \begin{array}{r} 3\{3(a+\cos\beta)^2+2\mu_1 \\ +3a^2\mu_3\} \end{array} \end{bmatrix} \tag{39}$$

---

[3] Shaffer, *J. Chem. Physics*, 1942, **10**, 1.

[4] Torkington, *ibid.*, 1949, **17**, 357.

where $\mu_1 = m_Y/m_X$, $\mu_3 = m_Y/m_Z$, $M = m_Y$.

With tetrahedral angles, the above reduce to

$$A_1 \begin{bmatrix} (1 + 3\mu_1) & -4\sqrt{2} & -1 \\ & 4(8 + 3\mu_1) & 4\sqrt{2} \\ & & (1 + \mu_3) \end{bmatrix} \quad . \quad . \quad (40)$$

$$E \begin{bmatrix} 2(4 + 3\mu_1) & 8\sqrt{2} & -2(3a + 1)\sqrt{2} \\ & (16 + 15\mu_1) & \{3\mu_1 - 4(3a + 1)\} \\ & & \{(3a + 1)^2 + 6\mu_1 + 9a^2\mu_3\} \end{bmatrix} \quad . \quad (41)$$

Only half the matrices are given, since they are symmetric.

Other cases, such as the asymmetric triatomic molecule, substituted ammonias, etc., can be treated in the same manner as the above two examples. By altering the subscripts in formulae (8) to (14) as one proceeds, systems of any complexity can be dealt with.

The author wishes to express his gratitude to Courtaulds Limited, and to Sir Cyril Hinshelwood; the above is part of a programme of work carried out while attached to the Research Laboratory, Maidenhead, at the Physical Chemistry Laboratory, Oxford.

Department of Physics,
King's College,
Strand, W.C.2.

THE KINETICS OF THE HYDRATION OF ACETALDEHYDE

BY R. P. BELL AND B. DE B. DARWENT

Received 25th July, 1949

The kinetics of hydration of acetaldehyde have been studied at 0° using a dilatometric method. The reaction is of the first order with respect to aldehyde and shows general catalysis by acids and by bases. The reaction mechanism is discussed.

There is much evidence that an aqueous solution of acetaldehyde contains at equilibrium a considerable amount of the hydrate $CH_3CH(OH)_2$ and that the equilibrium is not reached instantaneously when acetaldehyde is added to water. The evidence has been summarized in a previous paper [1] which also reports measurements on the rate of the reverse reaction

$$CH_3CH(OH)_2 \rightarrow CH_3CHO + H_2O$$

in 92·5 % aqueous acetone. This reaction was found to exhibit general acid-base catalysis, and for acid catalysis there is a general relation between the catalytic power of different catalysts and their dissociation constants in water. Deviations from this relation were related to variations in the electronic structure of the catalysts. It would be of interest to extend these measurements to aqueous solutions, so that catalytic power and dissociation constant can be compared in the same solvent. The present paper describes preliminary measurements of this kind, using dilute solutions of acetaldehyde in water. Lauder [2] has recently published data on the rate of attainment of equilibrium in mixtures of high aldehyde content, but his results were of low reproducibility and they differ considerably from ours.

---

[1] Bell and Higginson, *Proc. Roy. Soc. A*, 1949, **197**, 141.

In water it is necessary to study the forward reaction

$$CH_3CHO + H_2O \rightarrow CH_3CH(OH)_2,$$

and this is so fast that measurement by conventional methods is only possible at 0°, and then only with a limited range of catalysts. Acetaldehyde was freshly distilled in nitrogen and kept in an atmosphere of nitrogen with the addition of 0·2 % of hydroquinone to retard oxidation. For convenience in handling, the acetaldehyde was used in the form of a 20 % solution in pure acetone: in making a kinetic experiment 2 ml. of this solution was added to 25 ml. of aqueous buffer solution, and the presence of this amount of acetone in the final solution has no effect on the kinetic results. Buffer solutions were made up with freshly deaerated conductivity water, and enough sodium chloride added to make the final ionic strength up to 0·1. In spite of precautions it was not found possible to avoid the presence of small quantities of acetic acid in the acetaldehyde: this was estimated by titrating another portion of the acetone solution just before use. The concentration of acetic acid + acetate in the final solution derived from this source never exceeded 0·001 N, and was usually about one-tenth as great.

The reaction velocities were measured by the dilatometric method previously described,[1] the dilatometer having a capacity of 20 ml. and a capillary of 0·2 sq. mm. cross-section. Solutions were brought to 0° before mixing and reliable readings could be obtained 2-3 min. after mixing. The half-times of the reactions studied varied from 3 to 8 min. and they were strictly of the first order over at least 90 % of their course. Velocity constants were obtained graphically by the method of Guggenheim [3] and were in some cases checked by using the observed end-point.

Measurements were made in buffer solutions prepared from benzoic acid, acetic acid, cacodylic acid, *p*-nitrophenol and *m*-nitrophenol. Several series were carried out with each acid, each series with buffer solutions of fixed ratio. Owing to the presence of small quantities of acetic acid formed by oxidation the buffer ratios in the final reaction mixtures differed slightly within a given series: the concentrations given in Table I are corrected for the presence of acetic acid, and the observed velocities have been corrected for the small contribution from catalysis by acetic acid and acetate ion, estimated from the results in acetate buffers. The catalytic constants of the various species were derived from the observed velocities by the following method.[4] In a solution of buffer ratio $[HA]/[A^-] = r$, the observed velocity is given by

$$v = v_0 + k_{H^+}[H^+] + k_{OH^-}[OH^-] + (k_{HA} + k_{A^-}/r)[HA], \quad . \quad (1)$$

where v_0 is the " spontaneous " velocity and the k's are catalytic constants. In a given series r, $[OH^-]$ and $[H^+]$ are approximately constant, and a plot of v against $[HA]$ gives a straight line of slope

$$s = k_{HA} + k_{A^-}/r$$

and intercept

$$v' = v_0 + k_{H^+}[H^+] + k_{OH^-}[OH^-].$$

---

[2] Lauder, *Trans. Faraday Soc.*, 1948, **44**, 729.

[3] Guggenheim, *Phil. Mag.*, 1926, (7), **1**, 538.

[4] Cf. Bell and Lidwell, *Proc. Roy. Soc. A*, 1940, **176**, 88.

The separate values of k_{HA} and k_{A^-} can then be obtained by plotting s against $1/r$, where r is the average buffer ratio in a series. Similarly, the values of v_0, k_H and k_{OH^-} can be obtained from the values of v', $[H^+]$ and $[OH^-]$ for the different series. In calculating the latter the mean value of r in each series was used, and the dissociation constants at 0° were taken from *Landolt-Bornstein Tabellen* (1937), a small extrapolation from the range 10°-50° being necessary for the nitrophenols. K_w at 0° was taken as $0{\cdot}114 \times 10^{-14}$ and the activity coefficients of all univalent ions as 0·764.

Since in some cases the buffer ratios vary appreciably within a given series, the above procedure does not give very accurate values for the catalytic constants. The approximate values thus obtained can, however, be used to correct the observed values of v for the variation of r within each series, and the above procedure repeated. Fig. 1 gives typical plots of v (corrected) against [HA] for benzoic acid. Fig. 2 gives the plots of v' (corrected) against $[H^+]$ and $[OH^-]$ for all the buffers investigated. Catalysis by hydrogen ions is negligible in the *p*-nitrophenate and *m*-nitrophenate buffers, and catalysis by hydroxyl ions is negligible in the benzoate, acetate and cacodylate buffers. The values of the catalytic constants finally adopted are given in Table II, and the velocities calculated from eqn. (1) using these constants are given as v (calc.) in Table I. A somewhat better agreement could probably be obtained by further adjustment of the constants, but the accuracy of the data hardly warrants this.

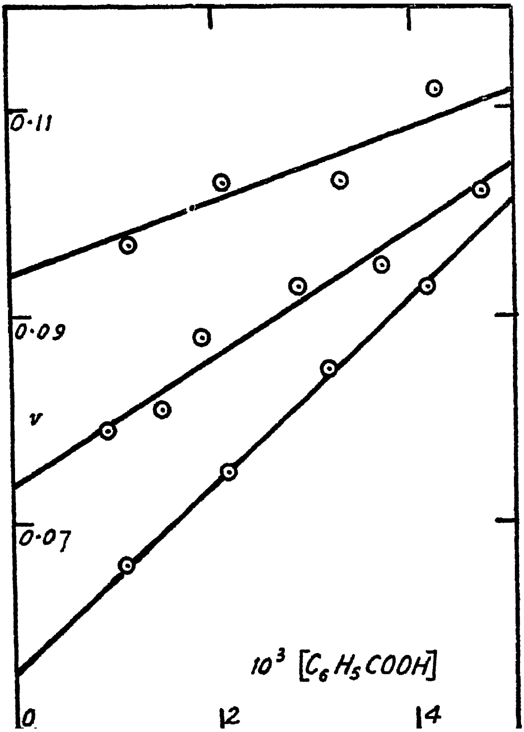

FIG. 1.

TABLE I

v denotes $\log_{10} e \times$ first-order constant in min.$^{-1}$

BENZOIC ACID

$r = 0{\cdot}057$, $[H^+] = 5{\cdot}80 \times 10^{-6}$ (mean)

10^5 [HA] (corr.)	110	212	314	411
10^4 [A$^-$] (corr.)	177	369	556	784
10^3 v (corr.)	69	76	86	92
10^3 v (calc.)	71	80	89	100

$r = 0{\cdot}114$, $[H^+] = 1{\cdot}15 \times 10^{-5}$ (mean)

10^5 [HA] (corr.)	95	146	188	284	367	466
10^4 [A$^-$] (corr.)	83	121	169	251	329	411
10^3 v (corr.)	79			93	95	102
10^3 v (calc.)		90	90	99	103	

$r = 0{\cdot}184$, $[H^+] = 1{\cdot}89 \times 10^{-5}$ (mean)

10^5 [HA] (corr.)	116	208	212	326	423
10^4 [A$^-$] (corr.)	61	114	119	169	237
10^3 v (corr.)	99	102	109	106	111
10^3 v (calc.)	106	108	107	117	118

ACETIC ACID

$r = 0{\cdot}118$, $[H^+] = 3{\cdot}36 \times 10^{-6}$ (mean)

10^4 [HA] (corr.)	27	49	69	90	109
10^4 (A$^-$) (corr.)	204	400	600	805	985
10^3 v (corr.)	66	87	99	116	127
10^3 v (calc.)	71	86	100	115	129

$r = 0{\cdot}140$, $[H^+] = 5{\cdot}02 \times 10^{-6}$ (mean)

10^4 [HA] (corr.)	27		50	96	144
10^4 [A$^-$] (corr.)	146	274	289	547	822
10^3 v (corr.)	73	84	91	110	135
10^3 v (calc.)	73	84	85	111	138

$r = 0{\cdot}308$, $[H^+] = 8{\cdot}78 \times 10^{-6}$ (mean)

10^4 [HA] (corr.)	30	47	74	87	113	152
10^4 [A$^-$] (corr.)	92	149	231	300	377	525
10^3 v (corr.)	82	93	102	106	123	134
10^3 v (calc.)	84	90	103	108	120	138

$r = 0{\cdot}505$, $[H^+] = 1{\cdot}44 \times 10^{-5}$ (mean)

10^4 [HA] (corr.)	54	81	107	138
10^4 [A$^-$] (corr.)	107	162	214	269
10^3 v (corr.)	111	124	128	145
10^3 v (calc.)	107	117	128	141

$r = 0{\cdot}732$, $[H^+] = 2{\cdot}09 \times 10^{-5}$ (mean)

10^4 [HA] (corr.)	25	45	71	91	111	131
10^4 [A$^-$] (corr.)	31	61	96	130	156	184
10^3 v (corr.)	116	128	132	150	148	157
10^3 v (calc.)	121	120	133	136	144	152

CACODYLIC ACID

$r = 0{\cdot}304$, $[H^+] = 2{\cdot}51 \times 10^{-7}$ (mean)

10^4 [HA] (corr.)	11·6	36	46
10^4 [A⁻] (corr.)	40	108	161
10^3 v (corr.)	64	89	111
10^3 v (calc.)	59	83	100

$= 1{\cdot}13$, $[H^+] = 9{\cdot}6 \times 10^{-7}$ (mean)

10^4 [HA] (corr.)	15·9	40	51	
10^4 [A⁻] (corr.)	12·9	36	46	83
10^3 v (corr.)	54	67	75	92
10^3 v (calc.)	53	65	70	

$r = 2{\cdot}18$, $H^+ = 1{\cdot}87 \times 10^{-6}$ (mean)

10^4 [HA] (corr.)	24	86	156
10^4 [A⁻] (corr.)	12·7	34	73
10^3 v (corr.)	60	80	108
10^3 v (calc.)	56	79	105

p-NITROPHENOL

: $0{\cdot}203$, $[OH^-] = 1{\cdot}75 \times 10^{-7}$ (mean)

10^4 [HA] (corr.)	5·0	9·1	9·5	15·0	21
10^4 [A⁻] (corr.)	25	37	55	73	106
10^3 v (corr.)	92	89	102	110	122
10^3 v (calc.)	96	90	111	110	125

$r = 0{\cdot}315$, $[OH^-] = 1{\cdot}17 \times 10^{-7}$ (mean)

10^4 [HA] (corr.)	11·0	17·5	29	41
10^4 [A⁻] (corr.)	34	56	93	132
10^3 v (corr.)	76	83	94	111
10^3 v (calc.)	82	91	104	119

$[OH^-] = 9{\cdot}5 \times 10^{-9}$ (mean)

10^4 [HA] (corr.)	70	290	318	444
10^4 [A⁻] (corr.)	16	51	87	123
10^3 (corr.)	53	68	86	98
10^3 (calc.)	56	68	81	96

m-NITROPHENOL

$r = 3{\cdot}13$, $[OH^-] = 1{\cdot}59 \times 10^{-7}$ (mean)

10^4 [HA] (corr.)	13·9	14·9	28	43	54	57
10^4 [A⁻] (corr.)	4·7	4·6	8·9	11·8	20	17
10^3 v (corr.)	99	92	106	109	122	105
10^3 v (calc.)	91	88	96	105	118	97

$r = 12{\cdot}9$, $[OH^-] = 3{\cdot}94 \times 10^{-8}$ (mean)

10^4 [HA] (corr.)	49	140	202
10^4 [A⁻] (corr.)	3·8	9·7	17·2
10^3 v (corr.)	61	68	85
10^3 v (calc.)	59	68	83

The results given above show definitely that the hydration of acetaldehyde is catalyzed by water molecules, hydrogen ions, hydroxyl ions, undissociated acid molecules and anion bases, thus confirming the observations made on the reverse reaction in aqueous acetone. Table II shows that there is, as usual, a general relation between catalytic power and acid-base strength, but the data are not sufficiently numerous to establish this relation quantitatively. It is planned to extend work on this reaction by using methods applicable to the study of still faster reactions.

TABLE II.—DISSOCIATION AND CATALYTIC CONSTANTS

Acid	K	k_{HA}	k_{A^-}
Water . . .	*$2{\cdot}05 \times 10^{-17}$	†$7{\cdot}7 \times 10^{-4}$	$2{\cdot}5 \times 10^{5}$
m-Nitrophenol . .	$2{\cdot}4 \times 10^{-9}$	0·10	16
p-Nitrophenol . .	$3{\cdot}3 \times 10^{-8}$	0·18	3·5
Cacodylic . .	$5{\cdot}7 \times 10^{-7}$	2·37	2·70
Acetic . . .	$1{\cdot}7 \times 10^{-5}$	3·20	0·43
Benzoic . . .	$6{\cdot}05 \times 10^{-5}$	3·25	0·35
H_3O^+ . . .	55·5	$3{\cdot}0 \times 10^{3}$	†$7{\cdot}7 \times 10^{-4}$

* $K = K_w/55{\cdot}5$.
† $k = v_0/55{\cdot}5$.

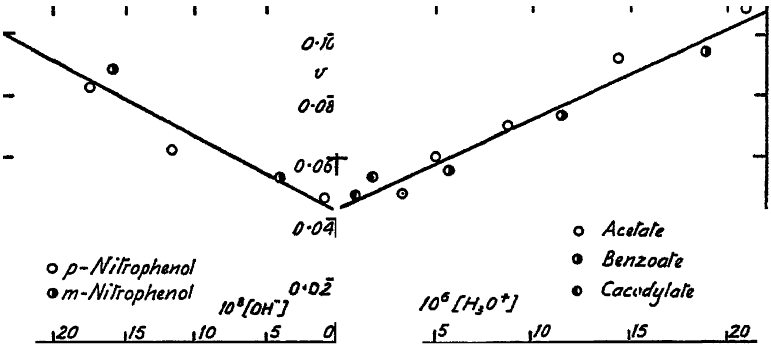

FIG. 2.

We are unable to reconcile our results with those of Lauder,[3] who also gives data for the rate of hydration, based on dilatometric and refractometric measurements. He did not realize the catalytic nature of the reaction, and worked in unbuffered solutions which presumably contained small but variable quantities of acetic acid : this may account for the erratic behaviour of his results, and the fact that his rates decrease with increasing temperature. It is more difficult to explain the fact that most of his recorded rates are considerably lower than the water-catalyzed rate which we have found at ·0°. His solutions contained a much greater proportion of acetaldehyde than ours, and a correspondingly smaller concentration of catalytically-active water molecules. It is also possible that in these concentrated solutions he may have been measuring the rate of formation of a hydrated form such as $(CH_3CHOH)_2O$; the analogue of this compound is stable in the case of monochloracetaldehyde,[5] and similar hemihydrates are believed to exist in aqueous formaldehyde solutions.[6] This suggestion may also account for the discrepancies in the equilibrium degrees of hydration given by different authors: thus Herold and Wolf[7] find 60 % hydration from ultra-violet absorption measurements, Schou[8] 26 % by the same method, and Lauder[2] a very small degree of hydration from measurements of refractive index.

---

[5] Natterer, *Monatsh.*, 1882, 3, 449.
[6] Walker, *Formaldehyde* (Amer. Chem. Soc. Monogr., 1944, Ch. iii).

The mechanisms proposed by Bell and Higginson[1] for the catalyzed hydration were as follows:

ACID CATALYSIS:

$$\mathrm{CH_3CHO + H_2O + HB \rightleftharpoons CH_3CH(OH)(OH_2^+) + B^-} \qquad \text{(i)}$$
$$\mathrm{CH_3CH(OH)(OH_2^+) + B^- \rightleftharpoons CH_3CH(OH)_2 + HB} \quad . \quad \text{(ii)}$$

BASIC CATALYSIS:

$$\mathrm{CH_3CHO + H_2O + B^- \rightleftharpoons CH_3CH(OH)O^- + HB} \quad . \quad \text{(iii)}$$
$$\mathrm{CH_3CH(OH)O^- + HB \rightleftharpoons CH_3CH(OH)_2 + B^-} \quad . \quad . \quad \text{(iv)}$$

Of these four steps, (ii) and (iv) involve simple proton transfers to and from oxygen atoms, and experience indicates that these equilibria will be set up instantaneously. The rate-determining steps then become (i) and (iii), which involve greater structural changes and are likely to be slow. They are both formally termolecular reactions, and it is interesting to enquire how far they can be split up into successive bimolecular steps, as is frequently the case.[9] The only possibilities are as follows:

Reaction (i)

$$\left\{\begin{array}{ll} \mathrm{HB + H_2O} & \mathrm{\rightleftharpoons B^- + H_3O^+} \quad . \quad . \quad . \quad (a) \\ \mathrm{CH_3CHO + H_3O^+} & \mathrm{\rightleftharpoons CH_3CH(OH)OH_2^+} \quad . \quad . \quad (b) \end{array}\right.$$

$$\text{or} \left\{\begin{array}{ll} \mathrm{CH_3CHO + HB} & \mathrm{\rightleftharpoons CH_3CH : \overset{+}{O}H + B^-} \quad . \quad . \quad (c) \\ \mathrm{CH_3CH : \overset{+}{O}H + H_2O} & \mathrm{\rightleftharpoons CH_3CH(OH)\overset{+}{O}H_2} \quad . \quad . \quad (d) \end{array}\right.$$

$$\text{or} \left\{\begin{array}{ll} \mathrm{CH_3CHO + H_2O} & \mathrm{\rightleftharpoons CH_3CH(O^-)\overset{+}{O}H_2} \quad . \quad . \quad (e) \\ \mathrm{CH_3CH(O^-)\overset{+}{O}H_2 + HB} & \mathrm{\rightleftharpoons CH_3CH(OH)\overset{+}{O}H_2 + B^-} \quad . \quad (f) \end{array}\right.$$

Reaction (iii)

$$\left\{\begin{array}{ll} \mathrm{B^- + H_2O} & \mathrm{\rightleftharpoons HB + OH^-} \quad . \quad . \quad . \quad (g) \\ \mathrm{CH_3CHO + OH^-} & \mathrm{\rightleftharpoons CH_3CH(OH)O^-} \quad . \quad . \quad . \quad (h) \end{array}\right.$$

$$\text{or} \left\{\begin{array}{ll} \mathrm{CH_3CHO + B^-} & \mathrm{\rightleftharpoons CH_3C : O + HB} \quad . \quad . \quad (j) \\ \mathrm{CH_3\bar{C} : O + H_2O} & \mathrm{\rightleftharpoons CH_3CH(OH)O^-} \quad . \quad . \quad . \quad (k) \end{array}\right.$$

$$\text{or} \left\{\begin{array}{ll} \mathrm{CH_3CHO + H_2O} & \mathrm{\rightleftharpoons CH_3CH(O^-)\overset{+}{O}H_2} \quad . \quad . \quad (l) \\ \mathrm{CH_3CH(O^-)\overset{+}{O}H_2 + B^-} & \mathrm{\rightleftharpoons CH_3CH(OH)O^- + HB.} \quad . \quad (m) \end{array}\right.$$

All these possibilities can be excluded by the following arguments. If reactions (*b*), (*d*), (*h*) or (*k*) were rate-determining the reaction would show specific catalysis by hydrogen or hydroxyl ions,[10] while if reaction (*e*) (identical with (*l*)) determined the rate there would be no catalysis by acids or bases. Both these conclusions are at variance with the general catalysis by acids and bases actually observed. On the other hand, reactions (*a*), (*c*), (*f*), (*g*) and (*m*) cannot be rate determining, since they are ordinary acid-base reactions involving the transfer of a proton to or from an oxygen atom, which is known to be a very rapid process. It is more difficult to predict the behaviour of reaction (*j*) but there is good experimental evidence that it cannot in fact take place at any measurable rate. If it could do so the hydrogen of the —CHO group should exchange with deuterium oxide, which is not the case, even under strongly alkaline conditions. Direct exchange experiments with acetaldehyde were inconclusive,[11] but it was later shown by Bonhoeffer and Walters [12] that in the aldol condensation of acetaldehyde by aqueous potassium carbonate, only the hydroxyl hydrogen has exchanged with the solvent: similarly, Fredenhagen and Bonhoeffer [13] showed that in the Cannizzaro reaction of benzaldehyde, formaldehyde or glyoxal in very concentrated alkali there was no isotopic exchange of the hydrogen bound to carbon.

---

[7] Herold and Wolf, *Z. physik. Chem. B*, 1929, **5**, 121; 1931, **12**, 165.

[8] Schou, *J. Chim. phys.*, 1929, **26**, 69.

[9] Cf. Hinshelwood, *J. Chem. Soc.*, 1947, 694.

[10] Cf. Bell, *Acid-base Catalysis* (Oxford, 1941), p. 122.

It thus appears that the termolecular reactions (i) and (iii) cannot be split up completely into consecutive bimolecular steps. However, this does not mean that we must imagine the unlikely event of three molecules arriving together simultaneously. In the first place, the concentration of water molecules is so high that the presence of a water molecule at a collision between two solute species is not a highly improbable event. In the second place, it is quite likely that two of the three reacting species may be loosely connected together by hydrogen bonding before reaction, for example, as in the following schemes:

Reaction (i):

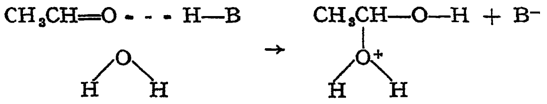

Reaction (iii):

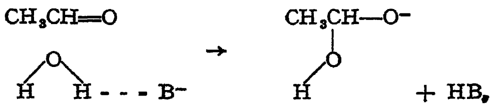

where the dotted lines represent hydrogen bonds. The formation of these bonds can be regarded as the initial stages of reactions (*c*) and (*e*) above, but, as already explained, these reactions cannot go to completion before the other reacting species approaches.*

Our thanks are due to Dr. J. E. Prue for helpful discussion.

One of us (B. de B. D.) wishes to express his gratitude to the National Research Council of Canada for leave of absence.

Physical Chemistry Laboratory,
Oxford.

---

[11] Klar, *Z. physik. Chem. B*, 1934, **26**, 335.

[12] Bonhoeffer and Walters, *Z. physik. Chem. A*, 1938, **181**, 441.

[13] Fredenhagen and Bonhoeffer, *ibid.*, 1938, **181**, 379.

* Exactly the same line of argument shows that the hydrolysis of orthoesters and the dimerization of hydroxy-aldehydes and ketones (Bell and Baughan, *J. Chem. Soc.*, 1937, 1947; Bell and Hirst, *ibid.*, 1939, 1777), must involve a termolecular step which cannot be resolved into two bimolecular ones.

THE THERMAL OXIDATION OF THE ALIPHATIC AMINES

By C. F. Cullis and L. S. A. Smith

Received 5th August, 1949

A study has been made of the vapour-phase oxidation of the four simplest primary aliphatic amines, and particular attention has been paid to the ways in which their behaviour resembles or differs from that of the corresponding paraffins. In general the reaction bears a close similarity to hydrocarbon oxidation. Attack of the amines is believed to occur at a point in the hydrocarbon chain, and reaction is thought to proceed through the formation of intermediate peroxides. In certain cases free NH_2 radicals appear to be liberated during the breakdown of these peroxides. These radicals may subsequently give rise to oxides of nitrogen, whose participation in the reaction mechanism may cause the oxidation of the amines to show certain differences in behaviour from that of the unsubstituted paraffins.

Although the vapour-phase oxidation of the paraffin hydrocarbons has received considerable study, that of their simple derivatives has not been so widely investigated. A comparative study of a number of chloroparaffins has recently been made,[1] and it appears that in the kinetics of their reaction with oxygen, primary and some secondary chloro-paraffins are generally similar to the corresponding hydrocarbons; the reaction seems to be essentially an oxidation of the hydrocarbon chain of the molecule The influence of chlorine is to increase the ease of oxidation (*a*) by impairing the symmetry of a methyl group into which it is introduced, and (*b*) by exerting a direct inductive effect of its own.

With the introduction of an amino group into a hydrocarbon molecule, a further possibility arises; for, apart from the ability of this substituent to exert influences of the type mentioned above, the amino group may itself be attacked by oxygen. It was considered of interest to investigate in what respects the oxidation of the amines is comparable in mechanism to that of the unsubstituted paraffins, and also to discover the part played by the amino group in the reaction.

The only previous study of the homogeneous thermal oxidation of an aliphatic amine appears to be that of Emeleus and Jolley,[2, 3] who investigated the oxidation of methylamine. Jolley [2] showed that the reaction possesses many of the characteristics of a chain reaction, and he noted in particular a striking similarity to hydrocarbon oxidation. The conclusion was reached that initial attack of the methylamine molecule takes place at the methyl group.

In the present work a comparative study has been made of the oxidation of the four simplest amines. With each of these, the following have been investigated:

(*a*) the temperatures at which pyrolysis and oxidation become appreciable;

---

[1] Cullis, Hinshelwood and Mulcahy, *Proc. Roy. Soc. A*, 1949, **196**, 160.

[2] Jolley, *J. Chem. Soc.*, 1934, 1957.

[3] Emeleus and Jolley, *ibid.*, 1936, 1524.

(*b*) the maximum rates of reaction of a standard amine-oxygen mixture;

(*c*) the variation of maximum oxidation rate with temperature.

Ethylamine and *n*-propylamine have been singled out for more detailed study, involving the determination of:

(*a*) the dependence of maximum oxidation rate on the initial reactant concentrations;

(*b*) the influence on the reaction of altering the amine/oxygen ratio, while the total pressure is kept constant;

(*c*) the effect of the surface;

(*d*) the influence of an inert gas;

(*e*) the influence of acetaldehyde and formaldehyde.

In addition, an investigation has been made of the products formed during the oxidation of these two amines.

Experimental

The apparatus resembled that used in this laboratory for the oxidation of hydrocarbons.[4] In essentials, it consisted of a silica reaction vessel (of 12 cm. length and 290 cm.^{3} capacity) suspended in a furnace, and connected both to a mercury manometer and to devices for admission of reactants and withdrawal of products. To prevent condensation of products and to facilitate admission of reasonably large pressures of the higher amines, the tubing leading to the reaction vessel was wound with electrically heated Nichrome wire. The furnace used gave a temperature uniform to 2° C over the length of the reaction vessel; the temperature was measured with a platinum-rhodium thermocouple and was automatically controlled to within ± 0·5° C.

Methylamine and ethylamine were prepared by dry distillation of their hydrochlorides with calcium oxide. The free base was dried by passage through a U-tube packed with calcium oxide, and condensed in a trap surrounded by solid CO_2; the middle fraction of the liquid was then distilled into a previously evacuated storage vessel. The purest available commercial samples of the higher amines were used, and these were subjected to careful fractionation. The liquid was placed in its storage bulb and dissolved air was removed by repeated freezing of the liquid followed by evacuation.

Oxygen and nitrogen were obtained from cylinders. Each gas contained 1-2 % of the other, and this impurity was neglected. The gases were dried by passage through a column of phosphorus pentoxide and were stored in 5-litre globes. Formaldehyde was obtained by gently heating paraformaldehyde, and acetaldehyde was purified in a manner similar to that used for the higher amines.

The course of the reaction was followed by pressure-time records and by periodic analysis for certain intermediate products. The analytical methods employed are discussed later.

Results

A Comparative Survey of the Oxidation of Methylamine, Ethylamine, *n*-Propylamine and *n*-Butylamine

(*a*) PYROLYSIS AND OXIDATION TEMPERATURES.—Jolley[2] showed that the rate of pyrolysis of methylamine is negligible at temperatures at which rapid oxidation occurs. In the present investigation, the temperatures were determined at which both pyrolysis and oxidation become appreciable for the four amines studied. The reactants were admitted to the reaction vessel at a standard pressure (75 mm. amine for pyrolysis, and 50 mm. amine + 200 mm. oxygen for oxidation) and at a temperature well below that at which reaction occurs. The temperature was then regularly increased, and the pressure was measured at frequent intervals. At first the pressure increases linearly with the absolute temperature, but at the reaction temperature the value of dp/dT rises markedly. The values of the pyrolysis and oxidation temperatures determined in this way are shown in Table I.

---

[4] Cullis, Hinshelwood, Mulcahy and Partington, *Faraday Soc. Discussion*, 1947, **2**, 111.

TABLE I

Substance	Pyrolysis Temp. (° C)	Oxidation Temp. (° C)
Methylamine	560	320
Ethylamine	496	293
Propylamine	478	275
Butylamine	470	290

The only important fact which emerges from these measurements is that in all cases the pyrolysis temperatures lie well above those at which oxidation commences. Since the above figures are highly dependent on such factors as the rate of heating and the length of the induction period preceding reaction, they do not, for example, provide any reliable indication of the relative ease of oxidation of the amines. For this purpose, it is preferable to compare the rates of oxidation in a constant temperature system.

(*b*) THE MAXIMUM RATES OF REACTION OF A STANDARD AMINE-OXYGEN MIXTURE.—For each of the four amines, the maximum oxidation rate ($\rho_{\max.}$) was measured under standard conditions. The pressure-time curves are shown in Fig. 1.* The rate of reaction increases rapidly with the length of the carbon chain, but the structural influence is not as marked as with the paraffin hydrocarbons.[4] In particular, the abnormally large difference in oxidizability of ethane and propane does not find a parallel in the case of ethylamine and propylamine.

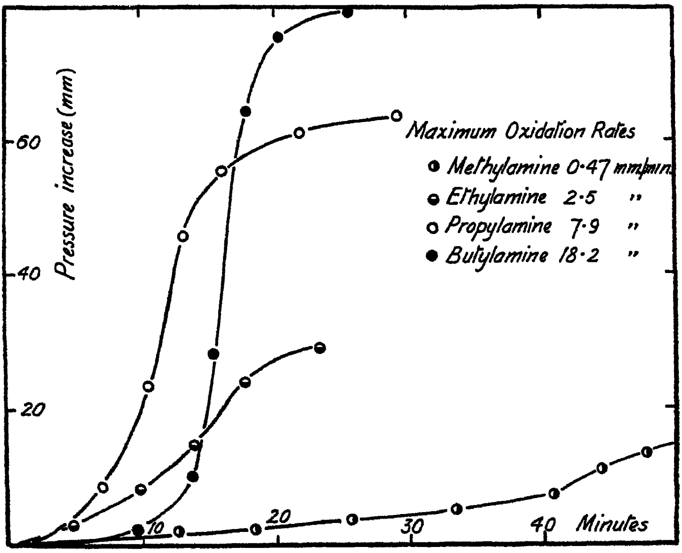

FIG. 1.—The oxidation of the amines at 280° C. Amine pressure: 50 mm.; oxygen pressure: 200 mm.

It appears from Fig. 1 that, as the series is ascended, the pressure-time curves show an increasing similarity to those obtained with hydrocarbons; with butylamine, there is an appreciable induction period before reaction sets in. It is of interest that the segmented pressure-time curve shown by methylamine at 280° C becomes smooth as the temperature is increased.

---

* Pressure readings were usually taken every 10 or 15 sec. Only a few experimental points are included in the diagram to identify the various curves with the compounds to which they refer.

(*c*) THE VARIATION OF MAXIMUM OXIDATION RATE WITH TEMPERATURE.—The maximum rates of reaction of a standard mixture were measured for each amine at a series of temperatures. The results are shown as log $\rho_{max.}$ against $1/T$ plots in Fig. 2. With methylamine and ethylamine, are uninterrupted straight lines in the temperature range investigated. With propylamine, however, there is a clearly-defined break at about 335° C; this is reminiscent of the behaviour of propane and some of its other derivatives,[5] which show transition from a low-temperature to a high-temperature mechanism in this region. With butylamine, cool flames appear at temperatures above 305° C; there is no return to slow reaction at higher temperatures. The occurrence of cool flames with this amine is a further indication that a lengthening of the carbon chain increases the similarity to hydrocarbon combustion.

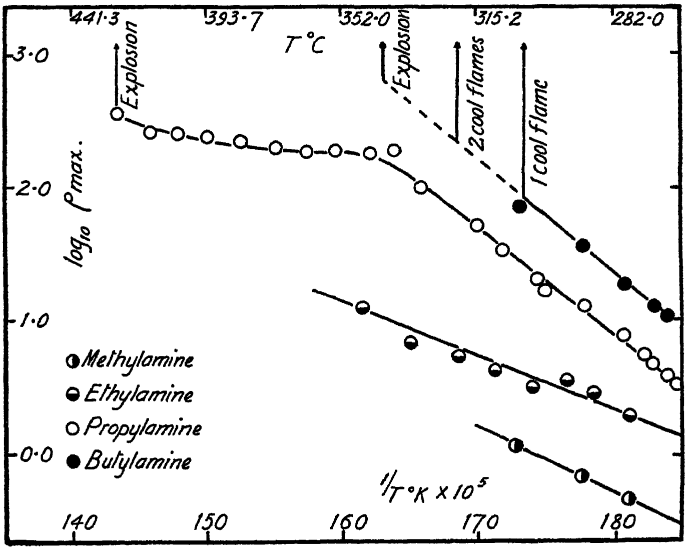

FIG. 2.—The variation of maximum oxidation rate with temperature. Amine pressure: 50 mm.; oxygen pressure: 200 mm.

It was found in this work that, with the amines, abnormally high rates of reaction are reached before explosion takes place. With ethylamine, a rate of 180 mm./min. can occur without explosion intervening, while with propylamine rates as high as 260 mm./min. have been observed. The explosions met with in amine oxidation are therefore probably largely thermal in character.

The Kinetics of the Oxidation of Ethylamine and *n*-Propylamine

(*a*) THE DEPENDENCE OF MAXIMUM OXIDATION RATE ON THE INITIAL REACTANT CONCENTRATIONS.—Fig. 3 shows the variation of $\rho_{max.}$ with reactant concentrations for both ethylamine and propylamine. The results are closely similar to those found for the higher paraffins. Comparison of these results with those obtained by Jolley[2] for methylamine shows that, as the amine series is ascended, the reaction becomes more strongly dependent on amine concentration and is decreasingly influenced by oxygen concentration.

(*b*) THE INFLUENCE OF THE AMINE/OXYGEN RATIO ON THE REACTION.—Mixtures of varying composition but of constant total pressure were allowed to react at 280° C. Fig. 4 shows the values of $\rho_{max.}$ as a function of the percentage of oxygen present for a series of experiments with ethylamine. In common with the higher paraffins,[6, 7] the mixture containing equal concentrations of the two reactants has the highest value of $\rho_{max.}$, though the time taken to acquire this rate is abnormally long in this particular case.

Closely similar results were obtained with propylamine at the same temperature.

[5] Mulcahy, *Trans. Faraday Soc.*, 1949, **45**, 537.

[6] Pidgeon and Egerton, *J. Chem. Soc.*, 1932, 661.

[7] Prettre, *Ann. Comb. Liq.*, 1936, **11**, 667.

If it is assumed (cf. Fig. 3) that over the range of concentrations investigated :

$$\text{Rate} = k\,[\text{Amine}]^2\,[\text{Oxygen}]^{\frac{1}{2}}$$

the maximum rate should occur for a 4/1 amine-oxygen mixture. Recent experiments in this laboratory with other organic compounds, whose behaviour is generally similar to that of the amines, have indicated that the influence of oxygen concentration, though small at high oxygen pressures, may be very marked in presence of a large excess of the organic compound ; while under the latter conditions the influence of the concentration of the organic compound may be quite small. Similar effects in amine oxidation would tend to shift the theoretical optimum composition in the direction of a higher proportion of oxygen. This is found to be the case experimentally, though the extent of this shift is surprisingly large.

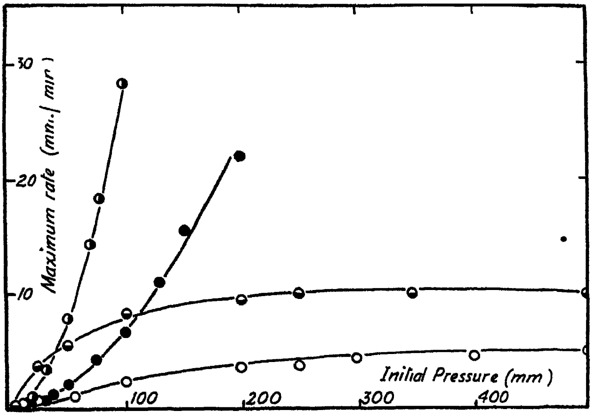

FIG. 3.—The variation of maximum rate with the initial pressures of reactants at 280° C.

○ Oxygen pressure varied ; ethylamine pressure : 50 mm.

● Ethylamine pressure varied ; oxygen pressure : 200 mm.

◒ Oxygen pressure varied ; propylamine pressure : 50 mm.

◑ Propylamine pressure varied ; oxygen pressure : 200 mm.

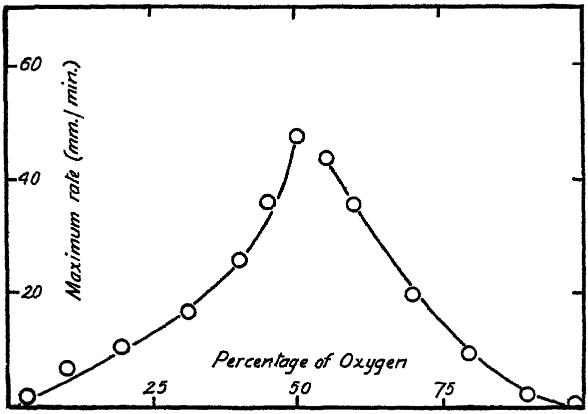

FIG. 4.—The variation of maximum rate with amine/oxyen ratio at 280° C. Total pressure : 500 mm.

(*c*) THE EFFECT OF THE SURFACE.—Amine oxidation is not nearly so sensitive to surfaces influences as hydrocarbon combustion. A frequent observation in the present investigation was that admission of air to the reaction vessel or leaving the vessel evacuated for some time causes the first subsequent run to show an abnormally long induction period, though little alteration in the value of $\rho_{max.}$ is observed. It is evident that the nature of the adsorbed gases affects the reaction, but uniformity of the surface can apparently be regained after only one or two runs. This is in striking contrast to the behaviour of the paraffins, where there is considerable difficulty in obtaining reproducible results.[8]

To investigate further the influence of the surface, the surface/volume ratio was considerably increased by filling the reaction vessel to one-third of its depth with fine silica chips. Neither with ethylamine nor with propylamine is any significant variation in the value of $\rho_{max.}$ caused by this procedure, though in some cases a slight lengthening of the induction period occurs.

(*d*) THE INFLUENCE OF AN INERT GAS.—In the slow combustion of hydrocarbons, addition of an inert gas sometimes shortens the induction period without much affecting the value of $\rho_{max.}$[4, 6] Some typical results for the addition of nitrogen to a standard propylamine-oxygen mixture are shown in Table II. It is evident that this gas has no appreciable effect on the reaction.

TABLE II

Temperature : 292° C ; Propylamine pressure : 50 mm. ; Oxygen pressure : 200 mm.

Nitrogen Pressure (mm.)	$\rho_{max.}$ (mm./min.)	Induction Period* (min.)
0	12·0	5·0
50	11·0	5·0
100	11·3	4·7
151	11·3	4·7
197	11·5	4·2
250	11·8	4·7
349	11·5	4·4

Similar results were obtained with ethylamine at 280° C.

(*e*) THE INFLUENCE OF ACETALDEHYDE AND FORMALDEHYDE.—Acetaldehyde has in many cases a marked accelerating effect on the oxidation of the paraffins,[9] whereas formaldehyde promotes oxidation by the high-temperature mechanism,[10] but has a powerful inhibiting effect on the low-temperature reaction.[4, 11] Both these additives were found to shorten the induction period in the oxidation of ethylamine and propylamine, and the value of $\rho_{max.}$ was slightly increased. Acetaldehyde has the greater accelerating influence, but its effect is by no means large.

Analytical Methods.—Jolley [2] showed that the final products of oxidation of methylamine are carbon monoxide, carbon dioxide, nitrogen, ammonia, hydrogen cyanide and formaldehyde, together with small amounts of hydrogen and unknown quantities of methane, ethane and ethylene. In this investigation, an analysis of some of the oxidation products of ethylamine and propylamine was attempted. These are considerably more numerous than those found with methylamine, and the problem is further complicated by the ease with which many of the species present interact with one another. In order to form some qualitative picture of the course of the reaction, attention was paid to intermediate rather than final reaction products. The analysis was only made quantitative for certain compounds considered to be of primary importance in the reaction.

(1) QUALITATIVE ANALYSIS.—The reacting gases were withdrawn from the reaction vessel by " sharing " with an evacuated gas-pipette after different

---

[8] Mulcahy, *Trans. Faraday Soc.*, 1949, **45**, 575.

[9] Pease, *Chem. Rev.*, 1937, **21**, 279 ; Harris and Egerton, *ibid.*, 287 ; Egerton and Young, *Trans. Faraday Soc.*, 1948, **44**, 575.

[10] Bone and Hill, *Proc. Roy. Soc. A*, 1930, **129**, 434 ; Bone and Allum, *ibid.*, 1932, **134**, 578 ; Norrish and Foord, *ibid.*, 1936, **157**, 503.

[11] Harris and Egerton, *Chem. Rev.*, 1937, **21**, 287.

* Defined here as the time taken for a pressure increase of 5 mm. to occur.

extents of reaction had occurred. The products were extracted with water and the resulting solution was analyzed, the following tests being applied :

(*a*) *Formaldehyde* : Schryver's test.[12]
(*b*) *Acetaldehyde* : Lewin's test.[13]
(*c*) *Alcohols* : The carbon disulphide test.[14]
(*d*) *Oxides of nitrogen* : Griess-Islovsky test.[15]
(*e*) *Ammonia* : Amines interfere with the tests for ammonia. Nessler's reagent, however, gives a reddish-brown precipitate with ammonia, pale yellow precipitates with methylamine and ethylamine, and a white precipitate with propylamine. These precipitates are turned black in presence of much formaldehyde, but in the dilute solutions used formaldehyde did not interfere. The marked difference in colour made possible a rough estimate of the ammonia present.
(*f*) *Hydrogen cyanide* : The Prussian Blue test.

All the above reactions were found to give strongly positive results with M/1000 test solutions.

(2) QUANTITATIVE ANALYSIS.—Since peroxides are thought to be of primary importance in the oxidation of many hydrocarbons, quantitative analysis for such compounds was carried out with ethylamine and propylamine. The thiocyanate method [16] was employed, and the refinements recently recommended by Widmaier and Mauss [17] were adopted. For peroxide estimations, the reacting gases were extracted with benzene instead of with water.

In the case of propylamine only, the total base concentration was determined at various stages of the reaction by titration with acid, using methyl orange as indicator. The only basic substances present are amines and ammonia, and no simple method could be devised of separating the relative contributions of each. In presence of excess oxygen, however, the amounts of ammonia are generally small, and the total base concentration gives an approximate estimate of the amount of unchanged amine.

Analytical Results.—(1) ETHYLAMINE. Qualitative tests were applied to the intermediate products mentioned at various stages of the reaction of a 1/1 amine-oxygen mixture. A strictly comparative technique was used throughout, the tests always being carried out according to a standard procedure. The results are classified as: negative (—), feebly positive (+), positive (++), and strongly positive (+++), and are shown in Table III.

TABLE III

Temperature : 280° C ; Ethylamine pressure : 250 mm. ; Oxygen pressure: 250 mm.

% Reaction Completed	0 %	5 %	10 %	25 %	50 %	75 %	100 %
Formaldehyde	—	+	+	+	++	++	+++
Acetaldehyde	—	+	++	++	++	++	++
Alcohols	—	—	—	—	—	—	—
Oxides of nitrogen	—	+	+	++	++	++	+
Ammonia	—	—	+	+	++	++	++
Hydrogen cyanide	—	—	—	—	—	—	—

Formaldehyde, acetaldehyde and ammonia develop continuously throughout the reaction. Oxides of nitrogen show similar behaviour, though their concentration decreases slightly in the fully reacted mixture. Alcohols and hydrogen cyanide are invariably absent.

[12] Schryver, *Proc. Roy. Soc. B*, 1910, **82**, 226.
[13] Lewin, *Ber.*, 1899, **32**, 3388.
[14] See Feigl, *Spot Tests* (New York, 1947), 324.
[15] See Ubbelohde, *The Science of Petroleum* (Oxford, 1938), **4**, 2938.
[16] Yule and Wilson, *Ind. Eng. Chem.*, 1931, **23**, 1254.
[17] Widmaier and Mauss, *Revue de l'Institut Français du Pétrole*, 1948, **3**, 151.

A further series of experiments was carried out to determine the variation of peroxide concentration during the reaction; the results are given in Fig. 5. As with certain hydrocarbons, the peroxide concentration runs approximately parallel with the rate of pressure increase. The maximum rate is reached very late in the course of the reaction (at about 85 % completion); similarly, the peroxide concentration acquires its maximum value at about this stage.

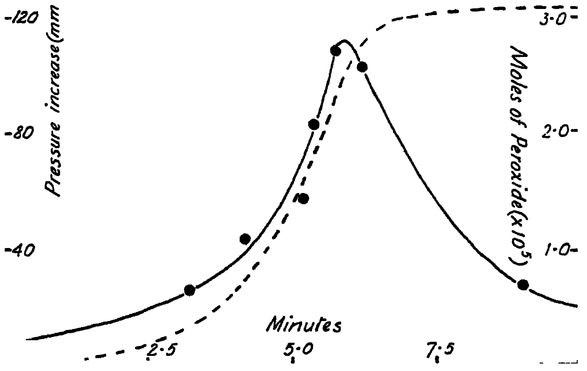

FIG. 5.—The variation of peroxide concentration during the oxidation of ethylamine at 280° C.

Ethylamine pressure : 250 mm. ; oxygen pressure : 250 mm.
●, Moles of peroxide ; - - - - Pressure-time curve.

(2) PROPYLAMINE.—Fig. 2 shows that the log $p_{max.}$ — $1/T$ plot for propylamine has a well-defined break at about 335° C, which may indicate that a change of mechanism is occurring in this temperature region. Two series of analyses were carried out at temperatures above and below 335° C, to see whether there was any marked difference in the nature of the reaction products.

(*a*) *Experiments at* 292° C.—The qualitative results are shown in Table IV.

TABLE IV

Temperature : 292° C ; Propylamine pressure : 70 mm. ; Oxygen pressure : 200 mm.

% Reaction Completed	0 %	10 %	25 %	50 %	75 %	90 %	100 %
Formaldehyde .	—	+	++	++	++	++	+
Acetaldehyde . .	—	—	—	—	—	—	—
Oxides of nitrogen .	—	+	+	++	++	++	+++
Ammonia . .	—	—	+	++	+	+	+
Hydrogen cyanide .	—	—	—	—	—	—	—

Formaldehyde but no acetaldehyde is present. Oxides of nitrogen appear in considerable quantity, though the amounts of ammonia are comparatively small. Hydrogen cyanide is always absent.

The variation of peroxide and total base concentrations is shown in Fig. 6. The peroxide concentration again runs parallel with the rate of pressure increase. The total base concentration may, in view of the small quantities of ammonia formed be taken as an approximate measure of the amount of unchanged amine.

It appears from Fig. 6 that the rate of pressure increase gives a good indication of the rate of destruction of propylamine.

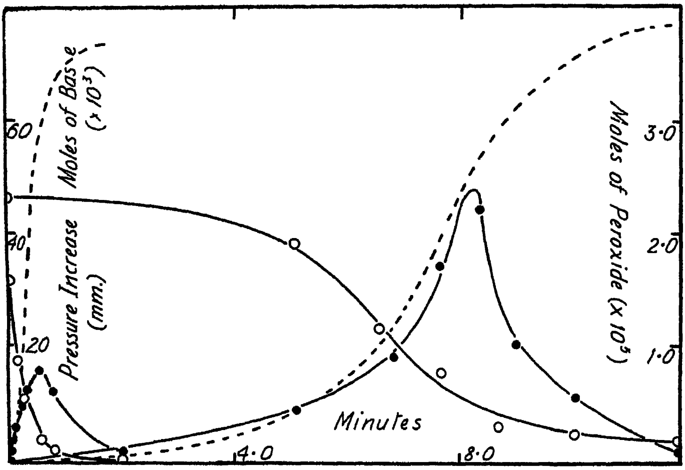

FIG. 6.—The variation of peroxide and total base concentrations during the oxidation of propylamine.

The curves on the right of the diagram refer to :
Temperature : 292° C ; propylamine pressure : 70 mm. ; oxygen pressure : 200 mm.

The curves on the left of the diagram refer to :
Temperature : 353° C ; propylamine pressure : 50 mm. ; oxygen pressure : 200 mm.

● Moles of peroxide ; ○ Moles of base ; - - - Pressure-time curves.

(*b*) *Experiments at* 353° C.*—Table V gives the principal qualitative results. These are similar to the results at 292° C except for the formation of appreciable quantities of hydrogen cyanide. Nitrogen oxides are again present in somewhat greater concentration than ammonia.

TABLE V

Temperature : 353° C ; Propylamine pressure : 50 mm. ; Oxygen pressure : 200 mm.

% Reaction Completed	0 %	10 %	27 %	50 %	73 %	88 %	100 %
Formaldehyde .	—	+	++	++	+++	++	+++
Acetaldehyde .	—	—	—	—	—	—	—
Oxides of nitrogen .	—	+	+	+	++	++	++
Ammonia . .	—	—	+	+	+	—	—
Hydrogen cyanide.	—	—	—	+	++	++	++

The variation of peroxide and total base concentrations at 353° C is also shown in Fig. 6. Comparison of the two series of experiments shows that, while the peroxide concentration in both cases runs approximately parallel with the rate of pressure increase, the stationary concentrations of such intermediates are considerably higher at 292° C ($\rho_{\text{max.}} = 25{\cdot}7$ mm./min.) than at 353° C ($\rho_{\text{max.}} = 112{\cdot}0$ mm./min.).

---

* A somewhat lower pressure of propylamine was used in this series, as the mixture employed at 292° C underwent explosion at this temperature.

(*c*) *The variation of peroxide concentration with temperature.*—To investigate this point more fully, analysis for peroxides was carried out at a series of temperatures between 266° C and 396° C using a standard amine-oxygen mixture. The peroxide concentration was measured when the rate of pressure change was a maximum.

The results shown in Fig. 6 indicate that at a given temperature :

Rate of reaction $\propto$ Peroxide concentration $= k$ [Peroxides]

or $\rho_{\text{max.}} = k$ [Peroxides (max.)].

If reaction occurs exclusively by a peroxidic mechanism over the whole range of temperature investigated,

$$\ln\left(\frac{\text{Peroxides (max.)}}{\rho_{\text{max.}}}\right) = \ln\left(\frac{1}{k}\right) = \text{constant} + \frac{E}{RT}$$

(where E is the activation energy of the decomposition of the peroxide) ; thus the graph of $\log_{10}$ Peroxides (max.)/$\rho_{\text{max.}}$ against $1/T$ should be linear. If, on the other hand, a non-peroxidic mechanism intervenes as the temperature is increased, the relationship will no longer be linear. Fig. 7 shows the values of $\log_{10} \rho_{\text{max.}}$ and of the logarithm of the above ratio as functions of temperature. The fact that the latter graph deviates markedly from a straight line suggests that the contribution of peroxidic mechanisms to the total rate of reaction decreases with temperature. Since the rate of reaction increases continuously in the temperature region investigated, another mechanism evidently comes into play as that involving peroxides dies away.

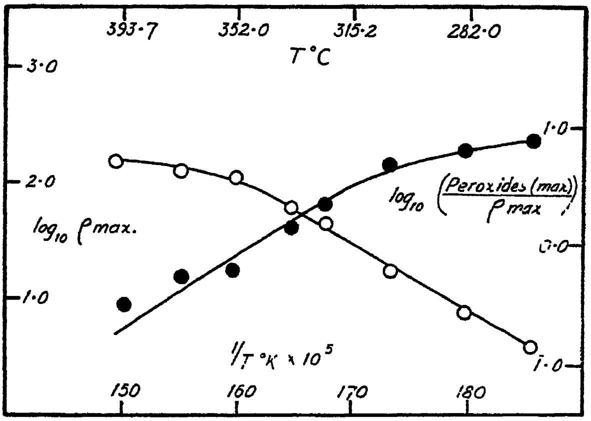

FIG. 7.—The variation of maximum oxidation rate and peroxide concentration with temperature.

Propylamine pressure : 50 mm. ; oxygen pressure : 200 mm.

● $\log_{10}\left(\frac{\text{Peroxides (max.)}}{\rho_{\text{max.}}}\right)$; ○ $\log_{10} \rho_{\text{max.}}$

As the temperature is increased, the autocatalytic nature of the reaction becomes less marked and the maximum rate is acquired at an increasingly early stage. Table VI shows the variation with temperature of the ratio : $\Delta p_{\rho_{\text{max.}}}/\Delta p_{\infty}$, i.e. the fraction of reaction which has occurred when the rate reaches its maximum intensity. This suggests that the reaction which sets in at higher temperatures is not autocatalytic in nature. In the temperature region where both mechanisms are operative, the resulting pressure-time curves therefore undergo a progressive change in shape.

TABLE VI

Propylamine pressure : 50 mm. ; Oxygen pressure : 200 mm.

Temperature (° C)	$\Delta p_{p_{\max.}}/\Delta p_{\infty}$
266	0·66
283·5	0·58
304	0·51
323·5	0·41
334	0·35
353	0·30
372	0·25
396	0·19

(*d*) *The variation of the nature of the reaction products with oxygen concentration.*—A comparative series of analyses was made for mixtures containing varying pressures of oxygen at 292° C. The reacting gases were withdrawn and analyzed (*a*) when the rate was at its maximum intensity, and (*b*) when reaction was complete. The results are principally of interest with regard to oxides of nitrogen and ammonia (Table VII).

TABLE VII

Temperature : 292° C ; Propylamine pressure : 70 mm.

Oxygen Pressure (mm.)	350		200		70		35	
% Reaction Completed	55 %	100 %	71 %	100 %	68 %	100 %	59 %	100 %
Oxides of nitrogen	++	+++	++	++	+	++	—	+
Ammonia . .	+	—	++	+	++	+	++	++

Excess oxygen evidently favours the production of nitrogen oxides, while excess amine promotes the formation of ammonia.

Discussion

A comparative study of the four simplest amines shows that their slow oxidation in many ways resembles the low-temperature combustion of the paraffins. It is found that (*a*) the temperatures at which oxidation commences lie in the same region (between 250° C and 300° C), and (*b*) a pronounced structural influence is apparent, there being a rapid but well-graded increase in ease of oxidation as the carbon chain is lengthened.

A more detailed study of the behaviour of ethylamine and propylamine indicates further similarities to the higher paraffins. Thus, (*a*) the influence on the reaction of varying the reactant concentrations is substantially the same, and (*b*) the reaction appears to proceed through the formation of intermediate peroxides. Unlike ethane and propane which show well-defined differences from one another,[4] ethylamine and propylamine closely resemble one another in the kinetics of their oxidation. This resemblance may be connected with the fact that the ethylamine molecule, unlike that of ethane, contains a CH_2 group, the presence of which (or of a CH group) is thought to be essential for a low-temperature oxidation mechanism to take place.[1, 5]

In contrast to the behaviour of the paraffins, however, (*a*) the oxidation of ethylamine and propylamine is remarkably little influenced by the surface, (*b*) added nitrogen has no appreciable effect on the reaction, (*c*) aldehydes do not exert powerful catalytic effects, and (*d*) though the reaction proceeds autocatalytically, the oxidation of these amines is not preceded by an appreciable induction period.

Nevertheless, the striking similarities to hydrocarbon combustion suggest that oxidation of the amines proceeds by a closely analogous mechanism, the reaction being essentially an oxidation of the hydrocarbon chain and involving the intermediate formation and breakdown of substituted alkyl peroxides. It appears, however, that with the amines :

(i) The chain-branching processes are more efficiently controlled than in paraffin combustion. The gradual increase of reaction rate from a vanishingly small to a very high value is rarely observed. Sharp explosion limits are not found, and it would appear from the very high rates of reaction encountered immediately prior to explosion that such explosions as do occur are largely thermal in nature.

(ii) The chain-breaking processes do not depend to any marked extent on the walls, but the reactive chain-carriers are destroyed mainly by chemical reaction in the gas phase.

These two effects might be caused by the production of a powerful chain-breaker in the course of the reaction. Since analysis shows that oxides of nitrogen are almost invariably present, traces of unoxidized nitric oxide may here be exerting a chain-terminating influence.

The analytical results show that the nitrogen of the NH_2 group is converted mainly into nitrogen oxides and ammonia, and that at low temperatures no appreciable quantities of hydrogen cyanide are formed. In other words, the C—N bond appears to be broken early in the reaction. Furthermore, with propylamine, nitrogen oxides and ammonia are formed at the expense of one another, according to whether oxygen or amine is in excess. This suggests that both products are formed by further reaction of the same intermediate species ; the obvious intermediate is an NH_2 radical.

The principal analytical data can be explained if, in the case of ethylamine, a series of reactions such as the following is assumed to occur :

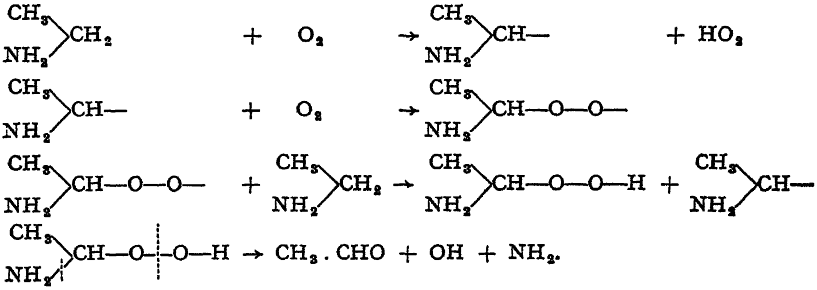

$$\left.\begin{array}{l}CH_3\\NH_2\end{array}\right\rangle CH_2 + O_2 \rightarrow \left.\begin{array}{l}CH_3\\NH_2\end{array}\right\rangle CH— + HO_2$$
$$\left.\begin{array}{l}CH_3\\NH_2\end{array}\right\rangle CH— + O_2 \rightarrow \left.\begin{array}{l}CH_3\\NH_2\end{array}\right\rangle CH—O—O—$$
$$\left.\begin{array}{l}CH_3\\NH_2\end{array}\right\rangle CH—O—O— + \left.\begin{array}{l}CH_3\\NH_2\end{array}\right\rangle CH_2 \rightarrow \left.\begin{array}{l}CH_3\\NH_2\end{array}\right\rangle CH—O—O—H + \left.\begin{array}{l}CH_3\\NH_2\end{array}\right\rangle CH—$$
$$\left.\begin{array}{l}CH_3\\NH_2\end{array}\right\rangle CH—O\,\vdots\,O—H \rightarrow CH_3.CHO + OH + NH_2.$$

The latter reaction may, in suitable circumstances, give rise to chain-branching, since the hydroxyl radical will cause the liberation of a further " hydrocarbon " radical :

$$OH + CH_3.CH_2.NH_2 \rightarrow CH_3.\overset{|}{C}H.NH_2 + H_2O,$$

whereas the amino radical may either continue the chain by reacting with amine or be effectively destroyed by reaction with oxygen :

$$NH_2 + CH_3.CH_2.NH_2 \rightarrow CH_3.\overset{|}{C}H.NH_2 + NH_3$$
$$NH_2 + O_2 \rightarrow \text{oxides of nitrogen.}$$

Such a scheme fails to account specifically for the formation of formaldehyde, but this substance may arise by further oxidation of acetaldehyde. The latter compound reacts readily with oxygen under the conditions of experiment, and formaldehyde is found to be a product of the reaction.

On account of the large number of secondary reactions which can occur, amine oxidation is considerably more complex than paraffin combustion. It does not seem profitable at this stage to attempt to propose a quantitative theory of the oxidation. By treatment analogous to that adopted in the case of the paraffins,[1] the simplified mechanism outlined above for the oxidation of ethylamine leads to substantially the same result, and can be made to explain many of the characteristics of the reaction, such as the autocatalytic development of the rate and the characteristic influence of reactant concentrations on the reaction.

With propylamine, the position is considerably more complicated, for there is evidence that more than one mechanism is in operation. The similarity of the behaviour of propylamine to that of ethylamine suggests that the mechanism is similar at low temperatures. The formation of nitrogen oxides and ammonia as reaction products makes it probable that in the molecule

$$CH_3 \,.\, \underset{(A)}{CH_2} \,.\, \underset{(B)}{CH_2} \,.\, NH_2,$$

attack occurs at (B) with subsequent formation of the peroxide

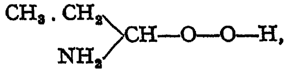

$$\begin{matrix} CH_3 \,.\, CH_2 \searrow \\ \\ NH_2 \nearrow \end{matrix} CH{-}O{-}O{-}H,$$

followed by liberation of an NH_2 radical and propionic aldehyde ; this would explain why no acetaldehyde is detectable during propylamine oxidation.*

As the temperature is increased, there is a change in the slope of the $\log \rho_{\max.} - 1/T$ plot (Fig. 2) as well as an alteration in the form of the pressure-time curves ; simultaneously the concentration of intermediate peroxides declines. All these facts indicate that a somewhat different mechanism is coming into play at higher temperatures, though qualitative analysis does not show any marked change in the nature of the products in the high-temperature region, except that free hydrogen cyanide becomes detectable.

The behaviour of butylamine is more closely akin to that of the unsubstituted hydrocarbons. The presence of an induction period and the existence of cool flames suggest that chain-branching is able to operate more efficiently in the oxidation of this amine. Initial attack probably occurs largely at the CH_2 groups not adjacent to the amino group, so that nitrogen oxides may not be formed in quantities sufficient to cause appreciable suppression of the branching processes.

The general similarity of the kinetics of hydrocarbon and amine oxidation suggests that attack of the amines takes place at a point in the hydrocarbon chain ; the reactions occurring are probably analogous to those in operation in the low-temperature oxidation of the paraffins, though the participation of NH_2 radicals in the mechanism may exert characteristic effects. The influence of structure on the ease of oxidation of the amines is therefore likely to be governed by factors similar to those operative in hydrocarbon oxidation. With the higher paraffins the introduction of an amino group would be expected to cause an increase in oxidizability comparable to that found with the chloro-paraffins. Such a group will tend to decrease the stability of the intermediate peroxides formed in the reaction, both by impairing the symmetry of a methyl group into which it is introduced, and by exerting an inductive effect similar to (though weaker than) that of chlorine.[18] With ethane, the introduction of an amino group has a profound influence in altering the characteristics of the reaction. The structural influence in this case would be expected to be much greater than that due only to factors of the type mentioned above; for the presence of a substituent in the ethane molecule provides a CH_2 group which may enable the resulting compound to undergo oxidation by a mechanism analogous to that in operation with the higher paraffins and their derivatives.

---

* Lewin's test [13] only detects propionic aldehyde in comparatively high concentration.

Although a direct comparison of the rates of oxidation of the amines and the corresponding paraffins has not been made, a study of the temperatures at which oxidation becomes appreciable does indicate that the increase in oxidizability caused by introduction of an amino group, while comparatively small with propane and butane, is very large indeed with ethane. The increase is, however, even more marked with methane. This latter fact is somewhat surprising, for the methylamine molecule, which contains no CH_2 group, would not be expected to undergo oxidation in the low-temperature region. This compound has received little attention in the present work, and its behaviour is shortly to be investigated in more detail.

Physical Chemistry Laboratory,
South Parks Road,
Oxford.

---

[18] See, for example, Dewar, *Electronic Theory of Organic Chemistry* (Oxford, 1949), p. 52.

EQUILIBRIA IN SOLUTIONS OF FERROUS IONS AND αα′-DIPYRIDYL

By J. H. Baxendale and Philip George

Received 15*th August,* 1949

The dissociation constant of the conjugate acid of the base αα′-dipyridyl has been determined at several temperatures. At 25° C, $I = 0{\cdot}025$, $pK_a = 4{\cdot}334$.

The red complex ion Fe $(Dipy)_3^{++}$ is shown to be formed through two intermediates according to the scheme:

$$\text{Fe}^{++} + \text{Dipy} \rightleftharpoons \text{Fe Dipy}^{++} \qquad K_1,$$
$$\text{Fe Dipy}^{++} + \text{Dipy} \rightleftharpoons \text{Fe (Dipy)}_2^{++} \qquad K_2,$$
$$\text{Fe (Dipy)}_2^{++} + \text{Dipy} \rightleftharpoons \text{Fe (Dipy)}_3^{++} \qquad K_3.$$

The overall equilibrium constant $K_1K_2K_3$ is found to be $1{\cdot}15 \times 10^{17}$ (mole/l.)$^{-3}$ at 25° C. The constant $K_1 = 1{\cdot}6 \times 10^4$ at 35° C., and whilst K_2 cannot be determined exactly, measurements show that at 35° C, $K_2 < 10^5$ (mole/l.)$^{-1}$ and hence $K_3 > 2 \times 10^7$ (mole/l.)$^{-1}$.

The heat of formation of Fe $(Dipy)_3^{++}$ from Fe^{++} and 3 Dipy is $24{\cdot}3 \pm 1{\cdot}3$ kcal. The heat of formation of the first intermediate Fe $Dipy^{++}$ is $7{\cdot}5 \pm 2{\cdot}0$ kcal.

The near u.-v. spectra of αα′-dipyridyl, the αα′-dipyridylium ion, Fe $Dipy^{++}$ and Fe $(Dipy)_3^{++}$ have been obtained.

The intense red colour which appears when the base αα′-dipyridyl is added to solutions of ferrous salts, was shown by Blau[1] in 1898 to be due to the complex ion Fe $(Dipy)_3^{++}$ formed by the reaction:

$$\text{Fe}^{++} + 3\ \text{Dipy} \overset{K}{\rightleftharpoons} \text{Fe (Dipy)}_3^{++}.$$

---

[1] Blau, *Monatsh.*, 1898, 19, 650.

Jaeger and Dijk[2] have shown that with many metal ions which form tris-dipyridyl complexes intermediates containing one and two molecules of the base can be prepared in well-defined crystalline forms by the simple addition of the requisite stoichiometric amounts of the metal salts and base in aqueous solution. This was not the case for the ferrous dipyridyl complexes, but they obtained a compound containing one molecule of dipyridyl by working with alcoholic solutions. The investigations of Bjerrum[3] on the equilibria in metal ammine systems have established that in these also intermediates containing from one to six ammonia molecules can be obtained with suitable concentration conditions. In a preliminary publication[4] we have shown that the formation of the Fe $(\mathrm{Dipy})_3^{++}$ is reversible and goes by consecutive additions of the free base to the ferrous ion as follows :

$$\mathrm{Fe^{++} + Dipy \overset{K_1}{\rightleftharpoons} Fe\ Dipy^{++}} \quad . \quad . \quad . \quad (1)$$

$$\mathrm{Fe\ Dipy^{++} + Dipy \overset{K_2}{\rightleftharpoons} Fe\ (Dipy)_2^{++}} \quad . \quad . \quad . \quad (2)$$

$$\mathrm{Fe\ (Dipy)_2^{++} + Dipy \overset{K_3}{\rightleftharpoons} Fe\ (Dipy)_3^{++}} \quad . \quad . \quad . \quad (3)$$

Reactions (1), (2) and (3) are extremely fast and the equilibria are well over on to the side of Fe $(\mathrm{Dipy})_3^{++}$ formation, but it is possible to bring them into a measurable region by decreasing the concentration of free αα′-dipyridyl in the solutions. This can be done by utilizing the basic character of αα′-dipyridyl, displacing the equilibrium

$$\mathrm{Dipy\ H^{+} \overset{K_a}{\rightleftharpoons} Dipy + H^{+}} \quad . \quad . \quad . \quad . \quad (4)$$

to the left by increasing the $\mathrm{H^+}$ ion concentration. We found that except in the more acid solutions only the free base is effective in forming the complex. By this method we have been able to elucidate the equilibria and kinetics of the system, and here we shall be concerned with the equilibria. The overall equilibrium constant K has been determined at one temperature by Dwyer and McKenzie[5] using a potentiometric method and Krumholtz[6] has recently reported the results of a colorimetric study of the system similar to that described in this paper. The analogous system ferrous ion + phenanthroline, examined by Lee, Kolthoff and Leussing[7] is comparable in many respects to the present one.

Algebraic Expressions for the System at Equilibrium.—Let c_1 represent the concentration of Fe $\mathrm{Dipy^{++}}$, c_2 of Fe $(\mathrm{Dipy})_2^{++}$, c_3 of Fe $(\mathrm{Dipy})_3^{++}$, f of total $\mathrm{Fe^{++}}$ present (combined and free), d of total dipyridyl (combined and free) and h of $\mathrm{H^+}$ ion. Then in general we have

$$\text{Free Fe}^{++} = (f - c_1 - c_2 - c_3),$$

$$\text{Total free dipyridyl} = (d - c_1 - 2c_2 - 3c_3),$$

$$\text{Total dipyridyl present as free base} = \frac{(d - c_1 - 2c_2 - 3c_3)K_a}{K_a + h}.$$

Now if dipyridyl is present in excess this will favour the formation of Fe $(\mathrm{Dipy})_3^{++}$, and provided that $c_3 \gg c_1 + c_2$ the expression for the overall equilibrium constant is simply

$$K = \frac{c_3}{(f - c_3)(d - 3c_3)^3} \cdot \left(\frac{K_a + h}{K_a}\right)^3 . \quad . \quad . \quad . \quad (1)$$

---

[2] Jaeger and Dijk, *Z. anorg. Chem.*, 1936, **227**, 273.

[3] Bjerrum, *Metal Ammine Formation in Aqueous Solution* (Haase & Son, Copenhagen, 1941).

[4] Baxendale and George, *Nature*, 1948, **162**, 777.

[5] Dwyer and McKenzie, *Proc. Roy. Soc. N.S.W.*, 1947, **81**, 97.

[6] Krumholtz, *Nature*, 1949, **163**, 724, and private communication.

[7] Lee, Kolthoff and Leussing, *J. Amer. Chem. Soc.*, 1948, **70**, 2348.

If Fe^{++} is present in excess it will favour the formation of Fe $Dipy^{++}$ at the expense of Fe $(Dipy)_3^{++}$, and it can be shown from the four equilibrium expressions for reactions (1) to (4) above that when $f \gg c_1 + c_2 + c_3$,

$$d = 3c_3 + 2K_1K_2f \cdot \left(\frac{c_3}{Kf}\right)^{\frac{2}{3}} + \left(K_1f + 1 + \frac{h}{K_a}\right)\left(\frac{c_3}{Kf}\right)^{\frac{1}{3}} . \qquad (2)$$

If K is known, measurements of c_3 for various values of d at constant f give simultaneous equations from which in principle K_1 and K_2 can be obtained. Whether they can be determined from actual experimental observations depends on their relative numerical values. Thus, if the second or third term on the right of eqn. (2) is negligible with respect to the other then only K_1 or the product K_1K_2 can be obtained.

Experimental

Materials.—The αα′-dipyridyl was a sample kindly supplied by Mr. F. H. Burstall. It was recrystallized from petroleum ether and the purity was shown to be greater than 99 % by acid titration and colorimetric estimation. Standard solutions of the base were made up in the necessary buffers. All other compounds were of A.R. grade.

Throughout the work acetate and phthalate buffers were used in such concentrations as to give solutions of ionic strengths $I = 0{\cdot}025$. Measurements of pH were made with a glass electrode which was standardized at the working temperature by phthalate buffers.[8]

Determination of K_a.—A solution of $3{\cdot}00 \times 10^{-2}$ M αα′-dipyridyl was titrated with 0·140 N HCl at 16·5° C, the pH being measured on a G.E.C. glass electrode pH meter after each addition of acid. Analysis of the pH titration curve showed that only one basic group is titrated down to pH 1·6, and the curve is of the form required by the titration of a monoacid base. Values of K_a at temperatures other than 16·5° C were obtained by measuring the pH of a half-neutralized solution (on the assumption of only one basic group) at various temperatures.

Determination of Fe $(Dipy)_3^{++}$.—The calculation of equilibrium constants from the equations given above is based on the determination of equilibrium Fe $(Dipy)_3^{++}$ concentrations in solutions of varying Fe^{++}, αα′-dipyridyl and hydrogen ion concentrations. These determinations were made on a colorimeter having balanced barrier-layer photo-cells in a circuit proposed by Brice.[9] Using a cuvette with 1 cm. light path, Beer's law was found to hold up to 8×10^{-5} M Fe $(Dipy)_3^{++}$, and in this region the accuracy was about ± 1 %. With a 4-cm. cuvette Beer's law held up to 2×10^{-5} M and this could be measured to ± 2 %. All measurements were made with a light blue filter (Chance OB2). For one set of determinations at 49·2° C a specially constructed cuvette with a 13-cm. light path was used. This was made to fit into a thermostat around which was built a colorimeter of the above type, and concentrations of Fe $(Dipy)_3^{++}$ could be measured *in situ*.

Preparation of Equilibrium Mixtures.—Except in the experiments just described using the 13-cm. cuvette, the mixtures were made up by allowing 100 ml. of buffer solution containing the required amount of αα′-dipyridyl to come to thermal equilibrium at the working temperature. To these solutions were then added ferrous sulphate, usually as 1 or 2 ml. of an appropriate stock solution. Measurements of Fe $(Dipy)_3^{++}$ were made at intervals until equilibrium was reached. At the higher pH's and temperatures the solutions were deoxygenated with nitrogen to prevent oxidation of Fe^{++}.

Results

K_a and Heat of Dissociation of the Ion, Dipy H^+.—From the titration curves K_a was found to be $4{\cdot}17 \times 10^{-5}$ at 16·5° C. The results of the determinations over the temperature range are given in Fig. 1, where pK_a is plotted against T^{-1}. From the slope, $\Delta H = 2{\cdot}0 \pm 0{\cdot}1$ kcal. Values of K_a required for the evaluation of the equilibrium constants described below, were read off

---

[8] Hamer and Acree, *J. Res. Nat. Bur. Stand.*, 1935, **35**, 381, 539; 1946, **36**, 47.

[9] Brice, *Rev. Sci. Instr.*, 1937, **8**, 279.

Fig. 1 at the appropriate temperature. K_a has been determined by other investigators but not its variation with temperature. At 25° C and at various ionic strengths our value of $pK_a = 4{\cdot}334$ ($I = 0{\cdot}025$) agrees well with that obtained by Krumholtz [6] $pK_a = 4{\cdot}335$ ($I = 0{\cdot}01$) but is a little lower than the value quoted by Dwyer and McKenzie, $pK_a = 4{\cdot}40$ ($I = 0{\cdot}007$).

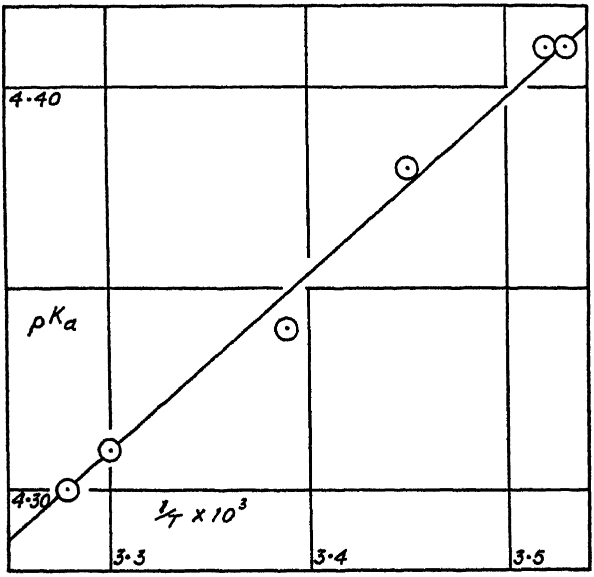

FIG. 1.—Variation of pK_a for Dipy H+ with temperature.

Overall Equilibrium Constant and Heat of Formation of Fe (Dipy)$_3^{++}$.—In solutions at pH 2·58 containing large excesses of αα′-dipyridyl over the Fe++, it was found that the equilibrium Fe (Dipy)$_3^{++}$ concentrations fitted an equation of the form :

$$K_{\text{obs.}} = \frac{c_3}{(f - c_3)(d - 3c_3)^3} \quad . \quad . \quad . \quad . \quad . \quad (3)$$

$K_{\text{obs.}}$ was found to vary with pH and experiments at 45° C with varying d at different pH's are recorded in Table I.

TABLE I.—DATA OBTAINED AT 45° C TO ILLUSTRATE THE CALCULATION OF $K_{\text{obs.}}$ AND THE EQUILIBRIUM CONSTANT K. $pK_a = 4{\cdot}24$ AT 45° C

Mean $K = 8{\cdot}73 \pm 0{\cdot}65 \times 10^{15}$

pH	$d \times 10^4$	$f \times 10^5$	$c_3 \times 10^5$	$K_{\text{obs.}} \times 10^{-10}$	Mean $K_{\text{obs.}}$	$K = K_{\text{obs.}}\left(\frac{H^+}{K_a}\right)^3$
2·58	1·67	4·35	1·03	12·1		
	2·50	4·29	2·00	12·7	$12{\cdot}7 \times 10^{10}$	$9{\cdot}2 \times 10^{15}$
	3·33	4·31	2·88	13·4		
2·45	2·5	4·37	1·28	4·35		
	3·33	4·26	1·84	4·46	$4{\cdot}36 \times 10^{10}$	$7{\cdot}8 \times 10^{15}$
	4·17	4·37	2·70	4·26		
2·24	3·33	4·37	1·10	1·25	$1{\cdot}22 \times 10^{10}$	$9{\cdot}2 \times 10^{15}$
	4·17	4·26	1·60	1·20		

Comparing eqn. (3) with (2) it is clear that under these experimental conditions $c_3 \gg c_1 + c_2$ and hence $K_{obs.}$ should be related to K by

$$K_{obs.} = K \,.\, \frac{K_a}{h + K_a}\,.$$

Since in this pH region $H^+ = K_a$, $K_{obs.}$ should thus be linear with respect to $(K_a/h)^3$. This plot is shown in Fig. 2 for values of $K_{obs.}$ determined at 25°, 35° and 45° C, the appropriate value of K_a being used at each temperature. The slope of these lines give K at the various temperatures (Table II), from which a mean ΔH of $-24{\cdot}3 \pm 1{\cdot}3$ kcal. is calculated for the formation of Fe $(\text{Dipy})_3^{++}$ from Fe^{++} and αα′-dipyridyl.

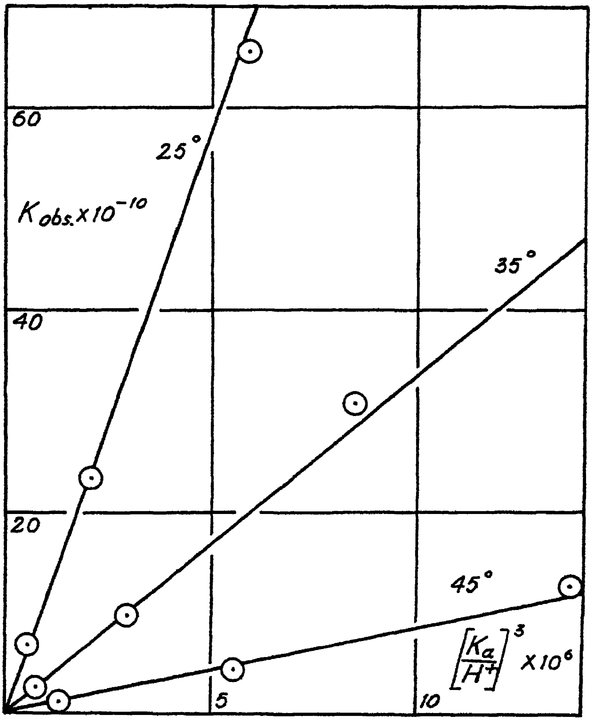

FIG. 2.—Variation of overall equilibrium constant $K_{obs.}$ with H^+.

TABLE II.—THE EQUILIBRIUM CONSTANT K AT DIFFERENT TEMPERATURES OBTAINED FROM DATA SIMILAR TO THAT IN TABLE I

T °C	K
25	115×10^{15}
35	$33{\cdot}6 \times 10^{15}$
45	$8{\cdot}7 \times 10^{15}$

$\Delta H = -24{\cdot}4 \pm 1{\cdot}3$ kcal.

Equilibrium Constants for the Formation of the Intermediates.—The determination of K_1 and K_2 requires appreciable amounts of Fe Dipy^{++} and Fe $(\text{Dipy})_2^{++}$ to be present in solution compared with the amount of Fe $(\text{Dipy})_3^{++}$ formed. The most favourable condition for this is a large excess of Fe^{++} over the dipyridyl. This was confirmed experimentally. Solutions of αα′-dipyridyl ranging in concentrations between 3·0 and 15·0 × 10^{-5} M were made up in pH 4·0 phthalate at 35° C. Ferrous sulphate was added to give 5·0 × 10^{-3} M ferrous ion in all cases except one with 15 × 10^{-5} M αα′dipyridyl in which the [Fe^{++}] was made equivalent, i.e. 5 × 10^{-5} M. In this case 99 % of the possible Fe (Dipy)$_3^{++}$ was formed, but in the others the amount decreased with increasing f/d, and with a value of 167 for the ratio, only 27 % of the possible Fe (Dipy)$_3^{++}$ was formed. These observations are recorded in Table III. With equivalent amounts of Fe^{++} and dipyridyl, 99 % of the possible Fe (Dipy)$_3^{++}$ was formed, so that even at this low Fe^{++} concentration the amount of free base present at equilibrium is small. It is therefore safe to conclude that at the much higher Fe^{++} concentration used for the results of Table III, the reason for the smaller amounts of Fe (Dipy)$_3^{++}$ formed is that the base is present as Fe Dipy^{++} and Fe (Dipy)$_2^{++}$.

TABLE III.—MEASUREMENTS OF Fe (Dipy)$_3^{++}$, (c_3), IN PHTHALATE BUFFER SOLUTION pH 4·00, I = 0·025 AT 35° C WITH CONSTANT Fe^{++} ION CONCENTRATION f = 5·0 × 10^{-3} M AND VARYING CONCENTRATIONS OF αα′-DIPYRIDYL (d)

$d \times 10^5$ M	$c_3 \times 10^5$ M	$\frac{d \quad 3c_3}{c_3^{\frac{1}{3}}} \times 10^4$	% of possible Fe (Dipy)$_3^{2+}$ $\frac{3c_3}{d} \times 100$
3·0	0·27	1·58	27
4·5	0·59	1·51	39
6·0	0·97	1·45	49
6·0	1·00	1·40	50
9·0	1·72	1·49	57
12·0	2·55	1·48	64
15·0	3·25	1·65	65

For the accurate colorimetric determination of Fe (Dipy)$_3^{++}$ in these solutions, it was necessary to show that the intermediates did not contribute to the light adsorption. It was observed that with 0·1 M Fe^{++} and 3·0 × 10^{-5} M αα′-dipyridyl, no Fe (Dipy)$_3^{++}$ was formed at all, but the solution had a pale yellow colour, due presumably to the intermediates. However, the optical density of this solution with the filters used in the Fe (Dipy)$_3^{++}$ determination, was negligible.

The results listed in the first two columns of Table III can now be analyzed using eqn. (2) for the condition $f \gg c_1 + c_2 + c_3$ is satisfied since $f \gg d$. The equation can be rewritten as

$$2K_1K_2f\left(\frac{c_3}{Kf}\right)^{\frac{2}{3}} + \left(K_1f + 1 + \frac{h}{K_a}\right)\left(\frac{c_3}{Kf}\right)^{\frac{1}{3}} = d - 3c_3. \quad . \qquad . \quad (4)$$

However, as can be seen from the third column of Table III the value of $\frac{d - 3c_3}{c_3^{\frac{1}{3}}}$ is independent of c_3 which implies that the first term in eqn. (4) is negligible. This term gives the concentration of Fe (Dipy)$_2^{++}$ and hence under these experimental conditions only the complexes Fe Dipy^{++} and Fe (Dipy)$_3^{++}$ are present in significant amounts. Similar results were obtained for f = 5 × 10^{-4} M and 10^{-3} M and 10^{-2} M. It can be seen from eqn. (4) that when $K_1f \gg 1 + \frac{h}{K_a}$, the ratio $\frac{d - 3c_3}{c_3^{\frac{1}{3}}}$ should vary as $f^{\frac{2}{3}}$. A plot of this ratio B for the above values of f is given in Fig. 3 when a straight line is obtained with slight deviations for the low values of f when the approximation $K_1f \gg 1 + \frac{h}{K_a}$ is no longer valid. We have calculated K_1 from (4) neglecting the first term. For $f = 10^{-2}$, 5 × 10^{-3}, 10^{-3} and 5 × 10^{-4}, K_1 is found to be 1·67, 1·60, 1·75 and 1·52 × 10^4 respectively, with a mean value 1·64 ± 0·1 × 10^4 at 35° C. Similar determinations with two values of f at 49·2° C gave K_1 = 1·92 ± 0·26 × 10^4. This would indicate that the formation of Fe Dipy^{++} is almost thermoneutral

Krumholtz[6] using a different method has reported values of 2·45 × 10⁴ at 25° C and 1·42 × 10⁴ at 45° C giving a positive heat of formation of some 6 kcal. In view of this we have extended our measurements to 0° C and 17° C and have obtained values of 7·9 and 2·9 × 10⁴ respectively, which lead to a value of 7·5 ± 2·0 kcal. for the heat of formation of Fe Dipy^{++}. We are unable to explain the discrepant value at 49·2° C.

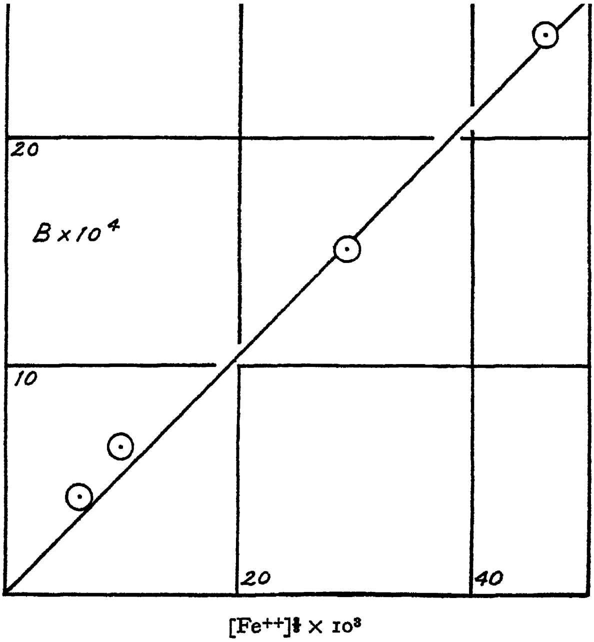

FIG. 3.

In order to determine K_2 we must choose conditions such that $2K_1K_2f\left(\frac{c_3}{Kf}\right)^{\frac{2}{3}}$ becomes larger with respect to $\left(k_1f + 1 + \frac{h}{K_a}\right)\frac{c_3}{Kf}^{\frac{1}{3}}$. One way is to make c_3 larger; this, however, is not experimentally possible, for still preserving the necessary condition $f \gg d$, calculation shows that it would require impossibly large concentrations of Fe^{++}. The other alternatives are to increase the pH so that h/K_a is negligible, to decrease f_1, or to decrease K by working at a higher temperature. The best approximation to these conditions which could be attained experimentally was to work at 50° C, at pH 5·14 and with Fe^{++} concentrations of about 4×10^{-6} M, in the special cuvette referred to previously. However, under these conditions it was found that the overall equilibrium (1) applied, which means that K_2 is too small with respect to K_3 for any appreciable amount of Fe (Dipy)$_2^{++}$ to be formed.

An upper limit for K_2 can be estimated by assuming that $2K_1K_2f\left(\frac{c_3}{Kf}\right)^{\frac{2}{3}}$ constitutes some 10 % to $d - 3c_3$, i.e. 10 % of the dipyridyl is present as Fe (Dipy)$_2^{++}$. This could certainly have been detected experimentally but the figure will suffice for an approximate calculation. Using the last observation in Table III it is found that $K_2 \sim 10^5$. Since 10 % represents a maximum value the calculation shows that $K_2 < 10^5$ at 35° C. With the previously determined values of $K(= K_1K_2K_3)$ and K_1 at this temperature it follows that $K_3 > 2 \times 10^7$.

Ultra-Violet Absorption Spectra.—As a further confirmation of the existence of the ion Fe Dipy^{++} we have obtained the u.-v. absorption spectra of aqueous solutions of Fe (Dipy)$^{++}$, Dipy H$^+$, the free base αα′-dipyridyl, and solutions which, from the equilibrium data, are expected to contain Fe Dipy^{++}.

For the latter we worked at pH 4·0 with $1{\cdot}24 \times 10^{-5}$ M αα′-dipyridyl and $1{\cdot}6 \times 10^{-2}$ M Fe^{++} and from the value of K_1 determined previously it is calculated that practically all the base is present as Fe $Dipy^{++}$ under these conditions.

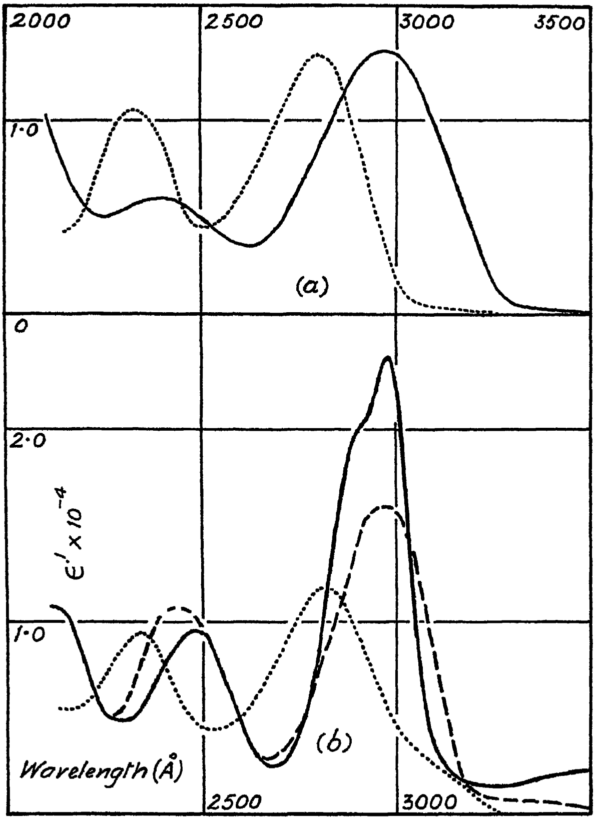

FIG. 4.—U.-v. absorption spectra of αα′-dipyridyl and complex ions.

(b) · · · · · · · · · · · · free base Dipy.

———————— Dipy H^+.

(b) · · · · · · · · · · · · Dipy at pH 4·92.

— — — — — — — Fe $Dipy^{++}$.

———————— Fe $(Dipy)_3^{++}$.

The absorption spectra were obtained with Beckmann Model DU spectrophotometer and are shown in Fig. 4 (a) and (b). For comparison between the various species we have plotted ϵ' the extinction coefficient per mole of dipyridyl per litre in each case, i.e. for Fe $(Dipy)_3^{++}$, $\epsilon' = \epsilon/3$, where ϵ is the true molar extinction coefficient. In Fig. 4 (a) the spectra of the free base and its conjugate acid are compared, and in Fig. 4 (b) the base at pH 4·92 with the complex ions Fe $Dipy^{++}$ and Fe $(Dipy)_3^{++}$ measured at this pH. Each spectrum has two maxima in the near ultra-violet and the wavelengths and molar extinction coefficients for these are listed below.

	Dipy	Dipy H^+	Fe $Dipy^{++}$	Fe $(Dipy)_3^{++}$
λ_1(Å) . . .	2325	2400	2475	2480
$\epsilon_1 \times 10^{-4}$ . .	1·05	0·590	1·03	0·965
λ_2 (Å) . . .	2800	2975	2975	2980
$\epsilon_2 \times 10^{-4}$ . .	1·34	1·36	1·61	2·38

Beer's law holds in each case. It can be seen that the shift of the maxima to longer wavelengths which results when Dipy H^+ is formed from the free base is also shown when the base is co-ordinated in the two complex ions. Moreover λ_2 is practically the same for all three ions. The complex ions differ from Dipy H^+ however, in that the peak at λ_1 is somewhat broader and that at λ_2 less pronounced in the latter.

The Blue Ferric Trisdipyridyl Complex Ion.—The analogous ferric complex to Fe $(\text{Dipy})_3^{++}$ is pale blue and can be prepared from the latter by direct oxidation. The two complex ions form a reversible redox system.[11] However, the ferric complex ion *cannot* be prepared by the simple addition of Fe^{+++} to αα′-dipyridyl. If this is attempted a brown solution is obtained[1] and from ethereal solutions of $FeCl_3$ and αα′-dipyridyl Simon and Haufe[10] have isolated a compound having the formula $FeCl_3$ (Dipy).

However, a value of the equilibrium constant K' for the reaction

$$\text{Fe}^{+++} + 3\,\text{Dipy} \overset{K'}{\rightleftharpoons} \text{Fe}\,(\text{Dipy})_3^{+++}$$

can be calculated from the following data at 25° C:

$$\text{Fe}^{+++} + \tfrac{1}{2}\text{H}_2 \rightleftharpoons \text{Fe}^{++} + \text{H}^+ \qquad E^\circ = 0{\cdot}77\ \text{V};\ \Delta G^\circ = -17{\cdot}7\ \text{kcal.},$$

$$\text{Fe}^{++} + 3\,\text{Dipy} \rightleftharpoons \text{Fe}\,(\text{Dipy})_3^{++} \qquad K = 1{\cdot}15 \times 10^{17};\ \Delta G^\circ = -23{\cdot}1\ \text{kcal.}$$

$$\text{Fe}\,(\text{Dipy})_3^{+++} + \tfrac{1}{2}\text{H}_2 \rightleftharpoons \text{Fe}\,(\text{Dipy})_3^{++} + \text{H}^+ \qquad E^\circ = 1{\cdot}06\ \text{V};^{11}\ \Delta G^\circ = -24{\cdot}4\ \text{kcal.}$$

Hence for

$$\text{Fe}^{+++} + 3\,\text{Dipy} \rightleftharpoons \text{Fe}\,(\text{Dipy})_3^{+++}, \quad K' = 1{\cdot}6 \times 10^{12};\ \Delta G^\circ = -16{\cdot}4\ \text{kcal.}$$

However, this value can only be regarded as approximate. The overall equilibria for the formation of Fe $(\text{Dipy})_3^{++}$ and Fe $(\text{Dipy})_3^{+++}$ as written above are independent of hydrogen ion concentration but we have observed that in the range of hydrogen ion concentration 0·01 to 2·0 M Fe $(\text{Dipy})_3^{++}$ dissociates more rapidly[4] and Fe $(\text{Dipy})_3^{+++}$ more slowly as the acid concentration incerases. Analysis of the results indicates the presence of species other than the simple complexes in these conditions, and since the E° of the Fe $(\text{Dipy})_3^{++}$ + Fe $(\text{Dipy})_3^{+++}$ system was obtained in such solutions, the ΔG° is not that for the simple oxidation-reduction written above. However, we find that the error from this source is not very great. It is interesting to note that in the case of the phenanthroline complexes only the oxidized form shows this behaviour in acid solution.[7]

We are grateful to Prof. M. G. Evans for his interest in this investigation.

Physical and Organic Chemistry Department,
The University,
Leeds.

[10] Simon and Haufe, *Z. anorg. Chem.*, 1936-7, **230**, 100.

[11] Hume and Kolthoff, *J. Amer. Chem. Soc.*, 1943, **65**, 1895.

RATE COEFFICIENTS IN THE POLYMERIZATION OF METHYL METHACRYLATE

PART II

By M. H. Mackay and H. W. Melville

Received 4th April, 1949

The benzoyl peroxide photosensitized polymerization of methyl methacrylate has been investigated and shown to be similar in mechanism to the direct photoreaction. The photopolymerization has been found to be retarded, not inhibited, by benzoquinone. Using the rate coefficients obtained in Part I, the approximate absolute value of the coefficient for interaction of polymer radicals with benzoquinone molecules has been calculated. Some experiments on the dark reaction are described, which are consistent with the photo-production of a substance capable of thermal dissociation at room temperature to produce radicals.

In Part I,[1] an account was given of the liquid-phase photopolymerization of methyl methacrylate, and rate coefficients and activation energies were evaluated for the propagation and termination reactions. In this paper some further experiments are described, dealing with the effect of benzoyl peroxide and of benzoquinone on the photopolymerization, and with the dark reaction which continues after the photopolymerization has been terminated by cutting off the illumination. All the experiments refer to the liquid phase, and the apparatus and methods used have been described in Part I.

The Benzoyl Peroxide Sensitized Polymerization

It is now well established[2] that the *initial* step in the decomposition of benzoyl peroxide in dilute solution is a fission of the molecule into two free radicals,

$$C_6H_5 . CO . O . O . OC . C_6H_5 \rightarrow 2C_6H_5 . CO . O . —$$

Such a radical can initiate polymerization by reaction with a monomer molecule to form an active centre which will be a monoradical,

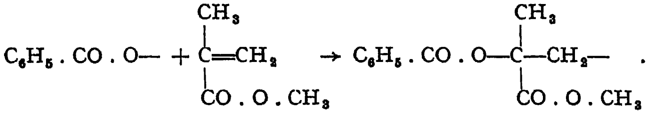

$$C_6H_5 . CO . O— + \overset{CH_3}{\underset{CO . O . CH_3}{C}}{=}CH_2 \rightarrow C_6H_5 . CO . O—\overset{CH_3}{\underset{CO . O . CH_3}{C}}—CH_2— \quad .$$

Photo-initiation on the other hand produces a diradical,[1]

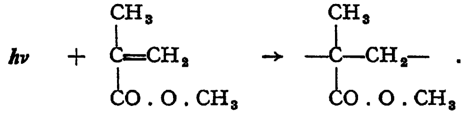

$$h\nu + \overset{CH_3}{\underset{CO . O . CH_3}{C}}{=}CH_2 \rightarrow —\overset{CH_3}{\underset{CO . O . CH_3}{C}}—CH_2— \quad .$$

The monoradical benzoyl peroxide catalyzed and photosensitized polymerizations of methyl methacrylate are here compared with the diradical photopolymerization and also with the corresponding reactions of vinyl acetate.[3]

Experimental and Results

Preliminary runs showed that there was a marked acceleration of polymerization in presence of benzoyl peroxide, although the sensitized rate was still of the same order of magnitude as the direct photo-reaction. Purified benzoyl peroxide was weighed out and dissolved in A.R. benzene to give a standard solution and a measured volume of this was added to the reaction vessels. Since benzoyl peroxide is not appreciably volatile at ordinary temperatures, the reaction vessels could be pumped out on the vacuum line after removal of benzene by a filter pump, without loss of benzoyl peroxide. An attempt was made to isolate the photosensitized reaction by using a series of Corning glass filters to cut out the light which excited the direct reaction while admitting light of longer wavelengths which would be absorbed by the benzoyl peroxide. It was found, however, that those filters which cut out the direct reaction also reduced the rate of the sensitized reaction more than 10-fold.

The benzoyl peroxide thermal-catalyzed polymerization of methyl methacrylate was first followed at 35·6° C for different catalyst concentrations for comparison with the sensitized reaction. The reaction showed no induction period and was apparently independent of the amount of polymer present over a considerable range, with a "gel" effect setting in later. The rate was proportional to the square root of the catalyst concentration as had been found by previous investigators.[4]

---

[1] Mackay and Melville, *Trans. Faraday Soc.*, 1949, **45**, 323.

[2] Barnett and Vaughan, *J. Physic. Chem.*, 1947, **51**, 926. Cass, *J. Amer. Chem. Soc.*, 1946, **68**, 1976. Bartlett and Nozaki, *ibid.*, 1946, **68**, 1495, 1686.

[3] Burnett and Melville, *Proc. Roy. Soc. A*, 1947, **189**, 481.

The photosensitized reaction (with simultaneous photopolymerization) was followed for a wide range of peroxide concentrations at 35·6° C. All the experiments, except where the intensity was varied as shown in Tables I, III and V, were carried out at a constant light intensity, which was approximately the same as that used for the absolute measurements described in Part I. This reaction also showed no induction period and was apparently independent of the amount of polymer present over a considerable range of conversion (Fig. 1). The effect of peroxide concentration on rate was complex and, at high concentrations, the rate became independent of peroxide concentration, as shown in Fig. 2 and 3. The observed rates were not corrected for the simultaneous photopolymerization. Owing to its strong absorption at the wave-lengths used,[5] the benzoyl peroxide probably exerts an internal filter effect so that at high sensitizer concentrations the photopolymerization may be reduced or eliminated on this account.

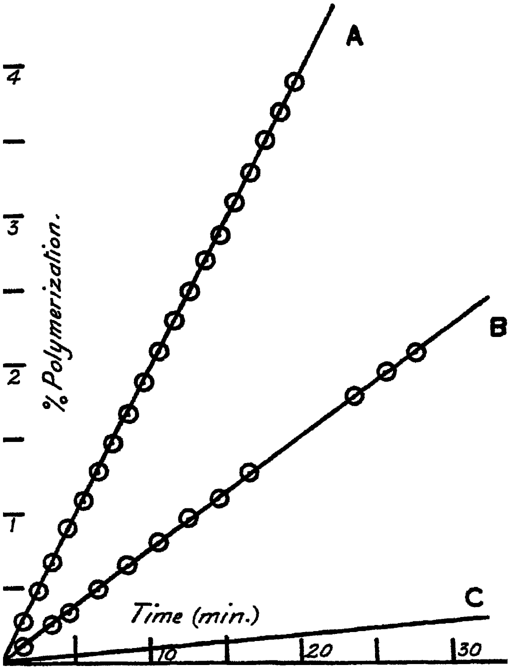

FIG. 1.—The sensitized polymerization as a function of time at 35·6° C. A and C benzoyl peroxide concentration 0·00495 mole/l.

A—sensitized reaction.
B—photo-reaction.
C—thermal catalyzed reaction.

The intensity exponent of the sensitized reaction was measured in the initial stages of the reaction. The polymerization rate was measured under different intensities obtained by insertion of successive calibrated screens.

---

[4] Brookman and Norrish, *Proc. Roy. Soc. A*, 1939, **171**, 147. Norrish and Smith, *Nature*, 1942, **150**, 336. Schulz and Harborth, *Makromol. Chem.*, 1947, **1**, 106.

[5] Burnett (J. D.), (unpublished observation).

At a peroxide concentration of 1·1 × 10⁻² mole/l. (see Fig. 3), the intensity exponent was found to be 0·67 (Table I), as compared with the value 0·48 previously obtained for the direct reaction.[1]

TABLE I.—RATE OF THE SENSITIZED POLYMERIZATION AS A FUNCTION OF INTENSITY

Temperature = 35·6° C; benzoyl peroxide concentration = $1{\cdot}1 \times 10^{-2}$ mole/l.

Relative Intensity I_r	Relative Rate R	Intensity Exponent x $(R \propto I_r^x)$
10·0	0·278	0·67
3·46	0·129	
2·11	0·098	
10·0	0·289	0·67
3·46	0·138	
2·11	0·101	

By measuring the intrinsic viscosities of the polymers formed in a series of runs carried out with the same concentration of benzoyl peroxide and under the same intensity, but each to a different measured conversion, it was found that the intrinsic viscosity increased during the course of the reaction, as shown in Table II.

TABLE II.—INTRINSIC VISCOSITY AS A FUNCTION OF CONVERSION

Temperature = 35·6° C; benzoyl peroxide concentration = $1{\cdot}0 \times 10^{-2}$ mole/l.

% Conversion	3·0	8·7	13·7	16·0
$[\eta]$	0·65	0·79	1·06	1·28

The intrinsic viscosities of the polymers were also measured for a series of runs carried out with the same concentration of benzoyl peroxide and to the same % polymerization, but under different light intensities obtained as above. Plotting $\log_{10} I_r$ against $\log_{10} [\eta]$ gave $[\eta] \propto I_r^{-0{\cdot}37}$, i.e. $\{[\eta] \, . \, I_r^{0{\cdot}37}\}$ is approx. constant, as in Table III.

TABLE III.—INTRINSIC VISCOSITY AS A FUNCTION OF INTENSITY

Temperature = 35·6° C; benzoyl peroxide concentration = $1{\cdot}0 \times 10^{-2}$ mole/l.; conversion = 3 %

Relative Intensity I_r	Intrinsic Viscosity $[\eta]$	$[\eta] \, . \, I_r^{0{\cdot}37}$
10·0	0·65	1·52
3·46	0·89	1·41
2·11	1·16	1·53

A further series of runs was carried out under the same intensity and to approximately the same % conversion but with different initial concentrations of benzoyl peroxide, and the intrinsic viscosities of the resulting polymers were again measured. This was then repeated for a different final % conversion. The results, given in Table IV, show that at the highest benzoyl peroxide concentrations used, the intrinsic viscosity of the polymer, as well as the rate of polymerization (Fig. 2 and 3), becomes independent of sensitizer concentration.

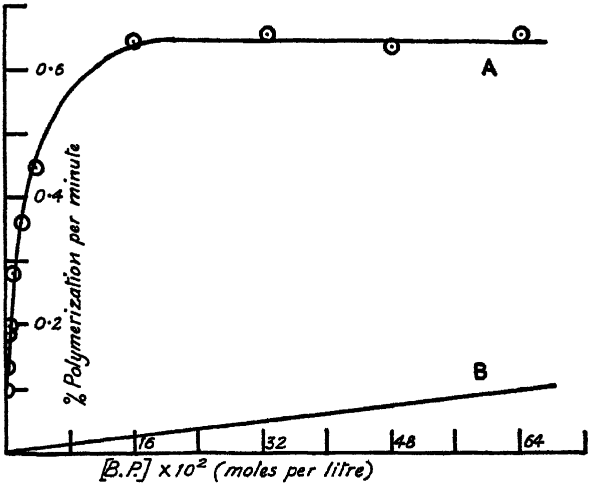

FIG. 2.—Rate of the sensitized polymerization as a function of sensitizer concentration at 35·6° C.

A—sensitized reaction ; B—thermal catalyzed reaction.

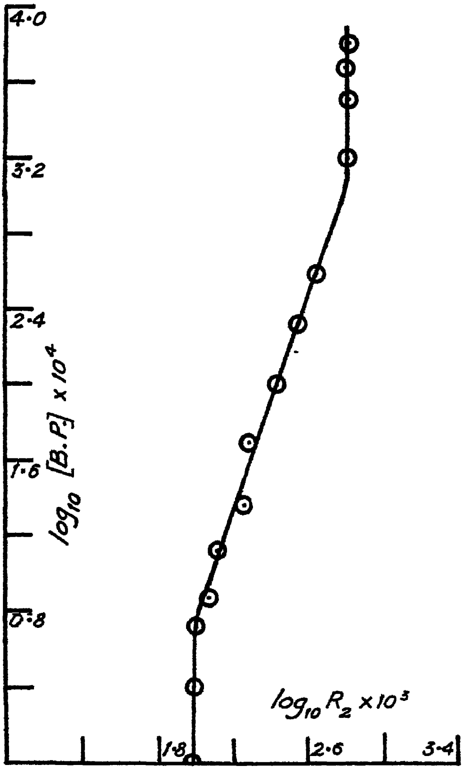

FIG. 3.—Rate of the sensitized polymerization as a function of sensitizer concentration at 35·6° C—log. plot.

TABLE IV.—INTRINSIC VISCOSITY AS A FUNCTION OF PEROXIDE CONCENTRATION

Temperature = 35·6° C

(*a*) Benzoyl Peroxide Concentration × 10^5 (mole/l.)	% Conversion	[η]
0	3·5	1·06
52·9	2·5	1·17
132·0	3·7	1·06
495·0	5·2	0·74
1000·0	4·0	0·67
2065·0	4·6	0·67

(*b*) Benzoyl Peroxide Concentration × 10^2 (mole/l.)	% Conversion	[η]
1·0	12·5	0·98
16·0	11·7	0·53
32·7	13·2	0·58
64·5	12·5	0·54

The above experiments show a close similarity between the photo, catalyzed and sensitized polymerizations of methyl methacrylate, indicating a similarity in mechanism in all three cases. On varying the light intensity to give approximately equal rates for the photo and sensitized reactions at 35·6° C, the intrinsic viscosities of the polymers formed were also found to be approximately the same, as shown in Table V.

TABLE V

Temperature = 35·6° C; conversion = 3 %

Relative Intensity	Benzoyl Peroxide Conc. (mole/l.)	Relative Rate	[η] of Polymer
10·0	$1·1 \times 10^{-2}$	0·289	0·65
3·46	$1·1 \times 10^{-2}$	0·138	0·89
2·11	$1·1 \times 10^{-2}$	0·101	1·16
10·0	0	0·104	1·02

The comparison is not strictly quantitative since the polymer formed in the sensitized reaction will contain some photo-polymer formed under a lower intensity and thus of higher molecular weight than in the parallel photo-reaction. The true value of [η] for the sensitized reaction will therefore be somewhat lower than the experimental value.

Compared with vinyl acetate,[3] methyl methacrylate is much less responsive to sensitization by benzoyl peroxide: whereas with vinyl acetate under similar conditions the sensitized polymerization is so large that the direct reaction is negligible by comparison, with methyl methacrylate the maximum sensitized rate obtainable is only about six times the photopolymerization rate. In the case of vinyl acetate, while the rate at the highest benzoyl peroxide concentrations falls off slightly with increase in sensitizer concentration, the mean molecular weight decreases so rapidly that the product (mol. wt. × [benzoyl peroxide]$^{\frac{1}{2}}$) also decreases with increasing sensitizer concentration. Also the intensity exponent rises from 0·5 in absence of sensitizer, tending to a value of one at high peroxide concentrations. Burnett and Melville,[3] by a kinetic analysis, showed that these observations were consistent with termination by benzoyl peroxide molecules. With methyl methacrylate, the evidence is less clear.

The increase in intensity exponent in presence of benzoyl peroxide and the rate being independent of peroxide concentration at high sensitizer concentrations suggest that termination by peroxide molecules is taking place, but this is hardly supported by the intrinsic viscosities. At moderate peroxide concentrations, the intrinsic viscosity shows a downward trend with increasing sensitizer concentration, which is consistent with the decrease in intrinsic viscosity with increasing intensity, but the simultaneous photo-reaction makes precise molecular weight measurements by this method difficult.

The Effect of Benzoquinone on the Photopolymerization

The action of quinones on free radical polymerizations has been discussed in a number of recent papers.[6, 7] A distinction has been drawn between reactions in which the active centres are (*a*) monoradicals, where retardation only takes place, as in the benzoyl peroxide catalyzed polymerizations of styrene and methyl methacrylate,[6] and of vinyl and allyl acetates ; [8] and (*b*) suitably spaced diradicals, where complete inhibition occurs, as in the photopolymerization of vinyl acetate [9] and also in the thermal polymerization of styrene,[6, 10] where the period of inhibition is followed by retardation.

Since the active centres in the photopolymerization of methyl methacrylate are believed to be diradicals ; [1] the effect of benzoquinone was expected to be similar to that in (*b*) above ; giving an inhibition period during which all the active centres produced were being consumed by reaction with quinone molecules and from which it might be possible to calculate the rate of initiation of such centres, as in the photopolymerization of vinyl acetate.[9]

Experimental and Results

A series of runs was carried out at the same temperature and light intensity, one with pure monomer and the others with different concentrations of benzoquinone. The purified benzoquinone was weighed out and dissolved in A.R.

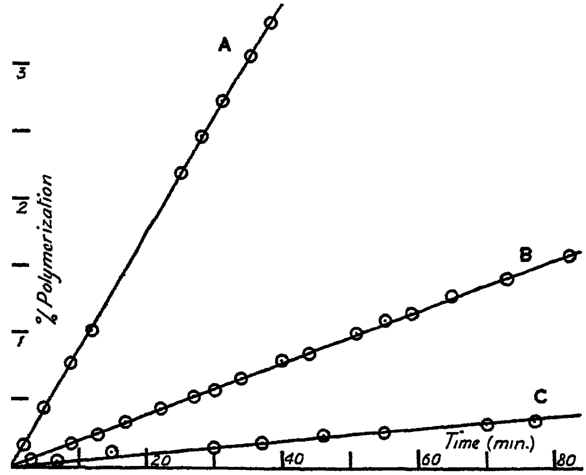

FIG. 4.—The effect of benzoquinone on the photopolymerization rate at 35·6° C (see Table VI).

---

[6] Melville and Watson, *Trans. Faraday Soc.*, 1948, **44**, 886.

[7] Price and Read, *J. Polymer Sci.*, 1946, **1**, 44. Price, *Faraday Soc. Discussions*, 1947, **2**, 304.

[8] Bartlett, Hammond and Kwart, *ibid.*, 1947, **2**, 342.

[9] Burnett and Melville, *Proc. Roy. Soc. A*, 1947, **189**, 456.

[10] Foord, *J. Chem. Soc.*, 1940, 48. Kern and Feuerstein, *J. prakt. Chem.*, 1941, **158**, 186. Goldfinger, Skeist and Mark, *J. Physic. Chem.*, 1943, **47**, 578.

benzene to give a standard solution. A measured volume of this was added by a pipette through a filler to the cleaned reaction vessel and the benzene was evaporated cautiously by means of a water pump. Before evacuating on the vacuum line, the reaction vessel was cooled in alcohol and solid CO_2, since benzoquinone is appreciably volatile at ordinary temperatures. It was found that in presence of benzoquinone there was no evidence of any inhibition period; polymerization proceeded at a reduced rate which remained constant so long as it was followed (Fig. 4) and the polymerizing mixture retained its yellow colour. Measurement of the intrinsic viscosities of the polymers formed showed that there was a sharp decrease in relative mean molecular weight in presence of benzoquinone (Table VI).

TABLE VI.—The Effect of Benzoquinone

Temperature = 35·9° C; $2f(I) = (7{\cdot}60 \pm 0{\cdot}23) \times 10^{-8}$ einstein l.$^{-1}$ sec.$^{-1}$

Concentration of Benzoquinone × 10^3 (mole/l.) (X)	Rate (% Conversion per Hour) (R)	Relative Rate (R_X/R_0)	Reciprocal Rate × 10^{-4} (R_X^{-1})	[η] of Polymer	In Fig. 4
0	5·25	1	0·74	1·02	A
3·37	1·18	0·224	3·29	0·33	B
9·25	0·285	0·054	13·6	—	C

The fact that, in presence of benzoquinone, the mean molecular weight decreases in approximately the same ratio as the rate means that the rate of initiation is not significantly affected by the benzoquinone, i.e. there is no internal filter effect and the influence of the benzoquinone is not on the initiation but on the termination step of the polymerization. The complete absence of any inhibition period shows that the Diels-Alder type of reaction between a diradical formed from two monomer molecules and a quinone molecule does not take place with methyl methacrylate, but that the quinone molecule apparently reacts with one end of a growing radical as with a monoradical.[6] For the diradical-quinone reaction to take place, a certain spacing of the diradical ends must be possible; in methyl methacrylate the presence of the α-methyl groups may alter the bond angles and prevent the diradical from taking up a suitable configuration.

If it is assumed that a benzoquinone molecule reacts with a growing chain-end by addition or transfer to form a radical which is relatively inert, the subsequent reactions of this radical may be disregarded and an approximate value obtained for the rate coefficient for interaction of a benzoquinone molecule and a growing chain.

In the notation of Part I, Q_r' represents an active " half-chain " of length r units, and Q_r represents an inactive " half-chain " of length r units.

If R_0 is the rate of polymerization in absence of benzoquinone,
R_X ,, ,, ,, ,, presence ,,
(X) ,, concentration of quinone,
k_X ,, coefficient for interaction of a benzoquinone molecule and a growing chain;

the kinetic scheme for the unretarded reaction will be,

$$\begin{aligned} M + h\nu &= Q_1' + Q_0' \quad f(I) \\ Q_r + M &= Q_{(r+1)}' \quad k_p \\ Q_r' + Q_n' &= Q_r + Q_n \quad k_t \end{aligned}$$

with, in presence of benzoquinone, the additional step,

$$Q_r' + X = Q_rX' \quad k_X.$$

The rate of production of " half-chains ", $2f(I)$, has been discussed in Part I and was obtained in the same way from rate and osmotic molecular weight measurements.

For the unretarded reaction, in the steady state,

$$R_0 = k_p(\mathrm{M}) \left[\frac{2f(I)}{k_t}\right]^{\frac{1}{2}}.$$

In presence of an excess of benzoquinone, the main reaction removing radicals Q_r' is that with benzoquinone, and in the steady state

$$2f(I) = k_{\mathrm{x}}(\mathrm{X}) \,.\, (\Sigma Q_r')$$

so that

$$R_{\mathrm{x}} = \frac{k_p(\mathrm{M}) \,.\, 2f(I)}{k_{\mathrm{x}}(\mathrm{X})}.$$

If R_0/R_{x} is plotted against (X), the slope S of this line is

$$k_{\mathrm{x}} \,.\, k_t^{-\frac{1}{2}} \,.\, [2f(I)]^{-\frac{1}{2}},$$

so that

$$k_{\mathrm{x}} = S \,.\, k_t^{\frac{1}{2}} \,.\, [2f(I)]^{\frac{1}{2}}. \quad \ldots\ldots \quad \text{(i)}$$

Also, if R_{x}^{-1} is plotted against (X), the slope T of this line is

$$k_{\mathrm{x}}/k_p \,.\, 2f(I) \,.\, (\mathrm{M}),$$

so that

$$k_{\mathrm{x}} = T \,.\, k_p \,.\, 2f(I) \,.\, (\mathrm{M}) \quad \ldots\ldots \quad \text{(ii)}$$

Plotting the appropriate data from Table VI gives,

$$S = (1{\cdot}91 \pm 0{\cdot}32) \times 10^3 \text{ l. mole}^{-1}$$
$$T = (1{\cdot}30 \pm 0{\cdot}36) \times 10^7 \text{ (l. sec. mole}^{-1})^2$$

Substitution of these figures and of the values previously obtained for the other coefficients in (i) and (ii) gives

$$k_{\mathrm{x}} = (4{\cdot}3 \pm 0{\cdot}9) \times 10^3$$

and

$$k_{\mathrm{x}} = (3{\cdot}7 \pm 1{\cdot}1) \times 10^3 \text{ l. mole}^{-1} \text{ sec.}^{-1}$$

respectively, i.e. a mean value of

$$k_{\mathrm{x}} = (4{\cdot}0 \pm 1{\cdot}0) \times 10^3 \text{ l. mole}^{-1} \text{ sec.}^{-1} \text{ at } 35{\cdot}9^\circ \text{ C.}$$

The Dark Reaction

Polymerization in the dark following the irradiation of monomer vapour was first discovered by Carothers [11] with chloroprene. Melville later observed the same phenomenon with methyl methacrylate, and made a study of this reaction [12] and also of that with chloroprene.[13] Methyl *iso*propenyl ketone has been found to behave similarly, and the phenomenon appears to be confined [14] to disubstituted monomers of the general formula $CH_2 = CXY$.

A similar dark reaction following the irradiation of liquid methyl methacrylate has been described by Bamford and Dewar,[15] who have deduced from their experiments that irradiation by ultra-violet light of either liquid or vapour produces a photo-catalyst, while an inhibitor is produced from the monomer on heating or spontaneously on standing. The dark reaction was also observed in the early stages of the present work and some experiments are described here which have been carried out independently on this reaction. These are consistent with the photochemical formation of some form of catalyst, as suggested by Bamford and Dewar, but the work done so far shows no evidence for inhibitor formation. Further experiments being done may help to clarify this point and characterize the reaction more precisely.

---

[11] Carothers, Williams, Collins and Kirby, *J. Amer. Chem. Soc.*, 1931, **53**, 4203.

[12] Melville, *Proc. Roy. Soc. A*, 1937, **163**, 511.

[13] Bolland and Melville, *Proc. Rubber Tech.Conf.* (London), 1938, 239

[14] Melville, *J. Chem. Soc.*, 1941, 414.

[15] Bamford and Dewar, *Nature*, 1946, **158**, 380; *Faraday Soc. Discussions*, 1947, **2**, 310, 317; *Proc. Roy. Soc. A*, 1949, **197**, 356.

Experimental and Results

In all the photopolymerization experiments described in Part I, it was found that polymerization did not cease on cutting off the light, but continued in the dark. There was an initial decay in rate over a few minutes (at 20–35° C), after which the rate appeared constant, within the accuracy of measurement, over approximately 20 min. Measurement over longer intervals, however, showed that there was in fact a continuous slow falling-off in rate with time (Fig. 5 and 6), although the polymerization was still measurable after several days.

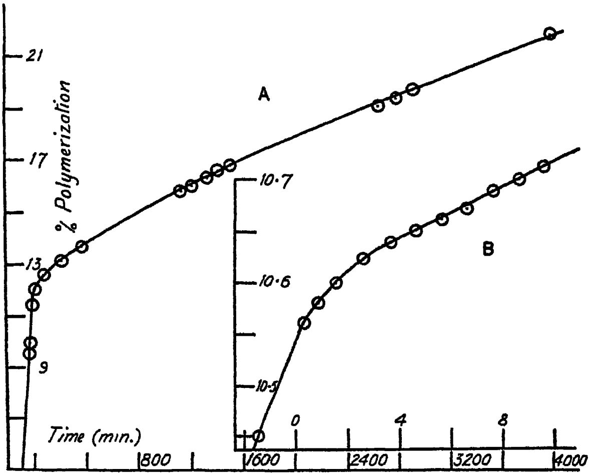

FIG. 5.—The dark reaction as a function of time.
A—20·9° C ; B—35·9° C.

The magnitude of this dark reaction was found to depend on temperature and amount of polymerization. The dark reaction set in as soon as a measurable amount of polymer had been formed and, for runs carried out at the same temperature and photopolymerized under the same light intensity, the dark rate over a given time range was proportional to the first power of the % polymer

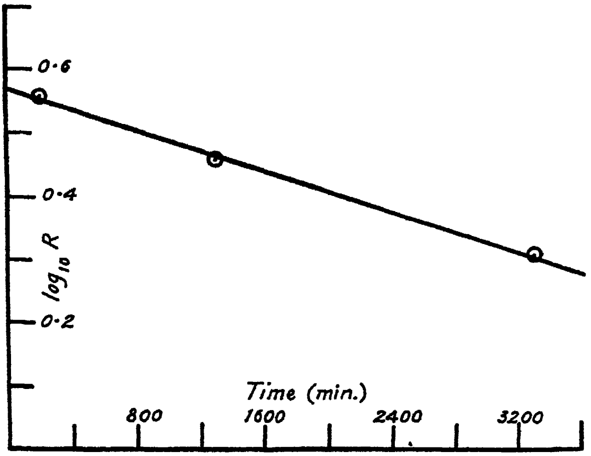

FIG. 6.—Decay of the dark reaction at 20·9° C. R is the dark rate (% polymerization per min.) $\times 10^3$.

present at the end of the photo-reaction, as shown in Fig. 7. In two runs carried out at the same temperature (35·9° C) to the same % conversion but under different light intensities (relative values 10 and 3·46), so that the final rates of photopolymerization and the mean molecular weights of the polymers and also the total number of quanta absorbed by the systems were different, the dark reactions appeared to follow the same course in each case (Fig. 8), showing that the dark rate is highly insensitive to the light intensity during irradiation.

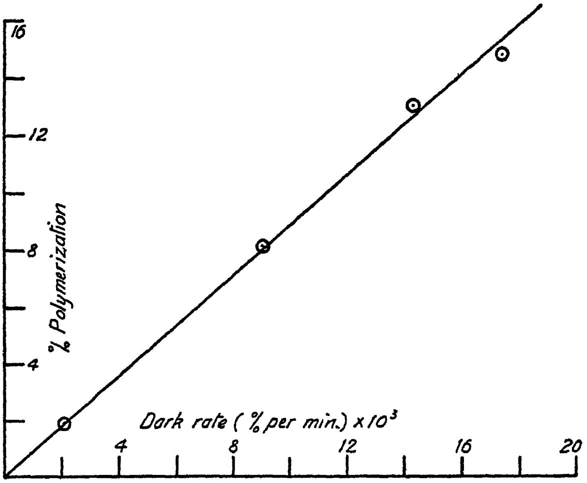

FIG. 7.—Dark rate as a function of conversion at 35·6° C. Dark rates measured over time range 5-15 min.

To find the effect of subsequent polymerization in the dark on the mean molecular weight of the polymer, photopolymerization was carried out in two reaction vessels at 35·9° C under the same intensity. One reaction vessel was removed after 12 % conversion, cooled immediately, the polymer-monomer mixture dissolved out and the polymer precipitated. With the other, the light was cut off after about 9 % conversion and the polymerization allowed to continue in the dark at the same temperature to about 12 % conversion (this took several days). The final meniscus reading was taken, the polymer-monomer

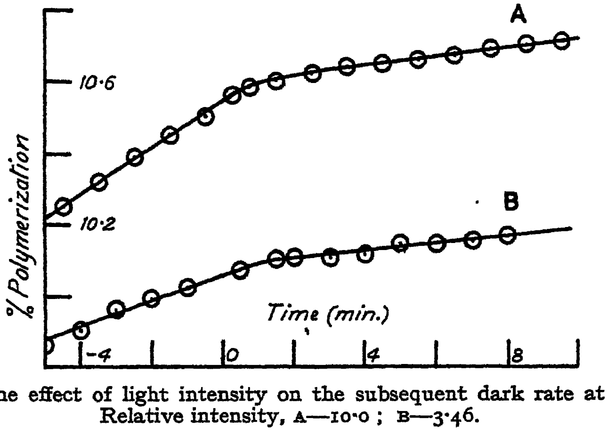

FIG. 8.—The effect of light intensity on the subsequent dark rate at 35·9° C. Relative intensity, A—10·0 ; B—3·46.

mixture dissolved out and the polymer precipitated in the usual way. The osmotic molecular weights and intrinsic viscosities of the two polymers were measured and gave the following results,

$$12\ \%\ \text{photopolymerization} \qquad \overline{M}_n = 336{,}000 \pm 10{,}000, \quad [\eta] = 1{\cdot}02$$

$$\left.\begin{array}{l} 9{\cdot}25\ \%\ \text{photopolymerization} \\ 2{\cdot}49\ \%\ \text{dark polymerization} \end{array}\right\} \quad \left\{\begin{array}{l} \overline{M}_n = 336{,}000 \pm 10{,}000 \\ [\eta] = 2{\cdot}01 \end{array}\right.$$

During polymerization in the dark, the number average molecular weight remained the same, whereas the mass of polymer increased some 20 %, so that new polymer molecules must have been formed. (The greater mean chain length of these new molecules will affect the intrinsic viscosity which is sensitive to high molecular weights but not the osmotic molecular weight which is sensitive to low molecular weights.) The constancy of the number average molecular weight could arise through a transfer reaction but it has already been shown [1] that transfer does not occur to any significant extent at this temperature.

To find the effect of air on the dark reaction, monomer was photopolymerized to about 12 % conversion at 35·9° C, the reaction vessel left in the dark at 25° C for about an hour and the rate of the dark reaction then measured. The end of the reaction vessel capillary was broken off and the contents exposed to the air for a few hours. The reaction vessel was closed with a small rubber stopper and the dark reaction again measured at the same temperature as before and was found to be practically unchanged, as shown in Table VII.

TABLE VII.—EFFECT OF AIR ON THE DARK REACTION

Temperature = 25·0° C

Before Exposure to Air			After Exposure to Air		
Time (min.)	Decrease in Height (cm. × 10³)	Relative Rate (cm./min. × 10³)	Time (min.)	Decrease in Height (cm. × 10³)	Relative Rate (cm./min. × 10³)
0	0	—	0	0	—
6	3	0·50	2	1	0·50
22	12	0·55	10	5	0·50
28	16	0·57	16	9	0·56
37	21	0·57	23	13	0·56
43	24	0·56	32	16	0·50

In order to obtain the overall activation energy of the dark reaction, monomer was photopolymerized in two reaction vessels at 35·9° C to about 12 % conversion; the reaction vessels were left in the dark at 25° C for a few hours to establish a steady rate and the rates of the dark reaction in both were then measured alternately at 45° C and 25° C, giving the results shown in Table VIII.

TABLE VIII.—ACTIVATION ENERGY OF DARK REACTION

	Temperature ° C		$\left(\frac{\text{Rate}_{45{\cdot}53}}{\text{Rate}_{25{\cdot}00}}\right)$	E (kcal./mole)
	25·00	45·53		
Mean relative rate (cm./min. × 10³ × conversion factor for experimental temperature)	0·415	3·55	8·55	19·7
	0·549	4·14	7·54	18·6

The overall activation energy for the dark reaction is thus about

19 (19·1 ± 0·6)kcal./mole.

To find the effect of heat on the dark reaction, photopolymerization was arried out to 12 % conversion in two reaction vessels exposed to the same intensity at 20·9° C, and the light cut off. One reaction vessel was kept at 20·9° C and the dark reaction followed. The other, after observing the dark reaction for 30 min., was immersed in a thermostat at 80° C for 30 min., then returned to 20·9° C and allowed to reach equilibrium. Polymerization was then found to continue, although at a slower rate than in the control experiment on account of the more rapid falling-off in the dark rate during the heating at 80° C. During the time range 5-15 min. after cutting off the light (before the heat treatment), the rate of polymerization was $9{\cdot}2 \times 10^{-3}$ % per min., and in the control experiment $11{\cdot}1 \times 10^{-3}$ % per min. During the time range 2500-3000 min. (after the heat treatment), the rate was $1{\cdot}12 \times 10^{-3}$ % per min., and in the unheated control $2{\cdot}20 \times 10^{-3}$ % per min. This result appears to conflict with Bamford and Dewar's observations [15] that heating either liquid or vapour to 100° C for a few minutes arrests the polymerization.

In the experiments on the benzoyl peroxide sensitized reaction described in this paper, a dark reaction was observed of the same form as that following the photo-reaction. The dark polymerization rate was corrected for the simultaneous catalyzed polymerization according to the method of Noyes and Leighton,[16] i.e.

$$R_D = (R_3^2 - R_1^2)^{\frac{1}{2}}$$

where R_D = rate of true dark reaction,
R_3 = „ observed dark reaction,
R_1 = „ benzoyl peroxide catalyzed reaction.

The corrected dark rate over a given time range was again proportional to the polymer concentration; the rate again showed a slow decay with time and was not sensibly dependent on the sensitizer concentration, as shown in Table IX.

TABLE IX.—Effect of Sensitizer Concentration on Dark Rate

Dark rates measured over range 5-15 min. from cutting off light; constant intensity as above; 35·6° C.

Benzoyl Peroxide Concentration × 10⁵ (mole/l.)	R_3 (% per min. × 10³)	R_1 (% per min. × 10³)	R_D (% per min. × 10³)
(i) At 3-5 % conversion			
0	8·2	0	8·2
25·3	9·0	2·3	8·7
231	11·7	6·3	9·9
495	15·0	8·9	12·1
2070	22·9	17·2	15·1

Benzoyl Peroxide Concentration × 10³ (mole/l.)	R_3 (% per min. 10³)	R_1 (% per min. × 10³)	R_D (% per min: × 10³)
(ii) At 10-12 % conversion			
3·83	37·5	23·2	29·5
16·0	49·3	44·0	22·2
32·7	65·0	61·0	22·4
48·2	77·1	71·6	28·6
64·5	90·2	82·5	36·5

Discussion

At the time when the vapour-phase process was studied [12] the two phenomena, light and dark reactions, appeared to be so dissimilar that it was considered that the reaction mechanisms must likewise be different. The present experiments indicate that the mechanisms of growth and termination of the polymers are essentially the same but that the initiation process differs markedly in the two cases. Besides virtually instantaneous production of radicals in the normal way, some other photo-reaction occurs which produces from the monomer or polymer a substance capable of generating radicals thermally over a long period of time at room temperature. The other possibility is the production of a relatively stable radical which reacts very slowly. There is no question that once growth is started it occurs very rapidly as in the ordinary radical reaction. There is no continuous growth of the polymer over a long period of time as was initially suggested when knowledge of polymerization was very rudimentary. The formation of new molecules, shown by the molecular weight measurements, implies that initiation is taking place; and the decay of the dark rate with time, shown in Fig. 6, would follow from the slow decay of a catalyst formed photochemically. The dependence of the dark rate on the first power of the polymer concentration (Fig. 7) and the low-intensity exponent (Fig. 8) are somewhat surprising and indicate that the polymer plays some part in initiating the dark reaction. Assuming that propagation and termination are as in the photo-reaction, the possible mechanisms may be outlined.

---

[16] Noyes and Leighton, *The Photochemistry of Gases* (Reinhold, 1941).

Let R_0 be the initial dark rate,
R_i the rate of initiation corresponding to R_0,
I the light intensity during irradiation,
T the irradiation time,
M a monomer molecule, (M) the monomer concentration, etc.,
P a polymer molecule, P′ a polymer radical,
C a catalyst molecule, C′ a catalyst radical,
$(\mathrm{C})_0$ the initial catalyst concentration after irradiation.

1 (*a*). *Catalyst is formed photochemically from the monomer,*

$$(2)\quad \mathrm{M} + h\nu \rightarrow \mathrm{C}.$$

Rate of catalyst formation = const. $I\,.\,(\mathrm{M})^{(2)}$ and total concentration $(\mathrm{C})_0$ = const. IT at constant (M), neglecting the decay of catalyst during irradiation.

A catalyst molecule reacts with a polymer molecule to form radicals,

$$\mathrm{C} + \mathrm{P} \rightarrow 2\mathrm{P}'$$

so that

$$R_i = \text{const.}\ (\mathrm{C})_0(\mathrm{P})$$

therefore

$$R_0 = \text{const.}\ R_i^{\frac{1}{2}} = \text{const.}\ [IT(\mathrm{P})]^{\frac{1}{2}}. \quad . \quad . \quad . \qquad \text{(iii)}$$

For constant I,

$$R_0 = \text{const.}\ (\mathrm{P}),$$

since $(\mathrm{P}) \propto T$ at constant I; for constant (P),

$$R_0 = \text{const.}\ I^{\frac{1}{2}},$$

since $T \propto I^{-\frac{1}{2}}$ for constant (P).

1 (*b*). *Catalyst is formed as in* 1 (*a*).

A catalyst molecule dissociates into radicals which can then react with polymer molecules,

$$\mathrm{C} \rightarrow 2\mathrm{C}'\ k_1; \qquad 2\mathrm{C}' \rightarrow \mathrm{C}\ k_2;$$
$$\mathrm{C}' + \mathrm{P} \rightarrow \mathrm{P}'\ k_i.$$

Assuming a radical recombination mechanism analogous to that applied by Matheson [17] to the decomposition of benzoyl peroxide, in the steady state,

$$\frac{d(\mathrm{C}')}{dt} = k_1(\mathrm{C}) - k_2(\mathrm{C}') - k_i(\mathrm{C}')(\mathrm{P}) = 0$$

and

$$(\mathrm{C}') = \frac{\dfrac{k_1}{k_2}(\mathrm{C})}{1 + \dfrac{k_i}{k_2}(\mathrm{P})}.$$

---

[17] Matheson, *J. Chem. Physics*, 1945, 13, 584.

If $k_1(\mathrm{P}) \gg k_2$, $(\mathrm{C}') = \text{const.}\ (\mathrm{C})/(\mathrm{P})$,

$R_i = \text{const.}\ (\mathrm{C}')_0(\mathrm{P}) = \text{const.}\ (\mathrm{C})_0$

and $R_0 = \text{const.}\ (IT)^{\frac{1}{2}}$. . . . . . (iii*a*)

For constant I, $R_0 = \text{const.}\ (\mathrm{P})^{\frac{1}{2}}$;

for constant (P), $R_0 = \text{const.}\ I^{\frac{1}{2}}$,

as in 1 (*a*) above. This, therefore, cannot apply in the present instance.

If $k_1(\mathrm{P}) \ll k_2$, $(\mathrm{C}') = \text{const.}\ (\mathrm{C})$,

so that this gives eqn. (iii) for R_0.

1 (*c*). *Relatively stable radicals are formed photochemically from the monomer,*

$$(2)\quad \mathrm{M} + h\nu \rightarrow 2\mathrm{C}'.$$

A radical reacts with a polymer molecule to form a polymer radical,

$$\mathrm{C}' + \mathrm{P} \rightarrow \mathrm{P}'.$$

This also gives eqn. (iii) for R_0.

2 (*a*). *Catalyst is formed photochemically from a polymer molecule,*

$$\mathrm{P} + h\nu \rightarrow \mathrm{C}.$$

Rate of catalyst formation = const. $I(\mathrm{P})$

and total concentration $(\mathrm{C})_0 = \int_0^T \text{const.}\ I(\mathrm{P})\ .\ \mathrm{d}t$

$= \text{const.}\ I^{3/2}\ .\ T^2$, since $(\mathrm{P}) = \text{const.} I^{\frac{1}{2}}\ (T.)$.

A catalyst molecule reacts with a monomer molecule to initiate polymerization,

$$\mathrm{C} + \mathrm{M} \rightarrow 2\mathrm{P}'$$

so that $R_i = \text{const.}\ (\mathrm{C})_0(\mathrm{M})$

and $R_0 = \text{const.}\ I^{\frac{3}{4}}T$ at constant (M) . . . (iv)

For constant I, $R_0 = \text{const.}\ (\mathrm{P})$;

for constant (P), $R_0 = \text{const.}\ I^{\frac{1}{2}}$, as in 1 (*a*) above.

2 (*b*). *Catalyst is formed as in* 2 (*a*).

A catalyst molecule dissociates into radicals which can then react with monomer molecules,

$$\mathrm{C} \rightarrow 2\mathrm{C}'\ k_1; \quad 2\mathrm{C}' \rightarrow \mathrm{C}\ k_2;$$
$$\mathrm{C}' + \mathrm{M} \rightarrow \mathrm{P}'\ k_i.$$

As in 1 (*b*) above, in the steady state,

$$\frac{\mathrm{d}(\mathrm{C}')}{\mathrm{d}t} = k_1(\mathrm{C}) - k_2(\mathrm{C}') - k_i(\mathrm{C}')(\mathrm{M}) = 0,$$

so that

$$(\mathrm{C}') = \text{const.}\ (\mathrm{C})$$

at constant (M) and this gives eqn. (iv) for R_0.

2 (*c*). *Relatively stable radicals are formed photochemically from the polymer,*

$$\mathrm{P} + h\nu \rightarrow 2\mathrm{C}'.$$

A radical reacts with a monomer molecule to form a polymer radical,

$$\mathrm{C}' + \mathrm{M} \rightarrow \mathrm{P}'.$$

This also gives eqn. (iv) for R_0 so that all these mechanisms, except 1 (*b*) in a certain case, yield the same approximate intensity and photopolymer concentration relationships. 2(*a*) — (*c*) appears more probable than 1(*a*)—(*c*). Since they require the presence of polymer as well as catalyst, the latter would also be inconsistent with Bamford and Dewar's observation [15] that the activity is volatile at 0° C.

The high overall activation energy of the dark reaction shows that the initiation process has a considerable activation energy. From data on the photopolymerization $E_p = (4{\cdot}4 \pm 1{\cdot}0)$ and $E_t = (0 \pm <2)$ kcal./mole., so that if $\bar{E}_i$ is the activation energy for the initiation reaction, then

$$E_{\text{total}} = \tfrac{1}{2}E_i + E_p - \tfrac{1}{2}E_t$$

and E_i is approximately 29 (29·4 ± 3·0) kcal./mole. This may be due to the energy required for addition of a relatively stable radical to a monomer or polymer molecule (but cf. $E_p = 4{\cdot}4$ kcal./mole) or more probably to the decomposition of a catalyst produced photochemically as in 1(*b*) and 2(*b*) above.

It has been suggested [15] that methyl methacrylate has a high rate of thermal polymerization. Prior to the photo-reaction, however, the monomer showed no measurable polymerization over long periods under our experimental conditions. This could arise through the presence in the monomer of some substance inhibiting a thermal reaction; but in the photopolymerization the rates were found to be completely reproducible and linear from the beginning, with no indication of initial retardation or inhibition, so that this possibility is discredited.

One of us (M. H. M.) is indebted to Messrs. Bakelite Ltd. for financial assistance during the course of this work (1946-48).

Chemistry Department,
The University,
Edgbaston, Birmingham.

Chemistry Department,
University of Aberdeen.

REVIEWS OF BOOKS

A New Dictionary of Chemistry (2nd Edition). Ed. S. MIALL AND L. M. MIALL. (Longmans, Green & Co., London, 1949). Pp. ix + 589. Price 60s.

The first edition of the dictionary appeared in 1940—the appearance of this second revised edition after nine years is associated with destruction of nearly all the existing stocks in 1940 during an air raid in December, 1940. It is, therefore, not as well-known as the appearance of the 2nd edition suggests. It is thought that this one-volume dictionary, containing nearly 6000 entries, will not prove of great value or interest to chemists generally. It certainly contains a mass of miscellaneous information ot general chemical matters, but this is not of the kind which will be of real use to the serious student of chemistry—they will have available in libraries other well-known reference books, dictionaries, etc., for consultation.

However, people other than chemists often require a handy book of reference—thus, works managers, patent agents, pharmacists, etc., should find it a welcome addition to their personal library. There is a useful table of physical constants of nearly 2000 organic compounds; this contains melting-points, boiling-points, density and specific rotations. And in the main body of the text, some short biographical articles on well-known scientists are included.

Physics and Chemistry of Cellulose Fibres (with particular reference to Rayon). By P. H. HERMANS (Elsivier Publishing Co., Inc., Amsterdam, London, New York, 1949; Distributors: Cleaver-Hume Press Ltd., London). Pp. xx + 534. Price 50s.

This book forms part of Elsivier's Polymer Series on the chemistry, physics and technology of high polymeric and allied substances. It is not intended to cover such a wide field as the title might suggest but rather to deal with those aspects of the physical chemistry of native and regenerated cellulose with which the author has been concerned, and to which he has contributed so many important papers during the last decade or so.

The book consists of three parts. The first part is primarily concerned with the molecular and super-molecular structure of cellulose in general and with the properties and size of the cellulose molecule. It contains a chapter of ten pages entitled " Chemical Reactions and Breakdown of the Chain Molecules " which opens with the sentence: " Discussion of the chemistry of cellulose molecules does not fall within the framework of this book ". Other subjects dealt with in Part I are cellulose solutions and gels, and the relationship and differences between regenerated and native cellulose.

The second part deals with the morphology and the general physical and chemical behaviour of cellulose fibres. The chapters on sorption and swelling, density, optical properties and the X-ray examination of cellulose fibres are a revised version of the contents of the valuable monograph, *Contribution to the Physics of Cellulose Fibres*, published by Elsivier in 1946 and reviewed in *Trans. Faraday Soc.*, 1946, **42**, 799. In the chapter on mechanical properties the author is preparing the reader for a more fundamental investigation of deformation to follow in Part III.

In the third part on artificial cellulose fibres the chemist who is concerned with the preparation of regenerated cellulose fibres will find much food for thought. After a few chapters devoted to the process of viscose production, isotropic monofils are studied in detail in an attempt to isolate some of the many factors which are involved in the technical spinning process. The molecular orientation produced by deformation of the cellulose gels with various degrees of swelling is measured by optical, X-ray and swelling anisotropy methods and the results obtained are used to test the theory that the material possesses a network structure with only a few chain elements between the junction points.

In a postscript the author explains that the manuscript of the book was almost complete by the end of 1941, that its publication was delayed by the war, and that it has been revised so as to take account of recent English and non-European literature and of the work carried out in 1943-44 by the author and his colleagues. In these circumstances it is perhaps not surprising that the text shows signs of the patching that has been necessary.

There are several minor errors such as g./cm. for g. cm. on p. 272, Ch. XIV for Ch. XIII on p. 398, v_f for q_i in eqn. (11.2) on p. 463, and a rather misleading heading in Table XXXV on p. 274 which should preferably read " degree of elongation " instead of " extension at break ".

The difficult task of translation into English has on the whole been well done, but there are numerous instances where the imperfect acquaintance of the translator with English usage and terminology is evident to the English reader.

In spite of the slight defects that have been mentioned, the book contains such a mine of information on the special aspects of cellulose which Dr. Hermans has studied that it can be recommended to physical chemists who are interested in the fundamentals of the viscose process and in the physical rather than the chemical properties of cellulose fibres.

R. M.

The Structure of Matter. By FRANCIS OWEN RICE AND EDWARD TELLER. (John Wiley & Sons, Inc., New York; Chapman and Hall Ltd., London, 1949.) Pp. viii + 361. Price 30s.

This book is the introductory volume in the Structure of Matter Series of which Maria Goeppert Mayer is the Advisory Editor, and its aim is to acquaint the reader with the scope and application of quantum mechanics using the minimum amount of mathematics. The standard is roughly equivalent to that expected of the Honours Student in Physical Chemistry in his final examination.

Many books have been written about Quantum Mechanics—most of the good ones are too mathematical for the average undergraduate in chemistry ; of the rest, which are claimed to be introductory in character, the treatment is usually severely limited in scope by the author's desire either to avoid the essential mathematics or by his inability to present the general arguments without including a large number of differential equations and their solution.

In the present book, however, the authors have succeeded in writing a broad and comprehensive survey of quantum mechanics virtually without mathematics. Starting with the hydrogen atom, they deal with the behaviour of atoms and molecules in electric fields, with van der Waals' forces, the chemical bond and forces in the solid state. A chapter on magnetic properties is followed by two on molecular vibrations and electronic spectra. The final chapters are on nuclear chemistry and the state of matter in the stars. And yet the Schroedinger equation is not explicitly stated anywhere in the text! This is an achievement which many chemists will applaud, since they are often dismayed by the immense amount of labour involved in the calculations of the theoretical physicists even when the problem is concerned with a very simple and highly idealized system ; and when the theoretician employs semi-empirical methods, often highly charged with empiricisms, the chemist may have grave misgivings about the validity of the procedure.

For these reasons, chemists of this mind should study this book. The arguments, somewhat general it is true, are clearly outlined ; abstruse discussions, metaphysical and philosophical, are absent. There is, of course, a loss of depth in some of the chapters but there is also a welcome absence of rigour, welcome because it lends clarity and vigour to many of the themes developed by the authors. This volume is an introductory text, not a book of reference ; it stresses the qualitative and practical results and the consequences of the quantum theory in an endeavour to help chemists to understand the chemical properties of matter.

There is certainly good value here for 30s. F.C.T.

CORRIGENDA

1949, Vol. **45.**

Page 722, 4th line above Table I

For 2 % (7 % S) *read* 0·2 % (0·07 % S).

Page 722, footnote, 2nd line,

For " due " *read* " assigned "

DIFFUSION PROPERTIES OF GASES

PART III. THE DIFFUSION AND THERMAL DIFFUSION COEFFICIENTS FOR ISOTOPIC GASES AND GAS MIXTURES

BY E. R. S. WINTER

Received 12*th May*, 1949

Recent calculations by Hirs[illegible]ird and Spotz of the Chapman and Enskog gas collision integrals, Ω_k^l, for the Lennard-Jones 12 : 6 model have been used to test the ability of the model to predict the diffusion and thermal diffusion properties of binary gas mixtures and of isotopic gases. For isotopic gases the model gives results in fair agreement with experiment, although there are not sufficient experimental data to enable a critical comparison to be made. For gas mixtures the use of

$$E(0)_{12} = \{E(0)_{11} \,.\, E(0)_{22}\}^{\frac{1}{2}}$$

and

$$r(0)_{12} = \frac{r(0)_{11} + r(0)_{22}}{2}$$

is preferred; these assignments of the interaction energies and diameters for the collision of pairs of unlike gas molecules give rise to close agreement between theory and experiment for rare gas mixtures, and fairly reasonable agreement for other gas mixtures.

The general results of the classical kinetic theory of gases were developed mainly by Enskog and by Chapman and are conveniently presented by Chapman and Cowling.[1] The results give the transport properties in terms of certain integrals Ω_k^l the values of which depend upon the force laws assumed to hold in the interaction of one molecule with another, and upon the temperature. These integrals have been evaluated for a number of molecular models and the predictions of these models compared with theory; thus Chapman and Cowling [1] summarize the work which had been done (by 1938) upon the inverse power, the Sutherland, and the various models of Lennard-Jones, as well as the simpler cases of rigid smooth elastic spheres and of rough spheres; more recently Furry and Jones [2, 3] and, in a briefer manner, Grew,[4] have discussed certain of these models with particular reference to the thermal diffusion constants of gases. None of the models considered are in general really satisfactory for calculating the physical properties of gases, and this applies particularly to the calculation of the thermal diffusion constant, which is the property most sensitive to the law of molecular interaction. The molecular model which has proved most successful in other applications [5] is the Lennard-Jones 12 : 6 model, more accurate models have been considered by Margenau,[6] Massey and Mohr [7] and Amdur,[8] but these are too complex for general use. The integrals Ω_k of Chapman and Cowling for the 12 : 6 model have recently been evaluated by Hirschfelder, Bird and Spotz[9] and their tables enable one to test this model more widely than has hitherto been possible. It is the purpose of this paper to compare with experiment the values of the diffusion coefficients and thermal diffusion ratios for isotopic gases and some gas mixtures, using the equations developed by Chapman and Enskog and the tabulated integrals for the 12 : 6 model of Hirschfelder *et al.*

---

[1] Chapman and Cowling, *The Mathematic Theory of Non-uniform Gases* (C.U.P., 1939).

[2] Jones, *Physic. Rev.*, 1941, **59**, 1019.

[3] Jones and Furry, *Rev. Mod. Physics*, 1946, **18**, 151.

[4] Grew, *Proc. Roy. Soc. A*, 1947, **189**, 402.

[5] Fowler and Guggenheim, *Statistical Thermodynamics* (C.U.P. 1939), Chap. 8.

[6] Margenau, *Physic, Rev.*, 1931, **38**, 747.

[7] Massey and Mohr, *Proc. Roy. Soc. A*, 1934, **144**, 188.

[8] Amdur, *J. Chem. Physics*. 1947, **15**, 482; 1948, **16**, 190.

Formulae for Thermal Diffusion and Diffusion.—For convenience of reference the relevant equations from Chapman and Cowling are given here. The first approximation to the thermal diffusion ratio $(k_T)_1$ for a gas of two components is given by

$$(k_T)_1 = 5(C - 1) \cdot \frac{s_1 n_{10} - s_2 n_{20}}{Q_1 n_{12} + Q_2 n_{21} + Q_{12}}, \quad . \quad . \quad . \quad (1)$$

where
$$s_1 = \frac{M_1^2 E}{(\mu_1)_1} - M_2\{3(M_2 - M_1) + 4M_1 A\},$$

$$s_2 = \frac{M_2^2 E}{(\mu_2)_1} - M_1\{3(M_1 - M_2) + 4M_2 A\},$$

$$Q_1 = \frac{M_1 E}{(\mu_1)_1} \cdot [6M_2^2 + 5M_1^2 - 4M_1^2 B + 8M_1 M_2 A],$$

with a similar expression for Q_2,

$$Q_{12} = 3(M_1 - M_2)^2(5 - 4B) + 4M_1 M_2 A(11 - 4B) + \frac{2E^2 M_1 M_2}{(\mu_1)_1(\mu_2)_1}$$

and $m_0 = m_1 + m_2,\ M_1 = m_1/m_0,\ M_2 = m_2/m_0,\ n_0 = n_1 + n_2;$

$n_{10} = n_1/n_0,\ n_{20} = n_2/n_0,\ n_{12} = n_1/n_2,\ n_{21} = n_2/n_1,$

where the *m*'s are the weights of the gas molecules and the *n*'s their number densities. $(\mu_1)_1$ and $(\mu_2)_1$ are the first approximations to the viscosities of the two components, given by $\frac{5kT}{8\Omega_2^2}$ in each case. The second approximation to the thermal diffusion ratio has not been given for the general case so that no estimate is readily made of the error to be expected by the use of $(k_T)_1$ for the 12 : 6 model except that it is likely to be less than 23 %.[10]

For diffusion we have the equations for the first and second approximations to the diffusion coefficient,

$$(D_{12})_1 = \frac{3E}{2nm_0}, \quad . \quad . \quad . \quad . \quad . \quad . \quad . \quad (2)$$

$$(D_{12})_2 = \frac{(D_{12})_1}{1 - \Delta}, \quad . \quad . \quad . \quad . \quad . \quad . \quad . \quad (3)$$

where
$$\Delta = \frac{5(C - 1)^2(P_1 n_{21} + P_2 n_{21} + P_{12})}{Q_1 n_{12} + Q_2 n_{21} + Q_{12}},$$

$$P_1 = \frac{M_1^3 E}{(\mu_1)_1};\ P_2 = \frac{M_2^3 E}{(\mu_2)_1};$$

$$P_{12} = 3(M_1 - M_2)^2 + 4M_1 M_2 A.$$

In the above equations,

$$A = \frac{\Omega_2^2}{5\Omega_1^1};\quad B = \frac{5\Omega_2^1 - \Omega_3^1}{5\Omega_1^1};$$

$$C = \frac{2\Omega_2^1}{5\Omega_1^1};\quad E = \frac{kT}{8M_1 M_2 \Omega_1^1};$$

and the various Ω_k^l refer to the interaction of a molecule of component 1 with one of component 2.

---

[9] Hirschfelder, Bird and Spotz, *ibid.*, 1948, 16, 968.

[10] Grew, *Proc. Roy. Soc. A*, 1941, 178, 390.

Molecular Model.—Values of functions bearing a close relationship to the various Ω_k^l, and of A, B and C for a wide range of $kT/E(0)$ have been tabulated by Hirschfelder *et al.*,[9] who wrote the interaction energy for two like molecules in the form

$$-E(r) = 4E(0)\left\{\left(\frac{r_0}{r}\right)^6 - \left(\frac{r_0}{r}\right)^{12}\right\}, \quad . \quad . \quad . \quad (4)$$

where r is the distance apart of the molecular centres, so that r_0 corresponds to the collision diameter for low velocity collisions. Using their tables and the appropriate Chapman-Enskog expression for $(\mu)_2$—the second approximation to the viscosity—they assigned values to $E(0)$ and r_0 for a number of gases, by fitting $(\mu)_2$ to the observed viscosity over a wide temperature range. In general, good agreement was found between calculated and observed values of the gas viscosities; for convenience of reference the values given by Hirschfelder, Bird and Spotz for $E(0)/k$ and r_0 for certain gases are reproduced in Table I.

TABLE I

Gas	$\frac{E(0)}{k}$	r_0(Å)
He	6·03	2·70
Ne	35·7	2·80
A	124	3·418
H_2	33·3	2·968
N_2	91·46	3·681
CO	110·3	3·590
O_2	113·2	3·433
CO_2	190	3·996
CH_4	136·5	3·822

Thermal Diffusion in Isotopic Gases.—When the gas consists of two components which are isotopic and of small mass difference, e.g. ^{20}Ne—^{22}Ne or $^{12}CH_4$—$^{13}CH_4$ eqn. (1) may be replaced by the general result obtained by Jones,[11]

$$\alpha = 45\left(\frac{m_2}{m_1} \quad \frac{m_1}{m_2}\right)\frac{(2\Omega_2^{\,1} - 5\Omega_1^{\,1})(15\Omega_1^{\,1} + 3\Omega_2^{\,2})}{3\Omega_2^{\,2}(165\Omega_1^{\,1} - 60\Omega_2^{\,1} + 12\Omega_3^{\,1} + 24\Omega_2^{\,2})}, \quad (5)$$

where α is defined by

$$\alpha = \frac{k_T}{c_1 c_2}, \quad . \quad . \quad . \quad . \quad . \quad (6)$$

where c_1 and c_2 are the concentrations of the two components ($c_1 + c_2 = 1$). Since to a close approximation isotopic molecules differ only in mass, the Ω_k^l of eqn. (5) will be those found by Hirschfelder *et al.* to describe the viscosity of the normal gas.

For the elastic sphere model we have, for isotopic molecules of the same radius,

$$\alpha_{e.s.} = \frac{105}{118}\cdot\frac{m_2 - m_1}{m_1 + m_2}, \quad . \quad . \quad . \quad . \quad . \quad (7)$$

so that we may conveniently use the function R_T,

$$R_T = \frac{\alpha}{\alpha_{e.s}}. \quad . \quad . \quad . \quad . \quad . \quad . \quad (8)$$

Using eqn. (5) and (7) together with the functions A, B, C and E given above, we see that

$$R_T = \frac{16{\cdot}9(C - 1)(1 + A)}{A(11 - 4B + 8A)}, \quad . \quad . \quad . \quad . \quad (9)$$

---

[11] Jones, *Physic. Rev.*, 1940, **58**, 111.

so that R_T is a function which is independent of the masses of the molecules and depends only on the law of molecular interaction. It should be noted that eqn. (5) is true only to a first approximation, being the first term in the expansion of eqn. (1) in powers of $\frac{(m_2 - m_1)}{m_2 + m_1}$; however, we have compared the two equations for small values (0·05 to 0·15) of this fraction and find the difference is negligible.*

Values of R_T calculated from eqn. (9) have been plotted against $kT/E(0)$ in Fig. 1 (the legend of which gives values of R_T for large values of $kT/E(0)$) and it is seen that the curve is very similar in form to that obtained for the 8 : 4 model by Jones.[2] The maximum value of R_T for isotopic gases on the 12 : 6 model is about 0·63 which is in much better agreement with observed values than the figure of 0·47 given by the 8 : 4 model. Since the only extensive figures upon the temperature variation of R_T for isotopic gases are those of Stier,[12] and since these do not agree with the results upon rare gas mixtures (cf. below) we do not consider that the accuracy of the 12 : 6 model can yet be assessed for the isotopic case.

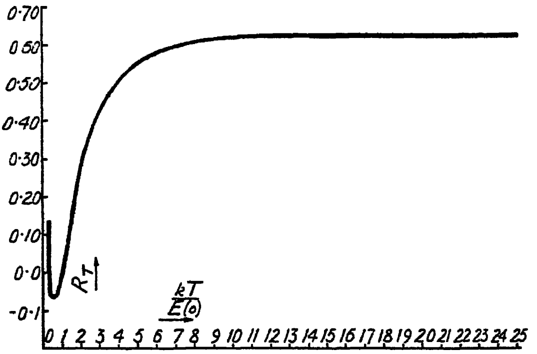

$\frac{kT}{E(0)}$	R_T
10	0·618
20	0·627
30	0·624
60	0·629
100	0·621
400	0·617

FIG. 1.—R_T as a function of $\frac{kT}{E(0)}$ for isotopic molecules of small mass difference.

The values of R_T predicted by eqn. (9) are compared with observation n Table II, where T_r is defined by [13]

$$T_r = \frac{T_1 T_2}{T_2 - T_1} \cdot \ln\left(\frac{T_2}{T_1}\right), \qquad . \quad . \quad . \quad (10)$$

T_2 and T_1 being the temperatures between which the thermal diffusion has been measured.

In order to calculate R_T and $(k_T)_1$ for H_2—D_2 mixtures an estimate of $E(0)$ and r_0 for the deuterium molecule had to be made, the mass difference for this case being so large that we cannot *assume* those constants are the same as for the more abundant isotope, which is what we have done for the other cases. However, from the viscosity data of Van Cleave and Maas [14] it appears that over the temperature range 150 to 350° K the viscosity of deuterium is moderately well represented if $E(0)$ and r_0 are given the values for ordinary hydrogen; the temperature range studied by Van Cleave and Maas is not extensive enough to allow a more accurate assignment and these values have therefore been used in our calculations.* We see that our values for R_T and $(k_T)_1$ are in excellent agreement with the work of Heath, Ibbs and Wild,[15] and with one of Murphey's figures,[16] although both ourselves and Ibbs disagree with Murphey's value for R_T at about 320° K; a redetermination at this temperature is clearly desirable. It may be noted that Grew[10] found that the value of k_T was approximately constant between 293° and 700° K, and also between 90° and 293° K; these measurements were not very extensive, but it is of interest that they do not agree with the theory or with Murphey's findings; further experimental work is necessary.

---

* More extensive calculations have been carried out by Dr. K. E. Grew (private communication).

[12] Stier, *Physic. Rev.*, 1942, **62**, 548. [13] Brown, *ibid.*, 1940, **58**, 661.

[14] Van Cleave and Maas, *Can. J. Res.*, 1935, **12**, 1.

TABLE II.—THERMAL DIFFUSION OF ISOTOPIC MOLECULES

Gas	% of Lighter Constituent	R_T		T_r° K	Ref.
		Obs.	Calc.		
H_2—D_2	50	0·583	0·587	327	15
„	~ 80·4	0·502	0·587	313	16
„	~ 80·4	0·445	0·463	118	16
^{20}Ne—^{22}Ne	90	0·382	0·485	129	12
„	90	0·550	0·592	238	12
„	90	0·713	0·620	432	12
„	90	0·816	0·627	712	12
^{36}A—^{40}A	0·307	0·0673	0·030	129	12
„	0·307	0·151	0·075	154	12
„	0·307	0·312	0·363	300	12
„	0·307	0·466	0·530	555	12
„	0·307	0·534	0·581	720	12
$^{12}CH_4$—$^{13}CH_4$	98·9	0·297	—	450	24
„	98·9	—	0·445	430	—
„	98·9	0·274	—	405	24
$^{32}O_2$—$^{34}O_2$	97·5	0·367	0·375	284	25
„	97·5	0·475	0·475	386	25
„	97·5	0·538	0·504	443	25
		$k_T \times 10^2$			
		Obs.	Calc.		
H_2—D_2	10	1·45	1·48	327	15
„	20	2·65	2·66	327	15
„	30	3·56	3·54	327	15
„	40	4·16	4·12	327	15
„	50	4·32	4·34	327	15
„	60	4·16	4·22	327	15
„	70	3·62	3·76	327	15
„	80	2·81	2·91	327	15
„	90	1·66	1·67	327	15

For argon and neon the calculations are compared with the results of Stier, whose figures for neon agree well with the earlier and less extensive work of Nier.[17] Only about two-thirds of Stier's results are quoted but this is sufficient to show the measure of agreement with our calculations.

---

* Since for H_2—D_2 mixtures $\frac{m_2 - m_1}{m_2 + m_1} = 0{\cdot}333$, eqn. (9) will not be a good approximation; the full equation (1) has therefore been used for this case.

[15] Heath, Ibbs and Wild, *Proc. Roy. Soc. A*, 1941, **178**, 380.

[16] Murphey, *Physic. Rev.*, 1947, **72**, 834.

[17] Nier, *ibid.*, 1940, **57**, 338 L.

We see that for both gases the agreement is very bad at low temperatures, is good in the middle of the temperature range, and becomes less satisfactory again at about 700° K. Stier found that his results for these two gases could be represented by the equation

$$R_T = 0{\cdot}25 \ln (T_r/b) \quad . \quad . \quad . \quad . \quad (11)$$

with $b = 26{\cdot}6$ for neon and $86{\cdot}9$ for argon; b is roughly proportional to the critical temperature.

The 12 : 6 model does not predict the linear relationship of eqn. (11) and Jones and Furry [3] have found a similar disagreement for the 8 : 4 model. The high temperature divergence of the 12 : 6 model is possibly due to the inaccuracy of the repulsive term in eqn. (4), since this will become more important as the molecular encounters become more energetic. The low temperature disagreement is due at least in part to the neglect of quantum mechanical effects. This question has been briefly discussed in general terms by Furry and Jones [3] who quote a correction factor, calculated for the elastic sphere model by Mott-Smith. Mott-Smith's correction factor adds a term

$$f(q) = \frac{25}{472} \cdot \frac{h}{d} \cdot \left(\frac{\pi}{mkT}\right)^{\frac{1}{2}} (c_2 - c_1) \quad . \quad . \quad . \quad (12)$$

to the right-hand side of eqn. (7), the sign being such that if it were the only term the rarer constituent would be more concentrated in the hotter part of the gas. In eqn. (12), h, k and T have their usual significance, m is the mean mass of the molecules, the c's are the concentrations of the two species and d is the molecular diameter. We see that if this correction factor were applied to our figures for the 12 : 6 model it would act in the correct sense, i.e. would decrease the calculated values of R_T for neon and increase them for argon. The size of this correction is, however, much too great if the elastic sphere diameter or values of r_0 from Table I are used; since no details of the derivation of eqn. (12) appear to have been published the discussion cannot be carried further at this stage. The agreement is good for oxygen, over the relatively restricted temperature range for which experimental figures are available; our three experimental results (Part I) fit a straight line of the same type as that for neon and argon:

$$R_T = 0{\cdot}37 \ln (T_r/110).$$

In general the predictions of the 12 : 6 model are definitely superior to those of all other models which have been examined. The inverse power and the Sutherland models are useful interpolation formulae provided that the exponent n of the former and the constant C of the latter are evaluated over the relevant temperature range from the viscosity of the gas; they have been discussed by Jones and Furry.[3]

The experimental values for methane are in serious disagreement with theory, and since all three models agree in predicting a higher value for R_T, a re-examination of this gas would be useful, and this is now being undertaken in these laboratories.

"Self-diffusion" in Gases.—The coefficient of self-diffusion proper is not observable experimentally; the nearest approach to its direct measurement is probably the work of Harteck and Schmidt [18] upon the inter-diffusion of ortho- and para-hydrogen. A very close approximation will be that obtained by measuring the inter-diffusion of two isotopic species of small mass difference and there has recently appeared an appreciable volume of work of this nature. A third method is the indirect one due to Kelvin,[1] in which the inter-diffusion of three dissimilar gases is studied, the gases being examined in pairs. From the resulting equations it is possible to deduce the self-diffusion coefficient of each gas.

---

[18] Harteck and Schmidt, *Z. Physik. Chem. B*, 1933, **21**, 447.

It has been usual to compare diffusion results with theory by writing

$$\left(\frac{\rho D_{11}}{\mu}\right)_{\text{obs.}} \approx \frac{\rho(D_{11})_1}{(\mu)_1} = 3A, \quad . \quad . \quad . \quad (13)$$

where ρ is the density of the gas. This expression is independent of pressure (except at very low pressures when the mean free path becomes large) and not very dependent upon temperature : A is given at the beginning of this paper, and may be calculated for the various molecular models. A closer comparison with theory could be made by using the second approximations to the viscosity and diffusion coefficients, but in general $\rho(D_{11})_2/(\mu)_2$ will differ from $3A$ by not more than 1 %. For cases when isotopic species of differing masses are used there is a further correction necessary to eqn. (13) since the experimental values of ρ and μ should be those corresponding to the mean gas composition during the course of the diffusion determination : in practice the values used appear to be those for the normal gas, i.e. one containing the natural isotope distribution. The correction to ρ and μ could readily be made and would involve in some cases the application of a correction factor of as much as 2-3 % to eqn. (13), but unfortunately the necessary concentrations are not given by some of the workers in this field. For this reason the observed values of the diffusion coefficients themselves are also compared with the calculated values of $(D_{11})_1$, since D_{11} is less dependent upon the gas composition than is the function $\rho D_{11}/\mu$. Table III compares theory with experiment for the cases that $E(0)$ and r_0 are known ; there are a few other experimental values of self-diffusion coefficients such as for UF_6, Xe and Kr, where these constants have not as yet been assigned.

TABLE III

Temperature		$\left(\frac{\rho D}{\mu}\right)_{\text{obs.}}$	$3A$	D_{11}		Ref.
Gas	°K			Obs.	Calc.	
H_2	293	1·37	1·33	1·285 ± 0·0025	1·243	18
,,	85	1·32	1·31	0·172 ± 0·008	0·167	18
,,	20·2	1·28	1·32	0·00816 ± 0·0002	0·0104	18
Ne	293	1·275	1·33	0·473 ± 0·002	0·491	26
A	295	1·31	1·31	0·178 ± 0·001	0·179	27
CH_4	293	1·33	1·31	0·174 ± 0·005	0·209	28
O_2	273	1·40	1·31	0·189	0·176	1
N_2	293	1·48	1·31	0·221 ± 0·009	0·199	35
CO	273	1·31	1·31	0·175	0·175	1
CO_2	273	1·49	1·32	0·104	0·092	1

All figures refer to a pressure of 760 mm. mercury, the experimental results being converted to that pressure on the assumption that the diffusion coefficient varies inversely with the pressure. We see that, with the exception of the figures for oxygen, nitrogen and carbon dioxide, the calculations are in reasonable agreement with observed figures. The values given in the table for oxygen and carbon dioxide were obtained by Kelvin's method from experiments upon the inter-diffusion of hydrogen, carbon monoxide, and oxygen or carbon dioxide ; that for nitrogen was obtained by following the diffusion of $^{14}N^{15}N$ molecules into normal nitrogen. We have recently measured the diffusion of $^{14}N^{15}N$, $^{16}O^{18}O$, and $C^{16}O^{18}O$, into the corresponding normal gases at two temperatures and find good agreement with theory for the first two gases ; carbon dioxide gives a high result, but not as high as Table III indicates ; these measurements will be reported in the next paper in this series.

Interaction of Unlike Molecules.—The calculation of the properties of gas mixtures cannot be performed until some estimate is made of the interaction energies for collisions between unlike molecules; these will be related to the corresponding energies for collisions between pairs of like molecules, but the type of relationship does not follow directly from eqn. (4). As Hirschfelder *et al.*[9] have pointed out, this problem is most easily approached by experimental determination of the diffusion coefficients of gas mixtures over a wide temperature range followed by a comparison of the results with the predictions of various interaction laws. In the absence of sufficient experimental results of this nature we must use other evidence to decide on the most probable form of the interaction energy. Since thermal diffusion ratios are much more dependent upon the form of interaction law used than are diffusion coefficients, the examination of the temperature variation of the former will provide a critical test of any chosen law. There exists a large body of suitable experimental figures upon the thermal diffusion of gas mixtures at many temperatures, but unfortunately the calculation of thermal diffusion ratios is laborious, and since no simple relationship exists between the assumed interaction law and the calculated thermal diffusion ratio we cannot use these experimental figures to find the correct interaction. In this paper we use only two of the many possible forms of interaction and show that one is far superior to the other, although even the best is not applicable to all the gas pairs examined.

Using the 8, 10 and 13½ : 4 models, Lennard-Jones and Cook[19] found that the isothermals of He—Ne and, less accurately, those of H_2—N_2 mixture could be accounted for by writing

$$\sigma_{12} = \frac{\sigma_{11} + \sigma_{22}}{2}, \quad . \quad . \quad . \quad . \quad . \quad (14)$$

where σ_{11} and σ_{22} are the collision diameters for the encounter of like molecules at 1° K and σ_{12} is the collision diameter for a pair of unlike molecules at the same temperature. These workers also used

$$\nu_{12}^{1/n} = \tfrac{1}{2}(\nu_{11}^{1/n} + \nu_{22}^{1/n}) \quad . \quad . \quad . \quad . \quad (15)$$

where n is the exponent of r in the equation

$$- E(r) = \frac{\mu}{r^4} - \frac{\nu}{r^n}. \quad . \quad . \quad . \quad . \quad (16)$$

Hirschfelder and Roseveare,[20] using the 12 : 6 model, found that the temperature variations of the low-pressure Joule-Thomson coefficients for several gas mixtures were excellently described by using eqn. (14) and

$$E(0)_{12} = \{E(0)_{11} \,.\, E(0)_{22}\}^{\frac{1}{2}}. \quad . \quad . \quad . \quad (17)$$

The same equations were found by Beattie and Stockmayer[21] to be satisfactory as a basis for calculating the second virial coefficients of methane–n-butane mixtures.

We will use these (empirical) equations (14) and (17), remarking that we may write (14) in our notation

$$r(0) = \frac{r(0)_{11} + r(0_{22})}{2} \qquad (18)$$

and also that for the gas mixtures which we shall consider, eqn. (18) is the same (to within better than 1 %) as

$$r(0)_{12} = \{r(0)_{11} \,.\, r(0)_{22}\}^{\frac{1}{2}} \quad . \quad . \quad . \quad . \quad (19)$$

---

[19] Lennard-Jones and Cook, *Proc. Roy. Soc. A*, 1927, **115**, 334.
[20] Hirschfelder and Roseveare, *J. Physic. Chem.*, 1939, 43, 15.
[21] Beattie and Stockmayer, *J. Chem. Physics*, 1942, **10**, 473.

The use of either eqn. (18) or (19) produces identical results in our calculations.

We also note that eqn. (17) is roughly equivalent to the procedure adopted by Grew,[4] who, following a suggestion by Jones,[2] plotted values of R_T for the rare gas mixtures against ln (T_r/T_c) where $T_c = (T_{1c}T_{2c})^{\frac{1}{2}}$, T_{1c} and T_{2c} being the critical temperatures of the two gases. Since we have the approximate relationship (ref. 5, p. 345) :

$$\frac{kT_c}{E(0)} = 1{\cdot}22 \quad . \quad . \quad . \quad . \quad . \quad (20)$$

for certain of the simple gases we would expect Grew's procedure to bring values of R_T for various gas mixtures on to one curve, as indeed it does to a fair approximation. The $E(0)$ of eqn. (20) is strictly that of the 12 : 6 model, and using the values assigned by (mainly) Lennard-Jones and Buckingham (column 4, Table IV) or by Hirschfelder *et al.* (column 3, Table IV), it is fairly true for O_2, N_2, Ne and A but does not apply for other gases, as is shown by Table IV. The procedure adopted by Grew is thus of limited use since quite a large shift is to be expected, for instance, in gas mixtures containing He or H_2 as one component.

TABLE IV

Gas	T_c° K	$\frac{kT_c}{E(0)}$(HBS)	$\frac{kT_c}{E(0)}$(BLJ)
H_2	33	0·997	1·08
He	5	0·8	0·834
Ne	44·3	1·24	1·25
A	151	1·22	1·26
O_2	154	1·36	1·31 *
N_2	126	1·38	1·31
CH_4	190·5	1·39	—
CO	134	1·22	1·41 †
CO_2	304	1·60	—

* Hirschfelder and Roseveare, *J. Physic. Chem.*, 1939, **43**, 15.
† Corner, *Proc. Physic. Soc.*, 1946, **58**, 737.

Thermal Diffusion in Gas Mixtures.—Using eqn. (17), (18), or (19) and Table I to obtain $E(0)_{12}$ and $r(0)_{12}$ in each case, we have calculated by means of eqn. (1) values of $(k_T)_1$ for a number of gas mixtures, the result being compared with the experimental figures in Table V for rare gas mixtures, and in Table VI for some other gas mixtures which were taken more or less at random from those which have been examined experimentally ; many more remain to be compared with theory. Since we wished to compare the observed values with those calculated, over a range of concentrations in many cases, we present the results in terms of k_T rather than in the more usual form of the thermal diffusion constant, α, which is very much less dependent upon concentration than is k_T.

Table VII gives for purposes of comparison some values of $(k_T)_1$ obtained by using the equation

$$E(0)_{12} = \frac{E(0)_{11} + E(0)_{22}}{2} \quad . \quad . \quad . \quad (21)$$

instead of eqn. (17) ; clearly the latter is to be preferred (cf. also ref.[3]).

We see that theory and experiment agree well for the rare gas mixtures in Table V, both the observed temperature variation and the concentration variation of k_T being faithfully followed by the use of eqn. (17) and (19) to evaluate the interaction energies and diameters. The only discrepancy of any magnitude is met with in the He—Ne mixtures where one set of workers get results above, and the other reports figures below, those calculated. Blüh[22] *et al.* also report figures higher than those of Grew; a careful re-examination of this pair of gases is desirable. In view of the good agreement for rare gas *mixtures* it is very surprising that for *isotopic* rare gases, e.g. Ne and A, Table II, there are much greater divergences in the corresponding temperature range: these differences are greater than the claimed experimental error, but since the work upon isotopic gases has been done by one worker only, whereas Grew's results upon rare gas mixtures are checked at several points by other workers, it is probably best to await further experimental material before finally assessing the 12 : 6 model.

Table VI shows less satisfactory agreement between observation and our calculations, although the general trend of k_T is satisfactory in all cases except that of N_2 and CO. The exact evaluation of $E(0)_{12}$ for these and other mixtures will probably have to await the determination of D_{12} over a wide temperature range. Since in all cases (except for N_2—CO) where there is serious disagreement in Table VI a relatively small change of $E(0)_{12}$ would bring the results into line, it is evident that eqn. (17) and (19) are not far from the truth for the gases so far examined.

TABLE V.—RARE GAS MIXTURES

Gas	% of Lighter Constituent	$k_T \times 10^2$		T_r° K	Ref.
		Obs.	Calc.		
He—Ne	53·8	7·65	8·15	205	4
,,	53·8	7·82	8·28	330	4
,,	53·8	7·83	8·39	365	4
,,	20	5·31	4·53	330	29
,,	30	7·24	6·21	330	29
,,	40	8·64	7·45	330	29
,,	50	9·70	8·15	330	29
,,	60	10·04	8·26	330	29
He—A	51·2	9·10	9·44	179	4
,,	51·2	9·20	9·57	205	4
,,	51·2	9·56	9·61	365	4
,,	10	2·50	2·59	330	29
,,	20	4·76	4·94	330	29
,,	30	6·60	6·98	330	29
,,	40	8·10	8·93	330	29
,,	50	9·31	9·79	330	29
Ne—A	51·2	3·50	3·47	179	4
,,	51·2	3·80	3·85	205	4
,,	51·2	4·15	4·25	261	4
,,	51·2	4·77	4·90	406	4
,,	20	2·33	2·57	324	29
,,	30	3·39	3·53	324	29
,,	40	4·07	4·24	324	29
,,	50	4·57	4·63	324	29
,,	60	4·67	4·68	324	29

Mention must also be made of a recent paper by Waldman[23] who has examined the thermal diffusion of $A—O_2$, $A—N_2$, and $O_2—N_2$ mixtures at low temperatures and reports a change of sign of α for $A—O_2$ and $A—N_2$ mixtures between 89° and 293° K. The sign of α is determined by the value of C in eqn. (1), and we find that these observations are in agreement with eqn. (17) since at 89° K, $\left(\frac{kT}{E(0)}\right)_{O_2/A} = 0{\cdot}752$ and

---

[22] Blüh and Puschner, *Phil. Mag.*, 1937, **24**, 1103.

[23] Waldman, *Z. Naturforsch. A*, 1947, **2**, 358.

$C = 0{\cdot}9897$, while $\left(\frac{kT}{E(0)}\right)_{N_2/A} = 0{\cdot}836$ and $C = 0{\cdot}9939$, but at 293° K, $C > 1$ in both cases. Waldman also finds no detectable separation of

TABLE VI.—OTHER GAS MIXTURES

Gas	% of Lighter Constituent	$k_T \times 10^2$		T_r° K	Ref.
		Obs.	Calc.		
H_2—He	22·2	2·39	1·98	46	30
,,	81	2·03	2·38	118	16
,,	81	1·79	2·31	358	16
,,	50	4·81	3·74	330	15
,,	60	4·42	3·56	330	15
,,	70	3·50	3·08	330	15
,,	80	2·84	2·31	330	15
,,	90	1·32	1·29	330	15
H_2—A	47	5·14	5·89	167	31
,,	55·6	5·73	6·25	167	31
,,	47	6·35	7·71	258	31
,,	55·6	7·12	8·17	258	31
N_2—He	34·5	7·42	7·12	145	32
,,	53·1	9·42	9·23	145	32
,,	34·5	8·31	7·65	261	32
,,	53·1	10·7 *	9·92	261	32
N_2—A	46	1·01	0·624	157	31
,,	62·5	0·842	0·596	157	31
,,	70	0·83	0·536	157	31
,,	46	1·82	1·32	252	31
,,	62·5	1·70	1·28	252	31
,,	70	1·53	1·16	252	31
H_2—N_2	29·4	3·95	3·97	143	31
,,	42·0	5·21	5·01	143	31
,,	77·5	4·84	4·44	143	31
,,	29·4	5·48	5·90	264	31
,,	42·0	7·49	7·37	264	31
,,	77·5	6·63	6·36	264	31
H_2—CO_2	53	6·89	8·39	300	33
,,	53	8·99	9·60	370	33
H_2—CO	24	3·70	3·21	142	31
,,	53	5·83	5·08	142	31
,,	24	4·45	4·81	246	31
,,	53	7·38	7·66	246	31
N_2—CO	50	1·53	0·05	324	34

* By extrapolation.

TABLE VII

Gas	of Lighter Constituent				T_r° K
		Obs.	Calc. eqn. (17)	Calc. eqn. (21)	
He—Ne	53·8	7·65	8·15	8·30	205
,,	53·8	7·82	8·28	8·43	330
He—A	51·2	9·10	9·44	6·75	179
,,	50	9·31	9·79	8·97	330
Ne—A	51·2	3·50	3·47	2·90	179
,,	51·2	4·15	4·25	2·94	261

O_2—N_2 mixtures at 89° K and this also is borne out by the theory, since here $\left(\frac{kT}{E(0)}\right)_{N_2/O_2} = 0{\cdot}875$, and $C = 0{\cdot}9963$ so that $\alpha \approx 0$, the mass difference being small.

TABLE VIII.—DIFFUSION CONSTANTS FOR GAS MIXTURES (cm.^{2}/sec.)

Gas	D_{12}(obs.)	$(D_{12})_1$	$(D_{12})_2$
H_2—CO_2 (3/1)	0·594	—	0·550
,, (1/1)	0·605	0·545	0·553
,, (1/3)	0·633	—	0·555
H_2—CO (1/1)	0·651	0·662	0·674
H_2—N_2 (1/1)	0·674	0·658	—
H_2—CH_4 (1/1)	0·625	0·619	0·628
N_2—CO (1/1)	0·192	0·173	0·174
He—A (1/1)	0·641	0·633	—

Diffusion in Gas Mixtures.—Using eqn. (17) and (19), (2) and (3), the coefficients of diffusion for certain gas mixtures have been calculated and are compared with the observed values in Table VIII. No attempt at a detailed comparison has been made, the experimental values being taken from Chapman and Cowling (p. 252) who state they are mainly average values, reduced to 273° K and 1 atm. In view of the difficulty of measuring the diffusion coefficients the agreement found in Table VIII may be regarded as satisfactory and as a further confirmation of the general correctness of eqn. (17) and (19), the largest difference being found for hydrogen-carbon dioxide; the experimental value for N_2—CO may well be inaccurate since these two gases are very similar and their self-diffusion coefficients are both about 0·175 cm.^{2}/sec.$^{-1}$ at N.T.P.

Inorganic and Physical Chemistry Department,
Imperial College,
London, S.W.7.

[24] Nier, *Physic. Rev.*, 1939, **56**, 1009.
[25] Whalley and Winter, *Trans. Faraday Soc.*, 1949, **45**, 1091.
[26] Groth and Sussner, *Z. physik. Chem.*, 1944, **193**, 296.
[27] Hutchinson, *Physic. Rev.*, 1947, **72**, 1256.
[28] Winn and Ney, *ibid.*, 1947, **72**, 77.
Atkins, Bastick and Ibbs, *Proc. Roy. Soc. A*, 1939, **172**, 142.
Van Itterbeck, van Paemel and van Lierde, *Physica*, 1947, **13**, 231.
Ibbs, Grew and Hirst, *Proc. Physic. Soc.*, 1929, **41**, 456.
Ibbs and Grew, *ibid.*, 1931, **43**, 142.
Bastick, Heath and Ibbs, *Proc. Roy. Soc. A*, 1939, **173**, 543.
Ibbs and Underwood, *Proc. Physic. Soc.*, 1927, **39**, 227.
[35] Winn, *Physic. Rev.*, 1948, **73**, 698 L.

THE IMPORTANCE OF SURFACE OXIDE FILMS IN THE FRICTION AND LUBRICATION OF METALS

PART I.—THE DRY FRICTION OF SURFACES FRESHLY EXPOSED TO AIR

By E. D. Tingle

Received 22nd June, 1949; as amended 25th October, 1949

A new " cutting " technique of surface preparation is used to demonstrate the effect of the surface oxide film on the friction and lubrication of metals. With unlubricated surfaces the oxide film generally produces a marked reduction in friction even though the period of exposure to the atmosphere of a freshly cut surface is only a few seconds. With subsequent growth of the film there is further reduction but the effect is less marked. The experiments indicate that the thin layer of oxide immediately adjacent to the surface plays a more significant part in reducing the friction than the thicker layers of oxide above it.

The experiments with lubricated surfaces emphasize the importance of chemical attack in boundary lubrication by fatty acids and demonstrate the essential part played by the oxide film in the formation of the lubricating layer. The combined action of water and atmospheric oxygen on the surface of a reactive metal is often able to produce a penetrable film which will react with a fatty acid to give an effective lubricating layer. On the basis of these experiments the lubricating properties of long chain fatty acids on three main classes of metals is explained.

Most metals when " cleaned " in air are covered with a surface film of oxide. This fact has not always been sufficiently considered when interpreting what happens when metals, dry or lubricated, slide over one another at slow speeds and under heavy loads. This paper describes an investigation of the effect of oxide films on the friction of metal surfaces sliding under these conditions. The first part deals with clean unlubricated surfaces, the second with surfaces which are lubricated with a thin " boundary " film of a polar, long-chain, carbon compound.

Experimental

Apparatus.—The Bowden-Leben apparatus was used throughout this investigation to study the friction between the sliding surfaces. This apparatus has been fully described elsewhere.[1] In essence it comprises a lower plane surface moving horizontally at controlled slow speeds against which is pressed, by a known load, an upper hemispherical slider of the same material. The slider is held in a light metal arm mounted on a bifilar suspension of stretched wires. The elastic deflection of the arm measures the friction, the low inertia and high natural frequency of the measuring system ensuring response to rapid fluctuations in the frictional force.

In this investigation the normal loading of the surface was 4 kg. and the speed of the lower plane surface was low, usually 0·01 cm./sec. At this low speed of relative movement the temperature rise due to frictional heating of the surfaces is negligibly small.

Preparation of Surfaces.—Apart from variation due to normal loading, relative sliding speeds and temperature, the friction between surfaces rubbing together dry or under conditions of boundary lubrication depends in an incompletely known way on several different surface conditions. A slight variation in one of these surface conditions may have a profound effect on the coefficient of friction. This is almost certainly the reason for the discrepancies in the coefficients of friction recorded in the literature and for the frequent wide scatter of results in experimental measurement. It is therefore important that frictional measurements should be reported with a detailed account of the preparation of the surfaces and the conditions under which the measurements were made It is of equal importance to adopt a technique of preparation that reduces possible variation in surface conditions to a minimum

---

[1] Bowden and Leben, *Proc. Roy. Soc. A*, 1939, **169**, 371.

The following simple method for preparing the surfaces was found to give reproducible results and was used throughout the investigation —

(1) Removal of heavy grease contamination by immersion in an *iso*propyl-ether acetone vapour bath

(2) Abrasion of the lower plane surfaces on a medium grade abrasive paper (Hydrodurexil 320) under a rapid stream of cold water The abrasion is carried out so as to leave the scratches all at right-angles to the future direction of sliding This is followed by thorough washing in a stream of carefully distilled water The surface is grease-free when water will spread over it in a continuous film which thins by drainage to give interference colours Finally the surface is dried by wiping lightly with clean filter paper

(3) Preparation of the upper slider by rotating it rapidly against fine abrasive paper (Hydrodurexil 600)

After preparation care was taken to manipulate both the surfaces with degreased implements only

The "Cutting" Technique of Surface Preparation.—It is clearly an advantage to know fairly precisely the period during which surfaces used in frictional measurements have been exposed to the surrounding atmosphere This was achieved by laying bare a smooth shallow track on the lower metal surface by means of a specially designed cutting tool The upper surface (slider) used in the measurement of friction passed over this track immediately behind the cutting tool so that the interval between exposure of the metal and measurement of friction was very short It was determined by the distance of the cutting edge from the point of contact of the slider and by the speed of the lower surface A diagram of the experimental arrangement is shown in Fig 1(*b*) The photograph (Fig 1(*a*)) shows the tool in position while cutting a track on the lower test surface

A tungsten carbide tipped tool clamped in a massive adjustable arm gave the best results A smooth shallow track, 0 4 cm wide and approximately 0 002 cm deep could be made at speeds from 0 01 to 0 1 cm /sec

The cutting technique was used in two main investigations —

(*a*) A study of the friction of newly cut metal surfaces exposed to the laboratory atmosphere for periods from 4 to 40 sec (Part I)

(*b*) An investigation of the ability of a lubricant to reduce the friction of surfaces freshly cleaned of all contaminant films (Part II) Tracks were cut under a pool of the applied lubricant In this case the perfectly clean metal surface could absorb only those substances which were present in the lubricant solution

The technique of cutting tracks on a metal surface described above was used to measure the friction on surfaces which had been exposed to air for small known periods after the track had been formed The results were compared with frictional measurements on abraded surfaces as normally prepared

Lower surfaces of copper, iron, cadmium and magnesium of high purity were used with sliders of the same metal as the lower surface All the surfaces were prepared grease free by the method described above

The tool was adjusted to make a shallow cut on the surface sliding beneath it a short distance ahead of the point of contact of the slider Comparison between the friction on the abraded and the cut surface was made simply by moving the slider from the cut track onto an uncut portion of the lower surface These comparisons were always made at the same sliding speed The tungsten carbide tipped tool gave very satisfactory results for cadmium and magnesium but there was some difficulty in producing smooth tracks on copper, aluminium and iron, particularly at higher speeds

Results

The Friction of Unlubricated Surfaces.—The results of the experiments are given in the Table (p 95) where comparisons between the abraded and the cut surfaces are made at sliding speeds of 0 01 and 0 1 cm /sec The distance between the cutting edge and the point of contact of the slider was 4 mm Consequently the periods of exposure to the atmosphere of the freshly cut surface at the two speeds were 40 and 4 sec respectively

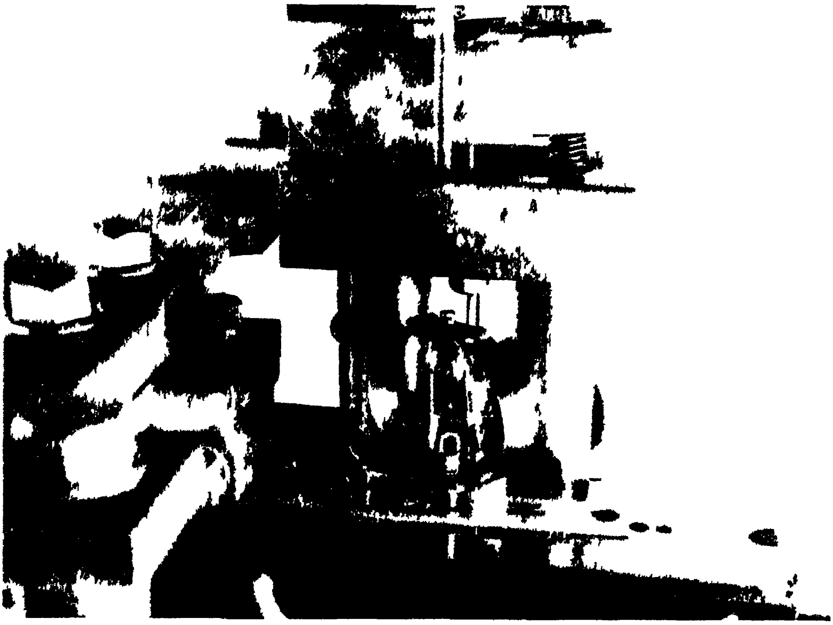

FIG 1(*a*)

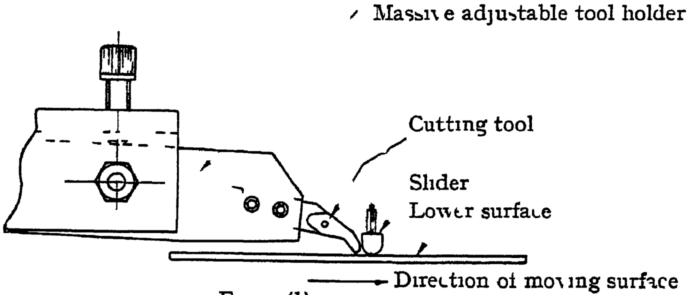

FIG 1(*b*)

[To face page 94

TABLE I.—COEFFICIENT OF FRICTION ON CUT AND ABRADED SURFACES

Metal	Sliding Speed 0·01 cm./sec. Exposure Time 40 sec.		Sliding Speed 0·1 cm./sec. Exposure Time 4 sec.	
	Abraded Surface $\mu_{max.}$	Cut Surface $\mu_{max.}$	Abraded Surface $\mu_{max.}$	Cut Surface $\mu_{max.}$
Copper . . .	1·20	1·40	1·40	1·60
Cadmium . .	0·50	0·50	0·50	0·60
Magnesium . .	0·50	0·60	0·45	0·50
Aluminium . .	1·15	1·10	—	—
Dural * . . .	0·70	0·75	0·70	0·80
Iron . . .	0·60	0·65	—	—

* Composition of Dural is 4 % Cu, 0·5 % Mg, 0·5 % Mn, remainder Al.

Sliding on the surfaces was usually of the stick-slip type, merging in some cases into the type of sliding in which the coefficient of friction fluctuates irregularly. The coefficient of friction ($\mu_{max.}$) recorded in the Table is that at the highest point of the stick or at the maximum value reached in the irregular fluctuations.

Discussion

The results show that for all the metals examined the friction on the cut surface is at most only a little higher than that observed for the abraded surface; nor is there much difference between the cut tracks exposed for 4 sec. and 40 sec.

Experiments by Bowden and Hughes,[2] and by Holm and Kirchstein [3] have shown that the oxide film formed on metals is the main agent in reducing the coefficients of friction to the value observed between normally clean metals. If this film is removed the value of the coefficient of friction is much higher (e.g. for outgassed copper surfaces Bowden and Hughes find that the coefficient becomes 4·8). The fact that coefficients of friction of this magnitude were not obtained in any of the experiments using freshly cut surfaces would therefore indicate than an oxide film capable of reducing the perfectly clean metal friction to the value for normally prepared surfaces is formed very rapidly. In the above experiments such a film is formed in less than 4 sec. on the metals examined. This is in agreement with the observation by Bowden and Hughes that a small quantity of oxygen admitted to outgassed copper surfaces reduces the coefficient of friction from 4·8 to 2·4 in a very short time.

Several workers (e.g. Evans and Miley,[4] Campbell and Thomas [5]) have investigated the growth of oxide films on copper exposed to air. Their techniques, however, could not be used to measure the thickness of oxide formed in the short periods involved in the present experiments. The thickness of these films must therefore remain a matter for conjecture. The thickness of oxide formed on a surface of copper abraded on fine emery under water has been measured by Campbell and Thomas.[5] From their figures we may conclude that the abraded surfaces used in the experiments have an oxide layer in the region of 40 Å thick. The thickness of the oxide films formed on the cut tracks will presumably be smaller than this.

Data relating oxide film thickness on copper and the coefficient of dry friction are collected in Table II where results obtained by the author are compared with those of other workers.

[2] Bowden and Hughes, *Proc. Roy. Soc. A*, 1939, **172**, 263.

[3] Holm and Kirchstein, *Wiss. Veroff. Siemens-Werk*, 1936, **15**, 122.

[4] Evans and Miley, *Nature*, 1937, **139**, 283

[5] Campbell and Thomas, *ibid.*, 1938, **142**, 253.

These results for copper show that by far the greatest reduction in the coefficient of friction occurs as the oxide film thickens from 0 to 40 Å. The rate of reduction with increasing thickness then becomes much slower and probably becomes zero at visible oxide thicknesses.

The reduction of the high values of friction between metal surfaces by oxide films can be readily explained in terms of the theory of metallic friction developed by Bowden and co-workers.[7] This theory suggests that the frictional resistance between both unlubricated and lubricated metals is due primarily to the shearing of metallic junctions formed by adhesion and welding at the points of contact. Where a film of foreign material is present on the metal surface it will bear part of the normal load. The amount of intimate metallic contact is reduced by a greater or less extent depending upon the mechanical properties of this film material. The resistance to motion is then the force necessary to shear junctions of metal and of the material of the film. If A is the area which supports the applied load, α is the fraction of the area over which complete metal-metal contact occurs and S_m, S are the shear strengths of the metal and of the film material we may write

$$F = A(\alpha S_m + (1 - \alpha)S). \quad . \quad . \quad . \quad . \quad (1)$$

There are then two possible causes of the reduction of F by the oxide film. If it be first assumed that the shear strength of the oxide is less than that of the metal, then the friction reduction can be brought about simply by reducing the total area over which metal-metal contact can occur by a fraction $1 - \alpha$. Alternatively the presence of the film may lead to formation of welded junctions which contain small " inclusions " of oxide. These might be expected to reduce the value of S_m in eqn. (1) above. It is possible that both mechanisms are operative.

We may now consider why a very thick oxide layer is little better in reducing friction than a very much thinner layer. Several investigations have shown (see Evans,[8] Chalmers and Quarrel[9]) that the thin layer of oxide immediately adjacent to the metal surface has different structural and mechanical properties from the layers formed above it. It is possible

TABLE II.—FRICTION OF COPPER SURFACES

Surface Treatment	Thickness of Oxide Film Å	Coeff. of Dry Friction	Coeff. of Dry Friction by Other Workers
Carefully outgassed . .	0	—	4·8 Bowden and Hughes [2]
Carefully outgassed, trace of oxygen admitted .	<40	—	2·4 Bowden and Hughes [2]
Cut surface exposed to air for 4 sec. . . .	<40	1·6	—
Cut surface exposed to air for 40 sec. . . .	<40	1·4	—
Abraded under water .	40	1·2	1·21 Campbell [6]
Heated to give thick oxide film *	1000	0·80	0·76 Campbell [6]

* The surface was heated in an air oven at 200° C until an even 2nd order yellow interference film of oxide was obtained. This film has a thickness[10] of approx. 1000 Å.

---

[6] Campbell, *Proc. Conf. Friction and Surface Finish* (M.I.T., 1940), 197.

[7] Bowden and Tabor, *Ann. Reports*, 1945, **42**, 20.

[8] Evans, *Symposium on Internal Stress in Metals and Alloys* (Inst. of Metals, 1947), p. 291.

[9] Chalmers and Quarrel, *Physical Examination of Metals*, Vol. II (Arnold, London, 1941).

therefore that this thin film has a much higher resistance to penetration than the crystalline oxide above it. The value of α in eqn. (1) may therefore be little affected when a relatively thick layer of oxide is formed above the primary thin surface-film. This would explain why a protective film capable of producing the major reduction in friction is so rapidly formed in the cutting experiment. The explanation is probably true for all the metals examined.

In any system where unlubricated metals slide on one another the rate of formation of the oxide film may have an important effect on the frictional behaviour. In sliding, contaminant films will be worn away and the shearing of minute metal junctions will expose fresh metal surfaces which give high friction and surface damage. If the rate of production of the friction lowering oxide film is less than that of the formation of naked metal, the above effect will be cumulative. The experiments show, however, that very small degrees of oxidation of metal surface lead to considerable lowering of the friction.

These results have a bearing on many metal-forming operations. In the dry cutting of metals one of the causes of poor finish is the formation of too large a " build-up edge " of cut metal welded to the nose of the cutting tool. Ernst and Merchant [10] have shown that it is the high friction between the tool and the freshly cut metal that facilitates and perpetuates the existence of the built-up edge. The experiments described above in which this high friction between a metal and a newly exposed surface of the same metal is measured have an obvious bearing on the problem.

PART II. THE FORMATION OF LUBRICATING FILMS ON METAL SURFACES

Bowden, Gregory and Tabor [11] have pointed out the importance of chemical reaction with the surface when long-chain fatty acids lubricate metals. Long-chain materials, when present as a solid film, reduce to a low value the friction between metal surfaces sliding under boundary conditions. This is true for all classes of such materials. Substances which are not normally able to react chemically with a metal, such as long-chain paraffins, alcohols and esters, only provide effective lubrication * while solid. On melting, the friction rises sharply, the sliding becomes irregular and damage of the surface increases abruptly. The same result is obtained with a fatty acid on a non-reactive surface. On the other hand, on a metal surface with which reaction can occur, a fatty acid will maintain low friction to temperatures considerably above its bulk melting point. This behaviour occurs not only with pure fatty acid but also with solutions as dilute as 0·1 % by weight. This has been explained by assuming that a surface film of a soap, which has a higher melting point than the acid from which it is derived, is formed by reaction with the metal. The transition from low friction to a much higher friction occurs when the soap film loses its solid structure, i.e. at a temperature considerably higher than the melting point of the acid.

A dilute solution of lauric acid ($C_{11}H_{23}COOH$) in a non-polar solvent such as liquid paraffin B.P. will provide good lubrication (coeff. of friction $\mu = 0{\cdot}1$) of copper surfaces to a temperature of approximately 110° C, which is well above the melting point (43° C) of the acid.[11] Since copper is an electro-positive metal the acid cannot react directly with the metal. Soap formation must, presumably, take place by reaction of the acid with the surface oxide layer. This assumption is supported by the work of Dubrisay[12] and Prutton[13] on the corrosion of metals by solutions of organic acids. If this view is correct, we should expect that a solution of lauric acid would not prove an effective lubricant on a copper surface from which the oxide layer has been removed.[14]

---

[10] Ernst and Merchant, *Proc. Conf. Friction and Surface Finish* (M.I.T., 1940), 76.

* Throughout this paper lubrication is considered effective only when sliding is smooth and the coefficient of friction μ is below 0·15.

[11] Bowden, Gregory and Tabor, *Nature*, 1945, **156**, 97.

Experimental and Results

The Lubrication of Freshly Exposed Metal Surfaces.—The following experiments were designed in the first place to test the hypothesis of soap formation by investigating the lubricating ability of a dilute fatty acid solution (1 % by weight of pure lauric acid in liquid paraffin B.P., a highly refined white mineral oil) on a copper surface from which the existing oxide film had been removed. A diamond-edged cutting tool laid bare a smooth shallow track on the lower copper surface under a pool of the lubricant solution. In this way the oxide-free surface was covered with lubricant without at any time being exposed to the air.* The friction between this surface and a slider of the same metal was then measured in the usual way.

It was found that the coefficient of friction μ measured in this experiment was very high ($\mu = 0{\cdot}7$-$1{\cdot}2$), the sliding was irregular in nature and the damage of the sliding surfaces very extensive. The friction remained high while the lower surface was heated to 100° C. Surfaces of copper for frictional measurements had normally been prepared by abrading on emery paper under water to remove grease; they were then washed in a stream of hot water for a short time and allowed to dry in air. A surface prepared in this way is successfully lubricated by the lauric acid solution under the same conditions of loading and speed of sliding as used in the experiment above. The friction is low ($\mu = 0{\cdot}1$) and sliding is smooth.

The explanation of the high friction when the fatty acid solution failed to lubricate the naked copper surface would appear to be simply that the acid cannot react directly with the metal. Thus the soap film which, it has been suggested, is essential for this type of lubrication, is not formed. Further experiments, however, showed the phenomenon to be one of greater complexity.

Conditions for Effective Lubrication.—A track bared by the cutting-tool on copper was exposed to the atmosphere for periods up to 24 hr. Under these conditions a surface oxide layer up to 100 Å thick is formed. Fatty acid solution applied to this surface did not give effective lubrication. Considerably thicker films of oxide (up to *ca.* 1000 Å thick) were prepared by heating identically prepared copper surfaces for increasing periods at 140° C followed by cooling to room temperature in a vacuum desiccator. None of these surfaces was lubricated by the fatty acid solution nor were surfaces prepared simply by abrasion under cold water. Only those copper surfaces which had been washed by boiling water for about 2 min. after abrasion gave the characteristic smooth sliding and low friction ($\mu = 0{\cdot}1$) with fatty acid solution. A cut track on copper could be similarly lubricated if exposed to the action of boiling water for not less than 2 min.

The experiments were then extended to a wide range of reactive and non-reactive metals. The friction was measured when fatty acid solutions were applied to surfaces prepared in three ways:

A. Surfaces abraded on fine emery paper under cold water and then washed with hot water.

B. Surfaces from which existing surface oxide film had been removed by cutting under a pool of the lubricant.

C. Tracks cut in air and then washed with cold, warm or boiling distilled water for varying periods until lubrication could be effected. The temperature of the water and the period of washing depended upon the metal.

The comparisons were made on the same test-pieces and under the same conditions simply by moving the slider to different regions of the lower surface while it was in motion. The results of these experiments are shown graphically in Fig. 2.

For the metals magnesium, cadmium, zinc, copper and iron the friction on the surface freed from surface oxide films (B) is much higher than on the abraded surface (A) or on the cut tracks which had been suitably wetted (C). The sliding on surface B is irregular and there is considerable plucking and tearing of the surface. It is clear then, that the surface film formed by the action of the atmosphere and water plays an important role in the effective lubrication of these metals, whether electronegative or electropositive. Aluminium shows a similar effect, although of a different magnitude. The friction with lubricant on the abraded surface is higher than with the metals already mentioned. However, the cut track (B) again shows a higher friction than the abraded surface (A) or the washed track (C). Bismuth is an exception to the general trend: the friction on the surface cut under the lubricant is lower than that on the abraded surface. As might be expected, with platinum and silver, where reaction in any case is impossible, the friction is high and has roughly the same value on surfaces prepared in the three different ways.

---

[12] Dubrisay, *Compt. rend.* 1940, **210**, 533.

[13] Prutton, *Ind. Eng. Chem.*, 1945, **37**, 901. [14] Tingle, *Nature*, 1947, **160**, 710.

* There is, of course, the possibility of slight surface oxidation by dissolved oxygen. Even so the oxide film will be formed under anhydrous conditions (see later).

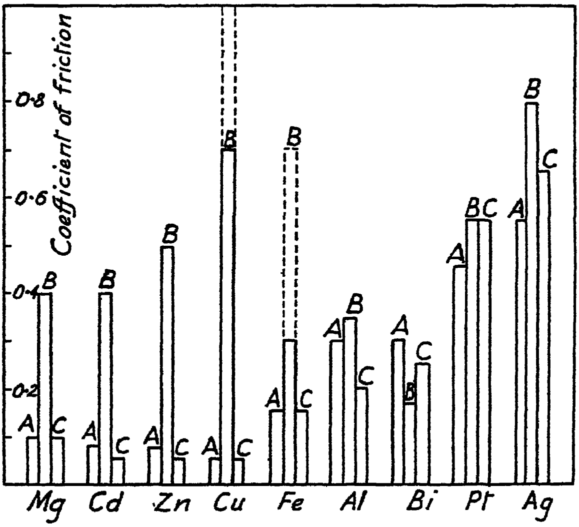

FIG. 2.—Friction of metals lubricated by 1 % lauric acid solution.
A—abraded surface, B—surface cut under lubricant, C—cut surface, wetted

TABLE III.—THE COEFFICIENT OF FRICTION OF SURFACES LUBRICATED WITH IN PARAFFIN OIL

Surface abraded under dry . . .	Cu	Cd	Mg	Steel	Bi
Kerosene . . .	1·2	0·3→0·50	0·40	0·40	0·3→0·4
Benzene . . .	1·2	0·30	—	—	—
Paraffin oil . .	0·7→1·0	—	—	—	—
Surface cut under lubricant . .	0·7→1·2	0·40	0·40	0·3→0·7	0·17

The conclusion that the action of water plays an important part in determining the effectiveness of lubrication of metals by fatty acids is borne out by a supplementary series of experiments. In these the lower test surface was prepared by abrading on the standard abrasive paper under the surface of a non-polar organic liquid that had been carefully dried over sodium wire. Kerosene, benzene and medicinal paraffin B.P. were used in this way. After abrasion, the surfaces were washed with some of the clean dry liquid. Excess liquid was then shaken off and the 1 % solution of fatty acid in paraffin oil applied without the metal surfaces having been exposed directly to the air. The friction was then measured in the usual manner. Results are given in Table III.

In these experiments, lubrication is again ineffective. The surfaces will almost certainly have an oxide layer, formed by attack from dissolved oxygen. For example, Campbell [3] finds that a copper surface freshly abraded under benzene has an oxide film of 37 Å thickness upon it. This oxide layer, however, will have been formed in the present experiments without the presence of water at any stage.

Discussion

It is clear from all these experiments that effective lubrication by fatty acid solutions depends upon the presence on the surface of the metal of a suitable oxide or hydroxide film. The observation has an important bearing on the boundary lubrication by fatty acid solutions of the metals examined. Where sliding takes place over the same portion of the surface (as in a journal and bearing), and boundary conditions prevail, abrasion of the surface will occur by continuous shearing of the minute metallic junctions formed through the lubricant film. Consequently the sliding process will give rise continuously to freshly exposed metal which, as we have seen, is not lubricated by the fatty acid solution. Effective lubrication occurs only when a film is formed capable of reacting with the fatty acid. Lubrication of the metal freshly exposed by the sliding process will remain poor until such a film is reformed upon it. The second observation of importance is that under the experimental conditions described only those surfaces which had been in contact with water at some stage of their preparation could be efficiently lubricated. Water appears to play an important part in the formation of a surface film which by reaction with the fatty acid will provide an efficient lubricating layer.

The Formation of the Lubricating Layer by Fatty Acids.—In order to discuss further the part played by water in the formation of an effective boundary lubricating layer we may consider some recent work which has thrown light on the ability of fatty acids to provide such a layer.

Several experimenters (Bowden and Leben,[15] Hughes and Whittingham,[16] Frewing [17]) using the Bowden-Leben apparatus and working with conditions of load and speed similar to those of the present investigation, have observed that a deposited monolayer reduces the friction as much as a thick layer interposed between the rubbing surfaces. It is noticeable, however, that all these workers used steel surfaces. Some more recent work by Gregory and Spink,[18] and by Greenhill,[19] has thrown doubt upon the effectiveness of the primary monolayer on other metal surfaces. Greenhill found that a deposited monolayer of soap would lubricate a steel surface but that all other metals examined required more than a single layer before lubrication was effective. Copper, nickel and silver required three layers, while platinum required about nine layers.

We have seen that long-chain paraffins, esters and alcohols provide effective boundary lubrication while present between the sliding surfaces as a solid film. When the temperature is raised to the melting point of these compounds there is a sharply defined breakdown in lubricating ability * despite the fact that, as shown by Zisman and co-workers,[20, 21] monolayers of such compounds may exist on a metal surface at temperatures above their bulk melting points. This is consistent with Greenhill's results that non-ferrous metals require more than a monolayer before lubrication is effective.

---

[15] Bowden and Leben, *Phil. Trans. A*, 1940, **239**, 1.

[16] Hughes and Whittingham, *Trans. Faraday Soc.*, 1942, **38**, 9.

[17] Frewing, *Proc. Roy. Soc. A*, 1942, **181**, 23.

[18] Gregory and Spink, *Nature*, 1947, **159**, 403.

[19] Greenhill, *Trans. Faraday Soc.* 1949, **45**, 631.

* On steel and iron surfaces, long-chain esters and alcohols maintain effective lubrication above their bulk melting point. This anomalous behaviour of ferrous metals which may be connected with their ability to be lubricated by a single adsorbed monolayer of long-chain carbon compounds is discussed in a communication to be published shortly.

A long-chain fatty acid, on the other hand, will effectively lubricate reactive metals to a temperature above its bulk melting point. There is evidence [11, 19] that fatty acids are able to do this by reacting with the lubricated surface to form a soap film. The experiments described earlier show that the presence of an oxide film is essential if lubrication by fatty acid solutions is to be effected. The chemical reaction of oxide with acid is probably complex, and will vary with the chemical nature of the oxide. Summing up the experimental evidence, it appears that fatty acids in solutions are, in general, able to provide effective boundary lubrication of a reactive metal by reacting with an appropriate surface oxide film to form a layer of " soap " of higher melting point and lower solubility than the acid and more than one molecular layer in thickness.

The Role of Water in the Formation of Lubricating Films on Metal Surfaces.—We may now consider anew the observation that the presence of water at some stage in the preparation of the surface appears essential for effective lubrication by the fatty acid solution. We have seen that mere thickness of oxide film is not the important factor. The role of water may then be either :

(i) to take part in the oxide-acid reaction. It is possible, for example, that the presence of a film of water may produce local ionization of the acid at the seat of reaction ; or

(ii) to determine the nature of the surface layer.

It is significant that different metals require different degrees of treatment with water before lubrication is effective. Magnesium and cadmium for example, require only a brief washing in cold water, while copper, on the other hand, requires washing with boiling water for 2 min. This fact argues in favour of role (ii).

We have seen that experimental evidence indicates that solutions of fatty acid provide good lubrication of metal surfaces only when a chemical reaction takes place to provide a layer of soap thicker than a monolayer. If the surface is non-reactive or will react only very slowly with the fatty acid then the formation of a thick layer of " soap " will not be possible. It was noticed, however, that lubrication was either immediately effective or ineffective even after the solution of fatty acid had been in contact with the surface for many hours. It appears unlikely, therefore, that the rate of chemical reaction of the oxide with the acid is the deciding factor.

Moreover, if the soap monolayer formed from an initial adsorbed monolayer of acid is compact and strongly adsorbed we might expect further reaction to be greatly retarded and lubrication to be ineffective on non-ferrous metals. We might expect this to happen when the surface presented to the lubricant solution was itself compact and impenetrable, e.g., the surface of a naked metal or one covered with a compact impervious oxide skin. On the other hand, a porous reactive oxide layer would allow penetration of the solution and reaction not only at the surface but in the volume of the layer. This would give rise to the solid, thick soap layer which we have seen is essential for effective lubrication.

It is suggested, therefore, that the action of oxygen and water together on the surfaces of copper, cadmium, magnesium and zinc among the metals examined, is able to provide this reactive, porous layer essential to the formation of an effective multimolecular layer of soap. Oxidation

---

[20] Bigelow, Pickett and Zisman, *J. Colloid Sci.*, 1946, **1**, 513.

[21] Bigelow, Glass and Zisman, *ibid.*, 1947, **2**, 563.

under anhydrous conditions leads to an oxide film which is too compact and continuous for the necessary penetration of the acid solutions.*

The Lubrication of Metals by Fatty Acid Solutions. — We have seen that dilute solutions of fatty acids will provide effective lubrication of metal surfaces if it is possible for them to react so as to form a metallic soap layer. This layer must, for non-ferrous metals, be effectively more than one monolayer thick. Furthermore, we have seen that formation of such a soap layer depends on the presence of a suitable oxide layer.

On the basis of the above argument metals can be divided into three categories to explain their behaviour in the experiments described earlier :

(i) metals which form a thick permeable layer of oxide capable of reacting with fatty acids to form a soap ;
(ii) metals whose oxides, although probably capable of reaction with fatty acid, are formed on the surface as tough, compact skins ;
(iii) metals which form no oxide film or only a very thin film.

Of the metals investigated in the present study, magnesium, cadmium, zinc, copper and iron † fall in the first class. These metals, provided that a suitable oxide layer is formed on their surface, can be lubricated efficiently (coeff. of friction μ is approximately 0·1) by dilute solutions of long-chain fatty acid up to temperatures which correspond to the bulk melting or softening point of the soap formed.

Aluminium and probably chromium and nickel will be in the second class above. The oxide of these metals, since it occupies more volume than the metal from which it is formed, is in a state of compression in the film. The high strength of these oxides prevents cracking and the film is therefore very tough and compact. Consequently, fatty acid solution cannot penetrate to form a multimolecular lubricating layer of soap. It is probable that a monolayer of soap is formed from the primary adsorbed monolayer of acid. This monolayer on the compact oxide surface will retard further soap-formation and will be insufficient in itself to provide effective lubrication. The coefficient of friction when metals of this class are lubricated with fatty acid solution is about 0·3 and sliding is normally intermittent (stick-slip) in type.

Platinum, gold and silver in the third category of metals have very thin oxide films or no film at all.[15] No soap formation and consequently no effective lubrication is possible. The coefficient of friction with dilute fatty acid solutions is of the order of 0·6.

The work described in this paper was carried out in the Research Laboratory on the Physics and Chemistry of Rubbing Solids, Department of Physical Chemistry, Cambridge, while the author was seconded there from the Royal Aircraft Establishment. The author thanks Mr. K. V. Shooter, Dr. Bowden, Greenhill and Tabor for helpful discussion during the course of the work, and the Ministry of Supply for permission to publish the paper.

Laboratory on the Physics and Chemistry of Rubbing Solids,
Department of Physical Chemistry,
Cambridge.

---

* It is interesting to note that Greenhill[22] has shown that sulphide films on copper in conjunction with a dilute fatty acid solution provide excellent lubrication. Such sulphide films are well-known from corrosion studies to be much more porous and discontinuous than oxide films on copper. It is possible that this enables ready penetration of the acid to allow formation of a thick soap layer.

† See, however, footnote on p. 100.

[22] Greenhill, *J. Inst. Petroleum*, 1948, **34**, 659.

INTENSITIES OF VIBRATION BANDS

PART II.—BENDING VIBRATIONS OF SUBSTITUTED BENZENES AND THE DIPOLE OF THE C—H LINK

By A. R. H. Cole and H. W. Thompson

Received 30*th June*, 1949

Earlier measurements on the intensities of some vibrational absorption bands of different classes of substituted benzenes, designed to calculate a value of the dipole moment of the C—H bond, have been revised and extended. The results suggest a mean value of about 0·57 D for this quantity, with the hydrogen atom positive with respect to carbon.

The dipole moment of the C—H bond is a quantity of some interest, but there is still uncertainty about its value and also argument as to which end of the bond carries the formal positive charge. Attempts have been made recently to investigate this from measurements on the intensities of some vibrational absorption bands ; this and other relevant work has been summarized critically by Gent.[1] In an earlier paper from this laboratory,[2] results were described on certain vibration bands associated with out-of-plane bending motions ot C—H bonds in substituted benzenes. It was found that a characteristic frequency exists for one such vibration, depending only upon the positions and within wide limits not upon the nature of the substituent groups. Assuming a simplified potential energy function for the vibrations, which reproduces satisfactorily the values for corresponding frequencies of benzene itself, the relative amplitudes for the vibrating mass-points were computed for the different modes, and thus a value could be obtained for the absorption intensity. Assuming values for the electric moments of the C—X bonds, X being a halogen carrying the excess negative charge, the polarity of the C—H bonds in this group of molecules was found to be $\overset{-}{\mathrm{C}}$—$\overset{+}{\mathrm{H}}$ with dipole moment close to 0·4 D.

Other results of Thorndike, Wells and Wilson [3] on the vibration bands of ethylene, methane and ethane, suggested a value near 0·4 D, but somewhat different values were obtained from different vibration bands of the same molecule. Foley [4] calculated a value 0·6 D from the bending mode in H—C≡N, and Rollefson and Havens [5] estimated a value of about 0·3 D from bands in the spectrum of methane.

In view of the general importance of this problem, the previous work of Bell, Thompson and Vago on the deformational modes of substituted benzenes has now been extended by reference to many more compounds, the experimental accuracy has been somewhat improved, and the theoretical treatment has been revised by a more satisfactory choice of the force constants. The principles of the whole method were fully explained in the previous paper, and only the main points will be given again here.

---

[1] Gent, *Quart. Rev.*, 1948, **2**, 383.

[2] Bell, Thompson and Vago, *Proc. Roy. Soc. A*, 1948, **192**, 498.

[3] Thorndike, Wells and Wilson, *J. Chem. Physics*, 1947, **15**, 157.

[4] Foley, *Physic. Rev.*, 1946, **69**, 628.

[5] Rollefson and Havens, *ibid.*, 1940, **57**, 710.

Calculation of Frequencies and Amplitudes.—For the out-of-plane motions of the substituted benzenes, a simple force system with only two force constants, suggested by Wilson[6] and modified by Bell,[7] has been used. This accounts for the observed frequencies of benzene within 10 %, and has been used successfully by Ingold and Leeke[8] in dealing with the excited states of benzene and hexadeuterobenzene. Fig. 1 shows the dimensions and co-ordinates of the molecular model used. Distances *e* and *f* can be either *a* or *d* according as the carbon atom is bonded to the substituent X or to a hydrogen atom, *r*, *x*, *w*, *y*, *q* and *z* represent small displacements perpendicular to the plane of the ring. An angle of deformation can be measured in terms of these displacements as follows:

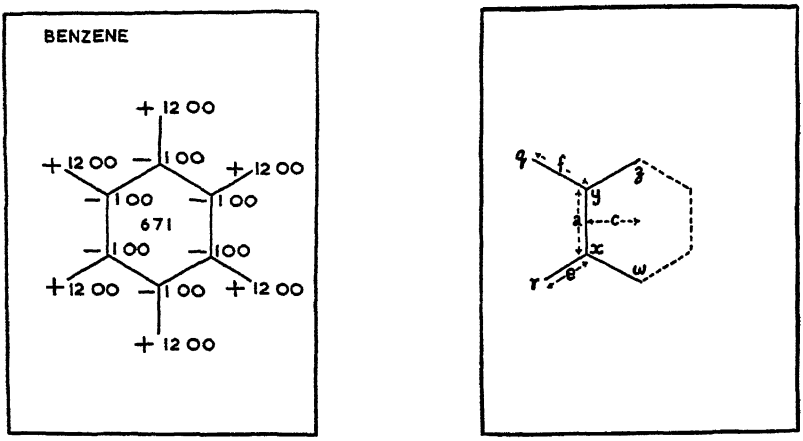

FIG. 1.

$$\mu = \frac{(r-x)}{e} + \frac{(y+w-2x)}{a} \quad . \quad . \quad . \quad (1)$$

and an angle of twist ϕ about a C—C bond is given by

$$c\phi = w + \frac{x(a-e)}{e} - \frac{y(a-f)}{f} - z - \left(\frac{ra}{e}\right) + \frac{qa}{f}. \quad . \quad (2)$$

The potential energy during a vibration is assumed to be given by

$$2V = hd^2 \sum_i \mu_i^2 + Qc^2 \sum_i \phi_i^2, \quad . \quad . \quad . \quad (3)$$

in which the force constants *h* and *Q* refer to bending and twisting.

Eqn. (1), (2) and (3) can now be used to set up the secular determinant for the vibrations of different substitution classes, these being solved numerically as described in the previous paper. The following constants were assumed:

$$h = 2{\cdot}44 \times 10^4 \text{ dyne/cm.}, \quad Q = 0{\cdot}40 \times 10^4 \text{ dyne/cm.},$$
$$d = 1{\cdot}08 \text{ Å}, \quad a = 1{\cdot}39 \text{ Å}.$$

The value of *h* was estimated from the vibration frequency of benzene at 671 cm.$^{-1}$ which involves no twisting; and that of *Q* adopted here is slightly larger than the value used earlier since it leads to a better general agreement with the observed frequencies.

---

[6] Wilson, *Physic Rev.*, 1934, **45**, 706.
[7] Bell, *Trans. Faraday Soc.*, 1945, **41**, 293.
[8] Ingold and Leeke, *Nature*, 1946, **157**, 46.

The relative amplitudes obtained from the above calculations were adjusted so as to represent a classical vibration of energy proportional

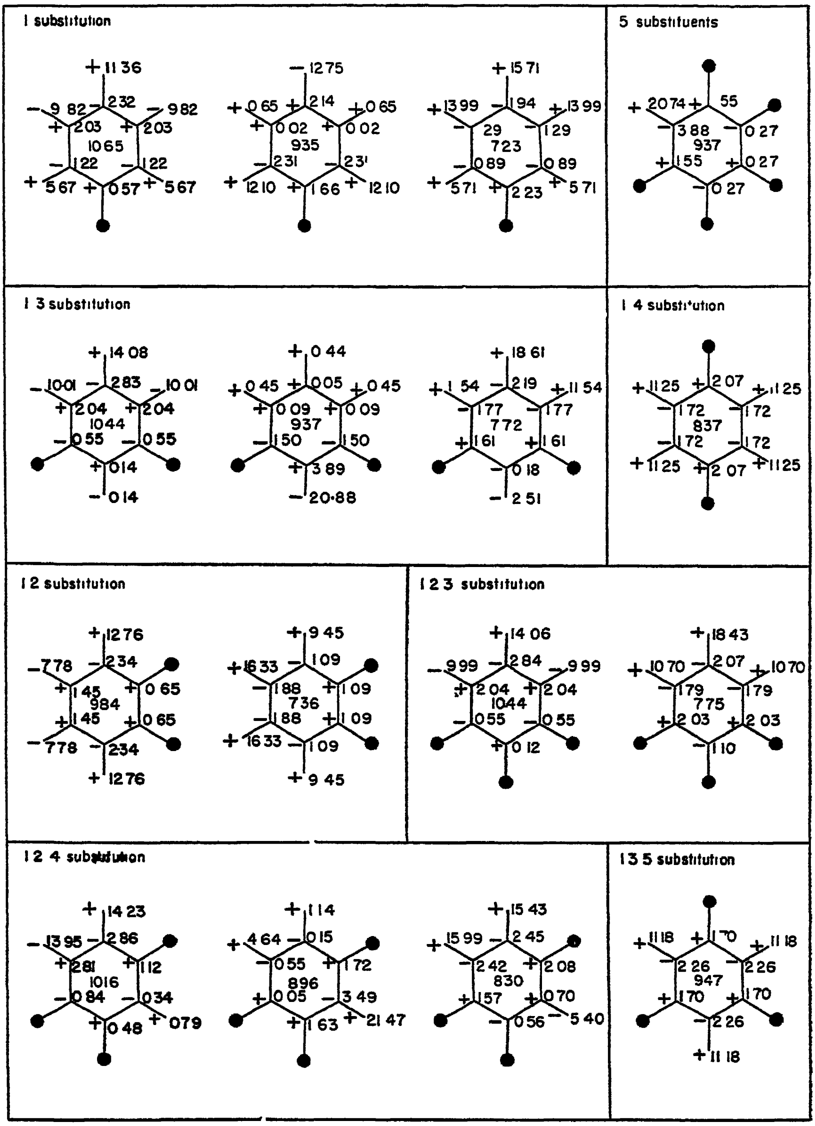

FIG. 2

to the frequency, the amplitude of the carbon atom in the 671 cm.$^{-1}$ vibration of benzene being taken as unity. The frequencies and amplitudes obtained are shown in Fig. 2, from which it can be seen that for each type of substitution the lowest frequency corresponds to a vibration in which all, or nearly all, the hydrogen atoms are displaced in the same sense. This would be expected since the amount of twisting is least in this mode. These vibrations will therefore correspond to the intense absorption bands, and the calculated frequencies shown in Table I together with mean frequency found experimentally for the substances measured in the different classes. Table I shows that there is reasonably good agreement between the observed and calculated frequencies except in the case of 1 : 3 : 5 trisubstituted compounds, but even here the discrepancy is not much greater than is usually found in this kind of simplified treatment. We can therefore regard the force field and calculated amplitudes as satisfactory.

TABLE I

Type of Substitution	$\nu_{obs.}$ (cm.$^{-1}$)	$\nu_{calc.}$ (cm.$^{-1}$)	% error
Mono . . .	742	723	− 2·5
1 : 2	750	736	− 1·9
1 : 3	774	772	− 0·3
1 : 4	809	837	+ 3·5
1 : 2 : 3 . . .	772	775	+ 0·4
1 : 3 : 5 . . .	849	947	+11·5
1 : 4 : 5 . . .	810	830	+ 2·5
Penta . . .	871	937	+ 7·6

Experimental and Results

The compounds used were specially purified. The hydrocarbons were from a collection of pure hydrocarbons obtained under the auspices of the Hydrocarbon Research Group of the Institute of Petroleum, and most of the other substances were commercial samples recrystallized or fractionally distilled, the m.p.'s and b.p.'s indicating satisfactory purity. A few were specially prepared for this work.

The spectra were measured on a single-beam recording spectrometer using a rock-salt prism over the range 9-14μ. The effective slit widths were adjusted for each compound so as to be the same (4 cm.$^{-1}$) at the wavelengths of the absorption band being studied. Measurements were made in bromoform solution since this solvent has a clear transmission over the region involved, is suitable as regards solubilities, and is unlikely to lead to complications due to intermolecular interactions. One rock-salt absorption cell was used throughout, being rather less than 0·1 mm. in thickness.

The values given in Tables II and III show that for each substitution type, the position of the key band (the out-of-plane vibration) is roughly constant. Each band was measured at several concentrations and the optical density was

TABLE II

Substance	ν(cm^{-1})	ε	$A\mu^2_{CH} \times 10^6$
Toluene	734	10·58	3·82
o-Xylene	748	11·00	4·45
m-Xylene	773	8·19	5·21
p-Xylene	799	8·34	3·88
1 : 2 : 3-Trimethylbenzene .	772	6·84	4·28
1 : 2 : 4-Trimethylbenzene .	810	5·57	7·54
1 : 3 : 5-Trimethylbenzene .	838	5·86	4·30
Pentamethylbenzene . .	867	1·75	4·33

Mean value of $A\mu^2_{CH} = 4·6$.

(Mean value if 1 : 2 : 4 derivative is omitted = 4·2.)

TABLE III

Substance	ν(cm.$^{-1}$)	ε	μ_{CH} (D)
Chlorobenzene	743	11·20	2·2
Fluorobenzene	756	11·82	1·1
Bromobenzene	739	11·40	1·4
o-Fluorotoluene	757	13·00	0·29
o-Chlorotoluene	751	11·71	0·89
o-Iodotoluene	747	9·72	—0·35
o-Dichlorobenzene . .	752	9·61	—0·78
o-Chloroiodobenzene . .	750	12·32	0·84
m-Fluorotoluene	778	8·50	2·8
m-Bromotoluene	773	7·24	—0·78
m-Dichlorobenzene . .	780	14·20	0·32
m-Chloroiodobenzene . .	773	7·34	—1·7
p-Fluorotoluene	818	10·92	0·38
p-Chlorotoluene	809	9·63	0·82
p-Bromotoluene	803	10·60	0·42
p-Iodotoluene	800	9·15	0·94
p-Dichlorobenzene . .	820	11·80	0·64
p-Dibromobenzene . .	811	10·60	0·87
p-Chlorobromobenzene .	816	10·64	0·91
p-Bromoiodobenzene . .	807	11·25	0·62
p-Chloroiodobenzene . .	811	10·00	1·1
2 : 4-Difluorotoluene . .	805	4·30	0·35*
1 : 2 : 4-Trichlorobenzene .	814	9·00	0·21*
1 : 2 : 4-Tribromobenzene .	810	7·03	0·26*
1 : 3 : 5-Trichlorobenzene .	853	10·44	0·55
1 : 3 : 5-Tribromobenzene .	850	10·35	0·51
Ethyl 1 : 3 : 4 : 5-tetrachlorobenzene	875	2·85	0·65

Mean value of μ_{CH} = 0·57 D.

* Calculated using mean value of 4·2 for $A\mu_{CH}^2$.

plotted against frequency (cm.$^{-1}$). In a few cases where slight overlapping of two bands occurred, graphical separation was used. Since the half-width of the bands varied for different compounds, band areas were used as a measure of the absorption rather than peak heights. For each solute the band area was plotted against concentration (mole/l.) and the slope of the line obtained was taken as a measure of the absorption coefficient. Although the individual band areas were probably only accurate to within 5 %, the errors in the slopes of the final plots were probably less than this, and they varied eightfold over the range of solutes used. The absorption coefficients are collected in Tables II and III.

Discussion

The methyl benzenes will be considered first. It is assumed that the electric moment between a methyl group and the ring carbon atom is zero. This assumption cannot lead to serious error, since the hydrogen atoms will in general have much larger amplitudes than the carbon atoms.

Fig. 2 shows that the motion of C—X bonds during a vibration is almost invariably opposite in phase to that of the C—H bonds. Hence if the C—X and C—H bond moments had similar directions, they would oppose each other in contributing to the total change in dipole moment which is responsible for the absorption of the infra-red radiation. Similarly, if these moments are opposite in sign they will reinforce one another, and increase the intensity of the absorption band. The present measurements show that in nearly all the compounds examined, the absorption coefficient of a halogen-substituted benzene is greater than that of the corresponding methyl benzene. This means that the C—X and C—H bond moments must be opposite in sign, and since it is generally agreed that the halogen atoms are negative with respect to carbon, the C—H bond must have a moment $\overset{-}{\mathrm{C}}—\overset{+}{\mathrm{H}}$.

Following the procedure of Bell, Thompson and Vago, the absorption coefficient ϵ of the methyl benzenes can be related to the calculated amplitudes by the equation

$$\epsilon = A\mu_{\mathrm{CH}}^2 . \nu\left\{\Sigma(a_{\mathrm{H}} - a_{\mathrm{C}})\right\}^2,$$

where μ_{CH} is the C—H bond moment,
ν is the frequency of the absorption peak,
a_{H} and a_{C} are the amplitudes of the hydrogen and carbon atoms, and
A is a constant for this series of measurements.

Using this equation, it is possible to obtain a value for $A\mu_{\mathrm{CH}}^2$ from the results with the methyl benzenes, as shown in Table II. The constancy of this factor is satisfactory for all compounds except the 1 : 2 : 4-trisubstituted type, and the fact that there is no progressive change as the number of methyl groups increases indicates that it is not serious to ignore the C—(CH_3) bond moment. Similarly, for a halogen-substituted compound

$$\epsilon = A\mu_{\mathrm{CH}}^2 . \nu\left\{\Sigma(a_{\mathrm{H}} - a_{\mathrm{C}}) + \Sigma(a_{\mathrm{X}} - a_{\mathrm{C}})\frac{\mu_{\mathrm{CX}}}{\mu_{\mathrm{CH}}}\right\}^2.$$

Inserting the amplitudes given in Fig. 2, we obtain the following equations for the different substitution classes:

MONO: $\epsilon = A\mu_{\mathrm{CH}}^2 . \nu\left\{61{\cdot}4 - 2{\cdot}23\frac{\mu_{\mathrm{CX}}}{\mu_{\mathrm{CH}}}\right\}^2,$

ORTHO: $\epsilon = A\mu_{\mathrm{CH}}^2 . \nu\left\{57{\cdot}5 - 2{\cdot}18\frac{\mu_{\mathrm{CX}}}{\mu_{\mathrm{CH}}}\right\}^2,$

META: $\epsilon = A\mu_{\mathrm{CH}}^2 . \nu\left\{45{\cdot}1 - 3{\cdot}22\frac{\mu_{\mathrm{CX}}}{\mu_{\mathrm{CH}}}\right\}^2,$

PARA: $\epsilon = A\mu_{\mathrm{CH}}^2 . \nu\left\{51{\cdot}9 - 4{\cdot}14\frac{\mu_{\mathrm{CX}}}{\mu_{\mathrm{CH}}}\right\}^2,$

1 : 2 : 3-SUBST.: $\epsilon = A\mu_{\mathrm{CH}}^2 . \nu\left\{45{\cdot}5 - 2{\cdot}96\frac{\mu_{\mathrm{CX}}}{\mu_{\mathrm{CH}}}\right\}^2,$

1 : 2 : 4-SUBST.: $\epsilon = A\mu_{\mathrm{CH}}^2 . \nu\left\{30{\cdot}2 - 3{\cdot}09\frac{\mu_{\mathrm{CX}}}{\mu_{\mathrm{CH}}}\right\}^2,$

1 : 3 : 5-SUBST.: $\epsilon = A\mu_{\mathrm{CH}}^2 . \nu\left\{40{\cdot}3 - 5{\cdot}10\frac{\mu_{\mathrm{CX}}}{\mu_{\mathrm{CH}}}\right\}^2,$

PENTA-SUBST.: $\epsilon = A\mu_{\mathrm{CH}}^2 . \nu\left\{24{\cdot}6 - 2{\cdot}83\frac{\mu_{\mathrm{CX}}}{\mu_{\mathrm{CH}}}\right\}^2,$

These formulae apply when the substituents are all identical, but may easily be modified for those compounds which have more than one type of substituent.

In Table III, values are given for the calculated C—H bond moment, assuming $\mu_{\mathrm{CF}} = -1{\cdot}25$ D, $\mu_{\mathrm{CCl}} = -1{\cdot}4$ D, $\mu_{\mathrm{CBr}} = -1{\cdot}3$ D and $\mu_{\mathrm{CI}} = -1{\cdot}1$ D, and using the measured frequency for the particular molecule and the appropriate value of $A\mu_{\mathrm{CH}}^2$ for the substitution type.

Although the individual values of μ_{CH} may vary rather widely, it is significant that nearly all are positive, and the variations are not unexpected in view of the simplified treatment. The mean value of about

0·57 D is rather higher than previously found, but falls into line with other values quoted above. It is indeed possible that the value may change somewhat in different molecules, although such differences will be small.

One of us (A. R. H. C.) thanks the University of Western Australia for a Hackett Studentship which enabled him to carry out the work.

The Physical Chemistry Laboratory,
Oxford.

SOME MOLECULAR ORBITAL CALCULATIONS ON THE SYSTEMS *o*- AND *p*-$C_6H_4X_2$

By V. Gold

Received 21*st July*, 1949

The π electron energies of the molecules *o*- and *p*-$C_6H_4X_2$ have been calculated by means of a molecular-orbital procedure, using a range of values for the Coulomb integral of X and the resonance integral for C = X. It is shown that, by assigning suitable values to these parameters, it is possible to explain quantitatively the difference in reduction potentials between *o*- and *p*-benzoquinone without assuming the intervention of any factors other than π electron energies.

I. Introduction.—During the last few years a number of papers has appeared in which the technique of the simple molecular-orbital method for conjugated carbon systems is extended to systems containing also one or more hetero-atoms.[1] In such treatments it is usual to neglect overlap and to allow for the difference of the hetero-atom by (i) assigning to it a different Coulomb integral α_X which is conveniently expressed in the form [1e]

$$\alpha_X = \alpha_C + h\beta_{C-C},$$

α_C being the Coulomb integral for C in an entirely conjugated carbon system and β_{C-C} the resonance integral in such a system; (ii) assuming a law for the variation of the Coulomb integral along the conjugated carbon chain attached to the hetero-atom, i.e. an inductive effect; (iii) assigning a different value to the resonance integral for C—X, conveniently expressed in the form [1e] $\beta_{C-X} = k\beta_{C-C}$; the C—C resonance integrals in the systems are assumed to be unaltered.

There is, however, only qualitative theoretical guidance in the choice of these parameters which therefore ought to be evaluated empirically by comparison with experimental data. Unfortunately, the complications which are introduced into the calculation by the hetero-atom mean that the systematic study of the effect of varying these parameters on the result of the calculation is a lengthy and tiresome problem. Also, there appear to be few experimental data which are both sufficiently accurate and sensitive to the choice of the parameters to promise their reliable evaluation even if the results of such systematic calculations were available. Most molecular-orbital calculations on hetero-systems have therefore proceeded from a more or less intuitive set of parameters. Whatever the theoretical status of this type of molecular-orbital procedure is, there is little doubt that it does provide a model which can be improved by the judicious selection of the "hetero-parameters".

---

[1] (*a*) Wheland and Pauling, *J. Amer. Chem. Soc.*, 1935, **57**, 2086; (*b*) Wheland, *ibid.*, 1942, **64**, 900; (*c*) Coulson, *Trans. Faraday Soc.*, 1946, **42**, 106; (*d*) Longuet-Higgins and Coulson, *ibid.*, 1947, **43**, 87; (*e*) Longuet-Higgins and Coulson, *J. Chem. Soc.*, 1949, 971.

The present calculations deal with the structures

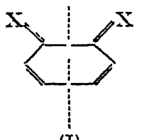

(I)

and

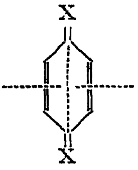

(II)

both of which are relatively simple and, because of their symmetry properties, the secular determinants can be factorized. According to the values of the hetero-parameters the calculations should include molecules such as

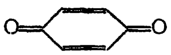

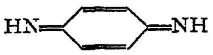

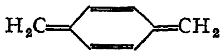

and perhaps also

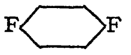

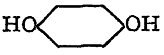

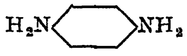

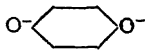

etc.

and their *o*-analogues. For the quinones fairly reliable experimental data can be found in the standard oxidation-reduction potentials. It was hoped in this way to discover a good set of hetero-parameters for O=, but the results permit only qualitative conclusions in this respect.

II. Method and Results.—The main block of calculations deals with the π electron energies for systematic variation of both h and k. The Coulomb integrals throughout the system can be expressed as

$$\alpha = \alpha_0 + \delta_n h \beta,$$

where $n = 0, 1, 2 \ldots$ according to whether the atom considered is X, next to X, one atom further removed from X, etc. It has been assumed that

$$\delta_n = f^n,$$

where f is a fraction for which the value $1/3$ has been chosen. This attenuation of the inductive effect is rather slower than has usually been assumed in this kind of calculation, but it is the type of law which acid dissociation constants show to hold for an inductive effect.[2] * Only positive values of h and values of $k > 1$ were considered.

In disubstituted derivatives we must also decide whether the effects of the two substituent groups are additive at any position in the ring. It would appear from general arguments that there should be additivity for small effects, whereas for a large inductive effect, amounting almost to saturation distortion, only the nearer substituent group need be considered in evaluating the Coulomb integral for that position. The difference between the two procedures is, in fact, very slight and of consequence only for the C atoms adjacent to X in the *o*-compounds, where, however, the saturation effect may be operative. Although the other procedure may probably be slightly preferable the calculations have been carried out on the assumption of non-additive effects on the Coulomb integrals in the ring but, for comparison, they were in one case also carried through for additivity. It has throughout been assumed that the groups X exert no appreciable influence on each other's Coulomb integrals.

---

[2] Derick, *J. Amer. Chem. Soc.*, 1911, **33**, 1181.

* The same value has recently been advocated by Dewar.[3]

[3] Dewar, *J. Chem. Soc.*, 1949, 463.

The results are summarized in Table I. E is the π electron energy of the molecule when it contains eight π electrons in the lowest four levels. The resonance energies R are relative to the conventional fixed bond formulae (I and II), but still using the appropriate values for h and k.

TABLE I.—π ELECTRON ENERGIES FOR o- AND p-$C_6H_4X_2$

h	k^2	Ortho			Para			$\frac{E_{ortho} - E_{para}}{\beta}$	$\frac{R_o - R_p}{\beta}$	Inductive Effect
		$\frac{(E\quad 8\alpha)}{\beta}$	$\frac{R}{\beta}$	Lowest Unfilled Root	$\frac{(E - 8\alpha)}{\beta}$	$\frac{R}{\beta}$	Lowest Unfilled Root			
0	1	9·954	1·954	+0·295	9·924	1·924	+0·311	+0·030	+0·030	Non-additive
0	4	$21·00_4$	1·00	+0·590	$20·78_8$	0·79	+0·884	$+0·21_6$	+0·21	,,
1	1	$13·13_2$	1·95	−0·358	13·270	1·94	−0·362	$−0·13_8$	+0·01	,,
1	2	$14·45_6$	1·68	−0·092	$14·56_0$	1·64	−0·106	$−0·10_4$	+0·04	,,
1	16	$24·03_0$	1·01	+0·452	$23·96_6$	0·80	+0·658	$+0·06_4$	+0·21	,,
2	1	$16·79_8$	2·05	−0·905	$17·05_8$	2·03	−0·918	$−0·26_0$	+0·02	,,
2	4	$19·86_0$	1·49	−0·234	$20·09_0$	1·44	−0·268	$−0·23_0$	+0·05	,,
2	9	$23·43_0$	1·20	+0·160	$23·57_6$	1·06	+0·172	$−0·14_6$	+0·14	,,
2	16	$27·18_8$	1·03	+0·303	$27·27_8$	0·84	+0·417	$−0·09_0$	+0·19	,,
2·7	1	$19·66_8$	2·27	−1·171	$19·91_6$	2·14	−1·243	$−0·24_8$	+0·13	,,
3	1	$20·97_8$	2·41	−1·257	$21·25_2$	2·26	−1·333	$−0·27_4$	+0·15	,,
3	4	$23·49_0$	1·63	−0·669	$23·86_4$	1·59	−0·709	$−0·37_4$	+0·04	,,
3	9	$26·82_8$	1·27	−0·121	$27·14_2$	1·16	−0·179	$−0·31_4$	+0·11	,,
3	16	$30·51_0$	1·11	+0·133	$30·72_0$	0·90	+0·156	$−0·21_0$	+0·21	,,
4	1	$25·53_2$	2·97	−1·467	$26·13_4$	3·03	−1·444	$−0·60_2$	−0·06	,,
6	1	$35·16_4$	4·34	−1·720	$36·06_0$	4·45	−1·667	$−0·89_6$	−0·11	,,
2	1	$17·28_8$	2·15	−0·992	$17·38_4$	2·06	−0·967	$−0·09_6$	+0·09	Additive

III. **Discussion.**—(*a*) INFLUENCE OF VALUES OF h AND k ON π ELECTRON ENERGIES. Increase in h lowers all levels because of the greater Coulomb stabilization, though not all of the levels are affected to the same extent and there is some change in the order of energy of the levels. When h is increased we get in all cases a stabilization of the lowest levels and a slight raising of some of the higher filled ones, the total effect on the π electron energy for four filled levels being stabilizing.

The effect of a small variation of h on the resonance energy, as defined above, is practically nil, but for larger values of h the resonance energy increases. This is presumably due to the fact that the greater localization of the electrons consequent upon an increase in h is more than compensated by greater Coulombic stabilization. Whereas in the fixed-bond structure only one pair of electrons can benefit from this increased attractive force of X, in the structure of minimum energy the group X draws a greater share of electrons to itself. This " resonance energy " is therefore not a delocalization stabilization but might—in a not too literal sense—be likened to the valence-bond " resonance " with ionic structures such as

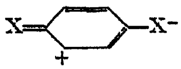

If k is increased, the C—X bonds become more and more fixed as double, without redeeming Coulombic compensation, and the resonance energy is decreased.

(*b*) OXIDATION-REDUCTION POTENTIALS OF QUINONES.—It was shown several years ago that it is possible by means of the molecular-orbitals technique to account quantitatively for differences in reduction potentials of quinones.[4] The basis of such treatments is the assumption that the only structure-sensitive contribution to the free energy of reduction comes from the attendant change in resonance energy. The resonance energy of the hydroquinone was assumed to be identical with that of the parent hydrocarbon and that of the quinone to be given by either (i) the resonance energy of the hydrocarbon obtained on replacing C=O by $C=CH_2$, i.e., setting $h = 0$, $k = 1$, [4a,b] or (ii) the resonance energy of the conjugated system left over after assuming the C=O bonds to be rigidly localized, i.e. setting k large.[4a] Although these assumptions are far removed from the truth in opposite directions, they both lead nevertheless to fairly satisfactory accounts of the structure dependence of the reduction potentials of either of the series *o*-quinones or *p*-quinones, but in each case there is a large discrepancy between the values calculated for the two series. Also it appears that, although the error introduced in the choice of these values for k does not have a significant effect on the comparisons within each series, the difference between the two series may be sensitive to the assumed values of the " hetero-parameters ".

Previous workers have attributed the discrepancy between the two series to the extra stability of *o*-hydroquinones due to hydrogen bonding,[4, 5] or to the extra instability of *o*-quinones due to electrostatic repulsion between neighbouring C=O dipoles.[4a] Concerning the first of these explanations it must be pointed out that in aqueous solutions both *o*- and *p*-hydroquinones will be stabilized by hydrogen bonding, either internal or external (to H_2O) and that the discrepancy between the two series could therefore only be attributed to the small energy difference between these two kinds of hydrogen bonding. The importance of repulsion between C=O groups is also difficult to assess, and it seems best to defer its discussion until direct thermochemical data on *o*-quinones are available. Thus, while it is possible that special effects operating in the *ortho* series only are the explanation of the discrepancy it seems worth while examining the results of the present calculations in order to see whether such a special explanation is essential for *o*- and *p*-quinone, and must be invoked for all values of the parameters h, k.

In this connection it is interesting to observe that Evans *et al.*[6] recently concluded that a modification of the method of calculation led to a much reduced difference between the *o*- and *p*-series, irrespective of the values of adjustable parameters h and k. A discussion of their detailed procedure, which is based on the extended application of approximate empirical additivity relationships in order to avoid the calculation of complicated quinones, is not relevant here. Their basic new suggestion is that the π electron energy change accompanying reduction to a hydroquinone is that obtained on feeding two extra electrons into the quinone energy levels. However, this leads to difficulties in an exact evaluation, such as the present one, owing to the changed value of the parameters h, k in quinone and hydroquinone. We know (i) that the group dipole moment of C—OH is smaller in phenols than in alcohols, which probably means that the π electron distribution in phenol is such as to leave a slight positive charge on O, thus reducing the magnitude of the moment, and a large positive value of h is therefore unlikely; (ii) that the C—OH bond lengths in phenols are $\sim 1\cdot36$ Å compared with $\sim 1\cdot14$ Å for C=O in quinone (cf. the increase in bond length of $\sim 0\cdot22$ Å on going from a double to a single C—C bond), i.e. the C—O bond in phenols can only have very slight double-bond character and, as the C—O distance is so long, a very low value for β_{C-O}. The force field required for hydroquinone is therefore probably not covered by the range of parameters studied, and it also appears probable that the original suggestion that the π electron energy of hydroquinone is identical with that of benzene or differs from it by the same amount for *o*- and *p*-hydroquinone is more reliable and it will be used in the following argument. Table I gives, however, all necessary data to carry through the analogous comparison on the Evans-Gergely-de Heer[6] model.

---

[4] (*a*) Diatkina and Syrkin, *Acta Physicochim.*, 1946, **21**, 21; (*b*) Evans, *Trans. Faraday Soc.*, 1946, **42**, 113.

[5] Branch and Calvin, *Theory of Organic Chemistry* (New York, 1941), p. 309.

The experimental datum which is to be used is the difference between the reduction potentials (E) for *o*- and *p*-benzoquinone, viz.,

$$E_o - E_p = 0{\cdot}098 \text{ volt.}$$

This result must now be expressed as an energy difference in units of β.

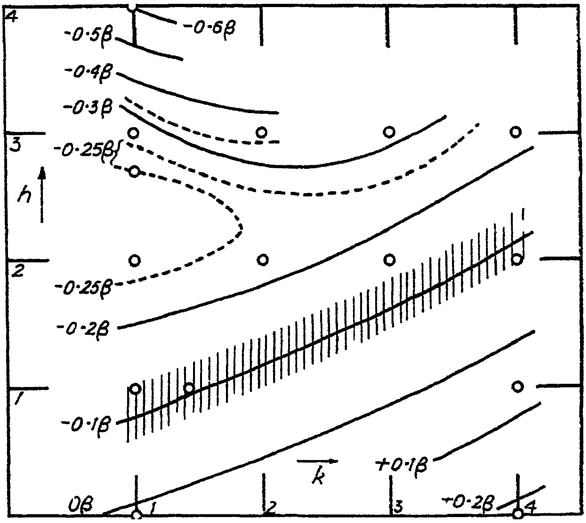

FIG. 1.
Circles : Calculated points.
Full lines : 0·1β contours.
Broken lines : 0·05 β contours.

According to our assumptions, we have for the reduction of a quinone

$$\Delta G = -\,2FE \qquad (F = \text{faraday})$$
$$\Delta H = -\,2FE - C_1$$
$$(E_{H_2Q} - E_Q) = -\,2FE - C_2 \qquad (C_1, C_2 = \text{constants})$$
$$\therefore \frac{dE}{d(E_{H_2Q} - E_Q)} = -\frac{1}{2F}.$$

Evans *et al.*[6] have shown that different assumptions about the hetero-parameters lead to the same value for the slope of a plot of E against $(E_{H_2Q} - E_Q)$. This may therefore legitimately be used to determine the value which is appropriate for β in this particular problem.

$$\text{Experimentally} \quad \frac{dE}{d(E_{H_2Q} - E_Q)} = -\frac{1}{2F} = 0{\cdot}82\ \beta^{-1} \text{ volt.}$$
$$\therefore |\beta| = 0{\cdot}82 \times 2F \qquad \text{(joules/mole).}$$
$$= 0{\cdot}82 \times 2^{*} \qquad \text{(eV/molecule)}$$
$$= 38 \text{ kcal./mole.}$$

---

[6] Evans, Gergely and de Heer, *Trans. Faraday Soc.*, 1949, **45**, 312.

* The value 0·82 eV given by Evans[4b] must be due to a slip

Taking this value of β, the experimental difference in reduction potentials corresponds to one of 0·12 β in π electron energies, i.e. since according to our assumptions, $(E_{H_2Q})_{para} = (E_{H_2Q})_{ortho}$,

$$(E_Q)_{para} - (E_Q)_{ortha} = 0{\cdot}12\ \beta.$$

In Fig. 1 the values of $(E_Q)_{para} - (E_Q)_{ortho}$ are plotted as a contour map for simultaneous variation of h and k and the shaded portion indicates the combinations of h and k which lead approximately to this energy difference between *o*- and *p*-benzoquinone. It is gratifying to find that some of these combinations are not unreasonable ones, according to Coulson, although not identical with his values.

Of course, it is possible and, in fact, probable, that other factors contribute to the difference in reduction potentials between *o*- and *p*-quinones, but it has been shown here that π electron energies, calculated by the molecular-orbital method with suitable additional parameters, may explain the whole phenomenon in benzoquinones. It would unfortunately be too laborious to see whether these parameters permit the whole problem of the difference between the *o*- and *p*-series to be resolved.

A similarly systematic study of the variation of the δ's has not been carried out, and the only comparison value which has been calculated, assuming an additive inductive effect, shows that the results *are* dependent on the δ values. In view of this, it is impossible to claim that the shaded region represents the only possible sets of hetero-parameters, but the difference does not appear to be large enough to upset the qualitative conclusions. Altogether the results do not fulfil the original hope that the calculations would lead to a more definite answer regarding the choice of hetero-parameters for oxygen.

Department of Chemistry,
King's College,
London, W.C.2.

THE KINETICS OF THE DEHYDROCHLORINATION OF SUBSTITUTED HYDROCARBONS

PART V.—THE MECHANISM OF THE THERMAL DECOMPOSITIONS OF 2-CHLOROPROPANE AND 1 : 2-DICHLOROPROPANE

BY D. H. R. BARTON AND A. J. HEAD

Received 29th July, 1949

2-Chloropropane decomposes in the temperature range 367-406° C by a nearly homogeneous first-order reaction to give propylene and hydrogen chloride. The relevant rate equation is

$$k = 10^{13{\cdot}4 \pm 0{\cdot}2}\, e^{-50{,}500 \pm 700/RT}\ \text{sec.}^{-1}.$$

There is no variation in rate constant with initial pressure. Additions of propylene and, in small amounts, of oxygen and chlorine do not affect the rate.

1 : 2-Dichloropropane decomposes in the temperature range 416-452° C by a nearly homogeneous first-order reaction, for which the relevant approximate rate equation is $k = 10^{13{\cdot}8}\, e^{-54{,}900/RT}$ sec.$^{-1}$. For both substances the mechanism of the decomposition is unimolecular, in agreement with the theory previously advanced.

Previous studies in this series [1], [2] have dealt with the thermal decompositions of ethyl chloride, 1 : 1- and 1 : 2-dichlorethanes and *tert.*-butyl chloride. Whilst there are still a number of minor features with regard to the 1 : 2-dichlorethane pyrolysis which require further examination, there can be no doubt in every case as to the correctness of the established mechanism of reaction. Three general mechanisms of dehydrochlorination have been detected, one of which is heterogeneous and most marked in clean-walled reaction vessels. The two homogeneous mechanisms are respectively unimolecular and radical chain in character. In Part IV of this series [2] we drew up a general theoretical scheme purporting to predict the mechanism of decomposition of a saturated chlorinated hydrocarbon merely by inspection of its molecular formula. This general scheme refers to the propagation steps in the hypothetical chain sequence and predicts whether the chain will, in fact, be propagated or not. Of course the existence of the necessary structural requirements for the propagation of the chain mechanism of decomposition does not of itself guarantee that a compound will decompose in such a manner, because for each substance there might be competition between the two different homogeneous mechanisms. The rigid application of the generalization enables us to predict which compounds *cannot* decompose by a chain mechanism, as contrasted with those which may. In actual fact it has been a common feature of our experience so far that saturated chlorinated hydrocarbons do decompose by the chain mechanism whenever the structural requirements are satisfied and inhibitors are absent.

---

[1] Barton and Howlett, *J. Chem. Soc.*, 1949, 155, 165.

[2] Barton and Onyon, *Trans. Faraday Soc.*, 1949, **45**, 725.

Continuing our work in directions already indicated [2] we have now turned our attention to 2-chloropropane and 1 : 2-dichloropropane. Both of these compounds should [2] decompose by the unimolecular mechanism, which prediction we have now proved to be correct.

Experimental

Materials.—Technical 2-chloro- and 1 : 2-dichloropropane were purified by the method used previously for other chlorinated hydrocarbons,[1] except that it did not prove possible to submit the dichloro-compound to fractional crystallization since it afforded a glass on cooling.[3] The following constants were recorded and are compared with the mean of the best literature values (in parentheses).

(*a*) 2-CHLOROPROPANE

B.p. 35·0° C corr. (34·8° corr.); from 34·8°.[4]

$d_{4^\circ}^{22^\circ}$ 0·8585 (0·8591 interpolated); from $d_{4^\circ}^{0^\circ}$ 0·8860,[4] $d_{4^\circ}^{15^\circ}$ 0·8680,[4] $d_{4^\circ}^{18\cdot6^\circ}$ 0·8657,[5] $d_{4^\circ}^{20^\circ}$ 0·8629,[5] $d_{4^\circ}^{30^\circ}$ 0·8491.[4]

$n_D^{22^\circ}$ 1·3770 (1·3772 extrapolated); from $n_D^{15^\circ}$ 1·38110.[4]

(*b*) 1 : 2-DICHLOROPROPANE

B.p. 96·1–96·2° C corr. (96·0° corr.); from 96·8°,[6] 96·4°,[7]

$d_{4^\circ}^{29^\circ}$ 1·1464 (1·1461 interpolated); from $d_{4^\circ}^{14^\circ}$ 1·1656,[6] $d_{4^\circ}^{20^\circ}$ 1·1578;[3] $d_{4^\circ}^{42\cdot1^\circ}$ 1·1294.[8]

$n_D^{22^\circ}$ 1·4389 (1·4391); from $n_D^{20^\circ}$ 1·4393,[8] $n_D^{20^\circ}$ 1·4388.[9]

Apparatus.—The apparatus and technique employed here have already been described in detail by Barton and Howlett.[1] Modifications were not found necessary in the present work.

---

[3] Cf. Timmermans, *Bull. Soc. chim. Belg.*, 1927, **36**, 504.
[4] Timmermans and Martin, *J. Chim. Phys.*, 1928, **25**, 422.
[5] Vogel, *J. Chem. Soc.*, 1943, 636.
[6] Linnemann, *Annalen*, 1872, **161**, 62.
[7] Nelson and Young, *J. Amer. Chem. Soc.*, 1933, **55**, 2429.
[8] Vogel, *J. Chem. Soc.*, 1948, 644.
[9] Goudet and Schenker, *Helv. chim. Acta*, 1927, **10**, 132.

Results

In Part IV of this series [2] we explained the difficulty of obtaining reproducible results in the pyrolysis of chlorinated hydrocarbons due to the variable catalytic activity of the surface of the reactor. Satisfactory reproducibility was only obtained after this heterogeneous reaction had been suppressed by the deposition of a uniform carbonaceous coating. Similar effects were noticed also in the thermal decompositions reported here, and the results outlined below were only obtained after the walls had been " aged " in the usual manner.[1, 2]

Stoichiometry.—Previous parts [1, 2, 10] in this series have established that the pyrolysis of saturated chlorinated hydrocarbons leads to the production of an olefin or chlorinated olefin and hydrogen chloride, in equimolecular amounts. The further pyrolysis of the olefin or chlorinated olefin under the same reaction conditions is slow enough to be neglected. That the reaction studied, in the case of 2-chloropropane, was the production of propylene and hydrogen chloride was confirmed by a series of long term (15-hr.) experiments in which the pressure finally attained was close to double the initial pressure (Table I). This also showed that the equilibrium position in the 2-chloropropane–propylene–HCl system was substantially 100 % on the side of the dissociation products over the temperature range employed.

Previously we had found [10] that up to 723° K the pyrolysis of 1 : 2-dichloropropane afforded a mixture of monochloropropenes and hydrogen chloride. In a series of long term (15-hr.) experiments the ratio of final to initial pressure was definitely greater than 2 (Table I) due, no doubt, as in the case of 1 : 2-dichlorethane,[1] to the splitting out of a second molecule of hydrogen chloride.

TABLE I

Temp. (°K)	Initial Pressure p_0 (mm.)	Final Pressure p_f (mm.)	p_f/p_0
2-Chloropropane			
640	123·8	241·7	1·95
663	56·3	110·0	1·95
663	80·3	159·9	1·99
663	55·6	107·9	1·94
663	61·1	122·6	2·01
664	70·1	136·5	1·95
664	38·6	75·3	1·95
664	86·1	170·8	1·98
665	66·0	132·2	1·99
665	108·5	210·6	1·94
665	38·7	77·5	2·00
665	77·7	153·3	1·97
675	65·5	129·0	1·97
1 : 2-Dichloropropane			
678	105·2	257·3	2·44
678	106·1	248·4	2·34
678	82·9	194·8	2·35
678	120·0	287·0	2·39
678	116·0	273·5	2·36
705	122·5	308·9	2·52
714	89·5	228·6	2·56
714	80·1	210·6	2·63

Kinetics.—Both thermal decompositions followed first-order kinetics, as illustrated by the data in Fig. 1 for 2-chloropropane and in Fig. 2 for 1 : 2-dichloropropane. In neither case was there any indication of the temperature-dependent induction periods which are a characteristic feature of the chain-type thermal dehydrochlorinations. Further, as is demonstrated in Table II, with neither substance was there any significant variation of velocity constant with initial pressure in the pressure ranges studied. This is a common feature of the reactions that we have examined so far in this series.

---

[10] Barton, *J. Chem. Soc.*, 1949, 148.

Having established these facts, the rate of decomposition of 2-chloropropane was determined at various temperatures in the range 367-406 using initial

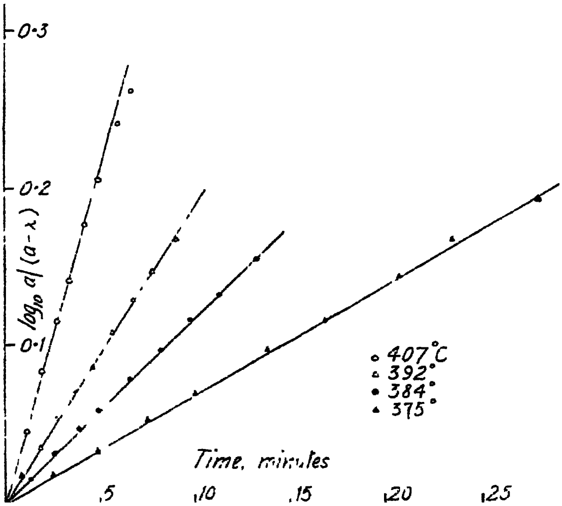

FIG. 1.

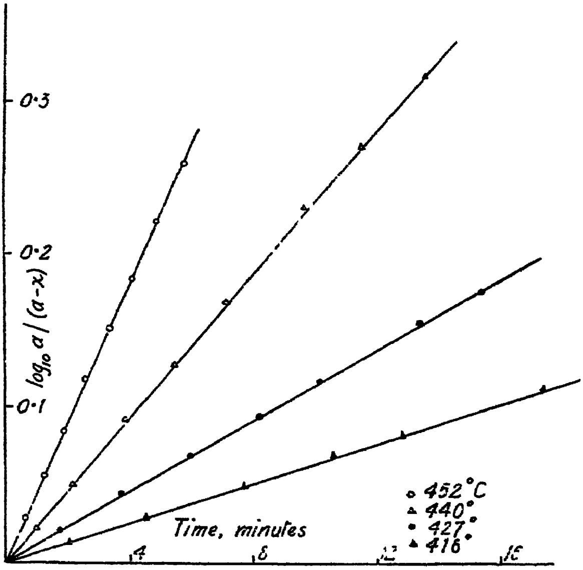

pressures of about 100 mm. The results obtained are summarized in Table III and it will be seen from the standard deviation of the mean (always $< 1·3$ %) that the reproducibility was satisfactory. The plot of $\log_{10} k + 4$ against the reciprocal of the absolute temperature gave a satisfactory straight line

(Fig 3), drawn by the least squares method, giving the same statistical weight to every run The relevant rate equation is

$$k = 10^{13\cdot 4 \pm 0\cdot 2} e^{-50{,}500 \pm 700/RT} \text{ sec}^{-1},$$

where the error limits are computed by the method described previously [2]

TABLE II

2 Chloropropane		1 2-Dichloropropane	
p_0 (mm)	k (sec $^{-1}$)	p_0 (mm)	k (sec $^{-1}$)
59·6	9·15 × 10^{-4}	51·4	9·34 × 10^{-4}
62·5	8·77	88·2	9·35
78·4	9·06	89·5	9·16
82·4	9·08	97·0	9·13
88·3	9·05	100·2	9·50
96·4	8·97	102·1	9·44
103·9	9·21	107·1	9·47
112·8	8·99	112·0	9·45
134·1	8·79	140·1	9·23

* All runs at 669·0° K, k (from rate equation) 8·85 × 10^{-4} sec $^{-1}$
† All runs at 713·5° K, k (from rate equation) 9·57 × 10^{-4} sec $^{-1}$

The reaction was shown to be substantially homogeneous by using a reactor packed with glass tubing in which the surface area/volume ratio had been increased by a factor of about four compared with the unpacked reactor Here the mean velocity constant was increased by 12 % over that computed for the same temperature from the above rate equation

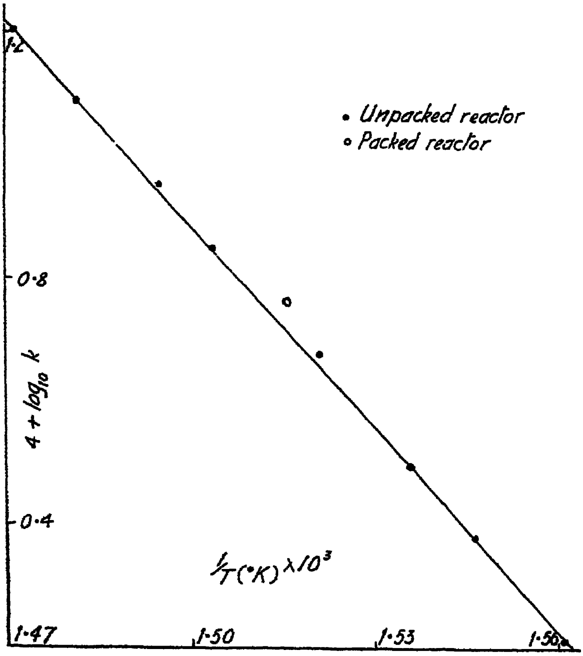

FIG. 3.

TABLE III

Temp. (° K)	No. of Runs	Mean Velocity Constant (sec.$^{-1}$)	Percentage Standard * Deviation of the Mean
2-Chloropropane			
640·6	7	0·162 10^{-3}	0·5
646·7	5	0·238	1·0
651·2	6	0·311	0·6
657·5	6	0·475	1·3
665·1	14	0·706	0·7
669·0	9	0·901	0·6
674·9	12	1·225	0·5
679·7	9	1·593	0·6
1 2-Dichloropropane			
689·5	8	0·253	0·8
699·7	8	0·443	1·2
713·5	13	0·942	0·5
725·1	11	1·821	0·9
Experiments in Packed Reactor.			
2-Chloropropane			
659·7	10	0·577	0·4
1 2-Dichloropropane			
682·7	13	0·205	2·5

* Given by $\frac{100}{\bar{x}}\sqrt{\frac{\Sigma(x-\bar{x})^2}{n(n-1)}}$, where the symbols have the obvious significance

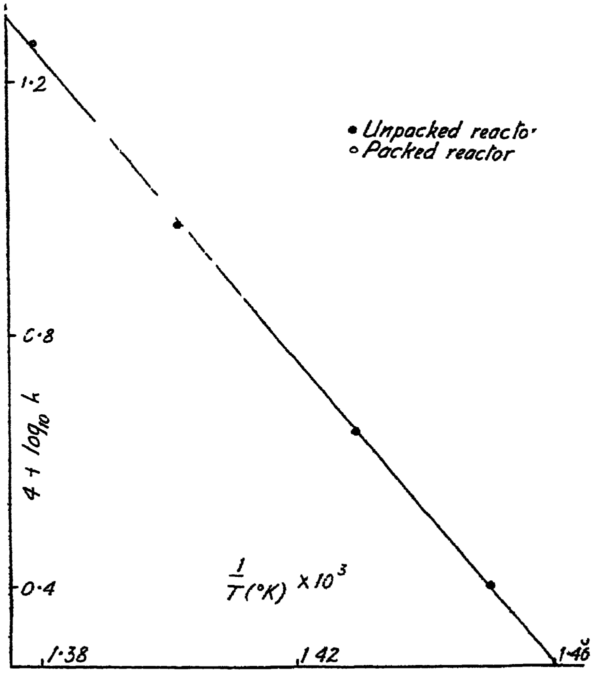

FIG. 4.

A similar, but more superficial, study has been made with 1 : 2-dichloropropane. The results are summarized in Table III and in Fig. 4. The relevant rate equation was found to be

$$k = 10^{13\cdot 8} e^{-54,900/RT} \text{ sec.}^{-1}.$$

Since the reaction was only examined at four temperatures we prefer not to attach any error limits to this equation. Packing the reactor in the same way as for 2-chloropropane led to the result shown in Table III, which represents an increase of 23 % over the rate calculated from the above rate equation. It must be concluded that the decomposition was substantially homogeneous.

Effect of Propylene.—In previous parts of this series[1] and elsewhere[11] we have shown that propylene constitutes a powerful inhibitor for those decompositions of chlorinated hydrocarbons which proceed by a chain mechanism. The effect of adding propylene to decomposing 2-chloro- and 1 : 2-dichloropropanes was therefore studied. As with ethyl chloride,[1] 1 : 1-dichlorethane[1] and *tert*.-butyl chloride,[2] propylene had no influence on the rate of decomposition. This is illustrated in Table IV where the 2-chloropropane initial pressure was 82 mm., and where the 1 : 2-dichloropropane initial pressure varied from 103 to 130 mm.

TABLE IV

2-Chloropropane *		1:2-Dichloropropane †	
Pressure of C_3H_6 × 100 / Init. Press. of 2-Chloropr.	k (sec.$^{-1}$)	Pressure of C_3H_6 × 100 / Init. Press. of 1 : 2-Dichloropr.	k (sec.$^{-1}$)
0 ‡	$4\cdot 76 \times 10^{-4}$	0 ‡	$4\cdot 78 \times 10^{-4}$
2·6	4·62	1·0	4·68
6·7	4·75	3·2	4·65
13·5	4·94	5·3	4·67
25·8	4·65	11·2	4·57
77·0	4·47	13·4	4·63

* All expt. corrected to 658·2° K; k (from rate equation) $4\cdot 75 \times 10^{-4}$ sec.$^{-1}$.
† All expt. corrected to 701·2° K; k (from rate equation) $4\cdot 86 \times 10^{-4}$ sec.$^{-1}$.
‡ Average value for normal runs carried out during these experiments.

Effect of Chlorine and Oxygen.—Small amounts of chlorine and oxygen are powerful inducing agents for the decomposition of 1 : 2-dichlorethane.[10, 12] As the data summarized in Table V (for chlorine) and Table VI (for oxygen)

TABLE V

2-Chloropropane *		1:2-Dichloropropane †	
Pressure of Cl_2 × 100 / Init. Press. of 2-chloropr.	k (sec.$^{-1}$)	Pressure of Cl_2 × 100 / Init. Press. of 1 : 2-Dichloropr.	k (sec.$^{-1}$)
0·1	$4\cdot 78 \times 10^{-4}$	0·2	$6\cdot 06 \times 10^{-4}$
0·5	4·63	0·5	6·01
0·9	4·99	1·5	5·81
1·4	Rapid—non-linear	3·3	5·73
0 ‡	5·63	0 ‡	5·79

* All expt. corrected to 658·2° K; k (from rate equation) $4\cdot 75 \times 10^{-4}$ sec.$^{-1}$.
† All expt. corrected to 704·7° K; k (from rate equation) $5\cdot 90 \times 10^{-4}$ sec.$^{-1}$.
‡ Normal run with no addition of chlorine, carried out immediately after the chlorine experiments were completed. The marked increase in rate with 2-chloropropane may mean that larger amounts of chlorine destroy the reactor coating and thus re-introduce the fast heterogeneous decomposition.

---

[11] To be published.

[12] Barton, *Nature*, 1946, **157**, 626.

show, these two elements, ***in small amounts and in coated reactors,*** have no significant effect on the rates of decomposition of 2-chloropropane and of 1 : 2-dichloropropane. In every case the initial pressure was in the range 65 to 135 mm.

TABLE VI

2-Chloropropane *		1:2-Dichloropropane †	
Pressure of O_2 × 100 / Init. Pressure of 2-chloropr.	k (sec.$^{-1}$)	Pressure of O_2 × 100 / Init. Pressure of 1 : 2-Dichloropr.	k (sec.$^{-1}$)
0·2	$4·70 \times 10^{-4}$	0·2	$5·31 \times 10^{-4}$
0·5	4·79	0·3	5·33
1·6	4·84	0·7	5·31
2·6	5·13 } Poor first order plots	1·7	5·22
5·0	5·78 }	3·6	5·08
0 ‡	5·02	0 ‡	5·32

* All expt. corrected to 658·2° K; k (from rate equation) $4·75 \times 10^{-4}$.
† All expt. corrected to 703·2° K; k (from rate equation) $5·43 \times 10^{-4}$.
‡ Normal run with no addition of oxygen, carried out immediately after the oxygen expt. were completed.

Discussion

The decompositions of 2-chloropropane and of 1 : 2-dichloropropane correspond by all experimental criteria with the similar reactions of ethyl chloride,[1] 1 : 1-dichlorethane [1] and *tert.*-butyl chloride.[2] Thus they are not inhibited by propylene, show no induction periods and are substantially homogeneous. Furthermore their rate equations have non-exponential terms (see further below) which are within a power of ten of 10^{13}, the value generally accepted as normal. Neither reaction, under the experimental conditions used here, was induced by the addition of chlorine or oxygen.* By the arguments given previously [1, 2] both reactions must be unimolecular in mechanism.

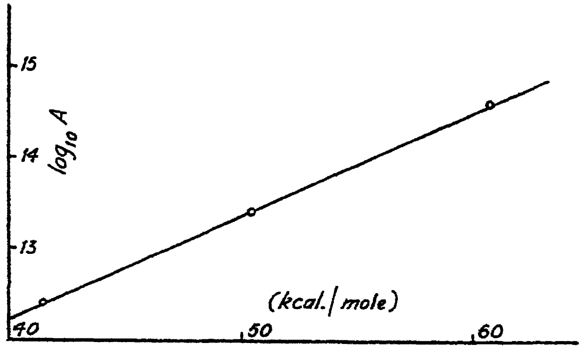

FIG. 5.

---

[13] Gregg and Mayo, *Faraday Soc. Discussions*, 1947, **2**, 328; cf. Fairclough and Hinshelwood, *J. Chem. Soc.*, 1937, 538, 1573; Cremer, *Experientia*, 1948, **4**, 349; Bamford and Dewar, *Nature*, 1949, **163**, 256; Moelwyn-Hughes, *Kinetics of Reactions in Solution* (Oxford University Press, 1933), p. 167; (1947 edition), p. 294.

* Cullis, Hinshelwood and Mulcahy (*Proc. Roy. Soc. A*, 1949, **196**, 160) noted that 50 mm. of 2-chloropropane decomposed at 343·5° C at 0·27 mm./min. This corresponds to a first-order velocity constant of $9·0 \times 10^{-5}$ sec.$^{-1}$, which

TABLE VII *

Substance Decomposed	Reaction Products	$\log_{10} A$	E (kcal./mole)
(*a*) *Normal Non-Exponential*	*Terms*		
C_2H_5Cl[1]	C_2H_4+HCl	14·6 ± 0·25	60·8 ± 0·8
$(CH_3)_2CHCl$	$CH_3 . CH : CH_2+HCl$	13·4 ± 0·2	50·5 ± 0·7
$(CH_3)_3CCl$[2]	$(CH_3)_2C : CH_2+HCl$	12·4 ± 0·2	41·4 ± 0·6
$CHCl_2 . CH_3$[1] †	$CH_2 : CHCl+HCl$	11·8 ± 0·3	48·3 ± 0·9
$CH_3 . CHCl . CH_2Cl$	Chloropropenes$+HCl$	13·8	54·9
$(CH_3)_3C(OH)$[14]	$(CH_3)_2C : CH_2+H_2O$	14·68	65·5
$(CH_3)_2(C_2H_5)C(OH)$[14]	Amylenes$+H_2O$	13·51	60·0
$(CH_3)_3C . OAc$[15]	$(CH_3)_2C : CH_2+CH_3 . CO_2H$	13·34	40·5
$(CH_3)_3C . O . CO . CH_2CH_3$[16]	$(CH_3)_2C : CH_2+CH_3 . CH_2 . CO_3H$	12·79	39·16
Cyclopentene [17]	Cyclopentadiene$+H_2$	13·04	58·8
(*b*) *Abnormal Non-Exponential*	*Terms*		
$CH_3 . CH(OAc)_2$ [18]	$CH_3 . CHO+Ac_2O$	10·3	32·9
$CH_3 . CH(OCOCH_2CH_3)_2$ [19]	$CH_3 . CHO+(CH_3CH_2CO)_2O$	10·4	32·9
$C_3H_7 . CH(OAc)_2$ [19]	$C_3H_7 . CHO+Ac_2O$	10·5	32·9
$Cl . CO_2 . C_2H_5$ [20]	$C_2H_5Cl+CO_2$	10·7	29·4
$Cl . CO_2 . CH(CH_3)_2$ [21]	$(CH_3)_2CHCl+CH_3CH : CH_2$ $+HCl+CO_2$	9·5	26·4

* It seems established that the thermal decompositions of paraldehyde (Coffin, *Can. J. Res.*, 1932, **7**, 75) and of related trimeric aldehydes (*idem.*, *ibid.*, 1933, **9**, 603 ; Bell and Burnett, *Trans. Faraday Soc.*, 1938, **34**, 420) are simple unimolecular reactions. In spite of this they have not been considered in Table VII, for their transition states are not, presumably, four-membered as in the other compounds discussed. The non-exponential terms of such thermal depolymerizations are in the region of 10^{13}. We have also not included the thermal decomposition of trichloromethyl chloroformate (Ramsperger and Waddington, *J. Amer. Chem. Soc.*, 1933, **55**, 214).

† The rate equation for 1 : 1-dichlorethane is slightly different from that given previously[1] for the same reason as in the preceding footnote. Again we are indebted to Dr. K. E. Howlett for making the necessary calculations.

It has been observed [13] that for a related series of rate processes a plot of the logarithm of the non-exponential term of the rate equation against the corresponding energy term often gives a straight line. Whatever the theoretical significance of such relationships may be, it was clearly of interest to examine the application of this correlation to the series ethyl chloride, 2-chloropropane (*iso*propyl chloride), *tert.*-butyl

is nearly three times greater than that computed from the rate equation found in the present paper. Since a clean-walled reactor was used it seems likely that the reaction observed by Cullis, Hinshelwood and Mulcahy was mainly heterogeneous. It also seems probable that the marked oxygen-catalyzed decomposition of 2-chloropropane, noted by these authors, was heterogeneous in origin. We have found that relatively large quantities of oxygen do catalyze the reaction, but the catalytic activity of the coated reactor walls, as judged by the rates of subsequent runs, is markedly increased in the process.

[14] Schultz and Kistiakowsky, *J. Amer. Chem. Soc.*, 1934, **56**, 395.

[15] Rudy and Fugassi, *J. Physic. Chem.*, 1948, **52**, 357.

[16] Warwick and Fugassi, *ibid.*, 1948, **52**, 1314.

[17] Vanas and Walters, *J. Amer. Chem. Soc.*, 1948, **70**, 4035.

[18] Coffin, *Can. J. Res.*, 1931, **5**, 636.

[19] *Idem.*, *ibid.*, 1932, **6**, 417.

[20] Choppin, Frediani and Kirby, *J. Amer. Chem. Soc.*, 1939, **61**, 3176 ; Choppin and Kirby, *ibid.*, 1940, **62**, 1592.

[21] Choppin and Compere, *ibid.*, 1948, **70**, 3797.

chloride, which differ structurally in a regular manner.* As Fig. 5 shows an excellent straight line is thereby obtained.

It is perhaps helpful at this stage in our investigations to summarize very briefly some of the more important literature with regard to unimolecular decomposition reactions. The latter can for the most part be divided into two types : (*a*) molecules which decompose to give two (or more) molecules by a single chemical transformation ; (*b*) molecules which decompose to give two radicals which then undergo a further series of reactions, very rapid compared with the rate of initial rupture of the molecule. Representative examples of the first type are further subdivided, as in Table VII into (*a*) reactions which have normal non-exponential terms, and (*b*) reactions where this term is abnormally low. The reactions included in both (*a*) and (*b*) must be regarded as proceeding through a cyclic four-membered transition state, exemplified by (I) for ethyl chloride and (II) for *tert.*-butyl alcohol.

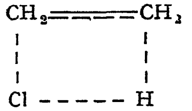

(I)

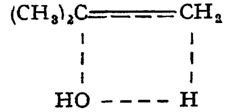

(II)

It has been suggested [21, 22] that reactions which involve transition states of this type having improbable configurations should have relatively large negative entropies of activation and thus rate equations with abnormally low non-exponential terms. However, this view cannot explain the absence of such anomalies for the compounds listed in the first part of Table VII. A possible explanation given by Rice and Gershinowitz [23] for the *tert.*-butyl alcohol dehydration is that the reaction proceeds in two steps, the first a migration of hydrogen from carbon to oxygen, the second a rupture of the oxygen-carbon bond. Apart from energetic considerations it seems to us that this mechanism is unlikely, since the requirement [24] of *cis*-stereochemistry in elimination reactions of the type discussed here cannot be explained easily on such a basis. Although reactions of both types (*a*) and (*b*) are elimination reactions, they do differ from each other in one respect. In type (*a*) reactions a $>C{=}C<$ linkage is formed whereas in type (*b*), a $>C{=}O$ linkage is produced. Correspondingly the $>C{=\!=}C<$ system is present in the transition state of type (*a*) but not in that of type (*b*).

The interpretation of the kinetics of reactions classified under type (*b*) and the proof of the absence of radical chains in their mechanisms is always difficult. Consequently it has been felt that discussion as for type (*a*) reactions is not justified at the present juncture. It is of interest in this connection, however, that recent work by Szwarc,[25] using a technique whereby these difficulties are largely eliminated, indicates that the non-exponential terms for the initial rupture of certain hydrocarbon molecules into two radicals are close to 10^{13}.

---

* The rate equation for ethyl chloride, $k = 10^{14.6\pm0.25}\,e^{-60,800\pm800/RT}$ sec.$^{-1}$ is slightly different from that given previously.[1] In the previous calculation of the best straight line by the least squares method the same statistical weight was given to each *mean* velocity constant. Dr. K. E. Howlett, to whom we are indebted, has now repeated the calculation giving the same statistical weight to *every* observed velocity constant and has further calculated the error limits by the method described previously.[3]

[22] Daniels, *Ind. Eng. Chem.*, 1943, **35**, 504 ; Glasstone, Laidler and Eyring, *The Theory of Rate Processes* (McGraw-Hill Book Co., New York, 1941), pp. 295-297.

[23] *J. Chem. Physics*, 1935, **3**, 479.

[24] Barton, *J. Chem. Soc.*, 1949, 2174.

[25] Szwarc, *J. Chem. Physics*, 1948, **16**, 128 ; 1949, **17**, 431.

We thank the Central Research Fund of London University for a grant in aid of this investigation. It was carried out during the tenure of an I.C.I. Fellowship by one of us (D. H. R. B.).

Imperial College,
London, S.W.7.

MEASUREMENTS ON THE ABSORPTION OF MICROWAVES

PART IV.[1]—NON-POLAR LIQUIDS

BY D. H. WHIFFEN

Received 2nd August, 1949

Benzene, carbon tetrachloride and similar symmetrical molecules which possess no permanent dipole moment are shown to have small dielectric losses which are proportional to the frequency in the range 0·3 to 1·2 cm.$^{-1}$. The experimental arrangement involves the measurement of the Q of a completely filled $H_{0,1,p}$ cavity resonator. The observed losses and their temperature coefficient are qualitatively explained on the basis of the existence of an average dipole moment in the liquid state of about 0·1 D per molecule, which is produced by molecular distortion.

In the course of testing materials for use as solvents for microwave loss measurements, it was observed that non-polar liquids such as benzene, carbon tetrachloride and carbon disulphide had a small, though definite, loss tangent near 1 cm.$^{-1}$ (30,000 Mc./sec.) which could not be removed by purification. A detailed study of such losses has been undertaken and the possible explanations are discussed in the later paragraphs.

Experimental

The loss tangents were derived from the Q of a fully-filled cavity resonator after the method of Bleaney, Loubser and Penrose.[2] A cylindrical $H_{0,1,p}$ cavity resonator was used at each wavelength range and these resonators were essentially the same as that shown in Fig. 2 of their paper, except that the input feeder was closed in each case with a reflecting plate half a wavelength from the axis of the resonator. The input and output guides were bent so that all the effective parts of the cavities could be immersed in a thermostat. All internal surfaces were electroplated with silver and thin mica windows were stuck over the insides of the coupling holes with De Khotinsky cement. Klystron oscillators were used as sources of radiation and silicon rectifying crystals as detectors. The galvanometer, found to be non-linear, was used merely as a null instrument, the crystal current being opposed by a known current derived with the aid of the standard resistances contained in a Cambridge Instrument Co. potentiometer. Measurements of the cavity Q, not only from the plunger travel between half-power points but also at lower transmissions, served to check the square-law nature of the crystal, which was found satisfactory on all but two occasions.

---

[1] Part III, Whiffen, *J. Amer. Chem. Soc.*, 1948, **70**, 2452.
[2] Bleaney, Loubser and Penrose, *Proc. Physic. Soc.*, 1947, **59**, 185.

In order to reduce interference at cross-over points [3] narrow cavities were used, the actual diameters being 3·50, 1·81 and 0·89 cm. for use near 0·3, 0·8 and 1·1 cm.$^{-1}$ respectively. Only the 1·81 cm. diam. cavity could be made resonant at a convenient frequency when filled with air; its Q was found to be 9,300 for the $H_{0,1,1}$ and 13,900 for the $H_{0,1,2}$ mode [3] at 0·87 cm.$^{-1}$. Theoretical values after allowing for the coupling holes and a 25 % decrease [4] from the direct current conductivity of silver, are 9,600 and 14,700 respectively. For fillings with very low loss tangent liquids it was possible to measure Q as a function of ν, the number of half-wavelengths in the cavity and to extrapolate $1/Q$, which is linear with $1/\nu$, to obtain a value for the Q of the $H_{0,1,\infty}$ mode. This depends only on the loss tangent of the liquid-filling and on the resistance losses in the side walls, which losses are small. Losses in the end wall, the plunger, in the mica windows, the cement and through the coupling holes are all inversely proportional to the number of wave-lengths and do not lower the Q for the $H_{0,1,\infty}$ mode. Subtraction of the theoretical value for the loss in the side wall from $1/Q$ leaves the loss tangent of the filling. This loss may then be used to obtain the total resistance and coupling losses at finite numbers of half-wavelengths and these values in their turn used to correct the Q values when extrapolation is not feasible because the absolute transmission of the cavity is too low at long cavity lengths with the higher loss fillings. In Table I are given the cavity diameters, the value of $1/Q$ for side wall loss only, $1/Q$ for the $H_{0,1,2}$ mode excluding losses in the liquid but including all resistance and coupling losses, and also given is the reproducibility in $1/Q$ with typical fillings. These are for average conditions of temperature, dielectric constant, exact frequency, etc., and corrections were applied for these factors where they were significant. This Table shows that the resistance loss is small compared with the losses of benzene as given in Fig. 1.

TABLE I

Frequency Region (cm.$^{-1}$)	Cavity Diameter (cm.)	$1/Q$ Side Walls	$1/Q$ for $H_{0,1,2}$ Mode	Reproducibility in $1/Q$
0·3	3·50	$0·15 \times 10^{-4}$	$0·45 \times 10^{-4}$	$0·1 \times 10^{-4}$
0·8	1·81	$0·2 \times 10^{-4}$	$0·9 \times 10^{-4}$	$0·3 \times 10^{-4}$
1·1	0·89	$0·8 \times 10^{-4}$	$1·5 \times 10^{-4}$	$0·5 \times 10^{-4}$

Materials.—BENZENE. A.R. thiophen-free benzene further purified by fractional freezing six times and dried over P_2O_5: n_D^{20} 1·5012, d_4^{25} 0·8740. A cooling curve taken with a thermocouple showed that 2/3 of this material froze within 0·04° C. Other pure samples dried over Na, over solid KOH, or redistilled from Na in dried air gave the same loss. A.R. benzene showed losses about 15 % higher and benzene saturated with water gave losses 50 % higher.

Trans-DECALIN. Commercial decalin was washed with H_2SO_4, NaOH and fractionally distilled twice under reduced pressure. The low boiling *trans* fraction was recrystallized three times from acetone, washed with water and dried with P_2O_5: n_D^{20} 1·4695, d_4^{25} 0·8642; 2/3rd froze within 0·5° C. The infrared spectrum showed no trace of any *cis* isomer. The rather large freezing range and the low density indicate that this material contains a trace of impurity, but there was insufficient *trans*-decalin for further recrystallizations.

CYCLOHEXANE. Frozen five times, dried P_2O_5, n_D^{20} 1·4264, d_4^{25} 0·7730.

CARBON TETRACHLORIDE. B.P. grade washed with H_2SO_4 and distilled in a Stedman fractionating column. Dried P_2O_5; n_D^{20} 1·4605, d_4^{25} 1·5841; 4/5th of this material froze within 0·04° C.

TETRACHLORETHYLENE. Commercial sample fractionally frozen ten times and dried K_2CO_3: n_D^{20} 1·5060, d_4^{25} 1·6144; 4/5th of this material froze within 0·02° C.

CARBON DISULPHIDE. Commercial CS_2 shaken with solid $KMnO_4$, with H_2SO_4, with H_2O and Hg. Redistilled and stored in the dark over $HgSO_4$: n_D^{20} 1·6290, d_4^{25} 1·2553.

---

[3] Nomenclature follows Lamont, *Wave Guides* (Methuen, 1942).

[4] Horner, Taylor, Dunsmuir, Lamb and Jackson, *J. Inst. Elect. Eng.*, Part III, 1946, **93**, 53.

"Mix". Results under this abbreviation refer to a mixture of equal volumes of benzene and carbon tetrachloride.

For each compound purification was continued until no further diminution of loss tangent could be obtained.

Results

Fig. 1 shows the loss tangent at 20° C plotted against frequency for the three hydrocarbons, benzene, *trans*-decalin and cyclohexane, and for a mixture of benzene and carbon tetrachloride. Fig. 2 shows the loss tangents of tetrachlorethylene, carbon tetrachloride and carbon disulphide treated in the same way. The centres of the vertical lines are the experimental points and their lengths are an indication of the experimental errors. No experimental point lies seriously off the corresponding straight line through the origin and the conclusion in each case must be that the loss is proportional to the frequency in this range. In no case is the loss greater than that found by Bleaney, Loubser and Penrose [2] and such differences as exist may reasonably be explained by impurities in their materials. Neither are the present results inconsistent with the loss values for benzene given by Powles.[5] Fig. 3 shows the variation of the loss tangents with temperature for benzene, carbon tetrachloride and the mixture at two frequencies, namely 0·72 and 0·33 cm.$^{-1}$. The two graphs are almost identical, except for the vertical scale, as would be expected if the loss is proportional to the frequency at each temperature for each liquid.

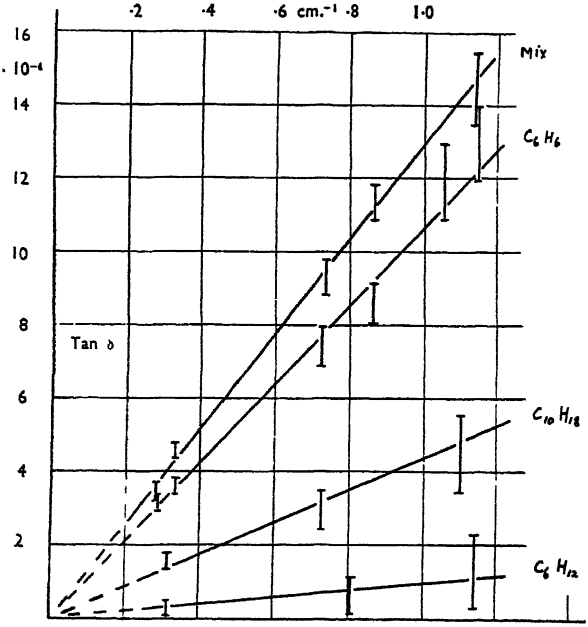

FIG. 1.—Loss tangent against frequency for the carbon tetrachloride-benzene mixture, for benzene, for *trans*-decalin, and for cyclohexane at 20° C.

A few measurements were also made with solutions of hexachlorbenzene, hexachlorethane, *p*-dichlorbenzene and *p*-dinitrobenzene dissolved in benzene and carbon tetrachloride. The indications were that these compounds when pure have loss tangents of the same order of magnitude as benzene. However, some of the solubilities are small and the changes of loss tangent were all less than 0·5 × 10^{-4} at 0·33 cm.$^{-1}$ and 20° C for the saturated solutions, so that a fuller investigation was not undertaken.

---

[5] Powles, *Trans. Faraday Soc.*, 1946, **42A**, 157.

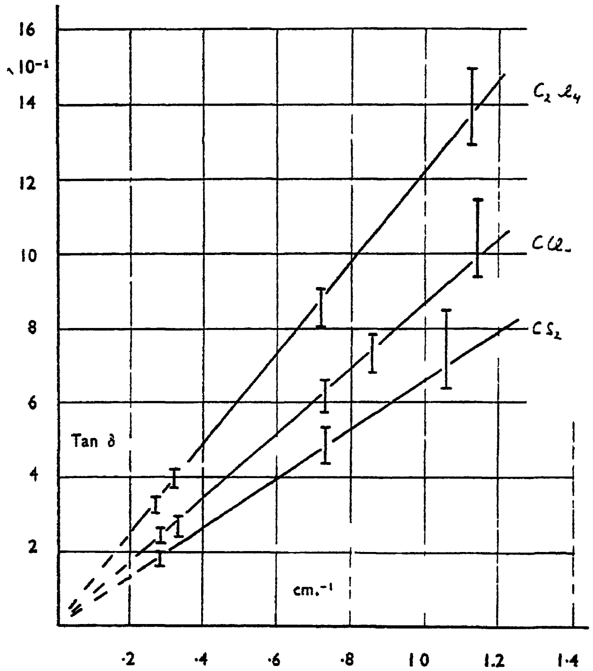

FIG. 2.—Loss tangent against frequency for tetrachlorethylene, for carbon tetrachloride and for carbon disulphide, at 20° C.

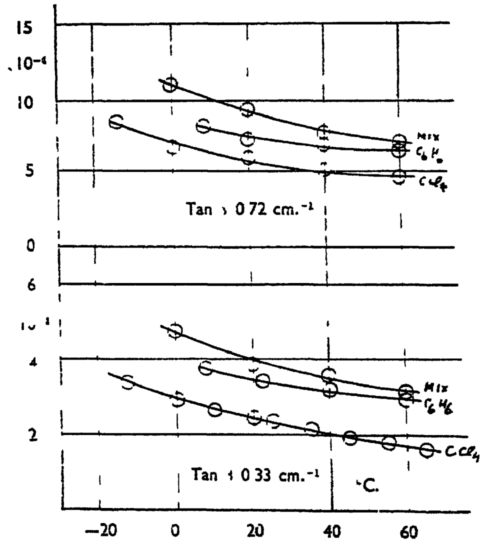

FIG. 3.—Loss tangent against temperature for the carbon tetrachloride-benzene mixture, for benzene and for carbon tetrachloride.
(*a*) at 0·72 cm.⁻¹, (*b*) at 0·33 cm.⁻¹.

Discussion

Any explanation of these losses must be consistent with their approximate magnitude, with the fact that the maximum loss lies above a frequency of 1·5 cm.$^{-1}$, and with the slight decrease of loss with increase of temperature.

Dielectric losses in the microwave region are normally explained as the relaxation losses of rotating dipoles, as first predicted by Debye.[6] All the molecules examined here have a centre of symmetry in their undistorted state and can, therefore, have no permanent dipole moment. This is not strictly true for molecules with different isotopes such as $CCl_3^{35}Cl^{37}$, etc., but the dipole moment is probably less than 0·02 D which is insufficient to account for the observed loss by a factor of 20 ; also for hydrocarbons the abundance of rare isotopes is too low for such an explanation to apply. The rotational transition is also permitted to appear in absorption as a consequence of the molecular quadrupole moment, except for carbon tetrachloride for which it is zero, but the magnitude of this effect is certainly too small at these frequencies and might be expected to depend on a higher power of the frequency.[7] Also apart from this complexity the maximum loss for a mechanism involving rotation would be expected to occur at the reciprocal of the relaxation time which is 0·8 cm.$^{-1}$ for toluene [8] and is unlikely to be above 1·5 cm.$^{-1}$ for benzene or solutions of impurity in benzene. Nor is any mechanism involving nuclear quadrupole moments applicable since C^{12}, H^1 and S^{32} all have zero moments.

Before suggesting that the observed losses are due to transient dipole moments, the possibility must be considered that it is the long wavelength tails of vibrational, infra-red absorption bands which are being observed. Indeed absorption from such a cause would quite possibly be proportional to the frequency as is predicted by both the Lorentz [9] and the Van Vleck and Weisskopf [10] formulae for line shapes in gases. But the absorption seems to be stronger than can be accounted for by such tails ; the quantitative evidence is scanty but some of these liquids transmit well [11, 12] at 70 cm.$^{-1}$ and the straight lines of Fig. 1 and 2 cannot extend to this frequency since they would predict too great absorption by a factor of about a hundred. There must then be a maximum in the loss before this frequency is reached. Furthermore the line breadths of infra-red bands increase with temperature so that an increase of the loss in the low-frequency tail would also be expected. This second argument applies even more strongly to difference bands, which are the only type of vibration bands with centres below 70 cm.$^{-1}$ for these molecules, since in these cases the population of the initial state, on which the intensity depends directly, increases rapidly with temperature by virtue of the Boltzmann distribution factor.

If the above arguments are accepted as showing that the loss is due to neither a rotational nor a vibrational transition, the consequences of the possibility that these molecules possess a dipole moment arising from distortion in the liquid state, must be considered. Quantitatively a contribution to the static polarization of about 0·15 cm.^{3} for benzene, and in proportion for the other liquids, dispersing according to the Debye form of the loss curve with a relaxation time of $1·0 \times 10^{-12}$ sec. would account for the observations. With the frequency dependence of the

---

[6] Debye, *Polar Molecules* (Chemical Catalogue Co., New York, 1929).

[7] Condon and Shortley, *Theory of Atomic Structure* (Cambridge University Press, 1935).

[8] Whiffen and Thompson, *Trans. Faraday Soc.*, 1946, **42A**, 166.

[9] Lorentz, *The Theory of Electrons* (Stechert & Co., New York, 1916).

[10] Van Vleck and Weisskopf, *Rev. Mod. Physics*, 1945, **17**, 227.

[11] Cartwright and Errera, *Proc. Roy. Soc. A*, 1936, **154**, 138.

[12] Barnes, Benedict and Lewis, *Physic. Rev.*, 1935, **47**, 129.

Debye formula, namely, loss proportional to $\omega\tau\ (1 + \omega^2\tau^2)$, where ω is the angular frequency and τ the relaxation time, the loss only departs from linearity with frequency by less than 5 % up to 1·2 cm.$^{-1}$ if the relaxation time is 1·0 × 10^{-12} sec.; this relaxation time is equivalent to a loss maximum at 7 cm.$^{-1}$. The value of 0·15 cm.^{3} suggested for the relevant polarization, is smaller than the reliability of gas measurements and a difference of this order of magnitude between gas and liquid polarizabilities would be difficult to observe, besides which it is not certain that the electronic and atomic contributions to the polarizability are constant to this accuracy. This liquid polarization of 0·15 cm.^{3} is equivalent to an average dipole moment of 0·1 D and it is suggested that such moments exist in the liquid state. This does not seem unreasonable since for carbon tetrachloride it would arise if one C—Cl link were bent through 6° from its equilibrium position; this would require 300 cal./mole, which is the potential energy in the force field at this distortion and is small compared with 7,500 cal./mole, which is the latent heat of evaporation and a measure of the cohesive energy of the liquid. The figures for carbon disulphide and tetrachlorethylene would be similar, but for benzene such a large moment is surprising. However, Le Fèvre and Le Fèvre [13] suggest that a dipole moment is able to induce a moment in liquid benzene of 0·4 times its own value, so that a suitable geometrical arrangement of C—H links of individual moment 0·4 D might induce a moment of 0·1 D.

The suggested relaxation time of 1·0 × 10^{-12} sec. is decidedly shorter than any value yet found for rotational relaxation. This can be explained if the dipole moment arises only as a result of the exact configuration of neighbouring molecules which are rapidly changing so that the dipole moment induced may change or vanish before the molecule in which it is situate can rotate appreciably. Thus, instead of changing direction by rotation of the molecule, the dipole moment will change direction by virtue of a new distortion produced at a later instant by another neighbour. The new direction of the dipole moment may be random in direction with respect to the earlier one, except that in the presence of a low frequency or static measuring field F each dipole moment μ will have a relative probability, $\exp(\mu F \cos\theta/kT)$, of being aligned at an angle θ to the field, this being the usual Boltzmann equilibrium factor. It is this extra probability of being aligned parallel to the electric field which gives rise to the low frequency polarization in a manner analogous to that obtained by the usual theoretical treatments of rotating molecules in a liquid. At a measuring field frequency comparable to the time required to establish the induced dipole moment, the field will change direction before the full polarization is set up and so dispersion and absorption will be present at these frequencies. Given the existence of a low-frequency polarization and a single relaxation time, the Debye form of dispersion curve follows quite generally [14] so that the linear dependence of the loss with frequency in the present instance is explained. That the relaxation time of such induced dipoles should be as short as 10^{-12} sec. is reasonable as this is the order of magnitude of the time between collisions in a liquid.

With such a collision picture of the process which leads to the polarization, it is difficult to predict the effect of an increase of temperature. The relaxation time probably decreases which is a factor tending to lower loss at 1 cm.$^{-1}$ but the change of the mean dipole moment is more difficult to assess and it is this quantity which controls the height of the maximum of the absorption curve. Since the dipole moment and the relaxation time arise from intermolecular effects, the loss of a mixture need not arise additively from the loss of the components according to their concentrations. Indeed, the losses of the carbon tetrachloride and benzene mixture are greater than those of either component at the same temperature (see Fig. 3).

---

[13] Le Fèvre and Le Fèvre, *J. Chem. Soc.*, 1936, 487.

[14] Yager, *Physics*, 1936, **7**, 434.

This mechanism for the loss can be considered from other aspects. It is a special case of the type discussed by Frank and Sutton [15] in which the solute and solvent molecule are identical. Furthermore, it is a case of the breakdown of the spectroscopic selection rules in the liquid state, since rotational absorption should be forbidden for non-polar molecules or it might even be described as a non-resonant translational spectrum. There should also be connection with the non-zero depolarization factor found for liquid carbon tetrachloride [16] which also implies an unsymmetrical molecule. However, in the absence of dielectric loss measurements at still higher frequencies where it should be possible to obtain the height and position of the absorption maximum, further discussion seems barren.

I am indebted to the Telecommunications Research Establishment, Malvern, for the loan of apparatus and to R. A. W. Hill for the loan of a pyknometer and for some samples of benzene. Also I wish to thank Dr. H. W. Thompson, F.R.S., for making available the equipment and for his encouragement and I wish most gratefully to acknowledge the award of a Senior Studentship by the Royal Commissioners for the Exhibition of 1851.

Physical Chemistry Laboratory,
Oxford University.

[15] Frank and Sutton, *Trans. Faraday Soc.*, 1937, **33**, 1307.
[16] Rank, *J. Opt. Soc. Amer.*, 1947, **37**, 798.

MEASUREMENTS ON THE ABSORPTION OF MICROWAVES

PART V.[1]—THE VARIATION OF RELAXATION TIME WITH SOLVENT

BY D. H. WHIFFEN

Received 2nd August, 1949

An account is given of an experimental method of measuring dielectric losses at 1·6 cm.$^{-1}$. Values of the loss at this and lower frequencies are given for some 25 systems of polar molecules dissolved in non-polar solvents. The results, which in the majority of cases are accurately expressed by a single Debye loss curve, are discussed in terms of the rotational relaxation times.

Since klystron oscillators have become available as radiation sources in the microwave region, several studies have been made on the rotational relaxation times of molecules in pure liquids and in solution. Such times, which are obtained essentially from the frequency of the peak of the Debye loss curves, have been measured for polar molecules dissolved in benzene,[2-6] in cyclohexane,[4, 6, 7] in heptane,[4, 8] and in paraffin ; [2, 4, 6] other solvents

[1] Whiffen, *Trans. Faraday Soc.*, preceding paper.
[2] Jackson and Powles, *ibid.*, 1946, **42A**, 101. [3] Powles, *ibid.*, 1948, **44**, 537.
[4] Whiffen and Thompson, *ibid.*, 1946, **42A**, 114 and 122.
[5] Cripwell and Sutherland, *ibid.*, 1946, **42A**, 149.
[6] Hall, Halliday, Johnson and Walker, *ibid.*, 1946, **42A**, 136.
[7] Whiffen, *J. Amer. Chem. Soc.*, 1948, **70**, 2452.
[8] Whiffen and Thomson, *Trans. Faraday Soc.*, 1946, **42A**, 166.

have been used at a single frequency.[6] In the present paper relaxation times for camphor in seven different solvents are given, as well as those of other polar molecules in various solvents.

Experimental

For loss measurements near 0·3 cm.$^{-1}$ a filled cavity resonator was used as described in Part IV.[1] For solution measurements it is unnecessary to know the wall resistance loss and the solvent loss separately and the loss tangent contribution due to the dissolved material alone is given by $(1/Q - 1/Q_0)$, where Q_0 is the Q of the solvent-filled cavity at the same resonance point and frequency.

For the range 0·6 to 1·6 cm.$^{-1}$ guide transmission methods were used. For the lower frequencies the details are already published,[3, 4] but at 1·6 cm.$^{-1}$ there are special features necessitated by the absence of klystron oscillators for this frequency. The radiation was generated by a crystal-doubler fed from a 0·8 cm.$^{-1}$ (*K*-band) klystron and it was detected with a superheterodyne arrangement by a crystal mixer which was also receiving radiation from the local oscillator, namely a second klystron. This oscillator was swept in frequency over a range of 10 Mc. sec. by means of an 800 c./sec. saw-tooth voltage injected to its reflector. When the two klystrons were 22·5 Mc. sec. apart in frequency, the 45 Mc./sec. beat frequency, produced from the overtone of the local oscillator and the 1·6 cm.$^{-1}$ signal which had traversed the test liquid, was amplified by a sharply tuned 45 Mc./sec. amplifier strip, detected and smoothed as regards the 45 Mc. sec. frequency. At this stage the signal consisted in a sharp pip of repetitive frequency 800 per sec., the amplitude of which was measured with a peak detector circuit with a long time constant. The steady output is thus proportional to the 1·6 cm.$^{-1}$ signal. The whole amplifier-detector system was calibrated by comparison with a modulated 45 Mc. sec. signal from a Mk V signal generator of the Marconi Instrument Co. which had a built-in calibrated attenuator. In this way the amplifier with its stepped gain control, the peak detector and its out-put meter, were all used as null instruments. With a good doubling crystal the full signal was 40 db in power above the noise level of the system. The sample of liquid for measurement was contained in a U-tube of silver wave guide of internal cross-section 0·45 × 0·25 cm., which was filled with a known volume of liquid the length of which was then calculated from

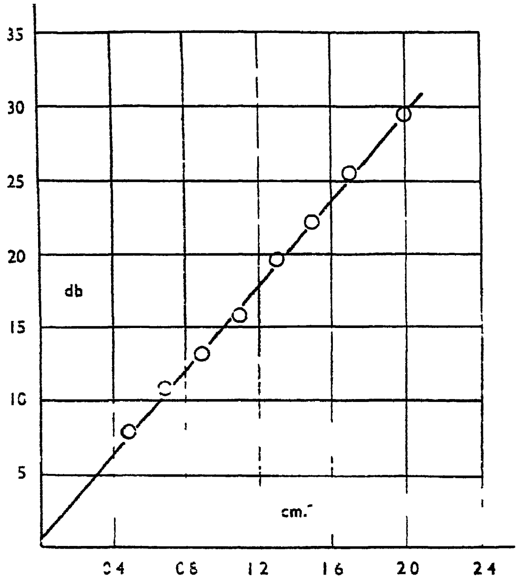

FIG. 1.—Db-loss against cm.$^{-1}$ filling of wave guide cell for toluene at 1·60 cm.$^{-1}$

the cross-sectional area. The accuracy of the method depends on the calibration of the signal generator and on the accuracy of the guide cross-section. Plots of the db-loss in the cell against volume of the filling give good straight lines and from their slopes the loss tangents are derived. One such line, for pure toluene, is shown in Fig. 1; the slope is 14·6 db/cm^3 which corresponds to a loss tangent of 0·0225 and a molecular loss tangent of 0·00238 at 20° C and 1·60 cm.$^{-1}$. A dipole moment of 0·32 D and a relaxation time of $6{\cdot}4 \times 10^{-12}$ sec. as suggested by Whiffen and Thompson[8] leads to a molecular loss tangent of 0·00231 under the same conditions.

All the chemicals used were commercial samples purified by recrystallization or redistillation and their purities were checked by means of their refractive indices or their melting points.

Results

The molecular loss tangents, that is the loss tangent of the solute referred to a concentration of 1 mole/l., observed at 20° C are given in Table I. These

TABLE I

Frequency (cm.$^{-1}$)	0·274	0·299	0·606	0·788	1·13	1·60
CHLOROFORM in						
Benzene	0·023	—	0·034	0·034	0·032	0·030
Cyclohexane	—	0·0118	—	0·029	0·033	0·034
Carbon tetrachloride	0·0157	—	0·030	0·032	0·034	0·031
Carbon disulphide	—	0·0100	—	0·025	0·030	0·034
CAMPHOR in						
Benzene	—	0·192	0·228	0·212	0·190	0·142
Cyclohexane	0·161	—	0·230	0·232	0·213	0·189
Carbon tetrachloride	—	0·211	0·235	0·212	0·178	0·130
Carbon disulphide	—	0·159	0·226	0·219	0·202	0·163
Methyl cyclopentane	—	0·131	—	0·245	0·237	0·198
Tetrachlorethylene	—	0·190	0·219	0·183	0·159	0·120
NITROBENZENE in						
Benzene	0·375	—	0·399	—	0·269	0·217
Cyclohexane	0·338	—	0·408	0·386	0·330	0·279
n-Heptane	0·262	—	0·409	0·417	0·378	0·335
Carbon tetrachloride	0·388	—	0·337	0·289	0·220	0·177
Carbon disulphide	0·290	—	0·412	0·389	0·312	0·270
CHLORBENZENE in						
Benzene	0·048	—	0·063	0·061	0·054	0·045
Cyclohexane	—	—	0·064	—	0·055	0·051
BROMBENZENE in						
Benzene	0·053	—	0·061	—	0·044	0·038
Cyclohexane	—	—	0·062	—	0·047	0·039
METHYL BENZOATE in						
Benzene	0·077	—	0·086	0·078	0·060	0·048
Cyclohexane	0·072	—	0·077	0·067	0·055	0·044
ETHYL BENZOATE in						
Benzene	0·088	—	0·085	—	0·057	0·046
Cyclohexane	0·082	—	0·074	0·065	0·053	0·043
BENZOPHENONE in						
Benzene	—	—	0·197	0·157	0·114	0·084
Cyclohexane	0·216	—	0·163	0·137	0·105	0·080

All loss tangents at a concentration of 1 mole/l. and at 20° C.

values are derived from measurements at several concentrations so chosen as to give a convenient loss tangent according to the method of measurement. The greatest concentration used was 0·8 mole/l. for chloroform in carbon tetrachloride but the majority of the solutions were five times more dilute ; for each system the loss was found to be proportional to the concentration.

Including loss tangents already published,[2-7] values of the loss for at least four frequencies are available for each of the systems of Table I. With such a range it is possible to say whether or not the loss curve follows the Debye shape for a single relaxation time. A direct graph of loss against frequency, or log frequency, is not very convenient for this purpose as it is difficult to choose the best values of the parameters for fitting a curve to the experimental points. This situation is made worse by the fact that the experimental errors are usually a constant fraction of the observed loss, rather than a constant absolute quantity, so that the points on the graph are not of equal accuracy as seen on a direct scale. If instead the product, loss tangent × frequency, is plotted against the ratio, loss tangent/frequency, a straight line should result. This follows from the Debye equation in the form [4]

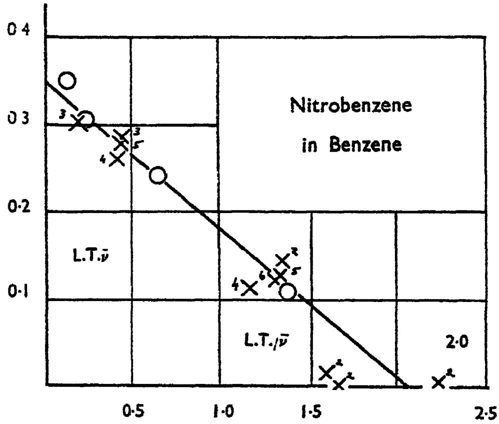

FIG. 2.—Loss tangent × frequency against loss tangent/frequency for nitrobenzene in benzene.

O loss from this paper ; X loss from reference as numbered.

$$L.T. = K\omega\tau/(1 + \omega^2\tau^2)$$

in which L.T. is the molecular loss tangent, ω is the angular frequency and τ the time of relaxation and K is given by

$$K = (\epsilon - 2)^2 4\pi N\mu^2/(27\epsilon kT)$$

where ϵ is the dielectric constant of the solvent and μ the dipole moment of the solute. This equation can be rearranged to give

$$(L.T./\omega) + \tau^2(L.T. \times \omega) = K\tau.$$

This shows that the graph of L.T. ω against L.T. $\times$ ω should be a straight line with slope τ^2; knowing τ then the intercept or any other point on the line gives a value of K from whence μ may be derived. An experimental error of 1 % at any frequency moves the corresponding point 1 % nearer or further from the origin and, provided the scales are chosen so that the slope of the line is approximately 45°, this error is an approximately constant distance at any part of the line. Furthermore the closeness of fit of a straight line to experimental points is easily judged by eye and the best straight line can be determined objectively by the method of least squares.

Factors which might cause a departure from strict linearity include the existence of a multiplicity of active relaxation times, such as would be expected for a molecule with a general frictional ellipsoid [9] or for a flexible molecule with a distribution of molecular shapes. In these cases the curve should be convex towards the origin, whereas a curve concave to the origin would indicate a loss peak narrower than the Debye shape and would be indicative of a resonance phenomenon. This latter would be unexpected for liquids except where the effect of the moment of inertia becomes important. Assuming[10] $I^{\frac{1}{2}}/\tau$ to be $2 \cdot 5 \times 10^{-8}$ c.g.s. units, visible departure of the L.T./ω against L.T. × ω graph from a straight line does not occur until frequencies at which L.T./ω has fallen to one hundredth of its value at $\omega = 0$, whereafter the value of L.T. × ω decreases rapidly and the curve falls to the origin. To detect the effect of the moment of inertia term would require a frequency of 6 cm.$^{-1}$ for benzophenone and even higher frequencies in the other cases. Actually the slope of the best straight line at low and intermediate frequencies is nearer $(\tau + \tau')^2$ than τ^2, where $\tau' = I/(2kT\tau)$ and is $\tau/100$ with the above value of $I^{\frac{1}{2}}/\tau$: this small correction has not been applied to the values of τ quoted below.

---

[9] Perrin, *J. Phys. Radium*, 1934, **5**, (vii), 497.

For each of the systems measured graphs of L.T./$\bar{\nu}$ against L.T. × $\bar{\nu}$ have been constructed including not only the measurements presented here but also the relevant loss values to be found in the literature.[2-7] $\bar{\nu}$ the frequency in wave numbers has been used in place of ω the frequency in radians/sec. for numerical convenience. In each case measurements at, or near, 1·6, 1·2, 0·8 and 0·3 cm.$^{-1}$ were available and in many cases values at 0·6 cm.$^{-1}$ and at low frequencies such as 0·1 cm.$^{-1}$ were also available. As examples of such graphs, Fig. 2 and 3 show the points for nitrobenzene in benzene and cyclohexane respectively. The circles refer to measurements reported in the present paper and the crosses to older values; the numbers against the crosses refer to the reference in which the loss measurement can be found. The previous measurements, both as shown in these graphs and in the others which are not published, lie above, on, and below the best straight lines and there are no strong indications of systematic differences.

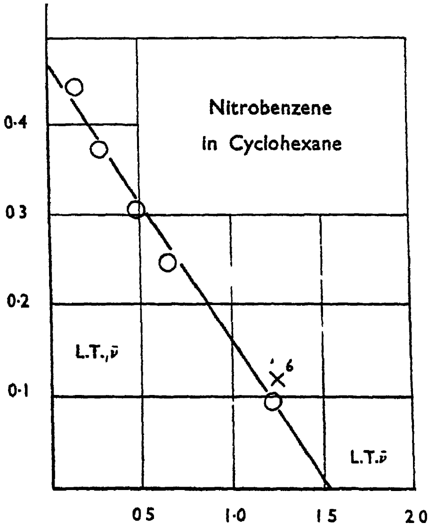

FIG. 3.—Loss tangent × frequency against loss tangent/frequency for nitrobenzene in cyclohexane.
O loss from this paper; X loss from ref. 6.

Discussion

From the slope and intercept of the graph, values of the relaxation time and the dipole moment of the solute were calculated in each case, with the results shown in Table II; this also includes values for chloroform and camphor dissolved in n-heptane[8] and the viscosities of the solvents at 20° C.

---

[10] Powles, *Trans. Faraday Soc.*, 1948, **44**, 802.

Except with a few cyclohexane solutions all the graphs were good straight lines and for these systems the Debye frequency dependence of the loss with one relaxation time must hold closely. For the cyclohexane solutions of methyl benzoate and benzophenone there are slight indications of curvature convex to the origin. For these two the curvature is of the same order of magnitude as the experimental errors, but for ethyl benzoate in cyclohexane there is a similar curvature which is rather more pronounced. The sum of two Debye loss terms with $\mu_1 = 1{\cdot}62$ D and $\tau_1 = 18{\cdot}5 \times 10^{-12}$ sec. and $\mu_2 = 0{\cdot}85$ D and $\tau_2 = 5{\cdot}3 \times 10^{-12}$ sec. leads to the full line in Fig. 4 which fits the experimental points better than a single loss term with $\mu = 1{\cdot}79$ D and $\tau = 13{\cdot}8 \times 10^{-12}$ sec. which gives the broken straight line : equally effective expressions with a continuous distribution of relaxation times could doubtless be devised. Possible reasons for the broadened dispersion include :

TABLE II

Solvent		Benzene	Cyclohexane	*n*-Heptane	Carbon Tetrachloride	Carbon Disulphide	Methyl Cyclopentane	Tetrachlor-ethylene	All at 20° C
Viscosity		0·65	0·97	0·42	0·97	0·37	0·50	0·9	cpoise
Chloroform	τ	7·1	3·2	3·1	5·0	2·7	—	—	$\times 10^{-12}$ sec.
	μ	1·12	1·13	1·09	1·11	1·12	—	—	D
Camphor	τ	9·5	7·1	6·5	10·7	7·5	5·8	10·7	$\times 10^{-12}$ sec.
	μ	2·90	2·95	2·99	2·90	2·84	2·90	2·78	D
Nitrobenzene	τ	12·8	9·5	6·8	15·2	8·6	—	—	$\times 10^{-12}$ sec.
	μ	3·92	3·92	3·90	3·81	3·79	—	—	D
Chlorobenzene	τ	8·3	7·8	—	—	—	—	—	$\times 10^{-12}$ sec.
	μ	1·52	1·55	—	—	—	—	—	D
Brombenzene	τ	10·6	10·4	—	—	—	—	—	$\times 10^{-12}$ sec.
	μ	1·54	1·55	—	—	—	—	—	D
Methyl benzoate	τ	11·4	11·9	—	—	—	—	—	$\times 10^{-12}$ sec.
	μ	1·79	1·72	—	—	—	—	—	D
Ethyl benzoate	τ	12·9	13·8	—	—	—	—	—	$\times 10^{-12}$ sec.
	μ	1·85	1·79	—	—	—	—	—	D
Benzophenone	τ	17·4	17·8	—	—	—	—	—	$\times 10^{-12}$ sec.
	μ	2·90	2·80	—	—	—	—	—	D

(i) Flexibility of the molecule leading to slightly different shapes in different individual molecules at any instant.

(ii) The activity of two or three relaxation times due to the distorted ellipsoidal nature of the molecule with a dipole moment not directed along a principal axis of the frictional ellipsoid.[9]

(iii) The existence in the liquid state of non-quantized internal rotation about the $C_6H_5CO—OC_2H_5$ bond which would lead to a contribution to the polarization with a different relaxation time from the rotation of the molecule as a whole.

The values of the dipole moment are all in agreement with the literature values,[11] at least to 5 %, the microwave values showing a tendency to be the lower. Exceptional in this respect is the present value of 3·79 D for nitrobenzene in carbon disulphide which is to be compared with the most probable value of 3·66 D given by Smith and Cleverdon.[12]

Concerning the exact values of the relaxation times, less can be said than might have been hoped. The times are not closely parallel to the solvent viscosities; for instance, camphor appears to rotate faster in cyclohexane than in carbon disulphide despite a 2·5-fold diminution of viscosity with the latter solvent. Neither is there any clear order of the solvents between themselves. The long relaxation time of $7{\cdot}1 \times 10^{-12}$ sec. for chloroform in benzene stands out amongst the shorter times for this solute in other solvents and it may be that the chloroform molecule is able to pack closely on the side of a benzene ring and is less able then to rotate about an axis perpendicular to the C—H link. At least this is an example of the fact that unknown and often specific interactions play an important part in determining times of relaxation.

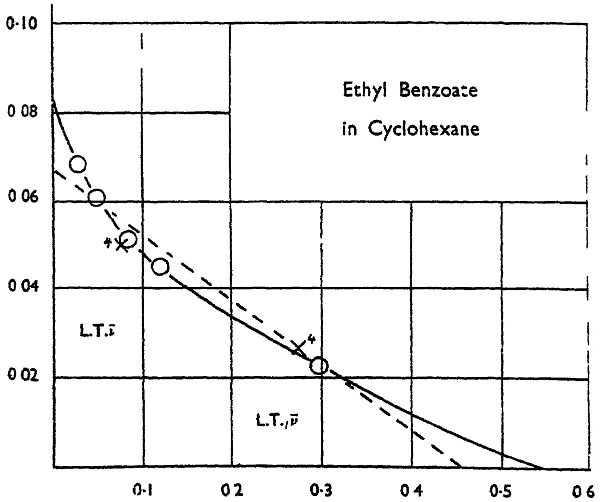

FIG. 4.—Loss tangent × frequency against loss tangent/frequency for ethyl benzoate in cyclohexane.

O loss from this paper ; X loss from ref. 4.

In the absence of any clear trend of the relaxation times with any physical property, apart from the size of the solute molecule, it is not profitable to discuss the exact values in greater detail. It is to be hoped that the general picture will become clearer when more measurements on very small and very large solute molecules are available.

In conclusion I would like to express my indebtedness to the Telecommunications Research Establishment, Malvern, for the loan of equipment and to Dr. L. E. Sutton for the loan of a signal generator. Furthermore, I would thank Dr. H. W. Thompson, F.R.S., for his encouragement and Mr. C. H. Miller for help in the design of electronic circuits. Also I acknowledge with sincere thanks the award of a Senior Studentship by the Royal Commissioners for the Exhibition of 1851.

Physical Chemistry Laboratory,
Oxford University.

---

[11] For dipole moments obtained from low frequency dielectric constant measurements see any table of moments such as Wesson, *Table of Dipole Moments* (Massachusetts Institute of Technology, 1947).

[12] Smith and Cleverdon, *Trans. Faraday Soc.*, 1949, **45**, 109.

MOLECULAR FORCE FIELDS

PART XII.—FORCE CONSTANT RELATIONSHIPS IN THE NON-METALLIC HYDRIDES

By D. F. Heath, J. W. Linnett and P. J. Wheatley

Received 16*th August*, 1949

The vibration frequencies of the saturated hydrides of the non-metallic elements of Groups IV, V, VI and VII have been used to calculate the force constants of these molecules. The potential energy function employed was based on the conception of bonding by overlap of atomic orbitals. It has been supposed, in addition, that changes of hybridization and of the spatial distribution of the orbitals could make certain distortions easier by a partial accommodation of the orbitals to the distortion. Comparisons have been made, within the various Groups and Periods of the Periodic Table of (i) the bond-stretching constants (ii) some bond-bond cross-term constants and (iii) the bending and orbital-following constants. The results have been discussed.

In Part I [1] we made a detailed examination of the potential energy (P.E.) function of the water molecule and concluded that hybridization changes in the atomic bonding orbitals during distortion were more important than HH repulsions. In Part VII [2] we studied the vibration frequencies of methane and its deuterated derivatives. We came to the conclusion that the orbital theory of directed valency combined with the conception of orbital following by change of hybridization [3] during certain distortions provided a satisfactory basis for constructing a potential energy function for this molecule. It seemed worthwhile to extend the conceptions provided by these detailed treatments to a wider range of molecules and to study the P.E. functions of the hydrides of the elements in Groups IV, V, VI and VII. There are rather less data available than we had hoped; but, nevertheless, some interesting regularities and irregularities are shown. Because of our results with CH_4 and H_2O we shall suppose that direct HH interaction forces are relatively unimportant and negligible (they cannot, of course, be non-existent). We shall examine (i) the bond stretching force constants and, where possible, consider these in relation to the bond lengths (ii) the bond–bond interaction constants and (iii) the bending constants, treating the bending on an orbital valency force field basis [4] combined with the conception of orbital following.[3] The molecules studied are CH_4, SiH_4, GeH_4, NH_4^+, NH_3, PH_3, AsH_3, H_2O, H_2S, H_2Se, HF, HCl, HBr and HI.

Results

The equations for the frequencies are given in the Appendix.

MH_4 Molecules.—For the tetrahedral molecules we used the P.E. function which had been tested for CH_4 in Part VII.[3] This involves a bond-stretching constant k_1, a bond bending constant k_H, and an orbital-following constant k_ϕ. The two stretching vibration frequencies (only one in GeH_4) are calculated in all molecules within 1½ % by one constant for each molecule. The two bending vibration frequencies enable k_H and k_ϕ to be calculated. The results are shown in Table I. The bond length is represented by r.

---

[1] Heath and Linnett, *Trans. Faraday Soc.*, 1948, **44**, 556.
[2] Linnett and Wheatley, *ibid.*, 1949, **45**, 39.
[3] Linnett and Wheatley, *ibid.*, 1949, **45**, 33.
[4] Heath and Linnett, *ibid.*, 1948, **44**, 873, 878, 884.

TABLE I

Molecule	$k_1 \times 10^{-5}$	$k_H/r^2 \times 10^{-5}$	$k_\phi/r^2 \times 10^{-5}$	r(Å)	$k_H \times 10^{11}$	$k_\phi \times 10^{11}$
CH_4 . .	4·95	1·302	0·798	1·094	1·630	0·955
NH_4^+ . .	5·38	1·680	0·799	(1·014)	(1·74)	(0·82)
SiH_4 . .	2·77	0·565	0·782	1·456	1·204	1·548
GeH_4 . .	2·61	0·515	0·507	1·478	1·125	1·108

k_1, k_H/r^2 and k_ϕ/r^2 are in dyne/cm. and k_H and k_ϕ in erg/radian^2

MH3 Molecules.—In these molecules all eight frequencies of NH_3 and ND_3 are known, seven of PH_3 and PD_3, and seven of AsH_3 and AsD_3. The four stretching frequencies of NH_3 and ND_3 can be calculated satisfactorily with one constant; the three of PH_3 and PD_3 and the three of the arsenic compounds can also be calculated satisfactorily with one bond stretching constant k_1. (For one vibration the percentage error is just over 2 %, but the average error is of the order of 1 %.) For each pair of isotopic molecules four bending vibration frequencies are available. The pair of symmetric vibration frequencies is used to calculate

$$\frac{3k_H\,\phi}{r^2(k_H + 3k_\phi)}$$

(see Appendix). The following constant is defined so that it is exactly equivalent to that used in the tetrahedral hydrides. This is possible for this vibration because, by virtue of the symmetry of the motion, the atomic orbital of the central atom occupied by the lone pair must remain directed along the symmetry axis throughout the vibration. The orbital distortion must therefore be exactly the same as in the corresponding vibration of the tetrahedral hydrides. The pair of degenerate bending vibration frequencies are used to calculate another bending constant k_G which is some unknown combination of the bond bending constant k_H and a following constant. This constant k_G is chosen so that, if the following constant becomes infinite (i.e. no orbital following), it would become equal to the bond bending constant ($k_G = k_H$), but if orbital following does occur k_G is less than k_H. The bending vibration frequencies are calculated with a maximum error of 2 % and an average error of less than 1 %. The results of the calculations are listed in Table II.

TABLE II

Molecule	$k_1 \times 10^{-5}$	$\frac{3k_Hk_\phi}{r^2(k_H+3k_\phi)} \times 10^{-5}$	$k_G/r^2 \times 10^{-5}$
NH_3	6·38	0·472	1·492
PH_3	3·2	0·553	0·742
AsH_3	2·7	0·483	0·595

The constants are in dyne cm.

MH2 Molecules.—For water, we have taken the figures from Part I.[1] These figures are therefore corrected for anharmonicity. The bond force constant, uncorrected for anharmonicity, is $7{\cdot}6 \times 10^5$ dynes/cm.[5] The three vibration frequencies each of H_2Se and D_2Se are known. In H_2S and D_2S the symmetric vibration frequencies are all known and values have been given for the two antisymmetric vibration frequencies, one for each molecule. However, the two antisymmetric frequencies do not satisfy the isotope ratio rule which is independent of the force field.[6] One must therefore be wrong. It seems likely to us that the antisymmetric vibration frequency in D_2S is somewhat in error because the bond–bond cross term constant calculated using the H_2S antisymmetric vibration frequency fits better into the sequence of the molecules in this group than if the D_2S frequency is used. The constant associated with bending (see Part VI),

---

[5] Linnett, *Quart. Rev.*, 1947, **1**, 73.

[6] Herzberg, *Infra-red and Raman Spectra* (van Nostrand, 1945), 229.

$$\frac{k_H k_F}{r^2(2k_H + k_F)},$$

is obtained from the two bending frequencies of the isotopic molecules. The frequencies are reproduced always more closely than 1½ %. The symmetric and antisymmetric stretching frequencies cannot be calculated satisfactorily by one constant and it is necessary to introduce a bond–bond interaction constant. So the P.E. function used for this molecule is

$$2V = k_1(\Delta r_1^2 + \Delta r_2^2) + k_{11}\Delta r_1 \Delta r_2 + 2k_H(\Delta\alpha - \Delta\beta)^2 + k_F\Delta\beta^2.$$

For the definition of the angle distortions $\Delta\alpha$ and $\Delta\beta$ see Part VI.[3] The values obtained for the constants are given in Table III.

TABLE III

Molecule	$k_1 \times 10^{-5}$	$k_{11} \times 10^{-5}$	$\frac{k_H k_F}{r^2(2k_H + k_F)} \times 10^{-3}$
H_2O, D_2O . .	8·424(7·6)	−0·2008	0·759
H_2S	4·03	−0·23	0·475
H_2S, D_2S . . .	(4·13)	(−0·34)	(0·484)
H_2Se, D_2Se . .	3·16	−0·25	0·330

The constants are in dyne/cm.

MH Molecules.—The force constants of the four molecules HF, HCl, HBr, HI corrected for anharmonicity are 9·7, 5·2, 4·1 and 3·1 × 10^5 dyne/cm.[5] Uncorrected for anharmonicity the constants are 8·9, 4·8, 3·8 and 2·9 × 10^5 dyne/cm.[5]

The bond–bond cross term constants do not seem to be necessary for the molecules MH_4 and MH_3 since sufficient agreement between calculated and observed frequencies can be obtained without using them. However, still better agreement would be obtained if cross-term constants of the following signs were introduced: CH_4: +ve; NH_4^+: +ve; SiH_4: +ve; GeH_4: frequency missing; NH_3: +ve; PH_3: −ve; AsH_3: −ve. So, if bond-bond cross term constants are to be introduced in these molecules, they must be small and of the signs listed above. These will be discussed later.

Discussion

We will discuss the results in the three parts listed in the Introduction.

(i) Bond Stretching Constants.—In Table IV are listed the force constants and bond lengths of the MH linkages in the saturated hydrides. The results are listed in the order of the Periodic Table. It will be seen that in every row and column of this Table the force constants increase from left to right and from bottom to top respectively. In Fig. 1 we have plotted log k against log r for all molecules where this is possible. It is found that the points for the four molecules in Group VII lie on a straight line of slope − 2, kr^2 = constant. This has been noted by others.[7] The three points for CH_4, SiH_4 and GeH_4 lie similarly on a straight line of the same slope. Moreover it is not unreasonable to draw a line of similar slope for the two points for H_2O and H_2S. No test at all can be made for the molecules of Group V since figures for NH_3 only are available. In addition the points for the four molecules CH_4, NH_3, OH_2 and FH lie on a straight line (slope − 3, kr^3 = constant) and the points for the three molecules SiH_4, SH_2 and ClH also lie on a straight line (slope − 4, kr^4 = constant). Thus, though further data are required to confirm this

[7] Glasstone, *Recent Advances in Physical Chemistry* (Churchills, 1938), 206.

conclusion, it appears that, for all Groups, kr^2 = constant and for each Period kr^n = constant, n being 3 for the first short Period, 4 for the second short Period and, if the relation persists, greater than 4 for the first long Period. We may use these regularities to obtain an approximate bond length for PH_3. For this molecule we have log k = log 3·2 = 0·51.

TABLE IV.—BOND-STRETCHING FORCE CONSTANTS AND BOND LENGTHS OF HYDRIDES. THE CONSTANTS ARE GIVEN IN DYNE CM. $\times 10^{-5}$ AND THE LENGTHS IN Å

CH_4	NH_3	OH_2	FH
k = 5·0	6·4	7·5	8·9
r = 1·094	1·014	0·958	0·917
SiH_4	PH_3	SH_2	ClH
k = 2·8	3·2	4·1	4·8
r = 1·456	—	1·334	1·275
GeH_4	AsH_3	SeH_2	BrH
k = 2·6	2·7	3·2	3·8
r = 1·478	—	—	1·414
			IH
—	—	—	2·9
—	—	—	1·504

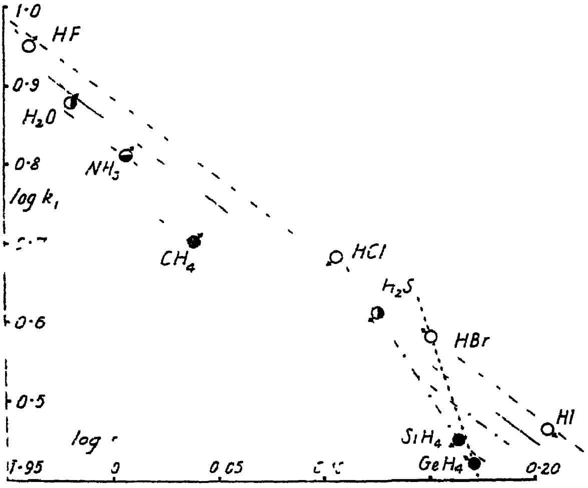

FIG. 1.—Plot of log k_1 against log r; k_1 is in units of 10^5 dyne/cm. and r in Å Group IV: black circles; Group V: half-black circles (horizontal division); Group VI: half-black circles (vertical division); Group VII: plain circles. Points for the same period are indicated by similar arrows attached to the circles.

From the line for Group V we get log r = 0·151, and for the line for the second short Period we get log r = 0·148. This suggests r = 1·41 Å. The two lines in fact cut at log k = 0·52 and log r = 0·145 which corresponds to k = 3·3 (in units of 10^5 dyne cm.) and r = 1·40 Å. The present data therefore suggest that r is close to 1·41 Å. In this conclusion we are, therefore, in agreement with Stevenson [8] who based his conclusions on evidence of a type similar, though not identical, to that used here. We think that it is unlikely that r can be as large as 1·46 Å as was suggested by Sutherland, Lee and Wu.[9] This value (1·46) would place PH_3 right out of its proper sequence in the second short Period. We do not feel that the data available justify any conclusions being made for the dimensions in AsH_3 and SeH_2. We agree with Stevenson that it seems very probable that, in these two molecules, the HMH angles are close to 90°.

It is interesting that the force constant of the GeH link in GeH_4 is only just smaller than the constants of the SiH link in SiH_4 (just above in the Periodic Table) and of the AsH link in AsH_3 (just to the right in the Periodic Table). The small change in force constant on passing from SiH_4 to GeH_4 is confirmed by the small change in the bond length in passing from SiH_4 to GeH_4, and it will be seen from Fig. 1 that the changes in force constant and bond length run parallel in the series CH_4, SiH_4, GeH_4. It is surprising that the change in bond properties from CH_4 to SiH_4 is more than ten times the change from SiH_4 to GeH_4. Considering the relation of GeH_4 to AsH_3 it seems that, if anything, the bond in GeH_4 is abnormally strong and short. This molecule seems to provide the only bond that is at all abnormal in relation to the others considered here. And, even in this case, the sequence of bond properties is maintained in both the Group and the Period.

(ii) Bond-bond Interaction Constants.—For the hydrides of O, S, and Se these are negative. Hoare and Linnett [10] have pointed out that this implies that the bond should be longer in the diatomic than in the triatomic molecule. For H_2O and H_2S this is, in fact, the case as can be seen from Table V. The lengths for H_2Se and HSe are not known. In Table V we have also listed the MH bond lengths in the polyatomic molecules CH_4, SiH_4, NH_3 and PH_3 (using the value given above) and the corresponding diatomic molecules. In all cases the bond length in the diatomic molecule is greater than in the polyatomic molecule. The cross-term constant in the hydrides of elements in Groups IV and V are uncertain but it seems that, if anything, for the Group IV hydrides the cross-term constants are positive; while for the Group V hydrides one is positive (NH_3) and two are negative (PH_3, AsH_3). The arguments of Hoare and Linnett relating bond lengths changes and cross-term constants really only apply to H_2O and H_2S, and should not be extended to the MH_3 and MH_4 molecules. However, it is worth remarking that the change of bond length on dissociation is in the same direction for all these molecules whereas the signs of the cross term constants are not always the

TABLE V

CORRESPONDING BOND LENGTHS IN DIATOMIC AND POLYATOMIC HYDRIDES

Bond	Diatomic Molecule (in ground state)	Polyatomic Molecule
CH	1·120 Å	1·094 Å
SiH	1·521	1·456
NH	1·038	1·014
PH	1·433	1·41
OH	0·971	0·9584
SH	1·35	1·334

---

[8] Stevenson, *J. Chem. Physics*, 1940, **8**, 285.

[9] Sutherland, Lee and Wu, *Trans. Faraday Soc.*, 1939, **35**, 1373.

[10] Hoare and Linnett, *Trans. Faraday Soc.*, 1949, **45**, 844.

same. It is interesting also that there appears to be some regularity in the cross term constants and it is possible that they would repay further investigation.

The values of the cross term constants in H_2O, H_2S and H_2Se are $-0{\cdot}20$, $-0{\cdot}23$ and $-0{\cdot}25$ respectively. That is the constant remains virtually the same. However, its proportion to the bond-stretching constant increases (2, 6 and 8 %) in the same sequence.

(iii) Bending and Following Constants.—The MH_4 molecules will be considered first. For all these, including NH_4^+, k_H/r^2 and k_H lie in the same sequence as the bond stretching constants. Moreover, the changes in k_H and k_1 run parallel as is shown by Fig. 2 in which log k_1 is plotted against log k_H (to calculate k_H for NH_4^+ it was supposed that the NH bond length was the same as in NH_3, since the values are not likely to be greatly different). Because the bonding orbitals in all these molecules must be of a uniform (sp^3) type this rough parallelism between

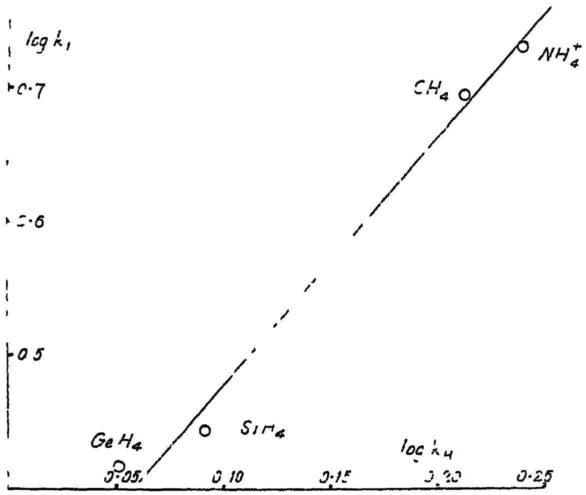

FIG. 2.—Plot of log k_1 against log k_H for tetrahedral hydride molecules. k_1 is in units of 10^5 dyne/cm. and k_H in units of 10^{-11} erg/radian^2.

k_H and k_1 might be expected on the conception of bonding by overlap of atomic orbitals. As the bonding orbital becomes more extensive and diffuse with increase in principal quantum number (i.e. going down the Periodic Table) it is likely that the restoring force for a given displacement, either along or perpendicular to the bond, will decrease. These changes are, in fact, found. In NH_4^+ the bond stretching and bond bending constants are greater than in CH_4 because of the greater effective charge on the central atom (i.e. greater electronegativity of the central atom).

As regards the constant k_ϕ which measures the power of the orbitals to accommodate their orientation to the movements of the atoms in certain distortions (see Part VI) the value of k_ϕ/r^2 is virtually constant for CH_4, NH_4^+ and SiH_4 but drops somewhat in GeH_4. The value of k_ϕ changes irregularly in the sequence CH_4, SiH_4, GeH_4 (see Table I). The reason for these changes is not apparent. We might have expected changes of hybridization to occur more easily for atoms lying lower in the Periodic Table (i.e. decrease in k_ϕ on going down the Periodic Table) because the difference in energy between s and p orbitals decreases. This decrease in k_ϕ definitely occurs from SiH_4 to GeH_2. The position regarding the constant k_ϕ is therefore rather unsatisfactory though it seems reasonable to us that we have found that k_ϕ is roughly the same order of magnitude for all the molecules.

The position for the molecules NH_3, PH_3 and AsH_3 is rather more complicated. Perhaps the most surprising observation is that

$$\frac{3k_H k_\phi}{r^2(k_H + 3k_\phi)}$$

does not vary regularly in this series of molecules being 0·472, 0·553 and 0·483 × 10^5 respectively. This irregularity does not appear to be a consequence of the particular force field we have assumed, for the frequencies of the symmetrical deformation vibrations of the hydrogen compounds (950, 991 and 906) also show the same irregularity in that the frequency is biggest in PH_3. We will return to consider this irregularity when we have examined the constant associated with the degenerate deformation of the molecules. This constant, k_G/r^2, is so defined that it has the value of k_H/r^2 if the orbital-following constant associated with the deformation is infinite (no following) but is less than k_H/r^2 if some following does occur (k_ϕ less than infinity). So k_H/r^2 must be greater than k_G/r^2, the latter having the following values for NH_3, PH_3 and AsH_3: 1·492, 0·742 and 0·595 × 10^5. (Incidentally, it is interesting that the ratio of k_G/r^2 to k_1 is virtually constant for these molecules: 0·23, 0·23 and 0·22 respectively.) Since k_H/r^2 must be greater than 1·492 and

$$\frac{3k_H k_\phi}{r^2(k_H + 3k_\phi)}$$

is 0·472 × 10^5 for NH_3, k_ϕ/r^2 must be less than 0·25 × 10^5. The minimum value it can have is one third of 0·472, which is 0·16 × 10^5 (if k_H/r^2 were very large). So k_ϕ/r^2 must lie between 0·16 and 0·25 × 10^5 and, since r is 1·014 Å, k_ϕ must lie between 0·16 and 0·26 × 10^{-11} dyne cm./radian². That is, it is much smaller than the similar constant in CH_4 and NH_4^+. The reason for this may be that, in NH_3, the fourth orbital of the nitrogen atom is occupied by a lone pair and does not therefore have to accommodate itself to an attached atom as in CH_4 or NH_4^+ where all four orbitals are engaged in bonding. This may mean that changes in hybridization can occur more readily in NH_3.

Similar arguments to those used in NH_3 result in the conclusion that k_ϕ/r^2 for PH_3 must lie between 0·18 and 0·7 × 10^5 and for AsH_3 between 0·16 and 0·8 × 10^5 dyne/cm. It seems probable that, in the series NH_3, PH_3, AsH_3, k_H/r^2 decreases on passing down the Group while k_ϕ/r^2 increases. It is very probable that this accounts for the irregularity in the variation of

$$\frac{3k_H k_\phi}{r^2(k_H + 3k_\phi)}$$

in the series for it is possible for k_H/r^2 and k_ϕ/r^2 to vary regularly but for the composite constant to change irregularly. It is impossible to obtain definite values for the constants k_H/r^2 and k_ϕ/r^2 because there is only one determined quantity (the composite constant). However, values that would satisfy the requirements are: $k_H/r^2 = 1·5$, 0·75 and 0·6 × 10^5 respectively; $k_\phi/r^2 = 0·25$, 0·7 and 0·8 × 10^5 dyne/cm. respectively. These change regularly but lead to the observed irregular change in

$$\frac{3k_H k_\phi}{r^2(k_H + 3k_\phi)}.$$

This is equivalent to saying that, in NH_3, the bending vibration frequency is low because orbital following is easy (k_ϕ small) while in AsH_3 the frequency is low because departure from orbital overlap is easy (k_H small). If these presumptions are correct k_ϕ/r^2 and k_ϕ increase in the series NH_3, PH_3, AsH_3.

It is interesting that the percentage difference between k_G/r^2 and

$$\frac{3k_H k_\phi}{r^2(k_H + 3k_\phi)}$$

decreases in the series NH_3, PH_3, AsH_3: 216 %, 34 %, 23 %. This measures the failure of the *simple* orbital valency force field to give a satisfactory account of the frequencies. It is interesting that, to some extent, the percentage failure parallels the difference between the MHM angle and 90°. The probable values of the MHM angles are: 108°, 93° 90 (Stevenson). It seems likely that both are a measure of the extent of hybridization between *s* and *p* orbitals in these molecules. In NH_3 this appears to be considerable for the angle is considerably different from 90° and the two bending constants are very different indicating that simple O.V.F.F. is inadequate and orbital following is considerable (confirmed by the small value of k_ϕ/r^2). The power of the central atom to vary the hybridization of its bonding orbitals seems to decrease on passing to PH_3 and AsH_3 which may be a result of the bonds being more nearly pure *p* in the equilibrium configuration (indicated by the HMH angle approaching 90°). The sequences of these various properties are mutually consistent on the basis of this explanation. However, it is not easy to see why there should be less hybridization in AsH_3 than in NH_3 since the binding of electrons in *s* and *p* orbitals is much more nearly the same in the arsenic atom than in the nitrogen atom. Mutual repulsion of the hydrogen atoms would explain the sequence of angles in these MH_3 molecules. However, our treatment of H_2O in Part I indicated that repulsion between the H atoms was not of major importance in this molecule. A similar result is also indicated by the fact that in CH_4, NH_3 and H_2O the bond length is less than in the corresponding diatomic molecule. If repulsion between the hydrogen atoms were the most important factor one would expect the change in bond length to be in the opposite direction.[11]

In the molecules H_2O, H_2S and H_2Se the composite bending constants,

$$\frac{k_H k_F}{r^2(2k_H + k_F)},$$

are 0·76, 0·48 and 0·33 × 10^5 respectively. This is the same sequence as that of the constant k_G/r^2 in the molecules NH_3, PH_3, AsH_3. Moreover, as in the MH_3 molecules, this composite bending constant is in almost constant ratio to k_1 in these MH_2 molecules. We cannot, of course, in these molecules, separate the two parts of the composite constant k_H and k_F. It seems probable that k_H decreases going down the Group, by analogy with the molecules in the other Groups; but nothing can be said about the following constant k_F.

An interesting feature of this study of bending constants is that, in each Group, if the stretching constant changes in one direction on passing from one molecule to another the bending constant changes in the same direction, the changes being roughly proportional to one another. This is definite only in the MH_4 molecules. In the MH_3 and MH_2 molecule it is impossible to separate the bending and following constants but the results indicate that the bending and stretching constants change roughly proportionately to one another within each Group. As stated earlier this is quite to be expected on a bonding theory based on the overlap of atomic orbitals.

APPENDIX

MH_4 Molecules.—The formulae for the tetrahedral hydrides are given in Appendix III of Part VII. The results for methane are given in that paper (Table II). The comparison of calculated and observed frequencies for NH_4^+,

---

[11] See also Pauling, *Nature of the Chemical Bond* (Cornell, 1945), § 13.

SiH_4 and GeH_4 are given below, the constants in Table I being used. The bending frequencies are reproduced exactly because two frequencies are used to calculate two constants, consequently only the stretching frequencies are listed :

	Symmetric		Degenerate	
	Calc.	Obs.	Calc.	Obs.
NH_4^+ . .	3011	3033	3157	3134 cm.$^{-1}$
SiH_4 . .	2159	2187	2212	2183
GeH_4 . .	2094	—	2114	2114

Because the calculated frequency is less than the observed for the symmetric vibrations and vice-versa for the degenerate vibrations the bond–bond cross term constant will be positive, if anything, in all these molecules.

MH3 Molecules.—The formulae for these molecules are :

SYMMETRIC : $\lambda_1 + \lambda_2 = k_1\left[\frac{1}{m_2} + \frac{3\cos^2\alpha}{m_1}\right] + \frac{3k_Hk_\phi}{r^2(k_H + 3k_\phi)}\left[\frac{1}{m_2} + \frac{3\sin^2\alpha}{m_1}\right]$,

and $\lambda_1\lambda_2 = k_1\frac{3k_Hk_\phi}{r^2(k_H + 3k_\phi)}\left[\frac{1}{m_2^2} + \frac{3}{m_1m_2}\right]$,

where $\lambda_i = 4\pi^2\nu_i^2c^2$.

DEGENERATE :

$$\lambda_3 + \lambda_4 = k_1\left[\frac{1}{m_2} + \frac{3\sin^2\alpha}{2m_1}\right] + \frac{k_G}{r^2}\left[\frac{1}{m_2} + \frac{3\sin^2\alpha}{2m_1(1+\cos^2\alpha)}\right],$$

and $\lambda_3\lambda_4 = k_1 \cdot \frac{k_G}{r^2}\left[\frac{1}{m_2^2} + \frac{3\sin^2\alpha}{m_1m_2(1+\cos^2\alpha)}\right]$.

In these formulae m_1 represents the mass of the central atom (N, P, As), m_2 the mass of the hydrogen atom, α the angle between the MH bond and the symmetry axis, and γ the frequency in cm.$^{-1}$. For the definition of the constants, see text. k_G becomes equal to the orbital bending constant k_H in the *simple* O.V.F.F. treatment. If orbital following is included, it is less than k_H by an amount dependent on the following constant. The values used for the constants are given in Table II. These lead to the results below (frequencies in cm.$^{-1}$).

	ν_1		ν_2		ν_3		ν_4	
	Calc.	Obs.	Calc.	Obs.	Calc.	Obs.	Calc.	Obs.
NH_3 . .	3323	3337	970	950	3434	3414	1636	1628
ND_3 . .	2384	2419	734	749	2538	2555	1185	1191
PH_3 . .	2355	2327	996	991	2361	2421	1127	1121
PD_3 . .	1690	1694	725	730	1698	—	804	806
AsH_3 . .	2147	2122	914	906	2147	2185	1005	1005
AsD_3 . .	1529	1534	655	660	1529	—	713	713

MH2 Molecules.—The figures for H_2O and D_2O are given in Part I. The algebraic formulae used for the other members of the Group are :

SYMMETRIC :

$\lambda_1 + \lambda_2 = (k_1 + \tfrac{1}{2}k_{11})\left[\frac{1}{m_2} + \frac{2\cos^2\alpha}{m_1}\right] + \frac{k_H \, . \, k_F}{r^2(2k_H + k_F)}\left[\frac{1}{m_2} + \frac{2\sin^2\alpha}{m_1}\right]$,

and $\lambda_1\lambda_2 = (k_1 + \tfrac{1}{2}k_{11})\left(\frac{k_H \, . \, k_F}{r^2(2k_H + k_F)}\right)\left[\frac{1}{m_2^2} + \frac{2}{m_1m_2}\right]$.

DEGENERATE :

$$\lambda = (k_1 - \tfrac{1}{2}k_{11})\left[\frac{1}{m_2} + \frac{2\sin^2\alpha}{m_1}\right].$$

α is half the HMH angle. The constants employed are given in Table III and the P.E. function is also given in the main text. The frequencies calculated are given below. Two sets are given for H_2S. Those marked (*a*) correspond to the unbracketted constants in Table III while those marked (*b*) correspond to the bracketted constants.

	ν_1		ν_2		ν_3	
	Calc.	Obs.	Calc.	Obs.	Calc.	Obs. cm.$^{-1}$
H_2S (*a*)	2607	2611	1285	1290	2685	2684
H_2S (*b*)	2621	2611	1297	1290	2735	2684
D_2S (*b*)	1882	1892	930	934	1965	1999
H_2Se	2275	2260	1060	1074	2361	2350
D_2Se	1620	1630	755	745	1685	1696

The bond lengths, angles and vibration frequencies of the polyatomic molecules are taken from *Infra Red and Raman Spectra* by Herzberg (van Nostrand, 1945) except in the following cases. In PH_3 and AsH_3 the angles given by Stevenson were used; and for the frequencies of SiH_4 and GeH_4 those given by Tindal, Straley and Nielsen were used.[12] The bond lengths and frequencies of the diatomic molecules were taken from *Molecular Spectra and Molecular Structure of Diatomic Molecules* by Herzberg (van Nostrand, 1939).

We wish to thank the Imperial Chemical Industries and the Royal Society for providing us with calculating machines. One of us (D. F. H.) wishes to thank the Department of Scientific and Industrial Research for a Maintenance Grant, and another (P. J. W.) the Harmsworth Trust for a Senior Scholarship.

Inorganic Chemistry Laboratory,
Oxford.

---

[12] Tindal, Straley and Nielsen, *Physic Rev.*, 1942, **62**, 151, 161.

A THEORETICAL STUDY OF SOME NON-BENZENOID HYDROCARBONS. PART II

BY R. D. BROWN

Received, 17th August, 1949

The atomic polarization energies, bond localization energies, resonance energies and electronic spectra of the hydrocarbons pentalene, heptalene, fulvalene and biphenylene have been considered. The chemistry of these molecules is discussed briefly in terms of the first two of these quantities revealing some unexpected results. Nucleophilic attack of fulvalene probably occurs at the position of highest π-electron density, and the reactive position in biphenylene is probably not that of highest free valence. Otherwise agreement with previous predictions based upon bond orders and π-electron densities is good.

The resonance energies are compared with those of related molecules and the electronic spectra are considered. It is concluded that the first three of these hydrocarbons are highly coloured, and the predicted spectrum of biphenylene is shown to be in accord with the observed spectrum.

In Part I of this series [1] the results of theoretical calculations of certain properties of the isolated molecule—π-electron densities, bond orders and lengths, free valences—were reported for four non-benzenoid hydrocarbons. Since three of these have not so far been prepared and the chemistry of the fourth (biphenylene) has not been investigated, the results were used to predict the probable chemical properties of these molecules. However, similar predictions based upon an approximate treatment of the structure of the activated complex [2] are probably more reliable (see later), and the results of such a treatment for the same four molecules are presented here. In addition the resonance energies and electronic spectra of these molecules are considered. Such results provide a means of determining the reliability of the LCAO method by subsequent experimental investigation particularly for the non-alternants, for which there are theoretical reasons [3] for expecting the method to be less reliable than for other molecules.

Symbolism and Method of Calculation.—The atomic polarization energies have already been discussed by Wheland,[2] who considered that they are probably no less reliable, and perhaps are more reliable, than π-electron densities for determining the most reactive position in a conjugated molecule. It is instructive to consider the structure of the activated complex for a substitution reaction in this connection. In the theory of absolute reaction rates [4] the rate constant may be expressed in terms of the potential energy of activation and partition functions of the reactants and the activated complex. For a given substitution reaction taking place at the various possible positions in a conjugated molecule it may be hoped that the partition functions of the various possible transition states involved are roughly the same except for cases which may be classified qualitatively under the heading steric hindrance. The relative success of qualitative electronic interpretations of organic reactions implies that, in the absence of more detailed information, the above assumption is reasonable.

The assumption is made then that the most reactive position in a conjugated molecule is that for which the potential energy of activation is smallest, unless the position is sterically hindered. In addition, as the partition functions are referred to the zero-point vibrational level it must be tacitly assumed that the various activated complexes have similar zero-point energies.

The atomic polarization energy represents an attempt to compute approximately the contribution of the π-electrons in the conjugated molecule to the potential energy of activation, and the use of this quantity to predict chemical reactivity involves the assumption that the other electrons make a constant contribution to the activation energy. The atomic polarization energy is the energy required to localize two, none or one π-electron upon a given carbon atom, depending upon whether electrophilic, nucleophilic or radical reactivities are being considered. It may conveniently be calculated by the LCAO method; [5] if the atomic orbitals are assumed to be orthogonal then the atomic polarization energies thus computed are represented by A_e, A_n, A_r, while if the overlap integral is taken to be 0·25 (as done by Wheland [2]) then the symbols A'_e, A'_n, A'_r are employed.

Now considering, for example, electrophilic substitution, if the actual π-electron activation is $\mathbf{A}_e$ then it is clear that A_e or A'_e will be greater than $\mathbf{A}_e$, quite apart from errors introduced due to approximations inherent in the LCAO method. In the transition state the two π-electrons which may be regarded as forming the incipient bond between the conjugated molecule and the attacking positive ion will not be completely localized in this bond (or alternatively upon the atom being substituted), so that $\mathcal{A}_\epsilon$ (or $\mathcal{A}'_\epsilon$) are greater than $\mathbf{A}_\epsilon$ by an amount which is the delocalization energy of the two π-electrons under consideration over the rest of the molecule plus the delocalization energy of the remainder of the π-electrons over the atom being attacked. Alternatively $\mathbf{A}_\epsilon$ can be regarded as the increase in π-energy of the conjugated system when the coulomb integral of a particular atom (and to a lesser extent its neighbouring atoms) is increased by a relatively large and undetermined amount. $\mathcal{A}_\epsilon$ represents an approximation to this which seems closer to the actual state of affairs than the alternative use of polarizabilities (the self-atom polarizability of Coulson and Longuet-Higgins [5]) which apply to a transition state for which the increase in coulomb integral is infinitesimally small. The use of π-electron densities in predicting chemical reactivity likewise requires the increase in π-energy to be related to these π-densities. Thus it is felt that predictions based upon atomic polarization energies are likely to be more reliable than those based upon π-electron densities, and when the two methods differ the former will be preferred.

---

[1] Brown, *Trans. Faraday Soc.*, 1949, **45**, 296.

[2] Wheland, *J. Amer. Chem. Soc.*, 1942, **64**, 900.

[3] Coulson and Rushbrooke, *Proc. Camb. Phil. Soc.*, 1940, **36**, 193.

[4] Glasstone, Laidler and Eyring, *The Theory of Rate Processes*, 1941, pp. 184-191.

[5] For a general account of the method see Coulson and Longuet-Higgins, *Proc. Roy. Soc. A*, 1947, **191**, 39.

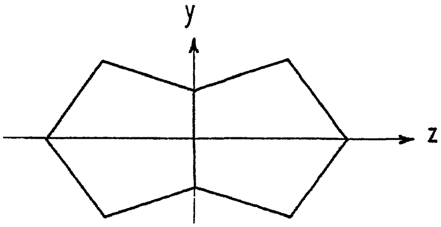

FIG. 1.

The calculation of bond localization energies has already been set out in detail elsewhere; [6] in the present case the resonance energies of the four hydrocarbons and the various residual molecules were all computed directly from the energies of the various occupied molecular orbitals, these latter energies being obtained by direct solution of the appropriate secular determinants. Although many of the residual molecules are non-alternants it is only for one of the bonds of fulvalene (see later) that two residual molecules were left, one of which (cyclopentadienyl) has a partly filled orbital with negative x_r. In such cases it has already been pointed out [7] that the possibility of a polar distribution of π-electrons among the residual molecules arises.

The bond localization energies are represented by B, B' according as they have been calculated employing $S = 0$ or $S = 0{\cdot}25$ respectively, and this also applies to the resonance energies R, R'. These and the atomic polarization symbols above conform to the convention that quantities computed assuming orthogonality of the atomic eigenfunctions are represented by block capitals, those calculated with an overlap integral of 0·25 by dashed block capitals, and the actual molecular quantities to which these quantities approximate are represented by script capitals. The values of B' and R' were also converted to kcal. mole^{-1} using the conversion factor $\gamma = -34$ kcal. recommended by Dewar.[8]

In the treatment of the electronic spectra the co-ordinate system used for the symmetry symbols was as follows. The molecular plane was taken to be the yz plane with the z axis along the longer axis of the molecule. This is illustrated for pentalene in Fig. 1. The symmetry symbols are those customarily employed.[9] and the various electronic transitions were investigated in the standard manner, as set out by Coulson [10] in his treatment of the polyacenes. The transition energies in every case have been computed for $S = 0{\cdot}25$. The numbering system is reproduced from a previous publication for convenience.

---

[6] Brown, *Austral. J. Sci. Res.*, *A*, 1949 (in press).

[7] Brown, ref. 6. The meaning of x_r, etc., is explained in this paper

[8] Dewar, *Trans. Faraday Soc.*, 1946, **42**, 767.

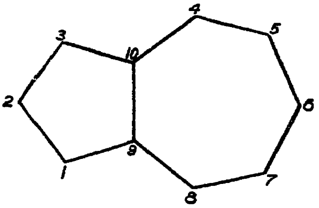

Results

1. Pentalene. –The atomic polarization energies are listed in Table I.

TABLE I.—ATOMIC POLARIZATION ENERGIES

Position	A_e	A_n (β)	A_r	A'_e	A'_n (γ)	A'_r
			Pentalene			
		1·538	1·959	1·692	0·931	
			2·027	1·436	1·430	
			Heptalene			
	1·660	2·193	1·926	1·001	1·573	1·287
	2·032	2·032	2·032	1·322	1·322	1·322
	1·715	2·357	2·026	1·035	1·710	1·373
			Fulvalene			
	1·987	1·365	1·676	1·416	0·839	1·127
	2·236	1·452	1·844	1·611	0·897	1·254
			Biphenylene			
1	2·408	2·408	2·408	1·739	1·739	1·739
2	2·352	2·352	2·352	1·672	1·672	1·672

The results are in good agreement with the π-electron densities previously reported, again predicting electrophilic substitution at position 2 and nucleophilic attack at position 1. In agreement with the free valences, radical attack is predicted to occur at position 1.

The bond localization energies, presented in Table II, predict that the 1 : 2 bond is the most reactive, in agreement with the bond orders,[1] but in contrast to the latter predict the 7 : 8 bond to be the least reactive. This seems to be the general rule for the bond localization energies of bonds common to two rings in a non-alternant hydrocarbon and will be considered more fully elsewhere.[11]

The resonance energy of pentalene is 37 kcal. (Table III) which suggests a reasonable stability, although the strain energy must be taken into account in this respect. The strain energy in benzpentalene has been investigated by Coulson [12] who concluded that it amounts to only a few kcal., and this will apply equally to pentalene. However, the relative unimportance of such considerations in special cases is illustrated by the stability of biphenylene (see later).

---

[9] Mulliken, *Physic. Rev.*, 1933, **43**, 279 ; Sponer and Teller, *Rev. Mod. Physics*, 1941, **13**, 75.

[10] Coulson, *Proc. Physic. Soc.*, 1948, **60**, 257.

[11] Brown, results in course of publication.

[12] Coulson, *Nature*, 1942, **150**, 577.

TABLE II.—BOND LOCALIZATION ENERGIES

Bond	B ($-\beta$)	B' ($-\gamma$)	B' (kcal. mole^{-1})
		Pentalene	
1 : 2	0·990	0·440	15
7 : 1	1·466	0·700	24
7 : 8	2·709	1·708	58
		Heptalene	
1 : 2	1·037	0·415	14
2 : 3	1·143	0·486	17
11 : 1	1·565	0·622	21
11 : 12	2·690	1·430	49
		Fulvalene	
1 : 2	0·748	0·280	9·5
2 : 3	1·124	0·604	21
10 : 1	2·167	1·342	46
9 : 10	1·855	0·855	29
		Biphenylene	
1 : 2	1·601	0·980	33
2 : 3	1·353	0·722	25
9 : 10	2·452	1·302	44
10 : 1	1·565	0·723	25
10 : 11	2·033	0·904	31

TABLE III.—RESONANCE ENERGIES

Molecule	R ($-\beta$)	R ($-\gamma$)	R' (kcal. mole^{-1})
Pentalene . .	2·456	1·087	37
Heptalene . .	3·618	1·465	50
Fulvalene . .	2·790	1·204	41
Biphenylene .	4·506	2·145	73

TABLE IV.—THE ELECTRONIC SPECTRUM OF PENTALENE

Transition	Upper Level	Energy ($-\gamma$)	Polarization
$N - V_1$	B_{1g}	0·421	Forbidden
$N - V_2$	B_{1u}	0·8	z
$N - V_3$	B_{2u}	1·015	y
$N - V_4$	B_{3g}	1·478	Forbidden

All things considered it is likely that pentalene is sufficiently stable, and not too reactive, to be isolated when a suitable synthesis has been devised.

The various possible electronic transitions for pentalene are tabulated, together with other relevant data, in Table IV. These results predict an absorption spectrum of rather a different type to that of its alternant homologue naphthalene. Thus the longest wavelength band is expected to be a forbidden transition, and the second band (permitted transition) has a transition moment in the z-direction. The transition energies are probably even less reliable than those computed for alternants, but it is likely that the forbidden transition will lie in the visible region of the spectrum and that pentalene like azulene is another coloured hydrocarbon of low molecular weight.

2. Heptalene.—The atomic polarization energies, recorded in Table I, again agree with the π-electron densities in predicting electrophilic attack at position 1 and nucleophilic reactivity at position 2. Also the position most reactive to radical reagents (i e. with smallest A_r, A'_r) is that which was found[1] to have the highest free valence. The bond localization energies (Table II) also fall qualitatively in the same sequence as the bond orders, but again from the magnitude of B' for the most reactive bond (the 1 : 2 bond) one would expect a greater reactivity in reactions such as ozonolysis, oxidation, etc., than with benzene, which would not be anticipated from the bond order. However, it is not yet certain that such semiquantitative considerations can be applied to bond localization energies of non-alternants.

The resonance energy of heptalene (50 kcal.) is considerably less than that of naphthalene (63 kcal.) or that of azulene (54 kcal.) even although it is a larger molecule than either of these two. Thus it seems likely that heptalene is a rather unstable molecule.

TABLE V.—THE ELECTRONIC SPECTRUM OF HEPTALENE

Transition	Upper Level	Energy (γ)	Polarization
$N - V_1$	B_{3g}	0·337	Forbidden
$N - V_2$	B_{1u}	0·855	z
$N - V_3$	B_{1u}	1·137	z
$N - V_4$	B_{2u}	1·328	y
$N - V_5$	B_{2u}	1·333	y

The theoretical data for the electronic spectrum of heptalene are given in Table V. Again a forbidden transition of unusually long wavelength is predicted so that heptalene is likely to be another coloured hydrocarbon. The spectrum should also resemble that of pentalene in that the first permitted band has a moment in the z-direction.

3. Fulvalene.—With fulvalene the atomic polarization energies (Table I) predict chemical properties rather different from those anticipated from the π-densities; they predict atom 1 to be the most reactive for all three types of reaction (electrophilic, nucleophilic, radical), whereas the π-electron densities predict nucleophilic reactivity to be the greatest at position 2. These two facts can be reconciled if position 1 has a greater polarizability than position 2 and computations of the polarizabilities of these positions are being carried through at present.

From the above it appears likely that fulvalene will be the first example of a molecule in which nucleophilic attack does not occur at the position of lowest π-electron density. Another possibility is that attack may take place at position 9; this has a greater positive charge than position 2, but as there is no hydrogen atom at position 9, addition is the only possible reaction. However, computation of A_n, A'_n ($-1·855\beta$; $-1·022\gamma$, resp.) reveals that this is unlikely.

The bond localization energies (Table II) agree with the bond orders in predicting that the 1 : 2 bond is the most reactive. However, the former indicate that the 2 : 3 bond will be more reactive than the 9 . 10 bond, a result contrary to the bond order data and contrary to qualitative concepts based upon the classical bond diagram shown in Fig. 2. Again this disagreement is possible if the self bond polarizabilities are sufficiently different; calculations of these quantities are at present in progress.

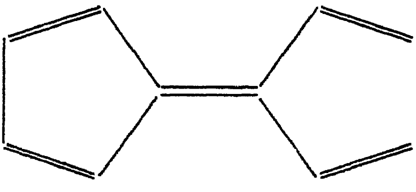

FIG. 2.

For the 10 : 1 bond of fulvalene the possibility of a non-uniform distribution of π-electrons in the residual molecule arises. The residual molecule here is cyclopentadienyl + allyl, and if five π-electrons are allotted to the former and three to the latter the bond localization energies shown in Table II obtain. However, the orbital thus singly filled in cyclopentadienyl has $x_r = -0{\cdot}618o$, and if it is assumed that six of the π-electrons are present in the cyclopentadienyl residue, two in the allyl residue, then it is found that $B = -1{\cdot}549\beta$, $B' = -0{\cdot}807\gamma$. However, this charge-transfer process probably requires a considerable amount of energy, and as there is no means of assessing this quantity at present it will be assumed to be prohibitive until evidence to the contrary is obtained.

From Table III we notice that the resonance energy of fulvalene, although considerably less than that of its very stable isomers naphthalene and azulene, is almost twice that of fulvene (22 kcal.) and it seems likely that fulvalene is reasonably stable and not too reactive chemically. Indeed the fact that it is so far unknown may be connected with the fact that no direct attempt to prepare it can be found in the literature.

TABLE VI.—THE ELECTRONIC SPECTRUM OF FULVALENE

Transition	Upper Level	Energy (γ)	Polarization
$N - V_1$	B_{2u}	0·296	y
$N - V_2$	B_{3g}	0·296	Forbidden
$N - V_3$	B_{1u}	0·561	z
$N - V_4$	A_{1g}	1·031	Forbidden
$N - V_5$	A_{1u}	1·223	z

The electronic spectrum (Table VI) is perhaps more interesting than either of the previous two molecules. The LCAO calculations predict the longest wavelength band system to be a *permitted* electronic transition of very long wavelength—perhaps extending into the infra-red.

4. Biphenylene.—Biphenylene is an alternant hydrocarbon, and consequently is a particular example of the following general principle. *In alternant hydrocarbons there is one position * in the molecule which is the most reactive in each of the three types of substitution reaction.* The removal of any atom from the conjugated system of an alternant hydrocarbon must necessarily give rise to an alternant radical; such radicals can be shown quite generally [13] to have their partly filled orbital with $x_r = 0$. This means that the corresponding singly positive and negative ions will have the same π-energy as the radical so that $A_e = A_r = A_{n}$ and similarly $A'_e = A'_r = A'_n$.

For biphenylene this position is predicted to be position 2 (Table I). This result is somewhat surprising in view of the fact [1] that the free valence is greater for position 1. For other more common alternant hydrocarbons such as naphthalene, anthracene and phenanthrene the positions of highest free valence [14] in each case are those of greatest chemical reactivity, and for azulene [15] and the three non-alternants just considered the position of highest free valence corresponds to that of smallest A_r (or A'_r). However, recently some doubt has been thrown upon the reliability of free valence in the prediction of chemical reactivity [16] and the predictions from the atomic polarization energies of biphenylene are borne out by computations of the self polarizabilities [5] of positions 1 and 2. The values obtained for $\pi_{1,1}$ and $\pi_{2,2}$ are 0·419 and 0·443 respectively; thus we feel confident in predicting that reactions such as bromination, nitration, amination, and other electrophilic, nucleophilic and homolytic reactions will occur preferentially at position 2, and, from comparison with the value of A' for benzene [2] ($-1{\cdot}849\gamma$) probably more readily than with the latter.

Experimental investigation of this matter is important in view of the rather widespread use of free valence for prediction and interpretation of chemical reactivity[17] and the recent introduction[18] of the essentially analogous residual affinities by Moffitt.

---

* In symmetrical molecules there may, of course, be several equivalent positions.

[13] Coulson and Rushbrooke, ref. 3; Coulson and Longuet-Higgins, *Proc. Roy. Soc. A*, 1947, **192**, 21.

[14] Coulson and Longuet-Higgins, *Rev. Sci.*, 1947, **85**, 929.

[15] Brown, *Trans. Faraday Soc.*, 1948, **44**, 984.

[16] Crawford and Coulson, *J. Chem. Soc.*, 1948, 1990.

The bond localization energies of biphenylene are listed in Table II. They are seen to agree in general with the bond orders previously reported,[1, 19] predicting the 2 : 3 bond to be the most reactive. It is interesting to notice that from the values of B' it would be expected that bonds 2 : 3 and 10 : 1 are almost equally reactive whereas the B values for these two bonds are relatively widely separated. It would be very useful to have experimental data on the relative reactivities of the bonds in biphenylene in the reaction with ozone or osmium tetroxide as a means of determining the usefulness of B or B' in predicting chemical reactivity.

The bond localization energies B, B', have been used to calculate the corresponding bond orders using for the purpose eqn. (33) and (34) of ref. 6. The results are shown in Table VII, p being the mobile bond order of Coulson[20] and the subscripts indicating the quantities used for the computation.

TABLE VII.—BOND ORDERS

Bond	p_B	$p_{B'}$	p
1 : 2	0·64	0·62	0·62
2 : 3	0·69	0·69	0·69
9 : 10	0·45	0·54	0·26
10 : 1	0·65	0·69	0·63
10 : 11	0·54	0·64	0·57

The agreement is similar to that usually observed[6] for alternants, with one or two exceptions. Thus the values of $p_{B'}$ for bonds 10 : 11 and especially 9 : 10 show unusually large divergences from p. Thus we might expect in particular the 9 : 10 bond to be more reactive than is indicated by its bond order.

The resonance energy of biphenylene is slightly greater than twice the resonance energy of benzene (i.e. 72 kcal.) and less * than that of biphenyl (76 kcal.). In addition the strain energy of the α-electrons in biphenylene is probably of the order of 100 kcal.[12] In spite of this biphenylene is relatively stable chemically,[21] indicating that arguments based on resonance energies, as expected, are not always valid when discussing stability.

TABLE VIII.—THE ELECTRONIC SPECTRUM OF BIPHENYLENE

Transition	Upper Level	Energy $(-\gamma)$	Polarization	Wavelength Å × 10⁵	
				Theor.	Obs.
$N - V_1$	B_{3g}	0·901	Forbidden	3·8	3·9
$N - V_2$	B_{1u}	1·222	z	2·8	3·6
$N - V_3$	A_{1g}	1·451	Forbidden	2·4	—
$N - V_4$	B_{2u}	1·519	y	2·3	--
$N - V_5$	B_{1u}	1·528	z	2·3	--

The electronic spectrum of biphenylene is considered in Table VIII. It is of interest that the calculations predict that the transition of longest wavelength is a forbidden transition. The spectrum of biphenylene has been determined by Carr, Pickett and Voris,[22] who consider that the bond observed in the ultraviolet is comprised of a low intensity band together with a higher intensity band of shorter wavelength. The present work suggests that this latter band is due to an $^1A_{1g} - {}^1B_{1u}$ transition.

---

[17] Daudel, Daudel, Buu-Hoi, and Martin, *Bull. Soc. Chim*, 1948, 1202.

[18] Moffitt, *Trans. Faraday Soc.*, 1949, **45**, 373.

[19] Waser and Schomaker, *J. Amer. Chem. Soc.*, 1943, **65**, 1451.

[20] Coulson, *Proc. Roy. Soc. A*, 1939, **169**, 413.

* This is only true when considering R'. R for biphenylene is actually greater than R for biphenyl ($-$ 4·383 β).

[21] Lothrop, *J. Amer. Chem. Soc.*, 1941, **63**, 1187.

The predicted wavelengths of bands listed in Table VIII have been calculated from the transition energies assuming $+ \gamma = - 3{\cdot}4$ eV, a value which gives reasonable agreement between predicted and observed positions of the longest wavelength bands of naphthalene, anthracene,[10] acridone, and pyridone.[23] The agreement between the predicted and observed positions of the forbidden transition of biphenylene is probably better than would be anticipated in view of the number of factors which have been neglected (e.g. interaction of electronic states of the same symmetry [24]).

In conclusion it may be noted that there seems little to choose between A and A' in predicting chemical reactivities, and the same applies to B and B' with the possible exception of the bond in biphenylene mentioned above. However, no definite statement of the usefulness of these quantities for such purposes can be made until a greater amount of experimental data for the relative reactivities of various positions is available for a greater number of unsubstituted conjugated hydrocarbons.

Chemical Laboratories,
University of Melbourne,
Victoria,
Australia.

---

[22] Carr, Pickett and Voris, *ibid.*, 1941, **63**, 3231.

* It is inherent in the present LCAO method that the values of γ which is best for computation of resonance energies is quite different from that which gives the best agreement with observed electronic transition energies.

[23] Brown, results in course of publication.

[24] Coulson and Fischer, *Phil. Mag.*, 1949, **40** (7), 386.

THE HEAT OF SOLUTION OF THALLOUS FLUORIDE AND THE DISSOCIATION ENERGY OF FLUORINE

By A. D. Caunt and R. F. Barrow

Received 26th August, 1949

The heat of solution of TlF to TlF ($800H_2O$) has been found to be exothermic to the extent of 0·5 ± 0·2 kcal./mole at 25° C. From this is derived the approximate upper limit of 45 kcal./mole for the heat of dissociation of F_2.

It was observed by Gaydon [1] that the dissociation energy of F_2 is linked with the properties of TlF in a thermodynamic cycle in which the steps are as follows:

$$\begin{aligned} &Tl_c + \tfrac{1}{2}F_{2g} + 800H_2O = TlF(800H_2O),\\ &TlF_c + 800H_2O = TlF(800H_2O),\\ &TlF_c = TlF_g,\\ &TlF_g = Tl_g + F_g,\\ &Tl_c = Tl_g. \end{aligned}$$

There is at least some information about the change in heat content for each of these processes, except that for the solution of thallous fluoride. We have therefore made some approximate measurements of this quantity. Consideration of the published data about the other steps leads then to the derivation of an upper limit for the dissociation energy of fluorine.

---

[1] Gaydon, *Dissociation Energies* (Chapman and Hall, 1947).

Heat of Solution of TlF.—The starting material was recrystallized thallous nitrate, free from lead. Two procedures were followed; in (1) thallium sulphide, precipitated by H_2S in presence of NH_4OH, was dissolved in aqueous HF; in (2) thallous carbonate, prepared by the sulphate-barium hydroxide method, was dissolved in aqueous HF. The latter method proved better, as the resulting solution in (1) was invariably acid. Dry samples of TlF were prepared by desiccation *in vacuo* over activated alumina using Pt vessels.

The heat of solution was measured in a simple Dewar flask calorimeter, waxed inside to prevent attack by free HF. Temperature changes were recorded on a Beckmann thermometer. After solution, the liquid was analyzed: Tl by titration with KIO_3 in concentrated HCl, and excess HF by titration with NaOH. The results are in Table I. A rough estimate of the effect of excess acid in (1) showed that it was less than 0·1 kcal; this effect was therefore neglected, so that with an accuracy sufficient for the present purposes, $\Delta H_{\text{soln.}} = -0{\cdot}5 \pm 0{\cdot}2$ kcal./mole for a solution of composition $TlF(800H_2O)$ at 25° C.

TABLE I

Composition of Solution	Temperature Rise °C	% Excess Acid (mole HF/mole TlF)	$\Delta H_{\text{soln.}}$ kcal./mole TlF
1. $TlF\ (1105H_2O)$ . . .	$0{\cdot}02_0$	4·2	$-0{\cdot}4_3$
2. $TlF\ (778H_2O)$ . . .	$0{\cdot}05_0$	0·90	$-0{\cdot}6_1$
3. $TlF\ (993H_2O)$ . . .	$0{\cdot}02_5$	0·0	$-0{\cdot}4_8$

Heat of Formation of TlF.—The heat of formation of $TlF(800H_2O)$ has been computed from two cycles, one through Tl_2O, the other through TlOH, which are in satisfactory agreement, viz.

$$\Delta H_{298} = -77{\cdot}3 \text{ kcal./mole.}$$

Heat of Sublimation of TlF.—The vapour pressure measurements of von Wartenberg and Bosse[4] for a small range of temperature near the boiling point (571° K) lead to $\Delta H_{\text{vap.}} = 25$ kcal. Then $\Delta H_{298} \sim 26$ kcal./mole. Neither the latent heat of fusion nor the melting point of TlF have been recorded, but the melting point must lie between 300° K and 571° K, and using the approximation $\Delta H_{\text{fus.}}.\ T_m \sim 6$, then $3{\cdot}5 > \Delta H_{\text{fus.}} > 1{\cdot}8$ kcal. Taking $\Delta H_{\text{fus.}} = 3$ kcal.,

$$\Delta H_{\text{subl.}} = 29 \text{ kcal. at } 25\ \text{C.}$$

Heat of Dissociation of TlF.—The absorption spectrum of TlF has been studied by Howell.[5] From well-marked predissociations, $D_0^{\circ} < 109$ kcal., so that $D_{298}^{\circ} < 110$ kcal./mole.

Heat of Sublimation of Tl.—Published estimates of this quantity vary over a rather wide range. We are inclined to believe that the best value for the present purpose comes from cycles involving TlCl and TlBr. The standard heats of formation of these substances are −50·0 and −41·2 kcal./mole.[3] The heats of sublimation have been determined by Niwa:[6] the values at 25° C are 28·8 and 32·9 kcal./mole. Now the heats of dissociation of both TlCl and TlBr are known with considerable accuracy.

---

[2] Bichowski and Rossini, *Thermochemistry of Chemical Substances* (Reinhold, 1936).

[3] *Selected Values of Chemical Thermodynamic Properties* (National Bureau of Standards, Washington, 1948).

[4] von Wartenberg and Bosse, *Z. Elektrochem.*, 1923, **28**, 384.

[5] Howell, *Proc. Roy. Soc. A*, 1937, **160**, 242.

[6] Niwa, *J. Chem. Soc. Japan*, 1939, **60**, 918; *J. Fac. Sci. Hokkaido Imp. Univ., Ser. III*, 3, 1940, No. 1, 17.

The latest investigation of TlCl by Miescher[7] gives $D_0'' = 89{\cdot}5$ kcal., from a very short extrapolation of vibrational levels in an excited state. Similarly, from the data of Howell and Coulson[8] on TlBr, $D_0'' = 74{\cdot}0$ kcal. mole. The values become 90·1 and 74·5 kcal./mole. at 25° C. Then, taking 29·0 and 26·7 kcal. for the standard heats[3] of formation of $Cl_g(^2P_{\frac{3}{2}})$ and $Br_g(^2P_{\frac{3}{2}})$, we have for the heat of sublimation of Tl at 25° C :

from TlCl, $\Delta H_{\text{subl.}} = -50{\cdot}0 + 28{\cdot}8 + 90{\cdot}1 - 29{\cdot}0 = 39{\cdot}9$ kcal./mole.
from TlBr, $\Delta H_{\text{subl.}} = -41{\cdot}2 + 32{\cdot}9 + 74{\cdot}5 - 26{\cdot}7 = 39{\cdot}5$ kcal./mole.
Thus $\Delta H_{\text{subl.}} = 39{\cdot}7$ kcal./mole.

Heat of Dissociation of F_2.—With the values considered above,

$$D(F_2),\ 298^\circ\ K < 2(-77{\cdot}3 + 0{\cdot}5 + 29 + 110 - 39{\cdot}7)$$
$$< 45\ \text{kcal./mole.}$$

This upper limit cannot be regarded as more than a rough estimate, but it does favour a low value of $D(F_2)$—e.g. about 40 kcal. as determined through ClF,* and is just compatible with the value 50 ± 6 kcal./mole, deduced recently from a study of the spectra of RbF and CsF.[11]

We are glad to acknowledge helpful discussion with Dr. H. A. Skinner.

Physical Chemistry Laboratory,
Oxford.

[7] Miescher, *Helv. physic. Acta*, 1941, **14**, 148.

[8] Howell and Coulson, *Proc. Physic. Soc.*, 1941, **53**, 706.

* From Schmitz and Schumacher,[9] $(D_{298})_{ClF} = 61{\cdot}2$ or $59{\cdot}8 \pm 0{\cdot}5$ kcal., thence with $(D_{298})_{Cl_2} = 58{\cdot}0$ kcal.,[3] $D_{F_2} = 64{\cdot}4$ or $61{\cdot}6 - 2\Delta H_{ClF}$, where ΔH_{ClF} is the standard heat of formation of ClF. For this quantity Wicke[10] obtained $-11{\cdot}6 \pm 0{\cdot}4$ kcal./mole. A recalculation of the results of Schmitz and Schumacher using values taken from Bichowski and Rossini[3] gives $13{\cdot}1 \pm 0{\cdot}5$ and 12 ± 2 kcal./mole. We therefore take the best value at present available for ΔH_{ClF} to be about $12{\cdot}3 \pm 1$ kcal/mole. Thus D_{F_2}, 298° K = $39{\cdot}8$ or $37{\cdot}0 \pm 0{\cdot}2$ kcal./mole.

[9] Schmitz and Schumacher, *Z. Naturforsch.*, 1947, **2a**, 362.

[10] Wicke, *Nach. Ges. Wiss. Göttingen*, 1946, 89.

[11] Caunt and Barrow, *Nature*, 1949, **164**, 753.

THE MAGNETIC SUSCEPTIBILITY OF CYCLO-OCTATETRAENE

II.—THE TEMPERATURE COEFFICIENT OF SUSCEPTIBILITY FROM 195° K TO 69° K

By F. R. M. McDonnell, R. C. Pink and A. R. Ubbelohde

Received 29*th August*, 1949

The magnetic susceptibility of cyclo-octatetraene has been measured in the range 195° K to 69° K. The results show no evidence for any paramagnetic component in the solid. There appears to be a decrease in diamagnetism on cooling through the transition point around 98° K which may be associated with tautomerism between different bond structures of the molecule.

Measurements on the magnetic susceptibility of liquid cyclo-octatetraene[1] indicated that at 20° C the molecular structure involved a system of conjugated single and double bonds, without " aromatic " electrons. However, a transition from yellow to white crystals observed in the solid at around 98° K made it desirable to confirm the above molecular structure,

[1] Pink and Ubbelohde, *Trans. Faraday Soc.*, 1948, **44**, 708.

since the presence of a small proportion of paramagnetic molecules might account for the yellow colour, and would upset the conclusions from the susceptibility measurements.

To test this possibility, the apparatus previously described was modified to permit measurements in the temperature range 195° K to 69° K, in which any paramagnetic contribution should become more pronounced than at 293° K. The sensitivity was also increased by replacing the analytical balance by a Bunge microbalance. Under good conditions, weighing errors with this balance did not exceed 0·003 mg. in these experiments.

Experimental

The cyclo-octatetraene was freshly redistilled from the sample previously used, and was contained in a sealed Pyrex tube as previously described. This tube was suspended by a 30-gauge copper wire from one arm of a Bunge microbalance, in such a position that the flat bottom of the tube was situated on the axis of the pole pieces of an electromagnet. The field used for the measurements was around 2,000 gauss. Control was obtained to ± 0·15% by adjusting the current through the coils of the magnet by means of a precision ammeter and a large rheostat.

The temperature of the sample (measured by a copper-constantan thermo-couple) was controlled by surrounding it by a thermostat the essential details of which are shown in Fig. 1 and 1A. The brass tube inside which the specimen swung had walls 1 mm. thick. It was closed with a brass plug at the bottom and provided with an inlet tube B. The diameter of the Pyrex vessel was 3 mm. less than that of the brass tube. Vacuum-tight joints were made at W, X, Y and Z with tight-fitting rubber collars (not shown on diagram). Measurements were made in an atmosphere of nitrogen at 195° K and 90° K, or hydrogen at 69° K.

The gases were freed from oxygen by passage over copper foil at 500° C, in the case of nitrogen, or over platinized asbestos at 500° C for hydrogen. After removal of oxygen the gases were freed from moisture by passage through a liquid-air trap, containing glass-wool.

Before a measurement the empty brass tube was flushed out by two streams of the required gas entering through the tube B and by an additional tube (not shown in the diagram) which reached to the bottom of the brass vessel. After flushing out, this additional tube was removed. When the specimen and the cap C had been placed in position the gas flow at B was stopped and a slow stream of the gas started through A. By this means the tube was maintained in a practically stagnant atmosphere permitting temperature equilibrium to be reached between the specimen tube and its surroundings, while the flow of gas at A prevented diffusion of atmospheric oxygen into the apparatus. Reproducible results could not be obtained unless the gas supply at A was also cut off during an actual weighing. Measurements were carried out at 195 ± 1° K (solid CO_2 and alcohol), 90 ± 1° K (oxygen boiling at atmospheric pressure) and 69 ± 1° K (oxygen boiling under reduced pressure).

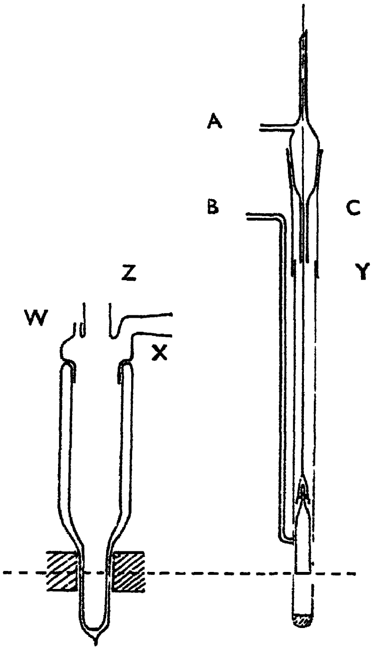

FIG. 1. FIG. 1A.

Vertical Scale—one-twelfth full size.
Horizontal Scale—one-sixth full size.
NOTE.—1A fits inside 1.

When cyclo-octatetraene was solidified in the Pyrex vessel *in situ*, two practical difficulties arose :

(i) Owing to the large decrease in volume on solidification, a " pipe " formed down the centre, which made it difficult to evaluate the density of the solid and hence to test for any absolute change in molecular susceptibility on passing from liquid to solid. To avoid the inconvenience, the substance was frozen *in situ* at the boiling point of oxygen, and after completing the measurements the next higher temperature or next lower temperature was used. Since no appreciable change had occurred in the space occupied by the solid, the ratio of the magnetic force on the solid at the two temperatures could be equated with the ratio of the magnetic susceptibilities, without serious error.

(ii) The Pyrex vessel containing cyclo-octatetraene apparently became electrified on cooling to 90° K, and could not be made to swing freely in the brass tube. This was overcome by silvering the sealed tube on the outside, which also helped to maintain uniformity of temperature of the specimen. It seemed likely that this phenomenon was due to the pyro-electric properties of crystals of cyclo-octatetraene, which would be expected from the space group proposed.[2]

Results

Results are summarized in Tables I-III. The temperature coefficient of the empty tube was determined at the end of the experiments.
Each result is the mean of ten determinations taken in groups of 3 or 4 at intervals.

TABLE I.—FORCE EXERTED ON EMPTY TUBE BY FIELD OF 2000 GAUSS

Temp. ° K	Force mg.
195	− 1·435 ± 0·005 (mean deviations)
90	− 0·207 ± 0·005
69	+ 0·435 ± 0·015

TABLE II.—CHANGE IN MAGNETIC SUSCEPTIBILITY OF CYCLO-OCTATETRAENE BETWEEN 195° K AND 90° K

Series	Net Force (mg.)		Diff. (mg.)
	90° K	195° K	
1	− 2·087	− 2·089	− 0·002
2	− 1·969	− 1·983	− 0·014
3	− 1·862	− 1·864	− 0·002

TABLE III.—CHANGE IN MAGNETIC SUSCEPTIBILITY OF CYCLO-OCTATETRAENE BETWEEN 90° K AND 69° K

Series	Net Force (mg.)		Diff. (mg.)
	69° K	90° K	
4	− 2·077	− 2·087	− 0·010
5	− 1·982	− 2·020	− 0·038
6	− 1·994	− 2·044	− 0·050
7	− 1·853	− 1·876	− 0·023

---

[2] Kaufman and Fankuchen, *Nature*, 1948, **161**, 165.

Discussion

Calibration of the Empty Vessel (Table I).—As often happens, the Pyrex glass appeared to contain a very small paramagnetic component. The probable error is somewhat larger at the lowest temperature owing to the bigger temperature fluctuations when the oxygen was boiled under reduced pressure.

Temperature Coefficient of the Susceptibility of Solid Cyclo-octatetraene (Table II).—Although the individual values in the different series vary owing to the variable "pipe" formation on cooling, the net change in susceptibility (right-hand column) is evidently very small between 90° K and 195° K. It may be noted that although 90° K is below the temperature of yellow → white transition, this transition does not occur at all rapidly unless the cooling is well below 90° K (cf. previous publication), and thus has no influence on the results in Table II.

The change in susceptibility in this temperature interval does not exceed an average of about − 0·006 mg. or 0·3 %. This is hardly outside experimental error.

Change of Susceptibility Associated with the Yellow → White Transition (Table III).—The probable error in Table III is greater than that in I or II owing to the larger fluctuations at the lowest temperature. The mean trend implies an average decreased diamagnetism of 0·030 mg. or 1·5 % on cooling through the transition point. Although the change of 0·030 mg. exceeds the mean error in this series of observations it does not exceed the *maximum* error which is 0·060 mg., so that the above result cannot be regarded as more than an indication of the order of magnitude and sign of any change in diamagnetic susceptibility on passing through the transition.

Significance of the Results for the Interpretation of Molecular Structure of Cyclo-octatetraene.—(*a*) POSSIBILITY OF A DIRADICAL FORM IN THE YELLOW LIQUID AND SOLID.—As was discussed in the previous publication [1] each of the various bond structures can in principle contribute to the molecular structure of cyclo-octatetraene. Alternative bond structures with the same electron multiplicity could be in resonance. A large shift in the relative importance of canonical forms in a resonance hybrid as the temperature changes would not be anticipated so far as present knowledge goes and will not be further discussed here. Where these bond structures are of different electronic multiplicity, tautomeric forms are to be expected, as for example in the possible equilibrium :

proportion ($1 - x$)   proportion (x)

As the temperature is lowered, the change in equilibrium constant, say from 195° K to 90° K, is given by

$$\ln [K_{195°}/K_{90°}] = \frac{-\Delta H}{1{\cdot}99}\left(\frac{1}{195} - \frac{1}{90}\right) = 0{\cdot}0030\,\Delta H \text{ cal.} \quad . \quad (1)$$

The effect on the magnetic susceptibility is twofold.

(*a*) Because of the Langevin temperature–orientation relationship of magnetic dipoles, the molar paramagnetic susceptibility due to the diradical form will be

$$\left[\frac{\mu}{2{\cdot}83}\right]^2 . \frac{1}{T} \text{ per mole.} \quad . \quad . \quad . \quad . \quad . \quad (2)$$

(*b*) The fraction x of diradical is in any case $\ll 1$ and must decrease with cooling if its heat content is greater than for the fully-bonded form.

Thus we may write

$$\log [K_{195^\circ}/K_{90^\circ}] = \log [\chi_{195^\circ}/\chi_{90^\circ}], \quad . \quad . \quad . \quad (3)$$

and the change in paramagnetic contribution over this temperature interval is

$$\Delta\chi_{\text{para.}} = \chi_{\substack{\text{para.}\\ 195^\circ\text{K}}} \left[1 - \frac{195}{90} \exp\left(- 0{\cdot}0030\ \Delta H\right) \right].$$

The experimental fact that $\Delta\chi_{\text{para.}} = 0$ over this temperature region means either that $\chi_{\substack{\text{para.}\\ 195^\circ\text{K}}}$ is zero or that the term in brackets becomes comparable with zero. This would require ΔH to be of the order 0·26 kcal./mole. It seems much more likely that $\chi_{\substack{\text{para.}\\ 195^\circ\text{K}}}$ is in fact zero, i.e. that the concentration of diradical is negligible. The alternative explanation of the new experimental data now obtained cannot be wholly excluded, but is not considered as a promising hypothesis.

(*b*) POSSIBLE BOND TAUTOMERISM AT THE TRANSITION POINT.—Other bond structures which must likewise be considered have been previously discussed.[1] The decrease in diamagnetism on passing through the transition point, so far as it exceeds experimental error, could in principle be due to an *increase* in volume on cooling. Such increases are not very likely in a hydrocarbon.

Alternatively the 1·3 % decrease in diamagnetism on changing from yellow to white solid could be explained

(i) by the disappearance of 3 % of benzenoid form below the transition point in the solid,

(ii) by either or both the transformations

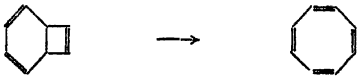

$\chi_m = - 51{\cdot}9.$ $\qquad$ $\chi_m = - 50{\cdot}24$

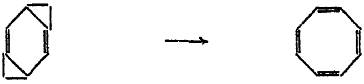

$\chi_m - 52{\cdot}24.$ $\qquad$ $\chi_m = - 50{\cdot}24.$

occurring in the sense that roughly half the molecules in the solid are in one or other of the forms on the left-hand side of the page, above the transition point, and change to the right-hand form below it.

Although the change in magnetic properties is not enough by itself to elucidate these rather subtle differences, the results so far obtained indicate the need for considering alternative bond structures in systems where tautomerism can occur even in the solid state. It may be that in other systems more pronounced effects on the physical properties will be found to be due to bond tautomerism.

Thanks are due to Messrs. I.C.I. Ltd. for the loan of a Bunge microbalance and for the gift of cyclo-octatetraene.

Department of Chemistry,
Queen's University,
Belfast.

REVIEWS OF BOOKS

The Colloid Chemistry of the Silicate Minerals. By C. EDMUND MARSHALL. (Academic Press Inc., 1949.) Pp. 195. Price $5.80.

This short but concentrated monograph will appeal chiefly to agronomists and physical chemists specializing in the study of clays. Some acquaintance with the field is implied, but, on the other hand, space has not permitted more than a sketchy account of some of the physicochemical problems concerned. The book consists of a critical survey of the more significant papers dealing with such properties of clays as the structure of their mineralogical constituents, optical properties of suspensions, their titration curves, ion exchange, electrokinetic properties, and rheology.

Prof. Marshall is the leading research worker in this field. His book, like his papers, is distinguished by a scientific soundness only too rare in the literature of clays. He wisely ignores altogether the mass of ill-conceived experiments which have been made with ill-defined clay materials, and concentrates on the work of his own school and that of authors such as R. Bradfield, W. F. Bray, E. A. Hauser, S. B. Hendricks, S. Mattson, and B. T. Shaw, who have contributed materially to our present knowledge of the fundamental properties of clays. Agricultural and industrial applications are not considered.

The monograph is notable for its salutary critical attitude. Cautious statements such as the following are common: " The only certain conclusion one can at present draw is that better experiments are needed." " The present situation with regard to clays is exceedingly confused." " It is evident that clear relationships to chemical structure and to the detailed mechanisms by which clays ionize have not yet been established." This critical treatment and the author's heavy style have resulted in a monograph which is unquestionably sound and useful, but for those who are not clay specialists it makes rather dull reading.

J. A. K.

An Advanced Treatise on Physical Chemistry. (Fundamental Principles, the Properties of Gases), VOL. I. BY J. R. PARTINGTON. (Longmans, Green & Co., 1949.) Pp. xlii + 943. Price 80s.

This volume is the first part of a comprehensive treatise on Physical Chemistry. It is a monumental work " in the pseudo-Teutonic tradition," to use the phraseology of the author. It begins with a Mathematical Introduction which assumes no knowledge of calculus or trigonometry and concludes with differential equations and Fourier series. Except for the material contained in the later section on Wave Mechanics, where the reader is introduced to spherical harmonics and other special functions, this Introduction comprising 114 pages is all that the average physical chemist needs. Section II (118 pages) gives an account of the Principles of Thermodynamics and the following 58 pages deals with the Kinetic Theory of Gases. Statistical Mechanics and Quantum Theory are crowded together into 83 pages and this chapter is followed by a short section of 42 pages on Wave Mechanics. The remaining 500 pages are devoted to

Thermometry, High and Low Temperatures, and to the Properties of Gases, including pressure-volume relationships, characteristic equations and critical phenomena, density, molecular weight, specific heat, viscosity, thermal conductivity, diffusion and the properties of gases at very low pressures.

There is an unusually large amount of valuable material in the form of tables of data and empirical equations ; the description of experimental methods are brief but the literature references are exceedingly full since they cover periodical publications, academy proceedings, dissertations, books and other sources. The total number according to the author is 18,145 and these are taken from over 500 different publications. There are also full lists of literature abbreviations and symbols so that uniformity is maintained throughout the text, e.g. equations given in the literature have been written in accordance with the author's systematic symbol list which follows in the main that adopted by the Joint Committee of the Chemical, Faraday and Physical Society of 1937. There is also a short subject index of 9 pages and a preface of 6 pages by the author.

No reviewer can do better than to quote some of the passages from this Preface since the author himself has so clearly expressed the purpose, character, scope and limitations of this first volume :

" It is not necessary, nor is it always desirable, to have a theoretical basis for *all* scientific knowledge, and those who have passed beyond the elementary stage know quite well how much valuable material will not fit in the shop-window display of the systematizer, yet often proves very handy in everyday laboratory or works experience." Writing of the large field covered and the body of information which has been presented in the book in a systematic form, the author continues : " Whether it will be useful to others must be judged by the reader. Those who have at their disposal all the large treatises and complete sets of journals and have the ability to find in them rapidly all the information they need, will probably judge the book of little value and may well make no use of it. Those less favourably situated may find it of use and it is mainly intended for such readers. It will not, therefore, be a valid criticism to say that all the information in it can be found in a better form elsewhere." " One tendency which has been avoided is to ' build ' the discussion of a topic around a theory which has been selected from among many alternatives. . . . In reading through the literature, old and new, many such attempts have been encountered, and in a large number of cases they have foundered on newer experimental data, so that the discussion gives a completely distorted and inaccurate view of the subject. It is hoped that readers who believe that some such procedure should have been adopted, and feel impatient with a less elegant treatment, will bear in mind that an author who has read far more literature than they have may have good reasons for his own procedure," and coupled with this, the author of the present book on the following page assures the reader that he has " read most of the literature, checked most of the references and wrote all the text."

Finally, " the ' advanced ' character of the work implies that the principal aim has been to give information to those in search of it and not to train students or even to ' make readers think.' "

F. C. T.

Luminescent Materials. By G. F. J. GARLICK. (Geoffrey Cumberledge, at the Clarendon Press, Oxford, 1949.) Pp. viii + 254. Price 21s.

In the last six years, three good books on the subject of luminescent materials have appeared; it might, therefore, be feared that there is no great demand at the moment for a further volume under this title. However, despite the apparent satisfactory state of the literature, there is, in fact, no co-ordinated account of this important and rapidly growing field of investigation. The present book represents an attempt—and, it is believed, a successful attempt—to remedy this defect, at least with respect to luminescence of inorganic solids. The author has necessarily had to restrict the scope and has concentrated on the more important theoretical and experimental investigations of fundamental processes. Since Dr. Garlick is a well-known research worker in this field it is natural that the treatment has a somewhat personal flavour, but this does not detract from the value of the book, and indeed gives it a degree of coherence often lacking in monographs.

Following an introductory chapter, there is an account of the mechanisms of luminescence in solids using the energy band theory of crystals for their interpretation. A greater part of Chapter III on classes of luminescent materials is devoted to those phosphors possessing high efficiency due to the presence of small concentrations of impurity. In Chapter IV recent work which assists in establishing more precise theoretical models to explain phosphorescence and thermo-luminescence is discussed. Then follows a chapter devoted to changes in electrical conductivity, dielectric constants and dielectric loss during luminescence, and to the production of luminescence by use of strong electric fields. The effects of infra-red radiation and the phenomenon of cathodo-luminescence are dealt with in the two subsequent chapters. Lastly, there is an excellent account of luminescence in organic molecules which includes a discussion on polarization and quenching of fluorescence, photochemical sensitization in relation to luminescence and the occurrence of long-period phosphorescence in molecular systems adsorbed on, or dispersed in, solids. There is a subject index and a list of references which is well selected and, in keeping with the general character of the book, right up-to-date.

The book is well and clearly written, a particularly useful feature at the beginning of each chapter being a precise indication of the material with which the author will be dealing, followed at intervals by short synopses of the present position of the subject. There are also suggestions for possible future experimental work which might lead to the elucidation of many of the problems confronting investigators. Many books on luminescence and allied phenomena degenerate at times into mere catalogues of results of empirical studies. This book, however, is concerned with the fundamental mechanisms particularly those associated with carefully prepared specimens of controlled constitution.

Because mistakes in proof reading so rarely occur in publications of the Clarendon Press, it is amusing to note that many of the author's collaborators have apparently no animate existence since he refers to them for example as, A. F. Wells, *et alia !*

Reports on Progress in Physics. Vol. XII, 1948-49. (The Physical Society, London.) Pp. 382. Price 42s. (non-Fellows), 25s. (Fellows).

These reports, which include developments to the end of 1948, are written by experts and each is accompanied by extensive references to the original literature. There is an impressive amount of information collected in the 380 pages of this book and one wonders how knowledge of recent work could be maintained without the help of these annual volumes of the Physical Society.

Readers of the *Transactions* will find a large number of the present reports of particular interest and value to them ; thus the theory of the oxidation of metals which is being largely developed at Bristol is summarized by Mott and Cabrera in a useful article ; phosphors and phosphorescence, certainly well-catered for these days by the recent appearance of three or four excellent monographs, is dealt with by Garlick ; but since the author confines himself mainly to work after 1940, there is plenty of new material thus indicating the rapid pace which this important branch is maintaining. The collision between atom and molecules at ordinary temperature by Massey is of a high standard but on comparison with the 1st edition of the book by the author and Mott, there does not appear to have been any spectacular advance.

Spectroscopists will not be disappointed with the report of Rubinowicz on multipole radiation in atomic spectra. Nuclear physicists are provided for in reports on mass spectrometry (Thode and Shields), nuclear paramagnetism (Rollin), high voltage X-rays in recent nuclear experiments (Bosley and Craggs), linear accelerators (Fry and Walkinshaw), and slow neutron absorption cross-sections of the elements (Ross and Story). Perhaps the most timely is the article by MacDonald on spontaneous fluctuations, which is mainly devoted to fluctuations analysis and a survey of recent developments, and that by Mendelssohn on low-temperature physics, which includes descriptions of recent techniques of superconductivity and superfluidity. Those concerned with the solid state will find much of interest in Orowan's excellent survey of the fracture and strength of solids, and also in the lecture survey by Jones on viscosity and related properties in glass.

It would be invidious to single out any one report, but it must be stated that the contribution by De Boer on molecular distribution equations of state of gases is outstanding. It is by no means easy reading but for those who are willing to make the effort there is a rich reward. The high standard of the Physical Society is well maintained in this volume. It is to be hoped that a sufficiently large number of copies were printed—so many excellent reports of previous years are unfortunately still out of print.

P. 168, line 2—

For of arranging N_1 solute molecules into a given set of clu..

Read of arranging N_1 solute molecules into a given set of clusters.

P. 168, line 7—

$$\textit{For}\quad \sum[N_1 - \sum(r-1)l_r + N_2]!\ p^{N_2 - zN_1}.$$

$$\textit{Read}\quad [N_1 - \sum(r-1)l_r + N_2]!\ p^{N_2 - zN_1}.$$

P. 168, line 12—

$$\textit{For}\quad N_1!\,\frac{\epsilon^{\Sigma(r1)l_r}}{N_1 - N_1} \approx \mathrm{e}^{-N_1},$$

$$\textit{Read}\quad N_1!\,\frac{\mathrm{e}^{\Sigma(r-1)l_r}}{N_1{}^{N_1}} \approx \mathrm{e}^{-N_1},$$

P. 168, eqn. (15)—

$$\textit{For}\quad \exp\left(\sum \kappa_r\xi^r\right) = \sum_{l_r} \xi^{\substack{\Sigma_r l_r \\ r}} \prod \frac{\kappa_r^{l_r}}{l_r!}. \qquad (15)$$

$$\textit{Read}\quad \exp\left(\sum \kappa_r\xi^r\right) = \sum_{l_r} \xi^{\substack{\Sigma_r l_r \\ r}} \prod \frac{\kappa_r^{l_r}}{l_r!}. \qquad (15)$$

P. 168, eqn. (19)—

$$\textit{For}\quad F(N_1, \kappa) = (1/2\pi i)\oint \exp\,[\psi_0(\xi, \kappa)]/\xi^{N_1 - 1}\mathrm{d}\xi, \qquad (19)$$

$$\textit{Read}\quad F(N_1, \kappa) = (1/2\pi i)\oint \exp\,[\psi_0(\xi, \kappa)]/\xi^{N_1 + 1}\mathrm{d}\xi, \qquad (19)$$

P. 169, eqn. (20)—

$$\textit{For}\quad \xi = \zeta\exp(i\phi),\ \mathrm{d}\xi = i\xi\exp(i\phi)\mathrm{d}\phi. \qquad (20)$$

$$\textit{Read}\quad \xi = \zeta\exp(i\phi),\ \mathrm{d}\xi = i\zeta\exp(i\phi)\mathrm{d}\phi. \qquad (20)$$

ORIENTATION EFFECTS IN BINARY SOLUTIONS *

By Arnold Münster

Received 16th May, 1949, in German

After a general discussion of the relations between molecular orientation and the entropy of mixing, a statistical theory is developed for non-[illegible] orientation of the solvent molecules. The thermodynamic properties [illegible] are in qualitative agreement with the experimental results for the [illegible] chloroform + acetone. It is shown that the assumptions of the calculation are approximately fulfilled here and that quantitatively satisfactory agreement can be obtained by using reasonable values of the parameters.

It has recently been shown [1] that it is impossible to account for the empirical thermodynamic properties of all binary liquid mixtures by the theory of strictly regular solutions. According to the theory of such solutions the sign of the excess entropy of mixing ($\Delta S_m^E < 0$), of the excess partial entropy of the solute ($\Delta S_1^E < 0$), and of the excess entropy of dilution ($\Delta S_2^E > 0$), is determined unambiguously and is independent of the sign of the heat of mixing, whereas experimentally the most varied combinations occur. Further, according to this theory, the excess partial entropy of the solute tends to the limit zero at infinite dilution, which is contrary to the experimental results in numerous cases. A discussion of the various effects which contribute to the excess entropy has shown that only two effects need be taken into account in order to explain the existing experimental results. These are the orientation of the molecules and the imperfection of the lattice in the liquid phase. In the following treatment the orientation effects will be discussed and examined more closely in a special case.

1. General Discussion.—The idea of orientation effects playing an essential part in the thermodynamic properties of binary solutions has been discussed recently by various authors.[2, 3, 4] It has not yet proved possible by strict statistical calculations, taking orientation into account, to derive thermodynamic functions which account for the required properties. Before we attack this problem, we propose to survey the possible types of orientation effects and their influence on the entropy of mixing. We shall only make use of the fact that an increase of the molecular order is accompanied by a decrease of the entropy. We denote the solute by 1 and the solvent by 2. Since orientation occurs through the interaction of neighbouring molecules we can classify the types of interaction as follows.

Type I. 1—1 Interaction.

Two solute molecules orient each other. At sufficiently low concentrations the theory of strictly regular solutions applies, i.e. $\Delta S_2^E > 0$.

---

* Dedicated, with respect, to Prof. W. Jost.

[1] Münster, *Z. Elektrochem.* (in press).

[2] Scatchard, Wood and Mochel, *J. Physic. Chem.*, 1939, **43**, 119.

[3] Goller and Wicke, *Angew. Chem. B*, 1947, **19**, 117.

[4] Wood, *J. Chem. Physics*, 1947, **15**, 358.

In certain cases, however, the cubed term in the expression for the excess entropy of dilution becomes negative, making the excess entropy itself negative [5] at higher concentrations.

Type II. 2—2 Interaction

In the pure solvent co-operative orientation takes place which is disturbed by the solute molecules. It may be expected here that the excess entropy of mixing and the excess partial entropy of the solute are positive. Characteristic examples of this occur in systems in which benzene is the solvent, e.g. benzene + cyclohexane,[6] benzene + carbon tetrachloride,[6, 7] benzene + carbon disulphide.[6]

Type III. 1—2 Interaction

The solvent molecules are oriented by the solute molecules whilst in the pure solvent free rotation occurs. Obviously in this case $\Delta S^E_m < 0$. On the other hand, it may be that $\Delta S^E_2 < 0$, because the number of molecules oriented on average by a solute molecule decreases when the latter form clusters at increased concentrations. This seems to be the case in the system chloroform + acetone.[6]

In this classification we are distinguishing between the solvent and solute and it is possible therefore that a given system will conform to different types in different concentration ranges. Thus it appears possible that the system benzene + methyl alcohol belongs to Type II ($\Delta S^E_m > 0$), at small methyl alcohol concentrations, but to Type I ($\Delta S^E_m < 0$) at higher methyl alcohol concentrations. The essential difference between Types II and III is due to the fact that in the latter the orientation has a non-co-operative character. These types are obviously limiting cases; in a given experimental system only the differences of the different kinds of interactions are significant. We shall now examine Type III statistically in greater detail.

2. The Model.—We shall use a model which, with one exception, is similar to that used earlier for strictly regular solutions.[1] We shall consider spherical particles of equal size, absence of long-range interaction forces, and the same number z of nearest neighbours for both kinds of molecules; but we shall no longer assume spherical symmetry of the interaction potential. We shall assume that the solvent molecules (index 2) can take up p orientations of equal energy in the pure phase, and we further assume that for those solvent molecules which are neighbours of a solute molecule (index 1) one of the orientations has an additional energy ϵ. We shall base the calculation again on the lattice model and assume that the partition functions of the intramolecular oscillations are the same for all lattice positions (standard configurations). We refer the potential energy of the standard configurations $E_{\text{min.}}$ to the infinitely dilute solution without orientation; then

$$E_{\text{min.}} = E_0 + E_s + E_{or} \quad . \quad . \quad . \quad . \quad (1)$$

Here E_0 is the energy of the standard configurations in which all solute molecules have only solvent molecules as their nearest neighbours and where these are not oriented. E_s is the additional energy of those standard configurations in which clusters of solute molecules occur, i.e. in which solute molecules occupy neighbouring lattice positions. E_{or} is the additional energy of the oriented solvent molecules.

Let the system contain l_r clusters of r molecules each; then

$$\sum_r r l_r = N_1, \quad . \quad . \quad . \quad . \quad . \quad (2)$$

where N_1 is the number of solute molecules. The energy of a cluster of

---

[5] Münster, *Kolloid-Z.*, 1948, **110**, 200.

[6] Kirejew, *Acta physicochim.*, 1940, **13**, 531.

[7] Scatchard, Wood and Mochel, *J. Amer. Chem. Soc.*, 1940, **62**, 712.

r molecules referred to the level E_0 is E_r; this energy can have different values within certain limits because there are several, say ν_r, possible ways of combining r molecules in a group so that each molecule has at least one other molecule of the group as its nearest neighbour. We can therefore write:

$$E_s = \sum_r \left(\sum_{i_r=1}^{l_r} E_{i_r} \right), \quad . \quad . \quad . \quad . \quad . \quad (3)$$

where E_{i_r} is the energy of the i_r-th group of r molecules. Whilst an isolated solute molecule has z solvent molecules as nearest neighbours, a solute molecule which belongs to a group of r molecules has only z_r of such neighbours, and z_r again depends on the configuration of the group. The energy of orientation is therefore

$$E_{or} = \sum \left(\sum m_{i_r} r\epsilon \right), \quad . \quad . \quad . \quad . \quad . \quad (4)$$

where m_{i_r} can assume all values from zero to z_r.

Let the partition function for the standard configurations and the orientations of the solvent molecules be

$$B'(T) = \sum \exp\,(-E_{\text{min.}}/kT) \quad . \quad . \quad . \quad (5)$$

(where k is Boltzmann's constant and T is the absolute temperature), and let the partition function for the orientation of single solute molecules be $\theta(z)$. The complete partition function for the orientation for any standard configuration is then

$$\Theta = p^{\,zN_1 - \sum\limits_r (\sum\limits_1^{l_r} z_r r)} \prod_r \prod_1^{l_r} \theta(z_r)^r, \quad . \quad . \quad . \quad (6)$$

(apart from a factor $p^{N_2 - zN_1}$ where N_2 is the number of solvent molecules), and we can write

$$B'(T) = \exp\,(-E_0/kT)(Q + Z). \quad . \quad . \quad . \quad (7)$$

Here

$$Q = (N_1 + N_2)!\, p^{N_2 - zN_1}\{\theta(z)\}^{N_1} \quad . \quad . \quad . \quad (8)$$

and

$$Z = \sum \left[\Theta \exp\,(-E_s/kT) - \{\theta(z)\}^{N_1} \right] \quad . \quad . \quad (9)$$

The sum in eqn. (9) is to be taken over all standard configurations. We shall now assume that all configurations which belong to a given set of the l_r have the same statistical weight g_{l_r} and we take for z_r its mean value over all configurations of a cluster. Each g_{l_r} belongs to an expression of the form:

$$\sum \ldots \sum \left\{ \Theta \exp\left[-\sum \left(\sum E_{i_r} \right) / kT \right] - \theta(z)^{N_1} \right\}, \quad . \quad (10)$$

where the sum is to be taken over all the ν_r configurations of the clusters. We now define

$$\phi_1 = 1,\ \phi_r = \sum \left\{ \left[\frac{p^{(z\quad z_r)}\theta(z_r)}{\theta(z)} \right]^r \exp\,[-E_r/kT] - 1 \right\} (r > 2), \quad . \quad (11)$$

where the sum is to be taken over all the configurations of a cluster of r molecules. Eqn. (10) then reduces[9] to

$$\{\theta(z)\}^{N_1} \prod \phi_r^{l_r}.$$

---

[8] Scatchard, Wood and Mochel, *J. Amer. Chem. Soc.*, 1946, 68, 1957.

[9] Münster, *Z. Naturforsch.*, 1947, 2A, 284.

The weight factor g_{l_r} has two components: the number of possible ways of arranging N_1 solute molecules into a given set of clusters,

$$N_1!/[\Pi l_r!\ \Pi(r!)^{l_r}]$$

and the number of standard configurations of the solution which belong to a given set of the l_r. If we treat the clusters as single molecules, i.e. neglecting their spatial extension,[1] we obtain for this

$$\sum[N_1 - \sum(r-1)l_r + N_2]!\ p^{N_2 - zN_1}.$$

We now apply Stirling's formula to this and neglect $\Sigma(r-1)l_r$ against $N_1 + N_2$ in the logarithmic term. Defining the quantities

$$\kappa_r = \frac{N_1^{r}\phi_r}{(N_1 + N_2)^{r-1} r!} \quad . \quad . \quad . \quad . \quad (12)$$

and taking, for not too high concentrations

$$N_1!\,\frac{e^{\Sigma(r1)l_r}}{N_1^{-N_1}} \approx e^{-N_1},$$

we obtain

$$B'(T) = \exp(-E_0/kT)(N_1 + N_2)!\ p^{N_2 - zN_1}\{\theta(z)\}^{N_1}\,.\,e^{-N_1}\sum\prod\frac{\kappa_r^{l_r}}{l_r!} \quad (13)$$

where the sum is to be consistent with eqn. (2)

3. Integral Representation of the Partition Function.—In order to evaluate the sum in eqn. (13) we shall use a method, the essence of which has been discussed thoroughly elsewhere.[10] We put

$$F(N_1, \kappa) = \sum_{\substack{l_r \\ \Sigma l r_r = N_1}} \prod_r \frac{\kappa_r^{l_r}}{l_r!}. \quad . \quad . \quad . \quad . \quad (14)$$

These functions are the coefficients of the expansion of

$$\exp\left(\sum \kappa_r \xi^r\right)$$

in powers of ξ, i.e.

$$\exp\left(\sum \kappa_r \xi^r\right) = \sum_{l_r} \xi^{\sum_r r l_r} \prod \frac{\kappa_r^{l_r}}{l_r!}. \quad . \quad (15)$$

If we take all sets of l_r together, for which $\Sigma r l_r = N_1$, it follows that

$$\exp\left(\sum \kappa_r \xi^r\right) = \sum_{N_1} \xi^{N_1} \sum_{\substack{l_r \\ \Sigma r l_r = N_1}} \prod_r \frac{\kappa_r^{l_r}}{l_r!}. \quad . \quad . \quad (16)$$

We now define new functions ψ_λ by the equations

$$\psi_\lambda(\xi, \kappa) = \sum \kappa_r \xi^r r^\lambda. \quad . \quad . \quad . \quad . \quad (17)$$

Hence

$$\exp\left(\sum \kappa_r \xi^r\right) = \exp[\psi_0(\xi, \kappa)] = \sum_{N_1} F(N_1, \kappa)\xi^{N_1}, \quad . \quad . \quad (18)$$

and $F(N_1, \kappa)$ can be expressed as a Cauchy integral

$$F(N_1, \kappa) = (1/2\pi i)\oint \exp[\psi_0(\xi, \kappa)]/\xi^{N_1-1}d\xi, \quad . \quad . \quad (19)$$

or

$$F(N_1, \kappa) = (1/2\pi i)\oint \exp[\psi_0(\xi,\kappa) - (N_1 + 1)\ln\xi]d\xi, \quad . \quad (19a)$$

where the contour of integration lies within the region in which $\exp[\psi_0(\xi_1\ \kappa]$ is regular and includes the point $\xi = 0$. The exponential is regular within the circle of convergence of $\psi_0(\xi, \kappa)$, with the exception of the point $\xi = 0$. The integral can be evaluated by the method of steepest descent.

---

[10] Münster, *Proc. Cambr. Phil. Soc.* (in press).

We take as the path of integration a circle round the origin and write :

$$\xi = \zeta \exp(i\phi),\ \mathrm{d}\xi = i\xi \exp(i\phi)\mathrm{d}\phi. \quad . \quad . \quad . \quad (20)$$

Then

$$F(N_1, \kappa) = (1/2\pi)\int_{-\pi}^{+\pi} \exp[f(\zeta, e^{i\phi})]\mathrm{d}\phi, \quad . \quad . \quad (21)$$

with

$$f(\zeta, e^{i\phi}) = \psi_0(\zeta e^{i\phi}, \kappa) - N_1 \ln(\zeta e^{i\phi}). \quad . \quad . \quad . \quad (22)$$

We now select ζ, the radius of the circle of integration, so that $f(\zeta, e^{i\phi})$, as a function of ϕ, has a maximum on the real axis ($\phi = 0$). It follows from eqn. (17) that

$$\frac{\partial}{\partial\phi}[\psi_\lambda(\zeta e^{i\phi}, \kappa)] = i\psi_{\lambda+1}[\zeta e^{i\phi}, \kappa]. \quad . \quad . \quad . \quad . \quad (23)$$

We thus obtain for ζ the equation

$$\left[\frac{\partial}{\partial\phi}f(\zeta, e^{i\phi})\right]_{\phi=0} = i[\psi_1(\zeta, \kappa) - N_1] = 0, \quad . \quad . \quad (24)$$

or

$$\psi_1(\zeta, \kappa) = N_1. \quad . \quad . \quad . \quad . \quad . \quad . \quad (25)$$

If we take into account that

$$\left[\frac{\partial^\nu}{\partial\phi^\nu}f(\zeta e^{i\phi})\right]_{\phi=0} = i^\nu\psi_\nu(\zeta, \kappa) \quad (\nu > 2), \quad . \quad . \quad (26)$$

we can expand the exponential in eqn. (21) about $\phi = 0$ and using eqn. (24) we thus obtain

$$F(N_1, \kappa) = \frac{1}{2\pi} \exp[f(\zeta)]\int_{-\pi}^{+\pi} \exp\left[-\psi_2(\zeta, \kappa)\frac{\phi^2}{2} + \sum_{\nu=3} i^\nu\psi_\nu(\zeta, \kappa)\frac{\phi^\nu}{\nu!}\right]\mathrm{d}\phi. \quad (27)$$

By the transformation

$$\phi^2 = 2y^2/\psi_2(\zeta, \kappa) \quad . \quad . \quad . \quad . \quad . \quad (28)$$

we obtain

$$F(N_1, \kappa) = \frac{1}{2\pi}\exp[f(\zeta)][2/\psi_2(\zeta, \kappa)]^{\frac{1}{2}}\int_{-\pi\sqrt{\frac{\psi_2}{2}}}^{+\pi\sqrt{\frac{\psi_2}{2}}} \exp\left[-y^2 + \sum_{\nu=3} i^\nu\psi_\nu(\zeta, \kappa)y^\nu/\nu!\left(\frac{\psi_2}{2}\right)^{\nu/2}\right]\mathrm{d}y \quad (29)$$

If we assume that

$$\frac{1}{\nu!}\frac{\psi_\nu(\zeta, \kappa)}{[\frac{1}{2}\psi_2(\zeta, \kappa)]^{\nu/2}} \ll 1 \quad (\nu > 3), \quad . \quad . \quad . \quad (30)$$

we can neglect the higher terms in the exponential and take the integral as an approximation from $-\infty$ to $+\infty$. Then, with eqn. (22), we get

$$F(N_1, \kappa) = \frac{\exp[\psi_0(\zeta, \kappa)]}{\zeta^{N_1}[2\pi\psi_2(\zeta, \kappa)]^{\frac{1}{2}}}, \quad . \quad . \quad . \quad (31)$$

and using eqn. (13), if we neglect the square root in the denominator of eqn. (31),

$$\begin{aligned}\ln B'(T) = {} \\ & -E_0/kT + \ln(N_1+N_2)! + (N_2 - zN_1)\ln p + N_1\ln\theta(z) - N_1 + \psi_0(\zeta, \kappa) \\ & -N_1\ln\zeta. \qquad (32)\end{aligned}$$

4. Development of the Partition Function.—For the sake of simplicity we shall take the calculations only to the first approximation ; this will show all the important characteristics. The quantity ζ can be calculated from eqn. (25) by a method of successive approximation. The first two terms of the solution are

$$\zeta = \frac{N_1}{\kappa_1} - 2\frac{\kappa_2}{\kappa_1}\left(\frac{N_1}{\kappa_1}\right)^2. \quad . \quad . \quad . \quad . \quad . \quad (33)$$

The weight factor g_{l_r} has two components: the number of possible ways of arranging N_1 solute molecules into a given set of clusters,

$$N_1!/[\Pi l_r!\ \Pi(r!)^{l_r}]$$

and the number of standard configurations of the solution which belong to a given set of the l_r. If we treat the clusters as single molecules, i.e. neglecting their spatial extension,[1] we obtain for this

$$\sum[N_1 - \sum(r-1)l_r + N_2]!\ p^{N_2 - zN_1}.$$

We now apply Stirling's formula to this and neglect $\Sigma(r-1)l_r$ against $N_1 + N_2$ in the logarithmic term. Defining the quantities

$$\kappa_r = \frac{N_1^r \phi_r}{(N_1 + N_2)^{r-1} r!} \quad . \quad . \quad . \quad . \quad (12)$$

and taking, for not too high concentrations

$$N_1!\,\frac{e^{\Sigma(r1)l_r}}{N_1{-}N_1} \approx e^{-N_1},$$

we obtain

$$B'(T) = \exp(-E_0{'}kT)(N_1 + N_2)!\, p^{N_2 - zN_1}\{\theta(z)\}^{N_1} \,.\, e^{-N_1}\sum\prod\frac{\kappa_r^{l_r}}{l_r!} \quad (13)$$

where the sum is to be consistent with eqn. (2)

3. Integral Representation of the Partition Function.—In order to evaluate the sum in eqn. (13) we shall use a method, the essence of which has been discussed thoroughly elsewhere.[10] We put

$$F(N_1, \kappa) = \sum_{\substack{l_r \\ \Sigma l r_r = N_1}} \prod_r \frac{\kappa_r^{l_r}}{l_r!}. \quad . \quad . \quad . \quad . \quad (14)$$

These functions are the coefficients of the expansion of

$$\exp\left(\sum \kappa_r \xi^r\right)$$

in powers of ξ, i.e.

$$\exp\left(\sum \kappa_r \xi^r\right) = \sum_{l_r} \xi^{\underset{r}{\Sigma} r l_r} \prod \frac{\kappa_r^{l_r}}{l_r!}. \quad . \quad . \quad . \quad (15)$$

If we take all sets of l_r together, for which $\Sigma r l_r = N_1$, it follows that

$$\exp\left(\sum \kappa_r \xi^r\right) = \sum_{N_1} \xi^{N_1} \sum_{\substack{l_r \\ \Sigma r l_r = N_1}} \prod_r \frac{\kappa_r^{l_r}}{l_r!}. \quad . \quad . \quad (16)$$

We now define new functions ψ_λ by the equations

$$\psi_\lambda(\xi, \kappa) = \sum \kappa_r \xi^r r^\lambda. \quad . \quad . \quad . \quad . \quad (17)$$

Hence

$$\exp\left(\sum \kappa_r \xi^r\right) = \exp[\psi_0(\xi, \kappa)] = \sum_{N_1} F(N_1, \kappa)\xi^{N_1}, \quad . \quad . \quad (18)$$

and $F(N_1, \kappa)$ can be expressed as a Cauchy integral

$$F(N_1, \kappa) = (1/2\pi i)\oint \exp[\psi_0(\xi, \kappa)]/\xi^{N_1 - 1} d\xi, \quad . \quad . \quad (19)$$

or

$$F(N_1, \kappa) = (1/2\pi i)\oint \exp[\psi_0(\xi,\kappa) - (N_1 + 1)\ln \xi] d\xi, \quad . \quad (19a)$$

where the contour of integration lies within the region in which $\exp[\psi_0(\xi_1\ \kappa]$ is regular and includes the point $\xi = 0$. The exponential is regular within the circle of convergence of $\psi_0(\xi, \kappa)$, with the exception of the point $\xi = 0$. The integral can be evaluated by the method of steepest descent.

---

[10] Münster, *Proc. Cambr. Phil. Soc.* (in press).

We take as the path of integration a circle round the origin and write:

$$\xi = \zeta \exp(i\phi), \quad d\xi = i\xi \exp(i\phi)d\phi. \quad . \quad . \quad . \quad (20)$$

Then

$$F(N_1, \kappa) = (1/2\pi)\int_{-\pi}^{+\pi} \exp[f(\zeta, e^{i\phi})]d\phi, \quad . \quad . \quad (21)$$

with

$$f(\zeta, e^{i\phi}) = \psi_0(\zeta e^{i\phi}, \kappa) - N_1 \ln(\zeta e^{i\phi}). \quad . \quad . \quad . \quad (22)$$

We now select ζ, the radius of the circle of integration, so that $f(\zeta, e^{i\phi})$, as a function of ϕ, has a maximum on the real axis ($\phi = 0$). It follows from eqn. (17) that

$$\frac{\partial}{\partial\phi}[\psi_\lambda(\zeta e^{i\phi}, \kappa)] = i\psi_{\lambda+1}[\zeta e^{i\phi}, \kappa]. \quad . \quad . \quad . \quad (23)$$

We thus obtain for ζ the equation

$$\left[\frac{\partial}{\partial\phi}f(\zeta, e^{i\phi})\right]_{\phi=0} = i[\psi_1(\zeta, \kappa) - N_1] = 0, \quad . \quad . \quad (24)$$

or

$$\psi_1(\zeta, \kappa) = N_1. \quad . \quad . \quad . \quad . \quad . \quad (25)$$

If we take into account that

$$\left[\frac{\partial^\nu}{\partial\phi^\nu}f(\zeta e^{i\phi})\right]_{\phi=0} = i^\nu\psi_\nu(\zeta, \kappa) \quad (\nu > 2), \quad . \quad . \quad (26)$$

we can expand the exponential in eqn. (21) about $\phi = 0$ and using eqn. (24) we thus obtain

$$F(N_1, \kappa) = \frac{1}{2\pi}\exp[f(\zeta)]\int_{-\pi}^{+\pi}\exp\left[-\psi_2(\zeta, \kappa)\frac{\phi^2}{2} + \sum_{\nu=3} i^\nu\psi_\nu(\zeta, \kappa)\frac{\phi^\nu}{\nu!}\right]d\phi. \quad (27)$$

By the transformation

$$\phi^2 = 2y^2/\psi_2(\zeta, \kappa) \quad . \quad . \quad . \quad . \quad (28)$$

we obtain

$$F(N_1, \kappa) = \frac{1}{2\pi}\exp[f(\zeta)][2/\psi_2(\zeta, \kappa)]^{\frac{1}{2}}\int_{-\pi\sqrt{\frac{\psi_2}{}}}^{+\pi\sqrt{\frac{\psi_2}{2}}}\exp\left[-y^2 + \sum_{\nu=3} i^\nu\psi_\nu(\zeta, \kappa)y^\nu/\nu!\left(\frac{\psi_2}{2}\right)^{\nu/2}\right]dy \quad (29)$$

If we assume that

$$\frac{1}{\nu!}\frac{\psi_\nu(\zeta, \kappa)}{[\frac{1}{2}\psi_2(\zeta, \kappa)]^{\nu/2}} \ll 1 \quad (\nu > 3), \quad . \quad . \quad . \quad (30)$$

we can neglect the higher terms in the exponential and take the integral as an approximation from $-\infty$ to $+\infty$. Then, with eqn. (22), we get

$$F(N_1, \kappa) = \frac{\exp[\psi_0(\zeta, \kappa)]}{\zeta^{N_1}[2\pi\psi_2(\zeta, \kappa)]^{\frac{1}{2}}}, \quad . \quad . \quad . \quad (31)$$

and using eqn. (13), if we neglect the square root in the denominator of eqn. (31),

$$\ln B'(T) = \\ -E_0/kT + \ln(N_1+N_2)! + (N_2 - zN_1)\ln p + N_1 \ln\theta(z) - N_1 + \psi_0(\zeta, \kappa) \\ -N_1 \ln\zeta. \quad (32)$$

4. Development of the Partition Function.—For the sake of simplicity we shall take the calculations only to the first approximation; this will show all the important characteristics. The quantity ζ can be calculated from eqn. (25) by a method of successive approximation. The first two terms of the solution are

$$\zeta = \frac{N_1}{} - 2\frac{\kappa_2}{}\left(\frac{N_1}{}\right)^2. \quad . \quad . \quad . \quad . \quad (33)$$

Further, from eqn. (12)

$$\kappa_1 = N_1,\ \kappa_2 = N_1\frac{\phi_2}{2}\cdot\frac{N_1}{N_1 + N_2}. \qquad (34)$$

We thus obtain

$$\psi_0(\zeta, \kappa) = N_1\left(1 - \tfrac{1}{2}\phi_2\frac{N_1}{N_1 + N_2}\right), \qquad (35)$$

and, expanding the logarithm,

$$N_1 \ln \zeta = -N_1\phi_2\frac{N_1}{N_1 + N_2}. \qquad (36)$$

We still need explicit expression for $\theta(z)$ and ϕ_2. Now

$$\theta(z) = \sum_{m=0}^{z} z!/[m!(z-m)!] \exp(-m\epsilon/kT)\,(p-1)^{z-m} = [\exp(-\epsilon/kT) + (p-1)]^{z} \quad (37)$$

and by eqn. (11), if w is the interaction energy of two solute molecules referred to E_0,

$$\phi_2 = z\{p^2[\exp(-\epsilon/kT) + (p-1)]^{-2}\exp(-w/kT) - 1\}. \qquad (38)$$

Hence

$$\psi_0(\zeta, \kappa) = N_1\left\{1 - \frac{z}{2}\left[\frac{p^3\exp(-w/kT)}{[\exp(-\epsilon/kT) + (p-1)]^2} - 1\right]\frac{N_1}{N_1 + N_2}\right\}, \qquad (35a)$$

and

$$N_1 \ln \zeta = -N_1 z\left\{\frac{p^3\exp(-w/kT)}{[\exp(-\epsilon/kT) + (p-1)]^2} - 1\right\}\frac{N_1}{N_1 + N_2}. \qquad (36a)$$

It follows from eqn. (32), (35*a*) and (36*a*), that

$$\begin{aligned}\ln B'(T) = {} & -E_0/kT + \ln(N_1 + N_2)! + (N_2 - zN_1)\ln p, \\ & + N_1 \ln[\exp(-\epsilon/kT) + (p-1)]^{z} \\ & + \frac{z}{2}\left\{\frac{p^2\exp(-w/kT)}{[\exp(-\epsilon/kT) + (p-1)]^2} - 1\right\}\frac{N_1^2}{N_1 + N_2}. \qquad (39)\end{aligned}$$

5. The Thermodynamic Functions.—The Helmholtz free energy is given by the equation

$$F = -kT\left[N_1\left(\ln\frac{v_1 f_1(T)}{N_1} + 1\right) + N_2\left(\ln\frac{v_2 f_2(T)}{N_2} + 1\right) + \ln B'(T)\right], \quad (40)$$

where $f_1(T)$ and $f_2(T)$ are the partition functions for the internal and kinetic energies, and v_1 and v_2 are the effective free volumes per molecule. We introduce the energy of the pure substances E_0' by the equation

$$E_0 = E_0' - \frac{z}{2}wN_1, \qquad (41)$$

with

$$E_0' = \frac{z}{2}(w_{11}N_1 + w_{22}N_2), \qquad (42)$$

where w_{11} and w_{22} are the interaction energies of two like molecules (referred to the ideal gas state). For the pure substances the Helmholtz free energy is

$$F_1 = -kTN_1\left[\ln v_1 f_1(T) - \frac{z}{2}\frac{w_{11}}{kT}\right],$$

$$F_2 = -kTN_2\left[\ln p v_2 f_2(T) - \frac{z}{2}\frac{w_{22}}{kT}\right]. \qquad (43)$$

We identify the Helmholtz free energy with the Gibbs' function G by neglecting the pressure term. We use R to denote the gas constant, x_1, x_2 are the mole fractions, n the total number of moles in the system.

We use W and W_{or} to denote w and ϵ, respectively multiplied by Avogadro's number. We thus have for the molar Gibbs' function of mixing

$$\frac{\Delta G_m}{RT} = x_1 \ln x_1 + x_2 \ln x_2 - \left[\frac{z}{2}\frac{W}{RT} + \ln\frac{\theta(z)}{pz} - \ln \zeta - 1\right]x_1 - \psi_0(\zeta, \kappa)/n, \quad (44)$$

or in explicit form,

$$\frac{\Delta G_m}{RT} = x_1 \ln x_1 + x \ \ln x_2 - z\left\{\frac{W}{2RT} + \ln\left[\exp(-W_{or}/RT) + (p-1)\right] - \ln p\right\}x_1$$
$$- \frac{z}{2}\left\{\frac{p^2 \exp(-W/RT)}{[\exp(-W_{or}/RT) + (p-1)]^2} - 1\right\}x_1^2. \quad (44a)$$

From this, we get for the molar entropy of mixing

$$\frac{\Delta S_m}{R} = -x_1 \ln x_1 - x_2 \ln x_2 + z\left\{\ln\left[\exp(-W_{or}/RT) + (p-1)\right] - \ln p \right.$$
$$\left. + \frac{W_{or}}{RT}\frac{\exp -(W_{or}/RT)}{[\exp(-W_{or}/RT) + (p-1)]}\right\}x_1$$
$$-\frac{z}{2}\left\{1 - \frac{p^2 \exp(-W/RT)}{[\exp(-W_{or}/RT) + (p-1)]^2}\left[1 + \frac{W}{RT} - \frac{W_{or}}{RT}\frac{2\exp(-W_{or}/RT)}{\exp(-W_{or}/RT) + (p-1)}\right]\right\}x_1^2. \quad (45)$$

For the molar heat of mixing we obtain

$$\Delta H_m = -z\left\{\tfrac{1}{2}W - W_{or}\frac{\exp(-W_{or}/RT)}{\exp(-W_{or}/RT) + (p-1)}\right\}x_1$$
$$+ \frac{z}{2}\frac{p^2 \exp(-W/RT)}{[\exp(-W_{or}/RT) + (p-1)^2]}\left[W - W_{or}\frac{2\exp(-W_{or}/RT)}{\exp(-W_{or}/RT) + (p-1)}\right]x_1^2. \quad (46)$$

6. The Partial Molar Quantities.—The chemical potentials referred to the pure substances are, from eqn. (44)

$$\frac{\Delta\mu_1}{RT} = \ln x_1 - z\left\{\frac{W}{2RT} + \ln\left[\exp(-W_{or}/RT) + (p-1)\right] - \ln p\right\}$$
$$- z\left\{\frac{p^2 \exp(-W/RT)}{[\exp(-W_{or}/RT) + (p-1)]^2} - 1\right\}x_1, \quad (47)$$

$$\frac{\Delta\mu_2}{RT} = \ln(1 - x_1) + \frac{z}{2}\left\{\frac{p^2 \exp(-W/RT)}{[\exp(-W_{or}/RT) + (p-1)]^2} - 1\right\}x_1^2. \quad (48)$$

For the partial molar entropy of the solute, eqn. (45) gives

$$\frac{\Delta S_1}{R} = -\ln x_1 + z\left\{\ln\left[\exp(-W_{or}/RT) + (p-1)\right] - \ln p \right.$$
$$\left. + \frac{W_{or}}{RT}\frac{\exp(-W_{or}/RT)}{\exp(-W_{or}/RT) + (p-1)}\right\}$$
$$- z\left\{1 - \frac{p^2 \exp(-W/RT)}{[\exp(-W_{or}/RT) + (p-1)]^2}\left[1 + \frac{W}{RT} - \frac{W_{or}}{RT}\frac{2\exp(-W_{or}/RT)}{\exp(-W_{or}/RT) + (p-1)}\right]\right\}x_1, \quad (49)$$

and for the entropy of dilution

$$\frac{\Delta S_2}{R} = -\ln(1 - x_1) + \frac{z}{2}\left\{1 - \frac{p^2 \exp(-W/RT)}{[\exp(-W_{or}/RT) + (p-1)]^2}\right.$$
$$\left.\left[1 + \frac{W}{RT} - \frac{W_{or}}{RT}\frac{2\exp(-W_{ro}/RT)}{\exp(-W_{ro}/RT) + (p-1)}\right]\right\}x_1^2. \quad (50)$$

For the partial heat functions we obtain

$$\Delta H_1 = -z\left[\tfrac{1}{2}W - W_{or}\frac{\exp(-W_{or}/RT)}{\exp(-W_{or}/RT)+(p-1)}\right]$$

$$+z\frac{p^2\exp(-W/RT)}{[\exp(-W_{or}/RT)+(p-1)]^2}\left[W - W_{or}\frac{2\exp(-W_{or}/RT)}{\exp(-W_{or}/RT)+(p-1)}\right]x_1, \quad (51)$$

and

$$\Delta H_2 = -\frac{z}{2}\cdot\frac{p^2\exp(-W/RT)}{[\exp(-W_{or}/RT)+(p-1)]^2}$$

$$\times\left[W - W_{or}\frac{2\exp(-W_{or}/RT)}{\exp(-W_{or}/RT)+(p-1)}\right]x_1^2. \quad (52)$$

Comparison of eqn. (36*a*) and (47) shows that the statistical parameter ζ, apart from a normalizing factor, is equal to the activity coefficient.

7. Discussion of the Results.—Eqn. (45) shows that the linear term in x_1 of the excess entropy of mixing (ΔS^E_m) is always negative, but that the quadratic term in x_1 is positive, when W_{or} is sufficiently large compared with W. The excess entropy of mixing is therefore negative at first and decreases to a minimum. Eqn. (46) shows that under the above conditions the heat of mixing is negative when $W_{or} < 0$. The heat of mixing also decreases to a minimum because the quadratic term in x_1 is positive. Thus ΔS^E_m and ΔH^E_m have the same sign and show

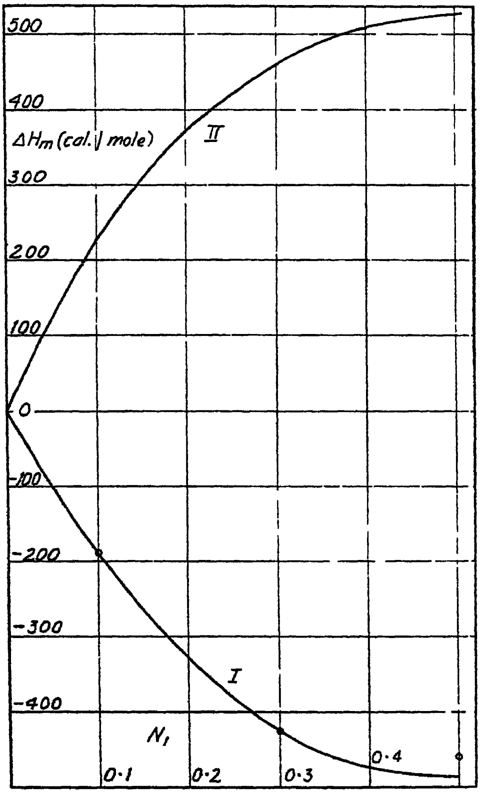

FIG. 1.—Heats of mixing. Curve I: Eqn. (46). Curve II: strictly regular solution. Circles: experimental values for the system chloroform + acetone.

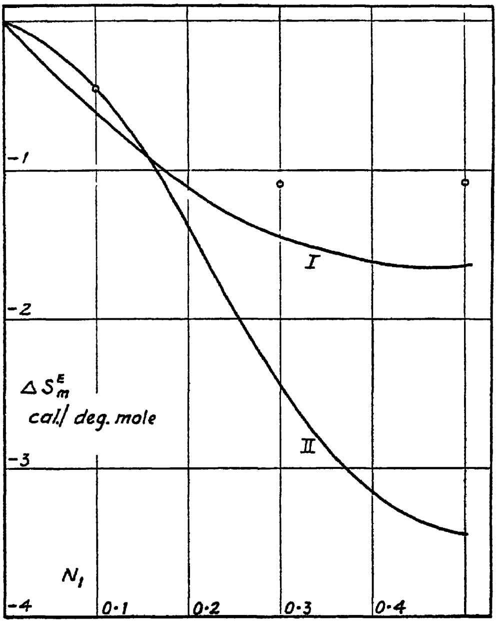

FIG. 2.—Excess entropy of mixing. Curve I : Eqn. (45). Curve II : strictly regular solution. Circles : experimental values for the system chloroform + acetone.

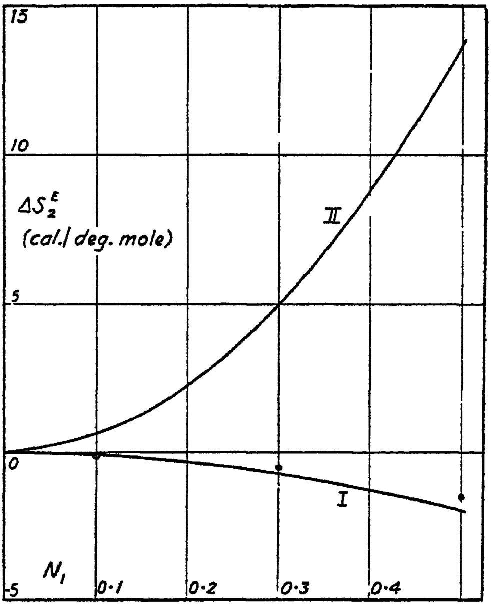

FIG. 3.—Excess entropy of dilution. Curve I : Eqn. (50). Curve II : strictly regular solution. Circles : experimental values for the system chloroform + acetone.

similar dependence on concentration; in some cases they may be practically proportional. It can also be seen that the value of ΔH_m is of the same order as that of $T \, . \, \Delta S^E_m$. The excess partial entropy of the solute has for $x_1 \rightarrow 0$ a finite negative limit and rises from this towards positive values. The excess entropy of dilution is also negative, but it decreases with increasing concentration towards larger negative values. The partial heat functions behave in a similar way as can be seen from eqn. (51) and (52).

The thermodynamic properties deduced here are all found experimentally in the system, chloroform + acetone. It appears that in this case the assumptions of the above calculation hold with sufficient accuracy. Let us consider chloroform as the solvent and acetone as the solute. Then it can be seen from the Trouton-Hildebrand constant of chloroform (= 21·7) that in the pure solvent there is little co-operative orientation.[11] In acetone the interaction is greater (Trouton-Hildebrand constant = 22·5),[11] but still much less than in methyl alcohol (Trouton-Hildebrand constant = 26·5).[11] On the other hand, the chloroform molecules should be strongly oriented by acetone because in the former the carbon-hydrogen bond is considerably loosened [12] and hydrogen bonding with acetone is probable.[13] Séguin [14] comes to the same conclusion on the basis of measurements of the magnetic susceptibility. Also, displacement of the CO bands in the absorption spectrum of the mixture [15] indicates that there is strong localized interaction between the chloroform and acetone molecules. This explains why they mix exothermically, whereas halides and hydrocarbons usually mix endothermically (e.g. cyclohexane and carbon tetrachloride).[16] We thus have here a marked 1–2 interaction. It must, however, be stressed that it is not the interaction between the molecules of the solvent and the solute (solvation) as such, which is the essential factor, but rather that the number of possible orientations of the solvent molecules is reduced by the neighbouring solute molecules. Whether this is regarded as compound formation, as recently advocated by Kirejew,[6] is merely a matter of terminology.

The functions ΔH_m, ΔS^E_m and ΔS^E_2, as given by eqn. (46), (45) and (50), are represented in Fig. 1-3 by the curves I. The following values were used for the parameters: $T = 298°\,\mathrm{K}$, $z = 4$, $p = 8$, $W_{or} = -1685$ cal./mole, $W = -1352$ cal./mole. The circles represent the experimental data for the system chloroform + acetone from Kirejew's results.[6] In view of the fact that our model contains many simplifications (particularly the neglect of the differences of molecular volumes and shapes, and imperfection of the lattice in the liquid phase) the agreement is satisfactory. It can be verified easily that for $W_{or} = 0$ the above equations reduce to those of the strictly regular solution. The functions for this case are shown as curves II in Fig. 1-3, according to eqn. (40), (38) and (44),[1] where second-order terms are taken into account; the same values of the parameters were used as in curves I. It can thus be seen that the orientation of the molecules affects the thermodynamic properties of the system in a decisive manner, and that the experimental results can only be explained by taking the orientation effects into account.

Faculty of Science,
University Frankfurt/M.

---

[11] Hildebrand, *J. Chem. Physics*, 1939, **7**, 233.

[12] Wicke, *Erg. exak. Naturwiss.*, 1942, **20**, 49.

[13] Eucken, *Lehrb. d. Chem. Physik*, Bd. 112 (Leipzig, 1944).

[14] Seguin, *Compt. rend.*, 1947, **244**, 928.

[15] Briegleb, *Zwischenmolekulare Kräfte und Molekulstruktur* (Stuttgart, 1937).

[16] Scatchard, Wood and Mochel, *J. Amer. Chem. Soc.*, 1939, **61**, 3206.

THE INFLUENCE OF STRESS UPON THE ELECTRODE POTENTIAL AND POLARIZATION OF IRON AND STEEL IN ACID SOLUTION

By M. T. Simnad and U. R. Evans

Received 30th May, 1949

The research described was designed to discover how far internal stress affects the true electrode potential of iron and steel. In acid solution, where no oxide film can survive, the unpolarized potential of cold-worked iron and steel is found to be anodic in relation to the same material in the annealed condition. The same difference is observed in experiments where a cathodic current (either greater or less than the protective value) is applied ; at any given current density, the potential of annealed specimens is about 25 mV nobler than that of the cold-rolled material. The cathodic polarization curves show a break at the point where the current reaches the protective value. The corrosion rate is affected by dissolved oxygen and by previous surface treatment.

1. The Nature of The Problem.—The main object of the research was to decide whether the *unpolarized* potential of a material is altered by internal stress. Some information is provided by previous researches on

(i) the effect of stress upon dissolution rate,
(ii) the latent energy in stressed metal,
and (iii) the corroding potentials of stressed and unstressed metal.

Although somewhat contradictory, the results justify the following conclusions :

(i) the rate of solution in acid is greatly increased by stress, as first shown by Osmond and Werth [1] and later confirmed by Barus,[2] Friend,[3] Garre,[4] Endo and Kanazawa,[5] Edwards,[6] Skapski and Chyzewski [7] and others. The increase has been ascribed either to a shift in potential or a redistribution of the cathodic elements on the surface. Friend [3] showed that in salt solutions the rate of solution is not increased by cold work ; here the attack is largely controlled by oxygen supply. Skapski and Chyzewski [7] confirmed this result, and noted that the effect of cold work only becomes appreciable below pH 4. Whiteley and Hallimond [8] showed that nitric acid, acting on strained iron, produced nitrogen compounds in proportions differing from those obtained with unstrained iron ; they ascribed this effect, which was independent of grain-size, to an increase in latent energy produced by strain.

---

[1] Osmond and Werth, *Ann. Mines*, 1885, **8**, 1.
[2] Barns, *Amer. J. Sci.*, 1886, **32**, 279.
[3] Friend, *Carnegie Schol. Mem.*, 1922, **11**, 150.
[4] Garre, *Korrosion und Metallschutz*, 1930, **6**, 200.
[5] Endo and Kanazawa, *Sci. Rep. Tohoku Univ.*, 1931, **20**, 124.
[6] Edwards, Phillips and Jones, *J. Iron Steel Inst.*, 1938, **137**, 223.
[7] Skapski and Chyzewski, *Metaux et Corrosion*, 1938, **13**, 21.
[8] Whiteley and Hallimond, *Carnegie Schol. Mem.*, 1918, 1.

(ii) The heat evolved during plastic deformation is found to be less than the work performed,[9] but there is wide discrepancy between the published values for the residual latent energy, which range between 0 and 70 % of the work of deformation. These numbers are equivalent to between 0 and 15 cal./g., and the calculated values of the change in potential which should result from cold-work present corresponding divergencies.

(iii) As shown below, the potential of a corroding metal usually bears no simple relation to the unpolarized potential; much controversy has originated from the neglect of this fact.[10] In neutral salt solutions it is difficult to distinguish between the effect of stress upon the oxide film and that upon the underlying metal, whilst in acid solutions the effect of polarization becomes the predominant factor.

Much past disagreement can be traced to different methods of surface preparation employed. The internal stresses present in cold-worked metal are masked by the usual methods of grinding with emery paper, whilst in annealed specimens the stress-free structure at the surface is destroyed by such treatment. Recent X-ray studies have shown that the distorted layer may extend an appreciable distance below the surface. Thus Vacher [11] removed successive layers from the surface by electropolishing and still detected the distorted structure at a depth of 95 μ; similar results have been obtained by Jacquet.[12] This surface distortion may be expected to shift the electrode potential of the metal to a less noble value. On cold-rolled metal, however, surface grinding modifies the internal stresses near the surface, since the local heating accompanying grinding probably relieves the stresses near the surface and replaces them by a different type of stress. Electropolishing of the metal has been used in many cases in order to overcome the objections raised to surface grinding. This method introduces no stresses and gives a flat, polished surface free from parasitic stresses, but it appears, in certain circumstances, to leave a resistant film on the surface which affects the time-potential curves.

These doubts and discrepancies make further study desirable; hence the present research was carried out.

2. Graphic Presentation of Results.—The electrochemical mechanism of corrosion by aqueous solutions has been established experimentally and will be assumed throughout the paper. The graphical construction, developed at Cambridge,[13, 14] for expressing the manner in which electrochemical factors determine the corrosion-rate and potential, will also be adopted. When current flows between the anodic and cathodic areas of a corroding specimen, both potentials, A and C (Fig. 1), are shifted towards one another. The corrosion velocity corresponds to a current of that strength I which will produce an intercept between the two curves equal to IR, where R is the resistance of the circuit; the corrosion velocity will then be I/F, where F is Faraday's number.

In acid solution, where the resistance is low and the anodic and cathodic areas generally close together, the intersection point P may be taken to represent the current flowing and the potential of the corroding specimen, If, in absence of stress, the anodic and cathodic curves (Fig. 2) are AP and CP, the corrosion current will be the abscissa of P. If stress shifts the anodic potential downwards to A′, the current will be increased to P′, whilst if stress diminishes anodic polarization, the anodic curve will become less steep (AP″) and the corresponding current will be the abscissa of P″. On the other hand, a reduction in the cathodic polarization will give a new cathodic curve CP‴, with a current corresponding to the abscissa of P‴. If both anodic and cathodic curves are affected, the potential may be almost unchanged by stress, although the current may be greatly increased.

---

[9] Elam, *The Distortion of Metal Crystals* (Oxford, 1935).

[10] Evans, *Metallic Corrosion, Passivity and Protection* (1946), p. 757.

[11] Vacher, *J. Res. Nat. Bur. Stand.*, 1942, **29**, 177.

[12] Jacquet, *Compt. rend.*, 1949, **228**, 1027.

[13] Evans, *J. Franklin Inst.*, 1929, **208**, 52.

[14] Evans and Hoar, *Proc. Roy. Soc. A*, 1932, **137**, 343.

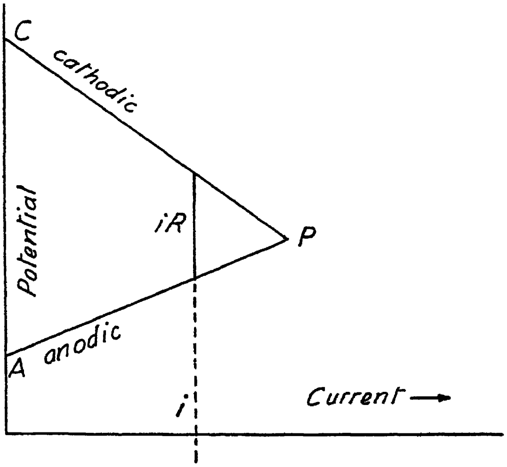

FIG. 1.

The graphical method was extended by Mears and Brown [15] and by Hoar [16] to interpret cathodic protection. If the cathodic current drawn from an external source is represented by the length YZ (Fig. 3) the corrosion current will be reduced from WP to XY. A current sufficiently strong to prevent corrosion altogether will depress the potential to the unpolarized value A. Thus the measurement of the potentials and

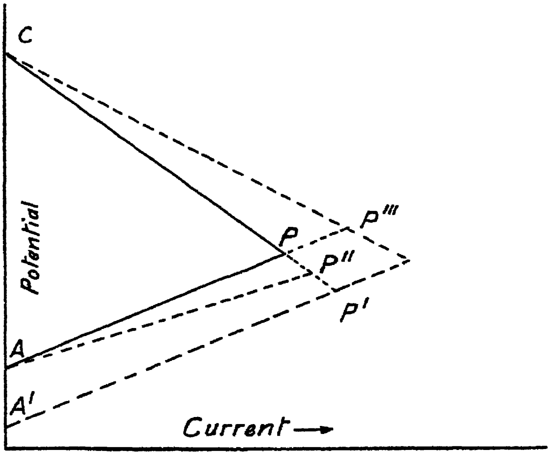

FIG. 2.

---

[15] Mears and Brown, *Trans. Electrochem. Soc.*, 1938, 74, 519.
[16] Hoar, *J. Electrodepositor's Tech. Soc.*, 1938, 14, 33.

corrosion rates with various applied cathodic currents should give a quantitative measure of the effect of stress on the polarization curves. It should then be possible to distinguish between the different theories on the effect of deformation on corrosion rate. In the present research this method has been applied to pure iron and mild steel in acid solution, both in the presence and absence of oxygen.

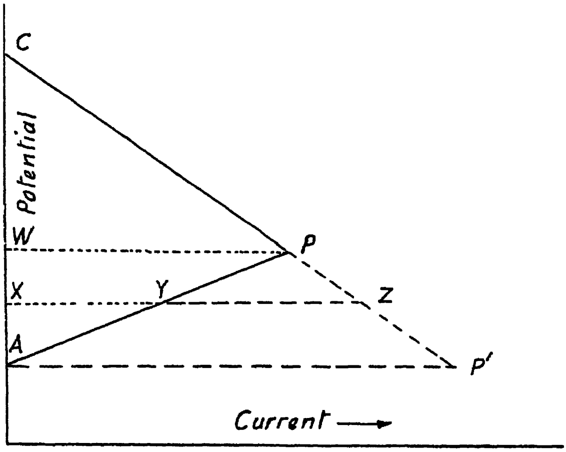

Fig. 3.

Experimental

Materials.—(*a*) Analysis. The materials used were pure iron sheet of 0·004 % carbon content, and steel of 0·26 % carbon. The analyses are given in Table I. The pure iron, SW47 (0·5 mm. thick), was obtained from Surahamma, Sweden ; the steel, U.S. 2 (0·3 mm. thick), was prepared by the late Dr. Swinden.

TABLE I.—Chemical Analysis of the Materials

Material	Pure Iron %	Mild Steel %
Carbon	0·004	0·19
Sulphur	0·012	0·03
Phosphorus	0·015	0·02
Silicon	—	0·07
Manganese	0·020	0·78
Copper	0·020	—
Nitrogen	0·020	—
Oxygen	0·150	—

(*b*) Annealing. The materials, as received, were in the cold-rolled condition. Specimens 1 in. by 3 in. were cut in a guillotine and degreased with acetone. Stress-free specimens were prepared by heating *in vacuo* (10^{-5} mm. mercury pressure), for 2 hr. at 650° C ; another set was heated at 1000° C. The surface remained bright after annealing. Several specimens which had been tinted by heating in air lost their colour during the annealing process—a change noticed also by Holm[17] and Gulbransen,[18] who ascribed it to reduction of oxide by carbon. (The superficial decarburation will introduce no error, since in the present research the surface layers are removed by anodic etching.)

---

[17] Holm, *J. Res. Nat. Bur. Stand.*, 1942, **28**, 569.

[18] Gulbransen, *Trans. Amer. Inst. Min. Met. Eng.*, 1948 (Tech. Publ. 2438).

(*c*) MICROSTRUCTURES. Microscopical examination showed freedom from inclusions. The effect of annealing on the microstructure was very marked. At both temperatures, recrystallization occurred, the original preferred orientations being changed. Heating at 1000° C involved passage through the critical point, and the phase change produced a large grain size. The distribution of cementite was altered in the usual manner upon annealing.

(*d*) HARDNESS. The hardness was measured in a Vickers diamond hardness-testing machine, using a load of 10 kg. The specimens were so placed in the machine that one of the diagonals of the diamond pyramid indenter was parallel to the direction of rolling. In the cold-rolled materials, the two diagonals of the indentation were found to differ significantly in length. The results, recorded in Table II, show that the hardness of the cold-rolled material, measured along the direction of rolling, is less than that at right-angles to the direction of rolling.

TABLE II.—VICKERS PYRAMID HARDNESS MEASUREMENTS

Material	Treatment	Hardness Number (10 kg. load)	
		Along *r-d*	Across *r-d*
Steel	*c-r*, emeried	220	248
,,	Emeried, *A* 1000° C	128	129
,,	*c-r*	236	252
,,	*A* 1000° C	130	130
,,	*A* 650° C	132	132
Pure iron	*c-r*	242	255
,,	*A* 1000° C	69	73
,,	*A* 650° C	86	86

In the above table the following abbreviations are used : *c-r* for cold-rolling ; *r-d* for rolling direction ; *A* for annealed.

The effect of orientation on hardness, noticed both on steel and pure iron, is to be expected. Although the steel and the iron are equally hard when cold-worked, annealing softens the iron more than steel, probably because of the absence of cementite in the iron. In both cases the hardness after annealing at 650° C is only slightly greater than at 1000° C. The slight preferred orientation remaining at 650° C, as shown by X-rays, is not large enough to affect the hardness. It would be of interest to correlate the degree of cold rolling, and the resultant preferred orientation, with the change in hardness along and across the rolling direction.

(*e*) CRYSTAL ORIENTATION. Through the courtesy of Dr. W. H. Taylor, the crystal orientations of the materials, in the cold-rolled and annealed conditions, have been studied by means of X-rays in the Cavendish Laboratory. The measurements were kindly carried out by Dr. P. Gay, who reports : " the cold-rolled specimens show preferred orientation, small grain-size, lattice strain. The specimens annealed at 650° C have a preferred orientation quite different from that of the cold-rolled, and their grain size is larger. There is no lattice strain in the annealed specimens, while the grain size is very large in those annealed at 1000° C."

The X-ray study of the specimens was made with unfiltered radiation since this was available and was most suitable for the transmission photographs. The pole figure constructed for the specimens, by comparison with standard photographs, appeared to be a (110) figure. The cold-worked specimens show definite preferred orientation and small grain size, and this bears out the microscopic appearance of the structure. The specimens annealed at 650° C give spotted rings, probably due to small particle size and also show some preferred orientation, but no stress. Here again, the result is in accord with that deduced from microscopic examination. The specimens annealed at 1000° C show only spots on the X-ray photographs and it has been impossible to get any preferred orientation from these. They showed a resolution of doublet, with absence of stress.

(*f*) Surface Preparation. Numerous trial experiments were carried out to test various surface treatments. The objection to using mechanically polished specimens is that such a process masks the inherent state of stress in the material by distorting the surface layers. At first sight it appeared that electro-polishing [20] might be the ideal method, but it was found that on the materials employed it developed a layer which was strongly adherent and unaffected by etching. Under suitable lighting the surface of the electro-polished metal showed a deep bluish purple film which could not be removed by cathodic reduction in acid solution. The method finally adopted was to etch the specimens anodically in a well-stirred solution of N HCl containing ferrous chloride. The current applied was 1 A/in.^{2} for 3 min. The resultant matte surface was free from pits and scratches.

(*g*) Masking of Specimens. The specimens were masked with polystyrene lacquer, except for an area of 2 cm. square to which the corrosion was confined. The polystyrene was applied twice, with an interval of a day between each application. It proved to be more satisfactory than wax since any hydrogen diffusing out through the back of the specimen merely caused a swelling in the coating, whereas wax and other brittle coatings would crack and fall off. The efficiency of the polystyrene was also tested by applying it to a tinted specimen which was then made cathode in an acid solution; any leaks in the coating would have resulted in the disappearance of the coloured oxide, but no such discoloration was observed.

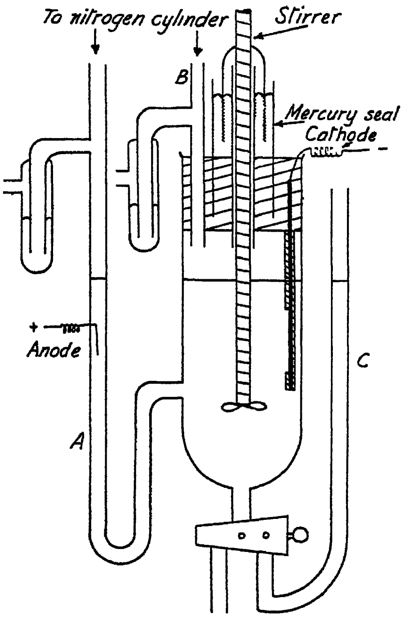

Fig. 4.

Solutions.—Two large reservoirs of N/10 HCl, one oxygen-free and the other saturated with oxygen, were prepared. The oxygen-free water was prepared by boiling for several hours and cooling under nitrogen. Pure nitrogen was bubbled through the acid solution in a fine stream, the space above the solution being alternately evacuated and filled with nitrogen (the progressive removal of oxygen by this method has been studied by Mears and Evans [19]). The reservoir was kept under slight pressure of nitrogen. The solution of oxygen-saturated N/10 HCl was stored under a slight pressure of oxygen. The pH of the solutions was measured with a glass electrode in conjunction with a Cambridge valve potentiometer, and found to be 1·3.

Apparatus.—The cell used in the experiments is shown diagrammatically in Fig. 4. It consists of a large glass tube in which the cathode, consisting of the material under study, is fixed in a slit made in the rubber stopper. The platinum wire anode is placed in a side arm, so as to prevent chlorine, evolved during electrolysis, from entering the part containing the specimen. A slight excess pressure of nitrogen is maintained in the cell through the tube B, which also serves as an exit for the hydrogen evolved during the experiments. To the bottom of the cell is attached a two-way tap which leads to the reservoir and also to the tube which makes communication through an agar-agar bridge with a calomel cell. The rubber bung at the top of the cell is provided with a glass tube in which the glass stirring rod rotates. To the outer end of the stirring rod is attached an inverted cup, which dips into a suitable mercury seal and prevents air from leaking into the cell. The motor used for stirring is of fractional horse-power and is fitted with a counter. Fluctuations in the mains voltage are corrected by means of a Raytheon voltage regulator, whilst a Variac auto-transformer is used to control the speed of the motor.

---

[19] Mears and Evans, *J. Soc. Chem. Ind.*, 1933, **52**, 349T.
[20] Jacquet, *Nature*, 1935, **135**, 1076.

When a current is to be applied to the specimen, a high external voltage is used in conjunction with a high external resistance, so that small changes in the resistance of the liquid portion of the circuit do not appreciably affect the current.

For taking electrode potential measurements the specimens are connected to a saturated calomel electrode through the tube C via an agar-agar bridge. Electrical connections lead to a Cambridge valve potentiometer, and potentials can be measured with an accuracy of ± 0·5 mV.

Procedure.—The specimens were degreased and masked with polystyrene except for an area 2 cm. square. The exposed area was then anodically etched, washed with distilled water and alcohol, dried and placed in a desiccator until required for an experiment. The specimens were placed in the cells through which nitrogen or oxygen was passed to displace the air. The stirrers were started, and the solution allowed to enter the cell by opening the taps at the bottom of the cell until it rose 2 cm. above the exposed area of the specimen. The current was adjusted to the required value and potential measurements were taken at intervals to the end of the test.

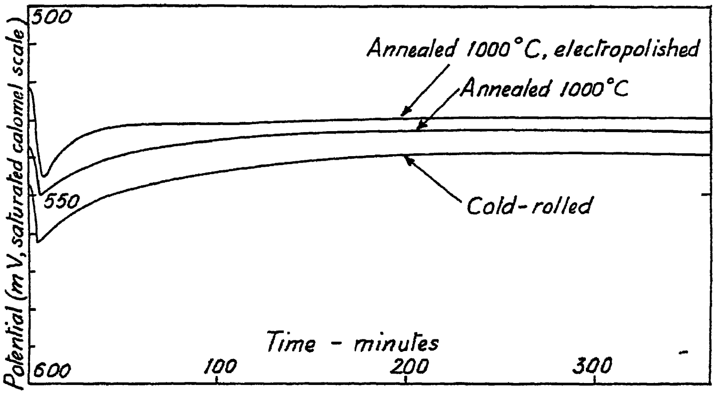

FIG. 5.—Time-Potential Curves for Steel in Aerated N/10 HCl.

The trial experiments showed that a steady potential was reached in about 1 hr. from the start of the test, and the main experiments lasted 150 min., during which time a reasonable amount of iron passed into solution in the absence of applied current. At the end of the experiments, the used solutions were collected, and their iron contents estimated by a colorimetric method based on thioglycollic acid. The use of a Spekker photoelectric absorptiometer made possible the determination of small quantities of iron.

Results

Preliminary Experiments.—The variation of potential with time for steel in air-saturated N/10 HCl, with no applied current, is indicated in Fig. 5. The curves show that the potential becomes less noble during the first few minutes, and then returns to a steady (nobler) value in about an hour. The marked effect of surface condition on rate of solution is brought out in Table III. Steel abraded with emery, annealed at 1000° C, and again abraded, is attacked 30 % more quickly than steel on which the final abrasion is omitted. Electropolishing gives the lowest rate of solution for any one material, probably because the true surface area is smallest, and also because a resistant film is present on its surface; (the time-potential curve is also different). Anodically etched metal suffers more rapid solution than the emery-treated surface, but the ratio of annealed to cold-rolled metal is much the same in both cases. There appears to be little difference in the behaviour of the steel annealed at 650° C compared with that annealed at 1000° C, despite large disparity in grain size.

Polarization Experiments.—In each series of experiments the results have been plotted as follows: for every applied current, the amount of iron

TABLE III.—INFLUENCE OF SURFACE TREATMENT ON RATE OF SOLUTION AND ON ELECTRODE POTENTIAL IN N/10 HCl

Material	Treatment	Solution N/10 HCl	Time (min.)	Iron Dissolved (mA)	Potential (mV)
Pure iron	*c-r*, etched	O_2-free	150	1·950	536
,,	*A* 650° C, etched	,,	150	0·980	541
,,	*A* 1000° C, etched	,,	150	0·940	545
,,	*c-r*, etched	O_2-sat.	150	2·550	550
,,	650° C, *A* etched	,,	150	1·550	547
,,	*A* 1000° C, etched	,,	150	1·480	545
,,	*c-r*, etched	,,	2	0·052	—
Steel	*c-r*, etched	O_2-free	150	0·635	540
,,	*A* 650° C, etched	,,	150	0·460	535
,,	*A* 1000° C, etched	,,	150	0·450	532
,,	*c-r*, etched	O_2-sat.	150	1·600	522
,,	*A* 650° C, etched	,,	150	1·250	515
,,	*A* 1000° C, etched	,,	150	1·320	514
,,	*c-r*, etched	,,	2	0·042	—
,,	*c-r*, emeried	O_2-free	150	0·350	541
,,	Emeried, *A* 1000° C	,,	150	0·171	535
,,	*c-r*, emeried	Aerated	360	0·760	540
,,	Emeried, *A* 1000° C	,,	360	0·370	534
,,	*c-r*, etched	,,	360	1·500	541
,,	*A* 650° C, etched	,,	360	0·750	536
,,	*A* 1000° C, etched	,,	360	0·710	536
,,	*A* 1000° C, electropolished	,,	360	0·355	531
,,	*A* 1000° C, emeried	,,	360	0·500	537

In the above table the following abbreviations are used : *A* for annealed ; *c-r* for cold-rolled.

estimated analytically in the solution has been converted into its equivalent current in mA and plotted logarithmically against its corresponding electrode potential, as, for instance, in Fig. 6. The curves (A_1 and A_2) slope downwards to the left, and represent the *anodic* polarization curves of the material under

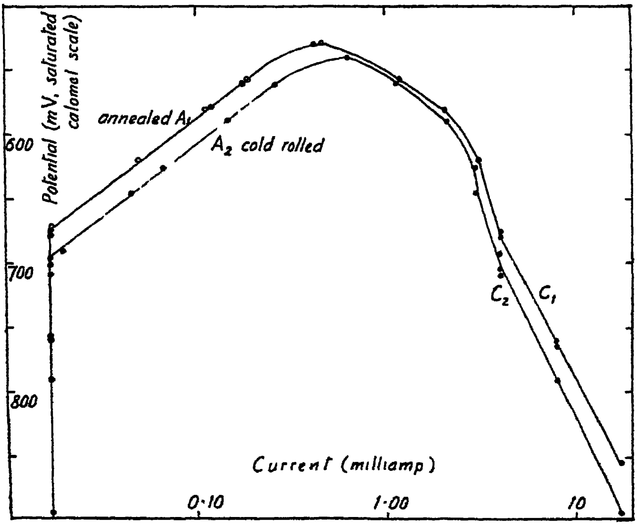

FIG. 6.—Steel in oxygen-free N/10 HCl. Relation between potential and current.

test—notwithstanding that the specimen was being subjected to cathodic treatment. The corrosion-rate provides a measure, not only of the anodic currents, but also of an equal cathodic current.[12] The *total* cathodic current is obtained by *adding* this to the *applied* cathodic current, and the curves obtained, plotted against potential, represent the *cathodic* polarization curve of the material. Such curves (C_1 and C_2) slope downwards to the right. They are, of course, the *prolongations* of the line CP of Fig. 1. The points at the apices, where the anodic and cathodic polarization curves meet, are obtained when no external currents have been applied.

The measured potentials were steady in the oxygen-free solution, but fluctuated by about ± 2 mV in the oxygen-saturated solutions ; in the latter, stirring had a pronounced effect on the potential.

(*a*) STEEL IN OXYGEN-FREE SOLUTION. The polarization curves obtained from the results plotted on a semi-logarithmic scale (Fig. 6) suggest certain relationships between the electrode potentials and currents. The points of the anodic polarization curve fall on straight, parallel lines which differ by about 22 mV, the stressed metal being the less noble. The curves obey the usual logarithmic equation

$$V = a - b \log i$$

where a and b are constants, V being the potential and i the current.

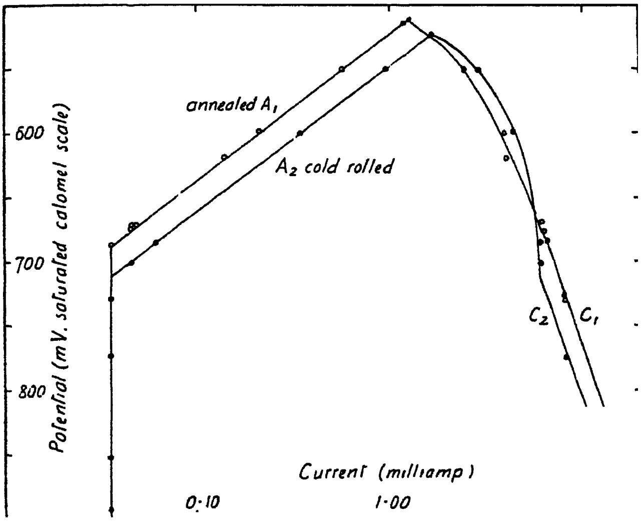

FIG. 7.—Steel in oxygen-saturated N/10 HCl. Relation between potential and current.

The total cathodic polarization curve, however, showed no simple relationship between potential and current until the point is reached at which the applied current is just " protective ".* Beyond that point, the curves show obedience to the equation

$$V = a + b \log i.$$

The slope is slightly greater for stressed than for annealed steel.

(*b*) STEEL IN OXYGEN-SATURATED SOLUTION. The curves are of similar type to those obtained in the oxygen-free solution, except for the following important differences (Fig. 7).

(i) The rates of solution, both in the presence and absence of stress, are appreciably greater than in the oxygen-free solution. The potentials obtained in the absence of applied currents are more noble than those in the oxygen-free solution.

(ii) The anodic polarization curves are lowered by about 50 mV, both for the annealed and the stressed specimens. The potential at which protection is just obtained differs by about 25 mV for the two materials.

---

* Even above the protective current density, a certain small quantity of iron is found in solution ; this does not arise from the corrosion of the metal but from reductive dissolution of the oxide film initially present.

(iii) The slopes of the curves C_1 and C_2 are greater than in the case of the oxygen-free solution.

(*c*) PURE IRON IN OXYGEN-FREE SOLUTION. The curves (Fig. 8) show only a few fresh features. The potential of the annealed iron in absence of applied current has actually a *less* noble value than that of the stressed metal, although it is corroding at an appreciably slower rate. The anodic polarization curve of the annealed iron lies about 22 mV on the noble side of the stressed iron. The slopes of these curves are practically the same as those for steel in oxygen-free solutions, but the potentials are about 50 mV less noble. The curves C_1 and C_2 again show breaks at potentials corresponding to those at which the

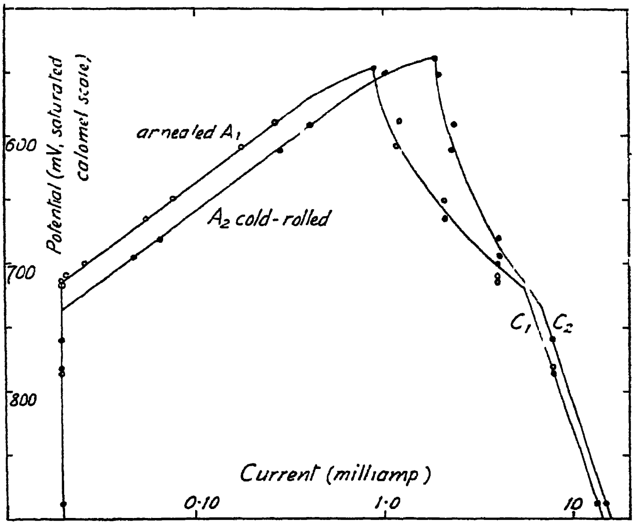

FIG. 8.—Pure iron in oxygen-free N/10 HCl. Relation between potential and current.

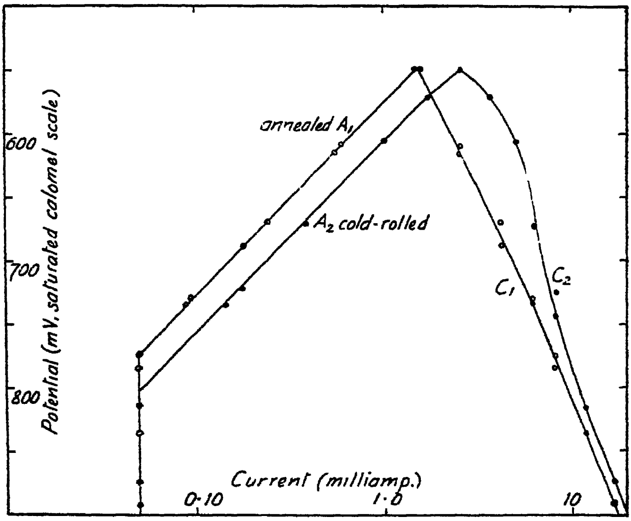

FIG. 9.—Pure iron in oxygen-saturated N/10 HCl. Relation between potential and current.

applied currents just become protective. The curve C_1 for the annealed material lies below curve C_2 for the stressed, although the corresponding slopes are the same.

(*d*) PURE IRON IN OXYGEN-SATURATED SOLUTIONS (Fig. 9). The potentials in the absence of applied current are the same for the annealed and the stressed specimens, but there is again a marked difference in their rates of solution. The anodic polarization curve of the annealed specimen lies about 25 mV on the noble side of the stressed. The curve C_1 for the annealed specimen lies below the curve C_2 for the stressed, and their corresponding slopes are the same. The rates of solution are appreciably greater than those in the oxygen-free solution. The anodic polarization curves A_1 and A_2 are both lowered by about 110 mV at 0·05 mA and 55 mV at 1 mA. The variation of potential with time at various applied currents is shown in Fig. 10.

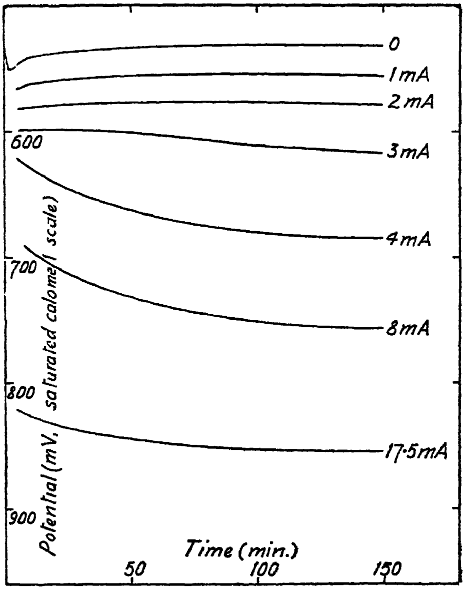

FIG. 10.—Time-potential curves for annealed steel in oxygen-free N/10 HCl. Figures denote applied current (mA).

TABLE IV.—ESTIMATION OF IRON IN OXIDE FILMS BY CATHODIC REDUCTION

Treatment of Specimen	Iron Estimated mg.
Anodic etch	0·044
Anodic etch, tinted blue, 1st order .	0·060
Anodic etch, tinted blue, 2nd order .	1·400
Emeried	0·022
Emeried, 1st-order blue . .	0·099
Emeried, vacuum annealed 1000° C .	0·010

Estimation of Iron in the Oxide Films.—It is well known that air-formed oxide films on iron can be reduced cathodically in acid solutions. Miley and Evans [21, 22] determined the thickness of oxide films on metals by measuring

---

[21] Miley, *Carnegie Schol. Mem.*, 1936, **25**, 197.

[22] Evans and Miley, *Nature*, 1937, **139**, 283.

the number of microcoulombs required for their reduction. In the present work, the actual amount of iron in the film was found by direct estimation in the solution after cathodic treatment *with current exceeding the protective value.* The results shown in Table IV bring out the effect of surface roughness on the amount of iron in the respective oxide films.

Discussion

Effect of Cold-work on Potential.—The contention that the potential of a freely corroding metal bears little relation to its unpolarized anodic potential in acid solution is justified by the results of the polarization experiments. The most striking demonstration of this is the fact that, in oxygen-saturated acid solution, the freely corroding potential of the cold-worked iron is actually more noble than that of the annealed, and there is little difference in the corresponding potentials in oxygen-free acid. This suggests that the cathodic polarization curve is less steep in the presence of internal stresses. On the other hand, the fact that the anodic polarization curves of the cold-worked iron and steel lie about 25 mV below their respective curves for the annealed condition is in harmony with the view that cold-worked metal is more "active" (in the electrochemical sense) than the corresponding annealed metal.

It is interesting to note that the polarization curves for steel are different in degree, though not in kind, from those for iron. The differences are probably due to the presence of cementite particles in the steel which act as local cathodes.

Effect of Oxygen.—The polarization curves, both for iron and steel, are lower in the presence of oxygen than the corresponding curves in oxygen-free solutions. With iron the presence of oxygen also increases the slope of the anodic polarization curves. The part of the cathodic polarization curves representing total hydrogen evolution (at currents above the protective value), follow the usual straight line logarithmic relation between overpotential and current. Here again, the corresponding curves for iron differ from those for steel. The curve for steel in oxygen-saturated solution is steeper than the corresponding curve in oxygen-free solution, but for iron it is slightly less steep. These results are in accord with the estimates, made by Hickling,[23] of the limiting current density below which the influence of oxygen on the polarization of metal electrodes in acid solutions becomes appreciable. The current densities represented by these curves are below the limiting values, and oxygen would, therefore, be expected to affect the results obtained.

General Conclusions.—The experiments seem to indicate that cold-work produces an appreciable change in the unpolarized potential, thus deciding a matter over which there has been much controversy. They also clarify our understanding of the corrosion of metal containing internal stresses, and confirm the main conclusions reached by the authors [24, 25] in their work on corrosion fatigue.

The authors would like to acknowledge the generous support of the British Iron and Steel Research Association and also the interest and encouragement of the Corrosion Committee; they wish to thank Dr. J. N. Agar, A. J. Gould, T. P. Hoar and J. E. O. Mayne for stimulating discussion, as well as Dr. W. H. Taylor and Dr. P. Gay, of the Cavendish Laboratory, for the X-ray examination of the materials used in the present research.

Department of Metallurgy,
The University,
Cambridge.

---

[23] Hickling and Salt, *Trans. Faraday Soc.*, 1941, **37**, 333.
[24] Evans and Simnad, *Proc. Roy. Soc. A*, 1947, **188**, 372.
[25] Simnad and Evans, *J. Iron Steel Inst.*, 1947, **156**, 531.

COVALENT RADIUS AND MOLECULAR STRUCTURE

By Jules Duchesne

Received 20th June, 1949

It is shown that hybridization is present to some extent in the halogen molecules as well as in carbon, oxygen and nitrogen. The evidence is based on a detailed study of the behaviour of the bond lengths in halogenated tetrahedral molecules. A correlation has been attempted using the data on the quadrupole moments in those molecules.

Schomaker and Stevenson[1] and Warhurst[2] have recently studied the important question of the determination of the lengths of bonds by means of atomic covalent radii. These authors have attempted to explain the discrepancies which occur, using a single set of revised covalent radii, by taking into account ionic bonding effects. They have advanced arguments for the view that resonance between ionic and covalent structures causes a contraction in bond lengths. Although this phenomenon certainly plays a part in determining bond lengths, difficulties remain in several cases, as noted by Pitzer[3] and Wells.[4] Furthermore, with halogenated methane CH_3X whose C—X bond lengths are now accurately known from microwave spectroscopy[5] marked discrepancies with respect to the predictions of the former authors[1, 2] are found. These considerations have convinced us that at least certain changes of bond lengths have an alternative origin.

Among other factors, repulsive effects of inner shells between bonded or non-bonded atoms have been shown to be important by Walsh,[6] Pitzer,[1] and Duchesne and Monfils.[7] As Pitzer has remarked, this factor may be of great help in explaining discrepancies in compounds for which the Schomaker and Stevenson scheme fails. However, it does not explain any anomaly and for that reason we have been led to consider the possibility of hybridization. Coulson[8] has shown how the covalent radius of carbon depends upon hybridization and has concluded that more *s* state in the *sp* hybrid the shorter are the bonds. This explains the shortening of the CH bonds in C_2H_2 (*sp*) with respect to CH_4 (sp^3). In these cases, the increased polarity of the bond cannot be responsible for the shortening. On account of the change of the sign of polarity in C_2H_2 with respect to CH_4, it is to be expected that the moment of the CH bond in C_2H_4 will be nearly zero. In spite of this, a shortening of the bond, though very small, has been observed. The idea of hybridization is therefore extended in this paper to other compounds where other factors seem inadequate.

A common feature to all the CH_3X and CX_4 molecules is the shortening of the C—X bond from the former to the latter. In spite of the relative smallness, this effect is very striking as the X—X repulsive forces should cause an increase of the CX bonds in CX_4. The C—Cl bond, for instance, equals respectively 1·755 Å and 1·786 Å in CCl_4 and CH_3Cl.[5] This property does not belong exclusively to the halogen derivatives of carbon; it also exists for silicon derivatives, e.g. for SiCl bond lengths values respectively equal to 2·00 and 2·048 Å in $SiCl_4$ and SiH_3Cl [5] are reported. On the other hand, the shortening of the CF bond with respect to the sum of covalent radii in CF_4 and CH_3F molecules must be noted (1·36 Å in the first and 1·385 in the second, instead of 1·49 Å). Such an effect is not apparent in other halogenated methanes, but is present again in the halogenated derivatives of silicon like $SiCl_4$ and SiH_3Cl (radius sum of Si and Cl equals 2·16 Å). Consequently there is a certain common behaviour of carbon and silicon though some discrepancy appears for the chlorinated derivatives.

---

[1] Schomaker and Stevenson, *J. Amer. Chem. Soc.*, 1941, **63**, 37.

[2] Warhurst, *Trans. Faraday Soc.*, 1949, **45**, 461.

[3] Pitzer, *J. Amer. Chem. Soc.*, 1948, **70**, 2140.

[4] Wells, *J. Chem. Soc.*, 1948, 55.

[5] Gordy, Simmons and Smith, *Physic. Rev.*, 1948, **74**, 243; Dailey, Mays and Townes, *ibid.*, 1949, **76**, 136; Simmons, *ibid.*, 1949, **76**, 686.

[6] Walsh, *J. Chem. Soc.*, 1948, 398.

[7] Duchesne and Monfils, *J. Chem. Physics*, 1949, **17**, 586.

[8] Coulson, *V. Henri Mem. Vol.* (Liège, 1948).

These facts have as yet not been explained theoretically. The interpretation given by Pauling [10] to justify the shortening of the CF bond in CF_4 based on a resonance effect with structures like $F^-C{=}F^+$ no longer seems satisfactory. Indeed, in the first place such an effect does not explain the same kind of shortening observed in CH_3F. In the second place, the contraction in the CF bond from CH_3F to CF_4 is 0·025 Å and for the CCl bond 0·031 Å contrary to what one would have expected. For the halogenated silicon derivatives the contraction is explained by Pauling as due to multiple bonds involving $3d$ orbitals, but Pitzer [4] has shown the difficulty in accepting this interpretation which is not confirmed by the dissociation energies. It is to be noted that structures such as $H_3Si^+Cl^-$ used to explain this effect are not excluded as they would increase the angle HSiH with respect to the tetrahedral value in agreement with recent observations (110° 57′).[5] Such a contraction is of the same order of magnitude as for CH_3F and this also is not in favour of the use of the $3d$ orbitals in the silicon compounds. On the other hand, using a similar argument to explain the contraction observed in $SiCl_4$ would be rather doubtful because in this case the part played by any ionic structure must be reduced. The reason lies in the fact that the repulsion between the chlorine atoms does not favour these structures. Furthermore, the contraction in the GeCl bond from GeH_3Cl to $GeCl_4$ is 0·067 Å. The difference is even larger than in the silicon compounds, and this cannot be explained by an increase of the multiple bonding. On the other hand the contraction with respect to the atomic radii is less in GeH_3Cl (0·063) than in SiH_3Cl (0·11). This result and the fact that the angles HSiH and HGeH are practically the same (which proves that the ionic character of SiCl and GeCl is not very different) indicates that the reason for the contraction in $GeCl_4$ is not to be found in ionic structures.

It therefore seems that neither multiple bonding nor the ionic character of the bonds are helpful in interpreting the structural behaviour of the halogenated derivatives of methane, silane and germane. The use of the new data for the bond lengths gives rise to too large deviations from the Warhurst theory. On the other hand, the Pitzer theory which certainly fits well with a number of facts seems to fail for others like those related to contractions for atoms in the same series of the periodic system as Si and Cl. It is desirable therefore to discover a more general reason for explaining the above peculiarities.

It is well known that in regular tetrahedral molecules like CF_4, CCl_4, $SiCl_4$, $GeCl_4$, the covalent radius of carbon, silicon and germanium must correspond by symmetry to an sp^3 state. If we disregard the ionic effects, which cannot be responsible here, we see no strong reason to believe that

---

[9] Sarbaugh, *Physic. Rev.*, 1948, 74, 1870.

[10] Pauling, *The Nature of the Chemical Bond* (Cornell University Press, Ithaca, N.Y., 1940).

the atomic radius of the central atom would be decreased. We are therefore led to a new hypothesis which has as yet not been suggested: that the halogen atom is itself contracted as compared to its covalent radius. This point of view leads to the possibility that the radius of the chlorine atom, for instance, can assume different values when linked with carbon, silicon and germanium.

By subtracting the covalent radius of carbon, silicon and germanium from the bond lengths in CH_3Cl, SiH_3Cl and GeH_3Cl, we find respectively 1·016, 0·88 and 0·93 Å for the radius of chlorine in these compounds. To understand these values, it is necessary to discuss the origin of the covalent radii. When we use half the interatomic distance of the X_2 molecule we obtain a covalent radius for the kind of bond between two X atoms. If we suppose that this bond has a pure *p* character, we get a covalent radius designed r_p. But, even independently of any hypothesis on the nature of the bond in X_2, there is no reason to suppose that the electronic state of X in X_2 is the same as in $CH_3X(CX_4)$, SiH_3X (SiX_4) or GeH_3X (GeX_4). This idea is supported by recent work on the absorption spectra of microwaves. The hyperfine structure of the rotational spectrum of a number of molecules has been interpreted as due to interaction of the nuclear quadrupole moment of one of the atoms with the molecular field. The resulting formula for the interaction energy has the form $eQ\,\partial^2V/\partial z^2$. According to Townes [11] the gradient of the electric field, $\partial^2V/\partial z^2$, is small when the electronic distribution in an atom of the molecule is spherical. Consequently, the contribution of $\partial^2V/\partial z^2$ to the quadrupole interaction is dependent upon the electronic symmetry around the atom to be considered. This expression determines, in other words, the total lack of symmetry of the electrons around the nucleus. $\partial^2V/\partial z^2$ has been evaluated at the chlorine nucleus of methyl chloride,[5] chlorosilane[9] and chlorogermane[5] to be 13×10^{15}, 7×10^{15} and $7{\cdot}2 \times 10^{15}$ E.S.U. respectively. This result, which shows a change in the electronic state of chlorine, is in good agreement with the earlier discussion of the distances. The increased electronic symmetry in SiH_3Cl and GeH_3Cl can be explained at least partly, either in terms of an increasing amount of ionic structures,[5] or in terms of more *sp* hybridization of chlorine, implied especially in the bonding electrons. The first assumption does not seem to provide a completely satisfactory interpretation, as the ionic structures (X^+Cl^-) cannot be responsible for a part of the effects. Therefore it must be admitted that the second assumption is justified, which means that hybridization plays a part in the halogens. The rather small dipole moment of SiH_3Cl (1·31 D)[5] may also be a consequence of hybridization. As a matter of fact, this phenomenon is the cause of a dipole moment in the molecule which is directed in the opposite sense to the main dipole moment. However, Dailey, Mays and Townes[5] have discussed the nature of the Si—Cl bond on the same basis and have explained the dipole moment peculiarity by assuming an ionic-covalent and double bond character. This seems an alternative solution of the problem. However, as a partial double bonding is rather uncertain, we believe that the use of hybridization is more appropriate. The same occurs for GeH_3Cl but the amount of hybridization is probably less than in SiH_3Cl, which is in agreement with the relative increase of the dipole moment (2·13 D). This result indicates that this factor might probably be used to follow the changes of the atomic radii in a series of chemical compounds of a particular atom.

On account of the part played by hybrids in halogenated polyatomic molecules it is perhaps to be expected that the diatomic molecules themselves would not be characterized by a pure *p* bond between the halogen atoms. This idea is reinforced by the fact that the C—Cl bond length in CH_3Cl is increased compared with the sum of the covalent radii. If

---

[11] Townes, *Physic. Rev.*, 1947, **71**, 909.

Cl_2 had a pure *p* bond, the covalent radius should have its maximum value and it would be impossible to explain any increase of C—Cl in CH_3Cl. We therefore might suppose that the molecules F_2, Cl_2, Br_2, I_2 have an *sp* hybridization which is more important when the molecule is heavy. As a result, fluorinated compounds like CF_4 would give rise to a contraction not found in the other halogenated derivatives, since for these the contraction would be expected to be in the diatomic molecule itself. This hypothesis would fit the well-known fact that the electronic *s* and *p* states converge when the atom becomes heavier, thus allowing an easier hybridization. However, a certain contradiction seems apparent between this assumption and the experimental data obtained with NH_3 and AsH_3.[12] In these cases the angle between the XH bonds decreases as the atomic mass increases, which would indicate a hybridization effect decreasing from NH_3 to AsH_3. This difficulty is not properly understood as yet.

This discussion does not mean that the ionic-covalent resonance structures do not play their part, but presumably the nature of the *s–p* hybridization in unconjugated system is an important factor to be considered, as the other factors do not explain all the observations. It is, of course, of interest to put these considerations on a more quantitative and theoretical basis. This is a matter for future development.

My thanks are due to Prof. C. A. Coulson for a helpful correspondence and to Dr. E. Warhurst for letting me know certain results before publication.

University of Liège,
Liège,
Belgium.

---

[12] Nielsen, *Physic Rev.*, 1949, **75**, 633.

THE STABILITY AND CHEMICAL REACTIVITY OF TITANIUM NITRIDE AND TITANIUM CARBIDE

BY F. H. POLLARD AND P. WOODWARD

Received 26th July, 1949

Titanium nitride has been shown to undergo a second-order decomposition in a vacuum at temperatures of 1000° C and higher, and the reactions of both nitride and carbide with various gases have been studied at 1200° C. Rapid oxidation occurs in presence of O_2, NO and CO_2, but N_2, H_2 and CO do not react. [illegible] first order.

The carbides and nitrides of the transition elements are among the hardest and most refractory materials known. Their chemical inertness at ordinary temperatures and unusual properties have given rise to many technical applications, but hitherto little has been known of their stability or chemical reactivity at high temperature.[1]

---

[1] Riley, *Quart. Rev.*, 1949, **3**, 160.

Experimental

Crystals of titanium nitride were prepared by growth on tungsten filaments from a gaseous phase, using the continuous-flow system described in an earlier paper.[2] Titanium carbide was produced similarly from a mixture of hydrogen/methane in the ratio 15/1, saturated with titanium tetrachloride vapour at 20° C, and passed over a tungsten filament at 1500° C. A deposit of uniform, metallic-looking, small, grey crystals was thus produced in convenient form for subsequent investigation. The electrode mountings, as shown in Fig. 1, were of tungsten seals with thick platinum leads to which the tungsten filament was directly spot-welded.

After the growth of a sample of nitride or carbide, the electrode was cleaned to remove deposits of lower chlorides of titanium produced during the crystal-growth process. Care was taken to avoid contact of solvents with the actual crystals, and the electrode was finally mounted in a water-cooled reaction vessel as shown in Fig. 1, using as joint grease a mixture of Apiezon-L with aluminium stearate. A small McLeod gauge, measuring from 10^{-3} to 5 mm. Hg pressure, was directly attached to the reaction vessel. Pressures greater than this could be measured on a glass spiral gauge also sealed directly on to the reaction vessel. Gases were introduced through a siphon. The crystals on the tungsten filament (which are themselves good conductors of electricity) were heated by A.C. at low voltage supplied from two step-down transformers, the first being of the Variac type to give accurate temperature control. The temperature of the specimen was measured with a disappearing-filament optical pyrometer. Since, however, nothing is known about the emissivity of the carbides and nitrides of titanium, only " brightness temperatures " were measured.

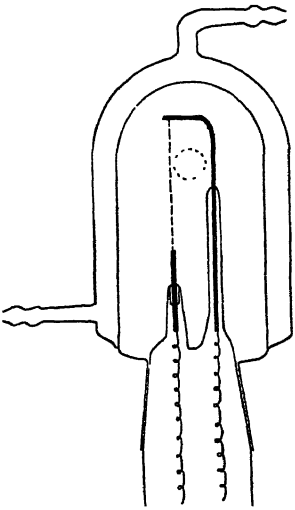

FIG. 1.—Reaction vessel with filament and electrodes in position.

Gases were analyzed by the following methods :

CO_2 : absorption in 50 % KOH solution.
CO : oxidation to CO_2 in a furnace containing CuO at 500° C, followed by absorption of CO_2.
H_2 : oxidation to H_2O in CuO-furnace at 500° C.
O_2 : absorption in alkaline pyrogallol at 20° C.
NO : absorption in chromous chloride solution.
N_2 : by difference.

The reaction vessel was of capacity 150 cm.³, so the quantities of gas to be analyzed were often considerably less than 1 cm.³. The analyses cannot, therefore, be regarded as highly accurate, since macro-methods were used for handling the gases. The reactivity of titanium nitride and titanium carbide with gases was measured at 1200° C, using pressures of a few mm. Hg. All volumes have been converted to N.T.P.

Results

Thermal Decomposition of Titanium Nitride.—When crystals of titanium nitride formed by gas-phase deposition are heated in an evacuated vessel at about 900° C, or any higher temperature, gas is evolved at a rate which can be determined by measurement of the pressure in the reaction vessel. Blackening of the surface occurs simultaneously.

The results obtained were not reproducible. The curves 1, 3, 4 and 5 included in Fig. 2 were all obtained by heating TiN at 1200°, and although the curves shown each use a different substrate metal as heating filament, the lack of reproducibility cannot be explained by this difference. Equally wide variations were observed with samples on filaments of the same metal, and at all temperatures below 1400° C curves of the same form were obtained. Moreover, although the gas was evolved at an ever-decreasing rate, no true equilibrium was reached.

---

[2] Pollard and Woodward, *J. Chem. Soc.*, 1948, 1709.

To investigate whether part of the gas emission was due to the filament itself, or the electrodes, or adsorbed gases on the vessel walls, experiments were done under similar conditions with a plain filament. The curve obtained is included in Fig. 2 (curve 6), the pressure increase being of an order of magnitude quite insufficient to account for the discrepancies in the results.

On analysis, at least 50 % of the gas was found to be H_2, and the variability of the pressure increase can be explained by the differences in the quantity of H_2 taken up during the original growth process. The residual gas, after removal of H_2, was identified as pure N_2 in a mass spectrometer, and arises from decomposition of the surface layers of the nitride crystals.

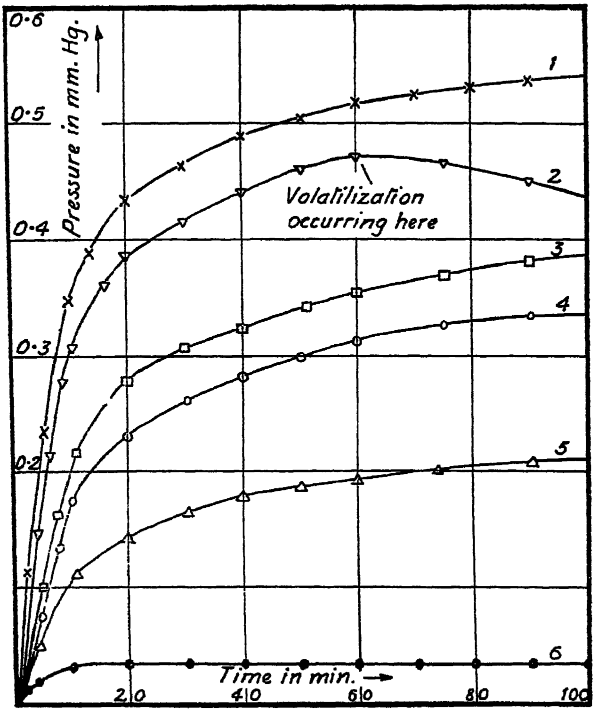

FIG. 2.—Gas evolution from titanium nitride crystals.

1. TiN on tantalum at 1200° C.
2. TiN on tungsten at 1450° C.
3. TiN on molybdenum at 1200° C.
4. TiN on tungsten at 1200° C.
5. TiN on platinum at 1200° C.
6. Tungsten wire only at 1200° C.

Kinetics of the Gas-evolution.—If the pressure in the reaction vessel is p, after a time of heating t, then it is found experimentally that, for any curve, t/p plotted against t gives a linear graph. Thus

$$t/p = 1/a + (b/a)t,$$

or

$$p = \frac{at}{1 + bt} \quad . \quad . \quad . \quad . \quad . \quad . \quad . \quad (1)$$

where a and b are constants. Such linear graphs have been drawn in Fig. 3 for curves 1, 3, 4 and 5 of Fig. 2.

Equation (1) represents values of p increasing as t increases, and approaching an upper limit as t becomes very large. Thus, the maximum pressure developed P can be calculated by putting $t = \infty$ into eqn. (1). Whence

$$P = p_{\text{max.}} = a/b, \quad . \quad . \quad . \quad . \quad . \quad . \quad (2)$$

the reciprocal of the gradient of the linear graph.

Now, for any reaction of order n, the rate at which the concentration c changes with time can be expressed by the equation :

$$-\mathrm{d}c/\mathrm{d}t = kc^n, \quad . \quad . \quad . \quad . \quad . \quad . \quad (3)$$

where k is the velocity constant. Hence, if c_1 and c_2 are the concentrations at times t_1 and t_2 respectively, we have

$$n = \frac{\log_{10}(-\mathrm{d}c_1/\mathrm{d}t) - \log_{10}(-\mathrm{d}c_2/\mathrm{d}t)}{\log_{10} c_1 - \log_{10} c_2}. \quad . \quad . \quad . \quad . \quad (4)$$

But $-\mathrm{d}c/\mathrm{d}t$ for the interstitial atoms, whether nitrogen or hydrogen, is measured by $\mathrm{d}p/\mathrm{d}t$ for the gas in the reaction vessel, and c_1 is measured by the difference between the ultimate pressure developed P and the pressure p_1 at time t_1.

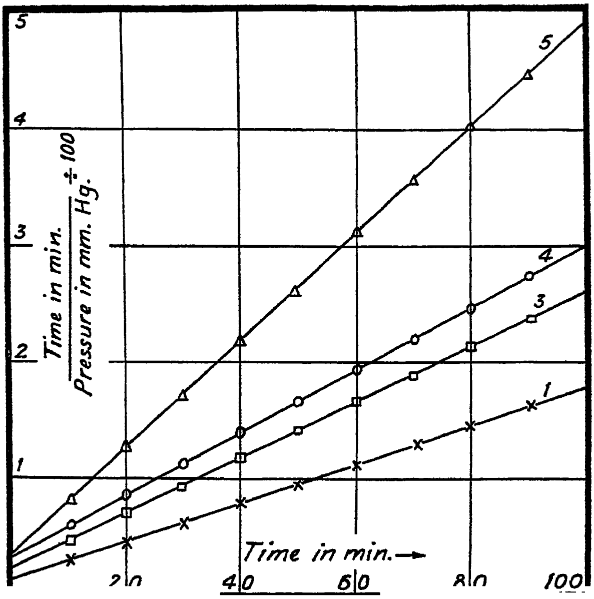

FIG. 3.—Relation between t and t/p for the thermal decomposition of titanium nitride. Curve numbers correspond with those in Fig. 2.

Thus
$$n = \frac{\log_{10}(\mathrm{d}p_1/\mathrm{d}t) - \log_{10}(\mathrm{d}p_2/\mathrm{d}t)}{\log_{10}(P-p_1) - \log_{10}(P-p_2)}. \quad . \quad . \quad . \quad . \quad (5)$$

But if
$$p = \frac{at}{1+bt},$$

then
$$\frac{\mathrm{d}p}{\mathrm{d}t} = \frac{a}{(1+bt)^2}, \quad . \quad . \quad . \quad . \quad . \quad . \quad (6)$$

which, on substituting in (5), gives $n = 2$. Consequently, using the value of P calculated from the t/p against t curve by means of eqn. (2), the gas evolution is a second-order process. This can be verified by calculation of the velocity constant for curves 1, 3, 4 and 5 of Fig. 2. In Table I the values calculated from curve 1 of Fig. 2 are shown. In the formula

$$k = \frac{1}{t} \cdot \frac{x}{a(a-x)}$$

a is measured by the calculated limiting pressure P, and x by the pressure p in the reaction vessel at any time t, giving k in units of (mm. Hg)$^{-1}$ min.$^{-1}$.

The values of k derived from different experiments were all of the same order of magnitude (between 0·1 and 0·3), though not identical. In general, larger values of k were associated with smaller values of P, and vice versa.

TABLE I.—SECOND-ORDER VELOCITY CONSTANTS FOR THE GAS EVOLUTION AT 1200° C FROM TITANIUM NITRIDE CRYSTALS

$P = 0{\cdot}59$ mm. Hg

t (min.)	5	10	20	30	40	50	60	70	80	90
p (mm. Hg)	0·218	0·340	0·431	0·463	0·489	0·510	0·520	0·528	0·536	0·543
k (mm. Hg^{-1} min.$^{-1}$)	0·19	0·23	0·23	0·22	0·22	0·23	0·22	0·22	0·22	0·23

If, at any stage in the primary thermal decomposition process the sample is cooled, the accumulated gas is not re-absorbed and can be pumped out of the reaction vessel. The nitride can then be reheated, and a second gas evolution obtained. Fig. 4 shows first, second and third decomposition curves for a particular nitride specimen on tungsten wire at 1200°. It also shows that the relation between t/p and t is still linear (except perhaps for values of $t < \sim 10$ min., where t/p appears to be constant), and in Table II, second-order velocity constants have been calculated for this curve.

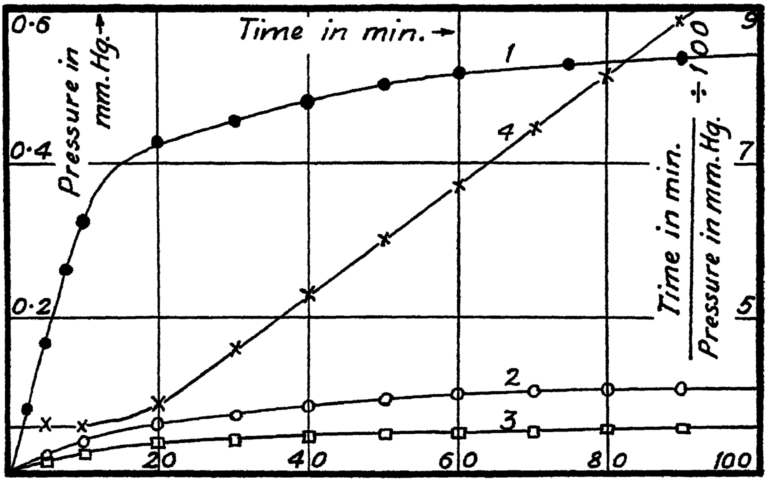

FIG. 4.—Successive heat treatments of titanium nitride. 1. Primary decomposition at 1200° C. 2 and 3. Successive decompositions at 1200° C. 4. Relation between t and t/p for curve 2, referred to the right-hand axis.

TABLE II.—SECOND-ORDER VELOCITY CONSTANTS FOR THE SECONDARY GAS EVOLUTION FROM TITANIUM NITRIDE CRYSTALS

$P = 0{\cdot}14$ mm. Hg

t (min.)	5	10	20	30	40	50	60	70	80	90
p (mm. Hg)	0·013	0·028	0·051	0·064	0·075	0·083	0·088	0·093	0·098	0·101
k(mm. Hg^{-1} min.$^{-1}$)	0·15	0·18	0·21	0·20	0·21	0·20	0·20	0·20	0·21	0·20

The agreement between the values of k for primary and secondary decompositions is reasonably good.

Thermal Decomposition above 1400°.—When titanium nitride is heated in an evacuated vessel at temperatures above 1400°, a dark-coloured film is produced on the vessel walls at a rate depending on the temperature of the specimen. The film is produced by particles travelling in straight lines, and the nitrogen simultaneously produced becomes partially "gettered" during the process, as shown in curve 2 of Fig. 2, which was taken at 1450°.

Unlike crystals of titanium nitride, the volatilized film dissolves fairly readily in hot 2N sulphuric acid. X-ray analysis of the film showed the structural arrangement of Ti atoms to be the same as that present in pure TiN (face-centred cubic). Hence it appears that the film is produced by thermal decomposition of the surface layers of the nitride, followed by volatilization of the titanium atoms thus produced. The initial desposit, being extremely active chemically, combines with sufficient nitrogen to retain the nitride crystal structure.

The critical volatilization temperature can be altered by the introduction of small amounts of gas into the reaction vessel. Table III gives values of the lowest temperature at which no visible film had been formed after 5 min. heating.

TABLE III.—CRITICAL VOLATILIZATION TEMPERATURES FOR TiN

Pressure in the Reaction Vessel	Critical Temperature °C.
Continuous evacuation ($= < 10^{-4}$ mm. Hg)	1450
3 mm. N_2	1800
3 mm. H_2	1600
5 mm. H_2	1800

Reactions of Titanium Nitride

(1) NITROGEN. No further absorption of gas occurs when titanium nitride is heated in pure nitrogen. On heating the filament, a slight, sudden increase of pressure occurs as a consequence of ordinary thermal expansion; this can be estimated and allowed for as necessary. A subsequent slow increase of pressure indicated slow evolution of gas by the nitride, as described earlier, with similar blackening of the surface layers of the crystals; the interior remained yellow.

(2) HYDROGEN. The behaviour is similar to that of nitrogen. No ammonia was detected in the residual gas which showed a small percentage of nitrogen from thermal decomposition of the nitride.

(3) OXYGEN. At 1200° C titanium nitride reacts rapidly with oxygen. In a closed vessel, the pressure of gas decreases to a minimum, then slowly increases, at which time the gas consists entirely of nitrogen. In a typical experiment, the pressure fell from 7·68 mm. to 3·90 mm. Hg during the first 15 min., and increased to 4·17 mm. during the next 25 min. In a series of experiments, the ratio oxygen admitted/nitrogen evolved was about 1·7, a considerable deviation from the equation

$$2\,TiN + 2\,O_2 \rightarrow 2\,TiO_2 + N_2.$$

It was observed that the layer of TiO_2, formed immediately upon heating the nitride, gradually disappeared, leaving a black lustrous surface on the specimen.

(4) NITROUS OXIDE and NITRIC OXIDE similarly react rapidly, but no kinetics or analyses of products have yet been carried out.

(5) CARBON MONOXIDE. Apart from the slight increases of pressure due to thermal expansion, and evolution of nitrogen and hydrogen by the titanium nitride crystals, no reaction occurs. Neither oxidation nor carbide-formation could be detected.

(6) NITROGEN-HYDROGEN MIXTURES are similarly unaffected by the presence of titanium nitride at 1200°.

(7) CARBON DIOXIDE appears to react very slowly with titanium nitride according to a second-order mechanism, and analysis of the products shows that the overall reaction can be represented approximately by the equation

$$2\,TiN + 4\,CO_2 \rightarrow 2\,TiO_2 + N_2 + 4\,CO.$$

Now if P = initial pressure of CO_2, and Δp = pressure increase after time t, then at the end of the reaction,

$$\Delta p = P/4,$$

and at any intermediate stage, the partial pressure of CO_2 is given by

$$p_{CO_2} = P - 4\Delta p.$$

The figures quoted in Table IV for the reaction between TiN and CO_2 give values for k, calculated from

$$k = \frac{4\Delta p}{Pt(P - 4\Delta p)}.$$

TABLE IV.—SECOND-ORDER VELOCITY CONSTANTS FOR THE REACTION OF CO_2 WITH TiN

t (min.)	0	10	20	30	40	50	60	70	80	90
p (mm. Hg)	2·75 $= P$	3·00	3·08	3·11	3·14	3·18	3·22	3·24	3·26	3·28
k (mm. Hg^{-1} $min.^{-1}$)		0·021	0·017	0·013	0·012	0·012	0·013	0·013	0.013	0·014

It is not possible at present to say which process is rate-controlling.

Thermal Decomposition of Titanium Carbide.—When crystals of titanium carbide, grown by gas-phase deposition, are heated above about 1000° C, gas is evolved, analysis of which shows a high percentage of H_2. As with the nitride, the surface changes from a shiny metallic to a dull black appearance. Measurement of the pressure increase with time gave results similar to those for the nitride, with a similar linear relation between t/p and t. Different samples evolved different quantities of gas, and calculation of the second-order velocity constants gave values varying by a factor of 10. Successive heat treatments also gave rather inconsistent values for k; specimen results are quoted in Tables V and VI.

TABLE V.—SECOND-ORDER VELOCITY CONSTANTS FOR THE PRIMARY AND SECONDARY GAS EVOLUTION FROM TITANIUM CARBIDE CRYSTALS

	t (min.)	5	10	20	30	40	50	60	70	80	90
Primary	p (mm. Hg)	0·250	0·337	0·410	0·457	0·459	0·521	0·540	0·551	0·557	0·863
decomposition	k (mm. Hg^{-1} $min.^{-1}$)	0·21	0·18	0·16	0·14	0·14	0·15	0·15	0·15	0·15	0·14
Secondary	p (mm. Hg)	0·075	0·102	0·131	0·150	0·163	0·174	0·183	0·192	0·196	0·199
decomposition	k (mm. Hg^{-1} $min.^{-1}$)	0·38	0·13	0·35	0·25	0·23	0·23	0·23	0·24	0·24	0·23

TABLE VI.—SECOND-ORDER VELOCITY CONSTANTS FOR THE GAS EVOLUTION FROM A DIFFERENT SPECIMEN OF TITANIUM CARBIDE CRYSTALS

	t (min.)	5	10	20	30	40	50	60	70	80	90
Primary	p (mm. Hg)	0·550	0·780	0·990	1·120	1·200	1·265	1·325	1·375	1·410	1·440
decomposition	k (mm. Hg^{-1}) $min.^{-1}$)	0·06	0·06	0·05	0·05	0·05	0·05	0·05	0·06	0·06	0·06
Secondary	p (mm. Hg)	0·075	0·110	0·160	0·195	0·225	0·250	0·275	0·295	0·320	0·330
decomposition	k (mm. Hg^{-1} min^{-1})	0·06	0·06	0·04	0·04	0·04	0·04	0·04	0·04	0·04	0·04

The relation between t/p and t departs from linearity for small values of t, giving values of t/p smaller than might be anticipated. This is different from the nitride, where t/p is approximately constant for small values of t (i.e. t/p is greater than anticipated).

Analysis of the gases evolved showed a high percentage of H_2. The residual gas showed a peak in the mass spectrometer at mass-number 16, suggesting methane. It was not proved, however, whether this arose by reaction of absorbed hydrogen with the carbon of the carbide consequent upon surface decomposition or whether methane had been directly adsorbed during the growth process.

Reactions of Titanium Carbide.—(1) NITROGEN. The only effect was a small pressure increase due to evolution of H_2 by the carbide crystals. The absence of chemical reaction was confirmed by analysis.

(2) HYDROGEN. A specimen of titanium carbide which had been successively subjected to heating at 1200° C for one hour, evacuation of the accumulated gas, reheating at 1200° C for another hour, etc., gave as maximum pressure at the eighth cycle, $4{\cdot}5 \times 10^{-2}$ mm. Hg. This treatment was followed by heating in 30 cm. of H_2 for several hours, after which the carbide was cooled, and the gas evacuated. On reheating the carbide, the maximum pressure developed was $5{\cdot}4 \times 10^{-1}$ mm. and analysis of this gas showed 90 % to be H_2. The residue was not identified, but was probably methane or some other hydrocarbon.

(3) OXYGEN. As with the nitride, reaction is rapid, the pressure of O_2 decreasing from 6·4 to 4·0 mm. within 12 min. followed by a slow increase. The final gas is almost entirely CO. Strickland-Constable[3] similarly found CO as the only product in the reaction between oxygen and carbon filaments above 1200°. Analysis of the gases during the reaction in the region of the minimum pressure revealed up to 50 % CO_2, but subsequent reheating of the carbide gave CO only. The complete reaction is in agreement with the equation

$$2\,TiC + 3O_2 \rightarrow 2\,TiO_2 + 2\,CO.$$

(4) NITROUS OXIDE. Again reaction is rapid, and occurs in agreement with the overall equation

$$TiC + 3\,N_2O \rightarrow TiO_2 + CO + 3\,N_2.$$

Moreover, if P = initial pressure of N_2O, and Δp = pressure increase after time t, then at the end of the reaction

$$\Delta p = P/3$$

and at any intermediate stage, the partial pressure of N_2O is given by

$$P - 3\Delta p.$$

The data in Table VII show that the reaction between TiC and N_2O takes place according to a first-order mechanism, as calculated from the formula

$$k = \frac{2{\cdot}303}{t} \log \frac{P}{\cdot\, 3\Delta p}.$$

TABLE VII.—FIRST-ORDER VELOCITY CONSTANTS FOR THE REACTION OF N_2O WITH TITANIUM CARBIDE

t (min.)	0	5	10	15	20	25	30	35
p (mm. Hg)	4·10 $= P$	4·60	4·80	4·96	5·08	5·22	5·32	5·41
k (min.$^{-1}$)	—	0·09	0·07	0·07	0·06	0·07	0·06	0·09

Strickland-Constable[3] similarly found a first-order reaction between N_2O and hot carbon filaments, with k-values of the same order of magnitude as those given here.

(5) CARBON MONOXIDE. No reaction occurs. The very slight increases in pressure observed could be attributed to evolution of gas from the crystals, as before, and analysis of the gas confirmed this view.

(6) CARBON DIOXIDE. Here reaction is relatively slow, but complete conversion to CO occurs. Successive reactions on the same carbide sample gave

---

[3] Strickland-Constable, *Trans. Faraday Soc.*, 1944, **40**, 333 ; 1947, **43**, 769.

consistent values for k, the reaction being of first order. This is again similar to the reaction on carbon filaments.[3] Analysis of the gases shows agreement with the equation

$$TiC + 3\ CO_2 \rightarrow TiO_2 + 4\ CO,$$

and the values of k given in Table VIII have been calculated as for the nitrous oxide reaction.

TABLE VIII.—FIRST-ORDER VELOCITY CONSTANTS FOR THE REACTION OF CARBON DIOXIDE WITH TITANIUM CARBIDE

t (min.)	0	5	10	20	30	40	50	60
p (mm. Hg)	4·10 $= P$	4·45	4·57	4·82	5·02	5·20	5·34	5·46
k (min.$^{-1}$)	—	0·06	0·04	0·04	0·04	0·04	0·05	0·05
p (mm. Hg)	3·40 $= P$	3·66	3·82	4·05	4·20	4·36	4·48	—
k (min.$^{-1}$)	—	0·05	0·05	0·04	0·04	0·05	0·06	—

Discussion

As the crystals of titanium nitride prepared by gaseous deposition contain appreciable quantities of H_2, it is not possible to measure a velocity constant for the direct decomposition. Below 1000° C, the evolution of gas is extremely slow; in the region 1000-1400° both H_2 and N_2 are evolved simultaneously, and at higher temperatures volatilization occurs. The values of k quoted are therefore composite, but suggest that both H_2 and N_2 are evolved by a second-order mechanism. Since the titanium atoms of titanium nitride are arranged as a face-centred lattice, with N atoms placed interstitially in the octahedral holes, H atoms could be accommodated in the tetrahedral holes of this lattice, from which they would presumably diffuse to the surface as atoms, recombine, and be de-adsorbed as molecular H_2.

The composite process of simultaneous diffusion of hydrogen and nitrogen does not necessarily involve the same mechanism for each component. Titanium hydride is known to be unstable above 600°,[4] so diffusion of hydrogen is probably rapid at 1400° C. On the other hand, the slowness of the colour change from yellow to black through the crystal suggests a slow rate of diffusion for N atoms. A second-order mechanism might well be involved in the recombination of atoms to form molecules on the crystal surfaces; this has been shown to be the case for the thermal decomposition of ϵ-iron nitride.[5]

Fast[6] has shown that zirconium will take up nitrogen into solid solution up to 20 atom-%, but that phases richer in nitrogen adopt the zirconium nitride structure. Evidence has here been presented, from the structure of the evaporated film, that the behaviour of titanium is similar. The evaporated film cannot contain sufficient nitrogen to be pure TiN, but nevertheless has the nitride crystal structure. This involves for titanium, a rearrangement from close-packed hexagonal to face-centred cubic structure.

From the similarity of the gas-evolution curves for titanium carbide to those of titanium nitride, it seems reasonable to suppose that the hydrogen in both materials is retained in the same state and is evolved by the same mechanism.

---

[4] Dushman, *J. Franklin Inst.*, 1931, **211**, 727.

[5] Goodeve and Jack, *Faraday Soc. Discussions*, 1948, **4**, 82.

[6] Fast, *Metallwirts.*, 1938, **17**, 641.

Titanium nitride and titanium carbide both react readily with oxidizing gases at high temperature. The reaction with O_2, does not show complete conversion of the titanium to TiO_2, however, and the existence of a minimum point in the reaction pressure curve implies that, at a certain stage in the reaction, both nitrogen and oxygen are simultaneously retained by the lattice, the nitrogen being subsequently released. Any hydrogen in the crystals is also oxidized at 1200°, so that in fact the deviation of the ratio oxygen admitted/nitrogen evolved from the expected value of 2 is rather greater than is implied by the experimentally determined value of 1·7.

The disappearance of the coating of TiO_2 produced during the early stages of the oxidation can be understood by analogy with the work of Fast on zirconium,[6] in which solid solutions of oxygen in zirconium were produced by heating the metal when coated with ZrO_2. The state of the oxygen after dissolving is not clear, but Dawihl and Rix [7] have shown that lower oxides of titanium TiO can form mixed crystals with titanium carbide in which, presumably, the oxygen is non-ionic and is placed interstitially like the carbon atoms.[8] This also explains the lack of agreement between the amount of oxygen absorbed and nitrogen evolved in comparison with the formal equation showing oxidation to TiO_2.

The authors wish to thank Dr. H. F. Kay for taking the X-ray powder photographs, and Mr. G. W. A. Fowles for the preparation of titanium carbide.

Department of Physical and Inorganic Chemistry,
University of Bristol.

---

[7] Dawihl and Rix, *Z. anorg. Chem.*, 1940, **244**, 191.

[8] *F.I.A.T. Review of German Science* (1939-1946). Part II (Wiesbaden, 1948).

SURFACE TENSION OF REGULAR SOLUTIONS

BY R. DEFAY AND I. PRIGOGINE

Received 27th July, 1949

The assumption of a unimolecular layer as the surface phase separating a strictly regular solution from its vapour phase, is in contradiction with the Gibbs adsorption formula.

When, however, one takes into account the possible presence of two unimolecular layers inside the surface phase, it is shown that the composition of the layer on the side of the solution differs but little from the composition of the solution itself, a circumstance which justifies the unimolecular layer model as a first approximation. The surface tension is not appreciably altered by this treatment, but the relative adsorption is modified significantly. The formulae thus obtained are no longer in contradiction with the Gibbs formula.

1. Unimolecular Layer on a Strictly Regular Solution.—The following model has been considered by Belton and Evans,[1] Schuchovitzky [2] and Guggenheim.[3] It is first assumed that the quasi-crystalline lattice is the same on the surface as in the bulk of the liquid phase. It is then assumed that the surface phase consists of a *unimolecular* layer the composition of which is, in general, different from that of the solution, the composition of the unimolecular layer itself being uniform.

---

[1] Belton and Evans, *Trans. Faraday Soc.*, 1945, **41**, 1.

[2] Schuchovitzky, *Acta Physicochim.*, 1944, **19**, 176.

[3] Guggenheim, *Trans. Faraday Soc.*, 1945, **41**, 150.

Let us call z the number of first neighbours of a given molecule inside the solution. A molecule in the unimolecular layer will be surrounded by $(l + m)z$ first neighbours of which lz lie inside the layer and mz lie in the liquid substrate. We must, of course, have

$$l - 2m = 1. \quad . \quad . \quad . \quad . \quad (1.1)$$

For regular solutions, including perfect solutions, the surface tension is then given by *

$$\begin{aligned} \gamma &= \gamma_1 + \frac{kT}{\omega}\log\frac{x_1'}{x_1} - \frac{m\alpha}{\omega}(x_2)^2 + \frac{l\alpha}{\omega}[(x_2')^2 - (x_2)^2] \\ &= \gamma_2 + \frac{kT}{\omega}\log\frac{x_2'}{x_2} - \frac{m\alpha}{\omega}(x_1)^2 + \frac{l\alpha}{\omega}[(x_1')^2 - (x_1)^2] \quad . \quad (1.2) \end{aligned}$$

In this formula, α is a characteristic constant (Fowler and Guggenheim's ω_{AB}), $\alpha = 0$ for a perfect solution ; ω is the " surface occupancy " assumed equal for both constituents, x_2' and x_2 are the mole fractions in the surface layer and in the liquid substrate.

We shall show now that (1.2) are incompatible with Gibbs' adsorption formula. In fact (1.2) gives at once

$$\left(\frac{d\gamma}{dx_2}\right)_{pT} = \frac{1}{\omega}\left[kT\left(\frac{x_1'}{x_1} - \frac{x_2'}{x_2}\right) - 2\alpha(1 - m)(x_2x_1' - x_1x_2')\right]. \quad (1.3)$$

One can now easily obtain the relative adsorption of component 2 with respect to 1 ; we have by definition (see ref. 6 and 4), neglecting the concentrations in the vapour phase in comparison with those in the liquid phase,

$$\Gamma_{21} = \Gamma_2 - \Gamma_1\frac{x_2}{x_1}, \quad . \quad . \quad . \quad . \quad (1.4)$$

in which Γ_1 and Γ_2 are the adsorptions on an arbitrarily chosen Gibbs' dividing surface. Putting this surface on the lower face of the monolayer and designating its area by Ω, (1.3) becomes

$$\left(\frac{d\gamma}{dx_2}\right)_{pT} = -\frac{\Gamma_{21}}{x_2}[kT - 2\alpha(1 - m)x_1x_2]. \quad . \quad . \quad (1.5)$$

On the other hand, Gibbs' formula may be written, for a regular solution (Hildebrand [5])

$$\left(\frac{d\gamma}{dx_2}\right)_{pT} = -\frac{\Gamma_{21}}{x_2}(kT - 2\alpha x_1x_2). \quad . \quad . \quad . \quad (1.6)$$

The formula (1.5) is inconsistent with (1.6) except when $\alpha = 0$, i.e. when the solution is perfect.

9. Surface Phase on a Strictly Regular Solution.—Let us now abandon the assumption of a monolayer and consider that the surface phase consists in general of several layers of different compositions. We shall perform the complete calculations for *two* molecular layers. As we shall see later, the composition of the lower layer is then already similar to that of the liquid, making the next approximation (i.e. that of three layers) unnecessary.

Let us represent by double primes $''$ the monolayer next to the liquid and by single primes $'$ the monolayer in contact with the vapour (see Fig. 1). These relations are the immediate extension of the energy of mixing used in the monolayer model (cf. Guggenheim [3]).

* Guggenheim,[3] formula (8.4).

[4] Defay, *Bull. Acad. roy. Belg.*, Cl. Sc., 1929, 1930, 1931. Travaux groupés dans l'ouvrage *Etude thermodynamique de la Tension superficielle* (Paris, Gauthier-Villars, 1934). *Mem. Acad. roy. Belg.* (in press).

[5] Hildebrand, *Solubility* (Rheinhold, New York, 1926), p. 190, formula (7).

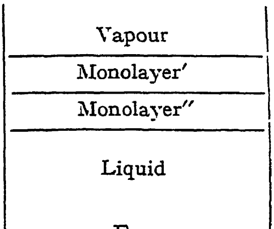

Fig. 1.

The energies of mixing are given by

$$W = \frac{N_1 N_2}{N}\alpha, \quad . \quad . \quad . \quad . \quad . \quad (2.1)$$

$$W'' = \frac{N_1'' N_2''}{N''}\alpha + N''(x_2 - x_2'')^2 m\alpha, \quad . \quad (2.2)$$

$$W' = \frac{N_2' N_2'}{N'}\alpha + N'(x_2' - x_2'')^2 m\alpha - N' x_1' x_2' m\alpha. \quad . \quad . \quad (2.3)$$

The total number of molecules N' and N'' in the layer ′ and layer ″ must necessarily be the same in view of the geometric model which we have adopted. Hence

$$N_1'' + N_2'' - N_1' - N_2' = 0. \quad . \quad . \quad . \quad (2{\cdot}4)$$

Now let us consider the partition function Ψ corresponding to the special choice * of the set of independent variables $p, T, \gamma, \mu_1 \ldots \mu_i$. We have

$$\Psi = \sum_{N_2', N_2'} \sum_{N_1'', N_2''} \sum_{N_1, N_2} \frac{N'!}{N_1'!\, N_2'!} \frac{N''!}{N_1''!\, N_2''!} \frac{N!}{N_1!\, N_2!}$$

$$\times (\lambda_1 f_1')^{N_1'} (\lambda_2 f_2')^{N_2'} (\lambda_1 f_1'')^{N_1''} (\lambda_2 f_2'')^{N_2''} (\lambda_1 f_1)^{N_1} (\lambda_2 f_2)^{N_2}$$

$$\times \exp\left(\frac{-W' - W'' - pV + \gamma\Omega}{kT}\right) = 1, \quad . \quad . \quad (2.5)$$

in which V is the volume, Ω the area of the surface and λ the absolute activities (according to Fowler and Guggenheim).

Using Stirling's formula, we can write (2.5), retaining only the largest term†

$$\log \Psi\dagger = N_1 \log \frac{\lambda_1 f_1}{x_1} + N_2 \log \frac{\lambda_2 f_2}{x_2} - \frac{N_1 N_2}{N} \frac{\alpha}{kT}$$

$$+ N_1'' \log \frac{\lambda_1 f_1''}{x_1''} + N_2'' \log \frac{\lambda_2 f_2''}{x_2''} - \frac{N_1'' N_2''}{N''} \frac{\alpha}{kT}$$

$$+ N_1' \log \frac{\lambda_1 f_1'}{x_1'} + N_2' \log \frac{\lambda_2 f_2'}{x_2'} - \frac{N_1' N_2'}{N'} \frac{\alpha}{kT}$$

$$- \frac{\alpha m}{kT} N''(x_2 - x_2'')^2 - \frac{\alpha m}{kT} N'[(x_2'' - x_2')^2 - x_1' x_2']$$

$$+ \frac{\lambda\Omega}{kT} - \frac{pV}{kT}. \quad . \quad . \quad . \quad . \quad . \quad . \quad . \quad (2.6)$$

Let us examine the extreme conditions of log Ψ† with respect to N_1, N_2, N_1'', N_2'', N_1', N_2', using (2.4). Multiplying (2.4) by the Lagrange factor χ, we get the six conditions

$$\left(\frac{\partial \log \Psi\dagger}{\partial N_i}\right)_{pT\gamma\lambda} = 0, \quad \left(\frac{\partial \log \Psi\dagger}{\partial N_i''}\right)_{pT\gamma\lambda} + \chi = 0, \quad \left(\frac{\partial \log \Psi\dagger}{\partial N'}\right)_{pT\lambda\gamma} - \chi = 0. \quad (2.7)$$

---

[6] Guggenheim and Adam, *Proc. Roy. Soc. A*, 1933, **139**, 218.

* Guggenheim,[7] Fowler and Guggenheim,[8] p. 254; μ_i chemical potential of component i.

[7] Guggenheim, *J. Chem. Physics*, 1939, **7**, 103.

[8] Fowler and Guggenheim, *Statistical Thermodynamics* (Cambridge University Press, 1939).

† Cf. Prigogine[9].

[9] Prigogine, *Trans. Faraday Soc.*, 1948, **44**, 626.

It is to be noted that the geometrical model here assumed gives

$$\Omega = N'\omega = N''\omega, \quad . \quad . \quad . \quad . \quad (2.8)$$

where ω is the area occupied by one molecule. In the derivatives (2.7) we shall assume that ω is a constant at given p, T and γ. In these derivatives we shall use the first one of the two forms (2.8). This choice only influences some intermediate calculations, but not the final results.

The first two conditions give, neglecting terms $pv\gamma/kT$,

$$\mu_1 = kT \log \frac{x_1}{f_1} + \alpha(x_2)^2 - 2\alpha m\frac{N''}{N}(x_2 - x_2'')x_2,$$

$$\mu_2 = kT \log \frac{x_2}{f_2} + \alpha(x_1)^2 + 2\alpha m\frac{N''}{N}(x_2 - x_2'')x_1, \quad . \quad . \quad (2.9)$$

So the values of the chemical potentials obtained when taking into account the presence of a surface phase, differ slightly from the values calculated when the influence of the surface phase is neglected. But one sees that the terms in N''/N which appear in (2.9) depend only on the difference between the composition of the liquid and that of the lower layer of the surface phase. By including a sufficient number of layers in the surface phase, this term can be made as small as desired.

3. Composition of the Lower Layer of the Surface Phase.—The second group of relations (2.7) gives, after some rearrangements, assuming $f_1'' = f_1$, $f_2'' = f_2$,

$$\log \frac{x_1 x_2''}{x_1'' x_2} - \frac{2\alpha}{kT}(x_2'' - x_2) - \frac{4\alpha m}{kT}\left(\frac{x_2 + x_2'}{2} - x_2''\right) = 0. \qquad (3.1)$$

This relation enables us to calculate x_2'' when x_2 and x_2' are known.

Setting

$$x_2'' - x_2 = \delta'', \quad x_1'' - x_1 = -\delta'' \quad . \quad . \quad (3.2)$$

and introducing these values of x_2'' and x_1'' in (3.1), and considering only linear terms in δ'', one obtains

$$\delta'' = \frac{\frac{2\alpha m}{kT}x_1 x_2(x_2' - x_2).}{1 - \frac{2\alpha l}{kT}x_1 x_2} \quad . \quad . \quad . \quad (3{\cdot}3)$$

Let us examine the magnitude of δ'': taking $x_1 = x_2 = 0{\cdot}5$, $m = 1/4$ and the following data for the acetone-ether system *

$$\frac{\alpha}{kT} = \frac{450}{600} = \frac{3}{4}, \quad x_2' - x_2 = 0{\cdot}1,$$ [4]

one obtains

The difference of composition between the liquid and the lower layer is as a matter of fact very small (1/10 of the total difference between the liquid and the upper layer).

4. Composition of the Upper Layer of the Surface Phase.—The third group of relations (2.7) gives, neglecting the terms in N''/N,

$$\log \frac{x_1 f_1'}{x_1' f_1} + \frac{\alpha}{kT}[(x_2)^2 - l(x_2')^2 - m(x_2'')^2] + \frac{\gamma\omega}{kT} - \chi = 0,$$

$$\log \frac{x_2 f_2'}{x_2' f_2} + \frac{\alpha}{kT}[(x_2)^2 - l(x_1')^2 - m(x_1'')^2] + \frac{\gamma\omega}{kT} - \chi = 0. \quad (4{\cdot}1)$$

---

* Computed by assimilating the surface phase to a monolayer.[9]

Subtracting, we have

$$\log \frac{x_1 x'_2}{x_2 x'_1} + \log \frac{f'_1 f_2}{f'_2 f_1} + \frac{\alpha}{kT}[2l(x_2 - x'_2) + m(x_2 - x_2) + 2m(x_2 - x''_2)] = 0. \qquad (4{\cdot}2)$$

Setting

$$x'_2 = x'_{20} + \delta', \quad x'_1 = x'_{10} - \delta' \quad . \quad . \quad . \qquad (4{\cdot}3)$$

where x'_{20} and x'_{10} obey (4.2) with $x_2 = x''_2$, one obtains

$$\log \frac{x_1 x'_{20}}{x_2 x'_{10}} + \log \frac{f'_1 f_2}{f'_2 f_2} + \frac{\alpha}{kT}[2l(x_2 - x'_{20}) + m(x_2 - x_1)] = 0. \qquad (4{\cdot}4)$$

This equation is identical with that obtained in the monolayer model by subtraction of the two equations (1.2) from each other. It shows that x'_{20} represents the equilibrium composition of the layer, computed in the monolayer model for the given value x_2 of the liquid.

Replacing in (4.3) and retaining only the linear terms in δ' we get

$$\delta' = \frac{\frac{2m\alpha}{kT}(x''_2 - x_2)x'_{10}x'_{20}}{1 - \frac{2l\alpha}{kT}x'_{10}x'_{20}} \quad . \quad . \quad . \quad . \qquad (4{\cdot}5)$$

This effect is entirely negligible (see (3.3)) being of the second order in α/kT.

5. Value of the Surface Tension.—Adding the first relations (4.1) and (3.1), one obtains

$$\frac{\gamma\omega}{kT} = \log \frac{x'_1 x''_1 f_1}{(x_1)^2 f'_1} + \frac{\alpha}{kT}[(x''_2)^2 - 2(x_2)^2 + l(x'_2)^2 + m(x''_2)^2] + \frac{\alpha m}{kT}\left[(x_2 - x''_2)^2 + y x''_2\left(\frac{x_2 + x'_2}{2} - x''_2\right)\right]. \qquad (5{\cdot}1)$$

Let us compare this value of γ to the value of γ_0 of the surface tension which would have been calculated in the monolayer model of composition x'_{20}.

By definition, γ_0 is the surface tension given by eqn. (1.2). The first of the equations (1.2) can be written in the form

$$\frac{\gamma_0\omega}{kT} = \log \frac{x''_{10} f_1}{x_1 f'_1} - \frac{\alpha}{kT}[l\{(x_2)^2 - (x'_{20})^2\} + m(x_2)^2]. \quad . \qquad (5{\cdot}2)$$

Subtracting (5.2) from (5.1), replacing x'_1 and x'_2 by their values (4.5) and x''_1 and x''_2 by their values (3.3), and neglecting terms of the second order in δ'' and δ', one obtains

$$(\gamma - \gamma_0)\frac{\omega}{kT} = \frac{2m\alpha}{kT}[- x'_{20}(x''_2 - x_2) - x_2(x'_2 - x_2) + x_2 x'_{20} - (x_2)^2 + x_2\delta' + x'_{20}\delta'']. \qquad (5{\cdot}3)$$

By using again (4.5) and (3.3) it is readily seen that all terms of the first order in δ'' and δ' disappear in this expression.

Hence the surface tension γ calculated in the two-layer model differs from the surface tension γ_0, calculated with the monolayer model only by terms of the second order in δ' and δ''. It means that they are practically equal to each other.

6. Value of Relative Adsorption.—In the monolayer model, formula (1.4) gives

$$(\Gamma_{21})_0 = \frac{x'_{20} - x_2}{\omega x_1}. \quad . \quad . \quad . \quad . \qquad (6.1)$$

With the two layer model, one obtains similarly

$$\Gamma \; = \; x'_2 - x_2 + x''_2 - x_2 \qquad (6.2)$$

Introducing (3.3) and (4.5) one has, neglecting terms of second order in α/kT,

$$\Gamma_{21} = (\Gamma_{21})_0\left[1 + \frac{2\alpha m}{kT}x_1x_2\right]. \qquad . \qquad . \quad (6.3)$$

Thus, from one model to the other, the calculated value of the relative adsorption undergoes a rather important modification which is of the first order in $\alpha\ kT$.

7. Comparison with the Gibbs Formula.—Since the surface tension γ, expressed as a function of x_2, has nearly the same value whether it is calculated according to the monolayer model or according to the two-layer model, it still obeys formula (1·3). This formula can also be written (see (1.5))

$$\left(\frac{d\gamma}{dx_2}\right)_{pT} = -\,kT\frac{(\Gamma_{21})_0}{x_2}\left[1 - 2\frac{\alpha}{kT}(1 - m)x_1x_2\right]. \qquad . \quad (7.1)$$

Let us replace $(\Gamma_{21})_0$ by its value obtained from (6.3). We get

$$\left(\frac{d\gamma}{dx_2}\right)_{pT} = -\,kT\,\frac{\Gamma_{21}}{x_2}\left[1 - \frac{2\alpha}{kT}x_1x_2\right] + O\left[\left(\frac{\alpha}{kT}\right)^2\right]. \qquad . \quad (7.2)$$

This expression differs from the Gibbs formula (1.6) only by the terms of the second order in α/kT. It may then be concluded that, within the limits of precision of the crude treatment of regular solutions used here, the two-layer model leads to results in conformity with the Gibbs formula.

8. Conclusions.—For *perfect* solutions, the monolayer model gives correct results. For *strictly regular* solutions, owing to the fact that the perturbation of the composition extends to deeper layers, this model is inadequate. Although it gives to a good approximation the surface tension, it leads to an incorrect estimate of the relative adsorption and is in disagreement with the Gibbs formula. The two-layer model corrects these defects. The statistical method used in this paper can be extended readily to a multilayer model.

We sincerely thank Prof. Guggenheim with whom we have had a most fruitful exchange of ideas concerning this problem. We also thank Prof. P. van Rysselberghe who has kindly reviewed the text of this paper.

Faculté des Sciences Appliquées
et Faculté des Sciences,
de l'Université Libre de Bruxelles.

THE TERMINATION OF BIRADICALS IN A POLYMERIZING SYSTEM

By R. N. Haward

Received 29th *July*, 1949

The possibility of a termination reaction occurring by a reaction between the two ends of a single polymeric biradical is considered. By applying Kuhn's statistical model of a polymeric chain to polystyrene polymerizing under certain assumed conditions, it is found that this self-termination process is a relatively probable event, as compared with true bimolecular termination between different polymer molecules. If long-chain biradicals do occur and polymerize, the present picture of the statistical chain in solution may require some amendment.

The nature of the role played by radicals having a single free valency in polymerizing systems has now been established in general terms, and quantitative measurement of the rates of the various steps of initiation, propagation and termination have been carried out in a number of cases. It is, therefore, natural that the possibility of other types of radical playing a part in polymerization reactions, and in particular a biradical having free valencies at each end, has become of interest. Such biradicals, if treated according to ordinary polymerization kinetics, are expected to polymerize to molecules of double the molecular weight of single radicals polymerizing in the same system. This suggestion has recently been put forward by a number of workers,[1, 2, 3] though it cannot be said that the evidence in favour of these biradicals is yet conclusive. In any case, it is necessary to distinguish between two types of biradical. Firstly, there are those which may be formed by the stepwise decomposition of a polyfunctional or polymeric catalyst. Here the two free valencies will not normally coexist. Secondly, there is the true biradical, which would be formed by the opening of a double bond and which logically leads to the idea of a polymeric molecule growing simultaneously at both ends. It is with the second type of biradical that this paper is concerned.

Now, if the possible termination reactions of biradicals are considered, a number of possibilities exist which are not applicable to the normal single radical. These modes of termination are summarized below for a particular case :

(1) Termination by disproportionation within the same molecule:

e.g. $—CH_2—CH_2—CH_2—CH_2 \longrightarrow CH_2{=}CH—CH_2—CH_3.$

(2) Termination by cyclization:

e.g.

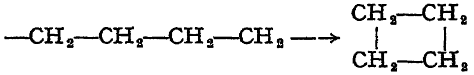

$$—CH_2—CH_2—CH_2—CH_2 \longrightarrow \begin{array}{c} CH_2—CH_2 \\ | \quad\quad | \\ CH_2—CH_2 \end{array}$$

(3) Termination by fracture of the molecule:

e.g. $—CH_2—CH_2—CH_2—CH_2 \longrightarrow 2C_2H_4.$

Although there is admittedly little evidence, it seems that reaction (3) cannot occur with high polymeric biradicals. Further, it may be noted that all the reactions (1) to (3) have been justified in experiments with normal molecules [4, 5].

(4) Termination by recombination between different molecules:

$$2(—CH_2—CH_2—CH_2—CH_2—) \longrightarrow —CH_2—(CH_2)_6—CH_2—$$

In this case, a new biradical is formed. If it were taken as a model for a polymerizing system, this type of termination would lead to a reduction of the rate of polymerization in the usual way, but polymers of very high molecular weight would result.

(5) Termination by disproportionation between different molecules:

$$2(—CH_2—CH_2—CH_2—CH_2—) \longrightarrow \begin{array}{l} —CH_2—CH_2—CH_2—CH_3 \\ \\ —CH_2—CH_2—CH—CH_2 \end{array}$$

i.e. two single radicals are formed from two biradicals.

There is also the possibility of termination by the cyclization of two or more biradicals ; however, this could also be regarded in terms of a sequence of reactions (4) and (2).

---

[1] Kern and Feuerstein, *J. prakt. Chem.*, 1941, **158**, 186.

[2] Melville and Watson, *Trans. Faraday Soc.*, 1948, **44**, 887.

[3] Bamford and Dewar, *Proc. Roy. Soc. A*, 1940, **192**, 309.

[4] Benson and Kistiakowsky, *J. Amer. Chem. Soc.*, 1942, **64**, 80.

[5] Bawn and Hunter, *Trans. Faraday Soc.*, 1938, **34**, 608.

It is intended to consider here the various possibilities applicable to high polymeric biradicals, and, in particular, the relative frequencies of reaction involving collisions between the two ends of the same molecule and those in which interaction between different molecules occurs. Obviously, the relative probability of these events will involve both the size of the molecule concerned and concentration of radicals in the polymerizing system, and in general one concentration will exist at which the rate of the two processes becomes equal. These questions have been discussed by Salomon[6, 7, 8] and Ziegler.[9] For example, it has also been shown by Ziegler that the probability of ring formation falls sharply after the 6 ring, and reaches a minimum for the 9-10-11 rings, after which the probability again increases. It may therefore be assumed that if biradicals are formed in a polymerizing system, they are likely to suffer self-termination in the initial stages of their growth. However, the effect of such early terminations would not be readily observed in a polymerizing system, since initiation is a rare event compared with the propagation reaction. For example, if x biradicals are initiated, and αx are terminated in the early stages by reactions of types (1), (2) and (3), then the observed result would normally be an initiation of $x(1 - \alpha)$ polymerizing biradicals. Thus, although the observed initiation would be less than the true biradical formation, and certain additional compounds would be formed in small quantities, polymerization would certainly take place so long as $\alpha < 1$.

In contrast to this process, the termination of a polymeric biradical by the mechanisms (1) and (2) would, if it were at all frequent, profoundly affect the course of the polymerization, since this possibility remains during the whole period of the growth of the biradical, i.e. until at least one of the free valencies is terminated. It is now intended to compare the relative frequency of this type of termination for a polymeric biradical with that for a bimolecular reaction of the type normally assumed, i.e. reactions (4) and (5).

The Probability of Termination of Polymerization by a Reaction between the Two Active Ends of a Single Long Chain Biradical.—If two polymeric radicals meet, it is assumed that the probability of a termination reaction is unaffected by the fact that they may or may not be part of the same polymer chain. Therefore, for a system consisting of long-chain biradicals polymerizing in solution, the following relations should apply:

$$\frac{\text{Rate of self-termination of biradical chains}}{\text{Rate of termination by different chains}}$$

$$= \frac{\text{Number of arrangements of pairs with opposite ends of the same chain}}{\text{Number of arrangements of pairs with the ends of different chains}} \quad . \; . \; . \quad (6)$$

The denominator of this ratio may be readily computed in terms of a conventional picture in which N long-chain molecules are assumed to be distributed among the s similar lattice sites of co-ordination number z. Then the number of pairs containing the ends of different chains

$$= \frac{z - 1}{2s} \,.\, 2N\,(2N - 2),$$

and when N is large this becomes

$$= \frac{2(z - 1)}{s} N^2.$$

---

[6] Salomon, *ibid.*, 1936, **32**, 153.

[7] Salomon, Rucicka and Meyer, *Helv. chim. Acta*, 1934, **17**, 882.

[8] Salomon, *ibid.*, 1934, **17**, 882.

[9] Ziegler, *Ber. A*, 1934, **67** (1), 139.

Further, if D_2 is the concentration of biradicals in mole/l., and all quantities are referred to the standard volume of 1 cm.^{3}, the term becomes

$$\frac{2(z - 1)}{\quad} N^2D_2^{\,2} \times 10^{-6},$$

where N is the Avogadro number.

The numerator of the ratio (6) is naturally only capable of being estimated in terms of a particular model for the configuration of a long-chain molecule in solution. However, the work of Kuhn [10], [11] enables a picture to be obtained in terms of certain assumptions. In practice, these assumptions involve replacing the long-chain molecule itself by a model consisting of a series of freely-moving linkages, which have the same total length as that calculated for the stretched polymer molecule. By assuming that free rotation occurs round all the joints in this artificial chain, the distance separating the ends may be calculated by statistical theory. It is found that this distance should be proportional to the square root of the extended chain length (or molecular weight), and this result has been confirmed by light scattering experiments with polystyrene. Furthermore, as will be seen later, it is possible to calculate the length of the assumed statistical units, either from light scattering or viscosity measurements, and these results are in reasonable agreement. Nevertheless, the utilization of these results to calculate the probability of an end-to-end configuration for the chain as a whole involves all the assumptions of Kuhn's statistical theory. Also the possibility undoubtedly exists that the configuration of a molecule could be affected because it is taking part in a polymerization reaction. However, it is thought that this effect will be small, provided that the changes in molecular configuration take place more quickly than chain propagation. Some evidence bearing on this point is discussed later.

In his statistical consideration, Kuhn [10] showed that the probability of the separation of the ends of a long chain molecule having components x, y, z, is given by

$$p(x, y, z)\mathrm{d}x\mathrm{d}y\mathrm{d}z = \frac{\beta^3}{\pi^{3/2}} \exp\left(-\beta^2(x^2 + y^2 + z^2)\right) . \mathrm{d}x\mathrm{d}y\mathrm{d}z,$$

where
$$\frac{1}{\beta^2} = \frac{2}{3} nA^2$$

if the chain consists of n freely moving links of length A.

From this, it follows, as shown by Kuhn,[10] that the probability of the chain having a ring form with one end being within a volume v close to the other end is

$$\frac{1}{(2/3\pi nA^2)}$$

Also if $\bar{r}^2$ is the root mean square distance between the ends of the chain $\bar{r}^2 = nA^2$.

In order to derive a term for the number of chains in the ring position, it is now only necessary to know v, and this may be put $= \frac{z - 1}{s}$ as in the earlier case. The formula for the number of chains with interacting ends per cm.^{3} now becomes

$$ND_2 \cdot \left(\frac{1}{(2/3\pi nA^2)}\right)^{3/2} \cdot \frac{z - 1}{s} \times 10^{-3},$$

and the original ratio,

$$\frac{\text{Rate of self-termination of biradical chains}}{\text{Rate of termination by different chains}}$$

$$\frac{10^3}{2ND_2(2/3\pi nA^2)^{3/2}}.$$

---

[10] Kuhn, *Kolloid-Z.*, 1934, 68, 2.

[11] Kuhn and Kuhn, *Helv. chim. Acta*, 1943, 26, 1394.

Finally, this calculation is not formally uniform. In one case a probability has been calculated from the model of a molecular lattice, and in the other case the model is that of a statistical chain containing a number of freely moving links.

Application of these Formulae to Styrene.—In order to apply this formula to any real polymerizing system, it is necessary to know D_2 and to estimate nA^2. It is obviously impossible to fix D_2 in a theoretical discussion; nevertheless, if k_p is known, it will be possible to make estimations of D_2 in terms of the rate of polymerization of a system, since

$$-\frac{\mathrm{d}(M)}{\mathrm{d}t} = 2k_pD_2(M).$$

For styrene at 25° C, the value of k_p has been estimated at 18·9 mole/l. sec. by Bamford and Dewar.[3] At present this seems the best value available, although Smith [12] has advanced reasons for believing it to be too low. It follows that if systems of styrene biradicals were polymerizing in pure monomer at 25° C, at rates which would bring about complete polymerization in 10, 100 and 1000 hr. . . . the values of D_2 would be approximately 10^{-6}, 10^{-7} and 10^{-8} mole/l. respectively. These values may, therefore, be used with a reasonable expectation that most styrene systems polymerizing at this temperature will be covered.

More difficulty arises over the evaluation of nA^2. As previously stated, this cannot be calculated from the molecular model assuming free rotation occurs round each valency bond, as the existence of restricted rotation and other factors would invalidate such results. However, following Kuhn,[11] the real molecular chain is replaced by a model, which consists only of freely moving links having a total length equal to that of the molecular chain. Each of these assumed freely moving links corresponds with several molecular linkages in the real polymer chain, and their length can be estimated from certain experiments.

For polystyrene dissolved in toluene, two groups of experimental work enable this to be done, and they may be applied to polystyrene dissolved in styrene monomer, provided that the configurations of polystyrene chains in styrene and toluene do not differ unduly. The first and most direct are the light scattering experiments of Doty, Affens and Zimm.[13] The second are the viscosity measurements on which the calculations of Kuhn [11] are based. Doty *et al.*[13] showed that when different polystyrene fractions are dissolved in butanone, the value of $\bar{r}^2$ was proportional to the molecular weight W, as predicted by Kuhn's theory. For toluene, a single result enables the slightly different constant of proportionality to be estimated and a proportionality to $\bar{r}^2$ has to be assumed. From this constant, the values of A and of s (the number of monomer units associated with one statistical freely moving link) may be estimated in terms of Kuhn's model. It may be noted that if the actual molecular linkages were used, instead of these longer units, then lower values of $\bar{r}^2/W$ would result, and the probability of ring formation would be increased.

Kuhn's calculations were based on the viscosities of dilute solutions of polystyrene in toluene at 20° C. The results of the two methods of treatment are given in Table I.

TABLE I

	A (Å)	s	$\bar{r}^2/W$ (Å^2)
Doty, Affens and Zimm .	58	23	1·4
Kuhn	35	14	0·84

---

[12] Smith, *J. Amer. Chem. Soc.*, 1948, **70**, 3695.

[13] Doty, Affens and Zimm, *Trans. Faraday Soc.*, 1946, **42B**, 66.

The results are in reasonable agreement with each other as to the order of magnitude. To apply these results it is only necessary to put

$$nA^2 = \bar{r}^2 = (\bar{r}^2/W)W \text{ in Å}^2$$
$$= (\bar{r}^2/W) \,.\, W \times 10^{-16} \text{ in cm.}^2$$

By interpolating these values in formula (1), a table may be constructed (Table II), showing the estimated ratio of self-termination to bimolecular termination for polystyrene biradicals present in the concentrations indicated, using the values of Doty, Affens and Zimm. In order to convert these to those which would have been obtained from Kuhn's data, it is only necessary to multiply by 2·2.

TABLE II.—THE CALCULATED RATIOS OF SELF-TERMINATION TO BIMOLECULAR TERMINATION FOR POLYSTYRENE BIRADICALS HAVING THE CONFIGURATIONS INDICATED BY DOTY, AFFENS AND ZIMM[7]

D_2 (mole l.) . . .	10^{-6}	10^{-7}	10^{-8}
Mol wt 10^4 . . .	165	1,650	16,500
10^5 . . .	5·2	52	520
10^6 . .	0·165	1·65	16·5

These figures indicate a relatively high probability for the self-termination reaction under the conditions named. This would seem reasonable if one end of a biradical is normally much nearer to the other end of the same molecule than to that of different molecules. Now for a polystyrene molecule of mol. wt. = 10^5 and a molar concentration of radicals of 2×10^{-7}, a simple estimation may be made. If the formula of Doty, Affens and Zimm[13] is used, the separation of the ends would be 375 Å, while with Kuhn's formula, the result would be 290 Å. On the other hand, distribution of this concentration of radicals at the corners of a cubic lattice would lead to a separation of the order of 2,000 Å. Thus quite simple considerations would seem to support the results previously obtained.

It now seems desirable to consider the effect of different parameters in the calculations. Here most of the figures have been chosen so as to bias the result against the self-termination reaction. For example, Bamford and Dewar[8] report a rate of polymerization of 3×10^{-8} mole/l. for the thermal polymerization of styrene at 25° C, leading to $D_2 = 10^{-10}$ and to a consequent increase in the figures quoted in Table II by a factor of 10^2. The values taken for the rate of polymerization at that temperature are, in fact, exceedingly high. Further, Bamford and Dewar's values of k_p are lower than that given by Smith[12] at 40° C, allowing for the difference in temperature. With regard to the parameters of the polystyrene molecule in solution, the formula involves A effectively to the power of 3/2 (nA being the total length of the molecule). Hence in order to reduce the ratio of self-termination to bimolecular termination to unity at $D_2 = 10^{-7}$ and mol. wt. = 10^{-5}, it would be necessary to increase s by a factor of 12, i.e. a polystyrene of mol. wt. = 10^4 would be quite straight. It seems very doubtful whether the work of Doty, Affens and Zimm could be in error by a factor of this magnitude. Indeed, the most recent work has tended to narrow the gap between these measurements and the configuration derived from viscosities. Using different methods of calculation both Debye and Bueche[14] and Kirkwood and Riseman[15] derive constants from the configuration of the polystyrene molecule which are close to those of Doty, Affens and Zimm. Again it might be suggested that there will be a space-filling effect at the centre of the sphere of distribution of the molecule which will prevent the two ends of the molecule from meeting. However, it does not appear that

[14] Debye and Bueche, *J. Chem. Physics*, 1948, **16**, 573.

[15] Kirkwood and Riseman, *ibid.*, 1948, **16**, 565.

the model requires the polymer actually to fill much of the space it occupies. For instance, for a molecule of mol. wt. = 10^5, this contains 10^3 molecules of styrene, but the sphere of radius 300 Å contains 10^5 molecules; therefore the access of the two ends to each other will apparently not be unduly impeded.

If the conclusions from these calculations are faulty it should derive from factors other than that of the configuration of the molecule. Such a condition could arise if the molecule would be slow in going through its configurations as compared with the lifetime of the growing polymer chain. In this connection it has been noted by Rideal[16] that if chain-twisting is the critical factor in gel rigidity, then rigidity should be proportional to the cube of the concentration C, whereas the entropy effect deriving from the configuration of the polymer chain leads to a square relationship. However, for polystyrene it has been shown by Ferry[17] that the rigidity is, in fact, proportional to C^3, provided the measurement is carried out in short periods to allow for a relaxation time of 4×10^{-4} sec. at 25° C. There is also a second relaxation time which is associated with changes in chain configuration and is dependent on the concentration, but in this case the relaxation time for a 15 % solution at 25° C is only $0{\cdot}73 \times 10^{-2}$ sec. For more dilute solutions it would be appreciably smaller. Therefore, since Bamford and Dewar,[8] working in very dilute solutions, find the lifetime of the growing polymer chain to be 2·8 min. at 25° C it does not seem that fresh difficulties can arise from this source, even allowing for a good deal of uncertainty in interpreting results of this type.

It seems reasonable to conclude that the probability of self-termination should be considered in all systems where polymerizing biradicals are considered. It also seems desirable to seek further and more direct evidence for the existence of the biradical than has been obtained so far. On the other hand, if it becomes apparent that biradicals do occur and polymerize, then the present picture of the polymer molecule in solution appears to require some amendment.

The writer is indebted to Prof. M. G. Evans and Dr. H. Steiner for many helpful discussions.

Petrocarbon Ltd., Research Laboratories,
Twining Road,
Trafford Park,
Manchester, 17.

---

[16] Rideal, *Nature*, 1949, **16**, 3665.
[17] Ferry, *J. Amer. Chem. Soc.*, 1942, **64**, 1330.

RATE COEFFICIENTS IN THE POLYMERIZATION OF STYRENE

BY H. W. MELVILLE AND L. VALENTINE

Received 1st *September*, 1949

The direct photopolymerization of styrene proceeded too slowly for accurate measurements with the usual dilatometric technique, so resource was had to the benzoyl peroxide photosensitized reaction. In this reaction, the rate of polymerization was proportional to the square-root of both the light intensity and the concentration of catalyst. The rate fell off gradually with time and this is attributed to wasteful decomposition of the catalyst. The rate coefficients for the polymerization were determined from a combination of life-time studies, using a modified sector technique, and measurements of the degree of polymerization. These coefficients, for propagation, termination, and transfer respectively, were found to be $k_p = 51{\cdot}9$, $k_t = 1{\cdot}05 \times 10^7$, $k_f = 1{\cdot}66 \times 10^{-3}$ l. mole^{-1} sec.$^{-1}$ at 30° C. These results are analyzed in the light of previous determinations, and it is suggested that the most probable values are $k_p = 39{\cdot}5 \pm 5$, $k_t = (7{\cdot}9 \pm 2{\cdot}0) \times 10^6$, $k_f = (1{\cdot}1 \pm 0{\cdot}5) \times 10^{-3}$ l. mole^{-1} sec.$^{-1}$ at 25° C. The question of whether polymer radicals disproportionate or combine is then discussed and finally some observations are made on radical reactivity, as adduced from the absolute values of the various velocity constants.

Although the free-radical polymerization of styrene has been investigated more extensively than that of any other monomer, it is only in recent years that the velocity constants for the separate stages of the polymerization have been evaluated. The nature of its polymerization characteristics is, however, well known, so that a study of this monomer is well suited for any determination of its rate coefficients. Apart from the intrinsic interest of such measurements, a knowledge of its kinetic coefficients would be very useful in any investigation of the correlation between the chemical structures of radicals and monomers, and their reactivity in free-radical polymerizations. Furthermore, an accurate knowledge of these rate constants is necessary for any kinetic investigations of copolymerizations in which styrene participates.

At the present moment, there is available a number of different techniques for measuring the rate coefficients of a polymerization reaction. The first method used [1, 2] involved the determination of the life-time of the active species by the use of intermittent illumination, obtained by a rotating sector. This information, together with a knowledge of the absolute rate of initiation, is all that is required in order to compute the velocity coefficients. This method has since been widely used both in these laboratories [3, 4] and elsewhere [5] and appears to give very satisfactory results. The main difficulty in its application lies in the accurate determination of the rate of initiation, which is usually obtained from either inhibition or molecular-weight studies. Internal filter effects in the former, and the presence of transfer in the latter subject these determinations to considerable difficulty.

Another method, based on the measurement of the rate of increase of viscosity of the polymerizing medium with time has been evolved recently.[6] The rate coefficients for styrene have been evaluated with this technique so that a comparison of the results obtained in that work with those determined by the sector technique would be of considerable interest. In the present work, the rate coefficients for the benzoyl peroxide photosensitized polymerization of styrene have been determined by a modified sector technique which avoids the difficulties, mentioned above, inherent in any determination of the rate of initiation.

Experimental

Following the usual procedure all reactions were performed *in vacuo*. A combination of a rotary oil-pump and a mercury two-stage diffusion pump produced a vacuum of 10^{-4} mm. Hg or better. In order to minimize contamination of the monomer by tap-grease, a silicone grease was used for all glass joints and stop-cocks. The reaction vessels were of the usual type employed in these laboratories [3] and were made of silica.

A G.E.C. Osira 125-W mercury-vapour lamp, fed through the usual choke and condensers from a constant voltage transformer, supplied the radiation.

---

[1] Burnett and Melville, *Proc. Roy. Soc. A*, 1947, **189**, 456.

[2] Swain and Bartlett, *J. Amer. Chem. Soc.*, 1946, **68**, 2381.

[3] Mackay and Melville, *Trans. Faraday Soc.*, 1949, **45**, 323.

[4] Bickel and Melville, *ibid.*, 1949, **45**, 1049.

[5] Matheson, Auer, Bevilacqua and Hart, *J. Amer. Chem. Soc.*, 1949, **71**, 497.

[6] Bamford and Dewar, *Proc. Roy. Soc. A*, 1948, **192**, 309.

This was focused on the reaction vessel by means of a pair of plano-convex silica lenses so that the image formed had the same cross-sectional area as the reaction vessel. Various glass filters were used in order to remove short-wave radiation ; the transmission characteristics of these, as determined with a Beckmann spectrophotometer, are shown in Fig. 1.

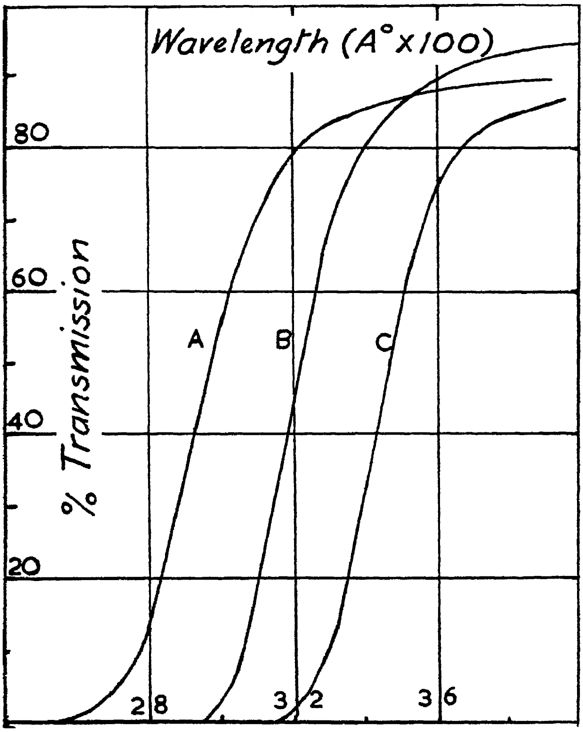

FIG. 1.—The transmission of various glass filters used.
A. Corning Corex D970, 2 mm.
B. Pyrex glass.
C. Plate window glass, 4 mm.

All reactions were carried out in a copper thermostat tank fitted with silica windows ; distilled water was used in order to prevent absorption of the activating radiation by impurities in the water. The temperature control of the thermostat, operated by a Thyratron relay, was better than ± 0·01° C. A travelling microscope which could be read to 0·01 mm. was used to follow the drop in meniscus level due to polymerization. With the reaction vessels used, this corresponded to 0·01 % polymerization. The data of Patnode and Scheiber [7] and the Dow Chemical Co. [8] were used for the densities of the polymer and monomer respectively. Using these figures, 100 % polymerization is equivalent to a volume contraction of 14·14 % at 25° C, 14·43 % at 30° C and 15·67 % at 50° C, the three temperatures used in these experiments. This relationship was checked by direct weighing of the polymer formed at 30° C and was found to hold up to at least 32 % conversion. When carrying out a run, the reaction vessel was placed in a definite position, allowed to reach temperature equilibrium, and then a screen was removed from the lamp.

In the determination of the life-times, the sector disc was made of sheet metal, painted black in order to avoid any reflection of the light. Sectors were cut out to a depth of 2 in., with an opening of $\pi/2$. Under the experimental conditions used, the styrene radicals had a life-time of the order of 1 sec. This means that the flashes of light must be of 1 to 10 sec. duration if the life-time is to be measured accurately. This is a difficult range to cover with the normal types of motors, since these are erratic at low speeds. The problem was finally solved by using a 220 volt D.C. motor to drive an intermittent relay type gear box (A.M. Rotary Transformer, Type 46, Ref. No. 10KB/409). This motor operates a suitable gear-box which then drives a cam. This in turn operates a circular disc which has a metal peg near the circumference. The peg engages in a slotted square cam once in every revolution and rotates it through 90°. Finally, the cam is connected to a spindle on which is fitted the sector disc. The duration of the flash was timed with a stop-watch reading to 0·1 sec., many observations being taken. This arrangement has several advantages over other types of sector drives. The actual time taken for the sector to rotate through 90° is only a small fraction (4-8 %) of the total length of a dark or light period. Once the square cam had made its rotation, it remained stationary until the peg had made another full revolution. As a result, the " wave form " of the incident light was virtually rectilinear, as required by sector theory.

---

[7] Patnode and Scheiber, *J. Amer. Chem. Soc.*, 1939, **61**, 3449.
[8] *Tech. Monog.* (Dow Chemical Co., 1946).

Molecular weights were determined in benzene solution at 21° C in a dynamic osmometer of the Fuoss and Mead type,[9] suitably modified.[10] The experimental technique was as described by these authors. As the concentrations were determined by evaporating a sample of the solution to constant weight, and this involves a small error due to residual solvent, a correction factor was applied to the concentrations. Experiments have shown [11] that with polystyrene the error is about 4 % ; all concentrations were corrected by this amount. The polymer samples for these determinations were prepared as follows. After polymerization, the contents of the reaction tube were quickly poured into a large excess (*ca.* 150 ml) of methanol at about — 10° C. By this treatment the polymer was precipitated as a fluffy mass which could be easily dried and re-dissolved. The samples were then filtered, washed with methanol and dried to constant weight in a vacuum desiccator. They were then re-dissolved in sufficient re-distilled benzene to give a 0·5-1·0 % solution and filtered through sintered glass before use.

Styrene (A. Boake Roberts, Ltd.) was separated from the phenolic inhibitor by washing three times with a 10 % solution of caustic soda, and the alkali removed by washing three times with distilled water. The styrene was then dried with calcium chloride and distilled under about 15-20 mm. of CO_2 (b.p. *ca.* 40° C at 18 mm. Hg). It was then stored at — 30° C until required.

Benzoyl peroxide was dissolved in chloroform and the aqueous layer removed. The solution was then concentrated at the water pump and the peroxide precipitated with methanol. It was then filtered, washed with methanol and stored over $CaCl_2$ in a vacuum desiccator. The catalyst was introduced into the reaction vessels as a solution in benzene, the solvent being subsequently removed under low vacuum. The catalyst-monomer mixture was stored in the dark over solid CO_2, for reasons given later.

The Direct Photo-Polymerization.—The reaction started immediately the tubes were illuminated with no detectable induction period, assuming its steady rate at once. In Pyrex reaction tubes, the reaction went at the rate of about 0·2 % per hour at 25° C, while Hysil reaction tubes absorbed the activating radiation to such an extent that the rate was reduced below 0·02 % per hr. In silica reaction tubes, the rate was about 0·3 % per hr. It was at first thought that these low rates might be due to the presence of a retarder, but this was disproved by heating a reaction tube for two hours at 90° C so that the thermal reaction would destroy any inhibitors. Styrene subjected to this treatment, however, showed exactly the same behaviour. This low rate of polymerization is thus not due to extraneous sources, but is inherent in the nature of the monomer. It is most probably caused by a low efficiency of the primary process, the overall quantum yield is about 6,[12] compared with one of over 900 for vinyl acetate under comparable conditions. As the primary quantum yield is 1 for vinyl acetate [1] that for styrene is hence probably $< 0{\cdot}01$.

Experiments at a higher temperature (50° C) yielded the value of 4·1 ± 1·5 kcal. for the overall activation energy ; this may be compared with the previously determined value of 5·1 ± 1 kcal.[6] The agreement is reasonably good, especially since the calculation is based on a relatively small number of experiments, and the experimental error in determining the rate is high, because of the low values.

---

[9] Fuoss and Mead, *J. Physic. Chem.*, 1943, **47**, 59.

[10] Masson and Melville, *J. Polymer Sci.*, 1949, **4**, 323, 337.

[11] Grassie and Melville, *ibid.* (in press).

[12] Taylor and Vernon, *J. Amer. Chem. Soc.*, 1931, **53**, 2527.

These rates were too low for any accurate determinations so that it was decided to use a photo-sensitizer, benzoyl peroxide, to increase the rate of polymerization, as it was known that this compound was an efficient photo-sensitizer for the polymerization of both vinyl acetate [1] and methyl methacrylate.[3]

The Benzoyl Peroxide Photosensitized Polymerization.—In the first experiments a Corex D 970 glass filter, with a cut-off value of 2500 Å (see Fig. 1) was used. The course of the reaction for various initial catalyst concentrations is shown in Fig. 2. In calculating the percentage volume contractions, allowance was made for the volume occupied by the catalyst itself; this correction never exceeded 2 %. It can be seen from Fig. 2 that there is a short induction period of not more than 3 min., after which time the reaction proceeds at a steady

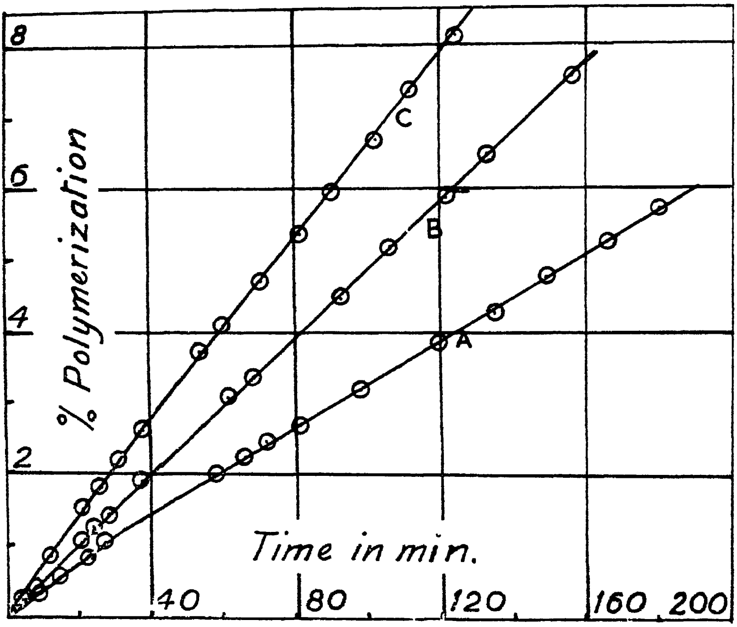

FIG. 2.—The course of the peroxide sensitized reaction.

A. $(B_p) = 1{\cdot}40 \times 10^{-2}$ mole/l.
B. $(B_p) = 4{\cdot}43 \times 10^{-2}$ mole/l.
C. $(B_p) = 7{\cdot}46 \times 10^{-2}$ mole/l.

TABLE I.—THE EFFECT OF CATALYST CONCENTRATION ON RATE AT 30° C ($\lambda > 2500$ Å)

Expt. No.	$B_p \times 10^2$ (mole/).l	R_i (%/hr.)	R_s (%/hr.)	R_s/R_i	P_s (%)	T_s (min.)
1	0·69	1·80	1·40	0·78	1·90	66
2	1·40	2·05	1·78	0·87	1·45	24
3	2·03	2·60	2·02	0·78	2·55	60
4	2·29	2·74	2·17	0·79	1·15	27
5	2·56	2·81	2·30	0·82	2·30	52
6	2·68	2·81	2·34	0·83	2·30	52
7	3·28	3·04	2·54	0·84	1·70	33
8	3·82	3·34	2·82	0·84	2·10	32
9	4·43	3·16	2·82	0·89	1·70	36
10	4·47	3·59	2·96	0·83	2·15	39
11	5·55	4·29	3·35	0·78	1·80	27
12	7·46	4·50	3·85	0·86	1·70	40

rate up to about 2 % conversion. The rate then decreases quite abruptly to about 85 % of its initial value and then remains quite constant up to about 8 % polymerization. This effect was found throughout the entire range of catalyst concentrations studied ($0{\cdot}7 - 7{\cdot}5 \times 10^{-2}$ mole/l.) as can be seen from Table I.

In this Table B_p represents the initial catalyst concentration, R_i and R_s the initial and steady rates of polymerization respectively; P_s and T_s denote the extent of polymerization (in %) and time (in min.) respectively at which the steady rate of polymerization commences.

It must be emphasized that these experiments were all done at low conversions, and the extent of conversion never exceeded 8 %; usually it was about 6 %. At high conversions, as was found later, the rate decreased still further, but this will be treated in a later section.

The value of R_s/R_i remains virtually constant throughout the experiments, with an average value of $0{\cdot}83 \pm 0{\cdot}05$, while the values for P_s and T_s fluctuate somewhat, and do not seem to have any definite connection with the rate or catalyst concentrations. The mean value of P_s is $1{\cdot}9 \pm 0{\cdot}5$ %. It was thought at first that this behaviour might be caused by the presence of traces of some catalyst, e.g. a peroxide, in the styrene, which would decompose under the action of ultra-violet light. This would cause an increase in the rate of polymerization which would persist until all the extraneous catalyst had been decomposed. In order to confirm this, the styrene was subjected to different methods of purification.

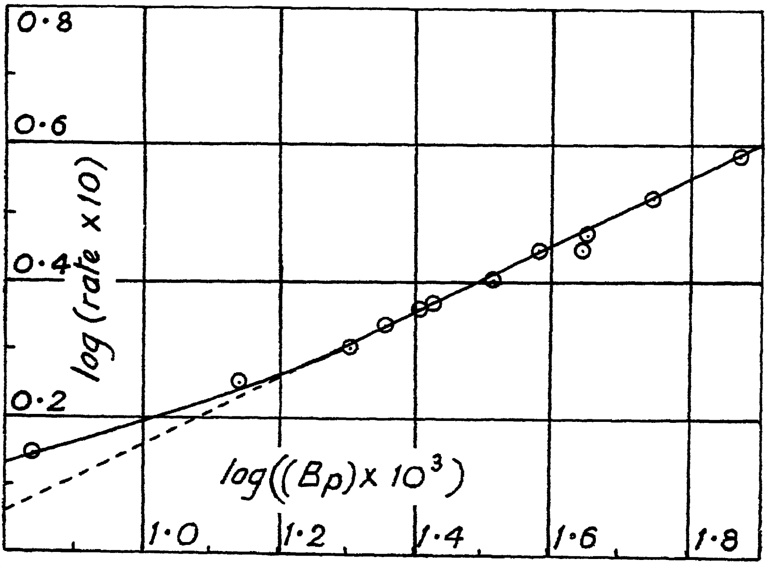

FIG. 3.—Logarithmic plot of rate against catalyst concentration for $\lambda > 2500$ Å.

In expt. no. (2), (8), (9) and (12), Table I, the monomer was given the normal routine purification. In expt. no. (1), (3) (6) the styrene was distilled over sodium hydroxide in an atmosphere of oxygen-free nitrogen, and then redistilled under nitrogen (b.p. *ca.* 40° C). In expt. no. (5) the styrene was distilled once under reduced pressure in nitrogen, and then illuminated *in vacuo* for 1½ hr., using the full light of the mercury arc. The residual monomer was then distilled off into the reservoir on the high-vacuum line. Finally, for expt. no. (7) and (11), the monomer was distilled once in air, about 1 % benzoyl peroxide added and the solution degassed in the norml way. This sample was then illuminated for about 1½ hr., and the remaining styrene distilled off into a reservoir.

In every case, exactly the same phenomenon was found. Expt. no. (5), (7) and (11) offer conclusive proof that traces of catalyst in the monomer are not responsible for the effect, since they would have been destroyed by the procedure employed. For example, in those cases where benzoyl peroxide was added, about 5 % polymer was formed, and this is beyond the point at which the reduced rate usually comes into operation. This explanation is also rendered rather unlikely by experiments on the effect of oxygen. It is well known that under certain conditions oxygen can attack styrene to form an unstable peroxide or hydroperoxide. However, in expt. no. (4) and (10), air was admitted to the reaction tubes before sealing off and yet the rates are in excellent agreement with the other values, as indicated by Table I and Fig. 3. Admittedly only a small volume of air was in contact with the monomer, but if a peroxide formed from the monomer was responsible for the fast initial rate, it might have been expected that there would have been a still greater increase in the presence of oxygen. It is possible, though very unlikely, that there is a more unstable peroxide present in the catalyst and that this causes the increased rate. However, since benzoyl peroxide purified in an exactly similar manner has been used in other investigations of this kind,[1, 3, 4] and no comparable effect has been found, this explanation can probably be discounted.

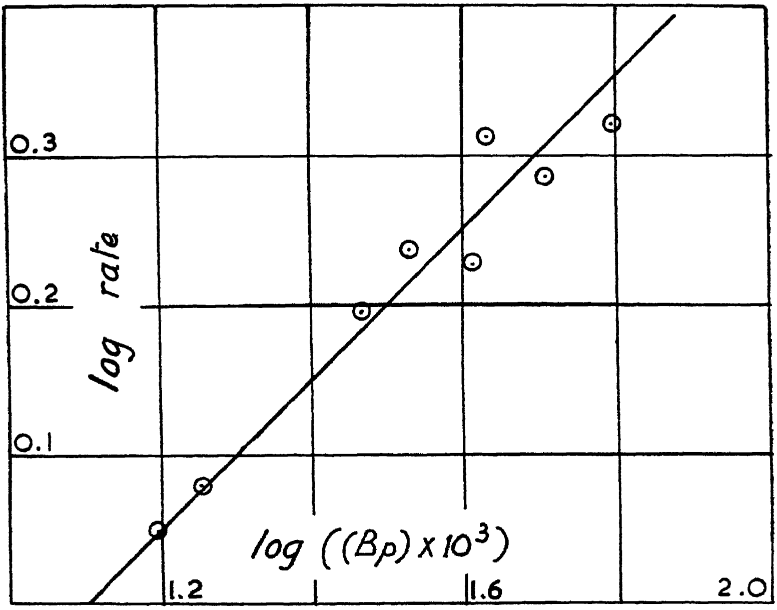

Fig. 4.—Logarithmic plot of rate against catalyst concentration for $\lambda > 2940$ Å.

A logarithmic plot of rate against catalyst concentration (Fig. 3) has a slope of 0·50, showing that the rate is proportional to the square root of the catalyst concentration. The relationship is not obeyed very closely at low catalyst concentrations, the rates being always higher than expected.

As it was thought that the various effects mentioned above might be due to some defects of the optical system used, e.g. internal filter effects at short wavelengths or abnormal decomposition of the peroxide, similar experiments were performed with light of much longer wavelength. A filter of Pyrex glass, with a cut-off at 2940 Å was used to remove the short-wave radiation. The transmission of this filter is depicted in Fig. 1. In order to make quite certain that in these circumstances radical concentrations were substantially uniform, the spatial interference method was used.* These experiments showed that the radiation was weakly absorbed in accordance with the kinetic requirements. In all the runs done with this set-up, exactly the same behaviour was found. The initial rate is linear up to about 2·5 % conversion, after which it changes quite suddenly and assumes a lower, but quite constant, value. The results of these experiments are tabulated in Table II and a plot of the logarithm of the rate against the logarithm of the catalyst concentration is given in Fig. 4. Almost exactly the same results were obtained as in the experiments at shorter wavelengths of the activating radiation. The mean value of R_s/R_t is 0·86 ± 0·06 and that of P_s is 2·3 ± 0·5 %. For some reason not known, there is a much wider scatter of points in these experiments, as can be seen from a study of Fig. 4. A calculation of the slope of this line, using the method of least squares, yielded a value of 0·47. In this case again, the rate is proportional to the square root of the catalyst concentration, indicating that termination arises from the collision of two growing radicals.* In Table II, all the symbols have the same meaning as in Table I.

---

* Burnett, Melville and Valentine, *Trans. Faraday Soc.* (in press).

TABLE II.—EFFECT OF CATALYST CONCENTRATION ON RATE AT 30° C FOR LONGER WAVELENGTHS

Expt. No.	$B_p \times 10^2$ (mole/l.)	R_i	R_s	R_s/R_i	P_s	T_s
29	1·58	1·33	1·12	0·84	2·7	110
25	1·80	1·49	1·20	0·81	1·9	83
27	2·92	1·91	1·57	0·82	2·5	80
30	3·20	1·74	1·60	0·92	—	—
24	3·39	1·95	1·73	0·89	1·9	64
33	4·08	1·86	1·70	0·91	2·4	80
28	4·25	2·48	2·06	0·83	2·75	69
26	5·12	2·27	1·93	0·85	2·2	60
23	6·23	2·48	2·10	0·85	1·7	44

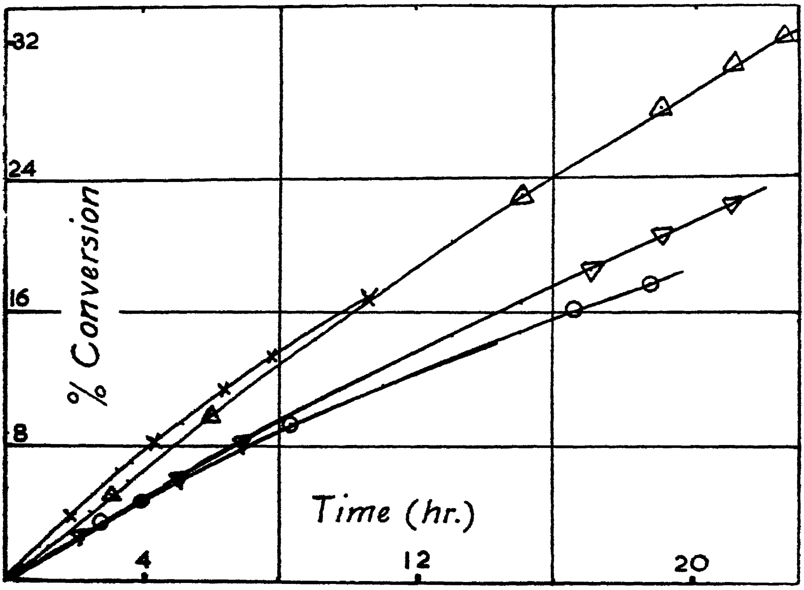

FIG. 5.—Experiments at higher conversion.

Expt. (29) ——⊙—— ; $\lambda > 2940$ Å, $(B_p) = 1{\cdot}58 \times 10^{-2}$ mole/l.
(30) ——△—— ; $\lambda > 2940$ Å, $(B_p) = 3{\cdot}50 \times 10^{-2}$ mole/l.
(31) ——×—— ; $\lambda > 2500$ Å, $(B_p) = 2{\cdot}46 \times 10^{-2}$ mole/l.
(36) ——▽ ; $\lambda > 3150$ Å, $(B_p) = 5{\cdot}14 \times 10^{-2}$ mole/l.

In order to ascertain the relationship between the intensity of the incident light and the rate of polymerization, the usual perforated screen technique was used. All measurements were made once the "steady" rate of polymerization had been attained. The mean of five determinations of the intensity exponent over the catalyst range $1{\cdot}4$-$7{\cdot}5 \times 10^{-2}$ M, was $0{\cdot}49 \pm 0{\cdot}02$, showing that the rate is accurately proportional to the square root of the light intensity over the entire range of catalyst.

---

* At the shortest wavelength, viz. 3021 Å and at the highest benzoyl peroxide concentration—6×10^{-2} mole/l.—the light is only absorbed to the extent of 50 %.

If the polymerizations were carried to higher conversions (> 10 %), some new features became apparent. The rate decreased slowly and regularly from 10-30 % conversion. Although the rate over the region 3-8 % conversion (R_s in the previous treatment) appeared to be constant, yet in reality it must have been decreasing slightly, as can be seen from Fig. 5. In this diagram, the course of the polymerization is illustrated for a variety of catalyst concentrations and wavelengths of light.

Certain features are at once apparent from a study of these results. With light of short wavelengths ($\lambda > 2500$ Å), the fall-off in rate is very much more rapid than in those experiments in which radiation of longer wavelengths was used (expt. (29) and (30)). Again, a comparison of expt. (29) and (36) show that longer wavelength radiation does not induce such a decrease in rate with time. Although these two runs have initially the same rate of polymerization, after 20 hr. there is a considerable difference between the two cases.

In the course of an investigation of the molecular weights of the polymers, it was found that the molecular weight of the polymer increased as the reaction proceeded. This could not be observed directly, but was deduced from a combination of rate and molecular weight data. This is most logically explained by a decrease in the rate of initiation; this would also explain the decrease in rate. It can easily be shown that the fall in rate is not due to a decrease in the monomer concentration. In order to explain the fall in rate, the rate would have to be proportional to about the thirtieth power of the monomer concentration, which is clearly impossible.

Discussion

The General Mechanism of the Polymerization.—It is convenient to split a discussion of the reaction into two parts, viz. the experiments at low and high conversions, since they illustrate rather different points. In the experiments at low conversions, since the rate is proportional to the square-root of both the catalyst concentration and the light intensity, then the polymer radicals are removed two at a time. This leads to the following mechanism, in which B represents a molecule of benzoyl peroxide, R a radical formed by its decomposition and the other symbols have their usual significance.

$$\begin{array}{rl} \mathrm{B} + h\nu = \mathrm{R} - & f(I) \\ \mathrm{R} - + \mathrm{M} = \mathrm{P}_1 & k_i \\ \mathrm{P}_r + \mathrm{M} = \mathrm{P}_{r+1} & k_{pr} \\ \mathrm{P}_r + \mathrm{P}_s = \mathrm{M}_r + \mathrm{M}_s & k_{mr} \,.\, k_{ms}. \end{array}$$

Transfer reactions have been omitted since, although they do occur to a slight extent, they do not enter into the kinetic expressions for the rate of polymerization. Applying the usual stationary state assumptions, we get

$$-\,\mathrm{d(M)}/\mathrm{d}t = (k_p/k_m)(\mathrm{M}) \,.\, (f(I))^{\frac{1}{2}}.$$

Since $f(I)$ will be a function of both the incident light intensity and the catalyst concentration, then the rate will be proportional to the square-root of both these quantities, in agreement with the experimental results. It should be noted that this result holds no matter what the precise mechanism of the disruption of the catalyst may be.

Certain results remain unexplained by the above mechanism, however. It has been seen that the rate of polymerization decreases rather suddenly after about 2 % conversion. Although the rate gradually declines throughout the reaction, this initial drop is much more pronounced than at any other stage of the reaction. The only reaction which bears any similarity is the influence of oxygen on the thermal polymerization of styrene.[13] Here the initial rate was maintained for a short time, but once the oxygen was used up the rate decreased abruptly. The oxygen presumably functioned catalytically by forming an unstable peroxide; once this was all decomposed the reaction attained the true thermal rate. Other investigators, however, found oxygen to be an efficient retarder of the polymerization,[14] while in the present work traces of air were found to exercise little influence on the rate. In any case, these experiments were done *in vacuo* ($p < 10^{-4}$ mm.), and it is most unlikely that oxygen at this pressure will have any effect.

---

[13] Goldfinger and Kane, *J. Polymer Sci.*, 1948, 3, 145

A possible explanation is that the peroxide forms a complex with the monomer and this complex is then destroyed to yield free radicals in the normal way. The formation of a complex between catalyst and monomer has been widely assumed,[15, 16] though it is still a controversial point. A high initial concentration of the complex might be established while the tube is warming up, shielded from the light, leading to a high initial rate. Afterwards, a "pseudo-equilibrium" would be set up and a steady rate maintained. Some confirmation of this view is provided by the fact that tubes which had been stored at − 20° C, when the monomer was still liquid, polymerized faster than those which had been stored over solid CO_2. Similar results were obtained with vinyl acetate.[17] In this case a higher initial concentration of the complex would be formed and thus a faster rate. However, since this did not form an integral part of the work being studied, the subject was not investigated further, and must remain a matter of speculation.

One other point remains to be discussed. It has been seen (Fig. 3) that the rate is apparently no longer proportional to the square-root of the peroxide concentration at low catalyst concentrations, being faster than the calculated value. Here again the reason is uncertain, although it is possible that at these low concentrations of peroxide the amount of wastage is less and so the rate of initiation will be increased above the calculated value. Again, the styrene itself may absorb some of the activating radiation at these low catalyst concentrations and hence the rate will be increased due to the direct photo-reaction.

With regard to the decline in rate at high conversions, an explanation for this phenomenon is not difficult to find. It has been widely recognized of recent years that the decomposition of benzoyl peroxide is by no means a simple unimolecular decomposition.[18, 19] It has been postulated that the radicals formed by the primary dissociation may subsequently attack the peroxide molecules, so that, in effect, not all the radicals which are formed initiate polymerization. In this way, a certain fraction of the decomposition is wasted as far as initiation is concerned. Redington[20] has confirmed this for a variety of diacyl peroxides in the system styrene peroxide. It was found that the wastage is considerably less at higher than at low temperatures and also that this wastage is greater for those peroxides which decompose at a more rapid rate.

A mechanism of this kind provides a complete explanation of the behaviour described here. The peroxide is destroyed too fast to be of value in initiating polymerization and a certain percentage is hence wasted. This proportion will naturally increase with increasing rate of decomposition of the peroxide if the radicals interact with each other. The increasing curvature of the conversion-time plot with decreasing wavelength of the activating radiation is thus explained. With these short wavelengths, the peroxide is decomposed faster (cf. Tables I and II), and so there will be a greater fraction of the peroxide wasted.

---

[14] Bovey and Kolthoff, *J. Amer. Chem. Soc.*, 1947, **69**, 2143.
[15] Kamenskaya and Medvedew, *Acta Physicochim.*, 1940, **13**, 559.
[16] Schulz and Harborth, *Die Makromol. Chem.*, 1947, **1**, 106.
[17] Burnett, *Thesis* (Aberdeen), 1947.
[18] Bartlett and Altschul, *J. Amer. Chem. Soc.*, 1945, **67**, 816.
[19] Nozaki and Bartlett, *ibid.*, 1946, **68**, 1686.
[20] Redington, *J. Polymer Sci.*, 1948, **3**, 503.

Determination of the Kinetic Coefficients

Theory.—Since there are three kinetic rate constants to be determined, viz. those for propagation, termination, and transfer, then three relationships between these quantities will be required before the individual values can be ascertained. Molecular weight data will yield the ratio k_p^2 k_t, while k_t can be determined from life-time studies, provided the rate of initiation is known. The usual methods for computing the rate of initiation derive from either molecular weight data or studies in inhibition. The latter method has several disadvantages, especially for the system being studied here. In a three-component system, e.g. styrene, benzoyl peroxide and inhibitor, the light absorption would become complicated and it would be difficult to avoid internal filter effects due to the absorption of light by the inhibitor molecules. This would be especially so for the normal types of polymerization inhibitors, e.g. amines, quinones and hydrazines, since these all possess strongly chromophoric groups. Since the possibility of using the inhibitor technique is ruled out, this leaves the method of molecular weight data. This again has its disadvantages. The usual procedure is to equate the number average molecular weight with the kinetic chain length, ignoring the effect of transfer, and then to calculate the rate of initiation from the relationship :

$$\nu = \frac{-\mathrm{d(M)}/\mathrm{d}t}{f(I)}$$

where ν = kinetic chain length and $f(I)$ = rate of initiation. This is at best a poor approximation, since transfer will undoubtedly occur to a greater or less extent in all polymerization systems.

In the present work a method was evolved which dispensed with the necessity of determining the rate of initiation the necessary relationships between the rate coefficients being found from the variations of life-time and degree of polymerization with the rate of polymerization.

The following simple scheme may justifiably be assumed to represent the course of the polymerization :

$$\begin{array}{ll} \mathrm{M} = \mathrm{P}_1 & f(I) \\ \mathrm{P}_r + \mathrm{M} = \mathrm{P}_{r+1} & k_p \\ \mathrm{P}_r + \mathrm{M} = \mathrm{M}_r + \mathrm{P}_1 & k_f \\ \mathrm{P}_r + \mathrm{P}_s = \mathrm{M}_r + \mathrm{M}_s & k_t. \end{array}$$

The initiation step consists of the photo-decomposition of a molecule of benzoyl peroxide to form free radicals and the subsequent attack of one of these radicals on the monomeric double bond. Since monoradicals are almost certainly formed from the decomposition of the peroxide, the growing polymer chains will also be monoradicals. The termination reaction has also been postulated as a disproportionation rather than a combination reaction. Although there is no direct evidence that this is so in the present system, the general weight of evidence from all sources is overwhelmingly in favour of this assumption. This point will be discussed more fully later.

On the basis of this reaction scheme, it is obvious that the mean degree of polymerization, $\overline{P}$, is given by

$$\overline{P} = \frac{k_p(\mathrm{P})(\mathrm{M})}{k_f(\mathrm{P})(\mathrm{M}) + k_t(\mathrm{P})^2}; \quad \frac{1}{\overline{P}} = \frac{k_f}{k_p} + \frac{k_t(\mathrm{P})}{k_p(\mathrm{M})},$$

where (P) = total concentration of polymeric radicals. Since $f(I) = k_t(\mathrm{P})^2$, and the overall rate of polymerization R is defined by

$$-\mathrm{d(M)}/\mathrm{d}t = R = k_p/k_t^{\frac{1}{2}} \,.\, (\mathrm{M}) \,.\, (f(I))^{\frac{1}{2}},$$

then

$$\frac{1}{\overline{P}} = \frac{k_t}{k_f} + \frac{k_t \,.\, R}{k_p^2(\mathrm{M})^2}. \qquad \text{. . . . . (1)}$$

Hence, from a plot of the reciprocal degree of polymerization against the rate, two of the three desired relationships between the kinetic coefficients may be obtained.

A third relationship is provided from life-time studies. The life-time, τ, is defined by

$$\tau = \frac{(P)}{f(I)} = \frac{1}{k_t[f(I)]^{\frac{1}{2}}}.$$

Combining this with the expression for the rate R we see that

$$\frac{k_t \,.\, R}{k_p(M)}. \qquad (2)$$

These three relationships provide the ratios k_t/k_p^2, k_t/k_p and k_f/k_p, from which the individual constants may be evaluated. Should the termination reaction be combination, then the slope of the plot of $1/\bar{P}$ against the rate will be $k_t/2k_p^2(M)$ and the intercept will be $k_f/2k_p$. As a result, the values for k_p and k_t would need to be halved.

Experimental

Various polymer samples were prepared as described above at 30° C and the rate of polymerization and molecular weight determined. The results are summarized in Fig. 6, in which π/c is plotted against c. Unfortunately it was not possible to measure molecular weights below about 45,000 with the membrane (bacterial cellulose) available, since the polymer diffused through and set up an opposing osmotic pressure.

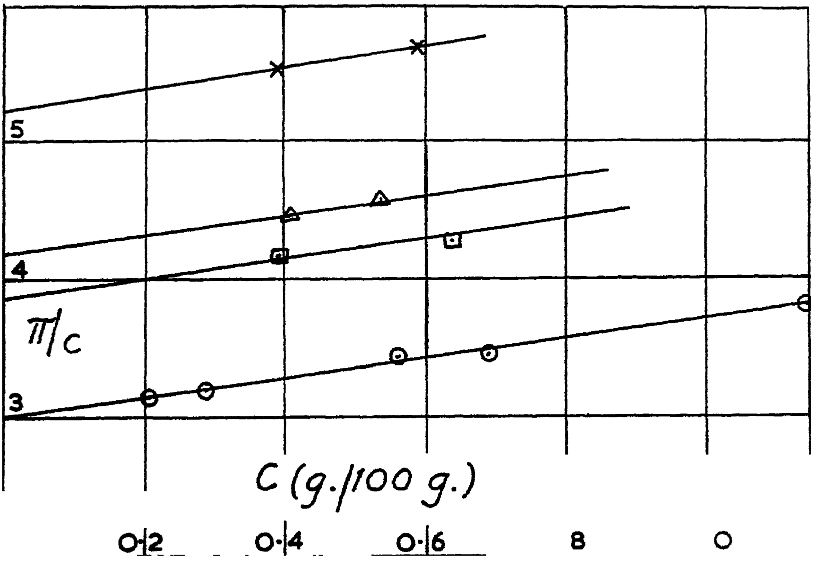

FIG. 6.—Variation of π/c with c for various polystyrenes (π in cm. benzene).
○—(29); ⊡—(25); △—(30); ×—(27).

It can be seen from Fig. 6 that the plot of π/c against c is linear over the extrapolation range $c = 0 - 1{\cdot}2$ g./100 g. As a result of this, the extrapolation to zero concentration is quite accurate and a much easier task than when the π/c curves have an upward concavity. A variety of formulations has been adduced to express the behaviour of solutions of high polymers, but that of Huggins[21] has proved the most useful. Considering that the reasons for deviations from ideal behaviour arose from the terms for entropy and heat of mixing, he obtained a simple formula to explain the relationship between osmotic pressure and concentration, e.g.

---

[21] Huggins, *Ind. Eng. Chem.*, 1943, **35**, 216, 980.

$$\frac{\pi}{c_2} - \frac{RT}{3m_1} \times \frac{d_1 c_2^2}{d_2^3} = \frac{RT}{m_2} + \frac{RT}{m_1}\,\frac{d_1}{d_2^2}\,(0{\cdot}5 - \mu)c_2,$$

where
c_2 = concentration of solute in g./ml.,
d_1, d_2 = densities of solvent and solute respectively,
m_1, m_2 = molecular weights of solvent and solute respectively,
μ = constant for any given polymer-solvent system,

and the other symbols have their usual meaning.

From the experimentally determined slope of these plots, the value of $\mu = 0{\cdot}47$ for this system is calculated; it is of some interest to compare this with previously determined values of μ for polystyrene. For polystyrene-toluene, it was found that very high molecular weight polymers gave a $\pi/c - c$ plot which was concave upwards.[22] The limiting value of the slope gave a value of $\mu = 0{\cdot}48$. Polymers prepared at higher temperatures (120 and 180° C) had μ values of 0·45 and 0·43 respectively, and for both the $\pi/c - c$ plot was linear.

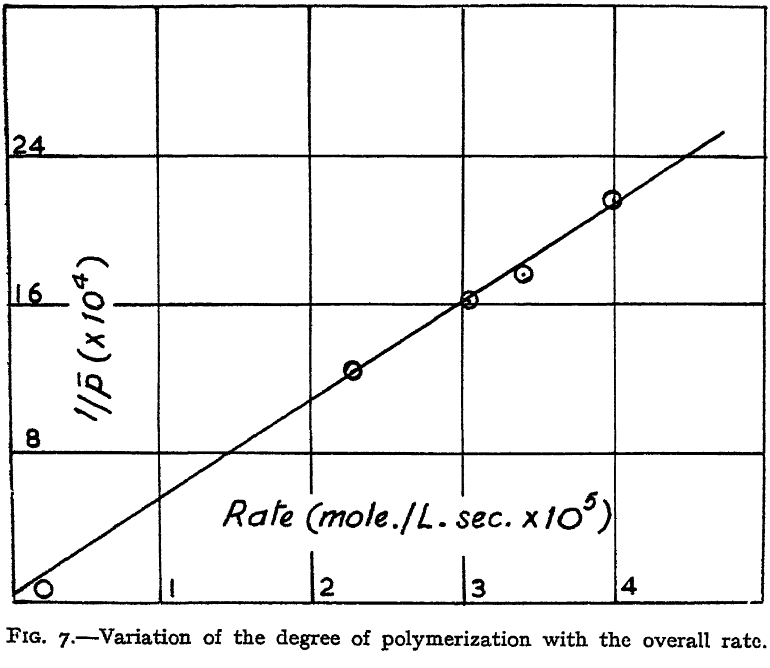

FIG. 7.—Variation of the degree of polymerization with the overall rate.

Hengstenberg and Schulz[23] investigated the system polystyrene-toluene and also polystyrene-methyl *iso*propenyl ketone. For both there was a linear plot between π/c and c, although the slope was much greater in toluene solution. In general it may be said that the better the solvent, the greater the slope of the $\pi/c - c$ curves and the lower the value of μ. In the present investigation, the value of μ (0·47) would indicate that benzene is a moderately good solvent for polystyrene in the thermodynamic sense. It is not possible to compare these results directly with the quoted values,[22] since these were given for fractionated polymers. Furthermore, fractions of the same molecular weight, but prepared at different temperatures (120 and 180° C), had different values of μ. The exact structure of the polymer chains must depend on the method of preparation and it may be that at these high temperatures there is a considerable amount of chain-branching or cross-linking. In the present work the value of μ remained constant over the entire range of molecular weights studied (48,000-83,000). Data on the variation of degree of polymerization with rate are provided in Table III and are illustrated graphically in Fig. 7.

---

[22] Alfrey, Bartovics and Mark, *J. Amer. Chem. Soc.*, 1943, **65**, 2319.
[23] Hengstenberg and Schulz, *Die Makromol. Chem.*, 1948, **2**, 51.

TABLE III.—VARIATION OF DEGREE OF POLYMERIZATION WITH RATE

Expt. No.	Rate × 10^5 (mole/l. sec.)	$\bar{P}$	$1/\bar{P} \times 10^4$
29	2·27	798	12·51
25	3·04	615	16·21
30	3·40	566	17·66
27	4·00	460	21·72

The figures quoted for the rate of polymerization need some comment. It will be remembered that at low conversions (up to 10 %) the rate could be split into two practically linear portions. In such cases (expt. (25) and (27)), the weighted average rate was calculated. Even in those experiments in which the conversion was as high as 30 % (expt. (29) and (30)), and in which the rate fell off gradually, the conversion-time curve could be split into short sections which were very nearly linear; here again, a weighted mean rate was calculated.

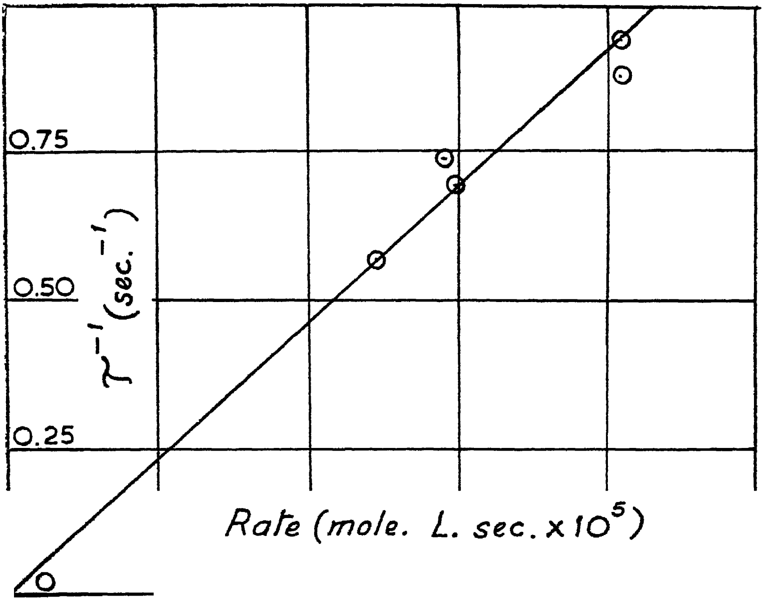

FIG. 8.—Variation of the life-time with the rate of polymerization.

Since the method of evaluating k_f/k_p involves a considerable back-extrapolation (cf. eqn. (1)), it is necessary to determine the equation of the line to a high degree of accuracy. This was done, using the method of least squares, and yielded the following values.

$$1/\bar{P} = 52{\cdot}4R + 3{\cdot}2 \times 10^{-5}$$

Hence $$k_t/k_p^2(\mathrm{M})^3 = 52{\cdot}4,$$

i.e. $$k_t^{\frac{1}{2}}/k_p = 62{\cdot}5\,;\quad k_f/k_p = 3{\cdot}2 \times 10^{-5}.$$

In the determination of the life-time, preliminary studies with a manually operated shutter had indicated that the life-times would be of the order of 1 sec. Accurate measurements were then made with the experimental set-up described above.

The experimental procedure was as follows. The rate of polymerization was measured under full intensity of the light and then the sector disc was set rotating; the flashes were timed with a stop-watch. Frequent counts of the sector speed were made and these were averaged over the whole of the run. The rate was again measured, allowing sufficient time for the rate to reach an equilibrium value. This was then repeated for various times of flash and the rate measured each time. After each run with the sector, the rate was determined again under full illumination.

In order to measure the life-time accurately it is necessary to determine the rate very precisely. Excellent illumination of the meniscus in the reaction tube is required. The rate was measured by finding the slope of a large-scale plot of conversion against time, and the life-time found from the theoretical curve.[1, 3] * These experiments were done with several different concentrations of benzoyl peroxide, at 30° C, using light of wavelength greater than 2940 Å. The results obtained are shown graphically in Fig. 8. The best line was drawn through the experimental points, utilizing the fact that this line will pass through the origin. This satisfied the equation (e.g. eqn. (2)).

$$\tau^{-1} = 2{\cdot}33 \times 10^4 R,$$

i.e. $k_t/k_p(\mathrm{M}) = 2{\cdot}33 \times 10^4$ and $k_t/k_p = 2{\cdot}03 \times 10^5$.

Combining this result with that obtained for $k_t^{\frac{1}{2}}/k_p$, then

$$k_p = 51{\cdot}9 \quad \text{l./mole}^{-1}\ \text{sec.}^{-1}$$

Hence $k_t = 1{\cdot}05 \times 10^7$ l./mole^{-1} sec.$^{-1}$

and $k_f = 1{\cdot}66 \times 10^{-3}$ l. mole^{-1} sec.$^{-1}$ at 30° C.

It is instructive to compare these values with those obtained by other workers, using wholly different techniques. A summary of all the available data for the kinetic coefficients is given below in Table IV.

TABLE IV.—THE KINETIC COEFFICIENTS FOR THE POLYMERIZATION OF STYRENE

Temp. °C	k_p	k_t ($\times 10^{-6}$)	k_f ($\times 10^3$)	E_p (kcal.)	E_t (kcal.)	Ref.
30	51·9	10·5	1·66	—	—	This work
25	18·7	2·79	0·67	6·5	2·8	6*a*
25	34·4	5·32	1·26	5·9	2·2	6*b*
25	33·8	5·15	—	—	—	24*a*
25	39·5	7·9	—	—	—	24*b*
25	101·0	—	—	11·7	—	25
30	36·0	—	—	10·5	—	26

Discussion

At first sight there does not seem to be close agreement between the various values quoted. There is a six-fold variation in the values of k_p and a four-fold one for k_t. It is possible, however, to bring these results into better agreement. The figures of Bamford and Dewar,[6] derived from measurements of the rate of increase of viscosity as the monomer polymerizes, are open to some doubt. The values for the rate constants vary appreciably with the value chosen for α, the exponent in the Staudinger equation relating viscosity to the molecular weight of the polymer. With $\alpha = 0{\cdot}67$, the value accepted by these authors as being correct, the results (6*a*) are obtained, while if $\alpha = 1{\cdot}0$, then the set (6*b*) results. As there is some doubt as to the correct values for α and K, their calculation of the rate coefficients must also be open to doubt. For example, they find $K = 4{\cdot}57 \times 10^{-3}$, $\alpha = 0{\cdot}65$, but Gregg and Mayo[27] report $K = 7{\cdot}53 \times 10^{-5}$, $\alpha = 0{\cdot}78$. The effect of an increase in α is to raise the values of k_p and k_t, but it is almost impossible to say what effect a decrease in K will have since Bamford and Dewars' expressions are so complicated. Their results with $\alpha = 1{\cdot}0$ are in quite good agreement with those reported here, however.

---

* The values of the life-time were determined from rate measurements at different sector speeds. They agreed with 10 % showing that the rate-sector speed relationship is normal.

[24] Burnett, unpublished work.

[25] Smith, *J. Amer. Chem. Soc.*, 1948, 70, 3695.

[26] Matheson, unpublished (quoted in [25]).

Burnett's results were obtained from a study of the non-stationary state which arises in the initial induction period and during the photochemical after-effect. It is possible to relate the induction period and decay time to the life-time of the radicals and hence calculate the coefficients. The set of results (24*a*) was calculated from a knowledge of the non-stationary state behaviour, using the rate of thermal initiation given by Bamford and Dewar[6] for $\alpha = 0{\cdot}65$; the results in (24*b*) are from a combination of the molecular weight data given here (Table III) and the life-time as deduced from the induction period. These values are in excellent agreement with the present values, the agreement for the propagation constant being particularly good.

The value for the propagation constant given by Smith[25] was calculated from a consideration of the emulsion polymerization and cannot be taken as a very accurate figure. It lies well above the other values and may safely be taken as incorrect. It is impossible to make any comment on the value of Matheson,[26] since no information is at present available as to his technique. As he has most probably assumed combination, his figure must be doubled in order to make a fair comparison with the others, which have all been calculated on the assumption of disproportionation. The activation energy for the propagation step quoted by these last two authors seems very high, but may be correct in view of the high degree of resonance stabilization exhibited by the styrene radical.

It would appear from a study of these figures that the values obtained in this work, those of Burnett and those of Bamford and Dewar, taking $\alpha = 1{\cdot}0$, are all in close agreement. There is a discrepancy factor of $1{\cdot}53$ for k_p and one of $1{\cdot}97$ for k_t.

The following values would hence appear to be the most accurate so far available, for the polymerization of styrene at 25° C:

$$k_p = 39{\cdot}5 \pm 5 \text{ l. mole}^{-1}\text{ sec.}^{-1}$$
$$k_t = (7{\cdot}9 \pm 2{\cdot}0) \times 10^6 \text{ l. mole}^{-1}\text{ sec.}^{-1}$$
$$k_f = (1{\cdot}1 \pm 0{\cdot}5) \times 10^{-3} \text{ l. mole}^{-1}\text{ sec.}^{-1}.$$

The variations seem to be rather large, but probably the agreement is as good as can be hoped for at the present stage of the development of this kind of work. An interesting point is that the values for the rate coefficients appear to be practically independent of the chain length, since all the results are in fair agreement, although the chain-lengths are vastly different. In the present work, $\overline{P} = 500$, while the results of Bamford and Dewar and also those of Burnett were found from experiments in which the chain length was of the order of 5,000 or greater. It may be, of course, that the constants do depend to some extent on the degree of polymerization. If such a situation exists, then it might be expected that the values of the rate constants would increase with decreasing size of the polymer radical. This might explain the fact that the present results are slightly higher than those of the other two authors. More probably, however, the variations are due to experimental error.

There is one major point which inevitably renders some doubt as to the validity of any results for the rate constants of polymerization processes. This is the vexed problem of whether chains disproportionate or combine. It may be useful at this stage to collect together most of the available evidence on the behaviour of various radicals. Both Evans

[27] Gregg and Mayo, *Faraday Soc. Discussions*, 1947, **2**, 328.

and Matheson favour combination for various reasons. Evans *et al.*[28] have shown that in the hydroxyl radical catalyzed polymerization of methyl methacrylate (using hydrogen peroxide in a redox reaction), the resulting polymer molecules contain two hydroxyl groups, and deduce from this that the radicals must have combined. However, it is possible that an additional terminal hydroxyl group may have been introduced by a transfer reaction, either with hydrogen peroxide or with water itself. Matheson [29] quotes experiments on such radicals as

$$\mathrm{MeO\,.\,C_6H_4\,.\,\overset{|}{C}H\,.\,CH_2\,.\,CH_3,}$$

which are reported to combine exclusively. However, other small radicals disproportionate, and it is by no means a safe assumption to suppose that large polymer radicals will behave in a manner similar to those comparatively small ones. For example, *p*-xylyl radicals

$$\mathrm{(CH_3\,.\,C_6H_4\,.\,CH_2—)}$$

are known to disproportionate in the gas phase [30] although they combine in the liquid state. Similarly, tri-*p*-tolymethyl radicals also disproportionate exclusively.[31]

It is also known that ethyl radicals disproportionate very readily.[32] Ethyl radicals formed by the dissociation of silver ethyl in alcohol readily undergo dismutation at − 30° C, so that the activation energy must be very low indeed. Weiss [33] has pointed out that for those radicals which have a dipole moment, and this includes most of the radicals found in polymerization reactions, disproportionation will be favoured. Again, radicals formed from primary alcohols ($\mathrm{R\,.\,\overset{|}{C}HOH}$) also disproportionate.[34] Further evidence in support of disproportionation comes from the work of Bolland and ten Have,[35] who found that semi-quinone radicals ($\mathrm{HO\,.\,C_6H_4\,.\,O—}$) disproportionate to form quinone and hydroquinone. Norrish,[37] in the course of a study of the photo-decomposition of ketones in paraffin solution, found that the initial radicals underwent a transfer reaction with the paraffin, forming paraffinic radicals. These then disproportionated to form unsaturated molecules and the amount of unsaturation produced could be measured quantitatively.

Evans [36] considers that the dismutation reaction, involving as it does the transfer of a hydrogen atom, should have a small activation energy. However, for vinyl acetate [1] there was no activation energy for the termination reaction, and yet the kinetics of the reaction point directly to disproportionation. Bamford [38] has shown that if disproportionation occurs the rate of increase of viscosity at high light intensities becomes proportional to $I^{(1-\alpha)/2}$, where α is the exponent in the viscosity equation, and this is followed experimentally with $(1-\alpha)/2 = 0{\cdot}10$, or $\alpha = 0{\cdot}80$, in excellent agreement with the published values ($0{\cdot}82$). If combination occurs, then the rate should be proportional to $I^{\frac{1}{2}}$, which is manifestly not so.

In any case, for all those systems which involve diradicals, termination must occur by disproportionation if finite molecular weights are to be attained. If combination occurs, then theoretically the final polymer should be one huge molecule of infinite molecular weight, apart from the polymers formed by chain transfer. Transfer reactions are not generally the limiting factor for the degree of polymerization, however.

---

[28] Baxendale, Bywater and Evans, *J. Polymer Sci.*, 1946, **1**, 237.

[29] Matheson *et al.*, ref. [5].

[30] Szwarc, *Faraday Soc. Discussions*, 1947, **2**, 46, 138.

[31] Marvel, Rieger and Mueller, *J. Amer. Chem. Soc.*, 1939, **61**, 2769.

[32] Bawn and Tipper, *Faraday Soc. Discussions*, 1947, **2**, 104.

[33] Weiss, *ibid.*, 1947, 138.

[34] Merz and Waters, *ibid.*, 1947, 179.

[35] Bolland and ten Have, *ibid.*, 1947, 257.

[36] Evans, *ibid.*, 1947, 275.

[37] Norrish, *Trans. Faraday Soc.*, 1939, **35**, 897.

[38] Bamford, *Faraday Soc. Discussions*, 1947, **2**, 401.

In conclusion, then, it may be said that the bulk of the evidence is in favour of disproportionation, and so the results obtained in the present work are likely to be correct within the experimental error.

Some Observations on Radical Reactivity.—From a comparison of the values of the absolute velocity coefficients for various monomers, it is possible to draw some interesting deductions regarding the reactivity of free radicals. In Table V, the best values for these constants are listed for five different monomers, the only ones for which data are available at present.

TABLE V.—THE ABSOLUTE RATE COEFFICIENTS FOR VARIOUS MONOMERS AT 25° C

Monomer	k_p	$k_t^{\frac{1}{2}}$ (× 10⁻³)	k_f (× 10³)	$k_t^{\frac{1}{2}}\ k_p$	k_f/k_p (× 10⁵)
Butyl acrylate[4] .	13·1	0·134	—	10·2	—
Styrene (*a*) . .	39·5	2·81	1·1	71·3	2·79
Methyl methacrylate (*b*) . .	122	2·84	—	23·2	—
Vinyl acetate (*c*) .	550	19·8	970·0 (*d*)	24·8	107·0
Vinyl chloride (*e*) .	—	—	—	—	~100

(*a*) This work.
(*b*) G. M. Burnett and H. W. Melville, unpublished work.
(*c*) Burnett, Melville and Valentine, *Trans. Faraday Soc.*, 1949, **45**, 960.
(*d*) Dixon-Lewis, *Proc. Roy. Soc. A* (in press). Calculated from his value at 0° C.
(*e*) Dr. Tuckett (private communication).

Some very interesting conclusions can be drawn from this Table. The values for k_p, $k_t^{\frac{1}{2}}$ and k_f all increase in a definite manner as one descends the series. This order is based on the reactivity of the various monomers in copolymerization studies,[29] styrene being the most reactive and vinyl chloride the least reactive. The position of butyl acrylate is based on the copolymerization of styrene and butyl acrylate, in which butyl acrylate adds on over twice as fast as styrene does to a styrene radical.[10] The value of $k_t^{\frac{1}{2}}$, rather than k_t, is taken as expressing the reactivity of the radicals in termination, since this does give a qualitative measure of the inherent terminating capacity of the radical concerned. Since the values increase in this series for the propagation, termination and transfer steps, it would seem that a determining factor in all these steps is the reactivity of the radical concerned. This is natural enough for the propagation and termination steps, but it seems rather surprising in transfer. For this step it might have been assumed that the limiting factor would have been the strength of the C—H bond, which would not alter appreciably from monomer to monomer.

Another point is that the value of the ratio $k_t^{\frac{1}{2}}/k_p$ does not alter very much, indicating that the relative reactivities of the radicals in termination and propagation is approximately constant for all the monomers.

One of us (L.V.) thanks the D.S.I.R. for the award of a Maintenance Allowance. We are grateful to Prof. A. C. Frazer for the opportunity of using a Beckmann Spectrophotometer.

Chemistry Department,
The University,
Edgbaston,
Birmingham 15.

---

[29] Mayo, Lewis and Walling, *Faraday Soc. Discussions*, 1947, **2**, 285.
[10] Arlman and Melville, unpublished work.

THE STABILITY OF STRUCTURES AT A FLUID INTERFACE

By D. J. Crisp

Received 5th September, 1949

An idealized array of parallel equidistant hairs, cylindrical in cross-section, can maintain a pressure difference across a liquid-vapour interface by virtue of the cylindrical bubbles formed when there is a finite angle of contact between the liquid and the surface of the hairs. A theoretical analysis of the forces operating upon such a system shows that when the bubbles are in their stable condition before the minimum radius of curvature is reached, then (i) if a hair is displaced in a direction perpendicular to the main direction of the surface there is a net restoring force bringing the displaced hair back towards the plane of the others; (ii) if a hair or group of hairs is displaced horizontally along the interface there will be (*a*) an increased vertical force in the direction of the applied pressure acting on these hairs which are spaced farther apart, (*b*) a horizontal displacing force acting in a sense which would increase the original displacement. The order of magnitude of these forces is shown to be similar to those due to the normal rigidity in structures of the dimensions discussed.

These conclusions emphasize the importance of rigidity among other requirements of a water-protecting structure and indicate the probable significance of certain grooming activities exhibited by insects which possess a water-protecting mechanism of this kind. The problem of rain-proofing or water-repellency calls for somewhat different and even contrasting requirements.

1. Introduction.—In the course of a study of the mechanism by which certain aquatic insects retain a layer of gas (" plastron ") over a part or whole of their body surface, it became necessary to consider the factors governing the stability of hairs lying at a fluid interface. In such insects it is usual to find that the retention of the gas is dependent upon the presence of a layer of very minute hydrofuge hairs, which prevent the water-air interface from invading the plastron.[1]

The efficiency of the system has been shown to be greatest when the hairs lie parallel to each other in the plane of the surface, each equidistant from its neighbour; any irregularities in the array will seriously impair its resistance to water penetration. When examined under conditions where the arrangement is solely determined by the normal rigidity of the structures themselves, morphological studies of the cuticle show that in every typical example, the hairs are in fact regularly arranged. It is of importance to consider what would be the effect of an excess pressure exerted on the water side of the meniscus, so causing it to be curved. Should a displacement of a hair or hairs relative to others give rise to forces which act in the same sense as the displacement, an element of instability would be present which if large enough compared with the rigidity of the hairs would destroy the regularity of the arrangement.[2] This paper shows that such forces do exist in simple structures, such as cylinders, lying at an interface. Similar considerations will hold for any system where water penetration is resisted by a flexible structure, and the principles described below may therefore have some bearing upon the behaviour of textiles in contact with water.

---

[1] Crisp and Thorpe, *Faraday Soc. Discussions*, 1948, **3**, 210.

[2] Crisp, *ibid.*, 1948, **3**, 282.

2. Conventions.—The same symbols are adopted as in an earlier publication in which the radius of curvature R of the cylindrical bubble formed by a pressure difference Δp on the water side of the interface between parallel cylinders of radius r and separation between centres l is given by

$$R = -\left[\frac{l/2 - r\cos\beta}{\cos(\beta+\theta)}\right]. \quad . \quad . \quad . \quad . \quad (1)$$

This relation is purely geometrical (Fig. 1). β represents the angle between the line joining the cylinder axes and the point of contact of the bubble with the cylinder surface, and θ is the contact angle of the bubble with the cylinder, employing the usual convention that θ is the angle between the solid liquid surface and the tangent of the air liquid (bubble) surface. β is assumed to be positive on the air side (lower side, Fig. 1) and negative on the water side of the line joining the axes of the cylinders. Then Δp the excess pressure on the water side will be

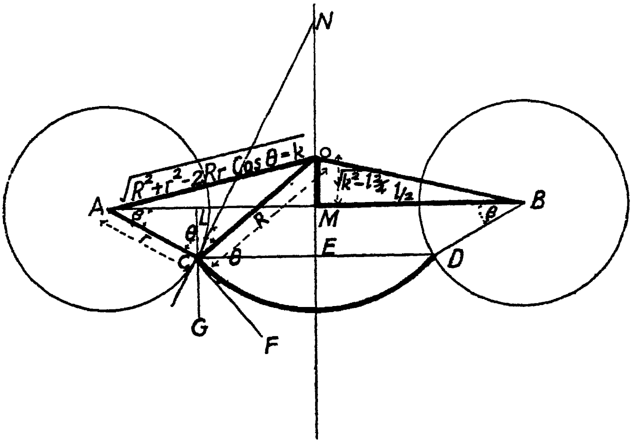

FIG. 1.—Cross-section of two adjacent hairs, centres A and B, radius r, with a cylindrical bubble, arc CD and radius R formed between them. In the treatment given, the water side of the interface lies to the upper side of CD.

$$\Delta p = \gamma/R, \quad . \quad . \quad . \quad . \quad . \quad . \quad (2)$$

while if

$$\sin\theta/\sin(\beta+\theta) = l/2r, \quad . \quad . \quad . \quad . \quad . \quad (3)$$

β and R are shown to have critical values, here termed β_m and R_m.[3]

There are two values of R_m and β_m satisfying (3), one corresponds to

$$3\pi/2 > (\beta_m + \theta) > \pi/2,$$

whence R_m and Δp_m are both positive; and the other where

$$-\pi/2 < (\beta_m + \theta) < \pi/2$$

giving negative values R'_m and $\Delta p'_m$. Both values of R_m are numerically minimal values, corresponding to maximum bubble pressures. Eqn. (3) may be expanded and substituted in (1) eliminating β and leading to a quadratic whose two solutions give explicitly:

$$R_m = r\cos\theta + \sqrt{l^2/4 - r^2\sin^2\theta}, \quad . \quad . \quad . \quad (4a)$$

$$R'_m = r\cos\theta - \sqrt{l^2/4 - r^2\sin^2\theta} \quad . \quad . \quad . \quad (4b)$$

It will be observed that since the cylinders cannot intersect, $l > 2r$ and the term inside the root sign is real and numerically greater than

---

[3] Thorpe and Crisp, *J. Expt. Biol.*, 1947, **24**, 227.

$r \cos \theta$, hence R_m is positive and R'_m negative as shown above. We shall not here be concerned with the negative values of R'_m, $\Delta p'_m$ or the corresponding β'_m, but the relations of these quantities are symmetrical with the positive values.

Eqn. (4) has been given by Baxter and Cassie [4] who derived it more elegantly from purely geometrical considerations. The fuller treatment here is, however, desirable in order to demonstrate the effect of varying the separation distance of the hairs.

3. Vertically Resolved Forces Sustained by Hairs.—Assuming a fixed regular array of cylindrical hairs there will be downward forces on each unit length of cylinders :

(*a*) due to unbalanced pressures $2\Delta p r \cos \beta$,

(*b*) due to surface tension $-2\gamma \cos (\beta + \theta)$.

Hence the vertical reaction V on unit length of the cylinder will be

$$V = 2\Delta p r \cos \beta - 2\gamma \cos (\beta + \theta). \quad . \quad . \quad . \quad (5)$$

Substituting (1) and (2),

$$V = \Delta p l. \quad . \quad . \quad . \quad . \quad . \quad . \quad (6)$$

The vertical force on each cylinder is seen to be independent of β but proportional to l if Δp is constant. Hence if a cylinder moves horizontally a distance dl to become placed at distances $l +$ dl and $l -$ dl from its neighbours, the vertical force on it remains unchanged. If, however, displacements occur causing a group of adjacent cylinders to be more widely spaced than the average, these will be subjected to a greater downward thrust (since l is increased) and will tend to be displaced relative to the remainder in the direction of Δp (Fig. 2).

(2)

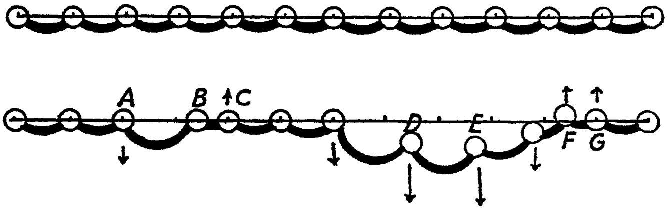

Fig. 2.—An array of hairs equidistant from one another (upper) and showing horizontal displacements (lower). The arrows represent the resultant changes in vertically resolved forces due to the displacements. Hairs A and C are in their original positions and B is displaced to the right. There is no change in the resultant vertical force on B.

4. Stability of Hairs in the Direction Perpendicular to the Surface Plane.—We shall now consider the effect of a small displacement of alternate hairs in an equidistant array, the displacement dx taking place in a direction perpendicular to the surface. The effect of this displacement is to increase the distance between the centres of the cylinders to $l/\cos$ dβ^*, where d$\beta^* =$ dx/l (Fig. 3). Since Δp is constant and R is

(3)

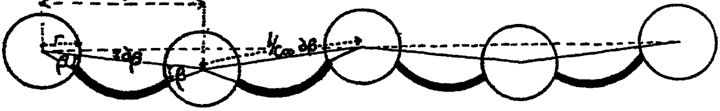

Fig. 3.—An array of equidistant hairs in which alternate members are displaced in a direction perpendicular to the interface.

---

[4] Baxter and Cassie, *J. Text. Inst.* 1945, *T.* 167.

unchanged, the value of β (the angle between the line joining the centres of the hair axes and the radius to the triple interface) is modified to β^*, β^* must satisfy

$$R = \frac{l/2 - r \cos \beta^*}{\cos (\beta^* + \theta)}.$$

The change noted in β is small and does not affect the argument below.

The difference in the vertical force on the displaced hairs (Fig. 3) tending to restore them to the plane of the others will be $2\mathrm{d}V/\mathrm{d}\beta^*$ since β^* is increased by $\mathrm{d}\beta^*$ for the odd, and decreased by $\mathrm{d}\beta^*$ for the even numbers.

Since

$$V = 2\Delta p r \cos \beta^* - 2\gamma \cos (\beta^* + \theta),$$

$$\mathrm{d}V/\mathrm{d}\beta^* = 2\gamma \sin \beta^* - 2\Delta p r \sin \beta. \qquad (7)$$

Hence reducing to a dimensionless form,

$$\frac{1}{2\gamma}\frac{\mathrm{d}V}{\mathrm{d}\beta^*} = \sin (\beta^* + \theta) - \frac{r}{R} \sin \beta^*. \qquad (8)$$

Clearly if the quantities in eqn. (8) are positive the force is a restoring force tending to align the hairs back into a coplanar array. To determine the sign, eqn. (4) is expanded to give β explicitly.

$$\sin \beta = \frac{1}{y^2 + w^2}\left[\frac{lw}{2} \pm y\sqrt{y^2 + w^2 - l^2/4}\right], \qquad (9)$$

$$\sin (\beta + \theta) = \frac{1}{z^2 + v^2}\left[\frac{lv}{2} \mp z\sqrt{z^2 + v^2 - l^2/4}\right], \qquad (10)$$

where

$$y = R \cos \theta - r,$$
$$z = r \cos \theta - R,$$
$$w = R \sin \theta,$$
$$v = r \sin \theta,$$
$$y^2 + w^2 = z^2 + v^2 = R^2 + r^2 - 2Rr \cos \theta = k^2.$$

It will be observed from Fig. 1 that k = OA, and $\sqrt{k^2 - l^2/4}$ = OM. At the minimum value for R, O is coincident with M.[4]

Substituting these values in (8) we obtain

$$\frac{1}{2\gamma}\frac{\mathrm{d}V}{\mathrm{d}\beta^*} = \pm \frac{1}{R}\sqrt{k^2 - l^2/4}. \qquad (11)$$

Now eqn. (9), (10) and (11) are roots of quadratics, which are real and equal when

$$R^2 + r^2 - 2Rr \cos \theta - l^2/4 = 0.$$

This, as will be seen from inspection of eqn. (4) and (12), implies $R = R_m$ and β having its unique value β_m. When R has any other value there are two values of β satisfying (9). One refers to the early state of the bubble before the critical point is reached. This condition is stable since, as β increases and the bubble moves in the direction of Δp, R decreases so that Δp can stabilize at a higher value. The other value of β refers to the condition where $\mathrm{d}R/\mathrm{d}\beta$ is positive and represents the unstable state. It will be seen either from inspection or by differentiation that the upper signs in eqn. (9) and (10) and therefore in (11) which is derived from (9) and (10) refer to the stable condition (e.g. in (9) if $\theta > \pi/2$, all terms are positive except y which is negative, hence the upper sign refers to the smaller value of $\sin \beta$, i.e. to the initial stable condition). Hence, since the term under the root sign of eqn. (11) is positive or zero, in the stable condition of the bubble $\mathrm{d}V/\mathrm{d}\beta^*$ is positive and a restoring force acts on any displaced hairs. As the bubble reaches its critical state this force diminishes to zero, and in the unstable condition the hairs, but for their inherent rigidity, would spontaneously be displaced relative to one another.

5. Stability of Hairs in the Direction of the Surface Plane.—The effect of a similar displacement in a horizontal direction is considered here. Resolving forces horizontally towards the centre of a cylinder the force acting on each half will be

$$H = \Delta pr(1 + \sin \beta) - \gamma \sin (\beta + \theta).$$

Reducing to a dimensionless form,

$$\frac{H}{\gamma} = \frac{r}{R} + \frac{r}{R} \sin \beta - \sin (\beta + \theta). \quad . \quad . \quad . \quad (12)$$

Using the previous method of eliminating β we obtain

$$\frac{H}{\gamma} = \frac{r}{R} \mp \frac{1}{R} \sqrt{k^2 - l^2/4}, \quad . \quad . \quad . \quad (13)$$

where $k^2 = R^2 + r^2 - 2Rr \cos \theta$.

To obtain the variation in H for a displacement ∂l differentiation gives

$$\frac{1}{\gamma} \cdot \frac{\partial H}{\partial l} = \pm \frac{l}{4R\sqrt{k^2 - l^2/4}}. \quad . \quad . \quad . \quad (14)$$

If F represents the horizontal force acting on a cylinder as a result of its displacement then

$$dF = 2\left(\frac{\partial H}{\partial l}\right) . dl. \quad . \quad . \quad . \quad . \quad (15)$$

Where F is assumed to act in the sense in which l is increasing, thus from (16) and (17)

$$\frac{dF}{dl} = \pm \frac{\gamma l}{2R\sqrt{k^2 - l^2/4}}. \quad . \quad . \quad . \quad (16)$$

Hence the horizontal force resulting from a displacement is in the same sense as the displacement when the bubble is in its stable (expanding) state. Thus the hairs will tend to segregate in a horizontal plane while the pressure difference Δp is increasing. As Δp approaches its critical value the denominator in eqn. (16) tends to zero, and the displacing force becomes increasingly pronounced. We conclude therefore that an array of equidistant hairs sustaining a pressure difference always has an element of instability and can only be maintained if it possesses a certain rigidity holding the cylinders apart at their appropriate distances.

The effect of a finite displacement Δl is shown by the difference equation:

$$\Delta F = \frac{\gamma}{R}\left[\sqrt{k^2 - \frac{(l - \Delta l)^2}{4}} - \sqrt{k^2 - \frac{(l + \Delta l)^2}{4}}\right]. \quad (17)$$

The displacing force ΔF clearly increases with Δl, at first linearly and then increasingly, reaching a maximum either when the second root term is zero, or when $\Delta l = (l/2) - r$. Fig. 4 shows how ΔF increases with Δl in a typical case.

Let us assume that the hairs are maintained in a regular array by a force E with an elastic constant ϵ defined by

$$\partial E/\partial l = - \epsilon. \quad . \quad . \quad . \quad . \quad . \quad (18)$$

This restoring force, assumed proportional to the displacement, can be equilibrated to the displacing force at a certain value of R termed R_s:

$$\left(\frac{\partial E}{\partial l}\right) dl + \left(\frac{\partial F}{\partial l}\right) dl = 0.$$

Hence from (16)

$$R_s\sqrt{R_s^2 + r^2 - 2R_s r \cos \theta - l^2/4} = l\gamma/2\epsilon \quad . \quad . \quad (19)$$

Eqn. (19) defines the minimum value for R for initial stability of the array. If $R < R_s$ the system is metastable, the array spontaneously segregating and allowing water to invade the wider spaces between the cylinders. Turning to eqn. (17), however, it will be observed that even if $R > R_s$, it is possible for the displacing force to exceed the restoring force if the displacement is sufficiently increased. Thus, in Fig. 4 the line OP represents an elastic restoring force of $\epsilon/\gamma = 0{\cdot}75$. Such a force would maintain a stable array at $R_s = 2{\cdot}0$, if θ is greater than 80° or thereabouts, but if θ were less than 60°, R_s would have to be greater than the figured value of 2 for stability. If $R_s = 2$, $\theta = 70$, the array is initially stable when $\Delta l = 0$, but if Δl exceeds 0·68, unstable conditions prevail since the lines cross at Q. The condition for complete stability will thus be

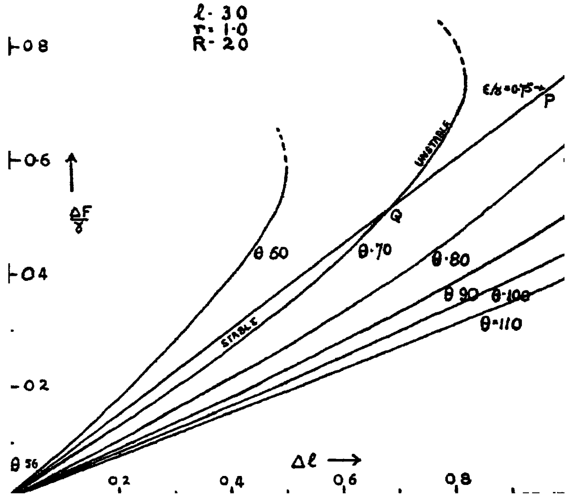

FIG. 4.—Plot of the lateral displacing force as a function of the displacement Δl of the cylinder from an equidistant position. This force is plotted as the non-dimensional quantity $\Delta F/\gamma$ for the particular case where $l = 3$, $r = 1$ and $R = 2$. Δp the downward pressure on the bubble is $= \gamma/R$. The maximum displacement possible is $\Delta l = 1$ when the cylinder touches its neighbour, but for the smaller contact angles figured ($\theta = 56°, 60°, 70°$) instability of the bubble sets in before this displacement can be attained (dotted line). The straight line OQP represents an elastic restoring force of constant $\epsilon = 0{\cdot}75\ \gamma$.

$$\frac{\epsilon\ .\ \Delta l}{\gamma} > \frac{1}{R_s}\left[\sqrt{R_s^2 + r^2 - 2R_s r\cos\theta - \frac{(l-\Delta l)^2}{4}} - \sqrt{R_s^2 + r^2 - 2R_s r\cos\theta - \frac{(l+\Delta l)^2}{4}}\right], \quad (20)$$

an expression most readily solved graphically as in Fig. 4.

The conclusion is therefore reached that when the elastic force is not greatly in excess of the displacing force the system becomes decreasingly stable as the displacement increases. A sufficiently large displacement might then lead to a breakdown of the structure. This explains the significance of the constant attention and grooming of waterproofing structures which has been observed to be performed by some insects and which has been described elsewhere.[5]

---

[5] Thorpe and Crisp, *J. Expt. Biol.*, 1949, **26**, 219.

6. Magnitude of Displacement Forces.—It is of interest to examine whether the forces discussed above are of an order comparable with the elastic forces likely to exist in such structures. The elastic forces are due to bending or torsional moments, in which the relevant dimensions are the radius of the hair r and its length h, and elasticity modulus Y. The force dW upon such a system causing a displacement dl will be

$$\mathrm{d}W \sim Y\frac{r^4}{h^3}\,\mathrm{d}l.$$

In the treatment above unit lengths have been considered, hence the constant ϵ will be $\frac{1}{h}\cdot\frac{\mathrm{d}W}{\mathrm{d}l}$, whence

$$\frac{\mathrm{d}E}{\mathrm{d}l} = \epsilon \sim Y\frac{r^4}{h^4}.$$

Using, eqn. (2) and (16) the displacing force may be rewritten as

$$\frac{\mathrm{d}F}{\mathrm{d}l} = \Delta p[l/2\sqrt{k^2 - l^2/4}] = \Delta p\, f(R, r, l, \theta),$$

where $f(R, r, l, \theta)$ is a non-dimensional function which, except for conditions where Δp is very small or where R closely approaches R_m, will be of the order of unity.

Hence $\mathrm{d}F/\mathrm{d}l \sim \Delta p.$

It will be noted that Y, ϵ and Δp all have dimensions $ML^{-1}T^{-2}$ and that the displacement and elastic forces are of the same order when

$$\frac{r}{h} \sim \left(\frac{\Delta p}{Y}\right)^{1/4}.$$

A group of insects which possess a waterproofing structure apparently requiring frequent grooming, the Elmidae, possess hairs in which $h = 10^{-3}$, $r = 0{\cdot}5 \times 10^{-4}$ and can resist a pressure difference of about 1 atm., hence if Y has a reasonable value of about 10^{11} the elastic and displacement forces would be of the same order. It is interesting to find in *Aphelocheirus* and in *Stenelmis crenata*, where r/h is about 0·2, that the hairs stand perpendicular to the surface with the very tip bent sharply at 90°, only this very short element is therefore subjected to displacement forces.

7. Rain Proofing.—Several authors have emphasized the different requirements of structures designed to prevent the penetration of water under pressure (water protecting) and those designed to promote run off of water droplets under effectively zero pressure (rainproofing or water repellency).[4, 6] Indeed the requirements of two mechanisms are shown to be in some respects incompatible.[5] It is relevant here to point out that the rigidity of the constituent structures is even more important in rainproofing than it is in water protection. In the latter case, where the liquid covers the whole of the surface, the displacement forces are difference terms due to the imposed pressure and to the displacement of the structures themselves. In uneven wetting of surfaces such as takes place with rainproofed materials, the displacement forces are absolute and have a maximum value of 2γ per unit length, as when, for instance, a thin film of liquid exists on one side only of a constituent hair. These materials must therefore be able to remain essentially in the same position when subjected to this force, and not mat together under its influence. As pointed out by Baxter and Cassie, the structure of ducks' feathers, which must be proof against uneven wetting, but not against any considerable penetration pressure, exemplifies this admirably. So also do the stiffer and larger hairs of numerous insect species which are protective

[6] Bartell, Purcell and Dodd, *Faraday Soc. Discussions*, 1948, **3**, 257.

against accidently wetting by rain or falling into water. Indeed, this may well be the significance of the many examples of hairs and bristles found on small sub-aerial anthropods, and in particular the short microtrichia which so frequently beset the wings.[5]

Manor Rd.,
Brixham, Devon.

THE SURFACE CHEMISTRY OF PROTEINS

BY C. W. N. CUMPER AND A. E. ALEXANDER

Received 7th September, 1949

I. Spread monolayers of the proteins, β-globulin, pepsin and insulin, together with the synthetic polymers, polymethacrylic acid, Nylon, polyalanine and polyphenylalanine, have been studied at a petrol ether-water interface. In addition to the force-area curves an oscillating needle technique was used to measure the interfacial viscosity and elasticity. Of these, the viscosity appeared to give the most detailed information about the structure of the film, since it only became appreciable when the molecules were close-packed, whereas the force-area curves were all of the expanded type.

Insulin behaved differently from the other proteins studied, as at the point of close-packing the film appeared to be two polypeptide chains in thickness. Polyphenylalanine behaved differently at the oil-water and air-water interfaces, an effect which has been ascribed to different orientations of the polymer molecules in the two cases.

No appreciable effect of pH was found with the proteins studied and, with pepsin, which was investigated in greater detail, the ionic strength and temperature were also without effect. Variation of pH did, however, influence the properties of polymethacrylate acid and Nylon films.

II. The adsorption at the oil-water interface of the proteins, β-globulin, pepsin and insulin has been studied as a function of protein concentration, nature of interface, pH, ionic strength, temperature and time by means of interfacial tension and interfacial viscosity measurements.

By making certain assumptions and using the data of Part I it is possible to calculate the thickness of the surface-denatured protein present at the interface. The marked effects of pH, ionic strength and temperature on the adsorption appear to be self-consistent and support the general picture that two consecutive processes occur on adsorption; firstly, surface denaturation involving an unrolling of the polypeptide chains and secondly, coagulation involving a regrouping of the surface denatured molecules with the formation of a coagulum largely devoid of surface activity. The above conclusions were strengthened by some experiments on the stabilization of oil-in-water emulsions by the proteins under different conditions of pH, ionic strength and temperature.

Over a century has passed since Ascherson published his classical paper entitled "The physiological role of the fats," in which he first pointed out that protein solutions tend to form, rapidly and spontaneously, visible elastic "skins" around the surfaces of oil droplets. The process involved is generally termed "surface denaturation," since the mere act of adsorption brings about changes in the native protein molecule with a marked loss in water solubility. Surface denaturation may thus be an important step in the formation of membranes in biological systems; it is also of considerable interest in connection with the stabilization of emulsions in biological systems and with the industrial use of proteins as foaming and emulsifying agents.

It is clear that all interfaces cannot possess equal powers for surface denaturation, for if this were the case the extensive interfaces in biological systems would soon remove all proteins from solution—with disastrous results! On the other hand it is quite conceivable that varied degrees of unfolding or denaturation might occur at interfaces differing for example in energy, chemical groupings, physical state, etc. This would open up many interesting possibilities for specific adsorption from solution and may have considerable bearing upon certain immunological reactions. Also the possibility of surface denaturing the protein in stages offers another line of approach to the problem of protein structure.

Viewed in relation to these industrial and biological applications the lack of fundamental knowledge concerning protein adsorption is striking. Some idea can be inferred from studies of spread monolayers at air-water and oil-water interfaces, but our detailed understanding of adsorbed films has advanced little since Ascherson's time.

In the present work the changes produced by adsorption upon various types of interface have been investigated by a number of physical methods. In addition certain serological studies have been carried out in collaboration with Dr. R. R. Coombs of the Department of Pathology, and will be presented in a later publication.

PART I. SPREAD MONOLAYERS AT OIL-WATER INTERFACES

Since 1926, when Gorter and Grendel [1] first made a systematic study of protein monolayers spread at an air-water interface, numerous papers have appeared, but most of those prior to 1939 do not deal with completely spread proteins. In spite of the greater biological significance attached to the oil-water as compared with the air-water interface, little work has been done in this field. The present study of spread monolayers of proteins and synthetic polymers at the oil-water interface was undertaken as a preliminary to an investigation of adsorbed films of proteins (see Part II). In addition to the usual force-area relationship, the surface viscosity and elasticity were determined as a function of the area.

Qualitative results for the viscosity of protein monolayers at the air-water interface have been obtained by Schaefer [2] from expansion patterns, and quantitative results by Langmuir and Schaefer [3] using an oscillating disc. They found considerable differences between different proteins. With most proteins the damping of the disc increased as the shearing stress decreased, indicating that the monolayers were behaving as plastic solids rather than viscous liquids. The results obtained in the present investigation for spread protein monolayers at the oil-water interface and for adsorbed films (Part II) indicate that the viscosity is Newtonian until it reaches a value of about three surface poises.

Experimental

The films were spread at a petrol ether (b.p. 90-100° C)-water interface in a glass dish of 12 cm. diam. by means of an all-glass micrometer syringe, the precautions recommended by Crisp [4] being observed. The force-area ($\pi - A$) curves were determined by measuring the interfacial tension with a platinum ring, as described by Alexander and Teorell.[5] The surface viscosity η_s of the film, defined as the change in viscosity of the interfacial layers produced by the insoluble film, was measured by oscillating a platinum needle, attached to a heavy metal bob, at the interface. If $\Delta(\lambda_{10}/P)$ represents the change produced by the film in the ratio of the logarithmic decrement λ_{10} to the period P of the oscillations, then the surface viscosity, in surface poises, is given by the expression :

---

[1] Gorter and Grendel, *Trans. Faraday Soc.*, 1926, **22**, 477.

[2] Schaefer, *J. Physic. Chem.*, 1938, **42**, 1089.

[3] Langmuir and Schaefer, *Chem. Rev.*, 1939, **24**, 181.

[4] Crisp, *J. Colloid Sci.*, 1946, **1**, 49, 161.

[5] Alexander and Teorell, *Trans. Farraday Soc.*, 1939, **35**, 727.

$$\eta_s = \Delta(\lambda_{10}/P)I/l^2 \times 4 \times 2\cdot3,$$

where I = the moment of inertia of the system and l = the length of the needle (4·00 cm.). Fourt[6] has defined an elasticity index E_s of the film by the relation :

$$E_s = \frac{4\pi^2 I}{l^3}\left(\frac{1}{P^2} - \frac{1}{P_0^2}\right),$$

where the subscript refers to the clean interface. This index is directly proportional to the contribution of the film to the restoring torque on the needle. The apparatus was water thermostatted at 25 ± 0·1° C and the phosphate and acetate buffers used as the aqueous phase kept at an ionic strength of 0·03 throughout, unless otherwise stated.

Three proteins were examined, bovine-β-globulin, crystalline pepsin and crystalline zinc-insulin (all from Armour & Co.). They were spread from 0·03 % solutions in 60 % *iso*propyl alcohol containing 0·5 M sodium acetate.[5] The synthetic polypeptides used were prepared by Dr. Dalgliesh ; the poly-*DL*-alanine was spread from a solution in 50 % *iso*propyl alcohol and the poly-*DL*-phenylalanine from pyridine. Nylon was spread from a solution in 2N H_2SO_4 + 50 % *iso*propyl alcohol and the polymethacrylic acid from 30 % pyridine.

Results

To assist in the elucidation of protein monolayers a number of linear polymers of known structure were first examined at the petrol ether-water interface. The compounds chosen, in order of increasing resemblance to the protein polypeptide chain, were

polymethacrylic acid 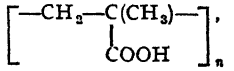

$$\left[\begin{array}{c}—CH_2—C(CH_3)—\\ \quad\;|\\ \quad COOH\end{array}\right]_n,$$

Nylon $[—(CH_2)_4 . CO . NH—]_n$,

polyalanine $[—CH(CH_3) . CO . NH—]_n$

and polyphenylalanine $[—CH . CH_2 . (C_6H_5) . CO . NH—]_n$.

The π, η_s and E_s results obtained with these synthetic polymers, plotted as a function of A (in A²/residue), are shown in Fig. 1, 2, 3 and 4. They all appear to be of the vapour-expanded type as usually found for oil-water monolayers.[5]

Polymethacrylic acid, although soluble in water, can be spread on acid substrates to give reasonably stable films. As seen from Fig. 1, the π—A and η_s—A curves vary with the pH : this we ascribe to some solution at the higher pH's (probably of the shorter chains) for, if the viscosities and elasticities are compared at equal surface pressures instead of at equal areas, good agreement is observed.

The force-area curves of Nylon (Fig. 2) depend markedly on the substrate, as found by Crisp[4] at the air-water interface. On the neutral substrate a marked surface viscosity was present at areas less than about 50 A²/residue, whereas on strong acid there was no detectable viscosity even at 5 Å²/residue, where the Nylon must be in the form of a thick collapsed polylayer.

The curves for the synthetic polypeptides (Fig. 3 and 4) resemble very closely those given by the proteins. Polyphenylalanine was also examined at the air-water interface and under these conditions it showed a rather unexpected, and very unusual, behaviour which will be discussed in more detail later.

The results for the proteins (β-globulin, pepsin and insulin) are shown in Fig. 5, 6, and 7. The influence of ionic strength, over the range 0·003 to 0·30, and of temperature, from 15 to 35° C, were examined for pepsin, but neither appeared to cause an appreciable change.

---

[6] Fourt, *J. Physic. Chem.*, 1939, **43**, 887.

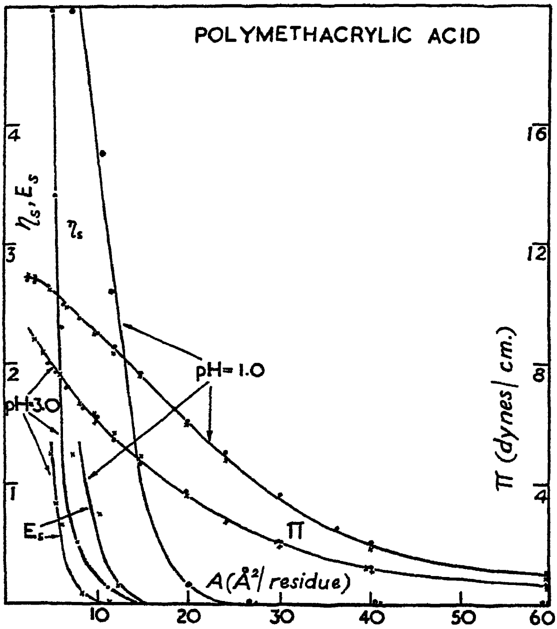

FIG. 1.—Spread monolayers of polymethacrylic acid at a petrol ether-water interface. Surface pressure π, interfacial viscosity η_s and elasticity index E_s as a function of the area per residue A.

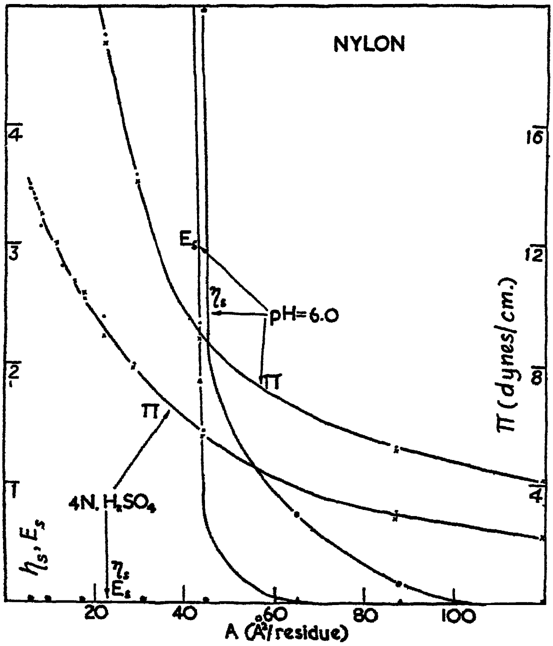

FIG. 2.—Spread monolayers of Nylon at a petrol ether-water interface. π_s, η_s and E_s as a function of A. Aqueous substrates, buffer pH 6·0 and 4N H_2SO_4.

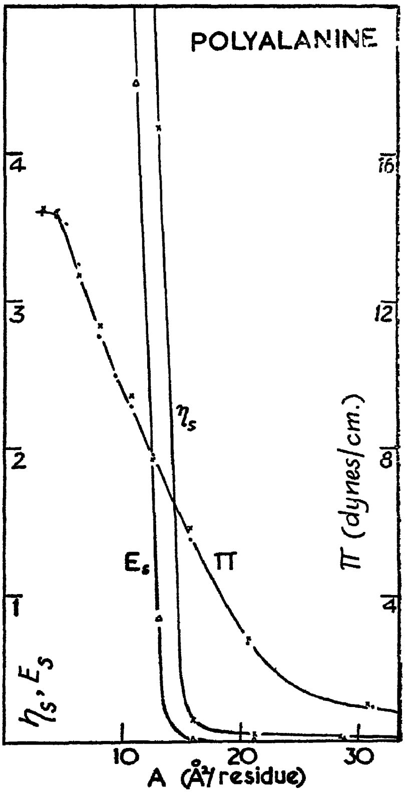

FIG. 3.—Spread monolayers of polyalanine at the petrol ether-water interface. π, η_s and E_s as a function of A.

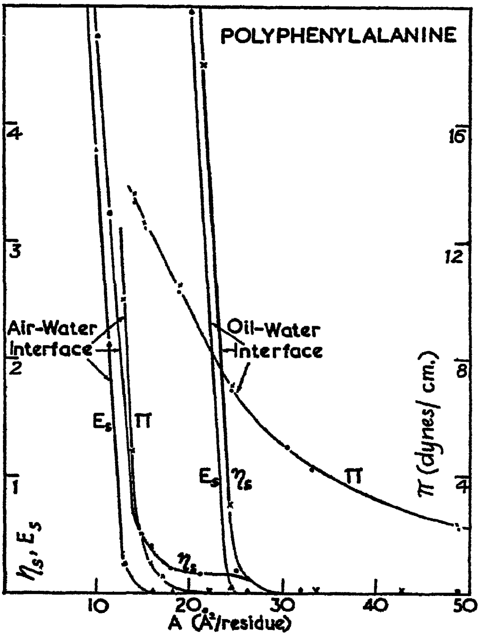

FIG. 4.—Spread monolayers of polyphenylalanine at the petrol ether-water and air-water interfaces. π, η_s and E_s as a function of A.

Discussion

Spread monolayers of proteins at the oil-water interface are believed to exist as unfolded polypeptide chains in the β-keratin configuration, oriented with as many of the non-polar side-chains in the oil phase and of the polar side-chains in the aqueous phase as is consistent with the steric configurations of, and lateral forces between, the main-chain and side-chains. The X-ray data of Astbury[7] gives the lengths of an amino-acid residue in the direction of the polypeptide chain as 3·5 Å and the inter-chain spacing as 4·5 Å. At an area of 15·7 Å^2 per residue therefore, the polypeptide chains are just close-packed and on further compression segments of the chains must leave the interface. The findings of the present investigation support this general picture.

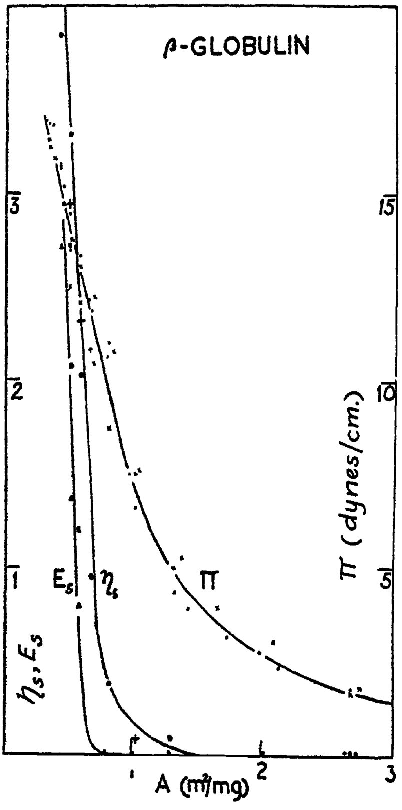

FIG. 5.—Spread monolayers of bovine β-globulin at the petrol ether-water interface. π, η_s and E_s as a function of A.

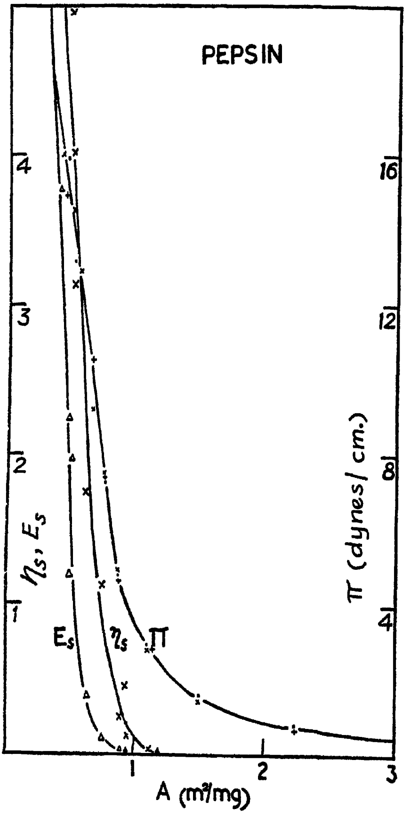

FIG. 6.—Spread monolayers of pepsin at the petrol ether-water interface. π, η_s and E_s as a function of A.

It is seen from the data shown in the Figures that an appreciable surface viscosity is only manifest when the molecules are close-packed at the interface. This point does not, however, show up as a discontinuity in the force-area curves which, as pointed out earlier, are of the vapour-expanded type. Not until the films have a surface viscosity of 1-2 surface poise (corresponding to a bulk value of *ca.* 10^7 poise), do they show detectable elasticity.

---

[7] Astbury, *Trans. Faraday Soc.*, 1933, **29**, 193; *Fundamentals of Fibre Structure* (Oxford, 1933).

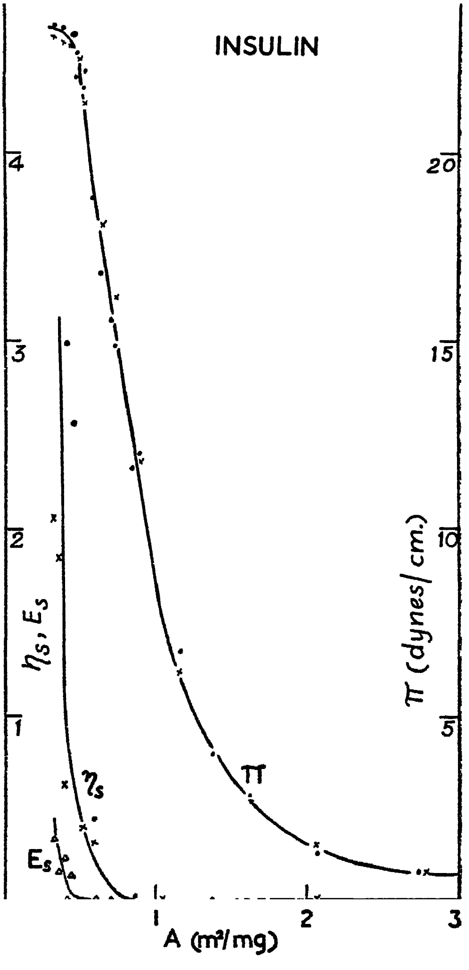

FIG. 7.—Spread monolayers of insulin at the petrol ether-water interface. π, η_s and E_s as a function of A.

Synthetic Polymers.—In polymethacrylic acid the appreciable surface viscosities at areas less than about 20 Å²/residue probably arise from two principal causes—mechanical entanglements between the polymer-chains, an effect accentuated by the rather rigid nature of the polymethacrylate chain, and some hydrogen bonding between the —COOH groups on adjacent chains.

With the Nylon monolayers, as with the proteins, there is believed to be hydrogen bonding between the C=O and N—H groups on adjacent chains. On strongly acid substrates this hydrogen bonding is greatly weakened or largely eliminated,[8] and since no surface viscosity is detectable in this case (see Fig. 2), it would seem that on neutral substrates the viscosity arises largely from hydrogen bonding.

---

[8] Alexander, *Proc. Roy. Soc. A*, 1942, 179, 470.

With polypeptides the viscosity is developed over a very small range of areas. Extrapolation of the surface viscosity curves gives areas of 14·7 Å^2/residue and 24·7 Å^2/residue for polyalanine and polyphenylalanine respectively. The onset of viscosity thus corresponds to close-packing of the chains in the former case, and to close-packing of the phenyl side-chains in the latter, since in air-water monolayers the cross-sectional area of the benzene nucleus is about 24 Å^2.[9, 10]

The structure of the polyphenylalanine monolayers was investigated further by spreading at an air-water interface: the surface viscosity curve now extrapolated to an area of 14·4 Å^2/residue and there was a small viscosity of *ca.* 0·2 surface poise up to an area of 25 Å^2/residue (see Fig. 4). The marked difference between the air-water and oil-water monolayers can probably be explained as follows: at the oil-water interface the energy requirements are best satisfied with all the phenyl groups in the oil phase and with the carbonyl groups in the aqueous phase. Examination of models shows that the molecule can easily pass into this configuration from the normal β-keratin structure and that the area per residue would be *ca.* 23 Å^2. This structure could have little direct hydrogen bonding, it being stabilized by the large energy decrease resulting from the transfer of half the phenyl groups from the aqueous to the oil phase. At the air-water interface this change is much less favourable energetically (*ca.* 300-1000 cal./g. residue less than in the former case), so the polypeptide chains take up a close-packed configuration instead, with equal numbers of phenyl groups in the air and aqueous phases. This configuration permits considerable hydrogen bonding between adjacent chains; some further stabilization may result from the phenyl groups of adjacent chains being in contact, thus reducing the hydrocarbon-water interface. When initially spread from pyridine the polyphenylalanine will assume the " oil-water " structure, thus accounting for the small but definite viscosity between 25 and 15 Å^2/residue.

Polyalanine in the " oil-water " configuration would occupy an area of 14·7 Å^2/residue. The energy change for the transfer of a methyl group from water to oil is much less than for phenyl and the hydrogen bonding tendency would favour the configuration with alternation of the side-chains. The actual structure taken up by polyalanine at the oil-water interface is thus unsettled at the moment; it could best be determined by interfacial potential measurements.

The effect of strongly acid substrates upon the polypeptide monolayers is much less than upon those of Nylon, both at the oil-water and also at the air-water interface (Glazer, private communication). The difference probably arises from the much greater surface density of —CO . NH— groups in the polypeptides, being separated by only one carbon atom as compared with four in Nylon.

Both these polypeptides were of the *DL* configuration: the *D*- and *L*-isomers alone could not be dissolved in suitable solvents for spreading, which demonstrates how large the forces between adjacent chains are in these regular structures.

Proteins.—In the proteins themselves it is unlikely that sufficient amino acids with bulky side-chains occur in adjacent positions along the polypeptide chains to cause the area per residue to exceed 15·7 Å^2, even if they were all polar or all non-polar and hence either all are in the aqueous or all in the oil phase. From X-ray data and molecular models the area per residue in the close-packed monolayers can be calculated. These values are compared in Table I with those obtained by extrapolating the surface viscosity–area curve to zero viscosity which, as pointed out above, indicates in our view the area for close-packing.

---

[9] Adam, *Proc. Roy. Soc. A*, 1923, **103**, 676.

[10] Adam, Berry and Turner, *ibid.*, 1928, **117**, 532.

The agreement is seen to be quite good with polyalanine, polyphenylalanine, β-globulin and pepsin, fair with polymethacrylic acid and very poor with Nylon and insulin. The low value with polymethacrylic acid can reasonably be explained as due to some of the low molecular weight polymer passing into solution. Nylon has a very flexible chain with four carbons between each polypeptide band and hence might form closed rings of various sizes by intramolecular hydrogen bonding, leading to a larger area per residue than for close-packing of the chains.

TABLE I

Substance	Mean Residue Weight	Area/Residue (Å^2)	
		From X-ray Analysis and Molecular Models	From the η_s - A Curves
Polyalanine			
" Oil-Water " configuration *	71	$\sim$14·7	14·7
" Air-Water " configuration *		15·7	
Polyphenylalanine			
Oil-Water interface	149	$\sim$23	24·7
Air-Water interface		15·7	14·4
Nylon	99	34	45
Polymethacrylic acid, pH=1·0	85	20	16·4
β-Globulin	$\sim$115	15·7	15·0
Insulin	113·6	15·7	7·9
Pepsin	$\sim$115	15·7	14·5

* See page 242.

With insulin the linear part of the η_s—A curve extrapolates to *ca.* 7·9 Å^2/residue, only about half the area expected from fully extended polypeptide chains. This would suggest that at the point of close-packing the " monolayer " of insulin is actually *two* polypeptide chains thick. Sanger [11, 12] has shown that the submolecule of insulin [13] of molecular weight 12,000, consists of four polypeptide chains held together by six disulphide bridges. Whether these four chains have a square configuration or a planar one in which two of the chains can leave the interface quite readily on compression is not known. Since the force-area curve is normal the latter hypothesis would seem the more plausible.

PART II. THE VISCOSITY, ELASTICITY AND THICKNESS OF ADSORBED FILMS

In order to analyze the effects of proteins upon the electrophoretic behaviour of colloidal particles and upon the stability of emulsions, it is clearly desirable to have some knowledge of the thickness and structure of the adsorbed layer. The study of the viscosity and elasticity of the adsorbed films, taken in conjunction with the same properties for spread monolayers (see Part I), provides one means of approach to this

---

[11] Sanger, *Biochem. J.*, 1945, **39**, 507.

[12] Sanger, *Nature*, 1947, **160**, 433.

[13] Chibnall, *Second Procter Memorial Lecture* (Inter. Soc. Leather Trades' Chemists).

problem. The effect of variables such as the type of protein and its concentration, the nature of the interface, pH, ionic strength, temperature, and time can readily be followed in this way as will be shown below. Some idea concerning the factors which influence, and the changes involved in, the process of surface denaturation can also be obtained.

The adsorption of proteins at interfaces can be considered to occur in three main stages :

(i) diffusion of the native protein molecules to the interface and their adsorption in the globular form ;

(ii) surface denaturation of the adsorbed globular protein, involving an unrolling of the polypeptide chains at the interface and hence a great increase in the asymmetry of the molecule ;

(iii) aggregation of the unrolled polypeptide chains into a coagulum largely devoid of surface activity, and consequently forced out of the interface by the spreading pressure of the native protein undergoing surface denaturation.

In some circumstances, depending upon the conditions, particularly the surface energy of the interface, either (iii) or both (ii) and (iii) may be absent.

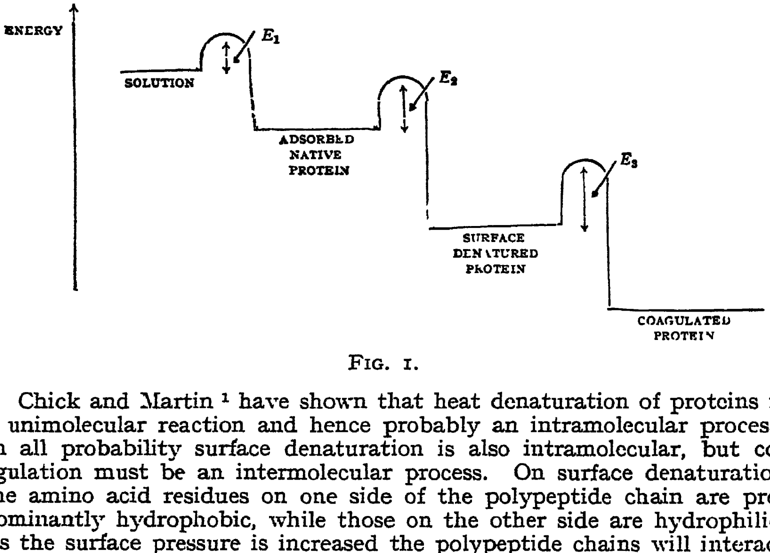

FIG. 1.

Chick and Martin [1] have shown that heat denaturation of proteins is a unimolecular reaction and hence probably an intramolecular process. In all probability surface denaturation is also intramolecular, but coagulation must be an intermolecular process. On surface denaturation the amino acid residues on one side of the polypeptide chain are predominantly hydrophobic, while those on the other side are hydrophilic. As the surface pressure is increased the polypeptide chains will interact with one another laterally, principally through hydrogen and salt bonds, and parts of the chains will be forced out of the interface. As still more protein becomes surface denatured this interaction between the unfolded chains will tend to form a three-dimensional coagulum with most of the polar groups in its interior and therefore having a low surface activity. Schulman and Rideal [2] found that *spread monolayers* of egg albumin cannot be heat coagulated, whereas both native protein [3, 4, 5] and heat-denatured protein [6] can be coagulated by shaking, the reaction occurring at the interface. This is easily explained if a three-dimensional structure is necessary for coagulation to occur. Wu and Ling [3] and Bull [7] report that the temperature coefficient of surface coagulation is much less than that of heat coagulation,[8] which is clearly in agreement with the above theory, since at an interface the polypeptide chains are already approximately aligned in one dimension. From an energy viewpoint the apparent energy of activation E_3 for the transition from the surface denatured to the coagulated state is probably much greater than for either of the other stages of adsorption, the energy diagram for adsorption being shown in Fig. 1, where $E_3 \gg E_2 > E_1$. We see from this diagram that a surface may act as a " catalyst " for protein coagulation, enabling a process with a high critical increment to proceed through a series of consecutive reactions each involving a lower energy barrier.

---

[1] *J. Physiol.*, 1911, **43**, 1.

[2] *Biochem. J.*, 1933, **27**, 1581.

[3] Wu and Ling, *Chinese J. Physiol.*, 1927, **1**, 407.

[4] Wu and Wang, *J. Biol. Chem.*, 1938, **123**, 439.

[5] Bull and Neurath, *ibid.*, 1937, **118**, 163.

[6] Bull, *ibid.*, 1938, **125**, 585.

[7] *Cold Spring Harb. Symp. Quant. Biol.*, 1938, **6**, 140.

From the above considerations coagulated protein should possess a certain degree of crystallinity with the polypeptide chains lying more or less parallel, in agreement with the X-ray studies of Astbury, Dickinson and Bailey [9] on heat-denatured albumins. When coagulation occurs the surface-denatured chains have to move relative to one another to give this partially oriented structure and enable the hydrogen and salt bonds to be formed. We therefore expect that anything which assists this process will increase the rate of coagulation.

Experimental

The viscosity and elasticity of the adsorbed films were measured with the same apparatus as used for spread monolayers (see Part I). In addition to the phosphate and acetate buffers used in Part I, it was found necessary to use unbuffered mixtures of HCl and NaCl below pH 3·7. Unless stated otherwise the ionic strength was 0·03, temperature 25° C and protein concentration 0·01 %. The proteins used were bovine β-globulin (Armour & Co.), insulin (two samples, Messrs. Boots and Armour & Co.), and pepsin (Armour & Co.). In addition polyacrylic and polymethacrylic acids (I.C.I. Ltd.) were studied for comparison with the proteins.

Results and Discussion

(i) EFFECT OF INTERFACE AND PROTEIN CONCENTRATION.—Two concentrations (0·01 % and 0·001 %) of bovine β-globulin were studied at pH 7·0, using three oil-water interfaces of very different character, namely white oil, white oil + 5 % oleyl alcohol, and tricresyl phosphate. The results (Fig. 2) show that when 5 % oleyl alcohol is added to white oil, thereby reducing the interfacial tension from 48 to 15·3 dynes/cm., the surface viscosity (and elasticity) of the adsorbed protein film is also reduced considerably and attains its maximum value much more rapidly. At a tricresyl phosphate-water interface (interfacial tension about 2 dynes/cm.) the surface viscosity and elasticity were both much greater than expected, and it seemed possible that the protein was reacting chemically with traces of free cresol in the oil phase. The protein concentration did not have such a marked effect as the nature of the interface, the values of the properties measured at the two concentrations, when plotted as a function of time, being approximately parallel to each other after adsorption for about 15 min.

(ii) EFFECT OF pH.—From the above results it was decided to use as oil phase the white oil + 5 % oleyl alcohol mixture (interfacial tension *ca.* 15·3 dynes/cm.), and a protein concentration of 0·01 %, for studying the effect of pH on adsorption. Fig. 3 and 4 show the results obtained at this interface for the adsorption of β-globulin and pepsin after 2 hr. Insulin was very similar to pepsin, the surface viscosity and elasticity rising to a fairly sharp maximum in the isoelectric zone with both proteins. β-Globulin, however, gave a rather blunt maximum at pH 3, three units below its isoelectric point. As was found with spread monolayers (Part I) no elasticity was detectable until the films had a viscosity of about one surface poise. The lowering of the interfacial tension produced by the adsorbed protein passed through a maximum near its isoelectric point in each case as found in previous investigations.

These results indicate that the isoelectric point of insulin lies between pH 5·0 and 5·4 and pepsin between pH 3·0 and 3·3. The isoelectric point of the insulin

---

[8] Lewis, *Chem. Rev.*, 1931, **8**, 81.

[9] *Biochem. J.*, 1935, **29**, 2351.

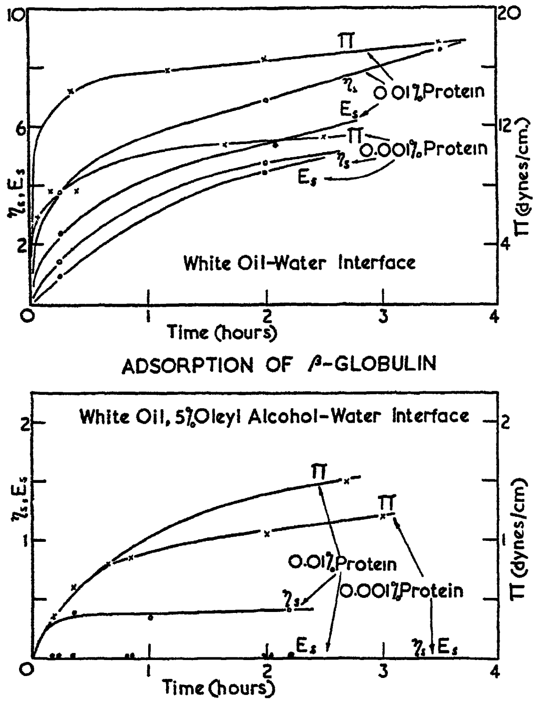

FIG. 2.—The adsorption of bovine β-globulin at the white oil-water and white oil, 5 % oleyl alcohol-water interfaces. Surface pressure π, interfacial viscosity η_s and elasticity index E_s as a function of time at two protein concentrations.

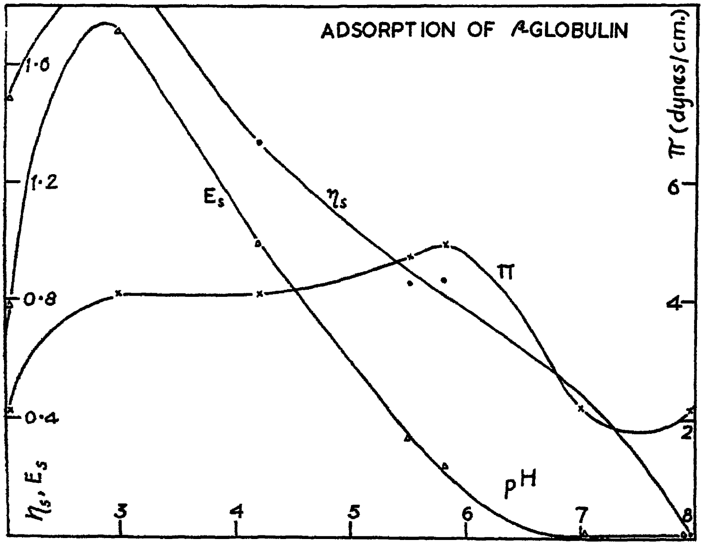

FIG. 3.—The adsorption of boving β-globulin at a white oil, 5 % oleyl alcohol-water interface. π, η_s and E_s as a function of pH.

was found to be pH 5·0 by electrophoretic measurements (to be published), and pepsin is reported either as having an isoelectric point at pH 2·8 [10, 11] or as being negatively charged right down to pH 1·0.[12, 13, 14]

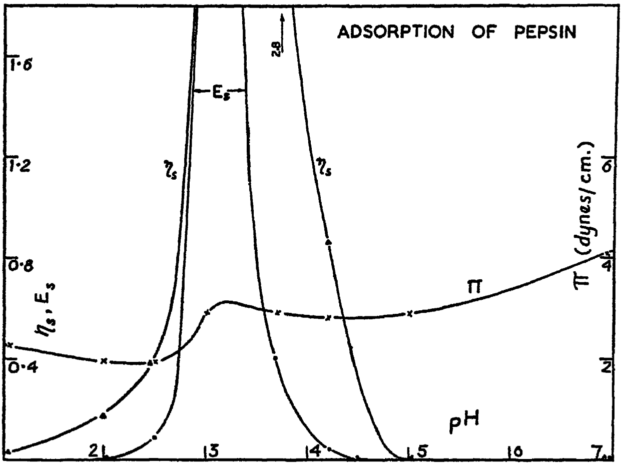

FIG. 4.—The adsorption of pepsin at a white oil, 5 % oleyl alcohol-water interface. π, η_s and E_s as a function of pH.

The adsorption from aqueous solution of the polymers, polyacrylic acid and polymethacrylic acid, was examined at a white oil interface, as their interfacial tension concentration curves for adsorption at the white oil + 5 % oleyl alcohol interface showed that little adsorption was occurring. From these results, and also from their effect on the mobility of a paraffin wax suspension, it was decided to use a concentration of 0·5 % for the polyacrylic and 0·1 % for the polymethacrylic acid. The lowering of the interfacial tension produced by both polymers (Fig. 5) increased as the pH of the aqueous phase was decreased,

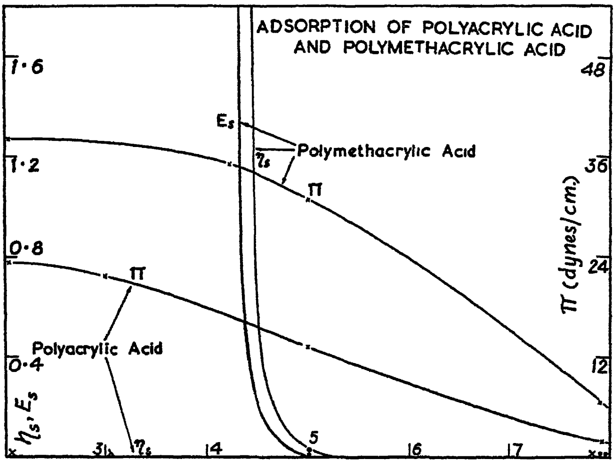

FIG. 5.—The adsorption of polyacrylic acid and polymethacrylic acid at a white oil-water interface. π, η_s and E_s as a function of pH.

---

[10] Northrop, *J. Gen. Physiol.*, **13**, 739, 767.

[11] Ågren and Hammersten, *Enzymologia*, 1937, **4**, 49.

[12] Tiselius, Henschen and Svensson, *Biochem. J.*, 1938, **32**, 1814.

[13] Northrop, *Crystalline Enzymes*, (New York, 1939).

[14] Herriot, Desreux and Northrop, *J. Gen. Physiol.*, 1940, **23**, 439.

but whereas the polyacrylic acid gave no surface viscosity over the pH range 2·0 to 8·0, the polymethacrylic acid showed a sudden increase from zero to a large value over the pH range 4·75 to 4·25. Polymethacrylic acid is more surface active than polyacrylic acid and an examination of molecular models shows that the difference in behaviour may also be due to the greater rigidity of the polymer chain in methacrylates.

(iii) Effect of Time at Constant pH.—Some typical curves showing the changes in surface viscosity, elasticity and surface pressure with time are shown in Fig. 6. Although over the pH range studied the variation of interfacial tension with time does not depend appreciably on pH, the surface viscosity and elasticity of the films do and are therefore more valuable criteria of the state of the film. After 2 hr. adsorption most of the curves have attained their

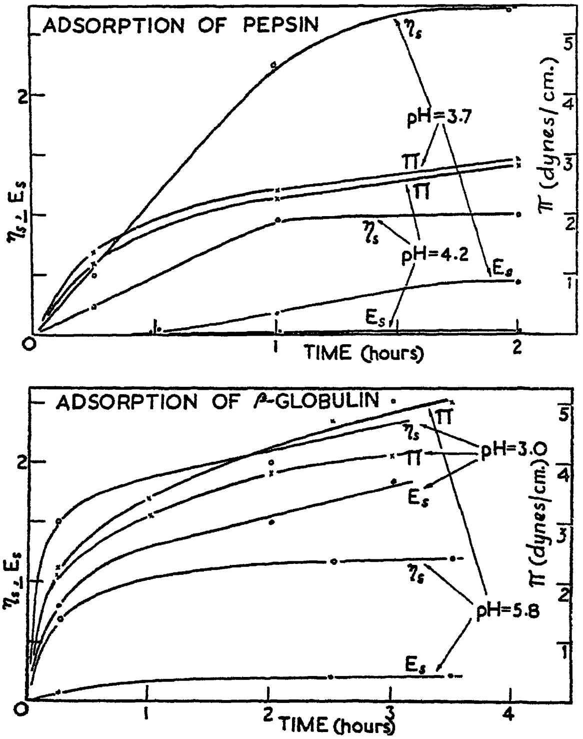

Fig. 6.—The adsorption of pepsin and bovine β-globulin at a white oil, 5 % oleyl alcohol-water interface. π, η_s and E_s as a function of time at two pH's.

maximum values, and it was for this reason that the effect of pH upon the surface viscosity and elasticity was studied after this time interval in the previous section. The results obtained for insulin were similar to those for pepsin, except in the region of its isoelectric point (pH 5·0) where the viscosity developed much more rapidly. At pH 5·5 for example, the surface viscosity and elasticity were too large to measure accurately (> 8 surface poises) after only 15 min. adsorption. The surface pressure, however, developed at the usual rate to a value of 6·2 dynes/cm., as compared with 5·6 dynes/cm. at pH 3·5 and 5·4 dynes/cm. at pH 7·5.

(iv) Effect of Ionic Strength and Temperature.—The effect of ionic strength and temperature upon the adsorption of pepsin at pH 3·7 was studied. Dilute acetate buffers alone were used to give the lower ionic strengths (0·003 and 0·03) and for the higher ionic strength (0·30) a mixture of acetate buffer (ionic strength 0·03) and salt (NaCl) since the surface activity of acetic acid is appreciable at high concentrations. From the effect of time upon the surface viscosity of adsorbed pepsin (Fig. 7) we see that by increasing the ionic strength

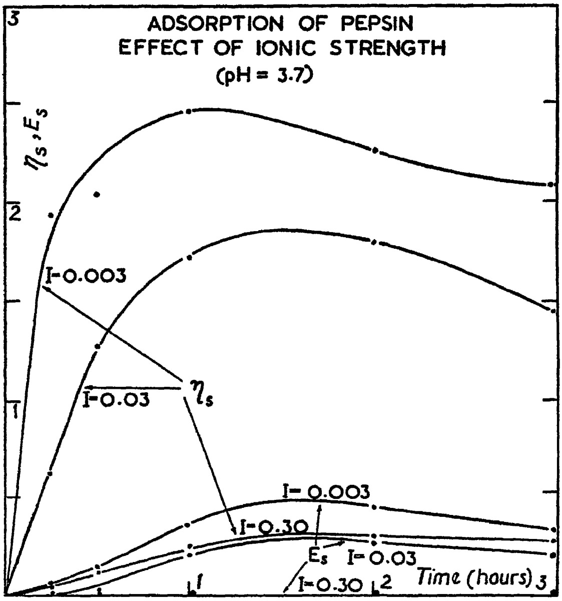

FIG. 7.—The adsorption of pepsin at a white oil, 5 % oleyl alcohol-water interface at pH 3·7. η_s and E_s as a function of time at three ionic strengths.

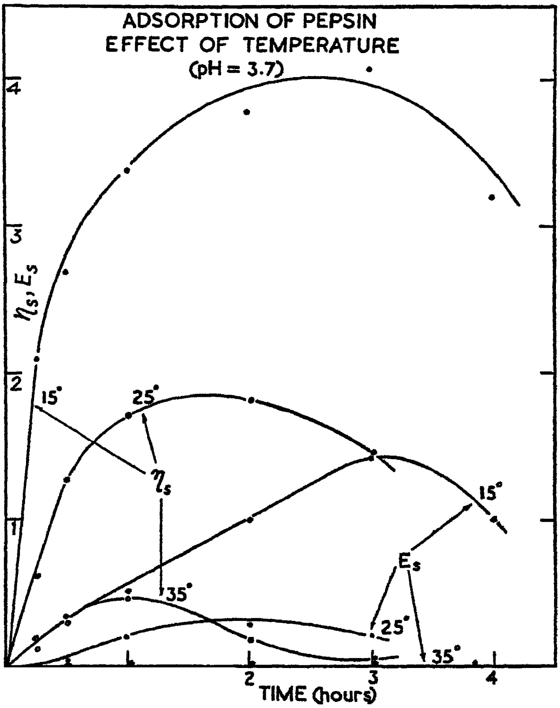

FIG. 8.—The adsorption of pepsin at a white oil, 5 % oleyl alcohol-water interface at pH 3·7. η_s and E_s as a function of time at three temperatures.

:e viscosity is reduced considerably and the time taken for it to reach its aximum value is increased.

Increasing and decreasing the temperature by 10° C also resulted in marked ıanges in the surface viscosity-time curves (Fig. 8). The lower the tem- ›rature the larger was the viscosity and the longer the time necessary for it › reach its maximum value.

The Apparent Thickness of Adsorbed Protein Films.—From the surface scosity of spread monolayers of proteins reported in Part I it is possible, after .aking certain assumptions, to estimate the thickness of films of the same roteins formed by adsorption from solution. The surface viscosity of the .onolayer is first plotted against its thickness, the latter being calculated irectly from the area occupied by the protein and its density. Using these ›sults we can now find the apparent thickness of the *adsorbed* films. Two ssumptions are necessary :

(*a*) that the surface viscosity is independent of the interfacial energy,

(*b*) that the structure of the spread monolayers and adsorbed films are essentially the same.

The first assumption is a reasonable one ; the second, however, will only be trictly true for the protein that has been completely surface denatured on ad- orption. Adsorbed films will probably contain, in addition to these fully nfolded molecules, some native protein, but the latter's contribution to the urface viscosity will be small, owing to its corpuscular shape. Surface- enatured protein which has aggregated into a coagulum will, because of its ›w surface activity, be largely displaced from the surface and hence make little r no contribution to the surface viscosity. The thickness of the adsorbed lms as calculated above should therefore give a reasonable indication of the hickness of the surface-denatured protein.

The thickness of adsorbed films found by deposition on prepared plates [15] ‚ill include that of the adsorbed native and coagulated protein, while du Noüy's ıethod [16] from surface tensions is based upon the rather unlikely assumptions hat all the protein in solution is adsorbed and that the same amount of protein s adsorbed per unit area at the protein solution-air interface as at the protein olution-glass interface.

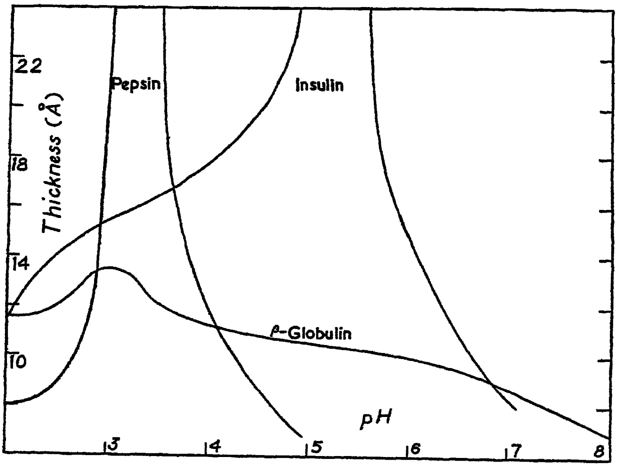

FIG. 9.—Apparent thickness of adsorbed protein films at a white oil, 5 % oleyl alcohol-water interface as a function of pH.

(i) EFFECT OF pH. The apparent thickness of films of β-globulin, pepsin and insulin, adsorbed for 2 hr. at the white oil + 5 % oleyl alcohol-water interface, are shown in Fig. 9 as a function of pH. Pepsin passes through a sharp maximum at about pH 3·2 when the thickness is more than 30 Å, falling to less than 8 Å on either side. Insulin also gives quite a sharp maximum and

[15] E.g. Blodgett, *Physic. Rev.*, 1939, **55**, 391.

[16] *Surface Equilibria of Biological and Organic Colloids* (Chem. Catalog Co., New York, 1926).

the thickest film of the three proteins. β-Globulin films rather surprisingly are never thicker than 13·5 Å under the conditions employed here. This might be explained by surface-denatured films of β-globulin coagulating more rapidly than the other proteins—actually it is doubtful whether insulin can be considered to coagulate at all.

The surface-denatured part of the adsorbed films of these proteins therefore seems to be never more than three or four polypeptide chains thick. If all the protein in solution had been adsorbed the total thickness of the films would have been about 1 μ (i.e. *ca.* 1000 layers), so it is clear that the process does not come to a halt for lack of protein.

(ii) Effect of Ionic Strength and Temperature. In Part I it was reported that the viscosity of spread monolayers of pepsin was independent both of ionic strength and of temperature, and so the results obtained with adsorbed films (Fig. 7 and 8) must presumably be due to changes in the thickness of the surface-denatured pepsin film. The apparent thicknesses calculated from these results are shown in Fig. 10. A layer 7 Å thick is built up in about 4 min. in each case, and it is only after this, when a second layer is forming, that differences appear. This is substantiated by the effect of pH and nature of the interface upon the apparent thickness. Bull,[17] by means of his roller technique, found that when the rate of diffusion to the air-water interface did not control the rate of the reaction, surface-denaturation occurred in less than 0·785 sec. Neurath[18] on the other hand found that a protein film continued to expand slowly for about 7 min. on dilute buffer.

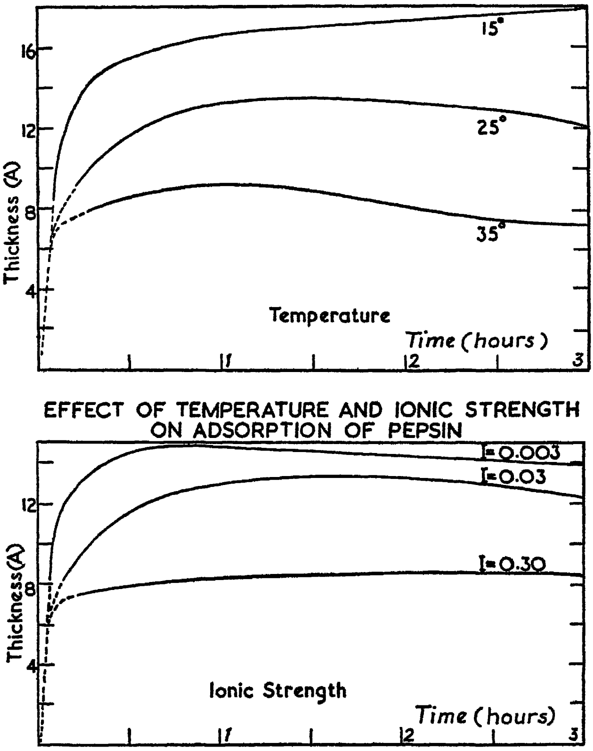

Fig. 10.—Apparent thickness of adsorbed pepsin films at a white oil, 5 % oleyl alcohol-water interface (pH 3·7) as a function of time at three temperatures and three ionic strengths.

---

[17] *J. Biol. Chem.*, 1938, **123**, 17.

[18] *J. Physic. Chem.*, 1936, **40**, 361.

According to the diffusion equation

$$n = 2n_0\sqrt{Dt/\pi},$$

where n_0 is the number of molecules/ml. in the solution and n the number/sq. cm. of surface, this first layer 7 Å thick should have been built up in 0·8 sec. if every molecule diffusing to the interface was surface-denatured immediately. The results indicate that on the average only about 1 in 17 did so during the first 4 min. If this is ascribed solely to an energy barrier between the globular and surface-denatured states, then its value would be about 750 cal., i.e. quite small. The conditions under which further denaturation occurs are completely different, depending on the state of the protein that has already been adsorbed.

An increase in the ionic strength of the solution will reduce the electrical forces between the protein molecules and thus have two main effects upon the adsorption. Firstly, the reduced force between the adsorbed pepsin at the interface and native molecules underneath will weaken the deforming forces tending to unfold the native protein. Secondly, and probably the more important factor, the forces between the surface-denatured chains will be reduced and so the rate of coagulation will be increased. The result of both these effects will be that the apparent thickness of the adsorbed films will be less the higher the ionic strength, and so provides a possible explanation of the experimental observations. The effect of salts upon the rates of denaturation and coagulation reported in the literature is rather confused and contradictory, due often to differences in the relative rates and extents of the two stages under different experimental conditions, as well as to inadequate pH control. In general it seems that with salt concentrations less than about 2N the rate of coagulation of denatured protein is increased (e.g. for heat coagulation,[19] surface coagulation[3]). Anson and Mirsky [20] found that the bulk viscosity of a protein solution increased on heat denaturation and increased further when salt was added until coagulation occurred.

In a similar way it seems probable that an increase in temperature will increase the rate of coagulation considerably, while having only a much smaller effect on the rate of adsorption and surface-denaturation, and hence the apparent thickness of the adsorbed films will be reduced. The thickness will also reach its maximum value more rapidly as found experimentally.

Stabilization of Emulsions.—As is well known, adsorbed proteins will stabilize oil-in-water emulsions. The following experiments were carried out in this connection.

TABLE I.—TIME OF SEPARATION OF EMULSION

Oil	Interfacial Tension (dyne/cm.)	No γ-globulin	0·01 % γ-globulin	0·00001 % γ globulin
White oil	48	1 min.	> 24 hr. (practically no change at the end of this period)	3 min.
White oil saturated with cetyl alcohol	27	¾ min.	Three main drops of oil separated by visible protein skins after four hours	1 min.
Oleyl alcohol	12	2 min.	3 min. (visible skin at interface)	2 min.

4 ml. of the oil were placed in a stoppered test-tube and a solution of the protein (about 16 ml.) in dilute buffer added so that all the air was excluded from the tube. In this way no denaturation of the protein at the air-water interface could occur. Three tubes containing (1) no protein, (2) 0·01 % protein and (3) 0·00001 % protein, were shaken simultaneously for 5 min. and the stability of the emulsion formed, as indicated by the time of separation, noted. Using bovine γ-globulin at pH 7·0 the results shown in Table I were obtained.

[19] Lepeschkin, *Biochem. J.*, 1922, **16**, 678.

[20] *J. Gen. Physiol.*, 1932, **15**, 341.

These results fit in well with the interfacial tension measurements on the same systems (to be published). There is practically no stabilization of the emulsion when the protein concentration is 0·00001 % due to the fact that there is not a complete film of γ-globulin at the interface. With a 0·01 % concentration of protein the degree of stabilization decreases as the interfacial tension of the oil-water interface alone decreases. The stabilization of these emulsions by the γ-globulin is due primarily to the mechanical properties of the denatured protein film and not to the lowering of the interfacial tension.[21] When insulin was used instead of bovine γ-globulin the results shown in Table II were obtained.

TABLE II

pH	Oil	Interfacial Tension (dyne/cm.)	No Insulin	0·01 % Insulin	0·00001 % Insulin
7·0	White oil	48	½ min. (Very little emulsification)	1¼ min. (Little emulsification but different from the other tubes)	¼ min. (Very little emulsification)
	White oil + 0·05 % oleyl alcohol	27	1 min.	1 min.	1 min.
	White oil + 5 % oleyl alcohol	14	1 min.	1 min.	1 min.
5·0	White oil	48	1¼ min.	Few droplets after 2 hr.: very few after 20 hr. Much better emulsification than at pH 7·0	1¼ min.
	White oil + 5 % oleyl alcohol	14	1 min.	Few droplets after 1½ hr.	1 min.

These results offer further proof that the stabilization is due to mechanical protection. Insulin does not form visible denatured skins at oil-water interfaces and is a very poor stabilizer. The surface viscosity of adsorbed insulin films is found to be much greater at pH 5·0 than at 7·0, and hence we would expect it to be a more efficient stabilizer, as found experimentally. The lowering of interfacial tension produced by the adsorbed insulin is practically the same at pH 5·0 as at 7·0.

The effects of ionic strength and temperature upon the stability of emulsions were also investigated, using a 0·01 % solution of pepsin at pH 3·7, and white oil + 5 % oleyl alcohol as the oil phase. An increase in ionic strength (0·003-0·3) or temperature (15° C-35° C) caused the emulsion to break more rapidly, a coagulated skin being formed, and over the range examined the former appeared to exert the greater influence. These findings are seen to be in good accord with the predictions made above from the studies of the thickness of the adsorbed films.

We should like to thank the following: Armour & Co., Boots Ltd., I.C.I. Ltd., and Dr. C. E. Dalgleish for gifts of the chemicals used in these investigations, and the Department of Scientific and Industrial Research for financial assistance to one of us (C. W. N. C.)

Department Colloid Science,
Cambridge.

---

[21] Alexander, *J. Oil Colour Chem. Assoc.*, 1949, 32, 51.

THE RELATIVE STRENGTHS OF BASES IN DIOXAN-WATER MIXTURES

By J. C. James and J. G. Knox

Received 15*th August*, 1949; *as revised* 4*th November*, 1949

Measurements of base strength are reported for *p*-toluidine, aniline, *p*-chloroaniline and *m*-nitroaniline in dioxan-water mixtures at 25° C. The effect of a substituent on the variation in relative strength with change in medium is that which is to be expected from the dipole moment of the substituent and the dielectric constant of the medium. Values of the acidity function H_0 have been derived for solutions of hydrogen chloride in dioxan water mixtures, and provide information as to the extent to which this quantity is dependent on the nature of the indicator base used.

Measurements of dissociation constants for conjugate acids of organic bases in mixed solvents are of interest in connection with acid strength and its dependence on solvent nature. Existing results are scanty, however, and relate mainly to media of high dielectric constant. In the present paper, pK_A measurements are reported for *p*-toluidine, aniline, *p*-chloroaniline and *m*-nitroaniline; these primary amines have widely differing constants in water, and may conveniently be studied down to a dielectric constant of about 10 in dioxan–water mixtures. Determinations have been made by conductimetric methods in preference to potentiometric titration, as it has been stated that the glass electrode becomes subject to errors in mixed solvents in which the proportion of water is small.[1, 2]

Experimental

MATERIALS. The amines and amine hydrochlorides used were purified by standard methods. 1 : 4-Dioxan was purified by prolonged refluxing with sodium, and distillation[3]

MEASUREMENTS. Conductivities were determined by means of a screened A.C. bridge, based on the designs given by Jones and Josephs,[4] and by Shedlovsky,[5] the precautions recommended by these authors for minimizing effects due to the inductance and capacity of various parts of the bridge network being followed. Temperature control was maintained by an oil filled thermostat at 25 ± 0·005° C; measurements were made at frequencies of 1000 and 3000 c./sec. A dipping electrode cell of the Hartley and Barrett type was used, standardization being effected using Jones and Bradshaw's 0·01 M potassium chloride solution.

For *p*-toluidine, aniline and *p*-chloroaniline, the method of Bredig[6] was used. Appropriate quantities of dioxan and water were weighed into the cell and the resistance of the solvent was determined; a suitable amount of amine hydrochloride was added and the resistance redetermined. Weighed additions of

---

[1] Goodhue and Hixon, *J. Amer. Chem. Soc.*, 1934, **56**, 1329.

[2] Dole, *The Glass Electrode*, p. 140.

[3] Kraus and Vingee, *J. Amer. Chem. Soc.*, 1934, **56**, 513.

[4] Jones and Josephs, *ibid.*, 1928, **50**, 1049.

[5] Shedlovsky, *ibid.*, 1930, **52**, 1793.

[6] Bredig, *Z. physik. Chem.*, 1894, **13**, 289.

the base were then made, resistance measurements being taken after each addition. Bredig has shown that the degree of hydrolysis of the amine hydrochloride is given by

$$x = (\Lambda - \Lambda_S)/(\Lambda_A - \Lambda_S),$$

where Λ is the observed conductivity of the hydrochloride solution, Λ_A the conductivity of HCl and Λ_S that of the unhydrolyzed salt all at a molar concentration c. Λ_A may be obtained from the data of Shedlovsky,[7] and of Owen and Waters;[8] Λ_S is obtained by the addition of sufficient free base to repress hydrolysis completely, the conductivity of the added weak base being negligible in presence of the salt. Then the conjugate acid dissociation constant is given by

$$K_A = \frac{[B][SH^+]}{[BH^+]} \cdot \frac{f_B f_{SH^+}}{f_{BH^+}},$$

where f's represent activity coefficients. Since f_B and f_{SH^+}/f_{BH^+} are effectively unity,

$$K_A = \frac{[B][SH^+]}{[BH^+]} = \frac{x^2c}{(1-x)}.$$

Slight changes in viscosity and dielectric constant are caused by addition of the base; measurements of the decrease in conductivity caused by the addition of amines to solutions of KCl in dioxan water mixtures indicate that for concentrations up to 0·05 M, the decrease is approximately given by $\Delta\Lambda = 0{\cdot}01m\Lambda$, where m is the molar concentration of the base. Values for Λ_S have accordingly been corrected on this basis; the correction is small, and normally corresponds to a possible error of less than 0·01 pK unit. Slight hydrolysis exists even after the addition of free base, and allowance has been made for this by the use of a method of successive approximations as to the value of pK_A. This correction, although negligible with *p*-toluidine, becomes appreciable with weaker bases, and corresponds to errors of the order of 0·1 pK unit with *p*-chloroaniline. The conductivity of the water used was normally about 2 gemmhos; measurements were made at concentrations of the order of 0·01-0·02 M, to minimize the uncertainty necessarily involved in solvent corrections. The results for a typical run are given in Table I in which

TABLE I.—THE HYDROLYSIS OF ANILINE HYDROCHLORIDE IN WATER AT 25° C

c_1 (g. equiv./l.)	c_2 (g. equiv./l.)	Λ	Λ_S	Λ_S (corrected)	Λ_A	x	pK_A
0·008027	0·01884	120·20	104·00	103·70	413·22	0·0533	4·618

c_1 is the aniline hydrochloride concentration and c_2 the concentration of added free aniline. The value obtained for Λ_S after correction for viscosity changes and incomplete repression of hydrolysis, is given in col. 5.

The complete results are summarized in Table II, each pK_A value being the mean of at least two independent determinations. The results obtained in water are in good agreement with accepted values from the literature and the accuracy, ± 0·01 pK unit, is of the same order as that obtained from the potentiometric titration method.

As *m*-nitroaniline is too weakly basic for the Bredig method to be applied, recourse has been made to a modification of the conductimetric method used by Pearson and Tucker[16] for the study of very weak bases. The resistance

---

[7] Shedlovsky, *J. Amer. Chem. Soc.*, 1932, **54**, 1411.

[8] Owen and Waters, *ibid.*, 1938, **60**, 2371.

[9] Hall and Sprinkle, *ibid.*, 1932, **54**, 3472.

[10] Hall, *ibid.*, 1930, **52**, 5115.

[11] Pring, *Trans. Faraday Soc.*, 1923, **19**, 705.

[12] Bronsted and Duus, *Z. physik. Chem.*, 1925, **117**, 299.

[13] Flexser, Hammett and Dingwall, *J. Amer. Chem. Soc.*, 1935, **57**, 2103.

[14] Pedersen, *Kgl. Danske Vidensk. Selskab*, 1937, **14**, 9.

[15] Philpot, Rhodes and Davies, *J. Chem. Soc.*, 1940, 84.

[16] Pearson and Tucker, *J. Amer.Chem. Soc.*, 1949, **71**, 749.

R_A of a solution of HCl in the mixed solvent was measured ; successive weighed additions of the base were then made, the solution resistance R being measured after each addition. If x is the fraction of base remaining uncombined,

$$x = (\Lambda - \Lambda_S)/(\Lambda_A - \Lambda_S) = R_A(R_\infty - R)/R(R_\infty - R_A),$$

where R_∞ is the resistance of the unhydrolyzed salt solution. Also,

$$K = x(a - xb)/(1 - x),$$

where a is the stoichiometric concentration of added base and b the initial HCl concentration, in mole/l. A value for R_∞ was selected, by a trial and error process, to give a dissociation constant which did not vary with concentration,

TABLE II.—DISSOCIATION CONSTANTS IN DIOXAN WATER MIXTURES

% Dioxan (w/w)	*p*-toluidine pK_A	Aniline pK_A	*p*-chloroaniline pK_A
0	5·11 [5·07,[9] 5·12[10] 5·12[11], 5·07[12]]	4·62 [4·58,[9] 4·64[6] 4·64[13], 4·59[11]]	4·00 [4·00[12], 4·00[1] 4·04[15]]
20	4·92	4·44	3·65
45	4·54	4·01	3·08
70	4·16	3·58	2·68
82	4·06	3·42	2·56

% Dioxan (w/w)	*m*-nitroaniline pK_A	% Dioxan (w/w)	*m*-nitroaniline pK_A
0	[2·60[17]]	50	1·38
20	2·08	60	1·13
30	1·83	70	1·03
40	1·60	82	1·03
45	1·44	—	—

this being taken as the correct value. The method is illustrated by the following figures obtained for a 60 % dioxan-water mixture.

TABLE III.—*m*-NITROANILINE IN 60 % DIOXAN-WATER
Hydrogen chloride 0·009774 M R_∞ 950 ohms

Total Base Added (mole/l.)	R (ohm.)	x	pK
—	296·6	-	
0·01180	324·6	0·8748	1·132
0·01480	330·7	0·8501	1·121
0·02863	360·9	0·7410	1·127
0·03620	376·2	0·6925	1·126
0·04356	390·6	0·6500	1·128
0·05301	409·3	0·5998	1·133
			Av. 1·

The results are summarized in Table III, resistance values having been corrected as before for viscosity and dielectric constant changes caused by base addition. The low solubility of *m*-nitroaniline in water has restricted measurements to mixtures containing not less than 20 % w/w of dioxan, and for aqueous *m*-nitroaniline solutions the value $pK_A = 2·60$ given by Bryson [17] has therefore been used. All dissociation constants given have been converted to the molality basis by increasing pK_A ($= -\log K_A$) by $\log d$, where d is the density of the solvent.

---

[17] Bryson, *Trans. Faraday Soc.*, 1949, **45**, 257.

Discussion

Changes in the relative strengths of acids and bases with change in solvent have been interpreted by Wynne-Jones [18] in terms of a theory which predicts a linear relationship, $\log K_R \alpha - 1/\epsilon$ (where K_R is the ratio of the dissociation constants of two acids, and ϵ is the dielectric constant of the solvent). Although the investigations of Kilpatrick and co-workers,[19, 20, 21] and of Wooten and Hammett,[22] indicate that in pure solvents the relationship is approximately followed down to a dielectric constant of about 25, Elliot and Kilpatrick,[23] and Harned [24] find that the relationship breaks down with mixed solvents such as dioxan-water. This failure of the Wynne-Jones relationship has been ascribed [23] to a preferential orientation of dioxan molecules around the solute, causing a lower dielectric constant in the vicinity of the acid molecules.

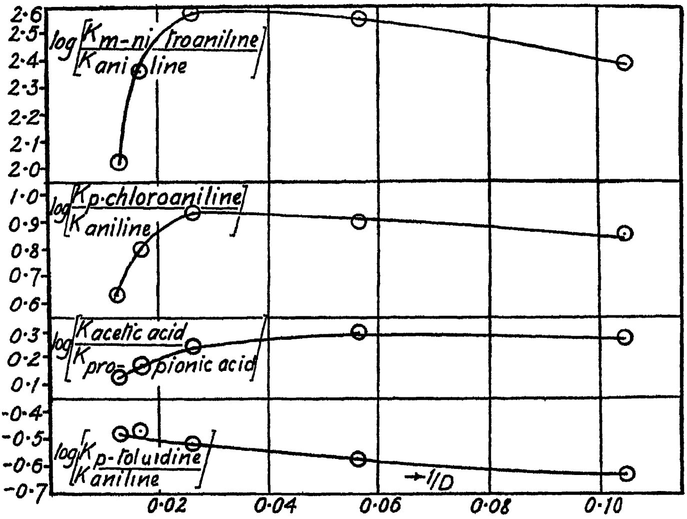

FIG. 1.—Variation of the logarithms of dissociation constants ratios with dielectric constant.

For cation acids of the type BH^+, Mason and Kilpatrick [25] have stated that no correlation with Wynne-Jones' relationship can be found from available data in pure solvents, and the present work indicates that this is also the case for dioxan-water mixtures. In Fig. 1, $\log K_R$ values obtained from the present work have been plotted against $1/\epsilon$; corresponding values given by Harned [26] for acetic and propionic acids are plotted for comparison. Marked curvature occurs at low dielectric constants, and it would appear that cation acids resemble uncharged acids in this respect.

The ionization of a cation acid is governed by the equilibrium

$$BH^+ + S = B + SH^+,$$

where BH^+ represents the conjugate acid of the base, and SH^+ the solvated proton. As the reaction involves a proton shift but not the creation of a new field, the variation in dissociation constant with dielectric constant may be expected to be relatively slight compared to that for an uncharged acid, for which the ionization reaction

---

[18] Wynne-Jones, *Proc. Roy. Soc. A*, 1933, **140**, 440.

[19] Minnick and Kilpatrick, *J. Physic. Chem.*, 1939, **43**, 259.

[20] Kilpatrick and Mears, *J. Amer. Chem. Soc.*, 1940, **62**, 3047, 3051.

[21] Elliot and Kilpatrick, *J. Physic. Chem.*, 1941, **45**, 454, 466, 472.

[22] Wooten and Hammett, *J. Amer. Chem. Soc.*, 1935, **57**, 2289.

[23] Elliot and Kilpatrick, *J. Physic. Chem.*, 1941, **45**, 485.

[24] Harned, *The Physical Chemistry of Electrolyte Solutions*, Chap. 15.

[25] Mason and Kilpatrick, *J. Amer. Chem. Soc.*, 1937, **59**, 572.

$$BH + S = SH^+ + B^-$$

involves both a proton shift and the creation of a new field. Thus, in the present work, passing from water to 70 % dioxan caused the conjugate acid of aniline to become approximately 1 pK unit stronger, whereas from the data of Harned,[24] an uncharged acid such as acetic acid, becomes about 4 pK units weaker. The increase in acidity thus shown by cation acids has been taken by Braude and Stern[26] to indicate that the proton affinity of water is greater in dioxan-water mixtures than in water.

It is perhaps unlikely that variation in the relative strengths of closely related acids should be dependent merely upon differences in ionic size, as is implied by the Wynne-Jones treatment, and an alternative explanation has been advanced by Schwarzenbach and Egli.[27] The additional work required to ionize a cation acid containing a substituent polar group, as compared with the unsubstituted acid, in a solvent of dielectric constant ϵ is given by

$$\Delta W = e\mu \cos \theta / \epsilon r^2,$$

where r is the distance from the dipole to the $-NH_3^+$ group, $\mu \cos \theta$ is the component of the dipole along r, and e is the charge on the ion. When an increase in ionization is caused by substitution, ΔW is negative in sign and an increase in strength relative to the unsubstituted acid should result on changing to a solvent of lower dielectric constant. The present work indicates that the extent of the increase in acidity which occurs on passing from water to a mixed solvent of lower dielectric constant is in the order *p*-toluidine < aniline < *p*-chloroaniline < *m*-nitroaniline (Table II). The corresponding dipole moments for these amines are 1·31,[28] 1·505,[29] 2·994,[30] and 4·25,[28] and thus substituents which cause an increase in absolute strength cause an increase in strength relative to the anilinium ion with decrease in dielectric constant, in accordance with the above theory. (Schwarzenbach and Egli [27] have emphasized that these considerations only apply to distantly substituted acids and are not adequate when the substituent is adjacent to the acidic group.)

The concept of acidity function H_0 has been introduced by Hammett,[31] and gives a quantitative measure of the tendency of a solution to donate a proton to a neutral base. The function may be defined by

$$H_0 = \log \frac{[B]}{[BH^+]} - \log K_A^{H_2O},$$

where $K_A^{H_2O}$ is the conjugate acid dissociation constant of an indicator base in dilute aqueous solution, which is taken as a reference state. Thence

$$H_0 = \log K_A^S - \log K_A^{H_2O} - \log [SH^+],$$

where K_A^S is the corresponding indicator constant in solvent S. In a solution containing acid of concentration c mole/l., $[SH^+] = \alpha c$, where α is the degree of dissociation of the acid, and

$$H_0 = pK_A^{H_2O} - pK_A^S - \log \alpha c.$$

The assumption here involved is that the ratio of different indicator constants is independent of the medium. In media of high dielectric constant this assumption is justified as the dissociation constant ratio is governed by an equation of the type [32]

$$\log K_R = a + b/\epsilon,$$

---

[26] Braude and Stern, *J. Chem. Soc.*, 1948, 1076.

[27] Schwarzenbach and Egli, *Helv. chim. Acta*, 1934, **17**, 1176.

[28] Tiganik, *Z. physik. Chem.*, 1931, **13**, 425.

[29] Few and Smith, *J. Chem. Soc.*, 1949, 753.

[30] Few and Smith (in press).

[31] Hammett, *Chem. Rev.*, 1935, **16**, 67.

[32] Hammett, *Physical Aspects of Organic Chemistry*, p. 265.

with values of the coefficient *b* such that the expression is practically constant and equal to *a* when the dielectric constant is of the order of 80 or more. For media of lower dielectric constant this assumption is questionable, however, and it has therefore been tested from the present results. Values of H_0 have been calculated for 0·1 M HCl solutions in dioxan-water mixtures, and are given in Table IV, the necessary values for α having been obtained from the dissociation constant data of Owen and Waters,[8] and the activity coefficient data of Harned.[33] (Braude and Stern[26] have determined acidity functions for similar solutions, using a spectrophotometric technique, with *p*- and *m*-nitroaniline as indicator bases. For comparison, H_0 values have been interpolated from these results and are given in Table III; corresponding results obtained in the present work are substantially higher.) It may be seen that for a given solvent composition, the value obtained for H_0 depends considerably on the nature of the indicator base, as is to be expected, since it has already been shown that $\mathrm{p}K_A^{\mathrm{H_2O}} - \mathrm{p}K_A^S$ is markedly influenced by polar substituents. It would appear that although proton acceptor tendencies of solutions may be compared using a single common indicator base, the values obtained in media of low dielectric constant ($<$ 80) are by no means absolute.

TABLE IV.—ACIDITY FUNCTIONS FOR 0·1 M HCl SOLUTIONS

Dioxan (w/w)	Acidity Function H_0				
	p-toluidine	aniline	*p*-chloroaniline	*m* nitroaniline (present work)	*m* nitroaniline (Braude)[26]
20	1·19	1·18	1·35	1·52	1·26
45	1·58	1·62	1·93	2·17	1·79
70	1·97	2·06	2·34	2·59	2·33
82	2·35	2·50	2·74	2·87	2·38

Harned[24] has emphasized that although dissociation constant ratios are often used for the comparison of acid strengths, the "relative strength" is a function of the medium and of the acids and is not a fixed quantity. The present investigation of cation acid behaviour in mixed solvents lends additional support to this view.

The authors wish to express their thanks to Dr. J. C. Speakman for many useful discussions and for his interest and advice throughout the work.

Chemistry Department,
The University,
Glasgow, W.2.

---

[33] Harned, *The Physical Chemistry of Electrolyte Solutions*, p. 548.

REVIEWS OF BOOKS

Psychical Physics. By S. W. TROMP. (Elsevier Publishing Co. Ltd., and Cleaver-Hume Press Ltd., London, 1949.) Pp. xvi + 534. Price $8.

The author of this book is a geologist, and his purpose in writing it is to discuss such evidence as there is for the objective reality of water-divining and kindred phenomena, and what experiments have in fact been performed in this field. Very appropriately, he is an investigator himself into these matters. He points out that the practice of water-divination has been going on for some seven thousand years, and that all the incredulity exhibited by its detractors has not shaken the confidence of those who have seriously studied it. Whatever else may be said on either side, this is in itself a rather remarkable state of affairs, and indicates the need for great caution on the part of scientists and others who may be inclined to reject the whole subject out of hand. In any event, it will be only prudent to avoid the impression of discarding something as meaningless because in effect it is difficult to reconcile with traditional concepts. Broadly, this is the position taken by Prof. Tromp himself who, wholly correctly, approaches the matter as a sceptic, but not as one with a pre-conceived bias towards discrediting dowsers and all their works. It is perhaps not irrelevant to recollect a remark of that profound philosopher, the late Prof. A. E. Taylor, to the effect that we shall never find something for which we have no interest in looking; in other words, there must be some measure of desire to lay bare a particular "unknown ". Just here lies the value of the present work; the author is critical, but not weighted in favour of negation. His verdict indeed is that dowsing is " real ".

We have now, it seems, reached a more advanced phase of enquiry than is commonly supposed. Quite recent work in Holland (at Leiden and at Delft) has provided a basis of physics and chemistry hitherto sadly lacking. In addition, the Einthoven string galvanometer has played a major part in carefully controlled tests. It looks as if up-to-date methods of detecting very weak electric and magnetic fields—in both animate and inanimate objects—are playing a conspicuous part in demonstrating at least the high plausibility, and possibly the certainty, of a whole host of complex effects to which there is no need to apply the adjective "para-normal". Unusual they may be, but not outside the natural order. One question which always arises concerns the relative scales of magnitude of the effect which is being sought, and that of the disturbances which must always be expected. Obviously the latter are large, necessitating heroic precautions to reduce them, even if they cannot be wholly eliminated.

Yet, it looks, on balance, as if the battle was going in favour of revealing some refinements of our whole being - and those of the world around us—previously either unsuspected or written off as irrational. The importance of all this for psychology and medicine needs no emphasis: indeed even the intractable states of suggestion and hypnotism appear to be in process of being brought under discipline. Physical chemists will note the predominant role played by colloids (and by cataphoresis) in many of the systems investigated.

In brief, the book is a mine of information about all kinds of things, some perhaps a trifle " off the record ". Nevertheless, so much careful scrutiny, and a bibliography of nearly fifteen hundred entries, deserves impartial attention and whole-hearted appreciation.

F. I. G. R.

CORRIGENDA

1919, Vol. 45

P. 1143, eqn. (1)

For $$(\partial^2 G/\partial n_1^2)\,.\,(\partial^2 G/\partial n_2^2)\quad(\partial^2 G/\partial n_1 \partial n_2) = 0 \quad . \quad . \quad (1)$$

Read $$(\partial^2 G/\partial n_1^2)\,.\,(\partial^2 G/\partial n_2^2) - (\partial^2 G/\partial n_1 \partial n_2)^2 = 0 \quad . \quad . \quad (1)$$

P. 1144, line 19—

At end of the paragraph, *for* mixtures.

read mixtures under the above conditions.

P. 1145, eqn. (6)—

For $$(\partial^2 G/\partial y_1^2)\,.\,(\partial^2 G/\partial y_2^2) - (\partial^2 G/\partial y_1 \partial y_2) = 0, \quad . \quad . \quad (6)$$

Read $$(\partial^2 G/\partial y_1^2)\,.\,(\partial^2 G/\partial y_2^2) - (\partial^2 G/\partial y_1 \partial y_2)^2 = 0, \quad . \quad . \quad (6)$$

P. 1148—

The diagrams (but not the legends) of Fig. 4 and Fig. 5 should be interchanged.

A SURVEY OF HEATS OF MIXING OF SOME ORGANIC COMPOUNDS WITH ALUMINIUM CHLORIDE

By M. H. Dilke, D. D. Eley and (Miss) M. G. Sheppard

Received 8th June, 1949; as revised 30th November, 1949

Heats of mixing of aluminium chloride and a number of organic liquids have been measured with an accuracy of 1 kcal. The liquids examined have included aldehydes, ketones, ethers and nitrogen bases. The heats of mixing have been related in a preliminary fashion to the energy of the co-ordinate link formed between the electronegative atom in the organic substance and the aluminium chloride. This bond energy would seem to be strongly influenced by the electronegative character of the atom concerned since it is affected by inductive and resonance effects in the rest of the molecule. Future developments are indicated.

Aluminium chloride in its anhydrous state has long been known to give stable molecular compounds with many types of organic molecule,[1] and it has been variously argued how far such stable complexes play a part in the catalytic action of aluminium chloride.[2, 3, 4] We have recently established the role that stable complexes of reaction product with aluminium chloride play in lowering the free energy change and activation energy for the Gattermann-Koch reaction.[5, 6] On the other hand, the work of Fairbrother [4] has firmly outlined the behaviour of *unstable* complexes. It is clear that the heat of formation and other physical properties of the bond X → $AlCl_3$, where X is an electron donor atom in some organic molecule, is of the greatest interest in Friedel-Crafts catalysis, and indeed more generally since the results suggest a speculation on problems of enzyme action.

Experimental

The Calorimeter.—The method used is a refinement of that used earlier in unpublished work.[7] The organic substance concerned, which must be a liquid, or in solution in an inert liquid, was run into a mixture of powdered aluminium chloride and the inert liquid, usually chlorobenzene. Where there was any possibility of reaction apart from complex formation, an analysis of the end products was made. There is one case, butylamine, in this paper, where some very small reaction may have occurred.

The calorimeter is shown in Fig. 1. It consisted of a transparent Dewar vessel 22 cm. × 4 cm. int. diam., immersed in a thermostat at 25° C. The temperature was measured by an F 3000 ohm thermistor (Standard Telephone and Cable Company, Ltd.), according to the method of Campbell and Hutchinson.[8] Its resistance was measured to better than 1 ohm in a Wheatstone bridge, using a current of 0·4 mA. Over the 2° C range used, log R was proportional to T within 1 % and this was used in all calculations. Over the same range the error in the law $R \propto T$ was 2 %. Since the resistance change was 150 ohm per degree, temperature was determined to 0·005° C. Some thermistors were found to maintain constant resistance at 25° C over several months, but others fluctuated at irregular intervals, and needed constant checking.

---

[1] For a list, see C. A. Thomas *et al.*, *Anhydrous Aluminium Chloride in Organic Chemistry* (Chemical Catalog Co., 1941), pp. 48-56.

[2] Boeseken, *Rec. trav. Chim.*, 1900, **19**, 19.

[3] Boeseken, *ibid.*, 1910, **29**, 85.

[4] Fairbrother, *J. Chem. Soc.*, 1937, 503.

[5] Campbell and Eley, *Nature*, 1944, **154**, 85.

[6] Dilke and Eley, *J. Chem. Soc.*, 1949, 2601, 2613.

[7] Eley, *Ph.D. Thesis* (Cambridge, 1941).

[8] See Hutchinson, *Trans. Faraday Soc.*, 1947, **48**, 443.

The water equivalent was determined with an 18-ohm coil of 38 s.w.g. Brightway wire, wound on a glass tube and encased in specially thinned glass tubing. The annular space containing the wire was filled with transformer oil to just over the resistance coil. The leads to the coil were of 38 s.w.g. copper. Thermal lags were negligible and the current was taken from a 4-V accumulator and read to 1 % on a Weston 0-500 milliammeter.

The stirrer was a glass paddle, diameter 2·5 cm. The glass delivery coil had a capacity of 5 cm.³ and was constructed of three three-quarter turns, diam. 3 cm., of a coil, so that it fitted alongside the heating coil and thermistor. Its nozzle came just over the level of the calorimetric liquid, and it was connected to a coil immersed in the thermostat, and thence to a calcium chloride tube.

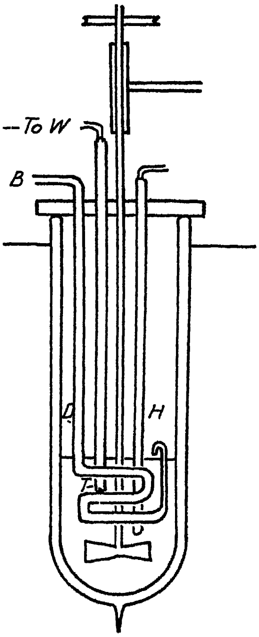

FIG. 1.—The calorimeter.
B Blow tube.
D Delivery tube.
H Heating coil.
T Thermistor.
W Wheatstone bridge.

Method.—All the apparatus was very carefully cleaned and dried. 5 ml. of the organic liquid under test was pipetted into the delivery tube, which was then attached to the calorimeter lid by a brass collar. About 0·5 g. of the halide under test was accurately weighed into a weighing bottle and kept in a desiccator. When ready it was rapidly transferred to the Dewar vessel, care being taken not to lose any on the sides, and the empty bottle reweighed. The measured volume of calorimetric liquid (60 ml. chlorobenzene) was then added, the top fitted and the whole apparatus clamped in the thermostat. The contents of the calorimeter were brought to 25° C using the heating coil, and then left 10 min. to reach equilibrium. Then by blowing through the calcium chloride tube and external coil at 25° C the organic liquid was mixed with the aluminium chloride plus calorimetric liquid, and resistance values of the thermistor taken thereafter at ½ min. intervals, using a ⅕ sec. stopwatch accurate to 1 part in 1000. The complex formation was complete in a few minutes, and after following the cooling curve for a sufficient time, a known current was switched on to the heating coil.

Calculation and Errors.—When complex formation occurred, the temperature rise was usually complete in 1-4 min. If any further reaction took place, the temperature rose over a longer period. This point, together with other relevant information, is discussed under the individual cases. Fig. 2 shows a typical run. The temperature-rises a and b are taken at the mid-points of the heating curve, according to White's approximate method for heat losses as outlined in the recent article by Sturtevant.[9] If x, the unknown heat of mixing, gives a temperature rise a, and a current i through the coil resistance R for t min. gives the rise b, then

$$x = 14{\cdot}34\, i^2Rt\, a/b,$$

where x is in cal., i in amp., R in ohms and t in min.[*]

Several runs were carried out with each organic liquid, using varying amounts of aluminium chloride. The slope of the straight line which resulted (see later) when the heat evolved x was plotted against weight of aluminium chloride w gave the heat of complex formation in cal./mole aluminium chloride. The intercept on the heat axis corresponding to zero added aluminium chloride gave s, the heat of solution of the organic liquid in the calorimetric liquid chlorobenzene. In many cases this was also measured in a separate experiment.

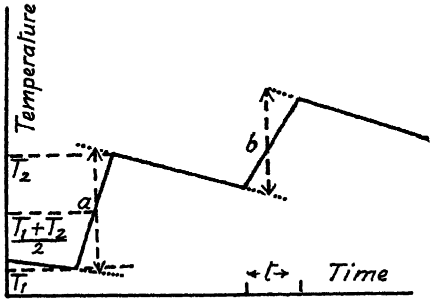

FIG. 2.—A temperature-time curve.

Thus if Q be the heat of mixing per mole of aluminium chloride, the molecular weight of which is taken as 133·3, then for a fixed amount of organic liquid (5 ml.),

$$x = s + \frac{w}{133{\cdot}3}Q,$$

and $$Q = 133{\cdot}3\, dx/dw.$$

The errors are in two groups, those concerned with the calorimeter itself and those concerned with the manipulation of the chemicals concerned, particularly the hygroscopic aluminium chloride. The total error in the calorimeter, arising from measurements of current, time and temperature is estimated to be at most 1 %. This is borne out by test measurements of the heat of neutralization. 10·5 ml. N NaOH were added to 10 ml. N HCl plus 40 ml. water. The measured heats were 133·0 and 134·0 cal. in two cases, to be compared with the standard value of Richards and Rowe of 133·9 cal.[10] A special set of experiments was made to show that 10 min. was sufficient time to obtain temperature equilibrium. The heat of solution of 1 ml. benzaldehyde in 60 ml chlorobenzene was measured after various times, with the results shown in Table I. This Table also shows the accuracy with which small amounts of heats may be determined. In general, the accuracy is about 0·1 cal. and we are usually concerned with heats of 10 to 100 cal.

The 5-ml. coil was found to deliver 4·26 ± 0·08 g. benzaldehyde, a reproducibility more than sufficient for our work, where the excess of organic liquid over aluminium chloride present ensured complete complex formation. The biggest error undoubtedly lies in the transference of aluminium chloride which will involve slight hydrolysis. The effect of this will not make itself felt on the heat of complex formation Q, as calculated from the slope of the straight line described before. Rather will it lead to an erroneous value of the heat of solution of the organic liquid in the chlorobenzene. The good reproducibility of the graphs of heat against weight of aluminium chloride suggests that the heats of complex formation per mole of aluminium chloride, reckoned as monomer, are accurate to ± 1 kcal.

---

[9] Sturtevant, *Physical Methods in Organic Chemistry*, vol. I (ed. Weissberger, Interscience, New York, 1945).

[*] Based on $4{\cdot}18_6$ joules/calorie.

[10] Richards and Rowe, *J. Amer. Chem. Soc.*, 1922, **44**, 684.

TABLE I

Experiment . .	36	37	38	39	40
Time, min. . .	60	30	90	30	90
Heat absorbed, cal. .	1·14	1·44	1·63	1·55	1·42

Materials.—Unless otherwise stated, the final treatment of all liquids involved drying with calcium chloride (with nitrogen bases, sodium hydroxide was used) and fractionating over a column of 7 theoretical plates. The refractive index values refer to the sodium *D* line, and comparison values from *Int. Crit. Tables* or other tables are given in brackets.

ALUMINIUM CHLORIDE.—A mixture of equal parts of B.D.H. aluminium chloride and aluminium powder was sublimed in a stream of dry HCl gas. The product was a white crystalline solid. It was then sublimed in a stream of dry nitrogen to remove adsorbed HCl.

CHLOROBENZENE.—The initial treatment involved washing with 50 % sulphuric acid and water. The product showed no reaction or coloration with pure aluminium chloride over half a day; b.p. 131·2-132·7° C, $n_{20°}$ = 1·5245 (1·5248).

ACETALDEHYDE.—B.D.H. paraldehyde was washed with caustic soda, water, dried with sodium sulphate and distilled. A drop of phosphoric acid was added to the purified paraldehyde and the liberated acetaldehyde removed by fractional distillation; b.p. 21·5° C.

BENZALDEHYDE.—Distilled in a stream of nitrogen; b.p. 178° C; $n_{17·6}$ 1·5460 (1·5463).

ACETOPHENONE.—B.D.H. recrystallized, m.p. 19·5° C.

BENZOPHENONE.—B.D.H., m.p. 48·0° C. It was dissolved in chlorobenzene, 1 g./ml., in order to use it in the delivery tube.

ANISOLE.—B.p. 153° C; n_{20} = 1·5181 (1·5179).

DIPHENYL ETHER.—Recrystallized from absolute alcohol; m.p. 27° C. It was used as a solution in chlorobenzene.

PYRIDINE.—B.p. 115·2° C. n_{22} = 1·5078 (1·5090).

PIPERIDINE.—B.p. 106·5° C. n_{20} = 1·4547 (1·4534).

QUINOLINE.—B.p. 123° C. (10 mm.). n_{21} = 1·6180 (1·6245).

DIETHYLAMINE.—B.p. 55° C. $n_{22·5}$ = 1·3880 (n_{18} = 1·3873).

TRIETHYLAMINE.—B.p. 88·5° C. $n_{20·5}$ = 1·4001 (n_{20} = 1·4003).

n-BUTYLAMINE.—B.p. 77·5° C. n_{22} = 1·4012 (1·4010).

DIPHENYLAMINE.—M.p. 53·5° C, used as a solution in chlorobenzene.

NITROBENZENE.—B.p. 209·0° C. $n_{23·5}$ = 1·5519 (n_{20} = 1·5526).

Results

The results of the calorimetry are listed in Table II. A group of typical graphs is plotted in Fig. 3. From these graphs we calculate Q, heat of mixing per mole of aluminium chloride reckoned as monomer, and s the heat of solution of approximately 5 ml. of the organic liquid in 60 ml. chlorobenzene.

Acetaldehyde.—Complex formation was too slow for a heat to be measured, the solvents chlorobenzene, carbon tetrachloride, benzene and nitrobenzene being tried. In the absence of a diluent, acetaldehyde reacted with aluminium chloride to give heat evolution but no HCl, and thus a complex may possibly exist.

Benzaldehyde.—Results obtained using aluminium chloride sublimed in nitrogen lie on the same graph with those obtained using aluminium chloride sublimed in HCl. The end product was a colourless solution from which the complex was partially precipitated as a white solid. In another paper[6] the complex is shown to be 1/1 in character, that is, $C_6H_5CHO \cdot AlCl_3$. Q = 24·7 kcal., $s = 5$ cal. (cf. two direct determinations, 5·4, 5·5 cal.).

Acetophenone.—The complex was completely soluble in benzene to give a golden solution. Its formula is $C_6H_5COCH_3 \cdot AlCl_3$.[11] Q = 19·2 kcal. $s = 7$ cal. (cf. 3·5 cal. directly).

---

[11] Kohler, *Amer. Chem. J.*, 1902, **27**, 241.

TABLE II

The third column gives the time required for complex formation, or more precisely, for the maximum temperature to be reached

g. $AlCl_3$	Heat (cal.)	Time (min.)
BENZALDEHYDE		
0·296*	49·5	2
0·538*	95·5	2
0·814*	144·1	1·5
0·221*	31·9	1·5
0·744	134·2	2·5
0·412	76·0	2·5
0·255	43·8	2·5
ACETOPHENONE		
0·678	88·9	7·5
0·570	72·5	4·0
0·368	44·0	4·5
BENZOPHENONE		
0·389	39·4	3·5
0·632	66·7	4·0
0·796	86·9	5·5
0·973	104·7	5·5
n-BUTYLAMINE		
0·203	131·8	1·5
0·097	58·7	2·5
0·075	39·4	2·5
0·133	88·0	3·0
ANISOLE		
0·412	23·3	2·0
0·789	47·0	2·0
0·613	35·5	2·0
1·064	62·9	2·0
DIPHENYL ETHER		
0·416	13·7	4·5
0·616	18·1	3·5
0·812	25·3	6·0
0·943	30·4	4·0
PYRIDINE		
0·605	181·9	3·5
0·357	94·8	2·5
0·534	157·6	7·5
QUINOLINE		
0·162	43·3	1·5
0·099	25·4	1·0
0·071	17·8	1·0
0·121	30·7	1·0
DIPHENYLAMINE		
0·211	16·3	6·0
0·401	29·8	3·5
0·606	48·3	4·0
0·780	59·7	4·0
PIPERIDINE		
0·217	92·4	1·5
0·142	70·1	2·5
0·110	42·3	1·0
0·089	36·8	1·5
0·167	72·0	1·5
0·139	57·9	1·5
TRIETHYLAMINE		
0·300	70·0	2·0
0·212	52·7	2·0
0·412	96·4	2·0
0·616	124·5	2·0
0·111	38·5	2·5
DIETHYLAMINE		
0·185	92·4	1·0
0·116	71·4	1·5
0·078	51·7	1·5
0·145	86·3	1·5
0·055	37·6	2·0
NITROBENZENE		
0·677	29·1	3·0
0·435	16·4	3·0
0·980	48·6	4·0
0·516	21·3	3·5

* $AlCl_3$ sublimed in HCl.

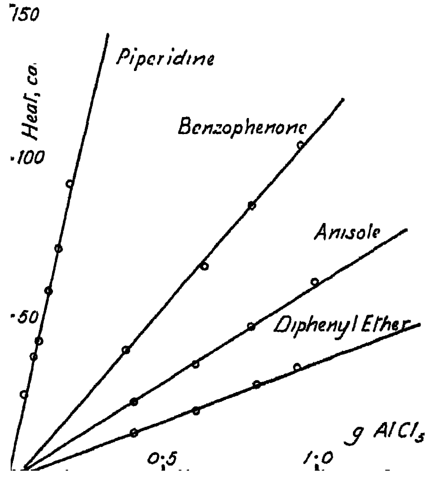

FIG. 3.—A selection of data.

Benzophenone.—The complex was formed as a yellow-green solution, a slight gelatinous precipitate forming on standing. It has been isolated and described as $(C_6H_5)_2CO \, . \, AlCl_3$.[1] $Q = 15{\cdot}4$ kcal.

Anisole.—The complex was formed as an orange solution with a very slight gelatinous precipitate. It has been previously isolated and described as $C_6H_5OCH_3 \, . \, AlCl_3$.[12] $Q = 8{\cdot}2$ kcal.

Diphenyl Ether.—The complex was completely soluble in chlorobenzene, giving an orange brown solution. A very slight gelatinous precipitate was present Kohler [11] gives it the formula $(C_6H_5)_2O \, . \, AlCl_3$. $Q = 4{\cdot}1$ kcal.

Pyridine.—The complex was precipitated as a white crystalline solid, the trace of HCl inevitably present giving some pyridine hydrochloride also, but the error was probably small. $Q = 47{\cdot}8$ kcal. $s = 28$ cal. (much greater than the directly measured value of $- 6$ cal.). Kohler [13] reports a crystalline complex $C_6H_5N \, . \, AlCl_3$, but the work of Watts referred to in the next section suggests the end product may not be simple.

Piperidine.—A white gelatinous precipitate was formed. $Q = 57{\cdot}1$ kcal.

Quinoline.—A relatively small amount of white apparently gelatinous precipitate was formed in a green solution. Further investigation indicated that this complex was probably crystalline, but because of the small amount of precipitate, it has not yet been further investigated. $Q = 36{\cdot}2$ kcal.

Diethylamine.—A white gelatinous precipitate. $Q = 70$ kcal.

Triethylamine.—A brown gelatinous precipitate in a brown solution. $Q = 24{\cdot}0$ kcal.

***n*-Butylamine.**—A white gelatinous precipitate. $Q = 94$ kcal.

Diphenylamine.—A brown gelatinous precipitate. $Q = 10$ kcal.

Nitrobenzene.—A golden solution resulted, containing some white precipitate. $Q = 7{\cdot}9$ kcal., $s = 9$ cal. (cf. direct value of $6{\cdot}5$ cal.).

Both $C_6H_5NO_2 \, . \, AlCl_3$ and $(C_6H_5NO_2)_2 \, . \, AlCl_3$ have been described in the solid state.[1] Plotnikow and Vaisberg [14] give $12{\cdot}2$ kcal. for the heat of solution of aluminium chloride in nitrobenzene. The difference from our value may be due to difference in molecularity of complex or heat of solution.

Other Substances.—No heat of complex formation was observed with aniline. A marked heat was observed with acetone, but its rapid evaporation precluded reproducible results. A similar effect was obtained with the volatile liquid, ethylamine.

The Nature of the Final State.—With the exception of pyridine which deposits a crystalline complex, and quinoline which deposits a small amount of apparently crystalline material, all the other nitrogen substances give as end states either solutions or solutions containing a *very small amount* of gelatinous precipitate. Separate experiments in which these substances were mixed and protected from the air have shown that these gelatinous precipitates can be attributed most probably to small amounts of hydrolysis due to access of moisture to the calorimeter, occurring subsequently to the initial rapid temperature rise and introducing a negligible error in the heat measurement. The precipitate resists filtration and is what one would expect of an organic alumina gel. There is necessarily a period of about ½ hr. before the end solution is removed for examination. The excellent reproducibility of the straight lines for the heat-weight relation over a 20-fold range of heats is emphasized as supporting the absence of side-reactions of any magnitude, in the 4 min. during which the complex is formed. We shall accordingly write for the reaction in the calorimeter :

$$\tfrac{1}{2}Al_2Cl_6\,(s) + nX(l) \rightarrow X_nAlCl_3\left(\begin{matrix} s \text{ or} \\ \text{solution}\end{matrix}\right) + Q,$$

where Q is the measured heat of mixing, and we neglect in our present discussion whether the complex remains in solution, or precipitates as for pyridine. We shall assume that the heat of solution differences are small enough to be neglected in considering the whole body of data.

The value of n is established as 1 for benzaldehyde as formed in the calorimeter.[6] Analyses quoted from the literature of crystalline complexes give $n = 1$ for oxygen compounds generally, which is probably relevant for the complex in solution. The evidence for nitrogen complexes is as yet less clear. Mr. Watts in our laboratory has prepared aluminium chloride-pyridine complexes with $n = 1$ and $n = 3$, but his results (to be published later) show that 70 %

---

[12] Walker and Spencer, *J. Chem. Soc.*, 1904, 1106.

[13] Kohler, *J. Amer. Chem. Soc.*, 1900, **24**, 385.

[14] Plotnikov and Vaisberg, *A. C. S. Abstr.*, 1941, **35**, 2405.

of the observed Q is associated with addition of the first molecule of pyridine, the two subsequent molecules being added with much smaller energies. It is possible that n may vary to some extent with these nitrogen bases, according to conditions (due to dissociation equilibria) and may vary from base to base. The detailed study of all these factors is in hand. Absence of evolved HCl gas or hydrolysis and recovery of the initial substance in most cases is satisfactory evidence for absence of side reactions, but with primary and secondary nitrogen bases, it might be asked how far the heat Q is due to reactions of the type

$$R \,.\, NH_2 + \tfrac{1}{2}\, Al_2Cl_6 \rightarrow R \,.\, NH \,.\, AlCl_2 + HCl$$

undetectable by these two methods. Mr. H. Watts has found evidence for side reactions when butylamine and aluminium chloride are held at 120°, but the effects are negligible at room temperature. Again, migration of alkyl groups in this system is negligible at room temperature,[15] and Nespital[16] has found $C_2H_5 \,.\, NH_2 \,.\, AlCl_3$ to be stable at relatively high temperatures.

"Bond Energy" of the Coordinate Link.—The results on the heats of mixing Q are presented in Table III. In addition we present values of a quantity E_n' where

$$E_n' = Q + D/2 = Q + 14,$$

and n refers to the molecularity of the complex, D being the heat of dissociation of Al_2Cl_6 into 2 $AlCl_3$ molecules, the most recent value for which is 28 kcal.[17] E_n' is the heat of the reaction

$$AlCl_3(s) + nX(l) \rightarrow X_n\, AlCl_3 \left(\begin{matrix} s \text{ or} \\ \text{solution} \end{matrix}\right) + E_n'.$$

TABLE III

Organic Molecule	Q (kcal.)	E_n' (kcal.)	μ D	R.E. (kcal.)	Basic Constant
Benzaldehyde .	24·7	39	2·75	47	—
Acetophenone .	19·2	33	2·9	54	—
Benzophenone .	15·4	29	3·0	93	—
Anisole . .	8·2	22	1·2	52	—
Diphenyl ether	4·1	18	1·1	—	—
n-Butylamine .	94	108	—	14*e*	$4{\cdot}1 \times 10^{-4}$
Diethylamine .	70	84	1·2	5	$1{\cdot}3 \times 10^{-3}$
Piperidine .	57·1	71	1·17*a*	2*e*	$1{\cdot}6 \times 10^{-3}$
Pyridine . .	47·8	62	2·26*a*	43	$1{\cdot}7 \times 10^{-9}$*b*
Quinoline .	36·2	50	2·16*a*	75	$1{\cdot}0 \times 10^{-9}$
Triethylamine .	24·0	38	0·9	13	$6{\cdot}0 \times 10^{-4}$
Ammonia .	—	40*g*	1·4*c*	0	$1{\cdot}8 \times 10^{-5}$*d*
Diphenylamine .	10	24	1·3	98*e*	$7{\cdot}6 \times 10^{-14}$
Aniline . .	—	—	1·5	51*e*	$3{\cdot}8 \times 10^{-10}$
Nitrobenzene .	7·9	22	3·95	—	—

R.E. = resonance energies, from Wheland, *Theory of Resonance* (New York, 1944).
μ = dipole moment, data, unless otherwise stated, from *Trans. Faraday Soc.*, 1934, **30**, 679.
a = Rau, *Z. physik. Chem.*, *B*, 1934, **26**, 23.
b = Hahn, *ibid.*, *A*, 1930, **146**, 389.
c = Le Fèvre, *Trans. Faraday Soc.*, 1947, **43**, 374.
d = Brown, *J. Chem. Physics*, 1943, **11**, 43.
e = Calculated according to Wheland's data, using heats of combustion from *Int. Crit. Tables*.
g = True E value for $AlCl_3(g) + NH_3(g) \rightarrow NH_3 \,.\, AlCl_3(g)$, based on data from Klemm *et al.*, *Z. anorg. Chem.*, 1931, **200**, 367.

It is possible by an energy cycle similar to that already given[6] to derive values of the bond energy E_n

$$AlCl_3(g) + nX(g) \rightarrow X_n\, AlCl_3(g) + E_n,$$

---

[15] Nozaki, *J. Amer. Chem. Soc.*, 1942, **64**, 2920.

[16] Nespital, *Z. physik. Chem. B*, 1932, **16**, 153.

[17] Fischer and Rahlfs, *Z. anorg. Chem.*, 1932, **205**, 1.

but to use this cycle it is necessary to know values of the sublimation energy (and also the solution energy in many cases) of the complex. We have given reasons for approximating E_1 by E'_1 [6] To this we may add that for $NH_3 . AlCl_3$ where we know the sublimation energy (Klemm) $E_1 - E'_1 - 1{\cdot}5$ kcal. only. There are grounds in other words for supposing in this first paper that differences in E'_1 and therefore Q also, will reflect fairly faithfully *differences* in the true bond energy E_1.

Since $n = 1$ may be assumed for the oxygen compounds, E'_n E'_1 here will give a relative measure of the strength of the $O \rightarrow Al$ link. In our discussion we shall assume that, as for the pyridine work cited, while the true value of n may be 3, or even vary from one substance to another, the first molecule attached largely determines the value of Q, and that E'_n gives not only an upper value for the strength of the $N \rightarrow Al$ link, in any particular case, but also a good relative measure of the $N \rightarrow Al$ bond energy in all cases. In making this assumption, we are neglecting completely the operation of steric effects, as while Q and E'_n correspond to $n = 3$ for pyridine, it is possible that for a large molecule like quinoline, n might not exceed 1, and the observed differences in Q and E'_n be due to this.

Discussion

Dipolar and Donor Bonds.[18]—Table III reveals no correlation between E'_n and the dipole moment of the added molecule. While a full discussion would bring in also the bond length and the polarizabilities of the molecules, to a first approximation this lack of correlation is strongly against the hypothesis of a dipole-dipole bond in the aluminium chloride–organic molecule complex. On the other hand, there is positive evidence in favour of a relation between E'_n and the " donor property " of the electro-negative atom in the organic molecule, which is best considered for the individual groups of compounds. We shall consider the donor property of the atom to be influenced by substituents according to well-known results on the inductive effect in the electronic theory of organic chemistry. In addition, we shall suppose that where the electrons on the electronegative atom resonate with the π electrons of a benzene ring, they are weakened in their power to form a donor link to aluminium chloride, and we shall take the measured resonance energies as a measure of this effect.

Aldehydes and Ketones.—We may suppose that the donor link is formed by the oxygen atom, e.g.

$$(C_2H_5)C{=}O \rightarrow AlCl_3$$

and the strength of this link to depend on the anionoid character of this atom. This will be increased by substitution of methyl for hydrogen and decreased by phenyl, so we should expect the following order of decreasing values of E'_n :

$$\text{acetophenone} > \text{benzaldehyde} > \text{benzophenone}.$$

However, we find the order

$$\text{benzaldehyde} > \text{acetophenone} > \text{benzophenone},$$

which, of course, is also the order of general reactivity of the carbonyl group in this series, so we may suppose that benzaldehyde is, in general, anomalous, the inductive effect of the H atom being enhanced in some way.

A consideration of the difference in resonance energy between the carbonyl compound, and the value of 39 kcal. for the benzene ring [19] leads to values of benzaldehyde 8, and acetophenone and benzophenone 15 each (in the latter case, one must subtract 78 kcal. for two benzene rings). Since the *lower* this resonance energy the more strongly electron-donating we may expect the oxygen atom to be, this method puts benzaldehyde at the head of the Table as found, but fails to distinguish the other two. Thus, we may conclude that there is no conflict between these results and the electron donor concept, but we shall not attempt any more quantitative discussion in the absence of any estimate of steric factors.

---

[18] Dilke and Eley, *Faraday Soc. Discussions*, 1947, **2**, 77.

[19] Pauling, *The Nature of the Chemical Bond* (Cornell, 1939).

Ethers.—The greater bond energy of the aldehydes and ketones suggests that the donor quality of oxygen in the C=O group is greater than the ether group, as we should expect on general grounds. The *difference* in E'_n between anisole and diphenyl ether, 4 kcal., is just that between acetophenone and benzophenone. Again, the effect arises probably from the greater inductive effect of methyl over phenyl, rather than from steric forces.

Nitrogen Bases.—The generally larger values of E'_n for nitrogen bases over the oxygen compounds probably reflects a true difference in bond energy outside any uncertainties due to the molecularity n. It is in line with the stronger basicity of the nitrogen compounds as shown with proton acids. Over the series of cyclic molecules, the decrease in bond energy piperidine > pyridine > quinoline > diphenylamine is found also with protons as shown in the values of the basic dissociation constants in Table III. This corresponds to a decreased availability of electrons at the nitrogen atom in so far as this is measured by the resonance energy of the compound. It is not clear how to reconcile these results with the molecular orbital calculation which gives a greater electronic charge on the N atom of quinoline than that of pyridine,[20] but a detailed discussion is out of place at present. The zero heat of mixing for aniline is anomalously low on the view taken here.

The series of decreasing bond energy for the aliphatic amines is $C_4H_9NH_2 > (C_2H_5)_2NH > (C_2H_5)_3N$. We shall not discuss ammonia, since this substance is anomalous as shown by its ability to give numerous higher compounds of great complexity (cf. Klemm, loc. cit.). The inductive effect at the N atom should increase with increased substitution of hydrogen, as is shown best by the series of decreasing ionization potential,[21] $NH_3 > CH_3NH_2 > (CH_3)_2NH > (CH_3)_3N$. Thus we cannot link up the bond energy to aluminium chloride with the negative charge on the N atom arising from the inductive effect. The basic dissociation constants give for the order of decreasing affinity for protons

$$(C_2H_5)_2NH > (C_2H_5)_3N > C_4H_9NH_2.$$

There is a close similarity between our series and that found by Brown[22] for the ethylamines and tributyl boron

$$NH_3 > C_2H_5NH_2 > (C_2H_5)_2NH > (C_2H_5)_3N,$$

which he supposes to arise from an increase in the steric effect from mono- to triethylamine. Even with HCl on this view triethylamine must exert a large steric effect, since the affinity is

$$(C_2H_5)_2NH > C_2H_5NH_2 > (C_2H_5)_3N > NH_3.$$

We are inclined to accept Brown's explanation and to apply it to our own results, but we are left still with the well-known result that only tertiary amines will form from an N → O link, in the amine oxides.* Does this mean that inductive influences in this case completely swamp the steric effects, in opposition to Brown's notion ? It is, however, not at all clear that failure to isolate an amine oxide from a secondary amine is due to a weakness of the $R_2HN \rightarrow O$ link. It may well be due to mobility of the H atom, which migrates to the O atom as being more electronegative, giving rise to the dialkyl hydroxylamine $R_2N \rightarrow OH$ usually obtained.

---

[20] Longuet-Higgins and Coulson, *Trans. Faraday Soc.*, 1947, **43**, 87.
[21] Price and Walsh, *Nature*, 1941, **148**, 372.
[22] Brown, *J. Amer. Chem. Soc.*, 1945, **67**, 1452.
* This point was raised by a referee.

It might perhaps be worth noting that if the main reaction between aluminium chloride and primary and secondary amines, were the elimination of HCl, subsequently bound as amine salts, this should be particularly marked with diphenylamine where the H atom will have the most marked electropositive character. In fact, the low E_n' value is against this view. The situation is thus rather different from that with boron trichloride which has a marked tendency to split off HCl.[23]

Conclusion.—In spite of uncertainties which centre mainly around n the molecularity of the complex, we believe there is a correlation between electron availability and bond energy, although the correlation does not hold for the aliphatic amines examined, where steric effects may come into play as suggested by Brown. To decide, however, the many points raised, further calorimetric work is necessary and this is proceeding along two lines. Firstly, we are preparing crystalline complexes and investigating their heats of hydrolysis. At the same time we are attempting to measure sublimation energies, so that true bond energy values may be obtained. Secondly, we are extending the heats of mixing along the line recently given[6] so as to obtain direct evidence on the value of n as the complex exists in solution.

It is interesting to speculate on the importance of the influence of molecular environment on N → metal links in biochemical specificity, particularly in enzyme and related systems. The specific action of the protein on the iron atom in haem presumably lies in the N → Fe link connecting the imidazole group on the protein to the iron atom. If the strength of this bond may be profoundly influenced by inductive and resonance effects in nearby parts of the globin molecule, does this not suggest an approach to the peculiarly specific action of globin in conferring oxygenation properties on the iron atom ? The specific action of proteins is commonly attributed entirely to the operation of short range van der Waals' forces necessitating a close steric fit of molecules, and the notion of transmitted effects on co-ordinate links offers an alternative approach, speculative but perhaps no more so than any other.

The authors' best thanks are due to the Distillers' Co., Ltd., for a scholarship to M. H. D., to Dr. H. Campbell and Mr. G. E. Coates for valuable advice and to Mr. H. Watts for permission to quote from some of his results on pyridine-aluminium chloride complexes.

Chemistry Department,
The University,
Bristol.

[23] Martin, *Chem. Rev.*, 1944, 34, 461.

THE FLOW OF AN AIR STREAM THROUGH A LAYER OF GRANULES

By J. R. Arthur, J. W. Linnett, Mrs. E. J. Raynor and E. P. C. Sington

Received 22nd July, 1949 ; *as revised 24th November,* 1949

An investigation of the flow of an air stream through a bed of granules is described. The work may be divided into two parts : (I) an examination of the pressure drop across the bed as a function of the flow rate and the condition of the granular bed ; (II) an examination of the distribution of flow rate across the bed by physical and chemical tests.

PART I

It has been shown[1] that, at low flow rates when the flow is viscous, the relation between the quantity of fluid flowing through a porous bed and the pressure drop is given by

$$F = \frac{A\Delta p}{\mu S_0^2 kl} \frac{E^3}{(1 - E)^2}, \qquad . \quad . \quad . \quad . \quad . \quad (1)$$

where F = volume penetrating the bed per second,
Δp = pressure drop across the bed,
A and l = cross-sectional area and length of bed respectively,
μ = viscosity of fluid flowing through the bed,
S_0 = specific surface area of the material of the bed,
E = porosity of the material of the bed (fractional free space),
k = a constant = 5·0 in c.g.s. units when the arrangement of granules in the bed is random.

Eqn. (1) holds for air if the volume changes in the bed are not great, as in the present work. It is equivalent to the relationship obtained by Kozeny[2] and by Fair and Hatch.[3]

Now if D_0 is the bulk density of the material of the bed and D is the apparent specific gravity of the bed as a whole, then

$$1 - E = D/D_0. \qquad . \quad . \quad . \quad . \quad . \quad (2)$$

Substitution of (2) and (1) gives

$$D_0 - D = \left[\frac{F}{\Delta p}\frac{l}{A} k\mu S_0^2 D^2 D_0\right]^{1/3}. \qquad . \quad . \quad . \quad . \quad (3)$$

Measurements of D and of $\Delta p/Fl$ (= Y) can be made for a given granular material in a given tube. If therefore $(D^2/Y)^{1/3}$ is plotted against D for the same granular material packed to different values of D in the same tube, a straight line should be obtained the intercept of which gives D_0 and from the slope of which S_0 can be calculated.

Experimental

Various samples of dry charcoal granules were used to form the beds, the gradings being 16-18, 7-18 and 10-18 B.S.S. The beds were supported on horizontal copper gauze in vertical glass tubes of diameters varying between 1·35 and 4·83 cm. Air was supplied to the top of the bed from a compressed air supply. This stream had been dried by calcium chloride and sulphuric acid, and its flow rate determined (to an accuracy of ± 1 %) by a meter measuring the pressure drop across a capillary. The pressure drop across the bed of granules was measured on an aniline sodium carbonate solution differential manometer. This had a sensitivity about 20 times that of a water manometer, so that pressure differences of 0·0025 cm. water could be detected. For higher pressure differences a water manometer was used.

In these experiments flow rates of less than 400 cm./min. in an open tube were used. Under these conditions it was found that if log Δp was plotted against log F a straight line was obtained within the error of the experiment (see Fig. 1). If the flow is fully stream-lined the slope of this line should be unity. In fact it was always found to be slightly greater than unity. For instance, using beds of 16-18 graded charcoal granules, the slopes of the logarithm plots were 1·03, 1·02 and 1·045 in tubes of diameter 4·83, 2·53 and 1·35 cm. respectively. The slopes showed no significant variation with porosity. Other charcoals gave slopes varying from 1·01 to 1·08 under similar conditions. Therefore, even at these low flow rates the flow does not seem to be wholly viscous. This presumably means that at certain places in the bed the flow is turbulent but that over most of the bed it is viscous. Of course at higher flow rates the turbulence increases. For the 16-18 graded charcoal in the 1·35 cm. tube the slope of the logarithm plot was found to be 1·28 at a flow rate of 1500 cm./sec. in the open tube and 1·6 at 4500 cm./sec. Other beds behaved similarly.

---

[1] Sullivan and Hertel, *Advances in Colloid Science*, Vol. 1, pp. 33-48.

[2] Kozeny, *Sitzber. Akad. Wiss. Wien, Math. naturw. Klasse* (*Abt IIa*), 1927, **136**, 271.

[3] Fair and Hatch, *J. Amer. Water Works Assoc.*, 1933, **25**, 1551.

Eqn. (1) to (3) applies to viscous flow which is the limiting condition as the flow rate is reduced towards zero. To apply these equations we need to know $Y = \Delta p/Fl$. Our procedure was to determine a series of values of Δp and F for a given bed of charcoal and then to calculate $\Delta p/F$ for each flow rate. A set of these figures for the 16-18 graded charcoal packed to a length of 12·3 cm. in a 1·35 cm. tube at an apparent specific gravity of 0·481 g./cm.^{3} is shown in Table I. The ratio, $\Delta p/F$, was then extrapolated to $F = 0$ which gave a limiting value of $3{\cdot}44 \times 10^{-3}$ in the present example. We then have $\Delta p/Fl$ equal to $2{\cdot}80 \times 10^{-4}$ when F is measured in cm.^{3}/min. and Δp in cm. of water. We will call this ratio Y'. The first part of Table II gives the values of Y'', D and $(D^2/Y')^{1/3}$ for a number of similar experiments with the same charcoal in the same tube, the charcoal having been intentionally packed to as wide a range of values of D as possible. The lengths of charcoal column used in these experiments ranged from 5 to 14 cm. The values of $(D^2/Y')^{1/3}$ are plotted against D in Fig. 2. The straight line is extrapolated to $(D^2/Y')^{1/3}$ 0 giving D_0 0·87 g. cm.$^{-3}$ This lengthy extrapolation will be discussed later. The slope of the line is 24·7. From the slope we have

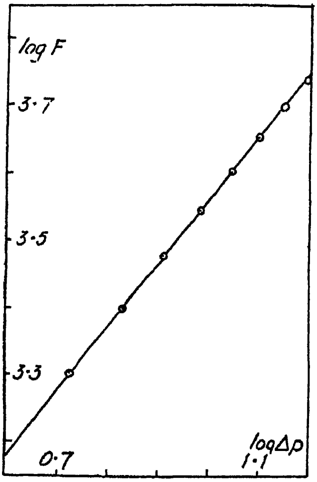

FIG. 1.—Relationship between F and Δp at low rates of flow.

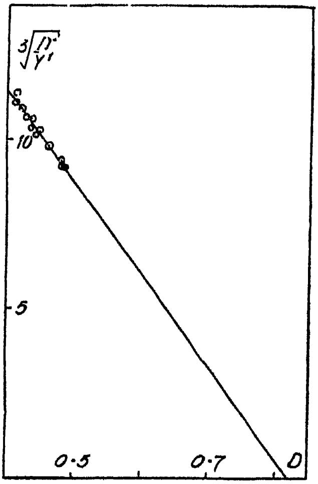

FIG. 2.—Method of obtaining D_0 and S_0.

TABLE I.—VARIATION OF PRESSURE DROP Δp AND OF THE RATIO $\Delta p/F$ WITH FLOW RATE F. PRESSURE DROP IN CM. OF WATER

Flow Rate cm.^{3}/min.	Pressure Drop	$\frac{\Delta p}{F} \times 10^3$	Flow Rate cm.^{3}/min.	Pressure Drop	$\frac{\Delta p}{F} \times 10^3$
200	0·706	3·53	400	1·453	3·63
250	0·893	3·57	450	1·647	3·66
300	1·077	3·59	300	1·838	3·68
350	1·267	3·62	550	2·037	3·70

$$1/(S_0^2 k\mu) = 0{\cdot}155.$$

The second part of Table II gives figures for the same charcoal in a tube of diameter 2·53 cm. Extrapolation of the graph of $(D^2/Y')^{1/3}$ against D gives $D_0 = 0{\cdot}86$ g. cm.$^{-3}$. The slope of the line is 36·9 giving $S_0 - 87$ cm.$^{-1}$. The third part of Table II gives figures for the same charcoal in a tube of diameter 4·87 cm. It was found impossible to obtain a wide range of porosities with this finely graded charcoal in the wider tube. The results for this case are therefore less suitable for graphical extrapolation than those obtained in the narrower tubes. In this case a line was drawn through the four points which gave a satisfactory value for the bulk density as compared with the results obtained in the narrower tubes. The density used was $D_0 = 0{\cdot}85$ g. cm.$^{-3}$. This gave a slope of 56·4 giving $S_0 = 88$ cm.$^{-1}$. The results obtained for the 16-18 graded charcoal are summarized in Table III. The values of D_0 and S_0 obtained from the three tubes are seen to be in good agreement with one another.

TABLE II.—VALUES OF Y', D AND $(D^2/Y')^{1/3}$ FOR THE 16-18 GRADED CHARCOAL

$Y' \times 10^4$	App. sp. grav. D	$(D^2/Y')^{1/3}$	$Y' \times 10^4$	App. sp. grav. D	$(D^2/Y')^{1/3}$
Tube diam. 1·35 *cm.*					
1·17	0·415	11·4	1·88	0·441	10·1
1·24	0·412	11·1	2·12	0·452	9·9
1·36	0·422	10·9	2·27	0·464	9·8
1·52	0·428	10·7	2·80	0·481	9·4
1·60	0·436	10·6	2·93	0·482	9·3
1·72	0·435	10·3	3·04	0·486	9·2
1·87	0·448	10·2	—	—	—
Tube diam. 2·53 *cm.*					
0·42	0·423	16·2	0·67	0·462	14·7
0·46	0·427	15·8	0·72	0·461	14·4
0·52	0·438	15·5	0·90	0·483	13·7
0·55	0·444	15·3	0·94	0·489	13·6
Tube diam. 4·87 *cm.*					
0·18	0·443	22·2	0·25	0·477	20·8
0·24	0·470	21·1	0·30	0·493	19·9

Taking $\mu = 1{\cdot}81 \times 10^{-4}$ in c.g.s. units and $k = 5{\cdot}0$ as recommended by Sullivan and Hertel we get $S_0 = 84$ cm.$^{-1}$.

TABLE III.—VALUES OF THE SPECIFIC SURFACE AREA S_0 AND BULK DENSITY D_0 DEDUCED FROM THE EXPERIMENTAL RESULTS

Tube diam. (cm.)	D_0(g./cm.^{3})	S_0(cm.$^{-1}$)
16-18 *Graded Charcoal*		
1·35	0·87	84
2·53	0·86	87
4·87	0·85	88
Mean	0·86	86
7-18 *Graded Charcoal*		
1·35	1·02	42
4·87	0·98	43
Mean	1·00	42·5
10-18 *Graded Charcoal*		
1·35	0·79	58
4·87	0·79	60
Mean	0·79	59

Experiments were also carried out on a 7-18 graded charcoal in tubes of diameter 1·35 and 4·83 cm. For the narrow tube the extrapolated value of

D_0 was 1·02 and the slope of the plot of $(D^2/Y')^{1/3}$ against D was 37·2 giving $S_0 = 42$ cm.$^{-1}$. For the wider tube D_0 was 0·98, the slope 86·5 and $S_0 = 43$ cm.$^{-1}$. The results are summarized in Table III which also gives a similar set for a 10-18 graded charcoal in the same two tubes.

Discussion

For the results at low flow rates it has been shown that plotting $(D^2/Y')^{1/3}$ against D gives straight lines. This demonstrates that the original equation accounts for the effect of porosity on the pressure drop. Rose[4] remarked that the main factor affecting resistance is " voidage " (i.e. porosity) and that voidage has an increasingly big percentage effect as E approaches unity, which is to be expected from the formula used here. Carman[5] has shown that the factor $E^3/(1 - E)^2$ accounts for the effect of changes in E. He used a wide range of particles and fluids (various organic liquids, water, as well as air). E varied from 0·26 to 0·89. Hatch[6] used with success the same porosity function for water flowing through sand beds. Fowler and Hertel[7] also found $E^3/(1 - E)^2$ was sufficient to take account of the effect of porosity in the flow of air through pads of various fibrous materials. Similar results have been obtained by Donat[8] and by Traxler and Baum[9] on the flow of air through beds of powders. Our results therefore confirm the conclusions of these other workers. Since the results were obtained for a range of column lengths, it must be concluded that the pressure drop is proportional to the column length as is given by the original equation. The bulk densities obtained from the results in different tubes agree well. It must be admitted that the extrapolation used was a dangerously long one, but the justification lies in the agreement between the results obtained for the same charcoal in different tubes.

The values of S_0 obtained from experiments in different sized tubes are in good agreement with one another. It is interesting that they seem to increase slightly on passing from narrow to wide tubes in all cases. A possible explanation of this is that, because the granules are not symmetrical, there is a less random arrangement of granules in the narrow tube than there is in the wide one, long granules tending to lie along the wall. Sullivan and Hertel[1] have shown that for glass fibres arranged parallel to the direction of flow, k is about 3·1. This is less than the value of 4·5 given by Sullivan and Hertel, or 5·0 given by Carman,[10] or 4·65 given by Muskat and Botset[11] for a random arrangement of surfaces. So it is possible that in a narrow tube a smaller value should be used for k than in a wide tube. However, the differences in the values of S_0 for different tubes are small. For the three charcoals the values of S_0 found were: 7-18, 43 cm.$^{-1}$; 10-18, 59 cm.$^{-1}$; 16-18, 87 cm.$^{-1}$. It will be seen that these values are very reasonable. For spheres $S_0 = 3/r$ where r is the radius. If $r = 0·05$ cm., $S_0 = 60$ cm.$^{-1}$; and if $r = 0·1$, $S_0 = 30$ cm.$^{-1}$. The areas measured refer only to the outer surface of the granules and do not include the pore areas. This means that the air flows over the outer surface only. If the granules are adsorbent, any gas adsorbed from the air stream must therefore be taken up at the outer surface, but since the high capacity of most adsorbents is due to inner pores, the majority of any material adsorbed must eventually be taken into these pores. Therefore the material adsorbed must migrate along the surface from the outer surface to the inner pores after its removal from the air stream.

---

[4] Rose, *Proc. Inst. Mech. Eng.*, 1945, **153**, 141, 148, 154.

[5] Carman, *J. Soc. Chem. Ind.*, 1938, **57**, 225; 1939, **58**, 1.

[6] Hatch, *J. Appl. Mechanics*, 1940, **7**, 109.

[7] Fowler and Hertel, *J. Appl. Physics*, 1940, **11**, 496.

[8] Donat, *Wasserkraft Wasserwintsch*, 1929, **24**, 225.

[9] Traxler and Baum, *Physics*, 1946, **7**, 9.

[10] Carman, *Trans. Inst. Chem. Eng.*, 1937, **15**, 150.

[11] Musket and Botset, *Physics*, 1931, **1**, 27.

We would stress here that nothing we have done here enables us to choose the best value that should be used for k. We find that, with $k = 5$, the values obtained for S_0 are reasonable but, since we have no independent determination of S_0, we cannot say whether k should be somewhat less than 5 as suggested by Sullivan and Hertel, and Muskat and Botset.

The general conclusions to be drawn from these results are therefore that, at low flow rates, the original equation represents the results very satisfactorily and, because of this, the results may be used to obtain the bulk density of the charcoal and an approximate value for the specific surface area of the granules.

PART II

It might be expected that the packing of the charcoal would be less good near the smooth walls of a wide tube than in the middle and that this would result in an increased linear flow rate near the wall for a given pressure drop across the bed. An investigation of the distribution of flow across the bed has been carried out by the follwing methods :

(i) By simultaneous measurement of the flow rate of air emerging from different parts of the same column of charcoal.
(ii) By chemical estimation of the products of reaction or adsorption on various parts of the charcoal when a stream of air containing a gas which is absorbed by or reacts with the charcoal is passed through the bed.
(iii) Qualitatively, by observing the passage of a gas-laden air stream through a bed of granules stained with an indicator.
(iv) By observing the concentration of emergent gas from the charcoal column at various parts of the cross-section by means of test papers, a gas-laden air stream being used.
(v) By suitable measurement of the temperatures attained at the side and in the middle of a wide column.

Experimental

(i) The measurement of the distribution of flow across the charcoal proved difficult because small changes of pressure in any section would cause considerable alteration in the linear flow rate through that section. It was therefore necessary to measure simultaneously the flow rate of air emerging from a column of charcoal in a circular middle section and in the annular space around, special care being taken that an equal resistance was offered to the air stream in each section.

Air, dried with calcium chloride and sulphuric acid, was supplied to the top of a bed of dried charcoal granules in a wide vertical glass tube. The bed rested on a copper gauze which filled the whole cross-section of the tube. This gauze was supported on the top of another tube inside and axially concentric with the main tube (Fig. 3). The air leaving the bed was therefore immediately divided into two parts, one flowing inside the inner tube and the rest between the inner tube and the main tube. The charcoal was introduced into the wide tube through a tube which was about the same diameter as the testing tube which had three very coarse gauzes across it, the middle one having its wires at 45° to the top and bottom ones. This packing device produced an even shower of charcoal granules falling into the tube when charcoal was poured in centrally at the top. It always gave a much more dense, tight and even packing in the wide tube than could be obtained by any other means. The flow of the air to the top of the bed was measured on a capillary flowmeter and the flow rates in the side and central sections were measured simultaneously with identical soap bubble measures. The latter measured the rate of flow by allowing the flow to drive a soap bubble along a tube and observing the time for the bubble to sweep out a calibrated volume. It was found to be of the utmost importance that the pressure drop beyond the charcoal should be the same for each section of the flow and that the total pressure should be as small as possible. Hence the soap bubble measurers were used since only a very small pressure was needed to drive the bubble along the tube. Wide tubing was used exclusively beyond the charcoal, except for chokes, to reduce the pressure loss.

The first method employed for ensuring this equality of pressure was by means of adjustable chokes F arranged so that the flow rates for the side and middle sections were unchanged when the measurers were interchanged. The diameter of the main tube was 4·87 cm. and of the middle section 3·54 cm. so that the areas of the two sections were not very different, the side being 7·99 sq. cm. and the control 9·29 sq. cm. The values obtained for the ratios of the linear flow rates in the side and middle sections are given in Table IV. A few experiments were carried out in the same manner with a wide tube the walls of which were corrugated, the ridges running round the tube. An experiment with a flow rate of 5000 cm.^{3}/min. in a tube with two corrugations gave the ratio of the linear flow rate in the side to that in the central section equal to 1·125. A similar experiment in a tube with three corrugations gave a ratio of 1·120 and when the flow rate was reduced to 3000 cm.^{3}/min. a ratio of 1·122. It will be seen that these ratios are virtually identical with those in Table IV and one can only conclude that corrugating the wall of the tube has no effect in reducing the linear flow rate in the outer section of the tube.

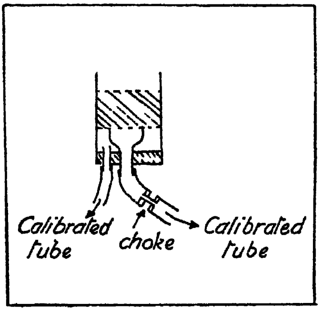

FIG. 3.—Device for measurement of flow rate across the charcoal column.

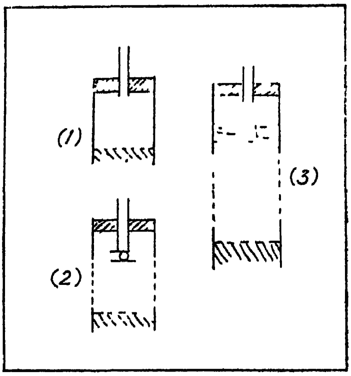

FIG. 4.—Methods of air introduction.

TABLE IV.—RATIO OF LINEAR FLOW RATE IN SIDE SECTION TO THAT IN CENTRAL SECTION

Diameter of main tube 4·87 cm. and of inner tube 3·54 cm.

(*a*) Charcoal grading 7-18 (*b*) Charcoal grading 10-18

Flow Rate (cm.^{3}/min.)	Ratio	Flow Rate (cm.^{3}/min.)	Ratio
3000	1·142	3000	1·131
4000	1·153	4000	1·138
5000	1·150	5000	1·135

The above technique of interchanging the soap bubble measurers could only be used when the volume flow rate through the side and central sections were approximately equal. To extend the measurements a new technique was adopted. In this the difference in pressure between the air below the side of charcoal bed and that below the centre of the charcoal bed was measured by a differential aniline-sodium carbonate solution manometer. The variable chokes between the bed and the two soap bubble measurers were then adjusted until there was no deflection on the manometer when the air flow was turned on and off. This meant that the pressure below the charcoal was uniform when the air was flowing, being equal in the central section and in the annular space around. Because of the sensitivity of the differential manometer used a difference in pressure between these two sections of 10^{-3} mm. Hg was easily detectable.

Three different variations of air inlet to the wide tube containing the charcoal were used. These are shown in Fig. 4. Inlet (1) was a tube and (2) was developed from this so that there should not be a central jet of air hitting the centre of the bed. However, later it was decided to obtain results with inlet (3). Here, the air, entering through a narrow inlet, impinged on a soldered circle in the middle of a gauze. This broke up the flow characteristic of the jet. Beneath the gauze was 2 cm. bed of small copper sulphate crystals on 1 cm. of 14-25 graded dry charcoal supported on another gauze and then about 25 cm. of empty tube before the charcoal surface. It was thought that this arrangement would ensure that there were no great irregularities in the flow to the charcoal bed.

In examining the flow across the charcoal with this arrangement three sets of experiments were carried out in a tube of diameter 4·86 cm., each set with an inner tube of a different diameter (3·12, 3·60 and 4·04 cm.). From the results obtained the linear flow rates in four sections could be calculated : (*a*) within a radius of 1·56 cm. ; (*b*) between 1·56 and 1·80 from the centre ; (*c*) between 1·80 and 2·02 from the centre ; (*d*) between a radius of 2·02 cm. and the wall at a radius of 2·45 cm. The results obtained using a charcoal graded 14-25 using the three different inlets are shown in Table V. Three different flow rates were used : 3000, 4000 and 5000 cm.^{3}/min. corresponding to average linear flow rates in an open tube of 160, 215, and 270 cm./min. The Table gives the linear flow rate in each section relative to the average linear flow rate. The last column gives the relative flow rate for the two outermost sections taken together.

The results for the inlet (3) will be considered first since the air is being introduced most evenly in this case. Because of the viscous effects near the wall, there will be a greater flow rate in the centre in the open part of the tube. This will tend to give a linear flow rate above the average through the middle of the charcoal. On the other hand, the charcoal will be less well packed near the wall and will therefore offer less resistance to the passage of the air. The flow rate through the middle of the bed was found to be slightly greater than in the regions adjoining it, and the flow within 0·6 cm. of the wall was also in excess (see Table V). This excess is mainly in the region between $r = 1·80$ and 2·02 cm., indicating that it is not due to a leakage down the wall itself but rather to an increased rate of flow through the less well-packed charcoal near the wall. The distribution of flow is practically independent of flow rate at the flow rates used.

TABLE V.—Variation of Linear Flow Rate across a Cylindrical Charcoal Bed. The Table Lists Relative Linear Flow Rates (R.L.F.R.) in Sections Defined by their Inner and Outer Radii

Inlet tube (1)					
Inner radius	0	1·56	1·80	2·02	1·80
Outer radius . . .	1·56	1·80	2·02	2·43	2·43
R.L.F.R., F = 3000 cm.^{3}/min. .	0·95	0·85	0·86	1·21	1·09
R.L.F.R., F = 4000 cm.^{3}/min. .	0·98	0·79	0·83	1·21	1·08
R.L.F.R., F = 5000 cm.^{3}/min. .	1·00	0·79	0·76	1·22	1·07
Inlet tube (2)					
Inner radius	0	1·56	1·80	2·02	1·80
Outer radius . . .	1·56	1·80	2·02	2·43	2·43
R.L.F.R., F = 3000 cm.^{3}/min. .	0·90	0·97	1·23	1·04	1·10
R.L.F.R., F = 4000 cm.^{3}/min. .	0·92	0·90	1·19	1·07	1·11
R.L.F.R., F = 5000 cm.^{3}/min. .	0·92	0·82	1·13	1·12	1·12
Inlet tube (3)					
Inner radius	0	1·56	1·80	2·02	1·80
Outer radius . . .	1·56	1·80	2·02	2·43	2·43
R.L.F.R., F = 3000 cm.^{3}/min. .	0·90	0·79	1·33	1·08	1·16
R.L.F.R., F = 4000 cm.^{3}/min. .	0·90	0·78	1·32	1·09	1·16
R.L.F.R., F = 5000 cm.^{3}/min. .	0·88	0·85	1·50	1·09	1·16

With a narrow inlet tube (1), the air impinges on the centre of the charcoal surface; there will be some spreading, but the increased pressure resulting from the impact of the air stream at the centre will cause a flow in excess of the average down the middle of the bed. The results in Table V show that there was an excess flow down the middle which increased with increasing flow rate. This is reasonable because the higher the flow rate the greater the force with which the jet will impinge on the middle of the charcoal surface. The results also show a much greater excess of flow rate in the section nearest the wall. This, again, must be due to the less dense packing near the wall, and may also be partly due to a slight excess of pressure due to lateral spreading of the air stream over the upper surface and its impinging on the side wall. The intermediate zone would thus have above it a pressure which is slightly less than that at the wall or at the centre, and the flow will be correspondingly less. With inlet (2) the air is thrown in four directions by the inlet tube and it is impossible to predict the nature of the flow at the top of the charcoal, this being greatest in the region slightly removed from the wall, as with inlet (3). The explanation is probably the same. It is seen therefore that the distribution of flow is very dependent on the type of inlet tube used but that it is always greatest somewhere near the outer wall of the tube even when the wall is corrugated.

(ii) A second method of studying the variation of flow across a bed of charcoal granules was as follows. A stream of air containing a small proportion of a gas adsorbed by the charcoal was passed through a bed in a glass tube. The bed was then divided into an inner and an outer portion and the amount of the gas removed per gram of charcoal in each section was estimated chemically This has been done for hydrogen sulphide on a coppered charcoal and for cyanogen chloride on coppered and silvered charcoals. In each case the diameter of the tube was about 4½ cm. Immediately the flow was stopped, the column was separated into two portions by forcing a thin-walled brass tube into it, this tube being concentric with the main tube. Each section was then analyzed for the products of removal. With hydrogen sulphide, S was produced by oxidation and determined by extraction with carbon disulphide, the latter being evaporated off and the sulphur weighed. The cyanogen chloride was extracted with hot NaOH, excess silver nitrate added and the excess titrated with thiocyanate. Previous blank experiments measured the very small amounts of S and chloride on the original charcoal. The weights of gas dealt with per gram of dry charcoal were then calculated after weighing the dried charcoal. The final result is the ratio of gas per gram of charcoal for the side and central sections. Typical runs are shown below.

(*a*) For cyanogen chloride.
Diameter of main tube, 4·2 cm. and that of middle section, 3·9 cm.

Ratio: Side/Central = 1·2/1·0.

(*b*) For cyanogen chloride.
Diameter of main tube, 4·2 cm. and that of middle section, 3·0 cm.

Ratio: Side/Central = 1·2/1·0.

(*c*) For hydrogen sulphide.

A slightly different technique was used, the middle section being separated during the whole experiment by a cylindrical muslin bag of 3·0 cm. diameter placed in the charcoal.

Diameter of main tube 4·5 cm.
Ratio: Side/Central = 1·29/1·0.

The results are in good agreement with those given in Part I where an entirely different method was used.

Similar experiments were made using wet charcoal and estimating the weight of water removed from each section by a dry air stream. The tube diameter was 4·5 cm. and the middle section was separated by a brass tube of diameter 3·0 cm. After 2 hr. the water content of the central section was reduced from 14·14 % to 11·44 % and that of the side portion to 10·77 % giving a ratio of water removed from the side and central sections as 1·24/1·0.

(iii) Sulphur dioxide was passed through a bed of silica gel granules coloured with alkaline phenolphthalein. A clear line of demarcation could be observed as the wave advanced. At places this was a little irregular due to small leaks ahead of the main front. When the visible wave had just reached the gauze at the end of the column the air stream was stopped. The silica gel was removed carefully so that the bottom layer was left undisturbed. It appeared as a ring of colourless gel surrounding a circle of pink gel, indicating that the gas had advanced at the side ahead of the main wave front. There was about 2 or 3 mm. difference in depth of penetration between the side and the centre at the bottom of a 6 cm. column. This provided additional confirmation that the flow rate at the side is in excess of the average.

(iv) A qualitative estimation was made of the position of initial penetration of hydrogen sulphide when air containing a small amount of that gas was passed through a bed of coppered charcoal in a tube of diameter 4·5 cm. A similar experiment was carried out for air containing a small amount of sulphur dioxide. Suitable test papers (lead acetate for hydrogen sulphide, and litmus for sulphur dioxide) were supported parallel to the air stream immediately beyond the charcoal, the paper extending diagonally from one wall to the other. With this arrangement the air flow in the bed was not disturbed. The papers changed colour at the side indicating that initially penetration occurred predominantly at the side. The effect persisted even if the charcoal was heaped at the side of the tube at the top surface of the bed (inlet end) to avoid any possibility of the column being shorter at the side. The middle of the test paper began to change colour about 10 min. after the side.

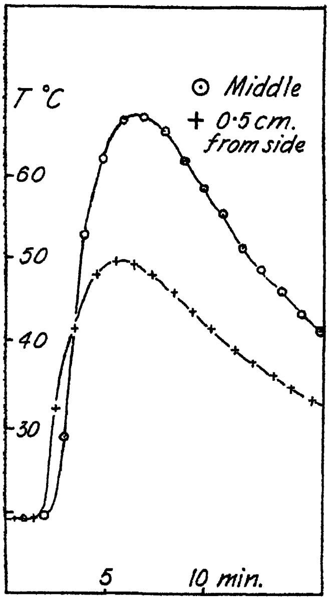

FIG. 5.—Rates of temperature rise at different distances from tube wall; 1 % H_2S, dry charcoal.

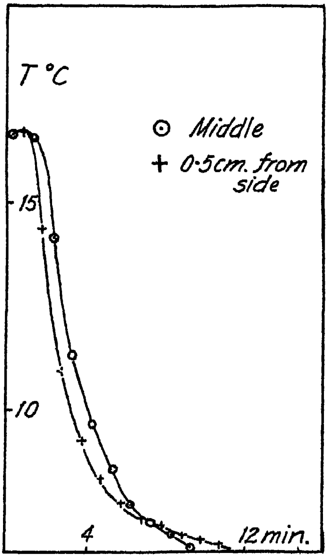

FIG. 6.—Rates of temperature rise at different distances from tube wall. Dry air, wet charcoal.

Separate experiments showed that corrugating the walls of the tube containing the charcoal did not affect the side leakage as detected by this method. The effect of preventing the air from entering or leaving the charcoal bed within 5 mm. of the wall by blocking out a ring 5 mm. wide at the edge of the top and bottom gauzes was found to prevent side leakage when tested by the present method. However, side leakage was only prevented if the device was placed at both ends of the charcoal.

(v) Evidence of the excess flow rate down the side has been obtained from the heating effects in the charcoal during the passage of an air stream containing either sulphur dioxide or hydrogen sulphide. At the beginning of the experiment the temperature is uniform and the rise in temperature at any place in or near the inlet surface will depend on the amount of gas removed at that place, which is a function of the amount of gas arriving at that place. If the flow rate at the side is greater than at the middle it will be expected that the rise in temperature at the side of the first layer of a charcoal column will be more rapid than at the middle. As soon as the limiting temperature is approached a temperature gradient will be set up across the column and the final temperature at the middle will be greater than at the side. Observations of this effect have been made in wide glass tubes for air streams containing 1 % of hydrogen sulphide and sulphur dioxide. A typical result for hydrogen sulphide is shown in Fig. 5, the thermocouples measuring the temperature of the charcoal being 0·5 cm. below the surface, one being in the middle of the bed and the other 0·5 cm. from the wall. The temperature rose more rapidly at the side than at the middle for the first few moments of the run, thus indicating that more gas was going on to the side portions than on to the central portion. In the steady state the expected temperature gradient is, of course, set up.

Similar experiments have been made by blowing dry air over charcoal saturated with water. Here a decrease in temperature occurs. Again, during the first moments of a run, the side region of the front surface changes in temperature more rapidly than the middle. A typical result is shown in Fig. 6, the thermocouples being placed in the same positions as in the experiment shown in Fig. 5.

In connection with the above, some experiments were carried out to determine the density of packing of two different charcoals in tubes of different diameter. The glass tubes used were of diameters 0·98, 1·51, 1·96, 3·02 and 4·79 cm. A known weight of charcoal was introduced into the tube, tapped to reduce it to the shortest length possible (in the 4·79 cm. tube the crossed gauze packing device was used) and the length measured. From this the apparent specific gravity could be calculated. A number of experiments were carried out with various lengths of each charcoal in each tube and averages taken. The results are summarized in Table VI for both the 7-18 graded charcoal and that graded 10-18 B.S.S. Taking the results for the 0·98, 1·51 and 1·96 cm. tubes it will be seen that the apparent specific gravity increases regularly on passing from the 0·98 to the 1·96 cm. tube. This indicates that the smooth wall interferes with the close packing of the charcoal granules near to it. This effect is greater with the coarser granules as would be expected. In tubes wider than 2 cm. the apparent specific gravity is less than in the 1·96 cm. tube and decreases on passing to wider tubes. It is believed that this occurs because no method of tapping the tube could be found which was capable of shaking the charcoal down fully in such large beds.

TABLE VI.—APPARENT SPECIFIC GRAVITIES OF TWO CHARCOALS IN TUBES OF DIFFERENT DIAMETERS—THE CHARCOALS WERE PACKED TO MAXIMUM POSSIBLE DENSITY

Tube diameters (cm.)	0·98	1·51	1·96	3·02	4·79
App. sp. grav.					
7-18 grading	0·722	0·752	0·767	0·754	0·740
10-18 grading	0·623	0·637	0·641	0·628	0·617

Discussion

The results described above lead to three main conclusions:

(*a*) The distribution of air-flow through the granular bed is dependent on the pressure conditions above the bed which are decided by the way in which the air is brought up to the surface. It is also greatly affected by small variations of pressure distribution beyond the bed. In general, it is very sensitive to the detailed pressure conditions above and below the bed.

(*b*) There is always an excess flow rate down the outer regions of the charcoal, though this is often greatest in the region slightly removed from the wall. There are strong indications that this occurs because the smooth wall reduces the density of packing near it.

(*c*) Neither of these conclusions are altered when the wall of the tube is corrugated.

The effect of the presence of the container wall on the density of packing near the wall and hence on the fluid flow in this region has also been considered by Furnas.[12] Working with lead shot and Cuyuna ore, he found the wall effect to be particularly important for low ratios of the container diameter d_t to particle diameter d_p. He gives curves expressing the wall effect as a function of d_p/d_t for packings having various proportions of voids. Furnas' detailed analysis of the wall effect was, however, questioned by Chilton and Colburn,[13] though these workers used Furnas' 50 % voidage curves in correlation of their own data. Gamson, Thodos and Hougen [14] also used Furnas' method for assessing the extent of wall leakage. None of these three researches attempted a direct measurement of the distribution of velocities across the granular beds used.

---

[12] Furnas, *U.S. Bur. Mines*, *Bull.* 307, 1929.

Saunders and Ford,[15] using a Pitot gauge, found that the flow of gas through a bed of spherical granules was greatest near the wall, being 50 % greater there than over the rest of the bed. These results indicated that the flow was greatest in the immediate vicinity of the wall but it is difficult to assess the condition of the air stream reaching the bed in these experiments (see (*a*) above). Rose [4] states that photographs of a bed show that the porosity is greater near the walls than in the rest of the bed. He suggests that wall effects in flow of fluids through beds are due to the combined effect of the greater porosity near the walls and that, in that region, the passages are less tortuous. Both these conclusions are consistent, in general form, with our results and conclusions.

The results obtained for the pressure fall through a bed of granules require that any material adsorbed from a gas stream must migrate over the surface of the granules from the outer surface where it is taken up to the inner pore surface where it is stored.

Finally, the results of Part I of this paper were obtained without regard to variations of flow across the charcoal bed. These variations, arising from a non-uniform porosity, do not cause the general equation (1) to be inapplicable to the average behaviour. The quantities S_0 and D_0, deduced from the experimental results, are presumably uniform across the bed and the values obtained for them should be reliable.

Acknowledgements are made to the Chief Scientist, Ministry of Supply, for permission to publish this work.

Inorganic Chemistry Laboratory,
Oxford University.

[13] Chilton and Colburn, *Trans. Amer. Inst. Chem. Eng.*, 1931, **26**, 178.
[14] Gamson, Thodos and Hougen, *ibid.*, 1943, **39**, 1.
[15] Saunders and Ford, *J. Iron Steel Inst.*, 1940, **141**, 1.

REACTIONS BETWEEN NITROGEN DIOXIDE AND FORMALDEHYDE

PART III.—THE DETERMINATION OF FLAME SPEEDS

BY F. H. POLLARD AND R. M. H. WYATT

Received 21*st September*, 1949

The spatial velocities of flames moving in mixtures of nitrogen dioxide and HCHO at initial pressures of 4-8 cm. Hg in a spherical vessel, have been measured using *Schlieren* photography. The velocity is independent of the initial pressure of the mixture, and reaches a maximum for a mixture containing 43·2 % HCHO, which is slightly higher than the stoichiometric mixture of 41·5 %. The relative importance of H, O, and OH in the flame processes is discussed and variations in the delay period are considered in relation to current theories of spark igntion.

As the first two papers [1, 2] of this series showed, nitrogen dioxide and HCHO react slowly in the temperature range 118-180° C, obeying a second-order law, and explosively, under certain conditions, above 160° C. It was also found that a mixture of the two gases could be ignited by a spark down to quite low pressures (a few mm. Hg). The determination of flame speeds in such mixtures is of considerable interest in providing a link in the series of reactions that take place during the burning of nitric esters. In the first stage,[3, 4] the molecules of nitric ester break up to give nitrogen dioxide, aldehydes and alcohols, which then react to give, amongst other products, CO, NO and H_2. Combustion involving these last three molecules constitutes the last stage.

It has long been known, too, that in the combustion of hydrocarbons, HCHO is an intermediate product which plays an important part in the mechanism of the flame, whilst nitrogen dioxide has a marked effect on the ignition limits. Hitherto no direct study of the reactions between nitrogen dioxide and HCHO under flame conditions has been made.

Experimental

The method of spherical flames at constant volume was chosen to determine the flame speeds, as the other methods, viz. the soap bubble method, the tube method and the burner method were not suitable. Preliminary experiments showed that the maximum spatial velocity was of the order of 1000 cm./sec., which is similar to that for ozone-oxygen mixtures analyzed by this method by Lewis and von Elbe,[5] and for CO and hydrocarbon-enriched air mixtures by Fiock and co-workers.[6] These experiments also showed that direct photography was of no use, for the nitrogen dioxide in front of the expanding sphere of flame filtered out the emitted light and only the last portion of the flame movement was recorded. So *Schlieren* photography was utilized and the usual spherical vessel was modified to include two plain glass windows and yet keep its spherical shape as far as possible. A 5-l. flask (no metal bomb being available) was taken and two large and parallel window flanges were blown in it so that two windows (20 cm. square × 1 cm. thick) could be sealed on by means of Picein and clamped by tie bars, B and B′ (see Fig. 1). The diameter of the vessel was 21·3 cm., and the distance between the two windows was 20·3 cm. Two other smaller flanges were added, one serving to fix on the assembly of ignition leads and gas inlet, and the other for the pressure indicator. This spherical vessel was housed in a cubical asbestos board oven O, thermostatically controlled at 57° C, to avoid polymerization of HCHO. The source of light H was a 250-W medium-pressure compact-source mercury lamp, and the rays from this lamp were focused on to knife edge K by means of lens L_1 and the aluminium front-surfaced mirror A inclined at 45°. The cone of light from the knife edge traversed the spherical vessel, was reflected back again through the vessel by the concave mirror M to another knife edge directly below the first (K), and through the lens L_2 and so on to the 35 mm. film rotating on the drum

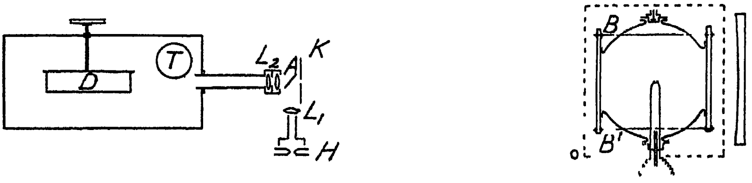

FIG. 1.—Apparatus for measuring flame speeds.

---

[1] Pollard and Wyatt, *Trans. Faraday Soc.*, 1949, **45**, 760.
[2] Pollard and Woodward, *ibid.*, 1949, **45**, 767.
[3] Phillips, *Nature*, 1947, **160**, 753.
[4] Adams and Bawn, *Trans. Faraday Soc.*, 1949, **45**, 494.
[5] Lewis and von Elbe, *J. Chem. Physics*, 1934, **2**, 283.
[6] Fiock, Marvin, Caldwell and Roeder, *Nat. Adv. Com. Aero. Reports*, 1939, No. 682.

D of the camera. The shutter on the lens of this camera was operated by a solenoid.

The pressure indicator was of the condenser type. The capacity changes due to deflection of its diaphragm (which was part of the main body of the indicator) caused corresponding changes in an oscillator frequency, which were converted into voltage variations and recorded by means of a cathode ray oscillograph. The optical arrangement only allowed the central half of the flame movement to be photographed. During this movement the pressure rises only by about 15 % and therefore has to be determined very accurately. The majority of the experiments were carried out at an initial pressure of 6·0 cm. Hg, as an initial pressure higher than 8·0 cm. Hg resulted in an explosion that jolted the windows from their seatings. The determination of a pressure increase from 6·0 cm. Hg to about 7 cm. Hg in the time interval of 5 millisec. was at first thought to be possible, but non-reproducibility led to the abandonment of pressure rise determination, and in most cases the values obtained were too low. A metal bomb with plane windows is now being made available, so that explosions can be carried out at higher pressures and it is hoped that satisfactory values of burning velocity will be obtained. On the other hand, at higher pressures, a substantial percentage of the nitrogen dioxide will be in the dimeric form and the photography of such flames will be more difficult even if a higher powered lamp is used.

Using the 250-W lamp, no image was formed on Ilford H.P.3 film, but by subjecting the exposed film to a low intensity lamp for 30 min. (the hypersensitization by uniform low intensity exposure method) before developing with a maximum energy developer at 24° C gave satisfactory traces as long as the partial pressure of nitrogen dioxide was not greater than 4·0 cm. Hg. Strips of 1/32 in. tape resistance wire were fixed to the front of the window of the bomb to act as reference markers. By measuring the distance from the knife edges to the front of the first window (i.e. to the plane containing the tape wires) and from the knife edges to the centre of the bomb, the distance between the inner edges of the tape wires as given by a still photograph of the tape wires and sparking points, could, by simple geometry, be translated into the real distance in the centre of the bomb. The timing was provided by an electrically maintained 1000 cycle tuning fork, the output of which was fed to a small cathode ray tube T, housed in the drum camera, and the circuit was so arranged that the first pulse from the fork fired the mixture, the firing unit being thyratron controlled.

Enlarged prints were made of the flame negatives and the still photograph of the tape wires and sparking points. Both were measured up with a Zeiss millimetre scale, and the flame radii values were redrawn on graph paper.

The materials were prepared and stored as given in Part I.[1] The argon used was of 96 % purity, the remainder being nitrogen. In any experiment, HCHO was admitted to the spherical vessel first to a predetermined pressure by using a spiral gauge, attached directly to the vessel via an explosion tap, as a null instrument. The nitrogen dioxide was then admitted, or if argon was to form part of the explosive mixture, this was admitted next, and nitrogen dioxide last.

Results

The Effect of Pressure on the Flame Speed.—The flame speed was shown to be independent of pressure in two ways. First, the explosion time (i.e. the time that elapses between the point of ignition and the maximum pressure attainable) was determined for equimolar mixtures of nitrogen dioxide and HCHO. At an initial pressure of 4·0 cm. Hg, three experiments gave explosion times of 13·2, 13·6 and 12·3 milliseconds; at 6·0 cm. Hg, two experiments gave 12·9 and 12·9 milliseconds, and at 8·0 cm. Hg, two experiments gave 13·1 and 12·8 milliseconds. (These seven values are for an auxiliary glass vessel of 3½ l. capacity, with no windows.) The maximum spatial velocity was also determined from the *Schlieren* photographs for equimolar mixtures. The values for initial pressures of 4·15, 4·29, 5·00, 5·13, 6·12, 6·17, 7·08 and 7·10 cm. Hg were 1110, 1020, 1080, 1120, 1120, 1090, 1090 and 1080 cm./sec.

It is estimated that the burning velocity for an equimolar mixture lies between 100 and 140 cm./sec. The maximum expansion ratio E (i.e. the ratio of the volumes of a certain mass of gas after and before explosion, measured at constant pressure) calculated from the theoretical flame temperature at

6·0 cm. Hg, is 12·4, and the maximum pressure developed in an explosion of an equimolar mixture was found to be 13·5 times the initial pressure. Some pressure records, as the flame travelled out from the centre, gave values approaching 140 cm./sec. for the burning velocity and assuming the expansion ratio at the beginning of the spread of flame to be between 8 and 10, this gives the burning velocity a value of 100-140 cm./sec. (as $S_b \simeq S_s/E$).

The Dependence of the Spatial Velocity on Composition. -The results of the determinations of the spatial velocity for different compositions of the two reactants are shown in Fig. 2. All were carried out at an initial pressure of 6·0 cm. Hg and 330° K. The maximum velocity of 1355 cm./sec. occurs at a composition of 43·2 % CH_2O + 56·8 % NO_2 (i.e. 1/1·3). The slow oxidation of formaldehyde by nitrogen dioxide [1] could be represented by the following overall equation,

$$5CH_2O + 7NO_2 \rightarrow 3CO + 2CO_2 + 5H_2O + 7NO,$$

which corresponds to a "stoichiometric" mixture of 41·5 % CH_2O + 58·5 % NO_2 (1/1·4). So this maximum speed concentration is in agreement with the usual findings that the fastest burning mixture contains slightly more oxidizable material than the "stoichiometric" mixture. The limits of propagation at this initial pressure of 6·0 cm. Hg lie between 22·5 and 25 % CH_2O and 61 and 67 % CH_2O.

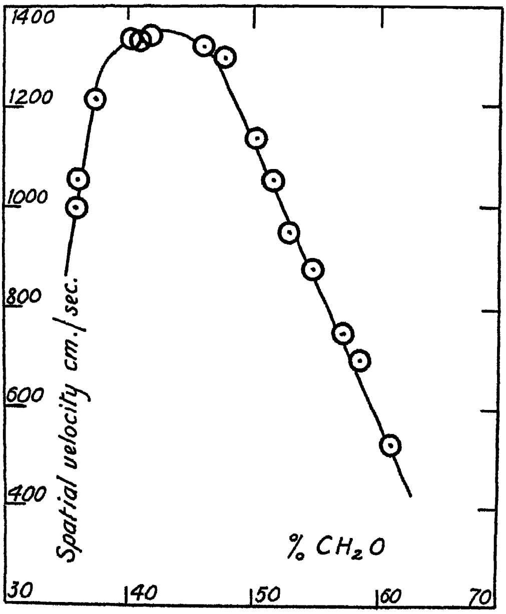

FIG. 2.—Variation in spatial velocity with the composition of CH_2O + NO_2 mixtures.

Addition of Argon to the Explosive Mixture.—A mixture of 42 % CH_2O + 58 % NO_2 was diluted with increasing amounts of argon and the spatial velocities of those mixtures are shown in Fig. 3. The partial pressure of the combustible gases was kept at 5·0 cm. Hg throughout. This graph is similar to that found by Fiock and Roeder [7] for A- and He-diluted CO + O_2 explosions. Argon was the only diluent used, because from a theoretical viewpoint it was not thought advisable to add nitrogen, since it is a major product of the combustion itself. This is in contrast to the usual case, where oxygen is the oxidant, with the nitrogen or other gas serving almost purely as a diluent.

Flame Temperatures.—Temperatures of the flames for mixtures of varying compositions at total initial pressures of 6·0 cm. Hg have been calculated at

[7] Fiock and Roeder, *Nat. Adv. Com. Aero. Reports*, 1936, No. 553.

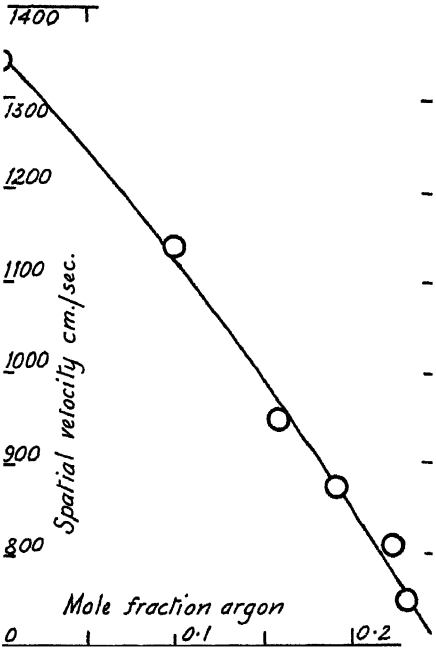

FIG. 3.—Effect of argon on the spatial velocity of a 42 % CH_2O + 58 % NO_2 mixture.

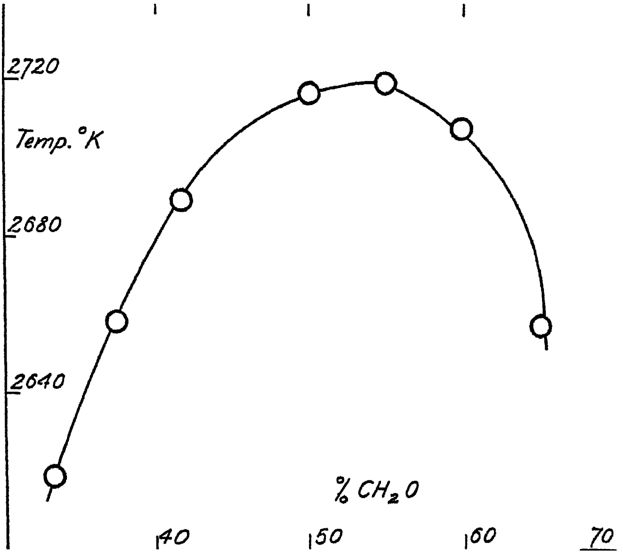

FIG. 4.—Calculated flame temperatures for varying $CH_2O + NO_2$ mixtures.

that pressure and are shown in Fig. 4. The following equilibria have been taken into account:

$$CO_2 + H_2 \rightleftharpoons CO + H_2O,^{8} \quad H_2O \rightleftharpoons OH + \tfrac{1}{2}H_2,^{9} \quad H_2O + \tfrac{1}{2}N_2 \rightleftharpoons NO + H_2,^{10}$$
$$2H_2O \rightleftharpoons O_2 + 2H_2,^{9} \quad \tfrac{1}{2}O_2 \rightleftharpoons O,^{11} \quad \tfrac{1}{2}H_2 \rightleftharpoons H.^{12}$$

The maximum temperature lies at a composition of 53 % CH_2O + 47 % NO_2, i.e. 1/0·9. Again the composition for maximum temperature is always slightly richer than the stoichiometric, due to dissociation at the flame temperature. Dissociation is increased as the pressure is decreased, and this may account for the rather large difference between the observed stoichiometric value of 41·5 per cent and the above value of 53 per cent CH_2O, though the theoretical flame temperature may follow the equation,

$$CH_2O + NO_2 \rightarrow CO_2 + H_2O + \tfrac{1}{2}N_2.$$

The partial pressures of H atoms, O atoms and OH radicals in equilibrium at these flame temperatures are given in Table I, together with the corresponding spatial velocity as read off from Fig. 2.

TABLE I

% CH_2O in Combustible Mixture	Temp. ° K	Partial Press H Atoms × 10^{-1} atm.	OH	O Atom	S_s cm./sec.
33·5	2618	12·2	36·2	29·2	780
37·5	2658	16·5	39·1	32·1	1265
41·5	2690	21·2	40·5	32·4	1345
50·0	2716	31·6	41·7	26·9	1145
55·0	2719	36·8	38·4	20·6	875
60·0	2707	40·5	31·3	14·4	606
65·0	2657	40·6	21·4	6·8	340

For the A-diluted mixtures, the temperatures are 2670, 2660, 2651, 2642° K when the corresponding mole fractions of argon are 0·000, 0·091, 0·167, 0·231. This gives a graph similar to Fig. 3.

Analysis of Gaseous Products.—A sample of the gases remaining in the bomb after the flame had traversed the mixture was taken and analyzed as shown in Part I. Table II gives the results for mixtures of varying composition, all at 6·0 cm. Hg initial pressure.

TABLE II

% CH_2O in Combustible Mixture	% N_2	% NO	% N_2O	% H_2	% CO	
34·7	34·6	27·2	2·6	0·0	2·	32·0
40·1	33·8	19·1	0·3	0·0	1·	44·0
45·3	33·1	9·9	0·2	0·0	2·	54·0
50·0	31·1	0·6	0·1	0·0	3·	64·8
55·0	28·1	0·0	0·1	3·6	23·	45·0
60·0	23·3	0·0	0·1	8·5	32·	36·1

It must be remembered that these analyses are of gases that have cooled down after a flame has traversed the mixture under a rapidly rising pressure and tem-

---

[8] Kassel, *J. Amer. Chem. Soc.*, 1934, **56**, 1838. Gordon, *J. Chem. Physics*, 1934, **2**, 549. Clayton and Giauque, *J. Amer. Chem. Soc.*, 1933, **55**, 5071. Davis and Johnston, *ibid.*, 1934, **56**, 1047.

[9] Dwyer and Oldenburg, *J. Chem. Physics*, 1944, **12**, 351.

[10] Johnston and Chapman, *J. Amer. Chem. Soc.*, 1933, **55**, 153. Giauque and Clayton, *ibid.*, 1933, **55**, 4875.

[11] Johnston and Walters, *ibid.*, 1933, **55**, 187.

[12] Giauque, *ibid.*, 1930, **52**, 4827.

perature. The absence of hydrogen, unless HCHO is in excess, is in agreement with the analyses of the products reported in the earlier paper on explosion limits.[3] If the assumption is made that all the nitrogen dioxide originally in the mixture is reduced to NO, N_2O and N_2 (the remaining gases are colourless over the range in Table II), then a measure of the carbon balance can be obtained. The values of the ratio C/N in the original mixtures, in the same order as that given in Table II, are 0·53, 0·67, 0·83, 1·00, 1·22 and 1·50. The values for this ratio in the resultant gases are 0·35, 0·54, 0·74, 1·08, 1·21 and 1·46. Satisfactory agreement is obtained for those mixtures originally containing more than 5 per cent HCHO, and it is reasonable to suppose that some HCHO survives, for mixtures containing less than 50 per cent.

Delay Period.—All the radius-time traces are curved just after the beginning of the flame movement, and are then straight for the remainder of the travel that is photographed. This initial acceleration has been observed before for other gaseous mixtures and the values of the delay period (i.e. the intercept on the time axis on producing back the straight portion of the radius-time trace, are given in Table III.

TABLE III

Spatial Velocity cm., sec.	Delay Period millisec.	Spatial Velocity cm./sec.	Delay Period millisec.
1340	0·15	1060	0·125
1330	0·05	1055	0·15
1330	0·10	1000	0·125
1330	0·15	955	0·225
1325	0·08	880	0·15
1290	0·225	754	0·475
1215	0·25	700	0·525
1140	0·20	530	1·00

The data in Table III correspond to the flame speeds and mixtures illustrated in Fig. 2.

Discussion

Mechanism of the Flame Reactions.—According to the theory of Zeldovich and Semenov[13] and Boys and Corner,[14] if the rate-controlling reaction in the flame is second order, then the linear burning velocity is independent of the pressure. Though we were only able to show that the spatial velocity is independent of pressure, it is very probable that the burning velocity is likewise independent of pressure. The decrease in temperature of the flame with decrease in pressure is to some extent compensated by an increase in the number of molecules, radicals and atoms in equilibrium at the flame temperature, i.e. the expansion ratio is probably not affected by pressure. Strictly, this integral order only holds if the flame temperatures throughout the series of experiments are identical. The second order dependence is in agreement with that found in the slow thermal reaction, in which the rate is first order with respect to HCHO and to nitrogen dioxide, but it does not necessarily imply that these two molecules are themselves concerned in the rate-controlling reaction or reactions.

Tanford and Pease[15] showed a close correlation between calculated values of the concentration of H atoms in equilibrium at the flame temperature, with burning velocities for moist CO flames, and it was logical to suppose that the combustion processes in those flames depended upon diffusion of H atoms. From Table I it can be seen that the H atom concentration increases as the % HCHO is increased, and, in fact, increases while the speed decreases. On the other hand, the OH radical and O atom concentrations increase and decrease, the latter having a maximum at the same mixture composition as the maximum in the spatial velocity. When the partial pressure of O atoms is plotted against the spatial velocity, two straight lines are obtained, one for the formaldehyde-rich mixtures and the other for the nitrogen dioxide-rich mixtures, intersecting at the maximum velocity values. This linearity must be fortuitous to some extent since the burning velocity is not exactly proportional to the spatial velocity over the range of compositions considered here. Now Tanford and Pease calculated the radical concentrations in the same mixtures for which Jahn [16] had previously determined the burning velocities. These mixtures contained CO, O_2, N_2, H_2O and H_2; but our calculations are for mixtures of only the two reactants, NO_2 and HCHO. One has to be careful in making deductions, since the burning velocity is not a function of one variable alone but depends on atom concentration, final temperature, diffusivity, conductivity, etc.; nevertheless, the correlation between the speed and the O atom concentration is very striking. The participation of O atoms in the flame reactions is highly probable, since they are readily available at the flame temperature; thus,

---

[13] Zeldovich and Semenov, *J. Expt. Theor. Phys. U.S.S.R.*, 1940, **10**, 1116.

[14] Boys and Corner, *Proc. Roy. Soc. A*, 1949, **197**, 90.

[15] Tanford and Pease, *J. Chem. Physics*, 1947, **15**, 431; 1947, **15**, 433; 1947, **15**, 861.

$$NO_2 \rightarrow NO + O,$$

and this initial step can be followed by such reactions [17] as

$$O + HCHO \rightarrow OH + CO + H,$$
$$H + HCHO \rightarrow H_2 + CO + H,$$
$$OH + HCHO \rightarrow H_2O + CO + H.$$

It also seems reasonable to suppose that, as the rate of diffusion of H atoms is much greater than that of O atoms, the rate-determining process may be O atom diffusion. Since no hydrogen is observed in the gaseous products, except for mixtures rich in HCHO, it would seem that the H atoms are rapidly removed by subsequent oxidation of hydrogen by either nitric oxide or nitrogen dioxide. The carbon monoxide must be similarly oxidized, since it is only present in small amounts when hydrogen is absent from the gaseous products (see Table II). A few experiments with hydrogen–NO_2 mixtures showed that under the same conditions, these flames propagate at a faster rate than formaldehyde + nitrogen dioxide mixtures, and carbon monoxide + nitrogen dioxide mixtures could not be ignited by the spark, whether dry or moist.

The addition of molecular O_2 to the initial mixture of formaldehyde and nitrogen dioxide would presumably have increased the partial pressure of O atoms, and also the flame speed, but no experimental data are yet available.

The Delay Period.—All the radius-time curves show a period just after ignition when the flame movement has a positive acceleration. Fiock and King [18] first noticed this for spherical flames with comparatively fast burning mixtures of moist CO and O_2. They thought the low initial spatial velocity resulted chiefly from subnormal values of the expansion ratio, which, in turn, could be associated with the establishment of an equilibrium depth and structure of the reaction zone. This explanation seems to require a rather large value for the depth of the reaction zone. Lewis and von Elbe [19] [20] suggested that this delay was due to greater heat dissipation through the relatively greater curved surface at the beginning of the spread of flame, and this has since been amplified in a theoretical paper on the subject of spark ignition. But *Schlieren* photographs of a mixture of 1 vol. hydrogen + 3 vol. oxygen at 6·0 cm. Hg pressure (obtained with the present apparatus) which might be expected to show a delay on account of the higher thermal conductivity of hydrogen, show little or no delay period.

---

[16] Jahn, *Der Zündvorgang in Gasgemischen* (Oldenburg, Berlin, 1942).

[17] Axford and Norrish, *Proc. Roy. Soc. A*, 1948, **192**, 518.

[18] Fiock and King, *Nat. Adv. Com. Aero. Reports*, No. 531, 1935.

[19] Lewis and von Elbe, *Combustion, Flames and Explosions of Gases* (Cambridge, 1938), p. 140.

[20] Lewis and von Elbe, *J. Chem. Physics*, 1947, **15**, 803.

The delay periods of nitrogen dioxide + formaldehyde flames may be explained along the lines of spark ignition work by Linnett and co-workers.[21] Their working hypothesis for the condition of ignition is the same as that assumed by Mole,[22] viz. the concentration of chain-propagating radicals should increase in an uncontrolled manner in the region around the spark. They concluded from their work that small amounts of inert gas aided ignition by showing up the diffusion of the chain radicals from the spark region. They showed also that the minimum ignition pressure rose when either CO or O_2 was in excess in a mixture of these two gases, containing a constant amount of water vapour. Table III shows that, with a few exceptions, for speeds greater than 1300 cm./sec., the delay period is not more than 0·15 millisec., for speeds between 1000 and 1300 cm./sec., the period lies between 0·15 and 0·25 millisec. and for smaller speeds, it progressively increases to 1 millisec. For HCHO + NO_2 explosions containing argon, the values for the delay period are all about the same, and none was greater than 0·175 millisec. Both of these series of results are in line with Linnett's results. The equilibrium state is reached as quickly as in the fastest mixtures, when argon is present to slow down the diffusion of the chain radicals from the spark ignition. The idea of hindering diffusion from the spark region and the idea of diffusion ahead of the flame front into the unburnt gas, as required for the flame propagation, are not necessarily contradictory. Until the equilibrium state is reached, the diffusion of active species from the spark region may be too fast for the necessary balance of diffusion and heat, according to the current theories of flame propagation, to be affected, mainly as a result of such thermal motion imparted to them by the spark. The violent conditions of the spark may also provide species which hinder the propagation processes, and until they are destroyed, the flame cannot attain its equilibrium state.

The authors wish to thank Prof. C. E. H. Bawn for helpful discussions, and Mr. J. D. Harris for some of the earlier experimental work. Acknowledgement is made to the Chief Scientist, Ministry of Supply, for permission to publish this work.

Department of Chemistry,
University of Bristol.

---

[21] Frost, Linnett and Raynor, *Trans. Faraday Soc.*, 1945, **41**, 487. Frost and Linnett, *ibid.*, 1948, **44**, 416.

[22] Mole, *Proc. Roy. Soc. A*, 1936, **48**, 857.

POLAROGRAPHIC BEHAVIOUR OF AROMATIC NITRO COMPOUNDS

PART II.—NITROSOBENZENE AND *N*-PHENYLHYDROXYLAMINE

By J. W. Smith and J. G. Waller

Received 14*th October*, 1949

The effects of pH value and of concentration on polarographic reduction of nitrosobenzene and oxidation of *N*-phenylhydroxylamine have been studied at 25° C. The results confirm that these two compounds form a reversible oxidation-reduction system. Between pH 4·0 and pH 10·0 the half-wave potentials vary linearly with the pH value, and at concentrations less than $2{\cdot}5 \times 10^{-3}$ M the diffusion currents are proportional to concentration. The heights of the polarographic waves for nitrosobenzene and *N*-phenylhydroxylamine are almost one-half the height of the reduction wave given by a nitrobenzene solution of equal molar concentration, confirming that the reduction of nitrobenzene requires four electrons at pH values greater than 3·0. The system nitrosobenzene–*N*-phenylhydroxylamine has also been studied potentiometrically.

In a previous paper[1] we have described the polarographic behaviour of nitrobenzene and a number of other nitro-compounds. Since that work was completed, Pearson[2] has published for nitrobenzene and the mononitrophenols polarographic data that are substantially in accord with our findings. Some recent results of Fields, Valle and Kane[3] and of Korshunov, Ryabov, Sazanova and Kirillova[4] for the half-wave potential of nitrobenzene are also in good agreement.

These investigations indicate that in neutral or alkaline solutions the reduction of nitrobenzene at the dropping mercury cathode requires four electrons, suggesting the formation of *N*-phenylhydroxylamine. In acid solutions, however, a second reduction wave occurs corresponding approximately to a two-electron process. In view of these results an investigation of the polarographic behaviour of nitrosobenzene and of *N*-phenylhydroxylamine was considered of interest. Conant and Lutz[5] have shown that these compounds form a reversible oxidation-reduction system, and Lutz and Lytten[6] have determined the oxidation-reduction potential of this system by titration with titanous chloride in 0·1 N HCl containing 50 % of acetone, with the object of ascertaining the effect of substituents in the aromatic ring on the redox potential. It should therefore be possible to compare any polarographic results for these two compounds with the results obtained from potentiometric titrations. The only published polarographic work on this system is a note[7] stating that *N*-phenylhydroxylamine gives rise to an oxidation wave in neutral solution. Levitan, Kolthoff, Clark and Tenenberg[8] showed that *N*-

---

[1] Page, Smith and Waller, *J. Physic. Chem.*, 1949, **53**, 545.

[2] Pearson, *Trans. Faraday Soc.*, 1948, **44**, 683, 692.

[3] Fields, Valle and Kane, *J. Amer. Chem. Soc.*, 1949, **71**, 421.

[4] Korshunov, Ryabov, Sazanova and Kirillova, *Zavod. Lab.*, 1948, **14**, 519.

[5] Conant and Lutz, *J. Amer. Chem. Soc.*, 1923, **45**, 1047.

[6] Lutz and Lytten, *J. Org. Chem.*, 1937, **2**, 68.

[7] Lester and Greenberg, *J. Amer. Chem. Soc.*, 1944, **66**, 496.

[8] Levitan, Kolthoff, Clark and Tenenberg, *ibid.*, 1943, **65**, 2265.

(*p*-sulphonamido)-phenylhydroxylamine in 0·1 N NaOH yields a polarographic reduction wave, but that it is not reducible at lower pH values. Some data for the polarographic behaviour of α-nitroso-β-naphthol have been given by Kolthoff and Langer,[9] who described the use of this compound for potentiometric titrations. The polarographic behaviour of *N*-nitroso-*N*-phenylhydroxylamine studied by Kolthoff and Liberti [10] shows no similarity to that of either nitrosobenzene or *N*-phenylhydroxylamine.

Experimental

The procedure for the polarographic investigation has been described in Part I.[1] Polarograms were recorded with a Cambridge polarograph, all measurements being carried out in a thermostat at 25 ± 0·1° C. The solutions examined all contained 10 % ethyl alcohol and 0·005 % gelatin was added as maximum suppressor. Half-wave potentials are reported in volts against the saturated calomel electrode (S.C.E.) and diffusion currents in microamperes. The dropping mercury electrode had the following characteristics on open circuit when immersed in 0·1 N KCl: at a pressure of 48 cm. Hg the drop time t was 3·50 sec., the weight of mercury m flowing per sec. was 1·604 mg. and $m^{\frac{2}{3}}t^{\frac{1}{6}}$ was 1·69.

In removing dissolved oxygen from nitrosobenzene solutions, it was observed that if nitrogen was bubbled through the solution too rapidly the step height obtained was lower than the expected value. This is probably due to the volatility of nitrosobenzene. No observable loss occurred if the nitrogen was passed slowly through the solution, although the oxygen was removed completely after 10 min. Alternatively, if the nitrogen was bubbled through a nitrosobenzene solution of the same concentration before passing through the polarographic cell, no loss of nitrosobenzene occurred.

It was reported previously [1] that attempts to measure the half-wave potential with greater accuracy by using the " expanded scale " technique of Werthessen and Baker [11] led to values that were consistently 0·035 V less negative than those obtained using the normal scale. This effect is probably due to a slight time lag of the galvanometer, which leads to innaccuracy with more rapid changes of potential. Schulman, Battey and Jelatus [12] have also reported that the rate of change of potential has a marked effect on the observed half-wave potential. It is therefore assumed that the half-wave potential measured by the expanded scale technique is more accurate than the value obtained by the normal technique, since the rate of change of potential with the former is one-third of that with the latter. This assumption has been tested by measuring the half-wave potential of nitrobenzene from a polarogram obtained manually, i.e. without using an automatic recording apparatus. As the galvanometer is allowed to reach equilibrium for each reading, errors due to any time lag of the instrument are avoided. It was found that the half-wave potential obtained in this way agreed exactly with the value obtained using the expanded scale technique. The accuracy of results measured on the expanded scale has been further checked by determining the half-wave potential for the reduction of cadmium ions. After applying corrections for the iR drop, the values obtained for solutions of cadmium sulphate in 0·1 N and in 1·0 N KCl (− 0·600 V and − 0·642 V, respectively, against the S.C.E.) agree with those published by Lingane [13] (− 0·599 V and − 0·642 V, respectively). Since it was intended to compare the polarographic half-wave potentials of nitrosobenzene and *N*-phenylhydroxylamine with the potentials measured by an electrometric titration method, all measurements on these compounds were carried out with the expanded scale technique. It should therefore be noted that the half-wave potentials recorded in Part I [1] should be corrected by subtracting 0·035 V before comparing them with the results quoted in this paper.

The potentiometric titrations were carried out in an atmosphere of nitrogen. The gas was admitted through a sintered-glass disc at the bottom of the cell so as to produce a fine " mist." A small glass stirrer immediately above this disc produced rapid mixing of the solution. A platinum wire sealed through a glass tube served as the indicator electrode for the titrations and a saturated calomel reference electrode was connected to the cell through a bridge of agar gel saturated with KCl. The reducing or oxidizing solution was added from a burette fitted into a hole in the rubber stopper with which the cell was closed. The cell contents were maintained at 25 ± 0·1° C by circulating water from a thermostat through the outer jacket of the cell. The potential difference between the two electrodes was measured with a Cambridge pH meter used as a millivoltmeter.

---

[9] Kolthoff and Langer, *J. Amer. Chem. Soc.*, 1940, **62**, 3172.
[10] Kolthoff and Liberti, *ibid.*, 1948, **70**, 1885.
[11] Werthessen and Baker, *Endocrinology*, 1945, **36**, 351.
[12] Schulman, Battey and Jelatus, *Rev. Sci. Instr.*, 1947, **18**, 226.
[13] Lingane, *J. Amer. Chem. Soc.*, 1939, **61**, 2099.

In carrying out the titrations, 75 ml. of buffer solution containing 10 % ethyl alcohol were introduced into the cell. After nitrogen had been passed through the solution for 10 min., approximately 10 mg. of nitrosobenzene or *N*-phenylhydroxylamine were rinsed into the cell with a little ethyl alcohol and the nitrogen was allowed to pass for a further 5 min. The rate of passage of nitrogen was then reduced, and the solution was titrated with the reducing or oxidizing agent in boiled-out water. Since a relatively small volume of the titrating solution was added, no other precautions were taken to exclude oxygen from the solution, except that the titanous chloride stock solution was stored as usual under N_2.

Reagents and Materials.—The buffer solutions used for the titrations were 0·2 M citric acid (pH 1·9) and 0·02 M sodium phosphate mixture of pH 7·3; those used for the polarographic work for the pH ranges indicated were as follows:[14]

pH	Solution
1·0-2·0	Sodium chloride and hydrochloric acid (Sörensen)
3·0-8·0	Sodium phosphate and citric acid (McIlvaine)
9·0-10·0	Glycine and sodium hydroxide (Sörensen)
11·0-12·0	Sodium hydroxide and sodium phosphate (Ringer)

The oxidizing agent used for the titrations was approximately 0·01 M bromine water, and the reducing solution was freshly diluted 1·25 % titanous chloride in 0·5 N HCl. It was shown that the pH values of the buffer solutions were unaltered at the end of the titrations.

N-PHENYLHYDROXYLAMINE was prepared by the reduction of nitrobenzene with Zn and ammonium chloride. The product was recrystallized from benzene immediately before use; m.p. 82° C (cf. Beilstein,[15] 82° C).

NITROSOBENZENE was obtained by oxidizing *N*-phenylhydroxylamine with chromic acid and distilling the product immediately in steam. The solid was dried on a porous tile and then washed with light petroleum; m.p. 68-69° C (cf. Beilstein [15] 69° C).

Results

Polarographic Investigation.– The effect of hydrogen ion concentration on the polarographic waves given by *N*-phenylhydroxylamine and nitrosobenzene is shown in Table I, in which the convention adopted is that reduction waves give positive diffusion currents, and oxidation waves negative diffusion currents. These results show that at pH values between 4·0 and 10·0 nitrosobenzene gives a reduction wave at almost the same potential as, and equal in height to, the oxidation wave given by *N*-phenylhydroxylamine. It should be noted that the diffusion current for *N*-phenylhydroxylamine at pH values greater than 8·0 is lower than the expected value. This is probably due to atmospheric oxidation, and it is suggested that the reduction waves obtained at pH 10·0 and at higher pH values are caused by the oxidation products. It is of interest that the half-wave potential of α-nitroso-β-naphthol between pH 4·0 and 10·0 [9] is close to that of nitrosobenzene. The fact that the sulphonamide complex of *N*-(*p*-sulphonamido-)phenylhydroxylamine,

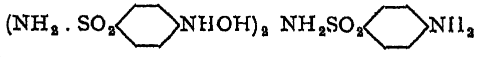

---

[14] Britton, *Hydrogen Ions*, 3rd ed. (Chapman and Hall, London, 1942).

[15] Beilstein, *Handbuch der Organischer Chemie*, **5**, **15** (Springer, Berlin, 1922, 1932).

is reducible in 0·1 N NaOH[8] suggests that this compound may be more stable in alkaline solution than is *N*-phenylhydroxylamine.

TABLE I.—EFFECT OF pH VALUE ON THE POLAROGRAMS FOR $5{\cdot}0 \times 10^{-4}$ M NITROSOBENZENE AND $5{\cdot}0 \times 10^{-4}$ M *N*-PHENYLHYDROXYLAMINE IN 10 % ETHYL ALCOHOL

pH Value	Nitrosobenzene				*N*-phenylhydroxylamine			
	First Step		Second Step		First Step		Second Step	
	Half-wave Potential in V	Diffusion Current in μA	Half-wave Potential in V	Diffusion Current in μA	Half-wave Potential in V	Diffusion Current in μA	Half-wave Potential in V	Diffusion Current in μA
1·0	—	—	−0·645	+0·7	—	—	−0·630	+1·6
2·0	—	—	−0·705	+1·9	—	—	−0·675	+1·8
3·0	—	—	−0·815	+0·9	—	—	−0·805	+1·3
4·0	+0·075	+2·3	—	0	+0·095	−2·6	—	0
5·0	+0·015	+2·5	—	0	+0·040	−2·6	—	0
6·0	−0·040	+2·6	—	0	−0·025	−2·7	—	0
7·0	−0·110	+2·7	—	0	−0·090	−2·7	—	0
8·0	−0·155	+2·6	—	0	−0·145	−2·2	—	0
9·0	−0·200	+2·6	—	0	−0·205	−1·7	—	0
10·0	−0·285	+2·5	—	0	−0·270 −0·750 −1·040	−0·8 +1·2 +1·5	—	0

Between pH 4·0 and 10·0, the reduction wave for nitrobenzene solutions of equal molar concentration is double the height of the wave given by nitrosobenzene and occurs at potentials that are approximately 0·45 V more negative than the nitrosobenzene wave. This result is in accord with the observation that the reduction of nitrobenzene at pH values greater than 3·0 requires four electrons.[1, 2] The fact that nitrosobenzene is reduced at a lower potential than nitrobenzene accounts for the direct reduction of nitrobenzene to *N*-phenylhydroxylamine. It is of interest to note that Astle and McConnell[16] found that *p*-nitrosophenol is reduced at a much lower potential than *p*-nitrophenol. This case is complicated, however, by the fact that *p*-nitrosophenol may exist in solution as *p*-quinone-monoxime.

TABLE II.—EFFECT OF CONCENTRATION ON THE POLAROGRAPHIC WAVES FOR NITROSOBENZENE AND *N*-PHENYLHYDROXYLAMINE AT pH 7·0 IN 10 % ETHYL ALCOHOL

Molar Concentration $\times 10^3$ (*C*)	Nitrosobenzene			*N*-phenylhydroxylamine		
	Half-wave Potential in V	Diffusion Current in μA (*i*)	*i*/*C*	Half-wave Potential in V	Diffusion Current in μA(*i*)	*i*/*C*
2·50	−0·120	10·3	4·1	−0·040	13·1	5·2
1·25	−0·115	6·8	5·4	−0·065	6·5	5·2
0·50	−0·100	2·6	5·2	−0·085	2·6	5·2
0·25	−0·095	1·20	4·8	−0·080	1·30	5·2
0·05	−0·095	0·30	6·0	−0·080	0·35	7·0

In acid solutions (pH < 4·0) the main polarographic waves for nitrosobenzene and *N*-phenylhydroxylamine occur at potentials that are too positive to measure, using the present base electrolytes. Each compound, however, gives rise to a second wave at the same potential as that of the second wave given by nitrobenzene in this pH range. This wave is not well-defined and exhibits a maximum that is not completely suppressed by 0·005 % gelatin. The height of this wave is rather less than that of the corresponding wave given by nitrobenzene.

---

[16] Astle and McConnell, *J. Amer. Chem. Soc.*, 1943, **65**, 35.

The effect of concentration on the polarographic waves for nitrosobenzene and *N*-phenylhydroxylamine at pH 7·0 is illustrated in Table II.

For solutions that are less than $2{\cdot}5 \times 10^{-3}$ M for the oxidizable or reducible compound, the diffusion current increases linearly with the concentration. The difference in half-wave potential is approximately equal to the fall in potential due to the current flowing, i.e. to iR, where i is the current flowing at the half-wave potential and R is the resistance of the cell. In these experiments the resistance was approximately 5000 ohms.

Potentiometric Titrations.—The oxidation of *N*-phenylhydroxylamine by bromine water at pH 7·3 and at pH 1·9, and the reduction of nitrosobenzene by titanous chloride at pH 1·9 were studied potentiometrically, and the oxidation-reduction potentials, i.e. the potentials corresponding to 50 % oxidation or reduction, are given in Table III.

TABLE III.—OXIDATION-REDUCTION POTENTIALS OF THE SYSTEM NITROSOBENZENE–*N*-PHENYLHYDROXYLAMINE

pH Value	Method of Determination	Redox Potential against S.C.E.
1·90	Reduction of nitrosobenzene	+0·245
1·90	Oxidation of *N*-phenylhydroxylamine	+0·220
7·30	Oxidation of *N*-phenylhydroxylamine	—0·095

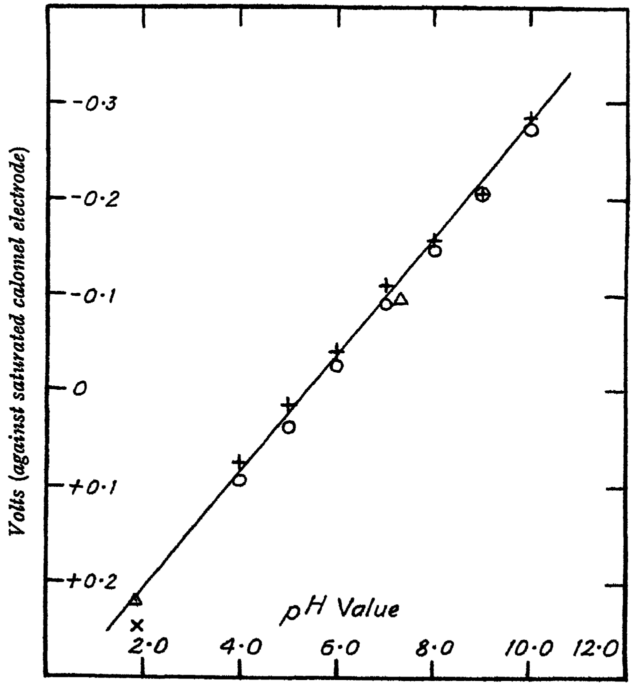

FIG. 1.—Effect of pH value on the half-wave potentials and on the oxidation-reduction potential of nitrosobenzene and *N*-phenylhydroxylamine.

+ Polarographic half-wave potential of nitrosobenzene.
⊙ Polarographic half-wave potential of *N*-phenylhydroxylamine.
× Oxidation-reduction potential of nitrosobenzene.
△ Oxidation-reduction potential of *N*-phenylhydroxylamine.

Discussion

The polarographic half-wave potentials for the reduction of nitrosobenzene and for the oxidation of N-phenylhydroxylamine are plotted against the pH value in Fig. 1, which also includes the oxidation-reduction potentials determined by potentiometric titration. The agreement is good, and the divergence between the results for the two compounds is practically eliminated if allowance is made for the iR drop in the cell. The observation[7] that N-phenylhydroxylamine shows at pH 6·3 an oxidation wave with a half-wave potential of − 0·02 V against the saturated calomel electrode is in accord with these results. Between pH 4·0 and pH 10·0 the half-wave potential E of the system can be represented approximately by the relation :

$$E = +0{\cdot}33 - 0{\cdot}061 \times \text{pH (in V against the S.C.E.)}.$$

Lutz and Lytten[6] give the reduction potential in 0·1 N HCl containing 50 % acetone as + 0·336 V (corrected to the S.C.E.). This value is not in agreement with the above equation, but our potentiometric titration results suggest that below pH 4·0 the reduction potential may be more positive than would be expected and the results in Fig. 1 suggest a value of about + 0·3 V at pH 1·0. In addition, the acetone used as solvent may have some effect on the value obtained.

Glaxo Laboratories Ltd.,
Greenford,
Middlesex.

Chemistry Department,
Battersea Polytechnic,
London, S.W.11.

THE PYROLYSIS OF HEXACHLOROETHANE

By F. S. Dainton and K. J. Ivin

Received 20th October, 1949

A preliminary investigation of the kinetics of the pyrolysis of hexachloroethane has been made between 300-420° C. The pyrolysis exhibits the characteristics of a chain reaction and is retarded by traces of nitric oxide and ammonia. Possible mechanisms are discussed.

In the course of another investigation, hexachloroethane was found to decompose at an appreciable rate above 300° C and in this paper the results of a preliminary investigation of the kinetics of the pyrolysis reaction will be presented.

Experimental

The apparatus was of conventional design, consisting of a cylindrical glass reaction vessel held in a horizontal electric furnace the temperature of which was automatically controlled to ± 0·5° C. Because of the low sublimation temperature of hexachloroethane, the manometer (a glass Bourdon gauge[1]) and connecting tubing were electrically heated to 180° C. The products of reaction were separated by fractional distillation *in vacuo* and the liquid products analyzed by means of their refractive index.

---

[1] Dainton and Ivin, *Trans. Faraday Soc.*, 1947, 43, 32.

Results

A typical pressure-time curve is shown in Fig. 1 (A). The pressure increased with time after a well-defined induction period τ during which there was little pressure change. The rate rapidly attained a maximum at the end of the induction period and then declined until a final steady pressure was reached. At high temperatures (400° C) and after prolonged heating the final pressure was $\frac{3}{2}p_0$ where p_0, = initial pressure of hexachloroethane. Under these conditions, the products were entirely liquid and consisted mainly of a mixture of tetrachloroethylene and carbon tetrachloride. At lower temperatures (350° C) or after brief heating, the products also contained chlorine and unreacted hexachloroethane. The initial reaction appears to be

$$C_2Cl_6 \rightarrow C_2Cl_4 + Cl_2 \quad . \quad . \quad . \quad . \quad . \quad . \quad (1)$$

followed by the slower reaction

$$C_2Cl_6 + Cl_2 \rightarrow 2CCl_4 \quad . \quad . \quad . \quad . \quad . \quad . \quad (2)$$

although we have not established with certainty the absence of carbon tetrachloride in the initial products. Reaction (2) has also been postulated by McBee *et al.*[2] The overall reaction at high temperatures may be represented by the equation

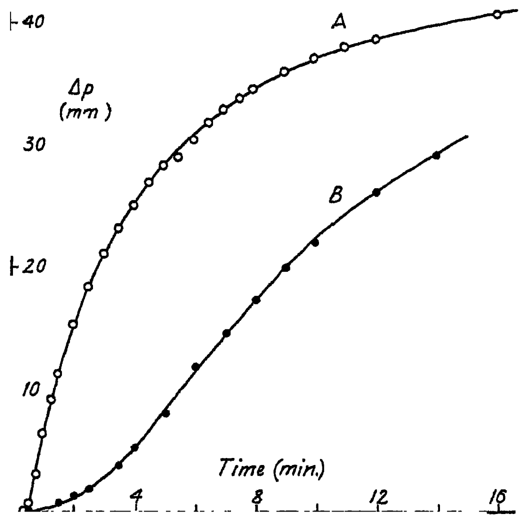

FIG. 1.—Increase of pressure with time and effect of adding ammonia.
Curve A, p_0 = 87·5 mm. C_2Cl_6;
Curve B, p_0 = 86·6 mm. C_2Cl_6 + 2·9 mm. NH_3.

$$2C_2Cl_6 \rightarrow C_2Cl_4 + 2CCl_4 \quad . \quad . \quad . \quad . \quad (3)$$

accounting for the rise of pressure to $\frac{3}{2}p_0$. Reaction (1) is endothermic and reversible. Some equilibrium constant measurements at low temperatures (< 350° C) were attempted, assuming (2) to be negligible, and a tentative value of $\Delta H = \sim 30$ kcal./mole deduced for reaction (1). This value is rather lower than that calculated from existing thermochemical data (see Appendix) but is subject to some uncertainty due to the possible occurrence of side reactions.

The induction period was always longer for the first of a series of runs under the same conditions, and was longer for the Pyrex vessel (diam. 45 mm.) than for the soda glass vessel (diam. 45 mm.). The cause of this ageing effect was not investigated. The induction period decreased rapidly with increasing temperature and pressure as shown in Fig. 2. Experiments in which hexachloroethane was heated in sealed tubes for varying periods of time established that the induction period was not due to the presence of the lubricating grease.

---

[2] McBee, Hass, Chao, Welch and Thomas, *Ind. Eng. Chem.*, 1941, **33**, 176.

The dependence of the maximum rate of pressure fall, $(\mathrm{d}p/\mathrm{d}t)_{\mathrm{max.}}$, on the initial pressure p_0 for reaction in the soda glass reaction vessel is shown in Fig. 3. The reaction is second-order at low pressure but shows a tendency to a lower order with increasing pressure and temperature. The second-order velocity constant increases exponentially with temperature. The results at low pressures are summarized by the equation

$$(\mathrm{d}p/\mathrm{d}t)_{\mathrm{max.}} = Ap_0^2 \,.\, e^{-E/RT},$$

where
$$A = 5{\cdot}1 \times 10^{-16} \text{ mm.}^{-1} \text{ min.}^{-1} \text{ (at } 398^\circ \text{ C)}$$
$$= 3{\cdot}6 \times 10^{10} \text{ mole}^{-1} \text{ l. sec.}^{-1}$$
$$E = 58 \pm 1{\cdot}5 \text{ kcal./mole.}$$

The kinetics of the pyrolysis in the Pyrex reaction vessel appeared to differ from those in the soda glass vessel, showing a lower order and lower energy of activation. However, the presence of a greased joint near the reaction zone, and the detection of HCl in the products made these results unreliable.

Small pressures (< 10 mm.) of NO or NH_3 lengthened the induction period and reduced the maximum rate as shown in Fig. 1(B). Nitrogen (taken direct from a cylinder) increased the maximum rate (for 79 mm. C_2Cl_6, 45 mm. N_2, 378° C).

Discussion

From the above results, it is evident that the decomposition of hexachloroethane between 300-420° C proceeds by a chain reaction. This conclusion is supported particularly by the existence of the induction period and by the effect of NO and NH_3, which are known to inhibit other chain reactions, involving chlorine atoms.[3] Furthermore, the value of A at 398° C calculated from the simple collision theory for a bimolecular reaction, taking the collision diameter of hexachloroethane as 5×10^{-8} cm., is 8×10^{10} mole^{-1} l. sec.$^{-1}$. This differs from the observed A by a factor of more than 10^8, which seems too large to be attributed solely to the existence of a large number of square terms in the activational process.

The initial act in the pyrolysis of hexachloroethane is probably either

$$C_2Cl_6 \rightarrow C_2Cl_5 + Cl \quad . \quad . \quad . \quad . \quad . \quad (4)$$

or

$$C_2Cl_6 \rightarrow 2CCl_3 \quad . \quad . \quad . \quad . \quad . \quad . \quad (5)$$

The process which predominates will be determined by the relative dissociation energies concerned. These will be slightly less than the *bond* energies of the CC and CCl linkages due to resonance stabilization of the entities C_2Cl_5 and CCl_3. However, no reliable estimates can be made of the bond energies in C_2Cl_6 from thermochemical data. Force constants have been calculated [1] for the various vibration frequencies from the Raman spectrum, assuming, however, that the bond lengths have their normal values (CCl = 1·76 Å; CC = 1·54 Å). While these data suggest that the CCl bond is the weaker, the probable stretching of the CC bond casts doubt on this inference. The lengths of the bonds in C_2Cl_6 are not known but in hexamethylethane [5] the CC bond is stretched to 1·58 ± 0·02 Å reducing the dissociation energy from 85 kcal./mole, to about 78 kcal./mole[6] (taking the latent heat of sublimation of carbon as 170 kcal./mole). The reduction in the dissociation energy of the CC bond in C_2Cl_6 is likely to be of a similar order of magnitude. The dissociation energy of the CCl bond will be close to that in CCl_4, namely 78 kcal./mole. Hence there

---

[3] Chapman and MacMahon, *J. Chem. Soc.*, 1909, **95**, 1717; 1910, **97**, 845.

[4] Hamilton and Cleveland, *J. Chem. Physics*, 1944, **12**, 249.

[5] Bauer and Beach, *J. Amer. Chem. Soc.*, 1942, **64**, 1142.

[6] Skinner, *Trans. Faraday Soc.*, 1945, **41**, 645.

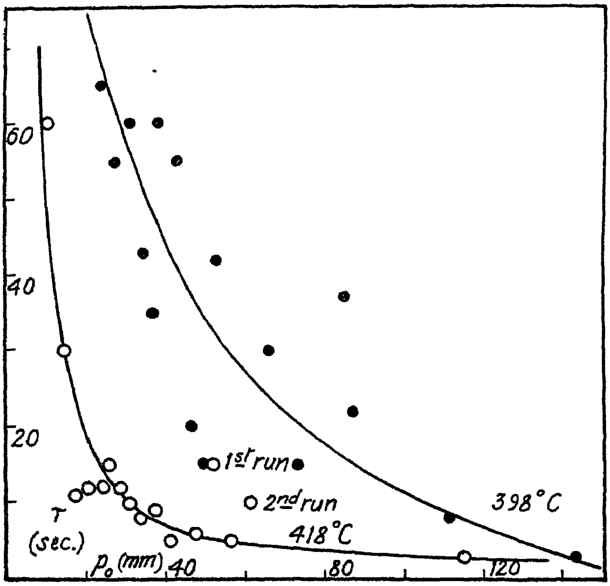

FIG. 2.—Effect of temperature and pressure on the induction period.

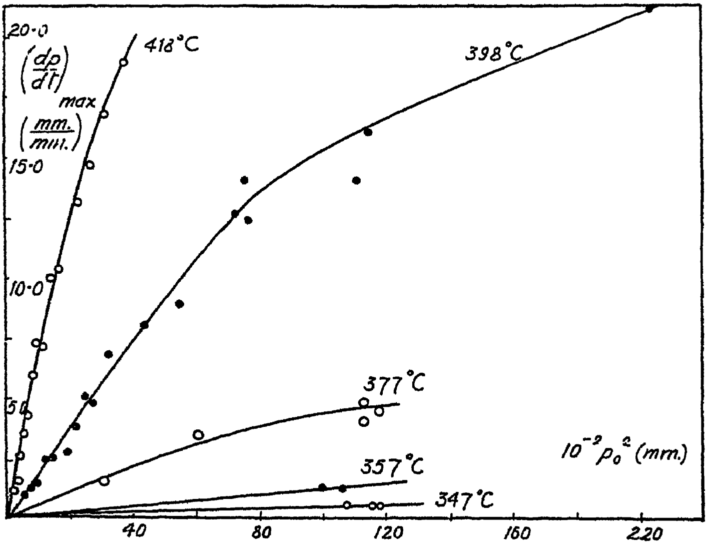

FIG. 3.—Dependence of maximum rate on initial pressure.

is probably little difference in the dissociation energies of the two types of bond in C_2Cl_6 and one cannot say which of the processes (4) and (5) will be favoured.

As soon as a small amount of chlorine has accumulated in the system the main source of chain centres will be by direct dissociation of the chlorine molecules since this requires only 58 kcal./mole. The reaction is thus autocatalytic, but whether the induction period is entirely due to the building-up of the chlorine concentration or whether it is due partly to the presence of traces of inhibitors has not been tested experimentally. The chlorine atoms may react with hexachloroethane in two ways :

$$Cl + C_2Cl_6 \rightarrow Cl_2 + C_2Cl_5 \quad \Delta H \sim 20 \text{ kcal./mole} \quad . \quad . \quad (6)$$

$$Cl + C_2Cl_6 \rightarrow CCl_4 + CCl_3 \quad \Delta H \sim 0 \text{ kcal./mole} \quad . \quad . \quad (7)$$

If (7) predominates, it is difficult to account for the production of appreciable quantities of chlorine, and carbon tetrachloride should be formed in the initial stages of reaction. If, on the other hand, (6) predominates, it may well be followed by the spontaneous dissociation of the C_2Cl_5 radical :

$$C_2Cl_5 \rightarrow C_2Cl_4 + Cl \quad . \quad . \quad . \quad . \quad (8)$$

Carbon tetrachloride will not then be found in the initial products but may be formed at a later stage by the secondary reaction (2). The reverse of reactions (6) and (8) are presumed to occur in the photochlorination of tetrachloroethylene at room temperature.[11]

While it is possible to account for the observed kinetics by making assumptions as to the relative importance of the various possible propagation and termination reactions, it seems desirable to obtain further experimental evidence to check these assumptions before embarking on a detailed consideration of the mechanism. A study of the rate of production of carbon tetrachloride and chlorine as a function of time would be of particular value.

Appendix

THE HEAT OF THE DISSOCIATION $C_2Cl_{6(g)} \rightarrow C_2Cl_{4(g)} + Cl_{2(g)}$

Since it proved difficult to achieve this equilibrium experimentally (see text), ΔH° for this reaction was estimated as follows :

	ΔH° (kcal./mole)	Ref
$C_2Cl_{6(s)} + 2O_{2(g)} \rightarrow 2CO_{2(g)} + 3Cl_{2(g)}$	− 110	7
$C_2Cl_{6(s)} \rightarrow C_2Cl_{6(g)}$	14·1	8
$2C_{(diamond)} + 2O_{2(g)} \rightarrow 2CO_{2(g)}$.	− 188·9	—
whence		
$2C_{(diamond)} + 3Cl_{2(g)} \rightarrow C_2Cl_{6(g)}$.	− 65	—

However, Kharasch[9] states that Berthelot's value for the heat of combustion of C_2Cl_6 is much too low and Bichowsky and Rossini estimate

	ΔH° (kcal./mole)	Ref.
$2C_{(diamond)} + 3Cl_{2(g)} \rightarrow C_2Cl_{6(g)}$.	- 37	10
Combining this with		
$2C_{(diamond)} + 2Cl_{2(g)} \rightarrow C_2Cl_{4(g)}$.	6	10
we obtain		
$C_2Cl_{6(g)} \rightarrow C_2Cl_{4(g)} + Cl_{2(g)}$ . .	43	—

Department of Physical Chemistry,
Cambridge.

---

[7] Berthelot, *Ann. chim. phys.*, 1893, **28**, 126.

[8] Dainton and Ivin, *Trans. Faraday Soc.*, 1947, **43**, 32.

[9] Kharasch, *J. Res. Nat. Bur. Stand.*, 1929, **2**, 359.

[10] Bichowsky and Rossini, *Thermochemistry of Chemical Substances* (1936)

[11] Dickinson and Carrico, *J. Amer. Chem. Soc.*, 1934, **56**, 1473.

ABSORPTION BY SIMULTANEOUS DIFFUSION AND CHEMICAL REACTION

By P. V. Danckwerts

Received 21st November, 1949

Equations are derived for the rate of absorption and the concentration distribution when a solute of limited solubility diffuses into a semi-infinite medium with which it undergoes a first-order or pseudo first-order reaction. Consideration is given to the case where the medium is a mixture, of which only one component reacts. A method is given for determining whether the above-mentioned equations can be applied in spite of local depletion of this component.

An equation is presented for the rate of absorption when the absorbed substance reacts instantaneously with a component of the medium which is present in limited concentration.

1. Introduction.—The problem here considered is the calculation of the rate of absorption of a substance (which will be called the "solute") which diffuses into a stagnant medium in which it has a limited solubility and with which it undergoes an irreversible first-order or pseudo first-order reaction. The medium has a plane surface and is of infinite depth (or, for practical purposes, is of such a depth that the concentration does not change appreciably at the bottom during the period of time considered). The surface of the medium is continuously saturated with the solute. As examples may be cited: the absorption of a gas into a liquid or solid, the dissolution of a solid into a supernatant liquid, or the absorption of one solid or liquid material into another. In each case the solute is assumed to be destroyed by a process which proceeds at a rate solely dependent on, and proportional to, its concentration in the medium.

If the medium is a fluid, the expressions developed here will only be valid if the density of the fluid always increases consistently in a downward direction (or, of course, if it remains uniform); otherwise convection currents will be set up and will increase the rate of absorption (as, for instance, when CO_2 is absorbed into a horizontal water surface). Even in the latter case, however, the fluid may be regarded as stagnant for a short initial period.

2. Exact and Approximate Solutions.—It is assumed that the ideal diffusion law expressed by (2.1) below holds for the diffusion of unreacted solute through the medium, and also that the mass of solvent per unit volume of the medium is virtually constant throughout, so that there are no volume changes in the medium when solute is absorbed. These conditions are the more likely to be fulfilled, the lower the solubility of the solute.

Let c^* be the saturated concentration of the solute reigning at the surface ($x = 0$), with c the concentration at a distance x below the surface, t the time, and k the velocity constant of the reaction between solute and medium. The initial concentration of solute in the medium is uniformly equal to zero.

Now the rate at which solute crosses unit area of any plane of constant x in the direction of increasing x is

$$\left(\frac{dQ}{dt}\right)_x = -D\frac{\partial c}{\partial x}, \quad . \quad . \quad . \quad . \quad . \quad (2.1)$$

(D being the diffusion coefficient of the solute in the medium) and the rate at which chemical reaction destroys the solute (per unit volume) is kc.

Consider an element of volume of unit cross-sectional area between planes x and $x + dx$. The following changes in its content of solute occur in time dt:—

Diffusing in : $-D\frac{\partial c}{\partial x}dt.$

Diffusing out : $-\left[-Ddt\left(\frac{\partial c}{\partial x} + \frac{\partial^2 c}{\partial x^2}dx\right)\right].$

Reacting : $-kcdt \,.\, dx.$

Net increase : $\left(D\frac{\partial^2 c}{\partial x^2} - kc\right)dt \,.\, dx.$

If the resulting increase in concentration is dc, the net increase above can be equated to $dc \,.\, dx$, giving

$$\frac{\partial c}{\partial t} = D\frac{\partial_2 c}{\partial x^2} - kc. \quad . \quad . \quad . \quad . \quad (2.2)$$

With the boundary conditions,

$$\begin{array}{lll} c = c^*, & x = 0, & t > 0 \\ c = 0, & x > 0, & t = 0 \\ c = 0, & x = \infty, & t > 0, \end{array}$$

the solution to eqn. (2.2) is

$$\frac{c}{c^*} = \frac{1}{2}\exp\left(-x\sqrt{\frac{k}{D}}\right) \,.\, \mathrm{erfc}\left[\frac{x}{2\sqrt{tD}} - \sqrt{kt}\right]$$
$$+ \frac{1}{2}\exp\left(x\sqrt{\frac{k}{D}}\right) \,.\, \mathrm{erfc}\left[\frac{x}{2\sqrt{tD}} + \sqrt{kt}\right], \quad (2.3)$$

where

$$\mathrm{erfc}\, z = 1 - \mathrm{erf}\, z = 1 - \frac{2}{\sqrt{\pi}}\int_0^z e^{-y^2}dy.$$

(The mathematical problem and its solution are identical with those for the conduction of heat along a thin rod which loses heat from its periphery at a rate proportional to its temperature.[1])

Differentiating (2.3) with respect to x and setting $x = 0$, we find

$$\left(\frac{\partial c}{\partial x}\right)_{x=0} = -c^*\sqrt{\frac{k}{D}}\left[\mathrm{erf}\sqrt{kt} + \frac{e^{-kt}}{\sqrt{\pi kt}}\right].$$

The rate of absorption dQ/dt per unit area of surface is given by

$$\frac{dQ}{dt} = -D\left(\frac{\partial c}{\partial x}\right)_{x=0} = c^*\sqrt{Dk}\left[\mathrm{erf}\sqrt{kt} + \frac{e^{-kt}}{\sqrt{\pi kt}}\right], \quad . \quad (2.4)$$

---

[1] Carslaw and Jaeger, *Conduction of Heat in Solids* (Oxford University Press, Oxford, 1947), p. 111.

whence the quantity Q absorbed in time t is

$$Q = c^* \sqrt{\frac{D}{k}}\left[(kt + \tfrac{1}{2})\operatorname{erf}\sqrt{kt} + \sqrt{\frac{kt}{\pi}}\,e^{-kt}\right] \quad . \quad . \quad (2.5)$$

The dimensionless quantities $\frac{Q}{c^*}\cdot\sqrt{\frac{k}{D}}$ and kt are plotted in Fig. 1, which enables the quantity absorbed at any time to be readily found.

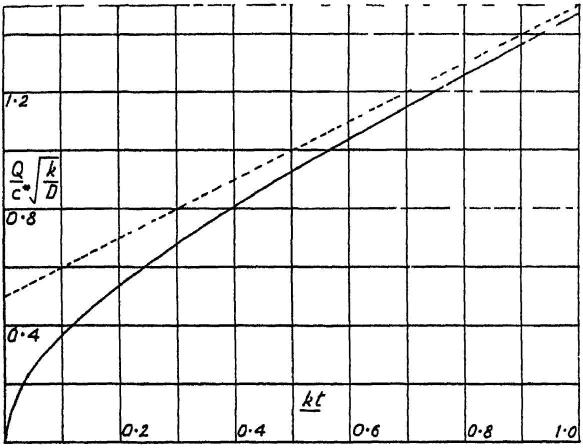

FIG. 1.

The function $\frac{Q}{c^*}\sqrt{\frac{k}{D}} = \left[(kt + \tfrac{1}{2})\operatorname{erf}\sqrt{kt} + \sqrt{\frac{kt}{\pi}}\,e^{-kt}\right]$ and asymptote

$$\frac{Q}{c^*}\sqrt{\frac{k}{D}} = (kt + \tfrac{1}{2}).$$

When kt is sufficiently large $\operatorname{erf}\sqrt{kt} \approx 1$, and eqn. (2.3), (2.4) and (2.5) become

$$\frac{c}{c^*} \approx \exp\left(-x\sqrt{\frac{k}{D}}\right), \quad . \quad . \quad . \quad . \quad (2.6)$$

$$\frac{dQ}{dt} \approx c^*\sqrt{Dk}, \quad . \quad . \quad . \quad . \quad . \quad (2.7)$$

$$Q \approx c^*\sqrt{Dk}\left(t + \frac{1}{2k}\right). \quad . \quad . \quad . \quad . \quad (2.8)$$

(The error in (2.7) and (2.8) is less than 2 % if $kt > 4$.) In other words, the rate of absorption and the concentration at any point tend to a steady value.

When kt is very small (a condition which is of interest in connection with the theory of absorption into agitated liquids) we find, on expanding $\operatorname{erf}\sqrt{kt}$ and e^{-kt} and neglecting powers of kt higher than the first, that (2.4) and (2.5) become

$$\frac{dQ}{dt} \approx c^*\sqrt{\frac{D}{\pi t}}\,(1 + kt) \quad . \quad . \quad . \quad . \quad (2.9)$$

$$Q \approx 2c^*\sqrt{\frac{Dt}{\pi}}\left(1+\frac{kt}{2}\right) \quad . \quad . \quad . \quad (2.10)$$

which reduce, when $kt = 0$, to the well-known values for diffusion without reaction.

3. Depletion of Second Reactant.—We may wish to apply the results to the case where the medium is a mixture, of which only one component, B, reacts with the absorbed solute, A, the reaction being first order with respect to both reactants. It is therefore of interest to determine the extent to which depletion of reactant B is likely to affect the rate of absorption.

Suppose the initial concentration of B in the medium is uniformly equivalent to c_0'. The concentrations, c and c', of A and B respectively at x at time t would be given by the solution, subject to the appropriate boundary conditions, of

$$\left.\begin{aligned}\frac{\partial c}{\partial t} &= D\frac{\partial_2 c}{\partial x^2} - k'cc'\\ \frac{\partial c'}{\partial t} &= D'\frac{\partial_2 c'}{\partial x^2} - k'cc'\end{aligned}\right\}, \quad . \quad . \quad . \quad (3.1)$$

where D' is the diffusion coefficient of component B in the medium, k' the second-order velocity constant ($k'c'$ is equivalent to k in eqn. (2.2) to (2.10).)

Putting

$$\partial c/\partial t = \partial c'/\partial t = 0$$

in (3.1), we find

$$D\frac{\partial_2 c}{\partial x^2} = D'\frac{\partial_2 c'}{\partial x^2},$$

whence

$$D\frac{\partial c}{\partial x} = D'\frac{\partial c'}{\partial x} + A, \quad . \quad . \quad . \quad (3.2)$$

where A is a constant. However, this is incompatible with the necessity that $\partial c'/\partial x = 0$ when $x = 0$, $\partial c'/\partial x = \partial c/\partial x = 0$ when $x = \infty$. This system, therefore, does not tend to a steady state, and we may suppose that the longer absorption proceeds the more widely does the rate of absorption depart from that given in (2.4). However, it is clear that if at a given time the quantity of B which has reacted per unit volume of the medium is at all points an insignificant fraction of its initial concentration c_0', then the quantity of A absorbed, and its concentration at any point, will not differ appreciably from that predicted by eqn. (2.3) and (2.5). Since the concentration of A, and hence the rate of reaction, is always greater at the surface ($x = 0$) than elsewhere, we may take the quantity of reaction occurring here as the criterion. In time t the quantity of B which has reacted per unit volume of the medium in the neighbourhood of the surface is Q_0, where $Q_0 < k'c_0'c^*t$, since the surface concentration of B will always be less than c_0'. A sufficient condition that the variation of c' may be ignored is, as we have seen, that $Q_0/c_0' \ll 1$. Substituting for Q_0 we have

$$k'c^*t \ll 1 \quad . \quad . \quad . \quad . \quad . \quad (3.3)$$

as a sufficient condition for the applicability of eqn. (2.3), (2.4) and (2.5). This condition may be unnecessarily stringent, particularly if $D' \gg D$, but should be a useful guide.

If the reaction between A and B is instantaneous, A and B cannot both be present in the same part of the medium at the same time; there will, in fact, be a zone near the surface containing A alone. It can be shown [2] that under these circumstances the rate of absorption is given by

$$\frac{dQ}{dt} = \frac{c^*}{\operatorname{erf}\,[\beta/\sqrt{D}]}\sqrt{\frac{D}{\pi t}}, \qquad \cdot \quad \cdot \quad \cdot \quad (3.4)$$

β being defined (so long as $\beta \neq 0$) by the relation

$$\left(\frac{n'c^*}{\sqrt{D'}}\right) \exp\left[\frac{\beta^2}{D'}\right] \operatorname{erfc}\left[\frac{\beta}{\sqrt{D'}}\right] - \left(\frac{nc_0'}{\sqrt{D}}\right) \exp\left[\frac{\beta^2}{D}\right] \operatorname{erf}\left[\frac{\beta}{\sqrt{D}}\right] = 0, \quad (3.5)$$

where n moles of A react with n' moles of B, and the concentrations are expressed in moles per unit volume.

To provide a clearer idea of the significance of (3.4) and (3.5) the coefficients of diffusion of A and B may be set equal (this will approximately represent the facts in many cases). Putting $D = D'$, eqn. (3.5) becomes

$$\operatorname{erf}\left[\frac{\beta}{\sqrt{D}}\right] = \frac{n'c^*}{n'c^* + nc_0'}, \qquad \cdot \quad \cdot \quad \cdot \quad (3.6)$$

so that (3.4) becomes

$$\frac{dQ}{dt} = c^*\left(1 + \frac{nc_0'}{n'c^*}\right)\sqrt{\frac{D}{\pi t}}. \qquad \cdot \quad \cdot \quad \cdot \quad (3.7)$$

If the initial concentration of B in the medium is equivalent to the saturated concentration of A at the surface, the rate of absorption will be twice as great as if there were no reaction taking place.

Department of Chemical Engineering,
Tennis Court Road,
Cambridge.

---

[2] Unpublished work by author.

THE STRUCTURE OF ALUMINIUM SOAPS

By G. A. Parry and A. J. Taylor

Received 29th April, 1949; as revised 20th June, 1949

Recent work on the structure of aluminium soaps is reviewed, and the structure of the soaps made by reaction between aluminium alcoholate and fatty acid is studied by means of the Karl Fischer reagent. The results obtained are applied to a study of the structure of aluminium soaps made by metathetic reaction between a sodium soap and a soluble aluminium salt.

The reaction between aluminium alcoholate and water has been studied and it is shown that one molecule of the alcoholate reacts with two molecules of water, and not with three molecules, which agrees with the results obtained by other investigators.

Since the war, the structure of aluminium soaps has been studied intensively by a variety of methods,[1–5] and although it seems now to be generally agreed that Lawrence's postulation of the existence of a tri-soap[17] is not supported by experimental evidence, an interesting observation has recently been made by McGee[11] that such experimental evidence may have hitherto been overlooked by virtue of the probable solubility of the tri-soap in the solvents employed. McGee's observation follows from his development of a theory originally put forward by Gray[7] in 1945. This theory postulates that the aluminium atom acts as a hexavalent co-ordination centre, and the same premise is made by Schulman and McRoberts[6] who develop the argument along different lines. The latter workers suggest that the co-ordinating valencies of the aluminium atom may be satisfied by groups such as water, fatty acid, fatty carboxylate, and hydroxy. Such a structure would account for the difficulty in obtaining duplicate samples of soaps of identical gelling characteristics due to the dependence of such a soap structure upon minutiae of experimental technique. Water is well known to have a potent peptizing effect upon aluminium soap-hydrocarbon gel systems, and an accurate knowledge of the exact amount present is important when assessing the gelling characteristics of any given sample. Moreover, assuming Schulman's conception of the soap structure to be valid, it is evident that free water will be more easily evolved and assessed than the molecularly bound water. This point has been tacitly appreciated by previous workers, who point out the dependence of the observed results upon the severity of the experimental conditions. In a study of the sorption of water by aluminium soaps, Shreve, Pomeroy and Mysels[8] examined the effect of exhaustive vacuum treatment at various temperatures, and also dehydration by benzene distillation. It was found, in the former case, that in an evacuated sorption balance, considerable decomposition took place at 100° C. The use made of the distillation method was to show that under these conditions, side reactions of the following type do not occur :

$$\mathrm{Al(OH)R_2 + HR = AlR_3 + H_2O} \quad . \quad . \quad . \quad (1)$$

$$\mathrm{Al_2O(OH)_2R_2 + 2HR = 2AlOHR_2 + H_2O} \quad . \quad . \quad (2)$$

---

[1] Smith, Pomeroy, McGee and Mysels, *J. Amer. Chem. Soc.*, 1948, **70**, 1053.

[2] Coe, Mysels and Smith, *J. Colloid Sci.*, 1948, **3**, 293.

[3] Galley and Puddington, *Can. J. Res.*, 1948, **26**, 155.

[4] McBain and Working, *J. Physic. Chem.*, 1947, **51**, 974.

[5] Sheffer, *Can. J. Res.*, 1948, **26**, 481.

[6] Schulman and McRoberts, *Nature*, 1948, **162**, 101.

[7] Gray, *Ph.D. Thesis* (Cambridge, 1945).

[8] Shreve, Pomeroy and Mysels, *J. Physic. Chem.*, 1947, **51**, 963.

but McGee[11] has since stated that the experimental evidence may be vitiated by the presence of methoxy groups in the soap used.

Shreve, Pomeroy and Mysels also apply the Karl Fischer method of moisture estimation to a sample of pure "dry" aluminium laurate prepared by metathesis, and obtain a result of 2·5 ± 0·4 % of moisture, corresponding to 0·62 ± 0·11 mole of water per mole of AlL_2OH. This figure is too far removed from unity to make a purely Schulman structure possible. The authors ascribe this moisture content to the fact that the conditions of the Fischer reaction induce side reactions of the type of equations (1) and (2) and also, presumably:

$$2AlR_2OH = R_2Al - O - AlR_2 + H_2O. \quad . \quad . \ (3)$$

There is no experimental certainty that these workers' so-called dry material does not contain traces of moisture. Indeed, as free acid had been extracted from the material they examine, eqn. (3) above is the only possible one to yield water, and the results they quote are only slightly higher than would correspond with this reaction.

A convenient method of testing these hypotheses of Shreve, Pomeroy and Mysels is presented by the reaction between aluminium alcoholate and a fatty acid. Thus, using carefully purified materials, we dissolved a quantity of aluminium *sec.*-butylate in very dry *sec.*-butyl alcohol, and added exactly two equivalents of 2-ethyl hexoic acid:

$$Al(OBu)_3 + 2HR = AlR_2OBu + 2BuOH. \quad . \quad . \ (4)$$

The exact amount of water, dissolved in *sec.*-butyl alcohol, to accord with eqn. (5), was then run in:

$$AlR_2OBu + H_2O = AlR_2OH + BuOH. \quad . \quad . \ (5)$$

At this stage, it is apparent that free water is not present. If, therefore, on analyzing this solution with the Karl Fischer reagent, water is obtained, it must be due to reaction according to eqn. (3). In point of fact, we found that water is recovered by the Fischer reagent, and obtained quantitatively, to a considerable degree of accuracy, in accordance with this equation. Typical results are given in Table I, wherein concordance between columns (*b*) and (*c*) shows the extent of agreement between observed and calculated results.

TABLE I

Water Added acc. to eqn. (5) mg. (*a*)	Water Available from eqn. (3) mg. (*b*)	Water found by K. F. Reagent mg. (*c*)
35	17·5	21
39	19·5	23
185	92·5	115
44	22	21
118	59	61
152	76	68
225	112·5	115
109	54·5	56
162	81	81
196	98	107

In order to ascertain whether reaction in accordance with eqn. (1) occurs, one equivalent of 2-ethyl hexoic acid was added to the resultants of eqn. (5). Titration with the Fischer reagent, showed that water was recovered only in accordance with eqn. (3), i.e. reaction (1) which should yield twice the amount of water, does not occur. In actual figures, of 105 mg. of water added to the system, the whole amount should have been recovered had eqn. (1) held, and 60 mg. if eqn. (3) is correct; in the result, 70·5 mg. were obtained on titration.

As a further check on the existence or otherwise, of the tri-soap, three equivalents of fatty acid were added to one mole of butylate. If the tri-soap exists, it should be formed according to the equation:

$$Al(OBu)_3 + 3HR = AlR_3 + 3BuOH. \quad . \quad . \quad (6)$$

If, now, one equivalent of water is added, and the product titrated with the Fischer reagent, provided the tri-soap is completely stable, all the water added should be recoverable on titration. On the other hand, if the tri-soap is easily hydrolyzed to the di-soap, or if the di-soap alone existed initially, titration should yield only one-half of a mole of water, in accordance with eqn. (3). This, in fact, is what was found. Full results are given in Table II which shows that the tri-soap is not formed at all, or that if it is, it is readily hydrolyzed.

TABLE II

Weight Water Recoverable According to eqn. (3) mg.	Water Estimated by K.F. Reagent mg.
143	152
143	156
28	33

A similar technique may be used for investigating the existence of mono-soaps. If one mole of fatty acid is added to one mole of aluminium butylate in solution in *sec.*-butyl alcohol, and two moles of water added, the mono-soap could conceivably be formed according to eqn. (7) and (8).

$$2Al(OBu)_3 + 2HR = 2AlR(OBu)_2 + 2BuOH \quad . \quad . \quad (7)$$

$$2AlR(OBu)_2 + 4H_2O = 2AlR(OH)_2 + 4BuOH. \quad . \quad (8)$$

This mono-soap would be expected to split off water as on titration with the Karl Fischer reagent:

$$2AlR(OH)_2 = Al_2R_2O_2 + 2H_2O, \quad . \quad . \quad . \quad (9)$$

so that from the 4 molecules of water added in reaction (8), two should be recovered from reaction (9). This, in fact, is what is observed, as is shown in Table III.

TABLE III

Weight Water Added eqn. (8) mg.	Weight Water Recoverable by eqn. (9) mg.	Weight Water Titrated by K.F. mg.
113	56·5	58·5
113	56·5	57·5

It is conceivable, however, that eqn. (9) does not represent the facts, and that the reaction proceeds according to the following scheme:

$$2Al(OBu)_3 + 2HR = AlR_2(OBu) + Al(OBu)_3, \quad . \quad . \quad (10)$$

this reaction taking place instead of reaction (7). On adding 4 moles of water (see eqn. (8), reaction would then take place as follows:

$$AlR_2(OBu) + H_2O = AlR_2OH \xrightarrow{\text{Karl Fischer}} \tfrac{1}{2}H_2O \quad . \quad (11)$$

$$\begin{array}{l} Al(OBu)_3 + 2H_2O = AlO\,.\,OH + 3BuOH \\ \qquad\qquad\qquad\qquad\quad \Big\downarrow \text{Karl Fischer} \\ \qquad\qquad\qquad\quad \tfrac{1}{2}Al_2O_3 + \tfrac{1}{2}H_2O. \quad . \quad . \quad . \quad . \quad (12) \end{array}$$

The two half-molecules of water from eqn. (11) and (12) together with the unused molecule from the 4 initially added would complete the 2 actually recovered. The above postulation of the reaction between aluminium butylate and water was suggested to the authors by T. S. McRoberts and J. H. Schulman, and in order to verify it, various amounts of water were carefully added to aluminium butylate in *sec.*-butyl alcohol, and the product titrated with the Fischer reagent. The results are given in Table IV and plotted in Fig. 1.

TABLE IV

Moles Water per mole Butylate (*a*)	Weight Water (*b*) = (*a*)	Weight of Water Recoverable by eqn. (12) (*c*)	Water Estimated by K.F. Reagent (*d*)
2·0	180	45	44·1
2·47	222	87	83
1·0	90	22·5	14
1·0	90	22·5	20
1·5	135	33·7	22·5
1·5	135	33·7	32·8
2·0	180	45	48·8
2·5	225	90	83
2·5	225	90	90
3·0	270	135	118
3·0	270	135	126

According to eqn. (12), if two moles of water are added to one mole of aluminium butylate, one quarter of that amount would be recovered on titration, and any water present over and above the stoichiometric quantity of water, should be recovered as such. This is amply borne out by the figure: thus, when 2 moles of water are added per mole of butylate, 0·5 mole of water is recovered. When, however, 2·5 moles of water are added, 0·5 + 0·5, i.e. 1·0 mole of water is recovered. This result accords with the evidence produced by Gray and Alexander[16] from the heat of reaction of aluminium alcoholate with water.

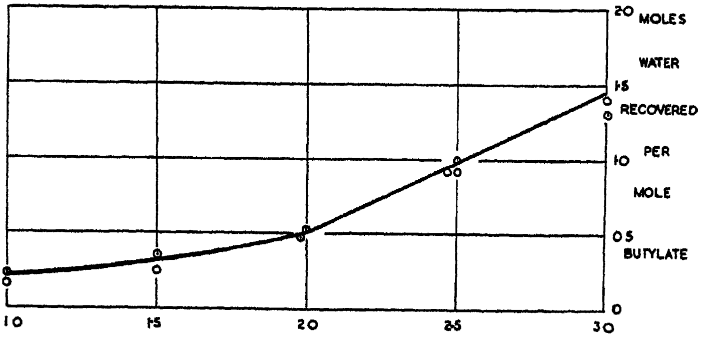

FIG. 1.—Moles of water added per mole butylate.

It is of interest to note that this reaction between aluminium *sec.*-butylate and water is found not to occur in methanol solution, presumably because of the strong affinity of the water for the methanol. Under these circumstances, all the water added is recovered on titration.

The above results appear to indicate that the use of the Karl Fischer reagent for determining the moisture content of commercial aluminium soaps would not be possible, due to the complication of reaction between hydroxy groups, and reaction between basic soaps and free acid to yield further free water. It was found, however, that when dried aluminium soaps made by the metathetic method were so examined, the amount of moisture obtained was considerably less than that which would be expected from the above reactions. This suggests that the structure of the latter soaps differ from those made metathetically, and this can be ascribed to a greater complexity of cross-linkaging in the metathetic soaps, as described by Sheffer.[5] It is possible, therefore, that in a " dried " metathetic soap, the moisture content determined by the Fischer reagent measures that proportion of the soap which has free hydroxyl groups capable of reacting with each other. This, in turn, tallies with recent work published by Mysels and McBain,[15] who found that part of metathetic aluminium laurate is soluble in cyclohexane, and part insoluble.

We propose to examine this aspect in greater detail.

Experimental

The conventional Karl Fischer technique was adopted [10, 11, 13] using a dead-stop end-point circuit with back-titration of excess reagent against a standard methanol-water solution. This technique calls for an exacting experimental procedure, with rigid exclusion of moisture vapour from all parts of the apparatus, but it was adopted after thorough trial in preference to the simpler adaptation of Johansson,[9] which, despite considerable modification of experimental conditions in an attempt to make it work, gave a badly-fading, and generally intransigent end-point.

The reagents employed were of the following purity :

(*a*) Pyridine.	Technical reagent, redistilled from quicklime.
(*b*) Iodine.	Pure resublimed.
(*c*) Methanol *sec.*-butyl alcohol.	Technical, dried to a water content of 0·01 % by the method of Gilman and Blatt.[14]
(*d*) Sulphur dioxide.	Laboratory reagent, dried by passage through calcium chloride.
(*e*) Aluminium butylate.	Prepared by reaction of pure aluminium foil with dried *sec.*-butyl alcohol in the presence of traces of mercuric chloride ; purified by distillation *in vacuo*.
(*f*) 2-Ethyl hexoic acid.	Technical 99 %, purified by redistillation *in vacuo*.
(*g*) Ether.	Technical reagent, dried by redistillation from sodium.

The Fischer reagent and the aqueous-alcoholic solutions were prepared in the customary strengths and standardized after an ageing period of 3 days. For the butylate-butanol solution, the *sec.*-butyl alcohol was dried to a moisture content of less than 0·5 %.

The alcoholate soaps were prepared in either of two ways :

(*a*) About 3 g. of aluminium butylate were weighed into a dried graduated 100 ml. receiver, and dissolved in 10-12 ml. of either *sec.*-butyl alcohol or ether. The calculated molar quantity of 2-ethyl hexoic acid-butanol solution was run in, the receiver stoppered, well shaken and left sealed for about 24 hr. It was then made up to volume with the appropriate solvent. A weighed amount of water from the dropping bottle was added and the receiver thoroughly shaken. As the " added " water never exceeded 350 mg. the alteration in volume could be ignored. The moisture obtaining from the solvent and 2-ethyl hexoic acid plus the " added " water made the total water present. 20 ml. aliquots were then withdrawn and estimated for moisture in the Fischer apparatus.

(*b*) Exact quantities of standard butanol solutions of both aluminium butylate and 2-ethyl hexoic acid were run into a clean dry reaction vessel, stirred thoroughly and left sealed for about 24 hr. The exact amount of butanol-water solution was then added, allowance being made for moisture already present, the bottle placed in position, stirred for 3 min. and the Fischer estimation carried out.

---

[9] Johansson, *Svenska, Traforskningsinstitutet, Tralemi och Pappersteknik*, 1947, **19**, 124.

[10] Smith, Bryant and Mitchell, *J. Amer. Chem. Soc.*, 1939, **61**, 2407.

[11] McGee, *ibid.*, 1949, **71**, 278.

[12] Foulk and Bawden, *ibid.*, 1926, **48**, 2045.

[13] Wernimont and Hopkinson, *Ind. Eng. Chem.* (*Anal.*), 1943, 272.

[14] Gilman and Blatt, *Organic Syntheses* (Vol. 1, 2nd Edn.), p. 219.

[15] Mysels and McBain, *J. Physic. Chem.*, 1948, **52**, 1471.

This latter method was found to yield more reproducible results than the former and was also easier to manipulate. It was found most important to allow sufficient time for reaction between butylate and acid to proceed to completion before adding the water.

Permission to publish has been given by the Chief Scientist, Ministry of Supply.

Ministry of Supply,
Langhurst,
Horsham.

24 *Randalls Road,*
Leatherhead,
Surrey.

---

[16] Gray and Alexander, *ibid.*, 1949, **53**, 23.
[17] Lawrence, *J. Inst. Petroleum*, 1945, **31**, 338.

THE THEORY OF COACERVATION

BY C. H. BAMFORD AND H. TOMPA

Received 6th October, 1949

The thermodynamic aspects of coacervation in non-electrolytes are completely explained in terms of the current statistical theories of polymer solutions. The system chloroform–alcohol–cellulose acetate is discussed in detail and the theoretical conclusions compared with experimental results. Finally, coacervation is discussed briefly from a molecular point of view.

1. Introduction.—Coacervation is the term introduced by Bungenberg de Jong and Kruyt [1] to denote a type of phase separation which occurs in colloidal solutions under suitable conditions. The main characteristic of coacervate systems appears to be that there are two liquid phases in equilibrium, both of which contain only small quantities of the solute (colloid). One phase, the coacervate, normally contains a few parts per cent. of the solute, while the other, the equilibrium liquid, is usually almost pure solvent. The coacervate, itself a dilute solution, thus appears to be immiscible with an excess of solvent (cf. Dobry [3e]), and this observation has been responsible for much of the attention which has been given to coacervation.

Coacervation has been observed both in solutions of electrolytes and non-electrolytes. The former have been studied extensively by Bungenberg de Jong and his collaborators,[2] and the latter by a number of French workers, notably Dobry.[3a–f]

It has been repeatedly pointed out, especially by Dobry, that in coacervation one deals essentially with systems in equilibrium. The thermodynamically relevant measurements which have been carried out in solutions of non-electrolytes include the determinations of polymer concentrations in both phases as a function of solvent composition [3a, e] or temperature,[3d] measurements of critical points as a function of molecular weight of the polymer,[3d] and determinations of osmotic pressures.[3b, f]

---

[1] Bungenberg de Jong and Kruyt, *Kolloid-Z.*, 1930, **50**, 39.
[2] Bungenberg de Jong, *ibid.*, 1937, **79**, 223, 334 ; 1937, **80**, 221, 350.

Several tentative explanations of coacervation have been suggested (Bungenberg de Jong,[2] Langmuir [1]), mainly based on ideas of solvation and electrostatic effects. It does not seem to be generally appreciated that the properties of coacervate systems, insofar as they are thermodynamically significant, are exactly those to be expected from current views of the statistical thermodynamics of polymer solutions. According to modern theory, the characteristic properties of these solutions are explicable in terms of the large differences in size between the solvent and solute molecules. We suggest that the basic feature of coacervation is similarly explicable as a size effect, both for electrolytes and non-electrolytes. Theory is at present hardly sufficiently advanced to deal with colloidal electrolytes adequately. Since with non-electrolytes the size effect alone is sufficient to account formally for the observations, we believe that the same explanation holds for colloidal electrolytes, although the detailed behaviour will be influenced by the presence of electric charges. In this paper we shall consider only coacervation in non-electrolytes.

2. Statistical Theories of Polymer Solutions. (*a*) GENERAL.—Expressions for the free energy of mixing of polymer and solvent, from which all relevant thermodynamic properties may be derived, have been obtained by the methods of statistical mechanics by Flory,[5] Huggins,[6] Orr,[7] and Guggenheim.[8] These calculations are based on a lattice model, which takes into account the difference in molecular sizes. Details of the calculations are well known, and need not be repeated here. The general correctness of the expressions has been amply confirmed by experiment.

The conditions under which phase separation takes place, together with the concentrations of coexisting phases and the critical points were first worked out by Flory [9] for binary systems, and later by Scott [10] and Tompa [11] for ternary systems. In all these calculations the polymer is regarded as a single component, and so the results apply strictly only to a homogeneous polymer. The main features of Flory's curves are shown in Fig. 1. The volume concentration of solute near the critical point is given by $1/(1 + r^{\frac{1}{2}})$, where r is the degree of polymerization. Thus for large r, this concentration is very small, amounting only to a few parts per cent. It is clear that the coexisting phases near the critical point are both dilute solutions, and except in the immediate neighbourhood of the critical point, one of the liquids is practically pure solvent. Fig. 1 also shows the increase in the critical temperature with increasing molecular weight. These features are essentially those of coacervation. We believe that coacervation is an extreme case of phase separation, and passes continuously with decreasing disparity in molecular sizes to the familiar features of partially miscible liquids. Fig. 1 gives an indication of this, and the experiments of Seyer and co-workers [12] provide evidence of the increase in solvent concentration in the critical state with increasing molecular size of the solute. These investigators measured critical temperatures and solvent concentrations in critical mixtures for a number

---

[3] (*a*) Dobry, *J. Chim. Phys.*, 1938, **35**, 387; (*b*) *ibid.*, 1939, **36**, 102; (*c*) *Bull. Soc. Chim. biol.*, 1940, **22**, 75; (*d*) *J. Chim. Phys.*, 1945, **42**, 92; (*e*) *ibid.*, 1945, **42**, 109; (*f*) *ibid.*, 1945, **42**, 114; (*g*) Gavoret and Duclaux, *J. Chim. Phys.*, 1944, **41**, 45; (*h*) Duclaux, *Cahiers Physique*, 1943, **13**, 1; (*j*) Dervichian, *Research*, 1949, **2**, 210.

[1] Langmuir, *J. Chem. Physics*, 1938, **6**, 873.

[5] Flory, *ibid.*, 1942, **10**, 51.

[6] Huggins, *Ann. N.Y. Acad. Sci.*, 1942, **43**, 190.

[7] Orr, *Trans. Faraday Soc.*, 1944, **40**, 320.

[8] Guggenheim, *Proc. Roy. Soc.*, *A*, 1944, **183**, 203, 213.

[9] Flory, *J. Chem. Physics*, 1944, **12**, 425.

[10] Scott, *ibid.*, 1949, **17**, 268.

[11] Tompa, *Trans. Faraday Soc.* 1949, **45**, 1142.

[12] Seyer and Gallagher, *Trans. Roy. Soc. Can.*, 1926, **20**, 343; Seyer and Todd, *Ind. Eng. Chem.*, 1931, **23**, 325.

of sulphur dioxide–*n*-paraffin mixtures. It was found that the volume percentages of sulphur dioxide increase continuously from a minimum of 39 % for the SO_2—C_8H_{18} system to 69·5 % for the SO_2—$C_{32}H_{66}$ system. The critical temperatures also increase from − 4·7° (C_4H_{10}) to 110° ($C_{32}H_{66}$).

(*b*) PHASE DIAGRAM FOR TERNARY MIXTURES.—We shall consider in more detail the system cellulose acetate, chloroform and ethyl alcohol which has been studied by Dobry.[3a, b] We have calculated a phase diagram for this system on the lines given by Scott [10] for ternary mixtures of which one component is a polymer. It is necessary to estimate values for the three interaction constants μ_{AO}, μ_{AP}, μ_{OP}, where A, C, P represent alcohol, chloroform, and polymer respectively. The interaction constant $\mu_{ij} = \mu_{ji}$ represents the excess interaction energy divided by kT of a molecule or segment of kind i surrounded by molecules or segments of kind j, together with a small correction term from the entropy expression. The system alcohol-chloroform has been investigated by Scatchard and Raymond.[13] Although the way in which the excess free energy of mixing splits up into heat and entropy contributions indicates that the mixture is not a regular one, nevertheless the excess free energy can be represented by an expression of the usual Hildebrand form. From the data of Scatchard and Raymond the value $\mu_{AO} = 1·13$ is obtained, and we have used $\mu_{AO} = 1·1$. Although the cellulose acetate used by Dobry was insoluble in chloroform, a very small amount of alcohol sufficed to take it into solution. It is clear therefore that the value of μ_{OP} is only slightly larger than the critical value 0·533 (for a polymer with $r = 935$). A value $\mu_{OP} = 0·56$ was finally adopted, since it gives a critical solvent composition near that of Dobry's.[3a] The third constant μ_{AP} was arbitrarily taken as 1, since this gives a value for the upper limit of alcohol in the solvent mixture near the observed one.[3b] We do not wish to suggest that these figures necessarily give the best representation of the system. In view of the limitations of the model as here applied quantitative agreement is hardly to be expected; all we wish to do is to show that reasonable values of the interaction energies lead to semiquantitative agreement with the observations, and that the system does not show any features which would be inconsistent with thermodynamic considerations based

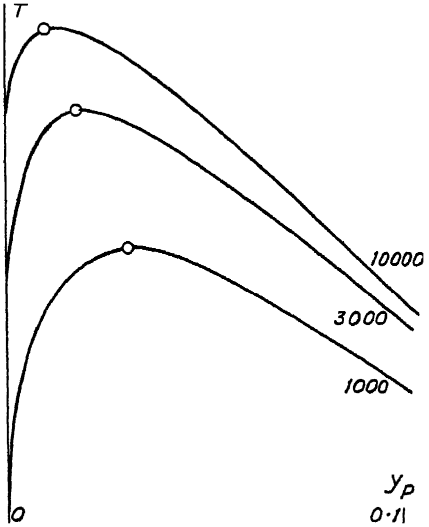

FIG. 1.—Composition of coexisting phases in the system solvent S and polymer P, for values of r indicated. Abscissa: volume fraction of polymer; ordinate: temperature. O: critical points.

---

[13] Scatchard and Raymond, *J. Amer. Chem. Soc.*, 1938, **60**, 1278.

on the model. From Dobry's figure [3b] for the limiting value of π/c, a molecular weight of $1{\cdot}01 \times 10^5$ was calculated. Thus the " chain length " is 935. This is not a true degree of polymerization, but is the ratio of the molar volumes of polymer and chloroform.

The critical points were calculated from Scott's eqn. (30) : [10]

$$1 - 2\mu_{AP}y_A - 2\mu_{CP}y_C + Qy_Ay_C = 0, \qquad (1)$$

in which the y's are volume fractions at the critical points, and

$$Q = 2\mu_{AC}\mu_{AP} + 2\mu_{AC}\mu_{CP} + 2\mu_{AP}\mu_{CP} - \mu_{AC}^2 - \mu_{AP}^2 - \mu_{CP}^2. \qquad (2)$$

Eqn. (1) gives the critical points for a polymer of infinite chain length, for which $y_P = 0$. Corrections to the values of the y's so obtained have

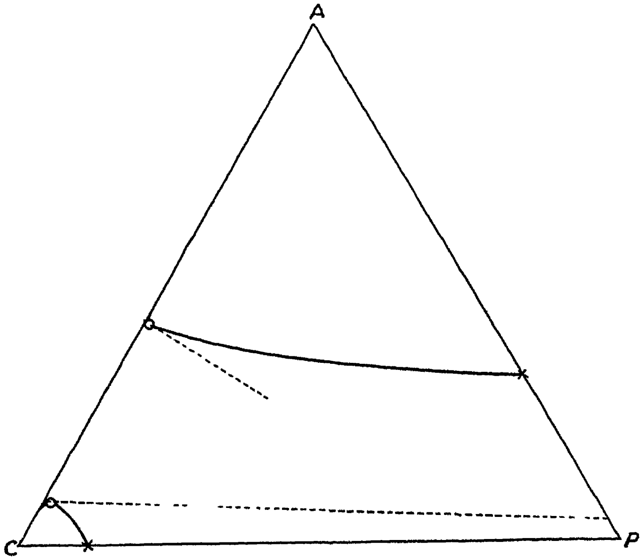

FIG. 2.—Phase diagram for the system chloroform C—alcohol A—cellulose acetate P, $r = 935$. O : critical points, - - - tangents at critical points.

been calculated by a method already described.[14] The following figures were obtained :

$$y_C' = 0{\cdot}912, \quad y_A' = 0{\cdot}057, \quad y_P' = 0{\cdot}031$$

and

$$y_C'' = 0{\cdot}511, \quad y_A'' = 0{\cdot}464, \quad y_P'' = 0{\cdot}025.$$

The former corresponds to a polymer concentration of 4·2 g./100 ml., compared to 3·2 % found experimentally by Dobry.[3a] The volume percentage of alcohol in the critical mixture is given by Dobry as 6·64 compared to our value of 5·9.

The tangents to the binodials (phase boundaries) at the critical points were calculated by differentiating Scott's eqn. (26). The points of intersection of the tangents and the AP axis are $y_A = 0{\cdot}033$ for the first critical point, and $y_A = -0{\cdot}611$ for the second.

The points of intersection of the binodials with the sides of the triangular diagram were next calculated by equating the expressions for the chemical potentials for the two components in the two phases (see Tompa [11]). The volume fractions of polymer in the coexisting phases are, in the system CP, approximately 0 and 0·180, and in the system AP, approximately 0 and 0·68.

With these data an approximate phase diagram has been constructed and is given in Fig. 2. It will be seen that the small binodial for chloroform-rich mixtures is very similar to the curve given by Dobry [3a] although it is not quite so symmetrical. Since the first tangent passes very near the apex P it is evident that the tie lines of the small binodial will all pass very close to P and therefore the solvent ratios in any two coexisting phases will be nearly identical. This is again in agreement with Dobry's results.

---

[14] Tompa, *J. Chem. Physics* 1949, 17, 1006.

(*c*) OSMOTIC PRESSURES OF TERNARY MIXTURES.—Scott[10] has derived an expression for the osmotic pressures of solutions of polymer in mixed solvents. Scott's eqn. (36) may be written

$$\pi V_0/RT = y_P/r + a_2 y_P^2 + \dots, \qquad (3)$$

where

$$\frac{1 - 2\mu_{AP}y_A - 2\mu_{CP}y_C + Qy_Ay_C}{2(1 - 2\mu_{AC}y_Ay_C)} \qquad (4)$$

Scott has discussed the uncertainties associated with osmotic pressure measurements in mixed solvents caused by non-equilibrium solvent distribution on the two sides of the membrane, and has shown that, on reasonable assumptions, the measured osmotic pressure is still given by eqn. (3) if a_2 is replaced by a_2^*;

$$a_2^* = \frac{1 - 2\mu_{AP}y_A - 2\mu_{CP}y_C + 2\mu_{AC}y_Ay_C}{2}. \qquad (4a)$$

Eqn. (3) gives the familiar linear relation between π/c and c; the slope of the line is proportional to a_2 (or a_2^*). It has already been pointed out by Scott that the numerator of eqn. (4) vanishes at the critical points for polymers of infinite chain length (cf. eqn. (1)), so that a_2 becomes zero.

Dobry[3b] has measured osmotic pressures of solutions of cellulose acetate in mixtures of chloroform and ethyl alcohol, and plotted $\pi/c - c$ curves for several different chloroform/alcohol ratios. She has observed that the slopes decrease with decreasing alcohol content, and become zero when the solvent composition is that of the critical mixture.

Since for infinite chain length the slope (a_2) vanishes at both critical points, the calculated curve relating the osmotic pressure and alcohol concentration at constant polymer concentration will have the shape observed by Dobry. For the polymer used by Dobry ($r = 935$). a_2 is zero for an alcohol concentration of 13·8 %, which is considerably higher than Dobry's observed value of 6·64 %. On the other hand a_2^* vanishes at 10·9 %. It must also be borne in mind that Dobry's polymers were not homogeneous. Since the values of the μ's and y's at the critical point depend on the weight average[15] the value of μ_{CP} chosen should strictly have been one appropriate to a polymer with $r > 935$, and having the observed critical point. Such a value of μ_{CP} would bring the concentration of alcohol at which a_2^* vanishes to below 10 %. The discrepancy between this and the observed value of 6·64 % is not unreasonable in view of the assumptions implicit in the model.

The decrease in the slope of the $\pi/c - c$ curve as one approaches the critical point has also been observed by Dobry[3c] in the system polystyrene, carbon tetrachloride and acetic acid, and by Weissberg *et al.*[16] in the system cellulose acetate, acetone and methyl alcohol.

(3) Conditions for Coacervation.—Objections to the above treatment of coacervation might be raised on the grounds that it seems to predict coacervation whenever a solution of a polymer passes from a homogeneous state to precipitation. In practice, however, coacervation is comparatively rarely observed. We believe that for homogeneous polymers coacervation will in fact usually occur. With heterogeneous polymers on the other hand this is not necessarily so. Fig. 3 represents the phase diagram for the simplest case, a single solvent and a heterogeneous polymer consisting of two species P_1, P_2 only. The diagram shows binodials for three different temperatures, together with the critical points and some tie lines. P represents the initial polymer, and S the pure solvent. The line SP represents all solutions of the polymer P. For the highest temperature at which phase separation can take place the line SP is tangential to the binodial, at the point F. However, F is not a critical point, and the composition of the coexisting phase is given by F′, which in general represents a swollen polymer, containing a comparatively high percentage of polymer. In this case, therefore, coacervation would not occur. Only if the point of contact F is near a critical point will the coexisting phases in this neighbourhood both be dilute solutions. If the polymer is homogeneous, the point F is always a critical point; for a heterogeneous polymer with a narrow molecular weight distribution F will be close to a critical point. In general the more heterogeneous the polymer, the further F will be from a critical point, and the less readily will coacervation be observed. It is, however, possible that, for a particular system, deviations from Flory's equation will allow the point of contact to remain in the neighbourhood of the critical point, thus making coacervation possible. If SP passes through a critical point without being a tangent to the binodial coacervation could occur, but would probably escape notice, since the temperature would be such that precipitation would be possible. This argument is easily extended to systems of more than two polymer components, and to mixed solvents.

---

[15] Tompa, in course of publication.

[16] Weissberg, Simha, Forsyth and Hanks, 113*th Amer. Chem. Soc. Meeting* (Chicago, 1948).

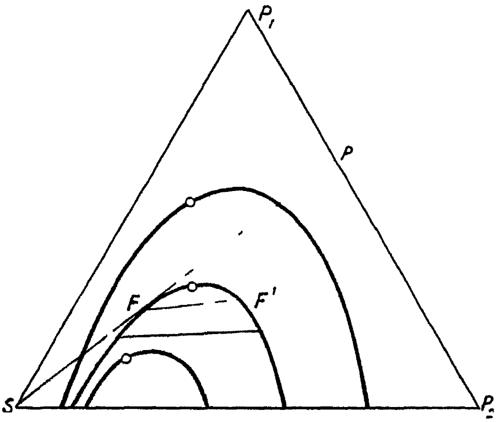

FIG. 3.—Phase diagrams for the system solvent S—polymer P_1—polymer P_2 at three different temperatures. O : critical points.

(4) Molecular Picture of Coacervation. — Although the statistical thermodynamical treatment can thus provide a formally satisfactory explanation of coacervation, it is desirable to consider, from the equivalent molecular kinetic point of view, how it is possible for a dilute polymer solution to be in equilibrium with practically pure solvent.

In binary systems of ordinary liquids A, B, of small molecular size, if the interaction energies of unlike molecules are less negative than those of like molecules, there will be a tendency towards aggregation of like molecules. This will be opposed by the thermal motion of the molecules, and mixing will occur provided the excess interaction energy is not too large. In other words, the escaping tendency of each constituent of such a mixture is less than in the pure state. If, however, the energy exceeds a certain value phase separation takes place and an equilibrium is established in which a limited number of molecules of A which can find their way into the bulk of the B molecules is balanced by those which are being continually pushed out by the larger attractive forces between molecules of the same kind. Thus a solution of A in B will be in equilibrium with one of B in A. It is in this way possible to visualize a situation in which the escaping tendency of a small number of A molecules mixed with a much larger number of B is equal to that of nearly pure A.

In a polymer solution the escaping tendency of the solvent is much higher than in the solution which would be obtained by replacing each polymer segment by a similar small molecule. This effect arises from the much greater restriction placed on the movement of the solvent molecules by the relative immobility of the large polymer molecules. It is already considerable in dilute solutions, so that in solutions containing only a few parts per cent. of polymer, the tendency towards phase separation produced by the excess interaction energy between polymer and solvent cannot be counterbalanced by thermal motion, and the escaping tendency can have a value equal to that in practically pure solvent. The solution in which this happens is then in equilibrium with nearly pure solvent, and the system corresponds to coacervate and equilibrium liquid. In solutions which contain more solvent than the coacervate the escaping tendency of the solvent would be larger than in the pure state. Such solutions would therefore be unstable and would separate into coacervate and equilibrium liquid.

Courtaulds, Limited,
Research Laboratory,
Lower Cookham Road,
Maidenhead, Berks.

SURFACE FILMS OF COPOLYMERS

By A. J. G. Allan and A. E. Alexander

Received 19*th October,* 1949

The surface pressure and surface potential characteristics of a series of copolymers derived from styrene and vinyl pyridine have been studied as functions of the polymer composition and the type of interface. An increase in the polar content appears to cause the molecule to lie flatter in the interface. When 25 % ammonium sulphate is substituted for water as the aqueous phase, the more highly polar water-soluble copolymers can be spread at both air-aqueous and oil-aqueous interfaces, and, in general, changing the non-aqueous phase from air to petrol ether stabilizes and expands the films. The observed changes in the surface pressure-area relationships are discussed in terms of the energy and entropy factors involved. From the surface potential measurements it is found that the maximum apparent surface moment decreases as the mole % of the polar grouping in the copolymer increases and this is attributed to steric factors becoming more pronounced as the styrene segments shorten.

Although the data available have been extended in recent years,[1, 2, 3] properties of surface films of polymers are not fully explained and there seems to be no record of any studies on films of synthetic copolymers. By copolymerizing monomers in different proportions a gradation in character of the polymer molecule results which is emphasized by its behaviour at interfaces. For example, it is possible to prepare polyelectrolytes with positive or negative " polyions " and to copolymerize an " iono-

---

[1] Crisp, *J. Colloid Sci.*, 1946, **1**, 49.

[2] *Idem.*, *ibid.*, 1946, **1**, 161.

[3] Benson and McIntosh, *ibid.*, 1948, **3**, 323.

genic " monomer with a hydrocarbon, varying the amount of the ionic grouping and hence controlling the hydrophobic-hydrophilic balance of the molecule.[4-7] In general, when such a compound is spread at an aqueous interface, it is to be expected that the ionic part of the molecule will be strongly bound to the water and the hydrocarbon easily removed.

Thus a wide range of designed characteristics become available by varying both the monomers, and the copolymerization ratio, besides the degree of polymerization. Such compounds should make particularly useful model systems for studying the much more complex copolymers and copolyelectrolytes occurring in nature.

This paper describes some surface studies of copolymers of styrene and 4-vinyl pyridine where the pyridine group has been converted to the *n*-butylpyridonium bromide :

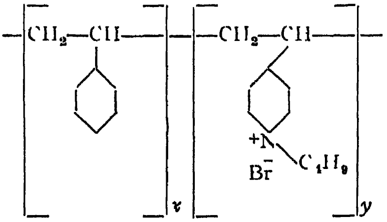

The behaviour at air-aqueous and oil-aqueous interfaces has been investigated for a series in which the pyridonium ion ranges from 1·5-90 mole % (i.e. $x/y = 66/1$ to $1/9$). Throughout the following paper the compounds are referred to on the basis of the mole % vinyl pyridine (ViPy) in the original copolymer, e.g. 25·6 %, 1·52 %, etc.

Experimental

Materials.—The preparation and purification of the copolymers is described in detail by Fuoss and Cathers,[6] who have kindly supplied the samples used in this investigation. The characteristics of this series are shown in Table I. (The molecular weights in column 3 are number average based on low surface pressure studies at the air-25 % ammonium sulphate interface).[8]

TABLE I

Copolymer Code No.	Mole % ViPy	Mol. Wt. (Approx. No. Average)
C51	1·52	97,000
B134 . . .	6·64	69,000
D41	13·00	58,000
B132 . . .	25·6	Not found
C125B. . .	58·3	14,700
C125C . .	77·8	58,000
C132 . . .	90·7	49,000

The first three compounds derived from 1·52, 6·64 and 13·0 % vinyl pyridine copolymers were dissolved in chloroform and spread from solutions containing about 0·5 mg./ml. The fourth, 25·6 %, was dissolved in a mixture of 60 % chloroform and 40 % *iso*propyl alcohol, the latter also assisting the spreading.[9]

---

[4] Fuoss and Cathers, *J. Polymer Sci.*, 1947, **2**, 12.
[5] Fuoss and Strauss, *ibid.*, 1948, **3**, 246, 602, 603.
[6] Fuoss and Cathers, *ibid.*, 1949, **4**, 97.
[7] Fuoss and Cathers, *ibid.*, 1949, **4**, 121.
[8] Allan and Alexander (to be published).
[9] Stallberg and Teorell, *Trans. Faraday Soc.*, 1939, **35**, 1413.

The 58·3 % compound was spread from 60 % *iso*propyl alcohol and water and the 77·8 % and 90·7 % were spread from solution in water alone. Spreading the 58·3 % compound from water alone did not affect the surface pressure-area curve.

Unless otherwise stated, the oil phase was redistilled petroleum ether (80°-100° C) and the aqueous phase either twice distilled water or a solution of 25 % by weight of A.R. ammonium sulphate, the latter being freed from any surface active material by previous shaking with adsorption charcoal.

Methods:—AIR-AQUEOUS INTERFACES. Surface pressures π were observed as functions of film area using the simple Langmuir trough with torsion strip and optical lever to measure the force on the mica boom.[10] The surface potentials ΔV were measured at the same time using the ionizing electrode method with a Lindemann electrometer.[11]

OIL-AQUEOUS INTERFACE. The ring method developed by Alexander and Teorell [12] was used, except that instead of a thick insensitive torsion strip to balance the whole of the pull on the ring, a thin strip was used and most of the force counterpoised by adding weights to a small scale pan on the arm which replaced the normal damping device. The maximum pull on the ring is calculated directly from the counterpoise and the optical deflexion, and the π-A curve built up by repeated addition of material to the same interfacial area.

SPREADING TECHNIQUE. The solutions were prepared in concentrations from 0·2-0·6 mg./ml. and were spread from a micrometer syringe fitted with an especially fine, obliquely levelled glass tip. At both interfaces the material was spread from the upper phase by just raising the aqueous phase with the syringe tip and allowing the material to run away from the needle down the meniscus and along the interface. The tip remained in the air or oil phase when solution was not being spread. The experiments were carried out at room temperature 19° C ± 2° C.

Results

Air-aqueous Interface.—With water as substrate, only two of the copolymers, 13·0 % and 25·6 %, gave stable films although the former collapsed slowly with time. The 1·52 % and 6·64 % compounds showed rapid collapse with no measurable pressure whereas those of highest vinyl pyridine content seemed to dissolve rapidly. The surface pressure π and surface moment μ

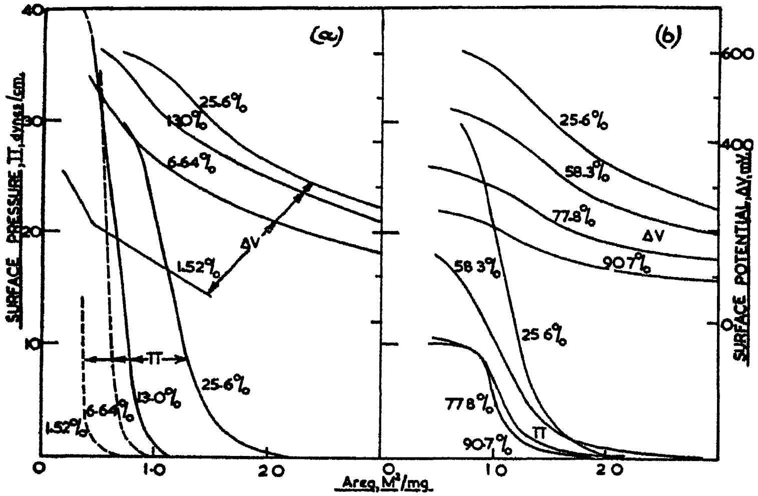

FIG. 1.—Surface pressures and surface potentials plotted against area in m.²/mg. for films spread at the air-25 % $(NH_4)_2SO_4$ interface.

---

[10] See, e.g., Alexander, *Surface Chemistry* (Butterworths, 1949).

[11] Schulman and Rideal, *Proc. Roy. Soc. A*, 1931, **130**, 259.

[12] *Trans. Faraday Soc.*, 1939, **35**, 727.

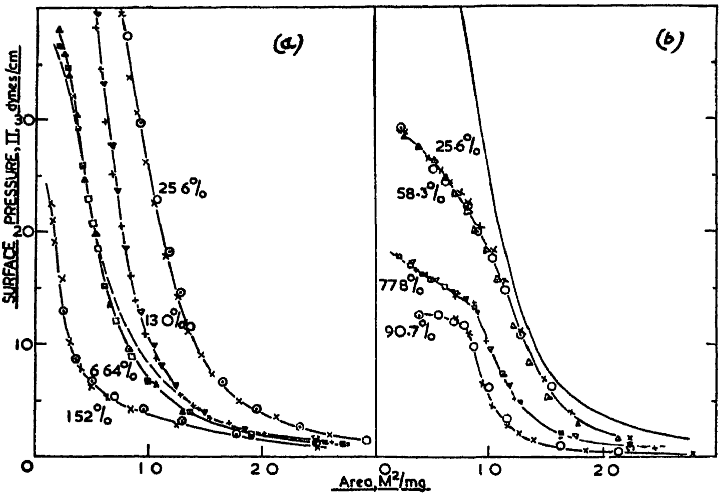

FIG. 2.—Surface pressures plotted against area in m.²/mg. for films spread at the oil-25 % $(NH_4)_2SO_4$ interface.

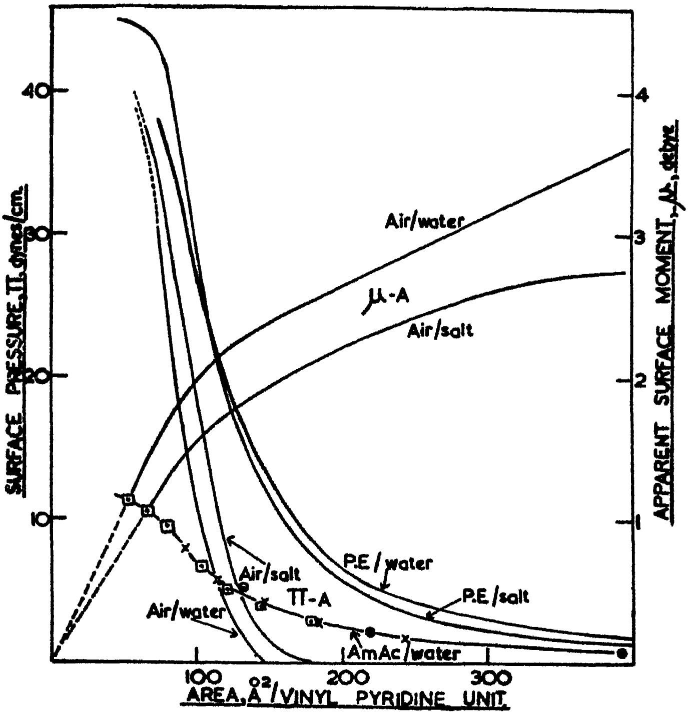

FIG. 3.—Surface pressure and surface moment plotted against area in Å²/ViPy unit for 13 % copolymer. For amyl-acetate-water interface,

⊙ Film in small ring, 8·8 cm. diam.

× Film in large ring, 11·7 cm. diam.

⊡ Film in dish, 16·4 cm. diam.

curves for the 13·0 % and 25·6 % compounds are shown in Fig. 3 and 4 plotted as a function of the area per vinyl pyridine unit in Å².

On replacing water by 25 % $(NH_4)_2SO_4$ solution as the aqueous phase, all the compounds could be examined. The water soluble compounds gave stable films showing no collapse with time and although the 1·52 % and 6·64 % compounds still collapsed they were considerably more stable than on water. The surface pressure and surface potential curves are plotted in Fig. 1(*a*) and (*b*), the areas being expressed in m.²/mg. The π-A curves for the 13·0 % and 25·6 % compounds are also shown in Fig. 3 and 4 for comparison with the values using water as substrate.

Oil-aqueous Interface.—With water as the aqueous phase, the compounds of high vinyl pyridine content were still soluble but the oil phase stabilized the first two compounds, 1·52 % and 6·64 %. Using 25 % $(NH_4)_2SO_4$ as the aqueous layer, the whole series became stable and gave the π-A curves shown in Fig. 2. The 58·3 %, 77·8 % and 90·7 % compounds could be spread from water alone at the oil-salt interface with no change in the shape of the π-A curve and thus no solubility in the aqueous phase. The dotted π-A curve for 6·64 % compound in Fig. 2 (*a*) shows its behaviour at the oil-water interface. There was no change in the curve for the 1·52 % compound, but similar effects for the 13·0 % and 25·6 % compounds were noticed. The π-A curves for oil-water and oil-strong salt are shown for comparison in Fig. 3 and 4. Substitution of the water by salt causes a decrease in pressure at corresponding areas in the low pressure region and an increase in pressure at smaller areas.

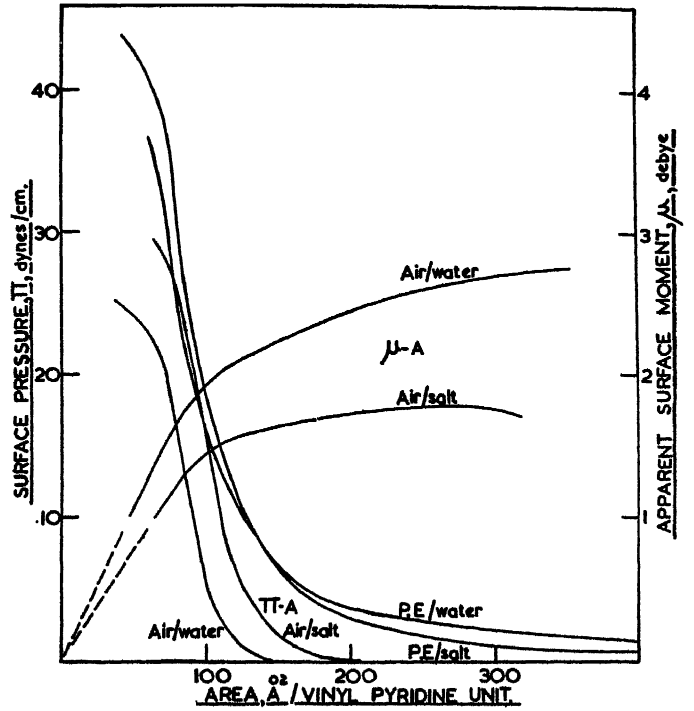

FIG. 4.—Surface pressure and surface moment plotted against area in Å²/ViPy unit for 25·6 % copolymer.

Mainly in order to test the efficiency of spreading at an interface of low interfacial energy, a π-A curve was obtained for the 13·0 % compound at the amyl acetate-water interface (γ_0 = 14 dynes/cm.).

By means of concentric glass rings of known diameter, it was possible to expand the film and then recompress by continuous addition, remove a second ring and recompress, finally to expand into the largest ring, i.e. the ordinary dish, and compress a third time by continuous addition. In this way the curve in Fig. 3 was built up, showing good spreading and no loss of material on removing the glass rings. It seems reasonable to conclude from this that spreading is complete in all the cases reported here.

Discussion

The film characteristics have been studied as functions of two series of variables, the type of interface and the polymer composition. While the hydrophobic-hydrophilic balance of the polymer molecule depends on its composition, the interactions between the ionic polar groups are governed mainly by the distances separating them along the chain and the interchain packing on the surface.

For the behaviour of polymer films, it might be anticipated that some general treatment should be possible, analogous to that already worked out for the bulk properties of polymer solutions.[13] In an attempt at such a treatment, an ideal model system has been used by Singer [14] to obtain an equation of state for polymer films by strict analogy to the calculations of Huggins [15] and Flory [16] for the three-dimensional solutions of polymers. As the equation developed only appears to allow for the divergence of the chain entropy from ideality, it seems desirable to consider other factors which must be involved in surface behaviour, although the data so far available are not amenable to more than semiquantitative discussion.

For the free energy of spreading of a polymer solution ΔG in terms of the two dimensional osmotic pressure π we can write

$$\Delta G = \int \pi \mathrm{d}A, \quad . \quad . \quad . \quad . \quad . \quad (1)$$

where A is the film area.

Since
$$\Delta G = \Delta H - T\Delta S, \quad . \quad . \quad . \quad . \quad . \quad (2)$$

it is clear that the surface pressure-area relationship can be discussed in terms of the energy and entropy factors involved, of which we consider the following to be the most important:

(i) van der Waals' interactions of the hydrocarbon portions of the copolymer (ΔH_{hc}),

(ii) electrostatic interactions of the ionic portions of the copolymer (ΔH_{es}),

(iii) entropy of the organic part of the molecule (ΔS_{ch}),

(iv) entropy of the gegenions (ΔS_{geg}).

ΔH_{hc} will be affected mainly by the polymer composition and by the nature of the non-aqueous phase, and ΔH_{es} by the composition of the aqueous phase. The high energy of attraction of the ionic groups to water indicates that these will all lie on the aqueous side of the interface except when the film is collapsing above its stability pressure. Fig. 5 gives some idea of the orientation of the constituent parts of the copolymer when spread at an aqueous interface.

Unlike earlier workers,[17, 18, 19] we believe that ΔH_{es} is a net attraction (i.e. $-$ve) owing to the Br^- ions being held in a two-dimensional lattice. There is evidence for this from the study of soap solutions [20] as well as the present monolayer work.

---

[13] See, e.g., Gee, *Reports Prog. Chem.*, 1942, **39**, 7; *Advances in Colloid Science*, Vol. II (Interscience, 1946).

[14] *J. Chem. Physics*, 1948, **16**, 872.

[15] (*a*) *J. Physic. Chem.*, 1942, **46**, 151; (*b*) *Ann. N.Y. Acad. Sci.*, 1942, **43**, 1.

[16] *J. Chem. Physics*, 1942, **10**, 51.

[17] Frumkin and Pankratov, *Acta Physicochim.*, 1939, **10**, 55.

[18] Donnison and Heymann, *Trans. Faraday Soc.*, 1946, **42**, 1.

[19] Cassie and Palmer, *ibid.*, 1941, **37**, 156.

[20] Stainsby and Alexander (in press).

Of the entropy terms, ΔS_{gig} is governed by the composition of both polymer and aqueous phase, whereas ΔS_{ch} is assumed constant, unaffected by polymer composition.

The Effect of Polymer Composition on the π-*A* Relationship.—On water, the solution of the higher % copolymers and rapid collapse of the two lowest members is perhaps the most striking effect of the change in hydrophobic-hydrophilic balance with % polar grouping. We ascribe the latter effect to the high van der Waals' attraction between the long styrene segments augmented by the net electrostatic attraction between the ions in the two-dimensional lattice, i.e.

$$T\Delta S_{ch} + T\Delta S_{gig} \lll \Delta H_{hc} + \Delta H_{eq}.$$

On 25 % ammonium sulphate, all the compounds give measurable π-*A* curves (Fig. 1) although the first two compounds, 1·52 % and 6·64 %, are rather unstable, indicated by the dotted curves. An expansion of the π-*A* curve with increasing ionic content of the copolymer would be expected owing to the great affinity of the ionic groups for the aqueous phase which tends to bring adjacent non-polar groups into the vicinity of the interface and thus to increase the area. Experimentally, this expansion is observed up to the 25·6 % and thereafter the limiting areas at low pressures are similar, owing to the molecules lying flat on the surface in all cases. The greater compressibility and the fall in stability pressure we believe to be caused by the greater ease of packing of the long chain molecules in the crystal. The limiting areas determined experimentally are shown in column 3 of Table II and these can be compared with the areas calculated (col. 2, Table II) assuming that the whole molecule lies flat on the surface with areas of 45 Å² per ViPy group and 24 Å² per styrene group.

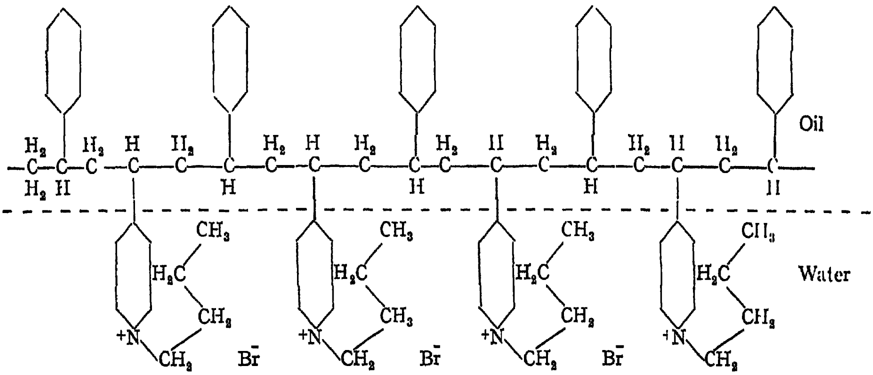

FIG. 5.—Configuration of copolymer units at an oil-water interface.

TABLE II

Compound Mole % ViPy	A_0 calcd. Lying Flat Å²/ViPy	A_0 Observed Å²/ViPy
1·52	5000	420
6·64	381	170
13·00	205	121
25·6	117	117
58·3	61	72
77·8	51	54
90·7	45	44

The experimental values are seen to check quite well for the higher members suggesting that, in these cases, the molecules are indeed lying flat on the surface. The marked deviations with the lower members can be very reasonably ascribed to the styrene segments being looped into the non-aqueous phase, although not to such an extent that all are out of the interface.

At the oil-25 % $(NH_4)_2SO_4$ interface (Fig. 2), the same marked expansion and fall in stability pressure is noticed as the % ionic grouping is increased and can be explained in the same way as above. In addition, the presence of the oil has stabilized the first two compounds, presumably due to the great reduction in the attractive forces between the hydrocarbon segments (ΔH_{hc}).

Effect of Variation of Interface on the π-A Relationship.—This is considered with reference to Fig. 3 and 4 which show the curves of two compounds at four different interfaces. These show a similar behaviour, but for clarity the discussion will be restricted to the 25·6 % compound. This copolymer, with approximately 1 polar to 3 non-polar groups, seems to have the best balance of hydrophobic-hydrophilic structure for monolayer work and for this reason is included in both families of curves in Fig. 1 and 2. The observed changes in π-A curves are discussed in relation to the energy and entropy factors involved in the expression for the free surface energy.

(i) TRANSITION AIR–WATER TO AIR–25 % $(NH_4)_2SO_4$. This expands the π-A curve without changing its shape. A similar effect was observed by Frumkin and Pankratov [17] and Donnison and Heymann [11] with unionized compounds such as cetyl alcohol and oleic acid. On water, the pyridonium ion and the bromide ion are considered to form a two-dimensional lattice so that there is a net electrostatic attraction. This can be calculated in a similar way to the calculation of the electrostatic lattice energy in the three dimensional crystal,[21] and it is found that for a square lattice

$$H_{es} = -\frac{7{\cdot}4 \times 10^2}{\epsilon\sqrt{A}} \text{ kcal./mole ViPy, } \quad . \quad . \quad . \quad (3)$$

where A = area per ViPy unit in Å^2 and ϵ = dielectric constant.

Assuming a dielectric constant of 80,

$$\Delta H_{es} = -\,9{\cdot}25/A^{\frac{1}{2}} \text{ kcal./mole ViPy. } \quad . \quad . \quad . \quad (4)$$

Now the difference in the free energy of spreading on water and on strong salt solution

$$\Delta G_{\text{salt}} - \Delta G_{\text{water}} = \int \left(\int_{A_1}^{A_2} \pi \mathrm{d}A \right)_{\text{salt}} - \left(\int_{A_1}^{A_2} \pi \mathrm{d}A \right)_{\text{water}} \qquad (5)$$

From the area between the π-A curves up to A = 100 Å^2/ViPy unit, for the 25·6 % compound, this gives

$$\Delta G_{\text{water}}^{\text{salt}} = 0{\cdot}35 \text{ kcal./mole ViPy.}$$

Using eqn. (2),

$$\Delta G_{\text{salt}} - \Delta G_{\text{water}} = (\Delta H_{hc} + \Delta H_{es} - T\Delta S_{geg} - T\Delta S_{ch})_{\text{salt}}$$
$$- (\Delta H_{hc} + \Delta H_{es} - T\Delta S_{geg} - T\Delta S_{ch})_{\text{water}} \qquad (6)$$

Now we assume that the addition of salt eliminates ΔH_{es} and also the entropy of the gegenions ΔS_{geg}, while ΔH_{hc} and $T\Delta S_{hc}$ remain constant so that

$$\Delta G_{\text{water}}^{\text{salt}} = -\,(\Delta H_{es})_{\text{water}} + (T\Delta S_{geg})_{\text{water}} \quad . \quad . \quad (7)$$

---

[21] Slater, *Introduction to Chemical Physics* (McGraw Hill, 1939), p. 385.

Assuming ideal entropies,

$$T\Delta S_{geg} = RT \ln (n_1/n_2), \quad . \quad . \quad . \quad . \quad (8)$$

where n_1 = concn. bromide ions at the area A_1,

n_2 = „ „ „ „ „ A_2.

For compression of the film from 200 to 100 Å^2/ViPy,

$$T\Delta S_{geg} = - RT \ln n_1/n_2 = -0{\cdot}4 \text{ kcal./mole ViPy.}$$

Now eqn. (4) gives

$$(\Delta H_{es})^{A\,=\,100}_{A\,=\,200} = -0{\cdot}28 \text{ kcal./mole ViPy.}$$

Thus, substituting in eqn. (7),

$$\Delta G^{\text{salt}}_{\text{water}} = -0{\cdot}12 \text{ kcal./mole ViPy,}$$

which does not show agreement with the observed value.

Part of the discrepancy may be ascribed to the assumption of ideal entropies, but it also seems likely that there is an additional factor contributing to the free energy of spreading. The work of Frumkin and Pankratov [17] and Donnison and Heymann [18] indicates that $\Delta G^{\text{salt}}_{\text{water}}$ is in fact positive for unionized compounds where ΔH_{es} and $T\Delta S_{geg}$ cannot be responsible for this change. They attribute this in part to the work of adsorption of the salt anions in the surface phase which is greater on the film covered surface than on the clean surface; presumably owing to the increase in polarizability of the contiguous phase.

At the air-aqueous interface this effect would presumably be involved with the ionic compounds studied by us, but, at the oil-aqueous interface where the polarizability is not appreciably altered by the film, the expansion effect is observed to be considerably smaller, which can then be reasonably attributed to the above electrostatic energy and gegenion entropy terms.

(ii) TRANSITION AIR-WATER TO PETROL ETHER-WATER. The expansion of the film on replacing the air phase by oil agrees well with the observations of previous workers. It seems clear that the ΔH_{hc} term (– ve and thus opposing spreading) is practically eliminated leading to an increase in ΔG (i.e. at a given A). This ΔH_{hc} term is comparatively large and would mask any change in $T\Delta S_{geg}$ at the air-aqueous interface. It is noted that the change of aqueous phase does not change the shape of the curve to the extent that a change from air-water to oil-water does.

In this case,

$$\Delta G_{\text{oil}} - \Delta G_{\text{air}} = \left(\int_{A_1}^{A_2} \pi \mathrm{d}A\right)_{\text{oil}} - \left(\int_{A_1}^{A_2} \pi \mathrm{d}A\right)_{\text{air}} \quad . \quad . \quad (9)$$

We assume that ΔH_{hc} is the only term affected and this is removed completely so that

$$\Delta G_{\text{oil}} - \Delta G_{\text{air}} = \Delta H_{hc} \quad . \quad . \quad . \quad . \quad (10)$$

From the areas under the π-A curves, up to A = 140 Å^2/ViPy,

$$(\Delta H_{hc})^{A\,=\,140}_{A\,=\,550} = -1{\cdot}25 \text{ kcal./mole ViPy, i.e. } 0{\cdot}42 \text{ kcal./mole styrene.}$$

On ammonium sulphate, the expansion of the film by oil is similar to the expansion on water, and considering the whole range of the π-A curves at the oil-aqueous interface with reference to the π-A curve at the air-water interface, the removal of ΔH_{hc} by the oil would appear to be almost the same and independent of the aqueous phase.

(iii) TRANSITION, PETROL ETHER-WATER TO PETROL ETHER.—25 % $(NH_4)_2SO_4$. Here addition of salt again eliminates ΔS_{geg} and, at large areas where ΔH terms are small this is observed as a decrease in the free energy of spreading, i.e. $\int \pi \mathrm{d}A$ is reduced.

From eqn. (8), compressing the film from 400 to 200 Å²/ViPy,

$$T\Delta S_{geo} = -\ 0{\cdot}4 \text{ kcal./mole ViPy.}$$

From the area between the π-A curves,

$$\Delta G_{\text{water}}^{\text{salt}} = \left(\int_{400}^{200}\pi dA\right)_{\text{salt}} - \left(\int_{400}^{200}\pi dA\right)_{\text{water}} = -\ 0{\cdot}2 \text{ kcal./mole ViPy.}$$

Again a discrepancy but the higher calculated value is presumably due to neglecting the removal of ΔH_{es} by the ammonium sulphate.
From eqn. (4),

$$(\Delta H_{es})_{400}^{200} = -\ 0{\cdot}2 \text{ kcal./mole ViPy.}$$

Substituting in eqn. (7),

$$\Delta G_{\text{water}}^{\text{salt}} = -\ (-0{\cdot}2) + (-\ 0{\cdot}4) = -\ 0{\cdot}2 \text{ kcal./mole ViPy,}$$

showing close agreement with the observed change in free energy.

In the high pressure region, i.e. when the film approaches close packing, the $T\Delta S$ terms will become less important compared with the ΔH terms. As pointed out above, salt eliminates ΔH_{es} and this probably explains the slight expansion also observed at the oil-aqueous interface at small areas (see also § (i)). Calculations on the basis of the simple theory above do not show good agreement at high pressures and we believe this is because the assumptions, such as the value of dielectric constant, become less valid.

(iv) EFFECT OF INTERFACIAL ENERGY. It has been pointed out by Bartell and Davies [22] that there is an " available energy for adsorption " at any interface depending on the interfacial tension of the clean interface and the final interfacial tension with a close packed film. They indicate that the larger this energy (which is in fact a measure of the collapse pressure of a film) the greater the tendency for the substance to spread and remain at the interface. The final interfacial tension is independent of the nature of the oil phase. This is observed with the 13·0 % compound which has been spread at petrol ether-water and amyl acetate-water interfaces ($\gamma_0 = 46$ and 14 dynes/cm. respectively). In each the final interfacial tension was about 3 dynes/cm.

Effect of Aqueous Phase and Polymer Composition on the Surface Potential and Surface Moment.—(i) AQUEOUS PHASE. So far, the only change made has been the substitution of 25 % $(NH_4)_2SO_4$ for distilled water. This results in a considerable reduction in μ, as shown in Fig. 3 and 4, which can be ascribed to the salt eliminating the diffuse double-layer of gegenions which give rise to a zeta-potential contribution to the surface potential. The magnitude of the reduction (*ca.* 120 mV) is consistent with this explanation.[23]

(ii) POLYMER COMPOSITION. In Fig. 6 is shown the effect upon the surface potential ΔV of increasing ionic content of the copolymer. The abscissae refer in all cases to an ionic group since the styrene can be regarded as essentially non-polar. The substrate, 25 % $(NH_4)_2SO_4$, should eliminate the zeta-potential contribution of the gegenions mentioned above.

The initial slopes of the ΔV-n curves have been obtained by extrapolation of the mean experimental curves to the origin and from these the maximum apparent surface moment μ_{max} has been calculated for each polymer. Each value of μ so obtained should give a measure of the mean contribution of the polar groups in the long chain molecule under conditions where intermolecular forces are absent. Its value is thus solely determined by intramolecular effects.

[22] *J. Physic. Chem.*, 1941, **45**, 1321.
[23] Powell and Alexander (to be published).

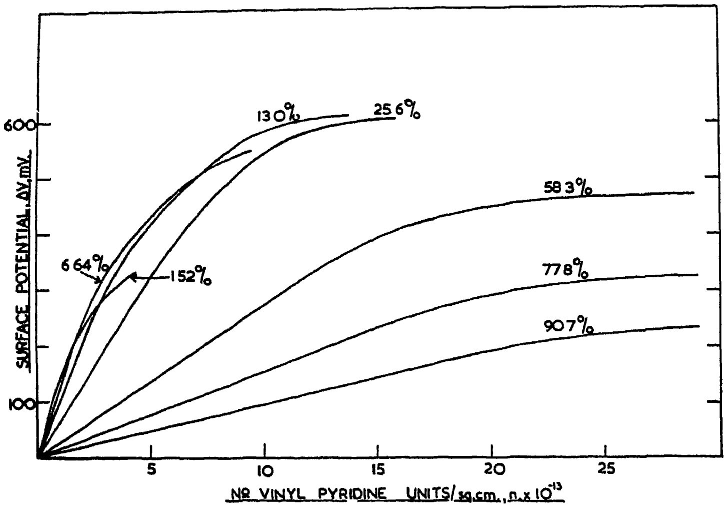

FIG. 6.—Surface potentials plotted against number of polar groups per sq. cm. at the air-25 % $(NH_4)_2SO_4$ interface.

The variation of the latter is illustrated by a plot of μ_{max} against polymer composition (Fig. 7), which shows a marked fall of μ_{max} as the ionic content increases. On the other hand, in the limit when the ionic content approaches zero, the value of μ_{max} should give a close approximation to the value of the apparent dipole moment for a single vinyl pyridonium ion when uninfluenced by others in the chain. In such a case,

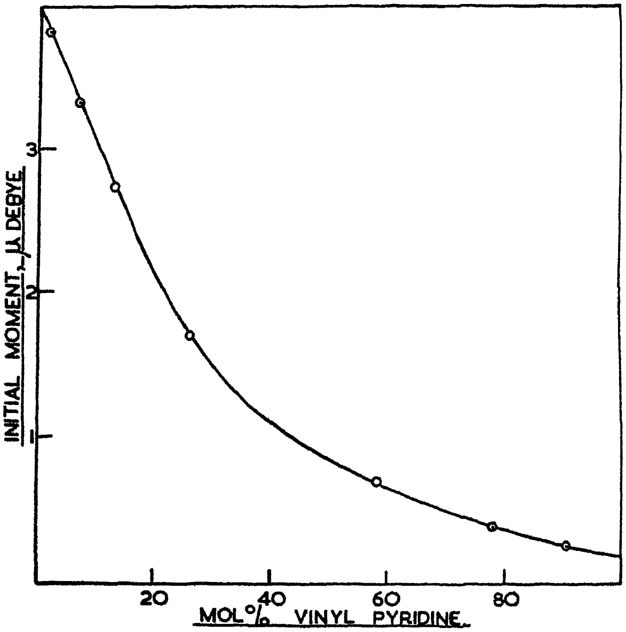

FIG. 7.—Maximum surface moment plotted against copolymer composition at the air-25 % $(NH_4)_2SO_4$ interface.

the dipoles would be free to orientate vertically to the surface, but, as the styrene segments separating the ionic groups become shorter, there is increasing steric hindrance between adjacent polar groups. It can be seen from models that this steric hindrance must force the pyridine rings away from their preferred orientation normal to the interface and thus bring about a fall in μ_{max}.

The curve in Fig. 7 shows a close resemblance to the equivalent conductance-composition curve given by Fuoss and Cathers. They ascribe the fall in equivalent conductance to a progressive binding of the gegenions to the chain, again an effect due to the proximity of the polar groups and their interaction.

To obtain further information about the surface behaviour of this series of copolymers, the experiments above for both air-aqueous and oil-aqueous interfaces are being continued to include the effects of temperature variation and also of type of salt and its concentration in the aqueous phase.

Department of Colloid Science,
Cambridge.

N.S.W. University of Technology,
Sydney, Australia.

THE POLYMERIZATION OF *ISO*BUTENE BY BORON TRIFLUORIDE

By Alwyn G. Evans and G. W. Meadows

Received 25th October, 1949 ; as revised, 2nd December, 1949

Experiments are described in which *iso*butene and boron trifluoride are very rigorously purified and condensed together at − 80° C for several hours without polymerization taking place. The necessity of a co-catalyst for the low-temperature high molecular weight polymerization of *iso*butene by boron trifluoride is thus established. The results are discussed.

In a recent paper [1a] we referred to experiments which showed that the low-temperature high molecular weight polymerization of *iso*butene by BF_3 requires a co-catalyst. These experiments are described in the present paper.

Experimental

Materials.—*iso*Butene was kindly given to us in cylinders by Messrs. Imperial Chemical Industries Ltd. (Billingham Division). Its normal routine purification before it was used in the present experiments was by distillation in a high-vacuum apparatus from − 80° C to liquid-air temperature, followed by further distillations over a sodium film heated to about 100° C until no permanent gas was produced. The last 5 to 10 % of the residue was discarded each time.

Boron Trifluoride was supplied by the Matheson Co., N.J., U.S.A. It was purified by several distillations *in vacuo* from − 80° C to liquid-air temperature.

As noted in earlier communications, the gases, purified in this way, could be mixed at room temperature without reaction occurring. On condensation at − 80° C, however, instantaneous polymerization to high molecular weight polymer occurred. Many different methods of purification of a more rigorous kind were used with only partial success in inhibiting the low-temperature reaction. Finally, the following procedure was found to be quite successful and reproducible.

[1a] Evans, A. G., and Meadows, *J. Polymer Sci.*, 1949, **4**, 359. In this paper references are given to the earlier publications in this field which have appeared since the original communication : (*b*) Evans, A. G., Holden, Plesch, Polanyi, Skinner and Weinberger, *Nature*, 1946, **157**, 102.

Intensive Purification of *Iso*Butene and BF$_3$.—The possibility was first considered of circulating the mixed gases over heated sodium in a closed system, and condensing the gases on to a sodium-covered surface. It was found, however, that BF$_3$ reacted readily with sodium at 90° C to give a black product, presumably boron. The reaction which occurred was probably analogous to that known to take place at a lower temperature with potassium : [2]

$$BF_3 + 3K = 3KF + B.$$

It was also shown that condensation of a gaseous mixture of *iso*butene and boron trifluoride, which had not been subjected to the intense purification described below, on to a sodium-coated glass surface, gave a solid polymer on warming to room temperature, thus showing that the presence of a sodium surface alone did not prevent the polymerization.

Apparatus and Method.—Several modifications of the apparatus have been used, but the essential arrangement is shown in Fig. 1. In this apparatus the *iso*butene was circulated over hot sodium and the BF$_3$ was allowed to stand in contact with cold sodium for 12-18 hr. before they were mixed. An approximately square closed circuit A made from Pyrex tubing, was connected with the main vacuum line by means of tap T. Sodium could be distilled into the vessel A from the tube F through a constriction G. The boron trifluoride purification tube C had a cone connecting it to the pumping system and a seal B leading into the vessel A. This seal could be broken by the magnetically operated glass covered breaker W to bring about mixing of the *iso*butene and the BF$_3$. Another glass seal I was introduced into vessel A so that later the gas mixture could be condensed into the vessel J, which had not been subjected to any sodium treatment, but had been well baked out with evacuation. Vessel J was connected to the vacuum system by a cone. The whole of vessel A was wound with Nichrome wire. Tappings were taken off the section marked L in Fig. 1, so that this portion could be heated to a higher temperature than the remaining part of the circuit, thus causing the gas in A to circulate by convection.

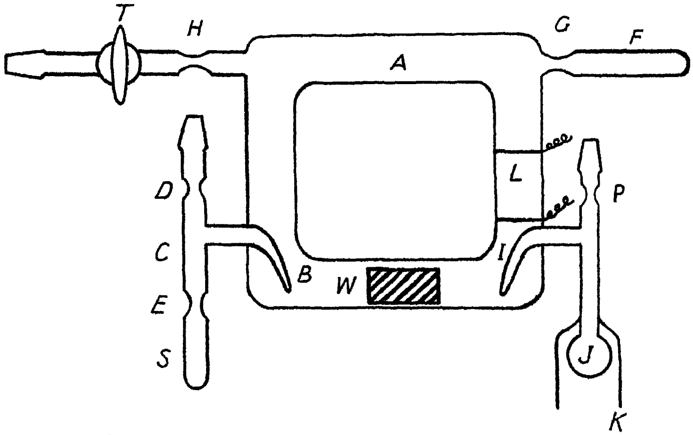

FIG. 1.—Purification of *iso*butene and boron trifluoride by treatment with sodium.

About 3 g. Na was sealed into both F and S, and the apparatus was evacuated for several hours, A being heated to free the surface from adsorbed material. The current heating A was switched off, and F was heated to 350° C by a furnace until sufficient sodium had distilled into vessel A, when tube F was drawn off at G. Tap T was then closed. In a similar way a sodium mirror was prepared in tube C, and S was drawn off at E. After sealing at E, a thin sodium film was deposited on the uncovered surface near the freshly made seal, by distilling the sodium down from the upper part of the tube.

---

[2] Ephraim, *Inorganic Chemistry* (Gurney and Jackson, 1943), p. 182.

About 400 mm. BF_3 were introduced into C, which was then sealed off at D. About 100 mm. *iso*butene were introduced into vessel A, and the vessel sealed off at H. The vessel A was then heated to 100°-110° C, while section L was heated to 230°-250° C to circulate the *iso*butene by convection over the heated sodium. The circulation was continued for 12-18 hr. and then the vessel cooled to room temperature. The seal B was then broken by the breaker W and the mixed gases were condensed into C using liquid air.

By shining a strong light through the lower part of tube C, where the sodium deposit was not very thick, it was possible to observe the behaviour of the condensed mixture on warming to room temperature. When the liquid air was removed, the solid melted and the liquid so formed evaporated completely. Condensation and re-evaporation was repeated in C several times with similar results. Then the condensed system was held at − 80° C for 4 hr. and at the end of that time the liquid evaporated completely on warming leaving no observable polymer. When tube C was opened later it was confirmed that there was no polymer present.

The mixed gases were next condensed on the surface of the circulator A by using a cold pad and, on warming to room temperature, the condensed solid liquefied and evaporated again without leaving any visible residue. This was repeated at several points on the surface of vessel A, which were free from sodium.

The seal I was then broken and the gas mixture was condensed into vessel J which had not been treated with sodium but which had been baked out with evacuation for about 12 hr. at 400° C prior to sealing at P. It was found that on warming the condensed gas mixture, all the *iso*butene evaporated leaving only a small trace ($< 1\%$) of polymer on the vessel wall. The mixture was again condensed in vessel J and then held at − 80° C for 2 hr., after which time all the *iso*butene evaporated on warming, without any apparent increase in the amount of polymer.

A trap with a breaker was then sealed on to the apparatus at point K. This trap was pumped out to 10^{-5} mm. for 1 hr. (without any baking) by an independent connection to the pumping system, and the system was then shut off from the pump by a tap. Bulb J was broken by the second breaker, and the mixed gases condensed in this new trap by cooling in liquid air. On warming up the condensed system, it was found that about one-third of the *iso*butene polymerized instantaneously to solid high moecular weight polymer. Condensing the remainder of the gas mixture at liquid-air temperature on a different part of the vessel and rewarming, brought about its instantaneous polymerization to solid high molecular weight polymer. On introducing moist air into the system, the apparatus became full with white fumes, thus confirming the presence of boron trifluoride.

Discussion

The experiments described show that the low-temperature high molecular weight polymerization of *iso*butene by BF_3 requires a co-catalyst. An extremely small amount of co-catalyst is required to cause the instantaneous polymerization of *iso*butene to solid polymer at low temperature. This is shown by the fact that a well-purified *iso*butene–BF_3 mixture was kept for 2 hr. at − 80° C without reaction in a vessel which had been well baked out on the pump and which had no taps, whereas the same mixture polymerized instantaneously in the condensed state in a vessel which had been pumped out without baking for 1 hr. only and which was closed by a tap.

The fact that the mixture was stable in a Pyrex glass vessel, which had not been treated with sodium, shows that if all the co-catalyst is removed, the *iso*butene–BF_3 mixture does not react on a Pyrex surface in the condensed state ; that is, Pyrex itself has no co-catalytic action.

There is thus no essential difference, between the room-temperature low molecular weight polymerization of *iso*butene and its low-temperature high molecular weight polymerization. Both processes require a co-catalyst. The fact that both the low and high molecular weight processes are essentially the same, is also borne out by the fact that the molecular weight of the polymer formed at room temperature can be increased by increasing the monomer pressure. When 100 mm. *iso*butene are mixed with 15 mm. BF_3 in the presence of co-catalyst, the average molecular weight of the product corresponds to about 5 monomer units. When the experiment is carried out at a constant *iso*butene pressure of 1500 mm., the average molecular weight of the product corresponds to about 30 monomer units. (These molecular weights were determined cryoscopically.)

Thus the low-temperature polymerization of *iso*butene does not proceed according to the mechanism

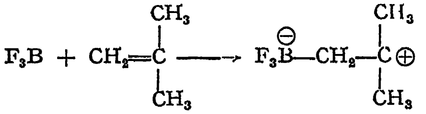

$$F_3B + CH_2{=}\overset{CH_3}{\underset{CH_3}{C}} \longrightarrow F_3\overset{\ominus}{B}{-}CH_2{-}\overset{CH_3}{\underset{CH_3}{C}}\oplus \quad . \quad . \quad . \quad (1)$$

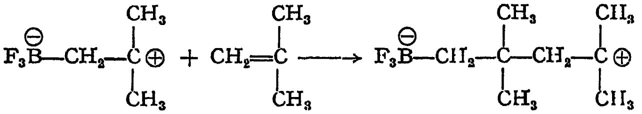

$$F_3\overset{\ominus}{B}{-}CH_2{-}\overset{CH_3}{\underset{CH_3}{C}}\oplus + CH_2{=}\overset{CH_3}{\underset{CH_3}{C}} \longrightarrow F_3\overset{\ominus}{B}{-}CH_2{-}\overset{CH_3}{\underset{CH_3}{C}}{-}CH_2{-}\overset{CH_3}{\underset{CH_3}{C}}\oplus \quad . \quad (2)$$

put forward by Hunter and Yohe[3] Price,[4] and Houtman.[5] The fact that we can mix BF_3 gas and *iso*butene vapour at room temperature to give a stable gas mixture the total pressure of which is equal to the sum of the partial pressures of the two components, (to $< 1\ \%$), shows that reaction (1) does not occur under these conditions.[1a] The "driving force" for opening up the *iso*butene double bond in the way shown in eqn. (1) would have to be supplied by the formation of the boron-carbon co-ordinate bond. The energy of formation of this bond is not known, but the values which have been obtained for the boron-oxygen[6] and the boron-nitrogen[7] co-ordinate bonds are small, being less than 20 kcal.

The low-temperature polymerization of *iso*butene by BF_3 requires a co-catalyst. The initiation of polymerization by co-catalyst complexes is attributed to the transfer of a proton from the complex to the olefin molecule.[8, 9, 1a] The energetics of the proton transfer reaction,

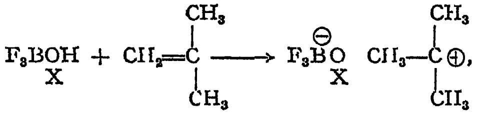

$$\underset{X}{F_3BOH} + CH_2{=}\overset{CH_3}{\underset{CH_3}{C}} \longrightarrow \underset{X}{F_3B\overset{\ominus}{O}}\ \ CH_3{-}\overset{CH_3}{\underset{CH_3}{C}}\oplus,$$

have been considered in some detail,[8, 1a] and the occurrence of proton transfer from a catalyst (conc. H_2SO_4, $BF_3.H_2O$ or floridin) to the olefin $\phi_2C{=}CH_2$ to give $\phi_2\overset{\oplus}{C}{-}CH_3$ has been demonstrated by absorption experiments in the near ultra-violet[10] (see also Dainton and Sutherland's work on the room-temperature polymerization of *iso*butene[11]).

The question as to whether in certain other Friedel-Crafts catalyzed olefin polymerizations, reaction occurs without the operation of a co-catalyst, was discussed at the Symposium on Friedel-Crafts Polymerization at Dublin,[12] and it appeared from this discussion that in no case was there direct evidence that the initiating agent is only the simple Friedel-Crafts catalyst.

---

[3] Hunter and Yohe, *J. Amer. Chem. Soc.*, 1933, **55**, 1248.

[4] Price and Ciskowski, *ibid.*, 1945, **60**, 2499.

[5] Houtman, *J. Soc. Chem. Ind.*, 1947, **66**, 102.

[6] Brown and Adams, *J. Amer. Chem. Soc.*, 1942, **64**, 2557. Laubengayer and Finlay, *ibid.*, 1943, **65**, 884.

[7] Brown, Taylor and Gerstein, *ibid.*, 1944, **66**, 431. Brown and Barbaras, *ibid.*, 1947, **69**, 1137. Brown and Taylor, *ibid.*, 1947, **69**, 1332.

[8] Evans, A. G., and Polanyi, *J. Chem. Soc.*, 1947, 252.

[9] Plesch, Polanyi and Skinner, *ibid.*, 1947, 257.

[10] Evans, A. G., and Hamann, *Symposium on Freidel-Crafts Polymerization, Proc. Roy. Dublin Society* (in press).

[11] Dainton and Sutherland, *J. Polymer Sci.*, 1949, **4**, 37.

Chemistry Department,
The University,
Manchester.

---

[12] *Proc. Roy. Dublin Society* (in press). See report on the Symposium by D. C. Pepper, *Nature*, 1949, **164**, 655.

CHANGES OF ENTROPY AND HEAT CONTENT DURING POLYMERIZATION

By F. S. Dainton and K. J. Ivin

Received 12th July, 1949

The interrelation of the values of the heats and entropies per mole of monomer polymerized under various experimental conditions is specified. Experimental methods for determining heats of polymerization are reviewed and the magnitude of various phase change corrections discussed, in relation to existing data on mono-olefins. Various empirical methods of evaluating ${}_{n}\Delta H^{\circ}_{gg}$ are outlined and use made of Anderson, Beyer and Watson's group method to calculate values of this quantity over a range of temperatures for ethylene, unconjugated vinyl and vinylidene compounds and styrene. The effects of resonance in the monomer and strain in the polymer are mentioned. Three experimental methods for measuring entropies of polymerization are described, namely (i) from equilibrium or "ceiling" temperatures, (ii) from standard entropies of polymer and monomer, and (iii) from the ratio of the frequency factors of the propagation and depropagation reactions. Empirical and statistical methods are then outlined, and phase change corrections and probable effects of monomer resonance and polymer strain described. Finally, the magnitude of the ratio $\Delta H/\Delta S$ for dimerization and high polymerization, and its temperature variation, are outlined. Comparisons with experiment are made and possible reasons advanced why certain vinylidene compounds polymerize only below room temperature and formaldehyde vapour below 100° C. The application of these ideas to copolymerization is briefly indicated.

In a recent paper [1] we have shown that the ceiling temperature observed in the formation of polysulphones from liquid mixtures of sulphur dioxide and olefines, is due to the reversal of the propagation reaction. The ceiling temperature T_x obtained by extrapolation of the rate–temperature or molecular weight–temperature curves, is the temperature at which the free energy of formation of the polymer from the reactants, under the given conditions specified by the subscript x, is zero. Hence

$$T_x = \Delta H_x/\Delta S_x,$$

where ΔH_x and ΔS_x are the increments at T_x of the heat content and entropy per mole of monomer polymerized. It can easily be demonstrated that, provided the chains are long, these increments also apply to the changes in heat content and entropy associated with the propagation reaction.

---

[1] Dainton and Ivin, *Nature*, 1948, **162**, 705.

In polysulphone formation the conditions for the observation of the ceiling temperature are particularly favourable. However, it is clear that in principle, all polymerization systems should exhibit this phenomenon under suitable conditions and that a study of polymerization reactions in this temperature region provides not only another method of determining heats of polymerization but also experimental values of entropies of polymerization. The latter quantities are of interest on general grounds and also because the frequency factor * A_d of the reverse of the propagation reaction can be calculated if ΔS° and the frequency factor A_p of the propagation reaction, are known. It is the purpose of this paper to review available data on heats and entropies of polymerization, particularly in relation to types of system in which the ceiling temperature is most likely to be observed.

Definitions.—Polymerization of a given monomer may occur under a variety of conditions and the following definitions will be employed.

REACTION	Monomer → Polymer	Limiting Values, $n \to \infty$, of :—		
EQUATION	$M \to \frac{1}{n}M_n$	HEAT CHANGE	ENTROPY CHANGE	CEILING TEMPERATURE (°K)
	gas (1 atm.) → gas (1 atm.)	ΔH°_{gg}	ΔS°_{gg}	T°_{gg}
	gas (1 atm.) → condensed (generally solid)	ΔH°_{gc}	ΔS°_{gc}	T°_{gc}
	liquid → condensed	ΔH°_{lc}	ΔS°_{lc}	T°_{lc}
	liquid → molar solution in monomer	ΔH°_{lsm}	ΔS°_{lsm}	T°_{lsm}
	liquid (molar solution) → molar solution	ΔH°_{ss}	ΔS°_{ss}	T°_{ss}

Except where otherwise stated the values of ΔH° and ΔS° are for 25° C. When a liquid monomer is only partially polymerized, or polymerized in solution, the concentration of polymer must also be stipulated since there will be small contributions, which may vary with dilution, to ΔH° and ΔS° from the heat and entropy of solution of the polymer. Since, as we have shown,[1] the chain initiation and termination reactions make their contribution to the values of ΔH° and ΔS°, these quantities will usually increase with the chain length n to limiting values. When n is small the actual value of n will be used as a prefix, e.g. ${}_2\Delta H^{\circ}$ for dimerization. When n is large, ΔH°_{gg} and ΔS°_{gg} are hypothetical quantities. ΔH° and ΔS° will also vary with temperature but this effect is found to be slight and in the same sense for both quantities. We therefore find the ratio $\Delta H^{\circ}/\Delta S^{\circ}$ to be only slightly dependent on temperature (see below) and hence the ceiling temperature may be put approximately equal to this ratio at 25° C.

The relations between the various heat and entropy changes at 25 C are given by eqn. (1) to (8).

---

* The frequency factor A is the non-exponential factor in the expression for the velocity constant. Thus for the propagation (subscript p) reaction and its reverse (called by us the "depropagation" reaction, subscript d) we have $k_p = A_p \cdot \exp(-E_p/RT)$ l. mole^{-1} sec.$^{-1}$ and $k_d = A_d \exp(-E_d/RT)$ sec.$^{-1}$, respectively. We have preferred to apply the term "depropagation" to the reverse of propagation because the word depolymerization applies to an overall reaction and therefore includes initiation and termination processes.

$$\Delta H^\circ_{gc} = \Delta H^\circ_{gg} - \frac{\lambda_n}{n}, \quad . \quad . \quad . \quad . \quad . \quad . \quad . \quad . \quad . \quad (1)$$

$$\Delta S^\circ_{gc} = \Delta S^\circ_{gg} - \left(\frac{\Delta S^\circ_n}{n}\right)_v \quad . \quad . \quad . \quad . \quad . \quad . \quad . \quad . \quad (2)$$

$$\Delta H^\circ_{lc} = \Delta H^\circ_{gc} + \lambda_1 = \Delta H^\circ_{gg} - \frac{\lambda_n}{n} + \lambda_1, \quad . \quad . \quad . \quad . \quad . \quad (3)$$

$$\Delta S^\circ_{lc} = \Delta S^\circ_{gc} + (\Delta S^\circ_1)_v = \Delta S^\circ_{gg} + (\Delta S^\circ_1)_v - \left(\frac{\Delta S^\circ_n}{n}\right)_v, \quad . \quad (4)$$

$$\Delta H^\circ_{lsm} = \Delta H^\circ_{lc} + \frac{L^\circ_n}{n} = \Delta H^\circ_{gg} - \frac{\lambda_n}{n} + \lambda_1 + \frac{L^\circ_n}{n}, \quad . \quad . \quad . \quad (5)$$

$$\Delta S^\circ_{lsm} = \Delta S^\circ_{lc} + \left(\frac{\Delta S^\circ_n}{n}\right)_s = \Delta S^\circ_{gg} + (\Delta S^\circ_1)_v - \left(\frac{\Delta S^\circ_n}{n}\right)_v + \left(\frac{\Delta S^\circ_n}{n}\right)_s, \quad (6)$$

$$\Delta H^\circ_{ss} = \Delta H^\circ_{gg} - \frac{\lambda_n}{n} + \lambda_1 + \frac{L^\circ_n}{n} - L^\circ_1, \quad . \quad . \quad . \quad . \quad . \quad (7)$$

$$\Delta S^\circ_{ss} = \Delta S^\circ_{gg} + (\Delta S^\circ_1)_v - \left(\frac{\Delta S^\circ_n}{n}\right)_v + \left(\frac{\Delta S^\circ_n}{n}\right)_s - (\Delta S^\circ_1)_s, \quad . \quad . \quad (8)$$

where λ_1 and λ_n denote the latent heats of vaporization at 25° C of the liquid monomer and condensed n-mer respectively and $(\Delta S^\circ_1)_v$ and $(\Delta S^\circ_n)_v$ the corresponding entropies of vaporization. L°_1 and L°_n denote the increase in heat content at 25° C when 1 mole of liquid monomer and 1 mole of condensed polymer respectively are dissolved in the solvent concerned, and $(\Delta S^\circ_1)_s$ and $(\Delta S^\circ_n)_s$ are the corresponding entropy changes.

In applying these relations it is noted that:

(*a*) if the vapours can be treated as ideal, the entropies of vaporization will be of the form $\frac{\lambda}{298 \cdot 1} + R \ln p$, and will thus be equal to Ri_1 and Ri_n, where i_1 and i_n are the integration constants of the vapour pressure equations of monomer and polymer respectively;

(*b*) if the solutions can be treated as ideal, $L^\circ_1 = L^\circ_n = 0$;

(*c*) if the solutions of monomer are either ideal or regular, the entropy of solution of the monomer will contain the term $(- R \ln N_1)$, where N_1 is the mole fraction of the monomer in the solution.

Heats of Polymerization.—Heats of polymerization may be either experimentally determined by each of three distinct methods or calculated by empirical methods.

(i) COMBUSTION OF THE MONOMER AND POLYMER SEPARATELY.[4, 7, 8, 25, 31] The difference in the heats of combustion gives ΔH°_{gc} or ΔH°_{lc} directly. Since the heats of combustion may be some 50 times that of polymerization, a high degree of accuracy in the experimental measurement is necessary if a moderate accuracy in the final result is to be obtained. However, the cooling corrections are reduced to a minimum and there are no corrections for temperature, heats of solution, etc. With monomers containing elements other than C, H and O the fate of these elements in combustion must be determined in each individual case. For example, we have found [3] that the combustion of 1-butene polysulphone proceeds according to the equation,

$$\frac{1}{n}(C_4H_8SO_2)_{n(s)} + 6\tfrac{1}{2}O_{2(g)} \rightarrow 4CO_{2(g)} + H_2SO_4 \, . \, 3H_2O.$$

(ii) DIRECT MEASUREMENT BY ISOTHERMAL OR ADIABATIC CALORIMETRY.[2, 3, 6, 6a, 8, 9, 10] The isothermal method has the advantage of practically eliminating cooling corrections and of integrating the heat evolved over a considerable period of time. A most satisfactory calorimeter has been described by Tong and Kenyon [2] in which the heat of reaction is used to vaporize weighable amounts of a solvent maintained at its boiling point. The adiabatic method is less satisfactory unless polymerization is rapid, and cooling corrections can be accurately determined.

In both cases it is necessary to estimate the amount of reaction which has taken place, either by direct analysis or by observation of some physical property. We have utilized the latter method in determining the heats of copolymerization of SO_2 with 1-butene or 2-butene, the maximum rate of volume contraction of the reaction system being compared with the maximum rate of rise of temperature of the calorimetric fluid.[3]

A number of reliable measurements of heats of polymerization have recently been made by the direct method, but due to lack of data on vapour pressures, heats of solution, specific heats, etc., these values cannot always be related with certainty to the idealized thermodynamic quantities given above. Fortunately, however, where such data do exist, the corrections to be applied are relatively small. For example, the values of ΔH°_{gg} at 127° C as calculated by Jessup [4] from the data of Rossini *et al.*,[5] is only 0·14 kcal./mole less than the value calculated for 25° C for ethylene. Again, the heat of polymerization of methyl methacrylate is independent,[2] within the experimental error ($\pm$ 0·2 kcal./mole), of temperature, catalyst concentration and the presence of CCl_4. Occasionally side reactions such as oxidation obtrude at high catalyst concentration, and in such cases it is necessary to extrapolate the results to zero catalyst concentration.[6]

(iii) KINETIC ANALYSIS IN THE REGION OF THE CEILING TEMPERATURE. For any polymerization reaction in which the propagation step is

$$M + P_r \underset{k_d}{\overset{k_p}{\rightleftharpoons}} P_{r+1}, \quad . \quad . \quad . \quad . \quad (9)$$

in which M denotes monomer, P_r growing polymer of length r, the rate of reaction under conditions where appreciable reversal of this reaction is occurring will be given by [1]

$$-\frac{d[M]}{dt} = f(x)\{A_p \exp(E_p/RT)[M] - A_d \exp((E_p - \Delta H^\circ_x)/RT)\}, \quad (10)$$

where $f(x)$ is a function depending on the initiation and termination processes,* E_p is the energy of activation of the propagation reaction. Rate measurements over a wide range of temperatures up to the ceiling temperature therefore enable ΔH° to be determined with an accuracy limited only by the accuracy of the rate determinations. The method has so far been applied only to the formation of polysulphones.[3]

---

[2] Tong and Kenyon, *J. Amer. Chem. Soc.*, 1945, **67**, 1278. Also see ref. 6, 9 and 10.

[3] Details of these experiments will be published elsewhere.

[4] Jessup, *J. Chem. Physics*, 1948, **16**, 661.

[5] Prosen, Johnson and Rossini, *J. Res. Nat. Bur. Stand.*, 1946, **37**, 51, where references to earlier work may be found.

[6] Tong and Kenyon, *J. Amer. Chem. Soc.*, 1947, **69**, 1402.

* $f(x)$ is the concentration of active centres and is solely a function of the initiation and termination processes only when the dead polymer does not undergo decomposition into two radicals. When such a reaction does occur $f(x)$ will contain in the numerator a positive term proportional to the polymer concentration. But even in this case $f(x)$ can never lead to a zero value of d(M)/dt. Should the dead polymer undergo depolymerization by splitting off successive monomer molecules by a non-chain process an extra negative term will appear in eqn. (10) and d(M)/dt may become zero even when $f(x)$ and the term in brackets are both positive. In this case, ΔH°_x cannot be obtained from kinetic analysis in the region of the ceiling temperature by applying eqn. (10), although the identity $\Delta H^\circ_x = T \cdot \Delta S^\circ_x$ will still apply at the ceiling temperature T.

TABLE I.—HEATS OF POLYMERIZATION OF MONO-OLEFINES

Monomer	Method and Temperature	$-\Delta H_x$	kcal./mole	Reference
Ethylene . .	(i) 25° C	$-\Delta H^\circ_{gc}$	25·4	4
	$\frac{1}{n}\lambda_n$ estimated[4] as 3·57 kcal./mole	$-\Delta H^\circ_{gg}$	21·8	4
	$\frac{1}{n}\lambda_n$ estimated as 2·57 kcal./mole	$-\Delta H^\circ_{gg}$	22·8	This paper
Propylene . .	(ii) 78° C, solvent *n*-butane, catalyst $AlBr_3$-HBr, polymer insoluble	$-\Delta H^\circ_{sc}$	~ 16·5	6*a*
Styrene † . .	(i) 25° C Final solution containing 6·9 % by weight of polymer	$-\Delta H^\circ_{lc}$ $-\Delta H^\circ_{gc}$ $-\frac{L^\circ_n}{n}$ $-\Delta H^\circ_{lsm}$	16·68 ±0·16 27·2 0·86 ± 0·05 17·54 ±0·16	7 This paper 7 7
o-Chlorostyrene .	(ii) B* 76·8° C Bz_2O_2	$-\Delta H^\circ_{lc}$	16·1 ±0·2	6
p-Chlorostyrene .	,, ,, ,,	,,	16·4 ±0·2	6
2 : 5-Dichlorostyrene	,, ,, ,,	,,	16·0 ±0·2	6
Ethyl vinyl benzene	,, ,, ,,	,,	16·5 ±0·2	6
Methyl methacrylate	,, ,, ,,	,,	16·3 ±0·2	6
	(ii) E, Room *T*, Fe^{++}-H_2O_2	approx. $-\Delta H^\circ_{lc}$	12·9 ±1·1	8
	(ii) B, 76·8° C, Bz_2O_2	$-\Delta H^\circ_{lc}$	13·0 ±0·2	9
	(ii) In CCl_4 solution ; 76·8° C	$-\Delta H^\circ_{ss}$	13·0	2
	(ii) In MeOH-H_2O solution polymer insoluble ; 76·8° C	approx. $-\Delta H^\circ_{lc}$	13·6	2
n-Butyl methacrylate . .	(ii) B, 76·8° C, Bz_2O_2	$-\Delta H^\circ_{lc}$	13·5 ±0·2	9
Cyclohexyl methacrylate . .	,, ,, ,,	,,	12·2 ±0·2	9
Benzyl methacrylate . .	,, ,, ,,	,,	13·4 ±0·2	9
Phenyl methacrylate . .	,, ,, ,,	,,	12·3 ±0·2	9
Methyl acrylate .	,, ,, ,,	,,	18·7 ±0·2	10
Vinyl acetate . .	,, ,, ,,	,,	21·3 ±0·3	10
Acrylonitrile . .	(ii) Polymer insoluble in monomer	,,	17·3 ±0·5	10
Vinylidene chloride	,, ,, ,,	,,	14·4 ±0·5	10
Acrylic acid . .	(ii) E, Room *T*, Fe^{++}-H_2O_2	approx. $-\Delta H^\circ_{lc}$	18·49 ±0·27	8
Methyl acrylate .	,, ,, ,,	,,	20·19 ±0·98	8
Methacrylic acid .	,, ,, ,,	,,	15·84 ±0·17	8
*iso*Butene . .	(i) Polymer was liquid (strictly $-\Delta H_{ll}$)	$-\Delta H^\circ_{lc}$	12·61	8, 25
,, . .	(ii) In solution in hexane	$-\Delta H^\circ_{ss}$	12·8	8, 25
SO_2+1-butene .	(iii) Excess SO_2 ; 40-65° C	$-\Delta H^\circ_{ss}$	20·7 ±1·4	1, 3
	(ii) Excess SO_2 ; 25-31° C	,,	22·0 ±0·7	1, 3
SO_2+2-butene .	(ii) Excess SO_2 ; 25-31° C	,,	20·5 ±1·7	1, 3 †

Footnotes to Table on pp. 336–7

(iv) CEILING TEMPERATURES AS A FUNCTION OF MONOMER CONCENTRATION. From eqn. (10) or by application of the isochore to the overall equilibrium it is evident that

$$\mathrm{d}\ \ln\ (\mathrm{M})/\mathrm{d}T = -\Delta H^\circ_{gc}/\boldsymbol{R}T^2$$

for systems in which the entropy of the polymer is constant. This latter condition is satisfied when the polymer exists as a pure condensed phase. Formaldehyde represents the only example where this method can be applied, and is a rather specialized case. The value obtained is

$$\Delta H^\circ_{gc} = -13{\cdot}3 \pm 1{\cdot}5 \text{ kcal./mole.}$$

A summary of all available data on heats of polymerization of olefines is given in Table I. The magnitude of the individual corrections for change of phase may be considerable, e.g. λ_1 for styrene is 10·5 kcal./mole,[11] and since $\Delta H^\circ_{lc} = -16{\cdot}7$, ΔH°_{gc} must be $-27{\cdot}2$ kcal./mole. Although there is no obstacle to the direct determination of λ_1 for all vinyl monomers, few published data exist. By contrast, direct measurement of $\frac{1}{n}\lambda_n$ is most unlikely, and for *iso*butene it has been assumed that $\lambda_1 = \frac{1}{n}\lambda_n$.[8] Such an assumption is unwarranted since the increment in λ_n per C_2H_4 unit in the paraffin series decreases to a limiting value of 1·36 kcal./mole * for the liquid hydrocarbons. When a polymer is formed as a crystalline solid, we must also include the contribution from fusion in λ_n. The only known example of $\frac{1}{n}\lambda_n$ including a fusion term is polythene, for which Jessup[4] gives the value 1·21 kcal./mole. Despite the fact that the monomers are generally liquids and the polymers solids, it is likely that in general, $\lambda_1 > \frac{1}{n}\lambda_n$ and hence $\Delta H^\circ_{lc} < -\Delta H^\circ_{gg}$; but the magnitude of the correction will probably be seldom in excess of 5 kcal./mole. Corrections for heats of solution will also be small, since molecular interactions with the solvent should be slight except when the monomer contains a highly polar group. This conclusion is well borne out by the observations (*a*) that the heat evolved per mole when polystyrene is dissolved in liquid styrene to 7 % by weight is only 0·86 kcal.[7] and (*b*) that, as already mentioned, the heat of polymerization of methyl methacrylate is independent of the solvent used.[2]

(v) EMPIRICAL ESTIMATION. All empirical methods of estimating heats of polymerization of vinyl compounds have been based on empirical relations between the heat of formation and structure of low molecular weight hydrocarbons. Thus, using the relations deduced by Rossini *et al.*,[5] Flory[13] obtained values of $\Delta H^\circ_{gg} = -22$ to -24 kcal./mole for a number of simple olefines. More recently, Jessup[4] has computed values of ΔH°_{gg} and ΔG°_{gg} for ethylene polymerization over a range of temperatures and chain lengths.

[6a] Fontana and Kidder, *ibid.*, 1948, **70**, 3745.

[7] Roberts, Walton and Jessup, *J. Polymer Sci.*, 1947, **2**, 420.

[8] Evans and Tyrrell, *ibid.*, 1947, **2**, 387.

[9] Tong and Kenyon, *J. Amer. Chem. Soc.*, 1946, **68**, 1355.

[10] *Idem.*, *ibid.*, 1947, **69**, 2245.

---

* Jessup[4] gives the value 2·36 kcal./mole based on measured heats of combustion of liquid and gaseous hydrocarbons. We have preferred the value 1·36 kcal./mole, which we have deduced from actual vapour pressure data of the normal paraffins from pentane to dodecane inclusive.[12]

[11] Pitzer, Guttman and Westrum, *ibid.*, 1946, **68**, 2209.

[12] These data were taken from Willingham, Taylor, Pignocco and Rossini, *J. Res. Nat. Bur. Stand.*, 1945, **35**, 219.

[13] Flory, *J. Amer. Chem. Soc.*, 1937, **59**, 241 ; pp. 249-250 especially.

The heat of polymerization of substituted olefines will be profoundly affected (*a*) by any resonance stabilization of the monomer brought about by conjugation of the substituent with the olefinic double bond and (*b*) by any distortion of normal valency dimensions and angles in the polymer. The former factor lowers the heat of polymerization to an extent equal to the resonance energy, which may be evaluated in the usual way, e.g. from the difference in heats of hydrogenation of ethylene and the vinyl compound.[13] ΔH°_{gg} for styrenes, vinyl cyanides, aldehydes and ketones should be lower than ethylene for this reason. The latter factor will also cause a reduction in heat of polymerization, but the magnitude of the effect is not directly calculable and is generally assumed to account for any difference between observed and calculated values of ΔH°_{gg} remaining after allowance has been made for monomer resonance effects.[8] The low value of ΔH°_{lc} for *iso*butene is attributed solely to this factor, whilst low values for the α-substituted acrylates and vinylidene ‡ chloride are probably due to a combination of both effects (see Table I).

A most useful empirical method of correlation of thermodynamic quantities with structure has recently been proposed by Anderson, Beyer and Watson.[14] The heats and entropies of formation of gaseous organic compounds in the standard state and the coefficients in the specific heat-temperature equation have been resolved by these authors into contributions attributable to atomic groups. The method is of very wide applicability, permitting ΔH°_{gg} to be evaluated for any temperature. Allowance is made for strong conjugation: and in our experience the method is reasonably accurate, leading to values of ΔH°_f and S° for hydrocarbons which compare favourably with those experimental values most recently published.[15] In Table II are presented values of ${}_n\Delta H^\circ_{gg}\,(T)$ for $n = 2$ and $n \rightarrow \infty$ for some typical monomers forming unstrained polymers. These were calculated from eqn. (11)

$$ {}_n\Delta H^\circ_{gg}(T) = {}_n\Delta H^\circ_{gg}\,(25^\circ\,\mathrm{C}) + \Delta a(T - 298{\cdot}1) + \frac{\Delta b}{2}(T^2 - 298{\cdot}1^2) + \frac{\Delta c}{3}(T^3 - 298{\cdot}1^3) \qquad (11) $$

where a, b and c are the coefficients in the specific heat equation

$$C_p = a + bT + cT^2.$$

For $n \rightarrow \infty$, ΔH°_{gg} (25° C) was taken to be the value of ΔH° (25° C) for the reaction

$$\mathrm{M}_{n(g)} + \mathrm{M}_{1(g)} \rightarrow \mathrm{M}_{(n+1)(g)}. \qquad . \quad . \quad . \quad (12)$$

* B bulk polymerization, generally approaching 100 % conversion.

E emulsion or aqueous phase polymerization. None of the quantities previously defined corresponds to the heat evolved under these conditions. It differs from $-\Delta H^\circ_{lc}$ mainly by the heat of solution of the monomer L°_1. This accounts for the differing values for methyl acrylate and methacrylate respectively.

The heats of polymerization of styrene, vinyl acetate and methyl methacrylate were first measured by Goldfinger, Mark and Josefowitz,[17] using method (ii) and the adiabatic calorimeter. The values, 15·0 ± 0·47, 8·0 ± 0·4 and 7·0 ± 0·4 respectively have not been included in the Table because the values there given are more accurate.

† This value is also consistent with the experimental log (rate)—1/T curve.

---

[14] Anderson, Beyer and Watson, *Nat. Petroleum News, Tech. Sect.*, 1944, **36**, R476.

[15] *Selected Values of Chemical Thermodynamic Properties* (*Nat. Bur. Stand.*, 1947, Series III) Table 23.

‡ Note in proof: In α-methyl styrene the resonance and steric effects are combined to give the very low value of 9·0 kcal. for ΔH_{lc} at 25° C. (Private communication from Dr. R. S. Jessup.)

[16] Richardson and Parks, *J. Amer. Chem. Soc.*, 1939, **61**, 3543.

[17] Goldfinger, Mark and Josefowitz, *ibid.*, 1943, **65**, 1432.

The value of this quantity determined by any of the empirical methods cited,[5, 14] is constant for $n > 2$.*

If the heat of formation of radicals by the reaction (13)

$$R + M_n \rightarrow P_n \quad . \quad . \quad . \quad . \quad . \quad (13)$$

is also constant for $n > 2$, then the heat of the propagation reaction (9) is the same as that of reaction (12) and also constant for $n > 2$. On the other hand, since ΔH°_{gg} for reaction $12 = (n + 1)\,{}_{n+1}\Delta H^\circ_{gg} - n\,{}_n\Delta H^\circ_{gg}$, it is *not* equal to ${}_n\Delta H^\circ_{gg}$ for low values of n. In fact, ${}_n\Delta H^\circ_{gg}$ increases slowly with n to the limiting value which is also the value of ΔH° for reaction (1) when $n > 2$ and for the propagation reaction (9) when $n > 2$ It is important that Table II be read in this sense.

Entropies of Polymerization.—The methods available for determining entropies include one direct experimental method, two indirect experimental methods, and one fairly satisfactory empirical method. In addition rough estimates based on statistical considerations are occasionally possible.

(i) DIRECT METHODS. MEASUREMENT OF CEILING TEMPERATURES: all direct methods involve the determination of either (*a*) equilibrium constants over a range of temperatures or (*b*) heat change and one equilibrium temperature. Both methods therefore require measurement of ceiling temperatures.

Method (*a*) is not easy to apply in practice since $K = (M_n)^{1/n}/(M_1)$ is usually difficult to measure, due to the fact that n has all values within a very wide range. If, however, the polymer formed separates as a pure condensed phase, $(M_n)^{1/n}$ can be taken as constant, and over short ranges of temperature

$$\ln (M_1) = -\frac{\Delta H^\circ_x}{RT} + \frac{\Delta S^\circ_x}{R},$$

provided ΔH°_x and ΔS°_x are substantially invariant and T is the ceiling temperature for the monomer concentration (M_1). In the special case where the polymer readily depolymerizes the equilibrium may be approached from the polymer side. Formaldehyde provides the only example of the application of this method, and we deduce

$$\Delta S^\circ_{gc} = -32{\cdot}5 \pm 4 \text{ cal./deg. mole}$$

for this monomer.

Method (*b*), which is based on the relation $\Delta S^\circ_x = \Delta H^\circ_x/T_c$, is only limited by the accuracy of the measurements of heats of polymerization and ceiling temperatures. Since ΔH is usually measured well below the ceiling temperature, the value of ΔC_p is necessary in order to obtain values of ΔS over a range of temperatures. The magnitude of the temperature corrections is not likely to be large (see (iv) below). Method (*b*) appears to be the most promising experimental approach but as yet has only been quantitatively applied to the copolymerization of SO_2 with 1- and 2-butenes. In these systems we[1, 3] find that the values of ΔS°_{ss} (standard state 1 mole l.$^{-1}$, excess SO_2) for 1-butene and 2-butene polysulphone formation are $71{\cdot}9 \pm 2{\cdot}0$ and $73{\cdot}1 \pm 5{\cdot}5$ cal./deg. mole respectively. A feature of this method, is that if the system behaves ideally, then

$$T_x = \frac{\Delta H_x}{\Delta S_x + R \ln (M_1)} \quad (\Delta S^\circ_x \text{ here refers to 1 mole l.}^{-1}) \quad . \quad (13)$$

We have been able to confirm the correctness of the corresponding expression for the copolymerization of 1 butene and SO_2, in which [M] is replaced by the product of the two monomer concentrations.[3]

(ii) FROM THE ENTROPIES OF MONOMER AND POLYMER. Standard entropies of monomers can be determined from specific and latent heat data, and the standard entropies of some gaseous monomers could be derived from spectroscopic data. Some of these data have been obtained for certain of the lower olefines and

---

* The method of ref. (14) gives ΔH°_{12} constant for $n > 2$.

$$\Delta S_x^\circ = \frac{1}{n} S_x^\circ(n) - S_{x(1)}^\circ$$

can therefore be evaluated for low values of n, in the special case of ethylene polymerization. For the more commonly used monomers and their associated high polymers both thermal and spectroscopic data are unfortunately almost non-existent. However, in the important case of styrene it is possible to obtain a value for ΔS_{lc}° as follows. Jessup * has measured C_p for monomeric styrene and polystyrene from 5° K to about 400° K from which, by graphical integration we have computed values of $\frac{1}{n} S_{n(c)}^\circ$ and $(S_{1(l)}^\circ - \Delta S_f)$, where ΔS_f is the entropy of fusion of styrene at 242·5° K. No direct measurement of this last-named quantity is to be found in the literature, but Smoker and Burchfield [30] have recorded the freezing points of solutions of xylene in styrene, and from these results $\Delta S_f^{242 \cdot 5} = 10{\cdot}1$ cal./deg. mole. The values of ΔS_{lc}° for styrene polymerization are thus (*a*) at 27° C, $- 25{\cdot}8$ cal./deg. mole, and (*b*) at 77° C, $- 27{\cdot}85$ cal./deg. mole. If, as we expect, $\left(\frac{\Delta S_n^\circ}{n}\right)_s$ for solution of polystyrene in monomer is small, then ΔS_{lsm}° will be only slightly less in magnitude than ΔS_{lc}°.

(iii) From the Ratio of the Frequency Factors of the Propagation and Depropagation Reactions. The value of the ratio A_p/A_d is exp $(\Delta S_x^\circ/R)$ and hence

$$\Delta S_x^\circ = R \ln (A_p/A_d),^1$$

where x denotes 1 mole/l. of monomer. Kinetic analysis of polymerization processes at low temperatures, where the depropagation reaction is not occurring to any extent, enables A_p to be determined. So far this frequency factor has only been evaluated in three cases, namely, for the bulk liquid-phase polymerization of methyl methacrylate,[18c] vinyl acetate [18a, b] and styrene.[19] Kinetic analysis of depolymerization reactions in which the propagation reaction is reduced to a minimum, either by continuous removal of monomer from the reaction system [20] or by maintaining the temperature above the ceiling temperature, may ultimately permit A_d to be measured. At present, no values of A_d are available for any reaction. However, the depropagation reaction is a unimolecular process and in such processes it is to be expected that the activated complex will resemble the initial state. Hence, in general, the entropy of activation should be small and the frequency factor of the order 10^{13} sec.$^{-1}$. Assuming this to be true for vinyl acetate and styrene we obtain $\Delta S_{lsm}^\circ = - 26{\cdot}2$ cal./deg. mole ($A_p = 1{\cdot}65 \times 10^6$ mole^{-1} sec.$^{-1}$) [18a] for the former and $- 27{\cdot}9$ cal./deg. mole ($A_p = 1{\cdot}0 \times 10^6$ mole^{-1} sec.$^{-1}$) for the latter. The closeness of the value $\Delta S_{lsm}^\circ = - 27{\cdot}9$ for styrene to $\Delta S_{lc}^\circ = - 25{\cdot}8$ cal./deg. mole, given in the preceding section appears to us to be significant. The data for methyl methacrylate are conflicting. Matheson *et al.*,[18c] from rotating sector measurements at 5, 30, 50 and 60° C and making use of earlier data of Schulz, give $A_p = 5{\cdot}13 \times 10^6$ l. mole^{-1} sec.$^{-1}$. On the other hand Bamford and Dewar [18c] give values for k_p at 25° and 0° C of 150 and 41·6 respectively, although not in the same paper, whence $A_p = 1{\cdot}76 \times 10^8$ l. mole^{-1} sec.$^{-1}$. Using the results of Matheson *et al.* we obtain $\Delta S^\circ_{tsm} = -24{\cdot}3$ cal./deg. mole.*

---

* Private communication to one of us (F. S. D.).

[18] (*a*) Burnett and Melville, *Proc. Roy. Soc. A*, 1947, **189**, 456 ; (*b*) Bartlett and Swain, *J. Amer. Chem. Soc.*, 1945, **62**, 2273 ; 1946, **68**, 2381 ; (*c*) Matheson, Auer, Bevilacqua and Hart, *ibid.*, 1949, **71**, 502 ; Bamford and Dewar, *Nature*, 1946, **158**, 380 ; *Faraday Soc. Discussions*, 1948, *44B*, 310.

[19] Bamford and Dewar, *Proc. Roy. Soc. A*, 1948, **192**, 309.

[20] E.g. methyl methacrylate degradation under the conditions described by Grassie and Melville, *Faraday Soc. Discussion*, 1948, *44B*, 378.

(iv) EMPIRICAL ESTIMATION. The methods available for evaluating ${}_n\Delta S^\circ_{gg}$ empirically are in principle the same as those for the estimation of ${}_n\Delta H_{gg}$. Thus Jessup[1] has utilized a relation connecting ΔG°_f for the formation of the mono-olefines and the number of carbon atoms to calculate ${}_n\Delta G_{gg}$ for the polymerization of ethylene. The values of ${}_n\Delta S^\circ_{gg}$ may then be obtained in the usual way. For other vinyl polymerizations the less accurate but more widely applicable group method of Anderson, Beyer and Watson[15] can be employed. Table II shows the values of ${}_n\Delta S^\circ_{gg}(T)$ calculated from eqn. (14) appropriate to $n = 2$ and $n \rightarrow \infty$.

$$
{}_n\Delta S^\circ_{gg}(T) = {}_n\Delta S^\circ_{gg}\,(25^\circ\,\text{C}) + \Delta a \ln T/298{\cdot}1 + \Delta b\,(T - 298{\cdot}1) + \frac{\Delta c}{2}(T^2 - 298{\cdot}1^2). \quad (14)
$$

The accuracy of the method may be judged by comparison of the values for the dimerization of ethylene in line 2 of Table II with the experimental values, which would read 15·7, 15·6, 15·4, 15·3, 15·16, 15·0.

(v) STATISTICAL CONSIDERATIONS. The factors which determine the magnitude of ${}_n\Delta S^\circ_{gg}$ may be appreciated by considering the translational, rotational and vibrational contributions separately.[22]

For the dimerization, the translational contribution ${}_2\Delta S^\circ_{gg(t)}$ is given by

$$
\begin{aligned}
{}_2\Delta S^\circ_{gg(t)} &= -\frac{1}{2}\left\{\frac{5}{2}R \ln 298{\cdot}1 - 2{\cdot}298\right\} + \frac{3}{4}R \ln (2m) - \frac{3}{2}R \ln m \\
&= -11{\cdot}967 - 3{\cdot}4305 \log_{10} m \text{ cal./deg. mole} \quad (15)
\end{aligned}
$$

where m is the molecular weight of the monomer. The external rotational contribution ${}_2\Delta S^\circ_{gg(r)}$ is given by

$$
{}_2\Delta S^\circ_{gg(r)} = -5{\cdot}80 + 2{\cdot}287 \log_{10} \frac{(I_AI_BI_C)_2^{\frac{1}{2}}}{(I_AI_BI_C)_1} - 4{\cdot}575 \log_{10} \frac{\sigma_2^{\frac{1}{2}}}{\sigma_1}, \quad (16)
$$

where σ denotes symmetry number, I_A moment of inertia in atomic mass Å^2 units and the subscripts 1 and 2 refer to monomer and dimer respectively. The vibrational contribution ${}_2\Delta$

$$
\begin{aligned}
{}_2\Delta S^\circ_{gg(v)} = \tfrac{1}{2}R \sum_2 \left\{\frac{a\nu_2}{e^{a\nu_2} - 1} - \ln (1 - e^{-a\nu_2})\right\} \\
- R\sum_1 \left\{\frac{a\nu_1}{e^{a\nu_1} - 1} - \ln (1 - e^{-a\nu_1})\right\}, \quad (17)
\end{aligned}
$$

where $a = 4{\cdot}827 \times 10^{-3}$ cm., ν denotes a vibration frequency and the summations are taken over all vibrations of the two molecules concerned.

Owing to the lack of values of the moments of inertia, symmetry numbers and vibration frequencies of the commonly used monomers and their dimers, expressions (15), (16) and (17) do not appear to be immediately useful. Furthermore, all internal rotational contributions to the entropies of the monomer and dimer have been included as vibrations in (17). Nevertheless, analysis of ${}_2\Delta S^\circ_{gg}$ in this way has advantages. Thus, a consideration of the vibration frequencies assigned to aliphatic hydrocarbons by Pitzer[23] immediately indicates that the

---

* Since this manuscript was completed the data of Melville and Mackay (*Trans. Faraday Soc.*, 1949, **45**, 323) have been published. These authors give $A_p = 5 \times 10^5$ l. mole^{-1} sec.$^{-1}$ whence $\Delta S^\circ_{tsm} = -28{\cdot}9$ cal./deg. mole.

[21] Kilpatrick, Prosen, Pitzer and Rossini, *J. Res. Nat. Bur. Stand.*, 1946, **36**, 559.

[22] For the appropriate formulae see standard text on statistical thermodynamics, e.g. Fowler and Guggenheim (Cambridge, 1939).

[23] Pitzer, *J. Chem. Physics*, 1937, **5**, 469; 1940, **8**, 711.

TABLE

Monomer	Temp. °K	298·1	400	500	600	700	800	900	Ceiling Temperature	
									Intersection of ΔH and $T\Delta S$	Ratio of $\Delta H/\Delta S$ values at 298° K
Ethylene	$-{}_2\Delta H^{\circ}_{gg}$	12,600	12,580	12,530	12,460	12,370	12,280	12,180	825	816
$CH_2{=}CH_2$	$-{}_2\Delta S^{c}_{gg}$	15·45	15·39	15·28	15·15	15·02	14·89	14·77		
	$-\Delta H^{c}_{gg}$	23,100	22,930	22,710	22,470	22,210	21,930	21,650	680	672
	$-\Delta S^{c}_{gg}$	34·40	33·90	33·43	32·99	32·58	32·21	31·88		
Vinyl compounds (unconjugated)	$-{}_2\Delta H^{c}_{gg}$	12,350	12,260	12,160	12,050	11·920	11,790	11,640	583	578
	$-{}_2\Delta S^{\circ}_{gg}$	21·35	21·09	20·87	20·66	20·47	20·29	20·12		
$CH_2{=}CHX$	$-\Delta H^{\circ}_{gg}$	22,900	22,360	22,090	21,660	21,220	20,780	20,360	585	575
	$-\Delta S^{\circ}_{gg}$	39·80	38·68	37·75	30·96	36·27	35·69	35·20		
Styrene	$-{}_2\Delta H^{c}_{gg}$	9,800	9,720	9,620	9,520	9,400	9,270	9,130	514	510
	$-{}_2\Delta S^{\circ}_{gg}$	19·20	18·96	18·76	18·58	18·41	18·24	18·09		
$CH_2{=}CH\,.\,C_6H_5$	$-\Delta H^{\circ}_{gg}$	17,800	17,400	16,990	16,560	16,110	15,680	15,260	508	502
	$-\Delta S^{c}_{gg}$	35·50	34·38	33·45	32·65	31·97	31·38	30·88		
Vinylidene compounds (unconjugated)	$-{}_2\Delta H^{\circ}_{gg}$	11,800	11,480	11,110	10,710	10,290	9,880	9,490	557	544
	$-{}_2\Delta S^{\circ}_{gg}$	21·70	20·77	19·96	19·22	18·58	18·03	17·58		
$CH_2{=}CX_2$ or	$-\Delta H^{c}_{gg}$	22,000	21,330	20,560	19,710	18,830	17,950	17,110	555	540
$CH_2{=}CXY$	$-\Delta S^{c}_{gg}$	40·70	38·77	37·05	35·51	34·15	32·97	31·98		

ΔH°_{gg} and ΔS°_{gg} for $n = 2$ and ∞ as functions of temperature (cal./mole and cal./mole °K respectively). Values are given to one more place of decimals than is justified, in order to recover small differences accurately.

total vibrational entropy, including internal rotational contributions, of most monomers or dimers at room temperature is only about 10-15 % of the total entropy. Also there will be little change in external rotational entropy on dimerization for those systems in which $\sigma_1 = \sigma_2 = 1$ and $(I_A I_B I_C)_2^{\frac{1}{2}} \simeq 350\,(I_A I_B I_C)_1$. In this case the main loss of entropy is due to the replacement of the translational entropy of the monomer by only half the translational entropy of the dimer. Eqn. (15) indicates that this loss is increased as the basic monomer ethylene is substituted, and we may associate the increase in the total entropy loss on substitution (see Table II ${}_2\Delta S^\circ_{gg}$ values) largely to this cause.

For the polymerization reaction we obtain

$$\begin{aligned}{}_n\Delta S^\circ_{gg} &= {}_n\Delta S^\circ_{gg(t)} + {}_n\Delta S^\circ_{gg(r)} + {}_n\Delta S^\circ_{gg(v)} \\ &= \left\{\frac{1-n}{n}(25{\cdot}98 + 6{\cdot}861 \log_{10} m) + \frac{6{\cdot}861}{n}\log_{10} n\right\} \\ &\quad + \left\{\frac{2{\cdot}287}{n}\log_{10}\frac{(I_A I_B I_C)_n}{(I_A I_B I_C)_1^n} + \left(\frac{1-n}{n}\right)11{\cdot}6\right\} \\ &\quad + \frac{R}{n}\sum^{y}(\Delta_n) - R\sum^{z}(\Delta_1), \qquad (18)\end{aligned}$$

in which $R\Delta$ = contribution to the entropy of one vibration; y and z denote the number of such terms appropriate to polymer and monomer respectively, and it will be noted that

$$\frac{y}{} - z = 6\frac{(n-1)}{}$$

When n is very large $\Delta S^\circ_{gg} = -\,{}_1S^\circ_g$ + the sum of the vibrational and internal rotational entropy of the monomer unit in the polymer. In ethylene $\Delta S^\circ_{gg} = -34{\cdot}1$ (Table II) whilst ${}_1S^\circ_g = 52{\cdot}5$ cal./deg. mole and we therefore conclude that this latter quantity is of the order of 18 cal./deg. mole.

The same problem has been considered by Baxendale and Evans,[24] who deduced the relation,

$$\frac{\Delta S^\circ_{lsm}}{R} = 1 - \log \gamma\sigma - \log (f_m/f_p), \qquad (19)$$

where γ is the co-ordination number of the space lattice, σ is the symmetry number of the polymer molecules and f_m and f_p are the respective partition functions of the free monomer units and of the monomer segments in the polymer. This expression refers to bulk polymerization and a standard state of 1 mole/l. The same difficulty arises, namely, that the vibration frequencies of the monomer units in the polymer chain are unknown, and therefore f_p and ΔS°_{lsm} cannot be evaluated. By assuming that there is no entropy of activation for the depropagation step (cf. § (iii)), Baxendale and Evans show that the observed value of A_p for vinyl acetate [18a] leads to reasonable values of internal vibration frequencies in the polymer molecule.

(vi) CORRECTIONS FOR PHASE CHANGE. The correction terms which serve to relate the various ΔS°_x values are listed in eqn. (2), (4), (6) and (8). As far as the latent heat terms are concerned, the remarks made in connection with ΔH°_x apply with equal force here. Unfortunately the vapour pressure data concerning both monomers and polymers are so rare that corrections under this heading can seldom be made. A possible line of progress in applying these corrections can be illustrated by ethylene.

---

[24] Baxendale and Evans, *Trans. Faraday Soc.*, 1947, 43, 210.

The correction term $-(\Delta S^\circ_n/n)_v$ for *liquid* polythene formation assuming that the vapour is ideal is

$$\frac{Ri_n}{n} = \frac{R}{n}\ln p_n + \frac{\lambda_n}{n298}.$$

Plotting the data of Rossini *et al.*[12] according to the approximate expression

$$\ln p = -\frac{\lambda}{RT} + i_n$$

we find that $i_n = 25{\cdot}53 + 0{\cdot}34n$ for $n > 4$, n being the number of C_2H_4 units in the normal paraffins to which the data refer. Hence, for n, $\frac{Ri_n}{n} = 0{\cdot}68$ cal./deg. mole. For solid polythene the correction term must be increased by $\frac{\lambda_n(f)}{n}$; Jessup[4] gives $\frac{\lambda_n(f)}{n} = 1{\cdot}21$ kcal./deg. mole and hence $\frac{1}{n}\frac{\lambda_n(f)}{298{\cdot}1} = 4{\cdot}06$. Accordingly $\Delta S^\circ_{gc} = \Delta S_{gg} - 4{\cdot}74$ cal./deg. mole for polythene.

(vii) RESONANCE IN THE MONOMER AND STRAIN IN THE POLYMER. Monomer resonance implies higher bond energies within the monomer and hence lower heats of polymerization. In practice the energies and vibration frequencies of the bonds in the monomers used are so large, that further increases will not bring about much decrease in the already small contributions which the bond vibrations make to the total entropy. For example, a bond which is increased in strength from 80 to 88 kcal. and in vibration frequency from 1000 to 1100 cm.$^{-1}$ will change its entropy contribution at room temperature from 0·094 to 0·065 cal./deg. mole. Any shortening of the bond associated with strengthening will result in a decreased rotational entropy contribution from the molecule, but here also, the effect will be small due to the relatively smaller percentage decrease in bond length for a given increase in strength when the bond involved is strong. Nevertheless, the total effect of monomer resonance will always be a reduction of the internal entropy of the monomer, which may be appreciable and may in some cases be greater than the increase in $\Delta S^\circ_{gg(t)}$ caused by changing the molecular weight of the monomer. The change of $-\Delta S^\circ_{gg}$ from 39·8 to 35·5 cal./deg. mole (Table II, col. 3) in passing from unconjugated vinyl compounds to styrene is probably largely due to the decreased total internal entropy of the latter compared with the former.

Steric strain in the polymer causes an abnormally low heat of polymerization. Only slight changes in bond vibrational entropy of the monomer segment in the polymer would be expected, but if the polymer chains are constrained into rigid configurations the lower torsional and skeletal vibrations might be so restricted as to cause a net decrease in internal entropy of the polymer. The magnitude of $-\Delta S^\circ_x$ would thus be increased.

Whichever of the two causes is responsible for a decrease in heat of polymerization, it would seem likely that percentage decrease in ΔH°_x will be considerably greater than the associated percentage change in ΔS°_x. Existing data on heats and ceiling temperatures are in support of this view. Table III summarizes the results of the application of methods (i) to (iv) whenever the data have justified it.

Calculated and Experimental Ceiling Temperatures.—It is evident from Table II and from Jessup's data[4] on ethylene, that the ceiling temperature as defined by the condition $\Delta G_x = 0$ decreases with the chain length. Such variation, however, appears to be appreciable only in ethylene. Experimental ceiling temperatures obtained by extrapolation † of the results of experiments in which the chain length of polymer formed is large will be the limiting values of T_c. Above this temperature very short chain polymers may still be formed and therefore actual viscosity–temperature and rate–[M] graphs, if determined in this

TABLE III —ENTROPIES OF POLYMERIZATION

Monomer	Methods and Comments	ΔS°_{c} (cal./deg. mole)	Reference
Ethylene (C_2H_4) .	(iv) at 25° C (iv) at 25° C and taking $(\Delta S^{\circ}_{n}/n)_{v} = 4·74$) (iv) at 25° C	ΔS°_{gg} − 34·0 ΔS°_{gc} − 38·74 ΔS°_{gg} = − 34·4	1 [1], 4 *
Vinyl cpd. (C_2H_3X) . unconjugated	(iv) at 25° C	ΔS°_{gg} = − 39·8	*
Vinyl acetate ($CH_2{=}CH.O.CO.CH_3$)	(iii) Room temperature, photochemical	ΔS°_{lsm} = − 26·2	[1], 18(*a*), 18(*b*)
Styrene ($CH_2 : CH . C_6H_5$)	(ii) at 27° C (ii at 77° C (iii) room temperature, photochemical (iv) at 25° C	ΔS°_{lc} = − 25·8 ΔS°_{lc} − 27·85 ΔS°_{lsm} − 27·9 ΔS°_{gg} = − 35·5	* * *, 10 *
Vinylidene cpds. ($CH_2{=}CX_2$ or $CH_2{=}CXY$)	(iv) at 25° C	ΔS°_{gg} = − 40·7	*
Methyl methacrylate $CH_2{=}C(CH_3)COOCH_3$	(iii) Room temperature, photosensitized by diacetyl	ΔS°_{lsm} = − 24·3	*, 18(*c*)
iso-Butene ($CH_2{=}C(CH_3)_2$	(*ib*) Assuming T_c 350° K Friedel-Crafts' catalysts	ΔS°_{lc} ~ 37	*
α-Methyl Styrene .	(*ib*) Assuming T_{lc} ~ 350	ΔS°_{lc} ~ − 26	*
Formaldehyde . .	(*ia*) 10°-58 C : to polyoxymethylene	ΔS°_{gc} 32·5 ± 4	*
Copolymerization SO$_2$+1-butene SO$_2$+2-butene	(*ib*) at 64° C (*ib*) at 40° C photochemical or catalyzed by Bz_2O_2 or $AgNO_3$ Standard state = 1 mole/l. in excess SO_2 as solvent	ΔS°_{ss} − 71·9 ± 2·0 ΔS°_{ss} − 73·1 ± 5·5	1 1

* Denotes this paper.

† Either (*a*) viscosity-temperature curves for a given [M] may be extrapolated to cut the temperature axis or (*b*) rate — [M] isotherms extrapolated to cut [M] axis. Details of the application of both methods will be given in subsequent papers.

region would be seen to approach the latter axes asymptotically. This view is confirmed in the 1-butene polysulphone formation by the following two experiments. Firstly, illumination at 70° C of a mixture of 1-butene and SO_2 for which the ceiling temperature was 63°, caused a certain amount of gum identified as short chain polysulphone to be formed in addition to the monomeric sulphonic acid formed by simple substitution. Secondly, in an experiment carried out 1° below the ceiling temperature using benzoyl peroxide as a catalyst a contraction corresponding to at least 50 % polymerization was reached after 25 hr. This is much in excess of that required to reduce the product of the concentrations of the reactants to its critical value for this temperature. Because of this dependence of ${}_nT_x$ on n at low values of n, the onset of the depropagation reaction is best detected by departures (in a negative direction) from the Arrhenius equation in the log (rate)–$1/T$ curve. If chain transfer is occurring to an increasing extent as the temperature is raised, this would be an additional reason for avoiding the use of viscosity–temperature curves.

Since both ΔH_x° and ΔS_x° are functions of temperature (see eqn. (11) and (14)) the correct method of evaluating T_x° is to plot ΔH_x° and $T\Delta S_x^\circ$ against temperature and identify the ceiling temperature with the points of intersection of these curves. The values so obtained are shown in the tenth column of Table II. Owing to the form of the temperature dependence of ΔH_x° and ΔS_x° an increase of ΔH_x° with temperature is always associated with an increase of ΔS_x° ; these two effects are of such a magnitude that the ratio of $\Delta H_x^\circ/\Delta S_x^\circ$ at 25° C is only very slightly different from the temperature of intersection of ΔH_x° and $T\Delta S_x^\circ$ curves. Comparison of the last two columns of Table II illustrate this.

The empirical method of Anderson, Beyer and Watson [14] for computing ΔS_{gg}° and ΔH_{gg}° leads to the conclusion that the ceiling temperatures for polymerization of the common monomers in the vapour at 1 atm. to hypothetical gaseous polymers (T_{gg}°) should lie in the range 200-300° C. The values of the ceiling temperatures for the different experimental conditions, i.e., T_{gc}°, T_{lc}° T_{lsm}°, and T_{ss}° will differ amongst themselves and also from T_{gg}°. For example, in the polymerization of styrene $\Delta H_{lsm}^\circ = -17{\cdot}5$ kcal.,[7] $\lambda_1 = 10{\cdot}5$ kcal.,[11] the integral molar heat of solution of polystyrene is only $-0{\cdot}8$ kcal., and hence,

$$\Delta H_{gc}^\circ = -17{\cdot}5 - 10{\cdot}5 + 0{\cdot}8 = -27{\cdot}2 \text{ kcal./mole.}$$

Vapour pressure data for styrene lead to $Ri_1 = 23{\cdot}9$ cal./deg. mole. Combining this with the value $-25{\cdot}8$ cal./deg. mole for ΔS_{lc}° calculated above we obtain $T_{gc}^\circ = 547°$ K. On the other hand if a frequency factor A_d of 10^{13} sec.$^{-1}$ is assumed, $\Delta S_{lsm}^\circ = -27{\cdot}9$ cal./deg. mole (see above) and we obtain $T_{lsm}^\circ = 625°$ K. In all cases the ceiling temperature will be lowered by reduction of monomer concentration according to eqn. (13). The order of magnitude of this effect in the liquid phase will be about 80° C for a tenfold reduction in monomer concentration. In the gas phase the magnitude will be somewhat smaller due to the higher standard entropy change.

We have argued that monomer resonance and polymer strain produce larger percentage changes in the heat than in the entropy. Accordingly, both the phenomena will cause ceiling temperatures to be lower than in systems where they do not occur. This is substantiated by several observations. For example, the order of decreasing ceiling-temperatures for formation of various polysulphones is also the order of increasing steric hindrance in the polymer.[1] Also, it is known that *iso*butene [25] and α-methyl styrene [26] probably both give sterically strained polymers and that both can only be polymerized to high molecular weight products below room temperature. This suggests that the ceiling temperature for these monomers is in the region of room temperature, a conclusion which is consistent with the observed low heat of polymerization of *iso*-butene (see Table I).

---

[25] Evans and Polanyi, *Nature*, 1943, **152**, 738.

[26] Hersberger, Reid and Heiligman, *Ind. Eng. Chem.*, 1945, **37**, 1073.

There appears to be only one case other than polysulphone formation where *quantitative* measurement of the dependence of $-d[M]/dt$ on temperature has revealed considerable deviation from the Arrhenius equation. This is the photochemical polymerization of vinyl acetate vapour studied by Melville and Tuckett.[28] At 50 mm. pressure, using filtered light, it was found that the log (rate)–$1/T$ curve was linear over the range 14° to 100° C corresponding to an apparent energy of activation of − 4·7 kcal./mole. Above 100° C the rate falls off and the authors remark " . . . the point at 128° C is obviously so far off (i.e. below) the straight line as to indicate a complete change of mechanism which has not been further investigated." Now

$$\Delta H^\circ_{gc} = \Delta H_{gg} - \frac{\lambda_n}{n} \text{ or } = \Delta H^\circ_{lc} - \lambda_1.$$

Taking ΔH°_{gg} from Table II as − 22·9 kcal./mole and assuming λ_n/n to be somewhat larger than the corresponding quantity for polythene,[1] say $\frac{\lambda_n}{n} = 4$ kcal./mole, we obtain $\Delta H^\circ_{gc} = -27$ kcal./mole. ΔH°_{lc} has been measured (Table I) as − 21·3 kcal./mole and, if we assume vinyl acetate to have a normal Trouton constant at its boiling point (72·3° C) then $\lambda_1 = 7$ kcal./mole, whence $\Delta H^\circ_{gc} = -28$ kcal./mole. Thus the value of ΔH°_{gc} may be safely assumed to be about − 27 kcal./mole. Similarly, ΔS°_{gc} may be estimated from either of the following relations

$$(a)\ \Delta S^\circ_{gc} = \Delta S^\circ_{gg} - \frac{Ri_n}{n},$$

and

$$(b)\ \Delta S^\circ_{gsm} = \Delta S^\circ_{lsm} - Ri_1 = \left(\frac{\Delta S^\circ_n}{n}\right)_s.$$

From Table II, $\Delta S^\circ_{gg} = -39{\cdot}8$ cal./deg. mole, whence taking $\frac{Ri_n}{n} = 0{\cdot}5$ of the value of Ri_1 for styrene, relation (*a*) gives that $\Delta S^\circ_{gc} = -52$ cal./deg. mole. The last term in eqn. (*b*) is not likely to be large (cf. calculation for styrene), and therefore neglecting this, writing $Ri_1 = 0{\cdot}8$ value for styrene, i.e. $Ri_1 = 19$ cal./deg. mole, and putting

$$\Delta S^\circ_{lsm} = R \ln\left(\frac{A_p}{A_d}\right) + R \ln \text{(molality of liquid vinyl acetate)}$$

we obtain $\Delta S^\circ_{gc} = -45$ cal./deg. mole. The actual entropy decrease in Melville and Tuckett's experiments which were carried out at 50 mm. pressure might be either 45 or $52 + R \ln \frac{76}{5} = 50{\cdot}4$ or $57{\cdot}4$ cal./deg. mole. Hence, the ceiling temperature under these conditions might be about 198 or 260° C and it is conceivable that these authors' observations may be explained by the onset of appreciable depropagation at 130° C without the necessity for the postulation of a complete change of mechanism.

Copolymerization reactions will also exhibit ceiling temperatures, the value being determined by the ratio $\Delta H/\Delta S$ for the particular copolymer resulting from a given monomer mixture. Let the two monomers be denoted by A and B and their respective ceiling temperatures for self-polymerization by T_A and T_B such that $T_A > T_B$ and the ceiling temperature for copolymerization of a given A + B mixture be T_{AB}. Below T_B, both A and B ends to growing chains will be able to add A and B monomers respectively, and probably also B and A monomers since it is most unlikely that $T_{AB} < T_B$. If T_{AB} lies between T_A and T_B we would expect that at temperatures between T_{AB} and T_B, B ends would only add A monomers, i.e. the reaction system would be one in which the apparent value of $k_{BB} = 0$; actually it would be that $(k_{BB(p)}[B] - k_{BB(d)})$ was negative. Such a state of affairs, in which copolymerization is occurring between two monomers one of which, B, will not polymerize alone is well known,[27] e.g. styrene (A) and diethyl maleate (B). It would not be expected that T_{AB} would exceed both T_B and T_A. At temperatures in excess of T_A, k_{AA} and k_{BB} would both be zero and hence any polymerization which did occur in this region would be bound to give rise to a polymer structure of the regular alternation —ABABA—, whatever the composition of the feed. It is difficult to envisage the structural requirements of the monomers and copolymer such that $(\Delta H/\Delta S)_{AB} > T_A$. Nevertheless such requirements are clearly fulfilled in the copolymerization of α-methyl styrene and maleic anhydride under conditions such that neither monomer will polymerize alone.[2, 29] The hypothesis of polar resonance [29] in the transition state of the propagation reaction, whilst leading to an enhanced value of k_p will not of itself account for the high value of $\Delta H/\Delta S$ implicit in the high ceiling temperature. Since the values of ΔH and ΔS refer to the reaction $A + B \rightarrow \frac{1}{n}(AB)_n$ an increase of ΔH, or a decrease of ΔS, or both, relative to $2\Delta H$ and $2\Delta S$ for $A \rightarrow \frac{1}{n}A_n$ is indicated. This could be accounted for by some strong interaction between adjacent A and B units in the polymer leading to its stabilization, despite the strongly disruptive influence of the steric strain. The nature of this interaction is at present obscure. Conceivably it might be due either to hyperconjugation effects or to large Coulomb-type forces due to incipient alternating polarity, positive on the styryl unit and negative on the anhydride.

The copolymerization of SO_2 and olefins might appear to be an extreme example of the last-named system. However, it will be shown elsewhere [3] that this reaction is best regarded as the self-polymerization of 1 : 1 molecular compounds of the reactants and for this reason, these reactions have been cited earlier as examples of 1-component polymerization.

The above examples are all characterized by formation of stable polymers. When the pure polymer depolymerizes rapidly, either alone or under the influence of the polymerization catalyst, the monomer ⇌ polymer equilibrium is mobile and ΔH and ΔS can readily be obtained from measurements of the equilibrium concentrations of monomer formed from the particular polymer at various temperatures [see methods (iv) and (1*a*)]. The formaldehyde-polyoxymethylene system is in this category,* and rough data exist for the dissociation pressures of gaseous formaldehyde over solid polymer in the temperature range 10-58° C,[31] which lead to values of $\Delta H^\circ_{gc} = -13{\cdot}3 \pm 1{\cdot}5$ kcal./mole and $\Delta S^\circ_{gc} = -32{\cdot}5 \pm 4$ cal./deg. mole. Thus $T^\circ_{gc} = 137^\circ$ C, in keeping with the observation of Norrish and Carruthers [32] that at 300 mm. pressure, no polymerization of gaseous formaldehyde can be detected at 100° C even when 32·4 mm. of formic acid, which is a powerful catalyst, are present. That the equilibrium had really been set up in Nordgren's experiments is shown by the fact that the values in the literature for the heats of combustion of $HCHO_{(g)}$ and $\frac{1}{n}(HCHO)_{n(s)}$ [33] indicate that ΔH°_{gc} lies between − 12·0 and − 13·3 kcal./mole.

---

[27] See account by Bawn, *The Chemistry of High Polymers*, 1948, p. 91.

[28] Melville and Tuckett, *J. Chem. Soc.*, 1947, 1201.

[29] Walling and Mayo, *Faraday Soc. Discussion*, 1948, 44*B*, 295.

[30] Smoker and Burchfield, *Ind. Eng. Chem.*, 1943, **35**, 128.

[31] Nordgren, *Acta Path. Microbiol. Scand.*, 1939, **40**, 21.

[32] Carruthers and Norrish, *Trans. Faraday Soc.*, 1936, **32**, 195.

* Dr. G. W. Meadows has informed us that he has experimental results which can only be interpreted on the assumption of some reversibility in the *iso*butene → poly*iso*butene system.

The authors wish to thank the Department of Scientific and Industrial Research for a maintenance grant to K. J. I.; the Royal Society and the Chemical Society for grants in aid of this and allied investigations. Thanks are also due to Prof. T. C. R. Fox for the loan of a calculating machine, and to Prof. R. G. W. Norrish and Prof. M. G. Evans for helpful discussions.

ADDENDUM. It has been pointed out to us that the recent publication of the Interscience reference book, *Monomers*, edited by Blout, Hohenstein and Mark, contains data on the physical properties of monomers which allow of refinement of some of our calculations. The alterations necessary are, with our original figures in parenthesis :—

(*a*) calculation of T°_{gc} for styrene,

$$\lambda_1 = 9{\cdot}05\ (10{\cdot}5)\ \therefore \Delta H^\circ_{gc} \doteq -25{\cdot}8\ (27{\cdot}2)$$

$$Ri_1 = 21{\cdot}2\ (23{\cdot}9)\ \therefore T^\circ_{gc} = 549^\circ\ (547^\circ)\ \mathrm{K};$$

(*b*) calculation of T°_{gc} for vinyl acetate,

$$\lambda_1 = 7{\cdot}8 \text{ or } 8{\cdot}2\text{—take } 8{\cdot}0 \text{ as mean } (7{\cdot}0)\ \therefore \Delta H^\circ_{gc} \quad -29\ (28)$$

$$Ri_1 = 23{\cdot}1\ (19)\ \therefore \Delta H^\circ_{gc} \doteq -49{\cdot}1.$$

Order of magnitude of T°_{gc} unaltered.

Department of Physical Chemistry,
Cambridge University.

---

[33] Bichowsky and Rossini, *Thermochemistry of Chemical Substances* (Reinhold, 1936), p. 236; Delepine, *Compt. rend.*, 1897, **124**, 1528; von. Wartenburg, *Z. angew. Chem.*, 1924, **37**, 457.

MELTING AND CRYSTAL STRUCTURE

PART II.—THE EFFECTS OF SOLID SOLUTION ON THE FREEZING OF BENZENE

BY F. W. THOMPSON AND A. R. UBBELOHDE

Received 2nd May, 1949; as revised 24th November, 1949

Freezing-point depressions have been measured for very dilute solutions in specially purified benzene, using as solutes the similar molecules cyclohexene, pyridine and thiophene, which might be expected to pack in the benzene crystals. Cyclohexane + benzene and benzene + cyclohexene have also been investigated in very dilute solutions ($N_2 \not> 0{\cdot}017$). The results can be interpreted with reference to the rotational entropy of fusion. The presence of foreign molecules in the benzene lattice appears, in at least one instance, to lower the latent heat of fusion to a marked degree, probably because the resulting lattice imperfections facilitate rotation of the benzene molecules in the crystal.

Although the melting and boiling points are closely similar, benzene and cyclohexane show a remarkable difference in their entropies of fusion, as shown in Table I.

TABLE I

	F.p.°C	B.p.°C	ΔS trans.	ΔS fusion	ΔS trans. + ΔS fusion
Benzene .	5·528	80·101	—	8·436	8·436
Cyclohexane	6·590	80·738	8·60	2·28	10·88

(ΔS in cal./mole deg.)

This difference may be accounted for as follows. There is evidence from polarization measurements that, just below the melting point, the molecules in benzene rotate about their hexagonal axes.[1] The molecules in cyclohexane probably rotate about at least one axis above the transition point at − 87·3° C in the solid.[2] Near the melting point, X-ray evidence indicates rotation about all three axes, although it must be admitted that the evidence for this latter statement is incomplete.[3]

In other crystals of cyclic organic compounds comparatively small imperfections have been found to modify to a notable degree the possibility of rotation.[4] It was decided to carry out a preliminary investigation on how far the introduction of other molecules into solid benzene might modify the behaviour on fusion, and, in particular, whether foreign molecules in the crystal could lower the entropy of fusion of benzene by promoting increased rotation in the solid.

To test this possibility, very pure benzene was prepared. Depression of its freezing-point was produced by the molecules (in order of decreasing size) cyclohexane, cyclohexene, pyridine and thiophene. Measurements of freezing-point depressions were restricted to very dilute solutions (mole fraction of solute $\not>$ 0·009). Comparison measurements were made of the freezing-point depression of very pure cyclohexane by benzene.

---

[1] Rousset, *Compt. rend.*, 1944, **219**, 485, 546.

[2] Parks, Huffman and Thomas, *J. Amer. Chem. Soc.*, 1930, **52**, 1032.

[3] Hassel and Sommerfeldt, *Z. physik. Chem. B*, 1938, **40**, 391.

[4] White and Bishop, *J. Amer. Chem. Soc.*, 1940, **62**, 8. White, Biggs and Morgan, *ibid.*, 1940, **62**, 16.

Experimental

Evaluation of Freezing Points.—Difficulties in obtaining large quantities of pure solvents imposed limitations on the choice of method with the dilute solutions involved. The use of a few milligrams of mixtures in sealed tubes[5] would in this instance call for a variable temperature bath controlled to about ± 0·002° C, which was not available. Differential methods such as that of Batson and Kraus[6] require about 500 ml. of solvent. As a compromise between various requirements, a refined Beckmann technique, which required from 15-20 ml. of solvent, was used. The apparatus is illustrated in Fig. 1. Features calling for special comment are :

(i) The Beckmann thermometer was almost entirely enclosed in the inner tube A. The temperature was read to ± 0·001° C using a microscope to avoid parallax.

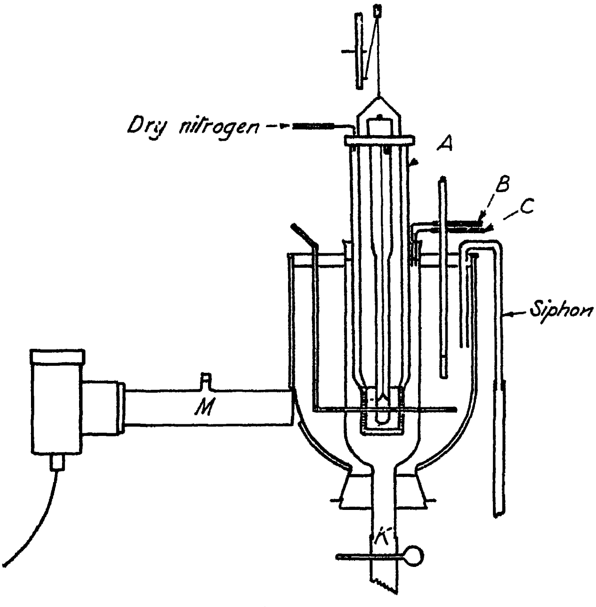

FIG. 1.

(ii) Provision was made for rapid cooling to the freezing point and for maintaining the subsequent jacket temperature only slightly below the freezing-point.

In a determination, the outer bath was first filled with ice + water. The sample was poured into the inner tube, which was protected from moisture by a cap and by a slow stream of dry nitrogen. This nitrogen was cooled to about the freezing-point of benzene to improve the steadiness of temperature of the Beckmann thermometer. In order to accelerate freezing, the air space was temporarily filled with cold water by means of the tube C. On the appearance of crystals this water was drained off by K. Next the Beckmann thermometer was removed from its special storage tube and placed in position. Mechanical stirring was commenced, and the reading of the Beckmann gave a rough value of the freezing point.

---

[5] Collett and Johnston, 1926 ; quoted by Weissberger, *Physical Methods of Organic Chemistry* (Interscience Publishers, Inc., New York, 1941), p. 32. Oldham and Ubbelohde, *Proc. Roy. Soc. A*, 1940, **176**, 50.

[6] Batson and Kraus, *J. Amer. Chem. Soc.*, 1934, **56**, 2017.

The inner glass stirrer had a clearance of 1-2 mm. from the walls of the tube (cf. Mair, Glasgow and Rossini,[7] but ct. Korvezee, Hertjes, Hessels and Knip [8]).

A stream of water from B, the amount of which was carefully controlled not to overheat the system and the Beckmann thermometer, was played on the outside of A until the crystals had practically all melted. The determination was then refined by adjusting the external bath temperature to $\not> 0{\cdot}3°$ below the rough freezing point. Cold water was allowed to trickle over the inner tube until the Beckmann temperature had dropped to the rough freezing point, when the stream of water was stopped and the lamp switched off. To prevent the marked heating of hydrocarbons by infra-red radiation,[5] the light of this lamp was filtered through a long column M of solvent. Readings of the Beckmann thermometer were taken at intervals.

In a successful determination, the temperature recorded by the Beckmann continued to fall for a few seconds after stopping the water stream and switching off the lamp ; it then started to rise. The rate of heat transfer was so slow that with benzene solutions with $N_2 \not> 0{\cdot}006$ the maximum temperature reached remained constant to within $\pm\ 0{\cdot}001°$ C for 5 min. In the present experiments the maximum supercooling was $\not> 0{\cdot}02 \pm 0{\cdot}01°$ C. From the analysis published by Glasgow, Streiff, and Rossini[9] who used supercooling of about 0·5° C it follows that any difference between the "true" freezing point and the "maximum temperature" could be neglected in our experiments so that their geometrical method of extrapolation was unnecessary.

Each freezing point was determined at least four times. The first value usually differed from those which followed by about 0·020° C due in part to the loss of air when rough freezing occurs for the first time. For pure solvents the mean of the remaining values was within ± 0·005° C. As more solute was added the spread rose to ± 0·007° for $N_2 \not> 0{\cdot}008$, and for the stronger solutions of benzene in cyclohexane to ± 0·010° C.

Treatment of the Beckmann Thermometer.—In using the Beckmann thermometer as a precision instrument a number of weaknesses call for special treatment.

(i) The calibration must be checked for uniformity of bore of the capillary, and the value of $dB/d\theta$ must be evaluated to check the scale interval, where B is the temperature on the Beckmann thermometer, and θ is the temperature in °C.

For the present experiments a large number of temperatures on the Beckmann thermometer were compared with a "coiled wire" platinum thermometer [10] the resistance of which could be measured to ± 0·0005 ohm (± 0·008° C). Both thermometers were immersed side by side in a Dewar flask of large capacity, filled with well-stirred water and the line of closest fit was evaluated for the plot of B against the resistance R over the six-degree range of the Beckmann thermometer. This gave $dB/dR = 16{\cdot}685\ B$ deg./ohm, with a higher precision than could be obtained from individual comparative readings. The platinum thermometer was calibrated at the temperatures of melting ice (frozen from air-free distilled water), the $Na_2SO_4 . 10H_2O$ transition (May and Baker, Chemical Reagent purity), and steam. This gave $dR/d\theta = 0{\cdot}06002$ ohm/°C whence $dB/d\theta = dB/dR \times dR/d\theta = 1{\cdot}0015 \pm 0{\cdot}0005$. This was only just outside the error of measurement over the extreme range of the Beckmann scale, so that departures of the Beckmann scale from the "true" centigrade scale could be neglected in determinations of the freezing point depressions of these dilute solutions. Where absolute values of freezing points are important, adjustment has been made in the uncertainty range to include any discrepancy between the Beckmann and true centigrade scales.

(ii) The ice point may change owing to thermal hysteresis in the glass of the thermometer bulb. Another cause of the change of ice point arises if the mercury in the stem enters the reservoir at the top. Distillation can then occur from this mercury to that already in the reservoir, or vice versa, according to the respective temperatures. Use was actually made of this distillation for precision setting of the Beckmann.

Both these sources of uncertainty were eliminated (*a*) by determining the ice point immediately before each freezing point series. This was done by carrying out freezing point determinations with freshly boiled distilled water. Traces of this water were then removed from the thermometer by washing twice with cold absolute alcohol, and three times with the cold solvent about to be used. By working quickly, the stem and bulb could be wiped with dry filter paper between each of these washings, without the mercury in the bulb heating up and so entering the reservoir.

---

[7] Mair, Glasgow and Rossini, *J. Res. Nat. Bur. Stand.*, 1941, **26**, 605.

[8] Korvezee, Heertjes, Hessels and Knip, *Chem. Weekblad.*, 1946, **42**, 363.

[9] Glasgow, Streiff and Rossini, *J. Res. Nat. Bur. Stand.*, 1945, **35**, 355.

[10] Stull, *Ind. Eng. Chem.* (*Anal.*), 1946, **18**, 234.

(*b*) The Beckmann thermometer when not in use was permanently stored in a clean dry tube immersed in ice in a Dewar flask. This helped to minimize any thermal hysteresis. With these precautions variations in the ice point did not exceed ± 0·005° C. As explained above, the Beckmann was never immersed in the solvent till this was already roughly at the freezing point.

TABLE II

No. of Freezings	F.p. of Crystals (°C) Benzene	Convergence (F.p. of crystals—f.p. of liquid) (°C)
0 (Analar)	4·620	—
1	5·110	—
2	5·465	0·675
3	5·521	0·214
4	5·520	0·000

(iii) Alterations due to changes in external pressure were neglected in the present experiments.[5] The calibration showed that alterations produced in the volume of the bulb could be neglected as long as the stem was kept vertical. Emergent stem correction was negligible, especially in view of the cooled nitrogen playing over the upper parts of the stem.

(iv) Sticking of the mercury was avoided by tapping the thermometer before reading, and by taking all important readings on a rising meniscus.

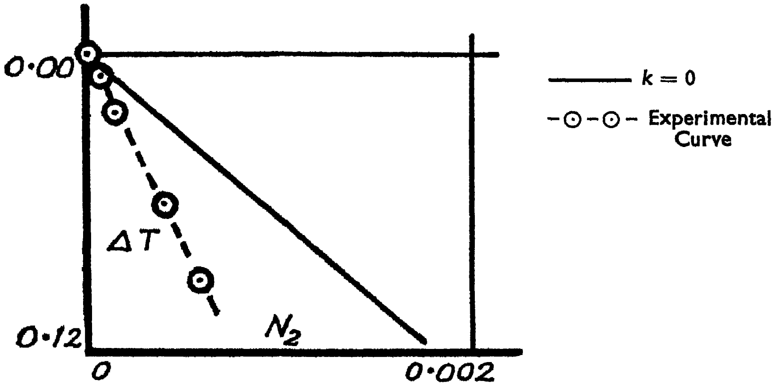

FIG. 2.—Solvent, benzene ; Solute, cyclohexane.

(v) Very complete shielding of the solvent and of the mercury in the bulb from radiation from lights, etc. was maintained in the final stages in taking readings.

Purification of Materials.—With the very dilute solutions used, the degree of purity required for the two solvents, benzene and cyclohexane, was about 100 times higher than that required for the solutes. For the solvents the principal methods were fractional distillation and fractional freezing, using the convergence test (Oldham and Ubbelohde [8]) to verify progress. This gave satisfactory results for benzene and rather less so for cyclohexane. The solutes were purified by fractional distillation.

Benzene.—A.R. benzene from the b.p. range 79·1-79·5° C was found free from thiophene (isatin test). It was fractionally frozen with vigorous mechanical stirring using a cooling bath of ice and salt. The solvents were protected throughout against diffusion of atmospheric moisture by a counter-current of dry nitrogen. Approximately half was frozen, and the mother liquor was then sucked off into a protected receiver.

TABLE III

No. of Freezings	F.p. of Crystals (°C) Cyclohexane	Convergence (F.p. crystals—f.p. liquid) (°C)
0	5·750	—
1	5·965	—
2	6·190	—
3	6·316	—
4	6·417	—
5	6·467	—
6	6·537	—
7	6·545	0·082
8	6·558	0·028
9	6·559	0·028
10	6·555	0·013
11	6·575	0·010
12	6·590	0·023

Before use the final fraction of benzene was further dried intensively by bubbling dry nitrogen through it for 90 min. at a temperature of 70 ± 5° C.[11] This raised the f.p. very slightly, but these last traces of water are difficult to keep out and the f.p. in four different runs ranged from 5·520° ± 0·010° C for the benzene used in the cyclohexane, cyclohexene and pyridine series to 5·541 ± 0·010° C for the benzene used in the thiophene series. The average

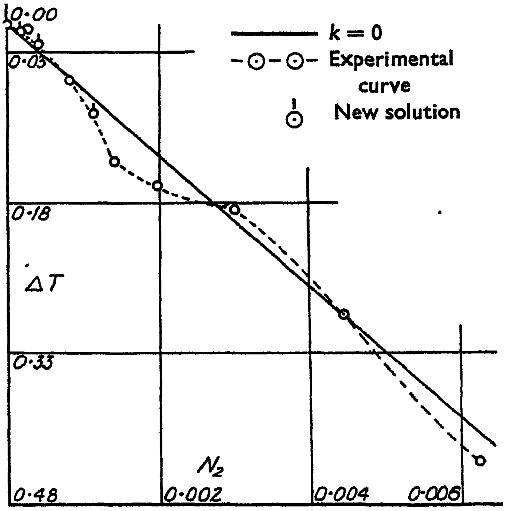

FIG. 3.—Solvent, benzene; Solute, cyclohexene.

---

[11] Fox and Martin, *Proc. Roy. Soc. A*, 1940, **174**, 273. Oldham and Ubbelohde, *J. Chem. Soc.*, 1941, 372.

value of the f.p. of the four samples was 5·528 ± 0·016° C. A depression of 0·021° C corresponds to about 74 microgram of H_2O per g. of benzene. This value of 5·528° C ± 0·016° C may be compared[12] with 5·50 ± 0·02° C (Gibbons *et al.*), 5·51 ± 0·01° C (Wojciechowski) and 5·533 ± 0·010° C (Glasgow *et al.*).

Cyclohexane.—Chemical Reagent cyclohexane (Howard) was purified by shaking for 3 hr. with 1/1 H_2SO_4/HNO_3, washed with water and alkali, dried and separated by fractional distillation (b.p. range 80·8-81·5 ± 0·1° C). The freezing points of the fractions were evaluated and the highest freezing portions were collected and further purified by freezing. As many as 12 fractional freezings were used but convergence was slow in the final stages.

The final sample 6·59° ± ·012° C compares with 6·68 ± 0·05° C (Aston, Szasz and Fink) and 6·554 ± 0·005° C (Glasgow *et al.*).[12, 13] As is discussed below, the slow convergence of freezing points at the final stages is probably due to the weak restraining forces in the cyclohexane lattice. It may just possibly be due to the presence of isomeric forms of the cyclohexane molecule. Unfortunately, the method of purification devised by Ashmore[14] came to our notice after this purification had been completed.

Cyclohexene.—This was prepared from cyclohexanol (b.p. range 161·2-162·3 ± 0·1° C at 771 mm.) according to the method of *Organic Syntheses* (Coll. Vol. I, p. 177), dried over anhydrous Na_2SO_4 and refluxed with Na for 7 hr. using a counter-current of dry nitrogen to protect it from moisture and oxygen, and finally fractionally distilled (b.p. 83·0 ± 0·1° C at 760 mm.). This compares[15] with 83·1° C obtained by Allsopp. Bromine absorption was used to verify that the product was 100 % cyclohexane.

Pyridine.—A.R. pyridine which had been standing over solid KOH for about 2 months was fractionally distilled (b.p. range 115·4 ± 0·1° C at 760 mm.). This compares with Timmerman's[16] value of 115·5° at 760 mm.

Thiophene.—Chemical Reagent thiophene (Hopkin and Williams) was fractionally distilled. The colourless distillate with b.p. range 84·5-84·6 ± 0·1° C at 772 mm. was used. This compares with 84·13 ± 0·1° C at 760 mm. and 85·8 ± 0·1° C at 800 mm. obtained by Fawcett and Rasmussen.[17]

Preparation of Solutions.—Due to the limited amount of pure solvents available, solutions were made by addition of small weighed amounts of a concentrated solution of the required solute to the dilute solution obtained from previous f.p. determinations. The main objection to this is the risk of cumulative absorption of moisture during transfers. To minimize this, transfers of solution were made as rapidly as possible. Particularly interesting parts of the freezing point curves were also checked by making up compositions *de novo*.

Results

The results are recorded in the following graphs, in which freezing point depressions ΔT, are plotted against the corresponding mole fraction of solute N_2. The ideal curves are calculated on the basis of the van't Hoff equation[18]

$$dT/dN_2 = (k - 1)RT^2/(\bar{H}_1 - \bar{H}_1'),$$

where T is the freezing point, k the distribution coefficient of the solute between the solid and liquid phases, $\bar{H}_1$ the partial molal heat content of the solvent in the liquid phase and $\bar{H}_1'$ the partial molal heat content of the solvent in the solid phase.

On account of the low mole fractions of solute in the present work, it was not possible to make direct analytical observations on the extent of solid solution. Distribution coefficients have been previously obtained for a range of considerably stronger solutions of thiophene in benzene and of pyridine in benzene, by the addition of a third substance soluble only in the liquid phase.[19] For thiophene in benzene, k is close to 0·4 over a wide range of concentrations. For pyridine k is less accurately known, but is about 0·18. (This difference between pyridine and thiophene is in the sense to be expected from the packing volumes, and the findings of Oldham and Ubbelohde,[5] that solid solutions occur more extensively when lattice defects are formed than when lattice bulges are involved.)

---

[12] Gibbons, *et al.*, *J. Amer. Chem. Soc.*, 1946, **68**, 1130. Wojciechowski, *J. Res. Nat. Bur. Stand.*, 1937, **19**, 347. Glasgow, *et al.*, *ibid.*, 1946, **37**, 141.

[13] Aston, Szasz and Fink, *J. Amer. Chem. Soc.*, 1943, **65**, 1135.

[14] Ashmore, *Analyst*, 1947, **72**, 206.

[15] Allsopp, *Proc. Roy. Soc. A*, 1934, **143**, 618.

[16] Weissberger and Proskauer, *Organic Solvents* (Oxford University Press, 1935).

[17] Fawcett and Rasmussen, *J. Amer. Chem. Soc.*, 1945, **67**, 1705.

[18] Lewis and Randall, *Thermodynamics* (McGraw-Hill Book Company, 1923), Chap. XX, eqn. (19).

For cyclohexane and cyclohexene in benzene, and for benzene in cyclohexane, k is unknown, and the unbroken lines are calculated on the basis $k = 0$. The slopes of the dotted lines in Fig. 4 and 5 were calculated using the values of k previously mentioned.

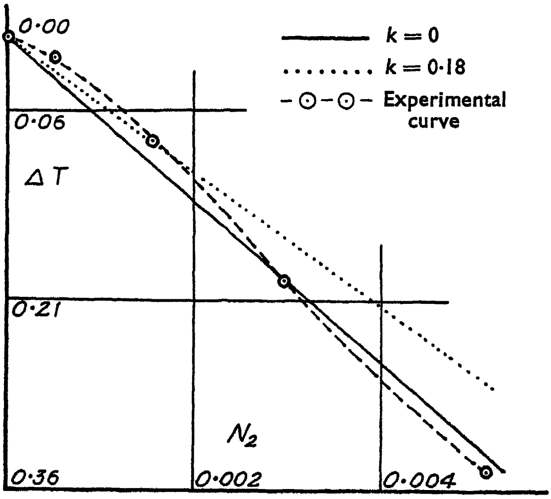

FIG. 4.—Solvent, benzene ; Solute, pyridine.

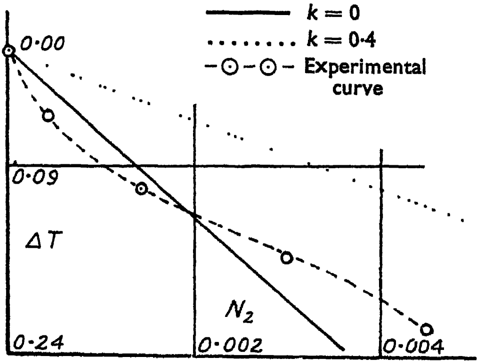

FIG. 5.—Solvent, benzene ; Solute, thiophene.

Discussion

Since we are concerned with the formation and behaviour of solid solutions in the systems studied, it is important to have as much information as possible on the space requirements of the molecules. So far as they are available, data have been collected in Table IV.

---

[19] Beckmann, *Z. physik. Chem.*, 1897, **22**, 609. Bury and Jenkins, *J. Chem. Soc.*, 1934, 688.

In the benzene crystal, thiophene almost certainly packs with a small volume defect, as is indicated from the collision areas and the parachors. The slightly larger volume occupied by thiophene in its own crystal lattice may be attributed to differences of crystal structure. Pyridine on the same basis would pack in the benzene crystal with a slight bulge.

TABLE IV.—SPACE REQUIREMENTS OF BENZENE AND RELATED MOLECULES[20]

Molecule	Vol. in crystal (cm.^{3} × 10^{-24})	Parachor	Collision area from viscosity of vapour (cm.^{2} × 10^{-16})
Cyclohexane . .	148·7 (*a*)	241·8 (*d*)	22·3 (*f*)
Cyclohexene . .	—	230·4 (*e*)	—
Pyridine . . .	—	199·7 (*d*)	20·0 (*f*)
Benzene . . .	117·75 (*b*)	192·1 (*c*)	19·0 (*f*)
Thiophene. . .	124·5 (*c*)	187·4 (*c*)	16·7 (*f*)

When cyclohexane is packed in the benzene crystal all the evidence indicates that the bulge would be considerably greater. The fact that the cyclohexane molecule is predominantly chair-shaped[21] would further hinder easy packing with the flat benzene molecules. Raman spectrum data, on which this conclusion is based, do not necessarily exclude small amounts of planar or boat-shaped cyclohexane present in equilibrium with the chair-shaped molecules. But even if these shapes were slowly formed in small amounts in the liquid according to the requirements of thermodynamics, the shapes would tend to be separated on fractional freezing. The slow convergence observed in the fractional freezing of cyclohexane may just possibly be attributed to some such effect. Cyclohexene is probably also puckered, and would not pack easily in the benzene crystal, though little is known about the size of the molecule. In cyclohexane, the space requirements of the (rotating) cyclohexane molecules are very considerably larger than those of the flat benzene molecules. Unless these also rotate in a similar fashion they would pack with a considerable lattice defect in the cyclohexane crystal.

The curve which is most easily interpreted is that shown in Fig. 6, where the solution appears to be ideal. In sharp contrast is Fig. 2, where the value of dT/dN_2 is -150, the ideal value being -66. This means that the value of $(\bar{H}_1 - \bar{H}_1')$ which gives the heat and entropy of fusion has been reduced by more than 50 %. It is highly probable that this reduction is almost entirely due to a large increase in $\bar{H}_1'$ due to rotation in the solid. The remaining graphs show similar effects, but after allowing for the experimental errors previously mentioned, and for the fact that the values were determined at relatively high concentrations, it is apparent that no definite proof of a decrease in $(\bar{H}_1 - \bar{H}_1')$ can be obtained from them, although the results are suggestive.

The most obvious explanations of the drastic reduction in the entropy of fusion of benzene due to the presence of foreign molecules are

(i) an increase in the number of molecules rotating about their hexagonal axes,

---

[20] (*a*) Lonsdale and Smith, *Phil. Mag.*, 1939, **28**, 614; (*b*) Cox, *Proc. Roy. Soc. A*, 1932, **135**, 491; (*c*) Morton, *Chemistry of Heterocyclic Compounds* (McGraw-Hill Book Co., 1946), pp. 41, 42; (*d*) Sugden, *The Parachor and Valency* (Routledge & Sons, Ltd., 1930); (*e*) Vogel, *J. Chem. Soc.*, 1938, 1332; (*f*) Lowry and Nasini, *Proc. Roy. Soc. A*, 1929, **123**, 686.

[21] Harrand, *Compt. rend.*, 1947, **224**, 462. Kohlrausch and Stockmayr, *Z. physik. Chem. B*, 1936, **31**, 382. Kohlrausch and Wittek, *ibid.*, 1940, **48**, 177.

(ii) the onset of rotation about axes at right-angles to the six-fold axis of symmetry,
(iii) a combination of both effects.

These appear to be the most probable means by which the benzene crystal can increase its entropy without actually melting.

The shape of the curves in Fig. 3 and 5 suggests that rotation in the solid is governed by two opposing factors:

(i) The presence of foreign molecules tending to reduce the forces opposing rotation.
(ii) The depression of the freezing-point tending to "freeze" the rotation.

Although the accuracy of individual points is not high enough to permit exact calculations, the experimental curves suggest definite trends in the freezing-points in accordance with this view. The variability in freezing-point depression claimed for benzene by Vrancker, Leach and Daniels,[22] may perhaps be attributed to the effects detailed above.

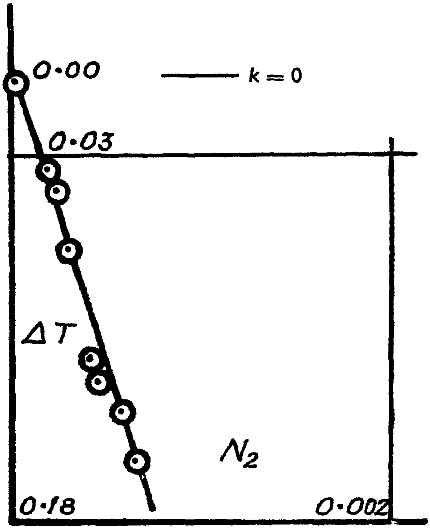

FIG. 6.—Solvent, cyclohexane; Solute, benzene.

It is obviously desirable that the above observations be supplemented by other experiments, such as measurement of latent heats of fusion by a calorimetric method, volume changes on fusion, and X-ray data on crystals just below the melting-point. In the meantime, they indicate some of the fundamental phenomena which may arise from the formation of solid solutions.

Department of Chemistry,
Queen's University,
Belfast.

---

[22] Vrancker, Leach and Daniels, *Nature*, 1944, **153**, 407.

KINETIC STUDIES IN THE CHEMISTRY OF RUBBER AND RELATED MATERIALS

VII.—INFLUENCE OF CHEMICAL STRUCTURE ON THE α-METHYLENIC REACTIVITY OF OLEFINS

By J. L. Bolland

Received 13th May, 1949; as amended 16th February, 1950

The efficiency of the radical reaction

$$RO_2\text{—} + RH \rightarrow RO_2H + R\text{—}$$

(representing the exchange of a hydrogen atom between an α-group of an olefin RH and a peroxide radical RO_2—) has been determined for the members of a series of twenty-four unsaturated hydrocarbons. The influence of certain structural features of olefinic groupings in determining the ease of α-methylenic hydrocarbon abstraction (and hence on the dissociation energy of α-β carbon-hydrogen bonds) have been identified : thus in the olefinic system

$$\underset{(a)}{CH_3}\text{—}\underset{(b)}{CH}\text{=}\underset{(c)}{CH_2}$$

the α-methylenic reactivity of the group (*a*) (as measured by the above exchange reaction) is unaffected by alkyl substitution at (*b*), but is increased by alkyl substitution at (*a*) and (*c*) (at 45° C by a factor of $3{\cdot}3^n$, where n is the total number of substituents introduced).

Olefins are attacked by oxygen at rates which are markedly dependent on the detailed chemical structure of the unsaturated grouping. In general such reaction rate differences could result from variations in the actual mechanism by which various olefins oxidize or could on the other hand reflect the influences of olefinic structure on one or more of the elementary reactions in a mechanism common to all olefins.

The former factor may be ruled out for the interaction of oxygen with a wide range of non-conjugated unsaturated hydrocarbons, as evidenced by the common mechanism carefully established for representative 1 : 4-dienic,[1, 2, 3] mono-olefinic (cf. ref. 4 and the Appendix to this paper) and hydroaromatic[5] molecules. The chain mechanism which holds[6] alike for oxidations initiated photochemically, by dissociable molecules (e.g. benzoyl peroxide) or by the α-hydroperoxidic oxidation product is reproduced here for convenience. If R— represents the radical obtained by abstraction of an α-methylenic hydrogen atom from an olefin (RH) and RO_2— the corresponding peroxide radical we may write :

$$\begin{array}{llll}
\text{Initiation} & \text{Production of R— or RO}_2\text{— radicals } R_i & & \\
\text{including} & \left.\begin{array}{l} 2RO_2H \longrightarrow \\ Bz_2O_2 \longrightarrow \\ RH + h\nu \longrightarrow \\ RO_2H + h\nu \longrightarrow \end{array}\right\} R\text{— or } RO_2\text{—} & \begin{array}{l} k_1 \\ k_7 \end{array} & \begin{array}{r} . \quad . \quad . \quad (R1) \\ . \quad . \quad . \quad (R7) \end{array} \\
\text{Propagation} & R\text{—} + O_2 \longrightarrow RO_2\text{—} & k_2 & . \quad . \quad . \quad (R2) \\
 & RO_2\text{—} + RH \rightarrow RO_2H + R\text{—} & k_3 & . \quad . \quad . \quad (R3) \\
\text{Termination} & \left.\begin{array}{l} R\text{—} + R\text{—} \\ R\text{—} + RO_2\text{—} \\ RO_2\text{—} + RO_2\text{—} \end{array}\right\} \rightarrow \begin{array}{c}\text{non-radical} \\ \text{products}\end{array} & \begin{array}{l} k_4 \\ k_5 \\ k_6 \end{array} & \begin{array}{r} . \quad . \quad . \quad (R4) \\ . \quad . \quad . \quad (R5) \\ . \quad . \quad . \quad (R6) \end{array}
\end{array}$$

---

[1] Bolland, *Proc. Roy. Soc. A*, 1946, **186**, 218.

[2] Bolland and Gee, *Trans. Faraday Soc.*, 1946, **42**, 230.

[3] Bolland, *ibid.*, 1948, **44**, 669.

[4] Bateman and Gee, *Proc. Roy. Soc. A*, 1948, **195**, 376.

[5] Bolland (in press).

[6] Bateman and Bolland, *Proc. XIth Int. Cong. Pure Appl. Chem.*, 1947.

R_i represents the rate of the initiation step and
k_1-k_7 the velocity constants of the elementary steps (R1)-(R7)

A systematic attempt to determine the effect of variations in RH on these various elementary reactions is made in this and two subsequent papers. Here the influence of structural factors on the propagation step (R3) is traced: in the second we deal with the other propagation process

$$R— + O_2 \rightarrow RO_2— ;$$

the third paper considers the type of chain initiation most likely to be intimately dependent on olefinic structure, namely hydroperoxide decomposition (R1).

Non-conjugated olefins undergo a variety of reactions in which the replacement of a hydrogen atom situated in an α-methylenic group occurs. One of the major factors controlling the rates with which individual olefins partake in this type of reaction will undoubtedly be the strength with which the replaceable α–β hydrogen atoms are attached to the α-carbon atoms. The reaction

$$RO_2— + RH \longrightarrow RO_2H + R—$$

affords an excellent opportunity of separating and studying this factor since here the α–β hydrogen atom is attacked by a radical the essential character and reactivity of which may safely be assumed insensitive to the identity of R. Variations in k_3 and the energy of activation of the reaction E_3 may thus be used to give quantitative information regarding α-methylenic reactivity in general and its relation to the architecture of olefins.

Determination of the relative efficiency of (R3) for different olefins rests on the following argument. Of the various possible oxidation conditions those best calculated to show up changes in k_3 require the presence of benzoyl peroxide as chain initiator and the use of high oxygen pressures: the former condition gives the best authenticated method of providing a rate of chain initiation which is independent of the nature of the olefin, while at high oxygen pressures the rate of oxidation consistent with the above mechanism assumes the simple form,[3]

$$\text{Rate} = k_7{}^{\frac{1}{2}}[Bz_2O_2]^{\frac{1}{2}}[RH]\left(1 + \frac{1}{\nu}\right) . k_3 k_6{}^{-\frac{1}{2}}. \quad . \quad . \quad (1)$$

The inclusion of ν, the chain length of oxidation, is of significance only in the case of the least oxidizable olefins. $k_3 k_6{}^{-\frac{1}{2}}$ may thus be determined if the rate of chain initiation is assumed (a) equal to the rate of decomposition of benzoyl peroxide and (b) independent of the nature of the olefin. Bartlett and Nozaki's[7] extensive kinetic measurements on the thermal decomposition of benzoyl peroxide indicate that these assumptions are unlikely to introduce any large uncertainty; these authors show that the unimolecular dissociation of peroxide molecules (into radicals) accounts for a large proportion of the observed peroxide decomposition. For example, even at the highest concentration of benzoyl peroxide here used in cyclohexene (Fig. 1) the rate of unimolecular dissociation accounts for some 60 % of the total peroxide decomposition observed at 80° C.

By application of the rotating-sector technique to the photo-oxidation of olefins, Bateman and Gee[8] have recently obtained absolute values for the efficiency k_6 and the activation energy E_6 of the chain terminating step (R6). The values of k_6 so obtained for four dissimilar olefins are sufficiently concordant to justify the assumption that k_6 is in fact independent of the nature of the olefin. On this basis the composite term $k_3 k_6{}^{-\frac{1}{2}}$ can be separated into individual k_3 and k_6 values. From measurements of the temperature dependence of k_6 Bateman and Gee suggest maximum and minimum figures for E_6 of 5 and 0 kcal. We have here arbitrarily taken E_6 as zero and have allotted k_6 Bateman and Gee's mean value of 6×10^5 mole^{-1} l. sec.$^{-1}$ to all olefins considered in this paper.* Hence, taking k_7 at 45° C as 5×10^{-7} sec.$^{-1}$, k_3 at this temperature is given by

---

[7] *J. Amer. Chem. Soc.*, 1946, **68**, 1686.

[8] *Proc. Roy. Soc. A*, 1948, **195**, 391.

$$k_3 = 1{\cdot}10 \times 10^6 \,.\, \frac{\text{Rate}}{[\text{Bz}_2\text{O}_2]^{\frac{1}{2}}} \,.\, \frac{1}{[\text{RH}]} \quad . \quad . \quad . \quad (1a)$$

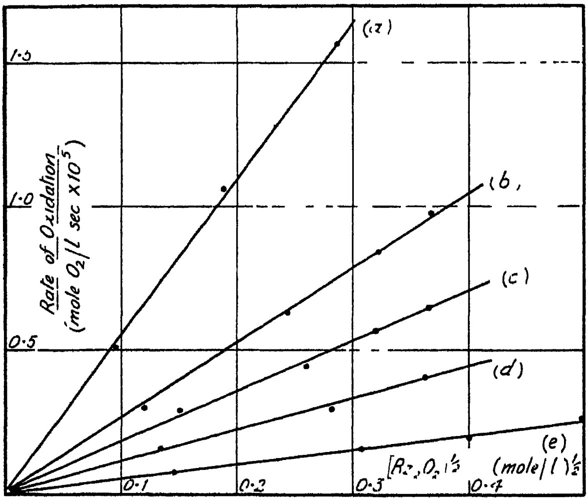

FIG. 1.—Variation of initial rate of oxidation with benzoyl peroxide at 45° C and 760 mm. oxygen pressure: (*a*) 1 : 3 : 5-trimethyl-cyclohexene; (*b*) 1-methyl-cyclohexene; (*c*) cyclohexene; (*d*) 4-methyl-heptene-3; and (*e*) allyl benzene.

Experimental

Rate Measurements.—Apart from substitution of a quill tubing glass spiral for the flexible connection between reaction vessel and gas burette system, the general method of oxidation rate measurement was that already outlined.[1] When dealing with relatively volatile olefins, the stem of the reaction vessel formed the inside wall of a condenser through which tap water (temperature *ca.* 10° C) was circulated. Where necessary the preliminary pumping out of the reaction vessel and gas burette system was carried out with the former maintained (by immersion in a CO_2-acetone bath) at a temperature sufficiently low to reduce the vapour pressure of the olefin to 10^{-4} mm. Measurements were carried out at oxygen pressures of approximately 760 mm. Hg.

Materials.—The methyl oleate, and ethyl linoleate samples were those used previously.[1, 3] The 2 : 4 : 4-trimethyl-pentene-1 was kindly provided by Dr. A. G. Evans of Manchester University. Fourteen of the other olefins used were drawn from pure samples prepared for other purposes in these laboratories: cyclohexene and 1-methyl cyclohexene (Dr. L. Bateman), 2-methyl-pentene-2 (Dr. J. I. Cuneen), diallyl (Mr. A. W. Kenchington), allyl benzene (Dr. H. P. Koch), crotyl benzene and γ-methyl crotyl benzene (Mr. J. A. Lyons), heptene-1, heptene-3 and 4-methyl-heptene-3 (Dr. C. G. Moore), 1 : 3 : 5-trimethyl-cyclohexene, and 2-methyl hepten-3-yl benzoate (Mr. A. L. Morris), 1 : 2-dimethyl cyclohexene-1 and ethyl linolenate (Dr. D. A. Sutton). Octene-1, hexadecene-1 and decane were commercial samples which were carefully fractionated on a

---

* We may note that the photo-oxidation chain lengths required in Bateman and Gee's deductions are derived from estimates of the chain length of the benzoyl peroxide initiated oxidation. It is readily shown that the individual rate constants deduced in this way are in fact αk_3 and αk_6, where α is the number of chains started by the decomposition of each benzoyl peroxide molecule.

15-plate column, small middle fractions being taken. 2 : 3 : 3-Trimethylbutene-1 was synthesized via pinacolone and 2 : 3 : 3-trimethyl butanol-2. The hexene-2 sample was obtained by careful fractionation of the dehydration product of hexanol-2.

The purity of the various olefins was examined by infra-red and ultra-violet spectrographic analyses (kindly carried out by Dr. H. P. Koch). Impurities were detected in only two cases : the hexene-2 and 4-methyl-heptene-3 samples contained not more than 10 % of their much less reactive isomers, hexene-1 and 2-propyl-pentene-1 respectively.

Results

The dependence of oxidation rate on the concentration of added benzoyl peroxide was found to conform for each olefin to a linear initial rate against $[Bz_2O_2]^{\frac{1}{2}}$ relation. Fig. 1 and data quoted elsewhere illustrate the accuracy with which the relation is obeyed. Values of the slope of the linear rate against $[Bz_2O_2]^{\frac{1}{2}}$ curves obtained for 24 olefins are collected in Table I. In most cases the slope was determined at at least three temperatures to give an accurate

TABLE I

Olefin	[RH] Mole/l.	Rate/$[Bz_2O_2]^{\frac{1}{2}}$ (Mole/l.)$^{\frac{1}{2}}$ sec.$^{-1}$ × 10^5					E_c
		35°	45°	55°	65°	75°	
1 2 : 3 : 3-Trimethyl butene-1	7·20	—	0·030	—	—	—	—
2 Heptene-1	7·12	—	0·085	0·275	—	—	(24·6)
3 Octene-1	6·40	—	0·079	0·333	1·40	—	26·8
4 Hexadecene-1	3·50	0·011$_5$	0·045	0·175	0·60$_2$	—	27·6
5 Diallyl	8·42	—	0·20$_1$(*a*)	—	—	—	(27·9)
6 2 : 4 : 4-Trimethyl-pentene-1	6·40	—	0·078	0·305	1·08	—	28·0
7 Hexene-2	8·00	—	0·49	—	—	—	—
8 Methyl oleate	2·96	—	0·32	0·95	2·83	8·0	23·5
9 Heptene-3	7·20	—	0·60	—	—	—	—
10 3-Methyl-pentene-2	8·33	—	0·75	—	—	—	—
11 Tetramethyl ethylene	8·40	—	3·20	—	—	—	—
12 2-Methyl-pentene-2	8·25	—	1·70	—	—	—	—
13 2-Me-heptenyl-benzoate	3·90	—	0·80	0·242	7·36	—	23·3
14 4-Methyl heptene-3	6·55	—	1·12	3·18	9·7	—	23·6
15 Allyl benzene	7·65	—	0·51	1·60	4·83	14·1	24·5
16 Crotyl benzene	6·67	0·74	2·33	6·83	—	—	22·3
17 γ-Methyl crotyl benzene	6·12	2·57	7·21	21·0	—	—	21·5
18 Ethyl linolenate	2·89	1·55	4·23	12·0	28·3	—	20·5
19 Ethyl linolenate	2·91	—	8·2	—	—	—	—
20 Cyclohexene	9·86	0·51	1·80	5·55	—	—	24·0
21 1-Methyl-cyclohexene	8·45	0·78	2·62	8·16	—	—	23·5
22 1 : 2-Dimethyl cyclohexene	7·47	1·41	4·58	13·7	—	—	23·0
23 1 : 3 : 5-Trimethyl cyclohexene	6·48	(*b*)	5·5	16·2	—	—	22·4
24 Tetralin	7·35	0·282	1·02	3·33	10·6	—	24·8
25 *n*-Decane	5·14	—	0·006	—	—	—	—

(*a*) Extrapolated value from 0·0167 at 28° C and 0·074 at 38° C.
(*b*) 0·49 at 25° C.

estimate of the overall energy of activation E_c. The oxygen pressure to which these data refer may be taken as infinite : the necessary small corrections have been applied to the slopes obtained at about atmospheric pressure.

Evaluation of k_3 for Individual α-Groups.—The presence of more than one α-methylenic site of reaction in many of the olefins examined implies that the observed k_3 [RH] is a composite factor which may be resolved into a number of such terms each expressing the efficiency with which a particular α-group

TABLE II

No	Type	Substitution*	Olefin	Reactive Grouping	$k_3 \times 10$ mole^{-1} l. sec.$^{-1}$				
					Calculated				Obs.
					(a)	(b)	(c)	Total	Total
A. Acyclic Olefins									
1	I	None	2 : 3 : 3-Tri-Me-butene-1	$CH_2 : C—CH_3$ (a)	0·42	—	—	0·42	0·46
2	II	1 Alkyl	Heptene-1	$CH_2 : CH . CH_2$ Alk. (a)	1·40	—	—	1·40	1·26
3	„		Octene-1	„	1·40	—	—	1·40	1·35
4	„		Hexadecene-1	„	1·40	—	—	1·40	1·41
5	„		Diallyl	„	1·40	—	—	2·80	2·63
6	„		2 : 4 : 4-Tri-Me-pentene-1	$CH_2 : C(CH_3) . CH_2$ Alk. (b) (a)	1·40	0·42	—	1·82	1·34
7	III	2 Alkyl	Hexene-2	$CH_3 . CH : CH . CH_2$. Alk. (b) (a)	4·6	1·4	—	6·0	6·7
8	„		Methyl oleate	Alk. $CH_2CH : CH . CH_2$. Alk. (a) (a)	4·6	—	—	9·2	11·9
9	„		Heptene-3	„ „	4·6	—	—	9·2	9·2
10	„		3-Methyl-pentene-2	$CH_3 . CH : C(CH_3)CH_2$. Alk. (a) (b) (a)	4·6	1·4	—	10·6	9·8
11	„		Tetramethyl-ethylene	$(CH_3)_2C : C(CH_3)_2$	4·6	—	—	18·4	42
12	IV	3 Alkyl	2-Me-pentene-2	$(CH_3)_2C : CH\ CH_3$. Alk. (b) (a)	15·2	1·4	—	18·0	22·6
13	„		2-Me-heptenyl benzoate		15·2	1·4	—	18·0	22·5
14	„		4-Me-heptene-3	Alk. $CH_2C(CH_3) : CHCH_2$Alk. (b) (c) (a)	15·2	4·6	1·4	21·2	18·7
—	V	4 Alkyl	—	—	—	—	—	—	—
15	VI	1 Phenyl	Allyl benzene	Ph .$CH_2CH : CH_2$ (a)	10·0	—	—	10·0	7·3
16	„		Crotyl benzene	Ph . $CH_2 . CH : CH . CH_3$ (a) (b)	33	1·4	—	34·4	38·3
17	„		γ-Me-Crotyl benzene	Ph . $CH_2 . CH : C . (CH_3)_2$ (a) (b)	109	1·4	—	112	129
18	VII	1 Vinyl	Ethyl linolenate	Alk. $CH_2CH : CH . CH_2 . CH : CH\ CH_2$ Alk. (b) (a) (b)	150	4·6	—	159	160
19	„		Ethyl linolenate	„ „ „ „ „	150	4·6	—	309	310
B. Cyclic Olefins									
20	III	2 Alkyl	Cyclohexene	Alk. $CH_2CH : CH\ CH_2$. Alk. (a) (a)	7·8	—	—	15·6	19·9
21	IV	3 Alkyl	1-Me-Cyclohexene	Alk. $CH_2 . C(CH_3) : CH\ CH_2$ Alk. (b) (c) (a)	25·7	7·8	2·4	35·9	34·0
22	„		1 : 2-Di-Me-Cyclohexene	Alk. $CH_2C(CH_3) : C(CH_3)CH_2$. Alk. (a) (b)	25·7	7·8	—	67·0	67·2
23	V	4 Alkyl	1 : 3 : 5-Tri-Me-Cyclohexene	Alk. $CH(CH_3)CH : C(CH_3)CH_2$ Alk. (a) (c) (b)	84·8	7·8	2·4	95	93·1
24	„	—	Tetralin	Ph . CH_2 . Alk.	—	—	—	—	15·2

* I.e., total substitution with reference to the most reactive α-group in the olefin (i.e. (a)) at the α-group itself and at the " far " end of the olefinic double bond.

reacts with RO_2— radicals. The olefins listed in Table I contain a wide variety of α-groupings each of which is distinguishable from the remainder by some feature of the unsaturated environment in which it occurs. All (apart from tetralin) can however be derived from the simplest possible type of α-group that encountered in propylene $\underset{(a)}{CH_3}\,.\,\underset{(b)}{CH}{=}\underset{(c)}{CH_2}$ (I) by substitution of methyl, alkyl, Alk. $CH{=}CH_2$— or phenyl groups at the three carbon atoms (Alk. = alkyl group). Such substitution may be expected to influence the reactivity (as measured by k_3) of the α-group (*a*) to a degree which is dependent on the identity of the substituting group and also on the particular carbon atom (*a*), (*b*), or (*c*) to which it is attached. Among the olefins examined the gradations from (I) in type and degree of substitution are sufficiently small and regular to allow quantitative evaluation of the specific influence of alkyl substitution at each of the three carbon atoms, and of substitution of Alk. CH=CH— and phenyl groups at the α-group (*a*). The conclusions may be summarized in the form of four rules, which refer to a temperature of 45° C.

(i) Effect of replacing one or two hydrogen atoms at (*a*) and/or (*c*) by methyl or other alkyl groups increases k_3 of α-group by $3{\cdot}3^n$, where n is the total number of alkyl groups *introduced at* (*a*) *and/or* (*c*). Replacement of the hydrogen atom at (*b*) has no effect.

(ii) Replacement of a hydrogen atom at (*a*) by a phenyl group increases k_3 23 times.

(iii) Replacement of a hydrogen atom at (*a*) by an Alk. CH=CH— group increases k_3 107-fold.

(iv) The k_3 value appropriate to an α-group contained in a cyclic structure is 1·7 times greater than that contained in the analogous acyclic olefinic group.

The applicability of these rules is tested in Table II, by using them to calculate the overall k_3 values for the complete range of olefins and making comparison with the figures actually found experimentally at 45° C. Taking k_3 for the standard propylene type of grouping as 0·042 the calculated k_3 values for individual α-groups (up to three in some cases) are inserted in columns 6-8, Table II. On the whole satisfactory agreement between calculated and observed overall k_3 data is obtained (though the deviation with tetra-methyl ethylene is to be noted). Closer agreement could of course be obtained [9] by introducing additional rules in which minor differences in the types of alkyl substitution are taken into account (e.g. as between methyl and other alkyl groups, between substitution at carbon atoms (*a*) and (*c*) and between substitution of the first and second hydrogen atoms at either of these two sites). An insufficient number of olefins has as yet been examined to identify such second-order effects with certainty.

We may note that the experimental justification for the conclusion that methyl substitution at the double bond has no influence on the reactivity of the " nearer " α-group rests on comparison of the k_3 values for 2 : 4 : 4-tri-methyl-pentene-1 and 3-methyl-pentene-2 with those for the Δ^1-olefins (No. 2-5) and hexene-2 respectively.

Discussion

It seems in the first place advisable to make it clear that the observed differences in the efficiency of (R3) arise primarily from variations in the energy of activation and not, for example, from random variations in the frequency factor, of a type not intimately connected with the structure of the unsaturated grouping. This point is made by the correlation between E_3 and $\log_{10} k_3$ shown in Fig. 2. E_3 is derived simply from the overall energy of activation of the oxidation E_0 since

$$E_0 = E_3 + \tfrac{1}{2}E_t - \tfrac{1}{2}E_6$$

(cf. eqn. (1)) and E_t and E_6 may be taken as 31 kcal./mole [10] and zero respectively. Departures from a linear relationship between E_3 and log k_3 do not exceed the estimated experimental error involved in the experimental determination of E_3.

---

[9] Bolland, *Quart. Rev.*, 1949, **3**, 1.

[10] This figure represents the mean of several determinations. McClure, Robertson and Cuthbertson, *Can. J. Res. B*, 1942, **20**, 103 ; Kamenskaya and Medvedev, *Acta Physicochim.*, 1940, **13**, 565 ; Nozaki and Bartlett, *J. Amer. Chem. Soc.*, 1946, **68**, 1690.

The frequency factor does, however, show systematic variation as the energy of activation alters. From the Arrhenius equation, $k_3 = PZe^{-E_3/RT}$ the slope of the $\log_{10} k_3$ against E_3 would be $(2{\cdot}3\ RT)^{-1}$ (equal to $6{\cdot}83 \times 10^{-4}$ at 45° C) if PZ remained constant throughout the series. The observed slope of $3{\cdot}3 \times 10^{-4}$ is only about half this value, indicating that PZ changes smoothly from 3×10^4 for the most reactive olefin (ethyl linoleate) to *ca.* 10^7 for the least reactive. A similar effect has been noted for several types of ionic reaction [11] and also for one other reaction involving radicals.[12] An explanation composed in general terms and so presumably applicable here also has been given by Fairclough and Hinshelwood [11] in which the importance of the time interval required for the necessary redistribution of energy accompanying chemical reaction is stressed. It should also be noted that the entire range of PZ found for ($R3$) lies well below the value (*ca.* 10^{11}) calculated from simple collisional kinetic theory and found to hold for numerous bimolecular reactions involving molecules and ions.[13]

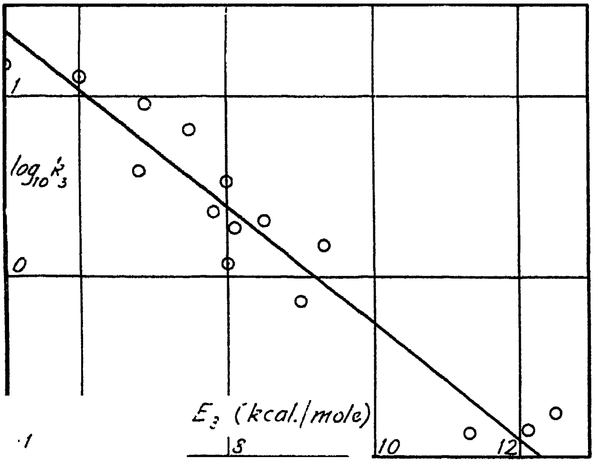

FIG. 2.—Relation between the velocity coefficients k_3 and the energies of activation E_3 of the reaction $RO_2— + RH \rightarrow RO_2H + R—$ based on data for fifteen olefins.

α-Methylenic Carbon-Hydrogen Dissociation Energies.—Within a series of similar reactions, the members of which are all exothermic, a close relationship is to be expected between the heat of reaction and the energy of activation. The exchange reaction

$$R\,.\,Cl + Na \longrightarrow R— + NaCl$$

(where variations in the hydrocarbon residue R in the alkyl chloride may be introduced) has been studied from this point of view. Evans and Polanyi [14] suggested on theoretical grounds that a simple linear relation

$$\Delta E = \alpha \Delta H \quad . \quad . \quad . \quad . \quad . \quad (3)$$

(where α is a constant having a value between zero and one) might exist between variations in energy of activation ΔE and corresponding variations in reaction heat ΔH. Using the dissociation energy of the alkyl iodides as a measure of ΔH, Butler and Polanyi [15] have provided an experimental basis for (3), finding a value of α of 0·27 for this particular reaction. Eqn. (3) was derived for reactions involving very small resonance energies in the transition state and it is to be expected that the reactions studied by Butler and Polanyi fulfil this requirement. Indications that the relation may also apply to exchange reactions involving appreciable transition state resonance have been obtained by Steiner and Watson [16] in their treatment of the substitutive reaction of chlorine with hydrocarbons.

---

[11] Fairclough and Hinshelwood, *J. Chem. Soc.*, 1937, 538.

[12] Gregg and Mayo, *Faraday Soc. Discussion*, 1947, **2**, 329.

[13] Moelwyn-Hughes, *The Kinetics of Reactions in Solution*, 2nd Edn., Chap. 3.

[14] *Trans. Faraday Soc.*, 1938, **34**, 11.

[15] *Ibid.*, 1943, **39**, 19.

A similar approach is possible with the general reaction, (R3). Here also the individual reactions are exothermic and variations in the heat of reaction can be directly related to differences in the dissociation energy of one bond—the α-β carbon-hydrogen bond severed in the course of reaction (R3). In the absence of an experimental study of the strengths of these α-β bonds in various unsaturated environments, we must turn to estimates of the dissociation energies based on calculations of resonance energies of various R— type radicals. Self-consistent calculations [17] for the radicals, which are derived from three main types of olefin examined here, $—\underset{|}{CH}—CH{=}CH_2$, $—CH{=}CH—\underset{|}{CH}—CH{=}CH—$ and —CH_2— give resonance energies of 18·7, 40·4 and 16·2 * kcal./mole respectively. These calculations are insufficiently refined to distinguish between, e.g., the radicals

$$\sim CH_2—\underset{|}{CH}—CH{=}CH_2 \text{ and } \sim CH_2—\underset{|}{CH}—CH{=}CH—CH_2 \sim,$$

though judging from the relative rates of oxidation of say the Δ^1 olefins and methyl oleate these two radicals have significantly different resonance energies. We have chosen to take the calculated resonance energies as corresponding to the latter radical. The differences in activation energy of reaction (R3) involving olefins from which these three radicals can be derived are best estimated from the linear log $k_3 - E_3$ relation in Fig. 2, taking for each type of olefin a k_3 value suggested by the rules given above. On this basis ΔE_3 as between linoleyl and allyl systems is 4·9 kcal./mole and that between linoleyl and benzyl systems 5·0 kcal./mole. The respective α values are thus 0·42 and 0·35 (mean 0·39).

Eqn. (3) may be used to estimate in approximate fashion the relatively small differences in heat of reaction for olefins which differ from these three basic types in methyl substitution only. Again ΔE is estimated from the linear log $k_3 - E_3$ relation in Fig. 2. Values of ΔH calculated from (3) taking $\alpha = 0{\cdot}39$ throughout and given in Table III, measure directly differences in the resonance energies E_{res} of the various radicals and in the dissociation energies $(D_{C-H})_{\alpha-\beta}$ of the various types of carbon-hydrogen bond. (The latter are taken simply as $(D_{C-H})_{\alpha-\beta} = (D_{C-H})_{\text{methane}} - E_{res}$).

The generalization has been made above that k_3 for an α-group is increased 3·3 fold for each methyl substituent introduced into either of two alternative positions [(*a*) and (*c*) in (I)]. Where the α-group becomes alkyl substituted, the frequency factor contained in k_3 must be reduced in sympathy with the reduction in replaceable β-hydrogen atoms. It is doubtful whether the frequency factor for any α-group will in fact be proportional to the number of β-hydrogen atoms contained therein. If however this (maximum) correction is applied, the relative ease of removal (by RO_2— radicals) of a hydrogen atom from primary, secondary and tertiary carbon atoms (as in Alk. $CH{=}CH . CH_3$,

---

[16] Steiner and Watson, *Faraday Soc. Discussion*, 1947, **2**, 88.

[17] Orr, quoted by Bolland and Gee, *Trans. Faraday Soc.*, 1946, **42**, 246.

* A recent estimate [18] of the resonance energy of the benzyl radical based on a study of the pyrolysis of toluene [19] suggests the rather higher value of 24·5 kcal./mole. The calculated resonance energies are employed here as giving the best comparative data for all three types of unsaturated systems in which we are interested.

[18] Swarc, *Faraday Soc. Discussion*, 1947, **2**, 39.

[19] Swarc, *J. Chem. Physics*, 1948, **16**, 138.

Alk. $CH{=}CH . CH_2$. Alk. and Alk. $CH{=}CH . CH (Alk)_2$.)

is in the ratio 1/4·8/32·7 (at 35° C). This suggests that an α-β carbon-hydrogen bond involving a primary carbon atom is 5·5 and 12·2 kcal. greater than that of similar bonds involving secondary and tertiary carbon atoms respectively.

The conclusion reached that a methyl substituent on an ethylenic bond activates the " far " rather than the " near " α-methylene group does not receive unanimous support from published chemical evidence. On the one hand are the observations of Cook,[20] Blumann and Zietschel,[21] and Hock and Lang [22] who identified products resulting from attack by oxygen at the α-methylene group *farther* from the alkyl substituent in methyl cyclohexene, α-pinene and *p*-menthene respectively. On the other hand, Dupont,[23] and Blumann and Zietschel [24] have isolated products from the auto-oxidation of methyl cyclohexene and limonene respectively, explicable only in terms of reaction occurring at the " near " α-methylenic group. Farmer and Sundralingam [25] recognized the formation of hydroperoxides at both the 6- and the 3-α-methylene groups in 1-methyl cyclohexene and expressed the opinion that the former (corresponding to attack at the nearer α-methylene group) predominated. In these various investigations, however, no serious attempt was made to account for all the reacted oxygen so that the products reported may well be those which are most readily recognized in a complex mixture of oxidation products and not necessarily those arising from the major cause of reaction.

TABLE III

Type of α-group	E_3	E_{res}	$(D_{C-H})_{\alpha-\beta}$
	(kcal./mole)		
I	12·2	10·3	88·2
II	10·6	14·5	84·0
III	9·0	18·7	79·8
IV	7·4	22·9	75·6
V	5·8	27·1	71·4

Complexity of Oxidation Products.—The k_3 values deduced for the three types of α-group in 1-methyl cyclohexene (Table II) may be used to illustrate the complexity of the primary oxidation product which may on occasion be encountered: in all, six α-hydroperoxides are to be expected, three corresponding to addition of oxygen to the allylic radical (eqn. (R2)) at the three original α-groups and three to the other end of the allylic systems with accompanying double bond shift. Since oxygen addition appears to occur in these two senses with equal ease, the two major products are

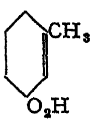

and

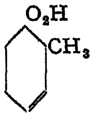

---

[20] *J. Amer. Chem. Soc.*, 1938, **60**, 1774.

[21] *Ber.*, 1913, **46**, 1178.

[22] *Ber.*, 1942, **75B**, 300.

[23] *Bull. Soc. Chim. Belg.*, 1936, **55**, 57.

[24] *Ber.*, 1914, **47**, 2623.

[25] *J. Chem. Soc.*, 1942, 121.

each in only 32 % yield. 14% and 4 % yields of the two analogous isomers resulting from initial attack at the 6-position, and the methyl group respectively complete the primary oxidation product.

Despite certain qualifications regarding their absolute accuracy the α-β-carbon-hydrogen dissociation energies listed in Table III do represent an advance toward a quantitative understanding of α-methylenic reactivity of olefins. The mechanisms by which olefins undergo other reactions resulting in substitution at α-groupings have not been determined in detail. Exceptions lie in the peroxidation reaction and the addition of certain maleic anhydride derivatives.[26] In so far as any general pattern can be distinguished, one step in the various schemes must involve removal of a hydrogen atom from the α-group concerned in the reaction ((R3) in the peroxidation mechanism). Provided this step has a determining influence on the overall rate of any given α-methylenic reaction, the structural effects outlined above will be of material importance.

The author wishes to express his gratitude to his colleagues who provided pure samples of olefines (as indicated in the test), to Dr. H. P. Koch for performing infra-red spectroscopic analyses, and to Dr. L. Bateman and Dr. G. Gee for valuable discussions during the course of the work. This work forms part of a programme of fundamental research on rubber undertaken by the Board of the British Rubber Producers' Research Association.

[26] Delalande, *Proc. XIth Int. Cong. Pure Appl. Chem.*, 1947.

APPENDIX

Benzoyl Peroxide Initiated Oxidation of Methyl Oleate.—The dependence of oxidation rate on the three concentration variables, $[Bz_2O_2]$, [RH] and oxygen pressure was found to conform to the following pattern :

(*a*) BENZOYL PEROXIDE CONCENTRATION.—Fig. 2 of Part II of the present series [2] contained data which showed that below the concentration limit imposed by the solubility of benzoyl peroxide in methyl oleate at 65° C, the rate of oxidation is proportional to $[Bz_2O_2]^{\frac{1}{2}}$.

(*b*) OLEFIN CONCENTRATION.—Oxidation rate data obtained with ethyl stearate as diluent are reproduced in Table IV. Over a ten-fold range of olefin concentration the ratio Rate/[RH] varies by only 40 %.

TABLE IV

$[Bz_2O_2] = 0{\cdot}14$ mole/l. Temp. 65° C

Mole Fraction		Rate × 10^6	Rate/oleate × 10^5	Rate $\frac{f_{R'H} \cdot \text{Rate}_{R'H}}{f_{RH}}$
Oleate	Stearate			
100	0	10·8	1·08	1·08
32·5	67·5	3·94	1·22	1·14
19·7	80·3	2·63	1·34	1·18
9·5	90·5	1·43	1·50	1·16
0	100	0·36	—	—

Rates are expressed in moles O_2 per l. per sec.

(*c*) OXYGEN PRESSURE.—The rate of oxidation of methyl oleate is insufficiently sensitive to variations in the oxygen pressure to permit an unequivocal decision as to the form the relation between these two quantities assumes. The data presented in Fig. 3 can however be regarded as being at least consistent with the relation established with much greater precision in the case of ethyl linoleate, viz. :

$$\text{Rate} = \text{const.} \frac{p}{p + \lambda}.$$

The kinetic evidence detailed above leads to the conclusion that the rate of oxidation of methyl oleate in presence of benzoyl peroxide may be represented by an equation equivalent in all respects to that obtained for ethyl linoleate.[3] An oxidation chain mechanism analogous to (R2)-(R6) must be considered as established with this mono-olefin also.

The relatively minor deviation from proportionality between oxidation rate and [RH] ((b) above) may be satisfactorily accounted for: the rate of oxidation of pure ethyl stearate itself is too great to justify treating it as an inert solvent at low methyl oleate concentrations. On the assumption that the reaction of oxygen with ethyl stearate occurs through reaction steps analogous to (R2) and (R3) ethyl stearate may be involved in the oxidation chain occurring in oleate-stearate mixtures without introducing any striking kinetic complication. The rate of such a coupled oxidation may be expressed in the simple form of eqn. (4) if the assumption is made that analogous reactions differing only in the peroxide radical involved (i.e. RO_2 – and $R'O_2$ –, if oleate and stearate are represented by RH and R'H) occur with equal efficiency.

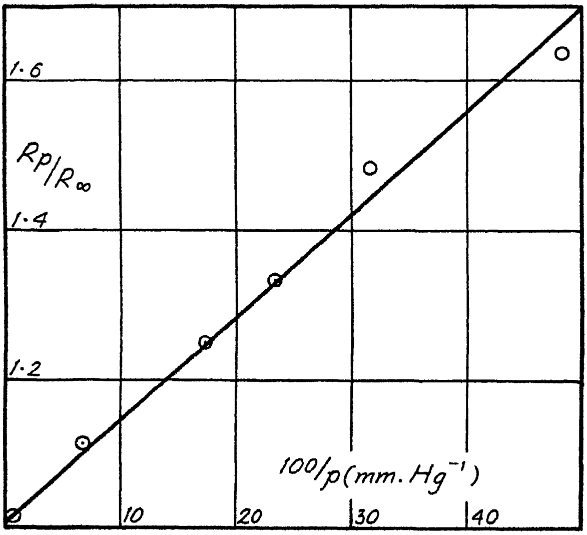

FIG. 3.—Variation of initial rate of oxidation of methyl oleate R_p with oxygen pressure p. Temperature 65° C. Concentration of benzoyl peroxide 0·02 mole/l. R_∞ represents the rate of oxidation at infinite oxygen pressure.

$$\text{Rate} = \frac{R_i^{\frac{1}{2}}}{\sqrt{k_6}} . (k_3[\text{RH}] + k_3'[\text{R'H}]). \quad . \quad . \quad . \quad (4)$$

R_i is the rate of chain initiation and k_3' the velocity coefficient of the reaction between R'H and $R'O_2$— (or RO_2—).

From eqn. (4)

$$\frac{R_i^{\frac{1}{2}}}{\sqrt{k_6}} k_3 . [\text{RH}] = \text{Rate} - \frac{R_i^{\frac{1}{2}}}{\sqrt{k_6}} k_3' . [\text{R'H}]$$
$$= \text{Rate} - f_{\text{R'H}}\, \text{Rate}_{\text{R'H}},$$

where $f_{\text{R'H}}$ is the mole fraction of stearate and $\text{Rate}_{\text{R'H}}$ the rate of oxidation of pure stearate under similar conditions of chain initiation.

The constancy of the figures contained in the fifth column of Table IV show that the variation in Rate/[RH] (column 4) can be accounted for adequately in this way.

46 *Moss Lane,*
Sale,
Manchester.

THE PRINCIPLE OF MAXIMUM OVERLAPPING

BY ALLAN MACCOLL

Received 23rd June, 1949; as amended 7th November, 1949

Assuming that the overlap integral between two carbon atoms gives a measure of the bond dissociation energy of a hybrid bond involving carbon, it is found that the bond strength of hybrid bonds increases in the order $sp > sp^2 > sp^3$. Figures are given showing the dependence of the overlap integral upon the state of hybridization. Some general considerations regarding the overlap integral and $s - p$ hybridization are also given.

In discussing the nature and bond-forming powers of atomic orbitals, Pauling [1] introduced the principle of maximum overlapping. This states that " of two orbitals in an atom the one that can overlap more with an orbital of another atom will form the stronger bond with that atom, and, moreover, the bond formed by a given orbital will tend to lie in that direction in which the orbital is concentrated." Noting that with respect to their angular dependence, p orbitals have a magnitude $\sqrt{3}$ times as great as that of an s orbital, Pauling suggests that bond energies of s—s, s—p and p—p bonds should be in the ratio $1, \sqrt{3}, 3$. He then goes on to define the bond strength of an orbital as the magnitude of the orbital in its angular dependence. Thus s and p orbitals have bond strengths of 1 and $\sqrt{3}$ respectively. In a similar fashion it may be shown that tetrahedral, trigonal and digonal orbitals have the bond strengths 2, 1·991 and 1·932.

Assuming that the bond strength as defined above is related to the bond dissociation energy, the above conclusions seem to be at variance with the experimental facts. Thus Walsh,[2] in order to account for the increasing bond dissociation energies of C—H bonds in the series CH, CH_4, C_2H_4 and C_2H_2 assumes that the greater the amount of s character, the stronger the bond. The experimental verification of this view is shown in Table I, the values being taken from Walsh's paper [2] in which the references will be found. Although there is some uncertainty attaching to the values of the bond energies, it is believed that the order is correct.

TABLE I

Molecule	C valency	r(C—H) (Å)	E(C—H) (kcal.)
CH	p	1·120	80
CH_4	sp^3	1·094	104
C_2H_4	sp^2	1·087	106
C_2H_2	sp	1·059	121

Further evidence relating to the strengths of bonds formed by carbon in various hybridization states comes from some calculations of Coulson.[3] This author has shown that the average distance of an electron from the nucleus is greater in a p than in an s orbital. Accepting that the shorter a bond is, the stronger is the bond, the data of Table I thus receive theoretical explanation.

---

[1] Pauling, *The Nature of the Chemical Bond* (Cornell University Press, 1940), p. 76.

[2] Walsh, *Faraday Soc. Discussion*, 1947, **3**, 18.

[3] Coulson, *V. Henri Memorial Vol.* (Liège, 1948), p. 15.

Since the principle of maximum overlapping seems inherently plausible, it must be assumed that the method of measuring the strength of an orbital by its magnitude in its angular dependence is at fault. Accepting the principle of maximum overlapping, an alternative criterion of the overlapping capacity of a given atomic orbital is suggested here. It is the overlap integral between two equivalent orbitals, distance R apart pointing towards each other in such a way as to have the same sign in the region of significant overlap. In this way given orbitals of various degrees of hybridization may be compared. If it may then be assumed that the overlap integrals calculated in this fashion retain the same order independently of the orbital overlapped, then they will form a reasonable measure of the bond-forming powers of orbitals.

This concept may be applied to carbon, by calculating the overlap integral for each type of C valency, for a C—C bond. The hybrid orbitals may be expressed in the form

$$\Psi = \psi_s \sin \rho + \psi_p \cos \rho, \quad 0 \leqslant \rho \leqslant \frac{\pi}{2} \quad . \quad . \quad . \quad (1)$$

while the overlap integral is defined by

$$S_\rho = \int \Psi_a \Psi_b d\tau, \quad . \quad . \quad . \quad . \quad (2)$$

in which Ψ_a and Ψ_b are two hybrid orbitals, distance R apart. Substituting (2) in (1) gives

$$S_\rho = S_{ss} \sin^2 \rho + S_{sp} \sin 2\rho + S_{pp} \cos^2 \rho, \quad . \quad . \quad (3)$$

where S_{ss}, S_{sp} and S_{pp} represent the overlap integrals $C_a(2s\sigma)$ $C_b(2s\sigma)$, $C_a(2s\sigma)C_b(2p\sigma)$ and $C_a(2p\sigma)C_b(2p\sigma)$. The hybridization parameter ρ in the various hybridization states has the values shown below :

ρ	90°	45°	35° 16′	30°	0°
Hybridization . .	s	sp	sp^2	sp^3	p

Using Slater eigenfunctions,[4] where Z is the effective nuclear charge and α is in atomic units, S_{ss}, S_{sp} and S_{pp} [*] may be calculated and tabulated as a function of

$$\alpha = ZR/2$$

R being the internuclear distance.

The results of such calculations are shown in Fig. 1, which shows the overlap integral in the various hybridization states as a function of α. The first point that emerges from the data is the vastly emphasized overlap that arises from hybridization. Secondly, the overlap in the observed range of α, 3 to 5, leads to the order $sp > sp^2 > sp^3 > s \sim p$.[†] Thus the rigidly applied principle of maximum overlapping is consistent with the data of Table I, assuming that the criterion suggested in this paper is a good one. This point will be returned to later.

In the case of C, $Z = 3{\cdot}18$ and $R = 2{\cdot}91$, $2{\cdot}50$ and $2{\cdot}26$ atomic units for sp^3, sp^2 and sp hybridization, and so α has the values 4·6, 4·0 and 3·6. At these distances the overlap integrals are respectively 0·67, 0·78 and 0·88. Thus the C—C(σ) bond dissociation energy in ethane, ethylene and acetylene should increase in that order. This is the opposite to what would be expected from Pauling's argument. The implication for thermochemistry is obvious. For it follows that a similar order of energy would be given by sp^3, sp^2 and sp bonds between C and, for example, H. Thus, in going from ethane to ethylene and acetylene, neglect of alterations in the

---

[4] Slater, *Physic. Rev.*, 1930, **36**, 57.

[*] The integrals required are to be found in a paper by Coulson, *Proc. Camb. Phil. Soc.*, 1941, **38**, 210.

[†] These points have also been noted by Mulliken and his collaborators (private communication, 1948). See also *J. Chem. Physics*, 1949, **17**, 510.

C—H energy will cause an accumulation of error in the estimate of the C═C and C≡C bond strengths.

The relatively poor overlap between *p* orbitals receives a ready explanation when it is remembered that the two lobes differ in sign. Thus when the positive regions of the two *p* orbitals are pointed towards each other so as to obtain the greatest positive value of *S*, there is still quite a large contribution from regions where the signs differ. For *s* orbitals, on the other hand, from all important regions the contribution is positive.

In order to verify the amended principle of maximum overlapping suggested in this paper, calculations were made of the overlap integral between C ($2s\sigma$) and C ($2p\sigma$) orbitals and a hydrogen ($1s$) orbital, the internuclear distance being taken as 1·080 Å. The hybrid overlap integral is given by

$$S_v = S_{sH} \sin \rho + S_{pH} \cos \rho \quad . \quad . \quad . \quad (4)$$

where S_{sH} and S_{pH} are the C($2s\sigma$) and C ($2p\sigma$), H ($1s$) overlap integrals. The necessary integrals may be obtained from the paper by Coulson referred to earlier. On carrying out the calculations it is found that

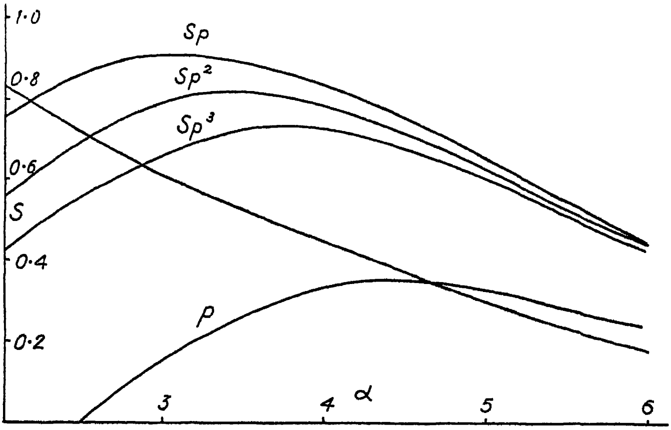

FIG 1.—The overlap integral for various hybrid orbitals.

$S_{sH} = 0{\cdot}59$, $S_{pH} = 0{\cdot}49$, and the hybrid overlaps are 0·72, 0·74 and 0·76 for sp^3, sp^2 and sp hybrids respectively. Thus the order is once again $S_{sp} > S_{sp^2} > S_{sp^3}$. Indeed Hirschfelder, as reported by Smythe,[5] has previously shown that $S_{sp^3} > S_{sH} > S_{pH}$. It may be thus concluded that the overlap of a given orbital with a similar one provides a reasonable measure of its bond-forming power. It must be noted, however, that hybridization appears to be much less efficient in the case of overlap between a hybrid and a non-hybrid orbital than it is in the case of two equivalent hybrid orbitals. This is attributable to the lack of a cross-term in (4) compared with (3).

In Fig. 2 are shown the C—C overlap integral for $\alpha = 4$ and the C—H overlap integral for $R = 1{\cdot}08$ Å as a function of the percentage *s* character ($\sin^2 \rho$). In both cases the overlaps of the hybrid orbitals are in the order $sp > sp^2 > sp^3$. Further, this order is retained in the observed range of C—C and C—H bond lengths.

Although it has been convenient to develop the inequality for the overlap integral, $sp > sp^2 > sp^3$ in a special case of great practical importance, the results may be obtained in a more general fashion. Consider the overlap between a hybrid orbital of parameter ρ centred on atom A and one of parameter τ centred on atom B. The overlap integral now takes the form

---

[5] Smythe, *J. Physic. Chem.*, 1937, **41**, 209.

$$S(\rho, \tau) = S_{ss'} \sin \rho \sin \tau + S_{sp'} \sin \rho \cos \tau + S_{ps'} \cos \rho \sin \tau + S_{pp'} \cos \rho \cos \tau, \qquad (5)$$

where

$$S_{ss'} = \int \psi_s^A \psi_s^B d\tau, \qquad S_{pp'} = \int \psi_p^A \psi_p^B d\tau,$$
$$S_{sp'} = \int \psi_s^A \psi_p^B d\tau, \qquad S_{ps'} = \int \psi_p^A \psi_s^B d\tau. \qquad (6)$$

$S(\rho, \tau)$ may be put in a more convenient form by defining the new hybridization parameters

$$\mu = \rho + \tau,$$
$$\nu = \rho - \tau. \quad . \quad . \quad . \quad . \quad . \quad . \qquad (7)$$

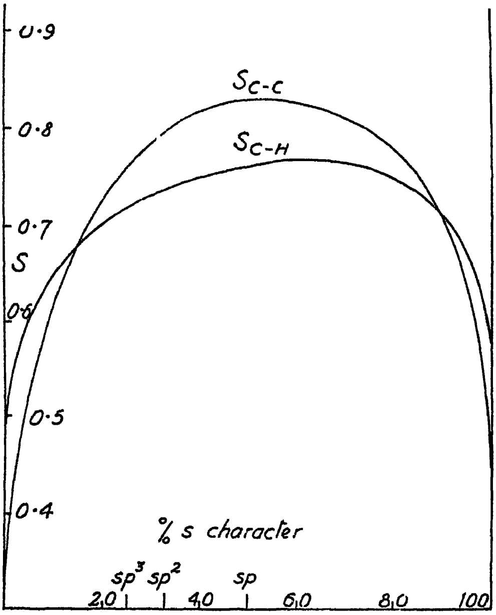

FIG. 2.—The overlap integral for C—C and C—H bonds as a function of % *s* character.

Substituting (7) in (5) and rearranging yields

$$S(\mu, \nu) = \tfrac{1}{2}(S_{sp'} + S_{ps'}) \sin \mu + \tfrac{1}{2}(S_{pp'} - S_{ss'}) \cos \mu + \tfrac{1}{2}(S_{sp'} - S_{s'p}) \sin \nu + \tfrac{1}{2}(S_{pp'} + S_{ss'}) \cos \nu. \qquad (8)$$

The turning point on this surface is given by

$$\frac{\partial S}{\partial \mu} = \frac{\partial S}{\partial \nu} = 0,$$

and these lead to the conditions

$$\tan \mu = \frac{S_{sp'} + S_{ps'}}{S_{pp'} - S_{ss'}},$$
$$\tan \nu = \frac{S_{sp'} - S_{ps'}}{S_{pp'} + S_{ss'}} \quad . \quad . \quad . \quad . \quad . \qquad (9)$$

for determining μ and ν and hence ρ and τ. Also if the S are all positive, and the orbitals can usually be oriented so that for internuclear distances of practical importance this criterion is satisfied, the turning point can be shown to be a maximum. The value of the maximum overlap is

$$S_{\max} = \tfrac{1}{2}\{[(S_{sp'} + S_{ps'})^2 \pm (S_{pp'} - S_{ss'})^2]^{\frac{1}{2}} + (S_{pp'} + S_{ss'})^2]^{\frac{1}{2}} + [(S_{sp'} - S_{sp'})^2\}. \quad (10)$$

Thus sp hybridization always increases the overlap integral, the increase being due to the cross terms $S_{sp'}$ and $S_{ps'}$.

Two simpler cases of overlap can also be discussed. The first is the overlap between two equivalent hybrid orbitals. The second is the overlap between a hybrid orbital on one atom and a simple atomic orbital. In the first case $S_{sp'} = S_{ps'}$ and equations (8), (9) and (10) reduce to

$$S(\rho) = \tfrac{1}{2}(S_{ss'} + S_{pp'}) + S_{sp'} \sin 2\rho + \tfrac{1}{2}(S_{pp'} - S_{ss'}) \cos 2\rho, \quad . \quad (11)$$

$$\tan 2\rho = \frac{2S_{sp'}}{S_{pp'} - S_{ss'}} \quad . \quad . \quad . \quad . \quad (12)$$

$$S_{\max} = \tfrac{1}{2}\{(S_{ss'} + S_{pp'} + [4S_{sp'}^2 \pm (S_{pp'} - S_{ss'})^2]^{\frac{1}{2}}\}. \quad . \quad (13)$$

From these equations the conditions on $S_{ss'}$, $S_{pp'}$, $S_{sp'}$ such that the order of increasing overlap is $sp > sp^2 > sp^3$ may be obtained. For this order will hold provided that $S_{\mathrm{di}} > S_{\mathrm{tri}}$, i.e., $S(45°) > S(35°\ 16')$. Explicitly, the condition is

$$S_{sp'} > 2{\cdot}9\ (S_{pp'} - S_{ss'}). \quad . \quad . \quad . \quad . \quad (14)$$

Now since in the 2-quantum case $S_{pp'} < S_{ss'}$ and $S_{sp'} > 0$, for values of α of physical interest, the result obtained earlier is recovered. Conditions for the reverse and intermediate orders may be written down in the same fashion.

The third case to be discussed is the overlap of a hybrid orbital with a simple atomic orbital, as for example in C—H bonds. In this case depending on whether the atomic orbital is an s or a p,

$$(a)\ S_{pp'} = S_{sp'} = 0,$$

or

$$(b)\ S_{ss'} = S_{ps'} = 0.$$

In these cases formulae (8), (9) and (10) reduce to

$$S(\rho) = S_{ss'} \sin \rho + S_{ps'} \cos \rho, \quad . \quad . \quad . \quad (15)$$

$$\tan \rho = \frac{S_{ss'}}{S_{ps'}}, \quad . \quad . \quad . \quad . \quad . \quad (16)$$

$$S_{\max} = (S_{ss'}^2 + S_{ps'}^2)^{\frac{1}{2}}, \quad . \quad . \quad . \quad . \quad (17)$$

and

$$S(\rho) = S_{sp'} \sin \rho + S_{pp'} \cos \rho, \quad . \quad . \quad . \quad (15a)$$

$$\tan \rho = \frac{S_{sp'}}{S_{pp'}}, \quad . \quad . \quad . \quad . \quad (16a)$$

$$S_{\max} = (S_{sp'}^2 + S_{pp'}^2)^{\frac{1}{2}}. \quad . \quad . \quad . \quad . \quad (17a)$$

Again the variation of the overlap integral with hybridization type may be investigated. For the order $sp > sp^2 > sp^3$,

$$S_{ss'} > 0{\cdot}84\ S_{ps'}, \text{ or } S_{sp'} > 0{\cdot}84\ S_{pp'}.$$

Another point that can be established in this case relates to the efficiency of hybridization. This can be examined by discussing the ratio $S_{\max}/S$, where S is the greater of $S_{ss'}$ or $S_{ps'}$ in case (a). Thus

$$\left.\begin{aligned} \frac{S_{\max}}{S_{ss'}} &= \left(1 + \frac{S_{ps'}^2}{S_{ss'}^2}\right)^{\frac{1}{2}} \qquad S_{ps'} < S_{ss'}, \\ \frac{S_{\max}}{S_{ps'}} &= \left(1 + \frac{S_{ss'}^2}{S_{ps'}^2}\right)^{\frac{1}{2}} \qquad S_{ss'} < S_{ps'}. \end{aligned}\right\} \quad . \quad . \quad (18)$$

Similar equations hold in case (b). Thus it can be seen that the hybridization is most effective when the two orbitals to be hybridized overlap equally with the atomic orbital of the second atom. Further, little is gained in the way of increased overlap unless $S_{ss'}$ and $S_{ps'}$ are of the same order of magnitude. The maximum value of the overlap integral in the case of $S_{ss'} = S_{ps'}$ is $\sqrt{2}S_{ss'}$.

In this treatment it has been assumed that the overlap integrals between atomic orbitals are independent of internuclear distance in so far as the different internuclear distances in the various hybridization states have not been taken into account. This is not so serious an omission as might at first appear, since the atomic radius of an atom decreases as the *s*-character increases. Hence this effect will only go to strengthen the inequality $sp > sp^2 > sp^3$.

It is not only with respect to carbon that the use of the concept of the bond strengths of orbitals runs into difficulties. For Duffey[6] has recently discussed the hybrid orbitals sp^3d leading to a trigonal bipyramidal configuration such as is observed for PCl_5. This author finds that the axial P—Cl bonds should be stronger than the equatorial, a fact that is difficult to reconcile with the observed distances. The examination of types of hybridization other than sp^3 is being undertaken.

The author is pleased to acknowledge discussions with Prof. C. K. Ingold, F.R.S., Prof. C. A. Coulson and with Dr. D. P. Craig.

Sir William Ramsay and Ralph Forster Laboratories,
University College, London, W.C.1.

---

[6] Duffey, *J. Chem. Physics*, 1949, **17**, 196.

THE PHOTOCHEMICAL FORMATION OF SULPHINIC ACIDS FROM SULPHUR DIOXIDE AND HYDROCARBONS

By F. S. Dainton and K. J. Ivin

Received 20th October, 1949

The reaction $RH + SO_2 \rightarrow R.SO.OH$ (where RH is an olefin or paraffin) occurs in the gas phase in the presence of ultraviolet light. In all cases the quantum yield is less than unity. The reaction affords a new method for the preparation of aliphatic sulphinic acids. The reaction proceeds most readily with long chain paraffins. It appears that tertiary carbon atoms are attacked more readily than secondary and secondary more readily than primary.

Olefins are less reactive than paraffins due to their high quenching ability with respect to excited sulphur dioxide molecules. They retard the reaction of paraffins.

The only reactions previously reported between sulphur dioxide and hydrocarbons[1] are those in which unsaturated hydrocarbons react to form a polysulphone, and with conjugated dienes, a cyclic monosulphone. In all cases reaction has only been reported in the liquid phase. During an investigation of the kinetics of olefin polysulphone formation, we have found that both paraffins and olefins will combine readily with sulphur dioxide in the gas phase under the influence of ultra-violet light to yield sulphinic acids. Paraffins also give sulphinic acids in the liquid phase while olefins normally give polysulphones.

---

[1] See Suter, *Organic Chemistry of Sulphur* (Chapman and Hall, 1944).

In this paper the results of a general investigation of the gas phase reactions and the relative reactivity of various hydrocarbons will be given, while in a succeeding paper the detailed kinetics of the *n*-butane and 1-butene reactions will be reported.

Experimental

Except in the cases mentioned below all hydrocarbons were obtained from cylinders. Propylene was prepared by dehydration of *n*-propyl alcohol with sulphuric acid and aluminium sulphate. *iso*Butene was a sample prepared by Mr. K. E. Russell by the dehydration of *tert*.-butyl alcohol over anhydrous oxalic acid at 80° C. The reaction of paraffins was found to be retarded by traces of olefins and precautions were therefore taken to remove the latter by allowing to stand over concentrated sulphuric acid for several hours, preferably overnight, before use. All the hydrocarbons were finally purified by distillation *in vacuo* at low pressure, the purity being checked when necessary by vapour pressure measurements. Sulphur dioxide was dried over phosphorus pentoxide and distilled *in vacuo*. Fractionation was not found necessary.

The apparatus for rate measurements was of the conventional type. The purified reactants were measured into a mixing bulb from which they could be admitted to the previously evacuated quartz reaction vessel. The latter was cylindrical in shape having a diameter of 7 cm. and depth of 2 cm. and was kept at constant temperature by immersion in a thermostat with quartz windows. The light source was a vertical quartz-mercury vapour lamp which was run hot, emitting mainly wave lengths $>$ 2300 Å, and an approximately parallel beam was passed into the reaction vessel with the aid of a convex lens and diaphragms. The voltage across the lamp was at first controlled by hand and later by means of a valve stabilizer. The reaction was followed by means of the pressure fall which was measured on a Bourdon gauge of the link type surrounded by a water jacket. At the end of an experiment, the gaseous products could be expanded into a bulb of known volume and analysis for sulphur dioxide performed by admitting an excess of iodine solution (obtained by adding potassium iodide and acid to a standard iodate solution) to the bulb, the excess being back-titrated with sodium thiosulphate solution. The gaseous products could be passed through a liquid air trap in order to test for the presence of any non-condensable gases. The total extent of reaction could be estimated both from the total pressure fall and from the weight of involatile product deposited in the reaction vessel.

An apparatus was constructed for the preparation of larger amounts of the products for identification purposes. This is shown diagrammatically in Fig. 1 and consisted essentially of a copper tank T with a central quartz chimney C, inside which was supported the quartz mercury lamp L (220 V tungsten anode type). The annular quartz reaction vessel R had an external diameter of 12 cm. and the internal distance between the walls was 1 cm. It was supported in the tank as shown and immersed in water which could be kept at constant temperature. (A cooling coil was necessary to dissipate the heat from the lamp.) The lamp was rigidly supported on a frame and could be lowered out of the chimney and started by tilting. The shutter S was used to control the illumination. Reaction in this apparatus proceeded some 20 to 30 times faster than that in the simple cell.

Analysis, Properties and Derivatives of Products.—In all cases reaction was accompanied by a pressure fall and the formation of a mist which on settling gave a colourless or pale yellow involatile oil with a disagreeable odour. The light scattered from the mist revealed convection currents which carried part of the product to the surfaces of the reaction vessel. The product from the *n*-butane reaction showed complete absorption below 3400 Å with a path length of 5 mm., but no photochemically induced decomposition of the product was observed. The oil desposited on the front surface of the reaction vessel tended to cut down the intensity of light absorbed by the reactants. With olefins, these oil droplets sometimes developed into a coherent film. This also showed strong absorption below 3650 Å and caused a marked retardation in the rate of reaction. This is shown for 1-butene in Fig. 2 : more oil was deposited on the front surface than on the back, due to the greater extent of absorption and reaction near the front surface and therefore on rotating the reaction

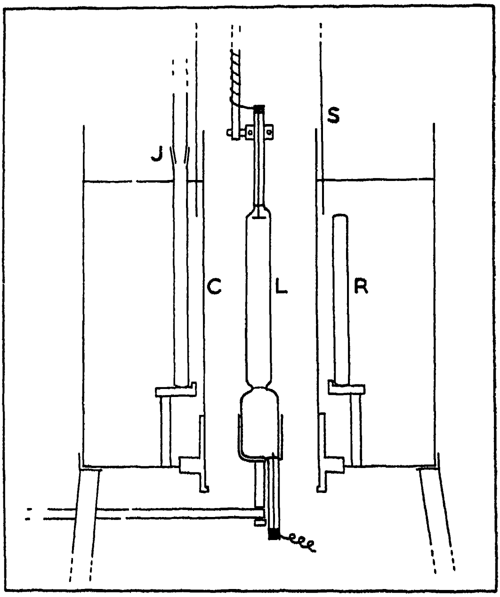

FIG 1.—Apparatus for preparation of products in quantity.

L = quartz mercury lamp (220 V type, tungsten anode).
C = quartz chimney (length 27 cm., diam. 7·5 cm.).
R = annular quartz reaction vessel (length 11 cm., depth of reaction space = 1·0 cm., external diam. 12·2 cm.).
J = B10 ground joint connecting to reservoir and vacuum line.
S = shutter.
T = copper tank (approx. 25 × 25 × 25 cm.).

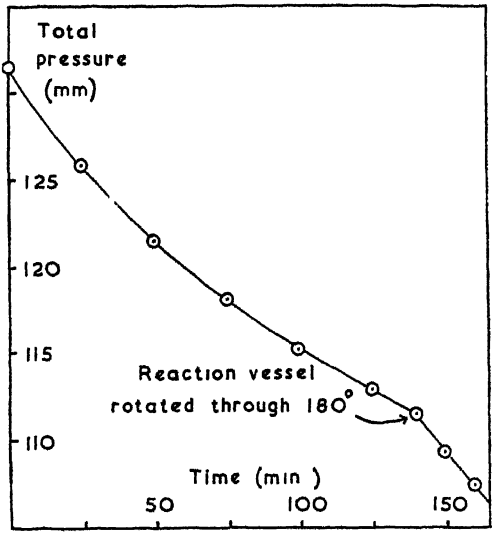

FIG. 2.—Retardation of 1-butene reaction by formation of absorbing film on front surface of reaction vessel. 65·8 mm. 1-butene + 65·8 mm. sulphur dioxide: $T = 24{\cdot}5°$ C.

vessel through 180°, there was a considerable increase in the rate of reaction. The formation of the film appeared to be due to secondary photopolymerization of the oil. Some of the oil was deposited on the bottom of the reaction vessel, out of the direct beam of the light. On evacuating the reaction vessel and exposing this oil to ultra-violet light, a certain amount of solid was formed. This solid, and the film formed on the front surface of the reaction vessel both resembled 1-butene polysulphone in being insoluble in ether and soluble in acetone, whereas the oil is soluble in both solvents. While not establishing the identity of the film and the polysulphone, the facts are not inconsistent with this possibility. The actual amount of film formed was never more than about 1 mg., and the ratio of film to oil was generally about 1/7, though this ratio probably changed with the extent of illumination.

Products from the *n*-butane reaction were prepared using different reactant ratios and gave the analyses shown in Table I. In the third experiment, the product had to be removed from the reaction vessel by extraction with ether which was then pumped off *in vacuo*. The low C/H ratio in this experiment is due to contamination by traces of water introduced in the extraction process. Even after allowance for this, the O/S ratio is still high and this is attributed to attack of the hydrocarbon by sulphur trioxide formed by decomposition of the sulphur dioxide (see later). The C/S ratio shows that some disulphonic acid is probably formed at all reactant ratios, but the variation is not large.

The molecular weight of the product of the *n*-butane reaction was determined ebullioscopically in acetone and gave a value of 139 ± 4. The value calculated for $C_4H_{10}SO_2$ is 122. This again indicates a certain amount of a disulphinic acid.

TABLE I

SO_2/C_4H_{40}*	Total Pressure (mm.)	% C	% H	% S	% O	Atomic Ratio		
						C/H	C/S	O/S
1·0	600	38·3	7·96	27·2	26·7	0·403	3·75	1·97
0·5-0·085	450-140	37·9	7·86	26·4	27·9	0·404	3·82	2·12
4·2-24	540-200	34·5	7·48	25·4	32·6	0·387	3·61	2·57
Calc. for $C_4H_{10}SO_2$		39·3	8·25	26·2	26·1	0·400	4·00	2·00

* When the initial ratio is not unity it changes as the reaction proceeds.

The presence of a hydroxyl group in the product of the 1-butane reaction was confirmed by its infra-red spectrum (determined by Dr. D. A. Ramsay), which shows very marked broad absorption at about 3·0 μ, characteristic of a hydrogen-bonded hydroxyl group.

The product of the 1-butene reaction could not be prepared in sufficient quantity for analysis owing to the low quantum yield and the rapid retardation of the reaction previously mentioned. However, its properties were very similar to that of the *n*-butane product. Also the kinetics of the two reactions were found to bear a close resemblance and it is reasonable to conclude that the reaction here is also a simple addition process.

The oils showed all the characteristics of aliphatic sulphinic acids, being slightly soluble in water, giving a solution acid to litmus which readily decolorized bromine water, iodine solution and acid or alkaline permanganate with equal facility. Some titrations were attempted but the end-points were never sufficiently clear to permit accurate measurements. However, the results indicated that not more than two atoms of bromine were consumed for one ($C_4H_{10}SO_2$) group in the *n*-butane product and a similar conclusion was drawn concerning the 1-butene product. Titration with alkali indicated an equivalent weight of the order 120-160 for the *n*-butane product.

The overall reaction may thus be written :

$$RH + SO_2 \rightarrow RSO_2H.$$

Analysis of the residual gases confirmed that the reactants were removed in equimolar amounts, provided the length of the hydrocarbon chain was not low and provided the reaction mixture was not too rich in sulphur dioxide. Some typical results are shown in Table II.

The pressure falls were in good agreement with the yield of sulphinic acid. For example, in one experiment with *n*-butane the yield of product calculated from the pressure fall was 49·4 mg. compared with the observed yield of 49·6 mg. In no case was any non-condensable gas formed when wavelengths $<$ 2400 A were excluded. The deviations from equimolar removal in the first and third sets of figures in Table II are to be attributed to photo-decomposition of sulphur dioxide which becomes appreciable when the hydrocarbon is unreactive as in ethane, or when an excess of sulphur dioxide is present. It may be noted at this point that sulphur dioxide alone decomposed extremely slowly to sulphur trioxide and sulphur even in the absence of wave lengths $<$ 3000 A ; we estimate the quantum efficiency as $<$ 0·01. It should also be mentioned that the data in Table II are rendered slightly inaccurate by the neglect of the slight solubility of the gaseous reactants in the liquid product. A few measurements indicated that sulphur dioxide was more soluble than *n*-butane in the product of their reaction and the main result of applying a correction to the above data is to lower by a few per cent. the pressure of hydrocarbon consumed.

TABLE II

$T = 25{\cdot}0°$ C

Hydrocarbon	Initial Partial Pressures (mm.)		Pressure Fall (mm.)	Pressures Consumed (mm.)	
	Hydrocarbon	Sulphur Dioxide		Hydrocarbon	Sulphur Dioxide
Ethane . .	151·8	148·0	34·0	13·2	20·8
n-Butane .	223·2	225·0	109·6	56·6	53·0
	18·0	103·0	25·0	9·0	16·0
	89·4	438·6	107·8	51·8	56·0
1-Butene .	188·8	207·4	39·6	19·8	19·8

It has been shown [2] that an excited 1-butene molecule, formed by collision of a normal molecule with an excited mercury atom, can isomerize to the more stable 2-butene. It was, therefore, of interest to find whether collision with an excited sulphur dioxide molecule would induce a similar process. However, on irradiating a mixture of sulphur dioxide and 1-butene in the annular vessel for a period calculated to enable every 1-butene molecule to undergo at least one collision with an excited sulphur dioxide molecule, no such effect could be detected. The vapour pressure method used to analyze the residual 1-butene was capable of detecting $>$ 3 % isomerization.

It is clear that in hydrocarbons other than methane, ethane and ethylene, substitution can occur on one of several types of carbon atom. Derivatives were made in an attempt to characterize the products, and to find which carbon atoms were preferentially attacked. Sulphones were made by the reaction

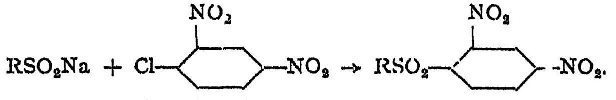

A solution of the sulphinic acid in alcohol, to which the calculated amount of sodium had been added, was refluxed for several hours with the calculated amount of 1-chloro-2 : 4-dinitrobenzene. The product was poured into water and after allowing to stand, the precipitate was filtered off and recrystallized from alcohol-water. Dry fusion of the sodium salt with the chloro compound was also successful. The results are shown in Table III.

Agreement between the observed and calculated analyses is good for the propane derivative, but the H, S and N values are unaccountably low for the *n*-butane derivative. The melting points indicate that the propane derivative consists of a mixture of the two isomers, whereas in the butane derivative the *sec.*-butyl compound predominates. Further evidence for the attack of a CH$_2$ group rather than a CH$_3$ group has been obtained from the rate data. An attempt to prepare a derivative from the product of the *iso*butane reaction was not successful. A solid which was isolated appeared to be 1-ethoxy-2 : 4-dinitrobenzene (obs. : 45·4 % C, calc. : 45·3 % C).

---

[2] Gunning and Steacie, *J. Chem. Physics*, 1946, **14**, 581.

No derivatives were made from the unsaturated sulphinic acids which are presumably formed from olefins, due to the difficulty of preparing them in appreciable quantity. It seems likely that both olefinic and saturated carbon atoms will be attacked and in the former case the resulting sulphinic acid will be conjugated and hence more prone to secondary polymerization. This would account for the fact that only part of the 1-butene product appears to undergo secondary polymerization. The question arises as to why a gaseous mixture of 1-butene and sulphur dioxide on irradiation gives a low molecular weight sulphinic acid whereas in the liquid phase a mixture of the same composition gives a high molecular weight polysulphone. Two possible causes may be suggested. Firstly, polysulphones are formed by a free radical mechanism and it seems probable that the initial centre is a diradical formed by the attachment of an excited sulphur dioxide molecule to an olefinic carbon atom, e.g.

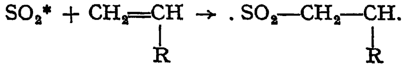

$$SO_2^* + CH_2{=}\underset{\displaystyle R}{\underset{|}{CH}} \rightarrow .\,SO_2{-}CH_2{-}\underset{\displaystyle R}{\underset{|}{CH}}.$$

In the gas phase such a diradical would rearrange to give an unsaturated sulphinic acid before further collisions could occur, whereas in the liquid phase the collision frequency is such that the chain is readily propagated. Secondly, the ceiling temperature for 1-butene polysulphone formation is only just above room temperature, and, as we have argued elsewhere,[3] the value for the vapour phase reaction should be lower. If it is, in fact, below the working temperature for the experiments described here, no high molecular weight polysulphone could be formed.

TABLE III

Hydrocarbon	Possible Group	Melting Points		Analyses				
		Lit.	Obs.		% C	% H	% S	N %
Propane .	*n*-Pr	127·5°	122°	Obs.	39·8	3·54	11·1	10·4
	sec.-Pr	140·5°		Calc.	39·4	3·68	11·7	10·3
n-Butane .	*n*-Bu	92°	117·5°	Obs.	41·4	3·88	9·7	8·8
	sec.-Bu	not known		Calc.	41·6	4·19	11·1	9·7

Comparison of Rates for Different Hydrocarbons.—Two sets of measurements were made and these are recorded in Tables IV and V respectively. Table IV consists mainly of data on paraffins and Table V mainly of data on olefins. Each set of measurements was made at 25° C at constant light intensity. The intensity for each set was different and for this reason 1-butene is given in both Tables. The measurements were made with a partial pressure of 150 mm. of each reactant, and at this pressure the influence of the hydrocarbon on the intensity of absorbed light is not appreciable. The quantum yields given are based on that of the *n*-butane reaction which was determined as described in the following paper. In all cases the full light of the Hg arc was used. No pressure fall was observed on illuminating a hydrocarbon by itself, and mercury vapour was without effect on the reactions. Also no dark reactions were observed after cutting off the light.

It will be seen from the Tables that the rate increases for each of the following series :

Methane < Ethane < Propane < *n*-Butane < Pentane . (1)
Ethylene < Propylene < 1-Butene . . . . . . (2)
Butadiene < 1-Butene < *n*-Butane . . . . . . (3)

---

[3] Dainton and Ivin, *Trans. Faraday Soc.* (in press).

It is clear that there may be two reasons for a low quantum yield in a given reaction. Either (i) addition to the hydrocarbon is difficult (reaction (4)), or (ii) the hydrocarbon possesses a high quenching ability with respect to excited sulphur dioxide molecules (reaction (5)).

$$SO_2^* + RH \rightarrow RSO_2H \quad . \quad . \quad . \quad . \quad (4)$$

$$SO_2^* + RH \rightarrow SO_2 + RH \quad . \quad . \quad . \quad . \quad (5)$$

In the latter case the hydrocarbon should inhibit the reaction of a second hydrocarbon with a higher quantum yield, whereas in the former case it should merely act as a diluent. The effect on the *n*-butane reaction, of small pressures of methane and 1-butene respectively, was therefore investigated. It was found that while methane had no significant effect, 1-butene caused a marked retardation. This shows that in series (1), the increasing rate is mainly due to the increasing ease of the addition reaction (4), which thus parallels the accepted order for the ease of rupture of the C, H bonds in hydrocarbons. In series (3) the increasing rate is mainly due to the decreasing quenching ability of the hydrocarbon. In the second series, the increase in rate is probably mostly due to the increasing ease of the addition reaction. The strong quenching ability of olefins, as compared with that of paraffins, has also been observed with sodium [4] and cadmium [5] and mercury [6] resonance radiations respectively, and the seat

TABLE IV.—PARAFFINS

Hydrocarbon	Partial Pressures (mm.)		Initial Rate of Pressure Fall (mm./hr.)	Estimated * Quantum Yield	Products and Remarks
	Hydro-carbon	Sulphur Dioxide			
Methane .	150	150	12 (initial) 2 (steady)	— 0·006	Rate fell off very rapidly to the steady value. Brown specks on walls, but fall in rate not due to decrease in intensity of absorbed light. Product had no distinctive odour.
Ethane .	150	150	10	0·025	Rather insoluble film formed on front surface of reaction vessel. Characteristic odour.
Propane .	150	150	42·5	0·125	Oil, characteristic odour.
n-Butane .	150	150	78	0·23	Ditto
iso-Butane.	150	150	63·5	0·18	Ditto
Pentane .	150	150	90	0·26	Oil, odour not as strong as for propane and butane products.
1-Butene .	150	150	15	0·044	Oil, characteristic odour. Film, insoluble in ether, soluble in acetone.
	—	150	approx. 1·5	<0·01	Decomposition of SO_2.

*Based on quantum yield of *n*-butane reaction (see next paper). The quantum yield increases with hydrocarbon pressure.

---

[4] Norrish and McFarlane Smith, *Proc. Roy. Soc. A*, 1940, **176**, 295.

[5] Steacie and Leroy, *J. Chem. Physics*, 1943, **11**, 164.

[6] Mitchell and Zemansky, *Resonance Radiation and Excited Atoms* (Cambridge Univ. Press, 1934).

of the quenching power is undoubtedly in the double bond. The detailed kinetics of the inhibition of the *n*-butane reaction by 1-butene and butadiene will be presented in a succeeding paper.

In the series of paraffins, the increment in the rate on introducing an additional CH_2 group is approximately constant. An approximate reactivity scale at 25° can be drawn up on the basis of the results in Table IV, as follows :

CH_4	CH_3	CH_2	CH
2	5	34	48

The rate for a given hydrocarbon may then be calculated by summing for the individual groups in the molecule. By this argument it would be expected that the secondary sulphinic acids would predominate in the products from propane and *n*-butane. The melting points of the derivatives give some support to this.

TABLE V.—UNSATURATED COMPOUNDS

Unsaturated Compound	Partial Pressures (mm.)		Initial Rate of Pressure Fall (mm./hr.)	Estimated * Quantum Yield.	Products and Remarks
	Unsat. Cpd.	Sulphur Dioxide			
Ethylene .	150	150	7·5	0·013	Oil, trace of film, faint characteristic odour.
Propylene .	150	150	11·5	0·020	Oil, characteristic odour No film observed after two hr. illumination.
1-Butene .	150	150	25	0·044	Oil, characteristic odour, and film.
2-Butene .	150	150	19	0·033	Oil, characteristic odour. No film after 10 min. illumination.
*iso*Butene .	approx. 150	approx. 150	approx. 8	—	Reaction was masked by thermal polymerization of the *iso*butene. The figure given is the increase in rate on illumination.
1 : 3-Butadiene	150	150	—	—	Rate irregular.

* Estimated from value for 1-butene.

One of us (K. J. I.) is indebted to the D.S.I.R. for a maintenance grant during the period (1945-48) in which this work was carried out. The authors wish to express their thanks to the Chemical Society and Royal Society for assistance in the purchase of apparatus.

Department of Physical Chemistry,
Cambridge.

THE KINETICS OF THE PHOTOCHEMICAL GAS-PHASE REACTIONS BETWEEN SULPHUR DIOXIDE AND *n*-BUTANE AND 1-BUTENE RESPECTIVELY

By F. S. Dainton and K. J. Ivin

Received 27th October, 1949

The kinetics of the gas-phase photochemical reactions between sulphur dioxide and *n*-butane and 1-butene respectively to form the corresponding sulphinic acids have been studied using wavelengths 2400-3340 Å, over the range of temperature 15-100° C. Excitation of the sulphur dioxide molecules is followed by the competitive processes: addition to hydrocarbon, quenching by hydrocarbon and internal deactivation. Quenching by normal sulphur dioxide molecules is not an efficient process, as indicated by the independence of the quantum yield of the *n*-butane reaction on sulphur dioxide pressure. The quantum yield of the *n*-butane reaction is only slightly dependent on wavelength within the experimental error and reaches a limiting value of 0·35 at high pressures of *n*-butane.

Both reactions have temperature coefficients less than unity and the pressure dependence of the apparent energies of activation suggests that the process of internal deactivation becomes more efficient as the temperature is raised. Experiments on the inhibition of the *n*-butane reaction by small amounts of 1-butene and butadiene indicate that the process of quenching of an excited sulphur dioxide molecule by a hydrocarbon is complex, the efficiency appearing to decrease with increasing pressure of hydrocarbon, but showing the usual dependence on unsaturation and conjugation.

In a previous paper [1] it was shown that sulphur dioxide will combine with aliphatic hydrocarbons in the gas phase under the influence of ultraviolet light to yield sulphinic acids. In the present paper, the results of a detailed kinetic investigation of the *n*-butane and 1-butene reactions will be presented.

Experimental

The reactions were followed by means of the pressure fall in the apparatus previously described.[1] The Bourdon gauge used to measure the pressure was sensitive to a change of 0·03 mm. A shutter, filter solutions and gauzes or perforated plates whose transmission had been measured with the aid of a photoelectric cell, could be placed in the beam to control the intensity and wavelengths of light reaching the reaction vessel. The intensity of the mercury lamp and the quantum yields of the reactions were too low to permit the use of monochromatic light, except in a few extended experiments. The kinetics of the *n*-butane reaction were studied using a nickel sulphate-cobalt sulphate filter solution to cut out wavelengths > 3340 Å. Relative light absorption curves were determined under these conditions with the aid of a lagged thermopile placed behind the thermostat. A constant fraction of the beam fell on the thermopile and the E.M.F. developed was measured using the circuit described by Nagai and Goodeve.[2] Absolute quantum yields were determined actinometrically using the uranyl oxalate actinometer of Leighton and Forbes.[3] The stock actinometer solution was 0·05 M with respect to oxalic acid, and 0·01 M with respect to uranyl oxalate. The procedure was as follows: a weighed quantity of actinometric solution was placed in a 2-cm. quartz cell, identical with the reaction vessel, behind which it was suspended in close contact. Three separate illuminations of equal length were necessary in any one determination.

[1] Dainton and Ivin, *Trans. Faraday Soc.*, 1950, **46**, 374.

[2] Nagai and Goodeve, *ibid.*, 1931, **27**, 508.

[3] Leighton and Forbes, *J. Amer. Chem. Soc.*, 1930, **52**, 3139.

Firstly, with the reaction vessel empty and evacuated, secondly, with the reactants in the reaction vessel, and thirdly, after pumping out the residual gases. The last illumination was rendered necessary by the fact that the oil deposited on the front surface of the reaction vessel absorbed some of the incident radiation. The amount of this deposit would not be expected to increase indefinitely but should approach a limiting value as the droplets coalesce and fall to the bottom of the reaction vessel. However, for a small extent of reaction such as that occurring in the quantum yield determinations, it was assumed that the intensity of light absorbed by the reactants decreased linearly with time, and a simple average between the initial and final values taken. The total pressure of reactants was maintained approximately constant during the second exposure by periodic admission of reactants from a reservoir. The actinometer solution was estimated by titration of a weighed quantity with potassium permanganate solution. Corrections were made for the absence of stirring, and for reflection and absorption losses. One experiment was made with a rare gas (neon) mercury lamp.

The kinetics of the 1-butene reaction were determined using the full light of the mercury lamp. No direct measurements of the quantum yield were made but fairly reliable estimates were obtained by comparison of the rate with that of the *n*-butane reaction under the same conditions.

The effect of the following added substances on the rate of the *n*-butane reaction was studied: nitrogen, iodine, phenol, 1-butene, butadiene, benzene. Nitrogen was prepared by passing cylinder gas over strongly heated reduced copper, followed by passage over phosphorus pentoxide and through a liquid air trap. It was premixed with the reactants in the mixing vessel. In the case of iodine and phenol, some of the pure solid was introduced into the reaction vessel, which was then pumped out for a short time, some of the solid material being left at the end of pumping. The effect of these substances was thus studied at partial pressures approximately equal to their respective vapour pressures at the temperature of reaction. 1-Butene and butadiene were prepared as described previously;[1] the benzene used was A.R. grade and was distilled *in vacuo*.

Results

(i) THE LIGHT ABSORPTION CURVE for 2 cm. depth of gaseous sulphur dioxide is shown in Fig. 1. This cannot be expressed in the form of an exponential since the light absorbed is not monochromatic. Fig. 2 shows that addition of the transparent *n*-butane increases the absorptive power of sulphur dioxide at low pressures while at high pressures where absorption is already virtually complete, there is relatively little effect.

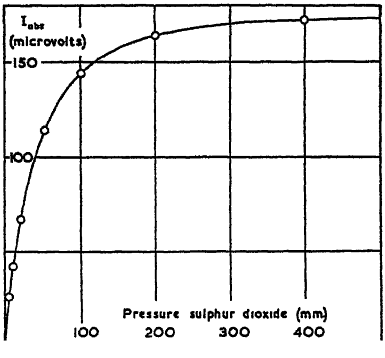

FIG. 1.—Absorption curve for sulphur dioxide. Hot mercury arc source, saturated $NiSO_4$—$CoSO_4$ filter (2 cm.). Path length 2 cm., $T = 25°$ C. $I_{abs.}$ measured in terms of microvolts generated on thermopile.

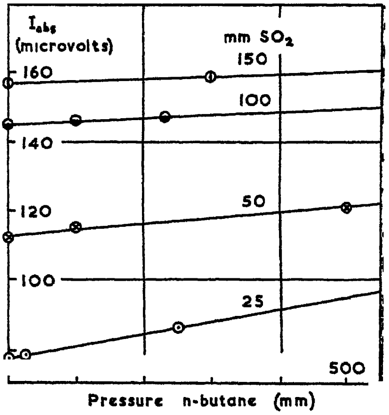

FIG. 2.—Effect of *n*-butane on absorption of light by sulphur dioxide. Hot mercury arc source, $NiSO_4$—$CoSO_4$ filter, $T = 24°$ C.

(ii) THE EFFECT OF INCIDENT LIGHT INTENSITY on the rate is the same for both reactions. Fig. 3 and 4 illustrate the first-power dependence in the two cases.

(iii) THE EFFECT OF PRESSURE on the initial rate for a constant reactant ratio is shown in Fig. 5. The decay of the rate with time in a given experiment was rather more rapid than Fig. 5 would indicate due to the accumulation of the product on the surface of the reaction vessel and the consequent reduction in incident intensity. This effect is even more pronounced in the 1-butene

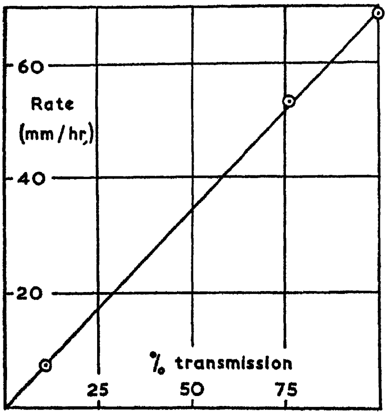

FIG. 3.—Effect of incident light intensity on initial rate of *n*-butane reaction. 204 mm. *n*-butane + 204 mm. sulphur dioxide, $T = 25°$ C. Percentage transmission refers to fraction of light passed by gauze filter.

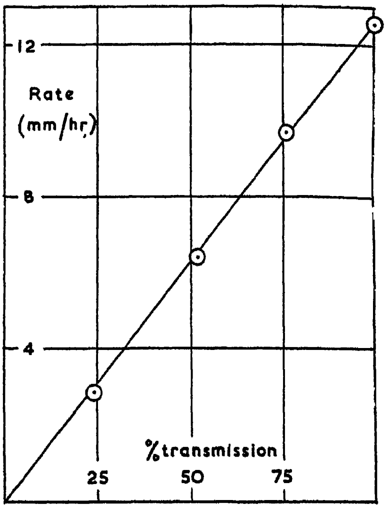

FIG. 4.—Effect of incident light intensity on 1-butene reaction. 6·5 mm. 1-butene + 65 mm. sulphur dioxide. Full mercury arc. $T = 24·3°$. Percentage transmission denotes fraction of light passed by gauze.

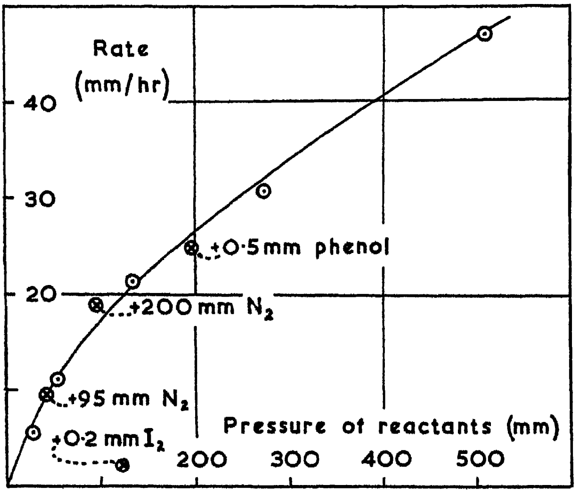

FIG. 5.—Effect of pressure on initial rate for a given reactant ratio. Effect of added amounts of nitrogen, phenol and iodine. $T = 25°$ C.

reaction.[1] A number of curves similar to that of Fig. 5 were obtained for different reactant ratios and from these the family of curves shown in Fig. 6 were constructed. Each curve represents the variation in rate with partial pressure of *n*-butane for a constant sulphur dioxide pressure. The intensity of light absorbed is not quite constant for each curve due to the slight pressure broadening effect (Fig. 2). On plotting log rate against log *n*-butane in Fig. 7, graphs are obtained which approximate to straight lines of slope 0·5 over their centre regions. Thus the order with respect to *n*-butane is fractional and decreases with increasing pressure of *n*-butane. It is also not very dependent on the sulphur dioxide pressure. The corresponding logarithmic plot for the 1-butene reaction is shown in Fig. 8. These measurements were made before the reaction with saturated hydrocarbons had been discovered and covered a restricted range of pressures. The plots approximate to parallel straight lines of slope 0·2 at low pressures of 1-butene. A later series of measurements was made over a wider pressure range at a somewhat lower light intensity (curve A) and it is seen that the order with respect to 1-butene increases appreciably at high pressures.

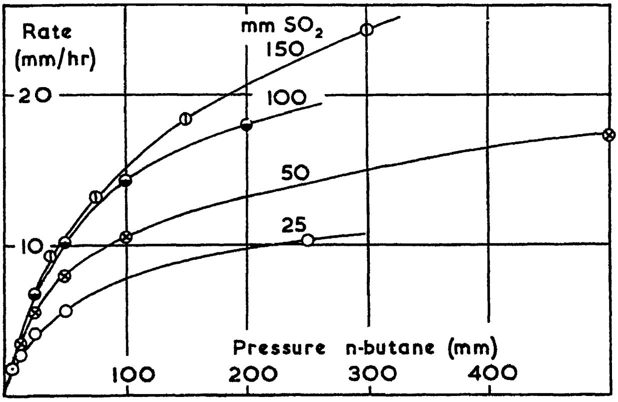

Fig. 6.—Effect of partial pressure of *n*-butane on initial rate. $T = 25°$ C.

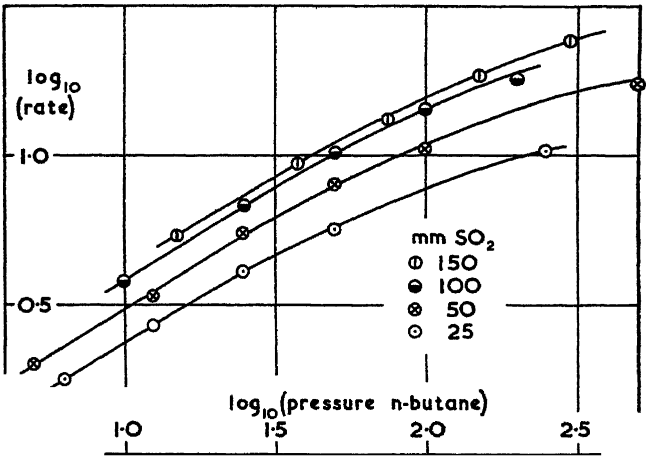

Fig. 7.—Effect of partial pressure of *n*-butane.

(iv) Quantum Yield Determinations and the Effect of Wave Lentgh.—In the initial stages of the investigation the effect of interposing various light filters was studied to find if there was any threshold wavelength above which reaction ceased. On irradiation of any mixture containing sulphur dioxide a small but reproducible initial pressure rise was always observed during the first few seconds. This was due to the conversion of the absorbed light into heat and the magnitude of the pressure rise formed a useful check on the amount of light absorbed. A smooth almost linear relation, shown in Fig. 9, was found to exist between the pressure rise and the subsequent rate of pressure fall for given pressures of reactants, irrespective of the method of variation of the incident light intensity and wavelength. This result indicates that the quantum yield is inversely proportional to the wavelength, and the data presented in the first three lines of Table I support this conclusion. Further, since the curve passes through the origin, light which is absorbed and causes a pressure rise

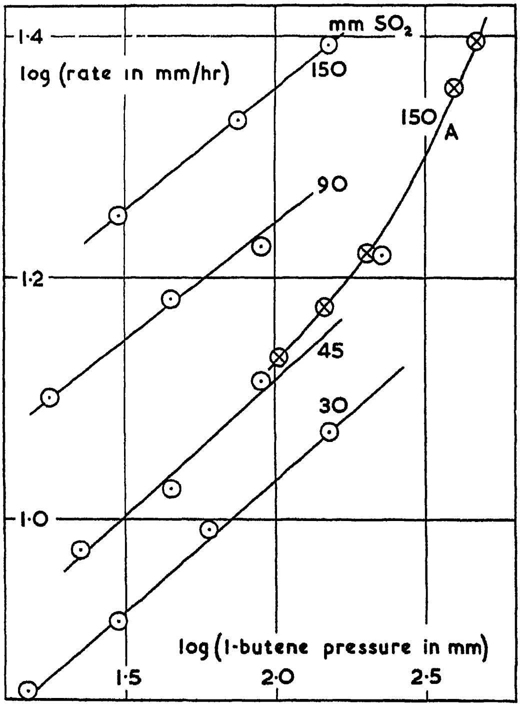

FIG. 8.—Effect of 1-butene and sulphur dioxide pressure on rate. Full mercury arc. Curve A, different intensity from other curves.

TABLE I

Light Source	Filters	Wave-length Å	Partial Pressures (mm.)		Quantum Yield	Rate (mm./hr.) / $I_{abs.}$ (μV)
			n-Butane	Sulphur Dioxide		
Hot Hg arc	$NiSO_4$—$CoSO_4$ K_2CrO_4	2967-3132	100	100	0·18 ±0·02	—
,,	$NiSO_4$—$CoSO_4$	2400-3132	100	100	0·19 ±0·02	0·095
Neon-Hg lamp	None	Mainly 2537	100	100	0·21 ±0·02	—
Hot Hg arc	$NiSO_4$—$CoSO_4$	2400-3132	200	100	0·26 ±0·03	0·12

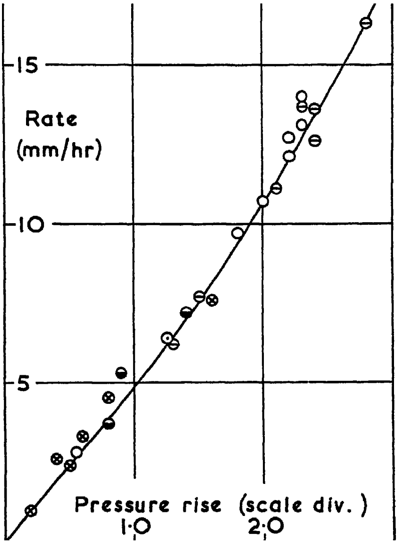

FIG. 9.—Relation between instantaneous pressure rise and subsequent rate on illumination of 65 mm. 1-butene + 65 mm. sulphur dioxide, $T = 25°$ C. 1 mm. = 3·21 scale division.

○ Light intensity varied by screens.
⊖ Voltage across lamp varied.
⊕ Filter solutions in beam.
◒ Film formed during reaction as filter.

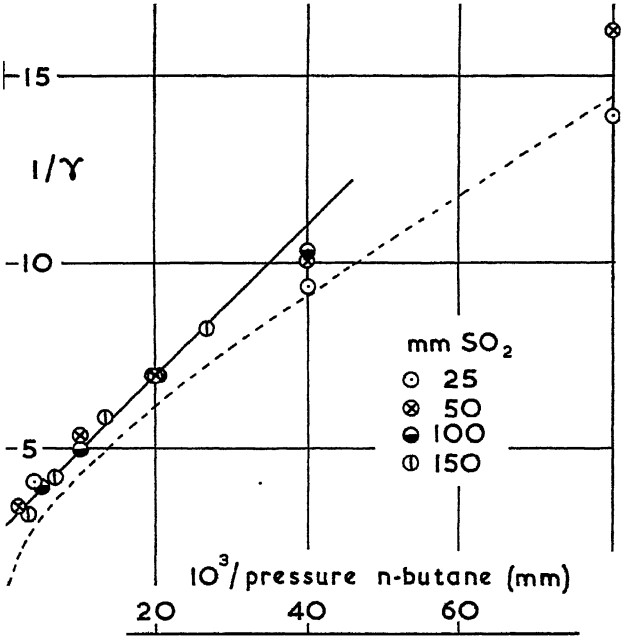

FIG. 10.—Relation between quantum yield and partial pressure of *n*-butane. $T = 25°$ C. Broken curve plotted from $1/\gamma = 1 + 23[RH]^{-0.5} + 87[RH]^{-1}$.

also causes some reaction and there can be no threshold wavelength for the reaction within the region of strong absorption of sulphur dioxide, i.e. wavelengths < 3200 A.

The results of four quantum yield determinations on the *n*-butane reaction are summarized in Table I.

The first three results indicate that for given pressures of reactants, the quantum yield is only slightly dependent on wavelength within the 10 % experimental error. The data which have been plotted in Fig. 2 and 6 may be used to calculate quantum yields on an arbitrary scale of mm. hr.$^{-1}$ μV^{-1}. The factor to convert these figures to absolute values is obtained from the second and fourth results in Table I and is 1 mm. hr.$^{-1}$ μV^{-1} = 2·05 molecules/quantum. The reciprocals of the absolute quantum yields so obtained are plotted in Fig. 10 against the reciprocal of the partial pressure of *n*-butane. The quantum yield is practically independent of sulphur dioxide pressure and a limiting quantum yield of 0·35 is attained at high pressures of *n*-butane.

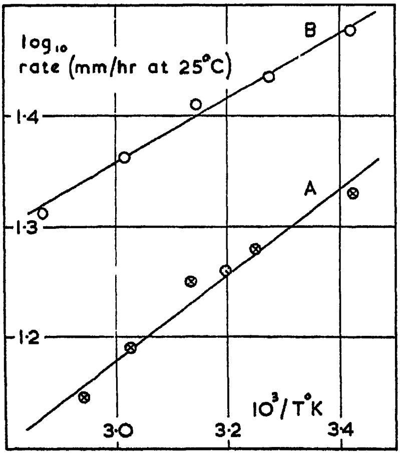

FIG. 11.—Effect of temperature on *n*-butane reaction.
A : 75 mm. *n*-butane + 75 mm. sulphur dioxide. $E = -1740 \pm 120$.
B : 150 mm. *n*-butane + 75 mm. sulphur dioxide. $E = -1380 \pm 100$.
(Pressures and rates corrected to 25° C; E in cal./mole)).

TABLE II

Hydrocarbon	% Hydrocarbon	Total Pressure (mm. at 25° C)	Temp. Range °C	No. of Points	$-E$ cal./mole
n-Butane (filtered light)	50	150	19-67	6	1740 ± 120
	50	300	19-76	5	1380 ± 100
1-Butene (unfiltered light)	50	130	24-100	3	1430 ± 250
	48	130	15-62	5	1700 ± 230*
	48	300	15-81	6	1000 ± 50

* This and the preceding set of measurements were made at different times and with different light intensities.

(v) EFFECT OF TEMPERATURE ON RATE.—No significant change in the amount of light absorbed by a given concentration of sulphur dioxide was detected between 10-100° C. The changes in rate are, therefore, to be attributed to changes in the velocity constants of the various processes. The results for an equimolar mixture of *n*-butane and SO_2 at concentrations corresponding to 150 mm. and 300 mm. respectively reduced to 25° C, are plotted in Fig. 11. Similar results were obtained for the 1-butene reaction. The apparent energies of activation obtained from the slopes of the log rate—1/T curves are summarized in Table II.

(vi) EFFECT OF ADDED SUBSTANCES ON THE *n*-BUTANE REACTION.—Nitrogen and phenol are without appreciable effect whereas iodine (see Fig. 5), 1-butene, butadiene and benzene (Fig. 12) exerted a marked retardation. It has previously been noted that 1-butene and butadiene affect the reaction by quenching the excited sulphur dioxide molecules and the same is equally true for iodine and benzene. The possibility that iodine retards the reaction by removing intermediate alkyl radicals is ruled out by the low quantum yield (which renders a chain mechanism improbable).

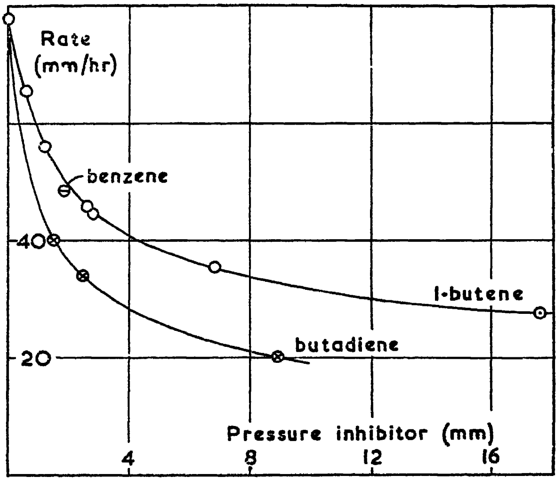

FIG. 12.—Retardation of *n*-butane reaction at 25° C.
150 mm. *n*-butane + 150 mm. sulphur dioxide + x mm. inhibitor.
Full mercury arc.

Discussion

The Mechanism of the Uninhibited *n*-Butane Reaction.—The relatively slight dependence of the quantum yield on wavelength indicates that the mechanism of reaction also does not change with wavelength, i.e. over the experimental range of 2400-3340 Å. The initial act is undoubtedly the excitation of a sulphur dioxide molecule, probably in a diradical state. Sulphur dioxide exhibits an apparent predissociation in the region of 2800 Å, which was at first supposed by Henri [4] to be a true predissociation. However, his estimate of the dissociation energy ($SO_2 \rightarrow SO + O$) was based on an incorrect value for the dissociation energy of SO and more accurate measurements by Martin [5] lead to a value of 136 ± 2 kcal./mole, corresponding to a wavelength of 2100 Å. While some of the quantities involved in this computation remain uncertain,[6] it seems improbable that direct dissociation of sulphur dioxide occurs under the conditions of our experiments and the slight photodecomposition of sulphur dioxide which was observed even with wavelengths > 3000 Å must be due to processes such as

$$SO_2^* + SO_2 \rightarrow SO_3 + SO.$$

Such side reactions are negligible in the *n*-butane reaction, except in mixtures rich in sulphur dioxide.[1]

---

[4] Henri, *Leipsiger Vorträge*, 1931, 131.

[5] Martin, *Physic. Rev.*, 1932, 41, 167.

[6] Gaydon, *Dissociation Energies and Spectra of Diatomic Molecules* (Chapman and Hall), 1947.

Price and Simpson[7] have suggested that absorption in the wave length region 2600-3400 Å causes excitation of a lone pair non-bonding $2p_0$ electron of one of the oxygen atoms into an anti-bonding orbital. The initial formation of a diradical in the polysulphone reaction (see later paper) and the formation of C—S rather than C—O links in all reactions between sulphur dioxide and hydrocarbons induced by light, are more easily accounted for if the excited sulphur dioxide molecule is regarded as reacting in the chemical form $O{=}\dot{S}{=}O$. The diradical formed in polymerization initiation would then be

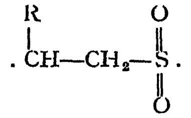

$$\cdot\overset{\overset{\mathrm{R}}{|}}{\mathrm{C}}\mathrm{H}-\mathrm{CH_2}-\underset{\underset{\mathrm{O}}{\|}}{\overset{\overset{\mathrm{O}}{\|}}{\mathrm{S}}}\cdot$$

and the sulphbinic acids formed by enolization reactions such as

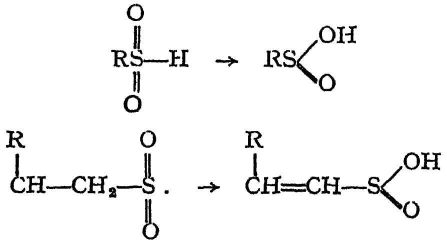

The simplest mechanism which may be written is as follows :

$$SO_2 + h\nu \rightarrow SO_2^* \quad . \quad . \quad . \quad . \quad . \quad . \quad (1)$$
$$SO_2^* + RH \rightarrow RSO_2H \quad (R = C_4H_9) \quad . \quad . \quad (2)$$
$$SO_2^* + RH \rightarrow SO_2 + RH \quad . \quad . \quad . \quad . \quad (3)$$
$$SO_2^* + SO_2 \rightarrow SO_2 + SO_2 \quad . \quad . \quad . \quad . \quad (3')$$
$$SO_2^* \rightarrow SO_2, \quad . \quad . \quad . \quad . \quad . \quad . \quad (4)$$

where SO_2^* represents the excited sulphur dioxide molecule. Steps (3) and (3′) are quenching processes and step (4) is the process of internal deactivation. Fluorescence in sulphur dioxide has only been observed below 2100 Å.[8] Assuming a stationary concentration of excited sulphur dioxide molecules, this mechanism leads to the following expression for the quantum yield γ :

$$\gamma = \frac{k_2\,[RH]}{(k_2 + k_3)\,[RH] + k_{3'}\,[SO_2] + k_4}, \quad . \quad . \quad (1)$$

the k's being the velocity constants of the various processes. Since it is found experimentally that the quantum yield is independent of the sulphur dioxide pressure (Fig. 10), $k_{3'}$ $[SO_2]$ may be neglected and eqn. (1) may be written

$$1/\gamma = 1 + k_3/k_2 + k_4/k_2\,[RH]. \quad . \quad . \quad . \quad (2)$$

This equation correctly predicts an intensity exponent of unity, a fractional order dependence on *n*-butane pressure, and a linear relation between $1/\gamma$ and $1/[RH]$. The deviations at low pressures of *n*-butane may be attributed to the side reactions. From the slope and intercept in Fig. 10 we have at 25° C

$$k_3/k_2 = 1{\cdot}9 \pm 0{\cdot}2,$$
$$k_4/k_2 = 207 \pm 17 \text{ mm.} = 0{\cdot}011 \pm 0{\cdot}001 \text{ mole/l.}$$

---

[7] Price and Simpson, *Proc. Roy. Soc. A*, 1938, **165**, 272.

[8] Lotmar, *Z. Physik.*, 1933, **83**, 765.

Mechanism of *n*-Butane Reaction Retarded by 1-Butene or Butadiene.—In the presence of small pressures of inhibitor B, we have the additional quenching process

$$SO_2^* + B \rightarrow SO_2 + B. \quad . \quad . \quad . \quad . \quad (5)$$

At low pressures of inhibitor, the corresponding substitution reaction may be neglected and the expression for the rate then becomes

$$\text{Rate} = \frac{k_2[\text{RH}]I_{\text{abs.}}}{(k_2 + k_3)[\text{RH}] + k_4 + k_5[\text{B}]} . \quad . \quad . \quad (3)$$

For a constant pressure of *n*-butane and sulphur dioxide, this expression reduces to

$$\frac{1}{\text{Rate}} - \frac{1}{\text{Rate}_0} = a[\text{B}], \quad . \quad . \quad . \quad . \quad . \quad (4)$$

where $a = k_5/k_2[\text{RH}]I_{\text{abs.}}$ and Rate_0 = rate for [B] = 0. On plotting the left-hand side of eqn. (4) against the inhibitor pressure, as in Fig. 13, it is found that the linear relation only holds at the lowest pressures, and considerable deviations occur above 1·5 mm. From the limiting slopes (as the inhibitor pressure tends to zero) values of k_5/k_2 may be deduced taking the quantum yield as 0·24 for [B] = 0. For 1-butene, k_5/k_2 = 210 and for butadiene 420. The relative quenching efficiencies *at low pressures* of *n*-butane, 1-butene and butadiene are thus 1·9/210/420. At inhibitor pressures above 1·5 mm. the rate is greater than expected. The reason for this is not clear. The pressures are too low for the substitution of the inhibitor to be important and the intensity of light absorbed cannot be appreciably affected. Similar results were obtained with 1-butene using a $NiSO_4$—$CoSO_4$ filter. Here no change in the intensity of light absorbed could be detected. The apparent explanation of the phenomenon is that the quenching efficiency of the inhibitors decreases with increasing pressure. This is contrary to the usual assumption that the quenching diameter of a gas is independent of pressure. Stuart's[9] data on the quenching of mercury resonance radiation showed deviations from the

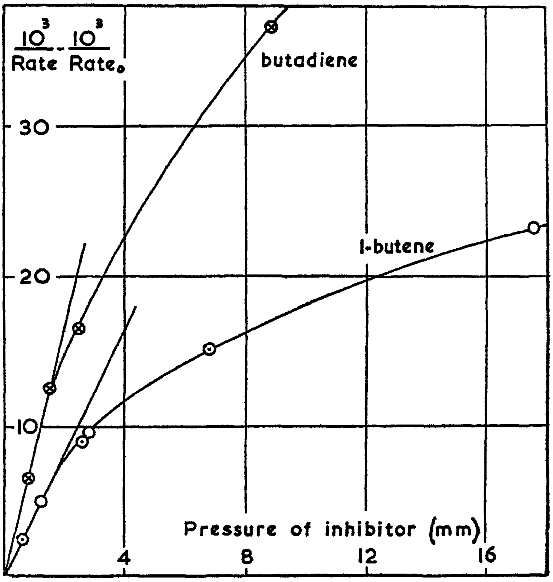

FIG. 13.—Retardation of *n*-butane reaction at 25° C.

---

[9] Stuart, *Z. Physik.*, 1925, **32**, 262.

simple laws which were at first attributed by Zemansky[10] to a variation in the quenching efficiency of the gas with pressure p. He computed that for a number of gases, the quenching rate was proportional to $p^{0\cdot 6}$. However, Zemansky subsequently considered that other explanations such as pressure broadening and diffusion of metastable mercury atoms to the walls, accounted better for Stuart's results. In the present system, pressure broadening effects are small and the absence of any effect of an inert gas on the rate shows that there are no important wall reactions. Hence it must be concluded that the quenching efficiencies of 1-butene and butadiene decrease with increasing pressure. The question arises as to whether a similar effect occurs with *n*-butane. Such an effect would make the graph of $1/\gamma$ against $1/[RH]$ concave towards the $1/[RH]$ axis. Inspection of Fig. 10 shows that a curve of this type can be drawn through the experimental points at least as well as a straight line. A plot of the curves of Fig. 13 on logarithmic scales shows that at the higher pressures of inhibitors, the quenching rate is approximately proportional to $[B]^{0\cdot 5}$. Let us assume that this relation also holds for *n*-butane ; eqn. (2) is then modified to

$$1/\gamma = 1 + \frac{k_3}{k_2}[RH]^{-0\cdot 5} + \frac{k_4}{k_2}[RH]^{-1}. \quad . \quad . \quad . \quad (5)$$

From the values of the rates at a constant partial pressure (150 mm.) of sulphur dioxide and three partial pressures (75, 150, 300 mm.) of *n*-butane respectively, it is possible to obtain the values of k_3/k_2 and k_4/k_2 in eqn. (5). From the data indicated, the equation

$$1/\gamma = 1 + 23[RH]^{-0\cdot 5} + 87[RH]^{-1} \quad . \quad . \quad . \quad (6)$$

was deduced, without reference to thermopile or actinometric measurements. This equation is plotted in Fig. 10 (broken curve) and it may be seen that while the calculated values of $1/\gamma$ are somewhat low, the general shape of the curve is correct, and adjustment of the constants and the exponent $-0\cdot 5$ in eqn. (6) would allow a better fit to be made.

Enough has been stated to indicate the complexity of the reactions between sulphur dioxide and hydrocarbons in the gas phase. The values of the velocity constant ratios must be accepted with reserve until more is known of the quenching processes involved in these reactions.

The apparent negative energy of activation requires comment. The molecules of butyl sulphinic acid when first formed possess a considerable excess of energy. It is possible that the excited molecules may re-dissociate unless stabilized by collision with other molecules. However, there are several objections to such an explanation. (i) The butyl sulphinic acid molecule is complex and any excess energy would be rapidly distributed between the many degrees of freedom. (ii) The product itself is quite stable to ultraviolet light. (iii) Kinetic treatment of the assumption leads to an expression which requires that

$$\text{rate} \propto (\text{total pressure})^2$$

at low pressures for a given reactant ratio. This is not in accordance with the experimental results. A second possibility is suggested by the analogy with gas-phase vinyl polymerizations. In these systems the apparent negative energies of activation have been attributed to adsorption effects. However, in the present case, there is no dark reaction and the solubility of the reactants in the product is also too small to account for the observed effect. A further possibility is that the velocity constants k_3 and k_4 are appreciably temperature dependent. Writing eqn. (2) in the form

$$\gamma = \frac{k_2}{k_2 + k_3 + k_4/[RH]} \quad . \quad . \quad . \quad . \quad (7)$$

---

[10] Mitchell and Zemansky, *Resonance Radiation and Excited Atoms* (Camb. Univ. Press, 1934).

then if k_3 is the most temperature dependent term in the denominator, increase of pressure will diminish the importance of the last term and the overall energy of activation will increase numerically. On the other hand, if k_4 is the most temperature dependent term, increase of pressure will result in decrease in the numerical value of the energy of activation. The latter is in accord with the observations, therefore it appears that the process of internal deactivation of an excited sulphur dioxide molecule is facilitated by an increase in temperature. In order to give an apparent negative energy of activation of 1740 cal./mole, E_4 must be somewhat greater than this value. In a diatomic molecule the process of internal deactivation involves the crossing of the potential energy curves of the excited and normal molecules. In polyatomic molecules such as sulphur dioxide, the simple curves are replaced by complex hyperfaces and internal deactivation becomes much more probable. As the temperature is raised, the average rotational and vibrational energy of the molecules in the lower state is raised and it is possible that the transitions which occur on absorption of light then result in a greater proportion of excited molecules near the cross-over points, so reducing the mean lifetime of the excited state and increasing k_4. This explanation of the temperature coefficient must be regarded as tentative and is only advanced in the absence of a more satisfactory solution.

An approximate estimate of the normal life-time τ of the excited sulphur dioxide molecule at 25° C may be made from eqn. (7), assuming τ to be the interval between collisions when $k_2 + k_3 = k_4/[\mathrm{RH}]$, i.e. when half the excited molecules disappear by collision processes. Taking the mean collision diameter as 3×10^{-8} cm., we may calculate the value of $\tau = 0{\cdot}3 \times 10^{-8}$ sec. It should be mentioned that if an equation of type (6) is adopted, a considerably larger value of τ is obtained.

Finally, it is of interest to note that collisions between normal and excited sulphur dioxide molecules do not generally result in quenching. Hence when sulphur dioxide is illuminated alone, most of the absorbed energy is converted into heat by internal deactivation of the excited molecules.

The Mechanism of the 1-Butene Reaction.—The possible steps in the reaction are :

$$\mathrm{SO_2} + h\nu \rightarrow \mathrm{SO_2}^* \qquad (1)$$

$$\mathrm{SO_2}^* \rightarrow \mathrm{SO_2} \qquad (4)$$

$$\mathrm{SO_2}^* + \mathrm{B} \rightarrow \mathrm{SO_2} + \mathrm{B} \qquad (5)$$

$$\mathrm{SO_2}^* + \mathrm{B} \rightarrow \mathrm{BSO_2} \qquad (6)$$

(B = 1-butene). The numbering of the steps is the same as in the n-butane reaction. By analogy with the n-butane reaction we have

$$\gamma = \frac{k_6[\mathrm{B}]}{(k_6 + k_5)[\mathrm{B}] + k_4} \qquad (8)$$

From the experiments on the inhibition of the n-butane reaction by 1-butene it is known that $k_5 \gg k_{3'}$. If, as is likely, $(k_5 + k_6) > (k_3 + k_2)$ the order with respect to the hydrocarbon will be smaller in the 1-butene reaction than in the n-butane reaction. This is true at low pressures. On increasing the pressure, the order with respect to 1-butene increases instead of decreasing as required by eqn. (8). This may be due to the falling away of the quenching efficiency of 1-butene at high pressures referred to in the previous section. Pressure broadening effects may also become important at high pressures of 1-butene due to the use of unfiltered light. The results in curve A of Fig. 8 may be expressed in the form

$$1/\mathrm{Rate} = 0{\cdot}026 + 7{\cdot}0/[\mathrm{B}] \qquad (9)$$

for [B] = 200 to 500 mm. Comparison of the rates of the 1-butene and *n*-butane reactions for 150 mm. hydrocarbon and 150 mm. sulphur dioxide (intensity of absorbed light assumed the same) gives

$$1/\gamma = 1 + 7 \cdot 4 + 2250/[\mathrm{B}]. \qquad (10)$$

Comparison of the constants of this equation with those of eqn (7) gives the ratio of quenching abilities of *n*-butane and 1-butene as

$$\frac{k_3}{k_5} = \frac{k_3k_2k_4k_6}{k_2k_4k_6k_5},$$
$$= \frac{1 \cdot 9}{207} \times \frac{2250}{7 \cdot 4} = 2 \cdot 8$$

This is contrary to the inhibition experiments. Hence no physical meaning can be ascribed to the constants in eqn. (10) and the linear relationship is fortuitous. This was to be expected from the foregoing discussion and further emphasizes the complexity of the system.

The explanation advanced to account for the apparent negative energy of activation or the *n*-butane reaction may again be put forward for the 1-butene reaction. Since $k_5 > k_3$, the term in [B] in the denominator of eqn. (8) is probably greater than the corresponding term in [RH] in eqn. (1). This reduces the effect of any variation of k_4 with temperature and the smaller numerical value of the energy of activation in the case of the 1-butene reaction (at a given pressure) is in accordance with this.

One of us (K. J. I.) is indebted to the D.S.I.R. for a maintenance grant during the period in which this work was carried out (1945-1948). We also wish to express our thanks to the Chemical and Royal Society for assistance in the purchase of apparatus.

Department of Physical Chemistry,
University of Cambridge,
Free School Lane,
Cambridge.

SOME DEVELOPMENTS OF GUGGENHEIM'S SIMPLIFIED PROCEDURE FOR COMPUTING ELECTRIC DIPOLE MOMENTS

BY J. W. SMITH

Received 1*st November*, 1949

Based on the treatment suggested by Guggenheim, a method has been devised which permits the calculation of the apparent orientation polarization and dipole moment of a polar solute in a non-polar solvent without the necessity of measuring the densities of the solutions. For aniline in various solvents the results are within 0·15 cm.^{3} and 0·002 D, respectively, of the values derived from the same data by the conventional method. A slight modification of Guggenheim's "further simplification" also leads to results which differ little from those deduced by the usual method except when the value of the dielectric constant of the solvent differs considerably from the square of its refractive index.

An interesting alternative to the usual method for computing dipole moments from dielectric constant, density, and refractive index measurements on dilute solutions of polar solutes in non-polar solvents has been suggested recently by Guggenheim.[1] He has pointed out that the usual formulae on which the dipole moments are calculated can be written in a form which, when expressed in the conventional terminology instead of the system used by him becomes

$$\frac{\epsilon_{12}-1}{\epsilon_{12}+2}-\frac{n_{12}^2-1}{n_{12}^2+2}\Big)=\Big(\frac{\epsilon_1-1}{\epsilon_1+2}-\frac{n_1^2-1}{n_1^2+2}\Big)+(P_{2A}-P'_{2A}+P_{2\mu})c_2, \quad (1)$$

where c_2 is the concentration of solute in moles per cm.^{3}, P_{2A} is the true atomic polarization of the solute, and P'_{2A} the value it would have if the atomic polarizations of the solute and solvent were in the ratio of their molar volumes, the other symbols having their usual significance. It follows, therefore, that if the quantity

$$D_{12}=\Big(\frac{\epsilon_{12}-1}{\epsilon_{12}+2}-\frac{n_{12}^2-1}{n_{12}^2+2}\Big)$$

is plotted against c_2, the initial slope gives the value of $P_{2A}-P'_{2A}+P_{2\mu}$. Guggenheim suggests that, in the absence of definite information regarding P_{2A} it is reasonable to suppose that $P_{2A}=P'_{2A}$, an assumption which permits the direct evaluation of $P_{2\mu}$, and thence of the dipole moment μ, by the relation

$$P_{2\mu}=\lim_{(c_2=0)}\partial D_{12}/\partial c_2. \quad . \quad . \quad . \quad . \quad (2)$$

As a further simplification, he shows that if $\epsilon_{12}-n_{12}^2$ is plotted against c_2, the initial slope gives approximately the value of

$$\frac{(\epsilon_1+2)(n_1^2+2)}{3}(P_{2A}-P'_{2A}+P_{2\mu}),$$

or, if it is assumed that

$$=P'_{2A},$$

the value of

$$(\epsilon_1+2)(n_1^2+2)P_{2\mu}/3.$$

Hence

$$P_{2\mu}=\frac{3\lim_{(c_2=0)}\partial(\epsilon_{12}-n_{12}^2)/\partial c_2}{(\epsilon_1+2)(n_1^2+2)}. \quad . \quad . \quad . \quad (3)$$

Developments of the Procedure.—One of the advantages of Guggenheim's approach is that the density values for the solutions are used only to compute c_2, and therefore need to be accurate only to about 1 %. He also points out that the values of c_2 are no more trouble to compute than the molar fractions. The solutions, however, are usually made up by weight, and hence the simplest form in which to express the concentration is the weight fraction w_2 of solute. Now this is related to c_2 by the expression

$$c_2=w_2/M_2v_{12},$$

where M_2 is the molecular weight of the solute and v_{12} the specific volume of the solution, and hence eqn. (1) can be written

$$D_{12}=D_1+(P_{2A}-P'_{2A}+P_{2\mu})w_2/M_2v_{12}. \quad . \quad . \quad . \quad (4)$$

Therefore, if D_{12} is plotted against w_2 the initial slope has the value

$$(P_{2A}-P'_{2A}+P_{2\mu})/M_2v_1,$$

which, if it be assumed that

$$P_{2A}=P'_{2A}$$

becomes

$$P_{2\mu}/M_2v_1,$$

and hence

$$P_{2\mu}=M_2v_1\,(\lim_{(w_2=0)}\partial D_{12}/\partial w_{12}) \quad . \quad . \quad . \quad . \quad (5)$$

---

[1] Guggenheim, *Trans. Faraday Soc.*, 1949, **45**, 714.

By utilizing this modification of Guggenheim's method, therefore, a value of the dipole moment of the solute molecule may be derived without the necessity of knowing the densities of the solutions.

Also since

$$\frac{\partial}{\partial w_2}\left(\frac{\epsilon_{12}-1}{\epsilon_{12}+2}-\frac{n_{12}^2-1}{n_{12}^2+2}\right)=\frac{3}{(\epsilon_{12}+2)^2}\cdot\frac{\partial\epsilon_{12}}{\partial w_2}-\frac{3}{(n_{12}^2+2)^2}\cdot\frac{\partial n_{12}^2}{\partial w_2},$$

an alternative approach is to determine the limiting values at infinite dilution of $\partial\epsilon_{12}/\partial w_2$ and $\partial n_{12}^2/\partial w_2$, say α and ν, respectively,[2] when $P_{2\mu}$ is given by

$$P_{2\mu}=3M_2v_1\left(\frac{\alpha}{(\epsilon_1+2)^2}-\frac{\nu}{(n_1^2+2)^2}\right). \quad . \quad . \quad . \quad (6)$$

This expression also follows directly from the usual relationships

$$P_{2E}+P_{2A}+P_{2\mu}=M_2\left\{\frac{3\alpha v_1}{(\epsilon_1+2)^2}+\frac{\epsilon_1-1}{\epsilon_1+2}(v_1+\beta)\right\},$$

and
$$P_{2E}=M_2\left\{\frac{3\nu v_1}{(n_1^2+2)^2}+\frac{n_1^2-1}{n_1^2+2}(v_1+\beta)\right\},$$

where β is the limiting value of $\partial v_{12}/\partial w_2$ when $w_2=0$, by assuming that

$$P_{2A}=M_2(v_1+\beta)\left(\frac{\epsilon_1-1}{\epsilon_1+2}-\frac{n_1^2-1}{n_1^2+2}\right),\text{ i.e. }P_{2A}=P'_{2A}.$$

The use of eqn. (6) involves less calculation than is required for the application of eqn. (2) or (5). Furthermore if there is a considerable error in one of the individual measurements of ϵ or of n this becomes more readily apparent by this method and it can be ignored in computing the values of α and ν.

The "Further Simplification".—Weight fractions can also be substituted for molar concentrations in Guggenheim's further simplification, when we obtain the expression

$$P_{2\mu}=3M_2v_1\,.\,\frac{\lim_{(w_2=0)}\partial(\epsilon_{12}-n_{12}^2)/\partial w_2}{(\epsilon_1+2)(n_1^2+2)} \quad . \quad . \quad . \quad (7)$$

It was pointed out by Guggenheim,[3] however, that this simplification implies the use of the term

$$\frac{\partial\epsilon_{12}}{\partial c_2}-\frac{\partial n_{12}^2}{\partial c_2}$$

instead of

$$\frac{\partial\epsilon_{12}}{\partial c_2}\left(1-\frac{\epsilon_1-n_1^2}{\epsilon_1+2}\right)-\frac{\partial n_{12}^2}{\partial c_2}\left(1-\frac{\epsilon_1-n_1^2}{n_1^2+2}\right).$$

As the second term in this expression is, for polar solutes, smaller than the first, no great error should be introduced by writing this as

$$\left(\frac{\partial\epsilon_{12}}{\partial c_2}-\frac{\partial n_{12}^2}{\partial c_2}\right)\left(1-\frac{\epsilon_1-n_1^2}{\epsilon_1+2}\right)\text{ or }\frac{\partial(\epsilon_{12}-n_{12}^2)}{\partial c_2}\,.\,\frac{n_1^2+2}{\epsilon_1+2}.$$

With this modification, eqn. (3) and (7) become, respectively,

$$P_{2\mu}=\frac{3\lim_{(c_2=0)}\partial(\epsilon_{12}-n_{12}^2)/\partial c_2}{(\epsilon_1+2)^2}, \quad . \quad . \quad . \quad . \quad (8)$$

and

$$P_{2\mu}=3M_2v_1\,.\,\frac{\lim_{(w_2=0)}\partial(\epsilon_{12}-n_{12}^2)/\partial w_2}{(\epsilon_1+2)^2}. \quad . \quad . \quad . \quad (9)$$

---

[2] Cf. Smith and Cleverdon, *Trans. Faraday Soc.*, 1949, **45**, 109.

[3] *Loc. cit.*, p. 716, footnote.

Eqn. (9) differs from (6) only in that $1/(\epsilon_1 + 2)^2$ has been substituted for $1/(n_1^2 + 2)^2$ in the second term. For a solvent of dielectric constant approximately 2, the maximum difference between ϵ_1 and n_1^2 is about 0·18; hence the error introduced in the second term as a result of this substitution is not greater than 9 %. Further, as this second term is generally only about one-tenth the value of the first, the whole result should be less than 1 % in error. For the same case the error arising from the use of eqn. (3) would be 4·5 %.

Application to Experimental Results.—Since the absolute values of the results obtained by the Guggenheim treatment are dependent upon the relative values of ϵ_1 and n_1^2 for the solvent, it is of interest to compare the values of P_μ and μ derived by these methods with those deduced by the more conventional procedure from experimental data for one solute in a series of different solvents. A suitable group of data is provided by the results recorded previously[4] for solutions of aniline in benzene, 1 : 4-dioxan, carbon tetrachloride, and n-heptane, a group of solvents of widely differing $\epsilon_1 - n_1^2$ values. From these results the values of the apparent dipole moment of aniline in the various solvents have been computed by Guggenheim's more exact and simplified methods and also by the various modifications here discussed. In Table I the values of $P_{2\mu}$ and of μ obtained by the various methods are compared with the results obtained by the more conventional procedure firstly without correction for P_A and secondly with the assumption that

$$P_{2E} + P_{2A} = 1{\cdot}05[R_D].$$

TABLE I.—ORIENTATION POLARIZATION AND APPARENT DIPOLE MOMENT OF ANILINE CALCULATED BY VARIOUS METHODS

Method	Solvent							
	Benzene		Dioxan		Carbon Tetrachloride		n-Heptane	
	P_μ cm.³	μ (D)	P_μ cm.³	μ (D)	P_μ cm.³	μ (D)	P_μ cm.³	μ (D)
Conventional								
Neglecting P_A .	47·65	1·528	64·19	1·773	44·90	1·484	46·10	1·504
$P_A = 0{\cdot}05$ [R_D] .	46·12	1·505	62·64	1·753	43·34	1·458	44·55	1·477
More exact methods								
G. 1 (Eqn. (2)) .	47·46	1·526	61·07	1·731	43·34	1·458	45·93	1·501
M.G. 1 (Eqn. (5))	47·40	1·525	61·06	1·731	43·38	1·459	46·05	1·503
M.G. 2 (Eqn. (6)	47·20	1·522	61·15	1·732	43·31	1·459	46·14	1·505
Simplified methods								
G. 2 (Eqn. (3)) .	47·69	1·529	64·86	1·784	44·82	1·483	46·03	1·503
M.G. 3 (Eqn. (7))	47·60	1·527	64·88	1·784	44·80	1·483	46·00	1·502
M.G. 4 (Eqn. (8))	47·35	1·524	61·96	1·743	43·75	1·465	46·15	1·505
M.G. 5 (Eqn. (9))	47·26	1·523	61·89	1·743	43·73	1·465	46·11	1·505

The derived data upon which the computations are based are shown in Table II, where the original methods detailed by Guggenheim are indicated by the prefix G. and the various modifications of Guggenheim's procedure by the prefix M.G.

As is to be expected, the methods M.G. 1, 2, 3, and 5, involving the use of weight fractions, lead to substantially the same results as the corresponding methods G. 1 and 2, and M.G. 4, in which molar concentrations are used in the computations, thus showing that, in so far as these methods are applicable, the density values of the solutions are not required for the calculation if the density of the pure solvent is known.

---

[4] Few and Smith, *J. Chem. Soc.*, 1949, 753.

The simplified procedures lead to values of P_μ and μ close to those derived by the more exact methods for solutions in benzene and *n*-heptane, but to much higher results for carbon tetrachloride and particularly for dioxan solutions; the amended equations for the simplified treatment (M.G. 4 and 5) lead to improvement of the agreement.

The values of P_μ and μ obtained for carbon tetrachloride solutions by the more exact treatments are very close to the results from the more conventional method, but for benzene and *n*-heptane solutions the values are higher, and for dioxan solutions are lower, than those obtained by the usual method. This difference is associated with the vexed question of the allowance which has been made for atomic polarization. Doubtless if one could only obtain data for the refractive index at infinite wavelength Guggenheim's assumption that $P_{2A} = P'_{2A}$ would be as good as any, in the absence of any direct data. However, the custom of measuring the refractive index for visible light leads to some anomalies; thus the values which have actually been assumed for the atomic polarization of aniline in these calculations range from 3·04 cm.^{3} in dioxan to $-$ 0·17 cm.^{3} in *n*-heptane. It is evident that so long as one is concerned only with the comparison of the moments of various solutes in one solvent Guggenheim's assumption is satisfactory, but that for the comparison of the apparent moments in different solvents the allowances for atomic polarization should be placed on a parallel basis. It is a factor which should not be ignored completely, and whilst the custom of assuming that $P_{2A} = 1{\cdot}05 P_{2E}$ is far from satisfactory, there is no better alternative in the present instance where the true value of P_{2A} is unknown.

TABLE II.—DERIVED POLARIZATION DATA FOR ANILINE IN VARIOUS SOLVENTS

	Solvent			
	Benzene	Dioxan	Carbon Tetrachloride	*n*-Heptane
lim $\partial D/\partial w_2$	0·4448	0·6740	0·7380	0·3360
a	2·933	4·520	5·030	2·050
ν	0·236	0·496	0·605	0·336
lim $\partial(\epsilon_{12} - n_{12}^2)/\partial c_2$	2881	3650	2606	2351
lim $\partial(\epsilon_{12} - n_{12}^2)/\partial w_2$	2·700	4·025	4·428	1·710
P'_{2A} (calc.)	0·425	3·038	1·585	$-$ 0·165
$P_{2A} - P'_{2A}$	1·11	$-$ 1·50	$-$ 0·05	1·70

Correction for Atomic Polarization.—It was suggested by Guggenheim that his method could still be used even if a different estimate of P_{2A}, such as a specified fraction of P_{2E}, were taken. Without measurements of the densities of the solutions, the actual value P'_{2A} which has been tacitly assumed cannot be calculated exactly, since the partial molar volume of the solute is not the same as its molar volume in the pure liquid state. As the term is small, however, an estimate can be made by assuming these two quantities to be the same, whence

$$P'_{2A} = M_2 v_2 \left(\frac{\epsilon_1 - 1}{\epsilon_1 + 2} - \frac{n_1^2 - 1}{n_1^2 + 2} \right). \qquad (10)$$

Also, although the electronic polarization in solution is not necessarily the same as in the pure liquid state, if one chooses to assume P_{2A} to be

5 % of P_{2E} no great error will be introduced by using the value of the latter derived from data for the pure liquid or even the value computed from the atomic or bond refractivities. A " correction " term for $P_{2A} - P'_{2A}$ can therefore be derived.

Such a correction term based on $P_{2A} = 0{\cdot}05 P_{2E}$ is shown in the last line of Table II. In computing P_{2A} and P'_{2A} the values of P_E and d_4^{25} for aniline were taken as 30·7 cm.^{3} and 1·0174 g. cm.$^{-3}$ respectively. When this is applied the values obtained by the more exact methods all lie within experimental error of the values deduced by the ordinary method. As is to be expected slightly more divergence is to be found in the corrected values computed by the simplified method, especially for solutions in dioxan. These results are illustrated by the " corrected " values shown in Table III.

TABLE III.—" CORRECTED " VALUES OF THE ORIENTATION POLARIZATION AND APPARENT DIPOLE MOMENT OF ANILINE, ASSUMING THAT $P = 0{\cdot}05\ [R_D]$

Method	Solvent							
	Benzene		Dioxan		Carbon Tetrachloride		n-Heptane	
	P_μ cm.^{3}	μ (D)	P_μ cm.^{3}	μ (D)	P_μ cm.^{3}	μ (D)	P_μ cm.^{3}	μ (D)
Conventional	46·12	1·505	62·64	1·753	43·34	1·458	44·55	1·477
G. 1 . .	46·35	1·508	62·57	1·752	43·39	1·459	44·23	1·472
M.G. 1 .	46·29	1·507	62·56	1·752	43·43	1·460	44·35	1·474
M.G. 2 .	46·09	1·504	62·65	1·753	43·46	1·460	44·44	1·476
G. 2 . .	46·58	1·511	66·36	1·804	44·87	1·484	44·33	1·474
M.G. 3 .	46·49	1·509	66·38	1·804	44·85	1·484	44·30	1·473
M.G. 4 .	46·24	1·506	63·46	1·764	43·80	1·465	44·45	1·476
M.G. 5 .	46·15	1·505	63·39	1·762	43·78	1·465	44·41	1·476

Conclusions.—From the calculations summarized above it may be inferred that a method by which the apparent dipole moment may be deduced accurately and with a minimum effort, without requiring a knowledge of the densities of the solutions studied, involves calculation of the value of $P_{2A} - P'_{2A} + P_{2\mu}$ from the relationship

$$P_{2A} - P'_{2A} + P_{2\mu} = 3M_2 v_1 \left\{ \frac{\alpha}{(\epsilon_1 + 2)^2} - \frac{\nu}{(n_1^2 + 2)^2} \right\} \quad . \quad (11)$$

followed by the evaluation of P'_{2A} from eqn. (10), the value of v_2 being taken as the specific volume of the pure solute if a liquid, or as its partial specific volume in any solvent if a solid or gas. Any appropriate comparable value is then assigned to P_{2A}; if this is based on a fraction of P_{2E} it is sufficient to deduce the latter from data for the pure substance or from atomic refractivities.

Alternatively, except where $\epsilon_1 - n_1^2$ for the solvent is large, good agreement with other methods is obtained by means of the approximate relationship

$$P_{2A} - P'_{2A} + P_{2\mu} = 3M_2 v_1 \,.\, \frac{\lim_{(w_2=0)} \partial(\epsilon_{12} - n_{12}^2)\partial w_2}{(\epsilon_1 + 2)^2}.$$

The value of $P_{2A} - P'_{2A}$ may then be deduced in the same way as for the more exact method.

The author is deeply indebted to Prof. E. A. Guggenheim, F.R.S., for valuable correspondence on this subject.

Department of Chemistry,
Bedford College, London.

DERIVATION AND DEVELOPMENT OF HÜTTIG'S MULTILAYER SORPTION ISOTHERM

By R. R. Fergusson and R. M. Barrer

Received 7th November, 1949

A statistical derivation has been given of the most generalized form of sorption isotherm based on Hüttig's view of the evaporation-condensation properties of a sorbed molecule. From this general equation a number of characteristic isotherm equations have been obtained analogous to the various modifications of the B.E.T. isotherm. From calculations based upon these Hüttig-type multilayer sorption isotherms it has been shown possible to obtain curves corresponding to isotherms of types I, III and to some extent V, of Brunauer's classiffication, but not to types II and IV. It is also possible to obtain limiting values of the sorption corresponding to less or much more than the two layers given by Hüttig's original isotherm equation.

Hüttig[1] and later Ross,[2] derived an isotherm for multilayer sorption, using kinetic methods involving detailed balancing which resemble those first used in deriving the B.E.T. isotherm.[3] The evaporation properties ascribed to sorbed molecules by Hüttig differ, however, from those which were attributed to the sorbate in deriving the B.E.T. isotherm. According to Hüttig a molecule in any layer evaporates just as well when covered by another molecule as when uncovered. On the other hand the B.E.T. postulate is that if a molecule in any lower layer is covered by a molecule in the next layer then the lower layer molecule cannot evaporate. One would expect Hüttig's assumption to be nearer the truth for a small extent of multilayer sorption and the B.E.T. assumption to be more correct for a denser and thicker multilayer film. Both B.E.T. and Hüttig theories assume that condensation occurs in any layer only on vacant sites in that layer, that is on top of uncovered molecules in the preceding layer. The isotherms obtained for unrestricted sorption are:

$$\theta = \frac{v}{v_m} = \frac{cx(1 + x)}{1 + cx} \text{ (Hüttig)} \quad . \quad . \quad . \quad . \quad . \quad (1)$$

$$\theta = \frac{v}{v_m} = \frac{cx}{(1 - x)(1 + \text{[illegible]}} \text{ (B.E.T.)} \quad . \quad . \quad (2)$$

(where x is the relative pressure, c is a constant, v the volume sorbed and v_m the volume required to complete a monolayer). It can be seen that in the Hüttig isotherm θ is never more than two. In the present paper a statistical derivation of Hüttig's isotherm will be outlined, and the isotherm extended in several directions.

Statistical Counterpart of Hüttig's Assumptions.—The total number of sorption sites available in the ith layer is equal to the number of molecules in the $i - 1$th layer. If, following Hüttig, evaporation from this ith layer is assumed independent of the presence of any higher layers, then at equilibrium the fractional coverage θ_i in that layer is independent not only of the number of molecules in the $i - 1$th layer but also of the number in any higher layers (i.e. $a_i p(1 - \theta_i) = b_i \theta_i$, where a_i and b_i are constants). Since θ_i is the only term involving concentration which affects the chemical potential of a molecule in the ith layer, this chemical potential, in contrast to the B.E.T. theory, is uninfluenced by the presence of molecules in any other layers. However, at equilibrium the chemical potential in each layer must be equal to the chemical potential, $\mu_g = kT \ln \alpha p$, of a molecule in the gas phase.* Thus at equilibrium:

---

[1] Huttig, *Monatsh.*, 1948, 78, 177.

[2] Ross, *J. Physic. Chem.*, 1949, 53, 383.

[3] Brunauer, *Physical Adsorption of Gases and Vapours* (O.U.P., 1945), p. 151.

$$\mu_1 = \mu_2 \ldots \mu_i = \mu_g, \text{ etc.} \quad . \quad . \quad . \quad . \quad (3)$$

If, therefore, we write down the partition functions $Q_1, Q_2, \ldots Q_i, \ldots$ etc., for the first, second, etc., layers, which contain $X_1, X_2, \ldots X_i$ molecules, then the chemical potential can be obtained from the series of relationships

$$-\frac{\partial \ln Q_1}{\partial X_1} = \frac{\mu_1}{kT}; \quad -\frac{\partial \ln Q_2}{\partial X_2} = \frac{\mu_2}{kT} \ldots; \quad -\frac{\partial \ln Q_i}{\partial X_i} = \frac{\mu_i}{kT}, \text{ etc.} \quad (4)$$

$Q_1, Q_2 \ldots Q_i$, etc. being differentiated separately and independently of each other.

The Isotherm.—Denote by q_1 the partition function of a molecule in the first layer. Then the partition function for this layer can be written:

$$Q_1 = \frac{B!}{(B - X_1)!\, X_1!}(q_1)^{X_1}, \quad . \quad . \quad . \quad . \quad (5)$$

where B denotes the number of sites available to the first layer molecules, i.e. the number of primary sorption centres. For the second layer:

$$Q_2 = \frac{X_1!}{(X_1 - X_2)!\, X_2!}(q_2)^{X_2}, \quad . \quad . \quad . \quad (6)$$

since the number of sites available to second layer molecules is X_1. One may similarly write down the partition functions for higher layers, and by differentiation according to eqn. (4), and equating μ_g to μ_1, μ_2, etc., one obtains the relationships:

$$\frac{B - X_1}{X_1} = \frac{1}{q_1 \alpha p}; \quad \frac{X_1 - X_2}{X_2} = \frac{1}{q_2 \alpha p}; \quad \frac{X_{i-1} - X_i}{X_i} = \frac{1}{q_i \alpha p}, \text{ etc.} \quad (7)$$

and thence

$$\frac{X_1}{B} = \theta_1 = \frac{q_1 \alpha p}{1 + q_1 \alpha p}; \quad \frac{X_2}{X_1} = \theta_2 = \frac{q_2 \alpha p}{1 + q_2 \alpha p}; \quad \frac{X_i}{X_{i-1}} = \theta_i = \frac{q_i \alpha p}{1 + q_i \alpha p}, \text{etc.}, \quad (8)$$

The total amount sorbed is

$$A = X_1 + X_2 + X_3 + \ldots, \quad . \quad . \quad . \quad . \quad (9)$$

whence

$$\theta = \frac{A}{B} = \frac{v}{v_m} = \frac{X_1}{B}\left(1 + \frac{X_2}{X_1} + \frac{X_3}{X_2} \cdot \frac{X_2}{X_1} + \ldots\right)$$

$$= \theta_1(1 + \theta_2 + \theta_3\theta_2 + \ldots) \quad . \quad (10)$$

Substitution of eqn. (8) in eqn. (10) then gives as the most general form of the Hüttig isotherm:

$$\theta = \frac{q_1 \alpha p}{1 + q_1 \alpha p}\left(1 + \frac{q_2 \alpha p}{1 + q_2 \alpha p} + \frac{q_3 q_2 (\alpha p)^2}{(1 + q_3 \alpha p)(1 + q_2 \alpha p)} + \ldots\right) \quad (11)$$

For a vapour,† since $q_L \alpha = \frac{1}{p_0}$, the isotherm (eqn (11)) may be rewritten as:

---

* The constant α in the equation $\mu_g = kT \ln \alpha p$ is given by

$$\alpha = \frac{1}{kT} \cdot \frac{h^3}{(2\pi mkT)^{3/2}} \cdot \frac{1}{Q_{int}},$$

where Q_{int} is the partition function for internal degrees of freedom of a molecule of mass m; k is Boltzmann's constant and T the absolute temperature.

† For the pure liquid in equilibrium with its vapour we have

$$\mu_L = \mu_g$$
$$- kT \ln q_L = kT \ln \alpha p_0,$$

so that $q_L \alpha = 1/p_0$. q_L is the partition function of a molecule in the liquid state.

$$v = \frac{}{1 + c_1x}\left(1 + \frac{c_2x}{1 + c_2x} + \frac{c_3c_2x^2}{(1 + c_3x)(1 + c_2x)} + \ldots\right), \quad . \quad (12)$$

where $c_1 = q_1/q_L$; $c_2 = q_2/q_L$; $c_3 = q_3/q_L$, etc.

The most general isotherm based on the B.E.T. assumptions, and corresponding to eqn. (12), has been obtained by Dole,[4] and is

$$\theta = \frac{x(c_1 + 2c_1c_2x + 3c_1c_2c_3x^2 + \ldots)}{(1 + c_1x + c_1c_2x^2 + c_1c_2c_3x^3 + \ldots)} \quad . \quad . \quad (13)$$

The constants, c_1, c_2, c_3, etc., have exactly the same significance in eqn. (13) as in eqn. (12). In these two equations if we make the simplifying assumption, common to both the original Hüttig and B.E.T. treatments, that

$$q_2 = q_3 = \ldots = q_L \quad . \quad . \quad . \quad . \quad (14)$$

then $c_2 = c_3 = \ldots = 1$ and eqn. (12), on summing the series in the bracket, becomes

$$\theta = \frac{c_1x}{1 + c_1x}(1 + x),$$

which is the Hüttig isotherm given in eqn. (1). Similarly, eqn. (13) reduces to the B.E.T. isotherm in eqn. (2)

$$v - \frac{}{(1 - x)(1 + (c - 1)x)}.$$

Special Cases.—In this section we will derive the counterparts, based on Hüttig's assumptions, of some of the modified B.E.T. type isotherms which have been derived in several attempts to improve on and diversify the original B.E.T. isotherm of eqn. (2). Firstly, it may be noted that when $q_1 = q_2 = q_3 = \ldots = c_1q_L$, eqn. (12) reduces to

$$\theta = c_1x \quad . \quad . \quad . \quad . \quad . \quad (15)$$

and Henry's law is obtained. Eqn. (13) with these assumptions becomes

$$\theta = \frac{c_1x}{1 - c_1x} \quad . \quad . \quad . \quad . \quad . \quad (16)$$

as pointed out by Dole.[4] If the sorption is restricted to a finite number of layers n then the assumptions which led to eqn. (15) now give

$$\theta = c_1x\left(1 - \left(\frac{c_1x}{1 + c_1x}\right)^n\right) \quad . \quad . \quad . \quad (17)$$

and the form of the isotherms is shown in Fig. 1. On the other hand if we make the same assumptions $q_2 = q_3 = \ldots = q_L$, and $q_1 = c_1q_L$ which transformed eqn. (12) to the Hüttig isotherm of eqn. (1), but if we also restrict sorption to a finite number n of layers as before, then (Fig. 2)

$$\theta = \frac{c_1x}{1 + c_1x}(1 + x)\left(1 - \left(\frac{x}{1 + x}\right)^n\right), \quad . \quad . \quad (18)$$

the B.E.T. counterpart to which is

$$\theta = \frac{c_1x(1 - (n + 1)x^n + nx^{n+1})}{(1 - x)(1 + (c - 1)x - c_1x^{n-1})} \quad . \quad . \quad . \quad (19)$$

As further examples of restricted adsorption one may include the case where $q_1 = c_1q_L$ and $q_2 = q_3 = q_4 = \ldots = kq_1 \neq q_L$. Similar assumptions were made in Anderson's[5] first modification of the B.E.T. isotherm of eqn. (2) and for the Hüttig isotherm for n layers they lead to

$$\theta = \frac{c_1x}{1 + c_1x}(1 + kc_1x)\left(1 - \left(\frac{kc_1x}{1 + kc_1x}\right)^n\right) \quad . \quad . \quad (20)$$

---

[4] Dole, *J. Chem. Physics*, 1948, 16, 25.

the exact B.E.T. analogue to which is

$$\theta = \frac{c_1x\,.\,(1 - (n+1)(kc_1x)^n + n(kc_1x)^{n+1}}{(1 - kc_1x)(1 + c_1x\{1 - k - (kc_1x)^n\})} \quad . \quad . \quad (21)$$

On letting n tend to infinity one obtains the isotherms for unrestricted

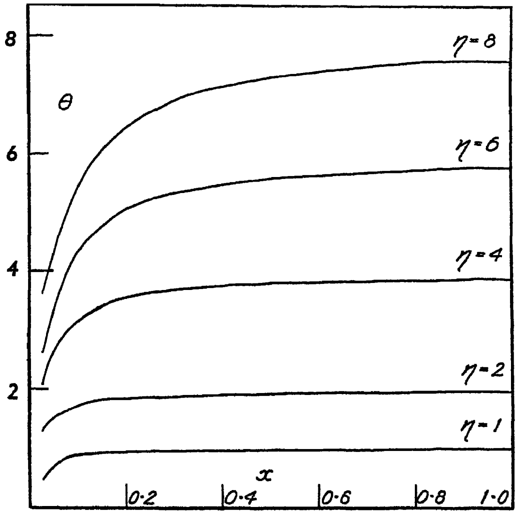

FIG. 1.—Restricted sorption, eqn. (17).
$q_1 = q_2 = q_3 = \ldots c_1q_L$;
$c_1 = 100$; $n = 1, 2, 4, 6, 8$.

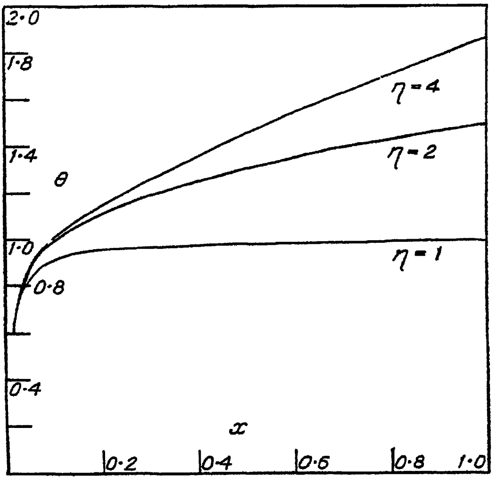

FIG. 2.—Restricted sorption, eqn. (18).
$q_2 = q_3 = \ldots = q_L$ and $q_1 = c_1q_L$;
$c_1 = 100$; $n = 1, 2, 4$.

adsorption but otherwise corresponding to eqn. (20) and (21). These are :

$$\theta = \frac{c_1x}{1 + c_1x}(1 + kc_1x) \text{ (Hüttig)} \quad . \quad . \quad . \quad . \quad (22)$$

$$\theta = \frac{c_1x}{(1 - kc_1x)(1 + c_1x(1 - k))} \text{ (B.E.T.)} \quad . \quad . \quad (23)$$

Isotherms according to eqn. (20) and (22) are plotted in Fig. 3 and 4.

A further example along the lines of Anderson's[5] third modification may be given. Let

$$q_1 = c_1 q_L\,;\; q_2 = q_3 = \ldots = q_r = c_2 q_L \text{ and } q_{r+1} = q_{r+2} = \ldots = q_L.$$

Substitution in the general Hüttig type isotherm eqn. (12) then leads to

$$\theta = \frac{c_1 x}{1 + c_1 x}\left[(1 + c_2 x)\left(1 - \left(\frac{c_2 x}{1 + c_2 x}\right)^{r-1}\right) + \left(\frac{c_2 x}{1 + c_2 x}\right)^{r-1}(1 + x)\right]$$

$$= \frac{c_1 x}{1 + c_1 x}\left\{1 + x\left[c_2 - \left(\frac{c_2 x}{1 + c_2 x}\right)^{r-1}(c_2 - 1)\right]\right\} \quad . \quad . \quad . \quad . \quad (24)$$

Typical isotherms corresponding to eqn. (24) are given in Fig. 5.

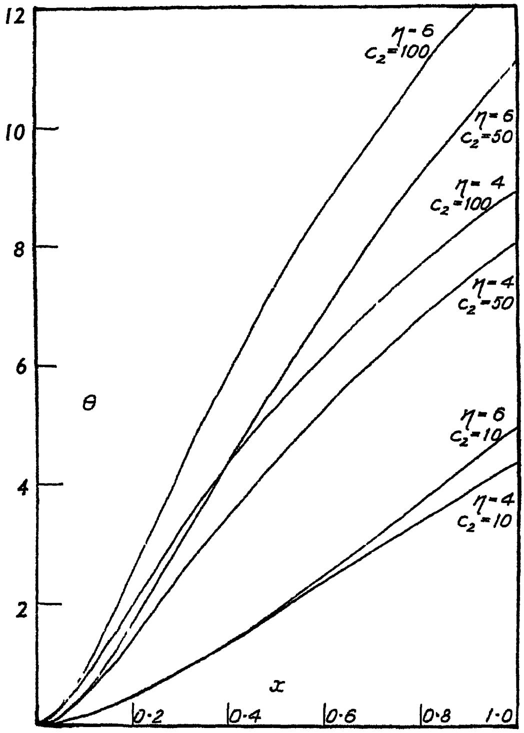

FIG. 3.—Restricted sorption, eqn. (20). $q_2 = q_3 = \ldots = kq_1 + q_L$ and $q_1 = c_1 q_L$; $c_1 = 1$; $c_2 = kc_1 = 10, 50, 100$; $n = 4, 6$.

Discussion

Several aspects of Fig. 1 to 5 are of interest. If one adopts the Hüttig assumptions then Fig. 1 in particular shows that Type I isotherms qualitatively similar in shape to those obtained for Langmuir monolayers are possible, in which, however, the sorption corresponds to a large number of layers. Surface areas then derived, assuming monolayers because of the form of the isotherm, could be seriously in error. One also sees that the several modifications of the Hüttig isotherms developed in this paper may give curves corresponding in Brunauer's classification[3] to Type I

---

[5] Anderson, *J. Amer. Chem. Soc.*, 1946, **68**, 686.

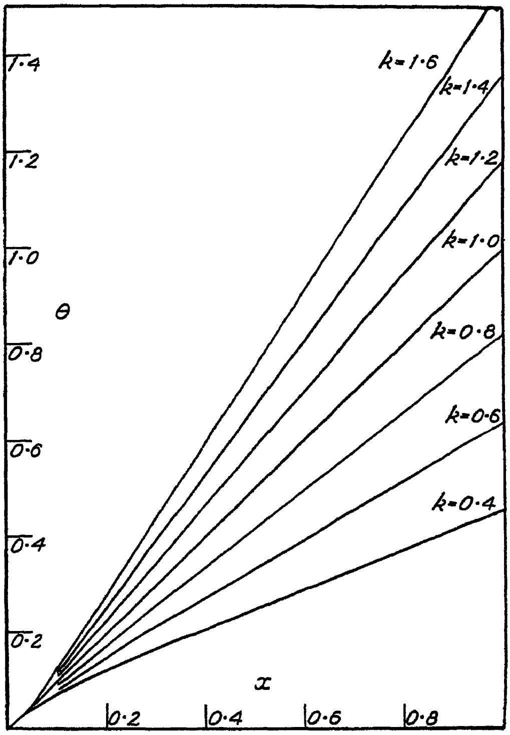

FIG. 4*a*.—Unrestricted sorption, eqn. (22). $q_2 = q_3 = \ldots = kq_1 + q_L$ and $q_1 = c_1 q_L$; $c_1 = 10$; $k = 0{\cdot}4, 0{\cdot}6, 0{\cdot}8, 1{\cdot}0, 1{\cdot}2, 1{\cdot}4, 1{\cdot}6$.

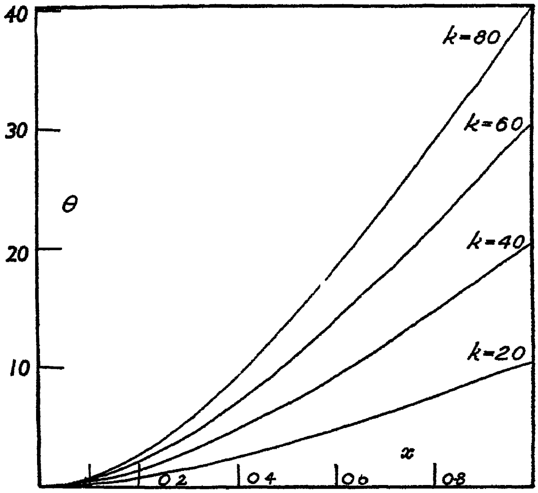

FIG. 4*b*.—Unrestricted sorption, eqn. (22). $q_2 = q_3 = \ldots = kq_1 + q_L$ and $q_1 = c_1 q_L$; $c_1 = 1$; $k = 20, 40, 60, 80$.

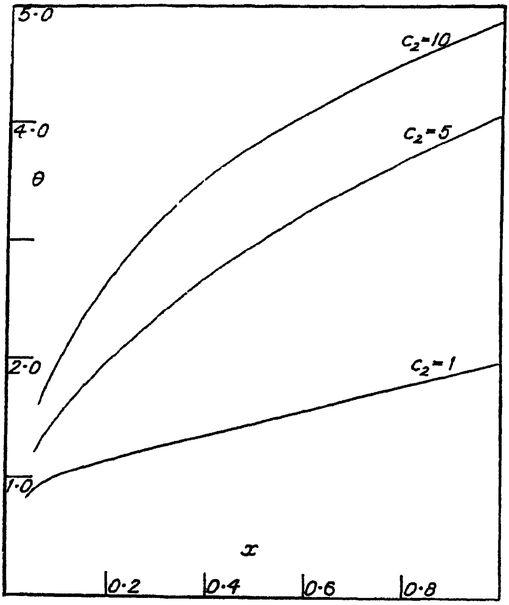

FIG. 5*a*.—Unrestricted sorption, eqn. (24).
$q_2 = q_3 = \ldots = q_r = c_2 q_L$;
$q_{r+1} = q_{r+2} = \ldots = q_L$; and $q_1 = c_1 q_L$;
$c_1 = 100$; $r = 5$; $c_2 = 1, 5, 10$.

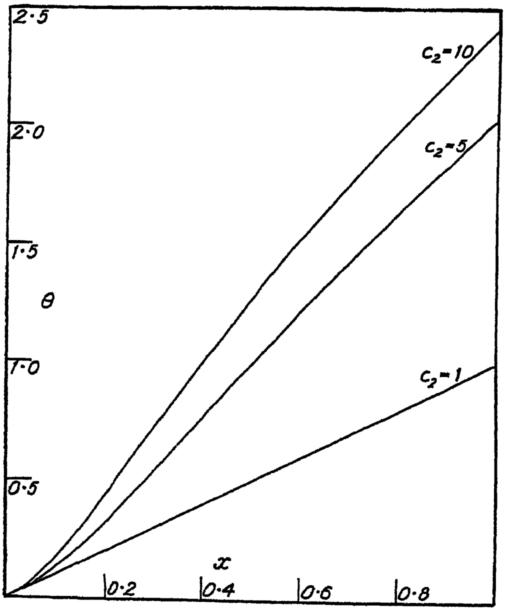

FIG. 5*b*.—Unrestricted sorption, eqn. (24).
$q_2 = q_3 = \ldots = q_r = c_2 q_L$;
$q_{r+1} = q_{r+2} = \ldots = q_L$ and $q_1 = c_1 q_L$;
$c_1 = 1$; $r = 5$; $c_2 = 1, 5, 10$.

isotherms (cf. Fig. 1 and 2); to Type III isotherms (cf. Fig. 4*b*); and to a limited extent those of Type V (Fig. 3 and 5*b*). It is not possible, however, to obtain curves corresponding to either of the isotherm Types II and IV. These results may be compared with calculations based on B.E.T. isotherm modifications, which may give curves similar in shape to experimental isotherms of Types I to V inclusive. However, this result cannot satisfactorily be used to decide which set of evaporation-condensation properties for a sorbed molecule (Hüttig's or B.E.T.'s) comes nearer to reality, because capillary condensation when combined with Hüttig isotherms can easily give compound isotherms of Types II or IV.

Another point of interest is that, whereas in Hüttig's original derivation (eqn. (1)) θ can never exceed two, the modifications now given can lead to a wide range of limiting values for θ both less than and much greater than two. In these various ways Hüttig's method of formulation is capable of considerable extension. A major objection to this, and to the B.E.T. method of treatment of multilayer sorption is undoubtedly the artificial picture of the multilayers as separate linear columns of molecules in which the molecules do not interact laterally with molecules in adjacent columns while they do interact with molecules in the same column.[6] No simple way of introducing these undoubtedly important lateral interactions has yet been devised.[7]

The Chemistry Department,
Marischal College,
The University,
Aberdeen.

---

[6] Hill, *J. Chem. Physics*, 1946, 14, 263.

[7] Hill, *ibid.*, 1946, 14, 441.

KINETICS OF THE AMINE-CATALYZED DECOMPOSITION OF NITRAMIDE

By R. P. Bell and G. L. Wilson

Received 15th November, 1949

Measurements have been made of the kinetics of decomposition of nitramide in aqueous solution at 25° C, using five primary and seven tertiary bases as catalysts. For each class of base there is a relation between catalytic power and basic strength, but the tertiary bases are more effective catalysts than primary bases of the same basic strength. This behaviour accords with the views previously advanced on the part played by hydrogen bonding between water molecules and amine cations in determining basic strengths in aqueous solution.

In previous kinetic work on the decomposition of nitramide in aqueous solution the systematic study of amine catalysts was confined to substituted primary anilines, for which there is a close relationship between catalytic effect and dissociation constant in water.[1] Isolated data for tertiary amines [2] do not conform to this relation, and a further study would be of interest. Bell and Trotman-Dickenson [3] measured the catalytic effect of 24 amine bases on the decomposition of nitramide in anisole solution. It was found that no single relationship between catalytic effect and dissociation constant in water was valid for all the bases studied, but that three separate relationships held for primary, secondary and tertiary aniline bases. A fourth relationship was valid for pyridine and quinoline bases. On the other hand, if the dissociation constants in water were replaced by basicity constants in the much less basic solvent *m*-cresol, then the data for mono- and di-methylaniline obeyed the relation valid for the primary anilines. It was therefore suggested that the distinction between primary, secondary and tertiary amines does not arise from any anomalies in their kinetic behaviour in anisole, but that their dissociation constants in water are affected differently by hydrogen bonding between the amine cation and the water molecule. The same concept serves to clear up many apparent anomalies in the effect of substituents on the basic strength of amines in water.[4]

---

[1] Brönsted and Duus, *Z. physik. Chem.*, 1925, 117, 299.

[2] Pfluger, *J. Amer. Chem. Soc.*, 1938, 60, 1513.

[3] Bell and Trotman-Dickenson, *J. Chem. Soc.*, 1949, 1288.

Since anisole has only very weak basic properties, it could be assumed that hydrogen bonding has no effect on the rate of the amine-catalyzed decomposition of nitramide in this solvent. In aqueous solution, on the other hand, hydrogen bonding may have an effect on the rate, since the amine cations must be partly formed in the transition state. This effect should, however, be less than the effect on the dissociation constants, which relate to complete separation of the cations. It might therefore be expected that the data for aqueous solutions would show the same distinction between primary, secondary and tertiary amines as was found in anisole, though to a smaller extent. The measurements described in this paper were designed to test this expectation. They were confined to primary and tertiary amines, for which the difference should be greatest.

Experimental

Nitramide was prepared as described by Marlies, La Mer and Greenspan.[5] Difficulties were caused by the presence in the final product of about 1 % of an acidic impurity : this was estimated by decomposing a specimen of nitramide by heating for 20 min. in pure water, and titrating the resulting solution with alkali. The use of various indicators showed that the impurity had a pK of less than 4. It probably consisted of unchanged nitro-urethane (pK = 3·3), resulting from incomplete conversion of ammonium nitro-urethane to potassium nitrocarbamate. This stage of the preparation involves the conversion of one solid into another, and it was in fact found that inefficient stirring in this operation gave a final product consisting largely of nitro-urethane (identified by mixed m.p.). The specimens of nitramide containing 1 % of acidic impurity gave on heating a small quantity of white residue which then charred, and it may be noted that the original discoverers [6] of nitramide found 0·43 % of carbon in their product. Further purification of nitramide by sublimation leads to great loss, and the kinetic measurements were therefore carried out with the material containing 1 % nitro-urethane, corrections being applied as described below. It is likely that a similar amount of acid impurity was present in the nitramide used in previous kinetic investigations, but no significant correction is involved unless the concentration of catalyst is very small compared with that of nitramide, as in the present investigation.

The purification of the amines used and the method of measuring the reaction velocity have been previously described.[3] All kinetic measurements were made at 25° C. First-order velocity constants were determined graphically for approximately the first half of the reactions : the logarithmic plots were usually straight, but showed a slight curvature with the strongest bases. The catalyst solutions were made by adding less than one equivalent of HCl to a solution of amine. The concentrations chosen were restricted (in some cases within rather narrow limits) by the solubility of the amine, the speed of the reaction, and the requirement that pH be less than 5, so as to ensure that almost all the nitramide is in the undissociated form.

[4] Trotman-Dickenson, *J. Chem. Soc.*, 1949, 1293.

[5] Marlies, La Mer and Greenspan, *Inorganic Syntheses* (New York, 1939), Vol. I, p. 68.

[6] Thiele and Lachmann, *Ber.*, 1894, **27**, 1909.

If C_B and C_A are the stoichiometric concentrations of base and acid taken, the concentration of free base in the solution is to a first approximation $[B] \sim C_B - C_A$. This needs correction for the presence of the nitramide in the solution. In the first place the concentration of nitro-urethane impurity C_X must be added to C_A since it will be almost completely dissociated at pH 4-5. Further, if the concentration of nitramide at any moment is C_N, denoting the nitramide ion by N^-, we have the equations

$$C_B = [B] + [BH^+], \quad C_N \simeq [NH]$$
$$[H^+] + [BH^+] = [N^-] + C_X + C_A \text{ (electroneutrality)}$$
$$\frac{[N^-][H^+]}{C_N} = K_N = 2{\cdot}55 \times 10^{-7}, \quad \frac{[B][H^+]}{[BH^+]} = K_A,$$

where K_N and K_A are the acidity constants of nitramide and the amine cation respectively. These equations can in principle be solved to give [B], [BH+], [N−] and [H+] in terms of the known quantities C_B, C_A, C_X, C_N, K_N and K_A, but in practice it is simpler to use a method of successive approximations, putting as a first approximation $[B] \sim C_B - C_X - C_A$. The nitramide concentration is of course varying throughout the course of each experiment, but since the velocity constants are average values for about the first half of the reaction, we have used in the calculation a value of C_N equal to two-thirds of the initial nitramide concentration. In a typical experiment with pyridine as a catalyst the figures were $C_B = 9{\cdot}43 \times 10^{-3}$, $C_A = 5{\cdot}99 \times 10^{-3}$, $C_N = 2{\cdot}76 \times 10^{-2}$, $C_X = 2{\cdot}8 \times 10^{-4}$ mole/l. The first approximation thus gives $[B] = 3{\cdot}16 \times 10^{-3}$ and the corrected value is $2{\cdot}89 \times 10^{-3}$ mole/l.

Results

In Table I the values given for the concentrations [B] and [BH+] have all been corrected as described above, and the first-order velocity constant k is expressed in min.$^{-1}$, decadic logarithms. The catalytic constant k_0 is determined from the equation

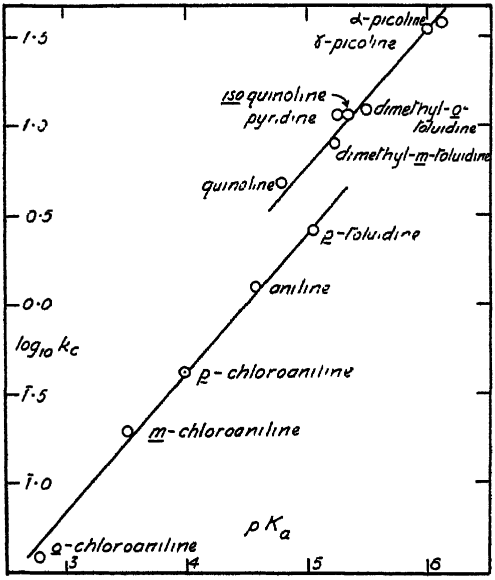

FIG. 1.

$$k = k_0 + k_c[B] + k_{N^-}[N^-],$$

where k_0 is the "spontaneous" rate at 25°, and k_{N^-} the catalytic constant of the nitramide ion. k_0 was measured in 0·07 N HCl solution and found to be

1·23 × 10⁻³, in exact agreement with the value previously obtained.[7] k_{N^-} was taken as 0·96, from the work of Tong and Olson,[8] and since the correction

TABLE I.—DECADIC LOGARITHMS; TIME IN MIN.

Base	10^4[B]	10^4[BH+]	10^4C_N	10^3k	k_c
o-Chloroaniline	90·1	8·93	495	1·62	0·037
,,	103·5	9·89	251	1·70	0·042
				Mean	0·039
m-Chloroaniline	373	101·0	290	8·80	0·200
,,	456	34·0	344	10·4	0·194
				Mean	0·197
p-Chloroaniline	17·27	6·42	255	2·11	0·417
,,	17·84	6·47	255	2·15	0·420
				Mean	0·416
Aniline	90·7	53·6	262	13·0	1·25
,,	103·7	103·1	250	14·8	1·28
				Mean	1·26
p-Toluidine	7·17	27·2	294	3·20	2·45
,,	9·64	37·5	322	4·10	2·72
,,	43·2	55·9	244	12·80	2·56
				Mean	2·56
Dimethyl-*m*-toluidine	12·55	62·0	148	10·5	7·47
,,	13·68	60·6	66	11·6	7·53
,,	30·8	123·0	69	26·4	8·15
,,	35·5	90·3	80	30·0	8·05
,,	35·8	90·0	71	30·5	8·13
				Mean	7·87
Dimethyl-*o*-toluidine	31·6	131	79	39·8	12·2
,,	32·7	130	20	42·5	12·6
,,	33·9	157	75	42·8	12·2
				Mean	12·3
Quinoline	26·6	14·3	83	14·1	4·80
,,	35·8	43·7	265	19·7	5·08
,,	38·4	52·8	308	19·6	4·68
,,	43·6	51·9	268	22·3	5·00
,,	57·2	98·4	115	27·3	4·54
,,	70·4	102·3	308	33·8	4·60
				Mean	4·78
Pyridine	16·8	47·5	144	19·9	11·1
,,	26·8	54·0	255	32·5	11·4
,,	28·9	65·4	276	35·5	11·7
				Mean	11·4

---

[7] Baughan and Bell, *Proc. Roy. Soc. A*, 1937, 158, 464.

[8] Tong and Olson, *J. Amer. Chem. Soc.*, 1941, 63, 3406.

TABLE I.—(*Contd.*)

Base	10^4[B]	10^4[BH$^+$]	10^4C_N	10^3k	k_c
*iso*Quinoline . .	26·2	113·3	286	32·8	11·5
,, . .	26·4	91·5	129	32·0	11·5
				Mean	11·5
γ-Picoline . .	5·93	165·6	269	21·8	34·2
,, . .	10·8	269·8	380	38·4	34·3
,, . .	14·2	227·7	294	51·0	34·7
				Mean	34·4
α-Picoline . .	2·63	152·0	290	11·3	37·7
,, . .	4·13	272·1	366	17·0	37·7
,, . .	5·04	266·4	308	20·0	37·0
,, . .	7·51	302·1	262	29·5	37·0
				Mean	37·4

for catalysis by nitramide ion was always a small one, [N$^-$] could be calculated from the mean nitramide concentration during the experiment.

Fig. 1 shows the values of $\log_{10} k_c$ from Table I plotted against the values of pK$_a$ for the amine cations. The pK$_a$ values and their sources have been given previously.[9] It will be seen that the primary and tertiary amines fall on two distinct lines, though their separation is not so great as when the reaction velocities in anisole are used. This confirms the views outlined in the introduction as to the part played by hydrogen bonding in the dissociation of amines in water. In anisole solution the heterocyclic bases behaved as more effective catalysts than tertiary aniline bases of the same dissociation constant, but this distinction does not appear in Fig. 1. The reason for the distinction in anisole solution is not clear.

Physical Chemistry Laboratory,
Oxford.

---

[9] Bell and Trotman-Dickenson, ref. 3. In Table II of this paper the pK$_a$ of dimethyl-*m*-toluidine was quoted erroneously as 5·34, but the correct value (5·24) was plotted in Fig. 2 of the same paper.

TWO FACTORS AFFECTING THE USE OF THE ROTATING SECTOR IN PHOTOCHEMICAL EXPERIMENTS

By W. G. Burns and F. S. Dainton

Received 21st November, 1949

The theory of the use of the rotating sector in the study of photochemically-initiated, unbranched chain reactions has been extended to include non-uniform light intensity. The value of corrections to be applied in a particular case are deduced and tabulated and illustrate the application of the method. The penumbra error, i.e. the error introduced by assuming that the light pulse is square, is discussed and its magnitude evaluated for a trapezoidal pulse. The error is very small and only important at very low sector speeds.

In photochemically-initiated, unbranched chain reactions, the rate of which depends on the intensity of absorbed light I_{abs} raised to some power n which is not unity, the use of light which is discontinuous in space or time, often enables valuable information to be obtained concerning the magnitude of the propagation and termination velocity constants. Of particular interest in this connection are chemical reactions, the course of which may be summarized in the three steps.

(1) Initiation $A_2 + h\nu \rightarrow 2A$ k_1,
(2) Propagation $A + B \rightarrow C + A$ k_2,
(3) Mutual termination $2A \rightarrow$ stable product, k_3,

where A is the reactive centre, B and A_2 are reactants and C is a product. Many photo-halogenation reactions and photo-polymerizations fall into this category and for all these reactions the steady reaction rate under continuous illumination is proportional to $I^{\frac{1}{2}}_{abs}$. When intermittent illumination is used, in which the fraction of the total space or time throughout which illumination occurs is f, the rate of reaction will be proportional to $I^{\frac{1}{2}}_{abs}/f^{\frac{1}{2}}$ when the interval between flashes is greater than the lifetime of the propagating chain (or the distance between the separated illuminated parts is greater than the mean distance travelled by the chain centres before destruction). When the intermittency is extremely rapid or the distance sufficiently minute for the converse to be true, the rate of reaction is proportional to $(I_{abs}/f)^{\frac{1}{2}}$, i.e. the state of affairs is equivalent to continuous illumination with intensity $= I_{abs}/f$.

The theoretical treatment of space discontinuity is especially difficult because the rate of diffusion of the centres into the dark space is also involved.[6] Time discontinuity has been considered fairly fully by a number of authors,[1] and achieved experimentally [2] by rotating circular discs with sectors removed about an axis parallel to the light beam. In all the theoretical treatments hitherto given, two assumptions have been made; (i) the light intensity throughout the reaction vessel is constant and (ii) the light reaches the reaction vessel in rectangular pulses. These assumptions are not justified and it is the purpose of the present paper to extend the theory to take account of this fact. Before doing so it should be remarked that the higher the transmissibility of the reaction cell and its contents, the more justified does assumption (i) become, and that many experiments have been conducted under conditions in which 90 % or more of the incident light was transmitted. Further, an approximation to rectangular light pulsing can be achieved by various devices such as a combination of large sector and small area of light beam or geared pairs of sectors rotating in opposite directions, etc.

The necessity for a theoretical examination of the errors involved in assumptions (i) and (ii) became apparent in the course of experimental work using a sector in an investigation of the photochemical formation of phosgene.[3]

(i) **Correction for Non-uniform Absorption.**—Using the simple reaction scheme given above, which is due to Rice [4] and following the treatment of Dickinson,[1] we obtain

$$\frac{\overline{[A]}}{[A]_s} = \frac{1}{f}\left[1 + \frac{1}{b_0}\ln\left(1 + \frac{(f-1)b_0}{1 + [A]_s/[A]_1}\right)\right], \quad . \quad . \quad (1)$$

---

[1] Briers, Chapman and Walters, *J. Chem. Soc.*, 1926, 562; Dickinson, from Leighton and Noyes, *Photochemistry of Gases*, (Reinhold, 1941), p. 202.

[2] Berthoud and Bellerot, *Helv. chim Acta*, 1924, 7, 307; Briers and Chapman, *J. Chem. Soc.*, 1928, 1802; Allmand and Style, *ibid.*, 1930, 506, 596; Burnett and Melville, *Proc. Roy. Soc. A*, 1947, **189**, 456; Matheson, Bevilacqua and Hart, *J. Amer. Chem. Soc.*, 1949, **71**, 497.

[3] Burns and Dainton (to be published).

[4] Rice, *J. Chem. Physics*, 1942, **10**, 440.

where $[\bar{A}]$ is the mean concentration of A during intermittent illumination, $[A]_s$ is the steady concentration of A during continuous illumination with light of the same incident intensity, $1/f$ = fraction of the total time during which light reaches the front face of the reaction vessel, $[A]_1$ is the value of [A] at the end of each light period and beginning of each dark period and b_0 is given by

$$b_0 = \frac{t_l}{\tau_0} = 2t_l k_3[A]_s = 2t_l(k_1 k_3 I_{abs})^{\frac{1}{2}},$$

where t_l/τ_0 is the ratio of the time of the light period t_l to the lifetime of the growing chain τ_0. It can also be shown that

$$\frac{[A]_1}{[A]_s} = \frac{(f-1)b_0 \tanh b_0}{2[(f-1)b_0 + \tanh b_0]}\left\{1 + \left[1 + \frac{4}{(f-1)b_0 \tanh b_0} + \frac{4}{(f-1)^2 b_0^2}\right]^{\frac{1}{2}}\right\} \quad (2)$$

and hence calculating $[\bar{A}]/[A]_s$ and $[A]_1/[A]_s$ from eqn. (1) and (2) for a fixed sector opening f, the ratio $2[\bar{A}]/[A_s]$ can be expressed as a function of the single parameter $b_0 = t_l/\tau_0$. Now $2[\bar{A}]/(A)_s$ which we shall denote by ρ is twice the ratio of the rate when the sector is running to the rate with the continuous light. Thus from measurement of ρ, b_0 and hence τ_0 can be determined. The lifetime of a chain is the concentration of centres divided by the rate of their destruction, i.e.

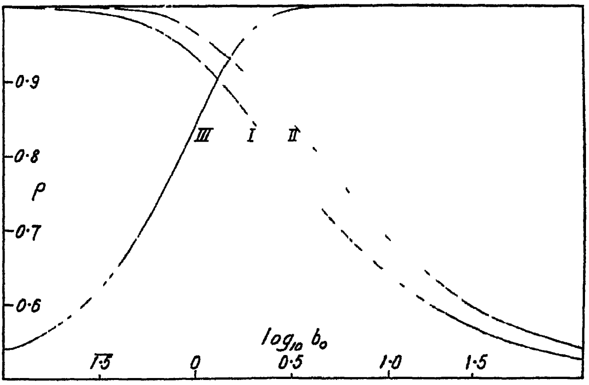

FIG. 1.—Dependence of chain centre concentration on b_0. I. ρ as function of b_0. II. ρ as function of b_0 (non-uniform absorption in 300 mm. Cl_2, 2 cm. depth at 25° C). III. $[A]_1$ $[A]_s$ as a function of b_0.

$$\tau_0 = 2k_3[A]^{-1}.$$

This, combined with rate measurements in continuous light enables k_2 and k_3 to be evaluated explicitly, provided that an estimate of k_1 the quantum efficiency of the primary act, can be made. In practice it is convenient to plot experimental values of ρ against

$$[\log_{10} 2t_l + \tfrac{1}{2}\log_{10} I_{abs}]$$

for different intensities and sector speeds and to fit over the points a movable graph of ρ against $\log_{10}b_0$. The position on the horizontal axis of this graph for the best fit will give the best value of τ_0 from which k_2 and k_3 can be evaluated. Alternatively from each value of ρ, b_0 can be found from the calculated curve and a value of τ_0 which should be constant, is obtained. A mean is then taken of the values for τ_0 giving greater weight to those points on the graph of ρ against $\log_{10} b_0$ where the slope is greatest. The values of $[A]_1/[A]_s$ and ρ for $f = 4$ and values of b_0 between 10^{-1} and 10^2 are given in Table I and plotted in Fig. 1.

Where the absorption is strong, the effect of non-uniformity of absorption becomes important, and it is necessary to integrate over the whole space of the reaction vessel the different local rates of reaction occurring in the different elements of volume. We deal first with continuous illumination. To simplify the conditions we assume that a uniform parallel beam enters a parallel plane-walled vessel perpendicularly to the plane, and is absorbed according to Beer's law, and that there is no diffusion of chain centres. Let I_0 = no. of quanta per cm.^{2} per sec. entering the cell, then the amount of light absorbed, I_{abs} in an element of volume of unit area of cross section, thickness dl, at l cm. from the front face is given by

TABLE I

b_0	$\log_{10} b_0$	$[A]_1/[A]_s$	$\rho = \phi(b_0)$	$\phi_0(b_0)$*	b_0	$\log_{10} b_0$	$\phi_0(b_0)$ †	ρ'
0·1	1·0000	0·539	0·9986	—	—	—	—	—
0·2	1·3010	0·577	0·9969	0·1999	0·16	1·204	0·160	1·000
0·4	1·6021	0·656	0·9859	0·3982	0·25	1·398	0·250	1·000
0·6	1·7782	0·729	0·9706	0·5939	0·4	1·602	0·798	0·996
0·8	1·9031	0·794	0·9523	0·7861	0·6	1·778	0·596	0·993
1·0	0·0	0·846	0·9327	0·9746	1·0	0·0	0·977	0·965
1·4	0·1461	0·922	0·8942	—	1·4	0·146	1·343	0·937
2·0	0·3010	0·973	0·8426	1·8699	2·0	0·301	1·870	0·902
3·0	0·4771	0·996	0·7839	2·6719	2·6	0·415	2·368	0·868
4·0	0·6021	1·000	0·7433	3·4438	3·0	0·477	2·687	0·852
5·0	0·6990	1·000	0·7142	4·1719	3·5	0·544	3·080	0·835
6·0	0·7782	—	0·6919	4·8761	4·0	0·602	3·458	0·813
7·0	0·8451	—	0·6746	5·5587	5·0	0·699	4·690	0·776
8·0	0·9031	—	0·6603	6·2261	6·0	0·778	4·893	0·756
9·0	0·9542	—	0·6486	6·8802	7·3	0·863	5·766	0·724
10	1·0000	—	0·6387	7·5238	8·5	0·929	6·574	0·707
15	1·1761	—	0·6053	—	10·0	1·000	7·543	0·687
20	1·3010	—	0·5859	13·606	16	1·204	11·250	0·642
30	1·4771	—	0·5638	19·344	25	1·398	16·480	0·602
40	1·6021	—	0·5313	24·915	40	1·602	24·88	0·572
50	1·6990	—	0·5433	30·388	60	1·778	35·74	0·558
60	1·7782	—	0·5376	35·790	100	2·000	56·94	0·540
80	1·9031	—	0·5300	47·460	—	—	—	—
100	2·0000	—	0·5251	57·014	—	—	—	—

* Obtained by calculation. † Obtained graphically.

$$I'_{abs} = -\frac{dI}{dl} = -\frac{d[I_0(1 - e^{-\alpha[A_2]l})]}{dl} = \alpha[A_2]I_0{}^{-\alpha[A_2]l} \quad . \quad (3)$$

If we put the reaction rate $= kI'^{\frac{1}{2}}_{abs}$ and $c = \dfrac{\alpha[A_2]}{2}$ we have:

$$\text{Rate (local)} = k(2c)^{\frac{1}{2}}I_0^{\frac{1}{2}}e^{-cl}, \quad . \quad . \quad . \quad . \quad (4)$$

$$\text{Rate (mean)} = \frac{1}{l}\int_0^l k(2c)^{\frac{1}{2}}I_0^{\frac{1}{2}}e^{-cl}dl, \quad . \quad . \quad . \quad (5)$$

$$= \frac{2k}{(2c)^{\frac{1}{2}}l}I_0^{\frac{1}{2}}[1 - e^{-cl}] \quad . \quad . \quad . \quad (6)$$

For the case of intermittent light the quantity ρ becomes

$$\rho' = \frac{2 \times \text{Rate with sector running}}{\text{Rate in continuous light}} = \frac{2\overline{\overline{\overline{[A]}}}}{\overline{\overline{[A]_s}}} = \frac{\frac{2}{l}\int_0^l \overline{[A]}dl}{\frac{1}{l}\int_0^l [A]_s dl}, \quad . \quad (7)$$

where the double bar represents the space average. From equations (1) and (2) ρ was calculated as a function ϕ of b_0, so that in terms of local rates we have

$$\rho(\text{local}) = \phi(b_0(\text{local})),$$

i.e.

$$\frac{2\overline{[\mathrm{A}]}_{(\text{local})}}{[\mathrm{A}]_{s(\text{local})}} = \phi(2t_l k_3[\mathrm{A}]_{s(\text{local})}),$$

where

$$[\mathrm{A}]_{s(\text{local})} = \left(\frac{\alpha I_0 k_1[\mathrm{A}_2]}{k_3}\right)^{\frac{1}{2}} \mathrm{e}^{-\frac{\alpha[\mathrm{A}_2]}{2}l}, \quad . \quad . \quad . \quad . \quad (8)$$

whence

$$2\overline{\overline{\overline{[\mathrm{A}]}}} = \frac{1}{l}\int_0^l \left(\frac{\alpha I_0 k_1[\mathrm{A}_2]}{k_3}\right) . \mathrm{e}^{-\frac{\alpha[\mathrm{A}_2]l}{2}} . \phi(2t_l(\alpha I_0 k_1 k_3 \mathrm{A}_2)^{\frac{1}{2}} . \mathrm{e}^{-\frac{\alpha[\mathrm{A}_2]l}{2}} dl \quad (9)$$

and

$$\overline{\overline{[\mathrm{A}]}}_s = \frac{2}{\alpha[\mathrm{A}_2]}\left(\frac{\alpha I_0 k_1[\mathrm{A}_2]}{k_3}\right)^{\frac{1}{2}}\left(1 - \mathrm{e}^{-\alpha[\mathrm{A}_2]l}\right). \quad . \quad . \quad . \quad (10)$$

Writing

$$[\mathrm{A}] = \frac{1}{2l}\left(\frac{\alpha I_0 k_1[\mathrm{A}_2]}{k_3}\right)^{\frac{1}{2}},$$

$$b' = 2t_l(\alpha I_0 k_1 k_3[\mathrm{A}_2])^{\frac{1}{2}},$$

we obtain

$$\rho' = c\frac{\int_0^l \mathrm{e}^{-cl}\phi(b'\mathrm{e}^{-cl})\mathrm{d}l}{(1 - e^{-cl})}, \quad . \quad . \quad . \quad . \quad (11)$$

and putting

$$\phi_0(b') = \int_0^l \phi(b')\mathrm{d}b',$$

we obtain

$$\rho' = \frac{\frac{\phi_0(b')}{b'} - \frac{\phi_0(b'\mathrm{e}^{-cl})}{b'}}{(1 - \mathrm{e}^{-cl})} \quad . \quad . \quad . \quad . \quad (12)$$

The numerator is obtained by plotting $\phi_0(b')$ against $\log_{10}b'$ and evaluating the difference $\phi_0(b') - \phi_0(b'\mathrm{e}^{-cl})$ in ordinates for the constant difference $\log_{10}\mathrm{e}^{-cl}$ in abscissae, and dividing this by b' in each case. The value of $(1 - \mathrm{e}^{-cl})$ is obtained from the extinction coefficient of the absorbing substance and the cell depth. Values of this function have been calculated for the case relevant to our experiments of a cell depth of 2 cm. and with 300 mm. of chlorine at 25° C absorbing light of wavelength 3650 Å. They are given in Table II and plotted in Fig. 1. It can be seen that there is a slight difference in shape between the curves for ρ and ρ'. For a determination of ρ', b' can be found, and the rate constants evaluated in the usual manner, since b' and b_0 differ only in the factor $(\alpha[\mathrm{A}_2]I_0/I_{\mathrm{abs}})^{\frac{1}{2}}$.

The values of the integrated function $\phi_0(b')$ were obtained by using the Gregory formula,[5] and by weighing graph paper, and the values agree to the first three figures, the Gregory formula being accurate to the fourth figure ; they are also given in Table I. This set of values, and the method given above will be of general application in the calculation of the effect of non-uniformity of absorption in sector experiments, the differences for different systems arising from the differences in cell depth and the extinction coefficient of the absorbing substance.

(ii) **The Penumbra Error.**—A close approximation to the state of affairs which obtains when a sector traverses a uniform light beam is obtained by considering a trapezoidal light pulse, i.e. a square light beam with the sector edge parallel to one side. Let the time of traverse of the beam by the sector edge be t_0 and put

$$2k_1 I_{\mathrm{abs}} = a, \; 2k_3 = g \text{ and } [\mathrm{A}] = y.$$

---

[5] Jeffreys and Jeffreys, *Methods of Mathematical Physics* (Cambridge, 1948), p. 259.

TABLE II.—VALUES OF y/y_0

No.	b_0	t_l/t_0	y_1/y_0	y_2/y_0	y_3/y_0	y_4/y_0	y_5/y_0
1	1	40	0·846	0·842	0·240	0·252	0·843
2	1	20	0·846	0·837	0·241	0·253	0·836
3	1	10	0·846	0·824	0·243	0·286	0·832
4	4	40	1·000	0·954	0·0773	0·126	1·000
5	4	20	1·000	0·915	0·0776	0·174	1·000
6	4	10	1·000	0·850	0·0782	0·266	1·000
7	10	40	1·000	0·895	0·9324	0·155	1·000
8	10	20	1·000	0·823	0·0326	0·273	1·000
9	10	10	1·000	0·726	0·0329	0·476	1·000

VALUES OF Areas/g

No. 1	Stage 1	Stage 2	Stage 3	Stage 4	Sum	Ideal	—	% Error
1	0·021	1·251	0·006	0·589	1·867	1·866	+0·001	0
2	0·042	1·244	0·012	0·568	1·866	1·866	0	0
3	0·085	1·234	0·026	0·526	1·871	1·866	0·005	0·27
4	0·100	2·511	0·010	3·326	5·947	5·944	0·003	0·05
5	0·200	2·466	0·023	3·268	5·957	5·944	0·013	0·22
6	0·397	2·396	0·056	3·142	5·981	5·944	0·037	0·62
7	0·240	3·320	0·018	9·201	12·78	12·78	0	0
8	0·459	3·233	0·057	9·049	12·80	12·78	0·020	0·15
9	0·833	3·091	0·190	8·696	12·81	12·78	0·030	0·23

Stage 1 denotes the light extinction process.
Stage 2 denotes the dark period.
Stage 3 denotes the light intensification process.
Stage 4 denotes the period of full illumination.

The equations which determine the concentration of centres for a 1-in-4 sector are then

(1) Light extinction process, y changes from $y_1 \rightarrow y_2$; time taken $= t_0$

$$\frac{dy}{dt} = -a\frac{t - t_0}{t_0} - gy^2.$$

(2) Complete extinction period, $y_2 \rightarrow y_3$ in time $3t_l - t_0$

$$\frac{dy}{dt} = -gy^2.$$

(3) Light intensification process, $y_3 \rightarrow y_4$ in time t_0

$$\frac{dy}{dt} = a\frac{t}{t_0} - gy^2.$$

(4) Complete illumination period $t_l - t_0$, $y_4 \rightarrow y_5$,

$$\frac{dy}{dt} = a - gy^2.$$

Eqn. (1) and (3) were integrated by putting $gy = \frac{1}{u}\frac{du}{dt}$, the solution for u being a power series which converges fairly rapidly. Since the error will depend on the extent of the traverse and on the sector speed, the magnitude of the penumbra effect has been calculated for three values of the ratio t_l/τ_0 ($= b_0$ of previous section) and for three values of t_l/t_0, i.e. the ratio of the sector width to the light beam width. The values chosen were those likely to occur in practice.

The effect of the penumbra on the mean radical concentration was evaluated by calculating the area beneath the $y - t$ curve for the full cycle $y_1 \rightarrow y_2 \rightarrow y_3 \rightarrow y_4 \rightarrow y_5$. For $b_0 = 4$ or 10 the value of y at the end of the light period is the equilibrium concentration in continuous light, i.e. y_0. For $b_0 = 1$, the value of y at the end of light period was taken to be $0{\cdot}846\ y_0$, which is the value y would have at the time b_0t_0 assuming ideal conditions, i.e. no penumbra. To calculate the area in the light extinction process, the approximation was made that $a - gy^2 = 0$ during this period. This gives slightly too small an area, but the effect is negligible except in the last case in the Table, where Area/g should be increased by 0·110 giving a error of 1·25 %.

The calculations show that fluctuations of y from the ideal value are caused by the penumbra but that the errors in the mean radical concentration due to the phases of light extinction and intensification compensate almost exactly. The net result is a small positive error, which is only appreciable at low sector speeds.

Note added in proof.—When two propagation steps each involving a different reactant, form part of the reaction mechanism, the variation of the experimental quantity ρ with mixture composition can be used to evaluate both velocity constants. An example of this will be given in a later paper.

We are indebted to the Department of Scientific and Industrial Research for financial aid to one of us.

Laboratory of Physical Chemistry,
Cambridge.

[6] See, for example, Jones and Melville, *Proc. Roy. Soc. A*, 1940, **175**, 392; and Burnett, Valentine and Melville, *Trans. Faraday Soc.*, 1949, **45**, 960.

ON THE EVALUATION OF ELECTRIC DIPOLE MOMENTS

BY K. B. EVERARD, R. A. W. HILL AND L. E. SUTTON

Received 24th November, 1949

The evaluation of the dipole moment of a substance from measurements of the dielectric constants, specific volumes and refractive indices of its dilute solutions in a non-polar solvent is discussed. The desirability of separately evaluating the total and the electron polarizations is considered, and difficulties in measuring the latter are discussed.

1. Introduction.—In recent years a number of papers dealing with the evaluation of electric dipole moments from dielectric measurements have appeared: Some of these are concerned with extrapolation procedure,[1, 2] and others with the question of what data are really necessary.[3, 4] While we are in substantial agreement with some of the views expressed, we think that there are qualifications and occasionally corrections which are worth mention.

[1] Halverstadt and Kumler, *J. Amer. Chem. Soc.*, 1942, **64**, 2988.

[2] Smith and Cleverdon, *Trans. Faraday Soc.*, 1949, **45**, 109.

[3] Guggenheim, *ibid.*, 1949, **45**, 714.

[4] Smith, *ibid.*, 1950, **46**, 394 (privately communicated before publication and after submission of this paper).

2. Notation.—The following notation will be used :

Subscripts 1 and 2 refer to the solvent and solute respectively; * symbols except ω bearing no subscript refer to the solution.† A symbol covered by a bar is an arithmetic mean.

$_Tp$, $_Ep$, $_Ap$, and $_Op$ are the specific total, electron, atom and orientation polarizations respectively; the capital P is used for molar polarizations ;

ω is the weight fraction of the solute ;

ϵ, v and n refer to dielectric constants, specific volumes and refractive indices ;

α, β, and γ are defined by the least square plots of eqn. (3.6), (3.5) and (5.2) respectively.

μ is the dipole moment, M the molecular weight, $[R]_D$ the molar refraction of the solute for the Na_D line and $[R]_\infty$ the same for infinite wave-length.

3. Basic Equations.—We shall first consider how $_Tp_{2\infty}$ the total polarization of the solute at infinite dilution is evaluated, taking as the basis of our discussion the Halverstadt-Kumler equation : [1]

$$_Tp_{2\infty} = 3\alpha v_1/(\epsilon_1 + 2)^2 + (v_1 + \beta)(\epsilon_1 - 1)/(\epsilon_1 + 2) \qquad . \quad (3.1)$$

which is derived algebraically from the five equations :

$$p_1 = v_1(\epsilon_1 - 1)/(\epsilon_1 + 2), \qquad . \quad . \quad . \quad (3.2)$$

$$p = v(\epsilon - 1)/(\epsilon + 2), \qquad . \quad . \quad . \quad (3.3)$$

$$p = (1 - \omega)p_1 + \omega p_2, \qquad . \quad . \quad . \quad (3.4)$$

$$v = v_1 + \beta\omega, \qquad . \quad . \quad . \quad . \quad . \quad . \quad (3.5)$$

$$\epsilon = \epsilon_1 + \alpha\omega. \qquad . \quad . \quad . \quad . \quad . \quad . \quad (3.6)$$

Eqn. (3.2) and (3.3) are based on the assumption that the internal field acting on a particle in the solution is given by the Clausius-Mosotti treatment, which assumption is known not to be adequate, but which we deliberately make because the more rigorous treatments devised by Onsager [5] and Kirkwood [6] can only be properly applied to spherical molecules, or require knowledge of further parameters ; so they are not very generally useful.

The absolute values of moments may consequently be in error by up to *ca.* 10 %, but for stereochemical applications of dipole moments absolute values are irrelevant ; it is only necessary that the values of component moments should be definite in a particular environment, and this is more likely to be the case.[7]

Eqn. (3.5) is a statement that volumes are additive. It is likely to be sufficiently accurate in the dilute solutions normally used. Eqn. (3.4) involves the assumption that p_1 and p_2 are independent of concentration. This latter is known not to be true. What is usually done, therefore, is to assume p_1 constant and to evaluate p_2 by some form of extrapolation to $\omega = 0$, because it is supposed that the discrepancy is caused by inter-dipolar forces. Goss disagrees with this procedure,[8] and evaluates both p_1 and p_2 by a method of intercepts.[9]

Eqn. (3.6) is introduced as an empirical truth. It must mean [1]

---

* This appears to be the more popular convention : the opposite one is used, however, in all the works of Le Fèvre.

†At the request of the Publications Committee we are not using the notation common in dipole moment literature. We omit the subscript 12 used to distinguish symbols relating to solutions. These appear simply as ϵ, v, n, etc., but where it is particularly necessary to distinguish general from particular functions this is done by words. We also omit the subscript 2 from the weight fraction of the solute, which appears as ω, that for the solvent therefore being $1 - \omega$. In order to make clear the meaning of quotations, we place our symbols in square brackets after those of the authors quoted.

[5] *J. Amer. Chem. Soc.*, 1936, **58**, 1486.

[6] *J. Chem. Physics*, 1936, **4**, 592.

[7] Sutton and Hampson, *Trans. Faraday Soc.*, 1935, **31**, 950.

[8] *J. Chem. Soc.*, 1937, 1915. [9] Orr and Butler, *Nature*, 1932, **130**, 930.

(i) that p_2 is not independent of ω, and (ii) that its relation to ω is not a simple linear one. It is not easy to give an experimental demonstration of these conclusions, because the requisite p_2 values have to be calculated from small differences between large numbers [p and $(1 - \omega)p_1$]. However, if the easily tested premise, eqn. (3.6), is valid, so also are the conclusions therefrom. Therefore, because it is easier to apply (3.6), involving only the use of a linear relation, than to find a curve of shape unknown fitting points which may scatter, the incorporation of it into (3.1) which automatically does the extrapolation is the better procedure.

The validity of (3.5) and (3.6) has recently been questioned by Smith and Cleverdon,[2] who advocate the addition of a term in ω^2 to each, claiming that " even at very low concentrations, the $\epsilon_{12} - \omega_2$ [now $\epsilon - \omega$] plot is definitely curved ". Whilst it is true that at high concentrations, as Smith and Cleverdon have shown, curvature is appreciable, especially with strongly polar solutes, other investigators,[1, 10, 11, 12] including ourselves, are agreed that in dilute solutions ($< \sim 1$ %) this effect is imperceptible. Although the accuracy of ${}_Tp_2$ may perhaps be greater if their procedure be followed, it is often impossible to do this for practical reasons; and if the aim is to obtain a dipole moment value it is usually unnecessary, because there is no point in obtaining molar polarizations (${}_TP_2$) to within 0·1 cm.^{3} unless atom polarizations are known with that order of accuracy, which they very rarely are. Deviations from linearity of $\epsilon - \omega$ and $v - \omega$ graphs corresponding to an uncertainty of *ca.* 1 cm.^{3} in ${}_TP_2$ can usually be tolerated (having regard to inevitable uncertainties), with consequent saving of time and materials. There are infrequent instances when, because there are no bonds likely to be very polar, and because vibration force constants are large (e.g. in unsymmetrical olefines or acetylenes), we can feel satisfied that the uncertainty in ${}_AP_2$ is less than 1 cm.^{3}: and then, of course, it may be worth while attempting to get greater precision in ${}_TP_2$.

At this point we may emphasize that our primary concern is the routine evaluation of electric dipole moments with a degree of accuracy appropriate to their applications, whereas Smith and his co-workers are particularly interested in studying small changes of moment from solvent to solvent and in assessing the ultimate limits of accuracy obtainable from solution measurements.

4. The Gradient α.—There has been some controversy about the method of obtaining α from the $\epsilon - \omega$ graph. Halverstadt and Kumler[1] advise that only values of ϵ for solutions be used to derive α; they discard the value of ϵ_1 on the grounds that (i) the " solutions may absorb more water vapour than the solvent ", and (ii) " each ϵ_{12} [ϵ] value for the different solutions depends on a single solvent measurement of ϵ_1 " which would thus be much more heavily weighted if the curve were drawn through it. Smith and Cleverdon,[2] on the other hand, say that in reliable work errors due to (i) do not occur, and that as for (ii) it is " usual to determine ϵ_{12} [ϵ] values with respect to an assumed value for ϵ_1, and this reference point is returned to repeatedly, especially when fresh batches of solvent are used, so that it is established very accurately ". Hence it should be more heavily weighted.

Each of these claims requires careful examination. It is true that in the most reliable work precautions are taken to exclude moisture; but this has not always been done, and in that event the Halverstadt-Kumler procedure is preferable. With regard to (ii), unless the apparatus is capable of absolute measurements, it is usual to calibrate it with benzene or some other solvent the dielectric constant ϵ_1 of which is assumed known, and to employ the following relation[13] for finding ϵ:

$$\epsilon = 1 + (\epsilon_1 - 1)C/C_1 \quad . \quad . \quad . \quad . \quad (4.1)$$

---

[10] Papers cited in ref. 1.

[11] Smyth (private communication).

[12] Li, An and Wu, *J. Amer. Chem. Soc.*, 1947, **69**, 2558.

[13] Cf. Le Fèvre, *Dipole Moments* (Methuen, 1938), p. 30.

in which C_1 is the amount, expressed in arbitrary scale units, by which the capacity of the dielectric constant cell increases when it is filled with solvent, and C with the solution. The "reference point" referred to by Smith and Cleverdon is not ϵ_1, which is not established at all* but is assumed, but C_1. Furthermore, C_1 is established no more accurately than C for a solution, if demountable cells are used, or if different batches of solvent are not purified to constant ϵ ($\pm$ 0·0001), which operation would be supererogatory so long as all the determinations on one solute are done with one batch.

Halverstadt and Kumler ignore ϵ_1 in finding α, for the reasons given above. If this be done, the fact that C_1 is not quite comparable with the values of C for the solutions hardly affects the slope α and, as will be shown in § 5, the slight error in absolute dielectric constant has a negligible effect upon the calculated dipole moment. The ϵ — ω graph is displaced, so that the dielectric constant ϵ_1' obtained by extrapolation to $\omega = 0$ differs from ϵ_1 by some quantity δ. It is ϵ_1' that Halverstadt and Kumler use for ϵ_1 in eqn. (3.1).

Now Smith and Cleverdon and also, in effect, Le Fèvre,[16] in deriving α work with a quantity $\Delta\epsilon = \epsilon - \epsilon_1$. The former define α as $(\Delta\epsilon/\omega)_{\omega=0}$, while the latter takes it as the average of the $\Delta\epsilon/\omega$ values.† This weighting of C_1 causes $(\Delta\epsilon/\omega)_{\omega=0}$ to become infinite if there is an error in C_1 which causes ϵ_1 to lie off the line through the solution points, in the way we have already considered. Evidently the correct procedure, *when solvent and solutions are treated alike and come from the same batch of solvent*, is to obtain α by fitting the best straight line to all values of ϵ, including the assumed value of ϵ_1.‡

If these conditions are not satisfied, then the value of ϵ_1 is probably best rejected. Only when the cell and the solvent have a very high degree of reproducibility and constancy is Smith and Cleverdon's use of ϵ_1 justified; and in our view the extra trouble is superfluous for routine measurements.

5. Degrees of Precision.—The next point to consider is what value to take for ϵ_1 in eqn. (3.1). We shall show in this section that it does not matter whether the assumed value is taken, or the value ϵ_1' obtained by extrapolation.

Eqn. (5.1), giving the electron polarization of the solute, may be derived in the same way as eqn. (3.1) for the total polarization:

$$_{E}p_2 = 6n_1\gamma v_1/(n_1^2 + 2)^2 + (v_1 + \beta)(n_1^2 - 1)/(n_1^2 + 2), \quad . \quad (5.1)$$

where γ is defined by eqn. (5.2), which is found to hold in dilute solution:

$$n = n_1 + \gamma\omega, \quad . \quad . \quad . \quad . \quad . \quad (5.2)$$

Now

$$\mu = \tfrac{3}{2}\sqrt{kTM\,_{O}p_2/\pi N} \quad . \quad . \quad . \quad . \quad (5.3)$$

and

$$_{O}p_2 = {_{T}p_2} - {_{E}p_2} - {_{A}p_2} = \frac{3v_1}{(\epsilon_1 + 2)} \cdot \alpha + \left(\frac{\epsilon_1 - 1}{\epsilon_1 + 2} - \frac{n_1^2 - 1}{n_1^2 + 2}\right)\beta - \frac{6n_1v_1}{(n_1^2 + 2)^2} \cdot \gamma$$

$$- \frac{\quad}{\epsilon_1 + 2} - \frac{\quad}{n_1^2 + 2} \qquad p_2. \quad (5.4)$$

---

* Benzene is usually used for calibration because its dielectric constant has been carefully determined [14], [15] but other liquids are quite often used as solvents, and in this case ϵ_1 is established in the same way as are the ϵ values for solutions.

[14] Hartshorn and Oliver, *Proc. Roy. Soc.*, *A*, 1929, **123**, 664.

[15] Sugden, *J. Chem. Soc.*, 1933, 768.

[16] Le Fèvre and Vine, *ibid.*, 1937, 1805.

† *Note added in proof.*—Since this paper was submitted, Le Fèvre (*Trans. Faraday Soc.*, 1950, **46**, 1), has explained that when α and β show a clear concentration dependence he extrapolates them to $\omega = 0$. Our remarks should therefore be considered *mutatis mutandis*.

‡ If the method of least squares is used,[1] then because we are concerned with the slope [$\alpha = \Sigma\epsilon(\omega - \bar{\omega})/\Sigma(\omega - \bar{\omega})^2$], greatest weight is attached to measurements

The accuracy with which the quantities in (5.4) must be obtained may be assessed by partial differentiation. For the usual solvent (benzene at 25°), putting ${}_{A}p_2 = 0$,

$$\delta\mu = 0{\cdot}0046\, M/\mu \,.\, \delta\alpha \tag{5.5}$$

$$\delta\mu = 0{\cdot}00008\, M/\mu \,.\, \delta\beta \tag{5.6}$$

$$\delta\mu = -\ 0{\cdot}014\, M/\mu \,.\, \delta\gamma \tag{5.7}$$

$$\delta\mu = (0{\cdot}0046 - 0{\cdot}0022\alpha + 0{\cdot}0040\beta)\, M/\mu \,.\, \delta\epsilon_1 \tag{5.8}$$

$$\delta\mu = (0{\cdot}00008 + 0{\cdot}0040\alpha - 0{\cdot}012\gamma)\, M/\mu \,.\, \delta v_1 \tag{5.9}$$

$$\delta\mu = (-\ 0{\cdot}014 - 0{\cdot}012\beta + 0{\cdot}010\gamma)\, M/\mu \,.\, \delta n_1, \tag{5.10}$$

where each $\delta\mu$ is a partial differential with respect to one variable at a time.

It will readily be seen, on trying typical values in these equations, that for errors in μ to become appreciable (say, $\delta\mu > \sim 0{\cdot}01$ D, where $\mu > \sim 0{\cdot}8$ D), β, which seldom exceeds $\pm\ 0{\cdot}5$, would have to be wrong in the first decimal place (i.e. it almost suffices to guess it), and ϵ_1, v_1 and n_1, each commonly measured to $\pm\ 0{\cdot}0001$ or less, in the second or sometimes the third place. Whilst accuracy in μ may occasionally be limited by accuracy in γ, by far the most important term in (5.4) is α.

It is therefore legitimate to ignore the small variations often observed in ϵ_1, v_1 and n_1, and to give them standard values. We may then write, simply, e.g.

$$\mu^2 = M(0{\cdot}00920\alpha + 0{\cdot}00015\beta - 0{\cdot}02790\gamma + 0{\cdot}00017) \tag{5.11}$$

for benzene at 25° as solvent. If the fourth term in (5.4), viz. the atom polarization of the non-polar solvent, were zero, the coefficient of β would also be zero, and there would be no need to measure specific volumes at all.[3, 4, 17]

The polarizations ${}_{T}p_2$ and ${}_{E}p_2$ are almost as insensitive as μ to reasonable variations in ϵ_1, v_1 and n_1, but in this case β needs to be known with much more accuracy.[18] Guggenheim[3] considers that to calculate polarizations is to waste effort. This is certainly true, provided that the sole purpose of measurements is to obtain dipole moments, and that there are no complications other than those already mentioned in deriving them. Electron and atom polarizations are, however, of interest in their own right;[19] and while the latter can only occasionally be determined by direct measurement, viz. when it is certain that the solute molecule is sufficiently symmetrical to be non-polar, the former are always available and may well be useful, more especially if the dispersion is measured (see § 6). If such observed values of ${}_{E}P_2$ are compared with the approximate ones derivable from tables of atomic and molecular refractions, new constitutional terms may be obtained when there are new groupings in the solute molecules, or the need for doing dispersion measurements may be revealed. Again, if the colour of the solute is so intense, or its solubility so little, that direct measurements are impracticable, then only estimated values of ${}_{E}P_2$ can be used: it is then essential to calculate ${}_{T}P_2$. For all these reasons, therefore, we still find it worth while to take the extra trouble of measuring specific volumes accurately.

One further practical point is that in checking observations it is

---

on the most and least concentrated solutions, and none at all to measurements on a solution of weight fraction $\overline{\omega}$. It is therefore advantageous from this point of view to cluster the concentrations of the solutions examined at each limit of the range of ω taken. On the other hand, linearity of the graphs is best tested with solutions of equally spaced concentrations. In practice a compromise must be reached.

[17] Cf. Henriquez, *Physica*, 1933, **1**, 41.

[18] Le Fèvre, *op. cit.*, p. 36.

[19] Sutton, *Faraday Soc. Discussion*, 1946, 170.

convenient to have separate plots of ϵ and n against ω because if a combined function is used, as recommended by Guggenheim, any error in measurement is liable to be disguised or obscured (cf. [2, 4]). The experimenter knows only too well that sure freedom from errors can never be attained.

6. Interferometers.—The use of an interferometer in evaluating dipole moments would appear to have much to commend it. It is quicker, more convenient, more accurate and simpler in use than a Pulfrich refractometer, and it gives the required values of Δn with the minimum of calculation.

On the other hand, there is a pitfall attending its use, viz. the " insidious " dispersion error, as it is described by Bauer.[20] This means that no solutes may be examined whose dispersions differ greatly from that of the solvent, for otherwise the zero-order band will not be achromatic, a property which is normally used in its identification. With benzene as solvent, solutes such as derivatives of naphthalene, styrene and stilbene may not safely be used, even in the very dilute solutions made up for dipole moment measurements; but simple derivatives of benzene, and compounds of an aliphatic nature, are usually satisfactory. A set of measurements is deemed to be " satisfactory " if, under the usual conditions, the molar refraction of the substance is within 1 or 2 cm.^{3} of that estimated from the tables (for the Na_D line), and if there is no abnormal scatter on the $\Delta n - \omega$ graph. (All our published refractions in papers subsequent to *J. Chem. Soc.*, 1949, 746, are " satisfactory ", and in this paper discrepancies are trivial.)

The following figures exemplify this point (practical details will be given in forthcoming papers).

Compound	$[R]_D$ (using interferometer)	$[R]_D^*$ (calc.)	$[R]_D$ (using refractometer)
Styrene	38·0	35·2	36·5
4-Dimethylaminostilbene †	112·1	80·3	87·8
4-Bromostilbene	88·1	73·4	72·8
4-Nitrostilbene	100·0	72·2	—
1-(4-Nitrophenyl)-4-phenyl-1 : 3-butadiene . .	139·4	79·2	—
1-(4-Dimethylaminophenyl)-4-phenyl-1 : 3-butadiene	—	87·2	109·1

7. Dispersion.—It is not unusual to find in the literature measured values of $[R]$ greatly exceeding calculated values,* even though obtained with a refractometer. Thus there are four examples of divergences of 15-20 cm.^{3} in a single paper by Bergmann and Weizmann [21] dealing with azobenzene derivatives, and one each of 229, 43, 18, 13 and 11 cm.^{3} in another,[22] dealing with stilbene and styrene derivatives.‡ De Gaouck and Le Fèvre [23] give $[R]$ for salicylidene anil as 66·4 cm.^{3}, yet for its 5-bromo-derivative as no less than 101·5 cm.^{3} (the increment due to the bromine should be 7·8 cm.^{3}). We give two examples in § 6.

---

[20] Weissberger's *Physical Methods of Organic Chemistry*, Vol. I (Interscience, 1945), p. 729.

* We have based the calculated values on the measured refraction of the parent hydrocarbon or azahydrocarbon.

† It was found that with a 1 % solution about the 40th order band was achromatic.

[21] *Trans. Faraday Soc.*, 1936, **32**, 1318.

[22] Bergmann, *J. Chem. Soc.*, 1936, 402.

‡ Bergmann stated that some of the measurements were carried out with an interferometer; but he did not state which.

[23] Bergmann, *J. Chem. Soc.*, 1938, 741.

Divergences as large as these are clearly serious in dipole moment calculations. Dispersion theory [24] correlates them with strong spectroscopic absorption in the near ultra-violet or visible frequencies, and shows that $[R]_\infty$ is larger than the sum of atomic $[R]_\infty$ terms, though the differences can only be calculated if the frequencies and transition moments for the absorption lines are known. The difference between $[R]_D$ (observed) and $[R]_\infty$ (correct) is likely to be greater than that between $[R]_\infty$ (correct) and $[R]_\infty$ (calculated).

Moments calculated with $[R]_D$ (observed) are therefore likely to be considerably smaller than the true values, and to be more in error, though in the opposite direction, than if $[R]_\infty$ (calculated) were used. In such cases, the best compromise is, in our opinion, to use $[R]_D$ (calculated) values which are somewhat larger than $[R]_\infty$ (calculated); and a further allowance for the exaltation may be made by starting from $[R]_D$ (observed) for the parent hydrocarbon. This still leaves the difficulty of allowing for ${}_AP_2$. When there is uncertainty in both ${}_EP_2$ and ${}_AP_2$ it is impossible to attain the usual degree of accuracy.

The authors thank the Department of Scientific and Industrial Research for a Special Research Grant (to L. E. S.) and for a Maintenance Grant (to K. B. E.).

Physical Chemistry Laboratory,
Oxford.

[24] Van Vleck, *Electric and Magnetic Susceptibilities* (Oxford, 1932), Chap. III.

THE VAPOUR PRESSURE OF 2 : 4 : 6-TRINITROTOLUENE

By G. Edwards

Received 8th December, 1949

Estimations of the vapour pressure of 2 : 4 : 6-trinitrotoluene have been made in the range 50-143° C by the Knudsen method. The results are in close agreement with those of Robertson [1] in the range 232-345° C and a general equation for the vapour pressure and latent heat of volatilization has been deduced. These equations enable an estimate to be made of the critical temperature.

A knowledge of the vapour pressure of trinitrotoluene is required for the evaluation of equations connected with the kinetics of its thermal decomposition and explosion, and to estimate the concentration of the explosive in the atmosphere of workrooms during its manufacture. The experiments described were conducted with these applications in view.

Experimental

Material.—2 : 4 : 6-trinitrotoluene was prepared by repeated crystallization of a commercial grade from concentrated sulphuric acid followed by water washing at 100° C and drying for the minimum period at this temperature.

---

[1] Robertson, *Trans. Faraday Soc.*, 1948, **44**, 977.

Apparatus.—The method used was that due to Knudsen,[2] measurements being made of the loss of vapour from a box with a hole of diameter less than the mean free path of the vapour molecules. The apparatus used in the present experiments is shown in Fig. 1. A pure liquid, the boiling point of which is known, was heated in the reboiler by passage of an electric current in the Nichrome coil A. Vapour from the liquid passed in a rapid stream up the inside of the funnel B and down the outer annulus to the vapour condenser C. The condensate re-entered the boiler at the base by way of the return pipe D. The outer shape of the upper section of the reboiler was constructed to conform accurately to the B.S.S. Joint B34[3] and was fitted to the Pyrex glass vacuum chamber as shown, lubrication being effected by Dow-Corning silicone lubricant. Approximately 1 cm. above the heater and concentric with it was a Pyrex glass condenser with a deep recess of the same internal diameter (0·375 in.) as the box heating chamber. The box containing the trinitrotoluene could be retained in this by the rotatable arm E until the apparatus was fully evacuated. Evacuation was effected by a pumping system consisting of three stages of oil-condensation pumps backed by a two-stage oil rotary pump. This system reduced the pressure to less than 10^{-5} mm. Hg (ionization gauge).

The box used was of polished aluminium and could be fitted with one of three lids with holes 0·0568, 1·068 and 1·250 mm. diam. respectively. The overall diameter of the box was 0·370 in. and height 0·375 in., and its weight almost exactly 1 g.

The mass of the box and trinitrotoluene were measured to 0·1 mg. on an analytical balance. The heater was removed from the glass vacuum chamber and the box pushed into the condenser recess and retained by the rotatable arm. The heater was brought up to its working temperature and inserted in the B34 joint of the vacuum chamber. Vacuum was applied and when conditions had stabilized the box was released from the condenser. The condenser was then charged with alcohol and powdered solid carbon dioxide. At the end of the test the vacuum was broken and the box removed for reweighing.

In early runs results were irreproducible. This was traced to poor heat transfer between the heating recess and the box. Careful re-machining of the box base and heating surface proved only a partial solution. In later runs contact was made through a small bead of Silicone grease placed on the base of the heater. This was carefully removed with a clean cloth before weighing. The error in weighing was shown by experiment to be less than 0·1 mg.

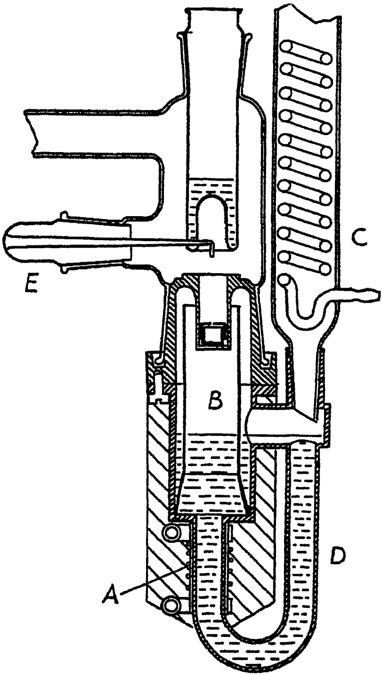

FIG. 1.

The temperatures shown in Table I were evaluated from the boiling points at 760 mm. by application of the Clausius-Clapeyron relationship. Times of heating were estimated by observation of the time required to melt pure substances under the same conditions as those applying in pressure-measuring tests. In all cases the substance in the box attained a temperature within 2° C of the reboiler temperature in less than 80 sec. No correction was applied for time of heating.

The results are shown in Table I. The vapour pressure was estimated using the relation

$$m^2/t^2 = p^2A^2M/2\pi RT,$$

where m is in g., t in sec., p in dyne/cm.^{2}, A in cm.^{2}, R in erg/deg. and M is the molecular weight in g. The results of Table I are shown graphically in Fig. 2,

---

[2] Knudsen, *Ann. Physik.*, 1909, **28**, 999.

[3] B.S.S., 572, 1934.

$\log_{10} p$ (cm.) being plotted against $10^3/T$. Treating the line representing the vapour pressure over the solid explosive as straight, its equation is

$$\log_{10} p = 14{\cdot}34 - 6180/T. \qquad (1)$$

The latent heat of sublimation is

$$L = 28{\cdot}3 \text{ kcal./mole.} \qquad (2)$$

TABLE I

Test No.	T.N.T. Lost, mg.	Time sec.	B.P. of Reboiler Liquid (corrected)	Hole Diameter (mm.)	Vapour Pressure (cm. Hg p)	$\mathrm{Log}_{10}\, p$	$10^3/T°$ K
1	1·7	10,800	53·0	1·250	$2{\cdot}64 \times 10^{-5}$	−4·579	3·068
2	7·7	24,000	60·1	1·250	$5{\cdot}43 \times 10^{-5}$	−4·265	3·002
3	5·4	19,000	60·8	1·068	$6{\cdot}32 \times 10^{-5}$	−4·199	2·998
4	9·7	24,000	61·5	1·250	$6{\cdot}86 \times 10^{-5}$	−4·164	2·990
5	5·3	19,800	61·0	1·068	$6{\cdot}22 \times 10^{-5}$	−4·206	2·994
6	16·6	12,600	72·1	1·068	$3{\cdot}11 \times 10^{-4}$	−3·507	2·898
7	17·1	12,840	72·1	1·068	$3{\cdot}14 \times 10^{-4}$	−3·503	2·898
8	16·6	12,600	72·3	1·068	$3{\cdot}11 \times 10^{-4}$	−3·507	2·896
9	27·6	10,200	78·5	1·068	$6{\cdot}44 \times 10^{-4}$	−3·191	2·845
10	26·6	10,800	78·5	1·068	$5{\cdot}88 \times 10^{-4}$	−3·231	2·845
11	32·9	12,600	78·3	1·068	$6{\cdot}22 \times 10^{-4}$	−3·206	2·846
12	14·8	5,400	79·8	1·068	$6{\cdot}55 \times 10^{-4}$	−3·184	2·834
13	28·7	10,800	80·1	1·068	$6{\cdot}37 \times 10^{-4}$	−3·196	2·832
14	27·0	9,000	80·2	1·068	$7{\cdot}16 \times 10^{-4}$	−3·145	2·831
15	29·9	9,000	82·4	1·068	$7{\cdot}96 \times 10^{-4}$	−3·099	2·814
16	35·4	7,200	86·9	1·068	$1{\cdot}19 \times 10^{-3}$	−3·926	2·778
17	33·6	7,200	86·9	1·068	$1{\cdot}13 \times 10^{-3}$	−3·949	2·778
18	24·6	5,400	99·5	0·568	$3{\cdot}92 \times 10^{-3}$	−2·407	2·681
19	26·8	5,400	99·5	0·568	$4{\cdot}07 \times 10^{-3}$	−2·390	2·681
20	53·5	3,900	99·0	1·068	$3{\cdot}37 \times 10^{-3}$	−2·473	2·688
21	34·2	3·600	110·6	0·568	$8{\cdot}26 \times 10^{-3}$	−2·083	2·607
22	21·9	2,400	110·5	0·568	$7{\cdot}96 \times 10^{-3}$	− 2·099	2·607
23	46·6	1·200	131·1	0·568	$3{\cdot}48 \times 10^{-2}$	− 1·459	2·475
24	46·3	1·200	131·5	0·568	$3{\cdot}45 \times 10^{-2}$	−1·462	2·473
25	82·2	1,200	141·4	0·568	$6{\cdot}21 \times 10^{-2}$	−1·207	2·413
26	81·7	1,200	142·0	0·568	$6{\cdot}58 \times 10^{-2}$	−1·182	2·410
27	81·5	1,200	142·5	0·568	$6{\cdot}17 \times 10^{-2}$	−1·210	2·407

Slight curvature is exhibited by the vapour pressure line for the liquid-vapour system. A tangent to this line at $10^3/T = 2{\cdot}80$ (i.e. a few degrees above the melting point) may be represented by

$$\log_{10} p = 10{\cdot}90 - 4960/T \qquad (3)$$

which yields for the latent heat of volatilization

$$L = 22{\cdot}7 \text{ kcal./mole,} \qquad (4)$$

and 5·6 kcal./mole for the latent heat of fusion. Fig. 3 shows graphically the relation of the results to those of Robertson,[1] Menzies[4] and Belajev and Yusephovich.[5] It is clear that taking into account the decrease of latent heat with increasing temperature, the present results are in good agreement with those of Robertson,[1] and a smoothly curved line can be drawn through these. The close relation

[4] Menzies, *J. Amer. Chem. Soc.*, 1920, **42**, 2218.

[5] Belajev and Yusephovich, *Compt. rend. U.R.S.S.*, 1940, **27**, 133.

of the results of Robertson and those of the present experiments appears to merit the application of a third term [6] to the vapour pressure equation, taking

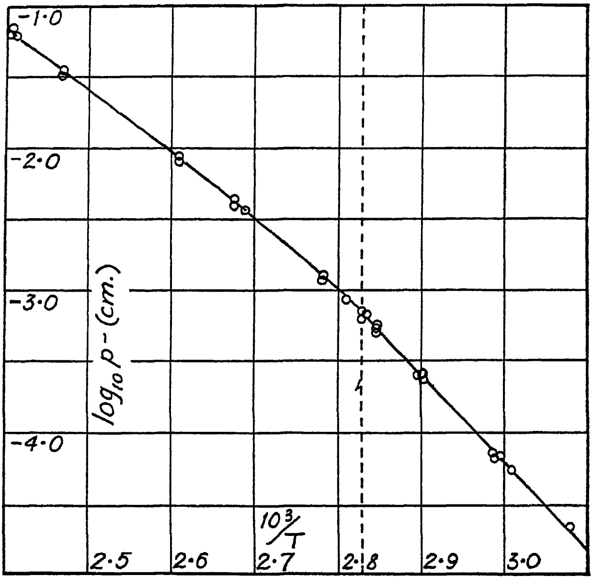

FIG. 2.

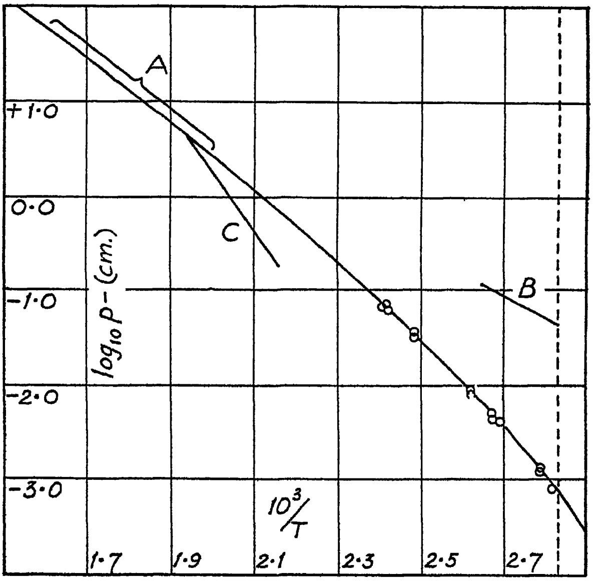

FIG. 3.—A Robertson, B Menzies, C Belajev and Yusephovich.

account of the curvature of the common line. Addition of the term $C \log_{10} T$ and solution of the simultaneous equations for the points

$(10^3/T = 1{\cdot}75, \log_{10}p \text{ (cm.)} = 1{\cdot}37)$, $(2{\cdot}30, -0{\cdot}70)$ and $(2{\cdot}83, -3{\cdot}14)$
yields the general equation

$$\log_{10}p \text{ (cm.)} = 73{\cdot}80 - 8240/T - 21{\cdot}05 \log_{10} T. \qquad (6)$$

---

[6] Henning and Stock, *Z. Physik*, 1921, 4, 226.

The Clausius-Clapeyron relationship may be applied to this equation to evaluate the latent heat of volatilization

$$LT = RT^2 \text{ d} \ln p/\text{d}t = 2{\cdot}303RT^2\text{d} \log_{10} p/\text{d}T \quad . \quad . \quad . \quad (7)$$
$$= 37{\cdot}680 - 41{\cdot}79T.$$

This yields a latent heat at the melting point of 22·9 kcal./mole, indicating a latent heat of fusion of 5·4 kcal./mole. On the assumption that the equation may be extrapolated indefinitely the latent heat at 0° K is 37·7 kcal./mole and the critical temperature 900° K.

The close agreement with the results of Robertson [1] suggests that the latter's estimation of accuracy (1000 cal. for L) is conservative. Considered collectively it would appear that an accuracy of 500 cal./mole can be ascribed to the results. This is substantiated by comparison of the calculated latent heat of liquefaction (5·6 from tangent measurements and 5·4 from the general equation) with that given by Perry,[7] viz., 5·1 kcal./mole.

The value of the critical temperature (627° C) by its method of estimation can only be regarded as indicating the order of the value. Its direct determination is not possible as the induction period prior to explosion at this temperature is only some milliseconds. The value may be of use in thermodynamic calculations involving the reduced temperature T/T_c.

The author wishes to acknowledge with thanks useful discussions with Dr. A. J. B. Robertson of The Royal Institution and with Prof. J. M. Robertson and Dr. J. C. Speakman of the University of Glasgow. This paper is published with the permission of The Chief Scientist of the Ministry of Supply.

The Royal Technical College,
George Street,
Glasgow.

[7] Perry, *Chemical Engineer's Handbook* (McGraw-Hill, New York, 1941), 2nd edn., p. 507.

REVIEW OF BOOK

Metals Reference Book. By C. J. Smithells (Ed.). (Butterworths Scientific Publications Ltd., 1949.) Pp. 735. Price £3.

This new British handbook will be very popular with practical and theoretical metallurgists, metal physicists and physical chemists. It is broader in range, more scientific, and far less technological than the well-known American *Metals Handbook;* it is also half the price. It can best be described in brief as a " pocket " encyclopaedia for the science of metals.

The value of a work of this kind depends chiefly on (*a*) the reliability of the data, (*b*) the range of topics covered, and (*c*) the effectiveness of the index. By all these tests *Metals Reference Book* is highly satisfactory. Above all, its reliability is assured by the names of the distinguished specialists who have contributed and edited. (Incidentally, the reviewer has looked for errors, but has not noticed any.) Nevertheless, it seems a pity that the names of the contributors appear only in a list at the front of the book. It is pertinent to ask who has been responsible for the various sections (cf. *International Critical Tables* or *Metals Handbook*). This is of interest because " the values given are those which contributors have selected as the most reliable ". Further, certain sections are particularly good, and the credit for them should go to the individual contributors who have put in the hard work (and vice versa, if applicable !).

The range of topics covered is remarkable, and it is impossible to do full justice to the scope of the work in a short review. Data are classified under 35 main headings, which are sub-divided into some 360 titles. Many of the sections contain numerous and often extensive tables, graphs, and diagrams. Among the more notable main sections are those dealing with the following subjects: atomic properties, line spectra, X-ray crystallography, crystal structure, crystal chemistry, geochemistry, metallography, phase equilibrium diagrams, gases in metals, and diffusion in metals. The last two are particularly good. Ordinary physical, mechanical and technological properties of metals are, of course, dealt with fully.

A section presenting theremodynamical data for metals and their more important compounds deserves especial mention; extensive and well-documented, it is probably unique as a condensed compilation of such data. In Table 8(*a*) the range of applicability of the equations for ΔG could usefully be added. In Table 19(*b*), which gives vapour pressure equations, and also in the heading of 8(*a*), one can only guess that log p and log T are presumably decadic logarithms.

There are more than 100 pages of phase diagrams, often six to a page. This collection will be very useful for quick reference, but it is disappointing to find that the diagrams have been merely collected from a number of sources such as *I.C.T.* and reproduced here without comment, reference, or even date. This explains why, for instance, the m.p. of iron is variously shown as 1528, 1530, 1535 and 1539° C. In future editions the source and date should be given at the very least, with preferably a few key references too. Incidentally, the Fe—O diagram, for one, is decidedly behind the times, as comparison with *Metals Handbook* (1948) would have shown.

Users of *Metals Reference Book* will have their own ideas for additional or alternative material which might have been included. Thus, nothing could be found on the heat treatment of less common metals and alloys such as tungsten and beryllium-copper, or the emissivity of non-metallic surfaces frequently encountered in metallurgy (e.g. slags and refractories). Similarly, 17 pages of integrals might have been more usefully devoted to some tables of erf x, etc., which are often needed in heat conduction and diffusion calculations, and which are not easy to come by. However, the selection of data provided is well balanced, and any improvements that may be effected in later editions—for which the editor invites suggestions—can only be minor if the *Reference Book* is to keep its present handy size (10 in by 6 in. by 1¼ in.). The high concentration of data has been secured by an economical lay-out and by use of small print that is, nevertheless, always legible. Paper and binding are adequate, and the book opens well. The edges of the pages are coloured and rounded at the corners to keep a neat appearance under heavy use. The price is very reasonable for such a mine of information. Demand for the book should be wide enough to permit the frequent revisions that will be required if *Metals Reference Book* is to maintain the high standard of reliability with which it has begun.

J. A. K.

THE VIBRATIONAL SPECTRA OF SOME ORGANIC SULPHUR COMPOUNDS AND THE CHARACTERISTIC FREQUENCIES OF C—S LINKAGES

BY N. SHEPPARD

Received 5th September, 1949

Infra-red spectra in the region 1500-500 cm.$^{-1}$ are reported for an extensive series of sulphur compounds that have not previously been investigated. Frequencies previously found in Raman spectra which are characteristic of SH, CS and SS linkages (2600-2550 cm.$^{-1}$, 710-570 cm.$^{-1}$ and *ca.* 500 cm.$^{-1}$ respectively) are found also in the infra-red spectra. A detailed study has been made of the variation of the CS stretching frequency with the nature of the saturated or unsaturated alkyl group attached to the sulphur atom. The frequency ranges characteristic of the CS linkage with the indicated alkyl substituents are as follows: methyl, 705-685 cm.$^{-1}$; primary alkyl, 660-630 cm.$^{-1}$; secondary alkyl, 630-600 cm.$^{-1}$; tertiary alkyl, 600-570 cm.$^{-1}$; cyclohexyl, 710-685 cm.$^{-1}$. The results are interpreted in terms of changes in the force constant of the C—S linkage in these compounds. Similar frequency and force constant variations occur with the corresponding alkyl chlorides and can be correlated with other bond properties.

As part of an infra-red spectroscopic study of the vulcanization of rubber,[1] a considerable number of organic sulphur compounds have also been investigated in this region of the spectrum. This work was undertaken with a view to the identification of the various types of sulphur linkages, viz. S—H, C—S, S—S and C=S, that might occur in vulcanizates. Complete analyses have been published previously of the spectra of the smaller molecules ethyl mercaptan[2] and thioacetic acid.[3] An earlier and complementary series of infra-red spectra of sulphur compounds over the range 3500-500 cm.$^{-1}$ has been obtained by Trotter and Thompson.[4] However, the increased range of compounds of which spectra are now available as a result of the present investigation together with the Raman spectra that have been available for several years[5-13] seemed to warrant a considerable extension of these authors' conclusions. In particular an attempt has been made to find out whether the detailed correlation rules, derived previously from the Raman spectra[14] for the identification of various types of C—S linkages, could be applied also to the infra-red data.

---

[1] Sheppard and Sutherland, *Trans. Faraday Soc.*, 1945, **41**, 261.

[2] Sheppard, *J. Chem. Physics*, 1949, **17**, 79.

[3] Sheppard, *Trans. Faraday Soc.*, 1949, **45**, 693.

[4] Trotter and Thompson, *J. Chem. Soc.*, 1946, 481.

[5] Kohlrausch, *Ramanspektren* (Akad. Verl. Becker und Erler, Leipzig, 1943), pp. 239 *et seq.*

[6] Hibben, *The Raman Effect and its Chemical Applications* (Reinhold, New York, 1939), pp. 256 *et seq.*

[7] Venkateswaran, *Indian. J. Physics*, 1930, **5**, 220.

[8] Venkateswaran, *ibid.*, 1931, **6**, 51.

[9] Thatte and Ganesan, *Phil. Mag.*, 1933, **15**, 51.

[10] Dadieu, Pongratz and Kohlrausch, *Monatsh.*, 1932, **61**, 409.

[11] Kopper, Seka and Kohlrausch, *ibid.*, 1932, **61**, 397.

[12] Pongratz and Kohlrausch, *ibid.*, 1932, **61**, 369.

[13] Koppl and Kohlrausch, *ibid.*, 1933, **63**, 255.

[14] Kohlrausch, *Ramanspektren*, p. 235.

16

Experimental

A Hilger D209 double-beam infra-red spectrometer was used under conditions described previously.[15] Rocksalt and potassium bromide prisms were used in their appropriate regions (3000-700, and 700-450 cm.$^{-1}$ respectively). A fluorite plate was used as a shutter in the potassium bromide region of the spectrum so as to allow for " false " energy. The cells used consisted of rocksalt or potassium bromide plates separated by lead washers of approximately 0·06 mm. thickness.

Most of the samples investigated were supplied by Dr. E. H. Farmer and Dr. R. F. Naylor of the British Rubber Producers' Research Association, Welwyn, Herts. The various compounds were subjected to physical and chemical examination at Welwyn, and samples sealed in nitrogen were then sent to Cambridge. These were run immediately after opening the glass sample tubes. The physical properties of compounds whose infra-red spectra are published here are as follows: di-*n*-propyl sulphide, b.p. 142° C; di-*n*-butyl sulphide, b.p. 182° C; di-*n*-butyl disulphide, b.p. 110-113° at 15 mm. pressure; di-*tert.*-butyl disulphide, 78-80° C at 16 mm; di-allyl sulphide, 138° C; di-crotyl sulphide, 78° C at 15 mm.; pentamethylene sulphide, 140° C; 2 : 2 : 6 : 6-tetramethyltetrahydrothiopyran, 66° C at 12 mm.; cyclohexyl mercaptan, 151-158° C; di-cyclohexyl sulphide, 74° C at 0·2 mm.; di-cyclohexyl disulphide, 100° C at 0·01 mm.; cyclohexyl-cyclohexenyl sulphide, 69-70° C at 0·1 mm.; di-cyclohexenyl sulphide, 81-82° C at 0·1 mm.; cyclohexene *epi*sulphide, 56-57° C at 15 mm.

The infra-red spectra of these compounds in the region 1500-500 cm.$^{-1}$ are given in Fig. 1 to 5. Both the infra-red and Raman data on the well-established C—S and S—S stretching frequencies of the simpler saturated sulphur compounds are collected together for comparative purposes in Table I. These frequencies all lie in the region 710-450 cm.$^{-1}$ which is well known to contain the strong frequencies in the Raman spectra associated with the stretching modes of the heavily weighted C—S and S—S linkages. The positions of the absorption bands in the infra-red spectra are given below:

TABLE I.—THE OBSERVED C—S AND S—S STRETCHING FREQUENCIES IN SATURATED ALKYL MERCAPTANS, SULPHIDES AND DISULPHIDES

Alkyl Group	Mercaptan		Sulphide		Disulphide			
	C—S frequency		C—S frequency		C—S frequency		S—S frequency	
	Raman §	Infra-red[4]	Raman §	Infra-red*	Raman §	Infra-red*	Raman §	Infra-red*
Methyl .	702	705	691	694	695	687	512	517
Ethyl .	657	660	648	640	640	639	509	510
n-Propyl .	651	653	652	648	—	628	—	—
n-Butyl .	653	658	655	649	—	631	—	—
*iso*Butyl	708	708	—	—	—	—	—	—
	668	672	—	—	—	—	—	—
*iso*Amyl .	658	—	—	—	—	—	—	—
sec.-Propyl	626	630	—	—	—	—	—	—
sec.-Butyl	617	—	—	—	—	—	—	—
tert.-Butyl	587	587	—	—	—	568	—	—
tert.-Amyl	575	—	—	—	—	—	—	—

The infra-red data * are taken from the present work and that of Trotter and Thompson;[4] the Raman data § from the compilations of Kohlrausch[5] and Hibben.[6]

DI-*n*-PROPYL SULPHIDE. 1463 (s), 1430 (w), 1379 (m), 1347 (w), 1291 (m), 1221 (s), 1095 (w), 1042 (w), 896 (m), 841 (w), 784 (m), 739 (m), 720 (w), 648 (m); (s) = strong; (m) = medium; (w) = weak.

DI-*n*-BUTYL SULPHIDE. 1461 (s), 1430 (w), 1376 (m), 1341 (w), 1300 (w),

---

[15] Sheppard and Sutherland, *J. Chem. Soc.*, 1947, 1540.

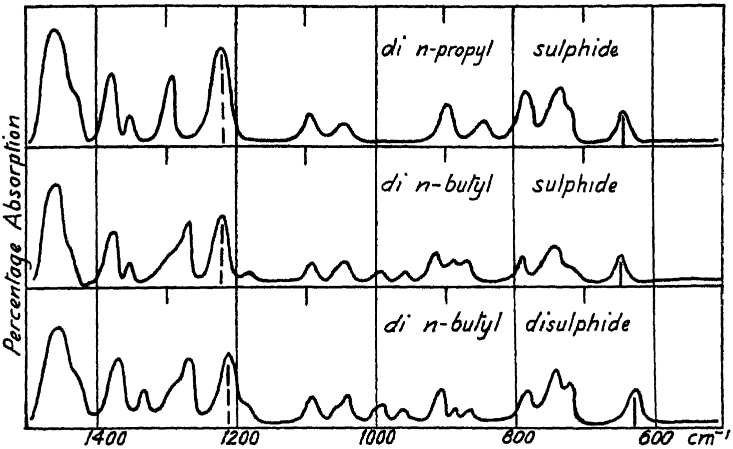

FIG. 1.—The infra-red spectra of some saturated alkyl sulphur compounds.

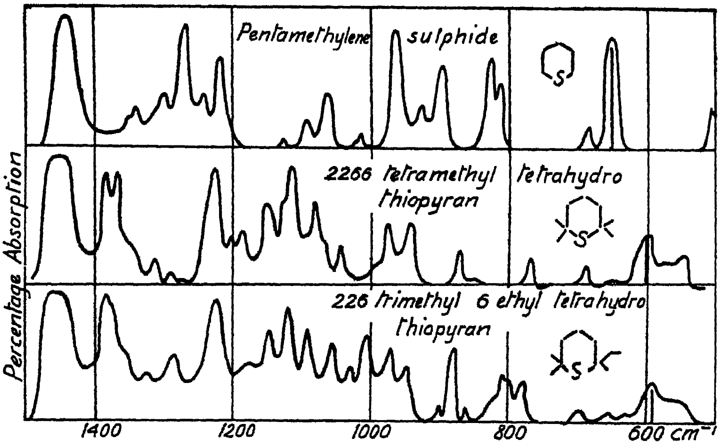

FIG. 2.—The infra-red spectra of some cyclic alkyl sulphur compounds.

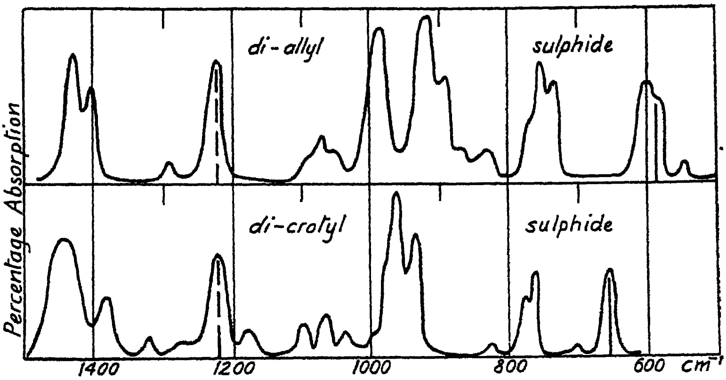

FIG. 3.—The infra-red spectra of some unsaturated sulphur compounds

1269 (m), 1219 (m), 1182 (w), 1094 (w), 1047 (w), 995 (w), 961 (w), 913 m), 889 (m), 872 (m), 786 (m), 745 (m), 704 (w), 649 (m).

DI-*n*-BUTYL DISULPHIDE. 1459 (s), 1425 (w), 1372 (m), 1332 (w), 1291) w), 1267 (m), 1211 (m), 1184 (w), 1090 (w), 1061 (w), 1048 (w), 993 (w), 963 (w), 907 (w), 889 (w), 865 (w), 778 (m), 742 (m), 723 (m), 631 (m).

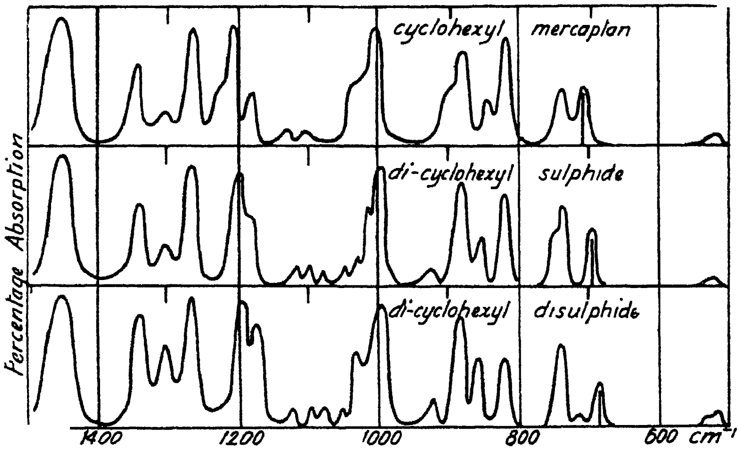

FIG. 4.—The infra-red spectra of cyclohexyl mercaptan, sulphide and disulphide.

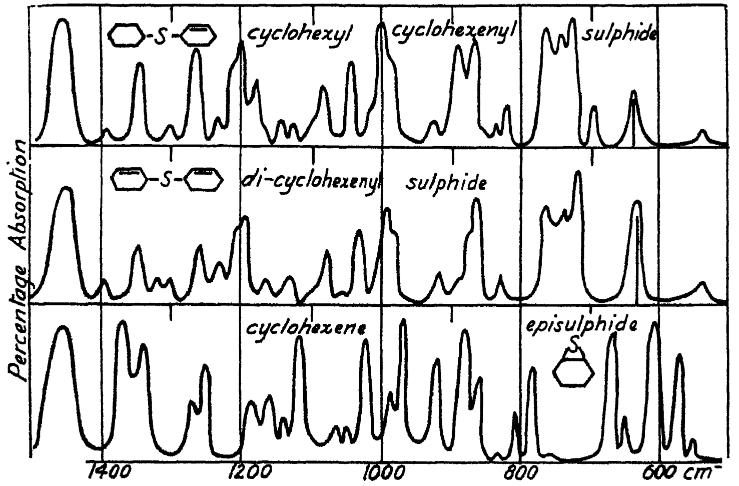

FIG. 5.—The infra-red spectra of cyclohexyl-cyclohexenyl sulphide, di-cyclohexenyl sulphide and cyclohexene *epi*sulphide.

DI-*tert*.-BUTYL DISULPHIDE. Not investigated in region 1500-700 cm.$^{-1}$ 568 (m).

DI-ALLYL SULPHIDE. 1637 (m), 1427 (m), 1403 (m), 1291 (w), 1220 (m), 1088 (w), 1070 (w), 1049 (w), 986 (s), 916 (s), 889 (m), 861 (w), 823 (w), 754 (m), 735 (m), 600 (m), 583 (m), 551 (w).

DI-CROTYL SULPHIDE. 1674 (w), 1440 (m), 1378 (m), 1307 (w), 1268 (w), 1217 (m), 1170 (w), 1094 (w), 1061 (w), 1033 (w), 992 (m), 961 (s), 933 (m), 826 (w), 776 (m), 760 (m), 700 (w), 658 (m).

PENTAMETHYLENE SULPHIDE. 1440 (s), 1339 (w), 1298 (w), 1269 (s), 1239 (w), 1216 (m), 1129 (w), 1092 (w), 1062 (m), 1014 (w), 965 (s), 929 (w), 900 (m), 828 (m), 814 (m), 685 (w), 654 (s), 505 (w).

2 : 2 : 6 : 6-TETRAMETHYLTETRAHYDROTHIOPYRAN. 1451 (s), 1381 (s), 1362 (s,) 1343 (w), 1307 (w), 1287 (w), 1224 (s), 1199 (w), 1181 (w), 1149 (m), 1120 (m), 1111 (s), 1079 (m), 1068 (w), 1036 (w), 971 (m), 942 (m), 868 (w), 769 (w), 691 (w), 654 (w), 603 (m), 574 (m), 547 (m).

2 : 2 : 6-TRIMETHYL-6-ETHYLTETRAHYDROTHIOPYRAN. 1459 (s), 1377 (s), 1368 (s), 1341 (w), 1313 (w), 1281 (w), 1222 (s), 1169 (w), 1142 (m), 1116 (s) 1087 (m), 1054 (m), 1028 (w), 1002 (m), 970 (m), 950 (w), 902 (w), 878 (m). 855 (w), 821 (w), 802 (m), 772 (m), 692 (w), 657 (w), 627 (w), 592 (m), 548 (m),

CYCLOHEXYL MERCAPTAN. 1450 (s), 1341 (m), 1301 (w), 1264 (s), 1224 (w), 1204 (s), 1184 (w), 1128 (w), 1103 (w), 1030 (m), 1000 (s), 916 (w), 885 (m), 839 (w), 819 (s), 734 (m), 707 (m), 524 (w).

DI-CYCLOHEXYL SULPHIDE. 1447 (s), 1335 (m), 1297 (w), 1264 (s), 1196 (s), 1180 (m), 1112 (w), 1096 (w), 1073 (w), 1043 (w), 1026 (w), 1007 (m), 998 (s), 918 (w), 886 (s), 855 (w), 820 (s), 743 (m), 737 (m), 696 (m), 516 (w).

DI-CYCLOHEXYL DISULPHIDE. 1447 (s), 1336 (m), 1297 (m), 1261 (s), 1197 (s), 1175 (m), 1119 (w), 1094 (w), 1075 (w), 1049 (w), 1027 (m), 996 (s), 919 (w), 887 (s), 856 (m), 817 (m), 737 (m), 713 (w), 689 (m), 516 (w), 510 (w).

CYCLOHEXYL-CYCLOHEXENYL SULPHIDE. 1640 (w), 1594 (w), 1446 (s), 1391 (w), 1339 (m), 1298 (w), 1265 (m), 1230 (w), 1210 (m), 1201 (s), 1180 (m), 1168 (w), 1140 (w), 1120 (w), 1104 (w), 1085 (m), 1042 (m), 1015 (w), 1000 (s), 988 (m), 922 (w), 888 (s), 869 (s), 856 (w), 840 (w), 822 (w), 759 (s), 735 (s), 723 (s), 695 (w), 634 (m), 534 (w).

DI-CYCLOHEXENYL SULPHIDE. 1642 (m), 1592 (w), 1442 (s), 1399 (w), 1342 (m), 1312 (w), 1301 (w), 1255 (m), 1228 (w), 1206 (m), 1195 (m), 1167 (w), 1134 (w), 1075 (m), 1055 (w), 1034 (m), 994 (m), 985 (m), 906 (w), 892 (w), 879 (m), 870 (m), 835 (w), 762 (s), 738 (s), 723 (s), 634 (s), 534 (w).

CYCLOHEXENE *epi*SULPHIDE. 1446 (s), 1371 (s), 1337 (m), 1268 (w), 1251 (m), 1187 (w), 1162 (w), 1137 (w), 1113 (s), 1063 (w), 1050 (w), 1024 (s), 986 (w), 970 (s), 916 (m), 881 (s), 858 (m), 834 (w), 805 (w), 784 (m), 666 (s), 640 (w). 604 (s), 574 (s), 551 (w).

The Interpretation of the Spectra

(*a*) SH Linkages.—The frequency associated with the stretching vibration of the SH linkage has previously been characterized in the infra-red by several workers.[16–18] In agreement with the earlier infra-red work and also the Raman results,[19] the present investigation has shown that this vibration is represented in absorption by a weak band between 2560 and 2590 cm.$^{-1}$. The question of the location of SH deformation vibrations has recently been discussed in detail elsewhere.[8] The in-plane SH deformation mode of the $C\overset{S}{\diagup\;\diagdown}H$ unit common to mercaptans appears to lie between 800 and 900 cm.$^{-1}$. However, because of its weakness in both types of spectra and its occurrence in a region of skeletal frequencies it cannot be unequivocally identified except in the simplest cases. The out-of-plane deformation mode is a restricted rotation with a frequency probably below 400 cm.$^{-1}$, and hence is not observable in the region of prism spectroscopy in the infra-red.

(*b*) C—S Linkages.—(1) SATURATED ALKYL DERIVATIVES. It can be seen from the compilation of results given in Table I that the same correlation rules apply to the frequencies characteristic of the stretching of the C—S linkage in both Raman [14] and infra-red spectra. On the grounds of these frequencies we can divide the compounds investigated into the four types CH_3—S—, RCH_2—S—, RR′CH—S—, and RR′R″C—S—, where R, R′, etc., represent saturated alkyl groupings. These correspond to methyl, primary, secondary, and tertiary alkyl groups attached to the sulphur atom, and their C—S stretching frequencies lie in the ranges :

Methyl	705-685 cm.$^{-1}$
Primary *.	660-630 cm.$^{-1}$
Secondary	630-600 cm.$^{-1}$
Tertiary	600-570 cm.$^{-1}$.

These correlation rules apply equally to mercaptans, sulphides or disulphides. However, for a given alkyl group there is usually a gradual decrease in the

---

[16] Bell, *Ber. B*, 1927, **60**, 1749.

[17] Bell, *ibid.*, 1928, **61**, 1918.

[18] Williams, *Physic. Rev.*, 1938, **54**, 504.

[19] Kohlrausch, *loc. cit.*, p. 211.

* This applies only if the hydrocarbon group is not branched close to the C—S linkage as, for example, in *iso*butyl compounds.

average value of the frequency on passing from mercaptan to sulphide to disulphide, although this effect is too small to warrant the formulation of separate rules for the three types of sulphur compound. The correlations obviously have direct use in the identification of such linkages in unknown compounds such as vulcanizates, and are more specific than those previously derived for infra-red work.[1] They seem to apply also to sulphides in which the C—S—C group is part of a ring formation (Fig. 2). They do not apply, however, to cyclohexyl derivatives (Fig. 4 and 5) and these will be discussed separately below.

The strong Raman lines and the corresponding infra-red absorptions listed for the mercaptans in Table I can clearly be assigned to the single C—S stretching mode in these compounds. In the spectra of the sulphides and disulphides two C—S stretching modes are possible in which these bonds vibrate in and out of phase with each other. With the sulphides the strength in the Raman effect of the characteristic frequencies listed above suggests that they represent the symmetrical mode, and this is confirmed by Thompson's detailed assignment of the spectrum of dimethyl sulphide.[4, 20] In this molecule the unsymmetrical frequency was only observable as a weak Raman line at 742 cm.$^{-1}$, and the corresponding mode in the larger molecules studied here cannot be picked out, particularly as CH$_2$ groups also give rise to rocking frequencies in the region 700-750 cm.$^{-1}$. The characteristic C—S frequencies in the disulphides also probably correspond to the in-phase vibration of the C—S linkages.

In addition to the characteristic C—S stretching modes considered in detail above, the primary compounds containing the linkage have strong absorptions between 1220 and 1230 cm.$^{-1}$ (*n*-propyl and *n*-butyl derivatives, see Fig. 1), or near 1270 cm.$^{-1}$ (ethyl compounds [3, 4]). In accordance with the detailed assignment given previously for ethyl mercaptan,[3] these absorptions can probably be attributed to the wagging modes of the CH$_2$ groups attached to the sulphur atom. Similar strong absorptions occur also in the spectra of the di-allyl and di-crotyl sulphides (Fig. 3) and can be accounted for in an analogous fashion.

(2) CYCLOHEXYL DERIVATIVES. The spectra of several cyclohexyl derivatives are given in Fig. 4 and it can be seen that they do not obey the above classification rules for the C—S stretching modes. A separate discussion is therefore required. If they were to be considered as normal alkyl compounds they would be classified as secondary derivatives, and the appropriate C—S frequencies would then be expected in the region 630-600 cm.$^{-1}$. In fact this region of the spectrum is transparent to radiation, and the nearest absorptions are close to 700 cm.$^{-1}$. Comparison of the spectra of cyclohexyl mercaptan, di-cyclohexyl sulphide, and di-cyclohexyl disulphide shows that absorption at 707, 696 and 689 cm.$^{-1}$ respectively can probably be assigned to C—S vibrations as they show the usual consecutive decrease in frequency in passing from mercaptan to sulphide to disulphide. The neighbouring absorption band near 735 cm.$^{-1}$ in cyclohexyl mercaptan remains in approximately the same position in all these three substances, and is presumably a frequency of the cyclohexyl group.

Fig. 5 also shows the spectra of some cyclohexenyl derivatives and of cyclohexene *epi*sulphide. The latter compound has several absorptions in the region 700-550 cm.$^{-1}$ and it is not clear which of these are to be assigned to C—S stretching frequencies. Cyclohexyl-cyclohexenyl sulphide shows an absorption at 695 cm.$^{-1}$ which is close to the C—S absorption of cyclohexyl sulphide and is probably also a C—S vibration. It has another new band at 634 cm.$^{-1}$ which may be the second C—S stretching mode. In the spectrum of di-cyclohexenyl sulphide the 695 cm.$^{-1}$ frequency disappears, but the other absorption is intensified (634 cm.$^{-1}$) in agreement with this assignment, although the possibility cannot be excluded that the latter is a frequency of the cyclohexenyl group itself.

(3) UNSATURATED DERIVATIVES. As representatives of this class the infra-red spectra of allyl, crotyl and cyclohexenyl sulphide have been examined in the present investigation (Fig. 3 and 5), and in addition Trotter and Thompson [4] give the spectrum of dibenzyl disulphide. In Table II are given the frequencies that can probably be assigned to C—S stretching modes in these molecules, together with the corresponding frequencies of their saturated analogues. The differences between the frequencies are given in the last column. With di-allyl sulphide the frequency at 583 cm.$^{-1}$ has been chosen as the C—S stretching mode in preference to that at 600 cm.$^{-1}$ because of its near coincidence with the

---

[20] Thompson, *Trans. Faraday Soc.*, 1941, **37**, 38.

strong Raman line[21] at 590 cm.$^{-1}$; for di-benzyl disulphide the C—S frequency of the analogous saturated compound is assumed to be a normal value for a primary alkyl disulphide. It is given in parenthesis so as to indicate that it is not an observed value.

TABLE II.—THE C—S STRETCHING FREQUENCIES OF SOME UNSATURATED AND SATURATED SULPHUR COMPOUNDS

Saturated		Unsaturated		ν_1 ν_2 (cm.$^{-1}$)
Name	C—S frequency (ν_1) (cm.$^{-1}$)	Name	C—S frequency (ν_2) (cm.$^{-1}$)	
Di-*n*-propyl sulphide	648	Di-allyl sulphide	583	65
Di-*n*-butyl sulphide	649	Di-crotyl sulphide	658	−9
Di-cyclohexyl sulphide	696	Di-cyclohexenyl sulphide	634	62
Primary disulphide	(630)	Di-benzyl disulphide	570	60

All the unsaturated substances investigated have the double bond separated from the C—S linkage by an intervening single bond. None have been investigated in which a double bond is next to the C—S link. As shown in Table II, with the exception of di-crotyl sulphide, the introduction of a double bond into the molecule in this position causes a decrease in the C—S stretching frequency of 60-70 cm.$^{-1}$. Although this conclusion must remain tentative because of the small number of examples and the discrepancy with the di-crotyl compound, there is other indirect evidence for this effect (see below). It is possible that our assignment of the C—S frequency of di-crotyl sulphide is incorrect, and indeed if any amount of the *cis* isomer were present the absorption at 658 cm.$^{-1}$ might be explained alternatively as a CH deformation mode about the double bond.[22]

(*c*) **S—S Linkages.**—The following disulphides have been examined in the region 800-450 cm.$^{-1}$: dimethyl disulphide, diethyl disulphide, di-*n*-propyl disulphide, di-*n*-butyl disulphide, di-*tert.*-butyl disulphide, and dicyclohexyl disulphide. The spectra of the first three of these have already been published by Trotter and Thompson[4] and our results are in excellent agreement with theirs except that our cell thickness was approximately 0·06 mm. and hence the weak bands near 500 cm.$^{-1}$ in di-*n*-propyl disulphide were not detected. The previously unpublished spectra are given in Fig. 1 and 4. The position of the C—S absorption has already been discussed.

In the Raman spectra S—S linkages in disulphides are usually characterized by strong lines in the neighbourhood of 500 cm.$^{-1}$. In the infra-red, absorptions at 517, 510 and 510 cm.$^{-1}$ have been observed for the dimethyl, diethyl, and dicyclohexyl disulphides respectively. These are clearly the counterparts of the Raman lines, and it is likely that an increased path length would show similar absorptions in this region for the higher molecular weight disulphides. As pointed out by Hibben[23] and others, these frequencies near 500 cm.$^{-1}$ are almost certainly the S—S valence stretching modes. Their low intensity in the infra-red may be attributed to the fact that the symmetrical vibration of the S—S link involves little change in electric moment (see below). If the assignment is correct, their appearance in absorption, however, is evidence against the presence of a centre of symmetry in all of the molecules present, and hence precludes the presence of only *trans* configurations of the type 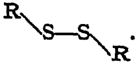 .

(*d*) **C=S Linkages.**—C=S linkages appear to be unstable in purely hydrocarbon surroundings,[24] and for this reason it was impossible to obtain a good series of reference compounds for the characterization of this linkage in the infra-red. However, about a dozen compounds were investigated in which the C=S linkage occurs, although usually in the immediate proximity of nitrogen or other sulphur atoms. Such compounds are used as accelerators in the commercial vulcanization of rubber. No useful correlations were found, however, and as the purity of some of the compounds was in doubt their spectra will not be discussed.

---

[21] Kohlrausch and Stockmair, *Z. physik. Chem. B.*, 1935, **29**, 292.

[22] See the infra-red spectrograms of *cis* olefines in the compilation of the *Amer. Petrol. Inst., Nat. Bur. Stand* (Washington, 1948).

[23] Hibben, *loc. cit.*, pp. 258, 259.

[24] Campaigne, *Chem. Rev.*, 1946, **39**, 1.

Discussion

(a) Intensity Considerations.—A notable difference between the Raman and infra-red spectra of these sulphur compounds lies in the fact that for conditions which bring up the spectra of the hydrocarbon parts of the molecules, the frequencies characteristic of S—H, C—S or S—S linkages are very strong in scattering, but relatively weak in absorption. The weakness in the infra-red limits their usefulness for qualitative or quantitative analysis of these groups, and explains why great difficulty was experienced in detecting such linkages in vulcanized rubber.[1] On the other hand they usually occur in unpopulated regions of the spectra and in favourable cases can be utilized by increasing the pathlength of the material investigated.

The cause of this difference of behaviour in these two types of spectra must be sought in the factors which determine the intensities in the two cases. In the infra-red the intensity of absorption due to a particular vibration will be proportional on the simple harmonic approximation to $(A\,dM/dQ)^2$, where A is a normalizing factor representing the amplitude of the vibration associated with the particular normal co-ordinate Q, and M is the vector representing the molecular dipole moment. The intensity of the same scattered frequency in the Raman spectrum on the other hand will be proportional to $(A\,d\alpha/dQ)^2$, where α is the tensor representing molecular polarizability, and A and Q have their previous meanings. To the approximation with which a normal mode of vibration can be considered as localized in a particular bond of the molecule, the normal co-ordinate Q can be approximated to as the bond length r and M and α can also be replaced by their bond analogues. This is probably a good approximation for the SH valence frequency, and a fair one for the stretching modes of C—S and S—S bonds the frequencies of which also occur in unpopulated spectral regions and are therefore affected to a moderate extent only by the presence of other neighbouring groups. It is also very likely that a bond with a high intrinsic dipole moment or polarizability will give a high value of dM/dr or $d\alpha/dr$ respectively, although the exact relationship depends on the shape of the M—r or α—r curves.[25] Thus the low dipole moment M of the S—H or C—S linkage (due to the small electronegativity difference between the constituent atoms) explains the weak intensity of these absorptions in the infra-red. With the S—S linkages the intensities will be further reduced because of the symmetry of the bond, and if the normal vibration were strictly localized in the S—S linkage the absorption would be " forbidden " on this diatomic approximation. However the polarizabilities α of these sulphur containing linkages will be large because of the presence of the large and easily polarizable sulphur atom, and the corresponding vibrations will show up as strong lines in the Raman effect. This is the explanation of the observation by Hibben[26] that the introduction of a heavy atom into a molecule usually gives rise to new strong lines in the Raman spectrum.

(b) The Force Constants of the C—S Linkages.—Characteristic " group " frequencies are often found to vary in position in different molecules containing the given structural unit. This may be caused by a change in the force constants of the group itself or by a change in the "effective" mass * of the neighbouring groups. In the present case we have experimental evidence for the decrease in the characteristic C—S stretching frequency in passing along the sequence methyl, primary, secondary and tertiary alkyl substituting groups. It would be of interest to find out whether the decrease in frequency is a reflection of a decreasing C—S stretching force constant. An accurate calculation of the C—S force constants from these spectra would require a complete normal co-ordinate analysis of a few of these large molecules, and this would be a very tedious algebraic task. Furthermore, the required frequency assignments for these molecules are not available. However, a solution to a first approximation can be achieved by a "diatomic approximation" of treating the C—S linkage (with its associated hydrogen atoms) as completely independent of the rest of the molecule. For this purpose the hydrogen atoms are assumed to be rigidly attached to the C and S atoms and their masses are accordingly added to those of the two atoms for the calculation of reduced masses.

---

[25] Herzberg, *Infra-red and Raman Spectra of Polyatomic Molecules* (Van Nostrand Co. Inc., New York, 1946), pp. 241, 261.

[26] Hibben, *loc. cit.*, p. 256.

As a second approximation the neighbouring heavy atoms can also be taken into account, the hydrogen atoms once again being allowed for as making their contributions to the masses of the heavy atoms. Thus the ethyl mercaptan molecule can be treated as a bent triatomic molecule with masses 15(CH_3), 14(CH_2) and 33(SH), and this has been carried out. On this approximation tertiary butyl mercaptan would be treated as an XYZ_3 type molecule. This should be a considerably better approximation than the simple "diatomic" one as it does take into account to some extent the effect of weighting the carbon atom of the C—S linkage with heavy groups.

In Table III are given the values of the force constants of the C—S linkage (k_{C-S}) in dyne cm.$^{-1}$ deduced by these two approximate methods. In the "heavy mass" approximation the relevant frequencies in the ethyl mercaptan spectrum have been taken as 966 cm.$^{-1}$ (C—C stretching), 659 cm.$^{-1}$ (C—S stretching) and 333 cm.$^{-1}$ $\left(\mathrm{C}\overset{\mathrm{C}}{\diagup\,\diagdown}\mathrm{S}\text{ bending}\right)$. The equations used have been derived by Lechner,[27] and Cross and Van Vleck.[28] Assignments for the spectra of *iso*propyl mercaptan and *tert.*-butyl mercaptan have not been made and hence the necessary experimental data are not available to make even "heavy mass" calculations for these molecules.

TABLE III.—SOME APPROXIMATE VALUES OF C—S STRETCHING FORCE CONSTANTS IN MERCAPTANS

Alkyl Group	Observed Frequency (cm.$^{-1}$)	$k_{C-S} \times 10^{-5}$ "Diatomic Approximation" (dyne cm.$^{-1}$)	$k_{C-S} \times 10^{-5}$ "Heavy Mass" Approximation (dyne cm.$^{-1}$)
Methyl	702	3·0	3·0
Ethyl	659	2·5	2·0
*iso*Propyl . . .	626	2·2	—
tert.-Butyl . . .	587	1·8	—

It can be seen from Table III that the decreasing C—S characteristic frequency is reflected by a decreasing value of k_{C-S} on the "diatomic" approximation, but that this is true for the "heavy mass" approximation also. Although the calculated values for k_{C-S} on even the "heavy mass" approximation should not be taken for comparison with other force constants derived from molecules by complete normal co-ordinate analyses, there seems to be little doubt of the qualitative decrease in the force constant in going from the methyl to the primary alkyl compounds. However, the apparent change of a whole unit in passing from the methyl to the ethyl compounds on the "heavy mass" approximation is almost certainly too great, and this serves to emphasize the relatively crude approximations involved. Similar force constant decreases probably occur on passing to secondary and tertiary alkyl derivatives, although these cannot be estimated in magnitude. The close parallel between the C—S stretching frequencies of these mercaptans and those of the corresponding sulphides and disulphides clearly means that the force constants of these linkages also vary in like manner with the nature of the substituent alkyl groups. It seems probable that the abnormally high values of the C—S stretching frequencies in the cyclohexyl compounds, and the low values of these modes in the unsaturated compounds can also be correlated with similar changes in the force constants of the C—S linkages involved.

---

* The "effective" mass will itself be a function of the masses, force constants, etc., of these groups.

[27] Lechner, *Wien Ber.*, 1932, **141**, 291.

[28] Cross and Van Vleck, *J. Chem. Physics*, 1933, **1**, 350.

(*c*) **Comparison with Related Molecules and with Other Bond Properties.**—In the preceding section the experimental results of the infrared investigation have been discussed from the point of view of the force constants of the C—S linkage. When the compilation of the spectra had been completed, chance reference was made to the Raman spectrum of a related chloride, and it was discovered that the Raman lines of the C—Cl stretching vibrations in these compounds run closely parallel to the C—S frequencies. In addition they can be similarly classified according to whether R in R—Cl is an alkyl group of a primary, secondary, tertiary or unsaturated nature.[14]

Dadieu, Pongratz and Kohlrausch and others [10–18] have made parallel Raman studies of chlorides and mercaptans, and Harkins and Bower,[29] and Harkins and Haun [30] have presented Raman data of series of chlorides and have drawn some tentative conclusions on the force constants of the C—Cl bonds in the different types of compounds. Although these last authors' calculations were based on the assumption that the C—Cl force constant is the same in methyl chloride and ethyl chloride—a conclusion which the more accurate treatment of the latter as a three-mass system has shown to be untrue—they did also conclude that the drop in C—Cl frequency in going from primary to secondary to tertiary groups corresponds to a decrease in the force constants.

It is interesting here to investigate in rather more detail the correspondence between the C—S and C—Cl stretching frequencies as there are a greater number of other data on the chlorides which can be correlated with the spectroscopic results.

In Table IV are given the frequencies of the C—S vibrations for a

TABLE IV.—A COMPARISON OF THE C—S AND C—Cl STRETCHING FREQUENCIES IN MERCAPTANS AND CHLORIDES

	$\nu_{C—S}$ (cm.$^{-1}$)	$\nu_{C—Cl}$ (cm.$^{-1}$)
Methyl	702	712
Ethyl	659	655
n-Propyl	652	651
2° Propyl	628	612
3° Butyl	587	570
Allyl	590*	594
Benzyl	570†	(556)

* From allyl sulphide. † From benzyl disulphide.

---

[29] Harkins and Bower, *J. Amer. Chem. Soc.*, 1931, **53**, 2425.

[30] Harkins and Haun, *ibid.*, 1932, **54**, 3920.

series of sulphur compounds (mercaptans unless otherwise indicated) and the C—Cl values for the corresponding chlorides. For consistency these are wherever possible taken from the spectra of the liquid, but it must be borne in mind that although these are approximately the same as values in the gaseous phase for the mercaptans, there are considerable shifts in passing from the vapour to the liquid states in the chloride spectra. The C—Cl frequencies of the saturated chlorides can be assigned with confidence because of their great intensity in the Raman spectra. In allyl chloride the value is taken from a fairly detailed assignment of this molecule [31] and is probably reliable. The benzyl chloride value is less certain as there are several strong bands in the region ; it is thus enclosed in brackets.

Assuming that a decreasing C—Cl stretching frequency corresponds to a decreasing force constant of the linkage, as has been previously discussed for the C—S frequencies, we can use these observed frequencies to arrange the C—Cl bonds in approximate order of force constant. This order is :

methyl $>$ ethyl $\bumpeq$ propyl $>$ secondary propyl $>$ tertiary butyl $\bumpeq$ allyl $\bumpeq$ benzyl chloride.

The same order is equally true for the C—S linkages in the mercaptans. The precise order of the *tert.*-butyl, allyl and benzyl compounds is uncertain because of difficulty in estimating the weighting effects of the more rigid unsaturated groupings.

In a recent review Walsh [32] has collected together much of the data on bond length, ionization potentials, bond energies, etc. of carbon halogen linkages and these agree well with the above conclusions regarding the order of strength of the C—Cl bonds. Walsh cited the Raman frequencies as being further evidence for this classification, but this evidence was of doubtful value until some attempt had been made, as has been done during this investigation, to separate force constant from mass effects. The bond properties are also of considerable importance from the point of view of the reaction mechanisms of related compounds of this sort and in this connection Butler and Polanyi [33] have recently estimated the bond dissociation energies of the C—I bonds in a similar series of iodides. In the order of decreasing dissociation energy they write :

methyl $>$ ethyl $>$ propyl $>$ 2° propyl $>$ 3° butyl $>$ benzyl $>$ allyl.

It can be seen that this order corresponds very closely to that deduced for the chlorides and the mercaptans from the spectroscopic data and lends considerable weight to our interpretation of these in terms of force constants. No significance can be attached to the reversal of order of the benzyl and allyl compounds when compared with the force constants deduced from the spectroscopic results, because of the crude approximations by means of which the force constants are estimated. However, the general trend is very satisfactorily in accord for the two bond properties.

The author would like to thank Dr. G. B. B. M. Sutherland, F.R.S., for many helpful discussions throughout the work, and Dr. R. F. Naylor and Dr. E. H. Farmer of the British Rubber Producers' Research Association for pure samples of the compounds studied.

He would also like to thank the Master and Fellows of St. Catharine's College for a Senior Research Studentship held during the period of this investigation, and the Dunlop Rubber Company Ltd., for a generous maintenance grant.

Department of Colloid Science,
Cambridge.

---

[31] Thompson and Torkington, *Trans. Faraday Soc.*, 1946, **42**, 432.

[32] Walsh, *ibid.*, 1947, **43**, 60.

[33] Butler and Polanyi, *ibid.*, 1943, **39**, 19.

THE EFFECT OF DIALYSIS ON THE PROPERTIES OF NUCLEAR GOLD SOLS

PART II.—THE NATURE OF THE COAGULATION INITIATED BY DIALYSIS

By A. K. Holliday

Received 16*th September*, 1949

Measurements of light absorption by nuclear gold sols over the wavelength range 670-430 $\mu\mu$ are made to determine particle size and to investigate the restricted coagulation initiated by dialysis, using theoretical absorption coefficients calculated by Mie and Gans. The particle size is determined by growing the nuclear particles to a point where the absorption coefficients are sensitive criteria of size. It is then shown that the change of absorption on coagulation must be due to a change of shape rather than of size, the data suggesting a change from spherical to ellipsoidal particles of axial ratio $\sim$ 0·5. The limiting values of the absorption coefficients, reached when coagulation is complete, support this conclusion, and indicate that the process is virtually restricted to one stage—the pairing of primary particles to form secondary doublets.

In a previous paper [1] it has been shown that dialysis of a nuclear gold sol, prepared by reduction with phosphine, causes a peculiar type of coagulation characterized by a colour change of the sol from red to blue without subsequent sedimentation, so that a stable blue sol is formed. In the present paper, a more detailed analysis of the colour change is reported, using an abridged spectrophotometer to measure the absorption coefficients of the sol at a number of wavelengths. Interpretation of these measurements in terms of particle size and shape enables both the course and extent of the coagulation process to be determined, and it will be shown that the stable blue sol results from the inhibition of the aggregation of the primary particles at an early stage in the process of coagulation. The effect of this inhibition of the coagulation upon the kinetics of the process is dealt with in a following paper.

Values of the absorption coefficients of gold sols at various wavelengths have been calculated theoretically by Mie [2] for spherical particles of different sizes. Gans [3] has made similar calculations for both ellipsoidal and plate-like particles, assuming the particle size to be small compared with the wavelength of the incident light. Experimental determinations of the absorption coefficients of gold sols by several investigators [4, 5, 6] have given results in general agreement with those of Mie, indicating that the assumption of a spherical particle is justified for sols prepared in the usual ways, or grown from nuclear sols by the method of Zsigmondy. No experimental test of Gans' values has been possible, since no direct method of producing the very small asymmetric particles is known. Moreover, although changes in the light absorption of gold sols occurring during coagulation have been measured,[7, 8] little attempt has been made to interpret the changes by means of the Mie-Gans theories, although the Mie theory has now been applied to the study of colloidal systems in general.[9] Any attempt to apply the theories to a process of coagulation demands, firstly, that the aggregated particles must be optically homogeneous with the same refractive index and bulk absorption coefficient as the primary particles, and secondly, that the shape of the aggregated particles must approximate to the spherical if they are large, or to an ellipsoidal or plate-like form if they are small. The complete irreversibility of the coagulation process in gold sols implies that the process is one of coalescence, involving recrystallization at the point of union of the particles, so that the bulk characteristics of the primary are reproduced in the aggregate. If the latter is large and spherical, it does not necessarily follow that it will be identical optically with a single uniform spherical particle of the same radius for the aggregate will probably possess a loose, sponge-like character, which will absorb or scatter light in quite a different manner to a homogeneous particle. Thus Kruyt and Troelstra have shown[10] that light absorption of silver iodide sols during coagulation is only a useful criterion of the process while the aggregates are small; for larger aggregates, the absorption of light is generally less than would be expected for homogeneous particles of equivalent size. Restricting the study of coagulation to the earlier stages makes change of shape an important factor. Electron microscopic examination of coagulated colloidal gold[11] shows that aggregation does not effect any noticeable distortion of the constituent primary particles; hence the first act of aggregation must produce an asymmetrical secondary or doublet. The latter, by further union with either primaries or secondaries, may produce aggregates with greater asymmetry (tending to become chain-like) or less asymmetry (tending to become roughly spherical). Assuming that any of these approximate in shape to ellipsoids of axial ratio between 0 (rods) and 1 (spheres), Gans' theory may be used to interpret light absorption changes in the earliest stages of coagulation. In later stages, it is unlikely that highly asymmetrical particles will persist; the aggregates will be more probably approximately spherical, and Mie's theory can be applied, provided that the aggregates are not so large as to lose optical homogeneity.

---

[1] Holliday, *Trans. Faraday Soc.*, 1947, **43**, 661 (Part I).

[2] Mie, *Ann. Physik*, 1908, **25**, 377.

[3] Gans, *ibid.*, 1912, **37**, 881.

[4] Steubing, *ibid.*, 1908, **26**, 329.

[5] Lange, *Z. physik. Chem.*, 1928, **132**, 1.

[6] Gribnau, *Kollid-Z.*, 1938, **82**, 15.

[7] Mukherjee and Papaconstantinou, *J. Chem. Soc.*, 1920, **117**, 1563.

[8] Rinde, *Dissertation* (Uppsala, 1928).

Experimental

Nuclear gold sols with a particle radius of $\sim 3\ \mu\mu$ were prepared by reduction of alkaline "gold chloride" with phosphine as described previously.[1] The approximate gold concentration was 60 mg./l., but to define absorption coefficients precisely, a more accurate value was necessary. The gold content of each sol was therefore determined colorimetrically, using the method described by Clabaugh[12] in which the gold is converted to a yellow complex by addition of *o*-tolidine. The intensities of the coloured solutions formed were determined by a Spekker photoelectric absorptiometer using dark blue filters. A colour intensity-concentration graph was obtained by using solutions of known gold content, prepared by dissolving gold metal in the minimum amount of aqua regia and diluting with water. The colloidal gold was likewise dissolved in aqua regia, evaporated nearly to dryness, dissolved in a known volume of water, *o*-tolidine added, and the colour intensity determined; the concentration of gold was then read off from the intensity-concentration graph.

The sols were dialyzed through a Cellophane membrane as previously described[1] against a stream of distilled water. Dialysis was accomplished at a rapid rate by increasing the ratio (membrane area)/(volume of sol) to a maximum, and under these conditions the colour change from red to blue was visually complete in about three days. While in the dialyzer, the gold content of the sols decreased somewhat due to deposition of gold on the membrane and to slight absorption of water. Hence the gold concentration in a sol undergoing dialysis was determined at intervals, and the absorption coefficients corrected accordingly.

---

[9] Oster, *Chem. Rev.*, 1948, **43**, 319.

[10] Kruyt and Troelstra, *Kolloidchem. Beih.*, 1943, **54**, 225.

[11] Von Borries and Kausche, *Kolloid-Z.*, 1940, **90**, 132.

[12] Clabaugh, *J. Res. Nat. Bur. Stand.*, 1946, **36**, 119.

A complete spectrophotometric analysis of the sols was not attempted, since theoretical absorption coefficients calculated by Mie and Gans are available only for seven wavelengths in the visible spectrum. Instead, the Spekker absorptiometer was used in conjunction with a set of eight spectrum filters as an abridged spectrophotometer. For each filter, the instrument gives a value of $\log_{10} I_0/I_t$ corresponding to the peak transmission wavelength of the filter, I_0 and I_t being the intensities of the incident and transmitted light respectively. This was verified by measuring $\log_{10} I_0/I_t$ with a Beckmann spectrophotometer for each peak transmission wavelength, using as a standard the coloured solution of inorganic salts described by Thomson,[13] which has approximately the same absorption at all wavelengths. Measurements with the absorptiometer on gold sols were first made at various concentrations of sol, to verify that the sols used here obey the Lambert-Beer law.[14] Values of $\log_{10} I_0/I_t$ were determined over a concentration range for two sols, one red and the other blue (formed by long dialysis), and with two filters transmitting at opposite ends of the spectrum. For each sol and each filter, $\log_{10} I_0/I_t$ plotted against concentration gave a straight line passing through the origin. Measurements were also made with each filter in turn to show that the absorption of a mixture of red and blue sol is the sum of the individual absorptions ; thus it was found that $\log_{10} I_0/I_t$ when plotted against percentage of red or blue sol in a mixture gave a straight line. In these determinations, the sols were protected by addition of 0·01 % of sodium protalbate, to prevent colour changes occurring during dilution or mixing. It was found that the presence of the protalbate itself altered the absorption of a sol slightly, so it was not added in the determinations of colour change during dialysis, as the latter occurred sufficiently slowly to make any change during the time of measurement negligible. It should also be mentioned that no tendency of the gold to deposit on the absorptiometer cells was ever observed, although behaviour of this kind has been observed by Lloyd and Evans in studies on colloidal gold.[15] A cell thickness of 1 cm. was found to be suitable for all readings during dialysis.

Results

Values of the absorption coefficients *k* were determined for the four nuclear sols used in the present studies, and are given in Table I. Values of *k* used in this paper are the values of $\ln I_0/I_t$ for a sol concentration of 19·3 mg./l., i.e. 1·0 cu. mm. Au/l., and for cell thickness 0·1 cm. These values are then directly comparable with the *k* values of Mie and Gans. The theoretical *k* values for the wavelengths appropriate to each filter have been interpolated from Mie's data—extended by calculation where necessary—and are plotted against particle radius in Fig. 1. The theoretical *k* values for a nuclear sol are quoted in Table I for comparison.

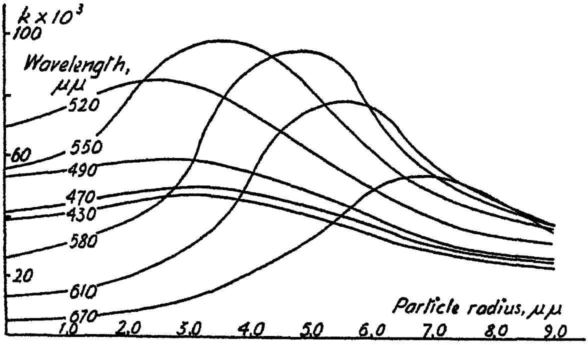

FIG. 1.

---

[13] Thomson, *Trans. Faraday Soc.*, 1946, 42, 663.
[14] Gribnau, Kruyt and Ornstein, *Kolloid-Z.*, 1936, 75, 262.
[15] Lloyd and Evans, *Trans. Faraday Soc.*, 1942, 38, 179.

TABLE I

Wavelength (μμ)	670	610	580	550	520	490	470	430
Designation of Sol	$k \times 10^3$							
A	6·1	15·7	27·7	45·8	76·5	64·1	56·9	54·0
B	8·6	18·3	29·4	44·9	60·1	57·7	50·8	48·7
C	6·9	15·7	27·5	45·9	76·8	63·9	56·1	52·7
D	7·5	16·0	28·3	46·0	76·1	60·6	53·9	51·7
Mie	5·0	13·5	26·7	55·5	69·6	52·7	41·0	38·9

The degree of reproducibility of the experimental k values is to be regarded as satisfactory when it is remembered that small differences in the mode of preparation may greatly affect the characteristics of the sols. The agreement between the determined k values and those of Mie is of the same order as that found by previous workers, the theoretical k values at the smaller wavelengths being rather lower than the experimental values. The agreement is sufficiently good to suggest that measurement of the absorption coefficients of a sol might give a means of determining particle size, provided that the coefficients are sensitive to changes in particle size, a condition which holds only for radii > 10 μμ. To investigate this possibility, the particles in nuclear sol B were grown to different sizes by the Zsigmondy method,[16] by adding a solution of hydroxylamine hydrochloride dropwise to a sample of the diluted nuclear sol containing an amount of potassium chloraurate necessary to produce growth to the required size. The absorption coefficients of each grown sol k_g were then measured, and a value of the radius r_g of the particles determined for each wavelength by interpolation in Fig. 1. The mean of the eight r_g values thus obtained was then converted to the nuclear particle radius r_n by using the relationship

$$r_n = r_g \, . \, c_0 V_0 / c_1 V_1,$$

in which c_0 and V_0 are the gold concentration and volume of the diluted nuclear sol, and c_1, V_1 the corresponding values for the grown sol. Table II shows the k_g, r_g and r_n values for four grown sols of different sizes, all grown from sol B.

TABLE II

Grown Sol No.		Wavelength (μμ)								Mean r_g (μμ)	r_n (μμ)
		670	610	580	550	520	490	470	430		
I	(1) $k_g \times 10^3$	36·2	57·8	80·1	94·2	75·7	56·8	51·4	52·3	—	—
	(2) $k_g \times 10^3$	33·4	56·8	82·9	100·5	78·6	59·3	53·5	53·8	—	—
	(3) $k_g \times 10^3$	33·8	54·4	77·2	94·9	76·7	57·9	51·3	52·3	—	—
	Mean $k_g \times 10^3$	34·5	56·3	80·0	96·5	77·0	58·0	52·1	52·8	—	—
	,, r_g (μμ)	51	41	36	30	38	35	34	34	37	3·1
II	Mean $k_g \times 10^3$	52·1	74·8	81·9	76·5	58·5	47·0	43·2	43·9	—	—
	,, r_g (μμ)	65	50	58	53	53	52	50	44	53	3·5
III	Mean $k_g \times 10^3$	23·1	42·2	68·7	99·1	91·3	67·1	57·5	57·4	—	—
	,, r_g (μμ)	42	37	33	35	25	30	34	34	34	3·6
IV	Mean $k_g \times 10^3$	59·4	59·1	54·9	49·9	40·9	35·1	33·1	33·6	—	—
	,, r_g (μμ)	70	69	70	69	70	67	67	62	68	3·4

---

[16] Zsigmondy and Thiessen, *Das kolloide Gold* (Leipzig, 1925), p. 64.

Three samples of each grown sol were prepared, and the Table shows the k_g values for each sample of one of the grown sols, to indicate the degree of reproducibility attained: for the other sols, only the mean k_g values are quoted. It should be noted that an approximate value of r_g must be known in order to interpolate the measured k_g values into Fig. 1 with reasonable certainty, since there may be two possible values of r_g for one value of k_g. Where the latter is found to lie above the maximum of the appropriate curve of Fig. 1, the value of r_g taken is that at the maximum.

The degree of concordance between the four values of r_n is sufficiently good to justify the use of the absorption measurements as a means of determining particle size, and the mean value of r_n, 3·4 ± 0·1 μμ, will be taken as the particle radius in all the nuclear sols used here, rather than the approximate value of 3μμ determined from the method of preparation, using data obtained by Usher.[17]

Effect of Dialysis on the Absorption Spectra of the Sol.—Changes in absorption during dialysis were followed straightforwardly by withdrawing samples of the sol from the dialyzer at successive times, and determining the values of $\log_{10} I_0/I_t$ and the sol concentration by the methods already described. As far as possible, conditions of dialysis were kept the same in all investigations to obtain comparable results. Table III shows the k values obtained with four nuclear sols. In some of the experiments, samples of sol were withdrawn from the dialyzer after the colour change had been initiated, and stored in quartz flasks at 25° C, the absorption being determined at intervals during the period of storage. The data for these experiments are given in Table IV.

TABLE III

Sol	Period of Dialysis (hr.)	Wavelength (μμ)							
		670	610	580	550	520	490	470	450
		$k \times 10^3$							
Mean	0	7·3	16·4	28·2	45·6	72·4	61·6	54·4	51·8
B	1	11·8	22·0	33·4	48·4	62·4	59·0	51·8	48·9
	2	12·4	23·6	35·1	49·4	61·8	58·1	50·6	48·2
	4	15·1	26·8	37·9	51·1	61·1	57·7	50·7	48·7
	7	16·5	28·2	39·0	51·9	61·3	57·1	50·0	47·7
A	12	27·3	42·2	53·1	62·8	67·6	62·5	56·2	54·8
	16	33·3	48·1	57·2	64·7	66·4	61·2	55·2	53·9
	24	39·4	54·4	61·9	67·4	66·7	61·1	55·3	54·3
	40	52·4	65·6	72·1	74·4	72·0	64·7	60·0	59·1
	70	53·9	66·8	71·7	72·2	69·4	63·6	58·4	58·2
	102	54·0	66·1	71·8	72·4	70·0	65·0	59·5	59·3
D	26	46·2	65·8	74·8	76·4	—	66·0	59·9	58·2
	70	53·6	69·4	74·8	75·4	—	65·1	60·7	59·3

Table III shows that dialysis causes a continuous increase in the k values at long wavelengths; at shorter wavelengths, k at first decreases, and then increases again to a value slightly higher than the original. Those k values which increase appreciably do so at first slowly, then more rapidly as the particle charge is reduced by dialysis, and finally tend towards limiting values, corresponding to a visually complete colour change from red to blue. If the sols are allowed to stand after an initial period of dialysis, Table IV shows that the k values change in the same way as during continuous dialysis, but the *rate* of change depends on the duration of the initial dialysis. After prolonged standing, the values of k again approach limits which appear to be the same as those approached in continuous dialysis, i.e. the characteristics of the final blue sols are the same irrespective of whether these are formed by continuous dialysis or by initial dialysis followed by prolonged standing.

---

[17] Usher, *Trans. Faraday Soc.*, 1940, 36, 549.

TABLE IV

Sol	Time of Dialysis (hr.)	Period of Storage (hr.)	Wavelength ($\mu\mu$)							
			670	610	580	550	520	490	470	430
			$k \times 10^3$							
A	12	37	31·0	46·4	55·2	63·6	66·7	61·1	55·5	54·0
		52	34·2	49·4	57·9	65·0	68·9	62·6	56·1	56·0
		81	35·5	50·3	58·4	64·9	65·7	60·2	55·6	54·6
		123	39·9	54·7	62·0	67·9	68·3	62·9	57·7	56·1
		199	41·4	55·6	62·9	66·4	67·1	62·1	55·4	55·3
		295	44·9	58·5	65·2	70·3	69·6	63·4	58·2	57·7
		314	44·8	58·4	62·4	67·9	68·0	62·6	57·0	57·0
		540	48·1	60·3	65·3	68·3	67·9	62·7	57·8	57·4
	130	446	55·3	66·1	69·4	69·9	68·0	61·9	56·5	58·2
		2430	56·9	66·9	69·9	71·4	68·7	64·9	58·9	60·8
		2990	56·9	66·6	70·6	72·4	71·2	64·3	62·5	60·3
C	1	3380	56·9	66·4	68·5	69·0	68·5	63·8	58·0	57·9
	4	3380	60·8	68·5	69·2	69·2	69·5	65·2	59·5	59·3
D	70	800	54·9	69·6	74·4	74·5	70·7	64·3	59·0	58·9

The changes in *k* on dialysis cannot be due solely to an increase in particle size, for the following reasons: firstly, the sols obtained after long dialysis appear blue by both transmitted and reflected light, whereas sols prepared by growing nuclear particles to a larger spherical size (e.g. the sols characterized in Table II), though blue by transmitted light, appear orange in reflected light. Secondly, if any increase of size does occur on dialysis, then it must be small, since a stable, non-sedimenting sol is formed; but Fig. 1 shows that a small increase in particle size cannot be the cause of the very large increases in *k* at long wavelengths. To obtain a more precise measure of the particle size actually attained on dialysis, samples of well dialyzed blue sols were examined with a Zeiss cardioid ultramicroscope. In every case, the concentration of visible particles in the blue dialyzed sols was the same as that in the initial red sols, where a very small number of visible particles (of dust, etc.) are observed. If the lower limit of ultramicroscopic visibility is taken as equivalent to a particle radius of 15 $\mu\mu$ (and this figure may be too high) then the number of particles formed by dialysis which exceed this radius must be negligible, since no increase in the concentration of visible particles occurs. It follows from Fig. 1 that practically the whole of the observed changes of *k* on dialysis must be due to a cause other than increase of particle size. This cause can only be a change in particle shape and therefore the changes in *k* produced by a change from spherical to ellipsoidal shape must be considered. In Fig. 2, theoretical *k* values for ellipsoidal particles are plotted against the axial ratio of the ellipsoid, for the wavelength used here. These values have been obtained by interpolation from Gans' data and by calculation from Gans' formula where interpolation is uncertain. A comparison of the data of Table III and IV with Fig. 2 suggests that the changes in *k* on dialysis are in fact due to a change in particle shape from spherical to ellipsoidal. The very large changes in *k* at long wavelengths indicate that the ellipsoidal particles formed must have an axial ratio in the neighbourhood of 0·5; the very small changes in *k* at the shorter wavelengths are in agreement with this hypothesis. Moreover, the absence of a maximum in any of the observed k values precludes the possibility that any appreciable number of particles with an axial ratio either $>$ or $<$ 0·5 can be formed *after* the particles of axial ratio $\sim$ 0·5 appear, because, if this were to occur, the values of k at the wavelengths 610, 580 and 550 μμ would necessarily fall from the high values attained in the formation of particles of axial ratio $\sim$ 0·5. Hence, since the first step in coagulation must be the union of two primary particles to form a doublet, which may be assumed to behave optically like an ellipsoid with an axial ratio near to 0·5, there can be little doubt that coagulation on dialysis ceases when this first step is complete, for any further aggregation of the doublets would involve the formation of particles with an axial ratio either $>$ 0·5 or, less frequently, $<$ 0·5.

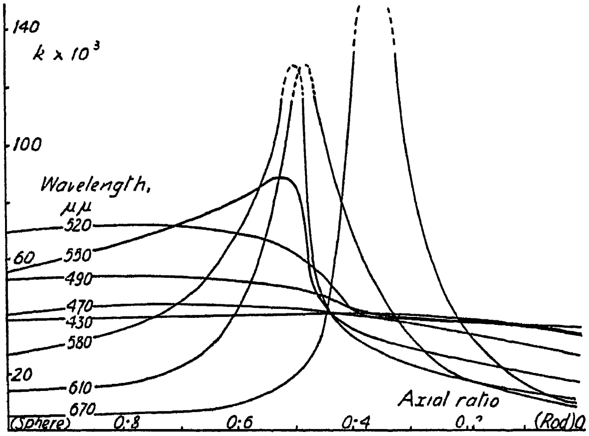

FIG. 2.

If the final blue sol formed after prolonged dialysis contains only doublet particles, then the limiting k values attained should all correspond to an axial ratio $\sim$ 0·5. Strictly, the true limiting values will be reached only after an infinite time of dialysis (or of subsequent standing) when all the primary particles have disappeared. In practice, these true limiting values must be obtained from the data of Tables I, II and IV. Limiting values can be obtained by plotting the k values against $1/t$ (where t = time of dialysis for Table III and time of standing for Table IV), and extrapolating to $1/t = 0$. For this purpose the k values in the Tables can be treated as referring to one mean sol, so that for each wavelength one limiting value of k, k_∞, is obtained instead of four values, each for a

TABLE V

Wavelength (μμ)	670	610	580	550	520	490	470	430
	$k \times 10^3$							
Axial ratio 0·7 (Gans) .	6·5	22·7	44·7	72·1	71·5	53·5	44·0	39·5
,, ,, 0·6 ,, .	9·5	41·9	68·8	80·1	68·7	52·3	43·5	40·0
,, ,, 0·5 ,, .	19·3	117	130	86·0	61·4	50·0	42·5	40·1
,, ,, 0·4 ,, .	115	69·0	33·1	35·5	40·2	42·7	40·0	39·8
Mean final blue sol (k) .	61	68	71	74	69	65	61	61
Axial ratio at k_∞ . .	0·43	0·55	0·59	0·67	0·60	$>$ 0·5		

particular sol. This procedure gives sufficiently accurate values of k for the wavelengths 520 to 430 $\mu\mu$, where the overall change in k is small, but is less accurate at the remaining four wavelengths.

Values of k for axial ratios 0·7-0·4, interpolated from Fig. 2, are given in Table V for comparison with k_∞ for the mean final blue sol. For the wavelengths 490-430 $\mu\mu$, the values of k_∞ lie above the maxima reached by the approximate curves of Fig. 2, and since these curves are very flat near their maxima, it is scarcely justifiable to assume a value of the axial ratio *at* the maxima ; all that can be reasonably assumed is that the axial ratio is not likely to be less than 0·5. The mean of the five definite axial ratios given by interpolating the k_∞ values on the Gans curves is 0·57, and this may be regarded as confirming that doublet particles preponderate in the final blue sol, since doublets, though possessing an axial ratio which must be very close to 0·5, cannot be expected to behave optically in exactly the same way as ellipsoids with an identical axial ratio.

The evidence presented above for the formation of doublet particles in coagulation by dialysis is necessarily qualitative, in that a comparison between observed and theoretical k values is made in the absence of any independent experimental check on the latter for asymmetric particles. Thus it is not possible to show unequivocally that there is no aggregation beyond the doublet stage, though it seems reasonably certain that any such aggregation cannot be appreciable. If the coagulation is in fact restricted to the formation of doublet particles by a single act of aggregation, then the rate at which the primary particles disappear should obey the rate law for a bimolecular reaction rather than the Smoluchowski equation for ordinary coagulation. In continuous dialysis, the particle charge—and therefore the energy of interaction of the particles—is continually decreasing, so that the velocity of coagulation at any instant is a function of both the energy of interaction and number concentration of the primary particles. If, however, the dialysis is stopped and the sol allowed to stand, then the subsequent coagulation should follow a bimolecular rate law with a velocity constant characteristic of the energy of interaction reached at the point when dialysis ceased. The kinetics of coagulation after different periods of initial dialysis are studied in the following paper.

Thanks are due to the Royal Society for a grant for the purchase of apparatus used in this work.

Department of Inorganic and
Physical Chemistry,
The University of Liverpool.

THE EFFECT OF DIALYSIS ON THE PROPERTIES OF NUCLEAR GOLD SOLS

PART III.—KINETICS OF COAGULATION AND APPLICATION OF THE THEORY OF COLLOID STABILITY

BY A. K. HOLLIDAY

Received 16*th September*, 1949

Measurement of the velocity of dialysis-initiated coagulation in a nuclear gold sol shows that the velocity follows a second-order rate law, confirming a previous conclusion that coagulation is restricted to primary-primary particle unions. The velocity increases with increasing period of dialysis, and the effect of temperature is also investigated ; with lengthy dialysis, coagulation at 50° C proceeds beyond the stage of primary-primary union. The theory of Verwey and Overbeek is used to calculate the double-layer potential ψ_0 from the coagulation rate, and ψ_0 is compared with the electrokinetic ζ-potential calculated from electrophoretic mobility. Reasonable agreement between the two potentials is found, ψ_0 being usually slightly greater than ζ. The theory is also used to explain the restricted coagulation ordinarily observed, and predicts the extension at 50° C. The assumptions made in applying the theory are discussed.

In Part II,[1] measurements of the light absorption of nuclear gold sols coagulating as a result of dialysis have indicated that the coagulation is restricted to the formation of secondary doublet particles by union of two primaries. In this paper, measurements of the coagulation velocity after given periods of dialysis are recorded and these are shown to support the conclusion of Part II. The effect of temperature on the coagulation rate is also investigated, to see if increased temperature can drive the coagulation beyond the limits ordinarily observed. The further purpose of this paper is to apply the Verwey-Overbeek theory of colloid stability [2] to the results obtained. Previously, theories of stability have been applied to sols coagulated by addition of electrolyte ; but it is believed that the restricted coagulation studied here is more particularly suitable for the application of theory for the following reasons. In electrolyte-initiated coagulations, primary particles disappear not only by union with one another, but also by union with the aggregates formed during coagulation. Hence, as soon as the concentration of aggregates becomes appreciable, the rate of primary disappearance (the coagulation rate) is determined by a number of different primary-aggregate interactions, each possessing a characteristic interaction energy (since the latter is a function of particle size). It follows that the rate of primary disappearance cannot be expressed solely in terms of one interaction energy calculated for one (primary) particle size. But in dialysis-initiated coagulation, only the one kind of union—primary-primary—takes place, and the rate of primary disappearance is then governed by one interaction energy. The latter is calculable from the observed coagulation rate and, using the Verwey-Overbeek theory, is expressed in terms of ψ_0, the potential drop across the particle double layers. ψ_0 is then compared directly with ζ, the electrokinetic potential, determined by measurement of the electrophoretic mobility of the coagulating particles ; the validity of ζ as a criterion of stability can therefore be directly assessed. The experimental evidence further requires that the interaction energies for primary-doublet or doublet-doublet unions must be sufficiently large to make the rate at which these unions occur negligibly small at ordinary temperatures, irrespective of the period of dialysis. These requirements are therefore considered in terms of the Verwey-Overbeek theory.

Experimental

Nuclear sols of known particle radius were prepared, characterized and dialyzed as described in Parts I [3] and II. After a given period of dialysis, samples of sol were transferred to stoppered quartz flasks and placed in the thermostat. The coagulation was followed by withdrawing samples and measuring the light absorption at wavelengths 670 and 610 $\mu\mu$. Conversion of each absorption measurement to primary particle concentration was made by use of the data in Part II, and the mean of each pair of results was taken. Possible errors in absorption measurements due to concentration changes arising from evaporation during the very long periods of coagulation were controlled by gold concentration determinations made at intervals during each run.

[1] Holliday (preceding paper).

[2] Verwey and Overbeek, *Theory of the Stability of Lyophobic Colloids* (Elsevier, Amsterdam, 1948).

[3] Holliday, *Trans. Faraday Soc.*, 1947, **43**, 661.

Electrophoretic mobilities were determined at 25° C by the moving boundary method referred to in Part I; as previously noted there, no detectable difference could be observed between the mobilities of the red primary and blue doublet particles. Changes in ionic strength during dialysis were determined from conductivity measurements (cp. Part I). No detectable change in either mobility or conductivity occurred during coagulation.

Results

Effect of Period of Dialysis.—Fig. 1 shows values of $1/n$ plotted against t for three different periods of dialysis, n being the number concentration of primary particles per ml. of sol and t the coagulation time (measured from zero time at the end of dialysis). The temperature of coagulation was 25° C. The slope of the line drawn through each set of points at first decreases with time, thereafter becoming constant, showing that the coagulation is then following a second-order rate law. The initially high rate of primary disappearance may be due to the presence of a few particles possessing a lower interaction energy than the remainder, these disappearing first at a rapid rate. (A similar phenomenon has been observed in electrolyte-initiated coagulation of gold sols.[4]) The period of dialysis has a marked effect on the coagulation rate, but the linear $1/n$ against t relationship is not altered; clearly, therefore, the primary particles disappear at a measurable rate only by union with one another in agreement with the conclusion reached in Part II. Examination of the absorption spectra of the coagulated sols confirmed that the coagulation had followed the course described in Part II, leading to a stable sol of doublet particles.

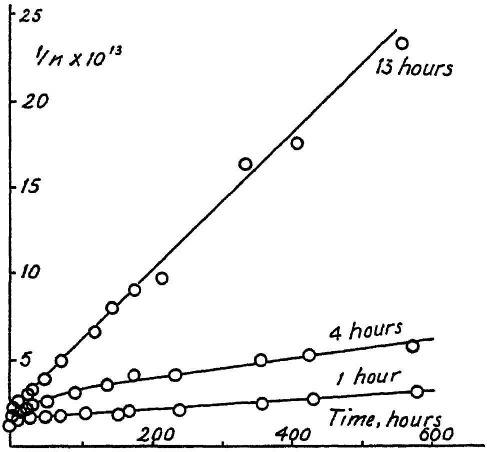

FIG. 1.

Effect of Temperature.—Fig. 2 shows the results obtained by coagulating at different temperatures for two different periods of dialysis (carried out at room temperature). For the shorter period of dialysis, increase of temperature produces no change in the velocity of coagulation; but on more prolonged dialysis increase of temperature from 25° to 35° C increases the coagulation rate, leaving the linear $1/n$ against t relationship unaffected. At 50° C, $1/n$ increases with t at a rate exceeding that for a second-order process, suggesting

TABLE I

Wavelength ($\mu\mu$)	670	610	580	550	520	490	470	430
$k_{50} \times 10^3$	70	72	72	71	70	65	62	61
$k_{\infty} \times 10^3$	59	71	74	75	71	65	61	61

---

[4] Lewis and Garner, *J. Physic Chem.*, 1926, **30**, 1401, 1410.

that primaries are disappearing here also by union with doublets. The absorption coefficients k_{60} for the sol used in this experiment were determined at the end of the coagulation run, and are compared with the k_∞ values for the "final blue sol" (coagulated at room temperature) in Table I. The change in absorption at 670 $\mu\mu$ supports the conclusion that particles other than doublets are formed at 50° C. (The n values at this temperature are calculated from the absorptions at 610 $\mu\mu$ only, because of the anomalous increase of k at 670 $\mu\mu$.)

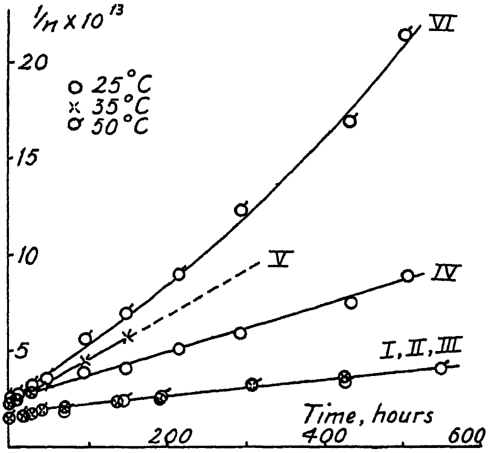

FIG. 2.—Effect of temperature on coagulation rate.
I, II, III : Dialyzed for 3 hr. IV, V, VI : Dialyzed for 7 hr.

Calculation of Double Layer Potentials from Coagulation Rates and Comparison with ζ-Potentials.—The methods described by Verwey and Overbeek [2] will be used throughout this section, and particular sections of their treatise are referred to by appropriate chapter and paragraph numbers.

The factor W by which the rate of rapid coagulation of a colloidal suspension is reduced due to a particle interaction energy V is given by Fuchs : [5]

$$W = 2\int_2^\infty e^{V/kT} ds/s^2,$$

where $s = R/r$, R being the distance between the particle centres, and r the particle radius. The rate of rapid coagulation c_f for primary-primary unions only is given by Smoluchowski [6] as

$$c_f = 8\pi r D n_0,$$

where n_0 is the initial number concentration of primary particles and D the diffusion coefficient. Since r and n_0 are known, c_f may be calculated, and thence

$$W = c_f/c_s,$$

where c_s is the observed rate of slow coagulation. The interaction energy V is the sum of two terms $V_R + V_A$, V_A being energy of repulsion due to double-layer interaction and V_A the van der Waals' energy of attraction. For a given value of s, V_R for spherical particles is a function of ϵ, the dielectric constant of the medium between the particles, κ the reciprocal double-layer thickness of Debye-Hückel, and ψ_0 the potential difference between the charged surface of the particle and the bulk of the surrounding electrolyte. The exact form of the function depends upon the magnitudes of ψ_0 and κr, and upon whether the particles approach at constant charge or at constant potential. The form used here is that for small values of ψ_0 and for $\kappa r \sim 1$, assuming approach at constant charge; the reasons for this selection, and for the value assigned to A in the expression for V_A below, are discussed later. The expression for V_R is then [7]

$$V_R = \psi_0^2 \epsilon r \frac{e^{-\kappa r(s-2)}}{s} \gamma,$$

---

[5] Fuchs, *Z. Physik*, 1934, **89**, 736.

[6] Smoluchowski, *Z. physik. Chem.*, 1917, **92**, 129.

[7] Ref. 2, Chap. X, § 3.

where γ is a function of s and κr. Numerical values of $V_R/\psi_0{}^2\epsilon r$ for different values of κr and s are given by Verwey and Overbeek.[8] The energy of attraction V_A has been given by Hamaker [9] as

$$V_A = -\frac{A}{6}\left(\frac{2}{s^2 - 4} + \frac{2}{s^2} + \ln\frac{s^2 - 4}{s^2}\right),$$

where A is a constant depending on the nature of the particles and the medium between. The value of A used here will be 10^{-12}.

The value of ψ_0 corresponding to a known W value is determined by trial and error, as follows. For a given coagulation run, an arbitrary value of ψ_0 is used and V_R calculated for a series of s values, using the experimental κr value and assuming ϵ to have the value for water at the appropriate temperature. V_A is also determined for the same s values, and V obtained; a plot of V against s gives a potential energy curve for the coagulation. A further plot of $e^{V/kT}/s^2$ against s enables graphical integration of the Fuchs expression to be carried out, and W determined. The whole procedure is repeated with different ψ_0 values until a W value equal to the experimental value is obtained; the corresponding ψ_0 is then the operative potential in the coagulation.

The ζ-potentials are calculated from the electrophoretic mobilities using the relationship due to Overbeek,[10] taking account of relaxation effects. The surrounding electrolyte is assumed to be uni-univalent, the particles to be non-conducting, and the effect of surface conductance to be negligible at the low κr values here.[11] Overbeek's extrapolations of his ζ-mobility relationship—strictly valid only for small ζ—are used to compute the large ζ values. In Table II, values of W, ψ_0 and ζ are given for the undialyzed stable sol and for the nine coagulation runs carried out. It should be noted that ψ_0 is referred to the temperature of coagulation, but ζ is determined only at 25° C, since moving boundary measurements are impracticable at higher temperatures.

TABLE II

Expt.	Temp. ° C (t)	W (expt.)	Mobility cm./sec./V/cm. × 10^4 (at 25° C)	Conductivity mhos × 10^{-6} (at 25° C)	κr (at t° C)	ψ_0 (mV) (at t° C)	ζ (mV) (at 25° C)
1	25	Stable	4·35	534	0·833	—	106
2	25	$3{\cdot}6 \times 10^7$	3·99	469	0·708	100	95
3	25	$1{\cdot}7 \times 10^7$	4·10	366	0·632	97	96
4	25	$2{\cdot}4 \times 10^6$	4·04	227	0·500	91	92
5	25	$2{\cdot}2 \times 10^7$	4·09	384	0·645	98	96
6	35	$2{\cdot}2 \times 10^7$	4·09	384	0·634	100	96
7	50	$2{\cdot}2 \times 10^7$	4·09	384	0·619	107	96
8	25	$8{\cdot}1 \times 10^6$	3·70	254	0·528	94	86
9	35	$4{\cdot}7 \times 10^6$	3·70	254	0·518	96	86
10	50	—	3·70	254	0·508	—	86

An attempt must now be made to apply theory to the problem of restricted coagulation. Qualitatively, it is easily seen that coagulation rate must decrease with increase of particle size because V increases with r. To apply the theory quantitatively, i.e. to calculate W_{pd} for primary-doublet unions, or W_{dd} for doublet-doublet unions, is difficult: firstly, because these unions involve non-spherical particles which may also have different sizes, and secondly, because ψ_0 for doublet particles is not necessarily the same as for primaries. The electrophoretic measurements, it is true, show that primaries and doublets have the same mobility, but this does not necessarily imply identical ζ (or ψ_0) values, since the shape factor may be important in the ζ-mobility relationship. Because of these difficulties, a crude calculation of W_{dd} only will be made, assuming the doublets to have a radius $r_d = (2r)^{1/3}$ and that ψ_0 is the same as for the primaries. Calculating for Expt. 4, where the primary-primary coagulation rate is a maximum, W_{dd} is 4×10^9, and the sol is obviously stable with respect to doublet-doublet unions. W_{pd} will presumably be less than W_{dd} and greater than W, but as W is already large, the rate at which primary-doublet unions occur will not appreciably affect the concentration of primaries over a measurable time interval. In Expt. 10 where "anomalous" coagulation is observed at 50° C, W_{dd} may be calculated by using ψ_0 from Expt. 9, at 35° C (a rather approximate, and probably slightly low value since ψ_0 appears to increase with temperature). W_{dd} is found to be 7×10^7, i.e. of the same order of magnitude as W. Hence coagulation beyond the primary-primary stage may be expected to occur at a measurable rate here, the behaviour which is in fact observed.

---

[8] Ref. 2, Chap. X, § 3. [9] Hamaker, *Physica*, 1937, 4, 1058.

[10] Overbeek, *Kolloidchem. Beih.*, 1943, 54, 287.

[11] Booth, *Trans. Faraday Soc.*, 1948, 44, 955; Henry, *ibid.*, 1021.

Discussion

It is clear from Table II that ψ_0 is always large. The correctness of calculating V_R by use of an expression valid only for small ψ_0 is therefore questionable, and, together with other assumptions made, requires discussion before any conclusions can be drawn from the results. V_R may be calculated from ψ_0 by the use of one of two relationships, one valid for small ψ_0 and small κr (~ 1), the other valid for large or small ψ_0 and large κr ($\gg 1$). Neither is strictly valid here, where ψ_0 is large and $\kappa r \sim 1$; the relationship actually used is that employed by Verwey and Overbeek in similar circumstances.[12] Calculations on the data of this paper kindly made by Prof. J. Th. G. Overbeek using the alternative relationship for large ψ_0 values give values of ψ_0 about 10 % larger than those of Table II, assuming approach at constant potential. The assumption of approach at constant charge has been preferred in the calculations given here, because approach at constant potential requires that the charge on the adjacent surfaces of two particles should decrease on approach.[13] While this may occur readily where the ions responsible for the surface charge can pass rapidly from surface to solution or vice versa, it is unlikely to occur in the case of colloidal gold, where the surface charge is an intrinsic part of the micelle and does not arise from ions common to both particle and electrolyte. Approach at constant charge leads to values of ψ_0 slightly *lower* than those obtained at constant potential.

The value used for the constant A in the calculation of V_A is 10^{-12}, the value chosen by Hamaker[9] and by Verwey and Overbeek[14] as generally applicable to aqueous colloidal systems; the latter authors quote some experimental evidence in support of their choice.[15] A depends upon the nature of the particles and the medium between them, and is determined ultimately by the polarizabilities of the atoms or ions concerned. Since the nature and composition of the colloidal gold particle are uncertain, a reasonable calculation of A is made virtually impossible. Fortunately, V is only affected to any appreciable extent by a change in the order of magnitude of A; thus, a change in A from 10^{-12} to 10^{-13} would decrease the given ψ_0 values by only ~ 5 %.

It seems clear that, while the assumptions made here appear to be the most reasonable in the prevailing circumstances, no marked change in ψ_0 would occur if other, and less reasonable assumptions were made. Therefore, the following conclusions, based on the results given in Table II, appear to be valid.

(i) Reasonable agreement exists between ψ_0 and ζ, the former being generally slightly larger. This would suggest that the greater part of ψ_0 is electrokinetically operative, and that ζ is therefore a reasonable criterion of colloid stability, if it is remembered that the product κr is also important in this respect. Necessarily, the range of ψ_0-ζ values which can be compared here is restricted by experimental considerations; the concordance might be less close at higher coagulation rates, i.e. at lower ψ_0 values.

(ii) Increase of temperature probably increases ψ_0; for a short period of dialysis (Expt. 6 and 7), the increase in V is sufficient to maintain

---

[12] Ref. 2, Chap. X, § 5.

[13] Ref. 2, Chap. III, § 4; X, § 2.

[14] Ref. 2, Chap. VI, § 2.

[15] Ref. 2, Chap. VII, § 2.

V/kT practically unchanged, and the rate of coagulation remains unaffected. Further dialysis (Expt. 8, 9 and 10) diminishes ψ_0, and the temperature increment is then no longer adequate to keep V/kT the same, with the consequence of an increased coagulation rate.

(iii) The application of theory to the phenomenon of restricted coagulation, though limited in validity by the approximations necessarily made, leads to conclusions in agreement with experimental observation. If a shape factor could be introduced into the Verwey-Overbeek expression for V, a more rigorous application of theory could be made not only to results like those given here, but to the more general type of electrolyte-initiated coagulation, where, in the case of colloidal gold,[16] aggregation seems to proceed at a rate dependent upon the number and nature of the aggregates formed.

Department of Inorganic and
Physical Chemistry,
The University of Liverpool.

[16] Tuorila, *Kolloidchem. Beih.*, 1926, **22**, 282.

THERMODYNAMICS OF ADSORPTION

PART I.—GENERAL CONSIDERATIONS

BY DOUGLAS H. EVERETT

Received 18th November, 1949

As a preliminary to a more detailed study of the thermodynamics of adsorption, the general methods of approach are discussed and it is concluded that a procedure closely akin to that employed in studying solutions is the most convenient both from the standpoint of analysis of experimental results and from that of theoretical interpretation.

1. Introduction.—An exact and at the same time useful thermodynamic treatment of adsorption of vapours by solids cannot be developed without assumptions as to the nature of the adsorbed phase. The various methods of approach differ in their choice of characteristic thermodynamic functions and in this paper we shall discuss their relative merits. This preliminary discussion is the more important since Hill [1] has recently examined this problem and reached conclusions with which we do not entirely agree. We consider that thermodynamic methods virtually identical with those employed in studying solutions are the more convenient and proceed in Part II to apply these methods to the localized monolayer and non-localized monolayer models of the adsorbed phase. In Part III we shall present the results of an analysis of experimental data in terms of the methods outlined in Part II. The main objects of these papers are (*a*) to stress that the mathematical forms of various adsorption isotherm equations can be derived on the basis of different physical models, and hence to point out that measurement of isotherms at one temperature can never distinguish conclusively between the various possible models; (*b*) to evaluate the thermodynamic quantities characterizing adsorption equilibria by analysis of isotherms obtained at several temperatures, and so obtain information on the nature of the

[1] Hill, *J. Chem. Physics*, 1949, **17**, 520; cf. Rowley and Innes, *J. Physic. Chem.*, 1942, **46**, 537, 548, 694; 1945, **49**, 411.

surface phase; (*c*) to show the importance of the entropy of adsorption in determining the exact shape of isotherms, and to discuss the relationship which appears between heats and entropies of adsorption.

2. Characteristic Functions.—As pointed out by Guggenheim[2] the introduction of surface effects into ordinary three-dimensional thermodynamics doubles the number of characteristic thermodynamic potentials. We normally have four such functions expressed in different sets of independent variables:

$$\left.\begin{aligned} E &= E(S, V, n_i) \\ H &= H(S, P, n_i) \\ F &= F(T, V, n_i) \\ G &= G(T, P, n_i) \end{aligned}\right\}\text{ where }\begin{aligned} H &= E + PV \\ F &= E - TS \\ G &= H - TS \end{aligned} \quad . \quad . \quad (1)$$

In applying thermodynamics to a surface phase we need a further variable to complete the specification of its state; we may choose either the surface area, A^σ, or the corresponding intensity factor ϕ (usually called the "spreading pressure"). To avoid confusion, and to stress that we are considering molecules in a surface phase we replace n_i by m_i the number of moles of the ith kind in the surface. We may now define eight characteristic functions for the surface phase:

$$\begin{array}{llll} E^\sigma = E^\sigma(S^\sigma, V^\sigma, A^\sigma, m_i) & . \ (2.1); & \mathscr{E}^\sigma = \mathscr{E}^\sigma(S^\sigma, V^\sigma, \phi, m_i) & . \ (2.5) \\ H^\sigma = H^\sigma(S^\sigma, P, A^\sigma, m_i) & . \ (2.2); & \mathscr{H}^\sigma = \mathscr{H}^\sigma(S^\sigma, P, \phi, m_i) & . \ (2.6) \\ F^\sigma = F^\sigma(T, V^\sigma, A^\sigma, m_i) & . \ (2.3); & \mathscr{F}^\sigma = \mathscr{F}^\sigma(T, V^\sigma, \phi, m_i) & . \ (2.7) \\ G^\sigma = G^\sigma(T, P, A^\sigma, m_i) & . \ (2.4); & \mathscr{G}^\sigma = \mathscr{G}^\sigma(T, P, \phi, m_i) & . \ (2.8)^3 \end{array}$$

In these H, F and G are defined as before by (1), while

$$\mathscr{E}^\sigma = E^\sigma + \phi A^\sigma \quad . \quad . \quad . \quad . \quad (3.1)$$

$$\mathscr{H}^\sigma = H^\sigma + \phi A^\sigma \quad . \quad . \quad . \quad . \quad (3.2)$$

$$\mathscr{F}^\sigma = F^\sigma + \phi A^\sigma \quad . \quad . \quad . \quad . \quad (3.3)$$

$$\mathscr{G}^\sigma = G^\sigma + \phi A^\sigma . \quad . \quad . \quad . \quad . \quad (3.4)$$

We use cursive capitals instead of Guggenheim's $\bar{E}$, $\bar{H}$, $\bar{F}$ and $\bar{G}$ as we wish to use the superscript bar to denote partial molar quantities. There is no accepted nomenclature for these functions and the terms surface energy, heat and free energy are often used ambiguously. Most authors[4] in applying thermodynamics to surface phases choose four of the above functions. Thus Hill employs E^σ, $\mathscr{H}^\sigma$, F^σ and $\mathscr{G}^\sigma$ (denoted by him as E_s, H_s, A_s and F_s).

The total differentials of the various functions may be written

$$\mathrm{d}E^\sigma = T\mathrm{d}S^\sigma - P\mathrm{d}V^\sigma - \phi\mathrm{d}A^\sigma + \sum_i \mu_i^\sigma \mathrm{d}m_i \quad . \quad . \quad (4.1)$$

$$\mathrm{d}H^\sigma = T\mathrm{d}S^\sigma + V^\sigma\mathrm{d}P - \phi\mathrm{d}A^\sigma + \sum_i \mu_i^\sigma \mathrm{d}m_i \quad . \quad . \quad (4.2)$$

$$\mathrm{d}F^\sigma = -S^\sigma\mathrm{d}T - P\mathrm{d}V^\sigma - \phi\mathrm{d}A^\sigma + \sum_i \mu_i^\sigma \mathrm{d}m_i \quad . \quad (4.3)$$

$$\mathrm{d}G^\sigma = -S^\sigma\mathrm{d}T + V^\sigma\mathrm{d}P - \phi\mathrm{d}A^\sigma + \sum_i \mu_i^\sigma \mathrm{d}m_i \quad . \quad (4.4)$$

[2] Guggenheim, *Modern Thermodynamics* (Methuen, London, 1933), chap. 12; cf. also Guggenheim, *Trans. Faraday Soc.*, 1940, **36**, 397.

[3] We assume mechanical and temperature equilibrium with the surroundings so that P and T are the pressure and temperature of the surroundings; we may thus omit the superscript σ.

[4] E.g. Hill, *loc. cit.*, Rowley and Innes, *loc. cit.*, Rideal, *Surface Chemistry* (Cambridge University Press, 1930), Alexander and Johnson, *Colloid Science* (Oxford University Press, 1948).

$$d\mathscr{E}^\sigma = TdS^\sigma - PdV^\sigma + A^\sigma d\phi + \sum_i \mu_i^\sigma dm_i \quad . \quad . \quad (4.5)$$

$$d\mathscr{H}^\sigma = TdS^\sigma + V^\sigma dP + A^\sigma d\phi + \sum_i \mu_i^\sigma dm_i \quad . \quad . \quad (4.6)$$

$$d\mathscr{F}^\sigma = -S^\sigma dT - PdV^\sigma + A^\sigma d\phi + \sum_i \mu_i^\sigma dm_i \quad . \quad (4.7)$$

$$d\mathscr{G}^\sigma = -S^\sigma dT + V^\sigma dP + A^\sigma d\phi + \sum_i \mu_i^\sigma dm_i \quad . \quad (4.8)$$

From these we see that ϕ and μ_i^σ may be defined by:

$$\phi = -\left(\frac{\partial E^\sigma}{\partial A^\sigma}\right)_{S^\sigma, V^\sigma, m_i} = -\left(\frac{\partial H^\sigma}{\partial A^\sigma}\right)_{S^\sigma, P, m_i} = -\left(\frac{\partial F^\sigma}{\partial A^\sigma}\right)_{T, V^\sigma, m_i} = -\left(\frac{\partial G^\sigma}{\partial A^\sigma}\right)_{T, P, m_i} \quad (5)$$

$$\mu_i^\sigma = \left(\frac{\partial E^\sigma}{\partial m_i}\right)_{S^\sigma, V^\sigma, A^\sigma, m_j} = \left(\frac{\partial H^\sigma}{\partial m_i}\right)_{S^\sigma, P, A^\sigma, m_j} = \left(\frac{\partial F^\sigma}{\partial m_i}\right)_{T, V^\sigma, A^\sigma, m_j} = \left(\frac{\partial G^\sigma}{\partial m_i}\right)_{T, P, A^\sigma, m_j}$$

$$= \left(\frac{\partial \mathscr{E}^\sigma}{\partial m_i}\right)_{S^\sigma, V^\sigma, \phi, m_j} = \left(\frac{\partial \mathscr{H}^\sigma}{\partial m_i}\right)_{S^\sigma, P, \phi, m_j} = \left(\frac{\partial \mathscr{F}^\sigma}{\partial m_i}\right)_{T, V^\sigma, \phi, m_j} = \left(\frac{\partial \mathscr{G}^\sigma}{\partial m_i}\right)_{T, P, \phi, m_j} \quad . \quad (6)$$

3. Definition of Heats of Adsorption.—It is well known that the term heat of adsorption has no exact meaning unless the conditions under which adsorption takes place are very carefully specified.[5] There are four heats of adsorption which can be expressed simply in terms of the above functions. For simplicity, we shall confine ourselves here to the adsorption of a single vapour on a solid surface.

If the heat evolved (at constant temperature) during the adsorption of m moles upon a surface initially clean, under certain specified conditions is Q, then the corresponding differential heat of adsorption q is defined by $\partial Q/\partial m$. Is is easily shown[6] that if V^G, V^σ and A^σ are constant during the process:

$$q = -\Delta\overline{\mathrm{E}} = \mathrm{E}^G - \overline{\mathrm{E}}^\sigma \quad . \quad . \quad . \quad (7.1)$$

if P and A^σ are constant

$$q = -\Delta\mathrm{H} = \mathrm{H}^G - \overline{\mathrm{H}}^\sigma \quad . \quad . \quad . \quad (7.2)$$

if V^G, V^σ and ϕ are constant

$$q = -\Delta\overline{\mathscr{E}} = \mathrm{E}^G - \overline{\mathscr{E}}^\sigma \quad . \quad . \quad . \quad (7.3)$$

if P and ϕ are constant

$$q = -\Delta\overline{\mathscr{H}} = \mathrm{H}^G - \overline{\mathscr{H}}^\sigma \quad . \quad . \quad . \quad (7.4)$$

where E^G and H^G are the molar energy and heat of the gas, and $\overline{\mathrm{E}}^\sigma$, $\overline{\mathrm{H}}^\sigma$, $\overline{\mathscr{E}}^\sigma$ and $\overline{\mathscr{H}}^\sigma$ are partial molar quantities defined by

$$\overline{\mathrm{E}}^\sigma = (\partial E^\sigma/\partial m)_{T, V^\sigma, A^\sigma} \quad (8.1) \qquad \overline{\mathrm{H}}^\sigma = (\partial^\sigma H/\partial m)_{T, P, A^\sigma} \quad (8.2)$$

$$\overline{\mathscr{E}}^\sigma = (\partial \mathscr{E}^\sigma/\partial m)_{T, V^\sigma, \phi} \quad (8.3) \qquad \overline{\mathscr{H}}^\sigma = (\partial \mathscr{H}^\sigma/\partial m)_{T, P, \phi} \quad (8.4)$$

The first two heats defined above are often called the differential heat of adsorption and isosteric heat of adsorption respectively, while the last is Hills' equilibrium heat of adsorption.[7]

---

[5] Cf. e.g. Williams, *Proc. Roy. Soc. Edin.*, 1917, **37**, 162; Hückel, *Adsorption und Kapillarkondensation* (Acad. Verlagsgesellschaft, Leipzig, 1928), Wilkins, *Proc. Roy. Soc. A*, 1938, **164**, 496, Brunauer, *Physical Adsorption of Gases and Vapours* (Oxford University Press, 1943), p. 218.

[6] Cf. Guggenheim, *loc. cit.*, p. 163.

[7] The nomenclature of these heats in the literature is inconsistent; isosteric is used by Freundlich and Hückel in a sense quite different from that used by Hill, Brunauer and others. We suggest that the "heats" listed above in (7) should be called differential energy, differential heat, equilibrium energy and equilibrium heat of adsorption respectively.

Equation (8.1) and (8.2) may be rewritten

$$\bar{\mathrm{E}}^\sigma = \mathrm{E}^\sigma + m(\partial \mathrm{E}^\sigma/\partial m)_{T,V^\sigma,A} \quad . \quad . \quad . \quad (9.1)$$

$$\bar{\mathrm{H}}^\sigma = \mathrm{H}^\sigma + m(\partial \mathrm{H}^\sigma/\partial m)_{T,P,A} \quad . \quad . \quad . \quad (9.2)$$

where $\mathrm{E}^\sigma = E^\sigma/m$ and $\mathrm{H}^0 = H^\sigma/m$ are mean molar quantities. Furthermore, since the partial molar quantities $\bar{\mathcal{E}}^\sigma$ and $\bar{\mathcal{H}}^\sigma$ are defined for a phase of one component at constant values of *all* the intensity factors, the partial molar and mean molar quantities are equal.

$$\bar{\mathcal{E}}^\sigma = \mathcal{E}^\sigma = \mathcal{E}^\sigma/m \quad . \quad . \quad . \quad . \quad (9.3)$$

$$\bar{\mathcal{H}}^\sigma = \mathcal{H}^\sigma = \mathcal{H}^\sigma/m. \quad . \quad . \quad . \quad . \quad (9.4)$$

The various heats of adsorption may now be written

$$-\Delta\bar{\mathrm{E}} = \mathrm{E}^G - \mathrm{E}^\sigma - \Gamma(\partial \mathrm{E}^\sigma/\partial \Gamma)_{T,V^\sigma} \quad . \quad . \quad . \quad (10.1)$$

$$-\Delta\bar{\mathrm{H}} = \mathrm{H}^G - \mathrm{H}^\sigma - \Gamma(\partial \mathrm{H}^\sigma/\partial \Gamma)_{T,P} \quad . \quad . \quad . \quad (10.2)$$

$$-\Delta\mathcal{E} = \mathrm{E}^G - \mathcal{E}^\sigma \quad . \quad . \quad . \quad . \quad . \quad . \quad . \quad (10.3)$$

$$-\Delta\mathcal{H} = \mathrm{H}^G - \mathcal{H}^\sigma \quad . \quad . \quad . \quad . \quad . \quad . \quad . \quad (10.4)$$

where we have introduced $\Gamma = m/A^\sigma$ in place of the separate variables m and A^σ; Γ may be called the surface concentration.

The heats of adsorption are related to the variation of equilibrium vapour pressure p of the adsorbed phase with temperature by a set of equations of the Clausius-Clapeyron type:

$$(\partial \ln n^G/\partial T)_{V^G,\Gamma} = -\Delta\bar{\mathrm{E}}/RT^2 \quad . \quad . \quad (11.1)$$

$$(\partial \ln p/\partial T)_{P,\Gamma} = -\Delta\bar{\mathrm{H}}/RT^2 \quad . \quad . \quad . \quad (11.2)$$

$$(\partial \ln n^G/\partial T)_{V^G,\phi} = -\Delta\mathcal{E}/RT^2 \quad . \quad . \quad (11.3)$$

$$(\partial \ln p/\partial T)_{P,\phi} = -\Delta\mathcal{H}/RT^2 \quad . \quad . \quad . \quad (11.4)$$

where n^G is the number of moles in a constant volume V^G of gas phase.

4. Relations between Heats of Adsorption.—The relationships between the four heats of adsorption defined above are readily obtained. We find that

$$\Delta\bar{\mathrm{E}} - \Delta\bar{\mathrm{H}} = P\mathrm{V}^G - P\mathrm{V}^\sigma + T\Gamma(\partial \mathrm{V}^\sigma/\partial \Gamma)_{T,P}(\partial p/\partial T)_{V^\sigma,\Gamma}. \quad . \quad (12)$$

The first term in (12) can usually be equated to RT, while the last two terms are usually negligible.

For the equilibrium energy and heat we have the simpler relation:

$$\Delta\mathcal{E} - \Delta\mathcal{H} = P\mathrm{V}^G - P\mathrm{V}^\sigma. \quad . \quad . \quad . \quad (13)$$

Again, for most purposes we may equate the right-hand side of (13) to RT.

The relation between $\mathcal{H}$ and H can be expressed in two alternative forms. For the mean molar quantities we have, by definition,

$$\mathcal{H}^\sigma = \mathrm{H}^\sigma + \phi/\Gamma$$

whence using (9.2) we obtain

$$\mathcal{H}^\sigma = \bar{\mathrm{H}}^\sigma + \phi/\Gamma - \Gamma(\partial \mathrm{H}^\sigma/\partial \Gamma)_{T,P}. \quad . \quad . \quad . \quad (14)$$

Eqn. (14) may be transformed as follows. We take the equation

$$\mathrm{G}^\sigma = \mathrm{H}^\sigma - T\mathrm{S}^\sigma,$$

and differentiate with respect to Γ, remembering that, because of (4.4),

$$(\partial \mathrm{G}^\sigma/\partial \Gamma)_{T,P} = -(\partial \mathrm{G}^\sigma/\partial \mathrm{A}^\sigma)_{T,P}/\Gamma^2 = \phi/\Gamma^2$$

while, from the two-dimensional analogues of Maxwell's equations,

$$(\partial \mathrm{S}^\sigma/\partial \Gamma)_{T,P} = -(\partial \mathrm{S}^\sigma/\partial \mathrm{A}^\sigma)_{T,P}/\Gamma^2 = (\partial \phi/\partial \mathrm{T})_{P,A}/\Gamma^2.$$

This leads to

$$\phi = \Gamma^2(\partial \mathrm{H}^\sigma/\partial\Gamma)_{T,P} + T(\partial\phi/\partial T)_{P,\Gamma} \quad . \quad . \quad . \quad (15.1)$$

which is the surface analogue of the well-known equation,

$$P = -(\partial \mathrm{E}/\partial \mathrm{V})_T + T(\partial P/\partial T)_\mathrm{V} \, . \quad . \quad . \quad (15.2)^8$$

Dividing (15.1) by Γ gives Hill's equation (71), except that we are using H^σ instead of E^σ. Substitution in (14) then gives

$$\mathscr{H}^\sigma = \bar{\mathrm{H}}^\sigma + \frac{T}{\Gamma}\left(\frac{\partial\phi}{\partial \mathrm{T}}\right)_{P,\Gamma}, \quad . \quad . \quad . \quad (16)$$

whence

$$\Delta\mathscr{H} = \Delta\bar{\mathrm{H}} - \phi/\Gamma + \Gamma(\partial \mathrm{H}^\sigma/\partial\Gamma)_{T,P} = \Delta\bar{\mathrm{H}} - \frac{T}{\Gamma}\left(\frac{\partial\phi}{\partial T}\right)_{P,\Gamma} \, . \quad (17)$$

Similarly

$$\Delta\mathscr{E} = \Delta\bar{\mathrm{E}} - \frac{T}{\Gamma}\left(\frac{\partial\phi}{\partial T}\right)_{\mathrm{V}^\sigma,\Gamma}. \quad . \quad . \quad . \quad (18)$$

Eqn. (17) is Hill's equation (80) while his (81) follows from (10.1) and (15).

In the special case in which $\phi = Tf(\Gamma)$, $(\partial\phi/\partial T)_{P,\Gamma} = \phi/T$ and

$$\Delta\bar{\mathrm{H}} = \Delta\mathscr{H} - \phi/T \quad . \quad . \quad . \quad . \quad (19.1)$$

$$\Delta\bar{\mathrm{E}} = \Delta\mathscr{E} - \phi/T. \quad . \quad . \quad . \quad . \quad (19.2)$$

It also follows that, in this case,

$$(\partial \mathrm{H}^\sigma/\partial\Gamma)_{T,P} = 0.^9$$

4. Discussion.—We now have to decide which set of thermodynamic functions is the more convenient, and in particular whether it is preferable to consider $\Delta\bar{\mathrm{H}}$ or $\Delta\mathscr{H}$ as the heat of adsorption most amenable to statistical mechanical interpretation.

At first sight $\Delta\mathscr{H}$, which is analogous to the heat of vaporization of a liquid at its saturated vapour pressure (and hence called the equilibrium heat) would seem to provide the best basis for theoretical treatment. This view has been adopted by Hill [1] who rejects $\Delta\bar{\mathrm{H}}$ as being " not of any great interest " because of the inclusion in it (eqn. (10.2)) of the term $(\partial \mathrm{H}^\sigma/\partial\Gamma)_{T,P}$, " which is difficult to interpret."

From a purely thermodynamic standpoint all four heats of adsorption $\Delta\bar{\mathrm{E}}$, $\Delta\bar{\mathrm{H}}$, $\Delta\mathscr{E}$, $\Delta\mathscr{H}$ are equally fundamental, and are in this respect to be preferred over some of the other heats of adsorption which have been defined from time to time.[10]

In practice, $\Delta\bar{\mathrm{E}}$ can be determined by calorimetric experiment [11] and

---

[8] Cf. Guggenheim, *loc. cit.*, eqn. (155·1). Note that the relation between H^σ and $\mathscr{H}^\sigma$ in terms of ϕ and A, is the same as that between E and H in terms of P and V, this is why H^σ appears in (15·1) while E appears in (15.2).

[9] Throughout we have dealt with general thermodynamic functions. If we limit ourselves to equilibrium states our equations need slight modification. In particular we should substitute

$$(\partial\phi/\partial T)_{P,\Gamma} = (\partial\phi/\partial T)_\Gamma - (\partial\phi/\partial P)_{T,\Gamma}(\partial p/\partial T)_\Gamma$$

$$(\partial \mathrm{H}^\sigma/\partial\Gamma)_{T,P} = (\partial \mathrm{H}^\sigma/\partial\Gamma)_T - (\partial \mathrm{H}^\sigma/\partial P)_{T,\Gamma}(\partial p/\partial T)_\Gamma.$$

These modifications refer to the effect of external pressure on the state of the surface phase. Normally this will be quite negligible, but if the adsorbed phase is in the form of a compressed gas, as is sometimes assumed in adsorption by porous solids, it may be important.

[10] Cf. Williams, Hückel, Wilkins, ref. 5.

[11] The calorimetric heat of adsorption $(\partial Q/\partial m)_{VG,A^\sigma}$ does not correspond accurately to $\Delta\mathrm{E}$ as defined by (7.1) since V^σ may not be constant. The exact equation is

$$\Delta\bar{\mathrm{E}} = (\partial Q/\partial m)_{VGG^\sigma} + \Gamma(\partial\bar{\mathrm{E}}^\sigma/\partial V^\sigma)_{T\Gamma}(\partial V^\sigma/\partial\Gamma)_T.$$

The correction term will usually be negligible.

$\Delta\bar{\mathrm{H}}$ can be obtained using eqn. (12), while $\Delta\bar{\mathrm{H}}$ may also be derived from the variation of saturation vapour pressure with temperature, when the surface concentration of adsorbed molecules is constant. Eqn. (11.2) is not strictly applicable since the pressure on the system (in the absence of a second gaseous non-adsorbable component) cannot be maintained constant, and gas imperfection is neglected; the exact relation corresponding to the usual experimental conditions is, of course

$$(\partial \ln p/\partial T)_{\Gamma} = \Delta\bar{\mathrm{H}}/pT(\mathrm{v}^{G} - \mathrm{v}^{\sigma}). \quad . \quad . \quad . \quad (20)$$

It is usually sufficiently accurate, however, to ignore v^{σ} in comparison with v^{G}, and to neglect gas imperfections so that in practice equation (11.2) can be employed.[12]

The other two heats of adsorption $\Delta\mathscr{E}$ and $\Delta\mathscr{H}$ cannot be measured calorimetrically since the processes to which they correspond involve the use of a hypothetical " surface piston " which varies the area of surface to maintain a constant value of ϕ. $\Delta\mathscr{H}$ can, however, be calculated from (11.4) (subject to the approximations mentioned in connection with (11.2)) by the method outlined by Hill.

The theoretical significance of heats of adsorption depends upon the ease or difficulty of interpreting the various terms in (17). Now, by (5)

$$\phi/\Gamma = \Gamma(\partial \mathrm{H}^{\sigma}/\partial \Gamma)_{S,P} \quad . \quad . \quad . \quad . \quad (21)$$

so that (17) may be written in the form:

$$\Delta\bar{\mathrm{H}} + \Gamma(\partial \mathrm{H}^{\sigma}/\partial \Gamma)_{T,P} = \Delta\mathscr{H} + \Gamma(\partial \mathrm{H}^{\sigma}/\partial \Gamma)_{S,P}. \quad . \quad . \quad (22)$$

We see that just as $\Delta\bar{\mathrm{H}}$ can be associated with a term $(\partial \mathrm{H}^{\sigma}/\partial \Gamma)_{T,P}$ so can $\Delta\mathscr{H}$ be associated with $(\partial \mathrm{H}^{\sigma}/\partial \Gamma)_{S,P}$. The argument in favour of $\Delta\mathscr{H}$ can be reduced to the consideration that while the second of these partial differentials can be interpreted physically in terms of the spreading pressure, the first has no such interpretation. Our comment on this is that the concept of spreading pressure only has a clear molecular kinetic interpretation when applied to non-localized surface films. If the adsorbed molecules are localized the concept of spreading pressure has no more physical significance than that of the surface tension of a solid, but is simply a function defined by eqn. (5). Thus, in the most general case, if we make no assumptions regarding the exact nature of the surface phase, we cannot assign a definite physical significance to either of the $(\partial \mathrm{H}^{\sigma}/\partial \Gamma)$ terms. Any detailed statistical mechanical theory should yield both terms, so that to this extent it matters little whether we choose $\Delta\bar{\mathrm{H}}$ or $\Delta\mathscr{H}$. However, in a less complete theory we should be able to calculate H^{σ} as a function of concentration of adsorbed molecules, in which case we obtain $\bar{\mathrm{H}}^{\sigma}$ directly by differentiation and do not need to concern ourselves with the physical interpretation of $(\partial \mathrm{H}^{\sigma}/\partial \Gamma)_{T,P}$.[13] To obtain $\Delta\mathscr{H}$ we should either have to obtain the adsorption isotherm first, and evaluate ϕ from the Gibbs' equation, or we might, in dealing with a non-localized surface phase obtain the equation of state as a first step in developing the theory. It is only in this latter case that $\Delta\mathscr{H}$ is as convenient a quantity as $\Delta\bar{\mathrm{H}}$.

In our view, the two statistical models considered by Hill in his Appendix I, illustrate this point. He considers (*a*) localized adsorption on a uniform surface without interaction between adsorbed molecules (Langmuir type) and (*b*) non-localized adsorption where the surface phase obeys the equation of state:[14]

$$\phi = \Gamma RT/(1 - \Gamma b). \quad . \quad . \quad . \quad . \quad (23)$$

---

[12] See Part II. A further assumption is also involved in (11.2) as it is normally employed. We usually interpret " constant Γ " to mean constant amount of adsorbed material on a given weight of adsorbent. This implies that the area of surface does not vary with temperature. If the change in area is caused only by thermal expansion the effect will usually be negligible; the assumption that (dA^{σ}/dT) is zero is not, however, necessary to our general arguments.

[13] Cf. e.g. A. R. Miller, *The Adsorption of Gases on Solids* (Cambridge University Press, 1949).

[14] Cf. Volmer, *Z. physik. Chem.*, 1925, **115**, 253.

To stress our point, we will make a further simplification and ignore for the moment the variation with temperature of the number of adsorption sites, and of b. In both instances $(\partial H^{\sigma}/\partial \Gamma)_{T,P} = 0$, so that if the potential energy of an adsorbed molecule, relative to its energy when an infinite distance from the surface, is ϵ, then $\Delta\bar{H}$ is immediately given by

$$(a)\ \text{localized adsorption}: \quad \Delta\bar{H} = \epsilon - \tfrac{1}{2}RT \quad . \quad (24.1)$$

$$(b)\ \text{non-localized adsorption}: \quad \Delta\bar{H} = \epsilon + \tfrac{1}{2}RT \quad . \quad (24.2)$$

The difference between cases (*a*) and (*b*) arises because of the retention by the molecules in the non-localized film, of two translational degrees of freedom, which are assumed to be completely frozen in a localized film.

The equilibrium heats of adsorption are, from (19.1),

$$(a)\ \text{localized adsorption}: \quad \Delta\mathscr{H} = \epsilon - RT + \phi/\Gamma \quad . \quad (25.1)$$

$$(b)\ \text{non-localized adsorption}: \quad \Delta\mathscr{H} = \epsilon + RT + \phi/\Gamma \quad . \quad (25.2)$$

In the second case, ϕ is given as part of the specification of the model so that we can immediately obtain $\Delta\mathscr{H}$ in the form given by Hill (eqn. (124), with $db/dT = 0$). On the other hand, for localized adsorption we have no physical picture of $(\partial H^{\sigma}/\partial \Gamma)_{s,P}$ so that we cannot calculate $\Delta\mathscr{H}$ without first obtaining the adsorption isotherm (or alternatively evaluating, $F(T, V, A, m)$ or $G(T, P, A, m)$).[15] We consider, therefore, that $\Delta\bar{H}$ which involves principally a consideration of the decrease of potential energy of molecules on adsorption, is a more useful quantity to study both experimentally and theoretically than $\Delta\mathscr{H}$, whose interpretation involves, *in addition*, a consideration of spreading pressures. Our belief that $\Delta\bar{H}$ is a more useful function than $\Delta\mathscr{H}$ is strengthened by the results of an extensive thermodynamic analysis of adsorption data which we have recently completed and which will be published shortly (Parts II and III).

In general we consider that the set of variables E, H, F and G is adequate to enable a comprehensive treatment of surface thermodynamics to be formulated. The use of $\mathscr{G}$ leads to a rather shorter derivation of the Gibbs' equation, but this equation can also be derived quite simply through G.

Chemistry Department,
University College, Dundee,
University of St. Andrews,
Scotland.

---

[15] The extra terms in Hill's equations (118) and (124) are easily seen to be equal to ϕ/Γ for the two models, when da/dT and $(db/dT) = 0$.

THE DIELECTRIC PROPERTIES OF POLYETHYLENE TEREPHTHALATE (TERYLENE)

BY WILSON REDDISH

Received 15*th December*, 1949

The permittivity and loss tangent of the polyester polyethylene terephthalate (Terylene) have been determined as functions of frequency (10^2-10^7 c./sec.) and of temperature (− 80° C to + 180° C), and the volume resistivity in the high temperature region has been studied.

Three alternating current dielectric processes have been distinguished, and effects associated with variations in the degree of crystallinity and in the water content of the material have been investigated. Tentative interpretations of the data are proposed; in particular, one dielectric process is correlated with mechanical and thermal properties of the polymer and is thought, therefore, to be due to relaxation of dipoles in the main polymer chain; a second process is attributed to the presence of — OH groups; and a third process, which occurs at low frequencies and high temperatures, is associated with the conduction of charge through the material.

Polyethylene terephthalate is a polyester which first attracted attention as a possible synthetic fibre.[1–5] In recent years processes have been developed to produce from it a yarn (Terylene) which can be woven to give a variety of fabrics characterized by their good strength, inertness to chemical attack and outstanding thermal stability (m.p. 260° C). This combination of properties suggests at once that if its electrical behaviour is promising Terylene in one form or another should be a useful addition to the existing range of electrical insulating materials.

Apart from these considerations, the subject of correlating the electrical —and as far as possible, the physical—properties of polymeric materials with their structure is one of great scientific and topical interest.[6, 11] Terylene, a polymer of known chemical composition and structure, is a suitable subject for a study of this type. Attention has been confined in the first instance to those properties (permittivity, power factor and resistivity) which are more readily correlated with the chemical constitution of a material, and properties such as electric strength and tracking resistance have not been considered.

Chemical and Physical Properties.—Terylene is a condensation product of terephthalic acid and ethylene glycol, the individual molecules consisting of long chains built up of one basic repeat unit with a " molecular weight " of 192.

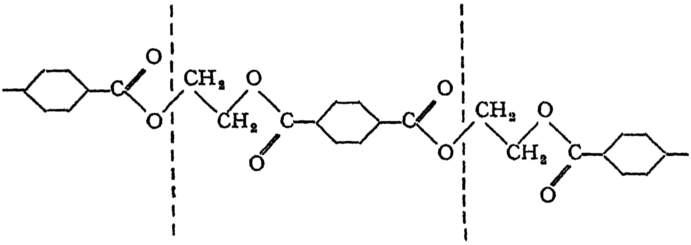

FIG. 1.—Repeat unit in polyethylene terephthalate.

The (weight average) molecular weight of the material used in this work is of the order of 30,000 so that the average length of a molecule is about 2000 Å. Although it is a polyester, Terylene is very resistant to hydrolytic attack, being quite unaffected by boiling water.

Terylene is a material consisting of intermingled crystalline and amorphous regions, the proportions of which are dependent on the mode of preparation. The structure of the crystalline regions has been elucidated by X-ray investigation, and from the dimensions of the unit cell the density of the crystallites has been estimated as 1·455 g./cm.^{3}.[7] Terylene as normally obtained has a density of about 1·38 g./cm.^{3} and in this

---

[1] Whinfield and Dixon, *Brit. Pat.* 578,079.
[2] Whinfield, *Chem. and Ind.*, 1943, **62**, 354.
[3] Whinfield, *Nature*, 1946, **158**, 930.
[4] Hardy, *J. Soc. Chem. Ind.*, 1948, **67**, 426.
[5] Hill and Walker, *J. Polymer Sci.*, 1948, **3**, 609.
[6] Forsythe and Jackson, *J. Inst. Elect. Eng.*, 1945, **92** (III), 23.
[7] Bunn and Daubeny (unpublished work).

form it is a white opaque solid. It can also be obtained as a completely amorphous transparent material (density *ca.* $1{\cdot}33$ g./cm.^{3}) by cooling rapidly from the melt; in this form it is stable only up to about 80° C, at which temperature it starts to crystallize. The "second order transition point" of the polymer is also at about 80° C, as shown by the increase at that temperature of the coefficient of expansion. Table I gives data which are typical of those obtained on crystalline material.

TABLE I.—VOLUME EXPANSION COEFFICIENTS OF TERYLENE

Average Volume Coefficient of Expansion	Temperature Range ° C
$3{\cdot}7 \times 10^{-4}$	+ 90 to + 190
$1{\cdot}6 \times 10^{-4}$	− 30 to + 60

The refractive index of the amorphous polymer at 25° C is

$$n_D = 1{\cdot}574, \text{ i.e. } n_D^2 = 2{\cdot}48.$$

It will be convenient to discuss these phenomena later in the light of the data presented below.

Experimental

Samples.—All measurements were carried out on discs, 53 mm. diam. and 0·5 mm. thick; these were dried initially and kept dry by storing at 60° C *in vacuo* (0·01 mm. Hg). The discs were cut from moulded sheets, some of which were amorphous and others (partially) crystalline. For the electrical measurements tin foil electrodes were stuck on to the discs using a trace of vaseline, although at the highest temperatures Aquadag colloidal graphite electrodes had to be used. In each case the electrode layer was backed by a brass plate under spring pressure.

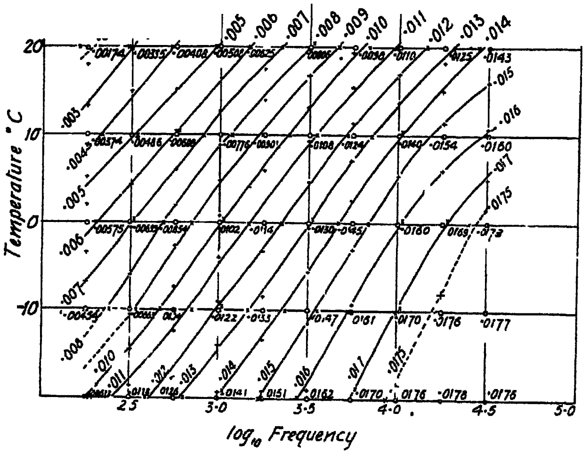

FIG. 2.—Examples of contour plotting.

O ·0123 Experimental data.

× × Interpolation points from tan δ $\log_{10} f$ plot.

+ + Interpolation points from tan δ, temp. plot.

Apparatus.—Permittivity and loss tangent were measured in the audio frequency range 10^2 to 3×10^4 c./sec. using a Schering type audio frequency bridge, and the radio frequency range 10^6 to 10^7 c./sec. was covered by the use of a resonance substitution method.[9] D.C. resistance of the sample was measured using a simple galvanometer circuit.

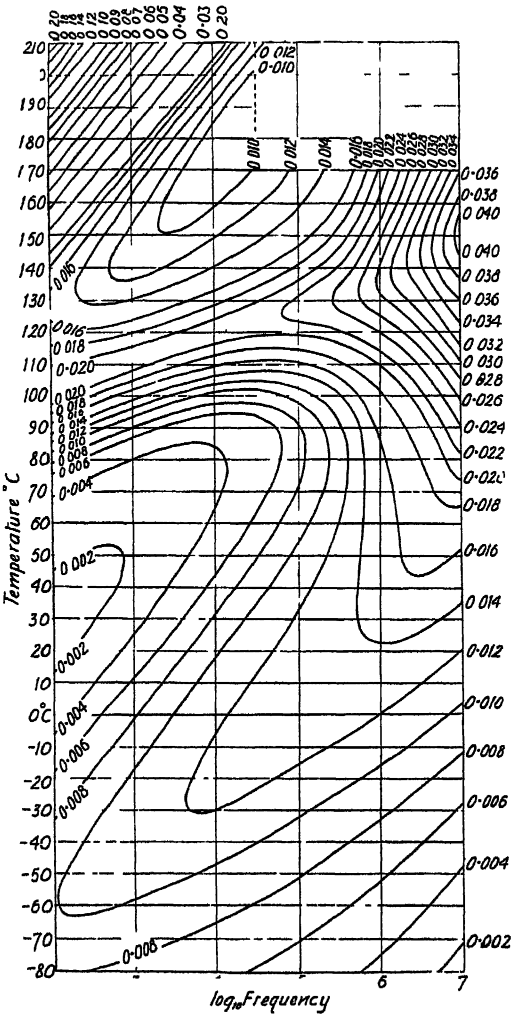

FIG. 3.—Tan δ contour map for dry crystalline Terylene.

Method of Presentation.—In the audio range, measurements of permittivity and of tan δ were made at constant temperature over the full frequency range. Frequency variation runs of this type were made at temperature intervals of 10°-15° from − 80° to + 170° C. In the radio frequency range it was more convenient to keep the frequency constant and vary the temperature over the entire range. The tan δ and permittivity data thus obtained were assembled as follows.

All the data were plotted using as co-ordinates temperature and $\log_{10}$ frequency ; the actual value, either of tan δ or of permittivity, was written alongside each point. Contour lines of constant permittivity or tan δ were then drawn

---

[8] Willis (unpublished work).

[9] Hartshorn and Ward, *J. Inst. Elect. Eng.*, 1936, **79**, 597.

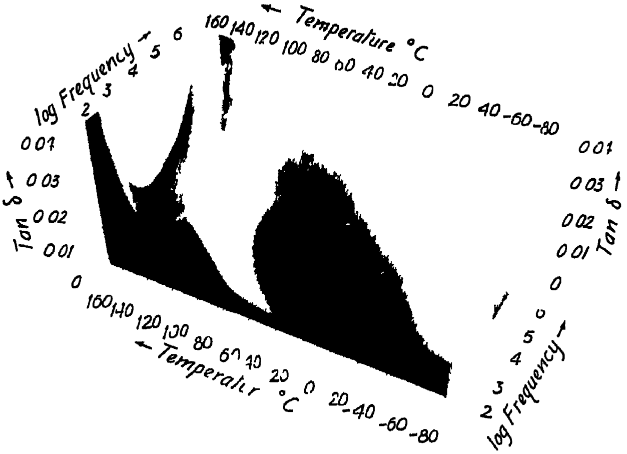

Fig. 5. Photograph of tan δ solid model

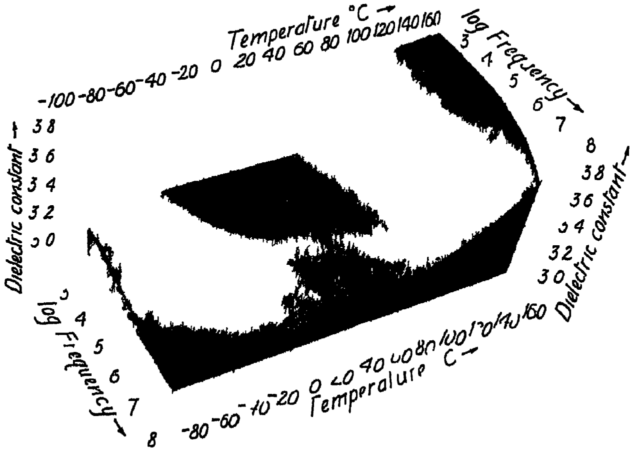

Fig. 6. Photograph of permittivity solid model

(To face page 463)

in, each line being a curve of best fit interpolated among the available points. Fig 2 shows one of these contour maps, and indicates the resolution obtained in the measurements

Results

Dry Crystalline Terylene.—The tan δ and permittivity contour maps obtained for dry crystalline Terylene are given in Fig 3 and 4 Solid models have also been constructed from the data, and photographs of these are given in Fig 5 and 6

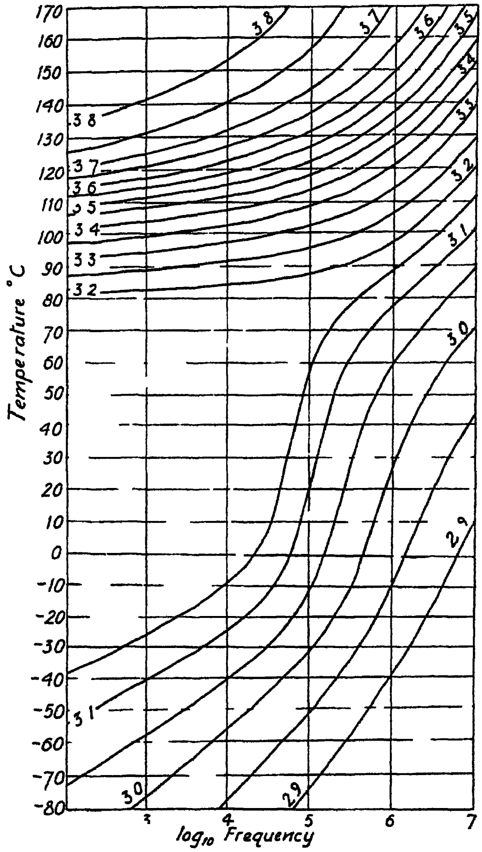

FIG 4 —Permittivity contour map for dry crystalline Terylene

It can be seen from Fig 3 that at 20° C tan δ has a maximum value of about 0 014 at 400 kc /sec $(\log_{10} f = 5\ 6)$ The frequency at which this maximum occurs shifts with temperature, so that the whole process appears as the low temperature ridge in the tan δ surface A second rather sharper ridge occurs at higher temperatures These two ridges merge at high frequencies and high temperatures because the frequencies at which the two maxima occur change with temperature at different rates A third dielectric loss process occurs in the low frequency, high temperature region it differs from the other two processes in that there is no observable maximum in tan δ Instead, tan δ increases sharply as the temperature is increased and as the frequency is reduced The effect of temperature on tan δ at 1000 c /sec is shown in Fig 7 Contributions from all three processes can be seen in this plot

Referring now to Fig 4 and 6, which show the variations of permittivity with frequency and temperature, it can be seen that there are two transition regions in the permittivity surface which correspond to the two ridges in the tan δ surface. The permittivity falls from the high level of 3·85, at low frequencies and high temperatures, to the lower level of 2·85, at high frequencies and low temperatures, in two stages, the intermediate level value of 3·15 being clearly defined. The contour lines on the permittivity map are approximately parallel to the ridges on the tan δ map; and the spacing of the permittivity contours is least, corresponding to maximum slope, along the axes of the tan δ ridges.

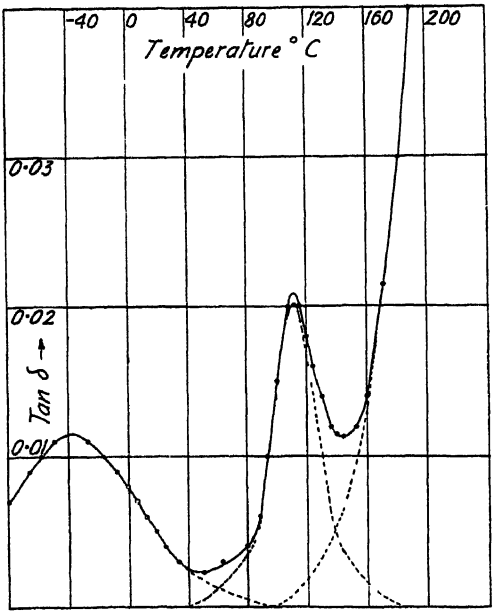

Fig. 7.—Variation of tan δ of dry crystalline Terylene with temperature at 1000 c./sec.

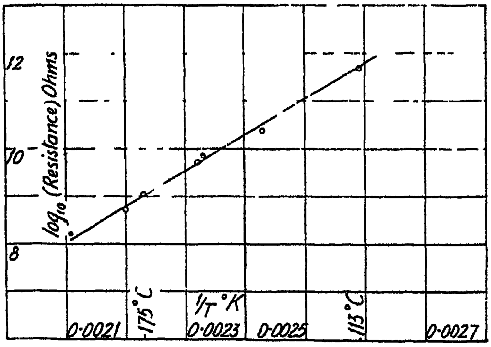

Fig. 8.—Plot of $\log_{10}$ (sample resistance) against $1/T$.

The effect of temperature changes on the d.c. resistance of a crystalline sample is shown in Fig. 8, in which $\log_{10} R$ is plotted against reciprocal absolute temperature. The geometrical factor for conversion from resistance R to resistivity ρ is $\rho/R = 260$ (based on room temperature dimensions).

Dry Amorphous Terylene.—Tan δ and permittivity have been measured over the temperature range − 80° C to + 70° C, and the frequency range

10^2 to 10^7 c./sec. The upper temperature limit is set by the fact that the amorphous material starts to crystallize at about 80° C. These results are not presented in full, but the essential details are given in Table II and in Fig. 11 and 12. These data show that amorphous Terylene also exhibits a low temperature process characterized by a tan δ ridge and permittivity transition; moreover the tan δ ridge occurs in the same position for amorphous as for crystalline material, as is clear from Fig. 11. The dielectric loss maximum is, however, greater for amorphous than for crystalline Terylene (Table II).

Effect of Water.—Dry samples, one crystalline and one amorphous, were weighed and then immersed in water at 20° C. Their weights were determined at intervals and the percentage weight increases are plotted in Fig. 9.

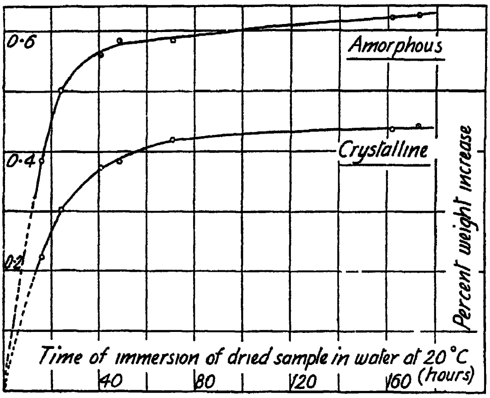

FIG. 9.—Water absorption curves.

The permittivity and tan δ of the wet samples were then measured over the audio frequency range 10^2 to 3×10^4 c./sec. and the temperature range − 80° C to + 20° C. The data are summarized in Table II and in Fig. 11 and 12; it can be seen that here again the positions of the tan δ ridges are unchanged although the heights are increased when water is present. The height for amorphous material is increased more than that for crystalline material.

TABLE II

State	Condition	ε at 100 c./sec. and 60° C	ε at 100 c./sec. and 20° C	ε at 10^5 c./sec. and 80° C	ε at 10^7 c./sec. and 80° C	Max. Value of tan δ at 10^5 c./sec. and 0° C
Crystalline	Dry	3·16	3·16	2·89	2·85	0·013
Crystalline	Wet	—	3·53	3·14	—	0·018
Amorphous	Dry	3·42	3·40	2·96	2·80	0·021
Amorphous	Wet	—	3·85	3·14	—	0·028

Water has no permanent effect on the dielectric properties of Terylene, as shown by the fact that a sample which was immersed in water for six months and subsequently dried was indistinguishable from an initially dry sample.

Discussion

The Frequency and Temperature Dependence of Dielectric Properties.—In this discussion the aim will be to show how the dielectric and certain physical properties of Terylene are inter-related, and then to make use of these correlations to identify as far as possible the molecular mechanisms responsible for the observed behaviour.

There are two main theories which have been advanced to account for the power loss maxima and associated permittivity transitions which characterize the variable frequency, variable temperature behaviour of many dielectric materials.[10, 11] They are the molecular theory first proposed by Debye,[12, 13, 14] in which the relaxation time of the significant dipolar molecules (or a constituent part of them) depends on the hindrance to free rotation imposed by the dipolar environment, and the structural inhomogeneity (or interfacial polarization) theory due to Maxwell and Wagner,[15] in which the relaxation time of the absorption process is governed by the relative permittivity and conductivity values which may be attached to the constituent microscopic regions of the material. The temperature dependence of the dielectric properties does not enter explicitly into either the Debye or the Maxwell-Wagner type of theory, and must be introduced by considering the effect of temperature on properties hitherto considered as constant. Debye used the temperature dependence of viscosity of the medium ; in the Maxwell-Wagner type of mechanism the resistivity must be considered as temperature dependent.

It is usually found that the temperature dependence of the relaxation time follows a simple exponential law, and this is true for both of the absorption processes which occur in Terylene, as may be demonstrated as follows.

(i) Fig. 11 is a plot of f_m (= frequency at which the tan δ maximum occurs) as a function of reciprocal absolute temperature. All the data for the low temperature process are assembled in this way, and it can be seen that for both crystalline and amorphous material, both wet and dry, all the points are grouped around a single straight line.

(ii) The data for the high temperature process occurring in crystalline material are presented in a similar way in Fig. 10. Thus the variations with temperature of the frequencies of maximum power factor are described by the Arrhenius equation,

$$f_m = A \exp(-E/RT). \quad . \quad . \quad . \quad . \quad (1)$$

The frequency factor A and the energy term E have been calculated from Fig. 10 and 11, both for the low temperature and the high temperature processes, and the results are given in Table III.

It can be seen from Fig. 8 that the temperature dependence of the D.C. resistance of crystalline material also obeys a similar law. Because the simple Arrhenius equation has been found to hold in cases such as this, the developments of chemical rate theory by Eyring and others [16] have been applied to dielectric phenomena. Using this approach the following relation for the temperature dependence of the relaxation time τ can be derived :

$$\frac{1}{\tau} = \frac{kT}{h} \exp\left(\frac{\Delta S^*}{R}\right) \exp\left(-\frac{\Delta H^*}{RT}\right) \quad . \quad . \quad . \quad (2)$$

where ΔH^* and ΔS^* are the energy and entropy of activation of the elementary transition involved. This means that, if a dipolar theory is considered, $1/\tau$ is the angular frequency at which a polar group acquires sufficient energy to surmount the energy barrier between two different configurations.

By use of eqn. (2), and by identifying ΔH^* with the experimental activation energy term E in eqn. (1), the experimental frequency factor

---

[10] Richards, *Faraday Soc. Discussion*, 1946, 194.

[11] Jackson and Saxton, *J. Inst. Elect. Eng.*, 1949, **96**, (III), 77.

[12] Debye, *Polar Molecules* (Dover Publications, New York, 1945, Chap. 5.)

[13] Jackson and Powles, *Faraday Soc. Discussion*, 1946, 101.

[14] Garton, *J. Inst. Elect. Eng.*, 1939, **85**, 625.

[15] Sillars, *ibid.*, 1937, **80**, 378.

[16] Glasstone, Laidler and Eyring, *The Theory of Rate Processes* (McGraw Hill, New York and London, 1941).

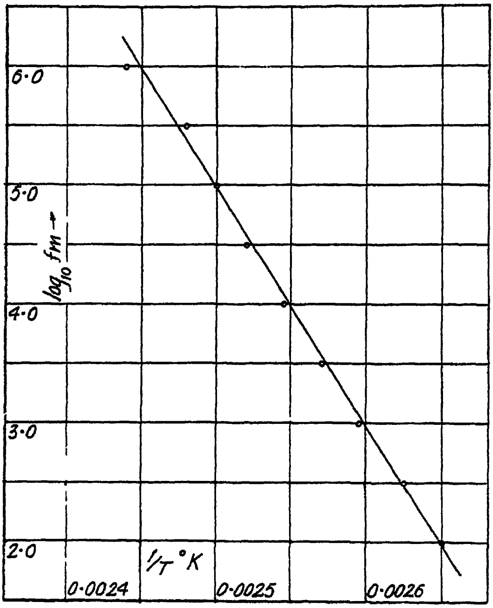

FIG. 10.—Plot of $\log_{10} f_m$ against $1/T$ for the high temperature absorption process in crystalline material.

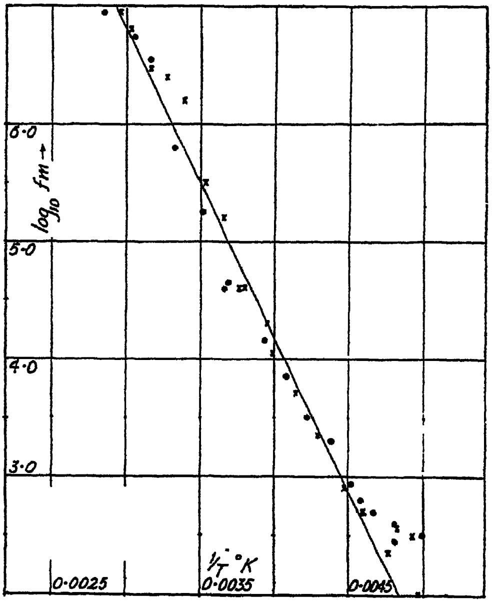

FIG. 11.—Plot of $\log_{10} f_m$ against $1/T$ for the low temperature absorption process in crystalline and amorphous material both wet and dry.

⧗ Crystalline (dry). ⧖ Crystalline (wet).

◓ Amorphous (dry). ◒ Amorphous (wet)

A has been split up and the value of the entropy term ΔS^* calculated. The data for the two dielectric processes are given in Table III.

TABLE III—Entropies and Energies of Activation

	A	$E \equiv \Delta H^*$ (kcal./mole)	ΔS^* (cal./mole deg.)
Low temperature process . .	10^{15}	12·4	12
High temperature process . .	10^{54}	90·4	190

The energy and the entropy of activation are low for the low temperature process and high for the high temperature process. In terms of a dipole mechanism, these results suggest that a small polar group in a not very restrictive environment is involved in the low temperature process, whereas a larger group, the motion of which is considerably hindered by its environment, is probably concerned in the high temperature process. Using the data presented, it will be convenient now to examine in detail the three dielectric loss processes, and to see to what extent it is possible to identify the molecular mechanisms responsible for them.

The Low Temperature Loss Process.—The most significant feature of this process is the way in which it is affected by changes in the water content of the material. The height of the loss maximum and the amount of the permittivity increment associated with the process are increased when water is absorbed (Table II), although the frequency of maximum loss remains unchanged (Fig. 11). It is clear that the additional loss and permittivity are due to a mechanism involving water. The problem of the cause of the residual loss in dried material then arises, for as the frequency of maximum loss is the same for wet as for dry material it would seem that all the loss is due to the same mechanism. This apparent paradox can be resolved in terms of the hypothesis, which is substantiated by several pieces of evidence, that the residual loss in dry material is due to the terminal —OH dipoles of the Terylene molecules. A dipolar mechanism is thus postulated in which the absorbed water molecules behave in a similar way to the terminal —OH dipoles.

The parameter ϵ'' ($= \epsilon \tan \delta$) is proportional to the rate of energy loss at each frequency, and may therefore be used to make quantitative comparisons. In Fig. 12, curves of ϵ'' against $\log_{10}$ (frequency) at 0° C are plotted for crystalline and amorphous materials, both wet and dry, and values of $\epsilon''_{\text{max.}}$ and of the areas under the curves are tabulated in Table IV. From these data and those of Table II it can be seen that the effect of absorbed water on dielectric properties is less for crystalline than for amorphous material. The difference can be expressed by the ratio of the increases on wetting of the areas under the ϵ''-$\log_{10}f$ curves for crystalline and amorphous materials. This ratio is 0·66, which is in good agreement with the ratio of the saturation water absorption of crystalline and amorphous material, 0·69 (Fig. 9). Moreover, from X-ray and density data the fraction of amorphous material present in the partially crystalline Terylene has been estimated to be about 0·6. The agreement among these figures shows that, as would be expected, water is absorbed by the amorphous polymer, or into the amorphous regions of the partially crystalline material.

Furthermore, it is significant that the ratio of the areas under the ϵ''-$\log_{10}f$ curves for *dry* crystalline and amorphous materials is also about 0·6 (0·59). This shows that it is only in the amorphous regions that the dielectric process operates which is responsible for the losses: in this case the residual losses which are attributed to the terminal —OH groups. The —OH terminal groups which must also be present in the crystalline

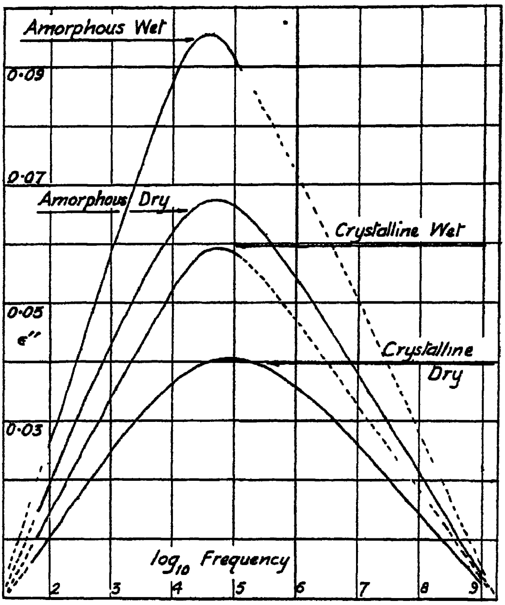

FIG. 12.—Plot of ϵ'' ($= \epsilon \tan \delta$) against $\log_{10}$ (frequency) at 0° C for crystalline and amorphous material both wet and dry.

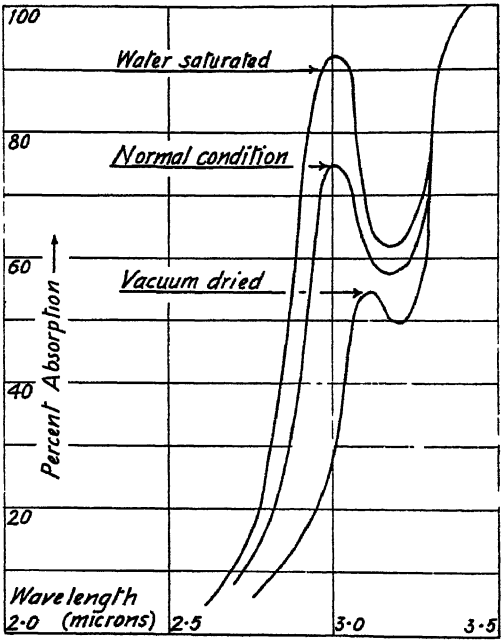

FIG. 13.—Effect of water content on part of the infra-red absorption spectrum of crystalline Terylene.

regions do not take part in the loss process in this frequency region, presumably because they are not free to move in the crystal, or because their relaxation time in the crystalline environment is very different from the relaxation time in the amorphous region environment.

With these considerations in mind, the infra-red absorption spectrum of a sample of crystalline Terylene was examined,[8] firstly in the normal (room storage) condition, then after drying, and finally after immersion in water for 14 days. The absorption data (corrected for scattering) for the relevant region of the spectrum are given in Fig. 13. There are two absorption bands attributable to the —OH stretching frequency perturbed by different degrees of combination. One band at 3·0 μ is seen to disappear on drying and must therefore be due to absorbed water. The other occurs at 3·1 μ and is typical of a combined —OH group. By comparing the intensity of this band with data for primary alcohols, a concentration of one —OH group per 88 repeat units, or 0·1 % by weight has been estimated. This is in greement with an estimate based on the assumption of two terminal —OH group per molecule of molecular weight 30,000. These infra-red data thus prove that the drying process is effective in removing absorbed water, and by showing the presence of combined —OH groups did in fact supply the clue that the residual loss might be due to terminal —OH groups.

As a further test of the dipole postulate, estimates of the concentration of —OH dipoles have been made using the equations of Debye and Sillars,[17] assuming the value 1·7 × 10[18] E.S.U. for the dipole moment of the —OH group.[18] Debye's equation for the dielectric loss factor ϵ'', for the case of a single relaxation time τ is

$$\epsilon'' = \epsilon \tan \delta = \frac{4\pi}{27kT} (\epsilon_0 + 2)^2 \mu^2 n \frac{\omega\tau}{1 + \omega^2\tau^2}, \quad . \quad . \quad (3)$$

where ϵ_0 is the low frequency value of ϵ, μ is the dipole moment, n is the number of dipoles per cm.^{3}, $\omega = 2\pi \times$ frequency, and $k =$ Boltzmann's constant $= 1{\cdot}38 \times 10^{-16}$ erg/deg. From this it may be derived that the maximum value of ϵ'', which occurs when $\omega\tau = 1$, is

$$\epsilon''_{\text{max.}} = \frac{2\pi}{27kT} (\epsilon_0 + 2)^2 \mu^2 n. \quad . \quad . \quad . \quad (4)$$

In order to take into account the spread of relaxation times which is usually observed experimentally, as this is not covered by eqn. (3) and (4), use is made of a relation which has been derived on very general grounds by Sillars.[17] This is that the area under $\epsilon'' - \ln f$ curves is in the same relation to the number of dipoles and their moment whatever the distribution of relaxation times. Sillars found that

$$\text{Area} = \int_{-\infty}^{+\infty} \epsilon'' \mathrm{d}\,(\ln f) = \frac{2\pi^2}{27kT} (\epsilon_0 + 2)^2 \mu^2 n. \quad . \quad . \quad (5)$$

From (4) and (5) the area under the Debye curve is $\pi\epsilon''_{\text{max.}}$, whereas for an experimentally determined $\epsilon'' - \ln f$ curve, with the same $\epsilon''_{\text{max.}}$ value, the area is larger due to the spread of relaxation times, thus the spread of relaxation times may be represented by the factor α, defined by

$$\alpha = \frac{\pi\epsilon''_{\text{max.}}}{\text{Area}}. \quad . \quad . \quad . \quad . \quad . \quad . \quad (6)$$

The results of these calculations are given in Table IV.

It is clear from a comparison of these estimates with the infra-red estimate of terminal —OH content, and with the measured water absorption, that the theory does not give a precise account of the situation, although the results are of the correct order of magnitude. As compared with the infra-red estimate, the dielectric estimate of terminal

---

[17] Sillars, *Proc. Roy. Soc. A*, 1939, **169**, 66.
[18] Le Févre, *Dipole Moments* (Methuen).

—OH content is too high, whereas the dielectric estimate of water absorption is too low when compared with measured values. From the nature of these disagreements it would seem that the terminal —OH groups are more effective in producing loss than the same weight of absorbed water. This effect is explicable in terms of association of the absorbed water molecules into small groups so that the effective dipole moment per molecule is reduced, as discussed by Argue and Maas.[19]

TABLE IV

Material	% Absorbed Water	ϵ'' max. at 0° C	Area under $\epsilon'' - \ln f$ Curve at 0° C	α	n = no. of OH Groups per cm.^{3}		Weight % of —OH	
					From (3) $n \times 10^{-19}$	From (5) $n \times 10^{-19}$	From (3)	From (5)
Crystalline	0	0·041	0·418	0·308	8·56	27·9	0·17	0·57
Crystalline	0·44	0·059	0·602	0·308	10·72	35·1	0·23	0·72
Amorphous	0	0·067	0·706	0·298	12·8	42·8	0·27	0·91
Amorphous	0·64	0·096	0·958	0·315	17·8	53·0	0·38	1·13

* The area under the $\epsilon'' - \ln f$ curve = 2·3 × area under the $\epsilon'' - \log_{10} f$ curve.

An alternative interpretation of the low temperature process, in which the absorbed water is considered to be present as droplets and as such would be described by a Maxwell-Wagner model as discussed by Sillars,[15] has been rejected for the following reasons.

(i) The dielectric results obtained for dry crystalline Terylene were stable and repeatable even after the sample had been raised to 200° C in the course of measurements, so that the residual loss could not be due to the same mechanism as the additional loss on this hypothesis.

(ii) No discontinuity was observed in the dielectric behaviour of wet materials at 0° C, whereas the absorption maximum for ice at just below 0° C occurs at a frequency which is 3 to 4 decades lower than the maximum for water at just above 0° C.

(iii) In modern theory of diffusion of water through polymers the water is considered to be present as single molecules or in small groups.

The High Temperature Loss Process.—There seems to be little doubt that a dipolar mechanism is the cause of the high temperature absorption process, in view of the following correlation. If an estimate be made of the temperature of loss maximum corresponding to a frequency of (say) 1 cycle in 10 sec., by extrapolation of the straight line of Fig. 10, a value near 80° C is obtained. Now, as mentioned above, this is near to the lowest temperature at which crystallization of amorphous material can be observed, and near also to the second-order transition temperature. It is above the second-order transition temperature that the typical high elastic behaviour of an amorphous polymer is developed,[20] and similar correlations between dielectric properties and bulk mechanical properties have been observed for polyvinyl chloride, polyvinyl acetate,[21] for chlorinated polythenes,[22] and for polythene and poly*iso*butene.[23] Where this correlation is observed the inference is that the dipole concerned is either one of the links in the main polymer chain or is so bound to the chain that independent movements of dipoles and chain segments are not possible.[21] It is generally accepted that second-order transition phenomena occur only in amorphous regions, and this is considered to be true for Terylene. By reason, therefore, of the association of the dielectric process with this transition it is reasonable to suppose that the dielectric process also occurs in the amorphous regions.

---

[19] Argue and Maas, *Can. J. Res. B*, 1935, **13**, 156.

[20] Tuckett, *Trans. Faraday Soc.*, 1942, 38, 310.

[21] Tuckett, *ibid.*, 1944, **40**, 448.

[22] Oakes and Richards, *Faraday Soc. Discussions*, 1946, 197.

[23] Plessner and Richards, *ibid.*, 206.

A consideration of the Terylene molecule shows that if the repeat unit is planar and centro-symmetric, as in Fig. 14(*a*), then there is no resultant dipole moment. It is known[7] that in the crystallites the units are arranged in this way.

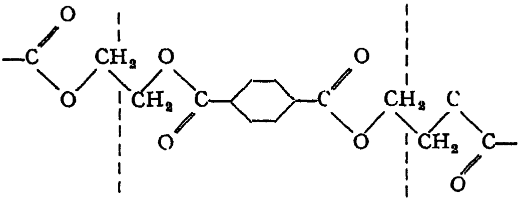

(*a*) Symmetrical arrangement of ester linkage : *trans* form.

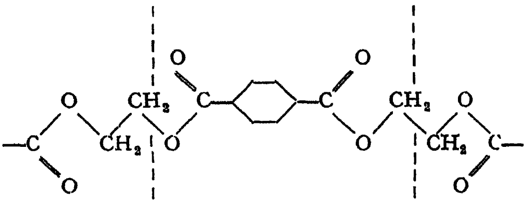

(*b*) Asymmetric arrangement of ester linkage : *cis* form.

FIG. 14.—Arrangements of a Terylene repeat unit.

In the amorphous regions, however, some distortion of this symmetric structure is likely. At high temperatures free rotation will take place around the bond joining the ester group to the benzene ring. The group centred on the benzene ring then has a resultant dipole moment, as is commonly experienced with *p*-substituted aromatic compounds with free rotation (as discussed for example by Le Févre[18]). Now the packing of the chains in the amorphous regions at low temperatures must be somewhat similar to that in the crystalline regions, for the densities of the two regions differ by only 10 %, so that it is likely that the benzene rings are parallel locally. This probably means that there will be two preferred positions for each of the ester linkages with the two oxygen atoms near the plane of the benzene ring. The arrangement of Fig. 14(*b*) is thus possible, and here the repeat unit has a large dipole moment perpendicular to the chain axis, and in the plane of the benzene ring. For the purpose of this argument, the symmetrical structure will be referred to as the *trans* form, and the asymmetric structure as the *cis* form.

Now, as stated above, amorphous Terylene starts to crystallize at a measureable rate when raised to 80° C. Thus at this temperature three phenomena may be correlated, and may be due to the same cause. Firstly, the onset, at 80° C, of transition between the *cis* and the *trans* configurations of the ester groups may be the additional degree of freedom to be associated with the second-order transition in the volume-temperature curve. Secondly, the occurrence of the *trans* configuration—the crystalline configuration—may be a factor limiting the rate of crystal growth. Finally, when transitions between the two configurations occur frequently enough, the repeat unit centred on the benzene ring will possess an average dipole moment, the relaxation time of which will be related to the average time between transitions, and is probably the cause of the dielectric absorption process.

The Low Frequency-High Temperature Process.—This process is evidently of a different type from the absorption processes discussed hitherto. The sharp frequency dependence in the low frequency region suggested that the A.C. behaviour might be associated with a D.C. conduction effect. It was in order to test this possibility that the conduction measurements given in Fig. 8 were made.

The simplest assumption which can be made is that, so far as this process is concerned, the specimen may be represented for a particular temperature by a parallel combination of a resistance R and condenser C, where R is the D.C. resistance, and C is the A.C. capacitance measured at the same temperature, and considered to be frequency independent. According to this model, the power factor tan δ is

$$\tan \delta = \frac{10^{12}}{RC\omega}, \quad . \quad . \quad . \quad . \quad . \quad (6)$$

where R is in ohms and C is in $\mu\mu$F and

$$\omega = 2\pi \times \text{frequency}.$$

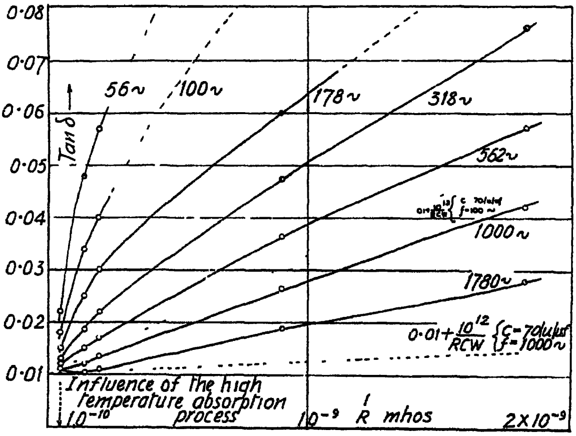

FIG. 15.—Cross plot showing tan δ in the low frequency–high temperature region as a function of $1/R$.

The results for crystalline Terylene have been tested against this formula. In Fig. 15 tan δ is shown as a function of $1/R$ for various frequencies. These data were obtained by means of a cross plot between data from Fig. 3 and Fig. 8. Curves based on eqn. (6) are also included. Even after allowing for the influence of the high temperature absorption process, it is obvious that the A.C. data are not completely explained in terms of the D.C. resistance. The effect is shown for a single temperature in Fig. 16, and it can be seen that the A.C. loss is always greater than the values predicted from eqn. (6), but tends to approach the theoretical behaviour asymptotically.

A plot of $\log_{10}$ tan δ against $\log_{10} f$ (Fig. 17) is almost a straight line with slope $-0{\cdot}51$. Thus tan δ is nearly proportional to $f^{-\frac{1}{2}}$ rather than f^{-1} as required by eqn. (6).

If the temperature dependence is now considered, it can be seen from Fig. 8 that the sample resistance depends on temperature according to a simple exponential law. In Fig. 18, $\log_{10}$ tan δ is also plotted against reciprocal absolute temperature for three frequencies, the data being taken from the contour map, Fig. 3. When the influence of the high temperature absorption process is allowed for, linear relations are again found, the slope being independent of frequency. The activation energies of D.C. resistance and of tan δ have been calculated from these plots, and the values are 38 kcal. and 14 kcal. respectively. This latter value also

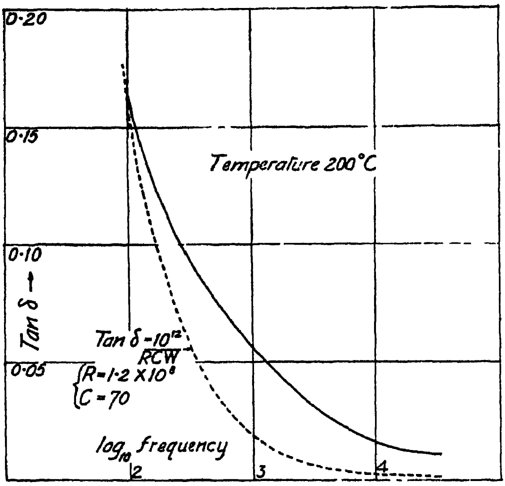

Fig. 16.—Plot of tan δ against $\log_{10} f$ in the low frequency region at 200° C. (R in ohms, C in $\mu\mu$F).

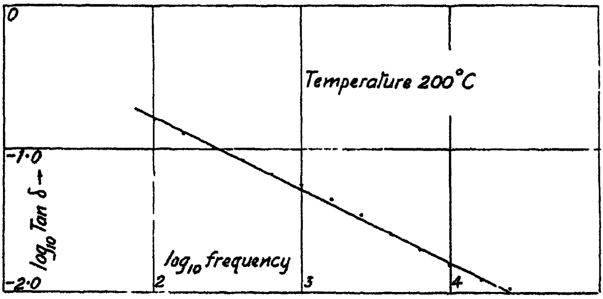

Fig. 17.—Log_{10} tan δ against $\log_{10} f$ at 200° C.

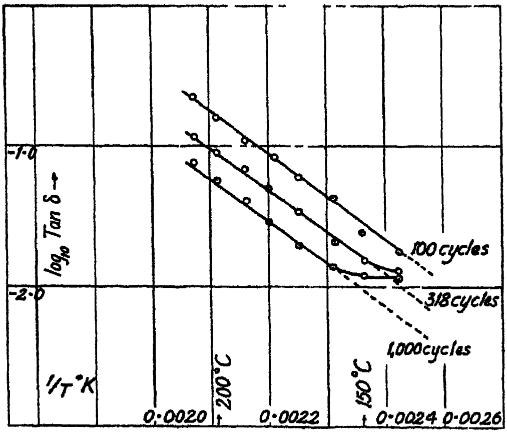

Fig. 18.—Plot of $\log_{10}$ tan δ against $1/T$ in the low frequency–high temperature region.

expresses the temperature dependence of the effective A.C. resistance of the sample calculated at each frequency from

$$R_{AC} = \frac{10^{12}}{C\omega \tan \delta}. \quad . \quad . \quad . \quad . \quad . \quad (7)$$

R_{AC} depends on frequency, being approximately proportional to $f^{-\frac{1}{2}}$. In order to account for the additional A.C. loss we may postulate that there are some charge carriers which cannot move all the way across the sample but are confined to zones which vary in size up to the specimen thickness and which may be the amorphous regions of the polymer. The Sillar's model [15] with ellipsoidal semi-conducting particles elongated in the direction of the field is perhaps appropriate here. Experimentally neither a maximum not a point of inflexion can be found in the loss curve in this region so that the system is not readily amenable to further analysis. The different values of the activation energy for D.C. and A.C. conduction processes suggest that there are two processes involved in the A.C. case.

Comparison of Permittivity and Refractive Index.—It has been shown (Table II) that at low temperatures and high frequencies crystalline and amorphous Terylene have approximately the same dielectric constant (i.e. 2·8). This value is larger than the square of the refractive index as measured in the visible region ($n_D^2 = 2{\cdot}48$). The difference is probably attributable to the infra-red dispersion processes. The single dielectric constant value for both crystalline and amorphous material implies that in any processes occurring at higher frequencies than those covered in this work, the vibrator cannot distinguish between crystalline and amorphous zones.

The author's thanks are due to Mr. E. R. S. Jones and Miss D. A. Thomas who carried out much of the experimental work recorded in this paper, to Dr. C. W. Bunn and Mr. H. A. Willis for their permission to use unpublished information on X-ray structure and infra-red absorption spectra, to Prof. Willis Jackson, and to the author's colleagues for many valuable discussions.

Imperial Chemical Industries, Limited,
Plastics Division,
Research Department,
Welwyn Garden City,
Hertfordshire.

METAL-MONOLAYER INTERACTIONS IN AQUEOUS SYSTEMS

PART I.—THE INTERACTION OF MONOLAYERS OF LONG-CHAIN POLAR COMPOUNDS WITH METAL IONS IN THE UNDERLYING SOLUTION

BY G. A. WOLSTENHOLME AND J. H. SCHULMAN

Received 23*rd December*, 1949

The effects on the mechanical properties of myristic acid monolayers, produced by the presence of salts of iron, aluminium, copper, cobalt, manganese, calcium and magnesium in the underlying solution have been investigated.

Two factors determine the nature of the interaction between metal and the film molecules: (*a*) the extent of ionization of the monolayer, and (*b*) the type of metal ions present in solution. Both these factors are dependent on the pH of the substrate.

There are three kinds of interaction between metal ions and the monolayer which are responsible for condensed solid film formation: (i) undissociated fatty acid—basic metal-ion interaction, (ii) dissociated fatty acid—basic metal-ion interaction, (iii) dissociated fatty acid—simple metal-ion interaction. Interaction (ii) is responsible for solid monolayers at areas per fatty acid molecule as high as $50 A^2$. Interaction (iii) results in soluble monolayers.

The selective flotation of minerals using soluble fatty acids as collecting agents, is the result of interactions at the mineral-water interface between the basic ionized mineral surface and the fatty acid. When there are no basic ions at an ionized mineral surface it is unlikely that a hydrophobic monolayer will be formed as the complex between ionized fatty acid and metal ion will be soluble, due to the absence of a basic ion network at the mineral surface. No monolayer condensation was observed with metal ions and associated fatty acids, although there were surface potential changes associated with induced dipoles.

The air-water monolayer technique has been applied to investigate the interaction between an insoluble amine monolayer and a silicate (in the underlying solution) with a view to determining the nature of the interaction between soluble cationic surface-active agents (e.g. amine hydrochloride, quaternary ammonium salts) and silica (or silicate) surfaces. The effects on the mechanical properties of a long chain amine monolayer produced by the presence of copper and silver salts in the substrate have also been investigated.

The formation of an adsorbed monolayer of amphipathic molecules at a solid-aqueous solution interface is responsible for the froth-flotation of finely ground mineral particles. Several theories have been put forward to explain the mode of action of a long-chain ion with a mineral surface. Taggart,[1] for example, has postulated an insoluble compound theory, whereas Wark [2] favoured a theory based on chemisorption (as applied to the xanthate ion).

In Part I of this paper, a new approach to this problem is made by using an air-water monolayer technique. These studies are confined mainly to fatty acid monolayers, which, when spread on salt solutions, interact with the metal ions in the substrate, producing changes in the mechanical properties of the monolayer. This technique in conjunction with flotation can show that the formation of an adsorbed monolayer of fatty acid molecules at a mineral-water interface is due to an interaction between fatty acid and metal ions, similar in type to the interaction between a fatty acid monolayer and metal ions at the air-water interface. Myristic acid is suitable for the air-water experiments, as on acid solution the force-area curves are extremely sensitive to the presence of metal ions in the substrate at room temperature. Caproic acid and caprylic acid which are soluble, are used for the flotation experiments.

A description is given of the different effects of ions produced by the salts of iron, aluminium, copper, cobalt, manganese, calcium and magnesium on myristic acid monolayers as a result of changes in the pH value of the underlying solution. The possible nature of the interaction between metal ions and ionic aggregates with monolayer molecules is discussed. The literature [3-7] mentions the effects of metal ions on the mechanical properties of insoluble monolayers, but stress has often been laid on the elimination of these effects rather than on their nature and cause.

---

[1] Taggart and Arbiter, *A.I.M.E. Metal Mining and Milling Methods* (1943), p. 500.

[2] Wark, *Principles of Flotation* (Austral. Inst. Min. Met. Eng., Melbourne, 1938).

[3] Harkins and Myers, *Nature*, 1937, **139**, 367.

[4] Blodgett, *J. Amer. Chem. Soc.*, 1935, **57**, 1007.

[5] Langmuir and Schaefer, *ibid.*, 1936, **58**, 284.

[6] Trapeznikov, *Acta Physicochim.*, 1939, **10**, 65.

[7] Mitchell, Rideal and Schulman, *Nature*, 1937, **139**, 625.

The technique is also applied to a monolayer of an insoluble cation-active compound with a view to determining the nature of the interaction between soluble cationic surface-active agents and silica (or silicate), silver and copper surfaces.

Experimental

Solutions were prepared in the pH range 3-9 from distilled water, saturated with carbon dioxide by adding N/10 NaOH or N/10 HCl. Hydrochloric acid alone was used to obtain pH values less than 3, and for pH values greater than 9 sodium bicarbonate and sodium hydroxide were employed. These procedures were adopted to eliminate contamination by small amounts of metallic impurities and salting-out effects by strong solutions of buffer salts. The salts investigated (of A.R. purity) were ferric chloride, aluminium sulphate, cupric chloride, cobaltous chloride, manganese chloride, calcium chloride and magnesium chloride. The solutions contained M/2000 of metal salt and were used within a few minutes of preparation. An enclosed Langmuir-Adam surface balance, with a torsion wire sensitive to 0·05 dyne/cm., was used.

The Effect of pH on Myristic Acid Monolayers.—*Fig.* 1 *shows that the* area at which the transition point occurred between the expanded and condensed states was dependent on the pH of the substrate. Similarly, the areas at which the monolayers collapsed on compression, and the areas to which the films tended at low compression, also decreased as the pH was increased. The pressure at which the transition took place was practically constant in the pH range 2 to 4·65.

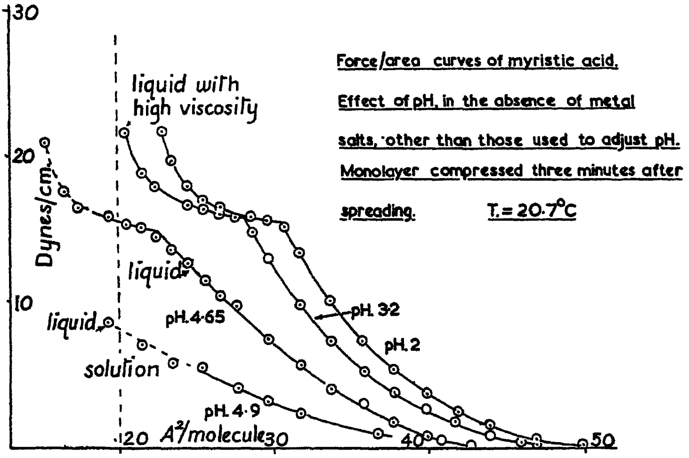

FIG. 1.—The effect of pH in the absence of metal salts.

When the pH of the substrate was greater than 4, the area per molecule at which the films collapsed was less than 20 Å². Thus at pH 4·65, at least a quarter of the film had gone into solution. At pH 4·9, a very unstable monolayer was obtained. This solution effect with increasing pH was due to ionization of the monolayer, and completely soluble films were obtained at pH 6 and on alkaline solutions. These experiments on the effect of pH in the presence of sodium ions are used as a basis for comparison with the force-area curves measured in the presence of divalent and trivalent metal ions.

The Effects of pH on Myristic Acid Monolayers in the Presence of Different Salts.—FERRIC CHLORIDE.—Fig. 2 shows that at pH 2·05 the force-area curve was affected very little by ferric chloride, whereas at pH 2·15 and pH 2·65 there were marked changes in the monolayer properties. The fully condensed film at pH 2·65 was a fragile solid at 0·1 dyne/cm. and became unstable at pressures above 1 dyne/cm. Monolayers of a similar type were obtained in the pH range (2·65-5), but at pH 5·5 the area of solidification was small, see Fig. 6. At pH 6 and on more alkaline solutions, the films were completely soluble.

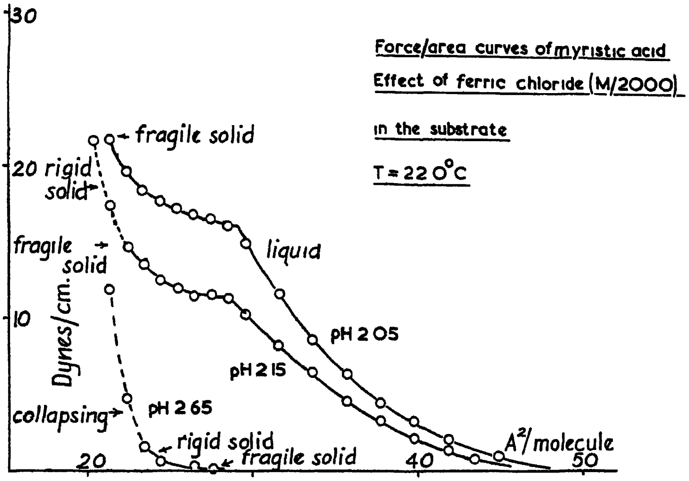

FIG. 2.—The effect of ferric chloride.

ALUMINIUM SULPHATE.—Force-area curves were not affected by this salt when the pH was less than 3·6. From Fig. 3 is can be seen that the monolayer was no longer liquid-expanded at pH 3·94 but solidified at a very low pressure

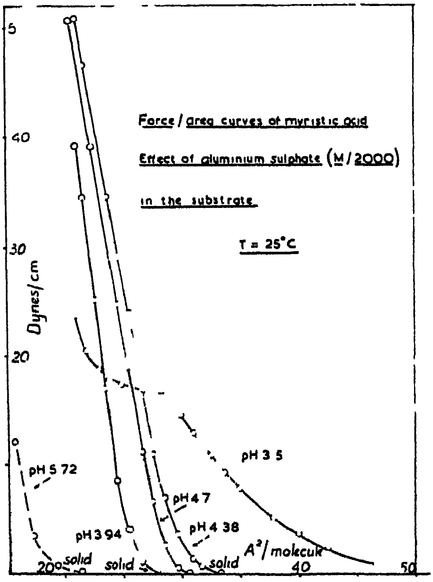

FIG. 3.—The effect of aluminium sulphate.

and remained solid up to the collapse pressure of approximately 40 dynes/cm. This monolayer was heterogeneous at areas greater than 28·6 Å². Slightly more stable films with higher areas of solidification were observed on increasing the pH to 4·38, but further increases in pH resulted in less stable films (see Fig. 6). No solid films could be formed on compression, when the pH exceeded 7·7.

CUPRIC CHLORIDE.—No effects attributable to this salt, were observed when the substrate pH was less than 4, but there were very striking effects with substrates more alkaline than pH 4·2 (Fig. 4). Exceptionally high areas of solidification were obtained at pH 5·20, 5·78 and 6·7, the values being 33 Å², 40Å² and 50Å², respectively. In addition, these monolayers were very stable, and were capable of withstanding pressures as high as 60 dynes/cm. before collapsing. A maximum area of solidification was attained at approximately pH 6·7 and on more alkaline solutions this area progressively decreased. At pH 9 it was exceedingly small (see Fig. 6).

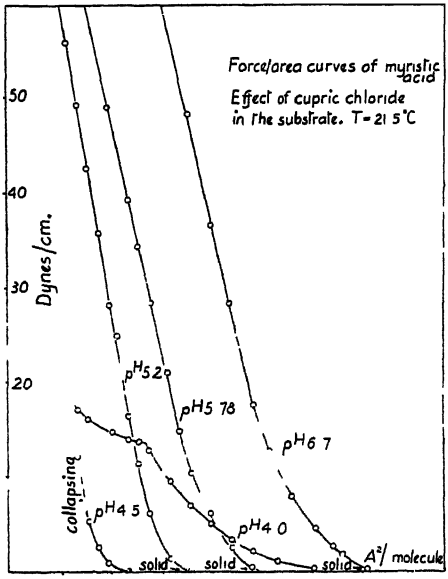

FIG. 4.—The effect of cupric chloride.

COBALTOUS CHLORIDE.—At pH 4, the force-area curves were identical in the presence and absence of cobalt salt. The solution effect observed (in the pH range 4·6-4·92) in the absence of salt (see Fig. 1) was eliminated by the presence of cobalt. Instead, a condensation of the liquid-expanded film took place (Fig. 5).

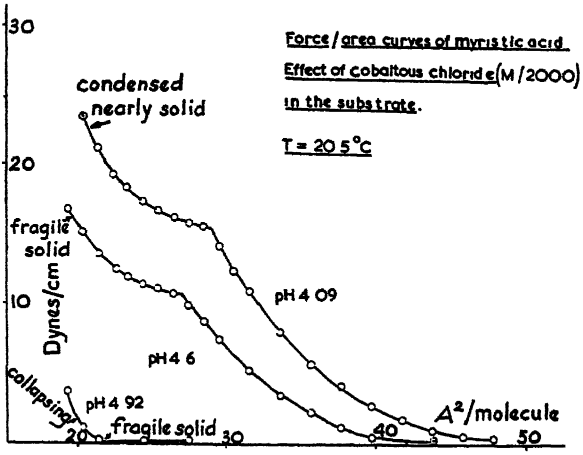

FIG. 5.—The effect of cobaltous chloride.

The properties of the condensed film were different from those observed in the presence of aluminium and copper (Fig. 3 and 4), a striking difference being the fragile nature of the solid film obtained above pH 4·92 which made measurements of force-area curves impossible. For example, at pH 4·92, the solid film started to collapse as soon as 1 dyne pressure was registered. Areas of solidification were also low in comparison (Fig. 6). At pH 9 no solid films were detected.

Manganese Chloride.—Solid films were obtained in the pH range (5·5-9·5) by compression of the monolayer, but force-area curves could not be obtained owing to the poor adhesion of these films to the water. These solid films were very similar to those obtained when cobalt was present and likewise showed no well-defined collapse pressure. Pressures of one dyne were sufficient to initiate slow collapse in the monolayer

Values of pH greater than 5, gradually reduced the area of solidification (Fig. 6) from 20 Å^2 at pH 5·5 to 10·5 Å^2 at pH 9·5. This indicates that although myristic acid films were partially stabilized by the manganese salt, the presence of manganese did not prevent the complete solubility observed in its absence. This is probably an instance of the reaction product between metal and film being soluble.

Calcium Chloride.—Solid films were produced in the pH range 5·5-10·5, which were of a fragile nature and slightly less rigid than those formed with manganese and cobalt salts. The area of solidification decreased as the pH value of the substrate increased in the manner shown in Fig. 6. Interaction at pH values greater than 10·5 could not be detected, as the product of reaction was soluble.

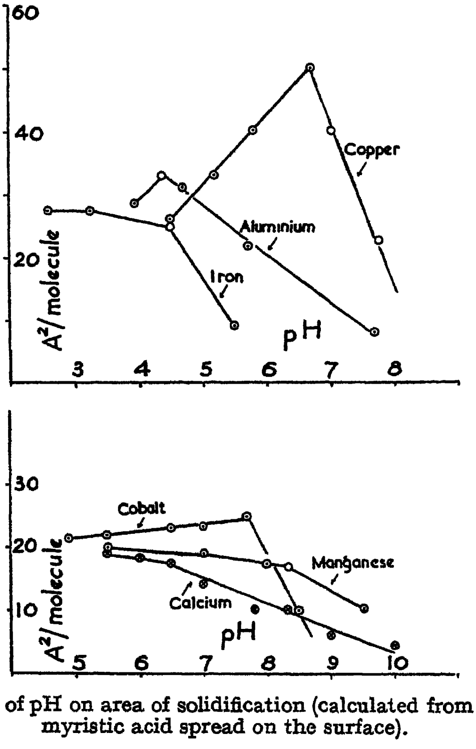

Fig. 6.—Effect of pH on area of solidification (calculated from the weight of myristic acid spread on the surface).

Magnesium Chloride.—No solid films were produced in the pH range (7·5-12). At these pH values the soluble monolayer could be compressed quickly without any rise in pressure down to very small areas.

Effect of pH on Area of Solidification of Myristic Acid Film with Metal Ions in Underlying Solution.—Fig. 7 shows (in diagrammatic form) the ranges of pH in which interaction between metal ions and monolayer has been detected. The pH value (pH_1) at which interaction was first detected, marks the extreme of this range on the acid side of neutrality and may be determined experimentally to within 0·1 pH. At a pH value (pH$_2$) condensation of the liquid-expanded film was complete. At higher pH values than pH$_2$, solid films formed at very low pressures, showing areas of solidification which decreased slowly, as the substrate was made more alkaline above a certain pH value (see Fig. 6), and finally at a pH value (pH$_3$) no solid film could be detected. The value pH$_3$ was not so well defined as pH$_1$ or pH$_2$, but was measured to within 0·5 pH. In Table I the values of pH$_1$, pH$_2$ and pH$_3$ are given for each metal.

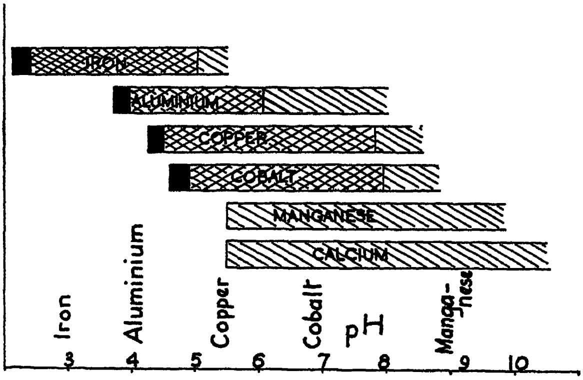

FIG. 7.—The effect of metal salts on myristic acid films.
Ranges of pH values in which interaction is detected between the myristic acid monolayer, and the metal salt in the substrate.

Vertical lines thus :— IRON| indicate hydroxide precipitation pH values.

■ pH range in which condensation of the liquid-expanded film takes place.

▩ Solid films with area of solidification > 20 A^2/mol.

▧ Solid films with area of solidification < 20 A^2/mol (calculated on amount of myristic acid spread).

TABLE I

Metal	pH_{HYD}	pH$_1$	pH$_2$	pH$_3$
Ferric	3·0*	2·10	2·60	5·5
Aluminium	4·20	3·70	3·94	8·00
Cupric	5·45	4·25	4·50	8·50
Cobaltous	6·90	4·60	4·92	9·00
Manganous	9·00	—	5·5	10·00
Calcium	—	—	5·5	10·5

* pH value at which solution became turbid. Other pH_{HYD} values from Britton.[9] pH_{HYD} is the pH for hydroxide precipitation.

Flotation Experiments.—Qualitative experiments were carried out to verify whether the pH ranges of interaction at the air-water interface also apply at the mineral-water interface. Approximately 1 g. of chalcocite (a copper mineral), ground under water, was *floated* by 100 ml. of caproic acid solutions at different pH values (2 to 10) containing 2 ml. of acid per litre. The tubes were shaken and allowed to stand for 1 min. and the amount of mineral in the

---

[8] Lamb and Jacques, *J. Amer. Chem. Soc.*, 1938, **60**, 967.
[9] Britton, *J. Chem. Soc.*, **127**, 2110, 2170, 2142, 2148.

froth was estimated. It was found that excellent flotation of the mineral was possible in the pH range (4·5-6·5), with maximum collection of the mineral in the froth at pH 5·5. Flotation was poor at pH 4·5 and ceased at pH 4·0. Similarly flotation at pH values greater than 6·5 was poor and diminished in more alkaline solutions until at pH 7·5-8 no mineral could be detected in the froth.

Two critical values at which flotation ceased were therefore obtained at pH 4·0 and at pH 7·5-8, which compare favourably with pH_1 and pH_3 in the monolayer experiments. Similar experiments using a caprylic acid solution containing 0·2 ml. acid/l. gave the same critical values. These pH values did not alter with fatty acid concentration, although the amount of mineral present in the froth and the frothing characteristics of the solution varied.

Iron pyrites in caproic acid solutions did not float at pH values higher than 6·5. It floated readily, however, at pH values less than 4, which is the critical value for chalcocite. For mixtures of pyrites and chalcocite at pH 3·0, pyrites floated leaving chalcocite behind, whilst at pH 6·5, chalcocite floated leaving pyrites in the residue.

The Application of the Monolayer Technique to a Cationic Compound.—Soluble cationic long chain compounds are used as collecting agents for quartz and silicates, consequently a monolayer of octadecylamine hydrochloride was spread on a M/20 phthalate-NaOH buffer solution at pH 6·2. At 24° C, the film was liquid-expanded (Fig. 8). A solution containing 200 mg. sodium silicate in buffer solution was injected into 800 ml. of solution in the trough.

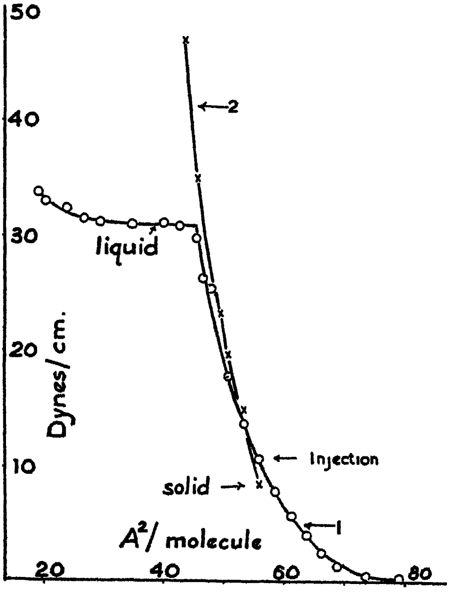

FIG. 8.

1. Force-area curve of octadecylamine hydrochloride M/20 phthalate/NaOH buffer.
2. Force-area curve 2 hours after injection of 200 mg. sodium silicate under monolayer.

The film was allowed to stand for 1 hr., after which it was found that portions of the film had solidified. After 2 hr., the whole film was a rigid solid at a pressure of 8 dynes (a value slightly lower than the initial pressure). This film remained solid on the injection of 5 mg. demonstrating the formation of a non-dispersible network in the adsorbed biomolecular layer.[14]

The compression curve of this solid film is shown in Fig. 8. A pressure of nearly 50 dynes/cm. was necessary to produce collapse in the film. Immediately after injection of the silicate, a large surface potential change was observed.[14] On alkaline solutions no solidification of the film occurred.

TYPES OF INTERACTION BETWEEN IONIZED AND NON-IONIZED MONOLAYERS, WITH METAL IONS, METAL ION AGGREGATES, AND NON-IONIZED AGGREGATES IN THE UNDERLYING SOLUTION.

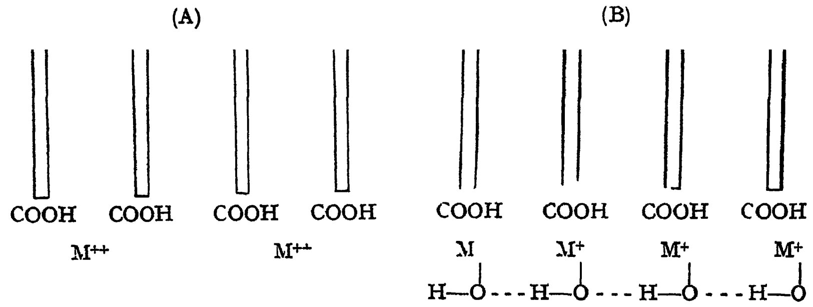

Induced dipole-ion interaction.
Surface potential change, no surface pressure charge.

Induced dipole-basic ion aggregate interaction.
Brittle solid films at large area per molecule and zero pressure.

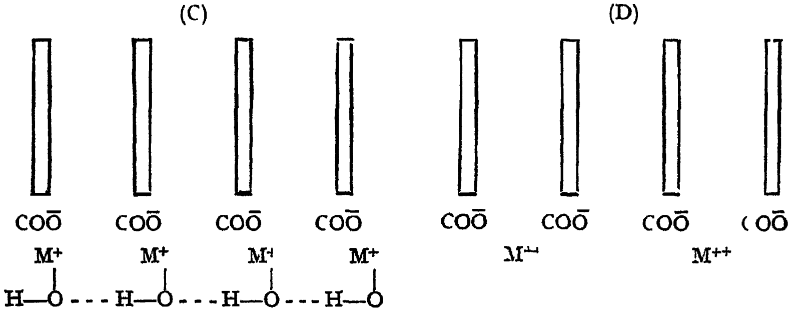

Ion-basic ion aggregate interaction.
Solid films at zero pressure, stable at high pressures and large areas per molecule.

$\bar{\text{Ion}}$-$\overset{+}{\text{ion}}$ interaction.
Brittle solid partially soluble.

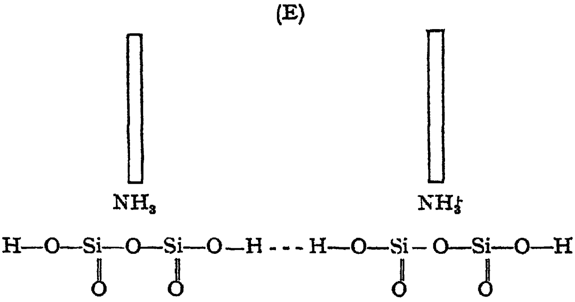

Ion-induced dipole in aggregate surface interaction.

FIG. 9.

Effects of Copper and Silver Salts in the Substrate on C_{20} Amine Hydrochloride Monolayers.—The lateral adhesion between the molecules in monolayers of long chain amines on acid substrates, is influenced very markedly by the types of anion present in solution.[10] Therefore a metal salt which contained the same anion as that present in the buffer solution was used.

Buffer solutions were prepared at pH 5 and at pH 6·2 with sodium acetate and acetic acid (total acetate concentration M/10). Solutions at these pH values were then made containing silver acetate (N/100 and N/1000) and cupric acetate (N/100 and N/1000) with the same total acetate concentration as the buffer solution containing no copper or silver. (pH values were individually checked.)

From Fig. 10 it will be seen that at pH 6·2 in the absence of silver and copper, the amine monolayer was vapour expanded. When copper was present in the underlying solution, no marked change in the force-area curve was measured. A concentration of M/1000 silver acetate in the substrate gave a marked lowering of the pressure of the transition and with M/100 silver acetate this effect was very pronounced. The condensed film obtained in this way did not solidify until the pressure reached 20 dynes/cm. (see Fig. 10). At pH 5, the force-area curves were identical in the presence and absence of silver and copper.

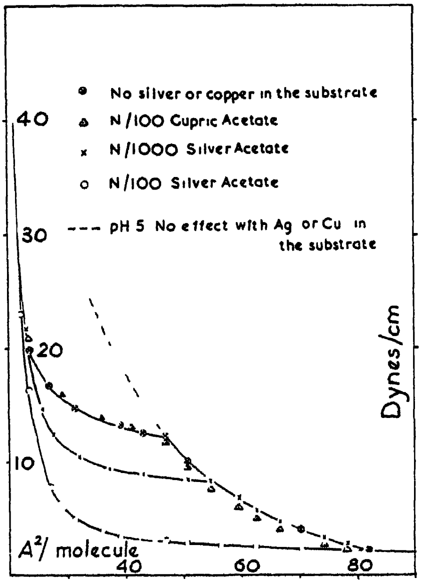

FIG. 10.—Force-area curves of eicosylamine hydrochloride on N/10 sodium acetate-acetic acid at pH 6·2.

Discussion

From surface potential measurements it is known that at pH 2, a myristic acid monolayer is composed of undissociated acid molecules and that at pH 10, ionization of this monolayer is almost complete.[11] At pH 5, approximately half the molecules are ionized, giving a monolayer which is unstable on compression (see Fig. 1). It will therefore be convenient to consider:

(*a*) the state of ionization of the monolayer at a given pH value ;

(*b*) the type of metal ions present in solution at the same pH value. In this way it may be seen whether conditions are favourable for interaction between the ions and the monolayer.

The Role of the Hydyoxyl Group in the Basic Metal Ion.—In the pH range 2 to 3 when very few ionized molecules exist in the monolayer, the only metal which has an effect on surface pressure measurements is iron, which it will be seen from Fig. 7 starts to precipitate from solution at pH 3 (see Table II). Therefore, as no surface pressure effects are present at pH 2, one may conclude that the metal ions responsible for the condensation of the monolayer in the pH range 2 to 3 are basic. Simple ferric ions produce no solid films, for at pH 1 there is no effect; however, they are able to induce dipoles in the monolayer molecules, which although not sufficient to alter the surface pressure characteristics, affect surface potential measurements (Fig. 9*a*).

---

[10] Adam, *Proc. Roy. Soc. A*, 1930, **126**, 532.

[11] Schulman and Hughes, *Proc. Roy. Soc. A*, 1932, **138**, 436.

Fig. 9*b* illustrates the mechanism of condensation of the film, due to basic ions interacting with undissociated molecules. The adhesion between these associated film molecules, which is responsible for solid film formation is possibly due to hydrogen bonding beneath the fatty acid monolayer between the hydroxyl groups present in the basic metal ions. Although aggregation of the basic metal ions and the subsequent precipitation of a metal hydroxide as a colloid may occur, a similar type of interaction at pH values greater than pH_{HYD} is not prevented, as presumably the basic ion is the main factor responsible for the interaction. When, however, complete flocculation of the colloidal aggregates takes place, these can no longer form a network underneath the monolayer. In addition, ionization of the precipitated hydroxide is suppressed and ionization of the monolayer is increased by increasing the pH value of the underlying solution to values higher than pH_{HYD}. Solid film formation therefore ceases at pH 5·5 approximately, in the case of iron.

It is known that the surface of a positively charged ferric hydroxide hydrosol is composed of a network of colloidal aggregates (or micelles) some hours after preparation and that multilayers of these micelles may be built up on a plate.[12] However, these aggregates are not by themselves responsible for solid film formation, for in the time taken to measure a force-area curve, a clean substrate surface pressure does not develop and remains liquid when the area is reduced. However, the presence of a monolayer which anchors the basic metal ions in the surface facilitates the interlinking process and the formation of a two-dimensional solid aggregate (Fig. 9*b*).

The formation of solid films in the presence of aluminium and copper salts may be explained by the same reasoning as that used for iron, but as the pH_{HYD} values of these metals are higher than for ferric iron (see Fig 7) the start of interaction might be expected at higher pH values than 2, as was in fact observed. The entire interaction ranges of aluminium and copper cannot be explained by the assumption that Type (*b*) interaction (Fig. 9) is the sole factor responsible for condensation effects. Two other types of interaction Type (*c*) and Type (*d*) (Fig. 9) are also present.

For example, at pH 4·5 in the presence of aluminium, and at pH 6 in the presence of copper, very high areas of solidification were measured in addition to high resistance to compression by the monolayers. This increased stability is possibly due to ionization in the monolayer (Type (*c*), Fig. 9) which produces a greater interaction between positively charged basic ions and negatively charged monolayers than is observed at pH 3 when interaction with basic ferric ions is due mainly to induced dipole effects.

Cobalt produces solid films of a different type from those already referred to. These show little adhesion to the substrate and from Fig. 6 it may be seen that the areas of solidification are smaller than for aluminium and copper, in the same pH ranges. Cobalt hydroxide does not precipitate until the pH value of the substrate is higher than 6·9. The interaction is therefore mainly Type (*d*), Fig. 9.

[12] Mokrushin, *Trans. Faraday Soc.*, 1947, **43**, 1.

[13] Schulman and McRoberts, *Nature*, 1948, **162**, 101; *Proc. Roy. Soc. A*, 1949 (Discussion on Gelation of Hydrocarbons).

Manganese and calcium produce solid films on very alkaline solutions, where interaction is wholly of the ionized monolayer-metal ion variety (Type (*d*)). At pH 5·5 manganese exists in solution as simple ions, so that even on acid solutions no hydrogen bonding enters into the structure of the monolayer. This is borne out by comparison of the areas of solidification of insoluble films in which hydrogen bonding is predominant with those in which ion-ion interaction is the major factor (see Fig. 9). For example, no areas of solidification greater than 20 Å^2/mole were measured with manganese in the substrate, which may be compared with values of 30 Å^2 found in the presence of iron at pH 2·5.

Magnesium ions, which according to theory should interact with the monolayer on alkaline solutions, fail to solidify the monolayer in the pH range 7·5 to 12. This may be attributed to the solubility of the reaction product, which in very alkaline solutions is the magnesium soap.

Interactions at the Solid-Liquid Interface.—The above three types of interaction at the air-water interface are very similar to those occurring at the mineral-water interface when a soluble fatty acid is used as a collecting agent. The experimental work on the flotation of chalcocite with caprylic and caproic acids has shown that the pH range of flotation is the same as the pH range of interaction observed between a myristic acid monolayer and copper ions in the substrate.

The analogy is permissible in this case because a chalcocite surface, which is readily oxidizable in air, or in water containing dissolved air, will provide an abundance of cupric ions at the mineral-water interface. Some of these ions will be free of the mineral surface, but some will be held to the lattice. Thus a reactive surface, consisting of interlinked basic cupric ions, will interact with the fatty acid molecules in solution in the manner outlined in Fig. 9. Flotation ceases at pH 7·4 to 8 when the surface of the mineral is converted to cupric hydroxide with the ionization suppressed.

Further support can be given to this concept by the flotation of iron-pyrites and chalco-pyrites with soluble fatty acids—thus the different stability pH ranges for the various basic metal ions would explain selective adsorption and flotation by soluble fatty acids. It is essential that the surface of the copper mineral be ionized in order that it may adsorb fatty acid molecules or ions to form a monolayer.

Chrysocolla (a copper silicate mineral) unlike chalcocite, is not floated by soluble fatty acids because of the very feeble surface ionization. Flotation may be obtained by treatment of this mineral surface with a very dilute ammonia solution and then by treatment with H_2S, which forms a readily ionizable sulphide layer on the mineral surface. The mineral is then easily floated with fatty acid and behaves as if it were chalcocite.

Interaction with Long Chain Amine Monolayers.—The experiment in which sodium metasilicate was injected beneath a long chain amine monolayer, held at a constant area on a slightly acid substrate, was designed to illustrate another type of interaction using the monolayer technique. Probably silicic acid is produced slowly from the slightly acid solution of sodium silicate, and molecules of this very feebly ionized acid attached themselves to the underside of the ionized amine monolayer,[14] mainly as the result of induced forces produced by the highly charged amine ions in the monolayer. A marked surface potential change observed immediately after the injection of the silicate, marks this first stage of the interaction. A slow polymerization of the silicic acid molecules then takes place, so forming a rigid network underneath the film which renders the monolayer completely solid after two hours, and non-dispersible by a non-complex-forming cationic detergent.

This interaction (Type (*e*)) is shown diagrammatically in Fig. 9. The polymerization of the silicic acid molecules is of course a very complex phenomenon and for the sake of clarity is represented in the diagram as inter- and intra-molecular condensation in two dimensions only. Polymerized aggregates of this kind do not by themselves build up a surface pressure in the absence of the monolayer, as is also the case with the metal hydroxides.

---

[14] Schulman and Rideal, *Proc. Roy. Soc. B*, 1937, **122**, 52.

It is known [14-16] that the solidification and non-dispersibility produced in an amine film by bimolecular-layer formation has direct analogies to the tanning of protein monolayers, and it is significant that some of the metal ions studied in this paper, e.g. iron and aluminium salts, are tanning agents similar to chromium salts, when in the form of basic ions. It is suggested, therefore, that a contributory factor to the tanning of proteins by inorganic agents is the association of the basic metal ions with the carboxyl groups, in the protein as demonstrated by their action on fatty acids in this paper, which may be compared with the tanning action of organic acids which associate with the amine groups in the protein.

Further support is given to this concept by the condensation of amine films in the presence of silver ions in the substrate at pH values higher than 6 and by the absence of these effects when copper ions are present in the substrate in the acid pH range (Fig. 10). These experiments indicate that positively charged basic metal ions do not interact with ionized amine films, but only with associated amines to give complex ions comparable to those produced with ammonia, e.g. $Ag(NH_3)_2^+$, $Cu(NH_3)_4^{++}$. Thus at pH 6·2, silver ions are available in the substrate, and interact with the non-ionized molecules in the monolayer. Under these conditions the basic copper complex is suppressed, consequently copper does not condense the film. At pH 5, neither copper nor silver produce condensation as the amine film is completely ionized, and this applies in more acid solutions.

The concept that the basic metal ions are reactive with fatty acids, either from solution of metal salts on monolayers or in analogous form at the surface of a mineral, has possible application to the fundamental forces involved in chromatographic absorption.

We wish to thank the Rhokana Corporation Ltd. for much material assistance. One of us (G. A. W.) is grateful to them for a personal grant, which has made this work possible. Our thanks are also due to Prof. N. K. Adam for samples of pure octadecylamine and eicosylamine hydrochlorides.

Department of Colloid Science,
University of Cambridge.

---

[15] Cockbain and Schulman, *Trans. Faraday Soc.*, 1939, **35**, 1.

[16] Cockbain and Schulman, *ibid.*, 1939, **36**, 1266.

METAL-MONOLAYER INTERACTIONS IN AQUEOUS SYSTEMS

PART II.—THE ADSORPTION OF LONG-CHAIN COMPOUNDS FROM AQUEOUS SOLUTION ON TO EVAPORATED METAL FILMS

By G. A. Wolstenholme and J. H. Schulman

Received 23*rd December*, 1949

Evaporated films of copper and silver with hydrophilic surfaces have been immersed in aqueous solutions of surface-active long-chain compounds, and the contact angles with these solutions have been measured under controlled conditions. Sodium dodecyl sulphate adsorbs on the surface of copper films which have been exposed to oxygen and the rate at which the contact angle increases depends on the temperature and on the concentration of long chain ions in solution. By assuming that the contact angle with these solutions is proportional to the number of molecules of long chain compound in the surface, a value of the activation energy for the surface reaction has been obtained.

Surface solubility or solubility of the complex between long chain ion and metal are factors which influence the formation of an adsorbed monolayer Soluble fatty acids form adsorbed monolayers on copper surfaces which have been exposed to air, but not to oxygen alone, and not on silver surfaces which have been exposed to oxygen or air. When soluble fatty acids adsorb on copper surfaces the rate of adsorption is too rapid to measure. Adsorption on to evaporated metal films is extremely sensitive to impurities from the air, in the possible form of carbon dioxide and sulphur containing compounds. Sodium sulphate accelerates and inhibits with increasing concentration the rate of adsorption of sodium dodecyl sulphate on to copper surfaces.

The kinetics of adsorption of long chain compounds at the solid-liquid interface resulting in the formation of hydrophobic surfaces has not been investigated to any extent, owing to the fact that suitable systems have not been found. A contributory factor to this has been the difficulty in preparing reproducible hydrophilic metal or mineral surfaces free from contamination and of measuring contact angles under equilibrium conditions.[1]

Experimental

The captive bubble method of Wark [2, 7] of measuring the contact angle at the solid-water interface ensures that the solid surface, when not covered by water is in a gas saturated with water vapour. Essentially, this method consists of lowering a gas bubble held on the end of a vertical tube immersed in water or aqueous solution on to the solid surface. If the surface is hydrophobic, the bubble of gas adheres to it and the air-water interface may be made to advance or recede over the surface, giving values of θ_A and θ_R respectively. When the solid surface is smooth, a value of contact angle θ_E, intermediate between θ_A and θ_R, may be established by gentle vibration after bringing the bubble into the advancing position. This is an equilibrium value, which with a very smooth surface, is the same whether from the advancing or receding positions.

Preparation of the Metal Surface.—Metal surfaces were prepared by evaporation in a Pyrex glass tube E (Fig. 1) henceforth referred to as the evaporation chamber. The upper end of this tube carried a large mercury seal, the

[1] Harkins and Fowkes, *J. Amer. Chem. Soc.*, 1940, **62**, 3377.

[2] Wark, *Principles of Flotation* (Austral. Inst. Min. Met., Melbourne, 1938).

[7] Siedler, *Kolloid-Z.*, 1934, **68**, 89.

mercury reservoir M and the cup N. Through N were sealed two tungsten wires on the end of which a spiral tungsten filament F was spot-welded, so that it was held approximately 3 cm. above the bottom of E. A small piece of the metal wire to be evaporated was placed inside the filament spiral and was surrounded by a small piece of thin walled quartz tubing, which prevented shorting of the filament coils.

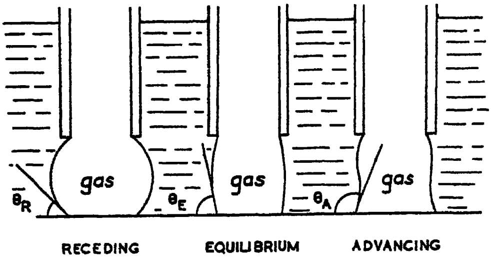

Bubble method for measurement of contact angle.

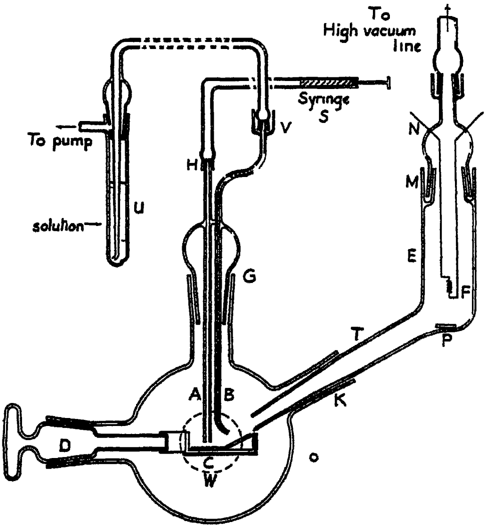

Contact angle apparatus.

Fig. 1.

A rectangular optically plane Hysil glass plate P (1 cm. by 2 cm.) rested on the bottom of the evaporation chamber in a horizontal position, but not directly underneath the filament. By heating the filament F *in vacuo* a thin metal film could be deposited on the surface of the plate P.

Transference of the Deposited Film.—The coated glass plate was transferred in a high vacuum down the tube T, which was arranged at such an angle that a gentle tap on the bottom of E would dislodge the plate from its former position, so that it slid slowly into the cell C, down a glass slide in the cell, and finally came to rest in a horizontal position directly underneath the vertical tube A. The specimen could now be viewed through an optically plane window W, held on the end of a tube sealed into the glass bulb O and parallel with the vertical sides of the glass cell C. This window was held internally, 1 cm. distant from the glass cell, in such a manner that the end of tube A inside the cell could be brought into focus using a microscope with a $1\frac{1}{2}$ cm. focal length objective. Another circular glass window was used to illuminate the surface of the plate. This window was sealed into O on the other side from W and parallel to it.

Introduction of the Solution.—The tube U contained the solution which was freed from air by evacuation through the side arm and the air was replaced by any desired gas. The vacuum in O was then let down by the same gas until the pressure was 1 atm. The capillary in U, was then broken and by applying a slight pressure to the side arm of tube U, the solution in the tube was siphoned over into the glass cell C, so as to immerse the plate completely.

Measurement of Constant Angle.—One end of tube A was sealed to an Agla glass syringe rendered air-tight by a film of high vacuum grease between the piston and the barrel. When the pressure in O was atmospheric a bubble of gas was blown on the end of the tube A in the solution, so that it came into contact with the evaporated metal film. Very delicate control of the piston was ensured by attaching it to a micrometer head. A specially adapted travelling microscope fitted with crosswires was used to observe the gas bubble, and to measure the contact angles with an accuracy of 1°.

Procedure.—Attention was given to cleaning and especially to the glass plate P, which after cleaning with chromic acid was rinsed with quartz-distilled water, heated and placed hot in the evaporation chamber. When the surface of the plate P was treated in the manner described, the film of metal adhered strongly to the glass, and even when wet with water was not detached by gently rubbing. All the ground joints were greased with silicone resin high vacuum grease, great care being taken to avoid grease extending below the ground joint of the tube holding the solution.

The whole apparatus was evacuated until the pressure fell to 10^{-5} mm. A typical metal film (of the order of 1/100 mm. thick) was deposited in 15 min. A surface prepared in this way had a very high reflectivity. After transferring the plate, which had been allowed to cool to room temperature, gas was introduced, followed by the solution made from quartz-distilled water, and contact angle measurements were taken.

Precautions Taken to Avoid Contamination.—Two liquid oxygen traps were placed between the high vacuum line and the evaporation chamber. One of the traps contained a filter which prevented dust particles from entering the apparatus when gases were introduced.

Control of Temperature.—The large glass bulb O, the syringe and the tube containing the solution were enclosed in a box air-thermostated to ±0·1° C. Three hours were allowed for the contents of the box to reach equilibrium with the surrounding air.

Materials.—The copper and silver wires were at least 99·99 % pure. The sodium dodecyl sulphate was of very high purity and gave a surface tension-concentration curve with no minimum.[11]

Results

Contact Angles with Water.—Copper and silver films which stood in oxygen, nitrogen and hydrogen, were completely wetted by water free of air, but containing the dissolved gases. After exposure to oxygen for periods of 10 min. or more, a copper film was covered by a cuprous oxide film about 90 Å thick.[17] In nitrogen and hydrogen it is very unlikely that the surface of the copper film was completely free of oxide. Dry specimens which stood unenclosed in laboratory air for short periods readily became contaminated and hydrophobic. When left inside the apparatus in air for periods up to 10 min. the contamination was not sufficient to make the surface hydrophobic. When cleaned gases were used, surfaces were hydrophilic even after 1 hr. exposure.[5]

Copper Surfaces in Fatty Acid Solutions.—Copper surfaces stood in oxygen for 10 min. They were then introduced into soluble fatty acid solutions, free of air, but containing oxygen, with the following concentrations : decanoic acid (C_{10}) 5-17·5 mg./l. ; caprylic acid (C_8) 50-150 mg./l. ; caproic acid (C_6) 150-1500 mg./l. No contact angles developed in these solutions at 20° C. The same solutions were then freshly prepared, but this time dissolved air was not expelled. Similarly, the copper surfaces were allowed to stand in air for 10 min.

Contact angles developed within ½ min. after immersion of the prepared surfaces. There was a fairly wide range of concentrations in which contact angles were the same and remained constant immediately after immersion.

[11] Miles and Shedlovsky, *J. Physic. Chem.*, 1944, 48, 57.

[17] Miley and Evans (see Evans, *Metallic Corrosion, Passivity and Protection*).

[5] Bartell and Cardwell, *J. Amer. Chem. Soc.*, 1942, 64, 494.

In order to obtain the maximum value of contact angle, the following concentrations of fatty acid were necessary:

C_{10} acid 13 mg./l., C_8 acid 110 mg./l., C_6 acid 1200 mg./l.

Weaker solutions gave erratic values of contact angle. The maximum values of contact angle observed were as follows:

Acid	θ_E	θ_A	θ_R
C_{10}	90	115-120	31
C_8	79	101	31
C_6	75	95	34

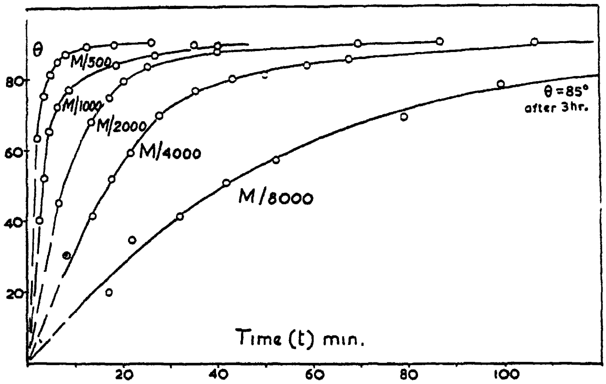

FIG. 2.—The effect of sodium dodecyl sulphate concentration on θ-t curves obtained with copper surface in oxygen. $T = 20°$ C.

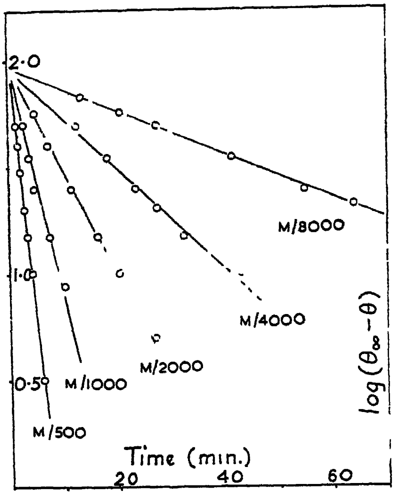

FIG. 3a.—Copper surface in oxygen: sodium dodecyl sulphate. $T = 20°$ C.

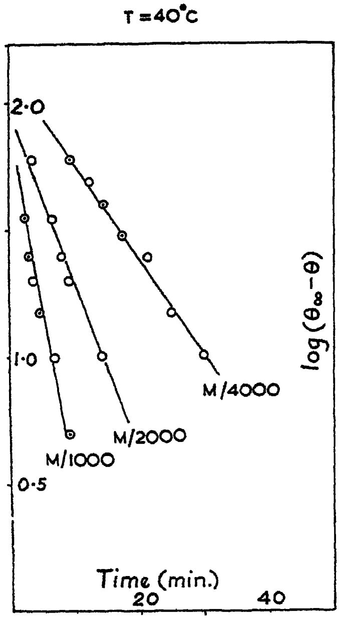

FIG. 3b.

SILVER SURFACES IN FATTY ACID SOLUTIONS.—When the concentrations of fatty acid were the same as those used previously, no contact angles developed after the silver films had been exposed to air or oxygen for 10 min.

COPPER SURFACES IN SODIUM DODECYL SULPHATE SOLUTIONS.—Copper surfaces stood for 10 min. in oxygen before immersion in sodium dodecyl sulphate solutions. For a given concentration, the contact angle θ_E increased with time of immersion, finally becoming constant at 90 ± 1°. Values of θ_E are plotted against time for different concentrations of sodium dodecyl sulphate in Fig. 2.

The rate of adsorption with M/250 solution was too rapid to measure accurately. θ_E was zero with a M/100 solution, although washing with distilled water restored the hydrophobic nature of the surface.

Mechanism of Adsorption.—If θ_∞ is the maximum value of the contact angle θ_E and θ is the contact angle θ_E at time t, then the series of curves obeyed the relationship:

$$\log(\theta_\infty - \theta) = kt \quad (k = \text{constant}).$$

This is shown by the straight line plots in Fig. 3*a* for a series of concentrations at 20° C. At 40° C the linear relationship still applied (Fig. 3*b*) and θ_∞ was the same as at 20° C, within experimental error (Fig. 4). The surface reaction therefore obeys a pseudo-unimolecular law, and it may be shown that the concentration of one of the reactants (i.e. the dodecyl sulphate ion) remains constant at the surface as the reaction proceeds. Similar equations have been developed for other surface reactions.[18]

CALCULATION OF THE ENERGY OF ACTIVATION FOR THE SURFACE REACTION.—From the variation of K with temperature (20° C and 40° C) at constant concentration, the energy of activation for the reaction may be calculated as K is proportional to k, the true velocity constant of the reaction (Fig. 5). By applying the Arrhenius equation, this energy of activation is 3200 ± 300 cal.

The Effect of Additions of Sodium Sulphate to Dodecyl Sulphate Solutions.—Copper surfaces stood in oxygen for 10 min. before immersion at 20° C in a M/2000 sodium dodecyl sulphate solution. Small salt additions up to M/200 increased the velocity constant of the surface reaction. Larger additions decreased K values and M/100 sodium sulphate suppressed adsorption completely (see Table I).

Values of K for salt concentrations up to M/2000 are calculated from the values of θ_E in the first 10 min. in solution, when the straight line relationship between $\log(\theta_\infty - \theta)$ and t was reasonably obeyed. Longer periods in solution produced deviations from this linear relationship, which could not be accounted for by experimental error alone. When salt concentrations greater than M/2000 were used the deviations were negligible.

M/250 was approximately the salt concentration required to suppress adsorption using M/2000 sodium dodecyl sulphate. M/500 salt was sufficient to suppress adsorption using M/4000 sodium dodecyl sulphate. $\theta_\infty = 90 \pm 1°$ remained unchanged for additions of salt up to M/500, and was the same as in the absence of salt. Films which were removed from solution after treatment with M/2000 sodium dodecyl sulphate containing M/100 sodium sulphate were hydrophilic when washed with distilled water.

THE EFFECT OF CHAIN LENGTH.—Sodium dodecyl and tetradecyl sulphate gave the same final contact angle θ_∞ of 90 ± 1°. For sodium decyl sulphate θ_∞ was 85 ± 1°. Increasing the chain length increased the rate of development of θ_E with the same molar concentration of each long chain sulphate. For M/500 solution, K values are given in Table II (20° C).

The value of K for the C_{14} compound is calculated from the value at M/2000. Adsorption was extremely slow for solutions of the C_{10} compound less than M/500; even after 3 hr. immersion in a M/1000 solution, contact angles were very small and too erratic to measure accurately.

THE EFFECTS OF IMPURITIES.—The surface reaction between an oxidized copper surface and sodium dodecyl sulphate was very sensitive to traces of metal ions in the distilled water, and to the presence of air. Only after taking rigorous precautions to ensure that the water was free from impurities and air were the experiments repeatable. For example, an evaporated film which was exposed to air for 10 min. behaved in a very erratic manner and in one case did not adsorb sodium dodecyl sulphate sufficiently to develop a contact angle, even after 30-min. immersion in a M/1000 solution.

---

[18] Hughes and Rideal, *Proc. Roy. Soc. A*, 1933, **140**, 253.

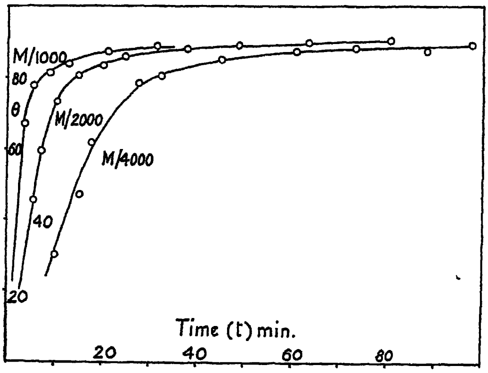

Fig. 4.—The effect of sodium dodecyl sulphate concentration on θ-t curves obtained with copper surface in oxygen. $T = 40$ C.

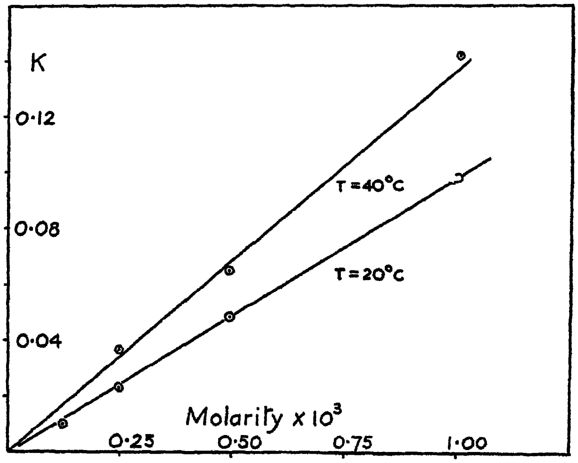

Fig. 5.—Plot of K against sodium dodecyl sulphate concentration.

TABLE I

Sodium Sulphate Concentration	$K = \frac{\log_{10}(\theta_\infty \quad \theta)}{t \text{ (in min.)}}$
0	0·049
M/4000	0·050
M/3000	0·065
M/2000	0·082
M/1000	0·024
M/500	0·014
M/250	Very small
M/100	0·000

TABLE II

Chain Length	$K = \frac{\log_{10}(\theta_\infty \quad \theta)}{t \text{ (min.)}}$
C_{10}	0·011
C_{12}	0·210
C_{14}	0·293

Carbon dioxide and nitrogen were not responsible for this peculiar behaviour, for when these gases were introduced into an oxygen atmosphere, the $\theta - t$ curves repeated as in pure oxygen. Sulphur compounds in the air were the most likely cause, for after some time in solution the copper film tarnished in the vicinity of the air bubble.

COPPER SURFACES IN OCTYLAMINE HYDROCHLORIDE SOLUTIONS.—Copper surfaces were exposed to oxygen for 10 min. and then immersed in air-free octylamine hydrochloride solutions. Contact angles developed and increased with time, finally becoming constant. In contrast with the copper | sodium dodecyl sulphate system, the values of θ_∞ were different for different concentrations (see Table III).

TABLE III

Conc. Octylamine Hydrochloride	θ_∞	Time to Reach Maximum Value (min.)
M/500	101	5
M/1000	92	25
M/1500	74	52
M/2000	~45	About 2 hr.
M/2500	Erratic No contact angle detected	

SILVER SURFACES IN OCTYLAMINE HYDROCHLORIDE SOLUTIONS.—Whereas a concentration of M/3500 was not sufficient to produce detectable adsorption on a copper surface, silver surfaces exposed either to air or oxygen developed contact angles rapidly in a solution of this strength. A maximum value of θ_E was reached in 10 min. and values of 70° to 80° were recorded. After the maximum value had been reached there was a fall in the value of θ_E to about 40° extending over a period of 20-40 min. This decrease was rapid at first, then diminished.

In M/1500 solution the maximum value of θ_E was reached in less than 1 min. at a value of 85° approximately. This remained constant for 2 min. then fell to 65° in another 5 min. θ_E remained fairly constant for 1 hr. at approx. 65°. The maximum contact angle with a concentration of M/7000 was reached in 30 min., and was followed by a slow decrease extending over a period of 2-3 hr.

Discussion

There are several experimental results which justify the view that the adsorption of dodecyl sulphate ions on to a copper surface after exposure to oxygen is the result of complex formation between the long chain ions and the metal, which is an irreversible process.

Firstly, the maximum number of long chain ions on the surface (measured by θ_∞) is not affected by the concentration of these ions in solution within wide limits. Secondly, θ_∞ is independent of the temperature in the range 20°-40° C. In addition, there is no appreciable change in the contact angle after a hydrophobic copper film, which has been removed from solution, is washed with distilled water. Also the surface reaction has an energy of activation of 3200 cal./g. mole (Fig. 5).

The formation of a monolayer of C_{10} fatty acid on a copper surface previously exposed in this case to air, may also be regarded as an irreversible process again involving chemical combination at the copper surface. Monolayers of this kind are not removed by washing with distilled water. Also the rapidity of the surface reaction may be explained by the assumption that the forces of interaction are basic ionic (see Part I).

Surface Solubility Effects.—There is no evidence to show for the two systems which have been discussed, that by a maintained chemical attack of the metal surface, the metal ions are removed from the surface into solution. That these solubility effects are negligible or completely absent does not always apply. For example, when copper and silver films are immersed in octylamine hydrochloride solutions θ_∞ differed for each concentration of this compound. (For copper surfaces, see Table III.)

Two explanations of these observations may be considered:

(i) The long chain amine molecules combine chemically with the surface, forming a soluble complex.

(ii) Side reactions, due for example to surface attack by hydrolysis products of the long-chain amine hydrochloride are constantly removing metal ions from the surface into solution, thereby hindering or completely preventing the formation of a monolayer.

For copper surfaces, it seems likely that hydrochloric acid, produced by hydrolysis of the long chain amine hydrochloride, dissolves away the surface layers of copper ions in the metal surface, so competing for the surface with the long chain amine molecules. In addition, the complex formed at the surface may be soluble. The different values of θ_∞ may therefore represent a balance between adsorption and solubility effects for each concentration of amine hydrochloride.

It has been shown that for M/1500 hydrochloride there is no contact angle on a copper surface. Presumably under these conditions, the rate of removal of long chain molecules from the surface in the form of a complex with the copper is equal to, or exceeds, the rate of adsorption.

For silver surfaces and long chain amine hydrochloride solutions, the $\theta - t$ curves show a maximum followed by a decrease in contact angle. Reasons for this behaviour are at present obscure, but it is likely that the different values for the maximum values of contact angle θ_E, corresponding to different octylamine hydrochloride concentrations are due to soluble complex formation, as distinct from surface attack by an acid hydrolysis product.

Solubility effects in the form of a maintained chemical attack of the copper surface are evident in high concentrations of C_6 acid and are present to a lesser extent for solutions of C_8 acid, although with a sufficiently high concentration of acid in solution, a hydrophobic surface can be maintained. Copper films which are removed from solutions of C_6 acid, containing 1500 mg./l., after several hours' immersion, are dull and appreciably thinner than initially. This observation lends further support to this view.

Salt Effects.—The effects of salt on the surface tensions and micelle formation of long chain electrolyte solutions have been investigated both theoretically and experimentally by several authors.[10, 12, 13, 16] The addition of sodium sulphate to M/2000 sodium dodecyl sulphate solutions affects the $\theta - t$ curve with copper surfaces. It has been shown that there are two effects. Small concentrations of sodium sulphate increase the rate of adsorption and salt concentrations exceeding M/2000 decrease this rate, finally preventing adsorption completely, when the salt concentration is approximately M/100. A decrease in the rate of adsorption might be accounted for by a reduction in the number of free long chain ions in solution by the incorporation of some of these ions into micelles. However, this is unlikely, for the following reasons:

(i) The tension lowerings of M/2000 sodium dodecyl sulphate by M/500 and M/100 sodium sulphate are 7 dynes and 11 dynes respectively—insufficient to indicate micelle formation.

(ii) A copper surface washed with water after immersion in M/2000 sodium dodecyl sulphate containing M/100 sodium sulphate was

---

[6] Kolthoff, *J. Physic. Chem.*, 1936, **40**, 1027.

[10] Powney and Addison, *Trans. Faraday Soc.*, 1937, **33**, 1246.

[12] Cassie and Palmer, *ibid.*, 1944, **40**, 116.

[13] Palmer and Rideal, *J. Chem. Soc.*, 1939, 573.

[16] Adam and Shute, *Trans. Faraday Soc.*, 1938, **34**, 758.

hydrophilic indicating that no adsorption has taken place, whereas a similar surface after immersion in M/100 sodium dodecyl sulphate containing no salt (i.e. at the micelle point) is hydrophobic after washing.[14, 15]

A more probable reason for this "depressant" effect of sodium sulphate is that there is a competition for the surface of the copper between long chain sulphate ions and sulphate ions. With high concentrations of sodium sulphate, the sulphate ion predominates on the surface. It should be emphasized that the additions of salt are not sufficient to salt out the long chain compound from solution.

At present, no satisfactory explanation can be given for the increase in the rate of adsorption observed with very small salt concentrations. Additions of sodium sulphate up to M/2000 have hardly any effect on the surface tension of sodium dodecyl sulphate solutions.

The Significance of the Absence of a Contact Angle.—Several reasons for the absence of a contact angle of a solution of a long chain compound on a metal surface have already been discussed, viz. : (i) micelle formation, (ii) surface solubility effects, (iii) the preferential adsorption of an ion with the same sign as the long chain ion. It has been shown that silver surfaces do not develop contact angles in fatty acid solutions. This is possibly due to a fourth reason, which is the poor ionization of a silver surface in distilled water and the absence of a chemical reaction between the fatty acid and the silver surface.

The Effect of Impurities from the Air.—Contact angles form on copper surfaces in fatty acid solutions in the presence of air, but not in the presence of oxygen. Although the precise nature of the observed effects is not known, it is possible that air containing sulphur dioxide or hydrogen sulphide forms mixed oxide+sulphide layers on the surfaces of the copper films. Also, the presence of carbon dioxide in the unbuffered solutions of long chain compounds influences the pH values of these solutions, so that a solution containing dissolved oxygen has a higher pH value than one containing dissolved air (see Part I). That impurities from the air have a marked effect on the surface reaction between copper and sodium dodecyl sulphate is also shown by the erratic results obtained in air which were absent in oxygen.

The Effects of Chain Length.—For the copper+sodium dodecyl sulphate system increasing the chain length above 10 carbon atoms, has very little influence on θ_∞. It seems certain therefore that increasing the chain length of the compound increases the rate of adsorption of the long chain ions on the copper surface. There is also evidence to show that increasing the chain length decreases solubility effects. For instance, these effects are absent for the system C_{10} acid+copper (in air), but very pronounced for the system C_6 acid+copper (in air). A comparison of the *K* values for the different long chain sulphates indicates that there were some solubility effects using the C_{10} sulphate.

The results obtained for all the systems studied indicate that the formation of an adsorbed monolayer at the interface between the metal and an aqueous solution of a long chain compound is due to a chemical reaction between the adsorbate molecules and the metal surface.[9] Consequently these systems are in no way comparable with those involving inert surfaces, e.g. noble metals,[3, 4] graphite,[8] paraffin wax, etc. Neither the Gibbs' equation nor equations of the Langmuir type may be applied,

---

[14] Wark and Wark, *Nature*, 1939, **143**, 856.

[15] Rogers, Sutherland, Wark and Wark, *Amer. Inst. Met. Min. Eng., Tech. Publ.* 2022, 1946

[9] Taggart, Taylor and Ince, *Trans. Amer. Inst. Min. Eng.*, 1930, **87**, 285.

[3] Bigelow, Picket and Zisman, *J. Colloid Sci.*, 1946, **1**, 513.

[4] Bigelow, Glass and Zisman, *ibid.*, 1947, **2**, 563.

[8] Corrin, Lind, Roginsky and Harkins, *J. Colloid Sci.*, 1949, **4**, 485.

when the final concentration of long chain molecules on the surface is independent of their concentration in the bulk.

We are indebted to the Rhokana Corporation Ltd., for much material assistance, and one of us (G. A. W.) is grateful to them for a grant which has made this work possible. We wish to thank Mr. C. C. Smith for constructing the glass apparatus.

Department of Colloid Science,
University of Cambridge.

THE INFLUENCE OF PRESSURE ON THE POLYMERIZATION OF STYRENE

By R. C. Gillham

Received 9*th January*, 1950

The effect of pressure on the polymerization of styrene is found to be an increase in rate of polymerization of about ten-fold at a pressure of 3000 atm. An increase of molecular weight of the polymer is also obtained. The failure to maintain isothermal conditions is considered to be largely responsible for the much greater effects obtained by previous investigators.

The influence of pressure on polymerization in the liquid phase has been investigated by many workers and, in some cases, large effects have been reported. A review of this work which is almost entirely qualitative or semi-quantitative is given by Bridgman.[1] The only previous quantitative investigation of the influence of pressure on the polymerization of styrene was by Tamman and Pape [2] who claimed very large effects. The method employed was to observe the rate of pressure drop in a steel cylinder, heated to 140° C, containing 4-5 g. of styrene confined in a glass tube by mercury. The free space in the cylinder was filled with mercury. From the results of their experiments, they deduced the approximate relationship between the rate constant and pressure to be $k_p = 0{\cdot}45 \times 10^{-8} p^2$. From this a value for k_{1500}/k_1 is given as $2{\cdot}24 \times 10^6$. Such a large effect led to a close examination of the experimental procedure and the results obtained. This revealed that the conclusions were based upon invalid assumption. A previous paper [3] describes the arrangement of Tamman's apparatus. From this it appears that only the temperature of the external surface of the steel cylinder was measured and that at equilibrium there was an unspecified temperature gradient through the sample. Serious doubt exists, therefore, as to the temperature control during the polymerization and any rise in temperature due to failure to dissipate heat of reaction would vitiate deductions from pressure-drop readings. The method assumes that the compressibility of the system is constant over the range 600-3000 kg. cm.$^{-2}$. This is extremely doubtful. Again, no mention is made of the purification process to which the styrene was subjected, beyond the fact that it was dry.

The results obtained were based on the assumption that, as the pressure drop is approximately proportional to the decrease in volume which is roughly proportional to the decrease in monomer concentration, it is, to a first approximation, proportional to the increase in polymer concentration. It was claimed that the logarithm of the observed pressure when plotted against time gave a straight line, the gradient of which gave a reaction velocity constant:

---

[1] Bridgman, *Rev. Mod. Physics*, 1946, **18**, 1.

[2] Tamman and Pape, *Z. anorg. Chem.*, 1931, **200**, 113.

[3] Tamman and Bandel, *ibid.*, 1930, **192**, 239.

$$k = \left\{\frac{\ln p_1 - \ln p_2}{t_2 - t_1}\right\}.$$

From results at initial pressures of 620, 1,010, 2,010 and 3,030 kg. cm.$^{-2}$ an approximate relationship for the variation of k_p with pressure was derived, and this was used to extrapolate to $p = 1$ kg. cm.$^{-2}$. It is clear from these results that even if this method of deriving the velocity constants is accepted, the extrapolation to $p = 1$ kg. cm.$^{-2}$ is quite unjustified. Again, the measurement of reaction velocity is made over a region of changing pressure (almost 400 kg. cm.$^{-2}$ in the observation at 3,030 kg. cm.$^{-2}$) and hence over a region of changing velocity.

Thus it would appear that Tamman and Pape's work can only be accepted as qualitative evidence of a large pressure effect on the rate of polymerization and that observation of the pressure drop is not a reliable method of following the course of the reaction. Beyond reporting that the densities of the end products were similar, Tamman and Pape do not mention any examination of the polystyrenes so produced. One of the objects of the present investigation described below is to obtain information on the effect, if any, of pressure on the molecular weight of the polystyrenes. A more absolute method is used to discover the influence of pressure on polymerization rate, the main object of the work. The actual degree of conversion to polymer at various stages throughout the reaction at constant temperature and pressure is determined. By this means, rate of conversion, i.e. rate of polymerization, is obtained directly.

I. BULK POLYMERIZATION

Experimental

The initial experiments were carried out by compressing styrene in vertical glass tubes closed at the upper ends, with the open ends under mercury contained in an outer glass tube. This glass part of the system fitted into a pressure vessel, the internal volume being 6 in. long by 1 in. diam. The remaining space in the bomb was filled with oil. This apparatus has been described previously.[4]

Pressure was applied by oil which was supplied either from a hand pump or from a mechanically driven pump delivering oil at 220 atm. Higher pressures were obtained by using a 14/1 ratio hydraulic intensifier so that a pressure of 3,000 atm. was easily obtained. The bomb itself was heated by a copper block furnace machined out to a close fit round the bomb. The furnace was heated by resistance windings on the outside and thermostatically controlled so that it could be maintained at any desired temperature with a variation of less than 1° C. This variation was smoothed out by heat transfer through the wall of the reaction vessel. The pressure throughout was measured by Bourdon gauges which were not further calibrated.

Styrene was dried over sodium sulphate and distilled in a stream of oxygen-free nitrogen at reduced pressure to remove hydroquinone stabilizer, rejecting the first and last 5 % of the distillate. The still was let up to atmospheric pressure with nitrogen. The reaction tubes were flushed with nitrogen and immediately filled from the still receiver, so that the styrene was at all times under a blanket of nitrogen. The tubes were quickly inverted under mercury.

The conversion of monomer to polymer was determined by dissolving in chloroform the syrup or plug obtained after polymerization and precipitating the polymer by pouring the chloroform solution into a large volume of methanol. The polymer was dried overnight at 80-100° C. This technique gave results reproducible within a few per cent. The molecular weight of the polymer was estimated by the relative viscosity of a 0·1 % solution in chloroform at 20° C in a No. 1 Ostwald viscometer. Results are reported as η_{sp}/c only.

The reaction tubes used were 4 mm. diam. and contained approximately 1 g. of styrene. Five of these could normally be held under mercury in the outer glass tube. During the polymerization the pressure was kept to within 50 atm. of the required pressure. At intervals during the course of the reaction the pressure was released, the bomb opened, one tube was removed, the bomb reassembled and heated again. Finally the full pressure was applied.

---

[4] Fawcett and Gibson, *J. Chem. Soc.*, 1934, 390.

Thermocouple Experiments—In order to ensure that the polymerizations were carried out isothermally it was necessary to follow the temperature of the reaction with a thermocouple. This involved bringing thermocouple leads out of the high-pressure system. A vessel fitted with insulated electrical contacts was incorporated next to the bomb in the high-pressure oil supply pipe-line. Thermocouple leads were taken from the bomb, threaded through the oil supply pipe and brought out of the system via the insulated contacts in the head of the vessel. The arrangement is shown in Fig. 1. The thermocouple was calibrated *in situ* before use. With the couple immersed in the styrene in one of the tubes, the temperature was observed from the beginning of a polymerization at 3,000 atm. with the furnace temperature set at 120° C. The internal temperature rose gradually to 120° C after 30 min. and remained there for the period of observation of 90 min. From this experiment and a similar one at 100° C it was established that the polymerizations could be carried out isothermally.

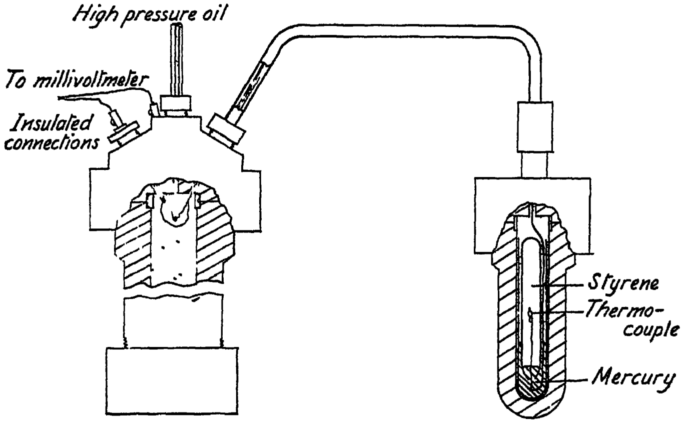

FIG. 1.

The reproducibility of the results obtained by the sampling method described above was shown to be satisfactory by comparing the conversions obtained in several tubes heated under pressure in the same bomb for the same time. Good agreement was obtained, as between the results of different experiments under similar conditions. With practice, the interruption to the normal course of the reaction was reduced to 15 or 20 min. The assumption that in this period the reaction virtually ceased, will be found to be justified when the reaction rates at atmospheric pressure and low temperature on the one hand and at high pressure and 100° C on the other, are compared. The conversion was determined for each tube. The commencement or resumption of the reaction was taken as the time of application or reapplication of full pressure, which was when the temperature reached 100° C as shown by the thermocouple.

Results and Discussion

Curves of conversion against time were plotted for pressures of 1, 1,000, 2,000, 3,000 and 4,000 atm. using this technique for isothermal polymerization with oxygen as far as possible excluded. Due to the speed of reaction only three points are available from the 4,000 atm. experiment, which was checked with the thermocouple. The results are given in Table I and Fig. 2.

In Fig. 2 the rate of polymerization is estimated by taking the gradient of the straight portion of each curve. In Table I the increase in rate at various pressures over the rate at 1 atm. is given. The result of excluding oxygen as far as possible and carrying out the polymerization under isothermal conditions is to show a greatly reduced effect compared with that reported by Tamman and Pape. An increase in molecular weight is observed with increased pressure of polymerization, by a factor of 1·55 at 3,000 atm.

TABLE I.—THE INCREASE IN RATE OF BULK POLYMERIZATION AND MOLECULAR WEIGHT OF POLYMER, WITH INCREASING PRESSURE

Temp. ° C	Pressure (atm.)	Maximum Rate (% Conversion/hr.)	-fold Increase over Rate at atm. Pressure	Viscosity of 0·1 % Chloroform Solution at 20° C	
				Conversion %	η_{sp}/c
100	1	3·40	1	44·9	1·50
				90·6	1·48
100	1,000	5·06	1·49	88·0	1·96
				90·3	2·03
100	2,000	15·9	4·64	60·6	2·09
100	3,000	34·3	10·1	71·6	2·32
				85·4	2·39
				77·6	2·30
100	4,000	50·0	14·7	49·9	2·52

The complex role played by oxygen in polymerization reactions is, of course, well known (see, for example, ref. 5 and 6 for the effect of oxygen on the polymerization of styrene). The reduction in rate on excluding oxygen from monomers to be polymerized at high pressure has been observed before with isoprene [7] and methyl methacrylate.[8] The effect of oxygen in the present case was shown by comparing the rates of isothermal polymerization of styrene distilled and kept under nitrogen and styrene through which oxygen had been passed. The latter showed twice the polymerization rate of the former.

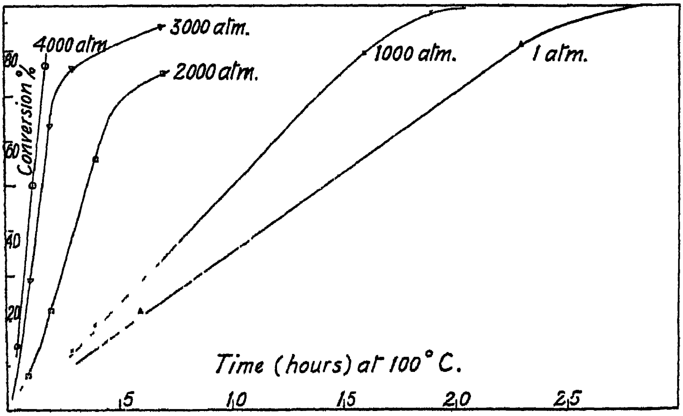

FIG. 2.

Of the two effects, that produced by uncontrolled oxygen concentration and by overheating, undoubtedly the latter is by far the greater

---

[5] Goldfinger and Lauterbach, *J. Polymer. Sci.*, 1948, **3**, 145.
[6] Bovey and Kolthoff, *J. Amer. Chem. Soc.*, 1947, **69**, 2143.
[7] Conant and Petersen, *ibid.*, 1932, **54**, 628.
[8] Vershchagin, Derevitskaya and Rogovin, *J. Phys. Chem. Soc. Russ.*, 1947, **21**, 233.

factor in producing a false impression of the reaction rate. To obtain an estimate of the magnitude of this effect the thermocouple was immersed in styrene contained in tubes of diameter 14 mm. and 9 mm. respectively. The wider tube contained about 15 g. of styrene and the narrower one, 5 g. This latter tube corresponded with the ones used by Tamman and Pape in diameter and volume. The attempted conditions in this case were 3,000 atm. and 120° C. In the experiment with the 14 mm. tube the temperature of the reaction mixture rose steadily as the contents of the bomb warmed up, and then rapidly to more than 300° C, 19 min. after heating was commenced. With the 9 mm. tube a similar phenomenon occurred, although not to the same extent : 25 min, after heating had begun the temperature had risen to a maximum of 170° C.

This emphasized the necessity for working with small diameter tubes in which it has been shown previously that no excessive rise in temperature takes place. The uncontrolled temperature rise when polymerization takes place in wider tubes is revealed by the properties of the product. For instance with a 14 mm. tube, whereas the value of η_{sp}/c for polymer made at 1 atm. at 140° C is found to be about 1·10, that at 1,500 atm. and 140° C is 0·7 and at 2,000 atm. is 0·31. At 120° C the η_{sp}/c value at 1 atm. is 1·32, at 1,000 atm. 1·58 and at 3,000 atm. is 0·42. The higher the initial temperature the more marked is this effect.

It has been found by experiment that there is no external manifestation of uncontrolled temperature rise in the form of an increase of pressure at the beginning of the polymerization. Thus in an apparatus such as Tamman's, there would be no indication of the non-isothermal conditions of the polymerization. The reduction in volume of the sample compensates for any expansion for this reason.

II. GRANULAR POLYMERIZATION

In order to confirm the results obtained by bulk polymerization it was considered desirable to test them using some different method of polymerization. The difficulty in pressuring such a system ruled out any method involving stirring, such as emulsion or the normal type of granular (" pearl ") polymerization.

Fortunately a new emulsifying agent, Promulsin, came to hand. On shaking styrene with a solution of Promulsin in water, a very stable dispersion of globules is obtained in a medium of jelly-like consistency,* and a granular polymerization can be carried out without the necessity for stirring. In effect the system consists of bulk polymerizations carried out in small droplets distributed throughout the jelly. From considerations of good heat transfer and the necessity for the isothermal condition of the reaction this would seem to be ideal for rapid polymerizations.

Experimental

A 2·5 % solution of Promulsin in 75 ml. of freshly boiled, distilled water was made in a 150 ml. flask, nitrogen was passed over the solution and the flask closed with a weighed stopper. The flask and contents were weighed. Styrene was purified as in the bulk polymerizations. 10 ml. were run into the flask under nitrogen, the flask was weighed, then shaken vigorously to disperse the styrene. An 80 ml. stainless steel reaction vessel was charged with this dispersion and the flask weighed again. From these weights the quantity of styrene transferred to the bomb was calculated. A bomb head with two pipe connections was used so that it was possible to fill the space above the suspension with water, after which the side connection was closed. Pressure was applied by oil and transmitted by a mercury seal to a reservoir of water connected to the reaction vessel (Fig. 3). A thermocouple pocket enabled the internal temperature to be observed. After the required length of time under polymerization conditions the bomb was opened and the contents washed out with distilled water. An equal volume of 2N sulphuric acid was added, with a few crystals of hydroquinone to stop polymerization of residual styrene. The mixture was then boiled for 5 min., when the Promulsin hydrolyzed and the polystyrene was precipitated. At high conversions the product was washed with water and methanol, but when there was much residual monomer it was necessary to precipitate the polymer from chloroform solution.

---

* The author is indebted for this information to Dr. K. W. Pepper of the Chemical Research Laboratory, Teddington, who developed this method for polymerizations at atmospheric pressure.

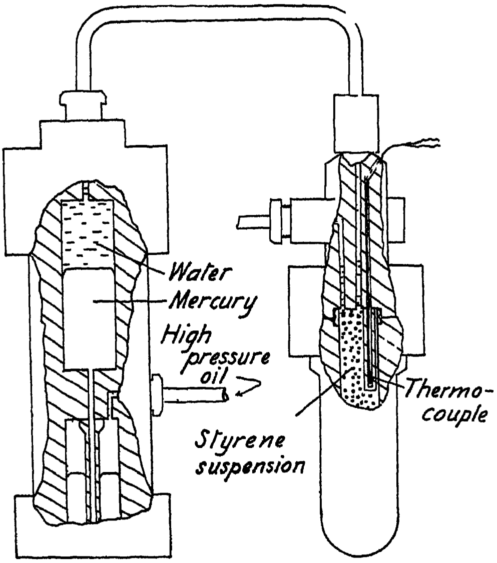

FIG. 3.

Results

The results of a few experiments at 100° C and 3,000, 2,000, 1,000 and 1 atm. using this technique are given in Table II, and Fig. 4.

TABLE II.—THE INCREASE IN RATE OF GRANULAR POLYMERIZATION AND MOLECULAR WEIGHT OF POLYMER WITH INCREASING PRESSURE

Temp. ° C	Pressure (atm.)	Maximum Rate (% Conversion/hr.)	-fold Increase over Rate at atm. Pressure	Viscosity of 0·1 % Chloroform Solution at 20° C	
				Conversion %	η_{sp}/c
100	1	2·5	1	69·5	1·71
				38·9	1·78
100	1,000	7·7	3·1	91·6	2·02
				38·9	1·96
100	2,000	16·0	6·4	75·1	2·04
				23·0	1·94
100	3,000	40·0	16	81·0	2·11
				73·9	2·10

As the value of the increase in rate at higher pressures is based on the rate at atmospheric pressure, this figure is very significant. The values obtained at 100° C agree reasonably well with values obtained by previous workers. For example, Mark and Raff [9] report a value of 2·39 % per hour for styrene polymerized in sealed tubes at 98·2° C. Schulz and Huseman [10] carrying out similar experiments obtained a figure of 3·03 % per hour at 100·5° C. Mayo and Gregg [11] report a rate of 2·23 % per hour for styrene polymerized at 100° C, yielding a polymer with a degree of polymerization of 4,030.

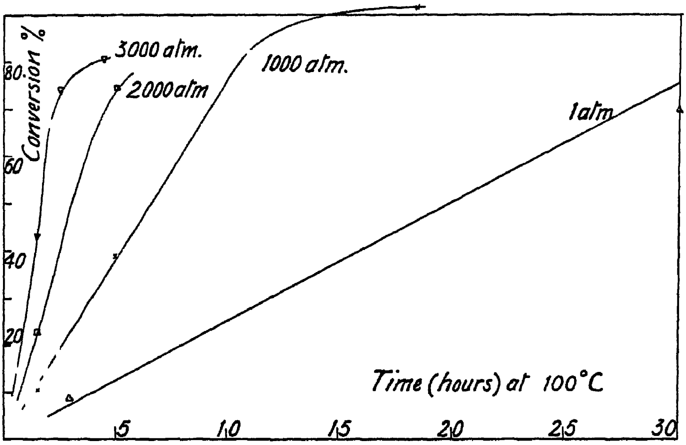

FIG. 4.

In putting forward an explanation of the effect of pressure on isoprene polymerization, Conant and Petersen [7] suggest the orientation of the molecules into more compact bundles, in which longer reaction chains would be propagated for each activation.

The rate of chain polymerization is given by $k_p m r$, where m and r are the monomer and free radical concentrations respectively. It has been suggested that the increase in rate of polymerization is partly due to the increase in monomer concentration brought about by the increase in density of the system, and partly by the effect of pressure on the velocity constant k_p. The increase in degree of polymerization or molecular weight can be explained by a similar process. For polymerization of a single monomer without transfer, the degree of polymerization K_0 in a steady state is given by

$$K_0 = \frac{\text{Rate of chain polymerization}}{\text{Rate of chain termination}}.$$

The smallness of the increase in degree of polymerization can, therefore, be partly explained by the corresponding increase in the value of the free radical term in the denominator.

This work was carried out in the laboratories of I.C.I. Plastics Division under the direction of Mr. H. J. Spencer Palmer whose assistance is gratefully acknowledged.

---

[9] Mark and Raff, *Z. Physik. Chem. B*, 1936, **31**, 275.
[10] Schulz and Huseman, *ibid.*, 1936, **34**, 187.
[11] Mayo and Gregg, *J. Amer. Chem. Soc.*, 1948, **70**, 284.

THE ADSORPTION OF GASES ON CALCIUM FLUORIDE

By V. A. Crawford and F. C. Tompkins

Received 16th January, 1950

Measurements of the adsorpton of SO_2, N_2O and CO_2 on CaF_2 crystals at various temperatures are given; these together with those already reported for the three gases and NH_3 on BaF_2 are considered in terms of the non-uniformity of the adsorbent surface. The validity of applying equations of state to adsorbed films and the concept of spreading pressures on non-uniform surfaces are discussed.

In a previous communication,[1] experimental values and theoretical calculations of the heat of adsorption and its variations with coverage of SO_2 (and other gases) on BaF_2 were reported. The decrease in heat with increasing amount adsorbed was attributed to (i) formation of multilayers, (ii) repulsion between similarly oriented dipoles, and (iii) the presence of three crystal planes, viz. (100), (110) and (111), having different adsorption potentials. It is now thought that the contributions from (i) and (ii) have been largely over-estimated. Thus Halsey [2] has shown that adsorption is mostly restricted to monolayers at all pressures (except at those approaching the saturation pressure of the liquid adsorbate) independent of the value of the parameter c in the B.E.T. equation; such a conclusion follows from the untenable assumption implicit in the deduction of the B.E.T. isotherm, that it is possible for a second molecule to be adsorbed on top of a *single* first-layer molecule with the full heat of liquefaction. Furthermore, our estimate of the repulsive contribution (ii) was too high since the mutual depolarizing influence of adsorbed polar molecules was neglected. We conclude therefore that the greater part of the observed decrease must be attributed to the effect of non-uniformity of the surfaces in addition to that arising from the presence of the different "ideal" planes already taken into account in (iii).

The problem of the *localized* adsorption of gases on non-uniform surfaces has been considered by Halsey and Taylor,[3] by Halsey,[2] and by Sips.[4] A more general approach to the problem shows that the procedure may be generalized provided that there is a wide distribution of adsorption sites.[5] In this circumstance the isotherm may then be largely characterized by the variation of heat with coverage.

In the present paper, some additional measurements of the adsorption of SO_2, N_2O and CO_2 on CaF_2 are given and these results, together with those already reported using BaF_2 as adsorbent, are considered in terms of the non-uniformity of the surface.

Experimental and Results

Calcium chloride was prepared by addition of slightly less than the stoichiometric quantity of conc. C.P. HCl to precipitated $CaCO_3$. After filtering and diluting the filtrate to M/10, the preparation of CaF_2 was similar to that of BaF_2. Details of the apparatus, procedure, etc., have been given in the previous paper.[1]

---

[1] Crawford and Tompkins, *Trans. Faraday Soc.*, 1948, **44**, 698.

[2] Halsey, *J. Chem. Physics*, 1948, **16**, 931.

[3] Halsey and Taylor, *ibid.*, 1947, **15**, 624.

[4] Sips, *ibid.*, 1948, **16**, 490.

[5] Tompkins (unpublished).

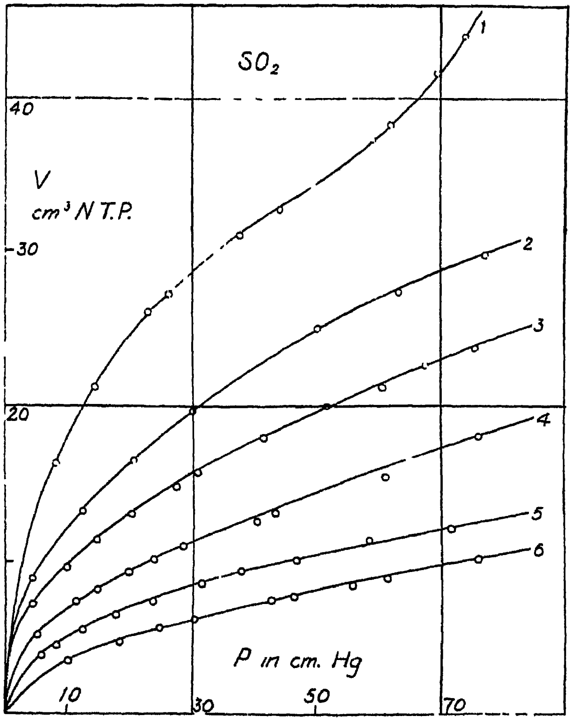

FIG. 1.—Adsorption of SO_2 on CaF_2.

Curve No. .	1	2	3	4	5	6
Temp. °C. .	0·0	19·1	32·9	55·9	74·9	98·5

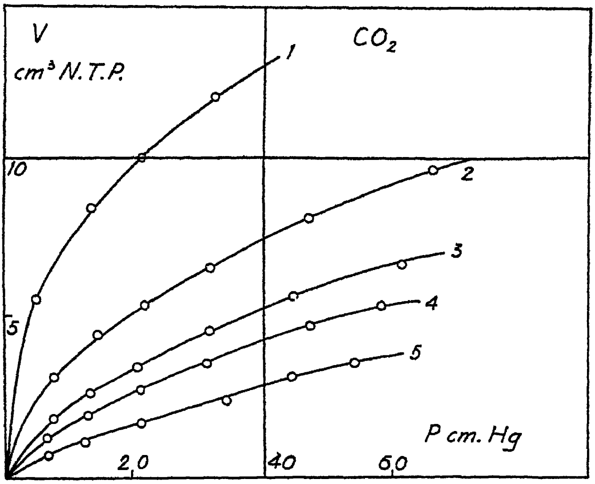

FIG. 2.—Adsorption of CO_2 on CaF_2.

Curve No. .	1	2	3	4	5
Temp. °C. .	—22·8	0·0	19·7	32·4	55·9

Fig. 1-3 summarize the amounts v of the various gases adsorbed at different temperatures. These have been corrected for adsorption on the glass walls

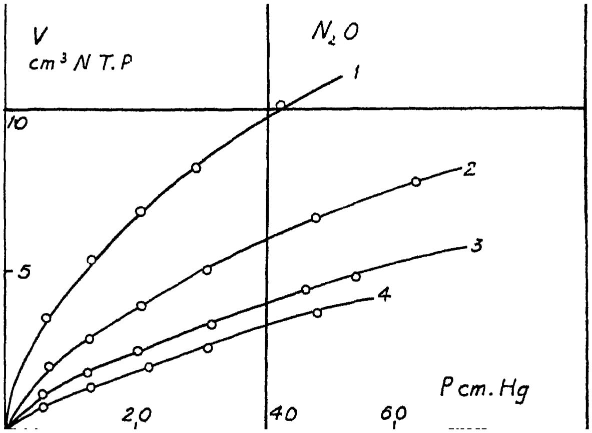

FIG. 3.—Adsorption of N_2O on CaF_2.

Curve No.	1	2	3	4
Temp. °C.	—22·8	0·0	19·4	35·5

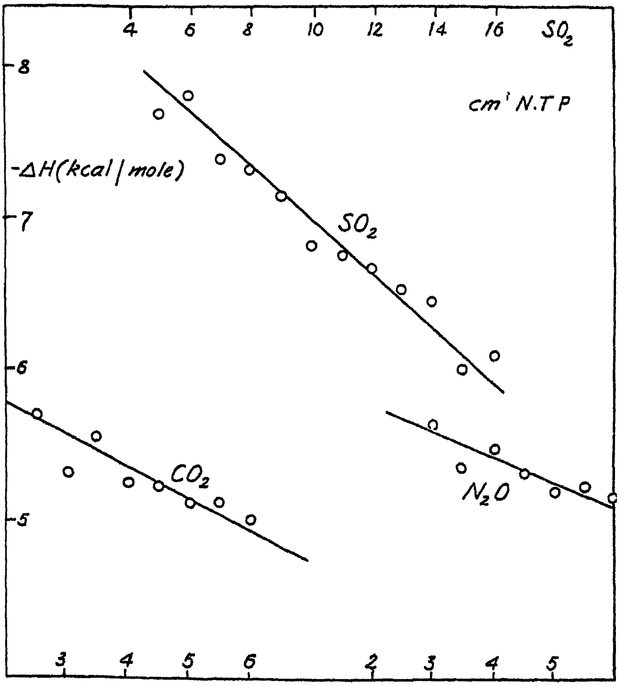

FIG. 4.—Variation of heats of adsorption with increasing v, averaged over the whole range of temperature.

and are expressed in cm.³ N.T.P.; equilibrium pressures p are given in units of cm. Hg. The accuracy of the v-values is better than 1 % at the lower p and 2 % at the highest p-value. The adsorption was reversible and complete within 3-4 min. of the admission of gas at all temperatures. There was definite evidence of chemical combination of NH_3 with CaF_2, as indicated by the occurrence of a rate process after the initial rapid adsorpton ; these results are therefore not considered here. Heats of adsorption in cal./mole adsorbate were calculated in the various temperature intervals from the Clausius-Clapeyron equation. The heat values decreased with increase of v for all gases but were sensibly independent of temperature. Fig. 4 is a plot of the heats as a function of v averaged over the whole temperature range for each adsorbate.

Discussion

In systems where lateral attractive interactions between the adsorbed molecules are small, the decrease in net free energy of adsorption $-\Delta G_n$, i.e. the free energy of transference of 1 mole from the bulk liquid adsorbate to the adsorbed phase, with amount adsorbed v can be expressed over a wide range in one of four ways, viz. :

(i) $-\Delta G_n$ is a linear function of v, or
(ii) of $\log v$;
(iii) $\log(-\Delta G_n)$ is a linear function of v, or
(iv) of $\log v$.

Since $$-\Delta G_n = RT \log p/p^\circ,$$

where p° = vapour pressure of liquid adsorbate at temperature T° K, this equation may be combined with (i)-(iv) to obtain relationship between the equilibrium pressure p and the amount adsorbed. Thus, we obtain (k_1, k_2, = constants) :

From (i), the Brunauer-Temkin isotherm or

$$\log p = k_1 v + k_2. \quad . \quad . \quad . \quad . \quad (1)$$

From (ii), the Freundlich isotherm or

$$\log p = k_1 \log v + k_2. \quad . \quad . \quad . \quad . \quad (2)$$

From (iii), the De Boer-Bradley-Palmer equation or

$$\log (RT \log p) = k_1 v + k_2. \quad . \quad . \quad . \quad (3)$$

From (iv), the Halsey " working isotherm " (k_1 variable), or the Harkins-Jura ($k_1 = -2$) equation, i.e.

$$\log (RT \log p) = k_1 \log v + k_2. \quad . \quad . \quad . \quad (4)$$

We note incidentally that both isotherms (3), and (4) with $k_1 = -2$, approximate to the B.E.T. equation over certain ranges of pressure.

Furthermore, if the amount adsorbed at different temperatures is expressed in units of volume at a standard temperature by equating the coefficient of expansion in the adsorbed layer to that of the bulk liquid adsorbate, then the entropy change accompanying the transfer of 1 mole of adsorbate from the liquid state to the adsorbed layer is often small compared with the average accuracy of adsorption heats. This is reasonably valid for non-uniform fine-grained surfaces having a random and wide distribution of adsorption sites.[5]

It follows (*a*) that in a first approximation the net free energy may be approximated to by the net heat of adsorption ($-\Delta H_n$) in such systems, (*b*) that there should be one characteristic curve for the relationship of $-\Delta G_n$ (or $-\Delta H_n$) with v independent of temperature for any particular system. Thus, it is generally found experimentally that the heat of adsorption is approximately temperature independent and there are many examples where $-\Delta H_n$ decreases with v in the manner described by eqn. (i)-(iv).*

If the decrease of heat with increase v is not large, function (iii) approximates to (i), i.e.

$$-\Delta H_n = -\Delta H_0 e^{-k_1 v} \rightarrow -\Delta H_0(1 - k_1 v) ;$$

---

* Cp. Brunauer, *The Physical Adsorption of Gases and Vapours* (O.U.P., 1943), p. 246.

similarly, (ii) and (iv) may be reduced to approximately equivalent forms for small variations of $-\Delta H_n$. Consequently it is often found that different isotherms describe the same experimental results equally well. If the $-\Delta H_n$ against v relationship is known, then in principle the distribution of adsorption sites on a non-uniform surface can be evaluated.

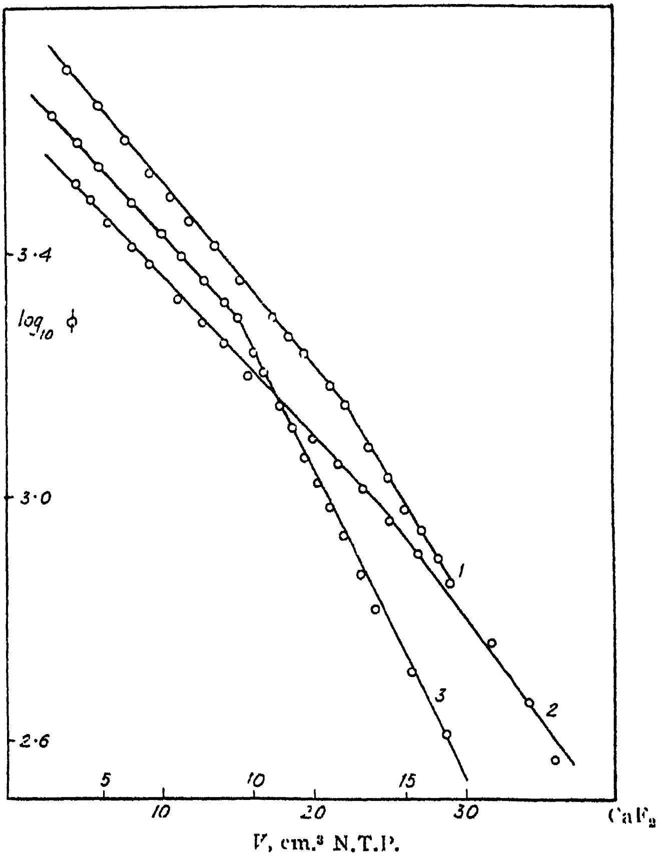

FIG. 5.—Test of Bradley-de Boer-Palmer equation ($\log \phi - V$).

Curve No. .	1	2	3
System .	NH_3—BaF_2	SO_2—CaF_2	SO_2—BaF_2

Thus an exponential distribution leads to the Freundlich equation, and a constant distribution to the Brunauer-Temkin isotherm ; unfortunately the distributions necessary to give isotherm (3) and (4) have, as yet, proved mathematically intractable. In other systems, however, where the entropy change is not negligible, the entropy can be an important factor in characterizing more exactly the isotherm.

An analysis of our results (Fig. 5 and 6) shows that the Bradley-de Boer-Palmer equation is most closely obeyed over the widest range pressures for SO_2 on CaF_2 and for SO_2 and NH_3 on BaF_2, whereas for the two non-polar gases on both CaF_2 and BaF_2 the Freundlich equation is the most satisfactory.

Now, if the non-uniformity of the solid adsorbent alone determines the distribution of sites then the same isotherm should be obeyed irrespective of the adsorbate. However, the nature of the adsorbate-adsorbent forces affects the distribution function. Thus, in the adsorption of a highly polar adsorbate where electrostatic forces predominate, the edges and corners of the crystal are low energy sites (high $-\Delta H$), whereas with non-polar gases dispersion forces are of prime importance and these positions correspond to high energy sites, and low adsorption potentials will be associated with cracks and re-entrant angles. Some such distinction as found above for polar and non-polar gases is therefore

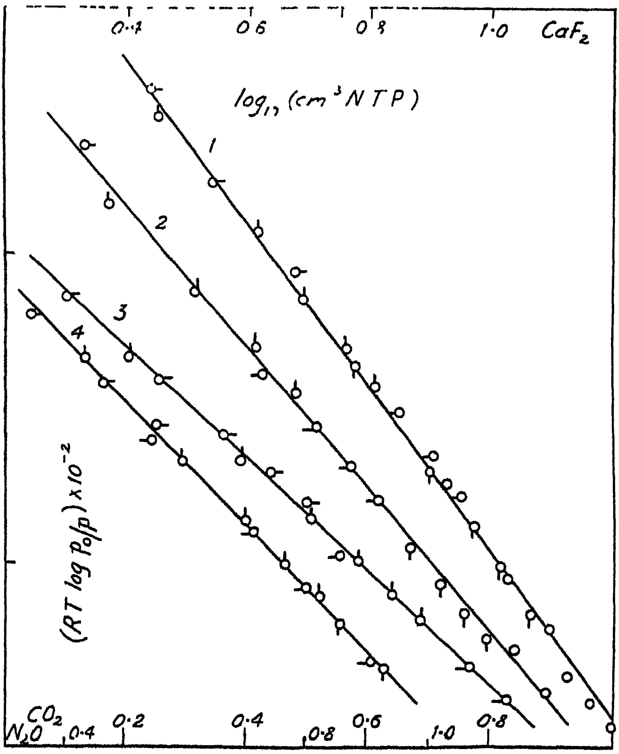

FIG. 6.—Test of Freundlich equation ($RT \log p_0/p - \log V$).

Curve No.	System.	
1	CO_2 –BaF_2	O– 55° C; –O 18·6° C; o —17·0° C. ⫰ 36° C; ⫯ 0·0° C;
2	CO_2—CaF_2	O– 55·0° C; –O 19·7° C; o —22·8° C. ⫰ 32·4° C; ⫯ 0·0° C;
3	N_2O—CaF_2	O– 19·4° C; –O —22·8° C. ⫰ 0·0° C;
4	N_2O—BaF_2	O– 23·7° C; –O —13·0° C ⫰ 0·0° C; ⫯ —22·8° C

expected. Further modification may arise by reason of interaction forces —thus, as in the present system, repulsive interaction between similarly oriented dipoles causes an increase in the adsorption potential of sites which are neighbours of occupied sites. Consequently, the distribution function evaluated from an experimentally determined isotherm refers to a distribution of "modified" sites, i.e., it also reflects the specificity of adsorbate-adsorbent forces and the effect of lateral interactions, and not solely the distribution of sites on the solid adsorbent. The calculations of Roberts[6] and of Miller[7] of the magnitude and variation of lateral interaction forces with coverage indicate that the contributions of these to the variation of heat is small, and that the specificity of adsorbate-adsorbent forces is the important factor.

The general theory from which equations (1), (2), (3) and (4) were derived is equally applicable to mono- or multilayer adsorption. However, at higher coverage the adsorbent sites become increasingly occupied and adsorption in the second layer commences, probably on triangular or square arrays of first-layer adsorbed molecules. Where there is marked difference between the average heat in the first layer and the heat of liquefaction of the adsorbate, then a distinguishable change in the distribution function is expected, and this will be reflected in the isotherm. It should be possible therefore to obtain some rough measure of the amount required to complete a " monolayer ".

In Fig. 5 are plotted the results for SO_2 on BaF_2 and on CaF_2 and for NH_3 on BaF_2 according to the De Boer-Bradley isotherm ; there is one characteristic curve independent of temperature indicating that the entropy term is small and that the net heat of adsorption is sensibly independent of temperature. The change of slope is associated with the change in the distribution function due to the production of first layer sites on which second layer adsorption is proceeding : this latter becomes marked only when the monolayer is nearly complete and thus the point of inflexion is an approximate measure of the amount present in the monolayer. The values are : 10 ml. for SO_2 on BaF_2 ; 13·5 ml. for NH_3 on BaF_2 ; and 23 ml. for SO_2 on CaF_2. These are to be compared with the average values obtained by use of the B.E.T. equation, viz.: 9·6 (SO_2), 10·5 (NH_3) for BaF_2 and 19·9 for CaF_2.

Now although the model on which the B.E.T. equation is based is unreal, the v values calculated from this equation agree well with other measurements using independent methods such as microscopic and electron microscopic examination, low-angle scattering of X-rays, and the use of Harkins-Jura method, etc. Emmett[8] has emphasized that the consistency is best with N_2 as adsorbate since its net heat of adsorption is sufficiently high to yield an isotherm with a pronounced " point B ", i.e. there is a marked diminution in the increase of amount adsorbed with increase of pressure at this point, which we interpret here as a marked change in the original distribution function. Many other gases have been used instead of nitrogen but the results yield areas which have to be multiplied quite arbitrarily by factors as high as 1·5 or in extreme cases by 2 or 3 ; in most of these systems there is no well-defined point B since the parameter c is low (less than 25), i.e. the net heat of adsorption is small. Apart from the criticism of Halsey on the basic postulates of the equation, it must be stressed that (i) physical adsorption is not completely localized even at − 192° C (another basic postulate of the theory) and (ii) even if it were, the lattice parameters of the adsorbent and not the molecular diameter of the adsorbate, should be used in the evaluation of surface areas. There are, in fact, so many untenable assumptions in the use of the B.E.T. equation, that consistency of v_m values calculated from the *equation* must be rather fortuitous. Values of v_m obtained from the use of point B have greater practical and theoretical significance but their absolute values may well be too high. Indeed, whenever there is a clearly defined point B, *any* multilayer theory gives v_m values in reasonable agreement with those derived from point B. This is because of the change in the distribution function leading to a much smaller increase in amount adsorbed (mainly in the second layer) as the pressure is increased. Thus, we may assume, with the authors of the B.E.T. equation, that a second-layer molecule on top of a first-layer molecule completely inhibits evaporation of the latter, or with Hüttig,[9] that evaporation of this molecule is not impeded, or even that there is a " liquid " monolayer and a simple Nernst distribution between gas and liquid phase is operative (i.e. Henry's law is obeyed in the higher layers), without materially altering the v_m values obtained. It is for this reason that we expect reasonable agreement between the amount adsorbed at the break in the De Boer-Bradley equation and point B since both indicate a change in a distribution function. Thus Brunauer has shown that point B and v_m values derived from the slope and intercept of the B.E.T. equation do not differ by more than 10 % : Ross[10] has likewise shown that v_m values derived from Hüttig's equation are normally within 10 % of the B.E.T. values, and the agreement here between point B and the inflection point in the De Boer-Bradley equation is of the same order.

---

[6] Roberts, *Some Problems in Adsorption* (C.U.P., 1939).

[7] Miller, *The Adsorption of Gases on Solids* (C.U.P., 1949).

[8] Emmett, *Adsorption and Kinetics of Heterogeneous Reactions* (Lyon, Sept., 1949).

The non-polar gases do not obey the De Boer-Bradley equation at low coverage but the Freundlich equation is well obeyed by both gases on both solids. The log plots at different temperatures when extrapolated to higher pressures intersect at some specific pressure (cp. [3]) but it must be stressed that there is no physical significance in the values of p or v at this intersection ; in particular, the v-value does not correspond to a saturated value because any individual $\log p - \log v$ plot has itself no saturation value except when p is infinity. This point of intersection is in fact a necessary corollary of the assumptions that the heat of adsorption is temperature independent and that the net entropy change is small at all temperatures. That these two assumptions are approximately valid is shown in Fig. 6 where it is shown that the $RT \log p_0/p - \log v$ plots for all temperatures fall on a single characteristic curve as the theory demands. Finally if the net heat of adsorption is large compared with that of liquefaction of the adsorbate, an inflection in the Freundlich plot corresponding to a change in the distribution function should be present. This certainly is the reason for the bending of the plot towards the pressure axis at high pressures normally found in such log plots. Unfortunately in the present measurements sufficiently high pressures have not been used, consequently evaluation of v_m values is not possible.

Where it is not possible to delineate isotherms at different temperatures by one characteristic curve, the marked divergences are a rough measure of the configurational entropy of the adsorbed layer ; this latter is appreciable if there are extentive areas of surface having the same adsorption potential.[5] In the present systems, the adsorbent surface must therefore possess a wide distribution of sites and this is in accord with the fact that the adsorbents are highly insoluble and were precipitated in a colloidal state. Later ageing, although apparently improving the quality and transforming the precipitate to a more crystalline form, was not sufficient to produce large areas of uniform potential.

Equation of State of the Adsorbate.—Harkins and Jura[11] in a series of papers have followed Gregg[12] in employing the same empirical equations to describe the physical state of films on solid surfaces and of insoluble films on water. This coincidence, which is a mathematical one only, has led to the use of such terms as condensed, liquid-intermediate, liquid expanded, etc., to describe the physical state of particular films, the nature of which, however, appears to be uncertain.

Let us consider localized adsorption on a uniform surface. The concept of localization arises from the periodic nature of the surface due to the regular array of ions (atoms) comprising the solid. Apart from evaporation-condensation processes, adsorbed molecules will possess mobility in the adsorbed layer in the sense that they jump frequently from site to site. This process may be regarded from the kinetic viewpoint as being responsible for the so-called spreading pressure as measured by the effect of the bombardment by these molecules of a hypothetical barrier placed perpendicular to the surface. The spreading pressure must therefore be dependent on the depth of the potential well which constitutes the (Langmuir) site such that the deeper the well, the less the spreading pressure. In the limiting case, that of an immobile layer, the spreading pressure is zero. Since the depth of the well is in general related to the average adsorption potential at the surface, the spreading pressure is a function of the heat of adsorption. Thus, very approximately, if the potential barriers responsible for the localization of molecules (1) and (2) are U_1 and U_2, the ratio of the spreading pressures ϕ_1 and ϕ_2 per mole is

---

[9] Hüttig, *Monatsh.*, 1948, **78**, 177.

[10] Ross, *J. Physic. Chem.*, 1949, **53**, 383.

[11] Harkins and Jura, *J. Chem. Physics* from 1944 onwards.

[12] Gregg, *J. Chem. Soc.*, 1942, 696.

$$\phi_1/\phi_2 = \exp\,((-U_1 + U_2)/RT),$$

assuming the same number of molecules of (1) or (2) per unit area.

For non-localized adsorption on a uniform surface, the free energy of the adsorbed layer in the simplest case of physical significance can be written as

$$F = -NkT \log \frac{N}{(A - NB)a(T)} - NkT,$$

where $a(T)$ is the partition function of the adsorbed molecule, B has the significance of a co-area, and A = total area of adsorbent surface. On a non-uniform surface, the corresponding free energy will be

$$F = -\sum_i \left(N_ikT \log \left(\frac{N_i}{(A - \sum_i N_iB_i)a_i(T)}\right) - N_ikT\right),$$

where the subscripts refer to molecules adsorbed at sites distributed singly and randomwise having an adsorption potential χ_i.

The spreading pressure of gas molecules adsorbed on the ith sites will be

$$\phi_i = N_ikT/(A - \sum_i N_iB_i),$$

and the chemical potential

$$\mu_i = kT\left(\log \frac{N_i}{(A - \sum_i N_iB_i)a_i(T)} + \frac{N_iB_i}{A - \sum_i N_iB_i}\right).$$

At equilibrium, the chemical potential on all sites is the same and equal to the partial potential in the gas phase, viz., $kT \log Cp$ (where C is a constant for the system at a definite temperature, and p the equilibrium pressure); consequently with $A \gg N_iB_i$,

$$kT \log \frac{N_1}{a_1(T)} + B_1\phi_1 = kT \log \frac{N_2}{a_2(T)} + B_2\phi_2 \ldots .$$

The spreading pressure associated with a given adsorption potential is thus a function of $a_i(T)$ and B_i, where (on extracting the adsorption heat)

$$a_i(T) = j_i e^{-\chi_i/kT}.$$

Equating to the partial potential in the gas phase then

$$\log Cp = \log \frac{N_1}{a_1(T)} + \frac{B_1\phi_1}{kT} = \log \frac{N_2}{a_2(T)} + \frac{B_2\phi_2}{kT},$$

and the total number of molecules adsorbed at a pressure p is

$$N = \sum_i N_i - Cp \sum_i e^{-\frac{B_i\phi_i}{kT}} a_i(T),$$

or the concentration

$$\Gamma \quad \frac{Cp}{D} \sum_i e^{\;\frac{B_i\phi_i}{kT}} \; a_i(T),$$

where D is a conversion factor involving the area of the adsorbent surface and Γ is the term which appears in the Gibbs' equation and which is used in deriving the so-called spreading pressure as used by Gregg. Denoting this pressure by ϕ_G then

$$\phi_G = kT \int_0^P \frac{Cp}{D} \sum_i e^{-\frac{B_i\phi_i}{kT}} a_i(T) \, \mathrm{d} \log (p).$$

Physically ϕ_G is the spreading pressure which would exist if the same number of adsorbed molecules N, assumed freely mobile, was distributed over the same area, of uniform potential, but this average spreading pressure cannot, however, be evaluated *theoretically* without a knowledge of the distribution function of the sites. For any distribution (e.g. using an exponential one in the terminology of Halsey and Taylor i.e. $N_\chi = c^* e^{-\chi/\chi_m}$) the total number of adsorbed molecules at a given p and T is related to the adsorption potential and thus to some function involving χ_m, where χ_m is the energy at which the sites are a fraction 1/e of those covered when $\chi = 0$.

This is perhaps made more obvious by reversing the argument. Experimentally it is found that the Freundlich equation is well obeyed for the two non-polar gases and approximately so for the two polar gases at higher coverage. This equation, which may be derived for a non-uniform surface assuming a wide exponential distribution of sites both for localized and non-localized[5] adsorption, may be written in the form given by Halsey and Taylor,[3] i.e.

$$\log N/N_0 = (kT/\chi_m) \log p + \text{const.},$$

where for non-localized adsorption $\chi = 0$ is the value of the adsorption potential at the liquid adsorbate surface at the temperature T. Writing $\sigma = A/N$, with σ = average area occupied by an adsorbed molecule, and A = area of adsorbent surface, then

$$(kT \log p)_T = \chi_m \log \frac{A}{\sigma N_0} + \text{const.}$$

Introducing Gibbs' equation

$$\partial\phi_G = \partial\left(\frac{kT}{\sigma} \log p\right)_T,$$

then

$$\sigma\partial\phi_G = -\chi_m \, \partial\sigma/\sigma,$$

or

$$\phi_G = \chi_m/\sigma + \text{const.},$$

i.e. the plot of ϕ_G against $1/\sigma$ is linear of slope χ_m (cp. Fig. 7 for the four gases on BaF_2). There is no simple relationship between the average net heat of adsorption ($-\Delta H_n$) and χ_m. However, the value of χ_0, the net heat at zero coverage obtained by extrapolation using the Clausius equation and subtracting the heat of liquefaction of the adsorbate, is independent of the distribution of sites. Hence providing the equilibrium distance of the adsorbate molecule from the adsorbent surface is independent of χ, and the effect of lateral repulsive forces is not high, then

$$\chi_0/\chi_m = \text{constant}.$$

The values obtained for the two non-polar gases are

N_2O, 2·7 CO_2, 2·8,

and for the two polar gases, both on BaF_2,

SO_2, 3·5 NH_3, 3·7.

The agreement is good; the ratio should not be the same for the two types of gases since the sites of importance at low coverage for polar gases are different from those for non-polar gases; this difference will be mainly reflected in the x_0 values.

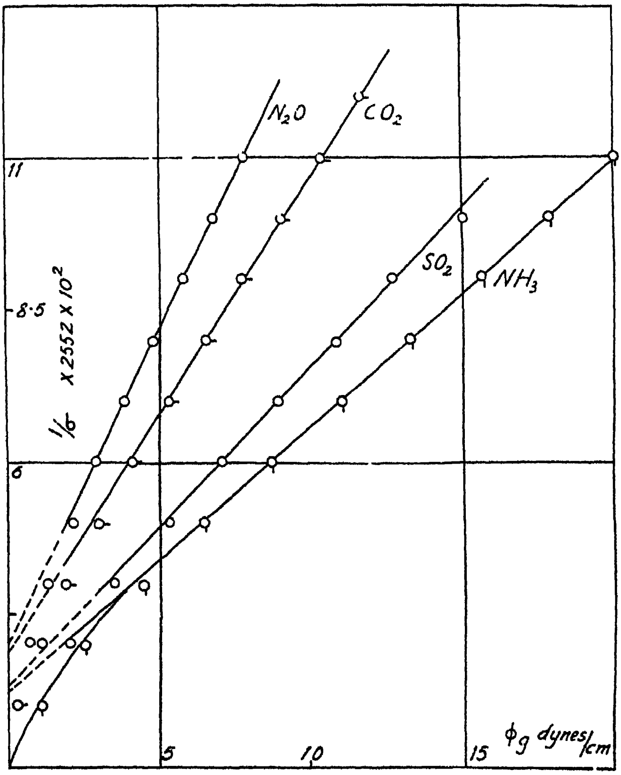

FIG. 7.—Test of $1/\sigma$—ϕ_g for the four gases on BaF_2.

It is seen that the ϕ_G—σ plots must involve the heat of adsorption as a parameter, whereas Harkins and Jura, and Gregg employ as the two variables only the limiting area of the molecule in the monolayer and the lateral cohesion between the adsorbed molecules. Furthermore, on non-uniform surfaces, it is difficult to accept the conclusions of Gregg in his later papers [18] in which the variation of compressibility of the surface layer (derived from the spreading pressure) is used as an indication of the existence of second- and third-order phase transitions.

Department of Chemistry,
Imperial College of Science and Technology,
London, S.W. 7.
and
Wheatstone Physics Laboratory,
King's College,
London, W.C. 1.

---

[18] Gregg and Maggs, *Trans. Faraday Soc.*, 1948, 44, 123.

REVIEWS OF BOOKS

Thermodynamics. By E. A. GUGGENHEIM. (North Holland Publishing Co., Amsterdam, 1949). Pp. xxiii + 395. Price 38s.

The announcement of a new book on thermodynamics by Guggenheim immediately raises the question of its relation to his earlier book published in 1933. In his preface to the latter, Donnan wrote: " I heartily commend Mr. Guggenheim's book to all students of physics and chemistry. They will find it an indispensable guide and lifelong friend, for age cannot wither the principles of thermodynamical science, enduring and incorruptible within their rightful domain." So many students have subsequently endorsed Donnan's remarks that the need for an entirely new book may not be obvious.

The answer to this query is that Guggenheim's new book really *is* new. Although naturally many subjects are discussed in essentially the same way as before, the approach differs in several important respects, and its scope is wider. It is specifically intended for both physicists and chemists, and therefore contains, in addition to very full accounts of the properties of solutions, chapters on electrostatic and magnetic systems, and on radiation. The most striking change made in the new book is in the prominent place now given to the statistical basis of thermodynamics. Chapter II is devoted to a " Digression on Statistical Mechanics ". This leads to the formulation of the third law of thermodynamics, which is then freely used throughout the book. All will welcome this new attempt by Guggenheim to bring to a wider range of readers the value of understanding the link between statistical mechanics and classical thermodynamics.

The book is described as " an advanced treatment " and is stated in the preface to be written for graduates. While it is doubtless true that no undergraduate could be expected to work through such a book, it should not be concluded that a previous knowledge of thermodynamics is assumed. On the contrary the basic principles of the science are very clearly discussed, and the argument of the book is logical and self-contained. Moreover, the author's style is, as always, a model of clarity, and the careful reader is left in no doubt as to the precise definition of the system under discussion and the nature of any approximations which may be introduced. As compared with its predecessor, the book contains an innovation in the shape of numerical illustrations of some of the mathematical results. Although still few in number, these have evidently been chosen with considerable care, and no attempt is made to provide lists of constants or numerical thermodynamic data. There are after all more appropriate sources of such material which will normally be in use alongside the textbook.

This is a book to be recommended without hesitation, and one likely to be extensively used as a standard text. Printing and binding are good, and the price does not appear excessive.

G. G.

Cosmic Radiation (COLSTON PAPERS BASED ON A SYMPOSIUM PROMOTED BY THE COLSTON RESEARCH SOCIETY AND THE UNIVERSITY OF BRISTOL, SEPTEMBER 1948). (London: Butterworth's Scientific Publications; New York: Interscience Publishers, Inc., 1949,) Pp. viii + 189. 25s. net.

This is a collection of some 30 papers on cosmic radiation; it is beautifully produced with that high standard of finish which we have been led to expect in work associated in one way or another with Prof. C. F. Powell. Although the flux of work on cosmic rays is perhaps at last beginning to crystallize it would still be dangerous and certainly invidious to select any one of these papers for special mention. It must suffice to say that brilliant contributions have come from France, Poland, Britain, America, Italy, Ireland, Denmark and Belgium. One notable feature is that attention has now begun to shift from the geophysical exploration of these radiations to the more fundamental question of the interactions of the radiations with atomic nuclei. In particular, the properties of the two well-established types of mesons and their interactions with matter are examined in both their experimental and theoretical aspects. It is a regrettable fact that it still appears to be true that what the gods give with one hand they take away with the other because the swift but sure way in which this field has been opened up by these brilliant contributors implies, in the words of the preface, that " In a subject which is evolving with such rapidity, it is perhaps inevitable that a published volume will soon become of little more than historical interest ".

F. C. C.

Gmelins Handbuch der anorganischen Chemie, 8th Ed. (System-Nummer 10, Selen, Teil B; Die Verbindungen des Selens.)

A volume covering part of the chemistry of selenium has been published as part of the eighth edition of Gmelin's *Handbuch der anorganischen Chemie* and should prove of real value to those chemists interested in this branch of the subject. Past editions of the work have provided a mine of useful and readily available information for teachers and research workers who need a first reference. The present volume which provides references up to the end of 1947 should prove just as useful.

The scheme of presentation adopted is that of employing major and sub-headings and dividing up the subject-matter into short paragraphs with references in the body of the text. It covers the chemistry of the compounds of selenium with hydrogen, oxygen, nitrogen, the halogens, and sulphur. Though brief, the treatment of these subjects is comprehensive. Thus under the heading *Selen und Wasserstoff* an excellent summary of the chemistry of hydrogen selenide is first given followed by an account of recent researches on the deuterium selenides and hydrogen perselenide. Where the literature is known to the reviewer it appears to be fully covered and this would seem to be true of all sections.

P. L. R.

THE ELEMENTARY THEORY OF THERMAL DIFFUSION

By E. Whalley * and E. R. S. Winter

Received 1st *August*, 1949

Fürth's elementary treatment of thermal diffusion has been applied to mixtures of elastic sphere gases with the help of certain simple assumptions concerning the transfer of momentum in collisions between dissimilar molecules. The results are in satisfactory agreement with the exact theory for elastic spheres except when the diameters and mass effects are in opposition with respect to thermal diffusion. In view of this agreement and the complexity of the exact theory of transport in multicomponent mixtures the elementary theory has been extended to such mixtures. The equations developed are comparatively simple and may be of value in a first analysis; they should give reasonable results if the masses and diameters act in the same direction.

The exact classical theory of transport phenomena in gases is extremely complex [1] and does not lead to any readily visualized physical interpretation of the processes occurring. Even the simplified treatment of Kennard[2] suffers from the same disadvantage. Fortunately, there are treatments of these phenomena available, which though approximate are comparatively simple and readily enable a visual picture of the phenomena to be obtained. The simplest of these is the familiar free-path theory, which is standard in texts on the kinetic theory of gases. Though free-path treatments of viscosity, thermal conductivity, and diffusion were given seventy years ago,[3] the rather more complex phenomena of thermal diffusion resisted attempts to formulate an elementary theory along the same lines [4] and it was not until 1939 that Gillespie,[5] using somewhat crude arguments, showed how thermal diffusion could be predicted in a simple manner; he assumed, however, that the free paths were the same for all molecules. In 1942 Fürth [6] gave a more elegant treatment and showed how the thermal diffusion ratio could be expressed in terms of the masses of the diffusing species and their free paths for the transfer of momentum and of number. He showed how the relations obtained were in qualitative agreement with observation and with the exact theory of Chapman and Enskog, but made no attempt to evaluate the free paths or to determine quantitatively the extent of the agreement between his treatment and the exact theory.

An alternative elementary approach to transport phenomena in gases, initiated by Stefan,[7] has been revived by Frankel [8] and been developed in detail by Cacciapuoti[9] and by Furry.[10] As pointed out by Furry this treatment is in some respects better than the mean free path treatment. Thus, for example, the coefficients of mutual diffusion of highly dissimilar molecules predicted by the Stefan-Frankel method are in much better agreement with the exact theory and with experiment than those predicted by the mean free path method. However, the theory is rather more complex than the free path theory.

---

* Present address: Dept. of Chemistry and Applied Chemistry, Royal Technical College, Salford.

[1] Chapman and Cowling, *Mathematical Theory of Non-Uniform Gases* (Cambridge, 1939).

[2] Kennard, *Kinetic Theory of Gases* (McGraw-Hill, 1938).

[3] See Meyer, *Kinetic Theory of Gases* (English translation, Longmans Green, 1899), or ref. 11.

[4] Chapman, *Phil. Mag.*, 1928, **5** (vii), 630.

[5] Gillespie, *J. Chem. Physics*, 1939, **7**, 530.

[6] Fürth, *Proc. Roy. Soc. A*, 1942, **179**, 461.

[7] Stefan, *Wein. Sitzungsber.*, 1872, **65**, 323.

[8] Frankel, *Physic. Rev.*, 1940, **57**, 660.

It is the purpose of this paper to show that Fürth's theory can be applied quantitatively to thermal diffusion in elastic sphere gases if certain simple assumptions are made concerning the transfer of momentum in collisions between dissimilar molecules. The results are in reasonably good agreement with the exact theory of Chapman and Enskog for elastic spheres, except when the diameters and mass effects are in opposition with respect to thermal diffusion. It is also shown that pressure diffusion follows from this treatment.

In view of the agreement obtained between the elementary and exact theories of thermal diffusion in binary mixtures, the elementary theory has been extended to diffusion in multicomponent mixtures. The exact theory of such systems is extremely complex,[17] and it is hoped that the elementary theory may be of value in a first analysis, provided that the masses and diameters act in the same direction, i.e. that the heavier molecules have the larger diameters.

It is important in considering the results given later to appreciate the difference between the mean free path and the exact treatments.

In the elementary kinetic theory of gases it is assumed that the gas is in a steady state and that the distribution of molecular velocities is that of Maxwell; from the theory one then calculates the transport properties by relatively simple dynamics based on the concept of the mean free path. In the Chapman-Enskog theory for non-uniform gases one uses a non-Maxwellian distribution which is derived by proper generalized summations of the equations resulting from consideration of a binary collision in the gas. These summations differ according to the molecular model used. From this more exact approach the equations for the transport properties follow directly without further appeal to the dynamics of molecular collisions. The Chapman-Enskog theory is the more correct but since we are here dealing with an unreal molecular model—the rigid elastic sphere—it is quite probable that in certain cases the free path approach may give the better agreement with observation. This is in fact the case, as is noted below.

Criticisms of the Mean Free Path Method.—The mean free path treatment of transport phenomena has been criticized on several grounds, particularly by Chapman[4] and by Furry.[10] As Chapman points out, if the gas is assumed to be at rest then the presence of a temperature gradient should lead to a pressure gradient, and it is necessary to introduce a small flow of gas to balance this effect. If it is legitimate to introduce this flow—and it readily follows from hydrodynamical considerations if the mean free path of the gas is much less than the diameter of the containing vessel—then the objection disappears. If the diameter of the vessel is such that hydrodynamical flow is impossible, i.e. if the diameter is much less than the mean free path, then a pressure gradient is set up as predicted, and the phenomenon is known as thermal transpiration.

A further criticism by Chapman is that values for the velocity of the flow mentioned above when deduced in two different ways are incompatible. This, however, is due to the use of the symbol w for two different quantities, that defined by Chapman's eqn. (7)[4] being a flow of mass, and that used in his eqn. (9), (10) and (13) being a linear velocity.

---

[9] Cacciapuoti, *Nuovo Cimento*, 1943, **1** (9), 126; *Brit. Abstr.*, 1944, **38**, 512.
[10] Furry, *Amer. J. Physics*, 1948, **16**, 63.

General Theory.—By applying Fürth's treatment to a mixture of s ideal gases of molar concentrations c_1, c_2, . . . c_s, and molecular masses m_1, m_2, . . . m_s, in which pressure and temperature gradients are maintained, we can readily show that the rate of mutual diffusion q_{12} of two gases (1) and (2) is given by

$$q_{12} = -\left(\frac{kT}{3}\right)^{\frac{1}{2}}\left\{\frac{l_1}{c_1 m_1^{\frac{1}{2}}} \cdot \operatorname{grad} c_1 - \frac{l_2}{c_2 m_2^{\frac{1}{2}}} \cdot \operatorname{grad} c_2\right)$$

$$-\left(\frac{l_1 - l_1'/2}{m_1^{\frac{1}{2}}} - \frac{l_2 - l_2'/2}{m_2^{\frac{1}{2}}}\right) \operatorname{grad} \ln T + \left(\frac{l_1}{m_1^{\frac{1}{2}}} - \frac{l_2}{m_2^{\frac{1}{2}}}\right) \operatorname{grad} \ln p\Big\}, \quad (1)$$

where l_1, l_2, . . . l_s, and l_1', l_2', . . . l_s', are the mean free paths for the transfer of number and of momentum respectively, p is the pressure, T the temperature, and k is Boltzmann's constant.

Evaluation of the Free Paths.—The free paths l and l' will differ mainly because of the different effects of the persistence of velocity after collision on number and momentum transfer. According to Jeans [11] the mean free path for number transfer in a gas composed of elastic spherical molecules (and the persistence concept is readily applicable only to such a gas) is given by

$$l_1 = \frac{}{\sum_{s} (1 - \theta_{1i}) n_i \sigma_{1i}^2 \sqrt{1 + \frac{m_1}{m_i}}},$$

where n_i is the number density of molecules (i), σ_{1i} is the mutual collision diameter for molecules (1) and (i) and θ_{1i} is the mean value of the persistence ratio for molecules (1) in collision with molecules (i) : the value of θ_{1i} is [1, 11]

$$\theta_{1i} = \tfrac{1}{2}M_{1i} - \tfrac{1}{2}M_{1i}^2 M_{i1}^{-\frac{1}{2}} \ln\left[(M_{i1}^{\frac{1}{2}} + 1)M_{1i}^{-\frac{1}{2}}\right], \quad . \quad . \quad (3)$$

where

$$M_{1i} = \frac{m_1}{m_1 + m_i}, \quad M_{i1} = \frac{m_i}{m_1 + m_i}. \quad . \quad . \quad . \quad (4)$$

The persistence ratio is defined as

$$\theta_{1i} = v_1/v_1^0$$

where v_1^0 is the velocity of a molecule (1) before collision with a molecule (i), and v_1 is the component of its velocity after collision, resolved along the direction of v_1^0.

Following Jean's treatment of the effect of persistence on momentum transfer we can show that

$$l_1' = \frac{1}{\pi \sum_{s} (1 - F_{1i}\theta_{1i}) n_i \sigma_{1i}^2 \sqrt{1 + \frac{m_1}{m_i}}}, \quad . \quad . \quad . \quad (5)$$

where F_{1i} is the mean fraction of the excess momentum of a molecule (1) which is not shared upon collision with a molecule (i). A rigorous evaluation of F_{1i} could undoubtedly be made along the lines adopted by Kuenen [12] in treating the viscosity of gas mixtures but the method is very involved and could not lead to completely accurate diffusion equations because of the approximations involved in the free path theory, and the analysis is not worth while. It would be of value, however, if we could obtain in a simple manner an approximate value for F_{1i}: values of the thermal diffusion ratio could then be calculated from truly elementary considerations.

[11] Jeans, *Kinetic Theory of Gases* (Cambridge, 1940).

[12] Kuenen, *Proc. Akad. Wetensch.*, 1914, **16**, 1162 ; 1915, **17**, 1068.

F will probably be a function of only the masses of the colliding molecules: we can guess at its form by considering the end and middle values of the function $F_{1i}\theta_{1i}$.

(i) As

$$m_1/m_i \to \infty, \quad F_{1i}\theta_{1i} \to 1,$$

since the motion of molecules (1) will be little effected by collisions.

(ii) Conversely as

$$m_1/m_i \to 0, \quad F_{1i}\theta_{1i} \to 0.$$

(iii) When $m_1/m_i = 1$ the assumption made by Jeans (ref. 11, p. 162) that the excess momentum above that appropriate to the point at which collision occurred is halved is most obvious, and gives good agreement with viscosity data. Thus as

$$m_1/m_i \to 1, \quad F_{1i} \to \tfrac{1}{2}.$$

The simplest value of F_{1i} which satisfies these conditions is

$$F_{1i} = \frac{m_1}{m_1 + m_i}. \quad . \quad . \quad . \quad . \quad . \quad (6)$$

For consistency, values of the σ_{ij}'s should be obtained from the free path formula for the coefficient of viscosity η which, corrected for persistence, is [11]

$$\eta = \frac{0{\cdot}401}{\pi\sigma^2}\left(\frac{3mkT}{2}\right)^{\frac{1}{2}} \quad (7)$$

From the measured value of η, the value of σ, the collision diameter for an encounter between two similar molecules, can be calculated. The value of σ_{ij} for use in eqn. (2) is then obtained from

$$\sigma_{ij} = \tfrac{1}{2}(\sigma_i + \sigma_j). \quad . \quad . \quad . \quad . \quad . \quad (8)$$

Binary Mixtures.—For mixtures of two kinds of molecules (1) and (2) we have

$$\text{grad } c_1 = -\text{grad } c_2, \quad . \quad . \quad . \quad . \quad . \quad (9)$$

and eqn. (1) reduces to

$$q_{12} = \frac{-D_{12}}{c_1c_1}(\text{grad } c_1 - k_T \text{ grad } \ln T + k_p \text{ grad } \ln p), \quad . \quad (10)$$

where

$$D_{12} = \left(\frac{kT}{3m_1m_2}\right)^{\frac{1}{2}}(l_1c_2m_2^{\frac{1}{2}} + l_2c_1m_1^{\frac{1}{2}}), \quad . \quad . \quad (11)$$

and is Meyer's equation for the coefficient of ordinary diffusion;

$$k_T = c_1c_2 \,.\, \frac{(l_1 - l_1'/2)m_2^{\frac{1}{2}} - (l_2 - l_2'/2)m_1^{\frac{1}{2}}}{l_1c_2m_2^{\frac{1}{2}} + l_2c_1m_1^{\frac{1}{2}}},$$

and

$$k_p = c_1c_2 \,.\, \frac{l_1m_2^{\frac{1}{2}} - l_2m_1^{\frac{1}{2}}}{l_1c_2m_2^{\frac{1}{2}} + l_2c_1m_1^{\frac{1}{2}}}, \quad . \quad . \quad . \quad (13)$$

k_T and k_p being known as the thermal and pressure diffusion ratios respectively. Eqn. (10) and (12) differ from those of Fürth in that k_T as here defined is the negative of Fürth's value. This is in accord with most of the recent discussions on thermal diffusion and has the advantage that molecules (1) are usually considered to be the lighter and thus k_T as defined above will usually be a positive quantity.

Eqn. (13) for the pressure diffusion ratio differs somewhat from that predicted by the exact theory, for which Chapman and Cowling (ref. 1, p. 244) give

$$k_p = c_1c_2 \,.\, \frac{m_2 - m_1}{c_2m_2 + c_1m_1}, \quad . \quad . \quad . \quad (14)$$

and should thus be independent of the molecular diameters. Since pressure diffusion is a rather unimportant phenomenon it will not be considered further.

The qualitative properties of the eqn. (12) have been discussed by Fürth.[6] To simplify the problem we consider the case where the differences between

$$2^{\frac{1}{2}}(1 - \theta_{11}),\ (1 + m_1/m_2)^{\frac{1}{2}}(1 - \theta_{12}),$$

and

$$(1 + m_2/m_1)^{\frac{1}{2}}(1 - \theta_{21}),$$

and between

$$2^{\frac{1}{2}}(1 - \tfrac{1}{2}\theta_{11}),\ (1 + m_1/m_2)^{\frac{1}{2}}\{1 - m_1\theta_{12}/(m_1 + m_2)\},$$

and

$$(1 + m_2/m_1)^{\frac{1}{2}}\{1 - m_2\theta_{21}/(m_1 + m_2)\},$$

are small enough to be negligible : this will be true to within about 10 % when the mass ratio is between about 0·7 and 1·4. By inserting these conditions into eqn. (2), (5) and (6) we justify Fürth's assumption that

$$l_1' = al_1, \quad l_2' = al_2 \quad . \quad . \quad . \quad . \quad (15)$$

the value of a being given by

$$a = \frac{1 - \theta_{11}}{1 - \frac{1}{2}\theta_{11}} = 0{\cdot}746. \quad . \quad . \quad . \quad . \quad (16)$$

Substitution of eqn. (15) into (12) gives [6]

$$k_T = c_1c_2(1 - a/2) \cdot \frac{a_1c_1 - a_2c_2}{b_1c_1^2 + b_2c_2^2 + b_{12}c_1c_2}, \quad . \quad . \quad (17)$$

where

$$a_1 = m_2^{\frac{1}{2}}\sigma_{12}^2 - m_1^{\frac{1}{2}}\sigma_1^2 ; \quad a_2 = m_1^{\frac{1}{2}}\sigma_{12}^2 - m_2^{\frac{1}{2}}\sigma_2^2, \quad . \quad (18)$$

$$b_1 = m_1^{\frac{1}{2}}\sigma_{12} ; \quad b_2 = m_2^{\frac{1}{2}}\sigma_2^2 ; \quad b_{12} = (m_1^{\frac{1}{2}} + m_2^{\frac{1}{2}})\sigma_{12}^2. \quad . \quad (19)$$

The qualitative properties of eqn. (17)-(19) have been discussed by Fürth.

Mixtures of Different Gases.—Values of k_T predicted by eqn. (2)-(5), (12) have been calculated for the following gas mixtures: hydrogen-helium, hydrogen-nitrogen, helium-neon, neon-ammonia, neon-argon, and nitrogen-carbon dioxide. The viscosity data used in calculating the diameters were those quoted by Chapman and Cowling (ref. 1, p. 229) for 0° C. The values of k_T predicted by both the Chapman-Enskog (elastic sphere) and the elementary theories for 0° C for mixtures of hydrogen-nitrogen, helium-neon, neon-argon, and nitrogen-carbon dioxide are plotted in Fig. 1. The full lines represent the predictions of the elementary theory and the broken lines represent the predictions of the exact theory for elastic spherical molecules.

The agreement with the exact theory is very satisfactory for mixtures of hydrogen-nitrogen, nitrogen-carbon dioxide, and neon-argon. For helium-neon, the elementary theory predicts values of k_T which are substantially less than those of the Chapman-Enskog theory, values which, in fact, are in considerably better agreement with the experimental data. Agreement is not nearly so good for hydrogen-helium and ammonia-neon mixtures as shown in Table I. The exact value of k_T for ammonia-neon was calculated from the equation,

$$k_T = -\frac{0{\cdot}0216\, c_1 + 0{\cdot}0312\, c_2}{4{\cdot}110\, c_1/c_2 + 1{\cdot}613\, c_1/c_2 + 1{\cdot}514},$$

obtained by substituting the masses and diameters into the Chapman-Enskog equation (ref. 1, p. 229) ; the subscript 1 refers, as usual, to the lighter molecule. It should be noted, however, that in both instances the heavier molecule has the smaller diameter, hence the mass and diameter effects are in opposition with respect to thermal diffusion, so that the error involved in the correction for persistence would have a larger relative effect than when the masses and diameter reinforce each other.

TABLE I.—THERMAL DIFFUSION IN H_2—He AND NH_3—Ne

Gas Mixture	k_T at $c_1 = c_2 = 0{\cdot}5$	
	Elementary	Exact
H_2—He	$-\,0{\cdot}009$	$+\,0{\cdot}0602$ [13]
NH_3—Ne	$-\,0{\cdot}071$	$-\,0{\cdot}00365$

Experimental values of k_T are all less than those predicted by both the elementary and exact theories for elastic spheres and show a considerable temperature dependence which cannot be accommodated in either theory.

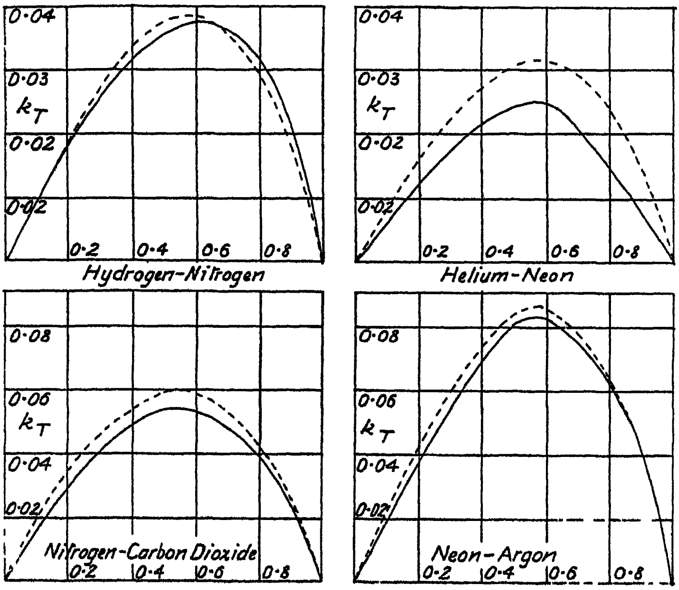

FIG. 1.—Thermal diffusion in gas mixtures.
Elementary theory ——; exact theory - - .

Mixtures of Isotopes.—If the diameters of the constituents of the mixtures are equal and the masses close enough for the approximations of eqn. (15) to be valid, then from (17)-(19) the thermal diffusion constant α, defined by

$$k_T = c_1 c_2 \alpha, \quad . \quad . \quad . \quad . \quad . \quad . \quad (21)$$

is given by

$$\alpha = 0{\cdot}627\,\frac{\sqrt{m_2} - \sqrt{m_1}}{c_2\sqrt{m_2} + c_1\sqrt{m_1}}, \quad . \quad . \quad . \quad . \quad (22)$$

which can be compared with the first approximation to the exact value [14]

$$\alpha = \frac{105}{118}\,\frac{m_2 - m_1}{m_2 + m_1}. \quad . \quad . \quad . \quad . \quad . \quad (23)$$

[13] Heath, Ibbs and Wild, *Proc. Roy. Soc. A*, 1941, **178**, 380.

[14] Furry, Jones and Onsager, *Physic. Rev.*, 1939, **55**, 1083.

The small concentration dependence of (22) is not incompatible with the exact theory as further approximations do indicate a small concentration dependence.[15]

If we neglect this small concentration dependence of α then the ratio of the elementary to the exact values of α, which we can denote by R_T, can be written

$$R_T = 1{\cdot}41 \frac{m_2 + m_1}{(\sqrt{m_2} + \sqrt{m_1})^2} . \qquad . \qquad . \qquad . \qquad (24)$$

For approximate purposes we can neglect the difference between $m_2 + m_1$ and $2m_1$ and eqn. (24) then becomes

$$R_T \cong 0{\cdot}70 . \qquad . \qquad . \qquad . \qquad . \qquad . \qquad (25)$$

Thus the elementary theory predicts values of α for isotopes which are considerably lower than the exact theory for elastic spheres and are in better agreement with experimental data.[16]

This is paralleled by the better agreement with experiment obtained [20] for the self-diffusion coefficient D_{11} using the mean free path theory, which predicts the relationship

$$D_{11} = 1{\cdot}34\ \eta/\rho,$$

while the exact theory predicts

$$D_{11} = 1{\cdot}2\ \eta/\rho.$$

In these equations η is the viscosity and ρ the density of the gas.

According to Jeans (ref. 11, p. 217) : " This suggests that for ordinary natural molecules the two simple theories (Meyer and Stefan-Maxwell) may represent the processes at work with as great an accuracy as the more elaborate theories of Chapman and Enskog, so long as we remain in ignorance of the exact molecular structure which ought to be assumed in the latter."

These remarks may also apply to thermal diffusion, but it should be noted that not all gas properties are better represented by the mean free path theory. Thus the coefficient of thermal conductivity K for molecules which possess no internal degree of freedom, is much better represented (ref. 1, p. 241) by the exact theory expression,

$$K = 2{\cdot}5\ \eta C_v,$$

than by the result of the mean free path theory,

$$K = 1{\cdot}6\ \eta C_v.$$

where C_v is the specific heat at constant volume.

We may conclude that the better agreement with experiment found by using the elementary theory for D_{11} and k_T has no fundamental significance since in any case we are here concerned with an unreal molecular model.

Multicomponent Mixtures.—The general theory of transport in multicomponent gaseous systems has been treated by Hellund and Uehling.[17] The equations they obtained, however, are very complex and it seems worth while in view of the agreement of the elementary theory of thermal diffusion with the exact theory, to apply the elementary theory to multicomponent systems. It would be expected that the equations obtained would indicate the general nature of the phenomena and might be useful in a first analysis of thermal diffusion in such a system.

---

[15] Chapman, *Proc. Roy. Soc. A*, 1940, **177**, 38.

[16] See, for example, Nier, *Physic. Rev.*, 1939, **56**, 1009 ; Grew, *Proc. Roy. Soc. A*, 1941, **178**, 390 ; Stier, *Physic. Rev.*, 1942, **62**, 548 ; Watson and Woernley, *ibid.*, 1943, **63**, 181 ; Murphey, *ibid.*, 1947, **72**, 834 ; Mann, *ibid.*, 1948, **73**, 412 ; Whalley and Winter, *Trans. Faraday Soc.*, 1949, **45**, 1085.

[17] Hellund and Uehling, *Physic. Rev.*, 1939, **56**, 818 ; Hellund, *ibid.*, 1940, **57**, 319, 328 ; Curtiss and Hirschfelder, *J. Chem. Physics*, 1949, **17**, 550.

For diffusion and thermal diffusion in a mixture of s ideal gases we have the $s - 1$ independent equations (1):

$$\left.\begin{aligned} q_{12} &= -\sqrt{\frac{kT}{3}}(\zeta_1 \text{ grad } c_1 - \zeta_2 \text{ grad } c_2 - \xi_{12} \text{ grad } \ln T), \\ q_{13} &= -\sqrt{\frac{kT}{3}}(\zeta_1 \text{ grad } c_1 - \zeta_3 \text{ grad } c_3 - \xi_{13} \text{ grad } \ln T), \\ &\ldots\ldots\ldots\ldots\ldots\ldots \\ q_{1s} &= -\sqrt{\frac{kT}{3}}(\zeta_1 \text{ grad } c_1 - \zeta_s \text{ grad } c_s - \xi_{1s} \text{ grad } \ln T), \end{aligned}\right\} \qquad (26)$$

where

$$\zeta_i = l_i/c_i\sqrt{m_i}, \qquad . \quad . \quad . \quad . \quad \text{(27}$$

$$\xi_{ij} = \frac{l_i - l_i'/2}{\sqrt{m_i}} - \frac{l_j - l_j'/2}{\sqrt{m_j}}, \qquad . \quad . \quad . \quad (28)$$

and by definition,

$$\sum_s \text{grad } c_i = 0. \qquad . \quad . \quad . \quad . \quad . \quad (29)$$

At equilibrium eqn. (26) equal zero, and under these conditions the solution of (26), (29) is

$$\text{grad } c_1 = \frac{\sum\limits_s \left[\xi_{ij} \prod\limits_s \zeta_j\right]}{\sum\limits_s \left[\prod\limits_s \zeta_j\right]} \text{ grad } \ln T. \qquad \begin{matrix} j \neq 1, i \\ \\ j \neq i \end{matrix} \qquad . \quad . \quad (30)$$

Mixtures of Isotopes.—For mixtures of isotopes eqn. (30) can be considerably simplified since, as for binary mixtures

$$l_1' = l_2' = \ldots = l_s' = al_1 = al_2 = \ldots = al_s. \qquad . \quad (31)$$

With this substitution, (30) reduces to

$$\text{grad } c_1 = \left(1 - \frac{a}{2}\right) \frac{\sum c_1 c_i(\sqrt{m_i} - \sqrt{m_1})}{\sum c_i\sqrt{m_i}} \text{ grad } \ln T. \qquad . \quad (32)$$

Since the masses are not very different we can put

$$\sum c_i\sqrt{m_i} = \sqrt{m}, \qquad . \quad . \quad . \quad . \quad (33)$$

where m is the mean mass, and (32) then becomes

$$\text{grad } \ln c_1 = \sum c_i \alpha_{1i} \text{ grad } \ln T, \qquad . \quad . \quad . \quad (34)$$

where

$$\alpha_{1i} = \left(1 - \frac{a}{2}\right) \frac{\sqrt{m_i} - \sqrt{m_1}}{\sqrt{m}}, \qquad . \quad . \quad . \quad . \quad (35)$$

and is identical with the thermal diffusion constant for a binary mixture of molecules (1) and (2) given by eqn. (22). Eqn. (34) is exactly similar to that given by Jones [18] obtained by specialization of the exact theory of multicomponent mixtures of Hellund.[17]

---

[18] Jones, *Physic. Rev.*, 1941, 59, 1019.

Ternary Mixtures.—If $s = 3$, eqn. (30) reduces to

$$\text{grad } c_1 = \frac{A_{12}c_1c_2 + A_{13}c_1c_3}{B_1c_1 + B_2c_2 + B_3c_3} \cdot \text{grad ln } T, \quad . \quad . \quad (36)$$

where

$$A_{12} = l_3\{(l_1 - l_1'/2)m_3^{\frac{1}{2}} - (l_2 - l_2'/2)m_1^{\frac{1}{2}}\}; \quad . \quad . \quad (37)$$

$$A_{13} = l_2\{(l_1 - l_1'/2)m_3^{\frac{1}{2}} - (l_3 - l_3'/2)m_1^{\frac{1}{2}}\}$$

$$B_1 = l_2l_3m_1^{\frac{1}{2}}; \quad B_2 = l_1l_3m_2^{\frac{1}{2}}; \quad B_3 = l_1l_2m_3^{\frac{1}{2}}. \quad . \quad . \quad (38)$$

When $c_3 = 0$, eqn. (36)-(38) reduce to (12) for binary mixtures.

If as previously we can neglect the difference between

$$2^{\frac{1}{2}}(1 - \theta_{11}), \quad (1 + m_1/m_2)^{\frac{1}{2}}(1 - \theta_{12}), \quad (1 + m_2/m_1)^{\frac{1}{2}}(1 - \theta_{21}), \text{ etc.},$$

and between

$$2^{\frac{1}{2}}(1 - \tfrac{1}{2}\theta_{11}), \ (1 + m_1/m_2)^{\frac{1}{2}}\{1 - m_1\theta_{12}/(m_1 + m_2)\}$$

$$(1 + m_2/m_1)^{\frac{1}{2}}\{1 - m_2\theta_{21}/(m_1 + m_2)\} \text{ etc.},$$

eqn. (36)-(38) can be put in the form

$$\text{grad } c_1 = \left(1 - \frac{a}{2}\right)$$

$$\frac{c_1c_2\{[a_{12}]_1c_1 - [a_{12}]_2c_2\} + c_1c_3\{[a_{13}]_1c_1 - [a_{13}]_2c_3\} + c_1c_2c_3d_1}{b_1c_1^2 + b_2c_2^2 + b_3c_3^2 + b_{12}c_1c_2 + b_{13}c_1c_3 + b_{23}c_2c_3} \cdot \text{grad ln } T \quad (39)$$

where the a's and b's are the same as those of eqn. (18), (19) for binary diffusion, thus

$$[a_{ij}]_1 = m_j^{\frac{1}{2}}\sigma_{ij}^2 - m_i^{\frac{1}{2}}\sigma_i^2, \quad [a_{ij}]_2 = m_i^{\frac{1}{2}}\sigma_{ij}^2 - m_j^{\frac{1}{2}}\sigma_j^2, \quad . \quad (40)$$

$$b_i = \sqrt{m_i}\sigma_i^2, \quad b_{ij} = (\sqrt{m_i} + \sqrt{m_j})\sigma_{ij}^2, \quad . \quad . \quad (41)$$

and d_1 is given by

$$d_1 = \sqrt{m_1}(\sigma_{12}^2 + \sigma_{13}^2) - \sigma_{23}^2(\sqrt{m_2} + \sqrt{m_3}). \quad . \quad . \quad (42)$$

The effect of the addition of a third gas on the separation of two gases by thermal diffusion is most conveniently studied for the separation of two isotopes in the presence of the third gas.

Mixtures of Two Isotopes in the Presence of a Third Gas.—This system is of interest in that thermal diffusion is used extensively for separating isotopes, and it is of value to determine whether the separation may be increased by the addition of a third gas. That the separation may be increased is indicated by the very approximate treatment of Gillespie,[5] but these predictions cannot be taken as quantitatively reliable. The exact theory of ternary mixtures [17] is very complex and it is difficult to draw general conclusions; numerical calculations were reported only for the separation of hydrogen and deuterium in the presence of helium, in which case the separation *decreased* by 59 % as the concentration of helium increased from zero to unity.

We consider for simplicity the limiting case as $c_3 \rightarrow 1$; (1) and (2) referring to the isotopes and (3) to the third gas. Under these conditions we find from (36)

$$\lim_{c_3 \rightarrow 1} \text{grad ln } c_1/c_2 = \left(1 - \frac{a}{2}\right)\frac{l_3^{(3)}(\sqrt{m_2} - \sqrt{m_1})}{l_1^{(3)}\sqrt{m_3}} \text{ grad ln } T, \quad . \quad (43)$$

where the superscript (3) indicates that the value of the quantity concerned is the limiting value as $c_3 \rightarrow 1$. Following Hellund we define the quantity

$$\Delta_{12} = \frac{\text{grad ln } c_1/c_2}{(\text{grad ln } c_1/c_2)_{c_3 = 0}} \quad . \quad . \quad . \quad . \quad (44)$$

For a binary mixture we have

$$\text{grad } c_1 = c_1 c_2 \alpha \text{ grad ln } T,$$
$$\text{grad } c_2 = - c_1 c_2 \alpha \text{ grad ln } T, \quad . \quad . \quad . \quad (45)$$

and by combining these with eqn. (22) we obtain

$$\text{grad ln } c_1/c_2 = \left(1 - \frac{a}{2}\right) . \frac{m_2^{\frac{1}{2}} - m_1^{\frac{1}{2}}}{m_1^{\frac{1}{2}}} \text{ grad ln } T. \quad . \quad . \quad (46)$$

From (43), (44) and (46)

$$\lim_{c_3 \to 1} \Delta_{12} = \frac{l_3^{(3)}}{l_1^{(3)}} . \left(\frac{m_1}{m_3}\right)^{\frac{1}{2}}, \quad . \quad . \quad . \quad . \quad (47)$$

or in terms of the masses and diameters

$$\lim_{c_3 \to 1} \Delta_{12} = \frac{\sigma_{13}^2(1 - \theta_{13})}{\sigma_3^2(1 - \theta_{11})} \left\{\frac{m_1(m_1 + m_3)}{2m_3^2}\right\}^{\frac{1}{2}}. \quad . \quad . \quad (48)$$

If $m_1 < m_3$ and $\sigma_1 < \sigma_3$, then $\Delta_{12} < 1$, and conversely, if $m_1 > m_3$ and $\sigma_1 > \sigma_3$, then $\Delta_{12} > 1$. Thus the separation of two isotopes can be increased by the addition of a lighter gas, or of a gas consisting of smaller molecules, and conversely the separation will be decreased by the addition of a heavier gas, or a gas consisting of larger molecules.

As numerical examples we consider the effect of helium on the separation of the neon isotopes, and of neon on the separation of the helium isotopes. For the former case we find

$$\lim_{c_3 \to 1} \Delta_{12} = 1{\cdot}77, \quad . \quad . \quad . \quad . \quad (49)$$

and for the latter

$$\lim_{c_3 \to 1} \Delta_{12} = 0{\cdot}427. \quad . \quad . \quad . \quad . \quad (50)$$

These values will not be exact but will probably indicate the order of magnitude of the effect, which is thus not very large.

No detailed experimental work on thermal diffusion in multicomponent mixtures has been published, but Chipman and Dastur [19] have reported the effect of the addition of a third (inert) gas to the steam-hydrogen mixture on the apparent equilibrium constant of the system

$$H_2(g) + O \text{ (in Fe)} \rightleftharpoons H_2O(g).$$

The results appear to be in qualitative agreement with the above equations, though it is difficult to draw sound quantitative conclusions from their work.

Thanks are due to the Department of Scientific and Industrial Research for a maintenance grant to one of us (E.W.).

Department of Inorganic and Physical Chemistry,
Imperial College,
London S.W.7.

---

[19] Chipman and Dastur, *J. Chem. Physics*, 1947, **16**, 637; *idem., Faraday Soc. Discussions*, 1949, **4**, 100.

[20] See Hutchinson, *Physic. Rev.*, 1947, **72**, 1256, for a summary of modern results.

THE INFRA-RED SPECTRA AND ASSIGNMENT OF THE FUNDAMENTAL FREQUENCIES OF THE ALKYL HALIDES

I. *tert.*-BUTYL HALIDES

By N. Sheppard

Received 21*st February*, 1950

The infra-red absorption spectra of *tert.*-butyl chloride, bromide and iodide have been obtained in the liquid state between 3500 and 450 cm.$^{-1}$. Nearly complete assignments have been made of the observed infra-red and previously published Raman frequencies to the normal modes of vibration of these molecules. Particular emphasis has been placed on the assignment of the frequencies of the *tert.*-butyl group between 1400 and 700 cm.$^{-1}$. Similar assignments have been given for the vibrational spectra of *tert.*-butyl mercaptan.

The identification of the fundamental modes of vibration of hydrocarbon groupings in different molecules is of considerable importance for the systematic interpretation of infra-red and Raman spectra. Studies have recently been made of the frequencies that can be assigned to ethyl [1] and *tert.*-butyl [2] groups in hydrocarbons. It seemed of value to undertake a similar investigation of the frequencies of these groups and of the *iso*propyl group in the alkyl halides. This communication presents the infra-red spectra of *tert.*-butyl chloride, bromide and iodide. Previously Lecomte[3a] has published the spectrum of *tert.*-butyl chloride in the form of a line diagram which seems to be in fair agreement with our results. Mortimer, Blodgett and Daniels [3b] have also studied the spectrum of *tert.*-butyl bromide between 700 and 500 cm.$^{-1}$. The Raman spectra have been available for some years,[4-8], the most recent work being that of Wagner [8] who made partial assignments from these data alone. Trotter and Thompson [9] have previously obtained the vapour-phase infra-red spectrum of *tert.*-butyl mercaptan, and its Raman spectrum has been observed by Kohlrausch and Koppl.[10] Because of its close spectral similarity to *tert.*-butyl chloride an attempt has been made to interpret the spectra of this compound also.

Experimental

The infra-red spectra between 3500 and 700 cm.$^{-1}$ were obtained using a model 12B Perkin Elmer spectrometer under standard conditions with a rock-salt prism as the dispersing element. The spectra between 700 and 450 cm.$^{-1}$ were investigated by means of a Hilger D209 spectrometer with a potassium bromide prism. The chemicals used were B.D.H. samples which were distilled shortly before taking the spectra. The *tert.*-butyl chloride and bromide boiled at 51° and 73° C respectively. The *tert.*-butyl iodide was distilled under reduced pressure. The substances were investigated in the liquid state using lead spacers between rocksalt or potassium bromide plates to form cells, the approximate thicknesses of which are given in Fig. 1.

---

[1] Sheppard, *J. Chem. Physics*, 1949, **17**, 74.

[2] Sheppard, *ibid.*, 1949, **17**, 455.

[3a] Lecomte, in *Traité de Chimie organique*, by Grignard and Baud (Masson, Paris, 1936), Vol. II, p. 190.

[3b] Mortimer, Blodgett and Daniels, *J. Amer. Chem. Soc.*, 1947, **69**, 822.

[4] Harkins and Haun, *ibid*, 1932, **54**, 3920.

[5] Dadieu, Kohlrausch and Pongratz, *Monatsh.*, 1932, **61**, 369.

[6] Harkins and Bowers, *Physic. Rev.*, 1931, **38**, 1845.

[7] Kahovec and Wagner, *Z. physik. Chem. B*, 1939, **42**, 123.

[8] Wagner, *ibid.*, 1940, **45**, 341.

[9] Trotter and Thompson, *J. Chem. Soc.*, 1946, 481.

[10] Kohlrausch and Koppl, *Monatsh.*, 1933, **63**, 255.

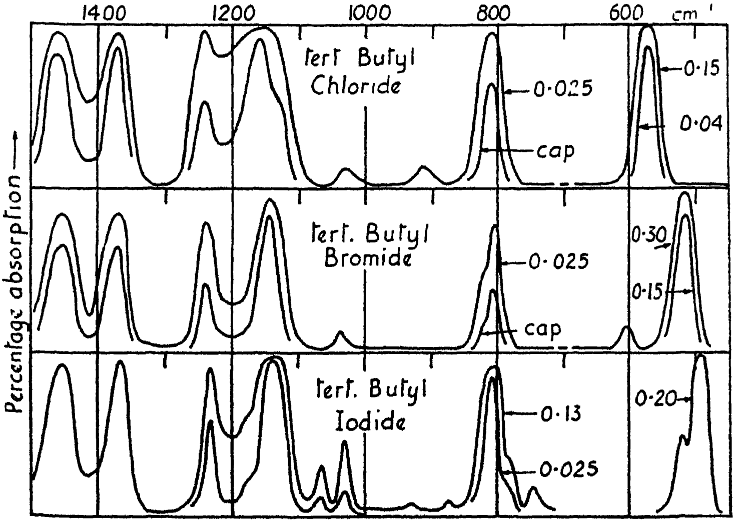

FIG. 1.—The infra-red spectra of *tert.*-butyl halides between 1500 and 450 cm.$^{-1}$: approximate thicknesses of liquid cells are given in mm. (cap.—capillary thickness).

Assignment of the Spectra. The *tert.*-butyl halides probably have C_{3v} symmetry and on this assumption the number and types of vibration of the different symmetry classes are those shown together with the selection rules in Table I. This Table has been drawn up on the generally accepted assumption that rotational isomerism does not occur in these molecules. It will be shown below that the spectra can be completely interpreted on this assumption.

TABLE I.—THE NUMBER, SYMMETRY TYPES, SELECTION RULES AND APPROXIMATE FREQUENCY RANGES FOR THE VIBRATIONS OF THE TERTIARY BUTYL HALIDES

Type of Vibration	A_1	A_2	E	Expected Frequency Range (cm.$^{-1}$)
CH_3 sym. stretching	1	—	1	*ca.* 2870
CH_3 asym. ,,	1	1	2	*ca.* 2960
CH_3 asym. deformation	1	1	2	*ca.* 1450
CH_3 sym. ,,	1	—	1	*ca.* 1375
C—C stretching	1	—	1	1300-700
CH_3 wagging	1	1	2	1300-700
C—X stretching	1	—	—	700-450
Skeletal deformation	1	—	3	<500
CH_3 restricted rotation	—	1	1	<300
Allowed in	I.R. & R(*p*)	—	I.R. & R(*dp*)	

I.R.—infra-red; R—Raman; *p*—polarized; *dp*—depolarized.

The C—C skeletal modes and the CH deformation vibrations occur at frequencies lower than 1500 cm.$^{-1}$. The C—C stretching and methyl wagging modes in particular overlap in the range 1300-700 cm.$^{-1}$ so that spectra observed in this region are usually very complex. From Table I it may be seen that the *tert.*-butyl halides should have ten fundamental allowed frequencies below 1300 cm.$^{-1}$. It has been found in practice that frequencies involving restricted rotation are very weak in both absorption and scattering spectra, so that nine Raman lines should be observed, of which four will be polarized. Just this number of frequencies is in fact found in the Raman spectrum of *tert.*-butyl chloride and bromide; with the chloride four of these are markedly polarized. The Raman spectrum of *tert.*-butyl iodide shows a few extra weak lines, but the nine Raman frequencies of the first two halides all have counterparts in the iodide spectrum. Furthermore, with one exception, all these frequencies of the three molecules are found in the infra-red spectra in the region investigated as shown in Fig. 1. It seems very probable that they are the expected fundamentals, and this assumption forms the basis of the assignment of the observed infra-red and Raman frequencies of these halides and of the mercaptan, shown in Table II, for this region of the spectrum.

The interpretation of the spectrum of *tert.*-butyl chloride as a typical member of the series will now be discussed in detail. For this molecule the two lowest polarized Raman frequencies at 570 and 372 cm.$^{-1}$ are clearly the C—Cl stretching and symmetrical skeletal deformation modes respectively. It remains to assign each of the polarized frequencies near 1156 and 811 cm.$^{-1}$ to either the remaining symmetrical C—C stretching or methyl wagging modes. The assignment given by Wagner [8] was based on a comparison of the calculated and observed skeletal modes of a series of molecules including *neo*pentane (tetramethyl methane) and *iso*butane as well as the *tert.*-butyl halides. The calculations showed that the triply degenerate C—C stretching vibration of *neo*pentane splits in the less symmetrical *tert.*-butyl halides to give a doubly degenerate vibration of about the same frequency and a symmetrical vibration at lower frequencies. At that time it was thought that the 921 cm.$^{-1}$ Raman line of *neo*pentane corresponded to the triply degenerate C—C stretching mode, so that Wagner assigned 811 cm.$^{-1}$ in the spectrum of *tert.*-butyl chloride to the symmetrical A_1 C—C stretching vibration, and 1156 cm.$^{-1}$ to the methyl wagging mode. More recently Simpson and Sutherland [12] have shown in a convincing manner that the triply degenerate C—C stretching mode in *neo*pentane lies at 1250 cm.$^{-1}$. It is thus much more reasonable to suggest that in *tert.*-butyl chloride the 1156 cm.$^{-1}$ frequency corresponds to the A_1 C—C vibration, and 811 cm.$^{-1}$ to the methyl wagging mode. Further, the depolarized Raman line at 1237 cm.$^{-1}$ may then be assigned to the degenerate C—C stretching mode.

These two C—C stretching frequencies together with the corresponding pairs for the bromide and iodide form a characteristic series of Raman lines which may now be successfully correlated with the spectra of *neo*pentane and *iso*butane. In the latter molecule Simpson and Sutherland [12] have assigned the 1172 cm.$^{-1}$ frequency to the C—C stretching mode. The pattern of lines of this group of molecules is in much better qualitative agreement with Wagner's calculations than the interpretation that he himself gives. Furthermore, it would be expected that the symmetrical C—C stretching mode of *tert.*-butyl chloride would be more affected than the methyl wagging mode by the change in the carbon-halogen stretching frequency on passing from one halide to the next. This is also in agreement with the above assignment.

The other two frequencies in this region of the spectrum (at *ca.* 918 and 1029 cm.$^{-1}$), which correspond to depolarized Raman lines, must be assigned to the remaining allowed doubly degenerate methyl wagging modes. As would be expected, these values are little changed in the various halides. The depolarized Raman lines at 406 and 304 cm.$^{-1}$ in the low frequency region are clearly the two doubly degenerate skeletal bending modes. The higher frequency fundamental of these two changes very little in value throughout the halides and can be regarded as mainly an internal mode of the *tert.*-butyl group, whereas the other two skeletal deformation modes are very considerably decreased in the bromide and iodide spectra and the vibrations probably involve more extensive changes in the $\mathrm{C}\diagup\overset{-}{}\diagdown\mathrm{X}$ angles. The assignments given above for *tert.*-butyl chloride in the region below 1300 cm.$^{-1}$ can be carried over in a straightforward manner for the other *tert.*-butyl halides. Every assigned fundamental

[11] Kohlrausch and Barnes, *Ann. Soc. Espan. Fis.-Quim.*, 1932, **30**, 732.

[12] Simpson and Sutherland, *Proc. Roy. Soc. A*, 1949, **199**, 169.

of the chloride has obvious counterparts in the observed frequencies of the bromide and iodide. The Raman spectrum of *tert.*-butyl mercaptan has been assigned in the same fashion, and because of the similar masses of the chlorine atom and mercaptan group there is a particularly close correspondence with the chloride spectra. An extra line at 2570 cm.$^{-1}$ in the mercaptan spectrum is the well-established SH stretching mode, and another line at 806 cm.$^{-1}$ has already been assigned [13] to the in-plane SH deformation frequency. The moderately strong 1177 cm.$^{-1}$ Raman frequency can probably be explained as the overtone of the C—S stretching mode, enhanced in intensity by Fermi resonance with the A_1 C—C stretching mode.

The other regions of the spectra can be assigned on lines previously well established though the overlap of neighbouring vibrations in CH stretching, CH_3 asymmetrical deformation, and CH_3 symmetrical deformation regions as given in Table I makes exact interpretation difficult. Suggested assignments in these regions of the spectrum are given in Table II. Frequencies which have to be assigned in a schematic manner because of overlapping are enclosed in brackets. In addition to the fundamentals assigned in Table II, each halide has three additional forbidden frequencies which are of the CH_3 asymmetrical stretching, CH_3 asymmetrical deformation, and CH_3 wagging types. These probably lie close to 2960, 1450 and 950 cm.$^{-1}$ respectively. The three degrees of freedom corresponding to restricted rotation of the methyl group cannot be assigned from the available experimental data.

There are several weak infra-red and Raman frequencies which have not been assigned to fundamentals in Table II but which can all be satisfactorily explained as overtone and combination bands involving the observed fundamentals. These interpretations are shown below where (R) denotes a Raman frequency and (I.R.) an infra-red frequency :—

tert.-Butyl chloride.

$2725 \equiv 2 \times 1361$ (R) ; $1130 \equiv 2 \times 570$ (I.R.) cm.$^{-1}$.

tert.-Butyl bromide.

$2723 \equiv 2 \times 1358$ (R) ; $814 \equiv 515 + 303$ (I.R.) ; $604 \equiv 2 \times 304$ (I.R.).

tert.-Butyl iodide.

$2711 \equiv 2 \times 1366$ (R) : $1300 \equiv 801 + 487$? (R) : $1177 \equiv 801 \equiv 386$ or $927 + 259$ (I.R. and R) ; $1066 \equiv 801 + 259$ (I.R.) ; $984 \equiv 2 \times 487$ (I.R.) ; $872 \equiv 487 + 386$ (I.R. ; $778 \equiv 2 \times 386$ (I.R.) ; $742 \equiv 487 + 259$ (I.R.) ; $516 \equiv 2 \times 259$ (I.R. and R).

tert.-Butyl mercaptan.

$2775 \equiv 1449 + 1369$? (R) ; $2714 \equiv 2 \times 1369$ (R) ; $1177 \equiv 2 \times 587$; $1103 \equiv 819 + 295$ (R) ; $445 \equiv$?

Discussion

It is of interest to compare these spectra and their assignments with similar results on other molecules containing the *tert.*-butyl grouping, particularly in the region 1300-700 cm.$^{-1}$ where the C - C skeletal stretching and CH_3 wagging modes occur. Assignments are available for several small hydrocarbons containing these groupings,[2] viz. 2 : 2-dimethyl butane, 2 : 2-dimethyl-3-butene, and 2 : 2-dimethyl-3-butyne, and more recently Simpson and Sutherland [12] have discussed in detail the skeletal stretching modes of saturated hydrocarbons containing the *tert.*-butyl group. The results of Simpson and Sutherland [12] necessitate a change in the assignment of the two high frequency C—C stretching modes near 1260 and 1210 cm.$^{-1}$ in the spectra of the small hydrocarbons [2] so that the higher frequency corresponds to the doubly degenerate mode and the lower frequency to the singly degenerate vibration. Otherwise, the previous assignments seem satisfactory. Hydrocarbons in which a carbon atom is attached to the *tert.*-butyl group have, in addition to the two skeletal stretching modes mentioned above, two doubly degenerate methyl wagging frequencies near 1025 and 930 cm.$^{-1}$ respectively, and a singly degenerate mode of the same type at about 880 cm.$^{-1}$. These

---

[13] Sheppard, *J. Chem. Physics*, 1949, 17, 79.

TABLE II.—THE ASSIGNED FUNDAMENTAL VIBRATION FREQUENCIES OF THE *tert.*-BUTYL HALIDES AND MERCAPTAN

3° Butyl Chloride		3° Butyl Mercaptan		3° Butyl Bromide		3° Butyl Iodide		Assignment
Infra-red	Raman[4, 5, 8]	Infra-red[9]	Raman[19]	Infra-red	Raman[5, 6, 8]	Infra-red	Raman[5, 7]	
2970 (*s*) — —	2978 (10) (2965) 2924 (12) *p*		2960 (10) (2960) 2924 (8)	2970 (*s*) — —	2982 (5) 2960 (5) 2918 (5) *p*	2970 (*s*) — —	2976 (2) 2955 (2) 2918 (2)	E E A_1 CH_3 asymm. stretching
2890 (*s*) —	2896 (4) 2870 (3)		2898 (6) 2864 (4)	2890 (*s*) —	2890 (3) (2870)	2890 (*s*) —	2896 (2) 2863 (2)	E A_1 CH_3 symm. stretching
1460 (*s*) —	— 1445 (8) 0·76	+	1449 (5) (1449)	1455 (*s*) —	1454 (5) *dp* (1445)	1456 (*s*) —	— 1448 (2)	E E, A_1 CH_3 asymm. deformation
1370 (*s*) —	— 1361 (1)	+	(1370) 1369 (½)	1370 (*s*) —	— 1358 (1) *p*	1370 (*s*) —	— 1366 (½)	E A_1 CH_3 symm. deformation
1240 (*m*) 1159 (*s*)	1234 (4) *dp* 1153 (6) *p*	+ +	1218 (3) 1160 (4)	1237 (*m*) 1145 (*s*)	1235 (3) *dp* 1142 (10) *p*	1230 (*m*) 1139 (*s*)	1223 (1) 1131 (8)	E A_1 C—C stretching
1031 (*w*) 910 (*w*) 810 (*m*)	1026 (2) *dp* 925 (3) *dp* 812 (7) *p*	+ + +	1030 (½) 930 (2) 819 (6)	1034 (*w*) — 802 (*m*)	1029 (2) 0·6 932 (1) *dp* 805 (6) 0·77	1029 (*w*) 928 (*w*) 804 (*s*)	1021 (½) 927 (½) 801 (4)	E E A_1 CH_3 wagging
570 (*s*)	570 (10) *p*	587	587 (10)	514 (*s*)	515 (10) *p*	490 (*s*)	487 (10)	A_1 C—X stretching
	406 (2) ? 372 (7) *p* 304 (6) *dp*		395 (1), 445 (½) 368 (5) 295 (3)		398 (2) 0·7 303 (12) *p* 268 (1)		386 (2) 259 (12) 227 (½)	E A_1 E Skeletal deformation
—	—	2580	2570 (7)	—	—	—	—	A_1 X—H stretching
—	—	+	866 (2)	—	—	—	—	A_1 X—H deformation

The numbers in brackets following the Raman frequencies denote the relative intensities of the lines.
p = polarized ; *dp* = depolarized ; (*w*) = weak ; (*m*) = medium ; (*s*) = strong.
+ denotes that an infra-red frequency is shown at roughly the frequency of the Raman line in the published curve of the spectrum [19]

are clearly the counterparts of the similarly observed methyl wagging modes of the *tert.*-butyl halides.

It would be expected [8, 13] that the replacement of the carbon atom by a halogen next to the *tert.*-butyl group would cause a general decrease of frequency of the A_1 singly degenerate modes as these are directly coupled to the lowered C—X stretching mode, and are not too different in frequency. Doubly degenerate E type modes in the 1300-700 cm.$^{-1}$ region are less likely to be affected, as the nearest varying frequencies of this symmetry will be the low frequency skeletal deformation modes. The experimental results are in agreement with these conclusions. For the C—C stretching modes the doubly degenerate frequency is lowered by only 20 cm.$^{-1}$ from an average value of *ca.* 1260 cm.$^{-1}$ in the three hydrocarbons to 1240 cm.$^{-1}$ in *tert.*-butyl chloride. The symmetrical C—C stretching mode on the other hand is lowered by 50 cm.$^{-1}$ for the same molecules and is further lowered in the bromide and iodide spectra. The methyl wagging modes show similar trends. Thus the two doubly degenerate modes in the hydrocarbons have frequencies almost identical with those of the *tert.*-butyl halides. The symmetrical methyl wagging mode, however, is lowered from *ca.* 880 cm.$^{-1}$ in the hydrocarbons to 810 cm.$^{-1}$ in *tert.*-butyl chloride, and to rather lower values in the other halides. This is presumably the result of considerable mechanical coupling between the vibration and the C—X stretching mode.

There is one experimental discrepancy between the present work and that of Mortimer, Blodgett and Daniels [3b] on *tert.*-butyl bromide. These authors find an extra infra-red frequency at 679 cm.$^{-1}$ but we have been unable to confirm this even with a considerable pathlength. The same authors find almost identical frequencies in *iso*propyl bromide and ethyl bromide at 678 and 681 cm.$^{-1}$ respectively, which again we have been unable to confirm. It appears that they are due to some experimental error ; this seems the more likely as the different molecules all show this extra frequency at approximately the same position. The above authors obtained two absorptions in the spectra between 700 and 500 cm.$^{-1}$ in many other bromides that they investigated in agreement with the Raman data on these molecules. On the other hand the Raman spectra of ethyl, *iso*propyl, and *tert.*-butyl bromide show only one strong line in this region whereas once again Mortimer, Blodgett and Daniels found two absorptions. Kohlrausch [14] has previously pointed out that the ethyl, *iso*propyl and *tert.*-butyl halides have rigid skeletons whereas the other halides which showed multiple lines in the Raman spectra could exhibit restricted rotation about carbon-carbon linkages. He concluded that as a result of these extra degrees of freedom different "rotational isomers" could exist and that these spectroscopically distinguishable molecules each contributed their own carbon-halogen stretching frequency to this region of the spectrum. Mortimer, Blodgett and Daniels [3b] conclude that their observed extra absorptions in the spectra of the rigid halides invalidate Kohlrausch's distinction between the spectra of the two types of molecules, and that some other explanation than rotational isomerism is required to explain the multiple frequencies in this region. However, our failure to find the second frequency observed by the above authors near 680 cm.$^{-1}$ in the infra-red spectra of the rigid halides is once again in agreement with Kohlrausch's hypothesis. Furthermore, recent work on hydrocarbons has shown that rotational isomerism is a necessary conception for the explanation of the complexity of the infra-red and Raman spectra of these molecules [15, 16] also.

The author is indebted to Dr. Delia M. Simpson for helpful discussions.

---

[14] Kohlrausch, *Z. physik. Chem.*, *B*, 1932, **18**, 61.
[15] Szasz, Sheppard and Rank, *J. Chem. Physics*, 1948, **16**, 704.
[16] Rank, Sheppard and Szasz, *ibid.*, 1949, **17**, 83.

He would also like to thank the Trustees and Advisory Council of the Ramsay Memorial Fellowships Trust for a Fellowship during the tenure of which this work was commenced, and the Commissioners for the Exhibition of 1851 for a current Senior Studentship.

Department of Colloid Science,
Cambridge.

THE INFRA-RED SPECTRA AND ASSIGNMENT OF THE FUNDAMENTAL FREQUENCIES OF THE ALKYL HALIDES

II.—*iso*PROPYL HALIDES

By N. Sheppard

Received 21st February, 1950

The infra-red absorption spectra of *iso*propyl chloride, bromide and iodide have been obtained in the liquid state between 1500 and 450 cm.$^{-1}$. Nearly complete assignments have been made of the observed infra-red and previously published Raman frequencies to the normal modes of vibration of these molecules. Particular emphasis has been placed on the assignment of the frequencies of the *iso*propyl group between 1400 and 700 cm.$^{-1}$. Similar assignments have been given for the vibrational spectra of *iso*propyl mercaptan.

This investigation forms part of a study of the vibrational spectra of the alkyl halides undertaken with a view to obtaining a systematic knowledge of the fundamental vibration frequencies associated with the ethyl, *iso*propyl and *tert.*-butyl groupings. The previous paper [1] gave an account of the spectra of the *tert.*-butyl halides. The infra-red absorption spectra of *iso*propyl chloride, bromide and iodide in the liquid state between 1500 and 450 cm.$^{-1}$ are described in the present paper. Lecomte [2, 3] has previously studied these compounds, presenting the results mainly in the form of line diagrams. His observations are rather less detailed, but are otherwise in good agreement with ours except for an apparent slight calibration difference between 1500 and 1000 cm.$^{-1}$. Mortimer, Blodgett and Daniels [4] have recorded the spectrum of *iso*propyl bromide between 700 and 450 cm.$^{-1}$. The Raman spectra of the *iso*propyl halides have all been well characterized in the literature.[5, 6, 7] Radinger and Wittek [7] have given a partial assignment of the Raman spectra and Wagner [8] has proposed alternatives to some of their conclusions. The Raman spectrum of *iso*propyl mercaptan has also been studied by Radinger and Wittek,[7] and the infra-red spectrum in the gaseous phase has been recorded by Trotter and Thompson.[9] An attempt is made to assign the observed frequencies in these spectra also by analogy with those of *iso*propyl chloride.

---

[1] Sheppard, *Trans. Faraday Soc.*, preceding paper.

[2] Lecomte in *Traité de Chimie organique,* by Grignard and Baud (Masson, Paris, 1936), Vol. II, p. 190.

[3] Lecomte, *Compt. rend.*, 1934, **198,** 65.

[4] Mortimer, Blodgett and Daniels, *J. Amer. Chem. Soc.*, 1947, **69,** 822.

[5] Harkins and Haun, *ibid.*, 1932, **54,** 3920.

[6] Kahovec and Wagner, *Z. physik. Chem. B*, 1939, **42,** 123.

[7] Radinger and Wittek, *ibid.*, 1940, **45,** 329.

[8] Wagner, *ibid.*, 1940, **45,** 341.

[9] Trotter and Thompson, *J. Chem. Soc.*, 1946, 481.

Experimental

The infra-red spectra were obtained in the manner described in the previous paper.[1] The redistilled B.D.H. samples of *iso*propyl chloride and bromide boiled at 37° C and 60° C respectively. The *iso*propyl iodide obtained from the same source was distilled under reduced pressure shortly before taking its spectrum.

Assignment of the Spectra.—(*a*) GENERAL CONSIDERATIONS. The maximum degree of symmetry that these molecules can possess is a single plane (point group C_s). The number, symmetry type, and expected frequency ranges for the various types of normal modes are summarized in Table I. All frequencies are allowed in both the infra-red and Raman spectra, although the restricted rotational modes of the methyl groups are likely to be weak or non-observable. The vibrations of symmetry type A' should give polarized Raman lines.

TABLE I.—THE NUMBER, SYMMETRY TYPES AND APPROXIMATE FREQUENCY RANGES FOR THE VIBRATIONS OF THE *iso*PROPYL HALIDES

Type of Vibration	A'	A''	Expected Frequency Range (cm.$^{-1}$)
CH_3 asymm. stretching . .	2	2	*ca.* 2960 [10]
CH_3 symm. stretching . .	1	1	*ca.* 2870 [10]
C—H stretching . . .	1	—	*ca.* 2890 [10]
CH_3 asymm. deformation .	2	2	*ca.* 1450
CH_3 symm. deformation . .	1	1	*ca.* 1375
C—H deformation . . .	1	1	1360-1200 [11]
C—C stretching . . .	1	1	1300-700
CH_3 wagging	2	2	1300-700
C—X stretching . . .	1	—	700-450
Skeletal deformation. . .	2	1	<500
CH_3 restricted rotation . .	2	1	<300

Fig. 1 shows the infra-red spectra of the liquid *iso*propyl halides between 1500 and 450 cm.$^{-1}$. The infra-red and Raman frequencies are assigned to the various normal modes of vibration of the molecules in Table II. These tabulated frequencies include all the strong infra-red and Raman data. The few weak frequencies not included are assumed to be overtone and combination frequencies and have been assigned below in terms of the fundamentals.

The usual overlapping of frequencies occurs in the regions of the CH stretching and CH_3 asymmetrical deformation vibrations. Accordingly semi-schematic assignments have been made for these vibrations. It was found that all the frequencies near 2900 cm.$^{-1}$ in the Raman spectra could be consistently explained as frequencies of the methyl group (cf. the spectra of the *tert.*-butyl halides [1]) and hence the stretching frequency of the lone C—H linkage has been schematically assigned to 2890 cm.$^{-1}$ as suggested by Fox and Martin.[10] Many of the hydrogen deformation and C—C stretching modes occur between 1360 and 700 cm.$^{-1}$, so that this is usually the most difficult region of the spectrum to analyze. The assignments shown in Table II for this region will therefore be discussed in detail for the *iso*propyl chloride molecule.

(*b*) THE ASSIGNMENT OF THE *iso*PROPYL CHLORIDE SPECTRA.—Table I shows that there should be twelve allowed fundamentals below 1360 cm.$^{-1}$ excluding methyl restricted rotations. The Raman spectrum of *iso*propyl chloride shows eleven lines in this region. All these frequencies have obvious counterparts in one or both of the Raman spectra of the other halides and hence they have been accepted as fundamentals. Weak extra frequencies at 949 and 1017 cm.$^{-1}$ are found in the infra-red spectrum of *iso*propyl chloride. The 949 cm.$^{-1}$ absorption has a counterpart in the *iso*propyl iodide spectrum and

[10] Fox and Martin, *Proc. Roy. Soc. A*, 1938, **167**, 257.
[11] Sheppard, *J. Chem. Physics*, 1948, **16**, 690.

TABLE II.—THE OBSERVED AND ASSIGNED FUNDAMENTAL VIBRATION FREQUENCIES OF THE *iso*PROPYL HALIDES AND MERCAPTAN

*iso*Propyl Chloride		*iso*Propyl Mercaptan		*iso*Propyl Bromide		*iso*Propyl Iodide		% Variation	Assignment	
Infra-red	Raman[5, 7]	Infra-red[9]	Raman[7]	Infra-red	Raman[5, 7]	Infra red	Raman[6, 7]			
	2982 (3) *p*		2968 (10) *p*		2984 (5) *dp*		2982 (1)	—	A'	CH_3 asymm. stretching
	2944 (6) *p*		(2950)		2956 (6)		2963 (3)	—	A'' (2)	
	2928 (8) *p*		2918 (10) *p*		2921 (7) *p*		2915 (4) *p*	—	A'	
	2865 (6) *p*		2866 (8) *p*		—		2872 (5) *p*	—	A'	CH_3 symm. stretching
	2909 (8) *p*)		(2900)		2894 (4) *p*		(2900)	—	A''	
	(2890)		(2890)		(2890)		(2890)	—	A'	CH stretching
1461 (*s*)	—	+	—	1465 (*s*)	—	1456 (*s*)	—	—	A' (2)	CH_3 asymm. deformation
1438 (*m*)	1455 (6) *dp*	—	1449 (7) *dp*	1442 (*m*)	1442 (4) *dp*	—	1448 (5) *dp*	—	A'' (2)	
1385 (*s*)	1388 (½)	+	1389 (½)	1385 (*s*)	1380 (1)	1382 (*s*)	—	—	A'	CH_3 symm. deformation
1372 (*s*)	—	+	—	1370 (*s*)	—	1369 (*s*)	1373 (1)	—	A''	
—	1337 (1)		1314 (1)	—	1325 (½)	1320 (*w*)	1313 (0)	1·8	A''	CH deformation
1261 (*s*)	1256 (2) *p*	+	1250 (2) *p*	1227 (*s*)	1219 (5) *p*	1201 (*s*)	1199 (7) *p*	4·8	A'	
1131 (*m*)	1126 (1) *dp*		1129 (½) *p*	1133 (*w*)	1119 (½) *dp*	1125 (*w*)	—	0·4	A''	C—C stretching
1062 (*s*)	1059 (4) *p*	+	1056 (3) *p*	1038 (*s*)	1038 (4) *p*	1018 (*s*)	1019 (2) *p*	4·2	A'	
1160 (*s*)	1161 (½)	+	1162 (½) *p*	1157 (*s*)	1154 (3) *p*	1147 (*s*)	1146 (8) *p*	1·3	A'	CH_3 wagging
949 (*w*)	—		955 (½)	—	946 (0)	941 (*w*)	—	0·8	A''	
932 (*w*)	937 (½)	+	—	931 (*w*)	—	928 (*w*)	925 (00)	0·9	A''	
881 (*s*)	884 (6) *p*	+	892 (4) *p*	877 (*s*)	879 (6) *dp*	872 (*s*)	874 (6) *dp*	1·1	A'	
615 (*s*)	612 (10) *p*	630	626 (10) *p*	536 (*s*)	536 (15) *p*	495(*s*)	489 (15) *p*	23	A'	C—X stretching
	424 (4) *p*		413 (4) *p*		407 (4) *p*		398 (5) *p*	6·4	A'	$\mathrm{C}\overset{\mathrm{C}}{\diagup\diagdown}\mathrm{C}$ deformation
	337 (5) *p*		336 (5) *p*		295 (12) *p*		265 (8) *p*	24	A'	$\mathrm{C}\overset{\mathrm{C}}{\diagup\diagdown}\mathrm{X}$ deformation
	326 (3)		—		—		—	—	A''	
—	—	2580	2567 (10) *p*	—	—	—	—	—	A'	X—H stretching
—	—	+	856 (2)	—	—	—	—	—	A'	X—H deformation

(*w*) weak; (*m*) medium; (*s*) strong; *p*, polarized; *dp*, depolarized. Frequencies in brackets have not been observed and are assigned schematically. The number in brackets after the Raman frequencies denotes the intensity of the lines. + indicates that an infra-red absorption is shown at approximately this frequency.[9]

has therefore been assumed to be the remaining fundamental, whereas the 1017 cm.$^{-1}$ absorption which has no counterpart in either of the other spectra is assigned (see below) as a combination frequency.

The detailed assignment of these chosen fundamentals can now be attempted. The previous assignment of Radinger and Wittek[7] as corrected by Wagner[8] was based on the observed Raman lines. Wagner's conclusions in the main seem acceptable, but will be reconsidered so as to include the extra infra-red data and to present a more complete picture of the methyl wagging modes. The three lowest Raman frequencies, viz. 326, 337 and 424 cm.$^{-1}$ can be assigned to the three skeletal deformation modes, two of which correspond to polarized Raman lines. In addition the very strong polarized Raman line at 612 cm.$^{-1}$ is well known to be the C—Cl stretching mode.[7] The two lone CH deformation modes would be expected to have high frequencies as in saturated hydrocarbons.[11] At least one of the hydrocarbon modes occurs consistently in the region 1340-1350 cm.$^{-1}$. The weak Raman line of *iso*propyl chloride at 1337 cm.$^{-1}$ is certainly

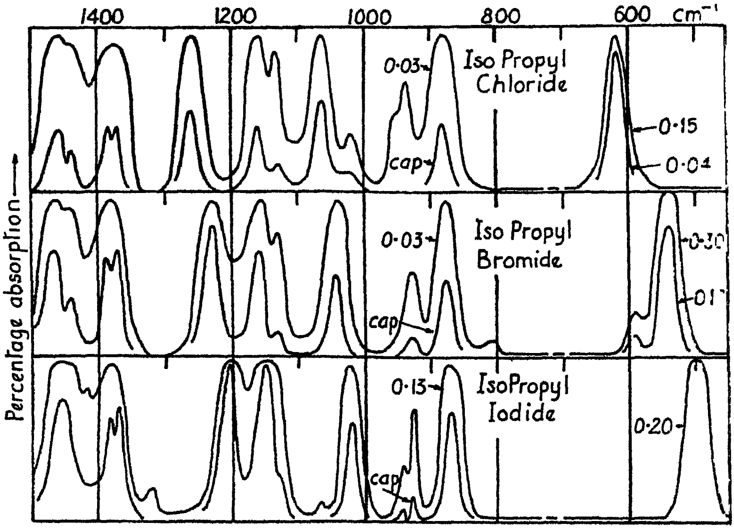

FIG. 1.— The infra-red spectra of *iso*propyl halides between 1500 and 450 cm.$^{-1}$: approximate thicknesses of liquid cells are given in mm. (cap. = capillary thickness.)

the A'' mode of this type, and the polarized Raman frequency near 1256 cm.$^{-1}$ is very probably the corresponding A' mode, in agreement with previous conclusions.[7, 8] The remaining six frequencies between 1200 and 800 cm.$^{-1}$ correspond to the two C—C stretching modes and four methyl wagging modes. Wagner[8] has made comparative calculations of the skeletal modes of the series of molecules *iso*butane, *iso*propyl chloride, bromide and iodide. These showed that the doubly degenerate C—C stretching mode in *iso*butane should split in the *iso*propyl halides to give a depolarized line of approximately the same frequency, and a polarized line at a slightly lower frequency. Similar calculations have been found to be in good agreement with the observed spectra of the *tert.*-butyl halides.[1] Recently Simpson and Sutherland[12] have shown that the Raman line at 1172 cm.$^{-1}$ in *iso*butane is the doubly degenerate C—C stretching mode. Accordingly in *iso*propyl chloride the only neighbouring depolarized Raman line at 1126 cm.$^{-1}$ is assigned to the A'' C—C stretching mode and the polarized line at 1059 cm.$^{-1}$ to the A' mode of this type. These assignments are in agreement with the work of Wagner for the *iso*propyl halides but not for *iso*butane, as the doubly degenerate C—C stretching mode of that molecule was put at 965 cm.$^{-1}$ by this author. The more recent interpretation[12] provides a consistent interpretation for the whole series. The only reasonable

[12] Simpson and Sutherland, *Proc. Roy. Soc. A*, 1949, 199, 169.

alternative to the above assignment for the A' C—C stretching mode would appear to be to assign the 1161 cm.$^{-1}$ Raman line to this vibration. This seems unlikely as Wagner's calculations show definitely that this C—C stretching mode should have a lower frequency than the A'' mode.

The remaining four frequencies at 1161, 949, 937 and 884 cm.$^{-1}$ must be the methyl wagging modes. The strong line at 884 cm.$^{-1}$ is polarized in the Raman spectrum, as is the corresponding line of *iso*propyl mercaptan, and is hence probably an A' mode. The strength of these Raman lines also favours their interpretation in this fashion, despite the apparent depolarized nature of the equivalent bromide and iodide frequencies. The 884 cm.$^{-1}$ frequency of *iso*propyl chloride is tentatively assigned to the symmetrical internal methyl wagging mode of the *iso*propyl group which takes place approximately in the plane. These lines are then analogous to the strong lines in the *tert.*-butyl halide spectra between 800 and 820 cm.$^{-1}$ which have been assigned to the symmetrical internal methyl wagging mode of the *tert.*-butyl group.[1] The Raman line at 1161 cm.$^{-1}$ is also one of a sequence of polarized lines and is assigned to the A' mode in which the methyl groups wag approximately perpendicular to the plane. The 949 and 937 cm.$^{-1}$ frequencies are hence the A'' methyl wagging modes.

(*c*) ASSIGNMENT OF THE SPECTRA OF THE *iso*PROPYL BROMIDE, IODIDE, AND MERCAPTAN.—The observed frequencies of the other *iso*propyl halides and of the mercaptan are assigned in a similar fashion as shown in Table II. The *iso*propyl mercaptan has an additional pair of frequencies near 2567 and 850 cm.$^{-1}$ which can be assigned to the SH stretching and the in-plane SH deformation modes respectively.[7, 13] The remaining observed frequencies which have not been assigned in Table II can be explained in terms of overtone and combination frequencies involving the chosen fundamentals ((R) denotes a Raman line, and (I.R.) an infra-red absorption) :—

isoPropyl chloride

2792 (R) ≡ 2 × 1388 ? ; 2727 (R) ≡ 2 × 1372 ; 1017 (I.R.) ≡ 612 + 424

isoPropyl bromide

2759 (R) ≡ 2 × 1385 ; 2727 (R) ≡ 2 × 1370 ; 590 (I.R.) ≡ 2 × 295.

isoPropyl iodide

2721 (R) ≡ 2 × 1369 ; 1061 (I.R.) ≡ impurity ?

isoPropyl mercaptan

2756 (R) ≡ 2 × 1389 ; 2723 (R) ≡ 2 × (1365) ; 1269 (R) ≡ 2 × 630 cm.$^{-1}$.

Discussion

The assignment of the spectra of these *iso*propyl halides has been accomplished by means of a detailed consideration of the *iso*propyl chloride spectrum, using the polarization data of the Raman lines, and previous results on related molecules. In the *tert.*-butyl halides such a procedure was sufficient to give a fairly unequivocal assignment because of the high symmetry of these molecules and the associated spectral simplicity. However, the *iso*propyl halides, although smaller molecules, have a much lower symmetry and correspondingly more complex spectra, so that it is desirable to attempt a check of the assignments proposed.

Examination of Fig. 1 or the frequencies shown in Table II reveals that some of the modes vary in frequency to a considerable extent on passing from the chloride to the iodide, while others are almost invariant in the different molecules. A group frequency will vary in position from molecule to molecule if other frequencies of the same symmetry type with which it is coupled change in value. Alternatively if the force constants controlling the vibration of the group are altered by changes in a neighbouring part of the molecule, this also will cause a shift in the group

---

[13] Sheppard, *J. Chem. Physics*, 1949, **17**, 79.

frequency. It seems probable that the most pronounced changes in frequency on passing from *iso*propyl chloride to the iodide will be caused by changes due to the coupling of changing C—X stretching and bending modes with the other vibrations of similar frequency and symmetry.

Little variation would be expected in the internal methyl group and CH frequencies above 1350 cm.$^{-1}$. On increasing the mass of the halogen atom (the force constants being assumed unchanged) the frequencies below 1350 cm.$^{-1}$ may be expected to vary in the following manner :

(*a*) the vibrations involving the C—X linkage will be greatly changed in frequency (these are the C—X stretching mode and the two deformation modes involving mainly changes in the $\mathrm{C}\overset{\mathrm{C}}{\diagup\;\diagdown}\mathrm{X}$ angle) ;

(*b*) the remaining *A'* vibrations in this region will be affected to a moderate extent, because of their proximity to and coupling with either the C—X stretching or *A'* $\mathrm{C}\overset{\mathrm{C}}{\diagup\;\diagdown}\mathrm{X}$ bending mode ;

(*c*) the remaining *A''* vibrations will be affected only to a small degree, because they are all very considerably separated in frequency from the *A''* $\mathrm{C}\overset{\mathrm{C}}{\diagup\;\diagdown}\mathrm{X}$ bending mode.

The percentage change in the various assigned modes of vibration have been computed by dividing the difference between the average frequencies (infra-red and Raman) of the chloride and the iodide, by the average value for the bromide frequency. These are given in Table II. All the changes correspond to a decrease in frequency on passing from the chloride to the iodide, as would be expected if the main factor were the change in the mass of the halogen. The frequencies involving the C—X linkage directly are almost certainly those assigned to 612, 337 and 326 cm.$^{-1}$ in *iso*propyl chloride. The percentage variations for the first two of these frequencies are over 20 %, but all the lines have not been observed in the third case. These are sharply differentiated from the remaining *A'* modes, for which the percentage changes in frequency vary from *ca.* 7 % for the skeletal deformation mode at 424 cm.$^{-1}$ to just over 1 % for the lower methyl wagging mode. Finally the *A''* modes all have still smaller percentage variations of less than 1 % with the single exception of the 1337 cm.$^{-1}$ CH deformation mode which shows a variation of *ca.* 2 %. Apart from these CH deformation modes which will be discussed later, the assigned frequencies thus behave in the predicted fashion. This provides general confirmation for the correctness of the assignments of frequencies to the different symmetry classes. Further, of the *A'* frequencies, the assigned C—C skeletal stretching and bending modes vary by the relatively large amounts of 4 and 7 % respectively, which would be expected as the bonds involved are directly attached to the C—X linkage. On the other hand the methyl wagging modes (both of types *A'* and *A''*) all vary by less than 2 % corresponding to the greater separation of these groups from the C—X linkage and the resulting much weaker coupling.

The CH deformation modes both exhibit abnormally large variations in frequency as shown in Table II. This behaviour of these modes cannot in this case be taken as evidence against the chosen assignments, as there is little doubt of their correctness in view of the high values of the frequencies concerned.[9] The large variation of these frequencies must therefore be due to some other cause, and it is probable that it is determined by a change in the force constant controlling the deformation vibrations of the CH linkage. This seems a reasonable explanation, since the CH linkage is attached directly to the C—X bond. A systematic study of such force constant changes in this and similar groupings will be presented in a forthcoming publication.

General Conclusions.—At the outset of this investigation of the *tert.*-butyl and *iso*propyl halides, it was hoped to achieve some systematic understanding of the C—C stretching and methyl wagging modes of the hydrocarbon groups. With the help of the extra data provided by the infra-red spectra of these halide molecules it has proved to be possible to make fairly complete and consistent assignments for the various normal modes of vibration.

It now seems clear that, at least for halides involving a single halogen atom and C—X linkage, the calculations made by Wagner[8] for the purpose of determining qualitative trends in the C—C skeletal stretching modes find good confirmation in the observed spectra. Wagner was not able to reach such convincing conclusions himself because of incorrect assumptions which were then prevalent on the assignment of certain key hydrocarbon frequencies. These appear to have been correctly assigned by Simpson and Sutherland.[12]

The identification of the C—C stretching modes has made possible in turn the characterization of most of the methyl wagging modes, and it is of interest to note the range of the spectrum covered by this type of vibration. In the *tert.*-butyl halides all of the allowed methyl wagging modes have been found in the region 800-1050 cm.$^{-1}$, and this holds true also for these modes in hydrocarbons containing the *tert.*-butyl group.[14] In the *iso*propyl halides three of the four modes occur in this region, and the remaining one lies near 1150 cm.$^{-1}$. It is possible that this last value is abnormally high because of mechanical resonance interaction between this mode and the C—C stretching mode near 1050 cm.$^{-1}$.* However, it must be concluded that in some cases methyl wagging modes can be found anywhere between 800 and 1200 cm.$^{-1}$, although the majority of them appear to occur below 1100 cm.$^{-1}$. It seems that a precise understanding of the features in the infra-red and Raman spectra caused by such modes can only be reached by a study of each type of polymethyl compound in turn. The present work provides the beginnings for such a classification.

The author is indebted to Dr. Delia M. Simpson for valuable discussions. He would also like to express his thanks to the Trustees and Advisory Council of the Ramsay Memorial Fellowships Trust for a Fellowship during the tenure of which this work was commenced, and to the Royal Commission for the Exhibition of 1851 for a Senior Studentship. The Perkin-Elmer Model 12B infra-red spectrometer was on loan to this department from Messrs. Aero Research Ltd., Duxford, Cambs.

Department of Colloid Science,
Cambridge.

[14] Sheppard, *J. Chem. Physics.*, 1949, 17, 455.

Note added in proof:

* When the frequencies of the same symmetry class are close in value their designation in terms of specific group frequencies is less valid, and the two normal vibrations will both involve considerable motions associated with each of the two group co-ordinates.

THE ABSORPTION OF ULTRASONIC WAVES IN PROPIONIC ACID

BY JOHN LAMB AND D. H. A. HUDDART

Received 4th October, 1949

The paper gives the results of measurements of the absorption and velocity of propagation of ultrasonic waves in propionic acid over the frequency range 1 Mc./sec. to 15 Mc./sec. and at temperatures from 7° C to 55° C. The occurrence of a relaxation process is confirmed, and the results are compared with previous measurements of a similar nature on acetic acid. The activation energy associated with the molecular equilibrium, which is perturbed by the ultrasonic vibrations, is evaluated as 7·5 kcal./mole.

It has previously been established [1] that the anomalous absorption of ultrasonic waves in acetic acid in the frequency range 0·5 to 67 Mc./sec. arises from a relaxation phenomenon. To recapitulate briefly, the relaxation can be attributed to the perturbation by the ultrasonic vibrations of a molecular equilibrium, the precise nature of which is as yet unknown. The process is assumed to involve a transition between two different energy states. Following Richards [2] and Herzfeld,[3] this is interpreted in terms of a relaxing component of the specific heat: * the activation energy associated with the relaxation can then be derived from the measured variation of relaxation time with temperature.

It has been suggested [4] that for acetic acid the equilibrium which is perturbed may be that existing between double and single molecules. The previous work has been extended to other carboxylic acids in order to yield further information about the process, and the results of measurements of the absorption and velocity of propagation of ultrasonic waves in propionic acid are given in this paper: the range of frequency covered by the experiments was 1 to 15 Mc./sec. and that of temperature, 7 to 55° C.

Experimental

Material.—A freshly distilled sample of propionic acid was used each day in order to minimize the effects of accumulated water absorption from the atmosphere.

Method.—The technique of measurement was similar to that employed in the previous work and has already been fully described.[1, 5] The temperature of the liquid was maintained constant to within 0·1° C during each set of observations required to determine the amplitude absorption coefficient α or the velocity of propagation V.

---

[1] Lamb and Pinkerton, *Proc. Roy. Soc. A*, 1949, **199**, 114.

[2] Richards, *Rev. Mod. Physics*, 1939, **11**, 36.

[3] Herzfeld, *J. Acous. Soc. Amer.*, 1941, **13**, 32.

* An alternative interpretation can be given in terms of a structural relaxation but this leads to an expression for the absorption coefficient similar to eqn. (1). See Hall, *Physic. Rev.*, 1948, **73**, 775.

[4] Spakowski, *C.R. Acad. Sci. U.R.S.S.*, 1938, **18**, 169.

[5] Pinkerton, *Proc. Physic. Soc. B*, 1949, **62**, 286.

Results

Observations were taken over the temperature range 7° C to 55° C and at nine frequencies between 1 Mc./sec. and 15 Mc./sec. The measured values of α and V are plotted in Fig. 1 and 2 respectively: no dispersion was recorded.

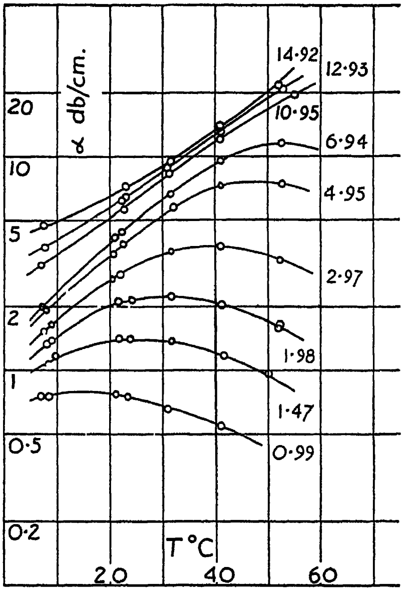

Fig. 1.—Absorption in propionic acid. Measured values of absorption α as a function of temperature. The figures against each curve refer to the corresponding frequency in Mc./sec.

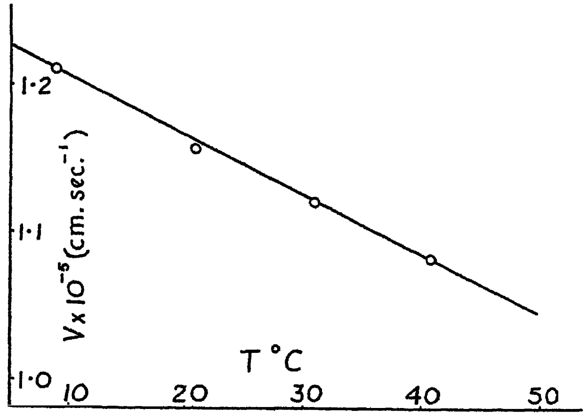

Fig. 2.—Variation of velocity of propagation V with temperature for propionic acid. The points represent the mean values taken at the different frequencies.

Analysis of Results.—It has been shown [1] that a relaxation mechanism, described by a single relaxation time τ, contributes to the total absorption coefficient an amount α' which can be represented at a frequency ν, by

$$\alpha' = A\nu^2/[1 + (\nu/\nu_m)^2], \quad . \quad . \quad . \quad . \quad . \qquad (1)$$

where

$$\nu_m \left[= \frac{1}{2\pi\tau} \right],$$

and A are parameters dependent upon temperature. The corresponding absorption per wavelength is

$$\mu' = \alpha' V/\nu = A V\nu/[1 + (\nu/\nu_m)^2] \quad . \quad . \quad . \quad . \quad (2)$$

Provided $\mu' \ll 1$*, the total absorption coefficient is given by

$$\alpha = B\nu^2 + A\nu^2/[1 + (\nu/\nu_m)^2], \quad . \quad . \quad . \quad . \quad (3)$$

in which the additional term, $B\nu^2$, includes the normal viscous absorption,[6] † and contributions from any possible further relaxation processes for which the relaxation times are much smaller than τ.

From eqn. (2) the relationship

$$\mu'/\nu + \mu' . \nu/\nu_m^2 = AV \quad . \quad . \quad . \quad . \quad (4)$$

is derived. Thus, if the absorption is characterized by a single relaxation time, a plot of μ'/ν against $\mu'\nu$ should give a straight line of slope $1/\nu_m^2$. This was found to be true at any particular temperature chosen within the range of the investigation, a typical plot being given in Fig. 3. The parameters occurring in eqn. (3) were evaluated at each temperature as described in the previous paper [1] with the exception of B which was estimated by a different procedure (see Appendix) owing to the fact that measurements were not available at frequencies considerably greater than ν_m. These parameters are listed in the Table for certain temperatures, while Fig. 4, in which the curves are calculated ones and the points represent the measured values taken from the smooth curves of Fig. 1, shows the variation of μ' with ν.

TABLE I

Temperature (° C)	Estimated Value of $B \times 10^{17}$ (sec.^{2} cm.$^{-1}$)	$A \times 10^{17}$ (sec.^{2} cm.$^{-1}$)	ν_m Mc./sec.	$\mu'_{\text{max.}}$ $(= AV\nu_m/2)$ $\times 10^2$
8	160	17,300	1·03	1·07
21	130	11,470	2·02	1·34
31	120	8,550	3·23	1·54
41	100	6,880	4·79	1·78
51	90	5,210	7·26	2·01

Discussion

It has been shown that the anomalous absorption in propionic acid can be ascribed to a single relaxation process within the respective frequency and temperature ranges of the present investigation. The absence of any recorded dispersion is consistent with the expression developed by Kneser [7] for the total change in velocity associated with a relaxation process, namely,

$$\Delta V/V = \mu'_{\text{max.}}/\pi.$$

At 31° C, for example, using the value of $\mu'_{\text{max.}}$ given in the Table,

$$\Delta V/V \approx 0·5\ \% :$$

the experimental accuracy ($\pm$ 0·5 %) of velocity determination was not

---

* The condition for the components of the absorption coefficient to be additive

[6] Stokes, *Trans. Camb. Phil. Soc.*, 1845, **8**, 287.

† See also Liebermann, *Physic. Rev.*, 1949, **75**, 1415, for measurement of dilatational viscosity; cp. also *ibid.*, 1949, **76**, 440.

[7] Kneser, *Ann. Physik, Lpz.*, 1938, **32**, 277.

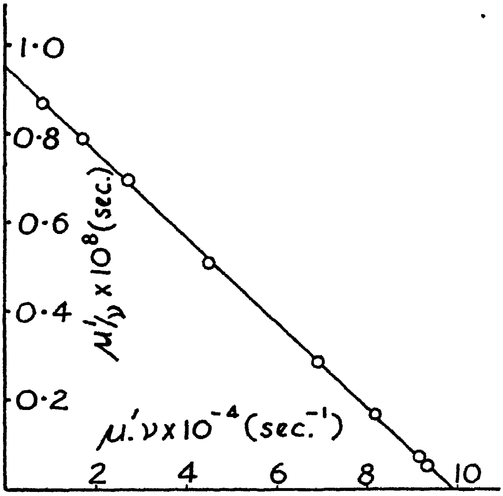

FIG. 3.—Experimentally derived values of μ' plotted in the form of μ'/ν against $\mu'\nu$ for a temperature of 31° C. The value of ν_m derived from the slope of this line is 3·23 Mc./sec. while the intercept on the μ'/ν axis gives $A = 8550 \times 10^{-17}$ sec.^{2} cm.$^{-1}$.

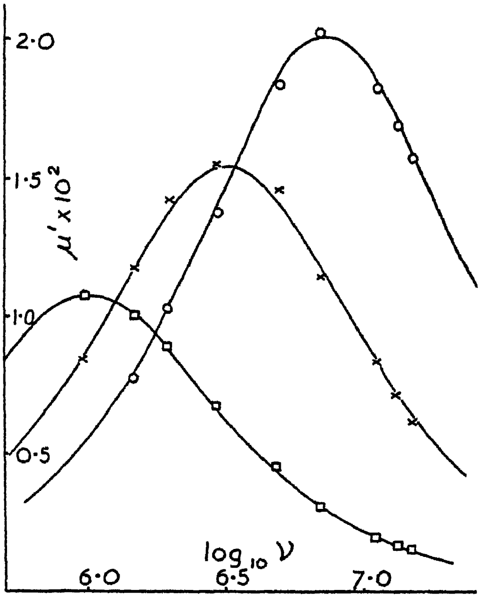

FIG. 4.—$\mu' = \alpha' V/\nu$, the absorption per wavelength due to the relaxation process, as a function of frequency. The curves are calculated ones using the parameters given in the Table and the points are measured values taken from the smooth curves of Fig. 1.

□ 8° C, × 31° C, ○ 51° C.

sufficient to discriminate between two velocity values differing by this amount.

If, following Eyring *et al.*[8, 9] the relaxation time is assumed to be given by an expression of the form

$$\tau = \frac{D}{T} \, . \, e^{\Delta E_a/RT}, \quad . \quad . \quad . \quad . \quad . \quad (5)$$

then

$$\nu_m = \frac{T}{2\pi D} \, . \, e^{\Delta E_a/RT}, \quad . \quad . \quad . \quad . \quad . \quad (6)$$

where D is a constant and ΔE_a is the activation energy associated with the equilibrium which is perturbed. The values of ν_m given in the Table can be used to test the validity of eqn. (6). Thus, Fig. 5 shows that the plot of $\log_{10} (\nu_m/T)$ against $1/T$ is a straight line and from the slope of this the activation energy is calculated to be $\Delta E_a = 7{\cdot}5$ kcal./mole. The agreement in order of magnitude between this value and that of 8·5 kcal./mole found previously for acetic acid does not conflict with the previous suggestion that the absorption is possibly due to the perturbation of the chemical equilibrium between double and single molecules.

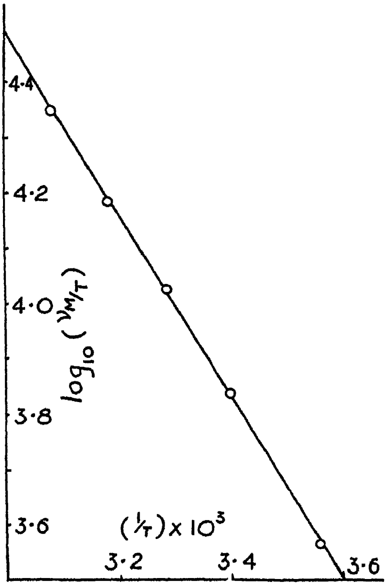

FIG. 5.—Log_{10} (ν_m/T) plotted against $1/T$. The slope gives the activation energy associated with the relaxation as
$\Delta E_a = 7{\cdot}51$ kcal./mole.

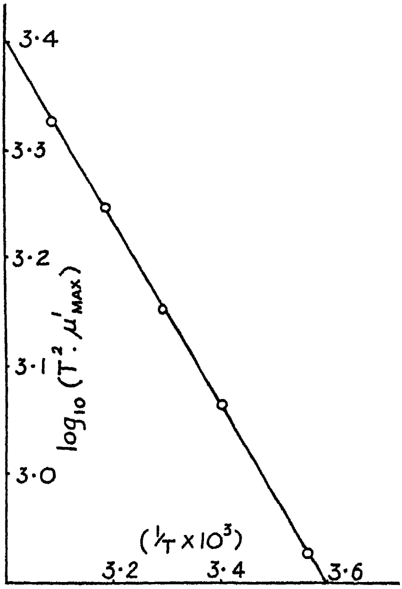

FIG. 6.—$\mathrm{Log}_{10}(T^2\mu'_{\mathrm{max.}})$ plotted against $1/T$. The points are derived from column 5 of the Table. From the slope of this line the difference of internal energy between the two energy states
$\Delta E_0 = 3{\cdot}86$ kcal./mole.

In addition, if ΔF represents the change in (Helmholtz) free energy between the two assumed equilibrium states of the molecule then, in general, this must be written,[1] $\Delta F = \Delta E_0 - T\Delta S_0$, where ΔE_0 and ΔS_0 are the corresponding changes in internal energy and entropy, respectively.

---

[8] Glasstone, Laidler and Eyring, *The Theory of Rate Processes* (McGraw-Hill, New York, 1941).

[9] Powell and Eyring, *Advances in Colloid Science*, 1941, **1**, 183.

Further, if $\mu'_{\text{max.}}$ is the maximum value of μ' at temperature T, then *

$$\mu'_{\text{max.}} = \frac{\pi}{2}\frac{(\gamma - 1)}{C_p} \cdot R\left[\frac{\Delta E_0}{RT}\right]^2 \cdot e^{\Delta E_0/RT} \cdot e^{\Delta S_0/R}. \qquad (7)$$

In this expression R is the gas constant and γ ($= C_p/C_v$) the ratio of specific heats. In accordance with this relationship the plot of $\log_{10}(T^2\mu'_{\text{max.}})$ against $1/T$ (cp. Fig. 6) is found to give a straight line from the slope of which ΔE_0 is calculated to be 3·9 kcal./mole: the corresponding value for acetic acid is 2·3 kcal./mole. In order to derive the entropy ΔS_0, and hence the free energy ΔF, from eqn. (7), it is necessary to know γ for the liquid phase: the value of the latter is 1·26 at 31° C, as calculated from the measured coefficient of thermal expansion and the measured velocity of ultrasonic waves (Fig. 2),[10, 11] Thus for a temperature of 31° C, taking $C_p = 33$ cal./mole deg.[12] and $\mu'_{\text{max}} = 1{\cdot}54 \times 10^{-2}$, substitution in eqn. (7) gives $\Delta S_0 = 4{\cdot}4$ cal./mole. deg. Thus

$$\Delta F = \Delta E_0 - T\Delta S_0 = 2{\cdot}5 \text{ kcal./mole}$$

as compared with the (approximate) value for acetic acid of 1·1 kcal./mole. Although it is not yet possible to define the precise nature of the energy change ΔF between the two equilibrium states, its evaluation is nevertheless an important step towards an understanding of the mechanism involved.

In conclusion, it is of interest to note that evidence of a relaxation process has been found also in formic acid. These measurements were not pursued, however, owing to the rapidity with which formic acid absorbs water from the atmosphere and the marked effect which this has on the absorption coefficient.

The authors wish to express their appreciation of the close interest which Prof. Willis Jackson has shown in the present work.

Appendix

Estimation of B.—Eqn. (3) can be rewritten as

$$\alpha/\nu^2 = B + A/[1 + (\nu/\nu_m)^2],$$

from which it follows that α/ν^2 approaches the value B at high frequencies ($\nu \gg \nu_m$). Further, it is evident from the experimental results that for $\nu < 3\nu_m$,

$$B \ll A/[1 + (\nu/\nu_m)^2]$$

and can be neglected in the determination of A and ν_m from a linear plot similar to Fig. 3. B can now be estimated by subtraction of the term $A/[1 + (\nu/\nu_m)^2]$ from the measured value of α/ν^2 at each of the higher frequencies employed, and ν_m redetermined using the results for all frequencies. The values of B given in the Table were estimated in this manner.

Electrical Engineering Department,
Imperial College,
S.W.7.

---

* See ref. 1, eqn. (19).

[10] Ubbelohde, *Modern Thermodynamics* (Oxford, 1937), p. 11.

[11] Bergmann, *Ultrasonics* (English trans.) (John Wiley, New York, 1938), p. 106.

[12] *Int. Crit. Tables*, 1929, **5**, 108.

CHEMICAL ACTION OF SOUND WAVES ON AQUEOUS SOLUTIONS

By N. Miller

Received 30*th January*, 1950

Experimental data are presented which confirm that the oxidative action of intense sound on dilute aqueous solutions of inorganic reducing agents is an "indirect" process, i.e. that it is due to reactive fragments produced in the disruption of water molecules by the sound. Possible methods by which a portion of the energy of the sound is degraded in this way are discussed briefly.

The chemical action of sound waves, both of audible and ultrasonic frequency, on dilute aqueous solutions has been examined by numerous investigators,[1] and bears a striking resemblance to that of ionizing radiation. For this reason it appears likely that the action of the sound waves is an "indirect" one, i.e. that the observed chemical changes are due to reactive fragments arising from the disruption of water molecules, rather than from any direct attack on the solute. It appeared desirable to the writer to carry out quantitative studies in this field with a view to providing further proof that the action is of this nature, and that it therefore provides an analogy with the well-known indirect effect of ionizing radiation on aqueous solutions.

Experimental and Results

Information on this point can readily be obtained from a study of the kinetics of the oxidation of inorganic reducing agents in solution, and although a number of experiments of this type have been carried out,[1-8] the results reported have been mainly qualitative. In order to permit of quantitative study of these changes, it has been noted by Weissler and Cooper [8] that careful account has to be taken of the dissolved gas content of the solution and the transmittance of the sound by the wall of the irradiation cell. Several investigators have established that the oxidation of reducing agents in solution is most pronounced when the solution is saturated with air or oxygen, less with nitrogen, and negligible with hydrogen. In all these cases the phenomenon of cavitation, with which the chemical action has been definitely associated,[9] takes place. In solutions saturated with carbon dioxide,[10] or in solutions freed from dissolved gas,[11] neither cavitation nor oxidation are observed.

The writer has followed the oxidation of ferrous ions in sulphuric acid solution by 500 kilocycle sound waves. The oxidation of this system under the action of ionizing radiation has been thoroughly examined, and in fact the techniques used in the preparation and analyses of the solutions were identical with those used in the writer's earlier work with ionizing radiation.[12] As was noted by Liu and Wu in the oxidation of potassium iodide by ultrasonics,[4] it was found that the behaviour of an air or oxygen-saturated solution is only reproducible within the first few minutes of irradiation, for the dissolved gas is rapidly driven out of solution as the irradiation proceeds, and the rise in temperature which ensues on prolonged irradiation leads to a change in the efficiency of the process. Reproducible results could only be secured for this system when one single cell was used, clamped in a rigidly fixed position relative to the source and never moved throughout the whole series of experiments. When this procedure was followed, the chief remaining source of irreproducibility was that due to changes in the surface of the liquid, which led to changes in the reflection of the sound back into the liquid phase. These changes led to large statistical variations in the chemical effects produced by a one-minute irradiation, but these were reduced to less than 10 % for irradiations of five min. duration.

---

[1] For a review of the literature, cf. Prud'homme and Grabar, *J. Chim. Phys.*, 1949, **46**, 323.

[2] Schmitt, Johnson and Olson, *J. Amer. Chem. Soc.*, 1929, **51**, 370.

[3] Beuthe, *Z. physik. Chem. A*, 1933, **163**, 161.

[4] Liu and Wu, *J. Amer. Chem. Soc.*, 1934, **56**, 1005.

[5] Flosdorf, Chambers and Malisoff, *ibid.*, 1936, **58**, 1069.

[6] Solov'eva, *J. Phys. Chem. U.S.S.R.*, 1937. **9**, 77.

[7] Kling and Kling, *Compt. rend.*, 1946, **223**, 33.

[8] Weissler and Cooper, *Manfg. Chemist*, 1948, **19**, 505.

[9] For most specific evidence, cf. Flosdorf, *et al.*[5], Polotskii, *J. Gen. Chem. U.S.S.R.*, 1947, **17**, 1048 ; Weissler and Cooper.[8]

[10] Liu and Wu,[4] Weissler and Cooper,[8] Prud'homme and Grabar.[1]

[11] Prud'homme and Grabar.[1]

The apparatus used consisted of a 500 kilocycle piezoelectric quartz oscillator specially designed by the National Research Council of Canada for the medical applications of ultrasonics. The quartz crystal, about 3 cm. in diameter, was placed directly against the bottom of a plastic beaker filled to a constant level with water, and the plane of contact between the crystal and the beaker was kept covered with oil to ensure the transmission of the sound across the interface. Inside the beaker was placed a flat-bottomed Pyrex irradiation cell, which was clamped in a fixed position with its base vertically above the crystal and in contact with the bottom of the beaker. The cell was filled to a constant level in each irradiation, and emptied and washed out by suction.

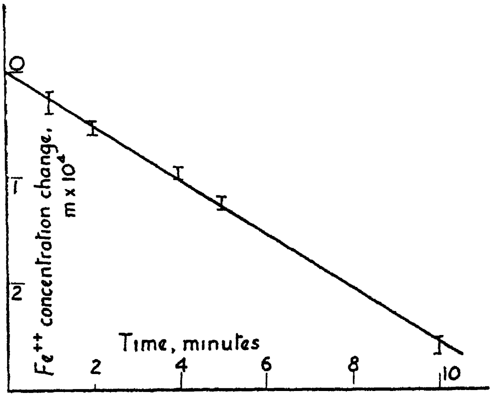

FIG. 1.—Air-saturated solutions—Fe^{++} concentration change against irradiation time at constant intensity of sound. Initial Fe^{++} concentration = 10^{-3} M.

Using this apparatus with the precautions observed above, and with the high tension supply to the oscillator kept constant at 2 kV, it was found that the oxidation of air-saturated 1/1000 M ferrous ammonium sulphate in N sulphuric acid was linear with time within the first 10-min. irradiation (Fig. 1). If after one six-min. exposure the solution was allowed to stand so as to become air-saturated once again, a further 6-min. exposure showed a further linear concentration change-time curve of identical slope to the first. The slope of such a curve provides an index of the chemical change per unit input of energy to the system, which will be referred to subsequently in this publication as the " yield " of the reaction.

When the initial Fe^{++} concentration of the solution was varied, and the yield determined in this way and plotted against initial Fe^{++} concentration, Fig. 2 was obtained. This shows a region of concentration independence extending from 5×10^{-4} M upwards, and is quite analogous to similar curves obtained using ionizing radiation.[13] Prud'homme and Grabar [1] have plotted a similar curve for the oxidation of potassium iodide solutions using ultrasonics, but the solutions used by these workers were of such high concentration that it is difficult to interpret their results on the basis of a purely indirect action.

---

[12] Fricke and Morse, *Phil. Mag.*, 1929, **7**, 129 ; Fricke and Hart, *J. Chem. Physics*, 1935, **3**, 60 ; Miller, *ibid.*, 1950, **18**, 79.

[13] Krenz, *Can. J. Res. B*, 1948, **26**, 647 ; Krenz and Dewhurst, *J. Chem. Physics*, 1949, **17**, 1337.

When the voltage of the power supply to the oscillator was varied between 1·5 and 2·8 kV, and the concentration change per unit time plotted against the sound energy output, i.e. the square of the voltage, another linear relation was observed (Fig. 3). A similar relationship has been observed by Weissler and Cooper in the oxidation of potassium iodide solutions containing traces of carbon tetrachloride by ultrasonic radiation.[8] Thus the further condition for the establishment of an indirect mechanism for the process is satisfied, i.e. that the yield of the reaction is independent of the intensity of the incident radiation.

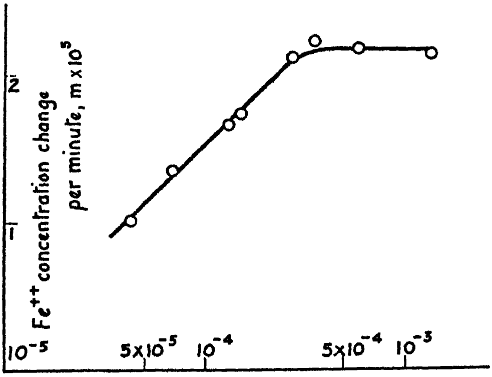

FIG. 2.—Air-saturated solutions—rate of Fe^{++} concentration change against initial Fe^{++} concentration at constant intensity.

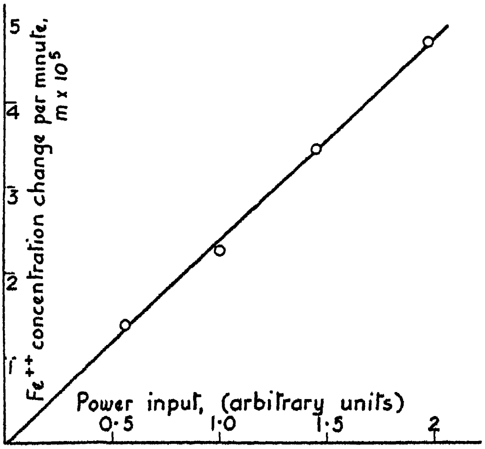

FIG. 3.—Air-saturated solutions—rate of Fe^{++} concentration change against intensity. Initial Fe^{++} concentration in each case = 10^{-3} M.

Discussion

We have, therefore, in seeking an explanation of these oxidations to look for a physical process by which a constant proportion of the energy of the sound waves is applied to the disruption of water molecules, presumably to give H atoms and OH radicals. Rough calorimetric measurements show that the proportion of the energy of the sound which is degraded in this way is very much lower than is the case with ionizing radiation. That the chemical change is associated with cavitation appears to be well established.[9] There appears to be a less well-established correlation between the " sonoluminescence " noted in aqueous solutions under ultrasonic irradiation and the chemical change observed.[14] The writer has found further evidence in support of this correlation in that the chemical change, like the sonoluminescence, has been found to be suppressed by raising the temperature of the solution to above 50° C.

---

[14] Harvey, *J. Amer. Chem. Soc.*, 1939, **61**, 2392 ; Bresler, *Acta physicochim.*, 1940, **12**, 323 ; Prud'homme, *J. Chim. Phys.*, 1949, **46**, 318.

The theory which is at present most widely accepted is that of Frenkel,[15] where the chemical change is attributed entirely to electrical discharges occurring on the growth of the cavities. If this is the case, the analogy with ionizing radiation is obvious. The most striking support for this theory is afforded by the fact that the yield observed in solutions saturated with different gases is related to the balloelectric potential built up on the surface of water droplets when water is atomized in the corresponding gaseous atmospheres, i.e. when the liquid-gas interface is rapidly expanded.[16] Thus, water atomized in a hydrogen atmosphere builds up very little charge,[17] while virtually no chemical change is noted in the irradiation of hydrogen-saturated solutions with ultrasonics, although copious cavitation is observed under these conditions. Another important piece of evidence supporting this theory is supplied by the observation of Flosdorf *et al.*[5] that the sonoluminescence originates from the surface of the cavities. Further hypotheses are that on the collapse of the cavities (i) oxygen molecules are raised to excited levels and thus disrupted,[18] or (ii) water molecules are similarly disrupted. The energy available, according to Lord Rayleigh,[19] is ample for these processes to occur. Finally, (iii) a "mechano-chemical" theory has been proposed by Marboe,[20] who suggests, in principle, that at the rapidly-forming surface of the cavities formed in water, some hydrogen-oxygen, rather than hydrogen, bonds are broken.

The following observations which the writer has made are not consistent with suggestions (i) and (ii) above. (i) The yield is independent of the oxygen concentration over a wide region of this concentration. This is evident both from the fact that the concentration-time curve is linear within the first few minutes of irradiation despite the rapid exhaustion of gas from solution during this period, and from the observation that this curve shows a very similar slope whether the solution is initially saturated with air or oxygen. If the activation of oxygen were the chief mechanism by which the chemical change occurred, the oxidation rate would be expected to be proportional to the oxygen concentration. (ii) The yield in solutions saturated with nitrogen is less than 1/10th that observed in air-saturated solution. If the activation of water molecules, leading to dissociation into H atoms and OH radicals, were predominant, the rate observed in nitrogen and hydrogen-saturated solutions would not be expected, by analogy with ionizing radiation, to be less than 1/2·5 of that observed in oxygen-saturated solution.[21]

These quantitative observations are consistent with the theory of Frenkel,[15] namely, that the chemical action observed is due to electrical discharges set free in the solutions. On this assumption, the conclusion is reached that if water molecules are raised to excited levels and disrupted by processes other than ionization and its consequences, the fragments must recombine quickly by a Franck-Rabinowitch process before they are able to escape from the shell of solvent molecules and react with the solute.

On the other hand, the mechano-chemical approach of Marboe is not ruled out by these findings. The ease of breaking of chemical bonds at an interface is known in certain cases to be dependent on the atmosphere in which the break takes place, and the solution of the problem may well lie in a combination of these two effects, the nature of the chemical bonds broken at the interface determining the charge which builds up across it. The importance of traces of different solutes in determining the charges built up in the disruption of water has been emphasized by Dorsey.[22]

---

[15] Frenkel, *Acta physicochim.*, 1940, **12**, 317.

[16] Fottinger, *Hydraulische Probleme* (Berlin, 1936).

[17] Thomson, *Phil. Mag.*, 1894, **37**, 341.

[18] Beuthe,[3]; Liu and Wu [4]; Flosdorf *et al.*[5]; Loiseleur, *Compt. rend.*, 1944, **218**, 876.

[19] Rayleigh, *Phil. Mag.*, 1917, **34**, 94.

[20] Marboe, *Chem. Eng. News*, 1949, **27**, 2198.

[21] Miller, *Nature*, 1948, **162**, 448; *J. Chem. Physics*, 1950, **18**, 79.

The writer wishes to record his gratitude to the National Research Council of Canada for the use of experimental facilities, and to Dr. G. Thyssen for advice and discussions.

Department of Natural Philosophy,
The University,
Drummond Street,
Edinburgh, 8.

---

[22] Dorsey, *Properties of Ordinary Water-Substance* (Reinhold, N.Y., 1940), p. 609.

OXYGEN OVERVOLTAGE

PART II.—THE INFLUENCE OF HYDROGEN ION CONCENTRATION, NATURE OF ELECTROLYTE, TEMPERATURE, AND ADDITION OF FLUORIDE

BY A. HICKLING AND S. HILL

Received 19*th September,* 1949

The influence upon oxygen overvoltage of wide variation of hydrogen ion concentration and nature of electrolyte, of temperature, and of the presence of fluoride ions, has been investigated for representative electrodes in the c.d. range 10^{-5} to 1 A/cm.^{2}. Decrease of pH and increase of temperature lower oxygen overvoltage by an amount which is in general greater the higher the overvoltage. Decrease of pH progressively reduces the slopes of the linear portions of the η—log I graphs and also favours the general approximation to linearity of these graphs.

Increase of temperature has little influence upon the slopes of the η—log I graphs, decreasing them slightly in some cases, but displaces any steps in the graphs to regions of higher c.d. Addition of fluoride produces an increase in overvoltage specific to platinum materials, which is greater the higher the overvoltage and the larger the concentration of fluoride; the increase is much greater in acid than in alkaline electrolytes.

In continuation of the work described in Part I of this series,[1] the effects upon oxygen overvoltage of wide variation of hydrogen ion concentration and nature of electrolyte, of alteration of temperature, and of the addition of fluoride to the electrolyte, have been investigated for representative electrodes in the current density (c.d.) range 10^{-5} to 1 A/cm.^{2}.

Experimental and Results

The general experimental procedure was the same as described in Part I.[1]

Influence of Electrolyte and pH.—Smooth platinum and gold were chosen as anodes for detailed study since they are relatively inert and can be used in acid solutions, and the previous work in alkaline solution had shown that they exhibited two different types of variation of overvoltage η with c.d. I. Measurements have been made at c.d.'s of 10^{-5}, 10^{-4}, 10^{-3}, 10^{-2}, 10^{-1} and

---

[1] Hickling and Hill, *Faraday Soc. Discussion*, 1947, **1**, 236.

1 A/cm.², and where necessary at intermediate c.d.'s, with these anodes in three electrolytes: (*a*) N KOH (results obtained in Part I [1]). (*b*) phosphate buffer composed of 0·2M KH_2PO_4 + 0·2 M Na_2HPO_4, pH 6·8, and (*c*) N H_2SO_4. The values of overvoltage obtained at each of the six standard c.d.'s are recorded in Table I, and in Fig. 1 are shown the corresponding $\eta - \log I$ graphs.

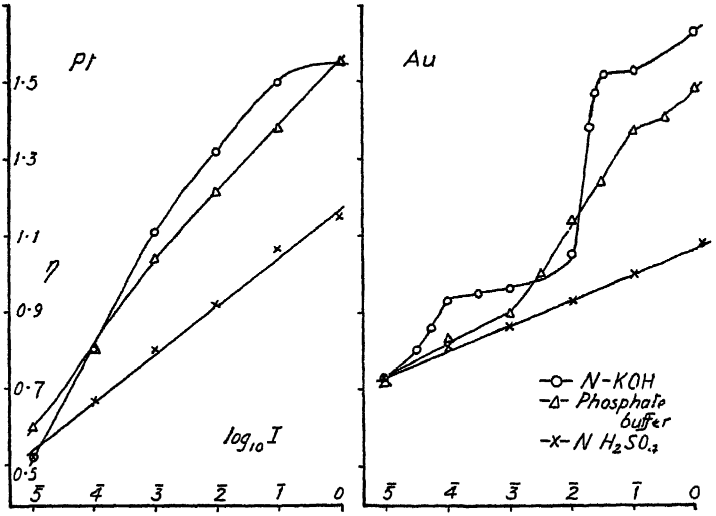

Fig. 1.—Influence of electrolyte.

For both platinum and gold, change of pH from 14 to 0 causes very little change in overvoltage at the lowest c.d., but at the highest c.d. the overvoltage is lowered by *ca.* 0·4 V for Pt, and 0·6 V for Au; with Pt there is a general tendency for the slope of the $\eta - \log I$ graph to decrease with decreasing pH from 0·30 in N KOH to 0·20 in phosphate buffer and to 0·13 in N H_2SO_4. With gold the most striking feature is the progressive elimination of the steps in the $\eta - \log I$ graph as the pH decreases. The steep rise of *ca.* 0·5 V in overvoltage which occurs in alkali at a c.d. slightly higher than 10^{-2} A/cm.² is much less abrupt in neutral solution, being spread over a range of *ca.* 10^{-3} to 10^{-1} A/cm.², and disappears completely in acid solution where a straight line graph of slope 0·07 is obtained.

TABLE I

Anode Material	C.d. A/cm.²	Overvoltage in Volts		
		N KOH	Phosphate Buffer	N H_2SO_4
Pt	10^{-5}	0·52	0·60	0·52
	10^{-4}	0·80	0·81	0·67
	10^{-3}	1·11	1·04	0·80
	10^{-2}	1·32	1·21	0·92
	10^{-1}	1·50	1·38	1·07
	1	1·55	1·56	1·15
Au	10^{-5}	0·73	0·72	0·73
	10^{-4}	0·93	0·83	0·81
	10^{-3}	0·96	0·90	0·86
	10^{-2}	1·05	1·14	0·93
	10^{-1}	1·53	1·37	1·00
	1	1·63	1·48	1·08

As in alkaline solution, the step in the $\eta - \log I$ graph for Au in neutral solution appeared to be associated with a change in the surface of the anode. Thus at 10^{-8} A/cm.^{2} the Au anode became covered with a reddish-yellow film which became a bright brown red at higher c.d.'s ; this film was soluble in dilute HCl with effervescence. In acid solution the Au anode developed a greenish coating (soluble in dilute HCl) which again became a bright brown red at high c.d.'s. The Pt anode was not visibly attacked in any of the solutions used.

Supplementary experiments with a Pd anode, which also gives a step in the η — log I graph in alkali, showed the same general tendencies as with Au. With decrease of pH the step became much less marked and the slopes of the linear portions of the graph were reduced. To ascertain if the nature of the cation present has any influence upon oxygen overvoltage, measurements were made at a Pt anode in N NaOH ; the overvoltages were not appreciably different from those obtained with a N KOH electrolyte.

Influence of Temperature.—Measurements of oxygen overvoltage were made at each of the six standard c.d.'s and, where necessary to define the η —log I graphs at intermediate c.d.'s, for anodes of Pt, Au, platinized Pt, and Co in N KOH at 70° C, and for anodes of Pt and Au in N H_2SO_4 at 70° C. Pt and Au were chosen as high overvoltage metals, Pt giving an approximately linear η — log I graph and Au typifying the step-like behaviour found for several anodic overvoltages ; platinized Pt was chosen as an anode of moderate overvoltage, and Co as one of low overvoltage, both metals becoming readily passive and giving steady overvoltages in a reasonable period of polarization. The electrolytic cell was suspended in a 1 l. beaker of heavy paraffin oil directly heated by a Bunsen flame, and by careful manual control it was found possible to maintain the temperature at 70 ± 1° C over long periods. The customary internal hydrogen reference electrode was used, and the E.M.F. of the hydrogen-oxygen cell was taken to be 1·19 V at 70° C ; this value was then subtracted from the measured anode-reference electrode potential to obtain the oxygen overvoltage of the working electrode. The electrodes were prepared in the usual manner ;[1] before use at 70° C a new measurement of oxygen overvoltage at 20° C was made in each case so as to obtain exactly comparable values, and these sometimes differ slightly from the earlier values quoted[1] although in general the reproducibility is highly satisfactory. The results are summarized in Table II, and the η — log I graphs are given in Fig. 2 and 3.

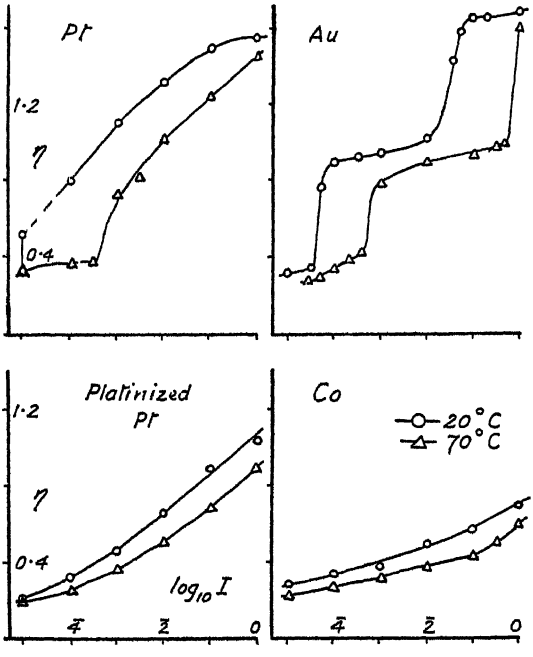

FIG. 2.—Influence of Temperature in N KOH.

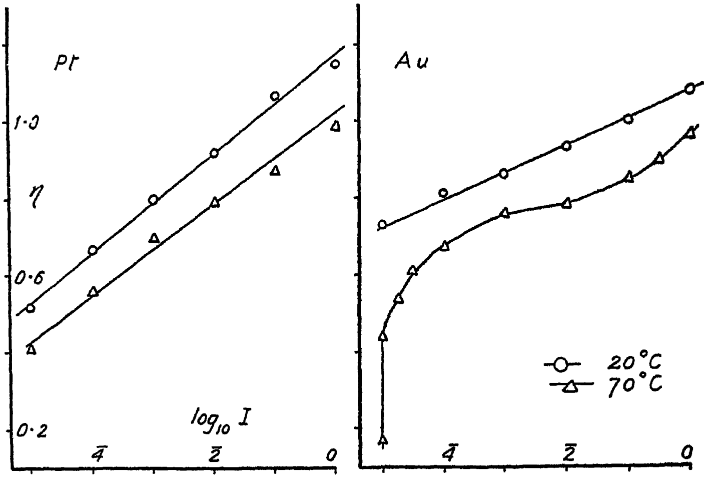

FIG. 3.—Influence of Temperature in N H_2SO_4.

TABLE II

Anode Material	C.d. A/cm.^{2}	Overvoltage in Volts			
		N KOH		N H_2SO_4	
		20° C	70° C	20°C	70° C
Pt	10^{-5}	0·33, 0·52	0·33	0·52	0·41
	10^{-4}	0·80	0·37	0·67	0·56
	10^{-3}	1·11	0·73	0·80	0·70
	10^{-2}	1·32	1·02	0·92	0·79
	10^{-1}	1·50	1·24	1·07	0·87
	1	1·55	1·46	1·15	0·99
Au	10^{-5}	0·32	—	0·73	0·17, 0·44
	10^{-4}	0·90	0·35	0·81	0·67
	10^{-3}	0·95	0·79	0·86	0·76
	10^{-2}	1·03	0·90	0·93	0·78
	10^{-1}	1·67	0·94	1·00	0·85
	1	1·70	1·62	1·08	0·97
Platinized Pt	10^{-5}	0·21	0·20	—	—
	10^{-4}	0·32	0·25	—	—
	10^{-3}	0·46	0·36	—	—
	10^{-2}	0·66	0·51	—	—
	10^{-1}	0·89	0·69	—	—
	1	1·14	0·90	—	—
Co	10^{-5}	0·28	0·23	—	—
	10^{-4}	0·34	0·27	—	—
	10^{-3}	0·38	0·32	—	—
	10^{-2}	0·50	0·37	—	—
	10^{-1}	0·58	0·43	—	—
	1	0·71	0·61	—	—

It is seen that in every case the oxygen overvoltage is lower at 70° C than at 20° C and there are appreciable changes in the shapes of the graphs. In the case of Pt in N KOH at 70° C there is a well-marked step in the η — log I graph at *ca.* 3×10^{-4} A/cm.^{2}; at 20° C no such step appeared, although at the lowest c.d. abnormally low values of overvoltage were occasionally observed.

With Au in N KOH at 70° C, there are two steps in the η − log I graph as at 20° C, but the steps now appear at c.d.'s about 20 to 30 times larger although between approximately the same values of overvoltage, so that the rise of temperature has effectively moved the whole graph laterally in the direction of higher c.d. The actual reduction in overvoltage at 70° C, between comparable portions of the graphs, is *ca.* 0·4 V at Pt, and *ca.* 0·15 V at Au, and the slope of the linear portion above the step for Pt is the same as at 20° C. The η − log I graphs for platinized Pt and Co in N KOH at 70° C have the same general shape as at 20° C but show a general decrease in overvoltage which becomes more marked as the c.d. increases. In N H_2SO_4 the effect of temperature seems somewhat less than in N KOH. With Pt there is a decrease in overvoltage of 0·1 to 0·2 V at 70° C, the decrease being greatest at high c.d.'s. Au shows a similar decrease over most of the c.d. range, but there seems to be some suggestion of a step at the lowest c.d.

Influence of Fluoride.—Addition of fluoride has been reported[2] to produce a considerable rise of oxygen overvoltage, and use is made of this in many technical electrolytic oxidation processes where a high anodic overvoltage is required. The phenomenon does not seem to have received any very detailed previous study and it has therefore been investigated in the present work. The experimental procedure was to polarize the anode under investigation at constant c.d. in pure electrolyte until its potential relative to an external hydrogen reference electrode became steady, the usual technique of potential measurement being employed; a measured quantity of N KF solution was then added, the electrolyte thoroughly mixed with a vigorous stream of oxygen, and the observation of the potential continued. Measurements were made using electrolytes 0·02 N and 0·1 N with respect to potassium fluoride for anodes of Pt, Au, Co, platinized Pt, and Pd in N KOH, and for Pt in N H_2SO_4, at c.d.'s of 10^{-5} and 1 A/cm.^{2} and at one intermediate c.d.

The surprising result was obtained that only with platinum anodes did any change of overvoltage occur on addition of fluoride; with all the other anodes investigated no appreciable alteration could be observed. With Pt an immediate rise of overvoltage was produced which was greater the higher the c.d., and was more marked in the acid than in the alkaline electrolyte; platinized Pt showed a much smaller effect, similar to that of smooth Pt at low c.d.'s. Some typical results are summarized in Table III.

TABLE III

Anode Material	Electrolyte	C.d. A/cm.^{2}	Elevation of Overvoltage V (V)	
			0·02N KF	0·1N KF
Pt	N KOH	10^{-5} 10^{-2} 1	0·01 0·06 0·03	0·01 0·11 0·16
Pt	N H_2SO_4	10^{-5} 10^{-2} 1	0·04 0·10 0·18	0·06 0·31 0·35
Platinized Pt	N KOH	10^{-5} 10^{-2} 1	0 0 0·02	0 0·01 0·08

Since the effect seemed to be specific to platinum, it was thought that it might be due to some change produced by the fluoride in the electrode surface. To test this, a new platinum anode was polarized in N KOH + 0·1 N KF at the highest c.d. of 1 A/cm.^{2} until the increased overvoltage had been established, and it was then removed, washed in distilled water, and transferred to a duplicate cell containing pure N KOH. On again polarizing at 1 A/cm.^{2} it gave its normal (lower) overvoltage, indicating that no change had been produced by the fluoride sufficiently permanent to survive the simple washing and transfer to fresh electrolyte. It thus appears that it is the presence of fluoride *in the electrolyte* which produces the elevation of overvoltage at platinum.

---

[2] Müller, *Z. Elektrochem.*, 1904, **10**, 776; Müller and Scheller, *Z. anorg. Chem.*, 1905, **48**, 112; see also Isgarischev and Stepanov, *Z. Elektrochem.*, 1924, **30**, 138.

Discussion

The present results indicate very clearly the importance of working over an extensive range of c.d.'s in attempting to ascertain the influence of experimental variables upon oxygen overvoltage. Thus while at 10^{-5} A/cm.^{2} the overvoltage is practically the same in acid and alkaline electrolytes, in agreement with the results of Hoar[3] who worked in the c.d. range 10^{-4} to 10^{-7} A/cm.^{2}, at higher c.d.'s the overvoltage is very greatly affected by change of electrolyte. The general conclusion to be drawn from the present work is that decrease of pH progressively reduces the slopes of the linear portions of the $\eta - \log I$ graphs and also increases the general approximation to linearity of these graphs. Where the Tafel equation

$$\eta = a + b \log I$$

is approximately obeyed, the values of b at 20° C, and the corresponding values of α derived from the equation

$$\frac{2 \cdot 303\, RT}{\alpha F} \log I,$$

are as follows

	N KOH		Phosphate Buffer		N H_2SO_4	
	b	α	b	α	b	α
Pt	0·30	0·20	0·20	0·29	0·13	0·45
Au	—	—	—	—	0·07	0·84

The value of b for platinum in acid solution is in good agreement with that previously obtained by Bowden[4] (0·12) and Roiter and Yampolskaya[5] (0·13), leading to a value of α in the vicinity of 0·5, but any general similarity to the phenomenon of hydrogen overpotential, such as has been claimed,[6] seems completely illusory, since for gold in acid solution and for platinum in other solutions quite different values of α are obtained. Bowden and Keenan[7] found that in alkaline solution α was greater than in acid solution and increased with increasing hydroxyl ion concentration, and Stout[8] reported a value of $\alpha = 1 \cdot 0$ in 0·1 N NaOH. These results are in complete contradiction to those found in the present work in which b increases and α decreases in passing from acid to alkaline solutions. The most likely cause of the discrepancy is to be found in the different experimental conditions employed; the authors quoted worked over rather limited ranges of low c.d.'s and appear to have ignored the influence of time of polarization, which is very great in alkaline solution,[1] in arriving at their results.

Increase of temperature has been found to produce in all cases a lowering of overvoltage, and in general this seems to be greater the higher the overvoltage; at the same time, any steps in the $\eta - \log I$ graphs are displaced to regions of higher c.d. This displacement, which is very well shown in the graphs for gold in N KOH, is of particular interest;

---

[3] Hoar, *Proc. Roy. Soc. A*, 1933, **142**, 628.
[4] *Ibid.*, 1929, **126**, 107.
[5] *J. Phys. Chem. U.S.S.R.*, 1937, **9**, 763.
[6] Bowden and Agar, *Ann. Reports*, 1938, 90.
[7] Unpublished work, quoted in ref. 6.
[8] *Faraday Soc. Discussion*, 1947, **1**, 246.

it seems unmistakably to imply that these sudden increases in overvoltage correspond to the attainment of limiting rates of reaction which are increased by rise of temperature. According to the conventional activation treatment of overvoltage, the slope of the $\eta - \log I$ graphs should increase with rise of temperature since $b = 2{\cdot}303\ RT/\alpha F$, and α is usually assumed to be constant. Results in agreement with this were reported by Bowden[4] for platinum in sulphuric acid, but Roiter and Yampolskaya[5] found that b was practically independent of temperature in this case. The present results are in agreement with those of the latter workers, and indicate that in general b is either constant or decreases somewhat with rise of temperature. From comparable sections of the $\eta - \log I$ graphs, the following very approximate values of the temperature coefficient of oxygen overvoltage at constant c.d. may be quoted :

	N KOH	N H_2SO_4
Pt	— 0·007	— 0·0025 V/deg.
Au	—	— 0·0025
Co	— 0·001 to — 0·003	—
Platinized Pt . . .	— 0·0002 to — 0·004	—

It has become fashionable in recent years to use the temperature dependence of overvoltage to derive the energy of activation W of the electrode reaction at the reversible potential using the relations

$$\left(\frac{\partial \eta}{dT}\right)_I = -\frac{(W - \alpha\eta F)}{\alpha FT}$$

$$\left(\frac{\partial \log_e I}{dT}\right)_\eta = \frac{W - \alpha\eta F}{RT^2}.$$

This practice appears to the present authors to be very open to criticism. It assumes that the activation theory treatment does represent accurately the relations at the electrode under investigation,[9] and this rarely seems to be in agreement with experimental observations on oxygen overvoltage, and furthermore the values are usually arrived at from very limited experimental data, a slight change in which may very markedly affect the calculated energies. Thus values of 18·7 kcal.[4] and 25·3 kcal.[8] have been reported for the deposition of oxygen on platinum in acid and alkaline solutions respectively. This apparent precision seems to be quite misleading. Calculations from the data obtained in the present work at each of the six standard c.d.'s give values ranging from 12 to 23 kcal. for platinum in acid solution, and 8 to 15 kcal. for platinum in alkaline solution, and for other electrodes even wider variations have been found.

The investigation of the influence of fluoride reveals the curious result that while a substantial rise of overvoltage occurs at platinum anodes at high c.d.'s, the effect is apparently specific to this metal. A platinized platinum anode behaves in this respect like smooth platinum polarized at a much lower effective c.d. The effect does not even seem to be shared by other metals of the platinum family, since no elevation was found with palladium, and Müller and Scheller[3] likewise could detect no effect with iridium. At the same time, as pointed out above, the phenomenon is not apparently due to any poisoning of the platinum surface. This strongly suggests that the mechanism of oxygen evolution at a platinum electrode may differ in some fundamental respects from that at other anodes. In support of this, it has recently been found[10] that the presence of low concentrations of oxidizable substances containing sulphur and/or nitrogen may also bring about very large elevations of oxygen overvoltage at a platinum anode, and again the effect is not shared by other electrode materials.

---

[9] See Agar, *Faraday Soc. Discussion*, 1947, **1**, 81 for attempts at a more general treatment.

[10] Hickling and Wilson, *Nature*, 1949, **164**, 673.

One of the authors (S. H.) gratefully acknowledges financial assistance received from Peter Spence and Sons Ltd. during the course of this work.

Department of Inorganic and Physical Chemistry,
Liverpool University.

OXYGEN OVERVOLTAGE

PART III.—A NOTE ON THE STANDARD POTENTIALS OF THE HYDROXYL RADICAL AND ATOMIC OXYGEN

BY A. HICKLING AND S. HILL

Received 3*rd February*, 1950

The standard potentials of the OH radical and of atomic O against OH^- ions have been calculated to be + 2·00 and 1·59 V respectively for these species at 1 atm. pressure. If the rate-determining step in the anodic evolution of oxygen responsible for the irreversibility is one involving OH radicals, then a range of pressures of 10^{-24} to 1 atm. would serve to account for the observed overvoltages. The supposition that atomic O is responsible for the polarization would require an impossibly high pressure of this substance at high overvoltage anodes.

As an approach to the problem of the mechanism of oxygen overvoltage, it is of interest to see if the accumulation at an anode of any unstable product, which may be formed as an intermediate between the discharge of the hydroxyl ion and the evolution of gaseous oxygen, could account for the high overvoltages which are experimentally observed. Two possible intermediates are the hydroxyl radical and atomic oxygen, and their standard potentials and the maximum overvoltages which they would produce can readily be calculated from thermodynamic data now available.

The Standard OH/OH^- Potential.—If one considers the hypothetical cell

$$\ominus \quad \underset{1\text{ atm.}}{H_2\,(g)} \;\Big|\; \text{Aqueous electrolyte} \;\Big|\; \underset{1\text{ atm.}}{OH\,(g)} \quad \oplus$$

then the electrode reactions when current flows will be :

at the anode	$H_2 - 2\,e \rightarrow 2\,H^+$,
at the cathode	$2\,OH + 2\,e \rightarrow 2\,OH^-$,
and	$2\,H^+ + 2\,OH^- \rightarrow 2\,H_2O$,

and the net cell reaction for the passage of 2 faradays of electricity will be

$$H_2(g) + 2\,OH\,(g) \rightarrow 2H_2O\,(l).$$

Thus the E.M.F. E of the cell will be equal to $-\,\Delta G^\circ/2F$, where $-\,\Delta G^\circ$ is the decrease in free energy for the reaction for the substances in their standard states. Now for the reaction

$$H_2(g) + 2\,OH\,(g) \rightarrow 2\,H_2O\,(g),$$

we have

$$\frac{\Delta G^\circ}{T} = \left(\frac{G^\circ - E_0^\circ}{T}\right)_{2H_2O} - \left(\frac{G^\circ - E_0^\circ}{T}\right)_{2OH} - \left(\frac{G^\circ - E_0^\circ}{T}\right)_{H_2} + \frac{\Delta E_0^\circ}{T}.$$

At 25° C the free energy functions of the reacting substances are :

H_2 − 27·191,[1] OH − 36·842,[2] and H_2O (*g*) − 37·179.[3]

Thus for the reaction at the same temperature

$$\Delta G^\circ = 7901 + \Delta E_0^\circ.$$

From data obtained from the spectrographic study of the dissociation of water vapour Dwyer and Oldenberg[4] have determined the change in zero-point energies ΔE_0° as − 133,800 (± 1300) cal. Hence for the reaction at 25° C, $\Delta G^\circ = -$ 125,000 cal. Allowing now for a free energy decrease of 2053 cal. per mole for the conversion of H_2O (*g*) to $H_2O(l)$, ΔG° for the reaction

$$H_2\,(g) + 2\,OH\,(g) \rightarrow 2\,H_2O\,(l)$$

is − 130,000 cal. Hence the E.M.F. of the hypothetical cell is given by

$$E = \frac{130{,}000 \times 4{\cdot}184}{2 \times 96{,}500} = 2{\cdot}82\ V.$$

This is therefore the potential of an OH electrode at 1 atm. pressure against a hydrogen electrode dipping into the same solution. For a solution containing unit activity of OH^- ions the hydrogen potential is − 0·82 V, and thus the standard potential of the OH radical is + 2·00 V on the hydrogen scale. A previous value of + 1·4 V was deduced by Latimer[5] based on a calculated value for the heat of formation of OH from gaseous atoms of 116,000 cal.,[6] but later work indicated that this datum required revision.[7]

The Standard O/OH⁻ Potential.—This can readily be deduced by considering the hypothetical cell

⊖		⊕
O_2 (*g*)	Aqueous electrolyte	O (*g*)
1 atm.		1 atm.

in which the net reaction for the passage of 4 faradays of electricity is $2\,O \rightarrow O_2$. $-\Delta G^\circ$ for this reaction at 25° C can be calculated as before from available data[8] and is found to be 110,170 cal. Hence the E.M.F. of the above cell is given by

$$E = \frac{110{,}170 \times 4{\cdot}184}{4 \times 96{,}500} = 1{\cdot}19\ V,$$

and taking the standard potential of molecular oxygen as + 0·40 V, the standard potential of atomic oxygen is + 1·59 V on the hydrogen scale. This value is in agreement with that implicit (but not stated) in results given by Latimer.[9]

---

[1] Giauque, *J. Amer. Chem. Soc.*, 1930, **52**, 4816. For a more recent value see Wilson, *Chem. Rev.*, 1940, **27**, 17.

[2] Johnston and Dawson, *J. Amer. Chem. Soc.*, 1933, **55**, 2744.

[3] Gordon, *J. Chem. Physics*, 1934, **2**, 65.

[4] *Idem.*, *ibid.*, 1944, **12**, 351.

[5] *Oxidation Potentials*, 1938, p. 43. See also Bray, *J. Amer. Chem. Soc.*, 1938, **60**, 82.

[6] Bates, *Z. physik. Chem.* (Bodenstein-Band), 1931, 329.

[7] Cf. Taube and Bray, *J. Amer. Chem. Soc.*, 1940, **62**, 3357.

[8] Johnston and Walker, *ibid.*, 1933, **55**, 172, 187.

[9] *Op. cit.*, p. 37.

Discussion.—From the measurements made in Part I[10] of this work, in which 12 different anodes were studied in alkaline solution over the current density (c.d.) range 10^{-5} to 1 A/cm.^{2}, it is apparent that oxygen overvoltages may range between the values of *ca.* 0·2 to 1·6 V, the latter very high value being approached only by platinum and gold at a c.d. of 1 A/cm.^{2}. Since the standard potential of the OH radical has been calculated to be + 2·00 V and the standard potential of oxygen is + 0·40 V, the maximum overvoltage which the OH radical could cause at 1 atm. pressure would be 1·6 V. If it is supposed that the potential of the OH electrode varies with pressure in the usual way for a gas electrode, then in the vicinity of room temperature the overvoltage (if due to OH radicals) would be given by

$$\eta = 1{\cdot}60 + 0{\cdot}058 \log p_{\text{OH}}.$$

Thus the overvoltage range 0·2 to 1·6 V would correspond to a variation of pOH between about 10^{-24} and 1 atm. Bearing in mind that the OH radical is relatively stable[11] and that it is being constantly formed at a working anode, it would appear that this range of pressures is not impossible if the rate-determining stage in the electrode reaction involves the OH radical.[12]

The overvoltage to which atomic oxygen at 1 atm. pressure could give rise would be 1·19 V, and this is much lower than the maximum overvoltages which have been observed. Assuming the usual variation of potential with pressure, an overvoltage of 1·6 V would correspond to a pressure of atomic oxygen of the order 10^{14} atm., which is hardly conceivable in practice. It thus appears that no rate-determining reaction dependent upon atomic oxygen, such as $2O \rightarrow O_2$, would account for the experimental overvoltages.

The authors are indebted to Prof. Wendell M. Latimer for helpful comments. One of the authors (S.H.) gratefully acknowledges financial assistance received from Peter Spence and Sons Ltd. during the course of this work.

Department of Inorganic and Physical Chemistry,
Liverpool University.

[10] Hickling and Hill, *Faraday Soc. Discussion*, 1947, **1**, 236.

[11] Cf. Oldenberg, *J. Chem. Physics*, 1935, **3**, 266.

[12] It is not of course implied that the OH radical would necessarily exist at low overvoltage anodes completely in the free state, but the pressure of free OH is a convenient index to the electromotive activity of any compound or adsorption complex which might be formed.

THE ELECTROKINETIC BEHAVIOUR OF ICELAND SPAR AGAINST AQUEOUS ELECTROLYTE SOLUTIONS

BY H. W. DOUGLAS AND R. A. WALKER

Received 8th February, 1950

An electro-osmotic method has been used to determine the zeta potential of pure Iceland Spar against CO_2-free water, its own saturated solution, and the effect of increasing concentration of dissolved electrolytes, $CaCl_2$, $BaCl_2$, $Pb(NO_3)_2$, $MgCl_2$, NaCl, NaOH, Na_2CO_3, $(NaPO_3)_6$ and others. The initial, negative zeta potential of the calspar, and its variation with dissolved electrolytes, was found to depend on its pretreatment. In particular, etching with very dilute mineral acid caused the potential to shift irreversibly to more negative values, an effect consistent with irregular pitting of the surface as shown by the electron microscope. The results have been considered in terms of an electrical double layer of the Stern type, of the crystal surface and hydration forces acting on the various ions, Ca^{++} and $CO_3^{=}$ in particular, and of the Paneth-Fajans rules for adsorption on to ionic lattices. The results indicate strong adsorption of positive ions to form a series $Ca^{++} > Ba^{++} > Pb^{++} > Mg^{++} >$ (Na^+ as reference), and of negative ions to form a series, Cl^- (as reference) $< OH^- < HCO_3^-$ or $CO_3^{=} < (PO_3^-)_6$.

Much work has been done relating the electrokinetic behaviour in aqueous media of a wide variety of insoluble and sparingly soluble substances with the ionic composition of the aqueous phase [1, 2] and the Gouy [3] and Stern [4] theories have proved of considerable value in interpreting the results obtained. Considerably less work has been carried out with a view to relating the electrokinetic behaviour with the physical and chemical nature of the insoluble substances.

The electrophoretic behaviour of members of various aliphatic homologous series (*n*-paraffins, alcohols, halides, carboxylic acids and esters) has been the subject of a number of investigations [5, 6, 7, 8] carried out in this Department, the results of which indicate that the electrokinetic behaviour of such compounds is related to the chemical structure and orientation of the surface molecules, though a satisfactory general theory has still to be formulated.

Sparingly soluble crystalline inorganic compounds, often occurring naturally in the form of highly crystalline minerals, constitute another group of compounds suited to the investigation of the relation between physical and chemical properties and electrokinetic behaviour. Capable of giving rise to ions themselves, in addition to adsorbing other ions from solution, the evaluation of their electrokinetic behaviour should be of material assistance in advancing electrical double layer theory. Much quantitative information exists concerning the crystal and chemical structures of many of these compounds and already one of the few pure crystals studied electrokinetically, silver bromide,[9] has been subjected to theoretical treatment in terms of its lattice structure.[10] Silver iodide has been studied experimentally by Kruyt and co-workers [11] whilst barium sulphate, both as barytes and in the form of prepared precipitates, has been the subject of a number of recent investigations.[12, 13, 14]

The present paper records some of the results obtained in an investigation of the electro-osmotic behaviour of a specimen of Iceland Spar, chosen for its high crystalline quality, low solubility, ionogenic nature and known structure, in various selected aqueous electrolyte solutions, as a contribution to the general problem of electrokinetic behaviour and structure.

[1] Freundlich, *Colloid and Capillary Chemistry*, trans. 2nd Edn. (Methuen, 1926), p. 255.

[2] Abramson, *Electrokinetic Phenomena* (Chemical Catalog Co., New York, 1934), Chap. 7 and 8.

[3] Gouy, *J. Physique*, 1910, **9**, 457.

[4] Stern, *Z. Elektrochem.*, 1924, **30**, 508.

[5] Dickinson, *Trans. Faraday Soc.*, 1941, **37**, 140.

[6] Douglas, *ibid.*, 1943, **39**, 305.

[7] Williams, *ibid.*, 1940, **36**, 1042.

[8] Price and Lewis, *ibid.*, 1933, **29**, 775.

[9] Julien, *Thesis* (Utrecht, 1933).

[10] Mott and Grimley, *Faraday Soc. Discussion*, 1947, **1**, 3.

[11] Kruyt and Verwey, *Z. Physik. Chem. A*, 1933, **167**, 137, 149 and 312.

[12] Ruyssen, *J. Physic. Chem.*, 1940, **44**, 265.

[13] Reyerson, Kolthoff and Coad, *ibid.*, 1947, **51**, 321.

[14] Buchanan and Heymann, *Proc. Roy. Soc. A*, 1948, **195**, 150.

Experimental

The Apparatus.—The apparatus used in determining the electro-osmotic flow of the various electrolyte solutions employed through plugs of Iceland Spar is shown diagrammatically in Fig. 1. It is a modification of the apparatus previously employed by Ham and Douglas.[15] The plug of spar crystals A was contained between discs of platinum gauze (40 mesh) B and C covered by circles of fine gauge bolting silk (150 mesh) to prevent leakage of the crystals (80-100 mesh). Three platinum spiral leads, from each of the discs were fused through glass connecting tubes and insulated from the solutions employed by coating with Robialac synthetic paint. By mercury connexion, the platinum discs served as reference electrodes for the adjustment of the operating P.D. across the plug, imposed by means of the reversible calomel electrodes E and F. The connecting tube for one of the reference electrodes B passed through a glass sleeve D (sealed by a length of rubber tubing), so that the plug length could be adjusted up to a maximum of approximately 5 cm. The electro-osmotic flow was determined by observing the rate of movement of a cylindrical air bubble, length approx. 5 × diameter,[16] introduced by means of a side tube I into the capillary tube GH, the bore and uniformity of which were accurately determined using a mercury thread. The plugs employed had a diameter of 1 cm. and were 3 cm. or more in length; the manipulation involved in forming the plugs, washing and filling the apparatus with the solutions was similar to that described by Ham and Douglas.[15] Tapping the walls of the containing tube with a rubber hammer was found to ensure reproducibility of packing of the plugs, within 1 %, as characterized by their specific hydrodynamic resistance to water and their specific electrical resistance to N/10 KCl solution. The total hydrodynamic resistance of the plugs was always at least 100 times that of the capillary tube for the same pressure head; so that the movement of the air bubble in the latter should correspond within 1 % to the full electro-osmotic flow through the plug. For uniform movement of the recording bubble and reproducibility of results the complete absence of grease from internal surfaces was found to be essential; this was assured by frequent cleaning with acid cleaning mixture followed by thorough washing with distilled water and the solution to be used.

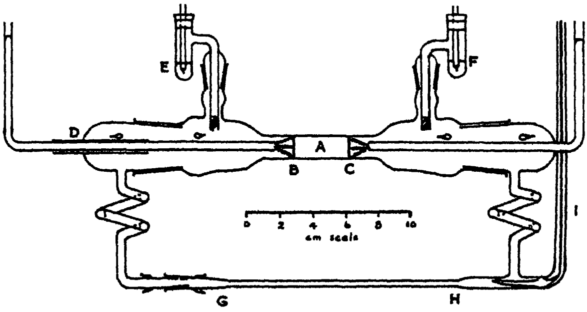

FIG. 1.

To conform with general electrokinetic practice the electro-osmotic data have been expressed in terms of the zeta potential, the necessary auxiliary electrical conductivity measurements being made using a modified Poggendorf bridge arrangement and 1000 cycle A.C. The apparatus was thermostated and all measurements made at 25 ± 0·1° C, the overall experimental error was estimated to be about 3 %.

Materials.—The Iceland Spar was initially in the form of colourless crystals, length of side half to 1 in. and having occasional internal "feather" fractures. They were crushed in a bright molybdenum steel percussion mortar and the product screened, using bolting silk sieves, into fractions of narrow size distribution. The fraction passing through the 80 mesh sieve and retained by the 100 mesh sieve, average diameter 2×10^{-2} cm., was used to form most of the plugs employed; slightly finer crystals were used for a number of the measurements and yielded the same zeta potential values.

---

[15] Ham and Douglas, *Trans. Faraday Soc.*, 1942, **35**, 404.
[16] Fairbrother and Stubbs, *J. Chem. Soc.*, 1935, **138**, 527.

Before use in the apparatus the sieved crystals were freed from adhering finer particles by agitating in water, allowing to stand for a few minutes and then decanting off the supernatant suspension. They were then boiled for an hour or more with distilled water in a covered quartz beaker, a treatment found to give reproducible behaviour from one batch of material to another, as shown by the constancy of the calculated zeta potentials towards water and N/10 Na^+ ion buffer of pH 9, and to regain the initial state after following through the effect of various electrolytes. Originally it was planned to clean the crystals by dissolving off the outside layers with limited amounts of dilute solutions of a mineral acid. However, such treatment was found to cause an irreversible change in behaviour, varying reproducibility with the concentration of the acid and the duration of treatment, and has only been carried out in a brief investigation of the effect. The various electrolytes used were all of A.R. quality and their solutions were made up using CO_2-free distilled water. Despite the slight solubility of calcite in water, the electro-osmotic behaviour of the crystals against distilled water and solutions of various salts was found to be independent of time for periods of observation on occasion up to several days. As measurements were normally made within 2 hr. of setting up the apparatus and filling with any solution, such solutions were not presaturated with calcite. Measurements of pH were carried out using either a glass electrode or a Hildebrand H_2 electrode and a valve potentiometer.

Evaluation of the Zeta Potentials.—According to Smoluchowski[17] the following equation holds for any porous diaphragm, independent of its structure,

$$\zeta = \frac{4\pi\eta v\kappa}{\epsilon i}. \qquad \qquad (1)$$

ζ is the electrokinetic potential, ϵ and η are respectively the dielectric constant and the viscosity within the double layer, v is the rate of electro-osmotic flow of liquid (volume per unit time) and κ is the specific conductivity of the liquid. In the present work the potential drop V across the diaphragm and its resistance R were measured and not the current i; substituting $i = V/R$,

$$\zeta = \frac{4\pi\eta v}{\epsilon} \cdot \frac{\kappa R}{V}. \qquad \qquad (2)$$

From the derivation, this equation is valid only if the effective diameter of the channels through which the liquid flows are large compared with the thickness of the electrical double layer. This condition should certainly hold for the diaphragms of 80-100 mesh crystals employed here, even for the most dilute solutions.

Further, no allowance is made for the existence of surface conductance in deriving eqn. (1) and (2). Owing to a significant contribution by surface conductance and possibly to slight solution of the plug material, the specific conductance of the more dilute solutions differed in the bulk, κ_B, and in the plug, κ_p, and the latter is the value appropriate to eqn. (2). If R_p is the measured resistance of the plug containing this solution, eqn. (2) may be written

$$\zeta = \frac{4\pi\eta v}{\epsilon} \cdot \frac{\kappa_p R_p}{V}, \qquad \qquad (3)$$

where κ_p is not known. According to the method adopted by Fairbrother[18] and by Briggs[19] this difficulty may be overcome as follows. Specific conductance and resistance are related by the general equation

$$R\kappa = (l/q), \qquad \qquad (4)$$

where q/l is the conductance capacity of the system and equal to the effective area cross-section q divided by the effective length l for a conductivity cell. Assuming the conductance capacity to be constant for a porous plug,

$$R_p\kappa_p = R_{KCl}\kappa_{KCl} \qquad \qquad (5)$$

R_{KCl} being the measured resistance of the plug to N/10 KCl solution, for which the surface conductance effect is negligible and the bulk specific conductance κ_{KCl} is accurately known. Thus the expression

$$\zeta = \frac{4\pi\eta v}{\epsilon} \cdot \frac{\kappa_{KCl} R_{KCl}}{V} \qquad \qquad (6)$$

should yield the true ζ values.

---

[17] Smoluchowski, *Graetz' Handbuch*, II, p. 374.

[18] Fairbrother and Varley, *J. Chem. Soc.*, 1927, **130**, 1584.

[19] Briggs, *J. Physic. Chem.*, 1928, **32**, 663.

In a recent paper, Overbeck and Wijga [20] have given details of an analysis which throws doubt on the validity of this method for allowing for the effect of surface conductance for a plug of granular material, as employed in the present work. According to their analysis, the conductance capacity of such a system is not a constant, and the ζ values calculated by means of eqn. (6) will still be lower than the true values, the difference being greatest in the most dilute solutions where surface conductance is most significant. Experimental figures quoted by these workers for granular diaphragms and for capillaries of the same Pyrex glass appear to confirm the analysis and show the effect to become significant for solutions below about 10^{-3} M. It is, however, assumed that the ζ potential of the glass employed is independent of its material form. Some of the data presented here, and the contemporary experimental findings of Buchanan and Heymann [14] for barium sulphate, suggest that the topography of a surface is an important factor in determining the magnitude of the ζ potential exhibited by it; the surface of a Pyrex capillary, intact and after crushing, will certainly differ somewhat in this respect.

In view of this uncertainty and others, including that of the appropriate values for the dielectric constant and the viscosity, eqn. (6) has been retained. It is to be borne in mind that in so far as such uncertainties exist the numerical ζ values recorded in this paper have a formal significance only, though they may more confidently be used in comparing the effects of the various electrolytes studied.

Results

The results obtained are largely summarized in Fig. 2, 3, 4 and 5, which record the zeta potential of samples of calcite as a function of the molar concentration of solutions of various electrolytes. Fig. 2 records the variation in the calculated zeta potential of two calcite samples, one treated with boiling water only, the other treated first with a limited amount of dilute HCl and then with distilled water, in aqueous solutions of the electrolytes $CaCl_2$ and Na_2CO_3, providing lattice ions in solution, and of NaCl, as a reference electrolyte not likely to show any specific effect but exerting its influence only in the diffuse part of the double layer. The ζ potential of the water treated calcite was found to be − 15 mV against its own saturated solution in CO_2-free water; the concentration of this solution has been taken as about 0·15 millimolar.[21]

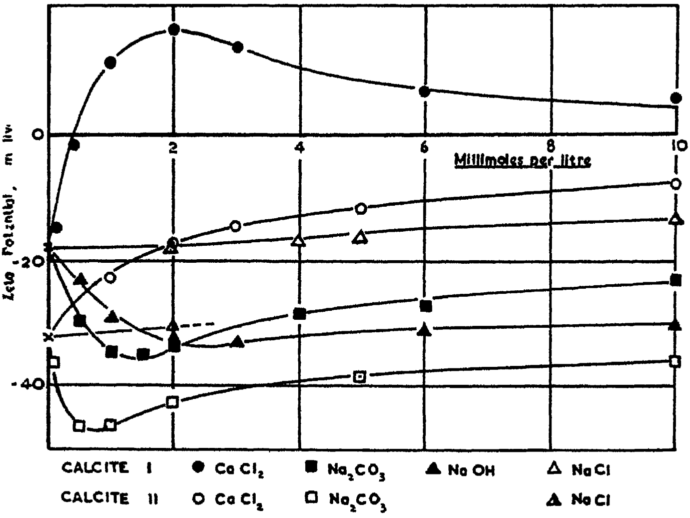

FIG. 2.

---

[20] Overbeek and Wijga, *Rev. trav. Chem.*, 1946, **65**, 556.

[21] Siedell, *Solubilities of Inorganic and Metal Organic Compounds*, 3rd Edn. (Van Nostrand, 1940).

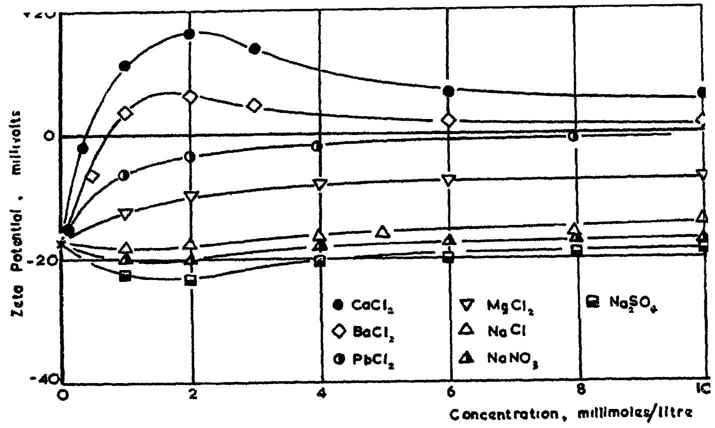

FIG. 3.

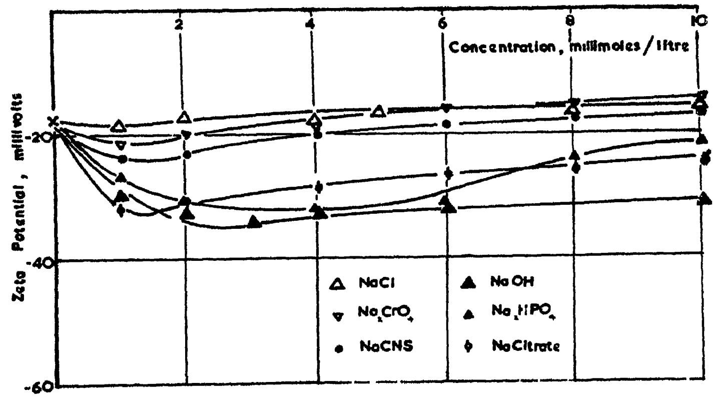

FIG. 4.

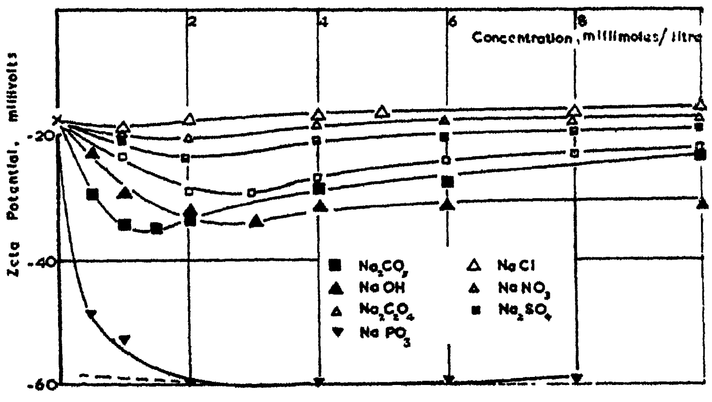

FIG. 5.

The curves for the water-treated calcite represent one observed limit to the behaviour of calcite; the curves for the acid-treated calcite are representative of, but do not mark the limit of, the change in behaviour for such material, though they do illustrate the shift to more negative zeta values which such treatment always produced. The change produced by successive treatments of any sample with limited amounts of dilute HCl and other mineral acids did, however, appear to reach a limit, dependent on the strength of the acid solution, at about − 40 mV against distilled water.

The ζ-potential-concentration curves obtained with electrolytes chosen with a view to determining the effect of a selection of +ve ions are shown in Fig. 3, whilst for −ve ions most of the curves are assembled in Fig. 4 and 5. Determinations made at decreasing salt concentrations, after the maximum, gave ζ curves which retraced those obtained for increasing salt concentrations, for all electrolytes except Na_2HPO_4 and glassy $NaPO_3$. For these two electrolytes the ζ potentials for the descending curve remained high at low concentrations, as indicated by the dotted curves in Fig. 4 and 5.

Discussion

The electro-osmotic measurements show the effective charge on the surface of calcite to be negative against water and its own saturated solution at 25° C. This is in agreement with the result obtained by Buzach and Dux [22] for microscopic particles; Malinowskaya and Gortikov[23] obtained the opposite result for some samples but their materials and technique seem doubtful.

When a calcite surface comes into contact with water or an aqueous electrolyte solution, two processes could conceivably operate to give rise to the electrical double layer of which the electro-osmotic effect is a manifestation: (*a*) either Ca^{++} or $CO_3^{=}$ might preferentially leave the crystal surface and pass into solution and result in the surface acquiring a charge of opposite sign which would tend to retain the ions lost against thermal agitation in the solution and so lead to the formation of an electrical double layer. (*b*) The surface might preferentially adsorb H^+, OH^- or other ions present in aqueous solution, and so acquire a net charge which would again lead to the formation of a diffuse double layer.

Considering process (*a*), the limited solubility of calcite shows that both Ca^{++} and $CO_3^{=}$ can and do leave the lattice. The relative tendencies of these ions to do so will be determined by two factors (i) the energy required to remove a Ca^{++} or $CO_3^{=}$ ion from the surface against the crystal forces, this will vary for successive ions of the same kind, and (ii) the hydration energies of Ca^{++} and $CO_3^{=}$ ions. The former quantities are not known; regarding the latter, the hydration energy of Ca^{++} will presumably not be very different from its heat of hydration, which is given as 17·7 eV (410 kcal. per mole) by Gurney.[24] An approximate value of 300 kcal. per mole is obtained for the hydration energy of $CO_3^{=}$ if an equivalent spherical radius of ~ 2 Å is used in the simple expression due to Born. The value of 2 Å is close to that obtained from the volume of the $CO_3^{=}$ ion in crystals calculated from details of its shape and dimensions as given by Bragg,[25] and is rather less than a value of 2·5 Å calculated from the limiting ionic mobility of $CO_3^{=}$ in water, assuming Stokes' law. The order of these heats of hydration is consistent with Ca^{++} leaving the lattice preferentially, which would thus acquire a negative charge.

Considering process (*b*) the ζ potential-concentration curves presented in Fig. 2, 3 and 4 show that the magnitude of the ζ potential varies very considerably in the presence of Ca^{++}, OH^- and $CO_3^{=}$ and certain other ions. As will be discussed later, this indicates strong adsorption of such ions from aqueous solution. Thus for calcite in CO_2-free distilled water, adsorption of OH^- ions might be a potential determining factor, operating also against competition in solutions containing other ions.

---

[22] Buzach an Dux, *Kolloid-Z.*, 1938, **83**, 279.

[23] Malinowskaya and Gortikov, *Colloid J. U.S.S.R.*, 1936, **2**, 429.

[24] Gurney, *Ions in Solution* (Cambridge, 1936), p. 202.

[25] Bragg, *Atomic Structure of Minerals* (Cornell U.P., 1937).

As a general interpretation the authors suggest that both processes operate in determining the electrokinetic behaviour of calcite, the electrical double layer former having a structure of the type formulated by Stern.[1] It is further suggested that process (*a*) essentially determines the charge on the calcite surface, this being negative as the result of a greater tendency of Ca^{++} than of $CO_3^{=}$ ions to pass into solution, whilst ions in bulk solution which markedly affect the electrokinetic behaviour (and therefore ζ) do so by being adsorbed to form a Helmholtz layer at some small but definite distance from the crystal surface. This is suggested in view of the reversibility of the ζ potential-concentration curves in general (phosphates excepted) and the high hydration energies for the positive ions which affect ζ potentials most. For the negative ions, hydration energies are much lower and it is conceivable that those showing the greatest effect on ζ may, because of large lattice forces acting on them near the surface, pass over against its negative charge and irreversibly increase this charge on the actual surface (e.g. phosphates).

The irreversible shift in the electrokinetic behaviour of calcite on treatment with acid, illustrated in Fig. 2, may be interpreted using the results of Hopkins.[26] By an electron optical technique he has shown that the dissolution of the surface layers of cleavage faces of calcite crystals, under similar conditions, proceeds unevenly and leads to pitting of the surface, the pits increasing in number and depth with increase in the strength of acid and the duration of treatment. Such pitting could modify the electrokinetic behaviour of calcite in a number of ways: (1) by increasing the extent of the actual charge-bearing surface relative to that of the hydrodynamic slip plane—as suggested by Bikermann;[27] (2) by changing the crystal forces acting on the Ca^{++} and $CO_3^{=}$ ions on their surfaces, and (3) by changing the adsorption forces acting on potential-determining ions in the rigid part of the double layer, as proposed. Factor (1) alone could account for the observed shift of the calculated ζ potential of calcite against distilled water towards more negative values on treatment with acid. The limit mentioned for successive treatments with acid of the same concentration requires the extent of pitting of the surface to reach a limit also.

Relative to sodium chloride as a reference electrolyte the ζ-concentration curves for $CaCl_2$ indicate much more intense adsorption of Ca^{++} ions from solution with the rigid part of the double layer for calcite I than for calcite II; the reversal of sign for calcite I arising from the adsorption of an excess of Ca^{++} ions, into the rigid (Helmholtz) part of the double layer, over the negative charge on the actual calcite surface. To continue on to the actual calcite surface, however, the heavily hydrated Ca^{++} ions would have to be stripped—and their hydration energy is high so that some such accumulation as suggested seems likely. The ζ-concentration curves for Na_2CO_3 are closely alike in form, that for the acid-treated calcite being displaced towards more negative ζ potential values. The sharper drop and earlier minimum of the latter curve suggests somewhat greater adsorption of $CO_3^{=}$ and OH^- ions by the acid-treated calcite. Hydroxyl ions are considered here in view of the hydrolysis of sodium carbonate solutions and the marked adsorption of OH^- ions as shown by the curve for NaOH.

For calcite crystals growing in solutions containing sufficient concentrations of Ca^{++} and $CO_3^{=}$ it is suggested that both are absorbed into the Helmholtz layer, whence Ca^{++} ions are pulled over by the combined surface charge and crystal forces and $CO_3^{=}$ ions, in equal numbers, by crystal forces against the surface charge.

The effects of Ba^{++}, Pb^{++} and Mg^{++} ions have been investigated as these also form sparingly soluble carbonates occurring naturally as crystals having either a calcite or aragonite type structure.[25] As anticipated in a general way from the Paneth–Fajans rules,[28] the results (Fig. 3) indicate marked adsorption of these ions, relative to NaCl as an electrolyte whose ions form soluble compounds with those of the lattice, and form a series

---

[26] Hopkins, *Phil. Mag.*, 1936, **21**, 820.

[27] Bikermann, *J. Chem. Physics*, 1941, **9**, 880.

$$Ca^{++} > Ba^{++} > Pb^{++} > Mg^{++}.$$

Solubility alone, however, does not account for this order, the order of solubility of their prepared carbonates in CO_2-free water [21] being

$$Ca^{++} \sim Mg^{++} > Ba^{++} > Pb^{++};$$

numerical values are given in Table I along with data relating to other possible factors determining adsorption. Ionic radius and lattice type (of the carbonate) do not appear to be determining factors, for a Mg^{++} ion, which is small enough to fit into the calcite lattice and maintain the crystal type, is adsorbed least whilst the barium ion, which is too big to fit without disrupting the existing structure, is adsorbed next most strongly after Ca^{++}. If a high polarizability and low heat of hydration for an ion were determining factors they would suggest a series

$$Ba^{++} > (Pb^{++}) > Ca^{++} > Mg^{++}.$$

A final factor is the net magnitude of the specific crystal and coulombic forces acting on the hydrated ions near the surface, and it is suggested that this is the factor which puts Ca^{++} at the head of the series.

TABLE I.—NUMERICAL DATA FOR FACTORS WHICH MAY DETERMINE ADSORPTION OF CERTAIN POSITIVE IONS BY CALSPAR

Ions in Order of Decreasing Adsorption	Ca^{++}	Ba^{++}	Pb^{++}	Mg^{++}
Solubility [1] of prepared carbonate, at 25° C (mole/l.) . . .	$1{\cdot}5 \times 10^{-4}$	10^{-4}	10^{-5}	$1{\cdot}5 \times 10^{-4}$
Ionic radius [2] in Å and lattice type: calcite	1·06	—	—	1·78
Ionic radius [2] in Å and lattice type: aragonite	1·06	1·43	1·32	—
Ionic polarizability [3] . . .	1·99	5·24	—	0·44
Heats of hydration [4] (kcal./mole)	421	347	—	498

[1] Siedell, *Solubilities of Inorganic and Metallic Organic Compounds* (Van Nostrand, 3rd Edn., 1940).

[2] Bragg, *Atomic Structure of Minerals* (Cornell U.P., 1937).

[3] Fowler, *Statistical Mechanics* (Cambridge, 1929).

[4] Butler, *Chemical Thermodynamics* (Macmillan, 4th Edn., 1946).

The adsorption of the negative ions also is in approximate agreement with the Paneth–Fajans rules; those which form moderately or very soluble calcium salts show the least variation of ζ potential with concentration as they are least adsorbed; those which form insoluble or only slightly soluble calcium salts will be adsorbed much more strongly. However, a striking divergence from these simple working rules is apparently afforded by the oxalate which shows much less effect than hydroxyl and phosphate ions forming, relatively, much more soluble calcium salts. The results for Cl^-, NO_3^-, CNS^-, $CrO_4^{=}$ and $SO_4^{=}$, as sodium salts, show no marked overall deviation one from another, over the same range of molecular concentrations. They suggest that adsorption of these ions is relatively low, though sufficient to offset the effect on ζ potentials of the decreasing thickness of the diffuse part of the double layer with increasing concentration.

For the other negative ions ζ moves to considerably more negative values and the curves are more distinct; after an initial relatively steep increase in ζ (numerically), the curves show more or less pronounced maxima at 1-2 millimolar and then fall off more slowly at higher concentrations. ζ potential-concentration curves of this type have frequently been observed in the past and a general explanation has been put forward by Abramson and Muller.[29] Calculation shows that for all such cases, including the present, the electrokinetic charge density-concentration curves are of typical adsorption isotherm form. The initial increase in ζ arises from the fact that, at low concentrations of electrolyte, the increase in the effective charge density resulting from preferential ion adsorption, outweighs the effect of decreasing double layer thickness; at higher electrolyte concentrations, the charge density tends to a limiting value whilst the thickness of the double layer continues to decrease and, in turn, predominates so that ζ then decreases and the ζ-concentration curve shows a maximum. Considering the individual curves further, the case of NaOH appears quite clear cut, indicating strong adsorption of OH^- ions. With sodium carbonate solutions, their greater ionic strength will tend to depress the ζ value at any concentration, as compared with NaOH, yet ζ reaches more negative values. Thus whilst the considerable OH^- content of carbonate solutions must make some contribution to the increase in ζ, its increase above the values for NaOH alone must arise from stronger adsorption of HCO_3^- and $CO_3^=$ ions. With the electrolytes sodium oxalate and sodium citrate, adsorption of OH^- formed by hydrolysis may account for part of the increase in ζ, but oxalate and citrate ions are strongly adsorbed also.

---

[28] Weiser, *Colloid Chemistry* (Wiley, 1939), p. 92.

Finally we consider the irreversible ζ-concentration curves for the phosphates Na_2HPO_4 and $(NaPO_3)_6$. For these it appears that the crystal surface forces acting on these phosphate ions are sufficiently strong to bind them on the actual crystal surface. Hexametaphosphate is of particular interest in connexion with the inhibition of the precipitation of calcium carbonate from aqueous solution by sodium hexametaphosphate. Reitemeier and Buehrer[30] found that the distorted calcite crystals deposited from solutions containing Ca^{++} and $CO_3^=$ ions, together with insufficient hexametaphosphate for complete inhibition, contained phosphorus. This is consistent with the irreversibility of the ζ-concentration curve for calcite in hexametaphosphate solutions. Further, the sign and magnitude of these ζ potentials render attractive the theory of colloid stabilization dismissed by Reitemeier and Buehrer on the grounds of their own ultramicroscopic studies and the electrokinetic work of Malinowskaya and Gortikov.[23] If colloidal calcium carbonate particles are then formed, the present results suggest that their ζ potential might be so enhanced by hexametaphosphate, even in minute amounts, that coagulation of this lyophobic sol would not take place.[31]

The Muspratt Laboratories,
Department of Inorganic and Physical Chemistry,
The University,
Liverpool.

---

[29] Abramson and Müller, *Cold Spring Harbor Symposia Quant. Biol.*, 1933, **1**, 29.

[30] Reitemeier and Buehrer, *J. Physic. Chem.*, 1940, **44**, 352.

[31] Verwey and Overbeek, *Theory of Stability of Lyophobic Colloids* (Elsevier, 1948), p. 172.

PHYSICAL ADSORPTION ON NON-UNIFORM SURFACES

BY F. C. TOMPKINS

Received 20th February, 1950

The effect of the non-uniformity of an adsorbent surface is discussed in relation to the isotherm obtained in physical adsorption, both for localized and non-localized monolayers. Subject to the approximation that the internal partition function of the adsorbed molecule $j_i(T)$ is independent of the adsorption potential χ_i at the ith sites, it is shown that log pressure against log amount adsorbed will be linear, no matter whether the adsorbed film is regarded as a polyphase or monophase system.

(1) Introduction.—Two recent papers [1, 2] have re-focused attention on the importance of surface heterogeneity in adsorption problems. In some systems [3] involving physical adsorption only, the decrease in adsorption heat with increasing coverage is considerably in excess of that which would result solely from the operation of lateral repulsive interactions between adsorbate molecules; thus, for SO_2 on BaF_2, the initial heat (extrapolated) is 11,000 cal./mole but this falls to 7,000 cal./mole at the completion of the monolayer as, calculated by the B.E.T.* method. The maximum decrease due to repulsive interactions is 1,900 cal./mole. A further decrease of 1,900 cal./mole it was estimated could be attributed to the different adsorption potentials existing at the (100), (110) and (111) planes of the crystal.

Finally a decrease of 1,500 cal./mole was attributed to the fact that on the B.E.T. model, the heat of adsorption calculated by the Clausius-Clapeyron equation is equal to

$$- x\Delta H_1 - (1 - x)\Delta H_2,$$

where x is the fraction of the total adsorption in the first layer, evaluated from the B.E.T. equation,

$-\Delta H_1$ is the adsorption heat in the first layer,
and $-\Delta H_2$ that in the second and higher layers.

Arguments subsequently put forward by Halsey [2] make it certain, however, that one assumption implicit in this equation, viz. that a molecule in the second layer can be absorbed on top of a molecule in the first layer with the full heat of liquefaction, is untenable. The calculated value of 1,500 cal./mole given above must therefore represent a gross overestimate.

It seems, therefore, that the measured decrease in the heat of adsorption must be to some considerable extent attributed to the non-uniform character of the actual surface planes, and it is the purpose of this paper to consider the effect of such heterogeneity on the variation of heats with coverage and on the character of the isotherm.

(2) Mobile and Immobile Films.—The variation of heat with coverage will be affected according to whether the adsorbate molecules are

---

[1] Halsey and Taylor, *J. Chem. Physics*, 1947, **15**, 624.

[2] Halsey, *ibid.*, 1948, **16**, 931.

[3] Crawford and Tompkins, *Trans Faraday Soc.*, 1948, **44**, 698.

* B.E.T. is used as an abbreviation for the names Brunauer, Emmett and Teller.

mobile or not. The concept of an immobile film as defined by Roberts[4] is one in which the adsorbate molecules remain fixed on the sites on which they were initially and randomly adsorbed; it implies that both the rate of evaporation of such molecules and the rate of jumping from site to site within the adsorbed layer is zero, or negligibly small. It is, in fact, a non-equilibrium state which changes slowly with time. Should such a film have significance, then because of the random distribution of the molecules, the heat of adsorption on a non-uniform surface will be, in the absence of interaction forces, independent of coverage. Since this concept of immobility has been used in physical adsorption studies, it must be stressed that nearly all films corresponding to this type of adsorption at room temperature possess mobility and, indeed, chemisorbed films will rarely be immobile.

Thus, on admission of gas to the adsorbent, the instantaneous configuration of the adsorbed layer is a random non-equilibrium one, but it will, however, attain its equilibrium state within the normal time interval (say 1 min.) between admission and measurement. Taking an average adsorption heat of 10 kcal./mole and noting that the adsorbate molecules acquire this energy mainly from the lattice vibrations of the atoms (ions) of the adsorbent, the average time that a molecule spends on the surface $= [\nu \exp(-\Delta H/RT)]^{-1}$, where ν is the lattice frequency, and $-\Delta H$ the heat of adsorption. Assuming that ν is 10^{12} sec.$^{-1}$ at room temperature, then any molecule is adsorbed and desorbed some 10^6 to 10^7 times during this 1-min. interval. On a non-uniform surface, the desorption rate is less from the low adsorption potential ($-\Delta H$ large) sites and considerably faster from sites of high energy, and the equilibrium distribution can be attained *solely* by desorption-adsorption processes. In physical adsorption there is abundant evidence than an adsorbate molecule has lateral mobility since it merely requires energy sufficient to surmount the potential barriers at the surface due to the periodic nature of the adsorbent force field. The calculations and the energy required to surmount such barriers (ΔU) show that it varies considerably, being as high as 6,500 cal./mole on the (100) plane of BaF_2 with SO_2 as adsorbate, and as low as 500 cal./mole for A on NaCl. Nevertheless this energy will rarely be as high as 50 % of the average adsorption heat and in most systems considerably less. Furthermore, only part of this energy need come from the lattice vibrations of the solid since the energy of the internal degrees of freedom of the " adsorption complex " (if the adsorbate molecule is polyatomic) is available. Thus Hill calculates that the mean " transition temperature " for a localized to non-localized layer is approximately $\Delta U/(10R)$. Consequently we conclude that immobile films are never formed in physical adsorption, and are far more rare in chemisorption than has been previously assumed.

(3) Localized and Non-localized Layer.—Confusion has been caused by the synonymous use of the terms, localized and immobile, in the description of adsorbed films. In localized adsorption the three translational degrees of freedom of the gas molecules have been converted to vibrational modes, i.e. a molecule is confined to a three-dimensional cell, the dimensions of the two sides in the plane of the surface being largely determined by the lattice parameters of the adsorbent and thus (unless the molecule is larger in cross-section than the area of the " solid " site, when it will occupy more than one site) largely independent of the dimensions of the adsorbate molecule. The dimension of the cell perpendicular to the surface is, however, dependent on temperature and on the magnitude of the adsorbate-adsorbent interaction.

Now the controlling factor for mobility is the maximum height of the surface barrier ΔU in the potential energy function restricting free migration of the adsorbate molecules over the surface. As noted above, Hill has calculated that the localized–non-localized transition occurs over a wide range of temperature and that the curve showing the heat capacity for two degrees of translational freedom passes through a maximum at T (°K) $= \Delta U/(10R)$. It is true that this value of the temperature may be considerably lower than the true one but there are nevertheless sound theoretical arguments for assuming that Robert's criterion of $\Delta U/R$ represents an upper limit for this temperature. If, however, we accept Hill's value, then since ΔU is normally 300-1500 cal./mole (the system $SO_2 + BaF_2$ is an exception), localized adsorption in physical adsorption would be rare, and even with SO_2 on BaF_2 there would be an appreciable amount of non-localized adsorption. The important conclusion is, however, that even where there is fairly complete localization, lateral mobility executed by a series of jumps can take place quite rapidly and freely.

---

[4] Roberts, *Some Problems in Adsorption* (C.U.P., 1939); and Miller, *Adsorption of Gases on Solids* (C.U.P., 1949).

[5] Hill, *J. Chem. Physics*, 1946, **14**, 263, 441; 1947, **15**, 767; 1948, **16**, 181.

(4) Adsorption Equilibrium for Localized Monolayers on a Non-uniform Surface with no Interaction.—The condition of minimum free energy of the system can be obtained by familiar methods, if we assume that the sites are independent of the presence of each other. Defining:

N_s, the total number of adsorption sites on the adsorbent surface (which is constant independent of temperature),

$\chi_1, \chi_2, \ldots \chi_n$, the minimum energy to evaporate an adsorbed molecule from the lowest energy states of the sites of different adsorption potential, 1, 2, . . . n,

$N_1, N_2, \ldots N_n$, the number of the different sites, 1, 2, . . . n, corresponding to the desorption energies of $\chi_1, \chi_2, \ldots \chi_n$,

$N_1', N_2' \ldots N_n'$, the number of sites 1, 2, . . . n occupied by adsorbed molecules at the equilibrium pressure p and a temperature T, and the N's are large;

$a_1(T), a_2(T), \ldots a_n(T)$, the partition function of the adsorbed molecule, including internal degrees of freedom, on sites 1, 2, . . . n. referred to the usual energy zero of the lowest state of the gaseous molecule at infinite dilution.

The complete partition function for the monolayer is

$$\prod_i \frac{N_i!\ a_i(T)^{N_i}}{(N_i - N_i')!\,N_i'!}, \qquad . \quad . \quad . \quad . \quad (1)$$

and the free energy of the adsorbed layer

$$kT\sum[-N_i\log N_i + N_i'\log N_i' + (N_i - N_i')\log(N_i - N_i') - N_i'\log a_i(T)].$$

The partial potential μ_i of molecules adsorbed on sites i is then

$$kT\log\left[\frac{N_i'}{(N_i - N_i')a_i(T)}\right], \qquad . \quad . \quad . \quad (3)$$

or with

$$\theta_i = N_i'/N_i,$$

$$kT\log\left[\frac{\theta_i}{(1-\theta_i)a_i(T)}\right]. \qquad . \quad . \quad . \quad . \quad (4)$$

At equilibrium, $\mu_1 = \mu_2 \ldots \mu_i = \mu_g$,

where μ_g is the partial potential in the gas phase and equals

$$kT\log\frac{p}{kT}\,\frac{h^3}{(2\pi mkT)^{3/2}\,.\,j(T)}$$

with $j(T)$ representing the partition function for the internal degrees of freedom of the gaseous adsorbate molecule. Consequently

$$\frac{\theta_i}{(1-\theta_i)a_i(T)} = \frac{p}{p^\circ} \quad . \quad . \quad . \quad . \quad (5)$$

with

$$p^\circ = kT(2\pi mkT)^{3/2} \, . \, j(T)/h^3$$

or

$$\frac{\theta_1}{(1-\theta_1)a_1(T)} = \frac{\theta_2}{(1-\theta_2)a_2(T)} \cdots \frac{\theta_i}{(1-\theta_i)a_i(T)} = \frac{p}{p^\circ}. \qquad (6)$$

The fraction of the total surface covered with adsorbed molecules at the pressure p and temperature T is

$$\Theta = \sum_i c_i \theta_i,$$

where

$$c_i = N_i \Big/ \sum_i N_i, \quad . \quad . \quad . \quad . \quad (7)$$

or

$$\Theta = \sum_i \frac{c_i a_i(T) p}{p^\circ + a_i(T) p}.$$

The partition functions, $a_i(T)$, etc., can be written as

$$e^{\chi_i/kT} \, . \, j_i(T), \text{ etc.,}$$

where $j_i(T)$ denotes the partition function for the internal degrees of freedom of the adsorbed molecule. The equation for the isotherm is therefore

$$\Theta = \sum_i c_i \left[e^{\chi_i/kT} \, . \, j_i(T) \, . \, p \right] \Big/ \left[p^\circ + e^{\chi_i/kT} \, . \, j_i(T) p \right], \quad . \quad (8)$$

which agrees, as it should do, with the equation of Halsey and Taylor who assumed that the surface could be regarded as a distribution of Langmuir patches.

The treatment above, however, emphasizes that there is the important restriction, viz. the adsorption has to be completely localized; but in practice, as has been stressed above, this condition is often absent, the layer being appreciably non-localized in physical adsorption except at very low temperatures. Provided $a_i(T)$ is known as a function of the number and desorption energies characteristic of the sites, this summation, in principle, can be effected. However, Halsey and Taylor in integration have assumed, for example, an exponential distribution involving χ_i, thereby implying that $j_i(T)$ is constant independent of χ_i. This will certainly be a crude approximation since Hill has shown that the rotation of an adsorbed molecule will be increasingly restricted as χ_i increases; similarly, both horizontal and the vertical vibration frequencies of the adsorbed molecule will be greater the larger χ_i. The conclusion therefore that an exponential distribution of sites leads to a Freundlich isotherm must be accepted with reserve. Finally, of course, the integration limits used, from $-\infty$ to $+\infty$, include a domain ($-\infty$ to 0) in which it is difficult to give any physical significance to χ.

It will be shown later that the Freundlich equation represents a reasonable approximation but it must be noted that this isotherm allows the amount of gas adsorbed to increase indefinitely with pressure and thus the number of sites available must be infinite—this, in fact, follows from Halsey and Taylor's integration. Consequently the log v against log p plot must depart from linearity at large p and the intersection of Freundlich isotherms at different temperatures should not be given any physical significance in terms of some saturation value (cp. Sips[6]).

(5) Adsorption Equilibrium on a Non-uniform Surface.—In dealing with non-uniform surfaces, two different types of surface may be recognized. A surface may have:

---

[6] Sips, *J. Chem. Physics.*, 1948, **16**, 490.

(*a*) sites of equal energy grouped in patches, i.e. the adsorbed film is a polyphase system; or

(*b*) sites of different energy distributed individually over the surface such that any small element of area contains a representative array of sites, i.e. the adsorbed film is a monophase system.

This distinction does not arise in localized adsorption since the sites are considered to be independent of one another to a first approximation.

(i) AN IDEAL NON-LOCALIZED LAYER, SITES OF DIFFERENT ENERGY DISTRIBUTED SINGLY OR IN GROUPS OVER THE SURFACE.—This presumes the absence of interaction forces and an area of adsorbent surface which is large compared with that occupied by adsorbed molecules (i.e. it is restricted to low coverage). With the same terminology the free energy of the adsorbed molecules at a pressure p and temperature T is

$$\sum_i \left[- N_i'kT \log a_i(T) + N_i'kT (\log N_i' - 1)\right]. \quad . \quad . \quad (9)$$

Consequently $\quad \mu_i = kT (\log N_i' - \log a_i(T)). \quad . \quad . \quad . \quad (10)$

At equilibrium $\quad \mu_1 = \mu_2 \ . \ . \ . = \mu_g,$

therefore $\quad a_1/N_1' = a_2/N_2' \ . \ . \ . \ a_n/N_n' = p^\circ/p \quad . \quad . \quad (11)$

The total adsorption is therefore $\sum\limits_i N_i' = N'$, and the coverage Θ is

$$\frac{N_1'}{a_1N_s}(a_1 + a_2 \ . \ . \ . \ a_n) = \frac{p}{p^\circ N_s}\sum_i a_i(T), \quad . \quad . \quad (12)$$

where N_s = the total number of adsorption sites. Since $a_i(T)$ is independent of p, a linear isotherm results just as if the surface were uniform. The three-dimensional analogue is a perfect gas subject to a force field such as a gravitational one, where the functional dependence of the force on depth replaces the distribution function of sites on the non-uniform surface.

(ii) A NON-LOCALIZED LAYER, ASSUMING THE ADSORBED LAYER TO BE A HIGHLY COMPRESSED GAS, AND SITES OF EQUAL ENERGY TO BE PRESENT IN GROUPS.—Since the area of the adsorbent surface is finite and because measurements are normally not concerned with the very low coverages demanded in the previous section, the adsorbed layer is now considered as a highly compressed gas. Although no general analytical solution is possible, this concept is developed since it has not been used either kinetically or statistically in adsorption theory although it is well known in the theory of liquids. It is assumed that each molecule of adsorbate is confined to a two-dimensional cell on the surface by its neighbours; the free area A_f is now taken as the average area in which the *centre* of the molecule can move.

The partition function of the adsorbed molecules is

$$\sum_i \left[\frac{1}{N_i'!}\left(\frac{2\pi mkT\,A_{f_i}}{h^2}\right)^{N_i'}(j_i'\,e^{\chi_i/kT})^{N_i'}\right], \quad . \quad . \quad (14)$$

where j_i' is the partition function for the internal degrees of freedom of the adsorbed molecule. The free energy is thus

$$kT\sum_i [N_i' \log N_i' - N_i' - N_i' \log Q_iA_{f_i}], \quad . \quad . \quad (15)$$

where $\quad Q_i = \dfrac{2\pi mkT}{h^2}\,j_i'\,e^{\chi_i/kT},$

and the partial potential of molecules on ith sites,

$$kT\left(\log N_i'/Q_i - \log A_{f_i} - N_i'\frac{\partial}{\partial N_i'}\log A_{f_i}\right). \quad . \quad . \quad (16)$$

Here A_{f_i} is the free area available to molecules which are adsorbed on groups of sites of adsorption potential χ_i, i.e.

$$A_{f_i} = (A_i^{\frac{1}{2}} - N_i^{\frac{1}{2}}\,cd)^2, \quad . \quad . \quad . \quad . \quad (17)$$

where d is the diameter of the adsorbate molecule, A_i the total area of surface with an adsorption potential χ_i and equals $c^2d^2N_i$. (N_i is the total number of adsorbed molecules on the area A_i when the monolayer is complete, and c is a shape factor). Finally

$$N_i'/N_i = \theta_i.$$

Hence $$\mu_i = kT\left[\log\frac{c^2d^2}{Q_i} + 2\log\frac{\theta_i^{\frac{1}{2}}}{(1-\theta_i^{\frac{1}{2}})} + \frac{\theta_i^{\frac{1}{2}}}{(1-\theta_i^{\frac{1}{2}})}\right]. \quad . \quad (18)$$

Writing $$x_i = \theta_i^{\frac{1}{2}}/(1-\theta_i^{\frac{1}{2}})$$

$$\mu_i = kT\,(\log Q_ic^2d^2 + \log x_i^2 + x_i). \quad . \quad . \quad . \quad (19)$$

Equating to μ_g, then

$$p/p_i^\circ = Kx_i^2\,e^{x_i},$$

where $$p_i^\circ = p^\circ\,e^{\chi_i/kT}, \quad . \quad . \quad . \quad . \quad (20)$$

and K is a constant at constant temperature and includes the partition function of the internal degrees of freedom of the adsorbed molecule. Since no general solution is possible for x_i in this equation, it is impossible

to sum for $$\sum_i \theta_i c_i,$$

where $$c_i = \frac{N_i}{\sum_i N_i},$$

analytically. Dropping the subscript i gives an equation for the isotherm on a uniform surface; a plot is given in Fig. 1 where it is clear that the log p — log v plot is linear up to $\theta = 0{\cdot}5$. As is well known, this type of relationship is fairly generally valid in many adsorption systems—the departure from linearity at higher coverage is, of course, necessitated by the finite number of sites on the area of the adsorbent, whereas the Freundlich equation fails to give a saturation value for finite pressures. The important conclusion is that a linear log p — log v plot is possible on a uniform surface if the not unreasonable assumption is made that the adsorbed layer corresponds to a 2-dimensional compressed gas for the range $\theta = 0 \rightarrow 0{\cdot}5$.

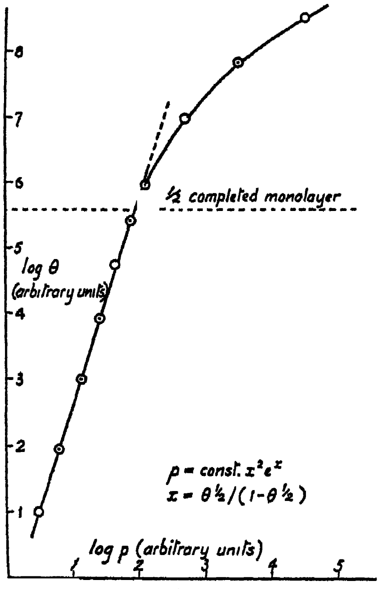

FIG. 1.

Since this approach leads to an intractable equation when applied to a non-uniform surface unless numerical or graphical methods of summation are used, we shall write the free energy of the adsorbed molecules in a two-dimensional mobile layer in a more crude form :

$$\sum_i N_i'kT\left(\log\frac{N_i'}{(A_i - N_i'B)a_i} - 1\right). \qquad (21)$$

Here B corresponds roughly to the co-area of the two-dimensional gas and is here approximated to twice the cross-sectional area of the adsorbed molecule following the normal procedure adopted in the three-dimensional van der Waals' equation ; B is assumed to be independent of the adsorption potential, and A_i = total area of the i sites.

The partial potential for the ith sites is then

$$\mu_i = kT\left(\log\frac{N_i'}{A_i - N_i'B} + \frac{BN_i}{A_i - N_i'B}\right). \qquad (22)$$

Writing $N_i\alpha = A_i$, $B = 2\alpha$, $\theta_i = \frac{N_i}{N_i'}$,

where α is the cross-sectional area of the adsorbed molecule (since the total area of the adsorbent surface is normally determined from adsorption measurements, $N_i\alpha = A_i$) and N_i is the total number of adsorbed molecules on ith sites in the completed monolayer. Equating to the partial potential in the gas phase,* then

$$\frac{p}{p_i^\circ} = \left(\frac{\theta_i}{1 - 2\theta_i}\right)\exp\left(2\theta_i/(1 - \theta_i)\right). \qquad (23)$$

An analytical solution for θ_i is again not possible, but we note that at low pressures when

$$\exp\left(2\theta_i/(1 - 2\theta_i)\right) \rightarrow 1$$

the solution is

$$\theta_i = \frac{p}{p_i^\circ + 2p}. \qquad (24)$$

For an exponential distribution of sites,

i.e. $p_i^\circ = p^\circ e^{\chi_i/kT}$

then, following Halsey and Taylor, we may write

$$\Theta = \int N_i\theta_i d\chi_i,$$

and $$\Theta = \tfrac{1}{2}(p_i^\circ/2p)^{kT/\chi_m} . ckT . f(kT/\chi_m), \qquad (25)$$

on $$\log\Theta = \frac{kT}{\chi_m}\log p + \text{const.}, \qquad (26)$$

i.e. the Freundlich equation is valid as for localized adsorption. It must be emphasized, however, that the validity is restricted to a very dilute range only.

This might be more clearly brought out by writing the partition function for the system for the mobile case and a uniform surface as

$$\frac{1}{N'!} . Q^{N'},$$

where Q refers to the partition function of a single molecule over the surface area A. For the immobile case the partition function for the system is

$$\frac{N_i!}{N'!\,(N - N')} . (Q_i)^{N'},$$

---

* The factor 2 in the exponential factor in eqn. (23) appears as a result of the assumption $B = 2\alpha$ which is true for dilute layers ; for highly compressed gases, $B \sim \alpha$; this merely alters the value of the coefficient in the denomination of eqn. (24) but otherwise does not affect the argument.

where Q_s is the partition function of a single molecule on a site, of which there are N_s in number.

In the very dilute range where $N_s > N'$, this reduces to

$$\frac{(N_s)^{N'}}{N'!} \cdot Q_s^{N'} = \frac{1}{N'!} \cdot (N_s Q_s)^{N'},$$

which is the same as for the localized case, since the condition

$$N_s Q_s = Q$$

accounts for the degeneracy in the localized case.

The range of applicability can be extended by assuming that the adsorbed layer obeys van der Waals' equation in two dimensions. Using the same nomenclature but introducing a' to account for attractive forces, the partition function for the ith molecules in the adsorbed layer is now

$$\frac{1}{N_i'!}\left[\frac{2\pi mkT}{h^2} \cdot (A - N_i'B) \exp\left(- a'N_i'/A_ikT\right)\right]^{N_i'} \quad . \quad (27)$$

leading to

$$\frac{p}{p_i^{\circ}} = \left(\frac{\theta_i}{1 - 2\theta_i}\right) \exp\left[\frac{2\theta_i}{1 - 2\theta_i} - \frac{2a'\theta_i}{\alpha kT}\right]. \quad . \quad . \quad (28)$$

However, although the equation

$$p = k'' \frac{\theta_i}{1 - 2\theta_i} \cdot \exp\left(2\theta_i/(1 - 2\theta_i)\right) \quad . \quad . \quad . \quad (29)$$

can only be reduced to the form

$$p = \frac{k'\theta_i}{1 - 2\theta_i} \quad (k'', k' = \text{const.})$$

for small values of θ, there is, however, surprisingly good agreement with an equivalent form

$$p = \frac{1 \cdot 3\theta_i}{1 - 3\theta_i} \quad \text{(for } k' = 1 \text{ in eqn. (29))}.$$

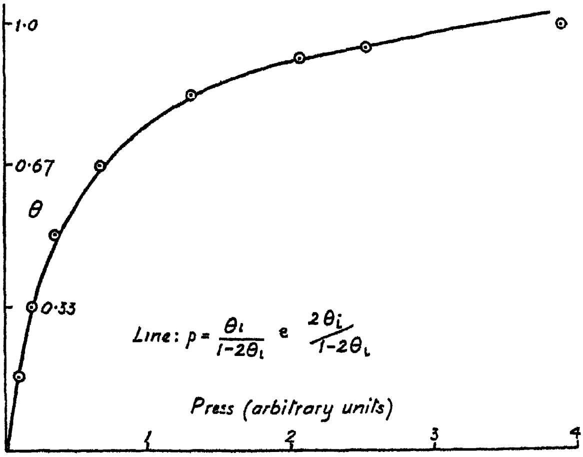

FIG. 2

(θ values adjusted so that maximum value is unity.)

In Fig. 2 values of p in arbitrary units as $f(\theta)$ calculated from

$$\text{(i)}\ p = \frac{\theta_i}{1 - 2\theta_i} \cdot \exp\left(2\theta_i/(1 - 2\theta_i)\right)$$

$$\text{(ii)}\ p = \frac{1{\cdot}3\theta_i}{(1 - 3\theta_i)}.$$

are plotted. It is clear that eqn. (ii) is a good approximation except when θ_i tends to zero, or is very large. It must be noted that θ_i is arbitrarily defined here through the relations

$$B = 2\alpha, \quad N_i\alpha = A_i, \quad \theta_i = N_i'/N_i$$

which determine the value of the constant ($= 2$ in (i)). However, other assumptions will only change the magnitude of this constant (e.g. it is unity for localized adsorption on highly compressed mobile layers) and it is always possible to set up an equation equivalent to (ii). There are also differences in the definition of θ in (i) and (ii). For the Langmuir treatment,

$$p = \text{const.}\ \frac{N}{N_s - N}$$

whereas for the equivalent treatment,

$$p = \text{const.}\ \frac{N}{N_s - \gamma N},$$

where $\gamma = B/\alpha$. Here $\alpha =$ the effective area occupied by the molecule in the completed layer and $B =$ the "exclusion" area analogous to the exclusion volume in the three-dimensional gas taken care of by b in the van der Waals' equation. On a heterogeneous surface we may now write

$$\theta = \sum c_i\theta_i = \sum_i c_i p/(1{\cdot}3p_i^\circ + 3p) \quad . \quad . \quad . \quad (30)$$

i.e. in the same form as Halsey and Taylor's summation. Using an exponential distribution

$$N_i = c\,e^{-\chi_i/\chi_m},$$

and the assumptions and approximations inherent in their method of summation, a Freundlich form of equation will again result when the integration is effected.

(iii) A NON-LOCALIZED LAYER, ASSUMING THAT THE SITES OF DIFFERENT ENERGIES ARE RANDOMLY DISTRIBUTED OVER THE SURFACE.—In this case the free energy of the adsorbed layer is

$$\sum_i N_i'kT\left[\log\frac{N_i'}{a_i(A - \sum_i N_iB)} - 1\right]$$

because the total area A is available to every adsorbed molecule except for the area $\sum_i N_iB$ covered by molecules already adsorbed. The partial potential μ_i of molecules associated with the ith sites is

$$kT\left[\log\frac{N_i'}{a_i(A - \sum_i N_i'B)} + \frac{BN_i'}{A - \sum_i N_i'B}\right]. \quad . \quad . \quad (31)$$

It is necessary to introduce the definitions

$$A = N_s\alpha, \quad B = 2\alpha, \quad \theta_i = N_i'/N_s$$

(cp. previous section), with $N_s =$ total number of adsorbed molecules in the completed layer, then

$$\mu_i = kT\left[\log\frac{\theta_i}{\alpha a_i(1 - 2\Theta)} + \frac{2\theta_i}{1 - 2\Theta}\right], \quad . \quad . \quad (32)$$

where
$$\Theta = \sum_i \theta_i = \sum_i N_i'/N_i.$$

Equating to the partial potential μ_g in the gas phase $= kT \log p/p^\circ$

then
$$\frac{p}{p^{\circ\prime}} = \frac{\theta_i}{a_i(1 - 2\Theta)} . \exp\left(2\theta_i/(1 - 2\Theta)\right), \quad . \quad . \quad (33)$$

where α has been absorbed into $p^{\circ\prime}$.

An analytical solution of θ_i is not possible but two limiting cases can be solved using certain approximations.

CASE (*a*). For small Θ,

where
$$\exp\left(2\theta_i/(1 - 2\Theta)\right) \rightarrow 1,$$

then, from (33),
$$\theta_1/a_1 = \theta_2/a_2 \;.\;.\;.$$

or
$$\Theta = \sum_i \theta_i = \frac{\theta_1}{a_1}(a_1 + a_2 \;.\;.\;.) = \frac{p}{p^{\circ\prime}}(1 - 2\Theta)\sum_i a_1.$$

Since $\sum_i a_i$ is a $f(T)$ but not of p, then at constant T,

$$\frac{p}{p^{\circ\prime}} = \frac{k'\Theta}{1 - 2\Theta} \quad (k' = \text{const.}), \quad . \quad . \quad . \quad (34)$$

i.e. a Langmuir type of equation obtains, which is independent of the distribution function. We note that in the adsorption of H_2 on tungsten, Frankenberg finds that a Langmuir equation is applicable at low coverage, but with increasing adsorption, the Freundlich equation is obeyed over a wide range.

CASE (*b*). Assuming a wide range of energies associated with the various sites such that at p_i all sites $\theta_1, \theta_2 \;.\;.\;.\; \theta_i$ are approximately completely filled and all sites $\theta_i, \theta_{i+1} \;.\;.\;.$ are empty, then at p_1, the free energy F_1 is

$$N_1'kT \log\frac{N_1'}{a_1(A - N_1'B)}, \quad . \quad . \quad . \quad (35)$$

and at p_i, the free energy is $\sum_i F_i$, or

$$\sum_i N_i kT \log\frac{N_i'}{a_i(A - N_i'B)}, \quad . \quad . \quad . \quad (36)$$

and the total amount adsorbed is $\sum_i N_i$.

Similarly, since $\mu_i = \mu_g$,

$$\mu_i = kT\left[\log\frac{N_i'}{a_i(A - N_i'B)} + \frac{BN_i'}{A - N_i'B}\right] = \mu_g = kT\log\frac{p_i}{p^\circ}. \quad (37)$$

where we note that

$$\mu_1 \neq \mu_2 \neq \mu_3 \;.\;.\;.\;.$$

Hence,

$$\frac{p_i}{p^\circ} = \frac{N_i'}{a_i(A - N_i'B)}\exp\left(\frac{BN_i'}{A - N_i'B}\right). \quad . \quad . \quad (38)$$

Since $\quad N_i'$ always $\ll N_i$,

then $\quad N_i'B \ll A$,

i.e. $\quad (A - N_i'B) \rightarrow A$

and $\quad \exp\left(BN_i'/(A - N_i'B)\right) \rightarrow 1$

$$\therefore \quad \frac{p_i}{p^\circ} = \frac{N_i'}{a_i A} = \frac{N_i'}{j_i A} \cdot \mathrm{e}^{\chi_i/kT} \quad . \quad . \quad . \quad (39)$$

The pressure p_i is the equilibrium pressure p when the sites 1 to i are filled.

Hence $$p = kN_i' \mathrm{e}^{-\chi_i/kT} \quad (\text{with } k = p^\circ/j_i A) \quad . \quad . \quad . \quad (40)$$

if $j_i(T)$ is assumed to be independent of i; the equilibrium pressure therefore varies exponentially with χ.

The distribution of number sites is not $f(\chi)$ since all sites up to and including the ith are presumed filled. Let us, therefore, assume that the number of sites with the same energy ΔN are equal and small, and also that $$\chi_i = \chi_0 \mathrm{e}^{-bi/m},$$

where b = const., and m = maximum value of i. These conditions probably describe the surface characteristics of adsorbents such as charcoal or silica gel.

$$\Theta = \sum_i N_i = i\Delta N/N_s \quad . \quad . \quad . \quad . \quad (41)$$

at p_i. At complete coverage

$$\Theta = 1 = m\Delta N/N_s \quad . \quad . \quad . \quad . \quad (42)$$

or $$\Theta = i/m \text{ at } p_i, \quad . \quad . \quad . \quad . \quad . \quad (43)$$

where m is the maximum value of i and thus the number of sites is finite.

From (40), and
$$\left.\begin{aligned} p_i &= k\Delta N \mathrm{e}^{-\chi_0 \exp(\ \ bi/m)/kT} \\ p_m &\sim k\Delta N \end{aligned}\right\}, \quad . \quad . \quad (43)$$

where m is large.

$$\therefore \quad \log \frac{p_i}{p_m} = -C\frac{\chi_0}{kT}\mathrm{e}^{-bi/m}, \quad . \quad . \quad . \quad (45)$$

or $$\log\left(kT \log \frac{p_i}{p_m}\right) = C'\frac{bi}{m} = C''\Theta, \quad . \quad . \quad . \quad (46)$$

where C, C', C'' are constants for a particular surface, which equation is the Bradley–de Boer–Palmer equation.

It may be noted that the original equation of this form was deduced by de Boer, who assumed multilayer adsorption brought about by the polarization of higher-layer molecules by those beneath. It is now known that this polarization effect was grossly over-estimated and that the formation of large numbers of higher layers is unlikely; the original postulates of this theory may therefore be regarded as untenable. Nevertheless, this form of isotherm has proved useful in describing experimental results and indeed has quite wide applicability. It is therefore of interest to note that the same form has been derived here for monolayers on non-uniform surfaces.

It is unfortunate that the type of distribution function of necessity used here, viz.

$$\chi_i = \chi_0 \mathrm{e}^{-bi/m},$$

and $$N_1, N_2 \ldots N_i = \text{constant},$$

differs somewhat from that used in the preceding sections, i.e.

$$N_i = c\,\mathrm{e}^{-\chi_i/\chi_m},$$

since we cannot conclude with certainty that adsorption on the two different types of surfaces (sites of equal energy grouped in patches and sites of different energy randomly distributed) will be characterized by the same isotherm. However, with a linear distribution, noting that χ_m is the lowest value of χ, and = 0,

$$\chi_i = (m - i)\Delta\chi, \; N_1 = N_2 \ldots = \Delta N.$$

Since $\sum_i' N_i = i\Delta N$ and hence $\Theta = i/m$, then, as before,

$$p_i = k\Delta N \mathrm{e}^{-\chi_i/kT},$$

and $$p_m = k\Delta N,$$

or $$p_i = p_m \mathrm{e}^{\chi_i/kT}. \qquad (47)$$

This may be written in the form

$$\log p_i/p_m = (i - m)\Delta\chi/kT = (\Theta - 1)m\Delta\chi/kT, \qquad (48)$$

or $$\log p_m/p_i = (1 - \Theta)\chi_0/kT, \qquad (49)$$

where χ_0 is the maximum value of χ on the surface.

This is the Brunauer-Temkin equation which can be deduced, as has been done by Sips, for localized adsorption using a linear distribution, and here for non-localized " patched " adsorption, by the method previously used. It may therefore be confidently anticipated that a linear log p — log v plot would be valid for an exponential distribution of the type

$$N_i = c\,\mathrm{e}^{\chi_i/\chi_m}$$

for random-site non-localized adsorption.

It is therefore concluded that the type of adsorption—whether localized, or the two types of non-localized—does not affect to any significant extent the character of the isotherm on a non-uniform surface. But it must be stressed that, with Halsey and Taylor, it has been assumed that the partition function $j_i(T)$ is independent of χ_i. Use may therefore be made of the concept of localization in setting up partition functions of adsorbed layers without serious error even though there may be definite experimental evidence pointing to non-localization of the adsorbed molecules. These ideas are further developed and generalized in the succeeding paper.

The author is indebted to Prof. D. H. Everett for valuable discussions.

Dept. of Inorganic and Physical Chemistry,
Imperial College,
S.W. 7.

ADSORPTION ISOTHERMS FOR NON-UNIFORM SURFACES

BY F. C. TOMPKINS

Received 20th February, 1950

A general approach to the problems of adsorption on non-uniform surfaces is outlined and, with certain restrictions regarding the magnitude of certain entropy changes, four well-known isotherms are deduced from the variation of heat of adsorption with coverage. A possible guide to the type of non-uniformity existing at the surface is suggested.

(1) The Adsorption Isotherm.—The approach in the preceding paper to the problem of adsorption is confined to consideration of a monolayer, i.e. it neglects sites created by gas adsorbed on top of the first layer. It is important to know what part is played by multilayer formation on a non-uniform surface. As stated previously, the considerations of Halsey show that the adsorption of a molecule on top of an isolated adsorbed molecule in the first layer with the full heat of liquefaction is impossible; at least a triangular array of molecules in the monolayer is necessary for second-layer adsorption. It is evident that on a uniform surface, whether the layer is localized or not, except when the equilibrium pressure approaches the saturation pressure of the liquid adsorbate, no considerable higher layer formation is probable. However, if the surface is non-uniform and the adsorption sites are grouped together such that a local high concentration in the monolayer is possible, then one can expect second layer formation before the higher adsorption sites (low $-\Delta H$) are filled; the effect would be to smooth out the almost stepwise isotherm expected on a uniform surface and make the determination of the area of the completed layer exceedingly difficult. In practice, since the distribution on many surfaces is not sufficiently wide there is usually found near $\theta = 1$, a sufficient change in the distribution function to allow an approximate estimation of the surface area; this, it is believed, is the reason why the B.E.T. point B method gives consistent results of the correct magnitude.

In order to obtain a working isotherm characteristic of a non-uniform surface, it is necessary to postulate an adsorption potential which increase with increase coverage; this variation must arise from the characteristics of the surface and consequently the distribution of adsorption sites will be largely independent of the temperature. Although such a distribution is a property of the adsorbent, the distribution function of the sites may also be, in part, dependent on the properties of the adsorbate since the forces responsible for the adsorption of different gases need not be the same. Thus, if the major contribution to the binding to the surface is due to dispersion forces, the adsorbate molecule will be most strongly held when it is " co-ordinated " with the maximum number of surface atoms (ions), i.e. low adsorption energy sites will be within sub-microscopic cracks or fissures or in re-entrant angles; conversely, positions at the corners and edges of crystals will represent sites of high energy. But if electrostatic forces predominate then the edges and corners are the low-energy sites, and within fissures, etc., will be found those of high adsorption potential. It is therefore possible that the distribution function of the same surface will be different when molecules of high dipole moment, e.g. SO_2, NH_3, etc., are adsorbed from that when non-polar molecules of low polarizability constitute the adsorbate. This would be (apart from possible interaction effects) reflected in part in the variation of adsorption heat with coverage and also in the general character of the isotherm unless the distribution function is wide and symmetrical about the average adsorption sites.

In setting up a working isotherm, let it be assumed that there is a maximum adsorption volume independent of temperature which in the simplest case, the monolayer, will correspond to a completed layer wherein the molecules are adsorbed on sites corresponding to the lattice constants of the solid surface if the adsorption is localized, or a close-packed array determined by the adsorption potential of adsorbent, the molecular dimensions and by other properties of the adsorbate which include interaction effects, if the layer is non-localized. The extension to multilayers introduces no difficulty provided the maximum adsorption is not linked to the concept of amount of adsorbate in the supposed monolayer and thereby to the surface area of the adsorbent. The term coverage, usually denoted by θ, would now refer to the fractional amount adsorbed relative to the maximum value. This latter is here defined as the total adsorption on all sites the adsorption potential of which exceeds that at the surface of the bulk liquid adsorbate, i.e. there may be empty adsorption sites on the solid surface the potential of which is greater than that on the surface of the liquid adsorbate at the same temperature; there may also be filled adsorption sites " created " by molecules in the first layer with a potential lower than that over the liquid adsorbate on which second-layer adsorption occurs. The adsorption potential distribution includes from the experimental viewpoint the effects of lateral interaction of adsorbate molecules induced by the solid, etc. It follows that the distribution function deduced from experimental measurements, e.g. from the variation of free energy or heat (see later) with coverage, or the nature of the isotherm will reflect the distribution of "modified" sites which is not solely a property of the non-uniformity of the adsorbent.

The maximum adsorption volume is made largely independent of temperature by replacing the equilibrium pressure p by p/p_s, where p_s - the relevant saturated pressure of the liquid adsorbate at the temperature of adsorption. This thus means that the adsorption potential is taken as zero over the surface of the bulk liquid adsorbate at all temperatures. It is convenient to replace the maximum adsorption volume by a "total available" surface of thickness corresponding to that of a one-molecule layer (τ). The total amount of gas adsorbed ($v_{\text{max.}}$) is

$$\int_0^{\tau_n \max.} (n_a - n_v)\mathrm{d}x,$$

where n_a is the number of molecules adsorbed/unit available area in the adsorbed phase and n_g the number of molecules in the gas phase per unit area in a volume of the same thickness parallel to, and at a distance from, the surface. Since

then, with negligible error,

$$V_{\text{max.}} = \int_0^{n_{\max}} n_a \,.\, \mathrm{d}x. \quad . \quad . \quad . \quad . \quad (1)$$

This can be evaluated if n_a is known as a function of the amount adsorbed, x. (The exact equation will be, of course, in terms of fugacities and not pressures.)

Now at any equilibrium pressure p the value of n_i, the number of molecules/unit area on the area A_i comprising all positions where the adsorption potential is given by ϵ_i will depend on the magnitude of ϵ_i, such that if $\epsilon_i > \epsilon_j$ . . ., etc., then $n_i > n_j$ . . . etc. Thus the non-uniformity of the surface determines the values of n_i, n_j . . . etc. for any equilibrium pressure p and temperature T; the change in energy on adsorption can therefore be calculated by evaluating the work required to compress n_x molecules from the gas phase at pressure p to the different concentrations which are present in the adsorbed phase. Here

$$n_x = \sum_0^x n_i$$

and equals the total number of molecules adsorbed at p and T. The total energy necessary to effect this compression is

$$\text{const.} \sum_0^x \left(\int_{n_g\tau}^{n_i\tau} V\mathrm{d}p \right) \delta x, \quad . \quad . \quad . \quad (2)$$

or

$$\text{const.} \sum_0^x \epsilon_i \delta x, \quad . \quad . \quad . \quad . \quad . \quad (3)$$

where ϵ_i is the adsorption potential on the i sites, or is the energy necessary to compress a mole of gas to the concentration existing in the adsorbed layer. Thus

$$\epsilon_i = \int_{n_g\tau}^{n_i\tau} V\mathrm{d}p. \quad . \quad . \quad . \quad . \quad . \quad (4)$$

It follows that the adsorption potential is a function only of the amount adsorbed. The evaluation of this integral requires an equation of state ; in the simplest case, we may write

$$\epsilon_i = \int_{p_s}^{p} RT\,\mathrm{d}p/p,$$

or for general use for a non-ideal gas equation,

$$(pV)_{n_gT}^{n_lT} - \int_{n_gT}^{n_lT} p\,\mathrm{d}V, \quad . \quad . \quad . \quad . \quad (5)$$

or
$$\epsilon_x = RT \log p_s/p + \text{a correction term}, \quad . \quad . \quad (6)$$

where the correction term is known to be small in most cases. The limit of integration at higher pressures is p_s, as noted above ; hence

$$\epsilon_x = RT \log p_s/p \quad . \quad . \quad . \quad . \quad (7)$$

to a good approximation. The term ϵ_x is the free energy difference between one mole of adsorbate as bulk liquid and the same quantity in the adsorbed layer. The (net) heat of desorption $-\Delta H_x$ which is defined for constant number of adsorbed molecules, is thus

$$-\Delta H_x = \epsilon_x - T(\delta\epsilon_x/\partial T)_x, \quad . \quad . \quad . \quad . \quad (8)$$

where, in general, $(\partial\epsilon_x/\partial T)_x$ is small, but not zero.

Providing the partition functions for the internal degrees of freedom of the adsorbed phase and the liquid state are assumed equal, then

$$(\partial\epsilon_x/\mathrm{d}T)_x = -(\partial\epsilon_x/\partial_x)_T \,.\, (\partial_x/\partial T)_{\epsilon_x}. \quad . \quad . \quad . \quad (9)$$

The term $(\partial x/\partial T)_{\epsilon_x}$ is proportional to the two-dimensional thermal expansion of the adsorbate if the adsorption is non-localized, or that of the adsorbent if localized, and in either is small. It follows that this entropy term is usually small so that

$$-\Delta H_x = RT \ln p_s/p. \quad . \quad . \quad . \quad . \quad (10)$$

It is better, however, to define a term $-\Delta H_x'$ with respect to constant adsorption volume by the introduction of the density of the adsorbed phase at the temperature of the adsorption. If, therefore, $-\Delta H_x'$ is independent of temperature as is usually so, then the plot of $RT \ln p_s/p$ against n_x/ρ_T to take care of the expansion term indicated above, where $\rho_T =$ the liquid density of the adsorbate at temperature T, should be a characteristic curve valid for all temperatures. The plot corresponds to the so-called affinity plot in the original Polanyi theory, i.e. it follows that if an isotherm is experimentally determined at one temperature, then isotherms at any other temperature can be calculated. Moreover, if the variation of net heat of adsorption with coverage is known either from theoretical calculations or experimentally from calorimetric measurements, the isotherm can be reasonably well characterized.

The data on the variation of heat with coverage show that, in absence of some special phenomena such as marked co-operative effects, the $-\Delta H_x'$ against x plots, where $x = n_x/\rho_T$, on (presumably) non-uniform surfaces monotonically decrease and can be expressed in one of four ways.

(i) $\quad -\Delta H_x' = -\Delta H_0(1 - kx), \quad k = \text{const.}$;

then $\quad RT \log p_s/p = -\Delta H_0(1 - kx)$

or $\quad \log p = k_1 x + \text{const.} \quad . \quad . \quad . \quad (11)$

for constant T.

This is the equation for the isotherm associated with the name of Brunauer and of Temkin and found to hold experimentally in certain systems of importance in catalytic processes. It has also been deduced by Halsey and Taylor, and by Sips, for localized adsorption when the distribution of sites is given by their nomenclature,

$$N(\chi_i) = \text{const.}$$

(ii) $$-\Delta H'_x = -\Delta H_0 e^{-k_2 x}, \quad . \quad . \quad . \quad . \quad (12)$$

then $$\log (RT \log p_s/p) = -k_2 x + \text{const.} \quad . \quad . \quad . \quad (13)$$

This is the equation found to be applicable by Palmer for adsorption on silica gel and deduced theoretically by de Boer and by Bradley assuming multilayer formation caused by transmission of polarization from lower to higher layers; incidentally this equation approximates closely to the B.E.T. equation under certain conditions.

(iii) $$-\Delta H_x = -\Delta H_0(1 - k_4 \log x), \quad . \quad . \quad . \quad (14)$$

or $$RT \log p_s/p = -k_5 \log x + \text{const.},$$

i.e. $$\log p = k_6 \log x + \text{const.}, (T \text{ const.}). \quad . \quad . \quad (15)$$

This is the Freundlich equation which has been deduced theoretically by Halsey and Taylor for localized adsorption and an exponential distribution of sites. As is well known it has a wide applicability as an empirical isotherm.

(iv) $$\log (-\Delta H'_x) = -\Delta H_0(1 - k_7 \log x), \quad . \quad . \quad (16)$$

or $$RT \log p_s/p = -k_8 \log x + \text{const.}$$

i.e. $$\log p = k_9 x^{k_8} + \text{const.} (T \text{ const.}). \quad . \quad . \quad (17)$$

This corresponds to the working isotherm proposed by Halsey assuming localized adsorption and an exponential distribution of sites, but including adsorption in higher layers on the groups of sites created by adsorption in the first or other lower layers. When $k_8 = 2$, the equation reduces to the Harkins-Jura equation which under certain circumstances approximates closely to the B.E.T. isotherm.

If, now, it is assumed that the fall in heat with coverage is due in the main to the non-uniformity of the surface then the problem becomes one of discovering the necessary distribution of sites on the adsorbent (where interaction terms etc. are important, the distribution of "modified" sites must be substituted). Sips has in part given a method of solution and has shown that an exponential distribution of sites lead to the Freundlich isotherm and that a constant distribution ($N(\chi_i) = \text{const.}$) yields the Brunauer-Temkin equation. Unfortunately his method cannot be used to find the distribution necessary to give isotherms (iii) and (iv). However, it has been shown that a distribution of the form

$$\chi_i = \chi_0 e^{-bi/m}, \; N_1 = N_2 \dots = \Delta N, \; (b, m = \text{const.}, \; i = 1, 2, 3 \dots)$$

leads to eqn. (iii).

It must be noted that the expression

$$RT \log p_s/p = f(x)$$

fails to yield the Langmuir equation, and in fact does not lead to any isotherm for a uniform surface when

$$-\Delta H'_x = \text{const.}$$

This latter conclusion is as it should be since the free energy of mixing of identical molecules among sites of equal energy has been neglected. This can be introduced by considering the configurational entropy. For localized adsorption with N as the number of available sites and N' molecules adsorbed on these, this entropy term is given by

$$R \log \frac{N!}{(N - N')!\,N'!}$$

which can be reduced to the usual form $R \log (\theta/(1 - \theta))$ for the partial molar localization entropy, providing the partition function for the internal degrees of freedom of a molecule in the liquid state is assumed equal to that of the molecule in the adsorbed phase at the same T. Consequently,

$$RT \log p_s/p = -\Delta H - RT \log (\theta/1 - \theta),$$

and where $-\Delta H$ is independent of θ,

$$\frac{p}{p_s e^{\Delta H/RT}} = \frac{\theta}{1 - \theta},$$

which is the Langmuir isotherm. In the non-localized system, a similar term of this form must be included. Generalizing for a non-uniform surface for non-localized adsorption, the partition function of the adsorbed layer may be written as

$$\sum_i \frac{1}{N_i'} \left[\frac{2\pi mkTj_i(T)}{h^2} \cdot \left(\frac{A - N_i'B_i}{N_i'}\right)\right]^{N_i'} \quad . \quad . \quad (18)$$

hence the free energy is

$$\sum_i kN_i'T\left[\log\left(\frac{N_i'}{A_i - N_i'B_i}\right) - 1\right] \quad . \quad . \quad (19)$$

and the internal energy

$$E = \sum_i kT^2N_i' \frac{\partial \log a_i}{\partial T}; \quad . \quad . \quad . \quad (20)$$

the entropy is therefore

$$S = \frac{E-F}{T} = \sum_i \left[kN_i'\left(T\frac{\partial \log j_i'}{\partial T} + \log j_i'\right) + \log\left(\frac{A - N_i'B_i}{N_i'}\right) - 1\right]. \quad (21)$$

In the first term the (net) heat of adsorption goes out leaving the partition function for the internal degrees of freedom of the adsorbed molecule $j_i'(T)$. The second term gives the configurational part and the first the non-configuration entropy. When referred to the liquid state, the first term is non-zero, but probably small; it arises from the fact that $j_i'(T)$ is $f(T, \chi_i)$, whereas in the liquid state $j(T)$ is merely a function of T; the assumption of equality of $j(T)$ and $j_i'(T)$ of the adsorbed state is thus without real meaning, although the differences are not large when summed. This is shown experimentally from the fact that there is good agreement between heat of adsorption as deduced from the Clausius-Clapeyron equation from (Langmuir) isotherms at different temperatures and that obtained by summing the heat of liquefaction of the adsorbate and the net heat of adsorption deduced from a single Langmuir isotherm at one (mean) temperature (cp. Foster[1]).

The configurational contribution to the entropy will depend on the number and extent of local patches of uniform adsorption potential; if the distribution is wide, then the second term is small. There will therefore in this case be no large error in equating the free energy to the heat content, whether the adsorption is localized or non-localized. Where the entropy term is significant, the affinity curves at different temperatures will not be coincidental and the magnitude of marked divergences to some extent parallels the number of sites possessing equal energies; it thus provides some rough guide to the degree of non-uniformity.

If one accepts the concept of non-uniformity of surfaces, then the interpretation of transformations of state in adsorbed films on solids (cp. Gregg[2a, b]) must be re-considered; it is no longer legitimate to draw analogies from the resemblance between these films and films of insoluble substances on water. Thus Gregg has inferred from the work of Mayer and Streeter that anomalous, diffuse and lambda first-order transitions indicate the co-existence of two phases over a range of pressure—the probability is that these represent simple first-order transitions on a heterogeneous surface over a range of pressures—clearly the transformation will take place at a lower equilibrium pressure at the sites of low adsorption potential and this will progressively include the higher adsorption sites as the amount adsorbed (and equilibrium pressure) increases. In fact where there appears evidence of the existence of a true first-order change (Fig. 1 (i), p. 124 in Gregg's paper [2a]) this suggests that a large extent of the available surface has uniform potential and this result should be reflected in marked divergences of affinity curves for the system at different temperatures.

---

[1] Foster, *J. Chem. Soc.*, 1945, 360.

[2] (a) Gregg, *J. Chem. Soc.*, 1942, 696; (b) Gregg and Maggs, *Trans. Faraday Soc.*, 1948, 44, 123.

The author is indebted to Prof. D. H. Everett for valuable discussion.

Dept. of Inorganic & Physical Chemistry,
Imperial College,
S.W. 7.

STUDIES OF SOAP SOLUTIONS

PART II.—FACTORS INFLUENCING AGGREGATION IN SOAP SOLUTIONS

BY G. STAINSBY AND A. E. ALEXANDER *

Received 23rd September, 1949

The change in heat content ΔH and the change in entropy ΔS have been calculated for the equilibrium :

soap molecule in solution $\rightleftharpoons$ soap molecule in a spherical micelle,

by considering the factors involved in the aggregation process. It is shown that ΔH is negative, is small and increases numerically with increasing temperature. Values of ΔH calculated from the temperature coefficient of the critical micellar concentration, and from the temperature dependence of the saturation solubility of soaps in water, are in reasonable agreement with the theoretical values. The aggregation of fatty acids in solutions of the fatty acid soaps is associated with a heat change of similar magnitude, i.e. when soap molecules aggregate the ions have little effect upon ΔH. This is contrary to previous considerations of the aggregation process. Ions, however, have a considerable effect upon ΔS.

The view is expressed that the main factors involved in the aggregation of soap solutions are the change in the hydrocarbon-water interface (the micelle having a considerable interface of this nature) and the change from a curled molecule in solution to a more flexible and extended molecule in the micelle. It is suggested that the bound gegen-ions lie *between* the long-chain ions forming the micelle, there being a net *attractive* coulombic force.

The theoretical treatment has been extended to cover the effects of simple salts and organic molecules upon the critical concentration for micelle formation and upon its temperature dependence. The conclusions are supported by experimental data.

One of the most striking and peculiar properties of aqueous soap solutions is the combination of low osmotic activity with high electrical conductivity. To account for this, McBain[1] proposed the idea of association of single soap ions into aggregates of colloidal dimensions, termed " micelles ". According to McBain two types of aggregate—neutral and ionic micelles—exist in equilibrium in solution, the proportions depending upon the concentration. Hartley,[2, 3] however, has shown that the observed properties of the dilute, clear, isotropic solutions are in keeping with the existence of only one type of micelle, the ionic micelle. This is approximately spherical in shape and is formed over a narrow range of concentration by the aggregation of about 50 simple ions for a C_{16} paraffin-chain soap. The radius of the micelle is a little less than the fully extended length of the hydrocarbon chain, the interior resembles a liquid hydrocarbon, and the charges from the ionic heads on the surface are largely (60-80 %) neutralized by binding of the gegen-ions. There is now considerable evidence that, at least in *dilute* soap solutions, Hartley's ideas are substantially correct.

---

* Present address : N.S.W. Univ. of Technology, Sydney, Australia.

[1] McBain, *Trans. Faraday Soc.*, 1913, **9**, 99.

[2] Hartley, *Aqueous Solutions of the Paraffin-chain Salts* (Hermann et Cie, Paris, 1936).

[3] Hartley, *Kolloid-Z.*, 1939, **88**, 33.

By extending Langmuir's treatment of interfacial energies,[4] Hartley [2, 3] has indicated some of the factors involved in the aggregation process. Aggregation was assumed to occur when the energy available from the hydrocarbon-water interface exceeded the electrical energy necessary to bring the ionic heads together in the spherical micelle. Furthermore, it was clearly shown from simple probability considerations that aggregation to spheres was more likely than aggregation to cylindrical or laminar micelles.

Ward [5] has extended Hartley's arguments to cover the addition of short-chain alcohols to simple soap solutions. Again ionic repulsion is supposed to be the dominant factor opposing aggregation. Ward, however, makes some allowance for the presence of a hydrocarbon-water interface within each micelle: in other words, the ionic heads do not constitute the entire surface of the aggregate.

Certain difficulties arise, however, when the above theories are examined quantitatively, for they predict the critical concentration for micelle formation c_s to be much less, and the temperature coefficient of c_s to be much greater, than the values actually observed. In addition, the aggregation of non-ionized molecules (e.g. fatty acids—Part I of this series [6]) does not find a ready explanation.

Debye [7] has recently considered the energetics of micelle formation using the cylindrical model of a micelle proposed by Harkins [8] from the results of X-ray studies of concentrated ($> 5\ \%$) soap solutions. Briefly, Debye's treatment differs from that of Hartley only in that short-range van der Waals' attractive forces are postulated as opposing the longer-range electrical repulsions.

The objects of the present paper are

(i) to calculate values of ΔH, the change in heat-content for the equilibrium:
single molecule in solution $\rightleftharpoons$ single molecule in the aggregate,
(ii) to consider the factors involved in the aggregation process in order to obtain theoretical estimates of ΔH (for comparison with (i)) and ΔS, the entropy change for the above equilibrium,
and (iii) to consider the effects of additives (simple salts and organic molecules) upon micelle formation, in the light of the analysis given in (ii).

As usual, the soap molecule is discussed in terms of the long-chain ion and the gegen-ion, and throughout the present paper the aggregate is assumed to be approximately spherical in shape, of structure outlined above.

Experimental Results.—Changes in heat content calculated on a concentration basis will be written as ΔH, whilst the thermodynamic values, using activities instead of concentrations, will be written as $\Delta H'$. $\Delta H_s'$ represents the true thermodynamic value of the change in heat content for the aggregation of soap molecules; $\Delta H_F'$ is the thermodynamic value of the change in heat content associated with the formation of fatty acid aggregates in dilute solutions of the fatty acid soaps. (The evidence for such aggregation has already been considered.[6]) In all cases the sign is negative if the aggregation process occurs with the liberation of heat.

Two methods of obtaining ΔH_s will be given, the first from the temperature coefficient of the critical concentration for micelle formation, and the second from the temperature coefficient of the saturation solubility of soaps in water. ΔH_F is calculated only from the first of these two approaches.

METHOD 1. VALUES OF ΔH FROM THE CRITICAL CONCENTRATION FOR AGGREGATION.

Consider the equilibrium:

soap molecule in solution $\rightleftharpoons$ soap molecule in the aggregate,

---

[4] Langmuir. [5] Ward, *Proc. Roy. Soc. A*, 1940, **176**, 412.

[6] Stainsby and Alexander, *Trans. Faraday Soc.*, 1949, **45**, 585.

[7] Debye, *J. Physic. Chem.*, 1949, **16**, 156; *Ann. N.Y. Acad. Sci.*, 1949, **51** (4), 575. [8] Harkins, *J. Chem. Physics*, 1948, **16**, 156.

and let
$$K_s' = \frac{\text{activity of a soap molecule in the aggregate}}{\text{activity of a soap molecule in solution}};$$

then
$$\frac{\mathrm{d}\ln K_s'}{\mathrm{d}T} = \frac{\Delta H_s'}{RT^2}.$$

If the activity of a soap molecule in the aggregate is constant, independent of temperature (i.e. if the micelles are regarded as a separate phase, and the process of aggregation as a phase-change),

then,
$$\frac{\mathrm{d}\ln a_s}{\mathrm{d}T} = -\frac{\Delta H_s'}{RT^2}, \qquad (1)$$

where a_s, the activity of the soap molecules in solution, is related to c_s, their concentration, by the usual equation $a_s = c_s f_s$, where f_s is the activity coefficient.

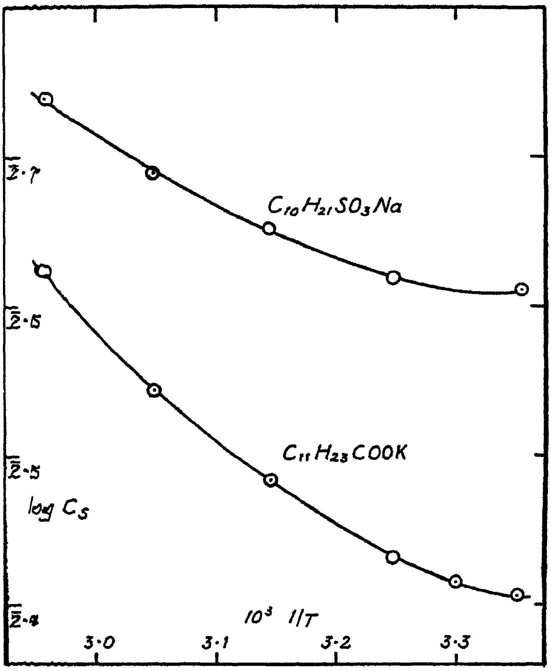

FIG. 1.—The temperature dependence of the critical concentration for micelle formation c_s.[11, 12]
(The unit of concentration is mole/l.)

As c_s is quite small (*ca.* N/1000 for a C_{18}-soap) it is unlikely that f_s is far from unity. In fact this has been demonstrated experimentally by dew-point [9] and by freezing-point [10] depressions. Thus ΔH_s, which is the value obtained by plotting log c_s against $1/T$ should not be very different from the true value, $\Delta H_s'$.

There is evidence that at a given temperature c_s is essentially constant once micelles are present, and is equal to the value of the soap concentration at which micelle formation occurs. The temperature coefficient of c_s is known reliably only in a very few instances, notably from the work of Powney and Addison [11] on the sodium *n*-alkyl sulphates, and that of Klevens [12] on two alkyl sulphonates and certain fatty acid soaps. As yet, values of c_s for soaps with more than 16 carbon atoms in the hydrocarbon tail have not been determined with sufficient accuracy for the present purpose. Two typical plots of log c_s against $1/T$ are shown in Fig. 1.

---

[9] McBain, Laing and Titley, *J. Chem. Soc.*, 1919, 1279.

[10] McBain and Bolduan, *J. Physic Chem.*, 1943, **47**, 94.

[11] Powney and Addison, *Trans. Faraday Soc.*, 1937, **33**, 1243.

[12] Klevens, *J. Physic. Chem.*, 1948, **52**, 130.

If c_F is the concentration at which fatty acid aggregates form[6] then, by analogy with the method already given for soaps,

$$\frac{d \ln c_F}{dT} = -\frac{\Delta H_F}{RT^2} \quad . \quad . \quad . \quad . \quad . \qquad (2)$$

Unfortunately, values of c_F are not known to an accuracy comparable with the experimental values of c_s for soap solutions, but plots of log c_F against $1/T$ are very similar to Fig. 1 in shape.

TABLE I.—EXPERIMENTAL VALUES FOR THE HEATS OF AGGREGATION OF SOAPS AND FATTY ACIDS IN AQUEOUS SOLUTIONS

Temperature Range	25°–35° C	35°–45° C	60°–80° C
$C_{11}H_{23}COOH$ . .	4	8	12
$C_{13}H_{27}COOH$ . .	4	18	20
$C_{15}H_{31}COOH$ . .	—	12	25
$C_{17}H_{35}COOH$ . .	—	5	25
$C_{12}H_{25}SO_4Na$ . .	1	1·8	5
$C_{14}H_{29}SO_4Na$ . .	—	1·5	5·5
$C_{12}H_{25}COOK$ . .	1	2·4	5
$C_{14}H_{29}COOK$ . .	1	1	2
$C_{10}H_{21}SO_3Na$ . .	0·5	1·4	3
$C_{12}H_{25}SO_3Na$ . .	—	1·8	4

All values are in kcal./mole and are negative.

In Table I values of ΔH_s and ΔH_F obtained by this method are collected together. It is clear from this data that

(i) ΔH_s and ΔH_F are very similar in magnitude, both being negative and small at room temperature. This is important since it shows that the ionic term for the former cannot be very important numerically; and (ii) both ΔH_s and ΔH_F increase numerically with increasing temperature.

METHOD 2. CALCULATION OF ΔH FROM THE SATURATION SOLUBILITY OF SOAPS IN WATER. Below a certain temperature, dependent mainly upon the chain-length of the soap and, to some extent, upon the nature of the head-group, the solubility increases very slowly with temperature. Above this temperature—called the Krafft point—the solubility rises very rapidly to high values. Murray and Hartley[13] have shown theoretically that this is to be expected if micelle formation occurs; the saturation solubility at the Krafft point should then be equal to the critical concentration. Tartar and Wright[14] have confirmed the theory for a series of sodium sulphonates and, at present, the only other accurate experimental determinations of saturation solubilities of soaps are those of Adam and Pankhurst,[15] using series of anisidine sodium sulphonates, pyridinium halides and trimethylammonium halides. The work of Tartar and Wright is the more amenable to further calculations and will be used here to illustrate this method of obtaining ΔH_s.

Consider the general equilibrium

$$\begin{tikzcd}
\text{solid} \arrow[rr, shift left, "\Delta H_1'"] \arrow[dr, shift left, "\Delta H_2'"'] & & \text{single ions} \arrow[ll, shift left] \arrow[dl, shift left, "\Delta H_s'"] \\
& \text{micelles} \arrow[ul, shift left] \arrow[ur, shift left] &
\end{tikzcd}$$

Let C represent the stoichiometric concentration of the soap solution (in terms of single molecules) and f its activity coefficient at T° K, g being the osmotic coefficient (Bjerrum) of the solution. If $\Delta H_2'$ is the heat absorbed on transferring one mole from the solid phase to the solution when micelles are present, then

$$\Delta H_2' = \Delta H_1' + \Delta H_s', \quad . \quad . \quad . \quad . \quad . \quad . \qquad (3)$$

---

[13] Murray and Hartley, *Trans. Faraday Soc.*, 1935, **31**, 183.

[14] Tartar and Wright, *J. Amer. Chem. Soc.*, 1939, **61**, 539.

[15] Adam and Pankhurst, *Trans. Faraday Soc.*, 1946, **42**, 523.

and
$$\frac{\mathrm{d}\ln Cf}{\mathrm{d}T} = \frac{\Delta H_2'}{RT^2}. \quad . \quad . \quad . \quad . \quad . \quad . \quad (4)$$

Also
$$\frac{g\,\mathrm{d}\ln C}{\mathrm{d}T} + \frac{\mathrm{d}g}{\mathrm{d}T} = \frac{\Delta H_2'}{RT^2}. \quad . \quad . \quad . \quad . \quad . \quad (5)$$

Making the not unreasonable assumption that g is independent of temperature, it follows that $\Delta H_2'$ may be obtained by plotting log C against $1/T$. The apparent heat of solution, ΔH_2, is related to $\Delta H_2'$ by the eqn.,

$$\Delta H_2' = g\Delta H_2.$$

Only a very limited amount of work is at present available upon the value of g. The sodium alkyl sulphonates, because of their very low solubility in water at 0° C, have never been investigated experimentally for this purpose. (The usual method employed is the depression of the freezing-point.) The temperature-dependence of g, if any, is not known either. However, the following classes of substances have received attention: Aerosols (di-alkyl sodium sulphosuccinates),[10] n-alkyl sulphonic acids,[16] n-alkylamine acetates,[17] fatty acid soaps.[10] For all these systems g is very close to unity when $C < c_s$, c_s being the critical concentration. At higher values of C, g falls rapidly and when $C \sim 4c_s$ it remains almost constant at about 0·16 to 0·20.

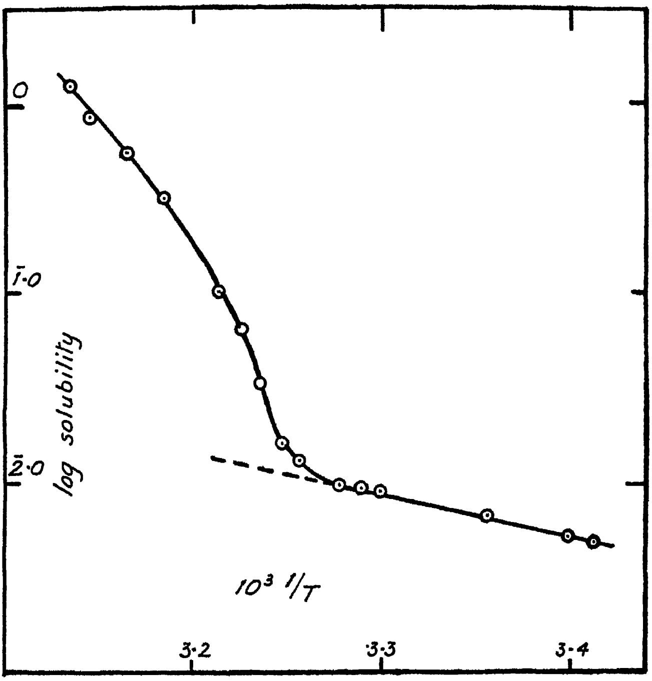

FIG. 2.—The saturation solubility of sodium dodecyl sulphonate at various temperatures.[11]

It is now possible to infer the general form of a graph of log C against $1/T$. Below the Krafft temperature, when no micelles are present, the slope of the graph should be approximately constant and equal to $\Delta H_1/2{\cdot}303R$. (Over a wide range of temperature ΔH_1 may be found to vary as the shape of the single molecules in solution, and thus their heat content will depend upon the temperature.) Above the Krafft point the slope of log C against $1/T$ will equal $\Delta H_2/2{\cdot}303Rg$. One might reasonably expect $\Delta H_2'$ to be less than $\Delta H_1'$, but the slope of the graph might well *increase*, not decrease, since g rapidly falls by a factor of 5 or 6, and soon becomes approximately constant. Fig. 2, which shows the plot of log C against $1/T$ for sodium dodecyl sulphonate—calculated from the solubility data of Tartar and Wright [11]—is in keeping with these inferences. This graph is typical for the series of sulphonates investigated, an increase in chain length merely displacing the curve to higher temperatures for similar values of the solubility.

---

[16] McBain, Laing, Dye and Johnston, *J. Amer. Chem. Soc.*, 1939, **61**, 3210.

[17] Ralston, Hoerr and Hoffman, *ibid.*, 1941, **63**, 2576.

Having found $\Delta H_1'$ and $\Delta H_2'$ by the above means, $\Delta H_s'$ follows from eqn. (3), but because of the uncertainty in the values of g, this method at present gives only very approximate values of $\Delta H_s'$. For example, from Fig. 2, $\Delta H_1'$ is about $+ 11$ kcal./mole. When C is *ca.* $5c_s$, $\Delta H_2'$ is about $+ 10$ kcal./mole, taking $g = 0{\cdot}18$. $\Delta H_s'$, therefore, is about $- 1$ kcal./mole (between 35 and 45° C), a value not very dissimilar from those obtained by Method 1.

THEORETICAL CONSIDERATIONS.—1. ΔH FOR THE AGGREGATION PROCESS. Although the aggregation of soaps is more complicated than the aggregation of fatty acid molecules, due to the ionic nature of the former, the structure of soap micelles in dilute solution is now well established, whereas the structure of fatty acid aggregates is still a matter of speculation. Accordingly, the former case will be considered first.

(1) *Soaps.* The initial state of heat content H_i is taken as the single molecule in dilute solution. As the concentration of single molecules in equilibrium with the micelles is very small (e.g. 0·001 M for a C_{16}-soap; 0·01 M for a C_{12}-soap, approximately), the constituent ions are very much farther apart than they are on the surface of a micelle. For the initial state, therefore, the interionic energy may be assumed to be zero.

Now consider the hydrocarbon tails of the long-chain ions. Because of the high interfacial tension between a hydrocarbon and water the tail assumes a spheroidal shape rather than the cylindrical (extended) form. If A_i is the surface area of the tail and γ' the *total* surface energy, then the interfacial energy is equal to $A_i\gamma'$. For all hydrocarbons, γ' is approximately constant [5] at 59 ergs cm.$^{-2}$.

In addition to the interfacial energy, the long-chain ion will have various forms of internal rotation, libration and vibration. The total energy from these sources may be written as L_i ergs per molecule. Both the long-chain ion and the gegen-ion will have translational energy, $3/2\,kT$ for each, and rotational energy again $3/2kT$. The total value of H_i per single soap molecule is, therefore,

$$H_i = A_i\gamma' + L_i + 6kT. \quad . \quad . \quad . \quad . \quad (6)$$

Now consider the final state, the single soap molecule in the micelle, of heat content H_f. Let there be n long-chain ions per micelle, and let nA_f be the total surface area of the micelle for which a hydrocarbon-water interface still exists. The interfacial energy per molecule in the micelle is then equal to $A_f\gamma'$. Ward [5] takes nA_f to be the difference between the total surface area of the micelle and the area covered by the long-chain ions. A crude picture, which is probably more representative of the real situation, is obtained if one imagines that there is water between each ionic head-group and extending into the outer parts of the micelle by being in contact with, say, the first two carbon atoms of each chain. Soaps with long hydrocarbon tails may not have a very large micellar hydrocarbon-water interface, but soaps with short chains or with branched chains (e.g. the Aerosols) may have a value of A_f which is quite a large fraction of A_i: it is not easy to visualize how short, relatively inflexible chains can form spherical aggregates with some considerable diminution in the hydrocarbon-water interfacial area. The value of $A_f\gamma'$ may well be the factor which determines whether aggregation occurs in solutions of short-chain salts, sulphonates of naphthalene, anthracene, etc. The interior of a micelle is believed to resemble a liquid hydrocarbon [2, 3] and the internal motions may be grouped in the internal energy term L_f per molecule, where $L_f \neq L_i$.

The long-chain ions in the micelle can, at most, rotate only about an axis along the length of the tail, i.e. the rotational energy per ion cannot exceed $1/2\,kT$. Because of the possibility of some movement of the long-chain ions within the micelle, even though the ionic head is fixed, each hydrocarbon tail may still have an energy of translation equal, at most, to $3/2\,kT$. As regards the gegen-ions, we believe that most of these are bound to the micelle and are thus without translational energy, although they may still have rotational energy of $3/2\,kT$ per ion.

Finally, the electrical energy of the ions in the micellar state requires consideration. Previous authors have not taken into account the gegen-ions, the majority of which must lie close to the micellar surface as the charge on a micelle is known to be quite small—say 4 or 5 units of charge, certainly not

40 or 50. If a fraction p of the gegen-ions are free, then $(1 - p)n$ gegen-ions are " bound " to the micelle, and have to be considered in calculating the net change in electrical energy upon aggregation. The maximum value of p seems to be about 0·30.

In contrast to earlier views we believe that the bound gegen-ions are situated *between* the long-chain ions, since sufficient water is present to maintain an aqueous environment, and this is their position of minimum potential energy. On this picture the total electrical energy of the micelle nE may be obtained in an approximate manner since it will lie between the values calculated for two extreme models : (1) all gegen-ions bound between the long-chain ions, (2) a fraction p ($p < 0{\cdot}3$) of the gegen-ions free, the rest bound as above. The former, in which all the gegen-ions are bound, leads to a net attractive force (i.e. E is negative), so that the electrical term assists aggregation. A precise calculation is not easy, but an estimate can be obtained from the similar problem for ionized monolayers. For example, at 50 Å^2/molecule, i.e. the gegen-ions about 7 Å apart (assuming a square lattice), E would be about 9×10^{-14} ergs per molecule, or 1·3 kcal./mole (Allan, private communication).

For the second of the above models, E may be estimated from the formula for the charging and discharging of a hollow sphere, which gives

$$E = \frac{np^2e^2}{2\epsilon r} \quad . \quad . \quad . \quad . \quad . \quad (7)$$

where r is the radius of the micelle, e the electronic charge and ϵ the dielectric constant of water. Due to the bound gegen-ions E is quite small. (Note—eqn. (7) is invalid when p is very small since it indicates that when $p = 0$, $E = 0$ also. This is certainly not true as there is then a net attractive energy.)

The total value of H_f per molecule is thus given by

$$H_f - A_f\gamma' + L_f + 7/2\,kT + E, \quad . \quad . \quad . \quad (8)$$

and the change in heat content (per molecule) on aggregation is deduced from the expression

$$H_f - H_i = \gamma'(A_f - A_i) + (L_f - L_i) + E - 5/2\,kT. \quad . \quad . \quad (9)$$

Only A_i, γ' and kT are known with accuracy, the most probable values of A for straight-chain hydrocarbons in water being given by Ward.[18]

An estimate of $(L_f - L_i)$ may be obtained from the latent heat of fusion of hydrocarbons, since the transfer of the hydrocarbon chain from the aqueous phase to the micelle may be taken as somewhat akin to the process of melting. This may well be an over-simplification, but should be more nearly true for the soaps with the longer chains. Values of L_f and L_i may conveniently be obtained from the empirical equations for the entropy of solid and liquid hydrocarbons. Such equations[19] reduce to

$$L_f - L_i = T(7{\cdot}0 + 1{\cdot}9b)/N \text{ cal./molecule,}$$

where N is Avogadro's number and b is the number of carbon atoms per chain.

To obtain an estimate of E, the number of molecules per micelle n must be known. Debye,[7] using the light-scattering technique, found the following values :

$C_{10}H_{21}.N.(CH_3)_3.Br$, $n = 36$; $C_{12}H_{25}.N.(CH_3)_3.Br$, $n = 50$;
$C_{14}H_{29}.N.(CH_3)_3.Br$, $n = 75$.

Addition of simple salts in very low concentrations (e.g. 0·013 M KBr) appeared to increase n considerably, the increase rising with the addition of more simple salt. This is not in keeping with the careful diffusion measurements of Hartley and Runnicles, which showed no marked changes in micelle size in the presence of electrolytes.[20] In view of the uncertainty in the experimental values of n, we employ here calculated values, obtained as follows. Let r be the total radius of the micelle and d the part due to the ionic group. Then the volume of hydrocarbon per micelle V is given by

$$V = \frac{4}{3}\pi(r - d)^3.$$

---

[18] Ward, *Trans. Faraday Soc.*, 1946, **42**, 399.

[19] Parks and Huffman, *Free Energies of some Organic Compounds* (Amer. Chem. Soc. Monograph No. 60 ; Chem. Catalog Co., N.Y., 1932).

[20] Hartley and Runnicles, *Proc. Roy. Soc. A*, 1938, **168**, 420.

If v is the volume of the hydrocarbon portion of a single molecule, then $n = V/v$. Clearly, r must be known accurately. Perhaps the best method of obtaining r is Hartley's method [21] applied to the X-ray diffraction patterns of strong soap solutions. Values of r somewhat *less* than the stretched length of the molecule * then result, and this is in keeping with the internal disorder of a micelle and with the idea that the ionic heads of the micelles, due to the large fraction of bound gegen-ions, are not "straining outwards" but, on the contrary, tend to cause shrinkage. (Experimental values are *ca.* 15 Å for potassium laurate and *ca.* 22 Å for cetyl pyridinium chloride, for which the calculated stretched lengths are *ca.* 17·5 Å and *ca.* 25 Å, respectively.)

It is now possible to make theoretical estimates of $\Delta H_s'$. Consider, for example, solutions of cetyl pyridinium chloride :

$A_t = 300 \times 10^{-16}$ sq. cm., $A_f = 80 \times 10^{-16}$ sq. cm. (see above). $(L_f - L_t) = +8{\cdot}4 \times 10^{-13}$ ergs per molecule at 25° C. $E = +0{\cdot}3 \times 10^{-13}$ ergs per molecule if $p = 0{\cdot}3$, $\epsilon = 78$ and $n = 55$ (calculated from $r = 22 \times 10^{-8}$ cm., which, in turn, is calculated from the data of McBain and Hoffman [22]).

Thus from eqn. (9), $\Delta H_s' = -7$ kcal./mole at 25° C. In a similar manner it may be shown that for sodium dodecyl sulphate (or sulphonate), $\Delta H_s' = -6$ kcal./mole at 25° C ($A = 80 \times 10^{-16}$ sq. cm. ; $E = 0{\cdot}3 \times 10^{-13}$ ergs per molecule).

Such theoretical values are definitely larger than the experimental values given earlier. This is at least partly due to the present uncertainty in many of the terms in the theoretical equation for $\Delta H_s'$. It must again be emphasized that the contribution from the ionic terms is not large numerically.

On the basis of the above ideas it is to be expected that $\Delta H_s'$ should become more negative as the temperature rises, since an increase in T will increase A_t and also reduce the net contribution from the internal rotations, etc. Experimentally, $\Delta H_s'$ does become more negative as the temperature is raised, but it is not yet certain how much the assumption of a constant micellar activity, independent of temperature, is affecting the observation.

(ii) *Fatty Acids.* At present there is no information available upon the structure of fatty acid aggregates. It is of some interest, however, to see what value of $\Delta H'_F$ is to be expected if we assume that the aggregate is spherical and rather like a soap micelle. $\Delta H_F'$ may then be found by using eqn. (9) and omitting the electrical energy term E. This makes very little difference numerically, and therefore it would seem that the values of $\Delta H_s'$ and $\Delta H_F'$ should be very similar at equal temperatures. This, indeed, is what has been found (see Table I).

The heats of solution of the higher fatty acids, when there are no soap ions present, show no marked change with increasing temperature, as may be seen by replotting the results of Ralston and Hoerr [23] on a graph of log (solubility) against $1/T$. This may be an indication that at least a few ions must be present for aggregation to occur (see Part I [6]). The aggregation of butyric acid in water noted by Grindley and Bury,[24] may be a form of temporary association due to the relatively high concentration (i.e. small average distance apart)

2. ΔS FOR THE AGGREGATION PROCESS.—We have been considering the equilibrium between soap molecules in solution and in the micelle (assumed spherical) and have calculated $\Delta H_s'$. The associated entropy change $\Delta S_s'$ should therefore be related to $\Delta H_s'$ by the equation,

$$\Delta H_s' = T\Delta S_s'.$$

Values of $\Delta S_s'$ may be estimated independently by evaluating the change in entropy on passing from an ideal dilute solution to a non-ideal liquid.

Let NaL represent a typical soap, L being the long-chain ion. If the subscript A refers to the aqueous solution and the subscript M to the micelle, then, ignoring any change in internal entropy (see below), the entropy change per molecule will be

$$-\Delta S = R \ln \frac{\mathrm{L}_M f_{\mathrm{L}_M}}{\mathrm{L}_A f_{\mathrm{L}_A}} + R \ln \frac{\mathrm{Na}_M f_{\mathrm{Na}_M}}{\mathrm{Na}_A f_{\mathrm{Na}_A}}, \quad . \quad . \quad . \quad (10)$$

where f is an activity coefficient and L_A, L_M etc. are mole fractions. The activity coefficients for the aqueous phase may be taken as unity since the concentration of single ions in solution is so small.

---

[21] Hartley, *Nature*, 1949, **163**, 767.

* Allowing for the chain and a reasonable contribution from the polar head-group.

[22] McBain and Hoffman, *J. Physic. Chem.*, 1949, **53**, 39.

[23] Ralston and Hoerr, *J. Org. Chem.*, 1942, **7**, 546.

[24] Grindley and Bury, *J. Chem. Soc.*, 1929, 679.

To a first approximation both L_M and Na_M may be taken as unity. (The latter is certainly less than unity, but this does not seriously modify the result obtained below.) The separate activity coefficients, f_{L_M} and f_{Na_M}, which cannot be measured, are replaced by the mean activity coefficient, $f_\pm$, which can be evaluated by applying two-dimensional thermodynamics[25] to the monolayer results for sodium cetyl sulphate at the benzene-water interface.[26] (This is the only such monolayer study at present available.) When the area per L^- is 100 Å^2, $f_\pm$ is 15, and at 40 Å^2, $f_\pm$ is about 100. (The area per molecule on the micelle surface is believed to lie within these limits.) These are considerably greater than the values found for unionized compounds,[25] and this is not surprising as the micelle surface is not very different from a two-dimensional ionic crystal and we have taken $f = 1$ for a very dilute gaseous film.

Values of ΔS may now be calculated from eqn. (10), which reduced to

$$\Delta S = -2R \ln (f_\pm/L_A). \qquad (11)$$

For a C_{16} soap, L_A is about 2×10^{-5} and hence $\Delta S = -54$ cal./deg. mole if the area per L^- is taken as 100 Å^2. This value of ΔS is not the quantity $\Delta S_s'$, which we want, as the change in internal entropy has not been allowed for. An approximate figure for the latter is obtained, as with the evaluation of the change in heat content, from the entropy of fusion of the liquid hydrocarbon forming the tail of the soap molecule. Hexadecane has an entropy of fusion of 39 cal./deg. mole, making $\Delta S_s'$, for a C_{16} soap, equal to -15 cal./deg. mole, i.e. $T\Delta S_s' = -4{\cdot}5$ kcal./mole when $T = 300°$ K, which compares reasonably with the value of $\Delta H_s'$ already determined (-7 kcal./mole). If the area per head group is taken as 40Å^2, for which $f_\pm$ is about 100, the final value of $T\Delta S_s'$ is $-6{\cdot}7$ kcal./mole.

The effect of temperature upon the value of $T\Delta S_s'$ may be seen by a qualitative examination of the two terms involved in the entropy. The entropy change due to the hydrocarbon tails will decrease as the temperature rises, whereas that due to the ionic heads will most probably be temperature independent as the size of the micelles varies but little over the range under consideration[20] (20° to 80° C). The net change in entropy should, therefore, become more negative as the temperature rises. A similar change in $\Delta H_s'$ has been predicted and observed.

These calculations have shown that, in the aggregation of soaps, the importance of the gegen-ions lies in the entropy term and not in the heat term. This is where the present treatment differs most markedly from those of previous workers.

The Effects of Additives upon Micelle Formation.—I. THE EFFECTS OF SIMPLE SALTS UPON THE CRITICAL CONCENTRATION c_s. From our earlier analysis it would seem reasonable to conclude that salts have little effect upon $\Delta H_s'$, and this is confirmed by the experimental work of Powney and Addison.[27] For this reason, certain treatments[28, 29] of the effects of simple salts upon c_s are open to serious criticism. The well-known fact that the addition of simple salts progressively lowers the critical concentration for micelle formation must, therefore, be an entropy effect.

Consider, as before, a soap of the type NaL, and let there be a simple salt NaX present. If $\Delta H_s'$ is constant for the equilibrium between the single soap molecules and the micelle, then $T\Delta S_s'$ must also be constant, i.e.

$$-\Delta S_s = R \ln \frac{L_M}{L_A} + R \ln \frac{Na_M}{Na_A} = \text{constant} \qquad (12)$$

if ideal behaviour is assumed. (The treatment may be made more general by the insertion of activity coefficients, but in the absence of any precise knowledge of the variation of such coefficients with the concentration of added simple salt, little can be gained by giving the more general equations.) The nomenclature is that of the previous sections.

Addition of NaX will alter L_A and Na_A, but to a first approximation, will not alter L_M or Na_M, since salts have little effect, if any, upon the size of the

[25] Ward and Tordai, *Trans. Faraday Soc.*, 1946, **42**, 408.

[26] Alexander and Teorell, *ibid.*, 1939, **35**, 727.

[27] Powney and Addison, *ibid.*, 1937, **33**, 1253.

[28] Cassie and Palmer, *ibid.*, 1941, **37**, 156.

[29] Palmer, *Surface Chemistry* (Butterworths, 1949).

micelles.[20] It should be noted that the hypothetical case in which all the gegen-ions are bound is being considered. Thus

$$\ln L_A + \ln Na_A = \text{constant}.$$

Without serious error these mole fractions may be replaced by concentrations,

i.e. $$\ln [L_A] + \ln [Na_A] = \text{constant}.$$

But $$[LA_A] = c_s,$$

and $$[Na_A] = [NaX] + c_s,$$

where [NaX] is the concentration of simple salt which has been added; i.e.

$$\log c_s = \text{constant} - \log ([NaX] + c_s) \quad . \quad . \quad . \quad (13)$$

There is considerable experimental evidence [12, 27, 30] that the relationship between c_s and the bulk concentration of the simple uni-univalent electrolyte is of this form. The fact that the experimental slope is less than unity (0·5 – 1·0, depending upon the soap) may well be due to some of the approximations made in deducing eqn. (13). [The above treatment can readily be extended to salts other than the uni-univalent type.]

II. THE EFFECTS OF ORGANIC ADDITIVES UPON c_s.—Let P represent the *total* concentration (i.e. bulk plus micellar) of the organic compound. Again, for the equilibrium between single molecules and micelles,

$$T\Delta S_s = \Delta H_s.$$

The presence of the organic compound will, in general, affect both ΔH_s and ΔS_s. ΔH_s is altered since organic molecules, especially if polar in character, reduce the contribution from the micellar hydrocarbon-water interface ΔH_s^{hc}. Since ΔH_s^{hc} opposes micelle formation the addition of organic molecules, both polar and non-polar, should lower the value of c_s. In general, it would seem reasonable to assume that

$$\Delta H_s^{hc} = kP_M,$$

where k is a constant which is less for non-polar molecules than for polar ones such as phenols and alcohols, and the subscript M refers to the micelle. To a first approximation, therefore,

$$\Delta H_s = \Delta H_s^0 + kP_M, \quad . \quad . \quad . \quad . \quad . \quad (14)$$

where ΔH_s^0 is the value of ΔH_s in the absence of the organic additive. The approximation arises because the total surface energy γ' depends upon the concentration of organic additive in the bulk of the solution. For non-polar molecules this may certainly be neglected, and for polar molecules the distribution ratio P_M/P_A is so much in favour of the micelles that no serious error is introduced by assuming that γ' is a constant.

As regards entropy changes it is unlikely that Na_M and Na_A are affected when the amount of organic additive is small. (At higher concentrations there may be changes in dielectric constant which modify the gegen-ion distribution.)

Thus $$\Delta S_s = \Delta S_L + \Delta S_{Na}$$
$$= -R \ln L_M/c_s + \text{constant}.$$

For small values of P_M we can take L_M as effectively constant and then

$$T\Delta S_s = RT \ln c_s + \text{constant}. \quad . \quad . \quad . \quad . \quad (15)$$

From eqn. (14) and (15) we therefore have

$$\Delta H_s^0 + kP_M = RT \ln c_s + \text{constant},$$

or, $$\log c_s = \text{constant} + kP_M. \quad . \quad . \quad . \quad (16)$$

Unfortunately, no data are available to test eqn. (16) for non-polar organic molecules. (Lingafelter, Wheeler and Tartar[31] have shown that saturation with benzene results in a decrease of c_s by about 14 %, the decrease depending a little upon the soap.) The equation has been tested for polar molecules, however, by determining c_s for the system Aerosol M.A.*-phenol, using a drop-volume technique. Fig. 3 shows the results plotted as log c_s against the *total* phenol concentration. This is justifiable since P_M should be proportional to P. The linear relation found accords well with the prediction of eqn. (16).

---

[20] Hartley, *J. Chem. Soc.*, 1938, 1968.

[31] Lingafelter, Wheeler and Tartar, *J. Amer. Chem. Soc.*, 1946, 68, 1490.

There is considerable experimental evidence recorded in the literature upon the effects of short-chain alcohols on c_s. At low alcohol concentrations a decrease in c_s is observed, but at much higher concentrations c_s increases. This is not contradictory to the present theory since at high alcohol concentrations γ' and ϵ will both be altered markedly. Unfortunately, the region of low alcohol concentrations has not been investigated sufficiently thoroughly to be able to use the results to test eqn. (16). Furthermore, straight-chain soaps were used, whereas a branched soap has been used here. The effects are expected to be far more pronounced in micelles formed from branched-chain soaps as the initial micellar hydrocarbon-water interface is so much greater. (This fact, in addition, is partly responsible for the much higher values of c_s for branched-chain soaps, and for their greater solvent-power for small organic molecules.[32])

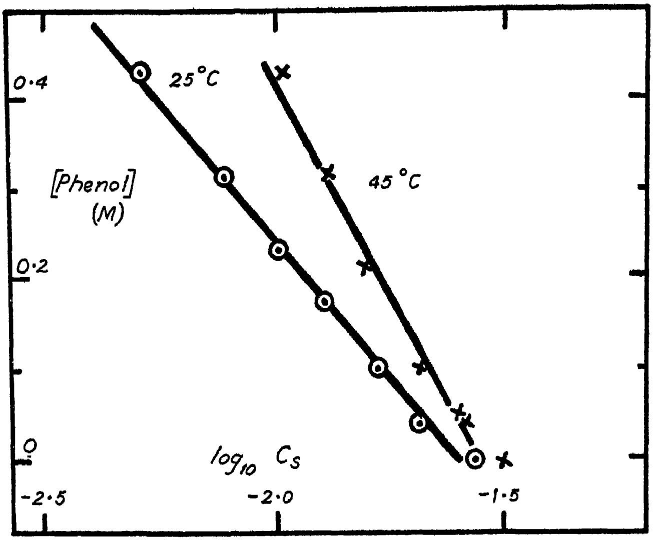

FIG. 3.—The dependence of the critical concentration for micelle formation c_s upon the total phenol concentration.
Soap : Aerosol M.A.

The effects of polar molecules upon ΔH_s should be reflected in the temperature coefficient of c_s for soap solutions containing such additives. ΔH_s is increased numerically as P increases, and therefore the temperature coefficient of c_s should also become increasingly greater. This is just what has been found for the system Aerosol M.A.-phenol, as Fig. 3 demonstrates.

We should like to thank Dr. G. S. Hartley for helpful discussions and the D.S.I.R. for financial assistance to one of us (G. S.).

Department of Colloid Science,
Cambridge.

* Aerosol M.A. is 2 : 2′-di(methyl-amyl) sodium sulphosuccinate.

[32] Unpublished work of the authors.

ELECTRICAL POTENTIAL DIFFERENCE AND RESISTANCE OF ISOLATED FROG GASTRIC MUCOSA AND OTHER SECRETORY MEMBRANES

By E. E. Crane and R. E. Davies

Received 22nd February, 1950

A P.D. was found across living isolated frog gastric mucosa (mean − 27 mV) and across other secretory membranes tested, which secrete under the experimental conditions but not across non-secretory membranes. The P.D. was reversibly abolished by anaerobiosis. When an applied current in either direction was passed through a secretory membrane (in the presence or absence of oxygen) the P.D. across it was a linear function of the current density up to a "breakdown" value at about 1 mA/cm.^{2}. At higher current densities the relationship was again linear but the resistance much less. Non-secretory membranes obeyed Ohm's law.

Both P.D. and resistance of isolated frog gastric mucosa depended little on the ionic composition of the secretory solution, but varied greatly with temperature. The "activation energy" was 16,000 cal./mole for both the rate of respiration (metabolic power) and (P.D.)^2/resistance (maximum electric power) of isolated frog gastric mucosae.

In 1834 Donné [1] first recorded the existence of a potential difference (P.D.) between the stomach and the blood stream, and raised the question of its function. Since then a considerable amount of work has been published on this problem.[2, 3, 4]

With isolated gastric mucosa it is possible to control the experimental conditions and also to measure both the electrical parameters and the metabolic activity. In particular the secretion of HCl can be measured and the minimum free energy required for its production can be calculated. Using live isolated frog and toad gastric mucosa at 25° C we have previously obtained the following results. (i) The addition of histamine was able to stimulate HCl secretion and produce an increase in the rate of respiration.[5] (ii) The secretory side was negative with respect to the nutrient side in an external circuit. The average P.D. across the mucosa was − 30 mV. Dead mucosae had no P.D.[6] (iii) The average resistance was about 210 Ω cm.^{2}; dead mucosae had a very much smaller resistance.[6] (iv) During acid secretion the P.D. was decreased and the resistance increased.[6] (v) The P.D.'s observed cannot be accounted for on the basis of simple diffusion potentials between the external solutions.[6] (vi) Anaerobically both P.D. and acid secretion were abolished and the electrical resistance increased.[6] (vii) Unstimulated mucosae could produce a current in an external circuit, maintaining an electric power output of the order of 1 μW/mg. dry wt., without appreciable polarization. About 10 % of the metabolic energy was thereby canalized into electrical energy.[6] (viii) In mucosae secreting HCl, currents ($\sim$1 mA/cm.^{2}) enhancing the natural P.D. (passed from nutrient to secretory side) greatly increased the rate of acid secretion. Similar opposing currents decreased this rate by the same order of magnitude; in many cases secretion was stopped.[7] (ix) In all cases, currents passed through non-secretive mucosae failed to initiate acid secretion. No other membranes examined (oesophageal, pyloric, duodenal and rectal mucosae, frogskin, Cellophane and dead frog gastric mucosa) produced HCl with any currents applied.[7]

---

[1] Donné, *Ann. Chim. Phys.*, 1834, **57**, 348.
[2] Biederman, *Elektrophysiologie* (Fischer, Jena, 1895).
[3] Rehm, *Amer. J. Physiol.*, 1944, **141**, 537.
[4] Rehm and Hokin, *ibid.*, 1947, **149**, 162.
[5] Davies, *Biochem. J.*, 1948, **42**, 609.
[6] Crane, Davies and Longmuir, *ibid.*, 1948, **43**, 321.

The present paper presents results relating to the electrochemistry of gastric mucosa and other secretory membranes including (*a*) their P.D. and their resistance and its dependence on current density and the ionic constituents of the secretory solution and on anaerobiosis, (*b*) the temperature relations of P.D., resistance and metabolic and electric power.

Experimental

Materials.—Most of the experiments were done on material prepared from frogs (*Rana temporaria*) and toads (*Bufo bufo*). The following species of animals were also used: rat (*Mus decumanus*), guinea pig (*Canis familaris*), polecat (*Mustela putorius*), hedgehog (*Erinaceus europaeus*), perch (*Perca fluviatilis*).

Preparation of Tissue.—Frog and toad oesophageal and gastric mucosa were washed and isolated according to the method of Davies.[5] Membranes from the duodenum and rectum were prepared similarly but with the muscle layers intact. Mammals were killed by a blow on the head and the required membrane (gastric mucosa, diaphragm, kidney capsule or atrium) dissected free at once. Perch were killed by crushing the skull and the swim bladder was dissected free from surrounding tissues.

Apparatus and Methods.—The apparatus, saline solutions and methods used during these experiments were similar to those previously described.[5, 6, 7] Membranes were mounted in Perspex holders held between two chambers containing nutrient or other saline solutions, gassed with the appropriate gas mixtures. Amphibian and fish membranes were maintained at 25° C and mammalian membranes usually at 38° C.

The Q_{HCl}* of acid-secreting membranes was estimated from changes in pH of the secretory solutions measured *in situ*. In most experiments the secretory solution was also changed periodically and its acid content determined, either manometrically by the addition of a bicarbonate solution, or by electrometric titration using a glass electrode and 0·01 N NaOH delivered from a Conway burette.

The P.D. between two saturated calomel electrodes, connected to the solutions bathing the two sides of the membrane by saturated KCl bridges with internal ground glass joints, was measured with a battery-operated Marconi pH meter and potentiometer, Type TF 511C. Electric current was passed through the membrane by means of zinc-zinc acetate electrodes separated from the solutions by the agar layers, as previously described.[6] The resistance was obtained from the slope of the P.D.-current graph, a correction being made for the resistance of the solutions.

Results

P.D.-Current Characteristics of Isolated Frog Gastric Mucosa.—RESISTANCE.—One of the most consistent electrical properties of isolated frog and toad gastric mucosa is the constancy of its resistance for current densities in either direction below about 0·5 mA/cm.^{2}; (here and elsewhere the area referred to is that of the hole in the Perspex holder, cf.[6]). This is referred to subsequently as the *low-current resistance*. Enhancing and/or opposing current densities up to this value were passed through 74 isolated frog and toad gastric mucosae, and in every case the graph obtained by plotting the P.D. across the mucosa against the current through it was a straight line. Moreover the resistance of a mucosa (given by the slope of the straight line) was not significantly different † for enhancing and opposing currents—there was no rectification (see Table I).

When the current density in the mucosa was increased above about 0·5 mA/cm.^{2} in either direction, the P.D. began to change less rapidly with current

[7] Crane, Davies and Longmuir, *Biochem. J.*, 1948, **43**, 336.

* Q_x = volume of x produced in µl. (expressed as a gas at N.T.P.)/(mg. dry wt. of tissue hr.). (22·4 × 10^6 µl. at N.T.P. = 1 mole).

† Here and elsewhere in this paper a 5 % level of significance is used.

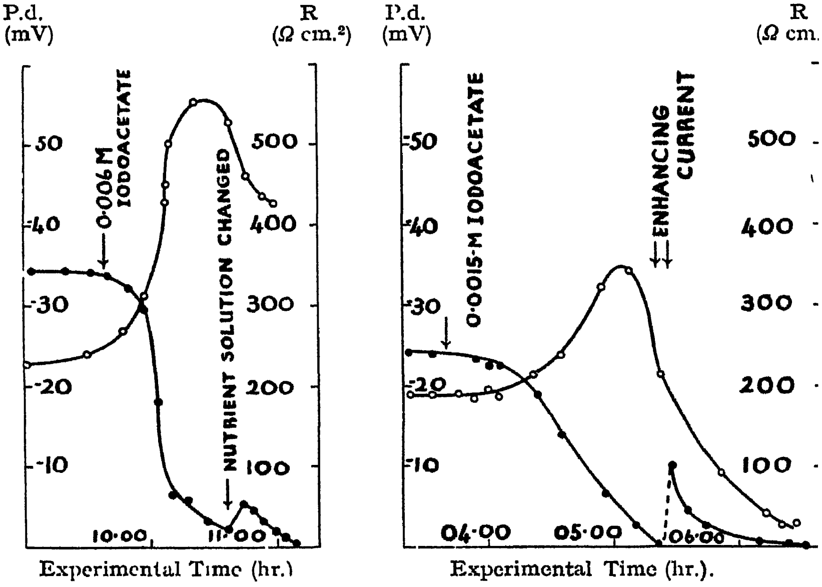

FIG. 1*a*.

FIG. 1*b*.

FIG. 1.—Effect of iodoacetate on the P.D. (●) and resistance (○) of two isolat frog gastric mucosae.

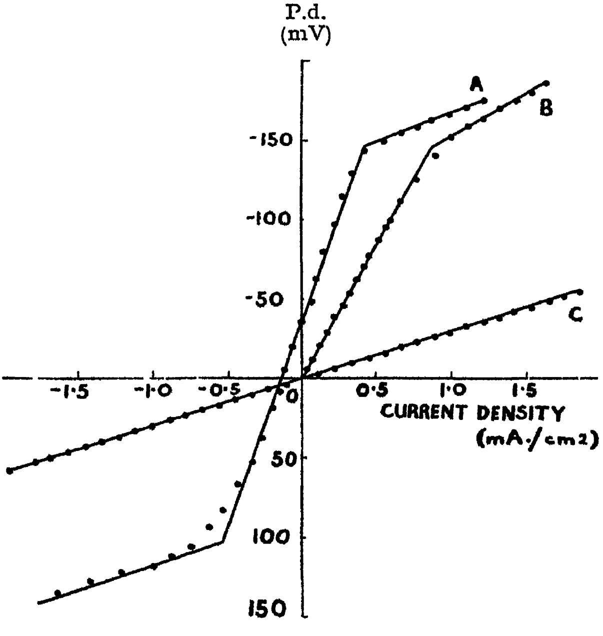

FIG. 2.—P.D.-current characteristics of isolated frog gastric mucosa: A, norm B, in the presence of iodoacetate; C, dead mucosa.

than previously, and finally the slope of the P.D.-current characteristic became constant again, at a much lower value than that with low currents. These characteristics are exemplified in Fig. 2, curve A, and Fig. 3, curve A. All of 39 frog and toad gastric mucosae examined gave characteristics of this type. For 24 of these mucosae (19 frogs and 5 toads) complete curves were obtained and the *high-current resistance*, the slope of the second linear part of the curve, was obtained for both enhancing and opposing currents. The combined results are given in Table I.

TABLE I.—MEAN VALUE OF LOW AND HIGH CURRENT RESISTANCES AND OF CONDITIONS AT BREAKDOWN OF 24 ISOLATED FROG (19) AND TOAD (5) GASTRIC MUCOSAE, WITH STANDARD ERRORS APPENDED

	Enhancing Current	Opposing Current
Low-current resistance R_1 (Ω cm.^{2}) .	207 ± 14	203 ± 12
High-current resistance R_2 (Ω cm.^{2}) .	35 ± 5·7	53 ± 5·4
Resistance R_2/R_1	0·18 ± 0·02	0·29 ± 0·04
Breakdown current density i_0 (mA/cm.^{2}) .	0·71 ± 0·06	0·67 ± 0·05
Breakdown P.D. V_0 (mV) . . .	−164 ± 10	+109 ± 8
Breakdown P.D.—natural P.D. (mV) .	−137	+136

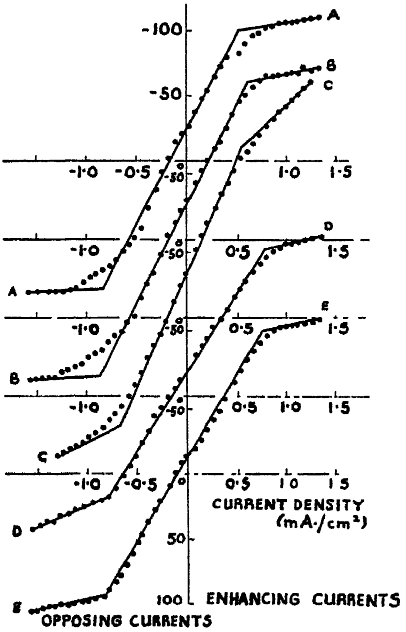

Ordinates: P.d. (mV)

FIG. 3.—P.D.-current characteristics of isolated frog gastric mucosae, with different ions in the secretory solution: A, 0·12 M NaCl; B, 0·12 M $NaNO_3$; C, 0·08 M phosphate buffer, pH 7·4; D, 0·12 M KCl; E, 0·08 M $CaCl_2$.

The average low-current resistance R_1 was 207 ± 14 Ω cm.^{2} for enhancing and 203 ± 12 Ω cm.^{2} for opposing current. These averages are not significantly different † from each other, nor from the mean resistance of frog gastric mucosa (210 ± 10 Ω cm.^{2}) reported earlier.[6] The average high-current resistances R_2 were 35 ± 5·7 Ω cm.^{2} for enhancing and 53 ± 5·4 Ω cm.^{2} for opposing current. The resistance to the passage of electric currents opposing the natural P.D. was thus nearly 50% higher than the resistance to currents enhancing the natural P.D. The standard error of the average difference (18 Ω cm.^{2}) between opposing and enhancing high-current resistances was 6 Ω cm.^{2}; the difference is significant.

The average ratios R_2/R_1 are also given in Table I, and again the value for opposing currents (0·29 ± 0·04) is about 50 % higher than that for enhancing currents (0·18 ± 0·02). The difference between these averages is 0·11 ± 0·05, which is just significant.

The results therefore show that partial rectification occurred at high, but not at low, current densities; it was observed in both secreting and non-secreting gastric mucosae. The effect varied widely in different mucosae however; the coefficient of variation (standard deviation/mean) of the difference between enhancing and opposing high current resistances was nearly 2.

RESISTANCE "BREAKDOWN".—The decrease in the resistance of the mucosa from its low-current to its high-current value was fairly sharp with enhancing currents, but more gradual with opposing currents (see Fig. 2*a*, and Fig. 1 of a previous paper[7]). In some mucosae (see Fig. 3) there appeared to be an intermediate linear portion of the characteristic with opposing currents, but characteristic A of Fig. 2 is more typical in this respect.

The "breakdown" point on the P.D.-current characteristic was defined as the point of intersection of the (produced) linear parts of the characteristic for low and high currents. The average current density at the breakdown point for enhancing currents was 0·71 ± 0·06 mA/cm.^{2} and for opposing currents was 0·67 ± 0·05 mA/cm.^{2}. The difference between the averages is not significant.

The average natural P.D. across the 24 mucosae represented in Table I was – 27 ± 2·1 mV, the secretory side being always negative with respect to the nutrient side in an external circuit. This is not significantly different from the mean of – 30 ± 0·9 mV reported earlier for 94 mucosae.[6] The average P.D. across the mucosa at the point of breakdown with enhancing currents was – 164 ± 10 mV, 137 mV numerically above the natural P.D. of – 27 mV. With opposing currents the average breakdown P.D. was 109 ± 8 mV, differing from the natural P.D. by 136 mV.

These results show that, for the mucosae studied, the breakdown point was independent of the direction of the current through the mucosa; both the breakdown current density and that part of the P.D. across the mucosa which was due to the applied current at the breakdown point were the same for enhancing and opposing currents.

Secreting and Non-secreting Gastric Mucosa.—Of the 24 mucosae included in Table I, eight were secreting HCl, but the remaining sixteen were not, when the P.D.-current characteristics were determined. The only apparent difference between these two groups was that the breakdown seemed to occur somewhat earlier (i.e. at lower P.D. and current density) in the 8 secreting than in the 16 non-secreting mucosae. There was certainly no remarkable change in R_2/R_1. The fact that R_1 and R_2 were not significantly different for the two groups is not inconsistent with the previously reported rise of resistance when acid secretion commences.[6] The coefficient of variation of the resistance of frog gastric mucosa was about 0·3 and the average fractional rise in resistance on secretion was less than 0·3. It is therefore unlikely that the present sample would show the rise in resistance on secretion, since different mucosae were used to obtain characteristics during, and in the absence of, acid secretion.

Results for other Membranes.—The above results show that the S-shaped characteristic is a property of the gastric mucosa itself, and not of the state of activity or inactivity of its secretory cells. Other membranes were studied in order to discover whether the S-shaped characteristic was peculiar to one class of membrane—that containing oxyntic cells—or whether it was common to membranes containing *any* secretory cells. The results obtained for secretory and non-secretory membranes are summarized in Table II.

Secretory Membranes. The secretory side of all amphibian secretory membranes studied was negative with respect to the nutrient side in an external circuit. All such membranes mounted without their muscular coat had P.D.-current characteristics similar to those of amphibian gastric mucosa. The three duodenal and rectal mucosae were mounted with the muscular coat attached; all these gave the S-shaped characteristic except one duodenal mucosa, which gave a linear curve with no breakdown.

Of the three isolated mammalian gastric mucosae used in the present experiments and listed in Table II, polecat mucosa was the only one which secreted acid, and the only one which developed a P.D. All four specimens examined had S-shaped P.D.-current characteristics. Isolated rat and hedgehog gastric mucosae did not secrete HCl, developed no P.D., and gave a linear characteristic through the origin. They obeyed Ohm's law for all currents applied (up to several mA/cm.^{2}).

The swim bladder of the perch was studied as an example of a membrane which secretes a gas. Two specimens containing the gas gland were used; neither showed any P.D., but both gave P.D.-current characteristics similar in shape to those of frog gastric mucosa. The breakdown current density was about 1 mA/cm.^{2} and R_2/R_1 was 0·5 to 0·6.

Non-Secretory Membranes.—No non-secretory amphibian membrane studied exhibited a P.D., all gave linear P.D.-current characteristics (Table II) even up to current densities many times the breakdown current density of amphibian gastric mucosa. Dead amphibian gastric mucosa behaved similarly. The muscular coat of the frog's stomach (3 cases out of 3) showed a slight breakdown effect at a current density of 5-6 mA/cm.^{2}, much higher than the breakdown current density of gastric mucosa.

TABLE II.—ELECTRICAL CHARACTERISTICS OF VARIOUS SECRETORY AND NON-SECRETORY MEMBRANES

Membrane (all Isolated)	Number Studied	Number giving S-shaped Curve	Number giving Linear Curve	Temp. (°C)	Approx. P.D. across Membrane (mV)
SECRETORY :					
Amphibian					
Gastric mucosa . . .	39	39	0	25	−30
Pyloric mucosa . . .	2	2	0	25	− 5
Duodenal mucosa (+muscle) .	2	1	1	25	− 2
Oesophageal mucosa . .	1	1	0	25	− 2
Rectal mucosa (+muscle) .	1	1	0	25	−17
Skin	5	5	0	25	−34
Mammalian					
Polecat gastric mucosa . .	4	4	0	25, 38	−10, −21
Hedgehog gastric mucosa .	2	0	2	25, 38	0, 0
Rat gastric mucosa . .	1	0	1	25	0
Fish					
Perch (*Perca fluviatilis*)					
Swim bladder (with gas gland)	2	2	0	25	0
NON-SECRETORY :					
Amphibian					
Dead gastric mucosa . .	28	0	28	25	0
Stomach muscle layer . .	3	3*	0	25	0
Mammalian					
Rat diaphragm . . .	7	0	7	38	0
Rat kidney capsule . .	1	0	1	25	0
Guinea pig atrium . .	2	0	2	38	0
Fish					
Perch (*Perca fluviatilis*)					
Swim bladder (no gas gland) .	1	0	1	25	0
Cellophane	1	0	1	25	0

* Slight breakdown at 5 mA/cm.^{2}.

Similarly no non-secretory mammalian membrane studied showed a P.D., and all obeyed Ohm's law for all current densities used (see Table II). The single example of non-secretory fish tissue used, part of the perch swim bladder not containing gas glands, gave a similar result.

SUMMARY. Every secretory membrane which was known to secrete under the conditions of the experiment, and which was detached from its muscular coat, gave an S-shaped characteristic. Every non-secretory membrane had a linear characteristic over the same range of current desities. It would therefore seem that a constant resistance at low current densities and a considerably lower constant resistance at higher current densities, together with an intermediate " breakdown " at a fairly well-defined current density, may be a specific property of tissues containing secretory cells.

Experiments in the Absence of Oxygen.—It has already been shown that in the absence of oxygen hydrochloric acid secretion did not take place in frog gastric mucosa, that the P.D. across it decreased reversibly to zero, and that there was a reversible rise in resistance.[6] The most noticeable other effect was the existence of an unstable electrical state at the breakdown point. In all of three experiments in anaerobiosis the P.D.-current characteristic was linear until a value of the current density was reached near the aerobic breakdown value, but after the next increase in current (say 10 sec. later) the P.D. *decreased* rapidly for a minute or more ; this " overshooting " effect was occasionally observed (to a much smaller degree) in experiments carried out in the presence of oxygen. Finally, after one or more minutes, the P.D. became steady and the readings could be continued; the anaerobic P.D.-current characteristic became linear again, with a much smaller slope than that at low current densities. Similar results were obtained with currents passing through the mucosa in either direction.

One specimen of frogskin was examined in the absence of oxygen; its resistance was also increased by anaerobiosis, but there was no overshooting, and the value of the high-current resistance was independent of the presence of oxygen. The P.D. characteristic of a single specimen of pylorus was not appreciably altered in shape by the absence of oxygen, but the anaerobic characteristic passed through the origin as there was no P.D. across the pylorus.

Effect of Iodoacetate.—Iodoacetate inhibits sulphydryl enzymes[8] and has been widely used to interfere with stages of the breakdown of glucose, although it also causes irreversible damage to other enzyme systems. Fig. 1 shows the effect of iodoacetate on two isolated frog gastric mucosae; other experiments gave similar results. The P.D. across the mucosa decreased to zero within 1 to 2 hr. after the addition of iodoacetate to 0·0045 M or 0·0015 M to the nutrient solution. On the other hand the resistance was at its maximum when the P.D. had almost reached zero; it fell subsequently to a value within the normal range for dead gastric mucosa (not shown in Fig. 1*a*).

Fig. 1*a* shows that, when the P.D. was already low, replacement of the nutrient solution by one not containing iodoacetate resulted in a temporary partial recovery of the P.D. The temporary 10 mV rise in P.D. (Fig. 1*b*) after the passage of a current through the mucosa from nutrient to secretory side (enhancing current) is interesting because such a rise was not observed except in the presence of iodoacetate. The P.D. across the mucosa had just reached zero (at 5.10) when an enhancing current up to a maximum of 1·8 mA/cm.^{2} was passed through the mucosa for a total time of 5 min. in order to obtain a P.D.-current characteristic (B of Fig. 2). The current was in such a direction as to carry negative iodoacetate ions from the mucosa back into the nutrient solution.

Fig. 2 shows P.D.-current characteristics for the gastric mucosa to which Fig. 1*b* refers, A before the addition of iodoacetate, B when the P.D. had just reached zero and finally C after the resistance had dropped to a fairly stable level (6.13-6.22); B is of a similar shape to A, although the P.D. had already reached zero. However, an hour later (C) the breakdown had completely disappeared, and the resistance at all current densities of the dead mucosa was about the same as that for high current densities in A. Several attempts were made to obtain a P.D.-current characteristic when the resistance was at its maximum value, but readings were too erratic while the mucosa was in this unstable state.

Effects of Different Ions in Isotonic Concentration in the Secretory Solution.—Experiments have been carried out to investigate the effects of replacing Na^+ and Cl^- in the solution S bathing the secretory side of isolated frog gastric mucosa by other ions, the total molarity being kept constant. While the composition of the solution S could be altered widely, the composition of a non-toxic nutrient solution could vary only within narrow limits.[9]

A remarkable result of these experiments with various ionic constituents of the solution S was the *lack* of effects on the electrical properties of the mucosa. Fig. 3 gives typical P.D.-current characteristics of an isolated frog gastric mucosa in the presence of histamine to 5×10^{-5} M, which failed to respond and did not secrete acid during the experiment; the pH of the unbuffered solution S was always between 6·7 and 6·0. The usual nutrient solution was used.

Characteristic A, taken at 2.28 hr. with 0·12 M NaCl as the solution S was the same as the characteristic taken before histamine was added at 2.05 hr. The points from which this characteristic was drawn show the commonly observed sharp breakdown with an enhancing current and more gradual breakdown with an opposing current. The points in the opposing-current breakdown region were linear in this case.

When the NaCl was replaced by 0·12 M $NaNO_3$ at 3.07 hr., the P.D. across the mucosa remained − 32 mV, and characteristic B was obtained. The low-current portions of B were the same as those of A. The high current portions were lines parallel to those of A; the high-current resistances were unaltered, but the breakdown current densities were higher by 0·2 (enhancing) and 0·05 (opposing) mA/cm.^{2}.

At 3.42 hr. the $NaNO_3$ solution was replaced by 0·12 M phosphate buffer, and the pH rose from 6·7 to 7·3. The P.D. across the mucosa was − 38 mV.

---

[8] Barron and Singer, *J. Biol. Chem.*, 1945, **157**, 221.

[9] Gray, Adkison and Zelle, *Amer. J. Physiol.*, 1940, **130**, 327.

The resistances were somewhat higher than with monovalent ions in the solutions, but the characteristic (C) was of the same type (see Fig. 3).

At 4·12 hr., 0·12 M KCl was substituted in the solution S. The P.D. across the mucosa was reduced to − 26 mV, and characteristic D was taken at 4.25 hr. The resistance for low current densities was 10 % lower than with NaCl and $NaNO_3$. With enhancing current the high-current resistance was the same as with these other solutions, and the breakdown current density intermediate between those with NaCl and $NaNO_3$. With opposing current the intermediate breakdown region was prolonged, but still linear.

At 4.55 hr., 0·08 M $CaCl_2$ was substituted for KCl as the solution S. The P.D. was − 16 mV, and the characteristic (E) showed very little change. At 5.36 hr., 0·12 M NaCl was again used as the solution S and the characteristic reverted almost exactly to characteristic A. The P.D. across the mucosa was now − 27 mV instead of − 32 mV. (A drop of 5 mV in the course of 3 hr. was common in our experiments.) All the small effects due to the different ions therefore appear to be reversible.

The mucosa was then killed by the addition of NaCN to the solutions. The resistance of the dead mucosa was subsequently measured with the five solutions used for characteristics A–E (Fig. 3) in turn in the secretory solution. The "dead" characteristics were all linear within the range used (± 1·5 mA/cm.^{2}); they are not plotted in Fig. 3 because in each case the resistance of the mucosa was so small in comparison with the resistance of the solutions that it could not be determined with any accuracy. It should be noticed in this connection that the high-current resistance of the mucosa was also very small, R_2/R_1 being very much lower than the average value (see Table I). It was generally found that the dead resistance of a mucosa was similar to its high-current resistance.

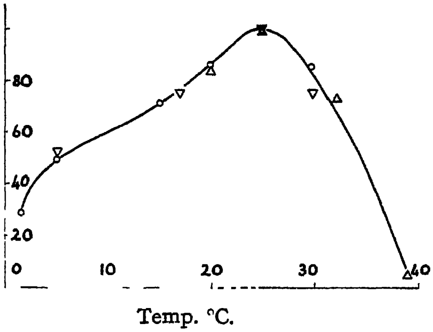

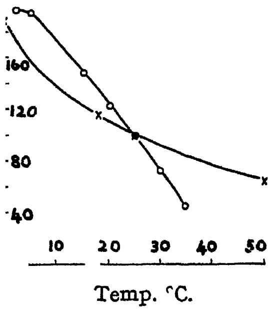

Ordinates: P.d. (percentage of value at 25° C).

FIG. 4*a*. FIG. 4*b*.

○ 4 Mucosae 25°→2°→30° C.
△ 2 Mucosae 25°→20→39 C.
▽ 3 Mucosae 5°→30° C.

Effect of Temperature.—The electrical properties and the rate of metabolism of isolated frog gastric mucosa were determined at temperatures between 2° C and 39° C, and an attempt was made to discover how the relationship between them varied with temperature. Temperature was controlled by heating or cooling the water bath. When the temperature was changed the P.D. did not become steady until the mucosa had been kept at the new temperature for about half an hour. Altogether about an hour was necessary in order to obtain a reliable P.D. level for each temperature.

POTENTIAL DIFFERENCE.—There was no consistent difference between results obtained when the bath was heated and when it was cooled, but P.D. showed less fluctuations in experiments when the bath was initially at 25° C and gradually cooled in 2° C than in experiments when the mucosa was put into a water bath at 2° C and gradually heated.

Fig. 4*a* shows combined results of experiments with nine isolated frog gastric mucosae whose average P.D. at 25° C was − 21 mV. The P.D. across a mucosa at each temperature is plotted as a percentage of the P.D. across the same mucosa at 25° C. Six of the points plotted (⊙) in Fig. 4*a* are average percentages for mucosae whose temperatures were varied from 25° C to 30° C, 15° C, 5° C, 2° C, 15° C, 25° C and 30° C, the whole process occupying 9 hr. Four points (▽) are average percentage P.D.'s for three mucosae which were immersed in a water bath at 5°, and after 2 hr. at this temperature they were maintained at 17° C, 25° C, 30° C, 22° C and 17° C over the next 6 hr. The remaining three points in Fig. 4*a* (△) represent averages for two mucosae kept at 25° C for 3 hr. and then at 20° C, 32° C, 39° C and 25° C over the next 5 hr. At 39° C the P.D. across one of these mucosae, A, was − 3 mV and across the other, B, 0 mV. They were both maintained above 38° C for 5 min. and the temperature then rapidly reduced to 25° C. The P.D. across B did not recover, but the P.D. across A rose to − 8 mV in 10 min. and remained steady until the end of the experiment (20 min.).

RESISTANCE.—Fig. 4*b* shows the average variation with temperature of the resistance of five isolated frog gastric mucosae, three with rising and two with falling temperature. The resistance of each mucosa at any temperature was calculated as a percentage of the resistance of the same mucosa at 25° C, and the points plotted in Fig. 4*b* represent the average of the percentages at each temperature. The average resistance (for 1 cm.^{2}) of the five mucosae at 25° C was 180 Ω cm. The variation of specific resistance of 0·12 M NaCl is also shown in Fig. 4*b* as a percentage of the value at 25° C.

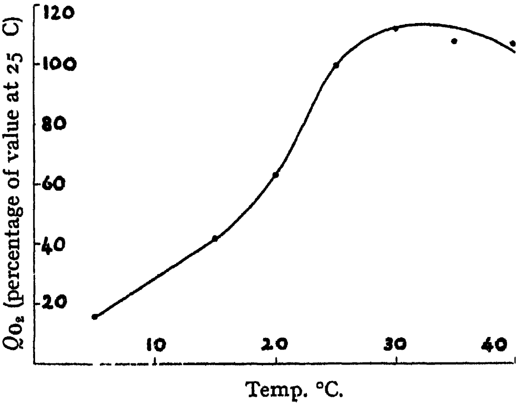

FIG. 4*c*.

Both the average P.D. V and the average resistance R at 30 were about one-third of their value at 25° C. However, while R increased continuously as the temperature decreased, becoming twice R_{25} at 2° C, V was a maximum at 25° C and at 2° C only one-third of V_{25}.

P.D.-CURRENT CHARACTERISTICS AT LOW TEMPERATURES.- A single experiment was carried out in order to discover any major effects of temperature on the P.D.-current characteristic. The curves were unaltered in shape at low temperatures and the values of the breakdown current density and of R_2/R_1 were not materially altered as the temperature of the mucosa was decreased from 25° C to 2° C, although R_1 and R_2 were both approximately doubled. Results of two experiments with frogskins showed that their P.D.-current characteristics were also essentially of the same shape at 2° C as at 25° C.

RATE OF RESPIRATION.—The Q_{O_2} of five isolated frog gastric mucosae was measured at temperatures increasing from 5° C to 40° C. As open sheets of mucosa were used in Warburg cups, acid secretion could not be measured.[5] However, the experiment was carried out in February and the mucosae were not stimulated with histamine, so it is most unlikely that any of them was secreting acid during the experiment.[11]

The average Q_{O_2} values (in μl./mg. (dry wt.) hr.) were determined as follows :

5° C	15° C	20° C	25° C	30° C	35° C	40° C	25° C
$-0{\cdot}1_9$	$-0{\cdot}5_1$	$-0{\cdot}7_6$	$-1{\cdot}2_1$	$-1{\cdot}3_5$	$-1{\cdot}3_0$	$-1{\cdot}3_0$	$-0{\cdot}9_8$

The Q_{O_2} increased numerically with temperature between 5° C and 30° C and thereafter remained fairly constant up to 40° C. After 35 min. at 40° C the

---

[10] *Int. Crit. Tables* (McGraw-Hill, New York), 1st ed., vol. vi, 233.

[11] Bradford, Crane and Davies, *Proc. Zool. Soc. Lond.* (in press).

temperature was reduced to 25° C when the Q_{O_2} was nearly 20 % less than its previous rate.

Electric and Metabolic Power. It seems likely [6] that the maximum electric power a mucosa could produce is $(\text{P.D.})^2/\text{resistance}$ or V^2/R. The metabolic power of a mucosa, i.e. the rate at which energy is liberated in the mucosa by metabolism, is proportional to the Q_{O_2}. Fig. 5*a* shows the relationship between the average values of V^2/R and Q_{O_2} (measured as percentages of the values at 25° C) for various temperatures. The points for 5° C, 15° C, 20° C and 25° C are nearly collinear, and the straight line through them passes almost through the origin. It seems that for any temperature between 5° C and 25° C the maximum electric power a mucosa could produce is nearly proportional to its metabolic power at that temperature—the efficiency of the utilization of metabolic power for electrical work appears to be independent of temperature within this range.

This is further shown in Fig. 5*b*, where $\log_{10} V^2/R$ and $\log_{10} Q_{O_2}$ (both percentages of values at 25° C) are plotted against the reciprocal of absolute temperature, after the method of Arrhenius [12] (see Höber,[13] Sizer [14]). The points representing temperatures between 5° C and 25° C are collinear within experimental error for both $\log_{10} V^2/R$ and $\log_{10} Q_{O_2}$, and may be represented by the same straight line. The gradient of the line is − 3,500 and the corresponding "energy of activation" is 3,500 × 4·58, i.e. 16,000 cal./mole.

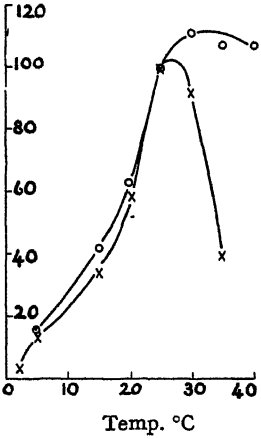

Fig. 5*a*.

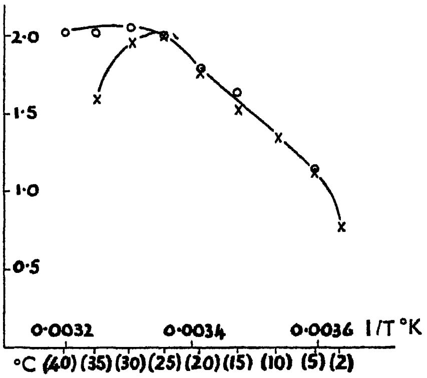

Fig. 5*b*.

Ordinates: (*a*) $\text{P.d.}^2/R$ and Q_{O_2} (percentage of value at 25° C)
(*b*) $\log_{10} \text{P.d.}^2/R$ and Q_{O_2} (percentage of value at 25° C)

The value of V^2/R at 2° C was less than that expected from the values above 5° C (Fig. 5*a* and 5*b*). Above 25° C neither the Q_{O_2} nor V^2/R continued to increase at the rate for temperatures below 25° C (Fig. 5*a* and 5*b*). The Q_{O_2} remained fairly constant from 25° C to 40° C, but V^2/R decreased rapidly; at 35° C it was only 40 % of its value at 25° C. Thus while between 5° C and 25° C a constant fraction of the metabolic energy of an isolated frog gastric mucosa could probably be used to produce electrical work, this fraction became very much smaller at temperatures above 25° C.

Comparative Results for Frogskin.—In order to discover whether the electrical properties of another secretory membrane varied with temperature in the same manner as those of frog gastric mucosa, three experiments were carried out with frogskin. All three gave similar results, which in some respects resembled those for gastric mucosa. Results of one experiment with abdominal skin, which was typical of all three, are shown in Fig. 6. Fig. *6a* should be compared with Fig. *4a* and *4b* and Fig. *6b* with Fig. *5b*. There were differences in the rate of variation with temperature of both P.D. and resistance, but the graph of $\log_{10} V^2/R$ against the reciprocal of the absolute temperature (Fig. *6b*) is linear for the range 2° C to 30° C. The gradient (−4,700) is greater than that for gastric mucosa, and the "activation" energy about 22,000 cal./mole. Two experiments with frogskin at 2° C gave similar P.D.-current characteristics to those for gastric mucosa at this temperature; there was no essential change in shape from the characteristic for frogskin at 25° C.

---

[12] Arrhenius, *Z. physik. Chem.*, 1889, 4, 226.

[13] Höber, *Physical Chemistry of Cells and Tissues* (Blakison, Philadelphia, 1945), p. 31.

[14] Sizer, *Adv. Enzymol.*, 1943, 3, 35.

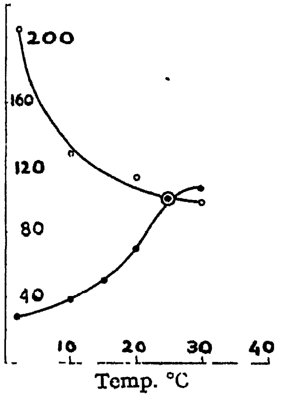

FIG. *6a*.

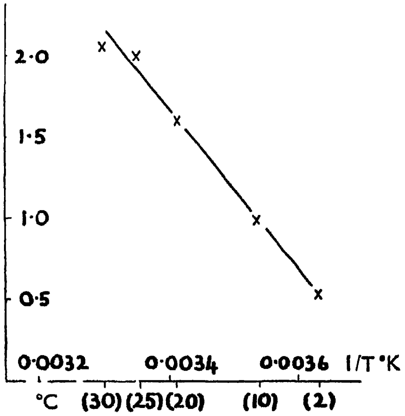

FIG. *6b*.

Ordinates: (*a*) P.d. and R (percentage of value at 25° C)
(*b*) $\log_{10}$ (P.d.^{2}/R) (percentage of value at 25° C)

Discussion

Electrical Properties of Secretory Membranes.—The electrical properties of all the secretory membranes studied were in many ways similar; and they differed from those of the non-secretory membranes which were investigated. A P.D. was developed across calomel electrodes connected by sat. KCl bridges to the fluid bathing both sides of most secretory membranes, but not across the non-secretory membranes. The occurrence of a characteristic breakdown of the resistance of the membrane also appears to be a property of, and confined to, secretory membranes.

A large *increase* in the resistance of isolated frog gastric mucosa, accompanied by a decrease of the P.D. across it, was observed (i) when respiration was stopped by the removal of oxygen, (ii) when respiration was inhibited by the addition of iodoacetate and (iii) when the rate of respiration was lowered by a reduction of the temperature. The result (i) is in agreement with results obtained by Rehm and Hokin [4] and by Rice and Ross,[15] who found that the P.D. across a dog's stomach wall was dependent upon an adequate supply of oxygen to the tissue. Francis and Gatty [16] found that the P.D. of frogskin was irreversibly reduced by iodoacetate even as dilute as 2 × 10^{-4} M.

The above results show that some stages of normal aerobic metabolism are needed to keep *down* the resistance of frog gastric mucosa tissue possibly by keeping open pathways for ion transport. On the other hand death of the mucosa is always associated with a major *fall* in the

[15] Rice and Ross, *Amer. J. Physiol.*, 1947, **149**, 77.
[16] Francis and Gatty, *J. Expt. Biol.*, 1938-9, **15**, 132.

resistance and with the disappearance of the breakdown. In this case permeability barriers normally maintained during life must be broken down ; ionic movements then occur much more readily.

It may be significant that the high-current resistance of gastric mucosa is similar to the dead resistance. It is possible that some of the barriers to ion transport are reversibly broken by the high potential gradients in gastric mucosa during the passage of the high currents.

Effect of other Ions on the Resistance and P.D. of Gastric Mucosa.—The P.D. across many non-living membranes is largely dependent on the nature and concentration of the ions in the solutions bathing the two sides.[17] However, the P.D. across the gastric mucosa was found to be remarkably independent of the composition of the secretory solution. The observed P.D. was thus not a physico-chemical effect directly dependent on the ionic composition of the solution bathing the membrane, but was a property of the tissue.[6] The results confirm those of Mond [18] who found that no significant changes occurred in the P.D. across a perfused frog stomach when isotonic solutions of NaCl, Na_2SO_4, $NaNO_3$, KCl or $CaCl_2$ were placed in contact with the secretory side. Teorell and Wersäll [19] also found that the secretory surface of isolated frog gastric mucosa was "insensitive towards the ionic composition of the solutions bathing it". Similar results were obtained by Rice and Ross on dogs ; [15] they found that a wide range of concentrations of various electrolytic solutions had only insignificant effects on the potential. These observations are in agreement with those of Goodman [20] and Quigley, Barcroft, Adair and Goodman.[21] Small rises in the value of the P.D. across isolated frog gastric mucosa occurred when hypotonic salt solutions were placed on the secretory side.[22]

The magnitude of the P.D. measured depends on the nature of the electrodes used. For instance with an isolated frog gastric mucosa (not secreting acid) separating a secretory solution of 0·012 M NaCl made up to 0·12 M with $NaNO_3$, pH 5·60 and a nutrient solution containing 0·095 M NaCl, pH 7·40, the P.D. between sat. calomel electrodes connected to the two solutions by sat. KCl bridges was −22 mV while between Ag/AgCl electrodes dipping in the two solutions it was + 30 mV and between glass electrodes in the two solutions + 84 mV.[22, 23]

Effects of Temperature.—No previous work has been published on the temperature variations of the P.D or Q_{O_2} of unstimulated gastric mucosa. Teorell has recently published preliminary results of the Q_{O_2} and Q_{HCl} of stimulated gastric mucosa.[24] Various workers have studied the temperature variations of the P.D. across living frog skin.[25, 26, 27, 28] Lund and Moorman [25] and Francis [26] investigated the temperature variations of the Q_{O_2} of frog skin. The only attempt to correlate the rate of respiration with the rate of production of electrical *energy* by frog skin at different temperatures was made by Francis.[26] He measured the electrical work done by three samples of frog skin, and the average rate of respiration of four others, and found that the average Q_{10} (temperature coefficient for a rise of 10°) of the electric power produced was 2·9 in the range of 0-10° C and 1·4 in the range 10-20° C. The average Q_{10} of the rate of respiration was 3·6 (0-10° C), 2·0 (10-20° C) and 1·9 (20-30° C). The total resistance in the circuit was 1500 Ω at room temperature; it must have been appreciably higher at low temperatures owing to the increase in resistance of the frog skin and solutions. The electric power produced was less than, and almost certainly not a constant fraction of, the electric power *available* from the tissue. The results indicate, however, that both the energy available from respiration, and the electric energy produced, decrease rapidly as the temperature decreases.

---

[17] Dole, *Principles of Experimental and Theoretical Electrochemistry* (McGraw-Hill, New York, 1935), 1st ed., chap. 22.

[18] Mond, *Pflüg. Arch. ges. Physiol.*, 1927, **215**, 468.

[19] Teorell and Wersäll, *Acta Physiol. Scand.*, 1945, **10**, 243.

[20] Goodman, *Surg. Gynec. Obstet.*, 1942, **75**, 583.

[21] Quigley, Barcroft, Adair and Goodman, *Amer. J. Physiol.*, 1937, **119**, 763.

[22] Davies and Ogston, *Biochem. J.*, 1950, **46**, 324.

[23] Crane, in *Progr. in Biophysics* (Butterworths, London, 1950).

[24] Teorell, *Experientia*, 1949, **5**, 409.

[25] Lund and Moorman, *J. Expt. Zool.*, 1931, **60**, 249.

[26] Francis, *Nature*, 1933, **131**, 805.

[27] Motokawa, *Jap. J. Med. Sci.* (III *Biophysics*), 1938, **5**, 93.

[28] Barnes, *Physiol. Zool.*, 1940, **13**, 82.

It seems likely [6] that the maximum electric power that could be produced by an isolated frog gastric mucosa is $(\text{P.D.})^2/R$ and it seems probable that the temperature variation of this function is of more significance in relation to the temperature variation of the rate of metabolism than that of the P.D. or resistance alone. Straight lines are obtained when either $\log_{10} Q_{O_2}$ or $\log_{10} (\text{P.D.}^2/R)$ is plotted against $1/T$; and these lines have the same slope (see Fig. 5*b*, 6*b*) in accordance with the Arrhenius equation.[12, 14]

Because of the complexity of the biological system it is not possible at present to interpret the exact significance of the value of the activation energy obtained from the slope of these lines (cf. Morales [29]). However, the observed similarity between the temperature variation of the Q_{O_2} and that of $(\text{P.D.})^2/R$ may be taken to support the view that there is a linkage or coupling between the metabolic power available to the tissue and the maximum electric power which the tissue can produce. The efficiency of the conversion of metabolic energy into electrical energy was found to be constant in the range 5-25° C. Some other aspects of the efficiency relations of certain metabolic and electrochemical processes in gastric mucosa have been discussed elsewhere.[30, 31, 32]

Medical Research Council Unit for Research in Cell Metabolism,
Department of Biochemistry,
The University,
Sheffield 10.

[29] Morales, *J. Cell. Comp. Physiol.*, 1947, **30**, 303.
[30] Crane and Davies, *Biochem. J.*, 1948, **43**, xlii.
[31] Crane and Davies, *ibid.*, 1948, **43**, xlii.
[32] Crane and Davies (in press).

REVIEWS OF BOOKS

Die Thermodynamik des Wärme- und Stoffaustausches in der Verfahrenstechnik. By DR.-ING. WERNER MATZ. (Steinkopf, 1949).

In this book, which is addressed to chemical engineers, Dr. Matz presents a coherent treatment of all countercurrent operations involving the transfer of heat and matter between phases. In common with previous authors, he is faced with the problem of linking up general thermodynamics with the specialized theories of heat and mass transfer in such a way as to make himself intelligible to mathematical amateurs. Although, in the opinion of the reviewer, this problem has not been fully solved, it must be admitted that Dr. Matz has faced up to it more boldly than many others and has not attempted to gloss over the difficulties.

An introductory chapter deals with analytical and geometrical methods of presentation, equations of state, thermodynamic principles and dimensional analysis. The second and perhaps most important chapter applies these principles to the theories of heat and mass transfer. The rest of the book, Chapters III to VII, is taken up with the application of these theories to problems of evaporation, distillation, adsorption, absorption and extraction. An appendix deals with the vector-analytical treatment of thermodynamic cycles.

Throughout the book very extensive use is made of a geometrical representation not very familiar in this country. The well-known linear relations employed in graphical heat balance calculations on an h—x diagram are considered as the expression of the First Law of Thermodynamics and are developed with the help of vectors in close analogy with the mechanical model of a system of forces. On this foundation is erected a geometrical theory of the exchange of heat and matter by way of polar triangles and the laws of harmonic projection. This leads not only to Ponchon's method of calculating distillation equipment by the use of a single " pole " (" reflux pole " in Dr. Matz's terminology), but to the use of two further " poles " (" transfer pole " and " mixing pole ") which appear as the two other points of the polar triangle and can be applied in the solution of other countercurrent problems.

In the chapter on distillation, a great deal of space is taken up with a qualitative discussion of the various types of phase equilibrium diagrams and thermodynamic surfaces, and critical phenomena are thoroughly discussed from the geometrical viewpoint. A similar method is used in the treatment of extraction problems.

As may be inferred from the above, Dr. Matz's treatment of thermodynamics is based primarily on the van der Waals' school. Little use is made of the methods now firmly entrenched in this country and which may be traced to G. N. Lewis and his interpretation of Willard Gibbs. Partial molar quantities are used only incidentally, fugacities and activities are not even mentioned. In spite of the extensive treatment of phase equilibria, no attempt is made to present, even in summary, a thermodynamic theory of solutions.

This is in itself no adverse criticism of a book intended for the use of chemical engineers. It must, however, be stated that the more theoretical portions of the book are more and not less exacting than the corresponding parts of comparable English and American text-books and, in many cases, more abstruse than is warranted by their practical application in later chapters. A considerable gap between theory and practice is evident throughout the book. Much theory is left unapplied, and therefore unjustified, and the practical problems, which are scattered rather sparsely in the text, are mostly solved without very much reference to the more fundamental theoretical considerations.

Though Dr. Matz's book contains many extremely interesting and stimulating ideas, enabling an English reader to broaden his outlook and to alter with advantage his accustomed line of attack, it is felt that the effort required to assimilate the unfamiliar treatment may be too great to attract even the more theoretically minded scientists and engineers in this country.

M. R.

Proceedings of the Technical Session on Bone Char Research, 1949. VICTOR R. DIETZ (Ed.) (The Bone Char Research Project, Inc.) Pp. 321.

This publication contains the papers presented at the "Technical Session" which was held at the National Bureau of Standards in January, 1949. The Bone Char Research Project was founded in 1939. It is supported by the leading sugar refining interests in the U.S.A., Great Britain and Canada, and the work of the Project is carried out at the N.B.S. Laboratory in Washington. At the 1949 "Session", which is intended to be the first of a series of two-yearly conferences, representatives of the sponsoring Companies presented the papers and contributed to the discussion.

The majority of the papers read were of technological rather than general scientific interest so that their appeal is limited mainly to the actual users and manufacturers of bone charcoal. At a conference of this kind the selection of material is necessarily somewhat arbitrary. However, the different phases of the bone char cycle are fairly well covered —decolorization, sweetening-off, regeneration and cooling, and decarbonization. Also basic investigations of the micro-structure of bone char by means of electron microscopy, and X-ray diffraction are reported, but the paper dealing with this aspect of the work does little more than indicate the methods of approach to the problem, as few definite conclusions are yet available. An interesting development is the introduction of a possible synthetic substitute designed to replace natural bone charcoal should the supply of the latter fail.

The investigations of the authors appear to have been influenced by the underlying belief that bone charcoal was designed specifically for sugar refining and that a substantially better adsorbent for the purpose is not to be expected. This is a defensible, but disappointing, proposition and one feels that it may, in the long run, impede progress.

Reproduction of the book is by the photo-lithographic process. The diagrams are uniformly clear and well arranged. The length of the text is such that the whole of the book can be read in a few hours. This, and the time necessary for further study of the controversial matters discussed, would be time well spent by anyone interested in the technology of bone charcoal.

S. H.

THERMODYNAMIC STUDIES OF SILICONES IN BENZENE SOLUTION

By M. J. Newing

Received 2nd March, 1950

The thermodynamic quantities ΔG, ΔH and ΔS of solutions of silicones in benzene have been obtained experimentally from measurements of molecular weights, lowering of vapour pressure in benzene and calorimetric determination of the heats of mixing. The values show large deviations from those expected from current theoretical treatments. The results suggest that in the pure silicone liquids the molecules are regularly coiled, but when dissolved in a solvent such as benzene, the coils are opened out and the molecules are in the form of extended flexible chains.

In general it is found that solutions of high molecular weight materials are not described by the ideal thermodynamic laws derived for solutions of small molecules. The deviations from ideality depend on the size and configuration of the dissolved molecules. Information on the state of the molecules may therefore be obtained from a study of the thermodynamic properties in solution. Summaries of the fundamental thermodynamic properties of binary liquid mixtures have been given by Meyer and van der Wyk [1] and Gee and Treloar.[2]

Extensive work has been done on the properties of polymers such as rubber in solution, but no systematic study of the thermodynamic properties of silicones in solution has been reported. This paper describes the determination of the thermodynamic quantities ΔG, ΔH and ΔS of solutions of silicones in benzene from (i) measurements of molecular weight; (ii) lowering of vapour pressure; and (iii) calorimetric determinations of the heat of mixing. In the discussion the values are compared with those expected from theoretical considerations.

Experimental

Materials.—The silicones used in these investigations were commercial Dow Corning dimethyl silicone liquids DC 500, 10 cstks. and 50 cstks., and DC 200, 350 cstks. These oils contain polymer chains of general form

$$CH_3[(CH_3)_2SiO]_nSi(CH_3)_3$$

over a narrow range of molecular weights.[3] They were heated under vacuum to remove any low-boiling polymers and used without further treatment.

Determination of Molecular Weights of Long Chain Silicones.—A cryoscopic determination was only practicable with the least viscous silicone. This gave an average molecular weight of 1140 in cyclohexane. The molecular weights of the two longer chain polymers were determined by measurement of their intrinsic viscosity $[\eta]$ in toluene. The average molecular weights M were obtained from the empirical equation

$$[\eta] = KM^{\alpha},$$

using the values, $K = 2{\cdot}00 \times 10^{-4}$ and $\alpha = 0{\cdot}66$ obtained by Barry [4] for the dimethyl polysiloxane homologous series.

---

[1] Meyer and van der Wyk, *Helv. chim. Acta,* 1940, **23,** 488.

[2] Gee and Treloar, *Trans. Faraday Soc.,* 1942, **38,** 147.

[3] Patnode and Wilcock, *J. Amer. Chem. Soc.,* 1946, **68,** 358.

[4] Barry, *J. Appl. Physics,* 1946, **17,** 1020.

The viscometer was of the U-tube type constructed according to British Standards' specifications. It had a time of flow for toluene of 5 min. and an eflux volume of 10 ml. The mean of four readings not differing by more than 0·2 sec. was taken for each point on the η_{sp}/c against concentration graph. The values for the intrinsic viscosities obtained by this method and the molecular weights calculated from them are given in Table I.

TABLE I

Silicone	Intrinsic Viscosity	Molecular Weight
DC 500 10 cstks. . . .	—	(1,140)
DC 500 50 cstks. . . .	0·465	3,850
DC 200 350 cstks. . . .	0·1175	15,700

Measurement of the Lowering of Vapour Pressure by Silicones in Benzene.—The partial molar free energies of dilution ΔG_0 for the three silicones were determined from the lowering of vapour pressure in benzene solutions. ΔG_0 is given by

$$\Delta G_0 = RT \ln a_0 = RT \ln (p_0/p_0^0), \quad . \quad . \quad . \quad (1)$$

where a_0 is the activity of benzene in the solution, p_0 is the vapour pressure of benzene above the solution, and p_0^0 is the vapour pressure of pure benzene. (In the subsequent work the subscript o refers to benzene and the subscript s refers to silicone.)

The vapour pressure apparatus used was a slightly modified form of that described by Gee and Treloar for the measurement of the vapour pressure of the rubber-benzene system.[2] A weighed sample of silicone was introduced into a narrow tube sealed to the apparatus. The tube was then sealed off and the silicone degassed by freezing and melting under vacuum several times. The apparatus was prepared for operation as described by Gee and Treloar.[2] The vapour pressure measurements were made at 25 ± 0·02° C, 1 hr. being allowed for the apparatus to come to equilibrium after immersion in the thermostat. Fig. 1 shows the vapour pressure curves obtained for the three silicones used. Values of ΔG_0 calculated from these curves are given in Tables II, III and IV.

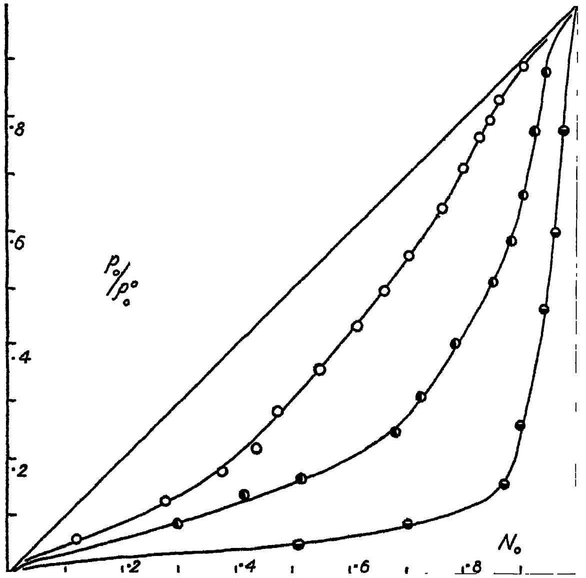

FIG. 1.—Relative lowering of vapour pressure of benzene-silicone solutions.

○ DC 500, 10 cstks. ◐ DC 500, 50 cstks. ◒ DC 200, 350 cstks.

TABLE II.—DC 500, 10 CSTKS. IN BENZENE

N_0	v_0	a_0	ΔG_0 cal. mole^{-1}	ΔH_0 calc. cal. mole^{-1}	ΔH_0 expt. cal. mole^{-1}	$T\Delta S_0$ expt. cal. mole^{-1}	$\frac{\Delta S_0 \text{ expt.}}{v_s^2}$ cal. mole^{-1} deg.$^{-1}$
0·1	0·0085	0·05	1789	−412	504	2293	—
0·2	0·0226	0·0925	1435	−470	485	1920	—
0·3	0·0318	0·143	1173	−461	472	1645	—
0·4	0·0487	0·225	917	−368	440	1357	5·08
0·5	0·0714	0·300	700	−285	423	1123	4·38
0·6	0·103	0·415	512	−206	377	889	3·71
0·7	0·151	0·550	356	−143	324	680	3·17
0·8	0·234	0·715	204	−71	253	457	2·61
0·85	0·302	0·810	126	—	195	321	2·20
0·9	0·408	0·885	73·1	−6·6	127	200	1·92
0·925	0·485	0·920	49·6	—	94	144	1·82
0·95	0·592	0·948	31·8	—	55·5	87	1·76
0·975	0·748	0·975	15·1	—	20·8	35·9	1·90
0·985	0·835	0·985	9·04	—	8·55	17·6	2·17
0·990	0·885	0·990	6·05	—	4·03	10·1	2·58

TABLE III.—DC 500, 50 CSTKS. IN BENZENE

N_0	v_0	a_0	- ΔG_0 cal. mole^{-1}	ΔH_0 calc. cal. mole^{-1}	ΔH_0 expt. cal. mole^{-1}	$T\Delta S_0$ expt. cal. mole^{-1}	$\frac{\Delta S_0}{v_s^2}$ cal. mole^{-1} deg.$^{-1}$
0·1	0·00255	0·033	2030	−610	461	2491	—
0·2	0·00574	0·065	1625	−655	459	2084	—
0·3	0·00981	0·095	1398	−662	454	1852	—
0·4	0·0151	0·135	1191	−636	447	1638	—
0·5	0·0225	0·176	1032	−588	438	1470	—
0·6	0·0335	0·225	890	−480	425	1315	—
0·7	0·0511	0·288	742	−424	403	1145	—
0·8	0·0843	0·400	546	−404	372	918	3·45
0·9	0·171	0·635	270	−193·8	293	563	2·74
0·925	0·221	0·779	152	—	251	403	2·23
0·94	0·266	0·850	96·7	—	218	315	1·96
0·95	0·305	0·890	69·4	—	189	258	1·81
0·96	0·356	0·940	36·9	—	156	193	1·59
0·97	0·427	0·955	27·4	—	118	145	1·49
0·98	0·530	0·974	21·7	—	72	94	1·43
0·99	0·695	0·99	6·02	—	27·5	33·5	1·21
0·995	0·820	0·995	2·98	—	8·0	11·0	1·14

Calorimetric Determination of the Heat of Mixing of Silicones with Benzene.—The apparatus consisted of a stout-walled transparent glass Dewar vessel of about 200 ml. capacity, provided with a well-fitting cork. Into this vessel were fitted a small heating coil (resistance 1·95 ohm), a mercury sealed stirrer, a thin-walled glass bulb of about 20 ml. capacity, which served to introduce the liquid to be diluted, and a thermistor[5] which measured the temperature change. The thermistor was arranged in one arm of a Wheatstone network, the ratio arms of which were both of 1000 ohms. The galvanometer had a sensitivity of 20 mm./ohm, and as the temperature coefficient of the thermistor in this region was about 100 ohms per degree, temperature changes of less than 1/1000° C were readily measurable.

A measured volume of benzene (about 50 ml.) was placed in the Dewar, and a measured volume of silicone (about 10 ml. in the first instance) in the

---

[5] Sillars, *J. Sci. Instr.*, 1942, **19**, 81.

TABLE IV.—DC 200, 350 CSTKS. IN BENZENE

N_0	v_0	a_0	ΔG_0 cal. mole^{-1}	ΔH_0 calc. cal. mole^{-1}	ΔH_0 expt. cal. mole^{-1}	$T\Delta S_0$ expt. cal mole^{-1}	$\frac{\Delta S_0 \text{ expt.}}{v_s^2}$ cal. mole^{-1} deg.$^{-1}$
0·1	0·000618	0·014	2540	−1163	440	2980	—
0·2	0·00139	0·025	2195	−1240	439	2634	—
0·3	0·00256	0·035	1985	−1270	438	2423	—
0·4	0·00368	0·045	1844	−1299	437	2281	—
0·5	0·0055	0·056	1715	−1303	435	2150	—
0·6	0·00825	0·068	1600	−1297	432	2032	—
0·7	0·0127	0·078	1515	−1303	423	1938	—
0·8	0·0217	0·104	1345	−1213	419	1764	—
0·9	0·0478	0·235	864	−801	390	1254	—
0·95	0·096	0·475	444	—	342	786	3·22
0·975	0·178	0·72	189	—	272	461	2·28
0·985	0·267	0·82	118	—	209	327	2·06
0·990	0·356	0·89	69·5	—	143	212·5	1·72
0·995	0·525	0·95	36·5	—	67	103·5	1·53
0·997	0·65	0·965	21·2	—	33	54·2	1·48
0·999	0·848	0·990	6·03	—	4·3	10·3	1·50

glass bulb. A magnetic device for breaking the bulb closed the silicone from the air. The assembled apparatus was left overnight in the thermostat at 25 ± 0·02° C. Stirring was started, and readings of the resistance were taken for 5-10 min. until a steady rise in temperature was being recorded. The bulb was then broken and the change in resistance of the thermistor followed. In these experiments the heat of mixing was positive, i.e. heat was absorbed, and the resistance of the thermistor increased. The total heat of mixing was absorbed in less than 1 min. Readings of the resistance were taken until a steady rise in temperature had been recorded for about 5 min. The heating coil was then switched on and the current flowing accurately measured by determining the potential drop across a standard 1 ohm resistance in the circuit. When the

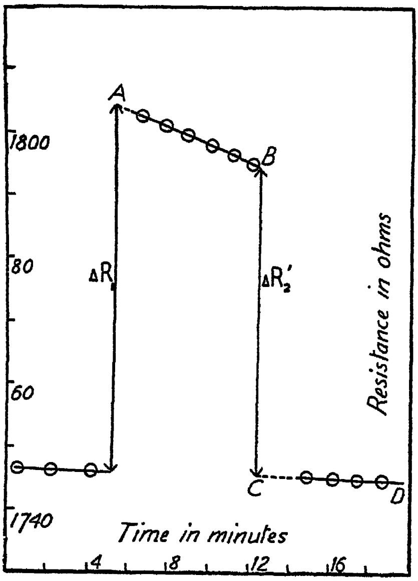

FIG. 2.

resistance of the thermistor was approximately the same as in its initial equilibrium state the heater was switched off, and readings of the resistance taken for a further 6 min.

Fig. 2 shows a typical graph obtained from such a series of measurements. The sudden rise and fall in resistance indicate mixing and heating respectively. The dotted lines give the extrapolation from the time of the first measurement after the operation to the time of mixing and turning on of the heater, and account for heat losses from the system. From the slope of the lines AB and CD it is obvious that the heat gains by the system are very much greater at the lower temperature. This difference is more important in the case of the measurement of the change in resistance with known electrical energy input ΔR_2 where the time involved is greater. (In general it was necessary to have the heater switched on for about 2 min.) In the final calculations of ΔR_2 in these cases, a small empirical correction was made to $\Delta R_2'$ to allow for this difference in heat gain. The heat of mixing was calculated from the change in resistance on mixing the two liquids, ΔR_1, using the heat capacity of the system obtained from the measured change in resistance ΔR_2 with known electrical energy input.

The experiment was repeated using a further volume of silicone (about 20 ml.) until after four dilutions an approximately equal volume mixture of silicone and benzene was obtained. The experiment was also carried out in reverse, i.e. about 50 ml. silicone were placed in the Dewar and diluted with four portions of benzene in the same way. The results obtained are shown graphically in Fig. 3.

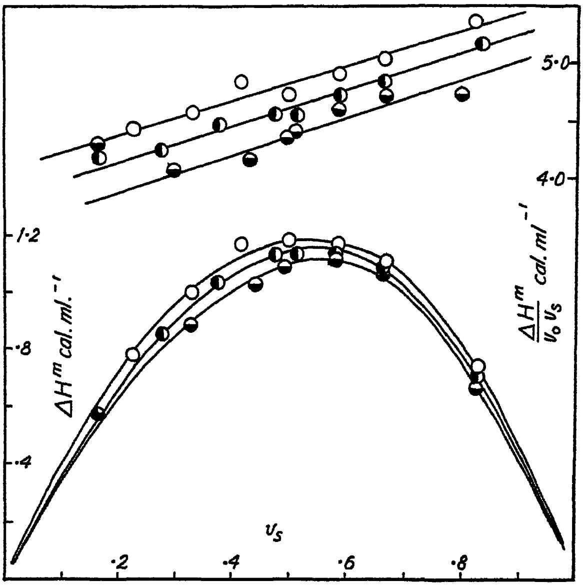

FIG. 3.—Heats of mixing of silicones with benzene at 25° C.

○ DC 500, 10 cstks. ◐ DC 500, 50 cstks. ◒ DC 200, 350 cstks.

The heat of mixing, ΔH^m is the heat absorbed on mixing v_s ml. silicone with $(1 - v_s)$ ml. benzene, where v_s is the volume fraction of silicone, and $(1 - v_s) = v_0$ is the volume fraction of benzene.*

Calculation of Thermodynamic Quantities.—(1) CALCULATION OF THE HEAT OF DILUTION ΔH_0.—The vapour pressure measurements, Fig. 1, show great departures from ideality, which increase with the molecular weight of the silicone. If these were regular solutions[6] (in which the heat of dilution determines the departure of the free energy of dilution from ideality) the heat of dilution could be calculated from the equation

---

* Measurements of the densities of solutions of various concentrations of the silicone DC 500 50 cstks. in benzene showed that any increase in volume on mixing was less than 0·1 % of the total volume of the mixture.

$$\Delta H_0 = \Delta G_0 + T\Delta S_0. \qquad (2)$$

Since the ideal entropy of dilution is given by

$$\Delta S_0 = -R \ln N_0$$

and further

$$\Delta G_0 = RT \ln a_0,$$

a_0 being obtained from the vapour pressure measurements, we have

$$\Delta H_0 = RT \ln (a_0/N_0). \qquad (3)$$

Since $a_0 < N_0$, ΔH_0 is negative. The values calculated from eqn. (3) are shown in Fig. 4. The calorimetrically determined values of ΔH_0 should agree with the calculated values if the solutions are regular.

The molar heat of dilution of the silicone solutions can be determined from measurements of the heat of mixing in the manner described by Ferry, Gee and Treloar:[7]

$$\Delta H^m = \alpha v_0 v_s, \qquad (4)$$

where v_0 and v_s are the volume fractions of benzene and silicone, and α is a constant dependent on the molar energies of evaporation of the components. Consequently the total heat of mixing N_0 moles of solvent with N_s moles of solute is given by

$$\Delta H = \alpha \frac{N_0 N_s V_0 V_s}{N_0 V_0 + N_s V_s}, \qquad (5)$$

where V_0 and V_s are the molar volumes of benzene and silicone.

The heat of dilution ΔH_0 is given by

$$\Delta H_0 = \left(\frac{\partial \Delta H}{\partial N_0}\right)_{N_s} \qquad (6)$$

It follows from (5) that if α is constant

$$\Delta H_0 = \alpha V_0 v_s^2, \qquad (7)$$

and if α is not constant

$$\Delta H_0 / v_s^2 = \left(\alpha - v_0 \frac{\partial \alpha}{\partial v_s}\right). \qquad (8)$$

The experimental values for ΔH^m are shown in Fig. 3. The curve is not a true parabola as it would be if α were constant. The values for α calculated from αH^m are shown in Fig. 3, and α is seen to increase with v_s. Values of ΔH_0 must therefore be calculated from eqn. (8) using a new value for α for each point. Table II, III and IV give the values of ΔH_0 determined in this way. These values are compared graphically (Fig. 4) with those calculated for a regular

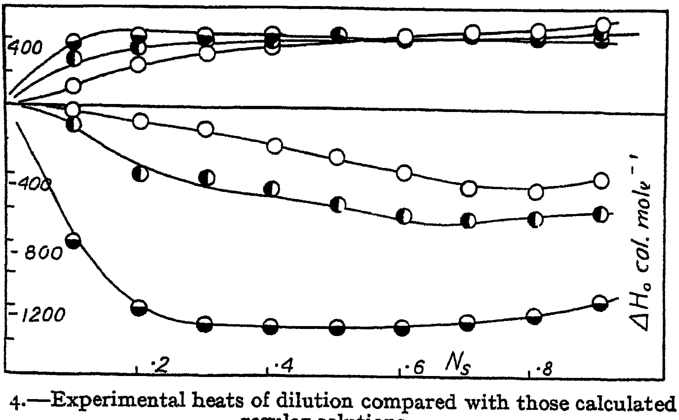

FIG. 4.—Experimental heats of dilution compared with those calculated for regular solutions.
Positive values of ΔH_0 are experimental.
Negative values of ΔH_0 are those calculated for regular solutions.

---

[6] Hildebrand, *Solubility* (Reinhold Publishing Co., N.Y., 1936), p. 65.

[7] Ferry, Gee and Treloar, *Trans. Faraday Soc.*, 1945, 41, 340.

solution. It is to be observed that ΔH_0 is positive. The comparison shows that the large deviations from ideality must be due mainly to a greater value of ΔS_0 than that given by $-R \ln N_0$, rather than the fact that $\Delta H_0 = 0$.

(2) CALCULATION OF THE ENTROPY OF DILUTION ΔS_0.—Statistical treatment of high polymers by Flory,[8] Huggins[9] and Miller[10] has led to equations for the partial molar entropy of dilution. Miller's equation gives

$$\Delta S_0 = -R\left[\ln(1 - v_s) - \frac{Z}{2}\ln\left\{1 - \frac{2}{Z}\left(1 - \frac{1}{n}\right)v_s\right\}\right], \quad . \quad . \quad (9)$$

where Z is the co-ordination number, and n is the number of submolecules equal in size to one solvent molecule, and normally is equal to the degree of polymerization.

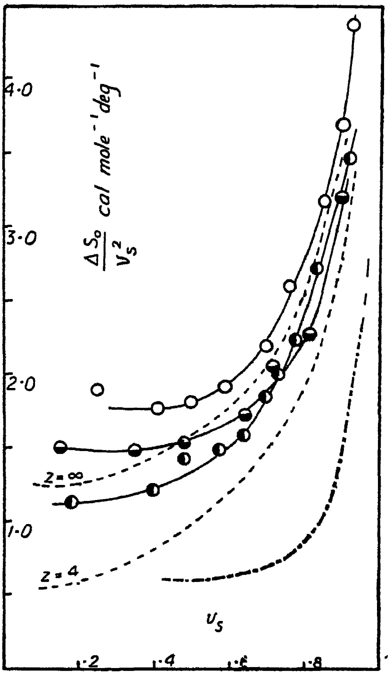

FIG. 5.—Experimental entropies of dilution compared with those calculated from eqn. (9) and with ideal values.

○ DC 500, 10 cstks. ◐ DC 500, 50 cstks. ◒ DC 200, 350 cstks.

– – – – – Curves calculated from eqn. (9).

– · – · – Ideal curve for DC 500, 10 cstks.

Theoretical curves calculated from eqn. (9) taking $Z = 4$ and $n = 100$ (a value lying between that for DC 500, 50 cstks. and DC 200, 350 cstks.) are shown in Fig. 5 together with the experimentally determined curves for the three silicones and the value of ΔS_0 for an ideal solution of DC 500 10 cstks. in benzene. Although the statistical theory appears to account for the order of magnitude of the entropies of dilution, it does not fully explain their departure from ideality, particularly at high dilution.

Discussion

The strong negative deviation of ΔG_0 from ideality in spite of a fairly large positive heat of dilution indicates a large entropy of dilution—greater than could be predicted for mixing two disoriented liquids (Fig. 5).

[8] Flory, (*a*) *J. Chem. Physics*, 1941, **9**, 660 ; (*b*) *ibid.*, 1942, **10**, 51.

[9] Huggins, (*a*) *ibid.*, 1941, **9**, 440 ; (*b*) *J. Physic. Chem.*, 1942, **46**, 1.

[10] Miller, (*a*) *Proc. Camb. Phil. Soc.*, 1942, **38**, 109 ; (*b*) *ibid.*, 1943, **39**, 54, 131.

A positive value for ΔH_0 suggests that some structural order in the pure liquid may be broken up by mixing. This change from an ordered liquid to a disordered solution would result in a large value of ΔS_0.

From the comparison of the experimental values for ΔS_0 and those calculated theoretically, Fig. 5, it can be seen that there must be a large degree of order in the pure silicone liquids. The silicones with their low energy of vaporization,[11] low energy for viscous flow,[12] and low surface tension,[13] exhibit remarkedly small intermolecular forces. Long range structural order in a liquid composed of these molecules would be impossible. Any order therefore will be within the molecules themselves in the pure liquid. If the polydimethylsiloxane molecules were coiled regularly in the pure liquid and were extended in solution by a suitable solvent such as benzene, the large values of ΔS_0 and ΔH_0 could be accounted for, and some of the anomalous properties of the pure liquids explained.

The values of the heat of mixing, ΔH^m cal./ml. (Fig. 3), are seen to be almost identical for the three silicones, in spite of the great differences in chain length of the compounds. If the heat of mixing is simply the energy necessary to uncoil the regularly coiled silicone molecules, the heat of mixing might be expected to be independent of the chain length of the molecules since the molar volume of the compounds is additive for each $((CH_3)_2SiO)$ unit.[11]

On the basis of measurements of force-area relations of monolayers of silicones on water and study of molecular models of such films, it has been suggested that silicone molecules may be coiled into helices.[14] These helices, which are thought to have 7 silicon atoms per turn, elongate with rise in temperature, and this elongation is advanced as the reason for the small change in viscosity with temperature which is characteristic of the silicones. With solutions, on the other hand, the value of 0·66 for α in the viscosity equation $(\eta) = KM^{\alpha}$ indicates long flexible chains in the dissolved state. The measurements of ΔG_0, ΔH_0 and ΔS_0 described in this paper, which indicate such a change of state on dissolution in benzene, support these views on the state of the silicone molecule in the pure liquid and in solution. Further work on this problem is in progress.

This work was carried out in the University Chemical Laboratories, Cambridge, under the supervision of Prof. H. J. Emeléus, F.R.S., whom the author wishes to thank for his help and encouragement. The author would also like to thank Dr. F. S. Dainton for most helpful discussions and the Commonwealth Scientific and Industrial Research Organization for an overseas studentship.

University Chemical Laboratory,
Pembroke Street,
Cambridge.

[11] Hurd, *J. Amer. Chem. Soc.*, 1946, **68**, 364.
[12] Wilcock, *Ibid.*, 1946, **68**, 691.
[13] Hunter, Warrick, Hyde and Currie, *ibid.*, 1946, **68**, 2284.
[14] Fox, Taylor and Zisman, *Ind. Eng. Chem.*, 1947, **39**, 1401.

THE HEAT OF SOLUTION OF IODINE IN SOME ORGANIC SOLVENTS

By K. Hartley and H. A. Skinner

Received 20th March, 1950

Values are reported for the heat of solution of solid iodine in 15 organic solvents. The heats of solution are examined in relation to the theory of regular solutions as developed (in particular) by Hildebrand, and approximate values are obtained for the heats of complex formation of iodine with various organic substances.

In the course of some measurements of the heats of iodination of metallic alkyls [1, 2] we required to know the solution heats of solid iodine in various organic solvents. The literature contains heat of solution data due to Pickering [3] and Waentig [4] which are, however, not always in close agreement, e.g. Pickering gave − 6·0 kcal. mole^{-1}, and Waentig −4·7 kcal. mole^{-1} for the heat of solution of I_2 in benzene. In this paper we report new measurements on the heat of solution of solid iodine in 15 common organic solvents. These heats were measured by the direct method.

Experimental

The heats of solution were measured in a Dewar vessel calorimeter, similar to that described by Pritchard and Skinner.[5] Temperature changes were followed by the change in resistance of a thermistor element; the iodine was contained in weighed glass ampoules, which were broken as required on a polytetrafluoroethylene platform immersed in the solvent inside the Dewar vessel.

TABLE I.—Heats of Solution and Colour of Iodine Solutions

Solvent	Conc. I_2 g./l.	Heat of Solution kcal. mole^{-1}	Colour of Solution
Cyclohexane	2·5	−5·8 ±0·2	Blue
Carbon tetrachloride	2·0	−5·8 ±0·2	Blue
Chloroform *	2·0	−5·1 ±0·2	Blue
Chlorobenzene	6·7	−4·75 ±0·05	Blue
Benzene	6·7	−4·25 ±0·05	Blue
Toluene	7·8	−3·85 ±0·05	Blue-brown
Methyl benzoate	5·7	−3·9 ±0·1	Brown
Ethyl acetate	5·7	−3·1 ±0·1	Brown
Methyl acetate	5·7	−2·45 ±0·1	Brown
Methyl alcohol	7·6	−2·07 ±0·05	Brown
1 : 4-Dioxan	7·8	−1·85 ±0·1	Brown
Diethyl ether	7·5	−1·80 ±0·1	Brown
Nitrobenzene	6·7	−1·70 ±0·1	Brown
Ethyl alcohol	7·7	−1·65 ±0·05	Brown
Pyridine	2·5	3·6 ±0·1	Yellow

* The chloroform contained 1½ % ethyl alcohol.

---

[1] Carson, Hartley and Skinner, *Proc. Roy. Soc. A.*, 1949, **195**, 500.
[2] Carson, Hartley and Skinner, *Trans. Faraday Soc.*, 1949, **45**, 1159.
[3] Pickering, *J. Chem. Soc.*, 1888, **53**, 865.
[4] Waentig, *Z. physik. Chem.*, 1909, **68**, 512.
[5] Pritchard and Skinner, *J. Chem. Soc.*, 1950, 272.

The solution heats in most solvents are negative, and it was possible to balance the negative heat of solution by simultaneously passing a measured amount of electrical energy through a calibration heater, so that the measurements were conducted under virtually isothermal conditions. In each experiment, the iodine was dissolved in 300 ml. of solvent. Corrections for small heat losses (evaporation, stirring) were made graphically.

The solvents were dried and fractionated prior to use, and A.R. iodine was used throughout. The results are summarized in Table I. The heats of solution are given in units of the kcal. mole.$^{-1}$ = $4{\cdot}1833 \times 10^3$ int. joules mole.$^{-1}$.

Discussion

The close parallelism between the *colour* of iodine solutions and the *heat of solution* is apparent from the results of Table I. Hildebrand[6] has previously shown that the solubility curves for iodine in solvents giving blue solutions form a regular family whose deviation from ideality can be related to differences of internal pressure (or cohesive energy density). The solubility curves of the brown solutions do not fall into a regular family of any kind, and the deviations are probably to be attributed to the formation of iodine-solvent complexes.

In the case of iodine forming an *ideal* solution, there is no heat and excess entropy of mixing of the liquid iodine with the solvent, and the heat of solution of solid iodine in this ideal case is negative and equal to the molal latent heat of fusion L_f of iodine. The solubility relationships holding for the blue iodine solutions are typical of so-called regular solutions, which deviate from the ideal only in that the heat of mixing is no longer zero. Hildebrand and Wood,[7] and Scatchard[8] have related the molal heat of mixing at constant volume ΔE_v for regular solutions to the concentrations of the components and their respective internal pressures, by the equation

$$\Delta E_v = \frac{x_1 V_1 x_2 V_2}{x_1 V_1 x_2 V_2} (d_2 - d_1)^2, \quad . \quad . \quad . \quad (1)$$

where x_1, x_2, and V_1, V_2 are the respective mole fractions and molar volumes of the two components, and d_1, d_2 are the internal pressures. These latter are defined by

$$d_1 = (\Delta E_1/V_1)^{\frac{1}{2}}\,; \quad d_2 = (\Delta E_2/V_2)^{\frac{1}{2}}, \quad . \quad . \quad . \quad (2)$$

where ΔE = molal internal energy of vaporization.

Accordingly, in the blue (regular) solutions, the overall heat of solution of solid iodine should be more negative than L_f, i.e. more negative than $-3{\cdot}74$ kcal. mole^{-1} (Frederick and Hildebrand[9]). In the non-regular brown solutions, a positive heat of combination due to iodine-solvent complex formation is likely to participate and render the overall heat of solution more positive than is calculated from internal pressure considerations alone.

For the regular solutions, the heat of solution is given by

$$Q_{\text{soln.}} = - L_f - q_R \quad . \quad . \quad . \quad . \quad (3)$$

in which q_R is related to eqn. (1) and (2). If the deviations from regular behaviour in the brown solutions are primarily due to the formation of iodine-solvent complexes, then the difference between an observed $Q_{\text{soln.}}$ and a calculated $-(L_f + q_R)$, would give a rough measure of the heat of this complex formation.

---

[6] Hildebrand, *Solubility of Non-electrolytes* (Reinhold, New York, 1936), 2nd ed.

[7] Hildebrand and Wood, *J. Chem. Physics*, 1933, **1**, 817.

[8] Scatchard, *Chem. Rev.*, 1931, **8**, 321.

[9] Frederick and Hildebrand, *J. Amer. Chem. Soc.*, 1938, **69**, 1436.

We have not attempted to evaluate the terms in q_R, as there are not data available on the volume changes accompanying the mixing of liquid iodine with the various solvents. These data would be required in order to compare the observed heats of solution at constant pressure with calculated values of ΔE_v at constant volume. Rather, we have examined the general relationship expressed in eqn. (1), (2) and (3) between $Q_{soln.}$ and the internal pressure term $(d_2 - d_1)^2$. The plot of $Q_{soln.}$ against $(d_2 - d_1)^2$ is shown in Fig. 1. It is seen that the solvents C_6H_{12}, CCl_4, $CHCl_3$, and C_6H_5Cl give points which lie reasonably close to a straight line intercepting the ordinate at $Q_{soln.} = - L_f$ when $(d_2 - d_1)^2 = 0$.

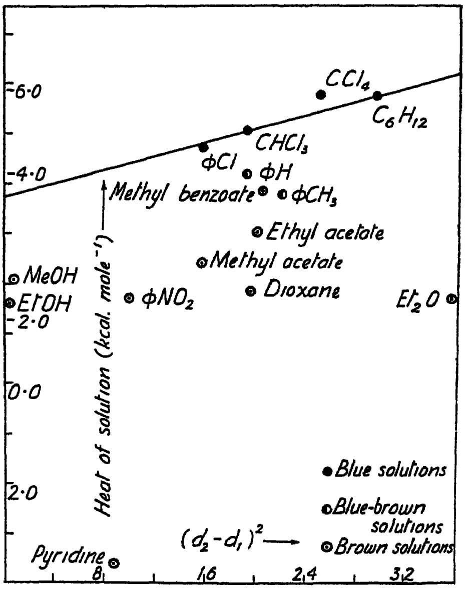

FIG. 1.

These solvents give blue solutions, and there is no evidence from other studies of complex formation in these instances. The solvents C_6H_6 and $C_6H_5 . CH_3$, which give blue or near-blue solutions, fall off the straight-line, toluene more so than benzene. We would interpret these deviations as evidence of I_2-benzene and I_2-toluene complex formation, and may refer to the work of Benesi and Hildebrand[10] confirming this conclusion. The brown solutions without exception deviate markedly from the straight line plot.

The values used for the internal pressures of the various solvents are listed in Table II. They were obtained, where possible, from experimental heats of vaporization; in some cases reliable heats of vaporization are not available and these are bracketed, but for the most part the data given in Table II should be accurate within a few per cent.

The internal pressure of liquid iodine was calculated from the value $\Delta E_{vap.} = 11{\cdot}2$ kcal. mole^{-1} given by Hildebrand,[5] and the molar volume $V = 59{\cdot}0$ ml. mole^{-1} obtained by extrapolation of the data of Drugman and Ramsey.[19] In the final column of Table II, the derived values of $(d_2 - d_1)^2$ are listed, d_2 being the internal pressure of iodine and d_1 referring to the solvent.

The large deviations of all the brown solutions from the simple linear dependence on $(d_2 - d_1)^2$, as shown by Fig. 1, strongly point to positive

---

[10] Benesi and Hildebrand, *J. Amer. Chem. Soc.*, 1949, 71, 2703.

TABLE II.—INTERNAL PRESSURES AT 20° C

Compound	$\lambda^{20}_{\text{vap.}}$ (ΔH) (kcal. mole^{-1})	V^{20} (ml. mole^{-1})	$\Delta E/V$ (cal. ml.$^{-1}$)	$(\Delta E/V)^{\frac{1}{2}}$	$(d_2 - d_1)^2$
Diethyl ether .	6·65[11]	103·7	58·5	7·65	35·4
Cyclohexane .	7·91[12]	108·7	67·3	8·2	29·1
CCl_4 . . .	7·85[12]	97·1	74·7	8·65	24·6
Toluene . .	9·08[12]	106·8	79·4	8·9	22·0
Methyl benzoate .	(10·8)	125·1	(81·5)	9·05	20·7
Ethyl acetate .	8·70[13]	97·8	83·0	9·1	20·1
Dioxane . .	(8·7)	96·9	84·1	9·17	19·6
Benzene . .	8·12[11]	88·9	84·8	9·2	19·3
Chloroform . .	7·47[12]	80·2	85·3	9·25	19·0
Methyl acetate .	7·96[15]	79·3	93·1	9·65	15·6
Chlorobenzene .	—	101·7	(93·4)[8]	9·65	15·5
Pyridine . .	9·71[16]	80·7	113·2	10·65	8·75
Nitrobenzene .	(11·7)[17]	102·0	(109·0)	10·44	9·98
Ethyl alcohol .	10·33[18]	58·2	171·0	13·1	0·27
Iodine . .	—	59·0[19]	190·0	13·6	0·0
Methyl alcohol .	9·01[12]	40·4	208·7	14·45	0·72

values for the heats of complex formation in these solvents. The magnitudes of the heats of complex formation can be obtained from the simple assumption that they are equal to the deviations from the linear plot of Fig. 1. The estimated values are then obtained as follows (in kcal./mole):

Benzene + 0·85; toluene + 1·45; methyl alcohol + 1·7; ethyl acetate + 2·05; ethyl alcohol + 2·1; methyl acetate + 2·4; nitrobenzene + 2·75; dioxane + 3·25; diethyl ether + 4·4; pyridine + 7·95.

Little is known from other sources of the heats of iodine-solvent complex formation; in case of iodine-ethyl acetate, Hildebrand and Glascock [20] measured the equilibrium constant at 12° C and 28° C of the reaction

$$\text{EtOOC . Me} + I_2 \rightleftharpoons \text{complex},$$

from which they were able to calculate the heat of the reaction as + 3·06 kcal./mole. Independent evidence for the formation of iodine-solvent complexes has been given by Hildebrand and Glascock for nitrobenzene and ethyl alcohol, and by Audrieth and Birr [21] with I_2-pyridine. Our data suggest that the I_2-pyridine complex is one of the most stable of the iodine-solvent complexes, and one is tempted in this instance to postulate salt-formation, in the manner

$$I_2 + \text{pyridine} \rightleftharpoons (C_5H_5\overset{+}{N}I)\overset{-}{I}\ (\text{pyridine}).$$

[11] Faust and Littman, *Z. physik. Chem.*, 1924, **113**, 482.
[12] *Selected Values of Chemical Thermodynamic Properties* (Bureau of Standards, Washington), 1948-49.
[13] de Kolossowsky and Alimow in *Landolt-Bornstein* (1936).
[14] Fiock, Ginnings and Holton, *J. Bur. Stand. Res.*, 1931, **6**, 881.
[15] Roth and Müller in *Landolt-Bornstein* (1936).
[16] Hieber and Woerner, *Z. Elektrochem.*, 1934, **40**, 252.
[17] Toral and Moles, *Ann. Soc. Espãn. Fis. Quim.*, 1923, **31**, 735.
[18] Bartoszewicz, *Rocz. Chem.*, 1931, **11**, 90.
[19] Drugman and Ramsey, *J. Chem. Soc.*, 1900, **77**, 1228.
[20] Hildebrand and Glascock, *J. Amer. Chem. Soc.*, 1909, **31**, 26.
[21] Audrieth and Birr, *ibid.*, 1933, **55**, 668.

The values quoted above for the heats of complex formation are, it should be emphasized, not strict measures of these heat quantities : nevertheless, they show a trend which is probably correct, even if the absolute values given are less reliable.

The authors wish to express their thanks to Prof. M. G. Evans, F.R.S., for his interest in this work and for his assistance in the interpretation of the results.

Department of Chemistry,
Manchester University.

THE ACTIVATION ENERGY AND THE STERIC FACTOR OF THE REACTION BETWEEN METHYL RADICALS AND TOLUENE

BY M. SZWARC AND J. S. ROBERTS

Received 20th February, 1950

Evidence obtained from the studies of various pyrolytic processes indicates that the activation energy of the reaction

$$C_6H_5 . CH_3 + CH_3 \longrightarrow C_6H_5 . CH_2 + CH_4$$

is between 10-15 kcal./mole, the most probable value being 12 ± 2 kcal./mole. It is shown also that the steric factor for the above reaction as well as that of the reaction $CH_3 + CH_3 \rightarrow C_2H_6$ is " normal ", i.e. the collision frequency of these reactions is of the order 10^{11}-10^{12} cm.^{3}/sec. mole. Thus an additional argument is brought against the idea of " low " steric factors in radical reactions.

The kinetics of the bimolecular reactions between methyl radicals and various hydrocarbons RH were studied by Taylor and his colleagues [1] who measured the rates of these reactions by determining the rates of formation of methane :

$$RH + CH_3 \longrightarrow R + CH_4. \quad . \quad . \quad . \quad (1)$$

The above workers succeeded in estimating the activation energies of reaction (1) corresponding to various hydrocarbons, and their work added valuable evidence supporting the idea that the C—H bond dissociation energy in hydrocarbons RH depends on the nature of the radical R. Thus, it was shown by Taylor *et al.* that the variation in the activation energy of reaction (1) is parallel to the usually assumed variation in the C—H bond dissociation energy of the respective hydrocarbon RH. Although this gradation is undoubtedly right, it may be possible that the numerical values of these activation energies require some corrections.

It was pointed out by Steacie *et al.*[2] that some difficulties arise from the mechanism proposed by Taylor in order to account for his experimental findings. Steacie suggested, therefore, that one might surmount these difficulties by assuming very low steric factors for reactions (1). The idea of low steric factors was opposed, however, by Evans and Szwarc [3] on the basis of other evidence pointing to the " normal " steric factors in radical reactions. Hence, it was necessary to look for an alternative explanation, and it would be possible to remove the discrepancy if the absolute values of activation energies of reaction (1) were higher than the values reported in the original papers.[1] It seems to us that this explanation is the correct one, and we intend to present in this paper evidence indicating that the activation energy of reaction (2)

---

[1] Cunningham and Taylor, *J. Chem. Physics,* 1938, **6**, 359 ; Smith and Taylor, *ibid.*, 1939, **7**, 390 ; Taylor and Smith, *ibid.*, 1940, **8**, 543.

[2] Steacie, Darwent and Trost, *Faraday Soc. Discussions,* 1947, **2**, 80.

[3] Evans and Szwarc, *Trans. Faraday Soc.*, 1949, **45**, 940.

$$C_6H_5 \, . \, CH_3 + CH_3 \longrightarrow C_6H_5 \, . \, CH_2 + CH_4 \qquad . \quad . \quad (2)$$

is likely to be 10-15 kcal./mole. Incidentally, this evidence demonstrates also that the steric factor of reaction (2) seems to be of the order of unity (0·1 to 1), and thus it supports the idea of "normal" steric factors in radical reactions.

The experimental material utilized in this paper was taken from the following investigations :

(*a*) Pyrolysis of ethylbenzene in a stream of toluene.[4]
(*b*) Pyrolysis of mercury di-methyl in a stream of toluene.[5]
(*c*) Pyrolysis of di-*tert.*-butyl peroxide in a stream of toluene.[6]
(*d*) Pyrolysis of di-*tert.*-butyl peroxide plus toluene in a static system.[6]

(*a*) Pyrolysis of Ethylbenzene.—It was demonstrated[4] that ethylbenzene decomposes into benzyl and methyl radicals as shown by eqn. (3) :

$$C_6H_5 \, . \, CH_2 \, . \, CH_3 \longrightarrow C_6H_5 \, . \, CH_2 + CH_3. \qquad . \quad . \quad (3)$$

Since the decomposition was carried out in a stream of toluene, methyl radicals were removed mainly by reaction (2) and the principal products of decomposition were dibenzyl and methane in a molecular ratio of 1/1. It was reported, however, that minute quantities of C_2 hydrocarbons (about 1-2 % of the amount of methane) were produced, and it is plausible to assume that they were formed in reaction (4),*

$$CH_3 + CH_3 \longrightarrow C_2H_6. \quad . \quad . \quad . \quad . \quad (4)$$

The stationary concentration of methyl radicals may be computed from the following equation :

$$k_3 \, . \, [C_6H_5 \, . \, CH_2 \, . \, CH_3] = k_2[CH_3][C_6H_5 \, . \, CH_3]$$

$$\therefore [CH_3] = \frac{k_3}{k_2} \frac{[C_6H_5 \, . \, CH_2 \, . \, CH_3]}{[C_6H_5 \, . \, CH_3]},$$

k_2 and k_3 denoting the rate constants of reactions (2) and (3) respectively.

The ratio $[C_2H_6]/[CH_4]$ may be computed from the relationship :

$$\frac{[C_2H_6]}{[CH_4]} = \frac{k_4[CH_3]^2}{k_2[CH_3] \, . \, [C_6H_5 \, . \, CH_3]},$$

k_4 denoting the rate constant of reaction (4).

$$\therefore \frac{[C_2H_6]}{[CH_4]} = \frac{k_4 k_3 [C_6H_5 \, . \, CH_2 \, . \, CH_3]}{k_2^2 \, . \, [C_6H_5 \, . \, CH_3]^2}.$$

It was estimated that :

$$[C_2H_6]/[CH_4] = 0{\cdot}01,$$
$$k_3 = 0{\cdot}1 \text{ sec.}^{-1} \text{ at } T = 710^\circ \text{ C},$$
$$[C_6H_5 \, . \, CH_2 \, . \, CH_3] = 4 \times 10^{-9} \text{ mole/cm.}^3,$$
$$[C_6H_5 \, . \, CH_3] = 2 \times 10^{-7} \text{ mole/cm.}^3.$$

Assuming that reaction (4) does not require any activation energy, we express $k_4 = s_4 \times 10^{12}$ cm.^{3}/mole sec., s_4 denoting the steric factor of reaction (4), while $k_2 = s_2 \times 10^{12} \times \exp(-E_2/RT)$, s_2 and E_2 denoting the steric factor and activation energy of reaction (2). Thus

---

[4] Szwarc, *J. Chem. Physics*, 1949, 17, 431.
[5] Szwarc, unpublished results, quoted by Gowenlock, see ref. 8.
[6] Szwarc and Roberts, *J. Chem. Physics*, 1950, 18, 561.
* An alternative source of the C_2 hydrocarbons was suggested in the original paper on ethyl benzene. Our other evidence has shown that reaction (4) is, in fact, more probable than was supposed.

$$E_2 \approx 14 + 2{\cdot}3 \log (s_2{}^2/s_4) \text{ kcal./mole.} \qquad (a)$$

(*b*) **Pyrolysis of Mercury Di-methyl.**—It was shown[7] that the pyrolysis of mercury di-methyl takes place according to eqn. (5) followed by a rapid reaction (6)

$$Hg(CH_3)_2 \longrightarrow HgCH_3 + CH_3 \qquad (5)$$
$$HgCH_3 \longrightarrow Hg + CH_3. \qquad (6)$$

When the reaction was carried out in a stream of toluene[5] it was found that for every methyl radical which was removed by reaction (4) four methyl radicals reacted with toluene according to eqn. (2). A treatment, identical to that described in (*a*) leads to the following result:

$$\frac{[C_2H_6]}{[CH_4]} = \frac{2k_4 \,.\, k_5[HgMe_2]}{k_2{}^2 \,.\, [C_6H_5 \,.\, CH_3]^2}.$$

Since

$$[C_2H_6]/[CH_4] = 1/4$$
$$k_5 = 0{\cdot}1 \text{ sec.}^{-1} \text{ at } 520° \text{ C},$$
$$[HgMe_2] = 5 \times 10^{-9} \text{ mole/cm.}^3,$$
$$[C_6H_5 \,.\, CH_3] = 2 \times 10^{-7} \text{ mole/cm.}^3,$$

we derive by a method similar to that used in (*a*) that

$$E_2 \approx 13{\cdot}0 + 1{\cdot}8 \log (s_2{}^2/s_4). \qquad (b)$$

(*c*) **Pyrolysis of di-*tert*.-butyl peroxide (Flow Method).**—The pyrolysis of di-*tert*.-butyl peroxide was shown[8] to take place according to eqn. (7) and (8) the latter being much faster than the former:

$$(CH_3)_3 . C . O . O . C(CH_3)_3 \longrightarrow 2(CH_3)_3 . CO . \qquad (7)$$
$$(CH_3)_3 . CO . \longrightarrow CH_3 . CO . CH_3 + CH_3. \qquad (8)$$

When the reaction was carried out in a stream of toluene[9] it was found that most of the methyl radicals were removed by reaction (4) producing ethane, while about 5 % reacted according to reaction (2) forming methane. Consequently, we calculate the stationary concentration of methyl radicals from the following equation:

$$2k_7 \,[\text{Peroxide}] = k_4[CH_3]^2,$$
$$\therefore\ [CH_3] = (2k_7\,[\text{Peroxide}]/k_4)^{\frac{1}{2}}.$$

The $[C_2H_6]/[CH_4]$ ratio is obtained from the equation

$$\frac{[C_2H_6]}{[CH_4]} = \frac{k_4[CH_3]^2}{k_2[CH_3] \,.\, [C_6H_5 \,.\, CH_3]}.$$
$$\therefore \frac{[C_2H_6]}{[CH_4]} = \frac{(2k_7)^{\frac{1}{2}}\,[\text{Peroxide}]^{\frac{1}{2}}k_4{}^{\frac{1}{2}}}{k_2\,[\text{Toluene}]}.$$

Since

$$[C_2H_6]/[CH_4] = 20,$$
$$k_7 = 0{\cdot}5 \text{ sec.}^{-1} \text{ at } 230° \text{ C}$$
$$[\text{Peroxide}] = 5 \times 10^{-9} \text{ mole/cm.}^3$$
$$[\text{Toluene}] = 5 \times 10^{-7} \text{ mole/cm.}^3$$

we derive, by a method similar to that used in (*b*), that

$$E_2 \approx 11{\cdot}9 + 1{\cdot}15 \log (s_2{}^2/s_4). \qquad (c)$$

[7] Warhurst and Gowenlock, see Gowenlock, *Ph.D. Thesis* (Manchester, 1949).

[8] Raley, Rust and Vaughan, *J. Amer. Chem. Soc.*, 1948, **70**, 88; **70**, 1336; **70**, 3259.

[9] Szwarc and Murawski (unpublished results).

(*d*) **Pyrolysis of di-*tert.*-butyl peroxide (Static System).**—The pyrolysis of di-*tert.*-butyl peroxide in a static system and in the presence of toluene has been investigated recently.[6] The mechanism suggested by Rust and Vaughan [8] was confirmed, and it was shown that methyl radicals either dimerize (most probably in the gas phase) or react with toluene according to eqn. (2) and produce methane. The amount of methane formed increased with the increasing toluene/peroxide ratio, as was required by the proposed mechanism. Since

$$d[C_2H_6]/dt = k_4[CH_3]^2$$

and

$$d[CH_4]/dt = k_2[CH_3][C_6H_5 \,.\, CH_3],$$

we derive

$$k_2^2/k_4 = \{d[CH_4]/dt\}^2/\{d[C_2H_6]/dt\} \,.\, [C_6H_5 \,.\, CH_3]^2.$$

Assuming that reaction (4) does not require any activation energy, we may compute the activation energy of reaction (2) by plotting log (k_2^2/k_4) against $1/T$. The results are represented in Fig. 1. The straight line corresponds to the value of E_2 of 13 kcal./mole, the uncertainty being ± 2 kcal./mole. The observed scattering of the experimental points is due, most probably, to some wall recombination which cannot be entirely excluded.

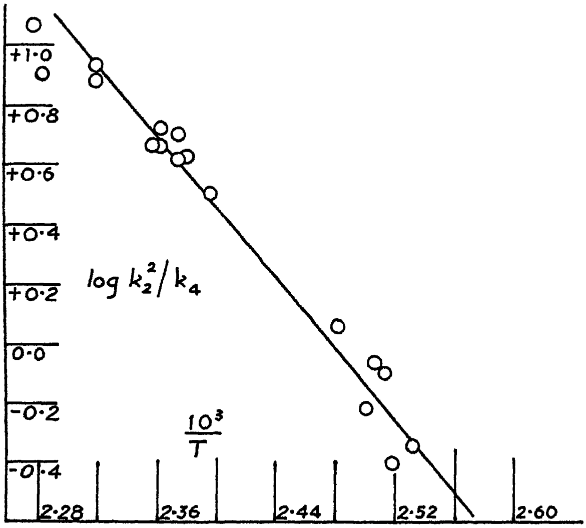

Fig. 1.

A treatment identical with that described in (*c*) leads to

$$\frac{[C_2H_6]}{[CH_4]} = \frac{(2k_7)^{\frac{1}{2}}k_4^{\frac{1}{2}}\,[\text{Peroxide}]^{\frac{1}{2}}}{k_2\,[\text{Toluene}]}.$$

Since

k_7 was determined at 10^{-5} sec.$^{-1}$ at 130° C,
[Peroxide] $= 7 \times 10^{-7}$ mole/cm.^{3},
[Toluene] $= 7 \times 10^{-6}$ mole/cm.^{3},
$[C_2H_6]/[CH_4] = 3$,

we derive, using the same reasoning as in (*c*) that

$$E_2 \approx 12{\cdot}6 + 0{\cdot}92 \log (s_2^2/s_4). \quad . \quad . \quad . \quad (d)$$

Let us summarize the results obtained above. The activation energy of reaction (2)

$$C_6H_5 . CH_3 + CH_3 \longrightarrow C_6H_5 . CH_2 + CH_4 \quad . \quad . \quad (2)$$

can be deduced from the studies of pyrolysis of:

(*a*) Ethylbenzene,* as

$$E_2 \approx 14 + 2{\cdot}3 \log (s_2^2/s_1) \text{ kcal./mole ;}$$

(*b*) Mercury di-methyl, as

$$E_2 \approx 13{\cdot}0 + 1{\cdot}8 \log (s_2^2/s_4) \text{ kcal./mole ;}$$

(*c*) Di-*tert*.-butyl peroxide (flow), as

$$E_2 \approx 11{\cdot}9 + 1{\cdot}15 \log (s_2^2/s_4) \text{ kcal./mole ;}$$

(*d*) Di-*tert*.-butyl peroxide (static), as

$$E_2 \approx 12{\cdot}6 + 0{\cdot}92 \log (s_2^2/s_4) \text{ kcal./mole ;}$$

and finally from the temperature coefficient of k_2^2/k_4, as

$$E_2 \approx 13 \pm 2 \text{ kcal./mole.}$$

Inspection of the equations given above shows that the best solution is obtained for log $(s_2^2/s_4) \approx -1$, namely:

(*a*) $E_2 = 11{\cdot}7$ kcal./mole,
(*b*) $E_2 = 11{\cdot}2$,,
(*c*) $E_2 = 10{\cdot}9$,,
(*d*) $E_2 = 11{\cdot}7$,,

which compares satisfactorily with that obtained from the temperature coefficient of k_2^2/k_4, i.e. 13 ± 2 kcal./mole. We conclude, therefore, that $E_2 = 12$ kcal./mole is the most probable value for the activation energy of reaction (2). The condition of log $(s_2^2/s_4) \approx -1$ means that $s_2^2/s_1 \approx 0{\cdot}1$. Since $s_2 \leqslant s_4$ and both are not greater than one, this condition leads to

$$0{\cdot}1 < s_2 < 0{\cdot}3 \text{ and } 0{\cdot}1 < s_4 < 1.$$

The above work therefore provides new evidence in favour of a " normal " steric factor for radical reactions.

Dept. of Chemistry,
The University,
Manchester.

---

* Since the amount of C_2H_6 was so small, and its origin may be debated, the discussion in (*a*) is justified only by an agreement with the further evidence derived from the other pyrolytic processes in which the amount of C_2H_6 was much greater.

THE REACTION BETWEEN PHOSPHORUS VAPOUR AND OXYGEN

By F. S. Dainton and H. M. Kimberley

Received 21*st November*, 1949, *as amended* 15*th May*, 1950

The kinetics of the " glow " of phosphorus have been extensively re-investigated. The results obtained and those of other investigators support a slightly modified form of a mechanism previously advanced namely:

(1) $P_4 + O_2 \rightarrow P_4O + O$,
(2) $P_4 + O + M \rightarrow P_4O + M$,
(3) $P_4O_n + O_2 \rightarrow P_4O_{n+1} + O (n = 1, 2, \ldots 9)$,
(4) $O + O_2 + M \rightarrow O_3 + M$,
(5) $O + X$ (= " poison ") → stable product,
(6) $O +$ wall.

Reaction (2) is strongly exothermic and has no energy of activation; but $E_4 = 4{\cdot}3$ kcal. Tests for the presence of oxygen atoms gave positive results. The most striking feature of the reaction is that if $[P_4]$ is constant the upper limit *decreases* with increasing temperature in agreement with $E_4 > E_2$, and is convincing evidence that the glow is an *isothermal* branched-chain explosion.

The reaction between elementary phosphorus and oxygen to form phosphorus pentoxide occurs in two distinct ways. Firstly, there is the cool flame reaction between phosphorus vapour and oxygen, which is characterized by the emission of a greenish glow and a small temperature increase; and secondly, there is a hot flame reaction for which the presence of solid or liquid white phosphorus is necessary, and which is characterized by an intense yellow flame, considerable temperature rise and conversion of some of the white phosphorus to the red modification. We are concerned solely with the first of these reactions.

The glow reaction is bounded by two sharply defined limits of oxygen pressure, which diverge with increase in the concentration of phosphorus and are affected by foreign gases and surface conditions in ways which indicate that it is an isothermal branched-chain reaction. This was first realized and stated by Semenoff,[1] but the detailed mechanisms prepared by him and by other workers[2] only partially account for the published data. These latter have recently been re-examined by Dainton,[3] who has proposed a scheme which seemed not only more successful in reconciling existing data concerning this reaction, but which could also be used to account for the salient features of the reactions of oxygen with arsenic and antimony respectively. The present experimental work was initiated in order further to test the applicability of this theory to the oxidation of each of these elements, but since our first experimental results with phosphorus were at variance with some of those of earlier workers, it was decided to make a complete re-investigation of the kinetics of the oxidation of this element. Our results have caused us to modify Dainton's scheme in one minor respect, and in its revised form it accounts for all the data of earlier workers and for the apparent inconsistencies between them. Some of these inconsistencies originated from the use of conflicting expressions for the vapour pressure of solid white phosphorus, and it was therefore necessary to redetermine the temperature dependence of the vapour pressure. This has been satisfactorily achieved by the use of a radioactive tracer (P^{32}) and has been described elsewhere.[4] Throughout the present work we shall take the latent heat of vaporization of white phosphorus in the temperature range concerned to be 14·04 kcal./mole P_4.

Experimental

Most of the data which were required were concerned with the variation of the upper and lower pressure limits with some experimental parameter such as temperature, phosphorus concentration, vessel diameter and surface condition, amount of inhibitor, etc. The usual methods of measuring these limits were employed, namely (*a*) the lower limit by the capillary leak method and (*b*) the upper limit by the withdrawal method. The apparatus used is shown diagrammatically in Fig. 1. Lower limits were determined in vessels attached at tap 1 and upper limits in vessels connected through tap 9. The vessel for the lower limit together with the mixing bulb and connecting tubing between the two was immersed in a water thermostat controlled to ± 0·05° C. Measurements on the upper limit were also made at temperatures below 0° C and when this was the case the reaction vessel was immersed in a cooling mixture contained in a half-silvered Dewar flask. All temperatures were measured on a standardized mercury thermometer.

[1] Semenoff, *Chemical Kinetics and Chain Reactions*, Oxford (1935), p. 163.

[2] Fishbeck and Eich, *Ber.*, 1938, **71**, 530.

[3] Dainton, *Trans. Faraday Soc.*, 1947, **42**, 244.

[4] Dainton and Kimberley, *ibid.* (in press).

In measurements on the lower limit when solid phosphorus was present, it was introduced as such or distilled *in vacuo*. Identical results were obtained in each case. The value of the upper limit is sensitive to traces of ozone and therefore the phosphorus was always distilled into the reaction vessel and particular care taken to clean the reaction vessel between each measurement.

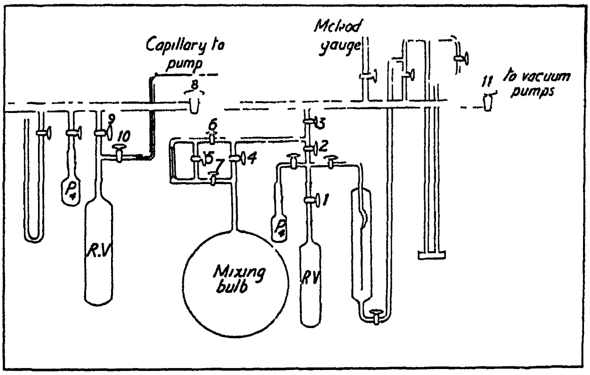

FIG. 1.—The Apparatus.

The reaction vessels were constructed of Pyrex, were cylindrical and about 15 cm. long with internal diameters varying from 1·0 to 7·3 cm. Other measurements were also made, e.g. analysis of the product, the rate of reaction above the upper limit, etc., and the methods used are described later.

White phosphorus was supplied by Messrs Albright and Wilson, Ltd., and specified free from sulphur, lead, iron and arsenic. The other materials were prepared by normal methods, dried and purified by well-established procedures.

Results and Discussion

Proposed Reaction Mechanism.—Since Miller's work[5] it has always been assumed that the products are largely the pentoxide (P_4O_{10}) with traces of ozone and lower oxides (P_4O_8 or P_4O_6). Recently it has been stated by Zagvozdkin and Barilko[6] that P_4O is a product of the reaction. It is assumed that it is formed by stabilization of the active centre formed in the reaction,

$$P_4 + O \rightarrow P_4O^*$$

and that this stabilization reaction accounts for the existence of the upper limit. P_4O is described as a stable, reddish, insoluble solid which constitutes up to 30 % of the product. Such a view is so obviously contrary to any mechanism hitherto proposed that we have repeated Miller's work and have confirmed her results. The product formed under the conditions of our kinetic work was about 80 % P_4O_{10} and all except $\sim$1·5 % of the remainder was soluble in water and accounted for in solution as phosphite. There is no evidence that the small insoluble residue is anything other than red phosphorus.

Addition of ozone markedly raises the upper limit[7] and ozone is formed whenever the glow is observed.[8] Therefore, whenever the glow reaction begins it will continue at pressures outside the normal limits. For example, at 0° C we found the upper limit in the presence of solid phosphorus to be 304 mm. of oxygen. If oxygen was then added, the glow could still be observed at a partial pressure of oxygen of 614 mm.

---

[5] Miller, *J. Chem. Soc.*, 1929, 1829.

[6] Zagvozdkin and Barilko, *J. Phys. Chem. Russ.*, 1940, 14, 505.

[7] Kovalsky, *Z. physik. Chem. B*, 1929, 4, 288.

[8] Downey, *J. Chem. Soc.*, 1924, 347.

Evidently ozone can accelerate the branching rate, most probably due to facile reactions of the type

$$P_4O_n + O_3 \rightarrow P_4O_{n+2} + O.$$

These facts raise the question as to whether it is justifiable to regard the ozone formation reaction

$$O + O_2 + M \rightarrow O_3 + M$$

as a chain terminating step. This should be considered in relation to the great sharpness of the limits. Within them the rate appears only to be limited by the supply and interdiffusion of the reactants. Outside, the rate is extremely small, and indeed has remained undetected by several observers. The minute amounts of ozone formed in the slow reaction above the upper limit therefore make an entirely negligible increase in the rate of branching and the reaction

$$O + O_2 + M \rightarrow O_3 + M$$

can be a part of the boundary condition determining the limits. Once the limit has been reached ozone is produced in relatively much greater quantity, sufficient to cause significant augmentation of the branching rate and thereby render the reaction autocatalytic.

The reaction scheme advanced by Dainton [3] requires modification in one respect. The propagation reaction involving oxygen atoms is written, $P_4 + O \rightarrow P_4O$, in that scheme. If an apical bond is formed as much as 156 kcal./mole may be liberated. We therefore consider that this reaction is only efficient when it is a 3-body process, and we accordingly represent the individual steps

1. $P_4 + O_2 \rightarrow P_4O + O$; initiation.
2. $P_4 + O + M \rightarrow P_4O + M$; propagation.
3. $P_4O_n + O_2 \rightarrow P_4O_{n+1} + O$ ($n \ngtr 9$) ; continuous branching.
4. $O + O_2 + M \rightarrow O_3 + M$; termination.
5. $O + X \rightarrow ?$; "
6. $O +$ wall $\rightarrow ?$; "

where M denotes a third body and may be a molecule of phosphorus, oxygen or added substance and X is an inhibitor or "poison". By the usual methods we obtain

$$\frac{d[P_4O_{10}]}{dt} = k_1[P_4][O_2] + \frac{10k_2[P_4][M]k_1[P_4][O_2]}{k_4[O_2][M] + k_5[X] + k_6 - 8k_2[P_4][M]} \qquad (1)$$

and the limits to the glow will be given by

$$8k_2[P_4][M] = k_4[O_2][M] + k_5[X] + k_6. \quad . \quad . \quad (2)$$

Assuming that the time for diffusion of oxygen atoms through a given distance in a given gas mixture is equal to the sum of the times required if each component were present alone, we can write

$$k_6 = k_6'[d^2(D^{-1}_{O_2}[O_2] + D^{-1}_{P_4}[P_4] + D^{-1}_{M}[M])]^{-1} \quad . \quad . \quad (3)$$

where D_x represents the diffusion coefficients of oxygen atoms through unit concentration of gas x, d is the diameter of the reaction vessel, and k_6' includes a factor for the ability of the surface to remove an impinging oxygen atom from the reaction. The term $k_4[O_2][M]$ is also composite and should be written

$$k_4[O_2][M] = e^{-E_4/RT}[O_2][A_4^{O_2}[O_2] + A_4^{P_4}[P_4] + A_4^{M}[M]] \quad . \quad (4)$$

in which the A terms are the frequency factors appropriate to reaction (4) for the various third bodies.

Experimental Verification of the Mechanism.—THE PRESENCE OF OXYGEN ATOMS.—The formation of ozone and the correlation between the inhibiting action of added gases and their reactivity towards oxygen atoms[9] provide substantial support for the assumption that oxygen atoms are chain centres. A more direct test for their presence is suggested by the recent work of Gaydon[10] and Whittingham,[11] but the low intrinsic brightness and the difficulty of maintaining the glow over long periods together with the ready mist-forming properties of the products make these tests difficult to apply in practice. Nevertheless, we have found that when nitric oxide is present, admission of oxygen to a pressure just exceeding that necessary for the establishment of a hot flame,[12] causes the emission of a much greener glow than in the absence of nitric oxide. The sulphur dioxide test was less satisfactory. No coloration of the glow was observed and, as already explained, the phosphorus pentoxide interfered with the detection of sulphur trioxide in this region. However, in the hot flame region, sulphur trioxide was identified in the products and purple wisps could easily be seen in the fringes of the flame. In assessing the validity of these observations it should be remembered that the most favourable conditions for positive results are when the reactants react relatively slowly with oxygen atoms, e.g. CO, H_2, CH_4, whereas phosphorus probably reacts extremely rapidly. We conclude that oxygen atoms are present in the glow reaction but have a very short lifetime.

THE PROPERTIES OF THE LOWER LIMIT (P_l).—From eqn. (2) and (3) we obtain eqn. (5) as the expression for the lower limiting concentration of oxygen :

$$[P_4]\{A_2^{O_2}[O_2] + A_2^{P_4}[P_4] + A_2^{M}[M]\}\{D_{O_2}^{-1}[O_2] + D_{P_4}^{-1}[P_4] + D_{M}^{-1}[M]\} = \frac{k_6'}{8d^2 \,.\, e^{E_2/RT}} \qquad (5)$$

This has been tested under a variety of conditions.

(*a*) TEMPERATURE DEPENDENCE when *no foreign gas is present* ($[M] = 0$) and $[P_4]$ is very small and constant. Under these conditions eqn. (5) leads to

$$P_l = \left(\frac{D_{O_2} k_6'}{8A_2^{O_2}[P_4]d^2}\right)^{\frac{1}{2}} . \, e^{-E_2/2RT} \quad . \quad . \quad . \quad (6)$$

The partial pressure of phosphorus in the reaction vessel was that of the saturated vapour at 0° C. The values of P_l observed at four temperatures between 0 and 30° C are given in Table I and show that the lower limit does not vary significantly with temperature when $[P_4]$ is maintained small and constant. The same result was obtained in the presence of foreign gases. Since neither of the terms D_{O_2} or $A_2^{O_2}$ are appreciably temperature dependent we conclude that $E_2 = 0$, a result fully in accord with expectation.

TABLE I.—TEMPERATURE DEPENDENCE OF LOWER LIMIT IN 3·35 CM. DIAM. VESSEL

P_l (mm. Hg) . .	0·0258	0·0258	0·0256	0·0249
Temp. °C . .	0·0	9·0	15·0	30·0

---

[9] Tausz and Görlacher, *Z. anorg. Chem.*, 1930, **190**, 95 ; Geib and Harteck, *Ber.*, 1933, **66**, 1815 ; Harteck and Kopsch, *Z. physik. Chem. B*, 1931, **12**, 327 ; Schacherl, *Coll. Czech. Chem. Comm.*, 1930, **2**, 665 ; Krejci and Schacherl, *ibid.*, 1932, **4**, 107 ; Schenk and Jablonowski, *Z. anorg. Chem.*, 1940, **244**, 397.

[10] Gaydon, *Trans. Faraday Soc.*, 1946, **42**, 292.

[11] Whittingham and Dooley, *ibid.*, 1946, **42**, 354.

[12] For the significance of the hot flame limits see Bevington and Dainton, *Trans. Faraday Soc.*, 1946, **43**, 377. The stationary concentration of oxygen atoms in the vicinity of these limits is probably higher than at any other part of the glow region.

(*b*) Dependence of P_l on $[\mathrm{P_4}]$. Eqn. (5) leads to different relationships between P_l and $[\mathrm{P_4}]$ determined by the relative magnitude of $[\mathrm{O_2}]$, $[\mathrm{P_4}]$ and $[\mathrm{M}]$. Thus when $[\mathrm{P_4}] \ll [\mathrm{O_2}]$ and $[\mathrm{M}] = 0$, eqn. (6) obtains and it would be expected that P_l would be inversely proportional to $[\mathrm{P_4}]^{\frac{1}{2}}$. Curve 1 of Fig. 2 shows the correctness of this. When, however, $[\mathrm{P_4}]$ exceeds $[\mathrm{O_2}]$ the equation for the limit becomes

$$[\mathrm{P_4}]^3\left\{A_2^{\mathrm{O_2}}D_{\mathrm{P_4}}^{-1} + A_2^{\mathrm{P_4}}D_{\mathrm{O_2}}^{-1}\frac{P_l}{[\mathrm{P_4}]} + A_2^{\mathrm{P_4}}D_{\mathrm{P_1}}^{-1}\right\}d^2 = \frac{k_6'}{8e^{-E_2/RT}} \quad . \quad (7)$$

and P_l should become dependent on a higher inverse power of $[\mathrm{P_4}]$ than $\frac{1}{2}$. This is in fact the state of affairs observed at higher temperatures in larger reaction vessels as curve 3 of Fig. 2 indicates. When a large excess of non-reactant gas is present such that $[\mathrm{P_4}] \ll P_l + [\mathrm{M}]$, eqn. (5) becomes

$$P_l = \frac{a+b}{2}[\mathrm{M}] + \left\{\frac{(a-b)^2[\mathrm{M}]^2}{4} + \frac{c}{[\mathrm{P_4}]}\right\}^{\frac{1}{2}}, \quad . \quad . \quad (8)$$

where *a*, *b* and *c* are constants. In agreement with (8) we have observed that when nitrogen or helium is added the dependence of P_l on $[\mathrm{P_4}]$ decreases regularly. When the former gas constitutes 90 % of the total the relationship

$$P_l \, . \, [\mathrm{P_4}]^{0 \cdot 2} = \text{const.}$$

holds, as may be seen from curve 2 of Fig. 2.

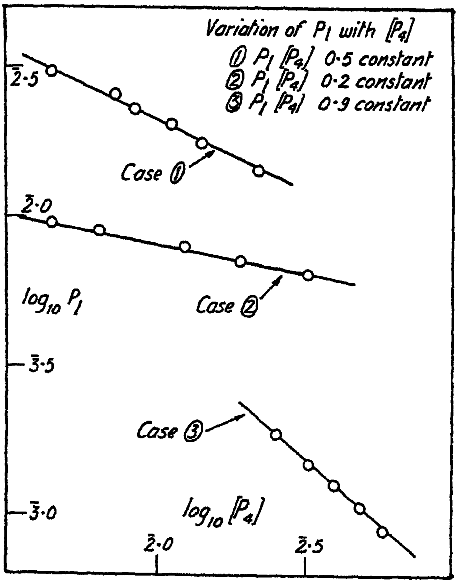

Fig. 2.—The Dependence of P_l on $[\mathrm{P_4}]$.

(*c*) The Influence of Vessel Diameter and Surface Condition.—We have stated that k_6' is dependent on the ability of the surface to remove from reaction any oxygen atoms which reach it. Replacement of a Pyrex surface by a long-chain "hydrocarbon surface" may be achieved by shaking cetyl-trimethyl ammonium bromide (Cetavlon) in a reaction vessel from which no precautions have been taken to remove moisture. The effect is to increase P_l by about 30 %, without affecting the temperature dependence, a result which is consistent with the anticipated action of the large number of methylene groups in increasing k_6'. If instead of methylene groups, a surface coating of methyl groups is formed (by the action of dimethyl silicon dichloride vapour on the moist Pyrex surface) the lower limit is unaffected in keeping with the known sluggish character of the reaction between methane and oxygen atoms at room temperature.

If the surface condition is maintained constant but the vessel diameter varied, the influence on the limit depends on the partial pressure of phosphorus. When this is small and whether or not a foreign gas is present, eqn. (5) leads to the prediction that P_l should be inversely proportional to d. Fig. 3 illustrates the truth of this over a wide range of conditions. As $[P_4]$ is increased the dependence of P_l on d should also increase (eqn. (7)) and this has been observed experimentally (curve 7 of Fig. 3). This change may be shown to be due to the increased proportion of phosphorus, because if foreign gas is now added to decrease the percentage of P_4 molecules without affecting the absolute values of $[P_4]$ the relation, $P_l \, . \, d =$ constant, is again found.

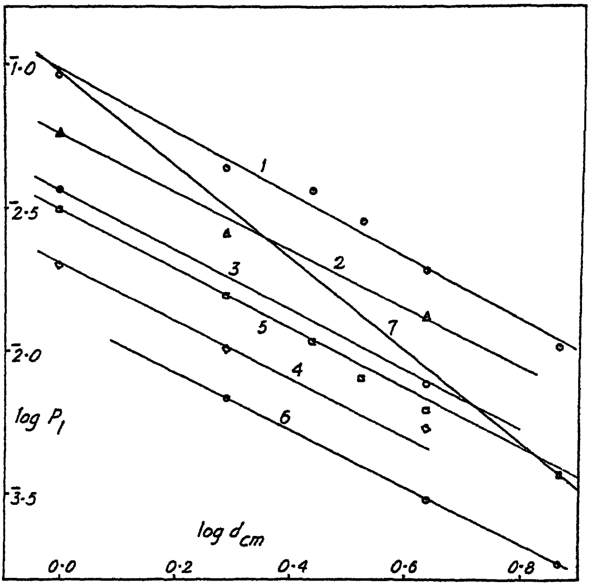

FIG. 3.—Dependence of the lower limit P_l on vessel diameter.

Curve 1.	Phosphorus at 0·0° C,	R.V. at 0·0° C.	Pure Oxygen	$P_l \cdot d^{1\cdot1}$=const.
Curve 2.	„ „ „	„ „ „	25% O_2+75% N_2	$P_l . d$ = „
Curve 3.	„ „ „	„ „ „	12·5%O_2+87·5%N_2	$P_l \cdot d$ = „
Curve 4.	„ „ „	„ „ „	4·75%O_2+95·25%N_2	$P_l \cdot d$ = „
Curve 5.	„ „ 15·0° C,	„ „ 15·0°C.	8·41%O_2+91·59%N_2	$P_l \cdot d$ = „
Curve 6.	„ „ 0·0 C,	„ „ 15·0°C.	Pure oxygen	$P_l . d$ = „
Curve 7.	„ „ 15·0° C,	„ „ 15·0°C.	„ „	$P_l . d^{1\cdot6}$= „

If $[P_4] \gg P_l$ an index n approaching 2 in the relation $P_l \, . \, d^n =$ constant, would be anticipated (eqn. (7)). Semenoff's experiments [13] in very large bulbs in which P_l varied from 0·005 to 0·0006 mm. are in this category and it is not surprising that he observed P_l to be proportional to d^{-2}.

(*d*) THE INFLUENCE OF FOREIGN GASES.—It is not possible to obtain a satisfactory test of eqn. (5) in so far as it summarizes the dependence of P_l on [M] for a given $[P_4]$ without making some assumption about the various coefficients of these quantities. For example, if the assumption is made that the reciprocals of the diffusion coefficients of oxygen atoms through O_2, P_4 and M are in the same ratio as the frequency factors of reaction (2) for each of these gases we may write

---

[13] Semenoff, *Z. Physik.*, 1927, **46**, 209.

$$\left(\frac{A_2}{D^{-1}}\right)^{\frac{1}{2}}(aP_l + b[P_4] + c[M]) = \left[\frac{k_6'}{8[P_4]d^2}\right]^{\frac{1}{2}} \quad . \quad . \quad (9)$$

where

$$a : b : c = D^{-1}_{O_2} : D^{-1}_{P_1} : D^{-1}_{M} = A_2^{O_2} : A_2^{P_1} : A_2^{M}.$$

This assumption is not so drastic as might at first sight appear, since both the ternary collision rate of $O + P_4 + M$ and the reciprocal of the diffusion coefficient will be proportional to

$$\left[{}_{O}\sigma^2_{M}\left(\frac{1}{16} + \frac{1}{m_M}\right)^{\frac{1}{2}}\right].$$

At constant partial pressure of phosphorus we can write

$$\left[P_l + \frac{b}{a}[P_4]\right]\left[1 + \frac{\frac{c}{a}[M]}{P_l + \frac{b}{a}[P_4]}\right] = \text{constant} \quad . \quad . \quad (10)$$

When $P_l \gg [P_4]$, eqn. (10) becomes identical with that proposed by Melville and Ludlam [14] both in form and in that the coefficient of [M] is inversely proportional to the diffusion coefficient of oxygen atoms through the gas M.

It is possible to calculate values of b/a and c/a based on known or assumed values of the collision diameters of the gases concerned. Substitution of these permits eqn. (10) to be tested graphically and we have found there is good agreement between theory and experiment. No great significance attaches to this agreement since the linearity of the plot is rather insensitive to the changes in the chosen values especially when $[M] \gg P_l > [P_4]$, i.e. at low temperatures in narrow reaction vessels.

THE PROPERTIES OF THE UPPER LIMIT (P_u).—Combining eqn. (2) and (4) and neglecting wall termination (i.e. $k_6 = 0$) we obtain eqn. (11):

$$\begin{aligned}8[P_4]\{A_2^{O_2}[O_2] + A_2^{P_1}[P_4] + A_2^{M}[M]\}e^{-E_2/RT} \\ = k_5[X] + [O_2]e^{-E_4/RT}\{A_4^{O_2}[O_2] + A_4^{P_1}[P_4] + A_4^{M}[M]\}, \quad (11)\end{aligned}$$

and since $[P_4]$ is always negligible, and we have shown $E_2 = 0$,

$$8[P_4]\{A_2^{O_2}[O_2] + A_2^{M}[M]\} = k_5[X] + [O_2]\{A_4^{O_2}[O_2] + A_4^{M}[M]\}e^{-E_4/RT}. \quad (12)$$

This equation was verified as follows.

(*a*) DEPENDENCE OF P_u ON TEMPERATURE.—If no gas other than oxygen is present the expression for the upper limit deduced from eqn. (12) is

$$P_u = \frac{8[P_4]A_2^{O_2}}{A_4^{O_2}}e^{+E_4/RT}, \quad . \quad . \quad . \quad . \quad . \quad (13)$$

and the variation of the upper limit with temperature when $[P_4]$ is maintained constant should give the value of E_4. It is of considerable interest that (13) does not allow of an increase of P_u with temperature, and if E_4 is not zero P_u should decrease. We thus have the possibility of the unusual phenomenon of an upper pressure limit to an explosion which decreases with temperature, i.e. a system which becomes *less* explosive as the temperature is raised. Such an explosion could not be thermal in origin, but could only be due to a decrease in the rate of termination as the temperature is reduced so that the net branching factor increases, becoming positive at the upper limit. It therefore became a matter of great importance to study the dependence of P_u on T when $[P_4]$ is constant. This proved to be difficult experimentally, and a slightly different technique had to be employed. The reaction vessel was filled with phosphorus vapour at the saturated vapour concentration at 15° C. The whole of the vessel was then cooled in liquid air and oxygen admitted to the required pressure. Finally the temperature was raised either to 17° or 70° C and the gases allowed time to mix before applying the withdrawal method, The fact that P_u does decrease with temperature was at once obvious, since, as the pressure was reduced, the glow appeared only in the connecting tubing to the reaction vessel which was at room temperature. On the other hand, if this tubing was heated electrically above the temperature of the reaction vessel the glow then appeared only in the vessel. Although there was thus no doubt of the existence of the effect it was clear that E_4 was small and that the results obtained were not sufficiently reproducible at the higher temperature to estimate E_4 with any accuracy. Upper limit data are much more reliable when solid phosphorus is present in the reaction vessel and it was therefore decided to obtain E_4 as described later.

---

[14] Melville and Ludlam, *Proc. Roy. Soc. A*, 1932, 135, 315.

(*b*) DEPENDENCE OF P_u ON $[P_4]$, T CONSTANT.—The chosen temperature was 17° C and the procedure was that described in the preceding paragraph. The results are given in Table II and it is evident that over the greater part of the range the relation $P_u/[P_4]^{0\cdot9}$ = constant is valid. At very low partial pressures of phosphorus this law is not obeyed.

TABLE II

Temperature = 17° C. Pyrex reaction vessel diameter 3·35 cm.

$[P_4]$ . .	0·01002	0·0108	0·00843	0·00673	0·0062	0·0061	0·0052	0·00425	0·00275	0·0026
P_u . .	494	492 482	437	340	325·5	308	278	266	214	203
$P_u/[P_4]^{0\cdot9} \times 10^{-4}$	4·93	4·56 4·46	5·18	5·06	5·24	5·06	5·34	6·26	7·78	7·8

No explanation of this is afforded by the present theory unless it is assumed that phosphorus vapour is adsorbed on the vessel walls. If the desorption is slow compared with the withdrawal rate the value of the upper limit which is observed will be that corresponding to a lower value of $[P_4]$ than is assumed from simple proportion. The experiments described elsewhere [4] using radioactive phosphorus indicate that in vessels containing oxygen a tightly bound layer of phosphorus at least one molecule thick is readily formed. Until this has been studied in more detail it is not possible to make quantitative allowance for it.

(*c*) DEPENDENCE OF P_u on T, SOLID PHOSPHORUS PRESENT.—When solid white phosphorus is present in the reaction vessel the variation of the upper limit with temperature should be given by

$$\frac{d\,(\ln P_u)}{dT} = \frac{\lambda_v - E_4}{RT^2}, \quad . \quad . \quad . \quad . \quad (14)$$

where λ_v is the latent heat of vaporization of solid white phosphorus in the temperature range concerned. Measurements of P_u at 25 temperatures in the range −23° to +20° C are plotted in curve 1 of Fig. 4. Eqn. (14) is obeyed in this region and from the slope of curve 1 we have that

$$\lambda_v - E_4 = 9\cdot6 \text{ kcal.}$$

Using the value $\lambda_v = 13{\cdot}9$ kcal., appropriate to 0° C we deduce that the value of E_4 is 4·3 kcal. Confirmation of the correctness of eqn. (12) is obtained from measurements of the temperature coefficient of the upper limit in the presence of either helium or carbon dioxide. These gases do not react with oxygen atoms but merely act as third bodies in reactions (2) and (4) and for a fixed ratio of $[M]/[O_2] = \alpha$ we obtain

$$P_u = 8[P_4]e^{-E_1/RT}\left\{\frac{A_2^{O_2} + \alpha A^{M}}{A_4^{O_2} + \alpha A_4^{M}}\right\}. \quad . \quad . \quad . \quad (15)$$

The slope of the log $P_u - 1/T$ plot should therefore be the same whether or not a non-reactant foreign gas is present. Curves 2 and 3 of Fig. 4 show this to be the case.

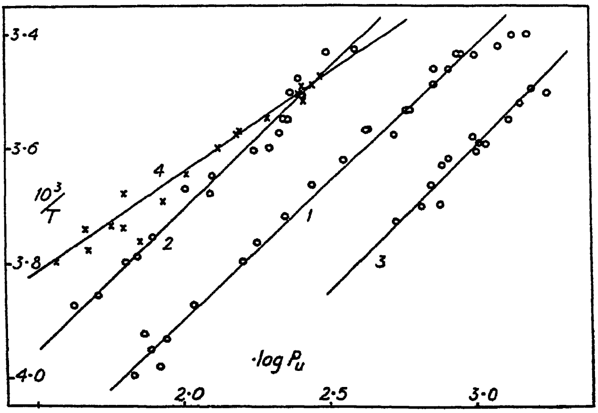

FIG. 4.—Temperature coefficient of the upper limit (P_u), when solid phosphorus is present.

Curve 1. Pure oxygen : P_u proportional to $[P_4]^{0{\cdot}66}$
Curve 2· 30% O_2, 70% He : P_u ,, ,, $[P_4]^{0{\cdot}66}$
Curve 3. 50% O_2, 50% CO_2 : P_u ,, ,, $[P_4]^{0{\cdot}66}$
Curve 4. 95% O_2, 5% 1-butene : P_u ,, ,, $[P_4]^{0{\cdot}93}$

If the foreign gas affects the upper limit principally by facile reaction with oxygen atoms it may be classed as a poison. The effect of small amounts of such substances as third bodies in reactions (2) and (4) can be neglected, but the term $k_5(X)$ must be included. When the ratio $[X]/[O_2] = \beta$ is fixed we obtain eqn. (16) :

$$P_u = \frac{8k_2[P_4] - k_5\beta}{k_4} \quad . \quad . \quad . \quad . \quad (16)$$

and when $E_5 < E_4$ the effect of the inhibitor will be to increase the dependence of the upper limit on temperature. Unsaturated aliphatic hydrocarbons behave as poisons in this way and curve 4 of Fig. 4 shows the increased temperature dependence in the presence of 1-butene. The relevant data of Bevington and Dainton [12] may be interpreted in a similar fashion.

(*d*) EFFECT OF SURFACE CONDITION AND VESSEL DIAMETER.—Eqn. (12) contains no term dependent on vessel diameter or surface condition and we have found that the upper limit is completely uninfluenced by these parameters.

(*e*) DEPENDENCE OF P_u ON [M], T CONSTANT.—The equation for the upper limit in terms of ratio $\alpha = [M]/[O_2]$ is

$$P_u = \frac{8[P_4]A_2^{O_2}}{k_4^{O_2}}\,\frac{1 + d\alpha}{1 + e\alpha}, \quad . \quad . \quad . \quad . \quad (17)$$

where $d = A_2^M/A_2^{O_2}$ and $e = k_4^M/k_4^{O_2}$; whence

$$\frac{\partial P_u}{\partial \alpha} = \frac{8[P_4]A_2^{O_2}}{k_4^{O_2}} \cdot \frac{d - e}{(1 + e\alpha)^2}. \quad . \quad . \quad . \quad (18)$$

In practice the limit is always reduced by addition of foreign gases, even when these cannot react with oxygen atoms, e.g. helium, and we therefore conclude that $e > d$, i.e. that oxygen is proportionately less effective in reaction (4) than in reaction (2).

(*f*) Dependence of P_u on [X], T Constant.—X is defined as reacting readily with oxygen atoms, i.e. k_5 is large. Small amounts of such substances bring about a marked lowering of the upper limit, and eqn. (16) now applies. The relative effectiveness of various inhibitors in depressing the upper limit of the glow of phosphorus is thus a direct measure of their relative velocity constants for reaction with oxygen atoms.

Of the gases whose effect on P_u has been studied, very few act exclusively as non-reactants (i.e. behaviour summarized by eqn. (17)) or as poisons. The inert gases are in the former category, together with N_2, CO, CO_2, and SO_2, all of which react very slowly with oxygen atoms at room temperature. Typical of the latter category are gases such as NO_2, Cl_2, Br_2, di- and cylic olefines. The bulk of the gases studied by Tausz and Görlacher[9] appear to exert their influence on P_u both by acting as a third body on the ozone formation reaction and by reaction with oxygen atoms. The appropriate equation in this case is

$$P_u = \frac{8[P_4]A_2^{O_2}}{k_4^{O_2}} \frac{1 - f\alpha}{1 - e\alpha}, \quad . \quad . \quad . \quad . \quad (19)$$

where $f = \left(\frac{k_5}{8[P_4]A_2^{O_2}} - \frac{A_2^M}{A_2^{O_2}}\right)$. It is easily shown that such an equation with suitable constants e and f can account for the data of Tausz and Görlacher at least as well as the two-constant equation proposed by Melville.[15]

The Slow Reaction Outside the Limits.—According to eqn. (1) there should be a slow reaction outside the limits. Ample evidence exists in support of this. Below the lower limit it is difficult to detect, presumably because the value of $[O_2]$ is so small as to make the rate of chain initiation $k_1[P_4][O_2]$ minute. However, Melville and Ludlam[14] have shown that when this rate of gas phase initiation is strongly augmented by initiation on the surface of a hot filament, the reaction rate below the lower limit attains a measurable value and has the usual characteristics of a chain reaction. The reaction rate above the upper limit is readily detectable provided a sensitive manometer is employed. We have observed that at 5° C and pressures *ca.* 100 mm. above P_u reaction rates of the order of 0·025 mm./min. are obtained. This rate increases slightly as the pressure is reduced and the upper limit approached. When this limit is reached the rate of pressure fall increases very sharply to values of the order of several mm./min. The rate just inside the limit is irreproducible and may be dependent on the surface area of solid phosphorus present. Owing to the difficulty of controlling and measuring this surface area, measurements of the rate of the glow reaction are not of quantitative significance. Nevertheless they provide support of qualitative value for the view that the glow reaction is only limited in velocity by the supply of phosphorus molecules to the reaction zone (cf. Fig. 7 of ref. (12)) and that the limit is the pressure at which the net branching factor is zero.

[15] Melville, *Trans. Faraday Soc.*, 1932, 28, 1.

Conclusions.—The new results presented and the results of previous workers constitute a satisfactory verification of the reaction mechanism proposed. The oxidation of phosphorus vapour may therefore be regarded as a continuously branched chain reaction in which the chain centres are oxygen atoms and P_4O_n ($n \ngtr 9$) units. From the temperature dependence of the pressure limits to the glow in the presence and absence of solid phosphorus it is concluded :

(*a*) that the reaction

$$P_4 + O + M \rightarrow P_4O + M$$

requires no energy of activation,

(*b*) that the energy of activation for the formation of ozone in a triple collision of the type

$$O + O_2 + M \rightarrow O_3 + M$$

is 4·3 kcal./mole and

(*c*) that self-heating plays no part in determining the conditions for transition from the stationary state of the slow reaction outside the limits to the non-stationary state of the glow within the limits. The last of these conclusions is most convincingly shown by the observation that if the concentration of P_4 molecules is fixed the upper limit *decreases* with temperature.

Conclusions (*a*) and (*b*) require further comment. From eqn. (13) and the observed values of $[P_4]$, P_u, E_4 the ratio of the frequency factors of reaction (2) and (4) at room temperature is about 10. It is unlikely that the collision rates in these two reactions would be so different and the reason may lie in different steric factors. The reaction

$$P_4 + O + M \rightarrow P_4O + M,$$

has no energy of activation and it is therefore unlikely that it is accompanied by any considerable rearrangement of PP bonds. This might be interpreted as signifying that the PO bond formed is an apical one. If this is so, the approach of an oxygen atom to the tetrahedral, P_4 molecule from almost any angle is likely to result in reaction, provided the third body M is also present. On the other hand $E_4 = 4·3$ kcal., the OO bond in O_2 is extended when O_3 is formed and it is likely that the reaction path to form the triangular O_3 molecule is associated with a fairly restricted angle between the line of approach of the oxygen atom and the figure axis of the O_2 molecule. Accordingly not every ternary collision for which the energy requirements are satisfied will result in reaction and we may expect $A_2^{O_2} > A_4^{O_2}$.

The velocity constant of reaction (4) may be considered from another viewpoint. Rodebush and Spealman [16] have shown that at 40° C the reaction

$$O + NO_2 \rightarrow NO + O_2$$

occurs once in every 10^5 collisions. From eqn. (19)

$$\partial P_u/\partial \beta = -\, k_5/k_4^{O_2}$$

and applying this to the data for the effect of NO_2 on the upper limit we obtain

$$k_4^{O_2} = 10^{-5} \,.\, Z_{O+NO_2} \times (1·5 \times 10^5 \text{ mm.})^{-1}$$

Since $E_4 = 4·3$ kcal.,

$$A_4^{O_2} \simeq 10^{-6} \,.\, Z_{O+NO_2}.$$

The anticipated ratio of the binary to ternary collision rates at 15° C is 10^4 for the species concerned and hence $A_4^{O_2} < Z_4^{O_2}$, i.e. not all the ternary $O + O_2 + O_2$ collisions which possess the 4·3 kcal. energy of activation result in reaction.

---

[16] Rodebush and Spealman, *J. Amer. Chem. Soc.*, 1935, **57**, 1474.

Irrespective of the absolute magnitude of $A_4^{O_2}$ the relative rates of reaction of poisons with oxygen atom may be obtained from a direct comparison of $\partial P_u/\partial \beta$ for different poisons.

We are indebted for financial aid to the Royal Society and the Rehabilitaton Dept., New Zealand Government.

Laboratory of Physical Chemistry,
Cambridge.

FURTHER OBSERVATIONS ON LATENT IMAGE FORMATION IN THALLOUS BROMIDE GELATIN SYSTEMS

BY MARGARET J. HARPER AND MOWBRAY RITCHIE

Received 31*st January,* 1950 ; *as revised* 9*th May,* 1950

Latent image formation in thallous bromide gelatin systems has been further investigated. As judged by the developed density, the use of a relatively unrestrained gelatin was characterized by a greater plate speed, unaffected by the addition of small amounts of sodium nitrite, by some sensitivity to green light, and by greater stability of the latent image centres in the dry emulsion. At low densities reciprocity relationships were unaffected.

Stationary characteristic curves, in which the rate of image formation was balanced by the rate of image destruction, were in evidence for both blue and green light ; for blue light, a linear relationship was established between developed density and light intensity in the lower intensity ranges. The desensitizing materials Malachite Green and Methylene Blue suppressed the image formation process.

The existence of both surface and internal latent image was demonstrated, the normal latent image being formed predominantly at the grain surface ; bleaching of latent image by low intensity blue light was not accompanied by any increase in the internal latent image. Under certain conditions, a reversal comparable to the Albert effect in silver bromide emulsions was observed.

The work of Farrer [1] and of Ritchie and Thom [2] has shown that latent image formation in thallous bromide-gelatin shows many similarities to that of the more extensively investigated silver bromide system. While spectral sensitivities extend over much the same regions, the former is characterized by a much lower plate speed and by the fact that a latent image produced by exposure to blue light may be bleached out entirely by a subsequent blue light exposure of sufficiently low intensity. Two distinct processes are thus to be recognized, the normal forward image building mechanism being inhibited by a reverse destruction of the image by light of the same wavelength. A " stationary " characteristic curve may thus be obtained. In this connection, Ritchie and Thom recognized with blue light the existence of a " bleaching limit " of intensity below which bleaching of an image produced by a pre-exposure could be observed, and above which, under certain conditions, an increase in density was obtained. If such bleaching limits be plotted against the primary densities brought about by suitable pre-exposures, then each point on the curve represents an equilibrium position at which illumination of the corresponding intensity will produce no further effect ; the curve is in

[1] Farrer, *Photo. J.*, 1936, **60**, 486.

[2] Ritchie and Thom, *Trans. Faraday Soc.*, 1946, **42**, 418.

fact a stationary characteristic curve. Establishment of such a curve by the method of direct exposure of a previously unexposed plate requires exceptionally long exposures, especially at the lower intensities, with consequent risk of oxidation of the thallium image; accordingly, stationary characteristic curves have been determined by the bleaching limit method for two types of emulsion, one made from normal photographic gelatin and the other from an unrestrained gelatin which required exposures less by a factor of approximately a thousand to give similar developed densities.

Experimental and Results

The preparation of the thallous bromide emulsions, exposure, development and measurement of developed densities were carried out by the methods previously detailed.[2] By " gelatin I " are denoted emulsions made with a " non-photographic " gelatin, as distinct from a " photographic " gelatin II (Nelson and Dale) and the " photographic " gelatin III, part of the same stock used initially by Ritchie and Thom. Incident light intensity measurements are normally quoted as galvanometer scale divisions as given by the photocell-galvanometer arrangement, where 1 scale division was equivalent to $9{\cdot}0 \times 10^{12}$ quanta ($\lambda = 4360$ Å) per sec. per sq. cm. of illuminated surface.

Stationary Characteristic Curves and General Comparison of the Gelatins.—Bleaching limits were determined as before by giving a series of plates primary exposures at constant times to gradually increasing intensities of light of wavelength 4360 Å. The uniform latent image obtained in each case was then immediately exposed through the calibrated sector wedge to light of the same wavelength. Provided the secondary light intensities were of the appropriate range, bleaching limits of intensity were recorded, below which bleaching occurred and above which an increased developed density was observed. These bleaching limits, in terms of the logarithms of the secondary incident intensity (in scale divisions) are plotted in Fig. 1 against the developed densities produced by the primary exposure. Curve I refers to the fast gelatin I; Curve II*a* to gelatin II immediately after emulsion manufacture, and Curve II*b* to the same emulsion, the speed of which had decreased considerably with time; Curve III represents recorded bleaching limits for a gelatin III emulsion. In all cases a

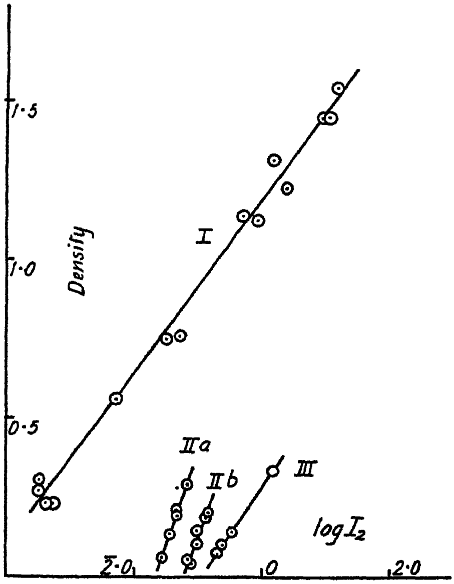

FIG. 1

linear relationship is evident, which holds down to the lowest densities concerned. The data * of Ritchie and Thom [2] show that at high densities a flat maximum is attained ; the shape of the stationary characteristic curve is therefore of the same type as that of the normal H and D curve, except that linearity exists at the lowest densities in the former. The slopes of the curves show the "photographic" gelatins to possess slightly greater photographic contrast, but gelatin I obviously gives an emulsion of much greater forward speed than the others. If the intercepts on the intensity axis be taken as a measure of the intensity just sufficient to produce a permanent latent image, then gelatin I is numerically 400 times faster than the most sensitive of the photographic varieties.

In contrast to the slow emulsions, the fast gelatin I emulsion was found to be sensitive to green light of wavelength 5460 Å at certain intensities, although the maximum developed density so produced was small. It appeared that a stationary characteristic curve was again in evidence. Because of the smallness of the maximum density, bleaching limits could not be determined accurately, but it was obvious that, as with blue light, the higher the density produced by a primary light exposure, the higher the bleaching limit as shown by a subsequent exposure.

Since desensitization by dyestuff will tend to oppose the image-forming process, attempts were made to confirm the corresponding alteration in the stationary curve in blue light with Methylene Blue and Malachite Green. The aqueous solutions used were 0·1 %, 0·01 % and 0·001 % in each case and the normal plates were dipped for 3 min., allowed to drain, and dried. Results were complicated by extensive fogging on normal development, but in terms of density above fog, no developed image was obtained on exposure except for the most dilute Malachite Green solution. Similarly, when a normal plate was exposed to give a high latent image density, then dipped in dye solution, dried and given a secondary exposure to blue light of different intensities, the primary image was rapidly removed. The forward process of latent image formation was thus completely inhibited by the dyestuff. Accurate comparison of results was again difficult because of fogging and because of the loss in primary latent image produced by a 3-min. immersion in water itself.

The latent image centres of this fast gelatin I dried emulsion were much more stable than in the slow "photographic" emulsions. After a normal drying process of 4 days after emulsion coating, no decrease in sensitivity was observed with gelatin I plates over a period of 10 months in one instance, in sharp contrast to the day-to-day fading observed by Ritchie and Thom. The latent image itself once formed was again regularly stable as judged by subsequent development, but for incompletely dried plates, as for example, those subjected to half the normal drying period, the developed density was observed to decrease from 0·32 to 0·05 in 45 min. after exposure and before development. Such effects must be ascribed to destruction of the thallium latent image by atmospheric oxidation under the moist conditions.

In contrast to Ritchie and Thom's results for the slow photographic emulsions, the corresponding addition of small quantities (of the order of 0·01 g. per 100 ml. liquid emulsion) of sodium nitrite produced no appreciable increase in plate speed. This was interpreted on the basis that the bromine atom acceptor action of gelatin I was large enough to render inappreciable the further action of small amounts of nitrite. At relatively long exposures, however, solarization was distinctly in evidence, more especially when the digestion period of manufacture was prolonged ; characteristic curves for 5-, 15-, 30- and 45-min. exposures of such an emulsion showed the 15-min. curve to possess at all intensities the greatest densities, the next being the 5-min. exposure, succeeded in turn by the 30- and 45-min exposures. At low intensities and short time exposures, reciprocity relationships remained approximately the same as for the slow gelatins.[2]

The relatively high speed of gelatin I plates and the accompanying solarization suggested that this gelatin was of the unrestrained type where the growth of crystal grains and of latent image centres was not greatly restricted. The test of Steigmann [3] was applied, based on the reduction of ammoniacal silver nitrate by ammonium sulphite. The solutions used were 0·50 g. gelatin in 5 ml. water at 60° C, 1 ml. 0·3 % sulphur dioxide solution, 1 ml. 0·1 N silver nitrate, 0·5 ml. dilute ammonia (25 ml. 0·88 ammonia + 75 ml. water). Gelatins I and II

* Ref. 2, p. 423, Fig. 4.

[3] Steigmann, *J. Soc. Chem. Ind.*, 1942, **61**, 67.

were thus compared by immersing the sample tubes in boiling water and observing visually the accompanying colour changes due to reduced silver. After 20 min. both samples were brown in colour, but at 7 min. gelatin I was orange, while gelatin II was only slightly yellow ; at 10 min. gelatin I was brown while gelatin II was orange-yellow. It thus appeared that gelatin I was an unrestrained gelatin as compared with the photographic gelatin II. In both cases suitable treatment with hydrogen peroxide decreased the rate of darkening, no change being observed in 20 min. Inasmuch as such a test has not been previously reported in relation to thallous bromide emulsions, a further similarity to the silver bromide system is thus indicated.

Internal and Surface Image Formation.—Attempts were made to determine the relative amounts of surface and internal latent image formation by means of surface and total developers as described by Stevens.[4] The surface developer consisted of a stock solution of 120 g. $Na_2CO_3 . 10H_2O$ per litre, to 50 ml. of which 1·2 g. *p*-hydroxyphenyl glycine were added as required. The total developer was made up by adding 10 ml. 10 % hypo to 50 ml. of the normal developer.

Consideration of possible surface and internal latent image in thallous bromide emulsions is complicated by the fact that the latent image produced initially by exposure was converted to the corresponding silver system by double decomposition. It was, however, established that potassium dichromate solution of suitable concentration could be used to remove surface image as judged by the above surface developer. This is shown in Fig. 2.

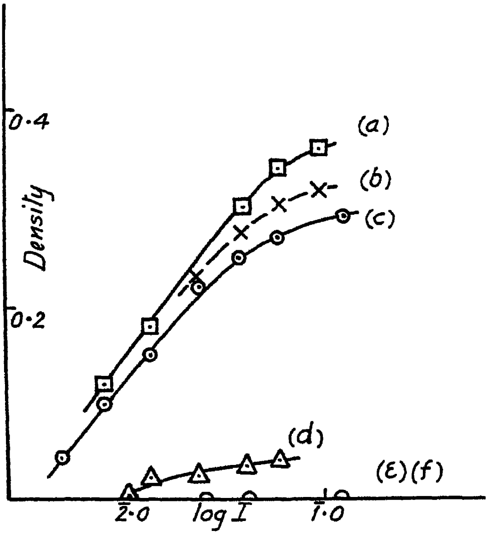

FIG. 2

Thallous bromide plates were suitably exposed, treated with silver nitrate solution and washed before being immersed for 2 min. in various dichromate solutions ; surface development followed further washing. The stock dichromate solution contained 0·75 g. potassium dichromate, and 0·5 ml. conc. H_2SO_4 in 100 ml. aqueous solution, and the various curves show the effect of the 2-min immersion in 50 ml. portions of solutions containing the following percentages of stock dichromate solution : (*a*) 0, (*b*) 0·16, (*c*) 3·1, (*d*) 6·25, (*e*) 12·5, (*f*) 25·0, (*g*) 100. For the concentrations of dichromate greater than (*c*), there is little evidence of residual surface image.

When two similar plates were exposed treatment of one with the surface developer produced a characteristic curve only slightly less in density for corresponding intensities than that given by the other by the total developer, and accordingly little internal image would appear to exist. A developed image of maximum density 0·2 was, however, produced by the total developer after a suitable bleaching solution (*e*) had been employed to remove the surface image.

---

[4] Stevens, *Phot. J.*, 1942, **82**, 42.

Attempts to remove surface latent image by suitably dilute bleaching agents, e.g. water itself, prior to double decomposition with silver nitrate, gave erratic and very low densities on subsequent total development.

Two similar plates were further exposed each to the same high intensity blue light. One half of each plate was then covered and the other halves given a secondary exposure to blue light of intensity below the bleaching limit. One plate was then surface developed and the other totally developed. Densities are recorded below. The differences are the same in each case; the amount of internal image is not appreciably increased, dispersal of the surface latent image by low intensity blue light being unaccompanied by any increase in the internal image.

Developed	Unbleached portion	Bleached portion
Surface	0·58	0·32
Total	0·65	0·39

It appeared that such internal latent image centres could be made available in circumstances comparable to those of the Albert effect in silver bromide systems. When plates were exposed to a blue light intensity range of 127 to 2·64 scale divisions for 12 min. by means of the step-wedge, this being succeeded by washing in running water for 10 to 30 min., subsequent exposure to a uniform intensity of 19 scale divisions for 5 min. showed a reversal in the sense that the lowest density produced normally by the first exposure was now the highest on normal development. This was attributed to the removal of the surface latent image by water containing oxygen, the grains being partly surface desensitized; further exposure increased the surface latent image only in those grains in which few internal latent image specks had been previously produced by the primary exposure, in accordance with the explanation of the Albert effect already advanced by Stevens.[5]

In the general treatment of thallous bromide by silver nitrate prior to development, the resultant disruption of the grains may reveal any internal image originally present, and will thus tend to present as surface image that latent image originally present in the grain interior. The final developed density of "internal" image will on such grounds be a minimum value.

Chemistry Department,
University of Edinburgh.

[5] Stevens, *Phot. J.*, 1939, **79**, 27.

ELECTROLYTES IN SOLUTIONS OF AMINO ACIDS

PART I.—THE CONDUCTIVITY OF POTASSIUM CHLORIDE IN AQUEOUS GLYCINE SOLUTIONS

BY C. B. MONK

Received 27th July, 1949; *as revised, 16th September*, 1949

The conductivity of KCl in 0·1, 0·25 and 0·5 M glycine solutions are reported, and the results are shown to agree, in dilute solutions, with those predicted by the Onsager equation.

Solutions which contain both electrolytes and amino acids (and related substances) are of particular interest with regard to their physical properties, since apart from their biological importance, they provide some of the relatively few cases where the dielectric constants are higher than those of ordinary aqueous solutions. In solutions where water and solvents of lower dielectric constants are used, the Debye-Huckel treatment is generally recognized as providing a reasonable interpretation of the results, but where amino acids are present in solution, it has been suggested that this theory possibly needs modification owing to the interaction between the dipolar ions formed by amino acids and ordinary ions from electrolytes. Kirkwood [1] and others have made extensions to the Debye theory in attempts to cover these particular cases, and a certain amount of success has been claimed where these modifications have been employed to interpret the solubilities of glycine in alcohol-water mixtures containing NaCl[2] and LiCl[3], and the solubilities of, e.g., $Ba(IO_3)_2$ and $Ca(IO_3)_2$ in aqueous glycine and alanine solutions.[4] Another aspect is that instanced by the work of Dunning and Shutt,[5] who concluded that the increased solubilities of AgCl and $PbCl_2$ in aqueous glycine could be explained, in a qualitative way, by coupling the Born equation [6] with the usual Debye-Hückel activity function. The Born equation deals with the effect of varying dielectric constants on the electrostatic forces between ions. The examples chosen by Dunning and Shutt were unfortunate, however, since both silver and lead form complexes with glycine,[7] and $PbCl_2$ is a comparatively weak electrolyte.[8] The enhanced solubility resulting from complex formation introduces a number of complications which will be discussed in a later paper. Failey,[9] who examined the solubilities of $TlIO_3$ and TlCl in amino acid solutions, discussed his results in terms of an expression developed by Scatchard; [10] this is on closely similar lines to the equation developed by Dunning and Shutt from Born's work. Again, in the case of thallium, although little or no complex formation occurs with amino acids (as shown by there being no significant pH change on adding glycine to a solution of $TlNO_3$), the agreement with theory is only qualitative. A weakness of these theories is that no account is taken of the possible variation in effective ionic radii on varying the composition of the solvent.

By far the greater number of studies on electrolytes in amino acid solutions have been concerned with complex formations, since with the exception of the alkali metals, and a few other cases, some complex formation takes place. Among the chief methods which have been used are solubility methods such as have been mentioned above and pH measurements. Conductivity methods have hardly been used at all, and this method should prove especially valuable when only small amounts of material are available, as for instance, with the higher polypeptides. Owing to the uncertainties which exist with regard to the interpretation of the results, a first contribution in this direction is made in the present paper, in which the conductivity of KCl in glycine solutions is reported.

Experimental and Results

A.R. glycine was dissolved, filtered and recrystallized twice from conductivity water, then dried to constant weight over KOH in vacuum. A.R. KCl was recrystallized three times from conductivity water, and after a preliminary heating heated to a dull red heat in a platinum dish. The conductivity apparatus and method of cell calibration have been described elsewhere.[11, 12] The temperature was kept at 25 ± 0·01° C. In making the measurements, the stock solution of glycine was made up by weight in conductivity water, the cell was rinsed with this several times, and then a suitable amount introduced into the cell. A weighed amount of KCl was dissolved in the remainder of the stock solution, and this solution was added in several small amounts from a weight-burette. In this way the concentration of glycine was kept constant. Buoyancy corrections were applied to all weighings, and the densities of the solutions were calculated from the equation of Wyman.[13] In some series the initial glycine solutions were equilibrated in contact with air, while for the rest, purified air was passed through the cell until the resistance became constant. All solutions were used within a few hours of making them, to avoid possible troubles due to bacterial action.

---

[1] Kirkwood, *J. Chem. Physics*, 1934, **2**, 351.
[2] Cohn, McMeekin, Greenstein and Weare, *J. Amer. Chem. Soc.*, 1934, **56**, 2270.
[3] Cohn, *Chem. Rev.*, 1936, **19**, 241.
[4] Keefer, Reiber and Bisson, *J. Amer. Chem. Soc.*, 1940, **62**, 2951.
[5] Dunning and Shutt, *Trans. Faraday Soc.*, 1938, **34**, 1192.
[6] Born, *Z. Physik.*, 1920, **1**, 45.
[7] Keefer and Reiber, *J. Amer. Chem. Soc.*, 1941, **63**, 689.
[8] Davies, *Trans. Faraday Soc.*, 1930, **26**, 592.
[9] Failey, *J. Amer. Chem. Soc.*, 1933, **55**, 4374.
[10] Scatchard, *Chem. Rev.*, 1927, **3**, 383.

Solvent Corrections.—Davies [14] has shown that when considering aqueous solutions containing CO_2, the ionization of the carbonic acid and the mobilities of the H^+ and HCO_3^- ions will be different when electrolyte is added to the solvent. In general these two effects oppose one another, since the increase in ionic strength will result in increased ionization of the carbonic acid, but at the same time it will decrease the mobilities of these two ions. Calculations show that the first effect is larger than the second, so that the specific conductivity due to the solvent is slightly larger when electrolytes are added. In the present case the solvent correction assumes considerable importance owing to the high concentrations of ionized glycine, but the same considerations apply, and provided that the pH of the solution is known, the true solvent correction can be calculated with the required accuracy. The pH of the solutions studied was in the neighbourhood of 6; the OH^- ion concentration can therefore be neglected, and the ions to be considered are H^+, HCO_3^-, H_2G^+ and G^- (the last two symbols representing the cation and anion respectively derived from glycine). The concentrations of all these can be calculated using the Debye-Hückel limiting equation, from the known pH and the known ionization constants of glycine [15] and carbonic acid.[16] The contribution of each to the conductivity of the solution can then be obtained from the appropriate mobility values. In water, at zero concentration, these are: H^+ 349·8,[17] HCO_3^- 44·5,[17] G^- 32·6,[18] and H_2G^+ 39·3,[18] but in the solutions considered these must be modified (*a*) to allow for viscosity changes by using Walden's equation [19]

$$\Lambda\eta^* = \Lambda(H_2O), \quad . \quad . \quad . \quad . \quad . \quad . \quad (1)$$

where η^* is the relative viscosity and (*b*) for alterations in the ionic strength, using Onsager's equation.

This was the procedure actually adopted, but for illustrative purposes, a more approximate method which gives virtually the same results may be quoted. In the electroneutrality equation

$$[H^+] + [H_2G^+] = [G^-] + [HCO_3^-]$$

the term $[H^+]$ is relatively small and may be neglected, and the mobilities of G^- and HCO_3^- are so nearly the same that these two terms need not be distinguished. The only concentration that need be determined therefore is H_2G^+, and this equals the sum of the other two. Consider the most dilute point of run 3(*b*) in Table I, in which the solvent correction is more than twice as important as for any other point in the Table. The concentration of the glycine is 0·5 M, the pH of the solution is 6·0, and K_A, the acid constant of H_2G^+ is $4{\cdot}47 \times 10^{-3}$. Therefore

$$[H_2G^+] = [H^+]\,[HG^{\pm}]/K_A = 0{\cdot}5 \times 10^{-6}/4{\cdot}47 \times 10^{-3} = 1{\cdot}12 \times 10^{-4}.$$

The mobilities of the H_2G^+ and G^- ions corrected for viscosity are 37·1 and 30·8 and the conductivity of the solvent, from Onsager's equation, is

$$\kappa = 10^{-3} \times 1{\cdot}12 \times 10^{-4}\,\{67{\cdot}9 - 76(1{\cdot}12 \times 10^{-4})^{\frac{1}{2}}\} = 7{\cdot}51 \times 10^{-6}.$$

---

[11] Davies, *J. Chem. Soc.*, 1937, 432.

[12] Davies and Monk, *ibid.*, 1949, 413.

[13] Wyman, *J. Amer. Chem. Soc.*, 1934, **56**, 536.

[14] Davies, *Trans. Faraday Soc.*, 1929, **25**, 129.

[15] Owen, *J. Amer. Chem. Soc.*, 1934, **56**, 24.

[16] Shedlovsky and MacInnes, *ibid.*, 1935, **57**, 1705.

[17] Harned and Owen, *The Physical Chemistry of Electrolytic Solutions* (Reinhold Publishing Corp., New York, 1943), Ch. 6, p. 172.

[18] Waind and Galliver (private communication, these laboratories).

[19] Walden, *Z. physik. Chem.*, 1906, **55**, 207; 1912, **78**, 257.

TABLE I.—CONDUCTIVITY OF KCl IN AQUEOUS GLYCINE SOLUTIONS AT 25°

Expt.	Glycine Molarity	$10^6\kappa_0$	10^4[KCl]	10^2[KCl]$^{\frac{1}{2}}$	Mobility Correction	Λ
1(*a*)	0·1000	2·907	3·1582	1·777	0·09	146·49
—	—	—	5·3758	2·319	0·06	145·96
—	—	—	8·3724	2·894	0·05	145·48
1(*b*)	0·1000	2·114	3·6787	1·918	0·08	146·37
—	—	—	6·1270	2·475	0·06	145·83
—	—	—	8·9950	2·999	0·05	145·42
—	—	—	11·650	3·413	0·04	145·04
1(*c*)	0·1000	3·377	16·325	4·040	0·03	144·42
—	—	—	21·821	4·671	0·03	143·91
—	—	—	28·133	5·304	0·02	143·39
—	—	—	34·203	5·848	0·02	142·95
2(*a*)	0·2500	5·706	3·4079	1·846	0·15	143·72
—	—	—	12·303	3·508	0·08	142·32
—	—	—	22·563	4·750	0·06	141·33
—	—	—	28·669	5·354	0·05	140·86
2(*b*)	0·2500	4·418	9·7391	3·120	0·10	142·60
—	—	—	18·858	4·343	0·06	141·64
—	—	—	27·079	5·204	0·05	140·95
—	—	—	32·895	5·736	0·04	140·52
2(*c*)	0·2500	5·442	4·5117	2·124	0·12	143·44
—	—	—	7·3267	2·707	0·10	142·92
—	—	—	10·433	3·230	0·09	142·50
—	—	—	15·675	3·959	0·07	141·99
3(*a*)	0·5000	9·590	6·5259	2·555	0·20	138·77
—	—	—	17·187	4·146	0·12	137·58
—	—	—	25·487	5·049	0·10	136·94
—	—	—	32·956	5·741	0·07	136·43
3(*b*)	0·5000	8·921	2·5305	1·591	0·28	139·58
—	—	—	5·2723	2·296	0·21	138·97
—	—	—	7·5992	2·757	0·18	138·60
—	—	—	10·521	3·248	0·15	138·22
—	—	—	15·547	3·943	0·12	137·75

pH of glycine solutions: (*a*) 5·9, (*b*) 6·0, (*c*) 6·0 for 0·1, 0·25 and 0·5 M respectively.

Ionic strengths of solvents: (*a*) $3·2 \times 10^{-5}$, (*b*) $7·2 \times 10^{-5}$, (*c*) $12·2 \times 10^{-5}$.

After adding KCl, the ionic strength is increased to $3·65 \times 10^{-4}$, and the concentrations of the solvent ions are increased by a factor f/f', where, by the Debye Hückel equation,

$$\log_{10} f/f' = 0·5(3·65^{\frac{1}{2}} + 1·12^{\frac{1}{2}}) \times 10^{-2}.$$

$[H_2G^+]$ hence becomes $1·13 \times 10^{-4}$, and

$$\kappa = 10^{-3} \times 1·13 \times 10^{-4} \{67·9 - 76(3·65 \times 10^{-1})^{\frac{1}{2}}\} = 7·51 \times 10^{-6}.$$

The two corrections therefore cancel out. The largest possible error is in the measurement of the pH of the solution. If we assume that this could amount to 0·1 unit and repeat the calculation for pH = 5·9, $[H_2G^+]$ becomes $1·41 \times 10^{-4}$, a significant difference; but the activity and mobility correction after adding KCl once more cancel out, so a simple subtraction of the initial solution conductivity represents the true solvent correction.

The influence of KCl on the pH of glycine solutions was followed by addition of 0·006 M KCl to 0·1 M glycine. A pH change of only 0·03 unit occurred, which is about that expected as a result of alteration in the ionic strength. King's work on the influence of NaCl on the ionization of glycine,[20] confirms this.

---

[20] King, *J. Amer. Chem. Soc.*, 1945, 67, 2178.

Since the increase in total ion concentration due to the solvent ions slightly lowers the mobilities of the KCl ions, corrections are necessary.[14] These have been calculated from

$$\Delta\Lambda = S\{(\mathrm{KCl} + I)^{\frac12} - I^{\frac12}\},$$

where S is the experimental slope of the curve obtained on plotting Λ, the equivalent conductivity of KCl, against the square root of the concentration, and I is the ionic strength of the solvent ions. These corrections are shown in Table I, together with the rest of the data. Fig. 1 represents a plot of the results, together with those for KCl in water.[21]

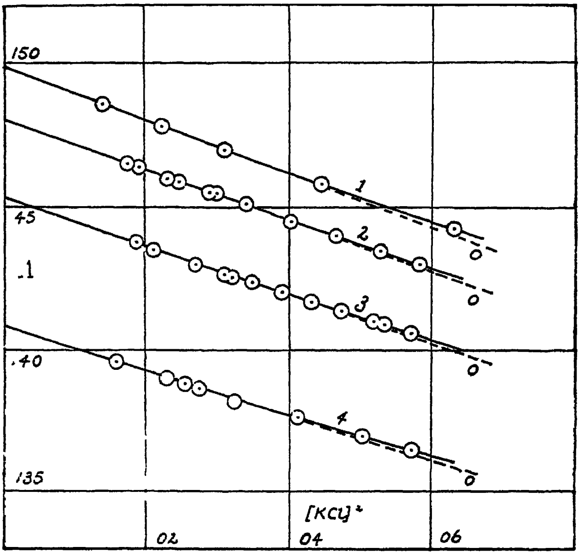

FIG. 1.—Conductivities of KCl. (1) in water; (2), (3) and (4) are in 0·1, 0·25 and 0·5 M glycine respectively. (Onsager slopes are indicated by O.)

Discussion

Using the most recent values for the constants involved,[22] the Onsager equation for a single electrolyte in solution at 25° is

$$\Lambda = \Lambda^\circ - \left[\frac{2\cdot8009 \times 10^6\, q z_1 z_2 \Lambda^\circ}{(1 + q^{\frac12})\,(\epsilon T)^{3/2}} + \frac{41\cdot247\,(z_1 + z_2)}{\eta(\epsilon T)^{\frac12}}\right] I^{\frac12}, \quad . \quad (2)$$

where q is 0·5 for electrolytes dissociating into two ions, z_1 and z_2 are the valencies of the two ions, ϵ is the dielectric constant of the solvent, η is its viscosity. The dielectric constants were obtained from the results of Wyman and McMeekin,[23] and the viscosities were interpolated from the figures of Conner and Smyth,[24] checking them as far as possible from those of Bell [25] and Hedestrand,[26] which are at other temperatures than 25°. The values of Λ° were obtained by a large-scale plot of Λ against the square root of the concentration. The relevant data together with the experimental and calculated limiting Onsager slopes are given in Table II.

It is seen that, within experimental error, the limiting experimental slopes agree with those calculated from Onsager's equation. At higher

---

[21] Shedlovsky, Brown and MacInnes, *Trans. Electrochem. Soc.*, 1934, **66**, 165.
[22] Birge, *Rev. Mod. Physics*, 1941, **13**, 233.
[23] Wyman, Jr., and McMeekin, *J. Amer. Chem. Soc.*, 1933, **55**, 908.
[24] Conner and Smyth, *ibid.*, 1942, **64**, 1870.
[25] Bell and Magden, *J. Chem. Soc.*, 1947, 74.
[26] Hedestrand, *Z. anorg. Chem.*, 1922, **125**, 153.

TABLE II.—CONDUCTIVITY DATA.

Glycine Molarity	ϵ	η	Λ°	Λ° (Calc.) Eqn. (1)	Λ° (Calc.) Eqn. (3)	Onsager Slope	Expt. Limiting Slope
0	78·54	0·008949	149·88	149·9	149·9	94·55	94·5
0·1000	80·80	0·00905	148·1	148·3	148·1	90·35	90
0·2500	86·19	0·00921	145·35	145·7	145·4	84·83	86
0·5000	89·93	0·00949	140·85	141·3	140·9	79·42	81

concentrations the curves begin to diverge upwards in a manner similar to that found when water alone is the solvent. The decreasing values of Λ° with increasing amounts of glycine fit in fairly well with Walden's rule (eqn. (1)), as is shown in column 5 of Table II. The empirical relation

$$\Lambda^\circ = \Lambda^\circ(H_2O) - 18(HG^\pm) \quad . \quad . \quad . \quad (3)$$

gives somewhat better values (column 6, Table II).

In the stronger glycine solutions, the concentrations of glycine ions are comparable with the concentrations of KCl. It has been shown by Onsager and Fuoss [27] that in a mixture of electrolytes, Kohlrausch's rule of the independent migration of ions does not apply and that conductivities are not additive. This might have had some influence in the present case. However, calculations on the particular solution discussed in connection with solvent corrections showed that, at the most, the Cl′ ion has a mobility change of about 0·02 unit, while the other ions are altered by less than 0·01 unit. The errors introduced by ignoring these effects are therefore negligible.

The author wishes to thank Prof. C. W. Davies and Prof. E. A. Guggenheim for their advice on the setting-out of this paper.

Edward Davies Chemical Laboratories,
University College of Wales,
Aberystwyth.

---

[27] Onsager and Fuoss, *J. Physic. Chem.*, 1932, 36, 2689.

ELECTRICAL AND STRUCTURAL PROPERTIES OF SOME ALKALINE EARTH AND NICKEL OXIDES SYSTEMS

BY M. G. HARWOOD, NORA HERZFELD AND S. L. MARTIN

Received 17th March, 1950

Selected compositions of the barium and/or strontium oxide - nickel oxide systems, including the pure components, have been examined. The variation of the electrical conductivity with temperature of pellets of the oxides has been investigated, generally *in vacuo*, and the results have been correlated with structural data obtained by X-ray diffraction.

Firing an equimolecular mixture of $BaCO_3$ and NiO *in vacuo* at 960° C gave a compound, barium nickelite, $BaNiO_2$, stable in air, and of higher conductivity than either BaO or NiO (measured *in vacuo*). The $\log_{10}\sigma - 1/T$ plot for this compound showed a kink at 770° K, indicating that two processes contributed to the observed conduction; these may have been caused by two bulk impurity levels in the crystal grains, or by a bulk and a surface level. Measurements of the Debye-Scherrer photograph of barium nickelite are given, as are the results of some subsidiary experiments carried out to determine some of its physical properties.

Barium nickelite was also formed when NiO was present in considerable excess in the original composition, but not when the pellet contained a large excess of $BaCO_3$; when equimolecular mixtures of $SrCO_3$ and NiO were fired under similar conditions, there was no reaction between the resulting SrO and NiO; and when the equimolecular mixed $BaCO_3$—$SrCO_3$ was used, only BaO formed a compound with NiO.

An examination has been made of the electrical conductivity of selected compositions of the barium and/or strontium oxide - nickel oxide systems, including the pure components, in the form of compressed powders. The results have been correlated with data obtained by X-ray diffraction.

The electrical conductivity of the alkaline earth oxides is of interest in the investigation of the mechanism of thermionic emission from oxide-coated cathodes, and consequently numerous studies of the conductivity of these oxides have been made.[1–13] Most of these were carried out on coatings of low density on a metal core; a ceramic base has recently been used by one investigator,[3] and for barium oxide there are some data on compressed powders.[9–13] The electrical conductivity of nickel oxide has been extensively examined by measurements carried out in a liberal supply of oxygen.[14, 15]

Our interest in the simple oxides was primarily confined to obtaining reference data regarding their behaviour *in vacuo* in the form of compressed powders, which would assist in the interpretation of the results obtained with the barium and/or strontium oxide nickel oxide mixtures.

Experimental

Preparation of Samples.—The starting materials were barium carbonate (total impurities less than 0·04 %), and strontium carbonate, precipitated with ammonium carbonate from a solution of $Sr(NO_3)_2$ (impurities: 0·6 % Ba, 0·6 % Si, and only spectroscopic traces of other metals). Barium strontium carbonate, containing 40·55 mole % $BaCO_3$, was co-precipitated with Na_2CO_3 from a solution of the nitrates. In certain cases equimolecular mechanical mixtures of the separate carbonates were used. (Impurities are proportional to those for the separate carbonates). Nickel oxide was supplied in two batches, one by the Mond Nickel Co. with the analysis: Ni 77·14 %, Co 0·55 %, Cu 0·09 %, Fe 0·22 %, SiO_2 0·33 %, S 0·35-0·5 % and the other containing Ni 76·1 %, Co 0·7 %, Al 0·1 %, Ba 0·5%, Ca 0·2 %, Mg 0·1 %, Fe 0·1 %, Si 0·1 %.

Impurities in nickel metal shown by spectrographic analysis were a trace of Si and small traces of Fe, Mn and Mg.

---

[1] Friedenstein, Martin and Munday, *Reports Prog. Physics*, 1946-47, **11**, 298.

[2] Wright, *Proc. Roy. Soc. A*, 1947, **190**, 394.

[3] Eisenstein, *Advances in Electronics* (Academic Press Inc., New York, 1948), p. 1; *J. Appl. Physics*, 1949, **20**, 776.

[4] Loosjes and Vink, *Philips Res. Reports*, 1949, **4**, 449.

[5] Nishibori and Kawamura, *Proc. Phys.-Math. Soc., Japan*, 1940, **22**, 378.

[6] Danforth and Goldwater, *J. Appl. Physics*, 1949, **20**, 163.

[7] Mahlman, *ibid.*, 1949, **20**, 197.

[8] Hannay, MacNair, and White, *ibid.*, 1949, **20**, 669.

[9] Blewett, *ibid.*, 1939, **10**, 668.

[10] Horton, *Phil. Mag.*, 1906, **11**, 505.

[11] Spanner, *Ann. Physik*, 1924, **75**, 609.

[12] Albricht, *Physica*, 1931, **11**, 146.

[13] Meyer and Schmidt, *Z. tech. Physik*, 1932, **13**, 137.

[14] v. Baumbach and Wagner, *Z. physik. Chem. B*, 1934, **24**, 59.

[15] Andrews and Wright, *Proc. Physic. Soc. A*, 1949, **62**, 446.

The materials, either singly or mixed in the desired proportions were milled with a small quantity of nitrocellulose binder in a steel mill, passed through a 60 mesh sieve, and pressed at 2000 lb./in.^{2} into pellets 1 cm. long and 1 cm. in diameter. With pure NiO, no binder was used. The pellets were fired *in vacuo* until the carbonates were completely decomposed ; the firing temperatures varied for the different substances and are given for each pellet together with the results of the conductivity and X-ray studies. A few experiments were also made with compositions fired in air. The dimensions of the individual pellets were measured after sintering and the pellets were all sealed off for storage in the atmosphere in which they were fired, i.e. generally *in vacuo*. The density of a BaO pellet thus produced was 4·5 g./cm.^{3} compared with 5·7 g./cm.^{3} for solid BaO.

Conductivity Measurements.—The ends of the pellets were coated with rhodium by sputtering under controlled conditions in argon. The coated pellet (B, Fig. 1) was placed between spring-loaded platinum electrodes AA, an arrangement found to give efficient contact. 50 μ diam. Pt/Pt—Rh thermocouple wires GG were welded to one electrode and were sufficiently long to ensure that the junctions could be maintained effectively at room temperature. The assembly was placed in a small tubular platinum-wound furnace F about 2·5 cm. diam. and 10 cm. long, mounted in a large cylindrical hard glass envelope the central portion of which was cooled by an air blast. All external electrical connections were made through tungsten-glass seals. Both the pellet-electrode and furnace assemblies were demountable through Picein seals SS effectively at room temperature. For measurements *in vacuo* the system was continuously pumped, through a liquid-air trap, by a mercury diffusion pump backed by a rotary oil pump, and a vacuum better than 10^{-6} mm. Hg could be maintained after the furnace, apparatus and pellet had been thoroughly degassed. In evaluating temperatures allowance was made for the resistance of the thermocouple. The temperature variation along the pellet was less than 20 deg. at a corrected thermocouple reading of 1000° C.

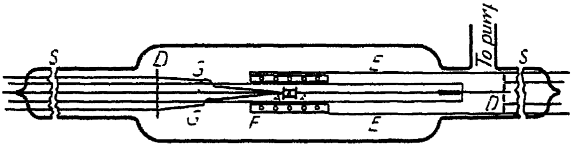

FIG. 1.—Diagram of apparatus for conductivity measurements *in vacuo*. AA, Pt electrodes ; B, pellet ; C, current leads ; DD, mica spacers ; EE, furnace leads; F, furnace ; GG, thermocouple wires ; SS, Picein seals.

Measurements on pellets of different length established that with the arrangement described contact resistances were negligible compared to the high pellet resistances. Hence, conductivity measurements were made with the simple D.C. circuit illustrated in Fig. 2, instead of by the method in which the potential difference between two points along the pellet is measured by probes carrying no current. Although on theoretical grounds the latter method is to be preferred, the use of potential probes is experimentally difficult and may introduce its own sources of error. Duplicate measurements were made at each temperature, the polarity being reversed between readings ; the constancy with time, reversibility with change of polarity, and reproducibility of the measurements showed that errors due to polarization introduced by the simplification in method were also quite negligible.

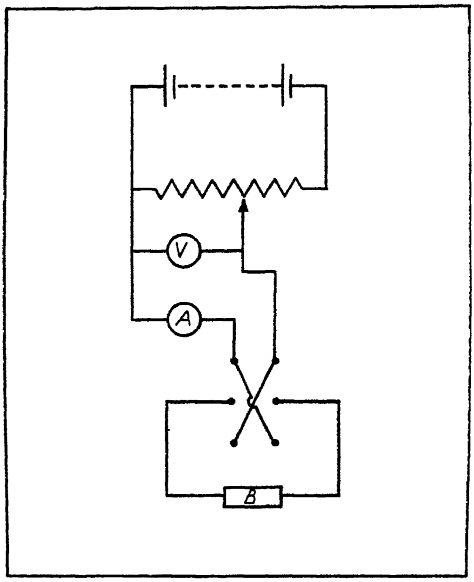

FIG. 2.—Circuit for conductivity measurements. B is the pellet.

With all pellets containing before firing less than 50 mole % NiO (including the pure alkaline earth oxides) some saturation of the current occurred at constant temperature as the applied voltage was increased from 2 to 100 V, as typified by the curve for a barium oxide pellet at two different temperatures in Fig. 3. This effect was quite independent of the electrode contacts. It was thus necessary to specify the measuring conditions in those cases and readings were taken at 100 V applied across the pellet 1 cm. long. In the other cases a more ohmic behaviour was observed, as shown in Fig. 3, for a pellet containing before firing 50 mole % NiO and 50 mole % $BaCO_3$ and the voltage applied across the pellet was varied between 2 and 100 V.

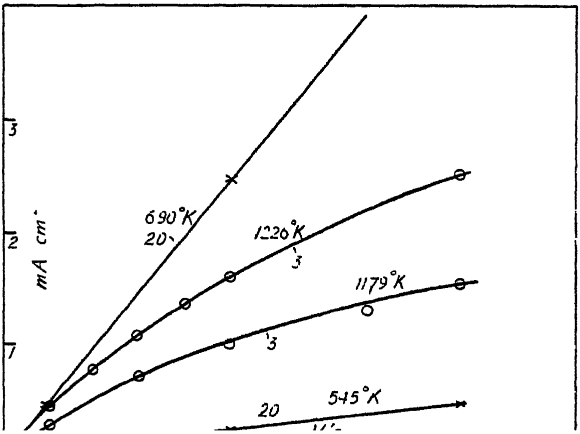

FIG. 3.—Examples of variation of conduction current with applied voltage at constant temperature: BaO, pellet No. 3; $BaNiO_2$, pellet No. 20.

After assembly in the measuring apparatus the pellet was heated up to the temperature at which it had previously been fired, and for experiments *in vacuo* was kept there for about 10 min. after gas evolution had ceased (total time, 15 to 60 min.). Measurements were then made both at decreasing and at increasing temperatures over the ranges indicated, allowing about 10 min. for reaching equilibrium at each temperature; unless otherwise stated, the results in both cases were reproducible. There was negligible variation in the conductivity values with time provided the pellets remained *in vacuo*.

X-Ray Diffraction Analysis.—The detection of reaction products in the system NiO—BaO was rendered difficult in the initial stages of this work on account of the fact that any free barium oxide admixed with them tended to react with water and carbon dioxide of the atmosphere. The structures of the hydrates, of which several are known, are quite complex, are of low symmetry and give powder diffraction patterns with a large number of lines. Barium carbonate too, gives quite a complicated pattern and although both carbonate and the hydrates can be identified fairly readily, their presence tends to mask that of other compounds for which a search was being made. It was considered desirable, therefore, to protect the sample from contact with the atmosphere during X-ray examination. To do this, the best procedure was found to be as follows. The pellets were ground in an agate mortar in an atmosphere of dry nitrogen; thin-walled tubes of cellulose nitrate of about 1 mm. ext. diam. specially made for the purpose and kept in a dry atmosphere were then filled with the powder and the ends sealed off with paraffin wax. Under these conditions, barium oxide was maintained for several hours before any hydrate could be detected in it. The samples were mounted in a Debye-Scherrer circular camera 11·46 cm. diam. and irradiated with X-rays from a copper target filtered through 19μ nickel. Lattice parameter measurements were made to an accuracy of ± 0·001 Å where these were considered vital to the work in hand.

Results

Conductivity.—The specific conductivity σ (ohm^{-1} cm.$^{-1}$) obtained from the measurements obeys the general relation

$$\sigma = A_1 \exp [- E_1/kT] + A_2 \exp [- E_2/kT], \quad . \quad . \quad . \quad (1)$$

where the A and E values are constants, T is the temperature in °K and k is Boltzmann's constant. At a temperature T_0, the contributions to the specific conductivity made by the two terms in eqn. (1) are equal, but at temperatures $T' \gg T_0$ and $T'' \ll T_0$, the specific conductivity is completely determined by one of the terms so that

$$\sigma' = A_1 \exp [- E_1/kT'] \text{ when } T' \gg T_0, \quad . \quad . \quad . \quad (2a)$$

$$\sigma'' = A_2 \exp [- E_2/kT''] \text{ when } T'' \ll T_0 \quad . \quad . \quad . \quad (2b)$$

$\text{Log}_{10}\, \sigma$ was plotted against $1/T$ for each pellet. In some cases a single straight line was obtained, showing that eqn. (2*a*) or (2*b*) was applicable over the temperature range used; for these pellets E and $\log_{10} A$ values were determined from all the experimental data, and they are summarized in Table I together with the relevant information about the individual pellets. In other cases, a curve was obtained which became linear at either end when the distance from $1/T_0$ on the $1/T$ scale became appreciable. For these pellets T_0 was determined graphically by finding the point of intersection of the two straight lines, as illustrated for pellet No. 20 in Fig. 6 by the dotted lines. The E and $\log_{10} A$ values in eqn. (2) which are summarized for these pellets in Table I were determined from straight line plots drawn through the points

$$[1/T_0, \log_{10} (\sigma_0/2)] ; \ [1/T', \log_{10} \sigma']$$

and $$[1/T_0, \log_{10} (\sigma_0/2)] ; \ [1/T'', \log_{10} \sigma''],$$

where $$1/T_0 - 1/T' > 4 \times 10^{-4} < 1/T'' - 1/T_0 ;$$

these lines are shown in Fig. 6 by alternate strokes and dots.

The reproducibility of the conductivity measurements at decreasing and increasing temperatures is illustrated for a pellet of barium oxide in Fig. 4. The reproducibility for different pellets of the same composition is shown by the duplicate and triplicate results in Table I and is demonstrated in Fig. 4 by the two sets of points for strontium oxide. For the alkaline earth oxides alone, one straight line was always obtained for the $\log_{10} \sigma$ against $1/T$ plot, as shown

TABLE I.—SUMMARY OF CONSTANTS IN EQN. (2) FOR VARIOUS COMPOSITIONS OVER THE SPECIFIED TEMPERATURE RANGES. MEASUREMENTS *in vacuo* UNLESS OTHERWISE STATED

No. of Pellet	Original Composition mole %	Firing Conditions	Final Composition	Temp. Range (°K)	E (eV)	Log$_{10}$ A (A in ohm^{-1} cm.$^{-1}$)
1	$BaCO_3$, 100	Vacuum 1000° C	BaO	1000-1280	1·86	3·23
2	,,	,,	,,	,,	2·08	3·45
3	,,	,,	,,	,,	1·85	2·82
4	$SrCO_3$, 100	Vacuum, 1120° C	SrO	1200-1400	2·01	2·46
5	,,	,,	,,	,,	1·87	2·00
6	$BaCO_3$, 50 $SrCO_3$, 50 Carbonates mech. mixed)	Vacuum, 1000° C				
7			BaO—SrO ,,	820-1160 ,,	0·91 1·01	$\bar{1}$·38 $\bar{1}$·96
8	$BaCO_3$, 40·5 $SrCO_3$, 59·5 (Carbonates co-pptd.)	,,	,,	820-1160	0·97	$\bar{1}$·40
9	NiO, 100	Air, 1000° C (Meas. in air)	NiO	500-730	0·96	3·21
10	,,	,,	,,	500-830	0·90	3·80
11	,,	Vacuum 1000° C	NiO+a little Ni	850-1250	1·32	$\bar{1}$·98
12	,,	,,	,,	,,	1·31	0·00
13	,,	,,	,,	,,	1·24	0·00
14	,,	,,	,,	930-1280	1·66	2·93
15	,,	,,	,,	1060-1230	1·82	3·58
16	NiO, 80 $BaCO_3$, 20	Vacuum 960° C	NiO+ $BaNiO_2$ + a little Ni	770-1250 470-770	1·05 0·39	3·04 $\bar{2}$·74
17	,,	,,	,,	750-1250 470-750	0·98 0·29	2·46 $\bar{3}$·85
18	NiO, 80 $BaCO_3$, 10 $SrCO_3$, 10	,,	NiO+$BaNiO_2$ +BaO—SrO + a little Ni	800-1250 510-800	1·10 0·37	2·86 $\bar{2}$·30
19	,,	,,	,,	740-1250 450-740	0·83 0·46	1·43 $\bar{2}$·93
20	NiO, 50 $BaCO_3$, 50	,,	$BaNiO_2$	810-1250 450-810	0·94 0·38	1·71 $\bar{2}$·11
21	,,	,,	,,	820-1250 450-820	0·93 0·39	1·67 $\bar{2}$·34
22	,,	,,	,,	700-1100 450-700	0·88 0·45	1·89 $\bar{2}$·76
23	NiO, 20 $BaCO_3$, 80	Vacuum 1000° C	NiO+BaO	850-1100	1·09	0·57
24	NiO, 20 $BaCO_3$, 40 $SrCO_3$, 40	,,	NiO+BaO—SrO	850-1100	1·04	0·00

by the examples in Fig. 4 for the pure and the equimolar mixed oxides. The non-ohmic current-voltage characteristics of these oxides have already been referred to.

The pellets of air-fired nickel oxide were taken from the second batch of material and gave straight line plots of $\log_{10} \sigma$-$1/T$ over the whole temperature range examined, as illustrated for pellet No. 10 in Fig. 5. Firing *in vacuo* gave pellets of lower conductivity; the highest values were obtained on pellets 11-13 which were taken from the same batch of material and were fired simultaneously for the same length of time; the lowest conductivity was observed

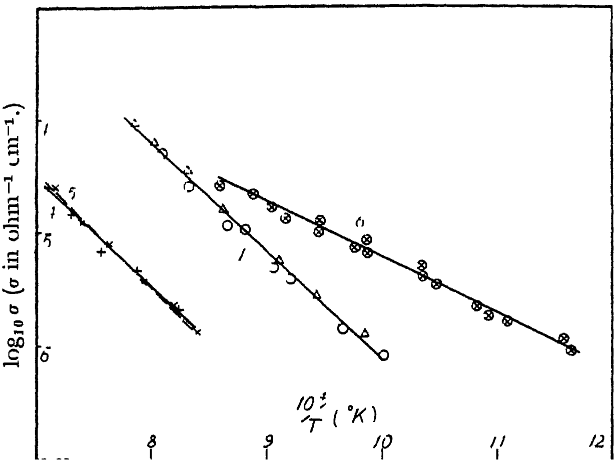

FIG. 4.—Variation of $\log_{10} \sigma$ with $1/T$ for pellet numbers 1, BaO ; 4 and 5, SrO ; 6, equimolar BaO—SrO. For pellet 1, O denotes measurements made at decreasing temperatures, Δ denotes measurements made at increasing temperatures. Measurements made *in vacuo* on vacuum-fired pellets.

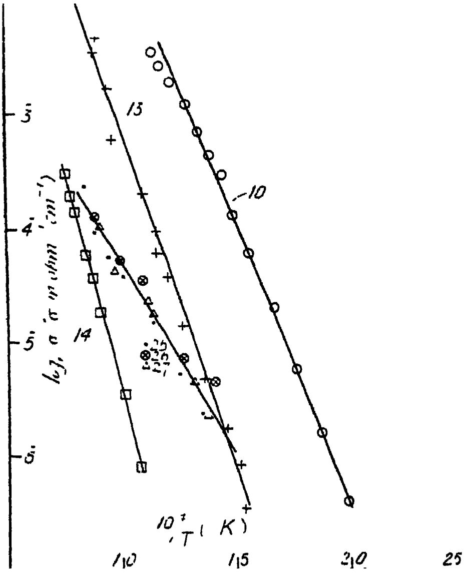

FIG. 5.—Variation of $\log_{10} \sigma$ with $1/T$ for pellet numbers:
10, NiO (air-fired, measured in air).
13, NiO (fired and measured *in vacuo*, batch 2).
14, NiO (fired and measured *in vacuo*, batch 1).
25, NiO (not pre-fired, measured *in vacuo* at increasing temperatures only).
26, NiO 95 mole % ; Ni 5 mole % (not pre-fired, measured as 25).
27, NiO 90 mole % ; Ni 10 mole % (not pre-fired, measured as 25).

with pellets 14-15 pressed from the higher purity material, which was used in the work on mixtures. X-ray examination of the powders after vacuum firing showed the presence of some metallic nickel (maximum concentration about 5 %). This, however, had a negligible effect on the conductivity of the pellets, as illustrated in Fig. 5 for pellets 25-27, containing respectively 0, 5 and 10 mole % of metallic nickel (of similar aggregate size) added to the nickel oxide powder. These pellets were not pre-fired, and measurements were made *in vacuo* at increasing temperatures only.

Pellets containing before firing 50 or more mole % NiO together with $BaCO_3$ or $BaCO_3$—$SrCO_3$ gave the type of $\log_{10} \sigma$-$1/T$ curve shown in Fig. 6. These pellets showed a remarkable resemblance which pointed to the presence of a common constituent responsible for the comparatively high conduction at low temperatures.

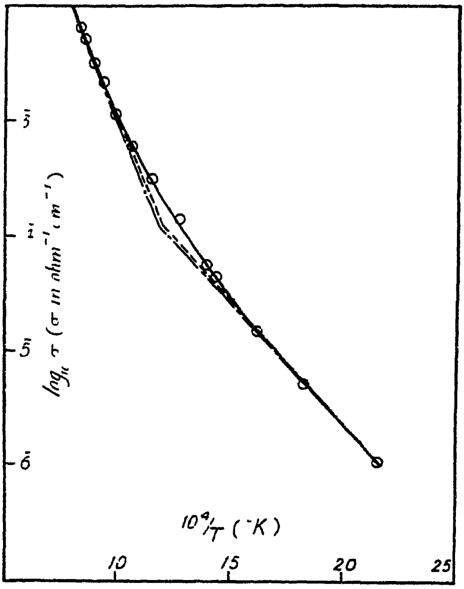

FIG. 6.—Variation of $\log_{10} \sigma$ with $1/T$ for pellet No. 20, $BaNiO_2$ (fired and measured *in vacuo*).

———————— drawn through experimental points.
. . . . extrapolation of straight lines at $T' \gg T_0$ and $T'' \ll T_0$.
—.—.—.—.— straight lines drawn through $[1/T_0, \log_{10} (\sigma_0/2)]$, $[1/T', \log_{10} \sigma']$ and $[1/T_0, \log_{10} (\sigma_0/2)]$, $[1/T'', \log_{10} \sigma'']$.

Structural and Other Data.—Barium and strontium oxides are known to form a complete series of mixed crystals with linearly varying lattice parameters.[1, 3, 9] Those determined for reference samples of BaO, SrO, and BaO—SrO containing 47 mole % BaO were 5·541, 5·157 and 5·339 ± 0·002 Å respectively, in fair agreement with the values of Huber and Wagener;[16] for nickel oxide we have obtained a value of 4·183 Å which compares with the value of 4·183 Å reported by Levi and Taccini.[17]

In pellets containing prior to vacuum firing 20 mole % $BaCO_3$ (similar to No. 16 and 17, Table I) or 10 mole % $BaCO_3$ and 10 mole % $SrCO_3$ (similar to 18 and 19 in Table I) nickel oxide, a little nickel, and a new compound A were detected, but no barium oxide, carbonate, or hydroxide; a barium strontium oxide with lattice parameter corresponding to (75 ± 5) mole % SrO was also detected in the pellets similar to No. 18 and 19. The approximate proportions of the various constituents indicated by the relative line intensities suggested the compound A was $BaNiO_2$. This was confirmed by examination of pellets prepared by firing equimolar mixtures of $BaCO_3$ and NiO *in vacuo* at 960° C for a sufficient time, when only compound A was detectable. The measurements

---

[16] Huber and Wagener, *Z. tech. Physik*, 1942, **23**, 1.
[17] Levi and Taccini, *Gazz. chim. ital.*, 1925, **55**, 28.

TABLE II.—MEASUREMENTS ON THE DEBYE-SCHERRER PHOTOGRAPH OF BARIUM NICKELITE

(θ = Bragg angle ; d = interplanar spacing ;

Wavelength $\lambda\begin{cases} K\alpha = 1{\cdot}5418\,; \\ K\alpha_1 = 1{\cdot}54050\,; \\ K\alpha_2 = 1{\cdot}54434\,; \end{cases}$

I/I_1 = relative intensity of lines, taking the strongest line as 1·0)

Line	I/I_1	θ	d(Å)
1	0·9	13·03	3·417
2	0·2	13·35	3·337
3	0·2	14·67	3·042
4	0·5	15·64	2·860
5	1·0	16·60	2·699
6	0·02	17·69	2·536
7	0·05	18·86	2·385
8	0·05	19·56	2·303
9	0·9	20·77	2·174
10	0·8	20·97	2·154
11	0·3	21·82	2·074
12	0·2	22·22	2·038
13	0·2	25·58	1·790
14	0·3	25·88	1·766
15	0·5	26·38	1·734
16	0·5	26·78	1·710
17	0·1	27·29	1·681
18	0·7	27·73	1·656
19	0·7	27·85	1·650
20	0·7	28·30	1·626
21	0·2	30·15	1·534
22	0·5	30·73	1·508
23	0·7	31·55	1·473
24	0·8	32·47	1·436
25	0·5	34·75	1·352
26	0·5	35·30	1·334
27	0·4	35·76	1·319
28	0·6	36·86	1·285
29	0·07	39·43	1·213
30	0·5	40·40	1·189
31	0·7	40·90	1·177
32	0·6	42·95	1·131
33	0·03	44·40	1·101
34	0·4	44·90	1·092
35	0·4	45·25	1·085
36	0·3	45·75	1·076
37	0·08	46·50	1·063
38	0·1	47·85	1·040
39	0·25	48·45	1·030
40	0·3	49·30	1·017
41	0·2	49·95	1·007
42	0·3	51·46	0·9856
43	0·05	52·89	0·9665
44	0·2	55·52	0·9352
45	0·05	55·86	0·9313
46	0·05	56·45	0·9249
47	0·6	57·14	0·9178
48	0·1	58·84	0·9008
49	0·3	59·53	0·8943
50	0·5	60·29	0·8875
51	0·2	61·07	0·8808
52	0·1	63·90	0·8584
53	0·2	65·00	0·8505
54	0·1	66·42	0·8411

TABLE II.—(*Cont.*)

Line	I/I_1	θ	d(Å)
55	0·5	68·45	0·8288
56	0·5	69·77	0·8215
57	0·6	71·55	0·8125
58	0·5 α_1	72·80	0·80631
59	0·25 α_2	73·06	0·80726
60	0·4 α_1	74·95	0·79762
61	0·2 α_2	75·23	0·79857
62	0·4 α_1	76·52	0·79208
63	0·2 α_2	77·10	0·79219
64	0·2 α_1	79·55	0·78326
65	0·1 α_2	80·45	0·78306
66	0·1 α_1	84·60	0·77376
67	0·05 α_2	85·65	0·77346

made on the powder photograph of A are given in Table II. A section of the X-ray diffraction pattern is reproduced schematically in Fig. 7.

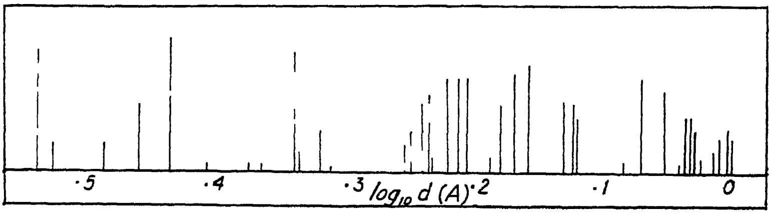

FIG. 7.—Schematic representation of a section of the Debye-Scherrer diffraction pattern of barium nickelite.

Firing the equimolecular mixture of $BaCO_3$ and NiO *in vacuo* at higher temperatures or for periods short of complete decomposition of the carbonate, sometimes produced another compound B mixed either with undecomposed barium carbonate or with A and always accompanied by the presence of free nickel. This compound was never obtained pure and was not further investigated; for conductivity work, conditions were always adjusted so that only compound A was obtained.

Compound A, barium nickelite, has also been prepared by firing equimolecular mixtures of barium peroxide and metallic nickel in air at 1000° C. Barium nickelite is stable in air over considerable periods; only slight decomposition was noticed after exposure to air for six weeks. Its approximate melting point *in vacuo* is 1330° K.

Subsidiary experiments were carried out to examine the thermionic emission properties of barium nickelite. If coated to a thickness of 30 μ on to a nickel core, this compound gave very low emission; the small currents observed may have been due to traces of barium oxide. After prolonged running (several days) at 1100° K under the application of an electric field, the current rose and subsequent examination showed that the coating consisted largely of barium oxide and metallic nickel.

When $BaCO_3$ or $BaCO_3$—$SrCO_3$ was present in considerable excess in the original composition, no reaction between the resulting BaO and NiO took place on firing *in vacuo* (i.e. pellets 23 and 24, Table I); nor was any evidence obtained for the formation of a Sr—Ni—O compound by firing $SrCO_3$ and NiO *in vacuo* at temperatures below 1100° C.

Discussion

COMPARISON WITH PREVIOUS RESULTS.—Of the earlier conductivity measurements on barium oxide, those of Horton [10] and Spanner [11] were made in air and probably apply to material not free from hydroxide or carbonate, and those of Albricht[12] at a single temperature do not give an E value. Meyer and Schmidt,[13] who made measurements on pellets pressed between nickel electrodes *in vacuo* using high-frequency A.C. to prevent electrolytic decomposition, obtained a break in the $\log_{10} \sigma$ against $1/T$ plot for "unactivated" barium oxide, finding an E value of 3·8 eV over the temperature range 1080-1180° K and an E value of 1·1 eV between 1180 and 1400° K. Our results are more closely in agreement with those of Blewett[9] from whose straight line plots of $\log_{10}\sigma$ against $1/T$ for pellets *in vacuo* the constants $E = 2$ eV, $\log_{10} A = 3{\cdot}7$ can be derived, but who does not state whether his pellets showed ohmic conduction or at what value of the potential gradient his measurements were made.

To our knowledge there are no published data on bulk samples (e.g. pellets) of strontium oxide or barium strontium oxide mixed crystals, or on barium oxide + nickel oxide mixtures. Results obtained on thin layers of strontium oxide[5] or barium strontium oxide[1, 3, 4-8] coated on to metal cores are not strictly comparable to those obtained on pellets; there are uncertainties regarding the effect of the reducing properties of the core metal in producing an excess of the metal constituent in the coating, regarding the influence of the probes used for measurement and the core-coating and probe-coating interfacial resistances, and the effect of the low density found with these coatings. The E value, 1·74 eV, found for strontium oxide[7] from such measurements, is, however, only slightly below those given in Table I. For barium strontium oxide solid solutions a wide range of E values, from 0·5-3·0 eV, has been given even when coated on to a ceramic core;[3] similar variations were found by Vink[4] using two coated surfaces pressed into contact to avoid the uncertainties present with probes. The investigations of Vink[4] and Eisenstein[3] gave evidence for breaks in the $\log_{10} \sigma - 1/T$ plots; in Vink's work these breaks occurred near the limits of the temperature range over which our measurements were carried out, and corresponding deviations from the straight line plot in our work might not have been noticed.

Our E and $\log_{10} A$ values for nickel oxide in air are in good agreement with those calculated from the data of v. Baumbach and Wagner[14] on two pellets, i.e. $E = 1{\cdot}07$ and 0·88 eV, $\log_{10} A = 3{\cdot}95$ and 3·00. Recently Wright and Andrews[15] have found a break in the $\log_{10} \sigma$ against $1/T$ plot for nickel oxide at temperatures between 560 and 650° K. Straight line plots were obtained both above and below this region giving E values of about 1·0 and 0·3 eV respectively, the former in agreement with v. Baumbach and Wagner. Our measurements extended down to 500° K and did not give any evidence for a similar break in the $\log_{10} \sigma - 1/T$ plot.

THEORETICAL CONSIDERATIONS.—The modern conception of the bulk conductivity of semi-conductors[18, 19] recognizes two types of impurity centres which may be responsible for the observed conduction; for polar compounds these are caused by an excess or a defect of the metal ion constituent over the stoichiometric composition. The alkaline earth oxides are generally assumed to be excess semi-conductors, although there is only indirect evidence for this statement;[3,*] nickel oxide absorbs excess oxygen when heated in air and behaves like a defect semiconductor.[15, 20]

---

[18] Fowler, *Statistical Mechanics* (Cambridge University Press, 1936), 2nd Ed., p. 397.

[19] Mott and Gurney, *Electronic Processes in Ionic Crystals* (Clarendon Press, Oxford, 1948), 2nd Ed., Chap. V.

[20] De Boer and Verwey, *Proc. Physic. Soc.*, 1937, **49**, 59.

[*] Recently, a preliminary communication has appeared by Wright (*Nature*, 1949, **164**, 714) to the effect that barium strontium oxide undergoes a P—N transition at 850° K.

The theory leads to an equation for the conductivity of the form

$$\sigma = Bln_i^{\frac{1}{2}} \exp -[\Delta E_i/2kT], \quad . \quad . \quad . \quad (3a)$$

where l is the mean free path of the free electrons (or positive holes) of concentration n_i, ΔE_i is the energy gap between the bottom of the conduction band (or the top of the full band) and the impurity level, and, provided certain simplifying assumptions hold, B is a constant. Comparing with the empirical equation (2)

$$\left.\begin{aligned} A &\equiv Bln_i^{\frac{1}{2}} \\ E &\equiv \Delta E_i/2 \end{aligned}\right\} \quad . \quad . \quad . \quad . \quad (3b)$$

In addition to bulk conduction, crystals may exhibit surface conduction of lower activation energy; this process arises from the presence of surface levels such as first described by Tamm [21] and recently by Bardeen.[22]

When applying the conductivity equations to our experimental data, it is useful to estimate whether each substance had come into equilibrium with the surrounding atmosphere at the temperatures at which measurements were made. In this respect Bevan, Shelton and Anderson [23] recognize three temperature ranges; one, above $0{\cdot}5T_m$ (where T_m is the melting point in °K), where bulk diffusion of lattice defects is sufficiently fast for true equilibrium to be established; a second range from $0{\cdot}3$-$0{\cdot}5\ T_m$ where only the surfaces of the crystal grains come into equilibrium with the surrounding atmosphere; and a range below $0{\cdot}3\ T_m$ where no reaction with the surrounding medium occurs. To facilitate discussion, the firing temperatures and the temperature ranges over which certain E values apply are given in Table III as a fraction of the melting point of the corresponding oxide in °K. The melting points of barium strontium oxide mixed crystals have not been measured, and the data on the equimolar mixed oxide could, therefore, not be included in this Table.

TABLE III.—RELATION BETWEEN THE FIRING AND MEASURING TEMPERATURES AND THE MELTING POINTS OF THE SUBSTANCES IN °K.

Compound	M.p.	Firing temp./m.p.	Atmosphere	Measuring temp./m.p.	E (eV)
BaO	2196[24]	0·58	Vacuum	0·45-0·58	1·85-2·08
SrO	2703[25]	0·52	,,	0·44-0·52	1·87-2·01
NiO	2263[26]	0·56	Air	0·22-0·36	0·90-0·96
NiO	2263[26]	0·56	Vacuum	0·38-0·56	1·24-1·82
$BaNiO_2$	1330	0·94	,,	0·58-0·94	0·88-0·94
				0·34-0·58	0·38-0·45

The E values observed for the alkaline earth oxides are sufficiently low to rule out the possibility of intrinsic conduction. On applying eqn. (3b) it becomes apparent that the number of impurity centres responsible for the observed conduction is much larger than could be accounted for by thermal dissociation. (The equilibrium pressure of oxygen above barium oxide in contact with the solid metal is 2×10^{-43} mm.[27]).

[21] Tamm. *Physik. Z. Sowjet.*, 1932, **1**, 733.
[22] Bardeen, *Physic. Rev.*, 1947, **71**, 717.
[23] Bevan, Shelton and Anderson, *J. Chem. Soc.*, 1948, 1729.
[24] *Int .Crit. Tables* (McGraw Hill Co., 1926), 1st Ed., **1**, 146.
[25] *Ibid.*, **1**, 147.
[26] v. Wartenberg and Reusch, *Z. anorg. Chem.*, 1932, **208**, 380.
[27] White, *J. Appl. Physics*, 1949, **20**, 856.

Reduction by carbon from the binder may have played a part in establishing the excess metal; electrolysis did not appear to be a factor, for at no time was any increase in conductivity noted on passing current. The straight line relation between $\log_{10} \sigma$ and $1/T$ indicated that the product of the concentration of the number of impurity centres and the mean free path of the electrons has remained constant during the period of measurement. Since *large* variations in the mean free path are unlikely, the concentration of impurity centres cannot have varied widely. The non-ohmic relation between current and voltage for these oxides, which has also been observed on oxide-coated cathodes, has led Loosjes and Vink [4] to put forward a mechanism involving conduction by an intergranular electron cloud, produced by thermionic emission from the grains.

The nickel oxide pellets were fired at 0·56 T_m, either in air or *in vacuo*. According to Bevan, Shelton and Anderson we should expect rapid diffusion of lattice defects and a response to the surrounding atmosphere at this temperature. This was borne out by the behaviour of pellets taken from the same batch of material, which was consistent with the concept of nickel oxide as a defect semi-conductor, giving lower E values and higher $\log_{10} A$ values for the air-fired compared to the vacuum-fired material. Pellets taken from the first batch of material were examined only *in vacuo*, and gave both higher E and higher $\log_{10} A$ values compared to the vacuum-fired pellets of the other batch, the overall result being a still lower conductivity over the temperature range investigated. Pellet 25 (Fig. 5) which was not pre-fired had a much higher conductivity at low temperatures than vacuum-fired pellets of the same batch of material (i.e. No. 14 and 15), but on heating to 0·5 T_m its conductivity was similar to that of the latter pellets and after subsequent cooling a $\log_{10}\sigma - 1/T$ plot similar to those for pellets 14 and 15 was obtained. It is also consistent with the concept of nickel oxide as a defect semi-conductor that the presence of small aggregates of metallic nickel, in a concentration much too low to form a continuous path, should not markedly affect the conductivity of the nickel oxide pellets; for only if another impurity level caused by excess nickel at some point in the nickel oxide lattice were created would any marked change in conductivity be expected.

Barium nickelite was heated to 0·94 T_m before conductivity measurements were made, and the lattice defects formed during firing should, therefore, have been uniformly distributed throughout the crystal grains. The $\log_{10}\sigma - 1/T$ plot obtained over the temperature range 0·34-0·94 T_m, illustrated by the example in Fig. 6, is evidence that two mechanisms are contributing to the observed conduction, one being predominant at high, the other at low temperatures. The mechanism previously suggested by Nijboer [28] to explain the occurrence of two straight lines is inapplicable here, since his conditions apply to the case where the ratio of the high temperature E value E_1 to the low temperature value E_2 is less than one; whereas the ratio derived from our data is greater than one. It is unlikely that the process predominant at high temperatures is intrinsic conduction, for the energy gap involved is too small for this mechanism; we may assume that the conduction is of the impurity type, being caused by a bulk level. The mechanism predominant at low temperatures must be caused by an impurity level, either in the bulk or on the surface of the crystal grains; the ratios of the E and A values for the high and low temperature conduction are in agreement with either explanation.

Regarding the possibility of two bulk impurity levels to account for the observed conduction, it should be noted that a similar suggestion for BaO—SrO was made by Eisenstein,[3] though without supporting evidence, namely that for each excess barium atom present two electrons should be available for excitation and that the first may require a lower activation energy than the second. However, the E and A values obtained for barium nickelite are in agreement with a postulation of two bulk impurity levels *only* if we consider the electrons which require a low activation energy to be excited from centres containing *two* electrons and those requiring a high activation energy from centres containing only *one* electron, and if there are always far more centres of the latter than of the first type. If such an explanation were correct, then the pre-firing temperature would be an important factor in determining the conductivity over any temperature range ; for it is during the pre-firing treatment that the relative abundance of the two types of centres would be fixed. The recent paper by Loosjes and Vink [4] gives evidence for this type of behaviour (i.e. a kink in the $\log_{10}\sigma - 1/T$ plot at 800° K in BaO—SrO on a nickel core, but the authors' explanation of the observed phenomenon is a different one. A mechanism similar to that proposed by Loosjes and Vink for barium strontium oxide cannot readily be applied to barium nickelite, since one would expect to be able to draw thermionic emission current from a cathode coated with a semi-conductor to which their theory applies.

---

[28] Nijboer, *Proc. Physic. Soc.*, 1939, 51, 575.

The failure of strontium oxide to form a nickelite under the same conditions as barium oxide can be understood if we consider the difference between the melting points of these oxides. It is well known that in many types of reaction between solids, the temperature at which measurable reaction starts is related to the absolute melting point of one of the reactants, and can in fact be represented by a common reduced temperature scale T/T_m. If we assume that the reaction between BaO and NiO begins at a measurable rate at 1200° K, the corresponding reaction between SrO and NiO would be expected to start at 1470° K which is 100° above the temperature to which the mixed oxides were heated.

We wish to thank Dr. J. A. M. van Moll and the Directors of Philips Electrical Ltd. for permission to publish this work.

Material Research Laboratory,
Philips Electrical Limited,
Mitcham Junction,
Surrey.

ACTIVITIES IN ALKALI OXIDE—SILICA MELTS

BY R. J. CALLOW

Received 1*st March,* 1950

The work of Preston and Turner on rates of volatilization of alkali oxides from binary silicate melts is the basis for a determination of the silica activities in such melts over a substantial part of the composition range.

The accuracy of the activity curves obtained is discussed. The bearing of the results on theories of the constitution of the melts is briefly indicated.

From a study of the phase diagrams, Rey [1] has made estimates of the silica activities in various binary silicate melts. These estimates suffer the uncertainties common to all such determinations from phase diagrams which extend over a wide temperature range. A more serious fault is that, due to the shape of the phase diagrams of binary silicate systems, it is not generally possible to determine activities except for molar fractions of SiO_2 close to unity. Although, as Bockris [2] has pointed out, thermodynamic properties do not give direct information on problems of structure, they act as an important check on structural theories derived from other data. It is therefore desirable to determine these properties as accurately as possible and over as wide a composition range as possible.

---

[1] Rey, *Faraday Soc. Discussions*, 1948, 4, 257.

[2] Bockris, *ibid.*, p. 321.

As Rey pointed out, in discussing his results, the most direct way of obtaining activities in liquids is from vapour pressure measurements. In an effort to obtain more accurate activities for the alkali oxide + silica systems, no comprehensive study of their vapour pressures could be found. The work of Preston and Turner [3] on rates of volatilization is, however, related to the vapour pressures and it has proved possible to use their results to calculate the activities reported in this paper.

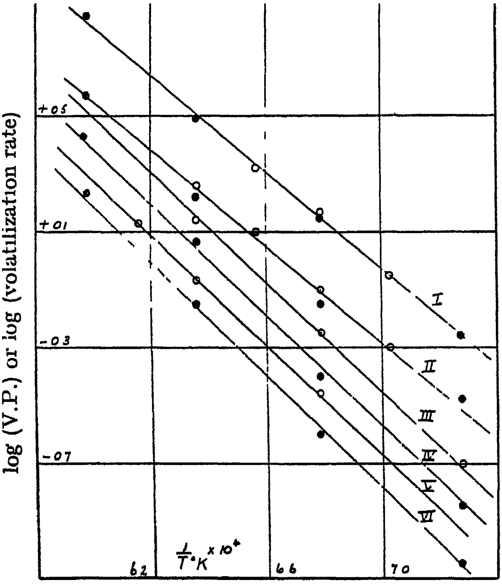

FIG. 1.—Temperature variation of vapour pressures and rates of volatilization in various alkali oxide + silica mixtures
● Rates of volatilization ; ○ Vapour pressures.

I. Vapour pressures and rates of volatilization of the mixture : SiO_2 0·61, K_2O 0·39.
II. Vapour pressures and rates of volatilization of the mixture : SiO_2 0·66, K_2O 0·34.
III. Vapour pressures of the mixture : SiO_2 0·52, Na_2O 0·48.
IV. Rates of volatilization of the mixture : SiO_2 0·52, Na_2O 0·48.
V. Vapour pressures of the mixture : SiO_2 0·56, Na_2O 0·44.
VI. Rates of volatilization of the mixture : SiO_2 0·56, Na_2O, 0·44.

The measurements made by Preston and Turner were of the weights lost by liquids of differing initial compositions when maintained at a constant temperature. By plotting the loss of weight as a function of time of heating, they were able to obtain initial rates of loss characteristic of the original composition. (More exactly, they obtained the average rate of loss over the first 20 hr. of heating. In those cases where the graph of loss of weight against time is markedly curved, it is necessary to re-plot their results and determine the slope at the origin. This has been done in the present calculations.) In a discussion of the experimental technique,[4] it was shown that the measured rate was affected by such factors as the shape of the containing crucible, the depth of liquid and the size of the furnace chamber. Nevertheless, in constant conditions, reproducible results were obtained. Thus, in any one series of experiments, the results for the different compositions would be comparable. The rates of volatilization will obviously be related to the vapour pressures of the solutions. The authors concluded that they were, in fact, directly proportional to the vapour pressures.[3, 5] To confirm this, they made several measurements of the vapour pressures of the more volatile liquids. Fig. 1 shows these results, together with the rates of volatilization for liquids of the same composition. It will be seen that the logarithms of the two quantities show the same temperature variation and that the proportionality between them is unaffected by changes in composition within the same system.

---

[3] Preston and Turner, *J. Soc. Glass Tech.*, (*a*) 1934, **18**, 143 (Li_2O—SiO_2) ; (*b*) 1932, **16**, 331 (Na_2O—SiO_2) ; (*c*) 1933, **17**, 122 (K_2O—SiO_2).

In the temperature range of Preston and Turner's work (1373° K to 1673° K), the vapour pressure of silica is negligible. The systems may be regarded as solutions of a volatile solute in an involatile solvent, so that an initial rate of volatilization is directly proportional to the vapour pressure of alkali oxide over the liquid, and, consequently, to the activity of alkali oxide in the liquid. The activity of silica may therefore be obtained by means of the Gibbs-Duhem equation, which, combined with the rectilinear relation between vapour pressure and rate of volatilization, leads to the expression,

$$\log\frac{a_1}{N_1} = -\int_0^{N_2}\frac{N_2}{N_1}\,d\left(\log\frac{r}{N_2}\right), \qquad . \quad . \quad . \quad (1)$$

where N_1 and N_2 are the molar fractions of silica and alkali oxide respectively, a_1 is the activity of silica and r is the rate of volatilization. The silica activity so obtained is referred to pure, supercooled liquid silica at the same temperature as that at which the rates of volatilization were determined. Fig. 2 to 4 show the experimental values of log r/N_2 plotted against N_2/N_1 for the systems $Li_2O—SiO_2$, $Na_2O—SiO_2$ and $K_2O—SiO_2$. It will be seen that all the systems give curves of the same type. There is nowhere any suggestion of an increase in log r/N_2 as N_2/N_1 tends to zero. However, the values of N_1 are not greater than 0·9, so that any increase in log r/N_2 at low values of N_2/N_1 would not be shown. As a preliminary step, we may ignore the possibility of such an increase and extrapolate the curves to $N_2 = 0$ as shown by the full lines of the figures. Graphical integration then yields values of a_1, within the composition ranges of the experimental results. These values are not recorded because, as will be shown below, they are not consistent with the phase diagrams for the appropriate systems.

To explain this inconsistency, it is necessary to consider the results obtained by the integration. The curves of N_2/N_1 against log r/N_2 are all nearly vertical for small values of the molar ratio. The area below any curve in this range is therefore negligible and, as the area measures log a_1/N_1, the latter will be nearly zero and a_1 will be almost equal to N_1. This ideal behaviour will continue until the curve begins to show a definite departure from the vertical. An examination of Fig. 2-4 shows that departures from ideality will become noticeable at a molar fraction of alkali oxide of about 0·75 in the system $LiO_2—SiO_2$, 0·85 in the system $Na_2—SiO_2$ and 0·95 in the system $K_2O—SiO_2$. According to the present calculations, therefore, the silica activity curves of all three systems should be ideal and so identical from $N_1 = 0$ to $N_1 = 0·95$. Beyond this point, the K_2O system will show deviations, while the other two systems will continue to be ideal down to $N_1 = 0·85$ when that containing Na_2O will

---

[4] Howes, Laithwaite, Preston and Turner, *J. Soc., Glass Tech.*, 1935, **19**, 104.

[5] Preston, *Trans. Faraday Soc.*, 1933, **29**, 1188.

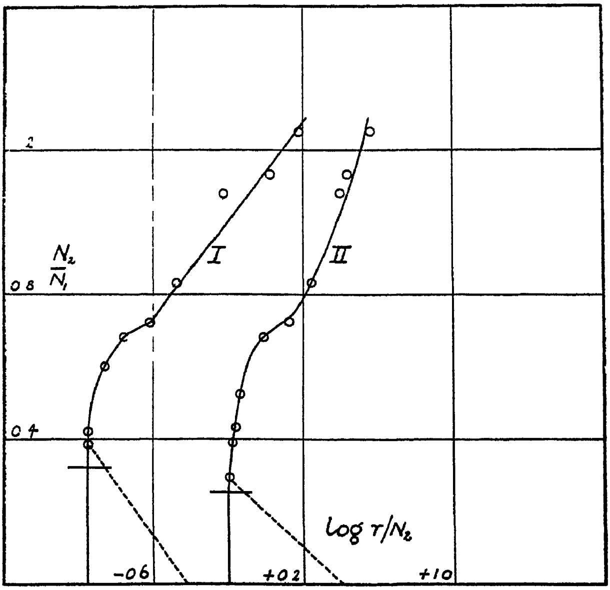

FIG. 2.—$\text{Log}_{10}\, r/N_2$ as a function of molar ratio at different temperatures.
Li_2O—SiO_2 I. 1573° K.
II. 1673° K.

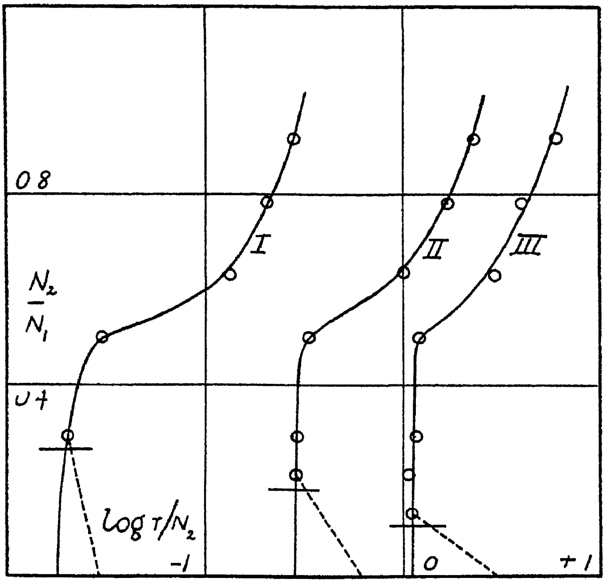

FIG. 3.—$\text{Log}_{10}\, r/N_2$ as a function of molar ratio at different temperatures.
Na_2O—SiO_2 I. 1373° K.
II. 1573° K.
III. 1673° K.

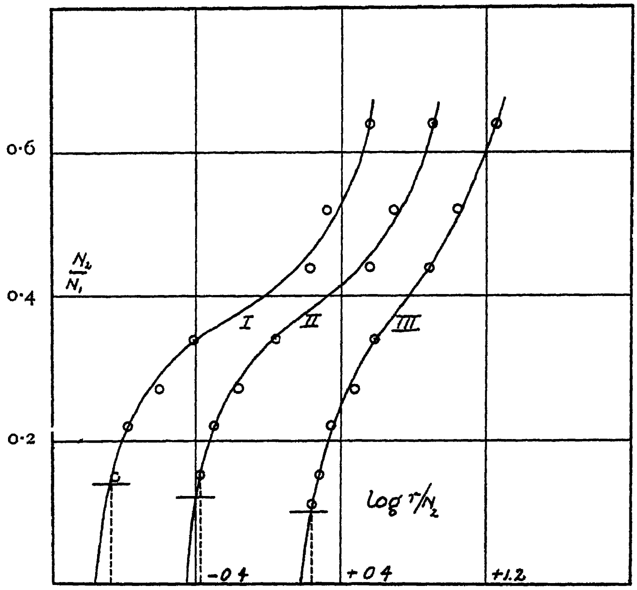

FIG. 4.—$\log_{10} r/N_2$ as a function of molar ratio at different temperatures.
K_2O—SiO_2 I. 1473° K.
II. 1573° K.
III. 1673° K.

begin to deviate. In these composition ranges, the phase diagrams show that, at its liquidus temperature, a solution is in equilibrium with solid silica. Below its melting point, the activity of solid silica is dependent only on the temperature while, if the solution is ideal, its silica activity is equal to its concentration of silica. The temperature at which the silica activity of a solution equals that of solid silica, i.e. the liquidus temperature, will thus depend only on the concentration of the solution. So long, then, as systems coincide in being ideal, they will coincide in liquidus temperatures. In other words, if the present silica activities are correct, the three systems should have identical phase diagrams in the composition range $N_1 = 1{\cdot}0$ to $N_1 = 0{\cdot}95$, while the systems Na_2O—SiO_2 and LiO_2—SiO_2 should further coincide down to $N_1 = 0{\cdot}85$. However, the phase diagrams obtained by Kracek[6] are not of this form.

This could be due to inaccuracies in the phase diagrams or in the results of Preston and Turner, to solid solubility of alkali oxide in silica, or to the data on rates of volatilization not extending to values of N_2 low enough to show up an increase in $\log r/N_2$ as N_2 tends to zero. The phase diagrams have been the subject of much careful work and are unlikely to be seriously in error. The work of Preston and Turner gives curves for $\log r/N_2$ which are mutually consistent, which show the departure from ideality to increase with fall in temperature and which give activity curves for the three systems in the order expected from the phase diagrams. In addition, minor changes in drawing the curves would have little effect on the activities obtained. We may therefore conclude that this work also is sufficiently accurate. To the author's knowledge, there is no evidence of solid solubility of alkali oxides in cristobalite. There is some information which suggests that both PbO and Na_2O dissolve in quartz,[7, 8] but the possibility remains that this is merely the formation of a surface layer of compound. Cristobalite and tridymite both occur as "stones" in glass, produced by devitrification. X-ray photographs of such stones show no signs of any dissolved material. As the stones are precipitated in conditions which would afford ample opportunity for solution, it appears unlikely that such solid solution does occur. The only remaining source of the discrepancy is that log r/N_2 increases as N_2/N_1 tends to zero, a fact which is obscured by the lack of experimental data for values of N_2/N_1 below about 0·1. (This is not the fault of the experimenters. The preparation and handling of such solutions is difficult and the rates of volatilization would have been too low to measure with any accuracy.) This conclusion is consonant with Kracek's opinion on the alkali oxide + silica systems. He considered that the $Rb_2O—SiO_2$ and $Cs_2O—SiO_2$ systems are ideal, at least in the region of very high silica. If this is so, the phase diagrams indicate that the remaining systems should all show initial positive deviations increasing from K_2O to Li_2O.

---

[6] Kracek, *J. Amer. Chem. Soc.*, 1930, **52**, 1436.
[7] Howarth, Maskill and Turner, *J. Soc. Glass Tech.*, 1933, **17**, 25.
[8] Preston and Turner, *ibid.*, 1941, **25**, 136.

Fortunately it is possible to estimate the correction due to this effect, if the heat of fusion of silica is known and if it can be assumed to vary only slowly with temperature. In this case, the activity of solid silica at a temperature T° K (referred to the supercooled liquid at the same temperature) is given by

$$\frac{\Delta G}{T} = - R \ln a_{\text{solid}} = \Delta H\left(\frac{1}{T} - \frac{1}{T_m}\right), \qquad . \quad . \quad (2)$$

where ΔG is the change in the Gibbs free energy on melting at a temperature T, ΔH is the heat of fusion (assumed independent of temperature) and T_m is the equilibrium melting temperature. T_m may be taken as 1986° K and ΔH as 1835 cal./mole (the value derived by Kracek assuming the systems $Rb_2O—SiO_2$ and $Cs_2O—SiO_2$ to be initially ideal). The activities of solid silica at different temperatures as derived from this equation are shown in Table I.

TABLE I.—ACTIVITIES OF SOLID SILICA AT DIFFERENT TEMPERATURES (REFERRED TO SUPER-COOLED LIQUID AT THE SAME TEMPERATURE)

Temp. °K	a_{solid}
1673	0·92
1573	0·89
1473	0·85
1373	0·81

In Table I, the effect of the transition from cristobalite to tridymite at 1743° K has been ignored, in view of the data of Mosesman and Pitzer.[9] These authors have shown that, in the temperature range 1743° K to 1373° K, the difference in heat content between cristobalite and tridymite is constant and equal to 50 cal./mole. From this it may be shown that the activity of cristobalite at 1573° K referred to tridymite at the same temperature is 1·000, the corresponding values for 1473° K and 1373° K being 1·005 and 1·008. Taking these values into account, the activities quoted for 1473° K and 1373° K would be reduced by 0·01. As these activities are derived by assuming that the heat of fusion of cristobalite is independent of temperature, the errors due to this assumption, at temperatures so far below the melting point, are probably greater than the correction.

From the phase diagrams, it is possible to determine the composition of the solution in a given system which is in equilibrium with solid silica at a particular temperature. In Table II this has been done for the temperatures of Table I.

---

[9] Mosesman and Pitzer, *J. Amer. Chem. Soc.*, 1941, 63, 2348.

TABLE II.—MOLAR FRACTIONS OF SiO_2 IN ALKALI OXIDE + SILICA SOLUTIONS WHICH ARE IN EQUILIBRIUM WITH SOLID SiO_2 AT THE TEMPERATURES SHOWN

Temp. °K	System		
	Li_2O–SiO_2	Na_2O–SiO_2	K_2O–SiO_2
1673	0·80	0·87	0·91
1573	0·76	0·84	0·89
1473	—	—	0·87
1373	—	0·79	—

The further procedure in estimating the corrections may be illustrated by the Li_2O—SiO_2 system at 1673° K. From Table II, it is seen that a solution of composition, $Li_2O = 0{\cdot}20$, $SiO_2 = 0{\cdot}80$, is in equilibrium with solid SiO_2 at 1673° K. At this temperature, Table I shows that the activity of the solid referred to the supercooled liquid at the same temperature, is 0·92. The activity coefficient of silica a_1/N_1 in the solution is therefore $0{\cdot}92/0{\cdot}80 = 1{\cdot}15$. The area under the curve of $\log r/N_2$ in the range $N_1 = 1{\cdot}0$ to $N_1 = 0{\cdot}80$, i.e. $N_2/N_1 = 0$ to $N_2/N_1 = 0{\cdot}25$ must, by eqn. (1), equal $-\log 1{\cdot}15$. The shape of the curve below the lowest experimental point at $N_2/N_1 = 0{\cdot}29$ is not known, but a comparison with other systems leads to the expectation that once $\log r/N_2$ begins to increase, it will do so continuously as N_2/N_1 tends to zero. In this case, the maximum area possible under the curve from $N_2/N_1 = 0$ to the lowest experimental point is given by a straight line drawn from this latter point of such a slope that the area beneath it from $N_2/N_1 = 0$ to $N_2/N_1 = 0{\cdot}25$ is equal to $-\log 1{\cdot}15$. In Fig. 2 the horizontal line drawn across curve II indicates the value of N_2/N_1 at which the activity is fixed by the phase diagram, i.e. 0·25, and the broken line is the completion of the curve by the method just described. The area beneath this broken line from $N_2/N_1 = 0$ to $N_2/N_1 = 0{\cdot}25$ is equal to $-\log 1{\cdot}15$. Whatever the shape of the actual curve, this area is known from the phase diagram. The course of the curve down to the lowest experimental value of $N_2/N_1 = 0{\cdot}29$ is also known. Between $N_2/N_1 = 0{\cdot}29$ and $N_2/N_1 = 0{\cdot}25$, $\log r/N_2$ may increase or it may follow the original extrapolation, only beginning to increase below $N_2/N_1 = 0{\cdot}25$. In the first case, the maximum area possible below the curve from $N_2/N_1 = 0$ to $N_2/N_1 = 0{\cdot}29$ is given by the area under the broken line; in the second case, the area beneath the curve between the same limits will be equal to $-\log 1{\cdot}15$ and this is the minimum value possible. The area beneath the broken line is found to correspond to $-\log 1{\cdot}21$. The area beneath the actual curve of $\log r/N_2$ from $N_2/N_1 = 0$ to $N_2/N_1 = 0{\cdot}29$ must therefore lie between $-\log 1{\cdot}15$ and $-\log 1{\cdot}21$. Previously, values of $\log a_1/N_1$ at any value of the molar ratio had been obtained by determining the area beneath the full line. These values may now be corrected, when N_2/N_1 is greater than 0·29, by subtracting the area beneath the full line from $N_2/N_1{=}0$ to $N_2/N_1{=}0{\cdot}29$ (which is, in this case, negligible) and adding an area between $-\log 1{\cdot}15$ and $-\log 1{\cdot}21$. This is equivalent to multiplying the activity values by a number between 1·15 and 1·21. The activity of silica in Li_2O—SiO_2 mixtures at 1673° K, referred to pure, supercooled liquid silica at the same temperature, in the composition range from $N_2/N_1 = 0{\cdot}29$ to $N_2/N_1{=}1{\cdot}22$ (beyond which there are no further experimental data on rates of volatilization) can therefore be obtained by determining the area under the full line of curve 2 and correcting the resultant activity values by multiplying them by a factor which lies between 1·15 and 1·21. Taking the correction factor to be 1·18, the values shown in Fig. 5, curve II, from $N_1 = 0{\cdot}45$ to $N_1 = 0{\cdot}75$ are obtained. This curve is extended towards $N_1 = 1$ using the value fixed by the phase diagram at $N_1 = 0{\cdot}80$ and is then completed by extrapolation.

Exactly analogous calculations may be made for each set of experimental results. These are illustrated in Fig. 2 to 4 by horizontal lines indicating the value of the molar fraction at which the silica activity is fixed by the phase diagram and by broken lines which indicate the maximum correction possible up to the lowest experimental value of N_2/N_1. The limiting values of the correction factors are shown in Table III. Using these, the activity curve, of Fig. 5 to 7 are obtained.

TABLE III.—Limiting Values of Correction Factors

Temp. °K	System		
	Li_2O–SiO_2	Na_2O–SiO_2	K_2O–SiO_2
1673	1·15–1·21	1·06	1·00–1·03
1573	1·17–1·25	1·06–1·09	1 00–1·02
1473	—	—	1·00
1373	—	1·03–1·09	—

Extrapolation of these curves to $N_1 = 0$ is not possible. From the shape of the graphs of log r/N_2 is seems probable, however, that a_1/N_1 decreases so rapidly as to make a_1 fall to extremely low values some distance from $N_1 = 0$. Because of this uncertainty in the curves of a_1, it is not possible to estimate the activities of the alkali oxides.

Discussion

It is possible to arrive at some estimate of the accuracy of the results of these calculations by considering the two sources of error, viz., the experimental results and the derivation of the correction factors.

The general shape of any curve of log r/N_2 against N_2/N_1 is unambiguous, although the experimental results are sufficiently scattered to leave some doubt as to the actual positioning of the curve. Nevertheless, the variations possible in drawing the curves make little difference to the areas beneath them and less to the activity values derived from these areas. From trials made with differently-drawn curves, it is considered unlikely that the error in the activity arising from uncertainty in the actual position of a curve would amount to more than ± 0·02.

One possible error in estimating the correction factors arises from doubt as to the heat of fusion of silica. The use of Kelley's [10] value of 2100 cal./mole for this quantity would alter the factor for the Li_2O—SiO_2 system at 1673° K by only 0·01. The main error in the correction factors is the uncertainty in the course of the curve of log r/N_2 between the lowest experimental value of N_2/N_1 and the point fixed by the phase diagram. Where this uncertainty is largest, it could alter the highest derived activity values by ± 0·03, but the error would rapidly decrease as the activity decreased. Combining these estimates of possible error, it is unlikely that the final result will be in error by more than ± 0·04, while, at low values of the activity, the error may be expected to be much less.

Fig. 8 shows the curves obtained for the three systems at 1673° K.

---

[10] Kelley, *U.S. Bur. Mines Bull.*, 393.

They are in general agreement with Rey's deductions, although the fall in activity is not so rapid as he has suggested. As was mentioned above, it appears probable that the fall continues to extremely low values: in Fig. 8, it is suggested, by the extrapolated broken lines, that the values are practically zero at the orthosilicate composition, when the solution probably consists largely of alkali metal and SiO_4^{4-} ions. The extrapolation is, however, purely conjectural. All that can be said, from the curves themselves, is that the addition of alkali oxides to supercooled liquid silica results in an initial positive deviation in the silica activity followed by a sharp fall to values showing very marked negative deviations. The amount of initial positive deviation decreases from Li_2O to K_2O, as does the sharpness of the fall and the molar fraction of alkali oxide at which it begins. It might be possible to account for the shape of the curves by some particular ionic model but this would be an arbitrary procedure in that several models might be found to fit the results. The proper use of activity values is as a check on constitutional theories derived from other data.

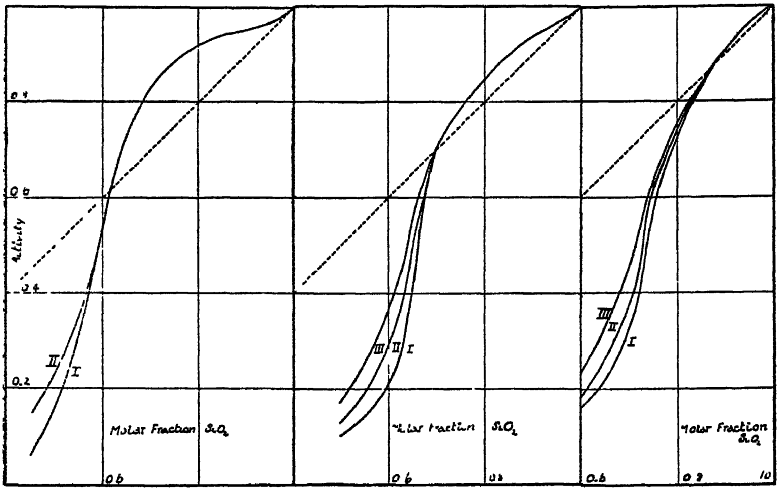

Fig. 5. Fig. 6. Fig. 7.

FIG. 5–7.—Activity of silica at different temperatures, referred to supercooled liquid silica at the same temperature.

FIG. 5.—$Li_2O—SiO_2$ I. 1573° K. II. 1673° K.

FIG. 6.—$Na_2O—SiO_2$ I. 1373° K. II. 1573° K. III. 1673° K.

FIG. 7.—$K_2O—SiO_2$ I. 1473° K. II. 1573° K. III. 1673° K.

When the present results are considered in relation to the "random network" theory of glass structure, it will be seen that they suggest this theory to be unsatisfactory for glasses of low silica content. The theory, founded mainly on the X-ray diffraction work of Warren and his school, considers a glass or the liquid to which it melts, to be a network of SiO_4 tetrahedra, arranged in a disordered fashion. In vitreous silica, this structure will resemble that of tridymite or cristobalite so that the corners of the tetrahedra are all shared and there are a number of large interstices. Into these interstices metal ions can be fitted, so that the introduction of an oxide is represented as the placing of the metal ions in interstices and the attachment of the oxygen ions to SiO_4 tetrahedra. This latter process results in an increasing number of tetrahedral corners being unshared until, at the orthosilicate composition, presumably all the tetrahedral corners are unshared and the liquid consists only of SiO_4^{4-} and metal ions. The general picture provided by the activity curves obtained above does not altogether agree with this theory, but suggests that the solutions may consist principally of alkali metal and SiO_4^{4-} ions well above the ortho-silicate composition.

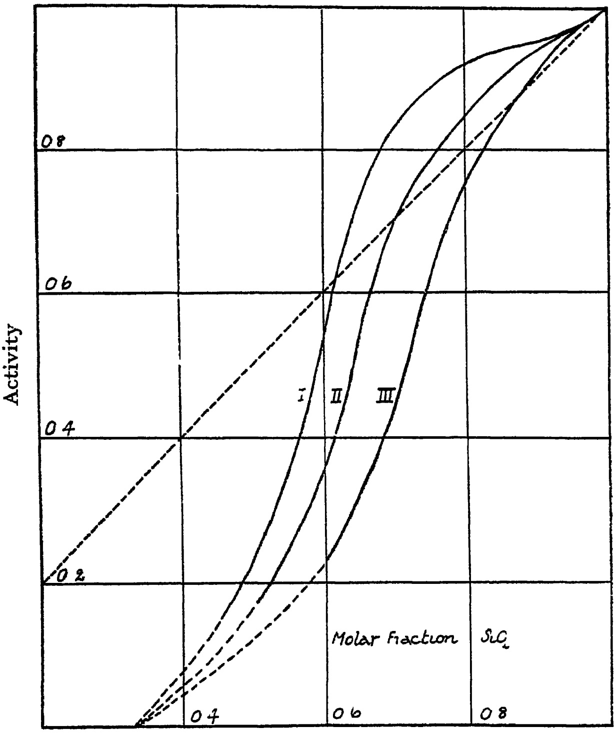

FIG. 8.—Activity of silica in alkali oxide — silica systems at 1673° K referred to supercooled liquid silica at the same temperature.
I. Li_2O—SiO_2. II. Na_2O—SiO_2. III. K_2O—SiO_2.

Increasing the " oxygen attraction " of the alkali-metal cation increases the initial positive deviation of the silica activity. The phase diagrams[6] of other oxide + silica systems show that, as the oxygen attraction is still further increased, immiscibility appears in the silica-rich composition range. In such cases, it is also apparent from the phase diagrams that the silica activity shows a very sharp fall just beyond the point at which immiscibility disappears. The higher the oxygen attraction of the foreign ion, the sharper is the fall in silica activity. In these cases also, it is possible that the fall gives rise to low activities at the ortho-silicate composition.

In the PbO—SiO_2 system, for which some preliminary calculations have been made (based on further results of Preston and Turner[11]), the tendency to immiscibility is still more marked than it is in the Li_2O—SiO_2 system and the fall in silica activity is sharper. It appears that the silica activity at the orthosilicate composition is only about 0·01, thus tending to confirm the opinion that the silica activities in these binary melts fall to very low values at the orthosilicate composition. It also appears probable that the activity of PbO in the composition range from pure PbO to the orthosilicate composition is fairly close to ideal. This suggests a resemblance to the FeO system in which Taylor and Chipman [12] found the FeO activity to be nearly ideal in the FeO-rich compositions. If this resemblance exists, Richardson's [13] suggestion for the silica activity of this system may well be incorrect and, here also, the silica activity may fall to low values at the orthosilicate composition.

---

[11] Preston and Turner, *J. Soc. Glass Tech.*, 1935, 19, 296.

The composition of the oxide-rich liquids in those cases where immiscibility occurs will differ considerably from the almost pure silica phase with which they are in equilibrium. The rapid fall in silica activities and the possibility of low values in the neighbourhood of the orthosilicate composition suggest that this effect is due primarily to the break-up of the silica lattice into SiO_4^{4-} ions. It is also probable that this break-up is a fairly sharp process, not the gradual one envisaged by the simple random-network theory. This would be more in accordance with viscosity data for those simple binary systems which show a rapid fall as foreign oxide is added to silica, followed by a slower decrease.[14]

Any more detailed picture of the structure must await further work of a non-thermodynamic kind. Of particular value will be work on the electrical conductivity and ionic mobility of the solutions. But, although thermodynamics cannot give any further immediate help, it will prevent the development of mistaken theories. For this reason, a knowledge of the activities is essential and it is greatly to be desired that they can be determined over the entire composition range and for other binary systems.

The author's thanks are due to the Directors of Pilkington Brothers Limited for permission to publish this paper.

Research Department,
Pilkington Brothers Limited,
St. Helens,
Lancashire.

[12] Taylor and Chipman, *Trans. Amer. Inst. Min. Met. Eng.*, 1942 (Tech. Pub. 1499).

[13] Richardson, *Faraday Soc. Discussions*, 1948, 4, 244.

[14] E.g. Morey, *Properties of Glass* (New York, 1938), p. 165.

Erratum

The Kinetics of Ionic Polymerizations, Parts I & II. By D. D. Eley and A. W. Richards (*Trans. Faraday Soc.*, 1949, **45**, 425).

Owing to a slip in the calculation of the third order velocity constants the values of these constants listed in Table I, p. 429, and in the first paragraph on p. 440 are all too high by a factor 10^6. Similarly, the values of log k in Fig. 5, p. 432, require 6 to be subtracted. None of the arguments are affected by these corrections. Our thanks are due to Dr. Plesch for drawing our attention to the error.

MONOLAYER PENETRATION AT THE OIL-WATER INTERFACE

PART I.—EFFECT OF SALTS ON EMULSIFICATION

By R. Matalon

Received 31st *March*, 1950

The enhancement of penetration in the presence of salts [1] previously demonstrated using the monolayer technique is now shown to induce spontaneous emulsification of Nujol in water at much lower concentration of alkyl sulphate when cholesterol is present in the oil phase. The stability to creaming and flocculation of the emulsion then produced is dependent on the salt concentration and on the valency of the added cation. The flocculation of the negatively charged lyophilic oil droplets studied here is attributed to a reduction in the ζ potential and degree of hydration of the interfacial layer.

Previous work [1] has shown that the presence of salts in an aqueous Na cetylsulphate solution enhances markedly the phenomenon of penetration of a cetyl alcohol monolayer spread at the air-water interface and that this effect was one of the major reasons for the experimental discrepancies in the results obtained by Schulman and Stenhagen,[2] and Harkins and co-workers.[3] This paper is an attempt to elucidate the effect of salts on penetration at oil-water interfaces.

Schulman and Cockbain [4] have shown that when a liquid complex such as cholesterol-cetylsulphate is present at the oil-water interface, it is possible to obtain spontaneous emulsification. If spontaneous emulsification is due to the presence of the complex formed *in situ*, it would be produced at much lower concentrations of the detergent in the presence of salts. The following investigation has been conducted for the system, cholesterol-sodium dodecylsulphate.

Cholesterol and sodium dodecylsulphate were dissolved in B.P. medicinal paraffin and water respectively. The water was twice distilled and free from any traces of metallic ions which enhance markedly the extent of penetration. Sodium dodecylsulphate was used instead of its higher homologue, sodium cetylsulphate, by reason of its greater solubility at ordinary temperatures. If sodium cetylsulphate is used instead, heating of the aqueous phase is necessary to obtain a clear solution, and mixing of the phases must be carried out with careful temperature control since the extent of the association sterol-alkylsulphate is temperature dependent. Thus a system sterol-alkylsulphate leading to spontaneous emulsification at 20° C is prevented from emulsifying at 80-90° C ; cooling in a stream of cold water (17° C) produces a spontaneous emulsion, shaking being unnecessary. To avoid complications due to differences in temperature sodium dodecylsuphate was therefore used in all cases, and mixing was done at ordinary temperature (20° C).

---

[1] Matalon and Schulman, *Trans. Faraday Soc.*, 1947, **43**, 479.

[2] Schulman and Stenhagen, *Proc. Roy. Soc. B*, 1939, **126**, 356.

[3] Harkins, Copeland and Gordon, *Surface Chemistry, Amer. Assoc. Adv. Sci.*, 1943, **21**, 79.

[4] Schulman and Cockbain, *Trans. Faraday Soc.*, 1940, **36**, 651.

Experimental and Results

The emulsion was prepared using 10 ml. of the aqueous phase and 2·5 ml. of oil. The oil contained in all cases an excess (20 mg.) of cholesterol, and the amount of sodium dodecylsulphate and salts were varied. Sodium chloride was used to investigate the effect of monovalent salts and copper sulphate used as a divalent salt. Emulsification was performed by pouring the aqueous phase into the oil phase and shaking ten times. All the emulsions of series III creamed the following day. The presence of NaCl in an aqueous solution of Na dodecylsulphate did not promote the emulsification of the oil in water in the absence of cholesterol, hence the results described in Table I may be attributed to the enhancement of the association cholesterol Na dodecylsulphate by NaCl. It is interesting to note the results obtained when the amount of salt is gradually increased. Whereas small amounts result in a better dispersion and stability, the emulsions obtained flocculate when the amount of salt present exceeds a certain value.

TABLE I.—OBSERVATIONS ON MIXING 10 ML. AQUEOUS SOLUTION WITH 2·5 ML. MEDICINAL PARAFFIN CONTAINING 20 MG. CHOLESTEROL

Na Dodecylsulphate (mg.)		NaCl (mg.)	Observations on Mixing
Series I	30	0	Spontaneous emulsion
	30	25	,, ,,
	30	50	,, ,,
	30	75	,, ,,
	30	100	Spontaneous, flocculated after 14 hr.
	30	150	Spontaneous, flocculated after 1-5 min.
Series II	15	0	Coarse emulsion
	15	25	Spontaneous emulsion, thick and milky
	15	50	,, ,, ,, ,, ,,
	15	100	Spontaneous emulsion, thick and milky, flocculation starting 40 min. after shaking
Series III	7·5	0	Extremely poor emulsion
	7·5	25	Good emulsion
	7·5	50	,, ,,
	7·5	100	,, ,,
	7·5	150	,, ,,

TABLE II

Sodium Dodecylsulphate (mg.)	Copper Sulphate (mg.)	Observations on Mixing
15	0	Coarse emulsion
	5	Spontaneous emulsion
	10	
	15	
	20	
	25	
	30	Spontaneous emulsion, flocculation 5-10 min. after mixing
	40	Spontaneous emulsion, flocculation 1-2 min after mixing

Table II summarizes the results obtained in connection with the effect of the presence of copper sulphate in the aqueous phase. It is evident that copper sulphate or sodium chloride enhances the emulsification, and that much smaller amounts of Cu^{++} are needed to produce the flocculation of the emulsions. Whereas with sodium chloride the flocculation started 40 min. after mixing in presence of 100 mg. of NaCl, with copper sulphate 30 mg. are sufficient to produce the flocculation of the emulsion 5 or 10 min. after mixing. It appears therefore that under these conditions flocculation is obtained by a monovalent salt when its molecular concentration is 32 times greater than that of the sodium dodecylsulphate, whereas a concentration only twice greater than that of the long-chain sulphate is needed to produce this result with copper salts.

In spite of an assertion to the contrary[5] it was found possible to prepare copper dodecylsulphate by mixing aqueous solutions of sodium dodecylsulphate with copper sulphate. It was necessary to let the mixture stand in a refrigerator for 10 to 15 min. before the copper dodecylsulphate was precipitated as pale blue plates.

Interpretation of Results.—It appears from the above results that these emulsions are sensitive to salts in the same way as a penetrated monolayer at the air-water interface. It can be shown that when salt is present a great part of the detergent is concentrated around the emulsion droplets.

Suppose that the droplet radius is 1μ when spontaneous emulsification is observed, it follows that the interfacial area $S = 3V/r$, (V, the volume of the oil = 2·5 ml.; r, the radius of the droplets = 10^{-4} cm.) is equal to $3 \times 2{\cdot}5 \times 10^{20}$ Å^2. If it is assumed that the interfacial layer is covered by the 1 : 1 complex, the area occupied by the sodium dodecylsulphate in the present emulsion would be $2{\cdot}5 \times 10^{20}$ Å^2. This area would be covered by 6 mg. of detergent assuming 20 Å^2 to be the area occupied by the long-chain sulphate.

In Table I it has been shown that in the presence of salt spontaneous emulsification can be obtained with 15 mg. of the long-chain sulphates in the aqueous phase, and that good emulsions can still be obtained with 7·5 mg. In the absence of salts the amount of detergent used is very much greater than that necessary to cover the interface. This may be explained by the following considerations.

Whereas it is known that salts do not effect the Π—A curve at the air-water interface of cholesterol, and therefore its adsorbing properties at the oil-water interface, salts have been found to produce a marked effect on the adsorption of the sodium dodecylsulphate, both at the air-water[6] and the oil-water interface.[7] Not only is the micellar concentration reduced, and the surface pressure of the adsorbed layer increased, but the slope of the γ—c curve increases also markedly, thus leading to a greater surface excess Γ of the long-chain ion in the adsorbing monolayer. In the particular case now investigated there is a greater number of sodium dodecylsulphate molecules near the cholesterol and hence the resulting interaction is enhanced. When the concentration of salts is too high flocculation of the emulsion is observed. This may be due to the action of two factors: (i) reduction of the droplet charge, and (ii) dehydration of the interfacial layer. If in the absence of salt, and at low concentrations of the long-chain sulphate in bulk, i.e. 15 mg., the droplet boundary may be pictured as a loose structure where only very few long-chain ions are associated with the cholesterol, the presence of salts would favour a greater packing at the interface. When the amount of salt exceeds a certain value the diffuse layer of gegenions approaches so close to the droplet that the droplet charge disappears almost completely. Flocculation is thus observed.

The flocculated emulsion is a thick mass, which suggests that during this process the droplets have been dehydrated. It appears that the oil droplets stabilized by cholesterol Na dodecylsulphate behave as a lyophilic colloid. Indeed the molecular concentration of monovalent salt necessary to produce the flocculation is 32 times greater than that of the detergent.

I wish to thank Dr. J. H. Schulman for his advice and stimulating criticism.

Department of Colloid Science,
The University, Cambridge.

---

[5] Lottermoser and Püschel, *Kolloid-Z.*, 1933, **63**, 175.

[6] Long, Nutting and Harkins, *J. Amer. Chem. Soc.*, 1937, **59**, 2197.

[7] Powney and Addison, *Trans. Faraday Soc.*, 1937, **33**, 1254; Cassie and Palmer, *ibid.*, 1941, **37**, 156.

HIGH POLYMER SOLUTIONS

PART I.—VAPOUR PRESSURE OF POLYSTYRENE SOLUTIONS

By C. E. H. Bawn, R. F. J. Freeman and A. R. Kamaliddin

Received 15*th March*, 1950

Measurements have been made of the vapour pressure of polystyrene solutions in toluene and methyl ethyl ketone at different temperatures. The heat of dilution of polystyrene by toluene is zero. The results are discussed in relation to the existing theories of the free energy and entropy of dilution of polymers.

Solutions of high polymers and other large molecules show striking departures from the laws of ideal solution. Theoretical considerations have shown that these effects are attributable to the differences in sizes and shapes of the species that make up the solution. From the point of view of thermodynamics the properties which are of particular interest in this respect are the free energy and heat of dilution and these quantities can be most conveniently determined from vapour and osmotic pressure measurements. These properties are related thermodynamically by the well-known expressions

$$\Delta G_1 = RT\ln(p_1/p_1^0) = -\Pi\overline{V}_1, \quad . \quad . \quad . \quad (1)$$

where p_1^0 is the vapour pressure of the pure solvent, p_1 the vapour pressure of the solution, Π the osmotic pressure and $\overline{V}_1$ the partial molar volume of the solvent in solution. Osmotic pressure measurements on solutions are usually made at very high dilution (up to 1 % concentration) whereas vapour pressure determination can be used to cover almost the whole range of concentration.

In recent years the application of statistical mechanics [1] to the calculation of the thermodynamic properties of polymer solutions has been largely successful in accounting for the difference in behaviour from ideal solutions. Numerical agreement between experiment and theory is not entirely satisfactory and the lack of reliable experimental data for different types of polymer-solvent systems has delayed a critical evaluation of existing theories. In view of the increasing tendency to use these theoretical relationships a searching examination of their validity is desirable. In the present and succeeding paper, vapour and osmotic pressure measurements of polystyrene solutions over a wide range of concentrations have been compared with current theories.

Experimental

The method of direct measurement of the difference in vapour pressures between a solution and the pure solvent was employed. The apparatus consisted of a U-tube connected at the bend to a mercury reservoir. One limb of the U-tube was closed by a small conical flask containing the solution. The other limb which led to a vacuum line was sealed to a calibrated side tube containing the solvent. Purified solvent was distilled *in vacuo* into the side arm from an external trap. Solutions were made by distilling known quantities of solvent on to the polymer. The manometer and mercury reservoir were immersed in a thermostat constant to ± 1/100° C, which could be lowered to allow access to the manometer.

---

[1] Huggins, *J. Chem. Physics*, 1941, **9**, 440 ; *J. Physic. Chem.*, 1942, **46**, 151 ; Flory, *J. Chem. Physics*, 1941, **9**, 660 ; *ibid.*, 1942, **10**, 51 ; *ibid.*, 1945, **13**, 453 ; Miller, *Proc. Camb. Phil. Soc.*, 1942, **38**, 109 ; *ibid.*, 1943, **39**, 54, 131 ; Guggenheim, *Proc. Roy. Soc. A*, 1944, **183**, 213.

Purification of Solvents.—For vapour pressure measurements it is essential to use carefully purified solvents. The main likely sources of error when an impure solvent is used are reaction of impurities with the mercury, and fractionation of the solvent during successive distillation from the solvent reservoir to the polymer, and vice versa.

TOLUENE was purified by the method of Richards and Barry.[2] Commercial "sulphur free" toluene was shaken 5 times with concentrated H_2SO_4, then washed with water, followed by 3 washings with 20 % KOH solution. After drying over $CaCl_2$, it was refluxed over clean sodium for about 10 hr., and twice fractionated. The final product distilled at a constant temperature of 110·62° C at 760 mm. Hg pressure. The isatin test for sulphur was negative. About 50 ml. of this fraction was collected in a trap, which was attached to the vacuum apparatus with the least possible exposure to air. The toluene was de-gassed and distilled slowly in vacuum. A middle fraction of about 15 ml. was selected for measurement. The homogeneity of this fraction was checked by measuring the vapour pressure of the first few drops obtained by a very slow distillation and also the vapour pressure of the last few drops left as a residue. The two pressures were identical.

The vapour pressure was measured at various temperatures, and the results agreed almost exactly with those given by the National Bureau of Standards.[3] The measured density was 0·8610 at 25° C which agreed closely with recent values reported.[4]

METHYL ETHYL KETONE.—Laboratory grade solvent was fractionated. A middle fraction was dried over anhydrous potassium carbonate and carefully refractionated. The product had a density of 0·7996 at 25° C in agreement with previous values.[5] The methyl ethyl ketone was refractionated in a vacuum, and its homogeneity checked in the same way as for toluene.

The vapour pressure-temperature relation was determined for the range 20-70° C. The plot of $\log p$ against $1/T$ was linear and represented by the equation

$$\log p \text{ (mm.)} = 7{\cdot}857 - 1754/T.$$

These results agreed with several sets of values reported in the literature.[5] The boiling point determined from the vapour pressure plot was 79·56° C.

POLYMER.—The polymer used was a close fraction obtained from polystyrene prepared by thermal polymerization of purified monomer as described in Part II. The molecular weight of the fraction as determined by osmotic pressure measurements in toluene and methyl ethyl ketone was 290,000.

Measurement of Vapour Pressure of Solutions.—The polymer was weighed into the conical flask, which was then sealed on to the apparatus. It was freed from gases by evacuation of the flask which was continuously heated in boiling water. The mercury in the U-tube was then raised, and solvent distilled *in vacuo* into the side arm attached to the limb of the manometer which was then sealed off from the remainder of the apparatus. The vapour pressure of the solvent was determined at a number of temperatures, and the results agreed with those obtained before the sealing-off of the system from the vacuum line.

Solutions of known concentration were made by distilling known amounts of solvent from the side tube into the conical flask, and vice versa. The difference in vapour pressure of solvent and solution were determined at various temperatures by direct reading of the mercury levels in the U-tube with a cathetometer.

All the thermometers used were calibrated by the National Physical Laboratory, and could be read to better than 0·01° C. The vapour pressures of the solutions were measured at the same temperatures as those at which independent measurements on the pure solvents had been made. The temperature variation was ± 0·002° C at 25° C and ± 0·01 at 80° C and the pressures were recorded over

[2] Richards and Barry, *J. Amer. Chem. Soc.*, 1915, **67**, 993.

[3] *Amer. Petroleum Inst. Res. Project* 44.

[4] Geist and Cannon, *Ind. Eng. Chem.* (*Anal.*), 1946, **18**, 611; *Int. Crit. Tables*, **3**, 28.

[5] Felsing, Shofner and Garlock, *J. Amer. Chem. Soc.*, 1934, **56**, 2252; Radulescu and Alexa, *Bull. Soc. chim. Rumania, A*, 1938, **20**, 89.

a period of time, and the mean value taken. The bore of the manometer tube was 1 cm. and meniscus corrections, which were small in all cases, were applied. The volume of the system was accurately calibrated; corrections were made for the mass of solvent in the vapour phase and for non-ideality of the vapour.

At the end of a series of measurements, all the solvent was distilled on to the polymer. The vapour pressure of the dilute solution was the same as that of the pure solvent and this showed that no volatile substances were produced in the system during the measurements.

For the calculation of volume fractions of the polymer, its density was determined in each solvent at 25° C and 60° C by measuring the densities of solutions of known concentration and assuming additivity of volumes. For toluene solutions at 25° C covering a range of weight fractions from 0·8293 to 0·9138 the determinations gave a constant polymer density of 1·083 ± 0·002 g./cm.^{3}, thus providing justification for the assumption of additivity of volume. Furthermore, the plot $1/\rho_{\text{sol.}}$ against weight fraction was linear and the partial molal volume of the solvent was found to be constant and equal to its molal volume. The densities of polystyrene in toluene and methyl ethyl ketone for a range of concentrations were: toluene 25° C, 1·083; 60° C, 1·070; methyl ethyl ketone 25° C, 1·091; 55° C, 1·092.

Results

Fig. 1 shows the plot of the ratio of the vapour pressure of the solvent over the solution p_1 to the vapour pressure of the pure solvent p_1^0 against the corresponding weight fractions W_1 of the solvent for toluene and methyl ethyl ketone. The results with toluene solutions at 25, 60 and 80° C show that dependence of p_1/p_1^0 on W_1 was independent of temperature. In these measurements no hysteresis effect was observed, the same values of p_1/p_1^0 were obtained independent of whether the concentration of the solution had been increased or decreased.

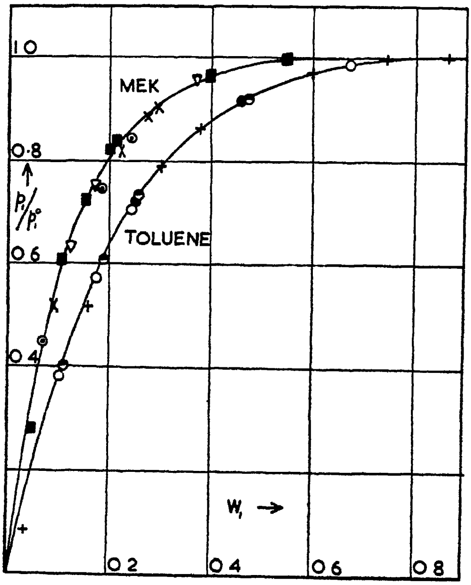

FIG. 1.—Variation of p_1/p_1^0 with W_1 for molecular weight fraction 290,000 in toluene and methyl ethyl ketone and at three temperatures.

Methyl ethyl ketone: weight fraction increasing ■ 25° ∇ 70° C.
,, ,, ,, ,, ,, decreasing × 25° ○ 70° C.
Toluene: weight fraction increasing ◒ 25° ● 60° ○ 80° C.
,, ,, ,, decreasing + 25° C.

The ratios p_1/p_1^0 for methyl ethyl ketone solutions were measured at 25° C and 70° C and a definite hysteresis effect was observed. Equilibrium was approached very slowly at 25° C, and the temperature dependence could not be determined with the accuracy attained with toluene. The magnitude of the error was small, and the maximum scatter in the values obtained at 25° C with increasing or decreasing concentration was about 4 %. The values obtained at 70° C showed much less scatter and equilibrium was reached more rapidly. Moreover, all the results at 25° C and 70° C, obtained with the weight fraction of solvent decreasing, lay on a smooth curve and it was considered that these results were more accurate than those obtained with the weight fraction of the solvent increasing, since, under the experimental conditions the distillation of solvent from the solution caused the solution to spread as a thin film over the surface of the bulb. A greater weight was given to these determinations when drawing the p_1/p_1^0 against W_1 curve.

Previous measurements on the vapour pressures of the polystyrene-toluene system at 20° have been reported by Baughan [6] using a technique which consisted of weighing a thin film of the polymer at measured vapour pressures of toluene. These results for an unfractionated polymer of average molecular weight 20,000 have been plotted together with our own data on a single graph (not reproduced). Baughan's results give a slightly higher p_1/p_1^0 than our measurements and the scatter of his points is considerable.

Free Energy, Heat, and Entropy of Dilution.—The molar free energy of dilution ΔG_1 was calculated using eqn. (1) and the heat of dilution from the temperature coefficient of the free energy by means of the thermodynamic relationship

$$\Delta H_1 = \left(\frac{\partial(\Delta G_1/T)}{\partial(1/T)}\right)_{p,N_2}.$$

The identity of the value of p_1/p_1^0 for the same weight fraction at different temperatures with toluene showed that ΔH_1 with this solvent was zero. With methyl

TABLE I.—Vapour Pressure of Solutions of Polystyrene Fraction (M = 290,000) in Toluene and Methyl Ethyl Ketone

Wt. Fraction of Toluene increasing 25° C		Wt. Fraction of Toluene decreasing 25° C		Toluene Temp. 60° C		Toluene Temp. 80° C	
W_1	p/p_1^0	W_1	p_1/p_1^0	W_1	p/p_1^0	W_1	p_1/p_1^0
0·111	0·403	0·033	0·084	0·102	0·383	0·246	0·706
0·191	0·611	0·156	0·523	0·179	0·576	0·458	0·914
0·273	0·740	0·236	0·704	0·261	0·725	0·671	0·984
0·476	0·918	0·304	0·791	—	—	—	—
—	—	0·380	0·866	—	—	—	—
—	—	0·599	0·969	—	—	—	—
—	—	0·744	0·997	—	—	—	—
—	—	0·918	~1	—	—	—	—

Wt. Fraction of Methyl Ethyl Ketone (M.E.K.) increasing 25° C		Wt. Fraction of M.E.K. decreasing 25° C		M.E.K. increasing 70° C		M.E.K. decreasing 70° C	
W_1	p/p_1^0	W_1	p_1/p_1^0	W_1	p/p_1^0	W_1	p_1/p_1^0
0·052	0·284	0·091	0·517	0·123	0·637	0·071	0·450
0·108	0·610	0·215	0·808	0·175	0·755	0·183	0·745
0·153	0·726	0·279	0·882	0·376	0·954	0·246	0·844
0·206	0·824	0·298	0·906	—	—	—	—
0·208	0·833	—	—	—	—	—	—
0·401	0·968	—	—	—	—	—	—
0·529	0·990	—	—	—	—	—	—

---

[6] Baughan, *Trans. Faraday Soc.*, 1948, **44**, 495.

ethyl ketone ΔH_1 was small and could not be accurately determined. The most reasonable estimation was about 20 cal./mole, but for the purpose of calculation of other thermodynamic quantities ΔH_1 may be taken as zero. The entropies of dilution derived by substitution of the value of ΔG_1 calculated from eqn. (1) in the expression

$$\Delta G_1 = \Delta H_1 - T\Delta S_1. \quad . \quad . \quad . \quad . \quad . \quad (2)$$

These values are not tabulated since they may be derived by simple arithmetic from the vapour pressure data summarized in Table I.

Discussion

The various theoretical treatments of the properties of polymer solutions are based on the quasi-crystalline model of a liquid, each cell of which may be occupied either by a solvent molecule or a segment of the chain molecule. The calculations of Huggins [1] lead to the following expression for the partial molal entropy of the solvent :

$$\overline{\Delta S_1} = -R\left[\ln(1 - V_2) - \left(1 - \frac{1}{n}\right)\frac{Z'}{2}\ln\left(1 - \frac{2V_2}{Z'}\right)\right], \quad . \quad (3)$$

where V_2 = volume fraction of solute,
n = number of segments in the polymer molecule.
$Z' \approx Z$ = co-ordination number of the lattice.

In combination with the heat of mixing $\Delta H_1 = \alpha V_2^2$ and expansion of the logarithm there is obtained the partial molal free energy

$$\overline{\Delta G_1} = RT\,[\ln(1 - V_2) + (1 - 1/n)V_2 + \mu V_2^2], \quad . \quad (4)$$

where

$$\mu = \frac{1 - 1/n}{Z'} + \frac{\alpha}{RT}. \quad . \quad . \quad . \quad . \quad (5)$$

This equation has given surprisingly good agreement with experiment if μ is assigned an arbitrary value not in agreement with that obtained from eqn. (4). In fact μ contains other factors,[1] besides those included in (4), and may also be dependent on solution composition. It has therefore been necessary to reformulate μ in the more general form

$$\mu = \beta + \alpha/RT, \quad . \quad . \quad . \quad . \quad (6)$$

where β is an empirical constant. The good agreement between experiment and theory is associated with this empirical μ since the partial molal entropies and heat of dilution independently do not agree with theory for dilute solutions.[8]

Before comparing the experimental data with eqn. (4) it is necessary to consider the units in which the volume fraction should be expressed. In the derivation of (4) in terms of the lattice model the volume fraction of polymer is defined as

$$V_2 = \frac{nN_2}{N_1 + nN_2}, \quad . \quad . \quad . \quad . \quad (7)$$

where N_1 = number of solvent molecules,
N_2 = number of polymer molecules,
n = number of segments in the polymer.

Experimentally the volume fraction of the polymer is usually expressed as the ratio of the volume of the polymer in solution to the total volume of solution, all volumes being measured before mixing

$$V_2' = \frac{V_2}{V_1 + V_2} \quad . \quad . \quad . \quad . \quad (8)$$

where V_1 and V_2 are the volumes of solvent and polymer respectively.

---

[7] Miller, *The Theory of Solutions of High Polymers* (Oxford, 1949).

[8] Ferry, Gee and Treolar, *Trans. Faraday Soc.*, 1945, **41**, 341 ; Gee, *J. Chem. Soc.*, 1948, 207.

These two volume fractions are not in general identical. It can be readily seen that if each repeating unit occupies one lattice site, which as shown below is reasonable for the present polymer-solvent systems, then

$$V_2 = \frac{w_2}{\frac{M_0}{M_1}w_1 + w_2} = \frac{w_2}{\frac{M_2}{nM_1}w_1 + w_2} \quad . \quad . \quad . \quad (9)$$

where w_1, w_2 are the weights of solvent and polymer and M_0, M_1, M_2 are the molecular weights of the repeating unit in the polymer and of the solvent and polymer respectively.

Similarly,

$$V_2' = \frac{w_2}{\frac{\rho_2}{\rho_1}w_1 + w_2}, \quad . \quad . \quad . \quad . \quad . \quad (10)$$

where ρ_1 and ρ_2 are the density of solvent and polymer. Only when

$$\frac{M_0}{M_1} = \frac{M_2}{nM_1} = \frac{\rho_2}{\rho_1}$$

is $V_2 = V_2'$ or when the volume of repeating unit and solvent molecules are of equal size as assumed in lattice theory.

Since
$$\frac{M_2}{nM_1} = \frac{PM_0}{nM_1} = \frac{\rho_2}{\rho_1}$$

where P is the degree of polymerization, the ratio P/n can be evaluated from the measured densities. In toluene and methyl ethyl ketone P/n had the values of 1·11 and 0·95 respectively. That is, the size of the polymer segment is so close to that of the structural unit that V_2 can be justifiably evaluated from eqn. (9).

From eqn. (1) and (4) and substituting $(1 - V_2) = V_1$ it follows that

$$\ln (p_1/p_1^0) = \ln V_1 + V_2 + \mu V_2^2. \quad . \quad . \quad . \quad (11)$$

This equation was tested by plotting $\ln (p_1/p_1^0) - \ln V_1 - V_2$ against V_2^2 taking V_2 as defined by (8), and a good straight line was obtained of slope corresponding to $\mu = 0·38$. This value applied over the whole range of composition at 25° C but at 60° C the results no longer fitted this equation, the plot showing a well-defined curvature. With methyl ethyl ketone as solvent no agreement with (11) was obtained for the results at either 25° C or 70° C.

According to (4) and (5) since the heat term for toluene was zero, the value of μ should be independent of temperature. This will not be so for (11) even when $\Delta H_1 = 0$ when the volume fraction V_2' is employed since V_2' depends on temperature in a manner determined by the coefficients of expansion of the components (eqn. (10)). In conformity with (7) the correct experimental volume fraction to use is (9) and with $\Delta H_1 = 0$ this satisfies the experimental observation that μ is independent of temperature for constant weight fractions. Furthermore, when (11) was compared with the experimental results using V_2 from (9) the equation was satisfied with a μ value independent of concentration and evidently of temperature. These results are plotted in Fig. 2 and the values of toluene and methyl ethyl ketone were 0·44 and 0·66 respectively.

A different theoretical approach has been made by Miller [1, 7] who used a more general statistical method but the same physical model. He deduced the free energy relationship

$$\frac{\overline{\Delta G_1}}{RT} = \ln (1 - V_2) - \frac{1}{2}Z \ln \left[1 - \frac{2}{Z}\left(1 - \frac{1}{n}\right) V_2\right] \quad . \quad (12)$$

for the case of zero energy of mixing. The equation is formally similar

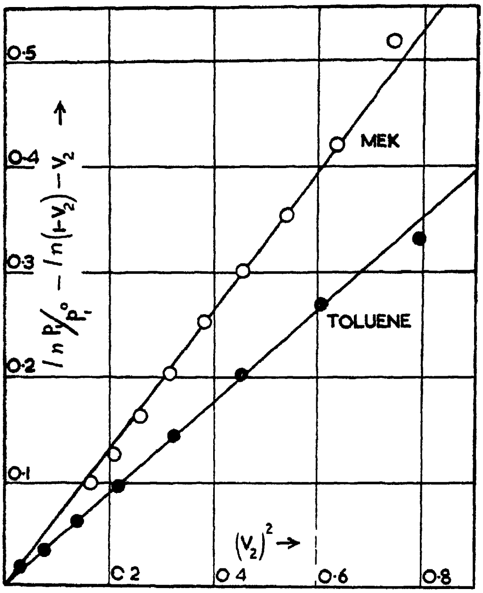

FIG. 2.—Showing validity of equation $\ln (p_1\ p_1^0) = \ln V_1 + V_2 + \mu V_2^2$ at temperatures 25, 60, 80 C, where $V_2 = \dfrac{w_2}{\dfrac{M_0}{M_1}w_1 + w_2}$. w_1, w_2 are weights of solvent and polymer and M_1, M_0 molecular weights of solvent and repeating unit in polymer.

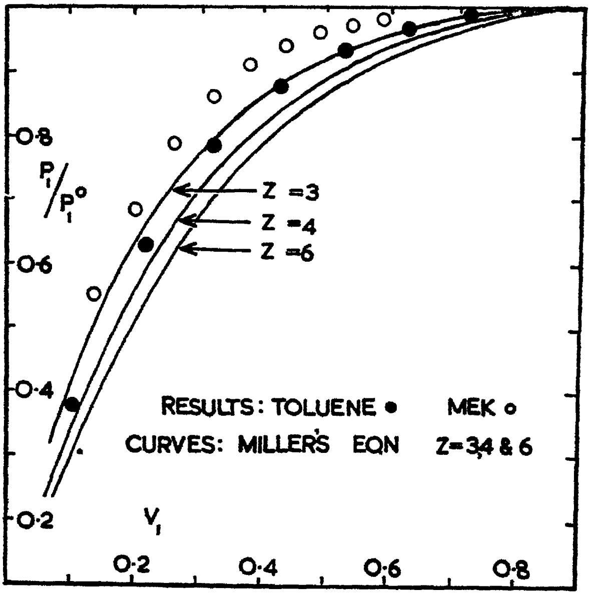

FIG. 3.—Comparison of experimental results with theoretical equation due to Miller.

to that of Huggins and both become identical with that of Flory when $z \to \infty$. The value of $p_1 \; p_1^0$ calculated from (12) for various values of the co-ordination number are compared with the experimental data in Fig. 3. It is seen that the agreement is poor unless co-ordination numbers not greater than 3 are assumed although the theory gives the correct order of magnitude and shape of the vapour pressure curve. In terms of the lattice model it is difficult to imagine Z values of this magnitude, and it is unlikely that difference in size between solvent and polymer segment would account for this discrepancy since it is reasonable to assume in the present system that either a polystyrene segment or a toluene molecule could be assigned to one site on the lattice.

The lack of precise data limits the comparison of the above results with other polymer systems and only with rubber and benzene are complete data available. With the latter system Gee and his co-workers[8] have clearly demonstrated that the theoretical free energy relationship (3) represents closely the experimental data when μ is treated as an empirical constant. It has been previously pointed out by Gee and by Flory that the partial molal entropy is not in accord with eqn. (2) and the present measurements confirm this conclusion. Only when the entropy includes the empirical constant μ or more precisely, the contribution to other than heat terms, are theory and experiment in accord. Since for the system polystyrene-toluene $\Delta H_1 = 0$ it follows from (3) that the entropy may be formulated as :

$$\Delta S_1 = - R(\ln (1 - V_2) + (1 - 1/n)V_2 + \mu V_2^2).$$

The success of this relationship in explaining our results is attributable to the term μV_2^2 which does not appear in the entropy relationship derived from the lattice theory. The origin of the latter term is not clear but among other factors includes the entropy of mixing arising from departure from perfect mixing. The absence of such an empirical term from Miller's eqn. (12) most probably accounts for the discrepancies with experiment.

Department of Inorganic and Physical Chemistry,
The University,
Liverpool.

THE DIFFUSION OF SOME HALO-METHANES IN POLYSTYRENE

By G. S. Park

Received 5th January, 1950

The overall rates of absorption of methylene chloride, chloroform, carbon tetrachloride, methylene bromide, bromoform and methyl iodide by polystyrene sheet have been measured at several surface concentrations. Diffusion coefficients obtained from these data are related to the penetrant concentration and are shown to satisfy approximately the relationship

$$\mathscr{D}_p = \mathscr{D}_0 e^{\alpha v_p}.$$

$\mathscr{D}_p$ and $\mathscr{D}_0$ are the diffusion coefficients for the penetrant when the volume fractions of the latter are v_p and 0 respectively. α is a parameter. In spite of the violent dependence of $\mathscr{D}_x$ on concentration the shape of any one absorption time curve does not deviate appreciably from that predicted for a constant, suitably chosen, diffusion coefficient.

Values of $\mathscr{D}_0$ and α are given for each penetrant at 25° C and for methylene chloride, chloroform and methyl iodide at 15° C or 35° C. $\mathscr{D}_0$ is shown to satisfy approximately the relationship

$$\mathscr{D}_0 = 3 \times 10^{-5} e^{0 \cdot 236 V_M}$$

where V_M is the molecular volume of the penetrant. α does not vary very much with the penetrant. The results are interpreted in terms of the theory of rate processes and energies and entropies of activation are obtained from coefficients obtained at different temperatures.

In a previous communication from this Laboratory[1] it has been suggested that the diffusion coefficient for polymer solvent systems may be expected to vary considerably with solvent concentration. Experimental work on a variety of such systems[2-6] supports this and it is of interest to see how far diffusion controlled phenomena are affected. In this introduction it is proposed to summarize the bearing of some previous work in this Laboratory on the effect of variable diffusion coefficients upon sorption rates before indicating the scope of the present paper.

The course of diffusion controlled absorption for various arbitrary, concentration dependent diffusion coefficients has been calculated by Crank and Henry.[7] Absorption-time curves were evaluated for infinite sheets of material maintained at a constant surface concentration C_0 of penetrant. These curves are only slightly different from curves constructed for constant diffusion coefficients provided the constant coefficients $\overline{D}$ are chosen to make the curves for constant and variable coefficients coincide exactly at the time corresponding to half the equilibrium sorption. For any one concentration dependent diffusion coefficient D the value of $\overline{D}$ depends, of course, on C_0 and is some average of D over the penetrant concentration range 0 to C_0. A knowledge of the kind of average permits the calculation of D from $\overline{D}$ if the latter is known as a function of C_0.

It is shown that[7]

$$\overline{D} \simeq I/C_0, \quad . \quad . \quad . \quad . \quad . \quad (1)$$

where $I \equiv \int_0^{C_0} D \, . \, dC$ and C is the penetrant concentration. In calculations of penetrant concentration as a function of the space co-ordinate[8] in sorption processes it has been shown that concentration dependence in the diffusion coefficient profoundly affects the results obtained. For this reason relationship (1), which enables the calculation of I and hence $D(C_0)$ from experimental data,[2, 3] is of considerable importance. The errors[*] in (1) fall between − 23 % and + 26 % for all the diffusion coefficients considered by Crank and Henry.[7] The value of I/C_0 predicted by (1) is too large for the cases in which D increases with C and is too small if D decreases with increasing C. In some later work the exact relationship between I/C_0 and $\overline{D}$ has been calculated for three types of diffusion coefficient increasing with concentration and data have been given to enable the approximate calculation of the relationship for other types of diffusion coefficient increasing with concentration.

---

[1] Hartley, *Trans. Faraday Soc.*, 1946, **42B**, 6.

[2] King, *ibid.*, 1945, **41**, 479.

[3] Rouse, *J. Amer. Chem. Soc.*, 1947, **69**, 1068.

[4] Liebhafsky, Marshall and Verhoek, *Ind. Eng. Chem.*, 1942, **34**, 704.

[5] Robinson, being prepared for publication.

[6] Crank and Park, *Trans. Faraday Soc.*, 1949, **45**, 240.

[7] Crank and Henry, *ibid.*, 1949, **45**, 636.

[8] Crank and Henry, *ibid.* 1949, **45**, 1119.

[*] By error is meant the difference between $\overline{D}C_0$ and I expressed as a percentage of I.

Crank and Park[6] have published experimental sorption time curves for the system chloroform-polystyrene which show that the rate of approach to equilibrium is a function of the concentration of chloroform at the surface. They concluded that the diffusion coefficient for chloroform in polystyrene is a function of concentration. Values of $\bar{D}$ were calculated for each value of the surface concentration C_0 and a first approximation to the integral I was obtained from relationship (1). An approximate D—C curve was found by graphical differentiation. Corrections to (1) could then be evaluated from the D—C curve and hence an improved D—C curve could be obtained. This process on further repetition eventually gave the true D—C relationship. The experimental investigations on the sorption of solvents by polystyrene have been extended in the present paper to include solvents other than chloroform. The method used for the calculation of D has been improved in several particulars and the values of D obtained for the several systems have been fitted to general mathematical expressions.

Experimental

Materials.—The polystyrene used was from the same stock of material as that used in the previous experiments[6] and hence had the same physical characteristics. A small quantity of polystyrene sheet only 0·025 mm. in thickness was, however, used for some experiments and it was found that this material had an intrinsic viscosity of 10·55 l. (base mole)$^{-1}$ which corresponds to a "viscosity average" molecular weight[9] of 280,000. It was found that all the polystyrene sheet obtained from the manufacturers had a high degree of orientation of the long axis of the molecules in the plane of the sheet; the 0·1 mm. sheet showed a 4-fold contraction in area above the second-order transition point. For some experiments the orientation was removed by allowing the material to relax under very slight tension or in the complete absence of tension at a temperature just above the second-order transition point of the material. The absence of orientation in this relaxed material was checked by examination in polarized light. The thin polystyrene sheet referred to above was used for the manufacture of this unoriented material and resulted in sheet of the order of 0·18 mm. in thickness.

The solvents used were of A.R. grade where available or were C.P materials obtained from British Drug Houses, Ltd., London. Except for chloroform, from which added stabilizer was carefully removed, no attempt was made to effect further purification. The butyl phthalate used was a technical grade and was purified as outlined in the previous paper.[6]

Procedure.—This was as already outlined[6] except that in the most rapid sorption of methyl iodide by polystyrene, the experiment was carried out in the absence of air and the uptake of methyl iodide was measured by the extension of a quartz spring. We have shown before[6] that, in the sorption of chloroform by polystyrene, the effect of still air on the sorption is negligible where the rate of sorption is less than 2 mg./hr. It is to be anticipated, however, that if the rate of sorption exceeds this value, as it does in the most rapid methylene chloride and methyl iodide experiments reported below, the effect of still air will distort the shape of the sorption-time curve and will lengthen slightly the sorption half-time. Other errors involved in the most rapid experiments are due to the disturbance of the system while the specimen is being weighed and to effects due to the heating of the specimen by condensation of solvent vapour. The former error is likely to be the most serious in experiments that are carried out at temperatures far removed from that of the room, e.g. the sorption of methylene chloride at 35° C.

It should be pointed out that all the errors will tend to make the observed value of the diffusion coefficient slightly too low at the high concentration end but will not otherwise affect the conclusion to be drawn from the experiments.

Results

Table I shows the properties of the halo-methanes used in the present series of experiments. The densities and molecular volumes are given at 20° C

[9] Bamford and Dewar, *Proc. Roy. Soc. A*, 1948, **192**, 329.

whereas the sorption experiments were carried out at 25° C. The densities and molecular volumes at 25° C will, however, be less than 1 % different from those at 20° C and so, for comparison purposes, the 20° C values will suffice.

TABLE I.—PROPERTIES OF THE HALO-METHANES USED

Compound	Density at 20° C	Molecular volume at 20° C (cm.^{3}/mole)	Boiling point (° C)
Methylene chloride	1·336	63·2	40·1
Chloroform	1·489	80·2	61·3
Carbon tetrachloride	1·595	96·6	76
Methylene bromide	2·495	69·7	98·2
Bromoform	2·890	87·5	149·5
Methyl iodide	2·279	62·3	42·5

Fig. 1 gives the absorption-time curves for methylene bromide at 25° C for various surface concentrations of the penetrant. The absorption-time curves for other penetrants are similar but the time scale varies considerably from one penetrant to another.

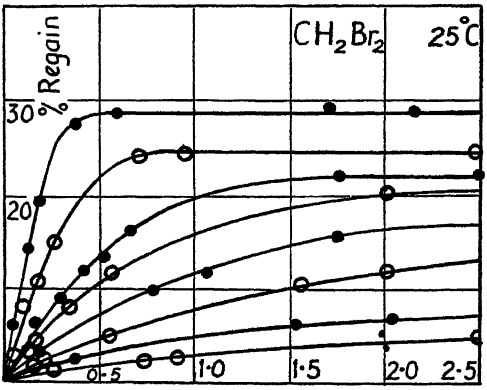

FIG. 1.—Regain–$t^{\frac{1}{4}}$ time curves for the absorption of methylene bromide by polystyrene. t is the time in sec. and l the thickness of the sheet in cm.

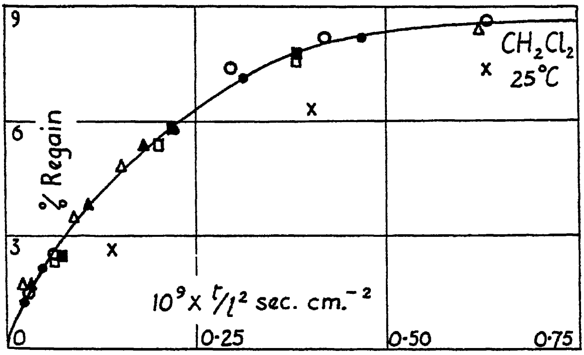

● Unoriented, l=0·186 mm. ○ Unoriented, l=0·160 mm.
△ Oriented, l = 0·103 mm. ■ Oriented, l = 0·113 mm.
■ Oriented, l = 0·071 mm. □ Oriented, l = 0.072 mm.
× Oriented, l = 0·023 mm.

FIG. 2.—Effect of thickness and orientation on sorption rate.

The work of Hartley[10] has shown the importance of molecular orientation in diffusion processes. Check experiments on polystyrene demonstrated that the effect was not likely to be important for the conditions of orientation and penetrant concentration obtaining in the present series of experiments. Fig. 2 showing the results of such a check also serves to indicate the degree of reproducibility obtained in duplicate absorption experiments. The deviation of the results for the very thin polymer sheet may be due to the systematic errors mentioned in the experimental section.

Discussion

Calculation of the Diffusion Coefficients.—The method for obtaining the diffusion coefficient-concentration relationship that has been published elsewhere[6, 7] and as mentioned in the Introduction, is unfortunately subject to error in two particulars. In the first place the identity

$$\bar{D} \equiv \mathrm{d}I/\mathrm{d}C_0 \quad . \quad . \quad . \quad . \quad . \quad (2)$$

is used to obtain the values of D by graphical differentiation. It has been found in most cases, e.g. where I approximates to an exponential function of C_0 and D varies considerably over the concentration range studied, that in practice the direct graphical differentiation is inaccurate. A more accurate method of differentiation involving a logarithmic plot has therefore been used. $\mathrm{Log}_{10} I$ is plotted against C_0 to give a straight line or a curve whose derivative is almost constant. $\mathrm{d}\log_{10} I/\mathrm{d}C_0$ is easily obtained by graphical differentiation and D is then obtained from the expression,

$$D \equiv \mathrm{d}I/\mathrm{d}C_0 \equiv 2{\cdot}303\, I\, \mathrm{d}\log_{10} I/\mathrm{d}C_0. \quad . \quad . \quad . \quad (3)$$

For the calculations of absorption-time curves, to give corrections to the successive approximations to the value of the diffusion coefficients,

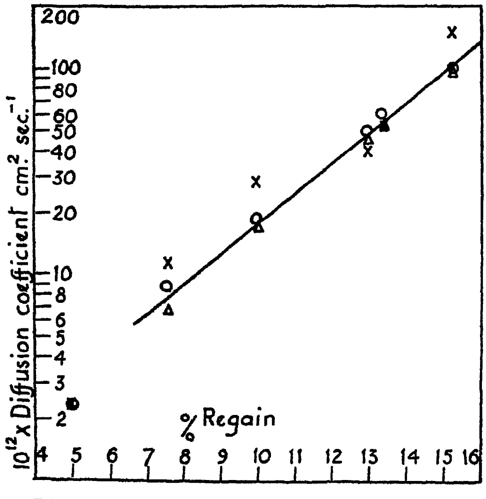

△ Linear extrapolation of log D assumed.
○ D assumed equal to $0{\cdot}024 \times 10^{-10}$ for $C < 5$ %.
× D assumed equal to $0{\cdot}024 \times 10^{-10}$ for $C < 5$ %, direct differentiation used.

FIG. 3.—A comparison of different calculations by Crank and Henry of the diffusion coefficient of chloroform in polystyrene.

---

[10] Hartley, *Trans. Faraday Soc.*, 1949, **45**, 820.

it is necessary to extrapolate these coefficients to concentrations below those of the slowest measured absorption-time curves. That the effect of the type of extrapolation is not very important is shown by Fig. 3 which also shows the decrease in scatter obtained by use of the refined method of graphical differentiation described above.

It might be thought that a test of the accuracy of the extrapolation would be afforded by a comparison of the shape of experimental and calculated absorption-time curves. Fig. 4 however, shows that within experimental error the observed points do not even distinguish between a constant and a variable coefficient.

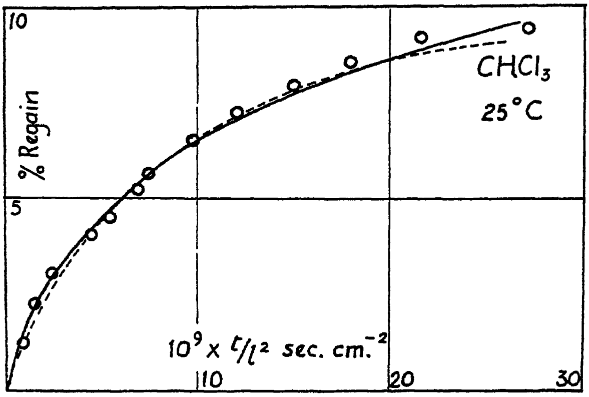

○ Experimental. —— Calc., variable D.
— — — Calc., constant D.

FIG. 4.—Calculated and experimental curves for the absorption of chloroform by polystyrene.

In view of the above arguments diffusion coefficient-concentration curves have only been reported over the range of concentration for which absorption measurements have been made. In all cases the extrapolation made for the purpose of calculation has been a linear one of the logarithm of the first approximation to the diffusion coefficient. The results are not greatly affected if this extrapolation is not correct.

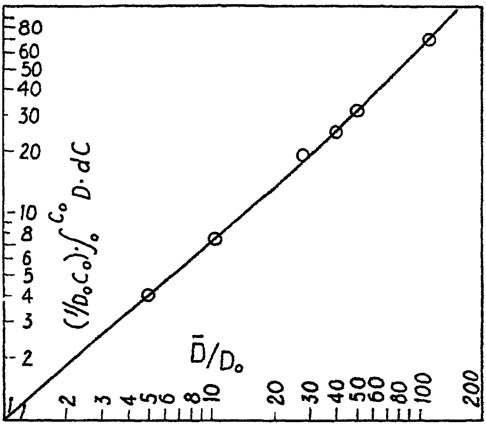

FIG. 5.—The $\bar{D} - I/C_0$ relationship.

After the dependence of D on C had been obtained in a few cases by evaluation of the successive approximations to the relationship between

$\bar{D}$ and I/C_0 it was realized that the D—C curves were all of approximately the same type. Hence it was possible to produce one curve, giving values of $I/(D_0C_0)$ in terms of $\bar{D}/D_0$, that held for all the systems investigated. Here D_0 is the diffusion coefficient at zero value of C.

This curve is reproduced in Fig. 5. The use of it dispenses with the method of successive approximation to the $\bar{D} - I/C_0$ relationship that had been used hitherto. It is of interest that the $\bar{D} - I/C_0$ curve for $D = D_0e^{lc}$ given in ref. 8 is almost identical with Fig. 5.

The procedure used for the subsequent calculation of diffusion coefficients is therefore as follows :

(i) $\bar{D}$ is deduced for each concentration of penetrant and an approximate value for D_0 is obtained by extrapolation of $d(\bar{D}C_0)/dC_0$ to zero value of C_0.

(ii) $\bar{D}/D_0$ values are then calculated and the corresponding values of $I/(D_0C_0)$ are found from Fig. 5.

(iii) Values of $\log_{10} I$ are calculated and plotted against C_0.

(iv) The slope of the above curve is then used to evaluate D by means of eqn. (3).

The diffusion coefficient concentration data obtained are shown in Table II together with the $\bar{D}$ values. It should be noted here that the rate of sorption of carbon tetrachloride by polystyrene, at concentrations of carbon tetrachloride where the polystyrene solvent system is still rigid enough to be handled, is very low. Even with polystyrene sheet only 0·025 mm. in thickness, sorption experiments lasted several months and had to be abandoned before equilibrium was reached. To obtain an idea of the value of the diffusion coefficient from these experiments it was necessary to obtain the equilibrium regains for carbon tetrachloride by extrapolation. A linear plot of molecular weight against equilibrium regain was made for each solvent+butyl phthalate composition, using the experimentally obtained points for CH_2Cl_2 and $CHCl_3$ and extrapolating values for CCl_4. In consequence the D—C curve for carbon tetrachloride can only be regarded as an approximation. An approximation to D has also been made for bromoform ; here only the experiments at very high surface concentration have reached equilibrium so a very narrow range of concentration is available for the construction of a C_0—I curve and a consequent low accuracy is to be expected in the D—C curve obtained.

Corrections to the Diffusion Coefficient for the Swelling and Overall Mass Flow of the Polymer.—It has been pointed out before[6] that the expression used for the calculation of D from the sorption half-time is based upon the assumption of a constancy of thickness of the polystyrene sheet at all times. If, however, the thickness increases as a result of the sorption of vapour, the sorption half-time is still given by the expression

$$\bar{D} = 0{\cdot}04939\ (t/l^2)_{\frac{1}{2}} \quad . \quad . \quad . \quad . \quad (4)$$

where $(t/l^2)_{\frac{1}{2}}$ is the value of t/l^2 when half the equilibrium sorption has been reached, provided that the diffusion coefficient is defined with reference to a unit of effective length in terms of which the thickness of the sheet is constant. A suitable scale of length has been defined by Crank and Hartley[11] and is such that equal increments of it mark off equal masses of polystyrene in a system of constant cross-sectional area. The cross-sectional area will be held at a constant value so long as the centre of the polystyrene sheet has not been swollen by penetrating vapour and it is fair to assume this up to at least the sorption half-time as has been shown in ref. 6, Fig. 5.

Crank and Hartley[11] have shown that, when there is no volume change on mixing, the diffusion coefficient D_p defined as above is related

---

[11] Hartley and Crank, *Trans. Faraday Soc.* 1949, **45**, 801.

TABLE II.—DIFFUSION COEFFICIENTS FOR VARIOUS SOLVENTS IN POLYSTYRENE

Penetrant and temperature	% Regain of penetrant	Volume fraction of penetrant	$D \times 10^{+9}$ cm.^{2} sec $^{-1}$	$D \times 10^{+9}$ cm.^{2} sec.$^{-1}$	$\mathcal{D}_v \times 10^{+9}$ cm.^{2} sec $^{-1}$
CH_2Cl_2 15° C	5·0	0·038	0·0585	0·093	0·083
	6·0	0·045	0·0698	0·127	0·111
	7·0	0·051	0·0845	0·174	0·149
	8·0	0·059	0·103	0·240	0·200
	9·0	0·066	0·127	0·327	0·267
	10·0	0·073	0·163	0·451	0·360
	11·0	0·080	0·216	0·619	0·483
CH_2Cl_2 25° C	5·0	0·038	0·139	0·205	0·181
	6·0	0·045	0·176	0·300	0·261
	7·0	0·051	0·226	0·442	0·378
	8·0	0·059	0·296	0·646	0·538
	9·0	0·066	0·396	0·963	0·785
	10·0	0·073	0·556	1·48	1·18
	11·0	0·080	0·843	2·59	2·02
CH_2Cl_2 35° C	5·0	0·038	0·325	0·568	0·500
	6·0	0·045	0·437	0·879	0·765
	7·0	0·051	0·593	1·37	1·17
	8·0	0·059	0·845	2·21	1·89
	9·0	0·066	1·30	3·56	2·91
	10·0	0·073	2·0	6·08	4·85
	11·0	0·080	2·8	12·3	9·6
CCl_4 25° C	8·5	0·053	0·000052	0·000086	0·000073
	11·5	0·071	0·000085	0·000179	0·000143
$CHCl_3$ 25° C	7·5	0·049	0·00437	0·0085	0·0073
	9·9	0·065	0·00797	0·0186	0·0152
	12·9	0·083	0·0171	0·0503	0·0388
	13·2	0·084	0·0199	0·0560	0·0431
	15·1	0·095	0·0326	0·160	0·0785
$CHCl_3$ 35° C	8·0	0·053	0·0088	0·0191	0·0162
	9·5	0·062	0·0133	0·0360	0·0298
	11·0	0·072	0·0211	0·0715	0·0566
	13·0	0·083	0·043	0·186	0·144
	15·0	0·095	0·107	0·491	0·364
CH_3I 15° C	6·7	0·030	0·0206	0·0206	0·0188
	9·8	0·043	0·0285	0·0349	0·0306
	17·1	0·073	0·0551	0·142	0·113
	21·6	0·090	0·120	0·394	0·297
	24·2	0·101	0·192	0·740	0·538
	26·3	0·108	0·345	1·59	1·13
CH_3I 25° C	9·6	0·042	0·0610	0·0731	0·0643
	12·7	0·056	0·0772	0·134	0·113
	15·6	0·067	0·112	0·270	0·219
	17·8	0·076	0·167	0·470	0·370
	20·6	0·087	0·282	1·00	0·761
	22·2	0·093	0·437	1·61	1·20
	24·4	0·102	0·667	2·73	1·98
CH_2Br_2 25° C	9·2	0·038	0·0251	0·026	0·023
	12·1	0·049	0·0309	0·051	0·044
	15·6	0·062	0·0466	0·113	0·093
	18·0	0·071	0·0681	0·193	0·155
	20·8	0·081	0·106	0·338	0·263
	21·7	0·083	0·139	0·446	0·344
	24·7	0·094	0·273	0·825	0·613
	28·7	0·108	0·457	1·75	1·24
$CHBr_3$ 25° C	25	0·083	0·00032	0·00133	0·00102
	30	0·098	0·00063	0·00345	0·00253
	35	0·113	0·00186	0·0099	0·0069

to the more usual diffusion coefficient D^v defined in terms of a normal length unit and with concentration expressed as mass per unit overall volume, by the expression

$$D^v = D_p(C_s^v V_s^0)^{-2}, \quad . \quad . \quad . \quad . \quad . \quad (5)$$

where V_s^0 is the specific volume of pure polystyrene and C_s^v is the concentration of polystyrene in mass per unit overall volume. The diffusion coefficients D^v or D_p alone give a measure of the real diffusion of the penetrant plus the mass flow of the whole system that must take place to maintain the correct mass-volume relationships.[1] Diffusion coefficients defined such that the influence of mass flow has been eliminated have been termed intrinsic diffusion coefficients.[11] The above authors [11] have shown that an expression can be given relating D_p to the intrinsic diffusion coefficients for polymer in penetrant and penetrant in polymer, $\mathscr{D}_s$ and $\mathscr{D}_p$ respectively. Except where one of the intrinsic diffusion coefficients is very much larger than the other, this expression alone will not enable us to calculate either intrinsic diffusion coefficient, but since we are dealing here with a polymer solvent system in which the long chain polymer will be relatively immobile, the relationship $\mathscr{D}_p \gg \mathscr{D}_s$ holds and the simple expression

$$\mathscr{D}_p = D_p(V_sC_s^v)^{-1}(V_s^0C_s^v)^{-2} \; . \quad . \quad (6)$$

results, where V_s is the partial specific volume of polystyrene at the concentration of polymer C_s^V. If we assume that there is no volume change on mixing polymer and liquid penetrant, $V_s = V_s^0$ and $V_sC_s^v = v_s$, the volume fraction of polymer. Hence we obtain

$$\mathscr{D}_p = D_p(1 - v_p)^{-3}, \quad . \quad . \quad . \quad (7)$$

where v_p is the volume fraction of the penetrant. Eqn. (7) enables us to evaluate $\mathscr{D}_p$ for all the systems investigated and this has been done in Table II.

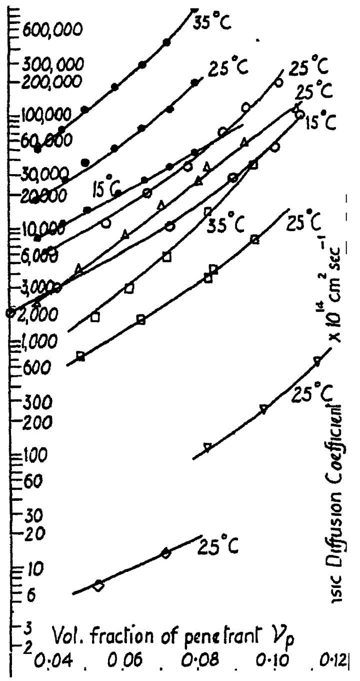

● CH_2Cl_2. □ $CHCl_3$. ◇ CCl_4.
△ CH_2Br_2. ▽ $CHBr_3$. ○ CH_3I.

FIG. 6.—Intrinsic diffusion coefficients for penetrants.

Values of Intrinsic Diffusion Coefficients as a Function of Concentration, Temperature and Penetrant Size.—A plot of $\mathscr{D}_p$ against v_p for all the penetrants has been made on a logarithmic scale in Fig. 6. It can be seen that the relationship between the intrinsic diffusion coefficient and concentration for most penetrants is approximately of the form

$$\mathscr{D}_p = \mathscr{D}_0 e^{\alpha v_p}, \quad . \quad . \quad . \quad . \quad . \quad (8)$$

where $\mathscr{D}_0$ and α are constant for any one penetrant at a fixed temperature. Values for $\mathscr{D}_0$ and α are given in Table III for each penetrant at 25° C and for methylene chloride, methyl iodide and chloroform at 15° C or 35° C. The effect of temperature on $\mathscr{D}_0$ and α is considerable but the range in temperature covered is not sufficient to allow any certain conclusions to be drawn about the form of the dependence of $\mathscr{D}_p$ on temperature.

TABLE III

Temperature	Penetrant	$10^{14} \times \mathscr{D}_0$ cm.^{2} sec.$^{-1}$	α	$RT\alpha$ kcal /mole
25° C	CH_2Cl_2	1950	56·3	33·6
	CH_3I	460	57·7	34·4
	CH_2Br_2	250	57·7	34·4
	$CHCl_3$	58	52·0	31·0
	$CHBr_3$	~ 2·3	~ 50	~ 30
	CCl_4	~ 0·9	~ 35	~ 20
15° C	CH_2Cl_2	1650	39·7	22·7
	CH_3I	475	46·3	26·5
35° C	CH_2Cl_2	2330	64·2	39·3
	$CHCl_3$	55	66·7	40·8

Fig. 6 illustrates the very great sensitivity of $\mathscr{D}_p$ to variation in penetrant molecular size. Thus, though the CCl_4 molecule has a volume only about 1½ times as great as the CH_2Cl_2 molecule, the difference in D_p is so large that it is almost impossible to measure sorption-time curves for the former. Table III shows how little α varies with molecular size but emphasizes how great is the variation of $\mathscr{D}_0$. In Fig. 7 values of $\log_{10} \mathscr{D}_0$ are plotted against molecular volume and fall roughly on a straight line satisfying the equation

$$\mathscr{D}_0 = Ke^{-\beta V_M}, \quad . \quad . \quad . \quad . \quad . \quad (9)$$

where K the diffusion coefficient for a penetrant of zero molecular volume at zero concentration in polystyrene is equal to 3×10^{-5} cm.^{2} sec.$^{-1}$, β is a constant equal to 0·235 cm.$^{-3}$ and V_M is the molecular volume at 20° C.

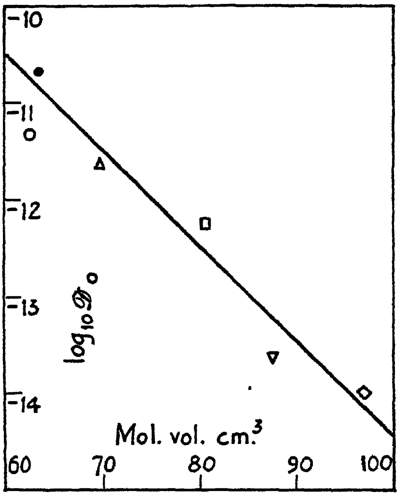

● CH_2Cl_2. ○ CH_3I. △ CH_2Br_2.
□ $CHCl_3$. ▽ $CHBr_3$. ◇ CCl_4.

FIG. 7.—Variation of diffusion coefficient with molecular size.

It is interesting that CH_2Cl_2 has a larger $\mathscr{D}_0$ than CH_3I though the molecular volumes would suggest the reverse order. This reversal may, as has been suggested by K. C. Smith [12] and by Hartley [13] for diffusion into cellulose acetate, be due to change in shape, CH_2Cl_2 being able to pass through a smaller opening than CH_3I, or it may be due to differences in packing in the liquid penetrants, the molecular volume of CH_2Cl_2 containing more free space than is the case for CH_3I. Alternatively, differences in interaction energy between penetrant and polymer may be large enough to play a part in determining $\mathscr{D}_0$.

---

[12] Smith, K. C., unpublished work in this Laboratory.

[13] Hartley, private communication.

The temperature dependence of the diffusion coefficients obtained here is somewhat greater than that reported by K. C. Smith[12] from measurements of overall penetration rates for various solvents and swellers in cellulose acetate. This is paralleled by the less violent dependence upon molecular size also reported by Smith and, though specific effects for cellulose acetate may operate, part of the difference may be ascribed to the different concentration range covered. The overall penetration rate leads to an average diffusion coefficient that includes values for the highly swollen mobile gel state as well as for the region of low penetrant concentration that has been dealt with by the present author. It is likely that diffusion in the highly swollen gel state will be more like that in simple liquids and hence less dependent upon molecular size and temperature than in the region of low penetrant concentration. This is in agreement with the small temperature dependence for diffusion in highly swollen cellulose acetate gels that has been obtained by Robinson.[5]

Before any interpretation of the facts given in this section in terms of current diffusion theory, a definition of the diffusion coefficient which seeks to eliminate effects of non-ideality must be mentioned. We will call the coefficient thus defined the thermodynamic diffusion coefficient. Non-ideality in solutions lead to an apparent concentration dependence of the intrinsic diffusion coefficient which may in some cases account for the whole of the observed effect.

The Thermodynamic Diffusion Coefficient.—It has been maintained by several authors[1, 11, 14, 15, 16] that diffusion in any system should be regarded as dependent upon the product of the concentration and the free energy gradient rather than upon the concentration gradient alone. Let a diffusion coefficient $\mathscr{D}_p{}^T$ be defined by the expression

$$\phi = \mathscr{D}_p{}^T \,.\, C_p{}^v/RT \,.\, \mathrm{d}\mu/\mathrm{d}x. \qquad . \quad . \quad . \quad (10)$$

Here ϕ is the flux of penetrant across a plane which moves in such a way that there is no real flow across it, and hence is the transfer rate due to true diffusion, $C_p{}^v$ is the concentration of penetrant in mass per unit overall volume, μ is the chemical potential per mole of penetrant and x is measured in ordinary units of distance, e.g. cm. It is then easy to show[11, 17] that

$$\mathscr{D}_p{}^T = \mathscr{D}_p \mathrm{d} \ln C_p{}^v/\mathrm{d} \ln a, \qquad . \quad . \quad . \quad (11)$$

where a is the activity of the penetrant.

In order that we may proceed further with the evaluation of $\mathscr{D}_p{}^T$ a knowledge of the activity concentration relationship is needed for the polystyrene-solvent system. In the absence of any data for the low values of $C_p{}^v$ with which we are dealing, we assume that the Huggins[18] equation

$$\ln a = \ln v_p + v_s + uv_s{}^2 \,. \qquad . \quad . \quad . \quad . \quad (12)$$

which has been shown[19] to hold for higher concentrations of penetrant in polystyrene, still holds. Baughan has shown that for polystyrene-solvent system u is a constant between ± 1.

---

[14] Barrer, *J. Soc. Dyers Col.* (Symposium on Fibrous Proteins), 1946, 108.

[15] Gilbert, *ibid.*, 1946, 114.

[16] Hartley, *ibid.*, 1946, 114.

[17] Glasstone, Laidler, Eyring, *The Theory of Rate Processes* (McGraw Hill Book Co., New York and London), 1941, Chap. 9.

[18] Huggins, *J. Amer. Chem. Soc.*, 1942, 64, 1712 ; *Ind. Eng. Chem.*, 1943, 35, 217.

[19] Baughan, *Trans. Faraday Soc.*, 1948, 44, 495.

If there is no volume change on mixing liquid penetrant and polymer then

$$v_p = V_p^0 C_p^v$$

and since

$$v_s + v_p = 1$$

it follows from eqn. (12) that

$$d \ln C_p^v / d \ln a = 1/[1 + v_p(2u - 1) - v_p^2], \qquad (13)$$

and hence

$$\mathscr{D}_p = \mathscr{D}_p^T/[1 + v_p(2u - 1) - v_p^2]. \qquad (14)$$

In all the work considered here the variation in v_p is from about 0·03 to 0·11 and if $u = 1$ this variation will only account for an increase in $\mathscr{D}_p$ of the order of 8 % whereas the observed increase is of the order of 8000 %. If u is less than a half, activity effects alone would lead to a decrease in $\mathscr{D}_p$ with increasing concentration. The conclusion is therefore reached that the variation in $\mathscr{D}_p$ with concentration is due to a variation in $\mathscr{D}_p^T$ and the activity effects are probably so small that to a first approximation $\mathscr{D}_p^T = \mathscr{D}_p$. Other reasons for the dependence of $\mathscr{D}_p$ on the concentration must therefore be sought.

Interpretation of $\mathscr{D}_p^T$ in Terms of Transition State Theory.—In terms of the transition state theory for rate processes[17] it is possible to express the diffusion coefficient $\mathscr{D}_p^T$ in terms of the free energy required to reach some transition state. Thus

$$\mathscr{D}_p^T = (\lambda^2 kT/h)e^{-\Delta G^*/RT} \qquad (15)$$
$$= (\lambda^2 kT/h)\, e^{-\Delta S^*/R}\, e^{-\Delta H^*/RT}, \qquad (16)$$

where k is Boltsmann's constant, h is Planck's constant, λ is the mean free path of the penetrant in the polymer and ΔF^*, ΔS^* and ΔH^* are the standard, free energy, entropy, and energy of activation for the diffusion process. It is significant that the curves shown in Fig. 6 are approximately exponential in character and it appears likely that the observed variations in $\mathscr{D}_p$ are due to an approximately linear variation of ΔG^* with composition. In fact it is easy to see that the quantity $RT\alpha$ given in Table III can be interpreted as the change in ΔG^* per unit change in volume fraction of penetrant. In terms of a theory of diffusion through channels, $RT\alpha$ is to be interpreted as a measure of the widening of channels with dilution of the polymer or as a measure of the lowering of the interaction between channel walls and the penetrant. In terms of a diffusion theory requiring hole formation in the polymer, $RT\alpha$ is a measure of the loosening of the polymer structure and is to be related to the change in viscosity or plasticity occurring as penetrant concentration increases. In any case it is of interest that $RT\alpha$ shows little variation with molecular size.

Fig. 7 referring to diffusion at zero concentration of penetrant can be interpreted as a linear dependence of the free energy of activation for diffusion in solvent free polystyrene ΔG_0^* upon molecular volume. Within the accuracy of the present results the free energy of activation could equally well be linear in (molecular volume)$^{1/3}$ i.e. in the molecular radius, or in (molecular volume)$^{2/3}$ i.e. in the molecular surface area.

From the slope of Fig. 7 (β of eqn. (9)), a value for $\partial \Delta G_0^*/\partial V_M$ can be obtained. This is found to be about 0·14 kcal./cm.^{3} which in terms of the theory of diffusion by formation of holes must be the free energy needed per cm.^{3} for hole formation in pure polystyrene. The free energy for making a hole of zero volume in the polymer matrix will be zero, and hence from eqn. (9) and (15),

$$\lambda^2 kT/h = K. \qquad (17)$$

On using the value for K of 3×10^{-5} given before, it is found that

$$\lambda \approx 0{\cdot}2 \text{ Å},$$

which is about one-tenth of the molecular radii of the penetrants used. This is not unreasonable when the approximate nature of the extrapolation used in obtaining the numerical value of K is taken into account.

The Energy and Entropy of Activation.—The expression

$$\mathrm{d}\,(\ln \mathscr{D}_p{}^T)/\mathrm{d}(1/T) = T + \Delta H^*/R \quad . \quad . \quad . \quad (18)$$

is easily obtained from eqn. (16) when ΔS^* and ΔH^* are temperature independent and enables one to calculate the activation energy for diffusion from the values of $\mathscr{D}_p{}^T$ measured at different temperatures. Values for $\mathscr{D}_p{}^T$ at 35° C for CH_2Cl_2 and $CHCl_3$ and at 15° C for CH_2Cl_2 and CH_3I together with the values at 25° C are given in Table II. The figures obtained for ΔH^* from eqn. (18) are given in Table IV. Owing to the low temperature range covered and the great dependence of $\mathscr{D}_p{}^T$ upon concentration no very great accuracy is claimed.

TABLE IV.—ACTIVATION ENERGY FOR DIFFUSION

Vol fraction of penetrant	Apparent activation energy in kcal. $= \Delta H^* \quad T(\mathrm{d}\Delta H^*/\mathrm{d}T) + T^2\mathrm{d}\Delta S^*/\mathrm{d}T$			
	CH_3I 15–25° C	CH_2Cl_2 15–25° C	CH_2Cl_2 25–35° C	$CHCl_3$ 25–35° C
0·04	14·1	14·3	18·6	—
0·05	13·9	14·7	22·0	13·2
0·06	15·1	16·5	23·4	18·4
0·07	15·7	20·0	24·4	17·1
0·08	16·9	24·7	26·8	21·6
0·09	18·3	—	—	26·2
0·10	18·3	—	—	—

The difference in the calculated values of ΔH^* for methylene chloride over two different temperature ranges indicates that the assumptions made in deriving eqn. (18) i.e. that ΔS^* and ΔH^* are temperature independent, are not strictly valid. In view of the considerable variations of ΔG^* with solvent concentration this is not entirely unexpected. It can be seen that eqn. (18) should then be replaced by (19).

$$\frac{\mathrm{d}\,(\ln \mathscr{D}_p{}^T)}{\mathrm{d}(1/T)} = T + \frac{\Delta H^*}{R} - \frac{T}{R}\frac{\mathrm{d}\Delta H^*}{\mathrm{d}T} + \frac{T^2}{R}\frac{\mathrm{d}\Delta S^*}{\mathrm{d}T} \quad . \quad . \quad (19)$$

The apparent activation energy values calculated from eqn. (18) then become equal to

$$\Delta H^* - T\mathrm{d}\Delta H^*/\mathrm{d}T + T^2\mathrm{d}\Delta S^*/\mathrm{d}T.$$

Until more data covering a larger temperature range are available it is not useful to speculate too much about the values of these quantities but it might be mentioned that the magnitude of the apparent activation energy values are of the order to be expected from the molecular size—activation energy relationship given by van Amerongen [20] for the diffusion of gases in rubber. A rough calculation of ΔS^* from eqn. (16) making use of the approximate value for $\lambda^2 kT/h$ of 3×10^{-3} and the apparent values of ΔH^* given in Table IV yields values between 20 and 50 cal./mole deg. Barrer [21] has pointed out that such high values for ΔS^* imply a considerable disturbance of the solid material in the formation of the transition state for diffusion. It is unlikely that the temperature variable factors of eqn. (19) will alter the order of magnitude of ΔS^* and so Barrer's conclusions probably hold for the diffusion systems studied here.

---

[20] van Amerongen, *J. Appl. Physics*, 1946, **17**, 972.

[21] Barrer, *Trans. Faraday Soc.*, 1939, **35**, 644.

The author wishes to acknowledge the considerable help given to him by the technical assistance of Mr. E. P. Cummins, the computational work of Miss M. E. Henry, and the mathematical discussions with Mr. J. Crank.

Courtaulds, Ltd.,
Research Laboratory,
Maidenhead, Berks.

REVIEWS OF BOOKS

Chemical Constitution and Biological Activity. By W. A. SEXTON. (E. & F. N. Spon, Ltd.) Pp. 412. Price 55s.

This book represents yet another attempt to bring order to a problem which has fascinated a large number of chemists for many years. In contrast to another recent publication which examined the basis of chemotherapy and therefore laid its main emphasis on the biochemical processes underlying the action of drugs, this one is principally concerned with types of chemicals and the physiological actions they possess, and biochemistry is subordinated to organic structures.

The book falls clearly into two sections. In the first, which occupies roughly a quarter of the book, the principal components, namely proteins, nucleic acids and polysaccharides, of biological fluids and tissues are briefly described. Emphasis is laid upon molecular size and spatial structure and on the various physico-chemical, as well as chemical, requirements with which a biologically active substance must conform. The very emphasis placed upon the physical chemistry of the systems concerned is in itself a pointer to the lack of real knowledge of the systems involved. Although the physical chemistry of drug action is a most actively debated subject, it is clear that this activity in debate is merely a cloak to cover ignorance of the processes involved. This is no criticism of this book, only a comment on the lack of data.

In the second section 16 short chapters are devoted to discussion on vitamins and antivitamins, sulphonamides, porphyrins, anthelminthics, antimalarials, trypanocides, plant growth regulators and kindred subjects, though in a book having the above title it is, perhaps, a little surprising that there is no reference to local anaesthetics or hypnotic drugs, two groups in which some relationships between constitution and activity could be constructed. In view of the vast amount of work done and of the author's own close association with antimalarials and trypanocides, it is not surprising that these two subjects receive somewhat more attention than others; on the other hand certain subjects, such as sympathomimetic drugs, seem to have been more cursorily treated than is consistent with their importance. This, however, is inevitable in any volume within the compass of which a large subject is being discussed and the virtue of wide range inevitably carries with it the counterbalancing vice of overcompression.

The book is very thoroughly indexed and on many of the points discussed reference is made to the original literature. It might, however, have been helpful to the enquiring reader if references to the many review articles on the various topics had been more liberally supplied.

In a volume in which so many complex formulae are accurately represented it is perhaps unfair to point to errors, but the formula of muscarine on page 186 appears to be wrong and it is unfortunate that on page 230 the suggested biogenesis of adrenaline ends with a compound which is not adrenaline and in which one of its most essential groups, namely the alcoholic hydroxyl group, is completely ignored.

The volume, however, contains a vast amount of information on a wide range of topics, for those interested in or concerned with this subject. The reviewer, when a student, was warned that, though he probably then thought he knew everything, the time would come when he would be glad to know where he could find anything. That time has now come and he is grateful to Dr. Sexton for writing a book in which he will be able to find, not perhaps everything, but at least a very great deal.

B. A. H.

Frontiers in Chemistry, Volume VII. Recent Advances in Analytical Chemistry. Edited by R. E. BURK and OLIVER GRUMMITT. (Interscience Publishers Inc., New York, 1949.) Pp. vii + 209. Price 27s.

The range of topics in analytical chemistry covered by this book is wide and somewhat scattered, but it is a fitting contribution to the *Frontiers in Chemistry* series, which aims at presenting to chemists intelligible information on the many borderline fields between chemistry and other sciences. The text incorporates seven independent monographs, the authors' names being a sufficient guarantee that they are up to date and authoritative.

Prof. I. M. Kolthoff writes on voltammetry (polarography) and amperometric titrations, surveying the basic principles of these techniques succinctly, and briefly outlining their applications. The increasingly important use of organic reagents in inorganic analysis is reviewed by Prof. J. H. Yoe, who resists a probable temptation to overemphasise selective organic reagents for detection of metals, and covers his field broadly, even discussing the use of organic wash-liquids and solvents. The same author surveys, in a separate section, recent colorimetric and gravimetric organic reagents, several specific reagents (for silver, palladium, iron, titanium, and tungsten) being considered. A less familiar topic, application of infra-red spectroscopy in analysis, is admirably introduced by Dr. O. Beeck, who describes the instrumental techniques and their quantitative and qualitative application, mainly with reference to hydrocarbons. An elegant exposition of electron microscopy (with a section on electron diffraction), well illustrated by typical micrographs, is furnished by Dr. J. Hillier. Refinements in fractionation methods and in the determination of freezing point, described by Dr. F. D. Rossini, aptly illustrate the considerable recent advances in analysis of complex hydrocarbon mixtures. A related field of analysis is reviewed by Dr. J. A. Hipple, who discusses the use of the mass-spectrometer, particularly in the study of hydrocarbons and their reactions.

Provided that it is realized that this book is a series of reviews on particular topics, rather than a broad survey of recent advances in analytical chemistry as a whole, it may be strongly recommended.

A. J. E. W.

Electricity in the Service of Man. By SYDNEY G. STARLING. 2nd Ed. revised by H. J. GRAY. (Longmans, Green & Co. 1949.) Pp. x + 255. Price 12s. 6d.

That a second edition of this book, first published in 1922, should be called for after a re-issue of the first edition in 1945, is evidence of its vitality. It is " designed to present to the general reader and to the student in other branches of science an appreciation of the subject of electricity as it appears to the physicist of to-day ", and it is a welcome addition to those works which have the important aim of bringing to the general community, as simply and as clearly as possible, a knowledge of the great achievements of science in enabling us to understand the phenomena of nature and in improving the amenities of our everyday life.

In twelve chapters, in the first of which is given an historical account of the discovery and early investigation of the phenomena of magnetism and electricity, there are discussed: the electromagnet, the dynamo, the electric motor, alternating currents, electric lighting, the electric telegraph, the telephone, electrolysis and batteries, electromagnetic theory and wireless telegraphy, gases and X-rays, radioactivity. Not only is fundamental theory explained in clear and simple language, demanding nevertheless the close attention of the reader, but most of the important everyday applications are also described.

In bringing the book up to date the reviser has, on the whole, been successful, and the reader will perhaps turn with special eagerness to the last three chapters of the book. Here, after an adequate discussion of electromagnetic theory, one is introduced to Hertzian waves and the early days of wireless telegraphy, followed by an interesting account of the thermionic valve, the triode valve and wireless telephony. The photoelectric cell and the development of the " talkie film " are also described. There then follow a discussion of the discharge of electricity through rarefied gases, the production of cathode rays and the use of the cathode ray tube in radar and television. From the discovery of X-rays there followed the discovery of radioactivity, and in the concluding chapter this very important property is discussed, the discussion ending with an account of nuclear energy, the atom bomb, the maintenance of the sun's temperature and the age of the earth.

On the whole the book can be warmly recommended, but the chapter on electrolysis and batteries is rather unsatisfactory and needs a very thorough revision. To seek to discuss the phenomena of electrolysis and the behaviour of voltaic cells except on the basis of the theory of ionization of electrolytes is surely mistaken. The short reference to the electrolytic dissociation theory is quite inadequate and there is no mention of ions. The discussion of the behaviour of batteries is therefore unsatisfactory and the chemical equations given are misleading.

A. F.

Haemoglobin. A Symposium based on a Conference held at Cambridge in June, 1948, in memory of Sir Joseph Barcroft. Edited by F. J. W. ROUGHTON and J. C. KENDREW. (London: Butterworth's Scientific Publications, 1949.) Pp. xii + 317. 40s. net.

This work comprises a series of contributions by some thirty participants in the Barcroft Memorial Conference on haemoglobin at Cambridge in June, 1948. In addition, eight distinguished colleagues of Barcroft provide personal tributes in the opening 31 pages.

The book is remarkable on the one hand for the narrowness of the subject a single protein and on the other for the variety of scientific skill and experience which is brought to bear on it. Since each contributor has an average of ten pages at his disposal, neither the matter nor the bibliography at the end of each article is comprehensive, nor are they intended to be. The reader will be well advised not to look for detailed knowledge but to read the book quickly for its overall impressions. It is by no means easy reading largely because of the number of authors and the absence of any attempt at editing. Nevertheless the book has general impressions of considerable value to convey and the reviewer ventures to predict that it will be laid down with the conviction that the field of proteins in general holds out a unique challenge and opportunity to research workers in numerous fields at the present time.

All the contributions are good and several are outstanding. Pauling makes a bold incursion into the electronic structure of haemoglobin in order mainly to explain the respiratory properties of the protein, and the same general ideas but with more attention devoted to the haem groups are pursued by Wyman. There is, of course, a great deal of spectrophotometry by several contributors, and Perutz and Kendrew do justice to the X-ray crystallography of the protein. The osmotic properties are largely left to Adair. There are several chapters on different aspects of the amino-acid composition of haemoglobin and myoglobin and Rimington writes on the biosynthesis of haem.

Jope, Dervichian and Roughton using different techniques have important evidence to offer concerning the physical state and kinetic relations of haemoglobin inside the erythrocyte. These articles naturally lead to more physiological chapters, including ones on foetal haemoglobin, methaemoglobin and even the behaviour of respiratory proteins of lower invertebrates.

There is only space here to mention a few of the contributors but enough have been named to vouchsafe for the quality of the book. At the same time it must be pointed out that many of the articles have a topical and provocative character befitting the conference atmosphere but not so suitable for the text book. This, taken in conjunction with the quality of reproduction, and including several printer's errors, makes the price rather high by comparison, for example, with a volume of *Recent Advances in Biochemistry*. This is a pity because the book clearly ought to be read by all concerned with proteins.

A. S. McF.

UNSTEADY-STATE DIFFUSION OR HEAT-CONDUCTION WITH MOVING BOUNDARY

By P. V. Danckwerts

Received 20th January, 1950

A general method of solution is described for a class of problems in unsteady-state linear heat conduction or diffusion, which involve two phases or regions separated by a moving plane interface.

The following examples are used to illustrate the method: the absorption by a liquid of a single component from a mixture of gases; tarnishing reactions; condensation of a vapour at the surface of a cold liquid or on a cooled surface; gas reacting at solid surface to form gaseous product; solution of a gas in a liquid, followed by reaction with solute; and progressive freezing of a liquid.

1. **Introduction.**—There is a category of problems in unsteady-state linear heat conduction or diffusion, involving contiguous phases or regions with a moving interface, for which special solutions have been produced from time to time. Among these have been (*a*) the progressive freezing of a liquid,[1] (*b*) the absorption by a liquid of a single component from a mixture of gases,[2] and (*c*) tarnishing reactions.[3] These are variants of a single mathematical problem, but have all been solved independently. The more general method of solution presented here may be of service in enabling solutions of new variants to be obtained with the minimum of fresh mathematical work. In addition, the method can be used to give a more general form of the solution to problem (*a*) above, and a more rigorous and highly-developed solution to (*b*), than appear to have been available hitherto.

In all the cases considered the two regions are separated by a plane surface, and diffusion or heat conduction takes place only along an axis perpendicular to this plane. The concentration or temperature is initially uniform in each region. The process of heat conduction or diffusion may cause changes which bring about the disappearance or appearance of matter at the interface in one or both of the regions, and a resulting bodily movement of the matter in one or both regions relative to the interface. As a simple example consider the melting of ice in contact with water; as heat flows from water to ice, ice disappears and water appears at the interface, so that both the ice and the water are in bodily movement with respect to the interface. In all the cases considered the rates of bodily motion of the matter in the two regions with respect to the interface are related by constant proportionality (e.g. the volume of ice melted is proportional to the volume of water formed). Variations in density (or partial density) of either medium due to variations in temperature or concentration are ignored.

In the next section the conditions of the problem will be stated in a form sufficiently general to include all likely applications of the solution. The extent to which various types of real system obey these conditions will be discussed in connection with the examples given later. The practical value of the results is limited by the fact that they cannot be applied to systems in which convection currents occur, or in which gradients of both temperature and concentration exist.

---

[1] Carslaw and Jaeger, *Conduction of Heat in Solids* (Oxford University Press, 1947), pp. 71, 227.

[2] Arnold, *Trans. Amer. Inst. Chem. Eng.*, 1944, **40**, 361.

[3] Booth, *Trans. Faraday Soc.*, 1948, **44**, 796.

2. Conditions of the Problem.—We consider two *media* which are stagnant in the sense that they are free from convection currents, but which may be in relative bodily motion along the x-axis (which is perpendicular to the interface). Location in medium 1 will be referred to co-ordinates of the x_1 system, which are stationary with respect to medium 1; location in medium 2 is referred to x_2 co-ordinates, which are stationary with respect to medium 2 (Fig. 1). The media are separated at time t

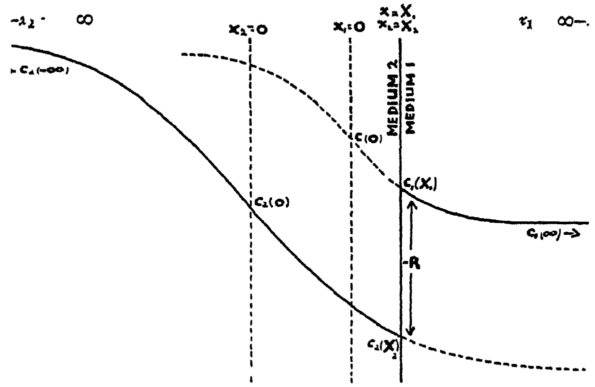

FIG. 1

by the plane $x_1 = X_1$, $x_2 = X_2$, which is initially at $x_1 = x_2 = 0$. Medium 1 occupies all or part of the space $X_1 < x_1 < \infty$, medium 2 all or part of the space $-\infty < x_2 < X_2$.

Present in both media is a *diffusant* (matter or heat); diffusional processes cause transport of the diffusant relative to the x_1 and x_2 co-ordinates, and transfer from one medium to the other. The concentration of the diffusant at time t is denoted by c_1 at x_1 and c_2 at x_2. Initially c_1 has the value $c_1(0)$ at $x_1 = 0$ and $c_1(\infty)$ for all $x_1 > 0$, c_2 the value $c_2(0)$ at $x_2 = 0$ and $c_2(-\infty)$ for all $x_2 < 0$. The following diffusion equations are obeyed in the two media:

$$\frac{\partial c_1}{\partial t} = D_1 \frac{\partial_2 c_1}{\partial x_1{}^2}, \quad . \quad . \quad . \quad . \quad . \quad (2.1)$$

$$\frac{\partial c_2}{\partial t} = D_2 \frac{\partial_2 c_2}{\partial x_2{}^2}, \quad . \quad . \quad . \quad . \quad . \quad (2.2)$$

D_1 and D_2 being the respective diffusivities, which are assumed to be independent of c_1 and c_2 respectively. (In diffusion in liquids, this assumption will be justified only if variations in the concentration of the diffusant are small.)

At any time the concentrations $c_1(X_1)$ and $c_2(X_2)$, at either side of the interface, are related by an equilibrium expression:

$$c_2(X_2) = Qc_1(X_1) + R, \quad . \quad . \quad . \quad (2.3)$$

where Q and R are physical constants (e.g. for absorption of a gas obeying Henry's law, Q = solubility of gas (in suitable units), $R = 0$).

The diffusant is conserved at the interface, as elsewhere, so that

$$D_1\left(\frac{\partial c_1}{\partial x_1}\right)_{x_1=X_1} - D_2\left(\frac{\partial c_2}{\partial x_2}\right)_{x_2=X_2} + c_1(X_1)\frac{\mathrm{d}X_1}{\mathrm{d}t} - c_2(X_2)\frac{\mathrm{d}X_2}{\mathrm{d}t} = 0. \quad (2.4)$$

Eqn. (2.4) merely expresses the fact that the quantity of the diffusant disappearing from medium 1 is equal to the quantity appearing in medium 2.

There is constant proportionality between X_1 and X_2 (since there is constant proportionality between the rates of movement of the two media relative to the interface—although one or both of these rates may be zero). Hence

$$X_2 = PX_1 \qquad . \quad . \quad . \quad . \quad (2.5)$$

where P is determined by the conditions of the problem.

At least two of the quantities $c_1(\infty)$, $c_1(0)$, $c_1(X_1)$, $c_2(-\infty)$, $c_2(0)$ must be specified in the data of the problem. In addition, in order to define the problem completely, it is necessary either that a third of these quantities should also be specified (solutions of Class B, see § 6) or that there should be constant proportionality of specified magnitude between the quantity of diffusant crossing the interface and the values of X_1 and X_2 (solutions of Class A, see § 5).

3. Solutions of Diffusion Equations for Infinite Media.—Consider an *infinite* medium in which eqn. (2.1) holds, together with the following boundary conditions:

$$\begin{array}{ll} c_1 = c_1(\infty),\ t = 0,\ \text{all } x_1 > 0, & c_1 = c_1(0),\ \text{all } t,\ x_1 = 0, \\ c_1 = c_1(-\infty),\ t = 0,\ \text{all } x_1 < 0, & c_1 = c_1(-\infty),\ \text{all } t,\ x_1 = -\infty, \\ 2c_1(0) = c_1(\infty) + c_1(-\infty), & c_1 = c_1(\infty),\ \text{all } t,\ x = \infty, \end{array}$$

where $c_1(\infty)$, $c_1(-\infty)$, $c_1(0)$ are all constant.

Employing the well-known solutions for the conduction of heat,[4] we find

$$\frac{c_1(\infty) - c_1}{c_1(\infty) - c_1(0)} = 1 - \operatorname{erf}\left[\frac{x_1}{2\sqrt{D_1 t}}\right] \qquad . \quad . \quad (3.1)$$

as the solution of (2.1), c_1 being the concentration of the migrant at x_1, t. Similarly the solution of (2.2) under analogous boundary conditions is

$$\frac{c_2(\infty) - c_2}{c_2(\infty) - c_2(0)} = 1 - \operatorname{erf}\left[\frac{x_2}{2\sqrt{D_2 t}}\right], \qquad . \quad . \quad (3.2)$$

which may be re-written as

$$\frac{c_2(-\infty) - c_2}{c_2(-\infty) - c_2(0)} = 1 + \operatorname{erf}\left[\frac{x_2}{2\sqrt{D_2 t}}\right]. \qquad . \quad . \quad (3.3)$$

We shall also have occasion to use the following results, applicable under the same sets of boundary conditions:

$$V_1 = 2[c_1(\infty) - c_1(0)]\sqrt{\frac{D_1 t}{\pi}}, \qquad . \quad . \quad . \quad . \quad (3.4)$$

$$V_2 = 2[(c_2(0) - c_2(-\infty)]\sqrt{\frac{D_2 t}{\pi}}, \qquad . \quad . \quad . \quad (3.5)$$

where V_1, V_2 are the quantities of diffusant crossing the planes $x_1 = 0$, $x_2 = 0$ respectively in direction of decreasing x in time t.

4. Application to Media bounded by Plane Surfaces.—Eqn. (3.1) and (3.3) refer to an infinite medium; however, each applies equally well to a region bounded by one or two x-planes, either stationary or moving, provided that (*a*) the *initial* concentration at every point in this restricted region is the same as for the same value of x_1 or x_2 in the infinite medium; and (*b*) the concentration at the boundary plane (or planes) is *at all times* the same as for the same value of x_1 or x_2 in the infinite medium.

The problems here discussed have the common feature that, although they concern media bounded by one or two planes, they fulfil the above conditions; the equations for infinite media can therefore be used. In other words eqn. (3.1) and (3.3) are, as will be shown, compatible with (*a*) eqn. (2.3), (2.4) and (2.5), and (*b*) the conditions determined by the data of the problem, which may be of Class A or Class B, as described below.

---

[4] Ref. (1), p. 43.

It may be noted that values of c_1 outside medium 1 and of c_2 outside medium 2 will have no physical significance.

5. Problems of Class A.—For this class of problem the conditions mentioned under (*b*) above are that two of the quantities $c_1(\infty)$, $c_1(0)$, $c_1(X_1)$, $c_2(-\infty)$, $c_2(0)$ should have specified values and that the magnitudes of X_1 and X_2 should at all times be proportional to the quantity of diffusant which has crossed the interface ($x_1 = X_1$, $x_2 = X_2$). Hence we may put X_1/S = (quantity of diffusant crossing interface in direction of decreasing x), whence

$$\frac{dX_1}{dt} = S\left[D_1\left(\frac{\partial c_1}{\partial x_1}\right)_{x_1=X_1} + c_1(X_1)\frac{dX_1}{dt}\right], \quad . \quad . \quad (5.1)$$

where S is a proportionality constant characteristic of the system. Combining this with (2.4) and (2.5) we have

$$\frac{dX_2}{dt} = PS\left[D_2\left(\frac{\partial c_2}{\partial x_2}\right)_{x_2=X_2} + c_2(X_2)\frac{dX_2}{dt}\right]. \quad . \quad . \quad (5.2)$$

Substituting (2.3), (2.5), (3.1) and (3.3) in (5.1) and (5.2)

$$\frac{dX_1}{dt}\left[\frac{1}{S} - c_1(X_1)\right] = [c_1(\infty) - c_1(0)]\sqrt{\frac{D_1}{\pi t}}\exp\left[\frac{-X_1^2}{4D_1t}\right], \quad . \quad . \quad (5.3)$$

$$\frac{dX_1}{dt}\left[\frac{1}{S} - PR - PQc_1(X_1)\right] = [c_2(0) - c_2(-\infty)]\sqrt{\frac{D_2}{\pi t}}\exp\left[\frac{-P^2X_1^2}{4D_2t}\right], \quad (5.4)$$

while, from (3.1), putting $x_1 = X_1$, $c_1 = c_1(X_1)$,

$$c_1(X_1) = c_1(0) + [c_1(\infty) - c_1(0)]\operatorname{erf}\left[\frac{X_1}{2\sqrt{D_1t}}\right]. \quad . \quad (5.5)$$

It is clear that (5.3), (5.4) and (5.5) can be simultaneously true for any value of t if, and only if, $X_1/\sqrt{t}$ is constant. Put

$$X_1 = 2\alpha\sqrt{D_1t}, \quad . \quad . \quad . \quad . \quad (5.6)$$

(5.3), (5.4) and (5.5) become respectively:

$$\sqrt{\pi}\,\alpha\exp[\alpha^2]\,.\left[\frac{1}{S} - c_1(X_1)\right] = c_1(\infty) - c_1(0), \quad . \quad (5.7)$$

$$\sqrt{\pi}\,.\,\alpha\sqrt{\frac{D_1}{D_2}}\exp\left[\frac{\alpha^2P^2D_1}{D_2}\right].\left[\frac{1}{S} - PR - PQc_1(X_1)\right] = c_2(0) - c_2(-\infty), \quad (5.8)$$

$$c_1(X_1) = c_1(0) + [c_1(\infty) - c_1(0)]\operatorname{erf}[\alpha]; \quad . \quad . \quad (5.9)$$

while from (3.3),

$$\frac{Qc_1(X_1) + R - c_2(-\infty)}{c_2(0) - c_2(-\infty)} = 1 + \operatorname{erf}\left[P\alpha\sqrt{\frac{D_1}{D_2}}\right] \quad . \quad (5.10)$$

Eqn. (5.7), (5.8), (5.9), (5.10) are independent and contain, besides physical constants and the parameters P and S, the six quantities, $c_1(0)$, $c_1(\infty)$, $c_1(X_1)$, $c_2(0)$, $c_2(-\infty)$, α. Hence if two of the concentrations are given the equations can be solved for the other three and for α. Those constant concentrations appearing in eqn. (3.1) and (3.3) which were not given explicitly in the data of the problem can now be substituted in terms of known quantities; the resulting equations for c_1 in terms of x_1 and t, and for c_2 in terms of x_2 and t, fulfil both the boundary conditions of the problem and the general diffusion equations, and hence constitute the required solution. Substitution for α in (5.6) gives X_1 (and hence X_2) in terms of t and known quantities.

It will be noted that the interfacial concentrations $c_1(X_1)$ and $c_2(X_2)$ are necessarily constant.

6. Problems of Class B.—Here the condition expressed by eqn. (5.1) and (5.2) no longer holds. Instead, the data of the problem require that three of the five concentrations $c_1(0)$, $c_1(\infty)$, $c_1(X_1)$, $c_2(0)$, $c_2(-\infty)$ should have specified values.

Substituting (2.3), (2.5), (3.1), and (3.3) into (2.4):

$$[c_1(\infty)-c_1(0)]\sqrt{\frac{D_1}{\pi t}}\exp\left[\frac{-X_1^2}{4D_1t}\right]-[c_2(0)-c_2(-\infty)]\sqrt{\frac{D_2}{\pi t}}\exp\left[\frac{-P^2X_1^2}{4D_2t}\right]$$
$$+\frac{dX_1}{dt}[(1-PQ)c_1(X_1)-PR]=0 \quad (6.1)$$

Taken with (5.5) this can be true for all values of t if, and only if, $X_1/\sqrt{t}$ is constant. Putting

$$X_1 = 2\beta\sqrt{t} \quad . \quad . \quad . \quad . \quad (6.2)$$

(6·1) becomes

$$\sqrt{\frac{D_1}{\pi}}[c_1(\infty)-c_1(0)]\exp\left[\frac{-\beta^2}{D_1}\right]-\sqrt{\frac{D_2}{\pi}}[c_2(0)-c_2(-\infty)]\exp\left[\frac{-P^2\beta^2}{D_2}\right]$$
$$+\beta[(1-PQ)c_1(X_1)-PR)]=0. \quad (6.3)$$

From (5.5)

$$c_1(X_1) = c_1(0) + [c_1(\infty) - c_1(0)]\operatorname{erf}\left[\frac{\beta}{\sqrt{D_1}}\right], \quad . \quad . \quad (6.4)$$

while from (3.3)

$$c_2(X_2) = Qc_1(X_1) + R = c_2(0) + [c_2(0) - c_2(-\infty)]\operatorname{erf}\left[\frac{P\beta}{\sqrt{D_2}}\right]. \quad (6.5)$$

Eqn. (6.3), (6.4) and (6.5) are independent; since three of the five quantities $c_1(\infty)$, $c_1(X_1)$, $c_1(0)$, $c_2(0)$, $c_2(-\infty)$ are known, the equations determine the values of the other two and of β. Hence X_1 can be found as a function of t from eqn. (6.2), and c_1 or c_2 as functions of t and x_1 or x_2 from (3.1) and (3.3).

7. Examples: Class A.—(*a*) ABSORPTION BY A LIQUID OF A SINGLE COMPONENT FROM A MIXTURE OF GASES.—An ideal mixture of a soluble gas A and an insoluble gas is in contact with a liquid. Initially the mole fraction of A in the gas is $c_1(\infty)$ and the concentration (vol. gas/vol. liquid) of dissolved A in the liquid is uniformly equal to $c_2(-\infty)$; $c_1(\infty)$ and $c_2(-\infty)$ are given. There is constant equilibrium between gas and liquid at the interface, where Henry's law is obeyed. There is no appreciable change in the partial volume or the temperature of the liquid when A is absorbed. Let the liquid be medium 2 and the gas medium 1. Provided the difference between $c_2(-\infty)$ and $c_2(X_2)$ (see below) is not too great, the law of diffusion expressed by (2.2) is obeyed in the liquid, dissolved A being the diffusant (Fick's law). If the x_1-origin moves so that there is no net flow of gas molecules across any plane of constant x_1, then equation (2.1) is obeyed in the gas (Stefan-Maxwell law). For this to be so, X_1 must be equal at all times to the volume of A absorbed by unit area of the liquid surface, i.e. $X_1 = V$. It can be seen that the conditions of the problem correspond to those specified for Class A, with $S = 1$ in eqn. (5.1) and (5.2).

The x_2 co-ordinate of the liquid surface does not change, hence $X_2 = 0$, $c_2(X_2) = c_2(0)$ for all t; in eqn. (2.5), $P = 0$. Eqn. (2.3) be-becomes

$$R = 0,\ c_2(X_2) = c_2(0) = Q \,.\, c_1(X_1),$$

where Q is the solubility of A in the liquid, expressed as volumes of gaseous A per unit volume of liquid per unit mole fraction of A in the gas.

Making the appropriate substitutions and eliminating the unknowns except for α, eqn. (5.7) to (5.9) become

$$\frac{\alpha\sqrt{\dfrac{\pi D_1}{D_2}} - Qc_1(\infty) + c_2(-\infty)}{\alpha\sqrt{\dfrac{\pi D_1}{D_2}} - Q + c_2(-\infty)} = \sqrt{\pi}\,.\,\alpha \exp\,[\alpha^2]\ \mathrm{erfc}\,[\alpha] = f(\alpha), \qquad (7.1)$$

where $$V = 2\alpha\sqrt{D_1 t} \quad . \quad . \quad . \quad . \quad . \quad (7.2)$$

Fig. 2 and 3 show f as a function of α, which can thus readily be found by trial, and used to find V as a function of t by means of (7.2).

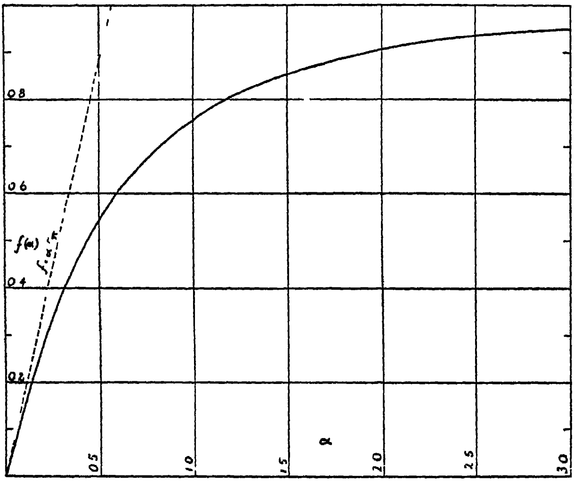

FIG. 2.—$f(\alpha) = \sqrt{\pi}\,.\,\alpha\,.\,e^{\alpha^2}\,.\,\mathrm{erfc}\,(\alpha)$ for positive values of α

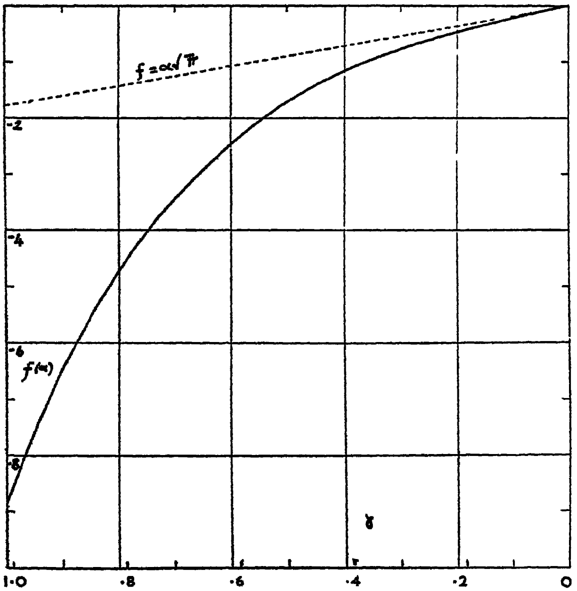

FIG. 3.—$f(\alpha) = \sqrt{\pi}\,.\,\alpha\,.\,e^{\alpha^2}\,.\,\mathrm{erfc}\,(\alpha)$ for negative values of α.

It is further easily shown that

$$c_1(X_1) = \frac{c_1(\infty) - f}{1 - f} = \frac{c_2(-\infty) + \alpha\sqrt{\dfrac{\pi D_1}{D_2}}}{Q} \quad . \quad . \quad (7.3)$$

$$c_1 = c_1(\infty) + [c_1(X_1) - c_1(\infty)]\,\frac{\operatorname{erfc}\left[\dfrac{X_1}{2\sqrt{D_1 t}}\right]}{\operatorname{erfc}\,[\alpha]}, \quad . \quad . \quad (7.4)$$

$$c_2 = Qc_1(X_1) + [Qc_1(X_1) - c_2(-\infty)]\operatorname{erf}\left[\frac{X_2}{2\sqrt{D_2 t}}\right]. \quad . \quad (7.5)$$

The same equations may be used, *mutatis mutandis*, for the escape of dissolved A from solution. In this case α will be found to be negative, and the quantity of A leaving the solution in time t is $-V$.

The solution to this problem obtained by Arnold [2] is in its essentials identical with that given above. However, Arnold's derivation is not mathematically rigorous, nor is the application to the general case, where $c_2(0) \neq c_2(-\infty)$, very clearly demonstrated.

It should be noted that the applicability of these equations to real systems depends on the absence of convection currents (this applies to all the systems discussed in this paper which contain fluids). For instance, if CO_2 is absorbed from air at a horizontal water surface the rate of absorption is very much higher than that given,[5] because changes in density cause convection in both gas and liquid (although, as will be shown, only the latter is of importance in this case). On the other hand, the escape of CO_2 from water into air, or the absorption of ammonia from air into water would produce systems in which the density consistently increased in a downward direction, and which would therefore remain stagnant.

It must also be assumed that the heat of solution and rate of absorption of A are not such as to cause serious departure from isothermal conditions, and that variations of the diffusion coefficient with concentration in the liquid will not be great enough to prevent the application of the diffusion equation (2.2). These assumptions are the more likely to be justified the smaller the value of $c_2(X_2) - c_2(-\infty)$ (i.e. when A is not very soluble, or the liquid is initially nearly saturated, or the mole fraction of A in the gas is small), but their validity should be considered in each case.

In cases where Henry's law does not apply, eqn. (2.3) may be assigned values of Q and R which will make it a good approximation to the facts in the neighbourhood of the expected value of $c_1(X_1)$. Eqn. (7.1) will then no longer apply, and eqn. (5.7) to (5.10) must be solved anew.

A special case arises when $c_1(X_1)$ (the interfacial concentration) is determined by some factor other than diffusion in a liquid. Examples are the isothermal evaporation of a liquid into still air ($c_1(X_1)$ determined by vapour pressure) or absorption of a gas into a liquid which is rapidly stirred without deforming the surface ($Q.\,c_1(X_1) = c_2(-\infty)$). For such cases, as is easily shown, (5.7) and (5.9) become

$$f(\alpha) = \frac{c_1(X_1) - c_1(\infty)}{c_1(X_1) - 1}, \quad . \quad . \quad . \quad . \quad (7.6)$$

where $f(\alpha)$ and α have the same significance as before.

(*b*) Effect of Presence of Insoluble Gas on the Rate of Absorption of a Soluble Gas.—This is an application of the previous solution. Considering the absorption of A into pure liquid ($c_2(-\infty) = 0$), we see from (3.5) that the quantity absorbed at time t will be

$$V = 2Qc_1(X_1)\sqrt{\frac{D_2 t}{\pi}}. \quad . \quad . \quad . \quad . \quad . \quad (7.7)$$

---

[5] Becker, *Ind. Eng. Chem.*, 1924, **16**, 1220.

It is of interest to see how widely, under typical conditions, the mole fraction of A at the surface departs from that in the body of the gas, that is, how closely the rate of absorption can be approximated by putting $c_1(\infty)$ for $c_1(X_1)$ in eqn. (7.7), and also the extent to which the presence of a small quantity of an insoluble impurity will slow down the absorption of a soluble gas.

The values of D_1 and D_2 will, in the case of most gases and liquids at ordinary temperatures, be in the neighbourhood of 0·1 and 2×10^{-5} cm.^{2}/sec. respectively, making $\sqrt{D_1/D_2} \approx 70$. Now suppose the value of Q is unity (a solubility comparable to that of CO_2 in water at ordinary temperatures); trial in eqn. (7.1) shows that α must be very small. Expanding exp $[\alpha^2]$ and erfc $[\alpha]$ we find that when $\alpha \ll 1$, $f \approx \alpha\sqrt{\pi}$. Hence from (7.1)

$$f \approx \frac{70f - c_1(\infty)}{70f - 1}, \quad . \quad . \quad . \quad . \quad (7.8)$$

whence $f \approx c_1(\infty)/70$. Thus, from (7.3), $c_1(X_1)/c_1(\infty) \approx 0{\cdot}986$, so the error involved in putting $c_1(\infty)$ for $c_1(X_1)$ in (7.7) will be less than 2 %.

In contrast to this, consider the case where $Q = 500$ (a value comparable with the solubility of ammonia in water at ordinary temperatures). If the bulk mole fraction, $c_1(\infty)$, of A is 0·95, $c_1(X_1)$ is found to be about 0·50.

This illustrates the well-known fact that diffusion in the gas does not play an important part in determining the rate of absorption unless the soluble gas has a fairly high solubility; with substances of low or moderate solubility, the concentration-gradient in the gas is small. Similarly, the "blanketing" effect of a small quantity of an insoluble gas will be appreciable only if the solubility of the soluble gas is fairly high.

(*c*) TARNISHING REACTIONS (GAS DIFFUSING).—A film of tarnish is formed on the surface of a metal by reaction with a gas. The reaction proceeds by diffusion of dissolved gas through the film to the surface of the metal, where its concentration $c_1(X_1)$ is assumed to be zero (i.e. the reaction is assumed to be so rapid that the rate of tarnishing is controlled entirely by the diffusion process). The outer surface of the film is constantly saturated with the gas.

Let the film be medium 1. Since $c_1(X_1)$ is not determined by diffusion in another medium, eqn. (5.8) and (5.10) are not required.

Let W be the mass fraction of the gaseous component in the compound which it forms with the metal, ρ the density of this compound (which is assumed independent of the concentration of the dissolved gas) and c_1 the concentration of dissolved gas (mass per unit volume of the film) at a distance x_1 beneath the surface of the film. The outer surface of the film is at $x_1 = 0$, the metal surface at $x_1 = X_1$, the film-thickness being X_1.

From eqn. (5.1)

$$S = -1/W\rho.$$

$c_1(0)$ is the saturated concentration of gas at the outer surface of the film; $c_1(X_1) = 0$. Then from (5.7) and (5.9)

$$\frac{c_1(0)}{W\rho} = \sqrt{\pi} \, . \, \alpha \exp[\alpha^2] \operatorname{erf}[\alpha] = g(\alpha) \quad . \quad . \quad (7.9)$$

while

$$X_1 = 2\alpha\sqrt{D_1 t} \quad . \quad . \quad . \quad . \quad (5.6)$$

where D_1 is the diffusivity of dissolved gas in the film. Fig. 4 gives g as a function of α, so that values of α corresponding to given values of $c_1(0)/W\rho$ can be found directly and used to calculate film thickness as a function of time from (5.6).

If $c_1(0) \ll W\rho$, expansion of exp $[\alpha^2]$ and erf $[\alpha]$ shows that $g \approx 2\alpha^2$, whence

$$X_1 = \sqrt{\frac{2D_1c_1(0)t}{W\rho}}. \qquad (7.10)$$

In other words, if the solubility of the gas in the film material is sufficiently small, the thickness may be calculated without appreciable error from the conventional " parabolic " formula which assumes that the concentration gradient in the film is uniform.

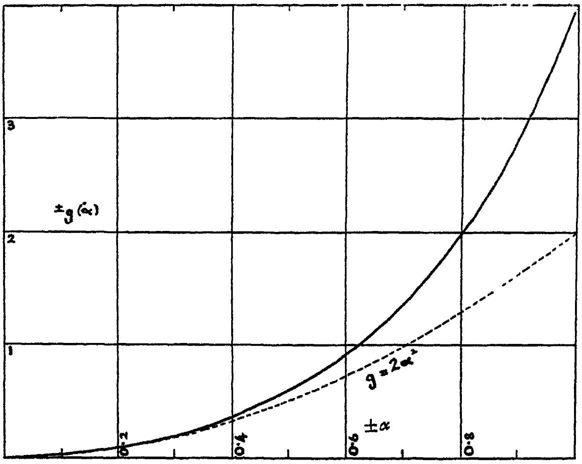

FIG. 4.—$g(\alpha) = \sqrt{\pi} . \alpha . e^{\alpha^2} . \text{erf}\ (\alpha)$.

Eqn. (7.9) and (5.6) are equivalent to the solution to this problem obtained by Booth,[8] who points out also that the approximate form will be very close to the exact one for the type of system normally encountered.

(*d*) TARNISHING REACTIONS (METAL DIFFUSING).—Eqn. (7.9), (5.6) and (7.10) will apply in this case also if $c_1(0)$ = saturated solubility of metal in film (mass/unit vol.), D_1 = diffusivity of metal dissolved in film, ρ = density of film, W = mass-fraction of metal in film-compound.

It may be noted that the methods of this paper could be used to deal with the case where both metal and gas diffuse through the film in opposite directions, provided that the reaction between them is fast enough to ensure that the concentration of one diffusant is virtually zero wherever the concentration of the other is appreciable.

(*e*) CONDENSATION OF A VAPOUR AT THE SURFACE OF A COLD LIQUID OF INFINITE DEPTH.—Here heat is the diffusant, and the liquid is taken to be medium 1. The vapour (which contains no uncondensable gases) is at its saturation temperature T_X, and is at equilibrium with the surface of the liquid at the same temperature. The heat content of the vapour is higher than that of the liquid at the surface by an amount equal to the latent heat of vaporization L (per unit mass). The liquid is initially at a uniform temperature T_∞.

The surface of the liquid is originally at $x_1 = 0$ and is at $x_1 = X_1$ at time t; X_1 is always a negative value of x_1, so that the depth of liquid which has condensed up to time t is $-X_1$, and the mass M condensed per unit area is $-X_1\rho$.

Taking the heat content of the liquid at the surface to be zero, we have

$$c_1(X_1) = 0, \quad c_1 = \rho\sigma(T - T_X),$$

where ρ, σ are the density and specific heat of the liquid (both taken to be independent of the temperature), and T is the temperature of the liquid at a depth x_1 below the surface. From (5.1) we see that

$$S = 1/L\rho.$$

Eqn. (5.7) and (5.9) become

$$\frac{\sigma(T_\infty - T_X)}{L} = f(\alpha), \quad . \quad . \quad . \quad . \quad (7.11)$$

where $f(\alpha)$ is the function of α given in (7.1) and plotted in Fig. 2 and 3. From (5.6)

$$M = -X_1\rho = -2\alpha\rho\sqrt{D_1 t}, \quad . \quad . \quad . \quad (7.12)$$

where D_1 is the thermal diffusivity of the liquid, being equal to $\kappa/\rho\sigma$, where κ is the thermal conductivity. Hence (7.12) can be written

$$M = -X_1\rho = -2\alpha\sqrt{\frac{\kappa t\rho}{\sigma}}. \quad . \quad . \quad . \quad (7.13)$$

For the temperature distribution in the liquid we have from (3.1)

$$T = T_X - (T_X - T_\infty)\left(1 - \operatorname{erfc}\left[\frac{X_1}{2}\sqrt{\rho\sigma/\kappa t}\right]\Big/\operatorname{erfc}\,[\alpha]\right) \quad (7.14)$$

When $\sigma(T_X - T_\infty) \leqslant L$, f is small, hence $f \approx \alpha\sqrt{\pi}$, and (7.12) becomes

$$M \approx \frac{2}{L}(T_X - T_\infty)\sqrt{\frac{\kappa t\rho\sigma}{\pi}}. \quad . \quad . \quad . \quad (7.15)$$

The same equations may be used for evaporation, in circumstances such that no convection currents arise.

(*f*) Vapour Condensing on a Cooled Surface.—The cooled surface ($x_1 = 0$) is assumed to be maintained at a constant temperature T_0. The depth of liquid which has condensed on the surface at time t is $-X_1$, and $-X_1\rho$ the mass condensed per unit area. Using the symbols of (*e*) above, we find

$$\frac{\sigma(T_X - T_0)}{L} = g(\alpha), \quad . \quad . \quad . \quad . \quad (7.16)$$

where $g(\alpha)$ is the function of α given in (7.9) and plotted in Fig. 4. Here α will give the value of M or X_1 when substituted in eqn. (7.12).

(*g*) Reaction of a Gas at a Solid Surface.—A pure gas A reacts with a solid to form a gaseous compound B. The reaction is so rapid that the concentration $c_1(X_1)$ of A at the interface is negligible. n_1 moles of A react to give n_2 of B. The gas is taken to be medium 1, and occupies the region $0 < x_1 < \infty$. The plane $x_1 = 0$ moves relative to the solid surface in such a way that there is no net flow of gas molecules across any plane of constant x_1. Hence

$$X_1 = V(1 - n_2/n_1),$$

where V is the volume of A reacted in time t, and X_1 is the x_1-co-ordinate of the surface of the solid. From (5.1) we see that

$$S = (1 - n_2/n_1).$$

c_1 is the mole fraction of A, $(1 - c_1)$ the mole-fraction of B, at x_1; the initial mole fraction of A in the gas $c_1(\infty)$ will be taken to be unity. Eqn. (5.7) and (5.9) now become

$$1 - n_2/n_1 = f(\alpha), \quad . \quad . \quad . \quad . \quad (7.17)$$

where $f(\alpha)$ is the function of α specified in (7.1) and plotted in Fig. 2 and 3.

Now if $n_1 \neq n_2$, from (5.6)

$$V = \frac{X_1}{(1 - n_2/n_1)} = \frac{2\alpha\sqrt{D_1 t}}{(1 - n_2/n_1)} \quad . \quad . \quad (7.18)$$

while if $n_1 = n_2$, then $c_1(X_1) = c_1(0) = 0$, and hence from (3.4)

$$V = 2\sqrt{\frac{D_1 t}{\pi}} \quad . \quad . \quad . \quad . \quad . \quad . \quad (7.19)$$

8. Examples : Class B.—(*a*) SOLUTION OF GAS IN A LIQUID, FOLLOWED BY REACTION WITH SOLUTE.—The surface of the liquid is constantly saturated with the gas B ; it is assumed either that the latter is undiluted with inert gases, or that the solubility of B is sufficiently small to permit the assumption that the composition of the phase is uniform (see example, § 7(*b*)). The case where this restriction is not imposed is discussed later.

The liquid contains a solute A which reacts virtually instantaneously and irreversibly with the dissolved gas. Laws of the form (2.1) hold for the diffusion of A and B in the liquid. Any part of the liquid will contain A or B but not both. There will be a plane, $x_1 = X_1$, $x_2 = X_2$, at which the concentrations of both will be zero. The part of the liquid containing A is taken to be medium 1, that containing B is medium 2. n_1 moles of A react with n_2 moles of B. The surface of the liquid is permanently at $x_1 = x_2 = 0$, so that $X_1 = X_2$, $P = 1$ (eqn. (2.5)). Also

$$c_1(X_1) = c_2(X_2) = 0,$$

hence $R = 0$ (eqn. (2.3)). In order to fulfil the conservation condition (2.4), put $c_1 = -m_1 n_2/n_1$, where m_1 is the concentration of A at x_1 (moles per unit volume). c_2 is the concentration of B at x_2 in the same units. $c_2(0)$ is the saturated concentration of B at the surface of the liquid. $m_1(\infty)$ is the initial concentration of A in the liquid.

Eqn. (6.3) and (6.5) then become

$$n_1 c_2(0) f\left[\frac{\beta}{\sqrt{D_1}}\right] - n_2 m_1(\infty) g\left[\frac{\beta}{\sqrt{D_2}}\right] = 0, \quad . \quad . \quad (8.1)$$

where f, g are the functions given (with α as variable) in eqn. (7.1) and (7.9) respectively, and plotted in Fig. 2, 3 and 4. Hence from (3.5), (6.5) we find the volume of gaseous B absorbed in time t to be

$$V = \frac{2c_2(0)}{\operatorname{erf}\left[\frac{\beta}{\sqrt{D_2}}\right]}\sqrt{\frac{D_2 t}{\pi}}. \quad . \quad . \quad . \quad (8.2)$$

The value of β can be found from (8.1) by trial, using Fig. 2, 3 and 4, and substituted in (8.2) to find V.

If the gas is diluted by an insoluble component, the surface concentration ($c_2(0)$) of B in the liquid will be determined by diffusion in the gas. In this case, to obtain an exact solution, (7.2) and (7.6) must be taken in conjunction with (8.1) and (8.2) ; by trial a value of the concentration at the surface of the liquid must be found which will make the rate of absorption the same when calculated from either set of equations. The quantities D_1, $c_1(\infty)$ and $c_1(X_1)$ in (7.2) and (7.6) will refer respectively to the diffusion coefficient in the gas and to the mole fraction of B in the bulk of the gas and at the interface

(*b*) PROGRESSIVE FREEZING OF A LIQUID.—Let the liquid be medium 1 and the solid medium 2. The temperature of the exposed surface of the solid is maintained constant at T_0 ; since no material crosses this boundary $x_2 = 0$ for all t at the surface. If there is a change in volume on freezing, there will be relative movement of the planes $x_1 = 0$, $x_2 = 0$.

The diffusant in this case is heat. L is the latent heat of fusion (per unit mass) ; ρ_1, ρ_2 are the densities, σ_1, σ_2 the specific heats and D_1, D_2 the thermal diffusivities of liquid and solid respectively. The variation of these quantities with temperature will be ignored. If κ_1, κ_2 are the thermal conductivities of liquid and solid respectively, then

$$D_1 = \kappa_1/\rho_1\sigma_1, \quad D_2 = \kappa_2/\rho_2\sigma_2.$$

The initial temperature of the liquid is uniformly equal to T_∞, and the solid-liquid interface ($x_1 = X_1$, $x_2 = X_2$) is always at the melting point T_X. The heat content of the solid at T_X is taken to be zero; hence that of the liquid at T_X is L. From (2.3), since $c_2(X_2) = 0$,

$$c_1(X_1) = -R/Q = L\rho_1.$$

Since $X_1/X_2 = \rho_2/\rho_1$, from (2.5)

$$P = \rho_1/\rho_2.$$

We also have

$$c_1 = \rho_1\sigma_1(T_1 - T_X + L/\sigma_1)$$

and

$$c_2 = \rho_2\sigma_2(T_2 - T_X),$$

where T_1 is the temperature at x_1 (in the liquid) and T_2 the temperature at x_2 (in the solid).

Eliminating $c_1(0)$, $c_2(-\infty)$ from eqn. (6.3) to (6.5), and substituting as above, we find

$$\frac{\sigma_1(T_\infty - T_X)}{f\left[\dfrac{\beta}{\sqrt{D_1}}\right]} + \frac{\sigma_2(T_0 - T_X)}{g\left[\dfrac{\rho_1\beta}{\rho_2\sqrt{D_2}}\right]} + L = 0, \qquad . \quad . \quad . \quad (8.3)$$

where f and g are the functions given (with α as variable) in (7.1) and (7.9) respectively, and plotted in Fig. 2, 3 and 4.

The thickness of the solid at time t is (from (6.2))

$$X_2 = X_1\rho_1/\rho_2 = 2\rho_1\beta\sqrt{t}/\rho_2 \qquad . \quad . \quad . \quad (8.4)$$

The temperature T_2 at any point in the solid is

$$T_2 = T_X - (T_X - T_0)\left(1 - \frac{\operatorname{erf}\,[x_2/2\sqrt{D_2t}]}{\operatorname{erf}\,[\rho_1\beta/\rho_2\sqrt{D_2}]}\right), \qquad . \quad (8.5)$$

while the temperature in the liquid is

$$T_1 = T_X - (T_X - T_\infty)\left(1 - \frac{\operatorname{erfc}\,[x_1/2\sqrt{D_1t}]}{\operatorname{erfc}\,[\beta/\sqrt{D_1}]}\right). \qquad . \quad (8.6)$$

Hence (8.3) may be solved by trial, with the aid of Fig. 2, 3 and 4, and the resulting value of β used to calculate the thickness of the solid and the temperature at any point in the system as functions of time.

If we put $\rho_1 = \rho_2$ in this solution (i.e. no change of volume on freezing) we obtain the form found in the text-books;[1] this form applies exactly to such phenomena as the freezing of damp soil, where there is in fact no appreciable change in volume on freezing.

It should be noted that a real system of liquid and solid will only behave in the way described by the formulae given above if the density increases consistently in a downward direction (or is uniform), as otherwise convection currents will arise. Thus the formulae could be used for the freezing from the top of water initially below 4° C, or for the freezing from the bottom of a liquid whose density increases consistently with decreasing temperature.

The above results apply, *mutatis mutandis*, to the melting of a solid which is initially at a uniform temperature.

Department of Chemical Engineering,
Tennis Court Road,
Cambridge.

THE DIFFUSION RATES OF SOME METALS IN COPPER, SILVER, AND GOLD

By O. KUBASCHEWSKI

Received 17*th March*, 1950

The diffusion rates of zinc, cadmium, and silver in copper (at temperatures between 710° and 860° C) and of silver in gold (800° to 1000° C) have been determined by a method which permitted the application of Stefan and Kawalki's tables. Analyses were carried out by a spectrographic method. These alloys containing zinc and cadmium, which have relatively high vapour pressures at the temperatures of experiment, were tightly enclosed in thick-walled iron cylinders in order to avoid effects due to evaporation of metal. The results are summarized by the equations:

$$\begin{aligned}
&\text{Ag in Cu } (1\ \%\ \text{Ag}): \ D = 0{\cdot}012 \exp(-35{,}600/RT),\\
&\text{Zn in Cu } (1\ \%\ \text{Zn}): \ D = 0{\cdot}0024 \exp(-30{,}200/RT),\\
&\text{Cd in Cu } (1\ \%\ \text{Cd}): \ D = 0{\cdot}0034 \exp(-29{,}200/RT),\\
&\text{Ag in Au } (3\ \%\ \text{Ag}): \ D = 0{\cdot}047 \exp(-38{,}500/RT).
\end{aligned}$$

The literature concerning the diffusion rates of nickel, palladium, platinum, copper, silver, gold, zinc and cadmium in copper, silver, and gold is reviewed, and the most probable constants of Arrhenius' equation for each system are derived from this survey. The low estimated accuracy of these figures reveals that most of the data require careful re-determination.

A large number of measurements of diffusion rates in metals has been made during the past 30 years. The information obtained has generally been presented in the form of Arrhenius' equation from which the activation energy can be derived. Hitherto, attempts to correlate either the absolute diffusion rates or the activation energies with other physical constants have proved unsatisfactory. In the opinion of the author, even Langmuir's more general equation is of too limited validity to be of real value. The reason for these difficulties in correlating diffusion data to other values is very probably the inaccuracy of the experimental results. Re-determinations often produce quite different data from those obtained in previous work, and activation energies especially have been subject to considerable changes. Diffusion rates are undoubtedly sensitive to a number of influences, and, what is worse, in our present state of knowledge we do not know the extent of some of them, or even whether we are taking all the variants into account. The best practical approach apparent at this stage seems to be to carry out measurements by as many different methods as possible, and to correlate the results critically, expressing them in equation form for further comparisons. This should assist materially toward establishing a general theory of diffusion.

While the present paper has as an object the presentation of some results obtained by the author's co-workers on the diffusion of zinc, cadmium, and silver in copper [1] and of silver in gold,[2] and to compare the results with earlier ones, the opportunity has been taken to survey the available data on diffusion of Ni, Pd, Pt, Cu, Ag, Au, Zn and Cd in copper, silver and gold. These systems have been selected since the rates of self-diffusion in copper, silver and gold are known with some accuracy, and as their thermochemical data are also known (for eventual correlation) more fully and accurately than those of any other metal.

---

[1] A. Klein, *Diss.* (Technische Hochschule, Stuttgart, 1948).

[2] H. Ebert and G. Trommsdorf (Stuttgart, 1944).

Experimental

The determinations of the diffusion rates of silver in gold and copper involved no special difficulties. The technique has been described in an earlier paper.[3] Small discs were made of 5 mm. diam., the thickness of the pure metal discs (gold or copper) being 1·5 mm., while those of the alloys (3·0 atomic % silver in copper or 8·77 atomic % silver in gold) were 0·5 mm. thick. The alloy discs were welded to the pure metals by the method originally described by Seith and Peretti.[4] The welded test-pieces were then annealed for suitable periods of time at the desired temperatures, and were then analyzed spectrographically. For this purpose the discs were used as the *upper* electrode,[5] the other electrode consisting of spectrochemically pure carbon. A Feussner type spark discharge was passed across the gap. A considerable oxidation of the metal electrode was observed when the carbon was used as the upper electrode. The optimum conditions for spark discharge were established for each metal system by preliminary experiments. The spectrometer used was a Zeiss type Q 24, with Jena quartz prism. The internal standard method was applied for analysis using for the copper-silver alloys the pairs Ag II 2413·22—Cu II 2486·0 ; Ag II 2437·77—Cu II 2506·4 ; Ag I 3382·89—Cu I 3307·95 Å. The calibration curves for analysis were derived from standard alloys containing 0·3, 1·0 and 3·0 at.-% Ag in Cu, whose composition was verified by chemical analysis.

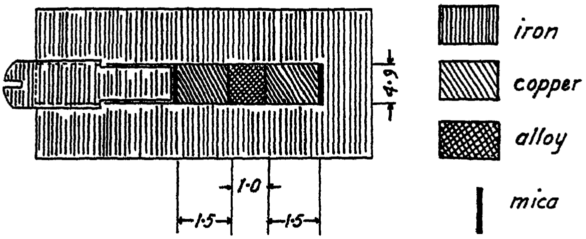

FIG. 1.

After sparking, a 1/10 mm. layer of the alloy disc was removed and a new pattern was taken. Since the thickness of the composite pellets was 2 mm., 20 of such analyses were made on each sample, and the curve for the atomic concentration of silver in the 1/10 mm. slices was drawn against the co-ordinate of distance from the original surfaces. From these curves diffusion constants were derived by using the tables of Stefan and Kawalki.

The great divergences in the values for diffusion rate in the copper-zinc system obtained by various observers are doubtless due to the considerable vapour pressure of zinc in brass at temperatures at which diffusion can be measured. Of the earlier observers, only Kirkendall, Thomassen and Upthegrove[6] used a method which eliminated the error due to evaporation. They used a copper-plated brass bar, so that diffusion occurred from the inside to the outside only. The concentration of zinc at the surface remained zero throughout the experiment.

For the investigation of the diffusion of zinc and cadmium in copper, Klein made up composite test pieces 5 mm. diam. in which a disc of alloy (3·0 at.-% Cd, or Zn in Cu) 1·0 mm. thick was sandwiched between two discs of copper 1·5 mm. thick (Fig. 1). Thus diffusion took place in two directions. The composition and homogeneity of the alloys were checked by chemical analysis of samples. The test pieces were pressed between mica discs into an iron cylinder with a bore 4·9 mm. diam. and 16 mm. deep. The outer 10 mm. were threaded, and the cylinder was closed with a screw with a 6 mm. cylindrical end fitting closely to the 4·9 mm. bore. Good contact between the test pieces and the iron cylinder was obtained by mechanical pressure alone. The connection between the surfaces was completed by smearing of the copper and by sintering on annealing, which made further welding unnecessary. The sealing was considered sufficiently effective to prevent the volatilization of cadmium or zinc. It was ascertained that the reduction in length of the pellets on compression did not exceed 2/100 mm.

---

[3] Kubaschewski and Ebert, *Z. Elektrochem.*, 1944, **50**, 138.

[4] Seith and Peretti, *ibid.*, 1936, **42**, 570.

[5] See van Calker, *Spectrochim. Acta*, 1944, **2**, 343.

[6] Kirkendall, Thomassen, and Upthegrove, *Trans. Amer. Inst. Min. Met. Eng.*, 1939, **133**, 186.

The iron cylinders were then sealed in evacuated vitreous silica tubes and placed in an electrical resistance furnace for periods between 11 and 26 days at temperatures varying from 600° to 860° C. The temperature was measured frequently by means of a calibrated thermocouple. The temperatures finally recorded were accurate to ± 4° C or less, corresponding to an average error in the diffusion constants of ± 5 %. After annealing, the samples containing cadmium were quenched in water.

The iron cylinders were then removed by turning, and the diameter of the diffusion samples was reduced by 1 mm. to eliminate any surface effects. The base and plug of the iron cylinder were analyzed spectrographically for cadmium and zinc, but no more than traces could be detected, if at all. In a few instances the iron cylinder wall was analyzed after reducing to 1/10 mm. thickness but no traces of zinc could be detected in the iron. Cadmium is insoluble in solid iron.[7]

The test cylinders were than analyzed spectrographically as outlined above. For analysis the following pairs were used : for copper-zinc alloys, Zn I 3345·02—Cu I 3337·85 and Zn II 2557·96—Cu II 2529·5, and for copper-cadmium alloys, Cd I 2288·02—Cu I 2303·12 and Cd II 2312·8—Cu II 2242·61 Å.

Results

Diffusion Rates.—Fig. 2-6 show the values of diffusion rates from the author's experimental work or from data published in literature. All these values for a certain system at a given concentration should lie on a straight line in the $\log D - 1/T$-plot, according to Arrhenius' well-known equation. In this equation,

$$D = Ae^{-Q/RT}; \quad . \quad . \quad . \quad . \quad . \quad (1)$$

D denotes the diffusion rate (given throughout in cm.^{2} sec.$^{-1}$), Q the activation energy, and A are constant. The dimensions of Q are in cal./mole and those of A are cm.^{2} sec.$^{-1}$. All percentages stated are atomic percentages.

There are two general methods of evaluating diffusion measurements, both based on Fick's laws. One is given, for instance, by the tables of Stefan and Kawalki, while the other method is the one worked out by Matano. Other methods are similar to these in principle. It must be born in mind that the Stefan-Kawalki method neglects the concentration dependency of diffusion for the range of concentration which is evaluated. Matano's method takes concentration dependency into account. By analogy with the treatment of thermochemical functions it is recommended that diffusion values obtained by the former method be known as " integral values " and those obtained by Matano's method as " partial values ". If the concentration dependency is small or if the concentration range evaluated by Stefan-Kawalki's method is small, the integral and partial diffusion rates do not differ much.

SILVER IN COPPER.—The diffusion rates measured by Klein are presented in Fig. 3. The temperature range was 717-867° C, the original concentration 3·0 % Ag and the average concentration 1 % Ag. The values accommodate closely enough to a straight line, from which the following values are derived :

Ag in Cu (1 % Ag) : $Q = 35{,}600 \pm 3{,}000$; $\log A = -1{\cdot}93 \pm 0{\cdot}15$.

ZINC IN COPPER (Fig. 2).—A large number of diffusion measurements have been carried out with α- and β-brasses. The results of the various observers are plotted as D against $1/T$ in Fig. 2. Only those published by Dunn[8] are omitted ; it is generally agreed that his evaporation method gave values which are much too low, because the rate was probably governed by another process, such as the evaporation of zinc from the (contaminated) surface, rather than the diffusion within the alloy. The rate of loss of zinc from an alloy (29·2 % Zn) was also used by Jenkins[9] for the determination of the diffusion rates in α-brass. This observer, however, found that at very low pressures the loss of zinc from the surface became independent of pressure, i.e. evaporation from the surface cannot be the factor governing the rate. Only these low pressure values were used for the calculation of diffusion constants.

---

[7] Wever, *Arch. Eisenhüttenwesen*, 1928-29, **2**, 739.

[8] Dunn, *J. Chem. Soc.*, 1926, **129**, 2973.

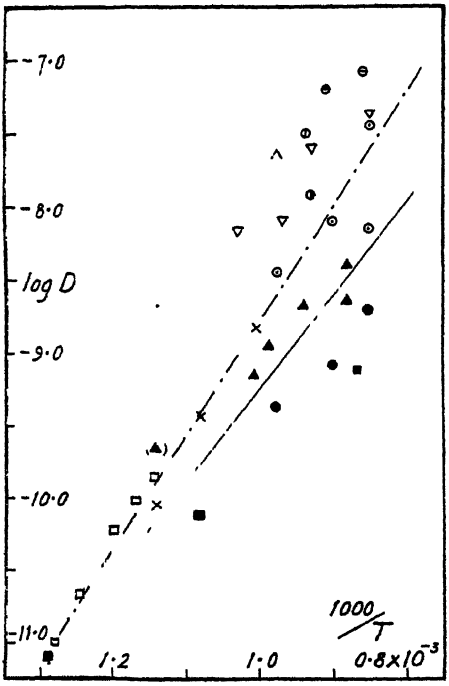

FIG. 2.—Diffusion of zinc in copper.

0-7 % Zn
● Rhines and Mehl.
■ Matano.
◑ Seith and Krauss.
▲ Present work.

24-29 % Zn
○ Rhines and Mehl.
□ Jenkins.
⊖⦶ Seith and Krauss.
× Kirkendall, Thomassen, Upthegrove.
▽ Bugakov and Rybalko.
Λ Hertsricken.

It is tempting to measure evaporation rates in such alloys as a method of determining the diffusion rate. A method of measuring the amount of zinc diffusing from a vapour phase into copper was developed on these lines by Seith and Krauss.[10] Insufficient agreement was found, however, between their equilibrium data for the zinc vapour pressures of brasses (which could also be calculated from their measurements) and those of other observers.[11] This was ascribed [11] to the faulty behaviour of their weighing system at the knife edge. It is therefore concluded that the diffusion rates calculated from their results may not be reliable. It is also seen from Fig. 2 that their log D values (⊖ ⦶) are higher than those of other observers. The values denoted ⊖ are rough estimates by Seith and Krauss, using another method. Bugakov and Rybalko,[12] and Hertsricken, Il'kewitch, Sakharov and Faingold[13] also used evaporation methods and claimed that they gave true diffusion constants. With this method, Bugakov and Rybalko found diffusion rates to be dependent on grain size This effect is, however, at least for α-brass, not due to a true grain boundary diffusion but probably originates in the shrinkage accompanying the loss of zinc and the resultant porosity of the specimens along the grain boundaries, as was observed by Mehl.[14] In Fig. 2, therefore, only those results obtained by Bugakov and Rybalko with single crystals of α-brass (29·4 % Zn) have been considered.

---

[9] Jenkins, *J. Inst. Metals*, 1947, **73**, 641.

[10] Seith and Krauss, *Z. Elektrochem.*, 1938, **44**, 98.

[11] See Weibke and Kubaschewski, *Thermochemie der Legierungen* (Berlin, 1943).

[12] Bugakov and Rybalko, *Tech. Physics U.S.S.R.*, 1935, **2**, 617.

[13] Hertsricken, Il'kewitch, Sakharov and Faingold, *Tech. Physics, U.S.S.R.*, 1941, **10**, 786.

[14] Mehl, *J. Appl. Physics*, 1937, **8**, No. 3.

The most reliable method for the measurement of the diffusion of zinc at high concentrations is undoubtedly that of Kirkendall, Thomassen and Upthegrove.[6] Experiments were carried out on brasses containing 27·7, 25·3 and 24·8 % zinc at the temperatures of 600°, 655° and 720° C respectively. The dependence on the concentration of zinc of its rate of diffusion at 750°, 840° and 900° C was determined by Rhines and Mehl.[15] The diffusion rate varies only slightly with alloys containing up to 10 % Zn, but then increases with zinc content. The deviations from the average value of log D were generally no more than ± 0·15 and became greater only at high concentrations of zinc. Though so low in absolute value, however, the deviations are too high to allow the derivation of accurate curves for the concentration dependence of the activation energy, as was attempted by Rhines and Mehl. Seith and Krauss found [10] that the diffusion rate in the α phase increases more rapidly with increases in concentration at low than with high zinc contents, thus disagreeing with Rhines and Mehl.

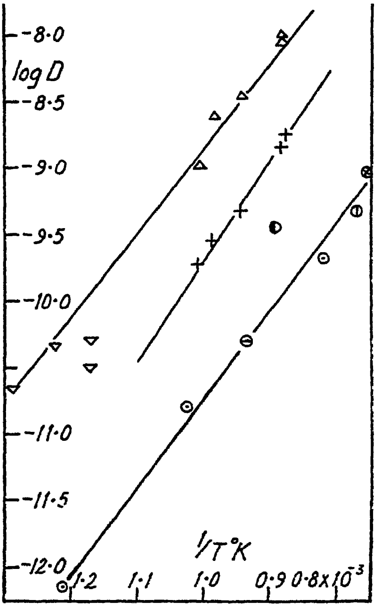

FIG. 3.

Nickel in Copper

○ Matano.
⊗ Johnson.
⌽ Grube and Jedele.
⊖ van Arkel.
◑ Hertsricken.

Cadmium in Copper

▽ Rhines and Mehl.
△ Present work.

Silver in Copper

+ Present work.

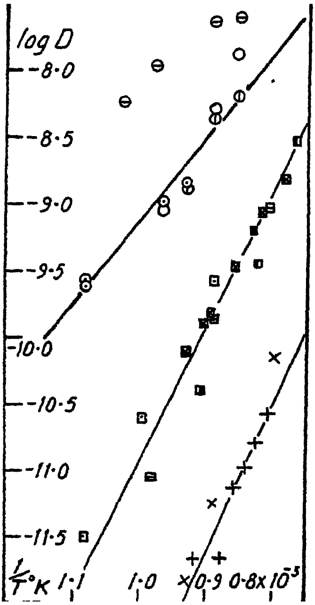

FIG. 4.

Copper in Copper

⊡ Raynor, Thomassen and Rouse.
⊟ Steigmann, Shockley and Nix.
◨ Rollin.
⊠ Maier and Nelson.

Gold in Gold

+ McKay.
× Sagrubskij.

Cadmium in Silver

○ Seith and Peretti.
⌽ Bugakov and Ssirotkin (5 % Cd).
⊖ Bugakov and Ssirotkin (10 % Cd).

---

[15] Rhines and Mehl, *Trans. Amer. Inst. Min. Met. Eng.*, 1938, **128**, 185.

The experiments of Klein described in the experimental section of the present paper were carried out with low concentrations of zinc (1 % as an average). Matano,[16] with a similar method but not ensuring loss of zinc vapour, used alloys with approximately 9 % Zn ; his results may be applied to an average zinc concentration of 4 %.

It is concluded that the results of Kirkendall, Thomassen and Upthegrove, Rhines and Mehl, Jenkins and of the present work, are the most reliable. In Fig. 2 two sets of data are plotted : those obtained at low concentrations of zinc (between 0 and 7 %), and those for the range 24-29 % Zn. For the latter concentrations the results of Jenkins, Kirkendall, Thomassen and Upthegrove, Rhines and Mehl can be well represented by a straight line. Bugakov and Rybalko's data, obtained with single crystals, are a little higher, and those of Hertsricken, Seith and Krauss are much higher. For the lower concentration there is some discrepancy between the figures of Rhines and Mehl, and Klein ; those of Matano are lower than those of Klein at high temperatures. The full line represents about the average of these measurements and is believed to be fairly correct. Thus we obtain the following values :

Zn in Cu (0-7 % Zn) : $Q = 30{,}200 \pm 5{,}000$; $\log A = -2{\cdot}62 \pm 0{\cdot}5$
Zn in Cu (24-29 % Zn) : $Q = 35{,}000 \pm 3{,}000$; $\log A = -1{\cdot}02 \pm 0{\cdot}2$.

It may be mentioned that the heats of activation hitherto reported are widely scattered, namely from 19,700 (Matano) to 42,000 (Dunn) below 10 % Zn, and from 28,000 (Bugakov) to 46,000 cal./mole (Jenkins) at 24-29 % Zn. The values adopted above represent approximately the average of these earlier values.

It may be noted finally that in a recent paper Darken[17] differentiates between the diffusion rate of zinc and copper in α-brass on the basis of the data given by Rhines and Mehl. It was calculated that zinc (at 22·5 % concentration) diffuses 2·3 times faster at 785° C than does copper. Birchenall and Mehl[18] were the first to introduce activities in Fick's equation, and to differentiate between the diffusion constants of the two constituent elements. These considerations are not of vital importance to the present paper.

Cadmium in Copper.—The diffusion rates of cadmium in its rather small solubility range in copper has been determined by Rhines and Mehl.[15] The investigation was carried out at a narrow low-temperature range only (500°-580° C), owing probably to the high vapour pressure of cadmium. An activation energy was calculated which was considered by those authors to be surprisingly low (6,800-8,200 cal.). The experiments of the present authors have been carried out at higher temperatures. Since the composition of the alloy discs was within a heterogeneous field with the high temperature experiments the evaluation of diffusion constants had to be modified in this particular case according to the rules which govern such systems.* It is seen from Fig. 3 that the straight line drawn using Klein's results also conforms with the values of Rhines and Mehl. Only their value for 580° C is somewhat too low for agreement, due possibly to evaporation of cadmium. It is believed that the constants derived from both these investigations should be quite reliable.

Cd in Cu (0·5 % Cd) : $Q = 29{,}200 \pm 3{,}000$; $\log A = -2{\cdot}46 \pm 0{\cdot}3$.

Silver in Gold (Fig. 6).—There are two recent independent investigations of this system, by Johnson,[19] and by Ebert and Trommsdorf.[2] Johnson studied an alloy containing 50 % of each element, using radioactive silver as an indicator (●) and also chemical analyses (■). Ebert and Trommsdorf worked on the range between 8·8 % Ag and pure gold, the average concentration being 3 % Ag. There is a difference between the values of the two works (see Fig. 6). which is easily explained by the difference in concentration, the rate of diffusion being higher in alloys of high gold content. The interesting feature of Johnson's results is the small but perceptible difference in the values when analyses are made by radioactive or chemical methods. This effect, however, needs further investigation and a line is drawn in Fig. 6 to conform most closely to all values.

---

[16] Matano, *Japan. J. Physics*, 1934, **9**, 41.
[17] Darken, *Amer. Inst. Min. Met. Eng., Metals, Tech.* (No. 2311), Jan. 1948.
[18] Birchenall and Mehl, *ibid.*, (No. 2168), June, 1947.
* For an example of this evaluation see for instance, Seith and Laird, *Metallkunde*, 1932, **24**, 193.
[19] Johnson, *Trans. Amer. Inst. Min. Met. Eng.*, 1942, **147**, 331.

The following constants are obtained for the two concentrations investigated:

Ag in Au (3 % Ag): $Q = 38{,}500 \pm 3{,}000$; $\log A = -1\cdot33 \pm 0\cdot2$;
Ag in Au (50 % Ag): $Q = 44{,}700 \pm 1{,}500$; $\log A = -0\cdot41 \pm 0\cdot15$.

Johnson[19] has also measured the diffusion of radioactive gold in a 50 % gold-silver alloy. The good agreement with the results of Weiss and Henry[20] and of Fraenkel and Houben[21] (see Fig. 6) may be fortuitous since these authors used a much less accurate method, namely the observation of the limits of resistance to chemical attack. Johnson's data should be the most reliable. Braune's measurements[22] were carried out at lower concentrations of gold. His values (○), corrected by a factor 4, are higher than those of Johnson.[19] It is doubtful whether this is due to a true concentration effect or whether Braune's data need correction. Since a straight line can be drawn through Braune's values and those obtained by Jost[23] at low temperatures (●), and since it is a general experience that activation energy becomes smaller at low concentrations of the diffusing element this line may be provisionally accepted. The following constants are obtained:

Au in Ag (*ca.* 3 % Au): $Q = 32{,}000 \pm 7{,}000$; $\log A = -2\cdot90 \pm 0\cdot5$;
Au in Ag (50 % Au): $Q = 43{,}500 \pm 2{,}000$; $\log A = -1\cdot02 \pm 0\cdot2$.

OTHER SOLUTIONS IN COPPER, SILVER AND GOLD.—The values of the constants Q and A in Arrhenius' equation evaluated above are given in Table I.

TABLE I

Basis Metal / Diffusing Metal	At.-%	Q (kcal./mole)	log A (cm.² sec.⁻¹)	Ref.
		Cu		
Ni	5	30·5 ± 1·5	−4·05 ± 0·15	16, 32, 33, 34
Pd	3	29·5 ± 2·0	−4·24 ± 0·2	16
Pt	2	28·0 ± 6·0	−4·76 ± 0·5	16
Cu	—	46·5 ± 3·5	−0·75 ± 0·2	28, 29, 30, 31
Ag	1	35·6 ± 3·0	−1·93 ± 0·15	1
Au	1·5	29·8 ± 5·0	−3·71 ± 0·3	16
Zn	0-7	30·2 ± 5·0	−2·62 ± 0·5	1, 15, 16
	24-29	35·0 ± 3·0	−1·02 ± 0·02	6, 9, 12
Cd	0·5	29·2 ± 3·0	−2·46 ± 0·3	1, 15
		Ag		
Ni	—	—	—	—
Pd	10	29·0 ± 8·0	−3·02 ± 0·5	37
Pt	—	—	—	—
Cu	1	(24·8)	−4·22 ± 0·6	4
Ag	—	46·0 ± 2·0	−0·05 ± 0·15	24
Au	*ca.* 3	32·0 ± 7·0	−2·90 ± 0·5	22, 23
	50	43·5 ± 2·0	−1·02 ± 0·2	19, 20, 21
Zn	*ca.* 5	(23·5)	(−3·36)	41, 42
Cd	0-5	(31·3)	(−2·33)	4, 41
		Au		
Ni	*ca.* 5	31·2 + 2·5	−2·75 ± 0·2	3
Pd	*ca.* 8	37·7 ± 3·0	−2·85 ± 0·2	37, 39, 40
Pt	10	40·3 ± 3·5	−2·65 ± 0·4	37, 39, 40
Cu	*ca.* 10	28·5 ± 5·0	−2·92 ± 0·6	37, 38
Ag	3	38·5 ± 3·0	−1·33 ± 0·2	2
	50	44·7 ± 1·5	−0·41 ± 0·15	19
Au	—	52·0 ± 3·0	−1·36 ± 0·3	26, 27
Zn	—	—	—	—
Cd	—	—	—	—

---

[20] Weiss and Henry, *Compt. rend.*, 1922, **175**, 1402.

[21] Fraenkel and Houben, *Z. anorg. Chem.*, 1921, **116**, 1.

[22] Braune and Hellweg, *Z. physik. Chem. A*, 1924, **110**, 147.

[23] Jost, *ibid.*, *B*, 1930, **9**, 75.

This Table contains also a number of further values which were derived from published work only. Most of the values of diffusion rates are plotted in Fig. 2-6. Some explanation of the method of evaluation is necessary.

Self-diffusion in silver was carefully studied by Johnson [24] in the range 1000° K to the melting point by the radioactive tracer method. His constants are accepted as reliable. They are supported by results calculated by Kuczynski [25] from sintering experiments with silver powder on a plane silver surface. This new method of determining rates of self-diffusion is, however, still open to criticism as it involves a number of simplifications.

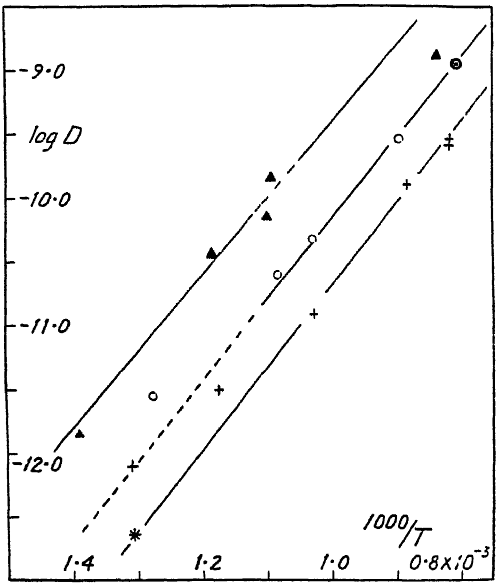

FIG. 5.

Gold in Copper
⊙ Matano.
Palladium in Copper
*+ Matano.

Palladium in Silver
▲ Jost.

Self-diffusion in gold was measured by Sagrubskij [26] and by McKay.[27] McKay tabulates his results in the dimensions mm.^{2} min.$^{-1}$, compares them in a diagram with those obtained by Sagrubskij, and emphasizes the good agreement. The re-calculation, however, shows a disagreement between Sagrubskij's original values and those plotted by McKay of 2 logarithmic units. It is believed that the disagreement between the results of the two series of experiments is not as great as that, but that a mistake occurred in McKay's calculation. Subtracting two units from McKay's logarithmic values the figures represented by the crosses in Fig. 4 are obtained which agree fairly well with Sagrubskij's measurements.

There are a number of determinations of self-diffusion in copper.[28, 29, 30, 31] among which there is no good agreement at the lower temperatures. The more recent values by Maier and Nelson,[28] and Raynor, Thomassen and Rouse [29] are preferred and the straight line in Fig. 4 is drawn mainly with their data.

[24] Johnson, *Trans. Amer. Inst. Min. Eng.*, 1941, **143**, 107.

[25] Kuczynski, *J. Metals*, 1949, **1**, 169.

[26] Sagrubskij, *Physik. Z. Sowjetunion*, 1937, **12**, 118 ; *Bull. Acad. Sci. U.R.S.S., Math. nat. Ser. Phys.*, 1937, 903.

[27] McKay, *Trans. Faraday Soc.*, 1938, **34**, 845.

[28] Maier and Nelson, *Trans. Amer. Inst. Min. Met. Eng.*, 1942, **147**, 39.

[29] Raynor, Thomassen and Rouse, *Trans. Amer. Soc. Metals*, 1942, **30**, 313.

[30] Steigmann, Shockley and Nix, *Physic. Rev.*, 1939, **56**, 13.

[31] Rollin, *ibid.*, 1939, **55**, 231.

Matano [16] has measured the diffusion rates of a number of metals in copper. Plotting his values as log D against $1/T$ shows that they do not conform to straight lines, but mostly lie on a curve. Matano has pointed out that the diffusion rate at low temperature varies according to whether the alloys are annealed before diffusion or not. This effect was not found at high temperatures, which suggests that a grain boundary effect is involved. At low temperatures recrystallization occurs slowly and thus the large area of grain boundaries facilitates diffusion. At high temperatures, recrystallization occurs rapidy and is generally completed during the first stages of diffusion measurements. It is seen from Fig. 5 that the value obtained with an annealed palladium-copper alloy (denoted by an asterisk) agrees well with the line extrapolated from the high-temperature values, but the low-temperature value obtained with an unannealed alloy does not. In the present evaluations therefore, more weight is generally placed upon high-temperature values than on low-temperature values (cp. Fig. for method used here).

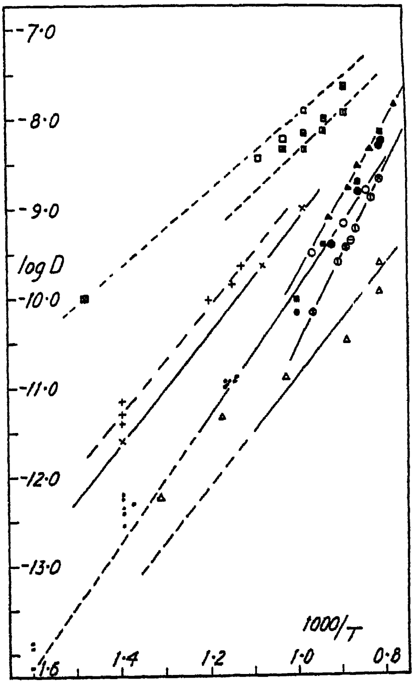

FIG. 6.

Gold in Silver.

⊗ Johnson.
• Jost.
○ Braune.
⦶ Weiss and Henry.
⊖ Fraenkel and Houben.

Silver in Gold.

● Johnson (radioact.).
■ Johnson (chem.).
▲ Present work .

Zinc in Silver.

◫ Bugakov and Ssirotkin (8 % Zn).
⊟ Bugakov and Ssirotkin (15·5 % Zn).
⊡ Bugakov and Ssirotkin (2·5 % Zn).
⊠ Bückle.

Platinum in Copper.

△ Matano.

Copper in Gold.

+ × Jost.

For the diffusion of nickel in copper the agreement between Matano and other observers [32-36] is good if a diffusion rate at 5 % Ni is selected from the diffusion rate-concentration curves given by Grube and Jedele [32, 33] (1025° C) and by Johnson [34] (1052° C). This is the average concentration in Matano's measurements. (Johnson [34] has measured separately the diffusion rates of the isotopes ^{58}Ni, ^{60}Ni, and ^{62}Ni.) From the line drawn in Fig. 3 only the value of Hertsricken and Faingold [36] shows deviation. This is probably not due to the higher original concentration of nickel (28·0 %) used, since the diffusion rate decreases with concentration; [32, 34] the Russian authors used compressed powders for their experiments, and though diffusion rate was found to be independent of pressure, a preferred diffusion along the grain boundaries is very likely in this case.

[32] Grube and Jedele, *Z. Elektrochem.*, 1932, **38**, 799.
[33] Matano, *Japan. J. Physics*, 1933, **8**, 109.
[34] Johnson, *Trans. Amer. Inst. Min. Met. Eng.*, 1946, **166**, 114.
[35] van Arkel, *Metallwirtsch.*, 1928, **7**, 656.
[36] Hertsricken and Faingold, *Mem. Phys. Kiew*, 1940, **8**, 127.

Other diffusion rates in gold have been investigated mainly by Jost [37, 38] and Kubaschewski and Ebert.[3] The constants given in Table I for platinum-gold, palladium-gold, copper-gold, and nickel-gold are almost the same as those derived in the original publications. Since Jedele's diffusion rates [39] (at 900° C) evaluated by Matano [40] were also considered slight alterations of the original constants became necessary. Only for nickel-gold is there a discrepancy between the data of Jedele and the author.

For palladium in silver, also investigated by Jost,[37] the original constants have not been accepted. It is seen from Fig. 5 that a straight line relationship is not very convincing. The line drawn is believed to give the best approximation. The value obtained for Q is, however, rather uncertain. Jost himself placed more weight on the high-temperature value than is done here and obtained a considerably lower value for Q, namely 20,200 cal./mole. In view of this ambiguity, the system Ag—Pd requires re-investigation. For copper in silver the constants given by Seith and Peretti [4] have been adopted. Their values are, however, scattered, and the temperature range of investigation (760°-895° C) is therefore too small to place much dependance on the equation derived from them.

Bugakov and Ssirotkin [41] have measured the diffusion rates of zinc in silver at 923°-1123° K with alloys containing 7·9, 15·5 and 22·5 % Zn, using the evaporation method. The diffusion rate was found to increase with zinc content (see Fig. 6), just as in the zinc-copper system. In view of the discussion on Bugakov's method and results on the copper-zinc alloys, these diffusion rates are possibly too high. Nor is the activation energy accurately determined since the temperature range investigated is relatively small. The values derived from the straight line in Fig. 5 (obtained from the values for 7·9 % Zn) and given in Table I therefore represent rough approximations only. For 400° C a value for D was derived by Bückle [42] from determinations of the rate of penetration of zinc into silver by micro-hardness measurements. His result is valid only for the *saturated* α solution and therefore is not in contradiction with the curve drawn with Bugakov and Ssirotkin's values.

Seith and Peretti [4] investigated diffusion of cadmium from silver alloys containing 2 % Cd into silver (650°-895° C). Bugakov and Ssirotkin [41] applied the evaporation method at concentrations 4·8, 9·6 and 14·5 % Cd. The values determined by Seith seem to fall on two straight lines, with a pronounced break between the two. The low-temperature line could be expressed by the relationship

$$D = 4{\cdot}84 \times 10^{-5}\, e^{-22,350/RT}.$$

An error was suspected in the high-temperature values due to evaporation of cadmium, though the test samples were protected by nickel and chromium coatings. Seith's results agree with those of Bugakov and Ssirotkin (4·8 % values) though the method employed by the latter should have obviated the error of which Seith's method was suspect. An increase in diffusion rate with cadmium content was again found in the experiments of the Russian authors. Since our present knowledge of diffusion in solid metals does not allow for a break in a $\log D - 1/T$ curve in the absence of a transformation a single straight line is drawn in Fig. 4 representing as well as possible all the experimental values. It is proposed that this curve should be generally accepted until further work clarifies these relations more completely.

The aim of this work has been to evaluate the most probable values of the constants in Arrhenius' equation for the diffusion of a number of metals in copper, silver and gold. No discussion of the data obtained is included, and it is intended that this should form the subject of a later paper.

The experiments described in the present paper were carried out at *Laboratorium für physikalische Chemie der Metalle am Max Planck-Institut für Metallforschung*, Stuttgart (Director: Prof. G. Grube). The author wishes to thank Dr. A. Pfeilsticker for his advice and assistance in carrying out the spectrographical analyses.

Metallurgy Division,
National Physical Laboratory,
Teddington, Middlesex.

---

[37] Jost, *Z. physik. Chem.*, 1933, **21**, 158. [38] Jost, *ibid.*, 1932, **16**, 123.

[39] Jedele, *Z. Elektrochem.*, 1933, **39**, 691.

[40] Matano, *Proc. Phys. Math. Soc. Japan*, 1933, **15**, 405.

[41] Bugakov and Ssirotkin, *Tech. Physics, U.S.S.R.*, 1937, **4**, 537.

[42] Bückle, *Metallforschung*, 1946, **1** (*Z. Metallkunde*, **37**), 175.

THE HYDROLYSIS OF ASPIRIN

A DETERMINATION OF THE THERMODYNAMIC DISSOCIATION CONSTANT AND A STUDY OF THE REACTION KINETICS BY ULTRA-VIOLET SPECTROPHOTOMETRY

By L. J. Edwards

Received 16*th March*, 1950

The ultra-violet absorption spectra of aspirin and salicylic acid have been determined over a pH range corresponding to 0 to 100 % dissociation of the acids. From these data the thermodynamic dissociation constant of aspirin has been calculated and a method evolved for the quantitative estimation of salicylic acid in the presence of aspirin. The kinetics of the aqueous hydrolysis at 17° C have been studied over the pH range 0·5 to 13; for the more rapid reactions occurring at the high pH values the velocity constants have been determined by a method in which a time base replaces the usual extinction base. The ordinary mechanism of acid-base catalysis needs modification to account for the results obtained; by regarding the hydrolysis as the sum of a number of bimolecular reactions the observed first-order velocity constant may be expressed as a function of several bimolecular constants which is in quantitative agreement with the measured values over the whole pH range.

The Absorption Spectra of Salicylic Acid and Aspirin.—The ultra-violet absorption spectra of salicylic acid in a variety of solvents and its sodium salt in aqueous solution have been recorded by a number of observers and are conveniently reviewed.[1] The spectra of *o*-acetylsalicylic

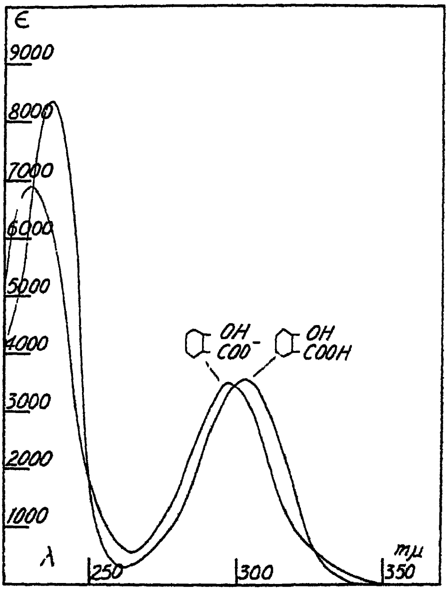

Fig. 1.—U.-v. absorption of salicylic acid and salicylate ion.

---

[1] *Int. Crit. Tables* (McGraw-Hill, 1933), 5, pp. 341, 362, 373.

acid in the fully dissociated and undissociated states are not on record, although Purvis[2] has reported the absorption of the acid and of its lithium salt in alcohol.

As a preliminary to the kinetic studies, both acids were examined at a number of pH values (Fig. 1 and 2). Below about pH 1 each of these acids could be regarded as undissociated to any appreciable extent, while above 6 the dissociation was substantially complete. The key points of the absorption curves are given in Table I.

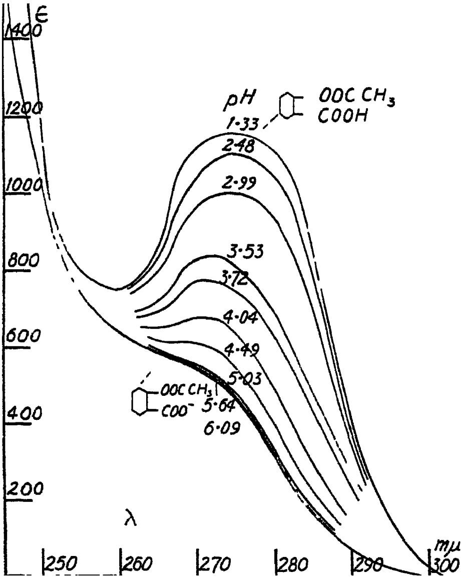

FIG. 2.—U.-v. absorption of aspirin at various pH values.

TABLE I.—KEY POINTS IN THE ABSORPTION SPECTRA OF SALICYLIC ACID AND ASPIRIN

		λ(mμ)	ε	
Salicylic acid	Molecular form	236	8350	Maxima
		302	3620	
		261·5	300	Minimum
	Ionic form	228·5	6920	Maxima
		296·5	3520	
		263·5	590	Minimum
		229·5	6890	Isobestic points
		249	1900	
		298·5	3470	
		327	510	
Aspirin	Molecular form	275	1160	Maximum
		259	760	Minimum
	Ionic form	None No isobestic points		

---

[2] *J. Chem. Soc.*, 1925, **127**, 2771 ; 1926, 775.

The Thermodynamic Dissociation Constant of Aspirin.—The pronounced difference in the absorption between the molecular and ionic forms of aspirin enabled the dissociation constant to be calculated by the method of Flexser, Hammett and Dingwall[3] based on the earlier work of Brode[4] in the visible range of the spectrum.

The extinction of a partly dissociated solution of a weak acid

$$HA \rightleftharpoons H^+ + A^-$$

is

$$\begin{aligned} \epsilon &= \epsilon(c_{HA} + c_A)d \\ &= (\epsilon_{HA}c_{HA} + \epsilon_A c_A)d, \end{aligned}$$

where ϵ_A, ϵ_{HA} and ϵ are the molecular extinctions of the dissociated, undissociated and mixed forms of the acid, respectively, concentrations being in mole/l.

Hence

$$\frac{c_A}{c_{HA}} = \frac{\epsilon_{HA} - \epsilon}{\epsilon - \epsilon_A}. \quad . \quad . \quad . \quad . \quad . \quad (1)$$

The thermodynamic dissociation constant of the acid is

$$K = \frac{a_H a_A}{a_{HA}} = \frac{c_H c_A}{c_{HA}} . \frac{f_H f_A}{f_{HA}}$$

or

$$pK = pH - \log_{10} \frac{c_A}{c_{HA}} . \frac{f_A}{f_{HA}} \quad . \quad . \quad . \quad . \quad . \quad (2)$$

Now f_{HA} may be taken as unity and the Debye-Hückel complete expression states that

$$-\log_{10} f_A = \frac{A\sqrt{I}}{1 + aB\sqrt{I}} - CI, \quad . \quad . \quad . \quad (3)$$

where A and B are constants whose values may be calculated at any given temperature, C is an empirical constant depending upon the salting-out effect at higher ionic strengths and a is the mean diameter of the ions involved.

Substituting (1) and (3) in (2), therefore,

$$pK = pH - \log_{10} \frac{\epsilon_{HA} - \epsilon}{\epsilon - \epsilon_A} + \frac{A\sqrt{I}}{1 + aB\sqrt{I}} - CI. \quad . \quad . \quad (4)$$

Using standard buffers of known composition all the terms on the right-hand side of (4) can be evaluated and K determined.

Experimental

The solvents of standard pH used in the determination of K were sulphuric acid, acetic acid, and acetic acid + sodium acetate solutions of known composition. It was desirable that the intermediate pH values for the partly dissociated aspirin should be fixed with some accuracy. Acetic acid was chosen for the buffer acid because its dissociation has been studied by several observers with considerable precision.[5]

The following expression, based on the complete Debye-Hückel equation, was used to calculate the pH of the acetate buffers at 17° C.

$$pH = 4{\cdot}756 + \log \frac{x}{100 - x} - \frac{0{\cdot}50\sqrt{\frac{mx}{100 + x}}}{1 + 0{\cdot}98\sqrt{\frac{mx}{100 + x}}} + 0{\cdot}015(x - 90)\frac{mx}{100 + x} \quad (5)$$

when 100 ml. of m-molar acetic acid was partly neutralized with x ml. of m-molar sodium hydroxide. In calculating the A and B constants the dielectric constant of water at 17° C was taken as 81·5 and the mean effective ionic diameter as 3·0 Å. The empirical constant C which is constant for different dilutions of the same mixture but varies for different mixtures,[6] could be expressed as a linear function of x more or less independent of temperature within the range 10° to 30° C; by putting $C = 0{\cdot}015\ (x - 90)$ good agreement was obtained with the bulk of the published data as well as with the author's own measurements on acetic acid buffers. Eqn. (5) gave values for pH which did not differ in the first two places of decimals from the most reliable data available when

---

[3] *J. Amer. Chem. Soc.*, 1935, **57**, 103.

[4] *Ibid.*, 1924, **46**, 581.

[5] E.g., La Mer and Parsons, *J. Biol. Chem.*, 1923, **57**, 622; Harned and Ehlers, *J. Amer. Chem. Soc.*, 1932, **54**, 1350; Cohn, Heyroth and Menkin, *ibid.*, 1928, **50**, 696; MacInnes, *Electrochemistry of Solutions* (Reinhold, 1939), pp. 274, 278.

$$5 < x < 95 \text{ and } 0{\cdot}01 < m < 0{\cdot}5.$$

Outside these limits it was less accurate.

In the absence of any sodium salt the pH at 17° C of a m-molar solution of acetic acid could be calculated from the empirical equation

$$a_{\mathrm{H}} = 0{\cdot}00448 m^{0{\cdot}517} \quad . \quad . \quad . \quad . \quad . \quad (6)$$

which was established experimentally over the range $0{\cdot}01 < m < 1{\cdot}0$. The usual approximation derived from $\sqrt{mK}$ would lead to

$$c_{\mathrm{H}} = 0{\cdot}00419 m^{0{\cdot}500}$$

In Table II the pH 1·33 solution was 0·1 N H_2SO_4. The absorption curve for aspirin in this solvent was identical with that in N H_2SO_4 at pH 0·53, indicating that the aspirin was present in molecular form below about pH 1·5. The solutions of pH 2·48 and 2·99 were prepared from 0·57 N and 0·057 N acetic acid, respectively, calculating the pH from eqn. (6); for these two solutions C in eqn. (4) was neglected. All the other solutions in Table II were prepared from 0·2 M acetic acid + 0·2 M sodium hydroxide in the appropriate proportions, calculating the pH from eqn. (5).

TABLE II.—MOLECULAR EXTINCTIONS OF ASPIRIN AT DIFFERENT DEGREES OF DISSOCIATION

pH	1·33	2·48	2·99	3·52	3·73	4·04	4·49	5·03	5·64	6·09
$\sqrt{I}$	0·270	0·058	0·032	0·110	0·135	0·182	0·245	0·290	0·308	0·312
λ(mμ)	ϵ_{HA}	ϵ								ϵ_A
265	850	825	790	720	695	650	625	605	600	600
270	1110	1060	980	825	780	675	615	580	570	565
275	1160	1100	1000	810	755	630	555	510	500	495
280	1115	1045	935	700	645	490	390	340	330	325
285	855	800	695	505	435	310	225	185	175	170

The ultra-violet absorption spectra were recorded on a Hilger medium quartz spectrophotometer. The density drum was calibrated from $E = 0$ to 2 using K_2CrO_4 as standard. All molecular extinctions in this paper are referred to $\epsilon_{\max.}$ 4816 at 371 mμ for K_2CrO_4. The calculated extinction never differed by more than 0·08 from the stated value at any point on the drum. It was considered advisable to make this calibration, however, as slight deviations from Lambert's law caused by instrumental errors might introduce quite serious errors into the calculation of the dissociation constant.

In all cases the aspirin concentration was of the order 3×10^{-3} M, insufficient to affect the calculated pH values of the buffer solutions. The absorptions were measured in 0·5 cm. quartz cells using the appropriate buffer solution in the comparison cell. The exposures were made as soon as all the aspirin had dissolved and before any appreciable hydrolysis had occurred.

The values for the molecular extinctions recorded in Table II are taken from the best curves representing a number of determinations. Substitution of these values in eqn. (4) gave a mean value of 3·565 for pK corresponding to a thermodynamic dissociation constant of $2{\cdot}72 \times 10^{-4}$ for aspirin at 17° C.

The maximum extinction of an aqueous solution ($3{\cdot}27 \times 10^{-3}$ M) of aspirin was 920 at 275 mμ, corresponding to about 27 % dissociation. In anhydrous alcohol a solution of the same concentration showed a slight medium shift of the maximum to 276 mμ with an extinction of 1100, corresponding to about 9 % dissociation.

---

[6] Cf. Cohn, *J. Amer. Chem. Soc.*, 1927, 49, 173.

Estimation of Salicylic Acid in the Presence of Aspirin.—It can be seen from Fig. 1 and 2 that in the neighbourhood of 300 mμ the absorption of aspirin is negligible whilst that of salicylic acid is at a maximum for all pH values. This afforded a most convenient method for measuring the degree of hydrolysis of aspirin at any stage. By estimating ϵ for the isobestic wavelength of 298·5 mμ the molar fraction of salicylic acid present could be obtained quite simply from $\epsilon/3470$ without any knowledge of the pH of the solution. When the latter was known it was preferred to measure ϵ at the wavelength of the salicylic acid maximum corresponding to that pH. The validity of the method was confirmed by measuring the absorptions of mixtures of known composition as illustrated in Fig. 3.

For the kinetic studies the solutions used in the calculation of K were maintained at 17° C and the progress of reaction followed by this spectrophotometric method from day to day. In addition to the buffer solutions already described, the pH range was extended by the use of other solutions as set out in Table III. At pH values higher than 12 the hydrolysis was too rapid to be measured in the usual manner. The total time necessary to record a complete absorption curve was normally 2-3 min.; during this time a fast reaction might go to more than 90 % completion so that the absorption results would be of no value. For such cases a special technique was devised whereby exposures were made with a fixed density drum setting (corresponding to a known degree of hydrolysis) at measured intervals of time. This technique is best illustrated by a specific example, viz., the reaction rate at pH 12·66.

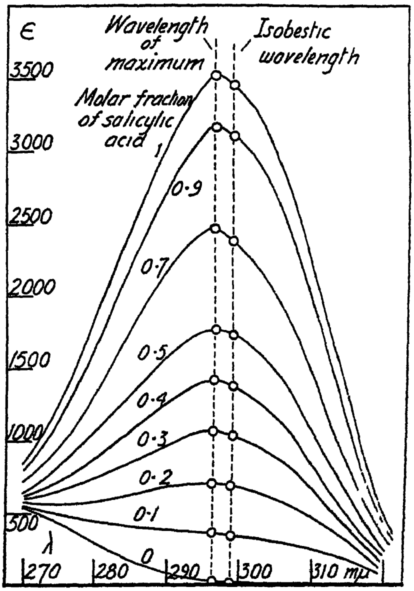

FIG. 3.—U.-v. absorption of mixtures of aspirin and salicylic acid at pH 7·0. Points ○ calculated from $\epsilon/3470$ at isobestic wavelength; from $\epsilon/3520$ at wavelength of maximum.

The buffer at this pH consisted of a solution of glycine (0·02 mole), NaCl (0·02 mole) and NaOH (0·08 mole). The aspirin was dissolved in water to which had been added the glycine and NaCl to give a solution at about pH 7. Under these conditions the rate of hydrolysis was only about 1/5000 of that attained on addition of the NaOH. At the moment of addition of the NaOH, therefore, a stopwatch was started and, after mixing the contents of the flask, a 0·1 cm. quartz cell was filled with the reaction mixture. The concentration of aspirin was chosen to give maximum absorption at about $\epsilon = 1\cdot 8$ (296·5 mμ) in a 0·1 cm. cell when hydrolysis was complete. A drum setting of 1·1 (calibrated value 1·04) corresponded to a mole fraction of salicylic acid of

$$\frac{1\cdot 04 \times 1000}{4\cdot 929 \times 0\cdot 1 \times 3520} = 0\cdot 599$$

at the moment when the absorption maximum at 296·5 mμ reached that point. Similarly, a drum setting of 1·5 (calibrated value 1·46) corresponded to a mole fraction of 0·841 of salicylic acid. From the rate at which the hydrolysis had occurred at lower pH values it was anticipated that these mole fractions would be reached in about 2-4 and 5-7 min. respectively after addition of the NaOH. Accordingly, with the drum set at 1·1, exposures were made at 15 sec. intervals from 2-5 min. after zero time. At this point the setting was changed to 1·5 and exposures were continued at the same rate until 10 min. after zero. The resulting absorption curves are illustrated in Fig. 4. The times at which absorption first occurred at 296·5 mμ were 2·7 and 5·7 min. respectively, corresponding to first-order velocity constants of 465 and 488 (mean $k = 476$). Whenever it was considered necessary to obtain more points on the reaction curve the hydrolysis was repeated with different drum settings. All the experimental determinations of k at pH values above 12 were made by this technique.

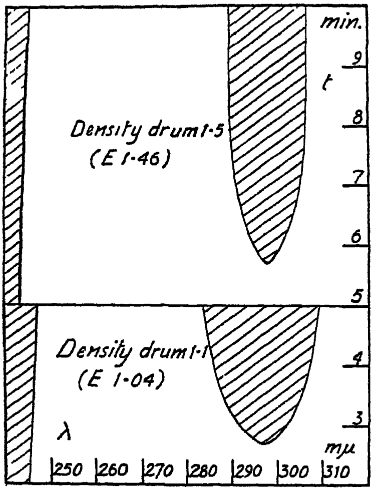

FIG. 4.—Time-absorption curves at fixed extinction values for 4·929 × 10^{-3} M aspirin in glycine buffer (pH 12·66, $\sqrt{I}$ 0·287).

The fastest reaction which could be followed by this method would be one that was 90 % completed in about 1·5-2·0 min., as the minimum time in which the reactants can be properly mixed and the cell filled is just over a minute.

Results

In all cases observed the rate of disappearance of aspirin (rate of formation of salicylic acid) followed a first-order course over at least the first 90 % of the reaction; Fig. 5 is typical of the results obtained. As most of the reactions studied were comparatively slow, points on the rate curves were usually measured at intervals of 24 hr. after the dissolution of the aspirin in the appropriate buffer. The velocity constants are reported in these units (days^{-1}) throughout this paper. The observed velocity constants, together with buffer data, are listed in Table III.

A plot of log k against pH (Fig. 6) demonstrated that the hydrolysis was catalyzed quite appreciably by H^+(AB) and strongly by OH^-(FG). Over the pH range 5-8 the velocity was constant apart from minor variations caused by salt effects. Between pH 2 and 3, however, there was a pronounced minimum C where the reaction velocity dropped to less than a quarter of the stationary value DE which is usually taken to represent the " spontaneous " reaction. At first it was thought that the rise in velocity from C to D might be caused by the change in concentration of the buffer solution. When the reaction was carried out in successive dilutions of the same buffer as indicated in Table IV, however, the variation in acetate ion concentration over a 64-fold range caused less than 10 % variation in the rate. Moreover, the rate appeared to increase with increasing dilution but this was probably the effect of the small increase in pH which occurred at each successive

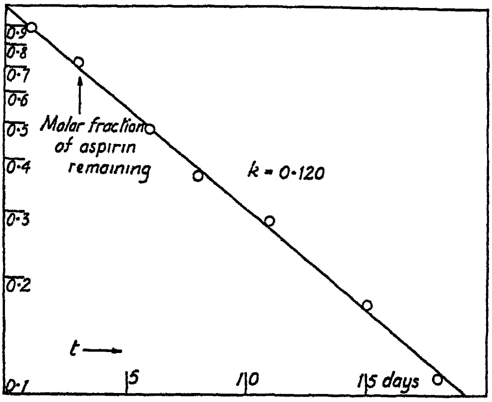

FIG. 5.—First-order disappearance of aspirin in acetate buffer at 17° C (pH 6·04, $\sqrt{I}$ 0·312).

TABLE III.—VELOCITY CONSTANTS FOR THE HYDROLYSIS OF ASPIRIN AT 17° C

Molarity of Buffer Components		pH	$\sqrt{I}$	k (days^{-1})
0·5022 M H_2SO_4		0·53	0·556	0·578
0·0502 M H_2SO_4		1·33	0·270	0·0835
0·0500 M KCl	0·1043 M HCl	1·00	0·387	0·190
0·0500 M KCl	0·0167 M HCl	1·80	0·256	0·0450
0·5700 M CH_3COOH		2·48	0·058	0·0267
0·0570 M CH_3COOH		2·99	0·032	0·0343
0·1878 M CH_3COOH	0·0122 M NaOH	3·53	0·110	0·0561
0·1667 M CH_3COOH	0·0333 M NaOH	4·04	0·182	0·0880
0·1399 M CH_3COOH	0·0601 M NaOH	4·49	0·245	0·125
0·1163 M CH_3COOH	0·0837 M NaOH	5·03	0·290	0·130
0·1047 M CH_3COOH	0·0953 M NaOH	5·64	0·308	0·130
0·1020 M CH_3COOH	0·0980 M NaOH	6·04	0·312	0·120
0·5135 M CH_3COOH	0·4865 M NaOH	6·06	0·698	0·120
0·1675 M KH_2PO_4	0·0335 M NaOH	6·21	0·485	0·113
0·1440 M KH_2PO_4	0·0577 M NaOH	6·64	0·509	0·110
0·1263 M KH_2PO_4	0·0758 M NaOH	6·98	0·528	0·107
0·1126 M KH_2PO_4	0·0901 M NaOH	7·40	0·541	0·108
0·1068 M KH_2PO_4	0·0961 M NaOH	7·75	0·547	0·116
0·1035 M KH_2PO_4	0·0994 M NaOH	8·10	0·550	0·134
0·0100 M KH_2PO_4	0·0080 M NaOH	7·35	0·161	0·115
0·0200 M KH_2PO_4	0·0160 M NaOH	7·37	0·226	0·120
0·0400 M H_3BO_3	0·0060 M NaOH	8·10	0·077	0·134
0·1744 M H_3BO_3	0·0262 M NaOH	8·19	0·162	0·154
0·1259 M H_3BO_3	0·0755 M NaOH	9·48	0·275	0·321
0·1033 M H_3BO_3	0·0982 M NaOH	10·52	0·314	1·97
0·1000 M Na_2HPO_4	0·0333 M NaOH	11·29	0·630	13·7
0·0714 M KH_2PO_4	0·1285 M NaOH	12·00	0·605	58·0
0·04 M glycine/NaCl	0·06 M NaOH	12·21	0·280	121
0·03 M glycine/NaCl	0·07 M NaOH	12·48	0·283	273
0·02 M glycine/NaCl	0·08 M NaOH	12·66	0·287	476
0·01 M glycine/NaCl	0·09 M NaOH	12·77	0·291	530
	Water	3·15	0·001	0·041

TABLE IV.—THE EFFECT OF ACETATE CONCENTRATION ON THE RATE OF HYDROLYSIS OF ASPIRIN AT 17° C

Half-neutralized ($x = 50$) acetic acid buffers

m	$[CH_3COO^-]$	$\sqrt{I}$	k	pH Calculated from (5)	pH Observed
1	0·333	0·576	0·112	4·37	4·55
1/2	0·167	0·408	0·116	4·51	4·56
1/4	0·0833	0·288	0·114	4·59	4·60
1/8	0·0417	0·204	0·114	4·65	4·65
1/16	0·0209	0·144	0·119	4·68	4·68
1/32	0·0104	0·102	0·115	4·70	4·70
1/64	0·00521	0·072	0·119	4·72	4·72

dilution of the buffer. It seemed that some other explanation was needed to account for the minimum at C; this was provided by a closer consideration of the reacting species taking part in the hydrolysis as set out in the following discussion.

Discussion

The usual mechanism of acid-base catalysis considers the observed velocity constant to be made up of a number of terms each of which is the product of a concentration and a catalytic coefficient for one of the species present in the reaction medium. Thus

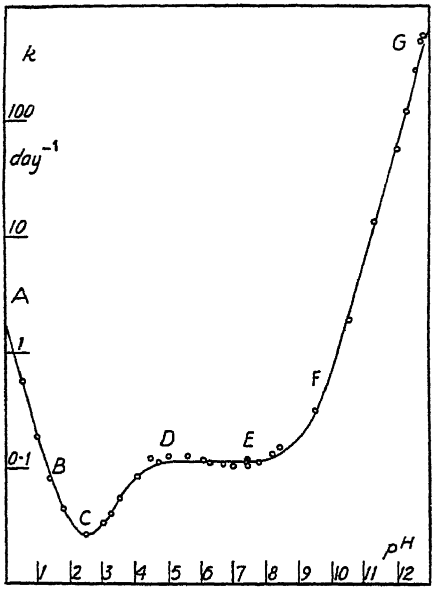

FIG. 6.—Overall velocity constant for aspirin hydrolysis at 17° C as a function of pH.

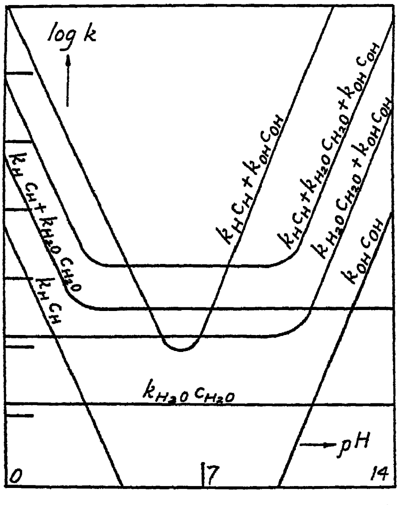

FIG. 7.—Possible forms of acid-base catalysis.

$$k = k_H c_H + k_{OH} c_{OH} + k_{H_2O} c_{H_2O} + k_{HX} c_{HX} + k_X c_X + k_{HY} c_{HY} + k_Y c_Y + \ldots \text{ etc.} \quad (7)$$

where HX, HY, etc., are the buffer acids and X, Y, etc., are the buffer anions. In dilute solutions the first three terms are usually large compared with the others so that a plot of log k against pH leads to one or another of the various possibilities set out in Fig. 7 according as k_H, k_{OH} or k_{H_2O} are the controlling factors. None of these possibilities suffices to account for the minimum at pH 2·5 in the experimental results illustrated in Fig. 6. This may be explained, however, if the hydrolysis is regarded as taking place via the six simultaneous reactions

$$\begin{aligned}
CH_3COOC_6H_4COOH + H_3O^+ &\xrightarrow{k_1} HOC_6H_4COOH + CH_3COOH + H^+\\
CH_3COOC_6H_4COOH + H_2O &\xrightarrow{k_2} HOC_6H_4COOH + CH_3COOH\\
CH_3COOC_6H_4COOH + OH^- &\xrightarrow{k_3} HOC_6H_4COOH + CH_3COO^-\\
&\quad\text{or}\quad HOC_6H_4COO^- + CH_3COOH\\
CH_3COOC_6H_4COO^- + H_3O^+ &\xrightarrow{k_4} HOC_6H_4COOH + CH_3COOH\\
CH_3COOC_6H_4COO^- + H_2O &\xrightarrow{k_5} HOC_6H_4COOH + CH_3COO^-\\
&\quad\text{or}\quad HOC_6H_4COO^- + CH_3COOH\\
CH_3COOC_6H_4COO^- + OH^- &\xrightarrow{k_6} HOC_6H_4COO^- + CH_3COO^-.
\end{aligned}$$

After time t let the number of moles of salicylic acid formed by each of these reactions be $x_1, x_2, \ldots x_6$. Then the aspirin concentration at that time will be $c_0 - \sum_1^6 x_n$, where c_0 is the initial concentration. Now at any time t

$$[CH_3COOC_6H_4COOH]_t + [CH_3COOC_6H_4COO^-]_t = c_0 - \sum_1^6 x_n,$$

and

$$\frac{[CH_3COOC_6H_4COO^-]_t}{[CH_3COOC_6H_4COOH]_t} = \frac{K}{c_H},$$

where K is the dissociation constant for aspirin. From these two relationships the molecular and ionic concentrations of aspirin can be found. Then

$$\frac{dx_1}{dt} = k_1 c_H \left(\frac{c_0 - \sum_1^6 x_n}{1 + K/c_H} \right)$$

$$\frac{dx_2}{dt} = k_2 c_{H_2O} \left(\frac{c_0 - \sum_1^6 x_n}{1 + K/c_H} \right)$$

$$\frac{dx_3}{dt} = k_3 c_{OH} \left(\frac{c_0 - \sum_1^6 x_n}{1 + K/c_H} \right)$$

$$\frac{dx_4}{dt} = k_4 c_H \left(\frac{c_0 - \sum_1^6 x_n}{1 + c_H/K} \right)$$

$$\frac{dx_5}{dt} = k_5 c_{H_2O} \left(\frac{c_0 - \sum_1^6 x_n}{1 + c_H/K} \right)$$

$$\frac{dx_6}{dt} = k_6 c_{OH} \left(\frac{c_0 - \sum_1^6 x_n}{1 + c_H/K} \right),$$

and the overall rate of hydrolysis is given by

$$\sum_1^6 \frac{dx_n}{dt} = \frac{d}{dt}\sum_1^6 x_n$$

$$= \left(c_0 - \sum_1^6 x_n\right)\left(\frac{k_1c_H + k_2c_{H_2O} + k_3c_{OH}}{1 + K/c_H} + \frac{k_4c_H + k_5c_{H_2O} + k_6c_{OH}}{1 + c_H/K}\right), \quad (8)$$

which at any fixed pH value integrates to give the apparent monomolecular reaction

$$\sum_1^6 x_n = c_0(1 - e^{-kt}),$$

where the observed first order velocity constant is a function of the six second-order constants

$$k = \frac{k_1c_H + k_2c_{H_2O} + k_3c_{OH}}{1 + K/c_H} + \frac{k_4c_H + k_5c_{H_2O} + k_6c_{OH}}{1 + c_H/K}.$$

If each of the six components on the right-hand side of (8) is plotted on the pH—log k diagram, four types of curve are obtained. In Fig. 8,

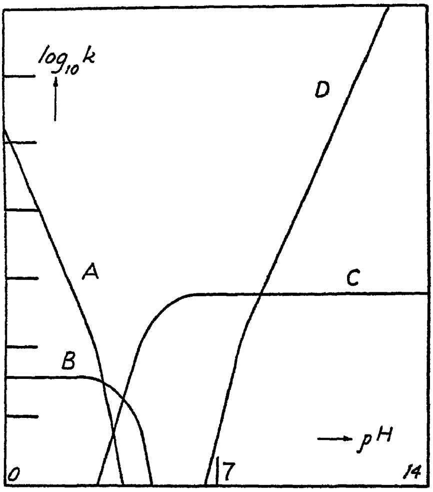

FIG. 8.—Possible forms of acid-base catalysis involving both the molecular and the ionic forms of the reactants.

Curve A represents $\dfrac{k_1c_H}{1 + K/c_H}$,

Curve B represents $\dfrac{k_2c_{H_2O}}{1 + K/c_H}$ or $\dfrac{k_4c_H}{1 + c_H/K}$,

Curve C represents $\dfrac{k_3c_{OH}}{1 + K/c_H}$ or $\dfrac{k_5c_{H_2O}}{1 + c_H/K}$,

Curve D represents $\dfrac{k_6c_{OH}}{1 + c_H/K}$.

A combination of these curves can be made to approximate to all the types particularized in Fig. 7; in addition they can be fitted to experimental data such as have been obtained in this investigation by giving appropriate values to the six bimolecular velocity constants and the dissociation constant of the compound undergoing hydrolysis.

Thus, in Fig. 6 the linear portion AB may be represented by

$$\frac{1\cdot9\, c_H}{1 + 2\cdot72 \times 10^{-4}/c_H}$$

using the thermodynamic dissociation constant determined in the first part of this investigation. This corresponds to the reaction between undissociated aspirin molecules and hydrogen ions (H_3O^+) with a second-order velocity constant of 1·9. It will be noted that while $c_H \gg K$ the expression reduces to $1\cdot9\, c_H$ with a slope of 1, comparable with the $k_H c_H$ term in the unmodified equation (7).

Similarly, the linear portion FG may be represented by

$$\frac{7500\, c_{OH}}{1 + c_H/2\cdot72 \times 10^{-4}}$$

corresponding to the reaction between aspirin ions and hydroxyl ions with second-order constant 7500. Here again, when $K \gg c_H$ the expression reduces to $7500\, c_{OH}$ with a slope of 1 analogous to the $k_{OH} c_{OH}$ term of eqn. (7).

The horizontal portion of the curve DE might be controlled by the reaction between aspirin molecule and OH^-, in which case

$$k_3 = 3\cdot18 \times 10^9 \quad \text{and} \quad k_5 \not> 10^{-5},$$

or the reaction between aspirin ion and H_2O might be the rate-determining factor, in which case

$$k_5 = 2\cdot11 \times 10^{-3} \quad \text{and} \quad k_3 \not> 10^6.$$

Now k_6 (aspirin ion and OH^-) is 7500 and it seems unlikely that the reaction between aspirin molecule and OH^- would be $4\cdot25 \times 10^5$ times faster than that between aspirin ion and OH^-; hence it is probable that the second alternative is correct and that $k_5 = 2\cdot11 \times 10^{-3}$ (i.e. $k_5 c_{H_2O} = 0\cdot117$ if $c_{H_2O} = 55\cdot5$) while k_3 might have any value below 10^6 (and probably below 10^3) without having any appreciable effect on the observed value of k.

At this stage, therefore we have

$k_1 = 1\cdot9$; $k_5 = 2\cdot11 \times 10^{-3}$;

$k_6 = 7\cdot5 \times 10^3$; $k_3 \ll 10^6$ and probably $< 10^3$.

At pH 2·5 the total contribution of these four reactions to the observed value of k is 0·0148 leaving a difference of 0·0117 to be accounted for. Now this difference may be made up by either the reaction between aspirin molecule and H_2O or aspirin ion and H_3O^+ or a combination of both. If it is caused entirely by the former reaction then at pH 2·5

$$55\cdot5\, k_2/1\cdot086 = 0\cdot0117,$$

$$\text{or} \quad k_2 = 2\cdot29 \times 10^{-4} \quad \text{and} \quad k_4 \not> 1.$$

If it is caused entirely by the latter reaction then at pH 2·5

$$3\cdot16 \times 10^{-3}\, k_4/12\cdot6 = 0\cdot0117,$$

$$\text{or} \quad k_4 = 46\cdot7 \quad \text{and} \quad k_2 \not> 10^{-6}.$$

Now it is unlikely that the reaction between molecular aspirin and H_3O^+ (whose velocity constant is 1·9) would be faster than that between aspirin ion and H_3O^+, hence the second alternative appears to be more acceptable.

The complete curve shown in Fig. 6 and defining the rate of reaction over the whole pH range is represented by

$$k = \frac{1\cdot9\, c_H}{1 + 2\cdot72 \times 10^{-4}/c_H} + \frac{46\cdot7\, c_H + 0\cdot117 + 7500\, c_{OH}}{1 + c_H/2\cdot72 \times 10^{-4}}. \quad (9)$$

The nearest approach to this that could be obtained by application of eqn. (7) would be

$$k = 1{\cdot}9\, c_H + 7500\, c_{OH} + 0{\cdot}117 \quad . \quad . \quad . \quad (10)$$

which does not account for the minimum at pH 2·5.

It is of interest to note that at the minimum at least three of the six reactions are making a measurable contribution to the overall velocity. Considering only the contributions of reactions (1), (4) and (5), we have

$$k = \frac{k_1 c_H{}^2 + k_4 K c_H + k_5 K c_{H_2O}}{c_H + K}, \quad . \quad . \quad . \quad (11)$$

and on differentiating

$$\frac{dk}{dc_H} = \frac{(c_H + K)(2k_1 c_H + k_4 K) - (k_1 c_H{}^2 + k_4 K c_H + k_5 K c_{H_2O})}{(c_H + K)^2}. \quad (12)$$

The condition for the minimum is therefore

$$k_1 c_H{}^2 + 2k_1 K c_H + k_4 K^2 - k_5 K c_{H_2O} = 0, \quad . \quad . \quad (13)$$

and the positive root of (13) is

$$c_H = K\left\{\left(1 + \frac{k_5 c_{H_2O}}{k_1 K} - \frac{k_4}{k_1}\right)^{\frac{1}{2}} - 1\right\}. \quad . \quad . \quad . \quad (14)$$

Substituting the numerical values mentioned above we have

$$c_H = 3{\cdot}6 \times 10^{-3}$$

or $\quad$ pH = 2·44 at the minimum.

A number of workers have studied the hydrolysis of aspirin under a variety of conditions. Rath[7] determined the rate in water at 100° C and obtained the first-order velocity constant $k = 7{\cdot}92$ days^{-1}. The temperature coefficient of the reaction has not been determined but Rath records the effect of temperature on the hydrolysis of diacetyl-tartaric acid, giving

$$(k_t + 10)/k_t = 1{\cdot}87.$$

If a similar factor is assumed to hold for aspirin, Rath's velocity at 17° C would be

$$7{\cdot}92/1{\cdot}87^{8{\cdot}3} = 4{\cdot}35 \times 10^{-2} \text{ days}^{-1}$$

compared with $4{\cdot}1 \times 10^{-2}$ reported in this paper.

La Mer and Greenspan[8] studied the bimolecular reaction between aspirin and NaOH at 25° C, obtaining $k = 8{\cdot}09$ min.$^{-1}$ (for $\sqrt{I} = 0{\cdot}218$). Converting to days^{-1} and reducing to 17° C this would correspond to

$$1440 \times 8{\cdot}09/1{\cdot}87^{0{\cdot}8} = 7{\cdot}05 \times 10^3 \text{ days}^{-1}$$

compared with $k_6 = 7{\cdot}50 \times 10^3$ found above.

Sturtevant[9] studying the same reaction as La Mer by a calorimetric method, found the bimolecular constant 15·42 min.$^{-1}$ at 35° C ($\sqrt{I}=0{\cdot}145$). At 17° C this reduces to

$$1440 \times 1542/1{\cdot}87^{1{\cdot}8} = 7{\cdot}2 \times 10^3 \text{ days}^{-1}$$

which is in even better agreement with the value of k_6 as found in this investigation.

Morton[10] followed the first-order hydrolysis of aspirin in potassium citrate buffer at laboratory temperature. Although the temperature was not controlled he obtained a good first-order rate with $k = 0{\cdot}103$ days^{-1} ($\sqrt{I} = 0{\cdot}547$). The pH of this buffer would be in the neighbourhood of 7 and his figure is in good agreement with that observed above, viz. 0·117.

[7] *Annalen*, 1908, **358**, 98.

[8] *J. Amer. Chem. Soc.*, 1934, **56**, 1492.

[9] *Ibid.*, 1942, **64**, 77.

[10] *Quart. J. Pharm. Pharmacol.*, 1933, **6**, 492.

Tsakalotos and Horsch[11] followed the hydrolysis in solutions of various acids. They reported minima in their concentration-time curves which they assumed to be caused by hydrogen ion catalysis but they gave no value for k_H.

Conclusion.—It has been shown that the hydrolysis of aspirin can be accounted for over the whole pH range by considering all the possible bimolecular reactions between the five species present in the equilibrium

$$2H_2O \rightleftharpoons H_3O^+ + OH^-$$

on the one hand, and the equilibrium

$$CH_3COOC_6H_4COOH \rightleftharpoons CH_3COOC_6H_4COO^- + H^+$$

on the other hand. The relatively minor variations in k caused by salt effects need not be taken into quantitative account in presenting a broad picture of the mechanism. It is worth noting, however, that the effect of an increase in I would be as follows:

Reactions 1, 3 and 5 (molecule and ion),	increase $\propto I$
Reaction 2 (molecule and molecule),	no effect.
Reaction 4 (ions of opposite charge),	decrease $\propto \sqrt{I}$
Reaction 6 (ions of the same charge),	increase $\propto \sqrt{I}$.

The curve ABCDEFG (Fig. 6) would therefore be slightly displaced at zero ionic strength in such a manner that it would lie below the existing curve along AB, crossing somewhere between B and C and continuing slightly above from C to D, crossing again near D to lie below the existing curve for the remainder of the pH range. The displacement at any point is unlikely to exceed a few per cent. and is probably of the same order of magnitude as the deviation of the experimental results from the horizonal line DE.

The extension of the general theory of aqueous hydrolysis in which both the ionic and the molecular form of the reactants are considered is, of course, not specific for aspirin. Expressions similar to eqn. (8) could be developed for any ionizing compounds undergoing hydrolysis and would probably account for deviations from the behaviour predicted by the more usual eqn. (7).

The author would like to record his thanks to Mr. K. L. Watling for his assistance in the laboratory and to the Directors of Beecham Research Laboratories Ltd. for their permission to publish this work.

The Physical Department,
Brockham Park,
Betchworth,
Surrey.

---

[11] *Bull. Soc. chim.*, 1914, **15**, 743.

THE KINETICS OF FORMATION AND DISSOCIATION OF THE FERROUS TRIS-DIPYRIDYL ION

By J. H. Baxendale and Philip George

Received 16th March, 1950

The formation of the complex ion $Fe(Dipy)_3^{++}$ from Fe^{++} and αα′-dipyridyl is first order in $[Fe^{++}]$ and third in [Dipy]. The fourth-order rate constant is $8{\cdot}4 \times 10^{14}$ and is temperature independent. The fourth order arises from the formation of the intermediates $FeDipy^{++}$ and $Fe(Dipy)_2^{++}$.

The dissociation of $Fe(Dipy)_3^{++}$ is first order and is independent of $[H^+]$ at low acidities but increases to a limiting value at higher $[H^+]$. The H^+ independent rate constant is given by

$$k_d = 3 \times 10^{17} \exp\left(-\frac{26{,}000}{RT}\right).$$

The increase with $[H^+]$ can be accounted for by the existence of the ion $Fe(Dipy)_3H^{+++}$ at high acidities.

In a previous publication [1] we have shown that the red complex ion $Fe(Dipy)_3^{++}$ formed by the addition of Fe^{++} to αα′-dipyridyl (Dipy) is in equilibrium with Fe^{++}, dipyridyl, and the intermediates $Fe(Dipy)^{++}$ and $Fe(Dipy)_2^{++}$ according to the equations :

$$Fe^{++} + Dipy \rightleftharpoons FeDipy^{++},\ K_1 \quad . \quad . \quad . \quad (1)$$

$$FeDipy^{++} + Dipy \rightleftharpoons Fe(Dipy)_2^{++},\ K_2 \quad . \quad . \quad . \quad (2)$$

$$Fe(Dipy)_2^{++} + Dipy \rightleftharpoons Fe(Dipy)_3^{++},\ K_3 \quad . \quad . \quad . \quad (3)$$

We were able to obtain values for K_1 and the overall equilibrium constant K where

$$K = K_1K_2K_3 = [Fe(Dipy)_3^{++}]/[Fe^{++}] \,.\, [Dipy]^3.$$

It was found that the equilibrium can be shifted by changes in pH and this is a consequence of the basic nature of the αα′-dipyridyl which forms the conjugate acid Dipy H^+, according to the equilibrium

$$Dipy\ H^+ \rightleftharpoons Dipy + H^+,\ K_a. \quad . \quad . \quad . \quad (4)$$

The determination of the above equilibrium constants was facilitated by this basicity since the concentration of free dipyridyl could be chosen at will simply by varying the pH of the solution. Hence even though K was of the order of 10^{16} indicating an extremely stable complex with very little free αα′-dipyridyl in equilibrium, by making use of the determined value of K_a it was possible to calculate this amount and hence K.

This technique has also been applied in a study of the kinetics of formation of $Fe(Dipy)_3^{++}$, a reaction which is extremely fast in neutral solutions but which is slowed down in more acid solutions. In addition we have examined the kinetics of dissociation of the complex ion. A preliminary report of this work has already been published.[2] Krumholtz [3] has also made an investigation of this system and the analogous phenanthroline system has been examined by Kolthoff *et al.*[4]

[1] *Trans. Faraday Soc.*, 1950, **46**, 55.

[2] Baxendale and George, *Nature*, 1948, **162**, 777.

[3] Krumholtz, *J. Amer. Chem. Soc.*, 1949, **71**, 3654.

[4] Lee, Kolthoff and Leussing, *ibid.*, 1948, **70**, 2340.

Experimental

Materials.—The same materials were used as for the equilibrium study and in all cases, except where indicated, M/40 phthalate buffers were used.

Measurement of Rates of Formation.—The formation of $Fe(Dipy)_3^{++}$ was followed colorimetrically.[1] As mentioned above, the rate of formation could be decreased considerably by working at low pH, and if the pH was low enough it was possible to have dipyridyl in such a large excess that it was essentially constant. Most observations were made under these conditions. After mixing the reactants, samples of the reaction mixture were poured into normal acid at appropriate time intervals to stop the reaction, and the $Fe(Dipy)_3^{++}$ concentration measured on the colorimeter. At the higher pH's where the reaction is extremely fast a different procedure was adopted. The reaction was begun by blowing the required amount of Fe^{++} into the buffer containing the $\alpha\alpha'$-dipyridyl which was being stirred vigorously. After an appropriate time a known volume of strong acid was poured into the mixture to stop the reaction and the concentration of $Fe(Dipy)_3^{++}$ measured soon afterwards. In this way it was possible to obtain points a few seconds after the reaction had begun, and enabled reactions with half times of only a few seconds to be followed.

In general, the initial concentrations of Fe^{++} were between 10^{-4} and 10^{-5} M and the dipyridyl varied from 2×10^{-3} M at low pH values to 3×10^{-5} M at the higher pH's. Formation rates were measured at 0° C, 17° C and 35° C, over the range pH 1·85 to pH 4·94.

Measurement of Rates of Dissociation.—A stock solution of M/100 $Fe(Dipy)_3^{++}$ was made up at a high pH where it was known to be formed almost quantitatively from equivalent amounts of Fe^{++} and dipyridyl. A small amount of this was then pipetted into a buffer solution having a lower pH, the value being chosen so that the complex dissociates due to removal of the dipyridyl in equilibrium with it as $DipyH^+$. The dissociation was followed colorimetrically. Rates were measured at 25° C, 35° C and 45° C.

We wish to thank Mr. D. Irvine and Mr. G. Hanania who carried out some of the experiments.

Results

Rates of Formation of $Fe(Dipy)_3^{++}$.—In the pH range 1·85 to 2·69 measurable rates of formation were obtained with concentrations of Fe^{++} about 10^{-5} M and concentrations of dipyridyl between 2×10^{-3} and 3×10^{-4} M. Thus the dipyridyl is essentially constant throughout the reaction. In these conditions the formation of $Fe(Dipy)_3^{++}$ was found to be first order in Fe^{++} and examples of the first-order plots at different pH's and dipyridyl concentrations are shown in Fig. 1. These first-order constants at the same pH and temperature but with varying concentration of dipyridyl were found to increase as the cube of the total dipyridyl concentration, $[Dipy]_T (= [Dipy] + [Dipy\,H^+])$.

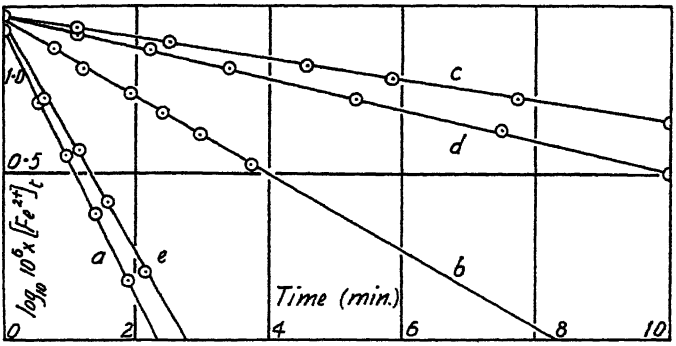

FIG. 1.—First-order formation of $Fe(Dipy)_3^{++}$ at 17° C with dipyridyl in large excess. $[Fe^{++}] = 9{\cdot}1\text{-}9{\cdot}6 \times 10^{-6}$ M.

a, b, c : pH 2·47, [Dipy] = 8·64, 5·76, 2·88 × 10^{-4} M.
d, e : pH 2·29, [Dipy] = 11·5, 5·76 × 10^{-4} M.

A plot of the first-order constants against $[\mathrm{Dipy}]_T^3$ is shown in Fig. 2 for reactions at different pH's.

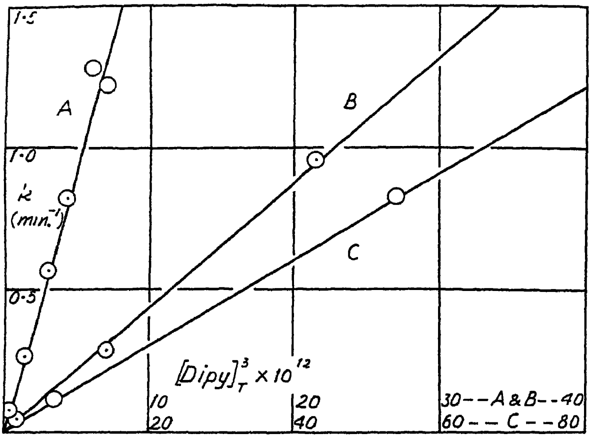

FIG. 2.—Variation of the first-order constant obtained when dipyridyl is in large excess at 17° C with $[\mathrm{Dipyl}]^3$.
A—pH 2·69 ; *B*—pH 2·47 ; *C*—pH 2.29.

Hence the reaction is fourth order, first in Fe^{++} and third in dipyridyl, and the fourth-order constants ($k_{\mathrm{obs.}}$) at different pH's can be obtained from the slope of the lines in Fig. 2. These constants vary with pH, as might be expected if the reaction goes through the free base, since at different pH's the presence of the acid-base equilibrium will give different concentrations of free dipyridyl from the same total concentration of the dipyridyl $(\mathrm{Dipy})_T$.

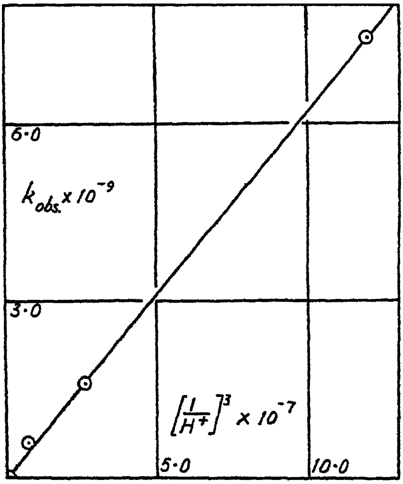

FIG. 3.—Variation of the observed fourth-order constant $k_{\mathrm{obs.}}$ with $[\mathrm{H}^+]$ obtained from the data in Fig. 2 at pH 2·69, 2·47 and 2·29 and from similiar data for experiments at pH 1·85 ($\mathrm{H_2SO_4}$ solution).

The concentration of free base is given by

$$[\mathrm{Dipy}] = [\mathrm{Dipy}]_T \,.\, K_a/(K_a + [\mathrm{H}^+]). \quad . \quad . \quad . \quad (5)$$

Thus assuming the reaction to go only through the free base with rate constant k_t we have

$$\mathrm{Rate} = k_t[\mathrm{Dipy}]^3[\mathrm{Fe}^{++}] = k_t[\mathrm{Dipy}]_T^3[\mathrm{Fe}^{++}] \,.\, K_a^3/(K_a + [\mathrm{H}^+])^3 = k_{\mathrm{obs.}}[\mathrm{Dipy}]_T^3[\mathrm{Fe}^{++}].$$

In which case the fourth-order constants $k_{\mathrm{obs.}}$ should vary with $[\mathrm{H}^+]$ according to the relation :

$$K_{\mathrm{obs.}} = k_t \,.\, K_a^3/([\mathrm{H}^+] + K_a)^3 \quad . \quad . \quad . \quad . \quad (6)$$

Since $K_a = 4{\cdot}2 \times 10^{-5}$, $K'' \ll [\mathrm{H}^+]$ in the low pH range, and hence $k_{\mathrm{obs.}}$ should be linear with $1/[\mathrm{H}^+]^3$. Fig. 3 shows that this relationship holds quite well.

These observations at low pH's are confirmed by experiments at higher pH's. Thus in a M/5 acetate buffer at pH 4·94 where the formation of $Fe(Dipy)_3^{++}$ is almost complete with $9{\cdot}6 \times 10^{-6}$ M Fe^{++} and $28{\cdot}8 \times 10^{-6}$ M dipyridyl (equivalent amounts) the rate of formation was measured using the acid quenching technique described above. The fourth-order kinetics require that $(1/[Fe^{++}])^3$ should be linear with time. This is actually observed as shown in Fig 4. At pH's 3·62, 3·63 and 4·06 where the dipyridyl had to be increased beyond the equivalent concentration to form the complex completely, but not so much that the change in dipyridyl concentration could be neglected, the general expression for different amounts of reactants in a fourth-order reaction of this type is found to apply.

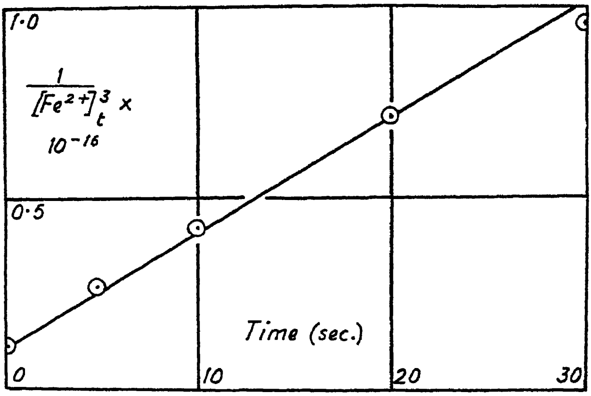

FIG. 4.—Fourth-order plot for the formation of $Fe(Dipy)_3^{++}$ at 17° C in 0·2 M acetate buffer pH 4·94 from equivalent concentrations of Fe^{++} ($9{\cdot}6 \times 10^{-6}$ M) and Dipy ($28{\cdot}8 \times 10^{-6}$ M).

TABLE I.—CALCULATION OF k_t FROM $k_{obs.}$ AT 17° C. PHTHALATE BUFFERS $I = 0{\cdot}025$; pK_a AT 17° C = 4·375

pH	$k_{obs.}$	$\frac{K_a}{K_a + [H^+]}$	$k_t \times 10^{-14}$
1·85	$2{\cdot}38 \times 10^{7}$	$2{\cdot}62 \times 10^{-8}$	9·1
2·29	$5{\cdot}79 \times 10^{8}$	$5{\cdot}38 \times 10^{-7}$	10·7
2·47	$1{\cdot}58 \times 10^{9}$	$1{\cdot}84 \times 10^{-6}$	8·6
2·69	$7{\cdot}45 \times 10^{9}$	$8{\cdot}22 \times 10^{-6}$	9·1
3·62	$2{\cdot}17 \times 10^{12}$	$3{\cdot}31 \times 10^{-3}$	6·6
3·635	$3{\cdot}28 \times 10^{12}$	$3{\cdot}61 \times 10^{-3}$	9·1
4·06	$1{\cdot}95 \times 10^{13}$	$3{\cdot}47 \times 10^{-2}$	5·6

Mean k_t at 17° C = $8{\cdot}4 \pm 1{\cdot}3 \times 10^{14}$ (moles/l.)$^{-3}$ (min.)$^{-1}$.

At these higher pH's the dependence of $k_{obs.}$ on $[H^+]$ is given by (6) above, but now K_a is of the same order as $[H^+]$ and must therefore be taken into account. Values of $k_{obs.}$ at these different pH's are listed in Table I and it can be seen that putting the known value of K_a into (6), reasonably constant values of k_t are obtained over the whole pH range at 17° C.

Temperature Dependence of the Formation Rate Constant.—Similar experiments to the above were done in the low pH range at 0° C and 35° C and values of k_t were calculated in the same way using the values of K_a appropriate to the temperature.[1] Table II shows that over this temperature range k_t is constant within the experimental error, indicating that the overall activation energy

TABLE II.—k_t AT VARIOUS TEMPERATURES

T °C	
0	$8{\cdot}5 \pm 2{\cdot}8$
17	$8{\cdot}4 \pm 1{\cdot}3$
35	$8{\cdot}9 \pm 0{\cdot}5$

for the formation of Fe(Dipy)_3^{++} is zero. We obtain $8·4 \times 10^{14}$ for k_t compared with $1·7 \times 10^{15}$ reported by Krumholtz.[3]

Rates of Dissociation of Fe(Dipy)_3^{++}.—Two sets of observations on the dissociation were made, one in phthalate buffers with pH between 2·2 and 2·8, and the other in various strong mineral acids with concentrations up to 5N.

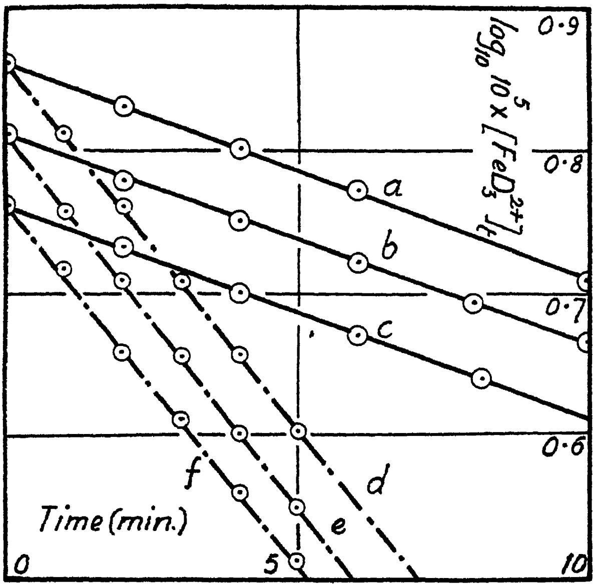

FIG. 5.—First-order plots for the dissociation of Fe(Dipy)_3^{++}, initial concentration about $7·0 \times 10^{-5}$ M.

35° C; *a*, *b*, *c*, pH's $2·25_5$, $2·44_5$, $2·59_5$ respectively.
44·6° C; *d*, *e*, *f*, pH's 2·28, 2·49, 2·62 respectively.

In the buffer solutions it was found that the rate of dissociation is first order in Fe(Dipy)_3^{++} as shown by Fig. 5, and the rate constant k_b is independent of pH over the range examined. The rate of fading has a marked temperature dependence and values of k_b at 25° C, 35° C and 44·6° C are given in Table III. These give an activation energy of 26·2 ± 2 kcal. for the dissociation. The value of $7·3 \times 10^{-3}$ min.$^{-1}$ for k_b at 25° C is in agreement with $7·45 \times 10^{-3}$ min.$^{-1}$ obtained by Krumholtz.[3]

TABLE III.—k_b AT VARIOUS TEMPERATURES IN PHTHALIC BUFFERS

pH 2·2 TO 2·8

T °C	$k_b \times 10$ (min.)$^{-1}$
25	7·3
35	36·0
44·6	117

In the mineral acids where the hydrogen ion concentration is much higher, the situation is rather different. Although the dissociation is again first order in Fe(Dipy)_3^{++} as is shown in Fig. 6, the first-order constants are bigger than those obtained as above, they increase with the acid concentration to a limiting value and they also differ with the acid used.

We have measured k_b in HClO_4, HNO_3, HCl and H_2SO_4 of varying concentrations at 35° C and 17° C. Up to acid concentrations of above 0·5 N, k_b is approximately the same for HCl, HNO_3 and HCl but above 0·5 N, k_b at a certain normality of acid varies with the acid in the order $\text{HNO}_3 > \text{HCl} > \text{HClO}_4$. At these higher concentrations of nitric acid we observed that Fe(Dipy)_3^{++} is oxidized to Fe(Dipy)_3^{+++}, and in similar concentrations of HClO_4 the perchlorate of Fe(Dipy)_3^{++} precipitates. Hence values of k_b obtained under these conditions will probably not give a true measure of the dissociation rates. No such complications are present in HCl and H_2SO_4, and the dependence of k_b on acid concentration for these solutions at 35° C is given in Fig. 7. Similar curves were obtained at 17° C, the only difference being the limiting value of k_b which at 17° C was found to be $12{\cdot}6 \times 10^{-3}$ min.$^{-1}$ and, as at 35° C, where the limit is 0·21 min.$^{-1}$, is the same for HCl and H_2SO_4.

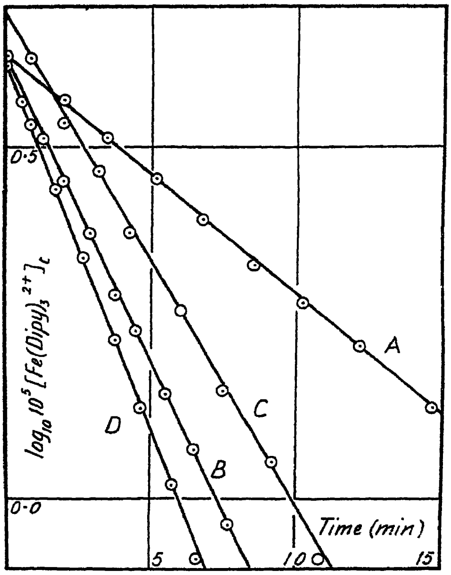

FIG. 6.—First-order plots for the dissociation of $Fe(Dipy)_3^{++}$, initial concentration about $4{\cdot}0 \times 10^{-5}$ M, in HCl and H_2SO_4 solutions at 34·8° C.

A, 0·22 N H_2SO_4;
B, 2·20 N H_2SO_4;
C, 0·48 N HCl; and
D, 10·0 N HCl.

The effect of addition of salts to the HCl and H_2SO_4 solutions was also examined. In 0·2 N HCl, addition of sodium chloride to bring the chloride ion concentration up to 2·0 M increased k_b from 9·8 to $10{\cdot}5 \times 10^{-3}$, at 35° C. Addition of sodium sulphate to 0·2 N H_2SO_4 solution to make it 2·0 M in sulphate decreased k_b from 7·8 to $3{\cdot}8 \times 10^{-3}$.

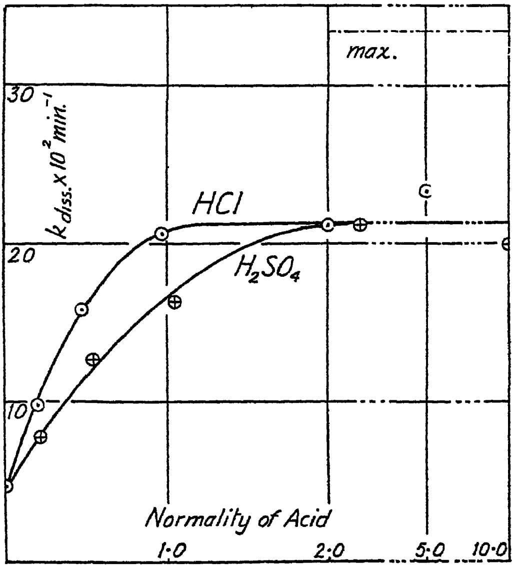

FIG. 7.—The variation of the first-order dissociation rate constant of $Fe(Dipy)_3^{++}$ at 34·8° C with the concentration of mineral acid. The maximum indicated should be reached if eqn. (9) holds.

Mechanism of Formation of $\mathrm{Fe(Dipy)_3}$.—The dependence of the rate of formation on the third power of the dipyridyl concentration obviously arises from the existence of intermediates $\mathrm{FeDipy^{++}}$ and $\mathrm{Fe(Dipy)_2^{++}}$ as indicated in eqn. (1) and (2). Under conditions where the forward reaction goes to completion we can rewrite (3) as

$$\mathrm{Fe(Dipy)_2^{++} + Dipy \xrightarrow{k_f} Fe(Dipy)_3^{++}}. \quad . \quad . \quad . \quad (7)$$

If now the equilibria (1) and (2) are set up very rapidly and (7) is the slowest step in the overall reaction we have :

$$d[\mathrm{Fe(Dipy)_3^{++}}]/dt = k_f[\mathrm{Fe(Dipy)_2^{++}}] \, . \, [\mathrm{Dipy}] = K_1K_2k_f \, [\mathrm{Fe^{++}}] \, . \, [\mathrm{Dipy}]^3.$$

Hence the overall formation rate constant k_t is given by

$$k_t = K_1K_2k_f = 8{\cdot}4 \times 10^{14} \text{ (moles/l.)}^{-3} \text{ (min.)}^{-1}.$$

Although K_1 is known [1] we were unable to obtain a value for K_2 in the equilibrium study, and so k_f cannot be obtained from this expression.

Mechanism of Dissociation of $\mathrm{Fe(Dipy)_3^{++}}$.—The observations indicate that $\mathrm{Fe(Dipy)_3^{++}}$ can dissociate in two ways. At low concentrations of $\mathrm{H^+}$ the rate is independent of $\mathrm{H^+}$ concentration and in these conditions presumably the rate of the reaction

$$\mathrm{Fe(Dipy)_3^{++} \rightarrow Fe(Dipy)_2^{++} + Dipy} \quad . \quad . \quad . \quad (8)$$

is being measured. This follows because, as will be seen later, the quotient of forward and back rate constants is in close agreement with the overall equilibrium constant. Since we have shown that the last addition of dipyridyl is the slowest step in the formation of $\mathrm{Fe(Dipy)_3^{++}}$, its reverse, i.e. reaction (8), must be rate determining in the dissociation.

Using the value of k_b at these low $\mathrm{H^+}$ concentrations, excellent agreement is obtained between the calculated overall equilibrium constant given by k_t/k_b and that actually observed.[1] This is shown in Table IV. The temperature dependence of k_b gives an activation energy of 26 ± 2 kcal., and within the experimental error this is the same as the overall heat of formation of $\mathrm{Fe(Dipy)_3^{++}}$, viz. 24 ± 1 kcal.

TABLE IV.—A COMPARISON OF THE OVERALL EQUILIBRIUM CONSTANT K, MEASURED DIRECTLY AND CALCULATED FROM THE RATIO OF FORWARD AND BACK RATE CONSTANTS

T °C	$K \times 10^{-15}$	$k_t/k_b \times 10^{-15}$
25	117	121
35	33·6	24·7
44·6	8·7	7·6

At the higher $[\mathrm{H^+}]$ obtaining in the dissociation by HCl and $\mathrm{H_2SO_4}$, the rate constant for dissociation increases at first with the acid concentration but ultimately becomes independent of it (see Fig. 7). This would be consistent with the formation of a complex $\mathrm{Fe(Dipy)_3H^{+++}}$ which dissociates more quickly than the simple $\mathrm{Fe(Dipy)_3^{++}}$ ion. Such a complex was suggested by Krumholtz [3] for this system and a similar suggestion was made by Kolthoff [4] to account for the increased stability of the ferric triphenanthroline ion at high acid concentrations. If the equilibrium

$$\mathrm{Fe(Dipy)_3H^{+++} \rightleftharpoons Fe(Dipy)_3^{++} + H^+}$$

is established quickly and the dissociation of $\mathrm{Fe(Dipy)_3H^{+++}}$ occurs with a rate constant k_b', simultaneously with that of $\mathrm{Fe(Dipy)_3^{++}}$, then the overall first-order dissociation rate constant k_{diss} will have the form :

$$k_{\mathrm{diss}} = (k_b'[\mathrm{H^+}] + k_bK)/([\mathrm{H^+}] + K_c), \quad . \quad . \quad . \quad (9)$$

where K_c is the classical acid dissociation constant of $\mathrm{Fe(Dipy)_3^{+++}}$. Hence at high [H$^+$], $k_{diss} = k_b'$ and should be independent of acid concentration, as is in fact observed.

However, we find that at 35° C and 17° C eqn. (9) does not hold over the whole range of [H$^+$] used if we substitute the normality of HCl for [H$^+$]. Krumholtz[3] on the other hand reported that at 25° C the observations in HCl solutions could be represented by eqn. (9), and he has given values for k_b' and K_e. We have confirmed that such is the case up to 0·5 N HCl if the acid normality is used for [H$^+$], but extending the observations to higher acid concentrations we find that k_{diss} becomes constant at $4{\cdot}4 \times 10^{-2}$ min.$^{-1}$ (k_b'). This does not agree with the value 8×10^{-2} min.$^{-1}$ which can be calculated from (9) using the data at the lower acid concentrations. Similar behaviour is found at 35° C (see Fig. 7) where the calculated and observed values for k_b' are $33{\cdot}4 \times 10^{-2}$ and $21{\cdot}6 \times 10^{-2}$ min.$^{-1}$ respectively.

The reason for these discrepancies does not seem obvious. It appears unlikely that it is salt effect since, as stated above, increasing the chloride ion concentration to 2·0 M in 0·2 N HCl changes the rate by only 7 %, and moreover this is an increase. The effect of added sulphate to the sulphuric acid, also given above, is almost certainly due to a different effect, viz. the depression of the dissociation of HSO_4^-, resulting in a lower [H$^+$].

In spite of these deviations from (9) it does appear that the existence of the ion Fe(Dipy)$_3$H^{+++} must be assumed to explain the observations qualitatively. Preliminary results obtained on the dissociation of the ferric tris-dipyridyl complex ion Fe(Dipy)$_3^{+++}$ indicate that a similar assumption is necessary in this case, but here the ion Fe(Dipy)$_3$H^{++++} is found to be a much weaker acid.

Discussion

Heats and Entropies of Formation of the Complex Ions.—We have found that the heats of formation of Fe(Dipy)$_3^{++}$ and FeDipy^{++} are 24 ± 1 kcal. and 7·5 ± 2 kcal. respectively. The entropies of formation are, within experimental error, zero in each case. Although the corresponding values for Fe(Dipy)$_2^{++}$ are not available, it would appear probable that for this also the entropy of formation is zero. Using this in conjunction with the maximum value of 10^5 estimated for K_2 it follows that the heat of formation of Fe(Dipy)$_2^{++}$ from FeDipy^{++} and dipyridyl is probably less than 7 kcal. Hence the heats evolved on the successive additions of dipyridyl to Fe^{++} are 7·5 kcal. for the first, ~7 kcal. for the second, and ~10 kcal. for the third.

The present system appears to be the only one for which the heats and entropies of formation of intermediates in tris co-ordination complexes have been determined. The Ni^{++}-ethylene diamine system has been examined[5] but only the heat and entropy for the formation of Ni(*en*)$_3^{++}$ has been reported. These are 25 kcal. and − 2 cal./mole deg. respectively, and are almost identical with those for Fe(Dipy)$_3^{++}$. Bjerrum[6] has made a detailed study of the intermediates in various metal ammine systems. In these it is found that the addition of successive NH$_3$ molecules to any one metal ion involves about the same heat of reaction which varies from 2 to 3 kcal. depending upon the particular metal ion. The entropy of addition of the NH$_3$ molecule becomes increasingly negative with successive additions, and in general the total entropy change is about − 20 cal./mole deg. It thus appears that the observed greater stability of the fully co-ordinated dipyridyl complexes over the ammines arises from a higher overall heat of formation of about 6 or 7 kcal. and a greater entropy of formation of about 20 cal./mole deg.

This greater entropy is due to the fact that the formation of the complexes is a substitution reaction. Thus the reactions should be written:

$$\mathrm{Fe(H_2O)_6^{++} + 3\ Dipy \rightarrow Fe(Dipy)_3^{++} + 6H_2O}$$

$$\mathrm{M(H_2O)_6^{++} + 6NH_3 \rightarrow M(NH_3)_6^{++} + 6H_2O.}$$

It can be seen in the latter reaction the translational entropy of six co-ordinating molecules is lost for the gain of the corresponding entropy of six water molecules. In the former, however, only three co-ordinating molecules lose this entropy, and although there is some compensation due to the larger mass, this is a small factor compared with that arising from the smaller number of molecules concerned. It is therefore to be expected that bidentate groups will lead to more stable complex ions from the standpoint of entropy. For tridentate groups the effect should be more pronounced, and the preliminary observations we have made on the Fe^{++}-bis-tripyridyl system confirm this.

---

[5] Calvin and Bailes, *J. Amer. Chem. Soc.*, 1946, **68**, 949.

[6] Bjerrum, *Metal Ammine Formation in Aqueous Solution* (Haase & Son, Copenhagen, 1941).

The zero entropy of formation of Fe(Dipy)$_3^{++}$ can be explained semi-quantitatively on the basis of its formation by the above substitution reaction. The main contributions to the entropy change are the loss of the translational and rotational entropy of three dipyridyl molecules in going from aqueous solution to the co-ordination shell, and the corresponding entropy gain by the liberation of the six co-ordinated water molecules. Eley and Evans[7] calculate that this latter process involves about 47 cal./mole deg. in the case of Fe^{++}. Now, since Fe(Dipy)$_3^{++}$ can be resolved into two optical isomers,[8] it would appear that the dipyridyl molecules are rigidly bound in this structure. Hence the co-ordination process is very similar to freezing as far as dipyridyl is concerned since it involves the same loss of rotational and translational freedom of the molecule. For diphenyl, a molecule of similar mass and dimensions, the entropy of freezing is -13 cal./mole deg., so that the co-ordination of three dipyridyls will probably result in a change of about -40 cal./mole deg. which is approximately balanced by the entropy gain in displacing the water of co-ordination.

The Dissociation Process.—We find that the dissociation of Fe(Dipy)$_3^{++}$ into Fe(Dipy)$_2^{++}$ and dipyridyl has an activation energy of 26 kcal. Expressing the rate constant in the usual way as $A\exp(-E/RT)$, the frequency factor A is found to be $10^{17.5 \pm 1.5}$. The process involves the replacement of a dipyridyl molecule by two water molecules and presumably the activation energy arises in the expansion of the structure to the extent necessary to accommodate the water molecules in the transition state. The positive entropy of activation implied by the rather high frequency factor would indicate that this expansion is accompanied by a certain amount of disorganization as might be expected.

As we have seen the higher rates of dissociation in strong acid solutions can probably be accounted for by the existence of the ion Fe(Dipy)$_3$H^{+++} which dissociates more quickly than Fe(Dipy)$_3^{++}$. The structure of this "protonized" complex is of some interest, and at least two possibilities suggest themselves. The proton could be combined with one of the nitrogen atoms which has become detached from the ferrous ion. One might expect this to result in considerable changes in the complex as a result of loss of the electrons from this nitrogen, but as far as we have been able to determine there is no change in the absorption spectrum and although the ion is less stable, the rate constant for dissociation is only increased by about four times. Another possibility is that the proton is attached to the aromatic hydrocarbon nuclei of the ion in much the same way as aromatic hydrocarbons and olefines form carbonium ions when dissolved in a strong acid.

It will be of interest to see how general is the occurrence of such ions in other systems. It is possible for instance that some of the acidic groups in the iron-porphyrin systems are attributable to this type of ion.

It is a pleasure to acknowledge many helpful discussions with Prof. M. G. Evans, F.R.S., during the course of this work.

Chemistry Department,
University of Leeds.

---

[7] Eley and Evans, *Trans. Faraday Soc.*, 1938, **34**, 1093.

[8] Werner, *Ber.*, 1912, **45**, 434.

THE SHADOW CAST BY A BUNSEN FLAME, ITS PRODUCTION AND USEFULNESS

By J. R. Grove, M. F. Hoare and J. W. Linnett

Received 17th March, 1950

The mode of formation of the shadow cast by the inner cone of a Bunsen flame has been studied. On the basis of a simple model the main features of the shadow picture have been accounted for both qualitatively and quantitatively. The method of Sherratt and Linnett for determining burning velocities gives results that are in error by an amount depending on the magnification employed and the level in the cone which is considered. With their particular experimental arrangement the measured burning velocity over the whole cone is about 4 % too high. Necessary modifications are suggested.

Direct shadow and *Schlieren* photographs are being used increasingly to locate and follow the movement of flame fronts.[1] Sherratt and Linnett [2] suggested, for example, that the direct shadow of the Bunsen cone could be used in employing the burner method for determining burning velocities. Garner, Long and Ashforth [3] have used both the shadow and visible cones in combination in a new method they have recently suggested. The burner method has many advantages as a means of determining the burning velocity V_b, and reasons were advanced by Sherratt and Linnett for using the shadow cone rather than the visible cone. Moreover, since the shadow cone does not depend on the light emitted from the flame for its formation, flames of low luminosity may be studied easily.

However, if the shadow photograph is to be used, it is essential that we should understand clearly how the shadow of the flame is produced. In the present work we have made a more detailed study than that carried out by Sherratt and Linnett of the way in which the shadow of a Bunsen flame cone is formed. As a result we have found that some modifications must be made in the method they suggest for calculating burning velocities. The values obtained for V_b using the new method are slightly lower than those resulting from the procedure suggested by Sherratt and Linnett.

The results obtained by Garner, Long and Ashforth,[3] using the simple shadow picture of a Bunsen flame, are different in form from those obtained by Sherratt and Linnett. This is exemplified by Fig. 5 of their paper.[3] It is difficult to understand the cause of the difference. The combustible mixtures used were not the same and may have had different burning properties. Differences in refractive indices in the two sets of experiments would lead to differences in the production of the shadow picture and this might account for the lack of agreement. Also the dimensions of the experimental arrangements may have been different. However, whatever the true explanation, we must come to the general conclusion that the differences between the results of Garner, Long and Ashforth and those of Sherratt and Linnett make it important that we should understand more fully how the shadow picture is produced.

---

[1] Keagy and Ellis, *Third Symposium on Combustion, Flame and Explosion Phenomena* (Williams and Wilkins, 1949), p. 667. Broeze, *loc. cit.*, p. 146. Wohl, Kapp and Gazley, *loc. cit.*, p. 3. Linnett and Hoare, *loc. cit.*, p. 195. Dery, *loc. cit.*, p. 235.

[2] Sherratt and Linnett, *Trans. Faraday Soc.*, 1948, **44**, 596.

[3] Garner, Ashforth and Long, *Nature*, 1949, **164**, 884 ; *Fuel*, 1949, **12**, 272.

1. Calculations for a Simple Flame Model.—The Bunsen flame consists of inner and outer cones of combustion. At the inner cone the premixed gases issuing from the burner tube undergo reaction; in the outer cone there is a mixing of the products of this reaction with the air, resulting in their further oxidation. Thus the outer cone is a diffusion flame.

In treating the production of a shadow by a Bunsen flame, we must consider the geometrical form of the flame and the refractive indices of the various portions. The shape is shown diagrammatically in Fig. 1*a*. There are three main regions marked A, B and C: A is unburnt mixture; C is the outside air; and B is the region of hot gases between the inner and outer cones. A section at the level xx will have the form shown in the plan illustrated in Fig. 1*b*, with the regions labelled as before.

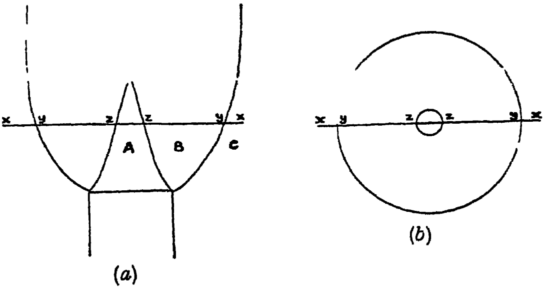

FIG. 1.—Elevation and plane of Bunsen flame (diagrammatic).

The controlling factor governing the refractive indices of the three zones will be their temperature. Pressure and mixture composition effects will be relatively small. Regions A and C will have a comparatively high refractive index relative to region B since they are at room temperature whereas B contains very hot gases. The regions will not, of course, be separated sharply though, at ordinary pressures, the change from the cold region A to the hot region B will be fairly well defined (normally the temperature will change over 1000° C within 1 mm.). The regions B and C will be less sharply separated than A and B.

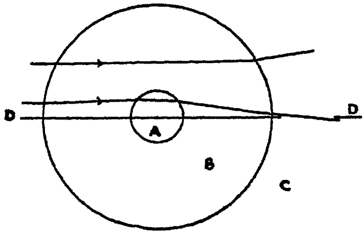

FIG. 2.—Course of light rays in horizontal plane on passing through flame model (diagrammatic).

Because, at the level xx, the edges of the inner and outer cones make only small angles with the vertical, we treat a system having the cross-section shown in Fig. 1*b* and which had cylindrical symmetry. Such a system will affect a beam of light passing through it in a manner similar to the Bunsen cone at the level xx. To simplify our calculations we supposed that the regions A, B and C, of different refractive index, were sharply separated. This is a good approximation for the surface between A and B and it is with the effect of this surface that we are mainly concerned. Although the approximation is less good for the BC boundary there is much less bending at this surface for the rays in which we are interested, and the approximation will certainly not affect the general form of our results.

In our calculations we took the diameters of the regions A and B to be 7 and 25 mm. respectively; these are reasonable dimensions in relation to flames on a burner tube of diameter 1 cm. The refractive indices of regions A and C were taken as 1·0003, and of region B, 1·00004 which are reasonable values for hydrocarbon air flames containing less than

10 % hydrocarbon. The calculations were made for a beam of parallel light.

The general course of the rays is indicated diagrammatically in Fig. 2. Changes in direction on refraction are exaggerated in order to make clear the direction of the bending. Calculations, using the ordinary methods of optics, were made for rays striking the system at distances of 1, 2, 3·2, 3·3, 3·4, 3·45, 3·46, 3·47, 3·48 and 3·49 mm. from the diameter DD. These calculations gave the distance from DD at which the various rays would leave the system at the interface of the regions B and C, and the angles these various emergent rays would make with DD. These results are given in Table I and shown diagrammatically in Fig. 3 for one side of the

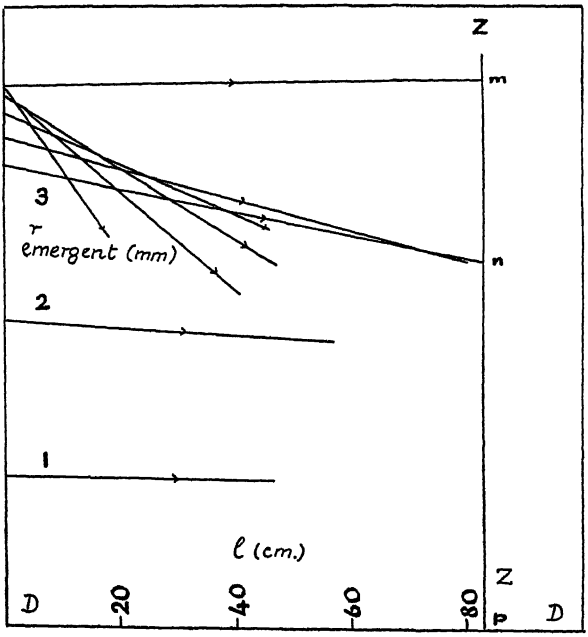

FIG. 3.—Course of rays (in horizontal plane) after passing through flame model (diagrammatic).

TABLE I.—CALCULATIONS FOR MODEL SHOWN IN FIG. 2 AND 3 LISTING THE DISTANCE OF INCIDENT AND EMERGENT RAYS FROM THE SYMMETRY PLANE. AND THE ANGLE THE EMERGENT RAY MAKES WITH THE SYMMETRY PLANE. THE INCIDENT RAYS ARE PARALLEL TO THE PLANE.

Distance from Sym. Incident Ray (mm.)	Plane of Emergent Ray (mm.)	Angle of Emergence (min.)
1·0	0·998588	0·3896
2·0	1·996572	0·9552
3·2	3·1874586	3·5677
3·3	3·2839173	4·5853
3·4	3·3761123	6·8290
3·45	3·4150660	10·0007
3·46	3·4201376	11·4123
3·47	3·4240828	12·1519
3·48	3·4229660	16·3412
3·49	3·4078687	22·6436

plane of symmetry DD It will be seen that the rays leaving the concentric cylinders A and B produce a caustic curve in the region beyond the cylinders It is important to know the exact form of the caustic because it is one of the most important features of the shadow picture We therefore calculated the shape of the caustic and the result is shown in Fig 4 which gives the distance of the caustic from the symmetry plane

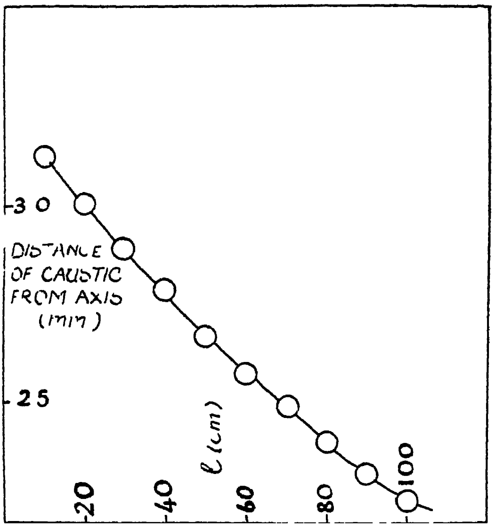

FIG 4 —Theoretical graph of position of caustic edge for varying distances beyond the flame model

at varying distances beyond the flame model Returning to Fig 3 the top line indicates the course of the ray that just fails to enter the region A but passes only through the region B, touching the edge of region A tangentially

From Fig 3 we may deduce the form of the shadow picture that would be obtained on a screen placed beyond the cylinders of gas A and B Suppose a screen (or photographic plate) were placed at ZZ perpendicular to the original light beam From *m* outwards there will be a general illumination of much the same intensity as in the absence of B because the rays of light in this region are only deflected slightly by the cylinder of gas B The deflection of the ray that is just outside *m* is, in fact, 0 1 minute as contrasted with the ray 0 01 mm inside it which just passes through A which is deflected 23 minutes From *m* to *n* there will be a complete shadow for all the light that would have reached this region will have been deflected towards the symmetry plane DD At *n* there will be the sharply-defined edge of the caustic, and, inside this, a band of much brighter illumination than exists elsewhere because of the concentration of the various deflected rays into this region Then, further inside towards *p*, the intensity will decrease towards the intensity that would have existed in the absence of A and B The same sequence of light and shade will be repeated on the other side of the symmetry plane, the whole shadow picture on ZZ having, of course a plane of symmetry If the screen ZZ were moved in toward A and B then, as will be seen from Fig 3, the region of shadow *mn* will become narrower and the position of the sharp outer edge of the bright caustic will move away from *p*

2. Comparison with Experimental Shadow Pattern.—It is important to compare the shadow picture of a flame with the calculated appearance A typical shadow picture of a flame is shown in Plate I.

PLATE I.—Shadow picture of Bunsen flame.

[*To face page* 748.

This is produced by a point source, and, hence, a divergent beam. The experimental set-up is shown diagrammatically in Fig. 5. However, the principles governing the formation of a shadow by the divergent beam will be the same as for a parallel beam, and the general form of the picture will be expected to be similar.

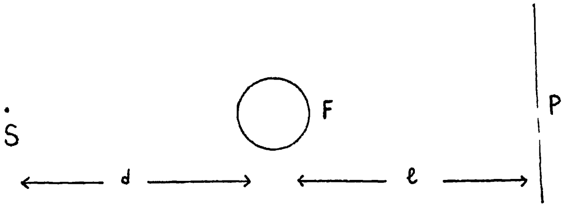

FIG. 5.—Diagram of experimental arrangement.

It will be seen that the shadow picture of the flame in Plate I is, in fact, the same in form as that indicated by a consideration of Fig. 3. The shadow corresponding to *mn* in Fig. 3 is clearly seen together with the sharply defined inner edge *n* which marks the position of the caustic curve. Inside this sharp edge is a region of greater brightness, as our theoretical considerations would lead us to expect (see above).

So we may say that the general form of the shadow picture is exactly that which would be anticipated from our calculations. This supports the view that the flame behaves as a region of gas of low refractive index (outer cone) surrounding a cone of gas of high refractive index (the unburnt gas). Separating these regions the reaction zone is considered to be of negligible thickness.

The observed shadow picture will next be compared quantitatively with the theory. To do this the following series of experiments was carried out, the object being to compare the observed caustic curve with that calculated (see Fig. 4).

The apparatus was set up as in Fig. 5, i.e. a point source and a divergent beam of light were used. A series of pictures was taken with a constant distance between the source and the burner d but varying distances from the burner to the photographic plate l. The magnification M of the arrangement is given by

$$M = \frac{l+d}{d}.$$

The distance between the sharp caustic edges at a height $M/2$ cm. above the burner top was measured. This is, in all cases, equivalent to the diameter of the shadow cone $\frac{1}{2}$ cm. above the top of the burner tube. This distance we will call $2r$. Allowing for magnification this is equivalent to a cone radius of $r_e = r/M$, $\frac{1}{2}$ cm. above the top of the burner tube. The relation between these quantities is shown in Fig. 6. Fig. 7 shows the way in which r_e, the equivalent radius, varies with l, the distance from the burner to the plate. All experiments in this set were carried out using a mixture of ethylene and air containing 5·9 % ethylene. A constant flow-rate was used. The burner tube was 1·0 cm. in diameter and d was 73 cm. throughout.

By calculating r_e, the equivalent radius of the shadow (caustic) cone at the burner, we have eliminated the effect of the divergence of the beam. Comparing Fig. 7, which gives the equivalent radii of the caustic cone at varying values of l, with Fig. 4 which gives the calculated form of the caustic using parallel light, we see that the form of the two curves is very similar indeed. Moreover, their slope is approximately the same.

In addition we measured the outer edge of the dark region of the shadow at a height $M/2$ above the top of the burner. This may be called R (see Fig. 6) and may be reduced to an equivalent radius at the top of the burner R_e, where $R_e = R/M$. The values of R_e are plotted as crosses in Fig. 7. Because the outer edge of the shadow is less well defined than the inner, caustic edge, the values of R are less easy to measure. It will be seen that R_e remains constant, within the limits of error of measurement. This is to be expected since R_e measures the radius of the ray ½ cm. above the top of the burner tube which just fails to enter the inner cone region and is not deflected. Moreover the extrapolations of the R_e and r_e curves meet at $l = 0$, which is again to be anticipated on the theory of the production of the shadow cone which has been outlined.

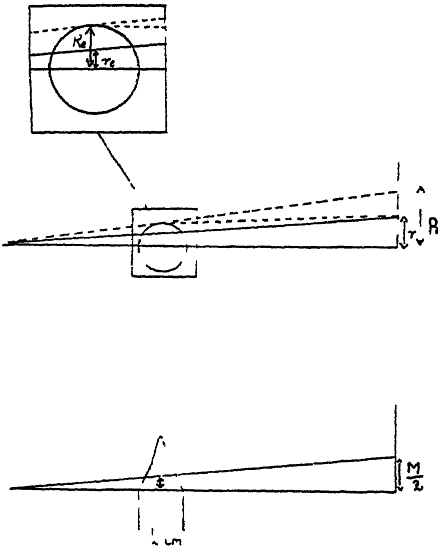

FIG. 6.—Diagram to illustrate relation between r and r_e and between R and R_e (see text).

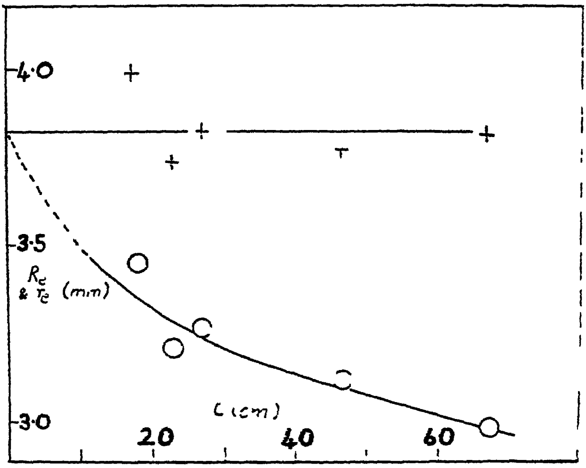

FIG. 7.—Graph of R_e and r_e against l, the distance from the burner to the photographic plate.

To summarize this section, we may say, therefore, that when a Bunsen flame casts a shadow a caustic curve of high-light intensity is produced by the inner cone of the flame, and that the form and dimensions of this shadow caustic are such as would be anticipated from the theory outlined in the last section.

3. Velocity Measurements.—Sherratt and Linnett measured the sharp inner edge of the shadow (i.e. the caustic) cone. It was assumed that this edge, the point source, and the inner edge of the flame zone lay on a straight line (see Fig. 6 in their paper). The considerations of the last two sections show that the assumption is not valid because the ray of light reaching the outer edge of the caustic has been refracted by the flame. If, however, we carry out the procedure of Sherratt and Linnett at varying distances from the flame, we see, from Fig. 3, 4 and 7, that as we move the photographic plate nearer the flame (decrease l) the inner edge of the shadow (the caustic) will approach closer and closer to the true position of the flame front. Thus, using their method for various values of l, we may expect the measured burning velocity to vary regularly, and to approach the true burning velocity as l approaches zero. Some results for such a series of measurements using an ethylene + air mixture containing 5·9 % ethylene are shown graphically in Fig. 8, the measured value of the burning velocity being plotted aginst l, the distance from the flame to the photographic plate.

It will be seen that, as l increases, the measured burning velocity increases. This is to be expected from the considerations of § 1, in which it was shown that the caustic edge moves further and further inwards from the outside edge of the shadow as we move away from the flame (cf. Fig. 3).[4] The consequences of this movement in relation to V_b, burning velocity, determination are discussed in § 5.

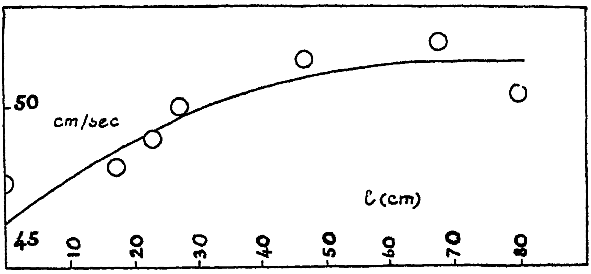

FIG. 8.—Variation with l of burning velocity measured using inner caustic edge.

Using the cone observed by *Schlieren* photography, the measured value of the burning velocity of a 5·9 % ethylene + air mixture is 47·5 cm./sec. This measurement was made on an entirely different apparatus by a different worker. For reasons which will be given in a paper by H. R. Conan and J. W. Linnett[5] we believe now that the values obtained for the burning velocity using the *Schlieren* cone are the most reliable. So the value of 47·5 has been plotted at $l = 0$ on the graph in Fig. 8. It will be seen that this point, together with the points for different values of l obtained by the shadow method, all lie reasonably near a smooth curve (all within 1 cm./sec.) forming a self-consistent set of results.

The general conclusion of this section is therefore that the method suggested by Sherratt and Linnett for determining burning velocities will lead to burning velocities which are somewhat bigger than the true value. The difference between the measured and true value is smaller the smaller the distance, l, between the flame and the photographic plate. It should be possible to obtain a true value of the burning velocity by making measurements at different values of l, and extrapolating to $l = 0$. However, this would prove somewhat laborious and several photographs would have to be taken and measured for each mixture. An alternative procedure is suggested in § 6.

---

[4] Wohl, *Third Symposium on Combustion, Flame and Explosion Phenomena* (Williams and Wilkins, 1949), p. 203.

[5] H. R. Conan and J. W. Linnett (to be published).

4. Vertical Displacement of Light Rays by Bunsen Cone.—It has been assumed that light rays are undeviated in a vertical direction, i.e. that, for the shadow cast by parallel light, there is no displacement of any ray out of its initial horizontal plane. This is not strictly the case. The calculations of § 1 were made for zones A, B and C which had cylindrical symmetry. The axis of these cylinders (assumed vertical) was at right-angles to the incident rays, so that these rays suffered no vertical deviation by the system. For the real flame, this is not true, and Fig. 9*a* shows how the axial ray will be bent downwards on passing through the inner cone. Similar deviation will occur when the ray traverses the boundary between the zone of hot gas and the cold surrounding air (called the outer cone).

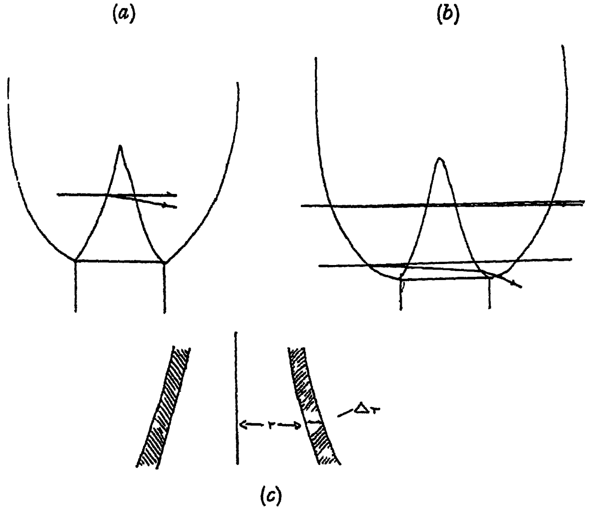

Fig. 9.—(*a*) and (*b*) show vertical deviation of rays passing through Bunsen flame; (*c*) shows meaning of r and Δr (see text).

The downward bending was demonstrated at the base of the cone in the following way. Using parallel light, a shadow photograph of the flame was taken 70 cm. from the burner tube. The flame was then extinguished and a separate shadow photograph of the burner tube alone was taken. The two photographs were enlarged to the same degree and superimposed by tracing. The image of the top of the burner was found to be depressed by the presence of the flame by about 0·5 mm.

The extent of the bending depends upon the shapes of both the inner and outer cones. The shape of the outer cone is by no means certain, but if the faint line which occurs on most shadow and *Schlieren* photographs be taken as a guide, we may suggest as a reasonable shape that shown in Fig. 9*b*. From this, it is seen that most of the bending takes place at the base of the outer cone as the angle of incidence is greatest there.

For the incidence of parallel rays near the outer edge of the inner cone (the rays responsible for the formation of the caustic discussed earlier) the downward deflection can be calculated and shown to be quite negligible (less than a tenth of the bending that is observed at the base). This means that the shadow will be distended downwards at the base, but over the rest of the cone the effect is very small. Since the rays which define the outer edge of the black shadow do not pass through the inner cone, whereas those marking the inner edge do, the inner cone will be displaced downwards relative to the outer, but again this will be only a small effect. With regard to burning velocity determination where measurements have always been neglected at the base the effect of this displacement will be insignificant, since the absolute height of the shadow cone above the burner top is not required. This means that it is not the displacement itself, but the change in the displacement as we go up the cone, which affects the measured burning velocity, and this is extremely small.

5. Comparison of Direct Shadow and *Schlieren* Photographs.—If a *Schlieren* picture of a Bunsen flame is taken, the inner cone appears quite sharply on the photograph (e.g. see photograph of Broeze [1]). The edge of this cone marks the position of the greatest rate of change of refractive index between the burnt and unburnt gases.[6] That is, it marks the surface between zones A and B in Fig. 1. Moreover the *Schlieren* photograph is a focused picture of the conditions at the flame. Therefore the *Schlieren* picture can be used to locate exactly the boundary surface between A and B. If this is compared with a shadow picture of the type shown in Plate I, but obtained using parallel light, it is found that the cone produced by the *Schlieren* photograph is exactly coincident with the outer edge of the shadow cone, except at points very close to the base. The deviation at the base is due to vertical displacement of the light rays and is precisely that to be expected from the conclusions of § 4.

6. Correction Method.—The striking fact about the shadow cone is the sharpness of the inner black-white edge, and the ease with which it can be measured. It would seem desirable therefore to see whether or not it could be employed, together with a correction factor, to determine burning velocity.

In Fig. 9*c*, if r is the radius of the inner edge of the shadow cone and $r + \Delta r$ the radius of the corresponding outer edge, a relationship between r and $r + \Delta r$ is needed as we pass up the cone. Δr increases relative to r as r gets smaller. To obtain the required relation at $l = 80$ a series of flames was considered in which the outer shadow edge was sufficiently sharp to measure. These flames were of varying hydrocarbon + inert gas + oxygen composition and height, and the values of r and $r + \Delta r$ were measured for various heights up the cone. The value of $r/(r + \Delta r)$ was plotted against percentage of the total height of the inner cone above the burner top on the photograph. Results are given in Fig. 10. The closeness of the points obtained from the different flames shows that it is feasible to employ a correction factor of this type. It is interesting to compare this experimentally determined correction factor with one calculated theoretically for parallel light from the simple picture of the flame used in § 1. Fig. 4 shows the plot of the theoretical position of the caustic at various distances from the flame. The conditions taken (inner cone radius 3·5 mm. outer 12·5 mm.) are those for a position about 29 % of the distance up a cone 20 mm. high. The graph shows that the position of the inner black-white edge at a distance 80 cm. will be at a radius of 2·4 mm. whereas the value of the outer edge is that of the true inner cone, i.e. 3·5 mm. Thus $r/(r + \Delta r)$ is 0·69. The vertical displacement of the caustic will be of the order of 0·03 mm. and equivalent to a negligible lateral shift. From Fig. 10 the experimental correction factor $r(r + \Delta r)$ is 0·75. Comparison between the calculated and experimental values is good.

---

[6] Klaukens and Wolfhard, *Proc. Roy. Soc. A*, 1948, 193, 512.

Burning velocities V_b are calculated, assuming a parabolic distribution of flow rate, from

$$= \frac{2V_f}{\pi R_t^2}\left[1 - \left(\frac{r}{MR_t}\right)^2\right] \sin \alpha,$$

where α is the angle of slope of the cone at a radius r measured on the photograph for which the magnification is M. V_f is the volume flow rate and R_t the radius of the burner tube. Since the angle α is derived from measured values of r (see Sherratt and Linnett) the correction to r as suggested above modifies both the r and α values in the above formula. The effect of the correction is to lower the measured burning velocity at large values of r and to raise it at small values of r. Table II shows a set of results for one flame and it will be seen that the corrected burning velocity is low at large r and high at small r as would be expected as a result of cooling at the wall and preheating at the centre respectively. The values over the middle region are practically constant. The uncorrected values of V_b are shown in Table II for comparison. The average value of the burning velocity for a given flame was decreased by about 4 % for each of several flames when the corrections were applied. It

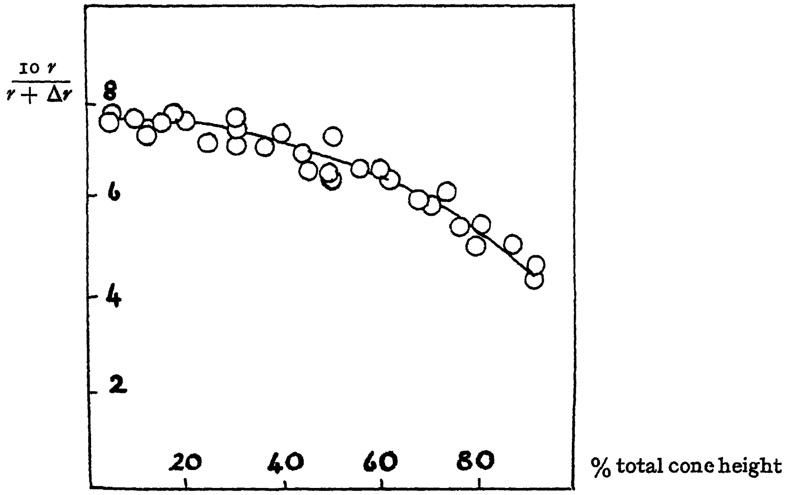

FIG. 10.—Graph showing variation of $r/(r + \Delta r)$ with cone height.

TABLE II.—CORRECTED AND UNCORRECTED BURNING VELOCITIES V_b FOR VARYING VALUES OF $r + \Delta r$ (SEE FIG. 9c), USING A 5·36 % ETHYLENE + AIR FLAME OF CONE HEIGHT 3·25 CM., $M = 2·365$ AND $l = 80$ CM.

r (corr.) i.e. $r + \Delta r$ (cm.)	V_b (corr.) (cm./sec.)	V_b (uncorr.) (cm./sec.)
0·8302	15·4	26·2
0·7090	21·6	27·7
0·6163	22·1	26·5
0·5091	23·4	25·4
0·3781	24·6	25·6
0·2437	26·7	25·3
0·1604	31·7	23·9

seems that this small correction factor (4 %) might even be used in practice (at least for $C_2H_4 + O_2 + N_2 + CO_2$ flames) for the particular experimental set-up that was being used.

7. Conclusions.—The main results of this study of the formation of a shadow by a Bunsen flame are :

(i) The form of the shadow cast can be explained on the basis of the simple model shown in Fig. 1, which consists of a region of relatively low refractive index (1·00004) between two regions of higher refractive index (1·0003).

(ii) The flame deflects rays of light in such a way as to form a caustic curve of high light intensity. This caustic has been identified with the sharp inner edge of the shadow of the inner cone.

(iii) Because the sharp inner edge of the shadow cone lies within the true cone measurement of it gives a high average value for the burning velocity.

(iv) The error decreases as the distance between the flame and the photographic plate decreases and approaches zero at zero distance.

(v) The *Schlieren* cone, which is considered to be the most satisfactory cone for use in determining burning velocities, corresponds closely with the outer edge of the shadow cone, which is, however, not well defined.

(vi) A modified method of using the sharp inner edge of the shadow cone has been suggested and, when applied to ethylene + air flames using our experimental arrangement, leads to a value for the burning velocity which is of the order of 4 % less than that obtained by the simple method of Sherratt and Linnett. The magnitude of the correction varies at different places up the cone (Table II).

We wish to thank Imperial Chemical Industries and the Royal Society for providing calculating machines, and H. R. Conan for many useful discussions.

Inorganic Chemistry Laboratory,
Oxford.

THE SURFACE PROPERTIES OF POLAR SILICONES

By M. J. Newing

Received 2nd March, 1950

An investigation has been made of the surface properties of some organo-silicon compounds, with particular reference to their orientation on a water surface and their efficiency as boundary lubricants. New silicones of the types $CH_3[(CH_3)_2SiO]_n . Si(CH_3)_2CH_2Cl$, $CH_3[(CH_3)_2SiO]_n . Si(CH_3)_2CH_2OH$ and $CH_2OH[(CH_3)_2SiO]_n . Si(CH_3)_2CH_2OH$ have been prepared, and their force-area and potential-area curves on water obtained. The results show that at low pressure all the silicone molecules are lying flat on the water surface. At a pressure of 8-10 dynes cm.$^{-1}$ collapse occurs, and the siloxane chain lifts out of the water. With the hydroxyl compounds the curves obtained show that the molecule is anchored by the —OH group. Close packing of the molecules does not occur even under a pressure of 25 dynes cm.$^{-1}$ because of the small lateral adhesion between the siloxane chains.

The behaviour of silicones as boundary lubricants on steel is discussed in relation to the possible orientation of the monolayers on the metal surface. Silicones are less effective than polar hydrocarbons in reducing metallic contact.

The thermal stability, chemical inertness, fairly high viscosity and small viscosity change with temperature of silicone oils make them very suitable hydrodynamic lubricants. Under conditions of boundary lubrication, however, when the moving parts are separated by a thin film of the lubricant, pure silicone oils are found to be very poor lubricants.[1] Boundary lubricating layers of silicones have indeed been formed by hydrolysis of the halosilanes on the metal surface [2] and by depositing monolayers on the metal by the Langmuir-Blodgett technique [3] and have been found to be similar in properties to hydrocarbon boundary lubricating films (for example, the lubrication depends on the length of the organic radical attached to silicon-oxygen network). However, such films are not of practical importance, as boundary lubricants are in general adsorbed from solution. Long-chain hydrocarbons with polar heads are effective boundary lubricants when applied in solution and it was thought that dimethylpolysiloxanes with reactive end-groups might form boundary lubricating films in the same way.

This paper describes an investigation of the surface properties of long-chain silicones with polar end-groups likely to be of use as boundary lubricants. Apart from the preparation of the materials (which have not previously been described) the work reported here consists of two parts :

(i) A study was made of the force-area and, in some cases, surface potential-area characteristics of monolayers of the silicones on water. The results of these experiments are relevant to the discussion of the orientation of the films in boundary lubrication.

(ii) The frictional properties of films of the silicones were investigated under conditions of boundary lubrication.

Experimental

Preparation of Silicones for use as Boundary Lubricants.—The most effective end-group in boundary lubricants is the carboxyl group, but repeated attempts to introduce a terminal Si—CH_2COOH group failed owing to the instability of such a group to hydrolytic cleavage. However, stable silicones of the type $CH_3[(CH_3)_2SiO]_n \cdot Si(CH_3)_2CH_2Cl$ and $CH_3[(CH_3)_2SiO]_n . Si(CH_3)_2CH_2OH$, which have not previously been reported in the literature, were prepared.

SILICONES WITH TERMINAL —Cl ATOM.—60 ml. of a mixture of compounds of the types $CH_3[(CH_3)_2SiO]_n \cdot Si(CH_3)_3$, $CH_3[(CH_3)_2SiO]_n . Si(CH_3)_2CH_2Cl$ and $CH_2Cl[(CH_3)_2SiO]_n . Si(CH_3)_2CH_2Cl$ were prepared from cyclic polymers of the type $[(CH_3)_2SiO]_n$, hexamethyldisiloxane and 1 : 3-*bis*-chloromethyltetramethyldisiloxane [4] by equilibrating with sulphuric acid according to the method of Patnode and Wilcock.[5] The molar ratio of the three starting materials was such that the main value of n in the resulting mixture was 7. Distillation did not give a satisfactory separation of the components in the relatively small amount of liquid. Compounds of the required type

$$CH_3[(CH_3)_2SiO]_n . Si(CH_3)_2CH_2Cl$$

where $n = 6$ and 7 were separated, but not in the pure state, as indicated by a high chlorine content. Data relevant to the two fractions obtained are given in Table I.

TABLE I

Compound	Molecular Weight		Chlorine Content	
	Calc.	Found	Calc.	Found
$CH_3[(CH_3)_2SiO)]_6Si(CH_3)_2CH_2Cl$ B.p. 175/20 mm.	566	561	6·3 %	7·2 %
$CH_3[(CH_3)_2SiO]_7Si(CH_3)_2CH_2Cl$ B.p. 167/5 mm.	640	642	5·5 %	6·4 %

---

[1] Kauppi and Pedersen, *S.A.E.J.*, 1946, 54, 121.

[2] Gregory and Newing, *Austral. J. Sci. Res. A*, 1948, 1, 85.

[3] Hunter, Gordon, Barry, Hyde and Neidenweich, *Ind. Eng. Chem.*, 1947, 39, 1389.

[4] Krieble and Elliott, *J. Amer. Chem. Soc.*, 1945, 67, 1810.

[5] Patnode and Wilcock, *ibid.*, 1946, 68, 360.

As some of the fractions from the distillation were small, the chlorine content was determined by a modification of the semimicro method of Sendroy,[6] after fusion with sodium peroxide. The molecular weights were determined by the elevation of boiling point of carbon tetrachloride.

SILICONES WITH TERMINAL —OH GROUP.—From the mixture of chlorinated silicones prepared above, a fraction in which the main values of *n* were 4, 5 and 6 and the chlorine content 6·4 %, was refluxed with glacial acetic acid and potassium acetate. After 4 hr. refluxing the oil was washed with distilled water and the chlorine content of the washings determined. It was found that 89 % of the chlorine had been replaced by the acetate radical. The acetate was converted to the alcohol by allowing it to stand at room temperature with a large excess of methanol and a drop of sulphuric acid.[7]

The components of the mixture which consisted of the types

$$CH_3[(CH_3)_2SiO]_n \, . \, Si(CH_3)_3, \qquad CH_3[(CH_3)_2SiO]_n \, . \, Si(CH_3)_2CH_2OH$$

and $$CH_2OH[(CH_3)_2SiO]_n \, . \, Si(CH_3)_2CH_2OH$$

were separated by chromatography. 1·2 g. silicone dissolved in 5 ml. 40-60 petroleum ether was poured on to a column of 30 g. " neutral alumina ", and diluted with 25 ml. aliquots. After the initial fraction, which contained the bulk of the unsubstituted silicone, small continuous fractions of silicone were obtained showing that there was no sharp separation of the components having one and two silyl methanol groups. Sufficient material for molecular weight and active hydrogen determinations could only be obtained by combining several of the smaller fractions. These measurements showed that the combined fractions contained mixtures of the mono- and dihydroxy compounds. Identification of some of the smaller fractions was effected from the force-area characteristics of a monolayer examined by spreading on a Langmuir trough. Comparison of the *F*—*A* curves for the initial fractions with those given by Fox, Taylor and Zisman [8] for dimethylpolysiloxane with methyl end-groups showed these fractions to be composed of the compounds $CH_3[(CH_3)_2SiO]_n \, . \, Si(CH_3)_3$. Comparison of the *F*—*A* curves of some of the later fractions with those published for ethoxy end-blocked dimethylsiloxanes [8] showed them to be composed of the dihydroxy compounds, $CH_2OH[(CH_3)_2SiO]_n \, . \, Si(CH_3)_2CH_2OH$. The intermediate fractions contained the desired compounds,

$$CH_3[(CH_3)_2SiO]_n \, . \, Si(CH_3)_2CH_2OH.$$

Apparatus.—Force-area relations were measured with a Langmuir-Adam surface balance of sensitivity 0·2 dyne. In some experiments the surface potential was measured simultaneously with a valve electrometer.[9] The silicones were spread on the water surface from benzene solution. Frictional measurements were made on the Bowden-Leben stick-slip apparatus.[10] The steel specimen and slider were freed from grease by rubbing on emery paper, the final abrasion being on Grade 600 Hydrodurexyl paper. They were washed with water and dried in *iso*propyl ether–acetone vapours. Steel was used since previous experience has shown it to be the metal most easily lubricated. Preliminary investigations of films of the silicone on copper showed no boundary lubrication. The silicones were applied to the surface as 1 % solution in cetane or in the pure state.

Results

Monolayers of Silicones at the Air-water Interface.—The orientation of the molecule is of primary importance if it is to be a good boundary lubricant.[11, 12] The orientation of the molecules on an aqueous surface may be studied with the aid of the force-area relationship of the monolayer. In view of the known correlation between the orientations observed on aqueous and on solid

[6] Sendroy, *J. Biol. Chem.*, 1937, **120**, 335.

[7] Spier, Daubert and McGregor, *J. Amer. Chem. Soc.*, 1948, **70**, 1117.

[8] Fox, Taylor and Zisman, *Ind. Eng. Chem.*, 1947, **39**, 1401.

[9] Harding and Adam, *Trans. Faraday Soc.*, 1933, **29**, 837.

[10] Bowden and Leben, *Proc. Roy. Soc. A*, 1939, **169**, 371.

[11] Fogg, *Proc. Physic. Soc.*, 1940, **52**, 239.

[12] Zorn, C.I.O.S. Microfilm No. 135 (Abt. VIII).

surfaces,[13] this method was adopted in the present investigation. Fig. 1 shows the force-area curve for two compounds of the type

$$CH_3[(CH_3)_2SiO]_n \,.\, Si(CH_3)_2CH_2Cl$$

where $n = 6$ and 7 spread on distilled water.

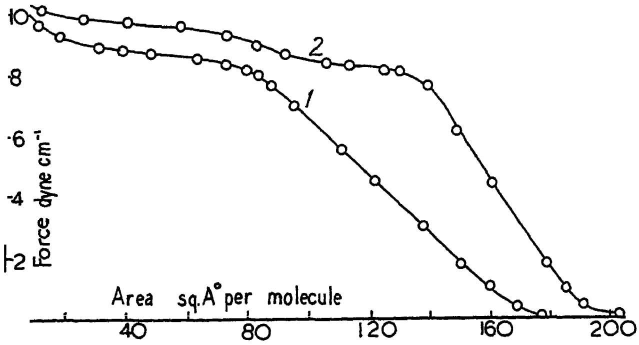

Fig. 1.—Force-area curves of silicones with stable terminal chlorine atom.
1. $CH_3[(CH_3)_2SiO]_6Si(CH_3)_2CH_2Cl$
2. $CH_3[(CH_3)_2SiO]_7Si(CH_3)_2CH_2Cl$.

The F—A and surface potential (ΔV)-area curves for the compounds of the type $CH_3[(CH_3)_2SiO]_n \,.\, Si(CH_3)_3$, $CH_3[(CH_3)_2SiO]_n \,.\, Si(CH_3)_2CH_2OH$ and $CH_2OH[(CH_3)_2SiO]_n \,.\, Si(CH_3)_2CH_2OH$ spread on N/1000 HCl are shown in Fig. 2.

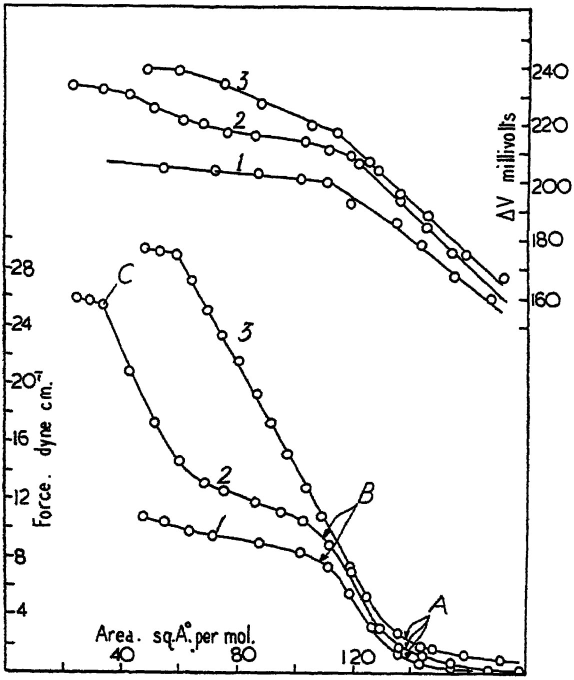

Fig. 2.—Force-area and surface potential-area curves of non-polar and polar silicones of the types
1. $CH_3 \ldots CH_3$,
2. $CH_3 \ldots CH_2OH$,
3. $CH_2OH \ldots CH_2OH$.

---

[13] Tingle, *Ph.D. Thesis* (Cambridge, 1948).

Each of the three substances was a mixture of the polymers $n = 4$, 5 and 6. Assuming that the area and surface potential are additive for each $[(CH_3)_2SiO]$ group,[8] n was taken to be 5 in each case.

The extrapolated values for the molecular areas and the areas per $[(CH_3)_2SiO]$ unit are given in Table II, together with the values at these areas for ΔV and for μ, the vertical component of the molecular dipole moment, calculated from ΔV. The values of μ are comparable at these areas since the molecules are all lying flat and close-packed on the water surface. At greater areas the films are gaseous.

For the compound $CH_3 \ldots CH_3$ the value of ΔV becomes constant and μ extrapolates to zero in the highly compressible region at about 10 dynes cm.$^{-1}$. For the compounds $CH_3 \ldots CH_2OH$ and $CH_2OH \ldots CH_2OH$ however, ΔV does not become constant nor does μ extrapolate to zero until the collapse of the film at 25·5 and 29·5 dynes cm.$^{-1}$ respectively. Only a small amount of hysteresis was obtained in the F—A curves if the films were not collapsed to a large degree.

TABLE II

Compound	Symbol	A Å^2	Area per $[(CH_3)_2SiO]$ Unit	B dynes/cm.	ΔV_A mV	$\mu_A \times 10^{20}$ (e.s.u.)
$CH_3[(CH_3)_2SiO]_6Si$—$(CH_3)_2CH_2Cl$	$CH_3 \ldots CH_2Cl$	167	23·9	8-10	—	—
$CH_3[(CH_3)_2SiO]_7Si$—$(CH_3)_2CH_2Cl$	$CH_3 \ldots CH_2Cl$	190	23·9	8-10	—	—
$CH_3[(CH_3)_2SiO)_5Si$—$(CH_3)_3$	$CH_3 \ldots CH_3$	138	23·0	8-11	181	666
$CH_3[(CH_3)_2SiO]_5Si$—$(CH_3)_2CH_2OH$	$CH_3 \ldots CH_2OH$	138	23·0	25·5	190	707
$CH_2OH[(CH_3)_2SiO]_5$—$Si(CH_3)_2CH_2OH$	$CH_2OH \ldots CH_2OH$	139	23·2	29·5	192	728

A (Å^2) = area at which molecules are lying flat and close-packed. (Fig. 2, Point A.)
B (dynes/cm.) = pressure of breakdown of film. (Fig. 2, Point B.)
ΔV_A = surface potential of the molecule at A.
μ_A = vertical component of the dipole moment of the molecule at A.

Lubrication.—Compounds of the types $CH_3 \ldots CH_2Cl$ and $CH_3 \ldots CH_2OH$ were applied to the steel surfaces as 1 % solutions in cetane. Retraction of the solution on the metal surface was observed, being more marked with the hydroxyl compound.* In neither case was smooth sliding obtained. The motion was irregular and consisted of small sticks and slips. The values of the coefficient of friction, with a load of 4 kg. and the temperature of breakdown, i.e. the temperature at which the friction rose sharply, are given in Table III.

TABLE III

Lubricant	Coefficient of Friction		Temp. of Breakdown, °C.
	Room Temp.	100° C	
1 % $CH_3 \ldots CH_2Cl$ in cetane	0·22-0·3	0·27	140-160
1 % $CH_3 \ldots CH_2OH$ in cetane	0·22-0·25	0·27	140-160
Pure $CH_3 \ldots CH_3$	0·6	—	—
Pure $CH_3 \ldots CH_2OH$	0·3	0·4	140

---

* Any impurities in these silicone samples consisted of silicones containing two or no polar groups. These would play no part in the lubrication.

The pure silicone of the type $CH_3 \ldots CH_2Cl$ gave slightly higher friction than a 1 % solution in cetane, although the temperature of breakdown of lubrication was still above 140° C. Very poor lubrication was obtained using a pure silicone of the type $CH_3 \ldots CH_3$ as lubricant.

Fig. 3 shows photographs of the tracks obtained on steel using $CH_3 \ldots CH_2OH$ in cetane and pure $CH_3 \ldots CH_3$ as lubricants. A marked improvement in boundary lubricating properties is to be observed on the addition of a polar end group to the silicone chain.

Discussion

Force-area Relations.—The behaviour of compounds of the type $CH_3 \ldots CH_3$ on water surfaces has been interpreted by Fox, Taylor and Zisman from comparison of *F—A* curves and molecular models.[8] It appears that at large areas the silicone molecules are lying flat on the surface with all their silicon and oxygen atoms in the water and the methyl groups in a plane above the water surface. The film may be compressed up to a value of 22·7 Å^2 per $[(CH_3)_2SiO]$ unit (point A in Fig. 2). On further compression some of the silicon and oxygen atoms lift out of the water until at the point B the molecules are in a highly compressible state and on further decreasing the area collapse occurs. It is to be observed from Table II that the value obtained for the area of one $[(CH_3)_2SiO]$ unit in the present investigations is about 23 Å^2 in all cases, in agreement with Fox, Taylor and Zisman. From the *F—A* curves it appears that the compounds of the type $CH_3 \ldots CH_2Cl$ behave in a similar way to those of the type $CH_3 \ldots CH_3$, presumably because the attraction of the halogen atom for the water is not great enough to enable it to act as an anchor.

In the case of the compound $CH_3 \ldots CH_2OH$ the siloxane chain lifts out of the water in the compressible region, but the terminal hydroxyl anchors it to the surface. The sharp rise in surface pressure with compression beyond 65 Å/molecule (Fig. 2) indicates that at this point the siloxane chains are out of the water and are as closely packed as possible at 13·5 dynes/cm. However, calculation of the cross-sectional area of a siloxane chain gives a value of 28 Å^2. It follows that at 65 Å^2/molecule the chains are not parallel close-packed, notwithstanding the sharp rise in pressure on further compression.

The van der Waals' forces of attraction associated with the siloxane chains are usually small as evidenced by the low boiling points, low surface tension, and small energy for viscous flow of the silicones.[14], [15] [16] Apparently the short-range intermolecular forces are prevented from being strongly operative by the free rotation of the methyl groups attached to the silicon atoms.[17] It may be inferred therefore that the thermal energy of agitation is greater than the forces of attraction and, at 35 Å^2 per molecule (point C in Fig. 2), is sufficient to overcome the forces by which the $—CH_2OH$ is anchored to the water.

The compound $CH_2OH \ldots CH_2OH$, which was identified by comparison of its *F—A* curve with that of ethyoxy end-blocked silicones,[3] is anchored at both ends by hydroxyl groups and shows no highly compressible region. The thermal agitations are curtailed by this double anchoring which may account for the fact that the film is stable up to a pressure of 29·5 dynes/cm.[2].

Surface Potential.—The value of μ for silicone films on distilled water is given by Fox, Taylor and Zisman [8] as $0{\cdot}89 \times 10^{-19}$ e.s.u. per $[(CH_3)_2SiO]$ group. The present measurements of surface potential made on N/1000 HCl lead to the value of $0{\cdot}95 \times 10^{-19}$ e.s.u. per monomer. The larger value may be due to improved orientation of the molecule on the acid substrate. Substitution of a single hydroxyl group for a terminal hydrogen

[14] Hurd, *J. Amer. Chem. Soc.*, 1946, **68**, 364.

[15] Wilcock, *ibid.*, 1946, **68**, 691.

[16] Hunter, Warrick, Hyde and Currie, *ibid.*, 1946, **68**, 2284.

[17] Roth, *ibid.*, 1947, **69**, 474.

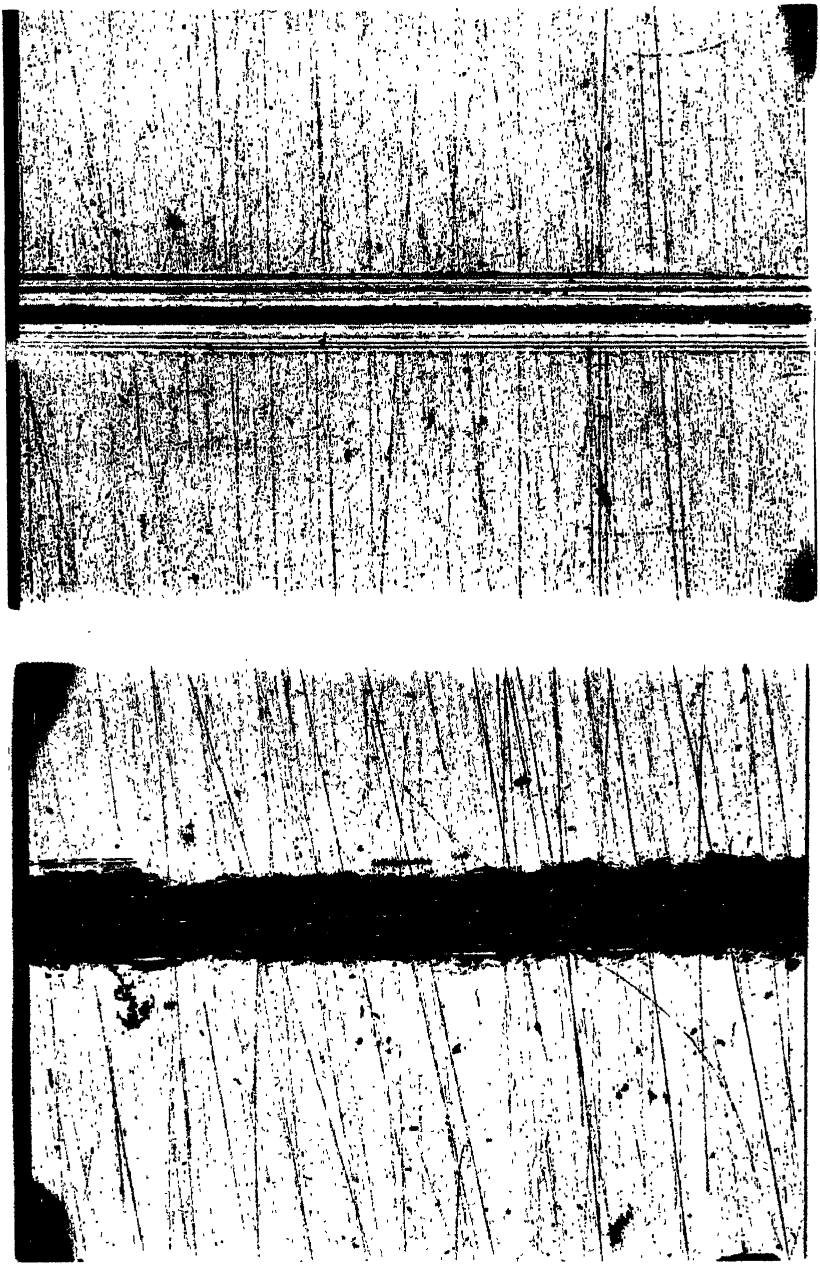

Fig. 3

1. Steel sliding on steel lubricated with silicones of the type $CH_3 \ldots CH_2OH$ in cetane. Load 2 kg.; coef. of friction = 0·13; temp. 120° C; magn. × 40.
2. Steel sliding on steel lubricated with pure silicones of the type $CH_3 \ldots CH_3$.

Load, 2 kg.; coef. of friction = 0·35; temp., 30° C; magn. × 40.

[*To face page* 760.

gives an additional 0·41 × 10^{-19} e.s.u. (Table I). If the —OH dipole were oriented perpendicular to the water surface its contribution to the dipole moment would be 2·0 × 10^{-19} e.s.u.[18] However, by consideration of molecular models of oriented monolayers of the types CH_3 . . . CH_3 and CH_3 . . . CH_2OH it may be shown that substitution of a hydroxyl group for a terminal hydrogen gives an almost horizontal direction to the —OH dipole. A vertical orientation of the —OH dipole can only be achieved by considerable distortion of the normal orientation of the siloxane chain.

The resultant configuration of the molecule then is due to the combined effect of two opposing forces :

(*a*) the attraction of the —OH dipole for the water and its tendency to orient perpendicular to the surface and
(*b*) the attraction of the silicon and oxygen atoms for the water.

The dipole moment of the molecule will be increased over that of the unsubstituted silicone by the addition of the —OH and decreased by the distortion of the siloxane chain, the sum of the two effects being to increase the value of μ by 0·41 × 10^{-19} e.s.u.

Addition of a hydroxyl group to the other end of the molecule does not double this value for the increase in dipole moment, the increase over the singly substituted compound being only 0·21 × 10^{-19} e.s.u. This may be due to a proportionally greater distortion of the siloxane chain on the addition of a second hydroxyl group to a molecule of this length, or perhaps to the mutual counteraction of the vertical orienting tendencies of the two OH groups.

Lubrication.—The work of Zorn[12] on the frictional properties of isomeric dibasic esters on steel and the investigations of Tingle[13] on the relation between the surface orientation (as measured by a Langmuir trough) and the frictional properties of a number of esters, have shown that close packing, i.e. good lateral adhesion, of the hydrocarbon chains is necessary for good lubrication. Consequently, the picture of the orientation of the silicon molecules on a water surface obtained from the above measurements, which shows little lateral cohesion between the chains, does not lead us to expect good boundary lubricating properties from films of these compounds on metals. Again, electron diffraction photographs taken by Dr. J. V. Sanders (unpublished) show that they are not regularly oriented in the manner characteristic of close-packed monolayers below their melting points.

The values of the coefficient of friction for the silicones (Table III) show that they do not form good boundary lubricating layers on steel. Steel is readily lubricated by normal long-chain hydrocarbon lubricants, e.g. long-chain fatty acids generally give a value for the coefficient of friction of less than 0·1 up to 180° C.

The fact that the chlorinated silicones lubricate at all indicates that they are adsorbed from solution on to the metal surface, even though the halogen is not polar enough to act as an anchor to monolayers of these silicones on water. This is understandable considering that the work of adhesion of halogen derivatives of hydrocarbons to metals, e.g. mercury, is much greater than to water,[19, 20] and moreover, that the halogen of the Si—CH_2Cl group is much more reactive than its carbon analogue.[21]

Conclusion.—As steel is easily and effectively lubricated by adsorption of common boundary lubricants under most conditions the polar silicones will not replace the hydrocarbon lubricants for general use. Their value as boundary lubricants lies in their resistance to high temperature oxidation and to chemical attack generally. It is in those special cases where it is not possible to use hydrocarbons that silicones may be useful.

---

[18] Schulman and Hughes, *Proc. Roy. Soc. A*, 1932, **138**, 430.

[19] Harkins, Brown and Davies, *J. Amer. Chem. Soc.*, 1917, **39**, 356.

[20] (*a*) Harkins and Grafton, *ibid.*, 1920, **42**, 2534 ; (*b*) Harkins and Ewing, *ibid.*, 1920, **42**, 2539.

[21] Whitmore and Sommer, *ibid.*, 1946, **68**, 481.

This work was carried out in the University Chemical Laboratories, Cambridge, under the supervision of Prof. H. J. Emeléus, F.R.S., whom the author wishes to thank for his help and encouragement. The author would also like to thank Dr. F. P. Bowden, F.R.S. and Dr. A. E. Alexander, for most helpful discussions, and the Commonwealth Scientific and Industrial Research Organization for an overseas studentship.

University Chemical Laboratory,
Pembroke Street,
Cambridge.

HYDROTROPY, SOLUBILIZATION AND RELATED EMULSIFICATION PROCESSES

PART IX.—THE ELECTRICAL CONDUCTIVITY AND THE WATER DISPERSIBILITY OF SOME SOLUBILIZED SYSTEMS

By P. A. Winsor

Received 9th February, 1950

The theory and classification applied to solubilized systems in Parts I-IX, has been used as a basis for an investigation of the electrical conductivities of a number of solubilized systems containing undecane-3-sodium sulphate as amphiphilic salt. The observed changes in conductivity which accompany changes in the composition and temperature of the systems are in close qualitative accord with the general theory developed earlier. A modification in the form of the diagram (Fig. 4, Part I) representing the intermicellar equilibrium appears, however, to be indicated.

Solubilized systems showing an extremely marked and reversible change of conductivity with temperature are described and their possible utilization in thermistor construction is suggested. The relationships between the electrical conductivities and the water dispersibilities of the systems investigated are described and discussed.

Much work has been done by McBain, Lottermoser, Hartley, Ralston, Tartar and by others on the electrical conductivity of aqueous solutions of both anionic and cationic long chain salts. This work has afforded information on the onset and progress of micelle development in these solutions and on its dependence on the structure of the dissolved salt.[1-4]

Considering measurements of transport numbers in conjunction with the conductivities of aqueous solutions of aliphatic amine hydrochlorides Ralston and Hoerr concluded[5] that their results were consistent with an equilibrium of the type :

$$\text{alkyl ammonium ions} \leftrightharpoons \text{ionic micelles} \leftrightharpoons \text{lamellar micelles}$$

which shifts towards the right with increasing concentration. These authors also found[6] that additions of *N*-methyl lauramide, lauro-nitrile

---

[1] McBain, *Z. physik. Chem.*, 1911, **179**, 766 ; *Colloid Chemistry*, ed. Alexander (Reinhold Publishing Corporation, 1944), Vol. V, p. 102

[2] Lottermoser *et al.*, *Kolloid-Z.*, 1933, **63**, 175 ; *Kolloid-Beih.*, 1937, **45**, 203.

[3] Hartley, *Aqueous Solns. of Paraffin Chain Salts* (Herman et Cie, Paris, 1936).

[4] Ward, *Proc. Roy. Soc. A*, 1940, **176**, 412.

[5] Ralston and Hoerr, *J. Amer. Chem. Soc.*, 1943, **65**, 976.

[6] *Idem, ibid.*, 1947, **69**, 883.

or *n*-dodecane reduce the conductivities and the critical concentration for micelle formation (*C*) in aqueous solutions of *n*-dodecylamine hydrochloride. Evidence supporting an inter-micellar equilibrium in aqueous solutions of anionic soaps is presented in a valuable and comprehensive paper by Hess[7] who considers X-ray data and the variations in the physical properties of the solutions with the concentration and molecular weight of the soap.

Investigations have been reported of the conductivities of long chain salts in aqueous alcohol solutions.[4] With aqueous ethanolic solutions of *n*-dodecylammonium chloride Ralston and Hoerr found[8] that *C* is increased with increasing ethanol content of the solvent. Also while ethanol lowers the specific conductivity below *C*, the specific conductivities of the more concentrated solutions are actually increased by the addition of small amounts of ethanol. This was attributed to the alcohol displacing the micellar equilibrium from lamellar micelles towards ionic micelles and simple ions. The addition of inorganic salt to aqueous solutions of both anionic[9] and cationic[10, 11] colloidal electrolytes has been observed to decrease the specific conductivity attributable to the colloidal electrolyte and to reduce *C*. The effect of inorganic salt is thus the opposite[12] of that of a water-soluble organic solvent such as methanol or ethanol. With dodecylammonium chloride in the presence of both sodium chloride (*ca.* 1·0 % w. in water) and methanol (25 % vol.) the effects are about mutually compensating.

Schulman and collaborators have reported that while certain soluble oils are conducting others are non-conducting.[13] They suggested that these systems are to be regarded as transparent emulsions in which water or oil respectively forms the continuous phase. " Anomalous " systems of intermediate conductivity were also encountered.[14]

In Part I of this series[15] a sequence of phase changes was described which was observed, for example, when cyclohexanol or *n*-nonylamine was added to a mixture of equal volumes (10 ml.) of cyclohexane and a 20 % wt./vol. solution of tetradecane-5 sodium sulphate in water. In order that the present paper shall be as self-contained as possible these phase changes, and the nomenclature and theory adopted earlier to denote them, will be briefly recapitulated here with the addition of slight modifications suggested by later work.

Classification of Phase Changes.—TYPE I SYSTEMS.—In the absence of added alkanol or amine the above mixture consists of an aqueous solubilized phase (S_1) containing the alkyl sodium sulphate and some solubilized hydrocarbon in equilibrium with an excess organic liquid phase containing only traces of water and alkyl sulphate. Systems containing S_1 in equilibrium with excess organic liquid are termed Type I Systems.

S_1-soln. On adding cyclohexanol or nonylamine to the above mixture at 19° C the solubilization of the organic liquid is increased until with 0·55 ml. cyclohexanol or 0·20 ml. *n*-nonylamine no excess organic liquid remains and clear water dispersible S_1-soln. are produced.

Gel G. On further addition of the polar organic liquid to S_1, phase discontinuity again appears and a birefringent gel *G* separates. With increasing addition of polar liquid *G* increases at the expense of S_1 and finally a homogeneous water dispersible gel, or liquid crystalline solution *G*, is produced (*ca* 0·75 ml. cyclohexanol or 0·28 ml. *n*-nonylamine).

S_2-soln. Further addition of alkanol or amine produces progressive breakdown of the gel with production of a second isotropic liquid phase S_2. The clear S_2 soln. obtained with cyclohexanol (1·05 ml.) disperses readily in water giving a very finely divided emulsion. However, the S_2 soln. obtained with *n*-nonylamine (0·38 ml.) does not disperse readily in water and has an electrical conductivity of an altogether smaller order than that of any of the S_1 or G systems already mentioned or than the S_2 system containing cyclohexanol.

---

[7] Hess, *Fette Seifen*, 1942, **49**, 81.

[8] Ralston and Hoerr, *J. Amer. Chem. Soc.*, 1946, **68**, 2460.

[9] Tartar *et al.*, *ibid.*, 1932, **61**, 549.

[10] Ralston, *et al.*, *ibid.*, 1948, **70**, 980. [11] *Idem, ibid.*, 1949, **71**, 2145.

[12] *Idem, J. Physic. Chem.*, 1948, **52**, 1494.

[13] Schulman and McRoberts, *Trans. Faraday Soc.*, 1946, **42B**, 165.

[14] Schulman and Riley, *J. Colloid Sci.*, 1948, **3**, 383.

[15] Winsor, *Trans. Faraday Soc.*, 1948, **54**, 376.

TYPE II SYSTEMS.—With more than 1·6 ml. cyclohexanol or 0·45 ml. *n*-nonylamine an aqueous phase separates from S_2. Such systems with an excess aqueous phase (containing only traces of sodium alkyl sulphate and organic liquid) in equilibrium with S_2 are termed Type II systems.

Phase Changes with Variations of Composition and Temperature.—The above sequence of changes

$$\text{Type I system} \leftrightharpoons S_1 \leftrightharpoons S_1 + G \leftrightharpoons G \leftrightharpoons G + S_2 \leftrightharpoons S_2 \leftrightharpoons \text{Type II system}$$

may be observed in many systems containing organic liquid (single substance or mixture), amphiphilic salt (single salt or mixture) and aqueous liquid (water alone or water with water-soluble organic liquid and/or inorganic salt) as the proportions of the components or the temperature of the system are varied.

The way in which changes in composition and temperature displace the above phase equilibria has been discussed in detail in Parts I to VIII.[16] Briefly the equilibria are shifted to the right by any change which would be expected to increase the ratio of the solvent attraction between the amphiphilic salt and organic liquid to the solvent attraction between the amphiphilic salt and aqueous liquid (Part I, Methods I *a-d*). Diminution of this ratio shifts the equilibria in the reverse direction (Part I, Methods II *a-d*).

Intermicellar Equilibria associated with Phase Changes.—Fig. 1 shows in slightly modified form, the intermicellar changes which it was suggested in Part I form the mechanism of the phase changes. In the original diagram (ref. (15), Fig. 4), the S_1-, G-, and S_2-micelles were represented in linear equilibrium. The triangular representation in Fig. 1 of the present paper is now preferred as being more suggestive of a close relationship between the spherical micelles in the S_1 and S_2 soln. and of a somewhat special stability for the lamellar micelle in the birefringent gel phase. The experimental evidence on these points will be considered below. In Fig. 1 the individual micellar forms, except the lamellar

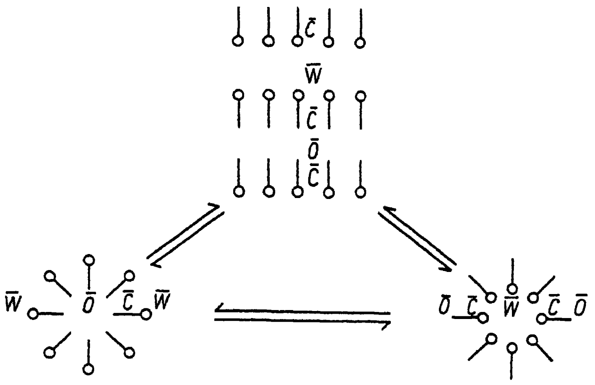

$R < 1$ — S_1 (isotropic soln.)

($S_1 + G$)

$R \simeq 1$ — G (gel or liquid crystalline soln.)

($G + S_2$)

$R > 1$ — S_2 (isotropic soln.)

$\bar{W}$ = Hydrophilic section of micelle.
$\bar{C}$ = Amphiphilic section of micelle.
$\bar{O}$ = Lipophilic section of micelle.
R = Ratio of dispersing tendencies on lipophilic and hydrophilic faces of $\bar{C}$ respectively.

FIG. 1.—Intermicellar equilibrium and associated phase changes shown by certain series of solubilized systems.

---

[16] Winsor, *Trans. Faraday Soc.*, 1948, **54**, 376, 451.

micelles when present in the liquid crystalline G systems, are visualized as quite temporary and rapidly interchanging. All the molecular species are supposed to be present in all sections of the micelles, $\overline{W}$, $\overline{C}$ and $\overline{O}$ merely indicating the types of species predominating in particular sections of the micelles. Thus the hydrophilic $\overline{W}$ section of the micelle will consist, in systems in which water is the only predominantly hydrophilic substance present, of water interspersed with a few ions derived from the amphiphilic salt. If inorganic salt or water soluble organic liquid are present they will also tend to concentrate in the $\overline{W}$ section of the micelles. The amphiphilic $\overline{C}$ section of the micelle will consist of amphiphilic salt ion-pairs together with a proportion of other amphiphilic molecules such as octanol-1 which may be present in the system.[13, 14, 17, 18] The lipophilic $\overline{O}$ section of the micelles will consist mainly of hydrocarbon together with a proportion of the less hydrophilic of the amphiphilic species present.

Clearly the various sections of the micelle will tend to interdisperse both on account of the thermal motion of the molecules and of those inter-molecular forces which are attractive in character. R represents the ratio of the interdispersing tendencies between $\overline{C}$ and $\overline{O}$ on the one hand, and between $\overline{C}$ and $\overline{W}$ on the other. So far no method is known of measuring R quantitatively but it is supposed to vary qualitatively as in Fig. 1. R may be regarded as the ratio of the spreading tendencies of the $\overline{C}$ layer on its lipophilic and hydrophilic faces respectively. Thus when $R < 1$ the $\overline{C}$ layer will tend to be convex towards $\overline{W}$, when $R > 1$ the $\overline{C}$ layer will tend to be convex towards $\overline{O}$ and when $R = 1$ the planar arrangement of the $\overline{C}$ layers will be the most stable.

Object of the Present Work.—In the present work measurements have been made of changes in specific resistance accompanying changes in the composition and temperature of S_1, G and S_2 phases. It was hoped to see how far these measurements would extend, modify or refute the idea of the existence of an inter-micellar equilibrium, such as that in Fig. 1. Also it was hoped to obtain information about the mechanism of the dispersibility of "soluble oils" in water by observing the relationships between specific resistance and water dispersibility in these systems. Undecane-3 sodium sulphate has been used as amphiphilic salt throughout the present investigation. This salt was chosen for reasons of convenience only, in particular (i) it has a high solubility in water; (ii) the G-region in the systems obtained with it are not extended as would be the case with a -1 sulphate (cf. Part IV); (iii) the viscosities of the S_1- and S_2-soln. are conveniently low for manipulation. Pentadecane-3 sodium sulphate, originally tried as amphiphilic salt for the investigation, was found to give inconveniently viscous systems.

Experimental

Apparatus.—Resistances were measured using a Mullard measuring bridge with magic eye indicator (Type GM 4140/1). The bridge was supplied with current from a Mullard 1000 c./sec. oscillator (Type GM 4260). Resistances could be measured with an accuracy of *ca.* 1 %. Temperatures were controlled using a thermostat and measurements of resistance were made at 20° C unless otherwise stated. The conductivity cell used is represented in Fig. 2. The electrodes (about 0·8 cm. square and 0·8 cm. apart) were of platinum deposited on Pyrex by the method of Coffin,[19] but instead of the solution of platinic chloride in a mixture of lavender and rosemary oils, a solution of $H_2PtCl_6 . 6H_2O$ (1 g.) in *n*-octanol (3 ml.) was used. This solution when painted on Pyrex, evaporated and ignited, yields a coherent film of platinum metal which adheres well to the glass. The electrodes were subsequently coated with platinum black.[20] This was found essential for getting clearly marked null points in the measurements of the lower resistances. The cell constant determined using standard potassium chloride solutions was 2·08.

[17] Schulman and Hughes, *Biochem. J.*, 1935, **29**, 1242.
[18] Harkins and Mittleman, *J. Colloid Sci.*, 1948, **4**, 367.
[19] Coffin, *Can. J. Res. B*, 1940, **8**, 318.
[20] Kohlrausch, *Ann. Physik*, 1975, **154**, 1, 215.

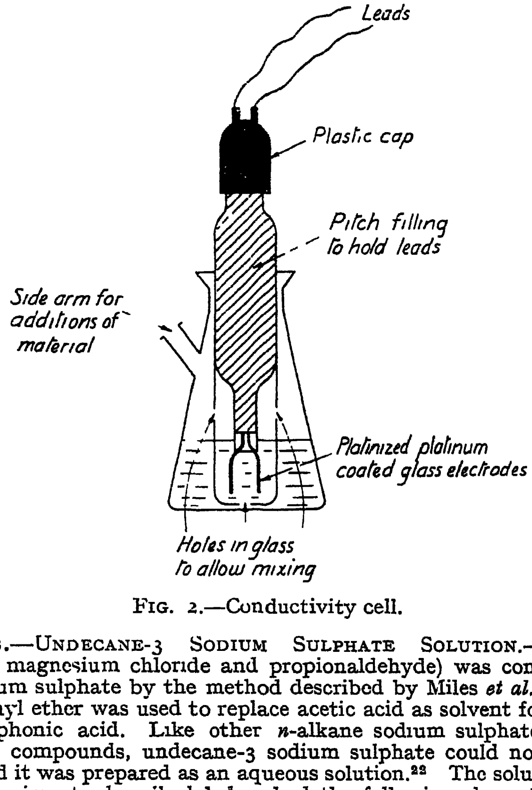
Leads
Plastic cap
Pitch filling to hold leads
Side arm for additions of material
Platinized platinum coated glass electrodes
Holes in glass to allow mixing

FIG. 2.—Conductivity cell.

Materials.—UNDECANE-3 SODIUM SULPHATE SOLUTION.—Undecanol-3 (from *n*-octyl magnesium chloride and propionaldehyde) was converted to undecane-3 sodium sulphate by the method described by Miles *et al.*[21] except that anhydrous ethyl ether was used to replace acetic acid as solvent for the reaction with chlorsulphonic acid. Like other *n*-alkane sodium sulphates, except the -1 and the -2 compounds, undecane-3 sodium sulphate could not be obtained crystalline and it was prepared as an aqueous solution.[22] The solution employed in all the experiments described below had the following characteristics :—

Alkyl sulphate content (Methylene Blue method [23])	20·12 %
,, ,, ,, (from sulphated ash)	20·07 %
Density	1·034
Refractive index n_D^{20}	1·3578
Specific resistance at 20° C	14·0 Ω

ORGANIC LIQUIDS.—The individual compounds were middle fractions from the redistillation of pure laboratory grade materials and had the following characteristics :

Substance	n_D^{20}	Specific resistance at 20° C. Ω
Cyclohexane	1·4278	$> 10^7$
n-Hexane	1·3812	$> 10^7$
Cyclohexanol	1·4648	$> 10^7$
n-Hexanol	1·4185	$4·6 \times 10^6$
n-Octanol	1·4304	$8·5 \times 10^6$
n-Dodecanol (m.p. 23° C)	1·4409	$> 10^7$
Ethylene glycol	1·4312	$3·0 \times 10^6$

Hydrocarbon B was a petroleum fraction which had been exhaustively extracted with oleum to remove aromatics: boiling range, 188°-213° C;

[21] Miles, *Ind. Eng. Chem.*, 1944, **36**, 610.
[22] Winsor, *Trans. Faraday Soc.*, 1948, **54**, 463.
[23] Epton, *ibid.*, 1948, **54**, 226.

D_4^{20} 0·777 ; n_D^{20} 1·4320 ; specific resistance $> 10^7$ ohm. Hydrocarbon B was used as hydrocarbon component in most of the experiments described in order to avoid losses due to evaporation such as would be likely with the more volatile C_8 hydrocarbons. The water used was laboratory distilled of specific resistance $2{\cdot}2 \times 10^5$ ohm.

Procedure.—The mixture was contained in a 50 ml. conical flask with the dip cell inserted through the neck (Fig. 2). A side arm served for addition of material. Stirring was done by moving the dip cell and by hand shaking. This was effective except perhaps with the thickest gels encountered. Additions were made by volume. Resistance measurements were confined to systems within the S_1, G, S_2 regions and the terminations of the resistance curves therefore correspond closely to the formation of Type I and Type II systems. At points where a fresh phase appears there should be a break in the resistance curve and an attempt has been made to indicate such breaks taking into account the phase changes in the system as observed visually. In general, the points where $S_1 \rightarrow (S_1 + G)$ and where $(G + S_2) \rightarrow S_2$ are readily noted but the transition points $(S_1 + G) \rightarrow G$, and $G \rightarrow (G + S_2)$ are less readily seen.

The resistance of a $(G + S)$ mixture will depend on the degree of mixing of the system and thus does not represent a definite physical characteristic of the system. However, such systems readily form emulsions stable during the time required for resistance measurement. The observed resistances therefore approximate to an average for the two phases present.

Results.—The experimental results are recorded graphically in Fig. 3-9. For convenience the model systems studied are given under the Fig. numbers in which the observations are recorded. D = dispersible in water; PD = poorly dispersible ; MD = giving milky dispersion ; ND = non-dispersible.

Discussion

The Form of the Inter-micellar Equilibrium.—In Fig. 1 emphasis is placed on the shapes which the $\bar{C}$ layers will tend to assume under various conditions. Within S_1 and S_2 soln. R is envisaged as varying from point to point with local fluctuations in composition due to the thermal motion of the molecules. However, R will be on an average < 1 in S_1 soln. and > 1 in S_2 soln. and the predominant forms of micelle will be those respectively shown at the left and right of Fig. 1. These types of micelle have

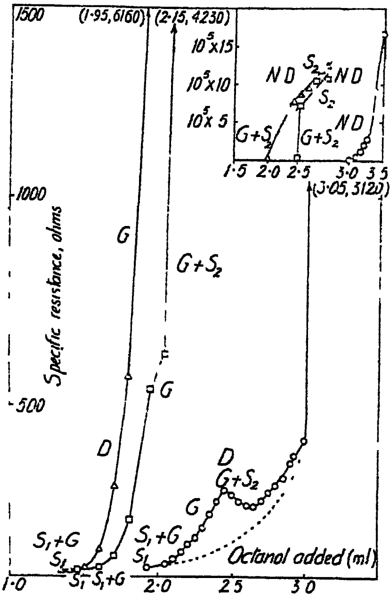

FIG. 3.—Changes in specific resistance when passing through S_1, G and S_2 stages on gradual addition of *n*-octanol to a mixture of undecane-3 sodium sulphate solution (10 ml., 20 % w.) with 10 ml. of △ cyclohexane, or ☐ *n*-hexane, or ○ aromatic-free hydrocarbon. (Boiling range 188 —213 C; D_4^{20} 0·777; n_D^{20} 1·4320.)

NOTE.—In Figures: D = Dispersible in water. P.D. = Poorly dispersible. M.D. = Giving milky dispersion. N.D. = Not dispersible.

recently been termed the hydrophilic oleomicelle and the oleophilic hydromicelle respectively by Schulman and Riley.[14] Continuous passage from S_1 into S_2 soln. occurs in certain systems without the appearance of gel (cf. e.g. Fig. 4 and 6). This indicates the possibility of an equilibrium between the two types of spherical micelle. In Fig. 3-9 it can be seen that the curves for the S_1 and S_2 soln. can always be connected by an (imaginary) smooth dotted curve which is not observed in practice on account of the appearance of the gel phase. This result probably indicates a continuity in the type of intermicellar equilibrium existing in both S_1 and S_2 soln. and it is for these reasons that Fig. 4 of Part I [15] has been revised in favour of Fig. 1. The relatively low specific resistance of certain of the S_2 soln., close in composition to the gel region, seems to indicate that they cannot be organized at all exclusively of oleophilic hydromicelles but must contain hydrophilic micelles in equilibrium with these.

A particularly high degree of molecular order in the gel systems is indicated by their liquid crystalline character. Also in Fig. 3-8 a distinct and separate curve is found for the specific resistance over the gel region. A high degree of order in the gel also appears likely from the refractive index-composition changes shown in Fig. 9. If the Lorentz-Lorenz molar refractions $\frac{n^2 - 1}{n^2 + 2}\frac{M}{d}$ of the various molecular species present are assumed to be unaffected by the production of gel, the increase in refractive index indicated by PQ corresponds to a contraction due to gel formation of about 1·6 %. The apparent continuity of the S_1 and S_2 sections of this refractive index composition curve is also noteworthy. For all these reasons it seems reasonable to assign to the gel phase a specially stable micellar organization as in Fig. 1.

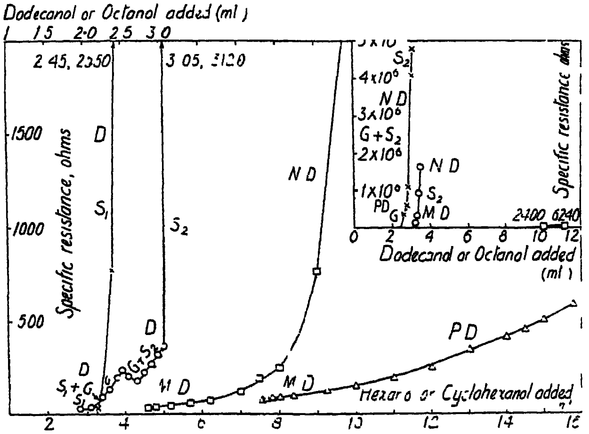

FIG. 4.—Changes in specific resistance on passing through S_1, G and S_2 stages on gradual addition to a mixture of hydrocarbon B (10 ml.) and undecane-3 sodium sulphate solution (10 ml.) of △ cyclohexanol, or ☐ *n*-hexanol, or ○ *n*-octanol, or × *n*-dodecanol.

Correlation between Observed Changes in Specific Resistance with displacements of the Intermicellar Equilibrium.—If the intermicellar equilibrium postulated in Fig. 1 is correct one would anticipate that in the S_1 and S_2 regions any change of composition (not directly introducing additional ions) which would be expected to increase R (cf. Methods I *a-d*, Part I [15]) should displace the equilibrium to the right and increase the specific resistance of the system. Similarly, changes tending to diminish R (cf. Methods II *a-d*,[15]) should decrease the specific resistance. Fig. 3-8 show that the qualitative accord with this expectation is complete.

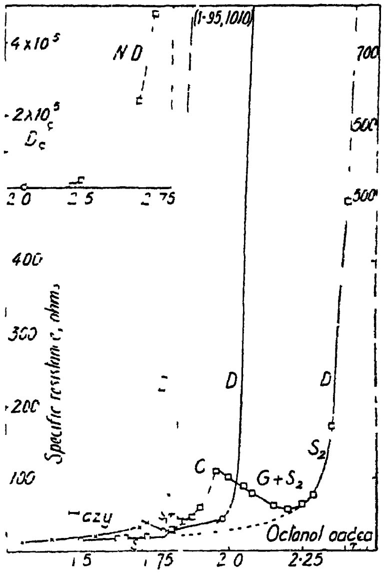

FIG. 5.—Changes in specific resistance on passing through S_1, G and S_2 systems on gradually adding *n*-octanol to mixtures of hydrocarbon B (10 ml.), and undecane-3 sodium sulphate solution (10 ml.) containing sodium sulphate: □ 0·1 g., or ○ 0·2 g., or × 0·4 g.

NOTE.—The curve corresponding to no added Na_2SO_4 is given in Fig. 4.

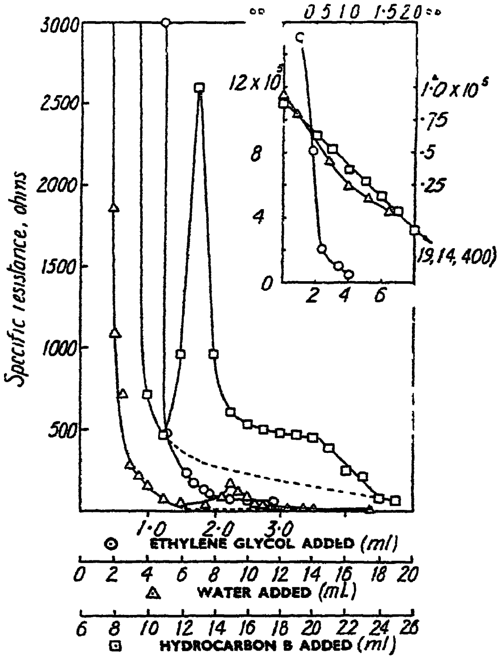

FIG. 6.—Changes in specific resistance on gradually adding—

○ Ethylene glycol to the S_2 solution obtained from *n*-octanol (3·7 ml.), hydrocarbon B (10 ml.), and undecane-3 sodium sulphate solution (10 ml., 20 % w.).

△ Water to the S_2 solution obtained from *n*-octanol (2·28 ml.), hydrocarbon B (10 ml.), undecane-3 sodium sulphate solution (10 ml. 20 % w.) and sodium sulphate (0·2 g.).

□ Hydrocarbon B to the S_2 solution obtained from *n*-octanol (3·7 ml.), hydrocarbon B (10 ml.), and undecane-3 sodium sulphate solution (10 ml., 20 % w.).

(The above S_2 solutions are such that any further addition of octanol would precipitate an aqueous phase.)

In a change which involves the production of gel, the alteration in conductivity to be expected is less clear. The lamellar micelle might afford facilities for ionic migration intermediate between those given by the S_1 and S_2 micelles. However, some reduction in conductivity might arise on account of the high viscosity of the gel systems. In practice the specific resistance curves obtained for the gel regions lie somewhat above the dotted curves drawn continuous with those for the S_1 and S_2 regions. There is also frequently a maximum in the specific resistance curve near the middle of the gel region. The experimental results thus again accord well with expectation. The changes of specific resistance with temperature shown in Fig. 7 and 8 are marked and on the basis of Fig. 1 correspond to a reduction of R with increase in temperature. This is the more usual apparent effect of increase of temperature on R as deduced from other evidence.[24] The extreme temperature dependence of the specific resistance of some S_2 soln. of specially selected composition (Fig. 8) appears to be of a strictly and rapidly reversible nature and might be of use for thermistor design.

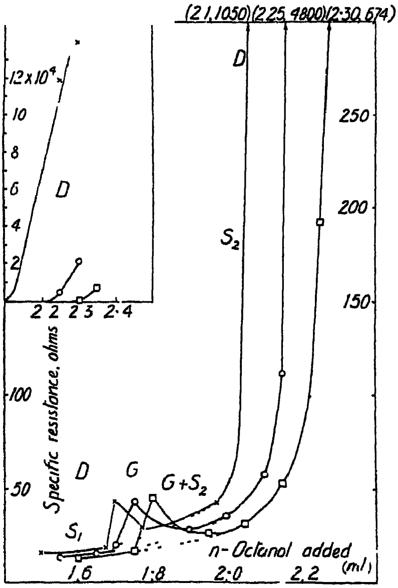

FIG. 7.—Changes in specific resistance on gradually adding *n*-octanol to a mixture of hydrocarbon B (10 ml.), undecane-3 sodium sulphate solution (10 ml.) and sodium sulphate (0·2 g.) at ⊡ 30° C, ⊙ 25° C, × 20° C.

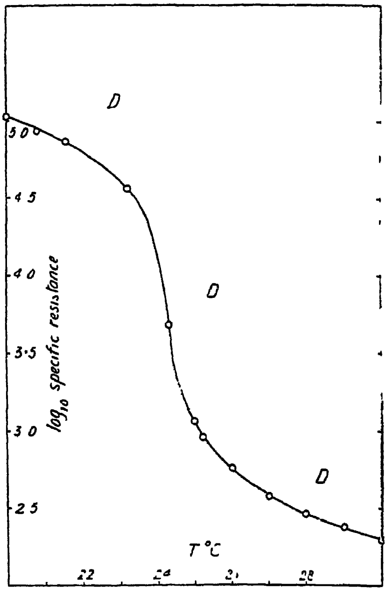

FIG. 8.—Changes in specific resistance with change of temperature of a solution containing hydrocarbon B (10 ml.), *n*-octanol (2.25 ml.), undecane-3 sodium sulphate solution (10 ml.) and sodium sulphate (0·2 g.).

This reversibility of the temperature-resistance effect has been studied by cycling the temperature of a small completely sealed cell over a range of 10° C for some days, the $Na_2SO_4 + Na_2SO_4 10H_2O +$ saturated solution equilibrium point being used as constant reference temperature. Within the limits of accuracy of the apparatus used the reversibility appeared complete.

---

[24] Winsor, *Trans. Faraday Soc.*, 1948, 54, 455.

Relationships between Water Dispersibility and Specific Resistance.—A close parallel is shown in Fig. 3-8 between water dispersibility and specific resistance. The S_2 soln. of high specific resistance are, in general, poorly dispersible. However, certain of the S_2 soln. containing sodium sulphate are more dispersible than S_2 soln. of similar specific resistance containing no sodium sulphate but an increased proportion of alkanol.

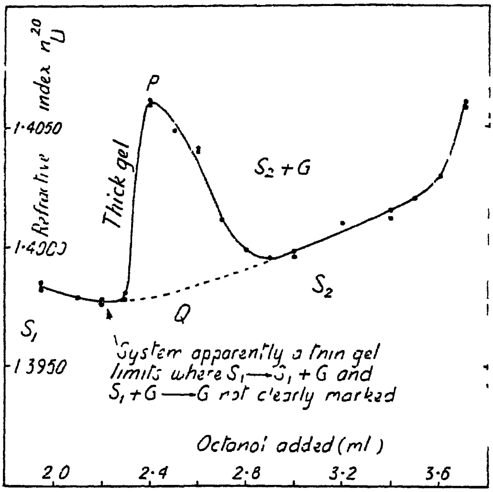

FIG. 9.—Changes in refractive index when passing through S_1, G and S_2 stages on gradually adding *n*-octanol to a mixture of hydrocarbon B (10 ml.) and undecane-3 sodium sulphate solution (10 ml.).

This result is to be expected since addition of water alone to an S_2 system containing sodium sulphate tends first to convert it to a readily dispersible G or S_1 system (cf. Fig. 6). In a somewhat complementary manner to this behaviour of S_2 soln. containing sodium sulphate, S_1 soln. containing ethylene glycol often disperse less readily in water than would be expected from their specific resistance. In this case, however, addition of water tends to convert the S_1 soln. to an S_2 soln. of high specific resistance and smaller water dispersibility.[25]

In Fig. 3-8 there are considerable differences among the dispersibilities of the dispersible systems. In most cases, when the system is added to water an opalescent, finely divided emulsion is produced. In other cases milky emulsions may form. The emulsions produced from the S_1 soln. containing hexanol-1 and cyclohexanol (Fig. 4) belong to this class.

The Individual Systems Investigated (Fig. 3-8).—The relative positions of these curves in Fig. 3 indicate, on the basis of Fig. 1, that the $\overline{C}$ layer of the micelles has a markedly greater tendency to become convex towards hexane or cyclohexane than towards the higher hydrocarbon.

In Fig. 4 the absence of gel in the systems containing cyclohexanol and *n*-hexanol and also the smaller effectiveness of these alcohols as compared with octanol and dodecanol in producing the change between Type I and Type II systems are probably due to their higher partial solubility in water. With these alcohols mutually opposing effects of an oil-soluble alcohol (Method I*b* [1]) and a water-soluble alcohol (Method II*b* [15]) may both be operative. The relatively very low specific resistances of the S_2 sols obtained with these alcohols may be due to a greater concentration of water and ions in the $\overline{O}$ portions of the S_2-micelles, $\overline{O}$ being rich in the C_6 alcohols which themselves exert a considerable solvency for water.

---

[25] Winsor, *Trans. Faraday Soc.*, 1948, **54**, 391, 453.

The gradual elimination of the gel kink in the specific resistance curve on addition of sodium sulphate (Fig. 5) is well marked (cf. [25]). The effect of the addition of sodium sulphate on the conductivity would be expected to be due to (1) increased conductivity due to added ions, (2) diminished conductivity due to displacement of the micellar equilibrium to the right (Method I*d*). The results indicate that (2) has a more pronounced effect than (1). However, the effect of (1) is also indicated in the lower resistances of the gel maxima and at the points of separation of an aqueous phase from the S_2 soln. in the systems containing the greater amounts of sodium sulphate.

The displacement of the micellar equilibrium to the left by addition of ethylene glycol (Method II*b* [15]), water (Method II*b* [15] when applied to a system containing sodium sulphate) or hydrocarbon (Method II*d* [15]) is well shown in Fig. 6. The absence of gelling during the S_2-S_1 change is noticeable in the systems containing added ethylene glycol. Although ethylene glycol reduces the gelling tendency it may not overcome it in cases where the tendency is otherwise strong. Thus, when ethylene glycol is added to a Type II system derived from undecane-3 sodium sulphate solution (10 ml.), hydrocarbon B (10 ml.) and *n*-dodecanol (3·7 ml.), 1·2 ml. gives a clear S_2 soln. (specific resistance 3×10^6 ohms), 3·2 ml. a clear gel (specific resistance 600 ohms), 4·5 ml. a clear S_1 soln. (specific resistance 70 ohms) and 5 ml. a Type I system. In this case the S_1 soln. disperse readily in water but the S_2 soln. do not. The effects of added hydrocarbon in increasing the water dispersibility and diminishing the specific resistance is shown in Fig. 6.

The effect of rise of temperature over the range 20-30° C on the systems shown may be interpreted as shifting the inter-micellar equilibrium to the left. As would be expected, in the region of the diagram where the specific resistance of the system shows the greatest sensitiveness to composition it also shows the greatest temperature dependency. The effect of rise of temperature in shifting the inter-micellar equilibrium to the left is also well shown by the phase changes observed on warming the Type II system obtained at 20° C from undecane-3 sodium sulphate solution (10 ml.), hydrocarbon B (10 ml.), and *n*-octanol (3·7 ml.). This system gave a clear S_2 soln. at 22·5° C, ($S_2 + G$) at 52° C, a clear gel G at 61·5° C, ($G + S_1$) at 63° C, S_1 at 65° C and a Type I system at 70° C.

The author wishes to thank Messrs. " Shell " Refining and Marketing Co. Ltd., for permission to publish this paper.

Thornton Research Centre,
Thornton-le-Moors,
Cheshire.

THE NON-STATIONARY PHASE OF CHAIN REACTIONS

PART I.—THE PHOTOPOLYMERIZATION OF STYRENE

BY G. M. BURNETT

Received 12th December, 1949

By means of an adaptation of the dilatometer of Schulz and Harborth, in order to operate *in vacuo*, and with a great increase in sensitivity it has been found possible to demonstrate the existence of a natural induction period in the photopolymerization of styrene. The method has been applied to the determination of the kinetic constants for styrene polymerization, the values obtained being in good agreement with those quoted in the literature.

From the nature of photochemical chain reactions it is evident that the so-called stationary state, which is usually studied, cannot be attained immediately the source of illumination is switched on, nor can the rate of reaction revert to zero immediately the exciting radiation is removed. The fact that such reactions should, in fact, show a "natural" induction period was first demonstrated by Weigert and Kellermann[1] in the hydrogen-chlorine reaction when it was shown that the maximum rate was not achieved until between 1/300 and 1/40 sec. after the start of the radiation.

The " after " effect has been studied with somewhat greater intensity. In a great many cases the after effect found in photochemical processes which was attributable to the adventitious formation of stable catalysts, etc., but with, for example, the hydrogen-chlorine reaction and also the photochemical interaction of iodine and potassium oxalate, a short true after effect was shown to exist. The latter reaction was investigated by the use of a rotating sector technique first by Berthoud and Bellenot[2] and then by Chapman, Briers and Walters,[3] the latter being successful in determining the life-time of the active centres formed during illumination.

Since 1945 attention has been focused on the use of methods of intermittent illumination to obtain the life-time of the chain carrying radicals in the addition polymerization of a number of monomers[4-7] and in photo-oxidation.[8] This followed the earlier attempts by Melville[9] to evaluate the life-time of the radicals involved in the vapour phase polymerization of methyl methacrylate. Bamford and Dewar[10] evolved a viscosity technique whereby they were able to show the existence of a photochemical after effect in polymerization reactions and also to measure its extent. This is essentially a method of defining the non-stationary stage of the reaction. Although their method has been applied only to the case in which two of the chain-carrying free radicals are simultaneously removed in the termination of the reaction chains, there is little doubt that it could be extended to the case in which only one such radical is involved.

The object of this paper is to present a method whereby the photo-initiation can be shown to give rise to a true induction period, and by the analysis of this induction period the rate constants for the various steps in the overall reaction can be deduced. The values for the rate constants for the thermal initiation, propagation, transfer and termination reactions for the polymerization of styrene monomer are recorded and compared with values already recorded in the literature. The theory can be extended to include the case of first-order termination but no experimental results on such reactions are given.

Theoretical.—Although the experimental technique which will be outlined is applicable in this case to a polymerization reaction there is little doubt that the theoretical argument is, in fact, true for any photochemical chain reaction. For convenience, however, a polymerization process will be assumed. In this case, it has to be pointed out that the values of the rate constants for the various steps of the reaction are taken to be independent of the chain-length, although this approximation will not hold in cases in which the chain-lengths are excessively low.[11] For comparatively long chains, on the other hand, there can be little doubt that this assumption is valid.[4] Using such a simplified picture the equations governing the reaction rates can be very much simplified since only the type of the radical and not its molecular weight needs to be considered. The following reactions are the most important in the polymerization process :

---

[1] Weigert and Kellermann, *Z. physik. Chem.*, 1923, **107**, 1.

[2] Berthoud and Bellenot, *Helv. chim. Acta*, 1923, **7**, 307.

[3] Chapman, Briers and Walters, *J. Chem. Soc.*, 1926, 562.

[4] Burnett and Melville, *Proc. Roy. Soc. A*, 1947, **189**, 456.

[5] Bartlett and Swain, *J. Amer. Chem. Soc.*, 1946, **68**, 2381.

[6] Matheson, Auer, Bevilacqua and Hart, *ibid.*, 1949, **71**, 497.

[7] Melville and Mackay, *Trans. Faraday Soc.*, 1949, **45**, 323.

[8] Bateman and Gee, *Proc. Roy. Soc. A*, 1948, **195**, 391.

[9] Melville, *ibid.*, 1937, **163**, 511.

[10] Bamford and Dewar, *ibid.*, 1947, **192**, 309.

[11] Mayo, *J. Amer. Chem. Soc.*, 1948, **70**, 3689.

Initiation . .	$M = P_1$	rate $= I$
Propagation .	$P_n + M = P_{n+1}$	rate $= k_p(P)(M)$
Termination .	$P_n + P_m = M_n + M_m$	rate $= k_t(P)^2$
Transfer . .	$P_n + M = M_n + P_1$	rate $= k_f(P)(M)$,

where M is a monomer molecule, P_n and M_n, the polymer radical and the corresponding deactivated molecule, k_p, k_f, k_t, the rate constants for the steps of the overall reaction. Since the overall conversion in the runs to be discussed was never allowed to exceed 1 % it is not necessary to take into account the possibility of chain transfer to the polymer, or branching or cross-linking. Neither will the polymerization be subject to any of the anomalous effects due to the increase in the viscosity of the medium as has been shown to be operative in the polymerization of methyl methacrylate.[12, 13] When in this chain reaction, the stationary state has been reached, it is known that

$$d(P)/dt = I - k_t(P_s)^2 = 0,$$

and hence the concentration (P_s) of the free radicals in the stationary state will be given by

$$(P_s) = (I/k_t)^{\frac{1}{2}}. \quad . \quad . \quad . \quad . \quad . \quad (1)$$

On the other hand, before the stationary state has been attained, i.e. during the initial stages of the reaction, the conditions governing the concentration of the active centres will be

$$d(P)/dt = I - k_t(P)^2.$$

Integration of this equation leads to

$$\tfrac{1}{2}(k_t I)^{-\frac{1}{2}} . \ln\left\{\frac{1 + (k_t/I)^{\frac{1}{2}}(P)}{1 - (k_t/I)^{\frac{1}{2}}(P)}\right\} = t + c,$$

or

$$\tanh^{-1}\{(P)/(P_s)\} = (k_t I)^{\frac{1}{2}}t = t/\tau,$$

since c is zero, as $(P) = 0$ when $t = 0$. τ is the life-time of the active centres which can be readily shown to be defined by

$$\tau = (k_t I)^{-\frac{1}{2}}.$$

Hence

$$(P) = (P_s) . \tanh(t/\tau).$$

The rate of polymerization at any instant will be given by

$$-d(M)/dt = k_p(P_s)(M)\tanh(t/\tau),$$

and integration of this equation gives

$$-\ln((M)/(M_0)) = (k_p/k_t)\ln\{\cosh(t/\tau)\}.$$

If F is the fraction of the monomer converted then

$$(M)/(M_0) = 1 - F,$$

so that

$$-\ln(1 - F) = (k_p/k_t)\ln\{\cosh(t/\tau)\},$$

and if $F \leqslant 1$, as it will be if the amount of conversion is kept low as has already been mentioned, then

$$-\ln(1 - F) = F,$$

so

$$F = (k_p/k_t)\ln\{\cosh(t/\tau)\}.$$

---

[12] Trommsdorff, *Colloquium on High Polymers* (Freiburg, 1944).
[13] Schulz and Harborth, *Die Makromol. Chem.*, 1947, **1**, 106.

When $t \gg \tau$, i.e. when the stationary state has been attained, it is easy to see that

$$F = (k_p/k_t)(t/\tau - \ln 2).$$

It is evident therefore that the plot of the fraction of monomer converted against the time will eventually give a straight line whose slope will be k_p/k_t and whose intercept t_i on the time axis is given by

$$t_i = \tau \,.\, \ln 2, \text{ or } \tau = 1{\cdot}44\, t_i.$$

Since the reaction requires a finite time in which to achieve its maximum rate it is evident also that when the source of initiation is removed some time will elapse before the reaction rate will fall to zero. The only possible practical method of achieving this sudden cessation of chain-starting is by a photochemical technique. After the source of illumination has been removed the equation governing the radical concentration will be

$$\mathrm{d(P)}/\mathrm{d}t = -\, k_t(\mathrm{P})^2,$$

which can be integrated to give,

$$(\mathrm{P})^{-1} - (\mathrm{P}_s)^{-1} = k_t t.$$

The rate of monomer conversion at any stage in this part of the reaction will be

$$R = k_p(\mathrm{P})(\mathrm{M}).$$

Substitution of the value of (P) from this relationship in the above equation will lead to

$$R^{-1} - R_s^{-1} = (k_t/k_p(\mathrm{M}))t.$$

Hence if the reciprocal of the rate during the dark period is plotted as a function of the time a straight line will result with a slope of $(k_t/k_p(\mathrm{M}))$. As a corollary of this the rate at a time equal to the life-time of the growing chains will be half of the steady state rate.

In some cases the chain termination mechanism will not be by the mutual destruction of two of the growing chains but may involve only one of the active radicals. This is stated to take place in the bulk polymerization of allyl acetate [14] and must also occur in those reactions in which inhibitors play an important role. If the termination mechanism is

$$\mathrm{P}_n + \mathrm{X} = \mathrm{M}_n, \text{ rate} = k_t'(\mathrm{P})(\mathrm{X}),$$

by a similar analysis to the above,

$$F = (k_pI/k_t'(\mathrm{X}))t - (k_pI/k_t'^2(\mathrm{X})^2)(1 - \mathrm{e}^{-k_t'(\mathrm{X})t}).$$

When t is very large the exponential term can be neglected, so

$$F = (k_pI/k_t'(\mathrm{X}))(t - (k_t'(\mathrm{X}))^{-1}).$$

Again this gives a straight line but in this case it is not possible to evaluate the separate constants without an exact determination of the rate of chain-starting. This line will give the value of $(k_t'(\mathrm{X}))^{-1}$.

The concentration of the chain carrier radicals during the after period will be governed by the relationship

$$\mathrm{d(P)}/\mathrm{d}t = -\, k_t'(\mathrm{P})(\mathrm{X}),$$

and following the same reasoning as before it can be shown that

$$\ln R = \ln K - k_t'(\mathrm{X})t,$$

where R is the rate of conversion of monomer, expressed as the fraction converted per sec. and $K = k_p(\mathrm{M})I/k_t'$, so that a linear relationship is possible and the slope of the line is $-\, k_t'(\mathrm{X})$.

Determination of Kinetic Constants in Polymerization.—From the definition of the life-time of the growing chain, viz. $\tau = (k_tI)^{-\frac{1}{2}}$, the following expression may be derived

$$\tau^{-1} = k_tR\ k_p(\mathrm{M}),$$

where R is the rate of monomer conversion expressed in mole $\mathrm{l.}^{-1}$ $\mathrm{sec.}^{-1}$.

---

[14] Bartlett and Altschul, *J. Amer. Chem. Soc.*, 1945, **67**, 816.

Hence there is a linear relationship between the rate and the reciprocal of the life time, and the slope of the line will be $k_t/k_p(\mathrm{M})$, so that the ratio of the kinetic constants can be computed.

In order to evaluate these constants explicitly it is necessary to obtain either another relationship between them or to determine the rate of chain-starting. Several methods for determining the latter have been used but all are open to criticism. If the effect of transfer is negligible then a measurement of the molecular weight will yield the rate of chain initiation. A second method in which the rate of initiation is deduced from a comparison of the rate of the photo-initiated reaction and the catalyzed polymerization has also been used[5] but since this assumes that the catalyst is wholly efficient the validity of the method is doubtful. The third technique depends on the fact that the polymerization of some monomers is completely suppressed by the additon of some substance such as benzoquinine. This was shown to be true in the photopolymerization of vinyl acetate[4] and the effect has also been shown in the photosensitized reaction.[15] Besides the possibility of an internal filter effect vitiating these results it is also uncertain that only one molecule of quinone is necessary for the cessation of each chain.[16]

The following scheme removes many of the difficulties which have been enumerated above and assumes only that the termination of chains is by dismutation. In the catalyzed polymerization the degree of polymerization $\overline{P}$ is given by

$$\overline{P}^{-1} = k_f/k_p + k_x(\mathrm{C})/k_p(\mathrm{M}) + k_t(\mathrm{P})/k_p(\mathrm{M}),$$

where (C) is the catalyst concentration and k_x the rate constant for the transfer reaction between catalyst and radical. Since in most cases the effect of the catalyst is negligible, the expression can be reduced to the form

$$\overline{P}^{-1} = k_f/k_p + (k_t/k_p{}^2(\mathrm{M})^2)R.$$

Hence the plot of $\overline{P}^{-1}$ against R will give a straight line with a slope of $k_t/k_p{}^2(\mathrm{M})^2$ and an intercept on the $\overline{P}^{-1}$ axis of k_f/k_p. In this way, therefore, a second relationship between the coefficients for the propagation and the termination reactions is obtained together with a direct measure of the ratio of the transfer to propagation rate constants.

Although it has been assumed that disproportionation is the only chain-stopping mechanism there appears to be a wealth of evidence to support both sides of the argument and, so far, there seems to be little in the way of conclusive evidence to support either side. For combination it is argued that in many cases involving small radicals there is almost complete recombination of these radicals. This has been demonstrated by Kharasch and others in the case of radicals such as

$$\mathrm{MeOC_6H_4\,.\,\dot{C}H\,.\,CH_2\,.\,CH_3}$$

and in the succinic acid synthesis in which the combination reaction

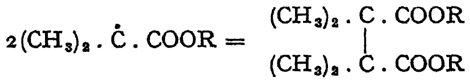

$$2(\mathrm{CH_3})_2\,.\,\dot{\mathrm{C}}\,.\,\mathrm{COOR} = \begin{array}{c}(\mathrm{CH_3})_2\,.\,\mathrm{C}\,.\,\mathrm{COOR}\\ |\\ (\mathrm{CH_3})_2\,.\,\mathrm{C}\,.\,\mathrm{COOR}\end{array}$$

has been established beyond all doubt. By analogy Price[17] points out that in methyl methacrylate the active radicals have a similar structure, i.e.

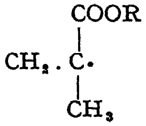

$$\begin{array}{c}\mathrm{COOR}\\ |\\ \mathrm{CH_2\,.\,C\cdot}\\ |\\ \mathrm{CH_3}\end{array}$$

---

[15] Matheson *et al.*, *J. Amer. Chem. Soc.*, 1949, **71**, 2610.

[16] Mayo, *ibid.*, 1948, **70**, 1284.

[17] Price, *Faraday Soc. Discussion*, 1947, **2**, 402.

and so should undergo a combination reaction. On the other hand, the investigation of the rate of change of viscosity for the photopolymerization of methyl methacrylate under high light intensities shows that the rate of change of viscosity is proportional to the tenth root of the light intensity which is in good agreement with the assumption of dismutation.[18] The analogy which Price uses is a dangerous one since it definitely appears from other work, notably that of Norrish,[19] that the size of the radical has a definite bearing on the ability to undergo combination and that the bigger the radical the less likely it is to do so. A method of determining which of these two possible termination reactions is predominant appears to be afforded most conclusively by a comparison of the number and weight average molecular weights. From kinetic analyses [20] it can be shown that in disproportionation the ratio of weight to number average is 2, while for combination it is 1·5. So far no measurements of this kind have been made with this end in view but in an investigation of the kinetic constants of vinyl acetate polymerization Bartlett and Kwart [21] have determined the molecular weight of the resulting polymer by both osmotic pressure and light-scattering measurements and found that the ratio of the two values is, in fact, 1·62, and therefore the evidence in this case appears to weigh heavily on the side of combination.

Experimental

In order that dilatometry could be used to follow polymerization reactions to high conversions Schulz and Harborth [22] evolved a dilatometer in which the recording liquid was mercury. This apparatus was adapted to give an instrument of very high sensitivity. The construction is shown in Fig. 1. The whole of the dilatometer is constructed of soda glass. The main reaction bulb A has a capacity of about 60 ml. and is connected to the capillary C whose internal diameter is 0·2 mm. The side tube D leads to a mercury reservoir, this being connected to the main apparatus by means of a length of pressure tube controlled by a pinch cock as close to D as possible. This arrangement proved to be very satisfactory and eliminated any manipulation of taps, etc., under the water of the thermostat. The dilatometer is connected to the high vacuum line at B and after being thoroughly evacuated mercury is allowed to enter the main bulb until it stands at a level of about 1 cm. in A. A measured volume of the monomer which has been thoroughly outgassed is poured from a second vessel to the dilatometer the operation being carried out *in vacuo*, and then the instrument is sealed off. After standing in a thermostat until the temperature of the bath is attained mercury is allowed to enter the dilatometer until the monomer is squeezed against the seal, and the mercury stands at a convenient height in the capillary. The tap E is then opened.

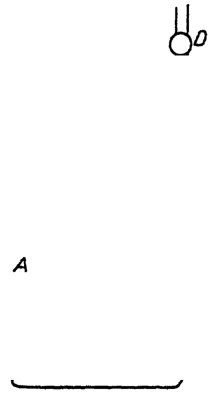

FIG. 1.—The dilatometer.

Commercial monomer was freed from stabilizer by washing with caustic soda and, after drying, was distilled at 18 mm. pressure in an atmosphere of CO_2, the fraction boiling at 40·2° C being collected, $n_D^{24} = 1{\cdot}54453$. This monomer was allowed to polymerize to about 4 % and redistilled before use.

The source of illumination was a 125 watt G.E.C. Osira lamp fed from a constant voltage transformer. The lamp was fitted with a soft glass envelope and the light passed through a further 6 mm. of soft glass in order to reach the reaction vessel. The total glass thickness in the light path was of the order of 8 mm. Tests showed that the light transmitted had a wavelength in excess of 3500 Å, at which wavelengths the absorption by styrene monomer is very little, so that the concentration of the radicals within the reacting system must be uniform. Such a condition is essential since it is tacitly assumed in the analysis that the free radicals active in propagating the chains are uniformly distributed throughout the volume.

---

[18] Bamford, *Faraday Soc. Discussion*, 1947, **2**, 401.
[19] Norrish, *Trans. Faraday Soc.*, 1939, **35**, 897.
[20] Melville and Gee, *ibid.*, 1944, **40**, 241.
[21] Bartlett and Kwart (unpublished work).
[22] Schulz and Harborth, *Angew. Chem.*, 1947, **59**, 90.

The following Table, constructed on the basis of data supplied by G.E.C. Research Laboratories, shows the energy output of the Osira lamp and the effective transmission through 8 mm. of soft glass. From this Table it is clear that there is little light of less than 3500 A being absorbed by the styrene.

TABLE I.—ENERGY OUTPUT OF G.E.C. OSIRA LAMP

Wavelength Å	Lamp Output W	Transmission through 8 mm. Glass (%)	Energy Transmitted through Glass W
5780	4·7	90	4·2
5460	4·1	90	3·7
4360	3·1	89	2·8
4060	1·9	88	1·7
3660	6·3	20	5·0
3340	0·5	0	0·1
3130	4·4	0	0
3020	1·9	0	0
2970	1·3	—	0
% radiation >3500	71·4	—	99·4

For measurement of the dark rate, i.e. the purely thermal polymerization, the reaction chamber was covered by means of a blackened glass tube in order to avoid any possible photoreaction initiated by stray light. This tube could be removed rapidly in order to allow measurement of the photoreaction.

Density of Polymer and Monomer.—The density of the monomer was measured at a number of temperatures using a pipette type pyknometer. At temperatures in excess of 30° C a small known weight of *p*-benzoquinone was

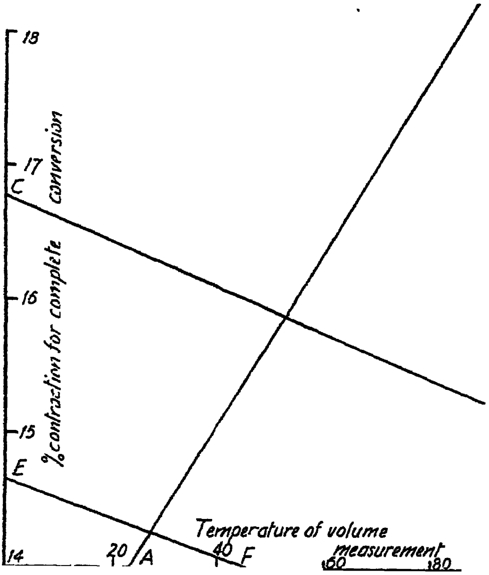

FIG. 2.—Relationship between contraction for 100 % polymerization and temperature at which volume of monomer is measured.

added to the monomer to prevent the formation of polymer during the determination. The results quoted in Table II are corrected to allow for this inhibitor. It will be seen that the results are in good agreement with those published by the Dow Chemical Company.[23] The density of polystyrene has already been reported in the literature [24] and the data have been used here. On the basis of these, Fig. 1 was constructed.

TABLE II.—DENSITY OF STYRENE MONOMER

Temperature °C	Density of Styrene	
	This Work	Dow
0	—	0·9238
10	—	0·9150
20	—	0·9063
25	0·9032	0·9019
30	0·8988	0·8975
35	0·8935	—
40	0·8880	0·8887
45	0·8837	—
50	0·8795	0·8800
55	0·8752	—

It is now possible to estimate the probable accuracy of the dilatometer in estimating the conversion and a volume of 40 ml. is used, then in a capillary of 0·2 mm. 100 % conversion corresponds to a movement of 1·78 × 10^4 cm. in the meniscus. Since the cathetometer readings were correct to 0·02 mm. this corresponds to a conversion of 10^{-5} % or 1 part in 10^7.

Results

Fig. 3 shows a typical run with styrene carried out at 25° C. The course of the reaction even during the non-stationary period has been delineated with some accuracy as can be seen from the curve. The predicted intercept on the axis has been obtained and shows that the lifetime of the active centres is 100 sec. Since it is not possible to carry out the extrapolation with the maximum accuracy the straight line giving the best fit was calculated by the method of least squares.

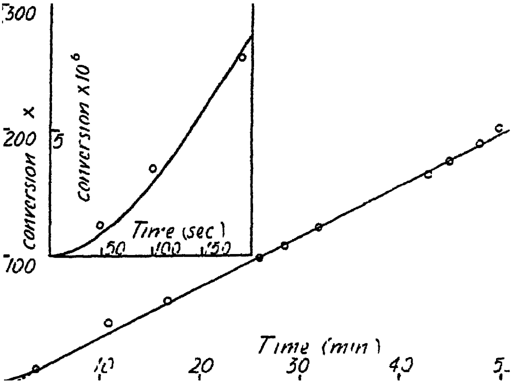

FIG. 3.—Course of reaction for photopolymerization of styrene.

---

[23] *Dow Chemical Company Technical Monograph*, 1946.

[24] Patnode and Scheiber, *J. Amer. Chem. Soc.*, 1946, 61, 3449.

Table III compares the experimental readings with those which are given by the best calculated curve and it will be seen that the agreement is exceptionally good. This, besides giving a good agreement with the theory, shows that the reaction was perfectly isothermal since otherwise much greater fluctuations would have been expected due to the rather large volume of liquid involved.

TABLE III.—CALCULATED AND EXPERIMENTAL RESULTS FOR THE POLYMERIZATION OF STYRENE AT 25° C

Time sec.	Conversion × 10^6		Error %
	Measured	Calculated	
1560	98	98·4	− 0·41
1710	108	108·4	− 0·37
1920	122	122·4	− 0·32
2580	165	165·9	− 0·54
2700	174	173·9	+ 0·06
2910	188	187·9	+ 0·05
3000	200	193·9	+ 3·05
3120	204	204·4	− 0·19
3360	218	217·4	+ 0·27

Runs were carried out for several light intensities and the life-time of the active species determined for each case. The reciprocal of the life-time is plotted against the rate of polymerization in Fig. 4, the slope of the line giving the value of k_t/k_p as $1{\cdot}51 \times 10^5$.

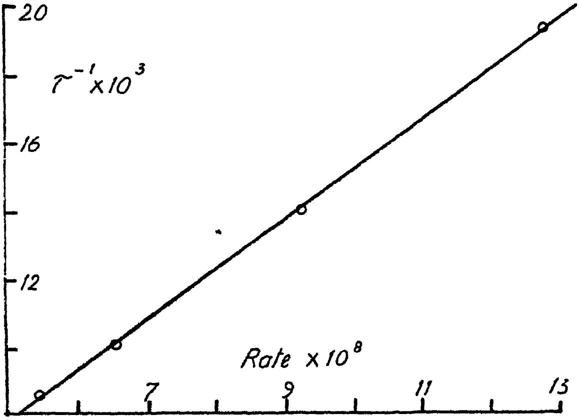

FIG. 4.—Reciprocal life-time as a function of rate of conversion.

The method of obtaining the energy of activation for the two steps is simple. The change in the ratio k_t/k_p gives, in effect, the difference in the energies of activation for the two steps, while the overall energy of activation for the photochemical reaction gives the value of $E_p - \frac{1}{2}E_t$, where E_p and E_t are the energies of activation for the propagation and termination reactions. This was found by direct measurement to be 5·30 kcal./mole. The temperature dependence of k_p/k_t reveals that the difference in the energies of activation is 4·30 kcal./mole, so that the energies for the individual parts of the reaction can be computed, and hence the frequency factors determined.

The investigation of the variation of the degree of polymerization with catalyst concentration is due to Melville and Valentine [25] and gives the value of k_t/k_p^2 as $3{\cdot}91 \times 10^3$, so that it is possible to deduce the individual values of the velocity coefficients at the temperatures used. The intercept obtained in these experiments was 3·19 × 10⁻⁵ so that transfer must have taken place and the relevant coefficient can be found. These results are brought together in Table IV, along with the calculated value of the rate constant for the purely thermal polymerization rate, assuming that the initiation step involves the combination of two styrene molecules to give a free diradical, viz. :

---

[25] Melville and Valentine, *Trans. Faraday Soc.* (in press).

$$2\phi\,.\,CH{=}CH_2 = \phi\,.\,\dot{C}H\,.\,CH_2\,.\,CH_2\,.\,\dot{C}H\,.\,\phi \qquad (\phi = C_6H_5).$$

The energy of activation and frequency factor for the transfer reaction has been deduced from the value of the degree of polymerization of thermally polymerized styrene at 100° C. This assumes that

$$\bar{P}^{-1} = k_f/k_p - k_i^{\frac{1}{2}}k_t^{\frac{1}{2}}/k_p$$

and since all the constants in the last term can be computed it follows that k_f can be found.

TABLE IV.—Rate Constants for Polymerization of Styrene

Temp. °C	k_i	k_p	k_t	k_f
		l. mole⁻¹ sec.⁻¹		
15	$1{\cdot}48 \times 10^{-16}$	29·2	$5{\cdot}55 \times 10^{6}$	$(5{\cdot}70 \times 10^{-4})$
25	$1{\cdot}34 \times 10^{-15}$	39·5	$5{\cdot}96 \times 10^{6}$	$1{\cdot}26 \times 10^{-3}$

Frequency Factors		Energies of Activation (kcal./mole)	
A_i	$4{\cdot}15 \times 10^{11}$	E_i	36·4
A_p	$1{\cdot}44 \times 10^{6}$	E_p	6·3
A_t	$1{\cdot}43 \times 10^{8}$	E_t	1·9
A_f	$4{\cdot}08 \times 10^{7}$	E_f	14·4

Since the most essential part of this method is the extrapolation of the linear portion of the conversion-time curve, it is necessary to estimate with what degree of accuracy the measurements can be made. In their investigation of the polymerization of methyl methacrylate in a dilatometer of the same type Schulz and Harborth found that under equilibrium conditions the temperature within the reaction vessel exceeded that of the thermostat bath by 0·1° C for a rate of reaction of 10 % per hour. Using these figures as a basis for calculation it is evident from the extremely low rate of polymerization used in these experiments (of the order of 2 × 10⁻² % per hour) the temperature elevation will be of the order of 2 × 10⁻⁴ °C. Although this is in fact less than the expected tolerance of the thermostat it is of interest to see to what extent such an increase in temperature will affect the results. The elevation will introduce an error of the order of 0·25 mm. in the readings which would make the life-time subject to an error of the order of 20 % so that it can be claimed that the ultimate determination of the rate constants are probably correct to within a factor of 2. A method has been devised to eliminate the temperature effect and work is at present proceeding along these lines.

Discussion

The results of Table IV are naturally subject to an uncertainty factor of 2 in the absolute values of the rate constants, arising from the assumption that the termination step is wholly disproportionation. This represents the maximum uncertainty since there is no valid reason for supposing that both of the possible termination steps can occur simultaneously. Some of the results which have already been published on this work are given in Tables V and VI.

Bamford and Dewar's results were obtained by using the viscosity method which they evolved for the determination of the rate constants of polymerization reactions, assuming that the constants for the Houwink

TABLE V.—COMPARISON OF RATE CONSTANTS FOR STYRENE POLYMERIZATION

Temp.	k_i	k_p	k_t	k_f	Source
25	$1{\cdot}34 \times 10^{-15}$	39·5	$5{\cdot}96 \times 10^{6}$	$1{\cdot}26 \times 10^{-3}$	This work
25	$1{\cdot}32 \times 10^{-15}$	18·7	$2{\cdot}79 \times 10^{6}$	$0{\cdot}67 \times 10^{-3}$	(10)
30	—	52·0	$1{\cdot}02 \times 10^{7}$	$1{\cdot}66 \times 10^{-3}$	(25)
50	—	39·0	3×10^{8} *	—	(26)

* Temperature 60°.

TABLE VI.—FREQUENCY FACTORS AND ENERGIES OF ACTIVATION FOR STYRENE POLYMERIZATION

A_i	$4{\cdot}15 \times 10^{11}$	$1{\cdot}23 \times 10^{12}$	—	—
A_p	$1{\cdot}44 \times 10^{6}$	$1{\cdot}02 \times 10^{6}$	$3{\cdot}5 \times 10^{10}$	$1{\cdot}20 \times 10^{8}$
A_t	$1{\cdot}48 \times 10^{8}$	$3{\cdot}07 \times 10^{8}$	—	$1{\cdot}20 \times 10^{10}$
A_f	$4{\cdot}08 \times 10^{7}$	$1{\cdot}50 \times 10^{7}$	—	—
E_i	36·4	37·0	—	—
E_p	6·3	6·5	11·7	9·0
E_t	1·9	2·8	—	3·0
E_f	14·4	14·2	—	—
Source	This work	(10)	(26)	(27)

equation were $\alpha = 0{\cdot}67$ and $K = 4{\cdot}57 \times 10^{-3}$. These values are somewhat at variance with those quoted by Mayo and Gregg [28] which were determined by the comparison of viscosity and osmotic molecular weights. Substituting the values of the latter workers would have the effect of slightly increasing the values in Table V, but even without this alteration the agreement between the two series of results is sufficiently good considering the very great difference in the methods of determination. Melville and Valentine [25] made use of the rotating sector technique with benzoyl peroxide acting as a sensitizer for the polymerization. The agreement between the results of this paper and those obtained by the more usual methods is exceptionally good and when it is borne in mind that the actual computation involves the determination of $k_i^{\frac{1}{2}}$ the discrepancy in the determination of this quantity is certainly not worse than a factor of 1·5. Smith [26] has evaluated the propagation constant for the emulsion reaction on the basis of a theory of emulsion polymerization due to Smith and Ewart.[29] In view of the great difference in conditions between the bulk and emulsion polymerization reactions any comparison of the results at this stage is probably without significance.

The author would like to record his thanks to Prof. H. W. Melville, F.R.S., for his continued interest and helpful advice during the prosecution of this work, and also to D.S.I.R. for a Senior Award (1947-48). The author also owes a debt of gratitude to Prof. P. D. Bartlett of Harvard University and Dr. M. S. Matheson of U.S. Rubber Company for granting permission for the use of results which have not yet been published.

Chemistry Department,
The University,
Edgbaston,
Birmingham, 15.

---

[26] Smith, *J. Amer. Chem. Soc.*, 1948, **70**, 3695.
[27] Matheson (unpublished results).
[28] Gregg and Mayo, *Faraday Soc. Discussion*, 1947, **2**, 329.
[29] Smith and Ewart, *J. Chem. Physics*, 1948, **16**, 592.

THE SWELLING OF CROSS-LINKED AMORPHOUS POLYMERS UNDER STRAIN

By L. R. G. Treloar

Received 11*th April,* 1950

The equilibrium swelling of vulcanized natural rubber in benzene and heptane was investigated experimentally as a function of the state of strain. Three types of strain were examined, i.e. simple elongation, 2-dimensional extension and uni-directional compression. The swelling ratios were determined either from measurements of linear dimensions, or by weighing, precautions being taken to ensure uniformity of the strain over the measured region. Measurements of swelling ratios were reproducible to about 1 %, and the swelling process was completely reversible (with respect to strain variations). Changes in swelling ratios of up to 50 % were observed, the swelling increasing under tensile stresses and falling under compressive stresses. The results were accurately accounted for by the author's extension of the Flory-Rebner statistical theory, using two independent parameters—one the μ-value in the Flory-Huggins equation for the free energy of mixing, which was obtained from vapour pressure data, and the other, the degree of cross-linking which was determined from the swelling of the unstrained rubber. It is concluded that for good swelling agents this theory is applicable to a homogeneous strain of the most general type.

That the equilibrium swelling of a cross-linked amorphous polymer in a suitable low-molecular liquid should depend on the strain to which it is subjected was shown theoretically by Flory and Rehner,[1] who also confirmed their result experimentally for butyl rubber under tension. Further confirmation was obtained by Gee [2] for natural rubber in good swelling agents (e.g. hydrocarbons), but with relatively poor swelling agents (e.g. esters) the agreement with the theory was only qualitative.

The theory was further developed by the author [3] to cover the more general case of a homogeneous strain of any type, and equations were derived for a number of particular types of strain, including simple elongation, two-dimensional extension (with two equal stretches) and uni-directional compression. It is the purpose of this paper to examine the swelling of vulcanized natural rubber under these three types of strain, and thus to provide a test of the more general theory. Two liquids, both good swelling agents, were used, i.e. benzene and heptane.

The Theoretical Relations between Swelling and Strain.—The theoretical derivation of the equilibrium degree of swelling makes use of quantitative expressions, derived by statistical methods, for the free energy of dilution of the polymer chains by the low-molecular liquid (A_{om}) and for the free energy associated with the elastic network of long-chain molecules (A_e). The former is given by the well-known Flory-Huggins equation [4, 5] which may be written in the approximate form (valid for $v_r > 0{\cdot}1$)

$$A_{om} = RT[\ln(1 - v_r) + v_r + \mu v_r^2], \quad . \quad . \quad . \quad (1)$$

where v_r is the volume fraction of polymer in the swollen gel, R the gas constant per mole, and T the absolute temperature, and μ a parameter which is specific to the particular polymer-solvent combination. The elastic network free energy is given by the statistical theory of rubber elasticity[6] as

---

[1] Flory and Rehner, *J. Chem. Physics*, 1944, **12**, 412.

[2] Gee, *Trans. Faraday Soc.*, 1946, **42**, 33.

[3] Treloar, *Proc. Roy. Soc. A*, 1950, **200**, 176.

[4] Flory, *J. Chem. Physics*, 1942, **10**, 51.

[5] Huggins, *J. Amer. Chem. Soc.*, 1942, **64**, 1712 ; *Ann. N.Y. Acad. Sci.*, 1942, **43**, 1.

$$A_e = \frac{\rho RT}{M_c}(l_1^2 + l_2^2 + l_3^2 - 3), \quad . \quad . \quad . \quad (2)$$

where l_1, l_2 and l_3 are the three principal extension ratios, referred to the unstrained unswollen dimensions, ρ is the density of the unswollen polymer, and M_c the molecular weight between successive points of cross-linkage (chain molecular weight). Using these expressions the relations given below are obtained for the swelling equilibrium under particular types of strain.

A modified formula for the entropy associated with the network expansion has recently been derived by Flory.[6a] This yields a slightly higher dependence of equilibrium swelling on strain, the difference amounting to about 10 % in the slope of the curves over the range covered by the present experiments. However, since the question of the relative merits of this and of other methods for the calculation of the entropy of mixing and of network expansion is still open to discussion, it was felt that it would not be appropriate, in the present context, to depart from the more usual formulae.

Simple Elongation (or Uni-directional Compression).—If l_1 is the extension (or compression) ratio, referred to the unswollen dimensions, and v_r is the volume fraction of polymer at equilibrium swelling, then[3]

$$\ln(1 - v_r) + v_r + \mu v_r^2 = -\frac{\rho V_0}{M_c}\cdot\frac{1}{l_1} \quad . \quad . \quad . \quad (3)$$

where V_0 is the molar volume of the solvent.

Two-dimensional Extension.—This is defined as a state in which tensile stresses produce equal strains in the directions l_2 and l_3, while the stress in the direction l_1 is zero. The condition for equilibrium is[3]

$$\ln(1 - v_r) + v_r + \mu v_r^2 = -\frac{\rho V_0}{M_c}\cdot\frac{1}{v_r l_2^4}. \quad . \quad . \quad (4)$$

Free Swelling.—Since v_r is the volume fraction of rubber in the mixture, it follows that $1/v_r$ is the volume in the swollen state corresponding to unit volume of the dry rubber. For unstrained swelling we have, therefore

$$l_1 = l_2 = l_3 = 1/v_r^{\frac{1}{3}}.$$

If in eqn. (3) $l_1 > 1/v_r^{\frac{1}{3}}$ the stress is tensile, while if $l_1 < 1/v_r^{\frac{1}{3}}$ it is compressive. The condition for free swelling may therefore be obtained by putting $l_1 = 1/v_r^{\frac{1}{3}}$ in eqn. (3), giving

$$\ln(1 - v_r) + v_r + \mu v_r^2 = -\frac{\rho V_0}{M_c}\cdot v_r^{\frac{1}{3}}. \quad . \quad . \quad . \quad (5)$$

A considerable amount of experimental evidence, which will not be reviewed here, has been adduced in support of the theoretical expressions (1) and (2) upon which the theory of the swelling equilibrium is based. In connection with (1) reference may be made to the work of Gee and Treloar[7] and of Gee and Orr,[8] which has been fully discussed,[9] while the elastic network formula (2) has been substantiated experimentally by the author.[10] More direct evidence relating to the swelling behaviour in the absence of strain, and the applicability of eqn. (5), has been provided by Flory,[11] Gee,[2] and Flory, Rabjohn and Shaffer.[12]

---

[6] Treloar, *Trans. Faraday Soc.*, 1943, **39**, 241.

[6a] Flory, *J. Chem. Physics*, 1950, **18**, 108.

[7] Gee and Treloar, *ibid.*, 1042, **38**, 147.

[8] Gee and Orr, *ibid.*, 1946, **42**, 507.

[9] Gee, *J. Chem. Soc.*, 1947, 280.

[10] Treloar, *Proc. Physic. Soc.*, 1948, **60**, 135.

[11] Flory, *Ind. Eng. Chem.*, 1946, **38**, 417.

[12] Flory, Rabjohn and Shaffer, *J. Polymer Sci.*, 1949, **4**, 225.

Experimental

The theoretical equations (3), (4) and (5) contain two adjustable parameters, μ and M_c, the derivation of which must first be considered. In this connection it is to be noted that while the value of μ depends on the solvent used, that of M_c is determined only by the rubber (i.e. for a given state of vulcanization). Moreover, if either μ or M_c is known, the other may be determined from a single measurement of the unstrained swelling equilibrium (eqn. (5)). The following procedure was therefore adopted.

The value of μ for rubber and benzene has been determined directly from vapour-pressure measurements,[9] and was taken as 0·41. From this, the M_c value for a particular sample of rubber swollen to equilibrium in benzene was calculated using eqn. (5). Another sample cut from the same sheet and having therefore the same M_c value, was swollen to equilibrium in heptane. From eqn. (5) the value of μ for heptane was thus found to be 0·42. This value was used in all subsequent experiments with heptane.

It should be noted that the values of μ and M_c were fixed either from vapour-pressure data or from the swelling equilibrium in the unstrained state. Their choice was thus entirely independent of the effect under investigation, i.e. the effect of strain on the swelling equilibrium. Once these two parameters are chosen, however, the theoretical formulae (3), (4) and (5) define unique relations between the swelling and the applied strain.

It may also be pointed out that the effect of strain is not sensitive to small variations in μ and M_c. For example, in a two-dimensional extension in heptane, a 10 % reduction in μ (with a corresponding reduction in M_c to fit the unstrained swelling equilibrium) was calculated to increase the rate of change of swelling with strain l_2 by only 5 %.

Of the three types of strain chosen for the present experiments, the most serious difficulties were encountered with the two-dimensional extension. This type of strain will therefore be discussed first.

Two-dimensional Extension.—The stretching in two dimensions of a sheet of rubber, weakened by a high degree of swelling, in such a way that both the swollen volume and the degree of strain could be measured, presented a number of difficulties. After numerous ineffective trials the following method was found to give a reasonably large strain before breaking occurred. The rubber sample was moulded in the form of a disc, as shown in Fig. 1, with a central portion 1 mm. thick and an outer region 2 mm. thick. The swollen rubber R (Fig. 2*a* and 2*b*) was gripped by means of eight clamps C having a rounded profile as in Fig. 2*b*, disposed around the circumference. The tightness of clamping was controlled by means of spacing washers of suitable thickness. (This was very critical: if clamped too tightly the rubber broke prematurely; if too loosely, it tended to slip out.) The mechanism for stretching the rubber consisted of an outer ring O which could be rotated with respect to the metal disc D by means of the ratchet mechanism M (details not shown).

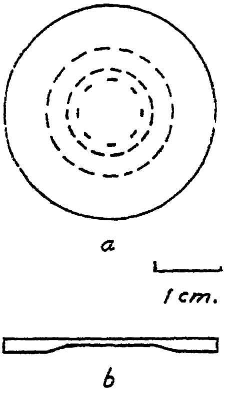

FIG. 1.—Rubber sample for 2-dimensional extension. (*a*) Plan; (*b*) Section.

The clamps were attached to points on the outer ring by means of stranded steel wires passing over eight pulleys P mounted on the inner disc; rotation of the outer ring in the direction of the arrow thus imparted an equal radial motion to each of the clamps. Means were provided for releasing the ratchet when it was desired to reduce the strain.

The swelling ratio was determined from measurements of the dimensions of the test piece in the strained swollen state. For the measurement of the thickness, the metal disc A (Fig. 2*b*) of 0·5 in. diam. was arranged so as to make a very light contact on the under surface of the strained sheet. A dial gauge, accurately mounted on the outer ring O by a reproducible 3-point support, was then brought down on to the upper surface, the difference of readings with and without the rubber in position giving the required thickness.

The dimensions in the plane of the sheet were obtained from measurements with a travelling microscope on references lines L marked on the sheet as shown in Fig. 2*a*. Some difficulty was experienced in obtaining a marking ink which would resist the solvent; the method adopted was to apply a solution of lead acetate in pyridine by means of a pen, and to develop this, before it had dried, in H_2S, thus producing insoluble lead sulphide.*

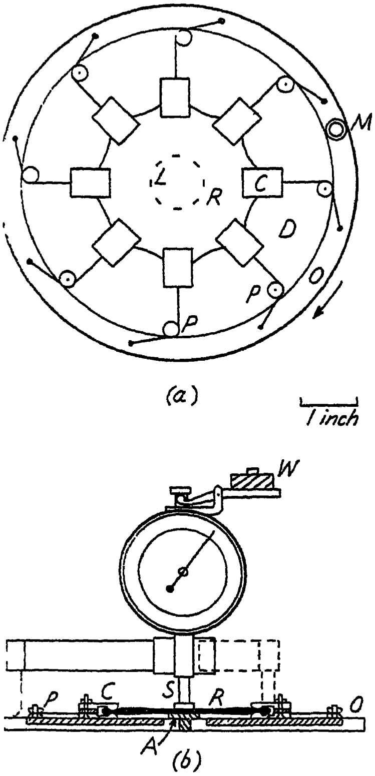

FIG. 2.—The stretching mechanism. (*a*) Plan; (*b*) Sectional elevation, showing gauge in position.

Accuracy of Measurement.—The least accurate dimensional measurement was the thickness measurement, and the reliability of this was the controlling factor in the accuracy with which the swelling ratio could be determined. Special attention was therefore given to possible errors in this measurement. The dial gauge itself was graduated to 0·01 mm. and readings could be estimated to 0·001 mm. To reduce the effect of compression of the rubber by the foot of the gauge, the spring which provided most of this pressure was removed. The residual pressure, due to the weight of the centre spindle S (Fig. 2*b*) and the hairspring, was partly counterbalanced by a weight W of 17 g. applied to the lever arm operating the gauge. The final mean pressure thus obtained (as measured by means of a balance) was 8 g.; this could not be further reduced because of the uncertain friction in the mechanism. A pressure of 8 g., corresponding to a stress of 12 g. cm.$^{-2}$, was found experimentally, in a typical strained swollen sheet, to lead to an error of 0·005 mm. in 1·4 mm. or 0·36 % in the thickness measurement, which was sufficiently small to be neglected. The overall accuracy in the measurement of the swelling ratio was probably rather better than 1 %.

Materials.—The rubber used in all these experiments was compounded according to the following formula:

Smoked sheet	100 parts by weight ;	M.B.T.S.	1 part by weight ;
Sulphur	2 ,, ,,	Stearic acid	0·5 ,, ,,
Zinc oxide	2 ,, ,,	Nonox S	0·5 ,, ,,

Vulcanized 45 min. at 140° C.

The values of M_c for different samples ranged from 7740 to 8520.

The benzene was of A.R. grade, while the heptane was of a commercial grade, stated to contain less than 0·5 % aromatics.

Procedure.—All the experiments were carried out with the apparatus immersed in solvent and placed in a water thermostat at 20° C. After an initial swelling (1-3 days), giving the equilibrium in the unstrained state, the sample was clamped and stretched, with periodical measurement of dimensions, for a sufficient time (generally not less than 5 hr.) for the attainment of equilibrium. From the final dimensions both the equilibrium swelling ratio and the stretch ratio in the sheet l_2 were calculated. The process was then repeated with increasing strains. One point was included, however, in which the equilibrium was approached from a higher value of strain in order to make sure that the points obtained were truly reversible. The rubber was then released, and the dimensions and swelling equilibrium in the unstrained state again measured;

---

* This technique was suggested and tried out by Dr. C. G. Moore, of the British Rubber Producers' Research Association, to whom my thanks are due.

these were very close to the original readings. The whole set of readings required 2 or 3 days for its completion. Finally the sample was dried and again measured.

Two minor corrections were introduced. Firstly, there was a loss of volume of about 2 % on re-drying, due to the removal of soluble ingredients. The swelling ratio was referred to the final, and not to the original volume of the dry rubber. Secondly, there was evidence of slight anisotropy in the original sample, since on swelling the thickness dimension increased a little more (1 or 2 %) than the lateral dimensions. Assuming that the swollen state most nearly represented the isotropic condition, the dimensions were corrected to take account of these small changes.

Typical results for both benzene and heptane are shown in Fig. 3. This gives the swelling ratio, i.e. the ratio of the volume of the swollen gel to the volume of the dry rubber, or $1/v_r$, as a function of the extension ratio in the plane of the sheet, referred to the unstrained *dry* rubber.

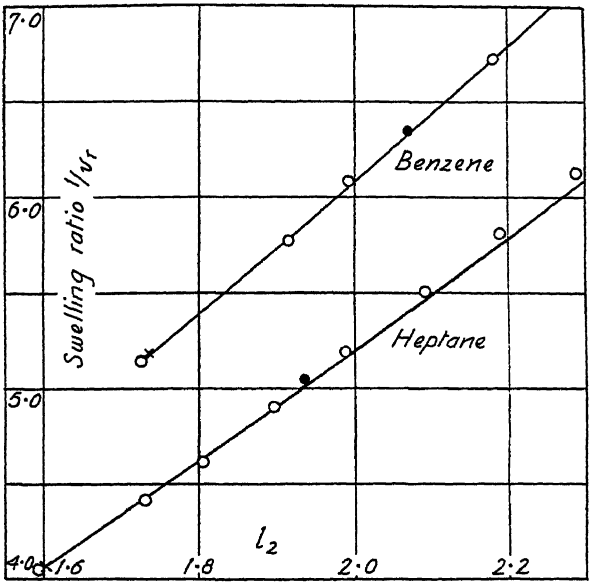

FIG. 3.—2-Dimensional extension. Swelling ratio as function of extended dimension l_2 referred to unstrained, unswollen state. ○ Strain increasing. ● Strain decreasing. × Final state on removal of stress. Curves theoretical.

Simple Elongation.—The technique of measurement of simple elongation was similar to that employed in the two-dimensional extension, except that the stretching device was simplified. The sample was in the form of a parallel-sided strip of approximate length 30 mm., width 7 mm. and thickness 1 mm. held in clamps having the form shown in Fig. 2*b*. The length measurement was made on a central region (12 mm. in length before swelling) marked out by two reference lines equidistant from the clamps. Both width and thickness were measured in the strained swollen state. (The latter was not essential, but comparison of the dimensional changes in these two directions provided a useful check on the general accuracy.)

The procedure was in all respects similar to that described above, except that a shorter time (3 hr.) was needed for the establishment of equilibrium. Corrections were applied as before for the slight anisotropy of the sheet, and for the removal of solids by the solvent. The results are reproduced in Fig. 4. Again, the agreement with the theory is very close.

Uni-directional Compression.—This proved to be the least accurate of the three measurements for two reasons. Firstly, the swelling ratios were determined by removal of the specimen from the solvent, superficially drying and weighing—a process not susceptible to the highest accuracy. Secondly, the samples used, being in the form of cylinders 1 cm. high and 1 cm. diam., required about 3 days to reach equilibrium, so that a total time of 2 weeks or more was required for a set of data. During this time there was a slow drift in the swelling ratio, which led to an appreciable uncertainty, particularly in benzene. This is discussed below.

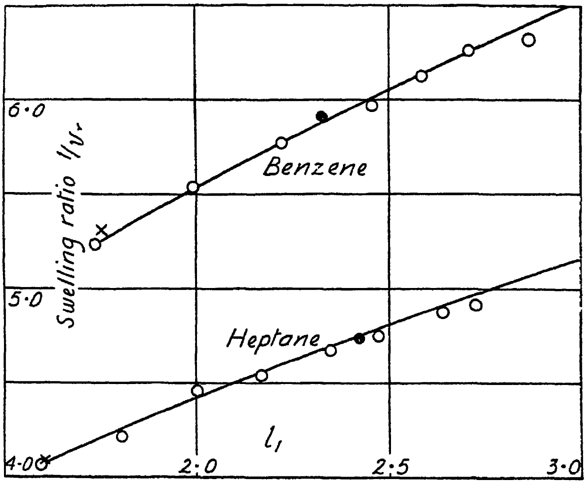

FIG. 4.—Simple elongation. Swelling ratio as function of extended dimension l_1 referred to unstrained, unswollen state. ○ Strain increasing. ● Strain decreasing. × Final state on removal of stress. Curves theoretical.

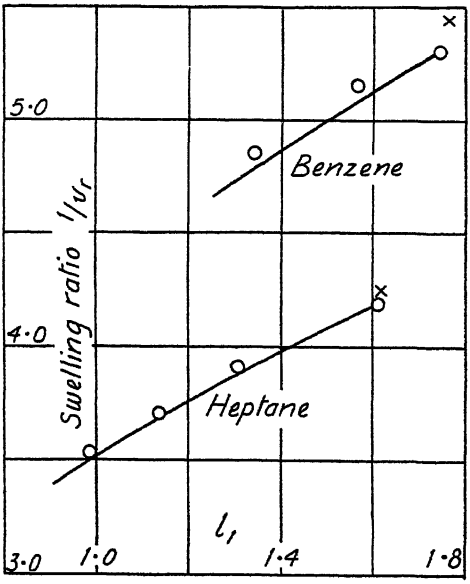

FIG. 5.—Compression. Swelling ratio as function of compressed dimension l_1 referred to unstrained, unswollen state. × Final state on removal of stress. Curves theoretical.

Apart from these difficulties, the application of a perfectly homogeneous compressive strain itself presents a problem, since on account of end friction a cylinder compressed axially between parallel plates tends to deform to a non-uniform barrel-like shape. This was largely avoided by the following device. The cylinder, after preliminary swelling in the unstrained state, was compressed while still immersed in solvent between parallel plates whose distance of separation could be adjusted by means of screws. The degree of compression was carried somewhat beyond that ultimately required, then slowly reduced to the final value. During the latter operation the "barrelling" was greatly reduced, and this tendency was enhanced by the subsequent outward diffusion of solvent due to the application of the compressive stress. Indeed, it was quite possible in this way to produce an opposite state in which the middle diameter was smaller than the end diameter. With a little adjustment, the conditions required for the attainment of a substantially uniform cross-section could thus be achieved.

The points on each of the curves of Fig. 5 were obtained with a single sample subjected to increasing compressions and finally returned to the unstrained state. After subsequent drying the weight and density of the sample were determined and these, in conjunction with the measured densities of the solvents, were used for the calculation of the swelling ratios. Figures are given in Table I for the change in the unstrained swelling ratio between the initial and final states, together with corresponding data for control samples not subjected to compression.

TABLE I.—CHANGES IN SWELLING RATIO WITH TIME

	BENZENE		
Compressed sample		*Control*	
Before straining, swollen 5 days .	$5{\cdot}30_4$	5 days . .	$5{\cdot}31_5$
Finally, total time 14 days .	$5{\cdot}44_2$	14 days . .	$5{\cdot}41_7$
Difference	2·6 %	Difference . .	1·9 %
	HEPTANE		
Before stretching, swollen 5 days	$4{\cdot}19_3$	5 days . .	$4{\cdot}02_7$
Finally, total time 31 days .	$4{\cdot}24_3$	26 days . .	$4{\cdot}06_4$
Difference	1·2 %	Difference . .	0·9 %

The difference between the increments of swelling for the strained and control samples is not significant. It is therefore reasonable to assume that the divergence between the experimental points and the theoretical curves of Fig. 5, which is relatively serious with benzene, may be attributed to this slow increase of swelling with time of immersion in the solvent, which occurs whether or not the rubber is under strain.

Conclusion.—It will be seen from Fig. 3, 4 and 5 that, for the liquids chosen in this investigation, the effect of strain on the swelling equilibrium is satisfactorily accounted for by the statistical theory, under the three entirely different types of strain examined. In view of the simplifying assumptions introduced into the model on which the statistical calculations are based, however, an exact agreement between theory and experiment is hardly to be expected, and the close agreement actually found (i.e. to within 5 % in the slopes of the swelling-strain curves) must be regarded as to some extent fortuitous. It is to be noted, for example, that in the study of the elastic properties of pure gum rubbers, significant departures from the theoretical form (2) for the network entropy have been observed.[10] With this reservation, however, the conclusion to be drawn from the present experiments is that the equations set out above provide a satisfactory quantitative interpretation of the dependence of the equilibrium swelling on a strain of the most general type.

The author desires to express his thanks to Dr. G. Gee for the provision of the rubber samples used in this work, and for a number of valuable discussions on the subject-matter of this paper.

The author is also indebted to the British Rayon Research Association for enabling the work, which was done in the Davy Faraday Laboratory of the Royal Institution, to be carried out.

The Royal Institution,
Davy Faraday Research Laboratory,
21 *Albemarle Street, W.*1.

THE PHYSICO-CHEMICAL PROPERTIES AND BEHAVIOUR OF THE NUCLEIC ACIDS

An informal discussion on this subject, arranged by the Colloid and Biophysics Committee of the Faraday Society and organized by Dr. J. A. V. Butler and Dr. D. O. Jordan, was held on 12th May, 1950, in the Institut Français du Royaume-Uni, Queensberry Place, London, by the kind permission of the Director, M. Jourdan. Two sessions were held: 10.30 a.m. to 12.30 p.m. and 2 p.m. to 5 p.m.; Prof. E. K. Rideal, F.R.S., was in the Chair during the morning session and Prof. R. Signer and Prof. V. Desreux during the afternoon. About 90 visitors and guests were present.

Short reports of all informal discussion meetings arranged by the Colloid and Biophysics Committee will in future be published in the *Transactions*. The following are abstracts of the papers which were read and discussed at the meeting held on 12th May, 1950.

Preparation and Physico-chemical Properties of Ribonucleic Acid from Different Sources. By V. DESREUX (*Liège*).

The ribonucleic acids which have been studied by several authors are heterogeneous and a complete purification is a difficult problem. Solubility curves demonstrate that the constant solubility sample of ribonucleic acid in one solvent is heterogeneous whereas in another solvent it probably forms a solid solution. It is impossible by means of solubility curves or by electrophoresis to distinguish ribonucleic acid prepared from yeast pancreas and that obtained from *E. coli*; the mobility also is practically the same. Both solubility and electrophoresis experiments show that the influence of the degradation products of ribonucleic acid on the solubility of these acids is great.

The diffusion constants of yeast D and *E. coli* ribonucleic acid are very similar (0·084 and 0·079 cm.^{2} day at 25° C), as are the sedimentation constants S and molecular weights (2·70 and 2·76 Svedberg units and 16,300 and 17,500 respectively). The acid obtained from the pancreas has, however, different values (D, 0·094; S, 2·15; m.wt., 11,500). The axial ratio of the acid is around 9·0

From the study of the electro-titration curves, it seems also that the pancreas acid is different from yeast and *E. coli* acid.[1]

Preparation and Properties of Desoxyribonucleic Acid (DNA) from Calf Thymus. By R. SIGNER and H. SCHWANDER (*Berne*).

Extremely high molecular weight DNA is obtained by (1) inhibiting nuclease activity, (2) repeated reprecipitation by dilution of 10 % NaCl solutions, (3) eliminating the protein by the Sevag method or the old Bang and Hamersten procedure, (4) drying from frozen state.[2]

All physical tests (viscosity,[2] sedimentation,[3] diffusion, double refraction of flow,[4] behaviour on addition of electrolytes) show that DNA so prepared behaves in dilute solutions as a polyvalent linear unbranched ion of molecular weight 1-2 × 10^6.

---

[1] Chantrenne, *Bull. Soc. chim. Belg.*, 1946, **55**, 5, 118; Ghuysen, Delcambe, Desreux, *Bull. Soc. chim. Belg.* (in press).

[2] Signer and Schwander, *Helv. chim. Acta*, 1949, **32**, 853; Vallet and Schwander, *ibid.*, 1949, **32**, 2508.

[3] Stern (in press).

[4] Schwander and Cerf, *Helv. chim. Acta*, 1949, **32**, 2356.

Sedimentation and Diffusion of Desoxyribose Nucleic Acid. By A. G. OGSTON (*Oxford*).

The deduction of the particle size and asymmetry, on the basis of published values of the sedimentation and diffusion constants,[5] is discussed, and values of the viscosity of solutions at low rate of shear are reported.

Molecular interaction makes it necessary to extrapolate the sedimentation and diffusion constants to zero concentration. The sedimentation constant S is satisfactorily extrapolated as 1 S against concentration, to give a limiting value of $13{\cdot}2 \quad 10^{-13}$. The extrapolation of the diffusion constant is performed with the aid of Flory's theory of the entropy of solutions of large particles, to give a value between $0{\cdot}55$ and $0{\cdot}7 \times 10^{-7}$. The particle weight then lies between $1{\cdot}0$ and $1{\cdot}3 \times 10^{-6}$ and the axial ratio of equivalent ellipsoids lies between 140 and 170. The last value agrees reasonably with the value of 190 obtained from the viscosity.

Some uncertainty about the extrapolated values remains. It is interesting that there is no large discrepancy between the results of sedimentation and diffusion and of viscosity, as there is for hyaluronic acid.

X-ray Studies on the Decomposition Products of the Nucleic Acids.* By S. FURBERG (*Oslo*).

Single crystal X-ray investigations have been carried out on some degradation products of yeast nucleic acid. The work on the pyrimidines[6, 7] has established that the six-membered ring of this molecule is flat while that on the purines[8] has established that the nine-membered ring is also flat. It was found that in a cytidine[9] the pyrimidine and ribose ring systems lay in planes approximately normal to each other. From preliminary X-ray investigations, this spatial relationship is suspected for the other nucleosides of yeast nucleic acid. An examination of cytidilic acid[10] suggests that the rings system have the same orientation with respect to one another and that the phosphoryl group is situated in the *trans* position to the ribose ring. From these findings two possible models of thymo nucleic acid have been built maintaining phospho-ester linkages. In one case the backbone of ribose rings and phosphate groups form a spiral enclosing the pyrimidines and purines; in the other the backbone is a zig-zag chain with the pyrimidines and purines pointing outwards. Both structures explain the strong 3·4 Å reflexion observed by Astbury[11] in fibrous sodium thymonucleate.

X-ray Diffraction Studies of Solutions of Desoxyribonucleic Acid (Na Salt). By D. P. RILEY AND G. OSTER (*London*).

X-ray photographs of nucleic acid solutions show three distinct regions of diffraction: 3 to 10 Å, 20 to 50 Å and 50 to 200 Å. The larger spacings vary as $1/\sqrt{c}$, where c is the volume concentration, which shows that the molecules are long cylinders which separate on dilution. The solutions or gels possess a pseudo-lattice structure in two dimensions and their paracrystalline nature, even under static conditions, is also demonstrated by their marked domain birefringence. An extrapolation to zero dilution gives a value of about 46 Å for the diameter of the cylindrical molecule in the dry state. The intensity and sharpness of the band of highest spacing is dependent on the source of the sample and on the method of preparation of a gel of given concentration. The intermediate spacing increases in the same way with dilution, but less markedly. This would suggest that the molecule possesses an internal structure on a moderately large scale which swells on addition of water. Extrapolation to zero dilution gives a value of about 12 Å for the dry repeat unit. The smaller scale structure (3 to 10 Å) remains essentially the same in all samples except for those thoroughly dried *in vacuo.*

---

[5] Cecil and Ogston, *J. Chem. Soc.*, 1948, 1382.

[6] Pitt, *Acta Cryst.*, 1948, **1**, 168.

[7] Clews and Cochran, *ibid.*, 1948, **1**, 4; 1949, **2**, 46.

[8] Broomhead, *ibid.*, 1948, **1**, 324.

[9] Furberg, *Acta Chem. Scand.* (in press).

[10] Furberg, (unpublished).

[11] Astbury, *Symp. Soc. Expt. Biology*, 1947, **1**, 66.

* Read by Dr. C. H. Carlisle.

Some Aspects on the Dielectric Properties of Desoxyribose Nucleic Acids. By G. JUNGER (*Stockholm*).

The dielectric dispersion of desoxyribose nucleic acid corresponds to a highly polar, rigid molecule rotating as a whole in an electric field.[12-14] The short relaxation times found (about 10^{-7} sec.) indicate orientation round the long axis of the molecule and are thus quite different from relaxation times obtained from hydrodynamic data [15] at orientation round a short axis.

In very dilute aqueous solutions (0·003-0·006 %) molecular weights of 600,000 and 200,000 are found for the specimens prepared according to Gulland *et al.*[16] and Hammarsten [17] respectively. The values are strongly dependent on the medium as electrolytes, etc., depolymerize easily. The depolymerization occurs with striking regularity and the same " specific " dipole moment (per average mononucleotide) is obtained independent of the molecular weight. In stronger solutions (0·05 % or stronger) the stability is greater but the products obtained after depolymerization are heterogeneous.

By precipitation of desoxyribose nucleic acid with ethanol in the presence of Mg ions very large artificial aggregates are obtained.

The Behaviour of Nucleic Acids as Polymeric Electrolytes. By D. O. JORDAN (*Nottingham*).

The nucleic acid polymer contains both strong and weak electrolytic groups and the presence of the former and ionization of the latter, effect the viscosity of its solutions and the shape of the titration curve. The viscosity of solutions of the sodium salt of desoxypentose nucleic acid shows structural character and has a value, at low pressures, which is very high.[18] The addition of sodium chloride reduces this high value considerably as has been shown to occur for simpler systems, e.g. polymethacrylic acid [19] and poly-*N*-*n*-butyl-4-vinyl pyridonium bromide.[20] The process is readily explained by the repulsion of the charged groups (PO^- at pH 7) maintaining a stretched polymer in aqueous solution. The addition of electrolyte reduces this repulsion permitting the molecule to coil, thereby giving a more symmetrical structure which accounts for the reduction in the viscosity, the structural character of the viscosity and the streaming birefringence.[18]

The analogy between nucleic acids and synthetic polymeric electrolytes cannot be carried too far since the number of gegenions absorbed

---

[12] Jungner, *Acta physiol. Scand.*, 1945, **10**, Supp. 32.

[13] Jungner, Jungner and Allgen, *Nature*, 1949, **163**, 849.

[14] Jungner, *Acta physiol. Scand.*, 1950, **20**, Supp. 69.

[15] Edsall, in Cohn and Edsall, *Proteins, Amino Acids and Peptides* (New York, 1943).

[16] Gulland, Jordan and Threlfall, *J. Chem. Soc.*, 1947, 1129.

[17] Hammarsten, *Biochem. Z.*, 1924, **144**, 383.

[18] Creeth, Gulland and Jordan, *J. Chem. Soc.*, 1947, 1141.

[19] Arnold and Overbeek, *Rec. trav. Chim.*, 1950, **69**, 192.

[20] Fuoss and Strauss, *J. Polymer Sci.*, 1948, **3**, 246, 602.

into the micelle must be large as indicated by the value of 550e for the charge per molecule in a solution of ionic strength 0·005 compared with the calculated value of 2664e for a molecule of molecular weight $8{\cdot}2 \times 10^5$. The presence of the gegenions in the micelle will reduce the number of effective ionized groups thereby decreasing the repulsion.

The dissociation constants are all found to be weaker when compared with the values for the monomer. Taking the —NH—CO— dissociations as an example, the back titration curve is typical of a weak polyacid. Calculation of the pK values at different degrees of ionization, however, although showing a decrease in acid strength as ionization increases, indicates that the initial limiting value at zero ionization is weaker than that of the nucleoside. This effect will be due to the presence of the PO^- groups. The case of the amino groups is more complicated, the field effect produced by ionization to $-NH_3^+$ and the effect of the PO^- groups acting in opposite senses.

The Anomalous Titration Curve of Deoxypentose Nucleic Acids. By D. J. Cosgrove and D. O. Jordan (*Nottingham*).

The acidic and basic groups of the sodium salt of deoxypentose nucleic acid of calf thymus prepared by various different methods, viz., those described by Gulland, Jordan and Threlfall,[21] Hammarsten [22] and by the authors, have been titrated electrometrically, employing hydrogen electrodes, and the data interpreted in terms of molecular and macromolecular structure. Addition of acid or alkali to a solution of the salt prepared by Gulland, Jordan and Threlfall [21] does not at first bring about the titration of groups in the pH range 5 to 11; the titration of groups is delayed until critical pH regions where the formation of ionized groups occurs rapidly. The back titration curves from pH 12 and 2·5 are more normal and show the presence of two —NH—CO— groups and three —NH_2 groups for each four atoms of phosphorus in the polynucleotide. The anomalous forward titration curves are explained by postulating the existence of hydrogen bonds between the —NH—CO— and —NH_2 groups of different purine and pyrimidine rings in the acids as initially prepared.

An anomalous titration curve was not previously obtained by titration of the material prepared by the Hammarsten method [22] but the authors have improved the Hammarsten technique so that the preparation titrates in a similar manner to that described by Gulland, Jordan and Taylor.[23]

Similar anomalous titration curves have been obtained for acids obtained from lamb thymus and herring sperm and it would appear that the anomalous titration curve is characteristic of all deoxypentose nucleic acids.

Alkali treatment of the acid obtained from calf thymus gives rise to a product with a titration curve resembling the back titration curve of the original substance. Heat treatment has a similar effect. Prolonged treatment with alkali produces a material of very low molecular weight which possesses rather more than two —NH—CO— groups for every four atoms of phosphorus.

The Electrometric Titration of Deoxypentose Nucleic Acids. By W. G. Overend and A. R. Peacocke (*Birmingham*).

Deoxypentose nucleic acids (DNA) have been isolated from calf thymus glands, soft herring roe, mouse sarcoma and wheat germ by methods involving saline extractions at pH 7. Several titrations at 25° of solutions of the first three DNA showed that there were, for every 4 g.-atoms of phosphorus, 3 groups with pK_a values between 2 and 7, and 2 with values between 7 and 12. The curves obtained on back titration with alkali from pH 2 and acid from pH 12 were never coincident (allowing for experimental error) either with the forward titration curve or with each other. The presence of 3 types of hydrogen bonds involving the titrating groups would explain this observation: (i) broken equally by acid at pH 2 or by alkali at pH 12; (ii) broken only by acid at pH 2; (iii) broken only by alkali at pH 12. Since previous investigators[24, 25] observed the existence of (i) only, different precipitation conditions and drying methods prior to titration, even in extractions at pH 7, may have a marked effect on the macromolecular structure of DNA.

---

[21] Gulland, Jordan and Threlfall, *J. Chem. Soc.*, 1947, 1129.

[22] Hammarsten, *Biochem. Z.*, 1924, 144, 383.

[23] Gulland, Jordan and Taylor, *J. Chem. Soc.*, 1947, 1131.

The Effect of Dialysis and Ultrasonic Irradiation on the Physical Properties of Deoxypentose Nucleic Acids. By W. G. Overend and A. R. Peacocke (*Birmingham*).

Dialysis caused no change in the number of titratable groups or in the pattern of the titration curves already described; the macromolecular structure, however, seemed to be more sensitive to acid and alkali. Ultrasonic irradiation of DNA resulted in a rapid fall in viscosity which was not regained on standing but continued to fall, though to a less extent than has been observed after X-irradiation of DNA.[26, 27] Irradiated solutions were of lower pH than those of the initial material. During irradiation no purine or pyrimidine bases were liberated and the product was still relatively insoluble in acid or ethanol. Extended irradiation resulted in small amounts of nitrogen (as ammonia) and acid-soluble organic bound phosphate being formed. The action of enzymes and titrations indicated that ultrasonic irradiation results initially in some general breakdown of hydrogen bonding in the DNA. Ultrasonic treatment to rupture the cells should be avoided in the isolation of DNA from micro-organisms since it also degrades the DNA.

Light Scattering Studies of Thymonucleic Acid. By G. Oster (*London*).

Light scattering measurements of diluted solutions of sodium thymonucleate with varying amounts of NaCl show that the three samples prepared by (i) Signer, (ii) Butler and Smith and (iii) commercial sample (B.D.H.) have weight average molecular weights (in millions) of (i) 3·23, (ii) 1·34 and (iii) 0·51 independent of salt concentrations up to 0·2 M. The particles are rods which repel one another by virtue of their ionic double layers. The rheological properties can be explained in terms of these results by analogy with those of other systems.[28]

Measurements of the angular scattering with incident and scattered light in polarizing conditions indicate that the particles are rods with strong negative birefringence and are not random chains. Viscosity measurements are in accord with light scattering results if the particle diameter is taken as being about 40 Å. Electron micrographs taken in collaboration with H. L. Nixon show that the particles are fibres with a diameter of about 50 Å.

The Degradation of Deoxyribonucleic Acid (DNA) by Chemical Agents and by Free Radicals. By J. A. V. Butler, B. E. Conway and K. A. Smith (*London*).

It was shown by Greenstein *et al.*[29] that DNA is degraded by X-rays, the action occurring (i) during the irradiation, (ii) continuing slowly for many hours after the irradiation. We have found that this "after-effect" does not occur in solutions irradiated in the absence of oxygen.

---

[24] Gulland, Jordan and Taylor, *J. Chem. Soc.*

[25] Cosgrove and Jordan, *ibid.*, 1949, 1413.

[26] Butler, Gilbert and Smith, *Nature*, 1950, **165**, 714.

[27] Taylor, Greenstein and Hollaender, *Cold Spring Harbor Symp. Quant. Biol.*, 1947, **12**, 237.

[28] Oster, *J. Gen. Physiol.*, 1950, **33**, 445.

[29] Taylor, Greenstein and Hollaender, *Cold Spring Harbor Symp. Quant. Biol.*, 1947, **12**, 237.

It is thus due to substances formed by the action of the primary radicals on oxygen. Since hydrogen peroxide cannot be detected in the solution, the after-effect is probably due to the formation of an unstable peroxide derivative of the nucleic acid. A similar degradation of the nucleic acid to that in (i) can be produced by free OH radicals formed by irradiation of hydrogen peroxide by u.-v. light and also by the Fe^{++}—H_2O_2 reaction.[30]

Similar changes are observed in the action of radiomimetic chemicals such as the sulphur and nitrogen " mustards ", which have been shown to produce mutations, chromosome abnormalities and in some cases are carcinogenic.[31] The nature of the degradation was discussed.

The Molecular Weights of Degraded Deoxyribonucleic Acids. By J. A. V. Butler, B. E. Conway and L. Gilbert (*London*).

Ultracentrifuge and diffusion studies have been made of the undegraded DNA and also of DNA degraded by X-rays and with the radiomimetic chemical HN2 (methyl-β-dichlorethylamine).[32] It is shown that the loss of the characteristic viscous behaviour and streaming birefringence is accompanied by a considerable reduction in the average molecular weight, which is of the order of 100,000. The products of these actions are, however, rather heterogeneous and include some rapidly diffusing material with quite low molecular weights. The degradation produced by these agents is not nearly so extensive as that caused by the action of deoxyribonuclease. Experiments have also been made on the chemical nature of the degraded products.

---

[30] Butler and Smith, *Nature*, 1950, **165**, 847.
[31] Butler, Gilbert and Smith, *ibid.*, 1950, **165**, 714.
[32] *J. Chem. Soc.* (in press).

REVIEWS OF BOOKS

Faraday's Discovery of Electro-Magnetic Induction: By Thomas Martin. (Edward Arnold & Co. Ltd., 1949.) Pp. 160. Price 9s.

This is a very readable account of one of the outstanding discoveries in " experimental philosophy ", namely Faraday's work on Electromagnetic Induction, which came to fruition in August 1831. The two varieties of the same fundamental principle gave to the world the essence of the transformer and of the dynamo. And all depended upon the observation of " make and break " by an exceptionally acute percipient. What is particularly refreshing is the way in which Mr. Martin has chosen his frame, to set off this classical landscape. We are told of holidays, of letters to friends, of " misunderstandings " and so on; in fact the common lot of many a leading research worker. Prizes of this magnitude—for there are several—do not drop into peoples' laps ; they follow long years of preparatory thought and practice. That Faraday was gifted to an unusual degree may be taken for granted, but his success is seen to be " inevitable ".

Characteristic too is his genius for finding the shortest way to the point. This appears from his sketches, many of which are reproduced, and add considerably to the interest of the whole theme.

Finally, Faraday did not hestitate to go outside his laboratory at the Royal Institution when there was something to be gained; attempts to study induction by the earth's magnetism using the Round Pond, Kensington Gardens, and Waterloo Bridge, illustrate this phase of his investigations.

Originally a chemist, Faraday's genius embraced metallurgy, glass technology and physics as life went on. As Mr. Martin so well shows, he had the supreme talent for knowing what problems to tackle, and which to reject.

F. I. G. R.

Electron Microscopy—Technique and Applications. By Ralph W. G. Wyckoff. (Published by Interscience Publishers, Inc., New York and London, 1949.) Pp. 248 Price £2.

The scientific value of the transmission-type electron microscope is widely known and such microscopes are now being manufactured in commercial forms suitable for routine work and for specialized research. Present users as well as potential purchasers of these instruments will welcome Wyckoff's new book which explains in detail the necessary adjustments, the preparation of suitable specimens and the types of problem which are suitable for attack.

The book begins with a brief non-mathematical account of the principles of the electron microscope and gives a critical review of the characteristics of the main commercial instruments produced in Europe and America. Although this chapter must inevitably become somewhat dated as new models appear, it remains valuable in indicating what the user may expect to obtain and what he should look for in a new instrument. The chapters on technique, which follow, are the main topic of the book and give full details of the methods of preparing suspensions, thin films, surface replicas, macromolecules and other types of specimen. Many of the recipes will be of interest to physical chemists and physicists, besides those working with electron microscopes, who also require to use such preparations. The accounts of the technique are accompanied by descriptions of a very large number of applications which have been made using electron microscopy in the fields of chemistry, biology and physics ; about 170 electron micrographs, excellently reproduced, accompany these descriptions ; full references to the literature are also given. The last chapter of the book gives an account of the work which has been done with the electron microscope on the arrangement of the macromolecules in a single crystal of a protein. The placing of the molecules in the crystal facets and the changes in these facets, as the crystal grows, are made visible. This work, arising from biochemical studies, is of great interest to the physical chemist and the crystallographer, who will hope for still further developments.

Technique and experimental methods are usually learnt from first hand, for it is difficult to explain such things in a book. Wyckoff has succeeded in overcoming the difficulty, however, mainly by giving adequate attention to detail. As an outstanding expert in this field, his account of the applications is convincing, critical and readable. The technique and applications fall together to give an entirely satisfactory book with which little, if any, fault can be found.

W. C.

THE VAPOUR PRESSURES OF CERTAIN LIQUIDS

By J. B. Matthews, J. F. Sumner and E. A. Moelwyn-Hughes

Received 25th January, 1950

The vapour pressures of the following liquids have been measured over a range of at least 100°, using the method of Ramsay and Young: 2-furfuraldehyde, symmetrical tetrachlorethane methyl salicylate, monoethanolamine, arsenious chloride, and *trans*-2-chlorvinyl-dichlorarsine (Lewisite). The results are summarized by means of the Kirchhoff-Rankine-Dupré equation, the three constants of which are briefly interpreted in terms of a kinetic theory of vaporization.

The thermodynamic expression for the saturation pressure p of a liquid in equilibrium with its vapour reduces to the form

$$\ln p = -\frac{L_0}{RT} + \int_0^T \frac{\mathrm{d}T}{RT^2}\int_0^T \Delta C_p \mathrm{d}T + \text{const.} \quad . \quad . \quad (1)$$

so long as the vapour obeys the ideal gas laws and has a molar volume overwhelmingly greater than that of the liquid. Even in this simplified form, however, the equation can hardly be called a convenient one: nor is it in any way a summarizing equation, for, in order to evaluate p, the difference ΔC_p between the specific heat of the liquid and that of the vapour must be known as a function of temperature. At the other extreme of the many methods employed for representing vapour pressures, we have the frequently used but over-simplified expression:

$$\log_{10} p = a - c/T, \quad . \quad . \quad . \quad . \quad (2)$$

which could only hold if the specific heats of liquid and vapour were equal at all temperatures. An equation of an intermediate type is that of Kirchhoff,[1] Rankine[2] and Dupré[3] which involves three constant terms:

$$\log_{10} p = a - b \log_{10} T - c/T. \quad . \quad . \quad . \quad (3)$$

It lacks the rigour of, but is more compact than, eqn. (1): and it avoids the physically unsatisfactory assumption upon which eqn. (2) is based. It is, accordingly, in terms of this equation that we represent the vapour pressures found for six of the numerous liquids which were examined in a programme of work which entailed a more careful specification of war chemicals than was possible from the literature up to 1940.

Experimental and Results

The experimental method used was that of Ramsay and Young,[4] with only minor modifications. To evaluate the constants a, b and c, we have used two methods which have been described in connection with a kindred problem.[5]

---

[1] Kirchhoff, *Pogg. Ann.*, 1858, **104**, 612.

[2] Rankine, *Phil. Mag.*, 1866, **31**, 200.

[3] Dupré, *Theorie Méchanique de la Chaleur* (1869), p. 96.

[4] Ramsay and Young, *Phil. Trans.*, 1885, **175**, 461.

[5] Moelwyn-Hughes, *Trans. Faraday Soc.*, 1940, **36**, 948. Kendrew and Moelwyn-Hughes, *Proc. Roy. Soc. A*, 1940, **176**, 352.

The data for furfuraldehyde and ethanolamine, however, have been analyzed by the method of least squares. All vapour pressures are given in mm. Hg 0° C.

2-Furfuraldehyde.—A specially purified sample supplied by B.D.H. was found to distil completely at a constant temperature under atmospheric pressure. A summary of boiling points at other pressures is given in Table I.

TABLE I.—THE VAPOUR PRESSURE OF 2-FURFURALDEHYDE
p IN mm. Hg 0 C.

T (°K)	*p* (obs.)	*p* (calc.)	*T* (°K)	*p* (obs.)	*p* (calc.)
329·02	13·25	13·24	391·55	203·9	204·7
329·22	13·45	13·39	394·00	223·1	223·1
337·73	20·90	20·90	397·90	256·1	255·0
340·85	24·91	24·44	399·20	263·0	266·4
348·20	35·1	34·86	399·50	271·0	269·1
349·62	37·76	37·76	405·30	326·9	325·8
358·10	54·41	54·71	406·95	339·8	343·6
360·53	61·8	60·83	409·10	367·1	367·8
365·30	74·7	74·53	411·50	399·5	396·6
366·20	77·32	77·40	413·10	422·8	416·9
369·92	90·46	90·40	416·95	462·3	468·5
375·28	113·1	111·7	420·00	517·8	513·3
376·46	117·8	117·0	422·80	538·0	557·2
378·24	127·6	125·3	424·85	579·4	591·3
380·42	137·2	136·2	427·10	618·6	630·4
384·80	162·4	160·5	428·25	641·0	651·1
389·40	185·5	189·6	433·90	764·2	761·3

Symmetrical Tetrachlorethane.—The commercial product was subjected to fractional distillation at atmospheric pressure, and the sample collected at 147·1-147·3° C/760·1 mm. was used for the vapour pressure measurements. From the results, plotted on a large-scale graph, vapour pressures were interpolated at even temperature intervals (Table II).

TABLE II.—THE VAPOUR PRESSURE OF SYMMETRICAL TETRACHLORETHANE

t°C	*p* (obs.)	*p* (calc.)
25	4·2	4·7
30	5·0	6·3
35	8·1	8·5
40	11·2	11·2
45	15·0	15·0
50	20·1	20·3
55	26·1	26·1
60	33·3	33·0
65	42·2	43·0
70	52·0	52·8
75	64·0	65·6
80	80·0	81·2
85	98·0	100·0
90	120·6	122·0
95	146·5	146·9
100	177·5	178·2
105	212·5	212·3
110	248·5	249·5
115	292·0	297·0
120	342·5	346·0
125	400·0	405·0
130	471·0	471·0

Methyl Salicylate.—A constant boiling fraction, obtained after repeated distillations, and retaining a refractive index of $n_D^{20} = 1{\cdot}52395 \pm 0{\cdot}00005$ during subsequent distillations was found to have the vapour pressures shown in Table III. These values are consistently higher than those obtained by Ramsay and Young.[6]

TABLE III.—THE VAPOUR PRESSURE OF METHYL SALICYLATE

T (°K)	p (obs.)	p (calc.)	T (°K)	p (obs.)	p (calc.)
352·1	4·28	4·329	425·3	107·7	109·1
357·3	5·675	5·758	429·2	123·1	124·7
361·0	7·27	7·006	432·8	136·8	140·6
362·3	7·37	7·499	439·2	173·0	172·9
366·0	9·06	9·067	443·5	195·3	197·7
366·2	9·27	9·158	451·1	248·8	248·8
369·1	10·55	10·59	457·3	293·4	297·7
374·0	12·94	13·45	464·1	352·8	359·8
376·6	15·04	15·23	466·1	374·6	380·0
377·6	16·32	15·96	468·9	402·0	409·6
380·1	17·93	17·93	473·2	456·8	458·5
383·8	21·01	21·21	473·2	460·1	458·5
387·5	24·60	25·01	475·1	489·3	481·4
387·7	26·61	25·23	477·0	499·4	505·4
390·7	28·77	28·74	479·1	529·5	532·5
396·5	37·34	36·70	480·9	556·5	557·3
403·2	48·28	48·16	481·3	579·8	562·7
405·5	53·57	52·71	483·4	593·9	592·7
408·8	62·82	59·89	487·1	642·2	648·2
414·1	73·43	73·11	493·1	762·0	746·4
417·2	81·91	81·93	493·6	760·5	755·0
421·5	94·84	95·57	—	—	—

Monoethanolamine.—Monoethanolamine was separated from diethanolamine, triethanolamine and other impurities found in the commercial product by fractionation in a 22-foot still. The fraction collected at 73° C/10 mm. froze sharply at 9·3° C under dry but otherwise atmospheric conditions. The density ρ, refractive index n, and viscosity η of the dry liquid were measured at 5° intervals between 20·0 and 40·0° C, with the following results :

$$\rho_4^t \text{ (g./ml.)} = 1{\cdot}0334 - 0{\cdot}000785t$$

$$n_D^t = 1{\cdot}4616 - 0{\cdot}000315t$$

and

$$\log_{10} \eta \text{ (g./cm. sec.)} = 1750/T - 6{\cdot}575.$$

t denotes temperature in degrees centigrade, and T in degrees absolute. By titration with standard hydrochloric acid, the sample was found to be 99·4 % pure. The vapour pressure determined at various temperatures and its logarithm are shown in Table IV.

TABLE IV.—THE VAPOUR PRESSURE OF MONOETHANOLAMINE

t° C	p	$\log_{10} p$ (obs.)	$\log_{10} p$ (calc.)	Deviation
65·4	6·7	0·8261	0·854	−0·028
65·5	7·1	0·8513	0·853	−0·002
69·5	8·7	0·9395	0·960	−0·020
70·8	9·4	0·9731	0·993	−0·020
71·0	9·8	0·9912	1·000	−0·009
72·1	10·8	1·0334	1·029	+0·004
73·3	11·2	1·0492	1·060	−0·011

---

[6] Ramsay and Young, *Trans. Chem. Soc.*, 1885, 48, 640.

TABLE IV.—*continued*

t° C	p	$\log_{10} p$ (obs.)	$\log_{10} p$ (calc.)	Deviation
75·1	13·2	1·1206	1·112	+0·008
76·9	14·0	1·1461	1·152	−0·006
78·4	15·4	1·1875	1·187	0·000
81·1	17·4	1·2405	1·253	−0·013
84·0	20·9	1·3201	1·324	−0·004
85·0	21·7	1·3365	1·347	−0·011
86·4	24·6	1·3909	1·381	+0·010
86·8	24·9	1·3962	1·390	+0·006
90·0	28·6	1·4564	1·461	−0·005
92·2	32·4	1·5105	1·514	−0·003
93·2	34·8	1·5416	1·537	+0·005
94·6	37·5	1·5740	1·567	+0·007
96·4	40·8	1·6107	1·605	+0·006
98·7	45·0	1·6532	1·656	−0·003
99·5	47·8	1·6794	1·672	+0·007
101·7	53·6	1·7292	1·720	+0·009
104·1	59·6	1·7752	1·768	+0·007
105·0	63·3	1·8014	1·788	+0·013
105·5	64·2	1·8075	1·796	+0·011
107·5	70·6	1·8488	1·839	+0·010
108·9	76·0	1·8808	1·868	+0·013
112·1	84·8	1·9284	1·929	−0·001
114·2	93·4	1·9703	1·970	0·000
117·3	105·1	2·0216	2·029	−0·007
121·0	122·9	2·0896	2·098	−0·008
125·0	145·9	2·1641	2·171	−0·007
126·9	159·4	2·2025	2·205	−0·002
128·8	171·4	2·2340	2·237	−0·003
132·0	193·3	2·2860	2·293	−0·007
133·3	205·5	2·3128	2·314	−0·001
136·0	227·2	2·3564	2·360	−0·004
137·9	242·0	2·3838	2·391	−0·007
141·5	280·0	2·4472	2·449	−0·002
144·6	316·8	2·5008	2·498	+0·003
147·1	340·7	2·5324	2·539	−0·007
150·8	406·5	2·6091	2·593	+0·016
154·7	445·3	2·6487	2·651	−0·002
158·5	518	2·7143	2·707	+0·007
161·4	554	2·7435	2·740	−0·004
167·0	652	2·8142	2·825	−0·011
170·9	751	2·8756	2·877	−0·001

Arsenious Chloride.—Arsenious chloride was purified by first freezing it, and discarding the first melt, and then by distillation from phosphorus pentoxide in an all-glass still. The alternate freezing and dry distillation were repeated five times, with continuous lowering of the vapour pressure, until finally a liquid was obtained which at 20° C possessed a constant vapour pressure which was lower by nearly 2 mm. than the lowest value published. High vapour pressures of only slightly impure samples were found to be due to hydrochloric acid, formed by hydrolysis of arsenious chloride, and accompanied by deposition of the crystalline oxide. The pure liquid froze at −19·8° C, in agreement with an earlier result.[7] The density at 20° C was 2·1570 ± 0·0005 g./ml. and the refractive index towards the *D* line of sodium was 1·5958. Chemical analysis gave 41·58 ± 0·05 % arsenic (theoretical 41·32) and 58·22 % chlorine. The total impurities probably did not exceed 2 parts in 1000. Vapour pressures interpolated at regular temperature intervals between 20° and 120° C are summarized in Table V.

---

[7] Pushin and Makuc, *Z. anorg. Chem.*, 1938, **237**, 177.

TABLE V.—THE VAPOUR PRESSURE OF ARSENIOUS CHLORIDE

t° C	p (obs.)	p (calc.)
20	6·9	6·9
25	10·0	9·5
30	12·8	12·9
35	17·7	17·3
40	23·3	22·9
45	30·3	30·1
50	39·7	38·9
55	50·6	49·8
60	63·5	64·9
65	79·0	79·1
70	97·8	98·0
75	120·8	121·1
80	146·4	147·6
85	177·3	178·7
90	215·0	215·3
95	257·5	256·5
100	307·0	303·4
105	362·1	356·5
110	417·7	417·9
115	482·2	485·3
120	559·6	559·8

***trans*-2-Chlorvinyldichlorarsine.**—Pure Lewisite, prepared by reducing 2-chlorvinylarsonic acid, conformed to the accepted standards of purity [8] and possessed the vapour pressures listed in Table VI.

TABLE VI—THE VAPOUR PRESSURE OF *trans*-2-CHLORVINYLDICHLORARSINE

t° C	p (obs.)	p (calc.)
50	2·3	2·5
55	3·4	3·4
60	4·6	4·7
65	6·2	6·1
70	8·1	8·2
75	10·6	10·7
80	13·9	13·9
85	17·9	17·9
90	22·8	22·0
95	28·8	28·8
100	36·1	36·1
105	45·1	44·8
110	55·7	55·2
115	67·5	67·3
120	81·0	81·7
125	96·3	98·2
130	113·7	117·5
135	136·9	140·0
140	163·2	165·2
145	194·1	194·1
150	228·0	227·0

---

[8] Whiting, *J. Chem. Soc.*, 1948, 1209.

Discussion

Vapour Pressure Constants.—The three constants of eqn. (3) derived for the liquids examined are given in Table VII. The figures given in the last colums of Tables I-VI indicate the extent to which eqn. (3) reproduces the experimental results. The latent heat of vaporization of the liquids supercooled to the absolute zero L_s and at the boiling point T_b are given in Table VIII, the bracketed values in which give some results of other workers. The figures in the last column indicate that all the liquids except ethanolamine are normal in Trouton's sense.

TABLE VII.—CONSTANTS OF THE EQUATION
$\log_{10} p$ (mm. Hg) $= a - b \log_{10} T - c/T$

Liquid	a	b	c
2-Furfuraldehyde . . .	29·3265	6·9418	3530·52
sym.-Tetrachlorethane . .	35·117	8·981	3646
Methyl salicylate . . .	36·5929	9·1999	4410·9
Monoethanolamine . . .	44·008	11·446	4809
Arsenious chloride . . .	46·714	12·926	4100·0
trans-2-Chlorvinyldichlorarsine .	48·660	13·297	4815

TABLE VIII.—LATENT HEATS OF VAPORIZATION (CAL./MOLE) AND BOILING POINTS (°K)

Liquid	L_s	L_b	T_b	L_b/T_b
2-Furfuraldehyde . .	16,160	9,224	433·8 (434·8)[9]	21·26
sym.-Tetrachlorethane .	16,683	9·184	420·4 (418·1)[10]	21·85
Methyl salicylate . .	20,190	11,155	493·9 (496·3)[11]	22·58
Monoethanolamine .	22,010	11,910	444·1 (444·4)[12]	26·81
Arsenious chloride .	18,758	8,368	404·54 (403·4)[13]	20·69
trans-2-Chlorvinyl-dichlorarsine . .	22,030	9,620	469·7 (469·7)[8]	20·48

Kinetic Interpretation.—The well-known kinetic theory of the vaporization of liquids [14] can be considerably extended in scope by postulating that the process of escape of a molecule from the surface resembles a unimolecular reaction, the energy of activation of which, ϵ, is distributed among a number, s, of harmonic oscillators.[15] We thus have the approximate relation:

Rate of evaporation from unit surface

$$= n_s(kT/h)e^{-\epsilon/kT}(\epsilon/kT)^{s-1}/(s-1)!, \quad . \quad . \quad . \quad (4)$$

where n_s is the number of molecules per unit area of liquid. In contrast to this complicated process, the process of condensation may still be regarded as simple, the rate being given by the relation:

$$\text{Rate of condensation on unit surface} = p\alpha/(2\pi mkT)^{1/2}, \quad . \quad . \quad . \quad (5)$$

where p is the saturation vapour pressure, α the accommodation coefficient, and m the molecular weight. Equating the two expressions, we have

---

[9] Evans and Aylesworth, *Ind. Eng. Chem.*, 1926, **18**, 24.
[10] Breuer, *J. Amer. Chem. Soc.*, 1936, **58**, 1289.
[11] Stull, *Ind. Eng. Chem.*, 1947, **39**, 517.
[12] Sivertz, Reitmeier and Tartar, *J. Amer. Chem. Soc.*, 1940, **62**, 1943.
[13] Baxter, Bezzenberger and Wilson, *ibid.*, 1920, **42**, 1386.
[14] Trautz, *Z. anorg, Chem.*, 1919, **105**, 97.
[15] Moelwyn-Hughes, *Trans. Faraday. Soc.*, 1937, **33**, 123.

$$p = n_s(2\pi mkT)^{1/2}(kT/h)(\epsilon/kT)^{s-1}\,e^{-\epsilon/kT}/(s-1)\,!\,\alpha \quad . \quad (6)$$

Comparison with eqn. (3) affords the following interpretation of its constants :

$$a = \log_{10}\left[\frac{n\,(2\pi mk)^{1/2}}{\alpha}\cdot\frac{k}{h}\cdot\frac{(\epsilon/k)^{s-1}}{(s-1)\,!}\right] - 3\cdot1253, \quad . \quad . \quad (7)$$

$$b = s - (5/2), \quad . \quad . \quad . \quad . \quad . \quad . \quad . \quad (8)$$

and

$$c = \epsilon/2\cdot303k. \quad . \quad . \quad . \quad . \quad . \quad . \quad . \quad (9)$$

It thus appears probable that, for the liquids examined here, the energy of activation of the escaping process is distributed among a number of oscillators ranging from 9 to 16. By eliminating ϵ and s from eqn. (7)-(9), the functional relationship between a, b and c is found, which is in general evident from the data of Table VII.

The work described here was done during 1940-43 in the Chemical Defence Research Establishment, Sutton Oak. Permission to publish the Report has been given by the Chief Scientist, Ministry of Supply.

Department of Physical Chemistry,

THE ABSORPTION SPECTRUM OF CF_2

By R. K. Laird, E. B. Andrews and R. F. Barrow

Received 11*th April*, 1950

Some of the ultra-violet bands of CF_2 have been observed in absorption. Qualitative study of the decay in intensity of absorption with time suggests that CF_2 has a half-life of the order of 1 sec. under the conditions of the experiment.

Uncondensed discharges through fluorocarbon vapours give rise to an emission spectrum which consists of (i) an extensive system of many-headed bands lying between 2340 and about 5000 Å, (ii) a system of violet-degraded double double-headed bands, of which the most prominent is at 2240 Å, (iii) a system of red-degraded bands, with marked sequences, lying in the range 1970 to 2210 Å. Both (ii) and (iii) are emitted by a diatomic molecule : vibrational analyses show that they have a lower state in common, which is probably the ground state, $^2\Pi$ of CF, and a rotational analysis [1] indicates that the transition in (ii) is $^2\Sigma-{}^2\Pi$.

The vibrational analysis of the shorter wavelength end of system (i) has recently been made by Venkateswarlu,[2] who gives good reasons for assigning it to non-linear CF_2. It seemed to us to be of interest to look for the absorption spectrum of CF_2, firstly to see if system (i) involved the ground state, and secondly in the hope of getting some information about the stability of this species.

Judging from the emission spectrum, much CF_2 is produced in an electrodeless discharge excited by a valve-oscillator operating at about

---

[1] Andrews and Barrow, *Nature*, 1950, **165**, 890.

[2] Venkateswarlu, *Physic. Rev.*, 1950, **77**, 676.

30 m in a stream of fluorocarbon vapour at a pressure of a few mm Hg According to a technique which we have used for study of the absorption spectrum of gaseous CS a stream of fluorocarbon was admitted to a 10 litre bulb and the pressure so controlled that the luminous discharge was confined to a region near to the walls of the bulb leaving a dark space along its axis Examination of the absorption spectrum along the axis with a Hilger medium quartz spectrograph showed bands in the region 2340 2660 A identical with some of those observed in the emission spectrum (Plate I) Pictures taken on a larger instrument (Hilger quartz Littrow E 478) showed the identity of the *K* structure of the absorption and emission bands at 2488 2519 and 2551 Å Thus system (1) involves the ground state of CF$_2$

Details of the absorption bands are given in Table I where the vibrational quantum numbers assigned by Venkateswarlu are also given It will be seen that the bands form a single progression with successive excitation of the bending vibration in the upper electronic state No bands have been observed which correspond to molecules in other than the ground vibrational levels so that it seems that Venkateswarlu s values of v_2 may have to be raised by 2 or perhaps 3 if the band at 2652 A proves to be genuine

TABLE I—ULTRA VIOLET BANDS OF CF$_2$

Absorption			Emission (Data of Venkateswarlu[9])				
λ_{air} (Å)	ν_{vac} (cm^{-1})	$\Delta\nu$ (cm^{-1})	ν_{vac} (cm^{-1})	v_1'	v_2'	v_1''	v_2''
?2345	42630		—	0	7	0	0
2371	42160	(470)	—	0	6	0	0
2399 0	41671	489	41667	0	5	0	0
2428 1	41172	499	41168	0	4	0	0
2457 6	40678	494	40677	0	3	0	0
2487 7	40186	492	40184	0	2	0	0
2518 7	39690	496	39692	0	1	0	0
2550 6	39195	495	39195	0	0	0	0
2583 3	38699	496	38695	(0	3	0	3)
2617	38200	499	—	—	—	—	—
?2652	37700	(500)	—	—	—	—	—

Notes—v_1' v_2' v_1'', v_2'' are the vibrational quantum numbers for symmetrical stretching and bending in the upper ( ) and lower ($''$) states respectively

The bands marked ? are doubtful

The band at 2617 is weak and difficult to measure accurately but it does not appear to be the same as that measured by Venkateswarlu at 2617 90 A The band at 2583 3Å is, however, very close to 2583 56, which he takes to be the head of the 0 3 0 3 band

It is our experience that the absorption spectra only of relatively long-lived species are observed with this technique Thus CS whose absorption appears strongly, has a half-life of the order of a minute under these conditions On the other hand careful examination of the absorption spectrograms shows that the $^2\Sigma-{}^2\Pi$ system of CF, which is likely to be a short-lived radical is not present, although it is probable that the $^2\Pi$ state is the ground state and although CF must be formed in concentrations at least comparable to those of CF$_2$ It therefore appears that CF$_2$ is relatively stable—at least in the gas phase at pressures of the order of 1 mm Hg

We have attempted to verify this conclusion in the following way With a steady stream of fluorocarbon vapour, the discharge was inter-

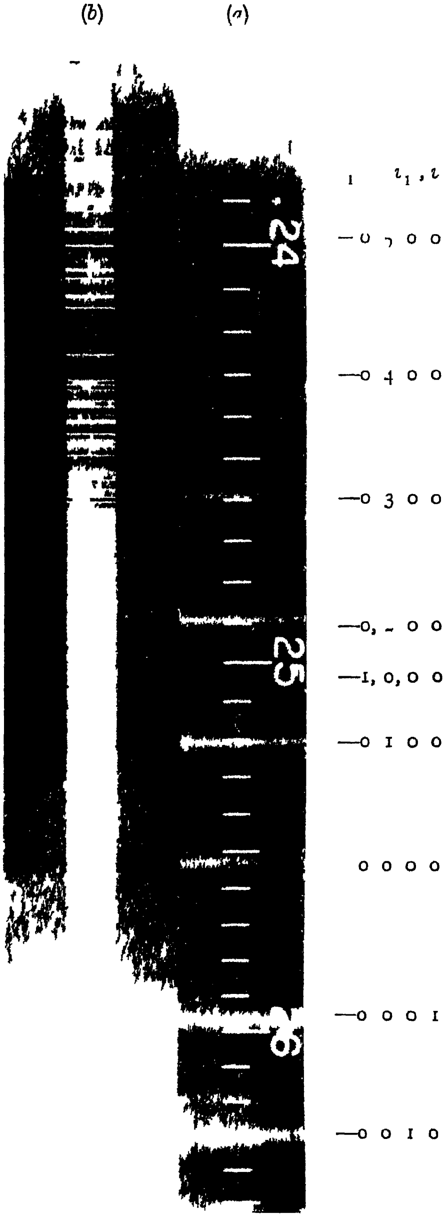

PLATE I.—Ultra-violet Cl₂ bands photographed on Hilger medium quartz spectrograph (a) emission (b) absorption with Fe arc comparison spectrum The assignment of vibrational quantum numbers is that of Venkateswarlu The wave-length scale is approximately correct at 2400 Å, and reads about 1 5 Å high at 2000 Å

[*To face p.* 804.

rupted, and about 0·25 sec. later, the absorption spectrum was photographed for a definite time, say 2 sec. This cycle was then repeated for a number of times sufficient to get adequate blackening of the photographic plate (about 10 min. in all). In different experiments the exposure time in the cycle was varied from 1 to 10 sec., while keeping the total exposure time constant. Even with the 10-sec. exposures, absorption could still be seen, and the 2-sec. absorption spectra were judged to be of roughly half the intensity of the 1-sec. absorption spectra. The decay-time of the exciting field is short compared with 1 sec., so that, provided that no CF_2 is formed in slow reactions initiated in the discharge, it may be concluded that the half-life of CF_2 under these conditions is of the order of 1 sec. The true half-life in the gas-phase may well be longer, for the decay at the walls appears to be rapid, so that we observed no absorption in 40-mm. tubes.

We should like to acknowledge our debt to Dr. Venkateswarlu for sending us an advance copy of his paper and to Messrs. I.C.I. (General Chemicals Division) Ltd., for the fluorocarbon.

Physical Chemistry Laboratory,
Oxford University.

A CORIOLIS PERTURBATION IN THE ULTRA-VIOLET SPECTRUM OF FORMALDEHYDE

BY J. C. D. BRAND

Received 18*th April,* 1950

The rotational structure of the principal progression of bands in the fluorescence spectrum of formaldehyde is affected by Coriolis coupling between the fundamental vibrations ν_5 and ν_6 in the levels of the electronic ground state. This coupling is strong between the fundamental frequencies, but is progressively much diminished between the combination levels $\nu_2 + \nu_5$ and $\nu_2 + \nu_6$, $2\nu_2 + \nu_5$ and $2\nu_2 + \nu_6$, etc. Approximate values of the coupling parameter have been evaluated. In this group of bands the electric moment is perpendicular to the symmetry axis, in the plane of the molecule.

The ultra-violet spectrum of formaldehyde contains a perpendicular band at 3700 Å, which is observed with moderate intensity in absorption [1] and is strong in the fluorescence spectrum.[2] This band is degraded rather sharply to the red and has not, therefore, the characteristic appearance of a perpendicular infra-red band, but the only differences arise from the fact that the rotational constants of the molecule are different in the upper and lower levels. The formaldehyde molecule is planar in the combining states and can be treated, in first approximation, as a symmetric top. With moderate resolving power, the most prominent features of the ultra-violet band are in the sequence of violet sub-bands

$$(K'' = K \rightarrow K' = K + 1),$$

where the heads formed by the ^RR-branches protrude above the unresolved background, and can be recognized easily from $K'' = 0$ to

---

[1] Henri and Schou, *Z. Physik*, 1928, **49**, 774. Schou, *J. Chim. Phys.*, 1929, **26**, 2. Sponer and Teller, *Rev. Mod. Physics*, 1941, **13**, 75.

[2] Herzberg and Franz, *Z. Physik*, 1932, **76**, 720. Gradstein, *Z. physik. Chem. B*, 1933, **22**, 384. Schuler, *Physik. Z.*, 1944, **45**, 61.

$K'' = 8$ (see Fig. 1). The ${}^{R}Q$-branches can be recognized, but are not very strong except near the centre of the band; the ${}^{R}P$-branches form heads, but are weak and can only be observed at the band centre and, owing to this difference of emphasis in the intensities, the pattern in the violet sub-bands is not reproduced in the red sequences. It is not permissible to ignore the fact that the two large moments of inertia are unequal, even when the rotational structure of the band is very incompletely resolved as in the present case, although the effect of the asymmetry on the appearance of the spectrum was only observed for transitions between the rotational states corresponding to the levels with $K = 0$ and $K = 1$ in the limiting case of the symmetric top. If the asymmetry is regarded as producing a perturbation of the levels of the symmetric top, the J_{-J} levels lie somewhat below their unperturbed values ($K = 0$) on an energy scale, and the J_{1-J} and J_{2-J} levels occur as a doublet placed almost symmetrically about the symmetric top level with $K = 1$. The splitting of the symmetric top levels with higher values of K is governed by an expression containing terms in b^2 and b^3 (where b is the asymmetry parameter) and can be neglected for the present purpose. The equations for the magnitude of the splitting have been given by several authors.[5, 8a]

Symmetrical Top Approximation: Evaluation of the Rotational Term Values.—Confining our attention, for the moment, to the violet sequences which obey the symmetric top formulae ($K'' > 2$), the heads of the successive sub-bands (Table I and Fig. 1) are observed to be separated by, in order, 19·5, 20·6, 20·6, 20·8, 20 and 19 cm.$^{-1}$. Without taking the interaction between vibration and rotation into account, the theoretical expression for the separation of the adjacent sub-band origins ($J = 0$) (to which, within the error of measurement, the same intervals apply) is

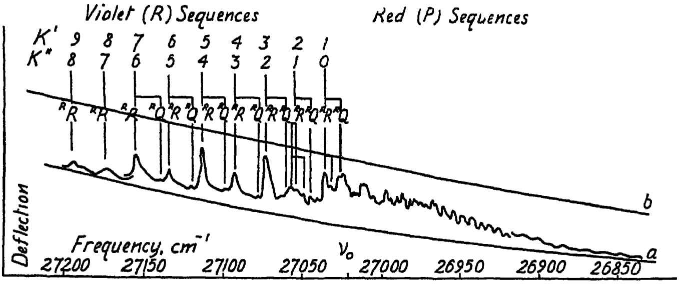

FIG. 1.—Microphotometer trace of the ultra-violet absorption band at 3700′ Å. The absorbing path was 10 cm. atm. at 150° C. The sub-bands are labelled in terms of the symmetrical top approximation.
Curve a: Deflection for $\log_{10} I_0/I = 0{\cdot}0$.
Curve b: Deflection for $\log_{10} I_0/I = 0{\cdot}22$.

$$\Delta\nu_0^{\mathrm{sub}} = 2\{A' - \tfrac{1}{2}(B'+C')\} - (2K+1)[\{A'' - \tfrac{1}{2}(B''+C'')\} - \{A' - \tfrac{1}{2}(B'+C')\}],$$
$$K = 0, 1, 2 \ldots, \quad . \quad . \quad . \quad . \quad (1)$$

where $A = h/8\pi^2 c I_A$, etc., and I_A, I_B and I_C are respectively the effective moments about the least, intermediate and greatest axes of inertia. Eqn. (1) affords no reasonable way of explaining the intervals in the violet sequences: in order to do so one would have to assume that the angle $\widehat{\mathrm{H{-}C{-}H}}$ is about 75° in the excited electronic state, whereas with an acceptable physical model ($110° < \widehat{\mathrm{H{-}C{-}H}} < 120°$) the interval between the sub-bands should not exceed about 15 cm.$^{-1}$, at least for the lower values of K. However, eqn. (1) is obeyed accurately by other bands in the ultra-violet absorption spectrum, and its failure in the present

TABLE I.—FREQUENCY OF SUB-BAND HEADS IN THE VIOLET SEQUENCES

A. TRANSITIONS WITH A COMMON LOWER STATE

$\frac{1}{2}(B'' + C'') = 1{\cdot}215$ cm.$^{-1}$. $A'' - \frac{1}{2}(B'' + C'') = 8{\cdot}19$ cm.$^{-1}$

K''	Band at 3700 Å $\frac{1}{2}(B' + C') = 1{\cdot}067$ cm.$^{-1}$ $A' \quad \frac{1}{2}(B' + C') = 7{\cdot}68$ cm.$^{-1}$ $\zeta = 0{\cdot}72 \quad \bar{\nu}_e = 28203$ cm.$^{-1}$ Sub-band Heads cm.$^{-1}$		Band at 3545 Å $\frac{1}{2}(B' + C') = 1{\cdot}056$ cm.$^{-1}$ $A' - \frac{1}{2}(B' + C') = 7{\cdot}64$ cm.$^{-}$ $\zeta = 0{\cdot}72 \quad \bar{\nu}_e = 29374$ cm.$^{-1}$ Sub-band Heads cm.$^{-1}$		Band at 3406 Å $\frac{1}{2}(B' + C') = 1{\cdot}046$ cm.$^{-1}$ $A' \quad \frac{1}{2}(B' + C') = 7{\cdot}61$ cm.$^{-1}$ $\zeta = 0{\cdot}72 \quad \bar{\nu}_e = 30528$ cm.$^{-1}$ Sub-band Heads cm.$^{-1}$	
	Obs.	Calc.	Obs.	Calc.	Obs.	Calc.
0	27035·9	27036·2	28207	28207	29359	29361
1	27053·9	27053·4	—	—	—	—
	27056·9	27056·2	28227	28227	—	—
2	27073·4	27073·1	28244	28244	29398	29398
	19·5	—	20	—	19	—
3	27092·9	27092·9	28264	28264	29417	29417
	20·6	—	21	—	22	—
4	27113·5	27113·5	28285	28284	29439	29437
	20·6	—	21	—	—	—
5	27134·1	27134·2	28306	28304	39	—
	20·8	—	18	—	—	—
6	27154·9	27154·6	28324	28324	29478	29476
	20	—	19	—	—	—
7	27175	27174·7	28343	28344	—	—
	19	—	19	—	—	—
8	27194	27193	28362	28363	—	—
	—	—	20	—	—	—
9	—	—	28382	28380	—	—
	—	—	18	—	—	—
10	—	—	28400	28396	—	—

B. TRANSITIONS WITH A COMMON UPPER STATE

$B' + C') = 1{\cdot}067$ cm.$^{-1}$. $A' - \frac{1}{2}(B' + C') = 7{\cdot}68$ cm.$^{-1}$.

K''	Band at 3950 Å $\frac{1}{2}(B'' + C'') = 1{\cdot}205$ cm.$^{-1}$ $A'' - \frac{1}{2}(B'' + C'') = 8{\cdot}15$ cm.$^{-1}$ $\zeta = 0{\cdot}5_8$ Sub-band Heads cm.$^{-1}$		Band at 4240 Å $\frac{1}{2}(B'' + C'') = 1{\cdot}195$ cm.$^{-1}$ $A'' - \frac{1}{2}(B'' + C'') = 8{\cdot}11$ cm.$^{-1}$ $\zeta = 0{\cdot}3_3$ Sub-band Heads cm.$^{-1}$		Band at 4570 Å $\frac{1}{2}(B'' + C'') = 1{\cdot}185$ cm.$^{-1}$ $A'' - \frac{1}{2}(B'' + C'') = 8{\cdot}07$ cm.$^{-1}$ $\zeta = 0$ Sub-band Heads cm.$^{-1}$	
	Obs.	Calc.	Obs.	Calc.	Obs.	Calc.
0	25296·8	25298·1	23578·7	23579·0	21880·6	21881
2	25332·7	25332·7	23612·3	23611·9	21912	21911
	18·3	—	15·0	—	11	—
3	25351·0	25349·9	23627·3	23626·9	21923	21924
	17·6	—	14·5	—	11	—
4	25368·6	25367·8	23641·8	23641·6	21934	21936
	17·3	—	15·8	—	—	—
5	25385·9	25385·7	23657·6	23656·2	25	—
	17·3	—	12·8	—	—	—
6	25403·2	25403·2	23670·4	23670·3	21959	21957
	—	—	27·5	—	—	—
8	—	—	23697·9	23697·2	—	—

The rotational constants have not been determined analytically, but are more in the nature of parameters adopted for the purpose of calculation.

case is due to the angular momentum generated about the symmetry axis by Coriolis coupling between two close-lying vibrational levels, of the type first discovered by Nielsen [3] in the infra-red spectrum. The sub-band intervals are determined by the *total* angular momentum about the symmetry axis, which is the sum of the vibrational and the rotational component.

For a perturbation of this kind to operate one quantum of the proper non-totally symmetrical vibration must be excited in one of the combining states. In the 3700 Å band, the transition originates from an excited vibrational level of the normal electronic state of the molecule. The variation with temperature of the intensity of absorption, which was difficult to measure because perceptible polymerization of the formaldehyde occurred at the pressure necessary for development of the band, corresponded to an excitation of approximately 800 cm.$^{-1}$,* the nearest infra-red frequency being at 1167 cm.$^{-1}$. Coriolis coupling occurs between the upper states of the fundamentals ν_6 (1167 cm.$^{-1}$) and ν_5 (1280 cm.$^{-1}$), in agreement with Jahn's rule, and the equation for the rotational energy levels has been obtained by Nielsen.[3] Because the coupling develops an angular momentum about the symmetry axis, only the dependence of the energy levels upon K is affected. Assuming that, in the combining states of the ultra-violet band, the Coriolis coupling is confined to the normal electronic state, the rotational term values of the upper and lower levels of the transition are given respectively by eqn. (2) and (3).

$$F'(K, J) = \bar{\nu}_e + \tfrac{1}{2}(B' + C')(J + 1)J + \{A' - \tfrac{1}{2}(B' + C')\}K^2 \qquad (2)$$

$$\begin{aligned} F''(K, J) = {} & \tfrac{1}{2}(\bar{\nu}_5 + \bar{\nu}_6) + \zeta^2 A'' + \tfrac{1}{2}(B'' + C'')(J + 1)J \\ & + \{A'' - \tfrac{1}{2}(B'' + C'')\}K^2 - [\{\tfrac{1}{2}(\bar{\nu}_5 - \bar{\nu}_6)\}^2 + \{2KA''\zeta\}^2]^{\frac{1}{2}} \end{aligned} \qquad (3)$$

In these equations, $\bar{\nu}_e$ is the height of the rotationless excited electronic level above the normal state of the molecule, and ζ is the Coriolis coupling parameter ; (3) is the equation derived by Nielsen, and referred to above.

The position of the heads in the violet sub-bands of the transition at 3700 Å can be calculated from eqn. (2) and (3), using rotational constants from Dieke and Kistiakowsky's analysis [4] of other bands in the ultra-violet absorption spectrum. Without the assistance afforded by these measurements very little progress could have been made. The 3700 Å band was not analyzed by Dieke and Kistiakowsky, but the rotational constants do not change much between one level and another in the upper electronic state, and the values for the transition at 28313 cm.$^{-1}$ will be assumed to hold approximately for the 3700 Å transition ($\bar{\nu}_e$ = 28189 cm.$^{-1}$). With this assumption the sub-band heads are found to be formed by the lines ${}^RR$ (7), the calculated positions of which are shown in Table I. Taking $\zeta = 0{\cdot}72$, the agreement is satisfactory. (Centrifugal stretching has been neglected.) Ebers and Nielsen [3] used the value of $\zeta = 0{\cdot}8$ to account for the structure of the infra-red bands, but the envelope of the band is not very sensitive to small changes of ζ, and the frequencies of the sub-band origins of the infra-red bands, recalculated with $\zeta = 0{\cdot}72$, are given in Table III.

Deviations from the Symmetrical Top.—To allow for the effect of asymmetry, one must replace K^2 in eqn. (1)-(3) by W_T. Because the asymmetry of the molecule is so slight, W_T is readily obtained from Witmer's equations [5] (as corrected by Wang). The details of the appearance of the central region of the band depend upon the axis of oscillation of the dipole moment. For the transitions which correspond approximately to the $K'' = 0 \rightarrow K' = 1$ sub-band of the symmetric top, the R-branch is formed by combination of the levels $J''_{-J''}$ and $J'_{1-J'}$ if the band is Type B, and by combination of $J''_{-J''}$ and $J'_{2\ J'}$ if the band is Type C. In each case, because we are dealing only with the R-branches, $J' = J'' + 1$. The consequence of this selection rule is that the R-branch is headless if the band is Type C, but inflects and forms a head at the frequency of the transition $J'' = 5_{-5} \rightarrow J' = 6_{-5}$ if the band is Type B. It is not difficult to decide between these possibilities. A sharp, intense maximum occurs at the frequency calculated on the second assumption (Table I and Fig. 1) and shows that the transition moment lies in the axis of intermediate inertia. The second violet sub-band, equivalent to the transition $K'' = 1 \rightarrow K' = 2$ in the symmetric top approximation, is split at the head by the asymmetry into a doublet, the source of the splitting being very largely in the lower state; the band envelope in this region is, therefore, the same for a Type B and a Type C band.

---

* Sponer and Teller [1] have reported that the temperature coefficient of absorption indicates an excitation of 600-700 cm.$^{-1}$.

[3] Nielsen, *J. Chem. Physics*, 1937, **5**, 818. Ebers and Nielsen, *ibid.*, 1937, **5**, 822.

[4] Dieke and Kistiakowsky, *Physic. Rev.*, 1934, **45**, 4.

[5] Witmer, *Proc. Nat. Acad. Sci.*, 1927, **13**, 60. Wang, *Physic. Rev.*, 1929, **34**, 243.

Coriolis Coupling between Combination Levels.—The 3700 Å system belongs to a progression which extends, in the fluorescence spectrum, from 3400 to 5000 Å. The interval between the bands which are members of this progression corresponds to one quantum of the totally symmetrical carbonyl-stretching vibration ν_2, the magnitude of which is 1749 cm.$^{-1}$ and 1180 cm.$^{-1}$ in the normal and electronically excited states respectively. The frequency of the first violet sub-band head is given in Table II, values calculated with eqn. (4) being entered for comparison :

$$\bar{\nu} = 27036{\cdot}0 + (1180{\cdot}4\,n' - 9{\cdot}4\,n'^2) - (1749{\cdot}2\,n'' - 10{\cdot}2_5\,n''^2)\ . \quad (4)$$

(n' and n'' are respectively the number of quanta of ν_2 in the upper and lower states). The movement of the first sub-band head with respect

TABLE II.—FREQUENCIES OF THE FIRST VIOLET SUB-BAND HEADS IN THE PRINCIPAL PROGRESSION OF THE FLUORESCENCE SPECTRUM

Intensity	Number of Quanta of ν_2 Excited		Frequency (cm.$^{-1}$)	
	Upper State	Lower State	Obs.	Calc.
4	2	0	27359·3	27359·3
—	—	—	1152·3	—
13	1	0	28207·0	28207·0
—	—	—	1171·0	—
170	0	0	27035·9	27036·0
—	—	—	1739·1	—
360	0	1	25296·8	25297·0
—	—	—	1718·5	—
1000	0	2	23578·7	23578·5
—	—	—	1698·1	—
220	0	3	21880·6	21880·5
—	—	—	1674	—
2^d	0	4	20207	20203

d = diffuse band.

Anharmonic Constants (cm.$^{-1}$)	Lower State	Upper State
x_{22}	−10·2	−9·4
x_{26}	− 4·5	—

to the band origin has not been allowed for, but it amounts to a few tenths of a wave-number only. In the ground state of the molecule, the stack of quanta of ν_2 is combined with a single quantum of ν_6, and the intervals are not quite the same if the ν_2 quanta are built up from the zero-point vibrational state (eqn. (5)), which is the case with the principal progression in the *absorption* spectrum :

$$\tilde{\nu} = 28312{\cdot}7 + (1191{\cdot}8\,n' - 9{\cdot}4\,n'^2) - (1753{\cdot}7\,n'' - 10{\cdot}2\,n''^2). \qquad (5)$$

Assuming that the vibrational term values obey an equation of the usual form (eqn. (6)) the anharmonic cross-term x_{26} can be evaluated (Table II).

$$G(n_1, n_2, \ldots n_6) = \sum_i n_i \nu_i + \sum_i \sum_{i>j} n_i n_j x_{ji} : i, j = 0, 1, 2 \ldots 6. \qquad (6)$$

Table I contains a list of the frequency of the sub-band heads of all the measurable bands in the fluorescence progression. The violet branches of the band at 4570 Å are overlapped by a band belonging to another progression and cannot be observed accurately, and the 4950 Å band is diffuse. The bands at 3406, 3545 and 3700 Å have a common lower level and the envelope of the violet sequences is practically the same in the three cases ; the position of the sub-band heads in the first two bands has been calculated (Table I) by the procedure employed for the 3700 Å band, using the same value for the Coriolis coupling parameter. The interval in the violet sequences falls from about 20 cm.$^{-1}$ in the bands just described to 17-18 cm.$^{-1}$ in the 3950 Å band, and to 14-15 cm.$^{-1}$ and about 12 cm.$^{-1}$ in the bands at 4240 and 4570 Å respectively. These observations demonstrate that the Coriolis coupling is confined to the levels of the normal electronic state. The three bands on the violet end of the progression are affected by the strong interaction between the fundamentals ν_5 and ν_6, the perturbation in the next two bands is successively diminished because of the reduced coupling between the combination levels $\nu_2 + \nu_5$ and $\nu_2 + \nu_6$, and $2\nu_2 + \nu_5$ and $2\nu_2 + \nu_6$, and the sub-band interval in the transition at 4570 Å is practically " normal " (eqn. (1)), showing that the levels $3\nu_2 + \nu_5$ and $3\nu_2 + \nu_6$ are uncoupled. Approximate values of the coupling parameter have been evaluated assuming, in the latter cases, that the difference between the frequencies of the interacting combination bands is the same as that between the fundamentals ν_5 and ν_6. This is only approximately true, but we do not know whether the interval grows larger or smaller by the addition of quanta of ν_2 and, in fact, a difference of several cm.$^{-1}$ in either direction has little effect on the result.

The interaction of the fundamentals ν_5 and ν_6 must bring about some mixing of the eigenfunctions, and a level in which either one of this pair of fundamentals is excited by a single quantum will possess to some degree the properties of both vibrations. One might expect to find, therefore, that each band of the progression is accompanied by a weak transition between the same levels which combine to produce the main band, except that the quantum of ν_6 in the lower state is replaced by ν_5. Unfortunately the region in question was always obscured by the red branches of the main system, and none of the satellite bands was observed with certainty. If it is accepted that the 1167 cm.$^{-1}$ frequency definitely belongs to the out-of-plane vibration $\nu_6(b_2)$,* the symmetry species of the total (electronic × vibrational) eigenfunction of the upper states of the progression has been determined, and is A_2. The intensity alternation, sub-bands with even values of K'' are strong, also shows that the symmetry species of the upper state is either A_1 or A_2, and the lower state either B_1 or B_2. The fluorescence spectrum contains two further progressions, which are comparatively strong, although weaker than the one discussed in this paper; all the associated bands are affected by Coriolis coupling, and in one case, at least, the perturbation is located in the levels of the electronically excited state.

---

* This is commonly assumed, although the identification of ν_5 and ν_6 with the frequencies 1280 and 1167 cm.$^{-1}$ respectively might have to be reversed.

Experimental

Formaldehyde was prepared by heating alkali-precipitated α-polyoxymethylene in an apparatus of the type described by Spence and Wild.[6] The α-polyoxymethylene, m.p. 175° (sealed tube), was prepared from paraformaldehyde according to the directions of Staudinger,[7] and was dried *in vacuo* before use.

Infra-red Measurements.—The infra-red spectrum of gaseous formaldehyde [3, 8b, 9] was re-measured between 5 μ and 20 μ using a single-beam recording prism spectrometer. In the region between 5 μ and 10 μ the absorption was well developed with an absorbing path of 0·5-1 cm. atm.: the resolving power of the rock-salt prism was about 10 cm.$^{-1}$. The Type *a* bands at 1743 cm.$^{-1}$ and 1503 cm.$^{-1}$ were observed as doublets, the *Q*-branches being unresolved. In each case the separation of the maxima in the *P*- and *R*-branches was about 55 cm.$^{-1}$, compared with the value of 50 cm.$^{-1}$ calculated by the formula of Gerhard and Dennison.[10] The frequency of the maxima in the perpendicular bands at 7-10 μ agreed with the measurements of Ebers and Nielsen [8] (Table III), which were obtained with a grating spectrometer and are more accurate than the present series: the latter have been recorded to show that extensive agreement has been obtained in this region of absorption, although in an early series of measurements [11] it was reported quite differently.

TABLE III.—*Q*-BRANCH MAXIMA IN THE INFRA-RED SPECTRUM OF FORMALDEHYDE, 7 μ-10 μ.

Frequency (cm.$^{-1}$)				Frequency (cm.$^{-1}$)			
Intensity Maximum, Obs.		Sub-band Origin, Calc.		Intensity Maximum, Obs.		Sub-band Origin, Calc.	
	Ebers and Nielsen	$\zeta = 0{\cdot}80$	$\zeta = 0{\cdot}72$		Ebers and Nielsen	$\zeta = 0{\cdot}80$	$\zeta = 0{\cdot}72$
1026	1027·0	1016·6	1023·0	—	1229·1	1229·2	1226·5
—	1051·0	1045·4	1050·1	1240	1239·3	1238·1	1240·7
1073	1075·9	1073·3	1077·4	1262	1259·0	1252·5	1262·0
1095	1099·7	1099·9	1101·5	1277	1275·2	—	—
1118	1121·8	1124·5	1124·8	1300	1300·8	—	—
—	1146·3	—	—	1324	1323·0	1318·1	1315·7
1165	1165·7	—	—	—	1339·4	1342·7	1338·9
1193	1193·4	1188·5	1190·3	1349	1347·0	—	—
1205	1204·6	1204·5	1207·4	1373	1370·5	1369·3	1364·0
1215	1213·8	1213·4	1219·6	—	—	—	—

$$A = 9{\cdot}4 \text{ cm.}^{-1}.$$
$$\nu_6 = 1167 \text{ cm.}^{-1}. \qquad \tfrac{1}{2}(B + C) = 1{\cdot}2 \text{ cm.}^{-1}.$$

The region between 10 μ and 20 μ was examined using a potassium bromide prism and, in agreement with the results of Singer,[9] no absorption was detected from a path of up to 10 cm. atm. of gaseous formaldehyde, or with liquid formaldehyde (*ca.* 0·2 mm. layer) at − 80° C. The liquid formaldehyde absorbed very strongly at 1740, 1500, 1245 and 1170 cm.$^{-1}$, the two latter frequencies being intense and fairly sharp maxima superimposed on a considerable background. No absorption was detected, however, at 2080 cm.$^{-1}$.

[6] Spence and Wild, *J. Chem. Soc.*, 1935, 338.
[7] Staudinger, Signer and Schweitzer, *Ber.*, 1931, **64**, 398.
[8] Herzberg, *Infra-red and Raman Spectra* (van Nostrand, New York, 1945), (*a*) Chap. I, § 4; (*b*) Chap. III, §3. [9] Singer, *Physic. Rev.*, 1947, **71**, 531.
[10] Gerhard and Dennison, *ibid.*, 1933, **43**, 197.
[11] Nielsen, *ibid.*, 1934, **46**, 117.

Ultra-violet Measurements.—The ultra-violet spectra were photographed with a Hilger medium spectrograph ($f/12$) on unsensitized or orthochromatic plates. The resolving power of the quartz and glass prisms was about 7 cm.$^{-1}$ and 2 cm.$^{-1}$ respectively. A tungsten lamp source was used for the absorption measurements, and a path of 1·5 m. was employed with pressures of formaldehyde up to 1 atm. The fluorescence spectrum was excited electrically.

The author wishes to thank Prof. F. J. W. Roughton, F.R.S., for permission to use the infra-red spectrometer, and acknowledges the pleasure and profit he has derived from discussions with Dr. A. G. Gaydon and Dr. N. Sheppard.

The University,
Glasgow, W.2.

THE DEPENDENCE ON STATE OF THE APPARENT DIPOLE MOMENTS OF ETHYLAMINE, DIETHYLAMINE AND TRIETHYLAMINE

By G. A. Barclay, R. J. W. Le Fèvre and B. M. Smythe

Received 26th January, 1950

Using the Debye-Clausius-Mosotti and other usual formulae the following moments are reported: $EtNH_2$, $1{\cdot}22_5$, 1·32, 1·09; Et_2NH, 0·920, 1·03, 1·11; Et_3N, 0·660, 0·91, 0·76 D. In each case the figures refer respectively to the gaseous, dissolved (C_6H_6), and liquid states. The new data are compared with those for NH_3 and the related methylamines. Each of the three ethylamines shows a *positive* solvent effect in benzene. As a class, the amines do not seem to fit equations which previously have satisfactorily connected true moments, obtained from gases, with their corresponding apparent values determined in solution. Disagreement is quantitative rather than qualitative. Possible reasons for this are mentioned.

This paper contains dielectric polarization data for the three ethylated ammonias: (*a*) as gases, (*b*) as solutes in benzene, and (*c*) as pure liquids. Since the work is a continuation of the programme outlined previously[1,2] we now record, without further preliminaries, relevant experimental details from which are drawn the apparent dipole moments in each of the states of aggregation. Finally, we compare our results with those for the series $MeNH_2$, Me_2NH, and Me_3N, and note the difficulties in making *a priori* calculations of the ratios $\mu_{soln.}/\mu_{gas}$ for these compounds.

Experimental

Materials.—Ethylamine was available as an anhydrous pure sample (Eastman Kodak Co.). It was further dried over KOH in the supply train (shown as Fig. 2 of ref. 2) leading to the " gas " cell and redistilled before use. Solutions were made up by weight using the procedure adopted with sulphur dioxide.[3]

Diethylamine was a pre-war Kahlbaum sample. After standing for 24 hr. over solid KOH it was fractionated, the portion of b.p. 55·5/761 mm. being retained for use.

We are indebted to Messrs. I.C.I.A.N.Z. for a gift of triethylamine; after KOH treatment, the bulk of the material had b.p. 88·9°/762 mm.

Benzene and carbon dioxide were purified as described previously.[1]

---

[1] Le Fèvre and Russell, *Trans. Faraday Soc.*, 1947, **43**, 374.
[2] Le Fèvre, Ross and Smythe, *J. Chem. Soc.*, 1950, 276.
[3] Le Fèvre and Ross, *ibid.*, 283.

Polarizations of the Amines as Vapours.—With experience, the *details* of the apparatus used in (1) have been changed although the fundamental principle remains the same. Particulars of the electrical arrangements may be found around Fig. 3 of ref. 2. The measurements on ethylamine were made with the oil-thermostat of ref. 2, those on di- and triethylamines with the vapour bath illustrated above Table II of ref. 4. Consequently it was necessary to determine separate CO_2-calibration equations for these two cases, respectively :

for $EtNH_2$: $\delta C/p = 1408{\cdot}123/T + 0{\cdot}0413$
for Et_2NH and Et_3N : $\delta C/p = 2294{\cdot}881/T - 0{\cdot}0129$.

Symbols and calculations are explained in ref. (1) and (2). It is sufficient here to mention that polarizations are estimated relatively to that of CO_2 (taken as 7·341 cm.^{3} and invariant with temperature) by $P = 7{\cdot}341\, x/x'$, where x' and x are the appropriate $(\delta C/p)_{p \to 0}$ values for CO_2 and the dielectric under examination.

Our observations are summarized in the following Tables.

POLARIZATIONS OF THE ETHYLAMINES AS VAPOURS

T (°K)	$(\delta C/p)_{p\to 0}$	P (cm.^{3})	P (calc.)	p range (cm.)	No. of Observation
		ETHYLAMINE			
303·0	30·95	48·44	48·10	27-69	10
321·8	27·88	46·30	46·33	25-70	11
351·3	24·1	43·79	43·95	25-65	12
355·0	23·7	43·38	43·68	24-70	12
380·0	21·0	41·89	41·98	20-61	13
410·0	19·0	40·08	40·22	22-70	9
431·0	17·6	39·03	39·14	29-56	12
446·5	16·9	38·89	38·40	27-69	13
		DIETHYLAMINE			
334·0	38·31	41·01	41·11	15-60	17
349·0	36·41	40·73	40·44	19-55	14
356·0	34·99	39·99	40·16	19-50	9
373·0	33·02	39·48	39·50	20-53	12
386·5	31·45	38·97	39·01	18-45	12
413·0	28·83	38·18	38·15	19-45	9
		TRIETHYLAMINE			
373·0	33·66	40·24	40·14	20-63	12
389·0	31·91	39·80	39·85	20-56	17
411·0	29·84	39·32	39·49	19-65	14
436·0	28·03	39·19	39·12	17-45	5
452·5	26·82	38·92	38·90	17-51	10

From the above, the relations between polarization and absolute temperature, and hence the dipole moments, may be evaluated (by least squares) as :

$EtNH_2$: $(P)_{T°} = 17{\cdot}9 + 9135{\cdot}2/T$, whence $\mu = 1{\cdot}22_5$D.
Et_2NH : $(P)_{T°} = 25{\cdot}67 + 5156{\cdot}7/T$, whence $\mu = 0{\cdot}92_0$D.
Et_3N : $(P)_{T°} = 33{\cdot}04 + 2649{\cdot}8/T$, whence $\mu = 0{\cdot}66_0$D.

The column headed P(calc.) shows the degree of agreement between quantities from these expressions and those from our actual recordings.

For comparison, the moments reported by previous workers have been :

$EtNH_2$: $\mu = 1{\cdot}31$, Højendahl-Pohrt ;[5] 0·99, Chatterjee and Ghosh.[6]
Et_2NH : $\mu = 0{\cdot}94$;[5] 0·90.[6]
Et_3N : $\mu = 0{\cdot}76$;[5] 0·82.[6]

---

[1] Le Fèvre, Mulley and Smythe, *J. Chem. Soc.*, 1950, 290.
[5] Højendahl, *Thesis* (Copenhagen, 1928) ; Pohrt, *Ann. Physik.*, 1913, **42**, 569.
[6] Chatterjee and Ghosh, *Physic. Rev.*, 1931, **37**, 427.

Since these agree neither among themselves nor with the present measurements, it is relevant to note that the distortion polarizations now found are close to the $(R_L)_D$ figures, as is the case for the methylamines :[1]

	$EtNH_2$	Et_2NH	Et_3N	$MeNH_2$	Me_2NH	Me_3H
${}_DP$ Expt. . .	17·9	25·7	33·0	10·6	15·0	20·0
$(R_L)_D$ . .	14·7 (Calc.*)	24·3 (Obs.)	33·1 (Obs.)	10·1 (Calc.*)	14·9 (Calc.*)	19·7 (Calc.*)

* Refractivity data from Vogel.[7]

Apparent Polarizations of the Amines as Solutes or as Pure Liquids.—Mixtures in benzene have been made up by weight as previously outlined.[1, 3] The apparatus for dielectric constant determinations described by Le Fèvre and Russell has, in Sydney, been replaced by the simpler arrangements noted by Calderbank and Le Fèvre[8] and Le Fèvre and Ross[3] for dilute solutions and polar liquids respectively. In other matters, standard procedures[9] have been followed.

The total molecular polarization of each solute at infinite dilution has been calculated[10, 11] via the equation :

$$_{\infty}P_1 = M_1p_2(1 - \beta) + M_1C\alpha\epsilon_2,$$

where

$$p_2 = (\epsilon_2 - 1)/(\epsilon_2 + 2)d_2,$$
$$C = 3/d_2(\epsilon_2 + 2)^2.$$

The P_1 at each w_1, evaluated as

$$P_1 = M_1[p_2 + (p_{12} - p_2)/w_1]$$

is shown, for comparison with $_{\infty}P_1$, in the last columns of the following Tables. Since all measurements have been referred to benzene of $d_{4°}^{25°} = d_2 = 0{\cdot}87378$ and $\epsilon_{1000kc}^{25°} = \epsilon_2 = 2{\cdot}2725$, the constants p_2 and C are 0·34086 cm.^{3} and 0·18809 respectively. Watch has been kept for variations of α and β with w_1 and where necessary, these two have been brought[11] to zero concentration. Our symbols are defined in several earlier papers (e.g. ref. [9, 10, 11]).

POLARIZATIONS IN BENZENE SOLUTION AT 25° C

$w_1 \times 10^5$	$\epsilon^{25°}$	$\alpha\epsilon_2$	$d_{4°}^{25°}$	βd_2	P_1 (cm.^{3})
			ETHYLAMINE		
677·11	2·3192	3·94	0·88256	− 0·2777	52·63
1393·6	2·3463	3·86	0·88068	− 0·2698	51·58
1401·2	2·3476	3·93	0·88066	− 0·2698	52·35
1929·1	2·3691	3·97	0·87923	− 0·2701	52·50
2552·4	2·3912	3·87	0·87766	− 0·2656	51·56
3289·8	2·4201	3·88	0·87580	− 0·2626	52·02
whence mean $\alpha\epsilon_2 = 3{\cdot}91$; mean $\beta d_2 = -0{\cdot}2687$.					
			DIETHYLAMINE		
3101	2·3199	1·53	0·87310	− 0·0219	46·8
5210	2·3499	1·49	0·87261	− 0·0225	46·2
8298	2·4009	1·55	0·87189	− 0·0228	46·9
10088	2·4269	1·53	0·87161	− 0·0215	46·5
·hence mean $\alpha\epsilon_2 = 1{\cdot}525$; mean $\beta d_2 = -0{\cdot}02217$.					

---

[7] Vogel, *J. Chem. Soc.*, 1948, 1830.

[8] Calderbank and Le Fèvre, *ibid.*, 1948, 1949.

[9] *Dipole Moments* (Methuen, 1948), 2nd edn., Chap. 2.

[10] Le Fèvre and Vine, *J. Chem. Soc.*, 1937, 1805.

[11] Le Fèvre, *Trans. Faraday Soc.*, 1950, **46**, 1.

POLARIZATIONS IN BENZENE SOLUTION AT 25° C—*continued*

$w_1 \times 10^5$	$\epsilon^{25°}$	$\alpha\epsilon_2$	$d_{4°}^{25°}$	βd_2	P_1 (cm.^{3})
		TRIETHYLAMINE			
2200	2·2817	0·418	0·86983	− 0·180	49·5
2860	2·2839	0·399	0·86866	− 0·179	49·2
3191	2·2849	0·389	0·86811	− 0·178	48·9
3410	2·2850	0·367	0·86730	− 0·190	49·0
4030	2·2882	0·390	0·86613	− 0·190	48·5
5724	2·2914	0·330	0·86363	− 0·177	47·8
6517	2·2927	0·310	0·86222	− 0·177	47·5
7396	2·2949	0·303	0·86070	− 0·177	47·3
8308	2·2981	0·308	0·85911	− 0·176	47·4
10220	2·2999	0·268	0·85549	− 0·182	46·8

whence (by least squares) $(\alpha\epsilon_2)_{w_1} = 0{\cdot}4468 - 1{\cdot}83\, w_1$; mean $\beta d_2 = - 0{\cdot}1806$.

TRIETHYLAMINE—MOLECULAR REFRACTIONS

$10^5\, w_1$	0	2200	2860	3191	4030	5724	6517	8308
$n_D^{25°}$	1·49331	1·49050	1·48964	1·48925	1·48788	1·48616	1·48514	1·48280
$(R_L)_D$	—	33·1	33·1	33·1	33·1	33·2	33·2	33·0

(cf. above Table for $d_{4°}^{25°}$ of these solutions).

RESULTS

	M_1	$(\alpha\epsilon_2)_{w_1=0}$	Mean β	$_\infty P_1$(cm.^{3})	$(R_L)_D$(cm.^{3}	μD
$EtNH_2$	45·1	3·91	− 0·307$_5$	53·3	14·7	1·3$_7$
Et_2NH	74·1	1·52$_5$	− 0·025$_4$	47·1$_5$	24·3	1·0$_6$
Et_3N	101·1	0·44$_7$	− 0·206$_7$	50·1	33·1	0·91

The moments shown at this stage are deduced as $\mu = 0{\cdot}221\ (_\infty P_1 - R_L)^{\frac{1}{2}}$, i.e. the common convention is adopted of taking $(R_L)_D$ as an approximation to $_DP$. The figure 14·7 cm.^{3} for $EtNH_2$ is calculated from Vogel's data,[7] while 24·3 cm.^{3} for Et_2NH is an actual determination by him; he records 33·8 cm.^{3} for Et_3N as a pure liquid. The above tabulated observations on benzene solutions were made in the divided cell of a Pulfrich refractometer and indicate a slightly lower refraction (33·1) which, being nearer to $_DP_{\text{Expt.}}$ (33·0), is here utilized. $(R_L)_D = 33{\cdot}8$ corresponds to $\mu = 0{\cdot}89$D.

Only one previous polarization measurement for dissolved ethylamine appears in the literature, i.e. that by Trunel,[12] who quoted $_\infty P_1 = 54 \pm 3$ cm.^{3} and $\mu = 1{\cdot}37$D. Di- and triethylamines have been examined by Fogelberg and Williams [13] and Higasi.[14]

	$_\infty(P_1)_{25°}$(cm.$^{-1}$)	$\mu\,D$	Solvent	Authors
Et_2NH	54	1·20	C_6H_6	F. and W.
	50·7	1·13	C_6H_6	H.
	47·1$_5$	1·0$_6$	C_6H_6	Present work
	49·4	1·10	Hexane	H.
Et_3N	51	0·90	C_6H_6	F. and W.
	46·6	0·79	C_6H_6	H.
	50·1	0·91	C_6H_6	Present work
	45·3	0·75	Hexane	H.

---

[12] Trunel, *Ann. Chim.*, 1939, **12**, 93.

[13] Fogelberg and Williams, *Physik. Z.*, 1931, **32**, 27.

[14] Higasi, *Inst. Phys. Chem. Res. Tokyo*, 1937, **31**, 311.

The dielectric constants of liquid di- and triethylamines at 25° were read as 3·782 and 2·408 from a calibration curve involving the "standard" condenser fillings specified by Le Fèvre and Ross.[3] Pre-war determinations by Mr. P. Russell (Univ. Coll., London) by the methods set out in ref. (1) were 3·93 and 2·48 respectively. Schlundt[15] had previously recorded 6·17 and 3·58 for $EtNH_2$ and Et_2NH at 21°, and Walden[16] 3·15 for Et_3N at the same temperature.

The densities of the three liquids, determined several times on different batches, fell within the ranges :

$$EtNH_2 : d^{25°}_{4°} = 0{\cdot}6761 - 0{\cdot}6778$$

$$Et_2NH : d^{25°}_{4°} = 0{\cdot}6981 - 0{\cdot}7016$$

$$Et_3N : d^{25°}_{4°} = 0{\cdot}7225 - 0{\cdot}7258.$$

These compare satisfactorily with the figures (0·6769, 0·6989 and 0·7227) given by Swift[17] which we have used therefore in compiling the following Table.

	$V^*_{25°}$	$\varepsilon^{25°}$	$(n^2_D)^‡_{25°}$	$_TP_{\text{Liq.}}$
$EtNH_2$	66·63	(6·17)†	1·849	42·2
Et_2NH	106·0	3·78	1·892	51·0
Et_3N	139·9	2·41	1·930	44·7

* Mol vol. at 25°.
† From ref. (15).
‡ From $(R_L)_D$, by $n^2 = (V + 2R)/(V - R)$.

Discussion

We begin by assembling our results in the forms used in other papers[1, 3, 4, 18] namely, showing the various polarizations at 25° together with the moments calculated therefrom when the temperature-invariant term of the Debye equation is taken as the true distortion polarization in each case.

P as cm.^{3} ; μ as D	EtNH	Et_2NH	Et_3N
$(_TP)_{\text{gas}}$	48·56	42·97	41·93
$_DP$	17·90	25·67	33·04
$(_OP)_{\text{gas}}$	30·66	17·30	8·89
$(_TP_\infty)\ C_6H_6$	53·3	47·1$_5$	50·1
$(_OP_\infty)\ C_6H_6$	35·4	21·5	17·0$_6$
$(_TP)_{\text{liq.}}$	42·2	51·0	44·7
$(_OP)^*_{\text{liq.}}$	24·3	25·3	11·7
$(_OP)^†_{\text{liq.}}$	44·7	33·1	12·2
μ_{gas}	1·225	0·92$_0$	0·66$_0$
$\mu_{C_6H_6}$	1·32	1·02$_6$	0·91$_3$
$\mu^*_{\text{liq.}}$	1·09	1·11	0·75$_8$
$\mu^†_{\text{liq.}}$	1·48	1·27	0·77

* Apparent values by the Clausius-Mosotti-Debye equations.
† Ditto by Onsager's equation.

---

[15] Schlundt, *J. Physic. Chem.*, 1901, **5**, 503.
[16] Walden, *Z. physik. Chem.*, 1910, **70**, 569.
[17] Swift, *J. Amer. Chem. Soc.*, 1942, **64**, 115.
[18] Barclay and Le Fèvre, *J. Chem. Soc.*, 1950, 556.

From the above we extract μ_1^2/μ_2^2 ratios ($= {}_0P_1/{}_0P_2$) and $\delta\mu/\mu_{\text{gas}}$ fractions * as follows :

	Liquid-gas		Solution-gas	
	${}_0P_{\text{liq.}}/{}_0P_{\text{gas}}$	$\delta\mu/\mu_{\text{gas}}$	${}_0P_{\text{soln.}}/{}_0P_{\text{gas}}$	$\delta\mu/\mu_{\text{gas}}$
$EtNH_2$	0·79	− 0·11	1·15	+ 0·08
Et_2NH	1·46	$+ 0{\cdot}20_8$	1·24	$+ 0{\cdot}11_5$
Et_3N	1·32	+ 0·15	1·92	+ 0·38

* $\delta\mu = (\mu_{\text{liq.}}$ or $\mu_{\text{soln.}})$ minus μ_{gas} ; in ref. (1) this subtraction was reversed.

It is seen that the apparent moment is *increased* by solution in benzene in all three cases, and that the secondary and tertiary derivatives *as liquids* each show a variation in the same sense. The present results thus resemble somewhat those previously[1] found for the series NH_3, $MeNH_2$, Me_2NH and Me_3N. Fig. 1 illustrates the degree of parallelism between the appropriate ${}_0P_1/{}_0P_2$ ratios, while Fig. 2 compares the modifications of the moment of ammonia caused by a progressive substitution of hydrogen by methyl—and ethyl—radicals.

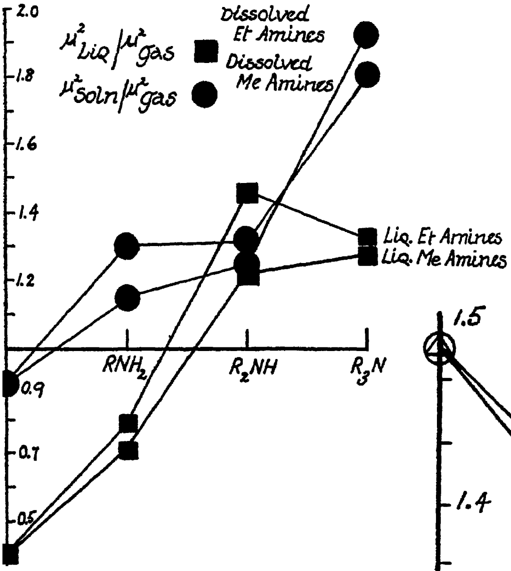

FIG. 1.

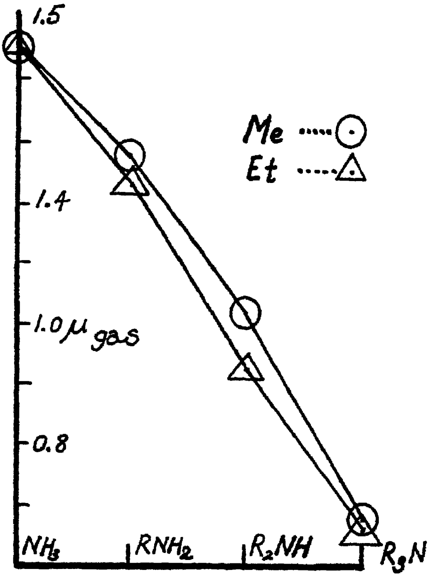

The Sign of the Solvent Effect.—The three ethylamines are recognized therefore as further instances of compounds where positive solvent effects are operative. Until recently [3, 18] it was thought that such molecules were characterized by *negative* Kerr constants [19, 20, 21] (cf. [1, 4]). Although Le Fèvre and Ross,[3] and Barclay and Le Fèvre [18] have since demonstrated that sulphur dioxide and methylene dichloride are exceptions to such a generalization, we may note, in passing, that the signs of the only two available relevant electric double refractions are: NH_3, positive,[23] Et_2NH, negative.[24] Unpublished measurements made in these Laboratories indicate, in accordance with elementary considerations, that trimethyl- and triethyl-amines resemble Et_2NH in this property. The later literature on the influence of a medium on μ_{apparent} is reviewed in ref. (3) and (18); that prior to 1936, by Glasstone.[22] The present position appears to be that none of the extant *a priori* theoretical approaches is *generally* satisfactory. The deficiencies of Onsager's equation,[25] when applied without modification, have been mentioned before [3] during comment on the work of Böttcher.[26] They are displayed in the following Table.

Substance	$\varepsilon^{25°}$	$(n_D^2)^{25°}$	$d_{4°}^{25°}$	${}_0P_{\text{Onsager}}$	${}_0P_{\text{gas}}$
NH_3	16·90	1·792	0·6028	62·6	43·7
$MeNH_2$	9·40	1·811	0·6539	54·4	34·3
Me_2NH	5·26	1·803	0·6386	39·6	21·6
Me_3N	2·44	1·808	0·6267	11·2	8·6
$EtNH_2$	6·17	1·849	0·6769	44·7	30·7
Et_2NH	3·78	1·892	0·6989	33·1	17·3
Et_3N	2·41	1·930	0·7227	12·2	8·9

Wilson's correction [20] cannot be made owing to the virtual absence of the necessary information concerning polarizability. (We have included NH_3 and its three methyl-derivatives in the above list because Table XI of ref. (1) contains clerical errors, although the μ_{Onsager} figures there shown agree substantially with those for ${}_0P_{\text{Onsager}}$ now given).

Barclay and Le Fèvre [18] found evidence, among a wide selection of *solution*-gas (as distinct from *liquid*-gas) data, that a formula of the following type has a useful applicability:—

$$\mu^2_{\text{soln.}}/\mu^2_{\text{gas}} = 1 + (\epsilon - 1)(\exp x^2 - n_2^2/n_1^2)/(\epsilon + 2).$$

Here x^2 reflects the geometry of the solute. (The remaining symbols have their conventional meanings.[9, 10, 11] The value of x^2 is obtained from scale drawings incorporating the *Wirkungsradien* of Stuart [27] superimposed upon the usual molecular dimensions known from X-ray or electron diffraction analysis.[28, 29]

If A is the maximum measurement parallel to $\mu_{\text{resultant}}$ and B and C those in the two perpendicular directions (C being put less than B if $B \neq C$), then

$$\begin{aligned} x^2 &= (C^2 - A^2)/A^2, \text{ when } A > B \geqslant C \\ &= (C^2 - A^2)/B^2, \text{ when } B > A > C \\ &= (C^2 - A^2)/C^2, \text{ when } B \geqslant C > A. \end{aligned}$$

---

[19] Le Fèvre and Le Fèvre, *J. Chem Soc.*, 1935, 1747.

[20] Goss, *Trans. Faraday Soc.*, 1934, **30**, 751.

[21] Higasi, *Inst. Phys. Chem. Res., Tokyo*, 1936, **28**, 284.

[22] Glasstone, *Ann. Reports*, 1936, **33**, 117.

[23] Breazeale, *Physic. Rev.*, 1935, 48, 237.

[24] Leiser, *Abhandlungen der Deutschen Bunsen-Gesellschaft* (Halle a. S., 1910), No. 4.

[25] Onsager, *J. Amer. Chem. Soc.*, 1936, **58**, 1486.

[26] Böttcher, *Physica*, 1939, **6**, 59.

[27] Stuart, *Z. physik. Chem. B*, 1935, **27**, 350.

[28] Pauling and Huggins, *Z. Krist.*, 1934, **87**, 205.

[29] Schomaker and Stevenson, *J. Amer. Chem. Soc.*, 1941, **63**, 37.

The examples listed by Barclay and Le Fèvre [18] were all molecules where $\mu_{\text{resultant}}$ lay on or about a symmetry axis. Of the present group only NMe_3 and NH_3 conform to this condition. A pyramidal structure for the first-named has been assigned by Brockway and Jenkins,[31] in which the C—N—C angles are 108 ± 4° and the C—N distances are 1·47 Å. Such specifications, although harmonious with the inferences of Thosar [32] relating to other amines, lead nevertheless to $\mu^2_{\text{soln.}}/\mu^2_{\text{gas}}$ ratios for the trimethyl- and triethyl-derivatives (1·2-1·3) which are too small. We note, moreover, that even if very flattened configurations are assumed, with the ethyl groups disposed to give maximum extension in the plane normal to $\mu_{\text{resultant}}$, the calculation is but little improved :

	A	*B*	*C*	μ_s^2/μ_g^2(calc.)	μ_s^2/μ_g^2(found)
NMe_3	4	7	7	1·21	1·80
NEt_3	4	9	9	1·32	1·92

The apical angle of ammonia has been usually quoted as *ca.* 109°, with the N—H distance from 1·02 to 1·06 Å ; [33, 34, 35] if the *Wirkungsradius* of hydrogen combined with nitrogen is roughly the same as in C—H, NH_3 should, by our " rule," show a positive solvent effect (calculated $\mu_s^2/\mu_g^2 = ca.\ 1{\cdot}1$). In fact, however, this is negative. By using an H—N—H angle of 85° (i.e. when the protuberances due to the hydrogens are beginning to cover completely one side of the sphere of radius 1·35 Å drawn around the centre of the N atom), an ${}_0P_s/{}_0P_g$ ratio of 0·94 is calculable and is of the order of the experimental value (viz. 0·93). Further, it is significant that the Kerr constant of ammonia is *positive*,[23] thus demonstrating a greater polarizability *along* the direction of the resultant dipole moment than across it. Stuart [36] estimates the three tensor components concerned as $24{\cdot}2 \times 10^{-25}$, $21{\cdot}8 \times 10^{-25}$, and $21{\cdot}8 \times 10^{-25}$ respectively ; by adopting these quantities in place of our *A* : *B* : *C* dimensions, we calculate ${}_0P_s/{}_0P_g = 0{\cdot}87$, i.e. somewhat smaller than that found.[1]

The consensus of evidence, nevertheless, is against any great departure from an approximately tetrahedral apical angle, although, as Coulson [37] points out, pure *p* binding of H to N could theoretically lead to one of 90°. An alternative explanation might be that the three hydrogen atoms are somewhat embedded in the electronic system of the nitrogen (as the H is thought to be in HCl (cf. Partington and Frank [38]). The ammonia molecule should then tend to present a more spherical shape (see Table below).

The direction of action of the resultant moments of the primary and secondary amines are difficult to predict although their structures are confirmed by various spectroscopic and other examinations,[39-44] their

---

[30] Wilson, *Chem. Rev.*, 1939, **25**, 377.

[31] Brockway and Jenkins, *J. Amer. Chem. Soc.*, 1936, **58**, 2036.

[32] Thosar, *J. Chem. Physics.*, 1938, **6**, 654.

[33] Sutherland, *Ann. Reports*, 1936, **33**, 56.

[34] Barker and Migestte, *Physic. Rev.*, 1936, **50**, 418.

[35] Sutherland, *Infra-red and Raman Spectra* (Methuen, 1935), p. 109.

[36] Stuart, *Z. Physik.*, 1929, **55**, 358 ; **59**, 13 ; 1930, **63**, 533.

[37] Coulson, *Quart. Rev.*, 1947, **1**, 144.

[38] Discussion remarks by Partington and Frank, *Trans. Faraday Soc.*, 1934, **30**, 871 ; cf. also Debye, *Polar Molecules* (Chem. Catalog. Co., U.S.A., 1929), p. 59.

[39] Thompson, *J. Chem. Physics*, 1939, **7**, 448.

[40] Cleaves and Plyler, *ibid.*, 563.

[41] Owens and Barker, *ibid.*, 1940, **8**, 229.

[42] Cleaves, Sponer and Bonner, *ibid.*, 784.

[43] Bailey, Carson and Daly, *Proc. Roy. Soc. A*, 1940, **173**, 339.

[44] Brown and Taylor, *J. Amer. Chem. Soc.*, 1947, **69**, 1332.

configurations are not conclusively decided. To investigate these points we have therefore reversed our calculations and computed x^2 for each compound from the ratios of the orientation polarizations actually observed. It will be noted that x^2 for NH_3 approaches the zero value to be expected were $A = B = C$:

	$_OP_s/_OP_g$	n_2^2/n_1^2	x^2
NH_3	0·93	1·251*	0·02
$MeNH_2$	1·30	1·238	0·81
Me_2NH	1·32	1·243	0·84
Me_3N	1·80	1·240	1·37
$EtNH_2$	1·15	1·212	0·54
Et_2NH	1·24	1·185	0·69
Et_3N	1·92	1·161	1·45

* $(n_D^2)^{25°}_{C_6H_6} = 2{\cdot}2417$.

Bailey, Carson and Daly [43] suggested for $MeNH_2$ a similarity with the D_{3h} model for ethane, yet neither on this or any other reasonable basis can a sufficiently *positive* x^2 be forecast for the two pairs of mono- and di-alkyl derivatives. If, for $A = B = C$, the dimensions of the " cavity " swept out by a rotation about the axis of $\mu_{resultant}$ are used, the situation appears better, but there seems no justification for such a procedure since we find that other molecules whose resultant moments are also " off " a symmetry axis obey the " rule " as originally worded. We quote $CH_3 . CH_2 . Br$ as an example: $A = 6{\cdot}0$, $B = 5{\cdot}4$, $C = 4$; exp $x^2 = 0{\cdot}574$; $n_D^2 = 2{\cdot}0178$; whence $\mu^2_{C_6H_6}/\mu^2_{gas} = 0{\cdot}84$ (calc.). Groves and Sugden [45] reported $\mu_{gas} = 2{\cdot}01$, and Cowley and Partington [46] $\mu_{C_6H_6} = 1{\cdot}88$, whence $\mu_s^2/\mu_g^2 = 0{\cdot}87$ (expt.). The agreement is satisfactory. Further observations on other alphyl- and aryl-amines are in hand.

Financial assistance from the Commonwealth Science Fund is gratefully acknowledged.

School of Chemistry,
University of Sydney,
N.S.W., Australia.

---

[45] Groves and Sugden, *J. Chem. Soc.*, 1937, 158.
[46] Cowley and Partington, *ibid.*, 1937, 130.

THE ANODIC BEHAVIOUR OF METALS

PART VI.—COBALT

BY S. E. S. EL WAKKAD AND A. HICKLING

Received 21*st February,* 1950

The initial build-up of anodic polarization at a cobalt anode over a wide range of conditions has been investigated using the cathode ray oscillograph. In alkaline solutions three stages of oxidation have been distinguished corresponding to the formation of CoO, Co_2O_3 and CoO_2. In general it appears that CoO is first formed but this is further oxidized to Co_2O_3 when the surface is only partly covered with the lower oxide. In hot concentrated alkali solutions continuous dissolution of CoO to give cobaltite ions may occur. In the passivation of a cobalt anode the Co_2O_3 forms a protective layer, essentially 1 molecule thick, which is further oxidized to CoO_2 before oxygen evolution commences. From the present work the standard Co_2O_3/CoO_2 potential is + 0·58 V.

In continuation of the work previously reported [1] in this series, the anodic polarization of cobalt has now been investigated by the oscillographic method which records the variation of potential with quantity of electricity passed prior to oxygen evolution As in previous studies with the base metals, attention has been directed primarily to the behaviour of cobalt in alkaline solutions, where passivity is almost at once set up, in order to detect the very rapid consecutive stages in polarization which occur. No previous work on cobalt from this point of view has been published, but other methods of investigation have yielded some indirect information. Grube and Feucht [2] studied the anodic behaviour of cobalt in alkali hydroxide solutions by plotting current density (c.d.) —potential curves ; in concentrated potassium hydroxide solution at high temperatures and low c.d.s cobalt was found to dissolve at negative potentials to give a blue solution containing cobaltite ions (CoO_2'' or $HCoO_2'$), but with decrease of concentration or lowering of temperature this process was soon replaced by passivation and rise of potential, and evolution of oxygen occurred. From a study of the oxidation of the cobaltite solution at a platinum anode, these workers inferred that the anodic oxidation of cobalt took place in three stages: at low potentials the oxide Co_3O_4 was formed ; at medium potentials Co_2O_3 was produced ; and at high potentials a solid solution of CoO_2 in the lower oxides was formed, oxygen evolution taking place by the decomposition of this unstable oxide to reform Co_2O_3.[3] Several studies of the anodic passivation of cobalt in acid solution have been made [4] which lead to the general conclusion that the passive metal is protected by a film of oxide.

Experimental

The electrical circuit and the electrolytic cell employed were fundamentally as previously described.[1] The cobalt electrodes used were made by plating cobalt at a c.d. of 5 mA/sq. cm. from a bath containing 140·5 g. $CoSO_4 . 7H_2O$, 14·5 g. NH_4Cl, and 15·5 g. H_3BO_3 per litre on to platinum wire electrodes of 0·05 sq. cm. area sealed directly into glass tubes. A fresh plating was used for each experiment. Observations have been made mainly with NaOH solutions of various concentrations as electrolytes ; additional experiments have been carried out in a number of buffer solutions. Except where otherwise stated, all experiments were made at 18° C. Initially the experiments were made with air-free solutions in an atmosphere of nitrogen, but it was subsequently found that the presence of air had no influence whatever upon the oscillograms and later experiments were therefore carried out in air.

The results are shown as photographed oscillograms in which the ordinates represent potentials and the abscissae are proportional to quantities of electricity passed. Suitable horizontal reference lines at intervals of 0·25 V were photographed immediately after recording the polarization tracks, so that significant potentials can be read directly from the oscillograms. The quantity of electricity passed at any stage in the polarization is computed from the known capacity of the condenser used in series with the electrolytic cell and the horizontal displacement which is governed by the voltage to which the condenser is charged

---

[1] Hickling, *Trans. Faraday Soc.*, 1945, **41**, 333 ; 1946. **42**, 518 ; Hickling and Spice, *ibid.*, 1947, **43**, 762 ; Hickling and Taylor, *Faraday Soc. Discussion*, 1947, **1**, 277 ; *Trans. Faraday Soc.*, 1948, **44**, 262.

[2] *Z. Elektrochem.*, 1922, **28**, 568.

[3] See also Mitselovskii and Ormont, *J. Gen. Chem. U.S.S.R.*, 1940, **10**, 161.

[4] Byers, *J. Amer. Chem. Soc.*, 1908, **30**, 1718 ; Byers and Thing, *ibid.*, 1919, **41**, 1902 ; Hedges, *Protective Films on Metals* (1932), p. 157 ; Georgi, *Z. Elektrochem.*, 1933, **39**, 209.

(on the original photographs, before reduction, 1 V on the condenser corresponds to an average displacement of *ca.* 1 mm.). Except where otherwise stated, a capacity of 9·3 μF was used in series with the cell. All potentials quoted are on the hydrogen scale.

Results

Behaviour in Alkaline Solution.—In Plate IA is shown the characteristic oscillogram in N NaOH for the anodic polarization of cobalt at 18° C with a polarizing c.d. of 0·02 A/sq. cm.; the spots on the left of the photograph indicate the steady hydrogen and oxygen evolution potentials at the same c.d. Three steps can be distinguished in the anodic polarization track. After a very rapid rise of potential from the hydrogen evolution value there occurs a short step beginning at $-$ 0·70 V, a longer and very definite step commencing at + 0·20 V, and a somewhat ill-defined step, indicated by a change in the slope of the track at about + 0·58 V, which passes ultimately into oxygen evolution. In Plate IB is shown an anodic track under the same conditions but with a higher series capacity of 13·5 μF which brings out more clearly the third step. These anodic tracks were very satisfactorily reproducible and only changed slightly with time, the first step becoming shorter if the pulsating electrolysis were very prolonged. Change of c.d. had no effect on the general form of the polarization or on the quantities of electricity passed in the steps, but there was a tendency for the starting potential of the second step to be raised somewhat at very high c.d.'s; this is illustrated in Plate IC by oscillograms taken at c.d.'s of 0·01 and 0·05 A/sq. cm. respectively. Increase of temperature also had only a slight influence on the anodic track as is shown in Plate ID where the upper curve is that obtained at a c.d. of 0·02 A/sq. cm. at 18° C and the lower curve is the corresponding track at 70° C; it may be noted that rise of temperature has lowered the potentials slightly throughout. In Plate IE are shown the anodic and cathodic polarization tracks in N NaOH at 0·02 A/sq. cm. under standard conditions. The cathodic track shows two sections, not very sharply separated, which appear to correspond to the second and third oxidation steps and are of approximately the same extent, but no reduction process is apparent at a potential near that of the first oxidation step; instead there occurs an arrest at a much more negative potential immediately prior to hydrogen evolution. Decrease of alkali concentration did not appreciably affect the general form of the anodic track, but the break potentials were slightly raised; thus Plate IF shows the oscillogram obtained under standard conditions at a c.d. of 0·02 A/sq. cm. in 0·1 N NaOH. Increase of alkali concentration likewise had little effect at 18° C, although there was a slight tendency for the first step to be lengthened, but in 8N NaOH at 95° C the first step extended across the whole plate as illustrated in Plate IIG which shows both anodic and cathodic tracks obtained under these conditions; it appears here that the metal is undergoing anodic dissolution and cathodic deposition almost reversibly.

Behaviour in Buffer Solutions.—The effect of decreasing the pH value on the anodic behaviour of cobalt was investigated using a variety of buffer and acid solutions as electrolytes. A c.d. of 0·02 A/sq. cm. and standard conditions were used throughout these experiments. In inert electrolytes such as N Na_2CO_3, pH 12, and 0·1 M $Na_2B_4O_7$, pH 9·2, the anodic track retained much the same form as in NaOH solutions, but the first step became less and less distinct with decrease of pH; this may be seen in Plate II, H and J, which record the oscillograms in these two solutions respectively. If, however, a mixture of N NH_4OH + M $(NH_4)_2SO_4$ was used as electrolyte, in which cobaltous hydroxide is freely soluble, the potential never rose above that corresponding to the first step, as is shown in Plate II I. In 0·2 M KH_2PO_4 + 0·2 M Na_2HPO_4 electrolyte, pH 6·8, the anodic and cathodic tracks shown in Plate II K were obtained. Here there is no sign of the usual arrests, and it appears that, as with nickel previously studied,[5] there is formed a protective film of the metal phosphate which is not reduced in the pulsating electrolysis; in support of this view, it was found that starting with a clean cobalt anode the anodic track initially indicated dissolution of metal but after a short time reverted to the form shown. In more acid solutions the oscillograms merely indicated anodic dissolution and cathodic deposition of cobalt as is illustrated by Plate II L, which shows the anodic and cathodic tracks in N CH_3COONa + N CH_3COOH, pH 4·6; it may be noted that the usual small cobalt overvoltage is involved in both processes.

[5] See Hickling and Spice, *loc. cit.*[1].

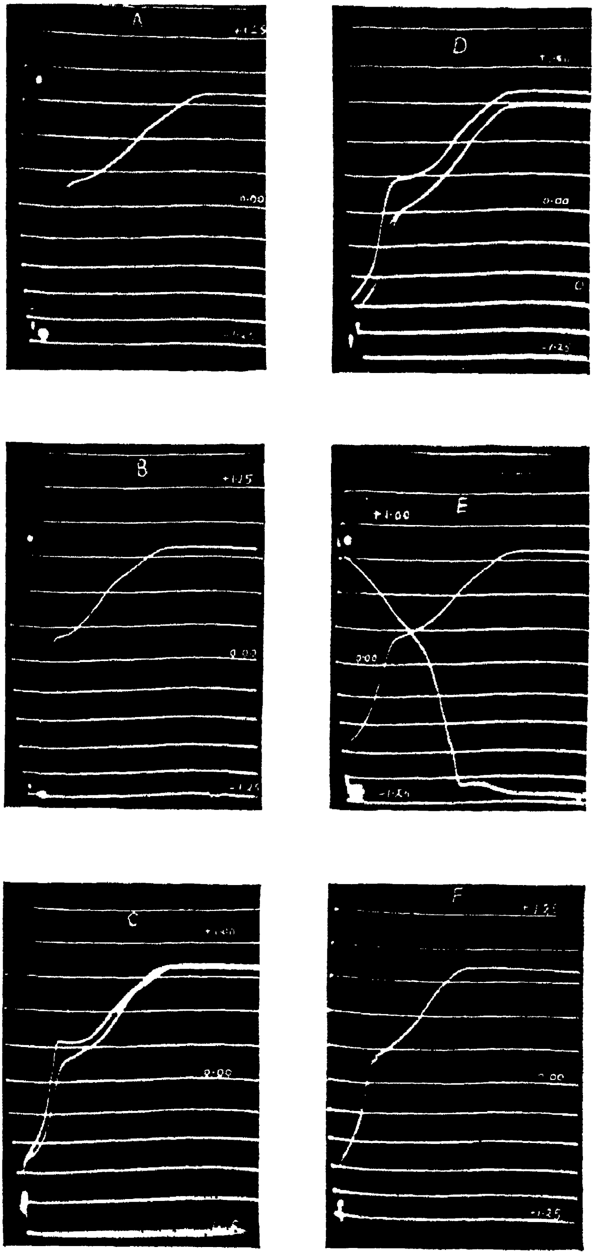

PLATE I.

[*Facing p.* 822.

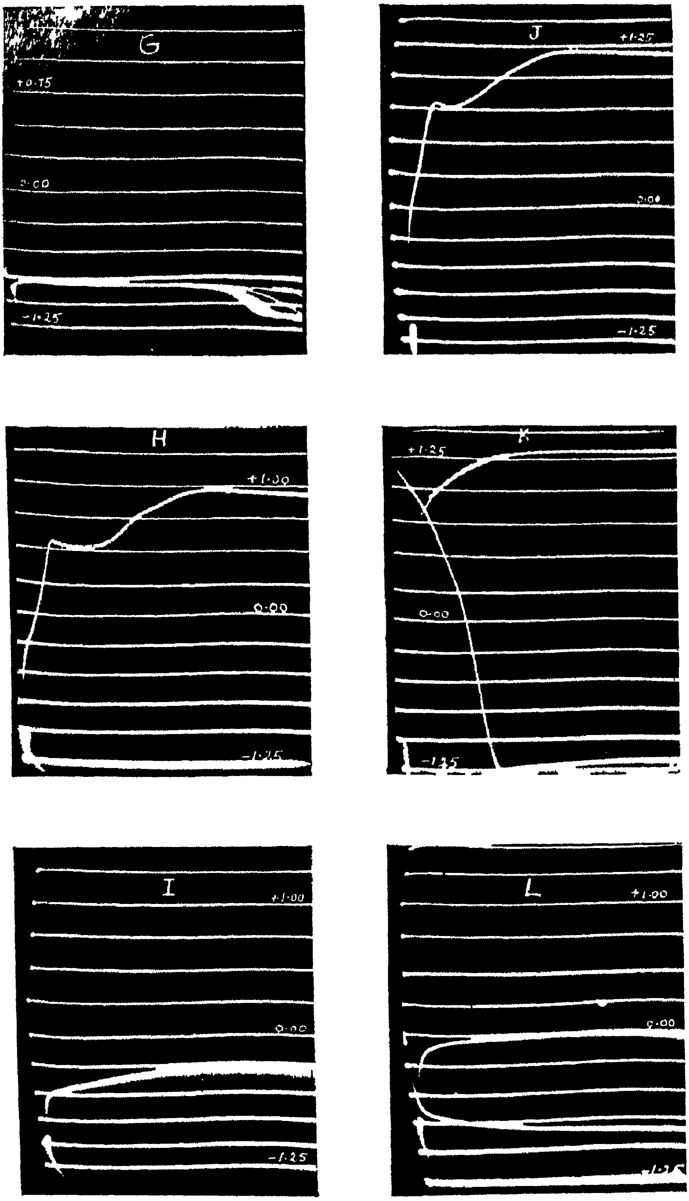
G
+0·75
0·00
−1·25
J
+1·25
0·00
−1·25
H
+1·00
0·00
−1·25
K
+1·25
0·00
−1·25
I
+1·00
0·00
−1·25
L
+1·00
0·00
−1·25

PLATE II.

Measurement of the True Area of the Cobalt Electrode.—For the complete interpretation of the oscillograms it is necessary to know the true area of the cobalt electrode used, and this involves the determination of the ratio accessible area/apparent area. No completely satisfactory method for the measurement of this ratio exists and, as has been previously emphasized,[6] this is a source of weakness in the oscillographic method of investigation. The only method which can be applied to small electrodes is that of Bowden and Rideal[7] in which the double layer capacity of the metal, when used as a cathode in acid solution, is measured and compared with that of mercury for which the accessible area is taken to be the same as the apparent area. This method was employed in the present work, using 0·1 N H_2SO_4 as electrolyte, and utilizing the usual oscillographic technique for the measurement of capacities. An average value of 81·5 μF was found for the minimum capacity per apparent sq. cm. of the cobalt electrodes prior to hydrogen evolution, while for mercury cathodes under identical conditions the average measured value was 11·5 μF/sq. cm. Thus it would appear that the ratio accessible area/apparent area for the electrodeposited cobalt electrodes is approximately 7.

Discussion

In alkaline solutions, cobalt gives a characteristic anodic polarization track, which is not very dependent upon experimental variables, and in which 3 steps can be distinguished. In the Table are shown the starting potentials for these 3 arrests in various electrolytes compared with the equilibrium potentials of the various cobalt oxides as calculated from data given by Latimer.[8] The very close agreement between the starting potentials of the 1st and 2nd arrests and the equilibrium values for the systems Co/Co$(OH)_2$ and Co$(OH)_2$/Co$(OH)_3$, leaves little doubt that these two steps in the anodic polarization correspond to the consecutive formation of cobaltous and cobaltic hydroxides or oxides.[9] The starting potential for the 3rd arrest is rather lower than the equilibrium values quoted for systems containing CoO_2, but it is to be noted that these latter values are doubtful and regarded by Latimer[8] as probably too high.

Electrolyte	pH	Starting Potentials			Equilibrium Potentials		
		(1)	(2)	(3)	Co $Co(OH)_2$	$Co(OH)_2$ $Co(OH)_3$	$Co(OH)_3$ CoO_2
N NaOH .	14	−0·70	+0·20	+0·58	−0·73	+0·20	+0·7 v.
0·1 N NaOH .	13	−0·65	+0·23	+0·65	−0·67	+0·26	+0·76
N Na_2CO_3* .	12	−0·60	+0·32	+0·75	−0·61	+0·32	+0·82
0·1 M $Na_2B_4O_7$*	9·2	−0·45	+0·50	+0·90	−0·45	+0·47	+0·97

* The values on the oscillograms in these solutions were displaced owing to the presence of a resistance error; the quoted values were obtained by extrapolation from observations at different currents.

The quantities of electricity passed in the 3 steps can be estimated approximately from the oscillograms, and in N NaOH the average values are *ca.* 2000, 4000 and 3000 microcoulombs per apparent sq. cm. severally, which would correspond to the formation of 6·3 × 10^{15}, 12·6 × 10^{15} and 9·2 × 10^{15} atoms of oxygen in each case. Taking the specific gravity of cobalt as 8·8, the diameter of the cobalt atom may be calculated to be approximately 2·2 × 10^{-8} cm., and hence there would be about 2 × 10^{15}

---

[6] Cf. Hickling, *Quart. Rev.*, 1949, **3**, 99.

[7] *Proc. Roy. Soc. A*, 1928, **120**, 80.

[8] *Oxidation Potentials* (1938), p. 198.

[9] The present considerations would apply equally well to the formation of hydroxides or oxides, and, in general, these possibilities cannot be satisfactorily distinguished.

atoms of metal per true sq. cm. or 14 × 10^{15} atoms of metal per apparent sq. cm. at a cobalt surface, assuming the measured value of 7 for the ratio accessible area/apparent area to be correct. The ratios atoms O to atoms Co at the end of each of the 3 steps are therefore approximately 0·5, 1·4 and 2·0. It would thus appear that CoO is formed in the 1st step but is further oxidized to Co_2O_3 when the surface is only partly covered with the lower oxide; an approximately unimolecular film of Co_2O_3 is then formed, which is in turn oxidized to CoO_2 before oxygen evolution commences. The extent of the 1st step varies with the nature of the electrolyte, and, as has been shown, in solutions in which cobaltous oxide is readily soluble, such as hot concentrated alkali or in ammoniacal solutions, it may be extended indefinitely. Even in N NaOH at 18° C it is possible that some dissolution occurs; this would account for the very negative step in the cathodic track which might be attributed to deposition of cobalt from cobaltite solution, and to the further shortening of the 1st anodic arrest in electrolytes of lower pH in which the oxide would be expected to be less soluble than in N NaOH. The extents of the 2nd and 3rd steps seem to be approximately the same in all the electrolytes of pH 9-14, and it would seem therefore that in these solutions cobalt owes its passivity primarily to the formation of a protective film of Co_2O_3, which is subsequently oxidized to CoO_2; in this respect it is analogous to nickel previously studied,[5] although here no other oxides than Ni_2O_3 were detected. From the present results the potential of the system Co_2O_3/CoO_2 is $+ 0·58$ V in N NaOH. To obtain further information as to the potential of CoO_2 and its stability, a 2 sq. cm. cobalt electrode was polarized anodically with a current of 0·04 A for 5 min. and the current was then interrupted and the potential of the electrode against a calomel reference electrode was followed on a valve voltmeter; the potential of the polarized cobalt anode dropped almost immediately to *ca.* $+0·6$ V, halted for a short time at $+0·59$ V and then dropped slowly over a period of more than an hour towards the CoO/Co_2O_3 value. This confirms the oscillograph value for the potential of CoO_2 and indicates that this oxide is essentially unstable.

Department of Inorganic and Physical Chemistry,
University of Liverpool.

EXPERIMENTS WITH COOL FLAMES

I—INDUCTION PERIODS

By F. E. Malherbe * and A. D. Walsh †

Received 6th March, 1950

Plots of cool flame induction period against total pressure in *n*-butane-oxygen mixtures are described. As the induction period tends to infinity, the plot becomes asymptotic to the line $P = P'$, where $P' >$ zero. P' is a function of temperature. Similar curves are shown for *n*-pentane and *n*-hexane. For these fuels the cool flame ceases to appear below a pressure at which the induction period is comparatively small: the time intervals to the maximum rate of slow oxidation plotted against pressure continue the curve of cool flame

---

* Present address: The Chemistry Department, The University of Pretoria, S. Africa.

† Present address: The Chemistry Department, The University of Leeds.

induction period against pressure. For all three fuels, plots of log (induction period) against $1/T$ do not give straight lines, but shallow curves whose slope falls off both as the temperature rises and as the total pressure increases. The induction period against pressure curves become more sharply bent as the temperature rises. On the basis of these facts an equation previously proposed by Russian workers for the variation of induction period with temperature and pressure is shown to be invalid and is replaced by a new equation that follows naturally from the theory of branched-chain reactions. The general theory is made specific by application to the autocatalytic formation of alkyl hydroperoxides and their breakdown to further products. All the above facts appear to be explicable in terms of these processes. The condition for a cool flame to arise is not simply that the net branching factor is greater than zero: a further condition, probably of thermal nature, has also to be satisfied.

A systematic study of combustion phenomena in ethers has already been reported.[1, 2, 3, 4] This study included a careful delineation of the cool flame pressure-temperature boundary and the effect upon it of a wide range of additives. It also included a study of the effect of certain additives on the time interval preceding the appearance of a cool flame. In general, however, the ethers are not convenient fuels for the study of cool flame induction periods since, under most conditions, the latter are too short to be easily measured. Attention was therefore turned to the *n*-paraffins, with which the induction periods preceding cool flames are more easily measured.

Experimental

The experiments reported here were carried out using an apparatus described elsewhere [2] and which in its final form was built by Dr. G. H. N. Chamberlain, to whom we should like to acknowledge our indebtedness. All times were measured with a stop-watch. The occurrence of a cool flame was noted either by watching a Bourdon pressure gauge or by direct observation through a window in the furnace. In our experience the secret of obtaining good reproducibility lies in rigid standardization of pumping times and other procedures (see [2]). In order to achieve this, all the curves reported for any one fuel were obtained on one day, If the routine *was* interrupted in any way, the series was started over again. The first few runs of a day were discarded. Two reaction vessels were used, one of quartz (25 cm. long and 3·9 cm. diam.) and one of Pyrex (22 cm. long and 3·3 cm. diam.). The hydrocarbons used were obtained as specially pure samples from the Phillips Petroleum Company (*n*-butane) and the Shell Petroleum Company (*n*-pentane and *n*-hexane). In each case they were further purified by distillations *in vacuo* from one liquid air trap to another, the middle fraction being taken at each step.

Results

Cool Flames in *n*-Butane.—The relationship between the induction period τ_1 preceding cool flames in a 50 % *n*-butane-oxygen mixture and the total pressure P of the mixture admitted to the reaction vessel is shown in Fig. 1. The Figure shows a family of $\tau_1 - P$ curves obtained with the Pyrex vessel and plotted at temperatures T°K ranging from 290° C to 360° C. These curves are typical of many that we have plotted. It is clear that as the pressure tends to infinity the curve becomes asymptotic to the line $\tau_1 = 0$, but that as the time tends to infinity the curve does not become asymptotic to the line $P = 0$. It is also clear from Fig. 1 that the curves become more sharply bent as the temperature rises. We discuss below the form of the mathematical equation required to represent the curves.

---

[1] Chamberlain and Walsh, *Rev. Inst. Français du Pétrole*, 1949, 4, 301.

[2] Chamberlain and Walsh, 3rd *Symp. Combustion, Flame and Explosion Phenomena* (Williams and Wilkins, Baltimore, 1949), p. 368.

[3] Chamberlain and Walsh, *ibid*, p. 375.

[4] Chamberlain and Walsh (in course of publication).

Plots of log τ_1 against $1/T$ at constant pressure give shallow curves rather than straight lines. Fig. 2 and 3 show, for example, plots for various constant total pressures. The slope ($\Delta \log \tau_1/\Delta(1/T)$) tends to fall off both as the temperature rises and as the total pressure increases.

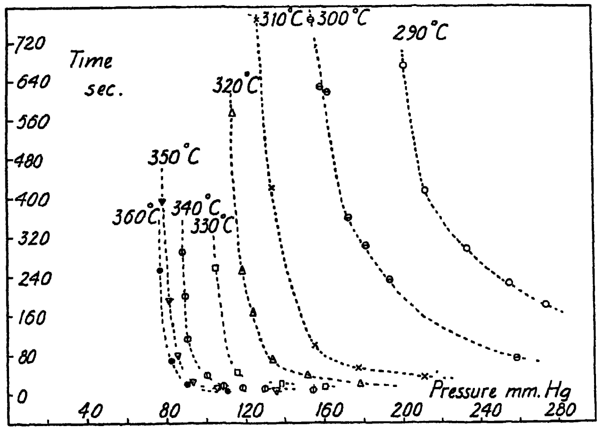

FIG. 1.—Cool flames in *n*-butane. Pyrex vessel. 50 % mixture. Temperatures from 290° C to 360° C.

Cool Flames in *n*-Pentane.—Fig. 4 shows a family of τ_1 against P curves plotted at various temperatures from 270° C to 330° C for a 50 % *n*-pentane-oxygen mixture in the Pyrex vessel. The family lies at much lower pressures and shorter time intervals than the corresponding one for *n*-butane.

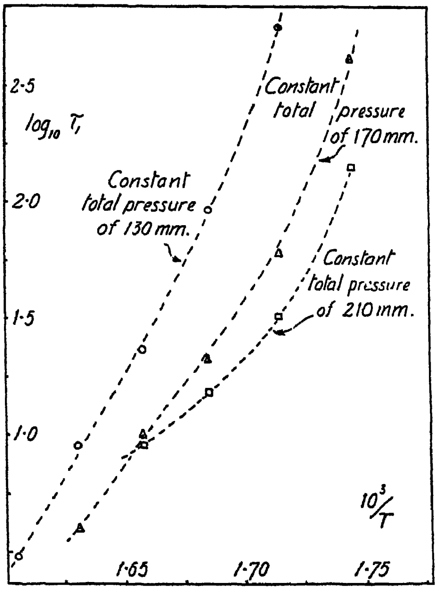

FIG. 2.—Cool flames in *n*-butane. Pyrex vessel. 50 % mixture.
Plots of log τ_1 against $1/T$ at different constant total pressures.

The *n*-pentane curves show an important feature that was not present with the *n*-butane curves. With *n*-butane, the curve of time interval τ_1 required for the appearance of a cool flame plotted against pressure could be continued apparently to indefinitely high values of τ_1. For *n*-pentane, however, as the curve is continued from high pressures towards lower pressures, there comes a point when the cool flame abruptly ceases to appear. In other words the pressure asymptote to which the $\tau_1 - P$ curve tends as $\tau_1 \rightarrow \infty$ is equal to the minimum pressure required for a cool flame at a particular temperature with *n*-butane, but lies at a pressure below the minimum pressure required for a cool flame at a particular temperature with *n*-pentane.

For *n*-pentane, at a pressure slightly below the minimum required for a cool flame at a particular temperature, rapid "slow oxidation" is observed after a certain time interval. If the time intervals τ_1' required for this slow oxidation to attain its maximum rate at various pressures are determined, the points are found to lie on a curve continuous with that of τ_1 against P. Such points are plotted in Fig. 4 which shows that the *n*-pentane $\tau_1 - P$ curves, like those for *n*-butane, become more sharply bent as the temperature rises. Fig. 5

shows plots of log τ_1 against $1/T$ for constant total pressures of 140 and 185 mm. of a 50 % n-pentane-oxygen mixture. The plots are not linear, but, as for n-butane, fall off in slope as either the temperature or pressure rises.

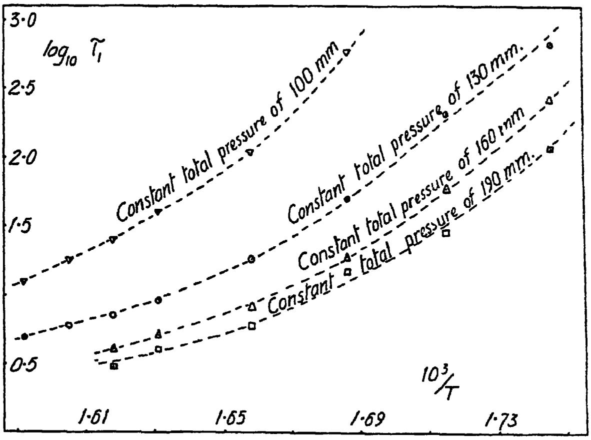

FIG. 3.—Cool flames in n-butane. Quartz vessel. 50 % mixture. Plots of log τ_1 against $1/T$ at different constant total pressures.

Cool Flames in n-Hexane.—Fig. 4 shows a family of curves plotted at various temperatures from 280° C to 330° C for a 30 % n-hexane-oxygen mixture in the Pyrex vessel. The law connecting τ_1 and P is obviously of the same form as for the n-butane and n-pentane curves. The curves become more sharply bent as the temperature rises. As for n-pentane, the cool flame fails to appear below a certain limiting pressure at any particular temperature, the time intervals to the maximum rate of slow oxidation then continuing the plot of τ_1 against P.

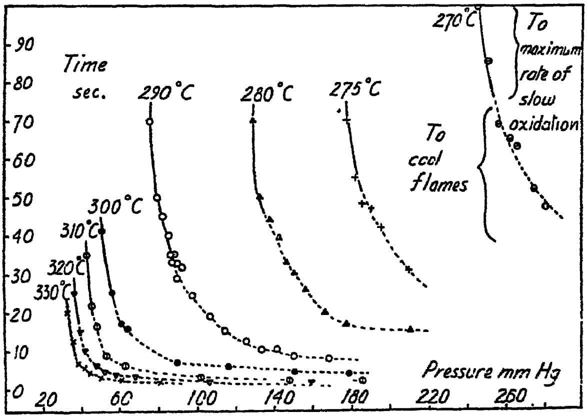

FIG. 4.—Cool flames in n-pentane. Pyrex vessel. 50 % mixture. Temperatures from 270° C to 330° C.

.... time to cool flame.

———— time to maximum rate of slow oxidation.

In Fig. 6 a line has been drawn to connect the pressure limits at different temperatures, so that at all points above this line the time interval represents that to attain maximum rate of slow oxidation and at all points below the line it represents the time to the appearance of a cool flame. Fig. 4 and 6 show that for n-pentane and n-hexane there is a finite time interval characterizing the

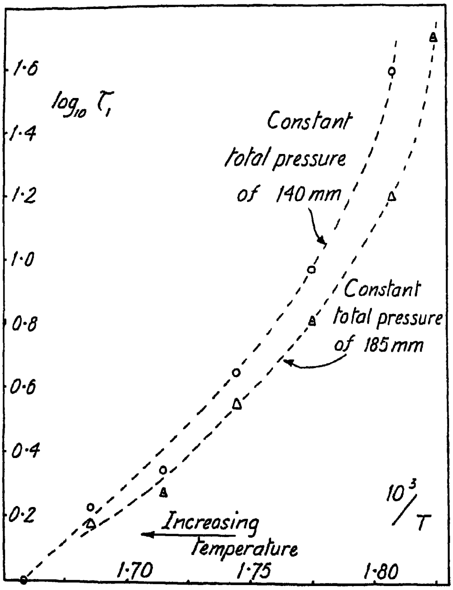

FIG. 5.—Cool flames in *n*-pentane. Pyrex vessel. 50 % mixture. Constant total pressure. Plots of log τ_1 against $1/T$.

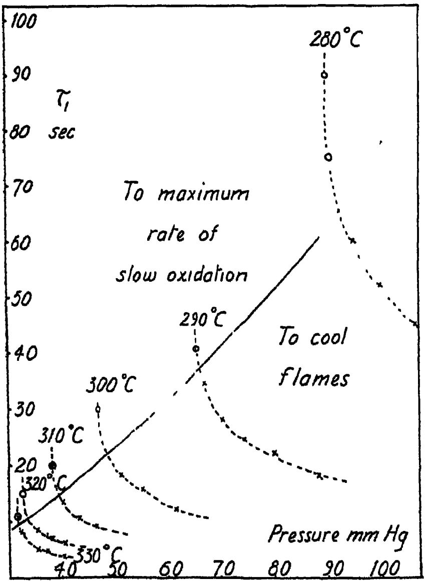

FIG. 6.—Cool flames in *n*-hexane. Pyrex vessel. 30 % mixture.

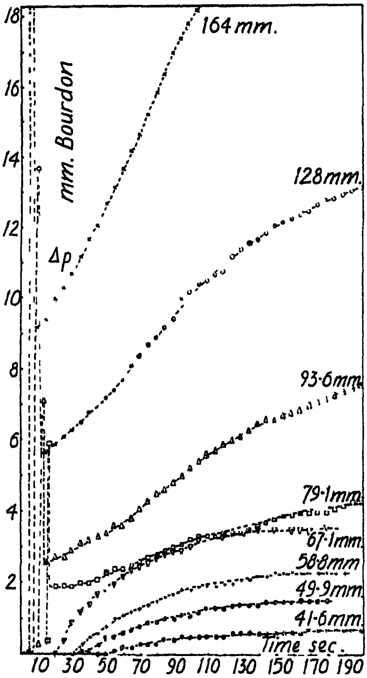

FIG. 7.—Cool flames and slow oxidation for *n*-hexane at 290° C. Pyrex vessel. 15 % mixture. 0·829 mm. Bourdon = 1 mm. Hg.

appearance of the cool flame at the limiting pressure, whereas under the conditions of our experiments the corresponding time interval for *n*-butane is apparently infinite. In the past, it has been common for investigators to write alongside cool flame limit curves values purporting to represent the induction period of the cool flame at the limiting pressure. It is clear from Fig. 1, 4 and 6 that these values are likely to differ considerably according to the limits between which the limiting pressure is bracketed: the only accurate way of obtaining them is to plot curves such as those of Fig. 4 and 6 and to bracket the critical pressure between narrow limits.

Fig. 7 shows pressure-time observations for a 15 % *n*-hexane-oxygen mixture in the Pyrex vessel at 290° C. At the four lowest initial pressures only slow oxidation occurred; at the higher initial pressures cool flames occurred, the pressure gauge showing a kick at the instant the cool flame occurred, followed by a smaller drop and slow oxidation thenceforward occurring at a roughly constant rate for some considerable time. The pressure against time plots when no cool flame occurred are reminiscent of these previously reported[3] for di-*iso*propyl ether in the cool flame temperature range. They show much longer induction periods than those for the ether but again a rather abrupt transition from a very low rate of pressure rise to the maximum rate, the rate then beginning and continuing to fall off with time.

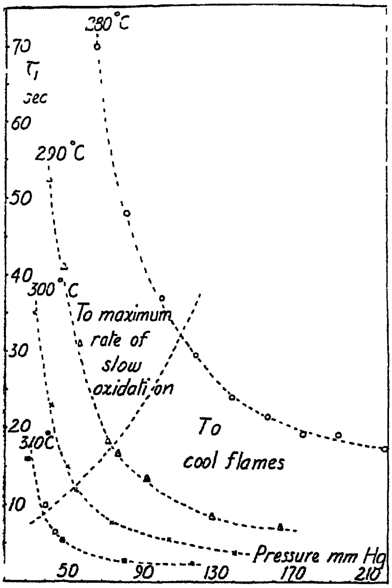

FIG. 8.—τ_1 against P plots for a 15 % *n*-hexane mixture at 280, 290, 300, 310° C.

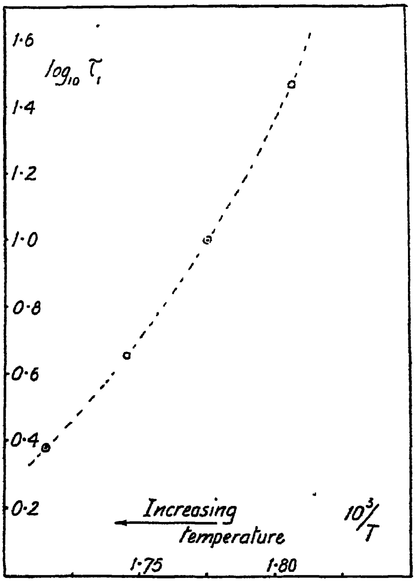

FIG. 9.—Plot of $\log_{10} \tau_1$ against $1/T$ at constant pressure of 120 mm. for a 15 % *n*-hexane mixture.

Fig. 8 shows plots of pressure against time interval to the cool flame or to the maximum rate of slow oxidation, the data being derived from Figures similar to 7. The curves become more sharply bent as the temperature rises. Again a line has been drawn to connect the cool flame pressure limits at different temperatures. Fig. 9 shows that for the 15 % mixture also the plot of $\log_{10} \tau_1$ against $1/T$ at constant pressure is not linear, but has a slope that falls off with rising temperature.

Plots of $\log_{10}$ (maximum rate of slow oxidation) against $\log_{10} P_{\text{total}}$ for those curves of Fig. 7 (and for similar curves at 280° C and 300° C) that did not lead to cool flames, reveal a dependence of the maximum rate of slow oxidation on a power of the total pressure varying between 3 and 4. Similarly, the maximum rate of slow oxidation of di-*iso*propyl ether at 220° C has been found[4] to depend on the 3·6th power of the total pressure.

Discussion

General Application of the Theory of Degenerate Branching.—The first point we wish to make is that the oxidation process responsible for the phenomena reported in this paper involves branching chains. The evidence includes (*a*) the suddenness with which reaction sets in as the pressure is gradually increased. At a pressure just below that corresponding to the asymptote as $\tau_1 \rightarrow \infty$ for any of the curves in Fig. 1, 4 and 8, the observed rate of reaction is very low. As the pressure is increased, measurable reaction sets in abruptly. (*b*) The two facts that oxidation in the cool flame temperature range is known to yield alkyl hydroperoxides as intermediate products [2, 5, 6] and that these are known readily to give rise to radical chain centres.

This being so, we may characterize the oxidation by the familiar equation [7]

$$dn/dt = \theta + \phi n, \quad . \quad . \quad . \quad . \quad (1)$$

where θ is the rate of initiation of chains, ϕ is the net branching factor and n is the number of chain centres. More specifically,

$$d(ROOH)/dt = \theta + \phi(ROOH). \quad . \quad . \quad . \quad (2)$$

Each ROOH molecule can be considered as a chain centre. Eqn. (2) then expresses the autocatalytic nature of the formation of alkyl hydroperoxides. Autocatalysis is assumed because of the known formation of the peroxides as products and their promoting effect when added to oxidation processes of the type discussed here.[8] At lower temperatures, using liquid di-*iso*propyl ether, the autocatalytic nature of peroxide formation has been directly observed.[9]

The observation that for *n*-pentane and *n*-hexane a plot of the time intervals to the maximum rate of slow oxidation against pressure is continuous with a plot of the induction periods to the cool flame against pressure (Fig. 4, 6 and 8) is important, for it shows that the cool flame is not an entirely separate phenomenon from the slow oxidation pressure rise that is commonly observed to precede it and which, for *n*-pentane and *n*-hexane, replaces it below a critical pressure. Rather, the cool flame is a phenomenon that arises out of the slow oxidation. As the pressure is increased, the rate of the slow oxidation increases, until at a critical pressure it gives rise to a form of explosion. The explosion is of a peculiar nature since it is quickly quenched by the formaldehyde to which it gives rise.[10, 11, 2, 3] It is this self-quenched explosion that is called the cool flame. To explain the continuity of the curves of τ_1 against P and τ_1' against P it is supposed that the cool flame arises when the rate of the slow oxidation (which increases with pressure) reaches a critical value. Below a certain pressure the maximum rate of the slow oxidation is less than the critical value and therefore no cool flame appears. Above that pressure the slow oxidation rate will attain the critical value before it reaches its maximum value, but the time interval to the attainment of the critical value (i.e. to the cool flame) will only be slightly less than that to the maximum value, since the reaction accelerates very rapidly just before the maximum rate is attained.

The pressure corresponding to the asymptote (as $\tau_1 \rightarrow \infty$) of a $\tau_1 - P$

---

[5] Walsh, *Trans. Faraday Soc.*, 1946, **42**, 269.

[6] For recent work showing the connection of peroxide formation with the cool flame process, see Friedlander and Grunberg, *J. Inst. Petr.*, 1948, **34**, 490; cf. Burgoyne, *Proc. Roy. Soc. A*, 1940, **175**, 539.

[7] Semenoff, *Chemical Kinetics and Chain Reactions* (Oxford, 1935).

[8] Blat, Gerber and Neumann, *Acta Physicochim.*, 1939, **10**, 283.

[9] Molodovskii and Neumann, *J. Physic. Chem. Soc. Russ.*, 1949, **23**, 30.

[10] Cullis and Hinshelwood, *Faraday Soc. Discussions*, 1947, 117.

[11] Walsh, *Trans. Faraday Soc.*, 1946, **42**, 321.

graph for hydrocarbons at " low " temperatures is, in certain ways, the analogue of the first pressure limit of explosion in hydrogen-oxygen mixtures. In both cases the reaction rate increases abruptly as the critical pressure is reached and in both cases the explanation is that ϕ, the net branching factor, has just become positive. But whereas in the hydrogen-oxygen reaction when ϕ becomes positive explosion invariably ensues, Fig. 4, 6 and 8 show that

$$\phi > 0 \quad . \quad . \quad . \quad . \quad . \quad (3)$$

is not a sufficient condition for a cool flame to occur.

The reason for this is primarily the much slower development with time of the hydrocarbon oxidation chains relative to the hydrogen chains. To explain this, Semenoff (ref. 7, p. 68) supposed that the branching in hydrocarbon oxidation was not of the " continuous " type encountered in the low pressure hydrogen-oxygen reaction (where branching is supposed to occur in every propagation cycle) but of an occasional type due to the reaction of a comparatively stable molecular product. Semenoff's idea fits the facts of hydrocarbon combustion very well. At " low " temperatures alkyl hydroperoxides play the part of the comparatively stable products that give rise to new chain centres. At higher temperatures, when alkyl hydroperoxides are no longer formed, aldehydes play a corresponding role.[1]

Semenoff pointed out that such a slowly branching reaction would probably never show a true branched-chain explosion, for by the time the number of reaction chains had developed to a considerable extent the consumption of reactants and their dilution with products would mean that only rapid reaction (a " degenerate explosion ") was likely to occur. Semenoff termed such a case a " degenerate branching " system. If explosion was encountered in a degenerate branching system, it was likely to be due to the heat produced exceeding that dissipated.

The relevance of this to the present facts is as follows. Eqn. (3) defines the pressure asymptote but not necessarily the cool flame limit. It is clear therefore that one cannot interpret the cool flame as a simple branching chain explosion. Evidently a further condition, as well as (3), has to be satisfied for the cool flame to arise. As we have stated, it is probable that a particular reaction rate, i.e. a particular concentration of centres n_0 has to be exceeded ; and the interpretation of n_0 is that it represents that concentration of centres which is required to cause the heat produced to exceed that dissipated. The appearance of a cool flame involves the satisfying of both a branched-chain and a thermal condition. For that reason, the explosion that occurs at the cool flame pressure limit is not necessarily an abrupt transition from negligible reaction as it is at the hydrogen-oxygen low pressure explosion limits : it may, as with *n*-pentane and *n*-hexane, be much more gradual. This links with the conclusion from studies of the propagation of cool flames [12, 13] namely, that both reaction chains and self-heating are important factors in the propagation.

The probable reason why, for *n*-butane, in contrast to *n*-pentane and *n*-hexane, the pressure asymptote on the $\tau_1 - P$ graph is identical with the cool flame pressure limit, is that the pressure asymptote lies at much higher pressures for *n*-butane than for *n*-pentane or *n*-hexane. It is plausible, therefore, that for *n*-butane, once ϕ becomes positive and oxidation starts, so much heat is produced per volume element that the thermal condition is automatically satisfied.

Since the normal flame at " low " temperatures is known only to arise after a prior cool flame, it is probable that three conditions have to be satisfied for a normal flame to occur at " low " temperatures : (i) ϕ, the

---

[12] Neumann, Rubin and Schnoll, *J. Physic. Chem. Soc. Russ.*, 1948, **22**, 641.

[13] Spence and Townend, 3rd *Symp. Combustion, Flame and Explosion Phenomena* (Williams and Wilkins, Baltimore, 1949), p. 404.

net branching factor for the increase of peroxide concentration, must be > 0; (ii) the peroxide concentration must rise beyond the critical value $(ROOH)_c$ which satisfies a thermal condition for the propagation of a cool flame; (iii) the rate of the cool flame reaction that ensues when (i) and (ii) are fulfilled must exceed some second thermally-dependent value. The second thermally-dependent critical pressure is much higher than the first because the hot flame propagation involves a much more intense oxidation process and temperature rise than the cool flame.

Applying the theory of branching chains,[7]

$$\phi\tau = \text{constant}, \qquad (4)$$

and

$$\phi = f - g - y, \qquad (5)$$

where f is the coefficient of linear branching, g and y are the coefficients of termination of chains by removal of centres singly in the gas phase (g) and at the wall (y). More specifically, ϕ from its definition in (2) must be of the form

$$\phi = f(P) - A, \qquad (6)$$

where $[f(P)]$ROOH gives the rate of chain formation of peroxides and A(ROOH) gives the rate of removal of peroxides. A may or may not vary with pressure, depending on the reactions whereby peroxides are destroyed. Consideration shows, however (cf. below), that $f(P)$ is likely to increase with pressure more rapidly than A. τ in eqn. (4) is the time to the occurrence of the degenerate explosion, i.e. of the maximum rate of slow oxidation. As explained above, this is practically synonymous with the time to the occurrence of a cool flame.

The Semenoff theory of degenerate branching implies that f, the coefficient of absolute branching, is much smaller for hydrocarbon-oxygen mixtures than for hydrogen-oxygen mixtures under similar conditions. Consequently, the pressure has to be raised to a much higher value in the former mixtures than in the latter to cause (by, for example, reduction of y) ϕ to become positive. This in turn may be the reason why the former mixtures do not usually show three pressure limits of explosion at constant temperature. The pressure for ϕ first to become positive is so high that gas-phase deactivation is simultaneously operative:[14] there is no separation of the pressure ranges in which surface and gas-phase deactivation control branching. (There is, however, separation of the temperature ranges in which these processes are dominant (see Part III)). The pressure required for ϕ to become positive in hydrocarbon-oxygen mixtures is the higher because of destruction of chains by the formaldehyde formed as a product. This probably occurs by interaction of formaldehyde with peroxide.[2, 3] The self-inhibition is another reason for the slowness of development of the hydrocarbon combustion chains even when ϕ is positive; and accounts also for the characteristic shape of the " low " temperature slow oxidation Δp against time curves (Fig. 7: cf. [2] and Fig. 8 of ref.[14]). The slope of the latter curves begins to fall off more rapidly and earlier than for the corresponding curves at " high " temperatures. Inhibition by formaldehyde (which increases in concentration as the reaction proceeds) is also a reason, in addition to consumption of reactants and dilution with products, why (3) is not a sufficient condition (as (1) or (2) suggests) for the number of centres to grow indefinitely.

Application to Results.—The form of the law connecting induction periods with pressure in oxidation reactions (e.g. in the oxidation of di-*iso*propyl ether at a temperature above its cool flame range [1] and in the oxidation of methane at 480° C [4]) has frequently been found to be

$$\tau P^n \doteqdot \text{constant}. \qquad (7)$$

Since, however, the $\tau_1 - P$ curves for *n*-butane (see Fig. 1) do not become even approximately asymptotic to the time axis as $\tau_1 \rightarrow \infty$, it is clear that the relationship between τ_1 and P cannot be represented by (7).

---

[14] Norrish and Reagh, *Proc. Roy. Soc. A*, 1940, 176, 429.

Russian workers,[8] have realized this and have sought to replace (7) by

$$\tau_1(P - P_0)^n = \text{constant}, \quad . \quad . \quad . \quad . \quad (8)$$

where P_0 is the asymptote to which the curve tends as $\tau_1 \rightarrow \infty$. It is difficult to test adequately eqn. (8) since, for the points at lower pressures, $P - P_0$ is very sensitive to the choice of P_0; and the extrapolation of the curve of τ_1 against P to $\tau_1 = \infty$ yields a rather uncertain value for P_0. In any case, however, it is difficult to see how the term $(P - P_0)$ can arise from kinetic equations which ultimately are an expression of the law of mass action.

The discussion in the previous section suggests that the correct expression is of the form

$$\tau_1(f(P) - A) = \text{constant}. \quad . \quad . \quad . \quad (9)$$

Provided that $f(P)$ increases with pressure more rapidly than A, (9) can account for the general form of the plots of τ_1 against P. Eqn. (9) requires that the value of P as $\tau_1 \rightarrow \infty$ be given by the solution of the equation

$$f(P) = A. \quad . \quad . \quad . \quad . \quad . \quad (10)$$

The Russian workers measured the values of τ_1 at constant pressure at different temperatures, found an approximate straight line plot for log $\tau_1 - 1/T$ and therefore expressed the dependence of τ_1 on temperature by the modified equation

$$\tau_1(P - P_0)^n e^{\gamma/T} = \text{constant}. \quad . \quad . \quad . \quad (11)$$

Fig. 1, 4 and 8, however, make it clear that this cannot be an adequate equation for the expression of the relation between τ_1, P and T—for, even if (8) were correct, it is clear from, say, Fig. 1 that P_0 is a function of temperature. Further, Fig. 2, 3, 5 and 9 show that the plot of log $\tau_1 - 1/T$ at constant pressure is a shallow curve rather than a straight line.

In terms of eqn. (9), the variation of τ_1 with temperature is expressed by making $f(P)$ and A functions of temperature. If $f(P)$ increases with temperature more rapidly than A, then (9) automatically effects a reduction with temperature rise not only of τ_1 but also of the value of P when $\tau_1 = \infty$. Suppose, for example, (9) has the particular form

$$\tau_1(Be^{-E_B/RT} . P^n - Ce^{-E_C/RT} . P) = D, \quad . \quad . \quad (12)$$

where B, C and D are constants independent of pressure and temperature. It is not suggested that this is necessarily the correct expression, but it exemplifies how an equation such as (9) can represent the observed changes with temperature. E_B is supposed greater than E_c. Then the value of P as $\tau_1 \rightarrow \infty$ is given by

$$P = \sqrt[n-1]{\frac{C}{B} \cdot e^{E_B - E_C/RT}} \quad . \quad . \quad . \quad . \quad (13)$$

This value decreases with rise of temperature in qualitative accord with Fig. 1. Furthermore,

$$\tau_1 = \frac{\dfrac{D}{B} \cdot e^{-E_B/RT}}{P^n - \dfrac{C}{B} \cdot e^{E_B - E_C/RT} . P} \quad . \quad . \quad . \quad . \quad (14)$$

and τ_1 decreases, at constant pressure, with rise of temperature, again in qualitative accord with Fig. 1.

Fig. 1, 4, 6 and 8 show that the $\tau_1 - P$ curves become more sharply bent as the temperature rises. It can readily be shown, by trying particular values of n, E and F in the equation

$$\tau_1(P^n - E) = F \quad . \quad . \quad . \quad . \quad (15)$$

that the plot of τ_1 against P becomes more sharply bent as F decreases.

Comparison of (15) with (14) shows that decrease of F takes place with rise of temperature. (14) can therefore account for the observed fact. (It is assumed that the effect of decrease of F upon the shape of the $\tau_1 - P$ curves is only partly offset by the simultaneous decrease of E that takes place : (14) and (15) show that E decreases less rapidly with rise of temperature than does F.)

From (14)

$$\ln \tau_1 = \ln (D/B + E_B/RT) - \ln (P^n - C/B \, . \, e^{E_B - E_C/RT} \, . \, P).$$

Hence

$$\frac{d \ln \tau_1}{d(1/T)} = E_B/R + \frac{(C/B) \, . \, e^{E_B - E_C/RT} \, . \, P \, . \, \dfrac{E_B - E_c}{R}}{P^n - (C/B) \, . \, e^{E_B - E_C/RT} \, . \, P}$$

$$= E_B/R + \frac{C(E_B - E_C)}{RB} \, . \left[\frac{1}{P^{n-1} \, e^{-(E_B - E_C)/RT} - C/B}\right] . \qquad (16)$$

which decreases both with increase of pressure and with increase of temperature in qualitative accord with Fig. 2, 3 5 and 9.

(3) **Chain Reaction Steps.**—Eqn. (2) and (6), and hence (9) in contrast to (8), are now shown to arise from an application of the law of mass action to the probable chemical equations governing the cool flame oxidation chains. It is not suggested that the following equations comprise an exhaustive and perfectly correct set of chemical reactions ; but they will serve to illustrate how (2) and (6) arise, even though some of them may have to be replaced by others as more knowledge accumulates. For initiation we write [1]

$$\mathrm{RH + O_2 \rightarrow R + HO_2} \quad . \quad . \quad . \quad (I)$$

and for propagation of the peroxide-producing chains,

$$\mathrm{R + O_2 \rightarrow RO_2^*} \quad . \quad . \quad . \quad . \quad (II)$$

$$\mathrm{RO_2^* + RH \rightarrow ROOH + R} \quad . \quad . \quad (III)$$

The R radical in these equations will be one derived from the parent hydrocarbon by removal of an H atom from a secondary C atom. (I) is a plausible example of a commonly found reaction, namely H removal by a radical from a molecule. (III) is of the same well-established type. (II) is an example of another common reaction, namely the association of two free radicals. The product of the association is written with an asterisk to denote that it must, in the first place, contain its own energy of formation. The peroxide formed in (III) may undergo a unimolecular breakdown to radicals. In the presence of O_2 molecules it is likely, however, that reaction with oxygen (to give a similar set of radicals) will be the faster. At any rate, partly for reasons that will be given in the following papers, we shall assume it here. The assumption is supported by the fact that the partial pressure of a peroxide required for ignition in air is much less than that required for explosion of the pure peroxide.[15] Reaction between ROOH and O_2 is likely to produce (cf. [5]) some, or all, of the following substances : formaldehyde, acetaldehyde, simple olefins, simple ketones, OH radicals, methyl or ethyl radicals, inert HO_2 radicals. Of these, the methyl or ethyl radicals will produce further OH radicals by reaction with oxygen. For the present purpose it is sufficient to simplify the reaction by writing

$$\mathrm{ROOH + O_2 \rightarrow OH} \quad . \quad . \quad . \quad . \quad (IV)$$

A plausible example would be

$$\mathrm{CH_3CH(OOH) \, . \, CH_3 + O_2 \rightarrow HO_2 + CH_3\overset{|}{C}(OOH) \, . \, CH_3 \rightarrow (CH_3)_2CO + OH.}$$

Reaction (IV) will be followed by

$$\mathrm{OH + RH \rightarrow R + H_2O} \quad . \quad . \quad . \quad (V)$$

---

[15] Harris, *Proc. Roy. Soc. A*, 1939, **173**, 126 ; 1938, **168**, 1.

Surface destruction of OH and RO_2^* radicals must be allowed for :

$$OH + \text{Surface} \rightarrow \text{destruction} \quad . \quad . \quad . \quad (VI)$$

$$RO_2^* + \text{Surface} \rightarrow \text{destruction} \quad . \quad . \quad . \quad (VII)$$

Surface destruction of R radicals will be less important because of their removal by the fast reaction (II).

Destruction of peroxide to products other than radicals must also be allowed for :

$$ROOH \underset{RH}{\rightarrow} \text{destruction} \quad . \quad . \quad . \quad . \quad (VIII)$$

This destruction is assumed to be particularly favoured by collisions with RH, whereas collisions with O_2 favour the branching reaction (IV).

These equations, if a steady state were maintained, yield the equation

$$\frac{d(ROOH)}{dt} = \theta + \phi\,(ROOH),$$

where
$$\theta = \frac{k_1k_3RH^2 . O_2}{k_7S},$$

$$\phi = \frac{k_3k_4\,RH . O_2}{k_7S(1 + k_6S/k_5RH)} - (k_4O_2 + k_8RH),$$

where S stands for the " concentration " of surface and will decrease with increase of pressure or with increase of vessel diameter. The condition for the steady state to cease to be applicable and (degenerate) explosion to ensue is $\phi > 0$. Evidently ϕ is of the form $f(P) - A$ and the example demonstrates how this form arises. Further, when $k_6S \ll k_5$ RH an equation of the form of (12) results.

Laboratory of Physical Chemistry,
Cambridge.

EXPERIMENTS WITH COOL FLAMES

II.—PRESSURE-TEMPERATURE LIMITS

By F. E. Malherbe and A. D. Walsh

Received 6th March, 1950

A search has been made for composite nature in the cool flame limit curves of *n*-hexane, *n*-pentane and *n*-butane. Breaks are found in these curves and shown to be present in curves plotted by other workers for propane. Each break is small and alone would not provide adequate evidence of a composite nature of the curve ; but cumulatively the extent and mutual consistency of the data make such a nature reasonably certain. This composite nature is reflected in hot flame limit curves, since at " low " temperatures the occurrence of a hot flame is dependent on the prior occurrence of a cool flame. In turn, the cool flame composite nature is a reflection of composite nature in the plot of maximum rate of slow oxidation (at constant initial pressure) against temperature. The latter is probably due to variations with temperature of the net branching factor ϕ. Increases in ϕ with temperature rise are interpreted as due to the onset of particular ways in which an oxygen molecule may attack an alkyl hydroperoxide molecule to give rise to free radicals. Since this attack is likely to result, in the first place, in abstraction of a hydrogen atom, increases in ϕ in separate temperature ranges are plausibly due to the different energies of activation which are required for O_2 attack at 1°, 2° and 3° CH bonds. In other words, the existence of composite nature in experimental quantities reflecting ϕ is correlated with the existence of different types of CH bond in the

alkyl hydroperoxide most readily formed by the fuel. This suggested correlation enables previously incoherent data on hot flame ignition curves in the " low " temperature region to be reduced to comparative, if still imperfect, order.

A number of workers have determined the pressure-temperature areas within which cool flames occur in a heated reaction vessel. In most cases these areas have been only roughly mapped and often no experimental points are recorded on the published figures. Maccormac and Townend[1] did, however, observe that the cool flame area for di-*iso*propyl ether appeared to be composite, a sharp break being visible in the limiting curve at a temperature of *ca.* 280° C. This observation was extended by Chamberlain and Walsh[2] who found the composite nature to be even more marked in the limit curve they plotted for diethyl ether. Fig. 1 reproduces a curve obtained by Chamberlain and Walsh. The curve is composed of two lobes separated by an inlet at *ca.* 275° C. The degree to which the inlet is accentuated depends upon the concentration of formaldehyde that is formed during the admission of the mixture to the reaction vessel and therefore upon the filling time. The two lobes correspond[2] to two maxima observed * in the plot of maximum rate of slow oxidation against temperature in the cool flame temperature region and to two lobes (observed both in pure ether-oxygen mixtures and especially in ether-oxygen-NO_2 or ether-oxygen-N_2 mixtures) found in the hot flame limit curve in the cool flame temperature region. If two lobes occur in the cool flame limit curve, they are likely to occur also in the limit curve for hot flames in the cool flame temperature region, since it has been shown (see ref. [2] for diethyl ether) that the hot flame at such temperatures only arises after the prior passage of a cool flame. In the presence of much inert gas (reducing surface-destruction of chains), the peak of the upper peninsula and the inlet in the cool flame limit curve are shifted to somewhat lower temperatures. The inlet is lowered by some 20° C in the change ether-oxygen to ether-air. Chamberlain and Walsh[2] have

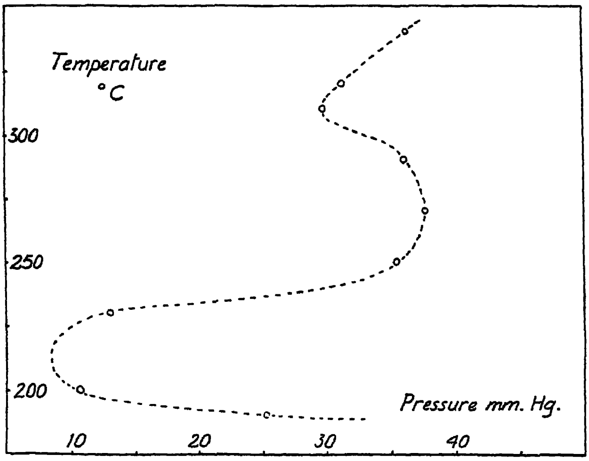

FIG. 1.—Cool flame limit curve for diethyl ether as plotted by Chamberlain and Walsh. 30 % ether—O_2. Quartz vessel.

---

[1] Maccormac and Townend, *J. Chem. Soc.*, 1938, 238.

[2] Chamberlain and Walsh, 3rd *Symp. Combustion, Flame and Explosion Phenomena* (Williams and Wilkins, Baltimore, 1949).

* These maxima have only been observed for di-*iso*propyl ether, but there is little doubt they exist also for diethyl ether.

shown how this can be understood. Consequently, since the hot flame limit curve lies at much higher pressures than the cool flame limit curve, the two lobes and inlet of the hot flame curve in the cool flame temperature region lie at somewhat lower temperatures than those of the cool flame limit curve. With 30 % diethyl ether-oxygen mixtures, the inlet in the hot flame curve lies some 20° C lower than in the cool flame curve. If the hot flame curve is plotted for hot flames arising in air instead of oxygen then the inlet lies even lower (230° C for 8·25 % diethyl ether-air as against 275° C for the 30 % ether-oxygen cool flame limit curve).

These observations for ethers provide a basis upon which an examination of the oxidation characteristics of other fuels can be founded. The particular question arises—are the cool flame limit curves for the paraffins also composite ?

On general grounds one might expect such composite nature, for, even with a fuel as simple as propane, more than one chain reaction path appears possible and it is probable that somewhat different mechanisms come into play in e.g. different temperature ranges. Turning to the hot flame limit curve, it is now well known that this is divisible into two main regions—a " high " temperature region above *ca.* 410° C and a " low " temperature region below that temperature.[3] Chamberlain and Walsh [2] showed that the " high " temperature hot flame ignition curve is further divisible into at least two regions, one above and one below *ca.* 450° C, the break at this temperature being due to the onset of a new initiation mechanism for the oxidation chains, namely the direct pyrolysis of the fuel vapour to radicals. In the " low " temperature region, the curves plotted by Townend and his co-workers [3] commonly show the presence of two lobes. Since, with diethyl ether,[2] the two lobes of the " low " temperature hot flame ignition curve have been shown to correspond to the two lobes of the cool flame limit curve, there is a strong suggestion that the two main lobes found in the " low " temperature hot flame ignition curve of paraffins, should also be found in the cool flame curves.

A main purpose of the present work was to test this expectation of composite nature in the cool flame limit curves for paraffins.

Experimental

It was realized that, since the inlet shown in Fig. 1 is only some 15 mm. Hg deep, in order clearly to show composite nature it would be necessary to measure the limits to a few mm. Doubtless it was because they only measured the limits to ± 38 mm. Hg that Townend and Chamberlain [4] did not observe the inlet with diethyl ether. They were, however, carrying out a pioneer survey of the field and naturally therefore were not concerned to measure limits to a high accuracy. For the present work, the cool flames have been observed either through a furnace window or by watching the movement of a Bourdon glass pressure gauge ; and the limits have been determined usually to ± 1 mm. The apparatus and the carefully standardized procedure to ensure reproducibility have already been described.[2] The reaction vessels were as described in Part I.

Results

Cool Flames in *n*-hexane-oxygen Mixtures.—Fig. 2 shows the pressure-temperature limits for the occurrence of cool flames in 80 %, 70 %, 50 % and 30 % *n*-hexane-oxygen mixtures in the Pyrex vessel. The limits were obtained from $\tau_1 - P$ curves such as shown in Fig. 6 and 8 of the preceding paper. The curves cannot be said to show a definite composite nature. It is possible, however, as has in fact been done, to draw them with a slight break at a temperature of *ca.* 330-350° C. The " break " is possibly observable in these curves, but if real it is most definite in the 30 % curve. This seemed possibly significant, since it was known that the upper lobe in the diethyl-ether cool flame curves became more prominent relative to the lower lobe in weak mixtures than in rich. Fig. 3, for example, shows limit curves plotted for various ether-oxygen mixtures.

---

[3] Townend, *Chem. Rev.*, 1937, **21**, 259.

[4] Townend and Chamberlain, *Proc. Roy. Soc. A*, 1937, **158**, 415.

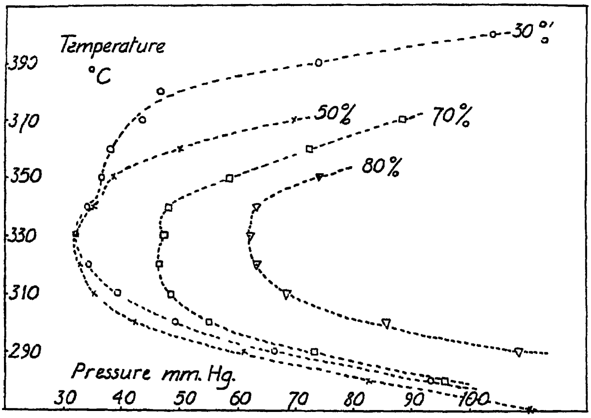

FIG. 2.—Cool flame limit curves for n-hexane mixtures of various compositions. Pyrex vessel.

The data on which they are based are taken from the published report by Chamberlain and Walsh.[2] It can be seen how the upper lobe varies much more with composition than does the lower and steadily increases in prominence relative to the lower lobe as one passes from the 80 to 70 to 50 to 30 to 20 % mixture. The reason for this has already been given.[2]

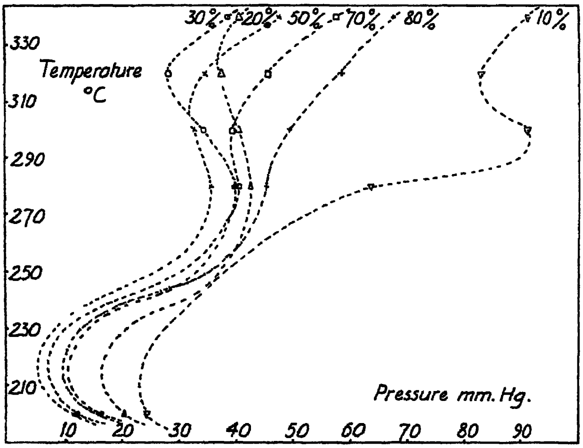

FIG. 3.—Cool flame limit curves for diethyl ether-oxygen mixtures. Quartz vessel.

Fig. 2 and 3 thus provided grounds for thinking an examination of the cool flame limits for a n-hexane-oxygen mixture weaker than 30 % might be profitable. Fig. 4 shows the results of such a study, by plotting the pressure-temperature limits for the occurrence of cool flames in a 15 % n-hexane-oxygen mixture. The curve shows two pressure minima, one about 340° C and one at about 360° C, separated by an inlet at about 348° C. This was consistent with the slight possibility suggested in Fig. 2 and the two diagrams *taken together* provide some confirmation of the idea that the cool flame limit curve for n-hexane is composite.

Nevertheless, the inlet in Fig. 4 is very small and barely outside the limits of experimental error. It was at this point, however, that we became aware of the work of Fréling.[5] Fréling has published cool flame limit curves for a 4·6 % *n*-hexane-air mixture in a quartz vessel 12·3 cm. long and 2·95 cm. diam. These curves show two peaks separated by a narrow inlet at 325-338° C and some 15-30° C wide according to the state of the surface. 4·6 % *n*-hexane-air corresponds to *ca.* 20 % *n*-hexane-oxygen. Moreover, the temperature of the inlet in Fréling's curves is some 15-20° C lower than the breaks or inlets of Fig. 2 and 4—which is just what would be expected from the comparison above of ether-oxygen and ether-air curves. Several small pieces of evidence, therefore, all fit together to show the composite nature of the *n*-hexane cool flame limit curve.

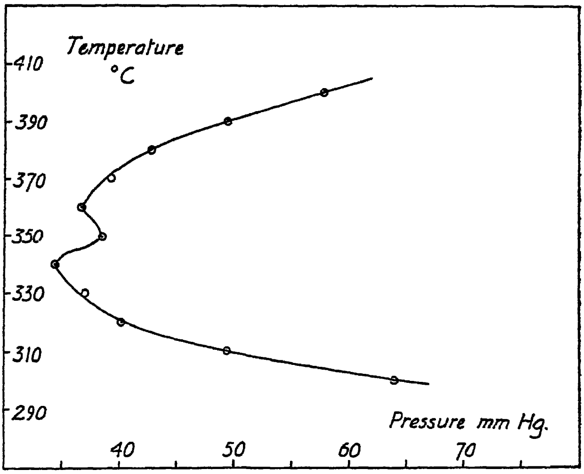

FIG. 4.—Cool flame limits for 15 % *n*-hexane—O_2. Pyrex vessel.

Townend, Cohen and Mandlekar[6] have published a hot flame limit curve for a 9·5 % *n*-hexane-oxygen mixture in a mild steel vessel. In the " low " temperature region this shows two main pressure minima at *ca.* 345° C and 290° C, with an inlet at *ca.* 325° C. In a glass (presumably Pyrex) vessel they find hot flame curves to lie *ca.* 20° C lower in temperature than in a mild steel vessel. The inlet therefore lies at a lower temperature for the hot flame curve than (as found here) for the cool flame curve under similar conditions —an observation in qualitative agreement with the facts discussed above for ethers. Townend, Cohen and Mandlekar[6] also give a hot flame curve for a 1·8 % *n*-hexane-oxygen mixture. This curve shows very well how much more prominent, relative to the lower lobe, the upper lobe becomes as the percentage *n*-hexane is reduced—again in agreement with these lobes being a reflection of lobes in the cool flame limit curve and with the behaviour of the ether cool flame limits. This is one of many examples of how systematic study of the combustion of ethers has provided some understanding of the detailed shapes of, and variation in, the many ignition curves plotted by Townend and his co-workers.

Cool Flames in *n*-pentane-oxygen Mixtures.—Fig. 5 shows a cool flame limit curve plotted for a 50 % *n*-pentane-oxygen mixture. This curve includes the data of Fig. 4 of the preceding paper together with data for 340-380° C. It suggests the presence of two lobes with a break between them at about 360° C. The effect is small and in itself would not provide adequate evidence of a composite nature for the limit curve. Taken in conjunction, however, with the evidence for *n*-hexane, *n*-butane and propane (see below) it is likely that the apparent composite nature is real. In further support, the hot flame limit curve given by Maccormac and Townend[1] for a 2·4 % *n*-pentane-air mixture shows two main lobes in the " low " temperature region, the temperature of the inlet being, as expected, considerably below 360° C.

---

[5] Fréling, *Colloque sur la Cinétique et le Mechanisme des Réactions* (Paris, April, 1948); see also Fréling and Laffitte, *Trans. Faraday Soc.*, 1946, **42**, 328.

[6] Townend, Cohen and Mandlekar, *Proc. Roy. Soc. A*, 1934, **146**, 113.

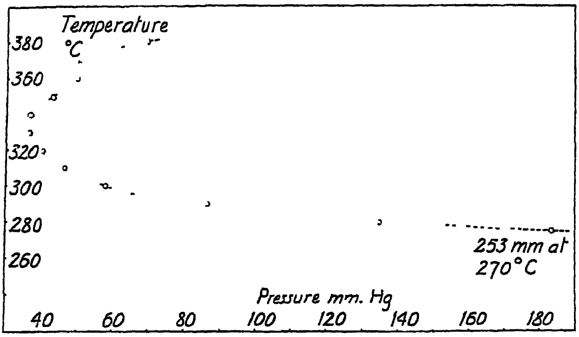

FIG. 5.—Cool flame limits for 50 % *n*-pentane—O_2. Pyrex vessel.

Cool Flames in *n*-butane-oxygen Mixtures.—Fig. 6 shows a cool flame limit curve plotted for a 50 % *n*-butane-oxygen mixture in the Pyrex vessel. This curve consists of the asymptotes (as $\tau_1 \rightarrow \infty$) of the curves in Fig. 1 of the preceding paper plotted against temperature (together with a curve at 370° C omitted, for the sake of clarity, from Fig. 1 of the preceding paper). It appears to show a break at a temperature of *ca.* 328° C. The break in the otherwise very smooth curve shows more definitely in a plot of log asymptote against 1/*T* (Fig. 7). Support is also found in a curve we have plotted for a 50 % *n*-butane-oxygen mixture in the quartz vessel. This curve (Fig. 8) suggests a break at *ca.* 335° C. It is noticeable that the limits of Fig. 6 are displaced much more to lower pressures in the wider quartz vessel (Fig. 8) if they lie at temperatures below the break than if they lie above. The hot flame curves of Townend, Cohen and Mandlekar[6] for *n*-hexane also show a much greater sensitivity of the lower lobe in the " low " temperature region than of the upper to surface/volume ratio, the limits tending to move to lower pressures with decreasing surface/volume ratio.

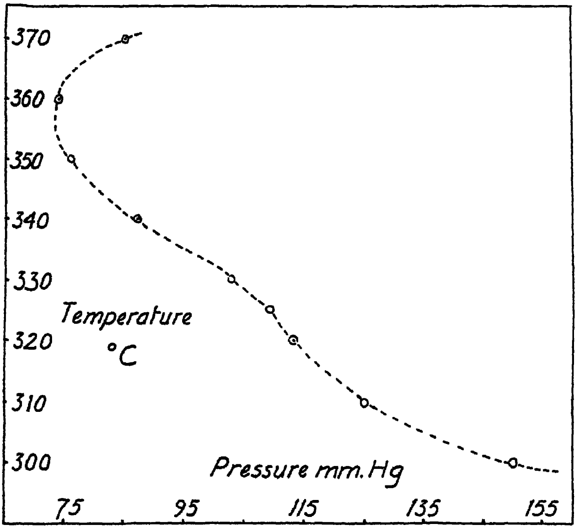

FIG. 6.—Cool flame limits for 50 % *n*-butane—O_2. Pyrex vessel.

Fig. 7 shows that the plot of log *P* against 1/*T* on the cool flame limit for *n*-butane over the temperature range given is not linear. Fig. 9 shows that the same is true for *n*-hexane except perhaps for the three lowest temperatures. A similar curve to Fig. 9 is obtained (Fig. 10) if the logarithm of the asymptote *P'* to which the curve of τ_1 against *P* tends as $\tau_1 \rightarrow \infty$ is plotted against 1/*T*.

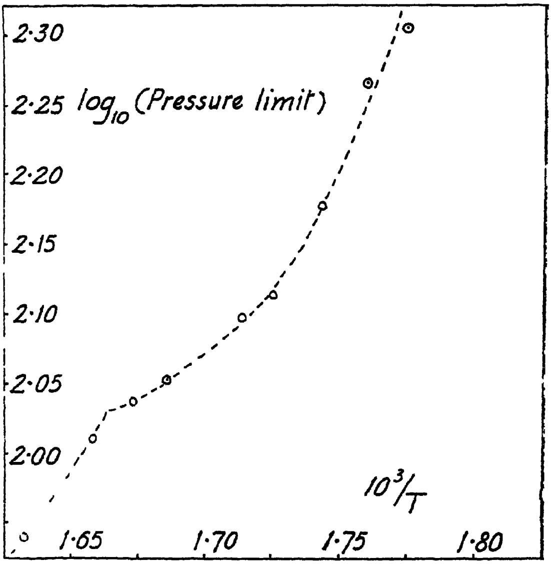

FIG. 7.—Cool flame limits for 50 % *n*-butane—O_2. Pyrex vessel.

Plot of log pressure limit – 1/*T*.

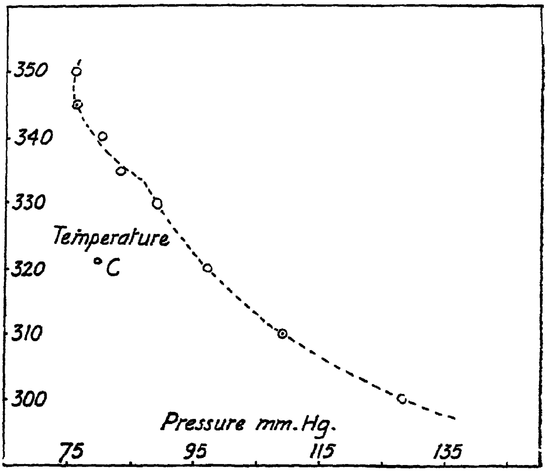

FIG. 8.—Cool flame limits for 50 % *n*-butane—O_2. Quartz vessel.

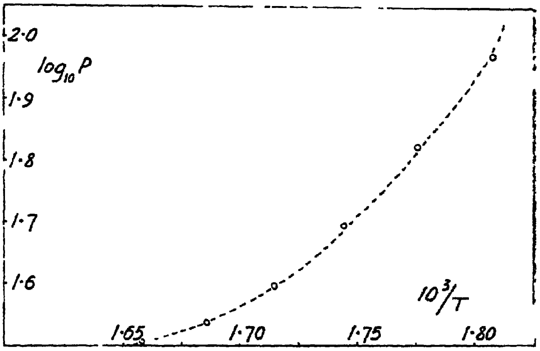

FIG 9.—Cool flames in *n*-hexane. 30 % mixture. Pyrex vessel. Plot of $\log_{10} P - 1/T$ on lower limit of cool flame ignition curve.

(For n-butane the asymptote and cool flame pressure limit are the same.) Similarly, for n-pentane the plot of log (cool flame pressure limit) or log asymptote against $1/T$ is approximately linear only at the lowest temperatures ($<290°$ C). This behaviour seems general. Guibiansky[7] has stated that

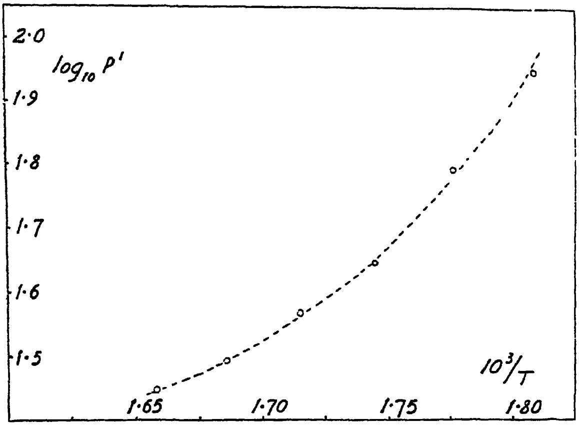

FIG. 10.—Cool flames in n-hexane. 30 % mixture. Pyrex vessel. Plot of $\log_{10} P' - 1/T$.

log P against $1/T$ gives a linear graph for the lower limit of the diethyl ether cool flame curve, but an actual plot of his values shows that only the three points at the lowest temperatures (i.e. those well below the first pressure minimum of the cool flame curve) are in an approximate straight line.

Cool Flames in Propane-oxygen Mixtures.—Newitt and Thornes[8] have already made a careful study of the cool flame limit curve of a 50 % propane-oxygen mixture in a quartz reaction vessel 28 cm. long and 5·5 cm. diam.

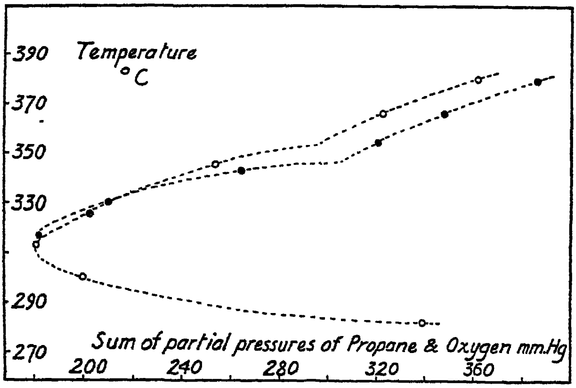

FIG. 11.—Cool flame limits for propane. Results of Newitt and Thornes replotted. —○—○— for 50 % propane—O_2. —●—●— for C_3H_8—O_2—N_2 mixture. Quartz vessel, 28 cm. long and 5·5 cm. diam.

On the evidence then available, they rightly drew a smooth curve through the experimental points of their graph; but close examination of their plotted points shows (Fig. 11) that, if each point is given due weight, the curve has to be drawn with a break at a temperature of about 358° C. If this were the only evidence for the break, it would be quite inadequate to establish the composite nature. However, several further pieces of evidence strongly support it. In the first place, an entirely independent set of results, obtained by Newitt

[7] Guibiansky, *Acta physicochim.*, 1938, **9**, 621.

[8] Newitt and Thornes, *J. Chem. Soc.*, 1937, 1656.

and Thornes[8] for a $C_3H_8+O_2+N_2$ mixture in the same reaction vessel, shows (Fig. 11), on close examination, a similar break at a temperature of *ca.* 350° C. As expected from the facts established for ethers, the addition of nitrogen lowers the temperature of the break. The amount of the lowering (for the addition of only one volume of nitrogen to one of oxygen) is naturally less than the lowering of the inlet in the case of diethyl ether (for the addition of four volumes of nitrogen to one of oxygen). In the second place, the points plotted and curve drawn by Newitt and Thornes[8] (Fig. 2 and 4 of their paper) for the hot flame limits in the "low" temperature region clearly show the existence of two lobes, the lower being the more pronounced and the temperature of the inlet between them being *ca.* 325° C.* As expected from the discussion above, this lies at a temperature below that of the break in the cool flame limit curve. Townend and Chamberlain[10] have also given a hot flame limit curve for propane (in admixture with air) showing two main peaks, at 375 and 325° C. These temperatures differ from those of the lobes or peaks of the diagrams due to Newitt and Thornes (*ca.* 360 and 290° C) because of the use of a reaction vessel of different dimensions (17 cm. long and 3·75 cm. diam.) and different material (mild steel, which raises the limits by some 20° C) and because of the use of air instead of oxygen. In the third place, by analogy with the facts established for ethers, one would expect the composite nature of the cool flame limit curve to show also in the curve of maximum rate of slow oxidation (at a constant initial pressure just below the cool flame minimum) against temperature. Such a curve has been given by Pease[11] for a 50 % propane-oxygen mixture oxidizing in a Pyrex reaction vessel (2·0 cm. diam.) and although he has drawn a smooth curve through the plotted points, there is one point which lies well below the curve—suggesting two peaks in the curve in the cool flame temperature region, one at *ca.* 320° C and one at *ca.* 340° C with an inlet between them at about 330° C. That the temperature of the inlet on Pease's curve is lower than that of the break in the curve of Newitt and Thornes is expected from the fact that Pease used a smaller reaction vessel than that of Newitt and Thornes. As already pointed out, the lower lobe of the cool flame limit curve is pushed to higher pressures more than the upper lobe by increase in the surface/volume ratio, so that the temperature of the observed inlet falls with increase in that ratio.

Discussion

The experiments described and discussed above make it reasonably certain that for the paraffins, as for the ethers, the cool flame limit curves are composite. Each piece of evidence is small and often doubtful in itself; but cumulatively the evidence is so consistent and so widespread as to leave little doubt that all the cool flame limit curves described are made up of at least two intersecting curves or lobes. The question arises, however, why should the effect be so difficult to detect with the paraffins in comparison with the ethers? This is due in the first place to the much smaller temperature range covered by the "irregularity" in the limit curve for *n*-paraffins than for ethers. Reference to Fig. 1 and 4, for example, shows that whereas the inlet in the diethyl ether curve extends over some 70° C or more, that in the *n*-hexane curve covers only some 20° C. In turn this is probably connected with the greater range of temperature covered by the whole ether-oxygen cool flame system outside the hot flame limits (*ca.* 170 to 360° C) compared with the *n*-paraffin-oxygen cool flame system (*ca.* 270 to 410° C). The reasons for this are indicated in Part III of this series of papers. In the following discussion hypotheses are tentatively put forward to explain the existence of the lobes.

The oxidation of any fuel involves the attack of free radicals (including

---

* The plotted points of Fig. 2, but not the curve drawn, for the hot flame limits in the "high" temperature region suggest also the break in the ignition curve at *ca.* 450-470° C expected from the study of ether oxidation and due to the onset of pyrolysis of propane molecules to free radicals. A similar break is shown very well at *ca.* 480° C in the ignition curves plotted by Townend and Mandlekar[9] for *n*-pentane.

[9] Townend and Mandlekar, *Proc. Roy. Soc. A*, 1933, **143**, 168.

[10] Townend and Chamberlain, *ibid.*, 1936, **154**, 95.

[11] Pease, *Equilibrium and Kinetics of Gas Reactions* (Princeton, 1942), p. 210.

O_2) on the fuel molecules. The most probable nature of this attack consists of hydrogen atom abstraction from a molecule by the radical.[12] The dissociation energies of (and therefore activation energies for attack on) 1°, 2° and 3° C—H bonds differ, increasing in the order $3° < 2° < 1°$. It therefore follows that, if the oxidation is studied over a range of temperature, the onset of attack on say 2° and 1° C—H bonds will occur at different temperatures and may give rise to two regions in the plot of an experimental measure of the oxidation against temperature. The first hypothesis is, therefore, that the two parts of the cool flame curves for *n*-paraffins and diethyl ether can be identified with these two regions. This hypothesis has already been adopted by Chamberlain and Walsh and evidence found to support it.[2] This evidence included a comparison of the cool flame limit curves for dimethyl [13] and diethyl ether.[2] The curve for dimethyl ether (with no 2° C—H bonds) does not extend below 240° C, i.e. the lower lobe of Fig. 1, for diethyl ether appears to be absent in the curve for dimethyl ether.

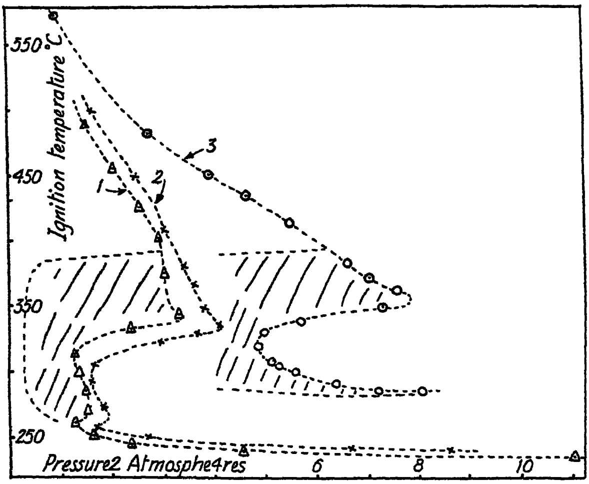

FIG. 12.—Ignition diagrams for corresponding mixtures with air of (1) *n*-octane, (2) *n*-heptane, (3) *iso*-octane. Cool flame range shaded. After Maccormac and Townend.

However, matters cannot be so simple. A particular difficulty is that the "low" temperature hot flame diagram for cyclohexane (containing only 2° CH bonds) shows two prominent lobes; [3, 14] and the presence of corresponding composite nature in the cool flame limit diagram is not incompatible with the points plotted by Burgoyne, Tang and Newitt.[14] The hot flame curve for *iso*-octane provides another difficulty. Whereas the molecule contains both 2° and 3° CH bonds (and also 1°), according to Fig. 12 (whose experimental points are taken from Fig. 1 of ref. (1)) the curve shows only *one* main lobe in the "low" temperature region. It is significant that this lobe corresponds to the upper of the two main lobes observed for *n*-paraffins (Fig. 12).

In the preceding paper it was shown that for a cool flame to arise it was necessary for the maximum rate of oxidation to exceed a critical value. The appearance of two lobes in the cool flame limit curve is due to a waxing and waning of the maximum rate of oxidation at constant initial pressure as the temperature changes. This has been shown directly for ethers (where two lobes certainly exist in the graph of maximum rate of oxidation against temperature) and this is probably true also for other fuels (cf. Pease's graph of maximum rate of propane oxidation against temperature [9]). The maximum rate of slow oxidation in turn depends upon ϕ, the net branching factor for the chain process. The greater ϕ, i.e. the more quickly the reaction develops, the greater the velocity attained before processes, such as consumption of reactants, can cause the falling-off that is characteristic of degenerate branching reactions. Indeed, at "high" temperatures (360° C for di-*iso*propyl ether [12] and 480° C for methane [15]) the maximum rate is directly proportional to ϕ. Therefore, in so far as the ease of the net branching process waxes and wanes with temperature rise, so the cool flame pressure limit (and hence the hot flame pressure limit) is likely to wax and wane.

---

[12] See Chamberlain and Walsh, *Rev. Inst. Français du Pétrole*, 1949, **4**, 301.

[13] Ermakova, Ermalova and Neumann, *Acta physicochim.*, 1939, **11**, 679.

[14] Burgoyne, Tang and Newitt, *Proc. Roy. Soc. A.*, 1940, **174**, 379.

Fairly direct evidence that the upper lobe is due to a change in ϕ is provided by measurement of the time interval between successive cool flames of diethyl ether occurring in a flow system.[16] A plot of this time interval against temperature shows a discontinuity at the lowest temperature of the upper lobe. Assuming it is ϕ that primarily determines the time interval ($\phi\tau$ = constant), this implies that ϕ changes as the upper lobe is reached.

We have identified the branching reaction as

$$ROOH + O_2 \rightarrow \text{radicals.}$$

We are therefore led to seek an explanation of the lobes observed in cool flame limit diagrams and in hot flame ignition curves at "low" temperatures in terms of the attack of O_2 on ROOH. If ROOH contains two types of CH bond, attack of O_2 on these will take place in two different temperature ranges. Certainly the existence of two lobes in the ignition diagram for cyclohexane suggests an explanation in terms of the structure of a product rather than of the original molecules. The peroxide from cyclohexane is expected to be

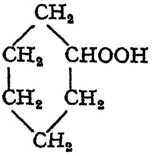

It should therefore react with O_2 in two distinct temperature ranges. The lower of these corresponds to attack on the 3° CH, the upper to attack on the remaining 2° CH bonds. Thus the observed two lobes in the "low" temperature ignition diagram may be explained.

From the high pressures required to cause ethane to ignite by the "low" temperature method, we may deduce that peroxide formation (and O_2 attack) at a 1° CH bond normally occurs with considerable difficulty. We therefore expect the peroxide from a *n*-paraffin to be of the type

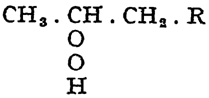

$$CH_3 . \underset{\substack{O\\O\\H}}{CH} . CH_2 . R$$

and *n*-paraffins should, in consequence, show two main lobes in their "low" temperature ignition diagrams. This is found experimentally (Fig. 12). The lower is due to attack at the 3° CH bond and the upper to attack at the 2° CH bond, as with cyclohexane.

One would expect *n*-paraffins to show also a third lobe lying at higher pressures and higher temperatures than the above two lobes. This would be due either to O_2 attack on the CH_3 groups of the above peroxide or to peroxide formation at the CH_3 group itself. It would probably be difficult to distinguish the composite nature because of (i) the smallness of the lobe and (ii) its proximity to the start of the " high " temperature part of the ignition curve.* It would partly correspond to the single ill-defined lobe shown by ethane [3] and acetone [1] in their " low " temperature ignition curves.

---

[15] Chamberlain and Walsh (to be published).

[16] Nixon (unpublished results).

Such a third small lobe for *n*-paraffins appears to be an experimental fact. In this connection it is unfortunate that experimental points have frequently not been recorded on published ignition curves. However, a third, relatively small, lobe lying at temperatures above those of the two main lobes, appears in a hot flame ignition curve plotted by Townend and Mandlekar [9] for *n*-pentane. It is shown particularly well on curves plotted by Maccormac and Townend for *n*-octane and *n*-heptane. These curves are reproduced in Fig. 12. The third lobe appears in the range *ca.* 340-390° C.

According to these views, propane should be a special case among the *n*-paraffins. The peroxide $CH_3CH(OOH)CH_3$ contains no 2° CH bonds. One would therefore expect the propane ignition diagram to show only one main lobe (corresponding to attack of O_2 on the 3° CH of the peroxide) and a second much less prominent lobe at higher temperatures. This expectation is borne out by the hot flame curves published by Newitt and Thornes [8] (Fig. 2 and 4 of their paper). It agrees also with a figure given by Maccormac and Townend [1] wherein propane is shown with only one important lobe but pentane, hexane and heptane with two. It is true that curves given by Townend and Chamberlain [10] show two lobes of almost equal importance, but this may perhaps be connected with the use of air instead of oxygen,† a steel instead of glass reaction vessel, and mixtures of much weaker composition than used by Newitt and Thornes.

In other ways propane is abnormal among the *n*-paraffins. The upper of the two cool flame lobes becomes more pronounced relative to the lower as one passes (under the same conditions of mixture strength and reaction vessel) from *n*-hexane to *n*-pentane to *n*-butane. The change can be seen from Fig. 2, 5 and 6. The upper lobe hardly shows for the 50 % *n*-hexane mixture, is more prominent for the 50 % *n*-pentane mixture and is more important than the lower for the n-butane mixture. (Similarly, the hot flame curves given by Townend (ref. (3) and references therein) and plotted under corresponding conditions show that the upper lobe becomes more pronounced than the lower as one passes from *n*-hexane to *n*-butane). For propane, however, according to Fig. 11, the lower lobe is again more important than the upper. In part this is no doubt due to the use of a wider reaction vessel for Fig. 9 than for Fig. 2, 5 and 6. That the lower lobe is more sensitive than the upper to variations in surface/volume ratio has been pointed out above. The sudden reversal of trend, however, is so marked that it is unlikely that it can be fully accounted for in this way. It is more probable that there is a real discontinuity. According to the present ideas, the upper lobe arises in different ways in *n*-propane and the higher paraffins. With the latter it is due to O_2 attack on the 2° CH bonds of ROOH, but with propane it is due to attack on the 1° CH bonds of ROOH and is therefore usually subsidiary to the lower lobe.

---

* Ignition curves for *iso*butane given by Townend, Cohen and Mandlekar,[6] however, show (i) a single main lobe (whose interpretation, we suggest, concerns formation of the 3° peroxide $(CH_3)_3COOH$ and (ii) a subsidiary lobe at higher temperatures, perhaps to be interpreted as involving peroxide formation at the CH_3 groups themselves. Two such lobes may be easier to distinguish in *iso*butane than in *n*-paraffins because (*a*) 3° and 1° peroxides are formed in temperature ranges more separated than those in which 2° and 1° peroxides are formed, (*b*) the absence of a prominent lobe due to O_2 attack at 2° CH bonds means less concealment of minor lobes.

† With diethyl ether inert gases inhibit hot flame ignition in the lower part of the " low " temperature region, but slightly promote ignition in the upper part.[2] Use of ether-air mixtures therefore tends to make the upper lobes of the ignition again lie at lower pressures relative to the lowest lobe than would be the case with ether-oxygen.

The peroxide given most easily by *iso*-octane should be

$$(CH_3)_3C \,.\, CH_2 \,.\, C(OOH)(CH_3)_2.$$[17]

iso-Octane should therefore show only one main lobe in its "low" temperature ignition diagram and this should lie in roughly the same temperature range as the upper of the two main lobes found for *n*-paraffins. Fig. 12 shows this to be true peroxide formation at the 2° CH bond probably only occurs at higher pressures. On the other hand, *iso*-octane should show a subsidiary lobe corresponding to the third, uppermost, lobe of *n*-paraffins. Inspection of the plotted points of Fig. 12 shows this to be true. The lobe is small, but its existence in all three curves of Fig. 12 strongly supports its reality.

The peroxide from diethyl ether is expected to be

$$CH_3 \,.\, CH(OOH) \,.\, O \,.\, CH_2 \,.\, CH_3.$$

The cool flame limit curve and the hot flame ignition curve at "low" temperatures should therefore show two main lobes (in agreement with Fig. 1) and also a small subsidiary lobe at higher temperatures. The latter is clearly to be seen in the hot flame curves already published (Fig. 6 of ref. (2)). It is quite plausible that it exists also in the cool flame limit curve for, on account of experimental difficulties, the latter has not been explored in the relevant temperature range.

With dimethyl ether, in fact, although there appears to be no analogue of the lowest lobe found for diethyl ether,* the cool flame limit curve plotted by Ermakova, Ermalova and Neumann [13] shows a break at *ca.* 375° C. The portion below this temperature can be ascribed to attack of O_2 on the 2° CH of the peroxide $HOOCH_2 \,.\, O \,.\, CH_3$ and the portion above to subsidiary attack on the 1° CH.

With di-*iso*propyl ether, the lower main lobe can be interpreted as due to O_2 attack on the 3° CH of the peroxide

$$(CH_3)_2C(OOH) \,.\, O \,.\, CH(CH_3)_2.$$

Owing to the strong inductive effect of the 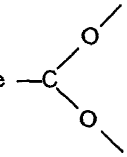 group, attack on the 1° CH bonds adjacent to the peroxide group may be easier with this molecule than is usually the case with 1° bonds. If so, this partly explains the observed pronounced upper lobe. Further reasons for a lobe interpreted as due to attack on 1° CH bonds showing more prominently with di-*iso*propyl ether than with *n*-paraffins may include (i) the absence of concealment by a lobe resulting from 2° CH attack, (ii) the greater range of temperature covered by the ether cool flame system than by the *n*-paraffin cool flame system.

In general, therefore, it is plausible to connect the number of lobes present in an ignition diagram with the types of CH bond present in the peroxide expected to be most readily formed. This supports the supposition of Part I that branching usually occurs by bimolecular reaction of ROOH and O_2 rather than by simple decomposition of ROOH. This does not imply that other processes may not also give rise to irregularities in ignition curves; nor that if more than one type of CH bond is present in the peroxide formed the ignition diagram must necessarily show two lobes. The ease of dissociation of the α-CH in *n*-alkyl aromatic compounds, for instance, may be such that (i) formation of the peroxide $C_6H_5CH(OOH) . R^{17}$ is overwhelmingly more probable than of any other, (ii) O_2 attack at the 3° CH bond of this peroxide is so much more probable than at any other CH bond that the ignition diagram (reflecting primarily the *easiest* mode of ignition) shows effectively only one lobe. This appears to be the experimental fact for *n*-propyl and *n*-butyl benzene.[14]

---

[17] Walsh, *Trans. Faraday Soc.*, 1946, **42**, 269.

* Cool flames are easier to observe at the temperatures of the lower than of the upper lobe.[2] A lower lobe for dimethyl ether is therefore unlikely to have been overlooked.

Laboratory of Physical Chemistry,
Cambridge.

INITIATION OF EXPLOSION IN LIQUIDS

MEASUREMENT OF THE TRANSIENT PRESSURES DURING IMPACT

BY PETER GRAY

Received, 4th April, 1950

The sensitivity to light impact of liquid explosives such as nitroglycerin is due to the presence of small trapped bubbles of gas. Under impact they undergo adiabatic heating during their sudden compression and give rise to local high temperatures which initiate explosion.

This paper describes measurements of the transient pressures developed in the trapped gas bubble during impact with an apparatus based on the piezo-electric effect which makes it possible for graphs of pressure against time to be recorded. Its behaviour has been examined with non-explosive liquids; it has been calibrated by a dynamic method and used to investigate liquid explosives.

The results obtained show that very high pressures are produced even by light blows; thus in a small trapped bubble temperatures of the order of 1000° C may be reached. Evidence is presented to support the view that explosion begins as a burning of the explosive vapour present in the gas bubble where, however, its concentration is extremely low. An examination of the ignition of greatly diluted explosive vapours confirms this suggestion.

The sensitivity to shock of liquid explosives is greatly increased by the presence of small bubbles of gas. Such bubbles may be trapped by spreading the explosive as a ring between flat surfaces or by striking it with a hammer having a small cavity in its impacting face; during the blow the trapped bubbles undergo sudden compression and rise rapidly in temperature. Such "hot spots" lead to the local inflammation of the explosive from which explosion may spread throughout the liquid.[1, 2]

In impact the pressure increase $(P_f - P_i)$ depends on the momentum and energy of the blow and the volume of the liquid, while the degree of heating $(T_f - T_i)$ during adiabatic compression is given by the relation

$$(T_f/T_i)^\gamma = (P_f/P_i)^{\gamma - 1},$$

(γ is the ratio of the principal specific heats of the gas, f final and i initial states) and for a detailed account of such initiation of explosion to be made the duration of impact and the transient pressures and temperatures must be known. Hitherto reliable estimates have not been available and more exact knowledge of these quantities is therefore necessary. Now, although these temperature rises are not only transient but also localized, the pressure increases though transient may be assumed uniform; from the variation of the pressure throughout the blow the variation of the temperature may be estimated.

---

[1] Bowden, Mulcahy, Vines and Yoffe, *Proc. Roy. Soc. A*, 1947, **188**, 291.

[2] Yoffe, *ibid.*, 1949, **198**, 373.

The construction and operation of an apparatus measuring simultaneously pressure and time throughout a blow are described ; it is found that even in light blows quite high pressures may be reached.

Initiation is physically due to the hot bubble. But the details may be more complex. The direct ignition by local heating of a liquid explosive has been shown to be difficult and it has been suggested [1, 2] that impact decomposition sensitized by gas bubbles begins as a burning of the small amount of explosive vapour in the bubble, heat liberated by chemical decomposition augmenting that produced physically. The confirmation of the possibility of inflammation of dilute explosive vapour [3, 4] strongly supports this view.

Measurement of Transient Pressure during Impact

The Impact Apparatus.—Previous measurements [1] have shown that the period of impact is brief and a recording device of small inertia is necessary to respond to the rapid variations in pressure. Use of the piezo-electric effect to reduce the problem from following transient mechanical stresses to measuring varying electrical changes has been made the basis of an apparatus [5] which records the transient impulses in a liquid under impact

Fig. 1 shows the arrangement of the apparatus. A quartz crystal was chosen as the piezo-electric source ; its size corresponds to a natural period of vibration much less than that of impact and ensures that it will not merely " ring " at its own natural frequency when struck suddenly. The crystal mount, which contains the explosive under examination, is shown in Fig. 2.

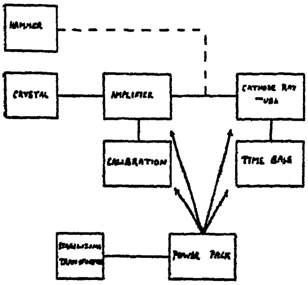

FIG. 1.—Block diagram of apparatus.

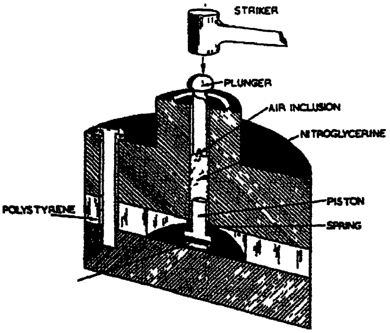

FIG. 2.—The crystal mount.

The crystal is placed on a brass block and the head of a piston pressed lightly against it by a spring washer. The upper and lower parts of the apparatus are in electric contact with the opposite faces of the crystal which are coated with conducting metallic layers and insulated from each other. The whole assembly is placed on an earthed plate between two insulating sheets to overcome stray capacity effects. A coaxial cable carries the transient charge from the crystal to the amplifier ; this cable acts as a condenser in parallel with the crystal so that the longer the cable the smaller the potential difference applied to the amplifier, which is so made as to have a uniform frequency response over a very wide range. Its amplification may be varied continuously.

The liquid explosive is confined between the piston and a plunger, and a small air bubble is trapped in the cavity in the plunger. An electromagnet is used to drop a hammer on to the plunger ; electrical contact between the hammer and the plunger triggers the single sweep of the cathode ray beam.

---

[3] Gray, *Revue de l'Insitut Français du Petrole et Annales des Combustibles Liquides*, 1949, **4**, 355.

[4] Gray and Yoffe, *Research*, 1949, **2**, 339.

[5] Gray, *ibid.*, 1949, **2**, 392.

The time taken for the beam to sweep across the screen can be varied from about 30 millisec. to 30 microsec. This trace on the screen is not very bright and does not last long; accordingly all stray light is excluded and a wide aperture lens of short focal length is used to focus an image on to a sensitive photographic plate.

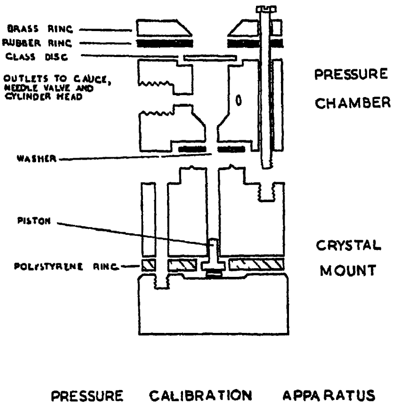

FIG. 3.—The pressure calibration apparatus.

Calibration.—The sensitivity of the crystal and amplifier units in terms of the pressure implied by a given deflection on the photographic plate may be calculated from the known piezo-constant of quartz and the characteristics of the apparatus or derived from the measurement of the response of the apparatus to a steady pressure (static calibration). However, a method simulating more closely the conditions of the impact experiments is to be preferred to these and a dynamic calibration has been made. The crystal is subjected to a sudden pressure change and the consequent transient charge is amplified and recorded.

The same crystal mount is used as in the impact apparatus; a column of air replaces the column of liquid and plunger (Fig. 3). A pressure chamber is fixed on to the crystal mount. The pressure chamber carries a gauge and a needle-valve and is joined to a nitrogen cylinder head. The other end of the pressure chamber is closed by a thin, circular disc of glass sealed in a shallow depression and pressed into place by the three bolts that join the pressure chamber to the crystal mount. The pressure is released by breaking this glass disc. The time-base was not used and calibrating traces were obtained as lines on the photographic plate perpendicular to the time axis. Because it was not possible to use very high pressures the most sensitive range of the amplifier was used. The calibrations showed some scatter; some typical results are summarized in Table I. The mean value of the sensitivity of the apparatus determined in this way is thus only a little less than the value calculated from the known piezo-electric constant of quartz. The sensitivity may be varied considerably and in particular depends on the length of the coaxial cable and on the cross-sectional area of the piston.

TABLE I.—THE SENSITIVITY OF THE IMPACT APPARATUS

Change in Pressure (atm.)	Measured Deflection (mm.) on Photographic Plate
26·7	22, 21, 17·5, 18·5
27·7	20·5
28·3	18·5
30	19·5, 24, 19, 21, 19·5

Mean sensitivity = 0·76 mm./atm.
Calculated sensitivity = 0·88 mm./atm.
(Estimated errors = 8 %)

Impact Pressures in Non-explosive Liquids.—When a non-explosive liquid is subject to impact in the apparatus the pressure increases to a maximum value as the plunger is brought to rest. As the liquid expands again the pressure falls. The pressure time graph displayed on the cathode ray tube screen and recorded on the photographic plate is a continuous line with a single maximum. In heavier blows there is a very marked oscillation of varying frequency superimposed on the trace.

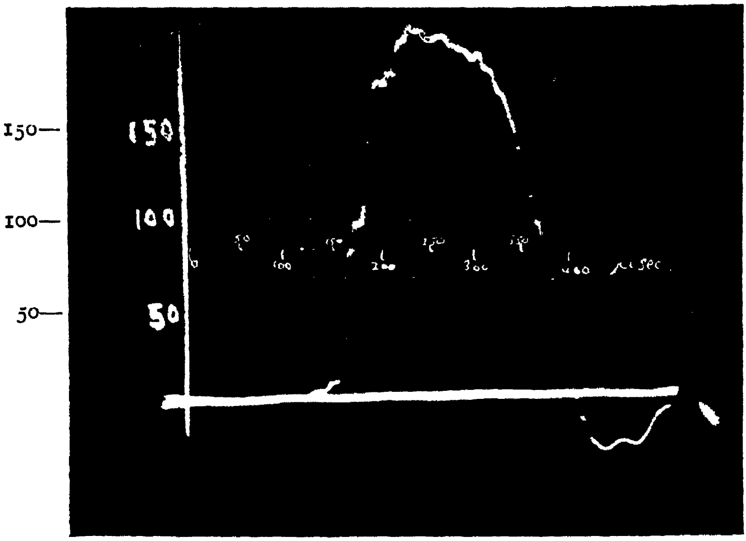

Time (microsec).

FIG. 4.—Pressures in atm. (ordinates) during impact on a non-explosive liquid.

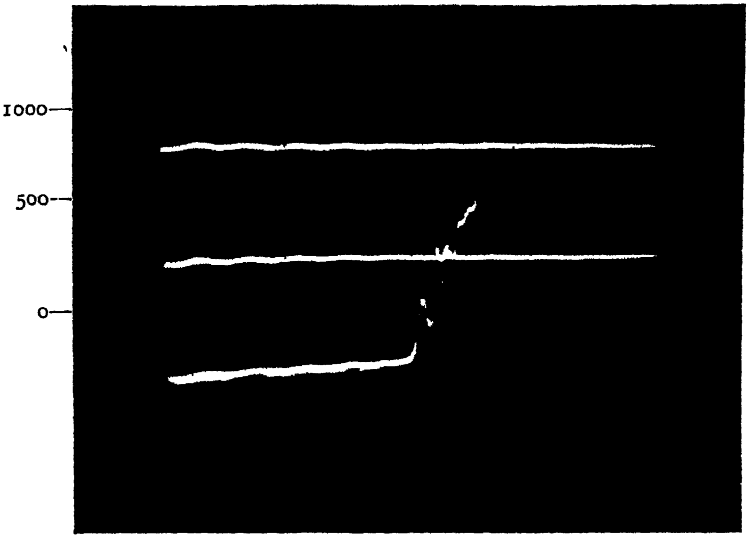

Time (microsec.).

FIG. 5.—Variation of pressure in atm. (ordinates) with time during impact on nitroglycerin. 70 g. hammer falling 4 cm. on to 0·006 ml. nitroglycerin. Volume of cavity 5×10^{-4} ml. Explosion occurred at 610 atm. 150 microsec. after appreciable pressure rise.

[*To face p.* 850.

Fig. 4 shows a typical quantitative result of impact on a non-explosive liquid. It is a record of the variation of pressure during impact on glycerol. The impulse was communicated by a 75 g. hammer falling about 7 cm. on to 1/50 ml. of liquid in the presence of a small air bubble. The maximum pressure is about 250 atm. The pressure ordinates marked are derived from the pressure calibration described previously. Independent confirmation of the pressure calibration may be derived from the times involved by applying the familiar equations of motion. If time is measured from the beginning of the trace the average pressure is about 200 atm. Such impulsive pressures in the liquid correspond to very high transient temperatures in the minute gas bubble trapped in the cavity.

Initiation of Explosions in Liquids

Impact Pressures in Explosive Liquids.—When a liquid such as nitroglycerin is detonated by impact in the apparatus the additional downward force due to the sudden release of the products of explosion causes a change in the gradient of the pressure-time graph. Previous work [1] with cavity strikers has demonstrated both the rapidity with which explosion follows impact and the speed at which it develops to such a rate as to become luminous. Values of 0-20 microsec. have been recorded for the time elapsing between impact and initiation of explosion in liquids whether explosion was detected by the shock wave or by the luminosity. Thus the gradient of the trace recorded on the photographic plate may be expected to show a discontinuity. This feature is clearly illustrated in Fig. 5, showing a typical explosion trace. In all the curves obtained breaks in the gradients occur within a millisec. of the beginning of impact and after pressures have been reached which vary from 750 to 360 atm. In one case explosion occurred after the pressure had passed its maximum value.

Discussion.—Pressures of this order for the initiation of explosions with cavity strikers are in accord with results obtained by Yoffe.[1] In these experiments films of liquid explosives spread on anvils of different materials were struck with hammers having cavities in their impacting faces. Though on hard materials explosions could be obtained, on the soft metal indium no decomposition was observed. The static flow pressure of indium is 100 atm.; its dynamic flow pressure has been estimated as 400 atm. and it appears that such values must be exceeded for impact by cavity strikers to lead to initiation. It is not impossible of course that the conditions for successful development of explosion control the incidence of observable decomposition and that these include factors such as on the degree of confinement.

The variations in pressure from experiment to experiment may be due to variations in the size of the air bubble. Though the size of the cavity in the end of the striker is known precisely its volume is not necessarily exactly that of the bubble. Robertson [6] has shown how the size of the hot spot affects the minimum value of the temperature it must reach to lead to an explosion in a solid, and similar problems are discussed by Jost [7] and by Lewis and von Elbe [8] in their examination of the spark initiation of explosion in gases. In all the experiments the pressures recorded are very high and even though part of the heat produced is lost by conduction, the gas bubble and hence the explosive vapour in it will easily rise in temperature by 1000° C. Such a value may explain why the sensitivity to shock of liquid explosives depends so little on their bulk temperature. Once the appropriate local temperature has been reached it seems that it is the amount of heat produced which controls initiation of explosion in experiments with these cavity strikers, and the results of experiments by Mulcahy [9] in which a decrease of explosion efficiency accompanies reduction of initial gas pressure may be due to the fact that the mass heated is less.

The Initiation of Explosion from the Gas Phase.—Though these transient pressures and temperatures are very high the actual amount of heat liberated physically is small (it has been estimated [1] to be $\sim 10^{-7}$ cal.) and may not be sufficient to ignite the cold liquid explosive in the brief time of impact. The initiation of explosion by direct heating of a liquid is not easy,[10, 11] and it is suggested that initiation occurs as a burning in the vapour phase of the heated explosive vapour in the bubble, the chemical energy of decomposition augmenting that produced physically. This view is supported by the importance of the chemical nature of the gas in the bubble.[1, 9]

---

[6] Rideal and Robertson, *Proc. Roy. Soc. A*, 1948, **195**, 135.

[7] Jost, *Explosion and Combustion Processes in Gases* (McGraw Hill, 1936).

[8] Lewis and von Elbe, *Combustion, Flame and Explosion in Gases* (C.U.P., 1938).

[9] Mulcahy, *Phil. Mag.*, 1948, **39**, 547.

[10] Bowden, Stone and Tudor, *Proc. Roy. Soc. A*, 1947, **188**, 329.

[11] Belajev, *Compt. Rend. U.S.S.R.*, 1938, **18**, 267.

The main difficulty about the suggestion, however, lies in the low concentration of explosive vapour on the gas bubble—only one part per million for nitroglycerin in a bubble of air at atmospheric pressure. The inflammation of very dilute mixtures with inert gases of nitroglycerin and of the analogous explosives methyl and ethyl nitrates has been examined by Gray and Yoffe.[12] It is found that all these nitrates when diluted from a thousand even to a million times with argon and nitrogen decompose with luminescence on admission to a hot quartz vessel. Table II summarizes some of these results.

TABLE II.—Total Pressure (mm. Hg) at which Mixture Glows on Admission to Quartz Vessel

Temperature approximately 420° C

Relative Concentration of Explosive Vapour in Mixture	Explosive Vapour Used		
	Methyl Nitrate	Ethyl Nitrate	Nitroglycerin
1 part in 100	0·5 (N_2)	0·2 (A)	—
1 part in 1,000	1·0 (N_2)	0·4 (A)	—
1 part in 10,000 . . .	5 (A)	1·0 (A)	5 (A)
1 part in 100,000 . .	50 (A)	—	50 (A)
1 part in 1,000,000 . .	60 (N_2) at 470° C	—	—

Symbols in brackets denote diluent used.

Thus, since at 400° C decomposition at a few mm. pressure of very dilute mixtures occurs with luminescence, in the more extreme conditions of the bubble where higher temperatures and pressures occur, similar behaviour is possible and chemical energy of decomposition in the vapour phase is available to facilitate initiation.

I wish to express my thanks to Dr. F. P. Bowden, F.R.S., for suggesting the problem and for his encouragement during the experiments, to Dr. G. C. Barker who designed the electronic parts of the apparatus and to Dr. A. D. Yoffe and Dr. J. R. Whitehead for their advice and help.

I also thank Gonville and Caius College for the award of the Dunlop Studentship, the Department of Scientific and Industrial Research for a maintenance grant and the Ministry of Supply (Air) for grants to the Laboratory for equipment.

Research Laboratory for the Physics and Chemistry of Rubbing Solids,
Department of Physical Chemistry,
Cambridge.

[12] Gray and Yoffe, *Proc. Roy. Soc. A*, 1949, **200**, 114.

INFLUENCE OF ION-EXCHANGE UPON INTRACRYSTALLINE SORPTION

By R. M. Barrer and D. W. Riley

Received 24th April, 1950

Measurements have been made of intracrystalline sorption of the inert gases Kr, A, Ne and He over a series of temperatures and pressures in chabazites rich in the ions (Ca^{++} + Na^{+}), Ba^{++}, Li^{+} and NH_4^{+}. Isosteric sorption heats sometimes agreed with those derived by an analysis of isotherm data for argon using a B.E.T. isotherm where n, the number of layers, is equal to one. Agreement using this method requires that the entropy of transfer of argon from liquid argon to the intracrystalline environment must be small. Isosteric heats of sorption show that there is inhomogeneity among sorption sites but that among ion-exchanged chabazites this inhomogeneity is not marked.

An analysis has been made of the interactions governing changes in sorption heat for a given gas in a series of ion-exchanged chabazites. The dominant interaction appears to result from polarization of the sorbate by the cation, and it may be inferred that cation and sorbate tend to be associated in the intracrystalline environment.

Chabazite ($(Ca, Na_2)O . Al_2O_3 . 4SiO_2 . 6H_2O$) was enriched by ion exchange in the manner described in another paper [1] in Li^+, Na^+, K^+, NH_4^+, Rb^+, Cs^+, Ag^+, Sr^{++} and Ba^{++}. Thus one obtained a series of sorbents all of which were true chabazites in which the aluminosilicate framework was virtually unchanged but in which cations were systematically replaced. Sorbed molecules are located in the same intracrystalline channels as the cations, and evidence has already been presented that there is a close association between cations and sorbed molecules.[2] The cation-exchanged chabazites now available form a group of crystals excellently suited to a further study of the influence of the cation upon the equilibria and energetics of this kind of zeolitic solid solution. As sorbates the simplest species were chosen, namely the inert gases He, Ne, A and Kr. A selection of the ion-exchanged crystals used included Ba^{++}, Li^{+}, and NH_4^{+}-rich and natural chabazites. Natural chabazite contains Ca^{++} and Na^{+} as cations. In a parallel study using ion-exchanged mordenites diffusion kinetics and energetics were examined, and it was established that ion exchange characteristically modified the crystals as diffusion media.[3] Thus a considerable amount of information is now available concerning the effects of exchange upon occlusion in rigid framework crystals. Earlier measurements along similar lines are confined to observations by Rabinowitsch and Wood [4] and by Lowenstein.[5] None of these workers attempted a quantitative interpretation of their data.

Experimental

The preparation of the ion-exchanged crystals has been described in another paper.[1] The apparatus and the origin and purification of gases has also been described elsewhere.[6] For measurement of low temperatures vapour pressure thermometers were constructed using the following gases and temperature ranges :

---

[1] Barrer, *J. Chem. Soc.*, 1950, 2342.

[2] *Idem.*, *Trans. Faraday Soc.*, 1944, **40**, 555.

[3] *Idem.*, *ibid.* 1949, **45**, 358.

[4] *Ibid.*, 1936, **32**, 947.

[5] *Z. anorg. Chem.*, 1909, **63**, 69.

Sulphur dioxide	− 10° C to − 53° C
Ammonia	− 34° C to − 77° C
Carbon dioxide	− 78° C to −110° C
Ethylene	−104° C to −150° C
Oxygen	−183° C to −210° C.

Standard refrigerants were used for some temperatures (liquid N_2 for −195° C, liquid O_2 for −183° C, and solid CO_2 for −78° C), but intermediate temperatures were obtained by a method described by Barrer.[7]

All the sorbents were initially outgassed for periods of 12 to 14 hr. at temperatures ranging from 450° for natural chabazite to 330° C for NH_4-chabazite. In the latter case care has to be taken not to cause decomposition with liberation of ammonia. Once the initial outgassing was completed subsequent outgassings between sorption runs could be carried out in about 2 hr. at 300° C or even less.

Isotherms.—Isotherms were determined as indicated in Table I.[7a] Typical isotherms are shown in Fig. 1*a*, *b* and *c*. It is seen that these isotherms are Type I in the classification of Brunauer.[8] Nevertheless they were not in quantitative agreement with the Langmuir equation, as was shown by a curvature in plots of p/v against p (p denoting the equilibrium pressure and v the amount sorbed). The curvature may be partly ascribed to inhomogeneity among the intracrystalline sorption sites (as indicated also by the sorption heats given in the next section, and as discussed by Barrer and Riley [6]). In such a crystal the first molecules occluded tend to be located on sites of highest sorption potential, positions of lower sorption potential being progressively filled as the charge of gas is increased. Even though heterogeneity among the sites were almost continuous it would not be far from the truth to express a given experimental isotherm as the sum of the sorptions on a number of groups of sorption

TABLE I

Mineral	Gas	Temperatures used (°K)
Natural chabazite	Kr	123, 153, 195, 221, 258, 273, 294
	A	81, 88·5, 123, 143, 195, 223, 258, 273, 293
	Ne	80, 88·5, 123
	He	80, 88·5
Lithium chabazite	Kr	123, 143, 195, 223, 258, 273, 291·5
	A	77·8, 89·3, 123, 140, 173, 195, 223, 258, 273, 293·5
	Ne	77·9, 89·2
	He	77·9, 89·3
Ammonium chabazite	Kr	195, 273, 294
	A	90·5, 195, 273, 290·5
	Ne	80, 90·3
	He	79·6, 90·3
Barium chabazite	Kr	195, 273, 294
	A	90·3, 195, 273, 290·5
	Ne	80, 90·3
	He	79·6, 90·3

---

[6] Barrer and Riley, *J. Chem. Soc.*, 1948, 133.

[7] *Idem*, *Proc. Roy. Soc. A*, 1937, **161**, 476.

[7a] Riley, *Thesis* (University of London, 1949) gives full details of these isotherms.

[8] *The Adsorption of Gases and Vapours* (O.U.P., 1944), p. 149.

sites each group being regarded as homogeneous and as giving rise to a B.E.T type of isotherm in which n (the number of layers) $= 1$. One may assume $n = 1$ because there is no room within the crystalline structure for multilayers to form.

TABLE II.—ISOTHERM OF ARGON IN LITHIUM CHABAZITE AT 89·3° K

Vol. (cm.^{3}) sorbed at N.T.P. per g.	Equilibrium pressure, p (in cm.)	p/v
10	0·0009	0·00009
20	0·0025	0·000125
30	0·0053	0·000177
40	0·0100	0·000250
50	0·0182	0·000364
60	0·0308	0·000513
70	0·0503	0·000719
80	0·0950	0·00119
90	0·140	0·00156
100	0·255	0·00255
110	0·450	0·00409
120	0·865	0·00721
130	1·64	0·0126
140	5·00	0·0357
148	37·5	0·254

The isotherm of argon within crystallites of lithium chabazite at 89·3° K will serve as an example of this method of analysis. The isotherm was plotted on a sufficiently large scale so that equilibrium pressures corresponding to successive increments of 10 cm.^{3} of argon could be read off (Table II). When p/v was plotted against p a curve rather than a straight line was obtained, as already noted. Tangents to this curve were then drawn for increments in v of 10 cm.^{3}. Each of these tangents was then regarded as a linear B.E.T. plot with $n = 1$ and from the slopes and intercepts values of the B.E.T. constants v_m and C were obtained. Thus $p/v = \frac{p_0}{cv_m} + \frac{p}{v_m}$ when $n = 1$ for the B.E.T. isotherm. Here p_0 denotes the saturation vapour pressure of argon at 89·3° K, and is taken as 93 cm. Hg. C is the equilibrium constant for the distribution of argon between the liquid phase and the chabazite crystals, and v_m is the amount of argon

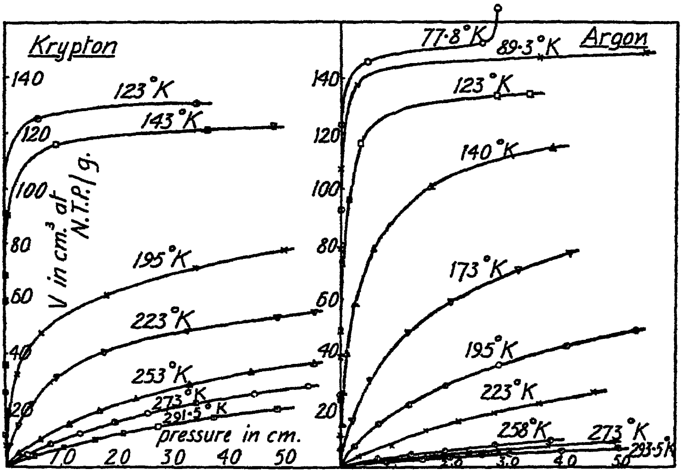

FIG 1*a*. .—Sorption of krypton and argon in lithium chabazite.

required to fill the intracrystalline sites involved. C is related to the standard free energy of transfer of argon from liquid argon to the intracrystalline sites by the equation

$$C = \exp\left(\frac{-\Delta A_0}{RT}\right) \simeq \exp\left(\frac{-\Delta G_0}{RT}\right).$$

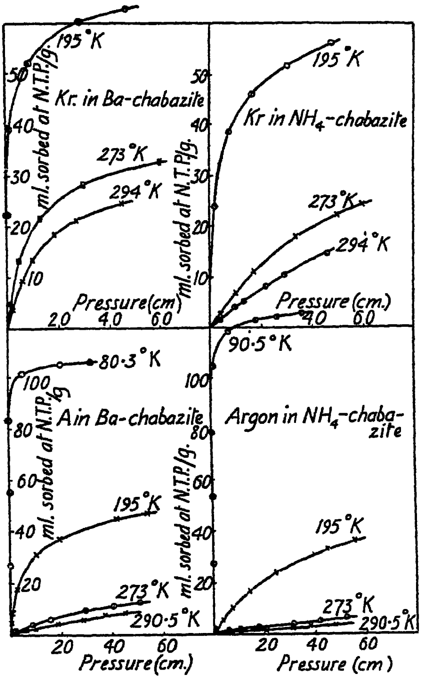

FIG. 1*b*.—Sorption of Kr and A in Ba-and NH_4-chabazite.

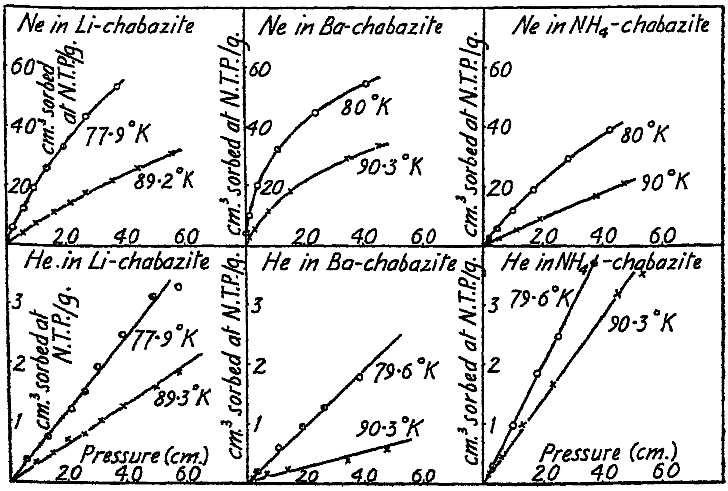

FIG. 1*c*.—Sorption of Ne and He in Li-, Ba- and NH_4-chabazites.

On the simplest assumption of a negligibly small entropy change for this transfer C takes the usual form given in the B.E.T. treatment:

$$C = \exp\left(\frac{-(E_1 - E_l)}{RT}\right)$$

where E_1 is the sorption heat from the gas phase, and $E_l = 1500$ cal./g. atom is the heat of liquefaction of argon. With these assumptions the following values of v_m, C, ΔG_0 and E_1 were obtained (Table III).

TABLE III.—ANALYSIS OF THE ISOTHERM OF ARGON AT 89·3° K IN LITHIUM CHABAZITE

Site Group (cm.^{3} sorbed)	v_m	C	$-\Delta G_0$ (cal. g. atom).	E_1 (cal./g. atom).
10-20	45·9	29400	1810	3310
20-30	53·9	22000	1760	3260
30-40	64·4	15300	1700	3200
40-50	72·0	11630	1650	3150
50-60	84·6	7380	1570	3070
60-70	94·7	5230	1510	3010
70-80	95·6	5050	1510	3010
80-90	120·8	1920	1330	2830*
90-100	116·2	2250	1360	2860
100-110	126·8	1350	1270	2770
110-120	133·0	985	1220	2720
120-130	143·2	555	1120	2620
130-140	145·3	478	1090	2590
140-148	149·2	277	990	2490

* There is a somewhat anomalous result for the site group 80-90, which has been carefully checked, but which may be due to a small error in the isotherm data.

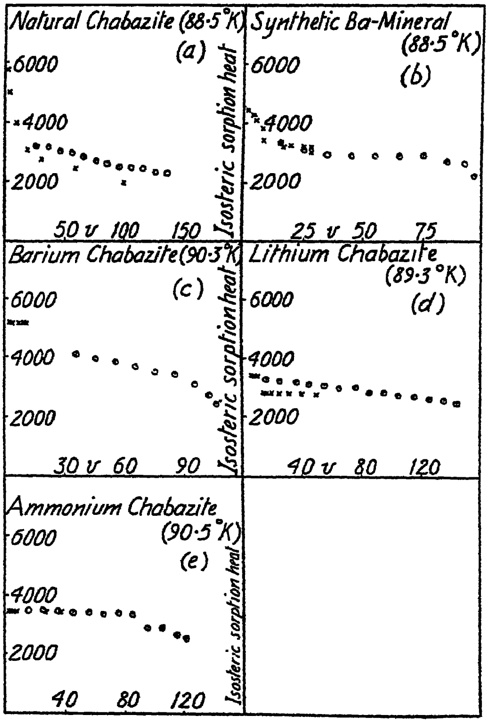

FIG. 2.—Isosteric heats (×) and values of E_1 (+) for argon in several ion exchanged chabazites and in a synthetic zeolite, plotted as functions of the amount of argon sorbed.

The v_m values increase with charge of gas. This means that the slopes and intercepts of the tangents give a measure of the saturation value for a heterogeneous sorbent only in the neighbourhood of saturation itself. The values of E_1 in column 5 of Table III decrease as the charge of gas increases, and are reasonably close to the isosteric sorption heats determined by means of the Clapeyron equation (see next section). When this is the case it may be taken as evidence for the assumption made in deriving E_1 that the entropy of transfer of argon from the liquid phase to the intracrystalline phase is small. Analogous determinations of E_1 were made also for argon at 89·3° K in a synthetic zeolite (Barrer and Riley[6]) and in ammonium, barium and natural chabazites. The extent of the correspondence between these values of E_1 and the isosteric heats is shown in Fig. 2. There is, of course, the same type of heterogeneity in terms of the free energy of sorption, ΔG_0, as for E_1. From the viewpoint of sorption equilibria in heterogeneous media the free energy distribution function among sites is more important than the energy distribution function. The affinities between the various gases and a given ion exchange chabazite are in the order Kr > A > Ne > He.

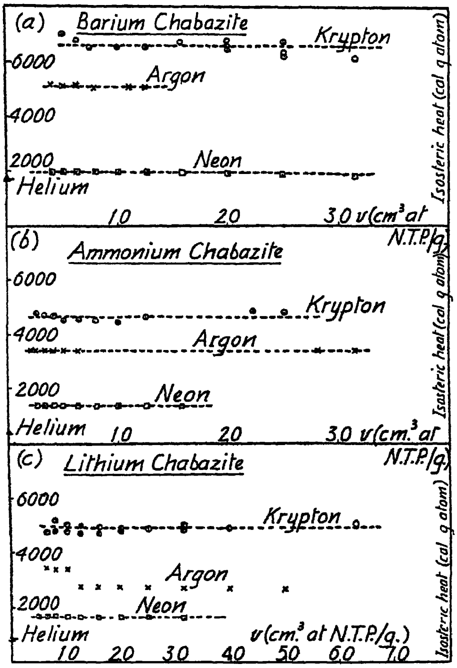

FIG. 3.—Isosteric sorption heats as a function of the amount sorbed.

Isosteric Sorption Heats.—The Clapeyron equation was used to derive isosteric heat of sorption, which may be identified with ΔH.[10] These sorption heats are shown as a function of the amount of gas occluded in Fig. 3. Table IV compares the *initial* heats of sorption for a natural Ca-rich chabazite, barium chabazite, a synthetic barium zeolite with sorptive properties similar to those of chabazite [9, 6] and lithium and ammonium chabazites.

TABLE IV.—SOME INITIAL ISOSTERIC HEATS OF SORPTION (cal./g. atom)

Crystal	Krypton	Argon	Neon
(Ca + Na)-chabazite . .	—~7200	−6150	−3300
Ba-chabazite . . .	— 6600	−5130	−1970
Synthetic zeolite . .	— 6700	−4400	−1800
Li-chabazite . . .	— 4890	−3500	−1670
NH_4-chabazite . . .	— 4670	−3430	−1400

A comparison of Fig. 3 with corresponding diagrams given by Barrer and Riley[6] for natural chabazite (Ca-rich) and for the synthetic zeolite of Table IV showed that Ba, Li and NH_4 chabazites were much more homogeneous than were natural chabazite and the synthetic product. In natural chabazite this may be due to the greater chemical homogeneity of the ion-exchanged forms (since natural chabazites contain both Ca^{++} and Na^+ ions), although other influences may also contribute (Barrer and Riley[6]). In Ba, Li and NH_4 chabazites the first 20 to 30 cm.³ at N.T.P. per g. are sorbed with little diminution in the sorption heat.

[9] Barrer, *J. Chem. Soc.*, 1948, 127.

[10] Hill, *J. Chem. Physics*, 1949, **17**, 520.

Discussion

There is a correspondence between the relative magnitudes of the isosteric sorption heats of the inert gases and their heats of liquefaction which suggests that the sorption energies might first be considered in terms of dispersion forces and hence of such physical properties as polarizability and diamagnetic susceptibility. The values of these constants which are employed here are summarized in Table V. The exothermic energy of interaction due to dispersion forces and to short-range repulsive forces can be written in terms of the Kirkwood expression [11] as

TABLE V

Ion or atom	$10^{24}\times$ polarizability (cm^3)	$10^{30}\times$ diamagnetic susceptibility (c.g.s. units)	$10^8\times$ radius (cm.)
Li^+	0·0292	− 1·05	0·78
Na^+	0·181	− 6·97	0·98
NH_4^+	—	—	1·43
Ca^{++}	0·471	−22·1	1·06
Ba^{++}	1·56	−76·4	1·33
He	0·20	− 3·12	~1·2
Ne	0·39	−11·0	1·60
A	1·63	−29·9	1·92
Kr	2·46	—	1·97

$$E = \sum 6mc^2\left\{\frac{1}{r_1^6} - \frac{1}{2}\frac{r_0^6}{r_1^{12}}\right\}\frac{\alpha_1\alpha_2}{\dfrac{\alpha_1}{\chi_1} + \dfrac{\alpha_2}{\chi_2}}, \qquad . \quad . \quad . \quad (1)$$

where m denotes the electronic mass, c is the velocity of light, α_1 and χ_1 are the polarizability and diamagnetic susceptibility of an atom or ion of the lattice and α_2, χ_2 are these quantities for the sorbate. r_0 denotes the equilibrium distance between lattice atom and sorbate atom and r_1 the actual distance. Exothermic energy changes are to be given a negative sign.

For maximum interaction $r_1 = r_0$, and r_0 may be taken as the sum of the radii of the interacting pair of atoms. For a given sorbate atom in a given crystal in which the anionic framework is unaltered but in which the interstitial cation alone is exchanged one may rewrite eqn. (1) as

$$E = E_0 + \sum 6mc^2 \cdot \frac{\alpha_1\alpha_2}{\dfrac{\alpha_1}{\chi_1} + \dfrac{\alpha_2}{\chi_2}} \cdot \left\{\frac{1}{r_1^6} - \frac{1}{2}\frac{r_0^6}{r_1^{12}}\right\}, \qquad . \quad . \quad (2)$$

where the first term E_0 denotes the interaction energy between the sorbate atom and the aluminosilicate framework which, to a first approximation, may be unaltered by simple ion exchange. The second term now denotes the contribution due to all interactions of a sorbate atom with cations only. If the mean positions of the sorbate atom and the cation are unaltered in the ion exchange then r_1 is also unaltered and the sorption energy takes the form :

$$E = E_0 + \text{const.}\ \frac{\alpha_1\alpha_2}{\dfrac{\alpha_1}{\chi_1} + \dfrac{\alpha_2}{\chi_2}}. \qquad . \quad . \quad . \quad . \quad . \quad (3)$$

On the other hand if the sorbate atom is in contact with a single cation ($r_1 = r_0$) its interactions with more distant cations may be neglected, and

$$E = E_0 + \text{const.}\ \frac{1}{r_0^6} \cdot \frac{\alpha_1\alpha_2}{\dfrac{\alpha_1}{\chi_1} + \dfrac{\alpha_2}{\chi_2}}. \qquad . \quad . \quad . \quad . \quad (4)$$

---

[11] *Physik. Z.*, 1932, **33**, 57.

In either event an alteration in sorption heat would arise from the different sorbate-cation interactions for the different ion-exchanged forms.* To explore these possibilities the terms $\frac{\alpha_1\alpha_2}{\frac{\alpha_1}{\chi_1}+\frac{\alpha_2}{\chi_2}}$ and $\frac{1}{r_0^6}\cdot\frac{\alpha_1\alpha_2}{\frac{\alpha_1}{\chi_1}+\frac{\alpha_2}{\chi_2}}$ involved in eqn. (3) and (4) respectively were derived for several sorbate-cation pairs (Table VI). These quantities vary by an order of magnitude for

TABLE VI

Atom-ion pair	$10^{43} \times \frac{1}{r_0^6}$	$10^{51} \times \frac{\alpha_1\alpha_2}{\frac{\alpha_1}{\chi_1}+\frac{\alpha_2}{\chi_2}}$	$\frac{10^8}{r_0^6}\cdot\frac{\alpha_1\alpha_2}{\frac{\alpha_1}{\chi_1}+\frac{\alpha_2}{\chi_2}}$	$\frac{3Nmc^2}{r_0^6}\cdot\frac{\alpha_1\alpha_2}{\frac{\alpha_1}{\chi_1}+\frac{\alpha_2}{\chi_2}}$ (cal)
A—Ca^{++}	1·43	10·1	1·44	− 505
Ne—Ca^{++}	2·82	3·23	0·94	− 370
He—Ca^{++}	7·55	1·10	0·83	− 330
A—Ba^{++}	0·85	33·5	2·84	−1010
Ne—Ba^{++}	1·40	10·9	1·53	− 540
He—Ba^{++}	3·82	3·69	1·41	− 495
A—Li^{+}	2·59	0·578	0·15	− 53
Ne—Li^{+}	5·53	0·180	0·10	− 36
He—Li^{+}	16·7	0·064	0·11	− 38

interaction with the ions Ca^{++}, Ba^{++} and Li^{+} and so much more widely than do the sorption heats themselves. In column 5 of Table VI the maximum interaction energies are given, and again these show that sorption heats should be greater in Ba^{++}-rich rather than in Ca^{++}-rich chabazites, the converse of the observations themselves. One may conclude that a simple explanation involving cation-sorbate dispersion forces is unlikely. Another kind of cation-sorbate interaction is considered to play an important part.

Additional cation-sorbate forces have been discussed by Barrer [12] who pointed out that polarization energies in the intense fields adjacent to any cation can account for the very marked effect of ion exchange on the affinity between a non-polar gas and its intracrystalline environment. The polarization energy per atom due to a cation-sorbate interaction is then

$$-E = \frac{\alpha_2 \cdot \epsilon^2}{2r^4}, \quad . \quad . \quad . \quad . \quad . \quad . \quad (5)$$

where ϵ is the ionic charge. The *maximum* values of E due to this cause arise if $r = r_0$ and are given in a number of cases in Table VII. It is seen that polarization could result in energies of interaction of considerable magnitude, and that these energies are in the same order as the experimental isosteric heats for a given gas in a group of ion-exchanged crystals. The range in the energies of Table VII over such a group of crystals is greater than the experimental range in isosteric heats for the same group (cf. Table IV). This is to be expected since the sorbate atom, because of thermal agitation and of polarization and dispersion forces originating from the anionic framework or even from other cations, will not continually remain in direct contact with one cation. Its average polarization energy is therefore likely to be less than the maximum values recorded in Table VII.

---

* In the case corresponding to eqn. (4) any shift in mean position of the sorbate could also modify E_0 to some extent.

[12] *Trans. Faraday Soc.*, 1944, **40**, 555.

TABLE VII.—MAXIMUM POLARIZATION ENERGIES

Atom-ion Pair	Polarisation Energy (cal./g.atom)	Atom-ion Pair	Polarization Energy (cal./g atom)
Ca^{++}—Kr	−19400	Ca^{++}—Ne	−5200
Ba^{++}—Kr	−13700	Ba^{++}—Ne	−3500
Li^{+}—Kr	− 7100	Li^{+}—Ne	−2000
NH_4^{+}—Kr	− 2900	NH_4^{+}—Ne	− 770
Ca^{++}—A	−13700	—	—
Ba^{++}—A	− 9700	—	—
Li^{+}—A	− 5100	—	—
NH_4^{+}—A	− 2000	—	—

If one compares the maximum contributions due to polarization for a series of gases in any given ion exchanged form one sees from Table VII that in all cases the polarizability of the sorbate and polarization energy increase together; while a comparison of the isosteric heats and the polarizabilities shows that they also increase together (Fig. 4). This parallelism is compatible with the polarization hypothesis and with a tendency for association between sorbate atoms and interstitial cations.

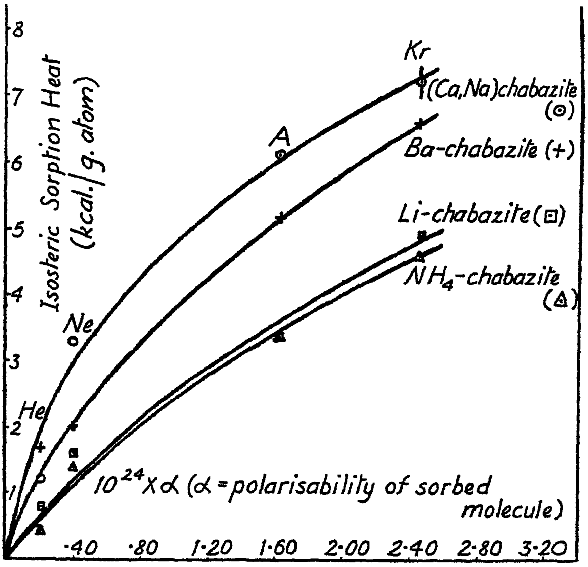

FIG. 4.—Empirical relation between polarizability and initial isosteric sorption heat.

Chemistry Department,
Marischal College,
The University,
Aberdeen.

Chemistry Department,
The University,
Sheffield.

HIGH POLYMER SOLUTIONS

PART II.—THE OSMOTIC PRESSURES OF POLYSTYRENE SOLUTIONS

By C. E. H. Bawn, R. F. J. Freeman and A. R. Kamaliddin

Received 15*th March,* 1950

Osmotic pressure measurements have been made on 10 molecular weight fractions of polystyrene in toluene and on 4 fractions in methyl ethyl ketone at 25° C. The results for toluene may be accurately represented by the equation

$$\frac{\Pi}{c_2} = \frac{RT}{M_2} + Bc_2 + Cc_2^2.$$

A graphical method of evaluating B and C is given and it is shown that there is a linear dependence of B on the reciprocal of the molecular weight for toluene solutions. The results are discussed in relation to the current theories of high polymer solutions.

The measurement of the osmotic pressure of dilute solutions of a polymer is the most commonly used, and probably the surest method for the absolute determination of its number average molecular weight. Osmotic pressure determination of polymer solutions show large deviations from the ideal behaviour expressed by the equation

$$\Pi = -\frac{\Delta G_1}{\overline{V}_1} = -RT \ln (1 - N_2), \quad . \quad . \quad . \quad (1)$$

where ΔG_1 is the molar free energy of dilution, $\overline{V}_1$ is the partial molar volume of the solvent, and N_2 is the mole fraction of the solute. Eqn. (1) is derived on the assumption that the heat of mixing is zero and that the entropy of mixing is that of a perfect gas. The non-ideal behaviour of the polymer solutions may be due either to non-ideal entropy of dilution, or to the existence of a finite heat of dilution or both. In many cases the heat of dilution of the polymer solution is small and the observed deviation from ideal behaviour is mainly due to the entropy term. In the theoretical derivation of (1) it is assumed that the molecules are similar in size and shape, and that the energy of interaction between the solute and solvent is small. This means that the molecules of solvent and solute can mix in a perfectly random manner. Molecules of polymer consist of large numbers of monomer units, and although the polymer molecules as a whole can be distributed randomly, there cannot be completely random mixing between the solvent molecules and the polymer segments. One theoretical method of approach has been to consider the polymer segments and solvent molecules as occupying points on a lattice, and to calculate the entropy of mixing of such a system.

Huggins,[1] using such a model, derived the formula :

$$\frac{\Pi}{c_2} = \frac{RT}{M_2} + \frac{RT}{M_1}\frac{d_1}{d_2^2}(\tfrac{1}{2} - \mu)c_2 + \frac{RT}{3M_1}\frac{d_1c_2^2}{d_2^3} + \dots \quad . \quad (3)$$

where d_1, d_2 are the densities, M_1 and M_2 the molecular weights of solvent and solute respectively, and μ is an empirical constant characteristic of a given solvent—polymer system at a given temperature. Similar expressions have been derived by Flory [2] and Miller.[3]

---

[1] Huggins, *J. Physic. Chem.*, 1942, **46**, 151 ; *Ind. Eng. Chem.*, 1943, **35**, 216, 980.

The osmotic pressure measurements on polystyrene solution in toluene and for other polymer-solvent systems show that the plot of Π/c_2 against c_2 is in general not linear and the terms in c_2^2 cannot be ignored.

As the value of Π/c_2 at infinite dilution is obtained by an extrapolation of the experimental $\Pi/c_2 - c_2$ curve, the accuracy of the determination of the molecular weight is profoundly affected by the method of extrapolation. For the present work a satisfactory extrapolation procedure has been employed and the constants B and C evaluated from measurements on a series of well-defined fractions of polystyrene.

Experimental

Measurements of osmotic pressure were made in modified Fuoss and Mead [4] osmometers. The half cells were made of forged stainless steel, each being 1 in. thick. Early measurements with an osmometer made of brass with half-cells ¾ in. thick showed that under the stresses of tightening the nuts, the cells tended to warp resulting in leakage round the membrane. With the thicker stainless steel blocks, and precision ground inner faces, no trouble due to leakage around the membrane was experienced, even with very thin, hard membranes.

The valve blocks were also made of stainless steel. In place of the needle valves used by Fuoss and Mead, a mounted ball-bearing was forced on to a seating inside the valve block. This proved more satisfactory than the needle valve when stainless steel was used for the blocks. These valves were quite leak-proof, although after long use the seat had to be re-made. The vertical stand pipes were made of ½ in. stainless steel tube, and one of them could be closed at the bottom by a needle valve thus isolating one-half cell. The difference in pressure across the valve was small and a needle valve was satisfactory.

Since accurate temperature control is essential for osmotic measurements, brass jackets were bolted to the back of the cells, covering most of the area inside the ring of fixing bolts. Water was circulated through the jackets from a thermostat regulated to 25·00 ± 0·02° C. The osmometers were kept in air thermostats fitted with double glass windows, and regulated to 0·1° C at the equilibrium temperature of the osmometers. The air thermostats were arranged so that direct sunlight did not fall on the osmometers. By this means not only was the effect of draughts eliminated, but no corrections were necessary for the exposed capillaries of the osmometer. The capillaries were 5 mm. diam. Veridia precision diameter tubing joined by glass-to-metal seals to brass plugs which were screwed into the top of the osmometer, using an aluminium washer. The threads were lightly coated with glycerine to ensure a leak-tight seal.

The osmometer was assembled with the membrane horizontal, one cell being supported in a cradle, and the membrane laid on and trimmed to size. At all times the membranes were kept wet with solvent, as drying caused shrinkage and rendered them unsuitable for use. The other cell was laid on top, the bolts inserted, and tightened by hand. The osmometer was then placed vertically on its stand and the nuts tightened as hard as possible. The membranes yielded under pressure and the nuts had to be re-tightened at intervals until they remained tight. The compression of the membranes was complete in about 24 hr., and caused no further trouble during the life of the membrane. Occasionally small bubbles of air were trapped in the cells during assembly, and these worked their way to the base of the capillaries. This bubble formation ceased after a few rinsings with solvent and was never experienced during measurements.

Two types of membranes were used : (i) denitrated collodion and (ii) alkali-treated commercial Cellophane membranes.

Collodion Membranes.—Various types of collodion were tested for use as membranes. Commercial collodion (B.D.H.) gave very variable membranes, the characteristics of which varied from sample to sample, even though the method of preparation was carefully standardized. It was finally decided that the most satisfactory membranes were those made from collodion solutions in ether-alcohol prepared in the laboratory. The grade of N/C had some effect on the membrane, and the type selected was HM 15/20 supplied by I.C.I. (Nobel Division). The N/C was dried in vacuum at room temperature for 24 hr. The alcohol used was dried with aluminium amalgam, and the ether with sodium wire. Traces of water may not have had any effect on the membranes, but it was considered that complete drying gave the most uniform product.

---

[2] Flory, *J. Chem. Physics*, 1942, **10**, 51 ; *ibid.*, 1945, **13**, 453.

[3] Miller, *Proc. Camb. Phil. Soc.*, 1943, **39**, 54.

[4] Fuoss and Mead, *J. Physic. Chem.*, 1943, **47**, 59.

The ratio alcohol/ether in the solvent for N/C had an appreciable effect on the resulting membrane, a high ether content giving thin, hard, and less uniform membranes. The stock solution of collodion was made by dissolving 30 g. of N/C in 600 ml. of alcohol + ether mixed in the ratio 2/1 by volume. This solution was filtered in order to remove dust and was stable for 2-3 months. The collodion deteriorated after long storage, and gave unreliable membranes. The membrane was prepared by pouring 20 ml. of the solution into a 7-in. diam. metal ring floating on mercury, previously cleaned by pouring a thin film of laboratory collodion over it, and removing the film when dry. The solution was left covered for ½ hr. before evaporation of solvent in order to allow any bubbles to disperse and to allow the formation of a uniform layer of collodion. The evaporation was carried out by drawing a slow stream of air through a funnel placed 1 in. above the solution. The time and uniformity of evaporation were found to have an important effect on the porosity of the membrane. Uniform membranes of pre-determined porosity were made by the addition of Cellosolve (ethylene glycol mono-ethyl ether). The control of membrane porosity by the addition of this and other reagents was extensively studied by Elford,[5] who found that the porosity decreased logarithmically with the increase in Cellosolve concentration. The amount of added Cellosolve was consequently critical in deciding the porosity of the resulting membrane. In agreement with Elford's results, it was found that while the addition of 1 ml. of Cellosolve to 40 ml. of solution produced membranes which were fairly porous and allowed serious polymer diffusion after some time, the addition of 3 ml. formed very slow and much less porous membranes, and the addition of 5 ml. rendered the membranes almost impermeable to solvent molecules. Quantities of Cellosolve varying from 2 to 3 ml. in 40 ml. solution, were therefore used. Cellosolve also improved the mechanical properties of the membrane, and rendered the conditions of evaporation much less important.

The denitration was carried out as described by Fuoss and Mead [4] following the method of Montanna and Jilk.[6] The ammonium sulphide used was 16 % concentration. After denitration the membranes were left overnight in running tap water. They were then conditioned by soaking for at least 2 hr. in each of the following liquids in order: 50/50 water + abs. alcohol, absolute alcohol, 50/50 abs. alcohol + solvent and pure solvent.

Cellophane Membranes.—These were used for measurements on low molecular weight materials and for checking results obtained with collodion membranes. The Cellophane employed was supplied by the British Cellophane Company, Bridgwater, and was free from preservatives. The wet material as taken from the rollers was never allowed to dry, and was swollen in 3-5 % NaOH solution according to the required porosity. Solutions exceeding 5 % in concentration were found to damage the membranes. About one week was allowed for the swelling as it was found that the porosity increased with the time of swelling. The swollen membranes were thoroughly washed with water before conditioning to solvents.

In the osmometer the membrane was held firmly round the edges, except with thick membranes, which were also supported by the internal rings. With very thin membrane movements of about 1/1000 in. occurred and this resulted in the levels in the two capillaries moving simultaneously over a short distance when the levels were adjusted. This rendered the initial adjustment more awkward, but did not affect subsequent operations, as, once the levels were set to approximately the correct osmotic pressure, the changes in pressure were not sufficient to move the membrane bodily.

Although some workers [6a] have reported effects due to adsorption of polymer in the membrane we have found no permanent change due to this cause. It was observed, however, that with a new membrane and with methyl ethyl ketone as solvent, low osmotic pressure values were registered at first, but after the membrane had been in contact with the solution for some time, consistent results

[5] Elford, *Trans. Faraday Soc.*, 1937, **33**, 1094.

[6] Montanna and Jilk, *J. Physic. Chem.*, 1941, **45**, 1375.

[6a] Fuoss and Mead [4]; McIntosh, Robertson and Grummitt, *Can. J. Res. B*, 1946, **24**, 150.

were obtained. Further conditioning to the solution was not necessary for subsequent determinations. In all cases, the original zero-difference of the membrane was re-established after rinsing with solvent a few times, showing that adsorbed polymer had no permanent effect on the membrane.

Checking of Mechanical Faults.—The only important mechanical fault which occurred was leakage through the valves and this was observed by measuring the zero difference of the osmometer, viz. the difference between the levels with solvent on both sides of the membrane with the solution half-cell sealed off by the vertical valve in the stand pipe. Owing to the stand pipe being permanently open on the solvent side, no trouble has been experienced due to leakage through the solvent drainage valve. If leakage through this valve occurred, the level on that side was lower than that on the solvent side, giving rise to a zero difference. Osmometers were not considered satisfactory unless the zero difference due to all causes was less than 0·025 cm. If the vertical valve was faulty, the zero difference depended on the level of the liquid in the solution stand pipe. Errors due to this were rarely encountered. As the net zero difference was dependent on variable factors, no attempt was made to introduce correction factors to account for this and measurements were made only in osmometers in which its magnitude was negligible. For this reason the zero difference was constantly used as a sensitive test of the mechanical reliability of the osmometer and efficiency of temperature control.

Temperature Effects.—Even when all reasonable precautions were taken in thermostating osmometers, the level of liquid in the sensitive solution side was rarely constant and oscillated about an equilibrium position. The amplitude of oscillation was rarely more than 0·005 cm., and in an actual measurement the upper and lower limits of pressure were recorded a number of times and their average taken.

In order to reduce evaporation of solvent from stand pipes and capillaries to a minimum, the pipes were fitted with caps with small holes, and dishes containing solvent were placed inside the air thermostat.

Preparation of Polymer Solutions.—All solutions were prepared by weighing. A concentrated solution was made and diluted by weight to give the lower concentrations. It was considered that errors due to the small amount of solvent which moved through the membrane were negligible compared with errors which would arise in determining the concentration by analysis. The toluene used was laboratory grade, dried over calcium chloride and fractionated. Commercial methyl ethyl ketone was dried with sodium sulphate and fractionated.

Measurement of Osmotic Pressure.—When the osmometer was known to be mechanically satisfactory, the membrane was first tested for diffusion by pouring into the solution side a concentrated solution of polymer of a molecular weight lower than that of the fractions to be subsequently measured. The solution was left for at least 24 hr., and the contents of the solvent cell tested for polymer, by draining the cell, and adding excess CH_3OH. If no cloudiness could be detected when the mixture was left to stand for a further 24 hr., and if the osmotic pressure remained constant, the membrane was considered satisfactory for use. Diffusion tests and zero difference measurements were carried out as often as possible while the osmometer was in use.

A static method of measurement was employed. Initially the cells were thoroughly rinsed with solution and solvent, the solution cell being drained and refilled at least 6 times. The solvent cell was then rinsed twice (whilst the solution cell was full) and both cells simultaneously drained and refilled with solvent and solution.

Equilibrium was then allowed to be established, the osmotic pressure recorded, and the cells drained, rinsed with solvent and solution and finally refilled. The osmotic pressure was then observed at intervals until equilibrium was reached. If this equilibrium value agreed with the one previously obtained and if it remained constant over a period of at least 12 hr., and further, if the diffusion test proved negative, the value was accepted. Equilibrium was attained in 1 to 5 hr. depending on the membrane porosity.

The most dilute solution was measured first, followed by the higher concentrations in order. No sign of membrane ageing was observed, and some membranes were in constant use for over a year without a detectable change of porosity. They were discarded only when the osmometer had to be dismantled.

Preparation of Polymer Samples.—Since the osmotic pressure measurements were carried out in conjunction with the determination of the viscosity-molecular weight relationship for polystyrene it was necessary to have carefully fractionated specimens of at least 1 g. These could have been obtained from commercial polystyrene, but in view of the observations that the structure of the polymer is dependent upon the conditions of polymerization it was desirable to prepare specimens of well-defined history. Moreover, since in commercial practice it is usual to take the polymerization as near to completion as possible it is very probable that these polymers contain branched or slightly cross-linked chains. In the present investigation it was desirable to confine the measurement to polymers of linear structure and with this object in view the extent of polymerization was not taken beyond 20 %. Polystyrene prepared by thermal polymerization of the monomer has a fairly sharp maximum in its size distribution curve which changes with the temperature of polymerization. In order to obtain adequate samples covering a wide range of molecular weights, polymers were prepared at several temperatures and separately fractionated.

Commercial monomeric styrene was washed free of inhibitor with potash, dried over A.R. $CaCl_2$ and fractionally distilled 3 times *in vacuo*. After the second distillation the sample was degassed *in vacuo* and finally distilled into a container to which were sealed a series of tubes. These tubes were thoroughly cleaned before sealing to the apparatus and all occluded gases were removed by flaming, with the tubes and connections evacuated. The styrene from the main reservoir was poured into the tubes by tilting, the tubes being sealed off whilst still evacuated. Monomer prepared in this way gave reproducible velocity measurements. The tubes were placed in thermostats at 60, 100 and 135° C and removed at times corresponding to not more than 20 % conversion. The contents were taken up in methyl ethyl ketone and the polymer precipitated by addition of a large excess of methyl alcohol. The polymer was redissolved in methyl ethyl ketone and reprecipitated. The separation into fractions was carried out by fractional precipitation from methyl ethyl ketone solutions by addition of methyl alcohol as described by Alfrey, Bartovics and Mark.[7] Each sample was separated into 6 reasonably sized fractions, each of which was separately refractionated into 4 or more fractions. In some cases a further refractionation was effected. The final fractions were always obtained from solutions not exceeding 0·1 % in concentration. These final fractions were reprecipitated with CH_3OH from dilute methyl ethyl ketone solutions, great care being taken to use conditions under which a flocculent precipitate, with the minimum of occluded solvent, was obtained. The precipitates were dried in a vacuum oven at 60° C for several days. No loss of weight was observed on further heating and there was no evidence of the retention of solvent by the polymer. In this way a range of fractions varying from 70,000 to 1,800,000 in molecular weight were obtained.

Results

The osmotic pressure measurements on 10 fractions in toluene and 4 in methyl ethyl ketone are summarized in Tables I and II. All measurements were made at 25·0° C. The unit of concentration used was g. cm.$^{-3}$ of solution and of pressure g. cm.$^{-2}$, and hence Π/c_2 was in cm. The plots of Π/c_2 against c for 4 fractions in both toluene and methyl ethyl ketone are shown in Fig. 1. In all cases the plots were non-linear, and could not accurately be described by the simple relationship which has been used for many systems. Extrapolations to $c_3 = 0$ were carried out both by free-hand drawing and by the graphical method described below and the extrapolated values are summarized in Table I.

Fig. 1 also shows the plot of Π/c_2 against c_2 for one fraction, in which alternate determinations were made using different osmometers and different types of membrane, one Cellophane, and the other collodion. The experimental points are clearly independent of both the osmometer and the membrane employed, and constitute a very satisfactory check on the general experimental procedure. In all, four osmometers were used, with both types of membrane, and no differences were detected which could be ascribed either to the osmometer or to the membrane.

When numerical values for toluene-polystyrene are substituted for the terms in Huggins' equation (3), the expression becomes

$$\frac{\Pi}{c_2} = \frac{RT}{M_2} + 2{\cdot}03 \times 10^5 \left(\tfrac{1}{2} - \mu\right) c_2 + 6{\cdot}27 \times 10^4 c_2^2.$$

Π is in g. cm.$^{-2}$, c_2 in g. cm.$^{-3}$ and $d_2 = 1{\cdot}08$ g. cm.$^{-3}$ as found experimentally.

---

[7] Alfrey, Bartovics and Mark, *J. Amer. Chem. Soc.*, 1942, 64, 2716.

TABLE I.—OSMOTIC PRESSURE OF SOLUTIONS OF POLYSTYRENE FRACTIONS IN TOLUENE AT 25° C

Fraction	$10^3 \times c_2$ g.cm.$^{-3}$	Π g.cm.$^{-2}$	(Π/c_2)	$(\Pi/c_2)_{c_2=0}$ Extrapolation	$(\Pi/c_2)_{c_2=0}$ Graphical Analysis	$M \times 10^{-4}$
S_1IB	4·27	0·22	51	—	—	—
	6·97	0·58	83	—	—	—
	9·00	1·00	111	14	14	180
	10·96	1·53	140	—	—	—
S_1ID	2·60	0·10	38	—	—	—
	5·07	0·32	64	—	—	—
	5·16	0·33	63	—	—	160
	6·54	0·52	80	17	16	—
	9·19	1·09	119	—	—	—
	9·50	1·17	123	—	—	—
S_1IIB	4·36	0·25	57	—	—	140
	7·26	0·68	94	19	18	—
	9·20	1·10	120	—	—	—
S_2IIA	4·54	0·30	66	—	—	—
	5·50	0·41	75	—	—	110
	7·36	0·74	101	23	23	—
	8·26	0·94	114	—	—	—
S_2IIB	3·18	0·17	54	—	—	90
	6·66	0·64	96	27	27	—
	10·00	1·47	147	—	—	—
S_2IVA	3·83	0·33	86	—	—	—
	5·50	0·56	102	50	49	50
	8·00	1·09	136	—	—	—
S_3IIA$_1$	1·55	0·16	105	—	—	—
	2·56	0·28	110	—	—	—
	2·93	0·32	110	—	—	29
	3·80	0·47	124	87	88	—
	5·38	0·77	143	—	—	—
	7·80	1·36	175	—	—	—
	8·68	1·60	184	—	—	—
S_3IIIA	1·75	0·31	177	—	—	—
	2·85	0·53	186	—	—	16
	4·35	0·88	202	—	—	—
	6·50	1·49	229	158	157	—
	8·85	2·36	267	—	—	—
S_3IVB	1·61	0·46	286	—	—	—
	2·42	0·70	290	—	—	9·4
	3·10	0·94	303	267	269	—
	4·91	1·62	330	—	—	—
	7·85	2·93	373	—	—	—
	10·16	4·16	409	—	—	—
S_3VB	1·65	0·61	370	—	—	7·2
	2·97	1·16	390	351	352	—
	4·80	2·00	416	—	—	—
	7·66	3·52	460	—	—	—

The plot of Π/c_2 against c_2 and $\Pi/c_2 - 6{\cdot}27 \times 10^4 c_2^3$ against c_2 for one fraction is shown in Fig. 2. If the Huggins equation were correct the latter plot should be linear. Obviously the correction term in c^2 is not sufficient in this case.

If the general expression

$$\Pi = \frac{RT}{M_2} c_2 + Bc_2^2 + Cc_2^3 + \ldots$$

is accepted, B and C can be evaluated from the experimental points by a simple graphical method. This also gives a satisfactory method for the extrapolation of N/c_2 to $c_2 = 0$.

TABLE II.—OSMOTIC PRESSURE OF SOLUTIONS OF POLYSTYRENE FRACTIONS IN METHYL ETHYL KETONE AT 25° C

Fraction	$10^3 \times c_2$ g.cm.$^{-3}$	Π g.cm.$^{-2}$	(Π/c_2)	$\Pi(/c_2)_{c_2=0}$	$M \times 10^{-4}$
S_1IB	2·67	0·04	15	—	—
	6·12	0·14	23	14	180
	8·91	0·31	35	—	—
S_3IIA_1	3·93	0·40	102	—	—
	8·08	0·95	118	87	29
	10·13	1·30	128	—	—
S_3IIIA	1·41	0·23	163	—	—
	2·90	0·48	166	158	16
	6·24	1·11	178	—	—
	8·57	1·63	190	—	—
S_3VB	2·49	0·87	349	—	—
	4·21	1·53	363	344	7·3
	5·56	2·03	365	—	—
	7·76	2·96	382	—	—

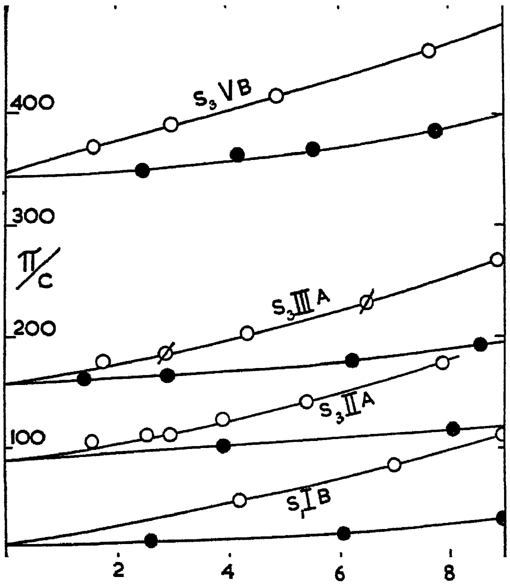

FIG. 1.—Variation of Π/c_2 with c_2 for four fractions.
○ Toluene. ● Methyl ethyl ketone.
Fraction S_3IIIA measured in two osmometers : ○ with collodion membrane ; ϕ with Cellophane membrane.

If any two values of c_2 and Π/c_2 are selected on the experimental curve, then by substitution

$$(\Pi/c_2) - (\Pi/c_2)_2 = B((c_2)_1 - (c_2)_2) + C((c_2)_1^2 - (c_2)_2^2)$$

i.e.

$$\frac{(\Pi/c_2)_1 - (\Pi/c_2)_2}{(c_2)_1 - (c_2)_2} = B + C((c_2)_1 + (c_2)_2).$$

By taking such pairs of points, and plotting the term on the left-hand side against $(c_2)_1 + (c_2)_2$ a straight line of intercept B and slope C should be obtained if the above expression is obeyed.

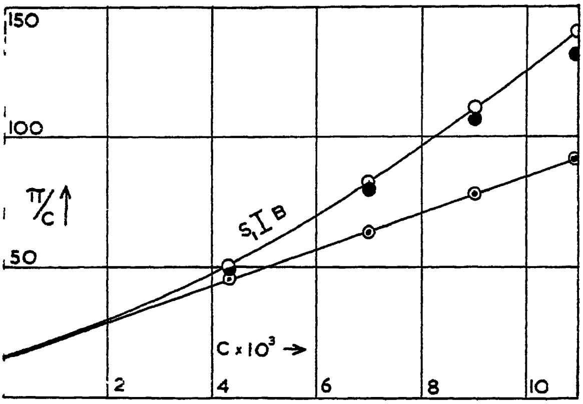

FIG. 2.—Variation of Π/c_2 with c_2 for fraction of molecular weight 1·8 × 10^6 at 25° C.

○ Experimental.
● $\Pi/c_2 - 6{\cdot}27 \times 10^4$ (Huggins [3]).
○ $\Pi/c_2 - 4{\cdot}1 \times 10^5\, c^2$.

Fig. 3 shows the result of such an operation for three fractions and in all other cases excellent straight lines were obtained. The values of C, so determined for the ten fractions, are summarized in Table III. Within the experimental error the values are constant, the average being $4{\cdot}1 \times 10^5$. This value was now used to reduce the experimental curve to a straight line, the quantity

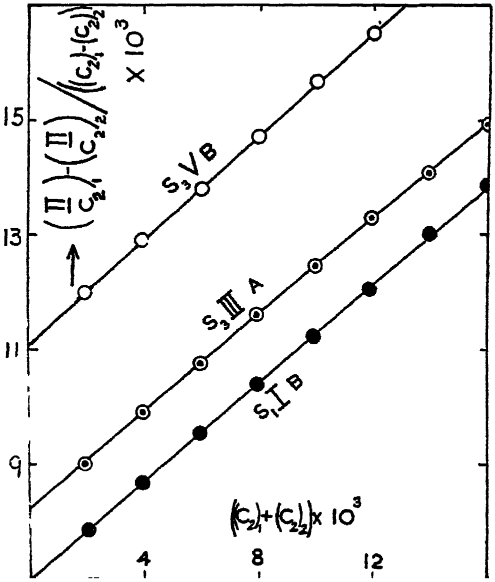

FIG. 3.—Variation of $\frac{(\Pi/c_2)_1 - \Pi(/c_2)_2}{(c_2)_1 - (c_2)_2}$ with $(c_2)_1 + (c_2)_2$ for three fractions.

($\Pi/c_2 - 4{\cdot}1 \times 10^5 c_2^2$) being plotted against c_2^2. The intercept of the linear plot which resulted with the axis gave the slope the value of B. The values of B are also summarized in Table III. The extrapolated values for the molecular weight obtained by this method were very close to the ones obtained by direct extrapolation of the Π/c_2-c_2 plot (Tables I and II).

TABLE III.—THE COEFFICIENTS B AND C

Fraction	$M \times 10^{-4}$	$10^{-3} \times B$	$10^{-5} \times C$
S_1IB . . .	180	7·0	4·3
S_1ID. . . .	160	7·3	4·7
S_1IIB . . .	140	7·3	4·1
S_2IIA . . .	110	7·6	4·3
S_2IIB . . .	90	7·7	4·1
S_2IVA . . .	50	7·6	3·8
S_3IIA1 . . .	29	7·8	3·6
S_3IIIA . . .	16	8·7	4·1
S_3IVB . . .	9·4	9·8	3·9
S_3VB . . .	7·2	11·0	4·5

Dependence of B and C on Molecular Weight and Concentration for Toluene Solutions.—The values of B and C summarized in Table III are only valid for concentrations up to 1 g./100 ml. Beyond this concentration the Π/c_2-c_2 plots decrease in curvature, indicating a decrease in the value of C. This is to be expected because if the above value of $4{\cdot}1 \times 10^5$ for C is valid at high concentrations, e.g. above 4 %, the deviation from ideality would be very much larger than observed in the region covered by vapour pressure measurements (Part I).[7a]

In order to estimate the effects of high concentrations, one fraction was measured up to a concentration of 2·5 g./100 ml. ($M = 1{\cdot}8 \times 10^6$). The graphical analysis was applied to the curve, and two distinct straight lines were obtained. For the concentration range up to 1·0 g./100 ml. the values of B and C were $7{\cdot}0 \times 10^3$ and $4{\cdot}3 \times 10^5$ respectively. For concentrations from 1·0 to 2·5 g./100 ml. the values were $B = 10 \times 10^3$ and $C = 1{\cdot}6 \times 10^5$. This effect has also been observed in other fractions, with the change occurring at about $C = 1{\cdot}0$ g./100 ml. Whereas the magnitude of C was independent of molecular weight, the values of B decreased with increase of molecular weight. As is shown in Fig. 4 the plot of B against $1/M$ is linear, and the scatter of points in high molecular weight regions fall within the experimental error of the determination of B.

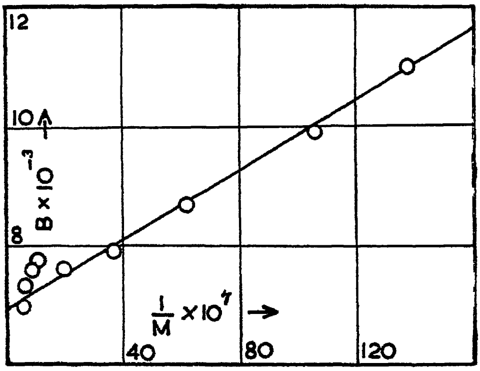

FIG. 4.—Variation of B in $\Pi/c_2 = \frac{RT}{M} + Bc_2 + Cc^2$ with $1/M$.

[7a] Bawn, Freeman and Kamaliddin, *Trans. Faraday Soc.*, 1950, 46.

Dependence of B and C on the History of the Polymers.—Although the above fractions were obtained from three samples of polymer prepared at different temperatures of polymerization, no effect of temperature of polymerization was apparent. This is confirmed by viscosity measurements described in Part III and it may be assumed therefore that there was no significant difference in molecular structure of the various fractions.

In order to estimate the effect of the conditions of polymerization of the polymer, fractions obtained from commercial polystyrene were also measured. A broad fraction obtained by removing the low molecular weight polymer (35,000 or below) had an average molecular weight of 210,000. The $\Pi/c_2 - c_2$ relationship for this polymer was linear, with $B = 14 \times 10^3$ and $C = 0$. The value of B corresponding to this molecular weight for a sharp fraction would have been equal to 8×10^3.

Another broad fraction extracted from commercial polystyrene by refluxing with acetone, and separating the part that was soluble in acetone had an average molecular weight of approximately 20,000 (a very slow Cellophane membrane was used in this case for the osmotic pressure determination). The plot of $\Pi/c_2 - c_2$ was also linear for this fraction with $B = 50 \times 10^3$. The corresponding value obtained by extrapolating our graph of B against $1/M$ (and assuming its linearity) was 20×10^3.

The system polystyrene-toluene has also been studied by Schulz[8] and by Alfrey, Bartovics and Mark.[7] Both of these authors obtained curved plots of Π/c_2 against c_2 similar to those reported here. Alfrey *et al.* used samples of polystyrene which, judging by their viscosity-molecular weight relationships, differed in properties from the samples used here. The data of Schulz have been analyzed for comparison with the present results. His values have been re-plotted and the best curve drawn through the points.

Plots of $\dfrac{(\Pi/c_2)_1 - (\Pi/c_2)_2}{(c_2)_1 - (c_2)_2}$ against $(c_1)_2 + (c_2)_2$ for the two middle fractions (m. wt. 160,000 and 180,000) were almost identical and were similar to our plot for the fraction of molecular weight $1{\cdot}8 \times 10^6$. The low concentration regions gave $B = 6{\cdot}5 \times 10^3$ and $C = 3{\cdot}7 \times 10^5$, the corresponding values for our fraction being 7×10^3 and $4{\cdot}3 \times 10^5$. For the higher concentration regions Schulz' data gave $B = 8{\cdot}0 \times 10^3$ and $C = 2{\cdot}3 \times 10^5$ compared with $B = 10{\cdot}0 \times 10^3$ and $C = 1{\cdot}6 \times 10^3$ for our fraction curves. It is interesting to note that Schulz' results indicate a change in value of the coefficients B and C at a concentration of 1·1 %, which is essentially the same as reported in the present work.

Other measurements of Schulz, reported in the same paper, show that the value of C at high concentrations is of the same order as in the two fractions calculated, i.e. about 2×10^5, and that the value of B for the low m. wt. fraction (60,000) is definitely higher than those for the other fractions. In general, the results of Schulz give curves of the same form as those obtained by us, and coefficients of the same order of magnitude. In addition, the coefficient B appears to vary with M in agreement with the present results.

Measurements in Methyl Ethyl Ketone as Solvent.—The results of measurements on four fractions in methyl ethyl ketone are summarized in Table I. The Π/c_2 plots are shown in Fig. 1, and were less definitely curved than the corresponding plots for the same fractions in toluene. The slope at low concentration is quite small, and the curve becomes almost normal to the Π/c_2 axis. The intercepts with this axis were almost identical with those obtained for toluene. This constitutes another check on the accuracy of the experimental results and the method of extrapolation.

The values of both B and C are much smaller than for solutions in toluene and their accurate evaluation was difficult owing to the small slope and curvature of the graphs. Consequently no conclusion could be drawn on the variation of these coefficients with concentration and molecular weight. The curvature of the Π/c_2 plots was, however, quite pronounced, especially at concentrations exceeding about 0·6 %. Consequently to treat these curves as straight lines in extrapolating to infinite dilution would cause a significant error.

Discussion

The statistical mechanical calculation of the thermodynamic properties of polymer solutions in terms of the lattice model has been remarkably successful in leading to an understanding of the properties of these solutions and the cause for the wide deviation from Raoult's law shown by these solutions. The results of this, and of the previous paper, show that quantitative agreement with theory is not entirely satisfactory and this may be a consequence of the idealized model of a solution which is assumed. Recently, McMillan and Mayer[9] have shown, by a statistical method using continuous distribution functions, that for non-ionic solutions the osmotic pressure is related to concentration by the convergent series

---

[8] Schulz, *Z. physik. Chem. A*, 1936, **176**, 317.

$$\Pi = RT(c_2/M_2 + Bc_2 + Cc_2^3 + \ldots)$$

and that the coefficients may be evaluated in terms of molecular distribution functions. Zimm[10] has extended this theory to polymer solutions and has calculated the value of *B* in terms of experimentally defined parameters. Although the theory at present is not suitable for quantitative use it does predict a dependence of *B* upon solute molecular weight, although the extent of this dependence is also determined by the stiffness of the chain and would be greatest in a molecular system with free rotation around all the bonds. Experimental measurements of Zimm[11] on the dependence of light scattering on concentration for polystyrene solutions show that with very high molecular weight polymer *B* decreases with molecular weight. Although the results support our experimental observations they were insufficient to provide an independent check of the inverse relationship established in the present work.

Most of this experimental work was carried out in the Chemistry Department of the University of Bristol (1946-48) and the authors wish to thank Mr. H. Banwell for his careful workmanship in the construction of the osmometer. One of us (A. R. K.) is indebted to the Iraq Government for a grant.

Department of Inorganic and Physical Chemistry,
University of Liverpool.

[9] McMillan and Mayer, *J. Chem. Physics*, 1945, **13**, 276.
[10] Zimm, *ibid.*, 1946, **14**, 164.
[11] Zimm, *J. Physic. Chem.*, 1948, **52**, 260.

THE TRANSFER OF SODIUM AND POTASSIUM BETWEEN MUSCLE AND THE SURROUNDING MEDIUM

PART II. THE SODIUM FLUX

BY E. J. HARRIS *

Received 5th May, 1950

The rate of loss of labelled sodium from frog sartorii has been studied under various conditions and following various treatments. The loss from muscles taken from frogs injected the previous day with radiosodium was usually a simple exponential process, but if the muscles were prepared by soaking in the radioactive solution the loss followed a law corresponding to the sum of two exponentials. This behaviour is shown to agree with that expected if the loss takes place in two stages, a transfer through the membrane and a desorption, the experimental result depending on the relative rates of the two processes. When the rate is limited by desorption the temperature coefficient is 2·7 for an 18° C change (from 0° to 18° C), but the temperature coefficient of the transfer

* With the technical assistance of G. P. Burn.

through the membrane is higher than this value. The loss to dextrose solution is slower than to Ringer's solution at 18° C. When the rate of loss has reached its lower value in Ringer's solution it can be increased if potassium phosphate solution be substituted. These facts are interpreted on the theory of the two-stage process.

The kinetics of the transfer of sodium and potassium ions between isolated frog sartorii and their surroundings has been shown, by the use of tracers, to follow a course consistent with a combined permeation and diffusion process.[1, 2] The delay imposed by the diffusion of the ions through the extracellular space makes it necessary to use an equation containing both diffusion and permeability constants when attempting to evaluate the permeability of the cell membrane to potassium, whereas, provided thin specimens are used, the diffusion of sodium through the extracellular space can be distinguished from the transfer through the membrane on account of the differing rates of the two processes.

Levi and Ussing[3] have studied the loss of both sodium and chloride from isolated muscles, and their findings for sodium are in agreement with ours. The flux of sodium from a cell, by which is meant the quantity of sodium leaving unit area of surface per unit time, is important because of its relation to the metabolism. As sodium is present in the cell in much lower concentration than in the external medium, and there is in addition a potential across the cell membrane which opposes the loss of a positive ion, the work required to expel the sodium is considerable. Ussing[4, 5] has discussed a mechanism which he calls " exchange diffusion " which would permit an exchange of internal sodium for external sodium by means of anchored groups in the membrane exposing more or less bound sodium ions alternately to the outside and the inside medium. This could operate without expenditure of energy, but there is no evidence for its existence. Any other mechanism will involve the expenditure of energy by the cell in order to expel sodium against the electrochemical potential gradient. The calculated heat equivalent of the work required to expel the sodium proves to be some 20 % of the resting heat production of the muscle.

The results given here for the sodium flux under various conditions include an account of a peculiar effect which appears when the muscles are prepared using rather strongly radioactive solutions. These were used because the earlier experiments had been limited in duration to about 1 hr. by the fact that insufficient radioactivity remained in the muscle at the end of this period. The higher radioactivity did certainly permit experiments to be continued for longer times, but it also exposed the complication that sometimes the exponent (k_2, in conformity with the terminology used in our previous paper) which determines the rate of loss of radioactive sodium (Na^x) according to the equation

$$Na^x = Na^x_{(t=0)} \exp(-k_2 t)$$

appeared to have two values during the experiment. However, it is still possible to evaluate the total sodium flux, which is the figure required. Whether the change in the value of k_2 is the result of exposure to radioactivity or not remains an open question.

Experimental

Methods.—The sartorii of *Rana temporia* were used exclusively. The frogs were of both sexes and were maintained in a moist tank. The experiments were in progress throughout the year. There was no evidence of bacterial action on the isolated muscles.

[1] Harris and Burn, *Nature*, 1948, **162**, 929.

[2] Harris and Burn, *Trans. Faraday Soc.*, 1949, **45**, 508.

[3] Levi and Ussing, *Acta Physiol. Scand.*, 1948, **16**, 232.

[4] Ussing, *Cold Spring Harbour Symp.*, 1948, **13**, 193.

[5] Ussing, *Physiol. Rev.*, 1949, **29**, 127.

In some experiments the sartorii were taken from a frog which had received an injection of 10 mg. radioactive sodium chloride, which was prepared from the carbonate in order to avoid the simultaneous presence of radioactive phosphorus formed from chlorine by transmutation. In other experiments the muscles were stored for various times in a Ringer's solution made up from radioactive sodium chloride. The muscle containing radioactive sodium was then transferred to a non-radioactive solution and the loss of radioactivity followed. For this purpose the muscle was attached to a support, which was sometimes the Geiger-Müller tube itself, and the support was immersed in the liquid. The advantage of attaching the muscle to the counter itself was that it enabled a continuous record to be made as liquid flowed round the tube, whereas the alternative procedure entailed interrupting the soaking-out for the counting periods. These, however, were not long (1 or 2 min.) so that no serious error is involved in the observation of the loss of sodium from the cells, which is relatively slow, compared with the loss from the extracellular spaces.

In order to obtain a measure of the amount of sodium associated with a certain radioactivity of the muscle the specimen was dissolved in a few drops of acid at the end of the experiment and the radioactivity of the solution compared with a suitable dilution of the original soaking in solution, or plasma, as the case might be. The counter used for the liquids held 2 ml. fluid.[6] Corrections for background, resolution time and decay were applied as necessary.

Results

The result of the preparation of the muscle by exposure to radioactive solution or plasma is to introduce labelled sodium in place of the ordinary sodium. If sufficient time has been allowed for equilibration it is convenient to regard the initial radioactivity as corresponding to all of the sodium being labelled.

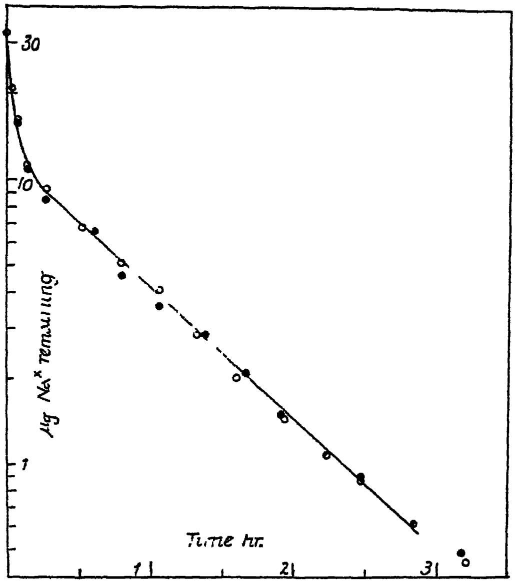

FIG. 1.—Records of loss of Na^x in two separate experiments, using the individuals of a pair of muscles. The muscles were prepared by soaking for 5 hr. in Na^xCl Ringer's soln., and were soaked out in Ringer's soln. at 18° C.

During the soaking-out the radioactivity measures the quantity of the labelled sodium remaining in the muscle and the unlabelled sodium which has entered in place of that part of the labelled sodium which has left is not observed. The quantity of labelled sodium, which will henceforth be designated Na^x, was plotted against time on semi-logarithmic paper, as in Fig. 1. The rapid phase of the loss, taking 15-20 min. if only one side of the muscle is exposed to the solution, is attributed to Na^x coming from the extra-cellular spaces, including any loosely adsorbed on the connective tissue. The quantity of Na^x found by subtracting the value of the ordinate at the intercept of the linear part of the curve from the initial measured amount, can be expressed in terms of the extra-cellular space of the muscle, assuming that the concentration in the extra-cellular fluid at $t = 0$ is equal to that in the soaking-in solution, or plasma, as the case may be. The exponent k_2 already mentioned is found by reading off the time for the sodium content of the muscle to diminish by e times, using the linear part of the curve.

---

[6] Harris, *J. Sci. Insts.*, 1949, **26**, 245.

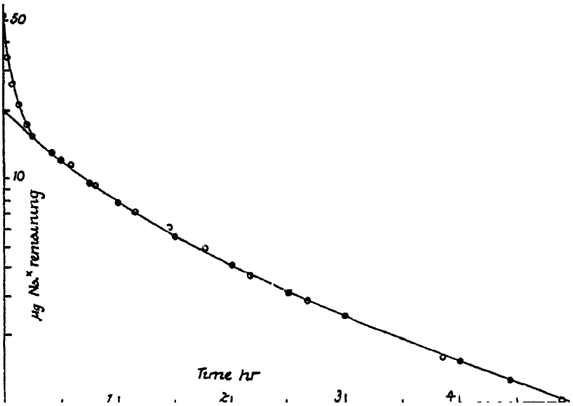

FIG. 2.—○ Na^x loss from muscle prepared by soaking 37 hr. in Na^xCl Ringer solution and then soaked out at 0° C in Ringer's solution. ● calculated from the equation $11{\cdot}4 \exp(-1{\cdot}62t) + 8{\cdot}4 \exp(-0{\cdot}43t)$. A further experimental point at 6 hr. agrees with the calculated value.

Fig. 2 illustrates the type of result which has frequently been obtained since more strongly radioactive sodium has been available. There is no longer a single value of k_2. Before proceeding it is worth considering the appearance of a plot on semi-logarithmic paper of a function composed of the sum of two exponentials. On Fig. 2, in addition to the experimental points, values of the function $11{\cdot}4 \exp(-1{\cdot}62t) + 8{\cdot}4 \exp(-0{\cdot}43t)$ have been indicated. It will be seen that apart from the initial 15 min. the function fits the results. As in the first 15 min. the Na^x in the extracellular space is diffusing into the external medium it is inevitable that the experimental values should include a diffusion fraction for this limited time, the exact value of which depends upon the dimensions of the specimen and whether one, or both, sides are exposed to the solution. It is clear that if an experiment can be continued for sufficiently long for the more rapidly varying function (here $\exp(-1{\cdot}62t)$) to have become negligible compared with the less rapidly varying one it is possible to obtain an accurate value of the k_2 of the latter, but it is much more difficult to arrive at an accurate measure of the higher k_2, particularly on account of the additional confusion introduced by the extra-cellular material.

It was at first thought that the slowly lost fraction was attributable to an impurity, but use of spectroscopically pure sodium carbonate as starting material led to similar results. The decay of the radioactivity of the slowly lost fraction agreed with that of Na^{24}.

Some results for the sodium flux have been summarized in Table I. The sodium leaving 1 ml. of cell fluid is given by the product $k_2(Na_i)$ per hr., and if two fractions are present the sum of the respective products is taken. To obtain the flux per unit area of cell surface the figure must be divided by the surface associated with unit volume of cell fluid, and in conformity with our previous paper 500 cm.^{2}/ml. has been used for the conversion.

Now the presence of a slowly lost fraction can only be revealed when all the rapidly lost fraction has gone, which takes 1-3 hr. It is therefore necessary to start with sodium of high specific activity in order to be able to observe the

TABLE I.—VALUES OF THE EXPONENTS, AND THE SODIUM FLUX FROM FROG SARTORII PREPARED EITHER BY INJECTION OF Na^{x}Cl OR BY SOAKING IN A RADIOACTIVE SOLUTION. THE LOSS OF Na^x IS TO RINGER'S SOLUTION AT 0° OR 18° C

Ref.	Treatment		K Content of Soln. used for Treatment m.moles/litre	Counts/min. x ml. Soln. at End of Treatment	Apparent Na Contents and Exponents				Total Flux μmole/cm.^{2} x hr.
	Method	Time Before Expt., and Temp. of Soln.			Fast Fraction		Slow Fraction		
					Na_t/Na_e	k_2 (hr.$^{-1}$)	Na_t/Na_e	k_2 (hr.$^{-1}$)	
	Measurements at 0° C.								
N3	Injected	Day previous	—	1·1 × 10^5	0·085	0·63	×	×	0·012
N29	,,	,, ,,	—	1·7 × 10^5	0·16	0·45	×	×	0·016
N42	Soaked	2 hr. at 18° C	2	21 × 10^6	0·086	0·88	×	×	0·017
N43	,,	,, ,,	12	21 × 10^6	0·086	0·88	×	×	0·017
N9	,,	,, ,,	2	4 × 10^5	0·03	1·8	0·054	0·42	0·017
N25	,,	3·2 hr. at 4° C	2	5·5 × 10^5	0·04	1·7	0·06	0·45	0·021
N26	,,	3·4 hr. at 4° C	2	5·5 × 10^5	0·045	1·6	0·08	0·25	0·020
N21	,,	18 hr. at 4° C	3	3·6 × 10^6	0·035	1·5	0·15	0·26	0·018
N44	,,	14 hr. at 4° C	2	9 × 10^6	0·05	1·5	0·16	0·11	0·015
	follow	ing N42							
N45	Soaked	14 hr. at 4° C	12	9 × 10^6	0·03	2·4	0·056	0·30	0·018
	follow	ing N43							
N60	Soaked	18 hr. at 4° C	2	12 × 10^6	0·19	0·30	×	×	0·013
							Mean flux	at 0° C {	0·017 ±0·0026
	Measurements at 18° C.								
N4	Injected	Day previous	—	1·1 × 10^5	0·10	1·54	×	×	0·034
N13	,	,, ,,	—	1·1 × 10^5	0·13	1·7	×	×	0·048
N29	,	,, ,,	—	1·7 × 10^5	0·16	1·1	×	×	0·039
N70	,,	,, ,,	—	2·2 × 10^5	0·17	1·3	×	×	0·048
N67	,,	,, ,,	—	1 × 10^6	0·064	2·0	0·087	1·0	0·049
N61	,,	2·2 hr before	—	1·3 × 10^6	(0·05)	2·5	0·18	0·45	0·046
147	Soaked	1 hr. at 18° C	3	1·7 × 10^5	0·04	2·0	0·16	0·61	0·047
N10	,,	2·3 hr. at 18° C	3	4 × 10^5	(0·015)	(3·0)	0·096	1·15	0·035
N65	,,	5 hr. at 18° C	2	5 × 10^6	0·146	1·0	×	×	0·032
N60	,,	18 hr. at 4° C	2	12 × 10^6	0·19	1·0	×	×	0·041
N73	,,	,, ,,	2	5·6 × 10^6	(0·078)	(2·5)	0·052	0·53	0·049
N74	,,	,, ,,	12	5·6 × 10^6	(0·054)	(3·0)	0·046	1·18	0·048
N46	,,	37 hr. at 4° C	2	6·5 × 10^6	0·094	1·6	0·069	0·43	0·038$_6$
N47	,,	,, ,,	12	6·5 × 10^6	(0·058)	(3·0)	0·031	0·61	0·043
N71	,,	20 hr. at 4° C	12	5·6 × 10^6	(0·045)	(3·0)	0·15	1·36	0·043
							Mean flux	at 18° C {	0·043 ±0·006

(*a*) The external sodium concn. [Na$_e$] was 111 μmole/l.

(*b*) When no change of slope was distinguished the sign × has been used, the allocation of the sodium is then arbitrary.

(*c*) In Expt. N60 the slope was measured successively at 0° and 18° C, so there was no occasion to observe a fast fraction at 18° C.

(*d*) Experiments made in duplicate on pair muscles usually gave similar results, and these have not been tabulated, this applies to N21, N25, N29, N61, N65.

(*e*) When considerable difficulty in separation of the components was experienced the doubtful figures have been bracketed.

tail end of the loss. There arises then the possibility that the radioactivity itself may bring about a changed rate of loss, possibly by damaging the cells. Accordingly, Table I includes a note of the radioactivity of the solution or plasma in which the muscle had been prepared. It is given in counts per min. per ml. of solution as counted in a liquid counter of about 20 % efficiency for β particles from Na^{24}.

If no change in the slope had been observed at the end of the experiment, which was usually determined by the radioactivity of the muscle having fallen to a few hundred counts per min., a single value of k_2 has been calculated. It is not possible to assert that no less rapidly lost Na^x is present in these cases, for referring to Fig. 2 if an imaginary experiment had ended after 2½ hr. it would have been very similar to the case of a single $\text{Na}_{t(0)} = 14{\cdot}5\ \mu\text{g}$. and $k_2 = 0{\cdot}64$ hr.$^{-1}$. It is necessary to anticipate the conclusion reached in the discussion at this point in order to state that although the results have been expressed in terms of the quantities of Na^x *apparently* associated with one or two exponential functions of time, say $A \exp(-at) + B \exp(-bt)$, the quantities A and B are not exactly equal to the amounts of sodium present initially on (or in) two different sites in the cells.

The Temperature Coefficient of Sodium Loss.—If it is desired to estimate the energy requirement of the sodium transfer it is necessary to compare the fluxes at two temperatures, for it is the flux and not k_2 which determines the energy. When similarly treated specimens are taken it transpires that their sodium contents are nearly equal, and in such cases the ratio of the fluxes is the same as the ratio of the k_2's. The presence of two sodium fractions complicates the interpretation of the experiments. In Table II some experiments are summarized which only show one fraction. As either pair muscles were used, or a single muscle was observed at the two temperatures, the ratio of the k_2's has been evaluated.

TABLE II.—EFFECT OF TEMPERATURE ON k_2 FOR SODIUM LOSS, MUSCLES IN WHICH NO SLOW FRACTION WAS OBSERVED

Potassium conc. in soaking-out soln.	2	2	2	12	12	m.mole
k_2 at 18° C hr.$^{-1}$	1·54	1·28	1·11	1·33	1·33	
k_2 at 0° C hr.$^{-1}$	0·63	0·45	0·45	0·46	0·46	
Ratio	2·44	2·85	2·46	2·89	2·89	
				Mean	2·76 ± 0·25	
Ref.	N3,4	N29	N30	N31	N32	

The effect of temperature on the loss of the *slow* fraction of the sodium was very variable. It was studied by making observations on a muscle at 0° C for sufficient time to establish that a constant k_2 had been reached, and then transferring to a similar solution at 18° C. Figures relating to these experiments are set out below.

Ref.	K conc. in Soln. used for Treatment m mole/l.	Constants for Slow Fraction				Flux Ratio
		k_2 at 0°C hr.$^{-1}$	Na_t/Na_e at 0° C	k_2 at 18° hr.$^{-1}$	Na_t/Na_e at 18° C	
N44	2	0·11	0·16	0·57	Same as 0° C	5·2
N45	12	0·30	0·056	0·71	„ „	2·4
N49	2	0·31	0·26	0·55	„ „	4·2
N59	2	0·33	0·19	1·0	„ „	3·0
N50	2	0·20	0·23	0·53	„ „	2·7
N9, 10	2	0·42	0·054	1·15	0·096	3·8
N60	2	0·30	0·19	1·0	Same as 0° C	3·3

It is clear that the effect of temperature on the rate of loss of the slow fraction is generally greater than its effect on the total flux which can be estimated from the ratio of the mean fluxes in Table I, and is 2·52. This value lies within the limits of error of the values of Table II.

The Influence of Various Media on the Sodium Loss.—Experiments were carried out on muscles prepared as described to see whether the medium affected the rate of sodium loss. When using media free from sodium it is clear that the diminution in labelled sodium does represent a net loss of sodium, and is not indicative of an exchange for unlabelled sodium such as is supposed to take place when using sodium containing media. In order to maintain electroneutrality either another cation must enter the cell in place of the sodium, or an anion must leave the cell. Fig. 3 illustrates experiments made on the individuals of a pair of muscles, one of which was put into isotonic potassium phosphate, and the other into dextrose solution containing 0·015 % each KCl and $CaCl_2$. Later in each case the muscle was transferred to Ringer's solution.

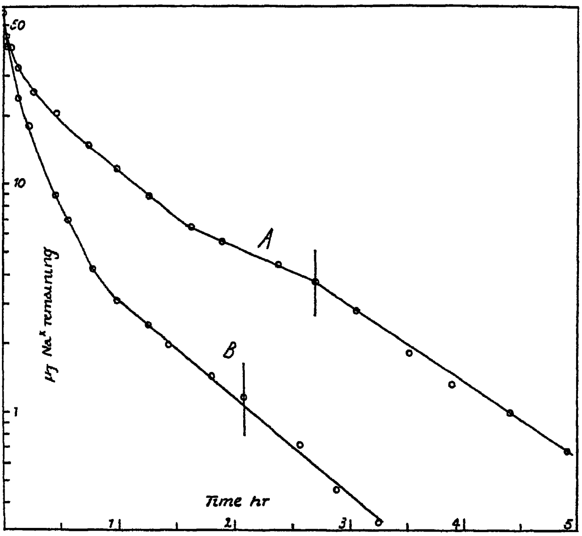

FIG. 3.—The loss of Na^x from the individuals of a pair of muscles, the initial part of curve A to isotonic dextrose, the initial part of curve B to isotonic potassium phosphate, and the parts to the right of the vertical line, in each experiment, to Ringer's solution. Temp. 18° C.

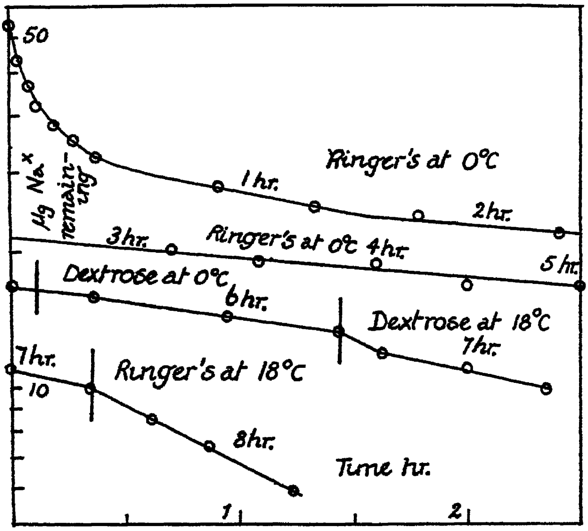

FIG. 4.—The loss of Na^x from a muscle to Ringer's solution at 0°, dextrose at 0°, dextrose at 18°, and Ringer's solution at 18° in succession. The time during which the experiment was in progress has been divided into intervals for convenience in plotting.

It will be seen that the loss of Na^x follows a composite course. The loss of potassium phosphate was faster than to dextrose solution and transfer to Ringer's solution did not affect the rate compared to potassium phosphate, but *increases* it compared to that in dextrose.

This typifies a general result, which is that the rate of loss of the slow fraction can be influenced by the medium. Fig. 4 shows how involved the relation may be. The rate of loss of the Na^x to Ringer's solution at 0° was followed for a considerable time, then dextrose at 0° was substituted, which made little difference. On transfer to dextrose at 18° C a temporary increase in rate took place, after which the loss was not much more rapid than at 0°. On substituting Ringer's solution at 18° a pronounced increase in rate was found—that is the ability of the rate to increase with temperature depends upon the medium. Even at 0° the rate of loss of the slow fraction could be increased by the substitution of potassium phosphate for Ringer's solution. The figures in Table III include the k_2 for both fractions found in Ringer's solution at 0°, and the new value of k_2 taken up on changing to potassium phosphate.

TABLE III.—EFFECT OF K PHOSPHATE ON k_2

Ref.	Constants in Ringer's Soln.				k_2 in K Phosphate hr.$^{-1}$
	Fast Frn. Na_t/Na_e	k_2 hr.$^{-1}$	Slow Frn. Na_t/Na_e	k_2 hr.$^{-1}$	
N20	0·04	1·7	0·19	0·22	0·66
N37	0·09	2·5	0·06	0·17	1·54

As before the quantities of Na are those associated with the respective exponentials. Other solutions investigated included sodium phosphate and choline chloride; these did not furnish any striking results.

Discussion

The use of more highly radioactive sodium shows that the loss of sodium from isolated muscles is not always, if it is ever, a simple exponential process as it previously appeared to be. The results can be fitted by the sum of two exponentials, and this raises two questions: (i) what determines the two functions and (ii) is the slowly lost fraction always present, or does it appear as a result of storage, particularly in radioactive solutions.

There is an element of inherent uncertainty in (ii) because in order to be able to label any slowly exchangeable sodium a time of treatment of order of the inverse of k_2 is required. In some experiments (e.g. 147, Table I) even rather short storage sufficed to show the presence of the slowly lost fraction, and it seems likely that the slow fraction appeared during storage and that it was derived from the Na^x in the solution, for had the slowly lost sodium been only partially equilibrated with the radioactive solution the muscle must have had an abnormally high sodium content. This example is not an isolated case. A further point supporting the suggestion that the slow fraction appears because the muscle is exposed to a medium different to the plasma is the fact that muscles dissected from an injected frog a few hours after the injection show a slow fraction (e.g. N61, Table I), whereas if left overnight before dissection it is rare to observe a slow fraction. The injection of 1 ml. of saline will considerably alter the concentrations of other substances in the lymph, and it may well take 12 hr. to restore normal conditions. It is true that the radioactivity of the plasma per unit weight of Na on the day following injection was usually some 10 times less than that of solutions used for treating the muscles, and this precluded continuing the experiments for as long as could be wished, because of the low radioactivity reached after 1½-2 hr., and in fact experiment N67, in which the activity was high, did have 2 fractions. However, further reference to Table I shows that in experiments using fairly similar and comparatively low radioactivities (compare 147 and N10 with N29 and N70, or N9 with N29) the slow fraction can be observed if the muscles have been prepared by soaking, but not by injection. Accordingly, it seems reasonable to conclude that the radioactivity is not the only factor leading to the appearance of the slow fraction, though it may be a contributory cause.

Expt. N44, 45 made on the same muscles respectively as N42, 43, show how an apparently simple process can be changed to a complex one merely by subjecting the specimens to longer storage. This would apparently rule out an explanation based on the two sodium fractions coming from cells of differing surface/volume ratios.

Comparison of the pairs, N46, N47 and N44, N45 and N73, N74, made with different potassium concentrations in the soaking-in solution shows that a high K concn. tends to keep the amount of the slow fraction low, and at the same time the value of k_2 for the slow fraction is higher. This supplies a partial answer to (i). It is that the sodium flux tends to be constant, and inspection of the final column of Table I shows that the total flux, made up of slow and fast fractions, is fairly constant at a given temperature. This means that the sodium loss is derived from one mechanism and not from two unrelated ones, as might be the case if one fraction came from, say, connective tissue. It is possible to envisage a sodium carrier system such as has been discussed by Ussing for muscle and frog skin, and by Hodgkin and Katz[7] for nerve, which would account for our results. Suppose Na^x ions are attached during the treatment to the carriers, some inside and some outside the membrane, and that the remaining internal sodium is also all labelled. When the specimen is put into an unlabelled medium it proceeds to lose Na^x in exchange for Na. Two cases arise, (1) if the loss from the surface to the solution is faster than the rate of supply of fresh Na from the inside of the cell, and (2) if the rate of loss from the surface is slower than the rate of supply from inside the cell. Case (1) corresponds to a slow "turnover" of the carrier, i.e. low metabolism, clearly the loss from such a muscle will take place in two phases; a rapid loss from the surface, followed by a slow loss from the interior. Case (2), corresponding to a high metabolism, will not be limited by the transfer through the membrane, but only by the rate of desorption, and will have only one time constant. Expressing this in the form of equations, with $[Na_i^x]$ being the inside concn. of Na^x, $[Na_s^x]$ the surface concn. of Na^x, which is measured as the quantity of surface Na associated with unit volume of fibre fluid, n_1 the rate of inward transfer, n_2 the rate of outward transfer, and n the rate of desorption, all per unit concn. of Na, we have

$$d[Na_i^x]/dt = n_1[Na_s^x] - n_2[Na_i^x]$$

and

$$d[Na_s^x]/dt = n_2[Na_i^x] - n[Na_s^x] - n_1[Na_s^x].$$

In addition the chemical concentrations irrespective of labelling are supposed to remain constant, so that $n_1[Na_s] = n_2[Na_i]$. The solution for Case (1) is readily obtained since the roots of the subsidiary equation for $[Na_i^x]$ are

$$\alpha, \beta = \frac{(n_1 + n - n_2) \pm (n^2 + n_1^2 + n^2 + 2nn_1 + 2nn_2 - 2n_1n_2)^{\frac{1}{2}}}{2}$$

and when n_1n_2 is small compared to $n(n_1 + n_2)$, which is equivalent when $n_1 \approx n_2$ and both n_1 and n_2 small compared to n, the admissible root is $- n_2$, and

$$[Na_i^x] = [Na_i^x]_{(0)} \exp [- n_2t].$$

---

[7] Hodgkin and Katz, *J. Physiol.*, 1949, 108, 37.

Solving for $[\mathrm{Na}_s^x]$ the result

$$[\mathrm{Na}_s^x] = \frac{n_2[\mathrm{Na}_i^x]_{(0)}}{n + n_1 - n_2} \exp(-n_2 t) - \frac{n_2[\mathrm{Na}_i^x]_{(0)}}{n + n_1 - n_2} \exp(-(n + n_1)t) + [\mathrm{Na}_s^x]_{(0)} \exp(-n + n_1)t$$

is obtained. As in the experiment the sum of $[\mathrm{Na}_s^x]$ and $[\mathrm{Na}_i^x]$ is observed the final equation is

$$[\mathrm{Na}_t^x] = [\mathrm{Na}_s^x] + [\mathrm{Na}_i^x] = [\mathrm{Na}_i^x]_{(0)}\left(1 + \frac{n_2}{n + n_1 - n_2}\right) \exp(-n_2 t) + \left\{[\mathrm{Na}_s^x]_{(0)} - \frac{n_2[\mathrm{Na}_i^x]_{(0)}}{n_1 + n - n_2}\right\}\exp(-(n + n_1)t)$$

which is made up of two exponentials, the latter varying more rapidly with t than the former since n_2 has been assumed smaller than n. The coefficients are not equal to $\mathrm{Na}_{i(0)}^x$ and $\mathrm{Na}_{s(0)}^x$, but as $n_2/(n + n_1 - n_2)$ must be numerically small to justify the assumption, the differences will not be serious. For the special case of all the n's equal it transpires that two exponents again are involved, one is about $2/7$ of the other, and the coefficient of the smaller is $1{\cdot}7\,[\mathrm{Na}_i^x]_{(0)}$, and of the larger $0{\cdot}3\,(\mathrm{Na}_s^x)_{(0)}$, so here the apparent quantities of the two fractions do not approximate to the quantities of internal and surface Na^x.

When the turnover between interior and surface is rapid compared with the rate of desorption the surface concn. of Na^x will be a constant fraction of the total Na^x, so put

$$[\mathrm{Na}_s^x] = f([\mathrm{Na}_s^x] + [\mathrm{Na}_i^x]),$$

f being a constant fraction. The integral form is then

$$[\mathrm{Na}_i^x] + [\mathrm{Na}_s^x] = ([\mathrm{Na}_i^x]_{(0)} + [\mathrm{Na}_s^x]_{(0)}) \exp(-fnt).$$

As f is a fraction, the exponent of the simple case, giving the single value, fn, will be less than the higher of the two exponents of the complex case which is $n + n_1$, supposing the value of n, the rate of desorption, is a constant. Reference to Table I shows that when a single exponent k_2 was found it is only about a half the higher of the two values when two values were obtained. This would be very difficult to explain on the basis of the slow fraction coming from less active cells, and the fast one from more active cells, for why should storage *increase* the metabolism of some cells and diminish that of others? The quantities apparently associated with the two exponents indicate that Na_s and Na_i have the same order of magnitude, i.e. f may have the value $\frac{1}{2}$. More accurate analysis does not appear possible at this stage, but the value of n seems to be about 3 $\mathrm{hr.}^{-1}$ at 18° C, and between 1·5 and 2 $\mathrm{hr.}^{-1}$ at 0° C.

The experiments made in dextrose and potassium phosphate can be considered in the light of this scheme. In the absence of a supply of ions from the external solution the desorption will be limited by the appearance of a counter E.M.F. and the rate may be limited by the rate at which the cell can provide anions, say phosphate, to accompany the sodium and so maintain a balance of electrical charge. At 0° the rate of production of anions may be maintained by desorption, making the rates equal in dextrose and Ringer's soln., but at 18° C the potential loss rate might exceed that at which anions are produced, so the loss would be accelerated if ions are supplied by the solution to replace those desorbed. An interesting possibility is that a substance furnishing alternative cations which can be adsorbed, but which are too large to enter the cell, might permit the measurement of $[\mathrm{Na}_s]$, the surface concn. In potassium phosphate the rate of loss of Na^x is no less than in Ringer's soln. (Fig. 3), and indeed, if the rate of loss has reached the slow phase in Ringer's soln., potassium phosphate accelerates it (Table III). This would indicate that potassium can replace sodium and that the reduction of the membrane potential brought about by a high potassium medium facilitates the outward transfer of sodium.

The temperature coefficient results obtained on specimens showing a single value of k_2 are to be interpreted on this theory as indicating the temperature coefficient of the desorption process, provided the factor f (the ratio of $[Na_s]/([Na_s] + [Na_i])$ remains unaltered. When dealing with two fractions the temperature coefficient of the loss of the faster fraction will be that of the desorption process, whereas that of the slower fraction will be that of the transfer through the membrane, which may be expected to be higher than that of a physical process. Some of the observed figures for the effect of temperature on the slow fraction do indeed indicate a high temperature coefficient, but the acceleration of the transfer brought about by raising the temperature may meet a limitation imposed by the rate of desorption which does not increase in proportion. Accordingly it does not follow that the full temperature coefficient of the transfer process will ever be manifest. This may account for the extreme variability of the effect of temperature on the slow fraction.

Finally, a comment on the energy consumption of the sodium transfer may be made. Conway,[8] and Levi and Ussing,[3] have discussed this matter. The flux used in the calculation of the latter authors does not differ to an important degree from the mean value in our Table I, but they appear to compare the heat equivalent of the sodium flux from unit volume of fibre fluid, with the resting heat of unit mass of muscle. If the comparison be made on equal terms, say for unit mass of muscle in each case, the figures are about 0·045 cal./hr. g. muscle for the sodium transfer, and 0·24 cal./hr. g. for the resting heat.[9] The intervention of the carrier system does not affect the result provided a one-for-one "exchange diffusion" process does not operate, and that the surface concentration remains unchanged.

I am indebted to Professor A. V. Hill for his support and helpful advice, to Prof. G. L. Brown for reading the manuscript, and to Dr. B. Katz for several discussions. Part of the expenses of this work were met by a grant from the Government Grants Committee of the Royal Society. The radiosodium was supplied by the Atomic Energy Research Establishment.

Biophysics Research Unit,
University College,
*London, W.C.*1.

---

[8] Conway, *Irish J. Med. Sci.*, 1947, Oct.-Nov.
[9] Hill, *Proc. Roy. Soc. B*, 1928, **103**, 138.

REVIEWS OF BOOKS

Etude Thermodynamique des Phénomènes Irréversibles. By I. Prigogine. (Liège, Belgique, 1947.) Pp. 144. Price 225 frs. belges.

This is an interesting and valuable book. Classical thermodynamics deals with equilibrium states and reversible processes; for irreversible processes it does not go beyond the statement that they are accompanied by an increase of the entropy. Attempts have been made in recent years to formulate this increase quantitatively and the book under review is the first systematic summary of both the author's and other workers' efforts. It must be mentioned that only such processes where the final or stationary state could also be reached by a reversible process are considered. It is, however, very useful to have one's attention drawn to such concepts as open systems, flow of entropy and local production of entropy, and to the connection between the rate of an irreversible process and the rate of increase of entropy. The reviewer regrets that more space has not been devoted to a discussion of the fundamental issues involved in extending the ideas of classical thermodynamics to irreversible processes. Especially the concept of heat of convection should have been defined with great care and discussed thoroughly, as the physical significance of its conventional meaning is not at all obvious, and it is not clear whether what is meant is not "energy of convection"; but heat and energy are not the same. The expression used in the book for the total heat, i.e. heat of conduction, convection and radiation (eqn. (4·3), (4·12)) leads to the conclusion that the addition to an ideal mixture of a small amount of one of its components is accompanied by heat of convection. Such a definition is, to say the least, inconvenient, but could presumably be used to give right results. But the care needed is shown by the fact that the author derives from it a finite difference between the compositions of two ideal gas mixtures which are held at different temperatures and have reached a stationary state by thermal transpiration, whereas it is easy to show from the kinetic theory of gases that there is no such difference; any difference observed experimentally must be due to deviations from the laws of ideal mixtures.

These criticisms of detail need not detract from the main value of the book which lies, in the reviewer's opinion, in drawing attention to a little known but much needed extension of the scope of thermodynamics. It is to be hoped that these defects will be eliminated in the more comprehensive treatise which the reviewer understands the author is preparing.

The price of the book in this country is very high; the reviewer is not competent to judge how far this is due to the rate of exchange.

H. T.

Tables of Sines and Cosines to Fifteen Decimal Places. (U.S. Dept. of Commerce, National Bureau of Standards, Applied Mathematics Series, No. 5, 1949.) Price 40 cents.

These Tables give the values of sin x and cos x at intervals of 0·01 degree, from 0° to 90°, all to 15 places of decimals. Second central differences are included, which are sufficient for interpolation to the full 15 decimals. The reliability of these tables, their cheapness and the fact that they fill a need recently stressed in the *Index of Mathematical Tables*, makes them exceedingly useful for those occasions when more than 6-figure accuracy is required.

C. A. C.

Advances in Catalysis and Related Subjects. Vol. II. (Academic Press, Inc., New York.) Pp. 292, Price $6.80.

This volume continues the work started in Vol. I, and contains eight articles, each by well-known writers in their particular fields. It is a very well-produced book, and can be recommended to all chemists interested in catalysis. It will be convenient to review each article separately in the order in which it occurs in the book.

" The Fundamentals of Catalytic Activity ", by F. Seitz. This is an elementary account of atomic forces and Eyring-Polanyi potential curve theory. It contains no reference to any actual reactions and is too generalized and vague to be useful to the expert, but it should be helpful to those who want a simple introduction to relevant theoretical concepts.

" The Mechanism of Polymerization of Alkenes ", by L. Schmerling and V. N. Ipatieff. A thorough and well-documented article dealing mainly with carbonium-ion mechanisms and demonstrating very well the power and simplicity of the Whitmore hypothesis.

" Early Studies of Multi-component Catalysts ", by A. Mittasch. An informative study of very important works by the man largely responsible, which contains many data of interest for theoretical consideration.

" Catalytic Phenomena related to Photographic Development ", by T. H. James. This article deals with the catalytic action of silver on silver ions by organic reducing agents.

" Catalysis and the Adsorption of Hydrogen on Metals ", by Otto Beeck. This article deals with the work of Beeck, Wheeler and their collaborators on the adsorption of hydrogen and other gases on evaporated films of metals. There is presented a wealth of important data, much of it for the first time. Dr. Beeck includes a critical comparison of his results with those of Roberts and Frankenburg. It is to be hoped that Dr. Beeck will continue to wield his pen as energetically as he has been conducting his experiments.

" Hydrogen Fluoride Catalysis ", by J. H. Simons. An authoritative account of the results of using this catalyst on all types of organic reactions.

" Entropy of Adsorption ", by Charles Kemball. This article gives the standard states and formulae for calculating entropies of adsorption and applies the method to distinguish the mobility or otherwise of a number of films.

" About the Mechanism of Contact Catalysis ", by George Maria Schwab. Prof. Schwab deals with the Langmuir kinetic equations, describing methods of arriving at adsorption coefficients and absolute velocity constants. He indicates his view that the " greater accuracy of the transition state method cannot at present yet be exploited in heterogeneous catalysis, as long as the really active surface is the main source of uncertainty ". The general discussion of experimental data is illuminating, and Schwab makes the interesting point that a first order reaction is intrinsically a thousand times slower than a zero order one.

It is hoped that enough has been said to indicate the diverse and interesting nature of the articles in this book.

D. D. E.

THE HOMOPOLAR BOND IN THE HYDROGEN MOLECULE

By M. F. Hoare and J. W. Linnett

Received 16th March, 1950

Using two wave functions for the hydrogen molecule, we have calculated the changes in the average electronic kinetic energy both parallel and perpendicular to the internuclear axis as the two hydrogen atoms approach one another. We have considered, also, the variations in average electronic and nuclear potential energy. The changes in electronic kinetic energy are related to changes in spreading and curvature of the wave function and an attempt is made to understand the changes in average potential and kinetic energy. At the equilibrium separation R_e the average potential energy is very much less than when the atoms are far apart, the average electronic kinetic energy parallel to the axis is slightly less, and that perpendicular to the axis considerably greater at R_e than when the atoms are far apart.

It is the purpose of this paper to examine why, when two hydrogen atoms are brought together, the total energy of the system decreases so that a stable H_2 molecule is formed. Pauling has said that " the interchange of electrons is, in general, the energy of the non-polar or shared electron chemical bond "[1] He advanced this view because the Heitler-London perturbation function,[2] which was considered to imply electron interchange between the two atoms, gave a much better value of the binding energy of H_2 than the simple function $\psi = \psi_a(1)\psi_b(2)$.

On the other hand the view is often expressed that the concentration of the electronic charge in the region between the two positively charged protons is responsible for the lowering of the energy of the system and for the production of a stable hydrogen molecule.[3] These two expressions of opinion seem to have different meanings, and it appears possible, therefore, that two distinct views are held regarding the explanation of the covalent bond that exists in the ground state of H_2. We propose to examine the energy changes occurring when two hydrogen atoms are brought together.

When considering valency it seems to us important that the following statement of Slater should be borne in mind : " The study of molecular structure has been too much based on particular models rather than on general principles."[4] There is no doubt that the statement of Pauling quoted above was based on the Heitler-London treatment of the hydrogen molecule. It is important to consider the extent to which the conception of the importance of " interchange of electrons " was based more on the particular model rather than on general principles. This is particularly the case since the concept of " interchange " tends to disappear with more detailed functions.[5]

---

[1] Pauling, *Chem. Rev.*, 1928, **5**, 185.

[2] Heitler and London, *Z. physik*, 1927, **44**, 455.

[3] Rice, *Electronic Structure and Chemical Binding* (McGraw-Hill, 1940), pp. 134-135. Dushman, *Elements of Quantum Mechanics* (Wiley, 1938), pp. 318-319.

[4] Slater, *J. Chem. Physics*, 1933, **1**, 687.

[5] Cook, *ibid.*, 1945, **13**, 262.

Coulson and Bell have used the virial theorem to separate the energy of the hydrogen molecule at various internuclear distances into two parts, the kinetic and the potential energies.[6] They have stressed that, when considering the changes of energy with distance in H_2 and H_2^+ and the attraction and repulsion forces at various separations in these two molecules, it is important to take into account the variation in electronic kinetic energy (K.E.) with changes in internuclear separation, as well as the variation in potential energy (P.E.). They have illustrated this clearly by a simple classical example pictured in Fig. 1 of their paper. This means that what is usually called the potential energy curve of a diatomic molecule is really made up of both potential energy and electronic kinetic energy. (We shall use E for the total energy, V for potential energy and T for kinetic energy. A bar over a letter will represent "average value of", and a subscript e will signify electronic, and a subscript n nuclear.) The so-called P.E. curve is a plot of E, the total energy, against R, the internuclear separation, it being supposed that, at each value of R, the nuclei are held at that distance apart by an external force.

In their paper Coulson and Bell give graphs for H_2 which show the variation of E, $\overline{V}$ and $\overline{T}_e$ with R for the real hydrogen molecule, and for the Wang variational treatment of the H_2 molecule. They find good agreement between the curves calculated using the Wang function and those derived from experimental data. Thus Coulson and Bell have divided the energy E for any value of R into $\overline{T}_e$ and $\overline{V}$. We have calculated, using two variation functions, the values, for a range of values of R, of the following: (i) the nuclear P.E., V_n; (ii) the electronic P.E., $\overline{V}_e$; (iii) the electronic K.E. parallel to the internuclear axis which we shall designate $\overline{T}_z$; (iv) the electronic K.E. perpendicular to the internuclear axis $\overline{T}_{xy}(=\overline{T}_x+\overline{T}_y)$. The two variation functions we have used are (*a*) that due to Wang,[7] which gives a binding energy which is 80 % of the true value, and (*b*) that due to Hirschfelder and Linnett,[8] which gives a binding energy which is 90 % of the true value. The former involves one and the latter four adjustable constants.

Results

We shall measure distance in atomic units of a_0, where $a_0 = 0{\cdot}52915$ Å, and energy in atomic units of e^2/a_0, e being the electronic charge. On this scale the total energy, mean potential and mean kinetic energy of the ground state of the H atom are $-\frac{1}{2}$, -1 and $+\frac{1}{2}$ respectively. The energies are obtained by the standard methods and the results for $\overline{T}_z$, $\overline{T}_{xy}$, $\overline{T}$, $\overline{V}_e$, V_n, $\overline{V}$, $\overline{E}_e$ and E using the Wang function are listed in Table I, and are graphed in various combinations in Fig. 1(*a*), 1(*b*) and 1(*c*).

TABLE I.—RESULTS OBTAINED USING THE WANG FUNCTION FOR H_2

R	t	$\overline{T}$	$\overline{T}_z$	$\overline{T}_{xy}$	$\overline{V}$	V_n	$\overline{V}_e$	E	$\overline{E}_e$
0·719	1·0	1·701	0·489	1·212	−2·609	1·391	−4·000	−0·908	−2·299
1·235	1·5	1·241	0·335	0·905	−2·373	0·810	−3·183	−1·132	−1·942
1·848	2·0	0·987	0·268	0·719	−2·106	0·541	−2·647	−1·119	−1·661
2·463	2·5	0·897	0·255	0·643	−1·970	0·406	−2·377	−1·073	−1·480
3·022	3·0	0·894	0·268	0·627	−1·936	0·331	−2·267	−1·042	−1·373
4·029	4·0	0·951	0·305	0·646	−1·968	0·248	−2·216	−1·016	−1·264
5·000	5·0	0·989	0·326	0·663	−1·992	0·200	−2·192	−1·003	−1·203

---

[6] Coulson and Bell, *Trans. Faraday Soc.*, 1945, 41, 141.

[7] Wang, *Physic. Rev.*, 1928, 31, 579.

[8] Hirschfelder and Linnett, *J. Chem. Physics*, 1950, 18, 130.

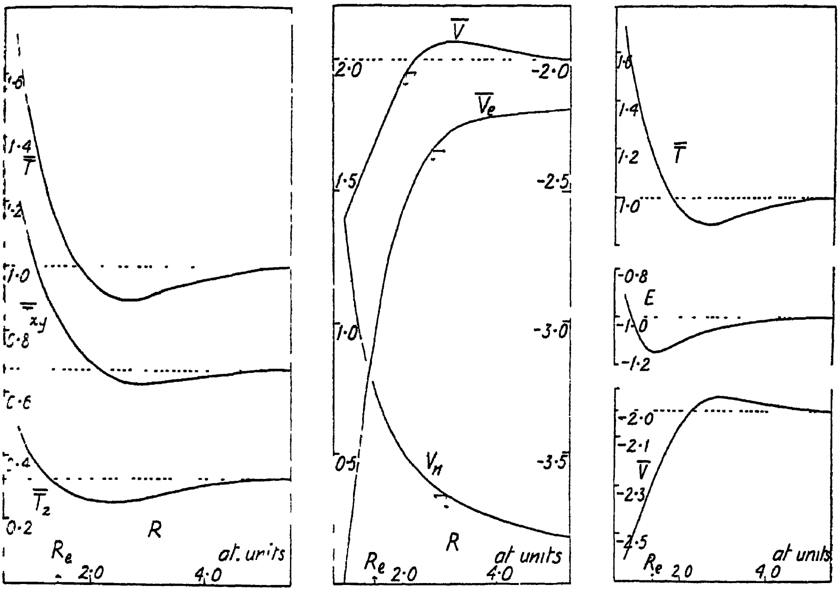

(a) (b) (c)

FIG. 1.—Graphs showing the variation with R, the internuclear distance, of $\overline{T}_z$, $\overline{T}_{xy}$, $\overline{T}$, $\overline{V}_e$, V_n, $\overline{V}$ and E. These were calculated using the Wang function.

The results for the same energy quantities obtained using the Hirschfelder-Linnett function are listed in Table II, and are graphed in various combinations in Fig. 2(*a*), 2(*b*) and 2(*c*).

TABLE II.—RESULTS OBTAINED USING THE HIRSCHFELDER-LINNETT FUNCTION FOR H_2

R	t	$\overline{T}$	$\overline{T}_z$	$\overline{T}_{xy}$	$\overline{V}$	V_n	$\overline{V}_e$	E	$\overline{E}_e$
0·734	1·0	1·624	0·465	1·160	−2·559	1·363	−3·921	−0·934	−2·297
1·210	1·5	1·258	0·325	0·933	−2·404	0·827	−3·231	−1·146	−1·973
1·798	2·0	0·986	0·250	0·736	−2·127	0·556	−2·683	−1·141	−1·697
2·417	2·5	0·868	0·226	0·642	−1·958	0·414	−2·372	−1·000	−1·504
3·000	3·0	0·853	0·237	0·616	−1·903	0·333	−2·236	−1·050	−1·383
3·5	3·5	0·902	0·268	0·633	−1·928	0·286	−2·214	−1·027	−1·312
4·0	4·0	0·942	0·295	0·648	−1·956	0·250	−2·206	−1·013	−1·263
4·5	4·5	0·969	0·313	0·657	−1·976	0·222	−2·198	−1·006	−1·229
5·0	5·0	0·984	0·323	0·661	−1·987	0·200	−2·187	−1·003	−1·203
6·0	6·0	0·996	0·331	0·665	−1·997	0·167	−2·164	−1·001	−1·167
7·0	7·0	0·999	0·333	0·666	−1·999	0·143	−2·142	−1·000	−1·143
8·0	8·0	1·000	0·333	0·667	−2·000	0·125	−2·125	−1·000	−1·125
10·0	10·0	1·000	0·333	0·667	−2·000	0·100	−2·100	−1·000	−1·100

Potential and Kinetic Energy.—The Schrödinger equation may be written, for one co-ordinate, in the form

$$-\frac{1}{\psi}\cdot\frac{h^2}{8\pi^2 m}\cdot\frac{d^2\psi}{dx^2}+V(x)=E.$$

For any particular value of x the value of the first term is equivalent to the K.E. of the particle. That is, the K.E. is related to the curvature of the wave function—the greater the curvature (with $d\psi/dx$ decreasing as

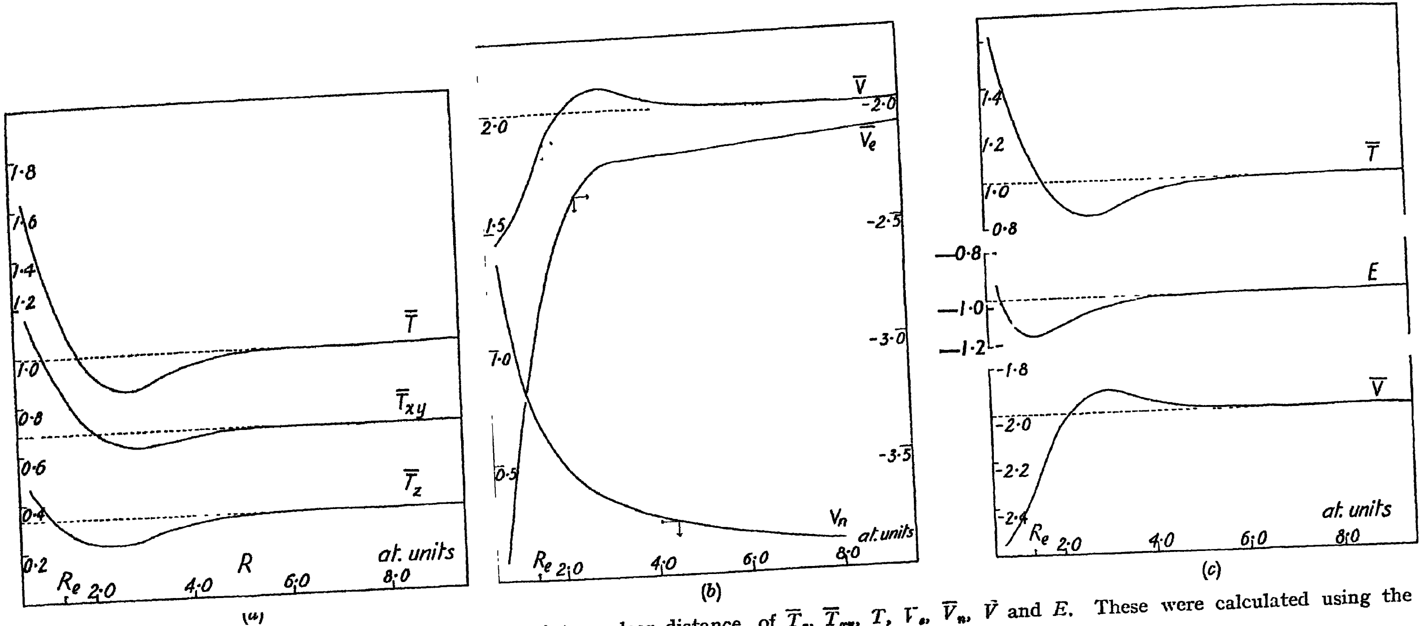

(a) (b) (c)

FIG. 2.—Graphs showing the variation with R, the internuclear distance, of $\overline{T}_z$, $\overline{T}_{xy}$, T, V_e, $\overline{V}_n$, $\bar{V}$ and E. These were calculated using the function of Hirschfelder and Linnett.

x increases, if ψ is positive) the greater is the equivalent K.E. This is well known for a particle in a box.

The same principle applies to other problems. Let us consider a particle moving in one direction, the P.E. varying proportionally to x^2 (the simple harmonic oscillator). The lowest state again is that for which the wave function is one half wave, but, in this case, the function spreads to infinity in either direction. However, it only has an appreciable value over a limited range. We may imagine the wave function spreading itself to the optimum extent, i.e. such that the energy is minimized. If it spreads over a greater range of x it can reduce its average curvature and hence T, but this increased spreading brings it into regions of higher P.E. and hence increases $\overline{V}$. On the other hand, if it restricts itself more, there will be an increase in curvature and hence in $\overline{T}$, and a decrease in V. We may suppose that the wave function adjusts its degree of spreading so that $E = \overline{T} + \overline{V}$ is minimized. The wave function for the first excited state consists of two half waves, so that the curvature is greater for a given degree of spreading. In fact the wave function spreads to a rather greater extent than in the ground state. Both $\overline{T}$ and $\overline{V}$ are therefore greater than for the ground state. However, E does not increase as rapidly with change in quantum number (proportional to $(n + \frac{1}{2})$) as does E in the case of a particle in a box (proportional to n^2). The reason is that the wave function increases its curvature less rapidly with increase in the number of nodes, because the wave spreads increasingly as the quantum number increases for the simple harmonic oscillation, whereas it is spread to the same extent for all levels of a particle in a box. We see that the more restricted the function is in space the greater is the average K.E.; the more spread the smaller is the average K.E. A rather similar approach has been made by Hellmann who has considered, in particular, the energy of a particle in a series of boxes of similar type and size.[9] We shall use these general ideas in the discussion of the H_2 molecule.

The Hydrogen Molecule.—We have used two wave functions. Comparison of Fig. 1 and 2 shows that the curves obtained using both are the same in general form. It seems probable, therefore, that the form of the various curves would be the same for the H_2 molecule. We shall therefore assume that we may regard the general form of the curves to be true, and that we may discuss these without fearing that they are the consequence of a particular model (cf. Slater [4]).

From Fig. 1(*c*) and 2(*c*) it will be seen that, as two H atoms are brought together, $\overline{T}$ first decreases while V increases. But, as they come still closer, $\overline{T}$ passes through a minimum and increases again, $\overline{V}$ at the same time decreasing and becoming less than in the two separated atoms. At the equilibrium separation (R_e), $\overline{T}$ is greater, and $\overline{V}$ is less, than in the separated atoms (required by the virial theorem). Let us consider the variation of T. The fall in this must be due to an increased spreading of the electronic wave function. Bowen [10] has stated that when the two nuclei come together the two electrons, if they have opposed spins, spread over the region of the two atoms instead of only over one "and the space in which each moves is about twice as great. This reduces the uncertainty of the momentum so that the combined system of two atoms has a lower electronic zero-point energy than that of two atoms separated from each other, i.e. energy is liberated when they combine." (Hellmann has also considered the changes in kinetic energy that occur when a homopolar bond is formed in similar terms.[11]) This is what we have termed in the last section the lowering of T_e by increased spreading of the wave function (the number of nodes remaining the same—here zero). But

[9] Hellmann, *Acta Physicochim.*, 1934, **1**, 333.

[10] Bowen, *Chemical Aspects of Light* (O.U.P., 1946), p. 103.

[11] Hellmann, *Z. Physik*, 1933, **85**, 180.

this lowering of $\bar{T}_z$ operates only at values of R greater than $1\frac{1}{4}R_e$, and $\bar{T}$ at R_e is greater than for the separated atoms. It seems, therefore, at first sight that this feature contributes to binding (or attraction) at large separations, but not at R_e.

However, it must be remembered that the spreading of the wave function which we and Bowen have been considering must occur mainly in the z direction, whereas T is the mean *total* K.E. It therefore seemed possible that the decrease in the mean K.E. for " motion " parallel to the internuclear axis $\bar{T}_z$ might be obscured by an even greater increase in the mean K.E. for " motion " perpendicular to the internuclear axis $\bar{T}_{xy}$. For this reason we carried out calculations to separate $\bar{T}$ into $\bar{T}_z$ and $\bar{T}_{xy}$. The results, for the two wave functions, are shown in Fig. 1(*a*) and 2(*a*)—the latter is likely to be nearer the truth. It will be seen that the curves of both ${}_z\bar{T}$ and $\bar{T}_{xy}$ have the same general form. However, $\bar{T}_{xy}$ has a minimum value at a greater value of R than $\bar{T}_z$, the minimum of which lies at about $1\frac{3}{4}$ R_e. Moreover, though $\bar{T}_{xy}$ is greater than $\bar{T}_z$ at all values of R, the maximum fall in T_{xy} from the value at $R = \infty$ (0·055 at. unit at $R = 2·9$) is less than the maximum fall in $\bar{T}_z$ from the value at $R = \infty$ (0·11 at. unit at $R = 2·4$). The figures are a consequence of the function used but the general picture is the same for both wave functions.

By separating $\bar{T}$ into $\bar{T}_z$ and $\bar{T}_{xy}$ we see that the main decrease in the mean K.E. is in $\bar{T}_z$ and that at R_e, $\bar{T}_z$ is less than at $R = \infty$. So, when the nuclear separation is R_e, the change in $\bar{T}_z$ from the value at $R = \infty$ is still contributing to binding, though, when R has decreased to R_e, $\bar{T}_z$ is increasing as R decreases, and at a value only slightly less than R_e becomes greater than the value at $R = \infty$.

The changes in $\bar{T}_{xy}$ are surprising. We might have expected $\bar{T}_{xy}$ to increase continuously as the atoms approach one another. However, there is an initial decrease before the inevitable increase. The increase is due to the effect of the two nuclei binding the electrons more closely to the internuclear axis and as a result, because the wave function spreads less in a direction perpendicular to the internuclear axis, $\bar{T}_{xy}$ increases. This is completely understandable, but *a priori* we would have expected it to operate at all separations. It will be considered further in a later section.

The graph of V against R is shown in Fig. 1(*c*) and 2(*c*). The nuclear P.E., V_n, can easily be separated from this since $\bar{V}_n = 1/R$ (using atomic units). $(\bar{V} - V_n)$ gives the mean electronic P.E., $\bar{V}_e$. V_n and $\bar{V}_e$ are plotted in Fig. 1(*b*) and 2(*b*). As the atoms approach $\bar{V}$ increases, passes through a maximum, and decreases but eventually it passes through a minimum and rises again without limit as $R \rightarrow 0$. (The final rise is not shown on our graphs, but see Coulson and Bell.[6]) This complicated sequence of changes is, to some extent, made more understandable if $\bar{V}$ is separated into $\bar{V}_e$ and V_n (Fig. 1(*b*) and 2(*b*)), for both change quite regularly, $\bar{V}_e$ always decreasing and V_n always increasing as R decreases from ∞ to 0. As the two atoms approach, V_n first increases more rapidly than V_e decreases. Then $\bar{V}_e$ decreases more rapidly than V_n increases. Finally as $R \rightarrow 0$, V_n approaches infinity whereas V_e falls to a limiting value (that for the helium atom) and so, as $R \rightarrow 0$, the increase in V_n outweighs the decrease in $\bar{V}_e$. The changes in $\bar{V}$ at separations less than R_e are easily understood, but the initial increase is less easy to understand. It seems that, at large values of R, the system lowers its total energy by spreading the electronic wave function into the region between the nuclei. However, the P.E. of an electron situated in that region is not sufficiently low to cause a lowering in $\bar{V}$, for V_n rises considerably in this range of R (down to about $2\frac{1}{2}$ at. unit). But the lowering of $\bar{T}$ resulting from the spreading of the electronic wave function into the central region and the accompanying decrease in curvature outweighs the rise in $\bar{V}$, and so E falls. As the nuclei come still closer the P.E. of an electron in the region between the nuclei falls so much as a result of their combined effect that the spreading of the wave function into this region results in such a lowering of $\bar{V}_e$ that $\bar{V}$ falls, and this is the condition when $R = R_e$.

In the above discussion we have ignored the P.E. arising from interelectronic repulsion. This increases steadily as R decreases. However, it does not alter the general conclusions being an additional positive factor in $\bar{V}_e$ which is small at large R and becomes considerable at small R. It is worth noting that the initial rise in V as the atoms approach cannot be ascribed to this factor, because the graph of $\bar{V}$ against R for the hydrogen molecule ion, with only one electron, has the same form (cf. Coulson and Bell [6]). The main feature of the changes in V are not due to interelectronic interaction but to the interaction of electrons and nuclei, and, at very small R, of the two nuclei.

The decrease in $\bar{T}_{xy}$ at large R remains puzzling. It may be associated with the rise in $\bar{V}$ because, as long as $\bar{V}$ is greater than at $R = \infty$, $\bar{T}_{xy}$ is less than at $R = \infty$, and at the point where $\bar{V}$ becomes equal to the value at $R = \infty$, $\bar{T}_{xy}$ also becomes the same as it was at $R = \infty$. We are unable to offer any explanation of this. Of course, it may be that this effect is a consequence of the functions we have used. However, the effect persists in much the same form and to much the same degree when the more flexible Hirschfelder-Linnett function replaces the Wang function. It seems probable that the effect is real, but an even more exact function would be necessary to prove this.

Let us trace the sequence of events as two H atoms approach one another.

(*a*) From $R = \infty$ to $R = 2{\cdot}9$. The electronic wave function, to decrease its curvature in the z direction, spreads into the region between the nuclei. The resulting decrease in $\bar{T}$ more than compensates the increase in $\bar{V}$. The main decrease is in $\bar{T}_z$, but $\bar{T}_{xy}$ decreases also.

(*b*) From $R = 2{\cdot}9$ to $R = 2{\cdot}4$. The P.E. of an electron in the region between the nuclei has now become so low that the drift of the electronic wave function into that region now lowers $\bar{V}$. $\bar{T}_z$ continues to decrease with this increased spreading in the z-direction. T_{xy}, on the other hand, increases because the dual effect of the two nuclei is to attract the electrons towards the internuclear axis. So the spread of the wave function perpendicular to the nuclear axis decreases, and T_{xy} increases.

(*c*) From $R = 2{\cdot}4$ to $R = R_e$ ($1{\cdot}4$). The P.E. of an electron in the region between the nuclei now becomes so low that the system lowers its total energy by lowering $\bar{V}$ at the expense of $\bar{T}$. Thus $\bar{T}_z$, as well as T_{xy}, begins to increase as R decreases. This is due to the fact that the lowering of P.E. in the region of the nuclei is so great that the energy of the system can be lowered to the greatest extent by the wave function becoming more restricted (in all directions) to this region of low P.E. So, over this range, $\bar{V}$ decreases but $\bar{T}$ increases. Moreover, V decreases more rapidly than T increases so that E continues to decrease.

(*d*) At R_e ($1{\cdot}4$). $\bar{V}$ is less than ($-$ 0·31 at. unit), $\bar{T}_z$ is slightly less than ($-$ 0·036), and $\bar{T}_{xy}$ greater than (+0·19), the values at $R = \infty$. (These figures satisfy the virial theorem.) The changes in $\bar{T}_{xy}$ and $\bar{T}_z$ agree with results given by Coulson.[12]

---

[12] Coulson, *Proc. Camb. Phil. Soc.*, 1941, 37, 65.

(*e*) From $R = R_e$ (1·4) to $R = 0{\cdot}6$. The wave function continues to become more and more restricted to the region of the nuclei and $\overline{V}$ decreases and $\overline{T}$ increases, but now the latter increases more rapidly than the former decreases, so E increases.

(*f*) As R approaches zero. $\overline{V}_e$ and $\overline{T}_e$ approach the values they have for the helium atom, while V_n increases towards infinity. Consequently E increases towards infinitely large values.

Slater has considered the changes in $\overline{T}$ and $\overline{V}$ that occur when two atoms approach one another in similar terms. However, he only considered the total average K.E., and, consequently, we have been able to consider some of the changes in more detail.

It is often said that the binding energy of a hydrogen molecule is largely exchange energy,[1] the implication being that the exchange energy is the energy arising from the ability of the electrons to spread over the region of both atoms. In this sense exchange energy appears to us to be most closely related to changes in $\overline{T}_z$ (because the spreading occurs largely in the z-direction), and we have seen that this contributes only slightly to bonding at R_e. So, to say that exchange, *in this sense*, is the main contributor to binding in the hydrogen molecule seems to be misleading. However, on many occasions, the word exchange is used in relation to certain terms, the exchange integrals, in the wave-mechanical expression for the energy. As such, it is an arbitrarily selected part of the energy expression, the selection depending on the type of treatment being used. In this latter sense (in association with exchange integrals) it is questionable whether exchange energy is a useful concept since it depends on the treatment employed and will vary according to the variation function that is used. Because it depends on the treatment it may be misleading for it may be more related to the particular treatment than to the essential properties of the system.

In our discussion of the changes in E, V and $\overline{T}$, summarized above, we have tried to use only general considerations and to avoid conceptions which are associated with some particular way of writing the molecular wave function.

Appendix.—The following integrals which do not occur in the literature had to be evaluated during the above calculations. They were evaluated by conversion to elliptic co-ordinates in the usual way.

Results are expressed in terms of the simpler functions $A_n(t)$ and $F_n(t)$ where

$$A_n(t) = \int_1^\infty \lambda^n \,.\, e^{-t\lambda} \,.\, d\lambda,$$

$$F_n(t) = \int_1^\infty \lambda^n \,.\, e^{-t\lambda} \,.\, Q_0(\lambda) \quad d\lambda,$$

where

$$Q_0 = \tfrac{1}{2} \ln \frac{\lambda + 1}{\lambda - 1}.$$

Recursion and " starting " formulae for the A and F functions, together with tabulated numerical values, are given by Rosen.[13]

$$P_1 = \int r_a \,.\, r_b \,.\, \cos^3 \theta_a \,.\, \cos \theta_b \,.\, e^{-Z(r_a + r_b)} \,.\, d\tau$$

$$= \frac{\pi R^5}{16}(4A_8 - \frac{20}{3}A_6 - \frac{34}{15}A_4 + 8A_2 - 2A_0 - 4F_9 + 8F_7 - 8F_3 + 4F_1).$$

$$P_2 = \int r_b \,.\, \sin^2 \theta_a \,.\, \cos \theta_a \,.\, \cos \theta_b \,.\, e^{-Z(r_a + r_b)} \,.\, d\tau$$

$$= \frac{\pi R^4}{8}(18A_7 - 22A_5 - 6A_3 + 10A_1 - 18F_8 + 28F_6 - 12F_2 + 2F_0).$$

[13] Rosen, *Physic. Rev.*, 1931, 38, 2109.

$$P_3 = \int r_a \, . \, r_b \, . \sin \theta_a \, . \cos^2 \theta_a \, . \sin \theta_b \, . \, \mathrm{e}^{-Z(r_a + r_b)} \, . \, \mathrm{d}\tau$$

$$= \frac{\pi R^5}{16}\left(4A_8 - \frac{44}{3}A_6 + \frac{296}{15}A_4 - \frac{156}{15}A_2 + \frac{4}{3}A_0 - 4F_9 + 16F_7 - 24F_5 + 16F_3 - 4F_1\right).$$

$$P_4 = \int r_b \, . \sin^3 \theta_a \, . \sin \theta_b \, . \, \mathrm{e}^{-Z(r_a + r_b)} \, . \, \mathrm{d}\tau$$

$$= \frac{\pi R^4}{8}(18A_7 - 50A_5 + 46A_3 - 14A_1 - 18F_8 + 56F_6 - 60F_4 + 24F_2 - 2F_0).$$

$$P_5 = \int r_a \, . \cos^3 \theta_a \, . \, \mathrm{e}^{-Z(r_a + r_b)} \, . \, \mathrm{d}\tau$$

$$= \frac{\pi R^4}{8}\left(4A_6 - \frac{32}{3}A_4 + 10A_2 - 2A_0 - 4F_7 + 12F_5 - 12F_3 + 4F_1\right).$$

$$P_6 = \int \sin^2 \theta_a \, . \cos \theta_a \, . \, \mathrm{e}^{-Z(r_a + r_b)} \, . \, \mathrm{d}\tau$$

$$= \frac{\pi R^3}{4}\left(14A_5 - \frac{76}{3}A_3 + \frac{34}{3}A_1 - 14F_6 + 30F_4 - 18F_2 + 2F_0\right).$$

$$P_7 = \int \frac{r_b}{r_a} \, . \sin^2 \theta_a \, . \cos \theta_b . \, \mathrm{e}^{-Z(r_a + r_b)} \, . \, \mathrm{d}\tau$$

$$= \frac{\pi R^3}{4}\left(-14A_5 + \frac{16}{3}A_3 + \frac{26}{3}A_1 + 14F_6 - 10F_4 - 6F_2 + 2F_0\right).$$

$$P_8 = \int r_b \, . \cos^2 \theta_a \, . \cos \theta_b \, . \, \mathrm{e}^{-Z(r_a + r_b)} \, . \, \mathrm{d}\tau$$

$$= \frac{\pi R^4}{8}\left(-4A_6 + \frac{8}{3}A_4 + \frac{14}{3}A_2 - 2A_0 + 4F_7 - 4F_5 - 4F_3 + 4F_1\right)..$$

In the above A_n and F_n represent $A_n(t)$ and $F_n(t)$, where $t = ZR$, in which R is the distance between the nuclei a and b. The co-ordinates are those used by Coulson and shown in a diagram in a paper dealing with similar one-electron integrals.[14] r_a and r_b are the distances of the electron from a and b. θ_a and θ_b are the included angles at a and b of the triangle formed by a, b and the electron.

We wish to thank the Imperial Chemical Industries and the Royal Society for providing us with calculating machines; R. P. Bell and E. J. Bowen for most helpful discussion and advice; and J. O. Hirschfelder for some Tables of integrals.

Inorganic Chemistry Laboratory,
Oxford.

---

[14] Coulson, *Proc. Camb. Phil. Soc.*, 1942, 38, 210.

THE VIBRATIONAL ASSIGNMENT AND THERMODYNAMIC FUNCTIONS OF TETRACHLOROETHYLENE

By P. Torkington

Received 29th August, 1949

The specific heat, free energy and heat content functions, and the entropy of tetrachloroethylene are calculated for eight temperatures over the range 298·15° to 1500° K, from assumed standard dimensions and from the most probable set of fundamental vibration frequencies. The errors introduced by uncertainties in the dimensions and in the vibration frequencies are compared with the differences caused by replacement of the B_{1g} fundamental at 1000 cm.$^{-1}$ by 512 cm.$^{-1}$. It is shown that if the estimated low frequencies are reasonably correct then measurement of the specific heat at room temperature can be employed to decide between these two frequencies; the magnitude of the specific heat will certainly show whether or not the non-planar vibrations are as low as recently suggested. The constants in the formulae for the translational and rotational contributions to the entropy and free energy are recalculated from the revised table of Birge.

Recently,[1] a complete vibrational assignment was suggested for tetrachloroethylene. Since it seemed rather unlikely that further spectroscopic work would lead to any definite solution, and since the molecule is an important key compound for the group of chlorine-substituted ethylenes, it was thought worthwhile to investigate the possibility of checking the assignment against experimental thermodynamic data. Previous assignments had been incomplete, and did not account satisfactorily for all the observed frequencies. The new assignment favoured lower frequencies for the non-planar vibrations and for the B_{1g} C—Cl stretching mode. These lower frequencies would have a considerable effect on the thermodynamic functions.

The following formulae were used for the estimation of the translational and rotational contributions to the entropy S° and free energy function $-(F^\circ - E_0^\circ)/T$, in cal./deg. mole.

$$\left.\begin{aligned} S^\circ_{trans} &= 2\cdot2870(5 \log_{10} T + 3 \log_{10} M) - 2\cdot3130 \\ S^\circ_{rot} &= 2\cdot2870(3 \log_{10} T + \log_{10} I_A I_B I_C - 2 \log_{10} \sigma) + 267\cdot5460 \end{aligned}\right\}(1)$$

$$\left.\begin{aligned} [-(F^\circ - E_0^\circ)/T]_{trans} &= 2\cdot2870 (5 \log_{10} T + 3 \log_{10} M) - 7\cdot2791 \\ [-(F^\circ - E_0^\circ)/T]_{rot} &= 2\cdot2870(3\log_{10} T + \log_{10} I_A I_B I_C - 2\log_{10} \sigma) + 264\cdot5663 \end{aligned}\right\}(2)$$

The constants in the above formulae are calculated from the revised table of Birge;[2] to correct data based on the values given by Herzberg,[3] the procedure is as follows. For $S^\circ_{trans+rot}$, subtract 265·2078, multipy the residue by the factor 1·000087, then add 265·2330; [for $-(F^\circ - E_0^\circ)/T]^\circ_{trans+rot}$, subtract 257·2625, multiply the residue by 1·000087, then add 257·2872. T is the absolute temperature, M the molecular weight, I_A, I_B and I_C the principal moments of inertia in g. cm.^{2} and σ the symmetry number.

---

[1] Torkington, *Trans. Faraday Soc.*, 1949, **45**, 445; *Proc. Physic. Soc. A*, 1950, **63**, 804.

[2] Birge, *Rev. Mod. Physics*, 1941, **13**, 233.

[3] Herzberg, *Infra-red and Raman Spectra of Polyatomic Molecules* (D. Van Nostrand Co., Inc., New York; London: Macmillan & Co., Ltd., 1945).

The following were accepted as standard masses and dimensions for tetrachloroethylene: $m_C = 12{\cdot}004$, $m_{Cl} = 35{\cdot}457$, $r_{C=C} = 1{\cdot}353$ Å, $r_{C-Cl} = 1{\cdot}69$ Å, and all angles 120°. The C=C bond-length is carried over from ethylene,[4] and the C—Cl bond-length from vinyl and vinylidene chloride.[5] With these values, the principal moments of inertia become as follows: $I_A = 504{\cdot}29$, $I_B = 563{\cdot}23$, $I_C = 1067{\cdot}52 \times 10^{-40}$ g. cm.^{2}; the least axis coincides with the C=C bond. For symmetry V_h, $\sigma = 4$, formulae (1) and (2) become,

$$\left.\begin{aligned} S^\circ_{trans} &= 11{\cdot}4350 \log_{10} T + 12{\cdot}9162 \\ S^\circ_{rot} &= 6{\cdot}8610 \log_{10} T + 9{\cdot}7499 \end{aligned}\right\} \quad . \quad . \quad . \quad (3)$$

$$\left.\begin{aligned} [-(F^\circ - E^\circ_0)/T]_{trans} &= 11{\cdot}4350 \log_{10} T + 7{\cdot}9501 \\ [-(F^\circ - E^\circ_0)/T]_{rot} &= 6{\cdot}8610 \log_{10} T + 6{\cdot}7702 \end{aligned}\right\} \quad . \quad (4)$$

The translational and rotational contributions to the entropy and to the free energy function are given in Table I.

TABLE I.—TRANSLATIONAL AND ROTATIONAL CONTRIBUTIONS TO THE ENTROPY AND TO THE FREE ENERGY FUNCTION; IN CAL./DEG. MOLE

T	298·15° K	300° K	400° K	600° K	800° K	1000° K	1200° K	1500° K
S°								
trans	41·2114	41·2421	42·6708	44·6844	46·1130	47·2212	48·1266	49·2348
rot	26·7270	26·7454	27·6026	28·8108	29·6680	30·3329	30·8762	31·5411
$(t+r)$	67·9384	67·9875	70·2734	73·4952	75·7810	77·5541	79·0028	80·7759
$-(F^\circ - E^\circ_0)/T$								
trans	36·2453	36·2760	37·7047	39·7183	41·1469	42·2551	43·1605	44·2687
rot	23·7473	23·7657	24·6229	25·8311	26·6883	27·3532	27·8965	28·5614
$(t+r)$	59·9926	60·0417	62·3276	65·5494	67·8352	69·6083	71·0570	72·8301

The increments 2·2870 $\Delta \log_{10} I_A I_B I_C$ to each of the rotational contributions are given in Table II for a series of variations in the structural parameters; the isotope effect is included for the sake of completeness and for comparison. The effect of these variations on the individual moments of inertia are tabulated in the Appendix.

TABLE II.—INCREMENTS 2·2870 $\Delta \log_{10} I_A I_B I_C$ FOR SELECTED VARIATIONS IN THE STRUCTURAL PARAMETERS

	Null Values	$\Delta\theta_{CCCl} = +2°$	$\Delta r_{C-Cl} = +0{\cdot}05$ Å	$\Delta r_{C=C} = +0{\cdot}027$ Å
For $m_{Cl} = 34{\cdot}981$	− 0·0396	− 0·0035$_4$	+ 0·0936	− 0·0117$_6$
For $m_{Cl} = 35{\cdot}457$	0	+ 0·0361	+ 0·1332	+ 0·0279
For $m_{Cl} = 36{\cdot}981$	+ 0·1234	+ 0·1596	+ 0·2567	+ 0·1512

The variations in the translational contributions caused by replacement of $m_{Cl} = 35{\cdot}457$ by 34·981 and 36·981 are − 0·0344 and + 0·1076 respectively.

---

[4] Gallaway and Barker, *J. Chem. Physics*, 1942, **10**, 88.

[5] Brockway, Beach and Pauling, *J. Amer. Chem. Soc.*, 1935, **57**, 2693.

The vibrational contributions to the specific heat C and to the internal and free energy functions are given in Tables III, IV and V. The data were calculated from the tables given by Taylor and Glasstone,[6] which are corrected to the basis of the new constants of Birge.

TABLE III.—VIBRATIONAL CONTRIBUTIONS TO THE SPECIFIC HEAT IN CAL./DEG. MOLE

ν, cm.$^{-1}$	298·15° K	300° K	400° K	600° K	800° K	1000° K	1200° K	1500° K
135	1·9180	1·9188	1·9484	1·9695	1·9770	1·9806	1·9825	1·9841
185	1·8600	1·8615	1·9151	1·9546	1·9685	1·9750	1·9786	1·9816
218	1·8134	1·8155	1·8881	1·9422	1·9615	1·9706	1·9754	1·9796
237	1·7838	1·7863	1·8708	1·9343	1·9571	1·9676	1·9734	1·9782
332	1·6116	1·6157	1·7667	1·8851	1·9289	1·9496	1·9607	1·9701
347	1·5814	1·5857	1·7479	1·8760	1·9236	1·9461	1·9584	1·9685
387	1·4979	1·5030	1·6949	1·8501	1·9085	1·9364	1·9516	1·9641
447	1·3677	1·3736	1·6092	1·8070	1·8831	1·9197	1·9400	1·9567
782	0·6811	0·6894	1·0685	1·4945	1·6895	1·7899	1·8474	1·8962
913	0·4829	0·4905	0·8668	1·3527	1·5950	1·7243	1·7998	1·8646
1571	0·0583	0·0604	0·2248	0·6835	1·0627	1·3202	1·4907	1·6502
Non-planar	5·5914	5·5958	5·7516	5·8663	5·9070	5·9262	5·9365	5·9453
Planar	9·0647	9·1046	10·8496	12·8832	13·9484	14·5538	14·9220	15·2486
Total	14·6561	14·7004	16·6012	18·7495	19·8554	20·4800	20·8585	21·1939
B_{1g} 512	1·2235	1·2305	1·5091	1·7551	1·8522	1·8994	1·9256	1·9475
B_{1g} 1000	0·3774	0·3844	0·7453	1·2569	1·5281	1·6770	1·7651	1·8412

TABLE IV.—VIBRATIONAL CONTRIBUTIONS TO THE INTERNAL ENERGY FUNCTION, $(E^\circ - E_0^\circ)/T$, IN CAL./DEG. MOLE

ν, cm.$^{-1}$	298·15° K	300° K	400° K	600° K	800° K	1000° K	1200° K	1500° K
135	1·4097	1·4128	1·5434	1·6826	1·7555	1·7996	1·8304	1·8608
185	1·2303	1·2342	1·3988	1·5788	1·6747	1·7341	1·7746	1·8158
218	1·1219	1·1261	1·3087	1·5128	1·6229	1·6914	1·7385	1·7864
237	1·0628	1·0674	1·2590	1·4756	1·5936	1·6674	1·7179	1·7696
332	0·8035	0·8085	1·0314	1·2999	1·4525	1·5501	1·6176	1·6873
347	0·7677	0·7727	0·9986	1·2737	1·4311	1·5321	1·6022	1·6746
387	0·6784	0·6834	0·9152	1·2057	1·3751	1·4849	1·5615	1·6409
447	0·5609	0·5658	0·8006	1·1088	1·2942	1·4162	1·5019	1·5914
782	0·1765	0·1777	0·3572	0·6750	0·9071	1·0746	1·1990	1·3340
913	0·1084	0·1108	0·2544	0·5485	0·7836	0·9596	1·0941	1·2424
1571	0·0077	0·0080	0·0397	0·1774	0·3540	0·5233	0·6713	0·8527
Non-planar	3·7619	3·7731	4·2509	4·7742	5·0531	5·2251	5·3435	5·4630
Planar	4·1659	4·1943	5·6561	7·7646	9·1912	10·2082	10·9655	11·7929
Total	7·9278	7·9674	9·9070	12·5388	14·2443	15·4333	16·3090	17·2559
B_{1g} 512	0·4535	0·4583	0·6898	1·0109	1·2107	1·3442	1·4392	1·5389
B_{1g} 1000	0·0776	0·0796	0·2017	0·4768	0·7093	0·8893	1·0285	1·1842

---

[6] Taylor and Glasstone, *Physical Chemistry*, Vol. I, (D. Van Nostrand, Co., Inc., New York; London: Macmillan & Co. Ltd., 1942).

TABLE V.—VIBRATIONAL CONTRIBUTIONS TO THE FREE ENERGY FUNCTION, $[-(F^\circ - E^\circ_0)/T]$, IN CAL./DEG. MOLE

ν, cm.$^{-1}$	298·15° K	300° K	400° K	600° K	800° K	1000° K	1200° K	1500° K
135	1·4639	1·4726	1·8987	2·5531	3·0494	3·4475	3·7788	4·1902
185	1·0471	1·0548	1·4341	2·0399	2·5082	2·8893	3·2092	3·6117
218	0·8539	0·8608	1·2121	1·7861	2·2377	2·6078	2·9203	3·3152
237	0·7625	0·7692	1.1046	1·6612	2·1036	2·4806	2·7762	3·1457
332	0·4473	0·4524	0·7174	1·1923	1·5888	1·9241	2·2130	2·5819
347	0·4126	0·4174	0·6726	1·1354	1·5249	1·8561	2·1417	2·5080
387	0·3337	0·3379	0·5681	0·9999	1·3718	1·6915	1·9693	2·3268
447	0·2444	0·2471	0·4444	0·8331	1·1794	1·4822	1·7484	2·0939
782	0·0462$_0$	0·0466$_2$	0·1231	0·3309	0·5587	0·7801	0·9874	1·2708
913	0·0244$_4$	0·0151$_2$	0·0759$_4$	0·2361	0·4279	0·6224	0·8099	1·0708
1571	0·0010$_1$	0·0010$_6$	0·0070$_0$	0·0465$_2$	0·1215	0·2190	0·3279	0·4981
Non-planar	3·3649	3·3882	4·5449	6·3791	7·7953	8·9446	9·9083	11·1171
Planar	2·2722	2·2968	3·7131	6·4354	8·8766	11·0560	12·9738	15·4960
Total	5·6371	5·6850	8·2580	12·8145	16·6719	20·0006	22·8821	26·6131
B_{1g} 512	0·1756	0·1784	0·3432	0·6892	1·0093	1·2949	1·5486	1·8814
B_{1g} 1000	0·0159$_9$	0·0165$_0$	0·0552$_6$	0·1895	0·3598	0·5382	0·7134	0·9603

TABLE VI.*—INCREMENTS TO THE VIBRATIONAL CONTRIBUTIONS TO THE SPECIFIC HEAT, FOR $\Delta\nu = \pm 10$ CM.$^{-1}$, IN CAL./DEG. MOLE

ν, cm.$^{-1}$	T = 298·15° K		400° K		800° K		1200° K	
	$\Delta\nu + 10$	-10	$+10$	-10	$+10$	-10	$+10$	-10
	$-\Delta C$	$+\Delta C$	$-\Delta C$	$+\Delta C$	$-\Delta C$	$+\Delta C$	$-\Delta C$	$+\Delta C$
135	0·0103	0·0097	0·0060	0·0053	0·0016	0·0014	0·0007	0·0006
185	0·0135	0·0129	0·0077	0·0074	0·0020	0·0020	0·0009	0·0009
218	0·0154	0·0148	0·0090	0·0085	0·0023	0·0023	0·0010	0·0010
237	0·0163	0·0157	0·0096	0·0092	0·0026	0·0023	0·0011	0·0011
332	0·0202	0·0196	0·0125	0·0122	0·0035	0·0034	0·0015	0·0016
347	0·0200	0·0201	0·0128	0·0127	0·0037	0·0035	0·0016	0·0016
387	0·0215	0·0211	0·0137	0·0136	0·0040	0·0039	0·0018	0·0017
447	0·0223	0·0219	0·0150	0·0148	0·0045	0·0045	0·0021	0·0020
782	0·0168	0·0172	0·0160	0·0160	0·0069	0·0068	0·0033	0·0034
913	0·0133	0·0134	0·0141	0·0146	0·0076	0·0075	0·0039	0·0038
1571	0·0022	0·0022	0·0052	0·0054	0·0078	0·0081	0·0052	0·0054
Non-planar	0·0392	0·0374	0·0227	0·0212	0·0059	0·0057	0·0026	0·0025
Planar	0·1332	0·1312	0·0989	0·0985	0·0406	0·0400	0·0205	0·0206
Total	0·1724	0·1686	0·1216	0·1197	0·0465	0·0457	0·0231	0·0231
B_{1g} 512	0·0222	0·0222	0·0157	0·0158	0·0051	0·0050	0·0023	0·0024
B_{1g} 1000	0·0109	0.0113	0·0133	0·0134	0·0079	0·0078	0·0042	0·0041

---

* The increments in Tables VI, VII and VIII have been given in full, since this is the first time possible errors due to frequency increments have been considered when calculating thermodynamic functions. The method of computing for ν, $\nu + 10$ and $\nu - 10$, gives both the increments and serves as a completely trustworthy check. In Tables recently drawn up by the author,[6a] these increments and the values of the functions themselves, can be read off for the vibration frequencies directly.

[6a] Torkington, *J. Chem. Physics* (in press).

TABLE VII.—INCREMENTS TO THE VIBRATIONAL CONTRIBUTIONS TO THE INTERNAL ENERGY FUNCTION, FOR $\Delta\nu = \pm 10$ CM.$^{-1}$, IN CAL./DEG. MOLE

ν, cm.$^{-1}$	T = 298·15° K		400° K		800° K		1200° K	
	$\Delta\nu = +10$	-10	$+10$	-10	$+10$	-10	$+10$	-10
	$-\Delta$	$+\Delta$	$-\Delta$	$+\Delta$	$-\Delta$	$+\Delta$	$-\Delta$	$+\Delta$
135	0·0374	0·0379	0·0297	0·0302	0·0164	0·0164	0·0112	0·0112
185	0·0336	0·0344	0·0278	0·0281	0·0158	0·0159	0·0109	0·0111
218	0·0314	0·0321	0·0264	0·0267	0·0155	0·0155	0·0109	0·0110
237	0·0300	0·0307	0·0256	0·0260	0·0154	0·0153	0·0107	0·0107
332	0·0240	0·0246	0·0220	0·0223	0·0142	0·0144	0·0102	0·0105
347	0·0232	0·0237	0·0214	0·0218	0·0141	0·0143	0·0102	0·0103
387	0·0208	0·0204	0·0201	0·0205	0·0137	0·0139	0·0100	0·0101
447	0·0179	0·0183	0·0179	0·0183	0·0132	0·0132	0·0097	0·0098
782	0·0063	0·0066	0·0090	0·0093	0·0101	0·0101	0·0082	0·0084
913	0·0041	0·0042	0·0067	0·0068	0·0089	0·0089	0·0078	0·0077
1571	0·00033	0·00031	0·0011	0·0012	0·0044	0·0046	0·0051	0·0053
Non-planar	0·1024	0·1044	0·0839	0·0850	0·0477	0·0478	0·0330	0·0333
Planar	0·1266	0·1288	0·1238	0·1262	0·0939	0·0947	0·0719	0·0728
Total	0·2290	0·2332	0·2077	0·2112	0·1416	0·1425	0·1049	0·1061
B_{1g} 512	0·0147	0·0154	0·0158	0·0162	0·0125	0·0125	0·0095	0·0096
1000	0·0029	0·0031	0·0053	0·0055	0·0082	0·0083	0·0074	0·0074

TABLE VIII.—INCREMENTS TO THE VIBRATIONAL CONTRIBUTIONS TO THE FREE ENERGY FUNCTION, FOR $\Delta\nu = \pm 10$ CM.$^{-1}$, IN CAL./DEG. MOLE

ν, cm.$^{-1}$	T = 298·15° K		400° K		800° K		1200° K	
	$\Delta\nu = +10$	-10	$+10$	-10	$+10$	-10	$+10$	-10
	$-\Delta$	$+\Delta$	$-\Delta$	$+\Delta$	$-\Delta$	$+\Delta$	$-\Delta$	$+\Delta$
135	0·0991	0·1099	0·1093	0·1199	0·1249	0·1363	0·1306	0·1416
185	0·0639	0·0693	0·0727	0·0786	0·0748	0·0937	0·0931	0·0999
218	0·0496	0·0534	0·0582	0·0620	0·0723	0·0763	0·0779	0·0828
237	0·0431	0·0465	0·0515	0·0550	0·0660	0·0688	0·0703	0·0737
332	0·0235	0·0249	0·0302	0·0323	0·0429	0·0446	0·0476	0·0500
347	0·0216	0·0229	0·0281	0·0296	0·0403	0·0422	0·0451	0·0473
387	0·0169	0·0180	0·0232	0·0242	0·0347	0·0363	0·0397	0·0415
447	0·0122	0·0129	0·0174	0·0184	0·0283	0·0297	0·0330	0·0340
782	0·00218	0·00233	0·0044	0·0047	0·0116	0·0117	0·0152	0·0154
913	0·00119	0·00122	0·00272	0·00285	0·0086	0·0087	0·0120	0·0120
1571	0·00005	0·00005	0·00024	0·00026	0·0021	0·0023	0·0041	0·0043
Non-planar	0·2126	0·2326	0·2402	0·2605	0·2720	0·3063	0·3016	0·3243
Planar	0·1207	0·1288	0·1578	0·1673	0·2345	0·2443	0·2670	0·2782
Total	0·3333	0·3614	0·3980	0·4278	0·5065	0·5506	0·5686	0·6025
B_{1g} 512	0·0086	0·0092	0·0132	0·0138	0·0234	0·0240	0·0276	0·0287
1000	0·00075	0·00082	0·00194	0·00206	0·0070	0·0072	0·0103	0·0102

In the tables, the contributions from the non-planar vibrations, and from the planar vibrations, excluding the B_{1g} C—Cl stretching mode, are summed separately, to facilitate any corrections subsequently found necessary. It will be noticed that the effect of the three non-planar vibrations is considerable; for the free energy below 800° K, the contribution is greater than that from the planar vibrations. Since there is some uncertainty in the values of the vibration frequencies, due to measurements having been made with vapour, liquid and solution, and to the estimation of the two low frequencies at 135 and 185 cm.$^{-1}$, tables of increments for $\Delta\nu = \pm 10$ cm.$^{-1}$ are given above (Tables VI to VIII), for four temperatures. The vibrational contributions to the entropy are the sum of the internal and free energy contributions. The total thermodynamic functions are given in Table IX, (*a*) with 512 cm.$^{-1}$, (*b*) with 1000 cm.$^{-1}$, assigned to B_{1g} C—Cl stretching.

TABLE IX.—TOTAL THERMODYNAMIC FUNCTIONS OF TETRACHLOROETHYLENE IN CAL./DEG. MOLE

	T	298·15° K	300° K	400° K	600° K	800° K	1000° K	1200° K	1500° K
With 512 cm.$^{-1}$	C	23·8255	23·8717	26·0562	28·4505	29·6335	30·3253	30·7300	31·0873
	$(H^\circ-E_0^\circ)/T$	16·3271	16·3715	18·5426	21·4955	23·4008	24·7233	25·6940	26·7406
	$-(F^\circ-E_0^\circ)/T$	65·8053	65·9051	70·9288	79·0531	85·5164	90·9038	95·4877	101·3246
	S°	82·1324	82·2766	89·4714	100·5486	108·9172	115·6271	121·1817	128·0652
With 1000 cm.$^{-1}$	C	22·9794	23·0256	25·2924	27·9523	29·3294	30·1029	30·5695	30·9810
	$(H^\circ-E_0^\circ)/T$	15·9512	15·9928	18·0545	20·9614	22·8994	24·2684	25·2833	26·3859
	$-(F^\circ-E_0^\circ)/T$	65·6457	65·7432	70·6409	78·5534	84·8669	90·1471	94·6525	100·4035
	S°	81·5969	81·7360	88·6954	99·3148	107·7663	114·4155	119·9358	126·7894

In Table X, the differences $[\phi(522) - \phi(990)]$ for the thermodynamic functions ϕ are compared with $\Sigma[\phi(\nu - 10) - \phi(\nu + 10)]$ for the remaining eleven frequencies.

TABLE X.—INCREMENTS AND ERRORS, IN CAL./DEG. MOLE

T	298·15° K		400° K		800° K		1000° K	
	(*a*)	(*b*)	(*a*)	(*b*)	(*a*)	(*b*)	(*a*)	(*b*)
C	0·8125	0·3410	0·7347	0·2413	0·3112	0·0932	0·1341	0·0462
$(H^\circ - E_0^\circ)/T$	0·3581	0·4622	0·4668	0·4189	0·4806	0·2841	0·3938	0·2110
$-(F^\circ-E_0^\circ)/T$	0·1502	0·6948	0·2726	0·8258	0·6189	1·0571	0·7974	1·1705
S°	0·5355	1·1570	0·7760	1·2447	1·1509	1·3412	1·2459	1·3815

Column (*a*): $[\phi(522) - \phi(990)]$; column (*b*) $\Sigma[\phi(\nu - 10) - \phi(\nu + 10)]$

From Table X, it is apparent that a measurement of the specific heat at room temperature will probably suffice finally to determine the vibrational assignment. The maximum probable error from the rotational contributions to the entropy and the free energy function can be estimated from Table II to be 0·1972 cal./deg. mole.

The author wishes to express his gratitude to Courtaulds Limited for making the present programme of work possible, and to Prof. C. A. Coulson for giving him facilities at the Department of Theoretical Physics, King's College, London.

APPENDIX.—INCREMENTS TO THE MOMENTS OF INERTIA OF TETRACHLOROETHYLENE, FOR VARIATIONS IN THE STRUCTURAL PARAMETERS

		Standard Dimensions	$\Delta\theta_{CCCl} = +2°$	$\Delta r_{C-Cl} = +0·05$ Å	$\Delta r_{C=C} = +0·027$ Å	
$m_{Cl} = 34·981$	ΔI_A	− 6·77	− 27·21	+ 23·10	− 6·77	$\times 10^{-40}$ g. cm.^{2}
	ΔI_B	− 7·32	+ 29·01	+ 10·50	+ 3·00	
	ΔI_C	− 14·09	+ 1·80	+ 33·60	− 3·77	
$m_{Cl} = 35·457$	ΔI_A	0	− 20·72	+ 30·28	0	
	ΔI_B	0	+ 36·83	+ 18·06	+ 10·45	
	ΔI_C	0	+ 16·11	+ 48·34	+ 10·45	
$m_{Cl} = 36·981$	ΔI_A	+ 21·68	+ 0·07	+ 53·26	+ 21·58	
	ΔI_B	+ 23·43	+ 61·83	+ 42·26	+ 34·29	
	ΔI_C	+ 45·10	+ 61·90	+ 95·52	+ 55·97	

Note added in Press.—Since this paper was completed, the infra-red spectrum of C_2Cl_4 has been re-examined,[7, 8] using a thallium bromide-iodide prism for the low-frequency region,[7] and a new vibrational assignment has been proposed.[8] The low-frequency bands have not yet been confirmed, and there is some confusion in the literature over the position of one of them.† As regards the assignment, 512 and 288 cm.$^{-1}$ seem much too high for the non-planar bending modes. (See the author's comparison of the force constants for non-planar bending of C_2Cl_4 and $COCl_2$.[1]) For these reasons, the present paper has been left in its original form; it should be a simple matter to bring it up to date at any time.

British Rayon Research Association,
Urmston, Lancs.

---

† For the band in question, Plyler[7] gives 347 cm.$^{-1}$, while Bernstein[8] quotes 318 cm.$^{-1}$. The former value coincides with a Raman line. The correct value appears to be 347 cm.$^{-1}$; the author is indebted to Dr. Phyler for a copy of the spectrum, not yet published.

[7] Plyler, *J. Chem. Physics*, 1948, **16**, 1008.

[8] Bernstein, *ibid.*, 1950, **18**, 478.

EQUILIBRIA BETWEEN SOLID, LIQUID AND GASEOUS PHASES AT LOW TEMPERATURES

THE BINARY SYSTEMS, ACETYLENE CARBON DIOXIDE, ACETYLENE ETHYLENE AND ACETYLENE ETHANE

By A. M. Clark and F. Din

Received 7th March, 1950

The general theory of equilibria between solid, liquid and vapour phases is presented and it is shown how the phase relations of an ideal system can be calculated from the vapour pressures of the components. The effects of deviations from ideal behaviour are qualitatively discussed. Phase diagrams of the three binary systems which have been studied experimentally are based on measurements of vapour pressures and solubility, or freezing point depression.

The system acetylene-carbon dioxide forms an azeotrope with a boiling point slightly above that of either component. The system acetylene-ethane forms an azeotrope with a low boiling point but in this case the appearance of the azeotrope is suppressed at pressures below 800 mm. by the appearance of more stable solid and liquid phases. The system acetylene-ethylene shows ideal behaviour in the equilibrium between liquid and vapour phases but the liquid-solid and solid-vapour equilibria are complicated by the formation of solid solutions. The triple point of acetylene has been found experimentally to be at 192·4° K and at a pressure of 962 mm. Hg.

Many experimental investigations have been reported concerning the relations between liquid and vapour phases of binary systems at various temperatures and pressures and many studies have also been made of liquid-solid relations in condensed systems. Few examples, however, are on record of systems in which the inter-relations of all three phases are concerned.and as far as the authors are aware the only binary system hitherto described in which there are comprehensive data for all three phases in equilibrium is that of carbon dioxide and hydrogen sulphide.[1] This paper describes an investigation of the three binary systems: (1) acetylene-carbon dioxide; (2) acetylene-ethane and (3) acetylene-ethylene, at temperatures near the boiling points of the components at atmospheric pressure.

As the triple-point of acetylene is very close to its normal sublimation point acetylene can occur as a solid phase within the range of conditions studied. In the case of the acetylene-carbon dioxide system both components are encountered as solid phases.

Theoretical.—The equilibria between solid, liquid and vapour phases were first described by Roozeboom [2] but appear to have received little attention. At a fixed pressure the phase diagram relating temperature and composition is usually of the form shown in Fig. 1(A). In this case the boiling points of both components at the given pressure are above their melting points and there is a wide region in which only the liquid phase occurs. At lower pressures the region of co-existence of liquid and vapour phases assumes a lower temperature level, but as pressure has little influence on the melting point or solubility of a solid phase, the position of the solid-liquid region remains practically unchanged. The effect of reducing pressure, therefore, is that the vapour-liquid region descends the temperature scale until it overlaps the solid-liquid region. The state of affairs thus set up is indicated by Fig. 1(B). It occurs at atmospheric pressure for components such as acetylene and carbon dioxide which have triple-points above their normal sublimation points.

---

[1] Klemenc and Bankowski, *Z. anorg. Chem.*, 1932, **209**, 225.

[2] Roozeboom, *Die heterogenen Gleichgewichte vom Standpunkte der Phasenlehre* (1904), Heft 2, Part I, p. 328.

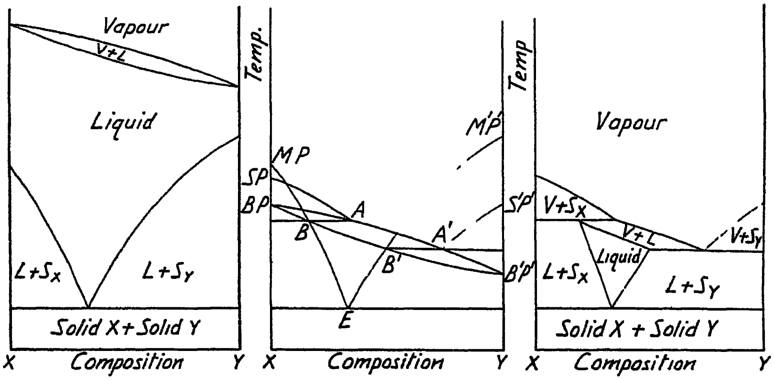

(A) (B) (C)

FIG. 1 (A), (B), (C).—Phase equilibria between solid, liquid and vapour for two components.

Fig. 1(B) includes a number of equilibrium relations which are metastable or unrealizable at the pressure in question. The curves MP–E and M'P'–E represent the solubility or the freezing point depression curves of the two components. The solutions which they represent have a stable existence only from the eutectic E to the points B and B'. The pure liquid components also cannot appear in stable form and the liquid-vapour region is limited to the area BAA'B'. Two new regions appear in which the pure solid components are in equilibrium with a vapour phase. These are bounded by the curves SP–A and S'P'–A'. These curves intersect the axes at the sublimation points SP and S'P' of the two components which are determined by the fixed total pressure of the system. It is assumed that no solid solutions are formed. In Fig. 1(C) the conditions which are metastable or which cannot be realized have been omitted and the diagram therefore represents the actual equilibrium relations which may be found in practice. The regions of co-existence of the various phases are indicated.

The case described is a general one for a system in which both components have triple points above their boiling and sublimation points and in which no solid solutions are formed. The form of the diagram is modified when only one of the pure components sublimes at the chosen pressure and it may be complicated by the appearance of an azeotrope, or by other deviations from ideal behaviour. This matter will be more fully discussed in connection with the systems acetylene-ethane and acetylene-carbon dioxide, both of which form azeotropes.

In spite of the well-known laws which express ideal behaviour, the fact appears to have escaped observation hitherto that it is possible to construct the complete phase diagram of an ideal system at a given pressure entirely from the vapour pressure data for the pure components. For this purpose the vapour must be assumed to behave as a perfect gas and no solid solutions or molecular complexes must be formed.

For a solution that behaves ideally with respect to the liquid-vapour equilibrium and also contains crystals of a pure solid component, not a solid solution, application of Dalton's and Raoult's laws leads to the following expressions :

$$P' = p = \pi y = Px,$$

in which

P' = the vapour pressure of the pure solid component at a given temperature,

p = partial pressure of the same component in the vapour phase,

P = vapour pressure of the same component as a supercooled liquid at the given temperature,

π = total pressure,

x = molar concentration of the component in the liquid phase,

y = molar concentration of the component in the vapour phase.

From these expressions,

$$y = P'/\pi \quad . \quad . \quad . \quad . \quad . \quad (1)$$

The position of a solid-vapour curve (e.g. SP–A, Fig. 1(B)) is thus fixed by the temperature and total pressure alone, and is independent of the nature of the second component.

The position of a solubility or freezing-point curve (e.g. MP–E, Fig. 1(B)) is given by

$$x = P'/P. \quad . \quad . \quad . \quad . \quad . \quad (2)$$

The concentration of a component in a solution with which it is saturated at a given temperature is thus determined by the ratio of the vapour pressures of its pure solid and liquid states at that temperature and is independent of the nature of the solvent as well as of the total pressure. As the solid state is the stable form under the conditions postulated the vapour pressure P of the liquid is for the metastable or supercooled condition.

The authors are not aware that this simple expression for the solubility or freezing curve of an ideal solution has been pointed out previously. There is no limitation that the solution must be dilute and no approximations are made as in the more familiar cryoscopic expressions for dilute solutions.

The liquid-vapour equilibrium boundaries (BP–B–B′–B′P′ and BP–A–A–′B′P′, Fig. 1(B)) may be calculated by applying the ideal expressions to each component separately. The following two well-known expressions are derived :

$$x_1 = 1 - x_2 = \frac{\pi - P_2}{P_1 - P_2}, \quad . \quad . \quad . \quad . \quad (3)$$

$$y_1 = 1 - y_2 = \frac{P_1(\pi - P_2)}{\pi(P_1 - P_2)}, \quad . \quad . \quad . \quad . \quad (4)$$

where subscripts 1 and 2 refer to the individual components. As already stated, at low temperatures the vapour pressures P_1, P_2, are for the supercooled pure liquid components.

When the behaviour of the system is not ideal the phase diagram cannot be constructed on the basis of the vapour pressures of the pure components but the result of deviations in a particular direction can be qualitatively predicted. When the system shows a positive deviation from Raoult's law, i.e. when the partial pressure of a component in the vapour is greater than the ideal value, the relationships become

$$P' = p = \pi y > Px.$$

In eqn. (1), y remains equal to P'/π and the course of the solid-vapour curves is therefore unaffected, but in eqn. (2), x becomes less than P'/P and the solubility of the component is therefore *below* the predicted value. The solubility curve thus lies *above* the predicted position on the temperature scale.

The direction of these displacements will be reversed by a negative deviation from Raoult's law. On thermodynamic grounds a deviation by one component must be associated with a similar deviation by the other and persist over the entire range of concentration.

If the two components form solid solutions the partial pressure of a component in the vapour phase in contact with the solid solution will be less than the vapour pressure of the pure solid component. The formation of solid solutions is an indication of molecular similarity and it is therefore likely that the liquid-vapour equilibrium will obey Raoult's law. In this case the pressure-concentration relationships become

$$P' > p = \pi y = Px.$$

Consequently eqn. (1) and (2) become respectively

$$y < P'/\pi \text{ and } x < P'/P.$$

The concentrations of the component are less than the ideal values in both cases and both the solid-vapour and solubility curves will be displaced above their ideal positions.

Previous Work.—The systems acetylene-ethylene and acetylene-ethane have been studied by Kuenen,[3] by Churchill, Collamore and Katz,[4] and McCurdy and Katz,[5] but only at temperatures around 0° C and at correspondingly high pressures. The only observations relevant to the present work are those of McMillan[6] who fractionally distilled acetylene-ethane mixtures at a pressure of 1 atm. He reported the existence of an azeotrope containing 40·8 % of acetylene boiling at − 94·5° C under atmospheric pressure. It will be shown subsequently, however, that McMillan was probably dealing with a mixture in which solid and liquid phases were both present and which therefore had a constant boiling point. Although his description of the distillation process is consistent with this explanation McMillan assumed that he was dealing with a true azeotrope. According to our observations, this system does not form a true azeotrope unless the pressure rises above 800 mm.

Experimental

PREPARATION OF THE GASES.—The gases were obtained from commercial cylinders, the acetylene being specially purified for this work and free from acetone. The gases were freed from carbon dioxide with potash solution and dried with phosphorus pentoxide before introduction to the apparatus. Permanent gases were removed by pumping.

APPARATUS AND METHOD.—The experimental procedure involved the measurement of the following properties of mixtures of known composition: (1) the initial freezing points of solutions, (2) the vapour pressures of liquid mixtures, and (3) the condensation pressures of vapours.

The apparatus, which was constructed in Pyrex glass, is shown in Fig. 2. The condensing vessel A was used as a receptacle for the incoming gases which had previously been purified and dried. The large bulbs B, B′, each of 5 l. capacity, were used as gas storage vessels for the pure components and the bulb C of 2 l. capacity was used for the preparation of gas mixtures. The small bulbs D and E, each of 5-ml. capacity, were connected to an absolute mercury manometer G. The bulb E was fitted with a magnetic stirrer. The manometer levels were measured within 0·05 mm. by means of a cathetometer.

The apparatus was first evacuated and a quantity of one of the pure components was slowly admitted and condensed in A by surrounding the bulb with liquid nitrogen. The condensed liquid was then distilled and the middle fraction was collected as gas in bulb B. The apparatus was then re-evacuated and the bulb B′ was charged with the other component by a similar procedure. Mixtures of the components were prepared by admitting each gas separately into bulb C using the changes in pressure shown by the manometer G to measure the composition of the mixture. As the maximum pressure concerned was usually less than $\frac{1}{3}$ atm. it was assumed that the mixture obeyed the perfect gas laws. A slight correction was necessary for the change of volume due to the movement of mercury in the manometer. The mixture was condensed completely into the bulb D by cooling with liquid nitrogen and the tap H was then closed. The mixture was finally distilled into the bulb E which was surrounded by a transparent Dewar vessel charged with liquid nitrogen to a level just below the bulb. In this way the outside of E was kept clean and free from frost which would have impaired the observation of the contents.

---

[3] Kuenen, *Phil. Mag.*, 1897, 44, (5), 174.

[4] Churchill, Collamore and Katz, *Oil Gas J.*, 1942, 41, (13), 33.

[5] McCurdy and Katz, *ibid.*, 1945, 43, (45), 102.

[6] McMillan, *J. Amer. Chem. Soc.*, 1936, 58, 1345.

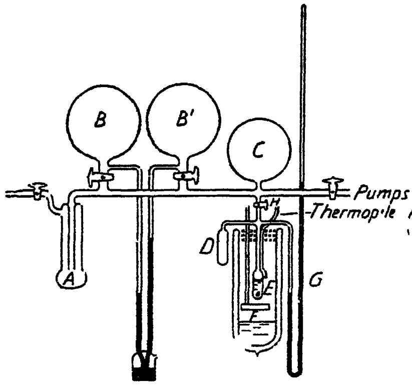

FIG. 2.—Apparatus for measuring vapour pressures.

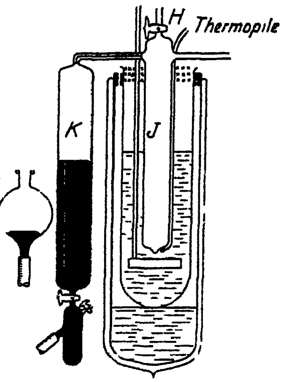

FIG. 3.—Apparatus for measuring condensation pressures.

Measurement of Freezing Point.—To measure the freezing point of a given mixture it was cooled gradually with constant stirring until the solid phase was observed to separate. For this purpose the level of liquid nitrogen was adjusted to a suitable distance below the bottom of the bulb E. The rate of cooling could be quite accurately controlled by this adjustment. The vapour pressure of the system at the moment that crystals were observed to appear in the bulb E was noted on the manometer. The temperature of the bulb was then allowed to rise slowly and the pressure at the moment of complete remelting of the crystals was noted. As the vapour pressure curve of saturated solutions was established independently, the vapour pressure at the point of crystallization served to determine the temperature of the system, the mixture thus acting as its own vapour pressure thermometer. By careful manipulation the temperatures of freezing and remelting for a given mixture could usually be made to coincide within 1° C, but owing to the possibility of delayed crystallization through super-cooling the temperature of remelting was generally considered the more reliable value.

As the volume of the vapour space was small, and as the composition of the vapour did not differ greatly from that of the liquid in equilibrium with it, it was assumed that the composition of the liquid was the same as that of the gas mixture from which it was condensed.

Measurement of Vapour Pressures.—For the measurement of vapour pressures the bulb E was immersed in a bath of *iso*pentane which was surrounded by a Dewar vessel containing liquid nitrogen. The temperature of the *iso*pentane was measured by a five-junction copper-constantan thermopile attached to a potentiometer. The ring magnet operating the stirrer in E also served to stir the *iso*pentane bath. By careful attention to the liquid nitrogen level the temperature of the bath could be maintained at any required value. When measuring the vapour pressures of saturated solutions it was not necessary to know precisely the composition of the mixture provided it contained the solid phase.

Measurement of Condensation Pressures.—For this purpose the apparatus was modified by substituting the arrangement shown in Fig. 3 for the bulbs D and E in Fig. 2. A small quantity of a gas mixture of known composition was condensed into vessel J. The mixture was allowed to evaporate and its pressure fixed initially by adjusting the level of the mercury in K. The tube J was then immersed in a bath of *iso*pentane which was slowly cooled by liquid nitrogen. The temperature of the *iso*pentane was measured by the thermopile and a record of the corresponding pressures and temperatures was made during the cooling process. A graph of these figures showed a sharp break at the initial condensation point, or dew point, of the mixture. The mixture was then allowed to re-evaporate and after thorough re-mixing the experiment was repeated starting from a different pressure but with the same mixture. A series of values was thus obtained for the condensation temperature of the given mixture at different pressures. The results were plotted and the condensation temperature at 760 mm., or any other fixed pressure, was obtained by interpolation. Some delay was noticed in condensation, particularly when the condensed phase was a solid, due apparently to supersaturation of the vapour. On raising the temperature the approach to equilibrium also appeared rather sluggish. In consequence the condensation temperatures could not be determined by this method with an accuracy better than 1° C.

Vapour Pressures of the Pure Components.—The vapour pressures of carbon dioxide and ethylene are well established, but published values for acetylene and ethane are not entirely consistent. Although the apparatus described was not designed for highly accurate measurements of vapour pressures it was considered desirable to re-determine the vapour pressures of acetylene and ethane in the course of the present work.

ACETYLENE.—Measurements of the vapour pressure of the pure solid confirmed the results of Burrell and Robertson [7] and the vapour pressure formula obtained by these authors has therefore been used. The formula is

$$\log_{10} p \text{ mm.} = 8{\cdot}84 - 1127{\cdot}1/T^\circ \text{ K},$$

from which the normal sublimation point is found to be 189·1° K. Burrell and Robertson did not measure the triple point. The pressure at the triple point was found by experiment to be 962 mm. which corresponds with a temperature of 192·4° K using Burrell and Robertson's formula. This temperature was confirmed by independent measurement using a carbon dioxide vapour pressure thermometer. These triple point figures are somewhat higher than those reported by previous authors. Volatile impurities in the acetylene might give a higher or lower pressure at the triple point than the true one but any impurity would depress the triple point temperature. As the value reported here is higher in temperature than those previously published it is considered to be more reliable.

The range of the manometers employed was insufficient for a wide investigation of the vapour pressure of liquid acetylene, and the following formula was therefore derived from a correlation of the measured value at the triple point with the value of 26·3 atm. at 0° C given in *International Critical Tables*:

$$\log_{10} p \text{ mm.} - 7{\cdot}4482 - 859{\cdot}27/T^\circ \text{ K}.$$

This gives a vapour pressure for the super-cooled liquid of 1 atm. at 188·1° K.

CARBON DIOXIDE.—The values for the vapour pressure of carbon dioxide were taken from the *Nat. Bur. Stand. J. Res.*[8] The following vapour pressure formula for liquid carbon dioxide, derived from the tabulated values, was used for extrapolation to low temperatures:

$$\log_{10} p \text{ mm.} = 7{\cdot}6771 - 885{\cdot}46/T^\circ \text{ K}.$$

The normal boiling point of the super-cooled liquid is thus calculated to be 184·7° K. It should be mentioned that this temperature is far below that to which liquid carbon dioxide can be supercooled in practice and it is therefore of theoretical significance only.

ETHYLENE.—The ethylene vapour pressure was adopted as the basis for the calibration of the copper-constantan thermopile, the formula of Stock, Henning and Kuss [9] being taken:

$$\log_{10} p \text{ mm.} = \frac{843{\cdot}13}{T} + 1{\cdot}75 \log T - 0{\cdot}008375T + 5{\cdot}3234.$$

ETHANE.—For ethane the vapour pressure results could be expressed adequately by the formula,

$$\log_{10} p \text{ mm.} = 7{\cdot}1809 - 794{\cdot}24/T^\circ \text{ K},$$

which gives excellent agreement with the results of Loomis and Walters.[10]

---

[7] Burrell and Robertson, *J. Amer. Chem. Soc.*, 1915, **37**, 2188.

[8] Meyers and van Dusen, *J. Res. Nat. Bur. Stand.*, 1933, **10**, 381.

[9] Stock, Henning and Kuss, *Ber.*, 1921, **54**, 1119.

[10] Loomis and Walters, *J. Amer. Chem. Soc.*, 1926, **48**, 2053.

Results

In Fig. 4 and 6 vapour pressure curves of the various pure substances in solid and liquid form are given. The dotted curves give the vapour pressures of the three-phase systems, i.e. of saturated solutions. Fig. 5, 7 and 8 are temperature-concentration diagrams for the binary systems showing the experimentally determined solubility curves and the interpolated data for the dew and bubble points. The unique points of the various diagrams are given in Tables I and II.

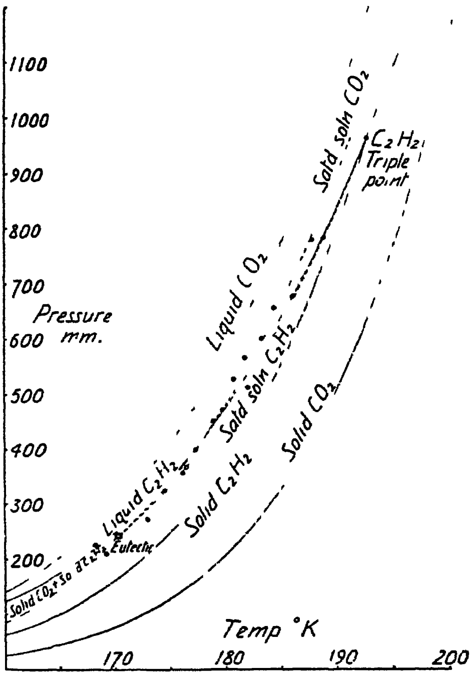

● Satd. soln. C_2H_2. ○ Satd. soln. CO_2.

FIG. 4.—The vapour pressures of carbon dioxide and acetylene and their solutions.

TABLE I.—VAPOUR PRESSURES OF PURE COMPONENTS

Component	p (mm.)	T °K
Acetylene triple point	962	192·4
Acetylene supercooled liquid	760	188·1
Acetylene supercooled liquid	900	191·2
Acetylene solid	760	189·1
Acetylene solid	900	191·5
Ethylene liquid	760	169·3
Ethane liquid	760	184·7
Ethane liquid	900	187·9
Carbon dioxide supercooled liquid	760	184·7

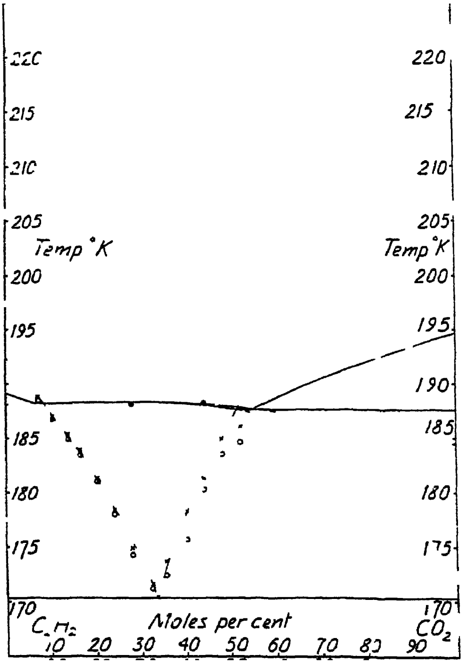

× Crystals disappear.
○ Crystals appear.
● Bubble points of unsaturated solutions.

FIG 5.—The system acetylene-carbon dioxide at 1 atm

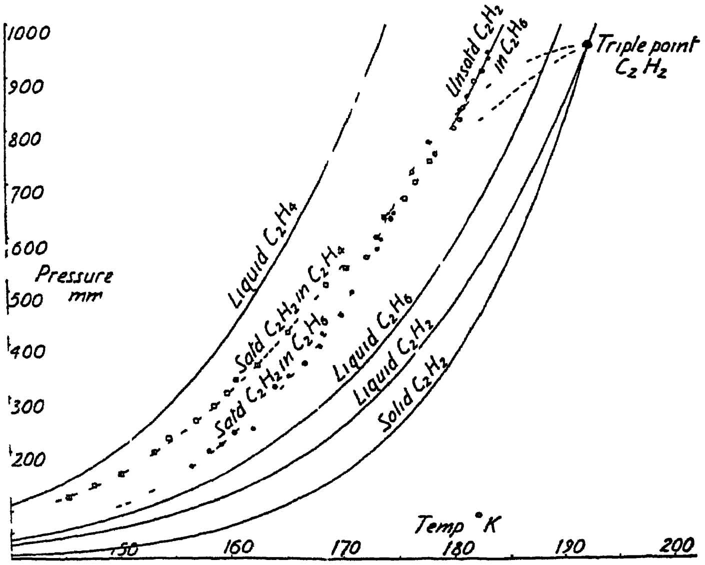

● C_2H_2, 66·7 %—C_2H_2, 33·3 %.
○ C_2H_2, 33·4 %—C_2H_6, 66·6 %
⊡ Saturated solution of acetylene in ethylene.

FIG 6.—The vapour pressures of acetylene, ethane and ethylene and their solutions.

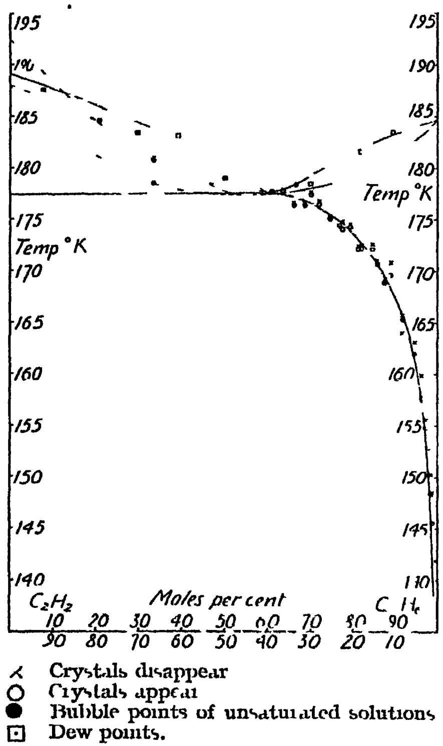

FIG. 7.—The system acetylene-ethane at 1 atm.

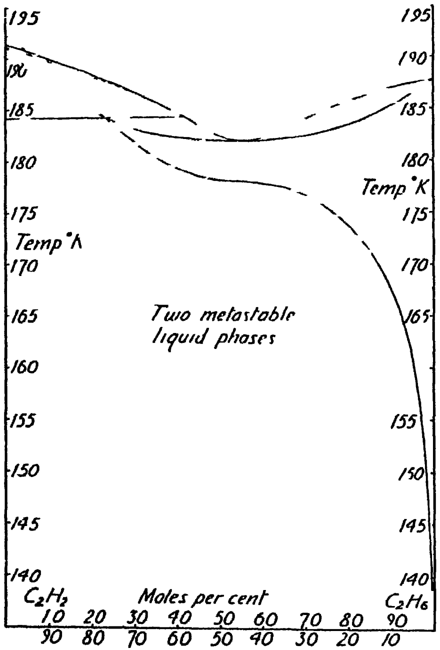

FIG 7a —The system acetylene-ethane at 900 mm.

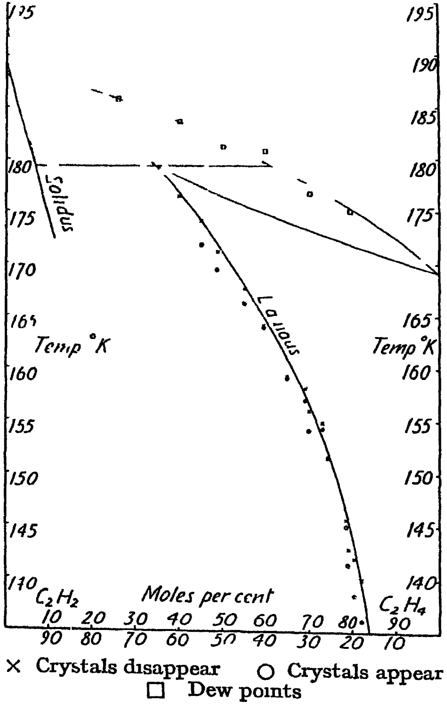

FIG 8 —The system acetylene-ethylene at 1 atm.

TABLE II.—Vapour Pressures of Saturated Binary Solutions

Molar Percentage of Components				p (mm.)	T °K
91·5	C_2H_2 †	8·5	CO_2	760	188·1
48·5	C_2H_2	51·5	CO_2 †	760	187·1
66·5	C_2H_2 * †	33·5	CO_2 †	242	170·3
37·5	C_2H_2 †	62·5	C_2H_6	760	177·4
77·0	C_2H_2 †	23·0	C_2H_6	900	184·2
65·5	C_2H_2 †	34·5	C_2H_4	760	179·4

* Eutectic. † Solid phase.

Discussion

The System Acetylene-Carbon Dioxide.—In Fig. 4 vapour pressure curves are given for solid carbon dioxide and acetylene and the supercooled liquids. The two dotted curves for the saturated solutions, one with acetylene as the solid in equilibrium, terminating at the acetylene triple point, the other with carbon dioxide as the solid in equilibrium, meet at the eutectic which lies on the curve representing the sum of the vapour pressures of the two solids; consequently no solid solutions are formed in this system. Pure liquid acetylene and all solutions containing carbon dioxide, both saturated and unsaturated, have a pressure of 760 mm. at a temperature close to 188° K (Tables I and II). However, the vapour pressure curve of the solution saturated with acetylene lies just below that of pure liquid acetylene. This is certain since the eutectic lies below the liquid acetylene curve and this point, where the vapour pressure remained constant at 242 mm. on freezing was very accurately established. At a given pressure, therefore, some solutions of acetylene have a higher boiling point than either of the components, and the system therefore forms a high-boiling azeotrope. At 1 atm. pressure the boiling-point of the azeotrope is only 0·1° C above that of liquid acetylene, as shown in Fig. 5. At the eutectic the ratio of the vapour pressures of the solids is 2/1 which is the same as the molar proportion of the components in the eutectic mixture. At this point, therefore, the vapour and liquid have the same composition, i.e. the eutectic liquid, under its own vapour pressure, behaves as an azeotrope. The composition of the azeotrope is unlikely to be much different at 760 mm. from its value at the eutectic pressure and this coincidence, which is quite accidental, enables the composition of the azeotrope at 760 mm. to be fixed fairly accurately.

As this system forms a high-boiling azeotrope there is a negative deviation from Raoult's law, i.e. the partial pressures of the components in the vapour are smaller than the law requires. This means that the freezing point curves must lie lower on the temperature-concentration diagram than would be predicted from the ideal relationships. This is confirmed by the experimental results.

The System Acetylene-Ethane.—From Fig. 6 the vapour pressure of a saturated solution of acetylene in ethane is seen to be higher at a given temperature than that of either of the two pure liquid components, except at the highest temperatures, i.e. at very high acetylene concentrations. The two unsaturated solutions measured also have higher vapour pressures than either component. This system therefore exhibits a very distinct tendency to form a low-boiling azeotrope. The course of the solubility or freezing point curve on the temperature-concentration diagram, Fig. 7, indicates that at 1 atm. the azeotrope would lie just inside the liquid-solid region and it is therefore suppressed. Nevertheless at this pressure a vapour of constant composition will be obtained on evaporation, since the system composed of solid, liquid and vapour phases in equilibrium at constant pressure is invariant. The vapour of constant composition contains 40 % acetylene at a temperature of 177·4° K (− 95·8° C) when the total pressure of the system is fixed at 1 atm. This composition agrees almost exactly with that reported by McMillan[6] although the temperature he observed, − 94·5° C, is over 1° above the present value. McMillan's pressures are not specified except by the statement that they varied between 752 and 766 mm. In Fig. *7a* the diagram has been constructed for a pressure of 900 mm. where it is seen that the azeotrope is fully realizable. The solubility or freezing point curve has a point of inflexion resulting from the same deviation from ideal behaviour which is responsible for the azeotrope. It is well known that the freezing point curve of systems of two immiscible or partially miscible liquids has a horizontal portion on the temperature-concentration diagram where the co-existence of vapour, solid and two liquid phases gives an invariant system. Azeotropism is associated with a tendency to immiscibility and the freezing point curve has a point of inflexion, but does not become horizontal in the absence of two liquid phases. In this system it can be predicted that two liquid phases would separate if the solution could be sufficiently supercooled. The hypothetical region of immiscibility is indicated by the dotted curve on Fig. *7a*. For further discussion of this point the reader is referred to Roozeboom's book.

As this system has a marked tendency to form a low boiling azeotrope the deviation from Raoult's law is strongly positive and, in accordance with the theory, the solubility or freezing point curve with acetylene as the solid separating is considerably above its ideal position on the temperature-concentration diagram.

The System Acetylene-Ethylene.—The vapour pressure curve of the saturated solution lies between those of the two pure liquid components over its whole course, Fig. 6. A saturated solution having a vapour pressure of 760 mm. has a temperature of 179·4° K and contains 65·5 % of acetylene, Fig. 8. Assuming ideal behaviour the concentrations in liquid and vapour phases at equilibrium can be calculated, as already described (eqn. (3) and (4)). At 760 mm. total pressure and a temperature of 179·4° K the concentration of acetylene in the liquid is thus found to be 65·5 % agreeing with the experimental value whilst in the vapour it is found to be 39·2 %. This value also agrees with experiment, but not with that calculated from the vapour pressure of the pure solid (eqn. (1)). It is also found by calculation (eqn. (2)) that the freezing point or solubility curve is not in the ideal position ; both this curve and the solid-vapour curve, when calculated, lie below the experimental curves. It must be concluded that this system is ideal as regards its liquid-vapour equilibrium, but also form solid solutions, with the result that the solid-vapour and freezing point curves are displaced from their ideal positions. The freezing point curve is in fact a liquidus curve ; a solidus curve has been drawn on Fig. 8, but its position is hypothetical.

This paper is published with the permission of the Directors of the British Oxygen Company. The work was carried out in the Gas Separation Research Laboratories of the Company.

The British Oxygen Company,
Research and Development Department,
Morden, London, S.W.19.

A RADIOACTIVE TRACER METHOD FOR THE DETERMINATION OF THE VARIATION OF VAPOUR PRESSURE WITH TEMPERATURE AND ITS APPLICATION TO WHITE PHOSPHORUS

By F. S. Dainton and H. M. Kimberley

Received 20th October, 1949; as amended 15th May, 1950

A static method of studying the variation of vapour pressure with temperature is discussed, which is based on " counting " a given volume of vapour at a fixed temperature in equilibrium with a sample of the condensed phase at a lower temperature when the latter is labelled with a radioactive isotope of one of the component elements. The application of the method to white phosphorus is described and combining the results obtained with the best literature value of the vapour pressure at 20° C it is found that

$$\log_{10} P \text{ (mm. Hg)} = -3529{\cdot}4/T - 3{\cdot}5 \log_{10} T + 19{\cdot}0923,$$

whence $\lambda_{25^\circ \mathrm{C}} = 14{\cdot}04$ kcal., $\Delta S_V^{25^\circ \mathrm{C}}{}_{(1 \text{ atm.})} = 27{\cdot}52$ cal. deg.$^{-1}$, and $\Delta C_P = -7{\cdot}0 \pm 0{\cdot}4$ cal. deg.$^{-1}$ over the temperature range concerned. The values of $\Delta S_V^{25^\circ \mathrm{C}}$ and ΔC_P are in good agreement with the values of $S^0_{\mathrm{P}_4(g)}$ (25° C, 1 atm.) and $C_{P\,\mathrm{P}_4\,(g)}$ calculated from spectroscopic data and the thermal capacity data of Stephenson and Maple for white phosphorus.

The accurate measurement of vapour pressures below 10^{-1} mm. Hg, by existing static or dynamic methods, is not easy. A possible static method, which does not appear to have been used before, would be to " count " a fixed proportion of the molecules in a given volume of the vapour when the compound being investigated contains a radioactive isotope of one of its component elements. Ideally, the isotope used should be capable of preparation in high concentration free from other isotopes, should emit only one type of radiation, which should be as hard as possible and possess a suitable half life. The concentration of molecules in the vapour will then be directly proportional to the counting rate after all due corrections have been made.* The constant of proportionality is most simply and accurately evaluated from measurements of the counting rate at a temperature where the vapour pressure is known by determinations using other methods. Alternatively it may be calculated by using a sample of known specific activity, a counting arrangement of known efficiency and from a knowledge of the geometry of the counter and counted volume together with the relevant stopping powers. An advantage of the method is that provided the dimensions of the system are fixed, this constant can be used for *any* compound containing the same isotope. Thus, in the experimental arrangement described below the factor determined for elementary phosphorus using P^{32} as a tracer, would be equally appropriate for an involatile phosphatic ester under conditions where self-absorption is negligible. In so far as it is desired to determine the variation of vapour pressure with change of conditions, e.g. temperature or mole fraction it is unnecessary to measure this constant. A further advantage of the tracer method is the wide range of values over which it may be employed because the magnitude of the counting rate is easily varied by adjustment of the volume counted, the specific activity and the stopping power of the windows. Moreover, if the temperature of the condensed form can be kept constant over long periods so that the total number of counts is considerable, even extremely low pressures may be measured with considerable accuracy.

---

* We have neglected the small differences between the vapour pressures of the solids formed from the five types of P_4 molecules, containing respectively 0, 1, 2, 3 and 4 P^{32} atoms, because their chemical constants are so close and it is unlikely that the solid forms differ appreciably. It also seemed probable that such differences would lie within our experimental error.

[1] De Witt and Skolnik, *J. Amer. Chem. Soc.*, 1946, **68**, 2305.

The isotope P^{32} is an almost ideal one with which to test the method. It is easily prepared by n, γ reaction on P^{31} or n, p reaction on S^{32}, and emits β-particles of high energy (max. 1·70 MeV) with a convenient half-life of 14·30 days. The range of the β-particles allows considerable latitude in the thickness of the window in front of the counter, and the absence of γ-rays reduces the shielding required. It was decided to use this isotope to determine the vapour pressure curve of elementary white phosphorus between $-23°$ C and its melting point. The reasons for this choice were: (*a*) red phosphorus containing P^{32} as the only radioactive species is now readily available, (*b*) an accurate value of the latent heat of sublimation of white phosphorus was required for the kinetic studies described in another paper, and existing data are highly unreliable (see discussion), (*c*) the affinity of phosphorus for traces of oxygen and the high rate of evaporation make for difficulties in application of a dynamic method.

Before the method was finally adopted it was necessary to establish that white phosphorus, which is rapidly converted to red by absorption of ultra-violet light, is either not so transformed by the absorption of its own β-particles, or that contamination of white by red phosphorus does not affect the vapour pressure measurements. There being no readily available source of β-particles the first point was tested by placing a sample of white phosphorus near a 400 mC radium source. After many hours exposure slight conversion to the red form was barely detectable. Indications of the correctness of the second point were obtained from experiments in which it was shown that white and red phosphorus are substantially immiscible and that the melting point of the white form is unaltered by the presence of large quantities of the red modification. When the first samples of phosphorus containing P^{32} were obtained it was shown directly that (*a*) any change of white to red induced by its own β-rays is extremely slow and (*b*) the counting rate of white phosphorus vapour is unaffected by the presence of the red form.

Experimental

About 1 g. of pure white phosphorus of the analytical quality described in a following paper, was distilled *in vacuo* into a cylindrical quartz tube 10 cm. long, 1·5 cm. external diameter. It was then wholly converted to the red variety by heating to 350° C for several hours. At this temperature the time required for 95 % conversion is 24 min. The tube and contents were then placed in an aluminium canister and subjected to pile radiation at A.E.R.E., Harwell, for the desired times.

The apparatus was constructed of Pyrex glass and is shown diagrammatically in Fig. 1. The quartz tube containing the red phosphorus was broken under water and placed in the tube R. After thorough evacuation, pure nitrogen or helium was admitted to a pressure of about 600 mm. Hg and the tube R and contents maintained at a dull red heat until all the phosphorous was converted and had condensed in the crystalline white form on the cooler parts of the walls. The whole system was then evacuated to at least 5×10^{-6} mm. Hg, as measured on a McLeod gauge and the phosphorus distilled into its ultimate container P, which was then sealed off from the main vacuum line at C and J. In any given experiment the temperature of P and its contents was controlled, below air temperatures by immersion in various freezing mixtures and above air temperatures by immersion in a small water thermostat. In all cases the bath temperature adjacent to the tube P was measured by a mercury-in-glass thermometer which had been standardized previously.

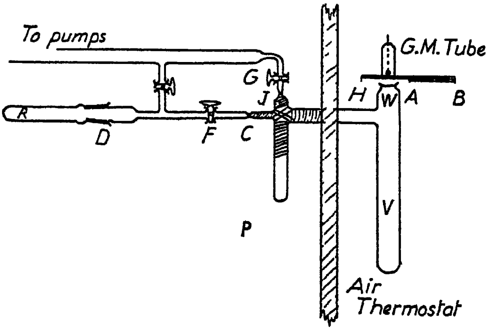

FIG. 1.

In order to ensure a satisfactory counting rate with the phosphorus samples of specific activity available a considerable volume of vapour was necessary, and to avoid counting any of the solid, the tube P was connected to a tube V about 3 cm. diam. and 25 cm. long through a side arm 2·0 cm. diam. as shown. It was also desirable that a portion of the wall of the tube V adjacent to, and at least as large in area as, the window of the Geiger-Müller tube should be sufficiently thin to permit the passage of a substantial portion of the β-particles. At first, mica windows waxed to the end of tube V were tried, but this always produced a high permanent counting rate due to phosphorus reacting either with the wax or alternatively with dissolved oxygen. Ultimately thin glass windows ($\sim$0·1 mm. thick) were found entirely satisfactory and were made by pressing the flame-softened perimeter of tube V against a bulb of thin glass. The window was then broken away from the bulb and its thickness determined by measurements on the projecting edges. The junction of the window with the tube was consolidated by running a small blowpipe flame round the edges. Such windows were fragile but after several attempts they could be made to withstand atmospheric pressure. We are indebted to Mr. F. Webber for developing the method of making these windows.

Since the counting rate is proportional to the concentration obtaining in the counted volume it was essential to maintain the temperature of this volume constant for all measurements. In order to carry out determinations on the white phosphorus at temperatures approaching the melting point, the counted volume, the counter and part of the connecting tubing were enclosed in an air thermostat working at 52·5 ± 0·4° C. The surface temperature of the wall of the tube V was checked by two fine thermocouples. That part of the connecting tubing which projected from the air thermostat and was not immersed in the liquid bath or water thermostat was heated electrically to about 60° C.

The tube V and the Geiger-Müller tube were both clamped to a single rigid steel framework, so that they were always in the same position relative to each other. A plastic sheet about 5 mm. thick was arranged to slide horizontally between the window W and the Geiger-Müller tube. A small copper disc about 1·5 cm. diam. fitted snugly in a circular depression of the same diameter in the plastic sheet at B. On this copper disc was a small deposit of uranium oxide, covered with a thin film of resin, which was used as a standard for the rate of counting. When the plastic sheet was pushed right over to the stop at H, this uranium source was directly beneath the window of the Geiger-Müller tube. A thin lead disc was placed under the copper disc, to ensure that, in this position, no β-particles from the tube V penetrated to the Geiger-Müller tube. The tube was a G.E.C.G.M. 4 tube of the suspended bead type in an argon-alcohol mixture, with a Duralumin window of thickness 6 mg./cm.^{2} and diam. 2·3 cm. and was operated at 1440 V. The high voltage supply was a power unit, type 200, as supplied by the Atomic Energy Research Establishment. The pulses were counted on a type X200 scaling unit, from the same source, which was connected through a probe unit, type 200, to the Geiger-Müller tube.

Six samples of phosphorus, with increasing specific activity up to a maximum of 13 mC/g. were employed. The usual counting sequence of (1) background, (2) uranium standard, (3) sample, (4) uranium standard, (5) background, was followed. As already stated, when mica windows were employed very high counts (up to 200/min.) were often observed even when the solid phosphorus was at liquid air temperatures. Although reduced, this count was still large when the first glass windows were used, and was only appreciably diminished when the tubes P and V and intermediate tubing had been carefully flamed out in a hard vacuum. This high liquid air count was ascribed to an involatile layer of phosphorus pentoxide formed from an adsorbed oxygen layer when the phosphorus vapour was admitted. This view is supported both by calculation which showed that a unimolecular layer of P_4 molecules could give rise to an even larger counting rate than was observed, and by the observation that admission of inactive phosphorus vapour to V before distilling the active white phosphorus into P reduced this liquid air count almost to the background value. There still remained the possibility that P_4 molecules might be adsorbed in appreciable amounts even on the flamed-out glass surface. The existence of a reversible adsorption of this kind would lead to apparent values of the latent heat of sublimation lower than the true values. Some experiments were therefore carried out with the inner surface of the counting vessel V coated with " methyl groups " or " hydrocarbon chains " by the method described in an earlier paper.[11] In each case no significant change in counting rate was observed, either at low temperatures (− 10° C) or at high temperatures (40° C). It therefore seems unlikely that adsorption of P_4 molecules is an important factor in these experiments.

The counting cycle (1)-(5) above was normally repeated once, and sometimes twice for greater accuracy. Errors due to the finite resolving time of the scaler and dead time of the counter were avoided by not permitting the counting rate to exceed 800/min. At temperatures and activities at which the counting rate would have exceeded this value perforated lead caps were placed over the window, thereby reducing the β-transmitting areas to about $\frac{1}{6}$th and $\frac{1}{16}$th respectively. The exact values of these ratios were determined extremely accurately at a fixed temperature.

Throughout the experiments the numbers of counts recorded of background, standard and sample were always arranged to keep the random errors of the background and standard counts less than that from sample. No correction was applied for self-absorption by the phosphorus vapour because even at the highest temperature used the column of saturated phosphorus vapour contains only $\sim$0·04 mg./cm.^{2}.

Results and Discussion

The counting rates C appropriate to the various temperatures are given in the Table together with the logarithms of the observed counting rate and of the rate calculated from eqn. (1)

$$\log_{10} C = -3529{\cdot}4/T - 3{\cdot}5 \log_{10} T + 23{\cdot}832. \qquad (1)$$

The agreement between eqn. (1) and the data is especially good above 10° C, but at − 23° C and − 9·74° C the observed counting rates appear to be larger than those given by eqn. (1) by an amount which is greater than the experimental error. Between − 10 and 0° C the curve joining the observed points lies very slightly above the line of eqn. (1), but the discrepancy is within the experimental error.

Assuming (*a*) that the difference between the specific heats at constant pressure of the vapour ($C_{P_4(g)}$) and the solid $C_{P(\alpha,\,\text{white})}$) is constant over the temperature range concerned and (*b*), that the pressure in the counted volume V is equal to the pressure over the solid in tube P, we can write

$$\lambda_T = A + \Delta C_P T, \qquad (2)$$

and hence

$$\log_{10} C = -\frac{A}{4{\cdot}571T} + \frac{\Delta C_P}{R} \log_{10} T + \text{a constant}, \qquad (3)$$

where λ_T is the latent heat of sublimation per mole of P_4 at T° K, $\Delta C_P = C_{P_4(g)} - 4C_{P(\alpha,\,\text{white})}$), and A is a constant. It is unlikely that assumption (*b*) is valid over the whole of the temperature range of measurement, since at pressures of about 0·0009 mm. Hg the mean free path of P_4 molecules is of the order of the diameter of the tube connecting P and V * and we may expect thermal transpiration effects to become noticeable. It is not possible to correct the observed pressures in V to give the real vapour pressures in this pressure region because the necessary data concerning P_4 vapour do not exist. It is easily seen, however, that at lower pressures where the mean free path considerably exceeds the diameter of the connecting tubing, eqn. (3) should be modified to

TABLE I

Temperature °C	Observed No. of Counts/min. ($C_{\text{obs.}}$)	Error = $\sqrt{N}$	$\text{Log}_{10}\, C_{\text{obs.}}$	$\text{Log}_{10}\, C_{\text{calc.}}$ [eqn. (1)]	$P_{\text{calc.}}$ (mm. Hg) *
40·84	7109	23	3·85181	3·85255	0·129
38·02	5818	28	3·76477	3·76443	0·1059
37·30	5522	27	3·74202	$3{\cdot}74173_5$	0·1005
34·25	4401	21	3·64355	$3{\cdot}64391_5$	0·0802
32·70	3929	19	3·59428	$3{\cdot}59334_5$	0·0714
31·10	3460	17	3·53908	$3{\cdot}54062_5$	0·0632
27·90	2712	14	3·43329	3·43339	0·0494
25·00	2169	16	3·33626	3·33451	0·0393
23·10	1851	7	3·26741	$3{\cdot}26795_5$	0·0337
21·34	1606	11	3·20575	$3{\cdot}20578_5$	0·0292
19·04	1332	8	3·12450	$3{\cdot}12394_5$	0·0242
17·03	1123	5	3·05038	$3{\cdot}05018_5$	0·0204
15·09	949	6	2·97727	$2{\cdot}97885_5$	0·0173
14·24	885·0	5·2	2·94694	$2{\cdot}94678_5$	0·0161
13·18	809·9	5·2	2·90843	2·90702	0·0147
11·47	692·3	4·7	2·83029	$2{\cdot}84205_5$	0·0127
9·90	603·0	3·1	2·78032	2·78162	0·0110
6·32	438·2	2·7	2·64167	2·64124	0·00797
3·45	336·6	3·1	2·52711	$2{\cdot}52595_5$	0·00611
0·00	243·0	1·1	2·38561	2·38383	0·00441
− 6·73	125·4	1·3	2·09830	2·09547	0·00227
− 9·74	101·3	0·9	2·00561	1·99629	0·00180
−23·0	23·5	0·4	1·37107	1·32963	0·000389

* Based on 0·0262 mm. Hg at 20·0° C.

$$\log_{10} C = -\frac{A}{4{\cdot}571 T} + \left(\frac{\Delta C_P}{R} - \tfrac{1}{2}\right) \log_{10} T + \tfrac{1}{2} \log_{10} T_g + \text{a constant} \qquad (4)$$

where T_g is the temperature of the gas in the counted volume. If thermal transpiration were occurring over the whole range of measurement, the effect in this instance would be to make the value of $\Delta C_P/R$ equal to -3 rather than $-3{\cdot}5$. In fact thermal transpiration effects are negligible in this system above 0° C where eqn. (1) is accurately obeyed. The points at $-23°$ C and $-9{\cdot}74°$ C differ from the values given by eqn. (1) by significant amounts and the reason is presumably associated with the onset of thermal transpiration.

Eqn. (1) therefore indicates that ΔC_P is -7 cal. deg.$^{-1}$ mole P_4^{-1} and λ (25° C) = 14·04 kcal. mole P_4^{-1}. The thermal capacity of white phosphorus over the range 0-40° C was measured by Young and Hildebrand[3] and over a much wider range by Stephenson and Maple.* No measurements are recorded of the specific heat of phosphorus vapour except that of C_P/C_V at 300° C,[4] but the structure and vibration frequencies of the P_4 molecule are well known[5] and $C_{P_4(g)}$ can therefore be calculated. At 250°, 273° and 298° K the external rotational contribution is 2·98 cal. deg.$^{-1}$ mole P_4^{-1}, and the vibrational contributions are 6·95, 7·53 and 8·07 respectively. The values of $C_{P_4(g)}$ at these temperatures are therefore 14·90, 15·38 and 16·02 cal. deg.$^{-1}$ mole P_4^{-1}. Using Young and Hildebrand's formula for $C_{P\,(\alpha,\,\text{white})}$ we then calculate ΔC_P to be $-6{\cdot}01$, $-5{\cdot}98$ and $-6{\cdot}18$ at these three temperatures, which values are smaller than the value of -7 given by eqn. (1). On the other hand if we take the data of Stephenson and Maple,* the corresponding values of ΔC_P became, $-6{\cdot}68$, $-6{\cdot}68$ and $-6{\cdot}75$, which represents very satisfactory agreement with our data.

---

* No data exist for the collision diameter of P_4, but from the structure of this molecule it is likely to be of the order 6 Å, and we have assumed this value.

[2] Weber, Keesom and Schmidt, *Comm. Kamerlingh Onnes Laboratory, Leiden*, 1936, **22**, no. 246*a*, *b*, *c*, *d*.

[3] Young and Hildebrand, *J. Amer. Chem. Soc.*, 1942, **64**, 839.

The value of λ (25° C) = 14·04 kcal. mole P_4^{-1} is at variance with the usually quoted value of 13·2.[6] This latter value must be regarded as incorrect for a reason which is quite separate from the fact that our value is the more accurate, namely, that existing data do not lead to the value of 13·2 kcal. Thus Joubert's values[7] for which no accuracy is claimed, lead to 13·7 kcal. Centnerswer's 5 values between 20° and 40° C obtained by a flow method do not give a linear log $P - T^{-1}$ plot.[8] Using a similar method, Fishbeck and Eich[9] have determined vapour pressures at 0°, 10° and 20° C, the value at 20° C being in fair agreement with Centnerswer's value, but the value of λ deduced from the data is 18·1 kcal. McCrae and Voorhis[10] have made accurate determinations of the vapour pressure of *liquid* phosphorus by the isotensiscope at 5 temperatures between 44° and 150° C but, contrary to reports, made no measurements on the solid. The equation for the vapour pressure of the liquid advanced by these authors, yields by extrapolation a value at the freezing point of 0·181. Despite the fact that their observed values at this temperature were 0·169 and 0·173 mm. they have combined the value of 0·181 with Centnerswer's "best" value at 20° C to deduce a vapour pressure equation for solid white phosphorus, from which we calculate λ (25° C) = 15·1 kcal.

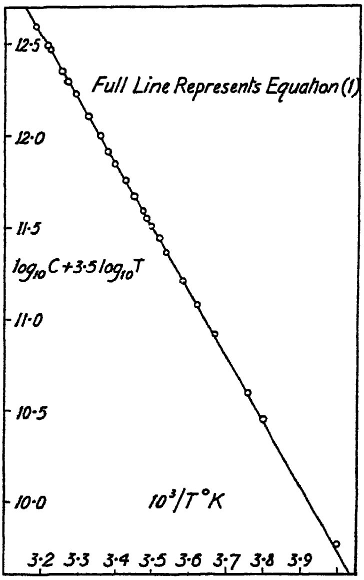

FIG. 2.

In order to transform the eqn. (1) into an absolute vapour pressure equation, the proportionality constant between the counting rate and pressure at 52·5° C in the counted volume, must be known (see first paragraph). Since this constant is a function of the design of the apparatus, we have used the direct comparison of the counting rate at 20° C as given by eqn. (1) with 0·0262 mm., which is the mean of 36 determinations by Centnerswer of the vapour pressure at 20° C. This compares well with the only other independent value at this temperature, namely 0·0269. We therefore obtain

---

* We are greatly indebted to Dr. C. C. Stephenson for making his unpublished data available for our use after our own experiments were completed.

[4] de Lucchi, *Nuovo Cim.*, (3), 1882, **11**, 11.

[5] Stevenson and Yost, *J. Chem. Physics*, 1941, **9**, 403.

[6] Bichowsky and Rossini, *Thermochemistry of Chemical Substances* (1936), p. 37.

[7] Joubert, *Compt. rend.*, 1874, **78**, 1853.

[8] Centnerswer, *Z. physik. Chem.*, 1913, **85**, 99.

[9] Fischbeck and Eich, *Ber.*, 1938, **71**, 520.

[10] McCrae and Voorhis, *J. Amer. Chem. Soc.*, 1921, **43**, 547.

$$\log_{10} P \text{ (mm. Hg)} = 3529{\cdot}4/T - 3{\cdot}5 \log_{10} T + 19{\cdot}0923. \quad . \quad (5)$$

The values of P calculated from this equation are given in the final column of the Table.

By combining eqn. (4) with the unpublished data of Stephenson and Maple on the thermal capacity of the solid, and assuming that P_4 vapour follows the ideal gas laws at pressures up to 1 atm. it is possible to evaluate the standard entropy of $P_{4(g)}$ at 1 atm. We obtain

$$S°_{P_4 \text{ (1 atm. gas at 25° C)}} = 4S°_{P\ (\alpha,\text{ white at 25° C})} + \frac{\lambda\,(25° \text{C})}{298{\cdot}16} - 4{\cdot}571 \log_{10} \frac{760}{P}$$
$$= 66{\cdot}72 \text{ cal./deg. mole.} \quad . \quad . \quad . \quad . \quad . \quad (6)$$

Owing to the uncertainty of the critical data for phosphorus it is not possible to evaluate a correction for non-ideal behaviour. This experimental value of $S°_{P_4(g)}$ may be contrasted with the value calculated by Stevenson and Yost of 66·92 cal. deg.^{-1} mole^{-1} from spectroscopic data, and in the derivation of which it is also assumed that phosphorus vapour behaves as a perfect gas.

It is a pleasure to record our indebtedness to Dr. A. G. Maddock for much help on the radiochemical side; and to the Royal Society and the Rehabilitation Department, New Zealand Government for financial aid.

Laboratory of Physical Chemistry,
Cambridge.

[11] Dainton and Kimberley, *Trans. Faraday Soc.*, 1950, **46**, 629; B. A. Rubin, *A.E.C.U.*—473 (reported in *Nuclear Science Abstracts*, 1949, **3**, 421) has also successfully used silicone coating of glassware to prevent any adsorption of P^{32} from aqueous solutions.

SOME ASPECTS OF THE MEASUREMENT OF HYDROGEN OVERPOTENTIAL

By A. M. Azzam, J. O'M. Bockris, B. E. Conway and Miss H. Rosenberg

Received 9th February, 1950

The rapid technique of measuring overpotential leads to the most reproducible results in acid solutions if the solutions are adequately purified. The negative deviations from the Tafel equation at high c.d.'s are spurious and caused by impurities such as H_2S (or a similar substance) in the electrolyte, which is adsorbed at the electrode only at potentials far from the electrocapillary maximum. The additions of O_2, H_2O_2, As_2O_3 have a qualitatively similar effect on the course of the potential—log c.d. relation. Equations are deduced for the potential during reductions as a function of i, pH and oxygen pressure.

The rate of removal of impurities by pre-electrolysis is controlled primarily by diffusion but the c.d. must be such that the electrode potential is sufficiently negative to reduce the impurities diffusing to the electrode. This condition is attained for low overpotential metals by pre-electrolyzing at the highest c.d.'s to be used in the subsequent measurements, whilst for mercury it is attained at c.d.'s between 10^{-6} and 10^{-3} A cm.^{-2}. In aqueous acid solutions the irreproducibilities of measurements at liquid and solid electrodes are considerably reduced by pre-electrolysis.

The measurement of hydrogen overpotential is noted for the irreproducibility of the results.[1, 2, 3] This is illustrated for an Ag cathode in Fig. 1. Results presented in the literature have been obtained by apparently arbitrary experimental techniques. Here, the aim is to clarify quantitatively the conditions necessary for the study of overpotential, and to establish whether the irreproducibility of results is due to the presence of impurities *in the solution.*

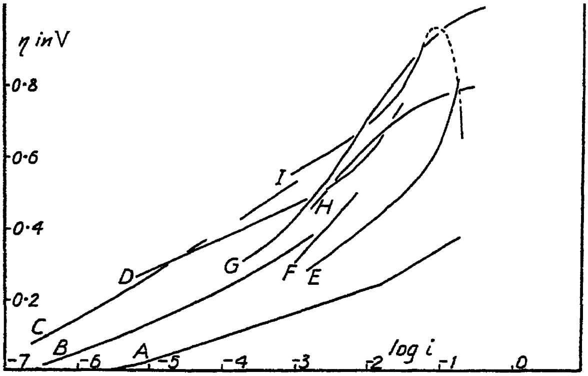

FIG. 1.—Overpotential at silver cathodes in aqueous acid solution.

A : Conway, N HCl, 1948.
B : Bowden and Rideal (etched), 0·5N H_2SO_4, 1928.
C : *Idem* (polished), 0·5 N H_2SO_4, 1928.
D : Harkins and Adams, NH_2SO_4, 1925.
E : Grant, N NaOH, 1928.
F : Cassel and Krumbeim, N H_2SO_4, 1934.
G : Knobel, Caplan and Eisemann, 2 NH_2SO_4, 1923.
H : Hickling and Salt, N HCl, 1940.
I : Bockris and Parsons, N HCl (in unpurified solutions), 1948.

Experimental and Results

Technique for Establishing a Tafel Line.—To examine the effect on the Tafel line of varying techniques of establishing it, comparative experiments of the rapid,[4] slow (the electrode is polarized at constant c.d. until the potential is constant) and resting[5] techniques were made with Hg, Cu, Ag, and Ni cathodes. For Hg cathodes the three techniques give the same results. For Ni and Ag, the slow and resting techniques give higher overpotentials for c.d.'s greater than 10^{-4} A cm.$^{-2}$ (see Fig. 2). The rapid technique gives a better reproducibility and agreement with the Tafel equation. The reproducibility of results with the rapid technique (± 0·01 V) is also better for Cu than that of the resting and slow techniques (± 0·08 V). The rapid technique is usually to be preferred, except when the variation of overpotential with time is not due to trivial causes. Thus, for Hg in alkaline solutions, where an equilibrium with a trace of alkali metal has first to be established, a slow technique would be preferable.

OVERPOTENTIAL AT HIGH C.D.'S.—The contention of Frumkin[6] that the decrease in slope of the Tafel line at high c.d.'s was due to incorrect extrapolation of the results obtained by Hickling and Salt[5] using their electronic commutator has been disproved by Bockris[7] who obtained by means of the direct method (using a similar solution and electrode preparation) results in good agreement

---

[1] Tafel, *Z. physic. Chem.*, 1905, **50**, 641.
[2] Jofa and Mikulin, *J. Physic. Chem.* (*U.S.S.R.*), 1944, **18**, 137.
[3] Béthune and Kimball, *J. Chem. Physics*, 1945, **13**, 53.
[4] Knobel, Caplan and Eisemann, *Trans. Electrochem. Soc.*, 1923, **43**, 55.
[5] Hickling and Salt, *Trans. Faraday Soc.*, 1940, **36**, 1224.
[6] Frumkin, *Acta Physicochim.*, 1943, **18**, 21.
[7] Bockris, *Trans. Faraday Soc.*, 1947, **43**, 417. Cp. Hickling, *Discussion Faraday Soc.*, 1947, **1**, 127.

with those of Hickling. However, using solutions carefully purified by pre-electrolysis, Azzam and Bockris[8] found that the Tafel equation for Hg is obeyed to c.d.'s above 10^{-2} A cm.$^{-2}$

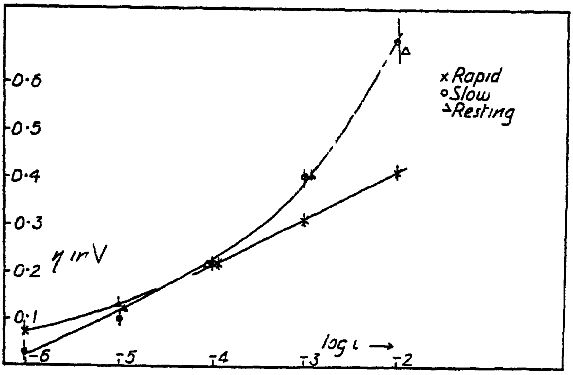

FIG. 2.—A comparison of rapid, slow and resting runs using a nickel cathode. ×—rapid. ○—slow. △—resting.

The "bend-over" of the Tafel line (which is an essential experimental support to the theory of Hickling and Salt[9]) may be of spurious origin in two possible ways. These are: (i) it may be due to a screening effect of the Luggin capillary on the current lines or (ii) to the presence of impurities adsorbed at the more negative potentials.

(i) SCREENING EFFECT.—Measurements were carried out using an Hg cathode in N/10 aqueous HCl in which system negative deviations from the Tafel line were observed at c.d.'s above $10^{-2.5}$ A cm.$^{-2}$. The distance of the Luggin capillary from the Hg surface was varied; the ohmic contribution to the potential was calculated * and subtracted from the measured overpotential. The activation overpotential was found to be independent of the distance of the Luggin capillary from the cathode surface. This result was confirmed in 1·66 N aqueous HCl (for which the ohmic contribution to the potential is less than that in N/10 solution) and in which the deviations are less, and in 5 N HCl for which the deviations are absent. Screening effects cannot therefore cause the negative deviations.

(ii) EFFECT OF IMPURITIES.—Addition of substances reducible at a mercury cathode causes no deviations of the type observed by Hickling anp Salt.[5] Hydrocarbons in petroleum greases caused marked but irreproducible deviations at high c.d.'s in the direction opposite to those observed by Hickling and Salt. Tafel lines with two distinct sections similar to those found by Bowden[10] were obtained. The adsorption of hydrocarbons at the mercury surface occurs slowly since these deviations were not observed until several hours after the addition had been made. Long-chain fatty acids neutralize the effect of the hydrocarbons but the overpotential remains irreproducible. However, the addition of traces of H_2S to a 5 N aqueous HCl solution (in which a linear Tafel line is initially observed) produces a deviation from the Tafel line identical with that found by

---

[8] Azzam and Bockris, *Nature*, 1950, **165**, 403.

[9] Hickling and Salt, *Trans. Faraday Soc.*, 1942, **38**, 474.

* Since no limiting current for hydrogen ion transport is observed in stirred solutions at c.d.'s less than 10^{-1} A cm.$^{-2}$,[11] the contribution of the p.d. in the diffusion layer to the total measured p.d. can be neglected under the conditions of the experiment referred to above. With this simplification the ohmic overpotential can be calculated from the resistance of the electrolyte contained in a right cylinder having the Hg surface as base and of height equal to the distance d between the Luggin capillary and the Hg electrode.

For a current density i and an electrolyte of specific conductivity κ, the ohmic overpotential η_r is given by

$$\eta_r = id/\kappa.$$

[10] Bowden, *Trans. Faraday Soc.*, 1928, **24**, 473.

[11] Parsons (unpublished); Frumkin.[6]

Hickling and Salt (Fig. 3). Hence, traces of H_2S or a similar impurity cause negative deviations from the Tafel equation.

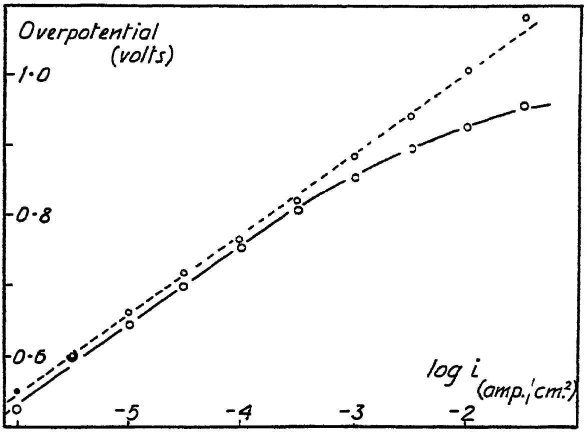

FIG. 3.—The effect of H_2S on the overpotential at a mercury cathode. O - - - O overpotential in pure 5N aqueous HCl, O———O the same after addition of a trace of H_2S.

The Effect of Traces of Oxygen in the Electrolyte.—Experiments were carried out using a Hg cathode under 6 different conditions. In Expt. I to IV a cell of the type employed by Bockris and Parsons,[12] and resting runs, were used, while in V and VI the technique developed for use at low c.d.'s was employed [13] (see Fig. 4). In Expt. I, the solution was saturated with oxygen; in II the solution was prepared as described by Bockris [7] using water of conductivity 10^{-6} mho cm.$^{-1}$. In Expt. III, the cell was deoxygenated by filling completely with conductivity water which was displaced by hydrogen, deoxygenated by passage through a furnace maintained at 600° C containing alternate packings of Cu rods and palladized asbestos. This hydrogen was then passed through the cell for 12 hr. The solution was prepared by passing HCl into conductivity water which had been twice distilled in a stream of hydrogen, the latter then being passed through the solution in the cell for a further 12 hr. In Expt. IV, the type of solution preparation described in III was used but the solution was finally purified by electrolysis with an auxiliary Hg cathode for 32 hr. at 10^{-4} A cm.$^{-2}$. In Expt. V the technique described by Bockris and Parsons [13] was used. In Expt. VI, after a run of type V had been carried out, known amounts of oxygen dissolved in pre-electrolyzed

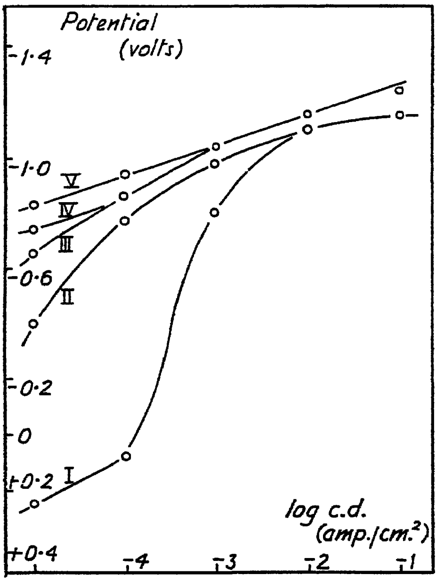

FIG. 4.—Overpotential at a mercury cathode in aqueous acid solutoin. Overpotential at a mercury cathode in presence of various quantities of oxygen. (For explanation of conditions I to V, see text.)

---

[12] Bockris and Parsons, *Trans. Faraday Soc.*, 1948, **44**, 860.

[13] Bockris and Parsons, *ibid.*, 1949, **45**, 916.

HCl solution were added to the catholyte by means of a dropper sealed into the top cap of the cathode compartment.

In the latter experiments a significant effect on the overpotential was obtained after 10^{-5} mole of O_2 (10^{-4} mole/l.) had been added (Fig. 5).* From

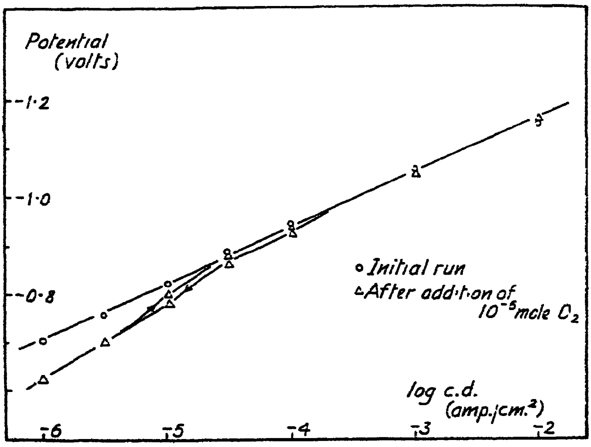

FIG. 5.—The effect of oxygen on overpotential at a mercury cathode.

this result, Hickling and Salt's "deoxygenated" solutions[14] contained a concentration of oxygen of the order of 10^{-4} mole/l. (assuming oxygen to be the only impurity present). If the cell used is not equipped with water-sealed joints and taps, with the most careful technique of solution purification (IV), the concentration of oxygen can be reduced only to about 10^{-4} mole/l. Similar experiments using copper and platinized platinum electrodes are reported in Fig 6. Results on the effects of other depolarizers or activators (H_2O_2, As_2O_3, $PtCl_4$) on a mercury cathode under conditions similar to VI are the same in form as those obtained when the depolarizer is O_2.

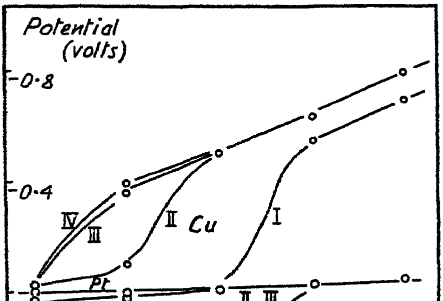

FIG. 6.—Overpotential at copper and platinized platinum cathodes in presence of various quantities of oxygen. (For explanation of conditions I to IV, see text.)

The electrode potential against log c.d. lines obtained in the presence of excess O_2 (Fig. 5, 6) show three sections for each of the three metals investigated. (*a*) At low c.d.'s there is an approximately linear region which represents a process involving the electro-reduction of O_2, the rate of which is large compared with that of hydrogen evolution. (*b*) At c.d.'s of the order 10^{-3} A cm.$^{-2}$ the electrode potential becomes rapidly more negative corresponding to the limiting current of the diffusion of O_2 from the solution to the electrode. The magnitude of this limiting current i_d, which is independent of the nature of the cathode material, is in satisfactory agreement with that calculated from simple diffusion theory (cp. ref. (14)) for O_2-stirred solutions. (*c*) At high c.d.'s the cathode potential becomes close to that observed in deoxygenated solutions and the deposition of H_2 becomes the principal electrode process.

---

* Fig. 5 and 7 are taken from Parsons, *Thesis* (London, 1948).

[14] Hickling and Salt, *Trans. Faraday Soc.*, 1941, **37**, 319.

Pre-Electrolysis.—The effects of time and c.d. on pre-electrolysis (or electrolytic purification of the solution) not previously investigated were studied using cathodes of Hg, Ag and Ni.

MERCURY.—Only general tendencies may be noted because it is difficult to obtain a comparatively pure solution in a reproducible state before commencement of the pre-electrolysis. Reproducible results (which do not alter on further pre-electrolysis) may be obtained after pre-electrolysis for 20 hr. at c.d.'s between 10^{-6} and 10^{-3} A cm.$^{-2}$. At higher c.d.'s the higher current passing through the cell introduces incidental complications (e.g. formation of bubbles in taps and in the electrical contact to the Hg, and local decrease of concentration in the anode compartment) which interrupt the polarizing current. Satisfactory results may sometimes be obtained by pre-electrolyzing for a short time (less than 1 hr.) at high c.d.'s (10^{-2} A cm.$^{-2}$). Longer pre-electrolysis times (e.g. 3 days) gave no conclusive results owing to the above-mentioned vitiating factors. Renewing the mercury electrode every 4 hr. during the pre-electrolysis does not affect the results.

The effect of depolarizers is markedly reduced by concluding the pre-electrolysis with a period of about 1 hr. during which the solution is not agitated (by hydrogen bubbling). The smaller negative deviations from the Tafel equation at high c.d.'s are not greatly reduced by pre-electrolysis. The impurity causing this effect would only be removed by pre-electrolysis at c.d.'s greater than 10^{-2} A cm.$^{-2}$ since it is presumably only present at the electrode at high negative potentials.

The presence of unpolarized Hg in the cathode compartment has no effect on the overpotential if the solution has been purified by pre-electrolysis. It does, however, have an effect in impure solutions (e.g. those containing oxygen) so that it is advisable to keep all Hg cathodically polarized during pre-electrolysis.

SILVER.—Fig. 7 shows results using a solution prepared without special purification. Pre-electrolysis was carried out on an auxiliary Ag cathode. Increase of time of pre-electrolysis at a constant c.d. of $1{\cdot}5 \times 10^{-1}$ A cm.$^{-2}$ led to a progressive lowering of overpotential to less negative values in the c.d. range 10^{-6} to 10^{-2} A cm.$^{-2}$. Runs conducted after 40 to 60 hr. pre-electrolysis on an auxiliary cathode gave more reproducible results and further increases of pre-electrolysis time did not change the results. In 0·01N HCl the effect of time of pre-electrolysis was less marked. In 0·01N HCl for passage of a constant quantity (10 coulombs) of electricity, variation of c.d. of pre-electrolysis in the range 10^{-6} to 10^{-1} A cm.$^{-2}$ led to a systematic lowering of overpotential values which reached a limit for the c.d. range of pre-electrolysis 10^{-2} to 10^{-1} A cm.$^{-2}$. During these changes in conditions of pre-electrolysis, the mean reproducibility of the values of overpotential improved from ± 0·05 to ± 0·02 V

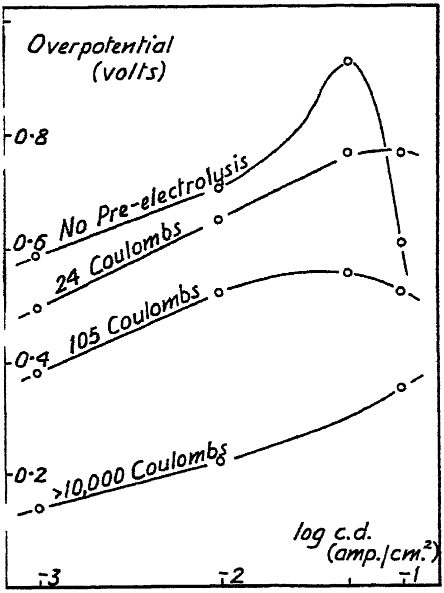

FIG. 7.—The effect of quantity of electricity passed during pre-electrolysis on the overpotential at a silver cathode in aqueous N HCl

NICKEL.—Increase of pre-electrolysis current density from 2×10^{-3} A cm.$^{-2}$ for 12 hr. to $4{\cdot}6 \times 10^{-2}$ A cm.$^{-2}$ for 15 hr. caused a marked reduction in the time variation of overpotential at Ni (see ref. (16)).

Pre-electrolysis is hence an essential method for the final purification of the solution.

Discussion

Consideration of previous work supports the experimental connection established between traces of H_2S in the solution and negative deviations from the Tafel equation. Thus, H_2 was formerly purified by passage through concentrated H_2SO_4. The latter is, however, reduced by H_2 gas to some extent. Direct experiment showed that H_2S in a $H_2 + H_2S$ mixture was incompletely removed at the normal rate of gas flow (3-4 l./hr.).* Reduction of H_2SO_4 might also occur in the HCl generator; since the HCl is purified using traps cooled in a CO_2-acetone mixture at − 78° C any H_2S (b.p. − 83° C) present would not be removed by this treatment. Thus, a slight tendency for negative deviations to occur is observed in Tafel lines obtained using the technique of Bockris and Parsons.[13] Bockris and Wetterholm [15] observed that the negative deviations from the Tafel equation were more pronounced in dilute solution. However, if the HCl gas [13] was carried forward from a saturated solution of HCl in a stream of H_2 into the conductivity water used in the cell, negative deviations from the Tafel equation were eliminated.

The work w required to replace a volume V_B of solvent A at an electrified interface by an equal volume of another molecular species B, i.e. the work of adsorption of B, was shown by Butler [18] to be

$$w = \tfrac{1}{2}[(\alpha_A - \alpha_B)E^2 + (p_A - p_B)E]\Delta V_B, \quad . \quad . \quad . \quad (1)$$

where E is the electric field at the interface, α's are the respective polarizabilities, p's are the permanent polarizations of the two molecular species and V_B is the molecular volume of B. Since the polarizability of water is $1{\cdot}44 \times 10^{-24}$ cm.^{3} and the dipole moment is 1·87 D, whilst the corresponding quantities for H_2S are $3{\cdot}64 \times 10^{-24}$ cm.^{3} and 1·1 D, the work of adsorption of H_2S at an Hg-aqueous solution interface will tend to be positive at low field strengths but will become negative at high field strengths. Hence the adsorption of H_2S at a mercury electrode will be more pronounced at potentials far from the electrocapillary maximum. A reaction occurring at the interface would thus be affected by H_2S only at high cathodic (or anodic) potentials as observed experimentally.

The decrease in the magnitude of the negative deviations from the Tafel equation at higher concentrations is explicable as follows. As the solution concentration increases the reversible hydrogen electrode becomes more positive with respect to the potential of the electrocapillary maximum in dilute solution. Since the overpotential at a given c.d. decreases with increase in concentration [13, 17] the potential of the working Hg electrode approaches that of the electrocapillary maximum. The field strength in the double layer at an electrode evolving hydrogen at a given c.d. will therefore decrease as the acid concentration increases, so that in more concentrated solutions a higher c.d. must be attained before H_2S becomes adsorbed at the electrode. Anion adsorption need not be considered as a factor affecting H_2S adsorption at the highly negative potentials concerned.[18]

---

[15] Bockris and Wetterholm (unpublished).

* The hydrogen purification train used by Bockris and Conway [16] and by Bockris and Parsons [13] contained no concentrated H_2SO_4 or other liquid reagents. It consisted of 30-40 cm. absorption tubes containing consecutively $MgClO_4$, Hopcalite (to convert CO to CO_2), sodalime; a furnace at about 500° C packed with palladized asbestos; and three traps cooled in liquid nitrogen, the second containing activated charcoal and the third packed with glass wool. The glass sections of the train were sealed directly together and Telcothene tubing was used for the connection to the cylinder to avoid contact of the hydrogen with rubber.

[16] Bockris and Conway, *Chem. Rev.*, 1949, **45**, 989; *J. Sci. Instr. A*, 1948, **19**, 23.

[17] Jofa, *Acta Physicochim.*, 1939, **10**, 903.

[18] Butler and Wightman, *J. Physic. Chem.*, 1931, **35**, 3293.

The lowering of overpotential occurring at high c.d.'s in the presence of H_2S is not connected with discharge from $H_3S^{\bullet}$ because the concentration of this ion will be minute in the presence of $H_3O^{\bullet}$, owing to the greater solvation energy of the latter. It is possible that the lowering is caused by commencement of proton transfer from H_2S, which is more probable than that from water, owing to the lower energy of dissociation of the S—H bond compared with that of the O—H bond (about 8 and 25 kcal. respectively).

The slope of the potential–log c.d. lines in the region of oxygen reduction for platinized Pt and Hg approximates to 0·12 V (Fig. 5 and 6). The same value was also observed by Krasil'schikov [22] for electro-reduction of oxygen at smooth Pt, Ag and Au cathodes; however, the corresponding slope for Cu electrodes is 0·03, indicating that the electrode process differs from that at the other cathodes.

Possible rate-controlling reactions in the electrolytic reduction of oxygen are (1) diffusion of oxygen to the electrode surface; (2) adsorption of oxygen on the electrode surface; and (3) reduction of adsorbed oxygen (*a*) by a reduction process not involving hydrogen atoms, and (*b*) by a reduction process involving hydrogen atoms. Jofa, Shimshelovich and Andreeva [23] have recently shown that the reduction at Hg occurs in two stages with intermediate formation of H_2O_2. The first stage can be assumed to be potential determining at least for curve I, Fig. 4, under the conditions of the present experiments. Thus, the following mechanism could account for the experimental results.

$$O_2 + H^+ + e \xrightarrow{\text{slow}} HO_2$$

$$HO_2 + H^+ + e \xrightarrow{\text{rapid}} H_2O_2.$$

The rate of reduction is hence given by

$$i = ka_{O_2}a_{H^+} \exp\left[-\psi\frac{F}{RT} - \frac{(e-\psi)F}{RT}\right] \quad . \quad . \quad (2)$$

or,
$$e = \text{const.} + \frac{(\alpha - 1)}{\alpha}\psi - \frac{RT}{\alpha F}[\ln i + \ln a_{O_2} + \ln a_{H^+}], \quad . \quad (3)$$

where e is the electrode potential at a c.d. of i A cm.$^{-2}$, ψ is the potential of the plane in which the reacting protons are situated, α is a proportionality constant, and a_{O_2} and a_{H^+} are activities. This equation accounts for the effect of potential on current density at Pt, platinized Pt, Au, Ag, and Hg if $\alpha = 0{\cdot}5$. It is also in agreement with the effect of oxygen concentration on the overpotential at Hg, the only metal for which this type of result is available.[23] The effect of pH is, however, more complex since besides affecting the term $\frac{RT}{F}\ln a_{H^+}$ it will also probably affect ψ. The metal surfaces are covered with an oxide film and the structure of the resulting electrode double layer is unknown. It can be assumed, however, that α is probably affected by pH to a different extent at different metals. Thus, the pH dependent term in eqn. (3)

$$\left(\frac{\alpha - 1}{\alpha}\psi + \frac{RT}{\alpha F}\ln a_{H^+}\right)$$

will depend on the nature of the cathode material as experimentally observed; for Hg $\left(\frac{\partial E}{\partial(\text{pH})}\right)_{i,\,O_2} = -\,0{\cdot}020$ to $-\,0{\cdot}030$ V,

---

[19] Jofa and Frumkin, *Acta Physicochim.*, 1943, **18**, 183.
[20] Hund, *Z. Physik*, 1925, **32**, 1.
[21] Bockris and Parsons (in course of publication).
[22] Krasil'schikov, *J. Physic. Chem.* (*U.S.S.R.*) 1949, **23**, 332.
[23] Jofa, Shimshelovich and Andreeva, *ibid.*, 1949, **23**, 828.

and for $$\mathrm{Pt}\left(\frac{\partial E}{\partial(\mathrm{pH})}\right)_{i,\,O_2} = -\,0{\cdot}055\ \mathrm{V}.$$

The low slope of section (*a*) of the curve for Cu electrodes may be explained using the equation of Haber and Russ [24] for reduction reactions,

i.e. $$e = \text{const.} - \frac{RT}{nF}\ln\left(\frac{i}{i_L - i}\right). \qquad (4)$$

The slope of the e against $\log i$ line at c.d.'s less than $i_L/10$ is then RT/nF where n is the number of electrons involved in the reduction process, i.e. for the electrode reactions

$$\mathrm{M - O} + 2e \rightarrow \mathrm{O^{=}},$$
$$\mathrm{O^{=}} + 2\mathrm{H^{+}} \rightarrow \mathrm{H_2O},$$

$n = 2$ and $RT/2F = 0{\cdot}029$ at 25° as observed.

Functions of pre-electrolysis at a cathode are (1) reduction of oxidizing agents (depolarizers) present in the solution, (2) removal of foreign cations by deposition, and (3) adsorption of capillary-active materials. A calculation of the concentration of ionic impurities in an aqueous HCl solution before pre-electrolysis, relevant to function (2), can be made from the ionic product of water from which, at 25°, $C_{\mathrm{H}^{\cdot}} = C_{\mathrm{OH}'} = 10^{-7}$. The specific conductivity of pure water is hence about $4{\cdot}89 \times 10^{-8}$ mho cm.$^{-1}$ at 25° C. The conductivity water used here had a κ value [13, 16] of 5×10^{-7} and assuming that this is due to simple cations and anions (mobility about 100 mho/g. equiv. at infinite dilution) the concentration of these is 5×10^{-6} N. The amount of alkali leached from Hysil glass during the distillation is approximately 5×10^{-7} g. equiv.[25, 26] and this corresponds to a concentration of 5×10^{-6} N in the cell. The electrical conductivity is hence virtually accounted for by the presence of alkali ions from the glass and the concentration of harmful ionic impurities is thus unlikely to be greater than 5×10^{-7} N. (Such quantities may affect hydrogen overpotential markedly.[16])

The rate of reduction of impurities during pre-electrolysis may be considered if the electrode can be assumed to be in a state of complete concentration polarization with respect to the impurities. The rate of decrease of concentration is given by

$$\frac{\mathrm{d}c}{\mathrm{d}t} = -\frac{i_L}{V}, \qquad (5)$$

where i_L, the limiting current due to the impurities, is DAC/δ, V is the volume of the solution, D is the diffusion coefficient of the impurity, A is the area of the electrode, δ is the thickness of the diffusion layer and C is the concentration of impurities. If C_0 is the concentration of impurity at the commencement of pre-electrolysis, then the concentration C after a time t is

$$C = C_0 \exp\left(\frac{-DAt}{V\delta}\right).*$$

The rate of transport is also affected by a force due to the electric field. This, however, increases D by a factor of approximately 2 which is not significant in the calculations given below; the value 10^{-5} cm.^{2}/sec. for D was hence adopted. The above equation shows that if the initial concentration of impurities is 5×10^{-7} g. equiv./l, the concentration of impurity left after pre-electrolysis of 40-hr. duration is about 3×10^{-10} g. equiv./1. Certain impurities [16] affect the overpotential when the concentration is of the order of 10^{-10} mole/l. so that the experimentally determined limit of poison concentration agrees well with the concentrations below which poison concentration is reduced by pre-electrolysis as exemplified above.

---

[24] Haber and Russ, *Z. physik. Chem.*, 1904, **47**, 257.

[25] Chance Bros., Ltd., Birmingham (private communication).

[26] Canwood, English and Turner, *J. Soc. Glass Tech.*, 1917, **1**, 153; van Niewenberg, *Chem. Weekblad*, 1917, **14**, 1034.

* Similar equations have been proposed by Agar and by Hickling (private communications).

During pre-electrolysis the potential of the auxiliary electrode must be kept more negative than the most negative value reached by the working electrode during the experiment. The duration of pre-electrolysis has to be empirically determined for each system, and may even vary for the same system owing to difficulties in achieving an absolutely reproducible initial state of the solution before pre-electrolysis ; the obvious higher efficiency of prolonged pre-electrolysis is off-set by diffusion of anode products to the cathode, etc. Increase of temperature clearly increases the efficiency, owing to the increase of the diffusion coefficient of the impurities towards the cathode.

The authors wish to thank Dr. R. Parsons for discussion and the following bodies for grants which have made this work possible : the Scholarships Committee of the University of London for a Postgraduate Studentship (B.E.C.) ; the Central Research Funds Committee of the University of London, and the Research Fund Committee of the Chemical Society of grants for apparatus used in this work.

Laboratories of Inorganic and Physical Chemistry,
Imperial College,
London, S.W.7.

THE CORROSION OF IRON COVERED BY A THIN FILM OF NEUTRAL SALT SOLUTION

BY W. I. WHITTON*

Received 11th April, 1950

The corrosion of iron covered by a thin film of neutral salt solution has been examined. In this paper, work with ½N NaCl solutions and oxygen atmosphere is described. Under these conditions unusual results are obtained, due to the combined effect of the high electrical conductivity of the liquid film and the unrestricted supply of oxygen reaching the metal surface. These results are dependent almost entirely on the corrosion properties of the metal itself. They indicate that acceleration of corrosion of the " oxygen absorption " type may be caused by the catalytic effect of certain impurities themselves, and not necessarily of oxide films, on the oxygen depolarization action. Several of the results obtained differ from those found for specimens corroding in a restricted supply of oxygen, and hence the need for careful differentiation between these two types of oxygen absorption corrosion is indicated. A simple apparatus which may be of use for industrial testing was developed for this work.

A study has been made of the corrosion of iron in oxygen atmospheres when covered by a thin film of neutral salt solution. Vertical specimens were used, and these were re-wetted once an hour by covering them completely with the liquid concerned. The corrosion rate was followed by measuring the oxygen consumption. These conditions produce a type of corrosion which has not been studied before. It will be referred to in this paper as the " liquid film " type. Palmaer [1] wetted vertical specimens initially and then did not rewet them. Kröhnke [2] and Arndt [3] studied specimens covered by a thin layer of condensed liquid. Both these conditions, however, produce corrosion differing from the liquid film type. The present conditions represent cases in practice where a surface is intermittently rewetted by a liquid, as by a swirling liquid, the waves of the sea or by showers of rain. In the past these conditions have been represented in the laboratory by the alternate wet and dry test; [4] this test is only of a semi-quantitative nature and does not permit a close examination of the corrosion action.

---

* Present address : Chemistry Dept., University College, Dundee.

[1] Palmaer, *Det 4de Nordiske Kjemi Kermøte, Oslo,* 1932, 183.

In this paper some of the characteristics of liquid film corrosion will be discussed. These have not been recognized before and for that reason the present theory of the corrosion of metals in neutral solutions is incomplete. Furthermore, there is evidence that cathodic impurities accelerate and direct corrosion under liquid film conditions. The evidence obtained may have a general application to all types of metallic corrosion in neutral salt solutions. Finally the use of the apparatus for laboratory and industrial testing is described.

Experimental

Apparatus and Procedure.—The complete apparatus is shown in Fig. 1. Essentially it consisted of two corrosion vessels C_1 and C_2 either of which could be connected to the gas burette B through the two-way tap T. The burette, thermostated by a water bath W, was connected to a levelling tube L and reservoir R. A gas reservoir *r* and outlet tube O were connected to the gas burette for supplying oxygen or oxygen-nitrogen mixtures. In the corrosion vessels the specimens were supported in Perspex stands S under glass hoods *h*. A photograph of a stand and specimens is shown in Fig. 2.

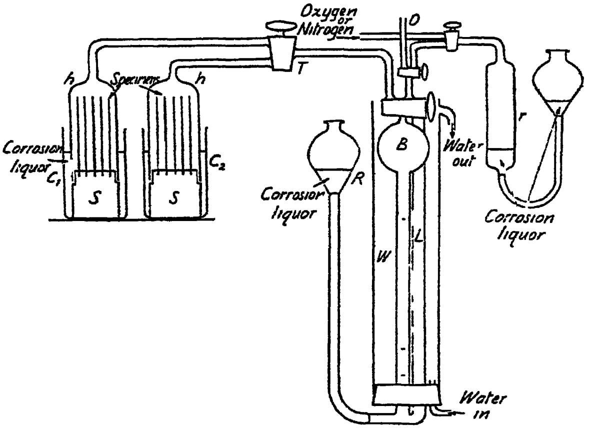

FIG. 1.—The apparatus.

To start an experiment the gas burette and levelling tube were filled with the corrosion liquor. The specimens were placed under the hoods and the corrosion vessel was filled with the liquor. All the air was drawn into the gas burette from the left-hand corrosion vessel and expelled through O. The required gas, usually oxygen, was drawn into the gas burette from the reservoir *r*. The volume was measured after drainage, and the gas was then passed to the corrosion vessel using R as the pump. Enough gas was supplied to ensure that the level of the corrosion liquor was always below the bottom of the specimens. The corrosion atmosphere under the hood was cut off from the outside atmosphere by a constant depth of corrosion liquor. Blank tests showed that no appreciable diffusion occurred into or out of the corrosion vessel in times considerably greater than those used in experiments. The right-hand corrosion vessel could be filled with the corrosion atmosphere in a similar manner. One hour after the specimens were first wet the volume of gas was re-read, by drawing it into the burette; it was replenished if necessary, and returned to the corrosion vessel. The specimens were therefore re-wet each hour. The liquid drained down the surface of the specimens, but it was found that the decrease in film thickness during one hour was not sufficient to affect the rate of corrosion. Longer periods without re-wetting of the specimens, however, did decrease this rate. The original film thickness cannot be maintained by a moist atmosphere as suggested by Palmaer.[1] This almost certainly accounts for the decrease in rate found during the early hours of Palmaer's experiments. It was not a retardation by corrosion product formation as he suggested—for in the present experiments even when large heaps of corrosion product covered the surface (see Fig. 2) the corrosion rate still remained constant.

---

[2] Kröhnke, *Stahl Eisen*, 1910, **30**, 1128.

[3] Arndt, *Chem. Zeit.*, 1910, **425-6**, 1078.

[4] *Proc. Amer. Soc. Test. Mat.*, 1924, **24** (I), 281.

To determine whether hydrogen was evolved during corrosion, the atmosphere was periodically withdrawn from the vessel containing the corroding specimens and passed into the other. Here it was submitted to the action of a heated platinum wire. The volume before and after this treatment was measured. Hydrogen was never detected as a product of corrosion.

A thermostat was not used for the whole apparatus, for although desirable in many ways, the construction was impracticable. Instead the apparatus was placed in a central room with a small weekly variation in temperature. Temperature coefficients were determined experimentally and applied to results where necessary.

Criterion for Corrosion.—The corrosion products were brown, so some oxygen was used in oxidizing ferrous iron to ferric iron

$$2FeO + [O] \rightarrow Fe_2O_3.$$

By analyzing the corrosion products and assuming the cathodic action to be

$$2e + [O] + H_2O = 2OH',$$

and the anodic action

$$Fe = Fe^{-+} + 2e,$$

it was found that of the total oxygen consumed, about 29 % was always used in oxidizing ferrous iron to ferric iron. It was assumed that this fraction was a constant and therefore the total consumption of oxygen per hour corrected to a definite temperature and pressure was considered to represent the corrosion rate. This is only a relative rate, and is used simply as a measure of the relative amounts of corrosion of different specimens under the same conditions.

In these rate measurements time was always measured continuously. No allowance was made for the short time the specimens were completely covered by liquid during the re-wetting process. During this time corrosion of the specimens proceeded at a similar rate to that when the specimens were covered by a thin film only, since the oxygen dissolved in the liquid was sufficient to maintain the rate of corrosion for this time interval.

Preparation of Materials:—(*a*) SPECIMENS.—Specimens in the form of thin sheets were used to give a maximum surface area for the space available. Large surface areas were used to minimize the effect of variations in the surface structure and to simplify the technique. Usually five specimens of the same metal 3 cm. × 9 cm. × 0·1 cm.) were used at once giving a total surface area of over 270 sq. cm.

In the present work four different steels were used (see Table I). The large sheets supplied (usually 18 gauge) were first cut approximately to shape in a guillotine. The specimens so obtained were surface-ground to accurate dimensions. For all grinding a silicon carbide wheel of medium grit size (No. 3746I) was used. Oil and grease were removed from the specimens with soap and water and the dried specimens were kept in a desiccator.

These surface ground specimens corroded slowly at first due to the presence of a protective oxide film ($Fe_2O_3 . H_2O$ and Fe_3O_4 or γ-Fe_2O_3). As this film was broken down the rate increased, and after a considerable time became steady. It was found, however, that this film could be removed by treating the ground specimens in hot 2N HCl at 75° C for 10 min. and washing in tap water for a further 10 min. Electron diffraction photographs showed that specimens after this treatment were almost free from oxide film. These specimens corroded at the steady rate eventually reached by the ground specimens,

TABLE I

Designation	Type of Steel	Composition (%)							
		C	Ni	Cr	Si	Mn	Cu	Sn	Pb
Steel VII	Enamelling iron .	0·02	0·03	0·015	0·005	0·16	0·09	*T*	*T*
Steel VIII	Spring steel	0·59	0·11	0·08	0·13	0·65	0·09	*T*	—
Steel IX .	Mild steel	0·07	0·02	0·015	0·06	0·33	0·05	—	—
Steel X .	Mild steel	0·11	0·05	0·03	0·07	0·57	0·09	*T*	—

T = trace.

not treated in acid. Furthermore, if specimens were cleaned in this manner, the steady rate was reproduced in successive experiments, provided corrosion had not continued so long that the surface was deeply pitted. In this case increase of surface area gave a corresponding increase of rate. In this paper the treatment with hot dilute HCl will be referred to as the " standard acid treatment ". Specimens were always subjected to this treatment before an experiment unless otherwise stated.

(*b*) CORROSION LIQUOR.—One set of experiments was carried out with NaCl solutions of varying concentration. In all other experiments the corrosion liquor was ½N NaCl. Distilled water was always used in preparing the solutions.

Results

A preliminary investigation of the corrosion process was carried out with an atmosphere of air. The results have a special significance and will be described elsewhere. Pure oxygen atmospheres were found to be more satisfactory for examining relative rates of corrosion and the results so obtained will now be described.

It was found that fairly reproducible results could be obtained in short times. Experiments were carried out in duplicate using firstly five specimens, secondly four specimens, and thirdly three specimens of each of the Steels VIIA and VIIB. (The A and B designations indicate specimens cut from different sheets or different areas of the same steel.) Each experiment lasted 10 hr. The results are shown in Table II. The maximum deviation from the mean of any one rate was 2·9 %.

TABLE II.—RATE OF CORROSION (ml. of oxygen consumed per hr.)

	5 Specimens	4 Specimens	3 Specimens
Steel VIIA . . .	6·91	5·76	3·98
	6·70	5·78	3·94
Steel VIIB . . .	6·69	5·77	3·88
	7·04	5·58	3·89
Mean	6·84	5·72	3·92
Rate per sq. cm. . . .	0·022	0·023	0·021

These results therefore show good reproducibility for short time experiments. This reproducibility was obtained in all results discussed in this paper. These results further showed that under these conditions the rate of corrosion is directly proportional to the surface area of the specimens.

As initial rates of corrosion are often misleading it was necessary to examine some rates over a much greater period of time. The corrosion of five specimens of Steel VIIA and five specimens of Steel VIIB was followed continuously for 60 hr. The rate gradually increased during the first 15 hr., slowed down slightly during the next 20 hr., and then became constant (see Fig. 3). The average rates per hour during various stages of the experiment are shown in Table III.

It is seen that even the rates obtained during the first 5 hr. compared favourably with the average rate over the whole 60 hr. It was evident from these results, however, that rates should only be compared over similar periods of the experiment.

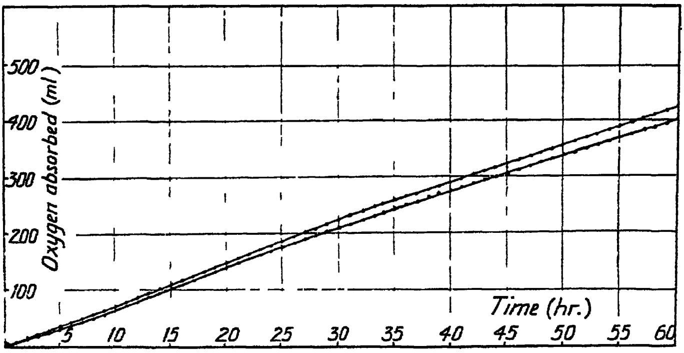

FIG. 3.—60-hr. experiments with Steel VII.

During these experiments the anodic points did not change their position even when corrosion deposits as high as 1 mm. (see Fig. 2) had formed over them, for when the corrosion products were removed, the areas beneath them were deeply pitted and the rest of the surface was relatively untouched. Thus, there was no redistribution of corrosion centres due to the presence of corrosion products as is sometimes found for fully immersed specimens.[5, 6]

TABLE III.—AVERAGE RATE (ml. of oxygen consumed/hr.)

Period	Steel VIIA	Steel VIIB
First 5 hr.	6·23	6·56
First 10 hr.	6·70	7·04
Last 30 hr	6·32	6·72
Total 60 hr.	6·73	7·11

The slight changes of shape of the curve during the whole 60 hr. appear to be due to the manner in which the heaps of corrosion products formed. These heaps first spread outwards giving an increase of rate due to differential aeration of the anodic and cathodic areas. The slight fall-off in rate after 20 hr. probably occurred as these heaps extended over some of the initial cathodic areas. The rate then became fairly constant, for the heaps finally tended to build upwards instead of outwards giving a crater form (see Fig. 2).

Variables and their Effects on Corrosion Rate:—(*a*) PARTIAL PRESSURE OF OXYGEN.—The corrosion rate of specimens in oxygen was less than 4·8 times the rate in air, indicating that the corrosion rate was not proportional to the partial pressure of oxygen. The rate of corrosion of Steel X was therefore investigated at different partial pressures. The partial pressure was controlled by placing a definite amount of nitrogen in the apparatus and replenishing the oxygen supply each hour. The results are shown in Fig. 4 (*a*). Each point is the mean of two experiments. The rate is proportional to the square root of the partial pressure of oxygen up to 12 cm. (see Fig. 4(*b*)). Above this pressure the rate increases very little with increase of pressure.

The ratio (rate in oxygen rate in air) was 1·4 for these specimens. Similarly, for Steels VII and VIII it was found to be 1·8 and 1·7 respectively. This result contrasts with that found for fully immersed specimens[7] and for partially immersed specimens.[8] In both these cases the rate is proportional to the oxygen

---

[5] Wormwell, *J. Iron Steel Inst.*, 1946, **154** (2), 219.

[6] Bengough, Lee and Wormwell, *Proc. Roy. Soc. A*, 1932, **134**, 308.

[7] Walker, Cederholm and Bent, *J. Amer. Chem. Soc.*, 1907, **29**, 1251.

[8] Mears, *Proc. Roy. Soc. A*, 1934, **146**, 162.

partial pressure (ratio = 4·8) Mears however found a curve resembling the present one using drops of salt solution on iron [9]

The corrosion rate under liquid film conditions with ½N NaCl and oxygen at atmospheric pressure is therefore not under oxygen control as it is with fully immersed and partially immersed specimens It appears that even with oxygen pressures well below 76 cm the cathodic areas receive as much oxygen as they can handle for as will be seen later although increase of oxygen pressure does not appreciably change the rate a change of the impurities or state of the impurities can do so

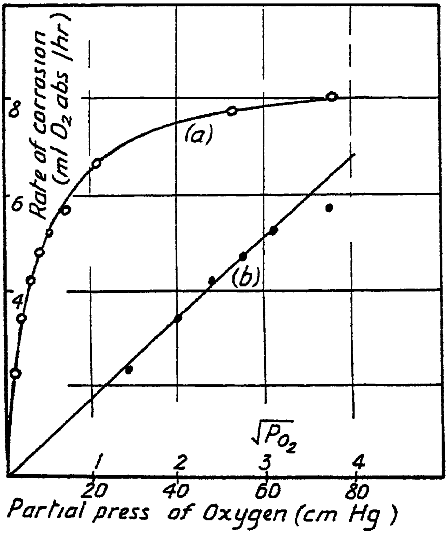

FIG 4—Relation between rate of corrosion and (a) partial pressure of oxygen, (b) the square-root of the partial pressure of oxygen

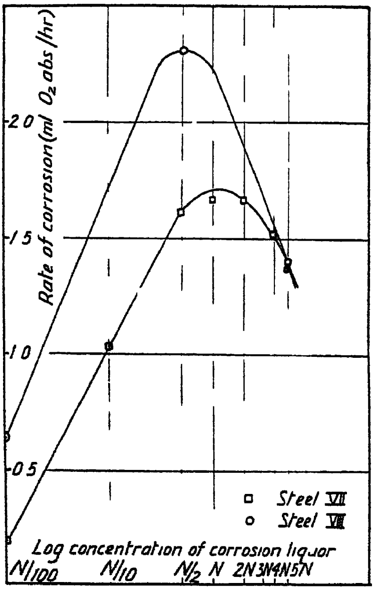

FIG 5—Effect of concentration of corrosion liquor on the corrosion rate

(b) COMPOSITION OF THE CORROSION LIQUOR—A set of experiments was carried out with Steels VII and VIII with NaCl solutions of concentrations varying from N/100 to 5N Four experiments were carried out for each metal at each concentration and the mean values for a single specimen of each steel are shown in Fig 5 It is seen that in dilute solutions the rate was slow but increased to a maximum value as the concentration increased and at higher concentrations decreased again The distribution of pitted areas varied In dilute solutions there were many very small pit marks As the concentration increased the area covered by each became larger so that in concentrated solutions there were fewer but bigger areas of attack Furthermore the colour of the products changed being very brown (ferric state) in dilute solutions and green to black (ferrous state) in the most concentrated solutions The only difference in behaviour between specimens VII and VIII was that in N/100 solutions the corrosion pits on specimens VII were definitely concentrated near the edges of the specimens whereas this was not the case with specimens VIII This is the only time any concentration of pits at the edges which are known to be strained, occurred in the present work This will be discussed later

These results are similar to those obtained for fully immersed specimens [6, 10] and for partially immersed specimens [11] They are explained by the increase of conductivity and decrease of oxygen solubility with increase of concentration Thus the conductivity increases by a factor of nearly 100 for an increase of concentration from N/100 to N, and the oxygen solubility is halved for an increase of concentration from N to 3N Qualitatively there is a continuous increase in

---

[9] Mears, *Trans Faraday Soc*, 1935 31, 527

[10] Bengough, Lee and Wormwell, *Proc Roy Soc A*, 1931, 131, 494.

[11] Evans and Hoar, *ibid*, 1932, 137, 343

Fig. [illegible] — Specimens of Steel VII at the end of [illegible]0 hr

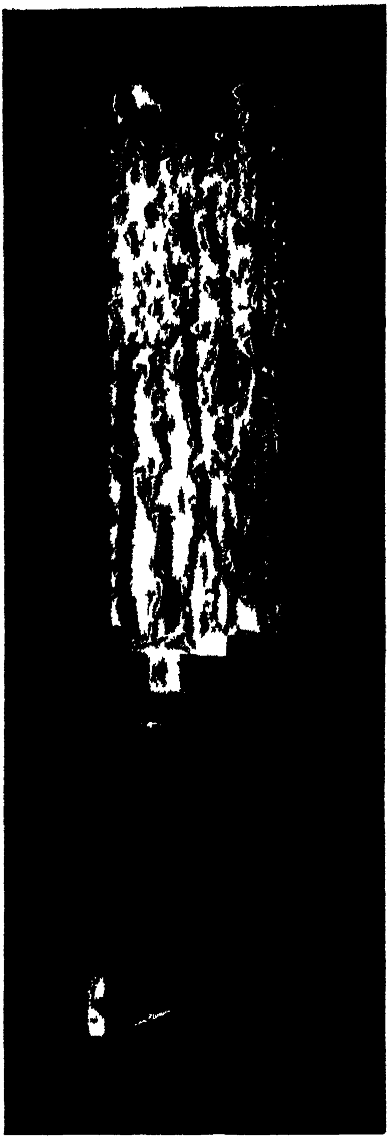

Fig. 2.—*Negative* Specimens of Steel VII at the end of 60 hr

[*To face p.* 962]

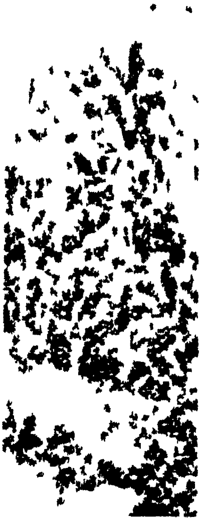

Fig 6(a) —Steel VII

Fig 6(b) —Steel VIII

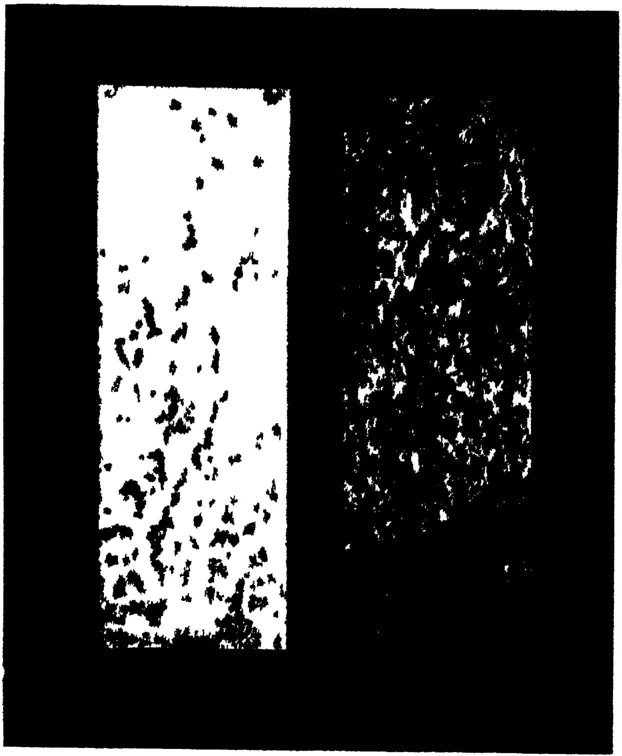

Fig 6(b) —*Negative* Steel VIII. Fig 6(a) —Steel VII the size of pitted area with increase of concentration, for with increased conductivity corrosion currents can flow over greater distances, i e between cathodic and anodic areas further apart Similarly the colour of the corrosion products becomes blacker and greener as less oxygen reaches them in more concentrated solutions Evidently the decrease of oxygen supply has little effect below concentrations of 1N, and the rate of corrosion increases with increase of conductivity. Above this concentration, however, the decreased oxygen supply becomes important and the rate of corrosion is decreased Furthermore, it can be seen that the rate of corrosion of Steel VIII approaches that of Steel VII This indicates that in solutions of higher concentration this liquid film type of corrosion must come under oxygen control

(*c*) VARIATION OF THE PROPERTIES OF THE METAL SPECIMEN —The corrosion of specimens of varying purity and subjected to various heat treatments was examined in oxygen at atmospheric pressure and a corrosion liquor of ½N NaCl The experiments described above, with varying partial pressure of oxygen and varying concentration of corrosion liquor, have indicated that specimens corroding under these conditions receive a free supply of oxygen at the metal surface

(1) VARIATION OF PURITY OF THE SPECIMENS —The general effect of impurities in iron was investigated by studying the behaviour of Steels VII, VIII, IX and X (see Table I) under the same conditions All specimens were initially surface-ground in the usual manner and grease was removed In the first series the freshly ground specimens were used without treatment For the second and third series the specimens from series 1 and 2 respectively were cleaned free from corrosion products with a bristle brush only In the fourth and fifth series specimens from series 3 and 4 respectively were subjected to the standard acid treatment, and in the sixth series the specimens were reground, given standard acid treatment and then tested Each series was carried out in duplicate for a period of 5 hr The mean rates for four specimens of each steel are shown in Table IV

TABLE IV —RATE OF CORROSION (ml O_2 consumed/hr)

	Steel VII	Steel VIII	Steel IX	Steel X
eries 1 .	3·61	4·83	5·32	4·80
ries 2 .	4·85	6·70	6·22	5·88
ies 3	4·88	7·20	6·79	5·57
ries 4	5·65	10·85	7·48	6·48
ries 5	5·59	11·49	7·65	6·45
eries 6	5·70	9·20	7·60	6·86

In the first three series the rates of corrosion increased for each type of steel This increase was evidently due to the slow breakdown of the oxide film known to be present on freshly ground specimens The standard acid treatment before series 4 removed the remaining portion of this film in each case, for when the acid treatment was repeated (series 5) only Steel VIII showed a further increase in corrosion rate This was due to an increase of the surface area of the specimens brought about by a much deeper pitting on these specimens than on any of the others Evidence for this was given by the series 6 results Only with Steel VIII was the rate slower after regrinding

There is no doubt from these results that different types of iron corrode at widely varying rates under these liquid film conditions Furthermore, the oxide film initially present on the surface of the specimens certainly retards the corrosion rate, but it does not change the order of the rates for the four types of steel Thus Steel VIII corroded at the fastest rate and Steel VII at the slowest rate in all six series There was one exception to this in series 1 where Steel IX corroded faster than Steel VIII.

The distribution of corrosion throughout the series was also different for the different metals The greatest variation was between the distribution of corrosion on specimens of Steels VII (the lowest C content) and VIII (spring steel) during the first three series On Steel VIII the anodic and cathodic areas remained in the same positions throughout. On Steel VII completely new pit marks formed in each new series At the end of series 3 Steel VII specimens had pit marks on nearly every part of the surface, whereas Steel VIII specimens had some very deep pit marks and the rest of the surface was almost untouched. This is shown in Fig. 6. Fig. 6*a* shows a typical specimen of Steel VII and Fig. 6*b* one of Steel VIII, photographed at the end of series 3 after the removal of corrosion products with a brush. Although nearly twice as much corrosion had occurred with Steel VIII during the three series, the number of pit marks on these specimens was far less than the number on Steel VII. As the permanent areas left on Steel VIII specimens must have been the cathodic areas it appears that these were directing corrosion, and furthermore these cathodic points must have been more cathodic than any new part of the surface uncovered as the pits deepened. With the purer steel, however, it appears that no such strong cathodic areas existed and as new surface was uncovered new cathodic and anodic points formed. Steels IX and X behaved more like Steel VII than Steel VIII.

Thus the impurities affect the distribution and rate of corrosion. It is interesting that the impurities in Steel VIII which order the distribution of corrosion to the greatest extent also have the greatest accelerating effect on the corrosion rate.

(*ii*) HEAT TREATMENT OF THE SPRING STEEL.—Specimens of spring steel ($C = 0{\cdot}59\ \%$) were hardened and tempered and the corrosion rates were measured of the martensite and tempered steels so formed. The work of Chappel[12] indicated that heat treatment of the metal had no effect on the rate of corrosion in neutral solutions. This worker used, however, fully immersed specimens. It was of interest to examine the behaviour of heat-treated specimens in neutral solutions under the liquid film conditions, where an unrestricted supply of oxygen reached the specimens.

Two sets of three specimens each were prepared for the measurement of the rate of corrosion of :

1. The normal steel.
2. Martensitic steel.
3. Steel tempered to 240° C.
4. Steel tempered to 450° C.
5. Steel tempered to 660° C.

The martensite was prepared by quenching the steel in iced water from a temperature of 900° C and the tempered steels were prepared from martensitic steel by heating at the appropriate temperature for 2 hr. All quenching and tempering processes were checked with Vickers hardness tests and photomicrographs. Two 5-hr. experiments were carried out with each set of specimens after standard acid treatment and the mean values of the four rates found for each state of the metal are shown in Fig. 7(*a*).

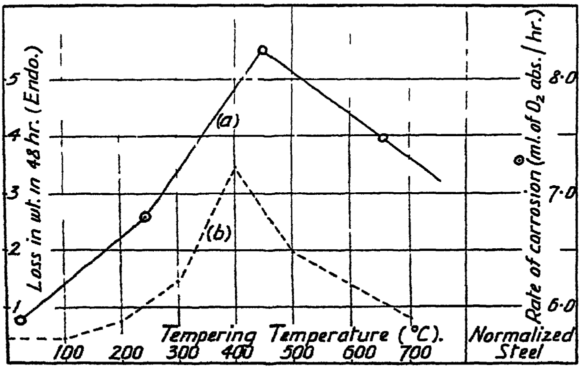

FIG. 7.—Effect of heat treatment of a high carbon steel on its rate of corrosion.
(*a*) Results obtained in present work in neutral solution.
(*b*) Results obtained by Endo in 1 % sulphuric acid.

The differences in rate observed clearly indicate that the martensite corroded at the slowest rate, the steel tempered to 450° C at the fastest rate and slowly cooled steel at a medium rate. The results resemble those obtained by Endo[13] for the corrosion of heat-treated steel in dilute acid solutions. Endo's results are shown dotted in Fig. 7(*b*). The present results can be interpreted in a similar fashion to that used by Endo. That is, the martensite is particularly homogeneous (being a solid solution), and therefore fewer variations of potential occur over the surface. A maximum heterogeneity occurs in steel tempered to about 450°. The coagulation of cementite when steel is tempered above this temperature must decrease the number of possible corrosion cells. Hoar and Havenhand, working with half-immersed specimens in citric acid and citrate buffers, also found that the presence of massive cementite in the metal may accelerate corrosion by assisting the cathodic process in acid solutions.[14]

---

[12] Chappell, *J. Iron Steel Inst.*, 1912, **85**, 270.
[13] Endo, *Sci. Reports Tohoku Univ.*, 1928, **17**, 1245.

It is clear from the present results that provided the supply of oxygen is not the controlling factor, heat treatment of carbon steels definitely affects the rate of corrosion in neutral solutions. Furthermore, the presence of massive cementite in specimens accelerates the corrosion in neutral solutions just as it does in acid solutions. As this massive cementite acts cathodically, it must be the cathodic process which is accelerated in each case.

Discussion

The Liquid-film Type of Corrosion.—The results described indicate that the corrosion of iron specimens when covered by a thin film of $\frac{1}{2}$N NaCl solution exhibits certain special characteristics. These are:

(i) Corrosion is entirely of the oxygen absorption type; there is no hydrogen evolution.

(ii) The rate is not proportional to the oxygen partial pressure.

(iii) Impurities in the metal have a very marked effect on the rate and distribution of corrosion.

(iv) Heat treatment of a high carbon steel affects its corrosion rate.

The theory of the corrosion of metals in neutral solutions has mainly been developed from results obtained with fully immersed and partially immersed specimens. Small differences of rate have been noticed with specimens of varying purity corroding in the partially immersed position, but apart from this none of the four characteristics described above are found. This difference of behaviour must be due to the free supply of oxygen reaching the metal surface under liquid film conditions, as compared with the controlled supply reaching specimens in the other two conditions. Differentiation must be made, therefore, between corrosion in neutral solutions which is under oxygen control and that which is not.

There is evidence in the literature that impurities have a very definite effect on the rate when there is not oxygen control. Thus Mears, working with specimens covered with drops,[9] and Evans and Lewis working with specimens shaken in tubes containing aerated liquid[15] showed that impurities change the corrosion rate. A significant set of experiments was carried out by the Institute of Civil Engineers.[16] They placed 14 different types of steel in each of 3 exposure conditions: (i) well above high-water level, (ii) at half-tide level, (iii) well below water level. The difference between the least and most corroded materials was greatest in the atmospheric tests and smallest in the complete immersion tests. The results of this set of experiments clearly indicate the difference between corrosion of specimens freely supplied with oxygen (condition (i)) and specimens corroding under oxygen control (condition (iii)). It is evident that the conditions studied in the present apparatus represent certain conditions found in practice more closely than do other laboratory tests that have been relied on in the past. Furthermore, the corrosion of metal surfaces covered by a thin film of liquid has many characteristics of its own. Some of these have been studied here, namely those connected with the corrosion of iron in $\frac{1}{2}$N NaCl solutions. The results obtained with solutions of varying concentration, however, indicate that the characteristics must be different in more concentrated solutions due to a restriction of the supply of oxygen to the metal surface. It is quite probable that these conditions then approach those of complete immersion

---

[14] Hoar and Havenhand, *J. Iron Steel Inst.*, 1936, **133**, 239.

[15] Evans and Lewis, *J. Soc. Chem. Ind.*, 1934, **53**, 25T.

[16] *2nd Report Corrosion Comm., Iron and Steel Inst.*, 1934, 148.

Further investigation of this liquid film type of corrosion using other metals and other solutions is required before a complete description of its characteristics can be given.

Role of Impurities in Corrosion in Neutral Solutions.—The present results throw some light on the role of impurities in corrosion in neutral solutions. The results with specimens VIII in the normal and heat-treated states indicate that it is the impurities which act cathodically that have the power to accelerate corrosion. The presence of an oxide film on a cathodic area does not seem to be as important as Brennert inferred.[17] Thus, the results given in Table IV show that the presence of an oxide film retards the rates but it does not change the relative effectiveness of the various impurities which accelerate corrosion. Furthermore, it was found that massive cementite in tempered steel accelerates the corrosion rate and this certainly would not be covered by an oxide film. Only in one instance was there any evidence that anodic areas were directing corrosion. That was during the corrosion of Steel VII in very dilute solutions when pits were concentrated about the edges of the specimens. Even under these conditions there seemed to be no concentration of pits on Steel VIII.

The observation that certain impurities were not equally effective in accelerating corrosion in acid and neutral solutions, led corrosion workers to consider the cathodic points active in the hydrogen evolution type of corrosion to be quite different from those active in the oxygen depolarization (oxygen absorption) type. Such a view is unnecessary. It is not likely that the catalytic effect of impurities would be the same in all cases because of the difference in mechanism of the oxygen depolarization and hydrogen evolution actions. Moreover, oxide films must often be present on cathodic areas in neutral solutions but not in acid solutions. The principal function of all cathodic areas is, however, to supply electrons, regardless of what process is absorbing them. It seems probable, therefore, that the catalytic effect of the cathodic impurities on the two actions might be similar in certain cases. This, in fact, is what has been found for heat-treated specimens where evidently the presence of massive cementite accelerates the corrosion rate in both types of attack.

The present results indicate, therefore, that certain areas on a metal surface are capable of accelerating the oxygen depolarization action, and these may or may not be covered with an oxide film. No systematic investigation of the acceleration of the depolarization action has been made. In 1944, Tomashov [18] tried to do this, but unfortunately used a method in which the specimens were under oxygen control. There is obvious need to carry out such an investigation with specimens receiving a free supply of oxygen. This would probably be possible by potential measurements on specimens covered with a thin film of liquid as in the present apparatus. It is envisaged that the electrode potential of a number of metals, containing various amounts of different impurities, could be found relative to a standard electrode of pure iron. Such results should show the relation between the oxygen depolarization action and the hydrogen evolution action and might throw light on the mechanism of both. Furthermore, the mechanism of hydrogen overvoltage might be elucidated by such results.

In the hydrogen evolution type of corrosion the overvoltage of the impurities is of importance in determining their effectiveness in accelerating corrosion. If the present explanation of the part played by impurities is correct, a more systematic tabulation of the relative effect of impurities in neutral solutions may also be possible.

---

[17] Brennert, *Trans. Amer. Electrochem. Soc.*, 1939, **76**, 231.
[18] Tomashov, *A.C.S. Abstr.*, 1944, **38**, 4555.

The Present Apparatus and its Uses.—The apparatus described has been found of use in indicating some of the characteristics of the liquid film type of corrosion. It has been especially useful for laboratory experiments because of the reproducibility of results obtained in short times. This has mainly been possible through the use of large surface areas, and also because of the uniform nature of the liquid film type of corrosion.

It may be thought that this type of corrosion should be very sensitive to film thickness for Bengough [10] showed that with liquid depths of less than 1·5 cm. the rate of corrosion is greatly affected by changes of the depth of immersion of specimens (see Fig. 8(*c*)). For this reason workers have not tried to use thin films for accelerated tests. The present results suggest, however, that if Bengough's curve could be extended for depths of immersion below 1 mm. that the curve would take on the shape shown in Fig. 8 (*a*) and (*b*). This is supported by the work of Vernon [19] who found that increase of the relative humidity above 80 % increased the corrosion rate due to the increased moisture forming on the surface. The increase was less than linear. This result would be represented by Fig. 8(*a*). Such a curve might be expected since decrease in thickness of the film must ultimately lead to increased electrical resistance in the external circuit and therefore a decrease of corrosion. This is supported by Palmaer's results.[1] It appears that the thickness of the liquid film left on the specimens in the present apparatus, when they are re-wet each hour, must correspond to a liquid depth in Fig. 8(*b*). That is, for a small range of depths the corrosion rate is fairly constant.

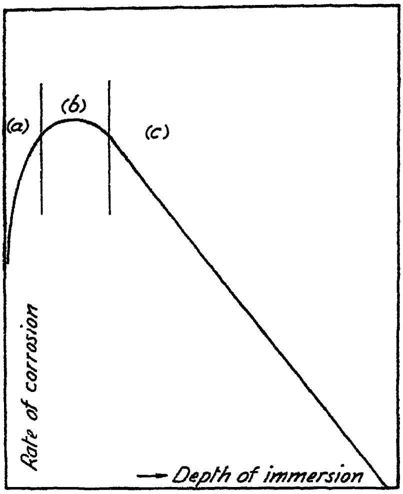

Fig. 8.—Proposed extension of Bengough's curve, of the relation between rate of corrosion and depth of immersion, at depths below 1 mm. Part (*c*) is a direct extension of Bengough's curve.

If the above theory of impurities acting as cathodic catalysts for the oxygen depolarization action is correct, the apparatus should not only be of use in examining the fundamental characteristics of the liquid film type of corrosion, but also in predicting the effect of impurities in all types of corrosion of the oxygen absorption type where there is a free supply of oxygen.

Furthermore, it is possible that the apparatus may have a use for industrial corrosion tests because reproducible results can be obtained in such short times. The results certainly should be applicable to corrosion of a metal periodically re-wetted either by the waves of the sea, by rain or by swirling liquids. In this respect it may be useful not only for examining clean metal surfaces, but also for testing the efficiency of various protective coatings.

I wish to thank Dr. A. L. G. Rees of C.S.I.R.O., Melbourne, for doing the electron diffraction work mentioned; Miss M. Gardiner of D.R.L.,

---

[19] Vernon, *Trans. Faraday Soc.*, 1935, **31**, 1628.

Melbourne, for analysing the specimens, and Mr. G. A. Ampt, University of Melbourne, and Prof. D. H. Everett, University College, Dundee, for very helpful advice. I would also like to acknowledge the valuable assistance of the late Assoc. Prof. E. Heymann of the University of Melbourne.

Chemistry Department,
University of Melbourne.

AN ELECTRON MICROSCOPE STUDY OF CRYSTAL SURFACES

BY J. AMES, T. L. COTTRELL AND AVIS M. D. SAMPSON

Received 28th March, 1950

A method of preparing crystal surface replicas for examination in the electron microscope is described. The majority of crystals studied show evidence of layer growth. When crystals are grown from solutions containing habit modificants, the layers become thicker and more numerous. Secondary surface phenomena include oriented ripples and ridges. Some possible modes of crystal growth are discussed in the light of the observations made.

An examination of strained [1] and habit modified [2] ammonium nitrate crystals carried out recently in this laboratory suggested that the electron microscope might find a useful application in the study of crystal growth and crystal habit modification generally. The electron microscope has two great advantages over the optical microscope in its superior resolving power and depth of field. The latter is especially useful in work of this type since the comparatively deep structures which occur on some crystal faces can be brought entirely into focus with little sacrifice in resolution, as, for example, in Fig. 4. Since only dry and very thin specimens can be examined in the electron microscope, however, the processes of crystal growth from solution cannot be observed directly. Crystals must first be removed from solution, dried, and subjected to some form of replica technique before an examination of the surface can be made. The possibility of effects not connected with normal growth contributing to surface structure is therefore present. In view of this, and the unfamiliar nature of many of the surface phenomena observed, attention was mainly directed towards aspects of crystal growth already established by means of the optical microscope. The observations of Bunn and Emmett [3] on layer growth were found to be particularly applicable, since layers or steps were visible on most ammonium nitrate crystals examined. These appeared to give a suitable basis for comparison between the optical and electron microscope techniques, and several crystals for which optical data were available were investigated for evidence of layers. The work here reported deals mainly with the appearance and behaviour of the surface layers under varying conditions of growth. Some aspects of secondary surface phenomena are also discussed.

---

[1] Fordham, *Faraday Soc. Discussions*, 1949, 5, 117.
[2] Butchart and Whetstone, *ibid.*, 1949, 5, 254.
[3] Bunn and Emmett, *ibid.*, 1949, 5, 119.

PLATE I

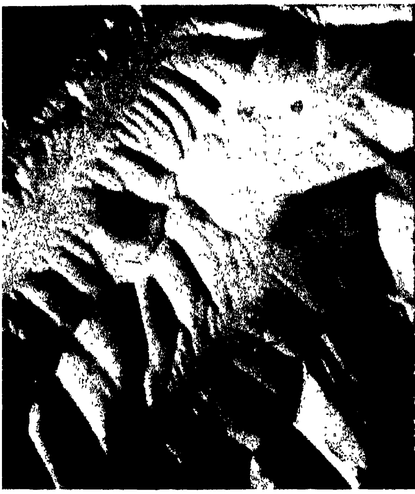

FIG. 1.—Ammonium sulphate. Chromium replica × 6000.

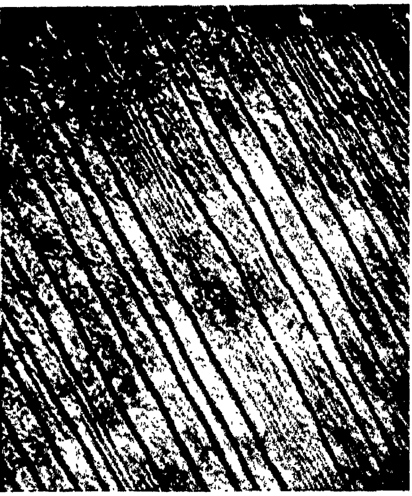

FIG. 2.—Ammonium nitrate (110 face). Gold-shadowed formvar replica × 10,500.

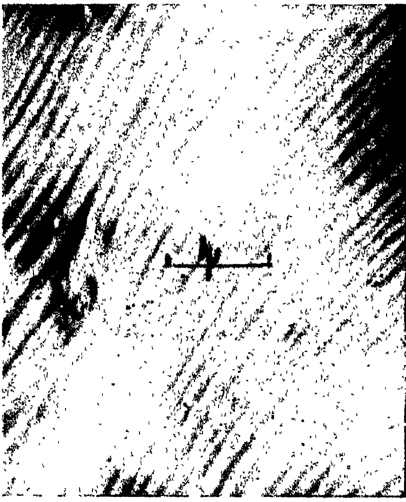

FIG. 3.—Acid magenta modified ammonium nitrate (100 face). Chromium replica × 16,000.

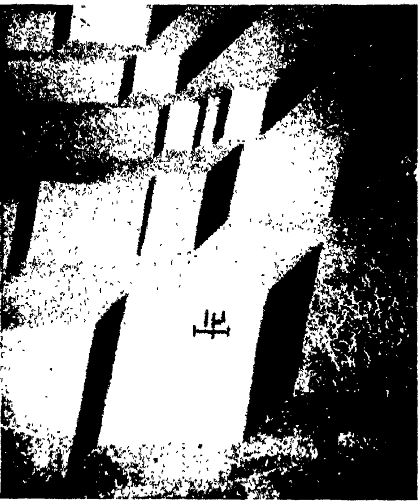

FIG. 4.—Acid magenta modified ammonium nitrate (high index face). Gold replica × 5500.

PLATE II

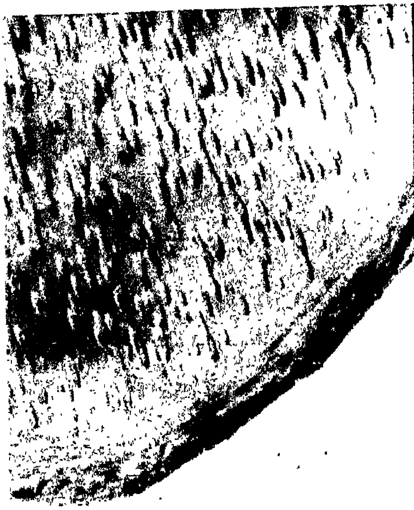

FIG. 5.—Ammonium sulphate (010 face). Chromium replica × 7500.

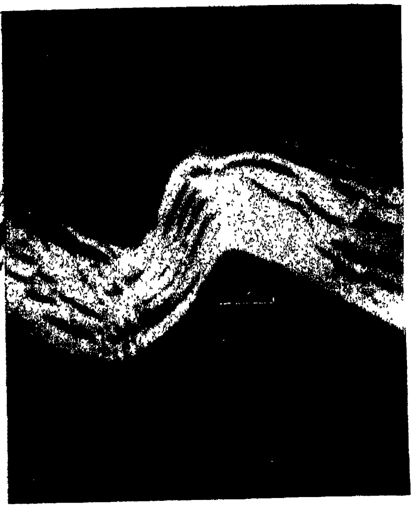

FIG. 6.—Magnesium sulphate. Formvar replica × 9000.

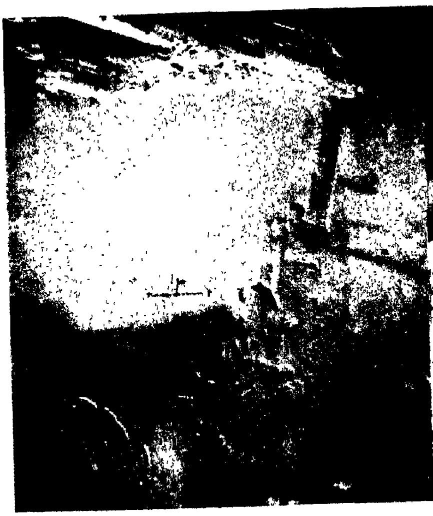

FIG. 7.—Potassium alum modified by Bismarck Brown (100 face). Chromium replica × 9500.

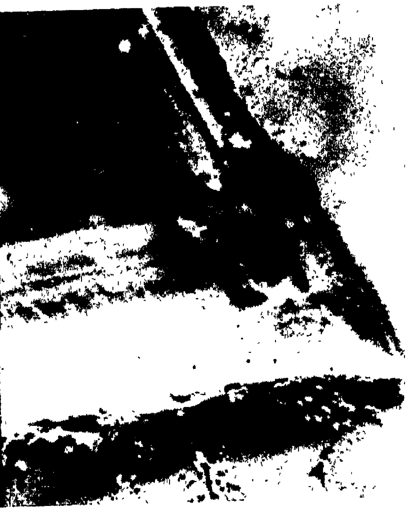

FIG. 8.—Potassium alum modified by Chlorazol Sky Blue (111 face). Chromium replica × 9000.

Plate III

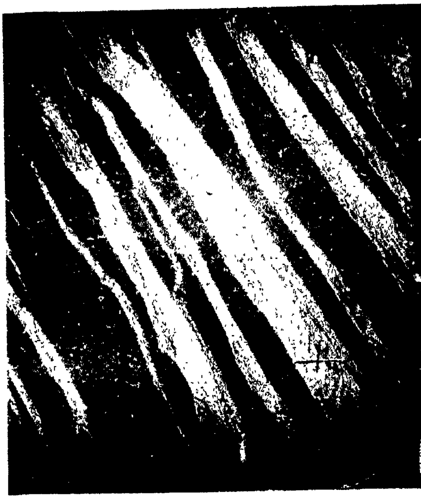

Fig. 9.—Potassium sulphate (111 face). Gold-palladium replica × 7500.

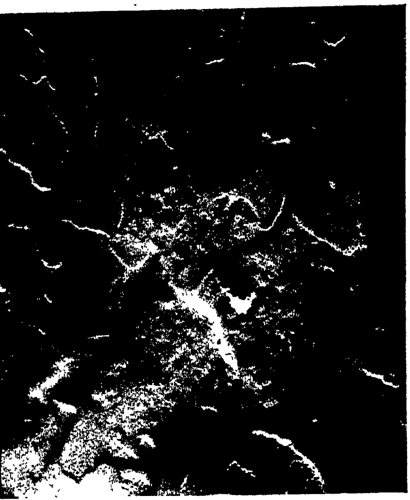

Fig. 10.—Sodium nitrate grown in 2 % solution of lead nitrate. Gold-palladium replica × 6000

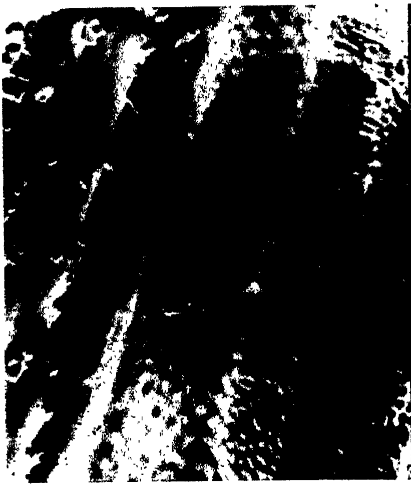

Fig. 11.—Sodium nitrate grown in 2 % solution of lead nitrate. Gold-palladium replica × 6500.

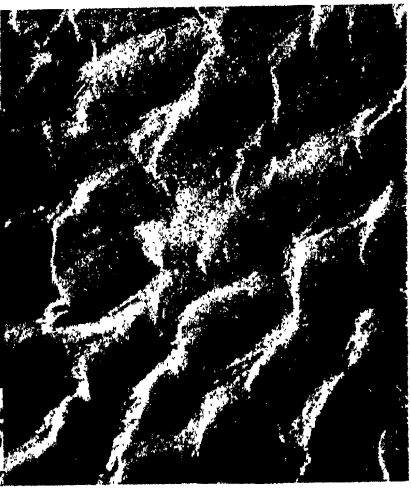

Fig. 12.—Sand ripples.

Experimental

Crystals were prepared by slow evaporation of saturated solutions at 26° C. Crystals having faces not less than 1 mm. square were desirable for convenient handling of the specimen. In general, crystals 5 to 10 mm. long were used, and these were usually grown in 1 to 2 days. Suitable crystals were removed from the mother liquor, dried rapidly on filter paper and mounted on microscope slides. Replicas of selected faces were prepared by an all-metal replica technique similar to that described by Williams and Wyckoff,[4] but requiring only a single evaporation. 20-30 mg. of the replica metal (gold, chromium or 60/40 gold-palladium alloy) were evaporated *in vacuo* with the specimen 8 cm. distant at an angle of 30° to the specimen plane. On lowering the coated crystal just below a water surface a coherent metal film floated off. Selected areas were then detached and mounted for examination in the electron microscope. No backing film was found necessary. Replicas obtained by this technique are positive replicas : in Fig. 5, 8 and 11 the prints have been reversed so that the " shadows " caused by surface projections appear dark.

Metal replicas obtained in this way can be expected to reproduce faithfully the contours of the crystal surface. The replica can be removed from the specimen without strain, and heating effects in the microscope are characterized by cracking and are easily recognizable. Where artefacts occur, they are most probably introduced into the crystal surface itself during the replica preparation. The following are each capable of contributing to the surface structure ; incomplete drying of the crystal, recrystallization of occluded mother liquor, heating due to the metal evaporation, mechanical distortion, and incomplete washing of the metal replica. These possibilities were investigated as far as possible. Thin films of saturated solution were allowed to crystallize rapidly on microscope slides, and surface replicas were prepared of the resulting material. An example of the type of result obtained is shown in Fig. 1. Although the method does not reproduce exactly the conditions on the surface of a partially dried crystal, it is nevertheless evident that from these conditions a variety of complex surface phenomena can arise. Heating effects due to the replica technique were not considered important, as apparently structureless replicas of many crystal faces could be obtained ; this was so even for ammonium nitrate IV, which undergoes considerable structural change at 32° C in its transition to ammonium nitrate III. Stained crystal surfaces have been investigated and reported upon previously.[1] Prolonged washing of replicas appears to be unnecessary, as they can usually be detached quite cleanly from the crystal. Occasionally, however, thin layers of material adhere to the replica, probably held in place by the surface contours. This results in the appearance of darker areas in the image, in which the surface contours are visible but with reduced contrast. The micrographs illustrating this work were obtained on a Metropolitan-Vickers E.M.2/1 (50 kV) electron microscope.

Results

Ammonium Nitrate IV.—Well-formed (110) faces were generally flat but a few examples of steps or layers were observed, as in Fig. 2. The surface of ammonium nitrate crystals grown from solutions containing acid magenta showed complex phenomena, some of which are illustrated in Fig. 3 and 4 The very regular layers of Fig. 4 were observed on a high index face lying between (110) and (010). Unfortunately no other examples of such depth and symmetry could be obtained ; interpretation of this feature is therefore uncertain, although it fits in well with the suggestion of Bunn that vicinal faces consist of systems of layers of low-index surfaces.

Crystals grown from solutions containing widely varying concentrations of acid magenta showed no great difference in surface fine structure although the (010) face development varied markedly.

Potassium Alum.—(110) and (111) faces of unmodified crystals were generally flat. When the crystals were grown from solutions containing Chlorazol Sky Blue or Bismarck Brown [5] layers were observed on both types of face (Fig. 7 and 8) though to a much smaller extent than with ammonium nitrate. Layers always appeared to originate in the centres of faces. From well-formed alum crystals it was possible to remove replicas extending over adjacent faces, and in no case were layers observed near edges or corners. Owing to the static nature of the observations the points of origin of layer systems were not easily identifiable but the absence of layers near edges and corners suggests that in fact they do not originate at these points.

---

[4] Williams and Wyckoff, *J. Appl. Physics*, 1946, **17**, 23.

[5] France, *Colloid Symp. Ann.*, 1929, **7**, 59.

The layer system of Fig. 7, though the most distinctive observed on alum crystals, shows some lack of uniformity. The layers do not appear to be discrete; it is, in fact, possible to trace a continuous path from the highest to the lowest layers without crossing a definite step. The appearance presented is that of steps which have been partially " silted up " by the deposition of further solute.

Sodium Nitrate.—The faces of unmodified crystals were mainly structureless. An extensive survey was made for evidence of layers, but none could be observed. When sodium nitrate is grown in solutions containing 2 % lead nitrate, however, considerable layer growth is visible, even under the optical microscope.[3] Fig. 11 shows that in addition a further granular growth occurs on the step edges. The oriented ripple-like structure of Fig. 11 was observed on a number of crystals, but was most marked with sodium nitrate grown from solutions containing lead nitrate.

Potassium Sulphate.—Layer growth can be observed optically.[3] Electron micrographs (Fig. 9) show that the layers are irregular, and a considerable amount of fine structure is visible on the layer edges. Layers were observed on (110), (111) and (010) faces.

Ammonium Sulphate.—A characteristic phenomenon was the appearance of a number of approximately circular areas, on the surfaces of which large numbers of oriented elliptical particles could be seen (Fig. 5). Layer or stepped structure was visible at the edges of the areas.

Other Salts.—No layers could be observed on sodium chlorate. Sodium chloride showed slight evidence of layers 1000-2000 Å thick, but in general the replicas obtained were structureless. Magnesium sulphate and zinc sulphate effloresced *in vacuo*, and the metal evaporation technique could not therefore be employed. Unshadowed formvar replicas were prepared but gave insufficient contrast for the detection of the thin layers. Some slight evidence of thicker layers was obtained from magnesium sulphate (Fig. 6), but insufficient to confirm Bunn's [3] interpretation of vicinal faces.

Discussion

In general the crystal faces studied in the electron microscope appeared relatively structureless, especially where the crystals were well-formed and unmodified. On most crystals, however, one or more of the surface phenomena described could be detected, though these often occurred only in isolated areas. Some of the phenomena observed were probably introduced by the specimen preparation technique and the results generally differed from crystal to crystal. Nevertheless, certain broad generalizations can be made. Step or layer-like irregularities were observed on the faces of a number of crystals: none could be detected in cases where the optical microscope did not show layer growth, apart from the inconclusive evidence of magnesium sulphate. However, the number of types of crystal examined was small, and high resolution micrographs could not always be obtained, owing to the difficulties of replica preparation. No observations were made inconsistent with the views of Bunn and Emmett [8] on layer growth: in particular, no evidence was obtained of layers originating at the edges on corners of crystal faces. The conditions of crystal growth studied by Bunn and Emmett were somewhat different from those under which the majority of the present work was carried out and correspond more to the work on rapid crystallization (Fig. 1). However, there appears to be little doubt that layers or steps are a feature of the growth mechanism.

In the presence of a crystal habit modificant the surface phenomena are more numerous and complex. Layers are generally thicker, and an increase in the number of visible layers is therefore to be expected. It seems probable that at least a part of the modification process involves a slowing-up of the layer spreading mechanism. This might well be effected by adsorption of the modificant on to advancing faces of the layers. The electron microscope does not show clearly whether or not these faces correspond to planar, low index surfaces. If they are in fact high index faces a mechanism of this type would explain why there appears to be little correlation between the dimensions of the molecule of the modificant and the distances in the modified crystal face. It is also supported by Whetstone's observation[6] that in ammonium nitrate crystals showing hour-glass inclusions of dyes, the pleochroism of the inclusions shows that the plane in which the dye molecules lie is normal or nearly normal to the plane on which habit modification took place.

In many of the micrographs, considerable departures from the generally accepted principles of crystal symmetry can be seen. As well as the expected linear phenomena of the Fig. 4 type, the micrographs show many examples of curved surfaces and edges. The replica thickness is several times that of the unit crystal cell, so that detail of this dimension would tend to be obscured in the specimen preparation process; it would in any case not be resolvable by the electron microscope. A series of irregularly-shaped dislocations of unit-cell dimensions would therefore appear as a surface or edge of irregular curvature. The addition of the solute ion by ion to the crystal surface is unlikely to produce such phenomena; where steady conditions of growth exist, surface irregularities tend to be smoothed out quickly. It seems improbable that the surfaces shown in Fig. 10 and 11 should arise from the same causes as those which produced, for example, the phenomena of Fig. 3 and 4. The overgrowths of Fig. 11 though possessing characteristic symmetry, show a lack of orientation which suggests that deposition occurred in the form of ionic aggregates of comparable size and symmetry. Berg[7] has observed that a higher concentration of solute arrives at crystal face centres than at edges, and, since the crystal face remains planar, is dissipated by some radial diffusion process. The kinetic treatment of Becker and Döring[8] suggests that under conditions such as these, where local fluctuations in concentration are likely to occur, there most probably exist in the diffusion stream ionic lattices of varying size. These might well be deposited on the crystal face in ripples and ridges of the type visible in Fig. 10 and 11. Analogous formations may be observed among large-scale phenomena. Fig. 12 shows a sand formation typical of those observable on sea-shores and river beds. According to Bagnold[9] the factors governing the shape of these formations are current strength and particle size distribution. Deposition at the crystal face is complicated by the powerful surface forces involved, and the analogy should not therefore be pressed. Nevertheless, there is such a marked correspondence between the sand formation of Fig. 12 and the surface phenomena of Fig. 10 and 11 that a process of this type might well cause the secondary phenomena described while making no overall contribution to crystal structure. It also offers a possible explanation for the "snow drift" appearance of the steps in Fig. 11 and the apparent "silting up" of parts of the stepped areas of Fig. 7.

Thanks are expressed to Dr. J. Whetstone and Dr. S. Fordham, for helpful discussion and to Mr. A. Fulton for Fig. 12.

Imperial Chemical Industries Limited,
Nobel Division, Research Department,
Stevenston.

---

[6] Whetstone, *Faraday Soc. Discussions*, 1949, **5**, 289.

[7] Berg, *Proc. Roy. Soc. A*, 1938, **164**, 79.

[8] Becker and Doring, *Ann. Physik.*, 1935, **24**, 719.

[9] Bagnold, *The Physics of Blown Sand and Desert Dunes* (Methuen, London 1941), Chap. 11.

THE THERMODYNAMICS OF ADSORPTION

PART II.—THERMODYNAMICS OF MONOLAYERS ON SOLIDS

By Douglas H. Everett

Received 11*th April*, 1950

A general thermodynamic treatment of adsorption equilibrium is proposed which follows the lines of the thermodynamics of solutions in that the properties of a real system are compared with those of an ideal reference system. For adsorption, two possible reference systems are the ideal localized monolayer and the ideal non-localized monolayer. These are examined and their range of usefulness is discussed generally; their application to experimental data is considered in the following paper of this series. A short discussion is also given of the relation between the present method and the Polanyi potential theory.

---

1. Introduction.—In a previous paper[1] we have given general reasons for preferring to treat the problems of the thermodynamics of adsorption in terms of the usual thermodynamic functions E, H, F and G in which the surface area A^{σ} is taken as an independent variable, rather than in terms of $\mathscr{E}$, $\mathscr{H}$, $\mathscr{F}$ and $\mathscr{G}$ in which the "spreading pressure" ϕ is the independent variable. This enables us to develop the thermodynamic argument along lines similar to those adopted in the study of solutions. Using this approach we are able to relate the behaviour of actual systems to the properties of an "ideal" or "perfect" system. The thermodynamics of surface phases is thus expressed in terms of the differences between the free energy, heat content and entropy of the actual system, and the corresponding functions for the reference system. If these "excess functions" are capable of theoretical interpretation in terms of a physical picture we may then be able to perceive what modifications are needed to the model upon which the reference system is based to bring it into closer agreement with real systems. The usefulness of this approach depends upon the choice of a physically reasonable simplified model, the properties of which provide a sensible basis for comparison with the properties of actual systems. For solutions this method has been successful because of the exact correlation between a simple statistical model and Raoult's law, which had already been recognized as representing the behaviour of mixtures of molecules of similar chemical properties. For adsorbed phases the problem is much more difficult because the physical state of adsorbed molecules is not known with any precision, and may vary from system to system.

In this paper we examine two possible reference systems, the ideal localized monolayer and the ideal non-localized monolayer. The problem of multilayer adsorption presents greater difficulty and will require closer examination.

2. Thermodynamic Equations for Adsorption Equilibrium.—We consider a vapour at a partial pressure p_{Γ} in equilibrium with a solid on which is adsorbed m moles of the vapour per gram of solid. We suppose that the solid adsorbent has a surface area A^{σ} cm.^{2}/g. which is independent of temperature, and denote the surface concentration in moles per unit area as $\Gamma = m/A^{\sigma}$. The chemical potentials of the adsorbed molecules and vapour will be equal so that the isothermal transfer of vapour from the standard gas state (unit pressure) to the surface will involve a change in chemical potential

---

[1] Everett, *Trans. Faraday Soc.*, 1950, **46**, 453.

$$\mu^{\sigma}_{\Gamma} - \mu^{\dagger G} = \Delta\mu^{\dagger}_{\Gamma} = RT \ln p^{*}_{\Gamma}, \quad . \quad . \quad . \quad (2.1)$$

where p^{*}_{Γ} is the fugacity of the vapour at a pressure p_{Γ}, μ^{σ}_{Γ} is the chemical potential of the sorbate in the adsorbed state at a surface concentration Γ; $\mu^{\dagger G}$ is the chemical potential of the vapour at unit pressure.*

We may now express the change in chemical potential in (2.1) in terms of heat and entropy contributions.

$$\Delta\mu^{\dagger}_{\Gamma} = \overline{\Delta \mathrm{H}}^{\dagger}_{\Gamma} - T\overline{\Delta \mathrm{s}}^{\dagger}_{\Gamma} \quad . \quad . \quad . \quad . \quad (2.2)$$

where

$$\left.\begin{aligned} \overline{\Delta \mathrm{H}}^{\dagger}_{\Gamma} &= \overline{\mathrm{H}}^{\sigma}_{\Gamma} - \mathrm{H}^{\dagger G} \\ \overline{\Delta \mathrm{s}}_{\Gamma} &= \overline{\mathrm{s}}^{\sigma}_{\Gamma} - \mathrm{s}^{\dagger G} \end{aligned}\right\} \quad . \quad . \quad . \quad . \quad (2.3)$$

$\overline{\mathrm{H}}^{\sigma}_{\Gamma}$ is the differential** molar heat content of the adsorbed molecules related to the total heat content of the surface (H^{σ}_{m}) by

$$\overline{\mathrm{H}}^{\sigma}_{\Gamma} = (\partial H^{\sigma}_{m}/\partial m)_{T,P,A^{\sigma}} \quad . \quad . \quad . \quad . \quad (2.4)$$

and $\mathrm{H}^{\dagger G}$ is the molar heat content of the vapour in the standard gas state. $\overline{\Delta \mathrm{H}}^{\dagger}_{\Gamma}$ is thus the differential molar heat content of the adsorbed molecules relative to the standard gas state, i.e. the molar heat of transfer of molecules from the standard gas state to an infinite surface containing adsorbed molecules at a concentration Γ. It is sometimes called the isosteric heat of adsorption.

Similarly

$$\overline{\mathrm{s}}^{\sigma}_{\Gamma} = (\partial S^{\sigma}_{m}/\partial m)_{T,P,A^{\sigma}} \quad . \quad . \quad . \quad . \quad (2.5)$$

and $\overline{\Delta \mathrm{s}}^{\dagger}_{\Gamma}$ is the differential molar entropy of the adsorbed molecules relative to the standard state.

Neglecting, for the moment, the difference between fugacity and pressure, we have for the equilibrium vapour pressure of the absorbed phase

$$\ln p_{\Gamma} = \frac{\overline{\Delta \mathrm{H}}^{\dagger}_{\Gamma}}{RT} - \frac{\overline{\Delta \mathrm{s}}^{\dagger}_{\Gamma}}{R} \quad . \quad . \quad . \quad . \quad (2.6)$$

If $\overline{\Delta \mathrm{H}}^{\dagger}_{\Gamma}$ and $\overline{\Delta \mathrm{s}}^{\dagger}_{\Gamma}$ can be expressed as functions of Γ, then (2.6) becomes the "adsorption isotherm" relating the amount of vapour adsorbed to the partial pressure of vapour.

Alternatively, choosing the pure liquid sorbate as standard state and considering the isothermal transfer of molecules from the liquid to the adsorbed state, we have

$$\ln (p_{\Gamma}/p^{\circ}) = \frac{\overline{\Delta \mathrm{H}}^{\circ}_{\Gamma}}{RT} - \frac{\overline{\Delta \mathrm{s}}_{\Gamma}}{R} \quad . \quad . \quad . \quad . \quad (2.7)$$

---

* If we employ as standard state the vapour as an *ideal* gas at *unit* pressure we must define p^{*} such that $p^{*}/p \rightarrow 1$ as $p \rightarrow 0$.

** *Note added in proof.*—The nomenclature employed in Part I for the quantities defined by (2.4) and (2.5) (cf. eqn. (8.1) . . . (8.4) of Part I) is unfortunate. Although these quantities are both *partial* and *molar*, the term *partial molar* is of course retained, by convention, for partial derivatives at constant intensity factors. To avoid confusion we have in this paper used the term *differential molar* for quantities, such as (2.4) and (2.5), which are defined at constant T and P, but not at constant surface pressure.

In Part I eqn. (9.3) is slightly inaccurate, but this does not affect any of the general arguments in the paper; nor will the inaccuracy be appreciable in practice. The following misprints also occurred in Part I: eqn. (7.2) should read

$$q = -\overline{\Delta \mathrm{H}} = \mathrm{H}^{G} - \mathrm{H}^{\sigma};$$

in eqn. (19.1) and (19.2) and in the line preceding them, for T read Γ; in footnote 11 the first term in the eqn. for $\overline{\Delta E}$ should read $(\partial Q/\partial m)_{V}{}^{G}{}_{A}{}^{\sigma}$.

where $\overline{\Delta\mathrm{H}}{}^{\circ}_{\Gamma}$ and $\overline{\Delta\mathrm{S}}{}^{\circ}_{\Gamma}$ are the differential molar heat and entropy relative to the pure liquid state, i.e. the heat and entropy of transfer of a mole of sorbate from the liquid to the surface. p° is the vapour pressure of the pure liquid at the temperature T; p_{Γ}/p° is frequently called the relative pressure. Eqn. (2.7) is sometimes more convenient than (2.6) but has the disadvantage of being inapplicable to the adsorption of a gas above its critical temperature or below its triple point (unless, of course, we employ extrapolated values of p°). Furthermore, if we wish to compare different sorbates, the use of (2.7) means that the standard states are different for each sorbate.

Eqn. (2.6) or (2.7) may now be employed to evaluate heat and entropy changes from measurements of adsorption isotherms at different temperatures and so to study $\overline{\Delta\mathrm{H}}{}^{\dagger}_{\Gamma}$ and $\overline{\Delta\mathrm{S}}{}^{\dagger}_{\Gamma}$ as functions of Γ. We see from (2.6) that

$$\frac{\mathrm{d}\ln p_{\Gamma}}{\mathrm{d}T} = -\frac{\overline{\Delta\mathrm{H}}{}^{\dagger}_{\Gamma}}{RT^{2}} \quad \text{(const. pressure)} \quad . \quad . \quad . \quad (2.8)$$

If we assume that the variation of pressure on the system, arising from the change of vapour pressure with temperature, has a negligible effect on its properties, then (2.8) may be applied directly to experimental results. This equation is approximate and assumes that the vapour behaves as a perfect gas, and that the molar volume of the adsorbed molecules v^{σ} is negligible compared with v^{g}, the molar volume of the vapour at pressure p_{Γ}. A discussion of these approximations, is given in Appendix I.

Isosteric heats of adsorption have been calculated from eqn. (2.8) by many authors, but very little attention seems to have been directed towards the corresponding entropy changes. One of the main objects of these papers is to emphasize the importance of entropies of adsorption in determining the shapes of adsorption isotherms. We may stress here that the above equations are quite general and involve no assumptions as to the nature of the adsorbed phase, they apply generally to monolayers, multilayers and to chemisorption.

Purely thermodynamic methods can take us no further and little useful information regarding the nature of adsorbed phases can be derived from the study of heat and entropy changes unless we can relate them to those predicted from a simple model. As pointed out above the choice of reference or standard system is more difficult than for solutions. We shall examine here two alternative models and discuss their value in the light of the experimental data in Part III.

3. Localized Monolayer Model.—The adsorption isotherm for a localized monolayer, in which the molecules or atoms are adsorbed on active sites on a homogeneous surface with no interaction between adsorbed molecules, was first obtained by kinetic reasoning by Langmuir.[2] Subsequently Fowler [3] showed that the same equation could be derived from a statistical mechanical consideration of the same model, the exact kinetic mechanism of adsorption and desorption being irrelevant. Various authors (Fowler;[4] Roberts;[5] Glasstone, Laidler and Eyring [6]) have extended the treatment to take account of interaction between adsorbed molecules. In these theories, however, no explicit account is taken of the possible variation of the entropy of adsorption with surface concentration of adsorbed phase. The resulting adsorption isotherms include the ratio of the partition functions of gaseous and adsorbed molecules but these are usually assumed to be the functions of T only, and this diverts attention from the possibility that they may also be functions of the concentration of molecules on the surface.

---

[2] Langmuir, *J. Amer. Chem. Soc.*, 1918, **40**, 1361.

[3] Fowler, *Proc. Camb. Phil. Soc.*, 1935, **31**, 260.

[4] Fowler, *ibid.*, 1936, **32**, 144; cf. Fowler and Guggenheim, *Statistical Thermodynamics* (C.U.P., 1939), p. 429.

[5] Roberts, *Some Problems in Adsorption* (Cambridge, 1939), p. 74.

[6] Glasstone, Laidler and Eyring, *J. Chem. Physics*, 1940, **8**, 659; cf. Glasstone, Laidler and Eyring, *Theory of Rate Processes* (McGraw Hill, 1941), p. 359.

Langmuir assumed that the surface could be regarded as an array of " active centres " each capable of adsorbing one molecule, so that at saturation the surface is covered by a unimolecular layer. The importance of this model is that it allows a calculation of the configurational, or localization, entropy of the surface phase. If we suppose there are M active sites and m of these are occupied by adsorbed molecules, then the number of arrangements of the system is $\frac{M!}{m!\,(M-m)!}$. If we assume that all these arrangements are equally probable, then the entropy of the system will include a term $k \ln \frac{M!}{m!\,(M - m!)}$, which, using Stirling's approximation, reduces to

$$-\,k[m \ln m/M + (M - m) \ln (M - m)/M].$$

The differential molar localization entropy of the adsorbed molecules $(\bar{s}_\theta^{\sigma,\,l})$ is obtained by differentiation with respect to m, and multiplication by Avogadro's number,

$$\bar{s}_\theta^{\sigma,\,l} = -\,R \ln \frac{\theta}{1-\theta}, \text{ where } \theta = m/M. \qquad . \quad . \quad (3.1)$$

The differential molar entropy of the adsorbed molecules will be the sum of the localization entropy and a contribution from the vibrational and rotational degrees of freedom $(s_\theta^{\sigma,\,*})$; we shall ignore for the moment internal degrees of freedom of the molecule :

$$\bar{s}_\theta^{\sigma} = \bar{s}_\theta^{\sigma,\,l} + \bar{s}_\theta^{\sigma,\,*} = -\,R \ln \frac{\theta}{1+\theta} + \bar{s}_\theta^{\sigma,\,*}. \qquad . \quad . \quad (3.2)$$

Hence from (2.3)

$$\Delta s_\theta^{\dagger} = \Delta s_\theta^{*} - R \ln \frac{\theta}{1-\theta}, \qquad . \quad . \quad . \quad (3.3)$$

where

$$\overline{\Delta s}_\theta^{*} = \bar{s}_\theta^{\sigma,\,*} - s^{\dagger,\,G} \qquad . \quad . \quad . \quad . \quad (3.4)$$

$\overline{\Delta s}_\theta^{*}$ is thus the entropy of adsorption leaving out the contribution from the localization term (3.1), it is analogous to the " excess entropy of mixing " employed in the study of the thermodynamics of solutions.

Substituting into (2.6) we have

$$\ln p_\theta = \frac{\overline{\Delta H}_\theta^{\dagger}}{RT} - \frac{\overline{\Delta s}_\theta^{*}}{R} + \ln \frac{\theta}{1-\theta}, \qquad . \quad . \quad . \quad (3.5)$$

whence

$$\frac{\theta}{1-\theta} = e^{-\frac{\overline{\Delta H}_\theta^{\dagger}}{RT} + \frac{\overline{\Delta s}_\theta^{*}}{R}} \cdot p_\theta. \qquad . \quad . \quad . \quad (3.6)$$

We see immediately that if $\overline{\Delta H}_\theta^{\dagger}$ and $\overline{\Delta s}_\theta^{*}$ are independent of θ, (3.6) reduces to Langmuir's equation

$$\frac{\theta}{1-\theta} = b p_\theta, \qquad . \quad . \quad . \quad . \quad . \quad (3.7)$$

where

$$b = e^{-\frac{\overline{\Delta H}_\theta^{\dagger} + T\overline{\Delta s}_\theta^{*}}{RT}} \quad . \quad . \quad . \quad . \quad . \quad (3.8)$$

Eqn. (3.5) and (3.6) may also be written in the alternative forms,

$$\ln p_\theta = \frac{\Delta \mu_\theta^{*}}{RT} + \ln \frac{\theta}{1-\theta}, \qquad . \quad . \quad . \quad (3.9)$$

or

$$\frac{\theta}{1-\theta} = e^{-\Delta\mu_\theta^*/RT} \cdot p_\theta \quad . \quad . \quad . \quad . \quad (3.10)$$

where $\Delta\mu_\theta^*$ is the differential molar free energy of adsorption minus the localization term $RT \ln [\theta/(1-\theta)]$.

Following Fowler and Guggenheim [7] we may call systems which obey (3.7) "ideal localized monolayers". Deviations from ideal behaviour can arise from the variation of $\overline{\Delta\mathrm{H}}_\theta^\dagger$, $\overline{\Delta\mathrm{s}}_\theta^*$, or both, with the surface coverage θ. Systems for which $\overline{\Delta\mathrm{H}}_\theta^\dagger$ only is dependent upon θ have been designated "regular monolayers" [8] but as we shall see, for adsorption on solids at least, the experimental evidence suggests that variations of $\overline{\Delta\mathrm{H}}^\dagger$ are always accompanied by changes in $\overline{\Delta\mathrm{s}}_\theta^*$.

Eqn. (3.6) may be regarded as the "generalized isotherm for localized monolayers", and demonstrates the part played by both heat and entropy terms in determining the shape of the isotherm. Many of the semi-empirical adsorption isotherms which have been proposed in the past correspond to fairly simple forms of $\Delta\mu_\theta^*$ as a function of θ.

For example, if

$$\Delta\mu_\theta^* = \Delta\mu_0^* + B\theta + C\theta^2 + \ldots \quad . \quad . \quad . \quad (3.11)$$

we have, expanding $\ln (1-\theta)$ in powers of θ

$$-\ln \theta + \ln p_\theta = \frac{\Delta\mu_0^*}{RT} + \left(\frac{B}{RT} - 1\right)\theta + \left(\frac{C}{RT} - \frac{1}{2}\right)\theta^2 + \ldots \quad (3.12)$$

Then if $C \sim RT/2$, $D \sim RT/3$ . . ., or in any case if θ is small,

$$\ln p_\theta/\theta = + \frac{\Delta\mu_0^*}{RT} + \left(\frac{B}{RT} - 1\right)\theta = \alpha + \beta\theta \quad . \quad . \quad (3.13)$$

which is the Williams-Henry-Wilkins [9] adsorption isotherm.

The variation of $\Delta\mu_\theta^*$ with θ is frequently approximately of the form (3·11) so that equations similar to (3.13) often give excellent representation of the experimental data.

4. Range of Validity of the Localized Monolayer Model.—The above general treatment of localized adsorption is based on two main assumptions which it will be wise to examine in more detail before proceeding.

ASSUMPTION 1.—The differential molar configurational entropy of localized adsorption is correctly given by $-R \ln [\theta/(1-\theta)]$.

First we may point out that it is immaterial whether a molecule, once adsorbed, remains on the same site or migrates from one site to another. This migration must always be possible by a desorption-adsorption mechanism, so if it occurs across the surface as well it will not affect our calculation of the entropy. The calculation of the entropy depends upon the assumption that the *sites* are localized, and is only concerned with the mobility of the molecules, in that, while in the adsorbed state, they must spend the bulk of their time attached to adsorption sites.

(*a*) *Effect of incomplete localization.*—The adsorbed molecules will vibrate parallel to, and normal to, the surface, and the amplitude of vibration will increase with temperature (or if we consider at constant temperature a series of systems of decreasing energy of adsorption). Provided the amplitude is not too large we may treat the entropy as the sum of the localization entropy $-R \ln [\theta/(1-\theta)]$ and the entropy of vibration (plus, for polyatomic molecules, the entropy of rotation or libration about the adsorption site) (cf. eqn. (3.2)). This approximation will begin to break down as the thermal energy kT approaches $\Delta\epsilon$, the height of the energy barrier separating one site from another, the molecules will then spend an appreciable time away from the "site" and the concept of localization will become blurred.

---

[7] Fowler and Guggenheim,[4] p. 426. [8] Fowler and Guggenheim,[4] p. 429.

[9] Williams, *Proc. Roy. Soc. Edin.*, 1918, **38**, 13; 1919, **39**, 48; *Proc. Roy. Soc. A*, 1919, **96**, 287, 298. (*b*) Henry, *Phil. Mag.*, 1938, 44 (6), 689. (*c*) Wilkins, *Proc. Roy. Soc. A*, 1938, **164**, 496.

The transition cannot be defined with any accuracy. The probability of finding a molecule in an interstitial position will be determined by the Boltzmann factor $e^{-\Delta\epsilon/kT}$. This factor only approaches unity when $T > \Delta\epsilon/k$, but at much lower temperatures there will still be appreciable mobility across the surface. For the present purposes our main concern is the accuracy of the procedure of dividing the entropy of the adsorbed phase into two independent terms. As shown by Hill[10] a consideration of the specific heat of adsorbed molecules suggests that the transition commences at about $T \sim \Delta\epsilon/10k$ but it will extend over a very wide temperature range probably to $T \sim \Delta\epsilon/k$. We consider that our calculation of the localization entropy will not be seriously affected until the temperature has reached at least $T \sim \Delta\epsilon/5$ under which conditions roughly 1 % of the molecules will at any instant be in interstitial positions. There is little reliable evidence relating to the height of energy barriers between adsorption sites, but if we adopt the suggestion[11] that they will be somewhat less than half the energy of adsorption, then our approximation should be adequate for most of the data we have examined. There is, however, some reason to expect our evaluation of the localization entropy to remain reasonably accurate at even higher temperatures. The monolayer, during the transition localized → non-localized is in a state rather akin to a two-dimensional liquid. Now the lattice model of a three-dimensional liquid when applied to entropies of solution gives remarkably good results even though the picture of the molecules as localized on lattice points can only be physically accurate for solid solutions; the localized monolayer treatment for adsorption may also give results with a validity outside the strict applicability of the physical model.

(*b*) *Effect of varying heat of adsorption.*—In deriving the localization entropy it was assumed that all arrangements of the m molecules on the M sites were equivalent. This will not be true if the energy of adsorption is different on different sites.

Two important cases arise, the variation of $\overline{\Delta H}^{\,l}_{\theta}$ with θ may be caused by molecular interaction, or to inhomogeneity of the surface. In the first instance it has been shown[12] that if w is the interaction energy between adjacent molecules then the configurational entropy is

$$\bar{s}^{\sigma,l} = -R\ln\frac{\theta}{1-\theta} - zR\ln\frac{2(1-\theta)}{\beta+1-2\theta} + \frac{4\theta(1-\theta)w\,e^{-2w/zRT}}{\beta(\beta+1-2\theta)T}, \qquad (3.14)$$

where

$$\beta^2 = 1 - 4\theta(1-\theta)(1-e^{2w/zRT})\,; \qquad . \quad . \quad (3.15)$$

and z is the number of nearest neighbours to a given site.

The second and third terms in (3.14) tend to cancel one another, and the correction to be applied to the regular localization entropy is found to increase roughly in proportion to $(2w/zRT)^{1.8}$; some typical values for the correction term are tabulated below.

Values for $z = 6$, $\theta = 0{\cdot}25$ (or 0·75 with sign changed).

$\frac{2w}{zRT}$	$2w$ at 300° K (cal./mole)	$\delta(s^{\sigma,l}_{\theta})$ (cal./mole deg.)	$\delta(s^{\sigma,l}_{\theta})$ as % of $-R\ln\frac{\theta}{1-\theta}$
0·10	360	− 0·008	0·4
0·167	600	− 0·030	1·4
0·50	1800	− 0·17	8·0
1·00	3600	− 0·56	25·0

---

[10] Hill, *J. Chem. Physics*, 1946, 14, 441.

[11] Tompkins, private communication.

[12] Cf. Fowler and Guggenheim[4], p. 441.

The deviation of the localization entropy from the " regular " entropy of adsorption is thus negligible except for powerful interactions between adsorbed molecules.

According to the above treatment of adsorption with interaction there is a linear variation in $\overline{\Delta H_\theta^\dagger}$ on passing from $\theta = 0$ to $\theta = 1$ the total change being $2w$; we see for example that to account for a variation in $\overline{\Delta H_\theta^\dagger}$ of 3600 cal. we must have $w = 3RT$. It is often held that the changes in $\overline{\Delta H_\theta^\dagger}$ observed experimentally are too large, and functionally of the wrong form, to admit of interpretation in terms of molecular interaction. These considerations, which we shall have occasion to examine in more detail later, suggest that variations in the heat of adsorption also arise from the heterogeneity of solid adsorbents.

Calculation of the localization entropy on a heterogeneous surface is more difficult. We assume that the M sites can be divided into groups $M_1, M_2 \ldots M_r (\sum_i M_i = M)$ which correspond to heats of adsorption $\Delta H_1, \Delta H_2, \ldots \Delta H_r$; the number of arrangements on the surface becomes

$$\prod_i \frac{M_i\,!}{(M_i - m_i)\,!\,m_i\,!},$$

where m_i is the number of molecules adsorbed on the ith set of sites. The total configurational entropy of the surface phase is then

$$S^{\sigma,l} = -kM[\sum_i c_i\{\theta_i \ln \theta_i + (1 - \theta_i) \ln (1 - \theta_i)\}], \quad . \quad (3.16)$$

where

$$c_i = M_i / \sum_i M_i = M_i / M. \quad . \quad . \quad . \quad (3.17)$$

To obtain the differential molar entropy we now require the derivative of (3.16) with respect to $m (= \sum_i c_i m_i)$. The various m_i's are not independent but are related by the fact that the whole system is in equilibrium with vapour at the same partial pressure. It is easily shown that each set of sites gives rise to a Langmuir type isotherm :

$$\frac{\theta_i}{1 - \theta_i} = e^{-\frac{\Delta H_i^\dagger - T\Delta S_i^\dagger}{RT}} \cdot p_\theta \quad . \quad . \quad . \quad (3.18)$$

so that if the distribution of heats and entropies over the surface is known we can in principle relate the m_i's and so obtain $\overline{\Delta S_\theta^l}$. There is, however, no general solution to the problem but there seems little reason to expect the term $- R \ln \theta_i (1 - \theta)$ to be separable from the expression for the differential molar localization entropy, and we may therefore find difficulty in applying the present analysis to heterogeneous surfaces.

ASSUMPTION 2.—The number of available sites is independent of the temperature.

This assumption has been criticized by many authors as being contrary to the experimental facts. It is frequently stated [13] that " saturation capacities " are dependent upon temperature, but before accepting these criticisms we must enquire how these saturation capacities are determined. Many statements appear to have been made on the basis of a qualitative inspection of experimental adsorption isotherms. This is a particularly unreliable procedure, especially when the isotherms at different temperatures do not cover the same range of relative pressures. The second method [14] is to determine the point of intersection of the isotherm with the ordinate drawn at the saturation vapour pressure of the sorbate. This assumes that $p_\theta = p^\circ$ when $\theta = 1$, which is contrary both to the mathematical form of the Langmuir equation for which $\theta \rightarrow 1$ as $p_\theta \rightarrow \infty$, and to the physical considerations involved. There is no particular reason to assume that the vapour pressure of a completed monolayer should be the same as that of the liquid state at the same temperature. Normally the sorbate vapour pressure will attain a value equal to the liquid while there are still a number of unfilled lattice points ; the " saturated " monolayer will contain " holes " in much the same way as we picture the presence of holes in the liquid state, or unoccupied lattice points in a crystal. There is of course no objection to the term " saturation adsorptive capacity " corresponding to equilibrium with saturated vapour at the same temperature, provided that it is not implied that this " saturation " corresponds to complete filling of the available adsorption sites. The most usual method of obtaining " saturation " values is to apply the Langmuir isotherm in the form,

---

[13] Cf. e.g. Goldmann and Polanyi, *Z. physik. Chem. A*, 1928, **132**, 313. McBain and Britton, *J. Amer. Chem. Soc.*, 1930, **52**, 2198. Wilkins, *Proc. Roy. Soc. A*, 1938, **164**, 510.

[14] E.g. Coolidge, *J. Amer. Chem. Soc.*, 1924, **46**, 596.

$$\frac{1}{\theta} = \frac{1}{bp} + 1,$$

or

$$\frac{p}{w} = \frac{1}{bw_s} + \frac{p}{w_s}, \qquad . \quad . \quad . \quad . \quad (3.14)$$

where w is the weight of sorbate, and w_s *the saturation value corresponding, in this case, to complete filling of the surface.* On plotting p/w against p the slope of the line should give $1/w_s$, provided that the Langmuir isotherm is obeyed. In practice a curve is nearly always obtained. Some authors [15] have taken the " limiting " slope at the highest values of p examined as giving the correct value of w_s. In many cases, however, this procedure is quite unreliable since there is no evidence that the curve is in fact approaching linearity, and at different temperatures the pressure ranges investigated do not correspond to comparable sections of the isotherm. The determination of the total number of sites presents the main difficulty in applying the present analysis ; we have taken the saturation value (i.e. for complete filling of adsorption sites) as temperature independent, and find that in most cases this is a satisfactory procedure (cf. Part III).

Summarizing these considerations we see that, taking the ideal localized monolayer as reference system, deviations from ideal may arise from :

(*a*) modification of the regular localization entropy caused either by interactions between adsorbed molecules (a relatively small effect) or by heterogeneity of the surface (for which no general conclusions can be drawn) ;

(*b*) variation of the heat of adsorption with degree of coverage arising from one or other, or both the causes under (*a*) ;

(*c*) variation of the vibrational and rotational degrees of freedom of the adsorbed molecules with degree of coverage, with a consequent variation of $\overline{\Delta s}{}^*_\theta$ with θ.

5. Non-Localized Monolayer Model.—The difficulties attached to a theoretical treatment of monolayers in the transition region between localized and non-localized are considerable and we shall proceed first to examine the properties of a film in which the molecules move freely in a potential field whose fluctuations over the surface are smaller than kT.

We may adopt two alternative although fundamentally equivalent approaches, both based on the concept of the non-localized monolayer as a two-dimensional gas exerting a " spreading pressure " ϕ. This model is of wide applicability to monolayers on a liquid surface but is

---

[15] E.g. Wilkins, ref. (9*c*).

TABLE I

Equation of State	Adsorption Isotherm	Integration Constant	$\bar{\mathrm{H}}^{\sigma}_{\Gamma}$	$\bar{\mathrm{S}}^{\sigma}_{\Gamma}$
1. $\phi = RT\Gamma = RT/\mathrm{A}^{\sigma}$	$p = c_1\Gamma$	$c_1 = \exp\left\{\frac{\Delta \mathrm{H}^{\dagger}}{RT} - \frac{\Delta \mathrm{S}^{\dagger}_1}{R} + 1\right\}$	$\bar{\mathrm{H}}^{\sigma}_{\Gamma} = \mathrm{H}^{\sigma} = \text{const.}$	$\bar{\mathrm{S}}^{\sigma}_{\Gamma} = \mathrm{S}^{\sigma}_1 - R(\ln \Gamma + 1)$ $= \bar{\mathrm{S}}^{\sigma}_1 - R \ln \Gamma$
2a. $\phi = nRT\Gamma = nRT/\mathrm{A}^{\sigma}$	$p = c_2\Gamma^n$	$c_2 = \exp\left\{\frac{\Delta \mathrm{H}^{\dagger}_1}{RT} - \frac{\Delta \mathrm{S}^{\dagger}_1}{R} + n\right\}$	$\bar{\mathrm{H}}^{\sigma}_{\Gamma} = \mathrm{H}^{\sigma}_1$ $- RT^2\left(\frac{\mathrm{d}n}{\mathrm{d}T}\right)(\ln \Gamma + 1)$	$\bar{\mathrm{S}}^{\sigma}_{\Gamma} = \mathrm{S}^{\sigma}_1$ $- R\left\{n + T\left(\frac{\mathrm{d}n}{\mathrm{d}T}\right)\right\}(\ln \Gamma + 1)$
2b. If in 2a $n = a/T$ $\phi = aR\Gamma$	$p = c_2'\Gamma^{a/T}$	$c_2' = \exp\left\{\frac{\Delta \mathrm{H}^{\dagger}_1}{RT} - \frac{\Delta \mathrm{S}^{\dagger}_1}{R} + \frac{a}{T}\right\}$	$\bar{\mathrm{H}}^{\sigma}_{\Gamma} = \mathrm{H}^{\sigma}_1 + aR(\ln \Gamma + 1)$	$\bar{\mathrm{S}}^{\sigma}_{\Gamma} = \mathrm{S}^{\sigma} = \text{const.}$
3. $\phi = \frac{RT\Gamma}{1 - b\Gamma} = \frac{RT}{\mathrm{A}^{\sigma} - b}$	$p = c_3\frac{\Gamma}{1 - b\Gamma}e^{b\Gamma/(1 - b\Gamma)}$	$c_3 = (1 - b)$ $\exp\left\{\frac{\Delta \mathrm{H}^{\dagger}}{RT} - \frac{\Delta \mathrm{S}^{\dagger}_1}{R} + 1\right\}$	$\bar{\mathrm{H}}^{\sigma}_{\Gamma} = \mathrm{H}^{\sigma} = \text{const.}$	$\bar{\mathrm{S}}^{\sigma}_{\Gamma} = \mathrm{S}^{\sigma}_1 - \frac{R}{1 - b\Gamma}$ $- R \ln \frac{\Gamma(1 - b)}{1 - b\Gamma}$
4. $\phi = \frac{RT\Gamma}{1 - b\Gamma} + a\Gamma^2$ $= \frac{RT}{\mathrm{A}^{\sigma} - b} + \frac{a}{(\mathrm{A}^{\sigma})^2}$	$p = c_4\frac{\Gamma}{1 - b\Gamma}$ $e^{b\Gamma/(1 - b\Gamma) + 2a\Gamma/RT}$	$c_4 = (1 - b)$ $\exp\left\{\frac{\Delta \mathrm{H}^{\dagger}_0}{RT} - \frac{\Delta \mathrm{S}^{\dagger}_1}{R} + 1\right\}$	$\bar{\mathrm{H}}^{\sigma}_{\Gamma} = \mathrm{H}^{\sigma}_0 + 2a\Gamma$	$\bar{\mathrm{S}}^{\sigma}_{\Gamma} = \mathrm{S}^{\sigma}_1 - \frac{R}{1 - b\Gamma}$ $- R \ln \frac{\Gamma(1 - b)}{1 - b\Gamma}$
5. $\phi = RT\Gamma(1 + B\Gamma + C\Gamma^2 + \ldots)$	$\ln \frac{p}{\Gamma} = c_5 + 2B\Gamma + \frac{3}{2}C\Gamma^2 - \frac{4}{3}D\Gamma^3 \ldots$	Depend on temperature dependence of $B, C, D \ldots$		
6. $\phi = RT\Gamma^{\circ}_s \ln(1 - \Gamma/\Gamma^{\circ}_s)$ $= RT\Gamma(1 + \Gamma/2\Gamma^{\circ}_s + \Gamma^2/3\Gamma^{\circ 2}_s + \ldots)$ $= RT\Gamma(1 + \frac{1}{2}\theta + \frac{1}{3}\theta^2 + \ldots)$	$p = c_6\frac{\Gamma/\Gamma^{\circ}_s}{1 - \Gamma/\Gamma^{\circ}_s}$ $= c_6\frac{\theta}{1 - \theta}$	c_6 $= \exp\left\{\frac{\Delta \mathrm{H}^{\dagger}}{RT} - \frac{\Delta \mathrm{S}^{\dagger}_{\Gamma^{\circ}_s/2}}{R} + 2\ln 2\right\}$ $= \exp\left\{\frac{\Delta \mathrm{H}^{\dagger}}{RT} - \frac{\overline{\Delta \mathrm{S}}^{\dagger}_{\Gamma^{\circ}_s/2}}{R}\right\}$	$\bar{\mathrm{H}}^{\sigma}_{\Gamma} = \mathrm{H}^{\sigma} = \text{const.}$	$\bar{\mathrm{S}}^{\sigma}_{\Gamma} = \mathrm{S}^{\sigma}_{\Gamma^{\circ}_s/2}$ $- R\left\{2 \ln 2 + \ln \frac{\theta}{1 - \theta}\right\}$ $= \bar{\mathrm{S}}^{\sigma}_{\Gamma^{\circ}_s/2} - R \ln \frac{\theta}{1 - \theta}$

---

[1] Henry's law.

[2a] Freundlich isotherm.

[2b] Cremer (*Monatsh.*, 1947, **77**, 126) suggests $n = a/T$; this leads to ϕ independent of temperature and s independent of θ.

[3] Volmer's isotherm, a is assumed independent of temperature.

[4] Magnus' isotherm, a and b assumed independent of temperature.

[5] When θ small this approximates to the Williams-Henry-Wilkins isotherm.

[6] Langmuir isotherm; note the heat and entropy terms are the same as those derived on the basis of localized monolayer model.

of less certain value when applied to adsorption on solids. The spreading pressure ϕ is related to the surface free energy by the equation

$$\phi = \left(\frac{\partial G^\sigma}{\partial A^\sigma}\right)_{T,P,m}, \quad . \quad . \quad . \quad . \quad (5{\cdot}3)$$

and this formal equation may be applied whether the film is mobile or not; but it is only for a non-localized film that we can give it a clear physical meaning in terms of a molecular-kinetic picture.

Our choice of reference system here is the ideal two-dimensional gas for which

$$\phi = \Gamma RT. \quad . \quad . \quad . \quad . \quad . \quad (5{\cdot}2)$$

Deviations from ideality may be represented either by the introduction of " cohesive " and " co-area " terms into the equation of state, by the use of virial coefficients, or by thermodynamic " excess functions ". We shall begin with a general investigation of the use of equations of state to represent the behaviour of surface phases.

We assume the non-localized film has an equation of state

$$\phi = \phi(T, \Gamma) \quad . \quad . \quad . \quad . \quad (5{\cdot}3)$$

and proceed to calculate its properties.

The use of the Gibbs equation

$$\mathrm{d}\phi = RT\Gamma \mathrm{d} \ln p \quad . \quad . \quad . \quad . \quad (5{\cdot}4)$$

to interrelate the equation of state with the adsorption isotherm is well known [16] and a series of conjugate equations of state and adsorption isotherms obtained in this way are given in Table I.

A second approach to the problem is to follow the methods outlined in § 2. Starting from the equation of state we employ the equations [17]

$$\left(\frac{\partial \phi}{\partial T}\right)_{P,\Gamma} = \left(\frac{\partial S^\sigma}{\partial A^\sigma}\right)_{T,P,m} = -\Gamma^2\left(\frac{\partial \mathrm{s}^\sigma}{\partial \Gamma}\right), \quad . \quad . \quad . \quad (5{\cdot}5)$$

and
$$-\left(\frac{\partial H^\sigma}{\partial A^\sigma}\right)_{T,P,m} = +\Gamma^2\left(\frac{\partial \mathrm{H}^\sigma}{\partial \Gamma}\right)_{T,P} = \phi - T\left(\frac{\partial \phi}{\partial T}\right)_{P,\Gamma}, \quad . \quad (5{\cdot}6)$$

where s^σ and H^σ are the mean molar quantities, to evaluate the molar entropy and heat of the surface phase. The differential molar quantities are then obtained and substituted in eqn. (2.3).

The procedure may be illustrated by considering the equation of state [18]

$$\phi = \frac{RT\Gamma}{1 - b\Gamma} + a\Gamma^2 \quad . \quad . \quad . \quad . \quad (5{\cdot}7)$$

in which a and b are analogous to the van der Waals' constants for an imperfect gas. We assume them to be temperature independent.

Now

$$\left(\frac{\partial \phi}{\partial T}\right)_{P,\Gamma} = \frac{R\Gamma}{1 - b\Gamma},$$

so that at constant T, P,

$$\mathrm{ds}^\sigma = \left(\frac{\partial \phi}{\partial T}\right)_{P,\Gamma} \mathrm{d}\mathrm{A}^\sigma = -\frac{R}{(1 - b\Gamma)\Gamma} \cdot \mathrm{d}\Gamma.$$

---

[16] Langmuir, *J. Amer. Chem. Soc.*, 1917, **39**, 1888. Bangham, *J. Chem. Soc.*, 1931, 1324; *Trans. Faraday Soc.*, 1937, **33**, 807. Gregg, *J. Chem. Soc.*, 1942, 696.

[17] See Part I for a detailed derivation of eqn. (5.6); (5.5) is the surface analogue of the Maxwell equation :—

$$\left(\frac{\partial S}{\partial V}\right)_T = \left(\frac{\partial P}{\partial T}\right)_V.$$

[18] Magnus, *Z. physik. Chem. A*, 1929, **142**, 401.

We may now integrate to obtain the molar entropy of the surface phase relative to that at unit surface concentration :

$$\mathrm{s}^{\sigma}_{\Gamma} = -R\ln\Gamma - R\ln(1 - b\Gamma) + R\ln(1-b) + \mathrm{s}^{\sigma}_{1}.$$

Thus

$$\bar{\mathrm{s}}^{\sigma}_{\Gamma} = \mathrm{s}^{\sigma}_{\Gamma} + \Gamma\left(\frac{\partial \mathrm{s}^{\sigma}_{\Gamma}}{\partial\Gamma}\right)_{T,P} = -R\ln\frac{\Gamma}{1-b\Gamma} - \frac{Rb\Gamma}{1-b\Gamma} - R\ln(1-b) - R + \mathrm{s}^{\sigma}_{1}$$

$$= \mathrm{s}^{\sigma}_{1} - \frac{R}{1-b\Gamma} - R\ln\frac{\Gamma(1-b)}{1-b\Gamma}. \qquad . \qquad . \qquad (5.8)$$

Also, from (5.6)

$$(\partial \mathrm{H}^{\sigma}_{\Gamma}/\partial\Gamma)_{T,P} = a,$$

so that

$$\mathrm{H}^{\sigma}_{\Gamma} = \mathrm{H}^{\sigma}_{1} + a(\Gamma - 1),$$

$$\bar{\mathrm{H}}^{\sigma}_{\Gamma} = (\mathrm{H}^{\sigma}_{1} - a) + 2a\Gamma = \mathrm{H}^{\sigma}_{0} + 2a\Gamma, \quad . \qquad . \qquad . \qquad (5.9)$$

where H^{σ}_{1} and H^{σ} are the molar heat contents of the surface phase at surface concentrations 1 and zero respectively.

Hence substituting (5.7) and (5.8) into (2.3) and (2.6) we obtain

$$\ln p = \frac{\Delta\mathrm{H}^{\dagger}_{0}}{RT} + \frac{2a\Gamma}{RT} + \ln\frac{\Gamma}{1-b\Gamma} + \frac{b\Gamma}{1-b\Gamma} - \ln(1-b) - \frac{\Delta\mathrm{s}^{\dagger}_{1}}{R} + 1,$$

whence

$$p = \frac{c\Gamma}{1-b\Gamma}e^{\frac{b\Gamma}{1-b\Gamma} + \frac{2a\Gamma}{RT}},$$

where

$$c = (1-b)e^{\frac{\Delta\mathrm{H}^{\dagger}_{0}}{RT} + \frac{\Delta\mathrm{s}^{\dagger}_{1}}{R} + 1}, \qquad . \qquad . \qquad . \qquad (5.10)$$

and

$$\Delta\mathrm{H}^{\dagger}_{0} = \mathrm{H}^{\sigma}_{0} - \mathrm{H}^{G}; \quad \Delta\mathrm{s}^{\dagger}_{1} = \mathrm{s}^{\sigma}_{1} - \mathrm{s}^{G}.$$

The second technique although generally a little longer than that employing the Gibbs equation, shows clearly how variations of heat and entropy of adsorption contribute to the isotherm, and also gives a value for the integration constant in the Gibbs equation. The values of $\bar{\mathrm{H}}^{\sigma}_{\Gamma}$ and $\bar{\mathrm{s}}^{\sigma}_{\Gamma}$ calculated from various equations of state are also included in Table I.

If the surface film behaves as a perfect two-dimensional gas, the vapour pressure of the film is proportional to the amount adsorbed (Henry's law). Volmer's isotherm corresponds to the introduction of a co-area,[19] and Magnus' to inclusion of both co-area and a van der Waals' *a* term in the equation of state. We may note that Magnus' isotherm was originally based on a particular theory of the forces involved in adsorption ; we observe that it could have been derived from more general considerations. If we employ a generalized equation of state involving successive " virial coefficients ", we obtain an equation essentially similar, at low coverages, to the equations suggested by Williams, Henry and Wilkins.[20] In this case we cannot evaluate the heat and entropy changes unless we know how the virial coefficients vary with temperature. If we assume the virial coefficients to be independent of temperature and to have the values $\frac{1}{2}\Gamma_s$, $\frac{1}{3}\Gamma_s$, $\frac{1}{4}\Gamma_s$ . . . or $\frac{1}{2}(\mathrm{A}^{\sigma}_{s})$, $\frac{1}{3}(\mathrm{A}^{\sigma}_{s})$, $\frac{1}{4}(\mathrm{A}^{\sigma}_{s})$ . . . (where $1/\Gamma_s = \mathrm{A}^{\sigma}_{s}$ the average area occupied by a molecule when the surface is " saturated "), then the Langmuir equation is obtained.[21] The heat and entropy contributions are in this instance the same as those derived earlier on the basis of a localized adsorbed phase. It is difficult to estimate whether these coefficients are of the magnitude to be expected for an imperfect two-dimensional gas, but they may be compared with those of Happell's equation of state [22] for a three-dimensional gas which have the values b, $0{\cdot}625b^2$, $0{\cdot}287b^3$, $0{\cdot}193b^4$, . . . where b is four times the volume of a rigid spherical molecule.

---

[19] Volmer, *Z. physik. Chem.*, 1925, **115**, 253 ; cf. Kemball, Rideal and Guggenheim, *Trans. Faraday Soc.*, 1948, **44**, 948.

[20] Cf. ref. (9).

[21] Rowley and Innes, *J. Physic. Chem.*, 1941, **45**, 158.

The equation of state $\phi = nRT\Gamma$ conjugate with the Freundlich isotherm is not one which can be derived on any simple theory of a two-dimensional gas, and the interpretation of the variation of $\overline{\mathrm{H}}^{\sigma}_{\Gamma}$ with Γ in terms of $(\mathrm{d}n/\mathrm{d}T)$ is not clear.

Taking the entropy of an ideal two-dimensional gas given in Table I we may now define the "excess entropy" for an actual system relative to this reference system.

$$\overline{\mathrm{s}}^{\sigma,\ddagger}_{\Gamma} = \overline{\mathrm{s}}^{\sigma}_{\Gamma} + R \ln \Gamma + (\mathrm{s}^{\sigma}_{1} - R).$$

Thus
$$\ln p = \frac{\overline{\Delta \mathrm{H}}^{\ddagger}_{\Gamma}}{RT} - \frac{\overline{\Delta \mathrm{s}}^{\ddagger}_{\Gamma}}{R} + R \ln \Gamma - (\mathrm{s}^{\sigma}_{1} - R).$$

$\overline{\mathrm{s}}^{\sigma,\ddagger}_{\Gamma}$ will in this case be related mainly to the decrease in entropy resulting from the reduction in accessible area caused by the finite size of the molecules. Examination of Table I shows that, on a simple picture, $\overline{\Delta \mathrm{s}}^{\ddagger}_{\Gamma}$ will include terms of the form $R \ln (1 - b\Gamma)$ and $Rb\Gamma/(1 - b\Gamma)$. Since b will be closely related to the effective area of a molecule :

$$b \sim \mathrm{A}^{\sigma}_{s} \sim 1/\Gamma_{s},$$

these terms will approximate to $R \ln (1 - \theta)$ and $\theta/(1 - \theta)$ and may in special cases lead to equations of form similar to the Langmuir equation. We have also seen that by a suitable choice of temperature independent virial coefficients the exact form of the Langmuir equation can be obtained. Thus it is clear that it may prove extremely difficult to distinguish between the properties of localized and non-localized models of a surface phase. This is perhaps not surprising since for liquids also it is not easy to distinguish between the thermodynamic properties derived from lattice models and highly compressed gas theories of the liquid state.

Since we have assumed the fluctuations in adsorption energy over the surface to be less than kT, variation of the heat of adsorption can, on this model, only arise from molecular interactions. In the simple theory these are introduced by the van der Waals' a term and the heat of adsorption will either increase or decrease (numerically) with Γ according as a represents an attractive or repulsive force. These conclusions will be considered in the light of the experimental data in Part III.

The extension of the non-localized monolayer treatment to lower temperatures where $\Delta\epsilon \sim kT$ involves a number of difficulties. Not only does the molecular kinetic interpretation of the "spreading pressure" become obscure, but one must consider two distinct cases when introducing the effect of heterogeneity of the adsorption sites.

(*a*) *The sites of each energy are grouped together in patches.*—The adsorbed layer is then to be regarded as a polyphase system. At equilibrium the adsorbed molecules on each patch will have the same chemical potential (i.e. vapour pressure). The surface concentrations to achieve this equality will be different in the different surface phases, and so also will be the "surface pressures". We can, in principle, define the surface pressure for each phase as

$$\phi_i = (\partial G^{\sigma_i}/\partial A^{\sigma_i})_{T,P,m},$$

but in practice the application of the Gibbs equation to the observed adsorption isotherm will yield an average ϕ :

$$\phi_m = \left(\frac{\partial G^{\sigma}}{\partial A^{\sigma}}\right)_{T,P,m} = \frac{(\partial G^{\sigma_1} + \partial G^{\sigma_2} + \ . \ . \ .)}{(\partial A^{\sigma_1} + \partial A^{\sigma_2} + \ . \ . \ .)_{T,P,m}},$$

[22] Happell, *Ann. Physik*, 1906, **21**, 342.

where the ∂G^{σ_i} terms arise from the variations ∂A^{σ_i} in the area of the phase σ_i. The ∂A^{σ_i} terms will be related to the total change in area, ∂A^{σ}, by the relations,

$$\partial A^{\sigma_i} = \frac{M_i}{\Sigma M_i}\partial A^{\sigma}.$$

(*b*) *The sites of different energy occur randomly on the surface* so that any chosen element of area, however small, will embrace a representative selection of sites. We can no longer regard this as a system containing distinguishable adsorbed phases, and we can only define ϕ in one way, $(\partial G^{\sigma}/\partial A^{\sigma})_{T,P,m}$. The theoretical treatment of this model is not simple. We have a rather special set of conditions in which the adsorbed molecules are non-localized and spend most of their time moving between lattice points, but the average concentration of molecules fluctuates rapidly from point to point on the surface because of the varying heats of adsorption on different sites. We shall not then expect the equation of state $\phi = \phi(\Gamma, T)$ to bear any simple relationship to the equations of state for imperfect three dimensional gases.

In both cases the differential heat of adsorption will vary with the amount adsorbed; the magnitude of the variation will depend upon the degree of heterogeneity of the surface.

6. The Polanyi Potential Theory.[23]—The present discussion of adsorption has some features in common with Polanyi's treatment and it seems useful to compare them. Both treatments direct attention in the first instance to the change in chemical potential on adsorption relative to some standard state. Polanyi employs the pure liquid as reference state, and in terms of this the graphs of $\Delta\mu_\Gamma^\circ$ against Γ at a series of temperatures have the general form shown in Fig. 1.

Equilibrium between the liquid and adsorbed states is given by the intercept of the free energy curve with the Γ-axis at Γ_s. As stressed in § 4, these "saturation" concentrations do not, in our view, correspond to complete filling of the available surface. This will correspond to Γ° which the curves approach at large positive values of μ_Γ°. The variation of Γ_s with temperature is not to be attributed to a variation of available surface with temperature but to an increasing number of vacant adsorption sites in the "equilibrium film" as the temperature increases. We may also picture the liquid state as containing an ever increasing number of "holes" as the temperature is raised[24] so that if the change with temperature of the percentage of "holes" is approximately the same for the adsorbed phase as for the liquid with which it is in equilibrium,

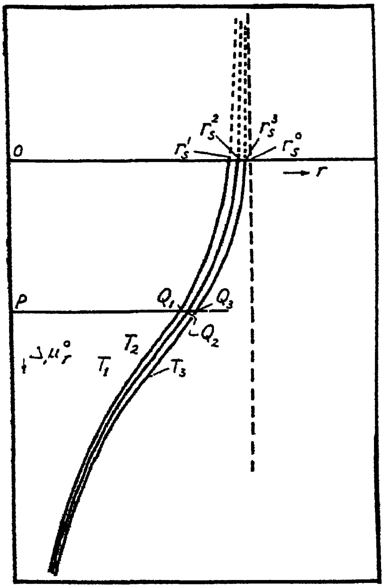

FIG. 1.—Chemical potential of surface phase at various temperatures, relative to pure liquid at same temperature (schematic).

---

[23] (*a*) Polanyi, *Verh. deut. physik. Ges.*, 1916, **15**, 55. (*b*) Goldmann and Polanyi, *Z. physik. Chem. A*, 1928, **132**, 313

[24] Frenkel, *Kinetic Theory of Liquids* (Oxford, 1946), p. 174. Eyring, *J. Chem. Physics.*, 1936, **4**, 283. Ewell and Eyring, *ibid.*, 1937, **5**, 726. Altar, *ibid.*, 1937, **5**, 577. Furth, *Proc. Camb. Phil. Soc.*, 1941, **37**, 252.

then we shall expect Γ_s (or w_s the weight of vapour adsorbed on 1 g. of adsorbent) to be proportional to the density of the liquid ρ, i.e. $w_s/\rho =$ constant. Furthermore, if the same is also true of adsorbed phases differing from the liquid by a constant difference of chemical potential such as Q_1, Q_2, Q_3, then the intercepts PQ_1, PQ_2, PQ_3 should also be proportional to the ρ's. This means that if we plot $\Delta\mu^{\circ}_{\Gamma}$ not against Γ, but against w/ρ (= the "volume of liquid adsorbed"), then the free energy curves should coincide to form a "characteristic curve" for the particular system. From the characteristic curve one can calculate the adsorption isotherm at any temperature at which the vapour pressure and density of the liquid is known. The existence of characteristic curves of the above type was deduced by Polanyi by a different argument, based, however, upon the assumed similarity between the liquid and adsorbed phases.

The argument we have given is qualitative, but it should be possible to derive from our general equations thermodynamic conditions for the Polanyi characteristic curve to be the same at all temperatures. We find, however, that this requires first the existence of a functional relationship between $\overline{\Delta H}^{\ddagger}_{\Gamma}$ and $\overline{\Delta S}^{*}_{\Gamma}$, and then the condition takes the form of a differential equation leading to a relationship between $\overline{\Delta H}^{\ddagger}_{\Gamma}$ and Γ. The direct solution of this equation is not straightforward but it may be possible, by carrying out an analysis of data for systems which conform to Polanyi's predictions, to derive the thermodynamic conditions for their validity.

7. Conclusions.—The above examination of possible "ideal" systems which might be employed as reference systems in a study of the thermodynamics of adsorption leads to the following important conclusions:

(i) The thermodynamics of adsorption on solids can be developed by standard methods, and free energies, heats and entropies of adsorption can be evaluated, subject to slight approximations.

(ii) The fact that a particular physical theory of adsorption leads to an adsorption isotherm which is observed experimentally is no evidence for the correctness of the model. This is an important point which has been overlooked too often in the past.

(iii) Even the correct prediction by a theory of the variation of heat and entropy of adsorption may not constitute a final proof, for we find that it is possible for quite different models to give very similar expressions for the heat and entropy changes, and the experimental data may not be sufficiently precise to distinguish between them.

(iv) Both the ideal localized monolayer and the ideal non-localized monolayer models may be used as reference systems. In general we shall expect the former to be more appropriate for systems at low temperatures, and especially where the adsorbent may be expected to possess definite active sites: while the latter model should be applicable to systems at high temperatures especially where the surface forces are expected to exhibit no strongly localized maxima. At intermediate temperatures it seems probable that the localized monolayer model will be more useful, as the extension of the theory of non-localized adsorption to heterogeneous surfaces presents considerable difficulties.

(v) In view of these conclusions it seems that, unless there is independent evidence that in a particular system the adsorbate behaves as a two-dimensional gas, then it is of doubtful significance to compare two-dimensional equations of state derived from adsorption isotherms with those of three-dimensional phases.[25]

(vi) An extensive and careful analysis of the experimental data is now required to assess the usefulness of the methods discussed and this will be presented in Part III.

[25] Gregg,[16]. Gregg and Maggs, *Trans. Faraday Soc.*, 1948, **44**, 123. Harkins and Jura, *J. Chem. Physics*, 1944, **12**, 112.

I have to acknowledge my indebtedness to the University of Oxford for an I.C.I. Fellowship (1945-47) during which period many of the ideas embodied in this paper were developed. I also wish to thank Dr. R. R. Smith for several valuable discussions, and Dr. F. C. Tompkins for letting me see some of his own papers[26] on this topic before publication.

Appendix

Exact Thermodynamic Equations.—In § 2 we have for convenience employed approximate equations. We give here the exact thermodynamic equations and discuss the nature of the approximations. Although analogous equations are well known for the equilibrium between liquid and vapour it seems worthwhile to state them explicitly for the case of adsorbed phases.

We have, for equilibrium,

$$\mu^{\sigma}_{\Gamma} - \mu^{\dagger G} = \Delta\mu^{\dagger}_{\Gamma} = RT \ln p^{*}_{\Gamma}, \quad . \quad . \quad . \quad (\text{A. 1})$$

where p^{*}_{Γ} is the fugacity of the vapour. If we choose as standard state the vapour at unit pressure

$$\ln p^{*}_{\Gamma} = \ln p_{\Gamma} + \frac{1}{RT}\int_{1}^{p_{\Gamma}} \beta \, \mathrm{d}p, \quad . \quad . \quad . \quad . \quad (\text{A. 2})$$

where $\beta = \mathrm{v}^{G} - \dfrac{RT}{p}$; v^{G} is the molar volume of the vapour at pressure p. With standard state, a perfect gas at unit pressure, the lower limit of integration will be zero.

Since for most vapours β is almost independent of pressure (for low pressures) it may be identified with the second virial coefficient and we may integrate immediately:

$$\Delta\mu^{\dagger}_{\Gamma} = RT \ln p^{*}_{\Gamma} = RT \ln p_{\Gamma} + \beta(p_{\Gamma} - 1). \quad . \quad . \quad (\text{A. 3})$$

Similarly,

$$\Delta\mu^{\circ}_{\Gamma} = RT \ln p^{*}_{\Gamma}/p^{\circ *} = RT \ln (p_{\Gamma}/p^{\circ}) + \beta(p_{\Gamma} - p^{\circ}). \quad . \quad (\text{A. 4})$$

Neglect of the correction terms in equation (A. 3) and (1. 4) will, for organic vapours such as benzene, lead to errors of the order of 1-2 % in the chemical potential.

The exact equation for the temperature coefficient of vapour pressure at constant Γ follows from

$$\frac{\mathrm{d}\left(\dfrac{\Delta\mu^{\dagger}_{\Gamma}}{T}\right)}{\mathrm{d}T} = \left(\frac{\partial\dfrac{\Delta\mu^{\dagger}_{\Gamma}}{T}}{\partial T}\right)_{P} + \left(\frac{\partial\dfrac{\Delta\mu^{\dagger}_{\Gamma}}{T}}{\partial T}\right)_{T} \cdot \frac{\mathrm{d}p_{\Gamma}}{\mathrm{d}T}. \quad . \quad . \quad (\text{A. 5})$$

The first term on the right-hand side is equal to

$$-\frac{\overline{\Delta \mathrm{H}}^{\dagger}_{\Gamma}}{T^{2}} = -\frac{\overline{\mathrm{H}}^{\sigma}_{\Gamma} - \mathrm{H}^{\dagger G}}{T^{2}}, \quad . \quad . \quad . \quad . \quad . \quad (\text{A. 6})$$

while in the second

$$\left(\frac{\partial\dfrac{\Delta\mu^{\dagger}_{\Gamma}}{T}}{\partial P}\right)_{T} = \frac{1}{T}\left(\frac{\partial\mu^{\sigma}_{\Gamma}}{\partial P}\right)_{T} = \frac{\mathrm{v}^{\sigma}_{\Gamma}}{T}, \quad . \quad . \quad . \quad (\text{A. 7})$$

where $\mathrm{v}^{\sigma}_{\Gamma}$ is the mean molar volume of the adsorbed molecules.

Thus

$$\frac{\mathrm{d} \ln p^{*}_{\Gamma}}{\mathrm{d}T} = -\frac{\overline{\Delta \mathrm{H}}^{\dagger}_{\Gamma}}{RT^{2}} + \frac{\mathrm{v}^{\sigma}_{\Gamma}}{RT} \cdot \frac{\mathrm{d}p_{\Gamma}}{\mathrm{d}T}. \quad . \quad . \quad . \quad (\text{A. 8})$$

But

$$\frac{\mathrm{d} \ln p^{*}_{\Gamma}}{\mathrm{d}T} = \left(\frac{1}{p} + \frac{\beta}{RT}\right)\frac{\mathrm{d}p_{\Gamma}}{\mathrm{d}T} = \frac{\mathrm{v}^{G}}{RT}\,\frac{\mathrm{d}p_{\Gamma}}{\mathrm{d}T}. \quad . \quad . \quad . \quad (\text{A. 9})$$

Hence

$$\frac{\mathrm{d}p_{\Gamma}}{\mathrm{d}T} = -\frac{\overline{\Delta \mathrm{H}}^{\dagger}_{\Gamma}}{T(\mathrm{v}^{G} - \mathrm{v}^{\sigma}_{\Gamma})}, \quad . \quad . \quad . \quad . \quad (\text{A. 10})$$

which is the exact form of the Clausius-Clapeyron equation for the system considered.

---

[26] *Trans. Faraday Soc.*, 1950, **46**, 569, 580.

The application of exact thermodynamics to surface phases on solids meets with difficulties when we attempt a precise determination of v_Γ^σ. From a thermodynamic standpoint it is defined by eqn. (A. 7), but there is no reliable experimental method of determining either v_Γ^σ, or ρ_Γ^σ the density of the adsorbed phase, although a number of methods have been suggested.[27]

It is probable, however, that in most instances v_Γ^σ will be small enough in comparison with v^G that we may neglect it in (A. 10), although vapours adsorbed in fine capillaries may have rather low densities and v_Γ^σ may be several per cent. of v^G. In general we may expect errors of less than ½ % in $\overline{\Delta\mathrm{H}}_\Gamma^\dagger$ to arise from neglect of v_Γ^σ.

If we make both the above approximations we obtain the well-known approximate formula

$$\frac{\mathrm{d}\ln p_\Gamma}{\mathrm{d}T} = -\frac{\overline{\Delta\mathrm{H}}_\Gamma^\dagger}{RT^2}. \qquad . \quad . \quad . \quad . \qquad (\text{A. 11})$$

The errors likely to arise in $\overline{\Delta\mathrm{H}}_\Gamma^\dagger$ from the approximations may be up to about 3 % for organic vapours below their normal boiling points.

We notice that we require the temperature coefficient of vapour pressure of the surface phase maintained at constant surface concentration; it is usually assumed that this can be interpreted as constant weight of adsorbate per gram of adsorbent, i.e. we assume the available surface area is independent of temperature. Wilkins [9c] has suggested that the vapour pressures at different temperatures should be taken for the same "fraction of saturation (θ)", the "saturation capacity" (determined by Wilkins from the "limiting slope" of the Langmuir plot) being allowed to vary with temperature. The above arguments show, however, that the "heat of adsorption" obtained in this way is not related in any simple manner to any thermodynamically defined heat (cf. Part I).

Chemistry Department,
University College, Dundee,
University of St. Andrews,
Scotland.

---

[27] Ewing and Spurway, *J. Amer. Chem. Soc.*, 1930, **52**, 4635. De Vries, *ibid.*, 1935, **57**, 1771. Danforth and De Vries, *ibid.*, 1939, **61**, 873. Morrison and McIntosh, *Can. J. Res. B*, 1946, **24**, 137. Tuck, McIntosh and Maass, *ibid.*, 1948, **26**, 20.

THE THERMODYNAMICS OF ADSORPTION

PART III.—ANALYSIS AND DISCUSSION OF EXPERIMENTAL DATA

BY DOUGLAS H. EVERETT

Received 11*th April*, 1950

An analysis on the lines suggested in Part II is made of published experimental data on the adsorption of gases. It is concluded that the thermodynamics of adsorbed monolayers may be discussed very satisfactorily by employing, as ideal reference system, the ideal localized monolayer model. Non-ideal behaviour arises from deviations of both the heat and entropy of adsorption from the ideal values. A linear relation exists between the non-ideal entropy and the heat of adsorption which for adsorption on charcoal at 0° C is identical with that between heats and entropies of condensation of vapours to pure liquids, or into solution. This relation suggests a method of calculating heats of adsorption from a single adsorption isotherm. The generality of the relation with respect to other adsorbates seems probable but the experimental data are not extensive enough to prove this conclusively.

The application of the present findings to problems of surface heterogeneity and multilayer adsorption is discussed.

1. **Introduction.**—In Parts I and II [1] we have outlined a general thermodynamic approach to adsorption equilibria and we now proceed to examine our proposed methods in the light of the data available in the literature. Published data suitable for detailed thermodynamic analysis are rare and, in the absence of reliable evidence on the accuracy of much of it, the conclusions reached in this paper must be to some extent tentative; we consider, however, that the method of analysis presented is a useful one which points the way for further investigation. Our object will be, in the first instance, to evaluate the partial molar free energy, heat and entropy of adsorption relative to the gas state at 1 mm. pressure. We shall then investigate the usefulness of the procedure of defining an ideal adsorbed phase as either (*a*) an ideal localized monolayer for which the heat of adsorption is independent of amount adsorbed, while the partial molar localization entropy of the phase is $-R\ln\theta/(1-\theta)$, where θ is the "fraction of surface covered" or (*b*) an ideal non-localized phase for which the spreading pressure follows the law $\phi = \Gamma RT$, where Γ is the surface concentration. Deviations from ideality will then be interpreted in terms of the "excess functions" [2] in a manner comparable to the treatment of solutions. The models we have chosen for ideal adsorbed phases are monolayer models, and we have therefore only analyzed data for systems which exhibit "Langmuir type" adsorption isotherms, and which may reasonably be supposed to form only a unimolecular film. The choice of an ideal system for the case of multimolecular adsorption will be much more difficult and we must await a more complete theory of adsorption of this type.[3] A possible approach to this problem is suggested by the results of the present analysis.

2. **Analysis of Experimental Data.**—The partial molar free energy of adsorption is given by

$$\Delta\mu_\Gamma^\dagger = RT\ln p_\Gamma, \quad . \quad . \quad . \quad . \quad (2.1)$$

when we take the gas state at unit pressure as standard state and ignore deviations from the perfect gas laws, or

$$\Delta\mu_\Gamma^\circ = RT\ln p_\Gamma/p^\circ, \quad . \quad . \quad . \quad . \quad (2.2)$$

relative to the adsorbate in the pure liquid state (vapour pressure $= p^\circ$).

The differential heat of adsorption may be evaluated by employing the Clausius-Clapeyron equation in its approximate form:

$$\frac{d\ln p_\Gamma}{d(1/T)} = \frac{\overline{\Delta H}_\Gamma^\dagger}{R} \quad . \quad . \quad . \quad . \quad . \quad (2\cdot3)$$

and the partial molar entropy $(\overline{\Delta S}_\Gamma^\dagger)$ obtained by combining the $\Delta\mu_\Gamma^\dagger$ and $\overline{\Delta H}_\Gamma^\dagger$ values.

The selection of data for analysis has been difficult. The theoretical study in Part II is concerned with monolayer adsorption, so we have only examined systems giving Langmuir type isotherms. We have also been obliged to restrict our analysis to work in which isotherms have been determined at several temperatures, and over a wide range of pressures, reaching, if possible, up to "saturation conditions". We have also limited ourselves to work for which the published data are given numerically. Unfortunately the majority of the vast literature on adsorption is eliminated on one or other of these grounds and our final selection includes only the work of Homfray,[4] Titoff,[5] Richardson,[6] Coolidge,[7] Goldmann and Polanyi,[8] and van Itterbeek and van Dingenen,[9] for the adsorption of gases on charcoal; the data of Frankenburg [10] (H_2 on tungsten), Wilkins [11] (N_2, A, O_2 on Pt), Keesom, Schmidt and Schweers [12] (H_2, Ne on glass) have also been analyzed but for various reasons they are not entirely suitable for thermodynamic analysis. The recent work of Tompkins and co-workers [13] on the adsorption of gases by ionic crystals will be discussed separately in a later paper.

---

[1] (*a*) Everett, *Trans. Faraday Soc.*, 1950, **46**, 453. (*b*) See preceding paper.

[2] The notation adopted for the various entropy terms is as follows:—

$\overline{\Delta S}_\Gamma^\dagger$ = entropy of isothermal transfer (per mole) from gas state at 1 mm. pressure to adsorbed phase.

$\overline{\Delta S}_\Gamma^\circ$ = entropy of isothermal transfer (per mole) from pure liquid to adsorbed phase.

$\overline{\Delta S}_\Gamma^{*}$, $\overline{\Delta S}_\Gamma^{c*}$ = excess entropies of transfer when ideal localized monolayer taken as standard reference system; standard states gas at 1 mm. pressure and pure liquid respectively.

$\overline{\Delta S}_\Gamma^{\ddagger}$, $\overline{\Delta S}_\Gamma^{c\ddagger}$ = excess entropies of transfer when ideal non-localized monolayer taken as standard reference system; standard states gas at 1 mm. pressure and pure liquid respectively.

[3] Cf. Hill, *J. Chem. Physics*, 1947, **15**, 767.

The method of analysis is perhaps best illustrated by presenting the results for two typical systems in detail, and for this purpose we have chosen Richardson's data for ammonia on charcoal and Goldmann and Polanyi's for ethyl ether on charcoal.

3. **Results of Analysis.**—(i) AMMONIA ON NUTSHELL CHARCOAL.—In Fig. 1 we show graphs of $\Delta\mu^{\dagger}_{T}$ against w (cm.^{3} adsorbed per g. of charcoal) for a range of temperatures taking the standard gas pressure as 1 mm. A family of curves is obtained which is typical of those for systems exhibiting Langmuir type isotherms. Complete filling of the surface will correspond to $w \sim 160$ cm.^{3} NH_3/g. Heats and entropies of adsorption ($\overline{\Delta \mathrm{H}}^{\dagger}_{T}$ and $\overline{\Delta \mathrm{S}}^{\dagger}_{T}$) at 273·1° K have been calculated from these results and are shown in Fig. 2. The heat of adsorption (curve (*a*)) falls (numerically) for the initial stages of the adsorption, but then remains constant, within the experimental error, from about 20 % coverage to the highest values examined. The entropy term (curve (*b*)) becomes steadily more negative following a slightly sigmoid curve. If we take the true saturation value for the surface to be 160 cm.^{3}/g. and evaluate $-R \ln \theta/(1-\theta)$ we obtain curve (*c*) for $T\overline{\Delta \mathrm{S}}^{*}_{T}$ at 273·1° K; $\overline{\Delta \mathrm{S}}^{*}_{T}$ is independent of the surface concentration of adsorbed molecules. $T\overline{\Delta \mathrm{S}}^{\ddagger}_{T}$ varies with surface concentration in the manner shown in Fig. 2(*d*). We thus conclude that except below 20 % coverage, this system follows the Langmuir equation.

Titoff's data for the ammonia-nutshell charcoal system are in excellent agreement with Richardson's, and show a similar initial fall in the heat of adsorption (cf. Fig. 9).

The ammonia-charcoal system is thus a good example of a system following the equations derived for an ideal localized monolayer.

(ii) ETHYL ETHER ON CHARCOAL.—Figs. 3 and 4 show the results of an analysis of Goldmann and Polanyi's data for the ethyl ether + Aussig A charcoal system. Here we have employed the pure liquid as standard state. In Polanyi's work the data at each temperature reach up to close to the saturation vapour pressure of the liquid. There is some indication that at lower temperatures multilayer formation commences close to the

---

[4] Homfray, *Z. physik. Chem.*, 1910, **74**, 129.

[5] Titoff, *ibid.*, 1910, **74**, 641.

[6] Richardson, *J. Amer. Chem. Soc.*, 1917, **39**, 1828.

[7] Coolidge, *ibid.*, 1924, **46**, 596.

[8] Goldmann and Polanyi, *Z. physik. Chem.*, 1928, **132**, 321.

[9] van Itterbeek and van Dingenen, *Physica*, 1937, **4**, 389, 1169; 1938, **5**, 529.

[10] Frankenburg, *J. Amer. Chem. Soc.*, 1944, **66**, 1827, 1838.

[11] Wilkins, *Proc. Roy. Soc. A*, 1938, **164**, 510.

[12] (*a*) Keesom and Schmidt, *Proc. Roy. Soc. Amsterdam*, 1933, **36**, 825; (*b*) Keesom and Schweers, *Physica*, 1941, **8**, 1007, 1020.

[13] (*a*) Crawford and Tompkins, *Trans. Faraday Soc.*, 1948, **44**, 698; (*b*) Young and Tompkins (unpublished).

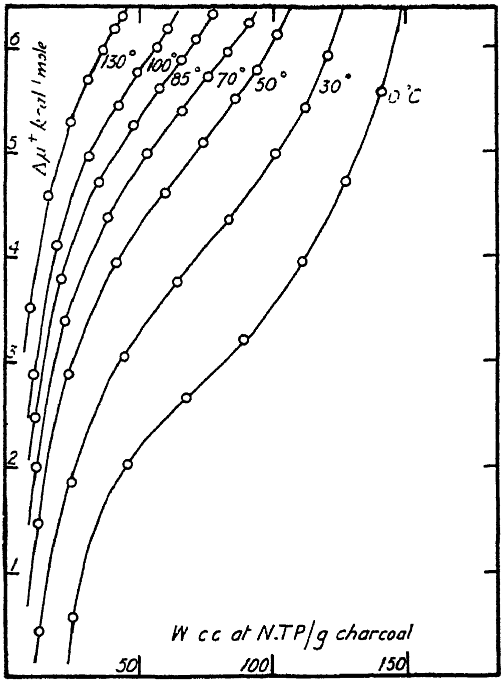

FIG. 1.—Chemical potential relative to standard gas state against surface concentration for $NH_3^\ddagger$ nutshell charcoal system at various temperatures.

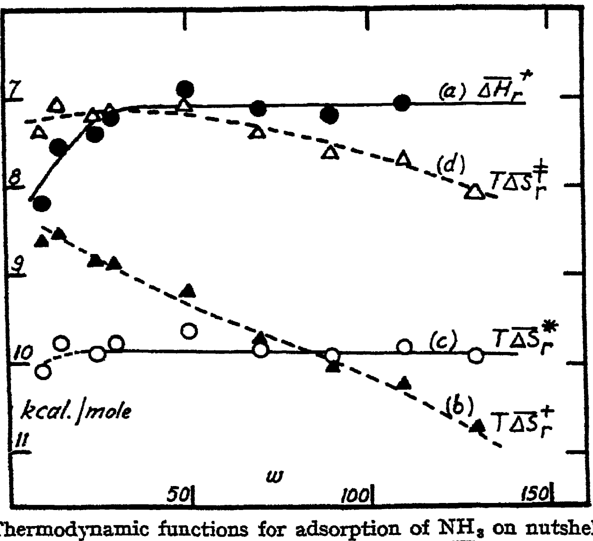

FIG. 2.—Thermodynamic functions for adsorption of NH_3 on nutshell charcoal.
Curve (*a*) $\overline{\Delta H}^\dagger$ against *w* Curve (*c*) $T \,.\, \overline{\Delta S}^*$ against *w*
(*b*) $T \,.\, \overline{\Delta S}^\dagger$ against *w* (*d*) $T \,.\, \overline{\Delta S}^+$ against *w*.

liquid vapour pressure; this is revealed by the sudden bend in the $\Delta\mu_\Gamma^\circ$ curves which become asymptotic to the Γ axis instead of cutting it. If we ignore this phenomenon and extrapolate the smooth, slightly sigmoid free energy curves we see that, in the absence of multilayer formation, equilibrium would be reached between liquid and adsorbed phase ($\Delta\mu_\Gamma^\circ = 0$) at slightly different values of Γ. This does not in our opinion mean that the available surface of the charcoal varies with temperature, but that as the temperature is raised, the adsorbed monolayer in equilibrium with liquid at the same temperature contains an ever increasing number of "holes" or vacant lattice sites (cf. Part II). The effective number of active sites corresponds to a saturation capacity of about 4·04 g. sorbate/10 g. charcoal for $p \to \infty$.

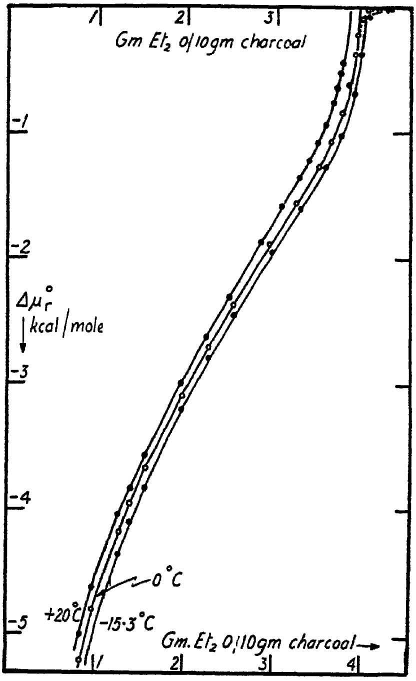

FIG. 3.—Chemical potential relative to pure liquid against surface concentration for ethyl ether + charcoal system at various temperatures.

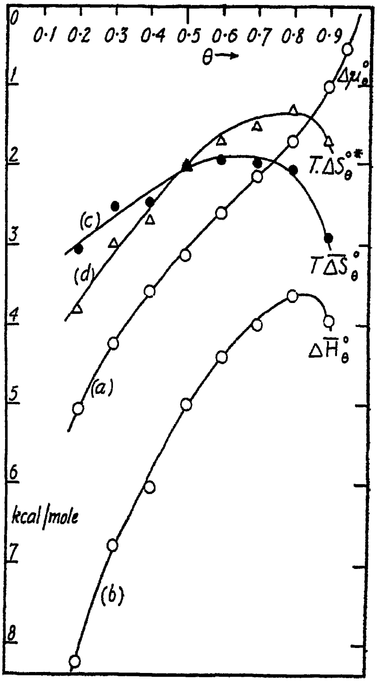

FIG. 4.—Thermodynamic functions for adsorption of ethyl ether on charcoal.

Curve (*a*) $\Delta\mu^\circ$ against θ.
(*b*) $\overline{\Delta H}^\circ$ against θ.
(*c*) $T\,.\,\overline{\Delta S}^\circ$ against θ.
(*d*) $T\,.\,\overline{\Delta S}^{\circ *}$ against θ.

The differential heat of adsorption falls steadily from $\theta = 0{\cdot}2$ to about 0·85, and then appears to rise sharply; $T\,.\,\overline{\Delta S}_\Gamma^\circ$ passes through a numerical minimum at about $\theta = 0{\cdot}6$. If we take the ideal localized monolayer as reference system with 4·04 g. sorbate/10 g. charcoal as the true saturation value then $T\,.\,\overline{\Delta S}_\Gamma^{\circ *}$ is found to lie parallel to the $\overline{\Delta H}_\Gamma^\circ$ curve. This parallelism is shown more clearly in Fig. 5 where both $T\,.\,\overline{\Delta S}_\Gamma^\circ$ and $T\,.\,\overline{\Delta S}_\Gamma^{\circ *}$ are plotted against $\overline{\Delta H}_\Gamma^\circ$. If we take the ideal entropy as $-R \ln \theta/(1-\theta)$ we reveal a linear relation between the excess entropy of adsorption and the differential heat of adsorption as the surface coverage varies. If we refer the system to the ideal non-localized monolayer no such parallelism is observed.

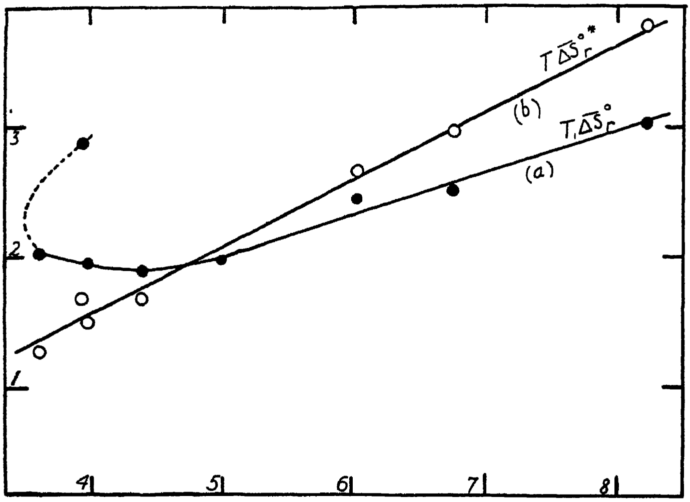

The ordinate is — $T\overline{\Delta s}$ and abscissae — $\overline{\Delta H}^\circ$.

FIG. 5.—Relation between heats and entropies of adsorption for ether on charcoal.

(*a*) $T\,.\,\overline{\Delta s}^\circ$ against $\overline{\Delta H}^\circ$. (*b*) $T\,.\,\overline{\Delta s}^{\circ *}$ against $\overline{\Delta H}^\circ$.

The ethyl ether-charcoal system is thus one which does not follow the ideal Langmuir equation, but deviates from it because of a simultaneous variation of both heat and entropy terms with surface concentration. The heat and non-ideal entropy terms are linearly related.

(iii) OTHER CHARCOAL SYSTEMS.—All the systems studied by Goldmann and Polanyi behave in a manner very similar to the ether-charcoal system except that the actual shapes of the $\overline{\Delta H}$ and $\overline{\Delta s}$ curves vary slightly. There is a linear relationship between $\overline{\Delta H}^\circ_T$ and $\overline{\Delta s}^{\circ *}_T$ for each gas-charcoal pair. Moreover, if we change the standard state from the pure liquid to gas at 1 mm. pressure so that the standard states are virtually identical for all systems and evaluate the entropy at 273·1° K then we find that the $\overline{\Delta H}^\ddagger_T$ against $\overline{\Delta s}^*_T$ curves for the various systems are superimposed. This remarkable correlation between the thermodynamic functions for the adsorption of different vapours on the same charcoal becomes more striking when we find that the data obtained for ammonia on a different charcoal fall on an extension of this same line. In fact (Fig. 6) all the gas-charcoal systems we have examined give points lying on the same general line. These points refer to gases differing as widely as H_2 and ether, and to a variety of different types of charcoal. Coolidge's results do not conform particularly well to the relation, but they scatter so much among themselves and are barely extensive enough for satisfactory analysis that we do not attach too much weight to them.

The best straight line through the experimental points has the equation

$$\overline{\Delta s}^*_T = -25{\cdot}5 + 0{\cdot}0014\,\overline{\Delta H}^\ddagger_T. \quad . \quad . \quad . \quad (3{\cdot}1)$$

Deviations from this average about ± 1·0 cal./mole deg. in $\overline{\Delta s}^*$ or about ± 100 cal. in the heat of adsorption ; this is well within the usual experimental error.

Moreover this equation is virtually identical with that observed by Barclay and Butler[14] between the heats and entropies of condensation of vapours both to pure liquids and into solutions. The Barclay-Butler line (at 25° C), as re-evaluated by Frank,[15] is shown dotted in Fig. 6.

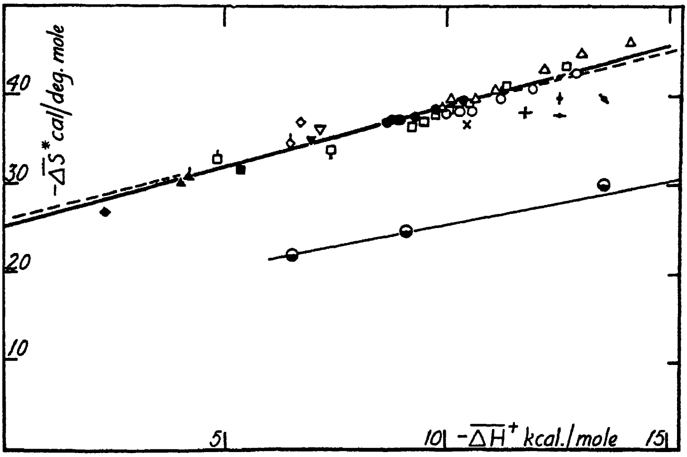

Fig. 6.—Relation between $\Delta\bar{H}^\dagger$ and ΔS^* for adsorption on charcoal at 0° C, and for hydrogen on tungsten at 300° C. Barclay-Butler relation at 25° C shown dotted.

Key :

○	Pentane	on Aussig A	(Goldmann and Polanyi)
●	Ethyl chloride	,, ,,	,, ,,
△	Ethyl ether	,, ,,	,, ,,
□	Carbon disulphide	,, ,,	,, ,,
⧫	Hydrogen	on coconut charcoal	(Titoff)
▲	Nitrogen	,, ,,	,,
◊	Carbon dioxide	,, ,,	,,
▼	Ammonia	,, ,,	,,
◊	Carbon dioxide	,, ,,	(Richardson)
▽	Ammonia	,, ,,	,,
■	Methane	on wood charcoal	(Homfray)
□	Ethane	,, ,,	,,
□	Carbon monoxide	,, ,,	,,
▲	Nitrogen	,, ,,	,,
×	Carbon disulphide	on coconut charcoal	(Coolidge)
+	Ethyl formate	,, ,,	,,
◆	Chloroform	,, ,,	,,
◆	Benzene	,, ,,	,,
●	Carbon tetrachloride	,, ,,	,,
●	Ethyl ether	,, ,,	,,
⊖	Hydrogen on tungsten		(Frankenburg)

In no case have we found any evidence that the use of an ideal non-localized monolayer as reference system would provide a more satisfactory analysis.

The data for the adsorption of He, H_2 and CO on charcoal at low temperatures are difficult to analyze satisfactorily ; the results are shown in

---

[14] Barclay and Butler, *Trans. Faraday Soc.*, 1938, 34, 1445.
[15] Frank, *J. Chem. Physics*, 1945, 13, 493.

Fig. 7. There is some indication that a linear relation still exists between the heat and excess entropy of adsorption, but that the slope increases as the temperature is decreased. The data are not reliable enough to allow us to investigate quantitatively the dependence of the slope on the temperature, since in most cases the analysis depends on rather uncertain estimates of the saturation values.

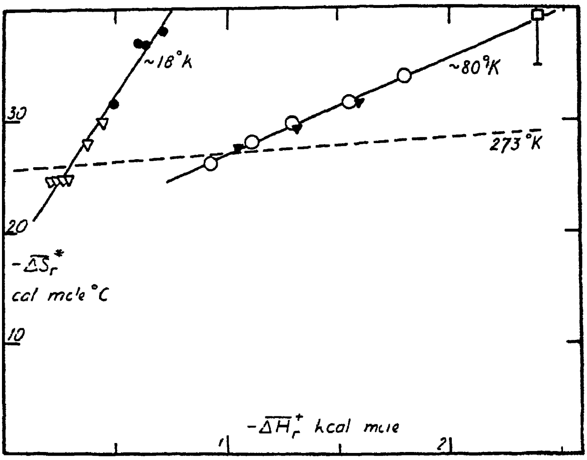

FIG. 7.—Relation between $\overline{\Delta H}$+ and $\overline{\Delta S}$* for adsorption at low temperatures.

○	Hydrogen on Carbotox	~ 80° K
▼	Hydrogen on Desorex B	~ 80° K
□	Carbon monoxide on Desorex B	~ 75° K
●	Neon on glass	~ 18° K
▽	Helium on Carbotox	~ 18° K

(iv) ADSORPTION ON GLASS AND METALS.—The data in the literature for adsorption on plane surfaces are also difficult to analyze. This is usually because no isotherms have been taken up to saturation conditions and it is therefore often quite impossible to obtain a reliable figure for the saturation value for the surface.

Data for $\overline{\Delta S}^*_r$ and $\overline{\Delta H}^\dagger_r$ for the systems H_2 on tungsten and Ne on glass are included in Fig. 6 and 7. They are rather scanty and do not form a very clear picture except to confirm that the slope of the ΔS^* against $\Delta H^\dagger$ line depends on the temperature. This is further confirmed by Tompkins and co-workers' data on adsorption on ionic solids which will be discussed later. It should be noted that for hydrogen on tungsten, since the adsorption reaction is $H_2(g) \leftrightharpoons 2H(\text{ads.})$, the ideal localization entropy term is $2R \ln \theta/(1 - \theta)$ and the heat and entropy terms are per mole of H_2.

4. **Discussion.**—Our object in carrying through the analysis of experimental results reported above was to investigate the relative merits of the localized and non-localized monolayers as ideal reference systems for the study of the thermodynamics of adsorption. For each system studied we find that by taking the ideal localized monolayer as reference system, the excess entropy is a linear function of the heat of adsorption. The alternative reference system leads to no such simple correlation between the excess thermodynamic quantities. On this basis we therefore consider that the former reference system is the more useful and we now proceed to discuss the consequences of this.

(i) GENERAL.—Perhaps the most important result of the present study is the demonstration that deviations from the ideal Langmuir equation occur by the variation of *both* the differential heat of adsorption and the partial entropy of adsorption with surface concentration. This means that any detailed statistical mechanical theory which attempts to take account of variations in the heat of adsorption must be inaccurate if it ignores the simultaneous variation in the entropy. It is only very recently that Hill[16] has drawn attention to this from a theoretical standpoint.

(ii) THE LOCALIZATION ENTROPY.—The above analysis suggests strongly that a term of the form $- R \ln \theta/(1 - \theta)$ plays a fundamental part in the entropy of adsorption, and this term is the partial localization entropy corresponding to the ideal localized monolayer model. We must not necessarily conclude, however, that the physical state of the adsorbed phase is thereby determined, for we have seen that an entropy term of similar form could arise on the basis of other physical models. In particular we have suggested that this term will be a reasonably accurate estimate for the configurational entropy of a phase in the transition region between localized and non-localized (i.e. a two-dimensional liquid state). The emergence of the above entropy term is, however, important when we come to discuss the question of surface heterogeneity (see below).

(iii) THE HEAT-ENTROPY RELATION.—Functional relations between heat and entropy changes are of frequent occurrence in physico-chemical phenomena, but it is unfortunately very easy to obtain spurious relationships from data of inadequate accuracy,[17(a)] while as Barrer and Skirrow[17(b)] have stressed, under certain circumstances they may have little fundamental significance. For example, if in a series of systems $\Delta\mu$ remains roughly constant in comparison with ΔH and $T\Delta\text{s}$, then the equation $\Delta\mu = \Delta\text{H} - T\Delta\text{s}$ ensures an approximately linear relation between Δs and ΔH, the slope of the line being $1/T$.

In the present instance we feel some confidence in our conclusions because (*a*) the changes in $\Delta\mu$, ΔH and Δs are often of about the same magnitude, (*b*) the linear relation is only obtained if account is taken of the localization entropy and (*c*) the final relation is identical with the Barclay-Butler relation between the standard heats and entropies of evaporation from liquids and solutions (cf. dotted line, Fig. 6), and suggests that they may have a common interpretation.

The heat-entropy relationship may be accounted for in rather general terms as follows.[18] The potential energy of a molecule approaching an adsorbing surface will vary with its distance from the surface in the manner shown in Fig. 8(*a*). If a molecule is adsorbed on an active site, then its motion parallel to the surface will be governed by potential energy curves of the type shown in Fig. 8(*b*). The vibrational entropy of the molecule arising from translation normal to, and parallel to, the surface depends upon the curvature of the potential minima; the present experimental results indicate that the deeper the potential well the greater the curvature at the potential minimum. Indeed, this is a characteristic of potential energy curves of the Morse type and the bireciprocal form. Presumably also entropy contributions arising from rotation of the adsorbed molecule, will also be more restricted the greater the energy of adsorption.[19]

Without a detailed theory of the forces acting between the surface and the adsorbed molecules it is difficult to attempt a theoretical derivation of the heat-entropy relation. A preliminary calculation, using classical mechanics, suggests, however, that on the basis of a Lennard-Jones and Devonshire bireciprocal potential field there should be a linear relation between the entropy of vibration and the logarithm of the energy of adsorption; over small ranges ΔH and Δs would be virtually linearly related and in any case could be made so by a small alteration to the model. However, the calculated slope appears to be much less than that observed. Further investigation of this problem is in hand.*

---

[16] Hill, *J. Chem. Physics*, 1949, **17**, 762.

[17] (*a*) See, for example, discussion in Hinshelwood, *Kinetics of Chemical Change*, (Oxford, 1940), p. 258; (*b*) Barrer and Skirrow, *J. Polymer Sci.*, 1948, **3**, 549, 564.

[18] See, for example, (*a*) Frank,[15] *loc. cit.*; (*b*) Bell, *Trans. Faraday Soc.*, 1937, **33**, 496.

[19] Hill, *J. Chem. Physics*, 1948, **16**, 181.

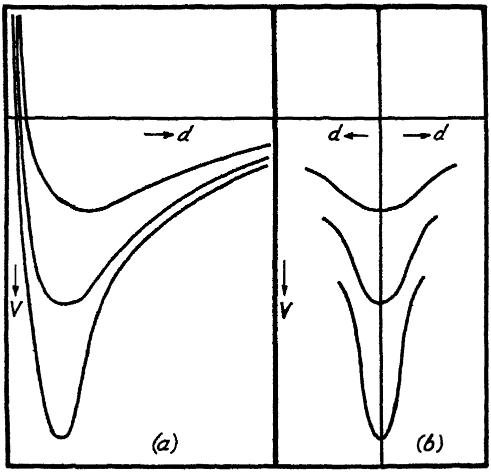

FIG. 8.—Potential energy curves for adsorbed molecule:
(a) for motion normal to surface;
(b) for motion parallel to surface.

On the basis of this general interpretation we may expect to observe specific deviations from the general equation just as there are specific deviations from the Barclay-Butler relation; it is, however, not clear whether the deviations shown in the figures are real, or are caused by experimental uncertainties which we cannot easily estimate.

(iv) THE VARIATION OF HEAT OF ADSORPTION WITH COVERAGE.—In several recent papers attention has been refocused on the causes of variation of heat of adsorption with surface concentration. The calculations of Roberts and Orr,[20] of Miller [21] and of Barrer [22] suggest that molecular interactions can only give rise to relatively small effects. The contribution of heterogeneity of the surface to the variation of heat of adsorption has therefore been regarded as important. We may first remark that if different molecules are adsorbed on the same heterogeneous surface, then provided the adsorption forces are similar in nature we should expect the heat against surface concentration curve to have roughly the same shape. In Fig. 9 we have collected together a typical set of heat curves, and this suggests strongly that it is the adsorbate rather than the adsorbent which determines the shape of the curve. Furthermore, as pointed out in Part II, the localization entropy for adsorption on a markedly heterogeneous surface will probably not contain the term $-R \ln \theta/(1-\theta)$.

---

* *Note added in Proof.*—A similar attempt to interpret heat-entropy relationships on the basis of the above considerations has been made by Eley (private communication). He finds, in agreement with the present conclusions, that to account for the observed relationship, the variation of the frequency of vibration with the depth of the potential energy minimum would have to be much more rapid than that derived from the accepted theories of intermolecular attraction. On the other hand, Evans and Longuet-Higgins (private communication) have succeeded in interpreting the Barclay-Butler relation in a very general manner by employing a similar model in conjunction with the law of corresponding states. It seems likely that their treatment can be extended to the case of adsorption.

[20] Roberts and Orr, *Trans. Faraday Soc.*, 1938, **34**, 1346.

[21] Miller, *The Adsorption of Gases on Solids* (C.U.P., 1949).

[22] Barrer, *Proc. Roy. Soc. A*, 1937, **161**, 476.

The fact that this term appears to be separable from the experimental entropy is perhaps evidence that surface heterogeneity is not important in the cases we have examined, i.e. for θ in the range 0·2-0·9. In this connection we may notice that in the ammonia + charcoal system the initial drop in $\overline{\Delta H}_\theta$ could be attributed to heterogeneity, since the constancy above $\theta = 0{\cdot}2$ indicates that there is no appreciable interaction between the adsorbed molecules; indeed, a sharp drop of this kind, probably caused by heterogeneity, is characteristic of almost all charcoal systems. A much more detailed experimental study of this problem is needed before we can be more definite on this point.

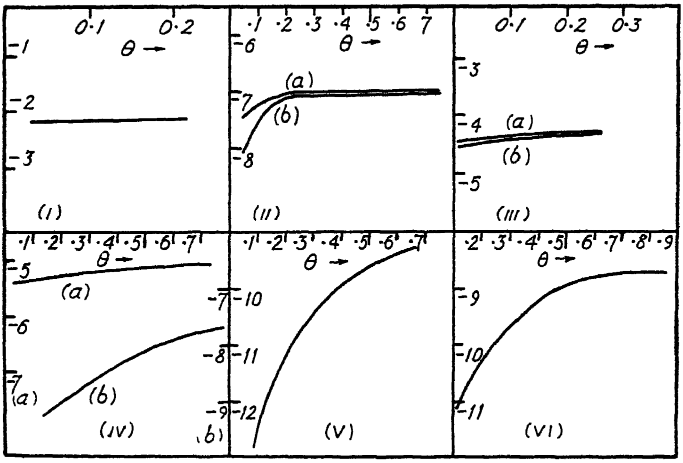

FIG. 9.—Dependence of differential heat of adsorption on fraction of surface covered.

(i)	Hydrogen on charcoal	(Titoff)
(ii)	Ammonia on charcoal	(a) (Titoff)
		(b) (Richardson)
(iii)	Nitrogen on charcoal	(a) (Titoff)
		(b) (Richardson)
(iv)	(a) Methane on charcoal	(Homfray)
	(b) Ethane on charcoal	,,
(v)	Carbon bisulphide on charcoal	(Polanyi)
(vi)	Ethyl chloride on charcoal	,,
	(Heats in kcal./mole.)	

If we assume that the variation of heat of adsorption with concentration at higher coverage than 0·2 is the result of intermolecular forces then we need a reasonable physical interpretation of their nature and magnitude. So far this is not forthcoming since all current theoretical treatments predict either that $\frac{d\overline{\Delta H}_\theta}{d\theta} \rightarrow 0$ as $\theta \rightarrow 0$; or that the limiting slope is not greater than the average slope between $\theta = 0$ and $\theta = 1$. It is perhaps relevant to observe that the surface upon which these large changes of $\overline{\Delta H}_\theta$ occur at relatively low θ are either charcoal or metal surfaces: in both cases we may have free electrons in orbitals covering large areas of the surface. If these electrons are involved in adsorption bonds then the effect may be considerable over a very wide area of surface; a somewhat similar interpretation has been suggested tentatively by Frankenburg.[23]

(v) CALCULATION OF HEATS OF ADSORPTION FROM ISOTHERMS AT A SINGLE TEMPERATURE.—The existence of a functional relation between

---

[23] Frankenburg,[10].

$\overline{\Delta \text{H}}^{\ddagger}_{\Gamma}$ and $\overline{\Delta \text{S}}^{*}_{\Gamma}$ enables us to eliminate $\overline{\Delta \text{S}}^{*}_{\Gamma}$ from eqn. (3.5) of Part II; using eqn. (3.1) of the present paper we have

$$\begin{aligned}\Delta\mu^{*}_{\Gamma} &= RT \ln p_{\Gamma} - RT \ln \theta/(1-\theta) \\ &= 25{\cdot}5T + (1 - 0{\cdot}0014 \,.\, T)\overline{\Delta \text{H}}^{\ddagger}_{\Gamma} \quad . \quad . \quad (4.1)\end{aligned}$$

or, at 273·1° K,

$$\overline{\Delta \text{H}}^{\ddagger}_{\Gamma} = \frac{\Delta\mu^{*}_{\Gamma} - 6900}{0{\cdot}618} \text{ cal./mole.} \quad . \quad . \quad . \quad (4.2)$$

Hence, if one isotherm is measured reaching sufficiently near saturation that $\Gamma^{\circ}_{\text{s}}$ and hence θ can be evaluated, then $\overline{\Delta \text{H}}^{\ddagger}_{\Gamma}$ can be calculated as a function of θ. When this relation is established adsorption isotherms can be calculated at other temperatures. We find that $\overline{\Delta \text{H}}^{\ddagger}_{\Gamma}$ evaluated by this method is always in very good agreement with that obtained from the Clausius-Clapeyron equation.

In effect the "characteristic function" for the adsorption system is the differential heat of adsorption and from a knowledge of this we can calculate the whole behaviour of the system.

(vi) Possible Extension to Multilayer Systems.—The present analysis indicates that the Barclay-Butler relation between the heat and entropy changes accompanying condensation processes embraces a very wide range of phenomena, provided that, for adsorption and solution, we take account of configurational entropy effects. Indeed, if we could estimate the configurational entropy terms which are involved in the condensation of "associated liquids" we might also be able to bring them into agreement with this generalization.[24]

We are led then to postulate that the entropy changes considered relate to changes in the translational and rotational degrees of freedom of the molecules under the influence of the intermolecular forces acting in the condensed phase. If this is so then we might expect the same equation to relate the heat and excess entropy for multilayer adsorption. We suggest therefore that a study of the configurational entropy of multilayers might be made by evaluating the heats and entropies of adsorption from the experimental data, and comparing the observed entropy with that which would be predicted from the observed heats on the basis of eqn. (3.1). The difference between the two will give the configurational entropy in the multilayer. Thus we propose simply to reverse the procedure we have employed for monolayer adsorption, for had we foreseen the wide applicability of the heat-entropy relation we could have used it to derive the term $- R \ln \theta/(1 - \theta)$ for the configurational entropy in the monolayer case.

At the moment we can only apply this proposed method at room temperature for we have insufficient data to define accurately the heat-entropy relation at other temperatures; nor are we yet certain whether the relation in fact applies accurately for adsorption on surfaces other than charcoal.

Summary and Conclusions.—The thermodynamic methods outlined in Part II are applied to published data on the adsorption of vapours on charcoal, glass and metals.

The following conclusions have been reached.

(i) The most convenient reference system for monolayer adsorption appears to be the ideal localized monolayer (Langmuir) model.

(ii) The excess partial molar entropies of adsorption are linearly related to the differential heats of adsorption. For adsorption on charcoal the relation coincides with that between heats and entropies of condensation of liquids, and of vapours and gases into solutions. An

---

[24] Cf. ref. 18(*b*).

interpretation in terms of the variation of vibrational and rotational degrees of freedom with the energy of adsorption is envisaged.

(iii) The simultaneous variation of the heat and entropy of adsorption means that many statistical mechanical theories of adsorption may need revision.

(iv) The applicability of the localized monolayer model, taken with the dependence of heats of adsorption on the vapour, nature of the adsorbent, and the surface concentration, suggests that charcoal surfaces may be more homogeneous than is usually thought. The data for other surfaces are not conclusive on this point.

(v) The above conclusions do not necessarily mean that the surface phases considered are physically identified with localized monolayers.

(vi) A possible method of determining the configurational entropy in multilayer adsorption is suggested.

(vii) There seems no reason why the present methods should not be applied to chemisorption, although no examination of the available data has yet been made. In this case, however, it will not be justifiable to assume that the adsorbent is inert, and that its energy and entropy are unaffected by the adsorbed molecules.

Chemistry Department,
University College, Dundee,
University of St. Andrews,
Scotland.

ON THE PRECIPITATION THRESHOLD OF SOLUTIONS OF HETEROGENEOUS POLYMERS

By H. Tompa

Received 22nd March, 1950

The precipitation threshold of heterogeneous polymers is calculated on the basis of the Flory-Huggins theory of polymers and the results applied to some existing data.

1. Introduction.—The solubility relationships of solutions of homogeneous high polymers have been worked out by Flory[1] on the basis of the statistical theory developed independently by himself[2] and Huggins.[3] He has also dealt with some aspects of the two-phase equilibrium of heterogeneous polymers. For homogeneous polymers, he has given explicit formulae for the lowest value of the interaction constant as a function of the chain length of the polymer, at which phase separation is at all possible, and for the composition of the solvent at this point. Since the interaction constant is a function of the temperature, the diagram showing the composition of co-existing phases for different values of the interaction constant is the equivalent of the familiar phase diagram for a two component system, in which temperature is plotted against concentration; the point at the maximum of the curve (minimum interaction constant) is a critical point, since the solution represented by it can be regarded as arising from the coincidence of two co-existing phases.

Solutions of heterogeneous polymers are systems of more than two components. For a given heterogeneous polymer there still exists a minimum interaction constant for phase separation such that all mixtures of the polymer form homogeneous phases at values of the interaction constant below this minimum, while phase separation can occur at higher values. The composition of the polymer in the two co-existing phases is not the same in general, and it has already been pointed out by the author[4] that the point in the phase diagram which represents the solution of the given polymer on the threshold of precipitation at the minimum interaction constant is not in general a critical point. Fig. 1 illustrates the case of a three component system consisting of a solvent S and two polymer components P_1, P_2 of the same homologous series but of different chain lengths. If P represents the given polymer, the line joining P and S represents all solutions of P. Several binodials, for different values of the interaction constant, are shown on the diagram, with tie lines and critical points; in particular, the binodial which touches PS corresponds to the minimum interaction constant. It is obvious that the point of contact F′ is not in general a critical point, and the composition of the co-existing phase is given by some point F″. The relationships are entirely analogous for a polymer consisting of n species, forming with the solvent a system of $(n + 1)$ components. An n-dimensional tetrahedron in n-dimensional space has to be used instead of the triangular diagram to represent the system, and the binodial curve is replaced by an $(n - 1)$-dimensional binodial surface. The given polymer is represented by a point P in the $(n - 1)$-dimensional face of the tetrahedron opposite the solvent corner S and the minimum value of the interaction constant is determined by the binodial surface, to which the line PS is a tangent. Again, the point of contact F′ is not, in general, a critical point.

---

[1] Flory, *J. Chem. Physics*, 1944, **12**, 425.

[2] *Idem, ibid.*, 1941, **9**, 660; 1942, **10**, 51.

[3] Huggins, *ibid.*, 1941, **9**, 440; *Ann. N.Y. Acad. Sci.*, 1942, **43**, 1.

[4] Tompa, *J. Chem. Physics*, 1949, **17**, 1003.

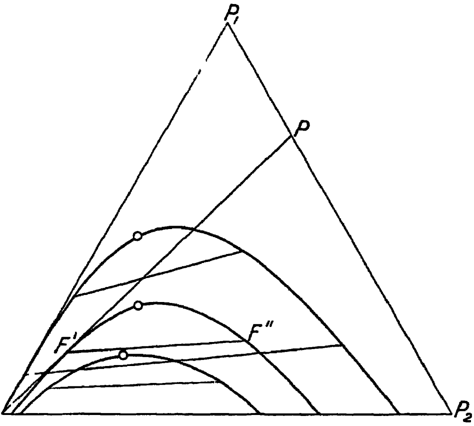

FIG. 1.—Binodials for the system solvent S and two polymers P_1 and P_2 for different values of α with tie lines. O, critical points.

It is the purpose of this paper to show how to calculate the minimum interaction constant and to apply the results to existing experimental data.

2. Theoretical Treatment.—The Flory-Huggins expression for the Gibbs' function of mixing of polymer solutions will be used as the basis of the calculation

$$\Delta G/kT = \sum_i n_i \ln y_i + \alpha y_0(1 - y_0) \sum_i r_i n_i. \qquad (1)$$

Here n_i is the number of molecules of kind i, r_i the number of sites occupied by a molecule of kind i, and y_i the site fraction defined by

$$y_i = \frac{r_i n_i}{\sum_i r_i n_i}. \qquad (2)$$

Within the limits of the Flory-Huggins theory the site fraction is identical with the volume fraction. The solvent is characterized by the suffix 0 $(r_0 = 1)$ and the polymer species by the indices 1 to n. The index i will always be used to denote any of the indices 0 to n, while the index j will be used for the indices 1 to n. Finally, α is the interaction constant, in Flory's theory equal to the excess interaction energy of a solvent molecule and a polymer segment, divided by kT, while in Huggins' theory it contains also a correction term from the entropy.

When two phases co-exist in equilibrium, the chemical potential μ_i of any component must have the same value in both phases. Denoting the value of the chemical potential referred to the pure substance by $\Delta\mu_i$, we obtain by differentiating eqn. (1)

$$\Delta\mu_0/kT = \ln y_0 + \sum_j \frac{r_j - 1}{r_j} y_j + \alpha(1 - y_0)^2, \qquad (3)$$

$$\Delta\mu_j/kT = \ln y_j + \sum (r_j - 1)y_j + r_j \alpha y_0^2. \qquad (4)$$

If we distinguish the two phases by primes and double primes, the equations determining the binodial surface are

$$\ln y_0' + \sum_j \frac{r_j - 1}{r_j} y_j' + \alpha(1 - y_0')^2 = \ln y_0'' + \sum_j \frac{r_j - 1}{r_j} y_j'' + \alpha(1 - y_0'')^2, \quad (5)$$

$$\frac{1}{r_j} \ln y_j' + \sum_j \frac{r_j - 1}{r_j} y_j' + \alpha y_0'^2 = \frac{1}{r_j} \ln y_j'' + \sum_j \frac{r_j - 1}{r_j} y_j'' + \alpha y_0''^2. \quad (6)$$

Instead of eqn. (6) we could use eqn. (7), obtained by subtracting eqn. (6) from eqn. (5):

$$\frac{1}{r_j} \ln y_j' - \ln y_0' + 2\alpha y_0' = \frac{1}{r_j} \ln y_j'' - \ln y_0'' + 2\alpha y_0''. \quad . \quad (7)$$

If the compositions of the two phases are changed by small amounts $\delta y_j'$, $\delta y_j''$ in such a manner that the phases remain co-existing, the following equations must hold:

$$\frac{\delta y_0'}{y_0'} + \sum_j \frac{r_j - 1}{r_j} \delta y_j' - 2\alpha(1 - y_0')\delta y_0'$$
$$= \frac{\delta y_0''}{y_0''} + \sum_j \frac{r_j - 1}{r_j} \delta y_j'' - 2\alpha(1 - y_0'')\delta y_0'', \quad (8)$$

$$\frac{1}{r_j} \frac{\delta y_j'}{y_j'} + \sum_j \frac{r_j - 1}{r_j} \delta y_j' + 2\alpha y_0' \delta y_0'$$
$$= \frac{1}{r_j} \frac{\delta y_j''}{y_j''} + \sum_j \frac{r_j - 1}{r_j} \delta y_j'' + 2\alpha y_0'' \delta y_0'' \quad (9)$$

At the point F′ a tangent to the binodial surface passes through the solvent corner S ($y_0 = 1$), so that there are values of $\delta y_j'$ possible such that

$$\delta y_j' = c y_j'. \quad . \quad . \quad . \quad . \quad . \quad (10)$$

Substituting into eqn. (8) and (9) and noting that

$$\delta y_0 = - \sum_j \delta y_j, \quad . \quad . \quad . \quad . \quad (11)$$

we obtain

$$c\left\{ \sum_j \frac{r_j - 1}{r_j} y_j' + \left[2\alpha(1 - y_0') - \frac{1}{y_0'} \right](1 - y_0') \right\}$$
$$= \sum_j \left[\frac{r_j - 1}{r_j} + 2\alpha(1 - y_0'') - \frac{1}{y_0''} \right] \delta y_j'', \quad (12)$$

$$c\left\{ \frac{1}{r_j} + \sum_j \frac{r_j - 1}{r_j} y_j' - 2\alpha y_0'(1 - y_0') \right\} = \frac{\delta y_j''}{r_j y_j''} + \sum_j \left[\frac{r_j - 1}{r_j} - 2\alpha y_0'' \right] \delta y_j''.$$
$$(13)$$

The $\delta y_j''$ and c can be eliminated from these equations by considering that they are $(n + 1)$ homogeneous linear equations for the $(n + 1)$ unknowns $\delta y_j''$ and c and that therefore the determinant of their coefficients must vanish. This determinant can be evaluated by using the identity

$$\begin{vmatrix} A + a_1, & B + b_1, & \cdot & \cdot \\ A + a_2, & B + b_2, & \cdot & \cdot \\ \cdot & \cdot & \cdot & \cdot \\ \cdot & \cdot & \cdot & \cdot \end{vmatrix} = \begin{vmatrix} a_1, & b_1 & \cdot & \cdot \\ a_2, & b_2 & \cdot & \cdot \\ & \cdot & \cdot & \cdot \\ & \cdot & \cdot & \cdot \end{vmatrix} + A \begin{vmatrix} 1 & b_1 & \cdot & \cdot \\ 1 & b_2 & \cdot & \cdot \\ & \cdot & \cdot & \cdot \\ & \cdot & \cdot & \cdot \end{vmatrix} + B \begin{vmatrix} a_1 & 1 & \cdot & \cdot \\ a_2 & 1 & \cdot & \cdot \\ & \cdot & \cdot & \cdot \\ & \cdot & \cdot & \cdot \end{vmatrix} + \quad . \quad (14)$$

The result obtained, after cancelling by a factor

$$1 - \left(2\alpha - \frac{1}{y_0''}\right) \sum_j \frac{r_j - 1}{r_j} y_j'',$$

is

$$(y_0' - y_0'')\left(2\alpha - \frac{1}{y_0'}\right)(1 - y_0) - \sum_j \frac{y_j'' - y_j'}{r_j} = 0. \quad . \quad (15)$$

Before proceeding further, it is instructive to consider that eqn. (15) can also be derived on the assumption of a continuous distribution of chain lengths in the polymer. Replacing y_j by $y\mathrm{d}r$ and summations over j by integrals, we obtain by differentiating eqn. (7) (which is more convenient to use than eqn. (6)) :

$$\frac{\delta y'}{ry'} - \frac{\delta y_0'}{y_0'} + 2\alpha\delta y_0' = \frac{\delta y''}{ry''} - \frac{\delta y_0''}{y_0''} + 2\alpha\delta y_0'', \quad . \quad . \quad (16)$$

If we make the substitutions equivalent to eqn. (10) and (11), this is transformed into an integral equation for $\delta y''/ry''$,

$$c\left[\frac{1}{r} - \left(2\alpha - \frac{1}{y_0'}\right)(1 - y_0')\right] = \frac{\delta y''}{ry''} - \left(2\alpha - \frac{1}{y_0''}\right)\int \delta y'' \, . \, \mathrm{d}r, \quad (17)$$

which is of a simple type and can be solved easily. Substituting the value of $\delta y''$ obtained into the equation equivalent to eqn. (12), we recover eqn. (15).

By introducing y_j^0, the site fraction of kind j in the pure polymer

$$y_j^0 = \frac{y_j'}{1 - y_0'}. \quad . \quad . \quad . \quad . \quad . \quad (18)$$

we can eliminate y_j' and y_j'' from eqn. (5) and (15) : firstly we write eqn. (7) in the form

$$y_j'' = y_j' \, . \, Y^{r_j}, \quad . \quad . \quad . \quad . \quad . \quad (19)$$

where

$$\ln Y = 2\alpha(y_0' - y_0'') - \ln y_0'/y_0''. \quad . \quad . \quad . \quad (20)$$

Eqn. (5) then reads

$$\ln \frac{y_0'}{y_0''} - (y_0' - y_0'') + (1 - y_0') \sum_j \frac{y_j^0}{r_j}(Y^{r_j} - 1)$$
$$- \alpha(y_0' - y_0'')(2 - y_0' - y_0'') = 0, \quad (21)$$

and eqn. (15) reads

$$(y_0' - y_0'')\left(2\alpha - \frac{1}{y_0'}\right) - \sum_j \frac{y_j^0}{r_j}(Y^{r_j} - 1) = 0. \quad . \quad (22)$$

These two equations, together with eqn. (23)

$$(1 - y_0') \sum_j y_j^0 . \, Y^{r_j} = 1 - y_0'' \quad . \quad . \quad . \quad (23)$$

determine α, y_0' and y_0'', if the y_j^0 are given. This α is α_m, the minimum value of the interaction constant for which phase separation is possible.

It is in general impossible to solve explicitly for α and numerical methods have to be used. The following scheme has been found to give α_m, y_0' and y_0'' without excessive labour : assume a trial value for Y and calculate $(1 - y_0'')/(1 - y_0')$ from eqn. (23). Put $1/(1 - y_0') = X$ and $\alpha(y_0' - y_0'') = A$ for the moment ; multiplying eqn. (21) by $1/(1 - y_0')$ and eqn. (22) by $y_0'/(1 - y_0')$ and subtracting gives a linear equation between X and A, while eqn. (22) can be transformed into a quadratic equation between them. It is found that only one of the solutions is physically significant and from this and the value of $(1 - y_0'')/(1 - y_0')$ the three quantities α_m, y_0' and y_0'' are calculated. It is now necessary to calculate Y and compare it to the trial value; the difference between these two figures can be used as a guide to a better trial value of Y and the whole process repeated to obtain values to any desired degree of accuracy. As the difference between the calculated and trial values of Y is usually very small, the calculation must be carried out to several more significant figures than are desired in α_m.

Values of α have thus been calculated for a polymer consisting of two species only, $r_1 = 10$, $r_2 = 100$, at intervals of 0·2 of the site fraction. These points, or rather the smooth curve drawn through them, are shown in Fig. 2, together with curves for α_n and α_w, the critical values for homogeneous polymers whose chain lengths equal the number and weight average chain lengths r_n and r_w of the given polymer respectively:

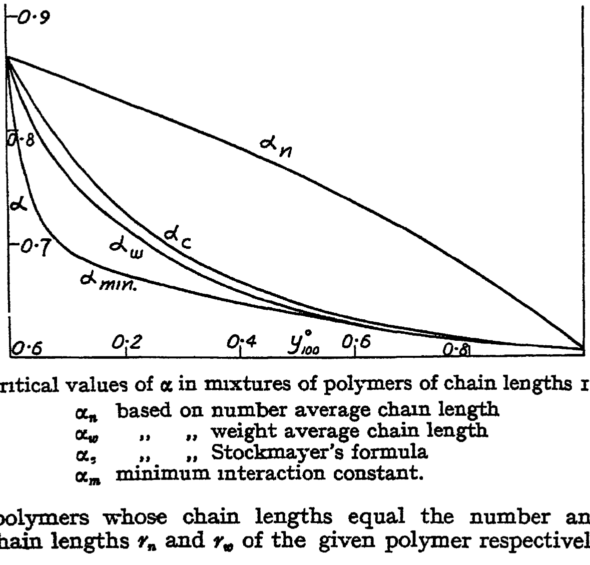

FIG. 2.—Critical values of α in mixtures of polymers of chain lengths 10 and 100.

α_n based on number average chain length
α_w „ „ weight average chain length
α_s „ „ Stockmayer's formula
α_m minimum interaction constant.

$$\alpha_n = \tfrac{1}{2}(1 + r_n^{-\frac{1}{2}})^2, \quad \alpha_w = \tfrac{1}{2}(1 + r_w^{-\frac{1}{2}})^2. \qquad (24)$$

The figure shows that α_m is always smaller than even α_w.

For a homogeneous polymer α_m is of course equal to the critical value given by one of eqn. (24), and $y_0' = y_0''$. For a narrow polymer fraction it is to be expected that y_0' will not be appreciably different from y_0''. Putting therefore $y_0' - y_0'' = \epsilon$, we can expand eqn. (21), (22) and (23) into a series of powers of ϵ, and can neglect the higher powers. Without going into the details of the calculation, which contains only elementary algebra, the result is

$$\epsilon = \frac{3(r_z - r_w)}{r_w^{\frac{1}{2}}(1 + r_w^{\frac{1}{2}})^2}, \qquad (25)$$

where r_z is the so-called z-average chain length. This value of ϵ is small if the relative dispersion of the chain lengths about the weight average

$$\frac{\overline{(\Delta r)^2}^{\frac{1}{2}}}{r_w} = \left(\frac{r_z - r_w}{r_w}\right)^{\frac{1}{2}} \qquad (26)$$

is small. The minimum interaction constant is then

$$\alpha_m = \alpha_w - \frac{(r_z - r_w)^2}{4r_w^{5/2}} = \alpha_w - \left[\frac{\overline{(\Delta r)^2}^{\frac{1}{2}}}{r_w}\right]^4 \cdot \frac{1}{4r_w^{\frac{1}{2}}}. \qquad (27)$$

It is interesting to compare this with the value of α_c, given by Stockmayer,[5] for which there is a critical point on the line SP. For small values of the relative dispersion this gives

$$\alpha_c = \alpha_w + \left[\overline{(\Delta r)^2}^{\frac{1}{2}}\right]^4 \cdot \frac{1}{8r_w^{\frac{1}{2}}}, \qquad . \quad . \quad . \quad (28)$$

so that the correction to α_w is half and of the opposite sign of that derived here. Values of α_c are also shown on Fig. 2. The figure shows that the correction to α_w is small even in regions where the number and weight average mole weights are still very different, thus confirming Stockmayer's assertion that the precipitation threshold is determined mainly by the weight average mole weight.

3. Application to Experimental Data.—The best experimental data for the precipitation threshold of heterogeneous polymers are those obtained by Gavoret and Magat.[6] These authors measured the amount of ethyl alcohol which has to be added to solutions of GR—S (butadiene-styrene copolymer) in toluene. Measurements were made on narrow fractions as well as on mixtures of narrow fractions. From the results on narrow fractions a relation between concentration of alcohol at the precipitation threshold and mole weight of the polymer was established and from this the results on mixtures were expressed as "experimental equivalent mole weight" (E.E.M.W.), i.e. the mole weight of a single polymer with the same precipitation threshold.[7] * Table I shows the E.E.M.W. and the number and weight average mole weights for four of the mixtures investigated, taken from Gavoret and Magat's paper.[7]

TABLE I

(All mole weights in thousands)

Mole Wt. of Fractions	% by Wt.	E.E.M.W.	M_n	M_w	$M_{\text{calc.}}$	M_{St}
20	90·38	30 ± 1	21·5	25·3	28	24·5
75	9·62	—	—	—	—	—
1	11·6	250 ±35	8·3	194·6	196·7	193·7
220	88·4	—	—	—	—	—
1	54·0	170 ±15	1·85	101·7	125	88·42
220	46·0	—	—	—	—	—
1	86·85	125 ±10	1·15	29·8	74	13·43
220	13·15	—	—	—	—	—

The minimum interaction constant was calculated for each of the four cases by the method of § 2, and to make comparison with Gavoret and Magat's data easier, these values were expressed as the mole weight M_{calc} of a single polymer with the same critical α, assuming the density to be unity and the mole volume of the solvent 100 cm³. These figures are also shown in Table I; the agreement with the experimental data is not unsatisfactory, considering that the model used in the calculations contains several simplifications, the most serious being the treatment of the toluene-alcohol mixture as a single liquid. It should also be noted that the experimental data were determined at a fixed polymer concentration of 0·01. It is very satisfactory that the E.E.M.W. is always larger than M_w, as predicted by the calculation. Values of M_{St} calculated by the formula given by Stockmayer[8] are always smaller than M_w, contrary to the figures of Gavoret and Magat, and are also given in Table I for the sake of comparison.

---

[5] Stockmayer, *ibid.*, 1949, **17**, 588.

[6] Gavoret and Magat, *J. Chim. Phys.*, 1949, **46**, 357.

[7] Gavoret and Magat, *J. Chem. Physics*, 1949, **17**, 999.

* The author is indebted to Dr. Magat for sending him the manuscript of this note before publication.

Courtaulds, Limited,
Research Laboratory,
Lower Cookham Road,
Maidenhead, Berks.

THE PHOTOPOLYMERIZATION OF VINYLIDENE CHLORIDE

PART I

By J. D. Burnett and H. W. Melville

Received 14*th March,* 1950

The direct photopolymerization of vinylidene chloride in the liquid phase and in hexane solution has been investigated over a temperature range of 15-35° C The reaction, like many others of this class, is of the typical chain type, mutual termination being the mechanism of stopping polymer growth. Under conditions where absorption of light is reasonably complete the rate is proportional to the concentration of monomer. The reaction is retarded by benzoquinone and from the rate of consumption of quinone an approximate estimate of the chain length may be obtained. By measuring the intrinsic viscosity of solutions of the polymer in hot trichlorobenzene it is shown that under the conditions of experiment no appreciable amount of transfer occurs. The life-time of the radicals has been measured by the rotating sector and the rate coefficients for growth and termination of growth obtained. While these values are comparable with other similar polymerizations, the temperature coefficients and temperature independent factors are abnormal. This is attributed to the fact that polymer is precipitated out of the monomer in an unswollen condition. The growth and termination reactions are in this respect heterogeneous.

The principles of the methods for the evaluation of the rate coefficients in radical addition polymerization are now well established and the results are available for a number of monomers. Analysis has naturally been done with homogeneous systems. When conditions are altered, for example by working in a mixture of liquids in which the polymer is more difficultly soluble, or if the viscosity of the solution rises, the termination process, i.e. radical-radical interaction, can be considerably diminished. These latter conditions often obtain in polymerization processes, for example in emulsions, and it is therefore important as a next step in the elucidation of these reactions to obtain more detailed quantitative data. The most extreme condition consists in carrying out the polymerization in the gas phase where the polymer, owing to its size and involability, soon forms a separate phase. When this happens conditions become extremely complicated because the monomer is probably absorbed by the polymer particle as a necessary preliminary to reaction. It is therefore a difficult matter to measure the effective concentration of monomer at the site of polymerization. Similarly, the mechanism of termination of growth is not clear although it is certain that the step involves the participation of two radicals as in the homogeneous reaction.

Conditions can be somewhat simplified if polymerization is carried out under such conditions that the polymer is precipitated during the reaction. Here again to get well-defined conditions it is essential to choose a reasonably simple system. In this respect the polymerization of vinylidene chloride seemed ideal since the polymer is not only precipitated from the monomer but it is in an unswollen state in a monomer environment. This paper describes the determination of the overall kinetics of the direct photopolymerization and also an attempt to evaluate the rate coefficients in this more complicated case in order to get information about the behaviour of a radical which is growing really as a separate phase in an environment of constant monomer concentration.

Experimental

It has long been known that the presence of oxygen has a considerable effect in many polymerization reactions.[1] The German chemical industry, as has been reported in a recent publication, found it necessary to carry out all chemical and physical processes with vinylidene chloride in an atmosphere of nitrogen.[2] Vinylidene chloride on contact with air readily forms, and decomposes to, phosgene and formaldehyde, accompanied by spontaneous polymerization; peroxides (presumably) of an explosive character have also been encountered in these reactions due to contact with air.

To avoid such complications with oxygen, and to ensure reproducible results, all experiments were carried out *in vacuo* and the reactants freed from oxygen before use (mercury diffusion and rotary oil pump). The purification train and monomer reservoir were contained in a secondary line sealed to the main vacuum line. It was found essential to keep the monomer stored in a bath of solid carbon dioxide and alcohol to prevent polymerization, and at such temperatures (approximately − 80° C) the vapour of vinylidene chloride is not of sufficient concentration to attack the tap greases, which were either Apiezon M or L.

Fused silica reaction vessels are most suitable for this work. Vessels made of Pyrex or Hysil were found to absorb too much of the activating radiation. The vessels were calibrated so as to act as dilatometers.

The source of radiation was a silica capillary mercury arc running at about 10 atm., fed from a constant voltage transformer. The lamp was encased in a watertight silica envelope for immersion in the thermostat. Due to the high working temperature of the lamp, it was found necessary to put a cooling oil (fed from a constant head and overflow water reservoir) in the thermostat. It was essential to use distilled water in the thermostat since the main activating radiation employed was below 2800 Å. A slit ($\frac{1}{8}$ in. by 2 in.) immediately in front of the small tubular light source, gave a suitable rate of reaction.

The monomer, as obtained from I.C.I., Blackley, contained Thymol as inhibitor and stabilizer; that from Distillers Co. Ltd., was stabilized by Carvacrol. The stabilized monomer was repeatedly washed with NaOH followed by distilled water. It was dried overnight by anhydrous sodium bisulphate in a specially light-proof bottle. The monomer was then distilled over fresh anhydrous sodium bisulphate; the fraction distilling at 31·5 to 31·7° C—the most reliable figures quote the vapour pressure of the compound at 760 mm. of mercury at 31·5° C,[2] and at 31·7° C [3]—was collected in a vessel, attached to the vacuum system, immersed in a solid carbon dioxide and alcohol mixture. A suitable quantity of the monomer was then transferred to a secondary reservoir on the high vacuum system, which was then sealed off. Subsequently the monomer was degassed in the normal manner. To remove any volatile impurity which may have been formed due to the contact of monomer with air, e.g. acetylene, hydrochloric acid, etc., but which could be frozen by liquid air, the reservoir was cooled in a solid carbon dioxide and alcohol mixture, and connected to the pumps for 5-10 min. When oxygen had been removed from the system (residual pressure approximately 10^{-4} to 10^{-5} mm. Hg) the monomer was distilled from a bath of solid carbon dioxide in alcohol to the primary reservoir cooled in liquid oxygen. This latter process is similar to the method used by Evans and Polanyi for the purification of *iso*butene,[4] and ensures the removal of low molecular weight polymer and also peroxides, formed in, and during, the previous processes. The monomer reservoir was from then on kept continually cooled at a temperature of approximately − 80° C, but allowed to warm gradually to room temperature when a tube was being filled. It was found desirable to purify about 100 ml. of monomer at any one time, since prolonged storage led to contamination. Frequent checks of the standard of purification were made by comparing the rate of polymerization of a sample with previous results obtained under the same experimental conditions.

---

[1] Taylor and Vernon, *J. Amer. Chem. Soc.*, 1931, **53**, 2527. Staudinger *et al.*, *Annalen*, 1031, **33**, 488; *Helv. chim. Acta*, 1929, **62**, 1127.

[2] *B.I.O.S. Report*, No. 1478.

[3] Staudinger, *Chem. and Ind.*, 1947, **45**, 685.

The Ultra-violet Absorption Spectrum of Vinylidene Chloride.—The extinction curve of vinylidene chloride, Fig. 1, was mapped in the usual manner, use being made of a Hilger Quartz Spectrograph. Samples of the monomer were investigated in solution of spectroscopic-quality cyclohexane, and from various methods of purification the results showed that the method outlined in the previous paragraph was adequate. No higher degree of purity was achieved or demonstrated either by the absorption spectrum or by actual results of polymerization reactions.

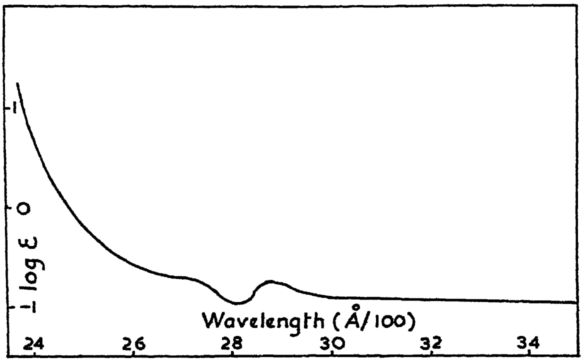

FIG. 1.—The u.-v. absorption spectrum of vinylidene chloride.

The Bulk Photopolymerization—The rate of reaction of a polymerization reaction may be, most conveniently, measured by the change in some physical property of the system, as the conversion of monomer to polymer takes place. Density differences between polymers and their parent monomers are usually sufficiently great to allow their use in following the course of a polymerization reaction. Starkweather and Taylor[4] have shown that the percentage contraction of the monomer is a linear function of the percentage polymerization which has been effected.

The dimensions of the reaction vessel were chosen, such that a reasonable drop in the meniscus level could be obtained for the rate of polymerization obtainable. A determination of the density of the polymer gave a value of 1·631 g. cm.$^{-3}$—the present experimental result compares favourably with the values given by Staudinger,[3] namely 1·605 for the amorphous material—increasing to 1·70 as crystallization of the polymer proceeds. This value compared with that of the monomer (1·2053 at 25° C)[2] indicates that for 100 % polymerization there should be a 26 % contraction in the original volume of the monomer at 25° C. In our apparatus a drop of 0·01 mm. in meniscus level corresponds to about 0·01 % polymerization.

The lack of a suitable solvent for polyvinylidene chloride at room temperatures was overcome by breaking open the tube at both ends and removing the residual monomer by a current of nitrogen—removal by heating, or by a stream of oxygen, proved inadvisable. The polymer can readily be scraped from the tube walls by a fine wire brush, and subsequently weighed, to give a check on the degree of conversion estimated from the decrease in volume. Such values, obtained in preliminary experiments, are tabulated in Table I; the two sets of results, as can be seen, are in good agreement.

When the liquid vinylidene chloride in bulk is exposed to ultra-violet light it polymerizes and the polymer, being insoluble, precipitates out almost immediately the light is switched on. The polymer forms as a flocculent white mass,

---

[4] Starkweather and Taylor, *J. Amer. Chem. Soc.*, 1930, **52**, 4708.

TABLE I.—MONOMER CONVERSION

Temperature	% Conversion	Volume of Monomer (ml.)	Weight of Polymer	
			Theory (g.)	Found (g.)
15° C	2·1	3·5	0·090	0·091
25° C	2·7	3·1	0·100	0·095
35° C	2·6	3·5	0·110	0·108

which does not discolour appreciably as the reaction proceeds, except on fairly long exposure. The course of the reaction over a normal time period is shown in Table II. (All experiments in Part I are at 25° C.) As can be seen from Table II, over a large extent of polymerization the rate is steady.

TABLE II.—THE COURSE OF THE POLYMERIZATION

Temperature = 25° C

Time (min.) (t)	Contraction %	Conversion % (C)	C/t
0	—	—	—
4	0·091	0·36	0·090
8	0·197	0·76	0·095
13	0·352	1·30	0·105
21	0·571	2·20	0·105
30	0·831	3·17	0·106
40	1·115	4·29	0·107
50	1·366	5·26	0·105

Experimentally it is undesirable to continue the reaction for more than 40 min. If the exposure time is prolonged there is a drop in the reaction rate as shown in Fig. 2, which can be attributed to two factors :

(*a*) The precipitated polymer, as would be expected, is most dense on the vessel wall nearest the light source. Thus light scattering would become more pronounced at high monomer conversions.

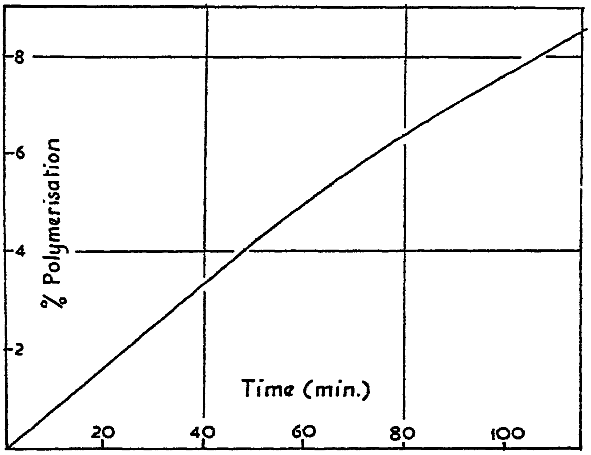

FIG. 2.—The effect of prolonged reaction.

(*b*) Some decomposition of the polymer apparently takes place on long exposure to short wavelength radiation. The freshly precipitated polymer remains quite white for a considerable period—up to 40-45 min., thereafter it tends to become brown, the degree of colour depending on the length of exposure. This is not unexpected, since the polymer evolves hydrochloric acid—more markedly than polyvinyl chloride—and turns brown in the process. More recently this polymer has been found to discolour on standing—more rapidly with increased temperature.[2] This colour change is thought to be due to the formation of polyene groups $(-CH{=}CH-)_n$.[5]

The absorption spectrum of vinylidene chloride, Fig. 1, was used with the view to a determination of the best range of ultra-violet to use for subsequent work. The effect of wavelength, using various filters, on the rate of polymerization was investigated. The filters used, and the transmission of these glasses (all of Corning manufacture), are indicated in Fig. 3. Table III gives the overall rates depending on the filters used.

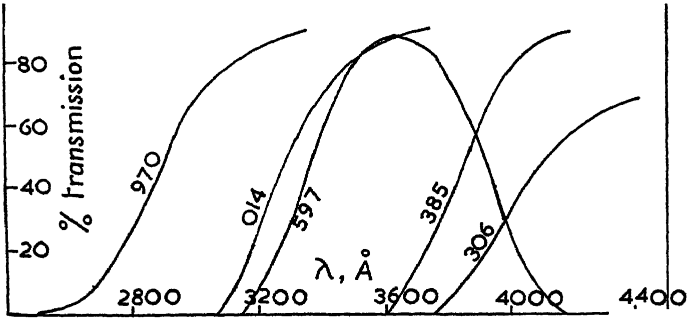

FIG. 3.—The transmission of the glass filters.

A peculiar effect was observed in using such filters. The normal procedure was to expose the system to the full radiation of the mercury lamp, measure the rate, insert the filters and measure the diminished rate. If, instead, the system was first exposed to the filtered light the rate observed was only 1/8th of that quoted in Table III. If, however, the system were exposed to the full radiation for a few minutes and the filter re-inserted the rate increased to the value quoted in Table III. This effect was not observed during intensity exponent experiments and is therefore not to be attributed to intensity changes but possibly to some effect of wavelength.

TABLE III.—THE EFFECT OF WAVELENGTH

Filter	Main Wavelength Transmitted from Hg Lamp	Overall Rate in mole $l.^{-1}$ $sec.^{-1} \times 10^5$
306 Noviol A . . .	—	—
597 R.P. Ultra . . .	3920	0·496
385 Nultra . . .	3920, 4360, 5480	1·614
014 Blue Fluorescing . .	3340, 3650, 3920 4360, 5480 } (2)	1·891
970 Conex D . . .	2805, 2895, 2970 3020, 3120 + } (2)	6·075
Whole emission spectrum of Osira lamp . . .	—	20·5
Dark rate	—	0·05

---

[5] Boyer, *Colloid Sci. Symp.* (Madison, 1946).

A sample of pure monomer was saturated with oxygen at atmospheric pressure before the reaction tube was sealed off for immersion in the thermostat. The rate was then found to have increased by approximately 15 %. Reduction of the light intensity gave a value of the intensity exponent as 0·49 ; which means that there is mutual termination of two growing chains and indicates that copolymerization probably takes place between the oxygen and the monomer; that is, the oxygen is incorporated in the polymer chain, presumably through peroxide formation.

Samples of monomer, which had been distilled such that peroxides formed in the purification would be present (that is, the monomer was not distilled carefully from a bath of solid carbon dioxide and alcohol to liquid oxygen before use), were found to give the same rates of polymerization as when oxygen was deliberately added to a sample of carefully purified monomer. The results are tabulated in Table IV for ease of comparison.

TABLE IV.—COMPARISON OF RATES

Sample	Rate × 10^5 (mole $l.^{-1}$ sec.$^{-1}$)	Intensity Exponent
Pure monomer	20·5	0·5
Pure monomer + oxygen . . .	24·0	0·49
Impure monomer	23·8	—
	24·4	0·52

Thus careful distillation from a solid carbon dioxide and alcohol bath to liquid oxygen is necessary in order to obtain the degree of monomer purity desirable for this investigation.

The value of the intensity exponent *n* was determined by varying the intensity of the incident light and noting the change in rate that was effected. The light intensity was reduced by inserting metal plates, which had holes bored at regular intervals, immediately in front of the light slit and before the reaction tube. In order to prevent any interference effects [6] the distance between the holes in the screen was not more than 1/10th of the linear dimensions of the reaction tube. The transmission of the resulting screen was measured by a photocell. Table V gives the rates under total radiation, and with the screen in position. When the intensity was suddenly changed in this way there was an immediate change in reaction velocity, no long photo after-effects or induction periods being observed.

TABLE V.—THE INTENSITY EXPONENT

Transmission of screen = 0·306

Initial Rate (1)	Rate with Screen in (2)	Final Rate (3)	*n* from	
			(2) and (3)	(1) and (2)
0·0103	0·00567	0·0104	0·52	0·51

This value of the intensity exponent implies that the termination reaction involves the mutual destruction of two of the growing polymer chains. But, as has been pointed out in many previous papers, no conclusion can be derived whether, firstly, the two chains combine to give one dead polymer, as in the scheme,

$$—CH_2—CCl_2— \; + \; —CH_2—CCl_2— \; \rightarrow \; —CH_2—CCl_2—CH_2—CCl_2— ;$$

or secondly, that one radical dehydrogenates the other so that both are stabilized thus

$$—CH_2—CCl_2— \; + \; —CH_2—CCl_2— \; \rightarrow \; —CH_2—CHCl_2 + CCl_2{=}CH—$$

---

[6] Jones and Melville, *Proc. Roy. Soc. A*, 1937, 163, 511.

No solvent being available for polyvinylidene chloride, at room temperature, the only method applicable for a determination of the rate dependence on monomer concentration was the use of cyclohexane of spectroscopic purity as a monomer diluent. A measured volume of the diluent was introduced into a reaction tube and attached to the vacuum line for degassing. Freezing of the cyclohexane was accomplished by a solid carbon dioxide and alcohol mixture. After degassing the tube was then filled by distilling into it a suitable volume of vinylidene chloride, and the rate of polymerization then measured in the normal manner. It must be noted that all the calculations are based on the volume of monomer only, it being assumed that the saturated hydrocarbon would have no influence whatsoever on the course of the reaction, apart from its role of monomer diluent. The results are shown in Table VI. Wherever possible the intensity exponent of a particular run was determined.

TABLE VI.—CONCENTRATION DEPENDENCE

Concentration mole/l. (C)	Rate (R) mole l.$^{-1}$ sec.$^{-1}$ × 10^{5}	Intensity Exponent n
12·4	20·5	0·5
8·93	16·7	—
7·61	14·2	0·5
6·1	8·0	—
5·77	11·3	0·5
4·67	7·8	0·5
3·67	5·2	0·5
2·78	3·3	—
2·8	3·5	—
1·51	2·28	0·5

The results are graphed logarithmically in Fig. 4, and calculation from the slope of the line shows the rate to be dependent on the first power of the monomer concentration. The intensity exponent once again indicates that termination is brought about by the mutual interaction of two of the active polymer molecules.

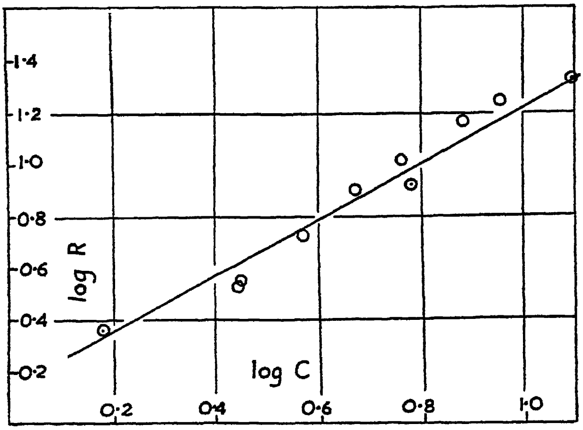

FIG. 4.—The dependence of rate on monomer concentration.

The fact that the rate of polymerization is proportional to the first power of the concentration would imply that the activating radiation is completely absorbed by the vinylidene chloride, since the rate would have been proportional to the 3/2 power if absorption were weak. Under these conditions it is not known, however, whether absorption occurs in a narrow layer or throughout the vessel. It is important, however, to ensure that the radical concentration is as uniform as possible so that when velocity coefficients are computed, reliable values may be obtained. When polychromatic light is necessarily used for such photo reactions it is not easy to calculate the rate of radical production at every point in the vessel even although the appropriate extinction coefficients are known. Moreover, the production of convection currents in the liquid, set up as a result of the heat liberated during polymerization, can lead to a more uniform distribution of polymer radical concentrations than would be calculated from extinction coefficients. These difficulties can be overcome by the spatial interference method in which the uniformity of radical concentration can be estimated. Briefly, two similar beams of radiation are arranged to strike the reaction vessel from opposite directions and the degree of interference from each source estimated by arranging three experiments, beam No. 1, beam No. 2, and the two beams together. Since the rate of polymerization is proportional to the square root of the intensity, then if complete interference occurs, i.e. when the radicals are uniformly distributed, the rate of polymerization will be equal to the square root of the sum of the rates for beams 1 and 2. If the radicals are confined to a thin layer close to the zone where the radiation enters the system, the rate will be equal to the sum of the rates for beams 1 and 2. The results are shown in Table VII. It will be seen that the observed rate, with the two beams operating simultaneously, is slightly greater than that calculated for complete interference, but much less than that for zero interference. The polymer radicals are thus distributed approximately uniformly throughout the vessel. The results of the previous section show that the activating radiation is absorbed fairly strongly by the monomer.

TABLE VII.—" SKIN EFFECT "

Rate_1	Rate_2	Rate_{1+2}	Theoretical Rate Interference	
			Full	None
0·0198	0·0178	0·0282	0·0266	0·0376

From these results it may be concluded that the rate of polymerization is proportional to the square root of the light intensity, and to the first power of the monomer concentration. Thus there is the relationship

$$-\,d(M)/dt = K(M)I^{\frac{1}{2}}$$

when K is a constant for a given temperature.

If it is assumed, for the present, that no transfer takes place in this reaction, the reaction steps may be formulated as usual as

$$M + h\nu = 2P_1 \text{ Initiation } 2I$$
$$P_1 + M = P_2 \text{ Propagation } k_{p_1}$$
$$. \quad . \quad . \quad . \quad . \quad .$$
$$P_n + M = p_{n+1} \text{ Propagation } k_{p_n}$$
$$P_n + P_m = M_n + M_m \text{ Termination } k_{t_n},\ k_{t_m},$$

where the symbols have their usual significance.

Since the reaction virtually ceases (it is to be recalled that a negligible thermal rate has been noted) when the light is removed, it follows that the stationary state method of analysis can be used. Assuming that the ratio of the kinetic constants (that is, k_{p_n}/k_{t_n}) is independent of the molecular size then

$$\frac{-\,d(M)}{dt} = \frac{(M)(2I)^{\frac{1}{2}}k_p}{k_t^{\frac{1}{2}}}$$

The experimental technique and theory used by Burnett and Melville[7] was followed in order to determine the life-time of the growing radical. The simplest method of obtaining intermittent illumination is by the use of discs, cut into sectors, which are rotated at a constant speed in the path of the light beam. In this particular case it was found most convenient to use an intermittent gear system, which operated a Maltese-cross cam to which a quarter-segment disc was directly attached. By this method it was possible to obtain a square

[7] Burnett and Melville, *Proc. Roy. Soc. A*, 1947, 189, 456

waveform. Since the sector had to be interposed between the light source and the reaction vessel, it was necessary to utilize another type of reaction system, the effective light intensity of which was smaller. In carrying out a run, the following procedure was adopted; the rate at uninterrupted illumination was observed, then the sector was rotated at a known speed and the rate again measured. If possible after 10-14 min., the sector speed was altered and the subsequent rate noted. Then to check the observed rates, the sector was removed and the rate of polymerization in an uninterrupted light beam observed, and correlated with the first observatiouns; naturally since linear rates, over a short period, have been demonstrated, the former and latter rates should be identical.

The rates of reaction, at varying sector speeds, were compared with the rate determined from uninterrupted illumination. For comparative purposes the results of this determination and the theoretical curve for an assumed lifetime of 4·5 sec. are plotted in Fig. 5. The agreement of theory and experimental results is good, though it appears that the lifetime may be slightly less than the value of 4·5 sec. taken. Once again it has been noted [7, 8] that deviations occur from the theoretical curve to a marked extent at large values of the flash-time; this deviation has been shown to be very marked in the kinetic analysis of butyl acrylate,[8] where the lifetimes are extremely high (of the order of 75 to 85 sec.).

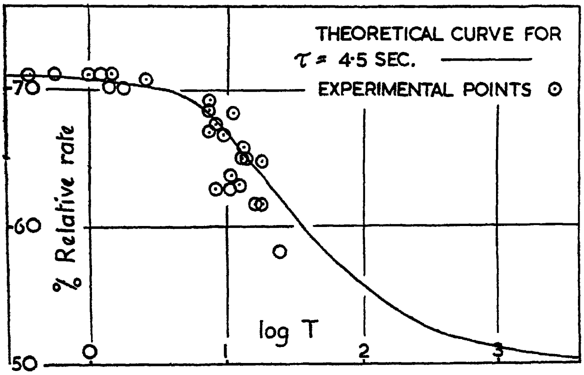

FIG. 5.—Rate of reaction as a function of duration of flash.

In order to complete the kinetic analysis it is necessary to devise a means whereby the number of chains started can be counted. The thermal polymerization of styrene is known to be inhibited by *p*-benzoquinone,[9] and Burnett and Melville [7] inhibited the photopolymerization of vinyl acetate with the same substance. With a similar end in view, the effect of *p*-benzoquinone on the polymerization of vinylidene chloride was investigated.

The absorption spectrum of benzoquinone shows a high intensity peak at about 2450 Å (Braude [10]). Reference to the absorption spectrum of vinylidene chloride and also to its rate of reaction depending on the wavelength of the activating light, implies that most of the activating energy is derived from wavelengths below 2400 Å. Below this wavelength the extinction coefficients of benzoquinone drop rapidly and are of the same order as that of the monomer. Thus with a concentration of benzoquinone of the order of approximately 10^{-3} M, the internal filter effect by this substance should be negligible compared with the overall absorption of the monomer. The benzoquinone was purified by steam distillation, and sublimed in a low vacuum. A solution was then prepared in dry ether so that suitable weights of the material could be introduced into the reaction vessels.

The effect of the benzoquinone is retardation—and not inhibition—as in the cases previously quoted.[7, 9] Table VIII shows the results of these experiments. These figures show that the ratio of reciprocal rate to benzoquinone concentration in constant, as is required by this theory of the action of retarders.

The intensity exponent was measured at various concentrations of retarder,

[8] Bickel and Melville, *Trans. Faraday Soc.*, 1949, 45, 1049.
[9] Foord, *J. Chem. Soc.*, 1940, 48.
[10] Braude, *ibid.*, 1945, 490.

TABLE VIII.—RETARDATION BY BENZOQUINONE

Concentration of Benzoquinone (B) moles/l. × 10^3	Rate mole $l.^{-1}$ $sec.^{-1}$ × 10^5	$1/R$	$\frac{1/R}{B}$	n
0	20·5	0·049	—	0·5
2·6	6·6	0·153	5·9	1·0
2·6	5·8	0·173	6·7	—
5·0	3·6	0·28	5·6	—
5·1	2·8	0·356	7·0	1·0
9·8	1·7	0·595	6·05	1·0
9·9	1·7	0·595	6·0	1·0
21·1	0·66	1·54	7·3	—

and as shown is unity. This, of course, indicates that no copolymerization takes place between the active chain carrier and the benzoquinone molecule; at the same time this result precludes the possibility of a transfer reaction being the predominant feature of the retarder in its action. Furthermore, these results mean that the benzoquinone must react with a growing chain and stop the chain propagation: and if benzoquinone had merely acted as an internal filter in cutting down the rate of initiation then the square-root intensity relationship would have been observed, and there would not have been a linear relationship between $1/R$ and benzoquinone concentration.

Hydroquinone also retards the polymerization. But, unlike *p*-benzoquinone, the reaction never attains a steady rate—the rate falls continuously. The hydroquinone was purified using the method of Bolland and ten Have,[11] by recrystallization from A.R. benzene three times under an atmosphere of nitrogen. The intensity exponent, estimated by comparing the rates obtained initially for two identical concentrations under different intensities, though far from accurate—approximately 0·45—indicates that copolymerization, or transfer, takes place and is the predominant feature of the action of hydroquinone. This case, apparently, is one of the transition cases referred to by Melville and Watson;[12] that is, the hydroquinone molecule reacts as in a copolymerization system, but the reactivity of the radical end so produced is less than that of vinylidene chloride due, in all probability, to its greater degree of stability.

The Determination of the Rate of Chain Starting.—Since benzoquinone only acts as a retarder in this polymerization, the determination of the rate of radical production can only be done by estimating the rate of removal of the quinone. Fortunately the fact that with sufficient quinone the intensity exponent attains a value of unity shows that the polymer radical growth is stopped by the action of the quinone. Thus at sufficiently high concentrations mutual termination may be neglected and the only significant termination reaction is

$$P_n + B \rightarrow M_n \; . \; . \; . \; k_q,$$

where k_q is the termination coefficient. Kinetic analysis then gives

$$-\,d(M)/dt = \frac{k_p(M)2I}{k_q(B)},$$

where (B) is the benzoquinone concentration. Support for this relation between $-\,d(M)/dt$ and (B) is given in Fig. 4 where log rate is a linear function of log $1/B$. Again in this circumstance $-\,d(B)/dt = 2I$ since it is presumed that the quinone only affects the terminal of polymer growth and not its initiation. If (B) is large enough to terminate all chains $-\,d(B)/dt$ will be constant and the disappearance of the quinone will be of zero order with respect to its own concentration. Thus two measurements of the concentration at $t = 0$ and after a reaction period suffice, provided that the quinone concentration has not fallen to a value such that mutual termination becomes of importance.

The colour of benzoquinone is characteristic of the substance, and if the reaction gave rise to no coloured end products, a determination based on the relative light absorption values of various concentrations of benzoquinone would give an analytical tool of the desired utility. Such a procedure is readily available with the aid of a Hilger absorptiometer. The greatest degree of accuracy is obtained by use of the Violet 601 filter; measurements with this filter are almost at the peak of the benzoquinone absorption at 4500 Å. It was also found possible to measure concentrations of the order of 10^{-3} to 10^{-4} molar. The most convenient solvent was A.R. benzene.

---

[11] Bolland and ten Have, *Trans. Faraday Soc.*, 1947, **43**, 201.

[12] Melville and Watson, *ibid.*, 1948, **44**, 886.

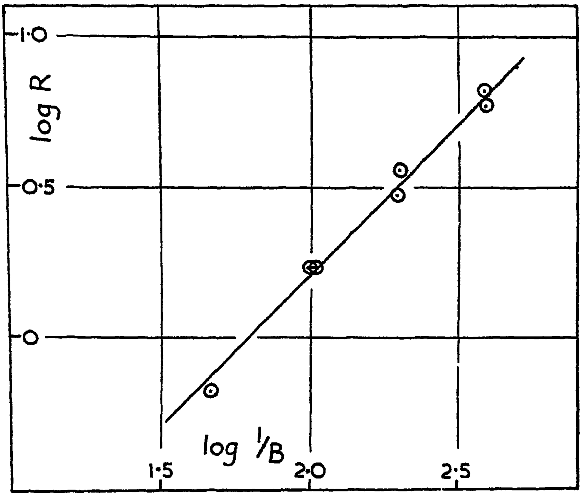

FIG. 6.—The relationship of the rate to the concentration of benzoquinone.

The cells as supplied with the instrument were found to require too large a volume of solution (at the expense of accuracy) for this work—viz. 4 ml. of solution (the volume of a reaction vessel) at 10^{-3} M. Smaller vessels were therefore constructed, the length of the absorption path remaining the same as that of the normal cells. The incident light of the absorptiometer consists of an intense beam, cylindrical in shape, about 10 mm. diam., and a highly diffuse light on the remaining area of the absorption cell. Two cells were made as shown in Fig. 7, with their cell mounts, which used only the light transmitted as an intense beam.

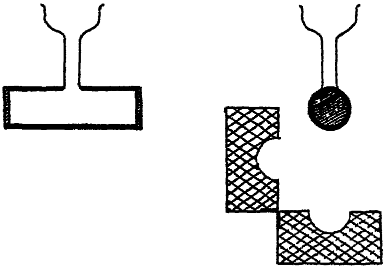

FIG. 7.—Micro cell and holder for Hilger absorptiometer.

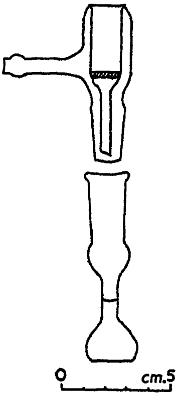

FIG. 8.—Standard 4 ml. flask with filter.

The cells proper were made from 10 mm. Veridia tubing, and were 38 mm. long. The windows, of plate glass, were sealed on to the tubing by means of polyvinyl alcohol in aqueous solution; this sealing surface gives satisfactory service, even with constant use. To mount the cells, the median height of the intense light beam above the cell carrier was measured, and the cells mounted in Bakelite blocks to the same height; the Bakelite cell-holders were machined to the same area dimensions as the normal cells. Each cell was fitted to its carrier individually, such that no light could pass to the photocell except via the cell proper. Care was exercised to ensure that they were always mounted in exactly the same positions, and in the same orientation. Experimentally it was found that the concentration of any benzoquinone solution could be estimated within ± 2 %, down to a concentration of 5×10^{-4} M, and with a solution of volume less than 4 ml.

Solutions of approximately 5×10^{-3} M benzoquinone in monomer were prepared as previously, and illuminated. After varied times of reaction, during which the rates of polymerization were checked, the tubes were taken from the thermostat, and immersed in a solid carbon dioxide and alcohol mixture to interrupt the reaction. After immersion in liquid oxygen the tube was then broken at both ends whilst the solution of monomer and benzoquinone was frozen. The solution was then allowed to thaw out into a filter stick, attached to a standard 4 ml. flask by a standard cone and socket, as shown in Fig. 8. By this means the solution was filtered from the polymer, formed in the reaction, and then the monomer could be quicky removed under suction. To prevent the removal of benzoquinone by sublimation, it was found advisable to replace some of the monomer in the flask, before total removal, by benzene. The empty reaction tube was washed out by benzene, and the solution concentrated, as necessary, in the standard flask. After all the benzoquinone had been removed into the standard flask, the solution was made up to the required volume, and its concentration measured on the absorptiometer with the use of the calibration curve.

Thus, knowing the initial weight of benzoquinone added and the final weight recovered, the difference in molar concentration could be estimated. The results of these determinations are tabulated below in Table IX.

TABLE IX.—DETERMINATION OF THE RATE OF INITIATION

Benzoquinone Concentration molar × 10^3		Time (min.)	$2I = -dB/dt \times 10^7$	Mean Rate moles l.$^{-1}$ sec.$^{-1}$ × 10^5
Initial	Final			
4·82	4·06	40	3·17	2·8
5·27	4·12	53	3·61	2·6
5·00	3·38	73	3·69	2·6
5·19	4·07	53	3·40	2·7
5·08	3·72	64	3·52	2·7

The rate of initiation $2I$ is expressed in mole radicals l.$^{-1}$sec.$^{-1}$, assuming that one benzoquinone molecule removes one polymer (mono) radical.

These figures are in good agreement, considering the magnitude of the errors that could be involved in the analysis of such small quantities, and since it was possible that some absorption of benzoquinone on the polymer might have taken place.

PART II

In Part I it has been shown that the general kinetics of vinylidene chloride polymerization fall into line with those of other similar reactions. It is now necessary to evaluate the velocity coefficients for the constituent reactions and to see how they are affected by change of temperature. Summarizing the results at 25° C:

(i) The overall rate of polymerization R_1 under steady illumination, in the optical system used for the determination of the rate of initiation, was $20{\cdot}5 \times 10^{-5}$ mole l.$^{-1}$ sec.$^{-1}$.

(ii) This was different from the overall rate R_2 found in the optical arrangement used in the determination of the average lifetime of the growing chain. In this case the rate was $13{\cdot}6 \times 10^{-5}$ mole. l.$^{-1}$ sec.$^{-1}$.

(iii) The measured rate of initiation, from the benzoquinone consumption technique, was $3{\cdot}48 \times 10^{-7}$ mole radicals l.^{-1} sec.^{-1} (reaction system 1).

(iv) The average lifetime of the growing polymer is, within experimental error, 4·5 sec.

It is necessary to reduce these values to the same experimental conditions. Since the lifetime factor is affected by the rate of initiation, it is most convenient to reduce the results in terms of the optical system used for the determination of the lifetime. It has been shown that the rate of reaction is proportional to the square root of the light intensity; therefore, denoting by subscripts 1 the factors in the system used in the benzoquinone experiments, and 2 those in the lifetime experiments, then

$$2I_2/2I_1 = (R_2/R_1)^2$$

and, substituting the known values,

$$2I_2 = \left(\frac{13{\cdot}6}{20{\cdot}5}\right)^{\frac{1}{2}} \times 3{\cdot}48 \times 10^{-7} = 2{\cdot}83 \times 10^{-7} \text{ mole radicals/l.}^{-1}\text{ sec.}^{-1},$$

that is, assuming that one molecule of the quinone is effective in stabilizing one radical. Henceforward $2I_2$ will be termed $2I$.

It is possible to show that under conditions of steady illumination,[1] the following equation holds

$$\text{Rate of initiation} = (P)/\tau,$$

where (P) is the total radical concentration, and τ the lifetime of the radicals.

For purposes of this kinetic analysis, it is assumed that insolubility of the growing chain would not prohibit applying an analysis which has been previously used for a system where the polymer formed a homogeneous solution in the monomer. With mutual termination of chains

$$(\mathrm{P})^2 = 2I/k_t,$$
$$(k_t 2I)^{\frac{1}{2}} = \tau$$
$$k_t^{-\frac{1}{2}} = \tau \times (2I)^{\frac{1}{2}},$$

and substituting the relevant values,

$$k_t = 1{\cdot}75 \times 10^5 \text{ l. mole}^{-1}\text{ sec.}^{-1}.$$

The overall rate of the reaction is defined by the expression

$$-\,\mathrm{d}(M)/\mathrm{d}t = k_p(\mathrm{M})(\mathrm{P}) = k_p(\mathrm{M})(2I)^{\frac{1}{2}}/k_t^{\prime\prime 2}.$$

Thus, rewritten, this expression can be used to find

$$k_p = \frac{-\,\mathrm{d}(\mathrm{M})/\mathrm{d}t \,.\, k_t^{\frac{1}{2}}}{(\mathrm{M})(2I)^{\frac{1}{2}}},$$

and by using the known values for these symbols

$$k_p = 8{\cdot}60 \text{ l. mole}^{-1}\text{ sec.}^{-1}.$$

From the calculated constants it is possible to determine the value of the kinetic chain length. This is done most simply from the relationship

$$\nu_k = \frac{-\,\mathrm{d}(\mathrm{M})/\mathrm{d}t}{2I},$$

where ν_k is the kinetic chain length. The relevant figures give the value of the chain length as 480.

From the results obtained in the retardation experiments at 25° C with benzoquinone, it is also possible to estimate the values of the kinetic coefficients in the termination of a growing chain by benzoquinone, that is, of

$$\mathrm{P}_n + \mathrm{B} \rightarrow \mathrm{Y}\ (\text{dead}) \ldots k_q.$$

---

[1] Jones and Melville, *Proc. Roy. Soc. A*, 1937, 163, 511.

Previously it was shown that the rate of conversion of monomer could be expressed by the equation

$$\frac{-\,\mathrm{d(M)}}{\mathrm{d}t} = \frac{k_p 2I(\mathrm{M})}{k_q(\mathrm{B})}.$$

From the results in the previous paper, and the known value of k_p at 25° C, k_q can be calculated. If it is assumed that the coefficient of propagation does not suffer much change with variation of rate of initiation at the same temperature, k_q is found to be $2{\cdot}2 \times 10^2$ l. mole^{-1} sec.$^{-1}$.

Under these conditions of retardation, say with an average retarder concentration of $5{\cdot}0 \times 10^{-3}$ mole/l., the concentration of active centres can be readily found. This is given by

$$\begin{aligned} (\mathrm{P}) &= 2I/k_q(\mathrm{B}) \\ &= 3{\cdot}2 \times 10^{-7} \text{ g. radical/l.} \\ \text{for} \qquad I &= 3{\cdot}48 \times 10^{-7} \text{ mole radical l.}^{-1} \text{ sec.}^{-1}. \\ \text{Thus,} \qquad k_q(\mathrm{P})(\mathrm{B}) &= 3{\cdot}5 \times 10^{-7} \text{ mole/l.}^{-1} \text{ sec.}^{-1} \\ k_t(\mathrm{P})^2 &= 1{\cdot}8 \times 10^{-8} \quad ,, \quad ,, \\ \text{and} \qquad k_p(\mathrm{P})(\mathrm{M}) &= 3{\cdot}4 \times 10^{-5} \quad ,, \quad ,, \end{aligned}$$

from which it is readily seen that the assumption that the benzoquinone rate of reaction is more rapid than the equivalent termination reaction of two active polymer chains, is justified. At the same time, it is seen that the propagation process is much faster, and this would account therefore for the lack of inhibition. Under these retarder conditions, it is estimated that the chain length is approximately 120, that is, compared to the unretarded value of 480 the chain length is appreciably reduced.

TABLE I.—THE AVERAGE LIFETIME AT 15° C

Duration of Flash (sec.)	Rate as %	Average Lifetime (τ) Calcd. from Graph (sec.)
6·2	70·3	11·2
8·2	70·3	14·9
11·8	70·0	14·3
14·1	69·2	13·9
16·8	68·6	13·0
18·4	68·5	13·2
18·4	67·8	10·8
21·0	68·0	13·2
21·6	67·5	12·1
21·7	67·0	10·9
23·5	67·0	11·7
26·3	66·5	11·0
36·4	65·0	12·1

A similar series of experiments was carried out at 15° C and 35° C. At 15° C the flocculated polymer particles are not deposited to such a great extent on the vessel walls nearest the light source; in addition the reaction could be continued for a longer period. At 35° C the polymer deposit is more marked on the vessel walls, and discoloration of the product sets in at an earlier stage in the reaction.

At both temperatures, however, linear rates were observed over the initial stages, and the dependence of the reactions on the square root of the light intensity was still operative and this permitted the determination of radical lifetimes. The average value of τ from these results is 12·4 sec. The overall rate for uninterrupted light in these experiments was found to be 2·94 %/hr., or $10{\cdot}3 \times 10^{-5}$ mole l^{-1} sec^{-1}. The results for the reaction at 35° C are given in Table II. The overall rate recorded for uninterrupted light, for this determination, was $17{\cdot}8 \times 10^{-5}$ mole l.$^{-1}$ sec.$^{-1}$.

TABLE II.—THE AVERAGE LIFETIME AT 35° C

Flash Time (sec.)	% Rate	τ (calc.) (sec.)
3·4	67	1·7
5·0	64·5	1·4
6·3	62·1	1·2
8·1	61·5	1·3
8·2	60·2	1·1
10·25	59·0	1·1

Average τ = 1·35 sec.

From the point of view of a complete kinetic analysis, it was necessary to determine the effect of temperature on the rate of initiation. As has been described above in detail, the analysis of the retarding influence of benzoquinone and its consumption was investigated. The results are tabulated below in Tables III and IV; the unretarded reaction rate under the same conditions was found to be $15{\cdot}2 \times 10^{-5}$ mole l.$^{-1}$ sec.$^{-1}$ at 15° C, and $27{\cdot}2 \times 10^{-5}$ mole l.$^{-1}$ sec.$^{-1}$ at 35° C. The rate of consumption of quinone which is equal to the rate of initiation (the assumption made in the analysis) is, within experimental error, the same value as determined previously. Thus it can be stated that there is no temperature coefficient for the rate of initiation.

TABLE III.—ANALYSIS OF THE INITIATION REACTION AT 15° C

Benzoquinone Concentration mole/l. × 10^3		Duration of Reaction (min.)	Rate of Consumption $= 2I \times 10^7$ mole l.$^{-1}$ sec.$^{-1}$	Rate $R \times 10^6$ mole l.$^{-1}$ sec.$^{-1}$	$R \times (B)$
Initial (B)	Final				
4·14	3·17	49	3·3	13·1	54
6·21	5·28	43	3·6	10·0	62
6·53	5·79	35	3·5	8·0	57
7·84	5·72	100	3·5	7·2	56
9·57	6·60	130	3·8	5·3	51

TABLE IV.—REACTION AT 35° C

Concentration of Benzoquinone × 10^3 moles/l.		Time (min.)	$2I \times 10^7$ mole l.$^{-1}$ sec.$^{-1}$	Rate × 10^5 mole l.$^{-1}$ sec.$^{-1}$
Initial	Final			
3·6	2·75	40·5	3·4	3·8
5·2	4·1	54·5	3·4	3·1
5·7	4·5	60	3·3	2·4
6·1	5·25	38	3·7	2·2
6·35	4·6	80	3·6	2·4

Comparison of Molecular Weights.—Polyvinylidene chloride has proved to be difficultly soluble; it can be swollen [2] at room temperature, but its solution can only be achieved at temperatures over 100° C in such substances as tetrachloroethane,[3] trichlorobenzene (probably a mixture of the isomers), etc. Thus to obtain the average number molecular weight, by osmometric measurements, it would be necessary to work at temperatures in the region of 120° C. This would have provided an absolute check on the results and indicate the possibility of transfer taking place during the chain reaction, but, at present, osmometric work at such temperatures gives rise to a number of technical difficulties. Therefore, recourse was had to the use of viscosimetric determinations of the relative molecular weight, since only comparative results were required to check the theoretical values of the chain length obtained. One trouble in this experiment was the tendency of the polymer to decompose rapidly at high temperatures. The kinetic chain lengths which can readily be calculated from the experimental results given previously are 365, 480 and 630 at 15° C, 25° C and 35° C respectively.

---

[2] *B.I.O.S. Report*, No. 1478.

Polymer was freshly made at 15° C, 25° C and 35° C, under the same experimental conditions as used previously, and a known concentration dissolved in hot trichlorobenzene rapidly. The resulting solution was rapidly transferred (without filtration) to the viscometer immersed in a high-temperature thermostat. All viscosity measurements were done under these crude conditions, since to prolong the solution at such temperatures for purification was inadvisable due to the decomposition of the polymer. The time of flow of the solutions was found to be measurable within ± 0·2 sec., which was considered reasonable in the circumstances. Usually 8-10 measurements sufficed to give an accurate mean value ; if the flow times were not fairly reproducible it was assumed that the solution was contaminated, and the experiment discarded.

TABLE V.—VISCOSITY MEASUREMENTS

Polymer made at	η Specific	Conc. g./100 ml.	η Intrinsic	ν Kinetic
288° K	0·038	0·55	0·069	360
298° K	0·05	0·60	0·084	480
308° K	0·081	0·81	0·100	630

These results, when plotted on a log-log scale, give a straight line relation in accord with the approximate relationship of Staudinger

$$\eta \text{ (intrinsic)} = K \, . \, m^{\alpha} = K \nu_k{}^{\alpha}$$

and thus

$$K = 1{\cdot}1 \times 10^{-3} \text{ and } \alpha = 0{\cdot}7.$$

This relation shows that no appreciable transfer takes place in the chain reaction, otherwise the intrinsic viscosity would have decreased rapidly with increasing temperature.

The thermal degradation of the polymer at 122° C was made evident by the change in viscosity of a solution after being kept for some time in the thermostat. At zero time η (intrinsic) was found to be 0·100, and an hour later viscosity measurements showed that the value of η (intrinsic) had fallen to 0·073 ; that is, the molecular weight had fallen by about a third.

Energies of Activation of the Elementary Steps.—It is a common observation that in photo gas-phase polymerization the overall temperature coefficient is negative. The corresponding homogeneous reactions in the liquid phase exhibit positive temperature coefficients. In the gas phase these results are undoubtedly due to the fact that the growing radical forms a separate phase. Thus the first act is adsorption of monomer on the growing particle. The concentration of monomer at the *site* of polymerization will thus be governed by the equilibrium set up between polymer and vapour. Thus on increasing the temperature of the system the concentration of monomer at the site of polymerization will decrease exponentially with temperature, being governed by the heat of absorption of monomer by polymer. With vinylidene chloride, in spite of the separation of polymer, this independent alteration of monomer concentration at the site of polymerization should not occur and the overall temperature coefficient should be positive. On the other hand, the polymer crystallizes so readily that the polymer radicals may well behave in a manner very different from a polymer chain that has a much greater mobility. The results are set out in Table VI.

---

[3] Staudinger and Feisst, *Helv. chim Acta*, 1930, 13, 382.

TABLE VI.—THE OVERALL ENERGY OF ACTIVATION

Temperature °K	Rate × 10^5 mole l.$^{-1}$ sec.$^{-1}$	*E* (calc.) kcal./mole
(*a*) $2I = 3{\cdot}48 \times 10^{-7}$ mole radicals l.$^{-1}$ sec.$^{-1}$.		
288	15·2	
298	20·5	5·1
308	27·2	5·2
(*b*) $2I = 2{\cdot}83 \times 10^{-7}$ g. mole radicals l.$^{-1}$ sec.$^{-1}$.		
288	10·3	
298	13·6	4·8
308	17·8	4·8

The overall energy of activation is of a reasonable order, and compares favourably with the previous results for the polymerization of vinyl compounds.[4, 5] But it is obvious from the results quoted at various temperatures, namely the variation of lifetime with temperature, that, unlike previously investigated reactions, the energy of activation of the termination process is not zero. This is more easily seen where for comparative purposes, the kinetic results are shown in Table VII.

TABLE VII.—THE KINETIC RESULTS

Temperature °K	$2I \times 10^{-7}$ mole l.$^{-1}$ sec.$^{-1}$	Rate × 10^5 mole l.$^{-1}$ sec.$^{-1}$	τ (sec.)
288	2·83	10·3	12·4
298	2·83	13·6	4·5
308	2·83	17·8	1·4

From this table there can readily be calculated the results of Table VIII.

TABLE VIII.—THE KINETIC CONSTANTS

Temperature °K	k_p (l. mole^{-1} sec.$^{-1}$	k_t (l. mole^{-1} sec.$^{-1}$)	Kinetic Chain Length
288	2·3	0·23 × 10^5	365
298	8·6	1·75 × 10^5	480
308	36·8	18·0 × 10^5	630

---

[4] Jones and Melville, *Proc. Roy. Soc. A*, 1940, **175**, 392.
[5] Burnett and Melville, *ibid.*, 1947, **189**, 456.

Thus a plot of k_p or k_t expressed in the logarithmic form against the reciprocal of the absolute temperature, should be a straight line. From the slope of this line, Fig. 1, it is easily calculated that

the energy of propagation = 25 kcal./mole,
and the energy of termination = 40 kcal./mole.

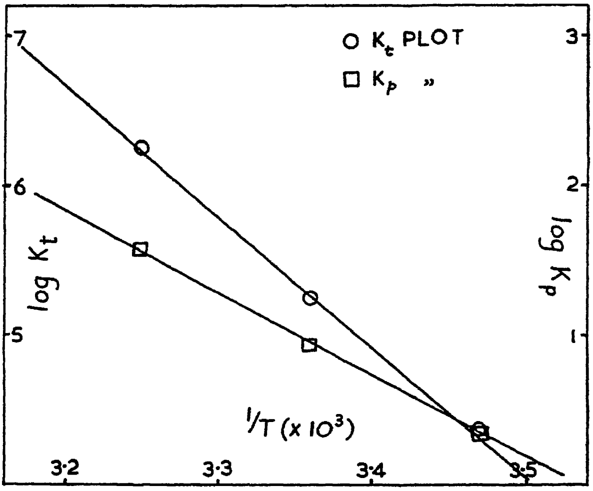

FIG. 1.—The plot of log (kinetic constants) against reciprocal temperature.

These values are phenomenally high, giving frequency factors

A_p of the order 10^{16},
A_t of the order 10^{30}.

In a similar way, by carrying out retardation experiments with benzoquinone at different temperatures, the temperature coefficient of the retardation reaction may be determined. k_q for retardation at 25° C is $2{\cdot}2 \times 10^2$ l. mole^{-1} sec.$^{-1}$., and the corresponding values for the reactions at 15° C and 35° C are $1{\cdot}8 \times 10^2$ and $11{\cdot}0 \times 10^2$ respectively. These values of k_q when plotted logarithmically against the reciprocal of the absolute temperature, Fig. 2, do not fall on even an approximately straight line, but increase very rapidly with increasing temperature.

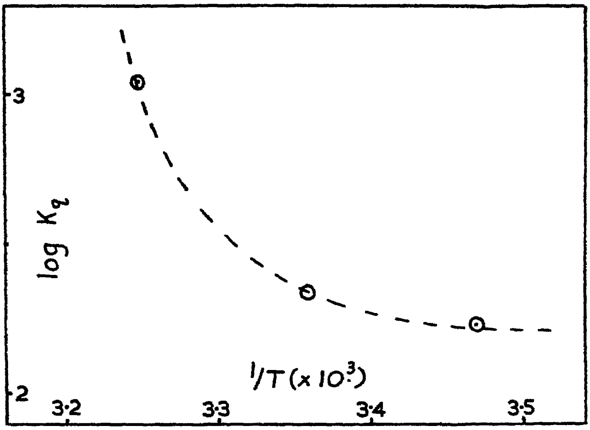

FIG. 2.

Discussion

The anomalously high values for the energy of activation of the separate steps in this polymerization and the impossibly high values for the temperature independent factors at once throw doubt on the assumption used to calculate these quantities. There is no doubt about the rate measurements; the rate of initiation of polymerization is measured by a chemical method about which there can be little doubt, except the uncertainty as to whether one or two radicals are destroyed per molecule of benzoquinone destroyed. Similarly the lifetime measurements are made by the sector method which now has independent confirmation of its reliability by developments in non-stationary treatments of kinetics. The calculation of the polymer radical concentration is made without further assumption from the relation

$$2I\tau = (\mathrm{P})$$

and consequently the value of k_t is calculated without further assumption assuming that the stationary state is established and that therefore

$$2I = k_t(\mathrm{P})^2$$

and

$$k_t = 2I^{-1}\tau^{-2}.$$

When a calculation of this kind is made, for a homogeneous polymerization, the numerical value of k_t is not dependent on temperature to any important extent, thus implying a very small energy of activation, but it is much smaller than that which would be expected for the interaction of small radicals. With vinylidene chloride the numerical value is of the order of 10^5, which is quite comparable with other radical-radical processes, Table IX. In view of the fact that the growing radical forms a separate phase in the monomer, the question arises as to whether it is legitimate to regard the interaction in the same way as in a homogeneous system. It may be that the rate-determining step is the collision between two colloidal particles and that therefore the theory of coagulation of such particles will be capable of predicting the rate of the termination reaction in this particular case. Calculations of this kind were made some time ago by Evans and co-workers[6] but at that time there were no numerical data to see whether this concept was in fact a sufficiently good approximation.

TABLE IX.—THE ABSOLUTE RATE COEFFICIENTS FOR VARIOUS MONOMERS AT 25° C

Monomer	k_p	$k_t^{\frac{1}{2}} (\times 10^{-3})$	$\frac{k_t^{\frac{1}{2}}}{k_p}$	Overall Energy of Activation kcal./mole
Butyl acrylate[7] . .	13·1	0·134	10·2	4·8
Styrene[8] . . .	39·5	2·81	71·3	5
Methyl methacrylate[9] .	122	2·84	23·2	4·4
Vinyl acetate[5] . .	900	22·3	24·8	4·5
Methyl acrylate[10] . .	—	—	2·3	4·5
Vinylidene chloride .	8·6	0·418	48·6	5·0

---

[6] Evans *et al.*, *Trans. Faraday Soc.*, 1947, **43**, 210; *J. Chem. Soc.*, 1947, 266; *Trans. Faraday Soc.*, 1946, **42**, 668.

[7] Bickel and Melville, *ibid.*, 1949, **45**, 1049.

[8] Melville and Valentine, *Proc. Roy. Soc. A*, 1950, **200**, 337.

[9] Burnett, *Trans. Faraday Soc.* (in press).

[10] Bagdasar, *J. Phys. Chem.* (*U.S.S.R.*), 1948, **22**, 1181.

The velocity constant for coagulation of spheres of radii r_1 and r_2 is

$$k = \frac{8RT}{3000\eta}\left(\frac{2 + r_1/r_2 + r_2/r_1}{4}\right) \text{ l. mole}^{-1}\text{ sec.}^{-1}$$

and therefore if the polymer chains of length x are coiled into spheres, then in terms of chain length

$$k_t = \frac{8RT}{3000\eta}\left(\frac{2 + (x_1/x_2)^{1/3} + (x_2/x_1)^{1/3}}{4}\right) \text{ l. mole}^{-1}\text{ sec.}^{-1} \quad . \quad (2)$$

In this latter equation the velocity constant is only very slightly dependent upon chain length, being independent of chain length when $x_1 = x_2$, and is only increased by 4 % when $x_1 = 10x_2$. It would appear justifiable therefore to consider k_t virtually independent of chain length.

Thus eqn. (2) can be used to calculate the termination constant for this reaction. It is to be remembered that hydrophobic sols have a viscosity close to water, and therefore it is justifiable to use the viscosity of vinylidene chloride at 25° C as the viscosity of the diffusing growing polymer in the system. No figures for the viscosity of pure vinylidene chloride are available, since it has been found that the viscosity varies during the determination, but figures for the aniline-stabilized product are available,[3] and for the purposes of this calculation are deemed sufficiently accurate.

At 25° C the viscosity (in centipoise) is 0·343, and assuming that the reacting chains are very nearly equal in length, there is obtained :

$$k_t = \frac{8 \times 8{\cdot}313 \times 10^7}{3000 \times 0{\cdot}343} = 6{\cdot}5 \times 10^5$$

(Experimentally, $1{\cdot}8 \times 10^5$) ;

at 15° C,

$$k_t = \frac{8 \times 8{\cdot}313 \times 10^7}{3000 \times 0{\cdot}377} = 5{\cdot}9 \times 10^5$$

(Experimentally, $0{\cdot}23 \times 10^5$) ;

and at 35° C,

$$k_t = \frac{8 \times 8{\cdot}313 \times 10^7}{3000 \times 0{\cdot}312} = 7{\cdot}1 \times 10^5$$

(Experimentally, $18{\cdot}0 \times 10^5$).

These theoretical values give an energy of activation for the termination process of 1·6 kcal., and a frequency factor of 10^7. Again the absolute values are in surprisingly good agreement with experiment and, it might be concluded, that collision of colloidal particles simply controls the velocity of the termination process.

There is unfortunately the complicating feature that, although it happens that the termination constants are reasonable in magnitude, the temperature coefficient is very high indeed, implying that considerable activation is needed before interaction will occur. This can hardly be attributed to any inherent unreactivity of the radicals themselves for if this energy of activation interacts, in the normal way, the frequency factor should be less than 10^{11} and never exceed it by many orders of magnitude. The only abnormal state of affairs is that the polyvinylidene chloride has a very marked tendency to crystallize. It may well be that the radical end of the polymer becomes embedded in a crystalline part of the polymer and in that respect becomes shielded from any radical or other molecule that might normally react with it. Even so, the energy required to make the radical available for reaction seems to be unduly high.

Similar difficulties arise in the interpretation of the rate of the growth reaction. Here there is an additional uncertainty. In the above calculation of the growth coefficient, it is assumed that the concentration of monomer at the site of polymerization is equal to that of the pure monomer on the reasonable assumption that the radical attached to the growing polymer particle is on the outside. Although, with this simplifying assumption, the numerical value of k_p is once again of the order of that obtained in homogeneous polymerizations. But the temperature coefficient and the temperature independent factors are so high as to throw doubt on this simple interpretation. It may be that the radical does become surrounded with crystalline polyvinylidene chloride and therefore becomes rather inaccessible. This leads to unusual frequency factors and energies. It is, however, surprising that although these abnormal values for the coefficients are obtained, the overall concepts of the reaction, such as rate dependence on concentration, light intensity and temperature coefficient, are so clearly similar to those in completely homogeneous processes.

In spite of these complications it is perhaps surprising that the absolute values of the coefficients, and the value $k_t^{\frac{1}{2}}/k_p$, lie quite reasonably in the range that is obtained for a variety of other systems (Table IX).

One of us (J. D. B.) is indebted to D.S.I.R. for a grant. The first part of this work was originally started in the University of Aberdeen and completed in the University of Birmingham.

Chemistry Department,
University of Birmingham.

THE ULTRASONIC DEGRADATION OF POLYMERS

BY H. W. MELVILLE AND A. J. R. MURRAY

Received 11*th April,* 1950

The ultrasonic degradation of dilute solutions of polymethyl methacrylate and polystyrene have been investigated under conditions in which no cavitation occurs. Degradation is much slower than when cavitation is allowed to take place. Osmotic pressure determinations of molecular weight show that true fission of polymers occur. Attempts have been made to find whether fission produces radicals or molecules by carrying out experiments in monomers in presence of iodine. The evidence shows that degradation into molecules seems to be preferred. Monomeric styrene is shown on the other hand to be induced to polymerize by ultrasonic radiation.

In 1933, Flosdorf and Chambers,[1] Szent Gyorgyi [2] and Szalay [3] succeeded in lowering the viscosity of solutions of some natural polymers by treatment with high-frequency sound waves. They attributed the viscosity fall to a breakdown of the polymer molecule and, in Szalay's experiments, a breakdown was also detected by chemical means.

In 1938, however, Freundlich and Gillings,[4] investigating the action of ultrasonic waves on aqueous solutions of gelatine and toluene solutions of rubber, found that the lowering of the viscosity was not permanent. They therefore concluded that the viscosity lowering was merely a thixotropic effect and was not due to molecular degradation. These experiments left some doubts as to the results of previous workers when viscosity measurements alone had been relied upon to give the proof of

[1] Flosdorf and Chambers, *J. Amer. Chem. Soc.*, 1933, **55**, 3051.
[2] Szent Gyorgi, *Nature*, 1933, **131**, 278.
[3] Szalay, *Z. physik. Chem. A*, 1933, **164**, 234.
[4] Freundlich and Gillings, *Trans. Faraday Soc.*, 1938, **34**, 649.

degradation. Moreover, in the previous year, Freundlich[5] had found that the liquefaction of thixotropic gels by ultrasonic waves could only be accomplished if the experiments were carried out at atmospheric pressure. The application of an external pressure prevented the liquefaction of the gels. Freundlich concluded therefore that the liquefaction was not being caused by the ultrasonic waves directly but by the mechanism of cavitation. Since the earlier experiments on degradation had all been carried out at atmospheric pressure, it is possible that, in these cases also, the breakdown was due to cavitation. The possibility of the viscosity fall being due to a thixotropic effect has been disposed of by Brohult's experiments with the degradation of haemocyanin[6] and more fully by the work of Schmid and Rommel[7] who worked with the chemically better defined synthetic polymers. Only with a benzene solution of polyethyl acrylate did these workers note any thixotropic effect and even here the effect was not the only cause of the viscosity fall.

Schmid and Rommel also investigated the possibility of the degradation being due to (*a*) oxidative fission or (*b*) cavitation. They excluded (*a*) by working in an atmosphere of nitrogen and obtaining the same rate of breakdown as in air. This result has been confirmed in the present work. The cavitation effect was investigated by Schmid and Rommel by working under sufficient pressure to prevent the formation of cavities. They concluded that there is a pressure effect which cannot be directly attributed to cavitation since there is still a pressure effect at pressures above that at which cavitation should be stopped.

The clarification of two main points in connection with the degradation has been attempted in this work. These are, the effect of cavitation and the nature of the products of degradation.

All workers are agreed that cavitation will occur in a solution through which ultrasonic waves of sufficient intensity are being passed. The usual method of preventing cavitation is to work under pressure[5, 7] so that the sound waves cannot produce cavities against the external pressure. Cavitation can also be prevented if there is no external pressure to collapse the cavities after formation. This method has been favoured in the present work since it has the dual advantage of preventing cavitation and also of permitting the experiments to be carried out in the absence of oxygen, which is essential for the investigation of the degradation products. The results obtained show that degradation can, in fact, be accomplished without the action of cavitation but it is not so marked as when cavitation is allowed to take place.

None of the previous workers has made any attempt to find out the nature of the ends of the new molecules formed by the rupture of the C—C bond. From a purely theoretical consideration it would appear likely that if a C—C bond in a polymer molecule is broken, then the two molecules thus formed would each have a free radical end which would have to be stabilized by some secondary reaction. In order to prove experimentally whether this is what really happens it is necessary to find a reaction which will detect the presence of radicals. It is well known that polymerization reactions can be initiated by free radicals and it was decided to use this reaction in order to detect the rate of production of free radicals during the degradation. If the overall rate of polymerization is measured and the various kinetic constants for the monomer being used are known, then the rate of radical production can be calculated.

Experimental

The ultrasonic waves (frequency 213 kc./sec.) were produced by the well-known method of driving a quartz crystal with the output from a valve oscillator. The circuit diagram of the oscillator is shown in Fig. 1.

---

[5] Freundlich, *J. Physic. Chem.*, 1937, 41, 1151.

[6] Brohult, *Nature*, 1937, 140, 805.

[7] Schmid and Rommel, *Z. physik. Chem. A*, 1940, 185, 98.

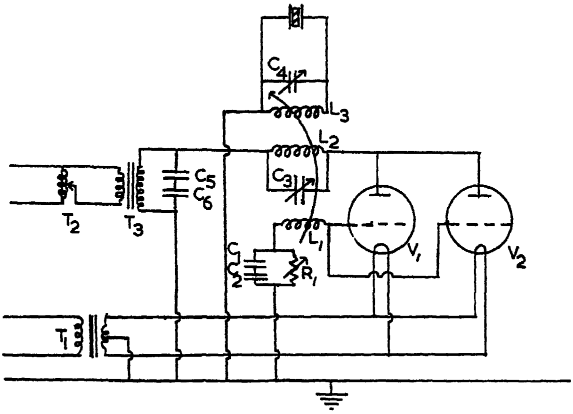

FIG. 1.—Circuit diagram of the oscillator.

Crystal Mounting.—When this work was first started, the crystal was mounted on a brass block which formed one electrode while the other electrode was a light ring of brass resting on the upper face of the crystal. The whole assembly was immersed in transformer oil to give better insulation between the electrodes and to damp the oscillations of the crystal to prevent fracture. This type of mounting has the disadvantage that half the output of the crystal is lost by absorption by the brass block. If, however, the bottom face of the crystal is in contact with a medium which is a poor conductor of sound the downward radiation will be reflected and after passing through the crystal, will emerge from the top face in phase with the radiation which is being emitted from that face and hence increase the intensity of the upward radiation.

The idea of reflecting the downward radiation was first put forward by Greutzmacher [8] who suggested having the bottom face in contact with air which is a relatively poor conductor of sound. Provided that one face of the crystal is in contact with oil there is no danger of the crystal fracturing since it is only possible for the crystal to vibrate symmetrically, and accordingly, damping of one face will automatically damp the other.

The designed crystal holder is shown in plan view in Fig. 2 and a partial section is shown in Fig. 3. The crystal as supplied by the Quartz Crystal Company was silvered on both faces to within 5 mm. of the edge. This portion was left unsilvered in order to increase the path-length between the two live surfaces. As a further precaution against sparking, the electrodes were made of circular cross-section. The electrodes were rings of copper wire of approximately ¼-in. diam. The rings were of such a size that they would make contact with the crystal at the edge of the silvered portion. The ends of the rings were soldered together and the excess solder filed away to leave as smooth a surface as possible. The leads to both electrodes consisted of 22 S.W.G. tinned copper wire soldered into small holes drilled into the electrodes.

In order to obtain maximum circulation of the oil at the edges of the crystal and prevent the collection of air bubbles, the holder was so designed that the crystal and electrodes were supported by lugs projecting from the main holder and was thus not in contact with the holder right round the circumference. In Fig. 2 the lugs A, B and C are those on the upper half of the holder; the lugs D, E and F, shown by dotted lines, are those on the lower half of the holder. By placing the lugs at 120° to each other and arranging the upper lugs to be at 60° to the lower, a secure support to the crystal is obtained and at no point are both faces of the crystal in contact with the holder. In Fig. 2 the outer continuous circle H represents the circumference of the crystal and the inner circles G_1 and G_2 represent the outer and inner edges of the upper electrode, the lower being directly below it. In Fig. 3 the method of cutting the lugs can be seen; only one upper (A, Fig. 2) and one lower (E, Fig. 2) lug is visible in the section but the others are identical. Two grooves are cut, one to locate the crystal and the other to locate the electrode. The depth of the electrode groove is so arranged that the crystal must rest on the electrode and not on the holder.

---

[8] Greutzmacher, *Z. tech. Physik.*, 1936, **17**, 166.

In use the crystal holder is supported by a ⅜-in. brass rod which can be seen at the left of Fig. 3. This brass rod is earthed to the case of the oscillator and forms one of the leads. The holder is immersed to a depth of about 4 in. in a bath of transformer oil contained in a cylindrical glass tank 15 in. long and 12 in. diam. A copper cooling coil is situated round the edge of the tank and the oil is continuously stirred. With this arrangement a fairly steady temperature (± 0·5° C) is obtained when the crystal is oscillating.

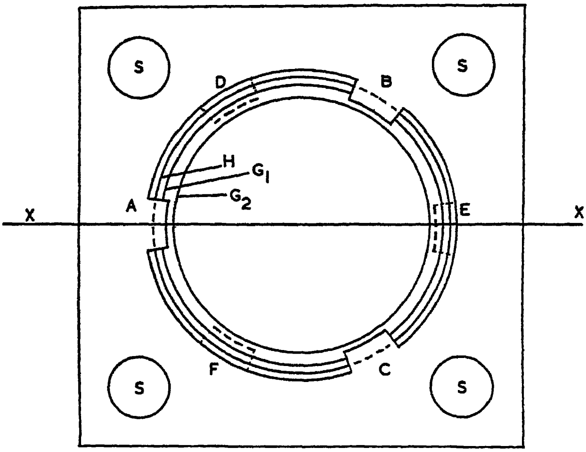

FIG. 2.—Plan view of the crystal holder.

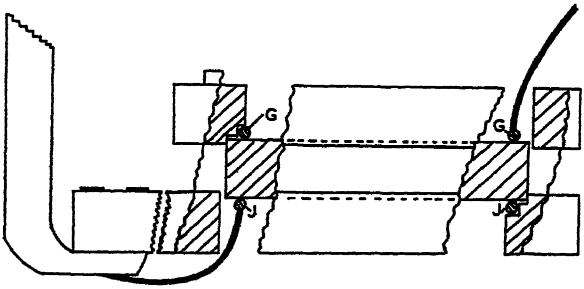

FIG. 3.—Partial section through XX (Fig. 2).

When the crystal is oscillating, air bubbles driven out of the oil by the ultrasonic waves from the lower face of the crystal are trapped by the crystal and the lower electrode, due to the fact that the lower electrode fits tightly against the crystal face. When the crystal has been running for about 30 min. sufficient bubbles have collected to cover completely the face of the crystal and thus provide an efficient reflector of the downward waves. Any air which escapes past the electrodes is swiftly removed by the circulating oil so that no danger of sparking between electrodes is introduced. As the air trapped below the crystal acts as a reflector, it will be seen that the intensity of the upward radiation will depend on the extent of the air bubble. Experiments were only carried out when the crystal was completely covered.

Tuning.—In order to obtain maximum sound energy from the crystal, it is necessary to supply the alternating voltage to the crystal at the same frequency as the fundamental frequency of the crystal. The fundamental frequency of the crystal is fixed by its dimensions and consequently the oscillator must be tuned to the frequency of the crystal. When a crystal is vibrating under oil, a fountain of oil is thrown up from the surface above the crystal face and this fountain forms a convenient tuning indicator. When the crystal is immersed as described above and the oscillator has been allowed to warm up, the latter can be brought into tune by adjusting the variable condensers in the anode and coupling tuned circuits, until a maximum fountain is obtained. This method of tuning has been tested by checking the output of the oscillator against a wavemeter and comparing the figure obtained with the makers' specifications for the crystal. The values obtained were never found to vary by more than 1 kc./sec. (0·5 %). The detailed points to be noted in tuning the oscillator described are dealt with more fully elsewhere.[9]

Intensity.—The intensity of a sound wave being transmitted through a liquid medium is given by

$$J = \rho\frac{v}{2}\,(\omega A)^2,$$

where J is the intensity in ergs/sec. cm.^{2}, ρ the density of the medium through which sound waves of frequency $\omega/2\pi$ c./sec. are travelling at a velocity v cm./sec. A is the maximum amplitude of the vibrating particle of the medium. For sound waves being generated by a piezoelectric quartz, the expansion produced is directly proportional to the applied voltage and the relationship for both the longitudinal and transverse effects was given by Voigt[10] as $\delta = 6{\cdot}36 \times 10^{-8}U$, where δ is the expansion in cm. produced by a voltage U E.S.U. When the quartz is vibrating the amplitude of the particles of the medium will be the same as the expansion of the quartz so that

$$\delta = A.$$

Introducing the values of $\rho = 0{\cdot}85$ and[11] $v = 1{\cdot}42 \times 10^5$ at a frequency of 213 kc./sec. the equations can be reduced to

$$J = 9{\cdot}72 \times 10^{-3} \times E^2 \text{ ergs/sec. cm.}^2,$$

where E is the root mean square applied voltage, the conversion to peak volts in E.S.U. being included in the value of the constant.

The value of the applied voltage in these experiments was about 25,000 V which, from the above equation gives a value of $J = 6 \times 10^6$ ergs/sec. cm.^{2}. The total effective area of both faces of the crystal was 39 cm.^{2} so that the total sound output should be about 23 W. The total dissipation of the oscillator is 400 W so that a conversion of about 6 % is being obtained.

Several methods of measuring the intensity of ultrasonic waves have been published[12-16] and some of these have been tried here. The only method with which any marked success was obtained was a modification of the method of Richards.[12] The absorbing medium used in this case was a block of polythene approximately 1 in. thick. This has been found by Hadfield[17] to have an acoustic impedance approximately equal to that of transformer oil so that there will be little reflection at the interface. The block was immersed in the oil bath above the crystal and the rate of heating under the influence of the ultrasonic waves and the rate of cooling were measured. From these measurements, the total heat input to the polythene was measured. In making these measurements, care must be taken to see that the face of the block next to the crystal is perfectly smooth and preferably chamfered, otherwise air bubbles will collect on the face of the block and reflect the sound waves. As the oil is being continuously cooled, direct radio frequency heating of the block can be ignored. The result of these measurements gave a total intensity of 30 W. Attempts were also made to use the method of Smith and Weimar[14] but they did not meet with success.

Apparatus.—The degradation reaction has to be followed by molecular weight determinations and it is highly desirable that this should be done by a method giving a number average. For convenience, however, in observing whether any effect exists or not, and especially in view of the fact that the reaction must be carried out *in vacuo*, the viscometric method was employed as a preliminary to osmotic measurements. In this way a vessel can be used in which the degradation and viscosity measurements can both be carried out.

[9] Murray, *Ph.D. Thesis* (Aberdeen, 1949).
[10] Voigt, *Abh. Ges. Wiss. Gottingen*, 1890, **36**, 1.
[11] Richards and Loomis, *J. Amer. Chem. Soc.*, 1927, **49**, 3086.
[12] Richards, *Proc. Nat. Acad. Sci.*, 1929, **15**, 310 ; 1931, **17**, 611.
[13] Sorensen, *Ann. Physik.*, 1936, **26**, (v), 121.
[14] Smith and Weimer, *Rev. Sci. Instr.*, 1947, **18**, 188.
[15] Hehlgans, *Ann. Physik.*, 1928, **86**, 587.
[16] Zvetkov *et al.*, *Acta Physicochim.*, 1946, **21**, 135.
[17] Hadfield (private communication).

The vessel used is shown in Fig. 4. It is a viscometer of the Ostwald type in which both the open ends have been sealed into a tube which is used as reaction vessel. After filling the viscometer was evacuated by a mercury condensation pump. The sealed vessel was clamped in position with the bottom of the reaction tube touching the surface of oil immediately above the crystal. This position was chosen as being the most easily reproducible. Some trouble was encountered with the viscometer cracking under the influence of the ultrasonic waves in the region of the clamp. This is due to the restriction imposed by the clamp on the vibration of the glass. It was found that this trouble could be overcome by inserting cotton wool between the vessel and the clamps.

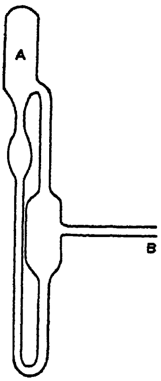

FIG. 4.—Vacuum viscometer.

The viscosity measurements were made in a bath thermostated to ± 0·01° C. It was found that the time of flow was reproducible to within ± 0·01 %.

The polymethyl methacrylate used was prepared from I.C.I. Kallodoc which had been freed from stabilizer by washing with caustic soda solution and washed and dried over calcium chloride. The polymer was prepared by heating with benzoyl peroxide as catalyst. Polystyrene was prepared by thermal polymerization of monomer which had been distilled at 15 mm. pressure. The monomer was supplied by A. Boake Roberts, Ltd. We are indebted to Dr. N. Grassie for samples of methyl methacrylate-acrylo nitrile copolymers, the preparation of which has been described elsewhere.[18]

Molecular weights, unless otherwise stated, were determined osmotically by the method described by Masson and Melville.[19] Since the π/c against c curves for benzene solutions of polymethyl methacrylate and polymethyl methacrylate-acrylo nitrile copolymers are well established, it is possible to estimate the limiting value at infinite dilution of π/c from a determination at one concentration. As there was only a small quantity of polymer degraded in the vacuum viscometer, this method had to be adopted when determining the end molecular weights of samples which had been degraded.

Degradation in presence of a gas.—With the initial crystal mounting described above, it was found that degradation could not be brought about *in vacuo*. Fig. 5 shows the effect of variation of experimental conditions. All runs were carried out at atmospheric pressure. The conditions for the various runs were as follows :

(I) In a 50 ml. flask : viscosity determined in an Ostwald viscometer.

(II), (III), (IV) : In vacuum viscometer sealed at atmospheric pressure.

In (II) the crystal was 0·5 cm. from the surface of oil and in the others it was at 1 cm. From the graphs it can be seen that in the runs using an open flask the degradation is much slower than where the viscometer is used. This is most likely due to the fact that there is a continuous loss of solvent during the run and this counteracts the fall in viscosity due to degradation.

In all the other runs, the variation of rate cannot be due to loss of solvent and, in fact, is a real one and must be due to an alteration of the arrangement of the crystal with respect to the vessel since the output of the oscillation was constant in all cases. In case (IV), the crystal had been embedded in the brass block before the run and a bubble of air had been trapped between the crystal and the block. Since air is known to be a good reflector of sound, the increase in the rate of breakdown can be attributed to the increased intensity due to reflection of the downward radiation.

The runs shown in (II) were carried out in exactly the same way as those in (III) with the exception that the crystal was 0·5 cm. instead of 1·0 cm. from the surface. This might be interpreted as indicating that the intensity of the waves was not the controlling factor in the rate of degradation. However, it was noticed that as the crystal was lowered into the oil, the fountain increased indicating there is a focusing effect which is more than counterbalancing the loss due to increased absorption.

It may be concluded that, under identical conditions, reproducibility can be obtained to within 2 %.

---

[18] Grassie, *Proc. Roy. Soc. A*, 1949, **199**, 1.

[19] Masson and Melville, *J. Polymer Sci.*, 1949, **4**, 323.

Effect of Nature of the Gas Present.—Since it had been found that the presence of a gas was necessary to obtain degradation with our initial apparatus, variation of the nature of the gas present was tried to see whether that gas was exerting a chemical or merely a physical influence. Runs were done in an atmosphere of air, oxygen and nitrogen (10 parts in 10^6 of O_2). In the case of the latter gases, the solution was completely evacuated and the appropriate gas admitted to atmospheric pressure. The gas was then pumped out again and the procedure repeated three times to make sure that the gas finally sealed up in the viscometer was as pure as possible.

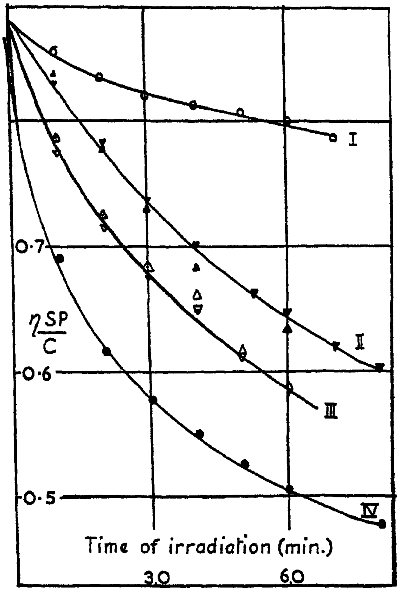

FIG. 5.—Effect of variation of experimental conditions.

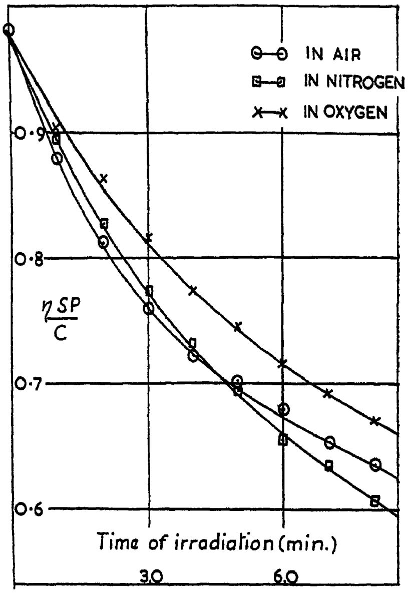

FIG. 6.—Effect of the nature of the gas present.

The results of the runs with these three gases are shown in Fig. 6. It would appear that there is a slight slowing-up of the degradation in presence of pure oxygen compared with air or nitrogen. If oxygen were to play any part in the breakdown, then the most likely role would be a reaction with any free radicals which may be produced. If free radicals are produced by the fission of a C—C bond then they must be stabilized by combination or disproportionation. If there is any tendency to combine this would be prevented by the oxygen and the rate of degradation would be apparently increased. The variation of rate with different gases is not very great and it can be assumed that the nature of the gas makes no significant difference and the presence of a gas is only necessary to permit cavitation to take place.

Degradation *in vacuo*.—(*a*) HIGH MOLECULAR WEIGHT MATERIAL.—A sample of very high molecular weight polymer was obtained by the thermal polymerization of methyl methacrylate *in vacuo*. The effect of ultrasonic waves on a 0·08 % solution in benzene of this polymer is shown in Fig. 7. As a comparison with degradation under the influence of cavitation another sample of the same solution was treated without previous evacuation. After 10-min. treatment this value of [η] was found to be 0·34, thereby showing the marked increase of efficiency of the cavitation mechanism.

(*b*) INTENSITY EFFECT.—As some discrepancy between similar runs had been noted, it was decided to investigate the effect of the intensity of the ultrasonic waves. As no means were available for the measurement of the intensity directly, the value of the anode current of the oscillator was taken as a relative measure of this quantity. A 0·1 % solution of polystyrene in benzene was used for this investigation. The molecular weight, from osmotic pressure measurements was 700,000. The results of this investigation are shown in Fig. 8, from which it can be seen that the degradation proceeds in a step-wise manner and from the first two runs it might be concluded that there is a limit to the extent of degradation which can be brought about with any intensity. The third run shows, however, that this is not the case and that the intensity only affects the rate of breakdown and not the limit. The variation of intensity carried out above is only over a very narrow range of possible intensities and it cannot be assumed that the results obtained can be applied over the whole range of intensities. It does, however, show the importance of maintaining a steady intensity if rates of degradation are to be studied.

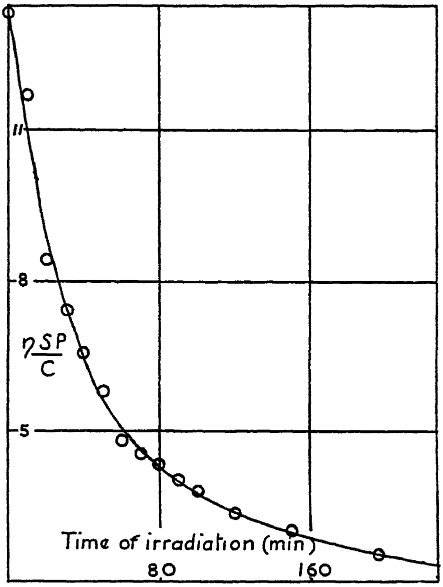

FIG. 7.—Degradation of high molecular weight polymethyl methacrylate *in vacuo*.

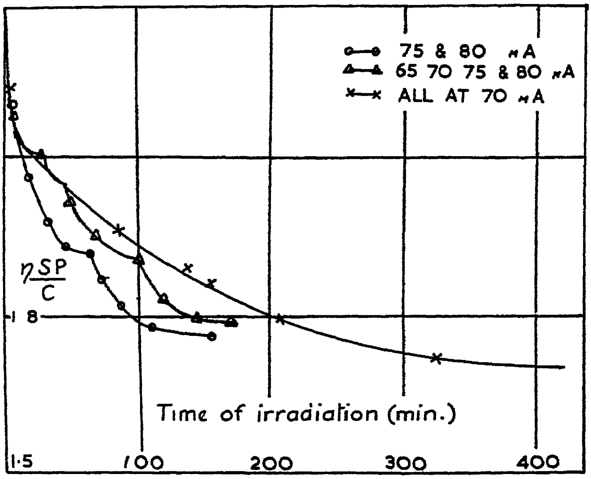

FIG. 8.—Effect of variation of the intensity.

(*c*) NATURE OF THE POLYMER.—Grassie and Melville [20] have found that the presence of acrylonitrile units in the methyl methacrylate chain alters the degradation characteristics. If a copolymer is formed with only a small amount of acrylonitrile, then the thermal breakdown occurs preferentially at the acrylonitrile units since these appear to be the weak points in the chain. Thus by performing experiments with a polymer of this kind it should be possible to see whether ultrasonic degradation preferentially occurs at the weak parts of the molecule or whether the fission of the chain occurs at an arbitrary point determined by other factors altogether.

---

[20] Grassie and Melville, *Proc. Roy. Soc. A*, 1949, **199**, 39.

Samples of the polymers used by Grassie and Melville were degraded in benzene solution at a concentration of 1 %. The polymers used were: (*a*) polymethyl methacrylate polymerized thermally with benzoyl peroxide—molecular weight 725,000; (*b*) polymethyl methacrylate-acrylonitrile copolymer in mole ratio of 411/1—molecular weight 615,000; (*c*) polymethyl methacrylate-acrylonitrile copolymer in mole ratio 40/1—molecular weight 547,000.

If there was to be any marked weakness in the molecule caused by the introduction of the acrylonitrile units then we should expect fission to occur at these bonds and that the molecular weight would fall to the average value of the methyl methacrylate chains, i.e. with the above copolymers to 41,000 and 4000 respectively. The experimental results are shown in Fig. 9 and it can be seen that there is no appreciable difference in the rate of degradation of the three polymers. In addition to the viscosity measurements shown in Fig. 9, the final molecular weight (after 350-min. treatment) of two samples each of the base polymer and the 411/1 copolymer were determined osmotically. The results obtained were:—

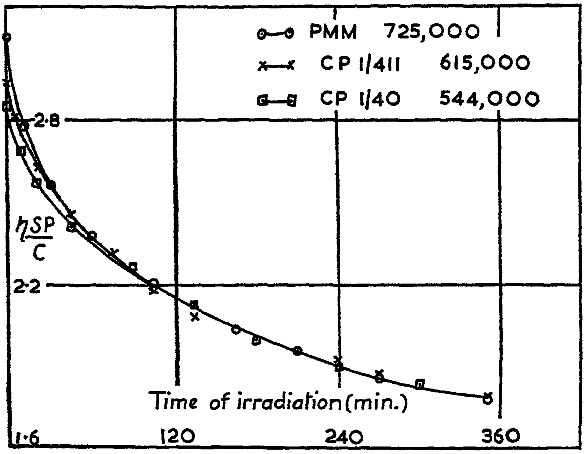

FIG. 9.—Variation of the nature of the polymer.

	Initial.	*Final.*
Methyl methacrylate	725,000	544,000 ± 40,000 460,000 ± 40,000
Copolymer	615,000	385,000 ± 25,000 395,000 ± 25,000

These molecular weights were calculated from osmotic pressure measurements at one concentration only, the extrapolation to zero concentration being done with the help of curves previously obtained for similar polymers.

Although the agreement between the final molecular weights is not very good, it is probably as close as can be expected from the method of measurement. In any case, the difference is much less than would be expected if the introduction of acrylonitrile units into the polymer chain were to cause any significant difference in the degradation characteristics.

It can be seen from Fig. 9 that the viscosities of the solutions are still falling fairly rapidly after 5-hr. treatment. One solution of polymethyl methacrylate was accordingly given prolonged treatment and after a period of 38 hr. the molecular weight had fallen to a value of 270,000.

(*d*) Comparison with Results of Previous Workers.—The most extensive work done to date on the subject has been that of Schmid and Rommell [7] and their experiments were carried out with toluene solutions of polystyrene. As we were mainly interested in the direct effect of the ultrasonic waves and not in the indirect cavitation effect, a comparison was made with the results obtained by the previous workers when working under 15 atm. pressure. The results of present experiments are shown along with those of Schmid and Rommel in Table I. This table gives the results of the degradation of an 0·1 % solution of polystyrene in toluene. The molecular weights given by Schmid and Rommel were calculated from the Staudinger equation $M = \frac{\eta_{sp}}{c\,.\,K_m}$, where c is the concentration of polymer in moles of monomer per litre. For comparative purposes the value of c has been recalculated in grams of polymer per 100 ml. and these values are given in Table I.

TABLE I.—Degradation of Polystyrene in Toluene Solution

This work (*in vacuo*)			Schmid and Rommel (under 15 Atm. Pressure)		
Time of Irradiation (min.)	$\frac{\eta_{sp}}{c}$		Time of Irradiation (min.)	$\frac{\eta_{sp}}{c}$	Mol. Wt. $\times 10^{-3}$
	Run 1	Run 2			
0	2·70	2·75	0	15·7	850
5	2·33	2·41	5·5	2·5	184
10	2·19	2·24	—	—	—
15	2·12	2·17	—	—	—
20	1·96	2·10	20	2·02	139
30	1·75	1·86	—	—	—
40	1·63	1·61	—	—	—
50	1·41	1·52	—	—	—
60	1·38	1·435	60	1·79	131
80	1·28	1·15	—	—	—
100	1·12	1·16	120	1·64	121

At first sight it would appear that the degradation obtained by Schmid and Rommel was much more effective than our own but there must be some discrepancy in the values given by Schmid and Rommel for the molecular weights. As the molecular weights of the polymers used here and by these workers were both measured from osmotic pressure, it is difficult to see where such a large discrepancy could have arisen. However, in spite of the wide variation in the absolute values obtained, the rate of fall in both cases is the same, viz. there is an initial rapid breakdown which merges into a slower rate as degradation proceeds.

Discussion

Schmid and Rommel investigated the effect of pressure on the ultrasonic degradation of nitrocellulose and of polystyrene. They found that (*a*) 5 atm. pressure slowed down and 8 atm. pressure completely stopped the degradation of nitrocellulose, and (*b*) 8 atm. and 15 atm. pressure slowed down the degradation of polystyrene to the same extent. From these results they concluded that there was a pressure effect which had nothing to do with cavitation, which should be stopped by 5 atm. overpressure, although a pressure effect could be obtained above this pressure. If the pressure amplitude is calculated for their system the value obtained is ± 4 atm. and as there may be a focusing effect due to the walls of the Bertholet bomb used by them, this figure may be exceeded and the pressure of 5 atm. may in fact not be sufficient to stop cavitation. If this is the case then the results agree qualitatively with those obtained here, viz., degradation can be accomplished by ultrasonic waves without the aid of the cavitation effect provided that the molecular weight of the starting material is high enough. Also the limiting size to which the molecules can be broken down is lower for breakdown involving cavitation than for simple ultrasonic degradation. The values for the limits found in this work and by Schmid and Rommel are given in Table II. The value of 226,000 is estimated from the apparent limit to which the molecular weight was tending when the degradation was carried out for 38 hr. It has already been seen that there is a wide discrepancy in the values of molecular weight given here and those given by Schmid and Rommel, probably due to errors in the method of measurement, so that no real comparison can be drawn from them.

TABLE II.—LIMITING MOLECULAR WEIGHT

This work		*Schmid and Rommel*	
In vacuo	Atm. pressure	15 atm.	Atm. pressure
226,000	47,000	121,000	28,000

One fact does emerge from Table II, however, and that is that in both cases the cavitation mechanism is more efficient than the shear brought about by ultrasonic waves themselves. In the experiments of Schmid and Rommel the difference between the two mechanisms is not so marked since they attained the value of 121,000 after 2 hr., whereas the value of 270,000 was only obtained in the present work after 38 hr. A possible explanation of the relative importance of cavitation is that at low intensities, the forces produced by the cavitation effect are much greater than the shearing forces associated with the ultrasonic waves. On the other hand, at higher intensities, the shearing forces exerted by the ultrasonic waves are much higher but the forces associated with the collapse of cavities do not increase in proportion to the intensity of the ultrasonic waves producing the cavities.

The fact that the breakdown depends on the shearing forces set up in the liquid by the ultrasonic waves is shown by the comparative ease with which the larger molecules are broken down. It was also found that the rate of breakdown increases with increasing intensity and velocity of the vibrating particles of the medium—which governs the rate of shear—also increases with increasing intensity. The effect of rate of shear has also been demonstrated by Evans [21] and his co-workers in the case of mechanical agitation.

From the negative effect of the introduction of acrylonitrile units into the polymethyl methacrylate chain it has been shown that the chemical structure of the molecule does not play a significant part in the liability to ultrasonic breakdown. The main factor in the construction of the molecule which affects its liability to ultrasonic breakdown is the chain length.

Nature of Fission Products.—The experiments described above and also those of Schmid and Rommel show conclusively that degradation of polymers may be brought about without causing cavitation in the liquid exposed to ultrasonic radiation. The next problem is to attempt to determine whether the polymer molecule is broken down into two radicals or two molecules and if possible the point at which fission occurs. The most sensitive method of detecting radicals in solution and of measuring their rate of production consists in carrying out the reaction in presence of a polymerizable monomer.

The polymer was dissolved in its own or another monomer for the above-mentioned test. Dilatometric procedures of detecting any polymerization proved not to be sufficiently accurate and the more laborious refractive index method was used in which samples of solution were periodically examined in a Pulfrich refractometer thermostated to ± 0·05° C. Refractive index changes linearly with the percentage polymerization in dilute solutions of polymer in monomer and hence no point-to-point calibration of the refractometer is necessary.

---

[21] Evans and Baxendale, *Faraday Soc. Discussion*, 1947, **2**, 404.

An approximate 1 % solution of the polymer of mol. wt. 725,000 previously used was made up in freshly distilled monomer, evacuated and irradiated for 2 hr. The results obtained are shown in Table III. From these figures, the rate of polymerization is 1·03 % per hr.

TABLE III.—POLYMERIZATION OF METHYL METHACRYLATE IN PRESENCE OF DEGRADING POLYMER

	n_D^{25}	Concentration of Polymer
Monomer	1·41219	—
Approx. 1 % soln. . . .	1·41288	0·885 %
After 2-hr. irradiation . . .	1·41448	2·94 %

From these experiments it would appear that the monomer is being induced to polymerize by the degradation of polymethacrylate. Blank experiments with the pure monomer gave under similar circumstances polymerization rates of 1·0 % and 1·6 % per hr. thus showing that ultrasonic radiation also may induce monomer to polymerize. This might readily be explained by assuming that the radiation merely heats the monomer to a high enough temperature to induce thermal polymerization. The use of an efficiently stirred and thermostated bath and the small size of the irradiation bulb together with the relatively low thermal rate of methacrylate rules out such a possibility. This ultrasonically-induced rate, however, is so high that methacrylate could not be conveniently used for the detection of radical production.

Similar experiments were made with styrene and vinyl acetate as monomers. With vinyl acetate there was no detectable polymerization; with styrene the rate was 0·2 % per hr. In view of the difficulty of measuring these small rates under the present conditions, experiments were made with benzoquinone to see if the rate of initiation of polymerization could accurately be measured. It is known that in the thermal polymerization of pure styrene the addition of benzoquinone gives rise to a well-defined induction period whereas in the monoradical produced reaction only retardation is observed under similar conditions.[9] In this case it was convenient to follow the course of reaction viscometrically. The addition of quinone completely suppressed the reaction, but at the end of a well-defined induction period the viscosity started to rise. The results are given in Table IV where it will be seen that the induction period increases with increasing concentration of quinone.

TABLE IV.—INHIBITION OF POLYMERISATION BY BENZOQUINONE

Concentration of Inhibitor (C) mole/l. × 10^6	Time of Inhibition (T) min.	Velocity of Initiation (C/T) mole/l. sec. × 10^{10}	Overall Rate % per Hour
2·59	8·0	5·4	0·12
3·06	11·0	4·63	0·108
5·08	27·0	3·14	0·09
		Mean 4·39	0·106

The velocity of radical production is then calculated from the rate of consumption of inhibitor. From the known values of the rate constants for propagation and termination the calculated value of the rate of polymerization of pure monomer is given in the last column. When the above-mentioned polymethacrylate was dissolved in styrene to make a 1 % solution by weight and the solution exposed to the ultrasonic radiation the rate of polymerization was 0·3 to 0·1 % per hr., which is hardly significantly higher than that of the polymerization of styrene itself. This would imply that degradation does not result in radical production.

The maximum possible rate of radical production from polymethacrylate may be approximately calculated in the following way. The initial molecular weight was 725,000. From the combination of osmotic and viscosity measurements it is estimated that the number average molecular weight is reduced to 500,000 after 2-hr. irradiation. Assuming as a first approximation that the rate of bond breaking is constant in this period then in 10 ml. of 1·00 % solution the number of moles of polymer produced by irradiation is $6{\cdot}3 \times 10^{-8}$. If each molecule is broken into two radicals then radical production is $1{\cdot}75 \times 10^{-9}$ mole/l. sec. The rate of polymerization that would be induced is then easily calculated from the usual rate equation

$$-\,\mathrm{d(M)}/\mathrm{d}t = k_p/k_t^{\frac{1}{2}}\,.\,(\mathrm{M})\,.\,I^{\frac{1}{2}}$$

where k_p and k_t are the propagation and termination rate constants and I the rate of radical production. At 25° C the values of $k_p/k_t^{\frac{1}{2}}$ are given in Table V. Since no polymerization, < 0·07 % per hr., of vinyl acetate could be detected in presence of degrading methacrylate the conclusion would be that less than 10 % of the radicals were produced from the methacrylate. With styrene the rate is quite comparable with the supersonically-induced polymerization rate and the result is therefore inconclusive.

TABLE V

	$k_p/k_t^{\frac{1}{2}}$	Rate of Polymerization % Hour
Methyl methacrylate	$4{\cdot}29 \times 10^{-2}$	0·64
Styrene	$1{\cdot}42 \times 10^{-2}$	0·21
Vinyl acetate	4×10^{-2}	0·60

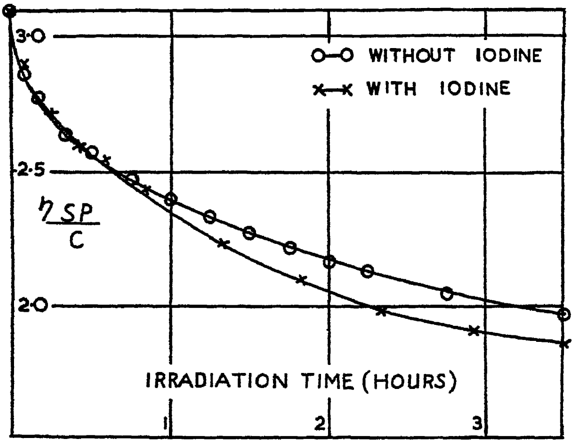

FIG. 10.—Degradation of polymethyl methacrylate in presence of iodine.

With methyl methacrylate the direct polymerization overshadows the polymer induced polymerization. The conclusion would therefore be that owing to the supersonically-induced polymerization of monomer the possibility of detecting radicals from degrading polymer is an extremely difficult matter.

Degradation in Presence of Iodine.—Having regard to the quite considerable amount of supersonic energy incident on the polymer solution the rate of bond fission is extremely small. This might in part be due to the fact that initial fission is into radicals but that normally there is no molecule ready to react with the radicals quickly enough to prevent their recombination within this cage of creation. Even with a monomer surrounding the cage the probability of an effective collision, e.g. with methacrylate, is only *ca.* 10^{-7} and the radicals in consequence might easily escape detection. Some experiments were made with iodine in benzene solution. A typical set of runs is shown in Fig. 10 with polymethacrylate where it will be seen there is no acceleration of degradation in presence of iodine.

This work was started in the Chemistry Department, University of Aberdeen, and completed in the Chemistry Department, University of Birmingham. One of us (A. J. M.) is indebted to Messrs. Bakelite for the award of a Scholarship.

Chemistry Department,
University of Birmingham.

REVIEWS OF BOOKS

Echanges Isotopiques et Structure Moleculaire. (Centre National de la Recherche Scientifique, Paris, 1948.) Pp. 108.

The proceedings of an international colloquium on this subject held in Paris in April 1948 (which have already appeared in the *J. Chim. Phys.*, 1948) have now reached us, published as Volume V in the series of *Colloques Internationaux du Centre National de la Recherche Scientifique.* The volume contains contributions from L. Pauling, S. Sugden, B. Pullman, G. A, Paneth, M. Haïssinsky, E. D. Hughes and C. K. Ingold, C. A. Coulson, G. Hevesy and others and, as may be inferred from this list of names, contains articles on a diversity of subjects (the most noticeable omission being references to the use of mass spectrometers). Indeed, isotope exchange has now become generally recognized as an adaptable tool in chemical investigations and it may soon be true that a discussion on " isotope exchange and molecular structure " will offer as unlimited scope as a discussion on chemical application of any common piece of laboratory equipment. However, this cannot be said yet, and this little omnibus pamphlet, like the more recent discussion of the Chemical Society in 1949, should stimulate and encourage work on these lines.

The articles and contributions to the discussion are, for the most part, printed in the author's language, i.e. either in French or English. To the reviewer's mind, this does not seem to and ought not to detract from the readability. On the other hand, this heterogeneity of languages, coupled with a heterogeneity of interests of the participants, seems to have made the actual discussion rather " tame " in comparison with the Discussions of the Faraday Society.

V. G.

Terrestrial Radio Waves. By H. Bremner. (Elsevier Publishing Co. Inc., 1949.) Pp. 343.

Those directly concerned with the influence of the spherical earth, the atmosphere, and the ionosphere on the propagation of radio waves will warmly welcome this book written by such a well-known contributor to the theory of the subject. The author has collated and presented as a connected account much of the theoretical work hitherto available only in numerous separate papers. The material is largely based on the methods instituted by Prof. Van der Pol and the author, but some reference is made to alternative treatments which have been proposed by other workers. Those who are aware of the scope of the theoretical problems of radio propagation will not be surprised that, in 340 pages, " the final results cannot make pretence of being exhaustive ". The main object of the book is to give a treatment of the mathematical-physical methods for the computation of transmitter fields, and this aim is well realized. Though much of the book is primarily of interest to the theoretician, the experimentalist and the communications engineer will be pleased to find that the theoretical applications and implications ot the theory have not been overlooked. Numerical results are well in evidence.

The introductory chapter is a short historical account of studies of the diffraction of waves by spheres and sets the radio problem against the wider background which includes the work of Rayleigh, Mie and Debye on the scattering of light and Airy's theory of the rainbow.

Part I of the book deals with radio waves propagating over a homogeneous spherical earth in a homogeneous atmosphere. The groundwave solution is first established as a series of zonal harmonics, and then Watson's transformation is applied to reduce the series to a form suitable for numerical calculation. Various applications are then discussed in detail and particular approximations valid for special cases are established. The final chapter of this part summarizes all the formulae necessary for computation of field strengths and includes much graphical information.

Part II extends the theory to include both atmospheric refraction and the effects of ionospheric reflections. The general case for a spherical earth surrounded by a medium whose refractive index is a spherically symmetrical arbitrary function of height is developed both by the W.K.B. approximation and by the method of residues whereby the field is expressed as a series of modes. The action of the earth's magnetic field is considered in the final chapter. The experimental worker will find Chap. X of particular interest. Here are discussed special applications of the theory and these include ionospheric reflection of long waves, ionospheric absorption and reflection of short waves, atmospheric superrefraction, and transmission of cosmic radio waves through the ionosphere.

The material is presented in a very logical manner, and this together with the clarity of exposition and the excellent balance maintained between the mathematical and practical aspects of the subject results in a book which will be of great value both to the post-graduate student and to the advanced worker in most fields of radio propagation. The usefulness of the book for reference purposes is enhanced by the excellent typography and format adopted.

N. E.

Makromolekulare Chemie und Biologie. By H. STAUNDINGER. (Wepf and Co., Basle, Switzerland.) SFr. 18.

Many books are now written about high polymer chemistry. The subject has enormous ramifications from a purely physical aspect right through chemistry to matters of biological interest. Almost anyone can write a book dealing with some aspect because there is plenty of material written in a way that may be readily understood. It is, therefore, refreshing to find a compact and interesting survey from one of the pioneers in the subject, H. Staudinger. It is difficult now to realize the opposition the author had to overcome some years ago in convincing other chemists of the novel concept of the structure and behaviour of high polymers of various types.

This book is a collection of a number of lectures delivered in Switzerland and in Germany dealing in a general but personal way about the chemistry of high polymers both natural and artificial. There is much emphasis on molecular structure as is to be expected, but only brief mention of the problem of synthesis. The phenomenon of viscosity of high polymer solutions naturally forms an important part of the book. Since the book is mainly descriptive in character, no mention is made of recent theories of the viscosity of high polymer solutions. This section leads naturally to a discussion of the shape of molecules in solution. There is too, philosophical speculation about the meaning of it all and especially in relation to the nature of living things of the lowest order. An excellent series of plates of the morphologcal features of fibres and other high polymers form a useful appendix to the book. It is an interesting and refreshing book to read, both for the specialist in high polymers who may know all about it already, and for all others with a general interest in matters of this kind.

H. W. M.

The Physics of Rubber Elasticity. By L. R. G. TRELOAR. (Geoffrey Cumberlege at the Clarendon Press, Oxford.) Pp. 255. Price 21s.

Although the basic cause of the elasticity of rubbers was correctly deduced by Joule as long ago as 1859, the modern theory is almost entirely a product of the last 15 years in which such a rapid growth in our knowledge of the physics and chemistry of high polymers has taken place. A quick development in any subject always produces a temporary surfeit of papers written by specialists for specialists and, until recently, very few general accounts of rubber-like elasticity existed outside the journals. The increasing mathematical complexity of subject has only underlined the need for an authoritative general account and the present book comes at a very opportune moment. Dr. Treloar is a particularly appropriate person to write such a book, not only through his own deceptively simple but decisive contributions in this field but also by reason of his many lectures designed to bring home its basic principles to non-specialist audiences.

Dr. Treloar's book succeeds admirably in its objective—it is both general enough to provide an up-to-date account of his subject to non-specialists yet at the same time exact enough to satisfy those who have more than a nodding acquaintance with its content. The first half of the book (Chapters I-VI) gives a straightforward and pleasing account of rubber-like elasticity of long molecules, the balance between theory and experiment being admirably kept; here it is demonstrated that, to a first-order approximation, the agreement between the two is very reasonable. A middle section (Chapter VII) will interest the specialist most because, here for the first time is an authoritative treatment of the second-order deviations which have been revealed by Treloar and his colleagues over the past few years—the account of Rivlin's and Mooney's theoretical work is especially valuable. The final chapters are concerned with the fruitful connection between optical and mechanical properties, the important effects of crystallization, the various time phenomena connected with viscous effects and the development of high elasticity. I am sure this book will be a standard work for many years to come.

R. F. T.

Organic Chemistry. By G. BRYANT BACHMAN. (New York: McGraw-Hill Book Company, Inc.) Pp. 432. Price 36s. 6d. net.

This volume is a standard text-book on systematic organic chemistry designed to cover a one-year course. It is written primarily for "non-chemistry majors", which may be taken to mean that it is suitable for students studying for a General degree or those taking chemistry as a subsidiary or ancillary subject. A wide field is covered, which obviously necessitates a lack of detail in many important topics, but this is intentional on the part of the author, who sets out to draw attention to the applications of organic chemistry to everyday life and to other fields of science, and to present broad generalizations rather than long lists of easily forgotten facts. Few would quarrel with this point of view, which has resulted in a very readable and attractive presentation of the subject for students who do not intend to make chemistry their profession in life. In many respects the work covers the familiar ground along conventional lines, but special attention is focused on such subjects as the petroleum industry, soaps and detergents, carbohydrates, biological processes, colour, physiological action, and polymers. There is also a useful chapter on the nomenclature of organic compounds, although the section on the pronunciation of organic names is likely to be less useful on this side of the Atlantic Ocean, where it is unusual to accent the second syllable in "amine" and "arsine", and where "methyl" is made to rhyme more frequently with "senile" than with "devil". The least attractive feature of the book is to be found in the photographic illustrations, which appear to be wholly out of place. The book can be recommended with confidence as providing a basis for a one-year course for students who are not taking chemistry as a main subject for their degree.

D. H. H.

CORRIGENDA

Trans. Faraday Soc, 1950, **46.**

P. 628, Fig. 1. *For* $\log k_2^{\frac{1}{2}}/k_4$

read $\log (10k_2\ k_4)$ cm ^{3} mole^{-1} sec.$^{-}$

EMPIRICAL METHODS OF ESTIMATING RESONANCE ENERGIES

PART I.—ANNELATION ENERGY

By R. D. Brown

Received 16th March, 1950

A molecular-orbital quantity termed the annelation energy is introduced to facilitate the empirical estimation of resonance energies of aromatic systems. The annelation energy is the loss in resonance energy accompanying annelation of two aromatic systems to produce a third. It is shown to be simply related to the mobile orders of the two bonds undergoing fusion. The statistics of the relationship are investigated and some resonance energies calculated by this method are listed.

Resonance energies of various molecules and molecular fragments play an important part in the localization theory of organic reactions.[1-4] For this reason it is useful to have simple empirical methods for deriving approximations to the resonance energies, R and R', when the direct LCAO calculation of these quantities becomes too laborious.[*] In the present paper one such empirical method of obtaining R and R' is discussed. A second method will be considered in Part II. In conjunction with other existing methods of computing these quantities [5] these form a powerful tool for the theoretical treatment of chemical properties of organic molecules by the localization technique.

Definition of Annelation Energy.—If an aromatic hydrocarbon H can be considered as formed by the fusion of two simpler aromatic hydrocarbons, A and B, then there exists a quantity K such that

$$K = R_A + R_B - R_H \quad . \quad . \quad . \quad . \quad (1)$$

which will be termed the *annelation energy* of the hydrocarbons A and B. The importance of this quantity lies in the empirical fact that if we use the LCAO quantities R and R' to define the corresponding LCAO annelation energies K and K' (adhering to the convention already suggested [2, 3] for the use of the prime), then K and K' are simply related to the mobile orders of the two bonds in A and B which undergo the fusion process. For which example, phenanthrene may be regarded as being formed by fusion of benzene to the $\alpha : \beta$-bond of naphthalene, and so we have

$$K = -2{\cdot}000\beta - 3{\cdot}683\beta + 5{\cdot}488\beta = -0{\cdot}235\beta,$$
$$K' = -1{\cdot}067\gamma - 1{\cdot}863\gamma + 2{\cdot}736\gamma = -0{\cdot}194\gamma,$$

and it is found (see later) that these quantities can be expressed reasonably well by a simple expression involving the mobile orders, 0·667 and 0·725, of the two bonds concerned in the fusion.

---

[1] Wheland, *J. Amer. Chem. Soc.*, 1941, **64**, 900.

[2] Brown, *Austral. J. Sci. Res. A*, 1949, **2**, 566.

[3] Brown, *Trans. Faraday Soc.*, 1950, **46**, 146.

[4] Brown, *J. Chem. Soc.*, 1950, 691.

[*] The symbolism employed throughout is that introduced in previous papers.[2, 3]

[5] Summarized by Brown, ref. (2).

A list of annelation energies for various fusions, together with other relevant data, is given in Table I. The requisite resonance energies which have not previously been recorded in the literature to so many significant figures are listed in Table II. Other figures used have been taken from the literature.[6, 7]

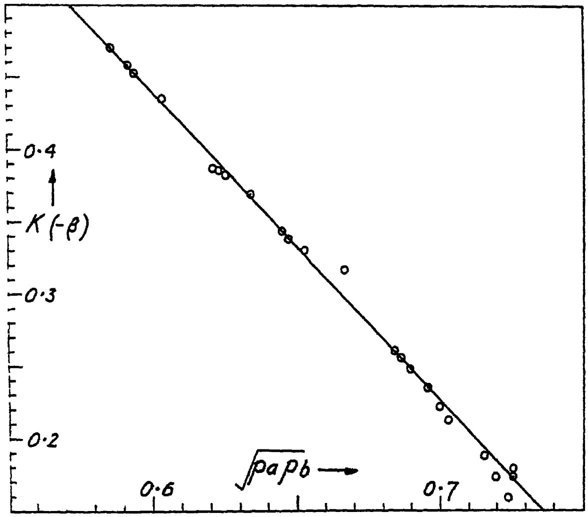

FIG. 1

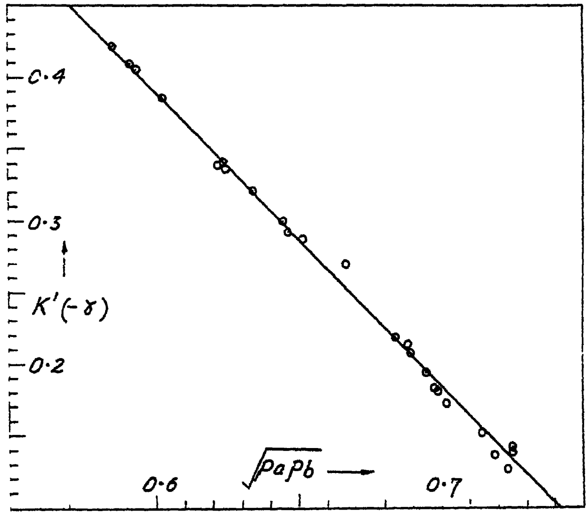

FIG. 2

Relation to Mobile Bond Orders.—It has been mentioned above that the annelation energy is related to the mobile orders of the two bonds undergoing the fusion, and a plot of K and of K' against $\sqrt{p_a p_b}$, is shown in Fig. 1 and 2 respectively, p_a and p_b being the mobile orders

---

[6] Berthier, Coulson, Greenwood and Pullman, *Compt. rend.*, 1948, **226**, 1906.
[7] Baldock, Berthier and Pullman, *ibid.*, 1949, **228**, 931.

of the two bonds. It is clear from these figures that the relationships between these quantities are in both cases closely linear. A relationship of the type $\mu\sqrt{p_a p_b} + \nu$ was fitted to each of the two sets of data by the method of least squares, the results being

$$K = (2{\cdot}1533\sqrt{p_a p_b} - 1{\cdot}7325)\beta, \quad . \quad . \quad . \quad (2)$$

$$K' = (2{\cdot}0674\sqrt{p_a p_b} - 1{\cdot}6319)\gamma, \quad . \quad . \quad . \quad (3)$$

the standard deviations for K and K' being $0{\cdot}00645\,\beta$ and $0{\cdot}00597\,\gamma$ respectively, and the standard deviations for the constants μ and ν being :

$$\text{for eqn. (2)}, \quad s_\mu = 0{\cdot}0313\,; \quad s_\nu = 0{\cdot}00138\beta\,;$$

$$\text{for eqn. (3)}, \quad s_\mu = 0{\cdot}0289\,; \quad s_\nu = 0{\cdot}00127\,\gamma.$$

TABLE I

Hydrocarbon	Components*	$K(-\beta)$	$K'(-\gamma)$	$\sqrt{p_a p_b}$
Naphthalene	B + B	0·317	0·270	0·667
Anthracene	B + N	0·370	0·322	0·634
Phenanthrene . . .	B + N	0·235	0·194	0·695
Naphthacene . . .	B + A	0·383	0·336	0·625
	N + N	0·436	0·387	0·603
Chrysene	B + P	0·256	0·214	0·686
	N + N	0·174	0·138	0·725
3 : 4-Benzophenanthrene .	B + P	0·261	0·218	0·684
	N + N	0·179	0·142	0·725
1 : 2-Benzanthracene . .	B + A	0·213	0·172	0·702
	B + P	0·347	0·300	0·645
Pentacene	B + Nc	0·387	0·340	0·623
	N + A	0·453	p·405	0·594
Picene	B + C	0·249	0·207	0·689
	N + P	0·188	0·151	0·715
1 : 2-3 : 4-Dibenzanthracene .	B + T	0·332	0·286	0·652
1 : 2-5 : 6-Dibenzanthracene .	B + Ba	0·221	0·180	0·699
1 : 2-7 : 8-Dibenzanthracene .	B + Ba	0·222	0·181	0·698
Pentaphene	B + Ba	0·339	0·292	0·647
Hexacene	B + Pe	0·388	0·341	0·621
	N + Nc	0·458	0·410	0·592
	A + A	0·471	0·423	0·586

* B : benzene
N : naphthalene
A : anthracene
Nc : naphthacene
Pe : pentacene
P : phenanthrene
Ba : benzanthracene
C : chrysene
T : triphenylene
Bp : 3 : 4-benzophenanthrene.

These results indicate that eqn. (2) and (3) give considerably more reliable results when used for the calculation of resonance energies of large polycyclic aromatic hydrocarbons from those of smaller ones than those obtained by the alternative empirical method of Carter.[8] Indeed the latter is of no use in the localization theory because it is generally necessary to know the relevant resonance energies to within ± 0·02 β (or γ).

Eqn. (2) and (3) are subject to some limitations, as is demonstrated by the data of Table III. In the latter the values of K and K' computed from eqn. (2) and (3) are compared with the actual values for some further hydrocarbons, the fusions in each case involving bonds such that the difference between their two mobile orders, δp, is more than 0·1 ; all fusions considered in Table I are such that δp is less than 0·1. In Table III the calculated values in all cases are greater than the actual values, the divergences showing a marked tendency to increase with δp. In view of this and the fact that no similar divergences have been found when δp is less than 0·1, it seems reasonable to relate the two. Presumably a more complicated function of p_a and p_b could be found which would reduce the discrepancies when δp is more than 0·1, but in practice this defect in the proposed formulae is usually avoidable, it generally being possible to find at least one fusion for which δp is less than 0·1. This will be illustrated for heptacene.

---

[8] Carter, *Trans. Faraday Soc.*, 1949, **45**, 597.

TABLE II

Hydrocarbon	$R(-\beta)$	$R'(-\gamma)$
Benzene	2·0000	1·0667
Naphthalene	3·6832	1·8631
Anthracene	5·3137	2·6077
Phenanthrene	5·4483	2·7359
Naphthacene	6·9308*	3·3389*
Chrysene	7·1922*	3·5883*
3 : 4-Benzophenanthrene . .	7·1875*	3·5842*
Pyrene	6·5055*	3·2121*
Hexacene	10·1560	4·7920

* These values should be compared with those quoted in ref. (6). The small discrepancies are presumably due to cumulative errors in the last significant figure. The values listed in the above Table were all computed retaining at least five decimals, and usually six.

TABLE III

Hydrocarbon	Components	$\sqrt{p_a p_b}$	δp	$K(-\beta)$			$K'(-\gamma)$		
				pred.*	act.†	δ	pred.*	act.†	δ
Benzanthracene	N + N	0·661	0·122	0·309	0·265	0·044	0·265	0·224	0·041
Triphenylene	B + P	0·719	0·108	0·184	0·174	0·010	0·145	0·137	0·008
1 : 2-3 : 4-Dibenzanthracene	N + P	0·684	0·172	0·260	0·189	0·071	0·218	0·152	0·066
	B + Ba	0·723	0·116	0·176	0·159	0·017	0·137	0·123	0·014
1 : 2-5 : 6-Dibenzanthracene	N + P	0·672	0·102	0·286	0·251	0·035	0·243	0·210	0·033
1 : 2-7 : 8-Dibenzanthracene	N + P	0·672	0·102	0·286	0·252	0·034	0·243	0·211	0·032
Pentaphene	N + A	0·667	0·135	0·296	0·234	0·062	0·253	0·193	0·060

* Values predicted using eqn. (2) and (3).
† Values calculated directly from the appropriate resonance energies.

The LCAO resonance energy of heptacene has not hitherto been computed by the direct method; for illustration of the application of eqn. (2) and (3) we shall now use these latter to estimate R and R' for this hydrocarbon. We may regard heptacene as formed by the following fusions:

(*a*) benzene + hexacene,
(*b*) naphthalene + pentacene,
(*c*) anthracene + naphthacene.

The mobile order of the 2 : 3 bond of hexacene has not been evaluated and in any case must be close to 0·57 so that for (*a*) δp would be very close to 0·1; consequently we need not consider (*a*) further. The other bond order data required for the calculations applicable to (*b*) and (*c*) are available [6, 7] and we find

$$(b)\ K = -0{\cdot}460\beta;\quad K' = -0{\cdot}471\gamma;\quad \delta p = 0{\cdot}024;$$
$$(c)\ K = -0{\cdot}476\beta;\quad K' = -0{\cdot}425\gamma;\quad \delta p = 0{\cdot}005;$$

TABLE IV*

No.	Hydrocarbon	Components	$(p_a p_b)^{\frac{1}{2}}$	$R(-\beta)$	$R'(-\gamma)$
I	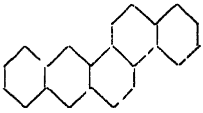	N + A	0·732	8·841	4·352
		B + C	0·642	8·841	4·349
		B + Ba	0·683	8·840	4·350
				8·841	**4·350**
II	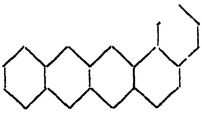	B + Ba	0·629	8·723	4·238
		N + P	0·613	8·719	4·234
		Nc + B	0·703	8·712	4·227
				8·718	**4·233**
III	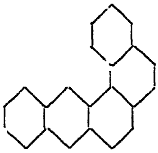	B + Ba	0·681	8·835	4·345
		N + A	0·732	8·841	4·352
		B + Bp	0·641	8·835	4·344
				8·837	**4·347**
IV	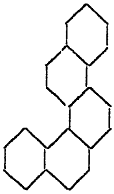	B + Bp	0·689	8·939	4·444
		N + P (1 : 2)	0·715	8·939	4·445
		N + P (3 : 4)	0·713	8·934	4·441
		B + C	0·687	8·938	4·443
				8·938	**4·443**
V	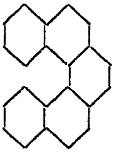	B + Bp	0·688	8·936	4·441
		N + P	0·713	8·934	4·441
				8·935	**4·441**
VI	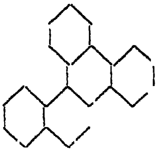	N + P	0·750	9·014	4·518
		B + C	0·709	8·995	4·489
		B + Bp	0·713	8·990	4·493
		B + T	0·678	9·003	4·503
				9·001	**4·501**
VII	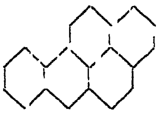	B + P	0·668	8·211	4·028
VIII	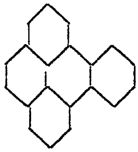	B + P	0·720	8·35†	4·17†

---

* Where several values are listed for a hydrocarbon they are followed by the mean value (black figures).

† For this fusion δp is 0·110 so a correction of $-0{\cdot}03\beta$ was added to R, of $-0{\cdot}03\gamma$ was added to R', these corrections being estimated from the data of Table III.

then, as $R = R_A + R_B - K$, we obtain

$$(b)\ R = -11{\cdot}767\beta;\quad R' = -5{\cdot}519\gamma;$$
$$(c)\ R = -11{\cdot}769\beta;\quad R' = -5{\cdot}521\gamma;$$
$$\text{Mean } -11{\cdot}768\beta \qquad -5{\cdot}520\gamma.$$

These mean values may be compared with the values obtained directly from the roots of the secular determinant for heptacene, viz.:

$$R = -11{\cdot}7675\beta;\quad R' = -5{\cdot}5175\gamma.$$

The fact that both mean estimates lie considerably closer to the directly calculated values than the limits imposed by the standard deviations previously computed, and also that the two estimates (*b*) and (*c*) are so concordant, is further confirmation of the reliability of the present method of estimation.

By essentially the same procedure the resonance energies of those of the fifteen possible hydrocarbons comprised of five fused benzene rings which have not already appeared in the literature[7] are listed in Table IV. Only fusions for which δp is less than 0·1 are included in Table IV, except in the case of 1 : 2-benzpyrene (VIII) for which no other possibility is available; in the latter case a correction of $-0{\cdot}03\beta$ and $-0{\cdot}03\gamma$ have been added to R and R', these figures being the approximate errors anticipated from the results listed in Table III. These results will be utilized elsewhere in discussions of the relative reactivities of these and other hydrocarbons towards ozone, osmium tetroxide, and other " bond reagents ", and also towards maleic anhydride.

Eqn. (2) and (3) have some interesting consequences, some of which can be confirmed by existing theoretical data. As the annelation energy depends only upon the mobile orders of the two bonds undergoing fusion, and for unsymmetrical fusions there will be two possible orientations of the two components, the two resultant isomeric hydrocarbons will have the same annelation energies and hence the same resonance energies. For example chrysene and 3 : 4-benzophenanthrene may both be considered as being formed by fusion of two naphthalene molecules through their $\alpha : \beta$ bonds; their resonance energies are seen from Table II to be very closely similar, and differ appreciably from those of the isomeric molecules naphthacene and benzanthracene. Another example is afforded by the data for the three dibenzanthracenes, pentacene, and pentaphene,[7] the 1 : 2-5 : 6- and 1 : 2-7 : 8-isomers both being derived by fusion of the $\alpha : \beta$ bond of naphthalene to the 2 : 3 bond of phenanthrene. These two molecules have very similar resonance energies which differ appreciably from those of the other isomers. It is proposed to term such isomeric molecules which for one particular fusion differ only in the sense in which the two bonds are fused *amphimeric*. Thus of the compounds listed in Table IV hydrocarbons (I) and (III) are amphimeric (with respect to the fusion N + A), as are (IV) and (V) (with respect to the fusion N + P, bond 3 : 4). Indeed the data there presented further confirm this principle, resonance energies of amphimeric compounds calculated using other than amphimeric fusions in all cases being very similar.

The present approximate method of obtaining resonance energies can be employed to proceed step by step to the resonance energies of extremely large polynuclear hydrocarbons almost without limit, the requisite bond orders being obtained from the corresponding bond localization energies, B and B', as discussed elsewhere.[8] The computation of B and B' may involve the resonance energies of large quinodimethanes. The empirical method of obtaining these is considered in Part II.

Chemistry Department,
University of Melbourne,
Victoria,
Australia.

---

[8] Brown, ref. (2), also further results in course of publication.

THERMOCHEMISTRY OF METALLIC ALKYLS

III.—MERCURY DIMETHYL AND MERCURY METHYL HALIDES

By K. Hartley, H. O. Pritchard and H. A. Skinner

Received 1st *June*, 1950

Measurements of the heats of reaction of mercury dimethyl with alcoholic solutions of bromine, iodine, mercuric chloride, mercuric bromide, and mercuric iodide (at 20° C) are reported. These data are combined with existing thermochemical values to give the relations :

(i) $Q_f(\mathrm{HgMe_2}, \textit{liq.}) = 2Q_f(\mathrm{MeBr}, g) - 31{\cdot}5\ (\pm 0{\cdot}85)$ kcal. mole.$^{-1}$.
(ii) $Q_f(\mathrm{HgMe_2}, \textit{liq.}) = 2Q_f(\mathrm{MeI}, g) - 18{\cdot}9\ (\pm 0{\cdot}64)$ kcal. mole^{-1}.

Accepting the value $Q_f(\mathrm{MeBr}, g) = 8{\cdot}6 \pm 0{\cdot}5$ kcal. mole^{-1} as correct, (i) leads to $-14{\cdot}3 \pm 1{\cdot}85$ kcal. mole^{-1} for the heat of formation of liquid $HgMe_2$, and (ii) gives $2{\cdot}3 \pm 1{\cdot}2$ kcal. mole^{-1} for the heat of formation of liquid methyl iodide. The heats of formation of the crystalline mercury methyl halides are measured as follows : HgMeCl, $27{\cdot}68 \pm 1{\cdot}45$; HgMeBr, $20{\cdot}46 \pm 1{\cdot}42$; HgMeI, $10{\cdot}20 \pm 1{\cdot}21$, all in kcal. mole^{-1}.

The dissociation-energies of the two CH_3—Hg bonds in $HgMe_2$ add up to $57{\cdot}4 \pm 4$ kcal., and the first and second CH_3—Hg bonds have unequal heats of dissociation, viz. $D(\mathrm{CH_3{-}HgCH_3}) \approx 51$ kcal., $D(\mathrm{CH_3{-}Hg}) \approx 6$ kcal. The CH_3—HgX bonds in the methyl mercuric halides have the following dissociation energies ; $D(\mathrm{CH_3{-}HgCl})$, $63{\cdot}4 \pm 2{\cdot}5$ kcal. ; $D(\mathrm{CH_3{-}HgBr})$, $60{\cdot}7 \pm 2{\cdot}6$ kcal. ; $D(\mathrm{CH_3{-}HgI})$, $59{\cdot}0 \pm 3{\cdot}3$ kcal.

Although mercury possesses an extensive organic chemistry,[1] little is known of the thermochemistry of organo-mercury compounds. It may be that the dialkyls of mercury are unsatisfactory compounds for study by the methods of combustion calorimetry, for in fact few data are available on this class of compounds, and it is our view that the limited published data are not reliable. For dimethyl mercury, in particular, there is a large discrepancy between the values for the heat of formation Q_f derived from the present research and from the heat of combustion given by Berthelot.[2] Nevertheless we consider the mercury dialkyls as suitable compounds for thermochemical study, since they undergo several simple reactions cleanly and easily at room temperature with halogens, halogen acids, and the mercuric halides.[3] In this paper we report some measurements of the heats of reaction of mercury dimethyl with iodine, bromine, and the halides of mercury, from which the values $Q_f(\mathrm{HgMe_2})$ and $Q_f(\mathrm{HgMeX})$ are obtained, and the dissociation energies of some Hg—CH_3 bonds can be derived.

Experimental

Preparation of Compounds.—$HgMe_2$ was prepared by the method of Gilman [4] from the interaction of $HgCl_2$ with the Grignard reagent. The crude product was carefully dried and purified by fractional distillation using a gauze-packed column : b.p. 92·3° C at 768 mm. Hg. The iodine, bromine and mercuric halides used were A.R. reagents ; the solvents were clinical ethyl alcohol and high-grade synthetic methanol.

Calorimeters.—The reactions with the halogens were studied in the calorimeter described previously by Pritchard and Skinner [5] but modified from the original by the replacement of all the rhodium-plated internal fittings by their glass equivalents. Reactions involving the mercuric halides, and various determinations of the heats of solution and mixing, were carried out in a similar, but smaller, calorimeter described by Hartley and Skinner.[6] The procedure in both sets of experiments involved the measurement of the change in resistance of a thermistor element (R_i = initial, and R_f = final resistance in ohms) occasioned by the breakage of a phial containing one of the reactants into a solution (in ethanol or methanol) of the second reactant. The calorimetric systems were calibrated electrically. The heats are given in units of the kcal. mole^{-1} ≡ 4·1833 × 10^3 int. joules mole^{-1}.

---

[1] See, e.g., Whitmore, *Organic Compounds of Mercury* (Chem. Catalog Co., New York, 1921).

[2] Berthelot, *Compt. rend.*, 1899, **129**, 918.

[3] Kharasch and Flenner, *J. Amer. Chem. Soc.*, 1932, **54**, 674.

[4] Gilman and Brown, *ibid.*, 1929, **51**, 928 ; 1930, **52**, 3314.

[5] Pritchard and Skinner, *J. Chem. Soc.*, 1950, 272.

Results

Mercury Dimethyl and Bromine.—Bromine reacts almost instantaneously at room temperature with an excess of $HgMe_2$ in alcohol solution, according to the equation :

$$HgMe_2 \text{ (alcohol soln.)} + Br_2 \ (liq.) \rightarrow HgMeBr \text{ (soln.)} + MeBr \text{ (soln.)} \quad . \quad (1)$$

The reaction was carried out by breaking thin glass phials containing known weights of bromine into dilute solutions of $HgMe_2$ in alcohol. Both ethyl and methyl alcohol were used as solvent, giving identical (± 0·2 kcal.) results. The $HgMe_2$ was present in excess in all experiments to eliminate the occurrence of a secondary reaction between the Br_2 and the HgMeBr, and the solutions were sufficiently dilute to keep to HgMeBr completely in solution. The results are summarized in Table I.

TABLE I.—Reactions of $HgMe_2$ with Bromine

Expt.	Wt. of Br_2 (g.)	R_i	R_f	Q (kcal. mole^{-1})
1	1·6665	1745·1	1663·4^5	44·81
2	1·8152	1734·4	1646·7	44·55
3	1·7332	1749·2	1664·3^5	44·71
4	1·7210	1704·6^5	1622·8^5	44·53
			Mean	44·65 ± 0·15

Mercury Dimethyl and Iodine.—The reaction of iodine in alcoholic solution with mercury dimethyl at room-temperature occurs less speedily than the similar reaction using bromine. We have found it most convenient to study this reaction by adding the mercury dimethyl to a solution of excess iodine in methanol—usually adding about 2 g. $HgMe_2$ to about 6 g. I_2 dissolved in 750 ml. alcohol. Under these conditions the reaction was completed in periods of less than ½ hr. Although these conditions correspond to a considerable I_2 excess, we have checked by independent studies that they do not lead to any significant occurrence of the secondary reaction between HgMeI and I_2, and that all the products of reaction remain completely in solution. The measured heats of the reaction

$$HgMe_2 \ (liq.) + I_2\text{(methanol)} \rightarrow \{MeI + HgMeI\} \text{ (soln.)} \quad . \quad . \quad (2)$$

are summarized in Table II.

TABLE II.—Reaction of $HgMe_2$ with Iodine

Expt.	Wt. $HgMe_2$ (g.)	R_i	R_f	Q (kcal. mole^{-1})
1	1·8120	1741·7	1709·1	24·45
2	1·9250	1735·6	1701·0	24·49
3	1·9914	1739·8	1704·0	24·48
				Mean = 24·47

---

[6] Hartley and Skinner, *Trans. Faraday Soc.*, 1950, **46**, 621.

Mercury Dimethyl and the Mercuric Halides.—The reactions between $HgMe_2$ and solutions of the mercuric halides in alcohol occur readily at room temperature. With $HgCl_2$ and $HgBr_2$ the reactions are reasonably fast if the mercuric halides are used in two or three-fold excess; the reaction with HgI_2 is rather sluggish and is better carried out in methanol than in ethanol as solvent.

The reactions were performed by breaking thin phials containing weighed amounts of mercury dimethyl into solutions of $HgCl_2$ in ethanol, $HgBr_2$ in ethanol, and HgI_2 in methanol. The measured heats of the reactions:

$$HgMe_2\ (\mathit{liq.}) + HgX_2\ (\text{soln.}) \rightarrow 2HgMeX\ (\text{soln.}) \qquad (3)$$

are summarized in Table III.

TABLE III.—REACTION OF $HgMe_2$ WITH MERCURIC HALIDES

Reaction	Expt.	Wt. $HgMe_2$ (g.)	Wt. HgX_2 (g.)	Ml. of Solvent	R_i (ohms)	R_f (ohms)	Q (kcal. mole^{-1})	Mean Q (kcal. mole^{-1})
$HgMe_2$ + $HgCl_2$	(i)	1·300	3·129	300	2132·0	2112·7	7·72	—
	(ii)	1·996	2·423	300	2121·4	2091·6	7·82	—
	(iii)	1·475	7·10	300	2166·0	2143·2	7·92	—
	(iv)	6·2652	11·0	750	1737·4	1699·0	8·02	**7·87 ±0·15**
$HgMe_2$ + $HgBr_2$	(i)	1·268	9·033	300	2212·2	2196·6	6·16	—
		1·928			2214·0	2190·2	6·19	—
	(ii)	1·368	8·987	300	2213·9	2196·5	6·37	—
	(iii)	6·4017	25·0	750	1744·1	1713·6	6·21	**6·24 ±0·10**
$HgMe_2$ + HgI_2	(i)	3·6482	—	750	1741·7	1732·2	3·51	—
	(ii)	4·0065	—	750	1730·7	1720·5	3·46	**3·48 ±0·03**

Heats of Solution.—The interpretation of the heats of reaction given above requires additional data on the heats of solution of both reactants and products in alcohol. These solution heats were measured in our smaller calorimeter, and the results are briefly summarized in Table IV.

TABLE IV.—HEATS OF SOLUTION

Solute	Solvent	Heat of Solution (kcal. mole^{-1})
$HgCl_2$ (cryst.)	EtOH	+0·04(±0·01)
$HgBr_2$ (cryst.)	EtOH	+0·35(±0·05)
HgI_2 (cryst.)	MeOH	−1·85(±0·15)
HgMeCl (cryst.)	EtOH	−4·15(±0·2)
HgMeBr (cryst.)	EtOH	−4·0(±0·3)
HgMeI (cryst.)	MeOH	−3·94(±0·1)
$HgMe_2$ (*liq.*)	EtOH	−0·6(±0·05)
I_2 (cryst.)	MeOH	−2·07(±0·05)
MeBr(*g*)	EtOH	+4·68 (±0·03)
MeI (*liq.*)	MeOH+HgMeI	−0·47(±0·05)

Calculation of Heats of Formation.—By combining the heats of reaction given in Tables I, II and III with the relevant heats of solution in Table IV, we can write the following set of thermochemical equations:—

$$HgMe_2\ (\mathit{liq.}) + Br_2\ (\mathit{liq.}) \rightarrow MeBr\ (\mathit{g}) + HgMeBr\ (\text{cryst.}) + 43{\cdot}37 \pm 0{\cdot}53\ \text{kcal.} \qquad (4)$$

$$HgMe_2\ (\mathit{liq.}) + I_2\ (\text{cryst.}) \rightarrow MeI\ (\mathit{liq.}) + HgMeI\ (\text{cryst.}) + 26{\cdot}81 \pm 0{\cdot}23\ \text{kcal.} \qquad (5)$$

$$HgMe_2\ (\mathit{liq.}) + HgCl_2\ (\text{cryst.}) \rightarrow 2HgMeCl\ (\text{cryst.}) + 16{\cdot}17 \pm 0{\cdot}55\ \text{kcal.} \qquad (6)$$

$$HgMe_2\ (\mathit{liq.}) + HgBr_2\ (\text{cryst.}) \rightarrow 2HgMeBr\ (\text{cryst.}) + 14{\cdot}59 \pm 0{\cdot}75\ \text{kcal.} \qquad (7)$$

$$HgMe_2\ (\mathit{liq.}) + HgI_2\ (\text{cryst.}) \rightarrow 2HgMeI\ (\text{cryst.}) + 9{\cdot}51 \pm 0{\cdot}38\ \text{kcal.} \qquad (8)$$

By subtracting eqn. (7) from twice eqn. (4), the additional equation

$$\mathrm{HgMe_2}\ (liq.) + 2\mathrm{Br_2}\ (liq.) \rightarrow \mathrm{HgBr_2}\ (\text{cryst.}) + 2\mathrm{MeBr}\ (g) + 72{\cdot}15 \pm 0{\cdot}61\ \text{kcal.} \quad (9)$$

is obtained. Similarly, subtraction of eqn. (8) from twice eqn. (5) gives

$$\mathrm{HgMe_2}\ (liq.) + 2\mathrm{I_2}\ (\text{cryst.}) \rightarrow \mathrm{HgI_2}\ (\text{cryst.}) + 2\mathrm{MeI}\ (liq.) + 44{\cdot}11 \pm 0{\cdot}44\ \text{kcal.} \quad (10)$$

The heat of formation of $HgMe_2$ can be obtained either from eqn. (9), assuming values for $Q_f(\mathrm{HgBr_2}, \text{cryst.})$ and $Q_f(\mathrm{MeBr}, g)$; or alternatively from eqn. (10), assuming values for $Q_f(\mathrm{HgI_2}, \text{cryst.})$ and $Q_f(\mathrm{MeI}, liq.)$. Considering the bromination data first, we have

$$Q_f(\mathrm{HgBr_2}, \text{cryst.}) = 40{\cdot}64 \pm 0{\cdot}24\ \text{kcal./mole}^{-1}\ (\text{Varet}^7)$$

and $$Q_f(\mathrm{MeBr}, g) = 8{\cdot}6 \pm 0{\cdot}5\ \text{kcal. mole}^{-1}.$$

The value for Q_f (MeBr, g) is based on the recommended value for Q_f (MeCl, g) given in the *Selected Values of Chemical Thermodynamic Properties* (Nat. Bur. Stand., Tables 23-7, 1949) and on measurements of the heat of the reaction $CH_3Br + HCl \rightarrow CH_3Cl + HBr$, reported by Bak.[8] Our estimate of ± 0·5 kcal. for the probable error in Q_f (MeBr) is perhaps optimistic; the combustion data of Thomsen[9] on MeBr correspond to $Q_f = 8{\cdot}2$ kcal., but Kharasch and Brown[10] suggest a correction to Thomsen's result which then gives $Q_f = 8{\cdot}8$ kcal.

Using the general thermochemical equation relating the heat of a reaction to the difference in the sums of the heats of formation of products and reactants, and eqn. (9), then

$$72{\cdot}15 \pm 0{\cdot}61 = Q_f(\mathrm{HgBr_2}, \text{cryst.}) + 2Q_f\ (\mathrm{MeBr}, g) - Q_f\ (\mathrm{HgMe_2}, liq.). \quad (11)$$

Substituting the values for $Q_f(\mathrm{HgBr_2})$ and $Q_f(\mathrm{MeBr})$ discussed above into eqn. (11) gives

$$Q_f(\mathrm{HgMe_2}, liq.) = -14{\cdot}31 \pm 1{\cdot}85\ \text{kcal.}$$

Turning to the iodination data, it is fortunate that one of the quantities we need is known with reasonably high accuracy, i.e. the heat of formation of HgI_2 (cryst. red), determined by Varet[7] by seven independent methods as $Q_f(\mathrm{HgI_2}, \text{cryst.}) = 25{\cdot}2 \pm 0{\cdot}2$ kcal. The corresponding equation to (11) for the iodination of $HgMe_2$ is

$$44{\cdot}11 \pm 0{\cdot}44 = Q_f(\mathrm{HgI_2}, \text{cryst.}) + 2Q_f(\mathrm{MeI}, liq.) - Q_f(\mathrm{HgMe_2}, liq.) \quad (12)$$

which, by substituting Varet's value for $Q_f(\mathrm{HgI_2}, \text{cryst.})$ becomes

$$18{\cdot}91 \pm 0{\cdot}64 = 2Q_f(\mathrm{MeI}, liq.) - Q_f(\mathrm{HgMe_2}, liq.). \quad (13)$$

If we now replace $Q_f(\mathrm{HgMe_2}, liq.)$ by the value obtained from our bromination experiments, eqn. (13) then yields

$$Q_f(\mathrm{MeI}, liq.) = 2{\cdot}3 \pm 1{\cdot}2\ \text{kcal. mole}^{-1}.$$

The heat of combustion data of Thomsen[9] on MeI correspond to the value $Q_f(\mathrm{MeI}, liq.) = 2{\cdot}0$ kcal. mole^{-1},* agreeing well with the value now obtained: the corrected Thomsen data of Kharasch and Brown[10] gave $Q_f = 3{\cdot}0$ kcal. Recently, however, Carson, Hartley and Skinner[11] reported $Q_f = 3{\cdot}85$ kcal., from studies of the heats of acid hydrolysis and iodination of cadmium dimethyl. As this latter value lies outside the estimated limits of error of the figure now recommended, we have re-examined the assumptions[5] implicit in the $Q_f = 3{\cdot}8$ determination, and are satisfied that it requires some amendment.

The results of Carson *et al.* may be expressed by the thermochemical equation:

$$(Q_3 - M - Q_2) = 2Q_f(\mathrm{CH_4}, g) + 2Q_f(\mathrm{I_2}, \text{ether}) + Q_f(\mathrm{CdSO_4}, 100)$$
$$-Q_f(\mathrm{H_2SO_4}, 100) - Q_f(\mathrm{CdI_2}, \text{ppt.}) - 2Q_f(\mathrm{MeI}, \text{ether}), \quad (14)$$

where Q_3, M and Q_2 have the meanings given previously.[11] The experimental results of Carson, Hartley and Skinner gave for the term $(Q_3 - M - Q_2)$ the value $- 2 \cdot 3 \pm 0 \cdot 7$ kcal. For the terms in Q_f on the right-hand side of eqn. (14), we have chosen the values recommended by the National Bureau of Standards[12] for $Q_f(CH_4)$, $Q_f(CdSO_4, 100)$ and $Q_f(H_2SO_4, 100)$, and the value $Q_f(I_2, \text{ether}) = - 1 \cdot 80 \pm 0 \cdot 2$ kcal. determined by Hartley and Skinner.[6] With these substitutions, eqn. (14) becomes

---

[7] Varet, *Ann. chim. phys.*, 1896, 8, 79.

[8] Bak, *Det Kgl. Danske Videns. Selskab*, 1948, **24**, 9.

[9] Thomsen, *Thermochemische Untersuchungen*, vol. 1-4 (Barth, Leipzig, 1882-1886).

[10] Kharasch and Brown, quoted by Wheland, *The Theory of Resonance* (John Wiley, New York, 1944).

* See *Selected Values of Chemical Thermodynamic Properties*, Table 23-11.

[11] Carson, Hartley and Skinner, *Proc. Roy Soc. A*, 1949, **195**, 500.

$$2Q_f(\text{MeI}) = 55 \cdot 3 \pm 1 \cdot 1 - Q_f(CdI_2) \quad . \quad . \quad . \quad (15)$$

The heat of formation of crystalline CdI_2 has been determined by various investigators and methods, and a selection of these is summarized below: 48·44 (Taylor and Perrott[13]), 48·22 (from Thomsen's[9] data), 48·86 (from Vosburgh's[14] data). The determination by Taylor and Perrott is the most direct, and for this reason we are inclined to give it the greatest weight. We adopt the value 48·5 ± 0·4 kcal. as one that covers the range in the various experimental data so far reported, and which lies close to the Taylor-Perrott value. With this substitution, eqn. (15) yields 3·4 ± 0·8 kcal. for the amended value of Q_f(MeI, *liq.*). Although within the limits of error of the present investigation, the amended value of Carson, Hartley and Skinner is subject to some uncertainty in that the precipitated CdI_2 obtained from the iodination of $CdMe_2$ was obtained as a fine microcrystalline powder, the heat content of which may well be influenced by the high surface area per unit weight.

The range in the published values for Q_f (MeI, *liq.*) corresponds to a range in the values of $Q_f(HgMe_2, \textit{liq.})$ from − 14·9 to − 12·1 kcal. mole^{-1}; we accept the value of − 14·3 kcal. obtained from the bromination data as the best in the light of present information on the heats of formation of the methyl halides. With this starting-point, the heats of formation of the crystalline methyl mercuric halides are obtained from the heats of the reactions given by eqn. (6), (7) and (8) as follows:

$$Q_f(\text{MeHgCl, cryst.}) = 27 \cdot 68\,^* \pm 1 \cdot 45 \text{ kcal. mole}^{-1}$$

$$Q_f(\text{MeHgBr, cryst.}) = 20 \cdot 46 \pm 1 \cdot 42 \text{ kcal. mole}^{-1}$$

$$Q_f(\text{MeHgI, cryst.}) = 10 \cdot 20 \pm 1 \cdot 21 \text{ kcal. mole}^{-1}.$$

Discussion

We have given details of the assumptions implicit in the present determination of $Q_f(HgMe_2, \textit{liq.})$ in order to assess the limits of error fairly and, we believe, generously. This is necessary in view of the serious divergence between the present value (− 14·3 ± 1·85) and the value of − 37·8 kcal. (quoted by Bichowsky and Rossini[15]) derived from the heat of combustion by Berthelot.[3] We understand that a re-examination of the combustion heats of the mercury alkyls is being undertaken by Springall and Carson,[16] and that the preliminary results confirm our conclusion of inaccuracies in Berthelot's data.

In previous papers of this series[11, 17] we have made use of the heats of formation of metal alkyls in order to derive values for the dissociation energies of metal-carbon bonds. In the present instance, we may derive the *sum* of the heats of dissociation of the first and second Hg—CH_3 bonds in $HgMe_2$ from the equation:

$$(D_1 + D_2) = Q_f(HgMe_2, g) - Q_f(Hg, g) - 2Q_f(CH_3, g), \quad . \quad (16)$$

and also the heats of dissociation of the bonds CH_3—HgX in the methyl mercuric halides from the equation:

$$D(CH_3 - HgX) = Q_f(\text{MeHgX}, g) - Q_f(\text{HgX}, g) - Q_f(CH_3\, g). \quad (17)$$

---

[12] *Selected Values of Chemical Thermodynamic Properties* (Nat. Bur. Stand. Washington, Tables 23–3, 32–5, 14–8).

[13] Taylor and Perrott, *J. Amer. Chem. Soc.*, 1921, **43**, 484.

[14] Vosburgh, *ibid.*, 1927, **49**, 2222.

* The value $Q_f(HgCl_2, \text{cryst.}) = 53 \cdot 5 \pm 0 \cdot 5$ kcal. (derived from Thomsen's[9] data) was assumed.

[15] Bichowsky and Rossini, *Thermochemistry of Chemical Substances* (Reinhold, New York, 1936).

[16] Springall and Carson (private communication).

[17] Carson, Hartley and Skinner, *Trans. Faraday Soc.*, 1949, **45**, 1159.

The terms in Q_f on the right-hand of eqn. (16) and (17) are now available, within relatively small limits of error, and are considered separately below.

(*a*) Q_f(HgMe$_2$, *g*).

This is obtainable directly from the measurement of the heat of formation of liquid HgMe$_2$ reported here, and the heat of vaporization of HgMe$_2$, $\lambda_{vap.} = 8{\cdot}1$ kcal.,[18] whence $Q_f(\text{HgMe}_2, g) = -22{\cdot}4 \pm 1{\cdot}9$ kcal.

(*b*) Q_f(Hg, *g*).

This is a well-established quantity. The National Bureau of Standards[18] recommends the value $Q_f(\text{Hg}, g) = -14{\cdot}54$ kcal.

(*c*) Q_f(CH$_3$, *g*).

In earlier papers[11, 17] we have used the value $Q_f(\text{CH}_3, g) = -32{\cdot}1$ kcal., based on the assumed value of 102·0 kcal. for $D(\text{CH}_3 - \text{H})$ at room temperature. Long[19] has recently revised the estimate by Kistiakowsky and van Artsdalen[20] of $D(\text{CH}_3 - \text{H})$, upgrading their value slightly. Accepting Long's amendment, we have used $Q_f(\text{CH}_3, g) = -32{\cdot}6 \pm 1$ kcal., corresponding to $D(\text{CH}_3 - \text{H}) = 102{\cdot}5 \pm 1$ kcal. at room temperature.

(*d*) Q_f(HgCl, *g*).

This may be derived from the spectroscopically determined value for the dissociation-energy of the HgCl molecule (Wieland;[21] $D°(\text{Hg} - \text{Cl}) = 24{\cdot}0$ kcal.); $Q_f(\text{HgCl}, g) = -18{\cdot}7$ kcal.

(*e*) Q_f(HgBr, *g*).

This may similarly be derived from Wieland's[22] determination of $D°(\text{Hg} - \text{Br})$ at 16·4 kcal.; $Q_f(\text{HgBr}, g) = -24{\cdot}0$ kcal.

(*f*) Q_f(HgI, *g*).

Gaydon[23] quotes $D°(\text{Hg} - I) = 7 \pm 1$ kcal.; whence $Q_f(\text{HgI}, g) = -32{\cdot}1 \pm 1$ kcal.

(*g*) Q_f(HgMeCl, *g*).

Charnley and Skinner[24] have obtained the preliminary value $\lambda_{sub}(\text{HgMeCl}) = 15{\cdot}6 \pm 0{\cdot}1$ kcal. for the heat of sublimation of room temperature, whence $Q_f(\text{HgMeCl}, g) = 12{\cdot}08 \pm 1{\cdot}55$ kcal.

(*h*) Q_f(HgMeBr, *g*).

Charnley and Skinner have measured λ_{sub}(HgMeBr) at $16{\cdot}35 \pm 0{\cdot}15$ kcal., whence $Q_f(\text{HgMeBr}, g) = 4{\cdot}11 \pm 1{\cdot}57$ kcal.

(*i*) Q_f(HgMeI, *g*).

Charnley and Skinner have measured λ_{sub}(HgMeI) at $15{\cdot}85 \pm 0{\cdot}15$ kcal., whence $Q_f(\text{HgMeI}, g) = -5{\cdot}65 \pm 1{\cdot}36$ kcal.

By substituting these values of the appropriate Q_f terms in eqn. (16) and (17), the following dissociation energies of Hg—CH$_3$ bonds are derived:

(i) $D(\text{CH}_3\text{—HgCH}_3) + D(\text{CH}_3\text{—Hg}) = (D_1 + D_2)$ in HgMe$_2$
$= 57{\cdot}3 \pm 4$ kcal.

(ii) $D(\text{CH}_3\text{—HgCl}) = 63{\cdot}4 \pm 2{\cdot}5$ kcal.

(iii) $D(\text{CH}_3\text{—HgBr}) = 60{\cdot}7 \pm 2{\cdot}6$ kcal.

(iv) $D(\text{CH}_3\text{—HgI}) = 59{\cdot}0 \pm 3{\cdot}3$ kcal.

---

[18] *Selected Values of Chemical Thermodynamic Properties* (Table 33-1, 33-2).

[19] Long, *Proc. Roy. Soc. A*, 1949, **198**, 62.

[20] Kistiakowsky and v. Artsdalen, *J. Chem. Physics*, 1944, **12**, 469.

[21] Wieland, *Helv. physic. Acta*, 1939, **12**, 295; 1941, **14**, 549; *Helv. chim. Acta*, 1941, **24**, 1285.

[22] Wieland; quoted by Werhli and Milazzo, *ibid.*, 1943, **26**, 1025.

[23] Gaydon, *Dissociation Energies* (Chapman and Hall, 1947).

[24] Charnley and Skinner (unpublished).

The thermochemical data on $HgMe_2$ are insufficient in themselves to give the individual values of the first and second bond dissociation energies, D_1 and D_2. The value of D_1 has, however, been obtained recently from kinetic studies on the pyrolytic decomposition of $HgMe_2$ by Warhurst and Gowenlock,[25] and by Szwarc. These experimenters have found $D_1 \approx 51$ kcal., which implies that the second bond dissociation energy is small, i.e. $D_2 \approx 6$ kcal., and that the radical $\cdot HgCH_3$ must be highly unstable, except in the circumstance that the reaction $Hg(^1S_0) + CH_3 \rightarrow \cdot HgCH_3$ requires a high activation energy.

The large difference between D_1 and D_2 in $HgMe_2$ follows the general trend in the D_1, D_2 values of HgX_2 molecules; one of us (Skinner[26]) has previously discussed this point in terms of the valence bonding in HgX, HgX_2 compounds. The values now reported for $D(CH_3—HgX)$, which show that the $CH_3—Hg$ bonds in the mercury methyl halides are more firmly held than the similar bonds in mercury dimethyl itself, raise several interesting questions on the character of metal-carbon bonds, but we reserve comment at the present time on these observations.

The authors wish to express thanks to Prof. M. G. Evans, F.R.S., for his interest and advice during the course of this research, and to Prof. H. D. Springall, Dr. E. Warhurst, and Dr. M. Szwarc for permission to quote their work prior to publication. We would also thank Prof. R. E. Lane of the Department of Occupational Health of Manchester University for the medical supervision of the experimenters handling the toxic materials. One of us (H. O. P.) thanks the D.S.I.R. for a maintenance grant.

Chemistry Department,
Manchester University.

---

[25] Warhurst and Gowenlock; Szwarc (private communications).

[26] Skinner, *Trans. Faraday Soc.*, 1949, **45**, 20.

THE ABSORPTION OF INTERRUPTED INFRA-RED RADIATION

By T. L. Cottrell

Received 14*th April,* 1950; *as revised* 26*th May,* 1950

It is shown that the rate of increase of translational energy in a gas illuminated by interrupted infra-red radiation is a function of the frequency of interruption, and it is suggested that in principle this provides a method of investigating the time constants involved in the interconversion of translational and vibrational energy.

1. Introduction.—It has been shown by measurement of the velocity of ultrasonic waves in gases that the transfer of energy from vibrational to translational modes is characterized by a time constant.[1, 2] At low frequencies the velocity corresponds to that calculated on the assumption that all degrees of freedom contribute to the specific heat; at high frequencies the velocity is that corresponding to non-excitation of vibration. It is interesting to consider what might happen in a gas illuminated by infra-red radiation interrupted at frequencies near the effective collision

---

[1] Kittel, *Reports Prog. Physics*, 1946-47, **11**, 205.

[2] Richards, *Rev. Mod. Physics*, 1939, **11**, 36.

frequency, and in particular to enquire under what conditions the attendant increase in translational energy (conveniently detected as a pressure increase in a constant volume system) is likely to be measurably dependent on the frequency of interruption.

Neglecting the effect of rotational excitation, for which the quanta involved are small, the mean rate of uptake of translational energy depends on the mean concentration of vibrationally excited molecules. The latter is expected to vary with the frequency of interruption of the incident radiation if either (i) the destruction of these species is proportional to a power of their concentration other than the first, or (ii) if this power is unity, provided that the coefficients of decay differ in the light and dark periods. It will be shown that the problem should be treated under heading (ii).

2. Description of the Model.—The absorption of interrupted infrared radiation under adiabatic conditions is treated as follows. A gas with only two relevant vibrational states, 0 and 1, of energy separation $h\nu$, is considered. The following processes are assumed to occur.

PROCESS	RATE	
(1) Induced absorption $0 + h\nu \rightarrow 1$	$\rho_\nu B_{01} n_0$	
(2) Induced emission 1 (in radiation field) $\rightarrow 0 + h\nu$	$\rho_\nu B_{10} n_1$	
(3) Spontaneous emission	$A_{10} n_1$	
(4) Degradative collision $0 + 1 \rightarrow 0 + 0$	$k_{10} n_0 n_1$	(2.1)
$1 + 1 \rightarrow 0 + 1$	$k_{10}' n_1^2$	
(5) Excitation by collision $0 + 0 \rightarrow 0 + 1$	$k_{01} n_0^2$	
$0 + 1 \rightarrow 1 + 1$	$k_{01}' n_0 n_1$	

It is clear that if $k_{10}' = k_{10}$ and $k_{01}' = k_{01}$, and since $N = n_0 + n_1$, we may write the rate of (4) as $f_{10} n_1$ and (5) as $f_{01} n_0$, where $f_{10} = k_{10} N$ and $f_{01} = k_{01} N$. Under these circumstances, case (ii) above applies.

The theory of the probability of energy transfer in collisions is not in a sufficiently advanced state to justify this assumption rigorously. Since the distribution of molecular velocities is unaffected by vibrational excitation, it seems likely that the approximation is fairly good. Kittel [1] has shown, using the method of impact parameters,[3] that a theoretical estimate of the exchange probability which is near the correct order of magnitude can be given. The probability P of exciting a state of energy $\hbar\nu$ in a collision is given by

$$P = \hbar^{-2} \left| \int^{\infty} F(t) e^{i\nu t} dt \right|$$

where x is the matrix element of the co-ordinate x connecting the initial and final states, and $F(t)$ is the force acting between the molecules. It is assumed that

$$F(t) = (w/a_0) e^{-v^2 t^2 / a_0^2},$$

where w has the dimensions of energy, a_0 is the Bohr radius, and v is the relative velocity of the molecules. The exchange probability thus depends on the initial and final states of the molecule to be excited or degraded, and the force between it and the exciting or degrading molecule. The former is clearly independent of the nature of the exciting or degrading molecule, and the latter depends on the relative velocity v, and on the parameter w, which also appears [1] to depend mainly on v. There is no obvious reason why w should depend on vibrational excitation, although the experimental result [2] that the efficiency of conversion of translational into vibrational energy by the collision of a molecule of one chemical species with one of another is highly specific shows that w must depend in some way on molecular structure. Moreover, there does not appear to be any experimental evidence to show that vibrational excitation modifies collision efficiency. Richards [2] has calculated the temperature coefficient of the transition probability in carbon dioxide on the assumption that o + 1 and o + o collisions are equally effective in causing the o → 1 transition, and obtained rough agreement with experiment. These considerations suggest that the assumption involved in treating the problem in case (ii) is tenable.

---

[3] Williams, *Proc. Roy. Soc. A*, 1933, **139**, 163.

3. Treatment of the Model.—The following notation is used, the definitions being those implied in (2.1):

ρ_ν	radiation density at frequency ν,
$B_{01} = B_{10}$	Einstein coefficients of induced absorption and emission,
A_{10}	Einstein coefficient of spontaneous emission,
f_{01}, f_{10}	effective collision frequencies for transfer of energy by collision,
N, n_0, n_1	Numbers of molecules, total, in state o, in state 1.

We have, since $N = n_0 + n_1$,

$$dn_1/dt = N(\rho_\nu B_{01} + f_{01}) - n_1(\rho_\nu \overline{B_{01} + B_{10}} + A_{10} + f_{10} + f_{01}). \qquad (3.1)$$

Putting

$$\alpha = (\rho_\nu B_{01} + f_{01})N,$$
$$\beta = (\rho_\nu \overline{B_{01} + B_{10}} + A_{10} + f_{10} + f_{01}),$$
$$\gamma = f_{01}N,$$
$$\delta = A_{10} + f_{10} + f_{01},$$

we have, from (1),

$$dn_1/dt = \alpha - \beta n_1 \text{ radiation on}$$
$$= \gamma - \delta n_1 \text{ radiation off.}$$

Consider $n_1 = n_1(0)$ at $t = 0$, and that the light is on and off alternately for a period τ.

Then if $e^{-\beta\tau} = b$, $e^{-\delta\tau} = d$,

and $\frac{\alpha}{\beta}(1 - b) = A$, $\frac{\gamma}{\delta}(1 - d) = B$,

we have

$$n_1(\tau) = n_1(0)b + A$$
$$n_1(2\tau) = n_1(\tau)d + B,$$

and in general,

$$\left.\begin{aligned} n_1(\overline{2m+1}\tau) &= n_1(2m\tau)b + A \\ n_1(2m\tau) &= n_1(\overline{2m-1}\tau)d + B \end{aligned}\right\} \qquad (3.2)$$

Hence $n_1(2m\tau) = B + Ad + bdn_1(\overline{2m-2}\tau)$

and

$$n_1(2m\tau) - x = bd[n_1(\overline{2m-2}\tau) - x] + B + Ad + (bd - 1)x.$$

Now let $x = \dfrac{B + Ad}{1 - bd}$.

Then

$$n_1(2m\tau) - x = bd[n_1(\overline{2m-2}\tau) - x]$$
$$= b^2d^2[n_1(\overline{2m-4}\tau) - x], \text{ etc.}$$

and finally $n_1(2m\tau) - x = b^m d^m[n_1(0) - x]$.

Treating $n_1(\overline{2m+1}\tau)$ similarly, and passing to the limits for m large, we have

$$\left.\begin{aligned} n_1(2m\tau) &\to x = \frac{B + Ad}{1 - bd} \\ n_1(\overline{2m+1}\tau) &\to \frac{A + Bb}{1 - bd} \end{aligned}\right\}. \qquad (3.3)$$

We now require $\overline{n}_1$, the mean value of n_1. In the interval $2m\tau$ to $\overline{2m+1\tau}$, the mean value of n_1 is

$$\frac{1}{\tau}\int_{2m\tau}^{\overline{2m+1}\tau} n_1 \mathrm{d}t = \frac{1}{\beta\tau}\Big[\alpha\tau - n_1(\overline{2m+1\tau}) + n_1(2m\tau)\Big]. \quad . \quad (3{\cdot}4)$$

Similarly in the interval $\overline{2m+1\tau}$ to $\overline{2m+2\tau}$, the mean value of n_1 is

$$\frac{1}{\delta\tau}\Big[\gamma\tau - n_1(\overline{2m+2\tau}) + n_1(\overline{2m+1\tau})\Big]. \quad . \quad . \quad . \quad (3{\cdot}5)$$

The mean value over the two sections of time is given by the average of (4) and (5). Thus

$$\overline{n}_1 = \tfrac{1}{2}\Big[\Big(\frac{\alpha}{\beta}+\frac{\gamma}{\delta}\Big) + \Big(\frac{1}{\delta}-\frac{1}{\beta}\Big)\Big(\frac{\alpha}{\beta}-\frac{\gamma}{\delta}\Big)\frac{(1-b)(1-d)}{\tau(1-bd)}\Big]. \quad . \quad (3{\cdot}6)$$

The limits for τ long and short are

$$\overline{n}_1 \rightarrow \tfrac{1}{2}\Big(\frac{\alpha}{\beta}+\frac{\gamma}{\delta}\Big),\ \tau \rightarrow \infty,$$

$$\rightarrow \Big(\frac{\alpha+\gamma}{\beta+\delta}\Big),\ \tau \rightarrow 0.$$

We are, however, interested in $\overline{E}_{tr}$, the mean translational energy of the gas, which we consider over a time long compared with τ. We have

$$\frac{1}{h\nu}\frac{\mathrm{d}\overline{E}_{tr}}{\mathrm{d}t} = -f_{01}N + (f_{10}+f_{01})\overline{n}_1,$$

where $\overline{n}_1$ is given by (3.6).

4. Discussion.—The effect of τ on $\overline{n}_1$, and hence on $\mathrm{d}\overline{E}_{tr}/\mathrm{d}t$ is only to be expected if the coefficients of decay in the light and dark periods, β and δ, differ appreciably, since when $\beta = \delta$, the second term in (3.6) is zero. It will be shown that under conditions when this is true

$$\alpha/\beta \gg \gamma/\delta,$$

and we may therefore rewrite equation (3.6) as

$$\overline{n}_1 \simeq \tfrac{1}{2}\frac{\alpha}{\beta}[1+\lambda]$$

$$\lambda = \Big(\frac{1}{\delta}-\frac{1}{\beta}\Big)\frac{(1-b)(1-d)}{\tau(1-bd)}.$$

In Fig. 1, λ is plotted against $\log_{10}x$, where $x = \delta\tau$, for various values of $\beta/\delta = n$. It will be noted that with $n = 3$, for example, $\overline{n}_1$ increases with increasing frequency of interruption (decreasing x) to 1·5 times its value for low frequencies of interruption. Under these circumstances, therefore, the effect should be detectable in any apparatus capable of measuring the heating of gases by infra-red radiation. It remains to show that such values of n may be expected under certain conditions in practice, and that under these conditions the relation $\alpha/\beta \gg \gamma/\delta$ also holds.

At thermal equilibrium,

$$f_{01} = f_{10}\mathrm{e}^{\,h\nu/kT}$$

and therefore at ordinary temperatures for most vibrations

$$f_{10} \gg f_{01}.$$

Since $\qquad B_{10} = B_{01}$, if $n > 2$

then $\qquad 2\rho_\nu B_{01} > A_{10} + f_{10} \gg f_{01}$

and $\qquad \alpha/\beta \gg \gamma/\delta.$

f_{10} is known to vary widely for different gases. In carbon dioxide, for example, there is a dispersion region at about 20 kc. sec.$^{-1}$ at N.T.P.[1] This means that f_{10} is about 2×10^4 sec.$^{-1}$ at N.T.P. and therefore about 3×10^2 sec.$^{-1}$ at a pressure of 1 cm. The Einstein coefficients are given by [4]

$$B_{nm}\rho_{\nu_{nm}} = B_{mn}\rho_{\nu_{mn}} = \frac{2\pi}{3\hbar^2}|R_{mn}|^2 \rho_{\nu_{mn}},$$

where R_{mn} is the matrix element for the electric dipole moment between the two states. We may put [1]

$$_{mn}|^2 = |(m|er|n)|^2 \sim (ea_0)^2 \sim 6.5 \times 10^{-36} \text{ c.g.s. units.}$$

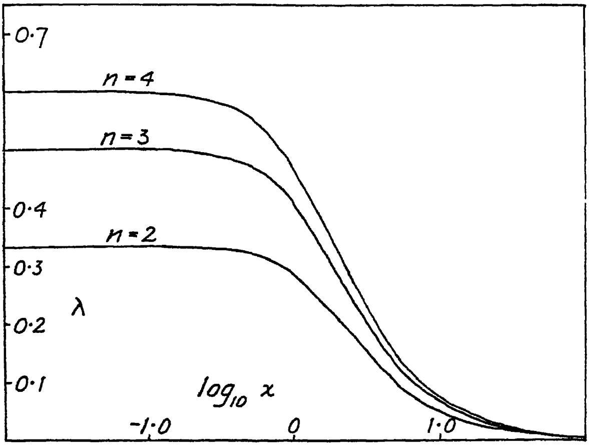

FIG. 1.—Plot of $\lambda = (1/\delta - 1/\beta)(1 - b)(1 - d)/\tau(1 - bd)$ against $\log_{10}x$, where $x = \delta\tau$, for various values of $\beta/\delta = n$.

The constant is approximately 2×10^{54} c.g.s. units, so $B_{10} = B_{01} \simeq 10^{19}$ c.g.s. units. A_{10} is given by [4]

$$A_{mn} = \frac{8\pi h\nu_{mn}^3}{c^3}B_{mn}.$$

Putting $\nu/c = 700$ cm.$^{-1}$, approximately the relevant vibration frequency for carbon dioxide, we have $A_{10} \sim 5 \times 10^2$. For $\rho_\nu B_{10}$ to be of the same order of magnitude as A_{10} and f_{10}, the radiation density ρ_ν must be about 10^{-17} erg. sec. cm.$^{-3}$ at $\nu/c = 700$ cm.$^{-1}$. A parallel beam of radiation from 1 cm.^{2} of a source at 1500° K dissipating 100 W cm.$^{-2}$ gives an energy density at this frequency of 6×10^{-17} erg. sec. cm.$^{-3}$. Under these conditions $\beta = 20 \times 10^2$ sec.$^{-1}$, $\delta = 8 \times 10^2$ sec.$^{-1}$, and thus $n = 2{\cdot}5$. Since the radiation density required is realizable experimentally. it should be possible to observe the effect in practice.

It is assumed that $d\overline{E}_{tr}/dt$ could be measured from the rate of increase in pressure of a suitable illuminated cell. This gives a quantity proportional to $\overline{n}_1$, which will depend on the frequency of interruption. A plot of this against the logarithm of the frequency of interruption should show a point of inflexion near $x = \delta\tau = 1$, the exact point depending on the value of n. n can be increased with increasing radiation density, and an extrapolation of the position of the point of inflexion to its position when $1/\rho = 0$ gives the case of n large, when the equation of the plot of interruption frequency against $\overline{n}_1$ is of the form $(1 - e^{-x})/x$. We can therefore obtain

$$\delta = A_{10} + f_{10} + f_{01} \simeq A_{10} + f_{10}.$$

---

[1] Eyring, Walter and Kimball, *Quantum Chemistry* (Wiley, New York, 1st ed., 1944), Ch. VIII.

Of these quantities f_{10} is pressure dependent and A_{10} is not, and it should thus be possible to separate them by determining δ at various pressures. Alternatively A_{10} could be determined by absolute intensity of absorption measurements in the infra-red, and subtracted from δ to give f_{10}.

Thanks are expressed to the author's colleagues for helpful discussion.

Imperial Chemical Industries Limited,
Nobel Division,
Research Department,
Stevenston, Ayrshire.

OXIDATION OF ALDEHYDES IN THE GASEOUS PHASE

PART IV.—THE MECHANISM OF THE INHIBITION OF THE GASEOUS PHASE OXIDATION OF ACETALDEHYDE BY NITROGEN PEROXIDE

BY C. A. MCDOWELL AND J. H. THOMAS

Received 27th March, 1950

It has previously been shown that nitrogen peroxide inhibits the low-temperature, thermal, gaseous-phase oxidation of acetaldehyde. A photoelectric method has now been used to measure the rate of disappearance of nitrogen peroxide during the induction period and the results so obtained show that nitrogen peroxide reacts with acetaldehyde to form nitric oxide in quantitative yield. The experimental results are best interpreted by assuming that the inhibition of the oxidation is due to the nitric oxide combining with the acetyl radical which normally initiates the oxidation chain.

The low-temperature oxidation of acetaldehyde in the gas phase is inhibited by small amounts of nitrogen peroxide,[1] and we have recently shown [2, 3] that a detailed study of the inhibition yielded information about the initiation process. An elementary theoretical treatment of the inhibition gave the familiar equation [4, 5]

$$I_0/\tau = r_i,$$

where I_0 is the initial concentration of inhibitor, τ the induction period and r_i the rate of initiation of chains. This equation was derived on the assumption that most, or all, of the inhibitor was used up during the induction period and as the deductions from it were so well obeyed by the experimental results it is reasonable to believe that the assumption is approximately correct. Nevertheless, it seemed desirable to have independent confirmation of this and it was also thought that if a means could be devised of following the rate of reaction of the inhibitor with the chain carriers, one might discover the actual mechanism by which nitrogen peroxide inhibited this oxidation.

Nitrogen peroxide absorbs strongly in the visible region of the spectrum and it was easy to devise a photoelectric method of following the rate at which it disappeared during the reaction. The experimental results obtained by using this method are of importance in elucidating the mechanism of the inhibiting action of nitrogen peroxide.

---

[1] McDowell and Thomas, *J. Chem. Soc.*, 1949, 2208.
[2] McDowell and Thomas, *J. Chem. Physics*, 1949, **17**, 588.
[3] McDowell and Thomas, *J. Chem. Soc.*, 1950, 1462.
[4] Goldfinger, Skeist and Mark, *J. Physic. Chem.*, 1943, **47**, 578.
[5] Melville and Watson, *Trans. Faraday Soc.*, 1948, **44**, 886.

Experimental

The apparatus was the same as that previously described [1] with the necessary modifications to enable the photoelectric estimation of the nitrogen peroxide to be conveniently carried out. The reaction vessel and ancillary apparatus for the estimation of nitrogen peroxide are shown diagrammatically in Fig. 1.

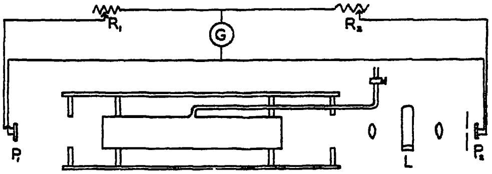

FIG. 1.

The vessel was 16·3 cm. in length, had a volume of 171 ml. and was made of Pyrex. The ends were optical flats in borosilicate glass fused to the Pyrex cylinder.

A parallel beam of light from a sodium lamp was passed through the reaction vessel and received on a EEL selenium photocell. On the opposite side of the lamp a parallel beam of light was directed through an iris diaphragm to another EEL cell which formed part of a bridge circuit with the first photocell and two variable resistances R_1 and R_2. With this arrangement it was easy to calibrate for nitrogen peroxide measurement by adding various amounts of the gas and noting the corresponding values of R_1 required to restore the balance of the bridge circuit.

When the external resistance is increased to about 1000 ohms the response curve of these selenium photocells becomes logarithmic and there are certain advantages in using them under these conditions. If the absorption of light by a substance follows Beer's law then

$$I = I_0 e^{-\epsilon cd},$$

where ϵ is the molar decadic extinction coefficient, c is the concentration in mole/l. and d the depth of the cell. If the response curve of the photocells is arranged to be logarithmic, then since

$$\log (I_0/I) = \epsilon cd,$$

the response under these conditions should be *linear* with the concentration of the absorbing substance. We found that a plot of the value of R_1 against the pressure of nitrogen peroxide was linear in agreement with the above requirements.

Results

Consumption of NO_2 during the Induction Period.—In Fig. 2 are plotted the pressure time curves for the inhibited oxidation of 106 mm. of acetaldehyde by 104·3 mm. of oxygen at 136° C in the presence of 4·2 mm. of nitrogen peroxide, and the rate of disappearance of nitrogen peroxide as measured by the photocell method. Examination of these curves shows that although the greater part of the nitrogen peroxide disappears during the induction period, there is still some unused inhibitor present when this ends. In the above experiment the induction period ends at 4·8 min., and at this time the value of R_1 is 901 ohms. The final value of R_1, i.e. the value when all the nitrogen peroxide has been consumed, is 1018 ohms, and the initial value of R_1 corresponding to the original concentration of inhibitor is 660 ohms. The concentration of nitrogen peroxide at any instant may be calculated from the equation

$$P_{NO_2} = \frac{R_0 - R_t}{R_0} . K, \quad . \quad . \quad . \quad . \quad . \quad . \quad (1)$$

where P_{NO_2} equals the pressure of NO_2 in the reaction vessel, R_0 is the value of R_1 when t is zero, and R_t is the value of R_1 at time t.

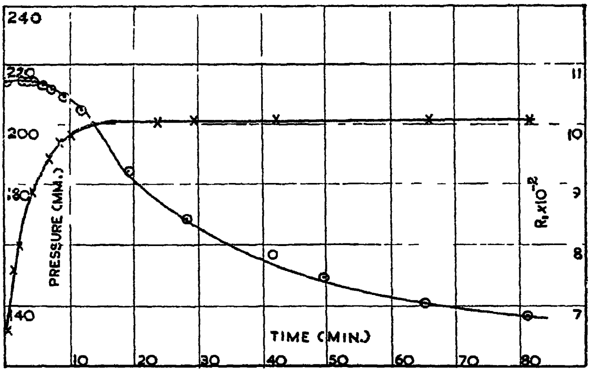

FIG. 2.

The initial value of P_{NO_2}, say, P_{iNO_2} is given by

$$P_{iNO_2} = \frac{1018 - 660}{1018} . K,$$

and the value of P_{NO_2} at the end of the induction period is

$$P_{tNO_2} = \frac{1018 - 901}{1018} . K,$$

hence the fraction of the initial amount of nitrogen peroxide left at the end of the induction period in this particular experiment is

$$\frac{P_{tNO_2}}{P_{iNO_2}} = \frac{1018 - 901}{1018 - 660} = 32 \cdot 7 \ \%$$

Kinetics of Inhibitor Action of Nitrogen Peroxide.—If the values of log $(R_0 - R_t)$ for any of these inhibition experiments are plotted against time a straight line graph is obtained (Fig. 3), which means that the rate of

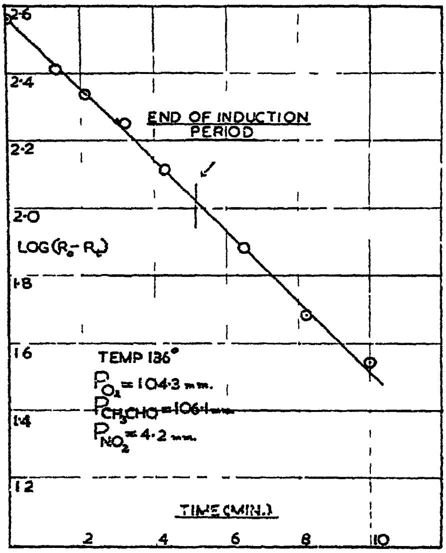

FIG. 3.—Rate of disappearance of NO_2.

disappearance of nitrogen peroxide is first order with respect to nitrogen peroxide. An interesting feature of this graph is that the nitrogen peroxide continues to react at the same rate *after* the end of the induction period.

The effect of temperature on the rate of disappearance of the nitrogen peroxide in this system has been studied for a mixture containing 104 mm. of acetaldehyde and 106 mm. of oxygen. The results are recorded in Table I.

TABLE I.—EFFECT OF TEMPERATURE ON THE RATE OF DISAPPEARANCE OF NITROGEN PEROXIDE IN ACETALDEHYDE–OXYGEN–NITROGEN PEROXIDE MIXTURES

Pressure of O_2 = 104 mm. Pressure of CH_3CHO = 106 mm.

Temp. °C	Pressure of NO_2 (mm.)	Period of Induction (min.)	d log $(R_0-R_t)/dt$
141	3·6	3·25	0·133
136	4·2	4·8	0·102
131	3·3	4·3	0·078
121·5	3·6	7·0	0·048
115·3	4·6	11·0	0·033

In Fig. 4 the logarithm of d log $(R_0 - R_t)/dt$ for each temperature has been plotted against the reciprocal of the absolute temperature and from the straight line obtained we calculate the activation energy for the reaction involving the consumption of nitrogen peroxide to be 16·8 kcal./mole. This is nearly 3 kcal. greater than the activation energy previously calculated [3] for the initiation reaction by the inhibitor technique. This discrepancy we consider to be outside the experimental errors of the methods used, and can only mean that two distinct reactions are involved.

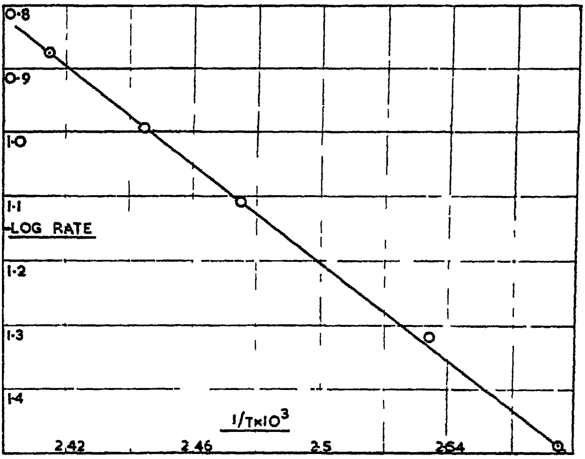

FIG. 4.—Effect of temperature on the rate of disappearance of NO_2.

Analysis of Products formed during the Induction Period.—In order to prove that the addition of nitrogen peroxide was inhibiting the main reaction which is the formation of peracetic acid,[1] a number of experiments were made at 138° C in which the reaction between a certain mixture of acetaldehyde, oxygen and nitrogen peroxide was stopped at intervals during the induction period and the products analyzed for peracetic acid. The products were as usual pumped through a cold trap at − 80° C by means of a Toepler pump. The condensible material was dissolved in water, diluted to 100 ml. and analyzed for peracetic acid by means of acidified potassium iodide and sodium thiosulphate solution. Before adding the potassium iodide to the solution a little urea was added to remove any residual nitrogen peroxide which might be present. A sample of the non-condensible gas was colourless, and gave no reaction with ferrous sulphate solution, thus showing that no nitric oxide was present. For comparison the reaction between the same mixture of acetaldehyde and oxygen, but without the addition of nitrogen peroxide was also examined by stopping it at the same time intervals and analyzing for peracetic acid. The results of the two sets of analyses are given in Table II.

TABLE II.—COMPARISON OF PRODUCTS FORMED IN PRESENCE OF AND ABSENCE OF NO_2

Temp. = 138° C. Pressure of CH_3CHO = 106 mm. Pressure of O_2 = 106·6 mm.

A 12·3 mm. NO_2 added		*B* No NO_2 added
Time min.	Conc. of Peroxide g. equiv./l.	Conc. of Peroxide g. equiv./l.
3	0·0	—
5	1·35 × 10^{-5}	14·8 × 10^{-5}
9	5·27 × 10^{-5}	32·8 × 10^{-5}
12	6·67 × 10^{-5}	37·9 × 10^{-5}

These results indicate that the nitrogen peroxide greatly reduces the amount of peracetic acid formed during the induction period.

Reaction between Acetaldehyde and Nitrogen Peroxide.*—During the experiments described above it was noticed that if acetaldehyde and nitrogen peroxide were mixed in the reaction vessel at the temperatures investigated, there was an immediate reaction during which the nitrogen peroxide disappeared. The reaction took place with practically *no change* in pressure, but could readily be followed by the optical method described earlier. It was obviously of importance to investigate this reaction from the point of view of the mechanism of the inhibition of the oxidation.

Order of Reaction with Respect to Nitrogen Peroxide.—The effect of varying the nitrogen peroxide concentration was examined for several different fixed concentrations of acetaldehyde. The rate of disappearance of nitrogen peroxide was measured as in the preceding experiments in terms of the value of resistance R_1 required to balance the bridge circuit at any particular instant. In Fig. 5 the values of log $(R_0 - R_t)$ are plotted against time for experiments at 128·5° C with a pressure of acetaldehyde of 57 mm. and different concentrations of nitrogen peroxide. It will be seen from the parallel straight lines obtained that the reaction is first order with respect to nitrogen peroxide.

Order of Reaction with Respect to Acetaldehyde.—In this series of experiments the effect of varying the concentration of acetaldehyde was examined at 128·7° C by following the rate of disappearance of nitrogen peroxide, the initial concentration of the nitrogen peroxide being kept constant throughout. Plotting log (R_0-R_t) against time for each reaction yielded straight lines from which the gradients d log (R_0-R_t) dt were measured. Table III gives the numerical results for the various values of d log $(R_0-R_t)/\mathrm{d}t$ together with the times for the half reaction calculated from the R_1 against time curves.

If either d log $(R_0-R_t)/\mathrm{d}t$ or $t_{\frac{1}{2}}$ be taken as a criterion of the reaction rate and the logarithm plotted against the logarithm of the acetaldehyde pressure a straight line is obtained with a gradient of approximately unity. The gradient is 0·94 if d log $(R_0-R_t)/\mathrm{d}t$ is used and 1·02 if log $t_{\frac{1}{2}}$ is used. Fig. 6 shows the graph of d log $(R_0-R')/\mathrm{d}t$ against the logarithm of the pressure of acetaldehyde. The reaction is thus first order with respect to both the reactants. A similar kinetic law has recently been shown[6] to govern the reaction between formaldehyde and nitrogen peroxide at temperatures below 180° C.

---

* This reaction is being studied also by Dr. Pollard at the University of Bristol. Dr. Pollard and his colleagues have carried out a most extensive series of investigations on the reactions of aldehydes with nitrogen peroxide and they will shortly be reporting their results on the acetaldehyde-nitrogen peroxide reaction.

[6] Pollard and Wyatt, *Trans. Faraday Soc.*, 1949, **45**, 760.

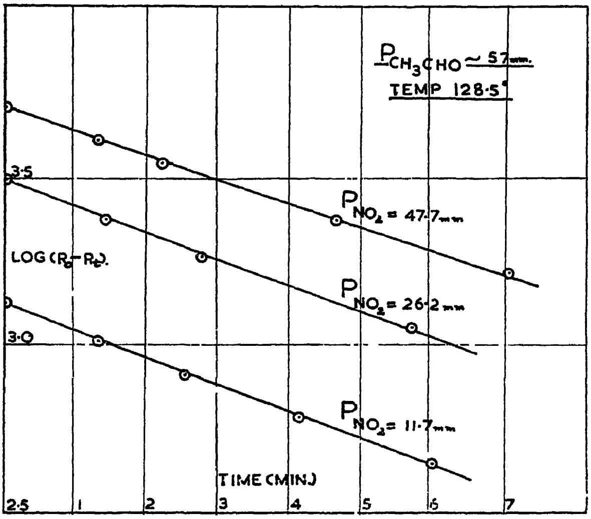

FIG. 5.—Effect on reaction rate of variation in NO_2 concentration.

TABLE III.—EFFECT OF VARIATION IN ACETALDEHYDE CONCENTRATION TEMPERATURE 128·7°

Pressure of NO_2 (mm.)	Pressure of CH_3CHO (mm.)	$d \log (R_0-R_t)/dt$	$t_{\frac{1}{2}}$ (min.)
48·5	132·8	0·16	1·72
46·2	104·5	0·14	2·10
48·7	85·5	0·106	2·78
47·7	57·7	0·071	4·0

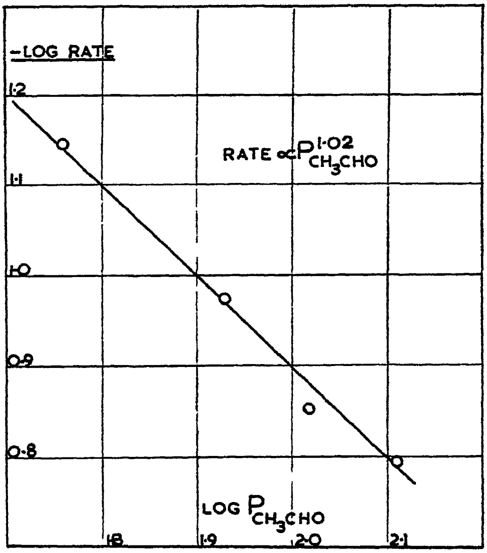

FIG. 6.—Order of reaction with respect to acetaldehyde.

Products of the Reaction.—The following simple analyses were made to determine the nature of the products of the reaction. At the end of a run the gaseous products were pumped off through a cold trap at − 80° C. 9·2 ml. of a colourless gas measured at 20° C and 754 mm. were collected. On adding ferrous sulphate solution, 90 % of this sample, i.e. 8·2 ml. were absorbed to give a brown solution showing the gaseous products to be almost entirely nitric oxide. The volume of the reaction vessel was 171 ml. and the pressure of nitrogen peroxide used in this experiment was 45·8 mm. at 128·7° C. This corresponds to a volume of ~8·0 ml. at 20° C and 754 mm. pressure. It would appear, therefore, that during the reaction the nitrogen peroxide is quantitatively converted to nitric oxide. A similar observation has been made for the low-temperature reaction between formaldehyde and nitrogen peroxide.[6]

The condensible products were acidic but did not liberate iodine from acidified potassium iodide solution. It would seem, therefore, that in addition to nitric oxide, an acid with no peroxide character is produced ; this acid is probably acetic acid.

Determination of the Velocity Constant and Activation Energy.—The rate of reaction of a certain mixture of acetaldehyde and nitrogen peroxide was measured at three temperatures and the values for the half-life times $t_{\frac{1}{2}}$ were read off the graphs of R_1 against time. From these values of $t_{\frac{1}{2}}$ the velocity constants given in Table IV were calculated.

TABLE IV.—VELOCITY CONSTANTS FOR BIMOLECULAR REACTION BETWEEN ACETALDEHYDE AND NITROGEN PEROXIDE

Temp. °C	c_{NO_2} (mole l.$^{-1}$)	c_{CH_3CHO} (mole l.$^{-1}$)	$t_{\frac{1}{2}}$ (sec.)	k (l. mole^{-1} sec.$^{-1}$)
118	$1·94 \times 10^{-4}$	$2·35 \times 10^{-4}$	453	9·08
128·7	$1·90 \times 10^{-4}$	$2·3 \times 10^{-4}$	240	16·8
143	$1·80 \times 10^{-4}$	$2·22 \times 10^{-4}$	132·6	31·3

Plotting log k against $1/T°$ K yields a straight line graph from which we obtain the kinetic expression

$$k = 10^{9·85} \exp\,(-\ 16{,}000\ \text{cal.}/RT)\ \text{l. mole}^{-1}\ \text{sec.}^{-1}\ ;$$

the error in the activation energy is probably not greater than ± 1000 cal. mole. It is of interest to note that Pollard and Wyatt [6] give the expression

$$k = 10^{7·1} \exp\,(-\ 15{,}100\ \text{cal.}/RT)\ \text{l. mole}^{-1}\ \text{sec.}^{-1}$$

for the reaction between formaldehyde and nitrogen peroxide.

Discussion

Since the activation energy for the reaction causing the disappearance of nitrogen peroxide in the inhibition experiments and that for the acetaldehyde-nitrogen peroxide reaction are approximately the same, it is probable that the same process is going on in both systems. Furthermore, in the acetaldehyde-nitrogen peroxide reaction, the latter compound is quantitatively converted to nitric oxide, and as this gas is not present in the gaseous products from the inhibition experiments, it would therefore seem that the inhibition by nitrogen peroxide of the oxidation of acetaldehyde is due to the nitric oxide produced in a side reaction between the aldehyde and the nitrogen peroxide. Nitric oxide is, of course, a well-known inhibitor of chain reactions.[7] A somewhat similar situation prevails in the inhibition of radical reactions by alkyl nitrites. Rice and Polly [8] find that these compounds show an inhibition which may be assigned to a dual action :

$$R + CH_3ONO \rightarrow RH + CH_2ONO \rightarrow RH + H_2CO + NO.$$

---

[7] See Hinshelwood, *Kinetics of Chemical Change* (Oxford, 1940).

[8] Rice and Polly, *J. Chem. Physics*, 1939, **6**, 273.

The molecules of nitrite themselves inhibit and *also* the nitric oxide produced inhibits according to the scheme [7]

$$R + NO = RNO.$$

The mechanism of the production of nitric oxide in the acetaldehyde–nitrogen peroxide reaction is not obvious. As shown above the kinetic laws governing this reaction being first order with respect to both reactants requires the rate of reaction to be governed by the equation

$$R = k[CH_3CHO][NO_2].$$

No satisfactory simple bimolecular process can be suggested which will account for the production of nitric oxide and a carboxylic acid (probably acetic acid). A similar situation is found in the reaction between formaldehyde and nitrogen peroxide.[6] Here also the nitrogen peroxide is quantitatively converted to nitric oxide, but instead of an acid being formed, Pollard and Wyatt find that the formaldehyde is quantitatively oxidized to carbon monoxide and carbon dioxide.

The reaction between formaldehyde and nitrogen peroxide is also of first order with respect to each reactant, and Pollard and Wyatt put forward two possible schemes :

SCHEME A

$$CH_2O + NO_2 = CH_2O_2 + NO \quad . \quad . \quad . \quad F\ (1)$$
$$CH_2O_2 = CO + H_2O \quad . \quad . \quad . \quad F\ (2)$$
$$CH_2O_2 + NO_2 = CO_2 + H_2O = NO \quad . \quad . \quad F\ (3)$$

Reactions (2) and (3), however, do not satisfy the experimental results, unless it is assumed that the breakdown of the intermediate is sensitized by nitrogen dioxide, when reaction (2) becomes

$$CH_2O_2 + NO_2 = CO + H_2O + NO_2 \quad . \quad . \quad F\ (2a)$$

SCHEME B

This alternative mechanism also assumes the sensitized decomposition of the product of the initiation on reaction :

$$CH_2O + NO_2 = (CH_2O\,.\,NO_2) \quad . \quad . \quad . \quad F\ (4)$$
$$(CH_2O\,.\,NO_2) + NO_2 = CO + H_2O + NO + NO_2 \quad . \quad F\ (5)$$
$$(CH_2O\,.\,NO_2) + NO_2 = CO_2 + H_2O + 2NO \quad . \quad . \quad F\ (6)$$

The application of the stationary state principle yields a rate equation which is in agreement with the experimental result.

Both of these reaction schemes have certain unsatisfactory features. The first, for example, assumes the formation of the compound CH_2O_2 which, the authors state, could be considered as either formic acid or a peroxide isomeric with formic acid. The former involves the formation of a carboxylic acid from an aldehyde in one step, a process which is not generally regarded as common in oxidation reactions.[9] A similar assumption in a recently proposed mechanism for the oxidation of formaldehyde has been shown to be unnecessary.[10]

It is highly probable that the reactions between aldehydes and nitrogen peroxide are free radical reactions and we, therefore, prefer reaction schemes involving radicals as intermediates. For acetaldehyde and nitrogen peroxide the following mechanism is suggested :

$$CH_3CHO + NO_2 = CH_3CO + HNO_2 \quad . \quad . \quad . \quad (1)$$
$$CH_3CO + NO_2 = CH_3CO_2 + NO \quad . \quad . \quad . \quad (2)$$
$$CH_3CO_2 + HNO_2 = CH_3COOH + NO_2 \quad . \quad . \quad (3)$$

---

[9] Hinshelwood *et al.*, *Faraday Soc. Discussions*, 1947, **2**.

[10] McDowell and Thomas, *Nature*, 1948, **162**, 367.

By applying the stationary state principle we obtain the following expression for the rate of reaction :

$$d[NO_2]/dt = k_1[CH_3CHO][NO_2]$$

which is in agreement with the experimental results. Reaction (1) is the rate-determining step. It is assumed that reactions (2) and (3) are very fast.

Before discussing the mechanism of the inhibition of the oxidation of acetaldehyde it is necessary to consider the oxidation reaction itself. We have recently shown [1] that the following mechanism satisfactorily accounts for the experimental observations :

$$CH_3CHO + O_2 = CH_3CO + HO_2 \quad . \quad . \quad . \quad A(1)$$
$$CH_3CO + O_2 = CH_3CO_3 \quad . \quad . \quad . \quad . \quad A(2)$$
$$CH_3CO_3 + CH_3CHO = CH_3CO_3H + CH_3CO \quad . \quad . \quad A(3)$$
$$CH_3CO_3 + O_2 = \text{chain ending} \quad . \quad . \quad . \quad A(4)$$

In the present discussion we are concerned only with the initiation reaction for the results of this paper show that the nitric oxide formed from the nitrogen peroxide inhibits the formation of peracetic acid. The inhibition is probably caused by the reaction of nitric oxide with the acetyl radical thus :

$$CH_3CO + NO = CH_3CONO \quad . \quad . \quad . \quad A(5)$$

At 143° C the velocity constant for the reaction between acetaldehyde and nitrogen peroxide is 31·3 l. mole^{-1} sec.$^{-1}$ whereas the velocity constant for the initiation reaction of the oxidation of acetaldehyde, i.e. reaction A(1), is 0·4 l. mole^{-1} sec.$^{-1}$ at 141° C.[3] Hence for concentrations of reactants used in the inhibition of the oxidation of acetaldehyde by nitrogen peroxide, the rate of formation of nitric oxide is about two and a half times faster than the rate of formation of acetyl radicals by reaction A(1). The fate of the acetyl radical in the inhibited oxidation reaction is governed mainly by two reactions namely :

$$CH_3CO + NO = CH_3CONO \quad . \quad . \quad . \quad A(5)$$
$$CH_3CO + O_2 = CH_3CO_3 \quad . \quad . \quad . \quad A(2)$$

So long as rate A(5) > rate A(2) few reaction chains will start and there will be inhibition, and the induction period will end only when the concentration of nitric oxide has fallen to such a low value that the rate of reactions A(2) and A(5) become equal. The time required for this state to be achieved will depend on the amount of nitric oxide present, and since this depends directly on the original amount of nitrogen peroxide, it is to be expected that the length of the induction period will depend directly on the original amount of inhibitor present. This was earlier shown to be the case.[3] The rate of formation of acetyl radicals will control the rate of consumption of nitric oxide and since rate of formation of acetyl radicals is simply the rate of initiation as shown by the reaction A(1), this means that for a fixed amount of nitrogen peroxide the length of the induction period is dependent on the rate of initiation ; and any factors which affect the rate of initiation will also affect the length of the induction period. This means that the temperature dependence of $I_0 t$ as a measure of the rate of initiation gives an estimate of the activation energy for the initiation reaction. This was previously shown to be 13·8 kcal./mole.[3]

The reaction between acetyl radicals and nitric oxide has previously been put forward by Anderson and Rollefson [11] to explain the decrease in the quantum yield of carbon monoxide in the photolysis of acetone vapour in the presence of nitric oxide. It is generally accepted [12] that the first step in the photolysis of acetone is the formation of acetyl and methyl radicals, and as the temperature is raised the acetyl radicals decompose to yield methyl radicals and carbon monoxide. The inhibition of the formation of carbon monoxide in the presence of nitric oxide is thought to be due to a reaction between acetyl radicals and the nitric oxide to form a relatively stable compound with the formula CH_3CONO.

---

[11] Anderson and Rollefson, *J. Amer. Chem. Soc.*, 1941, **63**, 816.

[12] See Steacie, *Atomic and Free Radical Reactions* (New York, 1946), p. 200 *et seq.*

Department of Inorganic and Physical Chemistry,
University of Liverpool.

REACTIONS IN LIQUID SULPHUR DIOXIDE

PART I.—EXCHANGE OF OXYGEN BETWEEN LIQUID SULPHUR AND THIONYL CHLORIDE

BY E. C. M. GRIGG AND I. LAUDER

Received 15*th January,* 1950; *as revised* 28*th June,* 1950

An investigation of the possibility of exchange of oxygen between liquid SO_2 and $SOCl_2$, using the heavy oxygen isotope ^{18}O as a tracer element, has been carried out. No exchange was found to occur. This result indicates that some aspects of Jander's theory of reactions in liquid SO_2 are not correct.

Jander's theory [1] of reactions in liquid SO_2 is based on the assumption that ionization of liquid SO_2 occurs according to the equation

$$2SO_2 \rightleftharpoons SO_3^{=} + SO^{++},$$

while thionyl chloride is assumed to ionize according to the equation

$$SOCl_2 \rightleftharpoons 2Cl^- + SO^{++}.$$

If these views are correct an exchange of oxygen between liquid SO_2 and $SOCl_2$ might be expected to occur via the common thionyl ion, SO^{++}. The procedure adopted to investigate the possibility of this exchange is outlined below.

Experimental

In brief the technique used was as follows. Sulphur dioxide, enriched in ^{18}O was mixed in the liquid state with $SOCl_2$. Subsequently the SO_2 was recovered and allowed to react with a slight excess of H_2S. The water formed was purified and its isotopic composition was determined by a density measurement.

THIONYL CHLORIDE was purified by a modification of a method described by Cottle.[2] 300 ml. of B.D.H. "redistilled" $SOCl_2$ was refluxed with 8·3 g. of pure sulphur for 6 hr. in an all-glass apparatus using a Widmer fractionating column with 37 turns. A middle fraction was collected and this was subjected to a second fractionation. Proper attention was paid, at all stages, to the exclusion of moisture. The product was colourless. It was thoroughly outgassed and stored *in vacuo*.

HYDROGEN SULPHIDE was prepared by direct union of hydrogen and sulphur. Pure sulphur was sublimed, under vacuum conditions, into a bulb of 1 l. capacity. Purified electrolytic hydrogen was introduced to a pressure of 55 cm. Hg. After heating for 20 hr. at 380° C, conversion to H_2S was almost complete. Connection to the vacuum system was made through a breakable glass seal and the gases were pumped through a trap cooled to $-183°$ C. The H_2S was subsequently allowed to evaporate from the trap into an evacuated storage bulb.

---

[1] Jander and Wickert, *Z. physik. Chem. A*, 1936, **178**, 57. Jander and Ruppolt, *ibid.*, 1937, **179**, 43, etc.

[2] Cottle, *J. Amer. Chem. Soc.*, 1946, **68**, 1380.

SULPHUR DIOXIDE was prepared by direct union of sulphur and oxygen. Pure sulphur was sublimed into a bulb of 1 l. capacity. Pure oxygen was introduced to a pressure of 38 cm. Hg. After heating for 50 hr. at 285° C conversion to sulphur dioxide was almost complete. The SO_2 was freed from any trace of oxygen and transferred to a storage bulb by a technique similar to that outlined above for H_2S. Experiment showed that the SO_2 prepared in this way was quite free from SO_3.

HEAVY OXYGEN used for preparing the SO_2 enriched in ^{18}O was obtained by the thermal diffusion method.[3]

The Reaction Mixture.—In all experiments, 0·192 g. of SO_2 were added to 0·384 g. of $SOCl_2$. All transfers were made under vacuum conditions. The reaction vessel, with tap attached, had a volume of approximately 20 ml. and, as the investigation was carried out at 0° C, approximately half of the SO_2 was in the liquid state.

The Recovery of SO_2 from the Reaction Mixture.—After the desired interval, the SO_2 was recovered by the following method. The reaction vessel was attached to the vacuum system and cooled to − 70° C. At this temperature, the vapour pressure of SO_2 is 20 mm. Hg while that of $SOCl_2$ is 1·25 mm. Hg. The tap to the reaction vessel was opened for 1 min. and the vapours given off were frozen in a trap cooled to − 183° C. The reaction vessel was then shaken gently for 2 min. to induce mixing of the reaction mixture before withdrawal of further vapour. The process was repeated for a total of 6 times. The distillate, consisting mainly of SO_2, was subjected to two further distillations as just outlined.

It was found, as already reported,[4] that SO_2 and H_2S do not react when dry. Accordingly, the SO_2 was mixed with H_2S in the presence of 3 mg. of water in a bulb of 1 l. capacity. After a period of 7 days, the water formed was isolated and placed in contact with 120 sq. cm. of silver foil in order to remove any excess H_2S present. After 4 days, this step in the purification process was repeated using a fresh piece of silver foil.

The density of the sample of water was then determined by the micropyknometer method of Gilfillan and Polanyi.[5]

Results

The results obtained are shown in Tables I and II. $\Delta\rho$ initial represents the excess density in parts per million (p.p.m.), of the water formed from the oxygen initially present in the SO_2; $\Delta\rho$ final (corrected) is that of the water subsequently formed at the end of the stated reaction periods corrected for the addition of 3 mg. of "normal" water as mentioned earlier; $\Delta\rho$ equilibrium represents the excess density in p.p.m., which the final water would have if the exchange proceeded to equilibrium. The error in the density measurements may be taken as ± 25 p.p.m.

TABLE I

No. of expt. .	1	2	3	4	5	6	7	8	9	10	11
$\Delta\rho$ final . .	175	38	27	29	5	0	3000	51	31	0	0

TABLE II

No. of Expt.	Reaction Time (days)	$\Delta\rho$ Initial	$\Delta\rho$ Final (corrected)	$\Delta\rho$ Equilibrium
12	6	2060	2050	1340
		2065	2050	1340
13	5	2065	1940	1340
		2065	2010	1340
14	9	2065	2030	1340
		2065	2025	1340

---

[3] Lauder, *Trans. Faraday Soc.*, 1947, **43**, 620.

[4] Matthews, *J. Chem. Soc.*, 1926, **129**, T2270.

[5] Gillfillan and Polanyi, *Z. physik. Chem. A*, 1933, **166**, 255.

Expt. (1) to (11) inclusive were carried out with reagents of normal isotopic compositions and so if the purification of the sample of water before the density measurement is made is satisfactory, $\Delta\rho$ final should be zero. The sample of water from Expt. (7) gave a decided test for chloride using $AgNO_3$, while the other samples up to Expt. (9) gave very faint tests for chloride. The samples of water obtained from Expt. (10) to (14) inclusive were treated with a thin film of sodium metal (0·6 mg.) prepared from sodium azide. Samples treated in this way did not give any test for chloride. All determinations of density for Expt. (12) to (14) were carried out in duplicate.

Discussion

The results show that, under the experimental conditions, no detectable exchange occurs between the oxygen of the SO_2 and that of the $SOCl_2$. (It should be mentioned that the value, 1940 p.p.m., Expt. (13), cannot be accepted with reliance as, during this determination, the " normal " readings with the pyknometer varied by an amount equivalent to 67 p.p.m.) Jander's view, therefore, that both liquid SO_2 and $SOCl_2$ are appreciably ionized cannot be correct. However, it is still possible that one of the reagents is appreciably ionized. An investigation of the possibility of exchange of oxygen between a dissolved sulphite and liquid SO_2 would help to decide this point. Further investigation along this line is proceeding.

We wish to thank Mr. L. Warrell for help with the experimental work.

Department of Chemistry,
University of Queensland,
Brisbane,
Australia.

THE CONDUCTIVITIES OF POTASSIUM AND LANTHANUM COBALTICYANIDES AND FERRICYANIDES

By J. C. James and C. B. Monk

Received 3rd May, 1950

Conductivity measurements on aqueous solutions of $K_3Fe(CN)_6$, $K_3Co(CN)_6$ and $LaCo(CN)_6$ at 18° and 25°, and of $LaCl_3$ at 25° are reported. The limiting mobilities of the La^{+++}, $Fe(CN)_6^{\equiv}$ and $Co(CN)_6^{\equiv}$ ions have been carefully evaluated, and the differences between the experimental conductivities and the theoretical Onsager equation for the first three of these salts have been discussed quantitatively in terms of incomplete dissociation. $LaCo(CN)_6$ behaves as a weak electrolyte, and its conductivity curve shows abnormal behaviour at higher concentrations. This is explained by assuming that the extent of dissociation passes through a minimum. Thermodynamic data for this salt have also been calculated.

Comparatively few electrolytes where both the cation and the anion have valencies of three or more are suitable for careful studies of the physical properties of their solutions, principally because they are either insoluble or they undergo hydrolysis. The second factor in particular is a major consideration so far as conductivity measurements are concerned, and hitherto $LaFe(CN)_6$, which has been reported by Davies and James [1] has been about the only electrolyte in the category under discussion, which has been thoroughly investigated by this method. It proved to be markedly different from salts formed by lower valency ions in that the conductivity curve in dilute solution is similar to that given by comparatively weak organic acids. This property is an extreme case of what has been found to be generally true, i.e., increase in the value of the valency-product of the two ions of an electrolyte is accompanied by a decrease in the dissociation constant.

$LaCo(CN)_6$ has also proved to be a salt of the 3—3 valency type suitable for conductivity measurements, and this has been pursued along the same lines as for $LaFe(CN)_6$. At the same time, in order to obtain independent figures for the mobilities of the individual ions at infinite dilution, measurements on dilute solutions of $LaCl_3$ and $K_3Co(CN)_6$ have also been made. It is necessary to know these limiting mobilities with a fair degree of accuracy for the quantitative evaluation of the dissociation constants and other properties. Direct extrapolation of the conductivities of higher valency electrolytes involves a considerable margin of uncertainty, although there are methods [1] which give satisfactory results in such cases. A puzzling feature which arose over this point occurred with $LaFe(CN)_6$, namely that Λ° calculated by these methods gave 168·9 (at 25°), whereas addition of the individual ion mobilities obtained from other sources gave 170·3. To settle this point, fresh measurements on $K_3Fe(CN)_6$ have also been included in this paper; these new results clear up the discrepancies.

Experimental

A.R. $K_3Fe(CN)_6$ was dissolved, filtered and recrystallized three times from conductivity water, and the crystals dried in vacuum over P_2O_5. Two separate batches were prepared. Each sample taken for a conductivity run was heated at 115-120° for 2 hr.; prolonged heating at this temperature showed the salt to be quite stable under this treatment.

$LaCl_3$ was prepared by conversion of B.D.H. pure $La(NO_3)_3$ to the oxalate, decomposing this by heat, and dissolution in A.R. HCl. This treatment was repeated 5 times. Crystals of $LaCl_3$ were finally obtained by passage of purified HCl gas into the solution in a platinum dish. The crystals were taken to 600° in a platinum boat in a Richards bottling apparatus, and pure dry HCl gas passed in during the heating, and finally dry N_2 when the temperature fell to 100°. This is essentially the treatment of Jones and Bickford [2] and others.[3]

$K_3Co(CN)_6$ was prepared by a method described by Bigelow.[4] The product was purified by repeated fractional precipitation with dioxan from conductivity water, and was dried in vacuum over P_2O_5 (purification methods involving evaporation of aqueous solutions were found to be unsatisfactory owing to the high solubility and the occurrence of slight decomposition).

$LaCo(CN)_6$ was made by the process of Willard and James.[5] A concentrated solution of $LaCl_3$ prepared from the pure oxide was mixed at 60° with a solution containing the correct amount of $K_3Co(CN)_6$. On cooling, fine white crystals of $LaCo(CN)_6$ separated out. These were drained, washed repeatedly with conductivity water and allowed to stand in a vacuum desiccator over a partially dehydrated specimen of the salt until the weight was constant. The composition of the salt was determined by electrolytic estimation of the Co content and corresponded to $LaCo(CN)_6, 5H_2O$ (Co : 13·23 % found, 13·27 % calc.).

Conductivity measurements were made at 18° and 25° with the apparatus described previously.[1, 6, 7] Several cells were used; for the most dilute solutions quartz cells of the Hartley-Barret type were employed, and for the intermediate solutions, Pyrex cells with fixed vertical electrodes entering through the cell walls. These were calibrated by the method of Davies.[8, 9] Pipette cells, designed on the lines recommended by Jones and Bollinger,[10] and calibrated with a 0·1 N solution of KCl [11] were used for the most concentrated solutions.

---

[1] Davies and James, *Proc. Roy. Soc. A*, 1948, **195**, 116.

[2] Jones and Bickford, *J. Amer. Chem. Soc.*, 1934, **56**, 606

[3] Longsworth and MacInnes, *ibid.*, 1938, **60**, 3070.

[4] Bigelow, *Inorganic Syntheses* (McGraw-Hill Book Co., London, 1946), Vol. II, 225.

[5] Willard and James, *J. Amer. Chem. Soc.*, 1916, **38**, 1497.

[6] Davies, *J. Chem. Soc.*, 1937, 432.

[7] Davies and Monk, *ibid.*, 1949, 413.

The density of $LaCo(CN)_6$ was determined for the purposes of buoyancy corrections and was found to be 2·058 at 25°. Density measurements on concentrated solutions of this salt at 25° were made; these may be represented by

$$\rho = 0{\cdot}9971 + 0{\cdot}090\ C,$$

C being the equivalent concentration. Densities of strong solutions of $K_3Fe(CN)_6$ at 25° were calculated from available data,[12] which can be expressed by

$$\rho = 0{\cdot}9971 + 0{\cdot}059\ C$$

over the range considered. Measured conductivities were corrected for the solvent conductivity, allowance being made in the correction for interionic attraction effects.[8] The equivalent conductivities Λ are in ohm.$^{-1}$ cm.^{2} g. equiv.$^{-1}$

Discussion and Results

Lanthanum Chloride.—The present measurements with $LaCl_3$ at 25° (which are given in Table I) agree excellently with those of Jones and Bickford [2] and those of Shedlovsky.[13] Our results extend into more dilute regions than those of the other workers, so that Λ° can be fixed with somewhat greater certainty. Using the Owen method of extrapolation,[14] as can be seen by Fig. 2, Λ° is 145·95 ± 0·05. Since the Cl^- ion has a limiting mobility of 76·34,[15] that of the La^{+++} ion is therefore 69·61, which may be compared with 69·5 obtained by Harned [15] using the same method of extrapolation. No measurements were made at 18°; those of Renholm,[16] which extend into dilute solutions, extrapolate to 125·2 ± 0·1. Interpolation from the transport numbers of Gunning and Gordon [17] shows that the limiting mobility of the Cl^- ion is 65·85 at 18°, so that of the La^{+++} ion is 59·35, comparable with the figure of 59·2 obtained independently.[18]

TABLE I.—CONDUCTIVITY OF LANTHANUM CHLORIDE AT 25°

$\kappa_{H_2O} \times 10^7$ (ohm^{-1} cm.$^{-1}$)	$C \times 10^4$ (g. equiv. l^{-1})	$C^{\frac{1}{2}} \times 10^2$	Λ (ohm^{-1} cm.^{2} g. equiv.$^{-1}$)
2·42	2·1037	1·450	141·81
—	3·7272	1·931	140·47
—	5·6568	2·378	139·21
—	8·2310	2·936	137·84
—	14·678	3·831	135·26

(pH of stock solution = 5·85)

Potassium Ferricyanide.—The data are given in Tables II and III. Application of Owen's method [14] to the more dilute solutions at 25° leads to Λ° of 172·6 ± 0·1, as can be seen from Fig. 2. Taking 73·52 as the mobility of the K^+ ion,[15] that of the $Fe(CN)_6^{\equiv}$ ion at zero concentration is consequently 99·1. This is 1·8 units lower than the value obtained

---

[8] Davies, *Trans. Faraday Soc.*, 1929, **25**, 129.

[9] Grindley and Davies, *ibid.*, 1929, **25**, 133.

[10] Jones and Bollinger, *J. Amer. Chem. Soc.*, 1931, **53**, 411.

[11] Jones and Bradshaw, *ibid.*, 1933, **55**, 1780.

[12] *Int. Crit. Tables* (McGraw-Hill Inc., New York, 1926), **3**, 92.

[13] Harned and Owen, *The Physical Chemistry of Electrolytic Solutions* (Reinhold Publishing Corp., New York, 1943, 339) (private communication).

[14] Owen, *J. Amer. Chem. Soc.*, 1939, **61**, 1393.

[15] Ref. 13, p. 172.

[16] Renholm, *Soc. Sci. Fenn. Comm. Phys. Math.*, 1927, **4**, No. 3, 17.

[17] Gunning and Gordon, *J. Chem. Physics*, 1942, **10**, 126.

[18] *Landolt-Bornstein Tabellen* (Springer, Berlin, 1936), 3rd suppl., 1059.

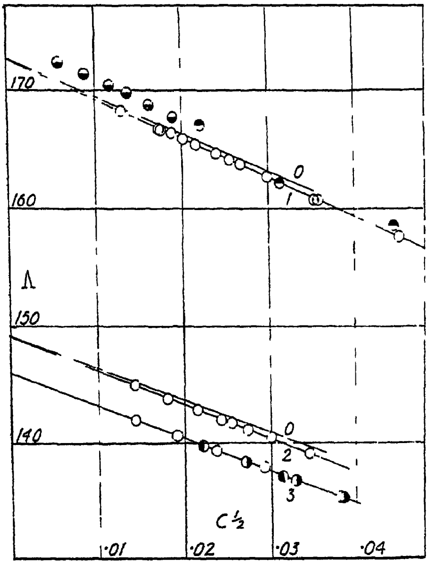

FIG. 1.—Conductivities of (1) $K_3Fe(CN)_6$ at 25°; (2) $K_3Fe(CN)_6$ at 18°; (3) $LaCl_3$ at 25°, O = Onsager slopes. Present work ○; ref. 19, ◓; ref. 20, ●; ref. 2, ◑; ref. 15, ◐.

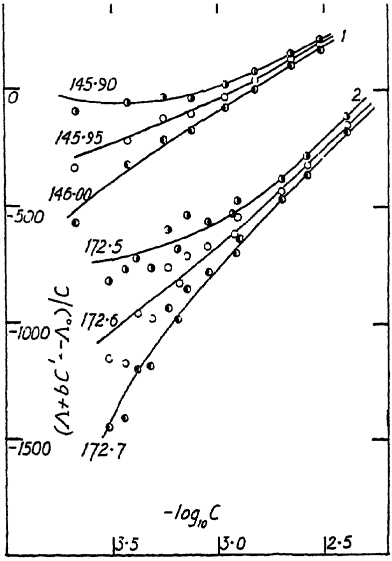

FIG. 2.—Owen's extrapolations for $LaCl_3$ at 25° (top set), and $K_3Fe(CN)_6$ at 25°. The figures attached to each curve represent various values of Λ^0 used in the ordinate function (b represents the Onsager slope). The data for $LaCl_3$ were taken from the present work and ref. (2), those for $K_3Fe(CN)_6$ were taken from the present work.

TABLE II.—CONDUCTIVITY OF POTASSIUM FERRICYANIDE SOLUTIONS AT 25°

Sample	$\kappa_{H_2O} \times 10^7$ (ohm^{-1} cm.$^{-1}$)	$C \times 10^4$ (g. equiv. l^{-1})	$C^{\frac{1}{2}} \times 10^2$	Λ (ohm^{-1} cm.^{2} g. equiv.$^{-1}$)	α	K
1	2·61	1·7470	1·322	168·19	0·0040	0·040
	—	3·1034	1·762	166·70	0·0046	0·057
	—	4·1650	2·041	165·84	0·0053	0·063
	—	5·8861	2·420	164·59	0·0060	0·077
2	2·15	3·1824	1·784	166·60	0·0058	0·046
	—	4·8041	2·192	165·30	0·0062	0·058
	—	6·6299	2·572	164·03	0·0073	0·070
	—	9·0761	3·013	162·60	—	—
	—	13·018	3·608	160·65	—	—
2	2·20	3·6575	1·913	166·35	0·0038	0·079
	—	7·2786	2·698	163·65	0·0072	0·077
	—	12·640	3·555	160·72	—	—
	—	20·620	4·541	157·55		—
	—	26·907	5·187	155·56	—	—
	—	41·195	6·418	151·95	—	—
1	15·0	0·0028274	0·05317	155·40	—	—
	—	0·014552	0·1206	138·71	—	—
	—	0·033808	0·1839	127·89	—	—
	—	0·075329	0·2745	118·70	—	—
2	15·0	0·0074494	0·08631	145·88	—	—
	—	0·013177	0·1148	139·69	—	—
	—	0·028394	0·1685	130·44	—	—
	—	0·057677	0·2403	121·72	—	—
	—	0·10333	0·3215	114·99	—	—

TABLE III.—CONDUCTIVITY OF POTASSIUM FERRICYANIDE SOLUTIONS AT 18°

Sample	$\kappa_{H_2O} \times 10^7$ (ohm^{-1} cm.$^{-1}$)	$C \times 10^4$ (g. equiv. l^{-1})	$C^{\frac{1}{2}} \times 10^2$	Λ (ohm^{-1} cm.^{2} g. equiv.$^{-1}$)	α	K
1	1·54	6·0142	2·452	141·85	0·010	0·046
	—	7·5591	2·749	141·00	0·011	0·051
	—	9·1418	3·024	140·29	—	—
	—	12·121	3·482	138·97	—	—
2	2·52	2·0703	1·439	144·83	0·0050	0·036
	—	3·3201	1·822	143·65	0·0078	0·036
	—	4·7462	2·179	142·69	0·0081	0·048
	—	6·5978	2·569	141·60	0·0091	0·056

by Hartley and Donaldson;[19] their figures are consistently higher than the present ones but there is good agreement between our figures and older data.[20] This is illustrated by Fig. 1. Hartley and Donaldson state that they found a steady change in the resistance readings with time, and they obtained their results by extrapolating back to zero time of stirring. With the present series, slight permanent drifts with time were found with solutions weaker than about 0·0003 C, but stronger solutions gave steady readings if the solutions were shaken each time a reading was taken, even over periods of 2 hr. or more. The change in the resistance on letting the solution remain steady in the cell is probably the result of adsorption at the electrodes, and has been noticed in a number of cases.[21]

At 18°, the $\Lambda°$ value obtained is 148·95 ± 0·1. For KCl at this temperature $\Lambda°$ is 129·67[8], whence from the Cl^- figure cited in connection with $LaCl_3$, we get 63·82 for the K^+ ion (as compared with the published value of 63·65 [18]), and 85·13 for the limiting mobility of the $Fe(CN)_6^{\equiv}$ ion.

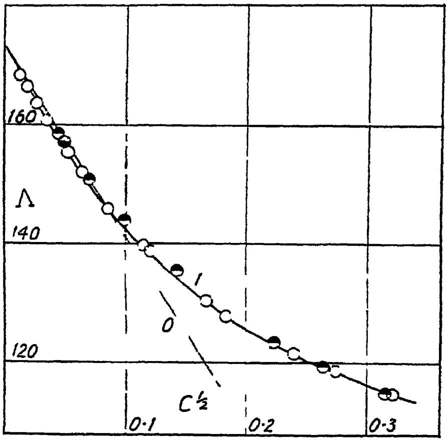

FIG. 3.—Complete conductivity curve of $K_3Fe(CN)_6$ at 25°. O = Onsager slope. Present work, ○ ; ref. 19, ◒ ; ref. 20, ◓.

Potassium Cobalticyanide.—The conductivities at 25° and 18° are given in Tables IV and V respectively and plotted in Fig. 4. Extrapolation gives $\Lambda°$ as 172·4 at 25° and 148·2 at 18°, so in the light of the values for the K^+ ion given above, the $Co(CN)_6^{\equiv}$ ion has mobilities of 98·9 and 84·4 at 25° and 18° respectively. These figures are only slightly less than those found for the $Fe(CN)_6^{\equiv}$ ion, which, considering the similarity in the two ions, is what one would expect to find.

---

[19] Hartley and Donaldson, *Trans. Faraday Soc.*, 1937, **33**, 465.
[20] Ref. 12, **6**, p. 253.
[21] James, *Trans. Faraday Soc.*, 1949, **45**, 855.

TABLE IV.—CONDUCTIVITY OF POTASSIUM COBALTICYANIDE SOLUTIONS AT 25°

Run	$\kappa_{H_2O} \times 10^7$ (ohm^{-1} cm.$^{-1}$)	$C \times 10^4$ (g. equiv. l.$^{-1}$)	$C^{\frac{1}{2}} \times 10^2$	Λ (ohm^{-1} cm.^{2} g. equiv.$^{-1}$)	α	K
1	3·56	0·7534	0·8680	169·44	—	—
	—	1·5666	1·252	158·23	—	—
	—	2·4893	1·578	167·11	0·0051	0·042
	—	3·3149	1·821	166·30	0·0058	0·048
	—	4·2188	2·054	165·61	0·0055	0·062
	—	5·2846	2·300	164·78	0·0062	0·067
2	4·20	0·8859	0·9412	169·32	—	—
	—	1·9240	1·387	167·96	—	—
	—	3·0240	1·739	166·73	0·0034	0·065
	—	4·2499	2·062	165·57	0·0055	0·062
	—	5·8474	2·418	164·25	0·0080	0·057
	—	7·9418	2·818	162·63	0·0109	0·055
3	3·92	1·3647	1·168	168·55	—	—
	—	2·4766	1·574	167·27	0·0030	0·070
	—	3·9270	1·982	165·81	0·0057	0·057
	—	5·1999	2·280	164·80	0·0069	0·060
	—	8·3829	2·895	162·62	0·0105	0·059
	—	10·514	3·243	161·36	0·0131	0·057

TABLE V.—CONDUCTIVITY OF POTASSIUM COBALTICYANIDE SOLUTIONS AT 18°

Run	$\kappa_{H_2O} \times 10^7$ (ohm^{-1} cm.$^{-1}$)	$C \times 10^4$ (g. equiv. l.$^{-1}$)	$C^{\frac{1}{2}} \times 10^2$	Λ (ohm^{-1} cm.^{2} g. equiv.$^{-1}$)	α	K
1	3·40	1·0633	1·031	145·37	—	—
	—	1·8831	1·372	144·26	—	—
	—	2·6615	1·631	143·58	0·0052	0·043
	—	3·4802	1·865	142·82	0·0075	0·038
	—	4·3817	2·093	142·32	0·0060	0·059
	—	5·4906	2·343	141·47	0·0091	0·047
2	1·86	0·7006	0·837	146·27	—	—
	—	1·4262	1·194	145·11	—	—
	—	2·1930	1·481	144·15	0·0024	0·079
	—	3·0301	1·742	143·35	0·0043	0·059
	—	3·9261	1·981	142·69	0·0047	0·069
	—	5·0447	2·246	141·79	0·0080	0·050

Ion-Association.—The experimental points for both $K_3Fe(CN)_6$ and $K_3Co(CN)_6$ in dilute solutions lie slightly below the limiting Onsager slopes. Ion-pair formation between a K^+ ion and the anion would appear to be the most probable cause of such deviations, since the mean diameter of the ions is considerably less than 10·5 Å, which is the value given by Bjerrum's theory[22] as the critical distance for this valency-type. For $LaCl_3$ the experimental and theoretical slopes coincide, indicative of the large effective radius of the La^{+++} ion, which is probably the result of heavy hydration.

The dissociation constants of the ion-pairs $KFe(CN)_6^{=}$ and $KCo(CN)_6^{=}$

---

[22] Bjerrum, *Kgl. Danske Vid. Selsk.*, 1926, 7, No. 9.

may be calculated by the method of Davies.[23] Taking the first of these salts, the corresponding Onsager equations for the stages representing complete dissociation and the dissociation of the ion-pair, are respectively

$$\Lambda_1 = 172{\cdot}60 - 220{\cdot}4I^{\frac{1}{2}} \text{ and } \Lambda_2 = 139{\cdot}3 - 149{\cdot}7I^{\frac{1}{2}}.$$

where I is the ionic strength. This is calculated from

$$I = C(2 - \alpha),$$

α being the fraction of $Fe(CN)_6^{\equiv}$ ions which associate with K^+ ions. The figure of 139·3 is derived from that of the K^+ ion (73·52) and by assuming that of the $KFe(CN)_6^{=}$ ion is 66·0, i.e. two-thirds that of the $(Fe(CN)_6^{\equiv}$ ion. This assumption is justified to some extent by the mobility of the $Fe(NO)(CN)_5^{=}$ ion being 69·4.[24] Combining the above equations using the mixture rule

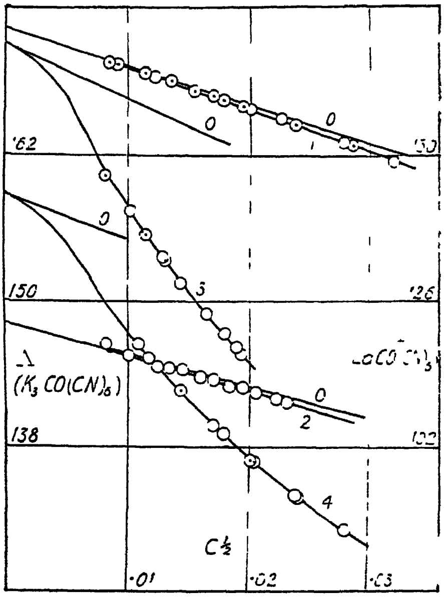

FIG. 4.—Conductivities of (1) $K_3Co(CN)_6$ at 25°; (2) $K_3Co(CN)_6$ at 18°; (3) $LaCo(CN)_6$ at 25°; (4) $LaCo(CN)_6$ at 18°. Onsager slopes represented by O.

$$3\Lambda = 3(1 - \alpha)\Lambda_1 + 2\alpha\Lambda_2,$$

we get $\Lambda = 172{\cdot}60 - 220{\cdot}4I^{\frac{1}{2}} - \alpha(79{\cdot}5 - 123{\cdot}9I^{\frac{1}{2}})$,

from which α may be calculated by approximations. The values of α are shown in the Tables. The dissociation constant

$$K = \frac{[K^+][Fe(CN)_6^{\equiv}]f_1f_2}{[KFe(CN)_6^{=}]f_3} = \frac{C(3 - \alpha)(1 - \alpha)f_{\pm}^6}{3\alpha},$$

where f_1, f_2 and f_3 are the ion activity coefficients, has been calculated for a number of points, and these are included in the Tables. For this purpose the Debye equation

$$-\log_{10}f_i = 0{\cdot}509z_i^2I^{\frac{1}{2}},$$

where z_i is the ion valency, has been used. Exactly similar treatment has been applied to the conductivities at 18° (using 0·503 for the Debye factor), and to the $K_3Co(CN)_6$ data. The calculations have been confined to the most dilute points, within the scope of the Onsager treatment. The K values are very sensitive to slight scattering in the experimental results, but the average results are of the same order for both salts. The results are summarized in Table VIII, in which the corresponding distances of closest approach of the ions, as calculated by Bjerrum's method,[22] are included. It is of interest to note that sodium trimetaphosphate, which is the only other salt of this valency type that has been studied,[7] has a dissociation constant of similar order to these two (0·068).

---

[23] Righellato and Davies, *Trans. Faraday Soc.*, 1930, **26**, 592

[24] Holzl and Stockmair, *Monatsch.*, 1931, **58**, 289.

Lanthanum Cobalticyanide.—The conductivity results obtained at 25° are given in Table VI, and the curve is compared with the theoretical one in Fig. 4 and 5. The experimental curve closely resembles that of $LaFe(CN)_6$,[1] and is similar to that of a comparatively weak electrolyte. The degree of dissociation for the points obtained with dilute solutions has been calculated from the relation

$$\alpha = \Lambda/\{168{\cdot}4 - 913{\cdot}41(\alpha C)^{\frac{1}{2}}\},$$

where 168·4 is the Λ° value obtained by addition of the individual ion mobilities cited previously. In Fig. 6 the logarithm of the apparent dissociation constant K' is plotted against $I^{\frac{1}{2}}$, where $I = 3\alpha C$, and a line has been drawn through the points with the slope required by the limiting Debye-Hückel function. Agreement with experiment is good except at the lowest concentrations (less than 0·00005 M), where the experimental points show a slight falling away. Thermodynamic dissociation constants have been derived for each point from the equation

$$\log_{10} K = \log_{10} [\alpha^2 C/3(1 - \alpha)] - 9{\cdot}164 I^{\frac{1}{2}}$$

and are given in Table VI.

TABLE VI.—CONDUCTIVITY OF LANTHANUM COBALTICYANIDE AT 25°

Run	$K_{H_2O} \times 10^7$ (ohm^{-1} cm.$^{-1}$)	$C \times 10^4$ (g. equiv. l.$^{-1}$)	$C^{\frac{1}{2}} \times 10^2$	Λ (ohm^{-1} cm.^{2} g. equiv.$^{-1}$)	$K \times 10^4$
1	2·63	0·7097	0·842	146·44	(1·606)
	—	1·0968	1·047	140·58	(1·679)
	—	1·7817	1·335	132·40	1·706
2	2·79	1·7482	1·322	133·03	1·732
	—	2·8390	1·685	123·63	1·740
	—	3·7112	1·927	118·08	1·743
	—	5·4794	2·341	109·76	1·747
3	4·17	2·1586	1·469	128·67	1·701
	—	3·8677	1·967	116·86	1·716
	—	5·2160	2·284	110·47	1·722
	—	7·1962	2·683	103·56	1·727
4	3·84	1·3817	1·175	136·70	(1·677)
	—	3·3334	1·826	120·43	1·745
5	—	44·756	6·690	68·41	—
	—	71·274	8·443	61·28	—
	—	72·688	8·525	61·15	—
	—	110·17	10·50	55·99	—
6	—	114·43	10·70	55·56	—
	—	114·52	10·70	55·53	—
	—	158·26	12·58	52·20	—
	—	203·99	14·28	50·43	—

The results at 18° are given in Table VII and Fig. 4, calculating the dissociation constants as before, using $\Lambda^\circ = 143{\cdot}7$, which again is based on the individual ion mobilities given in this paper. A plot of log K' against $I^{\frac{1}{2}}$ agreed satisfactorily with the theoretical Debye slope.

TABLE VII.—CONDUCTIVITY OF LANTHANUM COBALTICYANIDE AT 18°

Run	$K_{H_2O} \times 10^7$ (ohm^{-1} cm.$^{-1}$)	$C \times 10^4$ (g. equiv. l.$^{-1}$)	$C^{\frac{1}{2}} \times 10^2$	Λ (ohm^{-1} cm.^{2} g. equiv.$^{-1}$)	$K \times 10^4$
1	1·91	1·6050	1·270	114·83	(1·728)
	—	3·0007	1·732	105·15	1·802
	—	4·1713	2·042	99·47	1·821
	—	5·7523	2·398	93·74	1·838
2	3·24	1·2320	1·110	118·63	(1·714)
	—	2·1444	1·464	110·87	1·803
	—	3·2969	1·816	103·76	1·828
	—	4·2706	2·066	99·28	1·845
3	5·22	4·2419	2·060	99·12	1·818
	—	5·8893	2·427	93·29	1·836
	—	7·9448	2·819	87·95	1·852

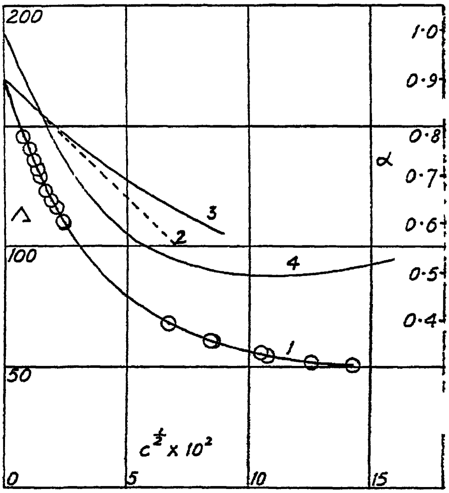

FIG. 5.—Complete conductivity curve of $LaCo(CN)_6$ at 25°. (1) experimental curve; (2) Onsager slope; (3) calculated true ionic mobilities plotted against the square root of the ionic concentration; (4) plot of calculated α values against $C^{\frac{1}{2}}$.

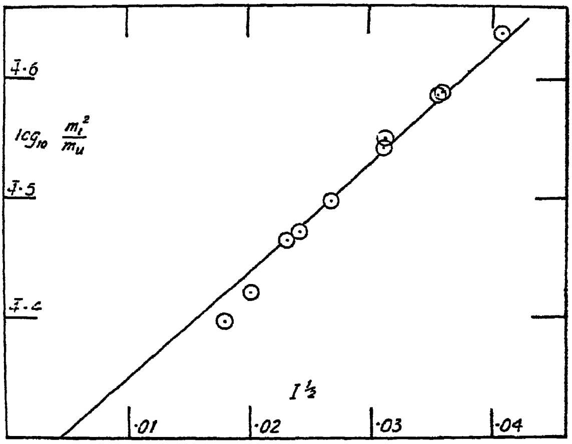

FIG. 6.—Plot of apparent dissociation constant of $LaCo(CN)_6$ against the square root of the ionic strength.

Introduction of the average dissociation constants at 18° and 25° (Table VIII) into the van't Hoff isochore gives $\Delta H = -1{\cdot}33$ kcal. between these two temperatures (assuming it does not alter over this range), while the free energy and entropy changes are $\Delta G = 5132$ cal. and $\Delta S = -21{\cdot}7$ cal./deg. respectively at 25°. The corresponding figures for $LaFe(CN)_6$[1] differ only slightly from these. As with $LaFe(CN)_6$, the constancy of closest approach of the ion centres, as derived from Bjerrum's equations (the data are given in Table VIII) indicates that Bjerrum's treatment satisfactorily relates the temperature variation of the dissociation constant with the variation in the dielectric constant of water. Conductivity measurements on $LaFe(CN)_6$ in aqueous solutions of dioxan, acetone, ethylene glycol and ethanol substantiate this view.[25]

TABLE VIII.—CONDUCTIVITY RESULTS

	$K_3Fe(CN)_6$	$K_3Co(CN)_6$	$LaCo(CN)_6$
Anion mobility (18°) . .	85·13	84·4	—
,, ,, (25°) . .	99·1	98·9	—
Average K (18°) . . .	0·05	0·055	$1{\cdot}825 \times 10^{-4}$
,, (25°) . . .	0·06	0·06	$1{\cdot}728 \times 10^{-4}$
Bjerrum distance (Å) (25°) .	8·0	8·1	7·18
,, ,, (18°) .	7·8	7·8	7·22

With the more concentrated solutions of $LaCo(CN)_6$ (which extend almost to the saturation point) at 25°, the curve (Fig 5) shows a marked flattening, resembling the curves for $LaFe(CN)_6$ and other high valency salts.[26] It has been shown by Davies [27] that a reasonable explanation for such behaviour can be given by supposing that the degree of dissociation passes through a minimum. Following this treatment, values of α have been calculated from

$$\log_{10}\frac{\alpha^2 C}{3(1-\alpha)} + \log_{10} f_{\pm}^2 = \log_{10} K \text{ (average)} = -3{\cdot}763,$$
$$\text{where } \log_{10} f_{\pm}^2 = -9\{I^{\frac{1}{2}}/(1+I^{\frac{1}{2}}) - 0{\cdot}20I\}$$

and are plotted against $C^{\frac{1}{2}}$ in curve 4 of Fig. 5. The empirical extension of the Debye-Hückel equation used above has been shown by Davies [28] to hold up to $I = 0{\cdot}1$. Curve 3 has been obtained from the equation $\alpha \Lambda_s = \Lambda$, and shows the calculated sum of the true ionic mobilities plotted against the square-root of the ionic concentration. The curve approaches the limiting Onsager slope asymptotically from above, just as in the case of the ferricyanide.

Lanthanum Ferricyanide.—The results given in this paper clear up the discrepancy previously noted.[1] Comparison shows that the methods used to obtain Λ^0 at 18° and 25° from the $LaFe(CN)_6$ data agree favourably with those obtained by addition of the individual ion mobilities given above, i.e. at 18°, 144·1 and 144·4, and at 25°, 168·9 and 168·7 respectively.

Summary of Data.—For convenience, the various limiting ion mobilities given in the above sections, the average dissociation constants and the corresponding Bjerrum distances have been collected and tabulated in Table VIII. In addition the following limiting ion mobilities have been calculated: La^{+++} (18°) 59·35, (25°) 69·61; Cl^- (18°) 65·85; K^+ (18°) 63·82.

The Edward Davies Chemical Laboratories,
University College of Wales,
Aberystwyth.

The University,
Glasgow.

---

[25] James, *J. Chem. Soc.*, 1950, 1094.
[26] Shoch and Felsing, *J. Amer. Chem. Soc.*, 1916, 38, 1926.
[27] Davies, *J. Chem. Soc.*, 1945, 460.
[28] Davies, *ibid.*, 1938, 2093.

MELTING AND CRYSTAL STRUCTURE

III.—LOW-MELTING ACID SULPHATES

By S. E. Rogers and A. R. Ubbelohde

Received 26th April, 1950 ; as revised, 20th June, 1950

A number of physico-chemical properties of the acid sulphates of sodium, potassium and ammonium have been correlated with the object of interpreting their low melting points and elucidating structural characteristics of solids and melts. It has been shown that the melts are ionic and that the low melting-points are associated with two effects :

(i) a large entropy of fusion (approx. 23 cal./mole deg.) ;
(ii) a comparatively low activation energy of flaw formation in the solid.

Results on electrical conductivity are as follows :

Salt	Temp. Range °C	σ ohm^{-1} cm.$^{-1}$	E_σ kcal./mole	A in $\sigma = Ae^{E_\sigma/RT}$
$KHSO_4$ melt . .	211·8-300·5	0·049-0·141	6·2	33
$KHSO_4$ solid *just* below f.p. .	93·0-168·0	$1{\cdot}282 \times 10^{-9}$- $3{\cdot}682 \times 10^{-8}$	15·3	6·8
$KHSO_4$ solid *well* below f.p. .	22·8-93·0	$2{\cdot}258 \times 10^{-10}$- $1{\cdot}282 \times 10^{-9}$	1·8	$3{\cdot}5 \times 10^{-7}$
$NaHSO_4$ melt . .	190·0-310·2	0·079-0·256	5·7	38
NH_4HSO_4 melt .	136·0-191·5	0·067-0·143	5·3	43

There is an anomalous increase in viscosity in the region of the freezing-point. E_η in the immediate neighbourhood of the freezing-point is 38·9 kcal./mole and at higher temperatures 12·0 kcal./mole. The volume change on freezing ($\Delta V/V_s = 0{\cdot}04$) is remarkably low. These observations indicate that the melt is polymerized near the freezing point.

Previous investigations on ionic melts have been rather scattered, and have been confined to certain specific properties, notably electrical conductivity and its relation to viscosity. In the present work an attempt has been made to give a broad correlation of the results of a number of physicochemical measurements with a view to clarifying ideas about the melting process of certain ionic salts. Special attention has been directed to what appeared to be anomalously low melting points. The acid sulphates of sodium, potassium and ammonium are dealt with in the present paper.

The main lines of investigation included the following physicochemical properties :

(*a*) Solid State—density, change in specific volume with temperature, change in electrical conductivity with temperature and preliminary X-ray studies on crystal structure.

(*b*) Molten State—viscosity, electrical conductivity, density and change of specific volume with temperature.

(*c*) Melting—changes in volume and heat content.

Striking results included the unusually low activation energies associated with electrical conductivity, the anomalously small change in volume on melting, and the slope of the viscosity-temperature curve of the melt. The entropy of melting was also unexpectedly high. The significance of these and of other experimental observations for the melting process is detailed in the discussion.

Experimental and Results

MATERIALS.—$NaHSO_4$ (A.R.) and $KHSO_4$ (A.R.) were used without further purification. Commercial $(NH_4)HSO_4$ was recrystallized twice from distilled water and dried between filter papers before use.

Chemical Decomposition.—In view of the confused statements in the literature, it was necessary to carry out tests on the chemical stability of these melts before attempting extensive physicochemical measurements. It was not found possible to carry out experiments on rates of decomposition *in vacuo* on account of frothing. After some trial, a simple set-up was used in which the salts were melted in a silica boat, and a constant surface area of melt was exposed to a stream of dry air. From analyses of the melt at intervals, and of the air, it was established :

(i) that the decomposition took place principally according to the equation

$$2MHSO_4 \rightarrow M_2S_2O_7 + H_2O \quad . \quad . \quad . \quad . \quad (1)$$

After some decomposition the pyrosulphate separated as a white solid (m.p. 414·2° C [1]). A trace of H_2SO_4 was detected ($\not> 0{\cdot}005$ % of reaction (1)). At the respective melting points, the relative rates of decomposition were

$$Na : K : NH_4 = 10 : 4 : 1.$$

A representative initial rate for $KHSO_4$ was 2×10^{-4} mole per mole salt per sq. cm. of surface per minute at 220° C. The temperature coefficients corresponded with relative activation energies of Na 3·3, K 6·8, NH_4 10·1 kcal/mole. These results verified that under the conditions used loss of water during the physicochemical measurements could be neglected, and that decomposition of the melt is fastest for the smallest cation. This is probably due to electrostatic effects in the abstraction process

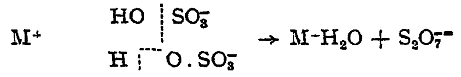

$$M^+ \quad \begin{array}{l} HO \,\vdots\, SO_3^- \\ H \,\vdots\, O.SO_3^- \end{array} \rightarrow M^-H_2O + S_2O_7^{--}$$

and helps to explain the instability of acid sulphates of the Group II ions in the solid state.[2] There was no evidence of large amounts of acid evolved from the melt as claimed in some published work.[3] The present results are in good agreement with those of Ishikawa, Masuda and Hagisawa[4] for $NaHSO_4$.

Electrical Conductivity.—The cell (Fig. 1) was designed to maintain the contents under a small positive pressure of dry N_2, since vacuum could not be used. The electrodes (cf. ref. (5)) consisted of a ring of platinum wire and a platinum disc gold-soldered to an upright platinum rod. The leads were of copper wire, hard-soldered to the platinum. Standard methods of using A.C. 800-2000 c./sec. and of temperature measurement to 0·1° C (Pallador thermocouple) were employed.

The salts were kept just molten in the cell for about 2 hr. before measurements were made to remove all bubbles from the electrodes. Measurements were made on the melts from about 25° to about 3° above the m.p. With this apparatus it was not possible to obtain results on the supercooled melt, which always crystallized at the f.p. Owing to the big increase in resistance, at the freezing point a change-over was made to D.C. measurements. The E.M.F. was only applied long enough to read the current through a galvanometer, since otherwise polarization caused very gradual creep.

The mean error in conductivity measurements on the melts did not exceed ± 0·7 % and in most cases was lower. In the solid state, however, precision was not as good, especially for the lower temperatures. At 200° C the mean

---

[1] Cambi and Bozza, *Ann. chim. appl.*, 1923, **13**, 221.

[2] Mellor, *A Comprehensive Treatise on Inorganic and Theoretical Chemistry* (Longmans & Co., 1922), Vol. III.

[3] Mellor, *ibid.*, Vol. II.

[4] Ishikawa, Masuda and Hagisawa, *Bull. Inst. Phys. Chem. Res.* (*Tokyo*), 1932, **11**, 1244.

[5] Biltz and Klemm, *Z. physik. Chem.*, 1924, **110**, 329.

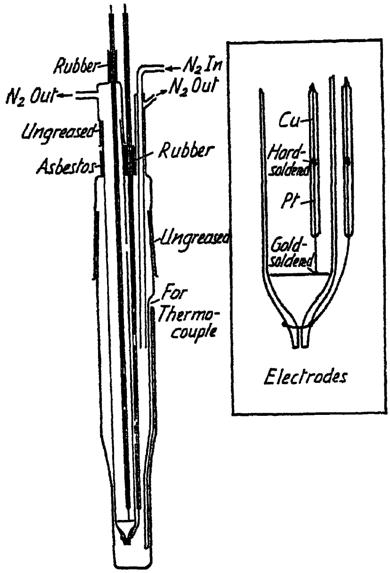

FIG. 1.—Electrical conductivity cell.

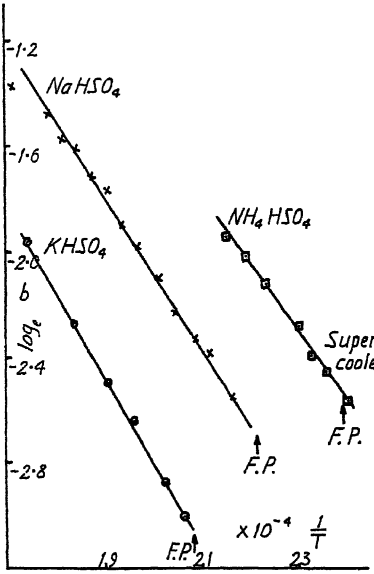

FIG. 2.—Log$_e$ σ against $1/T$ for acid sulphate melts.

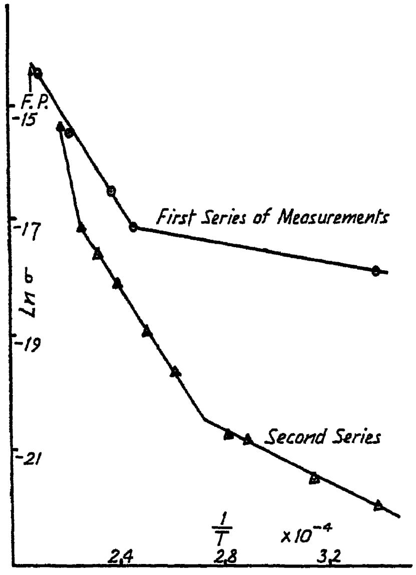

FIG. 3.—Log$_e$ σ against $1/T$ for solid $KHSO_4$.

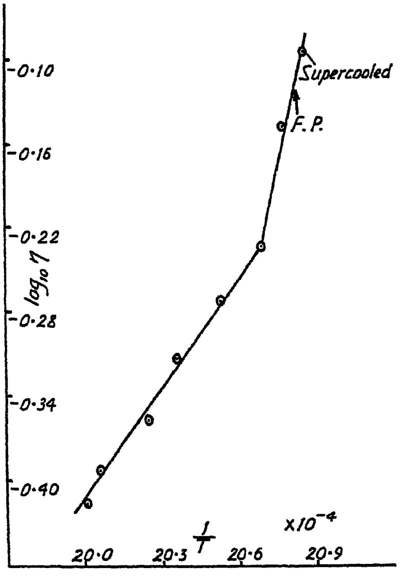

FIG. 4.—Log η against $1/T$ for $KHSO_4$ melt.

error was estimated at ± 0·4 % while at 134° it was ± 7·7 %. At room temperature it was possible to obtain results reproducible to ± 14 % when a series of measurements was taken without interruption. On leaving for some hours, variations of the extent of ± 80 % were found.

This is almost certainly to be attributed to changes such as migration of protons in the solid after passage of the current, which take time to disappear by diffusion at the lower temperatures. Changes of contact resistance at the electrodes may also occur on melting and re-freezing. The use of A.C. for these measurements of high resistances would have required special oscillators and bridges which were not available when the measurements were made, and would furthermore have introduced problems of dielectric behaviour of the solid which it was important to avoid.

Experiments showed that no simple interpretation of transport data could be made owing to the number of ions involved. Passage of current through the solids leads to visible whitening especially round the anode. Measurements of E.M.F. of primary cells showed normal behaviour and will not be described here in detail.

Plots of ln σ against $1/T$ for the three melts are given in Fig. 2. The plot of ln σ against $1/T$ for solid $KHSO_4$ is in Fig. 3. Calculated activation energies are dealt with in the Discussion.

Viscosity.—In order to avoid any risk of blocking capillaries by crystallites, near a fusion point, the method chosen for measuring relative viscosities was to time the rise of a float through the melt. The apparatus was essentially a simplified version of that described by Menary, Ubbelohde and Wright.[6] Measurements on molten $KHSO_4$ were repeated 4 or 5 times at the higher temperatures, about 8 times as the freezing-point was approached and 10 to 12 times in the immediate neighbourhood of the freezing-point where the mean deviation reached a maximum of ± 1·5 %.

Results are illustrated in Fig. 4 (log η against $1/T$). It will be seen that there is a rapid rise in viscosity in the region of the freezing-point. The activation energies for viscous flow have been calculated from the two straight portions of the curve and are given in Table I.

TABLE I.—ACTIVATION ENERGIES FOR VISCOUS FLOW IN $KHSO_4$

Temp. Range °C	E_η kcal./mole
207-210	38·9
210-226	12·0

Density.—A Pyrex dilatometer was used with solid $KHSO_4$. Medicinal paraffin was used as a confining fluid. This darkened very slightly after a few days' use. Absence of any lag in the expansion was verified by comparing heating with cooling curves. The maximum deviation between computed values from a straight line plot and experimental values was 0·12%. The density of $KHSO_4$ was calibrated in A.R. benzene at 18° C. The salt was freed from air-holes by melting and allowing to solidify *in vacuo*. The molar volume curve is shown in Fig. 5. Results may be summarized as follows :

Coefficient of expansion above m.p. = $7{\cdot}67 \times 10^{-4}$.
" " below m.p. = $5{\cdot}33 \times 10^{-4}$.
Molar volume of liquid at m.p. = 65·7 cm.^{3}.
" " solid at m.p. = 63·05 cm.^{3}.
$\Delta V/V_s$ at m.p. = 0·04
Density at 18° C = 2·374 ± 0·006 g. cm.$^{-3}$.

No evidence could be obtained on the volume curve for transition points in the solid.[7, 8] The reason why the polymorphism did not make itself evident in the present experiments is not clear. Nuclei would be necessary for the appearance of a new solid phase and the liquid paraffin may have inhibited their formation. If $\Delta V/V$ at the transition point in the dilatometer used is less than 0·002 it would not be observed. An analogous suppression of polymorphic transitions has been described.[9] The constancy of dV/dt for constant mass at various temperatures agrees with the observations of Volarovich and Leont'eva [10] on other ionic melts.

---

[6] Menary, Ubbelohde and Wright, *J. Chem. Soc.*, 1948, 454.
[7] Kendall and Landon, *J. Amer. Chem. Soc.*, 1920, **42**, 2131.
[8] Bridgmann, *Proc. Amer. Acad. Sci.*, 1916, **52**, 89.

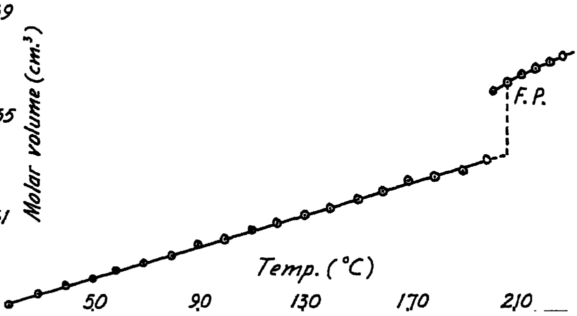

FIG. 5.—Thermal expansion of $KHSO_4$.

Analysis.—(*a*) X-RAY ANALYSIS.—$KHSO_4$ melt was smeared thinly over a glass cover slip and allowed to solidify. The large number of lines in the Debye-Sherrer photograph showed that the structure was more complex than the cubic, hexagonal, tetragonal or orthorhombic systems. Complete determination might prove a lengthy investigation. A precise comparison between the lattice density and the observed Archimedes density to determine the number of lattice flaws could not be made.

(*b*) QUANTITATIVE ANALYSIS OF THE SOLIDS showed that any systematic replacement of K by H or other lattice flaws was less than the scatter of the measurements (accuracy: K, ± 0·09 %; H, ± 0·002 %; SO_4, ± 0·14 %.)

(*c*) THERMAL DATA.—Conventional methods were used. A special feature was the insertion of an auxiliary heater in the melt to change dQ/dt under constant external conditions so as to calibrate the change in heat content during the arrest. A continuous stream of dry nitrogen was passed over the melt to prevent intake of moisture. Temperature readings to 0·1° C were taken using a mercury thermometer (stem at the temperature of the thermostat) at intervals of 10 sec. Results may be summarized as in Table II.

TABLE II.—THERMAL DATA

System	F.p. °C	Eutectic
$KHSO_4$	207·1	—
$NaHSO_4$	178·3	—
NH_4HSO_4	144·8	—
$KHSO_4$—$NaHSO_4$ . .	—	53·5 % $NaHSO_4$: 125° C
$KHSO_4$—NH_4HSO_4 .	—	83 % NH_4HSO_4 : 110·5° C

There was no evidence for compound formation. No arrests could be observed in the regions where polymorphic transitions have been reported by Kendall and Landon. Approximate entropies of fusion could be evaluated from the duration of the arrests. Owing, however, to the non-sharp change of slope at the end of the arrest, due to premelting, durations could not be assessed accurately. Various repeat experiments indicated that the entropy of fusion was of the order 14 to 20 cal./mole deg.

The occurrence of this premelting made a calorimetric method of obtaining more accurate heats of fusion rather unpromising. Detailed specific heat curves would have required more elaborate experiments than appeared to be warranted for the present purpose.

---

[9] Moesveld, *Z. physik. Chem. A*, 1937, **178**, 455.

[10] Volarovich and Leont'eva, *Compt. rend. U.R.S.S.*, 1935, **2**, 539.

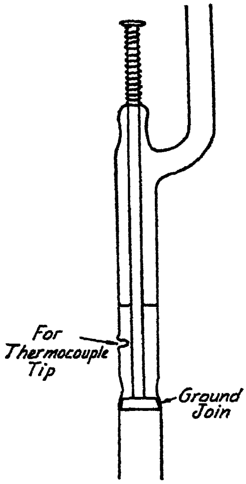

FIG. 6.—Method of mixtures apparatus.

For a closer estimate of the heat of fusion, the method of mixtures was applied. The release arrangement used is shown in Fig. 6. Some $KHSO_4$ powder was put in through the side-arm and the whole assembly weighed. It was heated by a metal tube furnace and the temperature of the melt was determined by a thermocouple in the pocket shown. After holding the melt at a convenient temperature for about 30 min. to promote uniformity, the spring was depressed and melt released into liquid paraffin in a Dewar flask. The rise in temperature was measured by a copper-constantan thermocouple. Continuous stirring was maintained. This rise was matched against the amount of electrical energy required to give the same rise in temperature (at about the same rate of heating) using a small immersion heater. The specific heat of solid $KHSO_4$ was taken from Kopp [11] and the specific heat of the melt was eliminated from pairs of experiments at different initial temperatures.

Although this mixture method is very approximate, it confirms the conclusion from the cooling curves that the entropy of fusion is high. From the times of duration of the arrests for the sodium and ammonium salts it is believed that they also have a high entropy of fusion.[11a] From this method the average of 6 results for $KHSO_4$ was 23·5 ± 3·2 cal./mole deg.

Discussion

Electrochemistry of the Melts.—CONDUCTIVITY.—Various types of behaviour have been described for ionic melts. For unassociated melts (e.g. alkali halides) an exponential relationship exists between conductivity and temperature: [12, 13]

$$\sigma = Ae^{-E/RT}, \quad . \quad . \quad . \quad . \quad (2)$$

where E is the energy necessary to effect the configurational change occurring in ionic migration and A is a constant.

For associated melts

$$\ln \sigma = B' - \frac{\beta'}{T}e^{b/T}, \quad . \quad . \quad . \quad . \quad (3)$$

where B', β' and b are constants.

Lowry [14] suggested that the high conductivity of molten AgCl is due to complex aggregates of ions carrying multiple electric charges, this probably representing an incomplete destruction of the lattice on melting (cf. the comparison between ionic melts and glasses [15]). The low conductivity of other melts is explained on a theory that on fusion the lattice breaks down into neutral ionic doublets (see also ref. (16)). This aggregation of ions in the melt has analogies with micelle formation and the melting may in the first instance be to micelles.

The results of the present work show that the conductivities of the acid sulphate melts have an exponential relationship with temperature as in (2) above (Table III). On this basis, the melts are substantially non-associated. However, viscosity results (see later) indicate micellar melting. This appears to have little effect on the values of E for the melt, since the E values for solid $KHSO_4$ are in any case small. But the A values are very different for $KHSO_4$ and for KCl (see Table VI).

---

[11] Kopp. *Phil. Trans. A*, 1865, **155**, 71.

[11a] Shemate and Naylor, *J. Amer. Chem. Soc.*, 1945, **67**, 72, who gave 8·2 cal./ mole deg. for $(NH_4)HSO_4$.

[12] Heymann and Bloom, *Nature*, 1945, **156**, 479.

[13] Evstrop'ev, *Bull. Acad. Sci. U.R.S.S., Classe sci. math. nat., Sér. phys.* 1937, **3**, 359.

[14] Lowry, *Phil. Mag.*, 1928, **5** (7), 1072.

[15] Kaneko, *J. Chem. Soc. Japan*, 1938, **59**, 673.

[16] Walden, *Z. physik. Chem. A*, 1931, **157**, 389.

[17] Biltz and Klemm, *Z. anorg. Chem.*, 1926, **152**, 267.

TABLE III.—ACTIVATION ENERGIES OF IONIC MIGRATION IN $MHSO_4$ MELTS

Melt	E_σ kcal./mole	A in $\sigma = Ae^{E_\sigma/RT}$ σ in ohm^{-1} cm.$^{-1}$
$KHSO_4$	6·2	33
$NaHSO_4$	5·7	38
NH_4HSO_4	5·3	43
KCl[17]	2·3	6·5

VISCOSITY.—Molten salts seem to fall into the categories of "normal" and "associated" with respect to their viscosity-temperature relation. Simple melts like NaCl and KNO_3 belong to the normal type [12, 18, 19] and are governed by the usual exponential formula

$$\eta = Ae^{-E_\eta/RT} . \quad . \quad . \quad . \quad . \quad . \quad (4)$$

Other melts such as silicates which may contain chain structures require more complicated expression.[18, 20, 21, 22] As yet no satisfactory equations seem to have been proposed.

Present results for $KHSO_4$ show that η is anomalous in the region of the freezing point. Two values for the activation energy of viscosity have been calculated, one well above and one just above the melting point. Comparisons with simpler melts are made in Table IV.

TABLE IV.—ACTIVATION ENERGIES OF σ AND η

Melt	E_σ kcal./mole	A_σ	E_η kcal./mole
$KHSO_4$ just above m.p.	6·2 over whole	33	38·9
$KHSO_4$ well above m.p.	temp. range studied		12·0
KCl [22]	2·3	6·5	7·8
$CaCl_2$ [22]	4·1	13·5	9·5

The value of E_η for $KHSO_4$ just above the melting point is of the same order as that for silicate melts studied by Bockris *et al.*,[22] suggesting the existence of chains of ions in the melt. The fact that E_η is greater than E_σ agrees with the observation of Heymann and Bloom [12] that this is generally the case. It may be that for $KHSO_4$ the energy barrier for viscosity involves the K^+, HSO_4^- and $SO_4^=$ ions, while the energy barrier for conductivity involves the very much smaller H^+ ions.

Properties of Lattice Flaws in $MHSO_4$ in Relation to Simpler Ionic Structures.—It seemed probable that the low melting-points of these acid sulphates might be attributed to the ease of formation of certain types of lattice defects in crystals containing protons. The simplest example is a *substitutional* defect, where a proton is substituted in the proper position for an alkali ion and the stoichiometric composition is altered to

---

[18] Volarovich, *Bull. acad. sci. U.R.S.S. Classe sci. math. nat.*, 1933, 1431.

[19] Ipatov, *J. Physic. Chem.* (*U.R.S.S.*), 1934, **5**, 790.

[20] Waller, *Phil. Mag.*, 1934, **18**, 579.

[21] Leont'eva, *J. Physic. Chem.* (*U.S.S.R.*), 1938, **11**, 310.

[22] Bockris, Kitchener, Ignatowicz and Tomlinson, *Faraday Soc. Discussions*, 1948, **4**, 265.

correspond. Since this would preserve electrostatic neutrality, and since the proton occupies less space than the M^+ ion, the energy change on substituting H^+ for M^+ might be expected to be small compared with the more familiar defect flaws in simple ionic lattices. Such substitutional flaws should therefore be numerous in acid salts.

Again, owing to the small size of the protons compared with the other alkali ions, it might be expected that H^+ could enter with particular ease into *interstitial* positions. It would be anticipated that electrical conduction in the solid and in the ionic melt of these acid salts would be largely due to migration of the protons.

It has been suggested that a measure of crystal imperfections may be obtained from the ratio σ (above m.p.)/σ (below m.p.). The larger the values the more perfect is the lattice.[23] Whatever interpretation is given to these figures it seems clear from Table V that the lattice flaws in $KHSO_4$ are exceptionally mobile but not very numerous.

TABLE V.—RATIO σ (ABOVE M.P.) σ (BELOW M.P.)

System	$\frac{\sigma \text{ above m.p.}}{\sigma \text{ below m.p.}}$
NaCl [22]	3×10^3
$CdCl_2$ [22]	2×10^2
AgCl [22]	3×10^1
1/1 CaO—SiO_2 [22]	2×10^2
1/1 MnO—SiO_2 [22]	3×10^2
$KHSO_4$	7×10^4

Energy Required for the Formation of Flaws and for their Migration in the Crystal.—Various kinds of defects generally recognized in a crystal lattice include Frenkel defects, Schottky defects, and co-operative defects.[24] The concept of lattice defects throws considerable light on the interpretation of the observed values of electrical conductivity σ in ionic crystals for which previous work has shown that the plot of log σ against $1/T$ consists of two different slopes, the high temperature slope being about three times that at low temperatures. All explanations of this effect involve two different physicochemical mechanisms of ionic transport in the solid. One view (cf. Mott and Gurney [25] and especially Seitz [26]) is that at low temperatures the observed activation energy is the energy required for the migration of flaws in the crystal, the number of flaws "frozen in" being unchanged with temperature. At higher temperatures work must be done in forming *fresh* flaws just below the melting-point. These ideas are represented quantitatively by the equations :

$$\sigma = A_{U_0} e^{-U_0/kT} \text{ (low temp.)}, \qquad (5)$$

$$\sigma = A_{W_0} e^{-(\frac{1}{2}W_0+U_0)/kT} \text{ (high temp.)}, \qquad (6)$$

where U_0 = potential barrier opposing ionic migration and
W_0 = energy of formation of fresh flaws.

The slopes of the log σ against $1/T$ curve enable calculation of U_0 and W_0 to be made. Alternative explanations in terms of motion over internal cracks or the effect of impurities are discussed by Mott and Gurney.[25]

The explanation given by Phipps, Lansing and Cooke [27] for Na halides was that at low temperatures only the Na^+ ion carried current, while for the higher temperature range both anions and cations were conducting. This was confirmed by subsequent transport measurements on NaCl by Phipps and Leslie.[28] For $KHSO_4$ the matter is more complicated, owing to the variety of ions which could take part at different temperatures.

---

[23] Bockris *et al., loc. cit.*; Hevesy, *Handbuch der Physik*, 1928, **13**, 289.

[24] Oldham and Ubbelohde, *Proc. Roy. Soc. A*, 1940, **176**, 50.

[25] Mott and Gurney, *Electronic Processes in Ionic Crystals* (Oxford, 1940), p. 26.

[26] Seitz, *Modern Theory of Solids* (McGraw-Hill Book Co., Inc., 1940), p. 555.

[27] Phipps, Lansing and Cooke, *J. Amer. Chem. Soc.*, 1926, **48**, 112.

Values of U_0, A_{U_0}, W_0 and A_{W_0} have been calculated for solid $KHSO_4$ for comparison with some typical values of other salts (comparison results in Table VI have been calculated from experimental data in the literature). The values of E and U_0 and W_0 are inter-related as follows :

$$\frac{E \text{ (lower)}}{R} = \frac{U_0}{k} \text{ (}E\text{ is in cal., }k\text{ is Boltzmann's constant).}$$

$$U_0 = \frac{E \text{ (lower)}}{N} \text{ (where }N\text{ is Avogadro's number)}$$

$$= E \text{ (lower)} \times 0{\cdot}693 \times 10^{-13} \text{ erg/molecule.}$$

$$\text{Similarly, } \tfrac{1}{2}W_0 + U_0 = E \text{ (upper)} \times 0{\cdot}693 \times 10^{-13} \text{ erg/molecule.}$$

TABLE VI.—FLAW ENERGIES (SOLIDS)

Salt	U_0 10^{13} erg mole	A_{U_0}	$W_0 \times 10^{13}$	A_{W_0}
$KHSO_4$ Sample (i) .	1·2	$3{\cdot}5 \times 10^{-7}$	19·0	6·8
Sample (ii) .	3·4	$11{\cdot}5 \times 10^{-7}$	12·5	0·35
KCl[29]	13·4	0·1	46·9	2×10^{7}
NaCl[27].	13·9	0·45	27·2	$9{\cdot}5 \times 10^{4}$
KBr[30]	15·4	$1{\cdot}1 \times 10^{-2}$	31·8	1×10^{6}
NaBr[27]	12·7	0·19	27·6	7×10^{5}
AgBr[29]	5·4	$4{\cdot}5 \times 10^{-3}$	10·3	$8{\cdot}5 \times 10^{3}$
TlCl (only one slope) [30]	11·5	4×10^{2}	—	—
$PbCl_2$ (,, ,,) [31]	7·4	1·4	—	—

A number of points appear about the conductivity in solid $KHSO_4$:

(*a*) The activation energy for migration at low temperatures appears to be the lowest yet observed. The fact that it varies from one sample to another for the lower slope has been previously reported for other salts.[29, 32] In this case it may be due to slight variations in the ratio of K^+ to H^+ in the salt.

(*b*) It is noteworthy that the small values of U_0 are associated with exceptionally small values of A_{U_0}. Similar correlation between the activation energy and the temperature independent term is found for other physicochemical properties, e.g. rates of reaction (cf. Hinshelwood [33]).

(*c*) The values of W_0 fall within the range exhibited by the other salts listed.

The present values do not permit a final distinction between the mechanisms :

(i) of flaw migration at low temperatures and flaw formation at high temperatures, and

(ii) the mechanism of transport by the single ion at low temperatures and by both ions at high temperatures. However, the very big ratio of A_{W_0} to A_{U_0} is more simply interpreted on the first of these hypotheses, particularly if transport is predominantly due to hydrogen ions at low temperatures.

---

[28] Phipps and Leslie, *J. Amer. Chem. Soc.*, 1928, **50**, 2412.

[29] Lehfeldt, *Z. physik*, 1933, **85**, 717.

[30] Phipps and Partridge, *J. Amer. Chem. Soc.*, 1929, **51**, 1331.

[31] Gyulai, *Z. physik*, 1931, **67**, 812.

[32] Smekal, *Handbuch der Physik*, 1933, **24**, 881.

[33] Hinshelwood, *The Kinetics of Chemical Change* (Oxford, 1940), p. 257.

Melting Parameters of $MHSO_4$ in Relation to Simpler Ionic Structures.—(*a*) CHANGE OF VOLUME ON MELTING.—Values now obtained for $\Delta V/V_s$ are compared with salts of simpler ionic structure in Table VII. The very small value of $\Delta V/V_s$ for $KHSO_4$ compared with NaCl and KCl is further evidence for structural anomalies in the region of the melting point and supports the conclusions drawn from viscosity data. Abnormally small values of volume increase on melting are found for example with crystals which maintain an open system of hydrogen bonds which collapse on melting, e.g. ice where the volume change on melting is actually negative and the behaviour of the liquid above the f.p. is anomalous, and resorcinol.[35] Although the structure of $KHSO_4$ is not known, it is likely that it involves a framework of hydrogen bonds.

TABLE VII.—VOLUME CHANGES ON MELTING

Substance	$\Delta V/V_s$
$KHSO_4$.	0·04
NaCl[34] .	0·30
KCl[34] .	0·23
Na metal[34]	0·027

(*b*) ENTROPY OF FUSION.—Determinations of latent heat of fusion give an indication of the relative change in order occurring on melting. The present value for $KHSO_4$ is compared with those for simpler salts in Table VIII.

TABLE VIII.—ENTROPY OF FUSION COMPARISONS

Salt	Melting Point (° C)	Entropy of Fusion (cal./mole deg.)
$KHSO_4$ . .	207·1	23·5 ± 3·2
NaCl[34] . .	800	3·35
KCl[34] . .	769	3·08
$NaNO_3$[36] . .	308	6·09
KNO_3[36] . .	333	4·42

Main Conclusions.—Two factors relating to the origin of the low melting points of $MHSO_4$ salts have been referred to:

(i) The energy of flaw formation is small compared, for example, with that of KCl. If $KHSO_4$ had the same simple ionic structure as KCl melting would follow a mechanism similar to that discussed for the inert gases by Lennard-Jones and Devonshire.[37] But the temperature of critical breakdown of the solid is lower the lower the energy of flaw formation.

(ii) The entropy of fusion of $KHSO_4$ is exceptionally large. It is a general rule that large entropies of fusion are correlated with lower melting points. Large entropy changes S_f on fusion permit equality of the free energies of liquid and solid at lower temperatures than with solids with the same heat of fusion but where $S_f (= R \ln (W_L/W_s))$ is smaller (cf. Ubbelohde[38]).

---

[34] Eucken, *Z. angew. Chem.*, 1942, **55**, 163.
[35] Robertson and Ubbelohde, *Proc. Roy. Soc. A*, 1938, **167**, 136.
[36] Goodwin and Kalmus, *Physic. Rev.*, 1909, **28**, 1.
[37] Lennard-Jones and Devonshire, *Proc. Roy. Soc. A*, 1939, **169**, 317.
[38] Ubbelohde, *Ann. Reports*, 1939, **36**, 150; *ibid.*, 1940, **37**, 167.

Till the detailed structure of $KHSO_4$ has been worked out it would be premature to interpret the large entropy change more closely. But it seems likely in view of the viscosity data that the protons in $KHSO_4$ maintain a rigid framework in the solid, by hydrogen bonding, and that the breakdown of configurational order of the SO_4 groups leads to additional entropy changes on melting, not available for simpler structures such as KCl where there is a change of positional entropy but no change of configurational entropy of the ions. The viscosity data suggest that the breakdown of configurational order on melting is not quite completed on melting but persists for a few degrees in the melt. This suggestion would imply that near the freezing point the structure of $KHSO_4$ is more complex than in the simple model of Lennard-Jones and Devonshire and has analogies with a molten glass.

Thanks are due to the Chief Scientist, Ministry of Supply, for permission to publish.

Chemistry Department,
Queen's University,
Belfast.

THE NATURE OF PRECIPITATED CALCIUM PHOSPHATES

By P. W. Arnold

Received 31*st March,* 1950 ; *as revised* 15*th June,* 1950

The absolute concentrations as well as the relative amounts of calcium and phosphorus determine the direction in which equilibrium conditions are approached in the $CaO—P_2O_5—H_2O$ systems examined. A solid of atomic ratio $Ca/P = 1{\cdot}33$ (octocalcium phosphate), was found to be the least basic of the apatite-like precipitates. It is probably a hydrated infinite two-dimensional complex with sheets held together by water molecules, $Ca_4H(PO_4)_3 . 3H_2O$. Solids with atomic ratios Ca/P ranging from 1·0 to 1·33 consist of at least two phases ; dicalcium phosphate and a solid at least as basic as octocalcium phosphate.

On structural grounds it appears possible that a continuous series of apatite-like solid solutions can exist between octocalcium phosphate and hydroxy- (or fluor-) apatite. In practice, no two preparations with composition lying between octocalcium phosphate and hydroxyapatite are likely to be identical.

The existence of precipitated calcium phosphates more basic than hydroxyapatite, the high loss on ignition of hydroxyapatites and the high fluorine contents of many natural sedimentary phosphates are explained on the hypothesis that thin sheets of apatite structure sorb hydroxyl or other anions where the calciums of the apatite lattice are exposed. Some evidence is obtained of complex ion formation in calcium phosphate solutions in which the atomic ratio Ca/P exceeds 0·5.

The interpretation of chemical data on phosphorus problems in soils and fertilizers is limited by lack of information on the fundamental equilibria of the calcium phosphates in water. Although sorption by soil colloids may be the principal factor responsible for the immobilization of water-soluble phosphates added as fertilizers, it is possible, at least in soils containing calcium carbonate, that dicalcium phosphate and more basic phosphates may be formed, perhaps with fluorapatite or hydroxyapatite as end-products. Further information on the composition, crystal structures and solubilities of the more basic calcium phosphates might throw new light on other fertilizer problems and also have some bearing on such questions as the formation of bone and the natural phosphorite deposits. As many of the calcium phosphates of agricultural and geochemical interest may be unstable, useful information may be provided from systems which have not reached equilibrium.

Crystalline mono- and dicalcium phosphates were recognized at an early date. Warington[1] was the first to establish that the prolonged hydrolysis of any calcium phosphate resulted in the formation of a solid of composition 10 $CaO . 3P_2O_5 . H_2O$ (or $Ca_5(PO_4)_3OH$) which he realized was an apatite. This material retained water even after strong ignition. The formation of a tricalcium phosphate by precipitation has been questioned by many workers. The arguments were reviewed by Eisenberger *et al.*[2] in 1940. Whereas Bassett[3, 4] supported the existence of a precipitated tricalcium phosphate, Trömel and Möller[5] regarded solids of the $Ca_3(PO_4)_2$ composition as hydroxyapatite with sufficient adsorbed phosphate to yield approximately this composition. Bredig *et al.*[6] thought it probable that precipitated tricalcium phosphate was composed of mixed crystals of hydrated $Ca_3(PO_4)_2$ of variable water content and hydroxyapatite with some adsorbed phosphate. Hendricks and his co-workers[7] concluded that precipitated tricalcium phosphate was an " aquo-apatite ", $Ca_9(PO_4)_6(H_2O)_2$, and that a complete series of solid solutions was formed between this material and hydroxyapatite. In their review Eisenberger *et al.* decided that the most satisfactory assumption was that " between dicalcium phosphate and lime there exists, in the ternary system, a continuous series of solid solutions having an apatite lattice ". It would follow, therefore, that tricalcium phosphate and hydroxyapatite do not exist in aqueous systems as unique stoichiometric compounds. Such a generalization requires further critical study. Various less basic calcium phosphates have received attention, including one of atomic ratio Ca/P= 1·33. Warington[8] drew attention to a material $Ca_4H(PO_4)_3$ which he termed octocalcic triphosphate or octocalcium phosphate. He encountered a solid of almost this composition when a surface film was formed during the slow loss of carbon dioxide from a calcium phosphate-rich solution. Bjerrum[9] referred to the same material as a theoretically important laboratory product and gave values for the solubility products of dicalcium phosphate, octocalcium phosphate and hydroxyapatite without, however, giving sufficient experimental evidence on their nature or conditions of formation. It is interesting to note that he was obliged to consider two values for the solubility products of both octocalcium phosphate and hydroxyapatite depending on whether the solids were precipitating or dissolving.

The extreme slowness with which equilibrium conditions are approached introduces the chief experimental difficulty in many of the investigations described in the literature. Other complications arise from the fact that calcium phosphate solutions tend to be supersaturated and to yield gelatinous solids difficult to isolate. In precipitating calcium phosphate solutions the trends in the pH values of the liquid phases may, perhaps, be taken as a rough index of the approach to equilibrium. Some pH determinations carried out by the writer on precipitating mixtures in which the atomic ratios Ca/P for the whole systems varied over the range 0·7 to 2·0 gave steady values in about one week. However, especially in the more basic systems small but significant changes in pH have been recorded over a period of a year.

---

[1] Warington, *J. Chem. Soc.*, 1873, **26**, 983.

[2] Eisenberger, Lehrman and Turner, *Chem. Rev.*, 1940, **26**, 257.

[3] Bassett, *Z. anorg. Chem.*, 1908, **59**, 1.

[4] Bassett, *J. Chem. Soc.*, 1917, **111**, 620.

[5] Trömel and Möller, *Z. anorg. Chem.*, 1932, **206**, 227.

[6] Bredig, Franck and Füldner, *Z. Elektrochem.*, 1932, **38**, 158.

[7] Hendricks, Hill, Jacob and Jefferson, *Ind. Eng. Chem.*, 1931, **23**, 1413.

[8] Warington, *J. Chem. Soc.*, 1866, **19**, 296.

[9] Bjerrum, *Skand. Naturforskermode, Helsingfors*, 1936, Beretning S., 344.

An examination was made of some partially equilibrated calcium phosphate water systems in which the solid was at least as rich in calcium as dicalcium phosphate. Attention was directed towards both the solid and liquid phases as far as possible.

Experimental

Phosphoric Acid-Calcium Hydroxide Titrations at Constant Volume.—Fixed quantities of either phosphoric acid or monocalcium phosphate solutions were treated with varying quantities of saturated calcium hydroxide and made up to a fixed volume (generally 100 ml.). The mixtures were rotated end-over-end for at least one week before the liquid phases were separated with the aid of an insertion filter and analyzed for calcium and phosphorus. Precautions were taken to prevent carbon dioxide from entering the mixtures. The Ca/P ratios in the solids were calculated from the differences between the total amounts of calcium and phosphorus used and the amounts found in the solutions. Calcium was estimated volumetrically after precipitation as oxalate at pH 4·5. The use of standard ceric sulphate and 0·02 N ferrous ammonium sulphate (orthophenanthroline ferrous ion indicator) was found to be preferable to a permanganate titration. Phosphorus was estimated by the molybdenum-blue method[10] using a Spekker photoelectric absorptiometer. The pH values

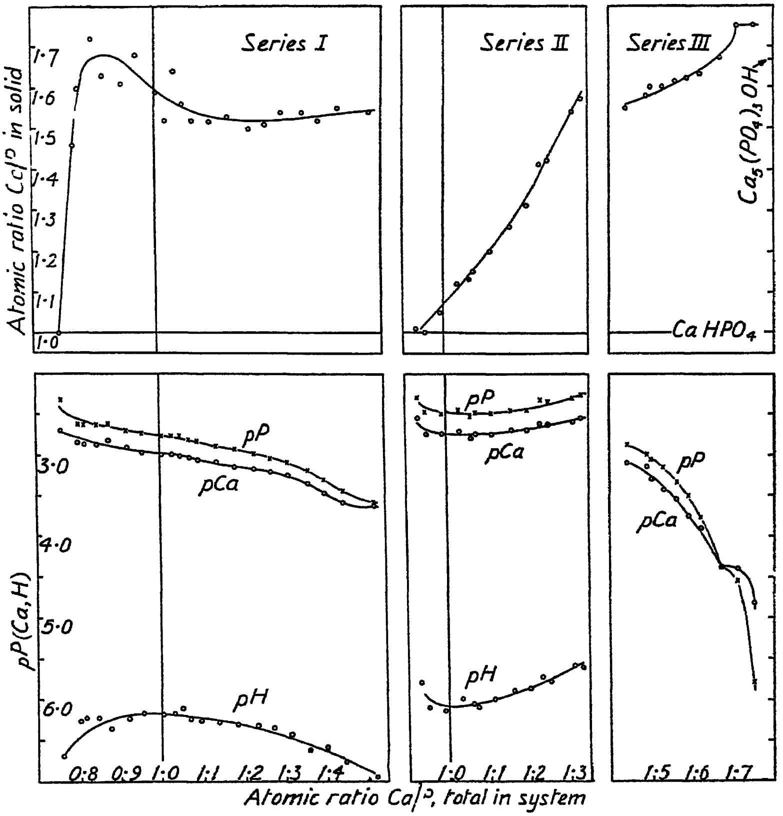

FIG. 1.

---

[10] Truog and Meyer, *Ind. Eng. Chem.* (*Anal. ed.*), 1929, **1**, 136.

of solutions were determined electrometrically (portable Cambridge pH meter; glass/saturated calomel standard electrode). The experiments were carried out at room temperature (15-22° C). The results from three series are summarized in Fig. 1, the total quantities of phosphorus in the systems being—

Series I, 3·1 milli-atoms per litre, initially as H_3PO_4.
Series II, 25·0 milli-atoms per litre, initially as $Ca(H_2PO_4)_2$.
Series III, 9·8 milli-atoms per litre, initially as H_3PO_4.

The pH values in Fig. 1 for series I and II may be regarded as titration curves at constant volume. The pH values in the more alkaline ranges of series III were too indefinite to be recorded. Fig. 1 also gives the atomic ratios for all solids and the compositions of the solutions expressed as the negative logarithms of gram-atoms per litre (pCa and pP). The data show that in systems approaching equilibrium after one week the composition of the precipitate depends on the absolute concentrations of the initial solutions as well as on their Ca/P ratios. Systems with total calcium and phosphorus in atomic ratios of between 0·9 and 1·0 gave precipitates approximating in composition to hydroxyapatite in the most dilute solutions (series I), but to dicalcium phosphate in the most concentrated solutions (series II). It is well known that precipitating systems of calcium hydroxide and phosphoric acid give more acid solutions than corresponding mixtures of sodium hydroxide and phosphoric acid because the calcium phosphate precipitates have a wider Ca/P ratio than the solutions from which they separate. This may be sufficient to account for curves with anomalous points of inflexion in the titration of phosphoric acid with calcium hydroxide (see e.g. 11, 12, 13). In Fig. 1 increasing additions of calcium hydroxide gave more acid solutions in the early stages of series I and the later stages of series II, i.e. in regions where the precipitates contain more calcium than dicalcium phosphate. If the atomic ratio Ca/P in a system is of the order 1·0 and a basic solid is precipitated, for example, hydroxyapatite,

$$Ca^{++} + HPO_4^{--} + XH_2O \rightarrow XCa_5(PO_4)_3OH + (1 - 5x)Ca^{++} + (1 - 3x)HPO_4^{--} + 4xH^+,$$

the Ca/P ratio of the solution changes from 1·0 to $(1 - 5x)/(1 - 3x)$. The increase in pH through the addition of more calcium hydroxide will be offset by acidification depending on both the composition and the amount of the calcium phosphate precipitated.

Complex Ion Formation.—For pH values below about 6·0 there was fair agreement between the observed pH values and those calculated from the calcium and phosphorus contents of the solutions and the second dissociation constant of phosphoric acid ($pK_2 = 7{\cdot}22$, neglecting effects of ionic strength). For pH values above 6·0 in series I the experimental values were always less than the calculated ones. As shown in Fig. 2 the discrepancies increased with the pH value. This anomaly might be explained by postulating the existence of a colloidal basic phosphate or a complex anion containing calcium. Bjerrum [9] suggested that an ion of the type $Ca(HPO_4^-)_2$ might account for up to 10 % of the dissolved calcium. To examine this possibility conductometric measurements were made on unsaturated solutions of dicalcium phosphate which behaved as a moderately strong electrolyte. A rough correlation between conductometric and potentiometric measurements was obtained if considerable proportions of some form of complex calcium phosphate ion were included in the equilibria. Postulating the existence of a complex of the type $CaPO_4^-$ (or $(CaPO_4^-)_m$), with an equivalent ion conductance similar to other charged complex ions (20-30 ohm^{-1} $cm.^2$), it appeared that the balance between the ionic entities in solutions of atomic ratio Ca/P = 1·0 (pCa = 3·4 approximately) would fall between the amounts in (1) and (2).

$$3Ca^{++} + CaPO_4^- + 2HPO_4^{--} + H_2PO_4^- \quad . \quad . \quad . \quad (1)$$

$$4Ca^{++} + CaPO_4^- + 3HPO_4^{--} + H_2PO_4^- \quad . \quad . \quad . \quad (2)$$

The fact that experimental Ca/P ratios in solution (where the values exceeded 0·5) were larger than the ratios calculated from the experimental pH values was in accord with the suggested formulation. A detailed study of the problem is necessary before any accurate conceptions regarding the equilibria in solution can be formulated.

[11] Wendt and Clarke, *J. Amer. Chem. Soc.*, 1923, **45**, 881.
[12] Holt, La Mer and Chown, *J. Biol. Chem.*, 1925, **64**, 509.
[13] Britton, *J. Chem. Soc.*, 1927, 614.

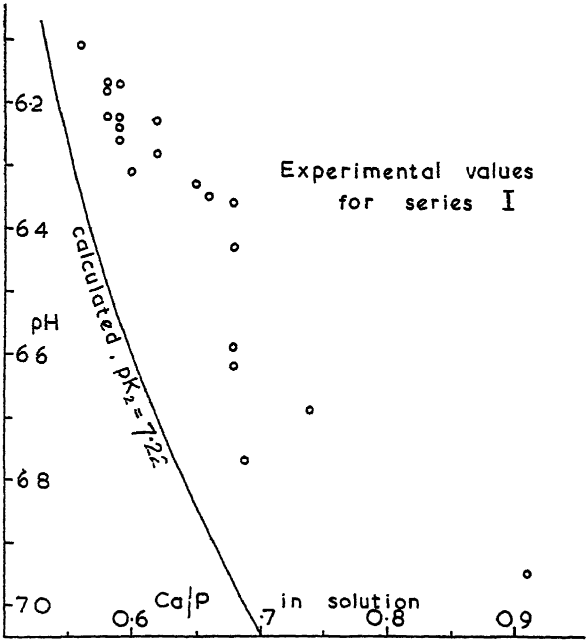

FIG. 2.

Preparation of Precipitated Calcium Phosphates.—A number of preparations were made under controlled conditions to provide precipitates for detailed study.

PRECIPITATED HYDROXYAPATITE.—An attempt was made to prepare a sample of hydroxyapatite using a modification of the slow crystallization process described by Kazakov.[14] Calculated quantities of solutions of calcium acetate and ammonium phosphate, containing additional free ammonia, were simultaneously introduced at a slow rate into about 10 l. of mechanically stirred CO_2-free ammonium acetate. Account was taken of the calcium and phosphate necessary to saturate the ammonium acetate which was M/20 with respect to acetate when the additions were complete. The pH of the system was maintained above 7·0 throughout the precipitation which was extended over 8 hr. The mixture was stirred for two days before the solid was withdrawn and washed with large quantities of distilled water. Analysis of the solid showed that the atomic ratio, Ca/P = 1·66, corresponded very closely with the theoretical hydroxyapatite composition. About 0·7 g. of solid were obtained from each litre of solution. After a preliminary drying at 100° C a sample of the solid was dehydrated in an electric muffle furnace. The temperature of the furnace was maintained at a series of suitable values until constant weight had been attained in each instance. The water remaining in the solid at each temperature, expressed as molecules H_2O per six P atoms, is shown in Fig. 3. A pronounced break in the dehydration curve is apparent. The loss in weight (2·07 %) between 1230° C and 1400° C is almost certainly due to the break-up of hydroxyl groups in the lattice. Above 1500° C a loss of P_2O_5 occurred. A sample of the solid dried at 100° C (S. 16) was included in the X-ray examination.

OCTOCALCIUM PHOSPHATE.—Although the addition of disodium phosphate Na_2HPO_4 to calcium chloride leads to the formation of dicalcium phosphate dihydrate, a reversal of the procedure produces a more basic solid. Warington [8] stated that octocalcium phosphate, $Ca_4H(PO_4)_3$, was formed in this way provided the mixtures remained alkaline. This has been confirmed by the writer. The pH values of mixtures remained substantially above 7·0 and solids of almost the theoretical octocalcium phosphate composition were obtained when the molar proportions of $CaCl_2$ to Na_2HPO_4 ranged from 1/3 to 1/12. The data in Table I indicate that the precipitates separated after various periods of equilibration (molar proportions of $CaCl_2/Na_2HPO_4$ = 1/12) contained more calcium than is required by the empirical formula $Ca_4H(PO_4)_3$, however, this was to be expected because the materials had been repeatedly washed with water.

---

[14] Kazakov, *Trans. Sci. Inst. Fertilizers and Insectofungicides* (U.S.S.R.), 1937, No. 139.

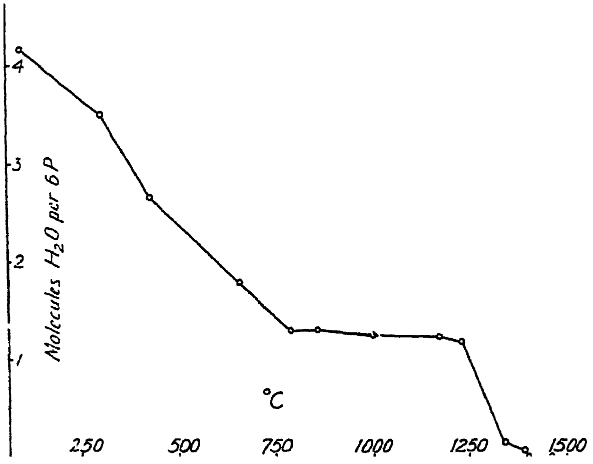

Dehydration of Hydroxyapatite (S. 16)

FIG. 3.

TABLE I.—ADDITION OF M/10 $CaCl_2$ TO M/10 Na_2HPO_4 (MOLAR PROPORTIONS 1/12) WITH VIGOROUS STIRRING

Time of Equilibration	Atomic Ratio Ca/P in Solid	% H_2O retained above 80° C
5 min.	1·38	9·20
6 hr.	1·46	8·50
12 „	1·41	8·78
2 days (S. 19)	1·34	11·45
8 „	1·39	10·40

It was interesting to note that when moist films of these solids were permitted to dry, the horny appearance of the dried films suggested that the solids might possibly possess a platey structure.

PRECIPITATES FORMED BY ADDING CALCIUM HYDROXIDE TO PHOSPHORIC ACID WITH RAPID MIXING.—The addition of saturated calcium hydroxide to phosphoric acid (20 millimolar) resulted in the formation of gelatinous precipitates which could usually be separated by centrifuging at 3000 rev./min. for 2 min. For mixtures with atomic ratios Ca/P ranging from about 0·8 to 0·95 the solids isolated within 2 min. of mixing ranged in composition from Ca/P = 1·22 to 1·48. One solid, Ca/P = 1·30 (S. 20), was dried below 100° C and reserved for X-ray powder diffraction examination. The rapid addition of large excesses of calcium hydroxide to dilute phosphoric acid resulted in the formation of basic precipitates which could occasionally be separated by centrifuging at 3000 rev./min. Two precipitates obtained in this manner were washed once with water and dried below 100° C. Both materials (S. 26 and S. 28), Ca/P = 1·95, which were considerably more basic than hydroxyapatite, were reserved for X-ray examination.

PARTIALLY EQUILIBRATED PRECIPITATES.—Solids for X-ray diffraction examination were prepared using the method outlined for obtaining the data in Fig. 1, series II. The mixes were rotated end-over-end for one week before the solids were separated and dried at 60° C (Table II). Sample S. 4 consisted entirely of well-defined crystals of dicalcium phosphate dihydrate (brushite).

TABLE II

Sample	Solution		Atomic Ratio Ca/P in Solid
	pCa	pP	
S. 10	2·65	2·43	1·34
S. 9	2·65	2·41	1·33
S. 8	2·66	2·42	1·21
S. 7	2·63	2·38	1·17
S. 4	—	—	1·00

X-RAY POWDER DIFFRACTION PATTERNS.—The following materials were examined :

S. 16, Ca/P = 1·66 precipitated hydroxyapatite.
S. 19, ,, = 1·34 from $CaCl_2$ and Na_2HPO_4.
S. 20, ,, = 1·30 calcium hydroxide and phosphoric acid.
S. 10, ,, = 1·34 calcium hydroxide and $Ca(H_2PO_4)_2$ solution.
S. 9, ,, = 1·33 ,, ,, ,,
S. 8, ,, = 1·21 ,, ,, ,,
S. 7, ,, = 1·17 ,, ,, ,,
S. 4, ,, = 1·00 dicalcium phosphate dihydrate.

S. 26 and S. 28, Ca/P = 1·95 calcium hydroxide and phosphoric acid.

The X-ray powder diffraction photographs of the finely ground solids were obtained using an X-ray tube operated with a copper target and nickel filter (CuK_α radiation, $\lambda = 1{\cdot}54$ Å). The *d* values were obtained in the usual manner. The relative intensities of the lines was estimated by eye. The results are represented graphically in Fig. 4, the *d* values being plotted as abscissae against the intensities of the diffraction pattern lines as ordinates. By a comparison of the positions and intensities of the lines on the diagrams it is possible to make the following generalizations. The precipitates approximating in composition to octocalcium phosphate exhibited diffraction patterns remarkably like that of hydroxyapatite (S. 16, Ca/P = 1·66). Sample S. 19 (Ca/P = 1·34) exhibited three faint lines (*d* = 2·26, 4·23 and 7·68 Å), which corresponded

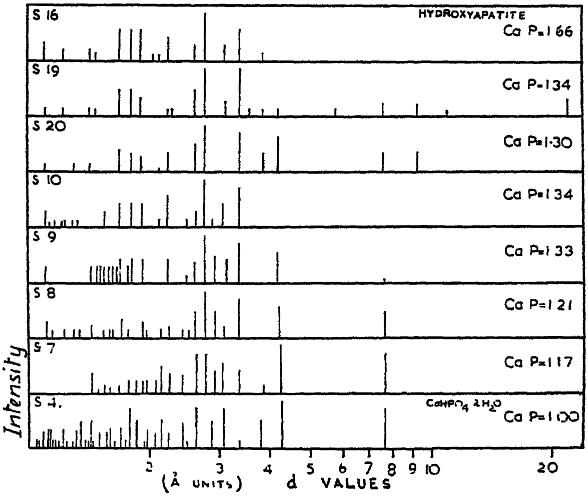

FIG. 4.

quite closely with intense lines of dicalcium phosphate dihydrate ($d = 2{\cdot}25$, 4·25 and 7·63 Å). Additional lines absent in both the dicalcium phosphate and hydroxyapatite patterns were found to represent d values of 2·31, 3·60, 5·86, 9·33, 11 and 22 Å. For sample S. 20 (Ca/P = 1·30) most of the lines characteristic of a hydroxyapatite were present together with four additional lines, three of which (2·14, 4·22 (diffuse) and 7·7 Å) agreed closely with lines present in dicalcium phosphate. The other line ($d = 9{\cdot}34$ Å) corresponded with the 9·33 line present in the pattern for sample S. 19. It is concluded that the two solids S. 19 and S. 20 of approximately octocalcium phosphate composition may possess lattice structures akin to that of apatite. The large d values (S. 19 : 9·33, 11 and 22 Å ; S. 20 : 9·34 A), which are not commensurable with the ordinary apatite structure, may be connected with the observation recorded earlier in this paper on the platey nature of dried octocalcium phosphate. A possible sheet-like hydrated structure for octocalcium phosphate is discussed later in the paper.

From a similar comparison of the diffraction patterns of solids S. 7 to S. 10 with those of dicalcium phosphate dihydrate and hydroxyapatite it was apparent that the solids S. 7 (Ca/P = 1·17) and S. 8 (Ca/P = 1·21) were mixtures of dicalcium phosphate and an apatite-like material. The proportion of dicalcium phosphate was much less in solid preparations S. 9 (Ca/P = 1·33) and S. 10 (Ca/P = 1·34), the latter giving a pattern very similar to that of an apatite, but with two or three faint lines characteristic of pure dicalcium phosphate. One of the dicalcium phosphate lines ($d = 4{\cdot}2$ Å) in solid S. 9 was fairly strong but most of the others were extremely faint or absent, again indicating the presence of only a small proportion of dicalcium phosphate. It was concluded that the partially equilibrated solids with Ca/P ratios ranging from 1·0 to 1·33 (approximately) were composed of at least two crystalline phases, one being dicalcium phosphate dihydrate and the other exhibiting an apatite-like powder diffraction pattern. Precipitates of octocalcium phosphate composition were the least basic of the materials in which apatite-like powder diffraction patterns predominated.

The two very basic solids S. 26 and S. 28 (Ca/P = 1·95) gave powder diffraction patterns indicating that an apatite lattice was present but with diffuse lines expected from poorly developed crystals. There was no evidence to suggest that any solid phase other than an apatite-like one was being dealt with.

Precipitated Calcium Phosphates and the Apatite Crystal Lattice.—The calcium-phosphorus-fluorine configuration accepted for fluorapatite has remained fundamentally unchanged since Mehmel [15, 16] and Náray-Szabó [17] first reached agreement on the subject. Recently Beevers and McIntyre [18] corroborated the accepted crystal structure of fluorapatite and were able to locate certain components in the unit of structure with greater accuracy than was formerly possible. Owing to the similarity in size of the fluoride and hydroxyl ions, hydroxyapatite would be expected to have a structure closely similar to fluorapatite. The findings of Beevers and McIntyre gave little support to an earlier view summarized by McConnell [19, 20] in the following words : " the structure of an apatite seems to be remarkably stable, permitting a number of rather unusual types of substitution and involving a considerable number of ions ". In view of the fact that the solid of atomic ratio Ca/P = 1·33, empirically $Ca_4H(PO_4)_3$, was the least basic of the precipitates found by the writer to possess an apatite-like diffraction pattern, it is of interest to consider a possible apatite-like structure for this material and a mechanism by which it can take up additional calcium. In the established fluorapatite structure the calcium and phosphorus arrangement (omitting the oxygens) could be illustrated by Fig. 5c in which more than the " unit cell " is drawn. There are two types of calcium, broadly described as " column " and " hexagonal screw ", which differ in respect

---

[15] Mehmel, *Z. Krist.*, 1930, **75**, 323.

[16] Mehmel, *Z. physik. Chem. B*, 1931, **15**, 223.

[17] Náray-Szabó, *Z. Krist.*, 1930, **75**, 387.

Beevers and McIntyre, *Min. Mag.*, 1946, **27**, 254.

McConnell, *Amer. Min.*, 1937, **22**, 977.

[20] McConnell, *ibid.*, 1938, **23**, 1.

to the number and positions of their neighbouring oxygens in the lattice. Layers of Ca and PO_4 in the planes $c/4$ and $3c/4$ are joined by column calciums at levels 0, $c/2$ and c. The F (or OH) ions are situated in the hexagonal screw channels in the main Ca and PO_4 layers. If, for theoretical considerations, the F (or OH) ions and the column calciums are omitted from the structure, the resulting positive charge deficiency could be satisfied by introducing six hydrogens per unit cell between alternate layers only. For the formation of the octocalcium phosphate it is possible for calcium ions to unite the main Ca and PO_4 layers at levels $c/2$. This would leave two hydrogens per unit cell as shown in Fig. 5A, although, here again, more than the unit cell is illustrated. The apparently independent sheets would probably be bound together by water molecules. It has been noted that as the Ca/P ratio in solids approaches 1·33, so the ratio of water molecules to PO_4 groups approaches 1·0. It is suggested that octocalcium phosphate is an infinite two-dimensional complex, $Ca_4H(PO_4)_3 . 3H_2O$, with sheets held together by O_{PO_4}—H_{H_2O} bonds. Uptake of calcium by octocalcium phosphate would proceed by the random elimination of hydrogens by column calciums resulting in ionic bonding of the sheets. Beyond the stage represented by Fig 5B, at which one-quarter of the column calcium sites are vacant, uptake of calcium may be accompanied by the introduction of anions (F or OH) into the hexagonal screw channels. In this manner a continuous series of compositions ranging from octocalcium phosphate to hydroxyapatite would be produced in which a gradually decreasing number of column calcium sites are left untenanted. Precipitates of tri-calcium phosphate composition (Fig. 5B) would merely represent the stage at which further uptake of calcium may be accompanied by the introduction of anions (F or OH) into the lattice. Data from Fig. 1, series II and III indicate that the transition from a solid of approximately octocalcium phosphate composition to solids slightly more basic than hydroxyapatite is a gradual one. Structural considerations allow solids covering the whole range of compositions from Ca/P = 1·33 to 1·67, but particles of a precipitate may well be heterogeneous. In this connection it is important to remember that the conditions governing the precipitation change as more solid separates. A solid formed in the early stages of a precipitation would not be in equilibrium with the solution at later stages. Through the low solubilities of the more basic calcium phosphates and their tendency to supersaturation readjustments of the equilibrium must necessarily be slow. Whether precipitated calcium phosphates of apatite structure are built up without discrete molecular types (continuous series of solid solutions) or are heterogeneous particles consisting of two or more fairly definite lattices, merging one with the other, the fact remains that, in practice, no two preparations with composition lying between octocalcium phosphate and hydroxyapatite are likely to be identical. It is possible that a relationship may be established later between the crystal structures of dicalcium phosphate dihydrate and hydrated octocalcium phosphate, but, so far, the writer has not encountered any solid of single phase with a composition intermediate between these two forms.

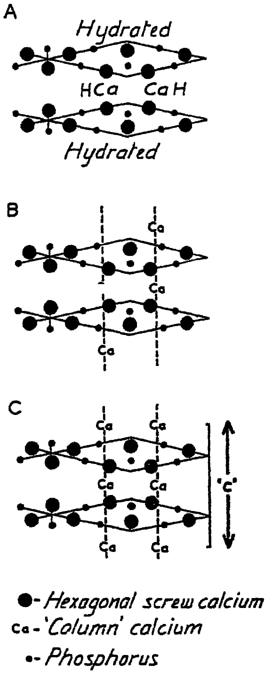

FIG. 5.

Solids more Basic than Hydroxyapatite.—The X-ray powder diffraction patterns of solids more basic than hydroxyapatite showed that they were poorly crystalline apatite-like materials. On structural grounds alone, it appeared to be unlikely that the uptake of calcium by an apatite-like lattice could proceed beyond the $Ca_5(PO_4)_3OH$ stage. Moreover, the sharp break in the pCa and pP curves in series III (Fig. 1) at the point where the Ca/P ratio of the solid was exactly that of hydroxyapatite, indicates that a change in the nature of the solid phase takes place at the hydroxyapatite composition. In this connection it is of interest to examine data concerning the actual amount of tightly bound constitutional water present in hydroxyapatite. According to Hendricks[7] the ignition of hydroxyapatite at 900° C resulted in the formation of oxyapatite. He stated that the X-ray powder diffraction pattern of the supposed oxyapatite was remarkably like that exhibited by the original hydroxyapatite. From the dehydration data presented in this paper (Fig. 3) it is evident that up to 900° C both the solids examined by Hendricks were hydroxyapatite. Warington[1] found from the difference between the combined CaO and P_2O_5 analyses and the total weight of solid that between 1·96 and 2·2 % H_2O was combined as hydroxyl in samples of hydroxyapatite. Bassett's[4] analyses ($CaO + P_2O_5$) for a series of solids approximating in composition to hydroxyapatite (atomic ratios Ca/P = 1·65 to 1·71) fell short of 100 % by amounts ranging between 2·21 and 2·25 %. Kazakov[14] concluded that a mean of 2·07 % hydroxyl water was present in his samples of hydroxyapatite. The sample S. 16 lost 2·07 % H_2O on ignition above 1230° C. (Fig. 3) All of these water contents are considerably larger than the theoretical one (1·79 % H_2O) calculated for the breakdown of the hydroxyl content of $Ca_5(PO_4)_3OH$.

McConnell[20] suggested that the monovalent hydroxyl group could substitute for oxygen in an apatite lattice. In this replacement a monovalent cation replaced a divalent cation and the electrostatic equilibrium was maintained. The synthetic sample of hydroxyapatite (S. 16) was thought to be free from contamination with monovalent cations and the suggestion that hydroxyl (equivalent to about 0·3 % H_2O by weight) substituted oxygen was not so plausible. The writer suggests that the very large specific surface of precipitated hydroxyapatite is responsible for the apparently high hydroxyl constituent and that the extra hydroxyls are surface anions required to balance the charge on the surface of the particles.

It is interesting to note that many Continental rock phosphate minerals contain considerably more fluorine, often up to 50 % more, than is required by the accepted fluorapatite formula $Ca_5(PO_4)_3F$. At present it is not possible to decide whether this extra fluorine is part of the apatite lattice or merely superficially associated with the particles.

In conclusion, a hypothesis may be advanced to account for the existence of calcium phosphates more basic than hydroxyapatite. The hydroxyapatite unit cell can be represented most simply by (I).

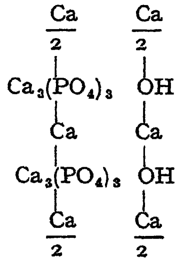

$$\begin{array}{cc} \frac{Ca}{2} & \frac{Ca}{2} \\ | & | \\ Ca_3(PO_4)_3 & OH \\ | & | \\ Ca & Ca \\ | & | \\ Ca_3(PO_4)_3 & OH \\ | & | \\ \frac{Ca}{2} & \frac{Ca}{2} \end{array}$$

(I)

i.e. $Ca_{10}(PO_4)_6(OH)_2$.

For an exposed surface the position may be represented by (II) or (III), depending upon whether the surface column calcium is absent or present.

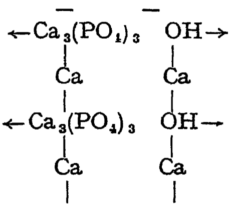
(II)

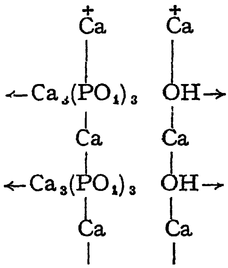
(III)

In either instance the surface would possess a charge and some form of ionically bound layer would be associated with it. The writer suggests that, at least for solids in neutral or alkaline solution, the position is that represented by (III), and hydroxyl ions are associated with the surface of the particles. Taking particles of n planes of phosphorus (considered at right-angles to the c axis) the composition of the material would be represented by the empirical formula $\{Ca_3(PO_4)_3OH\}_n \, . \, Ca_2(OH)_4$; the sorption taking place on the two surfaces where column calciums are exposed. When $n = 1$, we have sheet particles

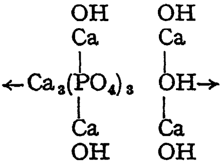

i.e. $Ca_7(PO_4)_3(OH)_6$ in which the atomic ratio $Ca/P = 2{\cdot}33$. So far as is known, no definite evidence has been obtained which indicates that a material as basic as this can be formed. However, if $n = 2$ we have

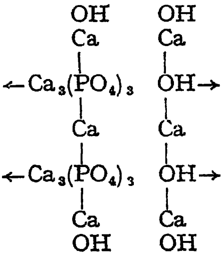

i.e. $Ca_2(PO_4)OH$, with an atomic ratio $Ca/P = 2{\cdot}0$. It has been found possible to isolate solids approaching this composition (see Greenwald [21]). The particles composing such a material would barely attain colloidal dimensions, the thickness being of the order 10 Å. The general growth of the particles may be visualized by postulating sheets of thickness equal to one unit cell of apatite with hydroxyl ions attached to their surfaces. As the plates thicken, base would be liberated, as is observed in the ageing of very basic solids. The atomic ratios Ca/P and OH/P can be calculated for various thicknesses from the general formula $\{Ca_5(PO_4)_3OH\}_n \, . \, Ca_2(OH)_4$

Referring to the dehydration of the precipitated hydroxyapatite (S. 16) (Fig. 3) it was found that 2·07 % water was lost above 1230° C.

---

[21] Greenwald, *J. Amer. Chem. Soc.*, 1944, **66**, 1305.

If the surface hydroxyls are held up to this temperature, as appears to be likely since they are more than 5 Å units apart, the constitutional water content corresponds to particles of an average thickness of 13 "apatite" unit cells ($n = 26$). For such a material the Ca/P ratio would be slightly greater than that of hydroxyapatite (1·69 as compared with 1·67), but the OH/P ratio would be considerably greater than in hydroxyapatite (0·38 as compared with 0·33). The Ca/P ratio could scarcely be determined with sufficient accuracy to decide whether the material was significantly more basic than hydroxyapatite, but the content of constitutional water from the hydroxyl, being about 15 % greater than for hydroxyapatite, would be easily determinable.

With the prospect of surface uptake of hydroxyl ions it is almost certain that other anions, including phosphate ions present in solution, would be sorbed (see Trömel [5]). Reference may be made to the solids formed in series I (Fig. 1) over the range of total Ca/P from 1·0 to 1·5. This type of complication in the chemistry of calcium phosphates would be difficult to treat rigidly, but it does at least provide a further possible explanation for the indefiniteness of many calcium phosphate precipitates recorded in the literature—an indefiniteness which has led many workers to dismiss them all merely as solid solutions.

The writer desires to thank Dr. E. M. Crowther for helpful criticism and advice received throughout the investigation. He is also indebted to the Agricultural Research Council for a grant during the tenure of which the work was carried out. Thanks are due to members of the Rothamsted Pedology Department for the use of X-ray apparatus and for the most willing assistance rendered.

Chemistry Department,
Rothamsted Experimental Station,
Harpenden,
Herts.

SORPTION OF WATER BY DEHYDRATED ALUM CRYSTALS

By A. Bielanski and F. C. Tompkins

Received 6th June, 1950

The sorption of water vapour on single crystals of potash alum dehydrated for 18 hr. at 55° C has been investigated in the temperature range 45-62° C at relative vapour pressures p/p_s between 0·04 to 0·95. First-layer adsorption on the easily accessible surface is reversible and complete at a relative pressure of 0·04. Second (and higher) layer adsorption proceeds at higher pressures and largely controls the rate of diffusion of water into the dehyrated alum. The heat of "desorption" is 11 kcal./mole water and the activation energy associated with the diffusion process is less than 500 cal./mole. The amount sorbed at time t is a linear function of $t^{\frac{1}{2}}$; there is, however, some evidence that the sorbent swells causing the diffusion coefficient to increase with increasing amount sorbed. At the composition $Al_2(SO_4)_3$ 9·4 H_2O a transformation occurs during hydration giving a "glassy" modification which is very stable to further hydration on dehydration. X-ray examination, however, indicates that this is not a new ordered phase.

Although the dehydration of hydrates [1] has been studied in some detail, less attention has been given to the reverse phenomenon, the "hydration" of dehydrated products, with the notable exception of the zeolites.[2] Seyewetz and Brissaud [3] classified the products of dehydration into five main groups according to whether rehydration proceeded (i) fully, (ii) partially and independently of the percentage relative water-vapour pressure ($p_r = 100p/p_s$) over the crystal, (iii) to an extent dependent on the value of p_r, (iv) until the product was deliquescent, or (v) not at all. Using hydrates all of which had been dehydrated at 120-140° C and rehydrating with air saturated with water vapour, they found that the velocity (and in many cases, the degree) of hydration depended on the relative pressure but not on the state of subdivision. The rate (at constant p_r and temperature) was constant over considerable periods but in some cases inflexions in the rate curves indicated possible formation of intermediate hydrates. Davis and Eyre [4] using $CuSO_4$ and $CaSO_4 . \frac{1}{2}H_2O$ and Ghosh [5] using $NiSO_4$, also reported a discontinuous sorption of H_2O but the "breaks" did not correspond to the compositions of any stable hydrates. The sorption of H_2O by (partially) dehydrated zeolites has been investigated by Tiselius; [2] using single crystals the inward diffusion of water was observed optically and the rate found to obey Fick's law. The sorption of other gases by zeolites has been comprehensively reviewed by Barrer.[6]

The object of the present work was to survey the main features of the processes occurring in the hydration of dehydrated potash alum. This compound was selected since the dehydration has been studied in detail by Garner *et al.*[1] But there is a lack of data concerning the influence of the properties of the dehydrated layer on the migration of water molecules. Moreover, for this salt the activation energy of dehydration is roughly the same (16 kcal./mole) as the heat of reaction, i.e. the activation energy for rehydration should be small provided no profound structural change takes place during dehydration. The rate-determining process would in such circumstances be a physical one involving the migration inwards of water molecules. Finally, the crystal structure of this alum has been elucidated.[7]

Experimental

Apparatus.—This consisted of (i) a reaction vessel for hydration and dehydration, (ii) a boiler system and (iii) a pumping system (Hyvac and Hg diffusion pump) (Fig. 1). Carbon tetrachloride vapour generated at a definite vapour pressure in (ii) was passed through the annular space of the double-walled reaction chamber for maintenance of constant temperature. The upper ground joint of (i), which was lubricated with silicone grease, carried a quartz spiral provided at the lower end with a cage to hold the crystal; this upper section was maintained at a temperature slightly above that of the reaction vessel by an auxiliary heater. Similarly, the tubing leading to the manometer was heated to 70° C and the manometer, used for measuring the water vapour pressure during hydration and also as a cut-off from the pumps, was steam-jacketed. The other manometer was used to measure the vapour pressure of the boiling CCl_4 and as a cut-off. The lower part of the reaction vessel contained about 2 ml. of thoroughly outgassed water; it was immersed in liquid N_2 during dehydration and surrounded by a well-lagged vessel through which water was circulated from a thermostat during hydration. Variation of the temperature of the thermostat allowed the production of a range of p_r values in the reaction vessel.

---

[1] E.g. Garner *et al.*, *Proc. Roy. Soc. A*, 1947, **189**, 392; 1940, **174**, 508; *Trans. Faraday Soc.*, 1936, **32**, 1739.

[2] E.g. Tiselius, *Z. physik. Chem. A*, 1934, **169**, 425; 1935, **174**, 401; *J. Physic. Chem.*, 1936, **40**, 40. Tiselius and Brohult, *Z. physik. Chem. A*, 1934, **168**, 248. Barrer, *Proc. Roy. Soc. A*, 1938, **167**, 392. Barrer and Ibbitson, *Trans. Faraday Soc.*, 1944, **40**, 206.

[3] Seyewitz and Brissaud, *Bull. Soc. Chem.*, 1930, **47** (1), 690; *Compt. rend.*, 1930, **190**, 690.

[4] Davis and Eyre, *Proc. Roy. Soc. A*, 1923, **104**, 1131.

[5] Ghosh, *J. Indian Chem. Soc.*, 1941, **18**, 472.

[6] Barrer, *Ann. Reports*, 1944, **41**, 31; *Quart. Rev.*, 1949, **3**, 293.

[7] Lipson and Beevers, *Proc. Roy. Soc. A*, 1935, **148**, 664.

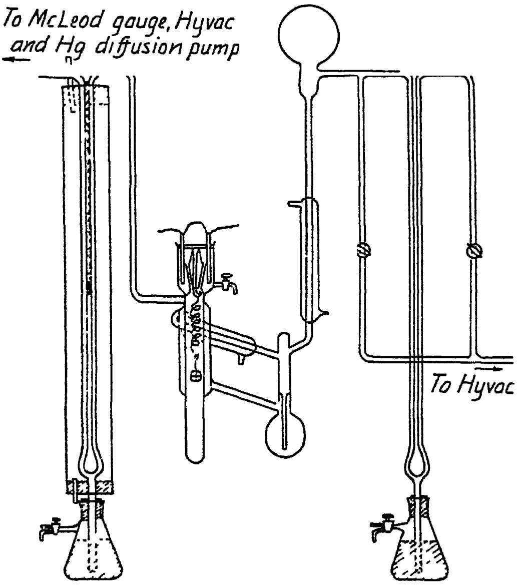

FIG. 1.

Calibrations.—During dehydration, the crystal was *in vacuo* and the lower part of the vessel in liquid N_2; during hydration it was in different V.P.'s of water and the lower limb was immersed in baths at different temperatures. Direct determination of temperature at the average position of the crystal showed, however, that this differed from that of the CCl_4 vapour by only ± 0·5° C under extreme conditions, i.e. a magnitude less than that due to the self-cooling of the crystal during dehydration. Calibration of the quartz spiral gave a satisfactory linear dependence of extension on load and the sensitivity (1·3 cm./0·1 g.) was practically temperature-independent.

PROCEDURE.—Good quality crystals of alum were obtained by slow crystallization from aqueous solution; these were carefully ground to parallelopipeds and the faces finally polished. All surfaces can therefore be assumed to be highly nucleated; the weight ($\frac{1}{2}$ g.) and dimensions (0·4 cm. side) of each crystal were recorded. Dehydration was effected at 55·0° C for 18 hr. with the lower limb in liquid N_2 and the pumps on. The pressure quickly fell to 5×10^{-5} cm. Hg and finally to less than 10^{-6} cm. Hg. The rate of loss of water after this treatment was negligible. The total loss of water was $21{\cdot}3_5 \pm 0{\cdot}2_5$ moles H_2O/mole alum. At the end of the dehydration period, the pressure over the CCl_4 was adjusted to correspond with the temperature required for rehydration, the cut-offs raised, the liquid N_2 bath replaced by the water-bath at the temperature corresponding to the p_r value to be used in hydration. Elongations of the spiral (± 0·02 mm.) were recorded at suitable intervals.

Results

Reproducibility.—A series of runs at 55° C at p_r 36·2 with crystals varying in weight from 0·32 to 0·62 g. showed that the probable error in the number of moles water/mole alum lost in the initial dehydration (55° C, 18 hr.) was 1 %; in the total gain during hydration, the error was 1·5 % and in the rate constants for the diffusion process (see later) 6 %. This was regarded as satisfactory in view of the extent of dehydration and the consequent damage to the original crystal.

Rate of Hydration.—A typical hydration curve showing the increase in weight Δw, expressed as extension of spiral in cm. as a function of time t and of $t^{\frac{1}{2}}$ within the p_r range 35 to 60 is shown in Fig. 2 and 3. The Δw against $t^{\frac{1}{2}}$ plot is linear over a considerable period, except initially where there is a concavity in the curve, but when Δw is about 6½, there is an abrupt change in the slope which is referred to here as the inflexion point. This point corresponds closely to a marked change in the appearance of the crystal. After the initial dehydration, the crystal appears white, opaque and porous although the original outer geometric shape is retained. At the inflexion point, the crystal becomes marble-like and then, usually within 10-15 min., it becomes glassy and transparent. After this transformation the rate of hydration at the same temperature and p_r is negligibly slow; furthermore, attempts to dehydrate this product *in vacuo* at 63° C over liquid N_2 for 20 hr. result in the loss of only 0·14 mole water/mole alum. This slow rate of hydration and dehydration was unaffected when the surfaces of the crystal were seriously damaged by scraping.

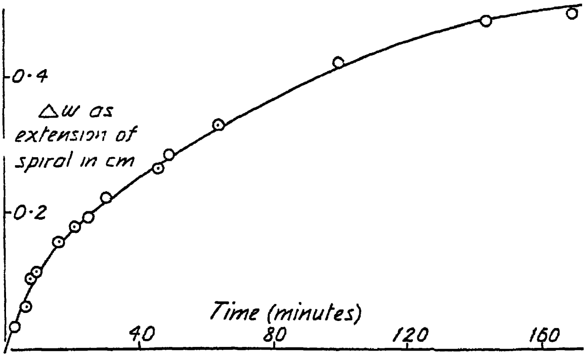

Temp. 55 C; $Pr = 56{\cdot}2$.

FIG. 2.

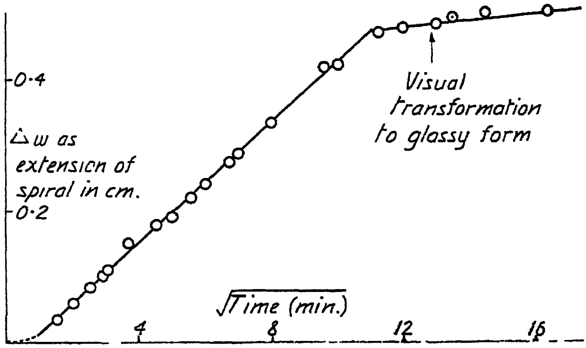

FIG. 3.

In contrast, if the hydration was interrupted before the transformation, fairly rapid, partial or complete dehydration (total loss of 21·25 moles water) was possible. Thus, if dehydration was commenced after 1·2 moles water had been added, all this additional water could be removed, but if dehydration was delayed until the crystal had gained 6 moles of water (i.e. at a time just preceding the transformation) 2·4 moles of water were quickly lost after which the rate of dehydration again became negligible.

In the p_r range 0 to 35, the Δw against t plots reached a " saturation " value ($\Delta w_{\max}$) which was dependent on the magnitude of p_r. The Δw against $t^{\frac{1}{2}}$ plots were again linear over a considerable range but there was no abrupt inflexion point, nor was it possible to convert the crystal to the glassy form. Partial dehydration was always possible but the amount removed depended on the value of p_r (or Δw_{max}) in the sense that at higher p_r values the ratio, moles water removed/Δw_{max} was smaller. Thus at 55° C and p_r 3·8, Δw_{max} was 1·18, and all could be removed in 5 hr. at 55° C *in vacuo*, whereas at the same temperature but with p_r 23·6 and Δw_{max} 3·75, the amount dehydrated under the same conditions was 2·80.

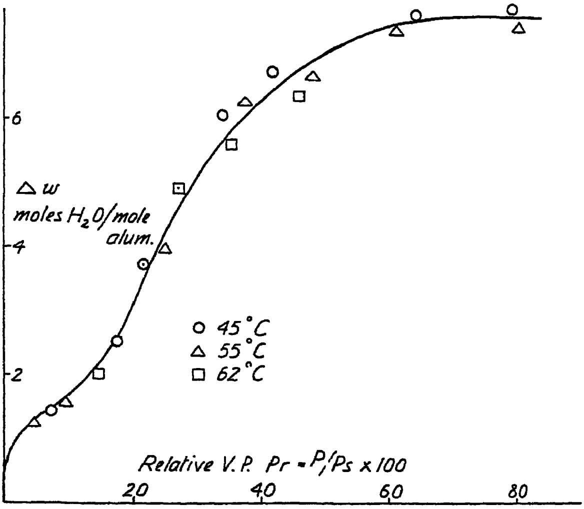

FIG. 4.

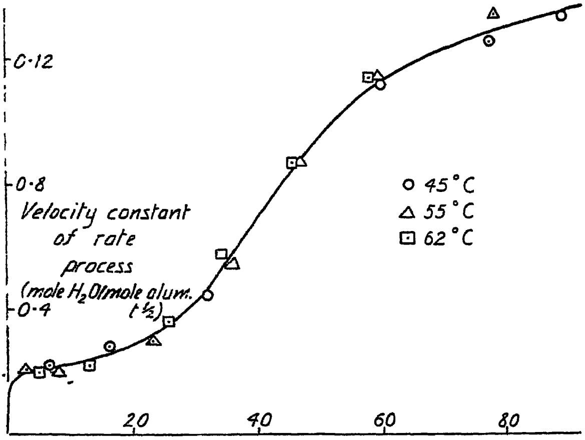

Relative V.P. = 100 p/p_s.

FIG. 5.

In the p_r range 60 to 100, hydration did not stop after the transformation; there was, however, still a well-marked inflexion point and unless p_r was greater than 80, the rate of hydration was much slower. This additional hydration was accompanied by changes in the appearance of the crystal; it became translucent and the surface had a gel-like texture. Below p_r 90, this hydration became negligible after about 30 min. and the additional amount of water taken up depended on the value of p_r, reaching a maximum for p_r less than 85 of about 1½ moles water/mole alum. Above p_r 90, hydration was reasonably rapid and continued until hydration was complete (24 moles water/mole alum), or even in excess of this by as much as 5 moles. In the initial stages the surfaces of the crystal became irregular and opaque; white incrustations were visible and at the same time dendritic growths outward from the surface began to be formed. It seemed clear that processes occurring after the transformation were markedly different from those taking place at the lower p_r values—they are therefore referred to as the secondary sorption to distinguish them from the primary process in which we are mainly interested.

In Fig. 4 has been plotted Δw_{max}, i.e. the saturation value if no transformation takes place, or the value of Δw at the inflexion point if such a change has occurred, as a function of p_r at three temperatures ; the plot resembles a sorption isotherm.

It has been noted that all Δw against $t^{\frac{1}{2}}$ plots, no matter the value of p_r, show well-defined linear portions obeying an equation therefore of the form

$$\Delta w = kt^{\frac{1}{2}} + B,$$

where k, the slope, is a rate constant and is a function of p and the temperature, and B is an arbitrary constant which would be zero if the linearity extended to zero time. The plot of k as a function of p_r at three temperatures is shown in Fig. 5 ; at constant p the rate constant is greatest at the lower temperature but at constant p_r, k is somewhat higher at the higher temperature.

Discussion

Sorption Rates.—The Δw against $t^{\frac{1}{2}}$ plots comprise three parts : (i) an initial concavity to the Δw-axis, preceding (ii) a linear portion ending rather abruptly at the inflection point, followed by (iii) a small increase of Δw with $t^{\frac{1}{2}}$ which is negligible, except at high p_r. Process (i), which is normally complete in 4 min., is ascribed to the experimental fact that $t = 0$ is arbitrarily taken as the time of removal of the liquid N_2 trap surrounding the inner tube of the reaction vessel and its replacement by a water bath at the temperature appropriate to the p_r value required in the subsequent hydration. A period of 5 min. is usually required before the vapour pressure attains the constant p_r value. Process (ii) is attributed to a diffusion process ; the period over which the $t^{\frac{1}{2}}$-law is valid is considerable and it terminates, for p_r values greater than 35, at a definite Δw value of 6·7 ± 0·2. Process (iii) only becomes significant when secondary sorption ensues.

The linear portion (ii) indicates (*a*) that the sorption (hydration) is not the inward progress of a well-defined hydrated-dehydrated interface (cp. the dehydration of $CuSO_4 . 5H_2O$) and (*b*) that the rate-determining process is not the rate of formation and growth of nuclei of the hydrated product since a sigmoid Δw against t plot would have been obtained. It is, however, consistent with diffusion along a network of interstitial channels such as are present in dehydrated zeolites.

The transition, process (ii) to (iii), takes place at the same time as the visual change of the alum from the opaque to the stable glassy form, i.e. the termination of diffusion is due to the occurrence of structural changes accompanied by the destruction, or blocking, of the network of channels through which diffusion proceeds. It is probable that reorganization ensues in the original channels and that the sorptive properties depend on their stability. In this connection, it may be noted that variation in conditions of initial dehydration (T, 35 to 70° C ; time, 18 to 66 hr.) has little effect on (i) the Δw-value at the transition, (ii) the rate of hydration, (iii) the water content of the "fully" dehydrated product (22·2 moles H_2O/mole alum lost). Furthermore, during the initial dehydration, the $(-\Delta w)$ against t plot is linear over a considerable period (i.e. consistent with an interface reaction) and there is no inflexion or abnormality in the plot at the $(-\Delta w)$-value corresponding to the transformation observed during rehydration. This latter fact suggests that the glassy form is not a definite crystalline hydrate. Confirmation of this is obtained from X-ray examination which indicates that the original alum lattice is largely destroyed during initial dehydration. The products obtained after rehydration at 55° C and p 5·9 mm. for (i) Δw 2, (ii) Δw 4, and (iii) Δw 7 (i.e. after transformation) all give diffuse low-angle bands with no sharp lines corresponding to either the original lattice or to any new ordered phase having linear dimensions of the order of 100 Å.

Despite this, the crystal retains its original external geometric form with only a 15 % decrease in volume following the loss of 22 moles H_2O/mole alum. (This loss would correspond to 74 % of original volume of the crystal assuming that a water molecule has a volume equal to that which it possesses in the liquid state.) The dehydrated product is probably a random array of minute blocks of varying dimensions in which the ions (and remaining water molecules) are displaced to varying extents from their original lattice sites. This type of structure is consistent with the desorption results.

As noted above, complete transformation occurs at a definite value of Δw; following this, dehydration (desorption) is not possible. However, at the lower Δw values, all the water added on hydration can be reversibly removed, but with increasing Δw, the ratio, moles H_2O added/moles H_2O desorbed, decreases. The amount of water irreversibly retained probably corresponds to the amount of transformation which has already taken place in localized volumes of the crystal, i.e. in this random structure the critical composition necessary for transformation in one of these localized regions is attained before the value Δw of 6·7 obtains for the whole mass. The ratio, reversibly bound to irreversibly bound water, therefore reflects the heterogeneous character of the product. Consistent with these ideas is the experimental observation that the transformation does not apparently proceed inwards from the outer surfaces.

Sorption Isotherms.—The experimental evidence shows (i) that sorption is reversible before *any* transformation takes place and (ii) that the transformation proceeds without change of Δw. This is taken as support for the assumption that the plots of Δw against p, up to Δw 6·7, represent equilibrium conditions. They are in fact sorption isotherms and are similar in form to those obtained in the sorption of vapours by porous solids, e.g. C_6H_6 by silica gel; the desorption branch is, of course, distinctly different: it is therefore possible to evaluate heats of sorption in the usual way. This heat is found to be 11 kcal./mole in the range 1 to 6·7 moles H_2O/mole alum, i.e. equal to the heat of liquefaction of water within our experimental error. This coincidence of values provides the reason why plots of Δw against p_r, but not those of Δw against p, are independent of temperature and suggests, but does not prove, that the process is associated with a condensation phenomenon.

Below Δw 1·2 or p_r 4, the plots could not be delineated with any accuracy using the present apparatus but since they must pass through the origin, the form of the curve in the region Δw 0 to 1·2, is not in doubt. The sharp initial increase of Δw at low p_r leading to an apparent saturation value at Δw 1·2 which is independent of T is almost certainly due to the formation of a complete " monolayer ". These 1st layer molecules are *not* tenaciously held by the " bare " ions of the dehydrated salt as might be expected, since they are rapidly removed on reducing p_r to zero; consistent with this, the rate constant against p_r plots also indicates that the layer is mobile (cp. later).

The rapid increase of Δw following 1st-layer adsorption is normally taken to mean that capillary condensation has occurred and the Kelvin equation

$$RT \ln p_s/p = 2\sigma V/r$$

(σ surface tension and V molar volume of liquid sorbate at temp. T; r radius of capillaries) is therefore used to evaluate the distribution of pores of different " Kelvin " radii. We have noted that the Δw against p/p_s plots are independent of T; it follows that the Δw against $RT \log p/p_s$ plots will be practically temperature independent over the small range used here (the error is about 3 % for 10° at 50° C, i.e. comparable with our experimental error). This means, as a first approximation, that at any p_r value all capillaries of radius less than a critical radius are filled and all above empty. Consequently Δw for a given p_r is independent of T

as found experimentally. Furthermore, if the rate process is diffusion of H_2O molecules from filled capillaries into the " lattice ", the rate constant at a definite p_r value will also be independent of T.

Experiments with methanol as sorbate suggest definite modifications of this view. The isotherms are similar to those using H_2O but, in agreement with a lower adsorbability, there is a much less sharp initial adsorption ; the saturation value is less definite and is reached at ½ mole CH_3OH/mole alum. The lower value is due to the larger cross-sectional area of CH_3OH (1·7/1) and the fact that H_2O can penetrate shallow gaps not accessible to the larger CH_3OH molecule. The Kelvin radius is calculated to be 5·3 Å at p_r 30 and 12·5 Å at p_r 60, whereas the diameter of the CH_3OH molecule is 4·6 Å. Apart from general considerations of the applicability of the Kelvin equation to such small capillaries, the excess energy of adsorption over that obtaining on the plane surface cannot be associated with meniscus formation. Nevertheless, in the secondary process, capillary condensation is believed to be an important factor at p values approaching p_s.

Thermodynamically, the shape of the isotherm requires an increase in the molal free energy of transference of the sorbate from the liquid to the adsorbed phase and this may be due to an increase in ΔH or a decrease in ΔS or both. If the capillary radius is not large compared with the radius of the adsorbate molecule the presence of nearby adsorbent ions will clearly cause ΔH to be higher than on a plane surface and furthermore, with increasing amounts sorbed, because of the attractive dipole interaction of sorbed H_2O molecules, clustering around an ion of the crystal causes ΔH to increase and ΔS to decrease. It is concluded therefore that condensation is not essential in explaining the shape of the isotherm. The latter concavity of the isotherm to the p_r-axis at high p_r is, of course, the consequence of a finite volume of the capillaries.

Mechanism of the Rate Process.—The rate constants,

and the relative rate constants, $R/\Delta w$, for constant p *decrease* with increase of T, but *increase* very slightly with T for constant p_r. It is therefore unlikely that the diffusion proceeds direct from the gas phase, otherwise a direct dependence on p at constant T would be expected. Furthermore, since the 1st layer is complete at Δw 1·2, the *increase* of R with p_r at constant T for larger Δw values is not controlled by the extent of 1st-layer adsorption. It follows that the rate of diffusion is dependent on the amount adsorbed in 2nd (and possibly higher) layers. Moreover, since in the region of interest, i.e. p_r less than 50, the amount adsorbed in higher layers must be less than that in the 1st layer, the magnitude of the measured Δw (at its maximum some 6 times larger than Δw due to the 1st layer) is also dependent on the amount adsorbed in higher layers. Now below Δw 1·2, 1st-layer adsorption proceeds ; this layer is mobile and molecules from it can proceed down capillaries at a definite rate, defined in terms of a rate constant R_1, until an equilibrium concentration in the capillaries, which is dependent on the extent of 1st-layer adsorption, is attained. At Δw 1·2, since 1st-layer adsorption is complete, the rate of diffusion of 1st-layer molecules is constant at a given T and the equilibrium amount within the capillaries is also fixed. The measured Δw is thus the sum of the weight due to 1st-layer adsorption which is designated Δw_1 (equals 1·2), and the amount within the capillaries which is related to it by an equilibrium constant. To find the effect of higher layer formation we may, without significant error, subtract Δw_1 from the total measured Δw (giving Δw_2) and R_1 from the measured R (giving R_2). Both R_2 and Δw_2 are controlled by the amount adsorbed in higher layers. Since for p_r less than 50, layers higher than the 2nd will be very sparsely filled, we may as a first approximation confine our attention to 2nd layer formation only. Noting that this takes place on a full 1st layer, then the adsorption heat is expected to be comparable with the heat of liquefaction of water (as is found), and the number of 2nd-layer sites is equal to the number of 1st-layer sites (neglecting edge effects).

Consequently, denoting by N_1, N_2, the number of molecules adsorbed in 1st and 2nd layers at a given p and T, and N_s the total number of (easily accessible) sites on the adsorbent, we may write

$$k_1 p(N_s - N_1) = k_2(N_1 - N_2), \quad . \quad . \quad . \quad (1)$$

$$k_3 p N_1 = k_4 N_2, \quad . \quad . \quad . \quad . \quad (2)$$

where k_1, k_3 are the condensation coefficients on the bare adsorbent and on 1st-layer molecules ; k_2, k_4 are the corresponding evaporation coefficients. In eqn. (2) it is assumed (i) that on average one 2nd-layer molecule prevents the evaporation of one 1st-layer molecule, (ii) that since (see later) the activation energy of mobility of 2nd-layer molecules is comparable with kT, then a molecule impinging from the gas phase on to a 2nd-layer molecule will normally have sufficient energy to push the latter aside. This means that the area available for condensation is proportional to θ_1, and not to $\theta_1 - \theta_2$.

Since $\quad k_1 \sim k_3 = k,$

then $\quad (N_1 + N_2)/N_s = kp(k_4 + kp)/[k_2k_4 + kp(k_4 - k_2)].$

At $p = p_s$, $\theta_1 = \theta_2$, therefore,

$$k_4 = kp_s,$$

and since the 1st layer is complete at very low p_r, then

$$k_4 \gg k_2.$$

Consequently

$$(N_1 + N_2)/N_s = p_r(1 + p_r)/(c + p_r),$$

where $\quad c = k_2/k_4$, and $p_r = p/p_s$.

Since $\quad c \ll 1,$

then $\quad (N_1 + N_2)/N_s = \Theta = (1 + p_r),$

and $\quad R = \text{const. } (1 + p_r),$

i.e. the rate should increase linearly with p_r at constant T as is found experimentally in the p_r range 30 to 60.

The above, however, neglects (i) the effect of sorbed molecules within the capillaries on the rate of diffusion and (ii) the finite capacity of the pores. The first factor may be overcome by the use of relative rate constants $R_2/\Delta w_2$, i.e. $(Q_t - Q_0)(Q_\infty - Q_0)$ in normal nomenclature. To take account of the second, let N_p equal the total number of molecules which can be sorbed in the pores, N_2' the number of molecules in the pores corresponding to the presence of N_2 molecules in the 2nd (easily accessible) layer at p and T, then at equilibrium

$$k_5 N_2(N_p - N_2') = k_5' N_2',$$

where k_5, k_5' have the nature of condensation and evaporation coefficients. On rearranging,

$$N_2 = k_5(N_p - N_2').$$

Further, $\quad \Delta w_2 = N_2 + N_2'$ and $N_2 \ll N_2'$,

therefore, as a first approximation,

$$N_2 = \frac{k_6 \Delta w_2}{1 - k_7 \Delta w_2},$$

where k_6, k_7 are constants. But R_2 is proportional to N_2, hence

$$\frac{R_2}{\Delta w_2} = \frac{\text{const.}}{1 - k_7 \Delta w_2},$$

i.e. the plot of $R/\Delta w_2$ against R should be linear. This is in accord with the results shown graphically in Fig. 6.

There is one further anomaly requiring explanation—the slopes of the $R_2/t^{\frac{1}{2}}$ plots remain constant for longer periods than is possible for diffusion down capillaries of finite length. It is believed that this is brought about by an increase in the magnitude of the diffusion coefficient D with increasing filling-up of the capillaries; this is a well-known result for diffusion into polymers which swell. No measurements of swelling

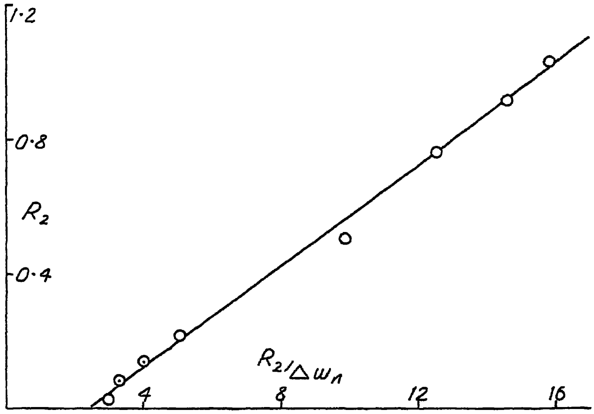

FIG. 6.

attending hydration have been made in the present investigation but we have already noted a shrinkage during dehydration. The increasing magnitude of D will offset the normal decrease in the slope of the $R_2/t^{\frac{1}{2}}$ plots at higher t, but the rather complete cancellation of these two opposite effects is, of course, fortuitous. We might further note that a relationship

$$\frac{R_2}{\Delta w_2} = \frac{\text{const.}}{1 - k_7 \Delta w_2},$$

such as deduced above, would (apart from the reasons given in its deduction) also be consistent with an increase of D with Δw_2, and the obedience of our results to this equation can mean that both factors are included.

Activation Energy E_2 of Rate Process.—The plots of R_2 against p_r are practically independent of T and consequently E_2 is approximately zero. The results do not allow an evaluation of E_1, the energy relating to mobility in the 1st layer, but its value cannot be large. Now the activation energy for viscous flow of water is 4-5 kcal./mole, but only 500 cal. is necessary for mobility, the rest being associated with hole formation. Below p_r 50, the 2nd layer is far from complete, so that the energy required for lateral mobility is of the order of kT, as we have found.

Secondary Sorption.—This has not been studied in detail but there is evidence that (i) at p_r 60 some hydrolysis occurs in the surface layers leading to the production of gelatinous aluminium hydroxide and that (ii) at still higher relative pressures appreciable capillary condensation takes place. This latter is followed by solution of the " alum " forming the boundaries of the channels and transport of ions through the solution then proceeds;[8] deposition of solute subsequently occurs at protuberances on the external surfaces, thereby accounting for the outward growth of " dendrites ".

One of us (A.B.) gratefully acknowledges a scholarship from the British Council during the tenure of which this investigation was made.

Imperial College of Science,
London, S.W.7.

[8] Cp. another possible mechanism proposed by Wagner, *Z. Elektrochem.*, 1941, **47**, 696.

THE INFLUENCE OF SUGARS ON THE ELECTROKINETIC POTENTIAL AND INTERFACIAL TENSION BETWEEN AQUEOUS SOLUTIONS AND CERTAIN ORGANIC COMPOUNDS

PART I.—THE ELECTROPHORETIC BEHAVIOUR OF ORGANIC DISPERSIONS

BY H. W. DOUGLAS

Received 29th March, 1950

A micro-apparatus has been used to investigate the mobility–pH behaviour of dispersions of a variety of organic compounds in buffered aqueous media at 25° C and also the effect of the addition of increasing amounts of the non-electrolytes sucrose, lactose and dextrose to the media. Addition of these sugars reduced the mobility values for all the dispersed substances, the reductions being greatest for paraffin hydrocarbons and least for *n*-alcohols; the effect appeared to be independent of pH. An analysis suggests that the variations in viscosity and dielectric capacity of the media produced by the addition of the non-electrolytes might by themselves account for the decreases observed with the *n*-alcohols, the charge on the alcohol particles being unaffected. With paraffins it is suggested that the reduction in mobility results from marked preferential adsorption of the added sugar molecules at the paraffin-water interface over the normal charging ions, the consequent reduced ionic adsorption giving a lower electrokinetic charge density and thus mobility. Evidence in support of this explanation is provided by measurements made, using a pendent drop apparatus, of the tensions at liquid paraffin—water and buffer solution and at alcohol-water interfaces and of the effect of sugars on these tensions.

The relationship between the electrophoretic behaviour of pure organic compounds dispersed in aqueous media and their chemical structure has been the subject of a number of investigations carried out in this laboratory.[1–5] These investigations were carried out by a moving boundary method using apparatus similar to that described by Price and Lewis.[1] As the OH$^-$ ion appears to be the most strongly potential determining ion for such systems electrophoretic mobilities were determined over the pH range 2 to 12 in buffered media N/100 to Na$^+$ ion. The purpose of this concentration of positive ion was sensibly to fix the thickness and thus the capacity of the electrical double layer round the negative dispersed particles; under these conditions, the variation in observed mobility with pH would be expected to run parallel with the variation in the electrokinetic charge density for the relatively coarse particles ($\alpha \sim 5 \times 10^{-4}$ cm.) in these dispersions. In order to produce and maintain sharp boundaries a small amount of sucrose (2 g./100 ml. of solution) was added to the dispersions in all cases. Overall, the results indicate that the electrokinetic behaviour of these compounds varies from one type of compound (homologous series) to another, being substantially the same for different members of the same series, e.g. for the paraffin hydrocarbons.[4, 5]

[1] Price and Lewis, *Trans. Faraday Soc.*, 1933, **29**, 775.
[2] Roberts, *ibid.*, 1936, **32**, 1705; *ibid.*, 1937, **33**, 643.
[3] Williams, *ibid.*, 1940, **36**, 1042.
[4] Dickinson, *ibid.*, 1941, **37**, 140.
[5] Douglas, *ibid.*, 1943, **39**, 305.

Even with the addition of sucrose or other supposedly inert substance to increase the density and lessen diffusion of their dispersions, many interesting compounds yield dispersions which form diffuse initial boundaries in the U-tube, and which sediment and break too rapidly for measurement. With a view to extend observations to such systems, often formed by members of homologous series below about C_{10}, and to make measurements on the more stable systems less time-consuming (without sacrificing accuracy), the author has built and operated a modified micro-apparatus for electrophoresis.[6] With this the migration of individual particles, through very small distances under an applied potential difference, is observed using a microscope. Mobility measurements, taking seconds only, may be made in rapid succession on the same or different particles and with systems which sediment too rapidly to be studied by the U-tube method, e.g., hexane, heptane, cyclohexane. Finally, the addition of any inert substance is unnecessary.

The present paper records mobility against pH curves obtained by the micro-method for a variety of dispersions in aqueous media, N/100 in Na^+ and containing 2 g. sucrose/100 ml. solution (2 % w/v), at 25° C, together with corresponding curves obtained by various workers using the U-tube method; in general these are in good agreement. It further records the curves obtained by the present micro-method in the absence of sucrose; these are quite distinct, the difference being most remarkable for the *n*-paraffins and *n*-alkyl halides. So far as it has been investigated, the electrokinetic behaviour again appears to be substantially the same for members of the same homologous series, e.g., *n*-paraffins, *n*-alcohols. Seeking an explanation of these differences with and without sugar, the effects of increasing w/v percentage of sucrose, lactose, dextrose and other substances on the mobility of representative *n*-paraffins and *n*-alcohols, both solid and liquid, have been determined at selected pH values and 25° C. The effects of these substances on the tension of a water-paraffin (liquid) and of a water-*n*-alcohol (liquid) interface have been determined (Part II) and certain of the results are recorded here. They indicate differing adsorptions of these non-electrolytes relative to one another, and to that of the potential determining ions, for any particular interface to be the main cause of the observed changes in electrokinetic behaviour.

Experimental

Materials and Purification.—In all cases special attention has been paid to purity of the compounds employed, and constancy of the electrophoretic behaviour on successive treatments appeared to afford the most sensitive test available. For several of the compounds, the author was fortunate in having purified samples used in earlier work, and these have been employed here after checking the electrophoretic behaviour and re-purifying where necessary.

Purified samples of dodecane (liquid) and paraffin wax, as used by Douglas,[5] were available and gave emulsions in N/100 Na^+ buffer of pH 9, containing 2 % w/v sucrose, having mobilities by the micro-method of − 1·06 μ sec. per volt/cm.* and − 1·10 units respectively at 25° C. Previous values by the macro-method for these samples in the same media were − 1·16 and − 1·0 units. In the absence of sugar, mobility values of − 5·8 and − 5·0 units were obtained for dodecane and paraffin wax respectively. These high mobility values were sensibly unaffected by treating the bulk samples with A.R. sulphuric acid, washing with alkali and with water, and subsequently distilling under reduced pressure (dodecane) or re-crystallizing (paraffin wax). The liquid paraffin (Nujol) as obtained had a mobility of − 5·65 units at pH 9 and showed no reaction with either conc. sulphuric acid or alkaline permanganate. It was therefore used as obtained, the constancy of its mobility being checked from time to time.

---

[6] Douglas, *J. Sci. Instr.*, 1946, **24**, 103.

* $\mu = 10^{-4}$ cm. The negative sign indicates that the particles bear a negative electrokinetic charge.

For cetyl iodide and octyl iodide samples of the material used by Dickinson[4] were available and were repurified to constant mobility as described by him. Mobility values of − 1·26 and − 1·30 units respectively were obtained at pH 9, in the presence of 2 % w/v sucrose by the micro-method as compared with the value of − 1·30 recorded by Dickinson for the macro-method.

The ethyl laurate used in the present work was a stored sample as purified and used by Williams.[3] A dispersion at pH 9 and 25° C gave a mobility of − 5·1 units by the micro-method in the presence of 2 % w/v sucrose as compared with the value of − 4·9 units found by Williams. Kahlbaum stearic acid was re-crystallized both from ethyl acetate (freed from acid and redistilled) and from redistilled petrol ether, giving products of the same limiting mobility, viz., − 3·7 units at pH 9 in the presence of sucrose by the micro-method.

Preparation of the Dispersions.—All the substances used were dispersed in distilled water using the modified steam jet method described by Douglas,[5] the compounds being initially floated as " oils " on the water which was heated above room temperature and the m.p. of the compound where necessary.

The Mobility Determinations.—The U-tube apparatus used in the determination of mobilities by the macro-method has been adequately described by Price and Lewis ;[1] the micro-method and apparatus have also been described elsewhere by the author.[6]

Results

Fig. 1 records the electrophoretic mobility against pH curves obtained by both the micro- and macro-methods for dispersions of a variety of compounds in buffered aqueous media, N/100 in Na$^+$ and containing 2 g. sucrose/100 ml. dispersion, at 25° C. The agreement between the results obtained by the two different methods is very satisfactory and substantiates the essential correctness of the observed mobilities.

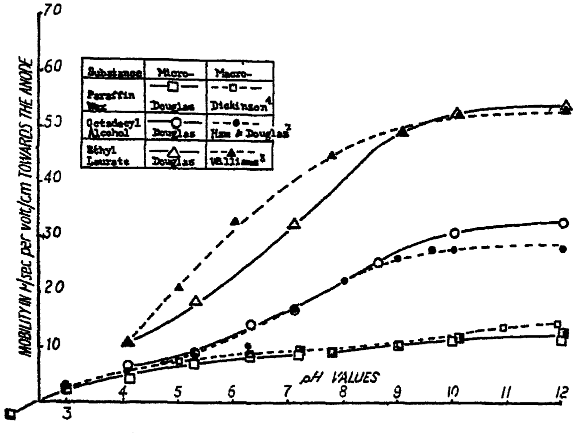

FIG. 1.—Comparison of mobility-pH curves obtained by the macro- and by the micro-methods, in N/100 Na$^+$ buffer solutions at 25° C containing 2 % w/v of sucrose.

Fig. 2 and 3 record the mobility against pH curves obtained by the present micro-method for the various compounds without and with 2 % w/v sucrose added. The effect of sucrose on the mobility–pH behaviour is most pronounced in the case of the *n*-paraffins and alkyl halides and least for the *n*-alcohols and ethyl stearate. The observed variations in the mobility of paraffin wax and liquid paraffin droplets with the amount of various sugars added to their buffered dispersions at selected pH's and 25° C are recorded in Fig. 4 and 5. The corresponding variations for *n*-octadecyl alcohol (solid) and for *n*-lauryl and undecyl alcohols (liquid) are recorded in Fig. 6 and 7. The effects of these sugars on the tension at liquid paraffin-water and *n*-undecyl alcohol-water interfaces at 25° C are recorded in Fig. 8 and 9.

---

[7] Ham and Douglas, *Trans. Faraday Soc.*, 1942, 38, 404.

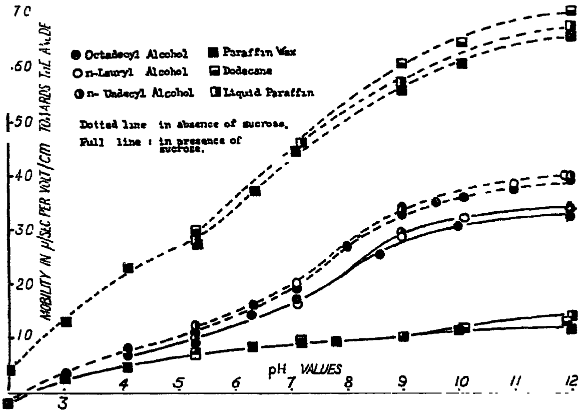

FIG. 2.—Mobility-pH curves, obtained in N/100 Na⁻ buffer solutions, at 25° C, with and without 2 % w/v sucrose added, for paraffins and *n*-alcohols.

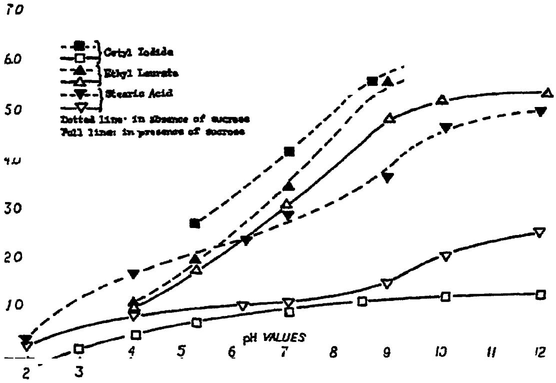

FIG. 3.—Mobility-pH curves, obtained in N/100 Na⁺ buffer solutions, at 25° C, with and without 2 % w/v sucrose added, for cetyl iodide, ethyl laurate and lauric acid. Micro-method.

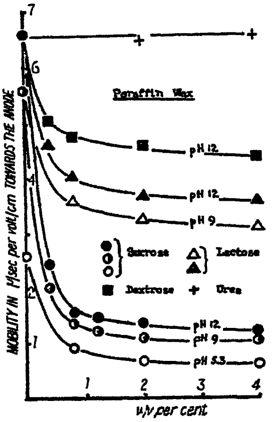

FIG. 4.

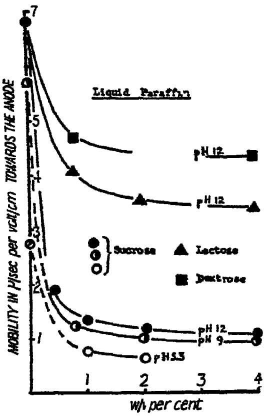

FIG. 5.

Effect of increasing w/v % of sugars on the mobility of paraffin wax and liquid paraffin at several pH's.

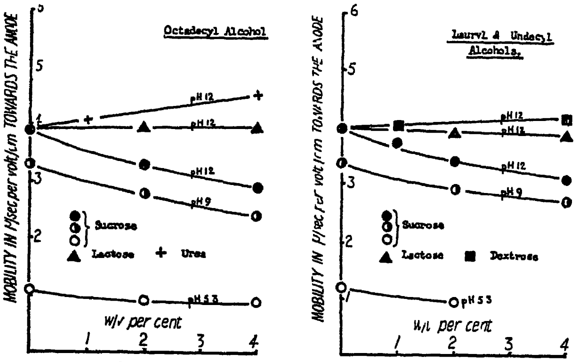

FIG. 6. FIG. 7.

Effect of increasing w/v % of sugars on the mobility of octadecyl (solid) and *n*-lauryl and undecyl (liquid) alcohols at several pH's.

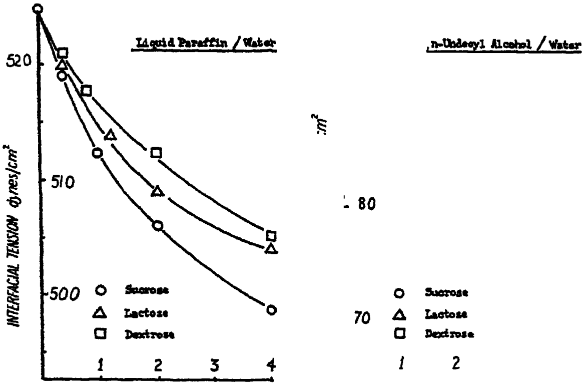

FIG. 8. FIG. 9.

The effect of increasing w/v % of sugars on the interfacial tension between water and a liquid paraffin and between water and *n*-undecyl alcohol, at 25° C.

Fig. 10 records the variation in electrokinetic charge density Q_E of dispersions of liquid paraffin in aqueous media at pH 12 and 25° C with increase in the amount of sugar added. It also shows the calculated Gibbs' excess concentration Γ_s of these sugars at the hydrocarbon-water interface in the absence of buffering electrolyte. The Q_E values have been calculated using Henry's equation[13] for the relation between the charge density and electrophoretic mobility of non-conducting particles, surface conductance and relaxation effects being neglected for the present relatively massive particles ($\alpha \approx 5 \times 10^{-4}$ cm.) in N/100 Na⁺ buffer solutions.[14] The surface excesses of the sugars have been evaluated using Gibbs' equation in the form

$$\Gamma_s = -\frac{c}{RT} \cdot \frac{d\gamma}{dc},$$

it having been shown experimentally that sucrose solutions are ideal up to *ca.* M/10. Finally in Fig. 11 the variation in the interfacial tension between medicinal paraffin and N/100 Na⁺ ion buffer at pH 9 with increasing amounts of sucrose added is recorded.

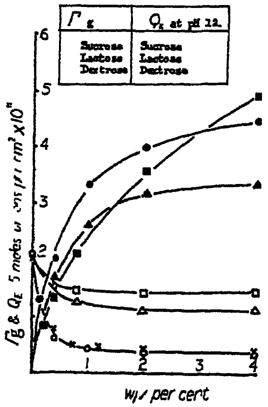

FIG. 10.—Γ_s and Q_E against w/v % added sugars for paraffin in aqueous media.

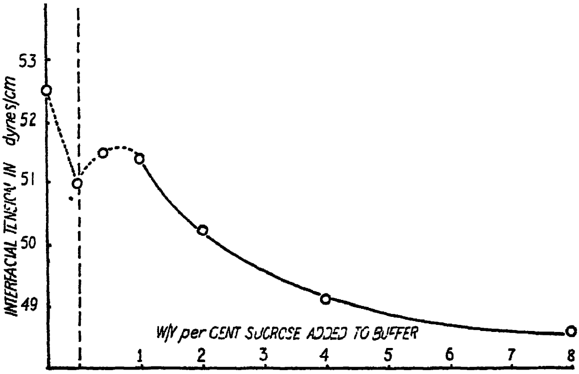

FIG. 11.—Interfacial tension of liquid paraffin against N/100 Na⁺ ion buffer solutions containing increasing w/v % sucrose, compared to water value at 25° C.

Discussion

From the results it is clear that whilst the electrophoretic behaviour of different members of the homologous series, *n*-paraffins, *n*-alkyl halides and *n*-alcohols, is substantially the same in particular aqueous media, this behaviour varies from one series to another and is differently affected by the addition of sugars. This is in contrast to the findings of Northrop and Cullen for certain bacterial and other suspensions,[8] the electrophoretic behaviour of which in aqueous media was unaffected by the presence of larger amounts of sugar than those recorded here. On the basis of their findings, mobilities obtained by the U-tube method in the presence of sucrose have previously been assumed to be the same as the unobserved mobilities in the absence of sucrose. The present observations on hydrophobic dispersions of organic compounds are, however, in agreement with the results of Kruyt and van Duin,[9] Freundlich and Rona,[10] Mukherjee [11] and others on hydrophobic solutions of inorganic substances (As_2S_3, $Fe(OH)_3$) ; this work has been concisely discussed by Rideal.[12]

No new hypothesis is required for the interpretation of the present results : in particular, the effect of different sugars on the mobility of *n*-paraffins and *n*-alcohols as recorded in Fig. 4, 5, 6 and 7. They may be accounted for in terms of the probable effect of the added sugars on the dielectric capacity and viscosity of the media and, for the paraffins, in terms of their preferential adsorption with consequent displacement of charging ions.

Henry [13] has derived the following general equation relating the electrophoretic mobility u of a non-conducting particle of radius α with its electrokinetic charge density σ,

$$\sigma = \frac{u\eta(1 + \kappa\alpha)}{\alpha} \cdot \frac{1}{f(\kappa\alpha)} . \quad . \quad . \quad . \quad . \quad (1)$$

In this equation η is the viscosity within the double layer and κ has the same definition and significance as in the Debye-Hückel theory of strong electrolytes (i.e. $1/\kappa$ is regarded as giving the effective thickness of the double layer). $f(\kappa\alpha)$ is a function which varies continuously from 2/3 to 1 as $\kappa\alpha$ varies from very small ($< 0{\cdot}1$) to very large (> 250) values. For particles of the size present in these dispersions ($\alpha \sim 5 \times 10^{-4}$ cm.) and in N/100 Na^+ buffers, $\kappa\alpha > 1000$ so that we may approximate eqn. (1) to give

---

[8] Northrop and Cullen, *J. Gen. Physiol.*, 1922, **4**, 635.
[9] Kruyt and van Duin, *Kolloidchem. Beihefte*, 1914, **5**, 269.
[10] Freundlich and Rona, *Biochem. Z*, 1917, **81**, 87.
[11] Mukherjee, *J. Indian Chem. Soc.*, 1928, **5**, 703.
[12] Rideal, *Surface Chemistry* (C.U.P., 1930), 2nd edn., p. 403.
[13] Henry, *Proc. Roy. Soc. A*, 1931, **133**, 124.
[14] Henry, *Trans. Faraday Soc.*, 1948, **44**, 1021.

$$\sigma = u\eta\kappa. \quad . \quad . \quad . \quad . \quad . \quad (2)$$

The dielectric capacity ϵ does not appear directly in this equation, nor does the ionic strength of the medium, $\frac{1}{2}\Sigma cz^2$; both may be introduced by writing

$$= \sqrt{\frac{4\pi e^2 N_A \Sigma cz^2}{1000kT}} = K\sqrt{\tfrac{1}{2}\Sigma cz^2/\epsilon}, \quad . \quad (3)$$

where K is a constant at constant temperature. Substituting (3) in (2), and expressing σ in e.s.u./cm.^{2}, η in poise, c in mole/l. and u in cm./sec. per volt/cm. the following equation is obtained :

$$\sigma = u\eta K\sqrt{\tfrac{1}{2}\Sigma cz^2/\epsilon} \times 3 \times 10^{-2}. \quad . \quad . \quad . \quad (4)$$

From this equation it follows that if, as for the curves plotted in Fig. 4, 5, 6 and 7, non-electrolyte is added to one of the dispersions at constant pH and ionic strength then any observed variation in mobility may be related to possible concomitant variations in the viscosity, dielectric capacity and charge density by the equation

$$u = K'\sigma\epsilon^{\frac{1}{2}}/\eta. \quad . \quad . \quad . \quad . \quad . \quad (5)$$

Assuming the electrokinetic charge density, and therefore the ionic adsorption process by which these non-ionogenic surfaces acquire their charge, to be unaffected by the addition of non-electrolyte and the relative variation in viscosity and dielectric capacity in the double layer to be the same as for the bulk medium, eqn. (5) predicts an approximately linear decrease in mobility with increasing w/v % sugar added, the relative decrease being the same for all dispersions. Table I records approximate values for the percentage lowering, relative to the value in the absence of added non-electrolyte, calculated from bulk viscosity and dielectric capacity data taken from the *Int. Crit. Tables*.

TABLE I

Added Substance	% Lowering in Mobility for			
	0	1	2	4 w/v %
Sucrose . . .	0	2	4	10
Lactose . . .	0	2	4	10
Dextrose . . .	0	2·5	5½	12

Some approximate percentage lowerings for 2·0 % w/v sucrose added at pH 12 are : ethyl laurate 10 %, *n*-alcohols 15 %, *n*-paraffins and alkyl halides 80 %, and for 4·0 % sucrose, *n*-alcohols 25 %, paraffins 90 %. It is estimated that the mobility values are accurate to ± 3 %, so that variation in viscosity and dielectric capacity alone could conceivably account for the variations observed with ethyl laurate and, possibly, the *n*-alcohols. For the paraffins and alkyl halides variation of these two factors alone appears quite inadequate, nor does it account for the change in effect from one sugar to another.

Matthews [15] and Strogonow [16] have shown respectively that sugars are adsorbed at a cyclohexane-water and at a liquid paraffin-water interface, lowerings of tension of several dynes being obtained for solutions of similar concentration to those employed in the present work. Such adsorption of non-electrolyte molecules, enhancing their concentration in the immediate neighbourhood of the interface, could considerably increase the viscous and dielectric capacity effects within the double layer and would also decrease the adsorption of ions from solution, the process which gives rise to the electrokinetic charge borne by the non-ionogenic surfaces of paraffins and *n*-alcohols. From this point of view, the present electrokinetic results indicate relatively strong adsorption of sugars by the paraffins and little, if any, by the *n*-alcohols. The interfacial tension data recorded in Fig. 8 and 9 for the effect of sugars on the interfacial tension against water at 25° C of the liquid paraffin and the *n*-undecyl alcohol used in the electrokinetic work, are in agreement with this. Sucrose, lactose and dextrose lower the equilibrium tensions of the paraffin-water interface to different extents and in the same relative order as they lower the electrophoretic mobility of paraffin dispersions in buffered media of fixed pH (Fig. 4 and 5); on the other hand the tension between *n*-undecyl alcohol and water, mutually saturated at 25° C, is little changed (cf. Fig. 6 and 7). The interfacial tension results for the paraffin-water interface are analyzed in detail in Part II, and Fig. 10 records the variation with w/v $^{\circ}_{0}$ in bulk of the amounts of sugar adsorbed Γ_g, as calculated by Gibbs' equation, along with the decrease in electrokinetic charge density Q_E of droplets of the same hydrocarbon at pH 12, calculated from eqn. (5) and allowing for variation in bulk viscosity and dielectric capacity. That the sugars are preferentially adsorbed, with consequent desorption of ions, is confirmed by the results presented in Fig. 11. This records the interfacial tension of the initial paraffin-water interface and the variation in equilibrium tension between the paraffin and N/100 Na$^+$ buffer of pH 9 with increasing w/v % of sucrose added. The tension for the system, buffer solution-hydrocarbon, is about 1·5 dynes lower than for the system, water-hydrocarbon, indicating adsorption of ions and consistent with the charging process. The subsequent increase in tension on addition of sugar is consistent with the absorption of sucrose molecules and the consequent desorption of *both* the primarily adsorbed ions and their partners in the diffuse part of the double layer. Subsequently the interfacial tension falls again as the sucrose continues to be reversibly adsorbed (see Part II) with increasing w/v % sugar added to the bulk solution. The limiting mobilities reached at the various pH's for the hydrocarbons may reflect the adsorptive capacities of the sugar monolayers formed (Part II) for negative ions and, in part, the possible ionization of these sugars as weak monobasic acids, $K_A \approx 5 \times 10^{-13}$, in alkaline media.[17]

---

[15] Matthews, *Trans. Faraday Soc.*, 1939, **35**, 1113.

[16] Stroganow, *Protoplasma*, 1935, **24**, 431.

Janssen [18] has observed a movement of sucrose and other sugar molecules in electrolyte solutions towards the anode in a Tiselius apparatus. He suggested that this movement resulted from the collision of the ions transporting the current with the uncharged sugar molecules, the net direction of movement being that of the ion of greater kinetic energy, usually the negative ion. The calculated "mobilities" [19] of the sucrose molecules in N/10, HCl, NaCl and other salt solutions lie between 10^{-6} and 10^{-5} cm./sec. per volt/cm.; for N/10 NaOH solution the mobility was rather higher *ca.* 2×10^{-5} cm./sec.: though the movement was not determined in N/100 NaOH, the mobility against concentration plot rises steeply with decreasing NaOH concentration. The possible dissociation of sugars in alkaline solution and the limiting mobility of *ca.* 10^{-4} cm./sec. per volt/cm. recorded for paraffin droplets which probably have a monolayer covering of sucrose molecules, suggest that the explanation of the effect recorded by Janssen may be an electrophoretic one.

[17] Hirsch and Schlags, *Z. physik. Chem. A*, 1929, **141**, 367.

[18] Janssen, *Rec. Trav. Chim.*, 1946, **65**, 564.

[19] Calculated by the author after private communication with Dr. Janssen.

PART II.—THE INTERFACIAL TENSION BETWEEN AQUEOUS SUGAR SOLUTIONS AND (1) A LIQUID PARAFFIN AND (2) *n*-UNDECYL ALCOHOL, AT 25° C.

The pendent-drop method has been used for the determination of the interfacial tensions between water and liquid paraffin and between water and *n*-undecyl alcohol, values of 52·5 ∓ 0·1 dynes/cm. and 8·61 ± 0·05 dynes/cm. respectively being obtained at 25° C. Furthermore, the effects of increasing concentrations of dextrose, sucrose and lactose on the tensions have been determined. The Π against A diagrams indicate gaseous films and the equation $\Pi(A - A_0) = xkT$ is obeyed; the slopes of the plots give values of 80 Å^2, 210 Å^2 and 225 Å^2 for dextrose, sucrose and lactose respectively, i.e. close to the X-ray values. It appears that under the conditions of these experiments the sugar molecules lie flat at the interface. The x values in the above equation are *ca.* 1·0, 0·93 and 0·88 for dextrose, lactose and sucrose respectively, indicating increasing cohesion between the film molecules in that order.

The interfacial tension measurements recorded in this paper were undertaken primarily to determine if the differing adsorption of sugars for hydrocarbon-water and alcohol-water interfaces could account for their effects upon the electrophoretic behaviour of dispersions of members of the paraffin and *n*-alcohol series in aqueous media; these showed, approximately, the greatest and least variation respectively of the different types of compound studied (Fig. 2 and 3, Part I). The tension results have been discussed from this point of view in Part I. They are also of interest in themselves; accurate values for the interfacial tension of the systems and information about the condition of the sugar molecules adsorbed are also obtained.

Experimental

Materials and Methods.—The liquid paraffin (Nujol) and the *n*-undecyl alcohol employed were portions of the samples used for the electrophoretic investigations previously described (Part I); the sugars of A.R. quality also were from the same samples.

The interfacial tension measurements were carried out using a pendent-drop apparatus already described in detail elsewhere.[1] In order to facilitate the attainment of temperature equilibrium between the "oil" and solution phases, with which the glass syringe and rectangular cell were respectively filled, the two phases were previously brought to the working temperature, 25·0 ± 0·1° C, in a separate thermostat. For *n*-undecyl alcohol-water, the two phases have an appreciable mutual solubility and this is further affected by the presence of dissolved sugars. Accordingly the two phases for each tension measurement were thermostated in a quartz flask for two or more days before use in the pendent-drop apparatus. It was not found possible to avoid completely the formation of a very thin emulsion of the alcohol in water, particularly when sugars were present; these very feeble dispersions were stable for days, and have been employed as the aqueous phases in the measurements recorded here. Auxiliary density measurements were made using an accurate pyknometer of 10 ml. capacity and having ground glass caps to cover the capillary ends after adjustment of the liquid levels.

Results and Discussion

The interfacial tensions have been calculated from the dimensions of drop silhouettes, recorded photographically and at known magnification, using the "selected-plane" equation

$$\gamma = \frac{(\rho_1 - \rho_2)gd_e^2}{H} \quad . \quad . \quad . \quad . \quad . \quad (1)$$

as derived by Hauser and others.[2] In this equation γ is the tension,

---

[1] Douglas, *J. Sci. Instr.*, 1950, **27**, 67.

[2] Andreas, Hauser and Tucker, *J. Physic. Chem.*, 1938, **42**, 1001.

g the gravitational constant, $(\rho_1 - \rho_2)$ the effective density of the pendent-drop, d_e its equatorial diameter and H is a function of the ratio d_s/d_e, d_s being the diameter of the drop at the selected plane height d_e from the tip of the drop, determined here from the tables computed by Fordham.[3]

The interfacial tensions between the hydrocarbon and the aqueous sugar solutions employed have been found to decrease with time reaching constant values after about 10 min. for dextrose and about 15 min. for sucrose and lactose; these "equilibrium times" are very large relative to calculated times for simple diffusion, and indicate the operation of some further process, giving rise to an energy barrier in the adsorption of the sugar molecules at the interface (this will be discussed later). Fig. 1 and 2 record the interfacial tensions of Nujol-water and *n*-undecyl alcohol-water, respectively, at 25° C, together with the change in the equilibrium tensions (for drops, 30 min. or more in age) effected by increasing w/v percentages (g./100 ml. solution) of the sugars, dextrose, sucrose and lactose dissolved initially in the aqueous phase.

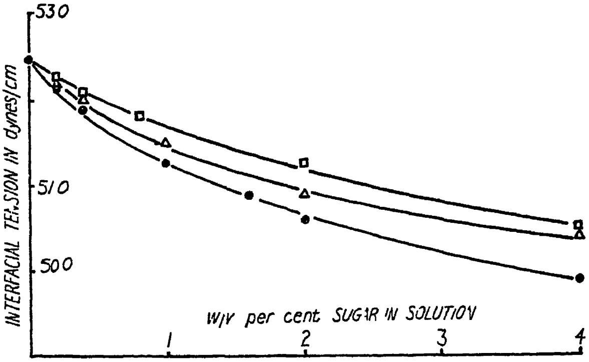

FIG. 1.—Variation of interfacial tension between liquid paraffin and aqueous sugar solutions with w/v % sugar dissolved, at 25° C.
● Sucrose △ Lactose ☐ Dextrose

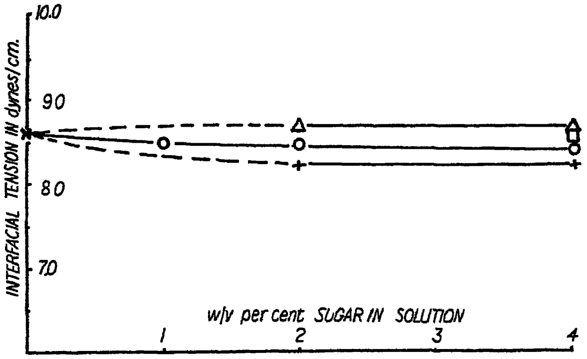

FIG. 2.—Variation of interfacial tension between *n*-undecyl alcohol and aqueous sugar solutions with w/v % sugar dissolved at 25° C. Phases mutually saturated.
○ Sucrose △ Lactose ☐ Dextose + Urea

No time effects were observed for undecyl alcohol which gave a tension of 8·61 dynes/cm. against water at 25° C, the two phases being mutually saturated. This value may be compared with the value of 8·52 dynes/cm. at 20° C, given by Harkins, Brown and Davies [4] for octyl alcohol-water.

---

[3] Fordham, *Proc. Roy. Soc. A*, 1949, 194.

[4] Harkins, Brown and Davies, *J. Amer. Chem. Soc.*, 1917, **39**, 354.

The small changes in tension resulting from the presence of sugars up to 4 w/v per cent. in the aqueous phase are not readily interpreted for this system of partially soluble phases. The mutual solubilities of the alcohol and water will be affected by the solution of sugars, and the surface tensions of the separate phases will also change; these changes have not been determined for the separate phases, but they could lead to either an increase or a decrease in the observed interfacial tension. However, in comparison with the hydrocarbon-water interface it appears that there is little adsorption of sugars at this alcohol-water interface.

The equilibrium tensions for liquid paraffin-aqueous sugar solutions recorded in Fig. 1 show a progressive decrease with increasing concentration for each of the sugars. The two phases being mutually insoluble and the sugars soluble in the aqueous phase only, these results are more readily analyzed. Before giving details of this analysis, the qualitative similarity of the present curves to those obtained by Matthews[5] for the cyclohexane-water interface, and by Stroganow[6] for a liquid paraffin-water interface, may be noted. The present tension lowerings are in the same relative order as those observed by Matthews but approximately twice as great: measurements now being made[7] indicate that the adsorption of other substances also is more pronounced at the Nujol-water interface than at cyclohexane-water interfaces.

Using the approximate form of the Gibbs equation,

$$\Gamma_s = -\frac{c}{RT}\cdot\frac{d\gamma}{dc}, \qquad . \quad . \quad . \quad . \quad . \quad (2)$$

the surface excesses Γ_s have been calculated from the estimated slopes of the interfacial tension against molar concentration curves for each of the sugars. This form of the equation has been used since the values for the tension lowerings recorded here are not accurate to more than 0·1 dyne/cm. and furthermore it has been shown by Perman[8] that sucrose solutions are ideal up to M/10. It is assumed here that the other two sugars, lactose and dextrose, also behave ideally in aqueous solution up to the same concentration. From the evaluated surfaces excesses the area per molecule A has been derived using the relation

$$A = 1/(\Gamma_s N_A). \qquad . \quad . \quad . \quad . \quad . \quad (3)$$

The corresponding force-area (Π against A) and ΠA against Π relations have been calculated by setting the surface pressure Π equal to the tension lowering and Fig. 3 records the Π against A curves. The dotted hyperbola indicates the theoretical curve for an ideal two-dimensional gas, obeying the equation

$$\Pi A = kT$$

at 25° C. It is clear that the assumed monomolecular sugar films are gaseous, the molecules themselves occupying a considerable area. The ΠA against Π plots for sucrose and dextrose are nearly linear and fit equations of the form

$$\Pi(A - A_0) = xkT\ ^{9}$$

reasonably well, with A_0 about 100 Å^2 for dextrose and about 250 Å^2 for sucrose; the values for lactose give a somewhat curved plot lying a little above that for sucrose.

The areas computed above relate to the Gibbs' excess only and take no account of the amounts normally present in the surface layer. The areas quoted for dextrose and sucrose molecules are quite close to the maximum areas of the molecules of these compounds calculated from the X-ray data of Cox, Goodwin and Wagstaff,[10] viz. about 90 Å² and 180 Å² respectively. It thus appears that the molecules lie flat and accordingly the thickness of this surface layer has been taken as 5 Å, i.e. the X-ray

---

[5] Matthews, *Trans. Faraday Soc.*, 1939, **35**, 1113.

[6] Stroganow, *Protoplasma*, 1935, **24**, 431.

[7] Unpublished measurements by E. Haythornthwaite in this laboratory, relating to the adsorption of simple amino acids.

[8] Perman, *Trans. Faraday Soc.*, 1928, **24**, 330; see also Butler, *Chemical Thermodynamics* (1946), 4th ed., p. 333.

[9] Rideal and Schofield, *Proc. Roy. Soc. A*, 1925, **58**, 109; see also Rideal, *Surface Chemistry* (1930), 2nd edn., p. 64.

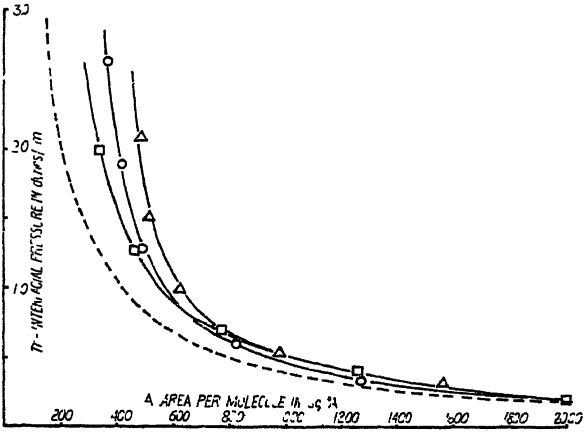

FIG. 3.—Force-area (Π—A) diagrams for sugars at liquid paraffin-water interface at 25° C.

$$\Pi = \gamma_0 - \gamma \qquad A = \frac{10^{16}}{N_A \Gamma_0} \text{ Å}^2.$$

○ Sucrose. △ Lactose. ☐ Dextrose.

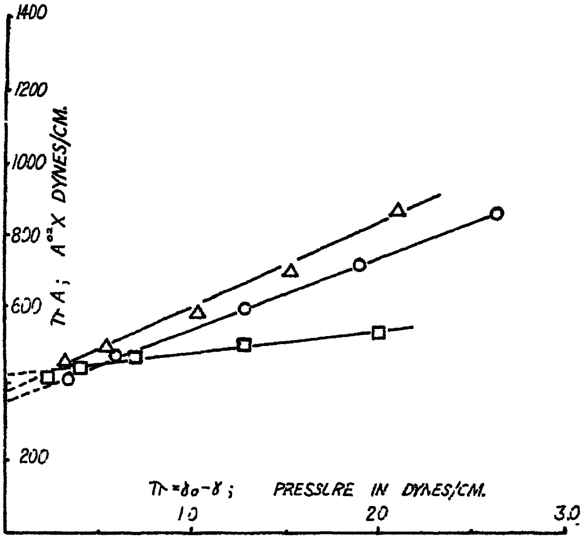

FIG. 4.—$\Pi A'$ against Π plots for sucrose, lactose and dextrose at liquid paraffin-water interface at 25° C, allowing for the amount normally present in the surface layer (5 Å).

○ Sucrose. △ Lactose. ☐ Dextrose.

---

[10] Cox, Goodwin and Wagstaff, *J. Chem. Soc.*, 1935, 1498.

value. Allowing for the amount of sugar normally present in this surface layer, the total surface amount Γ_T becomes

$$\Gamma_T = \Gamma_s + c/(2 \times 10^{10}), \quad . \quad . \quad . \quad . \quad . \quad (4)$$

where c is the bulk molar concentration ; the area per molecule is

$$A' = 1/(\Gamma_T N_A). \quad . \quad . \quad . \quad . \quad . \quad . \quad (5)$$

Fig. 4 records the $\Pi A'$ against Π plots which are now approximately linear for all three sugars and fit the following equations :—

Dextrose . . . $\Pi(A' - 80) = kT,$ . . . . . (7)
Sucrose . . . $\Pi(A' - 210) = 0{\cdot}88\,kT,$ . . . . . (8)
Lactose . . . $\Pi(A' - 225) = 0{\cdot}93\,kT$ . . . . . (9)

These results suggest that, in addition to the adsorbed sugar molecules lying flat at the interface, the cohesive forces between them are least for dextrose and greatest for sucrose.

The force-area behaviour of adsorbed films at " oil "-water interfaces has been derived for relatively few compounds ; these include fatty acids, dissolved both in the aqueous and non-aqueous phases,[11-18] n-alcohols,[13] sodium cetyl sulphate and certain protein films.[14] For these the force-area behaviour in general is consistent with the molecules themselves occupying an area A_0 close to the corresponding values derived for their oriented surface films on aqueous substrates. However, whether or not the interfacial films exhibit more gaseous or condensed behaviour than the surface films appears to depend on the nature of the " oil " phase.

Finally, in Fig. 5 the interfacial tension between Nujol and water, with and without 4 % w/v sugar added, is plotted as a function of time. The tension Nujol-water alone is independent of time whilst pronounced time effects are apparent for the sugar solutions, equilibrium tensions being reached in 5-10 min. for dextrose and 10-15 min. for sucrose and lactose. Similar time effects have been observed by Ward and Tordai[15] for the interfacial tension at 25° C between water and solutions of palmitic

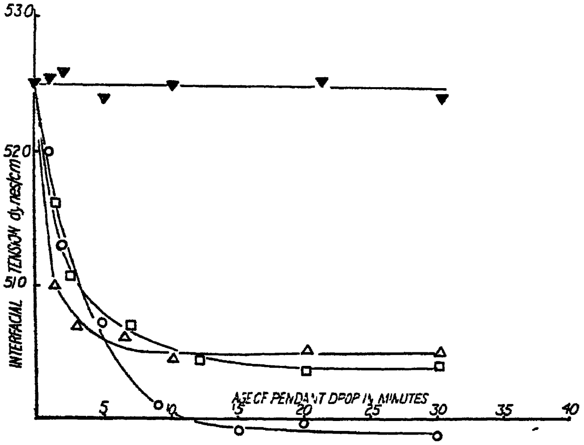

FIG. 5.—Variation of interfacial tension with time for liquid paraffin against water and 4 % w/v sugar solutions, at 25° C.

▼ Water. ○ 4 % Sucrose. △ 4 % Lactose. ⊡ 4 % Dextrose,

---

[11] Schofield and Rideal, ref. (9).
[12] Askew and Danielli, *Trans. Faraday Soc.*, 1940, **36**, 785.
[13] Hutchinson, *J. Colloid Sci.*, 1948, **00**, 21.
[14] Alexander and Teorell, *Trans. Faraday Soc.*, 1939, **35**, 727.
[15] Ward, *Surface Chemistry* (Butterworth), 1949, p. 55.

and lauric acids in hexane. Diffusion alone does not account for these effects [16] and, in the present instance at least, the results are consistent with the existence of an energy barrier, perhaps of the form suggested by Blair.[17] Using the equation derived by Blair for the formation of films obeying an Amagat equation against a constant energy barrier λ, values of λ of about 10 kcal./mole are obtained from the present data.

The Muspratt Laboratories,
The Department of Inorganic and Physical Chemistry,
University of Liverpool.

[16] Ward and Tordai, *J. Chem. Physics*, 1946, **14**, 453.

[17] Blair, *J. Chem. Physics*, 1948, **16**, 113.

THE FLOW PROPERTIES OF ELASTIC DISPERSIONS

By W. J. Dunning and D. Patterson

Received 2nd May, 1950; as revised 20th July, 1950

The flow properties of dispersions of latex rubber in Aroclor 4465 (a " liquid " with a viscosity of about 10^{10} poises) have been studied. The form of the compression-time curves and the order of magnitude of the strain relaxation time agree with the theory of Fröhlich and Sack.

Fröhlich and Sack [1] have developed a theory for the flow properties of elastic spheres dispersed in a Newtonian liquid. This theory appears to be as important as the corresponding theory of Einstein for dispersions of rigid spheres and it is desirable, therefore, to check its implications experimentally. It was the purpose of the present investigation to prepare systems which approximated as closely as possible to the idealized model studied by Fröhlich and Sack. If relaxation times of the order of minutes were to be obtained, consideration of the theory showed that the ratio of the viscosity of the liquid to the elastic modulus of the disperse phase should be about 10^2 or 10^3. Other theoretical considerations seemed to suggest that liquids with viscosities in the neighbourhood of 10^9-10^{10} poises would not be Newtonian. After an exhaustive search, it was found that certain grades of Aroclor—technical chlorinated diphenyl—have viscosities in this region, and within the accuracy of the experiments, they behave as Newtonian liquids. It is well known [2] that elastomers with elastic moduli of the order of 10^6-10^7 are not Hookean solids. There are no materials other than elastomers with moduli in this range. However, if the deformations of the dispersions were restricted to about 1 %, it was considered that the behaviour of the elastomers in them would be nearly Hookean and that hysteresis and other time effects would be negligible. Limitation of the deformations to this extent demanded accuracy in their measurement, whilst the time constants involved required that the observations were made over extended periods of time.

Some initial experiments were carried out with dispersions of synthetic elastomers. Their properties were qualitatively similar to those described below for dispersions of uncured rubber. The presence of low molecular weight plasticizers in these synthetic elastomers militated against their use.

---

[1] Fröhlich and Sack, *Proc. Roy. Soc. A*, 1946, **185**, 415.

[2] Treloar, *Trans. Faraday Soc.*, 1944, **40**, 59.

Experimental

Aroclor 4465 is a brittle " solid ". 25 lb. were melted and filtered at about 120° C. After cooling it was finely ground, carefully mixed and divided into representative samples. A quantity was weighed from each sample and to it was added an amount of uncured latex appropriate to the required percentage of elastomer. Since the volume of the latex varied with the percentage, the bulk of liquid was kept constant by addition of dilute ammonia where necessary. This facilitated the careful mixing of the latex and the powder. The water and ammonia were removed by drying *in vacuo* over sulphuric acid for three days. The dried mixture was placed in the stirred pan A (Fig. 1). The pan could be heated electrically and the mixture therein was melted under vacuum to avoid air bubbles. It is essential that the temperature be kept as low as possible; the temperature used here was 80-85° C. The trap E could be opened by a solenoid G and the mixture was released into the mould H. This mould consisted of three hinged parts (Fig. 2) and a base plate; it was chromium plated and it was necessary to clean and polish highly it each time to avoid adhesion. A cylindrical extension 2 in. high served to contain the cusp. After cutting off the latter and trueing the top surface of the sample in a lathe, the dimensions of the cylindrical sample were 5 in. high and 2·25 in. diameter. The

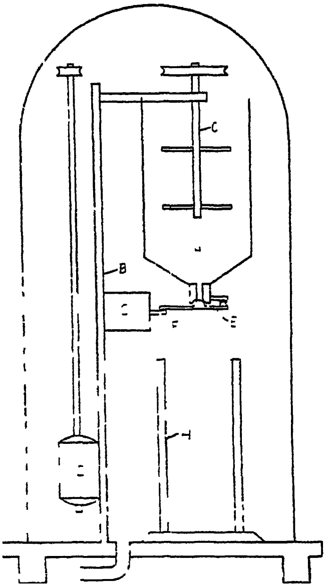

FIG. 1.

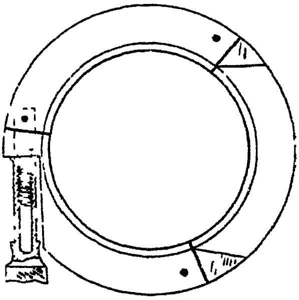

FIG. 2.

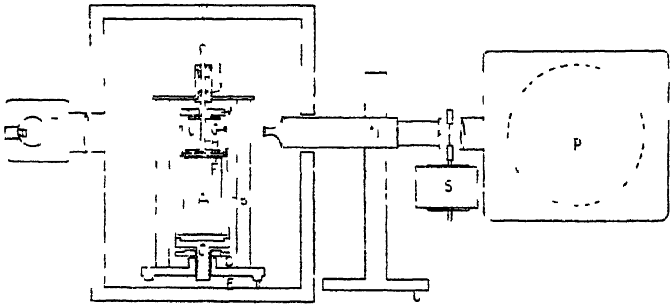

FIG. 3.

sample was supported in $BaClO_4$ solution of the same density and annealed in a thermostat at 25° C.

The plastometer is illustrated in Fig. 3. The sample A stood in a cylinder B which contained $BaClO_4$ solution to counter gravity, and thermostated water was circulated through the double jacket of B. In turn, B stood on a platform C which could be carefully raised and lowered by means of the knurled nut D. A light Perspex disc F just rested on the upper surface of the sample and carried two finely ruled glass scales GG. A light rigid piston H carried the weight W; the piston could be lifted clear for recovery measurements. The whole was placed in an air thermostat (25° ± 0·5° C).

The compression and recovery were followed by photographing the glass scale through the microscope M which was fitted with an eyepiece scale. Movements of 10μ could be observed. A valve relay circuit actuated by an electric clock operated the camera at fixed intervals of time (every 10 or 20 min.) for 48 hr.

Results

Viscosity of the Aroclor.—From the photographs, the height h of the sample was computed for each time. Fig. 4a shows the decrease in ln (h/h_0) with time under a total load of 233 g., h_0 being the original height of the cylinder.

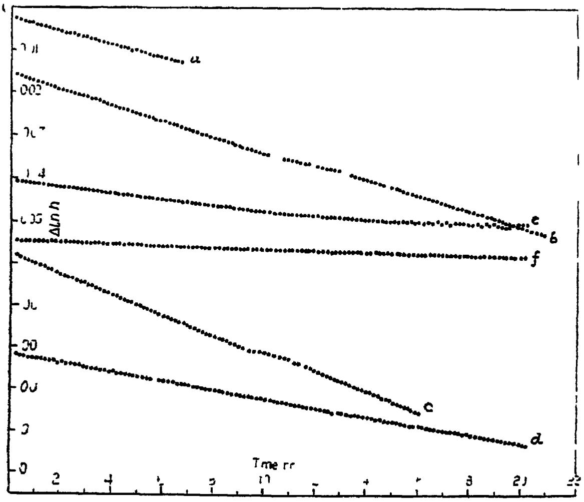

FIG. 4.

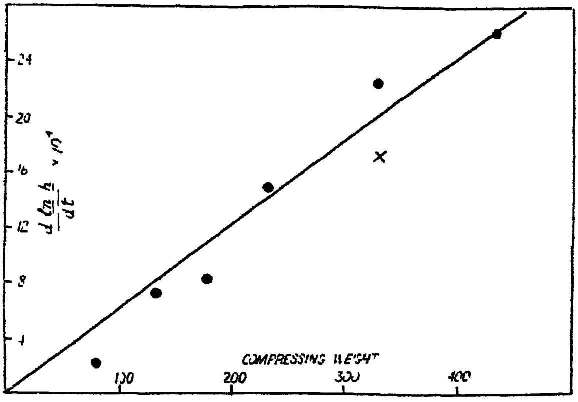

FIG. 5.

The first part of the compression is not shown since it was curved, owing to the difficulty in trueing-up the cylinder exactly. Plot *b* was obtained with 333 g., *c*, *d*, *e* and *f* were with 433, 183, 133 and 83 g. and were done in that order. The starting points of curves *d*, *e* and *f* have been moved upwards arbitrarily in the Figure to save space. The gaps between the termination of one compression and the beginning of the next were due to delays during which necessary adjustments were made.

Immediately at the end of the compression with 333 g. the piston and weight were lifted. The Perspex disc with its glass scales had been adjusted in weight and volume so that it just sank in the buoying solution, and thus exerted little or no restraint on any recovery by the sample. Although the total compression of the cylinder to this stage was about 8 %, no recovery was observed after 2 hr. If there was any recovery it was not greater than 0·1 % of the compression.

The gradients of the lines in Fig. 4 have been plotted in Fig. 5. A straight line could have been drawn through the points, cutting the weight axis at 60 g. This might indicate that the Aroclor is not a true Newtonian liquid, but is a Bingham plastic with a yield point corresponding to a load of 60 g. Another explanation would be that Aroclor shear hardens to a small extent. Indeed, the order in which the experiments were done was chosen to check whether shear hardening was important, but the lie of the points is not conclusive ; for example, the points at 333, 433 and 133 are too high to be consistent with shear hardening. A third explanation might lie in Eyring's theory of viscosity.[3] A more likely explanation than these would be the experimental difficulty of measuring such high viscosities at such low stresses to the precision required. This is indicated by the position of the cross in Fig 5, which is a repeat determination on a new sample.

After discussion with Dr. Fröhlich it was considered that Aroclor was sufficiently close to Newtonian behaviour to enable the theory of Fröhlich and·Sack to be tested. A straight line through the origin was drawn. From its slope the viscosity can be evaluated as 7·7 × 10⁹ poises, using the relation,

$$\frac{\mathrm{d}\ln h}{\mathrm{d}t} = \frac{S_{11}}{3\eta},$$

where S_{11} is the homogeneous compressive stress applied and η the viscosity. Poisson's ratio is assumed to be 0·5.

Modulus of the Rubber.—A strip of dried latex 8 × 3 × 1 cm. was extended by weights and the extension measured with a microscope. Up to a maximum extension of about 1 % the extension load plot was linear and no hysteresis was observed. From this the differential Young's modulus for zero stress was found to be $7{\cdot}1 \times 10^6$ dynes cm.$^{-2}$. Assuming that Poisson's ratio for rubber is 0·5, the modulus of rigidity is one-third of this.[4]

Flow Properties of the Dispersions.—The loads applied were such as to produce the same order of shearing stress as were used in obtaining the differential Young's modulus of the rubber. The compression against time curve for 5 % rubber dispersions was determined for a compressing weight of 83 g. (Fig. 6*a*). After 29 hr. the load was removed and the recovery curve obtained (Fig. 6*b*). The compression *e* in mm. is given by

$$e = 0{\cdot}0685t + 2{\cdot}8\,(1 - \mathrm{e}^{-t/7{\cdot}6}), \qquad (1)$$

with t in hours. The recovery curve is given by

$$e = 2{\cdot}58\mathrm{e}^{-\Delta t/8{\cdot}1} \qquad (2)$$

where Δt is the time elapsing after removal of the load.

Fröhlich and Sack give for the compression

$$e = \frac{S_{11}}{3\eta^*}\,t + \frac{S_{11}}{3\eta^*}\,(\tau_1 - \tau_2)(1 - \mathrm{e}^{-t/\tau_2}), \qquad (3)$$

and for the recovery,

$$e = \frac{S_{11}}{3\eta^*}\,(\tau_1 - \tau_2)(1 - \mathrm{e}^{-t'/\tau_2})(1 - \mathrm{e}^{-\Delta t/\tau_2}) \qquad (4)$$

---

[3] Glasstone, Laidler and Eyring, *Theory of Rate Processes* (McGraw-Hill, New York, 1941), p. 480.

[4] Lethersich, *J. Sci. Instr.*, 1944, **21**, 27.

where t' is the time at which the load is removed, S_{11} is the compressive stress, and

$$\eta^* = \eta(1 + 5\phi/2), \qquad (5)$$

$$\tau_1 = \frac{3\eta}{k}(1 + 5\phi/3), \qquad (6)$$

$$\tau_2 = \frac{3\eta}{k}(1 - 5\phi/2), \qquad (7)$$

where η is the viscosity of the pure Newtonian liquid, k the modulus of rigidity and ϕ the relative volume of the dispersed phase.

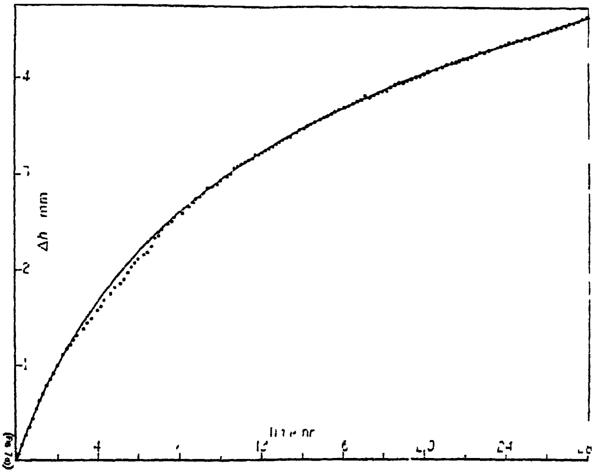

FIG. 6(a).

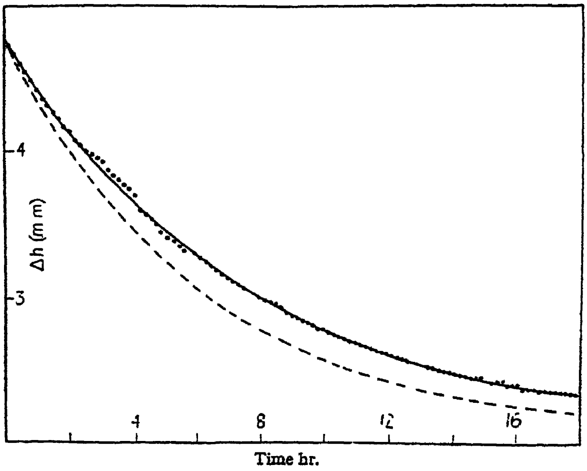

FIG. 6(b).

From eqn. (1) we obtain a value of 7·6 hr. for τ_2 (the strain relaxation time), and 2·8 for $\frac{S_{11}}{3\eta^*}(\tau_1 - \tau_2)$. These are in fair agreement with the values of 8·1 and 2·58 obtained from the recovery curve (eqn. (2)). The dotted line in Fig. 6b shows what the course of the recovery curve would have been with the first two values. Table I lists the values of the parameters derived from similar experiments.

TABLE I

Dispersion %	Load (g.)	η^*	τ_2 (hr.) (compression)	τ_2 (hr.) (recovery)
5	83	$7{\cdot}0 \times 10^9$	7·6	8·1
5	133	$7{\cdot}9 \times 10^9$	6·0	7·6
10	83	$6{\cdot}4 \times 10^9$	5·5	6·2
15	83	$5{\cdot}4 \times 10^9$	7·2 (0·42)	7·5 (0·35)

The curves for the 15 % dispersion could not be expressed by single exponential terms and it was necessary to use two exponential terms. The results were analyzed by Prony's method[5] and gave

$$e = 0{\cdot}089t + 6{\cdot}3e^{-t/7{\cdot}25} + 0{\cdot}87e^{-t/0{\cdot}42}$$

and

$$e = 5{\cdot}65e^{-t/7{\cdot}5} + 1{\cdot}0e^{-t/0{\cdot}35}$$

Many more compression and recovery experiments were carried out, some to elucidate and eliminate discrepancies and others to examine the influence of the variables. In general, it is concluded that the value of the deformation e is proportional to the compressing load (i.e. to S_{11}) and that small variations of η (the viscosity of the Aroclor) influence the parameters in the right direction.

Discussion

Using the values of $7{\cdot}7 \times 10^9$ poises for the viscosity of the Aroclor and $7{\cdot}1 \times 10^6$ for the Young's modulus of the rubber, the theoretical values of η^* and τ_2 can be calculated from Fröhlich and Sack's relations (5) and (7). The values are listed in Table II.

TABLE II

Dispersion %	η^*	τ_2 (hr.)
5	$8{\cdot}9 \times 10^9$	2·37
10	$9{\cdot}7 \times 10^9$	2·03
15	$10{\cdot}9 \times 10^9$	1·70

Comparison of Tables I and II indicates that the experimental and theoretical quantities agree satisfactorily as regards order of magnitude. This, together with the fact that the forms of the experimental and theoretical curves are identical, suggests that the theory is phenomenologically correct. It is difficult to decide the cause of the discrepancies in detail between the theoretical and experimental values of the quantities, and especially of their contrary trends with increasing concentration. We believe it does not lie in the theory or in the rheological measurements, but rather in the difficulty of dispersing the rubber in the Aroclor. The shortest possible heating times and the lowest possible temperatures were used for incorporation, but it is believed that the latex globules imbibe small amounts of the lower molecular weight molecules constituting the Aroclor and their bulk and modulus alter. To test this, two small strips of the rubber were heated under the molten Aroclor for 1 hr. at 120° C and 160° C. This is more drastic then the treatment during incorporation, but on the other hand the surface area of the droplets during incorporation is very much larger. The swelling of the strips was not noticeable, but they became less opaque. After removal and washing with acetone, they seemed softer to the touch. Attempts to measure the Young's modulus of similar strips whilst still submerged in the molten Aroclor were not successful. If dispersions were maintained at 120° for prolonged periods (hours) they became discoloured, the viscosity η^* decreased by about an order of 10, and the elastic recovery diminished. Further, the dispersions used were opaque whilst the pure Aroclor cylinders were transparent and glass-like.

---

[5] Whittaker and Robinson, *Calculus of Observations* (Blackie, London, 1944), p. 369.

It is concluded that the dispersions were certainly two-phase, and that disintegration and solution occurred only after prolonged heating at higher temperatures. There is still the question, however, of the nature of the dispersion. Was the rubber present as discrete globules, as long fibrils, or as a honeycomb of thin sheets enclosing small volumes of Aroclor ? In an attempt to decide this question, the Aroclor was dissolved away in a solvent and examination of the solution under a high-powered microscope revealed small spherical bodies of a similar size to the latex globules.

In the 15 % dispersion there is evidence of a second time constant of the order of 0·4 hr. The cause of this is difficult to find. If it is due to doublet formation of the droplets, it seems unlikely that this second time constant would be smaller than that of single droplets.

Our thanks are due to Miss J. Toogood for preliminary work on the flow properties of many substances and in particular, of the Aroclor. Thanks are also due to Dr. H. Fröhlich, Dr. R. Sack and Mr. W. Lethersich for much helpful discussion, and to the British Electrical and Allied Industries Research Association for financial assistance.

Chemistry Department,
The University,
Bristol.

VOLUME CHANGES IN THE STRETCHING OF VULCANIZED NATURAL RUBBER

By Geoffrey Gee, Jan Stern and L. R. G. Treloar *

Received 24th May, 1950

Measurements are presented of the volume changes accompanying small ($\not>$100 %) elongations of vulcanized natural rubber completely free from undissolved particles. The small expansions found agree with those calculated from the known compressibility of the rubber and the hydrostatic component of the stretching force. It is pointed out that this volume change mechanism applies generally to any isotropic body, and does not contribute significantly (in rubber) to the tensile stress.

The Significance of the Problem.—Previous studies [1] of the volume changes which accompany the extension of vulcanized natural rubber have shown that, using a compound as free as possible from mineral fillers, an elongation of at least 200 % can be attained without the volume changing by more than 0·2 %. At higher elongations, the volume diminishes, a phenomenon which can be quantitatively associated with the onset of crystallization.[1] There are, however, strong theoretical and indirect experimental reasons for believing that smaller extensions must be accompanied by finite though small *expansions*. The magnitude of these has been predicted [2] and in this paper their existence is confirmed by quantitative measurement.

---

* Present address, The Royal Institution, Albemarle St., W. 1.

[1] Holt and McPherson, *Bur. Stand. J. Res.*, 1936, **17**, 657 ; *Rubber Chem. Tech.*, 1937, **10**, 412. Fox, Flory and Marshall, *J. Chem. Physics*, 1949, **17**, 704.

The argument which led to the prediction of these expansions is of a very general nature, depending essentially on the possibility of resolving the tensile force into shear stresses and a hydrostatic tension. It is this latter which causes the material to expand, and this must happen for any isotropic material. If f is the force needed to elongate the material from l_0 to l and K its compressibility, the volume expansion ΔV is given by [2]

$$\Delta V = \tfrac{1}{3}K\int_{l_0}^{l} l\left(\frac{\partial f}{\partial l}\right)_{P,T} . \mathrm{d}l.$$

This equation applies so long as the material remains isotropic, and is therefore probably not seriously incorrect for the materials and elongations ($<$ 100 %) used in our experiments. By determining the stress-strain curve of the rubber and making use of its known compressibility, eqn. (1) enables us to calculate the expansion to be anticipated.

Previous indications that this analysis is correct rest on the further argument that the whole of the increase in internal energy observed in the stretching of such a rubber arises from the expansion, the internal energy being assumed to depend (at constant temperature) only on the volume, and not on the deformation. The most careful experimental studies of the thermodynamic properties of stretched rubber [2, 3] support this argument, and lead to two conclusions: (*a*) that vulcanized natural rubber stretched at *constant volume* would not change its internal energy, and (*b*) that the internal energy changes observed on elongation at *constant pressure* are those calculated from the volume changes given by eqn. (1). Additional confirmation comes from Meyer and Van der Wyk's demonstration [4] that rubber can be sheared without changes of internal energy, the result to be anticipated from the fact that a shear, having no hydrostatic component, will produce no volume change in an isotropic body.

Experimental

For the measurement of volume changes of the magnitude expected, i.e. of the order of one part in 10,000, the dilatometric method of Holt and McPherson [1] did not appear to be sufficiently sensitive. In the present investigation the method of hydrostatic weighing was adopted. The rubber was weighed immersed in water, first in the unstrained state, and then while stretched on a suitable frame. To obtain the necessary precision it was desirable to use as large a volume of rubber as possible, but the increase of volume beyond a certain point involved slow attainment of thermal equilibrium and also necessitated an undesirably bulky supporting frame to withstand the high tensile stresses. A compromise was effected by using 8 separate ring specimens cut from a single vulcanized sheet, mounted in parallel on the frame and having a total volume of about 6 cm.[3] Weighings could be made to 0·1 mg. which therefore corresponded to 1 part in 60,000 in volume. The first experiments were made on a pure gum vulcanizate of the type used in an earlier investigation by Gee.[2] This was found to give volume changes higher by about 100 % than the theory would require. This compound contained 2 % of zinc oxide, and it seemed not unlikely that the excessive volume changes might have been associated with this factor, since it is well known (Jones and Yiengst [5]) that the extension of rubbers containing inert fillers gives rise to a relatively large increase in volume, usually attributed to the formation of vacuoles around the filler particles. Further experiments showed the magnitude of the volume changes to depend markedly on the zinc oxide content. Since satisfactory vulcanizates of this type could not be made without zinc oxide, attention was given to an alternative method of cross-linking which did not require the introduction of solid ingredients. In this method best quality pale crepe was cross-linked by means of di-*tert.*-butyl peroxide, using a technique described elsewhere.[6] Two such compounds were investigated. Their degrees of cross-linking, or chain molecular weights (M_c) as determined by swelling in benzene and application of the Flory formula[7] with $\mu = 0{\cdot}39_5$ were 4900 and 9500 respectively. Their density at 20° C was 0·920 g. cm.$^{-3}$.

---

[2] Gee, *Trans. Faraday Soc.*, 1946, **42**, 585.

[3] Wood and Roth, *J. Appl. Physics*, 1944, **15**, 781; *Rubber Chem. Tech.*, 1945, **18**, 367.

[4] Meyer and Van der Wyk, *Helv. chim. Acta*, 1946, **29**, 1842.

[5] Jones and Yienst, *Ind. Eng. Chem.*, 1940, **32**, 1354.

The Volume Measurements.—The frame upon which the rings were stretched is shown in Fig. 1. The rings R of internal and external diameters approximately 3·8 and 4·2 cm. respectively, were mounted on 8 short brass rods of diameter ⅛th in. The 4 outer ones A were fixed; the others B could be positioned against one or other of a number of suitably spaced stops C, thus giving a succession of extensions. These rods were held in place by the rubber and could be simply removed by hand when required. The frame was suspended by means of 42 s.w.g. Eureka wire from the arm of an automatic analytical balance. The water temperature was *ca.* 22° C. This was not controlled thermostatically but differed only slightly from the temperature of the room, which was well screened from temperature fluctuations and draughts. To facilitate wetting a few drops of a detergent (Lissapol N) were added to the water.

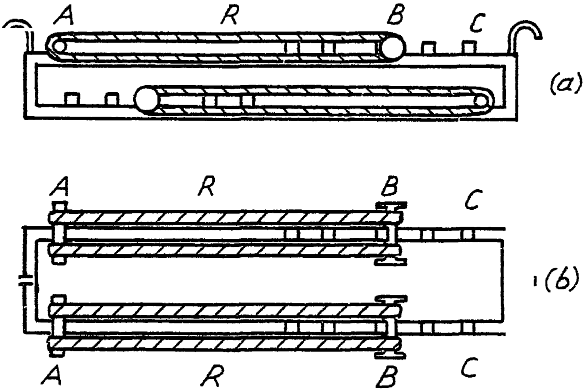

FIG. 1.—The stretching frame; (*a*) elevation, (*b*) plan.

The procedure adopted for the measurements was as follows. After immersion of the frame, with the specimens attached but not stretched, in the water bath, about 15 min. was allowed for thermal equilibrium to be established before recording the weight. The rings were then quickly stretched to the lowest extension, and after a few minutes the weight was again taken. Finally the rings were relaxed and the weight again determined. For the unstrained weight the mean of the initial and final readings was taken. The process was repeated, for the same strain, and in all at least six but usually eight readings of the required change in weight were taken; from these the average values of volume change for this strain were derived. During the time taken for a set of readings there was no appreciable change in the temperature of the water bath. The series of readings was then repeated at the higher extensions using the same rubber samples.

The results for the two differently cross-linked rubbers are represented in Fig. 2 in terms of the relative volume change $\Delta V/V$ as a function of the extension ratio $\alpha (= l/l_0)$. The extension ratios were calculated on the internal diameter of the rings.

The Tensile Measurements.—The force-elongation curves were measured on two of the rings actually used for the determination of the volume changes.

[6] Farmer, Moore and Morrell (unpublished work).

[7] Flory and Rehner, *J. Chem. Physics*, 1943, **11**, 521.

The length was measured to 0·5 mm. by means of a scale, and the tensions derived from the deformation of a calibrated flat steel spring. The rings were supported on brass rods of the same diameter as those fitted to the frame. The data obtained are shown in Fig. 3. There was a slight difference between figures for increasing and decreasing strain, especially for the lower modulus rubber, but this was never greater than 3 %. The curves shown represent the mean values.

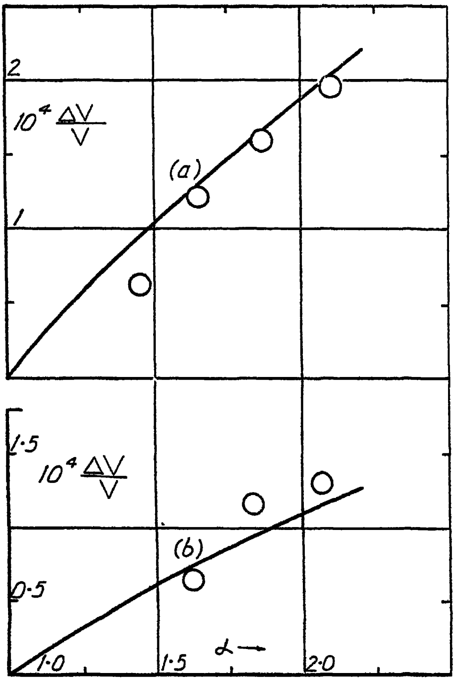

FIG. 2.—Volume changes on extension for two rubber samples : (a) M_c = 4900 ; (b) M_c = 9500 (curves theoretical).

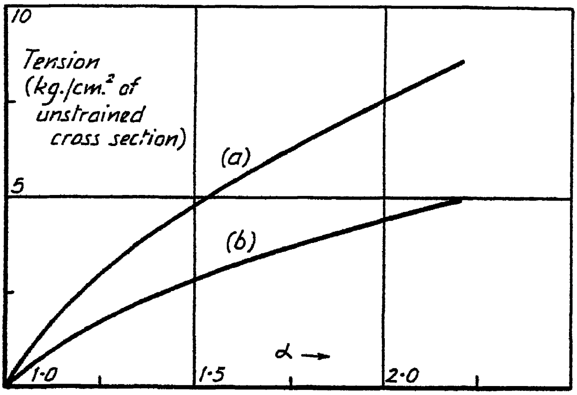

FIG. 3.—Force-elongation curves for the two rubber samples : (a) M_c = 4900 ; (b) M_c = 9500.

The calculation of the values of the integral in the expression (1) was carried out graphically using a figure of $5{\cdot}3 \times 10^{-5}$ bars^{-1} for the compressibility.[8] The theoretical volume-change curves thus derived are shown in Fig. 2.

There was some uncertainty with regard to the effective extension ratio for the rings, and the calculation of this quantity with reference to the internal diameter of the rings was arbitrary. However, since the same rings and the same method of holding were used in both the volume-change and tensile experiments, any error thus introduced would have had no effect on the relative values of the theoretical and experimental volume changes at a given extension ratio. In any case the accuracy of the tensile data is so much higher than that of the volume change data, that effects of this order may be neglected.

In view of the smallness of the volume change encountered, it is inevitable that the experimental errors in its measurement should be relatively large, probably in the neighbourhood of 10-20 %. To this degree of accuracy the data are in agreement with the calculated curves over the range of extension covered, i.e. up to 100 % extension.

Discussion

The evidence presented in this paper substantiates the interpretation put forward by Gee [2] and by Van der Wyk [4] to explain the internal energy and entropy changes which occur on stretching rubber. The conclusion to be drawn is that two distinct mechanisms are involved in the deformation : (1) a deformation of the molecular network, without change of volume, giving a *negative* entropy without change of internal energy for all extensions, in accordance with the basic assumptions of the statistical theory, and (2) a bulk expansion against intermolecular forces, due to the hydrostatic component of the applied stress, and giving rise to an *increase* of internal energy, with a corresponding *increase* of entropy. It should be repeated that the existence of the second mechanism, leading to an increase of volume, can be inferred from the fact that the material is compressible and initially isotropic ; that it should have been overlooked in some earlier thermodynamic studies is perhaps not surprising, in view of the smallness of the volume changes in question. What is surprising, at first sight, is that such relatively minute changes in volume should give rise to important internal energy and entropy changes.

It should be noted, however, that the contribution of the volume-change mechanism to the total stress or free energy of deformation is negligible, as may be seen from at least two independent arguments. (1) It has already been shown mathematically [2] that if a rubber, after extension at constant pressure, is compressed at fixed length to its original unstrained volume, the tension will remain practically unchanged. This means that the force-extension relation is essentially unaffected by the existence of the volume-change mechanism. (2) The work done by the applied tensile stress may be analyzed into two components, (*a*) the work done by the hydrostatic component of the stress in producing the change of volume, and (*b*) the work done by the shear stresses in producing the change of shape. Of these, it may be shown that in a typical case (*a*) is very small compared with (*b*). The effective hydrostatic tension is numerically equal to one-third of the tensile stress.[2] For one of the rubbers examined, the hydrostatic tension at 50 % elongation was *ca.* $2{\cdot}5$ kg./cm.^{2} and the corresponding expansion $\Delta V/V$ was $1{\cdot}25 \times 10^{-4}$, giving a contribution to the work (assuming ΔV proportional to P) of $1{\cdot}5_6 \times 10^{-4}$ kg. cm. per cm.^{3} of rubber. The total work done by the applied force is $\int_{l_0}^{l} f \, . \, dl$, which for an extension of 50 % was $\sim 1{\cdot}5$ kg. cm. This is about 10,000 times that due to the volume-change mechanism (*a*). It follows, therefore, that the latter makes no significant contribution to the total elastic stress.

This result may be regarded as a direct consequence of the fact that the bulk modulus of a rubber is higher than the Young's modulus by a factor of 10^4. The dimensional changes associated with the hydrostatic tension are therefore smaller, by a factor of this order, than the total dimensional changes accompanying the tensile stress. (Contrast the behaviour of a "hard" solid, for which the two moduli are of comparable magnitude.)

---

[8] Wood, *Proc. Rubber Tech. Conf., London,* 1938, p. 933.

From these arguments it must be concluded that the existence of an internal energy change on deformation does not necessarily imply that the mechanism with which the internal energy change is associated makes a significant contribution either to the elastic stress or to the elastic deformation.

The comparatively large internal energy changes found in the early stages of the extension of rubber may be regarded as arising from the expansion of the material against the *internal* pressure, which for natural rubber is about 4000 kg./cm.^{2}. If instead of a tensile stress one applies a unidirectional compressive stress, the volume is reduced, and the sign of the internal energy change reversed. The network entropy change is of course still negative. The total entropy change is therefore negative for all values of compression ; in particular the thermo-elastic inversion phenomenon, observed on extension,[9] whereby the stress-temperature coefficient and the entropy of deformation change sign (at about 10 % extension) does not appear. In shear also this effect is absent, but in this type of strain there is no volume change, and consequently no internal energy change.

It follows, therefore, that the changes in internal energy and entropy which accompany the elastic deformation of any material do not necessarily yield direct information regarding the mechanism of deformation, but must be interpreted with considerable caution and in the light of all the relevant facts. The analysis discussed in this paper appears to account in a natural way for the phenomena exhibited by amorphous rubber subjected to relatively small strains. It is, however, only valid for *isotropic* materials, and cannot therefore be applied to highly-extended rubber, in which the anisotropy due directly to the strain may be enhanced by crystallization. In this region the evidence of Wood and Roth [8] indicates that the negative internal energy and entropy changes due to crystallization completely obscure the primary effects due to the elastic network. Similar or even greater difficulties may arise in the investigation of highly-oriented crystalline fibres, such as wool,[10] hair,[11] Nylon [10] and cellulosic materials,[12] for which attempts have been made to interpret the thermo-elastic phenomena. If, as often happens, the fibre is hygroscopic, there is the added difficulty to which Woods [13] has drawn attention, that the water absorption may be a function not only of the temperature but also of the stress.

The investigation described in this paper forms part of the research programme of the British Rubber Producers' Research Association.

British Rubber Producers' Association,
48-52 *Tewin Road,*
Welwyn Garden City,
Herts.

[9] Meyer and Ferri, *Helv. chim. Acta*, 1935, **17**, 570.
[10] Woods, *J. Colloid Sci.*, 1946, **1**, 407.
[11] Bull, *J. Amer. Chem. Soc.*, 1945, **67**, 533.
[12] Busse, Lessig, Loughborough and Larrick, *J. Appl. Physics*, 1942, **13**, 715.
[13] *Nature*, 1949, **164**, 33.

HIGH POLYMER SOLUTIONS

III.—THE RELATION BETWEEN INTRINSIC VISCOSITY AND MOLECULAR WEIGHT FOR POLYSTYRENE FRACTIONS IN BENZENE, TOLUENE, CHLOROFORM, ETHYL BENZENE AND METHYL ETHYL KETONE.

By C. E. H. Bawn, R. F. J. Freeman and A. R. Kamaliddin

Received 2nd June, 1950

Measurements of the intrinsic viscosity of polystyrene fractions in five solvents at 25° C are in accord with the viscosity-molecular weight relationship $[\eta] = KM^{\alpha}$; α attains a limiting value of 0·73 in good solvents. The decrease in α as the solvent becomes poorer is accompanied by a corresponding increase in K and these two magnitudes are related.

The empirical equation (1) relating the intrinsic viscosity $[\eta]$ with the molecular weight M is now well established for many systems

$$[\eta] = KM^{\alpha}. \qquad . \quad . \quad . \quad . \quad . \qquad (1)$$

K and α are constants characteristic of the polymer-solvent system and except with very low molecular weight fractions the experimental evidence indicates that their values are constant and independent of molecular weight. For chain type molecules α assumes a value between $\frac{1}{2}$ and 1 for different polymer-solvent systems.

The many attempts to deduce eqn. (1) theoretically have been based on the hydrodynamic theory of viscosity combined with the statistical evaluation of the configuration of the chain. The original Staudinger equation ($\alpha = 1$) has been derived [1] for a free draining coil it being assumed that the resistance to flow of the solvent was the same for each element of the chain. Later, Debye and Bueche [2] showed that with a random coiled structure the outer elements disturb the flow inside the coil and that the inner elements are partly shielded from interaction with the solvent. Introducing hydrodynamic shielding these authors and Brinkman[3] independently. showed that eqn. (1) followed indirectly and that α should decrease from 1·0 to 0·5 as the molecular weight increases, the latter value applying to very large molecular weights. A similar conclusion has been reached by Kirkwood and Riseman [4] for a random coil structure with hindered rotation but using a different mathematical approach. Recently, Flory [5] has shown that special interferences between distantly connected segments of a chain neglected in the usual random flight approximation leads to the intrinsic viscosity law (1) with α between 0·5 and 0·8 depending on solvent and chain length, independent of permeability considerations. Thus besides their usefulness in molecular weight determination the values of K and α are important in assessing the influence of solvent on the configuration of the polymer chain. The present measurements refer to the viscosity-molecular weight relationships for polystyrene fractions (used for osmotic pressure measurements described in Part II) in five pure solvents. In the following paper the corresponding relationships are determined for mixed solvents, and the experimental results discussed in relation to the above theories.

---

[1] Huggins, *J. Physic. Chem.*, 1938, **42**, 911; *ibid.*, 1939, **43**, 439. Debye, *J. Chem. Physics*, 1946, **14**, 636.

[2] Debye and Bueche, *ibid.*, 1948, **16**, 573.

[3] Brinkman, *Appl. Sci. Res. A*, 1947, **1**, 27; *Physica*, 1947, **13**, 447.

[4] Kirkwood and Riseman, *J. Chem. Physics*, 1948, **16**, 565.

[5] Flory, *ibid.*, 1949, **17**, 303.

Intrinsic Viscosity-Molecular Weight Relations for Polystyrene.— Many measurements have been made of the intrinsic viscosity-molecular weight relationship for polystyrene. Staudinger[6] employing eqn. (1) with $\alpha = 1$ and using benzene as solvent observed that $K = 1{\cdot}7 \times 10^{-5}$ g./100 ml. of solution. (This unit of concentration is used throughout this paper and the relationships recorded refer to measurements at room temperature.) Schulz and Huseman[7] noted that K_{benzene} (taking $\alpha = 1$) varied from 0·4 to $1{\cdot}56 \times 10^{-5}$ for polymers covering the molecular weight range 24,000-550,000, samples being prepared by polymerization at 20° to 240° C. These workers[8] later found that for benzoyl peroxide catalyzed polymerization a sharp fraction gave a value of $K = 4{\cdot}6 \times 10^{-5}$, whilst the unfractionated sample had a K value of $6{\cdot}4 \times 10^{-6}$. Schulz,[9] in agreement with previous observations of Staudinger and Schulz,[9] concluded in later investigations that preparations carried out at different temperatures showed different degrees of chain branching and this was given as the reason for the variability of K for the samples prepared under different conditions. He stated that no branching occurred for polymerization at 20° C and was small for temperatures of 50-100° C. In later publications Schulz and Hengensburg,[10] still adhering to the original Staudinger equation, quote a range of values of K_{toluene} from 5·9 to $9{\cdot}0 \times 10^{-5}$ (average = 6·60) for a series of fractionated and unfractionated polymers prepared under varying conditions and at temperatures from 20-180° C. In methyl *iso*propyl ketone, however, Hengensburg and Schulz[10] conclude that the exponent α had the value 0·73. Using material of low degrees of polymerization from dimer up to molecular weight of 3000 and determining the molecular weight cryoscopically in benzene, Kemp and Peters[11] showed that the original Staudinger equation was obeyed with $\alpha = 1$ and $K = 5{\cdot}4 \times 10^{-5}$, a value 3·2 times greater than that found by Staudinger. Recently, Bamford and Dewar[12] have tested eqn. (1) for low molecular weight polymers (below the osmotic pressure range) made by a transfer reaction with a halogenated solvent, the molecular weight being determined by estimation of the chlorine content of the polymer. Their measurements satisfy

$$[\eta] = 4{\cdot}40 \times 10^{-4} M^{0{\cdot}65}$$

for unfractionated polymer in toluene and they state that K has this same value in styrene monomer and in benzene. These authors also state that this expression gave results which agree closely with the cryoscopic results for low molecular weight polymers. Examination of their data, however, shows that agreement is good only above molecular weights of 1100.

A detailed study of the thermal polymerization of styrene under varied conditions was carried out by Alfrey, Bartovics and Mark.[13] Samples prepared at 60, 120 and 180° C each to the extent of 40 % were fractionated and the viscosity-molecular weight relationships determined. The K's and α's for the three samples measured in toluene were $1{\cdot}6 \times 10^{-2}$, $6{\cdot}6 \times 10^{-3}$ and $4{\cdot}0 \times 10^{-4}$ and 0·70, 0·80 and 1·10 respectively. The authors attribute these differences to changes in the internal architecture of the macro-molecules. Recently Goldberg, Hohenstein and Mark[14] have redetermined the viscosity-molecular weight relationship for a fractionated polystyrene prepared by emulsion polymerization at 63° C. The results obtained for toluene and methyl ethyl ketone were

---

[6] Staudinger, *Die Hoch molekularen Organischen Verbindungen* (Berlin, 1932).

[7] Schulz and Huseman, *Z. physik Chem. B*, 1936, **34**, 194.

[8] *Idem. ibid.*, 1938, **39**, 246.

[9] Schulz, *ibid.*, 1939, **44**, 227. Staudinger and Schulz, *Ber.*, 1935, **68**, 2320.

[10] Hengensburg and Schulz, *Makromol. Chem.*, 1948, **2**, 5.

[11] Kemp and Peters, *Ind. Eng. Chem.*, 1942, **34**, 1097.

[12] Bamford and Dewar, *Proc. Roy. Soc. A*, 1948, **192**, 329.

[13] Alfrey, Bartovics and Mark, *J. Amer. Chem. Soc.*, 1943, **65**, 2319.

[14] Goldberg, Hohenstein and Mark, *J. Polymer Sci.*, 1947, **2**, 503.

$$[\eta]_{\text{toluene}} = 3{\cdot}7 \times 10^{-4} M^{0{\cdot}62},$$
$$[\eta]_{\text{MEK}} = 7{\cdot}0 \times 10^{-4} M^{0{\cdot}53}$$

In many recent American papers, relationships derived by Ewart and Tingey [15] have received wide acceptance. Since the details of these determinations do not seem to have been published we quote their relationship for benzene solution and molecular weight range 50,000-800,000, viz.,

$$[\eta] = 7{\cdot}54 \times 10^{-5} M^{0{\cdot}783}.$$

Further data were reported by Wales, Williams, Thompson and Ewart,[16] and by combination of these results with previous measurements by Ewart and Tingey and by Alfrey and others these authors conclude that α for benzene lies between 0·69 and 0·75. Gregg and Mayo [17] using chlorine analyses of transfer polymers prepared in carbon tetrachloride for molecular weight determination in the range 10,000-200,000 and osmotic pressure measurements for molecular weights 80,000-600,000 derive the relationship

$$[\eta] = 1{\cdot}935 \times 10^{-4} M^{0{\cdot}711}.$$

It is apparent that a wide divergence exists in the values of K and α determined by different workers for polystyrene fractions in identical solvents. These variations may be attributed to two main causes: (i) The polymers have been prepared to different extents of polymerization—an approach to complete polymerization may lead to chain branching and the resulting polymers would not obey the same viscosity law. High temperatures of polymerization also favour branching. (ii) Since the osmotic pressure measurements used for molecular weight determinations give a number average, comparison of osmotic and viscometric molecular weight (equal to weight average for homogeneous polymers) can only be satisfactorily made with well-fractionated samples.

It is desirable, therefore, in the determination of intrinsic viscosity-molecular weight relationships for linear polymers to use carefully fractionated samples of a polymer prepared by polymerization of monomer at relatively low temperature and to less than 20 % of the complete extent of polymerization.

Experimental

The solvents used were laboratory grade toluene, benzene, methyl ethyl ketone (MEK), chloroform and ethyl benzene. The methyl ethyl ketone was dried over anhydrous sodium sulphate, and the other solvents with calcium chloride. All solvents were fractionally distilled before use.

Measurements were made with a modified Ostwald viscometer, designed to have negligible kinetic energy corrections. Some results obtained in this viscometer were compared with results obtained in a viscometer the kinetic energy corrections of which had been carefully determined. The two sets of results agreed within the experimental error. Viscosities of the solution were determined at 25° C for at least four concentrations, and in most cases in the region 0·1-1 %.

The polystyrene fractions were prepared from monomer thermally polymerized to not greater than 20 % by procedures described in Part II. Molecular weights were determined by osmotic pressure measurements as previously described (Part II).

The intrinsic viscosities were determined by extrapolation of the plots η_{sp}/c against c (concentration expressed as g. 100 ml. of solution). The experimental curves were well representeed by Huggins [18] equation

$$\eta_{sp}/c = [\eta] + k'[\eta]^2 c \quad . \quad . \quad . \quad . \quad (2)$$

---

[15] Ewart and Tingey, quoted by Smith, *J. Amer. Chem. Soc.*, 1946, **68**, 2063.

[16] Wales, Williams, Thompson and Ewart, *J. Physic. Chem.*, 1948, **52**, 983.

[17] Gregg and Mayo, *J. Amer. Chem. Soc.*, 1948, **70**, 2373.

[18] Huggins, *ibid.*, 1942, **64**, 1557.

for the molecular weight range 70,000 to 2,000,000 and concentrations up to 1 % and for solutions in good solvents. For methyl ethyl ketone the η_{sp}/c against c curves departed from linearity, the curvature increasing with both concentration and molecular weight. An expression (3) initially proposed by Huggins and widely used by Schulz and his co-workers [19]

$$[\eta] = \frac{\eta_{sp}/c}{1 + K\eta_{sp}}, \qquad \ldots \ldots \quad (3)$$

or

$$\eta_{sp}/c = [\eta] + K[\eta]\,\eta_{sp},$$

is formally equivalent to the general expression (2) for low concentrations and the plot of η_{sp}/c against η_{sp} give the same intrinsic viscosity. The value of k' (eqn. (2)) was independent of molecular weight in a given solvent but varied with the solvent as shown in Table II.

Results

Table I summarizes the molecular weights and intrinsic viscosities of the polystyrene fractions in benzene, toluene, chloroform, ethyl benzene and methyl ethyl ketone at 25° C. The plot of log $[\eta]$ against log M (Fig. 1) shows that the results fit eqn. (1) with the values of the constant K and α given in Table II. The results show that the fractions obtained from samples polymerized to the extent of 20 % at temperatures 60, 100 and 135° C all fall on the same straight line and thus there is no reason to assume that the samples have different molecular characteristics.

TABLE I

Sample	$10^{-4}M$	C_6H_6	$CHCl_3$	$C_6H_5CH_3$	$C_6H_5C_2H_5$	MEK
S_1 I*b*	180	4·92	—	—	—	—
S_1 I*d*	150	3·85	3·76	3·39	2·89	1·69
S_1 II*b*	140	3·68	—	—	—	—
S_2 II*a*	110	2·72	—	—	—	—
S_2 II*b*	90	2·36	2·28	2·12	1·88	1·09
S_2 IV*a*	50	1·56	—	—	—	—
S_3 II*a*1	29	1·13	1·07	0·99	0·91	0·57
S_3 III*a*	16	0·71	0·69	0·66	0·63	0·40
S_3 IV*b*	9·4	0·48	—	—	—	—
S_3 V*b*	7·2	0·39	0·38	0·37	0·34	0·25

TABLE II.—VISCOSITY AND VISCOSITY-MOLECULAR WEIGHT CONSTANTS FOR POLYSTYRENE

Solvent	$K \times 10^4$	α	k'
Benzene	1·13	0·73	0·35
Chloroform . . .	1·12	0·73	0·36
Toluene . . .	1·34	0·71	0·38
Ethyl benzene . . .	1·76	0·68	0·39
MEK	3·05	0·60	(0·55)

Relationship between Viscosities in Different Solvents.—It follows from eqn. (1) that the intrinsic viscosities of a polymer fraction in two different solvents are related. Thus if $[\eta]_1$, K_1 and α_1 and $[\eta]_2$, K_2 and α_2 refer to any two solvents, then substitution in eqn. (1) gives

$$\log [\eta]_1 = \log K_1 - \frac{\alpha_1}{\alpha_2} \log K_2 + \frac{\alpha_1}{\alpha_2} \log [\eta]_2,$$

or

$$\log [\eta]_1 = A + B \log [\eta]_2.$$

The logarithms of the intrinsic viscosities in C_6H_6 were plotted against those in the other solvents, and resulting linear relationships satisfied the following equations :—

---

[19] Schulz and Blaschke, *Z. physik. Chem. B*, 1941, **50**, 305.

$$\begin{aligned} \log\,[\eta]_{C_6H_6} &= 0{\cdot}01_2 + 1{\cdot}00_4 \log\,[\eta]_{CHCl_3}, \\ &= 0{\cdot}03_5 + 1{\cdot}03_4 \log\,[\eta]_{\text{toluene}}, \\ &= 0{\cdot}08_7 + 1{\cdot}07_8 \log\,[\eta]_{C_6H_5\cdot C_2H_5}, \\ &= 0{\cdot}33_3 + 1{\cdot}22_9 \log\,[\eta]_{\text{MEK}}. \end{aligned}$$

These results agree very closely with the similar measurements of Goldberg, Hohenstein and Mark [14] for fractions in toluene and methyl ethyl ketone. The equations obtained were :

$$\begin{aligned} \log\,[\eta]_{\text{toluene}} &= 0{\cdot}28 + 1{\cdot}18 \log\,[\eta]_{\text{MEK}}\ ; && \text{(Goldberg } et\ al.\text{)} \\ &= 0{\cdot}29 + 1{\cdot}19 \log\,[\eta]_{\text{MEK}}\ ; && \text{(present investigation).} \end{aligned}$$

The value of K and α obtained by these authors were $3{\cdot}7 \times 10^{-4}$, $0{\cdot}62$ and $7{\cdot}0 \times 10^{-4}$, $0{\cdot}53$ for toluene and methyl ethyl ketone respectively and were not in satisfactory agreement with our measurements. The differences must be ascribed to an uncertainty in the molecular weights.

Discussion

The results of Fig. 1 show that the magnitudes of intrinsic viscosity of polystyrene fractions in different solvents are determined by the values

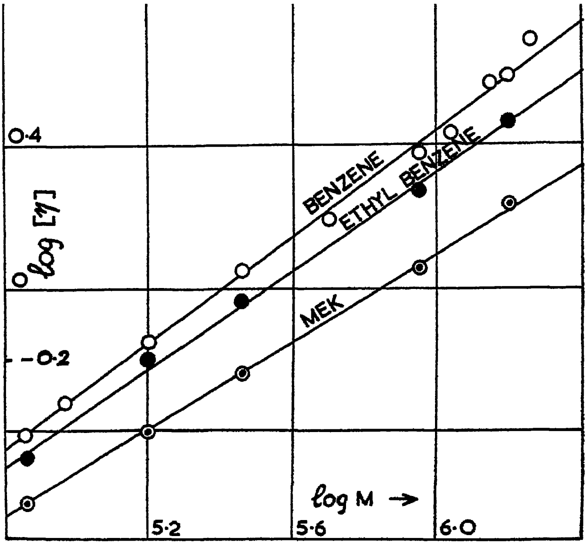

FIG. 1.—Viscosity-molecular weights relationship, ln $[\eta]$ = ln K + α ln M.

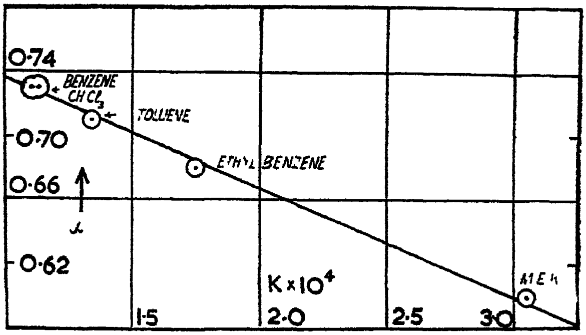

FIG. 2.—Variation of K with α ($[\eta] = KM^{\alpha}$) in pure solvents.

of both K and α. Furthermore, K and α for a single solvent are independent of molecular weights over the molecular weight range 70,000-2,000,000. The value of α in the best solvents for polystyrene yet known is 0·73 and there is no indication that α approaches the limited value of $\frac{1}{2}$ as predicted by theory [1, 2, 3] for very large molecular weights. It is interesting to note that both K and α have nearly equal values in the best solvents, and that there is an apparent linear relationship (Fig. 2) between α and K. Measurements on mixtures covering a wide range of solvent power (Part II) indicate a slightly curved plot of K against α, which approximates to a linear law over a narrow range of change of α. These results are extended and discussed in more detail in the following paper where it is shown that α is related to the internal configuration of the chain and approaches the limiting value of $\alpha = \frac{1}{2}$ (impenetrable spheres) at the precipitation point.

Department of Inorganic and Physical Chemistry,
University of Liverpool.

HIGH POLYMER SOLUTIONS

PART IV.—THE INTRINSIC VISCOSITY-MOLECULAR WEIGHT RELATIONSHIPS IN MIXED SOLVENTS

BY C. E. H. BAWN, T. B. GRIMLEY AND M. A. WAJID

Received 2nd June, 1950

The relation between the intrinsic viscosity and the molecular weight of polystyrene fractions (mol. wt. 72,000-1,600,000) in toluene-heptane and toluene-methyl alcohol mixed solvents, has been investigated. The relationship, $[\eta] = KM^{\alpha}$, was obeyed in all cases and with a constant value of α for any mixture. The value of α decreases in bad solvents reaching the value $\frac{1}{2}$ at the precipitation point. A single relationship exists between α and K for all pure and mixed solvents examined. The theories of viscosity advanced by Debye and Bueche and by Kirkwood and Riseman are used to evaluate the influence of the solvent on the average dimensions of a polymer molecule. At constant molecular weight the "effective bond length" b, in the equation $R^2 = b^2Z$ (R^2 is the mean square displacement of the chain ends and Z the degree of polymerization) decreases in bad solvents, but at the precipitation point, b is independent of the nature of the precipitating mixture. The importance of the so-called "volume effect" of coiling chain molecules and the difficulties in the way of its detection by viscosity measurements is briefly discussed.

The intrinsic viscosities of dilute solutions of a polymer vary with the nature of the solvent. Flexible chain polymers exhibit higher intrinsic viscosities in good solvents than in poor solvents and these effects may be interpreted in terms of the types of interaction between solvent and polymer molecules.[1] In the previous paper (Part III) [2] the effect on the viscosity of polystyrene solutions of the change from good solvents, benzene and toluene, to the poorer solvent, methyl ethyl ketone, have been summarized. Equally valuable information can be obtained from viscosity measurements in mixed solution provided that the solvents are carefully chosen. Thus the solvent power can be varied by adding either a poor or a non-solvent to a good solvent. In the present investigation

[1] Alfrey, Bartovics and Mark, *J. Amer. Chem. Soc.*, 1942, **64**, 1557.
[2] Bawn, Freeman and Kamaliddin, *Trans. Faraday Soc.*, 1950, **46**, 862.

the intrinsic-viscosity molecular weight relationships have been determined for polystyrene fractions in mixed solvent systems as far as the precipitation point. The influence of solvent medium on the dimensions of the molecule has been evaluated.

Experimental

Materials.—Five polystyrene fractions of molecular weights ranging from 72,000 to 1,600,000 prepared as described in Part II[3] were used. Recovery of these samples by precipitation by excess methyl alcohol from all solvents employed caused no change in the specific viscosity concentration curve for toluene and thus it may be assumed that the distribution function of individual fractions was unchanged.

Intrinsic Viscosity Measurements.—The intrinsic viscosities were determined as in the previous paper [2] from the plot of η_{sp}/c_2 against c_2. The Huggins equation

$$\eta_{sp}/c_2 = [\eta] + k'[\eta]^2 c_2$$

was obeyed in all cases and the plots showed no indication of curvature even at the highest proportions of non-solvent in the mixtures employed. (All measurements were carried out at 25° C.)

Precipitation Point.—The percentage of non-solvent to cause precipitation was determined by micro-titration of the non-solvent against 5 ml. of the solution of polymer of known concentration (made up by weighing). The titration vessel was thermostated at 25·0 ± 0·02° C. The titration point was taken as the first sign of permanent turbidity and was reproducible to within one drop of non-solvent. The percentage non-solvent γ to cause precipitation was found to be dependent on the initial concentration of the polymer in the solution and increased with increase in dilution. The value of γ at infinite dilution was determined by extrapolation of the plot of γ against percentage of polymer in solution. A typical plot is shown in Fig. 1, and in all mixtures and for all fractions used the plot showed similar curvature. The value of $[\eta]$ at the precipitation point was obtained by extrapolation of the curve of $[\eta]$ against percentage precipitant (Fig. 2).

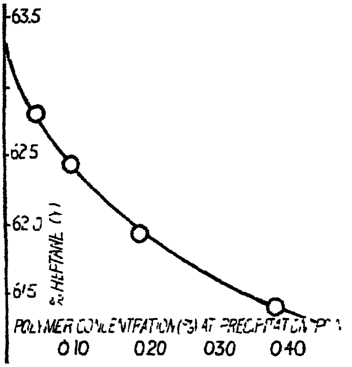

FIG. 1.—Precipitation point and polymer concentration (toluene-heptane).

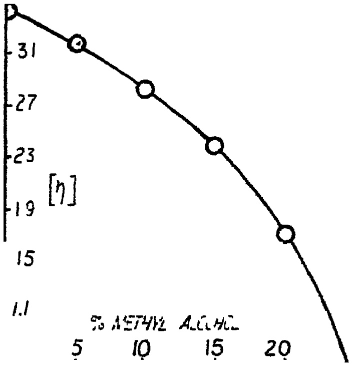

FIG. 2.—Variation of $[\eta]$ with % precipitant for toluene-methyl alcohol mixtures.

Results

INTRINSIC VISCOSITIES.—The addition of non-solvent caused a marked decrease in $[\eta]$ with all fractions. A typical plot of $[\eta]$ against percentage precipitant is shown in Fig. 2, and the results for all mixtures are summarized in Tables I and II.

The results confirm the previous observation by Alfrey, Justice and Nelson [4] for polystyrene and by Craggs and Rogers[5] for G.R.S. who showed that the intrinsic viscosity at the precipitation point for any fraction was independent of solvent composition. This indicates that the configuration of the molecular coil is similar in all solvents as the precipitation point is approached and this is in agreement with other results reported later.

---

[3] Bawn, Freeman and Kamaliddin, *Trans. Faraday. Soc.*, 1950, **46**, ref. to preceding paper, Part III.

[4] Alfrey, Justice and Nelson, *Faraday Soc. Discussion*, 1946, 50.

TABLE I

% Heptane by vol. at 25° C	Toluene-heptane mixtures $[\eta]$ for different fractions				
	M. wt. =				
	160×10^4	90×10^4	29×10^4	16×10^4	$7 \cdot 2 \times 10^4$
0	3·39	2·12	0·990	0·660	0·360
10	3·14	1·95	0·946	0·630	0·340
20	2·86	1·80	0·885	0·595	0·325
30	2·56	1·64	0·810	0·556	0·307
40	2·25	1·42	0·717	0·500	0·278
55	1·50	0·92	0·540	0·390	0·240
% Methyl alcohol by vol. at 25° C	Toluene-methyl alcohol mixtures				
0	3·39	2·12	0·990	0·660	0·360
5	3·18	2·02	0·976	0·645	0·352
10	2·85	1·84	0·915	0·620	0·340
15	2·40	1·56	0·795	0·555	0·310
20	1·75	1·19	0·640	0·470	0·280

TABLE II.—COMPOSITION OF PRECIPITATING MIXTURES AND VALUES OF EXTRAPOLATED INTRINSIC VISCOSITIES AT PRECIPITATION POINTS

Mol. wt.	Toluene-heptane		Toluene-methyl alcohol	
	% heptane	$[\eta]$	% MeOH	$[\eta]$
160×10^4	63·3	0·86 ± 0·05	24·3	0·86 ± 0·05
90×10^4	64·7	0·56 ± 0·05	25·0	0·57 ± 0·05
29×10^4	66·8	0·33 ± 0·02	26·4	0·32 ± 0·02
16×10^4	69·9	0·23 ± 0·02	27·7	0·25 ± 0·02
$7 \cdot 2 \times 10^4$	74·2	0·16 ± 0·02	31·3	0·16 ± 0·02

Viscosity-Molecular Weight Relationships.—The results of the measurement of the dependence of $[\eta]$ on molecular weight for a series of solvent-precipitant mixtures are shown in Fig. 3 and 4. In all cases the relationship

$$[\eta] = KM^{\alpha} \quad . \quad . \quad . \quad . \quad . \quad . \quad (1)$$

was obeyed and the values of K and α for a series of solvents are summarized in Table III.

The value of α at the precipitation point obtained by extrapolation of the plot of α against percentage precipitant (Fig. 5) was 0·5 within the experimental limits of determination of the precipitation point for both mixtures. A plot of the values of log $[\eta]$ at the precipitation point against log M was linear and of slope $\alpha = 0 \cdot 51$, ($K = 6 \cdot 1 \times 10^{-4}$). These results lead to the important conclusion that precipitation is characterized by a value of $\alpha = 1/2$.

It is noticeable that there is little change in K with the addition of 10-15 % heptane but with further amounts of precipitant its value increases rapidly. In contrast K increases considerably with addition of small amounts of methyl alcohol and this may be ascribed to the fact that methyl alcohol is a more effective precipitant than heptane. The decrease in α which occurs in both cases

---

[5] Craggs and Rogers, *Can. J. Res. B*, 1948, **26**, 230.

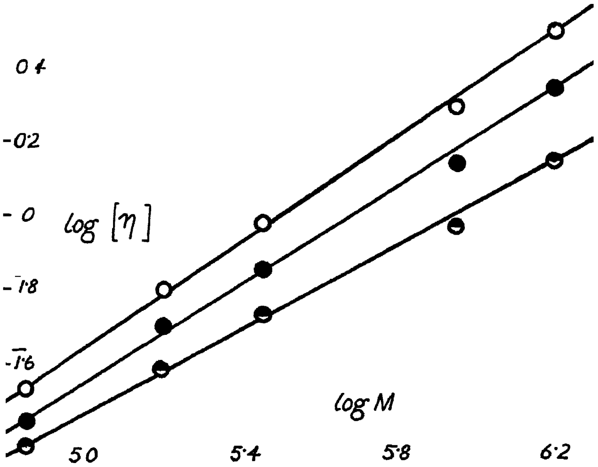

FIG. 3.—Viscosity-molecular weight relationships for toluene-heptane mixtures.

○ 10 % Heptane. ● 30 % Heptane. ⊖ 55 % Heptane.

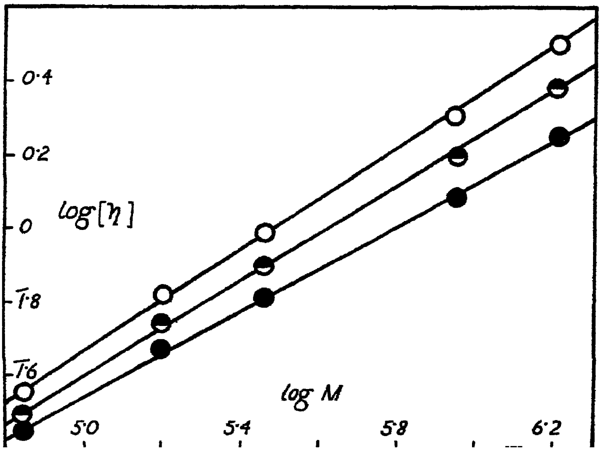

FIG. 4.—Viscosity-molecular weight relationships for toluene-methyl alcohol mixtures.

○ 5 % MeOH. ⊖ 15 % MeOH. 20 % MeOH.

TABLE III

Solvent	$K \times 10^4$	α
Toluene	1·34	0·71
+ 10 % Heptane	1·39	0·70
+ 20 % „	1·48	0·69
+ 30 % „	1·89	0·67
+ 40 % „	2·49	0·63
+ 55 % „	4·34	0·57
Toluene		
+ 5 % MeOH	1·50	0·70
+ 10 % „	1·75	0·68
+ 15 % „	2·22	0·65
+ 20 % „	3·98	0·59

as the solvent becomes poorer is accompanied by an increase in K' and a single relationship exists between α and K' (Fig. 6) for all pure and mixed solvents examined.

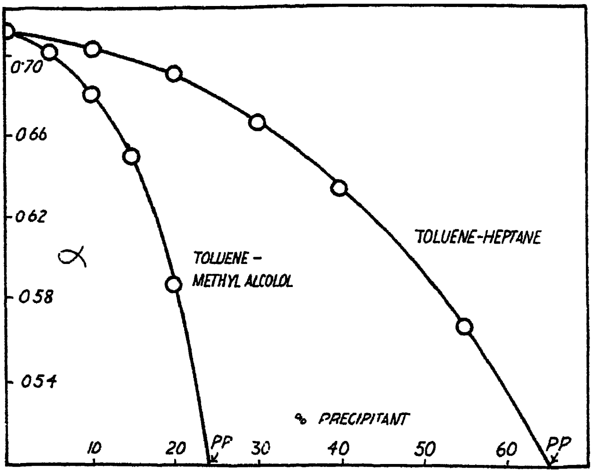

FIG. 5.—Decrease of α with % precipitant for toluene-heptane and toluene-methyl alcohol mixtures. (P.P. denotes precipitation point.)

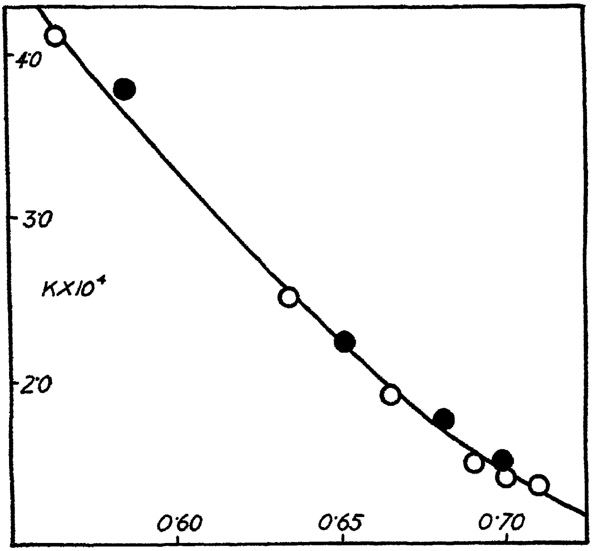

FIG. 6.—Variation of K' with α in $[\eta] = K'M^{\alpha}$.
● Toluene-heptane. ○ Toluene-MeOH. (Compositions as in Table III.)

Discussion

Theories of viscosity in relation to the size and shape of flexible macromolecules have recently been developed by Debye and Bueche,[6] Kirkwood and Riseman,[7] and by Brinkman.[8] The first-named authors consider

---

[6] Debye and Bueche, *J. Chem. Physics*, 1948, **16**, 573.
[7] Kirkwood and Riseman, *ibid.*, 1948, **16**, 565.
[8] Brinkman, *Appl. Sci. Res. A*, 1947, **1**, 27 ; *Physica*, 1947, **13**, 565.

the flow of solvent through a randomly coiled particle. Assuming the pearl necklace model they consider the disturbance of flow through the particle produced by its independent segments. The segments interfere with one another hydrodynamically with the result that the inner parts of the polymer molecule are shielded from the solvent by outlying portions. This shielding effect is greater for large molecules than for small ones.

The theories of both Debye and Kirkwood allow of the calculation of the effective length of the coil once the intrinsic viscosity-molecular weight relationship has been determined. The mathematical approach of these authors differs in that Kirkwood uses the statistics of the polymer chain with hindered rotation, whereas Debye replaces the polymer molecule by a hydrodynamically equivalent sphere of uniform segment density. It is thus necessary to consider separately the application of these theories to our results.

The Theory of Debye and Bueche.—The above-mentioned disturbance of flow appears in the theory of Debye and Bueche as a volume factor $\phi(\sigma)$ which is a function of the shielding ratio $\sigma = R_s/L$. R_s is the radius of the substituted sphere and L is a measure of the extent to which the velocity field of the solvent penetrates into the sphere. The formula for the intrinsic viscosity is

$$[\eta] = (4\pi R_s^3/3)(N/M_2)\phi(\sigma), \quad . \quad . \quad . \quad (2)$$

where N is Avogadro's number and M_2 the molecular weight of the polymer. Debye and Bueche show that for small values of the shielding ratio ($L \rightarrow R_s$), R_s is given by

$$R_s = 0{\cdot}527\,(<R^2>)^{\frac{1}{2}}, \quad . \quad . \quad . \quad . \quad (3)$$

where $<R^2>$ is the mean square separation of the chain ends. In these circumstances (free draining coil) eqn. (2) degenerates to

$$[\eta] = (\zeta/36\eta_0 m)<R^2>,$$

where ζ is the friction factor for one bead and m is the mass of a bead. Since $<R^2>$ for a random coil is proportional to the degree of polymerization, $[\eta]$ is proportional to M_2 and this is the Staudinger relationship. On the other hand, for large values of the shielding ratio ($L \rightarrow 0$), the polymer molecule approximates to a rigid sphere and it is shown that in this case eqn. (2) yields the Einstein relationship

$$[\eta] = 5/2(\Omega_s/Zm),$$

where $\Omega_s = 4\pi R_s^3/3$ and Z is the degree of polymerization.

In the intermediate case, the intrinsic viscosity is given by (2) and the viscosity-molecular weight law (1) follows somewhat indirectly. The theory predicts, as does that of Kirkwood and Riseman, that the value of the exponent α should decrease from 1 for low molecular weight polymers to 1/2 for very high molecular weights. To every value of Z (the degree of polymerization) and for a given solvent there belongs a definite exponent α, from which may be calculated a definite shielding ratio σ and hence a unique volume factor $\phi(\sigma)$. Simultaneous values of these last three quantities are tabulated by Debye and Bueche, so that using the measured values of $[\eta]$, the radius R_s of the equivalent sphere may be calculated from (2). In this connection it should be pointed out that since the experimental data is adequately represented in all cases by an equation of the form (1), we have followed Debye and Bueche in supposing that the value of α corresponds exactly to the average molecular weight (on a logarithmic scale) of the interval studied, i.e. to a molecular weight of 340,000. The results are summarized in Table IV which also contains values of $(<R^2>)^{\frac{1}{2}}$ calculated from (3) and values of b, the effective bond length calculated from the equation

$$<R^2> = b^2 Z. \quad . \quad . \quad . \quad . \quad . \quad (4)$$

Dependence of $< R^2 >$ on Solvent Composition.—The average configuration of a polymer molecule depends firstly on the bond lengths, bond angles and steric effects present in the molecule and secondly on the interactions between the molecule and the solvent environment. For any polymer fraction at a definite temperature, viscosity changes can be explained qualitatively[1] in terms of the contraction of the molecular coil as the solvent power decreases. The progressive decrease in the magnitude of $(< R^2 >)^{\frac{1}{2}}$ in going from good to bad solvents as exhibited in Table IV, gives quantitative expression to these ideas. In addition it should be remarked that the average dimension of the molecular coil at the precipitation point is the same in either solvent mixture.

TABLE IV.—MOLECULAR PARAMETERS FOR POLYSTYRENE OF MOLECULAR WEIGHT 340,000

Solvent	α	Debye-Bueche			Kirkwood-Riseman	
		R_s(Å)	$(<R^2>)^{\frac{1}{2}}$ Å	b (Å)	$(<R^2>)^{\frac{1}{2}}$ (Å)	b (Å)
Benzene	0·73	246	468	5·78	624	7·70
Toluene	0·71	233	443	5·46	586	7·25
Methyl ethyl ketone . .	0·60	170	323	3·99	431	5·32
90 % toluene, 10 % heptane	0·70	224	426	5·26	566	7·00
80 % ,, 20 % ,,	0·69	215	408	5·05	543	6·72
70 % ,, 30 % ,,	0·67	208	396	4·89	526	6·51
60 % ,, 40 % ,,	0·63	185	352	4·35	478	5·81
45 % ,, 55 % ,,	0·57	160	304	3·75	403	4·98
95 % ,, 5 % methyl alcohol	0·70	230	438	5·42	576	7·12
90 % ,, 10 % ,,	0·68	216	412	5·08	546	6·75
85 % ,, 15 % ,,	0·65	198	376	4·64	477	5·90
80 % ,, 20 % ,,	0·59	173	330	4·07	441	5·46
Precipitating mixture .	0·51	128	243	3·00	322	3·98

Dependence of Intrinsic Viscosity on Molecular Configuration.—Combination of the hydrodynamic theory of viscosity with the statistical theory of the average configuration of the polymer molecule indicates that the exponent α is a measure of the extent of coiling of the molecule. The variation of the calculated value of $(< R^2 >)^{\frac{1}{2}}$ with the value of $[\eta]$ corresponding to the average molecular weight 340,000 is shown in Fig. 7. These results clearly indicate that, for a given molecular weight, the predominant factor determining the influence of solvent on the intrinsic viscosity is the effect of the solvent on the average configuration of a polymer molecule.

The Theory of Kirkwood and Riseman.—In a treatment which differs from that of Debye in that the flexible molecule is considered in terms of a random coil model with hindered rotation rather than by the substitution of an equivalent sphere, Kirkwood and Riseman[7] have shown that the hydrodynamic behaviour of a flexible molecule may be described in terms of the two parameters b and ζ; b is the effective bond length defined by (4) whilst ζ is again the friction constant per monomer unit. The equation for the intrinsic viscosity is ($[\eta]$ in 100 ml./g.)

$$\left.\begin{aligned}[\eta] &= (N\zeta b^2/3600\,\eta_0 M_0)ZF(\lambda_0 Z^{\frac{1}{2}}),\\ \lambda_0 &= \zeta/(6\pi^3)^{\frac{1}{2}}\eta_0 b,\end{aligned}\right\} \quad . \quad . \quad . \quad (5)$$

where N is Avogadro's number, Z the degree of polymerization, M_0 the molecular weight of the monomer unit ($M_0 = 52$ for polystyrene) and η_0 the viscosity of the solvent.

Just as in the Debye-Bueche theory, the theory of Kirkwood and Riseman leads to a value of the exponent α in (1) which decreases from 1 to 1/2 as the degree of polymerization increases from zero to infinity. Simultaneous values of $x (= \lambda_0 Z^{\frac{1}{2}})$, $F(x)$ and α (x) are tabulated by Kirkwood and Riseman. To calculate b, (5) may be rearranged in the form *

$$b^3 = \{600\,M_0(6\pi^3)^{\frac{1}{2}}/N\pi^3\}\{[\eta]/Z^{\frac{1}{2}}xF(x)\}, \quad . \quad . \quad (6)$$

and in applying this equation to the experimental data, we have again assumed that the value of α in (1) corresponds exactly to the logarithmic average molecular weight of the interval studied. The results, together with the corresponding values of $(< R^2 >)^{\frac{1}{2}}$, the root mean square distance between the chain ends, are shown in the last two columns of Table IV. The relation between $(< R^2 >)^{\frac{1}{2}}$ and the value of $[\eta]$ corresponding to the logarithmic average molecular weight again appears to be linear (see Fig. 7).

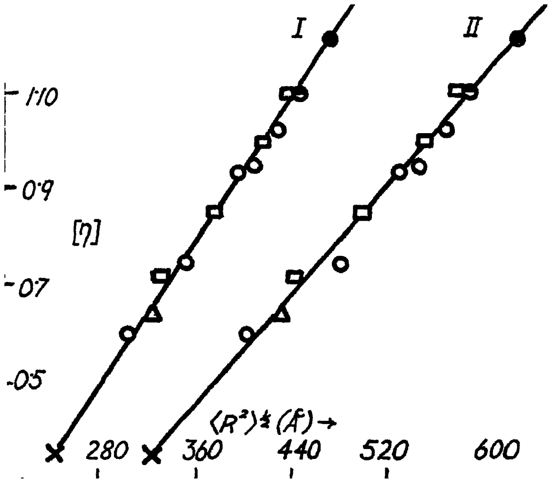

FIG. 7.—Relation between $[\eta]$ and $(<R^2>)^{\frac{1}{2}}$ for polystyrene of mol. wt. = 340,000 in different solvents. I Debye-Bueche theory. II Kirkwood-Riseman theory.

● Benzene. ◓ Toluene. ⊡ Toluene+MeOH.
○ Toluene+Heptane. Δ Methyl ethyl ketone. × Precipitation point.

Conclusion.—The experimental data presented in this series of papers are adequately represented by a formula of the form (1) with α depending only upon the composition of the solvent, whereas current theories of viscosity lead to the result that α varies from 1 to 1/2 as the degree of polymerization increases from zero to infinity. It must not be concluded, however, that these theories are in need of revision. The usual way of exhibiting the experimental data is to plot $\ln\,[\eta]$ against $\ln M$. To within a change of origin, the equivalent plot, according to the theory of Kirkwood and Riseman, is that of $\ln x^2F(x)$ against $2 \ln x$. This curve is shown in Fig. 8 where the interval covered by the present series of experiments is

---

* As $Z \rightarrow \infty$, $xF(x) \rightarrow 1{\cdot}588$ and (6) may be written

$$b^3 = \{2267/(6\pi^3)^{\frac{1}{2}}N\} \lim_{Z \rightarrow \infty} \{[\eta]Z^{-\frac{1}{2}}\}.$$

Kirkwood and Riseman suggest therefore that b may be determined by plotting $[\eta]Z^{-\frac{1}{2}}$ against $Z^{-\frac{1}{2}}$ and extrapolating the resulting curve to obtain the intercept on the $[\eta]Z^{-\frac{1}{2}}$ axis. However, the curve rises steeply as $Z^{-\frac{1}{2}} \rightarrow 0$ so that this procedure is very unsatisfactory. We verified that the data of Ewart and Tingey, quoted by Kirkwood and Riseman, shows the same behaviour.

also indicated. It is at once apparent that very accurate measurements of viscosity and molecular weight over a wide range of the latter will be necessary if the curvature of the plot of ln $[\eta]$ against ln M is to be detected.* It is not surprising, therefore, that at present, no experimental evidence indicating such curvature is available.

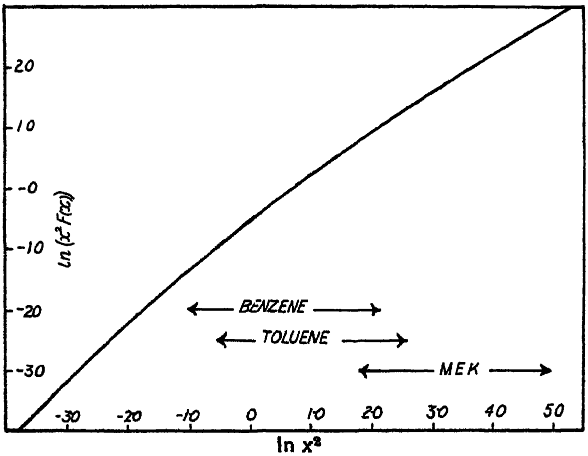

FIG. 8.—Viscosity-molecular weight relationship according to the theory of Kirkwood-Riseman. The experimental range investigated in benzene, toluene and methyl ethyl ketone is indicated on the diagram.

With regard to the dependence of b on the composition of the solvent we note that, in the simplest case, b would be regarded as a function of the torque hindering free rotation about the C—C bonds in the molecule and would not be expected to depend markedly on the nature of the solvent. We believe therefore that the variation of b with solvent composition must be attributed to the existence of *generalized forces* acting between monomer units which are not nearest neighbours in the chain. In the " random flight " model of a chain molecule, the presence of such forces gives rise to the so-called " volume effect ". The change which this brings about in the dimensions of the molecules has recently been considered theoretically by Flory [9] and Hermans.[10] In any given solvent, this volume effect leads to a variation of the parameter b in (4) with the degree of polymerization, but it seems probable on theoretical grounds [10] that for large values of Z, b approaches a constant value characteristic of the particular polymer-solvent system. *A priori*, this constant value may be approached either from above or from below (for polystyrene, there are some grounds for the belief that the second alternative is never in fact realized), but in any case, the effect of such variations on the theory of Kirkwood and Riseman is to modify the curvature of the plot of ln $[\eta]$ against ln M. Since the curvature of the original Kirkwood-Riseman plot (b constant) is apparently too slight to show up in measurements over a considerable range of molecular weights, it is clear that, at present, viscosity measurements are not capable of yielding information on the molecular weight dependence of the volume effect in coiling chain molecules.

Department of Inorganic and Physical Chemistry,
University of Liverpool.

---

* The same conclusion may be reached on the basis of the theory of Debye and Bueche.

[9] Flory, *J. Chem. Physics*, 1949, **17**, 303.

[10] Hermans, *Rec. trav. chim.*, 1950, **69**, 220.

REVIEWS OF BOOKS

The Chemical Elements and their Compounds. Vol. I and II. By N. V. Sidgwick. (Geoffrey Cumberlege, at the Clarendon Press, Oxford, 1950.) Pp. xxxii + 1703. Price 70s.

Dr. N. V. Sidgwick's previous book, *The Electronic Theory of Valency*, is one of the most important publications in the development of the modern approach to the problems of inorganic chemistry. In the present two volumes the author has undertaken the task of co-ordinating the chemistry of all the elements and their compounds in terms of the modern concepts of atomic and molecular structure. It is interesting to compare the treatise on inorganic chemistry of 20-30 years ago with the present book, and so to realize what great advances have been made in transforming this subject from a mass of seemingly unrelated and disconnected facts into a reasonably well-ordered system—it is fitting that it has been left to Dr. Sidgwick to present the transformation in this magnificent book at a price which is so remarkably moderate.

The interests of the author are happily confined to the academic aspects of the subject and his concern is primarily with theoretical relations. Within these limits the text forms a clear, balanced and complete account of our present understanding of the structure and reactions of practically all inorganic compounds. The survey is made with sound judgement by one who obviously has a mastery of detail yet preserves a critical appreciation of the whole field. Books on inorganic chemistry so often degenerate into chemical encyclopediae of preparations and properties ; readers, however, will find that these two volumes, although they contain sufficient detailed information as to merit the description of a complete reference book, make fascinating reading. There are nearly 3000 references to the literature and in addition, excellent subject and author indexes. It is regretted that these latter are confined to Vol. II and that no indication is given, e.g. by the use of bold figures, as to which volume the page number refers except that Vol. I ends at p. 853. However, with such excellent value for money, it would be churlish to emphasize the small amount of extra trouble which this omission involves.

The Introduction, is concerned with the " definition " of what is meant by resonance, electronegativity, heats of linkage, etc., and there are tables which include International Atomic Weights, Atomic Structure, Atomic and ionic radii, etc., conveniently placed for reference at the beginning of Vol. I, but the reader may be disappointed to find that there is no general preliminary account of atomic and molecular structure. This would have formed a useful preliminary to the more detailed considerations given in the separate chapters, the order of which is based on the Periodic Classification. An unusual, but welcome, feature is the inclusion of other compounds of carbon in addition to the simplest ones—carbon, in fact, is put in its proper place.

Here at last, then, is an account of the elements and their compounds which physical chemists will find eminently readable and one which he must possess for his own personal library. As yet no typographical error has been spotted, and though one may on rare occasions disagree with interpretation of some of the facts presented, the standard of factual accuracy is very high. Chemists in general owe Dr. Sidgwick a debt of gratitude for placing on record his many years of experience, thought and labours in this field.

Fluorescence and Phosphorence. By P. PRINGSHEIM. (Interscience Publishers, Inc., New York and London, 1949.) Pp. xvi + 794. Price 120s.

This book will undoubtedly prove to be the indispensable reference book for all interested in the theoretical and academic aspects of photoluminescence. Not only does it provide a balanced and objective account of our present knowledge of the subject—and, in fact, represents the most complete survey that is available—but it also gives detailed information on all important branches of the subject. Included is a bibliography of nearly 90 pages containing a list of books together with references to nearly 2000 original papers up to May 1948 ; in addition there are author, subject and reference number indexes.

Unlike most recent books on this subject, the fluorescence and phosphorence of gases and of solutions form an important part of the book: with the present, very natural, emphasis on the technical and practical importance of luminescent solids, it is essential to realize that there are many problems concerned with the fluorescent spectra of gases which require elucidation and that much information about collisional and energy transfer effects can be obtained by a careful study of this complex subject. The author has also allowed himself space to consider in some detail such matters as quenching processes in solution, the polarization of fluorescence, and "slow fluorescence" at low temperatures. The fluorescence of organic compounds occupies about 50 pages and is marked by the careful assessment of the present state of our understanding of this interesting branch of the subject.

Because of the excellent character of the whole book, because of its importance to students of this field, and because it is the kind of book to which one will constantly turn for quick and easy reference, it is almost tragic to learn that the English price is 120s.

The Swelling of Wood under Stress. By W. W. BARKAS. (H.M.S.O., 1949.) Price 6s.

This book, based on a series of lectures given by Dr. Barkas in Sweden, is characterized by simplicity of treatment and spiced by comments of the kind with which Dr. Barkas's audiences will be familiar.

Although "wood" appears in the title of a book which reviews a section of the work at the Forest Products Research Station, the subject matter relates more generally to gels, with illustrations taken from the data on wood. An increase in the volume of a gel accompanies its adsorption of vapour, and it is the author's intention to relate this adsorption swelling (which may be anisotropic) to the elastic constants of the gel.

On the mechanism of adsorption the author tries to take a non-partisan view, with the result that an original treatment is developed. From the author's standpoint, adsorption from the saturated vapour would continue to infinite dilution were it not for the restraint imposed by the rigidity which differentiates gels from liquids. From the similarity which the author sees between gels and liquids he derives his theoretical basis for adsorption : the solution of adsorbate in adsorbent will exert an osmotic pressure for which the thermodynamic equation of Porter, relating vapour pressure, osmotic pressure, concentration and hydrostatic pressure can apply. The Porter equation is also amenable to the introduction of direction stresses by which the " solution " becomes a " gel." Thus gels, and wood in particular, possess no definite internal surface on which adsorption can take place. If one asks why gels exhibit adsorption swelling, no molecular hypothesis is provided by this thermodynamic approach ; the theory shelters behind the Porter equation and the thermodynamics of solutions.

Whilst the scope of the book precludes the full mathematical analysis of the mechanical properties of anisotropic systems, problems such as that of plastic deformation are boldly faced and consideration of the respective contributions of the gross wood, fibre and gel is not shirked. This book stresses an important aspect of adsorption which is appreciated by few, and may be read with profit by both those interested in adsorption and in the rheology of gels.

F. A. P. M.

Synthetic Methods of Organic Chemistry. A Thesaurus by W. THEILHEIMER. Vol. II. Translated from the German by A. INGBERMAN. (New York: Interscience Publishers, Inc., 1949.) Pp. 324. Price 60s. net.

This volume is a translation into English of *Synthetische Methoden der Organischen Chemie, Repertorium II.* The third and fourth volumes in this series are not to be made available in the English language, but it is planned to continue the series in English with the fifth volume. These volumes are devoted to the publication of " new methods for the synthesis of organic compounds, improvements of known methods, and also old proved methods that are now scattered about in the original papers of the periodicals ". Such reactions are systematically classified on a simple formal basis with the aid of a number of novel reaction symbols. The present volume consists mainly of entries from British, French and Swiss journals published in 1945 and 1946, the flow of American journals to Switzerland having almost completely ceased at the time when the compilation was in hand. The present volume contains a useful cumulative subject index for Volumes I and II.

It is by no means clear on what basis the selection of material is based, but if there are any serious omissions some allowance must be made for the fact that the author had to collect his material without the aid of *Chemisches Zentralblatt* and presumably also of *Chemical Abstracts.* It is clear that this volume, like its predecessor, will be of considerable value to all engaged in preparative organic chemistry and, as a lexicon of reactions rather than of compounds, it will frequently provide the research worker with information which might otherwise be difficult to locate. Once again, however, it is to be regretted that carelessness in preparation or proof reading has left many inaccuracies. A glance through the pages will reveal the mis-spelling of many an author's name, and not infrequently strange and unfamiliar initials are assigned to well-known names. Such errors, trivial in themselves, leave the reader with the feeling that the text may contain other and more serious errors which, unlike the former, are not obvious without reference to the original paper.

D. H. H.

Physikalische Chemie in Medizin und Biologie. By W. BLADERGROEN 2 Auflage (Wepf & Co., Verlag, Basel, 1949). Pp. 675. 45 Swiss Francs.

The contents may be judged from the chapter headings: I. Atome, Ionen und Moleküle, II. Kinetik und Energetik, III. Materie und Strahlung, IV. Kernphysik, V. Die wässerige Lösung, VI. Das Säuere-Basen-Gleichgewicht, VII. Grenzflächenerscheinungen, VIII. Die Lehre der dispersen Systeme, IX. Strukturen der levbenden Substanz, X. Kolloidchemische Vorgänge im Körper, XI. Wichtige, osmotische Vorgänge, XII. Das Oxydoreduktionspotential, XIII. Stoffwechselprobleme, XIV. Die biologische Oxydation.

The borderline field between medicine, biology and physical chemistry is so vast that what an author chooses to put into a book of 675 pages on the topic can only be a matter of taste, and the treatment is bound to be rather uneven. In the present book, Chapters IV, VI, IX, XI and XII are very well done. Chapters XIII and XIV are good also, though they contain more ordinary biochemistry than physical chemistry. Generally speaking, the thermodynamic aspect is well treated. The treatment of reaction kinetics is, however, rather skimped, as is also that of photochemistry, which only receives the barest minimum of exposition in connection with photosynthesis. In Chapter II the author passes on the ancient and incorrect idea that a contact catalyst acts through the increase in concentration of the reactants in the adsorbed film. The treatment of insoluble films in Chapter VII is much too cursory in view of its importance for biological chemistry, and the treatment of colloid stability in Chapter VIII is very dated, no mention being made of the Flory-Huggins work on lyophile polymers or the Hamaker-Verwey theories of lyophobe stability.

Any book of this kind must have a physicochemical or biological bias, and this particular one lays emphasis on the biological side. It presents a great deal of interesting material on a number of *applications* of physical chemistry. On the fundamentals of the subject in some cases (*particularly the kinetic aspects*) it is rather out of date. Since, however, the thermodynamic applications of physical chemistry are, in general, more developed than the kinetic applications to biology, the emphasis on this side may be understood. The book may be recommended for departmental libraries. It is well printed and produced.

D. D. E.

Transactions of the Faraday Society

SUBJECT INDEX—VOLUME 46, 1950

PAGE

Absorption by Simultaneous Diffusion and Chemical Reaction. P. V. Danckwerts 300
—— of Interrupted Infra-red Radiation. T. L. Cottrell 1025
—— of Microwaves, Measurements on the. Parts IV and V. D. H. Whiffen 124
—— of Ultrasonic Waves in Propionic Acid. John Lamb and D. H. A. Huddart 530
—— Spectrum of CF_2. R. K. Laird, E. B. Andrews and R. F. Barrow. . 803
Acetaldehyde by Nitrogen Peroxide, The Mechanism of the Inhibition of the Gaseous Phase Oxidation of. C. A. McDowell and J. H. Thomas 1030
—— The Kinetics of the Hydration of. R. P. Bell and B. de B. Darwent . 34
Acetylene Carbon Dioxide, Acetylene Ethylene and Acetylene Ethane, The Binary Systems. A. M. Clark and F. Din 901
Activities in Alkali Oxide-Silica Melts. R. J. Callow. 663
Adsorption of Gases on Calcium Fluoride. V. A. Crawford and F. C. Tompkins 504
—— Isotherms for Non-uniform Surfaces. F. C. Tompkins 580
—— of Long Chain Compounds from Aqueous Solution on to Evaporated Metal Films. G. A. Wolstenholme and J. H. Schulman . . 488
—— on Non-uniform Surfaces, Physical. F. C. Tompkins . . . 569
—— Thermodynamics of. Part I. Douglas H. Everett 453
—— The Thermodynamics of. Parts II and III. Douglas H. Everett . . 942
Adsorbed Films, The Viscosity, Elasticity and Thickness of. C. W. N. Cumper and A. E. Alexander 243
Aggregation in Soap Solutions. G. Stainsby and A. E. Alexander . . 587
Alcohol, at 25° C, The Interfacial Tension between Aqueous Sugar Solutions and (1) A Liquid Paraffin and (2) *n*-Undecyl. H. W. Douglas . 1090
Aldehydes in the Gaseous Phase, Oxidation of. Part IV. C. A. McDowell and J. H. Thomas 1030
Alkali Oxide-Silica Melts, Activities in. R. J. Callow 663
Alkaline Earth and Nickel Oxide Systems, Electrical and Structural Properties of Some. M. G. Harwood, Nora Herzfeld and S. L. Martin 650
Alkyl Halides, The Infra-red Spectra and Assignment of the Fundamental Frequencies of. Parts I and II. N. Sheppard 527
Alkyls, Thermochemistry of Metallic. Part III. K. Hartley, H. O. Pritchard and H. A. Skinner 1019
Aluminium Chloride, Heats of Mixing of some Organic Compounds with. M. H. Dilke, D. D. Eley and Miss M. G. Sheppard . . . 261
—— Soaps, The Structure of. G. A. Parry and A. J. Taylor . . . 305
Alum Crystals, Sorption of Water by Dehydrated. A. Bielanski and F. C. Tompkins 1072
Amine-Catalyzed Decomposition of Nitramide, Kinetics of the. R. P. Bell and G. L. Wilson 407
Amines, The Thermal Oxidation of the Aliphatic. C. F. Cullis and L. S. A. Smith 42
Amino Acids, Electrolytes in Solutions of. Part I. C. B. Monk. . . 645
Annelation Energy. Part I of Empirical Methods of Estimating Resonance Energies. R. D. Brown 1013
Anodic Behaviour of Metals. Part VI. S. E. S. El Wakkad and A. Hickling 820
Aspirin, A Determination of the Thermodynamic Dissociation Constant and a Study of the Reaction Kinetics by Ultra-violet Spectrophotometry. The Hydrolysis of. L. J. Edward 723
Bases in Dioxan-Water Mixtures, The Relative Strengths of. J. C. James and J. G. Knox 254
Benzene and the Dipole of the C—H Link, Bending Vibrations of Substituted. A. R. H. Cole and H. W. Thompson 103
—— The Effects of Solid Structure on the Freezing of. F. W. Thompson and A. R. Ubbelohde 349
—— Solution, Thermodynamic Studies of Silicones in. M. J. Newing. . 613

PAGE

Benzene, Toluene, Chloroform, Ethyl Benzene and Methyl Ethyl Ketone, The Relation between Intrinsic Viscosity and Molecular Weight for Polystyrene Fractions in. C. E. H. Bawn, R. F. J. Freeman and A. R. Kamaliddin 1107
Biradicals in a Polymerizing System, The Termination of. R. N. Haward. 204
Bond in the Hydrogen Molecule. The Homopolar. M. F. Hoare and J. W. Linnett 885
Boron Trifluoride The Polymerization of *iso*Butene. Alwyn G. Evans and G. W. Meadows 327
Buffer Systems, Kinetic Studies in Heterogeneous. Parts I and II. R. P. Bell and J. E. Prue 5
***n*-Butane** and 1-Butene respectively, The Kinetics of the Photochemical Gas-phase Reactions between Sulphur Dioxide and. F. S. Dainton and K. J. Ivin 382
***iso*Butene** by Boron Trifluoride, The Polymerization of. Alwyn G. Evans and G. W. Meadows 327
1-Butene, The Kinetics of the Photochemical Gas-phase Reactions between Sulphur Dioxide and *n*-Butane, and. F. S. Dainton and K. J. Ivin 382
***tert.*-Butyl** Halides, The Infra-red Spectra and Assignment of the Fundamental Frequencies of the Alkyl Halides. N. Sheppard 527
Calcium Fluoride, The Adsorption of Gases on. V. A. Crawford and F. C. Tompkins 504
—— Phosphates, The Nature of Precipitated. P. W. Arnold 1061
Carbide, The Stability and Chemical Reactivity of Titanium Nitride and Titanium. F. H. Pollard and P. Woodward 190
Carbon Dioxide, Acetylene Ethylene and Acetylene Ethane. The Binary Systems, Acetylene. A. M. Clark and F. Din 901
CF_2, The Absorption Spectrum of. R. K. Laird, E. B. Andrews and R. F. Barrow 803
Chain Reactions, The Non-Stationary Phase of. Part I. G. M. Burnett 772
Chloroform, Ethyl Benzene and Methyl Ethyl Ketone, The Relation between Intrinsic Viscosity and Molecular Weight for Polystyrene Fractions in Benzene, Toluene. C. E. H. Bawn, R. F. J. Freeman and A. R. Kamaliddin 1107
2-Chloropropane and 1 : 2-Dichloropropane, The Mechanism of the Thermal Decompositions of. D. H. R. Barton and A. J. Head 114
Coacervation, The Theory of. C. H. Bamford and H. Tompa 310
Coagulation and Application of the Theory of Colloid Stability, Kinetics of. A. K. Holiday 447
—— Initiated by Dialysis, The Nature of the. A. K. Holiday 440
Cobalt. Part VI of The Anodic Behaviour of Metals. S. E. S. El Wakkad and A. Hickling 820
Cobalticyanides and Ferricyanides, The Conductivities of Potassium and Lanthanum. J. C. James and C. B. Monk 1041
Colloid and Biophysics Committee Discussions—The Physico-chemical Properties and Behaviour of the Nucleic Acid 790
Colloid Stability, Kinetics of Coagulation and Application of the Theory of. A. K. Holiday 447
Conduction with Moving Boundary, heat. Unsteady-State Diffusion or. P. V. Danckwerts 701
Conductivity and the Water Dispersibility of Some Solubilized Systems, The Electrical. P. A. Winsor 762
—— of Potassium and Lanthanum Cobalticyanides and Ferricyanides. J. C. James and C. B. Monk 1041
—— of Potassium Chloride in Aqueous Glycine Solutions. C. B. Monk. 645
Copolymers, Surface Films of. A. J. G. Allan and A. E. Alexander 316
Copper, Silver and Gold, The Diffusion Rates of Some Metals in. O. Kubaschewski 713
Coriolis Perturbation in the Ultra-violet Spectrum of Formaldehyde. J. C. D. Brand 805
Corrosion of Iron Covered by a Thin Film of Neutral Salt Solution. W. I. Whitton 927
Covalent Radius and Molecular Structure. Jules Duchesne. 187
Crystal Structure, Melting and. Part II. F. W. Thompson and A. R. Ubbelohde 349
—— Structure, Melting and. Part III. S. E. Rogers and A. R. Ubbelohde 1051

PAGE
Crystal Surfaces, An Electron Microscope Study of. J. Ames, T. L. Cottrell and Avis M. D. Sampson 938
***Cyclo*-octatetraene**, The Magnetic Susceptibility of. Part II. F. R. M. McDonnell, R. C. Pink and A. E. Ubbelohde 156
Degradation of Polymers, The Ultrasonic. H. W. Melville and A. J. R. Murray 996
Dehydrochlorination of Substituted Hydrocarbons, The Kinetics of the. Part V. D. H. R. Barton and A. J. Head 114
Dialysis on the Properties of Nuclear Gold Sols, The Effect of. Part II. A. K. Holiday 440
1 : 2-Dichloropropane, The Mechanism of the Thermal Decompositions of 2-Chloropropane and. D. H. R. Barton and A. J. Head. . . . 114
Dielectric Properties of Polyethylene Terephthalate (Terylene). Wilson Reddish 459
Diffusion and Chemical Reaction, Absorption by Simultaneous. P. V. Danckwerts 300
—— or Heat Conduction with Moving Boundary, Unsteady-State. P. V. Danckwerts 701
—— of some Halo-methanes in Polystyrene. G. S. Park 684
—— Properties of Gases. Part III. E. R. S. Winter 81
—— Rates of Some Metals in Copper, Silver and Gold. O. Kubaschewski . 713
Dimethyl and Mercury Methyl Halides, Mercury. Part III of Thermochemistry of Metallic Alkyls. K. Hartley, H. O. Pritchard and H. A. Skinner 1019
Dioxan-Water Mixtures, The Relative Strengths of Bases in. J. C. James and J. G. Knox 254
Dipole Moment Measurements, Extrapolation Formulae. R. J. W. Le Fèvre 1
—— of Ethylamine. Dimethylamine and Trimethylamine. G. A. Barclay, R. J. W. Le Fèvre and B. M. Smythe 812
—— On the Evaluation of Electric. K. B. Everard, R. A. W. Hill and L. E. Sutton 417
—— Some Developments of Guggenheim's Simplified Procedure for Computing Electric Dipole Moments. J. W. Smith 394
—— of the C—H Link, Bending Vibrations of Substituted Benzenes and the. A. R. H. Cole and H. W. Thompson 103
$\alpha\alpha'$-Dipyridyl, Equilibria in Solutions of Ferrous Ions and. J. H. Baxendale and Philip George 55
Dispersions, The Electrophoretic Behaviour of Organic. Part I. H. W. Douglas 1082
—— The Flow Properties of Elastic. W. J. Dunning and D. Patterson. . 1095
Elasticity and Thickness of Adsorbed Films, The Viscosity. Part II of The Surface Chemistry of Proteins. C. W. N. Cumper and A. E. Alexander. 243
Electrode Potential and Polarization of Iron and Steel in Acid Solution. The Influence of Stress upon the. M. T. Simnad and U. R. Evans 175
Electrokinetic Behaviour of Iceland Spar against Aqueous Electrolyte Solutions. H. W. Douglas and R. A. Walker 559
—— Potential and Interfacial Tension between Aqueous Solutions and certain Organic Compounds. H. W. Douglas 1082
Electron Microscope Study of Crystal Surfaces. J. Ames, T. L. Cottrell and Avis M. D. Sampson 938
Electrophoretic Behaviour of Organic Dispersions. Part I. H. W. Douglas 1082
Emulsification, Effect of Salts on. R. Matalon 674
—— Processes, Hydrotropy, Solubilization and Related. Part IX. P. A. Winsor 762
Energy and the Steric Factor of the Reaction between Methyl Radicals and Toluene, The Activation. M. Szwarc and J. S. Roberts . . . 625
—— Annelation. Part I of Empirical Methods of Estimating Resonance Energies. R. D. Brown 1013
—— Fluorine, The Heat of Solution of Thallous Fluoride and the Dissociation. A. D. Caunt and R. F. Barrow 154
Entropy and Heat Content during Polymerization, Changes of. F. S. Dainton and K. J. Ivin 331
Equilibria between Solid, Liquid and Gaseous Phases at Low Temperatures. A. M. Clark and F. Din 901
—— in Solutions of Ferrous Ions and $\alpha\alpha'$-Dipyridyl. J. H. Baxendale and Philip George 55
Ethane, The Binary Systems, Acetylene Carbon Dioxide, Acetylene Ethylene and Acetylene. A. M. Clark and F. Din 901

PAGE

Ethyl Benzene and Methyl Ethyl Ketone, The Relation between Intrinsic Viscosity and Molecular Weight for Polystyrene Fractions in Benzene, Toluene, Chloroform. C. E. H. Bawn, R. F. J. Freeman and A. R. Kamaliddin . . . 1107
Ethylene and Acetylene Ethane, The Binary Systems, Acetylene Carbon Dioxide, Acetylene. A. M. Clark and F. Din . . . 901
Explosion in Liquids, Initiation of. Peter Gray . . . 848
Ferricyanides, The Conductivities of Potassium and Lanthanum Cobalticyanides and. J. C. James and C. B. Monk . . . 1041
Ferrous Ions and αα′-Dipyridyl, Equilibria in Solutions of. J. H. Baxendale and Philip George . . . 55
—— *tris*-Dipyridyl Ion, The Kinetics of Formation and Dissociation of the. J. H. Baxendale and Philip George . . . 736
Flame, Its Production and Usefulness, The Shadow Cast by a Bunsen. J. R. Grove, M. F. Hoare and J. W. Linnett . . . 745
—— Experiments with Cool. Parts I and II. F. E. Malherbe and A. D. Walsh . . . 824
—— Speeds, The Determination of. Part III of Reactions between Nitrogen Dioxide and Formaldehyde. F. H. Pollard and R. M. H. Wyatt . . . 281
Flow of an Air Stream through a Layer of Granules. Mrs. E. J. Raynor and E. P. C. Sington . . . 270
—— Properties of Elastic Dispersions. W. J. Dunning and D. Patterson . 1095
Fluorine, The Heat of Solution of Thallous Fluoride and the Dissociation Energy of. A. D. Caunt and R. F. Barrow . . . 154
Formaldehyde, A Coriolis Perturbation in the Ultra-violet Spectrum of. J. C. D. Brand . . . 805
—— Reactions between Nitrogen Dioxide and. Part III. F. H. Pollard and R. M. H. Wyatt . . . 281
Freezing of Benzene, The Effects of Solid Solution on the. F. W. Thompson and A. R. Ubbelohde . . . 349
Frequencies of C—S Linkages. The Vibrational Spectra of Some Organic Sulphur Compounds and the Characteristic. N. Sheppard . . 429
—— of the Alkyl Halides, The Infra-red Spectra and Assignment of the Fundamental. N. Sheppard . . . 527
Friction and Lubrication of Metals, The Importance of Surface Oxide Films in the. Parts I and II. E. D. Tingle . . . 93
Gases, Diffusion Properties of. Part III. E. R. S. Winter . . . 81
—— on Calcium Fluoride. The Adsorption of. V. A. Crawford and F. C. Tompkins . . . 504
Gelatin Systems, Further Observations on Latent Image Formation in Thallous Bromide. Margaret J. Harper and Mowbray Ritchie . 641
Glycine Solutions, The Conductivity of Potassium Chloride in Aqueous. C. B. Monk . . . 645
Gold Sols, The Effect of Dialysis on the Properties of Nuclear. Part II. A. K. Holiday . . . 440
—— The Diffusion Rates of Some Metals in Copper, Silver and. O. Kubaschewski . . . 713
Heat Content during Polymerization. Changes of Entropy and. F. S. Dainton and K. J. Ivin . . . 331
—— of Solution of Iodine in some Organic Solvents. K. Hartley and H. A. Skinner . . . 621
—— of Solution of Thallous Fluoride and the Dissociation Energy of Fluorine. A. D. Caunt and R. F. Barrow . . . 154
—— of Mixing of some Organic Compounds with Aluminium Chloride. M. H. Dilke, D. D. Eley and Miss M. G. Sheppard . . . 261
Heterogeneous Buffer Systems, Kinetic Studies in. Parts I and II. R. P. Bell and J. E. Prue . . . 5
—— Polymers, On the Precipitation Threshold of Solutions of. H. Tompa . 970
Hexachloroethane, The Pyrolysis of. F. S. Dainton and K. J. Ivin . . 295
Hydration of Acetaldehyde, The Kinetics of the. R. P. Bell and B. de B. Darwent . . . 34
Hydrides, Force Constant Relationships in the Non-metallic. D. F. Heath, J. W. Linnett and P. J. Wheatley . . . 137
Hydrocarbons, A Theoretical Study of Some Benzenoid. Part II. R. D. Brown . . . 146

PAGE

Hydrocarbons, The Kinetics of the Dehydrochlorination of Substituted. Part V. D. H. R. Barton and A. J. Head 114
—— The Photochemical Formation of Sulphinic Acids from Sulphur Dioxide. F. S. Dainton and K. J. Ivin 374
Hydrogen Ion Concentration, Nature of Electrolyte, Temperature, and Addition of Fluoride. The Influence of. Part II of Oxygen Overvoltage. A. Hickling and S. Hill 550
—— Molecule, The Homopolar Bond in the. M. F. Hoare and J. W. Linnett 885
—— Overpotential, Some Aspects of the Measurement of. A. M. Azzam, J. O'M. Bockris, B. E. Conway and Miss H. Rosenberg. . . . 918
Hydrolysis of Aspirin: A Determination of the Thermodynamic Dissociation Constant and a Study of the Reaction Kinetics by Ultra-violet Spectrophotometry, The. L. J. Edwards 723
Hydrotropy, Solubilization and Related Emulsification Processes. Part IX. P. A. Winsor 762
Hydroxyl Radical and Atomic Radical and Atomic Oxygen, A Note on the Standard Potentials of the. A. Hickling and S. Hill 557
Iceland Spar against Aqueous Electrolyte Solutions, The Electrokinetic Behaviour of. H. W. Douglas and R. A. Walker. 559
Induction Periods. Part I of Experiments with Cool Flames. F. E. Malherbe and A. D. Walsh 824
Infra-red Radiation, The Absorption of Interrupted. T. L. Cottrell . . . 1025
—— Spectra and Assignment of the Fundamental Frequencies of the Alkyl Halides. M. Sheppard 527
Inhibition of the Gaseous Phase Oxidation of Acetaldehyde by Nitrogen Peroxide. C. A. McDowell and J. H. Thomas 1030
Interaction of Monolayers of Long-chain Polar Compounds with Metal Ions in the Underlying Solution. G. A. Wolstenholme and J. H. Schulman 475
Interface, The Stability of Structures at a Fluid. D. J. Crisp 228
—— Tension between Aqueous Solutions and certain Organic Compounds. H. W. Douglas 1082
Iodine in Some Organic Solvents, The Heat of Solution of. K. Hartley and H. A. Skinner 621
Ion-Exchange upon Intracrystalline Sorption, Influence of. R. M. Barrer and D. W. Riley 853
Iron and Steel in Acid Solution, The Influence of Stress upon the Electrode Potential and Polarization of. M. T. Simnad and U. R. Evans . 175
—— Covered by a Thin Film of Neutral Salt Solution. The Corrosion of. W. I. Whitton 927
Isotopic Gases and Gas Mixtures, The Diffusion and Thermal Diffusion Coefficients for. E. R. S. Winter 81
Kinetics by Ultra-violet Spectrophotometry, The Hydrolysis of Aspirin: A Determination of the Thermodynamic Dissociation Constant and a Study of the Reaction. L. J. Edwards 723
—— of Formation and Dissociation of the Ferrous *tris*-Dipyridyl Ion. J. H. Baxendale and Philip George 736
—— of the Amine-Catalyzed Decomposition of Nitramide. R. P. Bell and G. L. Wilson 407
—— of the Dehydrochlorination of Substituted Hydrocarbons. Part V. D. H. R. Barton and A. J. Head. 114
—— of the Hydration of Acetaldehyde. R. P. Bell and B. de B. Darwent . 34
—— Studies in Heterogeneous Buffer Systems. Parts I and II. R. P. Bell and J. E. Prue 5
—— Studies in the Chemistry of Rubber and Related Materials. Part VII. J. L. Bolland 358
Lanthanum Cobalticyanides and Ferricyanides, The Conductivities of Potassium and. J. C. James and C. B. Monk 1041
Latent Image Formation in Thallous Bromide Gelatin Systems. Margaret J. Harper and Mowbray Ritchie 641
Liquids, Initiation of Explosion in. Peter Gray 848
—— The Vapour Pressures of Certain. J. B. Matthews, J. F. Sumner and E. A. Moelwyn-Hughes 797
Lubrication of Metals, The Importance of Surface Oxide Films in the Friction and. Parts I and II. E. D. Tingle 93
Melting and Crystal Structure. Part II. F. W. Thompson and A. R. Ubbelohde 349
Membranes, Electrical Potential Difference and Resistance of Isolated Frog Gastric Mucosa and Other Secretory. E. E. Crane and R. E. Davies 598

PAGE

Mercury Dimethyl and Mercury Methyl Halides. Part III of Thermochemistry of Metallic Alkyls. K. Hartley, H. O. Pritchard and H. A. Skinner 1019
Metal Films, The Adsorption of Long Chain Compounds from Aqueous Solution on to Evaporated. G. A. Wolstenholme and J. H. Schulman 488
—— Ions in the Underlying Solution, The Interaction of Monolayers of Long-chain Polar Compounds with. G. A. Wolstenholme and J. H. Schulman 488
—— The Anodic Behaviour of. Part VI. S. E. S. El Wakkad and A. Hickling 820
Methacrylate, Rate Coefficients in the Polymerization of Methyl. Part II. M. H. Mackay and H. W. Melville 63
Methyl Ethyl Ketone. The Relation between Intrinsic Viscosity and Molecular Weight for Polystyrene Fractions in Benzene, Toluene, Chloroform, Ethyl Benzene and. C. E. H. Bawn, R. F. J. Freeman and A. R. Kamaliddin 1107
—— Halides, Mercury Dimethyl and Mercury. Part III of Thermochemistry of Metallic Alkyls. K. Hartley, H. O. Pritchard and H. A. Skinner 1019
—— Methacrylate. Rate Coefficients in the Polymerization of. Part II. M. H. Mackay and H. W. Melville 63
—— Radicals and Toluene, The Activation Energy and Steric Factor of the Reaction between. M. Szwarc and J. S. Roberts. 625
—— Thiol, Vibration-Rotation Bands in the Spectrum of. H. W. Thompson and C. H. Miller 22
Microwaves, Measurements on the Absorption of Parts IV and V. D. H. Whiffen 124
Molecular Force Fields. Part XII. D. F. Heath, J. W. Linnett and P. J. Wheatley 137
—— Orbital Calculations on the Systems o- and p-$C_6H_4X_2$. V. Gold . . 109
—— Structure, Covalent Radius and. Jules Duchesne. 187
—— Weight for Polystyrene Fractions in Benzene, Toluene, Chloroform, Ethyl Benzene and Methyl Ethyl Ketone. The Relation between Intrinsic Viscosity and. C. E. H. Bawn, R. F. J. Freeman and A. R. Kamaliddin 1107
Monolayers of Long-chain Polar Compounds with Metal Ions in the Underlying Solution, The Interaction of. G. A. Wolstenholme and J. H. Schulman 475
—— at Oil-Water Interfaces, Spread. Part I of The Surface Chemistry of Proteins. C. W. N. Cumper and A. E. Alexander . . . 236
—— Penetration at the Oil-Water Interface. Part I. R. Matalon . . 674
Mucosa and Other Secretory Membranes, Electrical Potential Difference and Resistance of Isolated Frog Gastric. E. E. Crane and R. E. Davies 598
Multilayer Sorption Isotherm, Derivation and Development of Hüttig's. R. R. Fergusson and R. M. Barrer 400
Nickel Oxides Systems, Electrical and Structural Properties of some Alkaline Earth and. M. G. Harwood, Nora Herzfeld and S. L. Martin . 650
Nitramide, Kinetics of the Amine-Catalyzed Decomposition of. R. P. Bell and G. L. Wilson 407
Nitride and Titanium Carbide. The Stability and Chemical Reactivity of Titanium. F. H. Pollard and P. Woodward 190
Nitrogen Dioxide and Formaldehyde, Reactions between. Part III. F. H. Pollard and R. M. H. Wyatt 281
—— Peroxide. The Mechanism of the Inhibition of the Gaseous Phase Oxidation of. C. A. McDowell and J. H. Thomas . 1030
Nitrosobenzene and *n*-Phenylhydroxylamine. Part II of Polarographic Behaviour of Aromatic Nitro Compounds. J. W. Smith and J. G. Waller 290
Nucleic Acids. The Physico-Chemical Properties and Behaviour of the. . . 790
Oil-Water Interface. Monolayer Penetration at the. Part I. R. Matalon . 674
—— Water Interfaces, Spread Monolayers. Part I of The Surface Chemistry of Proteins. C. W. N. Cumper and A. E. Alexander . . . 236
Olefins, Influence of Chemical Structure on the α-Methylenic Reactivity of. J. L. Bolland 358
Orientation Effects in Binary Solutions. Arnold Münster 165
Osmotic Pressures of Polystyrene Solutions. R. F. J. Freeman and A. R. Kamaliddin 862

PAGE
Overpotential, Measurement of Hydrogen. A. M. Azzam, J. O'M. Bockris, B. E. Conway and Miss H. Rosenberg 918
Overvoltage, Oxygen. Parts II and III. A. Hickling and S. Hill . . 550
Oxidation of Aldehydes in the Gaseous Phase. Part IV. C. A. McDowell and J. H. Thomas 1030
—— of the Aliphatic Amines. C. F. Cullis and L. S. A. Smith . . . 42
Oxide Films in the Friction and Lubrication of Metals. Parts I and II. E. D. Tingle 93
Oxygen between Liquid Sulphur and Thionyl Chloride, Exchange of. E. C. M. Grigg and I. Lauder 1039
—— Overvoltage. Parts II and III. A. Hickling and S. Hill . . . 550
—— The Reaction between Phosphorus Vapour and. F. S. Dainton and H. M. Kimberley 629
Paraffin and (2) *n*-Undecyl Alcohol, at 25° C., The Interfacial Tension between Aqueous Sugar Solutions and (1) A Liquid. H. W. Douglas . . 1090
Perturbation in the Ultra-violet Spectrum of Formaldehyde. A Coriolis. J. C. D. Brand 805
***n*-Phenylhydroxylamine**, Nitrosobenzene and. Part II of Polarographic Behaviour of Aromatic Nitro Compounds. J. W. Smith and J. G. Waller 290
Phosphates, The Nature of Precipitated Calcium. P. W. Arnold . . . 1061
Phosphorus, A Radioactive Tracer Method for the Determination of the Variation of Vapour Pressure with Temperature. F. S. Dainton and H. M. Kimberley 912
—— Vapour and Oxygen, The Reaction between. F. S. Dainton and H. M. Kimberley 629
Photochemical Experiments, Two Factors affecting the use of the Rotating Section in. W. G. Burns and F. S. Dainton 411
—— Formation of Sulphuric Acids from Sulphur Dioxide and Hydrocarbons. F. S. Dainton and K. J. Ivin 374
Photopolymerization of Styrene. Part I of The Non-Stationary Phase of Chain Reactions. G. M. Burnett 772
—— of Vinylidene Chloride. Part I and II. J. D. Burnett and H. W. Melville 976
Polarization of Iron and Steel in Acid Solution, The Influence of Stress upon the Electrode Potential and. M. T. Simnad and U. R. Evans . 175
Polarographic Behaviour of Aromatic Nitro Compounds. Part II. J. W. Smith and J. G. Waller 290
Polyethylene Terephthalate (Terylene), The Dielectric Properties of. Wilson Reddish 459
Polymerization of Methyl Methacrylate, Rate Coefficients in the. Part II. M. H. Mackay and H. W. Melville 63
—— Changes of Entropy and Heat Content during. F. S. Dainton and K. J. Ivin 331
—— of *iso*Butene by Boron Trifluoride. Alwyn G. Evans and G. W. Meadows 327
—— of Styrene, Rate Coefficients in the. H. W. Melville and L. Valentine . 210
—— of Styrene. The Influence of Pressure on the. R. C. Gillham . . 497
—— System, The Termination of Biradicals in a. R. N. Haward . . 204
Polymer Solutions, High. Part I. C. E. H. Bawn, R. F. J. Freeman and A. R. Kamaliddin 677
—— Solutions, High. Part II. C. E. H. Bawn, R. F. J. Freeman and A. R. Kamaliddin 862
—— Solutions, High. Part III. C. E. H. Bawn, R. F. J. Freeman and A. R. Kamaliddin 1107
—— Solutions, High. Part IV. C. E. H. Bawn, T. B. Grimley and M. A. Waiid 1112
—— On the Precipitation Threshold of Solutions of Heterogeneous. H. Tompa 970
—— The Ultrasonic Degradation of. H. W. Melville and A. J. R. Murray . 996
—— under Strain. The Swelling of Cross-linked Amorphous. L. R. G. Treloar 783
Polystyrene, The Diffusion of some Halomethanes in. G. S. Park . . 684
—— Solutions, Vapour Pressure of. C. E. H. Bawn, R. F. J. Freeman and A. R. Kamaliddin 677
—— Solutions, The Osmotic Pressures of. C. E. H. Bawn, R. F. J. Freeman and A. R. Kamaliddin 862
—— Fractions in Benzene, Toluene, Chloroform, Ethyl Benzene and Methyl Ethyl Ketone, The Relation between Intrinsic Viscosity and Molecular Weight for. C. E. H. Bawn, R. F. J. Freeman and A. E. Kamaliddin 1107

PAGE

Potassium and Lanthanum Cobalticyanides and Ferricyanides, The Conductivities of. J. C. James and C. B. Monk 1041
——— between Muscle and the Surrounding Medium, The Transfer of Sodium and. Part III. E. J. Harris 872
—— Chloride in Aqueous Glycine Solutions, The Conductivity of. C. B. Monk 645
—— Sulphate, The System Quinine, Quinine Sulphate and. Part II of Kinetic Studies in Heterogeneous Buffer Systems. R. P. Bell and J. E. Prue 14
Potential and Interfacial Tension between Aqueous Solutions and certain Organic Compounds. H. W. Douglas. 1082
—— Difference and Resistance of Isolated Frog Gastric Mucosa and other Secretory Membranes, Electrical. E. E. Crane and R. E. Davies . 598
—— of the Hydroxyl Radical and Atomic Oxygen. Part III of Oxygen Overvoltage. A. Hickling and S. Hill 557
Precipitation Threshold of Solutions of Heterogeneous Polymers. H. Tompa 970
Pressure during Impact, Measurement of the Transient. Initiation of Explosion in Liquids. Peter Gray 848
—— on the Polymerization of Styrene, The Influence of. R. C. Gillham . 497
—— Temperature Limits. Part II of Experiments with Cool Flames. F. E. Malherbe and A. D. Walsh 824
Principle of Maximum Overlapping. Allan Maccoll 369
Propionic Acid, The Absorption of Ultrasonic Waves in. John Lamb and D. H. A. Huddart 540
*iso***Propyl** Halides, The Infra-red Spectra and Assignment of the Fundamental Frequencies of the Alkyl Halides. N. Sheppard . . 533
Proteins, The Surface Chemistry of. Parts I and II. C. W. N. Cumper and A. E. Alexander 236
Pyrolysis of Hexachloroethane. F. S. Dainton and K. J. Ivin . . . 295
Quinine, Quinine Sulphate and Potassium Sulphate, The System. Part II of Kinetic Studies in Heterogeneous Buffer Systems. R. P. Bell and J. E. Prue 14
Radioactive Tracer Method for the Determination of the Variation of Vapour Pressure with Temperature. F. S. Dainton and H. M. Kimberley. 912
Rate Coefficients in the Polymerization of Methyl Methacrylate. Part II. M. H. Mackay and H. W. Melville 63
—— Coefficients in the Polymerization of Styrene. H. W. Melville and L. Valentine 210
Reactivity of Titanium Nitride and Titanium Carbide. The Stability and Chemical. F. H. Pollard and P. Woodward 190
Relaxation Time with Solvent, The Variation of. Part V of Measurements on the Absorption of Microwaves. D. H. Whiffen . . . 130
Resistance of Isolated Frog Gastric Mucosa and Other Secretory Membranes. Electrical Potential Difference and. E. E. Crane and R. E. Davies 598
Resonance Energies. Empirical Methods of Estimating. Part I. R. D. Brown 1013
Rotating Sector in Photochemical Experiments, Two Factors affecting the use of the. W. G. Burns and F. S. Dainton. 411
Rubber and Related Materials, Kinetic Studies in the Chemistry of. Part VII J. L. Bolland 358
——— Volume Changes in the Stretching of Vulcanized Natural. Geoffrey Gee, Jan Stern and L. R. G. Treloar 1101
Silica Melts, Activities in Alkali Oxide-. R. J. Callow. 663
Silicones in Benzene Solution, Thermodynamic Studies of. M. J. Newing . 613
—— The Surface Properties of Polar. M. J. Newing 755
Silver and Gold, The Diffusion Rates of Some Metals in Copper. O. Kubaschewski 713
Soap Solutions, Studies in. Part II. G. Stainsby and A. E. Alexander. . 587
—— The Structure of Aluminium. G. A. Parry and A. J. Taylor. . . 305
Sodium and Potassium between Muscle and the Surrounding Medium, The Transfer of. Part II. E. J. Harris 872
Solid Solution on the Freezing of Benzene, The Effects of. F. W. Thompson and A. R. Ubbelohde. 349
Sols, The Effect of Dialysis on the Properties of Nuclear Gold. Part II. A. K. Holiday 440
Solubilization and Related Emulsification Processes, Hydrotropy. Part IX. P. A. Winsor 762
Solutions, Binary, Orientation Effects in. Arnold Münster 165
—— Chemical Action of Sound Waves on Aqueous. N. Miller . . . 546
—— Surface Tension of Regular. R. Defay and I. Prigogine . . . 199

PAGE

Sorption, Influence of Ion-exchange upon Intracrystalline. R. M. Barrer and D. W. Riley 853

—— Isotherm. Derivation and Development of Hüttig's Multilayer. R. R. Fergusson and R. M. Barrer 400

—— of Water by Dehydrated Alum Crystals. A. Bielanski and F. C. Tompkins 1072

Sound Waves on Aqueous Solutions, Chemical Action of. N. Miller . . 546

Spectrum of CF_2, The Absorption. R. K. Laird, E. B. Andrews and R. F. Barrow 803

—— of Formaldehyde, A Coriolis Perturbation in the Ultra-violet. J. C. D. Brand 805

—— of Methyl Thiol, Vibration-Rotation Bands in the. H. W. Thompson and C. H. Miller 22

—— of Some Organic Sulphur Compounds and the Characteristic Frequencies of C—S Linkages, The Vibrational. N. Sheppard . . . 429

Stability and Chemical Reactivity of Titanium Nitride and Titanium Carbide. F. H. Pollard and P. Woodward 190

—— of Structures at a Fluid Interface, The. D. J. Crisp 228

Steel in Acid Solution, The Influence of Stress upon the Electrode Potential and Polarization of Iron and. M. T. Simnad and U. R. Evans . 175

Steric Factor of the Reaction between Methyl Radicals and Toluene. M. Szwarc and J. S. Roberts 625

Strengths of Bases in Dioxan-Water Mixtures, The Relative. J. G. Knox and J. C. James 254

Structure of Aluminium Soaps. G. A. Parry and A. J. Taylor . . . 305

—— Melting and Crystal. Part II. F. W. Thompson and A. R. Ubbelohde. 349

—— on the α-Methylenic Reactivity of Olefins, Influence of Chemical. Bolland 358

Styrene, Rate Coefficients in the Polymerization of. H. W. Melville and L. Valentine 210

—— The Influence of Pressure on the Polymerization of. R. C. Gillham . 497

—— The Photopolymerization of. Part I of The Non-Stationary Phase of Chain Reactions. G. M. Burnett 772

Sugars on the Electrokinetic Potential and Interfacial Tension between Aqueous Solutions and certain Organic Compounds, The Influence of. Parts I and II. H. W. Douglas 1082

Sulphates, Low-melting Acid. Part III of Melting and Crystal Structure. S. E. Rogers and A. R. Ubbelohde 1051

Sulphinic Acids from Sulphur Dioxide and Hydrocarbons, The Photochemical Formation of. F. S. Dainton and K. J. Ivin 374

Sulphur and Thionyl Chloride. Exchange of Oxygen between Liquid. E. C. M. Grigg and I. Lauder 1039

—— Compounds and the Characteristic Frequencies of C—S Linkages. The Vibrational Spectra of Some Organic. N. Sheppard . . . 429

—— Dioxide and *n*-Butane and 1-Butene respectively, The Kinetics of the Photochemical Gas-phase Reactions between. F. S. Dainton and K. J. Ivin 382

—— Dioxide and Hydrocarbons. The Photochemical Formation of Sulphinic Acids from. F. S. Dainton and K. J. Ivin 374

—— Dioxide, Reactions in Liquid. Part I. E. C. M. Grigg and I. Lauder 1039

Surface Chemistry of Proteins. Parts I and II. C. W. N. Cumper and A. E. Alexander 236

—— Films of Copolymers. A. J. G. Allan and A. E. Alexander . . . 316

—— Oxide Films in the Friction and Lubrication of Metals. Parts I and II. E. D. Tingle 93

—— Properties of Polar Silicones, The. M. J. Newing 755

—— Tension of Regular Solutions. R. Defay and I. Prigogine . . . 199

Susceptibility of Cyclo-octatetraene, The Magnetic. Part II. F. R. M. McDonnell, R. C. Pink and A. R. Ubbelohde 156

Swelling of Cross-Linked Amorphous Polymers under Strain. L. R. G. Treloar 783

Terylene, The Dielectric Properties of Polyethylene Terephthalate. Wilson Reddish 459

Tetrachloroethylene, The Vibrational Assignment and. Thermodynamic Functions of. P. Torkington 894

Thallous Bromide Gelatin Systems. Latent Image Formation in. Margaret J. Harper and Mowbray Ritchie 641

—— Fluoride and the Dissociation Energy of Fluorine. The Heat of Solution of. A. D. Caunt and R. F. Barrow 154

PAGE

Thermal Decompositions of 2-Chloropropane and 1 : 2-Dichloropropane, The Mechanism of the. D. H. R. Barton and A. J. Head 114
—— Diffusion, The Elementary Theory of. E. Whalley and E. R. S. Winter . 517
Thermodynamics of Adsorption. Part I. Douglas H. Everett 453
—— of Adsorption. Parts II and III. Douglas H. Everett. 942
—— Dissociation Constant and a Study of the Reaction Kinetics by Ultraviolet Spectrophotometry, The Hydrolysis of Aspirin: A Determination of the. L. J. Edwards 723
—— Functions of Tetrachloroethylene, The Vibrational Assignment and. P. Torkington 894
—— Studies of Silicones in Benzene Solution. M. J. Newing 613
Thionyl Chloride, Exchange of Oxygen between Liquid Sulphur and. E. C. M. Crigg and I. Lauder 1039
Thiol, Vibration-Rotation Banks in the Spectrum of Methyl. H. W. Thompson and C. H. Miller 22
Titanium Nitride and Titanium Carbide, The Stability and Chemical Reactivity of. F. H. Pollard and P. Woodward 190
Toluene, Chloroform, Ethyl Benzene and Methyl Ethyl Ketone, The Relation between Intrinsic Viscosity and Molecular Weight for Polystyrene Fractions in Benzene. C. E. H. Bawn, R. F. J. Freeman and A. R. Kamaliddin 1107
—— The Activation Energy and the Steric Factor of the Reaction between Methyl Radicals and. M. Szwarc and J. S. Roberts 625
2 : 4 : 6-Trinitrotoluene, The Vapour Pressure. G. Edwards 423
Ultrasonic Degradation of Polymers. H. W. Melville and A. J. R. Murray . 996
—— Waves in Propionic Acid, The Absorption of. John Lamb and D. H. A. Huddart 540
Ultra-violet Spectrophotometry. The Hydrolysis of Aspirin: A Determination of the Thermodynamic Dissociation Constant and a Study of the Reaction Kinetics by. L. J. Edwards 723
—— Spectrum of Formaldehyde, A Coriolis Perturbation in the. J. C. D. Brand 805
Valence-Force Displacement Co-ordinates, General. P. Torkington . . 27
Vapour Pressures of Certain Liquids. The. J. B. Matthews, J. F. Sumner and E. A. Moelwyn-Hughes 797
—— of Polystyrene Solutions. C. E. H. Bawn, R. F. J. Freeman and A. R. Kamaliddin 677
—— of 2 : 4 : 6-Trinitrotoluene. G. Edwards 423
—— with Temperature, A Radioactive Tracer Method for the Determination of the Variation of. F. S. Dainton and H. M. Kimberley . . 912
Vibration Assignment and Thermodynamic Functions of Tetrachloroethylene. P. Torkington 894
—— Bands, Intensities of. Part II. A. R. H. Cole and H. W. Thompson . 103
—— Rotation Bands in the Spectrum of Methyl Thiol. H. W. Thompson and C. H. Miller 22
—— Spectra of Some Organic Sulphur Compounds and the Characteristic Frequencies of C—S Linkages. N. Sheppard 429
Vinylidene Chloride, The Photopolymerization of. J. D. Burnett and H. W. Melville 976
Viscosity, Elasticity and Thickness of Adsorbed Films. Part II of The Surface Chemistry of Proteins. C. W. N. Cumper and A. E. Alexander. 243
—— and Molecular Weight for Polystyrene Fractions in Benzene, Toluene, Chloroform, Ethyl Benzene and Methyl Ethyl Ketone. The Relation between Intrinsic. C. E. H. Bawn, R. F. J. Freeman and A. R. Kamaliddin 1107
Volume Changes in the Stretching of Vulcanized Natural Rubber. Geoffrey Gee, Jan Stern and L. R. G. Treloar 1101
Water, by Dehydrated Alum Crystals, Sorption of. A. Bielanski and F. C. Tompkins 1072
—— Mixtures, The Relative Strengths of Bases in Dioxan-. J. C. James and J. G. Knox 254
Zinc Hydroxide and Zinc Sulphate, The System. Part I of Kinetic Studies in Heterogeneous Buffer Systems. R. P. Bell and J. E. Prue. . 5

AUTHOR INDEX—VOLUME 46, 1950

PAGE

Alexander, A. E. See *Allan, A. J. G.*, and
—— See *Cumper, C. W. N.*, and
—— See *Stainsby, G.*, and
Allan, A. J. G., and **Alexander, A. E.** Surface films of copolymers . . 316
Ames, J., **Cottrell, T. L.**, and **Sampson, A. M. D.** An electrical microscope study of crystal surfaces 938
Andrews, E. B. See *Laird, R. D., Andrews, E. B.*, and *Barrow, R. F.*
Arnold, P. W. The nature of precipitated calcium phosphates . . . 1061
Arthur, J. R., **Linnett, J. W.**, **Raynor, E. J.**, and **Sington, E. P. C.** The flow of an air stream through a layer of granules 270
Azzam, A. M., **Bockris, J. O'M.**, **Conway, B. E.**, and **Rosenberg, H.** Some aspects of the measurement of hydrogen overpotential . . 918
Bamford, C. H., and **Tompa, H.** The theory of coacervation . . . 310
Barclay, G. A., **Le Fevre, R. J. W.**, and **Symthe, B. M.** The dependence on state of the apparent dipole moments of ethylamine, diethylamine and triethylamine 812
Barrer, R. M., and **Riley, D. W.** Influence of ion-exchange upon intracrystalline sorption 853
—— See *Fergusson, R. R.*, and
Barrow, R. F. See *Laird, R. K., Andrews, E. B.*, and
—— See *Caunt, A. D.*, and
Barton, D. H. R., and **Head, A. J.** The kinetics of the dehydrochlorination of substituted hydrocarbons. Part V: The mechanism of the thermal decompositions of 2-chloropropane and 1 : 2-dichloropropane . . 114
Bawn, C. E. H., **Freeman, R. F. J.**, and **Kamaliddin, A. R.** High polymer solutions. Part I: Vapour pressure of polystyrene solutions . . 677
—— Part II: The osmotic pressures of polystyrene solutions 872
—— Part III: Intrinsic viscosity of polystyrene solutions 1107
Bawn, C. E. H., **Grimley, T. B.** and **Wajid, M. A.** High polymer solutions. Part IV: Intrinsic viscosity in mixed solvents 1112
Baxendale, J. H. and **George, P.** Equilibria in solution of ferrous ions and αα′-dipyridyl 55
—— and **George, Philip.** The kinetics of formation and dissociation of the ferrous *tris*-dipyridyl ion 736
Bell, R. P., and **B. de B. Darwent.** The kinetics of the hydration of acetaldehyde 34
—— and **Prue, J. E.** Kinetic studies in heretogeneous buffer systems. Part I: The system zinc hydroxide and zinc sulphate . . . 5
—— Part II: The systems quinine, quinine sulphate and potassium sulphate . 14
Bell, R. P., and **Wilson, G. L.** Kinetics of the amine-catalyzed decomposition of nitramide 407
Bielanski, A., and **Tompkins, F. C.** Sorption of water by dehydrated alum crystals 1072
Bockris, J. O'M. See *Azzam, A. M., Bockris, J. O'M., Conway, B. E.*, and *Rosenberg, H.*
Bolland, J. L. Kinetic studies in the chemistry of rubber and related materials. Part VII: Influence of chemical structure on the α-methylenic reactivity of olefins. 358
Brand, J. C. D. A Coriolis perturbation in the ultra-violet spectrum of formaldehyde 805
Brown, R. D. Empirical methods of estimating resonance energies. Part I: Annelation energy 1013
—— A theoretical study of some non-benzenoid hydrocarbons. Part II. . 146
Burnett, G. M. The non-stationary phase of chain reactions. Part I: The photopolymerization of styrene 772
Burnett, J. D., and **Melville, H. W.** The photopolymerization of vinylidene chloride. Part I 976
Burns, W. G., and **Dainton, F. S.** Two factors affecting the use of the rotating sector in photo-chemical experiments 411
Callow, R. J. Activities in alkali oxide-silica melts 663
Caunt, A. D., and **Barrow, R. F.** The heat of solution of thallous fluoride and the dissociation energy of fluorine 154

PAGE

Clark, A. M., and **Din, F.** Equilibria between solid, liquid and gaseous phases at low temperatures. The binary systems, acetylene carbon-dioxide, acetylene-ethylene and acetylene-ethane . . . 901
Cole, A. R. H. and **Thompson, H. W.** Intensities of vibration bands. Part II: Bending vibrations of substituted benzenes and the dipole of the C—H link . . . 103
Conway, B. E. See *Azzam, A. M., Bockris, J. O'M., Conway, B. E.*, and *Rosenberg, H.*
Cottrell, T. L. The absorption of interrupted infra-red radiation . . . 1025
—— See *Ames, J., Cottrell, T. L.*, and *Sampson, A. M. D.*
Crane, E. E., and **Davies, R. E.** Electrical potential difference and resistance of isolated frog gastric mucosa and other secretory membranes . . . 598
Crawford, V. A., and **Tompkins, F. C.** The adsorption of gases on calcium fluoride . . . 504
Crisp, D. J. The stability of structures at a fluid interface . . . 228
Cullis, C. F., and **Smith, L. S. A.** The thermal oxidation of the aliphatic amines . . . 42
Cumper, C. W. N., and **Alexander, A. E.** The surface chemistry of proteins. Part I: Spread monolayers at oil/water interfaces . . . 230
—— Part II: The viscosity, elasticity and thickness of adsorbed films . . . 243
Dainton, F. S. See *Burns, W. G.*, and
—— and **Ivin, K. J.** Changes of entropy and heat content during polymerization . . . 331
—— The pyrolysis of hexachloroethane . . . 295
—— The photochemical formation of sulphinic acids from sulphur dioxide and hydrocarbons . . . 374
—— The kinetics of the photochemical gas-phase reactions between sulphur dioxide and *n*-butene and 1-butene respectively . . . 382
—— and **Kimberley, H. M.** The reaction between phosphorus vapour and oxygen . . . 629
—— A radioactive tracer method for the determination of the variation of vapour pressure with temperature and its application to white phosphorus . . . 912
Danckwerts, P. V. Absorption by simultaneous diffusion and chemical reaction . . . 300
—— Unsteady-state diffusion or heat-conduction with moving boundary . . . 701
Darwent, B. de B. See *Bell, R. P.*, and
Davies, R. E. See *Crane, E. E.*, and
Defay, R., and **Prigogine, I.** Surface tension of regular solutions . . . 199
Dilke, M. H., **Eley, D. D.**, and **Sheppard, M. G.** A survey of heats of mixing of some organic compounds with aluminium chloride. Heat of mixing. Part I . . . 201
Din, F. See *Clark, A. M.*, and
Douglas, H.W. The electrophoresis behaviour of organic dispersions. Part I 1082
—— The interfacial tension and film behaviour of sugars . . . 1090
and **Walker, R. A.** The electrokinetic behaviour of Iceland spar against aqueous electrolyte solutions . . . 559
Duchesne, J. Covalent radius and molecular structure . . . 187
Dunning, W. J. and **Patterson, D.** The flow properties of elastic dispersions 1095
Edwards, G. The vapour pressure of 2 : 4 : 6-trinitrotoluene . . . 423
Edwards, L. J. The hydrolysis of aspirin: a determination of the thermodynamic dissociation constant and a study of the reaction kinetics by ultra-violet spectrophotometry . . . 723
Eley, D. D. See *Dilke, M. H., Eley, D. D.*, and *Sheppard, M. G.*
El Wakkad, S. E. S., and **Hickling, A.** The anodic behaviour of metals. Part VI: Cobalt . . . 820
Evans, A. G., and **Meadows, G. W.** The polymerization of *iso*butene by boron trifluoride . . . 327
Evans, U. R. See *Simnad, M. T.*, and
Everard, K. B., **Hill, R. A. W.**, and **Sutton, L. E.** On the evaluation of electric dipole moments . . . 417
Everett, D. H. Thermodynamics of adsorption. Part I: General considerations . . . 453
—— Part II: Thermodynamics of monolayers on solids . . . 942
—— Part III: Analysis and discussion of experimental data . . . 957
Fergusson, R. R., and **Barrer, R. M.** Derivation and development of Hüttig's multilayer sorption isotherm . . . 400

PAGE

Févre, R. J. W. Le. Extrapolation formulae in dipole moment measurements 1
Freeman, R. F. J. See *Bawn, C. E. H., Freeman, R. F. J.*, and *Kamaliddin, A. R.*
Gee, G., Stern, J., and **Treloar, L. R. G.** Volume changes in the stretching of vulcanized natural rubber 1101
George, P. See *Baxendale, J. H.*, and
Gillham, R. C. The influence of pressure on the polymerization of styrene . 497
Gold, V. Some molecular orbital calculations on the systems *o*- and *p*-$C_6H_4X_2$ 109
Gray, P. Initiation of explosion in liquids: measurement of the transient pressures during impact 848
Grigg, E. C. M., and **Lauder, I** Reactions in liquid sulphur dioxide. Part I: Exchange of oxygen between liquid sulphur and thionyl chloride 1039
Grimley, T. B. See *Bawn, C. E. H., Grimley, T. B.*, and *Wajid, M. A.*
Grove, J. R., Hoare, M. F., and **Linnett, J. W.** The shadow cast by a Bunsen flame, its production and usefulness 745
Harper, M. J., and **Ritchie, M.** Further observations on latent image formation in thallous bromide gelatin systems 641
Harris, E. J. The transfer of sodium and potassium between muscle and the surrounding medium. Part II: The sodium flux . . . 872
Hartley, K., Pritchard, H. O., and **Skinner, H. A.** Thermochemistry of metallic alkyls. III: Mercury dimethyl and mercury methyl halides 1019
— — and **Skinner, H. A.** The heat of solution of iodine in some organic solvents 621
Harwood, M. G., Herzfeld, N, and **Martin, S. L.** Electrical and structural properties of some alkaline earth and nickel oxide systems . . 650
Haward, R. N. The termination of biradicals in a polymerizing system. . 204
Head, A. J. See *Barton, D. H. R.*, and
Heath, D. F., Linnett, J. W., and **Wheatley, P. J.** Molecular force fields. Part XII: Force constant relationships in the non-metallic hydrides 137
Herzfeld, N. See *Harwood, M. G., Herzfeld, N.*, and *Martin, S. L.*
Hickling, A. See *El Wakkad, S. E. S.*, and
—— and **Hill, S.** Oxygen overvoltage. Part II: The influence of hydrogen ion concentration, nature of electrolyte, temperature, and addition of fluoride 550
—— Part III: A note on the standard potentials of the hydroxyl radical and atomic oxygen 557
Hill, R. A. W. See *Everard, K. B., Hill, R. A. W.*, and *Sutton, L. E.*
Hill, S. See *Hickling, A.*, and
Hoare, M. F. See *Grove, J. R., Hoare, M. F.*, and *Linnett, J. W.*
—— and **Linnett, J. W.** The homopolar bond in the hydrogen molecule . 885
Holliday, A. K. The effect of dialysis on the properties of nuclear gold sols. Part II: The nature of the coagulation initiated by dialysis . . 440
—— Part III: Kinetics of coagulation and application of the theory of colloid stability 447
Huddart, D. H. A. See *Lamb, J.*, and
Ivin, K. J. See *Dainton, F. S.*, and
James, J. C., and **Knox, J. G.** The relative strengths of bases in dioxan-water mixtures 254
—— and **Monk, C. B.** The conductivities of potassium and lanthanum cobalticyanides and ferricyanides. 1041
Kamaliddin, A. R. See *Bawn, C. E. H., Freeman, R. F. J.*, and
Kimberley, H. M. See *Dainton, F. S.*, and
Knox, J. G. See *James, J. C.*, and
Kubaschewski, O. The diffusion rates of some metals in copper, silver and gold 713
Laird, R. K., Andrews, E. B., and **Barrow, R. F.** The absorption spectrum of CF_2 803
Lamb, J., and **Huddart, D. H. A.** The absorption of ultrasonic waves in propionic acid 540
Lauder, I. See *Grigg, E. C. M.*, and
Le Févre, R. J. W. See *Barclay, G. A., Le Févre, R. J. W.*, and *Smythe, B. M.*
Linnett, J. W. See *Arthur, J. R., Linnett, J. W., Raynor, E. J.*, and *Sington, E. P. C.*
—— See *Grove, J. R., Hoare, M. F.*, and

PAGE

Linnett, J. W. See *Heath, D. F.*, *Linnett, J. W.*, and *Wheatley, P. J.*
—— See *Hoare, M. F.*, and
Maccoll, A. The principle of maximum overlapping 369
Mackay, M. H., and **Melville, H. W.** Rate coefficients in the polymerization of methyl methacrylate. Part II: The benzoyl peroxide sensitized polymerization 63
Malherbe, F. E., and **Walsh, A. D.** Experiments with cool flames. Part I: Induction periods 824
—— Part II: Pressure-temperature limits 835
Martin, S. L. See *Harwood, M. G.*, *Herzfeld, N.*, and
Matalon, R. Monolayer penetration at the oil-water interface. Part I: Effect of salts on emulsification 674
Matthews, J. B., **Sumner, J. F.**, and **Moelwyn-Hughes, E. A.** The vapour pressures of certain liquids 797
Meadows, G. W. See *Evans, A. G.*, and
Melville, H. W. See *Burnett, J. D.*, and
—— See *MacKay, M. H.*, and
—— and **Murray, A. J. R.** The ultrasonic degradation of polymers . . 996
—— and **Valentine, L.** Rate coefficients in the polymerization of styrene . 210
Miller, C. H. See *Thompson, H. W.*, and
Miller, N. Chemical action of sound waves on aqueous solutions . . . 546
Moelwyn-Hughes, E. A. See *Matthews, J. B.*, *Sumner, J. F.*, and
Monk, C. B. Electrolytes in solutions of amino acids. Part I: The conductivity of potassium chloride in aqueous glycine solutions . . 645
—— See *James, J. C.*, and
Münster, Arnold. Orientation effects in binary solutions 165
Murray, A. J. R. See *Melville, H. W.*, and
McDonnell, F. R. M., **Pink, R. C.**, and **Ubbelohde, A. R.** The magnetic susceptibility of cyclo-octatetraene. Part II: The temperature coefficient of susceptibility from 195° to 69° K 156
McDowell, C. A., and **Thomas, J. H.** Oxidation of aldehydes in the gaseous phase. Part IV: The mechanism of the inhibition of the gaseous phase oxidation of acetaldehyde by nitrogen peroxide . . . 1030
Newing, M. J. Thermodynamic studies of silicones in benzene solution. . 613
—— The surface properties of polar silicones 755
Park, G. S. The diffusion of some halo-methanes in polystyrene . . . 684
Parry, G. A., and **Taylor, A. J.** The structure of aluminium soaps . . 305
Patterson, D. See *Dunning, W. J.*, and
Pink, R. C. See *McDonnell, F. R. M.*, *Pink, R. C.*, and *Ubbelohde, A. R.*
Pollard, F. H., and **Woodward, P.** The stability and chemical reactivity of titanium nitride and titanium carbide 190
—— and **Wyatt, R. M. H.** Reactions between nitrogen dioxide and formaldehyde. Part III: The determination of flame speeds . . . 281
Prigogine, I. See *Defay, R.*, and
Pritchard, H. O. See *Hartley, K.*, *Pritchard, H. O.*, and *Skinner, H. A.*
Prue, J. E. See *Bell, R. P.*, and
Raynor, E. J. See *Arthur, J. R.*, *Linnett, J. R.*, *Raynor, E. J.*, and *Sington, E. P. C.*
Reddish, W. The dielectric properties of polyethylene terephthalate (Terylene) 459
Riley, D. W. See *Barrer, R. M.*, and
Ritchie, M. See *Harper, M. J.*, and
Roberts, J. S. See *Szwarc, M.*, and
Rogers, S. E., and Ubbelohde, A. R. Melting and crystal structure. III: Low-melting acid sulphates 1051
Rosenberg, H. See *Azzam, A. M.*, *Bockris, J. O'M.*, *Conway, B. E.*, and
Sampson, A. M. D. See *Ames, J.*, *Cottrell, T. L.*, and
Schulman, J. H. See *Wolstenholme, G. A.*, and
Sheppard, M. G. See *Dilke, M. H.*, *Eley, D. D.*, and
Sheppard, N. The vibrational spectra of some organic sulphur compounds and the characteristic frequencies of C—S linkages 429
—— The infra-red spectra and assignment of the fundamental frequencies of the alkyl halides. I: *tert.*-Butyl halides 527
—— II: *iso*Propyl halides 533
Simnad, M. T., and **Evans, U. R.** The influence of stress upon the electrode potential and polarization of iron and steel in acid solution . . 175
Sington, E. P. C. See *Arthur, J. R.*, *Linnett, J. W.*, *Raynor, E. J.*, and

PAGE

Skinner, H. A. See *Hartley, K., Pritchard, H. O.*, and
—— See *Hartley, K*, and
Smith, L. S. A. See *Cullis, C. F.*, and
Smith, J. W. Some developments of Guggenheim's simplified procedure for computing electric dipole moments 394
—— and **Waller, J. G.** Polarographic behaviour of aromatic nitro compounds. Part II: Nitrosobenzene and *N*-Phenylhydrophylamine . . 290
Smythe, B. M. See *Barclay, G. A., Le Fevre, R. J. W.*, and
Stainsby, G., and **Alexander, A. E.** Studies of soap solutions. Part II: Factors influencing aggregation in soap solutions 587
Stern, J. See *Gee, G. Stern, J.*, and *Treloar, L. R. G.*
Sumner, J. F. See *Matthews, J. B., Sumner, J. F.*, and *Moelwyn-Hughes*, E. A.
Sutton, L. E. See *Everard, K. B., Hill, R. A. W.*, and
Szwarc, M., and **Roberts, J. S.** The activation energy and the steric factor of the reaction between methyl radicals and toluene . . . 625
Taylor, A. J. See *Parry, G. A.*, and 305
Thomas, J. H. See *McDowell, C. A.*, and
Thompson, F. W., and **Ubbelohde, A. R.** Melting and crystal structure. II: The effects of solid solution on the freezing of benzene . . 349
Thompson, H. W. See *Cole, A. R. H.*, and
—— and **Miller, C. H.** Vibration-rotation bands in the spectrum of methyl thiol 22
Tingle, E. D. The importance of surface oxide films in the friction and lubrication of metals. Part I: The dry friction of surfaces freshly exposed to air 93
—— Part II: The formation of lubricating films on metal surfaces . . 97
Tompa, H. On the precipitation thresholds of solutions of heterogeneous polymers 970
—— See *Bamford, C. H.*, and
Tompkins, F. C. Physical adsorption on non-uniform surfaces . . . 569
—— Adsorption isotherms for non-uniform surfaces 580
—— See *Bielanski, A.*, and
—— See *Crawford, V. A.*, and
Torkington, P. General valence-force displacement co-ordinates . . . 27
—— The vibrational assignment and thermodynamic functions of tetrachloroethylene 894
Treloar, L. R. G. See *Gee, G., Stern, J.*, and
—— The swelling of cross-linked amorphous polymers under strain . . 783
Ubbelohde, A. R. See *McDonnell, F. R. M., Pink, R. C.*, and
—— See *Rogers, S. E.*, and
—— See *Thompson, F. W.*, and
Valentine, L. See *Melville, H. W.*, and
Wajid, M. A. See *Bawn, C. E. H., Grimley, T. B.*, and
Walker, R. A. See *Douglas, H. W.*, and
Waller, J. G. See *Smith, J. W.*, and
Walsh, A. D. See *Malherbe, F. E.*, and
Whalley, E., and **Winter, E. R. S.** The elementary theory of thermal diffusion 517
Wheatley, P. J. See *Heath, D. F., Linnett, J. W.*, and
Whiffen, D. H. Measurements on the absorption of microwaves. Part I: The variation of relaxation time with solvent 130
—— Part IV: Non-polar liquids 124
Whitton, W. I. The corrosion of iron covered by a thin film of neutral salt solution 927
Wilson, G. L. See *Bell, R. P.*, and
Winsor, P. A. Hydrotropy, solubilization and related emulsification processes. Part IX 762
Winter, E. R. S. Diffusion properties of gases. Part III: The diffusion and thermal diffusion coefficients for isotopic gases and gas mixtures . 81
—— See *Whalley, E.*, and
Wolstenholme, G. A., and **Schulman, J. H.** Metal-monolayer interactions in aqueous systems. Part I: The interaction of monolayers of long-chain polar compounds with metal ions in the underlying solution . 475
—— Part II: The adsorption of long-chain compounds from aqueous solutions on to evaporated metal films 488
Woodward, P. See *Pollard, F. H.*, and
Wyatt, R. M. H. See *Pollard, F. H.*, and

INDEX TO REVIEWS—VOLUME 46, 1950

PAGE

Advances in Catalysis and Related Subjects. Vol. II 883

Bachman, G. Bryant. Organic Chemistry 1012

Barkas, W. W. The swelling of wood under stress 1122

Bladergroen, Dr. W. Physikalische Chemie in Medizin und Biologie . . 1124

Bone Char, Proceedings of the Technical Session on. Edited by Victor R. Deitz 612

Bremner, H. Terrestrial radio waves. 1010

Cosmic Radiation. Symposium promoted by Colston Research Society and University of Bristol, 1948 516

Echanges Isotopiques et Structure Moleculaire. (C. N. R. S.) . . 1009

Frontiers in Chemistry. Vol. VII. Recent advances in analytical chemistry. Edited by R. E. Burk and O. Grummitt 698

Garlick, G. F. J. Luminescent materials 163

Gmelins Handbuch der Anorganischen Chemie. System-Nummer 10: Selenium. Teil B: Die Verbindungen des Selens, 1949 . . 516

Guggenheim, E. A. Thermodynamics—an advance treatment for chemists and physicists 515

Haemoglobin. A symposium based on a conference held at Cambridge in June 1948 in memory of Sir Joseph Barcroft. Ed. J. F. W. Roughton and J. C. Kendrew 700

Hermans, P. H. Physics and Chemistry of Cellulose Fibres . . . 79

Marshall, C. Edmund. The colloid chemistry of the silicate minerals . . 161

Martin, Thomas. Faraday's discovery of electro-magnetic induction . . 795

Matz, Werner. Die Thermodynamik des Warme- und Stoffaustausches in der Verfahrenstechnik 611

Miall, S., and Miall, L. M. A new dictionary of chemistry (2nd edn.) . . 78

Miall, L. M. See *Miall, S.*, and

Partington, J. R. An advanced treatise on physical chemistry. (Fundamental principles, the properties of gases), Vol. I 161

Physical Society. Reports on progress in physics. Vol. XII, 1948-49. . 164

Prigogine, I. Etude thermodynamique des phénomènes irréversibles . . 882

Pringsheim, P. Fluorescence and phosphorescence 1122

Rice, F. O., and Teller, E. The structure of matter 80

Sexton, W. A. Chemical constitution and biological activity . . . 697

Sidgwick, N. V. The chemical elements and their compounds. Vol. I and II 1121

Smithells, Colin J. Metals reference book 427

Starling, Sydney G. Electricity in the service of man 699

Staudinger, Prof. Dr. Hermann. Makromolekulare chemie und biologie . 1011

Table of Sines and Cosines to Fifteen Decimal Places at Hundredths of a Degree. U.S. Department of Commerce. National Bureau of Standards. Applied Mathematics Series 5 883

Teller, E. See *Rice, F. O.* and

Theilheimer, W. Synthetic methods of organic chemistry. Vol. II . . 1123

Treloar, L. R. G. The physics of rubber elasticity 1011

Tromp, S. W. Psychical physics 259

Wyckoff, Ralph W. G. Electron microscopy. Technique and application . 796

MINUTES OF THE 44TH ANNUAL GENERAL MEETING

Held on Tuesday, 26th September, 1950, at The University, Cambridge.

The President, Sir John Lennard-Jones, F.R.S., was in the Chair.

1. The Minutes of the 43rd Annual General Meeting, which had already been circulated, were taken as read and were confirmed.

2. ANNUAL REPORT AND STATEMENT OF ACCOUNTS.

   In presenting the Annual Report for the year 1949 (Session 1949-50), the President reminded the Members that at the last Annual General Meeting it had been resolved that a new class of membership be instituted, that of Honorary Life Membership, as some way of recognizing the eminence of some of its distinguished members. The actual election had been left to Council, and it was now his pleasure to announce that the following members had been selected for this honour : Prof. C. H. Desch, Prof. F. G. Donnan, Prof. Allan Ferguson and Prof M. W. Travers. This was received with acclamation.

   The President drew the attention of Members to a printing error on page 3 of the Report, where it appeared that the Chemical Society was a committee of the Royal Society.

   MARLOW MEMORIAL FUND. The sum of £106 had been collected, and a memorial cup had been purchased to be used at the Guest Night Dinners in memory of Mr. Marlow and other benefactors of the Society. They were greatly indebted to Prof. Garner for giving expert advice on the purchase of an antique silver cup of George II period.

   FINANCE. The Hon. Treasurer was unfortunately prevented by illness from making his report personally, but in his absence, the President said, he would like to take the opportunity of saying how extremely fortunate the Society had been in having secured Dr. O. H. Wansbrough-Jones as Hon. Treasurer. Various changes had been made in the Society's investments, following expert advice which, he was glad to say, would also be available in the future. It had unfortunately been necessary to increase the subscription from the beginning of the year, but it was an inevitable step and had made a great difference in the Society's finances.

   The Annual Report and Statement of Accounts were then unanimously adopted

3. ELECTION OF COUNCIL.

   The Officers were elected to take office on the list of October 1950 as follows :

President

SIR CHARLES GOODEVE, O.B.E., D.Sc., F.R.S.

Vice-Presidents who have held the Office of President

PROF. M. W. TRAVERS, D.Sc., F.R.S.
PROF. E. K. RIDEAL, M.B.E., D.Sc., F.R.S.
PROF. G. W. GARNER, C.B.E., D.Sc., F.R.S.
PROF. A. J. ALLMAND, D.Sc., F.R.S.
PROF. SIR JOHN LENNARD-JONES, K.B.E., D.Sc., F.R.S.

Vice-Presidents

PROF. C. E. H. BAWN, PH.D.	PROF. M. G. EVANS, D SC., F.R.S.
SIR ALFRED EGERTON, M.A., D.SC., F.R.S.	G. GEE, SC.D.
	G. S. HARTLEY, SC.D
PROF. H. J. EMELÉUS, D.SC., F.R.S.	PROF. H. W. MELVILLE, PH.D., F.R.S.

Hon. Treasurer

DR. O. H. WANSBROUGH-JONES, C.B., O B.E., M.A , PH.D.

The next item on the agenda was the election of Ordinary Members of Council, and the President explained that there were four vacancies, for which six nominations had been received. On the motion of Prof. A. R. Ubbelohde, seconded by Dr. K. G. Denbigh, a postal ballot was demanded, Dr. D. W. G. Style and Dr. W. C. Price being appointed as scrutators The results of the ballot would be announced in the *Transactions* for November.

4. AUDITORS.
The Society's auditors, Messrs. Knox, Cropper & Co , were re-appointed.

5. Prof. Garner proposed a vote of thanks to Sir John Lennard-Jones on his retirement from the Presidency of the Society during the years 1948-49 and 1949-50. There had been many difficult problems to solve during his two years of office and he had been unsparing of his time and efforts. The Society owed him a debt of gratitude for his help and guidance during the past two years. This was received with acclamation.

This concluded the business of the meeting.